GTT-Technologies

Slagatlas

HotVeGas

Version 15

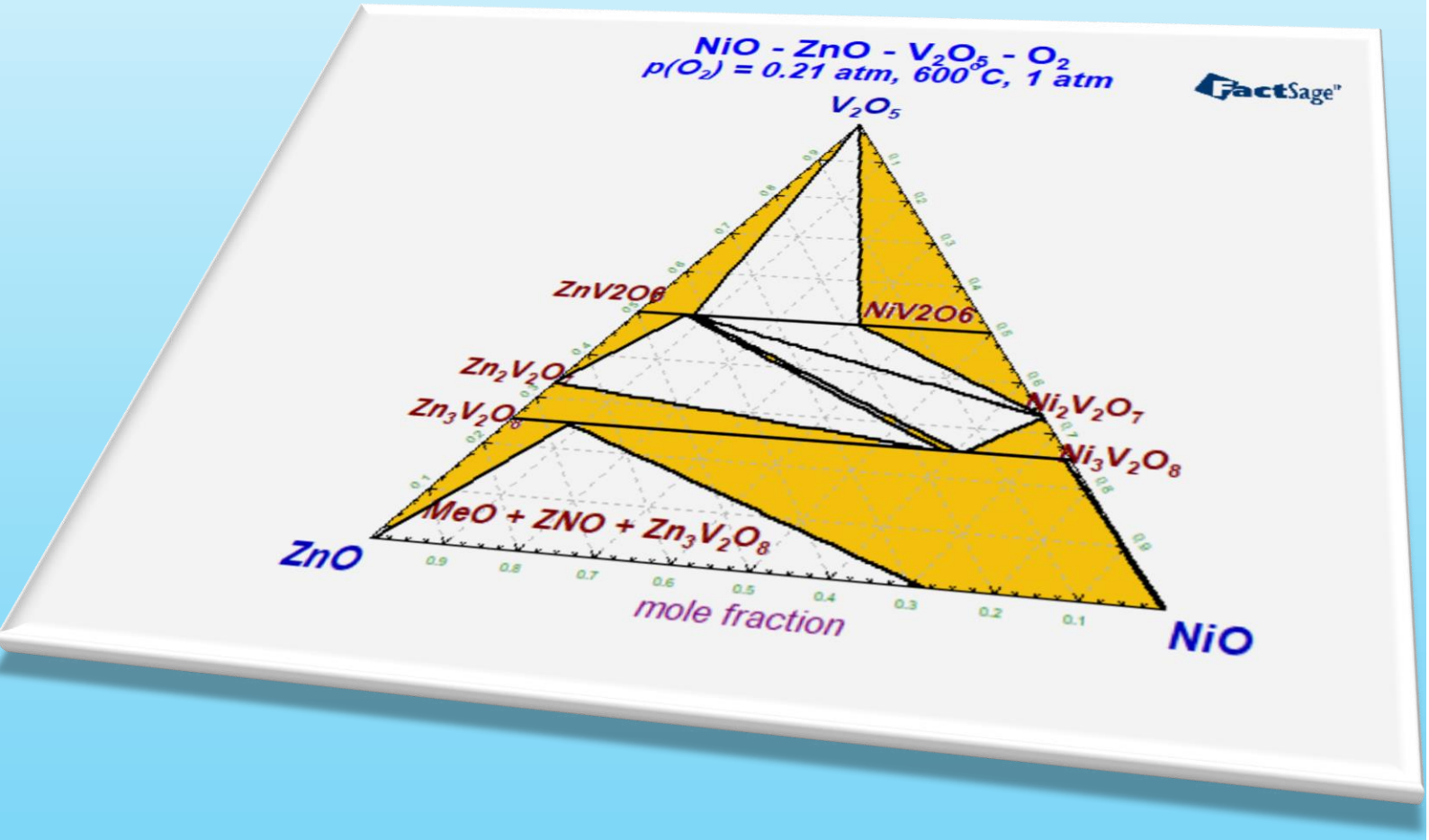

Introduction

The present collection of phase diagrams for binary, ternary and quaternary sub-systems among the components Al_2O_3-Al_2S_3-CaO-CaF_2-CaS-Cr_2O_3-CrS-FeO-Fe_2O_3-FeS-MgO-MgS-MnO-Mn_2O_3-MnS-K_2O-K_2S-Na_2O-Na_2S-NiO-NiS-P_2O_5-SO_3-SiO_2-SrO-TiO_2-Ti_2O_3-V_2O_3-V_2O_5-ZnO is the result of thermochemical data assessments (Gibbs energies) for the respective phases in each system. These assessments have been carried out in the framework of the HotVeGas project (parts I, II and III) in close collaboration with Forschungszentrum Jülich. The phase diagrams have all been calculated using the method of Zero Fraction Line tracing, in other words, there are no “hand drawn optimal” lines through a set of experimental data points as is still customary in parts the literature. Nevertheless, where available experimental information has been plotted into the calculated diagram. This enables the reader to check at any time on the quality of the data assessments. It must be mentioned especially at this point, that in some cases phase diagrams which have been produced in the classical “by hand” way have been used for controlling the thermochemical data assessments. These cases can usually be recognized from the fact that the “experimental points” follow the lines which have been draw by the classical phase diagram assessor.

The phase diagrams have been reproduced both in terms of mole fraction and weight-percentage axes in order to improve their usability both by thermochemists and users in industrial practice. The experimental points have been plotted into the diagram which uses the axes variables of the respective publication. For binary systems with Fe, which should in general be treated as proper ternary systems, one diagram each for a low (i.e. contact with Fe) and for a high oxygen potential ($p(O_2)$=0.21atm) has been generated. Note, that the diagram for low oxygen potential does not represent a fixed oxygen potential but holds for the Fe-activity fixed to be 1. The oxygen potential thus varies with temperature in these diagrams. The solid phases of Fe dissolve only negligible amounts of O, but the metallic melt takes up increasing amounts of oxygen with increase of temperature. This behavior has been incorporated in the present database. Also, the resulting miscibility gap between liquid metal and liquid oxide (slag) has been fully incorporated. Thus, some of the diagrams with Fe show in the range of the liquid phases a phase boundary (miscibility gap) which is not given in most of the literature phase diagrams.

For ternary systems, in order to give an overview as complete as possible, in most cases a set of phase diagrams has been generated. Isothermal sections for two standard temperatures (500°C and 1000°C) as well as for a temperature just below the liquidus surface are given. In addition, the liquidus surface itself is given, with isotherms in °C. For ternary diagrams too, mole fractions and weight-percentages are used as

axes variables. Also, the experimental information is inserted into the diagrams according to the above-mentioned method.

For quaternary systems, it would be necessary to use a three-dimensional composition tetrahedron. Temperature would then have to be treated as a constant parameter. Since perspective drawings of three-dimensional relationships do not lead to diagrams which can be used for quantitative reading it was decided to use for the present work two-dimensional representations, i.e. sections through the respective quaternary system. Also, it must be said that only a limited number of experimental data is available which permits to show comparisons between calculated and experimental phase boundaries. Thus, the number of quaternary phase diagrams in this Slag Atlas (Schlackenatlas) is at present still limited.

Finally, it should be noted that the HotVeGas project is still ongoing, at present in phase III. While the project is still running there will be changes and additions in the thermochemical database. These will be incorporated into the Slag Atlas in the form of new or modified diagrams in due time. It is thus recommended to keep close contact with GTT if you are interested in the most recent state of the database and the phase diagrams.

Your GTT-Team, August 2019

Einleitung

Die vorliegende Sammlung von Phasendiagrammen zu binären, ternären und quaternären Teilsystemen mit den Komponenten Al_2O_3-Al_2S_3-CaO-CaF_2-CaS-Cr_2O_3-CrS-FeO-Fe_2O_3-FeS-MgO-MgS-MnO-Mn_2O_3-MnS-K_2O-K_2S-Na_2O-Na_2S-NiO-NiS-P_2O_5-SO_3-SiO_2-SrO-TiO_2-Ti_2O_3-V_2O_3-V_2O_5-ZnO ist entstanden als Ergebnis von thermochemischen Datenauswertungen (Gibbs-Energien) zu den einzelnen Phasen in den jeweiligen Systemen. Diese Arbeiten wurden im Rahmen des HotVeGas-Projektes (Teile I, II und III) in enger Zusammenarbeit mit dem Forschungszentrum Jülich durchgeführt. Die Phasendiagramme sind allesamt mit Hilfe der Methode der Zero Phase Fraction Lines berechnet worden, es gibt also keine wie in der Literatur üblichen „von Hand“ eingezeichneten „optimalen“ Linien durch einen Satz von experimentellen Punkten. Dennoch sind experimentelle Informationen, wo vorhanden, in die hier vorliegenden Diagramme mit einbezogen worden. Dadurch ist eine Qualitätskontrolle der berechneten Phasengrenzen jederzeit möglich. Es sei an dieser Stelle aber darauf hingewiesen, dass in einigen Fällen Phasendiagramme, die nach der klassischen „von Hand“-Methode ausgewertet in der Literatur vorlagen, zur Kontrolle der thermochemischen Datenauswertungen genutzt wurden. Diese Fälle sind meist daran zu erkennen, dass die „experimentellen“ Punkte genau den Linien folgen, die der ursprüngliche Phasendiagramm-Auswerter gezeichnet hatte.

Die Phasendiagramme sind zur besseren Nutzbarkeit sowohl durch Thermochemiker als auch durch Anwender aus der industriellen Praxis jeweils mit Molenbruch- und mit Gewichtsprozent-Achsen dargestellt. Die experimentellen Punkte sind jeweils in dem Bild eingetragen, das die Achsen des experimentellen Bildes trägt. Bei binären Systemen mit Eisen, die eigentlich immer als ternäre Systeme betrachtet werden müssen, wurde jeweils ein Bild mit dem hohen ($p(O_2)$=0.21 atm) und niedrigen (Kontakt mit Fe) Sauerstoffpotential berechnet. Man beachte, dass die Bilder niedriges Sauerstoffpotential NICHT für ein fixiertes O-Potential, sondern für die Eisenaktivität 1 erzeugt wurden. Das Sauerstoffpotential variiert also in diesen Bildern. Dazu kommt, dass diese Bilder speziell für hohe Temperaturen oft anders sind als aus der Literatur gewohnt. Die festen Phasen des Eisens lösen vernachlässigbar wenig Sauerstoff, die Schmelze nimmt aber bei steigender Temperatur immer mehr Sauerstoff auf (siehe dazu auch das Fe-O Phasendiagramm). Die entstehende Mischungslücke zwischen der Fe-Metallschmelze und der Oxidschmelze (Schlacke) ist in den vorliegenden Berechnungen vollständig berücksichtigt worden. Daher enthalten einige der Phasendiagramme im Bereich der flüssigen Phase eine Phasengrenze (Mischungslücke), die man aus den bisherigen Veröffentlichungen nicht kennt.

Für die ternären Systeme ist jeweils ein Satz von Bildern erstellt worden, um einen möglichst vollständigen Überblick zu erhalten. So sind die isothermen Schnitte für zwei Standardtemperaturen (500°C und 1000°C) sowie eine Temperatur gerade unterhalb der Liquidusfläche gegeben. Dazu wird auch die Liquidusfläche selbst mit den Isothermen (Temperatur in °C) gegeben. Auch für die ternären Diagramme gilt, dass

sowohl Molenbruch als auch Gewichtsprozent für die Achsen verwendet werden. Auch die experimentellen Punkte sind nach dem schon oben erklärten Verfahren in die Bilder eingetragen worden.

Für quaternäre Systeme benötigt man eigentlich eine dreidimensionale Darstellung in einem Zusammensetzungstetraeder. Dabei wäre dann die Temperatur bereits eine Konstante. Da perspektivische Darstellungen von dreidimensionalen Zusammenhängen aber nicht quantitativ ablesbar sind, werden hier zweidimensionale Darstellungen, also Schnitte durch die quaternären Systeme dargestellt. Es gibt nur eine begrenzte Anzahl von experimentellen Informationen, die es erlauben, Vergleiche zwischen gerechneten und experimentellen Phasengrenzen vorzunehmen. Daher ist die Anzahl der quaternären Phasendiagramme in diesem Schlackenatlas im Augenblick noch eingeschränkt.

Es bleibt anzumerken, dass dieser HotVeGas-Schlackenatlas ein fortlaufendes Projekt ist. Solange es läuft, werden sich Änderungen, speziell aber Ergänzungen ergeben. Diese werden von Zeit zu Zeit in den Atlas ein gepflegt. Rücksprache mit den Editoren bei GTT bezüglich des jeweils neuesten Stands wird daher empfohlen.

Das GTT-Team, August 2019

Content

New systems in GTOX database 45

The solid solution phases, their description and modelling 46

Description of oxide melt 55

Description of liquid metal 57

Stoichiometric phases 58

Binary systems: 62

Al-O, Mole fraction 63

Al-O, Weight percent 64

Al-O, Mole fraction with isobars 65

Al-O2, Temperature vs. log P(O2) diagram 66

Al2O3-Al2S3, Mole fraction compared with experimental data 67

Al2O3-Al2S3, Weight percent 68

Al2O3-CaF2, Mole fraction 69

Al2O3-CaF2, Weight percent 70

Al2O3-CaO, Mole fraction 71

Al2O3-CaO, Weight percent compared with experimental data 72

Al2O3-CaS, Mole fraction 73

Al2O3-CaS, Weight percent 74

Al2O3-Cr2O3-O2, Mole fraction 75

Al2O3-Cr2O3-O2, Weight percent compared with experimental data 76

AlO1,5-FeO-Fe, Mole fraction 77

AlO1,5-FeO-Fe, Weight percent compared with experimental data 78

Al2O3-Fe2O3-O2, Mole fraction 79

Al2O3-Fe2O3-O2, Weight percent compared with experimental data 80

Al2O3-K2O, Mole fraction compared with experimental data 81

Al2O3-K2O, Weight percent 82

Al2O3-MgO, Mole fraction compared with experimental data 83

Al2O3-MgO, Weight percent 84

Al2O3-Mn2O3-O2, Mole fraction 85

Al2O3-Mn2O3-O2, Weight percent 86

Al2O3-MnO-Mn, Mole fraction compared with experimental data 87

Al2O3-MnO-Mn, Weight percent 88

Al2O3-Na2O, Mole fraction compared with experimental data 89

Al2O3-Na2O, Weight percent 90

Al2O3-NiO, Mole fraction 91
Al2O3-NiO, Weight percent 92
Al2O3-P2O5, Mole fraction 93
Al2O3-P2O5, Weight percent, compared with experimental data 94
Al2O3-SO3, Mole fraction 95
Al2O3-SO3, Weight percent 96
Al2O3-SiO2, Mole fraction in Kelvin compared with experimental data 97
Al2O3-SiO2, Weight percent 98
Al2O3-SrO, Mole fraction compared with experimental data 99
Al2O3-SrO, Weight percent 100
Al2O3-TiO2, Mole fraction 101
Al2O3-TiO2, Weight percent compared with experimental data 102
Al2O3-Ti2O3, Mole fraction 103
Al2O3-Ti2O3, Weight percent 104
Al2O3-Ti2O3, Mole fraction, P(O2)=10^{-1}5 bar compared with experimental data 105
Al2O3-V2O3, Mole fraction 106
Al2O3-V2O3, Weight percent 108
Al2O3-V2O5-O2, Mole fraction compared with experimental data 109
Al2O3-V2O5-O2, Weight percent 110
Al2O3-ZnO, Mole fraction compared with experimental data 111
Al2O3-ZnO, Weight percent 112
Al2S3-K2S, Mole fraction compared with experimental data 113
Al2S3-K2S, Weight percent 114
Al2S3-Na2S, Mole fraction compared with experimental data 115
Al2S3-Na2S, Weight percent 116
Al2(SO4)3-Na2SO4, Mole fraction compared with experimental data 117
Al2(SO4)3-Na2SO4, Weight percent 118
CaF2-CaO, Mole fraction 120
CaF2-CaO, Weight percent compared with experimental data 121
CaF2-Fe2O3-O2, Mole fraction 122
CaF2-Fe2O3-O2, Weight percent 123
CaF2-FeO-Fe, Mole fraction 124
CaF2-FeO-Fe, Weight percent 125
CaF2-MgO, Mole fraction 126
CaF2-MgO, Weight percent 127

CaF2-SiO2, Mole fraction 128
CaF2-SiO2, Weight percent compared with experimental data 129
Ca-O, Mole fraction 130
Ca-O, Weight percent 131
Ca-O, Mole fraction with isobars 132
Ca-O2, Temperature vs. log P(O2) diagram 133
CaO-CaS, Mole fraction 134
CaO-CaS, Weight percent 135
CaO-Cr2O3-O2, Mole fraction 136
CaO-Cr2O3-O2 Weight percent compared with experimental data 137
CaO-Cr2O3-O2 Weight percent compared with experimental data, $P(O_2)$=0.001 atm 138
CaO-CrO-Cr, Mole fraction compared with experimental data 139
CaO-CrO-Cr Weight percent 140
CaO-Fe2O3-O2, Mole fraction 141
CaO-Fe2O3-O2, Weight percent compared with experimental data 142
CaO-FeO-Fe, Mole fraction 143
CaO-FeO-Fe, Weight percent compared with experimental data 144
CaO-K2O, Mole fraction 145
CaO-K2O, Weight percent 146
CaO-Mn2O3-O2, Mole fraction compared with experimental data 147
CaO-Mn2O3-O2, Weight percent 148
CaO-Mn2O3-O2, P(O2)=1 atm Mole fraction compared with experimental data 149
CaO-Mn2O3-O2, P(O2)=1 atm Weight percent 150
CaO-MnO-Mn, Mole fraction 151
CaO-MnO-Mn, Weight percent compared with experimental data 152
CaO-MgO, Mole fraction 153
CaO-MgO, Weight percent compared with experimental data 154
CaO-Na2O, Mole fraction 155
CaO-Na2O, Weight percent 156
CaO-NiO, Mole fraction 157
CaO-NiO, Weight percent 158
CaO-P2O5, Mole fraction 159
CaO-P2O5, Weight percent compared with experimental data 160
CaO-SiO2, Mole fraction compared with experimental data 161
CaO-SiO2, Weight percent 162

CaO-SO3, Mole fraction compared with experimental data 163
CaO-SO3, Weight percent 164
CaO-SrO, Mole fraction 165
CaO-SrO, Weight percent 166
CaO-TiO2, Mole fraction 167
CaO-TiO2, Weight percent compared with experimental data 168
CaO-V2O3, Mole fraction 169
CaO-V2O3, Weight percent compared with experimental data 170
CaO-V2O5-O2, Mole fraction 171
CaO-V2O5-O2, Weight percent compared with experimental data 172
CaO-ZnO, Mole fraction 173
CaO-ZnO, Weight percent 174
Ca-S, Mole fraction 175
Ca-S, Weight percent 176
CaS-FeS, Mole fraction 177
CaS-FeS, Weight percent compared with experimental data 178
CaS-MgS, , Mole fraction compared with experimental data 179
CaS-MgS, Weight percent 180
CaS-MnS, Mole fraction compared with experimental data 181
CaS-MnS, Weight percent 182
CaS-SiO2, Mole fraction 183
CaS-SiO2, Weight percent 184
CaSO4-K2SO4, Mole fraction 185
CaSO4-K2SO4, Weight percent compared with experimental data 186
Weight percent compared with experimental data 187
CaSO4-MgSO4, Mole fraction 188
CaSO4-MgSO4, Weight percent compared with experimental data 189
CaSO4-Na2SO4, Mole fraction compared with experimental data 190
CaSO4-Na2SO4, Weight percent 191
Cr-O, Mole fraction compared with experimental data 192
Cr-O, Weight percent 193
Cr-O, Mole fraction with isobars 194
Cr-O2, Temperature vx. log P(O2) diagram 195
Cr2O3-Fe2O3-O2, Mole fraction compared with experimental data 196
Cr2O3-Fe2O3-O2, Weight percent 197

Cr2O3-K2O-O2, Mole fraction 198
Cr2O3-K2O-O2, Weight percent 199
Cr-K-O, Mole fraction 650°C 200
Cr-K-O, Mole fraction 380°C 201
Cr-K-O, Mole fraction Isopleth K2Cr2O7-K2CrO4 202
Cr2O3-MgO-O2, Mole fraction 203
Cr2O3-MgO-O2, Weight percent compared with experimental data 204
Cr2O3-MnO-CO-CO2, Mole fraction 205
Cr2O3-MnO-CO-CO2, Weight percent compared with experimental data 206
Cr2O3-Mn2O3-O2, Mole fraction compared with experimental data 207
Cr2O3-Mn2O3-O2, Weight percent 208
Cr2O3-Na2O-O2, Mole fraction 209
Cr2O3-Na2O-O2, Weight percent 210
Cr-Na-O, Mole fraction 380°C 211
Cr2O3-P2O5-O2, Mole fraction compared with experimental data 212
Cr2O3-P2O5-O2, Weight percent 213
Cr2O3-SiO2-O2, Mole fraction 214
Cr2O3-SiO2-O2, Weight percent 215
Cr2O3-V2O5-O2, Mole fraction compared with experimental data 216
Cr2O3-V2O5-O2, Weight percent 217
Cr2O3-ZnO-O2, Mole fraction 218
Cr2O3-ZnO-O2, Weight percent 219
CrO-SiO2-Cr, Mole fraction 220
CrO-SiO2-Cr, Weight percent compared with experimental data 221
Cr-S, Mole fraction compared with experimental data 222
Cr-S, Weight percent 223
Fe-O, Mole fraction in Kelvin compared with experimental data 224
Fe-O, Weight percent in Kelvin 225
Fe-O, Mole fraction with isobars 226
Fe-O2, Temeprature vs. log P(O2) diagram 227
Fe-S, Mole fraction compared with experimental data 228
Fe-S, Weight percent 229
FeO-FeS, Mole fraction 230
FeO-FeS, Weight percent 231
FeO-K2O-Fe, Mole fraction 232

FeO-K2O-Fe, Weight percent 233
Fe2O3-K2O-O2, Mole fraction compared with experimental data 234
Fe2O3-K2O-O2, Weight percent 235
FeO-MgO-Fe, Mole fraction compared with experimental data 236
FeO-MgO-Fe, Weight percent 237
Fe2O3-MgO-O2, Mole fraction 238
Fe2O3-MgO-O2, Weight percent compared with experimental data 239
FeO-MnO-Fe, Mole fraction 240
FeO-MnO-Fe, Weight percent compared with experimental data 241
Fe2O3-Mn2O3-O2, Mole fraction 242
Fe2O3-Mn2O3-O2, Weight percent compared with experimental data 243
Fe3O4-Mn3O4-O2, Mole fraction 244
Fe3O4-Mn3O4-O2, Weight percent 245
FeO-Na2O-Fe, Mole fraction 246
FeO-Na2O-Fe Weight percent compared with experimental data 247
Fe2O3-Na2O-O2, Mole fraction 249
Fe2O3-Na2O-O2, Weight percent compared with experimental data 250
FeO-NiO-Fe, Mole fraction 251
FeO-NiO-Fe, Weight percent compared with experimental data 252
Fe2O3-NiO-O2, Mole fraction compared with experimental data 253
Fe2O3-NiO-O2, Weight percent 254
FeO-P2O5-Fe, Mole fraction 255
FeO-P2O5-Fe, Weight percent compared with experimental data 256
Fe2O3-P2O5-O2, Mole fraction compared with experimental data 257
Fe2O3-P2O5-O2, Weight percent 258
Fe2O3-SO3, Mole fraction 259
Fe2O3-SO3, Weight percent 260
FeO-SiO2-Fe, Mole fraction 261
FeO-SiO2-Fe, Weight percent compared with experimental data 262
FeO-SiO2-Fe, Weight percent 263
Fe2O3-SiO2-O2, Mole fraction 264
Fe2O3-SiO2-O2, Weight percent compared with experimental data 265
FeO-SrO, Mole fraction compared with experimental data 266
FeO-SrO, Weight percent 267
Fe2O3-SrO-O2, Mole fraction 268

Fe2O3-SrO-O2, Weight percent compared with experimental data 269
FeO-TiO2-Fe, Mole fraction 270
FeO-TiO2-Fe, Weight percent 271
Fe3O4-TiO2-O2, Mole fraction 272
Fe3O4-TiO2-O2, Weight percent compared with experimental data 273
FeO-V2O3-Fe, Mole fraction 274
FeO-V2O3-Fe, Weight percent compared with experimental data 275
Fe2O3-V2O5-O2, Mole fraction compared with experimental data 276
Fe2O3-V2O5-O2, Weight percent 277
FeO-ZnO-Fe, Mole fraction 278
FeO-ZnO-Fe, Weight percent compared with experimental data 279
Fe2O3-ZnO-O2, Mole fraction compared with experimental data 280
Fe2O3-ZnO-O2, Weight percent 281
FeS-MgS, Mole fraction compared with experimental data 282
FeS-MgS, Weight percent 283
FeS-MnS, Mole fraction compared with experimental data 284
FeS-MnS, Weight percent 285
K2O-MgO, Mole fraction 286
K2O-MgO, Weight percent 287
K2O-Mn2O3-O2, Mole fraction 288
K2O-Mn2O3-O2, Weight percent 289
K2O-Na2O, Mole fraction 290
K2O-Na2O, Weight percent 291
K2O-P2O5, Mole fraction compared with experimental data 292
K2O-P2O5, Weight percent 293
K2O-SiO2, Mole fraction compared with experimental data 294
K2O-SiO2, Weight percent 295
K2O-TiO2, Mole fraction compared with experimental data 296
K2O-TiO2, Weight percent 297
K2O-V2O5, Mole fraction compared with experimental data 298
K2O-V2O5, Weight percent 299
K2S-K2SO4, Mole fraction compared with experimental data 301
K2S-K2SO4, Weight percent 302
K2S-Na2S, Mole fraction compared with experimental data 303
K2S-Na2S, Weight percent 304

K2SO4-MgSO4, Mole fraction *305*
K2SO4-MgSO4, Weight percent compared with experimental data *306*
K2SO4-Na2SO4, Mole fraction compared with experimental data *307*
K2SO4-Na2SO4, Weight percent *308*
K2S2O7-Na2S2O7, Mole fraction compared with experimental data *309*
K2S2O7-Na2S2O7, Weight percent *310*
Mg-O, Mole fraction with isobars *311*
Mg-O, Temperature vs. log P(O2) diagram *312*
MgO-MgS, Mole fraction *313*
MgO-MgS, Weight percent *314*
MgO-Na2O, Mole fraction *315*
MgO-Na2O, Weight percent *316*
MgO-P2O5, Mole fraction *317*
MgO-P2O5, Weight percent compared with experimental data *318*
MgO-TiO2, Mole fraction compared with experimental data *319*
MgO-TiO2, Weight percent *320*
MgO-SO3, Mole fraction *321*
MgO-SO3, Weight percent *322*
Mg-S, Mole fraction *323*
Mg-S, Weight percent *324*
MgO-Mn2O3-O2, Mole fraction *325*
MgO-Mn2O3-O2, Weight percent compared with experimental data *326*
MgO-MnO-Mn, Mole fraction *327*
MgO-MnO-Mn, Weight percent compared with experimental data *328*
MgO-SiO2, Mole fraction compared with experimental data *329*
MgO-SiO2, Weight percent compared with experimental data *330*
MgO-SrO, Mole fraction compared with experimental data *331*
MgO-SrO, Weight percent *332*
MgO-TiO2, Mole fraction compared with experimental data *333*
MgO-TiO2, Weight percent *334*
MgO-V2O3, Mole fraction *335*
MgO-V2O3, Weight percent compared with experimental data *336*
MgO-V2O5-O2, Mole fraction compared with experimental data *337*
MgO-V2O5-O2, Weight percent *338*
MgO-ZnO, Mole fraction *339*

MgO-ZnO, Weight percent *340*
Mg-S, Mole fraction *341*
Mg-S, Weight percent *342*
MgS-MnS, Mole fraction *343*
MgS-MnS, Weight percent *344*
MgSO4-Na2SO4 , Mole fraction compared with experimental data *345*
MgSO4-Na2SO4 , Weight percent *346*
Mn-O, Mole fraction *347*
Mn-O, Weight percent *348*
Mn-O, Mole fraction with isobars *348*
Mn-O2, Temperature vs. log P(O2) diagram *350*
MnO-MnS, Mole fraction *351*
MnO-MnS, Weight percent compared with experimental data *352*
Mn2O3-Na2O-O2, Mole fraction *353*
Mn2O3-Na2O-O2, Weight percent *354*
MnO-P2O5-Mn, Mole fraction compared with experimental data *355*
MnO-P2O5-Mn, Weight percent *356*
Mn2O3-P2O5-O2, Mole fraction compared with experimental data *357*
Mn2O3-P2O5-O2, Weight percent *358*
MnO-SiO2-Mn, Mole fraction *359*
MnO-SiO2-Mn, Weight percent compared with experimental data *360*
MnO-TiO2-Mn, Mole fraction compared with experimental data *361*
MnO-TiO2-Mn, Weight percent *362*
MnO-TiO2, Mole fraction, P(CO)/P(CO2)=1, compared with experimental data *363*
Mn2O3-TiO2-O2, Mole fraction, *364*
Mn2O3-TiO2-O2, Weight percent, *365*
Mn2O3-SiO2-O2, Mole fraction *366*
Mn2O3-SiO2-O2, Weight percent compared with experimental data *367*
MnO-V2O5-Mn, Mole fraction compared with experimental data *368*
MnO-V2O5-Mn, Weight percent *369*
MnO-V2O3, CO/CO2=1, Mole fraction compared with experimental data *370*
MnO-ZnO, Mole fraction compared with experimental data *371*
MnO-ZnO, Weight percent *372*
Mn2O3-ZnO-O2, Mole fraction *373*
Mn2O3-ZnO-O2, Weight percent *374*

Mn-S, Mole fraction 375
Mn-S, Weight percent 376
MnS-SiO2, Mole fraction 377
MnS-SiO2, Weight percent 378
Na2O-P2O5, Mole fraction compared with experimental data 379
Na2O-P2O5, Weight percent 380
Na2O-SiO2, Mole fraction compared with experimental data 381
Na2O-SiO2, Weight percent 382
Na2O-TiO2, Mole fraction compared with experimental data 383
Na2O-TiO2, Weight percent 384
Na2O-V2O5, Mole fraction compared with experimental data 385
Na2O-V2O5, Weight percent 386
Na2SO4-NiSO4, Mole fraction compared with experimental data 388
Na2SO4-NiSO4, Weight percent 389
Na2S-Na2SO4, Mole fraction compared with experimental data 390
Na2S-Na2SO4, Weight percent 391
Ni-O, Mole fraction compared with experimental data 392
Ni-O, Weight percent 393
Ni-O, Mole fraction with isobars 394
Ni-O, Temperature vs. log P(O2) diagram 395
Ni-S, Mole fraction compared with experimental data 396
Ni-S, Weight percent 397
NiO-MgO, Mole fraction compared with experimental data 398
NiO-MgO, Weight percent 399
NiO-NiS, Mole fraction 400
NiO-NiS, Weight fraction 401
NiO-SO3, Mole fraction compared with experimental data 402
NiO-SO3, Weight fraction 403
NiO-SrO, Mole fraction compared with experimental data 404
NiO-SrO, Weight percent 405
NiO-TiO2, Mole fraction 406
NiO-TiO2, Weight percent compared with experimental data 407
NiO-V2O5-O2, Mole fraction compared with experimental data 408
NiO-V2O5-o2, Weight percent 409
NiO-SiO2, Mole fraction compared with experimental data 410

NiO-SiO2, Weight percent *411*
NiO-ZnO, Mole fraction compared with experimental data *412*
NiO-ZnO, Weight percent *413*
O-Sr, Mole fraction compared with experimental data *414*
O-Sr, Weight percent *415*
O-Sr, Mole fraction with isobars *417*
O2-Sr, Temperature vs. log P(O2) diagram *418*
O-Ti, Mole fraction compared with experimental data *419*
O-Ti, Weight percent *420*
O-Ti, Mole fraction with isobars *421*
O2-Ti, Temperature vs. log P(O2) diagram *422*
O-V, Mole fraction *423*
O-V, Weight percent *424*
O-V, Mole fraction with isobars *425*
O2-V, Temperature vs. log P(O2) diagram *426*
O-Zn, Mole fraction *427*
O-Zn, Weight percent *428*
O-Zn, Mole fraction with isobars *429*
O2-Zn, Temperature vs. log P(O2) diagram *430*
P2O5-SiO2, Mole fraction compared with experimental data *431*
P2O5-SiO2, Weight percent *432*
P2O5-SrO, Mole fraction compared with experimental data *433*
P2O5-SrO, Weight percent *435*
P2O5-TiO2, Mole fraction *436*
P2O5-TiO2, Weight percent compared with experimental data *437*
P2O5-ZnO, Mole fraction *439*
P2O5-ZnO, Weight percent compared with experimental data *440*
SiO2-TiO2, Mole fraction compared with experimental data *441*
SiO2-TiO2, Weight percent *442*
SiO2-V2O3, Mole fraction *443*
SiO2-V2O3, Weight percent compared with experimental data *444*
SiO2-V2O5-O2, Mole fraction *445*
SiO2-V2O5-O2, Weight percent compared with experimental data *446*
SiO2-ZnO, Mole fraction compared with experimental data *447*
SiO2-ZnO, Weight percent *448*

SrO-SiO2, Mole fraction compared with experimental data *450*
SrO-SiO2, Weight percent *451*
SrO-V2O5-O2, Mole fraction compared with experimental data *452*
SrO-V2O5-O2, Weight percent *453*
SrO-ZnO, Mole fraction *454*
SrO-ZnO, Weight percent *455*
TiO2-VO2, Mole fraction compared with experimental data *456*
TiO2-VO2, Weight percent *457*
TiO2-V2O3, Mole fraction *458*
TiO2-V2O3, Wight percent compared with experimental data *459*
TiO2-V2O5-O2, Mole fraction compared with experimental data *460*
TiO2-V2O5-O2, Weight percent *461*
TiO2-ZnO, Mole fraction compared with experimental data *462*
TiO2-ZnO, Weight percent *463*
V2O5-ZnO-O2, Mole fraction compared with experimental data *464*
V2O5-ZnO-O2, Weight percent *465*
Ternary systems: *466*
Al-O-Ti *467*
Al-O-Ti, Mole fraction 1100°C 467
Al-O-Ti, Mole fraction 1400°C 468
Al2O3-CaF2-CaO *469*
Al2O3-CaF2-CaO, Mole fraction, 1100°C 469
Al2O3-CaF2-CaO, Mole fraction, 1600°C 470
Al2O3-CaF2-CaO, Mole fraction, 1800°C 471
Al2O3-CaF2-CaO, Weight percent, Isopleth C11A7F-C3A3F 472
Al2O3-CaF2-CaO, Weight percent, Isopleth C3A3F-CaAl4O7 473
Al2O3-CaF2-CaO, Weight percent, Isopleth C3A3F-CaAl4O7 474
Al2O3-CaF2-CaO, Mole fraction Liquidussurface 475
Al2O3-CaF2-CaO, Weight percent Liquidussurface 476
Al2O3-CaF2-CaO, Invariant equilibria on the liquidus surface 477
Al2O3-CaO-CaS, *478*
Al2O3-CaO-CaS, Weight percent, 1500°C 478
Al2O3-CaO-CaS, Weight percent, 1550°C 479
Al2O3-CaO-CaS, Weight percent, 1600°C 480
Al2O3-CaO-CaS, Mole fraction, Liquidussurface 481

Al2O3-CaO-CaS, Weight percent, Liquidussurface 482
Al2O3-CaO-CaS, Invariant equilibria on the liquidus surface 483
Al2O3-CaF2-MgO, *484*
Al2O3-CaF2-MgO, Mole fraction, Liquidussurface 484
Al2O3-CaF2-MgO, Weight percent, Liquidussurface 485
Al2O3-CaF2-MgO, Invariant equilibria on the liquidus surface 486
Al2O3-CaF2-SiO2 *487*
Al2O3-CaF2-SiO2, Weight percent, Liquidus lines at 1380°C and 1460°C 487
Al2O3-CaF2-SiO2, Weight percent 1425°C 488
Al2O3-CaF2-SiO2, Weight percent 1500°C, 1600°C and 1700°C 489
Al2O3-CaF2-SiO2, Mole fraction, Liquidussurface 490
Al2O3-CaF2-SiO2, Weight percent, Liquidussurface 491
Al2O3-CaF2-SiO2, Invariant equilibria on the liquidus surface 492
Al2O3-CaO-Cr2O3 *493*
Al2O3-CaO-Cr2O3, Mole fraction, Isopleth CaAl2O4-CaCr2O4 493
Al2CaO4-CaO-CaCr2O4, Mole fraction, Liquidussurface 494
Al2CaO4-CaO-CaCr2O4, Weight percent, Liquidussurface 495
Al2CaO4-CaO-CaCr2O4, Invariant equilibria on the liquidus surface 496
Al2CaO4-CaCr2O4-CaO-O2, Weight percent 1100°C 497
Al2CaO4-CaCr2O4-CaO-O2, Weight percent 1300°C 498
Al2O3-CaO-CaCrO4-O2, Weight percent 1300°C 499
Al2O3-CaO-CaCrO4, Mole fraction, Liquidussurface 500
Al2O3-CaO-CaCrO4, Weight percent, Liquidussurface 501
Al2O3-CaO-CaCrO4, Invariant equilibria on the liquidus surface 502
Al2O3-CaO-Fe2O3 *503*
Al2O3-CaO-Fe2O3, Weight percent 1145 C° 503
Al2O3-CaO-Fe2O3, Weight percent 1330°C 504
Al2O3-CaO-Fe2O3, Mole fraction Liquidussurface 505
Al2O3-CaO-Fe2O3, Weight percent Liquidussurface 506
Al2O3-CaO-Fe2O3, Invariant equilibria on the liquidus surface 507
Al2O3-CaO-K2O *508*
Al2O3-CaO-K2O, Mole fraction 1100°C 508
Isopleth KAlO2-CaAl2O4 (proposed calculation) 509
Al2O3-CaO-K2O, Mole fraction Liquidussurface 510
Al2O3-CaO-K2O, Weight percent compared with experimental data Liquidussurface 511

Al2O3-CaO-K2O, Invariant equilibria on the liquidus surface 512
Al2O3-CaO-MgO, *513*
Al2O3-CaO-MgO, Mole fraction 500 C° 513
Al2O3-CaO-MgO, Mole fraction 1000°C 514
Al2O3-CaO-MgO, Mole fraction 1320 C° kurz unterhalb Liquidussurface 515
Al2O3-CaO-MgO, Mole fraction 1600 C° compared with experimental data 516
Al2O3-CaO-MgO, Mole fraction in Kelvin x(Al2O3)=0.5 compared with experimental data 517
Al2O3-CaO-MgO, Mole fraction Liquidussurface 518
Al2O3-CaO-MgO, Weight percent Liquidussurface 519
Al2O3-CaO-MgO, Invariant equilibria on the liquidus surface 520
Al2O3-CaO-Na2O *521*
Al2O3-CaO-Na2O, Mole fraction 1200°C 521
Al2O3-CaO-Na2O, Mole fraction 1400°C 522
Isopleth Na2Al2O4-CaAl2O4, Mole fraction compared with experimental data 523
Al2O3-CaO-Na2O, Weight percent kurz unterhalb Liquidussurface 524
Al2O3-CaO-Na2O, Mole fraction Liquidussurface 525
Al2O3-CaO-Na2O, Weight percent Liquidussurface 526
Al2O3-CaO-Na2O, Invariant equilibria on the liquidus surface 527
Al2O3-CaO-P2O5, *528*
Al2O3-CaO-P2O5, Weight percent 475°C 528
Weight percent, Isopleth Al2P6O18-Ca2P2O7 compared with experimental data 529
Al2O3-CaO-P2O5, Weight percent, Isopleth Al2P6O18-CaP2O6 530
Al2O3-CaO-P2O5, Weight percent, Isopleth Al2P2O8-Ca2P2O7 531
Al2O3-CaO-P2O5, Weight percent, Isopleth Al2P2O8-Ca3P2O8 532
Al2O3-CaO-P2O5, Mole fraction Liquidussurface 533
Al2O3-CaO-P2O5, Weight percent Liquidussurface 534
Al2O3-CaO-P2O5, Invariant equilibria on the liquidus surface 535
Al2O3-CaO-SiO2, *536*
Al2O3-CaO-SiO2, Mole fraction 500C°, 536
Al2O3-CaO-SiO2, Mole fraction 1000 537
Al2O3-CaO-SiO2, Mole fraction 1185C° kurz unterhalb Liquidussurface 538
Al2O3-CaO-SiO2, Weight percent 1400 C° compared with experimental data 539
Al2O3-CaO-SiO2, Weight percent 1500 C° compared with experimental data 540
Al2O3-CaO-SiO2, Weight percent 1600 C° compared with experimental data 541
Al2O3-CaO-SiO2, Mole fraction x(Al2O3)=0,25 compared with experimental data 542

Al2O3-CaO-SiO2, Weight percent Al2CaSi2O8-SiO2 compared with experimental data 543
Al2O3-CaO-SiO2, Weight percent Ca2SiO4-Ca12Al14O33 compared with experimental data 544
Al2O3-CaO-SiO2, Mole fraction Liquidussurface 545
Al2O3-CaO-SiO2, Weight percent Liquidussurface 546
Al2O3-CaO-SiO2, Invariant equilibria on the liquidus surface 547
Al2O3-CaO-ZnO, *548*
Al2O3-CaO-ZnO, Mole fraction 1000°C 548
Al2O3-CaO-ZnO, Mole fraction Liquidussurface 549
Al2O3-CaO-ZnO, Weight percent Liquidussurface 550
Al2O3-CaO-ZnO, Invariant equilibria on the liquidus surface 551
Al2O3-Cr2O3-Fe2O3, *552*
Al2O3-Cr2O3-Fe2O3, Weight percent 1250°C 552
Al2O3-Cr2O3-Fe2O3, Weight percent 1350°C 553
Al2O3-Cr2O3-Fe2O3, Weight percent 1500°C 554
Al2O3-Cr2O3-MgO, *555*
Al2O3-Cr2O3-MgO, Mole fraction 1700°C 555
Al2O3-Cr2O3-SiO2 *556*
Al2O3-Cr2O3-SiO2, Weight percent 1550°C 556
Al2O3-Cr2O3-SiO2, Weight percent 1700°C 557
Al2O3-Cr2O3-SiO2, Weight percent 1800°C 558
Al2O3-Cr2O3-SiO2, Mole fraction Liquidussurface 559
Al2O3-Cr2O3-SiO2, Weight percent Liquidussurface compared with experimental data 560
Al2O3-Fe2O3-K2O *561*
Al2O3-Fe2O3-K2O, Isopleth FeKO2-AlKO2 561
Al2O3-Fe2O3-MgO, *562*
Al2O3-Fe2O3-MgO, Mole fraction 1250°C 562
Al2O3-Fe2O3-MgO, Weight percent 1600°C 563
Al2O3-Fe2O3-MgO, Mole fraction Liquidussurface 564
Al2O3-Fe2O3-Mn2O3 *565*
Al2O3-Fe2O3-Mn2O3, Mole fraction, 700°C 565
Al2O3-Fe2O3-Mn2O3, Mole fraction, 1500°C 566
Al2O3-Fe2O3-Mn2O3, Mole fraction, Isopleth Al2FeO4-Al2MnO4 567
Al2O3-Fe2O3-Na2O *568*
Al2O3-Fe2O3-Na2O, Isopleth FeNaO2-AlNaO2 compared with experimental data 568
Al2O3-Fe2O3-SiO2, *569*

Al2O3-Fe2O3-SiO2, Weight percent 1000°C 569
Al2O3-Fe2O3-SiO2, Weight percent 1600°C 570
Al2O3-Fe2O3-SiO2, Weight percent Solidusfläche 571
Al2O3-Fe2O3-SiO2, Mole fraction Liquidussurface 572
Al2O3-Fe2O3-SiO2, Weight percent Liquidussurface 573
Al2O3-Fe2O3-SiO2, Invariant equilibria on the liquidus surface 574
Al2O3-Fe2O3-TiO2, *575*
Al2O3-Fe2O3-TiO2, Weight percent 1000°C 575
Al2O3-Fe2O3-TiO2, Weight percent 1300°C 576
Al2O3-FeO-MnO, *577*
Al2O3-FeO-MnO, Weight percent, Liquid lines at 1550, 1600 and 1650°C 577
Al2O3-FeO-SiO2, *578*
Al2O3-FeO-SiO2, Weight percent 1000°C 578
Al2O3-FeO-SiO2, Weight percent 1700°C 579
Al2O3-FeO-SiO2, Mole fraction Liquidussurface 580
Al2O3-FeO-SiO2, Weight percent Liquidussurface 581
Al2O3-FeO-SiO2, Invariant equilibria on the liquidus surface 582
Al2O3-FeO-TiO2, *583*
Al2O3-FeO-TiO2, Weight percent 1000°C 583
Al2O3-FeO-TiO2, Weight percent 1300°C 584
Al2O3-FeO-TiO2, Mole fraction, Liquidus surface 585
Al2O3-FeO-TiO2, Weight percent, Liquidus surface 586
Al2O3-FeO-TiO2, Invariant equilibria on the liquidus surface 587
Al2O3-FeO-V2O3, *588*
Al2O3-FeO-V2O3, Mole fraction 600°C 588
Al2O3-FeO-V2O3, Mole fraction 1000°C 589
Al2O3-FeO-V2O3, Mole fraction 1500°C 590
Al2O3-Fe2O3-V2O5, *591*
Al2O3-Fe2O3-V2O5, Mole fraction 600°C 591
Al2O3-Fe2O3-V2O5, Mole fraction, Liquidus surface 592
Al2O3-Fe2O3-V2O5, Weight percent, Liquidus surface 593
Al2O3-Fe2O3-V2O5, Invariant equilibria on the liquidus surface 594
Al2O3-K2O-MgO, *595*
Al2O3-K2O-MgO, Mole fraction 1400°C 595
Al2O3-K2O-MgO, Mole fraction Liquidussurface 596

Al2O3-K2O-MgO, Weight percent Liquidussurface 597
Al2O3-K2O-MgO, Invariant equilibria on the liquidus surface 598
Al2O3-K2O-Na2O, *599*
Al2O3-K2O-Na2O, Mole fraction 700°C (proposed calculation) 599
Al2O3-K2O-Na2O, Mole fraction 1000C° (proposed calculation) 600
Al2O3-K2O-Na2O, Isopleth AlKO2-AlNaO2 (proposed calculation) 601
Al2O3-K2O-Na2O, Mole fraction Liquidussurface (proposed calculation) 602
Al2O3-K2O-Na2O, Weight percent Liquidussurface (proposed calculation) 603
Al2O3-K2O-Na2O, Invariant equilibria on the liquidus surface 604
Al2O3-K2O-SiO2, *605*
Al2O3-K2O-SiO2, Mole fraction 645°C 605
Al2O3-K2O-SiO2, Mole fraction 1000C° kurz unterhalb Liquidussurface 606
Al2O3-K2O-SiO2, Weight percent KAlO2-SiO2 compared with experimental data 607
Al2O3-K2O-SiO2, Weight percent K2Si2O5-AlKSi2O6 compared with experimental data 608
Al2O3-K2O-SiO2, Weight percent K16SiO2-Al6Si2O13 compared with experimental data 609
Al2O3-K2O-SiO2, Weight percent KAlSi3O8-K2Si4O9 compared with experimental data 610
Al2O3-K2O-SiO2, Weight percent KAlSi2O6-Al2O3 611
Al2O3-K2O-SiO2, Weight percent KAlSiO4-K2Si2O5 612
Al2O3-K2O-SiO2, Mole fraction Liquidussurface 613
Al2O3-K2O-SiO2, Weight percent Liquidussurface compared with experimental data 614
Al2O3-K2O-SiO2, Invariant equilibria on the liquidus surface 615
Al2O3-MgO-Na2O, *616*
Al2O3-MgO-Na2O, Mole fraction 1500C° 616
Al2O3-MgO-Na2O, Mole fraction 1600C° 617
Al2O3-MgO-Na2O, Mole fraction 1700°C, compared with experimental data 618
Al2O3-MgO-Na2O, Mole fraction Liquidussurface 619
Al2O3-MgO-Na2O, Weight percent Liquidussurface 620
Al2O3-MgO-Na2O, Invariant equilibria on the liquidus surface 621
Al2O3-MgO-P2O5, *622*
Al2O3-MgO-P2O5, Mole fraction 1200°C 622
Al2O3-MgO-P2O5, Mole fraction, Isopleth Mg(PO3)2-Al(PO3)3 623
Al2O3-MgO-P2O5, Mole fraction, Liquidussurface 624
Al2O3-MgO-P2O5, Weight percent, Liquidussurface 625
Al2O3-MgO-P2O5, Invariant equilibria on the liquidus surface 626
Al2O3-MgO-SiO2, *627*

Al2O3-MgO-SiO2, Mole fraction 500C° 627
Al2O3-MgO-SiO2, Mole fraction 1000C° 628
Al2O3-MgO-SiO2, Weight percent 1350 C° compared with experimental data 629
Al2O3-MgO-SiO2, Mole fraction 1380C° kurz unterhalb Liquidussurface 630
Al2O3-MgO-SiO2, Weight percent 1450 C° compared with experimental data 631
Al2O3-MgO-SiO2, Weight percent Al4Mg2Si5O18-SiO2 compared with experimental data 632
Al2O3-MgO-SiO2, Mole fraction Liquidussurface 633
Al2O3-MgO-SiO2, Weight percent Liquidussurface 634
Al2O3-MgO-SiO2, Invariant equilibria on the liquidus surface 635
Al2O3-MgO-TiO2, *636*
Al2O3-MgO-TiO2, Weight percent 1000C° 636
Al2O3-MgO-TiO2, Weight percent 1100C° 637
Al2O3-MgO-TiO2, Weight percent 1300C° 638
Al2O3-MgO-TiO2, Weight percent 1400C° 639
Al2O3-MgO-TiO2, Weight percent 1550C° 640
Al2O3-MgO-TiO2, Isopleth Al2MgO4-Mg2TiO4, Mole fraction compared with experimental data 641
Al2O3-MgO-TiO2, Isopleth Al2TiO5-MgTi2O5, Mole fraction compared with experimental data .. 642
Al2O3-MgO-TiO2, Mole fraction Liquidussurface 643
Al2O3-MgO-TiO2, Weight percent Liquidussurface 644
Al2O3-MgO-TiO2, Invariant equilibria on the liquidus surface 645
Al2O3-MnO-MnS, *646*
Al2O3-MnO-MnS, Weight percent, 646
Al2O3-MnO-MnS, , Weight percent, Co-saturated compositions at various temperatures 647
Al2O3-MnO-MnS, Mole fraction Liquidussurface 648
Al2O3-MnO-MnS, Weight percent, Liquidussurface 649
Al2O3-MnO-MnS, Invariant equilibria on the liquidus surface 650
Al2O3-MnO-SiO2, *651*
Al2O3-MnO-SiO2, Mole fraction 800°C 651
Al2O3-MnO-SiO2, Mole fraction 1550°C 652
Al2O3-MnO-SiO2, Weight percent, Liquid lines compared with experimental data 653
Al2O3-MnO-SiO2, Mole fraction Liquidussurface 654
Al2O3-MnO-SiO2, Weight percent Liquidussurface 655
Al2O3-MnO-SiO2, Invariant equilibria on the liquidus surface 656
Al2O3-Na2O-SO3, *657*
Al2O3-Na2O-SO3, Mole fraction, Liquidussurface 657

Al2O3-Na2O-SO3, Weight percent, Liquidussurface 658
Al2O3-Na2O-SO3, Invariant equilibria on the liquidus surface 659
Al2O3-Na2O-SiO2, *660*
Al2O3-Na2O-SiO2, Mole fraction kurz unterhalb Liquidussurface 660
Al2O3-Na2O-SiO2, Mole fraction 1000C° 661
Al2O3-Na2O-SiO2, Weight percent in K NaAlSi3O8-Al2O3 compared with experimental data 662
Al2O3-Na2O-SiO2, Mole fraction in Kelvin AlNaO2-SiO2 compared with experimental data 663
Al2O3-Na2O-SiO2, Weight percent Na2Si2O5-AlNaSiO4 664
Al2O3-Na2O-SiO2, Weight percent Al2O3-AlNaSiO4 665
Al2O3-Na2O-SiO2, Weight percent Na2SiO3-AlNaSiO4 666
Al2O3-Na2O-SiO2, Mole fraction Liquidussurface 667
Al2O3-Na2O-SiO2, Weight percent Liquidussurface compared with experimental data 668
Al2O3-Na2O-SiO2, Invariant equilibria on the liquidus surface 669
Al2O3-Na2O-V2O5, *670*
Al2O3-Na2O-V2O5, Mole fraction 500°C 670
Al2O3-Na2O-V2O5, Mole fraction, Isopleth Al_2O_3-$NaVO_3$ 671
Al2O3-Na2O-V2O5, Mole fraction , Isopleth AlVO4-NaVO3 672
Al2O3-Na2O-V2O5, Mole fraction , Liquidus surface 673
Al2O3-Na2O-V2O5, Weight percent, Liquidussurface 674
Al2O3-Na2O-V2O5, Invariant equilibria on the liquidus surface 675
Al2O3-NiO-SiO2, *676*
Al2O3-NiO-SiO2, Mole fraction, Isopleth NiAl2O4-SiO2 676
Al2O3-NiO-SiO2, Mole fraction, Isopleth NiAl2O4-Ni2SiO4 677
Al2O3-NiO-SiO2, Mole fraction, Liquidus surface 678
Al2O3-NiO-SiO2, Weight percent, Liquidus surface 679
Al2O3-NiO-SiO2, Invariant equilibria on the liquidus surface 680
Al2O3-P2O5-SiO2, *681*
Al2O3-P2O5-SiO2, Mole fraction, Isopleth AlPO4-SiO2 compared with experimental data 681
Al2O3-P2O5-SiO2, Mole fraction Liquidussurface 682
Al2O3-P2O5-SiO2, Weight percent, Liquidussurface 683
Al2O3-P2O5-SiO2, Invariant equilibria on the liquidus surface 684
Al2O3-P2O5-ZnO, *685*
Al2O3-P2O5-ZnO, Mole fraction, 500°C000°C 685
Al2O3-P2O5-ZnO, Mole fraction, 1000°C000°C 686
Al2O3-P2O5-ZnO, Mole fraction, Liquidusfläche 687

Al2O3-P2O5-ZnO, Weight percent, Liquidusfläche 688
Al2O3-P2O5-ZnO, Invariant equilibria on the liquidus surface 689
Al2O3-SiO2-TiO2, *690*
Al2O3-SiO2-TiO2, Weight fraction, Isopleth section Al2TiO5-SiO2000°C 690
Al2O3-SiO2-TiO2, Weight fraction, 1800°C°C 691
Al2O3-SiO2-TiO2, Mole fraction, Liquidus surface 692
Al2O3-SiO2-TiO2, Weight percent, Liquidus surface 693
Al2O3-SiO2-TiO2, Invariant equilibria on the liquidus surface 694
Al2O3-SiO2-V2O5, *695*
Al2O3-SiO2-V2O5, Mole fraction, 600°C 695
Al2O3-SiO2-V2O5, Mole fraction, 1200°C 696
Al2O3-SiO2-V2O5, Mole fraction, Liquidus surface 697
Al2O3-SiO2-V2O5, Weight percent, Liquidussurface 698
Al2O3-SiO2-V2O5, Invariant equilibria on the liquidus surface 699
Al2O3-SiO2-ZnO, *700*
Al2O3-SiO2-ZnO, Mole fraction, 500°C 700
Al2O3-SiO2-ZnO, Mole fraction, Liquidussurface 701
Al2O3-SiO2-ZnO, Weight percent, Liquidussurface compared with experimental datacom0 702
Al2O3-SiO2-ZnO, Invariant equilibria on the liquidus surface 703
CaF2-CaO-MgO, , *704*
CaF2-CaO-MgO, Mole fraction, Liquidussurface 1000°C 704
CaF2-CaO-MgO, Weight percent, Liquidussurface 1000°C 705
CaF2-CaO-MgO, Invariant equilibria on the liquidus surface 706
CaF2-CaO-SiO2, *707*
CaF2-CaO-SiO2, Mole fraction 1060°C 707
CaF2-CaO-SiO2, Weight percent, Isopleth Cuspidine-CaF2 708
CaF2-CaO-SiO2, Weight percent, Isopleth CaSiO3-CaF2 709
CaF2-CaO-SiO2, Weight percent, Isopleth Ca2SiO4-CaF2 710
CaF2-CaO-SiO2 Weight percent,, Isopleth Ca3SiO5-CaF2 711
CaF2-CaO-SiO2 Mole fraction, Liquidussurface 712
CaF2-CaO-SiO2 Weight percent, Liquidussurface 713
CaF2-CaO-SiO2, Invariant equilibria on the liquidus surface 714
CaO-CaS-SiO *715*
CaO-CaS-SiO2, Weight percent 1500°C 715
CaO-CaS-SiO2, Weight percent 1550°C 716

CaO-CaS-SiO2, Weight percent 1600°C 717
CaO-CaS-SiO2, Mole fraction, Liquidussurface 718
CaO-CaS-SiO2, Weight percent, Liquidussurface 719
CaO-CaS-SiO2, Invariant equilibria on the liquidus surface 720
CaO-Cr2O3-CrO, *721*
CaO-Cr2O3-CrO, Mole fraction 1000°C 721
CaO-Cr2O3-Fe2O3, *722*
CaO-Cr2O3-Fe2O3, Mole fraction CaCr2O4-CaFe2O4-O2 722
CaO-Cr2O3-SiO2, *723*
CaO-Cr2O3-SiO2, Weight percent CaSiO3-Cr2O3 an der Luft 723
CaO-CrO-SiO2, *724*
CaO-CrO-SiO2, Mole fraction 1290°C 724
CaO-CrO-SiO2, Mole fraction Liquidussurface 725
CaO-CrO-SiO2, Weight percent Liquidussurface 726
CaO-CrO-SiO2, Invariant equilibria on the liquidus surface 727
CaO-Fe2O3-FeO, *728*
CaO-Fe2O3-FeO, Weight percent Liquidus lines at 1200° and 1300°C 728
CaO-Fe2O3-FeO, Weight percent 1300°C 729
CaO-Fe2O3-FeO, Weight percent 1450°C 730
CaO-Fe2O3-FeO, Weight percent 1550°C 731
CaO-Fe2O3-FeO, Mole fraction Liquidussurface 732
CaO-Fe2O3-FeO, Weight percent Liquidussurface 733
CaO-Fe2O3-FeO, Invariant equilibria on the liquidus surface 734
CaO-Fe2O3-MgO, *735*
CaO-Fe2O3-MgO, Weight percent 1500°C 735
CaO-Fe2O3-MgO, Weight percent 1500°C $P(O_2)=10^{-9}$ bar 736
CaO-Fe2O3-MgO, Mole fraction Liquidussurface 737
CaO-Fe2O3-MgO, Weight percent Liquidussurface 738
CaO-Fe2O3-MgO, Invariant equilibria on the liquidus surface 739
CaO-FeO-MgO, *740*
CaO-FeO-MgO, Weight percent 1600°C 740
CaO-FeO-MnO, *741*
CaO-FeO-MnO, Weight percent 1150°C 741
CaO-FeO-MnO, Weight percent 1350°C 742
CaO-FeO-MnO, Liquid lines 743

CaO-FeO-P2O5, *744*
CaO-FeO-P2O5, Weight percent, Isothermal section at 1600°C 744
CaO-FeO-P2O5, Weight percent, Isopleth section at Ca3P2O8-FeO 745
CaO-FeO-SiO2, *746*
CaO-FeO-SiO2, Weight percent in Kelvin Ca2SiO4-Fe2SiO4 compared with experimental data 746
CaO-FeO-SiO2, Weight percent CaSiO3-FeSiO3 compared with experimental data 747
Weight percent CaSiO3-FeO-Fe compared with experimental data 748
Weight percent Ca2SiO4-FeO-Fe compared with experimental data 749
Weight percent 1600°C compared with experimental data 750
CaO-FeO-SiO2, Weight percent Liquiduslines 1200°C, 1300°C, 1400°C, 1650°C 751
CaO-FeO-SiO2, Mole fraction Liquidussurface 752
CaO-FeO-SiO2, Weight percent, Liquidussurface compared with experimental data 753
CaO-FeO-SiO2, Invariant equilibria on the liquidus surface 754
CaO-Fe2O3-SiO2, *755*
CaO-Fe2O3-SiO2, Weight percent CaSiO3-Ca2Fe2O5 compared with experimental data 755
CaO-Fe2O3-SiO2, Mole fraction Liquidussurface 756
CaO-Fe2O3-SiO2, Weight percent, Liquidussurface compared with experimental data 757
CaO-Fe2O3-SiO2, Invariant equilibria on the liquidus surface 758
CaO-Fe2O3-TiO2, *759*
CaO-Fe2O3-TiO2, Weight percent CaTiO3-Ca2Fe2O5 compared with experimental data 759
CaO-Fe2O3-TiO2, Weight percent CaTiO3-Ca2Fe2O5 760
CaO-Fe2O3-TiO2, Mole fraction, Liquidus surface 761
CaO-Fe2O3-TiO2, Weight percent CaTiO3-Ca2Fe2O5 762
CaO-Fe2O3-TiO2, Invariant equilibria on the liquidus surface 763
CaO-Fe2O3-V2O5, *764*
CaO-Fe2O3-V2O5, Mole fraction, 600°C 764
CaO-K2O-P2O5, *765*
CaO-K2O-P2O5, Ternary phases 765
CaO-K2O-P2O5, Weight percent, Isopleth CaP2O6-KPO3 766
CaO-K2O-P2O5, , Weight percent, Isopleth Ca2P2O7-CaKP3O9 767
CaO-K2O-P2O5, Weight percent, Isopleth Ca2P2O7-K4P2O7 768
CaO-K2O-P2O5, Weight percent, Isopleth K2CaP2O7-KPO3 769
CaO-K2O-P2O5, Weight percent, Isopleth K2CaP2O7-K5P3O10 770
CaO-K2O-P2O5, Weight percent, Isopleth CaKPO4-CaK2P2O7 771
CaO-K2O-P2O5, Weight percent, Isopleth CaKPO4-K4P2O7 772

CaO-K2O-P2O5, Weight percent, Isopleth CaO-CaKPO4 773
CaO-K2O-P2O5, Weight percent, Isopleth CaO-K4CaP2O8 774
CaO-K2O-P2O5, Weight percent, Isopleth CaO-K3PO4 775
CaO-K2O-P2O5, Weight percent, 500°C 776
CaO-K2O-P2O5, Mole fraction, 1000°C 777
CaO-K2O-P2O5, Mole fraction, Liquidussurface 778
CaO-K2O-P2O5, Weight percent, Liquidussurface 779
CaO-K2O-P2O5, Invariant equilibria on the liquidus surface 780
CaO-K2O-SiO2, *781*
CaO-K2O-SiO2, Ternäre Phasen 781
CaO-K2O-SiO2, Weight percent Isopleth CaSi2O5-K2Si2O5 782
CaO-K2O-SiO2, Isopleth CaSiO3-K2Si4O9 compared with experimental data 783
CaO-K2O-SiO2, Weight percent Isopleth K2Si2O5-K2CaSiO4 compared with experimental data 784
CaO-K2O-SiO2, Isopleth CaSiO3-K2SiO3 compared with experimental data 785
CaO-K2O-SiO2, Mole fraction 300°C 786
CaO-K2O-SiO2, Mole fraction Liquidussurface 787
CaO-K2O-SiO2, Weight percent Liquidussurface 788
CaO-K2O-SiO2, Invariant equilibria on the liquidus surface 789
CaO-MgO-MnO, *790*
CaO-MgO-MnO, Mole fraction 1500C° 790
CaO-MgO-P2O5, *791*
CaO-MgO-P2O5, Mole fraction 1000°C 791
CaO-MgO-P2O5, Weight percent, Isopleth Ca3P2O8-Mg3P2O8 792
CaO-MgO-SiO2, *793*
CaO-MgO-SiO2, Mole fraction 500C° 793
CaO-MgO-SiO2, Mole fraction 1000C° 794
CaO-MgO-SiO2, Mole fraction 1315C° kurz unterhalb Liquidussurface 795
CaO-MgO-SiO2, Mole fraction CaSiO3-MgSiO3 (CS-MS) compared with experimental data 796
CaO-MgO-SiO2, Mole fraction in Kelvin Ca2SiO4-Mg2SiO4 compared with experimental data 797
CaO-MgO-SiO2, Mole fraction Ca2SiO4-Akermanite compared with experimental data 798
CaO-MgO-SiO2, Weight percent CaSiO3-Akermanite compared with experimental data 799
CaO-MgO-SiO2, Mole fraction Liquidussurface 800
CaO-MgO-SiO2, Weight percent Liquidussurface 801
CaO-MgO-SiO2, Invariant equilibria on the liquidus surface 802
CaO-MgO-TiO2, *803*

CaO-MgO-TiO2, Mole fraction, 1300°C 803
CaO-MgO-TiO2, Mole fraction, Liquidus surface 804
CaO-MgO-TiO2, Weight percent, Liquidus surface 805
CaO-MgO-TiO2, Invariant equilibria on the liquidus surface 806
CaO-MgO-V2O5, *807*
CaO-MgO-V2O5, Mole fraction, 550°C 807
CaO-MgO-V2O5, Mole fraction, Isopleth section CaV2O7-Mg2V2O7 808
CaO-MgO-V2O5, Mole fraction, Liquidus surface 809
CaO-MgO-V2O5, Weight percent, Liquidus surface 810
CaO-MgO-V2O5, Invariant equilibria on the liquidus surface 811
CaO-MnO-SiO2, *812*
CaO-MnO-SiO2, Weight percent, Metasilicate section CaSiO3-MnSiO3 812
CaO-MnO-SiO2, Weight percent, Orthosilicate section Ca2SiO4-Mn2SiO4 813
CaO-MnO-SiO2, Mole fraction, Liquidussurface 814
CaO-MnO-SiO2, Weight percent, Liquidussurface 815
CaO-MnO-SiO2, Invariant equilibria on the liquidus surface 816
CaO-Na2O-P2O5, *817*
CaO-Na2O-P2O5, Ternary phases 817
CaO-Na2O-P2O5, Mole fraction, Isopleth CaP2O6-NaPO3 818
CaO-Na2O-P2O5, Mole fraction, Isopleth CaO-Na3PO4 819
CaO-Na2O-P2O5, Weight percent, Isopleth Na4CaP2O8-Na4P2O7 820
CaO-Na2O-P2O5, Weight percent, Isopleth NaCaPO4-Na4CaP2O8 821
CaO-Na2O-P2O5, Mole fraction, 300°C 822
CaO-Na2O-P2O5, Mole fraction, 1000°C 823
CaO-Na2O-P2O5, Mole fraction, Liquidussurface 824
CaO-Na2O-P2O5, Weight percent, Liquidussurface 825
CaO-Na2O-P2O5, Invariant equilibria on the liquidus surface 826
CaO-Na2O-SiO2, *827*
CaO-Na2O-SiO2, Ternäre Phasen 827
CaO-Na2O-SiO2, Weight percent 600°C 828
CaO-Na2O-SiO2, Weight percent 770°C 829
CaO-Na2O-SiO2, Orthosilicate isopleth compared with experimental data 830
CaO-Na2O-SiO2, Mole fraction Liquidussurface 831
CaO-Na2O-SiO2, Weight percent, Liquidussurface compared with experimental data 832
CaO-Na2O-SiO2, Invariant equilibria on the liquidus surface 833

CaO-NiO-SiO2, *834*
CaO-NiO-SiO2, Mole fraction 1340°C 834
CaO-NiO-SiO2, Mole fraction 1390°C 835
CaO-NiO-SiO2, Mole fraction 1475°C 836
CaO-NiO-SiO2, Mole fraction 1550°C 837
CaO-NiO-SiO2, Mole fraction, Liquiudussurface 838
CaO-NiO-SiO2, Weight percent, Liquiudussurface 839
CaO-NiO-SiO2, Invariant equilibria on the liquidus surface 840
CaO-NiO-V2O5, *841*
CaO-NiO-V2O5, Mole fraction 600°C 841
CaO-NiO-V2O5, Mole fraction , Isopleth Ca2V2O7-NiO-O2 842
CaO-NiO-V2O5, Mole fraction , Liquidus surface 843
CaO-NiO-V2O5, Weight percent , Liquidus surface 844
CaO-NiO-V2O5, Invariant equilibria on the liquidus surface 845
CaO-P2O5-SiO2, *846*
CaO-P2O5-SiO2, Weight percent, Isopleth Ca2SiO4-Ca3P2O8 846
CaO-P2O5-SiO2, Weight percent, 1000°C 847
CaO-P2O5-SiO2, Weight percent, 1225°C 848
CaO-P2O5-SiO2, Weight percent, 1600°C 849
CaO-P2O5-SiO2, Weight percent, Isopleth Ca3P2O8-SiO2 850
CaO-P2O5-SiO2, Weight percent, Liquidussurface in CaO-Ecke 851
CaO-P2O5-ZnO, *852*
CaO-P2O5-ZnO, Mole fraction 500°C 852
CaO-P2O5-ZnO, Mole fraction, Isopleth section Ca3P2O8-Zn3P2O8 853
CaO-P2O5-ZnO, Mole fraction, Isopleth section Ca2P2O7-Zn2P2O7 854
CaO-P2O5-ZnO, Mole fraction, Liquidussurface 855
CaO-P2O5-ZnO, Weight percent, Liquidussurface 856
CaO-P2O5-ZnO, Invariant equilibria on the liquidus surface 857
CaO-SiO2-V2O3, *858*
CaO-SiO2-V2O3, Mole fraction 1000°C 858
CaO-SiO2-V2O3, Mole fraction 1500°C 859
CaO-SiO2-V2O3, Mole fraction, liquidus surface 860
CaO-SiO2-V2O3, Weight percent, Liquidussurface 861
CaO-SiO2-V2O3, Invariant equilibria on the liquidus surface 862
CaO-SiO2-V2O5, *864*

CaO-SiO2-V2O5, Mole fraction 1500°C 864
CaO-SiO2-ZnO, *865*
CaO-SiO2-ZnO, Mole fraction 1000°C 865
CaO-SiO2-ZnO, Mole fraction Isopleth section Ca2SiO4-Zn2SiO4 866
CaO-SiO2-ZnO, Mole fraction Isopleth section CaSiO3-ZnO 867
CaO-SiO2-ZnO, Mole fraction Liquidussurface 868
CaO-SiO2-ZnO, Weight percent Liquidussurface compared with experimental data 869
CaO-SiO2-ZnO, Invariant equilibria on the liquidus surface 870
CaS-FeS-MgS, *871*
CaS-FeS-MgS, Mole fraction 700°C 871
CaS-FeS-MgS, Mole fraction 800°C 872
CaS-FeS-MgS, Mole fraction 900°C 873
CaS-FeS-MgS, Mole fraction, Liquidussurface 874
CaS-FeS-MgS, Weight percent, Liquidussurface 875
CaS-FeS-MgS, Invariant equilibria on the liquidus surface 876
CaS-FeS-MnS, *877*
CaS-FeS-MnS, Mole fraction 700°C 877
CaS-FeS-MnS, Mole fraction 800°C 878
CaS-FeS-MnS, Mole fraction 900°C 879
CaS-FeS-MnS, Mole fraction, Liquidussurface 880
CaS-FeS-MnS, Weight percent, Liquidussurface 881
CaS-MgS-MnS, *882*
CaS-MgS-MnS, Mole fraction, Isotherms 800°, 900 and 1000°C700°C 882
CaS-MgS-MnS, Mole fraction, Liquidussurface 883
CaS-MgS-MnS, Weight percent, Liquidussurface 884
CaSO4-K2SO4-MgSO4, *885*
CaSO4-K2SO4-MgSO4, Weight percent K2SO4-CaMg3S4O16 compared with experimental data 885
CaSO4-K2SO4-MgSO4, Weight percent K2Mg2S3O12-K2Ca2S3O12 886
CaSO4-K2SO4-MgSO4, Mole fraction, Liquidussurface 887
CaSO4-K2SO4-MgSO4, Weight percent, Liquidussurface compared with experimental data 888
Ca2SO4-MgSO4-K2SO4, Invariant equilibria on the liquidus surface 889
CaSO4-K2SO4-Na2SO4, *890*
CaSO4-K2SO4-Na2SO4,, Mole fraction 500°C 890
CaSO4-K2SO4-Na2SO4,, Mole fraction 700°C 891
CaSO4-K2SO4-Na2SO4,, Mole fraction, Liquidussurface 892

CaSO4-K2SO4-Na2SO4,, Weight percent, Liquidussurface 893
Ca2SO4-K2SO4-Na2SO4, Invariant equilibria on the liquidus surface 894
CaSO4-MgSO4-Na2SO4, *895*
CaSO4-MgSO4-Na2SO4, Mole fraction 500°C 895
CaSO4-MgSO4-Na2SO4, Mole fraction 700°C 896
CaSO4-MgSO4-Na2SO4, Mole fraction Liqudussurface 897
CaSO4-MgSO4-Na2SO4, Weight percent, Liqudussurface 898
Ca2SO4-MgSO4-Na2SO4, Invariant equilibria on the liquidus surface 899
Cr-Fe-S, *900*
Cr-Fe-S, Mole fraction Cr2FeS4-Cr3S4 900
Cr-Fe-S, Weight percent 600°C 901
Cr-Fe-S, Weight percent 700°C 902
Cr-Fe-S, Weight percent 950°C 903
Cr-Fe-S, Weight percent 1090°C 904
Cr-Fe-S, Weight percent 1300°C 905
Cr-Fe-S, Weight percent, isopleth section at ~50 mol% S 906
Cr-Mn-S, *907*
Cr-Mn-S, Mole fraction Cr2MnS4-Cr3S4 907
Cr-Mn-S, Mole fraction CrS-MnS 908
Cr-Mn-S, Mole fraction 800°C 909
Cr2O3-Fe2O3-FeO, *910*
Cr2O3-Fe2O3-FeO, Mole fraction 1300°C 910
Cr2O3-Fe2O3-MgO, *911*
Cr2O3-Fe2O3-MgO, Weight percent 1300°C 911
Cr2O3-Fe2O3-MgO, Weight percent 1700°C 912
Cr2O3-Fe2O3-MgO, Weight percent Liquidussurface 913
Cr2O3-Fe3O4-SiO2, *914*
Cr2O3-Fe3O4-SiO2, Weight percent 1400°C 914
Cr2O3-Fe3O4-SiO2, Weight percent 1500°C 915
Cr2O3-Fe3O4-SiO2, Weight percent 1700°C 916
Cr2O3-Fe3O4-SiO2, Weight percent 1850°C 917
Cr2O3-K2O-Na2O, *918*
Mole fraction Isopleth K2CrO4-Na2CrO4 918
Mole fraction Isopleth K2Cr2O7-Na2Cr2O7 919
Cr2O3-MgO-SiO2, *920*

Cr2O3-MgO-SiO2, Weight percent 1540°C 920
Cr2O3-MgO-SiO2, Mole fraction Liquidussurface 921
Cr2O3-MgO-SiO2, Weight percent Liquidussurface 922
Cr2O3-MgO-SiO2, Invariant equilibria on the liquidus surface 923
CrO-MgO-SiO2, *924*
CrO-MgO-SiO2, Mole fraction 1300°C 924
CrO-MgO-SiO2, Mole fraction , Liquidussurface 925
CrO-MgO-SiO2, Weight percent, Liquidussurface 926
CrO-MgO-SiO2, Invariant equilibria on the liquidus surface 927
Fe-Mn-S, *928*
Fe-Mn-S, Mole fraction 800°C 928
Fe-Mn-S, Mole fraction 1100°C 929
Fe-Mn-S, Weight fraction 1300°C 930
Fe-Mn-S, Weight fraction 1600°C 931
Fe-Mn-S, Weight fraction 1600°C, solubility of Mn and S in Fe-rich liquid 932
Fe-Mn-S, Weight fraction, isopleth section Fe/Mn=97/3 933
Fe-Mn-S, Mole fraction 1100°C, relationship between S potential and Mn fraction 934
Fe-Ni-S, *935*
Fe-Ni-S, Weight percent 550°C 935
Fe-Ni-S, Weight percent 650°C 936
Fe-Ni-S, Weight percent 900°C 937
Fe-Ni-S, Weight percent 1100°C 938
Fe-Ni-S, Weight percent, Isopleth FeS2-NiS2 939
Fe-O-S, *940*
Fe-O-S, Mole fraction, Liquidus lines at 1000°-1500°C 940
Fe-O-S, Mole fraction, 1324°C 941
Fe-O-S, Mole fraction, 1100°C 942
Fe-O-S, Mole fraction, 900°C 943
Fe-O-S, Mole fraction, 550°C 944
Fe2O3-FeO-MgO, *945*
Fe2O3-FeO-MgO, Weight percent 1300°C 945
Fe2O3-FeO-MgO, Weight percent 1400°C 946
Fe2O3-FeO-MgO, Weight percent 1500°C 947
Fe2O3-FeO-MgO, Weight percent 1600°C 948
Fe2O3-FeO-P2O5, *949*

Fe2O3-FeO-P2O5, Mole fraction 900°C 949
Fe2O3-FeO-SiO2, *951*
Fe2O3-FeO-SiO2, Weight percent 1200°C 951
Fe2O3-FeO-SiO2, Weight percent 1300°C 952
Fe2O3-FeO-SiO2, Weight percent, Liquidus lines at 1500-1650°C 953
Fe2O3-FeO-SrO, *954*
Fe2O3-FeO-SrO, Mole fraction 1000°C 954
Fe2O3-FeO-SrO, Mole fraction 1500°C 955
Fe2O3-FeO-SrO, Mole fraction, Liquidussurface 956
Fe2O3-FeO-SrO, Weight percent, Liquidussurface 957
Fe2O3-FeO-SrO, Invariant equilibria on the liquidus surface 958
Fe2O3-FeO-TiO2, *959*
Fe2O3-FeO-TiO2, Mole fraction 1300°C 959
Fe2O3-FeO-TiO2, Isopleth section FeTi2O5-Fe2TiO5, mole fraction 960
Fe2O3-FeO-TiO2, Isopleth section Fe3O4-Fe2TiO4, mole fraction 961
Fe2O3-FeO-V2O3, *962*
Fe2O3-FeO-V2O3, Mole fraction 1227°C 962
Fe2O3-Fe-V2O3, Mole fraction 1227°C 963
Fe2O3-FeO-V2O3, Mole fraction, Liquidussurface 964
Fe2O3-FeO-V2O3, Weight percent, Liquidussurface 965
Fe2O3-K2O-SiO2, *966*
Fe2O3-K2O-SiO2, Mole fraction 600°C 966
Fe2O3-K2O-SiO2, Mole fraction 850°C 967
Fe2O3-K2O-SiO2, Mole fraction, FeKO2-SiO2 compared with experimental data 968
Fe2O3-MgO-TiO2, *969*
Fe2O3-MgO-TiO2, Mole fraction, 1000°C MgO-TiO2, 969
Fe2O3-MgO-TiO2, Mole fraction, 1300°C 970
Fe2O3-Mn2O3-SiO2, *971*
Fe2O3-Mn2O3-SiO2, Mole fraction 1200°C 971
Fe2O3-Mn2O3-SiO2, Mole fraction 1400°C 972
Fe3O4-Mn3O4-SiO2-O2, Mole fraction, Liquidussurface 973
Fe3O4-Mn3O4-SiO2-O2, Weight percent, Liquidussurface 974
Fe3O4-Mn3O4-SiO2-O2, Invariant equilibria on the liquidus surface 975
Fe2O3-Na2O-SiO2, *976*
Fe2O3-Na2O-SiO2, Weight percent 700°C 976

Fe2O3-Na2O-SiO2, Weight percent 825°C 977
Fe2O3-Na2O-SiO2, Weight percent, Isopleth Acmite-Na2SiO3 978
Fe2O3-Na2O-SiO2, Weight percent, Isopleth Acmite-Na2Si2O5 979
Fe2O3-Na2O-SiO2, Weight percent, Isopleth Fe2O3-Na2Si2O5 980
Fe2O3-Na2O-SiO2, Mole fraction, Isopleth FeNaO2-SiO2 981
Fe2O3-Na2O-SiO2, Weight percent, Isopletale Schnitte mit 5Na2O Fe2O3 8SiO2 982
Fe2O3-Na2O-SiO2, Mole fraction, Liquidussurface 983
Fe2O3-Na2O-SiO2, Weight percent, Liquidussurface 984
Fe2O3-Na2O-SiO2, Weight percent, Liquidussurface Fe2O3-Na2SiO3-SiO2 985
Fe2O3-Na2O-SiO2, Invariant equilibria on the liquidus surface 986
Fe2O3-Na2O-V2O5, *987*
FeO-Na2O-V2O5, Mole fraction, Subsolidus surface 987
FeO-Na2O-V2O5, Mole fraction, Isopleth FeVO4-NaVO3 988
FeO-Na2O-V2O5, Mole fraction, Liquidus surface 989
FeO-Na2O-V2O5, Weight percent, Liquidus surface 990
Fe2O3-Na2O-V2O5, Invariant equilibria on the liquidus surface 991
FeO-MgO-SiO2, *992*
FeO-MgO-SiO2, Mole fraction 1300°C 992
FeO-MgO-SiO2, Weight percent 1450°C 993
FeO-MgO-SiO2, Weight percent 1550°C 994
FeO-MgO-SiO2, Mole fraction in Kelvin Mg2SiO4-Fe2SiO4 compared with experimental data 995
FeO-MgO-SiO2, Mole fraction in Kelvin MgSiO3-FeSiO3 compared with experimental data 996
FeO-MgO-SiO2, Mole fraction MgFe2O4-Mg2SiO4-O2 997
FeO-MgO-SiO2, , Mole fraction, Liquidussurface 998
FeO-MgO-SiO2, Weight percent, Liquidussurface compared with experimental data 999
FeO-MgO-SiO2, Invariant equilibria on the liquidus surface 1000
FeO-MgO-TiO2, *1001*
FeO-MgO-TiO2, Mole fraction, 1000°C 1001
FeO-MgO-TiO2, Weight percent 1300°C compared with experimental data 1002
FeO-MnO-P2O5, *1003*
FeO-MnO-P2O5, Weight percent, Part of liquidus surface 1003
FeO-MnO-P2O5, Mole fraction, Liquidus surface 1004
FeO-MnO-P2O5, Weight percent, Liquidus surface 1005
FeO-MnO-P2O5, Invariant equilibria on the liquidus surface 1006
FeO-MnO-SiO2, *1007*

FeO-MnO-SiO2, Weight percent, Isopleth metasilicate section FeSiO3-MnSiO3 1007
FeO-MnO-SiO2, Weight percent, Isopleth orthosilicate section Fe2SiO4-Mn2SiO4 1008
FeO-MnO-SiO2, Weight percent, 1170°C 1009
FeO-MnO-SiO2, Weight percent, 1240°C 1010
FeO-MnO-SiO2, Weight percent, 1300°C 1011
FeO-MnO-SiO2, Mole fraction, Liquidus surface 1012
FeO-MnO-SiO2, Weight percent, Liquidus surface 1013
FeO-MnO-SiO2, Invariant equilibria on the liquidus surface 1014
FeO-Na2O-SiO2, *1015*
FeO-Na2O-SiO2, Mole fraction 580°C 1015
FeO-Na2O-SiO2 Mole fraction, Isopleth FeO-Na2SiO3 1016
FeO-Na2O-SiO2 Mole fraction, Liquidussurface 1017
FeO-Na2O-SiO2 Weight percent, Liquidussurface 1018
FeO-Na2O-SiO2, Invariant equilibria on the liquidus surface 1019
FeO-SiO2-V2O3, *1020*
FeO-SiO2-V2O3, Mole fraction 1100°C 1020
FeO-SiO2-V2O3, Mole fraction, Liquidussurface 1021
FeO-SiO2-V2O3, Weight percent, Liquidussurface 1022
FeO-SiO2-V2O3, Invariant equilibria on the liquidus surface 1023
FeO-SiO2-ZnO, *1024*
FeO-SiO2-ZnO, Mole fraction 1085°C 1024
FeO-SiO2-ZnO, Mole fraction, Isopleth Fe2SiO4-Zn2SiO4-Fe 1025
FeO-SiO2-ZnO, Mole fraction, Liquidussurface 1026
FeO-SiO2-ZnO, Weight percent, Liquidussurface compared with experimental data 1027
FeO-SiO2-ZnO, Invariant equilibria on the liquidus surface 1028
FeO-TiO2-Ti2O3, *1029*
FeO-TiO2-Ti2O3, Mole fraction 1600°C 1029
FeO-TiO2-Ti2O3, Mole fraction 1500°C 1030
FeS-MgS-MnS, *1031*
FeS-MgS-MnS, Mole fraction, Isotherms at 600°, 700°, 800°, 900° and 1000°C 1031
FeS-MgS-MnS, Mole fraction, Liquidussurface 1032
FeS-MgS-MnS, Weight percent, Liquidussurface 1033
K2O-MgO-P2O5, *1034*
K2O-MgO-P2O5, Ternary Phases 1034
K2O-MgO-P2O5, Weight percent, 25°C 1035

K2O-MgO-P2O5, Weight percent, Isopleth K3PO4-MgO 1036
K2O-MgO-P2O5, Weight percent, Isopleth KMgPO4-MgO 1037
K2O-MgO-P2O5, Weight percent, Isopleth KPO3-MgP2O6 1038
K2O-MgO-P2O5, Weight percent, Isopleth K4P2O7-KMgPO4 1039
K2O-MgO-P2O5, Weight percent, Isopleth K3PO4-KMgPO4 1040
Weight percent, Isopleth K4P2O7-K4MgP2O8 1041
Weight percent, Isopleth KMg4P3O12-MgO 1042
K2O-MgO-P2O5, Mole fraction, Liquidussurface 1043
K2O-MgO-P2O5, Weight percent, Liquidussurface 1044
K2O-MgO-P2O5, Invariant equilibria on the liquidus surface 1045
K2O-MgO-SiO2, *1046*
K2O-MgO-SiO2, Ternäre Phasen 1046
Weight percent , Isopleth K2SiO3-K2MgSiO4 compared with experimental data 1047
K2O-MgO-SiO2, Mole fraction, Isopleth 0.5(K2MgSiO4)-SiO2° 1048
K2O-MgO-SiO2, Weight percent , Isopleth Mg2SiO4-K2MgSi3O8 1049
K2O-MgO-SiO2, Weight percent , Isopletalet Schnitt MgSiO3-K2Si7O15 Weight percent , Isopleth Mg2SiO4-K2MgSi5O12 compared with experimental data° 1050
Weight percent , Isopleth K2MgSi5O12-K2Si2O5 compared with experimental data° 1053
Weight percent , Isopleth K2MgSiO4-K2Si2O5 compared with experimental data 1054
Weight percent , Isopleth K2MgSi5O12-K2Si4O9 compared with experimental data 1055
K2O-MgO-SiO2, Mole fraction 600°C 1056
K2O-MgO-SiO2, Mole fraction 1000°C 1057
K2O-MgO-SiO2, Mole fraction , Liquidussurface 1058
K2O-MgO-SiO2, Weight percent , Liquidussurface 1059
K2O-MgO-SiO2, Invariant equilibria on the liquidus surface 1060
K2O-Na2O-P2O5, *1061*
K2O-Na2O-P2O5, Mole fraction 400C° 1061
K2O-Na2O-P2O5, Mole fraction Isopleth KPO3-NaPO3 compared with experimental data 1062
K2O-Na2O-P2O5, Mole fraction Isopleth K2P2O7-Na2P2O7 compared with experimental data 1063
K2O-Na2O-P2O5, Mole fraction Isopleth K3PO4-Na3PO4 compared with experimental data 1064
K2O-Na2O-P2O5, Mole fraction, Subsolidus surface 1065
K2O-Na2O-P2O5, Mole fraction, Reciprocal liquidus surface Na-K-P3O9-PO4 1066
K2O-Na2O-P2O5, Mole fraction, Liquidus surface 1067
K2O-Na2O-P2O5, Weight percent, Liquidus surface 1068

K2O-Na2O-P2O5, Invariant equilibria on the liquidus surface K2O-Na2O-P2O5, Invariant equilibria on the liquidus surface 1069
K2O-Na2O-SiO2, *1070*
K2O-Na2O-SiO2, Mole fraction 600C° 1070
K2O-Na2O-SiO2, Mole fraction 800C° 1071
K2O-Na2O-SiO2, Mole fraction 595C° kurz unterhalb Liquidussurface 1072
K2O-Na2O-SiO2, Weight percent K2Si2O5-Na2Si2O5 compared with experimental data 1073
K2O-Na2O-SiO2, Weight percent K2SiO3-Na2SiO3 compared with experimental data 1074
K2O-Na2O-SiO2, Mole fraction Liquidussurface 1075
K2O-Na2O-SiO2, Weight percent Liquidussurface compared with experimental data 1076
K2O-Na2O-SiO2, Invariant equilibria on the liquidus surface 1077
K2O-Na2O-TiO2, *1078*
K2O-Na2O-TiO2, Mole fraction, Isopleth K2TiO3-Na2TiO3 compared with experiments 1078
K2O-Na2O-TiO2, Mole fraction Liquidussurface, 1079
K2O-Na2O-TiO2, Weight percent Liquidussurface, 1080
K2O-Na2O-TiO2, Invariant equilibria on the liquidus surface 1081
K2O-Na2O-V2O5, *1082*
K2O-Na2O-V2O5, Mole fraction, Isopleth KVO3-NaVO3 compared with experiments 1082
K2O-Na2O-V2O5, Mole fraction, Liquidussurface 1083
K2O-Na2O-V2O5, Weight percent, Liquidussurface 1084
K2O-Na2O-V2O5, Invariant equilibria on the liquidus surface 1085
K2O-P2O5-ZnO, *1086*
K2O-P2O5-ZnO, Mole fraction, Isopleth KZn4P3O12-ZnO 1086
K2O-P2O5-ZnO, Mole fraction, Isopleth KPO3-ZnO 1087
K2O-P2O5-ZnO, Mole fraction, Isopleth Zn2P2O7-K2ZnP2O7 1088
K2O-P2O5-ZnO, Mole fraction, Isopleth Zn2P2O7-K4P2O7 1089
K2O-P2O5-ZnO, Mole fraction, Isopleth ZnP2O6-KPO3 1090
K2O-P2O5-ZnO, Mole fraction, Subsolidus 1091
K2O-P2O5-ZnO, Mole fraction, Liquidus surface 1092
K2O-P2O5-ZnO, Weight percent, Liquidus surface 1093
K2O-P2O5-ZnO, Invariant equilibria on the liquidus surface 1094
MgSO4-K2SO4-Na2SO4, *1095*
MgSO4-K2SO4-Na2SO4, Mole fraction, 500°C 1095
MgSO4-K2SO4-Na2SO4, Mole fraction, 700°C 1096
MgSO4-K2SO4-Na2SO4, Mole fraction, Liquidussurface 1097

MgSO4-K2SO4-Na2SO4, Weight percent, Liquidussurface 1098
K2SO4-Mg2SO4-Na2SO4, Invariant equilibria on the liquidus surface 1099
MgO-MnO-SiO2, *1100*
MgO-MnO-SiO2, Weight percent, Orthisilicate section Mg2SiO4-Mn2SiO4 compared with experimental data 1100
MgO-MnO-SiO2, Weight percent, Metasilicate section MgSiO3-MnSiO3 compared with experimental data 1101
MgO-MnO-SiO2, Mole fraction, Liquidussurface 1102
MgO-MnO-SiO2, Weight percent, Liquidussurface 1103
MgO-MnO-SiO2, Invariant equilibria on the liquidus surface 1104
MgO-Na2O-P2O5, *1105*
MgO-Na2O-P2O5, Ternary phases 1105
MgO-Na2O-P2O5, Mole fraction, 300°C 1106
Weight percent, Isopleth NaPO3-Na8Mg6P10O35 compared with experimental data Weight percent, Isopleth Na3PO4-Mg3P2O8 compared with experimental data 1107
MgO-Na2O-P2O5, Weight percent, Isopleth MgO-Na3PO4 1109
Weight percent, Isopleth MgP2O6-NaPO3 compared with experimental data 1110
MgO-Na2O-P2O5, Mole fraction, Liquidussurface 1111
MgO-Na2O-P2O5, Weight percent, Liquidussurface 1112
MgO-Na2O-P2O5, Invariant equilibria on the liquidus surface 1113
MgO-Na2O-SiO2, *1114*
MgO-Na2O-SiO2, Mole fraction 600°C 1114
MgO-Na2O-SiO2, Mole fraction 800°C 1115
MgO-Na2O-SiO2, Mole fraction 1200°C 1116
MgO-Na2O-SiO2, Mole fraction Liquidussurface 1117
MgO-Na2O-SiO2, Weight percent Liquidussurface 1118
MgO-Na2O-SiO2, Invariant equilibria on the liquidus surface 1119
MgO-P2O5-SiO2, *1120*
MgO-P2O5-SiO2, Weight fraction, Isopleth Mg3P2O8-SiO2 1120
MgO-P2O5-SiO2, Gewichtsanteil, Isopleth Mg3P2O8-Mg2SiO4 1121
MgO-P2O5-SiO2, Gewichtsanteil, Isopleth Mg3P2O8-MgSiO3 1122
MgO-P2O5-SiO2, Mole fraction, Liquidussurface 1123
MgO-P2O5-SiO2, Weight percent, Liquidussurface 1124
MgO-P2O5-SiO2, Invariant equilibria on the liquidus surface 1125
MgO-P2O5-ZnO, *1126*
MgO-P2O5-ZnO, Mole fraction, 500°C 1126

MgO-P2O5-ZnO, Mole fraction, Isopleth MgP2O6-ZnP2O6 1127
MgO-P2O5-ZnO, Mole fraction, Isopleth Mg2P2O7-Zn2P2O7 1128
MgO-P2O5-ZnO, Mole fraction, Isopleth Mg3P2O8-Zn3P2O8 1129
MgO-P2O5-ZnO, Mole fraction, Liquidussurface 1130
MgO-P2O5-ZnO, Weight percent, Liquidussurface 1131
MgO-P2O5-ZnO, Invariant equilibria on the liquidus surface 1132
MgO-SiO2-TiO2, *1133*
MgO-SiO2-TiO2, Mole fraction, 1400°C 1133
MgO-SiO2-TiO2, Weight percent, Isopleth section Mg2SiO4-Mg2TiO4 1134
MgO-SiO2-TiO2, Mole fraction, Liquidus surface 1135
MgO-SiO2-TiO2, Weight percent, Liquidus surface 1136
MgO-SiO2-TiO2, Invariant equilibria on the liquidus surface 1137
MgO-SiO2-V2O5, *1138*
MgO-SiO2-V2O5, Mole fraction, 1450°C 1138
MgO-SiO2-V2O5, Mole fraction, Solidus surface 1139
MgO-SiO2-V2O3, *1140*
MgO-SiO2-V2O3, Mole fraction, 1400°C 1140
MgO-SiO2-V2O3, Mole fraction, Liquidus surface 1141
MgO-SiO2-V2O3, Weight percent, Liquidus surface 1142
MgO-SiO2-V2O3, Invariant equilibria on the liquidus surface 1143
MgO-SiO2-ZnO, *1144*
MgO-SiO2-ZnO, Mole fraction, 1200°C 1144
MgO-SiO2-ZnO, Mole fraction, 1600°C 1145
MgO-SiO2-ZnO, Mole fraction, Isopleth Mg2SiO4-Zn2SiO4 1146
MgO-SiO2-ZnO, Mole fraction, Liquidussurface 1147
MgO-SiO2-ZnO, Weight percent, Liquidussurface compared with experimental data 1148
MgO-SiO2-ZnO, Invariant equilibria on the liquidus surface 1149
MgO-TiO2-Ti2O3, *1150*
MgO-TiO2-Ti2O3, Mole fraction, 1500°C 1150
MgO-TiO2-Ti2O3, Mole fraction, Liquidus surface 1151
MgO-TiO2-Ti2O3, Weight percent, Liquidus surface 1152
MgO-TiO2-Ti2O3, Invariant equilibria on the liquidus surface 1153
MnO-Mn2O3-TiO2, *1154*
MnO-Mn2O3-TiO2, Mole fraction, 1200°C 1154
MnO-Mn2O3-TiO2, Mole fraction, 1400°C 1155

MnO-MnS-SiO2, *1156*
MnO-MnS-SiO2, Weight percent, 1200°C 1156
MnO-MnS-SiO2, Weight percent, 1250° 1157
MnO-MnS-SiO2, Weight percent, 1300°C 1158
MnO-MnS-SiO2, Weight percent, Isopleth MnS-MnSiO3 compared with experimental data 1159
MnO-MnS-SiO2, Mole fraction, Liquidussurface 1160
MnO-MnS-SiO2, Weight percent, Liquidussurface 1161
MnO-MnS-SiO2, Invariant equilibria on the liquidus surface 1162
MnO-SiO2-ZnO, *1163*
MnO-SiO2-ZnO, Mole fraction, 1200°C 1163
MnO-SiO2-ZnO, Mole fraction, Isopleth Mn2SiO4-Zn2SiO4 1164
MnO-SiO2-ZnO, Mole fraction, Liquidussurface 1165
MnO-SiO2-ZnO, Weight percent, Liquidussurface 1166
MnO-SiO2-ZnO, Invariant equilibria on the liquidus surface 1167
MnO-TiO2-Ti2O3, *1168*
MnO-TiO2-Ti2O3, Mole fraction, 1200°C 1168
MnO-TiO2-Ti2O3, Mole fraction, TiO2-TiO1.6-Mn.33Ti.67O1.6, 1200°C 1169
MnO-TiO2-Ti2O3, Mole fraction, 1400°C 1170
MnO-TiO2-Ti2O3, Mole fraction, Liquidussurface 1171
MnO-TiO2-Ti2O3, Weight percent, Liquidussurface 1172
MnO-TiO2-Ti2O3, Invariant equilibria on the liquidus surface 1173
Na2O-P2O5-SiO2, *1174*
Na2O-P2O5-SiO2, Mole fraction, ternary phases 1174
Na2O-P2O5-SiO2, Mole fraction Isopleth $2Na_3PO_4$-Na_2SiO_3 compared with experimental data 1175
Na2O-P2O5-SiO2, Mole fraction Isopleth $2Na_3PO_4$-$Na_2Si_2O_5$ compared with experimental data 1176
Na2O-P2O5-SiO2, Mole fraction Isopleth $Na_{18}P_4Si_6O_{31}$-$Na_4P_2O_7$ compared with experimental data 1177
Na2O-P2O5-SiO2, Mole fraction Isopleth $Na_4P_2O_7$-SiO_2 compared with experimental data 1178
Na2O-P2O5-SiO2, Mole fraction Isopleth $NaPO_3$-SiO_2 compared with experimental data 1179
Na2O-P2O5-SiO2, Mole fraction Isopleth $Na_{18}P_4Si_6O_{31}$-Na_2SiO_3 compared with experimental data 1180
Na2O-P2O5-SiO2, Mole fraction, Subsolidus surface 1181
Na2O-P2O5-SiO2, Mole fraction, Liquidus surface 1182
Na2O-P2O5-SiO2, Weight percent, Liquidus surface 1183
Na2O-P2O5-SiO2, Invariant equilibria on the liquidus surface 1184

Na2O-P2O5-ZnO, *1185*
Na2O-P2O5-ZnO, Mole fraction, Ternary phases 1185
Na2O-P2O5-ZnO, Mole fraction, Isopleth ZnO-$Na_2Zn_5P_4O_{16}$ 1186
Na2O-P2O5-ZnO, Mole fraction, Isopleth ZnO-$NaPO_3$ 1187
Na2O-P2O5-ZnO, Mole fraction, Isopleth ZnP_2O_6-$NaPO_3$ 1188
Na2O-P2O5-ZnO, Mole fraction, Isopleth $Zn_3P_2O_8$-Na_3PO_4 1189
Na2O-P2O5-ZnO, Mole fraction, Isopleth $Na_4P_2O_7$-$Zn_2P_2O_7$ 1190
Na2O-P2O5-ZnO, Mole fraction, Subsolidus surface 1191
Na2O-P2O5-ZnO, Mole fraction, Liquidus surface 1192
Na2O-P2O5-ZnO, Weight percent, Liquidus surface 1193
Na2O-P2O5-ZnO, Invariant equilibria on the liquidus surface 1194
Na2O-SiO2-ZnO, *1195*
Na2O-SiO2-ZnO, Mole fraction, 700°C , 1195
Na2O-SiO2-ZnO, Mole fraction, 900°C , 1196
Na2O-SiO2-ZnO, Mole fraction, 1000°C , 1197
Na2O-SiO2-ZnO, Mole fraction, 900°C , 1198
Na2O-SiO2-ZnO, Mole fraction, Liquidussurface , 1199
Na2O-SiO2-ZnO, Weight percent, Liquidussurface , 1200
Na2O-SiO2-ZnO, Invariant equilibria on the liquidus surface 1201
NiO-V2O5-ZnO, *1202*
NiO-V2O5-ZnO, Mole fraction, 600°C , 1202
NiO-V2O5-ZnO, Mole fraction, Liquidussurface , 1203
NiO-V2O5-ZnO, Weight percent, Liquidussurface , 1204
NiO-V2O5-ZnO, Invariant equilibria on the liquidus surface 1205
P2O5-SiO2-ZnO, *1206*
P2O5-SiO2-ZnO, Mole fraction, 500°C , 1206
P2O5-SiO2-ZnO, Mole fraction, Liquidus surface , 1207
P2O5-SiO2-ZnO, Weight percent, Liquidus surface , 1208
P2O5-SiO2-ZnO, Invariant equilibria on the liquidus surface 1209
SiO2-TiO2-Ti2O3, *1210*
SiO2-TiO2-Ti2O3, Mole fraction, Liquidus surface 1210
SiO2-TiO2-Ti2O3, Weight percent, Liquidus surface 1211
SiO2-TiO2-Ti2O3, Invariant equilibria on the liquidus surface 1212
Sr-Fe-O, *1213*
Sr-Fe-O, Mole fraction, 400°C 1213

Sr-Fe-O, Mole fraction, 800°C 1214
TiO2-Ti2O3-V2O3, *1215*
TiO2-Ti2O3-V2O3, Mole fraction, 1200°C 1215
TiO2-Ti2O3-V2O3, Mole fraction, Liquidus surface 1216
TiO2-Ti2O3-V2O3, Weight percent, Liquidus surface 1217
TiO2-Ti2O3-V2O3, Invariant equilibria on the liquidus surface 1218
Quaternary systems: *1219*
Al2O3-CaO-Cr2O3-SiO2, *1220*
Mole fraction, Isopleth Uvarovite-Grossularite 1220
Al2O3-CaO-K2O-Na2O, *1221*
Mole fraction 600°C, Isothermischer Schnitt im AlKO2-AlNaO2-CaAl2O4 System 1221
Mole fraction 1100°C, Isothermischer Schnitt im AlKO2-AlNaO2-CaAl2O4 System 1222
Mole fraction 1700°C, Isothermischer Schnitt im AlKO2-AlNaO2-CaAl2O4 System 1223
Al2O3-CaO-MgO-SiO2, *1224*
Weight percent, Isopleth MgAl2O4-CaAl2Si2O7 1224
Weight percent, Isopleth MgAl2O4-Ca2Al2SiO7 1225
Weight percent, Liquidusoberfläche bei 10 mass.% Al2O3 1226
Weight percent, Liquidusoberfläche bei 15 mass.% Al2O3 1227
Weight percent, Liquidusoberfläche bei 5 mass.% MgO 1228
Weight percent, Liquidusoberfläche bei 10 mass.% MgO 1229
Weight percent, Liquidusoberfläche im Ca2SiO4-Al2O3-Mg2SiO4 System 1230
Weight percent, Liquidusoberfläche im Al2CaSi2O8-CaMgSi2O6-CaSiO3 System 1231
Weight percent, Liquidusoberfläche im Al2CaSi2O8-CaMgSi2O6-Mg2SiO4 System 1232
Weight percent, Liquidusoberfläche im Al2O3-Al2Ca2SiO7-MgAl2O4 System 1233
Al2O3-CaO-V2O3-SiO2, *1234*
Mole fraction, Isopleth Ca3V2Si3O12-Ca3Al2Si3O12 1234
Al2O3-Fe2O3-K2O-SiO2, *1236*
Mole fraction, Isopleth KFeSiO4-KAlSiO4 1236
Mole fraction, 1050°C 1237
Al2O3-K2O-Na2O-SiO2, *1238*
Weight percent, Isopleth AlNaSi3O8-AlKSi3O8 1238
Weight percent, Isopleth NaAlSiO4-KAlSiO4, (proposed calculation) 1239
Weight percent, Liquidussurface NaAlSiO4-KAlSiO4-SiO2 1240
Mole fraction, 1200°C in NaAlSiO4-KAlSiO4-SiO2 (proposed calculation) 1241
Mole fraction, 600°C in NaAlSiO4-KAlSiO4-SiO2 (proposed calculation) 1242

Mole fraction, Liquidussurface NaAlSiO4-KAlSiO4-SiO2 (proposed calculation) 1243
Al2O3-MnO-MnS-SiO2, , *1244*
Weight percent, MnS saturation boundaries at 1200°C with various wt pct Al2O3 1244
Cr-Fe-Mn-S, *1245*
Mole fraction, Isopleth section FrCr2S4-MnCr2S4 1245

New systems in GTOX database

(additions to the previous version November 2019, Slagatlas 14.0)

Binary systems

New systems	Reassessed systems
1. *Ni-S*	*Al_2O_3-V_2O_3*
2. *O-Sr*	*FeO-FeS*
3. *FeO-SrO*	*SiO_2-ZnO*
4. *Fe_2O_3-SrO*	*Fe_2O_3-V_2O_5-O_2*
5. *SrO-P_2O_5*	*Fe_2O_3-Na_2O-O_2*
6. *CaO-SrO*	*CaO-ZnO*
7. *Al_2O_3-SrO*	*CaO-V_2O_5*
8. *SrO-ZnO*	
9. *SrO-SiO_2*	
10. *MgO-SrO*	
11. *CaO-V_2O_3*	
12. *V_2O_5-ZnO*	
13. *SrO-V_2O_5*	
14. *NiO-TiO_2*	
15. *NiO-ZnO*	
16. *NiO-SrO*	
17. *NiO-MgO*	

For the Me-O systems the following two diagram types are added: Me-O phase diagram with the isobars, and also oxygen potential- temperature phase diagram.

Ternary systems

New systems	Reassessed systems
1. *CaO-V_2O_3-SiO_2*	*CaO-P_2O_5-SiO_2*
2. *FeO-Fe_2O_3-SrO*	*CaO-P_2O_5-ZnO*
3. *Al_2O_3-Na_2O-V_2O_5*	*CaO-SiO_2-ZnO*
4. *Fe_2O_3-Na_2O-V_2O_5*	*P_2O_5-SiO_2-ZnO*
5. *NiO-V_2O_5-ZnO*	
6. *Fe-Ni-S*	
7. *Fe-O-Sr*	

New quaternary system - *Al_2O_3-CaO-V_2O_3-SiO_2*

The solid solution phases, their description and modelling

System components:

1: Al 2: Ca 3: Cr 4: F 5: Fe 6: K 7: Mg 8: Mn 9: Na
10: Ni 11: O 12: P 13: S 14: Si 15: Sr 16: Ti 17: V 18: Zn

	Phase	Name	Model	Description
1.	Al3M_D022	AL3M	SUBL	(Al, Ti)$_3$ (Ti)
2.	Alfa	ALFA	SUBL	(Ca^{+2},K^{+1}, Mg^{+2},Na^{+1},Va)(SO$_4^{-2}$)
3.	AlPO4-HT	ALPH	SUBL	(Al^{3+},Si^{4+})$_1$(P^{5+},Si^{4+})$_1$(O^{2-})$_4$
4.	AlPO4-MT	ALPM	SUBL	(Al^{3+},Si^{4+})$_1$(P^{5+},Si^{4+})$_1$(O^{2-})$_4$
5.	BCC_A2	BCC	SUBL	(Al, Ca, Fe, O, Si, Cr, P, Mn, S, Zn, Ti, TiO$_3$, V, VO$_3$)$_1$ (Va)$_3$
6.	Beta-Alumina	BETA	SUBL	(Al^{3+})$_9$(Na^{1+},K^{1+})$_1$(O^{2-})$_{14}$
7.	Beta-prime	BET2	SUBL	(K^{1+},Na^{1+})$_2$ (Al^{3+},Va)$_2$ (Mg^{2+},Va)$_3$ (Al$_{10}$O$_{19}^{8-}$)$_1$
8.	Beta-tri	BET3	SUBL	(Al$_{40}$Na$_4$Mg$_5$O$_{70}^{6-}$, Al$_{40}$K$_4$Mg$_5$O$_{70}^{6-}$)$_1$ (O^{2-},Va)$_3$ (Al^{3+},Na^{1+})$_2$ (Al^{3+},Mg^{2+})$_2$
9.	BETA V-O	BETV	SUBL	(V)$_1$(O, Va)$_1$
10.	Bixbyte	BIXB	SUBL	(Fe^{3+}, Mn^{3+},Cr^{3+})$_2$ (O^{2-})$_3$
11.	Brezinaite	BREZ	SUBL	(Cr, Fe, Mn) (Cr)$_2$ (S)$_4$
12.	12CaO·7Al$_2$O$_3$	C12A	SUBL	(Ca^{2+})$_{12}$ (Al^{3+}, Fe^{3+})$_{14}$ (O^{2-})$_{33}$

13.	$CaO{\cdot}2Al_2O_3$	C1A2	SUBL	$(Ca^{2+})_1$ ($\underline{Al^{3+}}$, $Fe^{3+})_4$ $(O^{2-})_7$
14.	$CaO{\cdot}6Al_2O_3$	C1A6	SUBL	$(Ca^{2+})_1$ ($\underline{Al^{3+}}$, $Fe^{3+})_{12}$ $(O^{2-})_{19}$
15.	C1V1	C1V1	SUBL	($\underline{Ca}$, Mg)($\underline{V}$)$_2$(O)$_6$
16.	$2CaO{\cdot}Fe_2O_3$	C2F	SUBL	$(Ca^{2+})_2$ (Al^{3+}, $\underline{Fe^{3+}})_2$ $(O^{2-})_5$
17.	$Ca_2P_2O_7$-MT	C2P	SUBL	($\underline{Ca^{2+}}$,$Mg^{2+})_2(P^{5+})_2$ $(O^{2-})_7$
18.	C2S-C3P	C2SA	SUBL	($\underline{Ca^{2+}}$,Cr^{2+}, Mg^{2+},$Mn^{+2})_3(\underline{Ca^{2+}},\underline{Va})_1(\underline{P^{5+}},\underline{Si^{4+}})_2$ $(O^{2-})_8$
19.	α´- Ca_2SiO_4	C2SP	SUBL	($\underline{Ca^{2+}}$,Mg^{2+},Fe^{2+},Mn^{2+},$Zn^{2+})_3$ ($\underline{Ca^{2+}}$, $\underline{Va})_1$ $(\underline{P^{5+}},\underline{Si^{4+}})_2(O^{2-})_8$
20.	$3CaO{\cdot}Al_2O_3$	C3A1	SUBL	$(Ca^{2+})_3$ ($\underline{Al^{3+}}$, $Fe^{3+})_2$ $(O^{2-})_6$
21.	C3M3P2	C3M3	SUBL	($\underline{Ca^{2+}}$,$Mg^{2+})_3(Mg^{2+})_3(P^{5+})_4(O^{2-})_{16}$
22.	β-$Ca_3P_2O_8$	C3PL	SUBL	($\underline{Ca^{2+}}$,Mg^{2+},$Zn^{2+})_3(P^{5+})_2$ $(O^{2-})_8$
23.	α-$Ca_3P_2O_8$	C3PM	SUBL	($\underline{Ca^{2+}}$,Mg^{2+},$Zn^{2+})_3(P^{5+})_2$ $(O^{2-})_8$
24.	CAF2	CAF2	SUBL	$(Ca^{2+})_1$ (Al^{3+}, $Fe^{3+})_6$ $(O^{2-})_{10}$
25.	$CaO{\cdot}Cr_2O_3$-alpha	CAO1	SUBL	$(Ca^{2+})_1$ (Al^{3+}, $\underline{Cr^{3+}}$, $Fe^{3+})_2$ $(O^{2-})_4$
26.	$CaO{\cdot}(Al,Cr,Fe)_2O_3$ -beta	CAO2	SUBL	$(Ca^{2+})_1$ ($\underline{Al^{3+}}$, $\underline{Cr^{3+}}$, $\underline{Fe^{3+}}))_2$ $(O^{2-})_4$
27.	Oldhamite	CAS	SUBL	($\underline{Ca}$,Fe,$\underline{Mg}$, $\underline{Mn}$) S

28.	CBCC_A12	CBCC	SUBL	(Al, Cr, Fe, Mg, Mn, Si, Ti)
29.	Carnegieite	CGKS	SUBL	$(Al^{3+}, Si^{4+})_2\ (Va)_1\ (Na^{1+}, K^{1+}, Va)_1\ (O^{2-})_4$
30.	Clinopyroxene	CLIN	SUBL	$(Ca^{2+}, Fe^{2+}, \underline{Mg^{2+}})_1\ (Fe^{2+}, \underline{Mg^{2+}})_1\ (Si^{4+})_2\ (O^{2-})_6$
31.	CMP	CMP	SUBL	$(Ca^{2+}, \underline{Mg^{2+}})_1 (Ca^{2+})_1 (P^{5+})_2 (O^{2-})_7$
32.	Cordierite	CORD	SUBL	$(Al_2Si_5O_{18}^{10-})_1 (Fe^{2+}, Mg^{2+}, Mn^{2+})_2 (\underline{Al^{3+}}, Mg^{2+})_1$ $(\underline{Al^{3+}}, Si^{4+})_1$
33.	Corundum	CORU	SUBL	$(\underline{Al^{3+}}, Cr^{2+}, \underline{Cr^{3+}}, \underline{Fe^{3+}}, \underline{Mn^{3+}}, Fe_{0.5}Ti_{0.5}^{3+})_2$ $(Cr^{3+}, \underline{Va})_1\ (O^{2-})_3$
34.	CUB-A13	CUB	SUBL	(Al, Cr, Fe, Mg, Mn, Si, Ti)
35.	CZ2P-HT	CZ2P	SUBL	$(\underline{Ca^{2+}}, Zn^{2+})_1 (\underline{Zn^{2+}}, Ca^{2+})_2 (P^{5+})_2 (O^{2-})_8$
36.	FCC_A1	FCC	SUBL	(Fe, Ca, V, O, Si, Cr, P, Mn, S, Mg, Zn, Al, Ti, Ni)$_1$ $(Va)_1$
37.	$FeNaO_2$-delta	FENA	SUBL	$(\underline{Fe^{3+}}, Si^{4+})_1\ (\underline{Na^{1+}}, Va)_1\ (O^{2-})_2$
38.	Feldspar	FSPA	SUBL	$(\underline{Al^{3+}}, \underline{Fe^{3+}})_1 (\underline{K^{1+}}, \underline{Na^{1+}})_1\ (Si^{4+})_3 (O^{2-})_8$
39.	GAMMA V-O	GAMV	SUBL	$(\underline{V})_1 (\underline{O}, Va)_{0.5}$
40.	Garnet	GARN	SUBL	$(Ca^{2+})_3\ (\underline{Al^{3+}}, \underline{Cr^{3+}})_2\ (Si^{4+})_3\ (O^{2-})_{12}$
41.	Glaserite	GLAS	SUBL	$(\underline{K^{+1}}, Na^{+1})_3 (Na^{-+1})_1 (SO_4^{-2})_2$
42.	Hatrurite	HATR	SUBL	$(\underline{Ca^{2+}}, Cr^{2+})_3\ (Si^{4+})_1\ (O^{2-})_5$

43.	HCP_A3	HCP	SUBL	$(Al, \underline{Ti})_2\ (O, Va)$
44.	Hexagonal	HEXA	SUBL	$(Ca^{+2},\underline{K^{+1}}, Mg^{+2},\underline{Na^{+1}},Va, Ni^{2+},Al^{3+})(S^{-2}, \underline{SO_4^{-2}})$
45.	Sulfide hexagonal	HEXB	SUBL	$(\underline{K^{+1}}, \underline{Na^{+1}})_2(\underline{S^{-2}}, SO_4^{-2})$
46.	High-Sigma	HIGH	SUBL	$(Fe, Mn)_8(Cr)_4(Cr, Fe, Mn)_{18}$
47.	K3P-LT	K3PL	SUBL	$(K_2O)_2(P_2O_5)(K_2O,CaO,K_2CaO_2,MgO,K_2MgO_2)$
48.	K3P-MT	K3PL	SUBL	$(K_2O)_2(P_2O_5)(K_2O,CaO,K_2CaO_2,MgO,K_2MgO_2)$
49.	K3P-HT	K3PL	SUBL	$(K_2O)_2(P_2O_5)(K_2O,CaO,K_2CaO_2,Na_2O,$ $MgO,K_2MgO_2)$
50.	KAF4S3	KAF4	SUBL	$(\underline{Al^{3+}},\underline{Fe^{3+}})_4\ (K^{1+})_4\ (Si^{4+})_3(O^{2-})_{14}$
51.	Kaliophilite-HT	KALH	SUBL	$(\underline{Al^{3+}},\underline{Fe^{3+}})_2\ (K^{1+},Na^{1+})_2\ (Si^{4+})_2(O^{2-})_8$
52.	Kaliophilite-LT	KALL	SUBL	$(\underline{Al^{3+}},\underline{Fe^{3+}})_2\ (K^{1+})_2\ (Si^{4+})_2(O^{2-})_8$
53.	K_2MgSiO_4	KMS	SUBL	$(\underline{Mg^{2+}},Si^{4+})_1(Si^{4+})_1\ (\underline{K^{1+}},Va)_2(O^{2-})_4$
54.	$(K,Na)_2CrO_4$-LT	KN21	SUBL	$(\underline{K^{1+}},\underline{Na^{1+}})_2\ (Cr^{6+})(O^{2-})_4$
55.	$(K,Na)_2CrO_4$-HT	KN22	SUBL	$(\underline{K^{1+}},\underline{Na^{1+}})_2\ (Cr^{6+})(O^{2-})_4$
56.	$(K,Na)_2Cr_2O_7$	KN23	SUBL	$(\underline{K^{1+}},\underline{Na^{1+}})_2\ (Cr^{6+})_2(O^{2-})_7$
57.	(K,Na)2P-HT	KN2P	SUBL	$(\underline{K_2O},\underline{Na_2O})_2(P_2O_5)$

58.	KP-HT	KP_H	SUBL	$(\underline{K^{+1}},Na^{+1})(P^{+5})(O^{-2})_3$
59.	Langbeinite	LANG	SUBL	$(K^{+1})_2(Ca^{+2},Mg^{+2})_2(SO_4^{-2})_3$
60.	Leucite	LEUC	SUBL	$(\underline{Al^{3+}},\underline{Fe^{3+}})_2\ (K^{1+})_2\ (Si^{4+})_4(O^{2-})_{12}$
61.	Lowclinopyroxene	LOWC	SUBL	$(\underline{Ca^{2+}},\ Mg^{2+})_1\ (Mg^{2+})_1\ (Si^{4+})_2\ (O^{2-})_6$
62.	M1V1	M1V1	SUBL	$(Ca,\ \underline{Mg})(\underline{V})_2(O)_6$
63.	$M_2P_2O_7$	M2P	SUBL	$(Ca^{2+},\underline{Mg^{2+}},\underline{Zn^{2+}})_2(P^{5+})_2\ (O^{2-})_7$
64.	$Mg_3P_2O_8$	M3P	SUBL	$(Ca^{2+},\underline{Mg^{2+}},Zn^{2+})_3(P^{5+})_2\ (O^{2-})_8$
65.	M4O7	M4O7	SUBL	$(\underline{Ti},\ \underline{V})_4(O)_7$
66.	M6O11	M6O11	SUBL	$(\underline{Ti},\ \underline{V})_6(O)_{11}$
67.	M8O15	M8O15	SUBL	$(\underline{Ti},\ \underline{V})_8(O)_{15}$
68.	Melilite	MELM	SUBL	$(Al^{3+},\ Mg^{2+})_1\ (Al^{3+},\ Si^{4+})_1\ (Ca_2SiO_7^{\ 6-})_1$
69.	MeO	MEO	SUBL	$(Al^{3+},\underline{Ca^{2+}},\underline{Fe^{2+}},Fe^{3+},\underline{Mg^{2+}},Va,\ Cr^{3+},Na^{+1},\ \underline{Mn^{+2}},\ Mn^{+3},\underline{Ni^{2+}},\ \underline{Sr^{2+}},\ Ti^{4+},\ V^{3+},\ V,\ V^{2+},\ Zn^{2+})_1\ (O^{2-})_1$
70.	MeVO4	MEVO	SUBL	$(Al^{3+},\ Fe^{3+})_1(V^{5+})_1(O^{2-})_4$
71.	MgP2O6	MP	SUBL	$(\underline{Mg^{+2}},Zn^{+2})(P^{+5})_2(O^{-2})_6$
72.	Mullite	MULL	SUBL	$(Al^{3+})_1\ (Al^{3+})_1\ (Al^{3+},\ Cr^{3+},\ \underline{Si^{4+}},Fe^{3+})_1\ (Va,\ \underline{O^{2-}})_5$

73.	(K,Na)2C3A5	N2C3	SUBL	$(K^{1+},Na^{1+},Va)_1\ (Ca^{2+},K^{1+},Na^{1+})_1\ (Al^{3+})_2(O^{2-})_4$
74.	N3P-LT	N3PL	SUBL	$(\underline{Na_2O},K_2O)_2(P_2O_5)(Na_2O)$
75.	N3P-HT	N3PH	SUBL	$(\underline{Na_2O},K_2O)_2(P_2O_5)(Na_2O)$
76.	N3P-MT	N3PH	SUBL	$(\underline{Na_2O},K_2O)_2(P_2O_5)(Na_2O)$
77.	(K,Na)(Al,Fe)O_2-HT	NAFH	SUBL	$(\underline{Al^{3+},Fe^{3+}},\ Si^{4+})_1\ (\underline{K^{1+},Na^{1+}},Va)_1\ (O^{2-})_2$
78.	(K,Na)(Al,Fe)O_2-LT	NAFL	SUBL	$(\underline{Al^{3+},Fe^{3+}},\ Si^{4+})_1\ (\underline{K^{1+},Na^{1+}},Va)_1\ (O^{2-})_2$
79.	NC2S3	NC2S	SUBL	$(Na^{1+},Va)_2(Ca^{2+},Va)_1(CaNa_2Si_3O_9^{2-})_1$
80.	Nepheline	NEPH	SUBL	$(Al^{3+},\ Si^{4+})_2\ (Va)_1\ (Na^{1+},\ K^{1+},Va)_1\ (O^{2-})_4$
81.	$(Na,K)_2Si_2O_5$	NKS2	RKMP	$(K_2Si_2O_5,\ Na_2Si_2O_5)$
82.	NP-HT	NP_H	SUBL	$(K^{+1},\underline{Na^{+1}})(P^{+5})(O^{-2})_3$
83.	Olivine	OLIV	SUBL	$(\underline{Ca^{2+},Fe^{2+}},\ \underline{Mg^{2+},Mn^{2+}},Zn^{2+})_1(\underline{Ca^{2+},Fe^{2+},Mg^{2+}},\ \underline{Mn^{+2}})_1\ (Si^{4+})_1(O^{2-})_4$
84.	Orthopyroxene	ORTH	SUBL	$(\underline{Ca^{2+}},\ Mg^{2+},\ Fe^{2+})_1\ (Mg^{2+})_1\ (Si^{4+})_2\ (O^{2-})_6$
85.	Perovskite	PERO	SUBL	$(Ca^{2+})_2(Ti^{+4},\ Fe^{3+})_2(O^{2-})_5(O^{2-},\ Va)_1$
86.	Perovskite Sr-Fe	PESR	RKMP	$(Sr_2Fe_2O_5,\ Sr_2Fe_2O_6)$
87.	Protoenstatite	PROE	SUBL	$(Cr^{2+},\underline{Mg^{2+}})_1\ (Si^{4+})_1\ (O^{2-})_3$

88.	Protopyroxene	PROT	SUBL	$(\underline{Ca^{2+}}, \underline{Mg^{2+}}, Mn^{2+}, Fe^{2+}, Zn^{2+})_1 (Si^{4+})_1 (O^{2-})_3$
89.	PSbrookite	PSBR	SUBL	(Al, Mg, Fe, Ti, V) (Al, Ti, Fe) (Ti) $(O)_5$
90.	Pseudowollastonite	PSWO	SUBL	$(\underline{Ca^{2+}}, Cr^{2+})_1 (Si^{4+})_1 (O^{2-})_3$
91.	K2S2O7-HT	PYRO	SUBL	$(\underline{K^{+1}}, Na^{+1})_2 (S_2O_7^{-2})$
92.	Pyrrhotite	PYRR	SUBL	(Fe, Cr, Mg, Mn, Ni,Va)(S)
93.	Rankinite	RANK	SUBL	$(\underline{Ca^{2+}}, Cr^{2+})_3 (Si^{4+})_2 (O^{2-})_7$
94.	Rhodonite	RHOD	SUBL	$(Mg^{2+}, \underline{Mn^{2+}}, Ca^{2+}, Fe^{2+})_1 (Si^{4+})_1 (O^{2-})_3$
95.	Rutile	RUTI	SUBL	$(Ti, V)_1 (O, Va)_2$
96.	Sapphirine	SAPP	SUBL	$(Al_{36}Mg_{14}Si_3O_{80}^{12-})_1 (Al^{3+}, \underline{Si^{4+}})_3 (Al^{3+}, \underline{Va})_1$
97.	SIGMA	SIGM	SUBL	$(Fe, Mn)_8 (Cr)_4 (Cr, Fe, Mn)_{18}$
98.	SiO2-HT	SIOH	SUBL	$(Al^{3+}, \underline{Si^{4+}})_1 (P^{5+}, \underline{Si^{4+}}, Ti^{+4})_1 (O^{2-})_4$
99.	SiO2-MT	SIOM	SUBL	$(Al^{3+}, \underline{Si^{4+}})_1 (P^{5+}, \underline{Si^{4+}})_1 (O^{2-})_4$
100.	Spinel	SPIN	SUBL	$(Al^{3+}, Cr^{2+}, Cr^{3+}, Fe^{2+}, Fe^{3+}, Mg^{2+}, Mn^{2+}, Zn^{2+}, Ti^{4+}, Ni^{2+})_1 (Al^{3+}, Ca^{2+}, Cr^{3+}, Fe^{2+}, Fe^{3+}, Mg^{2+}, Mn^{2+}, Mn^{3+}, Mn^{4+}, Va)_2 (Cr^{2+}, Fe^{2+}, Mg^{2+}, Va)_2 (O^{2-}$
101.	Ti5O9	T5O9	SUBL	$(\underline{Ti}, V)_5 (O)_9$
102.	Tetragonal-Spinel	TETR	SUBL	$(Mn^{2+}, Mn^{3+}, Cr^{2+}, Cr^{3+}, Zn^{2+}, Ti^{+4})_1$ $(Mn^{2+}, Mn^{3+}, Cr^{3+}, Al^{3+}, Fe^{3+}, Va)_2 (O^{2-})_4$

103.	Thiospinel	THIO	SUBL	$(Fe, Mn)\ (Cr)_2\ (S)_4$
104.	Ti3Al	TI3A	SUBL	$(Al, Ti)\ (Al, Ti)\ (O, \underline{Va})_2$
105.	TiAl	TIAL	SUBL	$(Al, Ti)\ (Al, Ti)\ (O, \underline{Va})_2$
106.	TIOX	TIOX	SUBL	$(Ti^{+2}, Ti^{+3}, Va)(Ti, Va)(O^{-2})$
107.	Titania Spinel	TISP	SUBL	$(Fe^{2+}, Fe^{3+}, Mg^{2+}, Mn^{2+}, Ti^{+4+}, Al^{3+})_1(Al^{3+}, Fe^{2+}, Fe^{3+}, Mg^{2+}, Mn^{2+}, Mn^{3+}, Ti^{3+}, Va, V^{3+},)_2(Va)_2\ (O^{2-})_4$
108.	V3O5	V3O5	SUBL	$(\underline{V}, Ti)_3(O)_5$
109.	V5O9	V5O9	SUBL	$(\underline{V}, Ti)_5(O)_9$
110.	V-Garnet	VGAR	SUBL	$(Ca, Mg)_{0.5}\ Ca_{1.5}\ Mg\ V_2O_8$
111.	Willemite	WILL	SUBL	$(\underline{Zn}^{+2}, Mg^{+2}, Fe^{+2})(Si^{+4})_2(O^{-2})_4$
112.	Wollastonite	WOLL	SUBL	$(\underline{Ca}^{2+}, Fe^{2+}, Mg^{2+}, Mn^{2+})_1\ (Si^{4+})_1\ (O^{2-})_3$
113.	$Zn_3P_2O_8$-HT	Z3PH	SUBL	$(\underline{Zn}^{+2}, \underline{Ca}^{+2})_3(P^{+5})_2(O^{-2})_8$
114.	$Zn_3P_2O_8$-LT	Z3PL	SUBL	$(\underline{Zn}^{+2}, \underline{Ca}^{+2})_3(P^{+5})_2(O^{-2})_8$
115.	Zincite	ZNO	SUBL	$(Ca^{2+}, Cr^{3+}, Fe^{2+}, Fe^{3+}, Mn^{+2}, Mn^{+3}, Mg^{+2}, Va, Zn^{2+})\ (O^{2-})$
116.	ZnP_2O_6	ZP	SUBL	$(Mg^{+2}, \underline{Zn}^{+2})(P^{+5})_2(O^{-2})_6$
117.	Spinel Ni_2TiO_4	SPNT	SUBL	$(NiO)_2\ (NiO, TiO_2)$
118.	NiV_2O6	NIV	SUBL	$(\underline{Ni}^{+2}, Zn^{+2})(V^{+5})_2(O^{-2})_6$

119.	ZnV_2O6	ZNV	SUBL	$(\underline{Zn^{+2}}, Ni^{+2})(V^{+5})_2(O^{-2})_6$
120.	Ni3S2	N3S2	SUBL	$(\underline{Ni}, Fe, Va)_2\ S$
121.	$Me_3V_2O_8$	M3V	SUBL	$(\underline{Zn^{+2}}, \underline{Ni^{+2}})_3(V^{+5})_2(O^{-2})_8$
122.	$(Fe, Ni)\ S_2$	MES2	SUBL	$(\underline{Fe}, \underline{Ni})\ S_2$
123.	Pentlandite	PENT	SUBL	$(\underline{Fe}, \underline{Ni})_9\ S_8$

Description of oxide melt

1:	**Na_2O**	**2:**	**Al_2O_3**	**3:**	**K_2O**
4:	$KAlO_2$	**5:**	$(K_2Al_4O_7)$:3	**6:**	(K_4Si_2O6):3
7:	$(K_2Si_2O_5)$:2	**8:**	(K_2Si_4O9):3	**9:**	Si_2O_4
10:	$(Si_2Na_8O_8)$:5	**11:**	$(Si_2Na_4O_6)$:3	**12:**	$(Si_2Na_2O_5)$:2
13:	$(Si_2Al_6O_{13})$:4	**14:**	$(Si_2Al_2Na_2O_8)$:3	**15:**	$(Si_6Al_2Na_2O_{16})$:5
16:	$(Al_4Na_2O_7)$:3	**17:**	$NaAlO_2$	**18:**	(KSi_2AlO_6):2
19:	$(K_2Si_2Al_2O_8)$:3	**20:**	Ca_2O_2	**21:**	Mg_2O_2
22:	$CaSiO_3$	**23:**	(Ca_2SiO_4):1.5	**24:**	$SiMgO_3$
25:	$(Si_2Mg_4O_8)$:3	**26:**	$(CaAl_2O_4)$:1.5	**27:**	$(Ca_2Si_4Al_4O_{16})$:5
28:	$(Al_4Mg_2O_8)$:3	**29:**	$(Si_5Al_4Mg_2O_{18})$:5.5	**30:**	$(Ca_3Al_{10}Na_4O_{20})$:8.5
31:	$(Fe_2Si_5Al_4O_{18})$:5.5	**32:**	(Fe_3O_4):1.5	**33:**	Fe_2O_3
34:	Fe_2O_2	**35:**	(Al_2FeO_4):1.5	**36:**	Cr_2O_3
37:	(Cr_2FeO_4):1.5	**38:**	Cr_2O_2	**39:**	$(CaFe_2O_4)$:1.5
40:	$(CrAl_2O_4)$:1.5	**41:**	(Fe_2MgO_4):1.5	**42:**	(Fe_2SiO_4):1.5
43:	$FeNaO_2$	**44:**	$(FeNa_2O_2)$:1.5	**45:**	$FeKO_2$
46:	$(FeSiNa_2O_4)$:2.0	**47:**	$(Na_2Ca_3Si_6O_{16})$:5	**48:**	$FeSiO_3$
49:	$(Fe_2Ca_2Si_4O_{12})$:4	**50:**	$(Fe_2Si_4Mg_2O_{12})$:4	**51:**	CrS
52:	$CrCaO_4$	**53:**	(K_2CrO_4):1.5	**54:**	$(K_2Cr_2O_7)$:2
55:	(Na_2CrO_4):1.5	**56:**	$(K_2Si_5MgO_{12})$:4	**57:**	(K_2SiMgO_4):2
58:	(CaK_2SiO_4):2	**59:**	$(Ca_3Cr_2Si_3O_{12})$:4	**60:**	Ca_2F_4
61:	$CaSiF_2O_2$	**62:**	(Cr_3O_4):1.5	**63:**	P_2O_5
64:	FePO4	**65:**	$(Fe_2P_2O_7)$:2	**66:**	(FeP_2O_6):1.5
67:	$(Fe_3P_2O_8)$:2.5	**68:**	$(Ca_2P_2O_7)$:2	**69:**	(CaP_2O_6):1.5
70:	$(Ca_3P_2O_8)$:2.5	**71:**	$(Mg_2P_2O_7)$:2	**72:**	(MgP_2O_6):1.5
73:	$(Mg_3P_2O_8)$:2.5	**74:**	AlPO4	**75:**	CrPO4
76:	(P_2SiO_7):1.5	**77:**	NaPO3	**78:**	(Na_3PO_4):2
79:	$(Na_4P_2O_7)$:3	**80:**	$(P_2Al_2Mg_3O_{11})$:3.5	**81:**	(Mn_3O_4):1.5
82:	CaS	**83:**	FeS	**84:**	MgS
85:	Al_2S_3	**86:**	SiS_2	**87:**	$CrNaO_2$
88:	(Cr_2MgO_4):1.5	**89:**	MgF_2	**90:**	(Mn_2MgO_4):1.5
91:	MnS	**92:**	Mn_2O_2	**93:**	SO_3
94:	**Mn_2O_3**	95:	**$MnSiO_3$**	96:	**$(Mn_2SiO_4)1.5$**
97:	(Al_2MnO_4):1.5	**98:**	(Cr_2MnO_4):1.5	**99:**	(Fe_2MnO_4):1.5

100:	**$(Mn_2Al_4Si_5O_{18})$:5.5**	101:	**$(Mn_3Al_2Si_3O_{12})$:4**	102:	**$(MgMnSi_2O_6)$:2**
103:	$(CaMn_2O_4)$:1.5	**104:**	$(Mn_2P_2O_7)$:2	**105:**	$(Mn_3P_2O_8)$:2.5
106:	(MnP_2O_6):1.5	**107:**	$MnPO_4$	**108:**	K_2S
109:	$(KAlS_2)$:2	**110:**	Na_2S	**111:**	$(Ca_9V_6O_{18})$:7.5
112:	$(MnCaSi_2O_6)$:2	**113:**	$(FeMn_2O_4)$:1.5	**114:**	$(NaAlS_2)$:2
115:	(Fe_2CrO_4):1.5	**116:**	(K_2SO_4):1.5	**117:**	(Na_2SO_4):1.5
118:	$CaSO_4$	**119:**	$MgSO_4$	**120:**	$(K_2S_2O_7)$:2
121:	$(Na_2S_2O_7)$:2	**122:**	$CrKO_2$	**123:**	KPO_3
124:	(K_3PO_4):2	**124:**	$(K_4P_2O_7)$:3	**126:**	$MnNaO_2$
127:	$MnKO_2$	**128:**	(Mn_2CrO_4):1.5	**129:**	Fe
130:	Cr	**131:**	Mn	**132:**	$(CaKP_3O_9)$:2.5
133:	$(CaP_2Na_4O_8)$:3.5	**134:**	$(CaPNaO_4)$:1.5	**135:**	(ZnO):0.5
136:	(Zn_2SiO_4):1.5	**137:**	(Al_2ZnO_4):1.5	**138:**	$(Zn_3P_2O_8)$:2.5
139:	$(Zn_2P_2O_7)$:2	**140:**	(ZnP_2O_6):1.5	**141:**	(Fe_2ZnO_4):1.5
142:	Zn	**143:**	(Cr_2ZnO4):1.5	**144:**	$(ZnMn_2O_4)$:1.5
145:	$(KMgPO_4)$:1.5	**146:**	$(KMgP_3O_9)$:2.5	**147:**	$(Na_8Mg_6P_{10}O_{35})$:12
148:	$NiTiO_3$	**149:**	$(Na_4MgP_2O_8)$:3.5	**150:**	S
151:	Al	**152:**	$(KZnPO_4)$:1.5	**153:**	Ti
154:	(Al_2TiO_5):1.5	**155:**	Ti_2O_2	**156:**	Ti_2O_3
157:	Ti_2O_4	**158:**	$MgTiO_3$	**159:**	(Mg_2TiO_4):1.5
160:	$(MgTi_2O_5)$:1.5	**161:**	$(MgTi_2O_4)$:1.5	**162:**	$FeTiO_3$
163:	(Fe_2TiO_5):1.5	**164:**	$(Na_2ZnP_2O_7)$:2.5	**165:**	$(Na_2Zn_5P_4O_{16})$:5.5
166:	Mg	**167:**	Ca	**168:**	(Mn_2TiO_4):1.5
169:	$MnTiO_3$	**170:**	$(MnTi_2O_4)$:1.5	**171:**	(Fe_2TiO_4):1.5
172:	(Zn_2TiO_4):1.5	**173:**	$CaTiO_3$	**174:**	$(Cr_2Ti_2O_7)$:2
175:	V	**176:**	V_2O_2	**177:**	V_2O_3
178:	V_2O_5	**179:**	V_2O_4	**180:**	(MgV_2O_4):1.5
181:	(FeV_2O_4):1.5	**182:**	(MnV_2O_4):1.5	**183:**	(K_4TiO_4):2.5
184:	(Na_4TiO_4):2.5	**185:**	$NiSO_4$	**186:**	NiS
187:	Ni	**188:**	NiO	**189:**	$Al_2(SO_4)_3$:2.5
190:	(TiP_2O_7):1.5	**191:**	$(NiAl_2O_4)$:1.5	**192:**	$(NiFe_2O_4)$:1.5
193:	$(Fe_2S_3O_{12})$:2.5	**194.**	KVO3	**195:**	(K_3VO_4):2
196:	$(K_4V_2O_7)$:2	**197:**	NaVO3	**196:**	(Na_3VO_4):2
199:	$(Na_4V_2O_7)$:2	**200:**	Sr	**201:**	Sr_2O_2
202:	$(Sr_2Fe_2O_5)$:2	**203:**	$(SrAl_2O_4)$:1.5	**204:**	(Sr_3SiO_5):2
205:	(SrP_2O_6):1.5	**206:**	$(Sr_3P_2O_8)$:2.5	**207:**	$(Sr_2P_2O_7)$:2
208:	(Sr_2SiO_4):1.5	**209:**	$SrSiO_3$		

Description of liquid metal

1:	**Fe**	2:	**Mn**	3:	**Cr**
4:	P	**5:**	CaS	**6:**	S
7:	FeS	**8:**	MgS	**9:**	Ca
10:	Mg	**11:**	MnS	**12:**	(SiS_2):2
13:	Na_2S	**14:**	K_2S	**15:**	CrS
16:	K	**17:**	Na	**18:**	Al
19:	AlO	**20:**	CaO	**21:**	Al_2O
22:	Ti	**23:**	C	**24:**	O
25:	PO	**26:**	CrO	**27:**	Cr_2O
28:	MnO	**29:**	MgO	**30:**	V
31:	Sr	**32:**	Ni	**33:**	NiS
34:	(Ni_3S_2):2				

Stoichiometric phases

ALL compounds

Al2O3-CaO-CaF_2-CrO_x-FeO_x-K_2O-MgO-MnO_x-Na_2O-NiO-P_2O_5-SO_3-SiO_2-SrO-TiO_2-Ti_2O_3-VO_x-ZnO-CaS, CrS, FeS, MgS, MnS, NiS

```
Stoichiometric Condensed Phases:
  1: C_S1(s)                2: C_DIAMOND(s2)          3: CO2_S1(s)
  4: Na_s1(s)               5: Na2O_s1(gamma)(s)      6: Na2O_(s2)
  7: Na2O_s3(alpha)(s3)     8: Mg_hcp-A3(s)           9: MgO_S1(s)
  10: F2Mg_S1(s)            11: Al_S1(s)              12: Al2O3(s)
  13: AlNaO2_LT(s)          14: AlNaO2_HT(s2)         15: Al9NaO14
  16: Al12Na2O19_beta2-alu  17: Si_s1(s)              18: SiO2(s2
  19: SiO2_quartz_beta(s3)  20: SiO2(s4)              21: SiO2(s5)
  22: SiO2_tridymite_alpha  23: SiO2_tridymite_beta(  24: SiO2_cristobalite_al
  25: SiNa2O3_solid(s)      26: SiNa4O4_LT(s)         27: SiNa4O4_HT(s2)
  28: SiNa10O7_solid(s)     29: Si2Na2O5_LT(s)        30: Si2Na2O5_MT(s2)
  31: Si2Na2O5_HT(s3)       32: Si2Na6O7_solid(s)     33: Si8Na6O19_solid(s)
  34: MgSiO3_clinoenstatit  35: MgSiO3_low-clinoenst  36: MgSiO3_orthoenstatit
  37: MgSiO3_protoenstatit  38: MgSiO3_wollastonite(  39: Mg2SiO4_forsterite(s
  40: SiMgNa2O4_Na2O_MgO_S  41: Si3MgNa2O8_NMS3(s)    42: Si3Mg2Na4O10_N2M2S3(
  43: Si4MgNa2O10_NMS4(s)   44: Si6Mg2Na2O15_NM2S6(s  45: Si12Mg5Na2O30_Roedde
  46: Si2Al2Na2O8_S1(s)     47: Si3AlNaO8_low-albite  48: Si3AlNaO8_high-albit
  49: Al18Mg7Si3O40_sapphi  50: Al4Mg2Si5O18_cordier  51: P_S1(s)
  52: P_RED(s2)             53: P2O5_HEXAGONAL(s)     54: P2O5_ORTHORHOMBIC(s2
  55: P2O5_O'-Phase(s3)     56: NaPO3_solid(s)_LT(s)  57: NaPO3_solid(s)_HT(s2
  58: Na3PO4_solid(s)_LT(s  59: Na3PO4_solid(s)_MT(s  60: Na3PO4_solid(s)_HT(s
  61: P2Na2O6_solid(s)_LT(  62: P2Na2O6_solid(s)_HT(  63: Na4P2O7_S1(s)
  64: Na4P2O7_S2(s2)        65: Na4P2O7_S3(s3)        66: Na4P2O7_S4(s4)
  67: Na4P2O7_S5(s5)        68: Na4P2O7_S6(s6)        69: Na4P2O7_S7(s7)
  70: Na5P3O10_S1(s)        71: Na5P3O10_S2(s2)       72: MgP2O6_S1(s)
  73: Mg2P2O7_s1(s)         74: Mg3P2O8_S1(s)         75: PMgNaO4_R(s)
  76: P2MgNa4O8_T2(s)       77: P2MgNa4O8_S2(s2)      78: P2MgNa4O8_S3(s3)
  79: P2MgNa6O9_N3P-LT(s)   80: P2MgNa6O9_N3P-MT(s2)  81: P2MgNa6O9_N3P-HT(s3)
  82: P3MgNaO9_B1(s)        83: NaMg4P3O12_J(s)       84: P4MgNa2O12_B2(s)
  85: P6MgNa4O18_B3(s)      86: Na8Mg6P10O35_S1(s)    87: AlPO4_LT(s)
  88: AlPO4_MT(s2)          89: AlPO4_HT(s3)          90: Al6P2O14_3Al2O3_P2O5
  91: Al2P6O18_S1(s)        92: Na3Al(PO4)2_S1(s)     93: Na3Al2(PO4)3_S1(s)
  94: P2SiO7_solid_lt(s)    95: P2SiO7_solid_mt(s2)   96: P2SiO7_solid_ht(s3)
  97: P4Si3O16_s1(s)        98: Na5PSi2O9_S1(s)       99: Na18P4Si6O31_S1(s)
 100: Na15P5Si3O26_S1(s)   101: P3Si2AlO13_S1(s)     102: S1(s)
 103: S2(s2)               104: SO3_solid(s)         105: Na2S_S1(s)
 106: Na2SO4_S1(s)         107: Na2SO4_S2(s2)        108: Na2SO4_S3(s3)
 109: Na2S2O7_S1(s)        110: MgS_Niningerite(s)   111: MgSO4_S1(s)
 112: MgSO4_S2(s2)         113: Na2MgS2O8_LT(s)      114: Na2MgS2O8_MT(s2)
 115: Na2MgS2O8_HT(s3)     116: Na6MgS4O16_S1(s)     117: Na2Mg3S4O16_S1(s)
 118: AlS_solid(s)         119: Al2S3_S1(s)          120: Al2S3_S2(s2)
 121: Al2(SO4)3(s)         122: NaAlS2_S1(s)         123: Na2Al20S31_S1(s)
 124: Na3Al(SO4)3_S1(s)    125: SiS2_S1(s)           126: K_s1(s)
 127: K2O_s1(solid)(s)     128: K2O_s2(solid)(s2)    129: K2O_s3(solid)(s3)
 130: KAlO2_LT(s)          131: KAlO2_HT(s2)         132: KAl9O14_k-beta-alumi
 133: K2Al12O19_k-beta2-al 134: K2SiO3_solid(s)      135: K2Si2O5_LT(s)
 136: K2Si2O5_MT(s2)       137: K2Si2O5_HT(s3)       138: K2Si4O9_LT(s)
 139: K2Si4O9_HT(s2)       140: K2MgSiO4_solid(s)    141: K2Si3MgO8_solid(s)
 142: K2Si3MgO8_S2(s2)     143: K2Si5MgO12_solid(s)  144: K2Si12Mg5O30_roedder
 145: K4Si5Mg2O14_ortho(s) 146: K10Si11Mg5O32_tetrag 147: KSiAlO4_kaliophyllit
```

148: KSiAlO4_kaliophyllit 149: KSi2AlO6_leucite-LT(150: KSi2AlO6_leucite-HT(
151: KSi3AlO8_microcline(152: KSi3AlO8_k-feldspar(153: KSi3AlO8_sanidine(s3
154: K4Si3Al4O14_S1(s) 155: KPO3_S1(s) 156: KPO3_S2(s2)
157: KPO3_S3(s3) 158: KPO3_S4(s4) 159: K3PO4_S1(s)
160: K3PO4_S2(s2) 161: K3PO4_S3(s3) 162: K3PO4_S4(s4)
163: K4P2O7_solid(s)_LT(s 164: K4P2O7_solid(s)_MT(s 165: K4P2O7_solid(s)_HT(s
166: Na2KP3O9_S1(s) 167: K4P2Na2O8_S1(s) 168: KPMgO4_S1(s)
169: KMgP3O9_B1(s) 170: KMg4P3O12_J(s) 171: K2MgP2O7_T1(s)
172: K2P4MgO12_B2(s) 173: K4P2MgO8_K3P-LT(s) 174: K4P2MgO8_K3P-MT(s2)
175: K4P2MgO8_K3P-HT(s3) 176: K4P6Mg4O21_W(s) 177: K6MgP2O9_K3P-LT(s)
178: K6MgP2O9_K3P-MT(s2) 179: K6MgP2O9_K3P-HT(s3) 180: K2S_S1(s)
181: K2SO4_S1(s) 182: K2SO4_S2(s2) 183: K2S2O7_S1(s)
184: K2S2O7_S2(s2) 185: KNaS_S1(s) 186: KNaS2O7_S1(s)
187: K2S3Mg2O12_S1(s) 188: KAlS2_S1(s) 189: K2Al8S13_S1(s)
190: K2Al20S31_S1(s) 191: Ca_FCC_A1(s) 192: Ca_BCC_A2(s2)
193: CaO_solid(s) 194: CaF2_s1(s) 195: CaMg2(s)
196: CaAl2O4_Al2CaO4(s) 197: CaAl4O7_Al4CaO7(s) 198: CaAl12O19_Al12CaO19(
199: Ca3Al2O6_Al2Ca3O6(s) 200: Ca12Al14O33_Al14Ca12 201: Ca4Al6F2O12_3CaO_3Al
202: Ca12Al14F2O32(s) 203: Ca3Al16Na2O28_S1(s) 204: Ca8Al6Na2O18_Na2O_8C
205: CaAl16Mg2O27_(solid) 206: Ca2Al28Mg2O46_(solid 207: Al4Ca3MgO10_Al2Ca3Mg
208: CaSiO3_wollastonite(209: CaSiO3_pseudowollast 210: Ca2SiO4_olivine_gamm
211: Ca2SiO4_alpha-prime(212: Ca2SiO4_alpha(s3) 213: Ca3SiO5_hatrurite(s)
214: Ca3Si2O7_rankinite(s 215: Ca4Si2F2O7_Cuspidine 216: Ca5Si2F2O8_4CaO_2SiO
217: Ca10Si3F2O15_9CaO_3S 218: CaSiNa2O4_Na2CaSiO4(219: Na4CaSi3O9(s)
220: Na2CaSi5O12(s) 221: Ca2Si2Na2O7_Na2Ca2Si 222: Na2Ca2Si3O9(s)
223: Na2Ca3Si6O16(s) 224: Ca2Si2MgO7_akermanit 225: Ca3Si2MgO8_merwinite
226: Al2CaSi2O8_ANORTHITE 227: Al2Ca2SiO7_Gehlenite 228: Al2Ca3O12Si3_GROSSUL
229: Al26Ca20Mg3Si3O68_Pl 230: CaP2O6_S1(s) 231: CaP4O11_S1(s)
232: Ca2P2O7_s1(s) 233: Ca2P2O7_s2(s2) 234: Ca2P2O7_s3(s3)
235: Ca2P6O17_S1(s) 236: Ca3P2O8_beta(s) 237: Ca3P2O8_alpha(s2)
238: Ca3P2O8_alpha_prime(239: Ca4P2O9_S1(s) 240: CaPNaO4_S1(s)
241: CaP2Na2O7_CNP(s) 242: CaP2Na4O8_S1(s) 243: CaP2Na6O9_S1(s)
244: CaP2Na6O9_S2(s2) 245: CaP2Na6O9_S3(s3) 246: CaP6Na4O18_S1(s)
247: CaP2MgO7_CMP(s) 248: Ca3P4Mg3O16_Ca3Mg3(P 249: Ca5P2SiO12_Silicocar
250: Ca7P2Si2O16_7CaOP2O5 251: CaS_Oldhamite(s) 252: CaSO4_S1(s)
253: CaSO4_S2(s2) 254: Na2CaS2O8_S1(s) 255: Na6CaS4O16_S1(s)
256: CaS4Mg3O16_S1(s) 257: Ca3K4Al10O20_K2C3A5(258: CaK2SiO4_solid(s)
259: CaK4Si3O9_S1(s) 260: CaK4Si6O15_solid(s) 261: CaK8Si10O25_solid(s)
262: Ca2K2Si9O21_solid(s) 263: Ca3K2Si6O16_solid(s) 264: Ca3K2Si6O16_S2(s2)
265: CaKPO4_C2KP(s) 266: CaKP3O9_KC2P(s) 267: CaK2P2O7_CKP(s)
268: CaK4P2O8_K3P-LT(s) 269: CaK4P2O8_K3P-MT(s2) 270: CaK4P2O8_K3P-HT(s3)
271: CaK6P2O9_K3P-LT(s) 272: CaK6P2O9_K3P-MT(s2) 273: CaK6P2O9_K3P-HT(s3)
274: Ca2K2S3O12_S1(s) 275: Ca2K2S3O12_S2(s2) 276: Ca2K2S3O12_S3(s3)
277: Ti_hcp-3(s) 278: Ti_bcc-a2(s2) 279: CTi_S1(s)
280: TiO_<ALPHA>(s) 281: TiO2_Rutile(s) 282: Ti2O3(s)
283: Ti2O3_S2(s2) 284: Ti3O2_S1(s) 285: Ti3O5_<Gun+Trans>(s)
286: Ti3O5_S2(s2) 287: Ti4O7_<Gun>(s) 288: Ti5O9(s)
289: Ti6O11(s) 290: Ti7O13(s) 291: Ti8O15(s)
292: Ti9O17(s) 293: Ti10O19(s) 294: Ti20O39(s)
295: Na2TiO3_S1(s) 296: Na2TiO3_S2(s2) 297: Na4TiO4_solid(s)
298: Na2O5Ti2_S1(s) 299: (Na2O)(TiO2)3_solid(300: Na8Ti5O14_solid(s)
301: (Na2O)(TiO2)6_solid(302: MgTiO3_S1(s) 303: TiMg2O4_Mg2TiO4(s)
304: MgTi2O4_Spinel(s) 305: MgTi2O5_S1(s) 306: TiAl2_Al2Ti(s)
307: Ti8Al17_Al11Ti5(s) 308: TiAlO3_S1(s) 309: Al2TiO5_S1(s)
310: TiP2O7_S1(s) 311: TiP2O7_S2(s2) 312: Ti2P2O9_S1(s)
313: Ti5P4O20_S1(s) 314: K2TiO3_solid(s) 315: K4TiO4_solid(s)
316: K2Ti2O5_solid(s) 317: K2Ti3O7_solid(s) 318: K4Ti3O8_S1(s)

```
319: K2Ti4O9_S1(s)          320: K2Ti6O13_solid(s)     321: (K2TiO3)(Na2TiO3)_S1
322: (K2TiO3)2(Na2TiO3)_S   323: CaTiO3_CT(s)          324: Ca3Ti2O7_S1(s)
325: Ca5Ti4O13_S1(s)        326: CaSiTiO5_SPHENE(s)    327: V_S1(s)
328: VO_S1(s)               329: VO2_S1(s)             330: VO2_S2(s2)
331: V2O3_S1(s)             332: V2O5_S1(s)            333: V3O5_S1(s)
334: V3O5_S2(s2)            335: V3O7(s)               336: V4O7(s)
337: V5O9_S1(s)             338: V6O11_S1(s)           339: V6O13(s)
340: V7O13(s)               341: V8O15(s)              342: V52O64_Delta_prime(s
343: NaVO3_solid(s)         344: NaVO3_solid(s2)       345: Na3VO4_solid(s)
346: Na4V2O7_S1(s)          347: Na5V3O10_S1(s)        348: NaV6O15_S1(s)
349: Na2V6O15_S1(s)         350: MgV2O4_Spinel(s)      351: MgV2O6_(MgO)(V2O5)(s
352: Mg2V2O7_(MgO)2(V2O5)   353: Mg3V2O8_(MgO)3(V2O5)  354: AlVO4(s)
355: NaAlV2O7_S1(s)         356: KVO3_S1(s)            357: K3VO4_S1(s)
358: K4V2O7_S1(s)           359: K4V2O7_S2(s2)         360: KV3O8_S1(s)
361: K5V3O10_S1(s)          362: K3V5O14_S1(s)         363: KV6O15_S1(s)
364: K2V8O21_S1(s)          365: KNa(VO3)2_S1(s)       366: K2Na(VO3)3_S1(s)
367: KNa3(VO3)4_S1(s)       368: Sr8Fe6O17_S1(s)       369: CaV2O6_(CaO)(V2O5)(s
370: Ca2V2O7_(CaO)2(V2O5)   371: Ca3V2O8_(CaO)3(V2O5)  372: Ca7V4O17_Ca7Va4O17(s
373: Ca9V6O18_S1(s)         374: Ca10V6O19_S1(s)       375: CaMgV2O7_S1(s)
376: Ca3V2Si3O12_Goldmani   377: Ti2VO5_TI2VO5(s)      378: Cr_BCC-A2(s)
379: CrO2_S1(s)             380: CrO3_S1(s)            381: Cr2O3_Rho(s)
382: CrNa2O4-LT(s)          383: CrNa2O4-HT(s2)        384: Cr2Na2O4_S1(s)
385: Cr2Na2O7_solid(s)      386: Cr2SiO4_2CrO_SiO2(s)  387: CrPO4_S1(s)
388: Cr6P2O14_S1(s)         389: Cr10P2O20_S1(s)       390: CrS_S1(s)
391: CrS_S2(s2)             392: 'Cr2S2'_Cr1.03S(s)    393: Cr2S3(s)
394: Cr2S3_S2(s2)           395: Cr3S4(s)              396: Cr5S6(s)
397: Cr7S8(s)               398: CrKO2_S1(s)           399: CrK2O4-LT(s)
400: CrK2O4-HT(s2)          401: CrK3O4_S1(s)          402: CrK4O4_S1(s)
403: Cr2K2O7_solid(s)       404: CrKNaO4_KNaO_CrO3(s)  405: CrCaO4_S1(s)
406: CaCr2O4_beta(s)        407: CaCr2O4_alfa(s2)      408: Cr3Ca5O12_S1(s)
409: Cr4Ca6O16_S1(s)        410: Cr13Ca2O20_S1(s)      411: CrCa4Al6O16_4CaO_3Al
412: Cr2Ca6Al4O15_6CaO_2_   413: CrCaSi4O10_Gillespit 414: Cr2Ca3Si3O12_Uvarovi
415: Cr2Ti2O7(s)            416: CrVO4(s)              417: Cr2V4O13_CR2V4O13(s)
418: Mn_cbcc-a12(s)         419: Mn_cub-a13(s2)        420: Mn_fcc-a1(s3)
421: Mn_bcc-a2(s4)          422: MnO_S1(s)             423: MnO2_S1(s)
424: Mn2O3(s)               425: Mn3O4_Tetragonal-Spi  426: Mn3O4_Cubic-Spinel(s
427: Al2MnO4_Galaxite_(Sp   428: MnSiO3_RHODONITE(s)  429: Mn2SiO4_TEPHROITE(s)
430: Mn7SiO12_Braunite(s)   431: Mn2Al4Si5O18_Mn-cord 432: Mn3Al2Si3O12_Mn-Pyro
433: MnPO4_s1(s)            434: MnP2O6_s1(s)          435: Mn2P2O7_s1(s)
436: Mn2P2O8_S1(s)          437: Mn3P2O8_S1(s)         438: MnS_S1(s)
439: MnS2_S1(s)             440: Mn9SSi3O14_8MnO_MnS_  441: Mn26SSi9O43_25MnO_Mn
442: CaMnO3_s1(s)           443: Ca2MnO4_s1(s)         444: CaMn2O4_s1(s)
445: Ca3Mn2O7_s1(s)         446: CaMn3O6_s1(s)         447: Ca2Mn3O8_s1(s)
448: Ca4Mn3O10_s1(s)        449: CaMn4O8_s1(s)         450: CaMn7O12_s1(s)
451: MnTiO3_S1(s)           452: MnTi2O4_Cubic(s)      453: MnTi2O4_S2(s2)
454: MnTi2O5_Mn-pseudobro   455: Mn2TiO4_Spinel-Tetra  456: Mn2TiO4_Spinel-Cubic
457: MnV2O4_S1(s)           458: MnV2O6_S1(s)          459: Mn2V2O7_S1(s)
460: Cr3Mn5_CR3MN5(s)       461: MnCr2O4(solid)(s)     462: MnCr2S4_S1(s)
463: Fe_bcc_a2(s)           464: Fe_fcc_a1(s2)         465: FeO_Wustite(s)
466: Fe2O3_CORUNDUM(s)      467: Fe3O4_MAGNETITE(s)    468: FeNaO2_s1(s)
469: FeNaO2_LT(s2)          470: FeNaO2_HT(s3)         471: FeNaO2_delta(s4)
472: FeNa2O2_S1(s)          473: FeNa3O3_S1(s)         474: FeNa4O3_S1(s)
475: Fe2Na8O7_S1(s)         476: Fe16Na10O29_S1(s)     477: Fe2MgO4_S1(s)
478: Al2FeO4_S1(s)          479: Fe2Al2O6_S1(s)        480: FeSi(s)
481: FeSiO3_S1(s)           482: Fe2SiO4_FAYALITE(s)   483: FeSiNa2O4_Na2FeSiO4(
484: Fe2Si2Na2O8_S1(s)      485: Fe2Si4Na2O12_Acmite(  486: Fe2Si6Na2O16_S1(s)
487: Fe2Si8Na10O24_5Na2O_   488: Fe8Si5Na12O28_6Na2O_  489: Fe2Si5Al4O18_Iron-Co
```

```
490: FeP_FEP(s)           491: Fe2P_FE2P1(s)        492: Fe3P_CU3P1(s)
493: Fe3P_FE3P1(s2)       494: FePO4_S1(s)          495: FePO4_S2(s2)
496: FePO4_S3(s3)         497: FeP2O6_FeO_P2O5(s)   498: Fe2P2O7_2FeO_2O5(s)
499: Fe2P6O18_3P2O5_Fe2O3 500: Fe3P2O8_3FeO_P2O5(s) 501: Fe4P2O10_W2FP(s)
502: Fe4P6O21_2Fe2O3_3P2O 503: Fe6P2O14_3Fe2O3_P2O5 504: Fe7P6O24_W3F2P3(s)
505: Fe10P6O26_W8FP3(s)   506: Fe18P2O24_16FeO_Fe2O 507: FeS_TROILITE(s)
508: FeS_TROILITE(s2)     509: FeS_Pyrrhotite(s3)   510: FeS2_PYRITE(s)
511: Fe7S8_S1(s)          512: Fe9S10_S1(s)         513: Fe10S11_S1(s)
514: Fe11S12_S1(s)        515: FeKO2_LT(s)          516: FeKO2_HT(s2)
517: Fe12K2O19_S1(s)      518: Fe22K2O34_S1(s)      519: Fe2K2Si2O8_Kaliophil
520: Fe2K2Si2O8_Kaliophil 521: Fe2K2Si4O12_Iron-Leu 522: Fe2K2Si6O16_Iron-Ort
523: Fe4K4Si3O14_K2F2S3(s 524: CaFe2O4_beta(s)      525: Ca2Fe2O5(s)
526: Fe3CaO5_CaFe3O5(s)   527: Fe4CaO7(s)           528: Fe5CaO7_CaFe5O7(s)
529: Fe9Ca4O17_Ca4Fe9O17( 530: Fe17Ca4O29_Ca4Fe17O2 531: Ca3Fe2Si3O12_Andradi
532: FeTiO3_S1(s)         533: FeTi2O5_Pseudobrooki 534: Fe2TiO4_Spinel(s)
535: Fe2TiO5_Ferric_Pseud 536: FeVO4(s)             537: FeV2O4_S1(s)
538: Fe2V4O13_Fe2O3_2V2O5 539: NaFeV2O7_S1(s)       540: NaFe3V4O15_S1(s)
541: Ca6Fe7V3O24_S1(s)    542: FeCr2S4_Daubreelite( 543: Fe2MnO4_S1(s)
544: Ni_fcc-A1(s)         545: NiO_S1(s)            546: NiO_S2(s2)
547: NiCO3_S1(s)          548: Al2NiO4_S1(s)        549: Ni2SiO4_S1(s)
550: NiS_Millerite(s)     551: NiS2_Vaesite(s)      552: Ni3S2_heazlewoodite(
553: Ni3S4_thiospinel(s)  554: Ni7S6_solid(s)       555: Ni9S8_solid(s)
556: NiSO4_S1(s)          557: NiSO4_S2(s2)         558: Na2Ni(SO4)2_S1(s)
559: Na6Ni(SO4)4_S1(s)    560: Na2Ni3S4O16_S1(s)    561: NiCaSi2O6_Ni-clino-p
562: NiTiO3_S1(s)         563: NiV2O6_(NiO)(V2O5)(s 564: Ni2V2O7_(NiO)2(V2O5)
565: Ni3V2O8_(NiO)3(V2O5) 566: Ca5Ni4V6O24_S1(s)    567: Cr2NiO4_S1(s)
568: Fe2NiO4_S1(s)        569: Fe2NiO4_S2(s2)       570: Zn_S1(s)
571: ZnO_S1(s)            572: Al2ZnO4_S1(s)        573: Zn2SiO4_2ZnO_SiO2(s)
574: ZnSiNa2O4_Na2O_ZnO_S 575: ZnSi2Na2O6_S1(s)     576: Zn2Si2Na2O7_Na2O_2Zn
577: Zn2Si3Na4O10_S1(s)   578: ZnP2O6_S1(s)         579: ZnP4O11_S1(s)
580: Zn2P2O7_S1(s)        581: Zn2P2O7_S2(s2)       582: Zn3P2O8_S1(s)
583: Zn3P2O8_S2(s2)       584: NaZnPO4_S1(s)        585: NaZnPO4_S2(s2)
586: Na2ZnP2O7_S1(s)      587: NaZnP3O9_S1(s)       588: Zn5P4Na2O16_S1(s)
589: KZnPO4_LT(s)         590: KZnPO4_MT(s2)        591: KZnPO4_HT(s3)
592: KZn(PO3)3_S1(s)      593: K2ZnP2O7_S1(s)       594: K2Zn(PO3)4_S1(s)
595: K2Zn3(P2O7)2_S1(s)   596: KZn4(PO4)3_S1(s)     597: ZnCa3Al4O10_S1(s)
598: Zn3Ca6Al4O15_C6Z3A2( 599: Ca2ZnSi2O7_Hardyston 600: CaZn2P2O8_CaO_2ZnO_P
601: CaZn2P2O8_S2(s2)     602: CaZn2P2O8_S3(s3)     603: ZnTiO3_S1(s)
604: Zn2TiO4_S1(s)        605: ZnV2O6_S1(s)         606: Zn2V2O7_S1(s)
607: Zn3V2O8_S1(s)        608: Zn4V2O9_S1(s)        609: Cr2ZnO4_S1(s)
610: ZnMn2O4_S1(s)        611: Fe2ZnO4_Spinel(s)    612: Sr_fcc-a1(s)
613: Sr_bcc-a2(s2)        614: SrO_solid(s)         615: SrO2_s1(s)
616: SrAl2O4_Solid(LT)(s) 617: SrAl2O4_Solid(HT)(s2 618: SrAl4O7_solid(s)
619: SrAl12O19_hexagonal( 620: Sr3Al2O6_solid(s)    621: Sr4Al2O7_Solid(LT)(s
622: Sr4Al2O7_Solid(HT)(s 623: Sr4Al14O25_solid(s)  624: Sr5Al2O8_solid(s)
625: SrSiO3_Ps-Wollastoni 626: Sr2SiO4_beta(s)     627: Sr2SiO4_alpha'(s2)
628: Sr2SiO4_alpha(s3)    629: Sr3SiO5_solid(s)     630: SrP2O6_SP-beta(s)
631: SrP2O6_SP-alpha(s2)  632: Sr2P2O7_S2P-beta(s)  633: Sr2P2O7_S2P-alpha(s2
634: Sr3P2O8_S3P-alpha(s) 635: Sr3P2O8_S3P-beta(s2) 636: Sr3P4O13_Sr3P2O13(s)
637: Sr4P2O9_S4P(s)       638: SrV2O6_S1(s)         639: Sr2V2O7_S1(s)
640: Sr3V2O8_S1(s)        641: Sr4V2O9_S1(s)        642: SrFe12O19_SrO_6Fe2O3
643: Sr2Fe2O5_Perowskite( 644: Sr2Fe2O6_Perowskite( 645: Sr3Fe2O6_3SrO_Fe2O3(
646: Sr4Fe2O7_S1(s)       647: Sr4Fe6O13_4SrO_3_Fe2
```

Binary systems:

Mole fraction

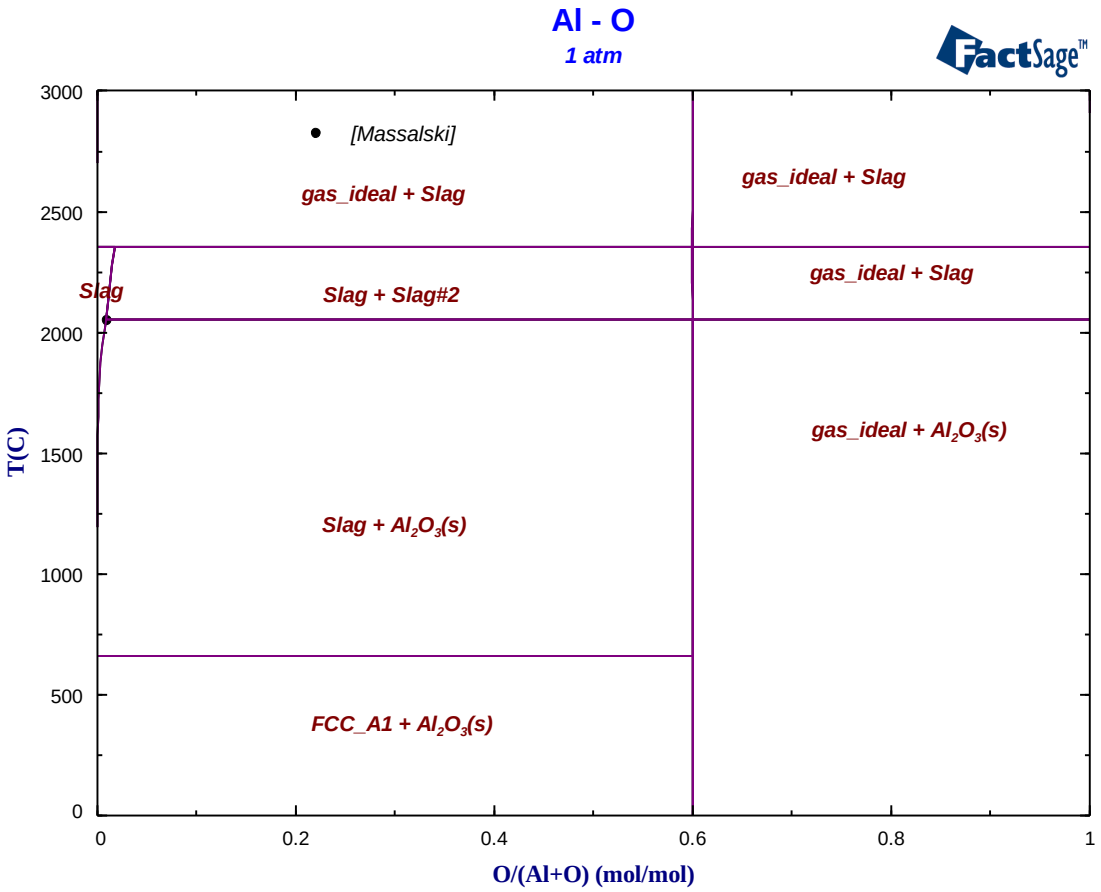

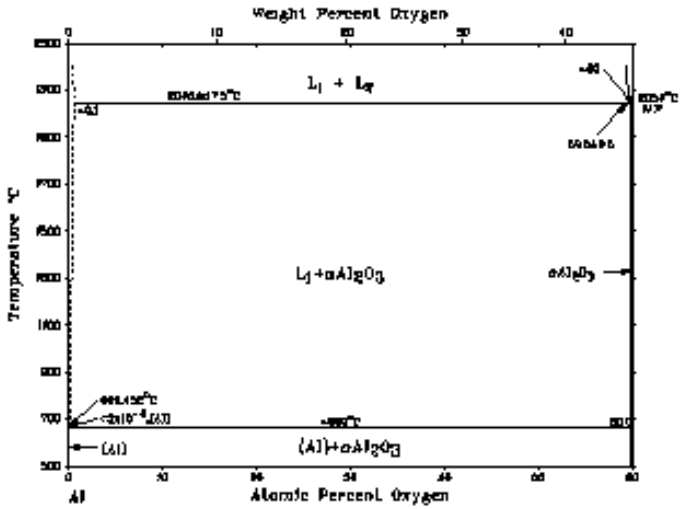

T.B. Massalski (ed), Binary Alloy Phase Diagrams, Second Edition, ASM International, Metals Park, OH 1990.

Weight percent

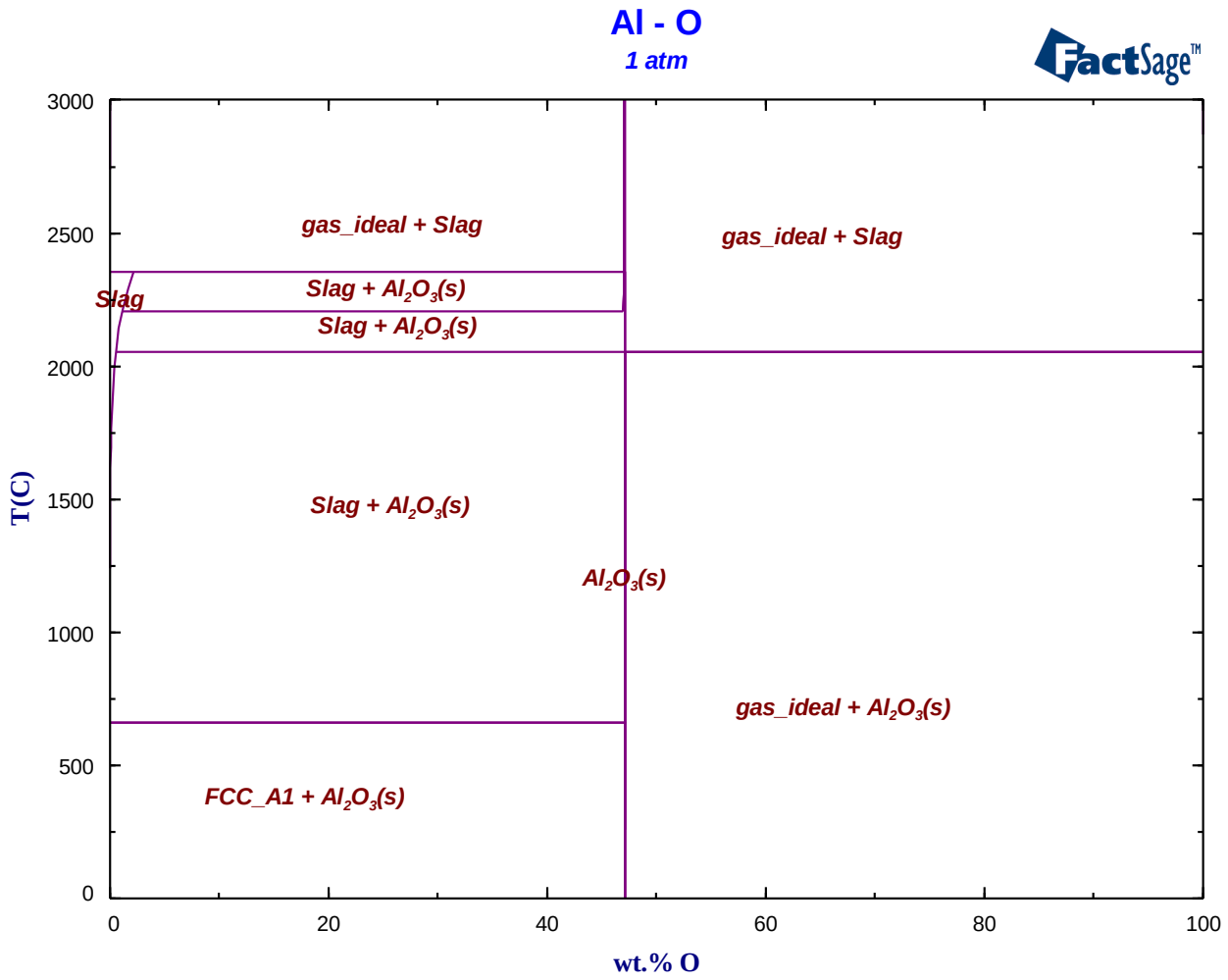

Mole fraction with isobars

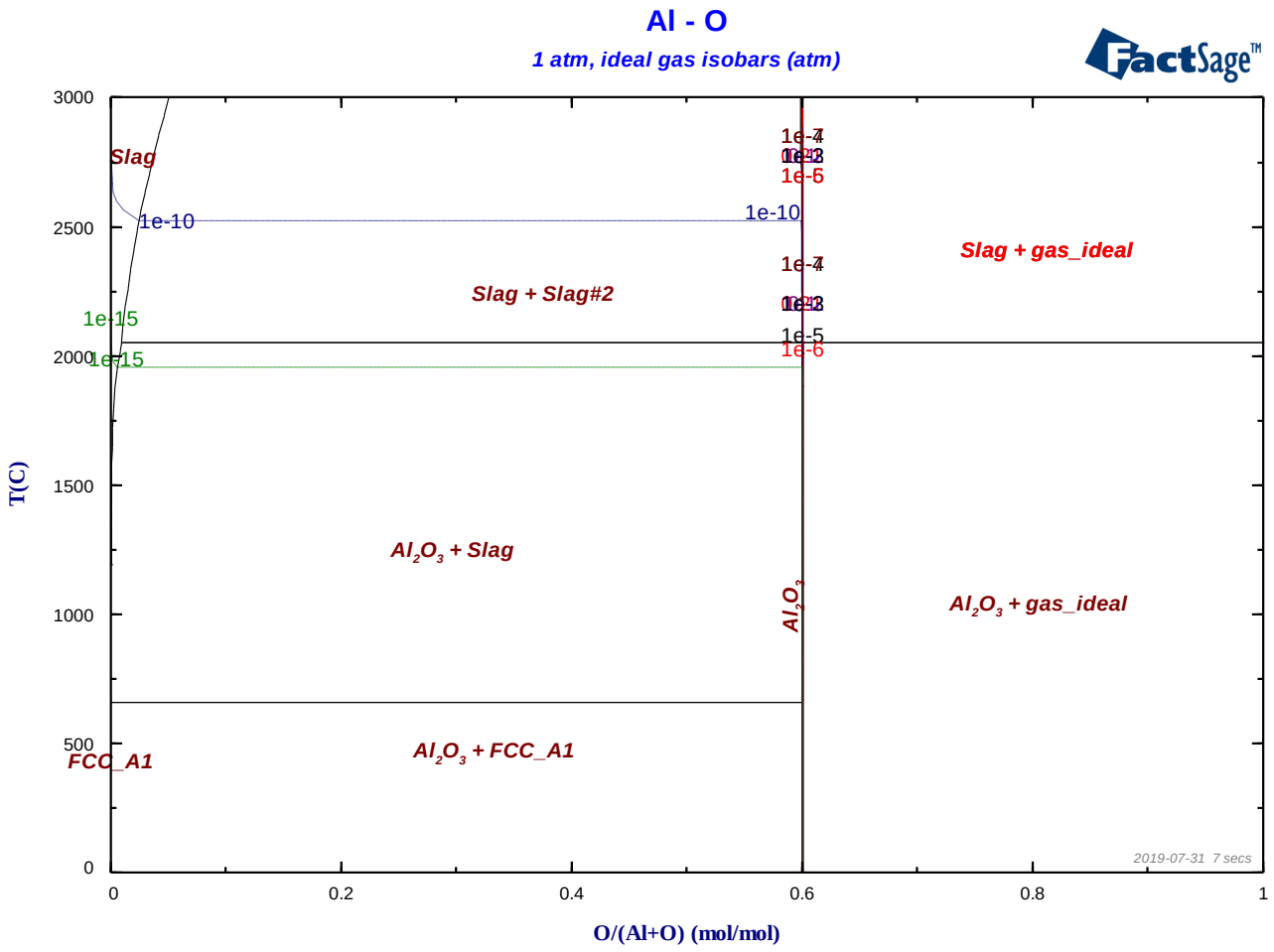

Al-O2,

Temperature vs. log P(O2) diagram

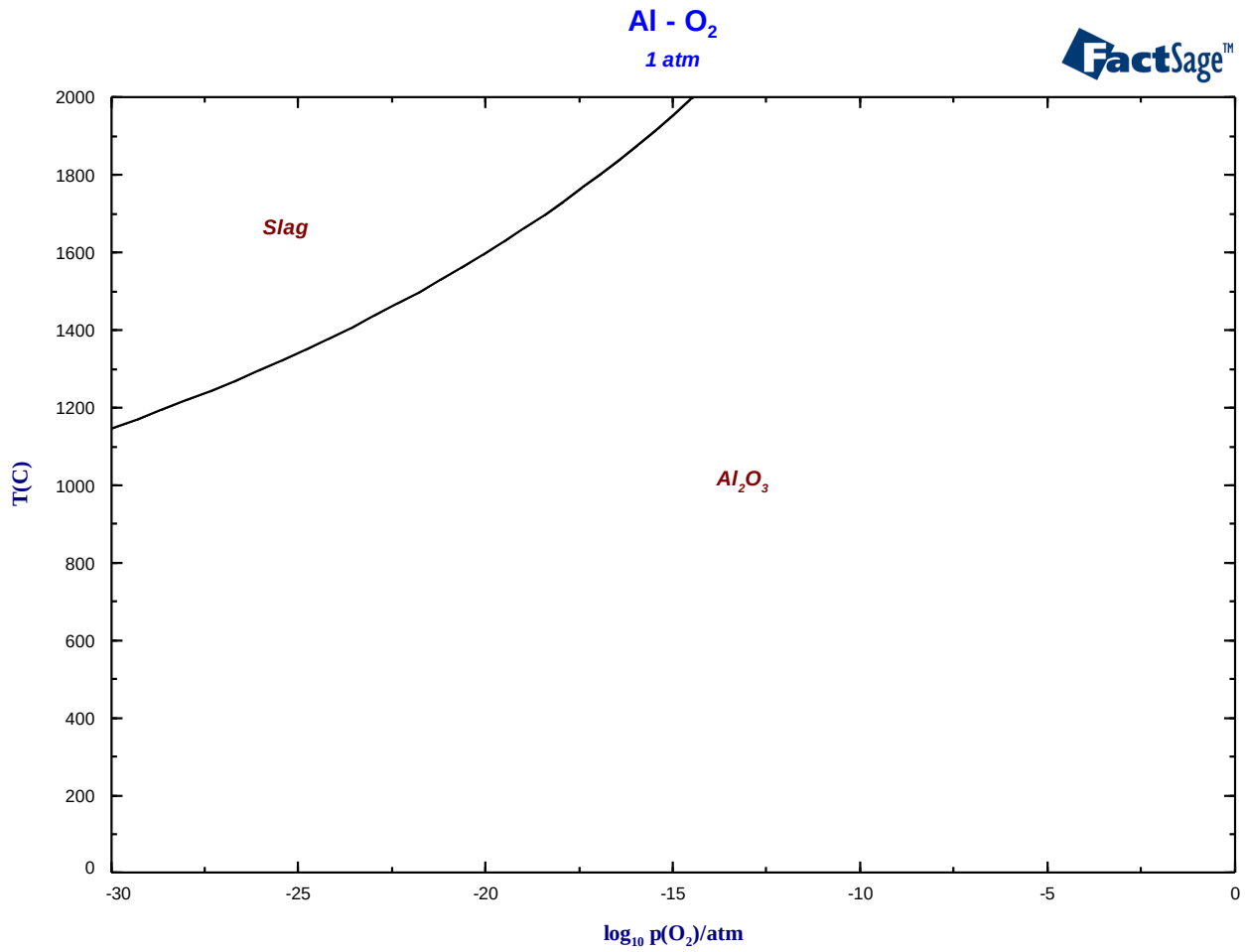

Mole fraction compared with experimental data

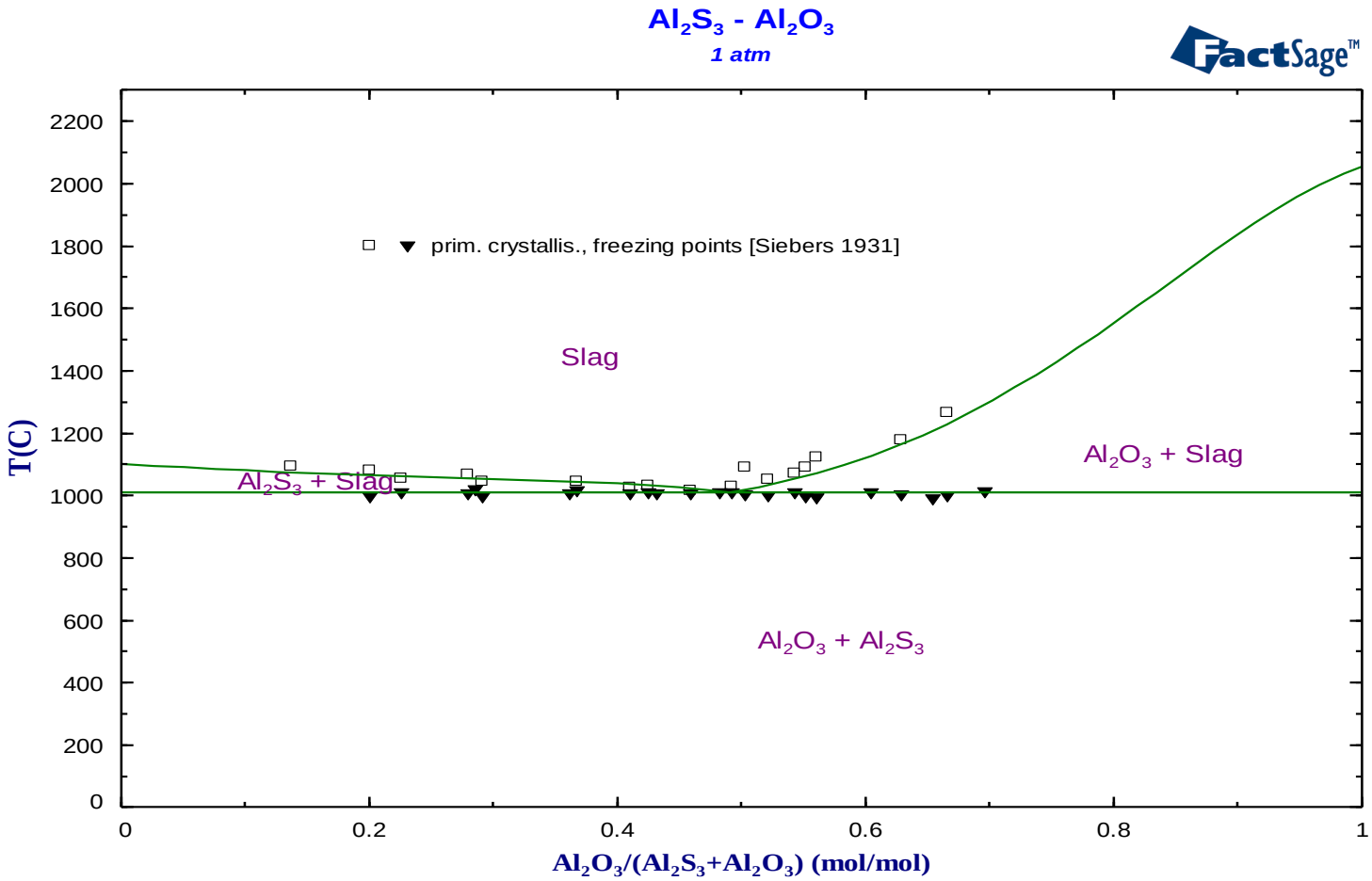

Weight percent

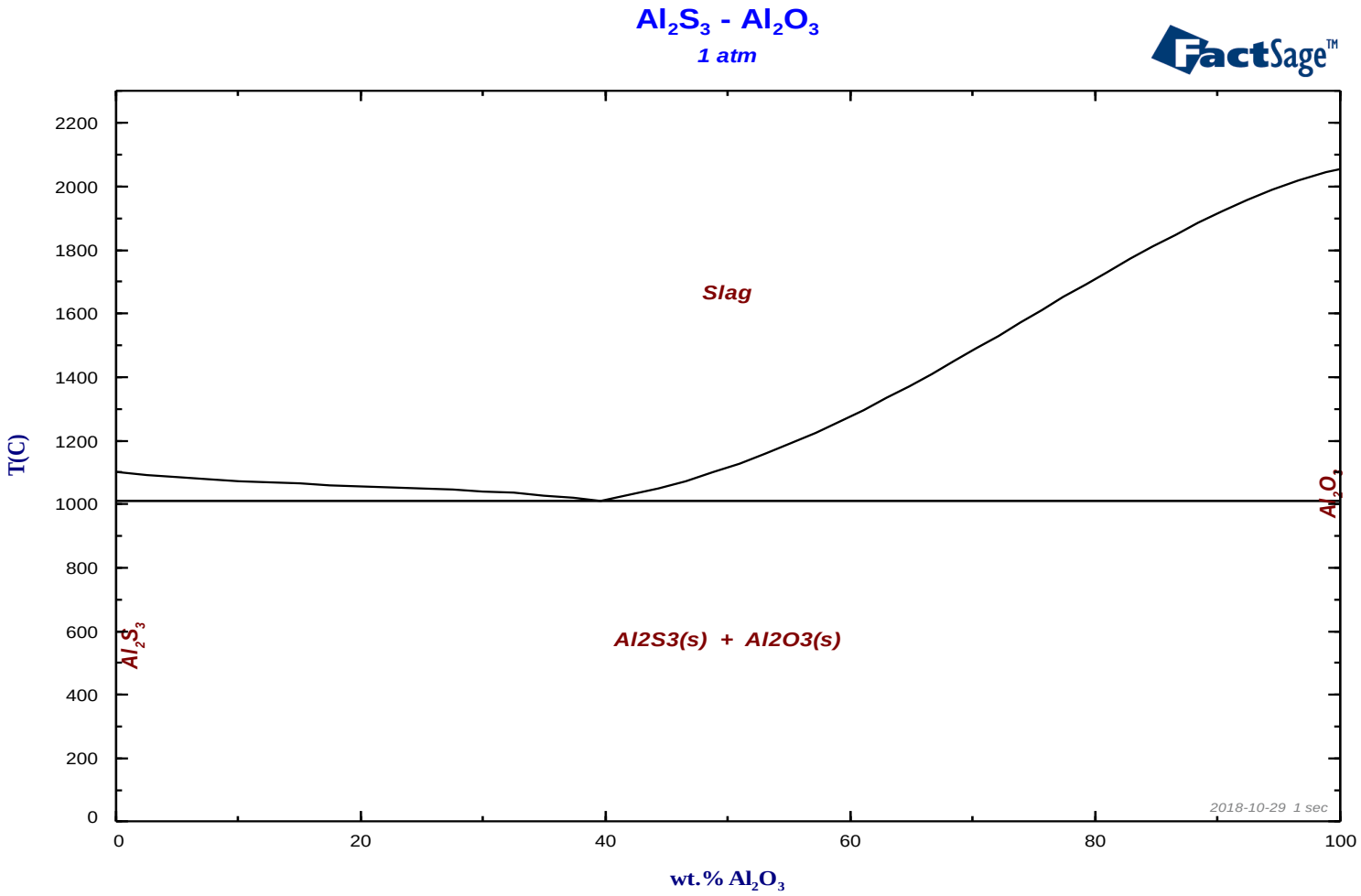

Mole fraction

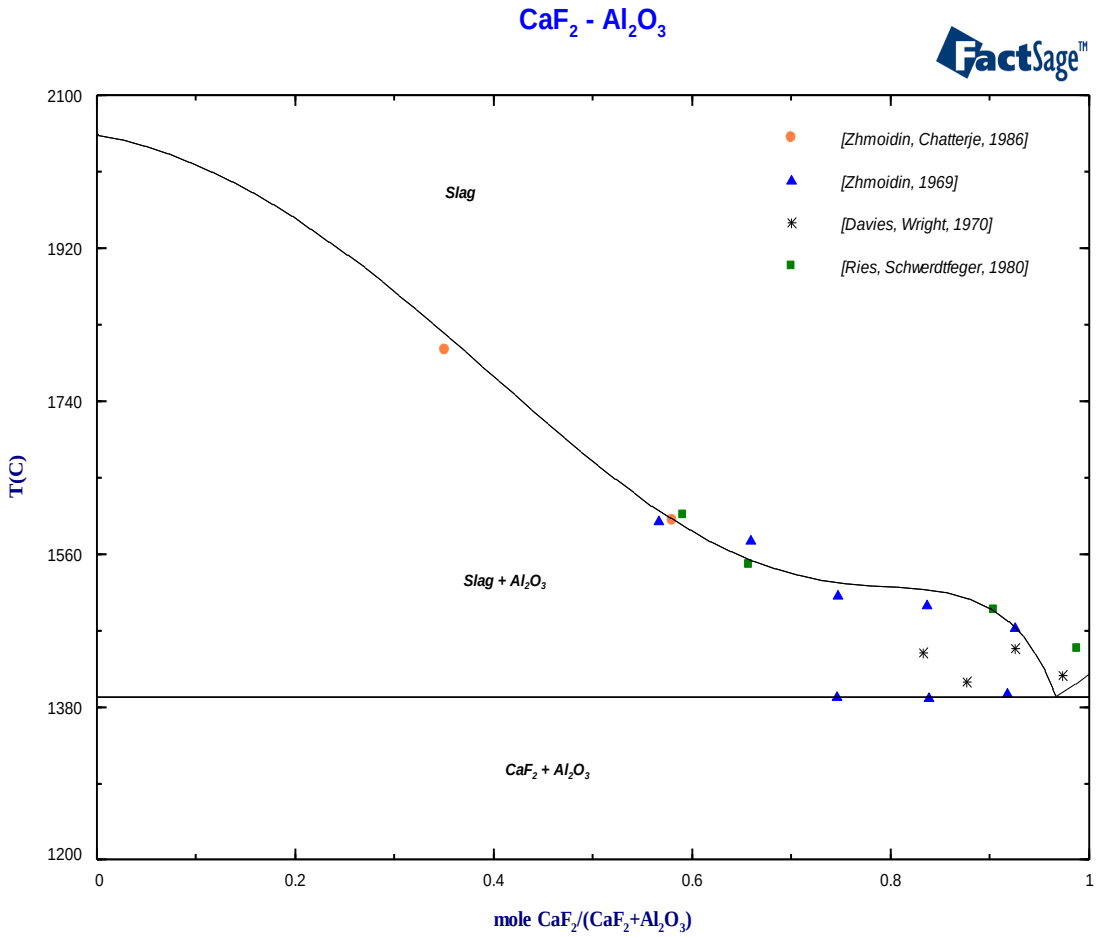

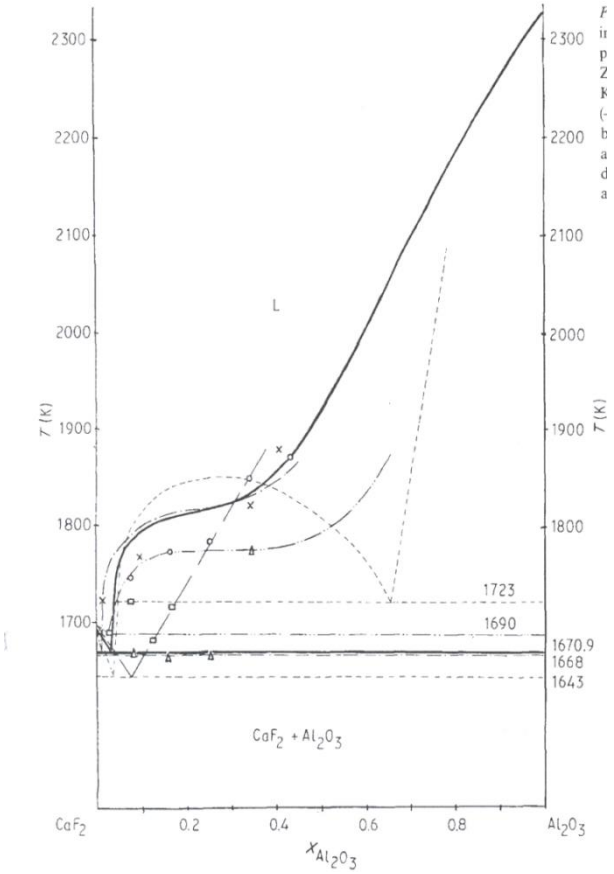

A.I. Zaitsev, N.V. Korolyov, B.M. Mogutnov, Journ. Mater. Scien., 26 (1991), pp.1588-1600.

Weight percent

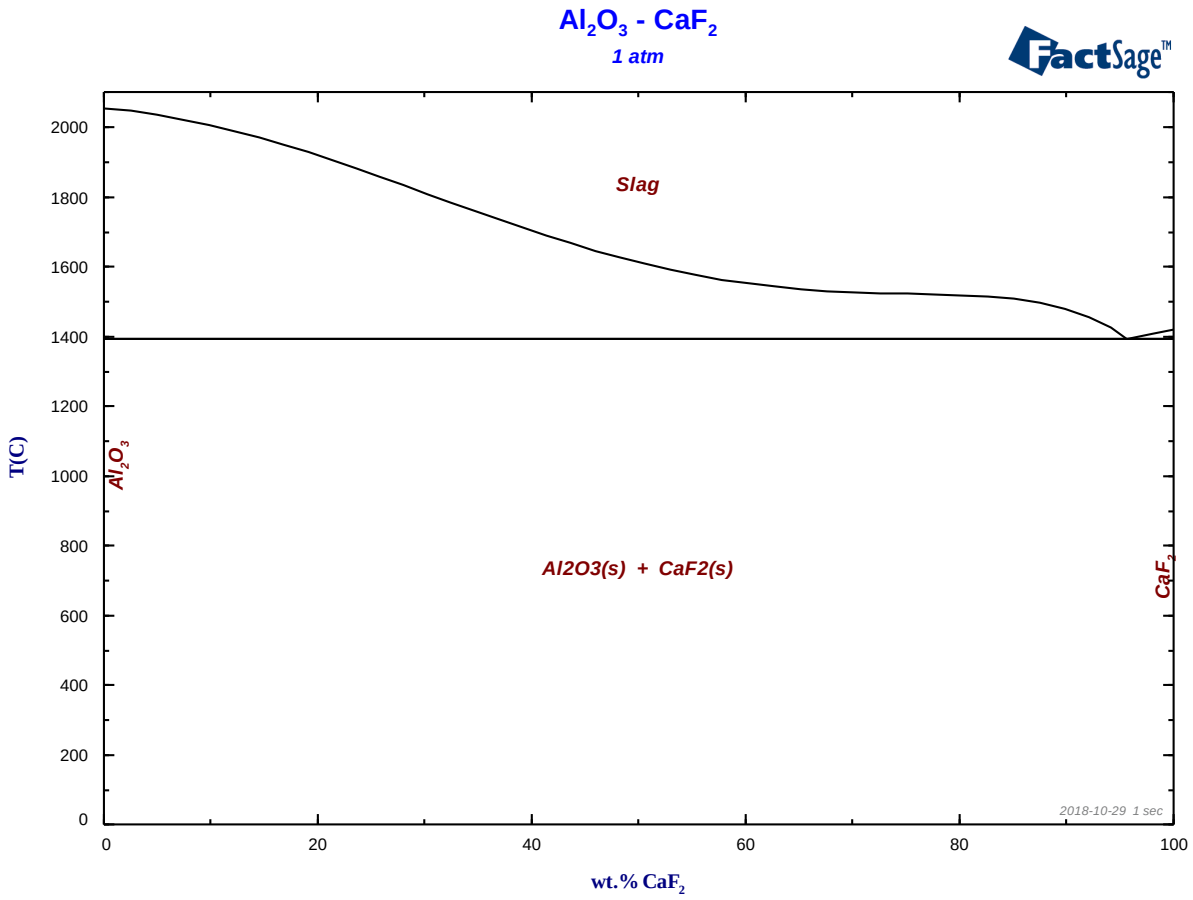

Mole fraction

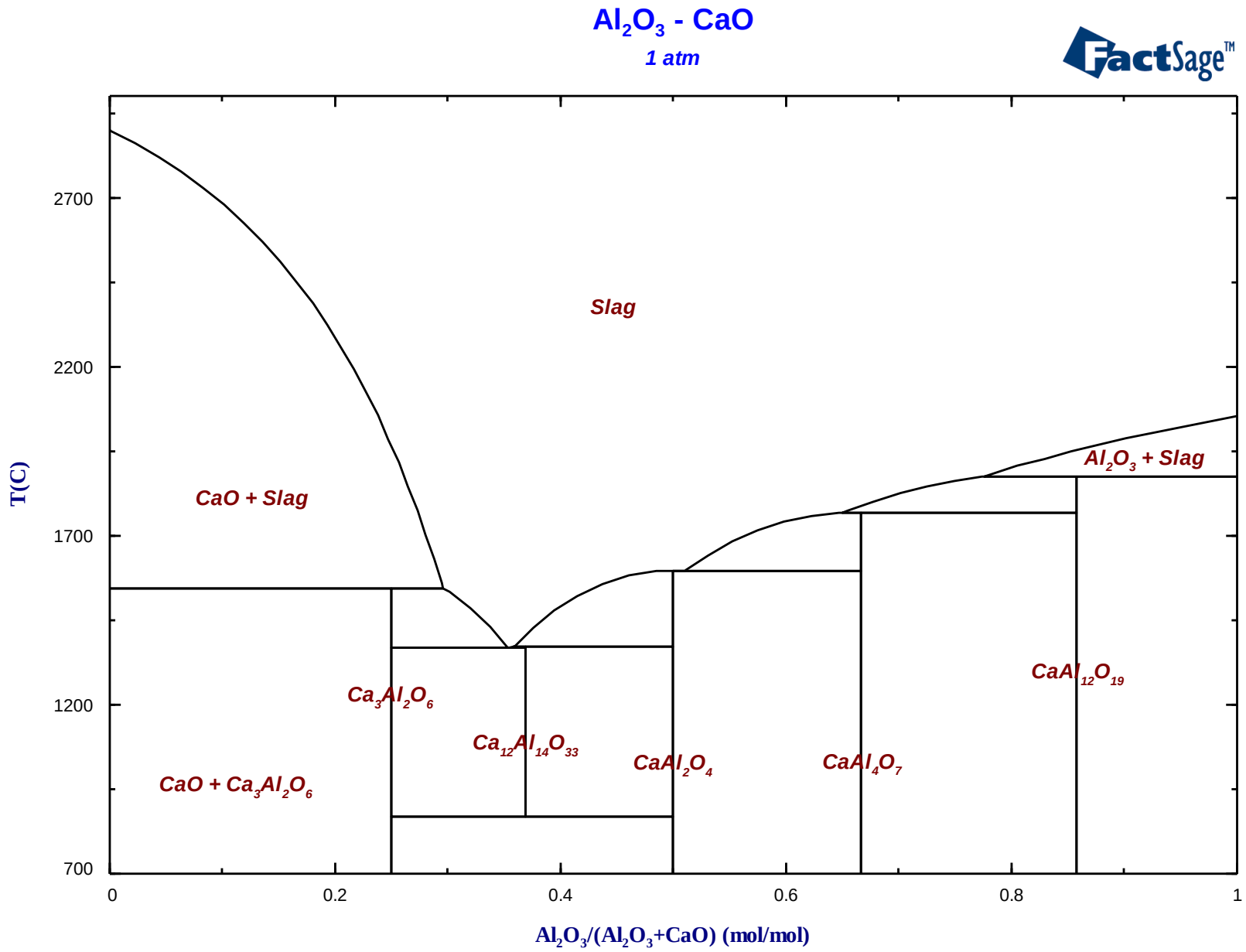

Weight percent
compared with experimental data

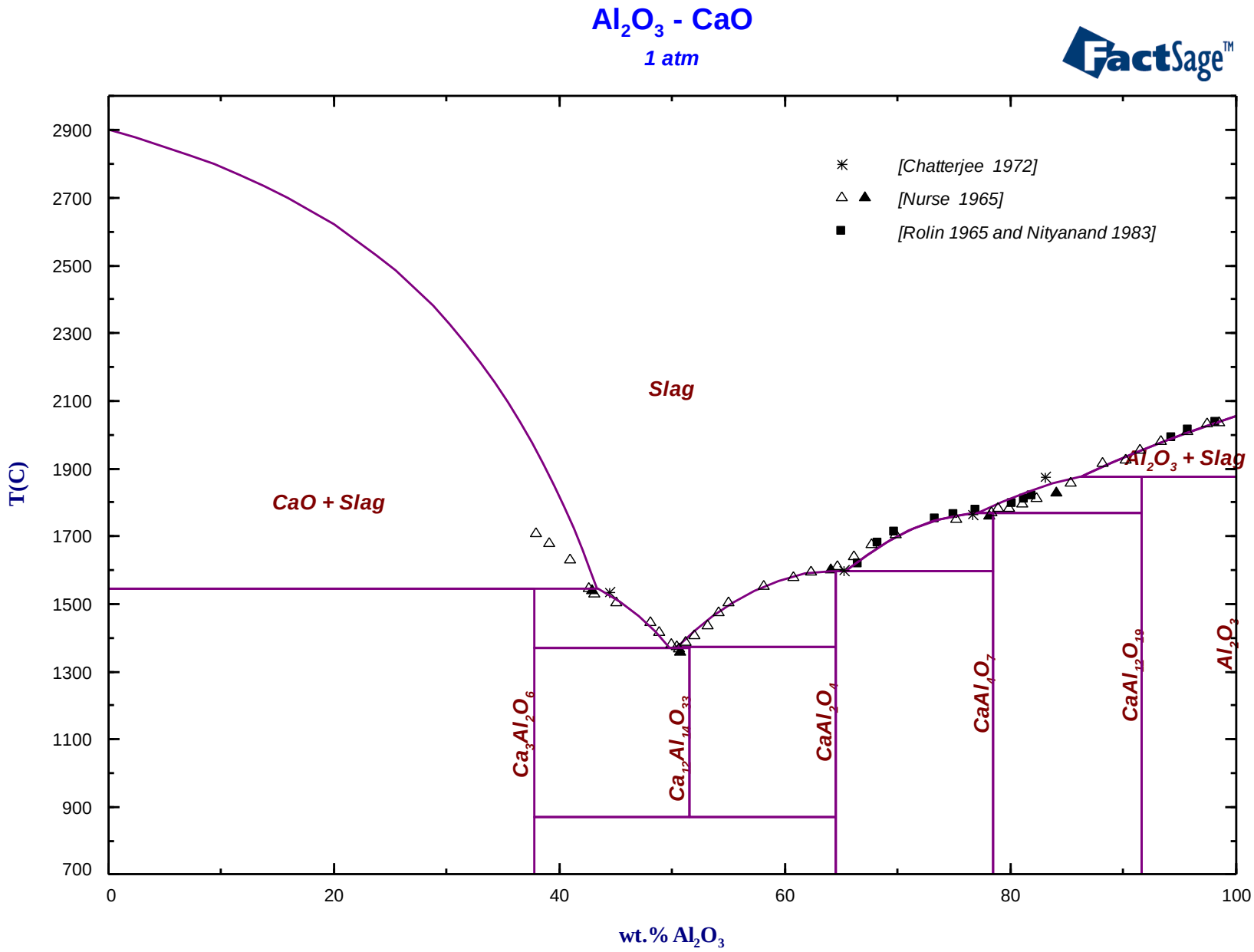

Mole fraction

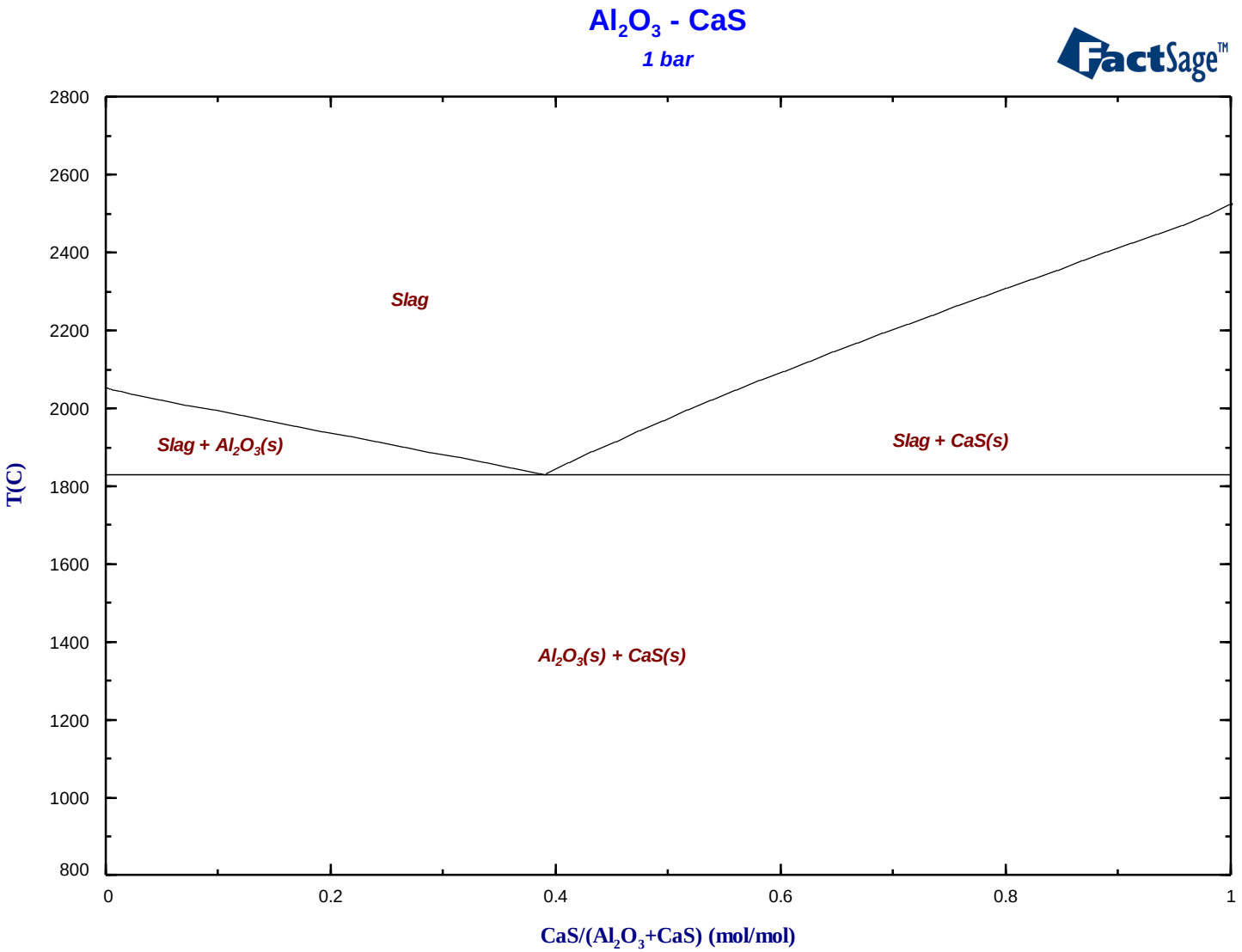

Weight percent

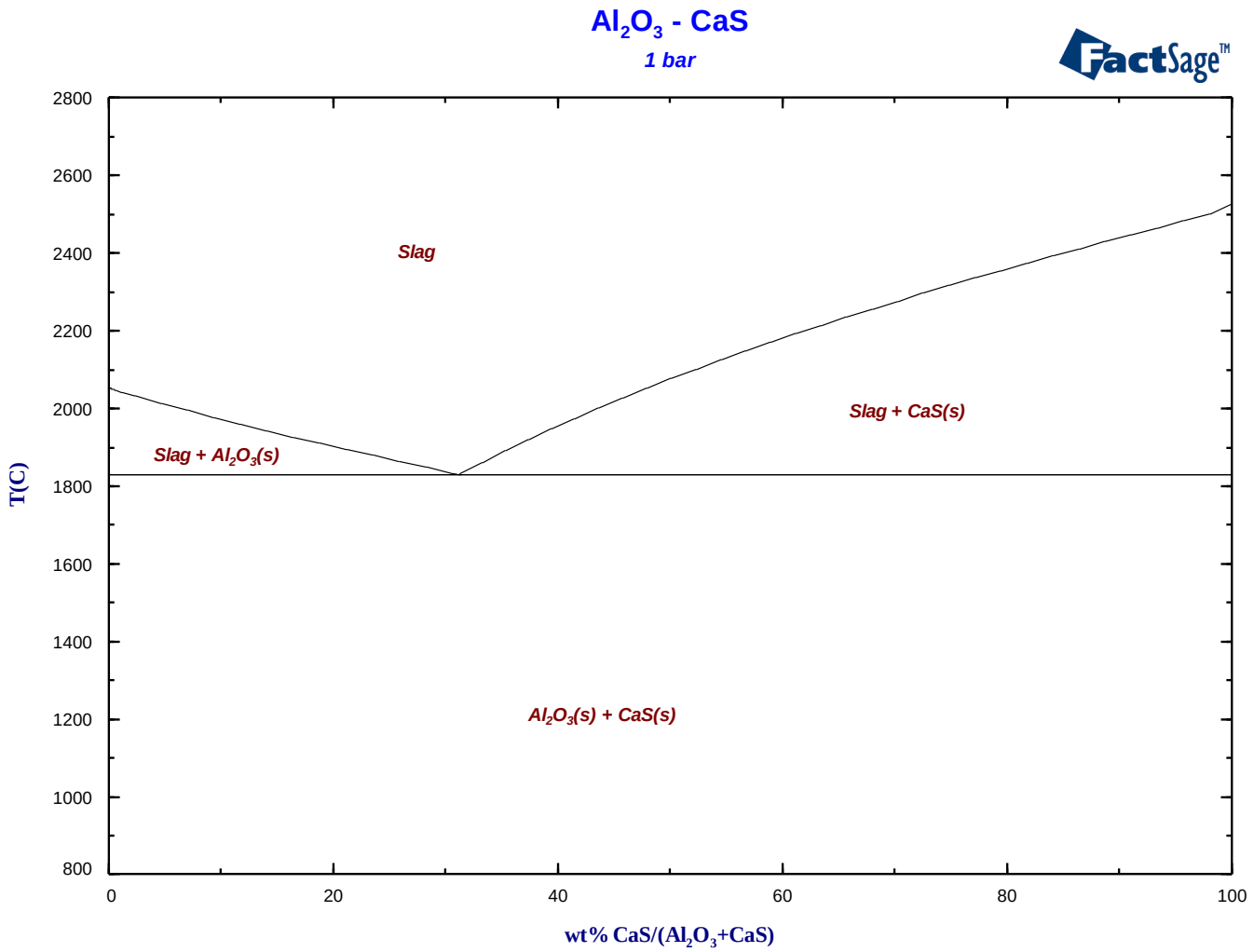

Mole fraction

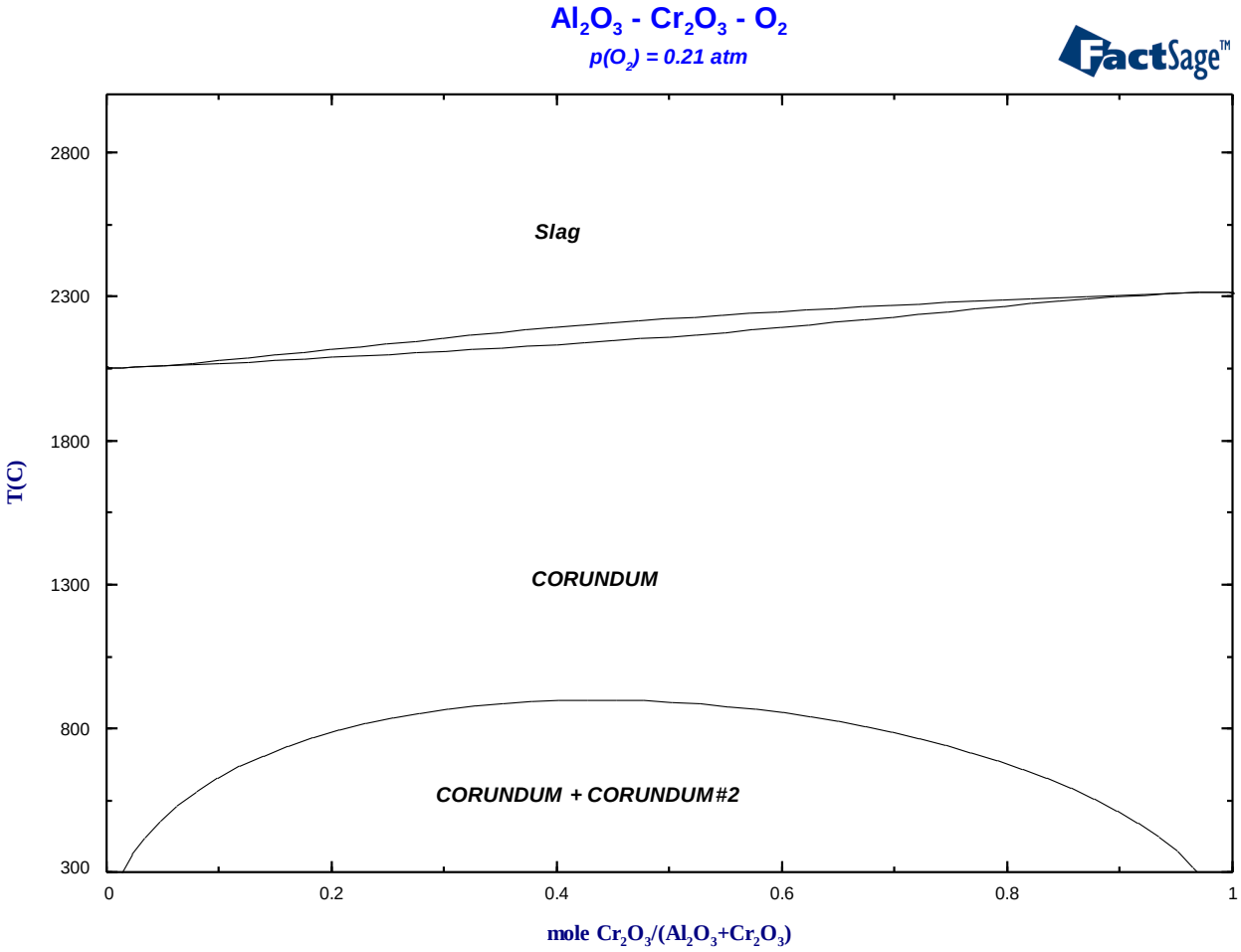

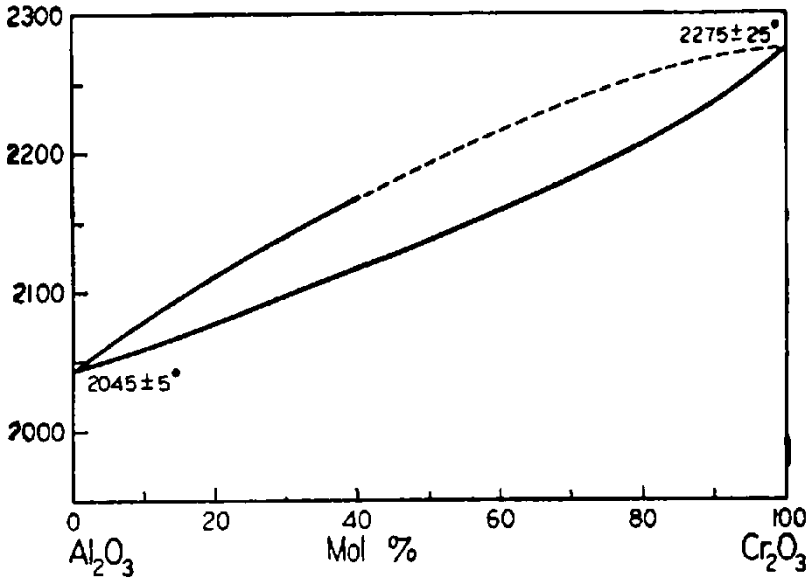

E.N. Bunting, J. Res. Natl. Bur. Stand. (U.S.), (1931), pp.947-949

Weight percent compared with experimental data

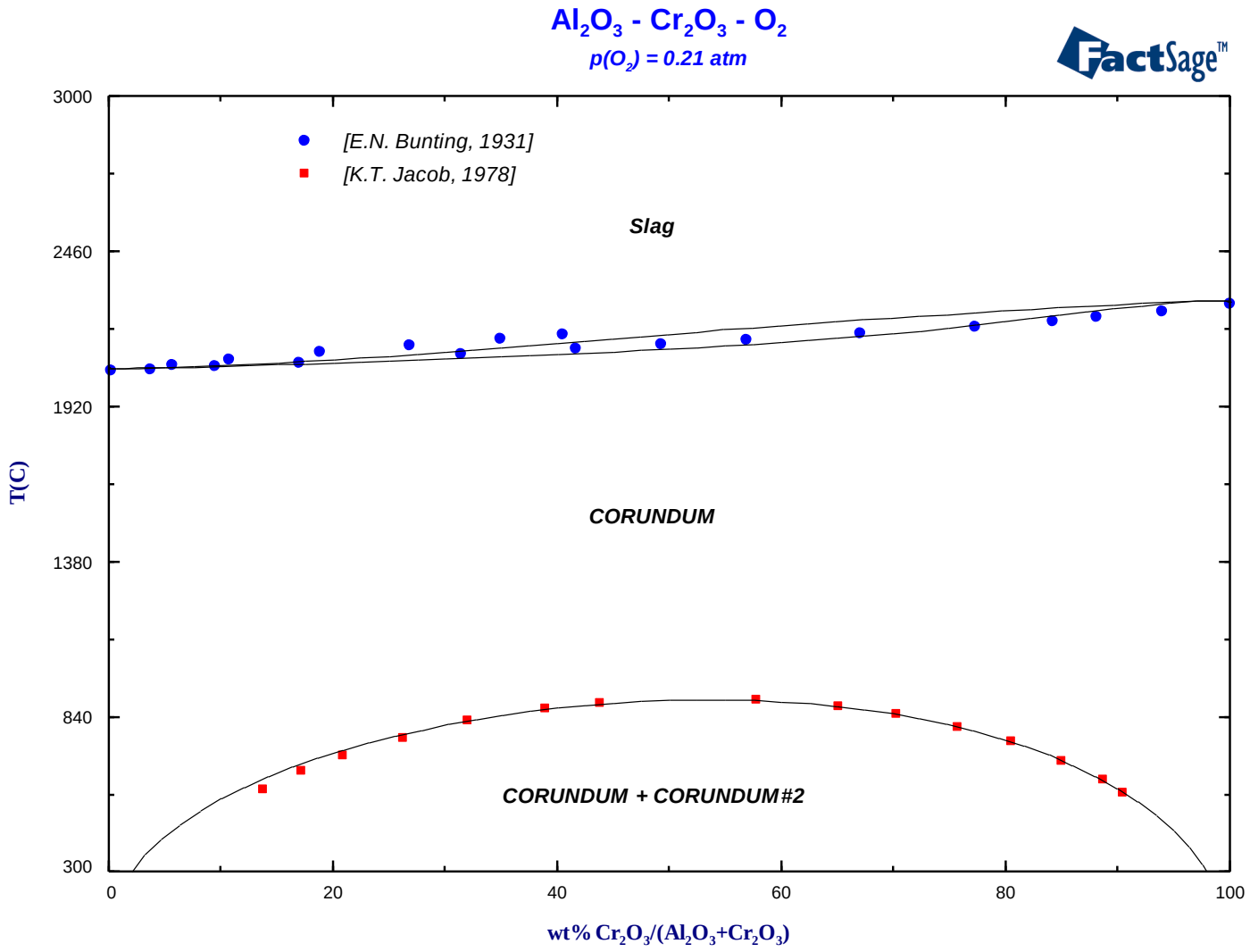

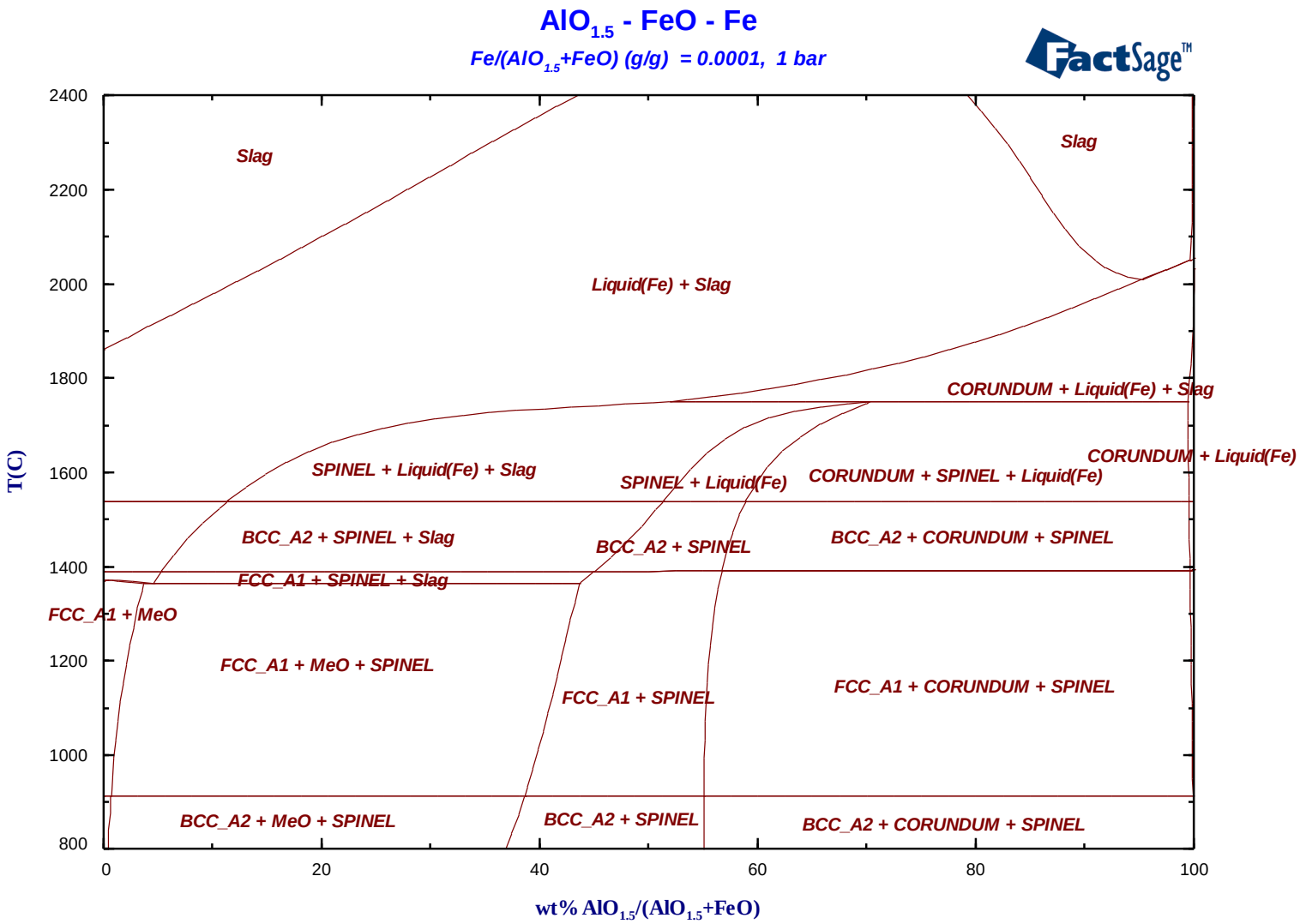
AlO1.5 - FeO - Fe
Fe/(AlO1.5+FeO) (g/g) = 0.0001, 1 bar
FactSage™
Slag
Slag
Liquid(Fe) + Slag
CORUNDUM + Liquid(Fe) + Slag
CORUNDUM + Liquid(Fe)
SPINEL + Liquid(Fe) + Slag
SPINEL + Liquid(Fe)
CORUNDUM + SPINEL + Liquid(Fe)
BCC_A2 + SPINEL + Slag
BCC_A2 + SPINEL
BCC_A2 + CORUNDUM + SPINEL
FCC_A1 + SPINEL + Slag
FCC_A1 + MeO
FCC_A1 + MeO + SPINEL
FCC_A1 + SPINEL
FCC_A1 + CORUNDUM + SPINEL
BCC_A2 + MeO + SPINEL
BCC_A2 + SPINEL
BCC_A2 + CORUNDUM + SPINEL
T(C)
2400
2200
2000
1800
1600
1400
1200
1000
800
0
20
40
60
80
100
wt% AlO1.5/(AlO1.5+FeO)

Weight percent compared with experimental data

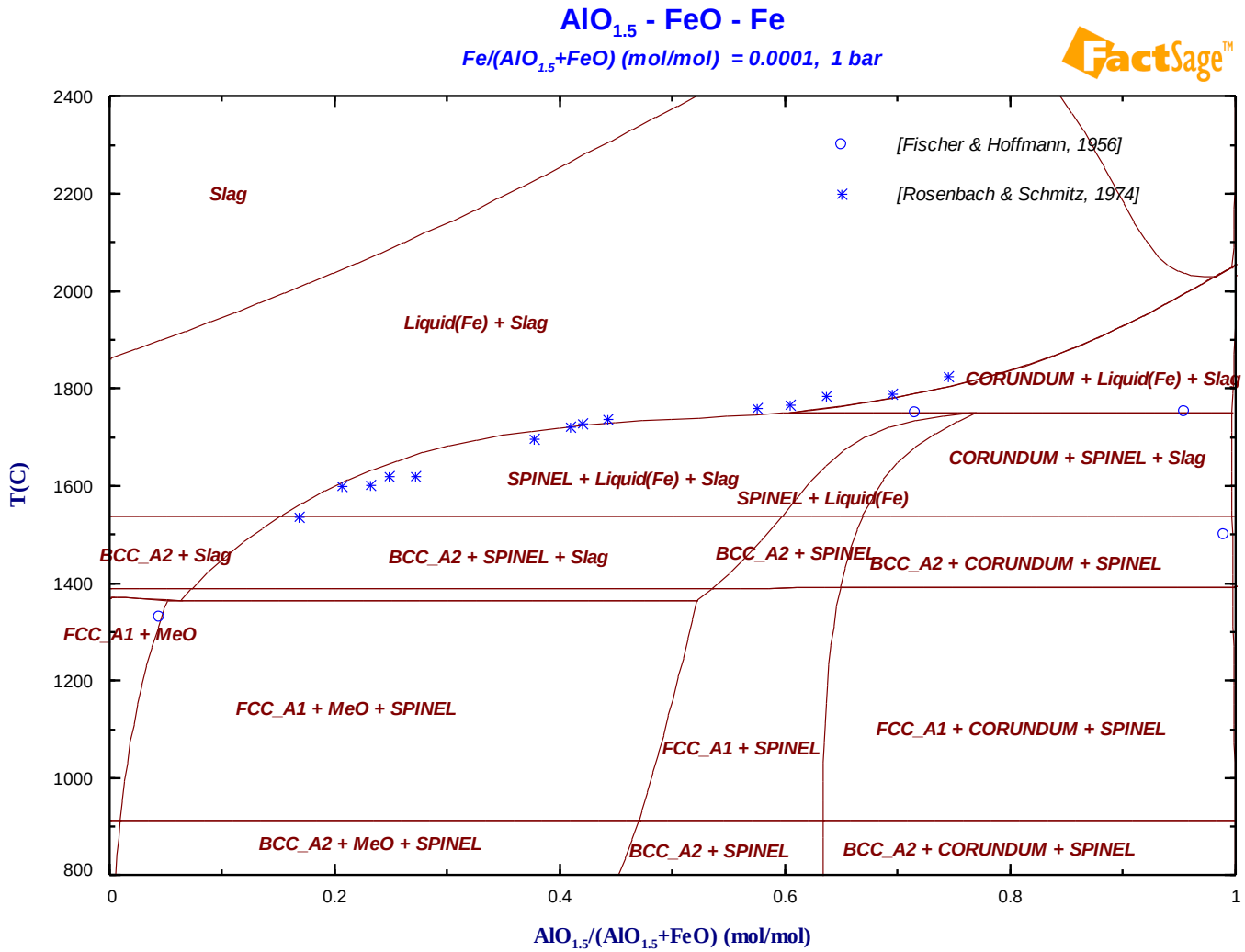

Mole fraction

Al_2O_3 - Fe_2O_3 - O_2

$p(O_2)$ = 0.21 atm

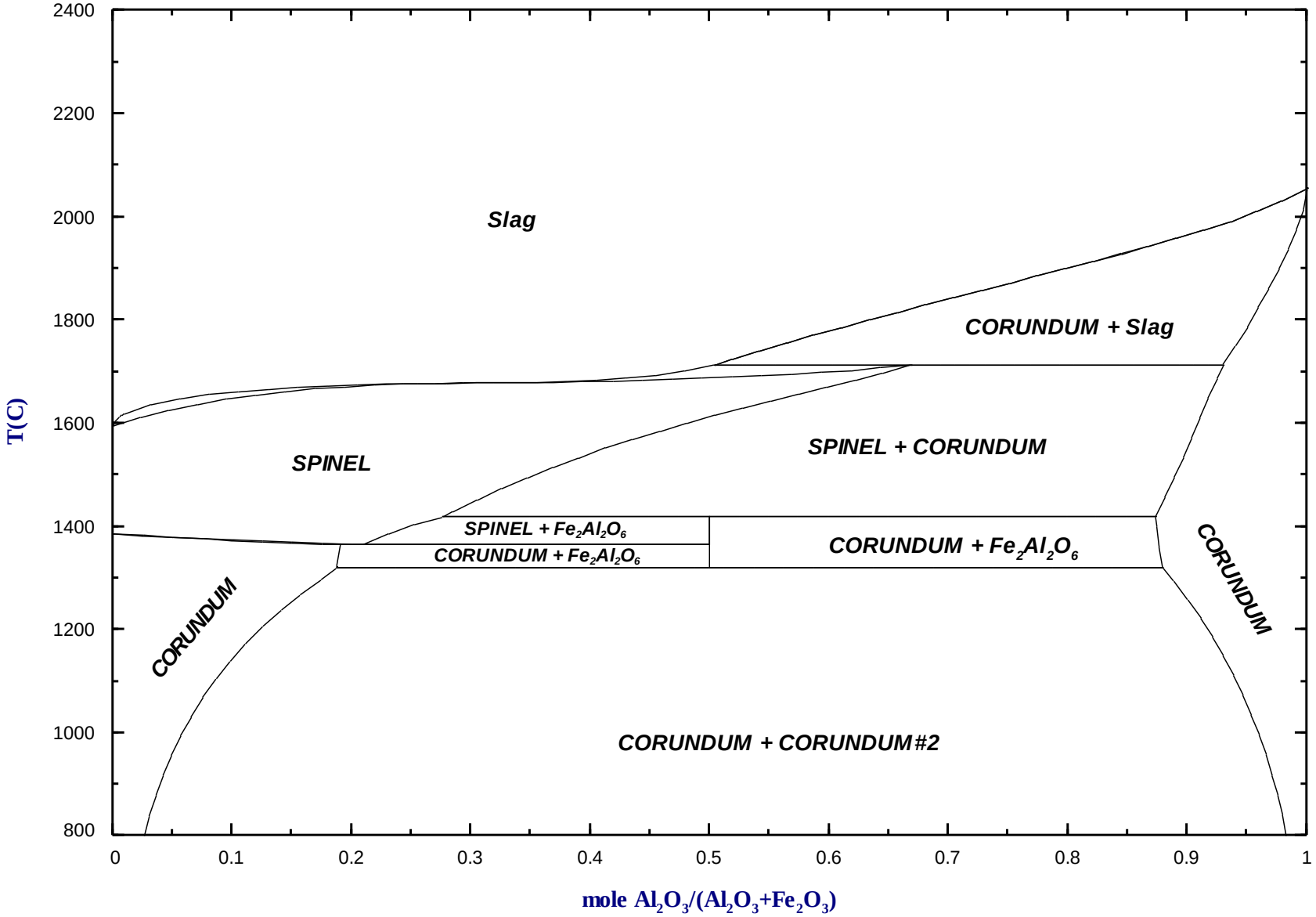

Weight percent
compared with experimental data

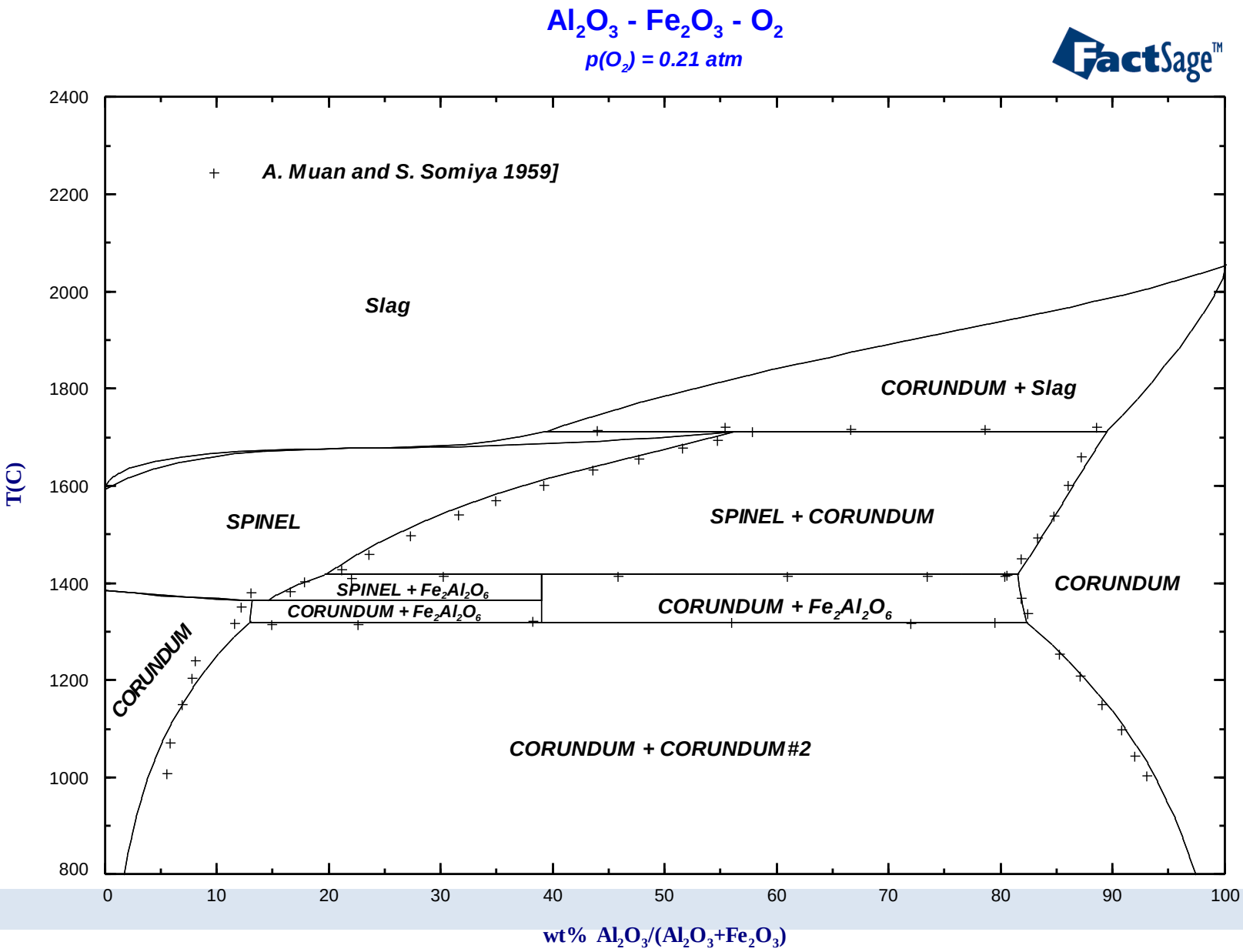

Mole fraction
compared with experimental data

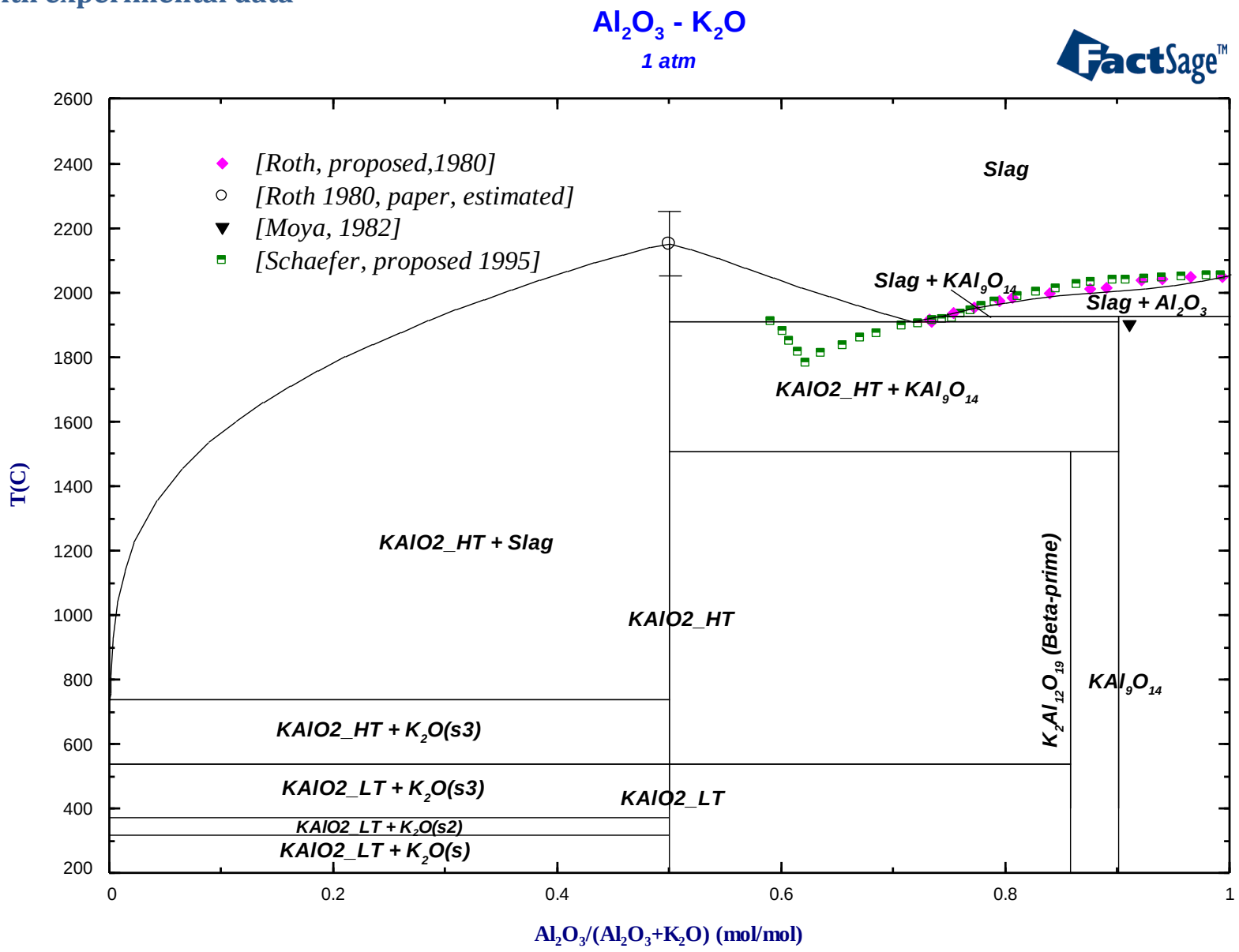

Weight percent

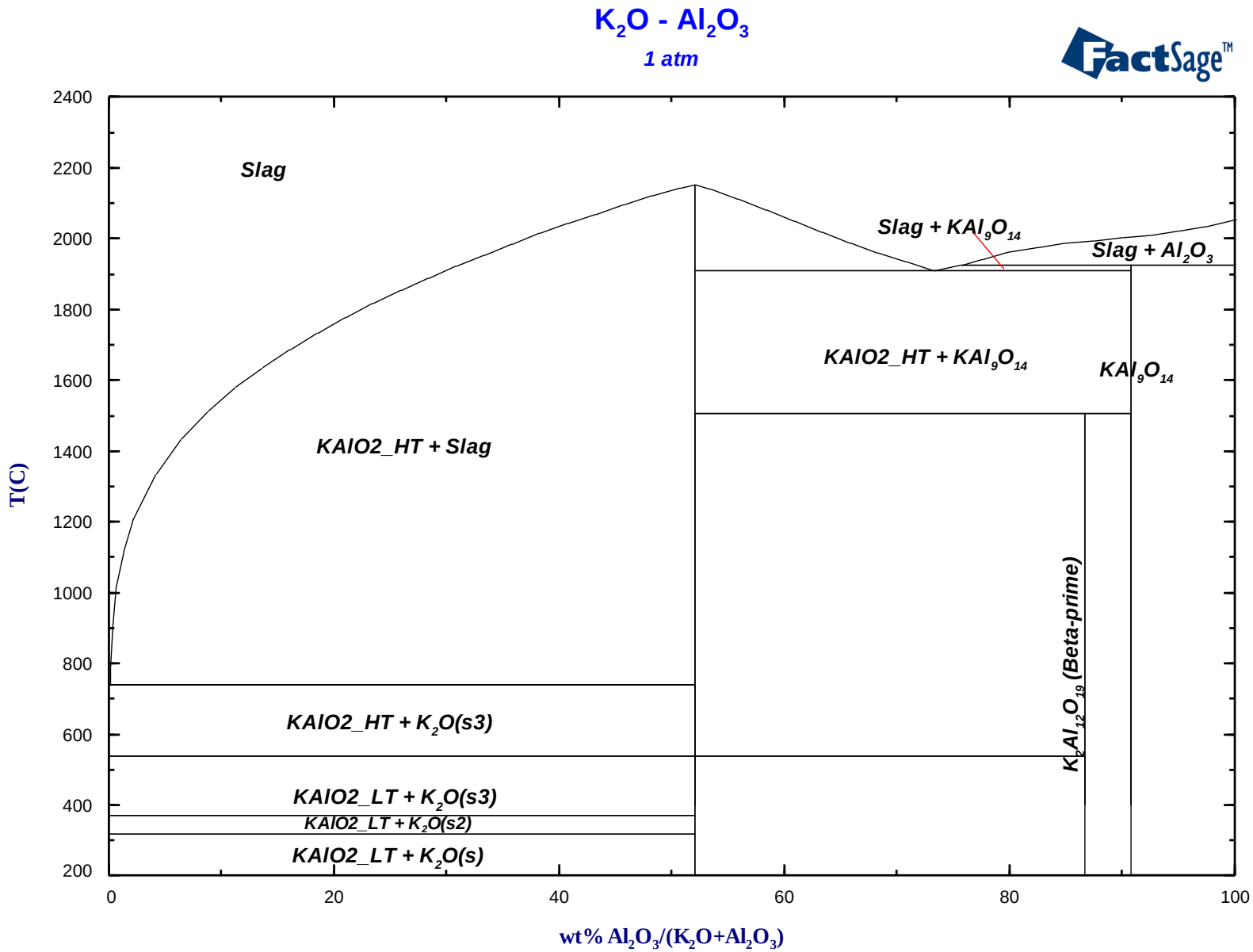

Mole fraction compared with experimental data

Al_2O_3 - MgO

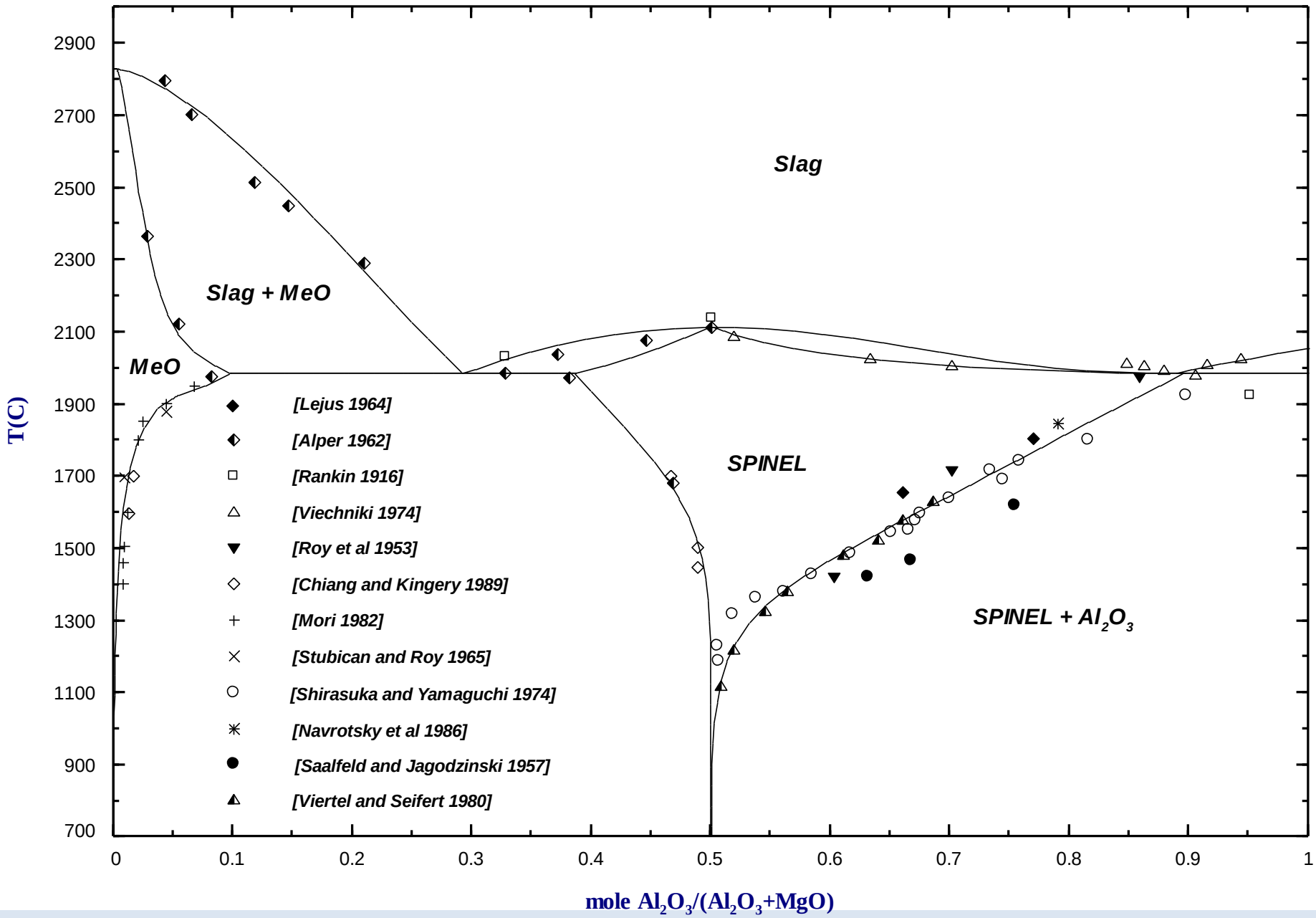

Al_2O_3 - MgO

Weight percent

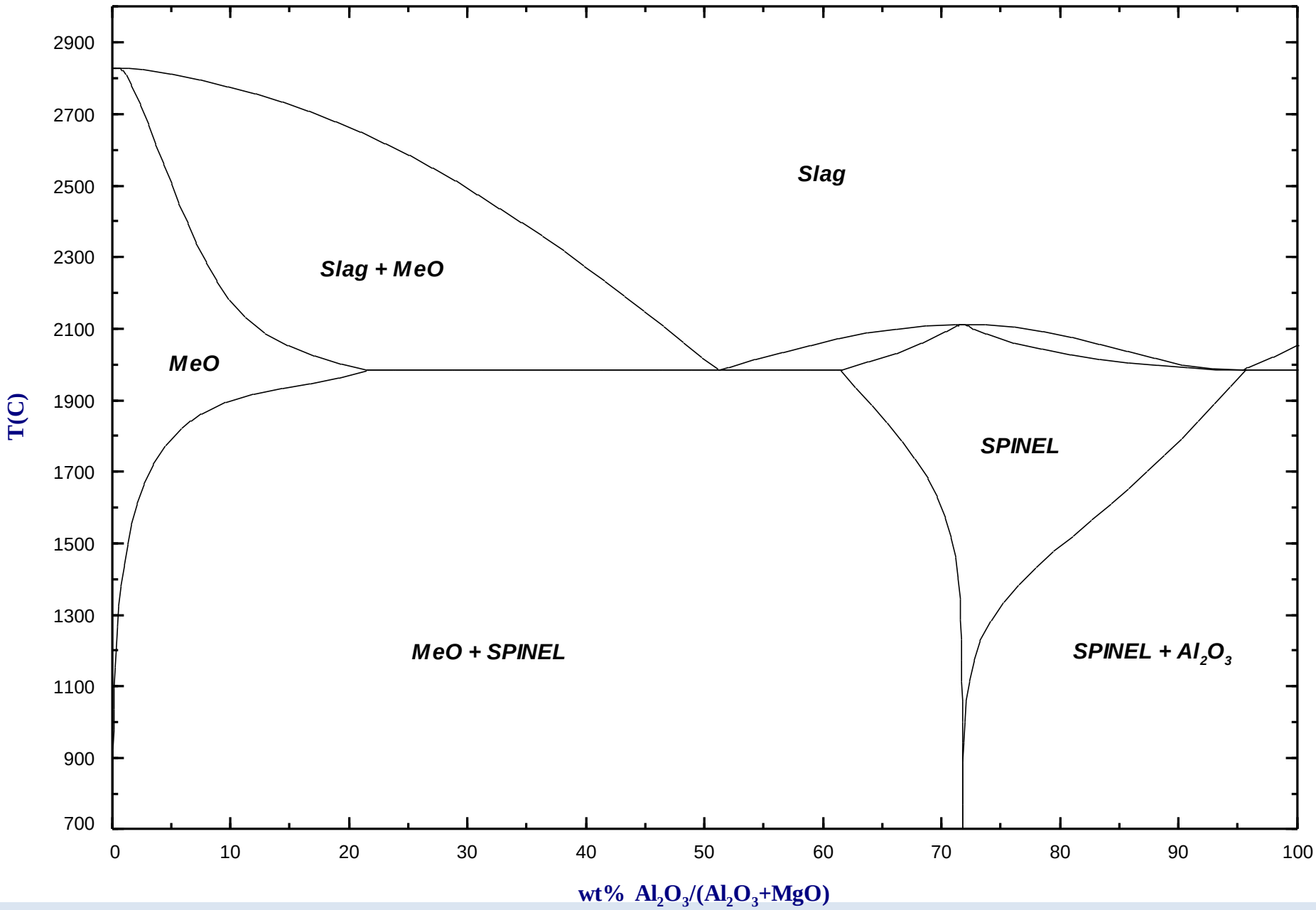

Mole fraction

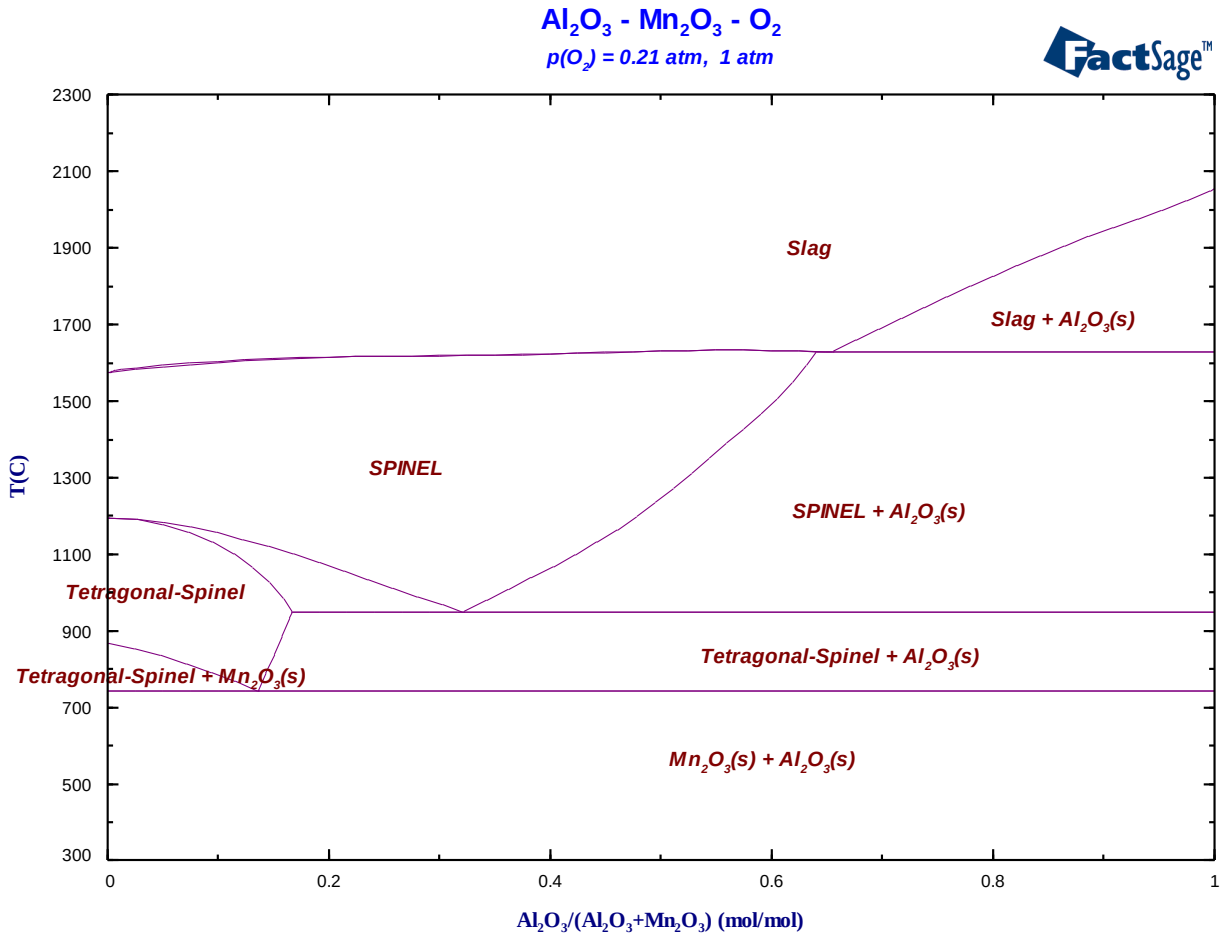

Weight percent

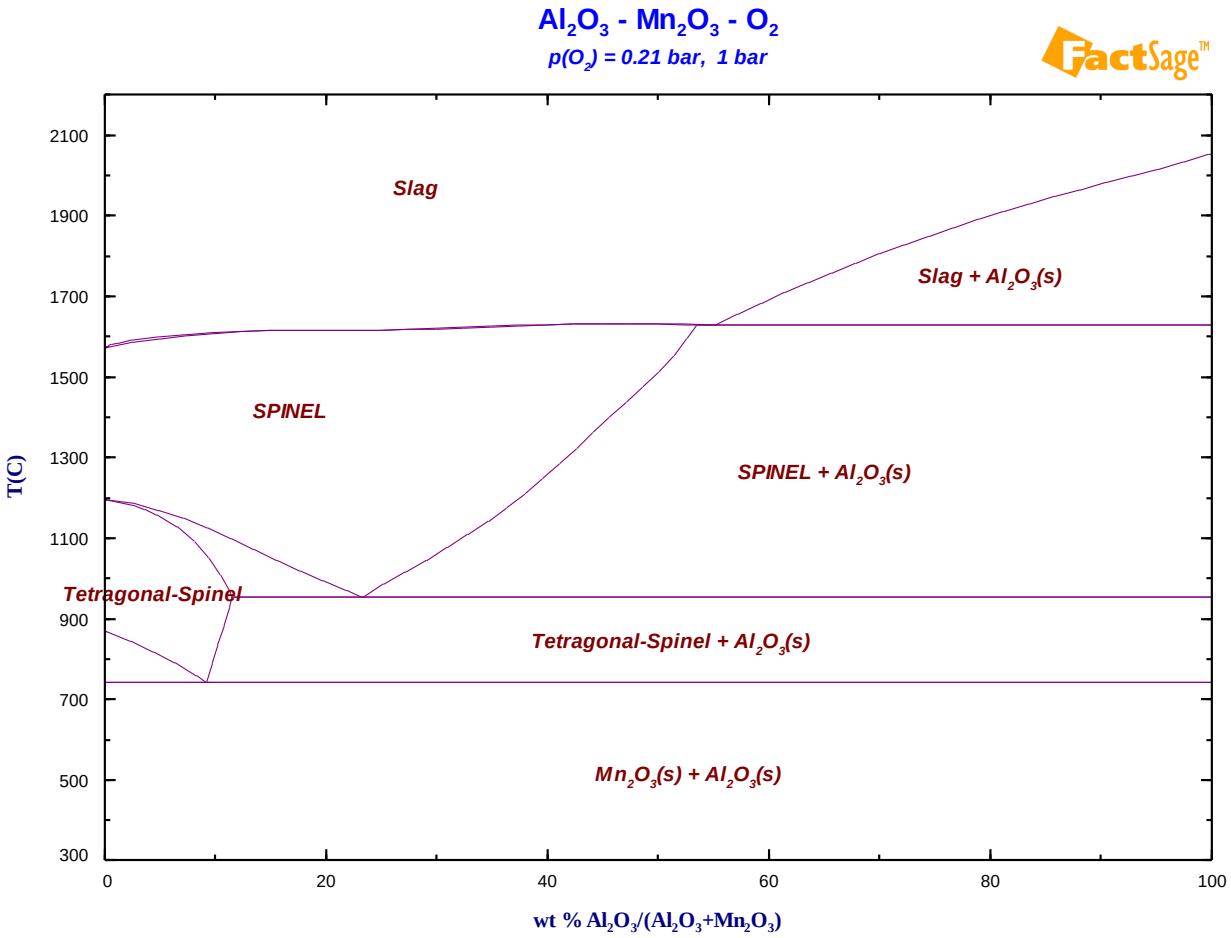

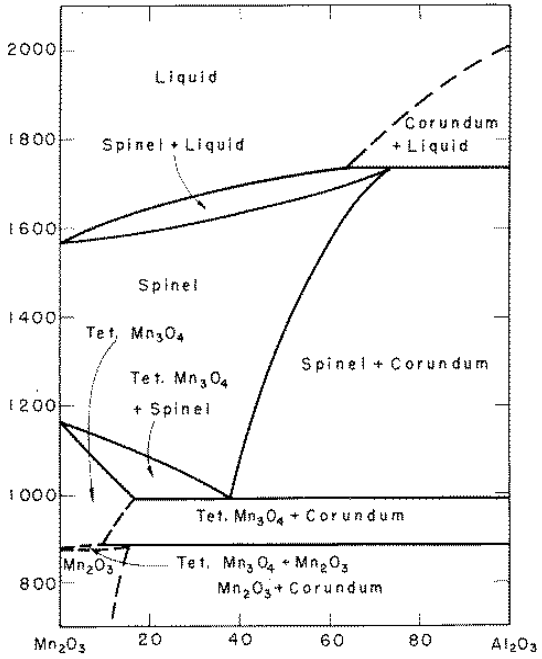

I.A. Novokhatskij, L.M. Lenev, A.A. Savinskaya, A.V. Gorokh, Zh. Neorg. Khim., 11 [2], (1966), pp. 427-428.

Mole fraction
compared with experimental data

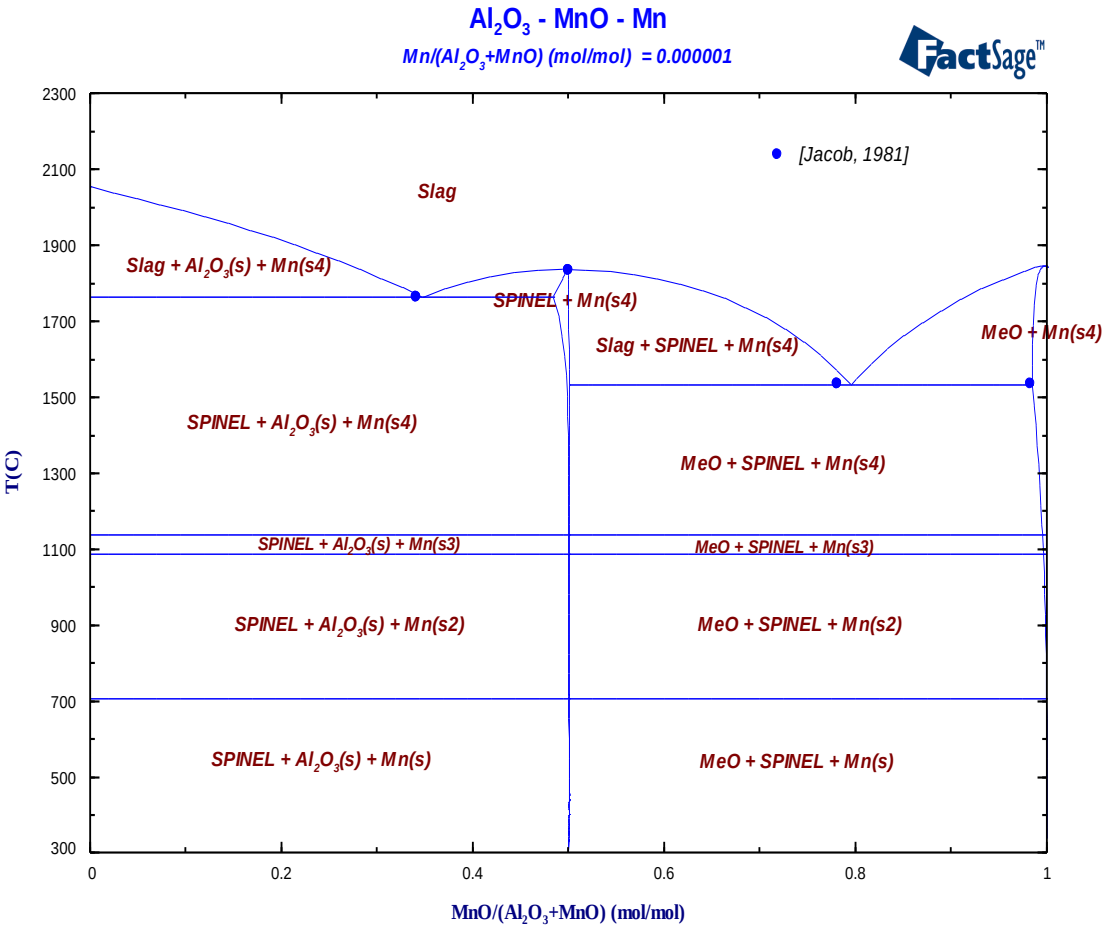

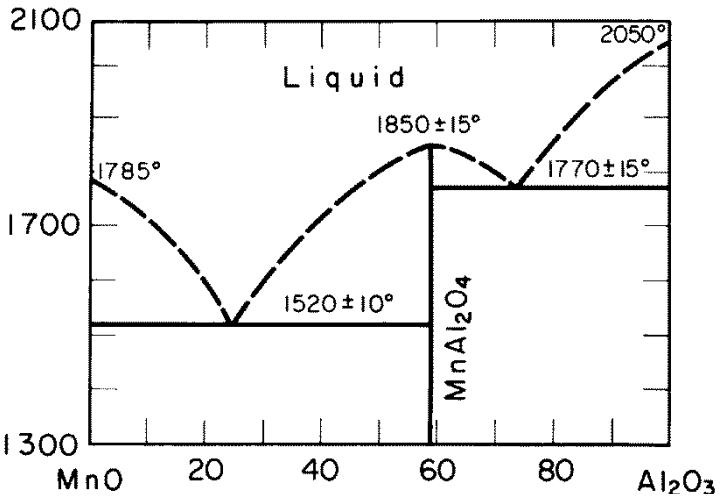

I.A. Novokhatskij, L.M. Lenev, A.A. Savinskaya, A.V. Gorokh, Zh. Neorg. Khim., 11 [2], (1966), pp. 427-428.

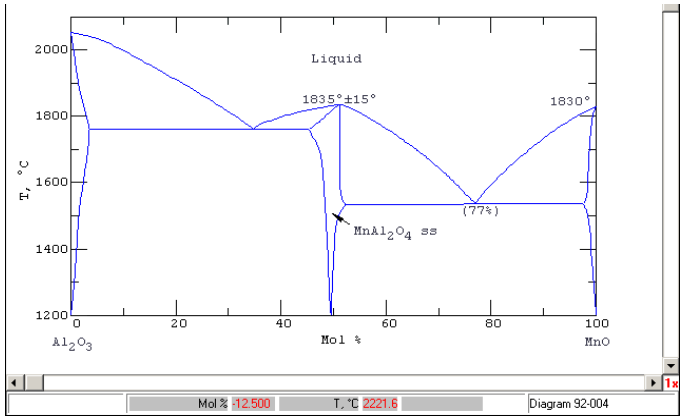

K.T. Jacob, Can. Metall. Q., 20 [1], (1981), pp. 89-92.

Weight percent

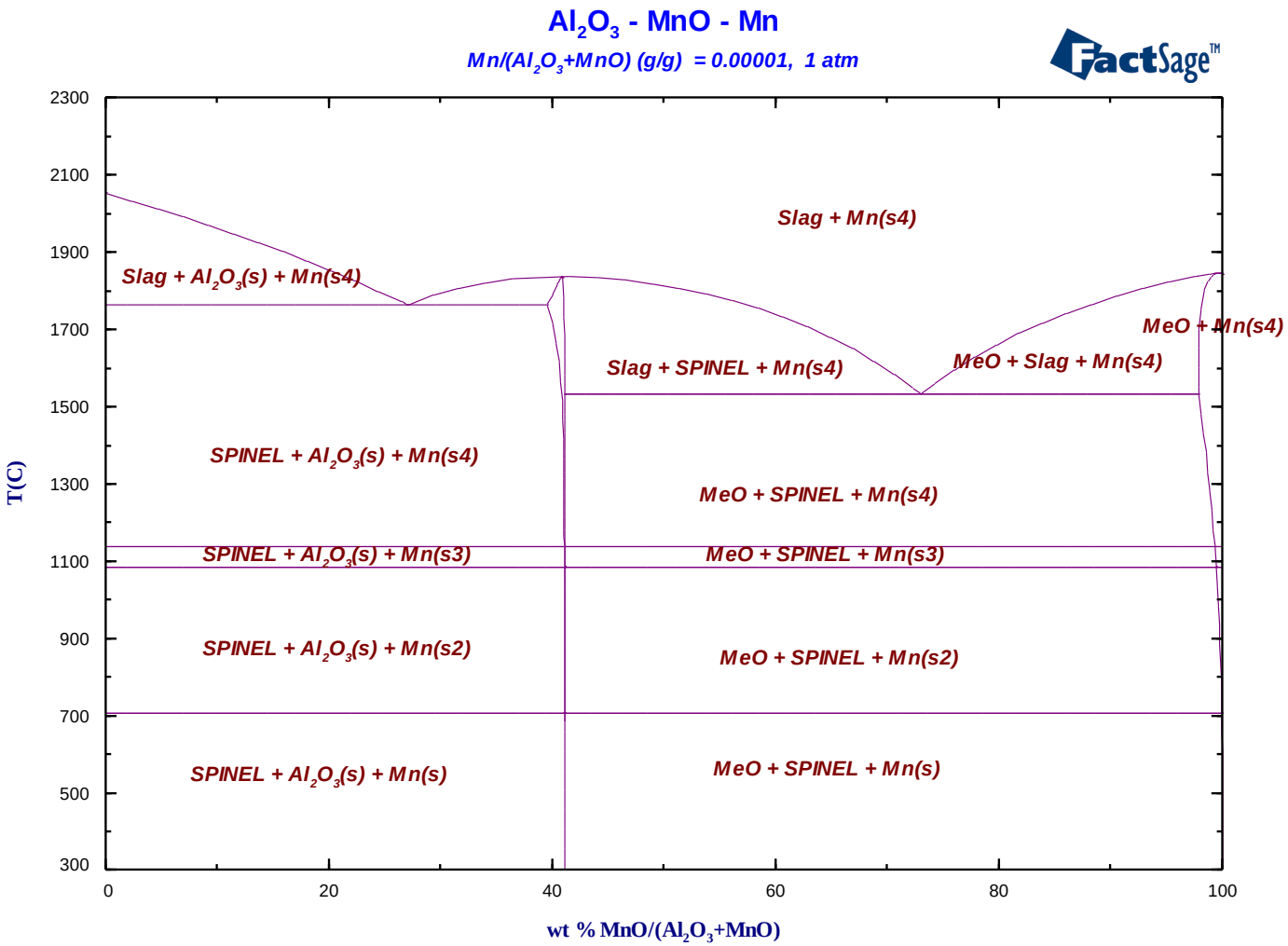

Mole fraction
compared with experimental data

Al_2O_3 - Na_2O

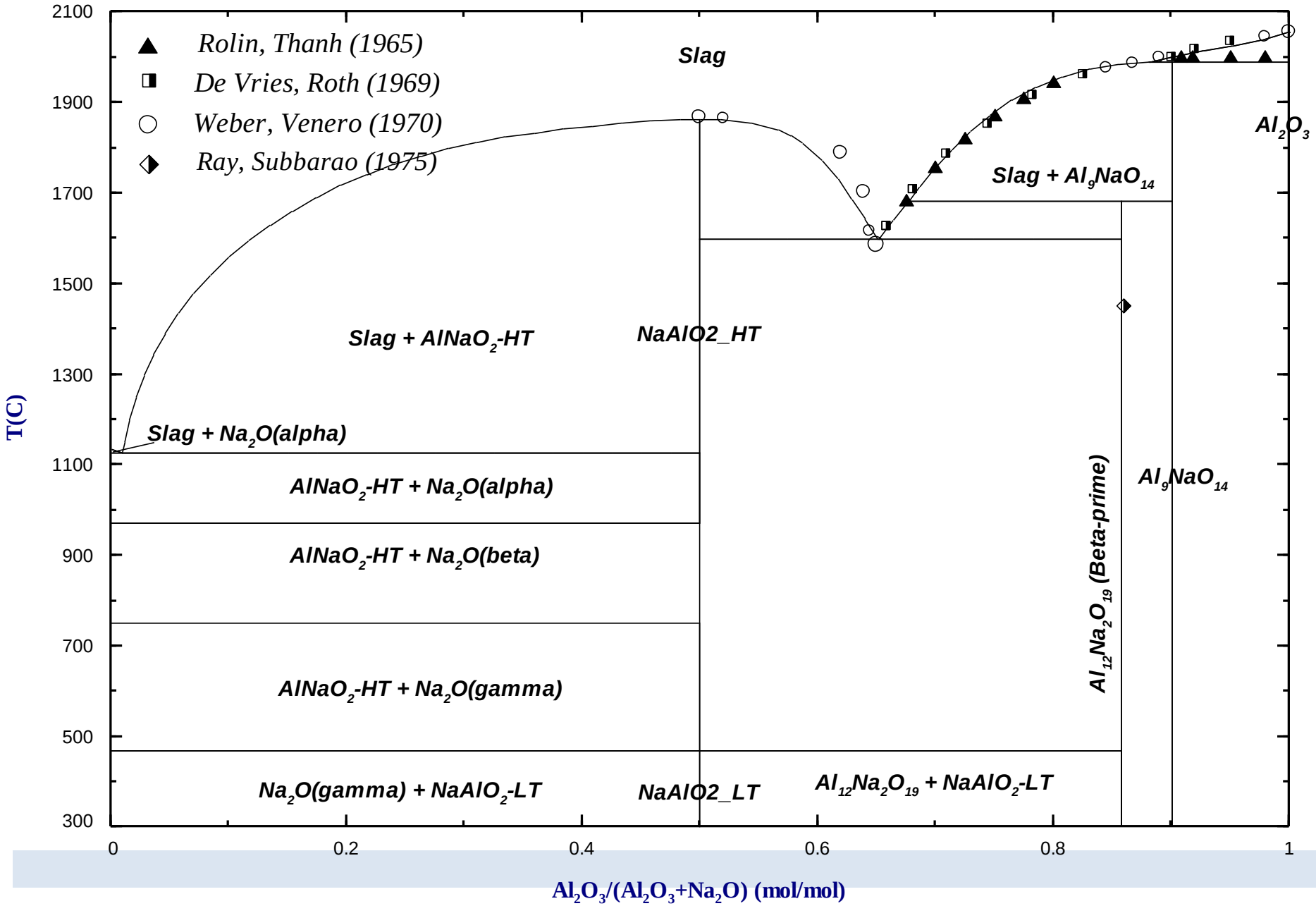

Weight percent

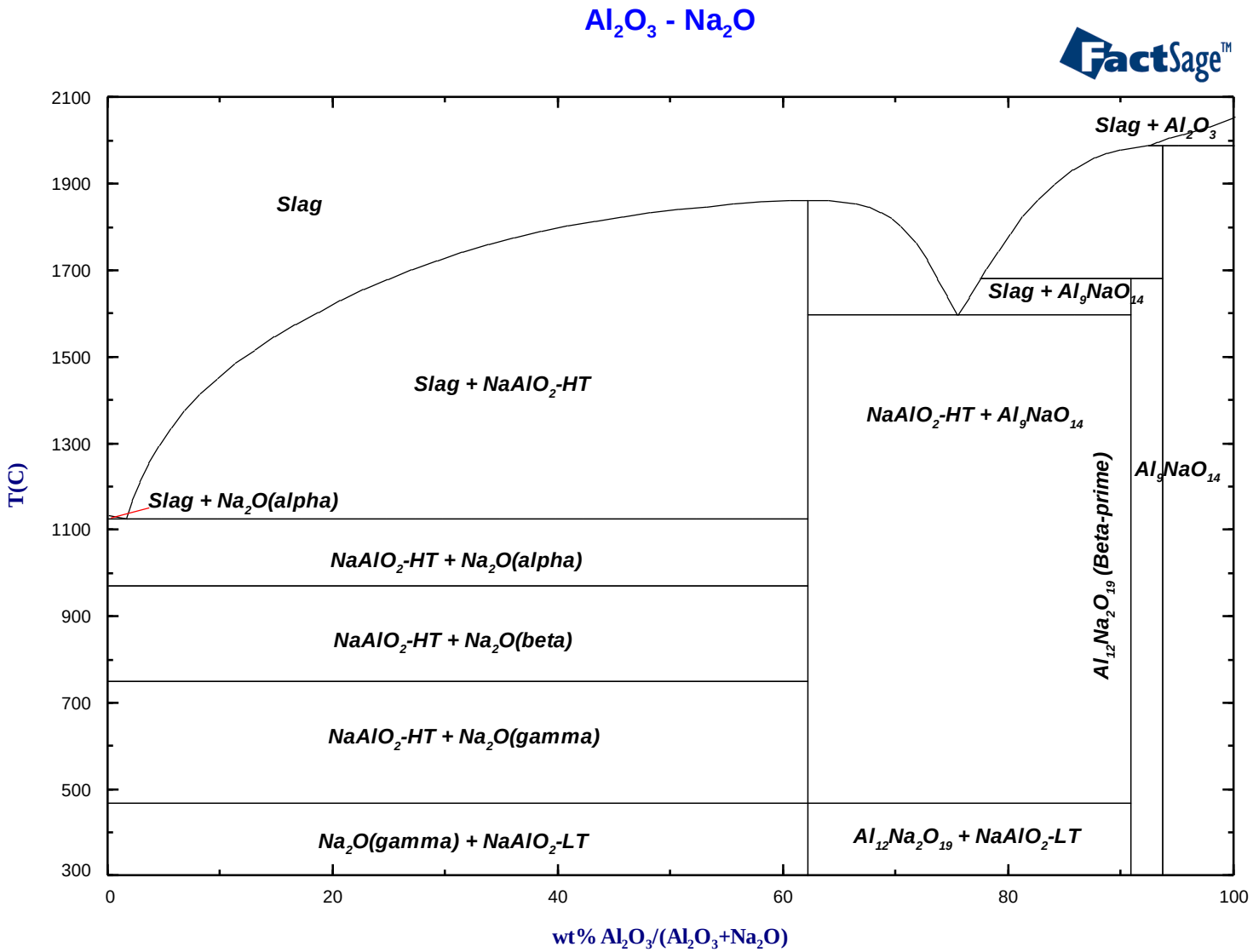

Mole fraction

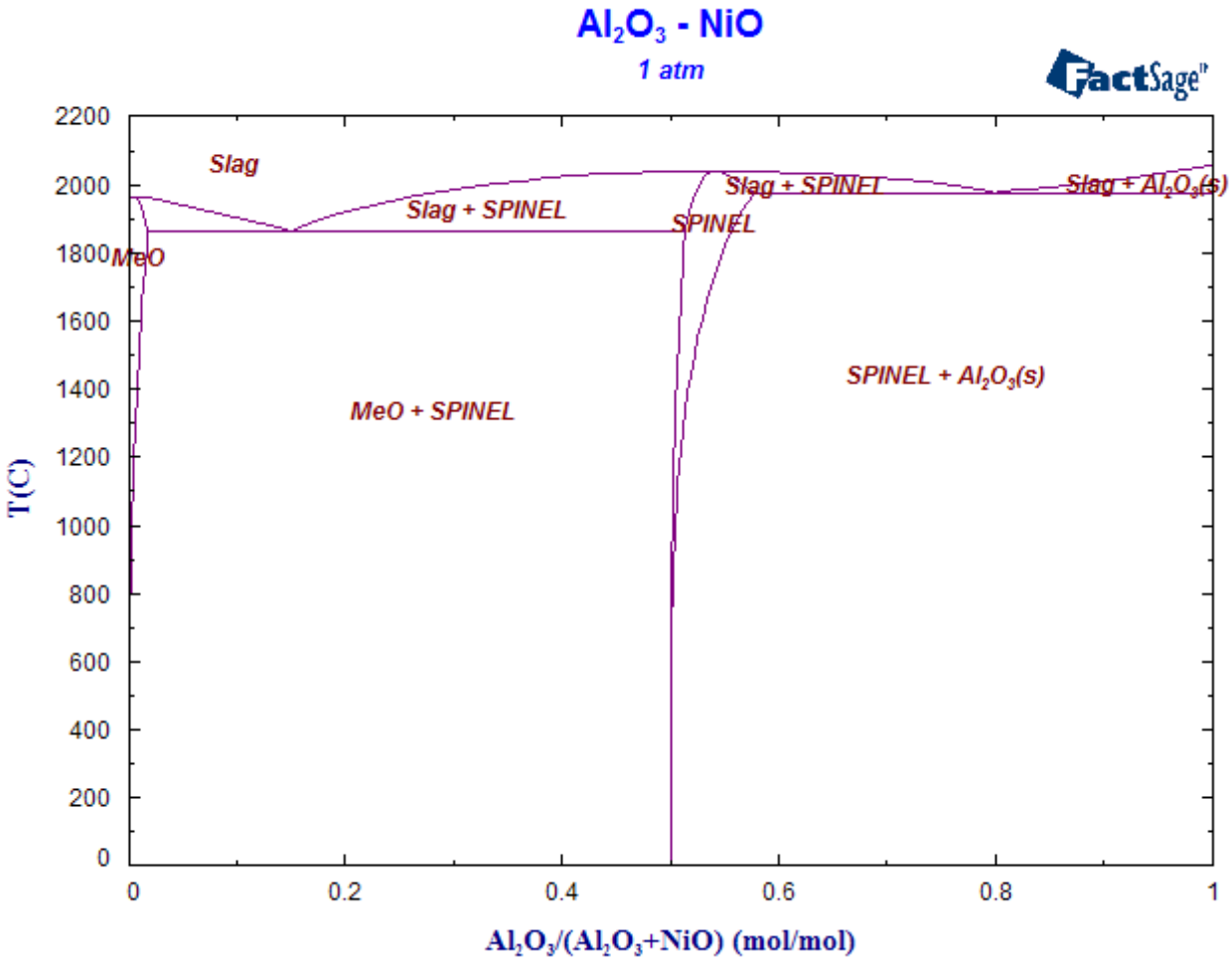

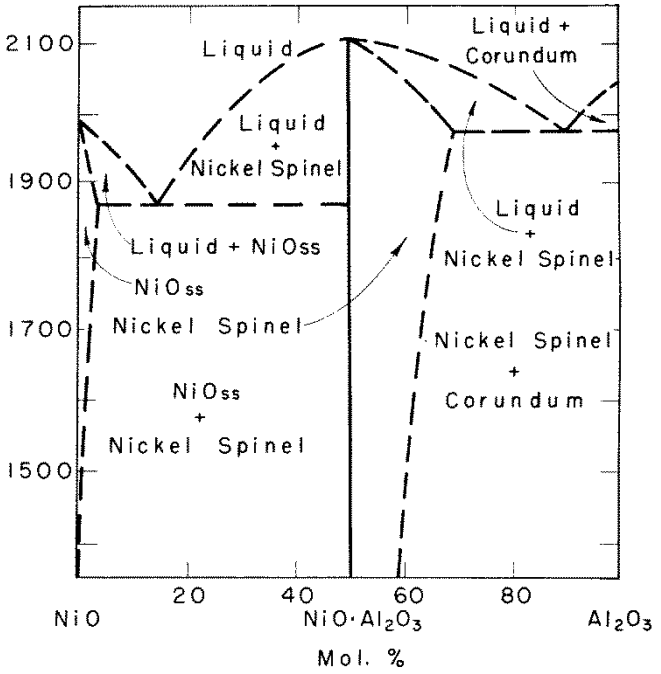

B. Phillips, J.J. Hutta, I. Warshaw, J. Am. Ceram. Soc., 46 [12], (1963), pp.579-583.

Weight percent

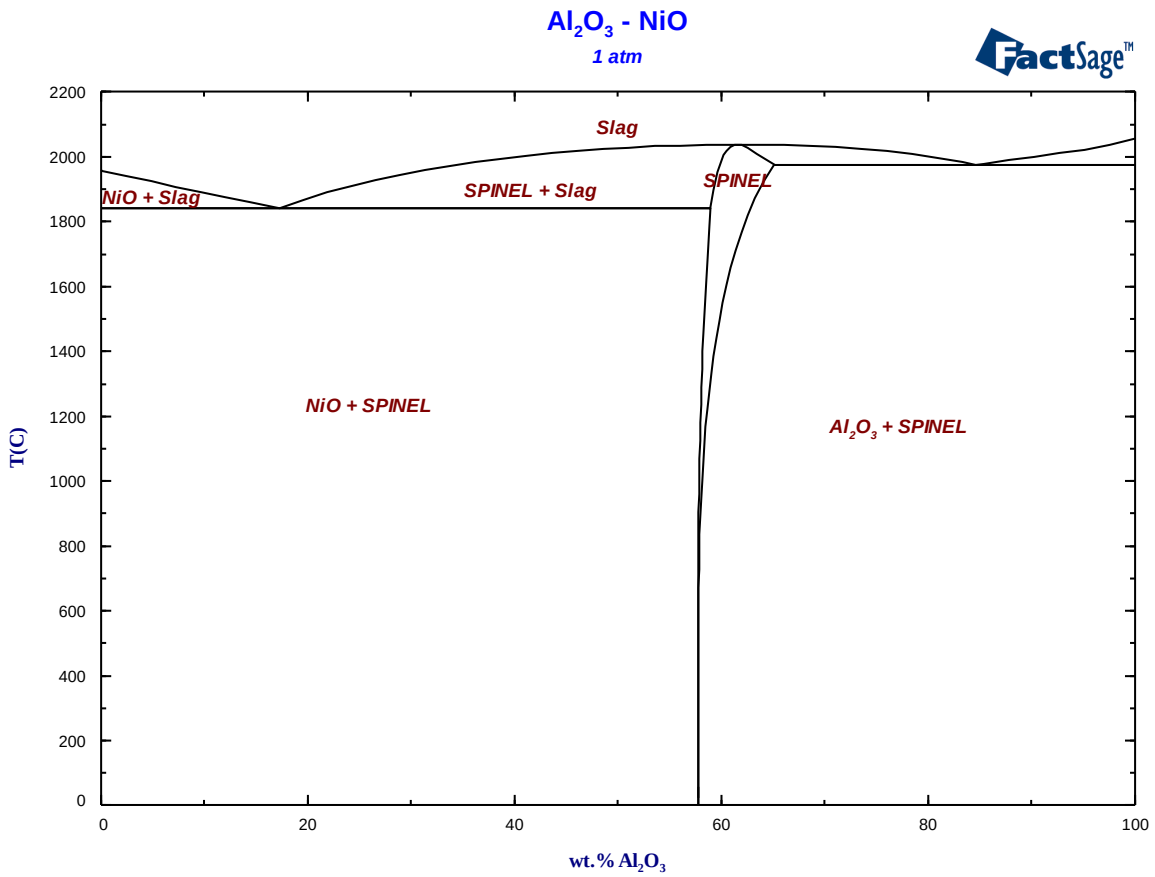

Mole fraction

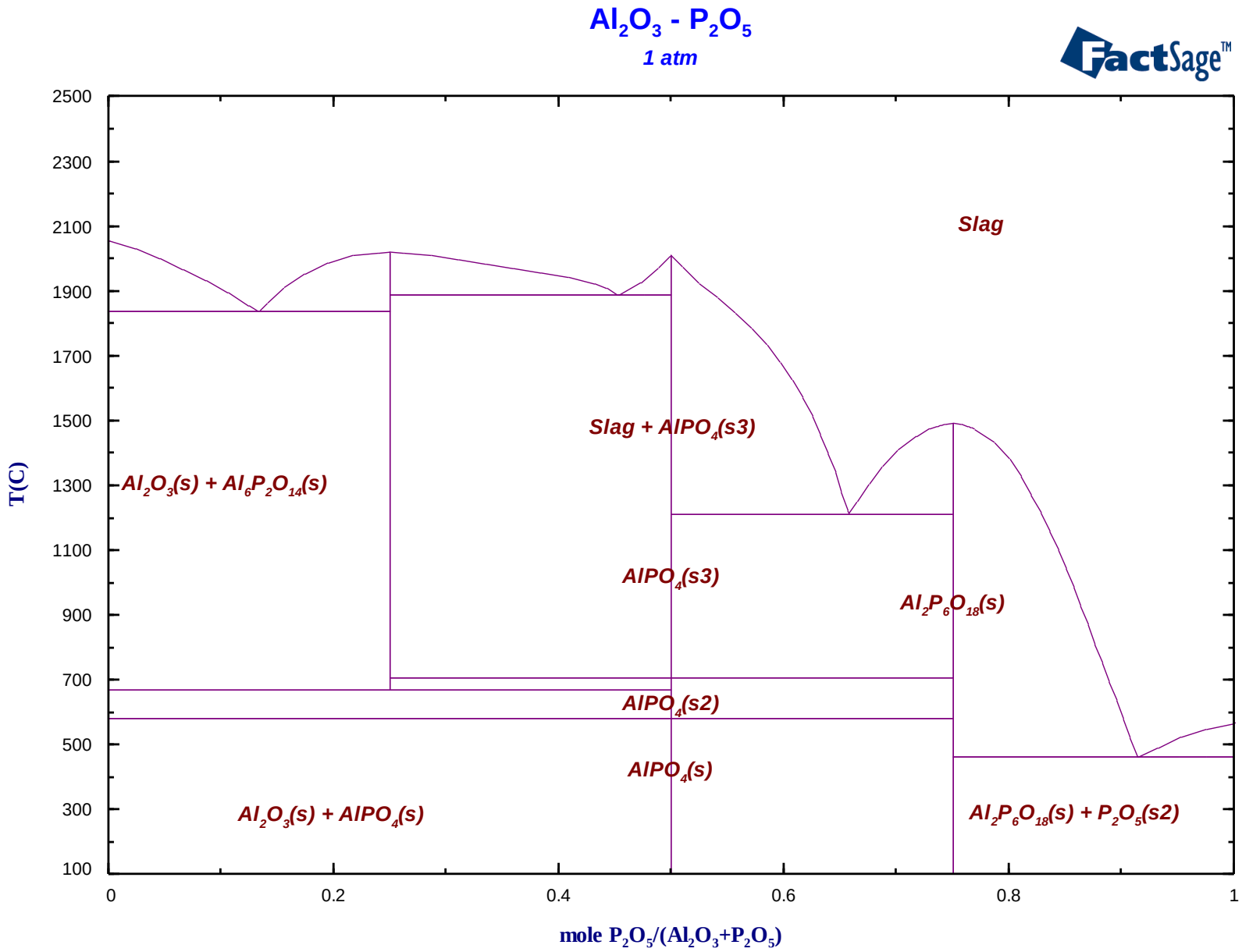

Weight percent,
compared with experimental data

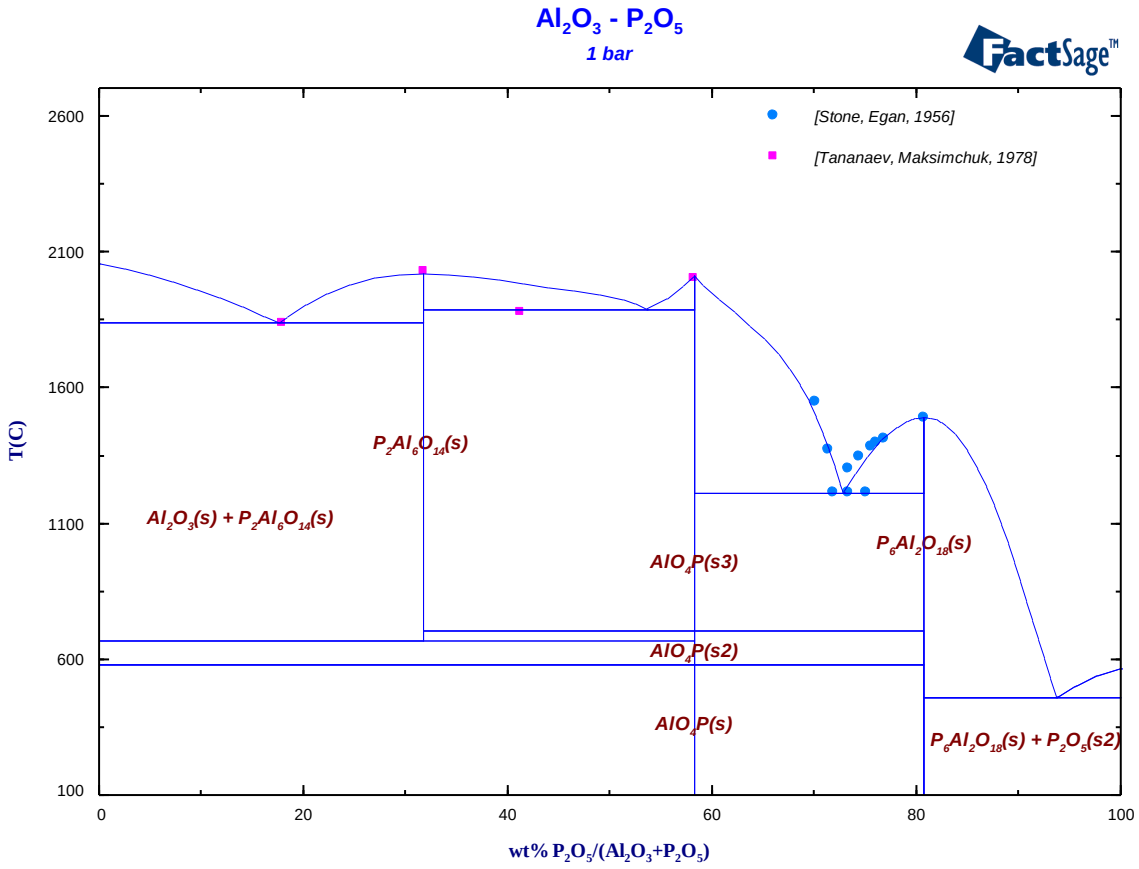

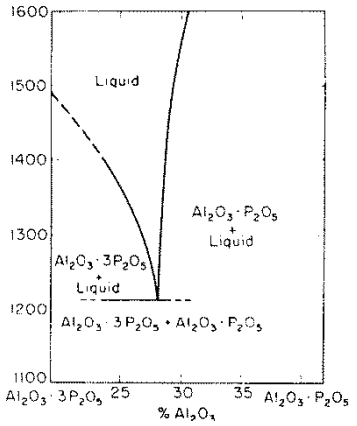

P.E. Stone, E.P. Egan, J.R. Lehr, J. Am, Ceram. Soc., 39 [3], (1956), pp.89-98.

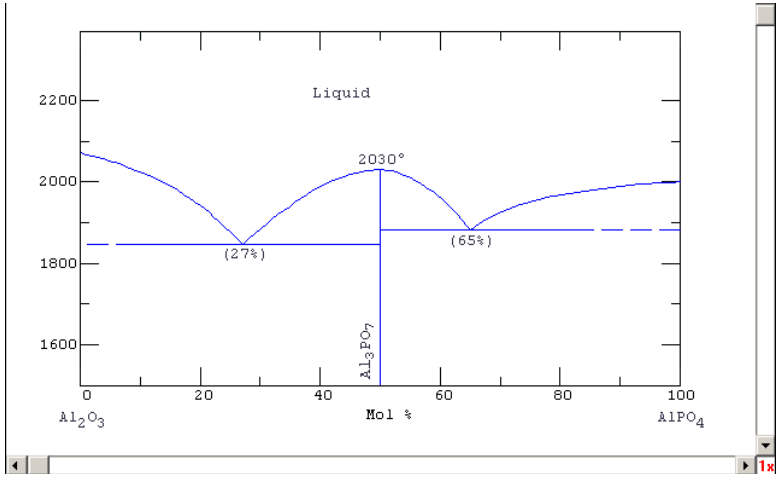

I.V. Tananaev, E.V. Maksimchuk,Y. G. Bushuev, S.A. Shestov, Izv. Akad. Nauk SSSR, Neorg. Mater., 14 [4], (1978), pp.719-722.

Mole fraction

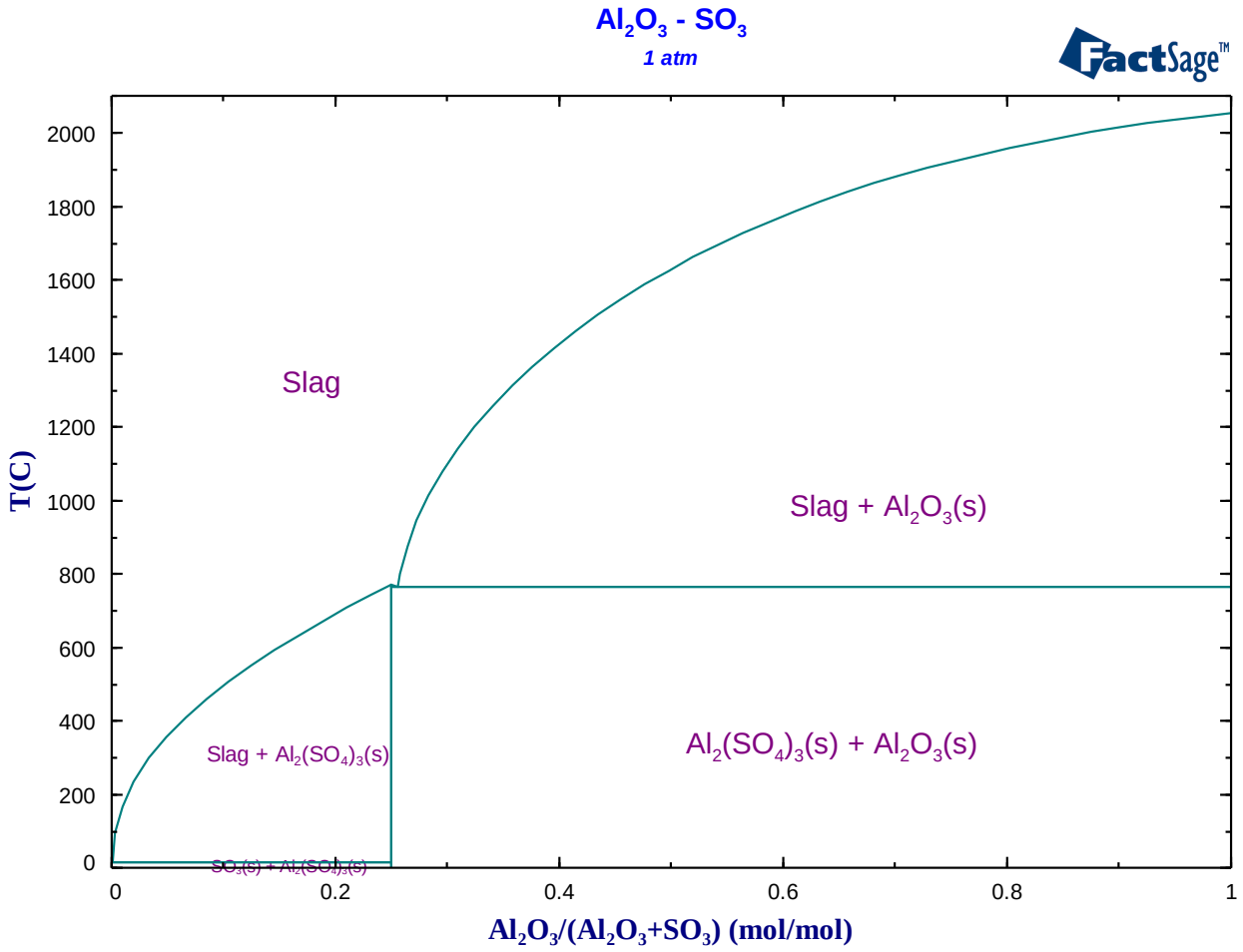

Weight percent

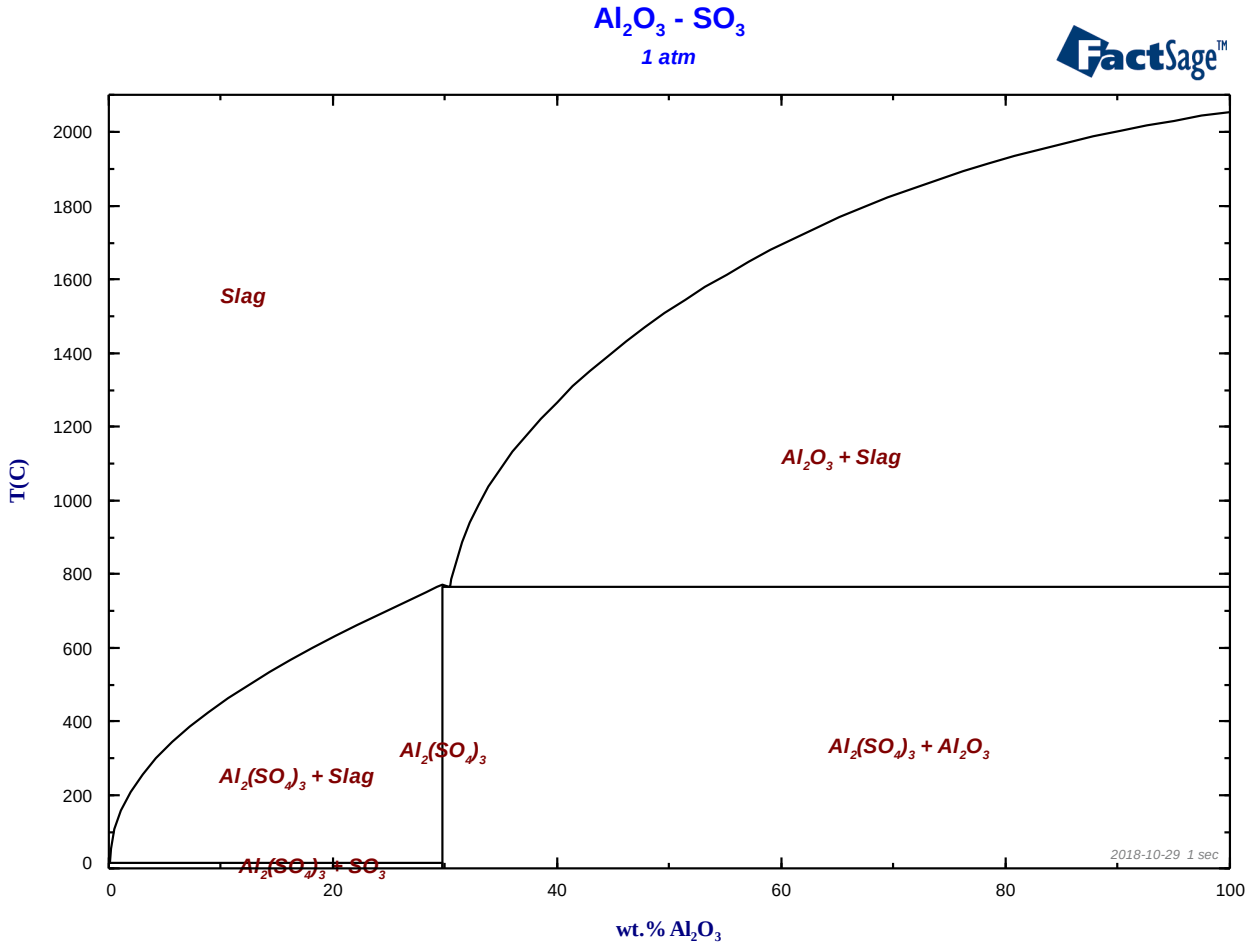

Mole fraction in Kelvin compared with experimental data

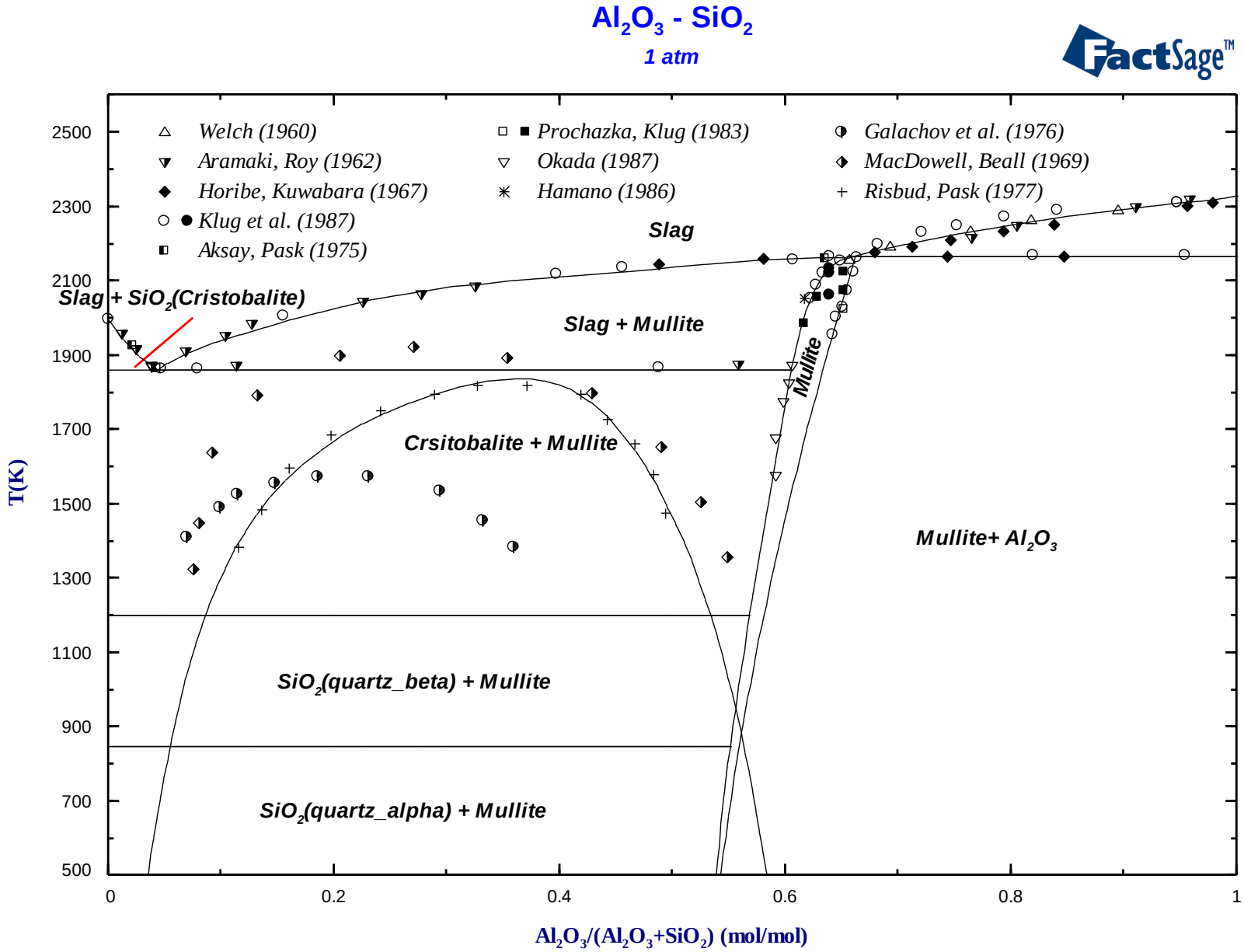

Weight percent

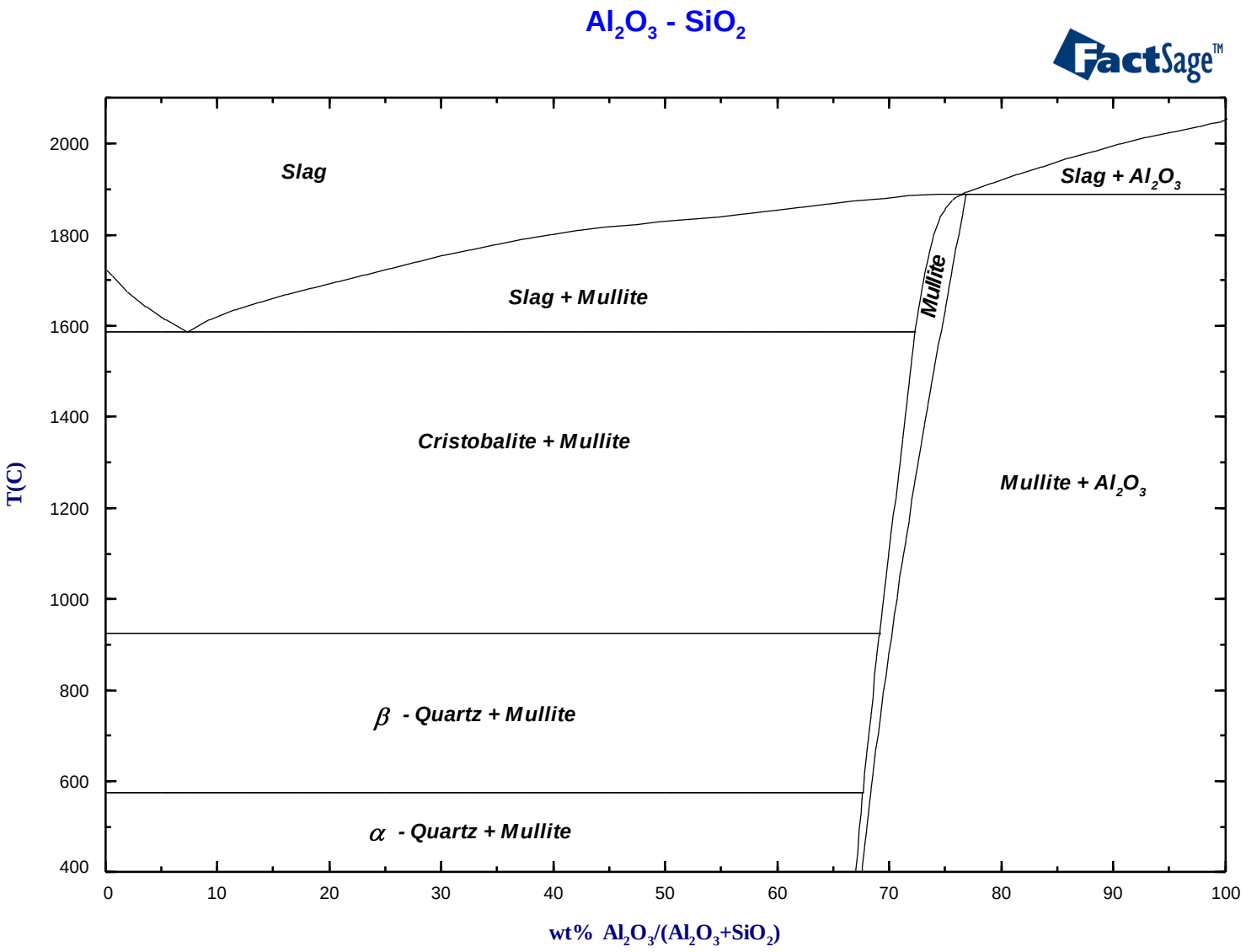

Al2O3-SrO,
Mole fraction compared with experimental data

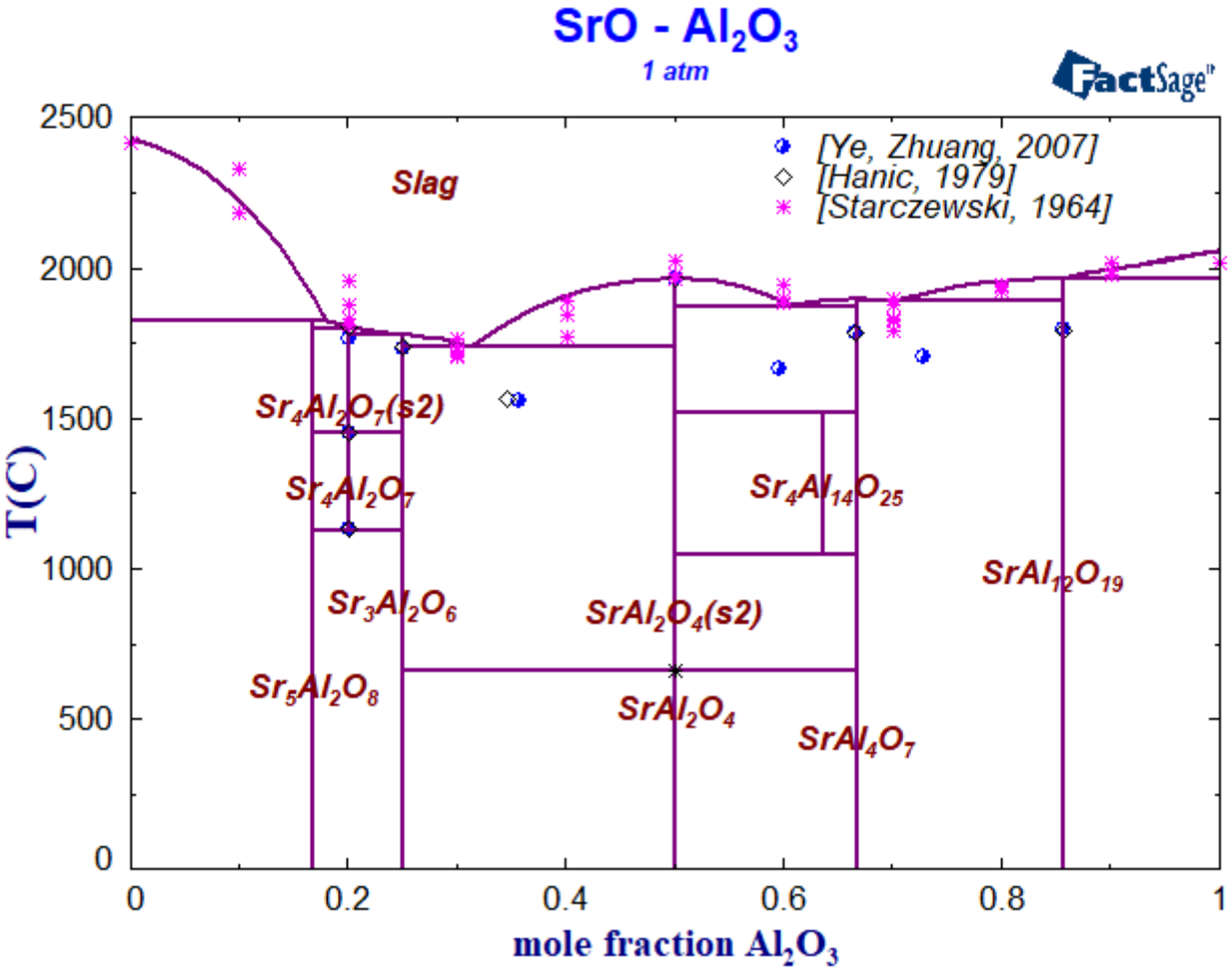

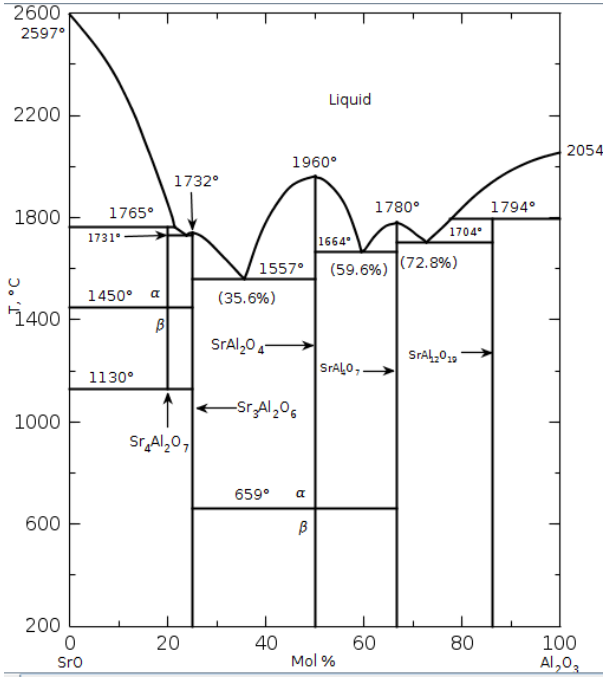

X. Ye, W. Zhuang, J. F. Wang, W. Yuan, Z. Qiao, J. Phase Equilib. Diff., 28 [4] 362-368 (2007).

Al2O3-SrO,
Weight percent

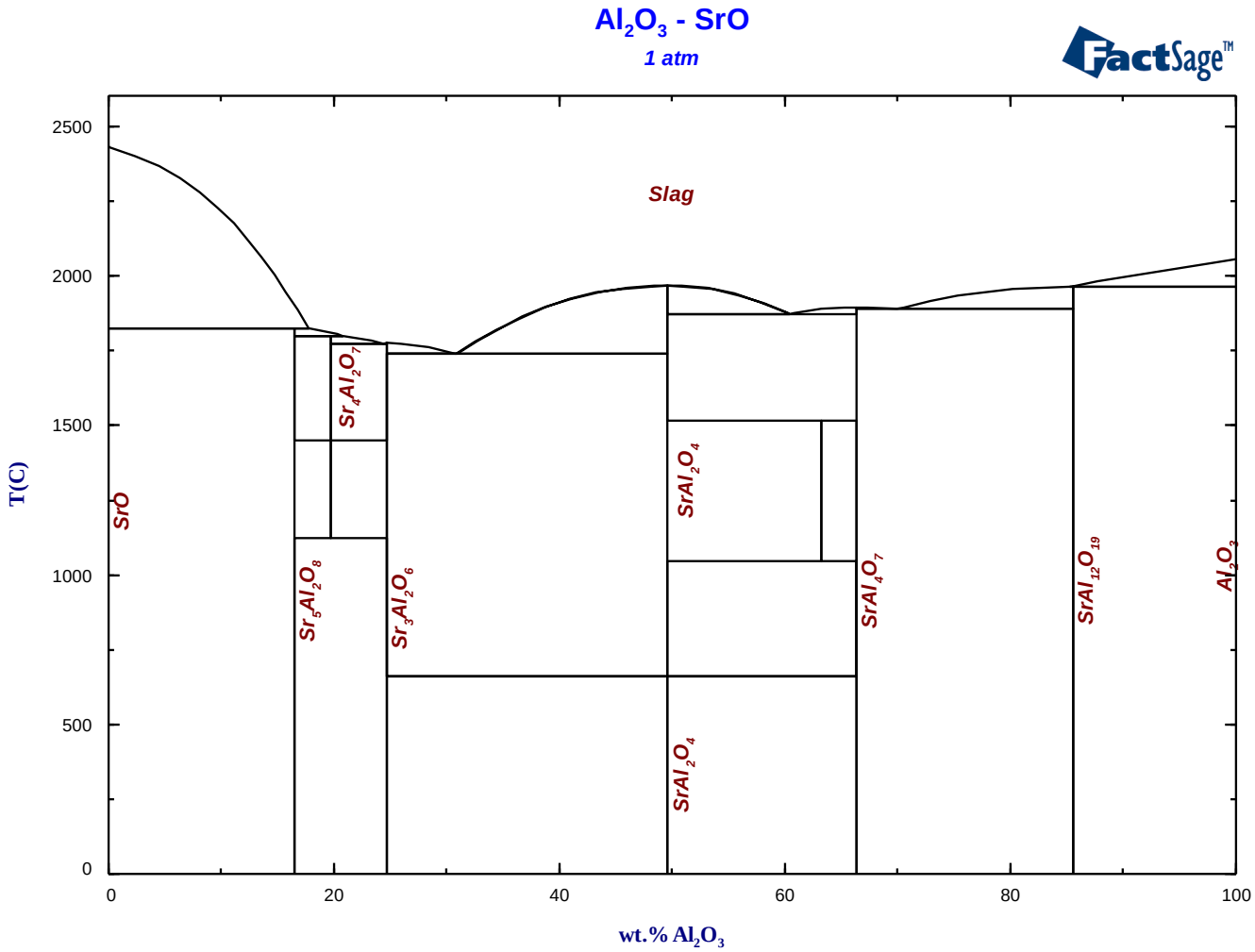

Mole fraction

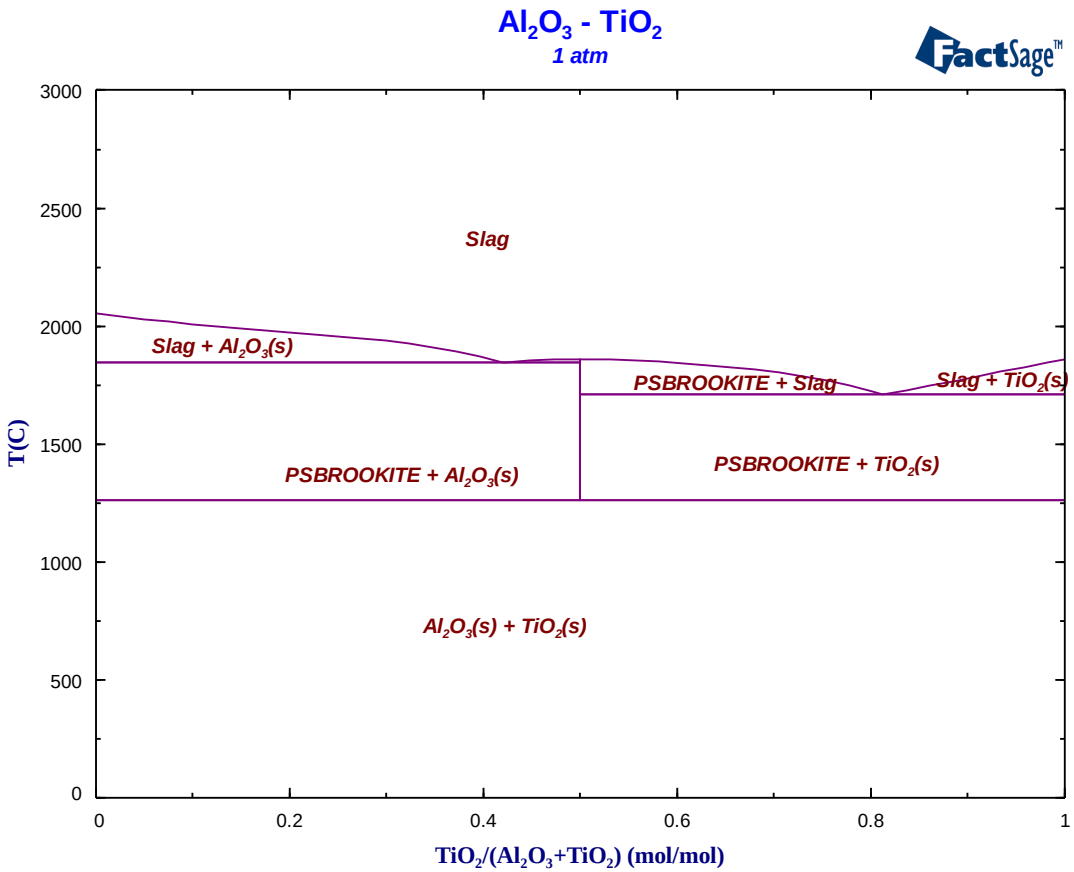

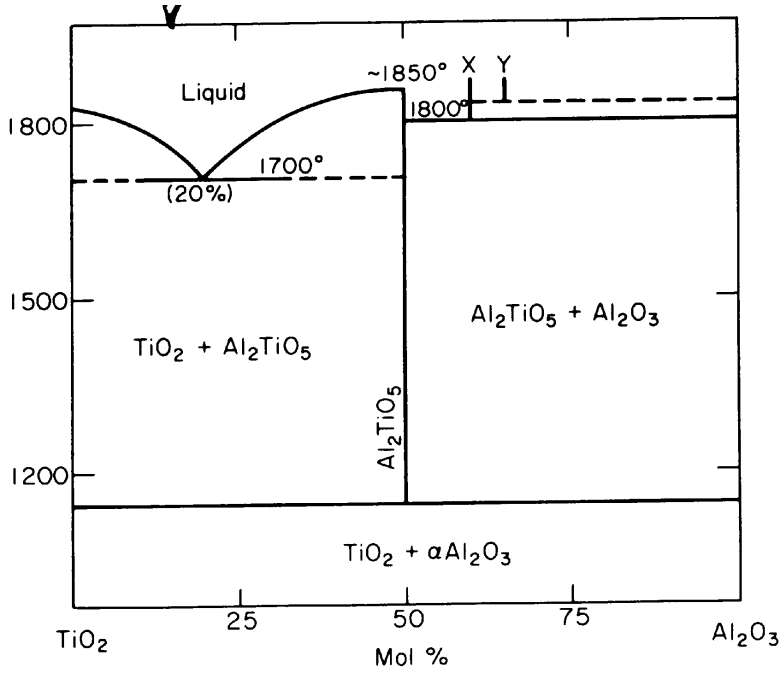

A.M. Lejus, D. Goldberg, A. Revcolevschi, C.R. Seances Acad. Sci., Ser. C, 263 [20], (1966), pp.1223-1226.

Weight percent
compared with experimental data

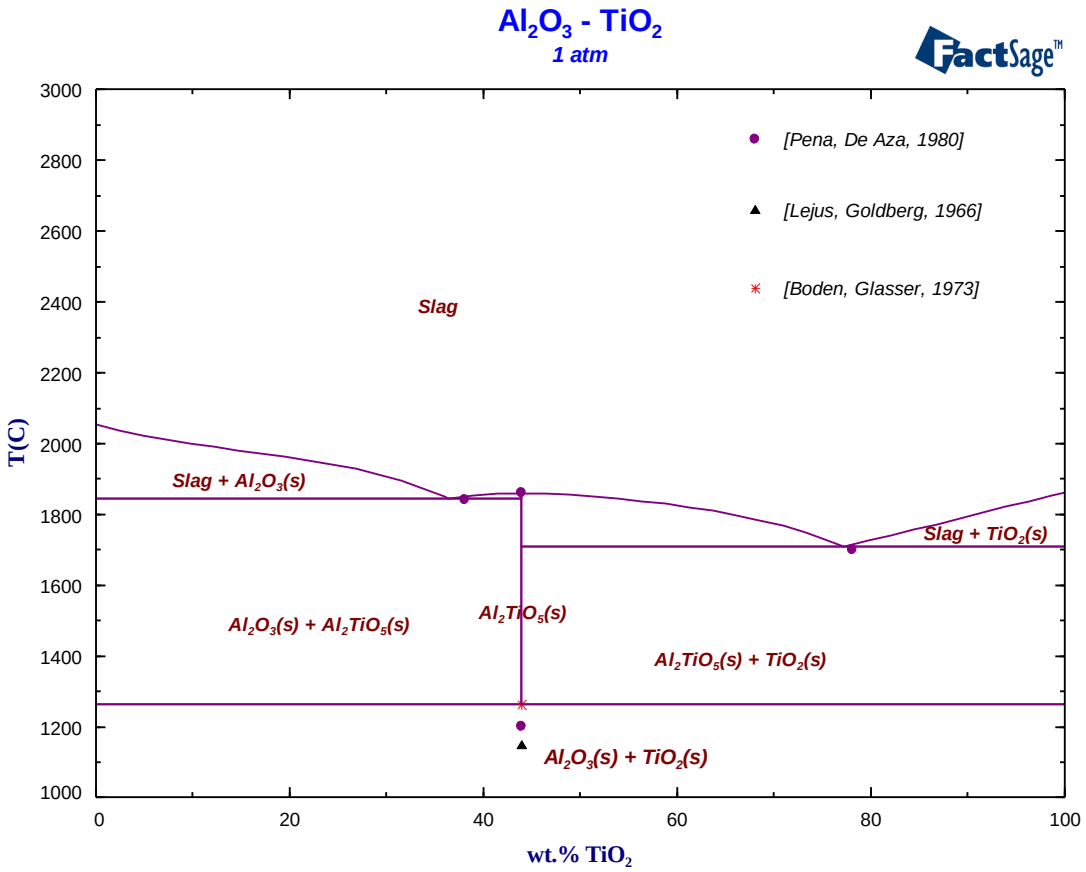

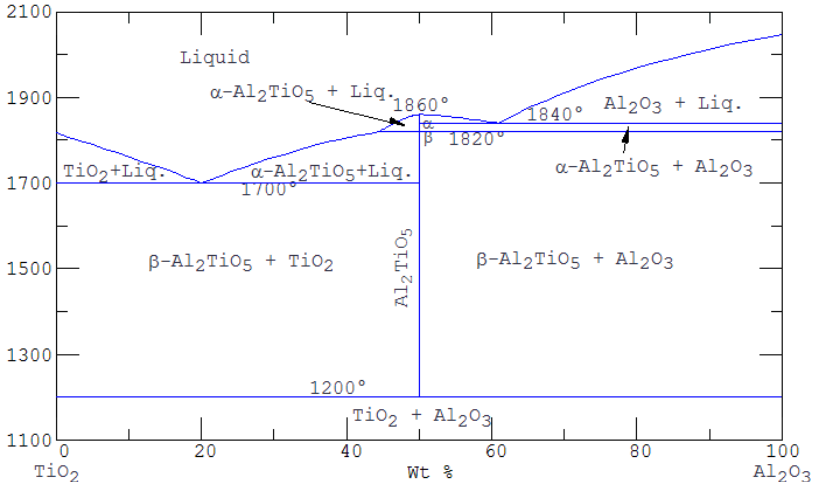

P. Pena, S. DeAza, Ceramica (Florence), 33 [3], (1980), pp. 23-30.

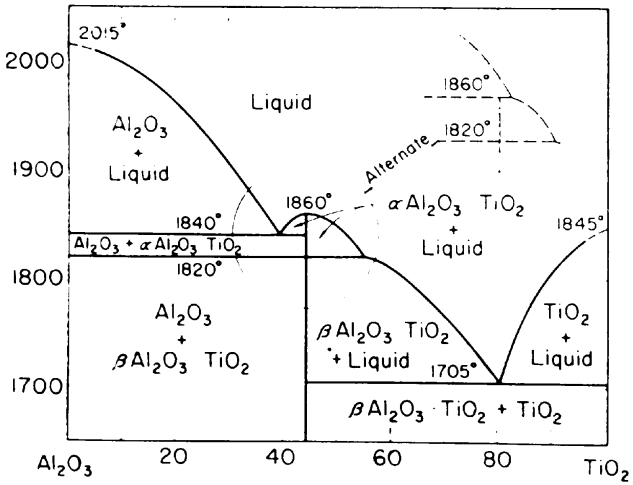

S.M. Lang, C.L. Fillmore, L.H. Maxwell, J. Res. Natl. Bur. Stand. (U.S.), 48 [4], (1952), pp. 298-312.

Mole fraction

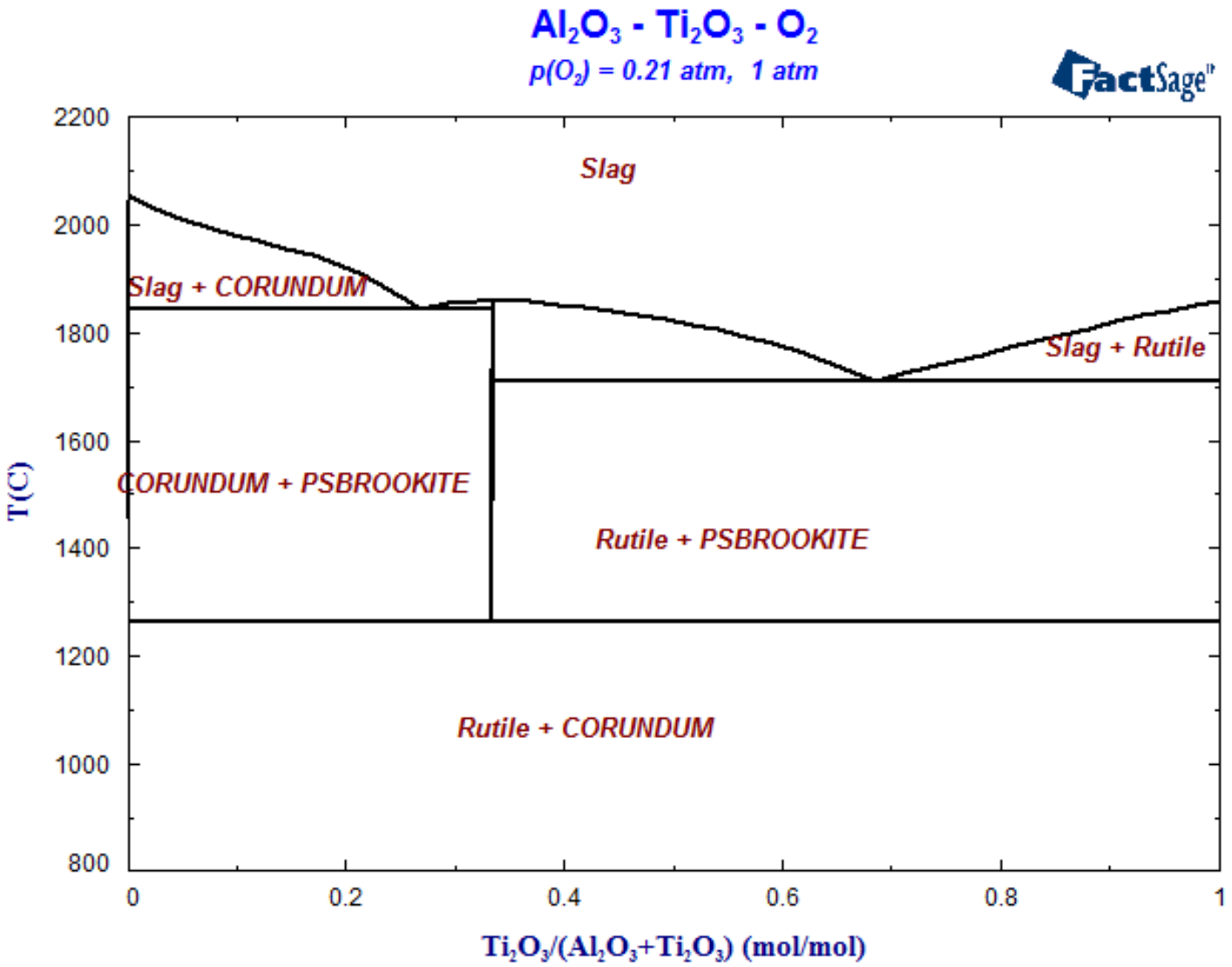

Weight percent

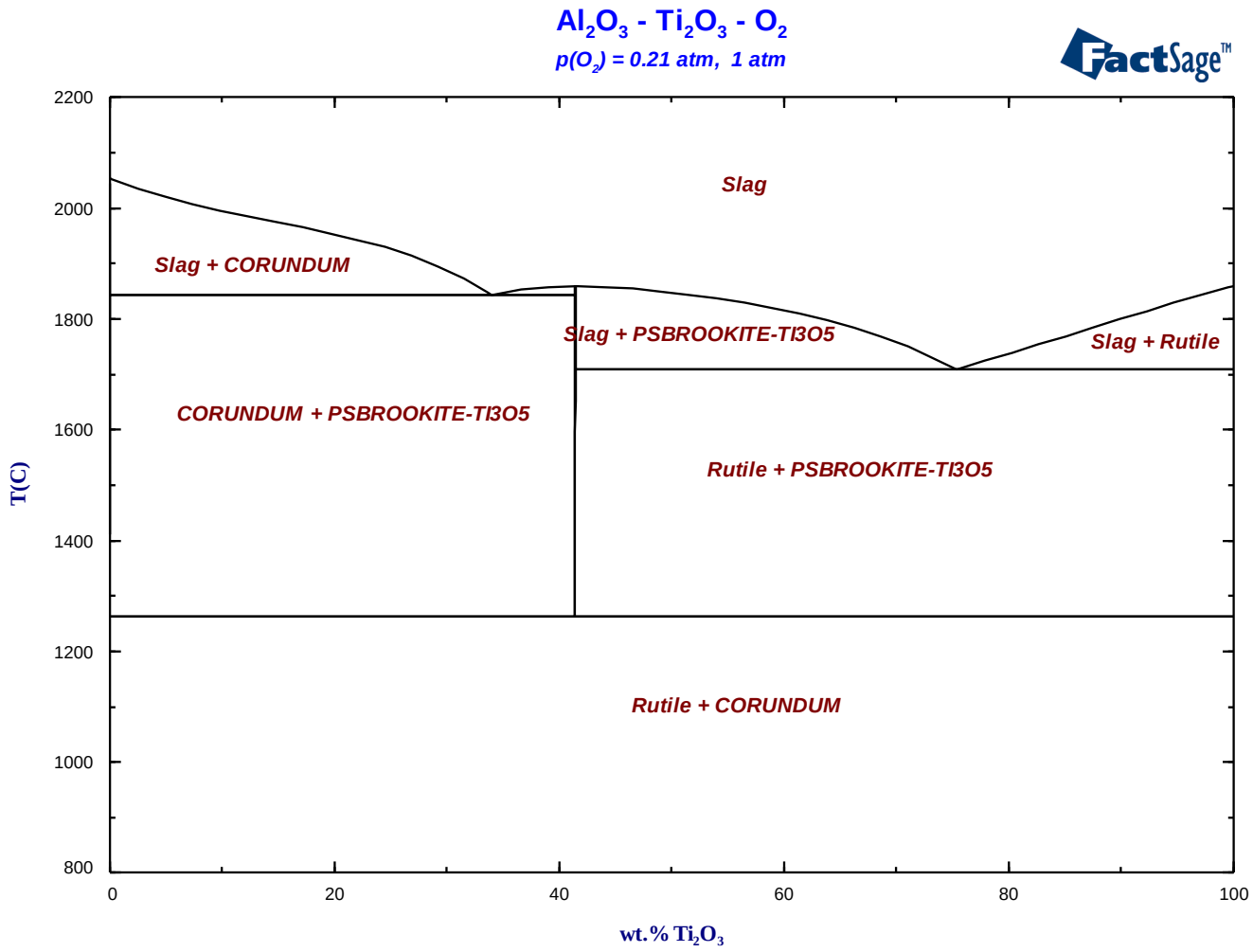

Mole fraction, P(O2)=10^{-15} bar compared with experimental data

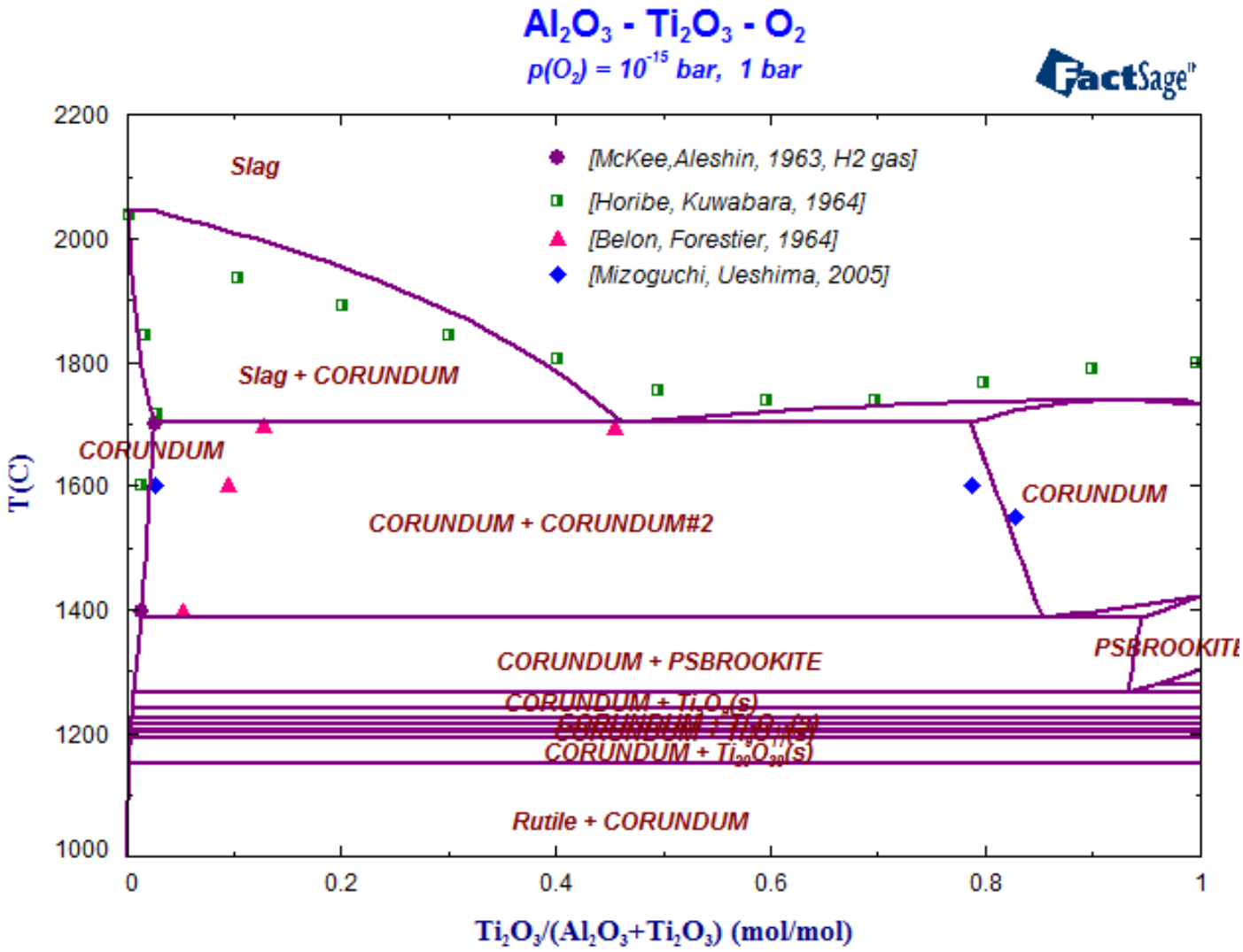

Al2O3-V2O3, Mole fraction

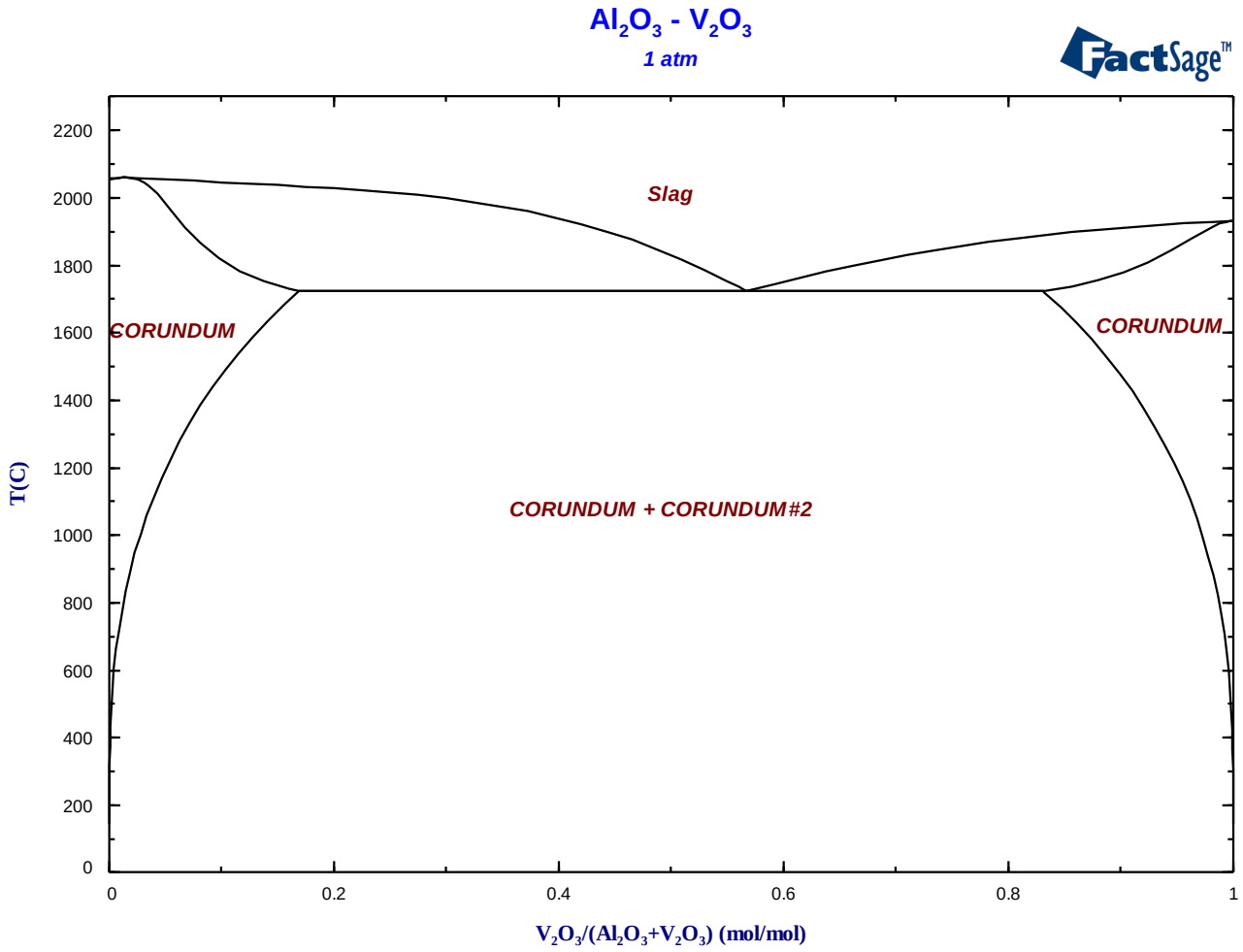

Al2O3-V2O3,
Weight percent

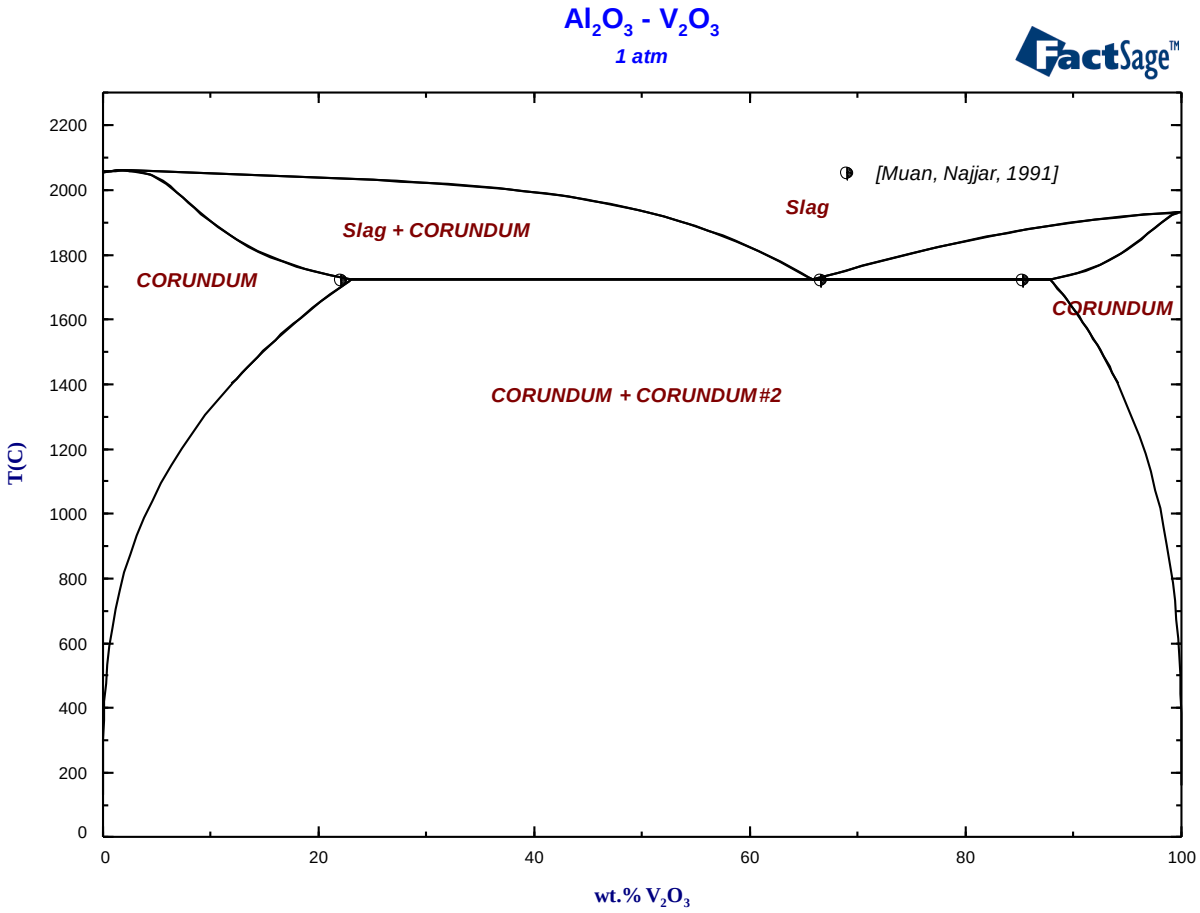

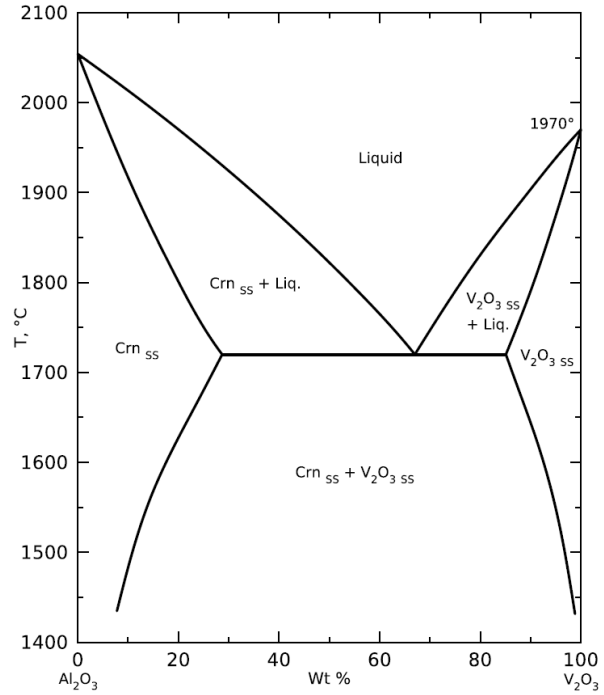

A. Muan and M. S. Najjar, "Compositions involving V2O3-Al2O3-CaO", US Patent 5,070,065, December 3, 1991.

Al2O3-V2O5-O2,
Mole fraction compared with experimental data

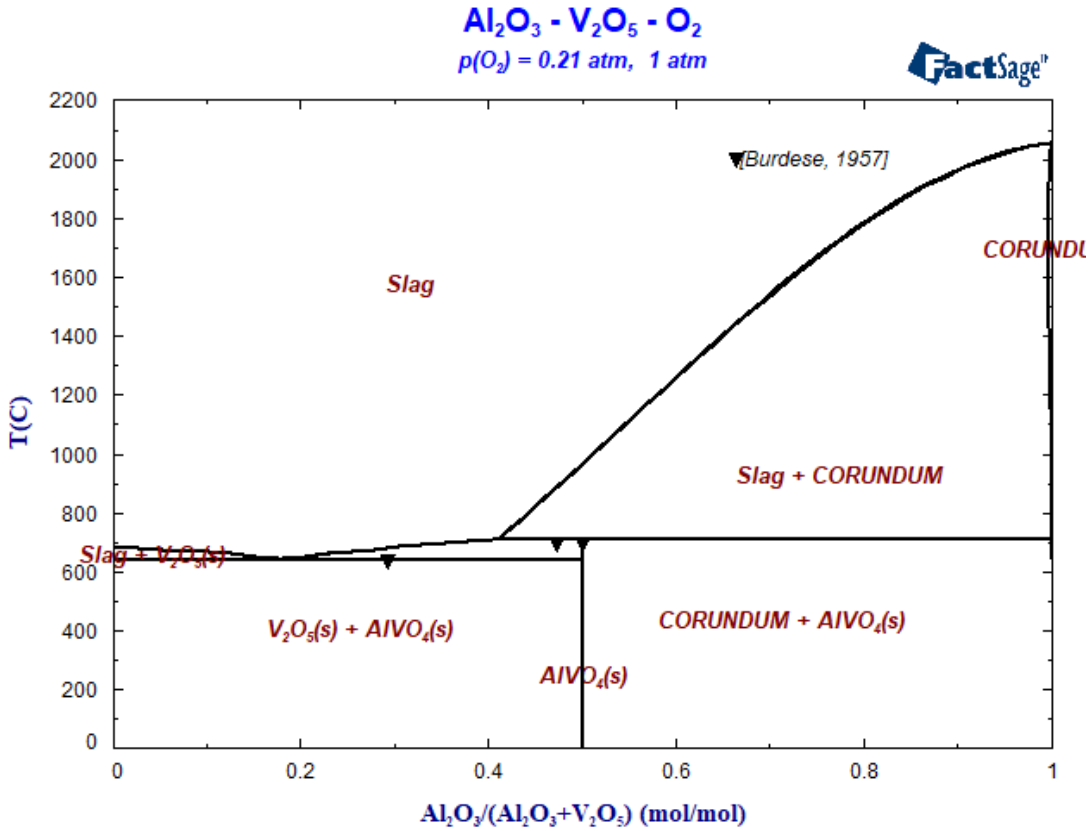

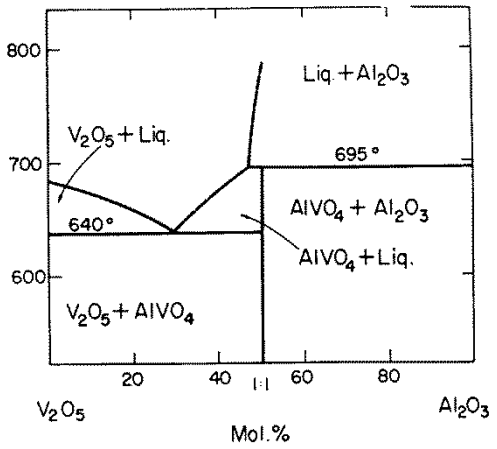

A. Burdese, Ann. Chim. (Rome), 47 [7-8], (1957), pp. 797-805.

Al2O3-V2O5-O2, Weight percent

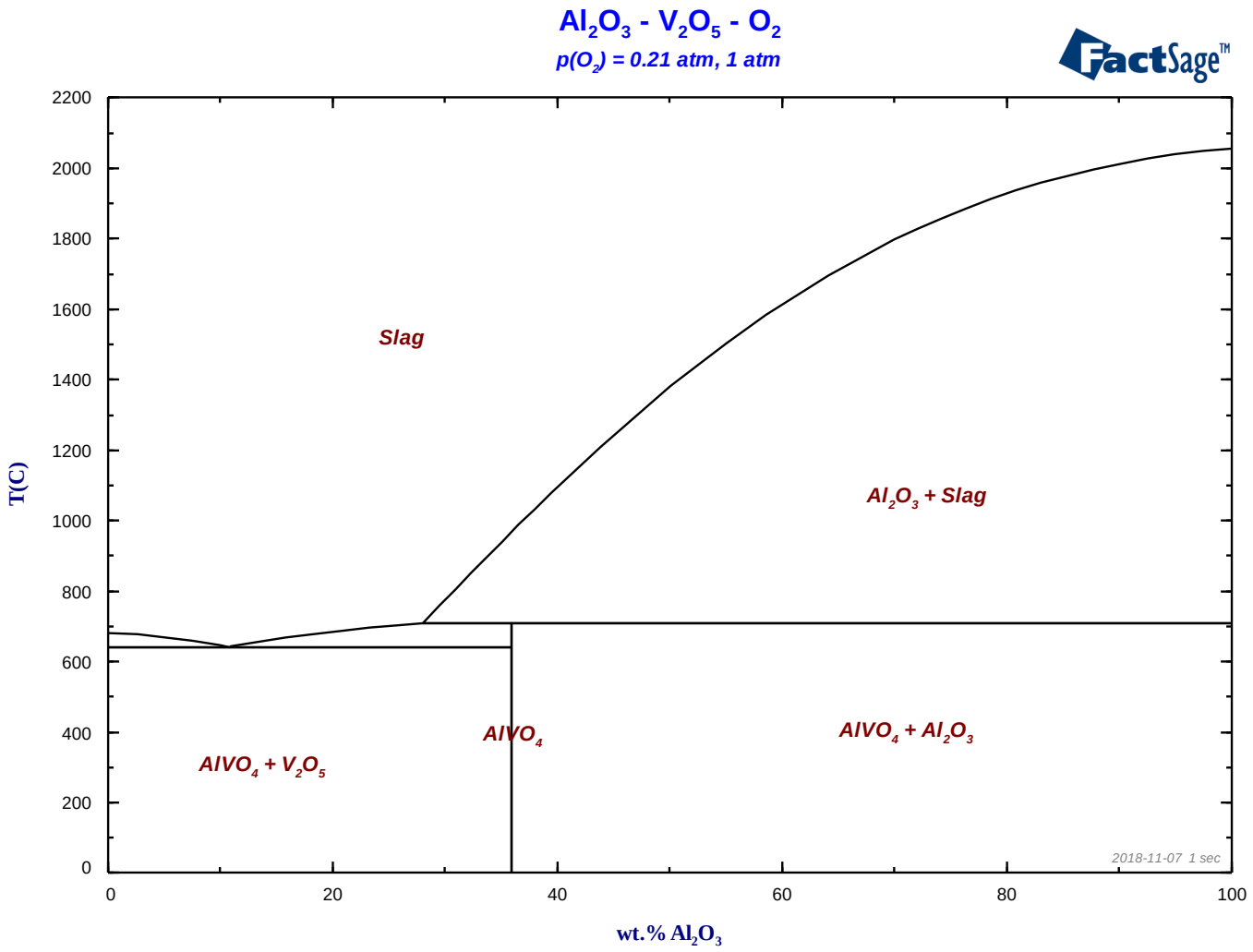

Mole fraction
compared with experimental data

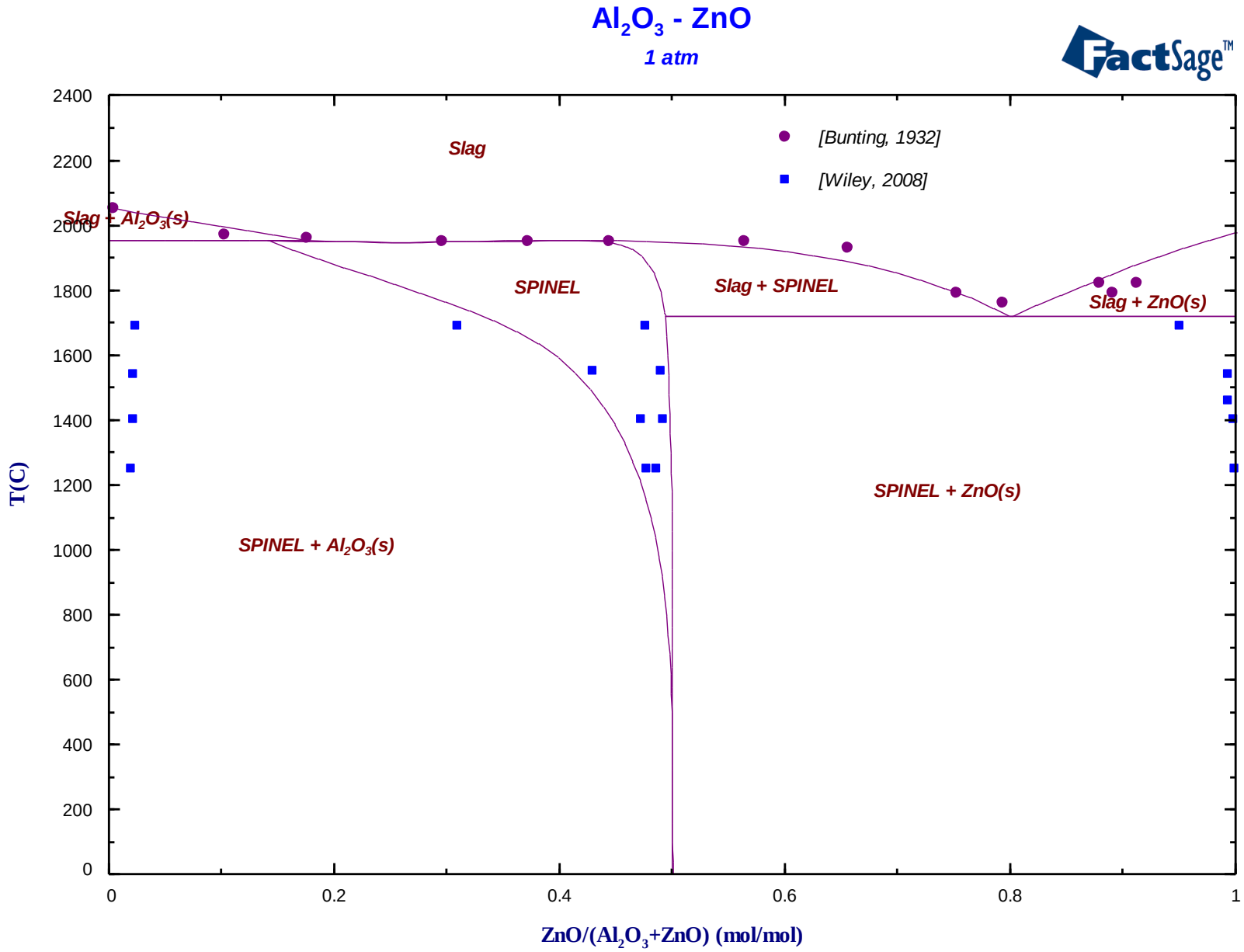

Weight percent

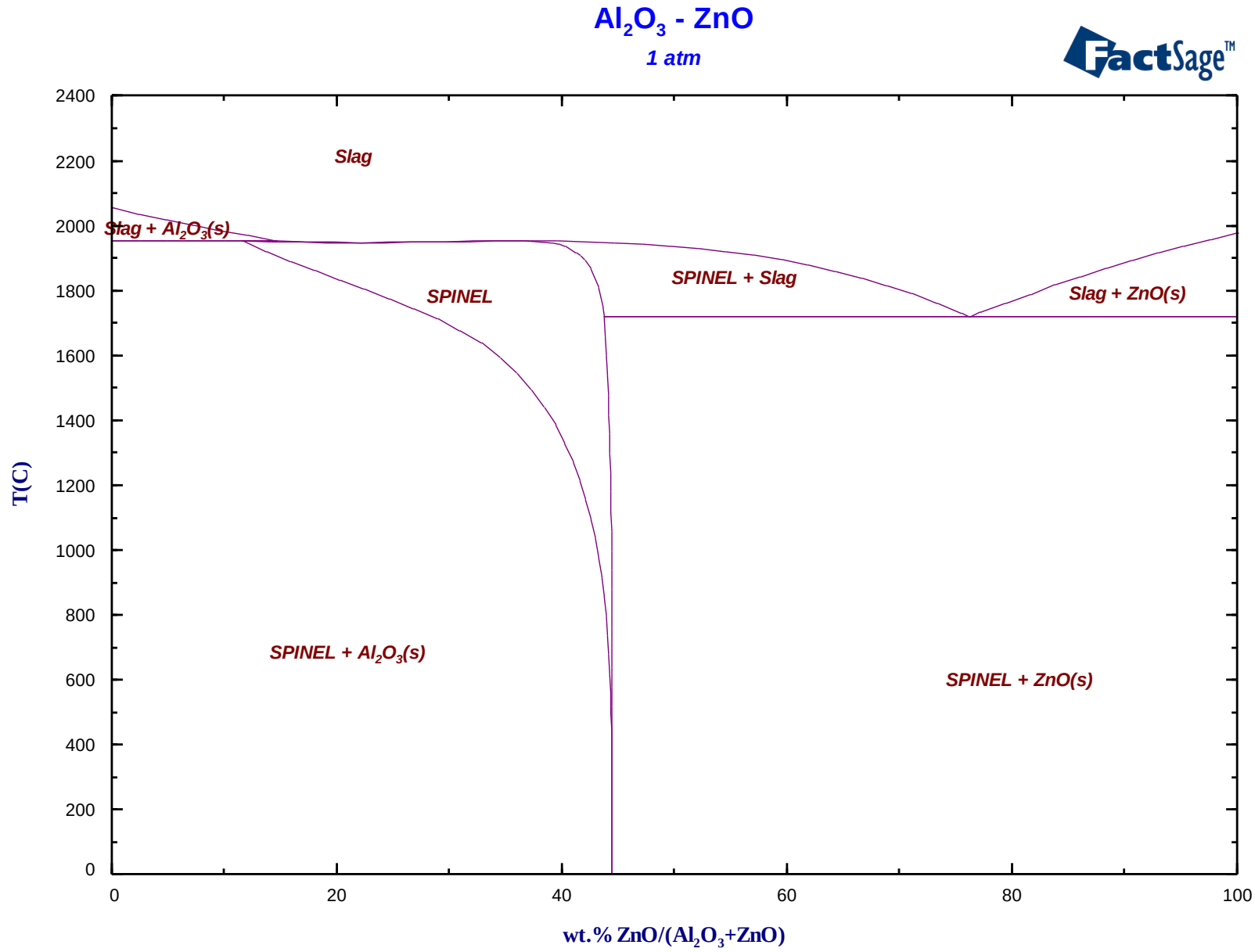

Mole fraction
compared with experimental data

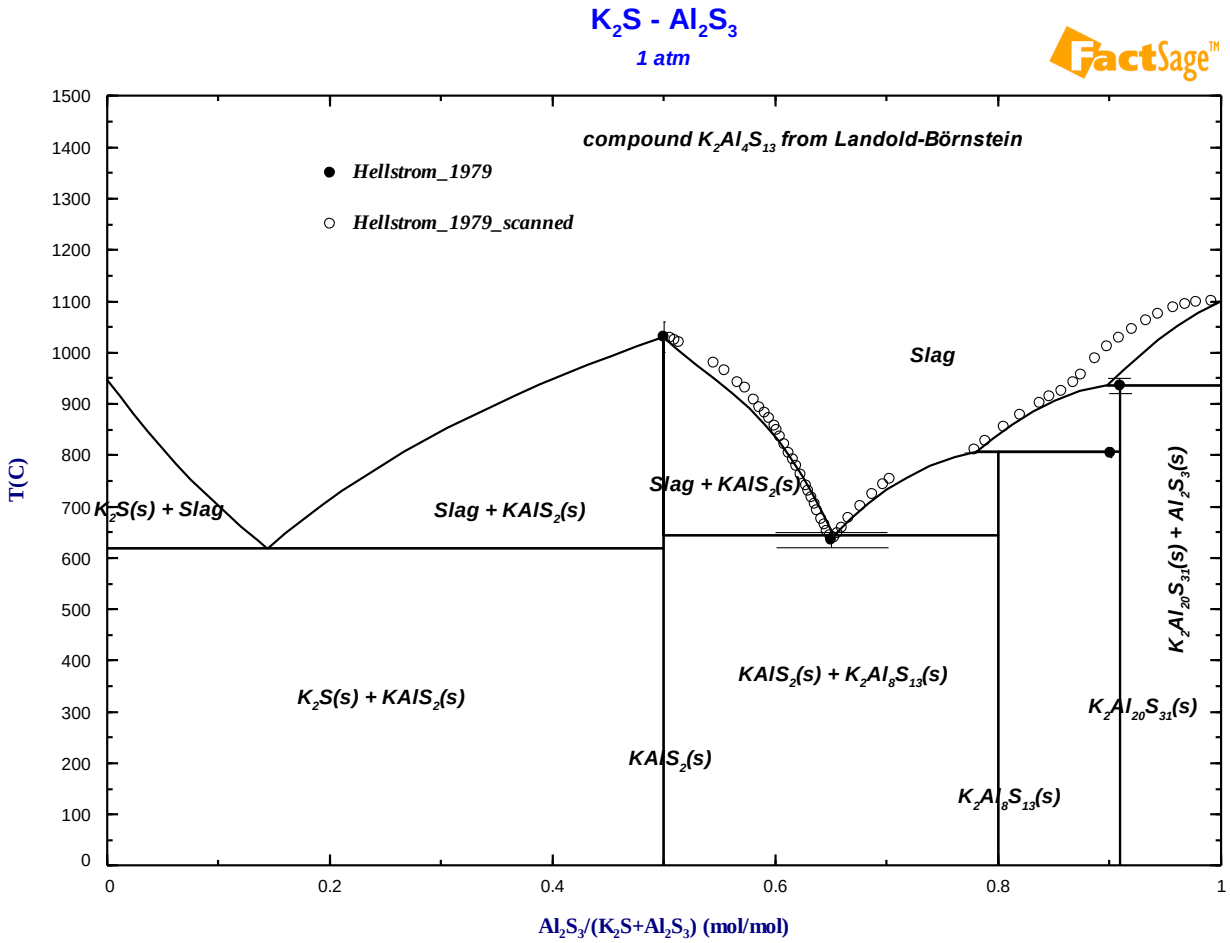

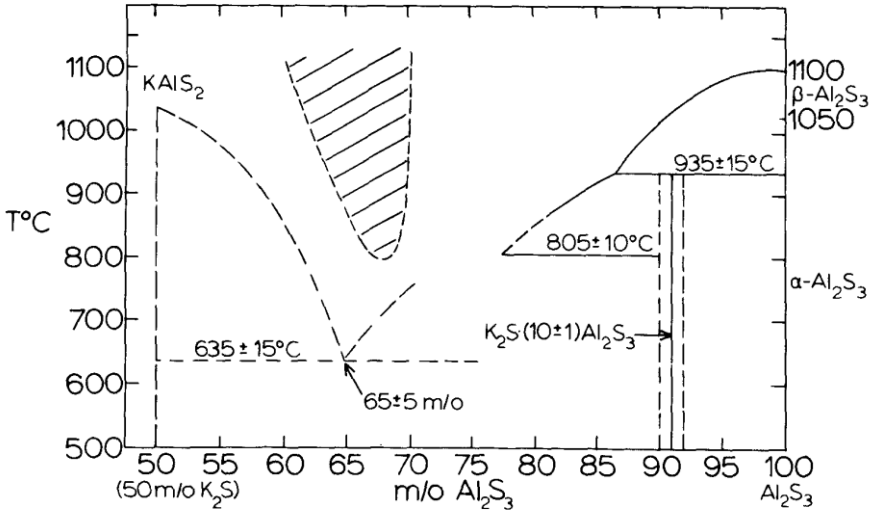

E.E. Hellstrom, R.A. Huggins, A study of the system M_2S-Al_2S_3, M=Li, Na, K; preparation, phase study and electrical conductivity, Mater Res Bull, 1979; 14: 881-9.

Weight percent

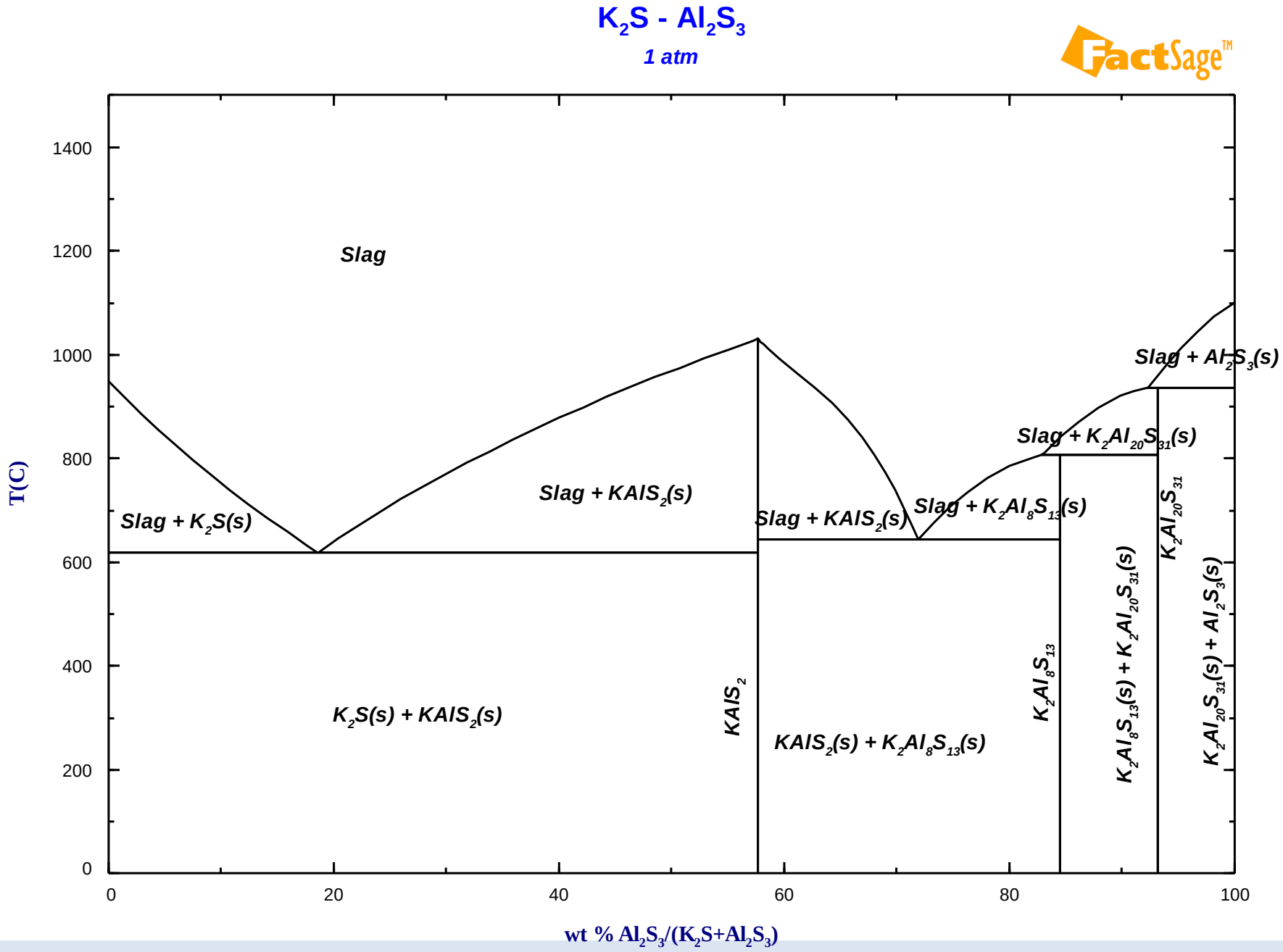

Mole fraction
compared with experimental data

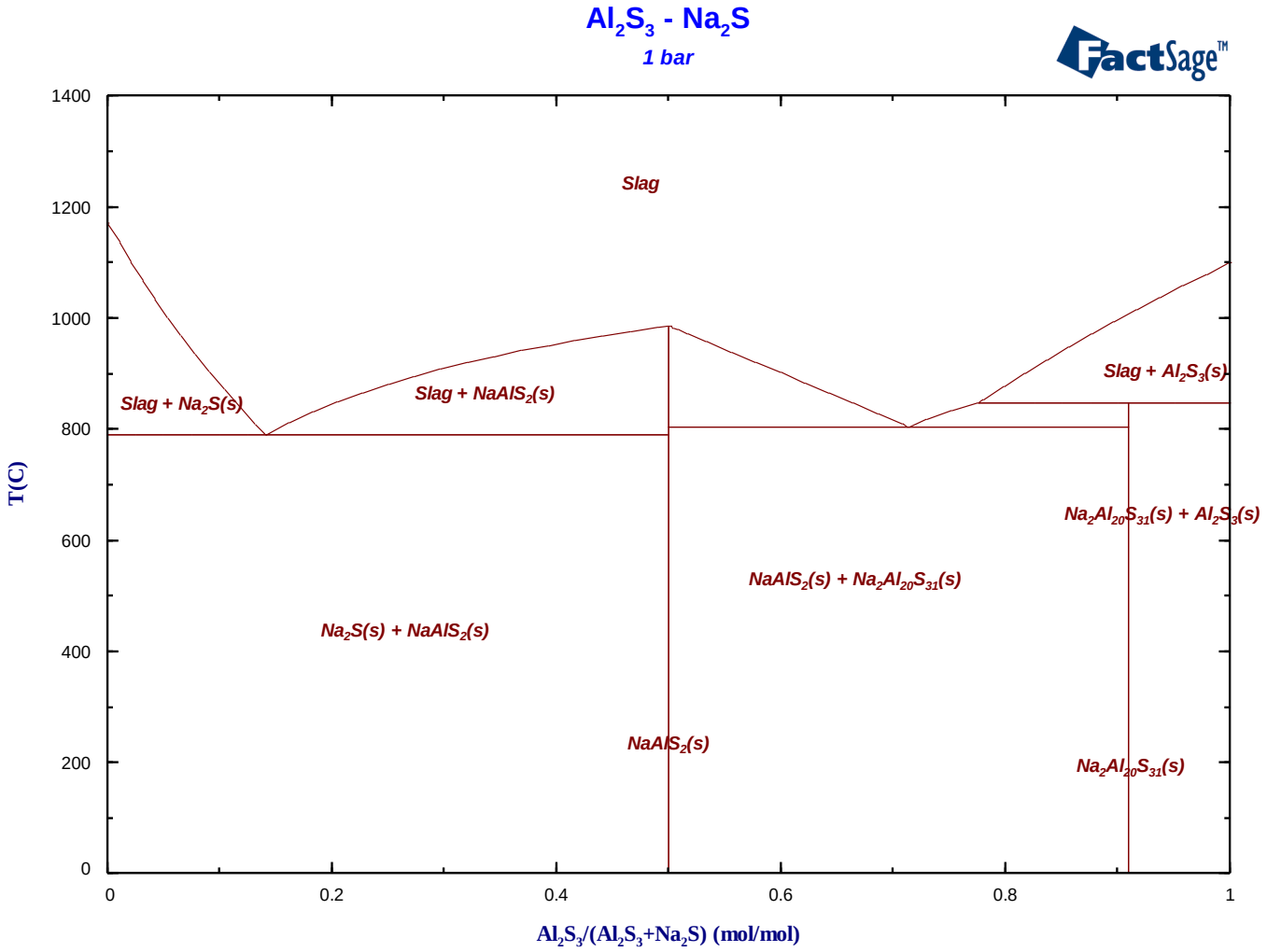

Weight percent

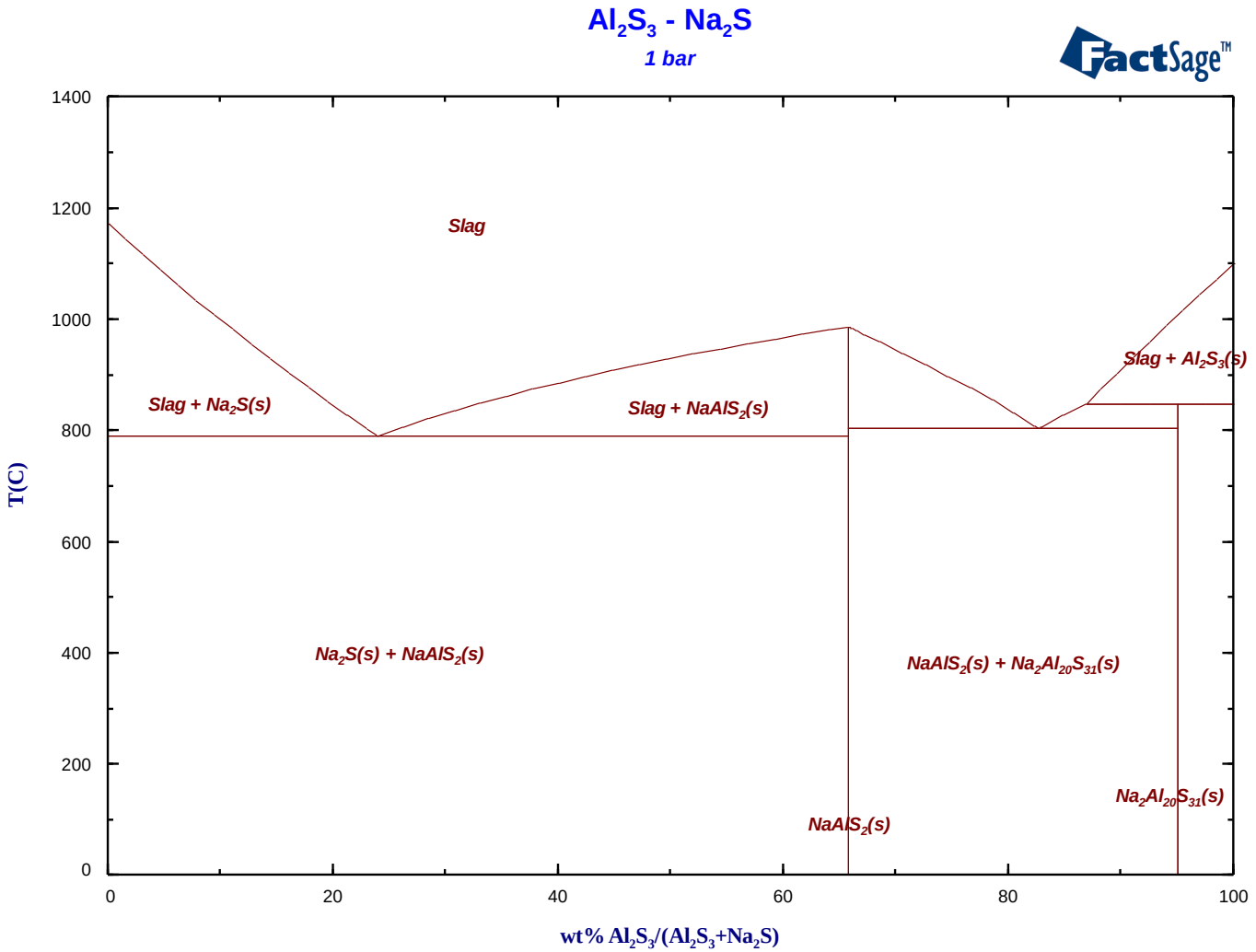

Mole fraction compared with experimental data

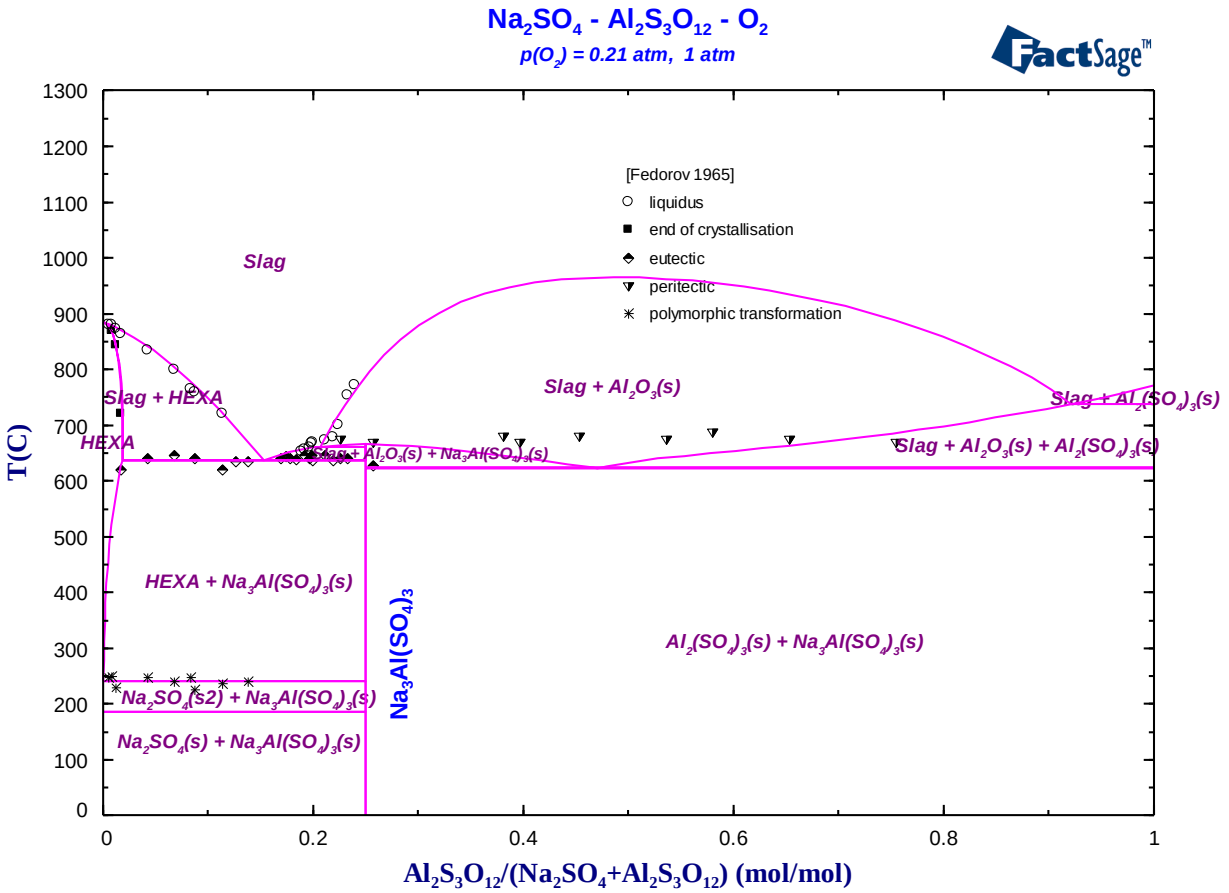

Al2(SO4)3-Na2SO4,

Weight percent

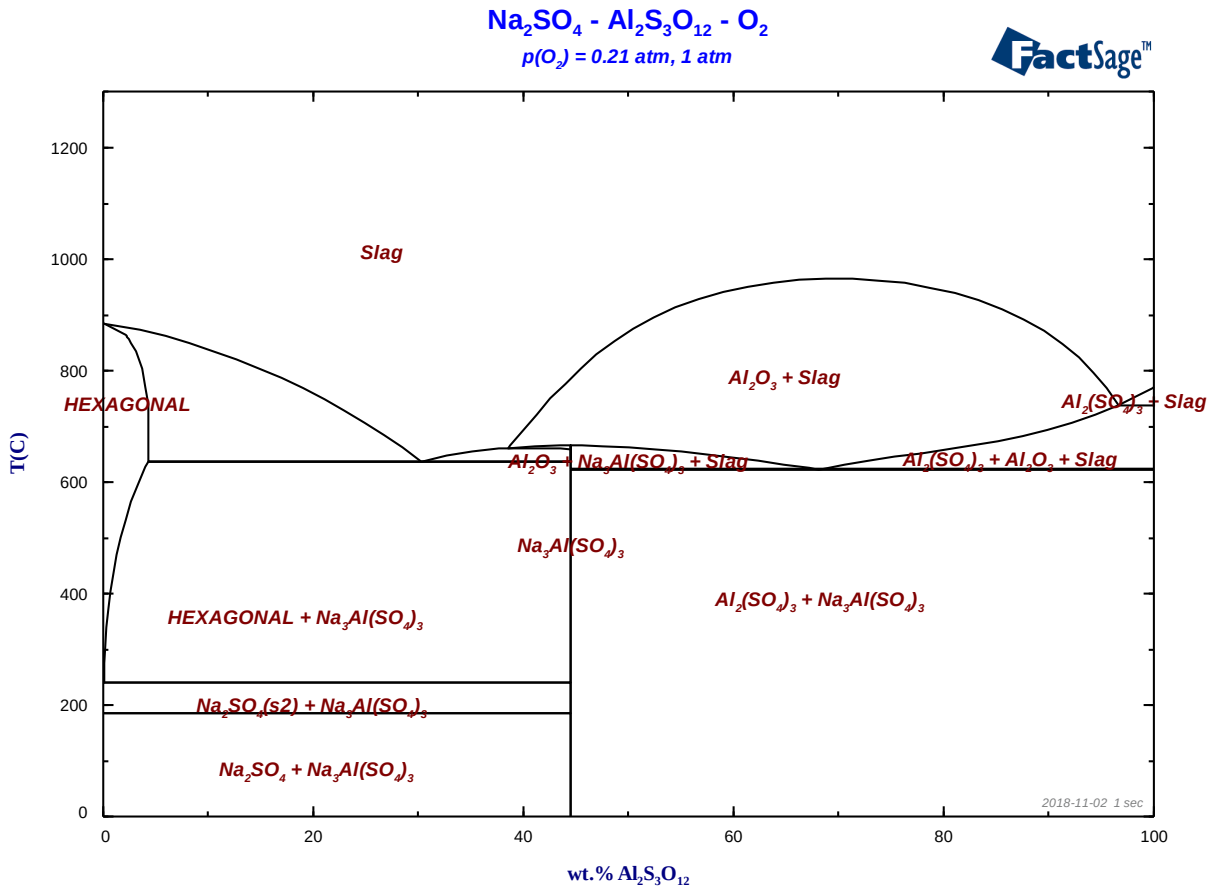

Mole fraction

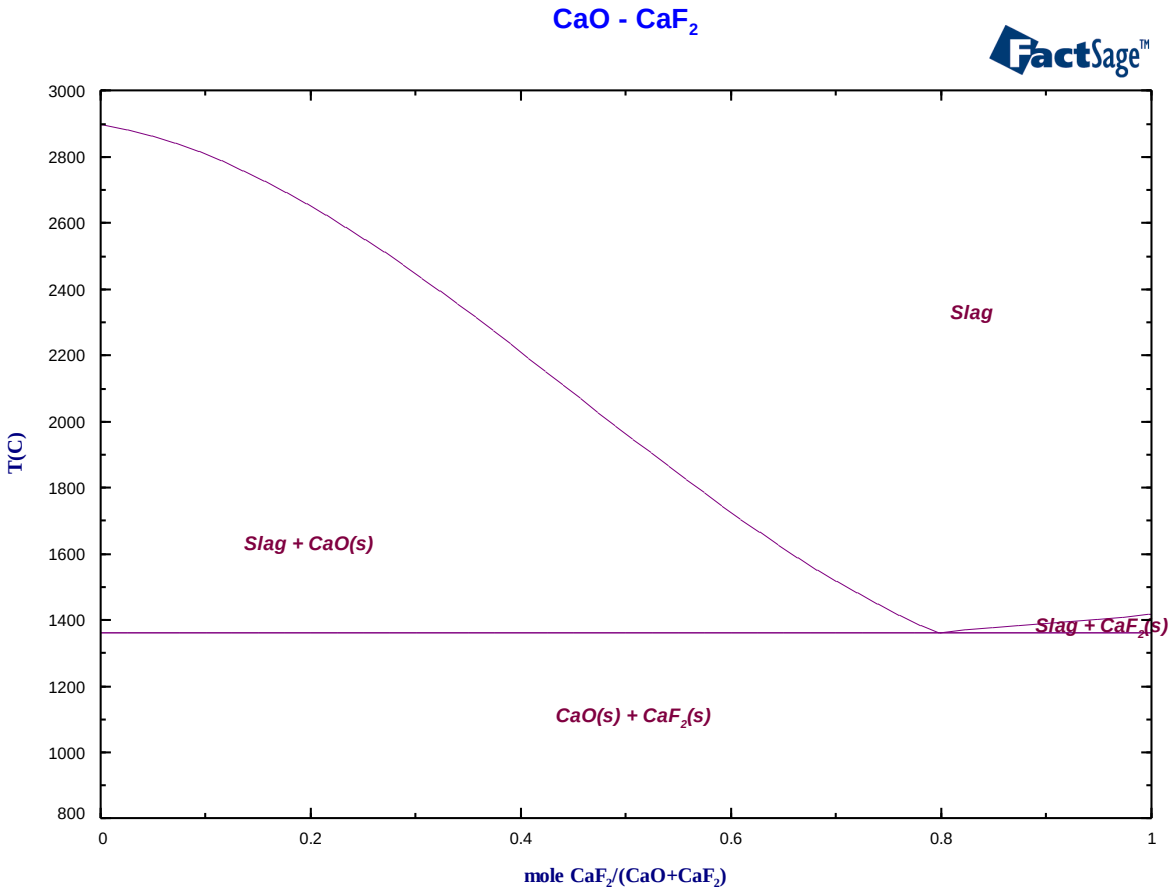

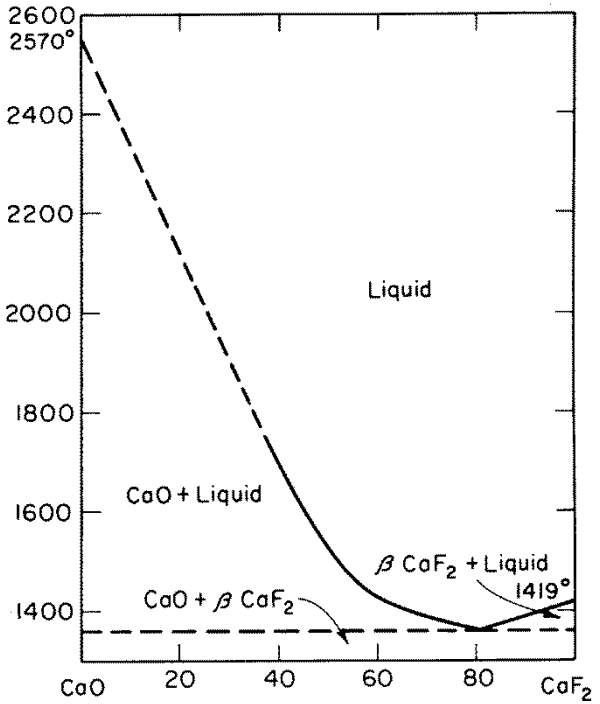

J. Mukerji, J. AM. Ceram. Soc., 48 [4], (1965), pp. 210-213.

Weight percent
compared with experimental data

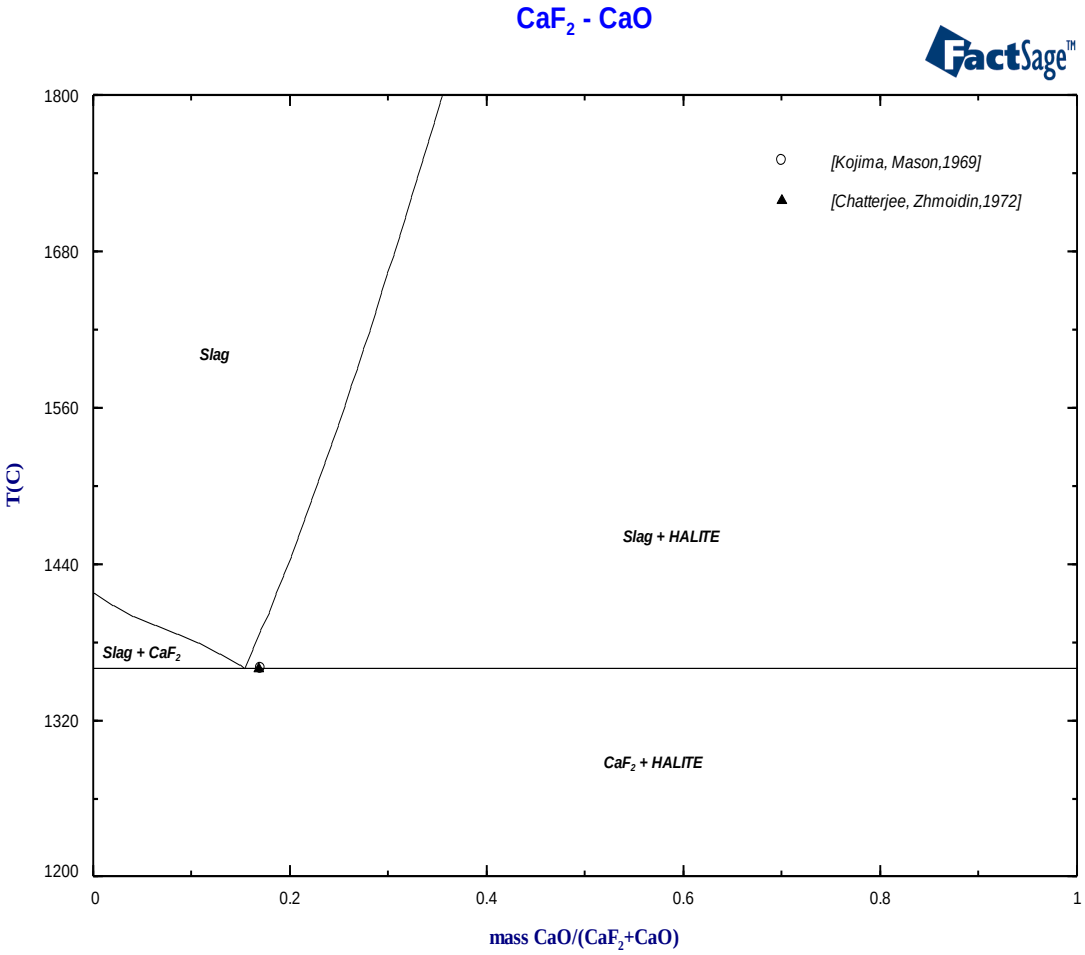

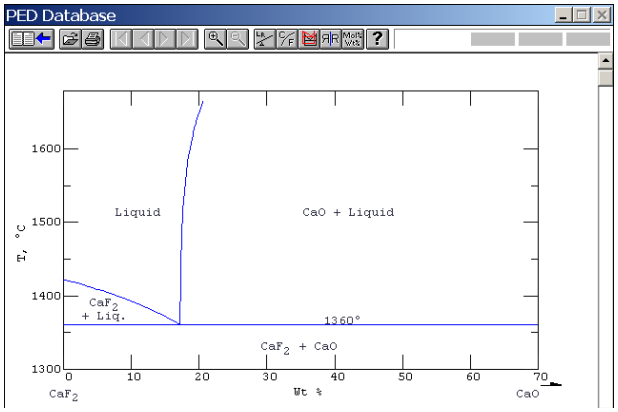

R. Ries, K. Schwerdtfeger, Arch. Eisenhuettenwes., 51 [4], (1980), pp. 123-129.

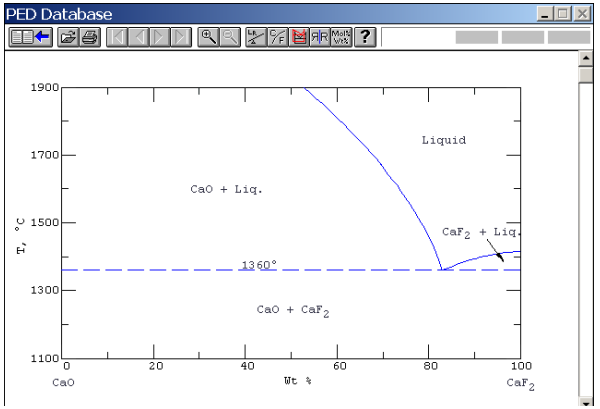

A.K. Chatterjee, G.I. Zhmoidin, J. Mater. Sci., 7 [1], (1972), pp. 93-97.

Mole fraction

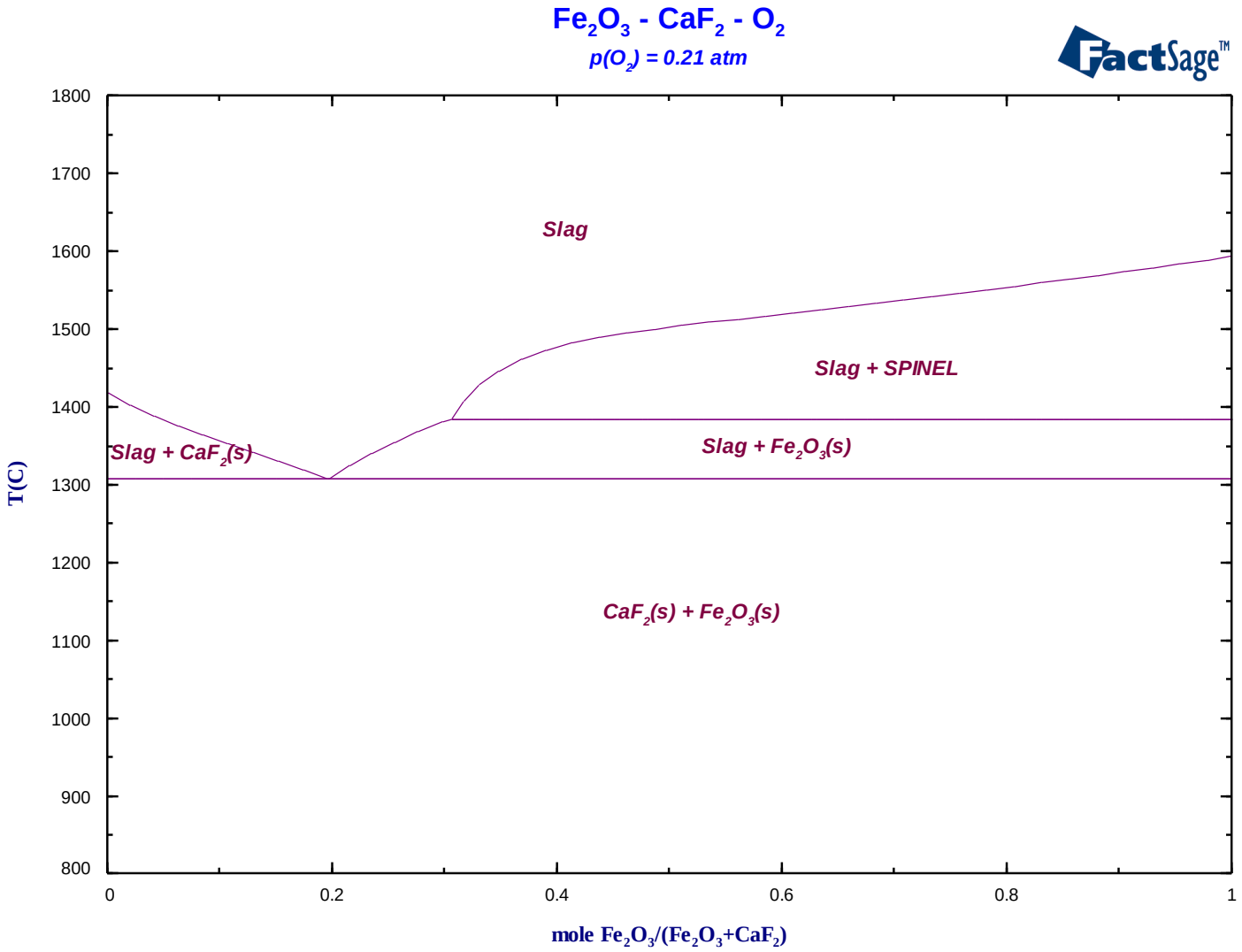

Weight percent

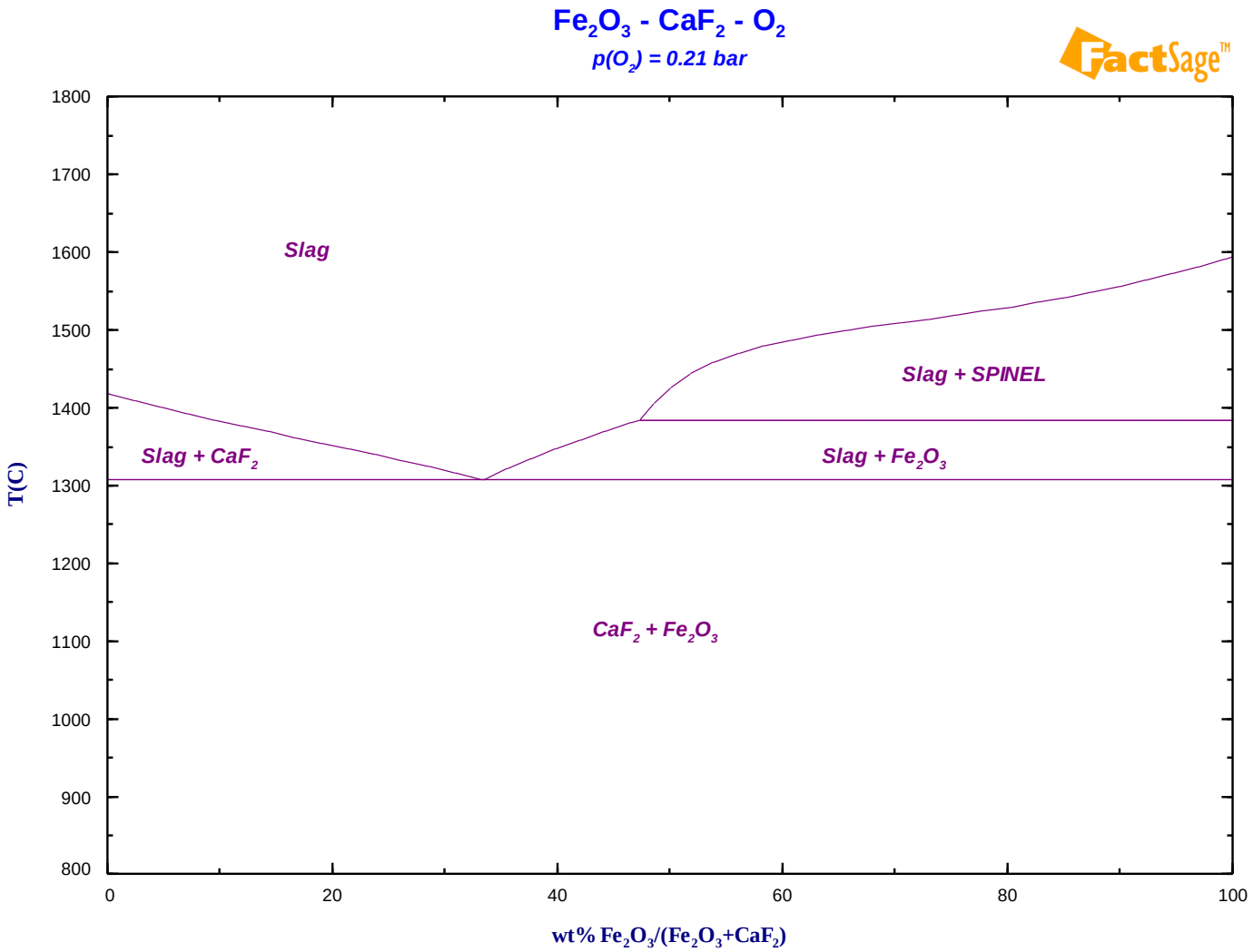

Mole fraction

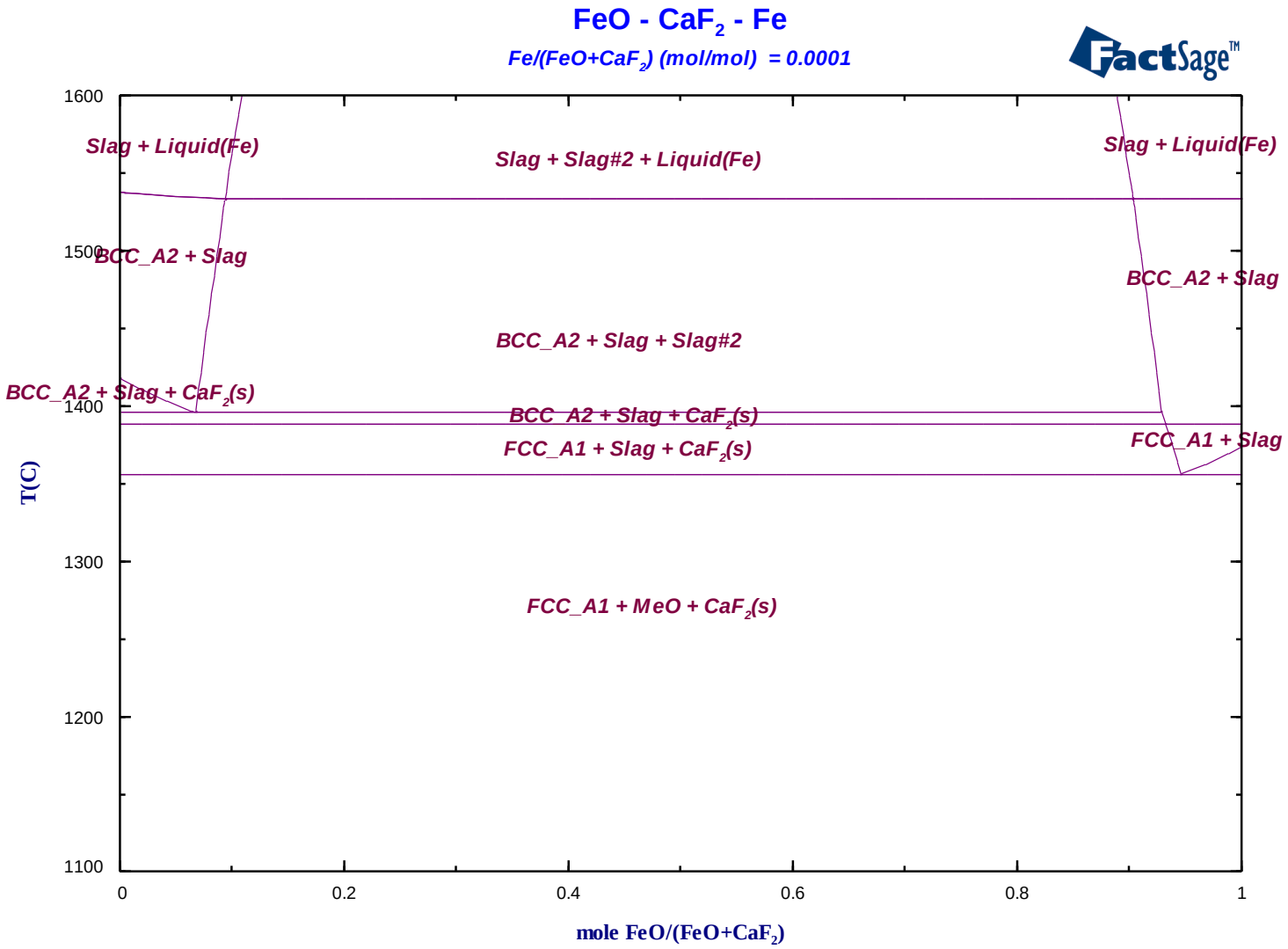

Weight percent

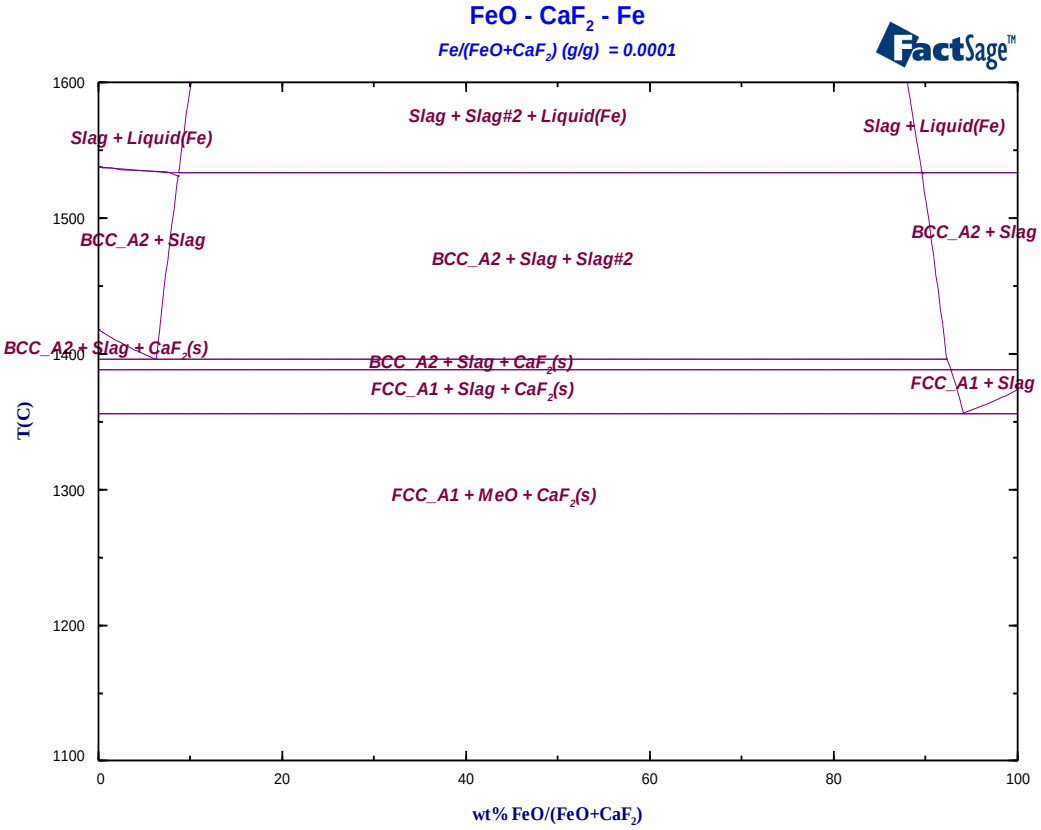

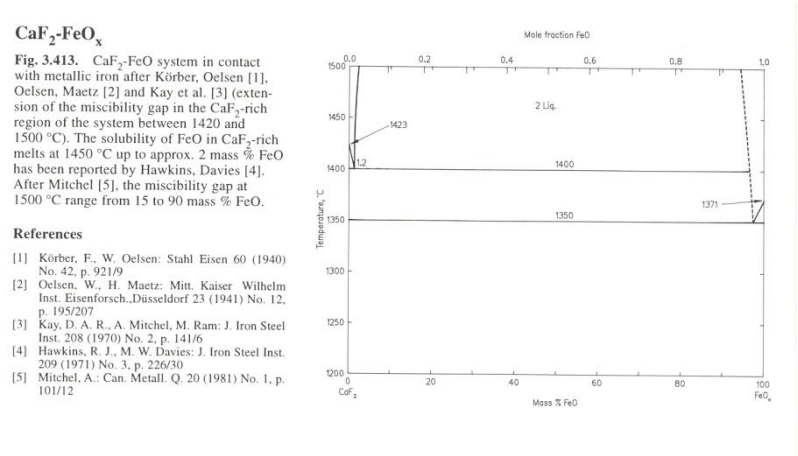

CaF_2-FeO_x

Fig. 3.413. CaF_2-FeO system in contact with metallic iron after Körber, Oelsen [1], Oelsen, Maetz [2] and Kay et al. [3] (extension of the miscibility gap in the CaF_2-rich region of the system between 1420 and 1500 °C). The solubility of FeO in CaF_2-rich melts at 1450 °C up to approx. 2 mass % FeO has been reported by Hawkins, Davies [4]. After Mitchel [5], the miscibility gap at 1500 °C range from 15 to 90 mass % FeO.

References

[1] Körber, F., W. Oelsen: Stahl Eisen 60 (1940) No. 42, p. 921/9
[2] Oelsen, W., H. Maetz: Mitt. Kaiser Wilhelm Inst. Eisenforsch.,Düsseldorf 23 (1941) No. 12, p. 195/207
[3] Kay, D. A. R., A. Mitchel, M. Ram: J. Iron Steel Inst. 208 (1970) No. 2, p. 141/6
[4] Hawkins, R. J., M. W. Davies: J. Iron Steel Inst. 209 (1971) No. 3, p. 226/30
[5] Mitchel, A.: Can. Metall. Q. 20 (1981) No. 1, p. 101/12

Slag Atlas, 2nd Ed., Verlag Stahl-Eisen, Düsseldorf, 1995.

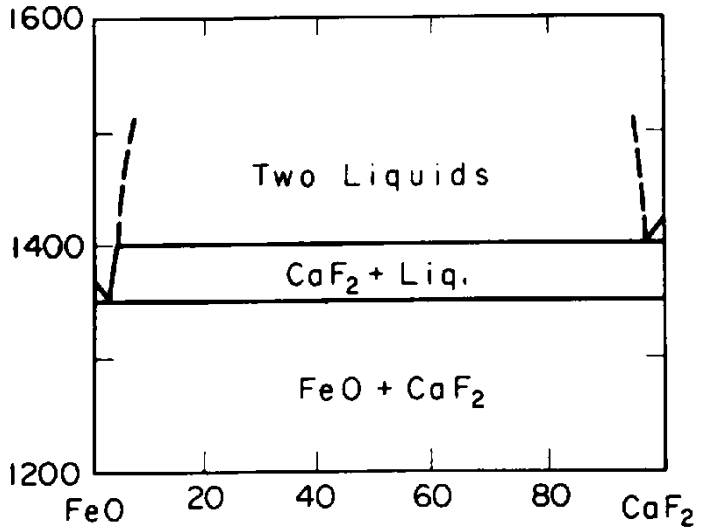

F. Koerber, W. Oelsen, Stahl Eisen, 60[42], (1940), pp.921-929.

Mole fraction

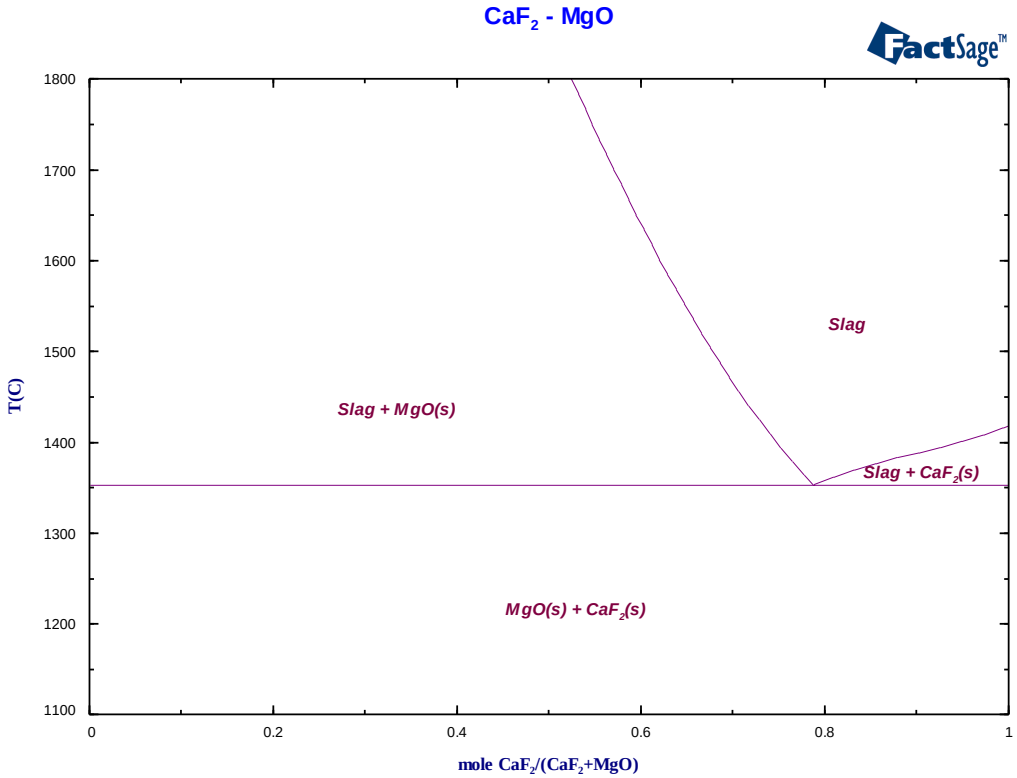

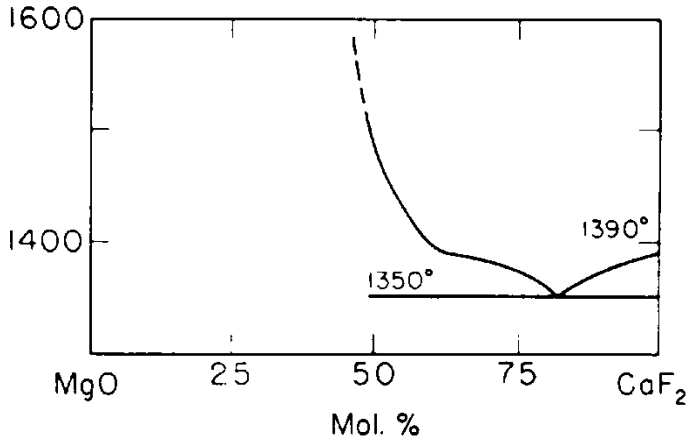

P.P. Budnikov, S.G. Tresvyatskii, Ukr. Khim. Zh. (Russ. Ed.), 19 [5], (1953), pp.552-555.

Weight percent

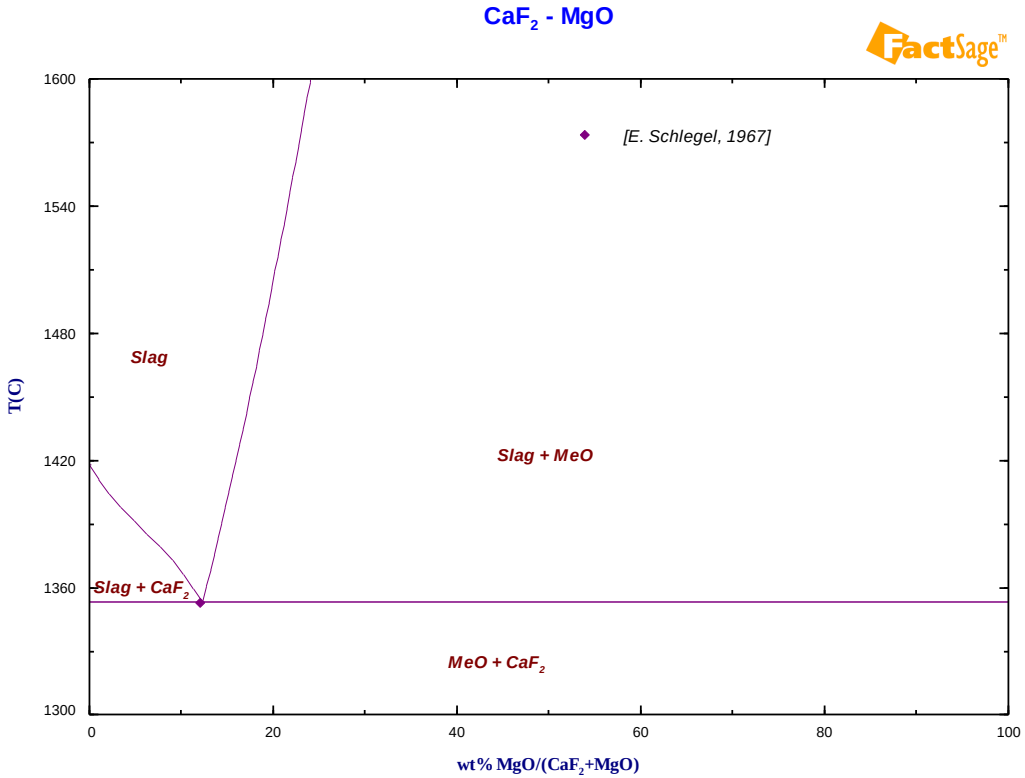

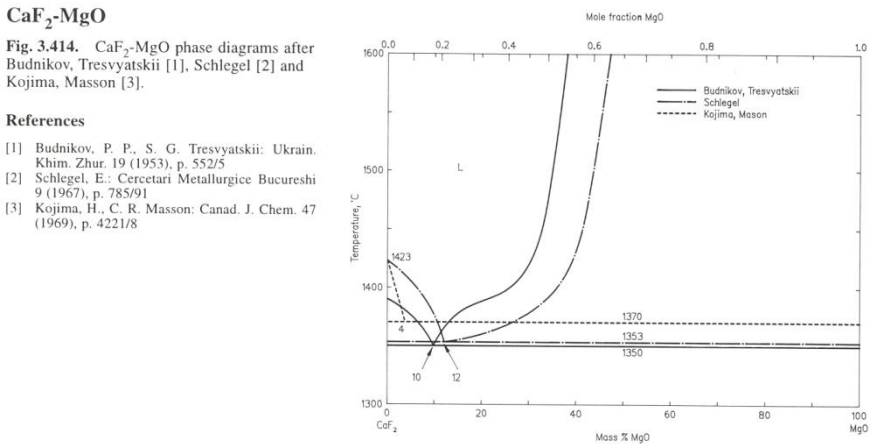

CaF_2-MgO

Fig. 3.414. CaF_2-MgO phase diagrams after Budnikov, Tresvyatskii [1], Schlegel [2] and Kojima, Masson [3].

References

[1] Budnikov, P. P., S. G. Tresvyatskii: Ukrain. Khim. Zhur. 19 (1953), p. 552/5
[2] Schlegel, E.: Cercetari Metallurgice Bucureshi 9 (1967), p. 785/91
[3] Kojima, H., C. R. Masson: Canad. J. Chem. 47 (1969), p. 4221/8

Slag Atlas, 2nd Ed., Verlag Stahl-Eisen, Düsseldorf, 1995.

Mole fraction

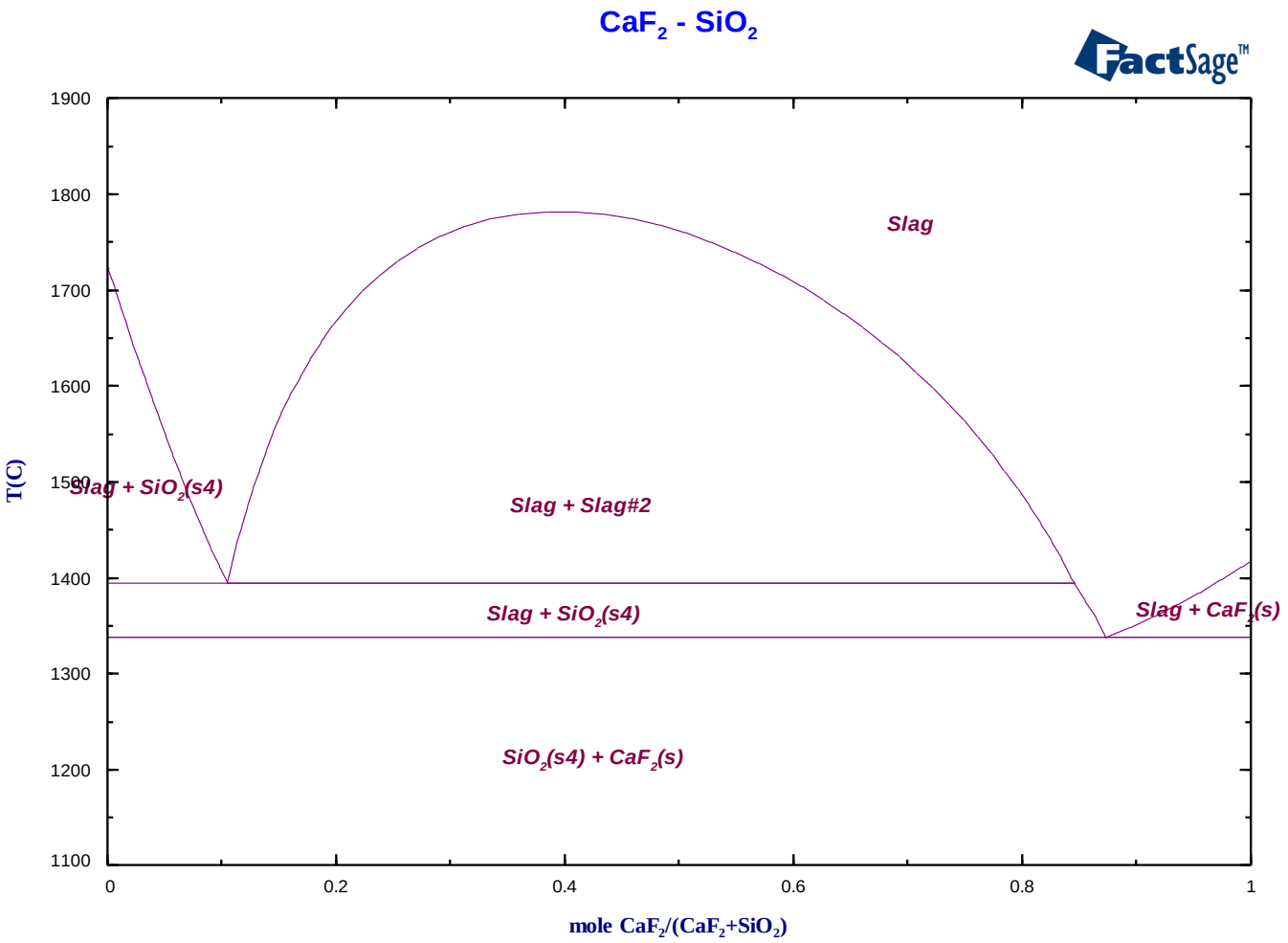

Weight percent
compared with experimental data

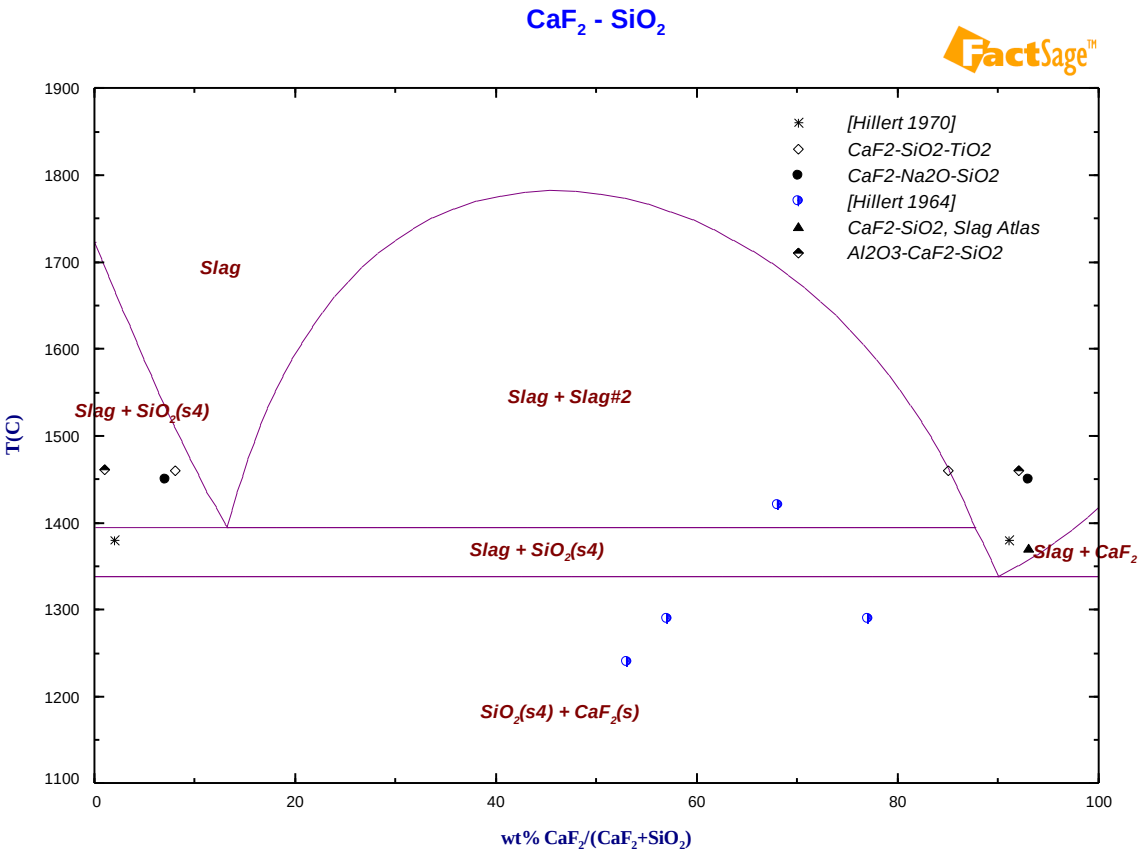

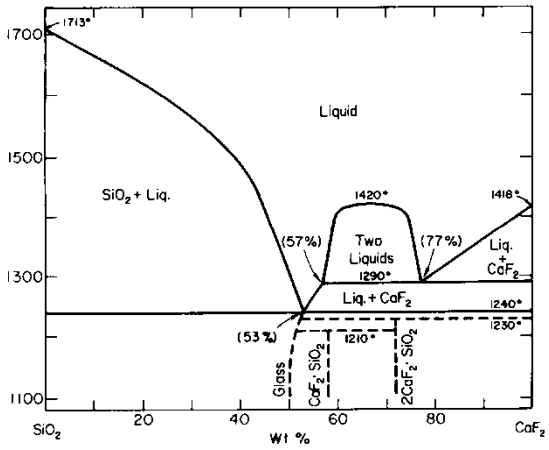

L. Hillert, Acta Chem. Scand., 18 [10], (1964), pp. 2411-2411.

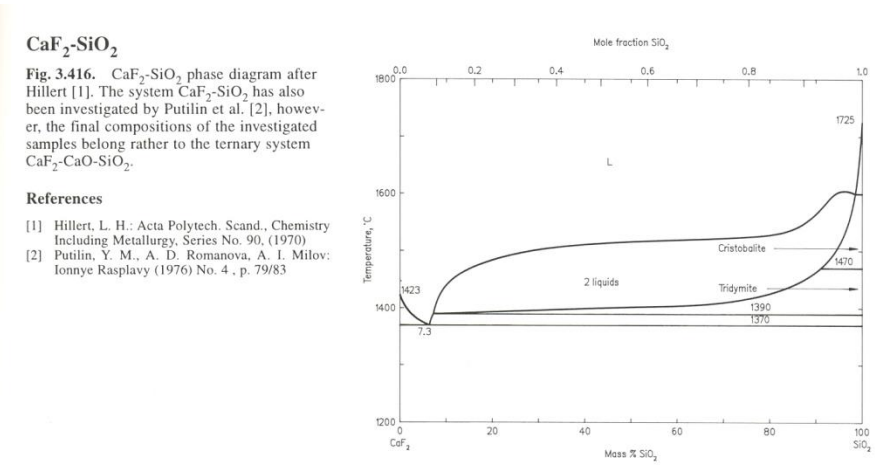

CaF_2-SiO_2

Fig. 3.416. CaF_2-SiO_2 phase diagram after Hillert [1]. The system CaF_2-SiO_2 has also been investigated by Putilin et al. [2], however, the final compositions of the investigated samples belong rather to the ternary system CaF_2-CaO-SiO_2.

References

[1] Hillert, L. H.: Acta Polytech. Scand., Chemistry Including Metallurgy, Series No. 90, (1970)
[2] Putilin, Y. M., A. D. Romanova, A. I. Milov: Ionnye Rasplavy (1976) No. 4 , p. 79/83

Slag Atlas, 2nd Ed., Verlag Stahl-Eisen, Düsseldorf, 1995.

Mole fraction

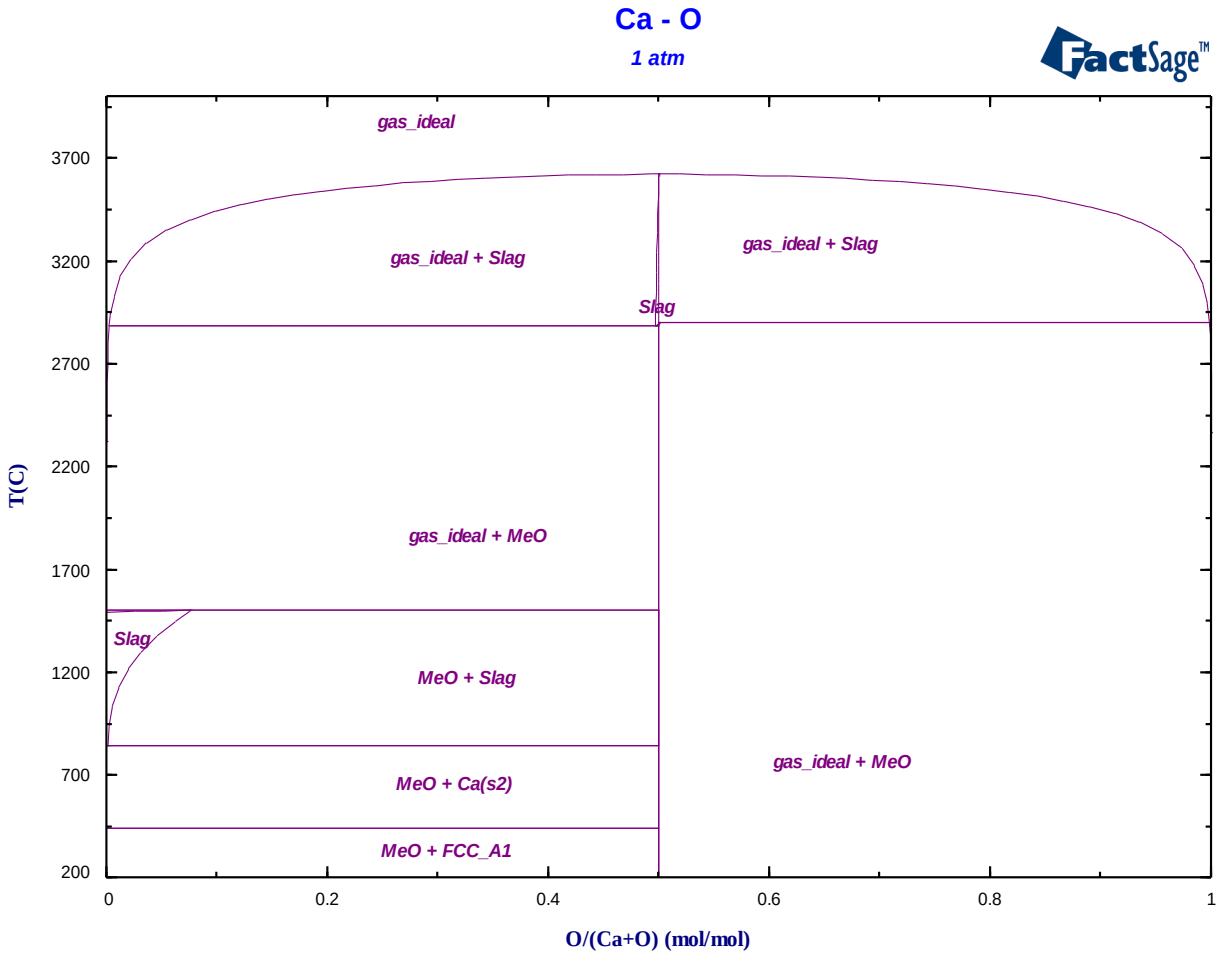

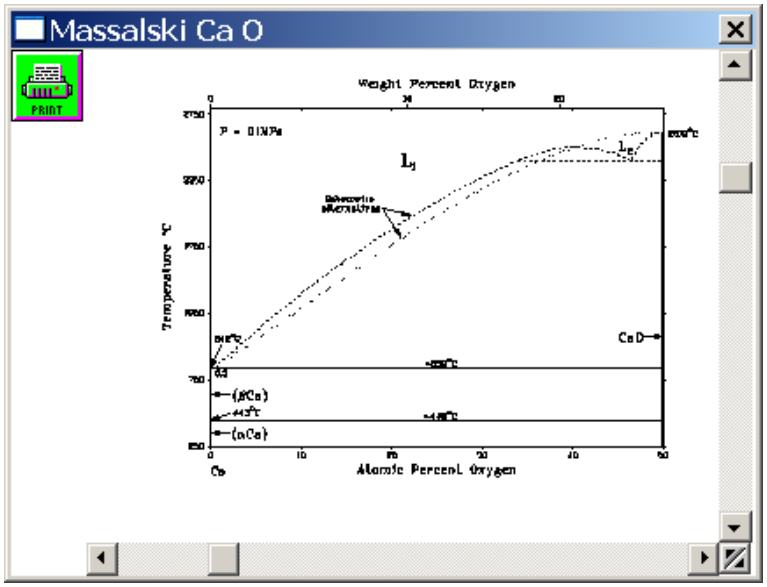

Weight percent

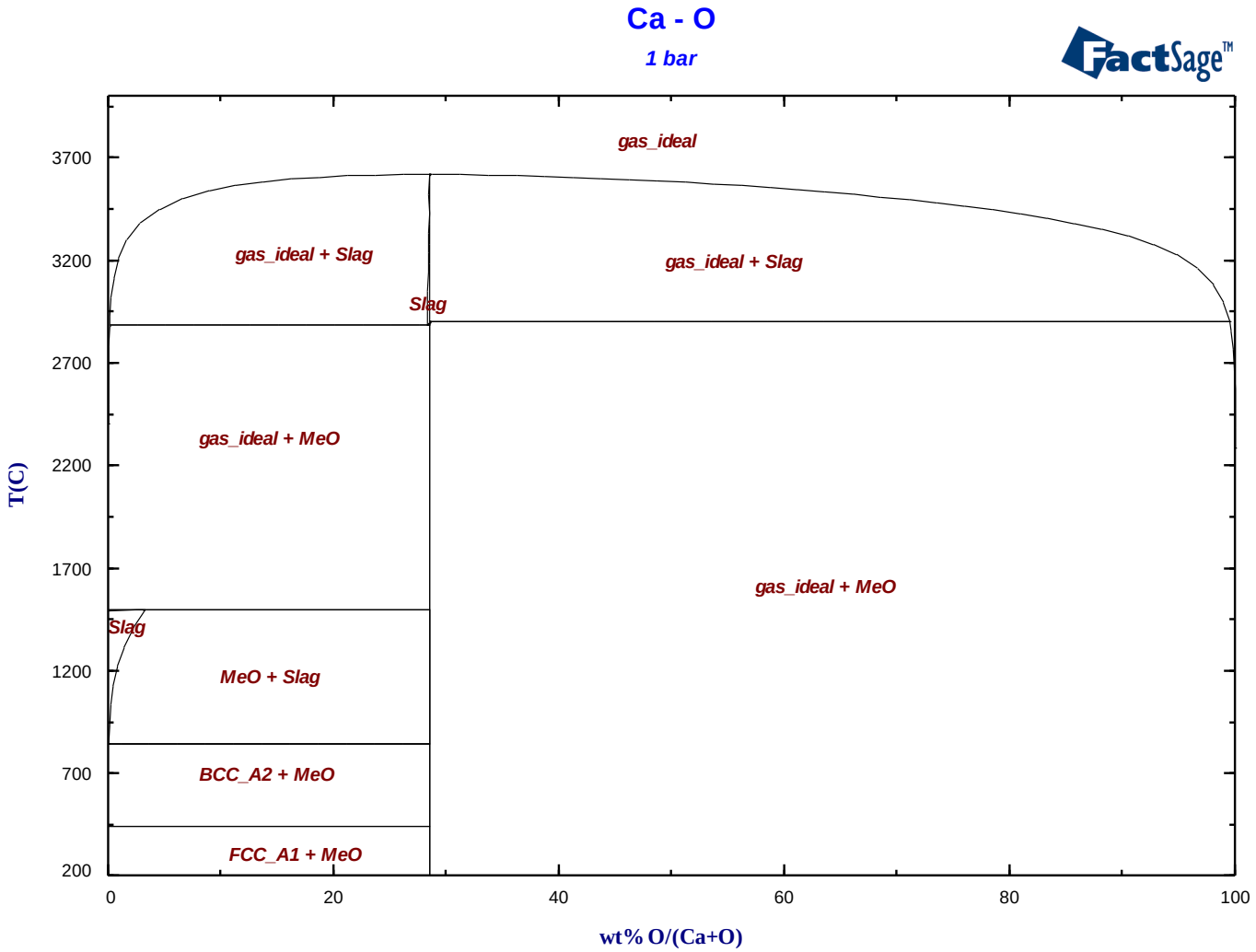

Mole fraction with isobars

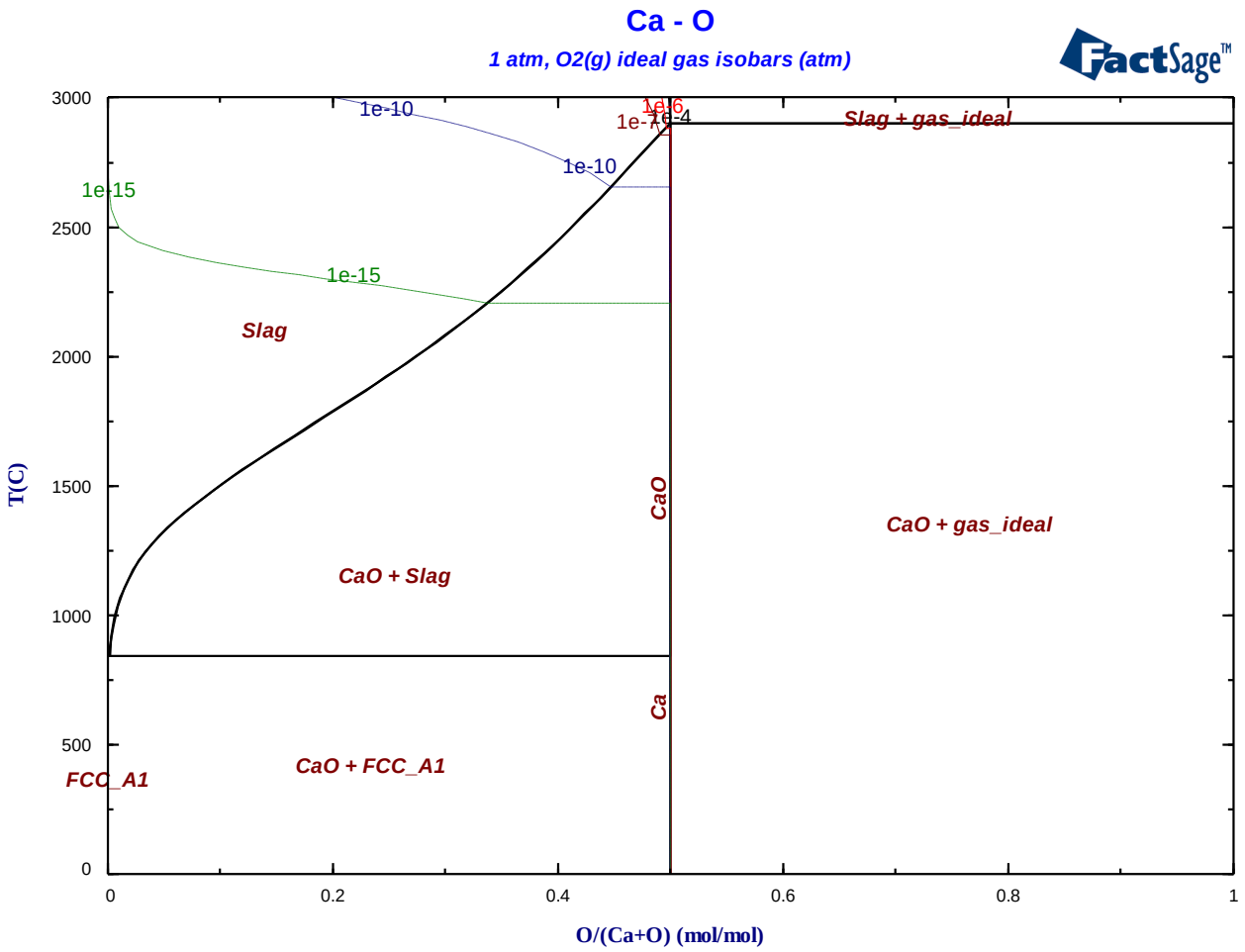

Ca-O2,

Temperature vs. log P(O2) diagram

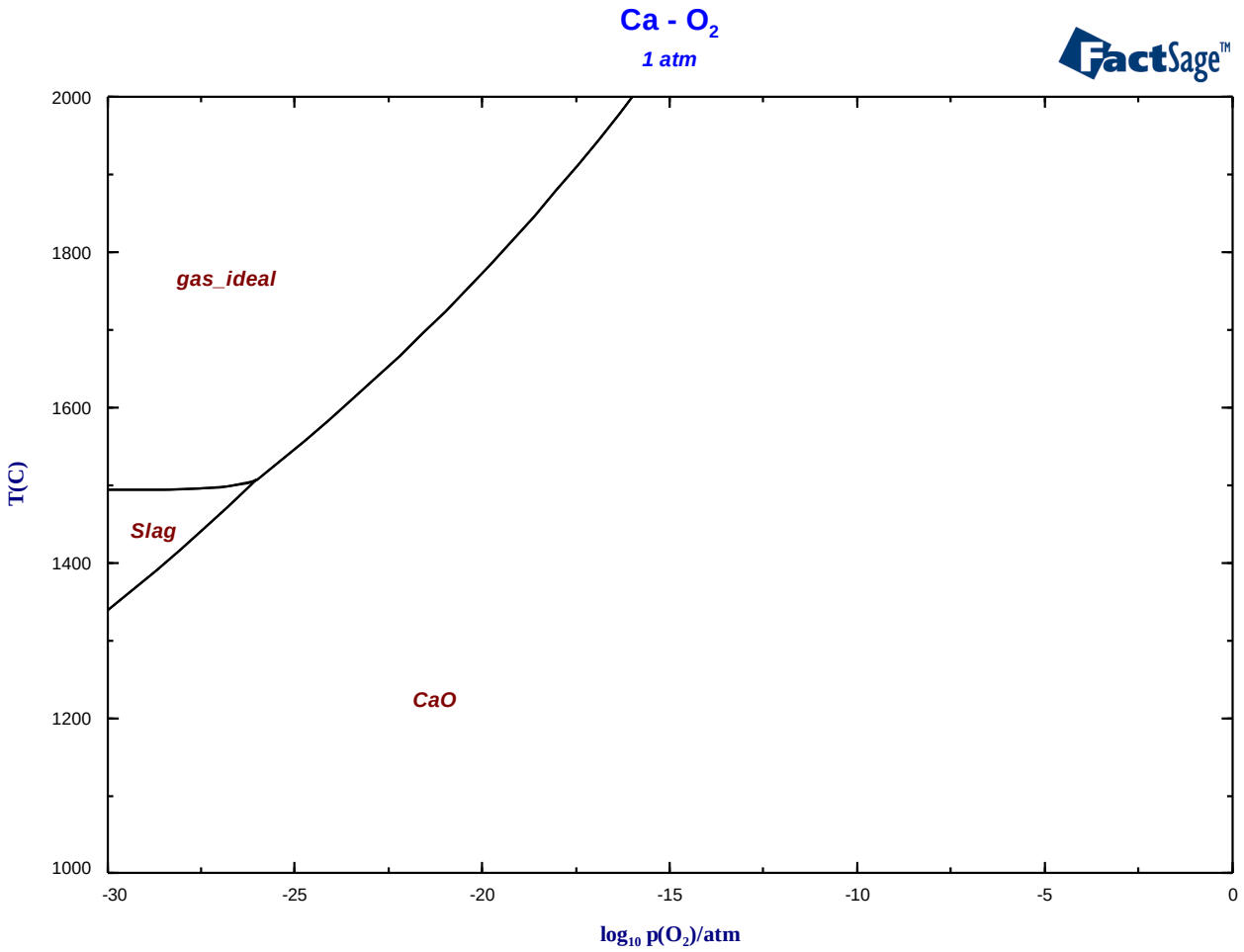

Mole fraction

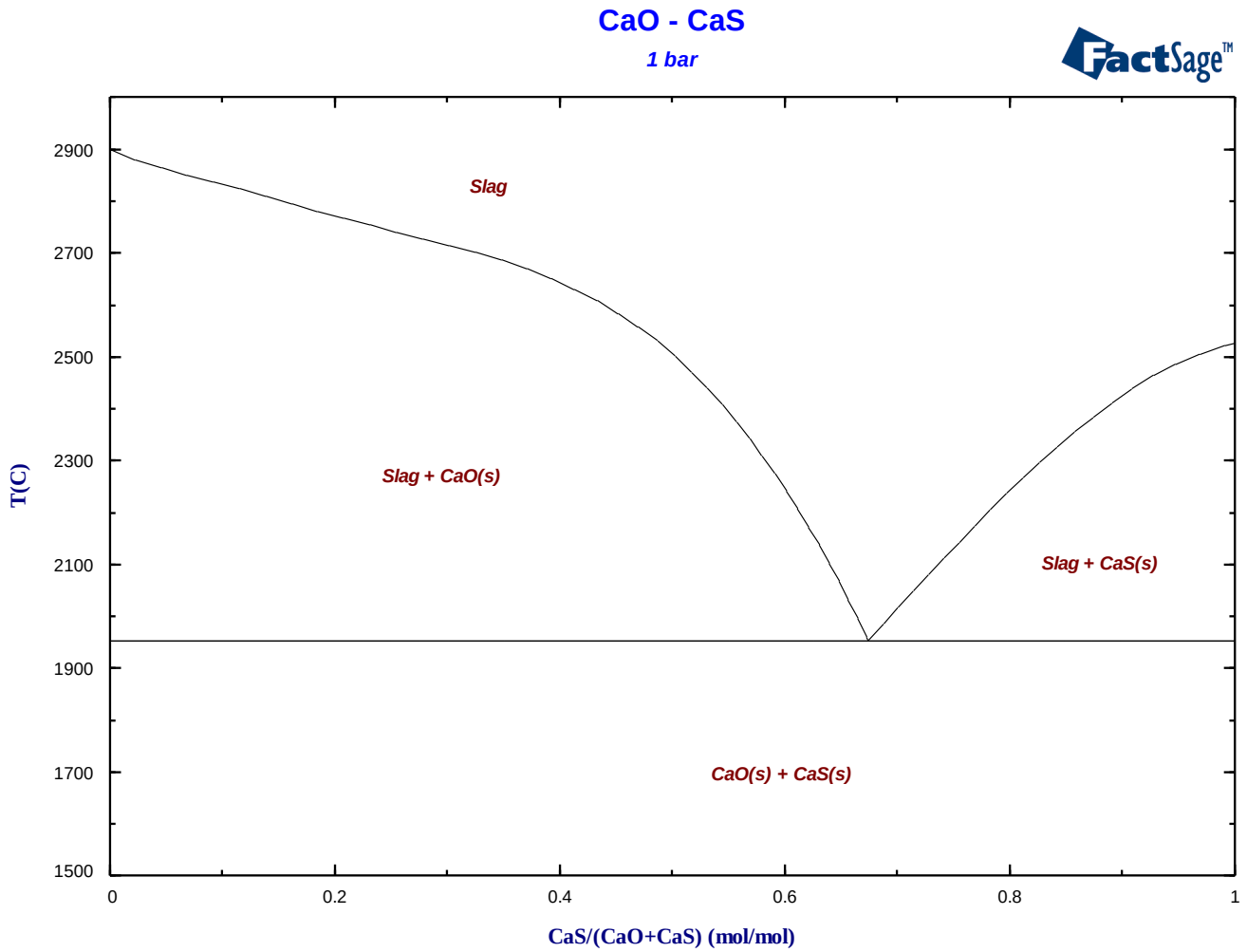

Weight percent

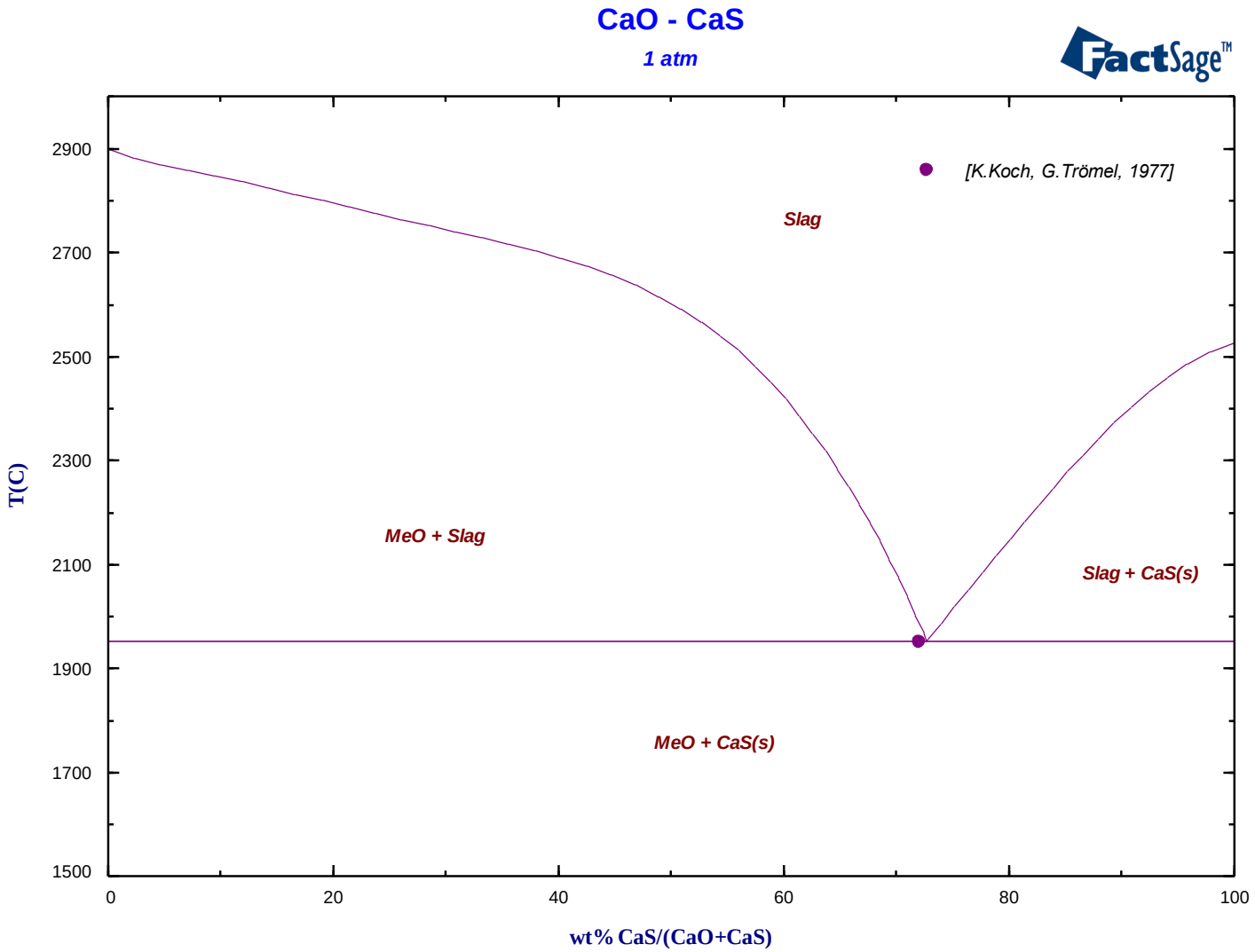

Mole fraction

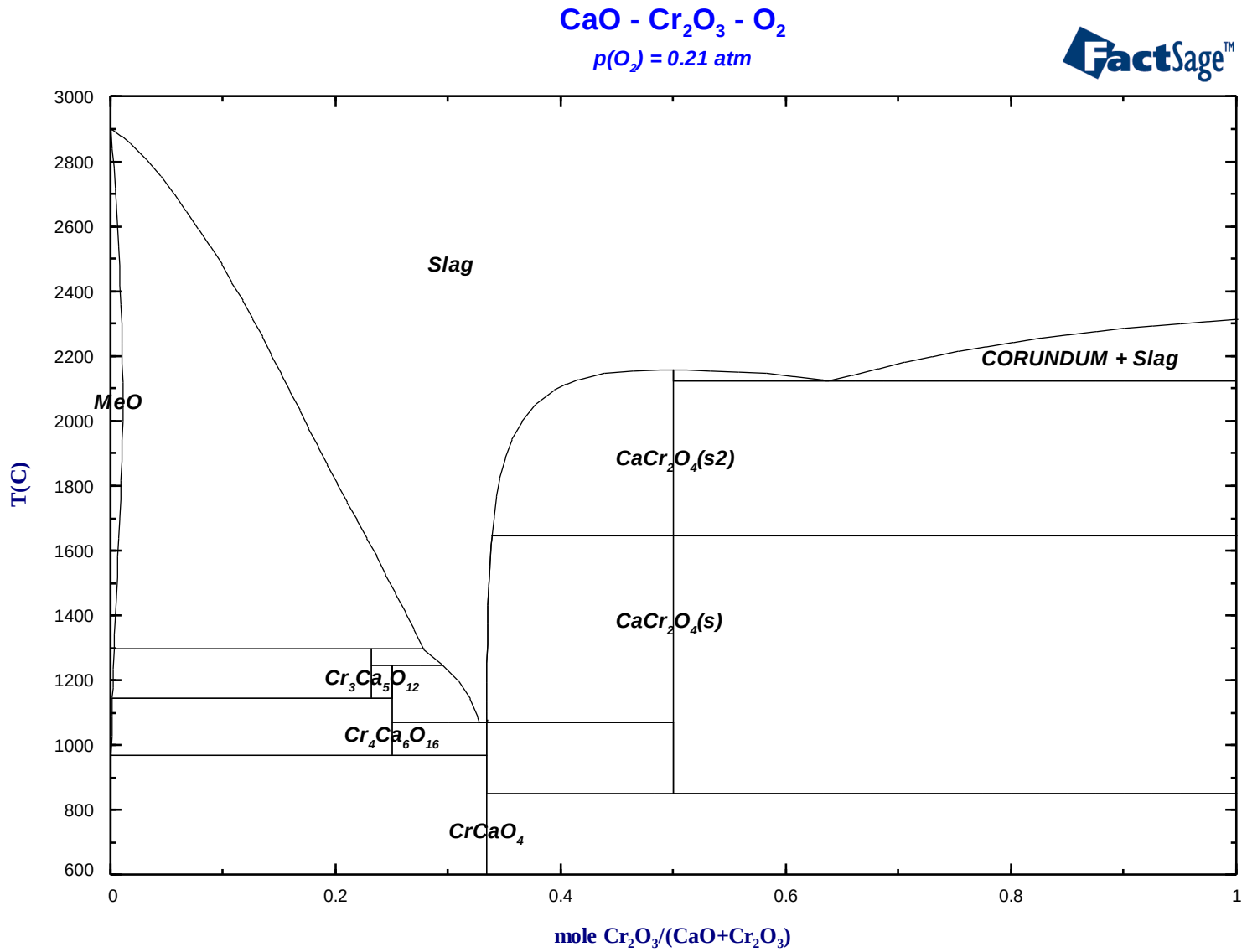

Weight percent
compared with experimental data

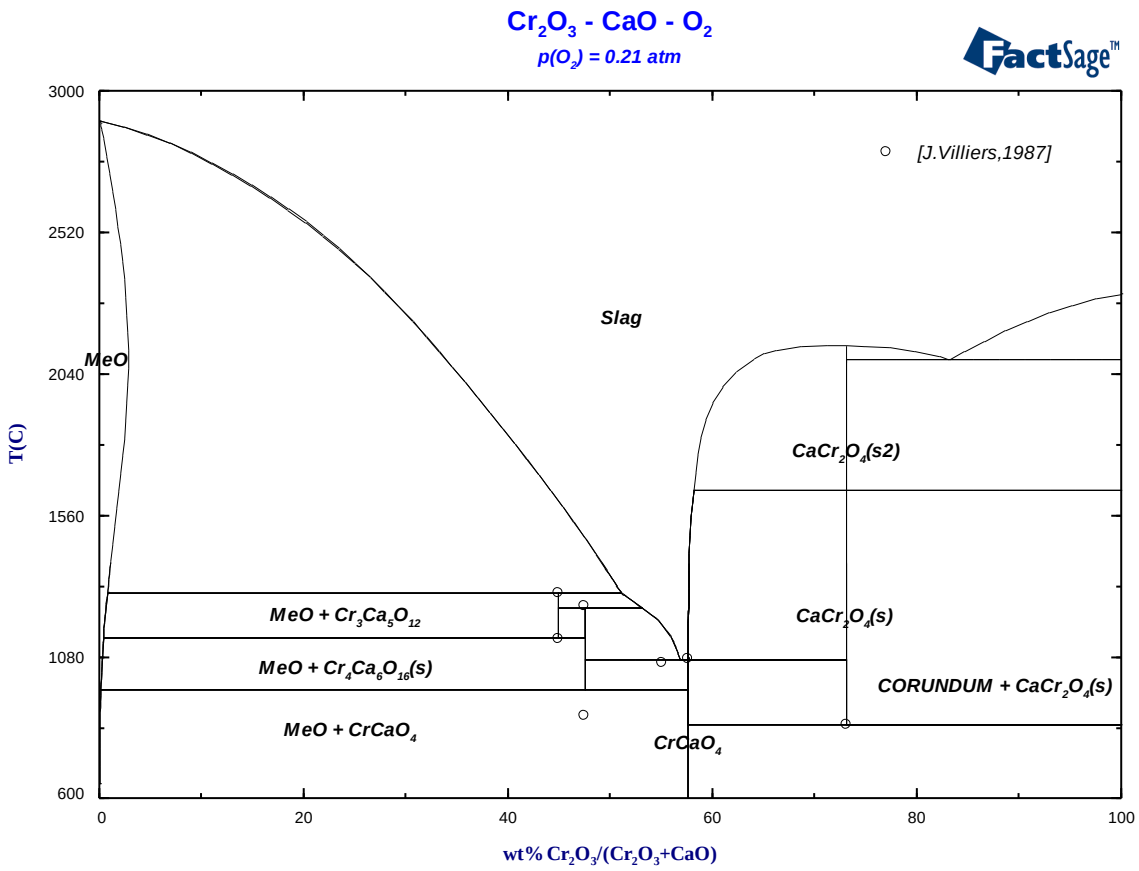

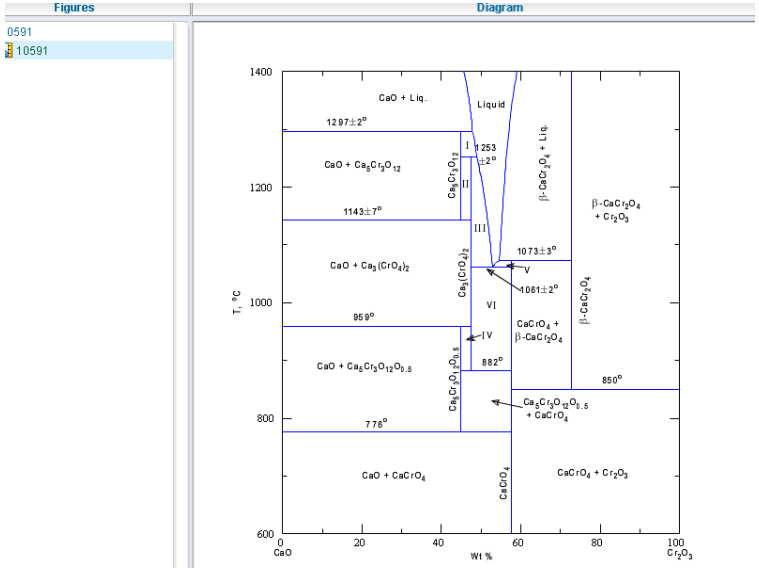

J. P. R. DeVilliers, J. Mathias, and A. Muan, Trans. - Inst. Min. Metall., Sect. C, 96, C55-C62

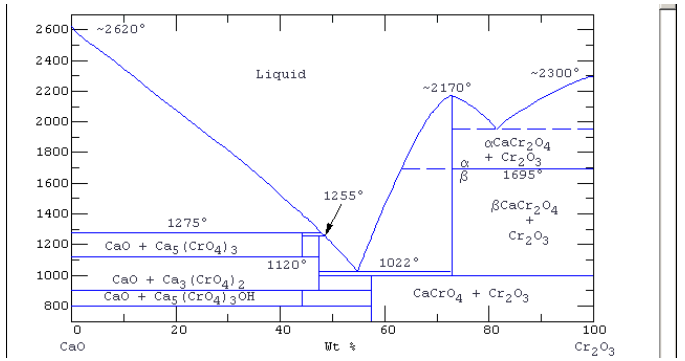

Z. Panek, Silikaty (Prague), 20 [1] 1-12 (1976).

Weight percent
compared with experimental data, $P(O_2)=0.001$ atm

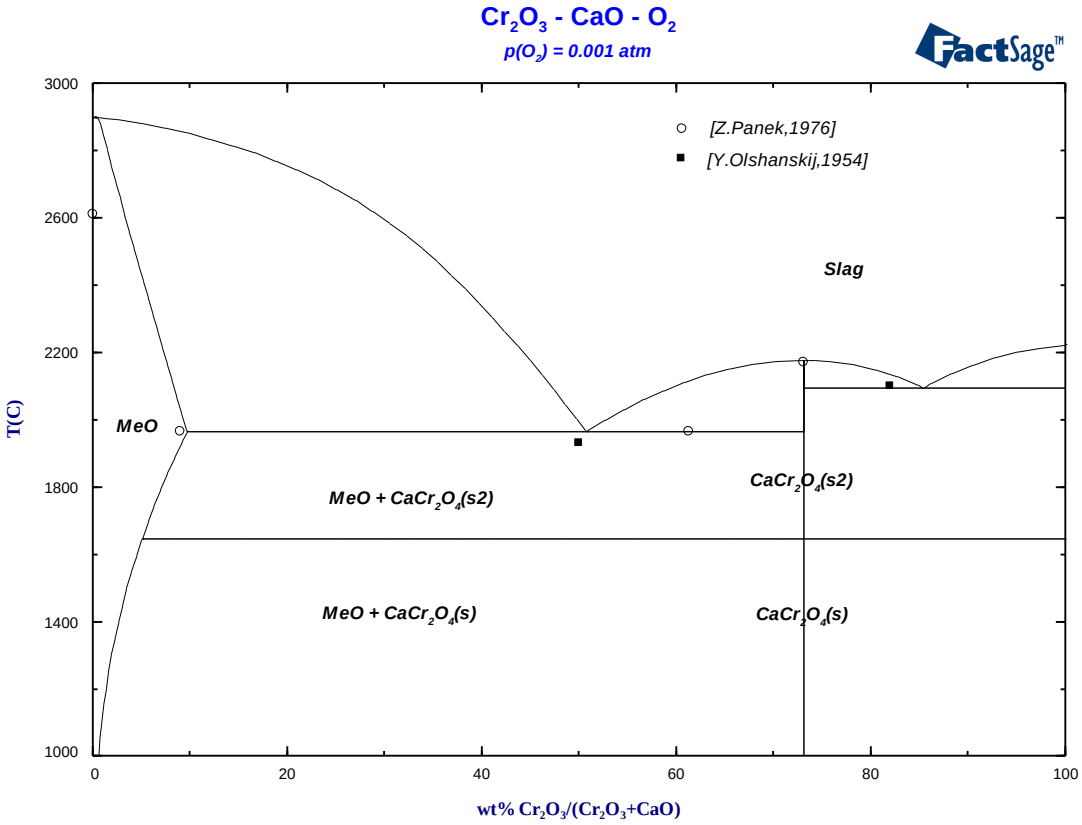

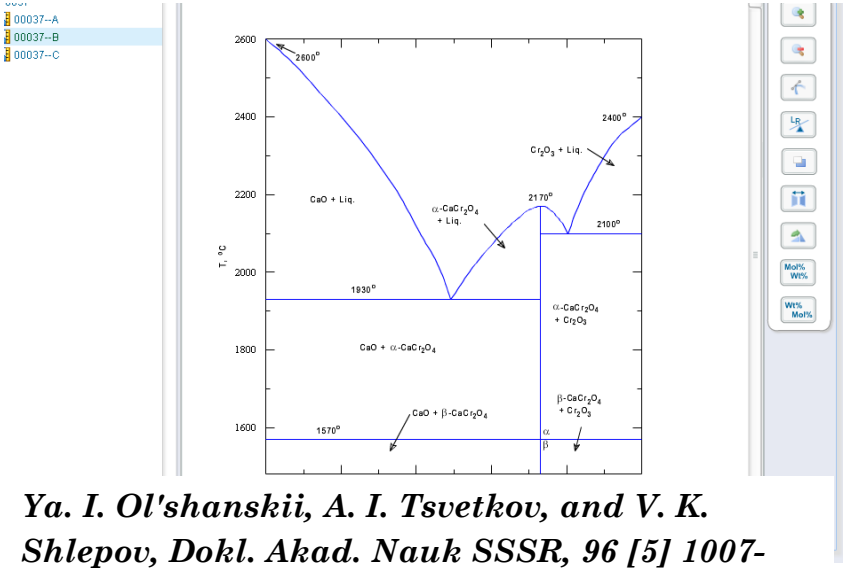

Ya. I. Ol'shanskii, A. I. Tsvetkov, and V. K. Shlepov, Dokl. Akad. Nauk SSSR, 96 [5] 1007-1009 (1954).

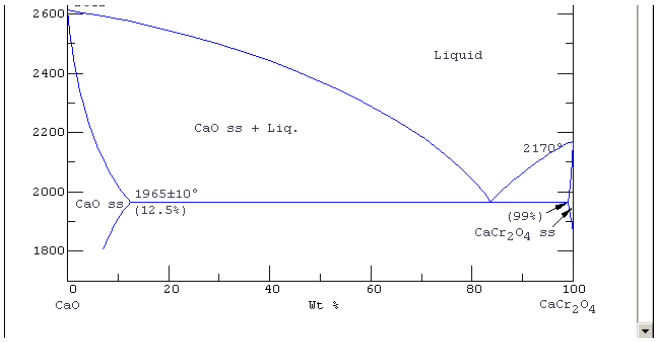

Z. Panek, Silikaty (Prague), 20 [1] 1-12 (1976).

Mole fraction
compared with experimental data

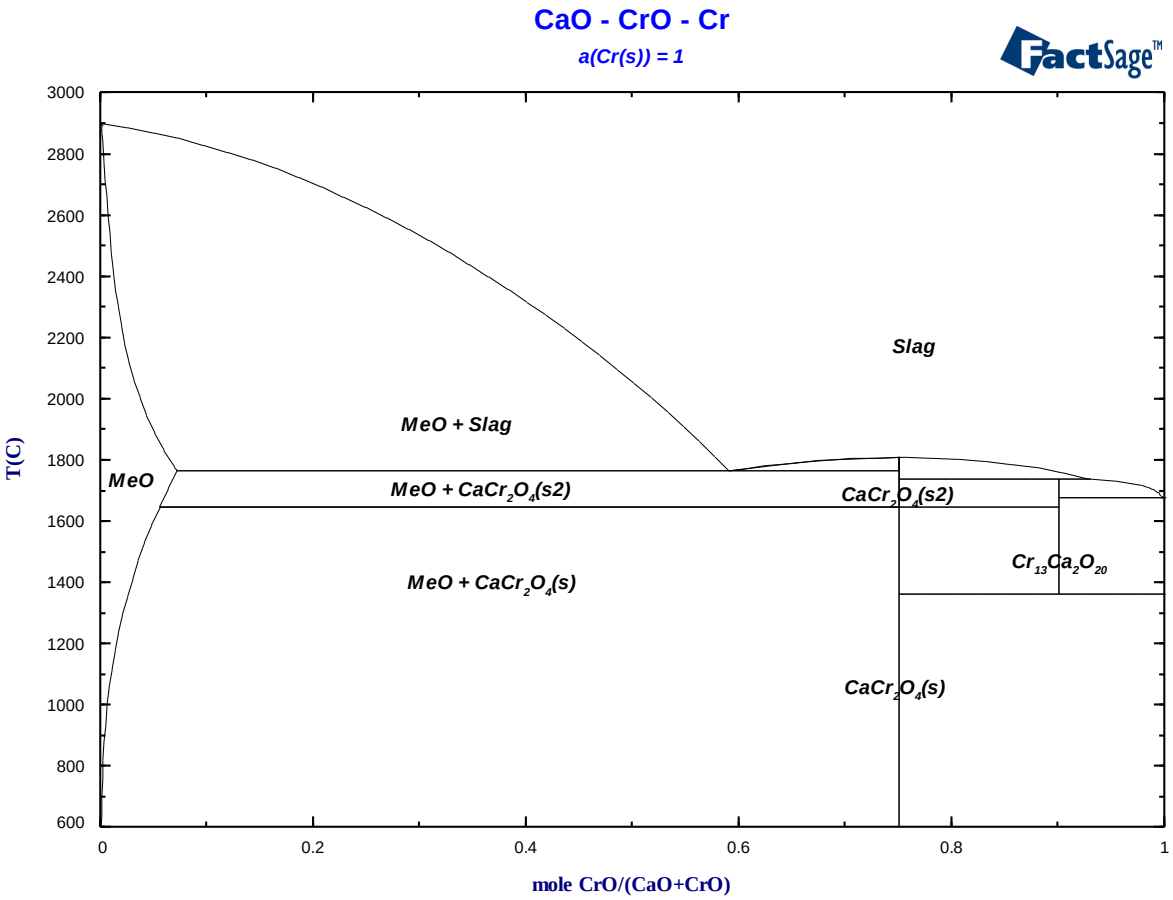

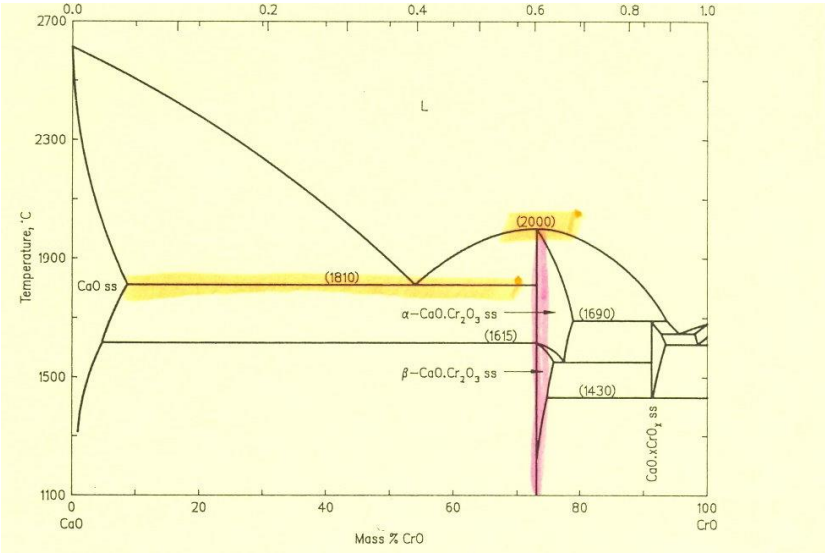

A.Muan, Spec. Publ. Geol. Soc. S. Afr. 7 (1983), pp. 325-336.

Weight percent

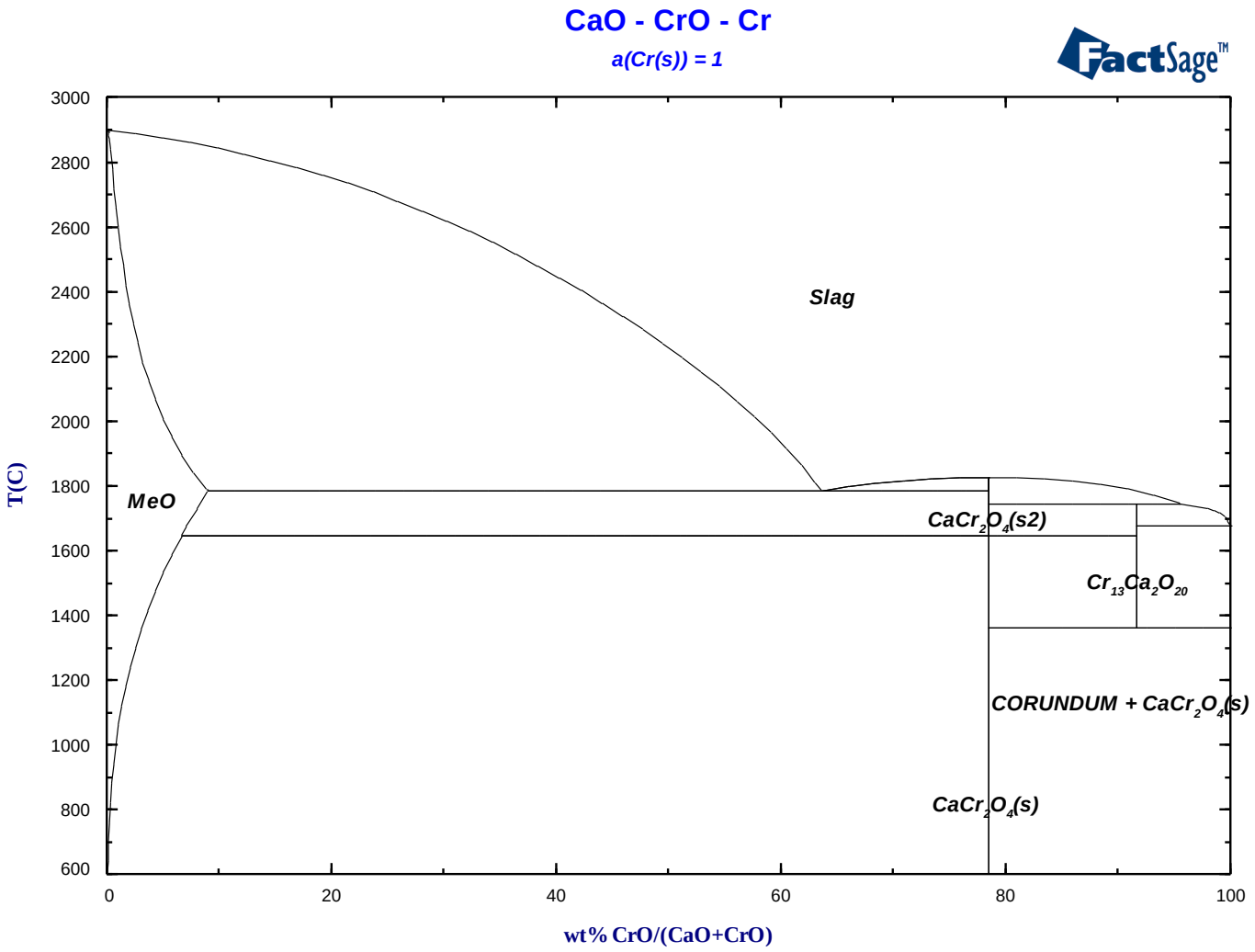

Mole fraction

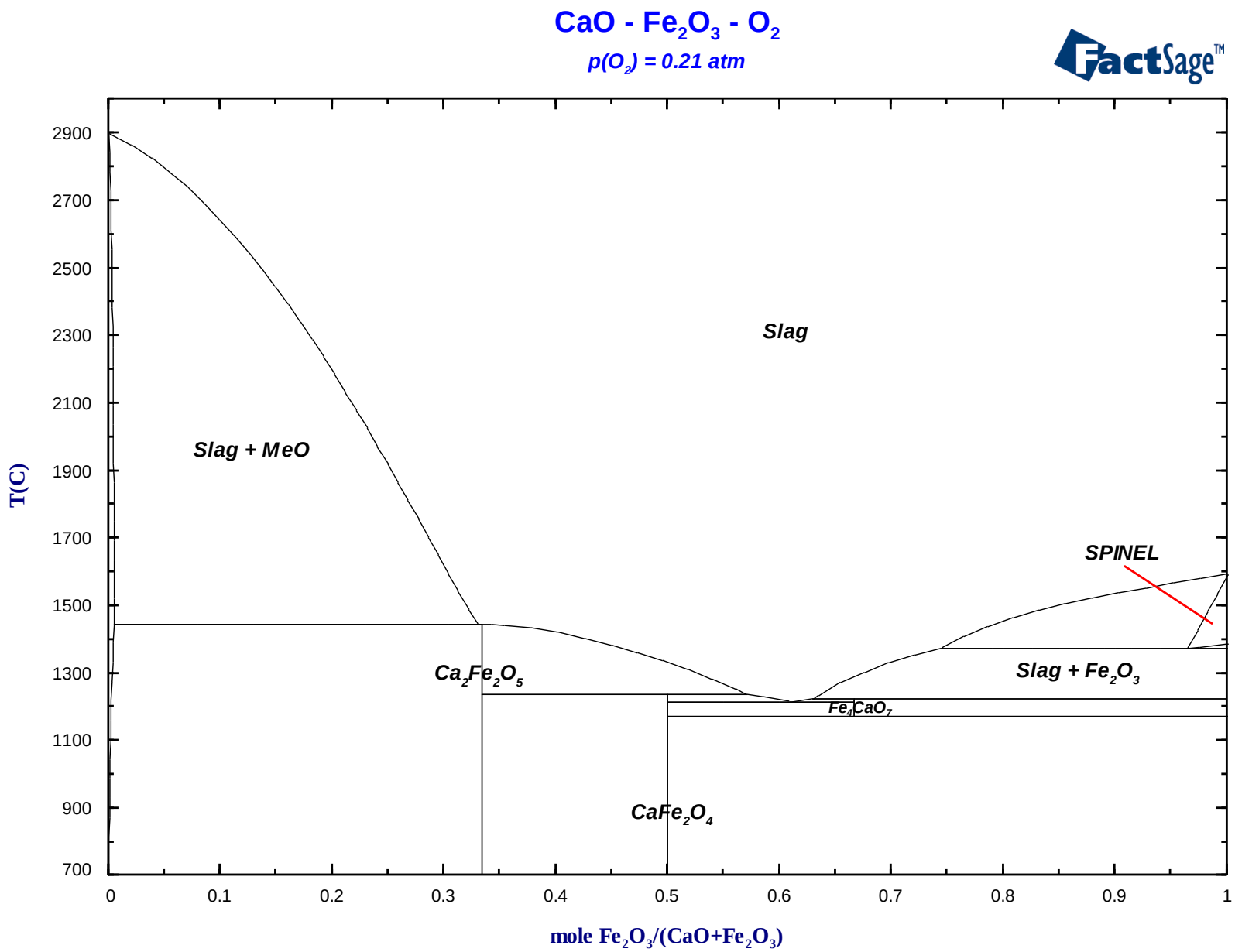

Weight percent
compared with experimental data

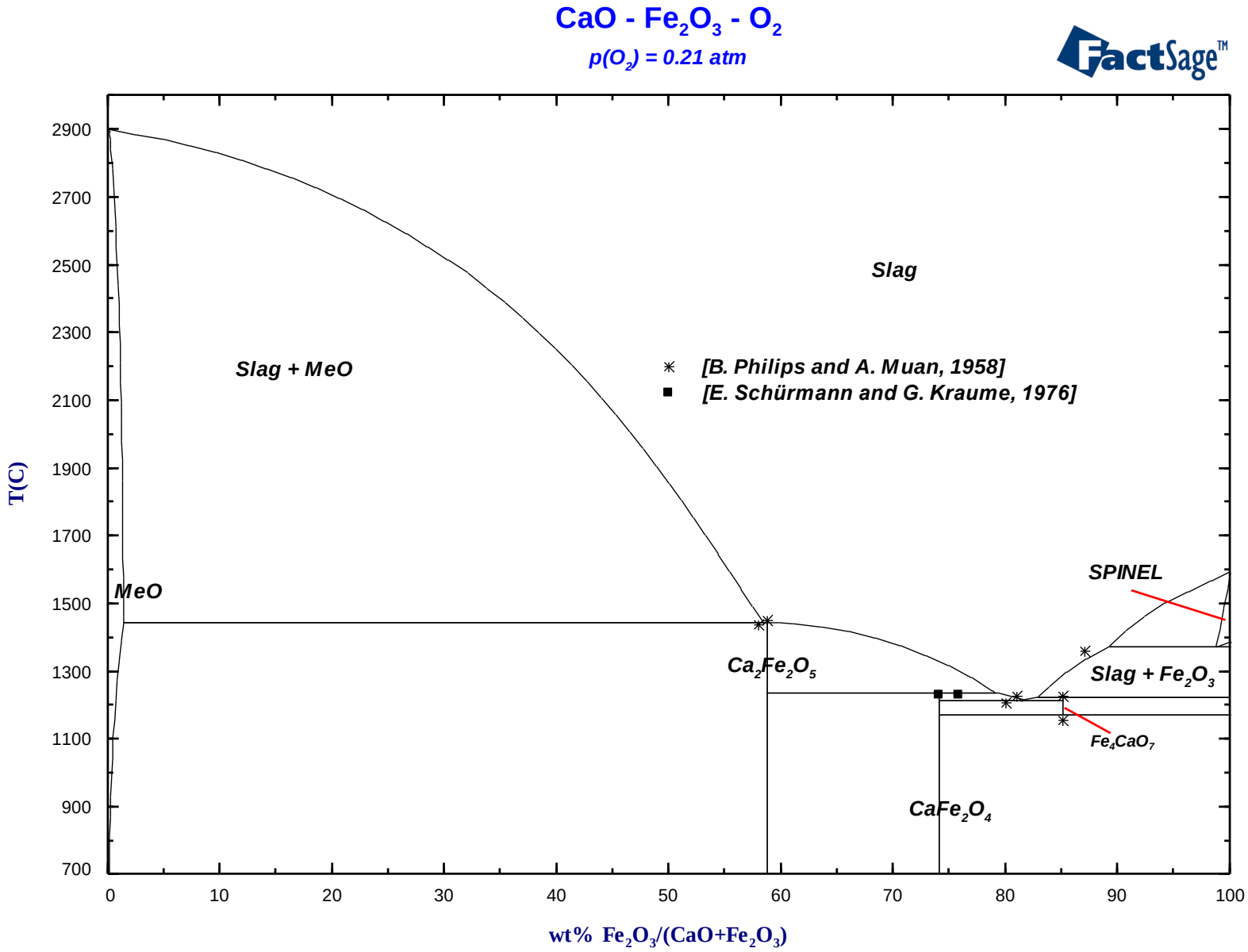

Mole fraction

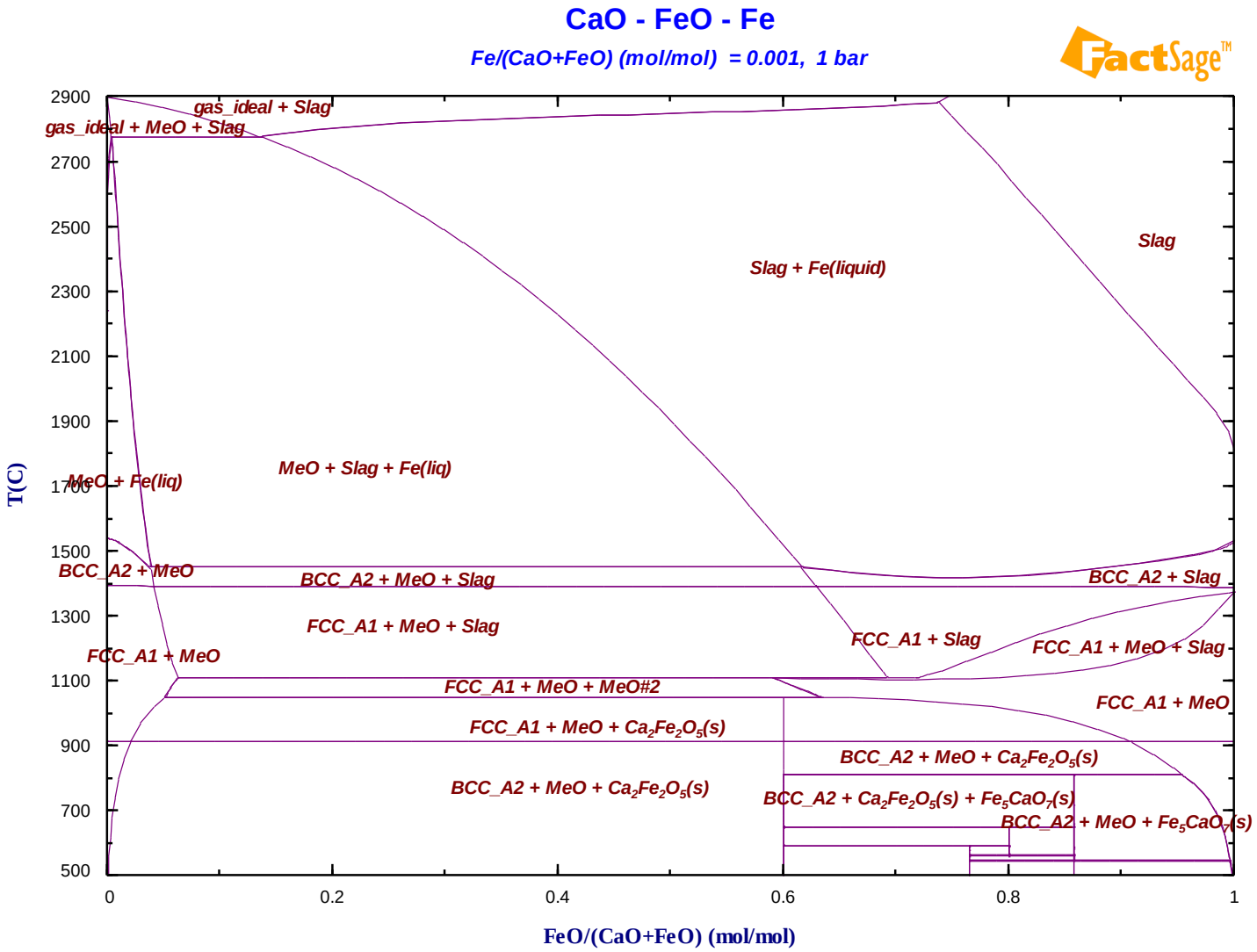

Weight percent
compared with experimental data

CaO - FeO - Fe

mass Fe/(CaO+FeO) = 0.001

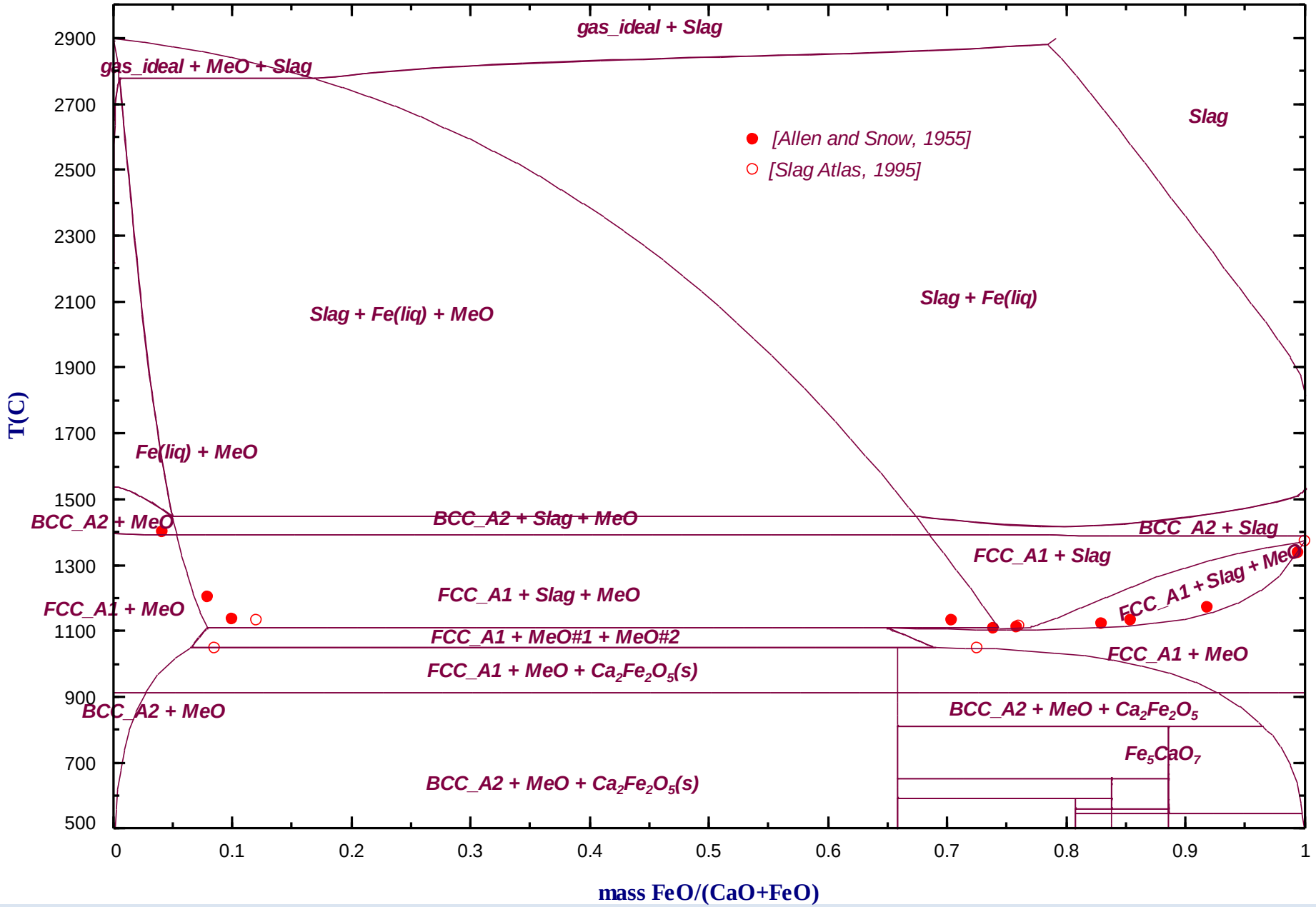

Mole fraction

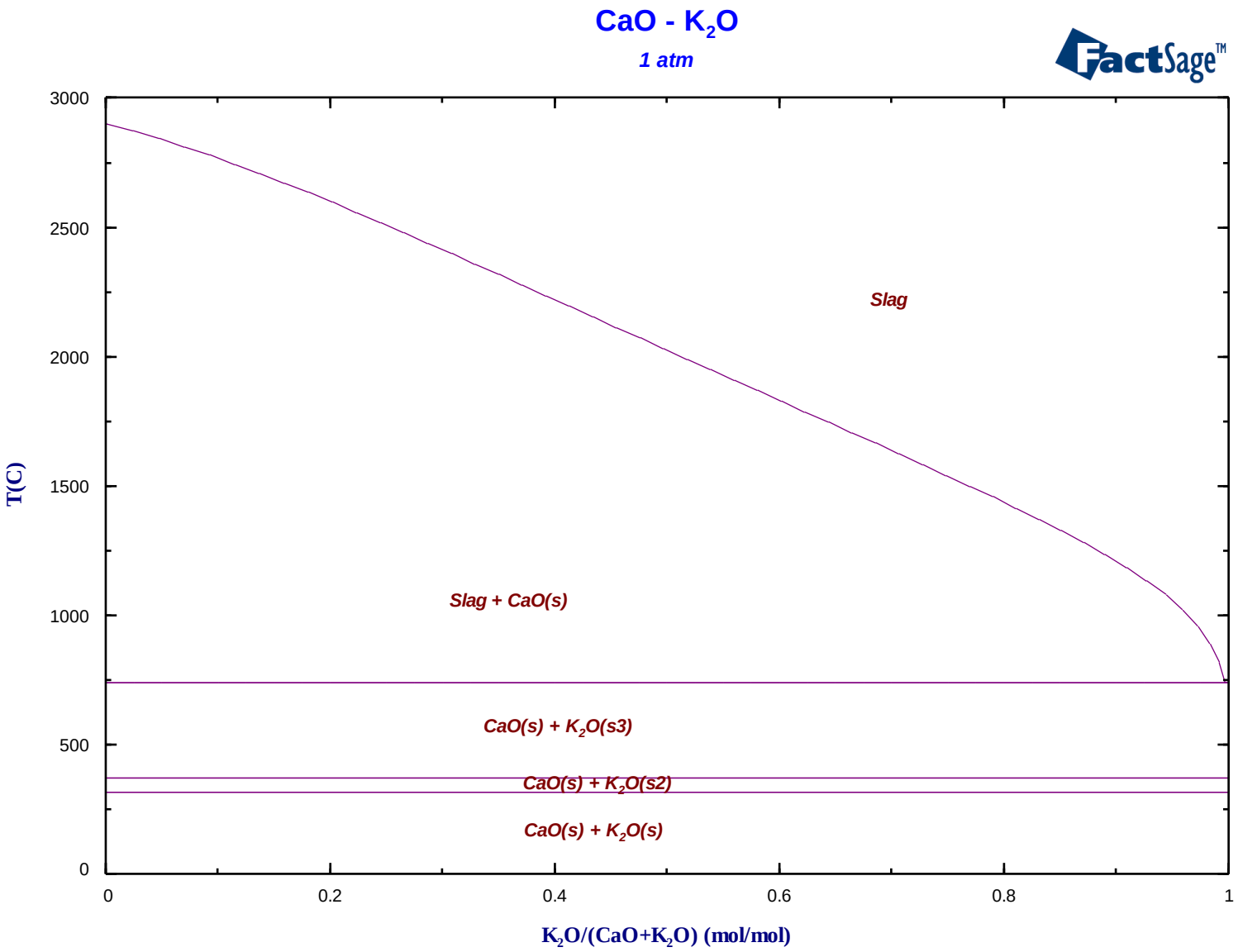

Weight percent

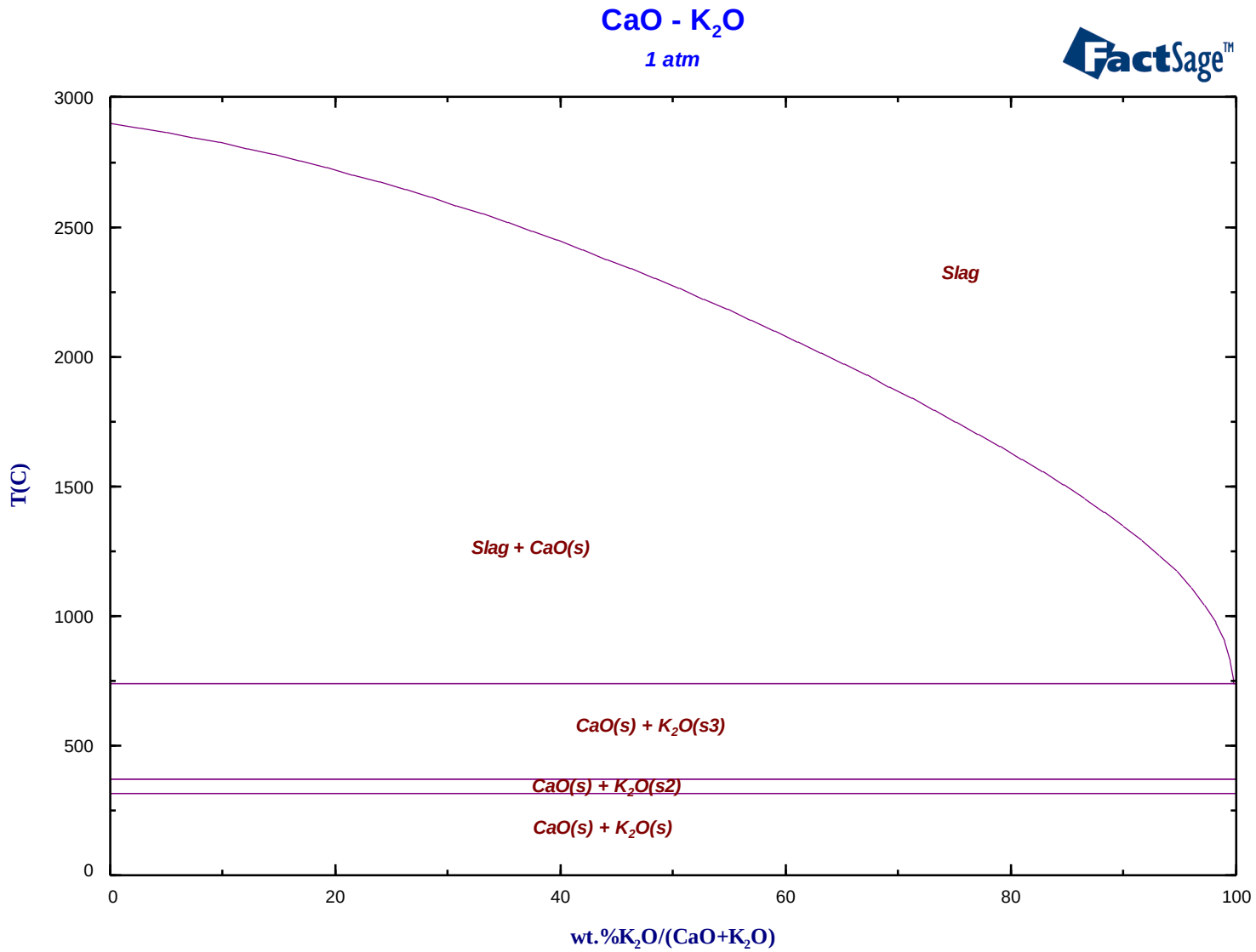

Mole fraction compared with experimental data

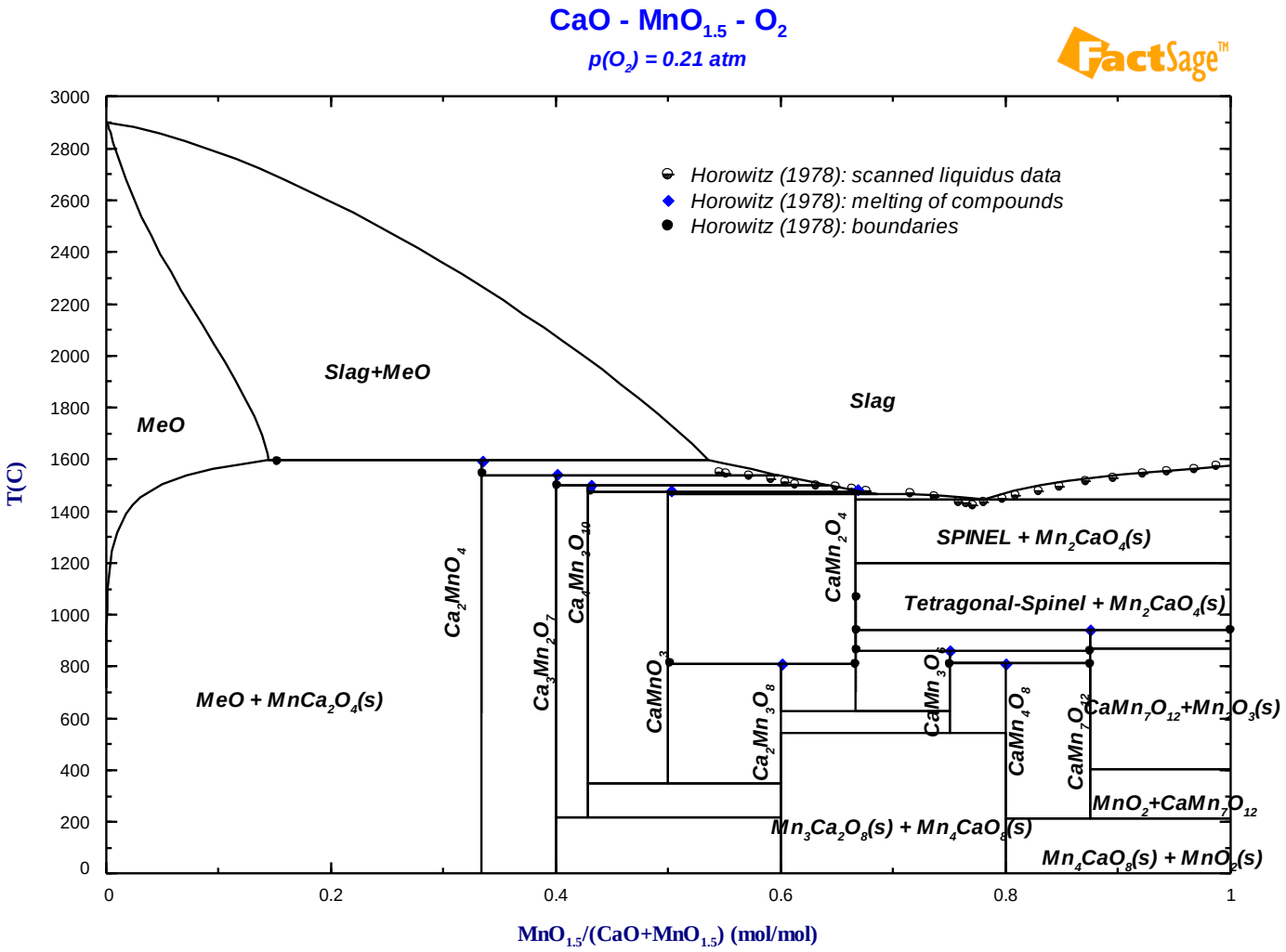

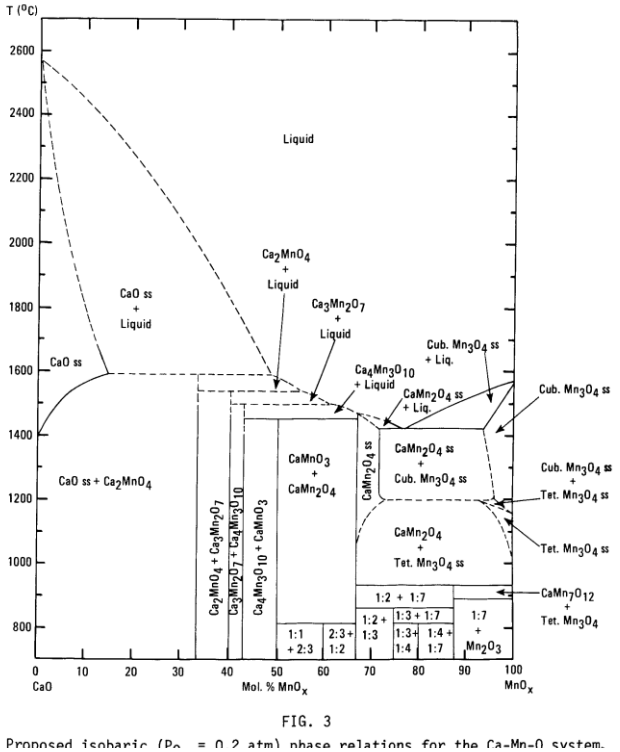

FIG. 3

Proposed isobaric (Po = 0.2 atm) phase relations for the Ca-Mn-O system.

H.S. Horowitz, J.M. Longo, Phase relations in the Ca-Mn-O system, Mater Res Bull, 1978; 13: 1359-69.

Weight percent

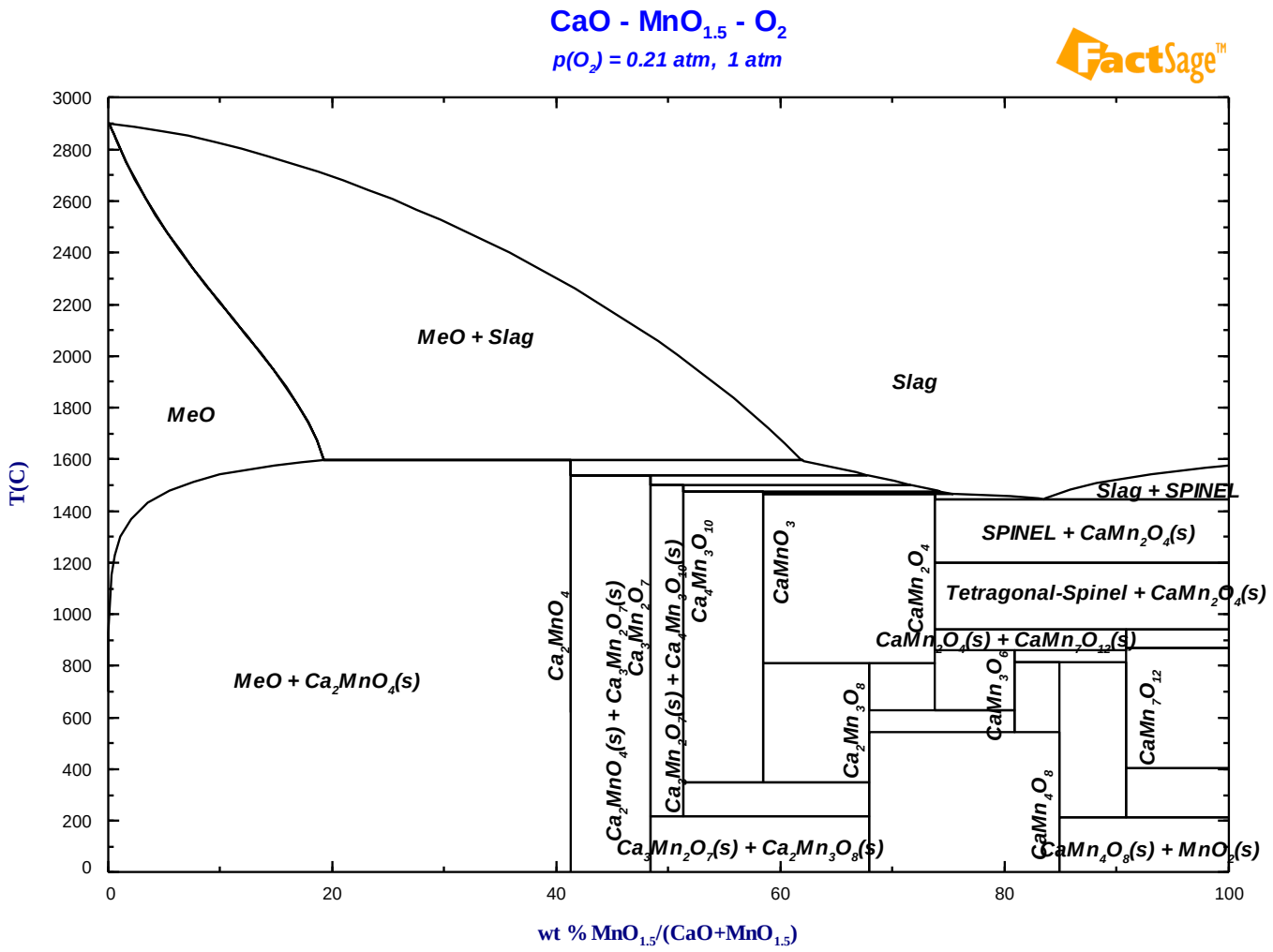

Mole fraction compared with experimental data

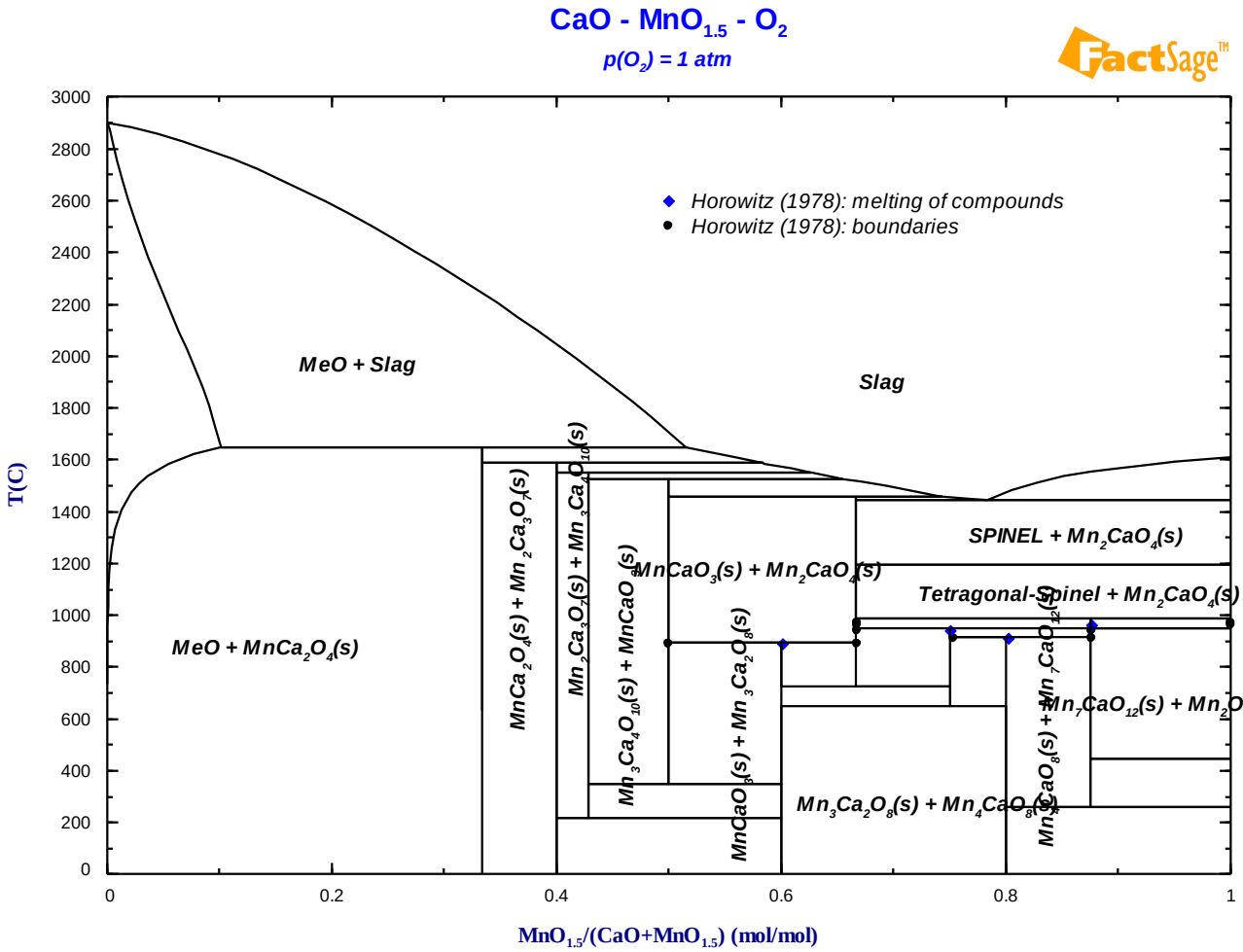

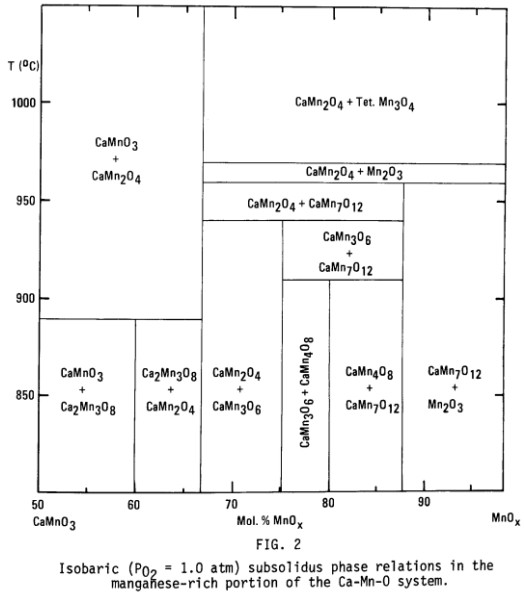

H.S. Horowitz, J.M. Longo, Phase relations in the Ca-Mn-O system, Mater Res Bull, 1978; 13: 1359-69.

Weight percent

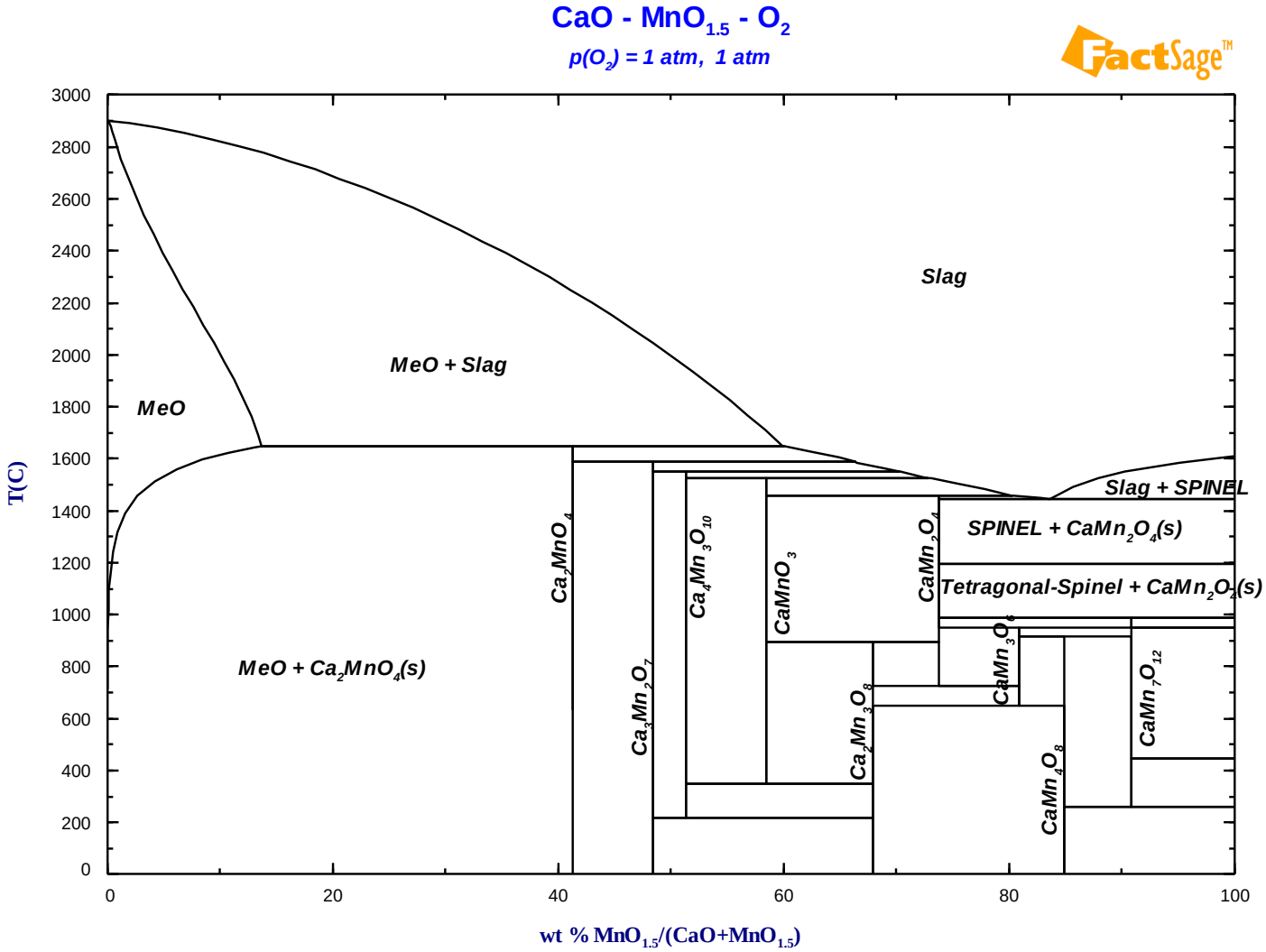

Mole fraction

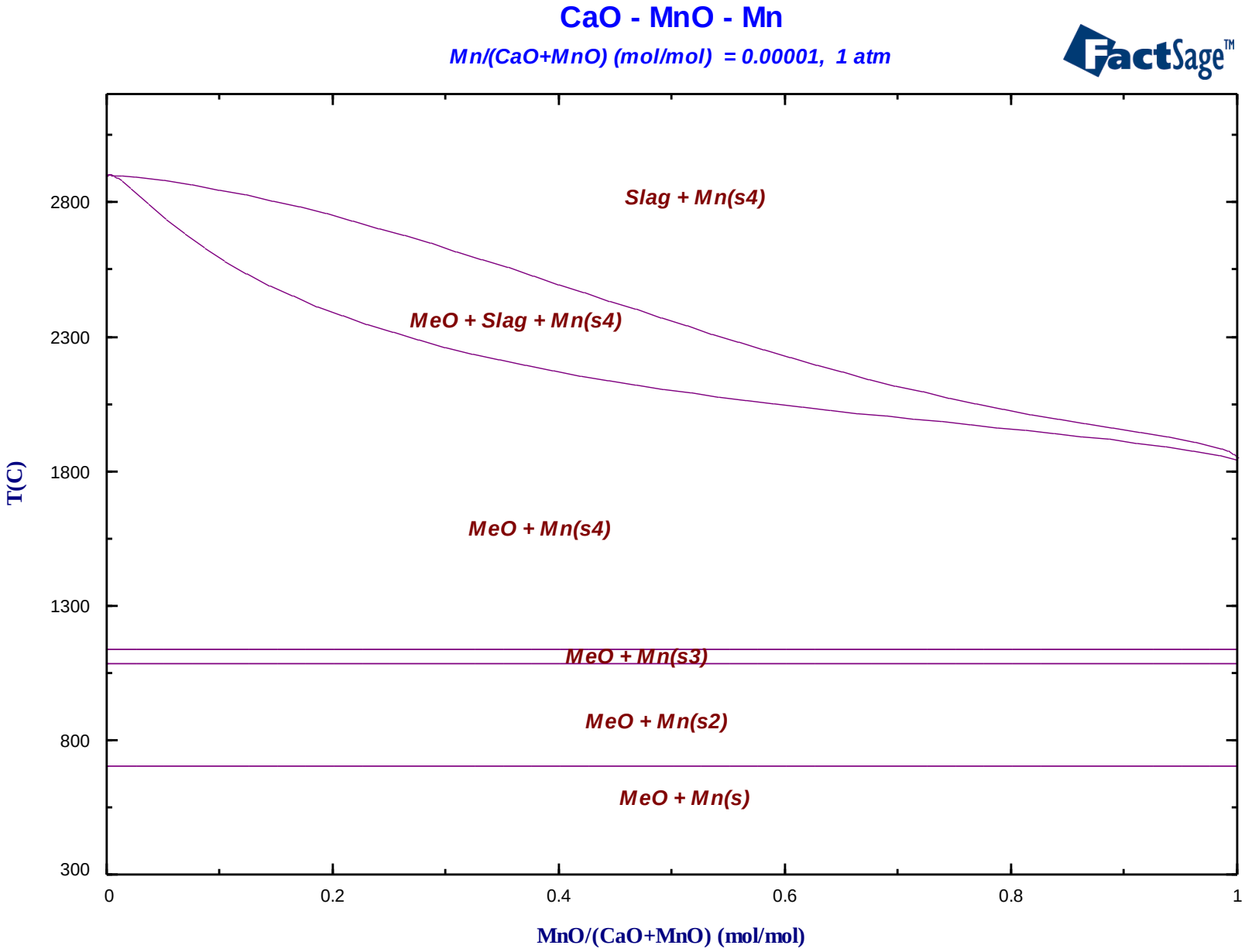

Weight percent
compared with experimental data

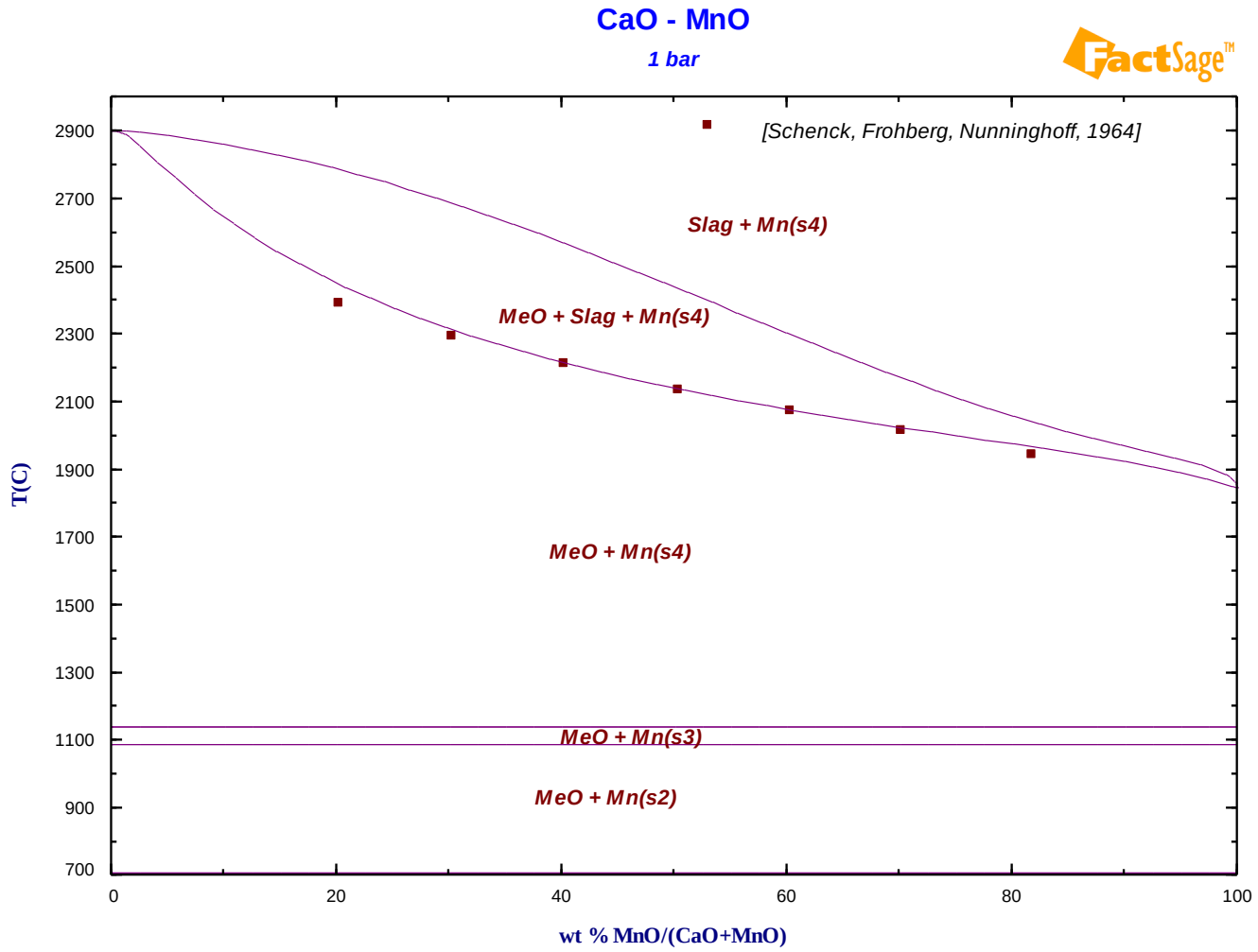

CaO - MgO

Mole fraction

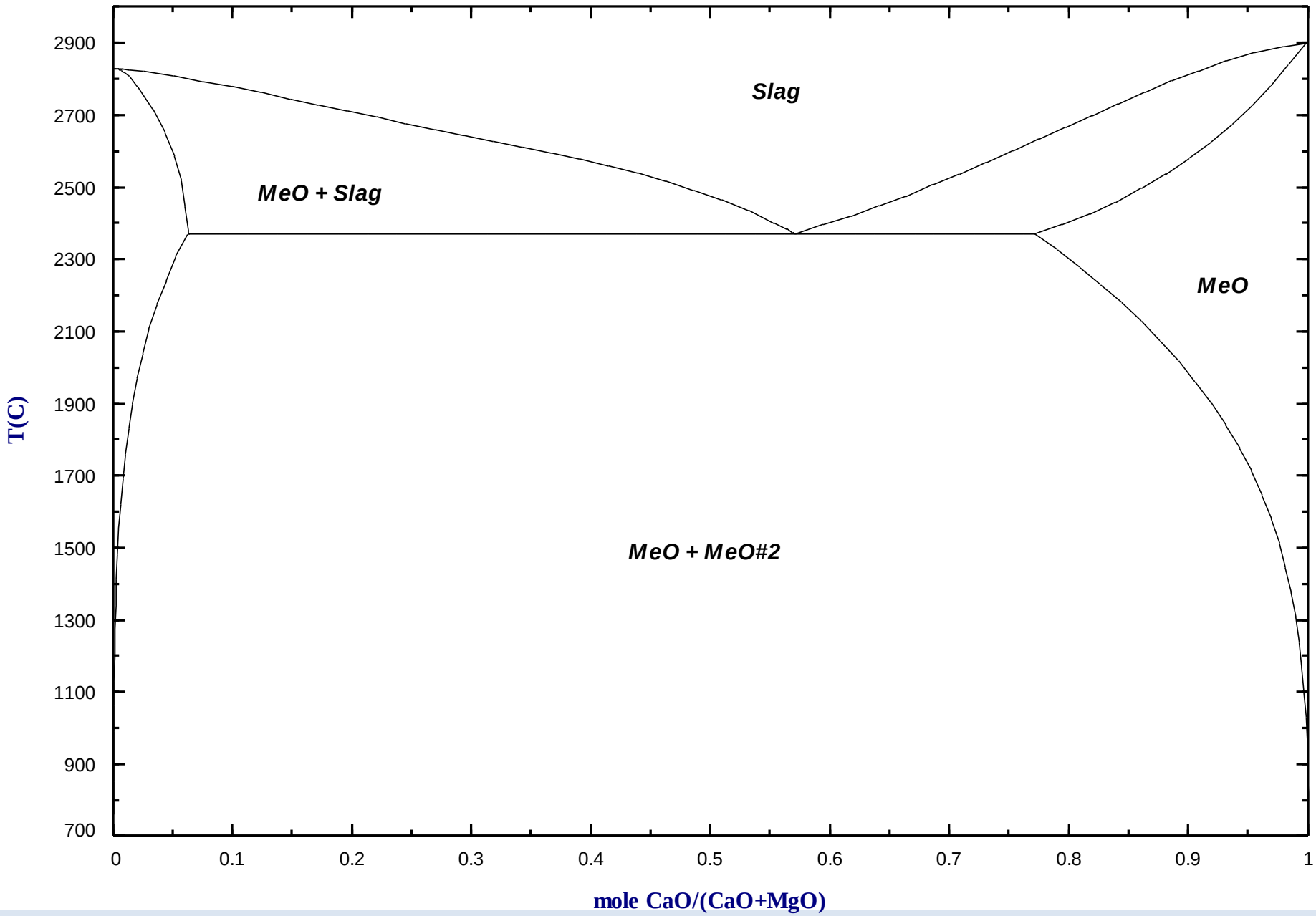

Weight percent
compared with experimental data

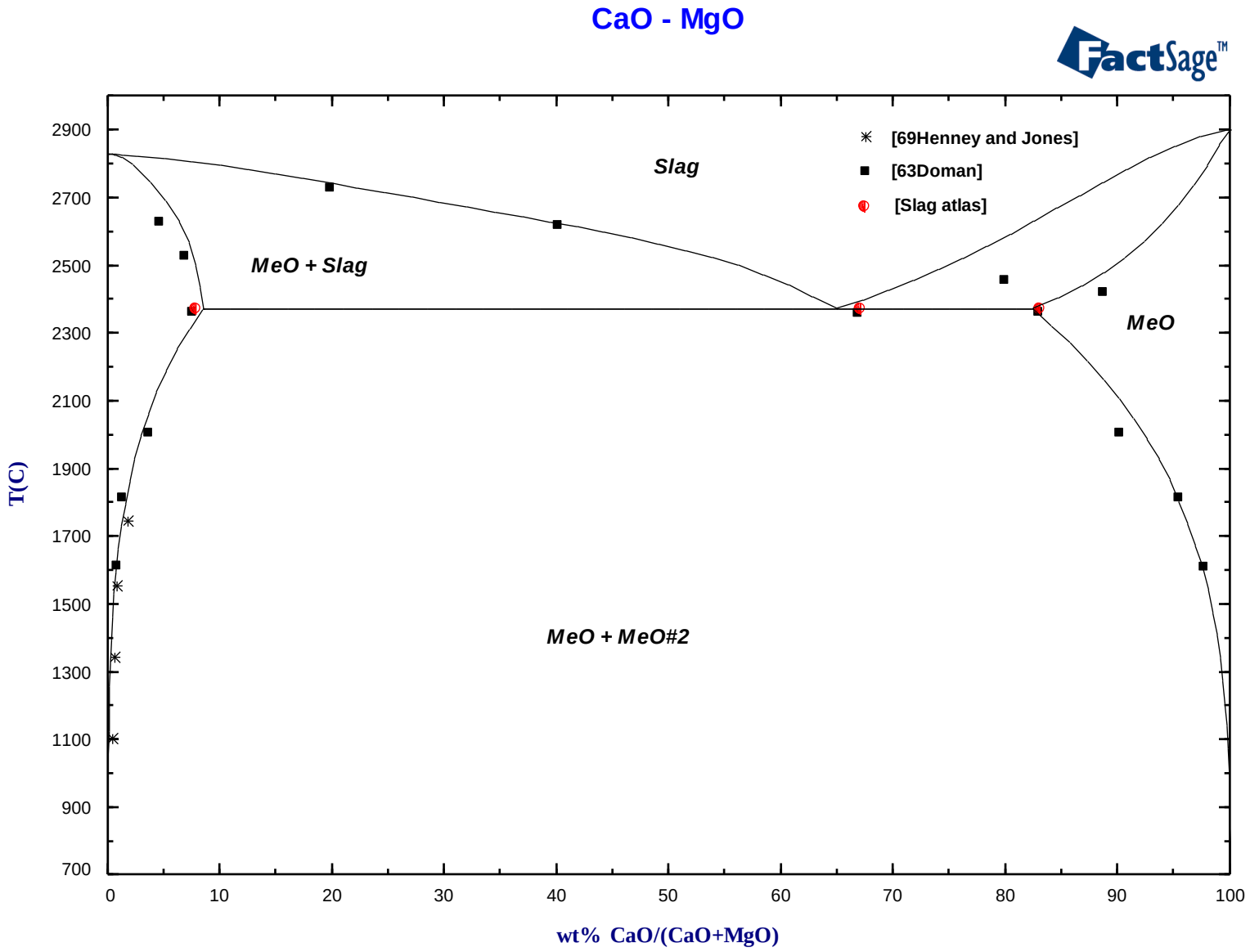

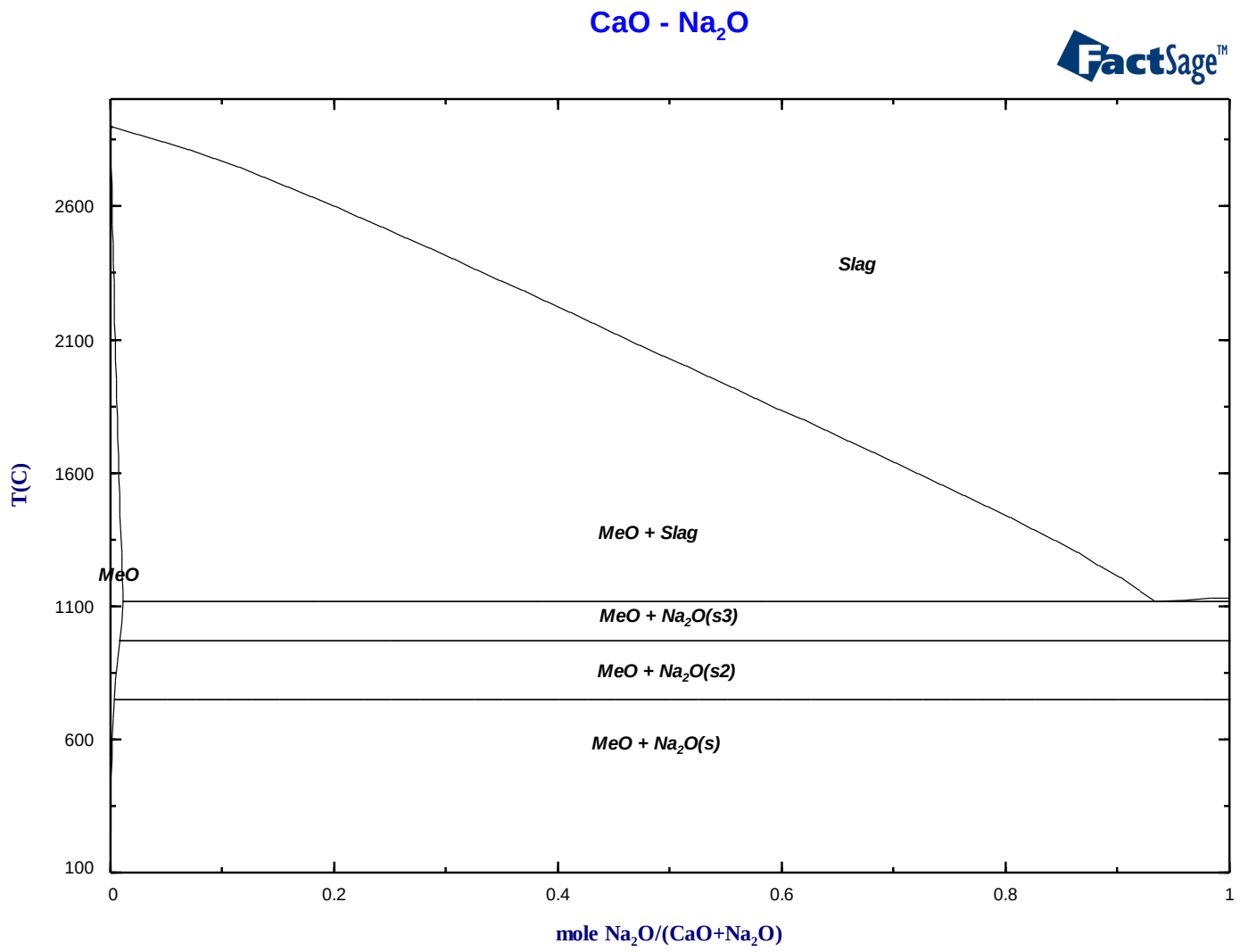
CaO - Na2O
FactSage™
2600
2100
1600
1100
600
100
T(C)
Slag
MeO + Slag
MeO
MeO + Na2O(s3)
MeO + Na2O(s2)
MeO + Na2O(s)
0
0.2
0.4
0.6
0.8
1
mole Na2O/(CaO+Na2O)

CaO-Na2O,
Weight percent

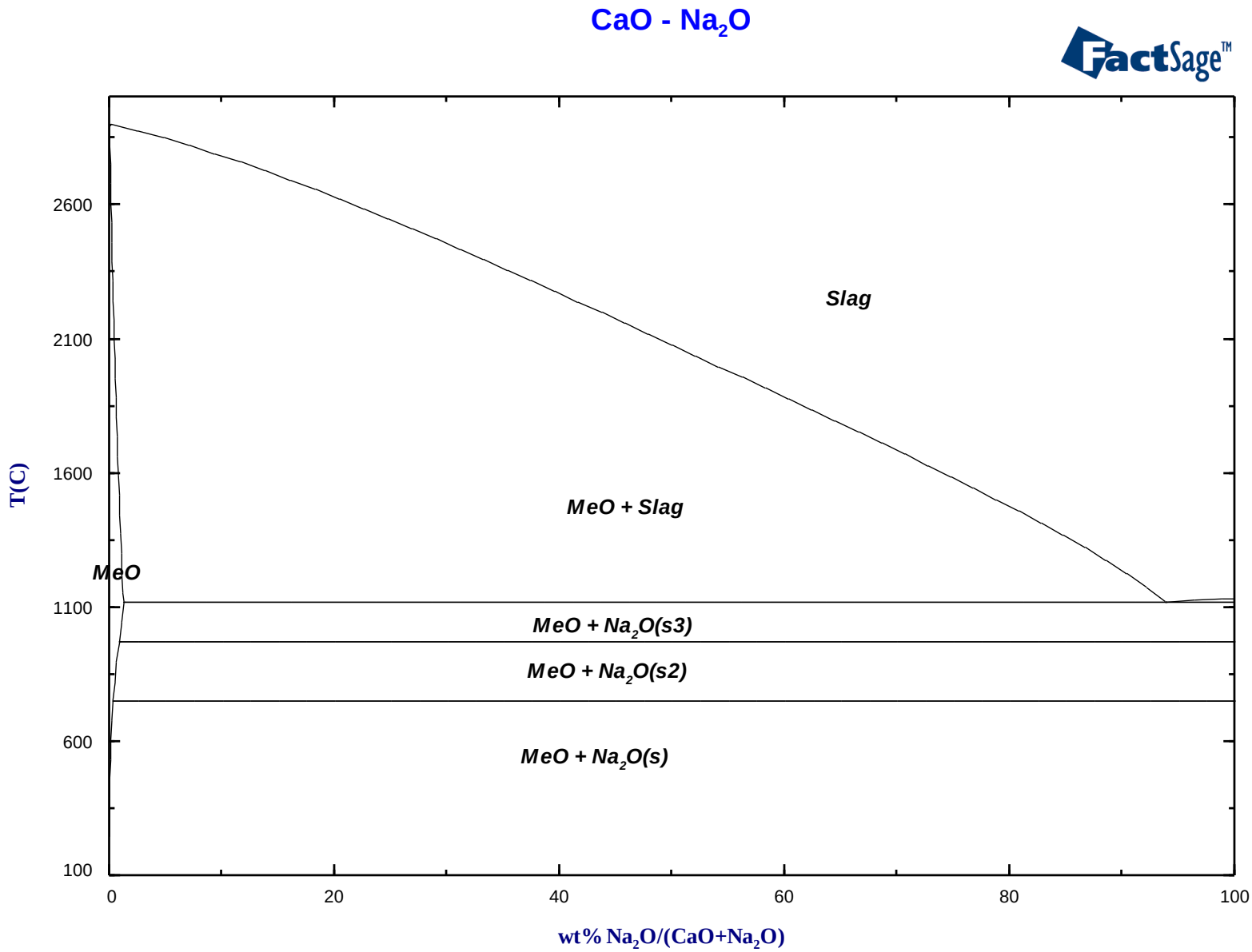

Mole fraction

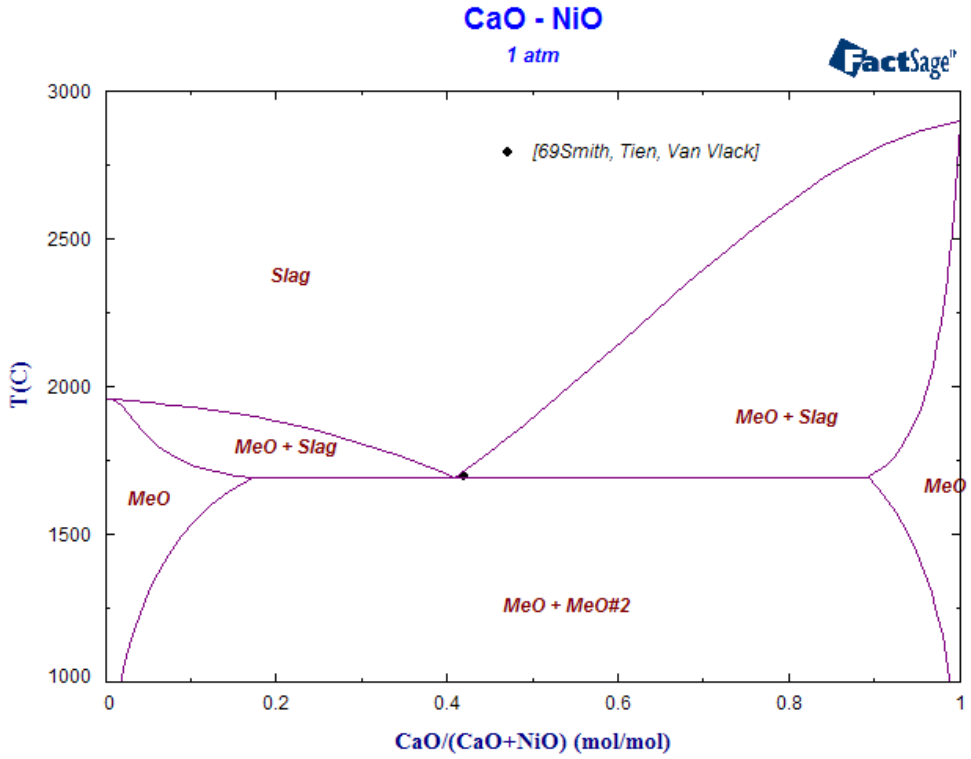

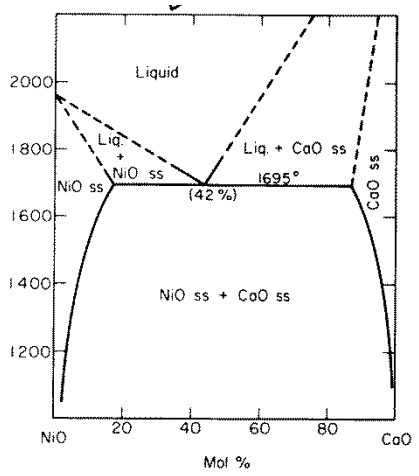

D.E. Smith, T.Y. Tien, L.H. Van Vlack, J. Am. Ceram. Soc., 52 [8], (1969), pp. 459-460.

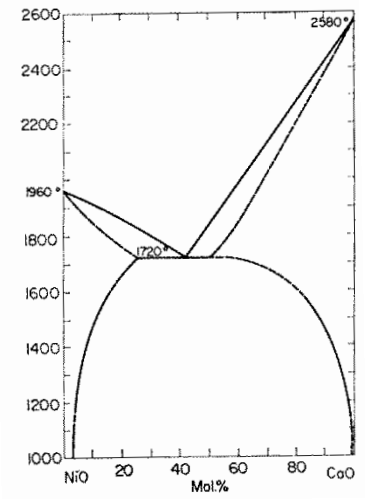

M.H. Tikkanen, private communication, 1962.

Weight percent

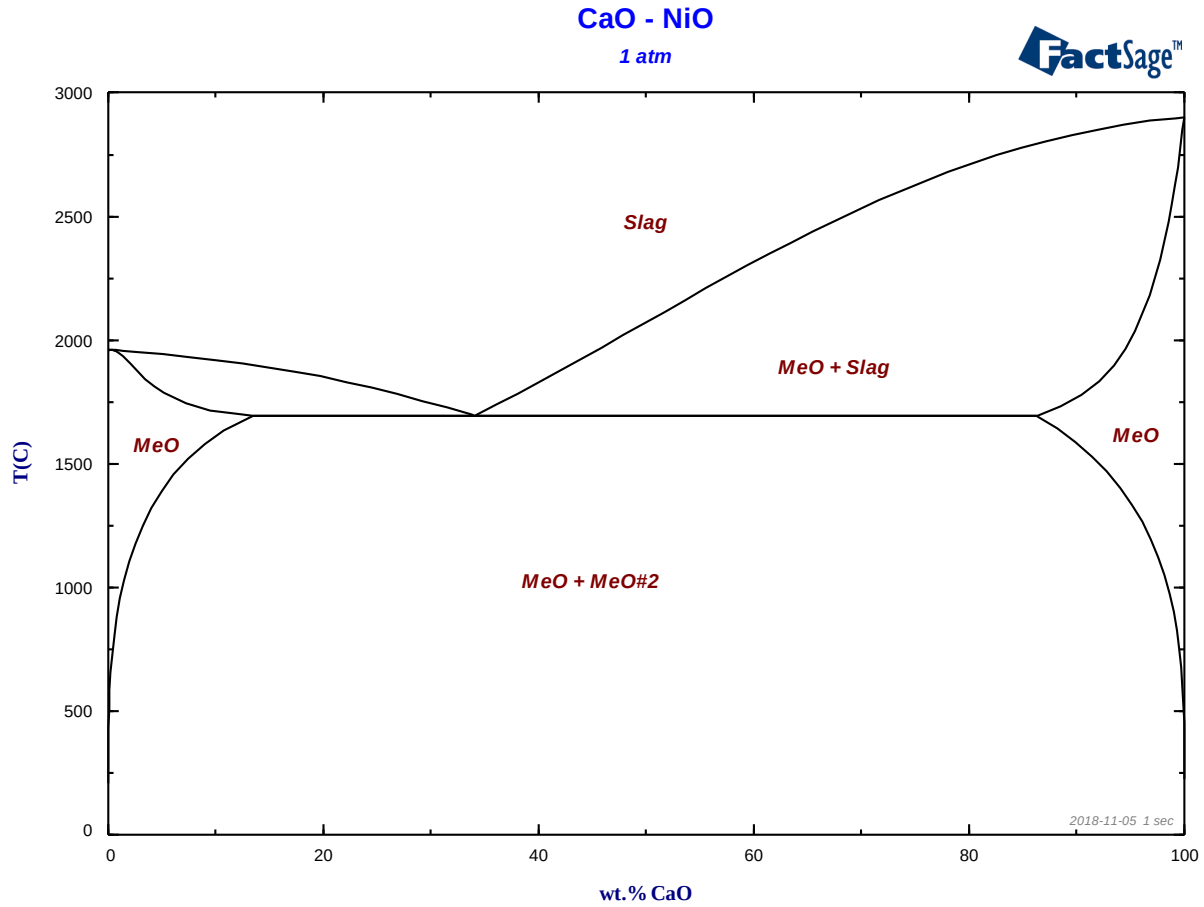

Mole fraction

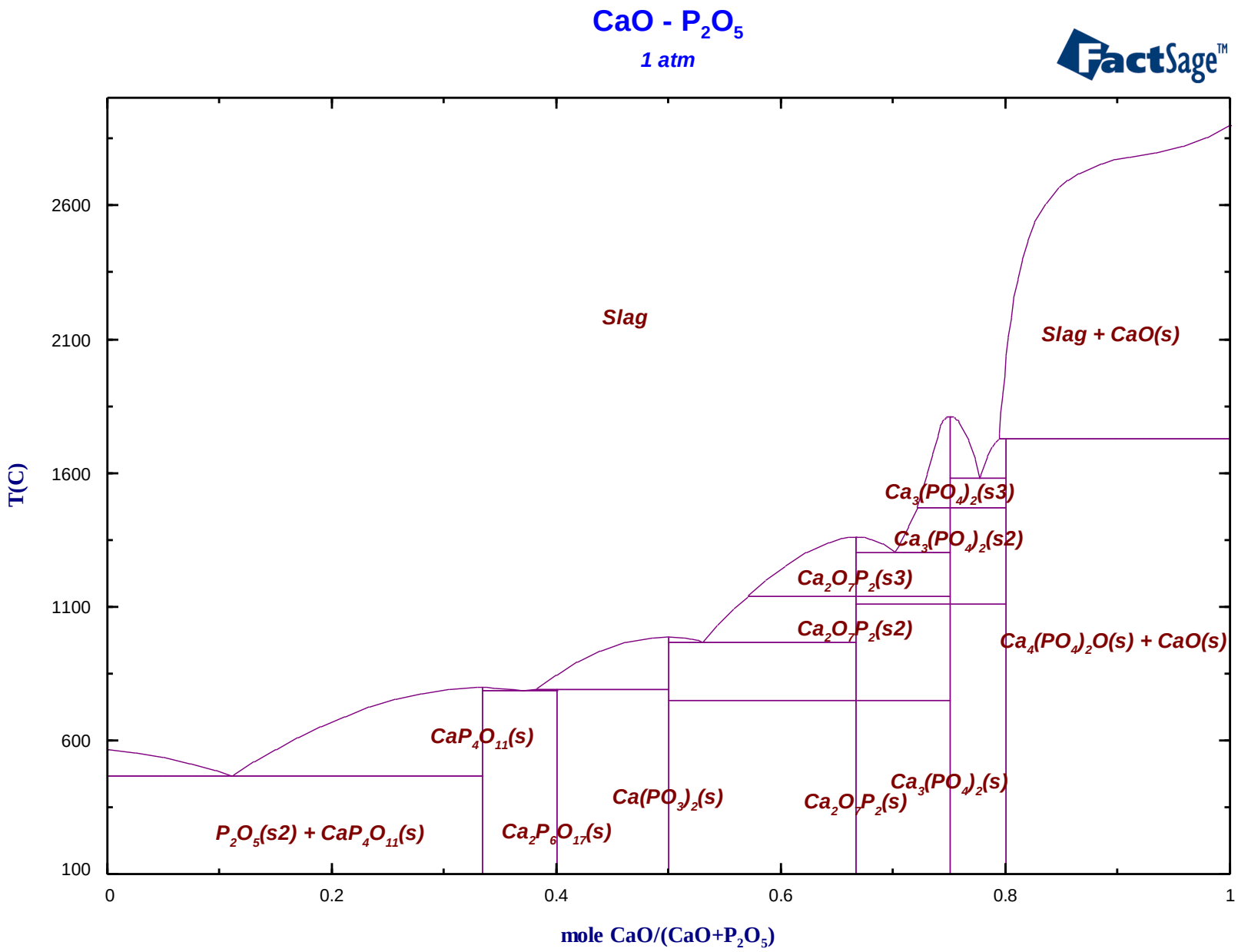

Weight percent
compared with experimental data

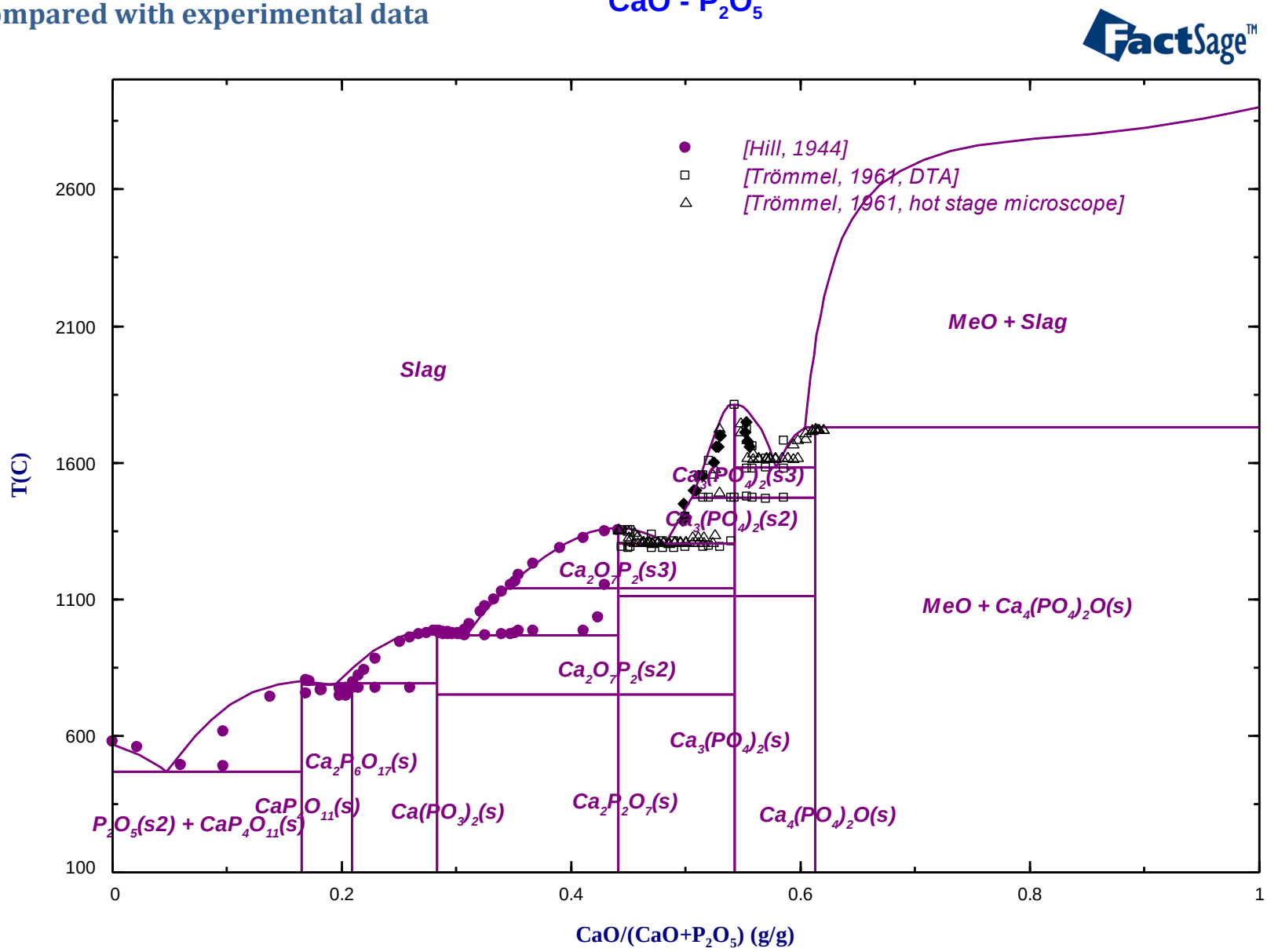

Mole fraction
compared with experimental data

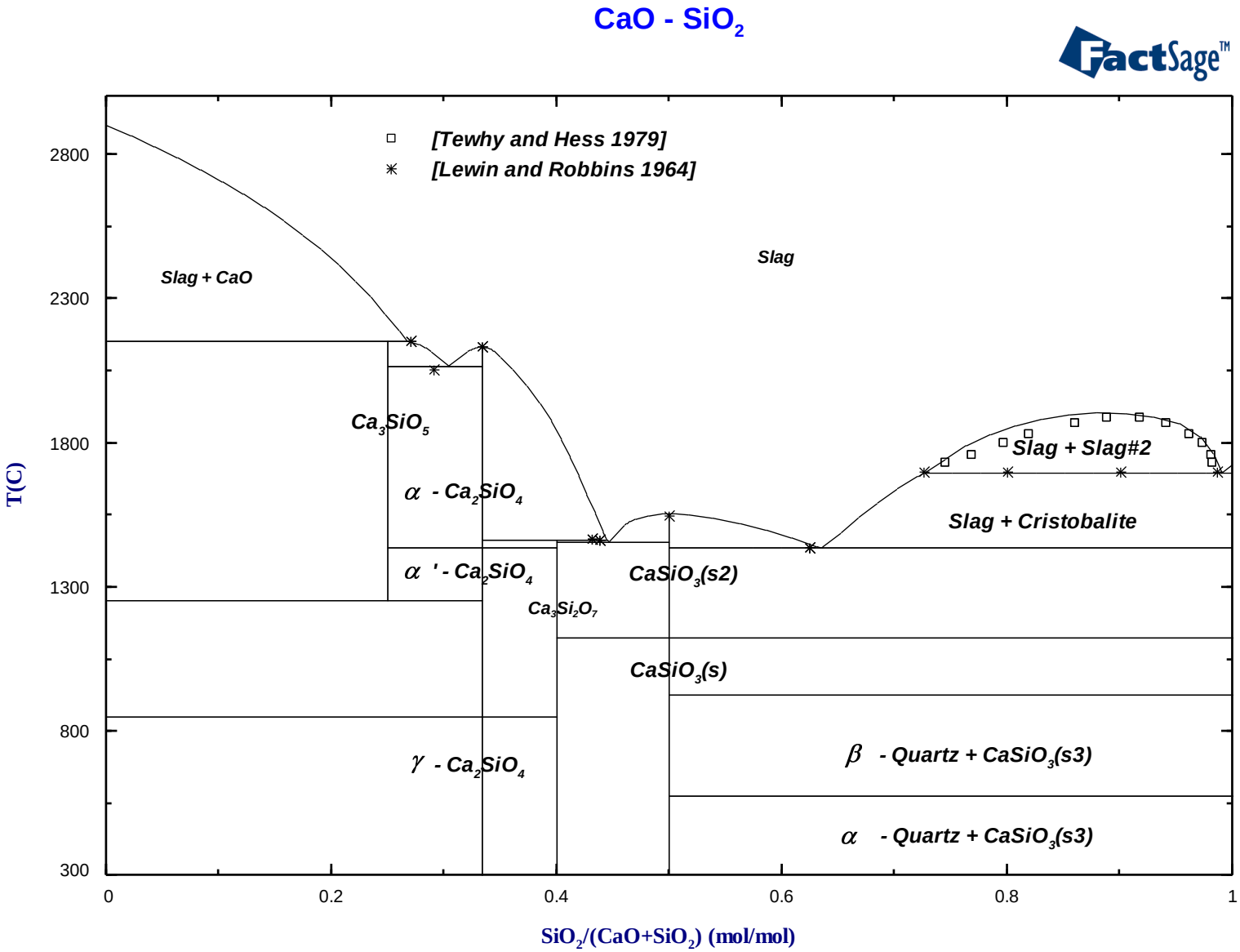

$CaO - SiO_2$

Weight percent

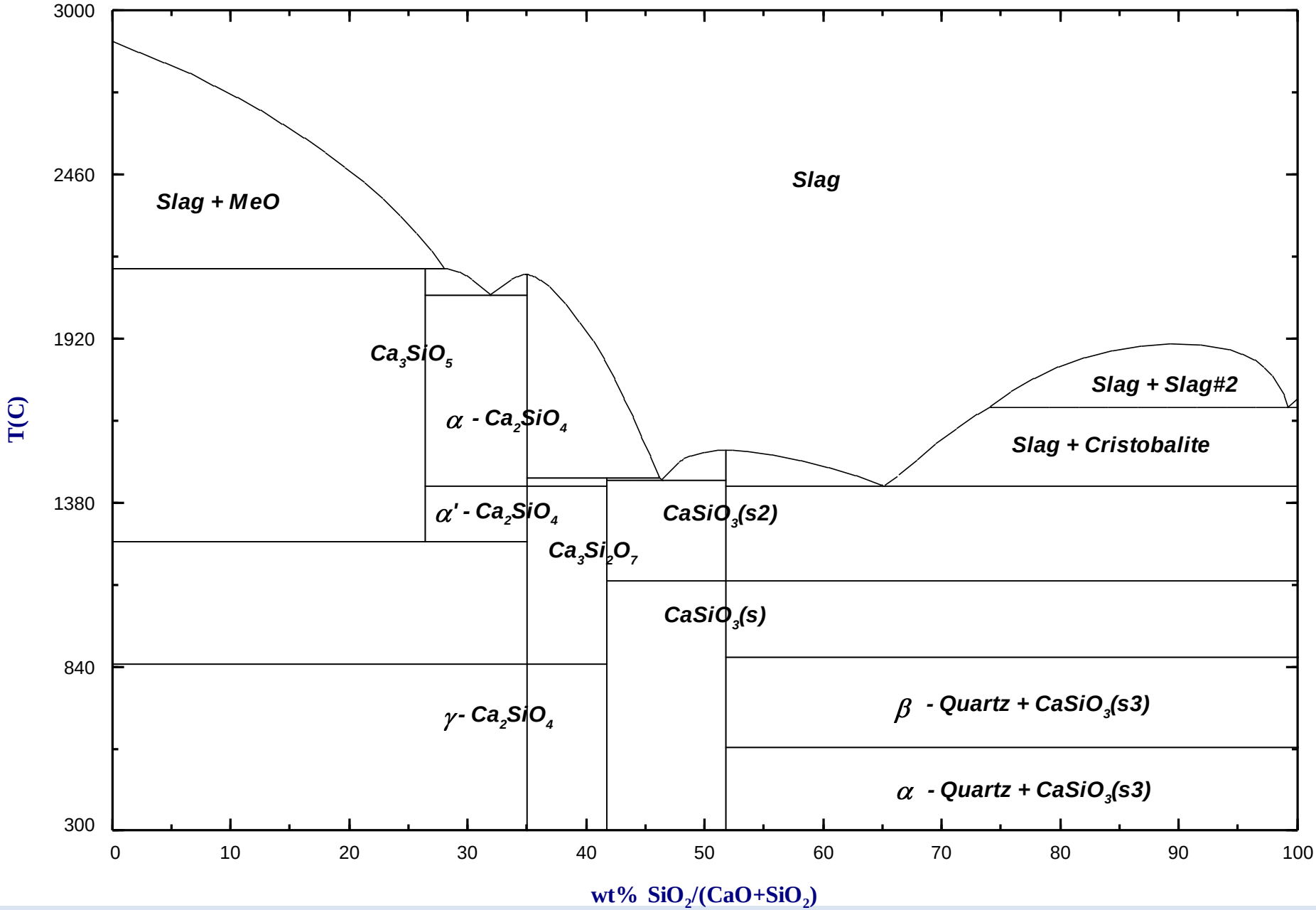

Mole fraction
compared with experimental data

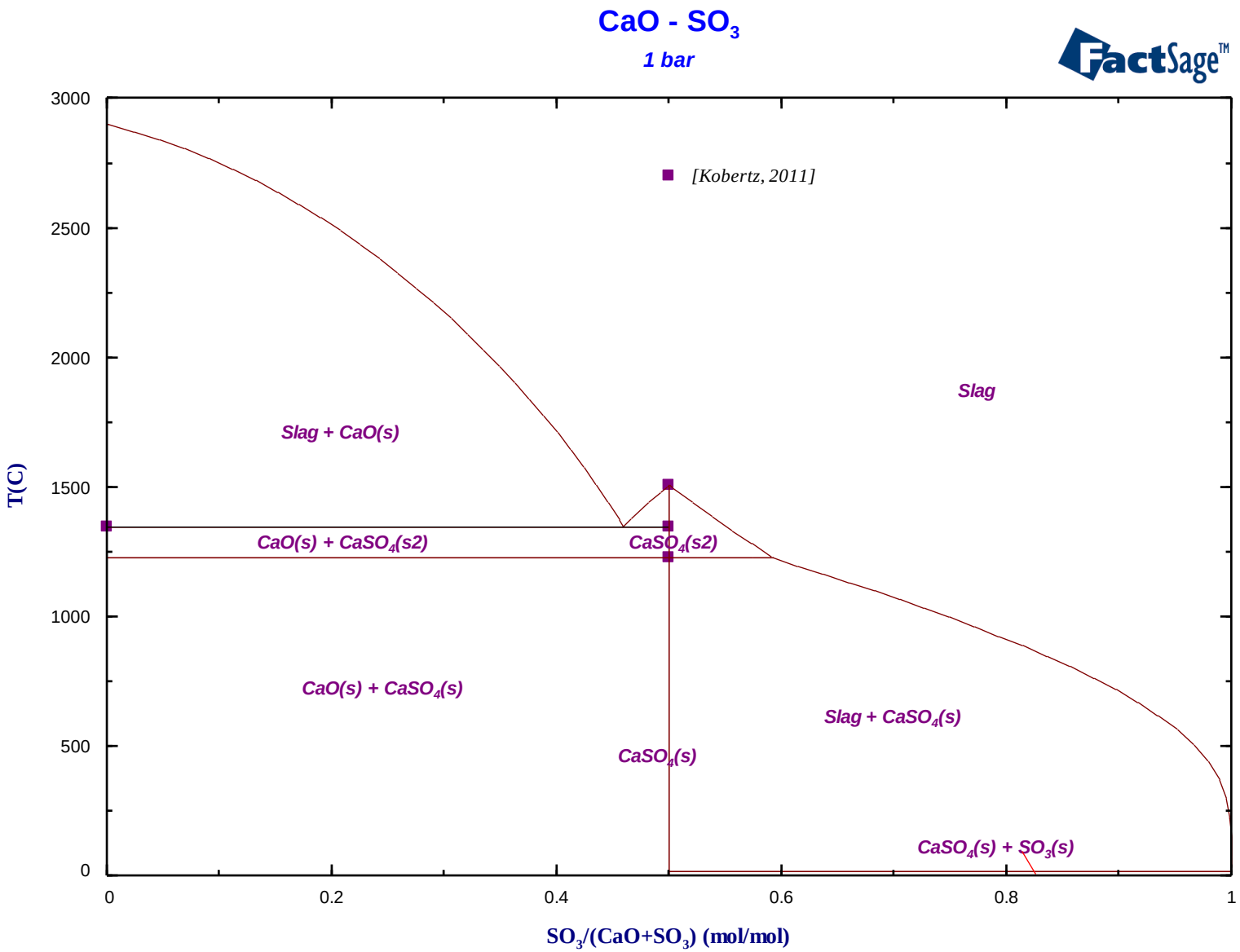

Weight percent

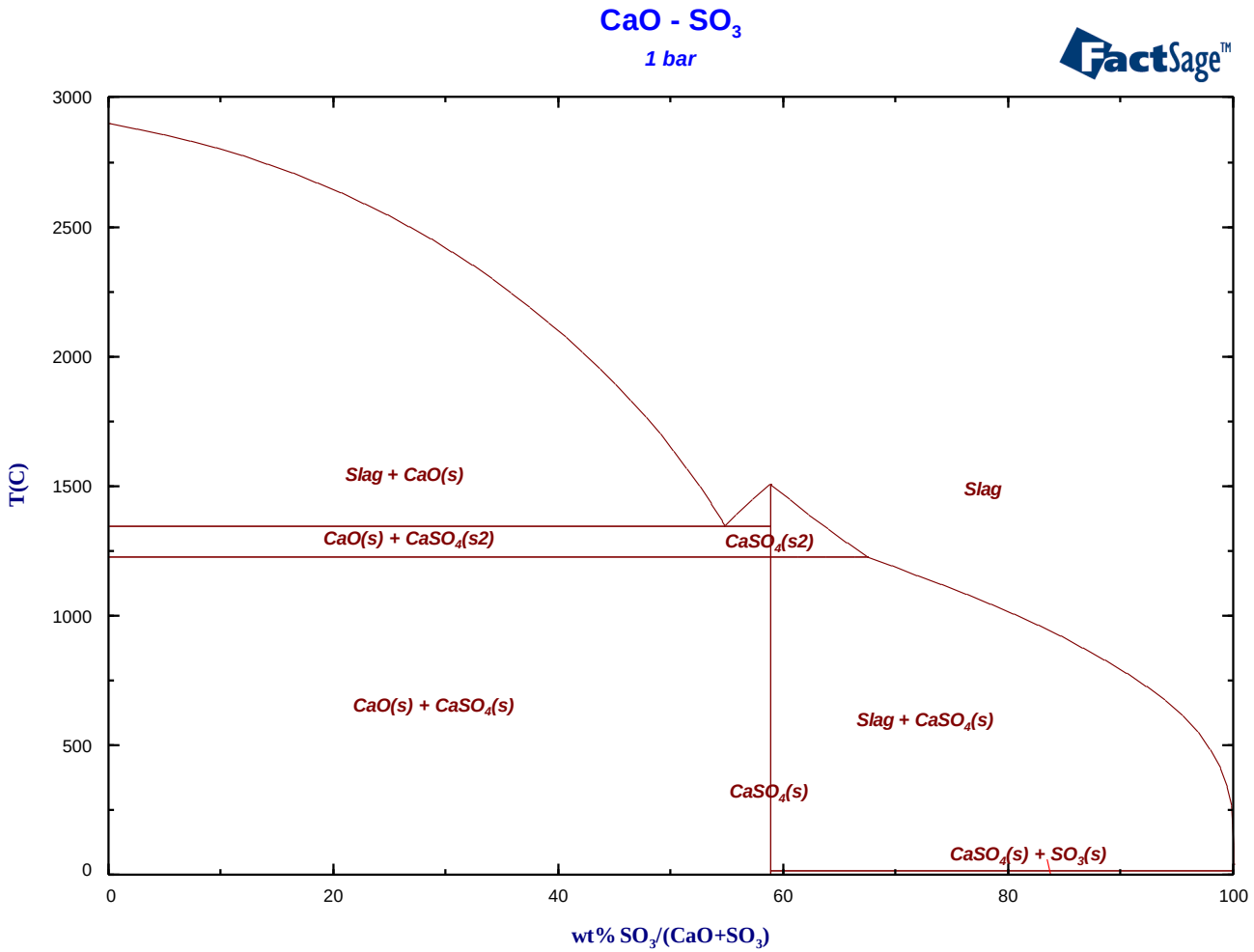

Mole fraction

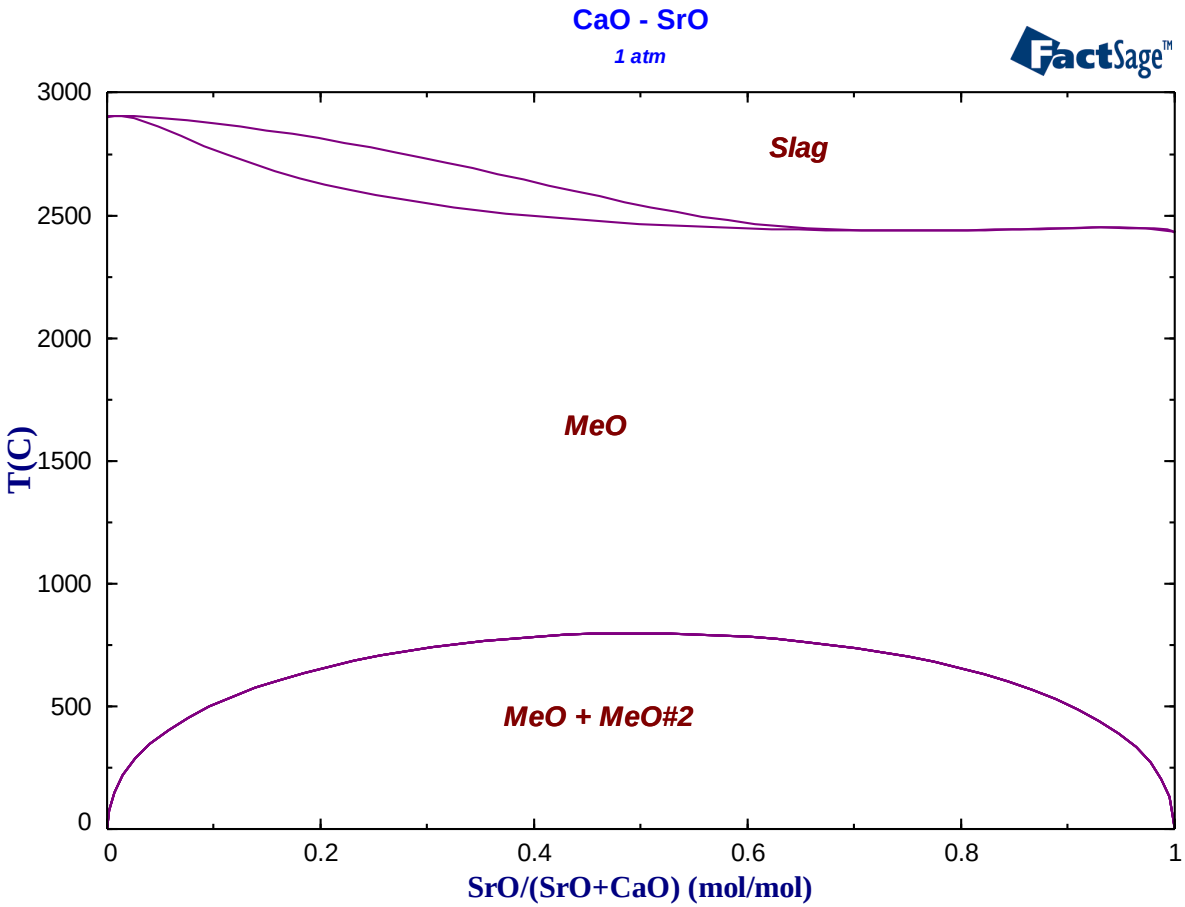

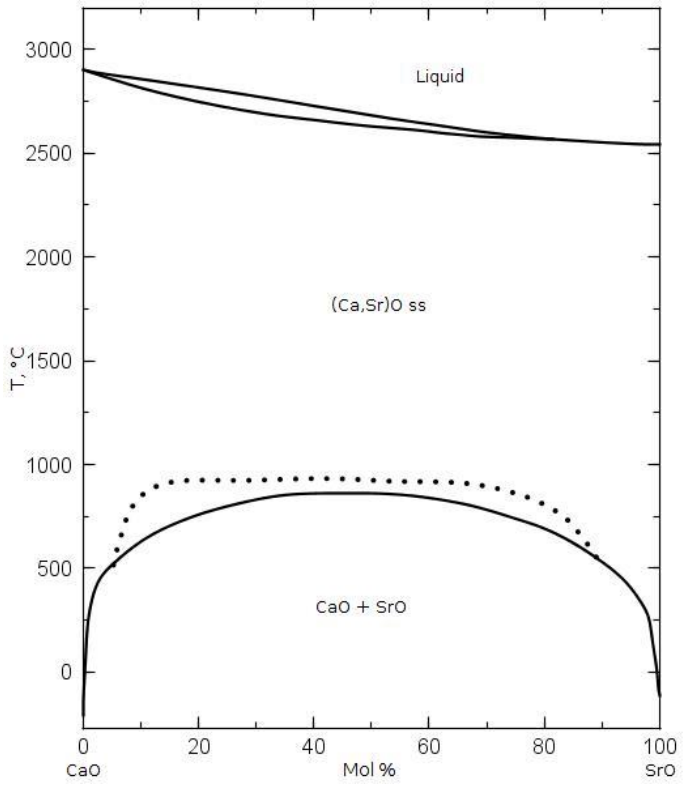

Van der Kemp, W. J. M., Blok, J. G., Van der Linde, P. R., Oonk, H. A. J., Schuijff, A., Verdonk, 1994.

Weight percent

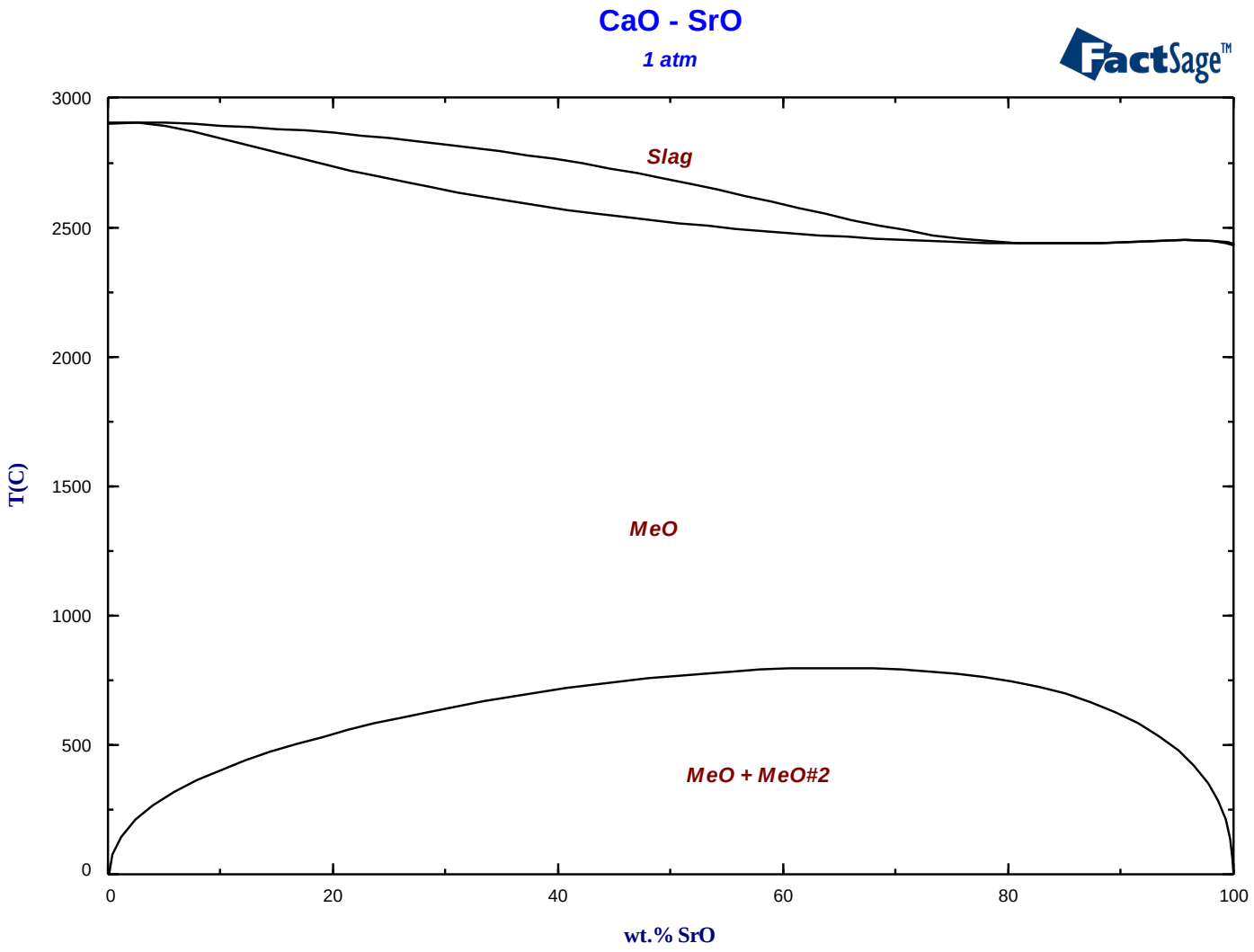

Mole fraction

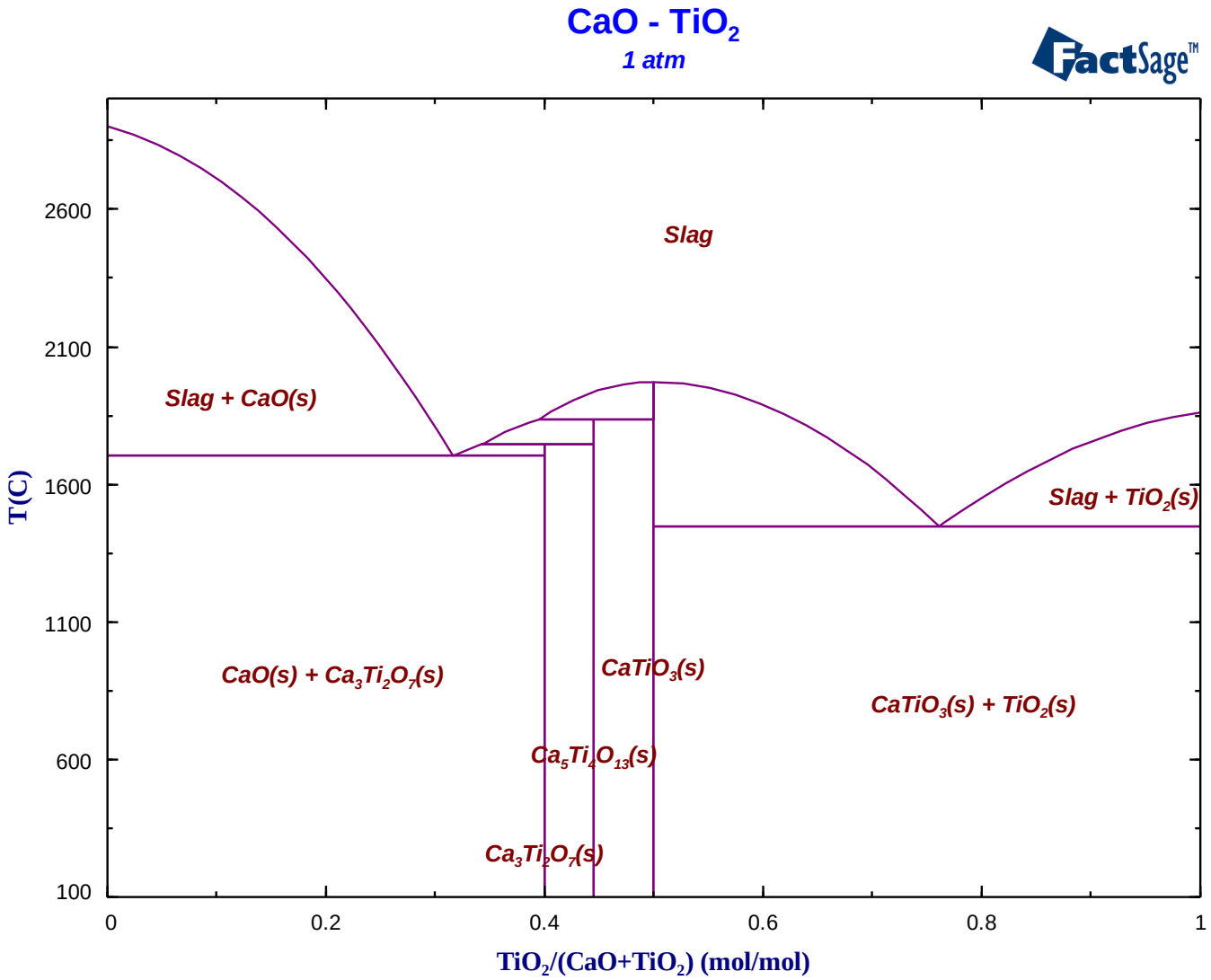

Weight percent compared with experimental data

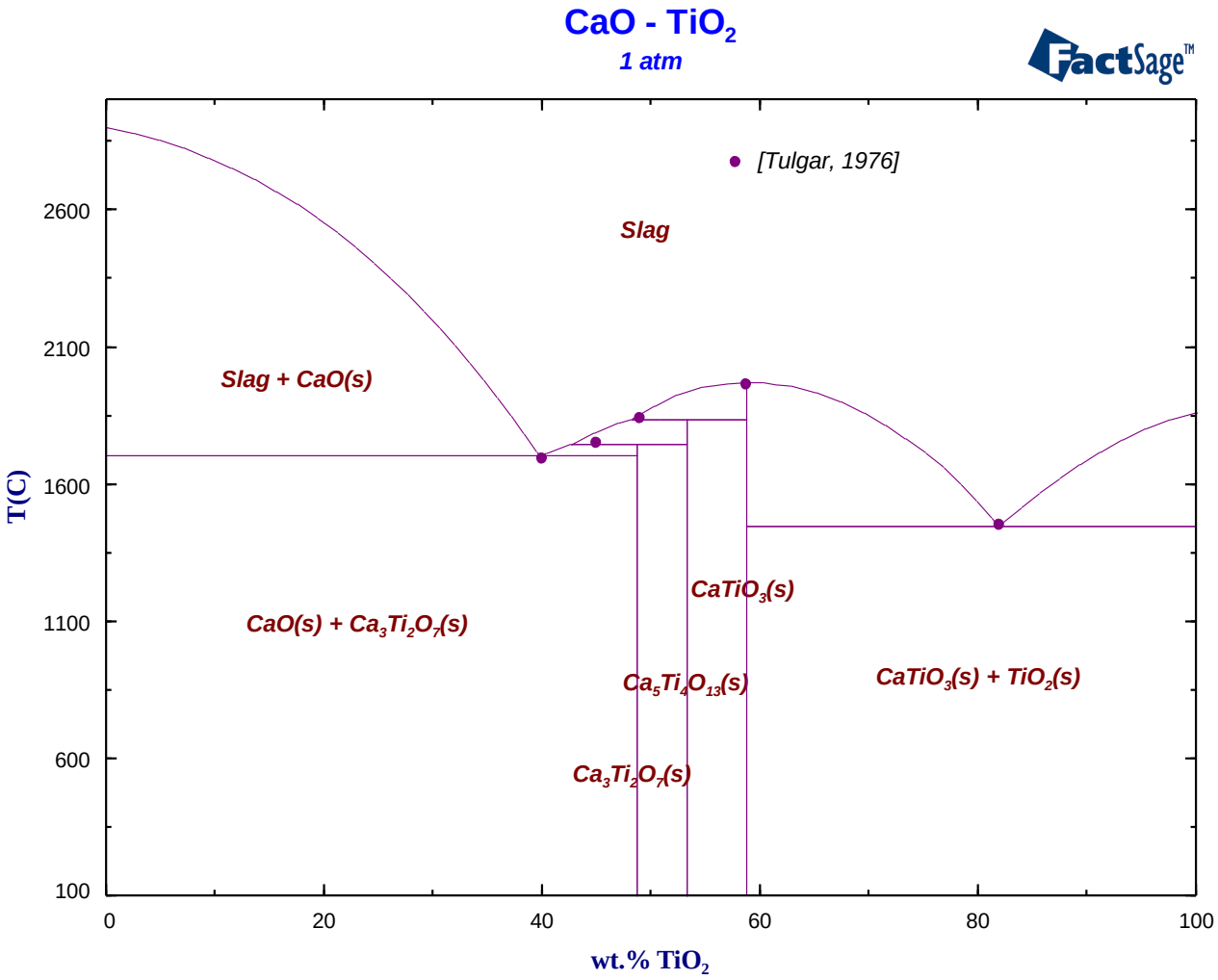

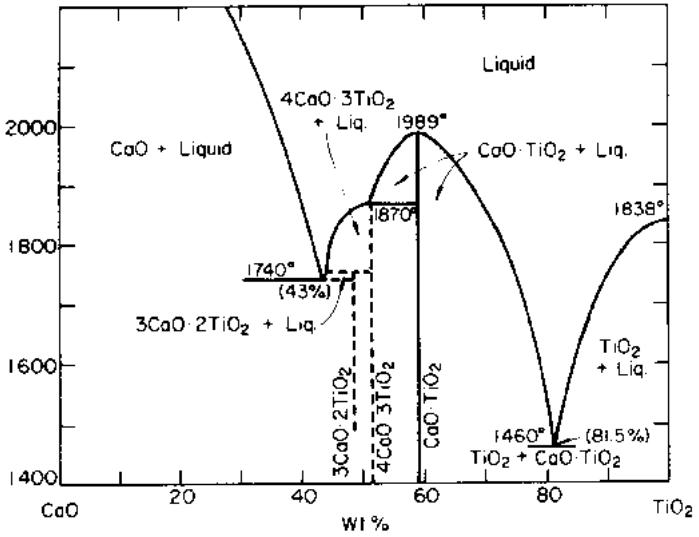

A. Jongejan, A.L. Wilkins, J. Less-Comon Met., 20 [4], (1970), pp. 273-279.

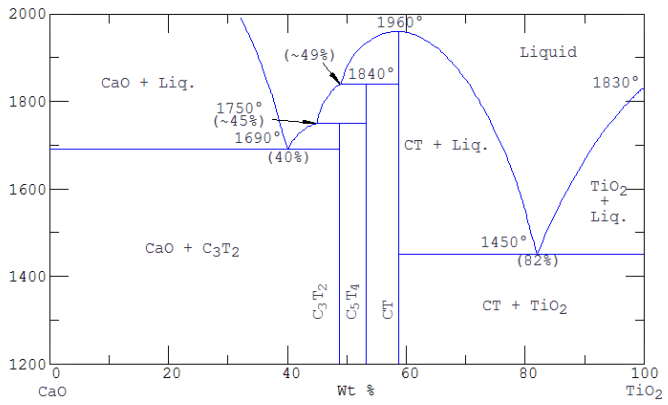

H.E. Tulgar, Istanbul Tek. Univ. Bul., 29 [1], (1976), pp. 111-129.

CaO-V2O3,
Mole fraction

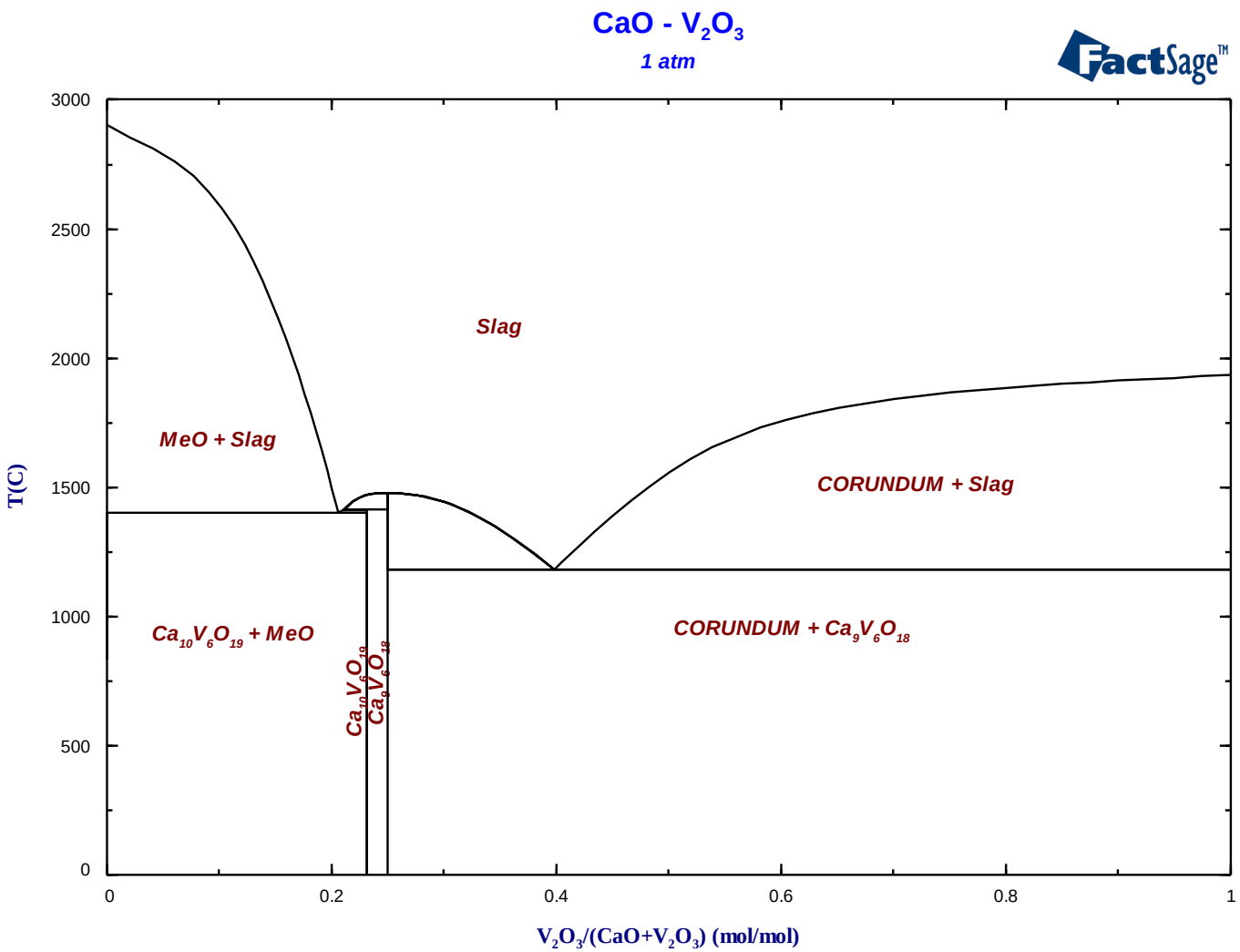

CaO-V2O3,
Weight percent compared with experimental data

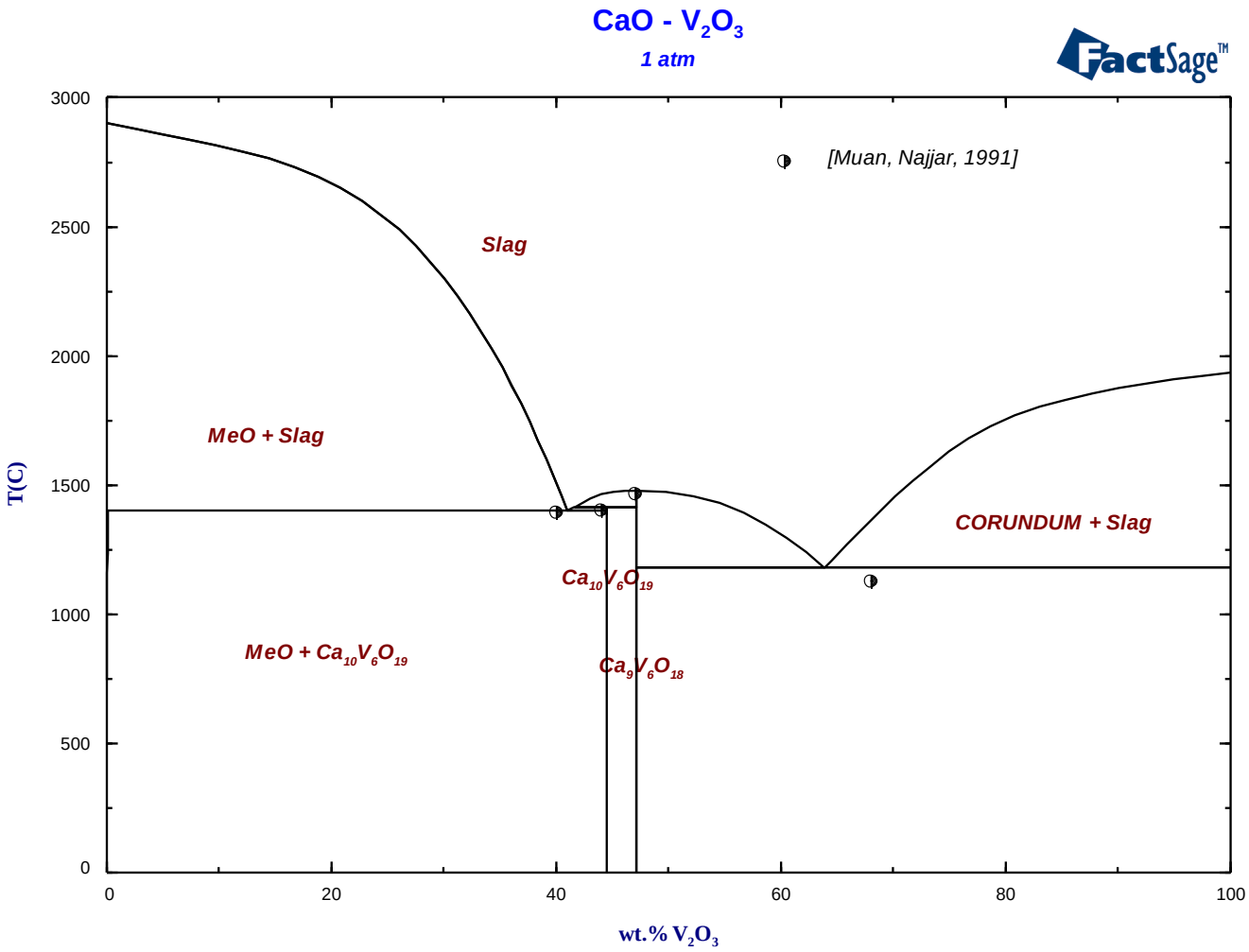

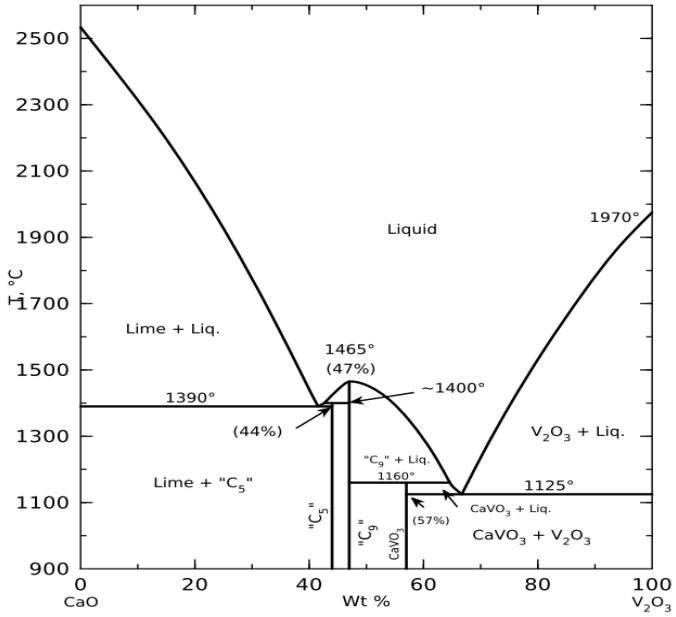

A. Muan, M. S. Najjar, "Compositions involving V2O3-CaO", US Patent 5,077,260, December 31, 1991.

CaO-V2O5-O2, Mole fraction

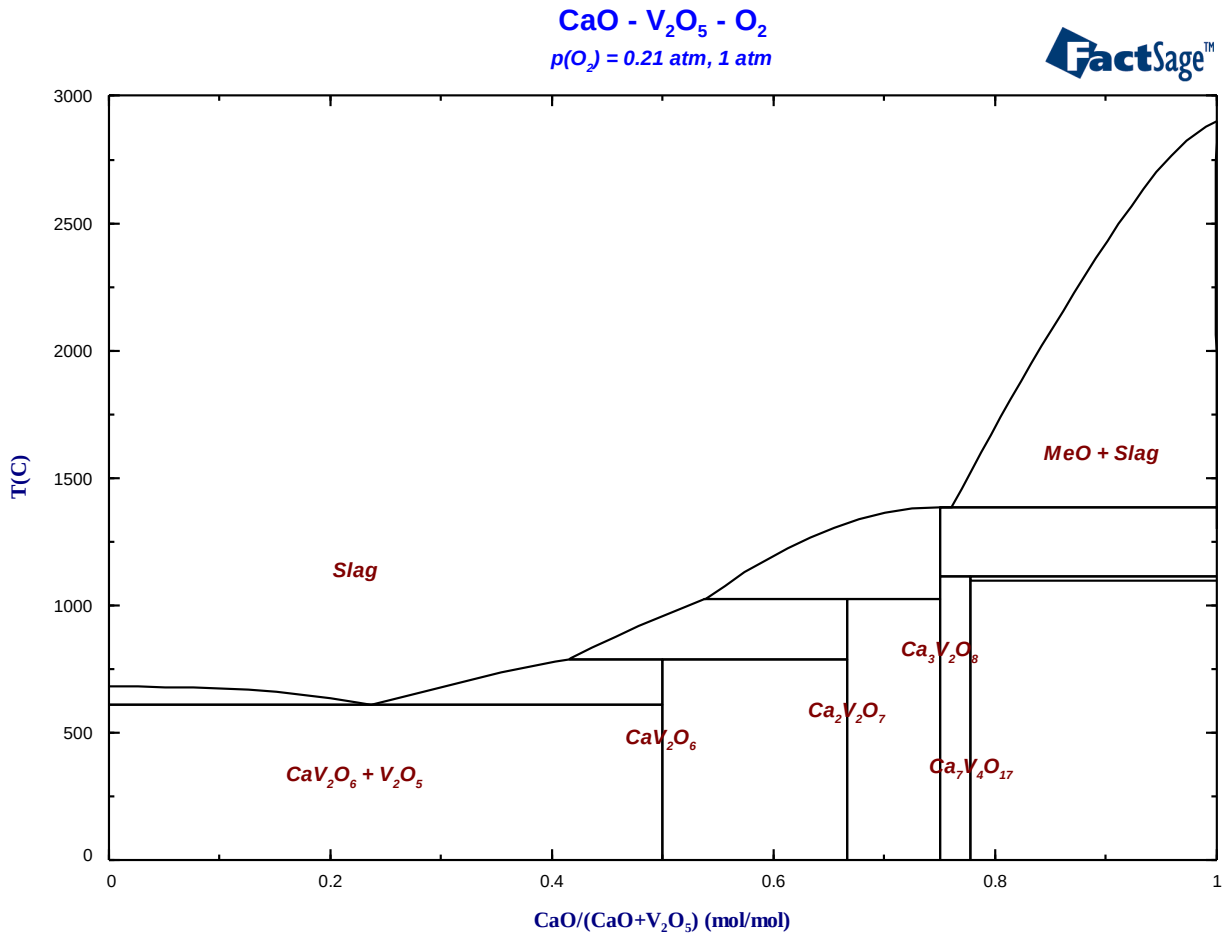

CaO-V2O5-O2,
Weight percent compared with experimental data

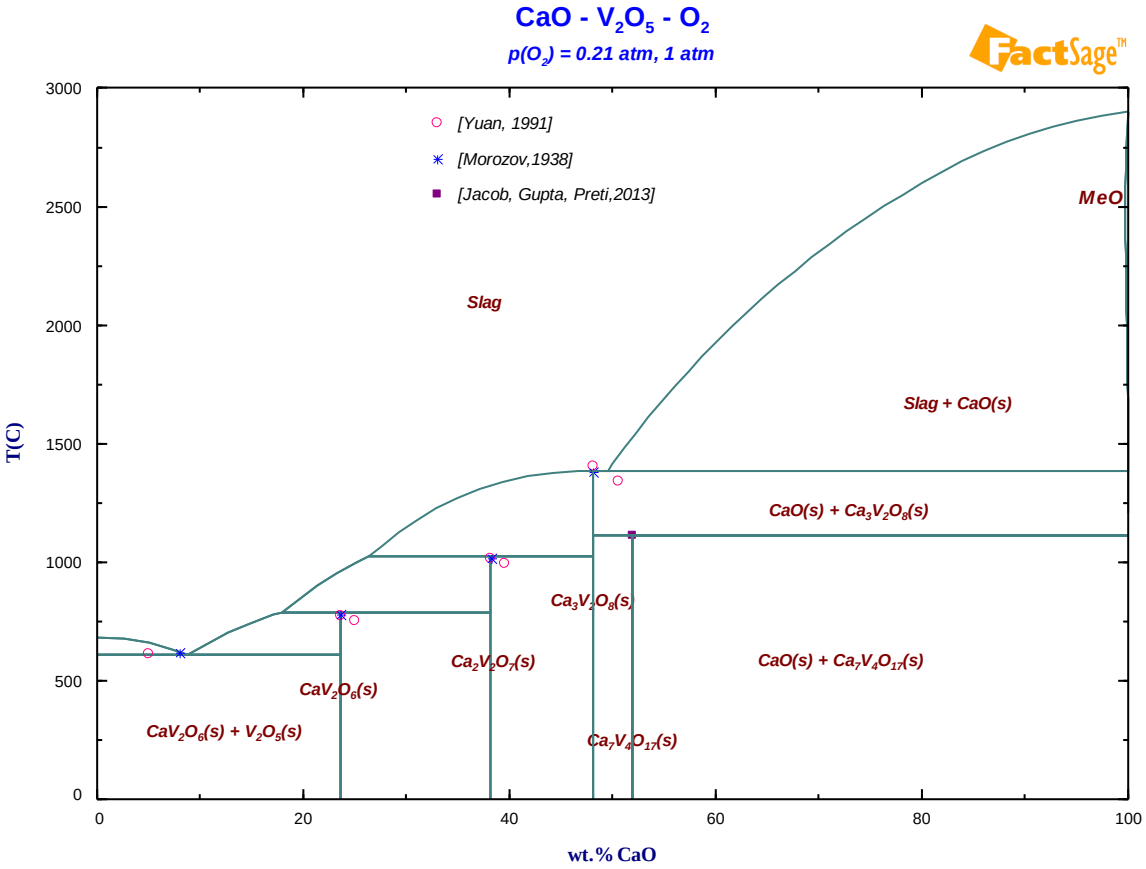

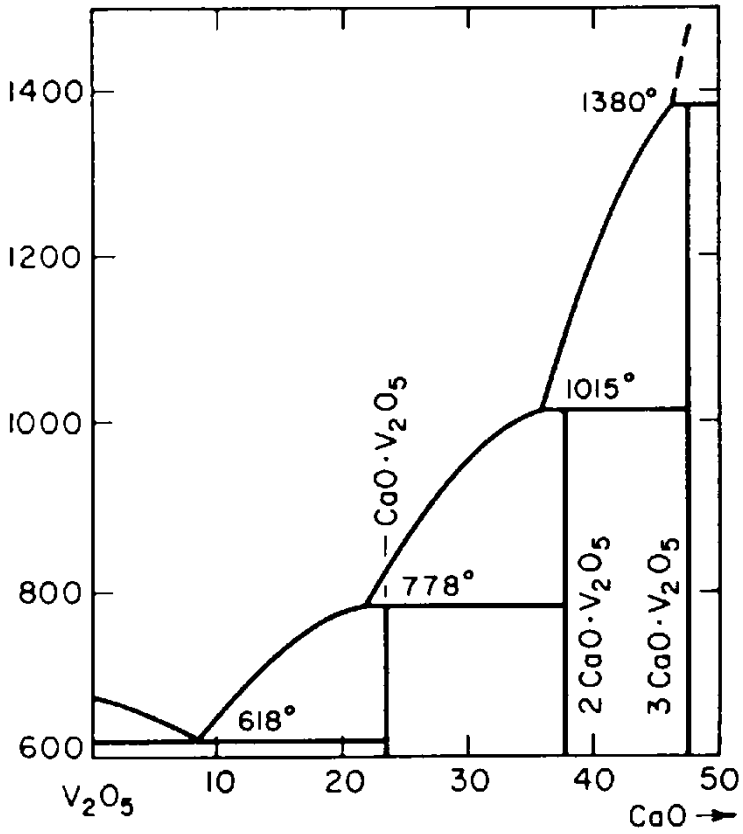

V.L.Volkov, A.A. Fotiev, L.L. Surat, Zh. Fiz. Khim., 49 [6], (1975), pp.1575-1577.

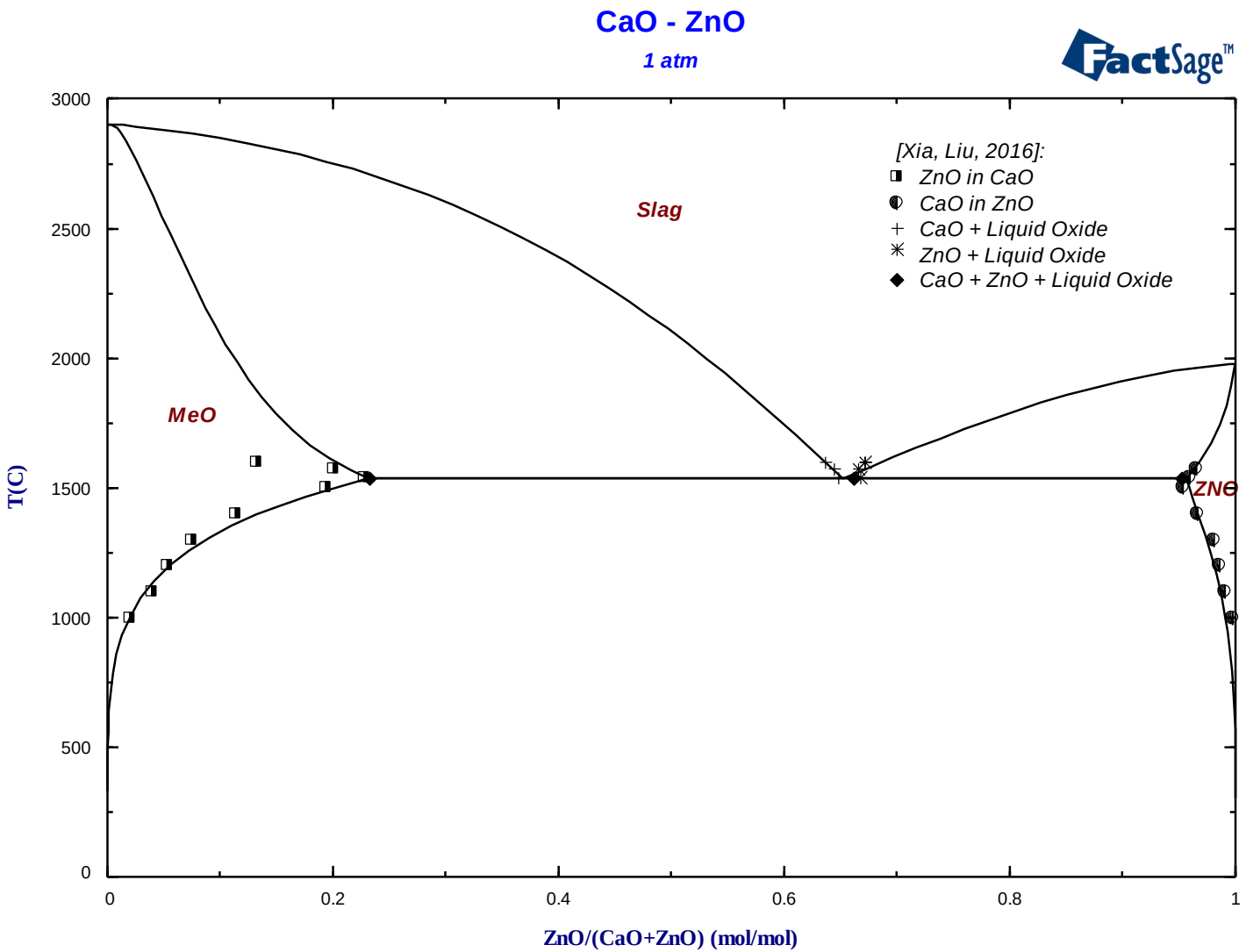
CaO - ZnO
1 atm
FactSage™
[Xia, Liu, 2016]:
ZnO in CaO
CaO in ZnO
CaO + Liquid Oxide
ZnO + Liquid Oxide
CaO + ZnO + Liquid Oxide
Slag
MeO
ZNO
T(C)
3000
2500
2000
1500
1000
500
0
0
0.2
0.4
0.6
0.8
1
ZnO/(CaO+ZnO) (mol/mol)

Weight percent

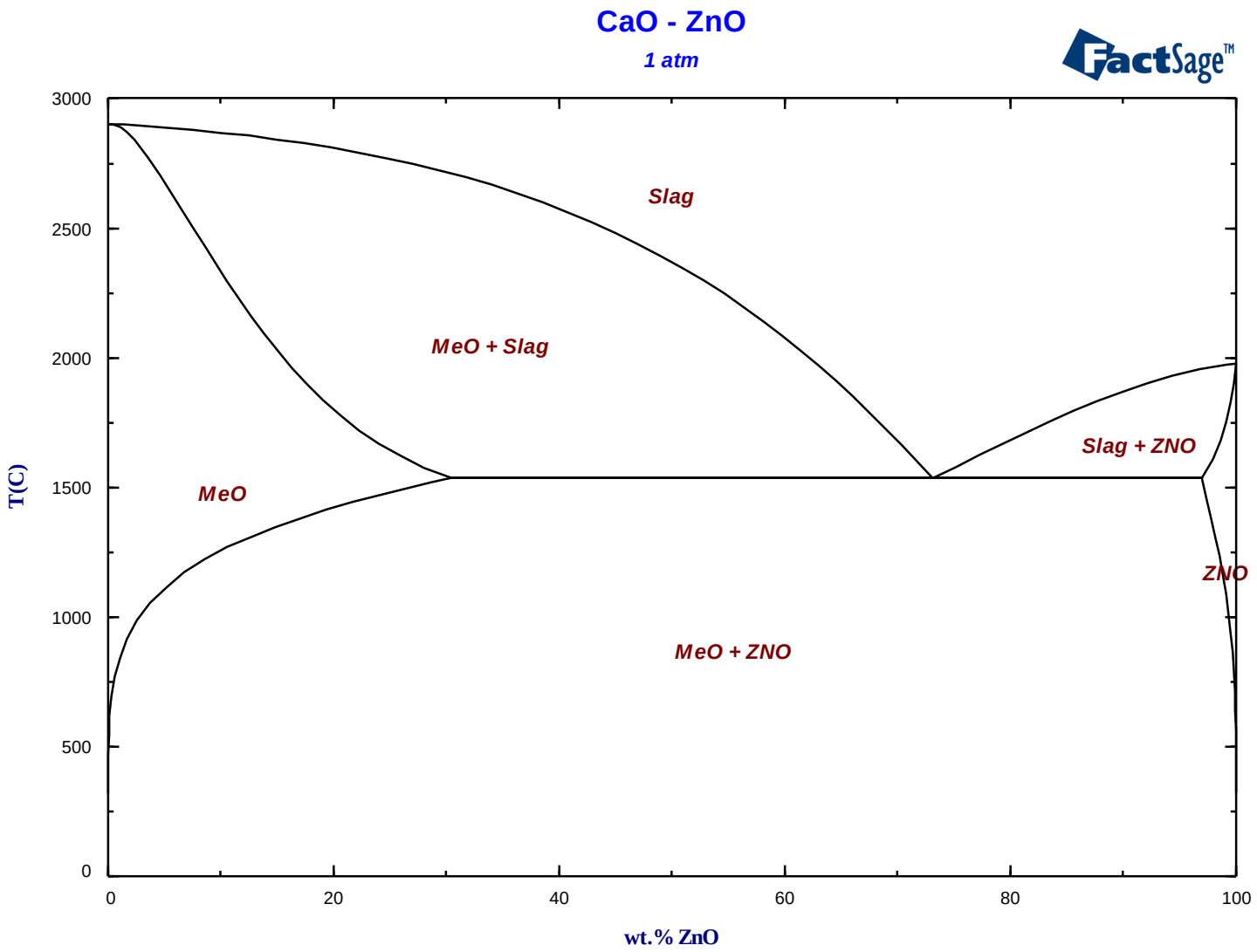

Mole fraction

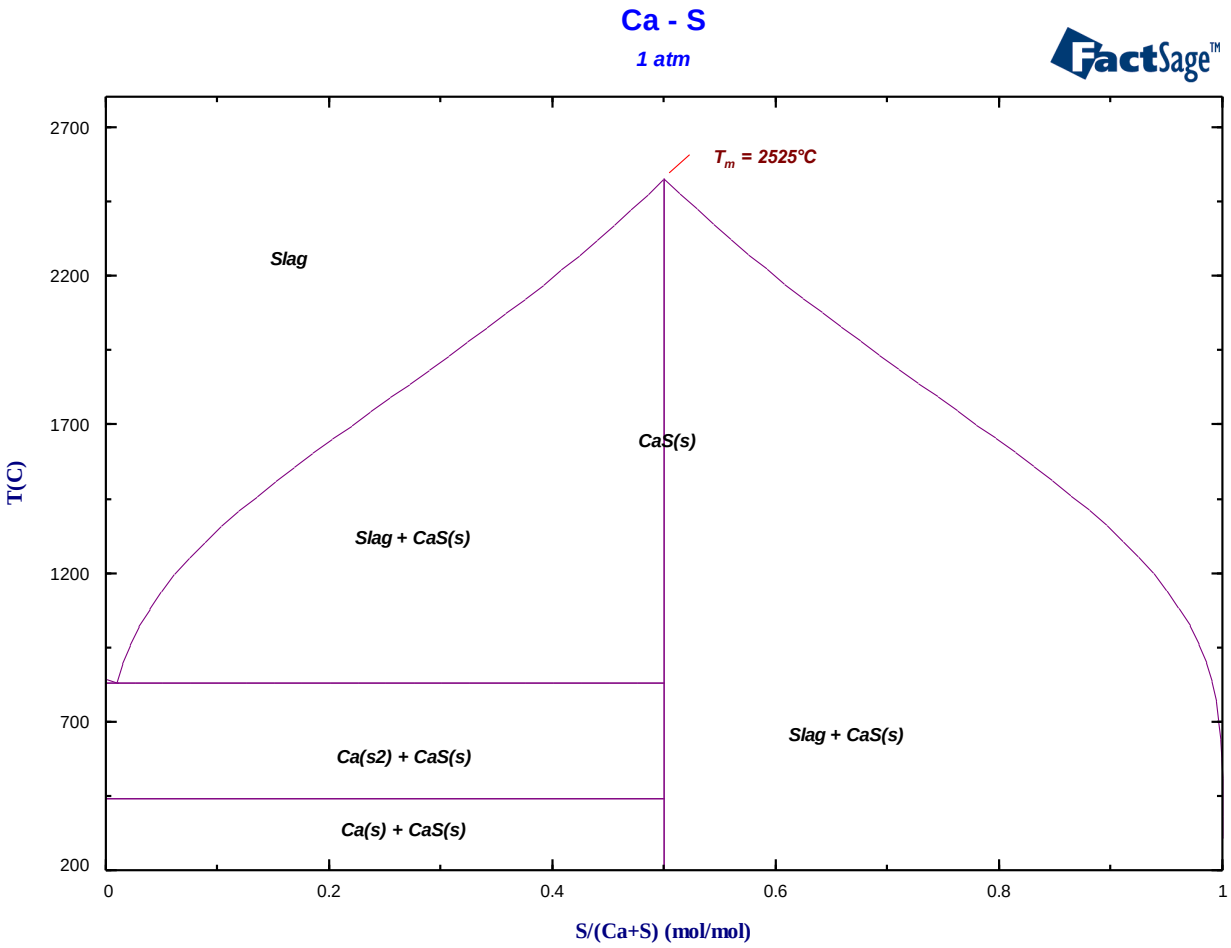

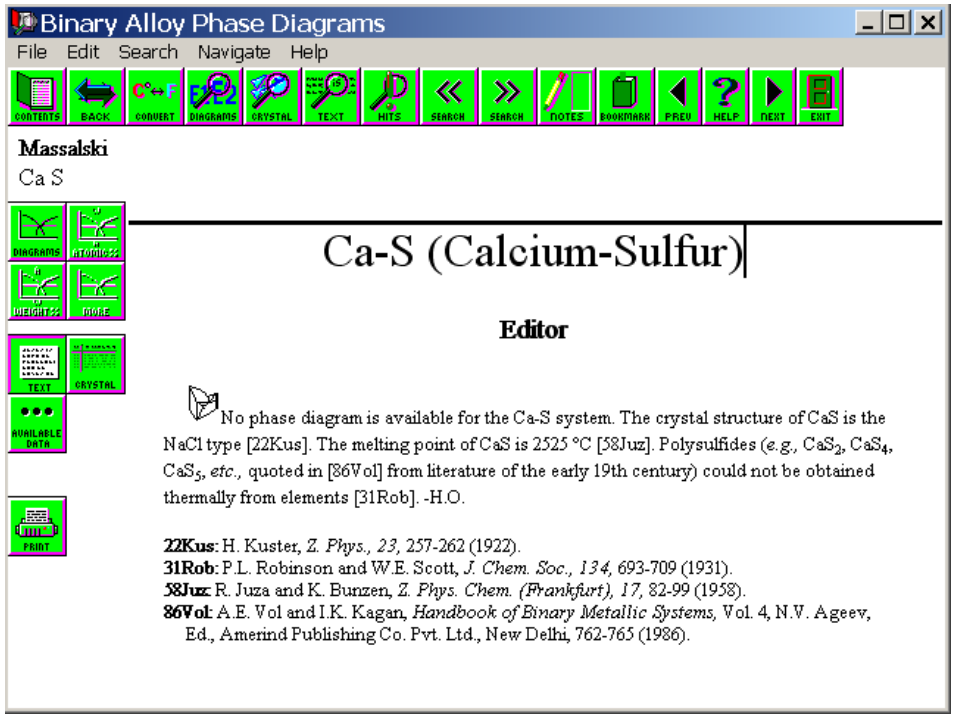

Weight percent

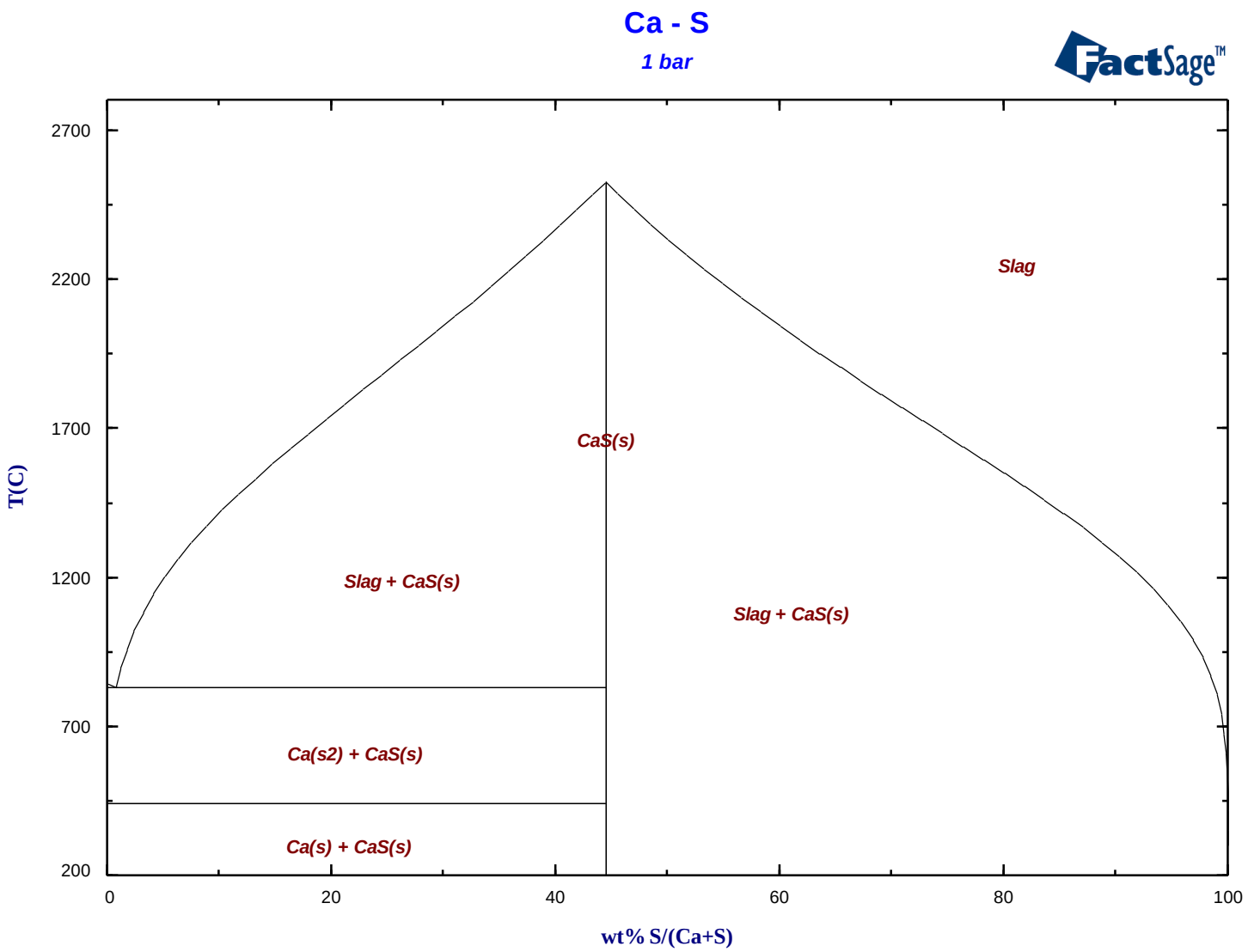

Mole fraction

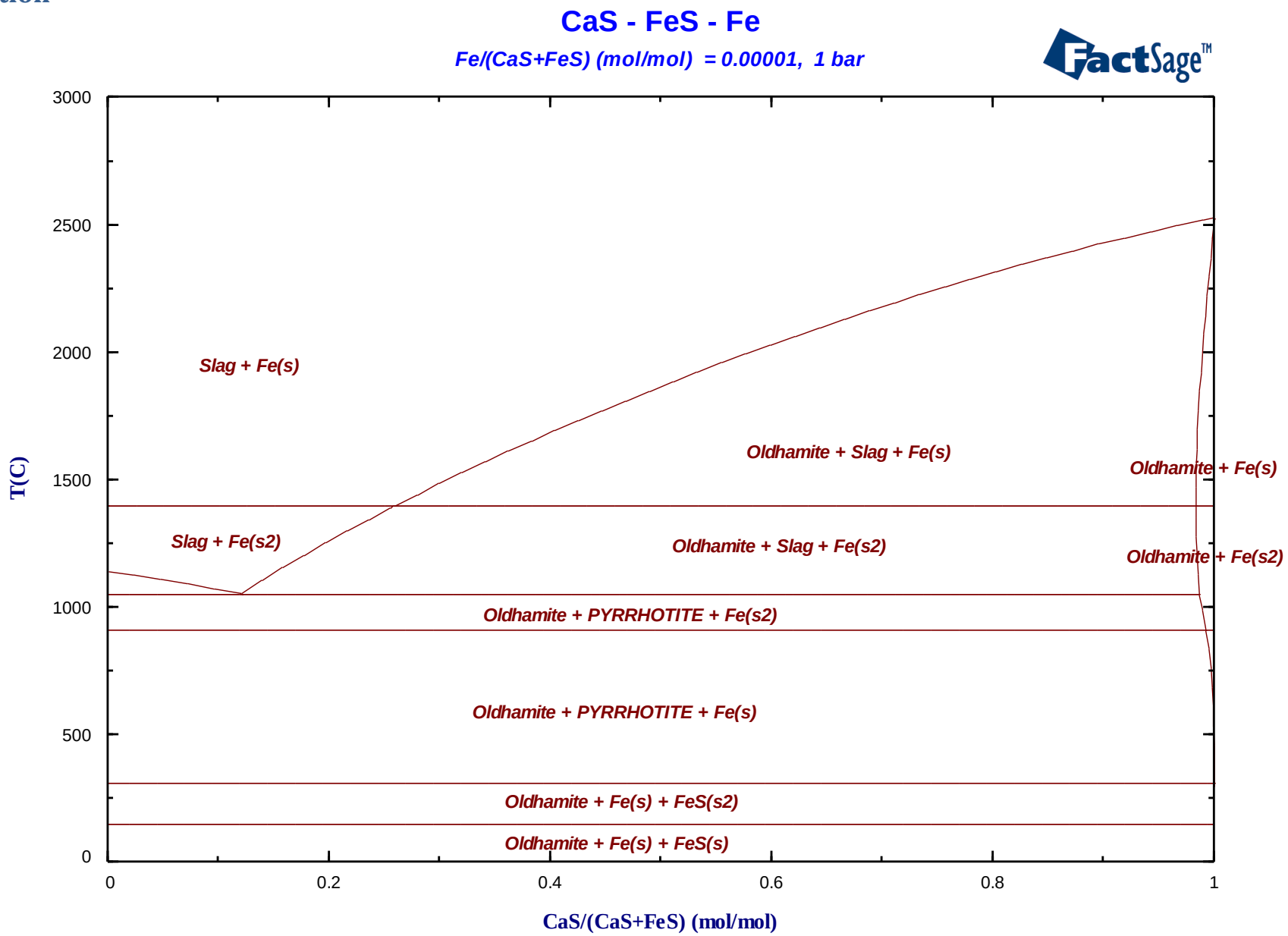

Weight percent
compared with experimental data

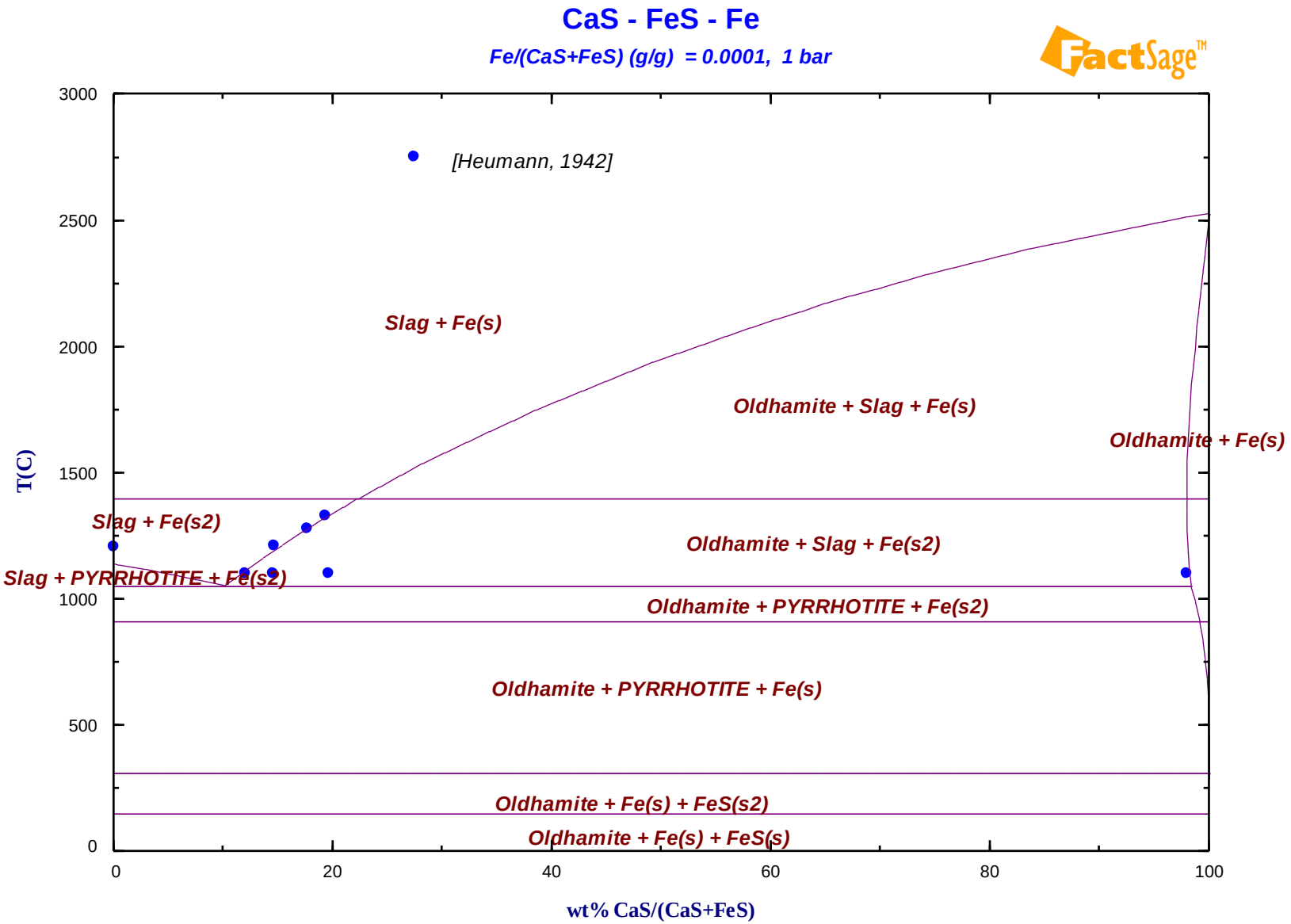

Mole fraction
compared with experimental data

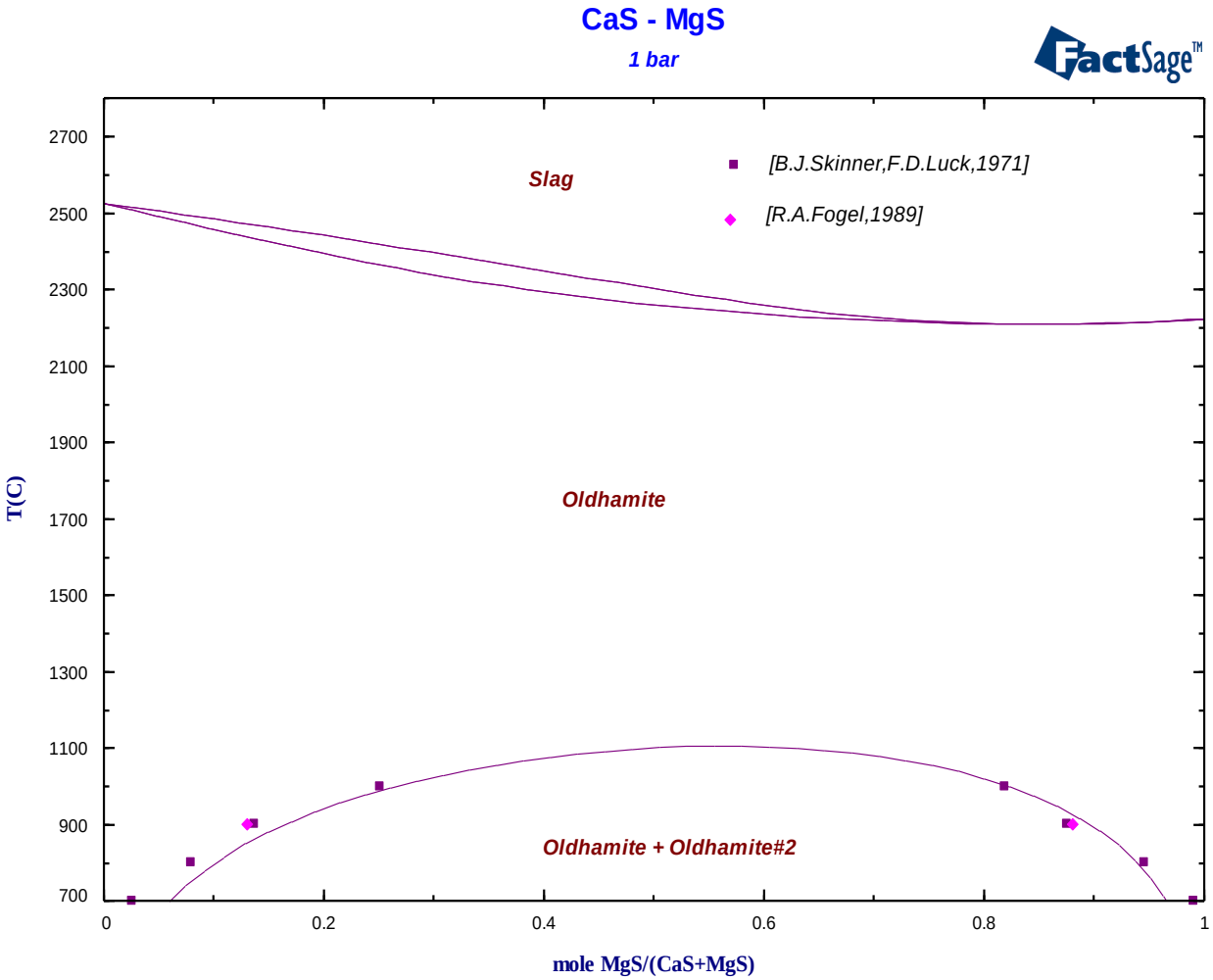

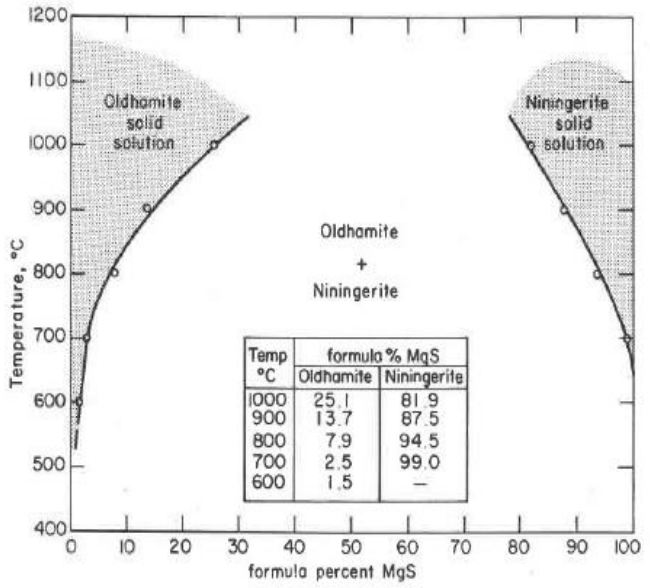

B.J. Skinner, F.D. Luck, Amer. Mineral., Vol.56 (1971), pp. 1269-1296.

Weight percent

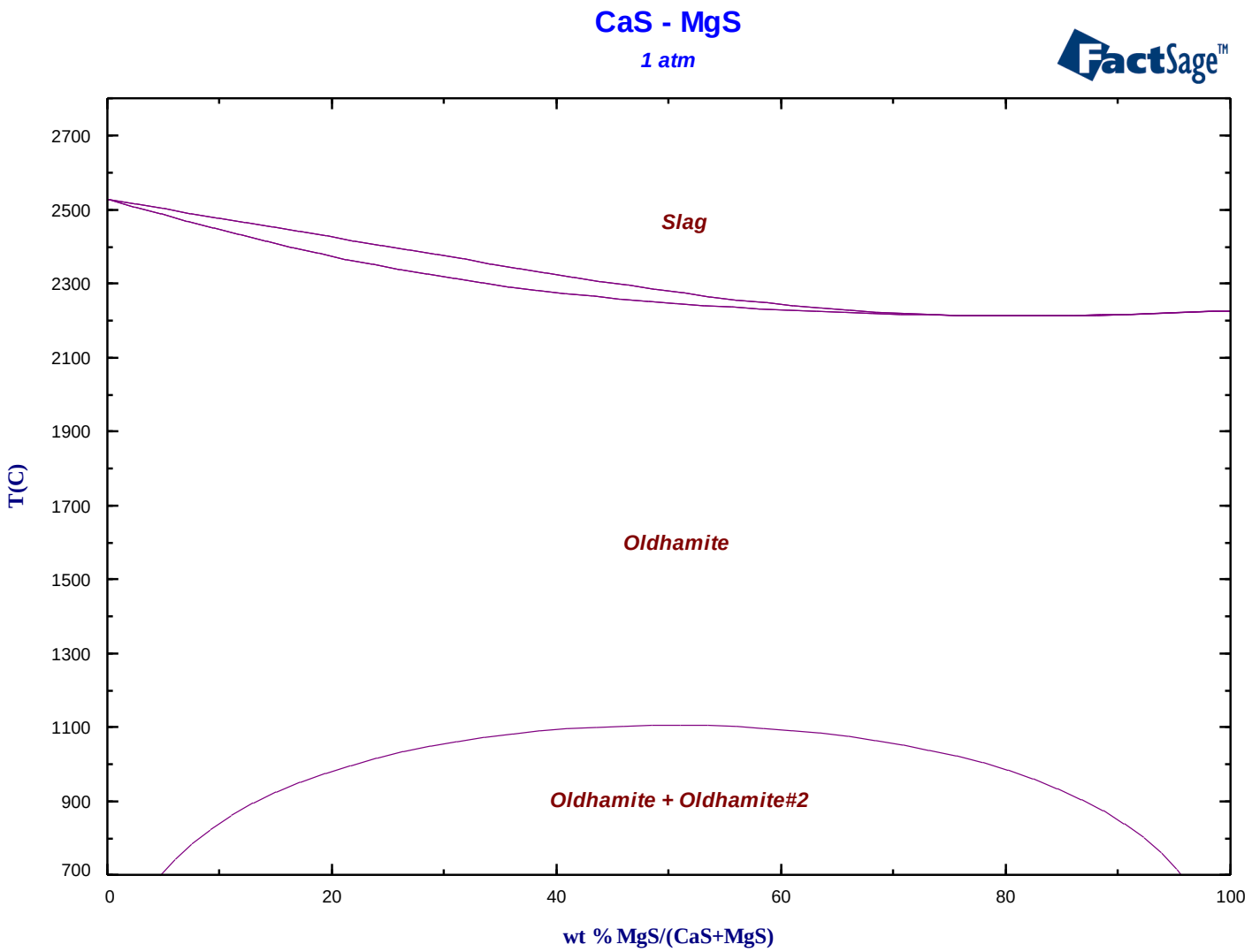

Mole fraction
compared with experimental data

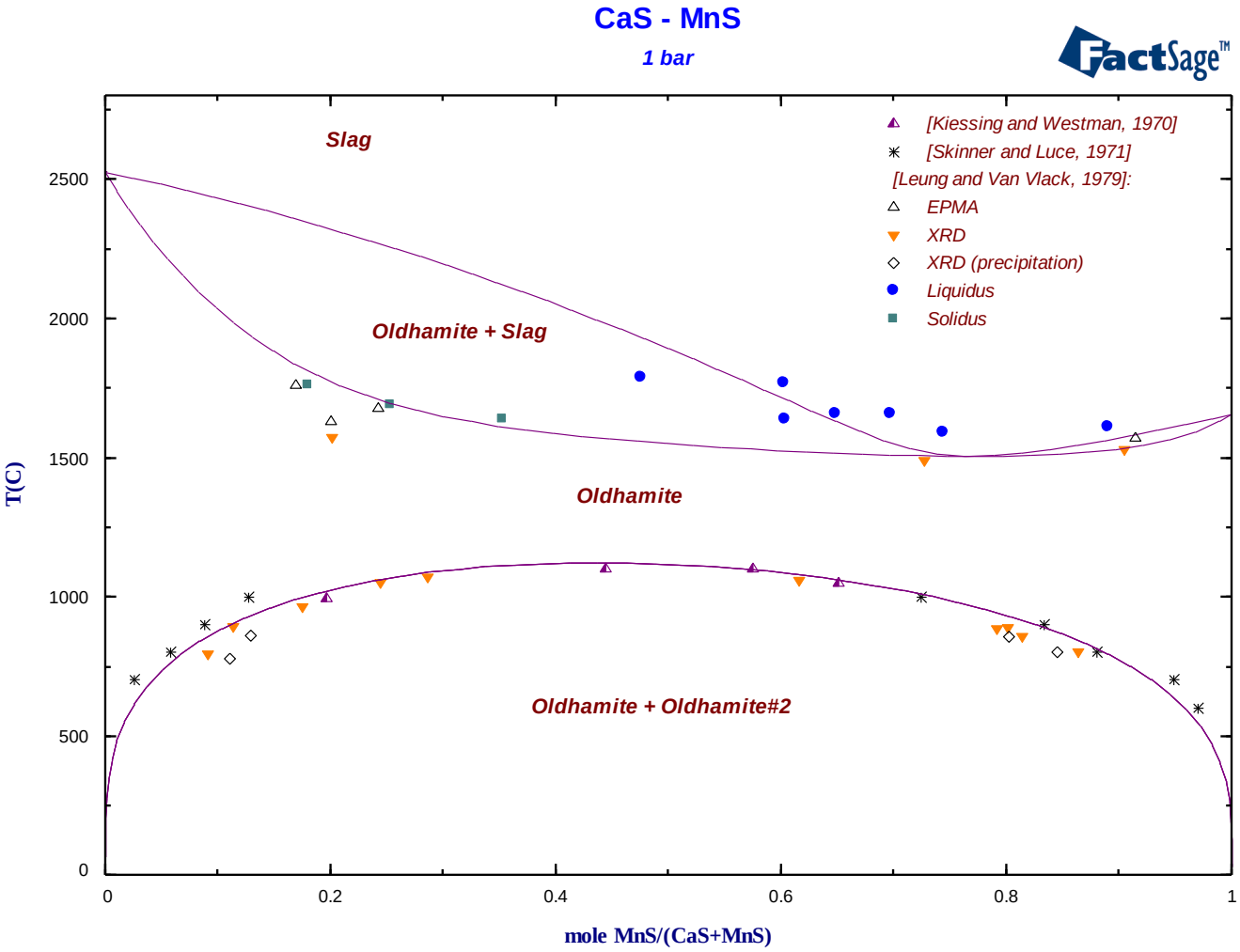

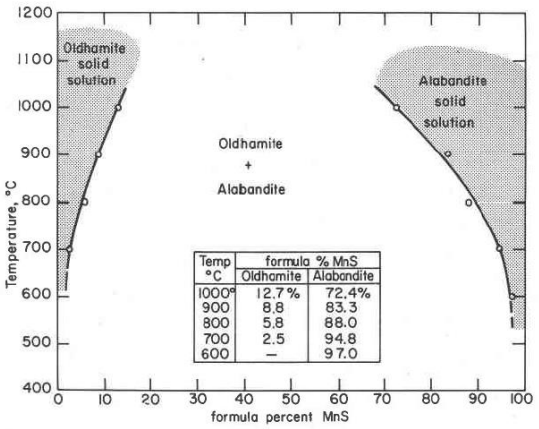

B.J. Skinner, F.D. Luck, Amer. Mineral., Vol.56 (1971), pp. 1269-1296.

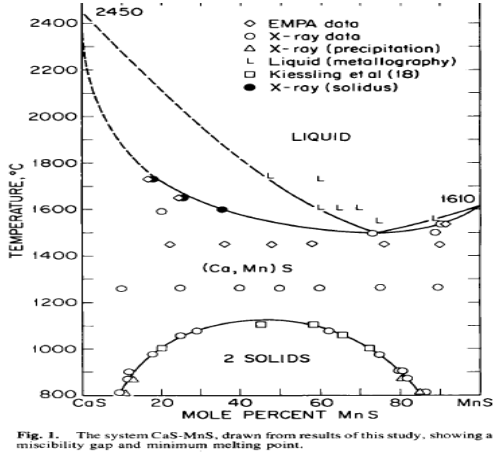

Fig. 1. The system CaS-MnS, drawn from results of this study, showing a miscibility gap and minimum melting point.

C.-H. Leung and L-H. van Vlack, J. Am. Ceram. Soc., 62 [11-12], (1979), pp.613-616.

Weight percent

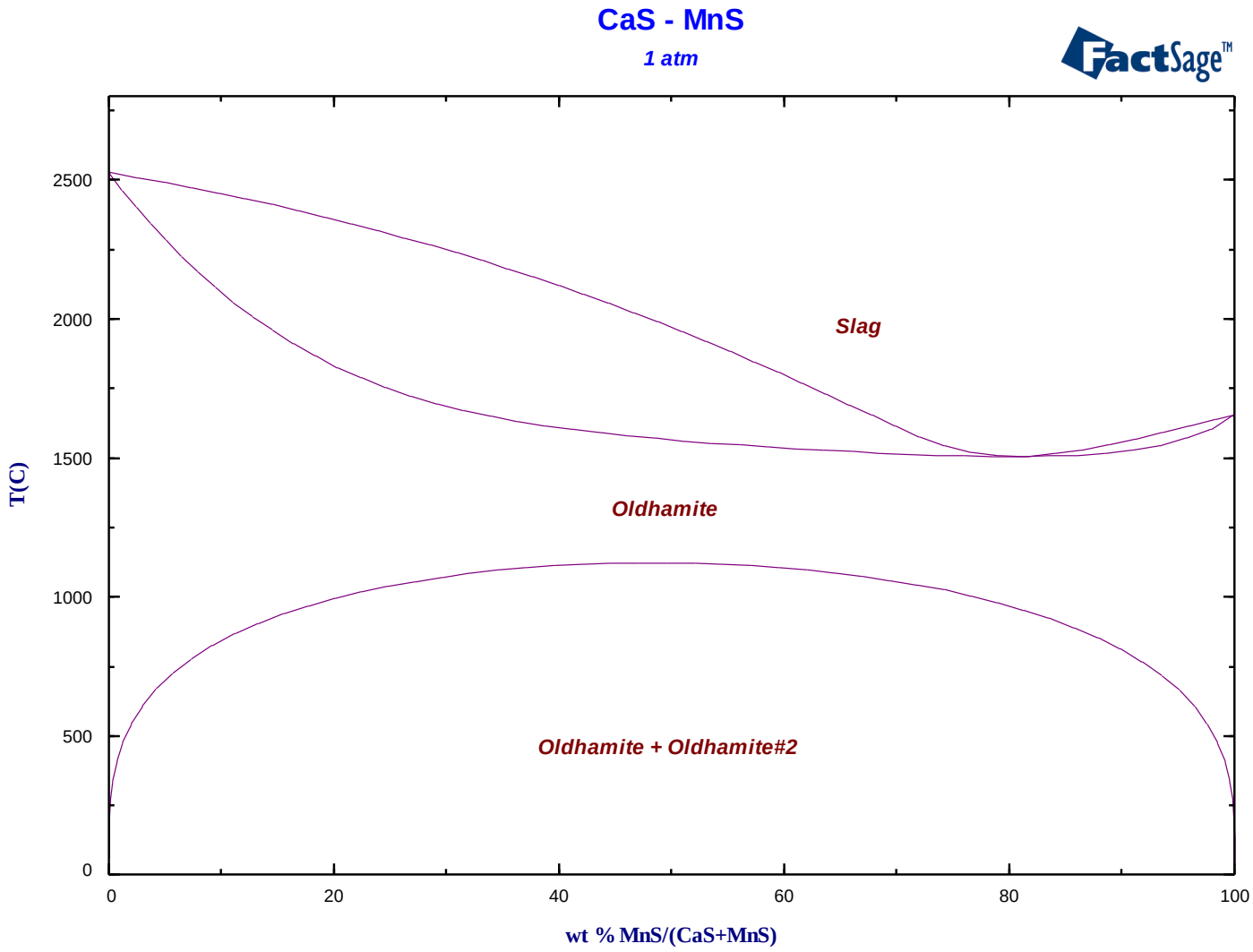

Mole fraction

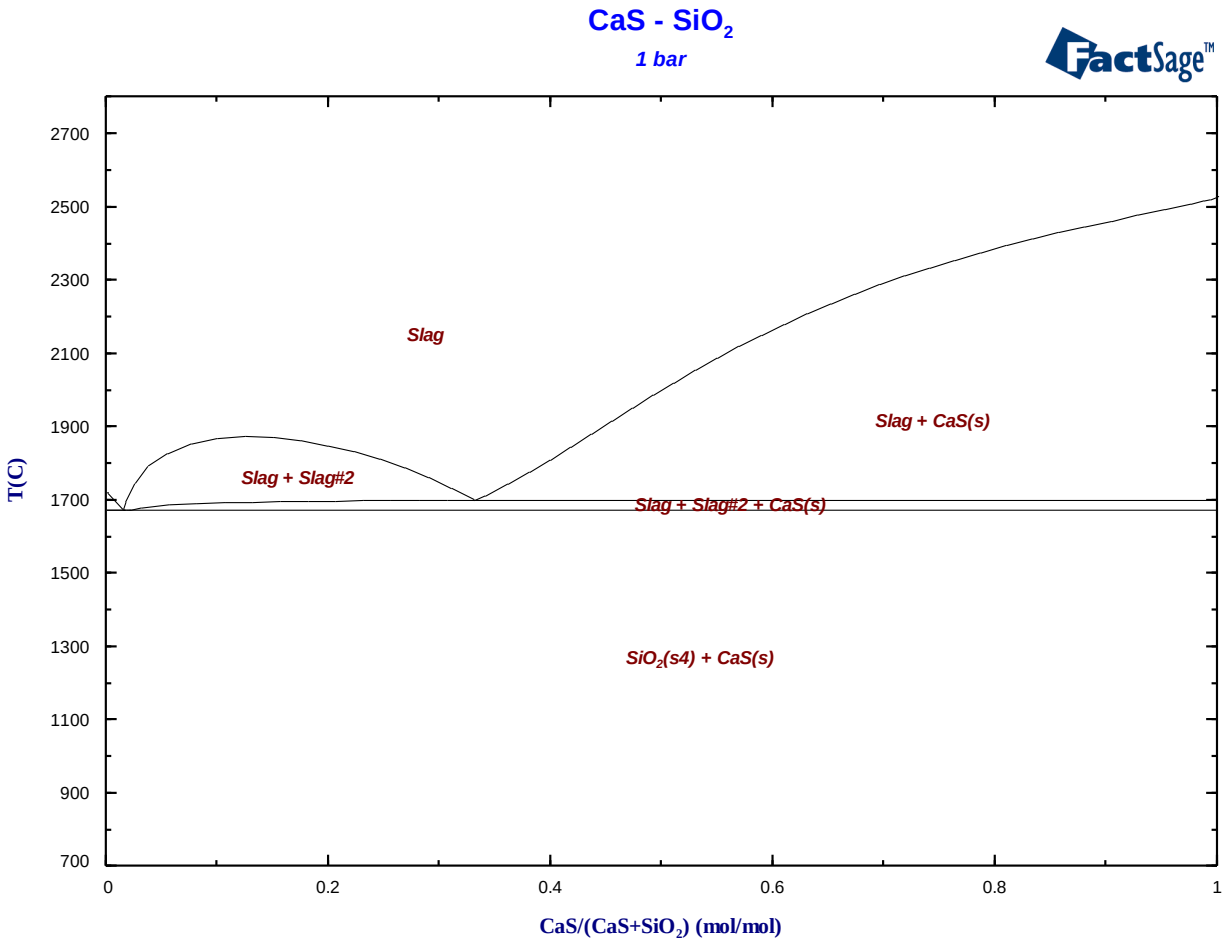

Weight percent

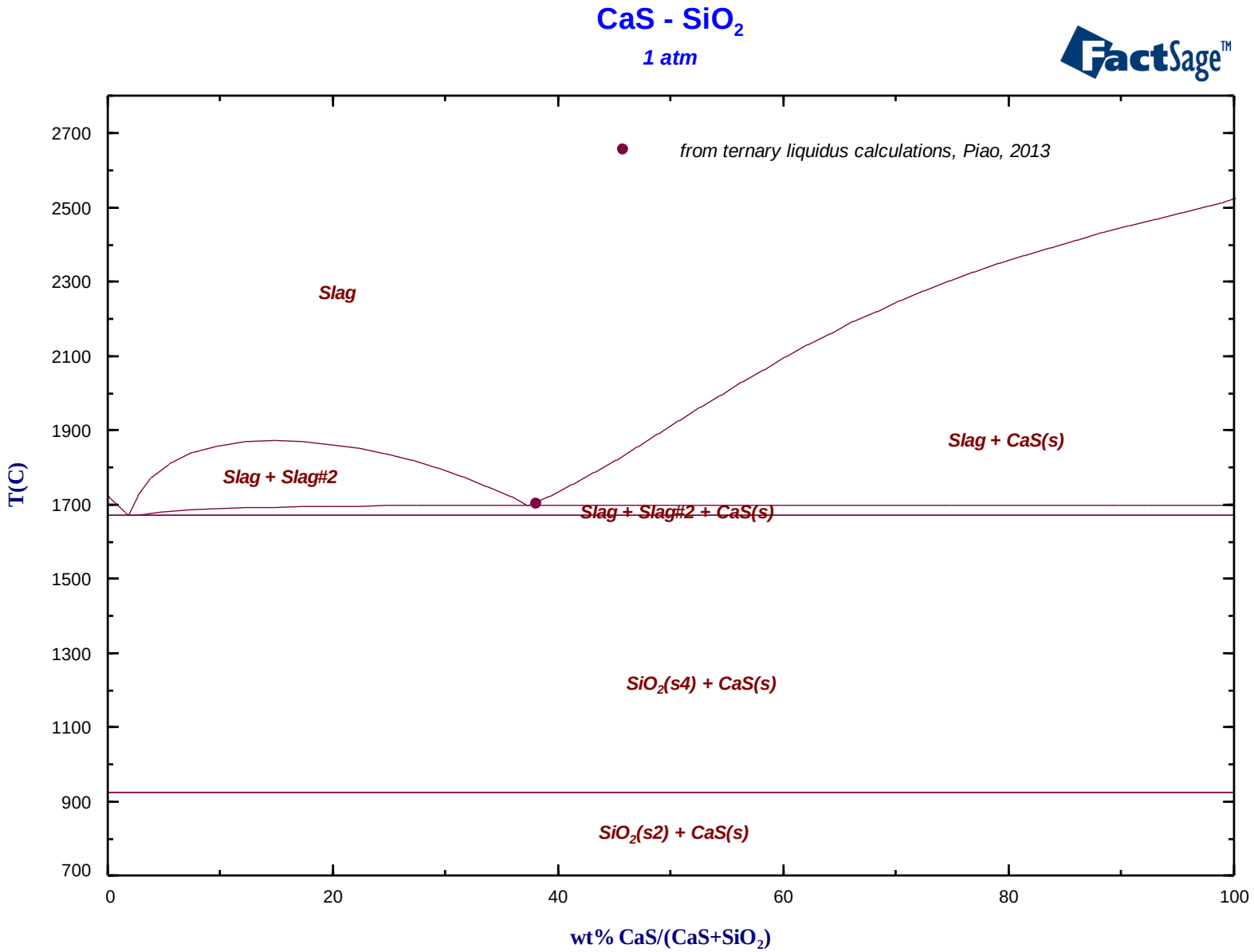

Mole fraction

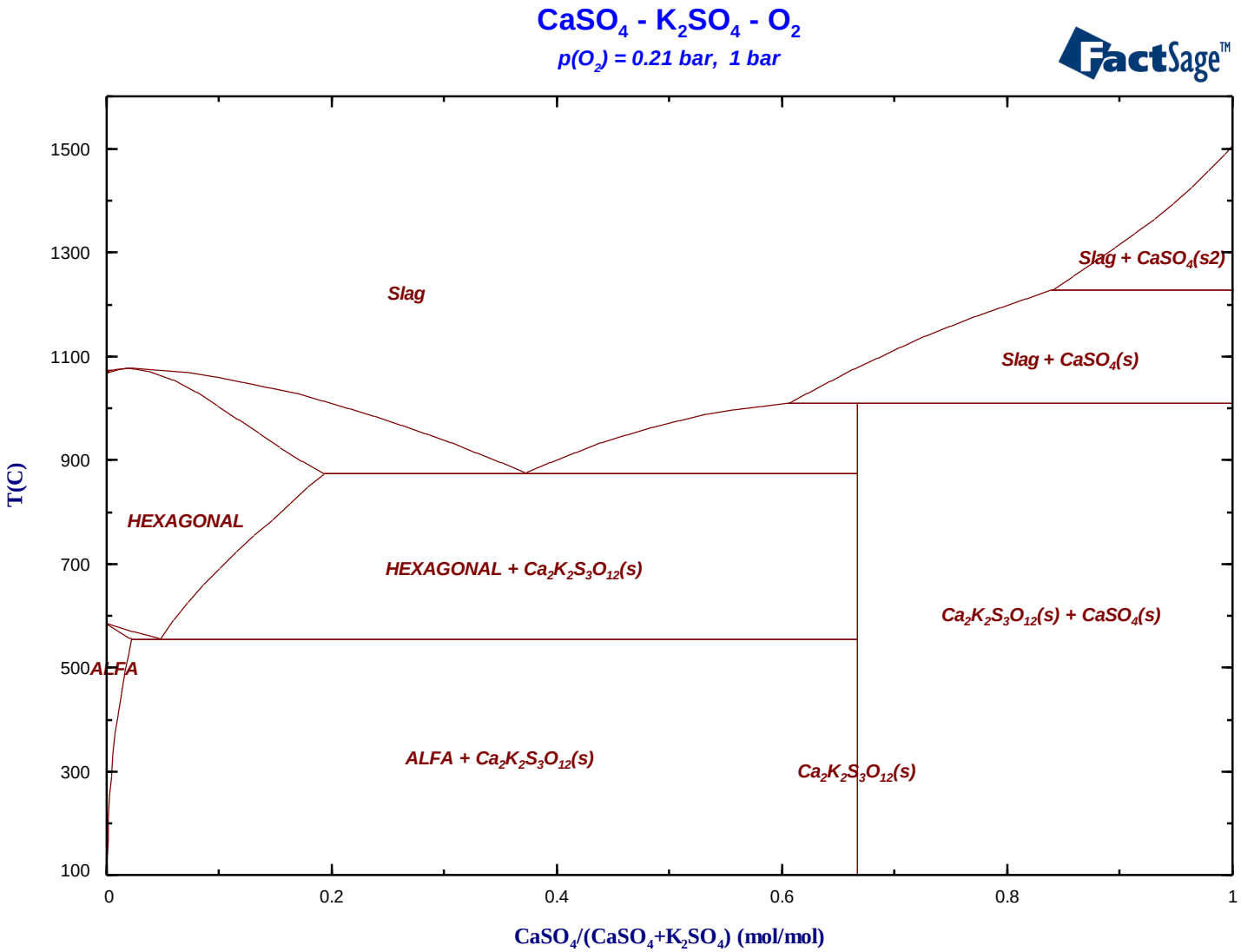

Weight percent
compared with experimental data

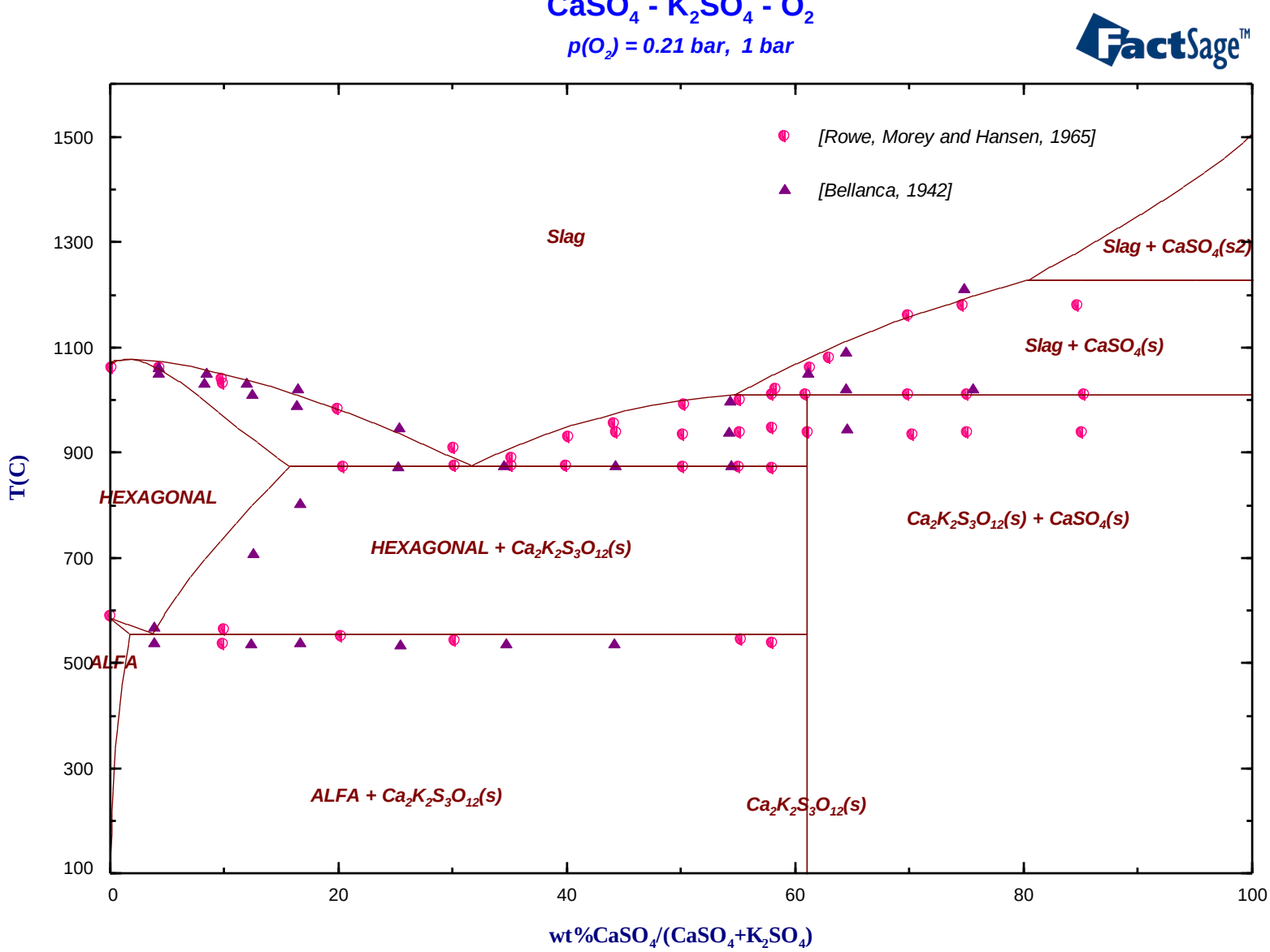

Weight percent
compared with experimental data

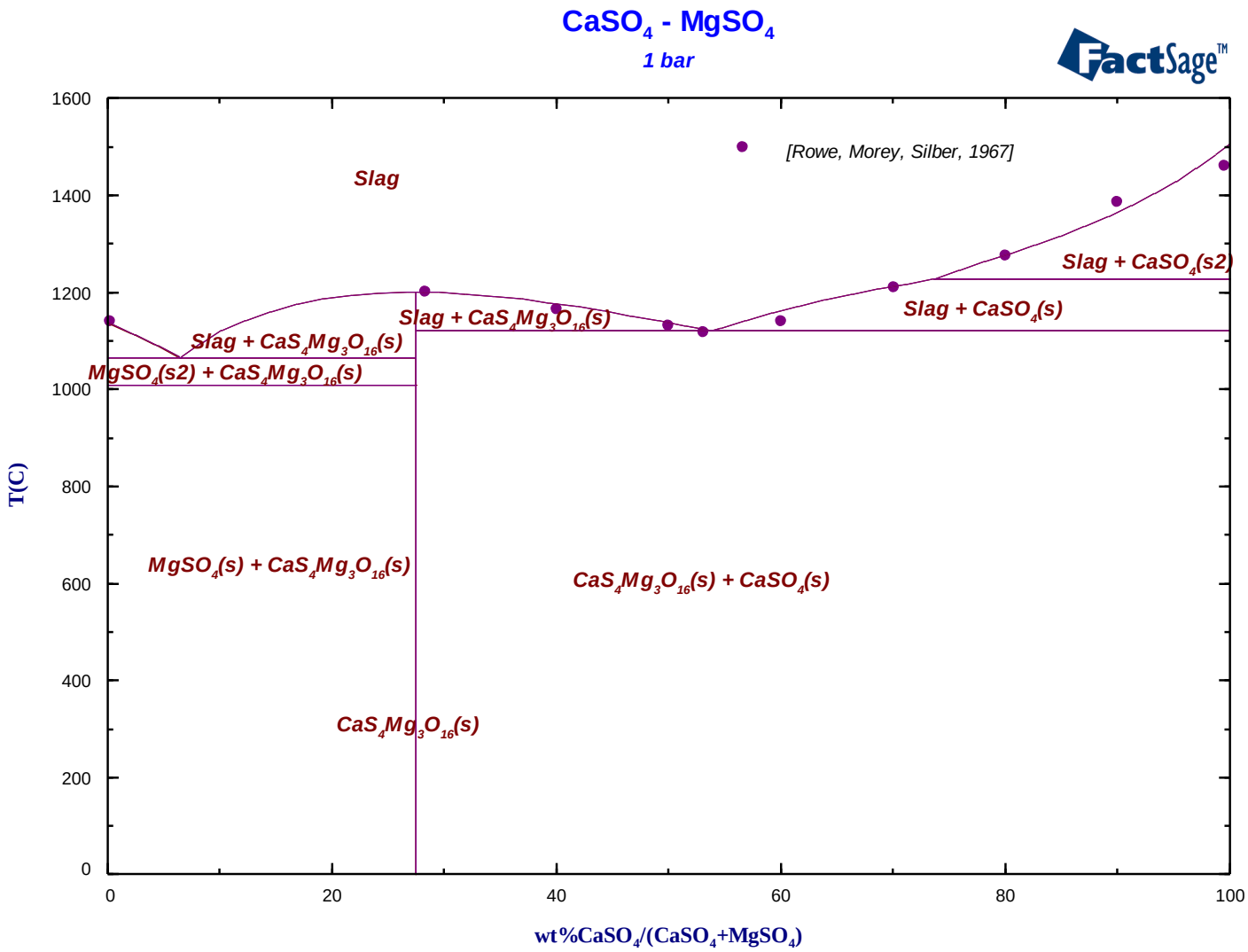

Mole fraction

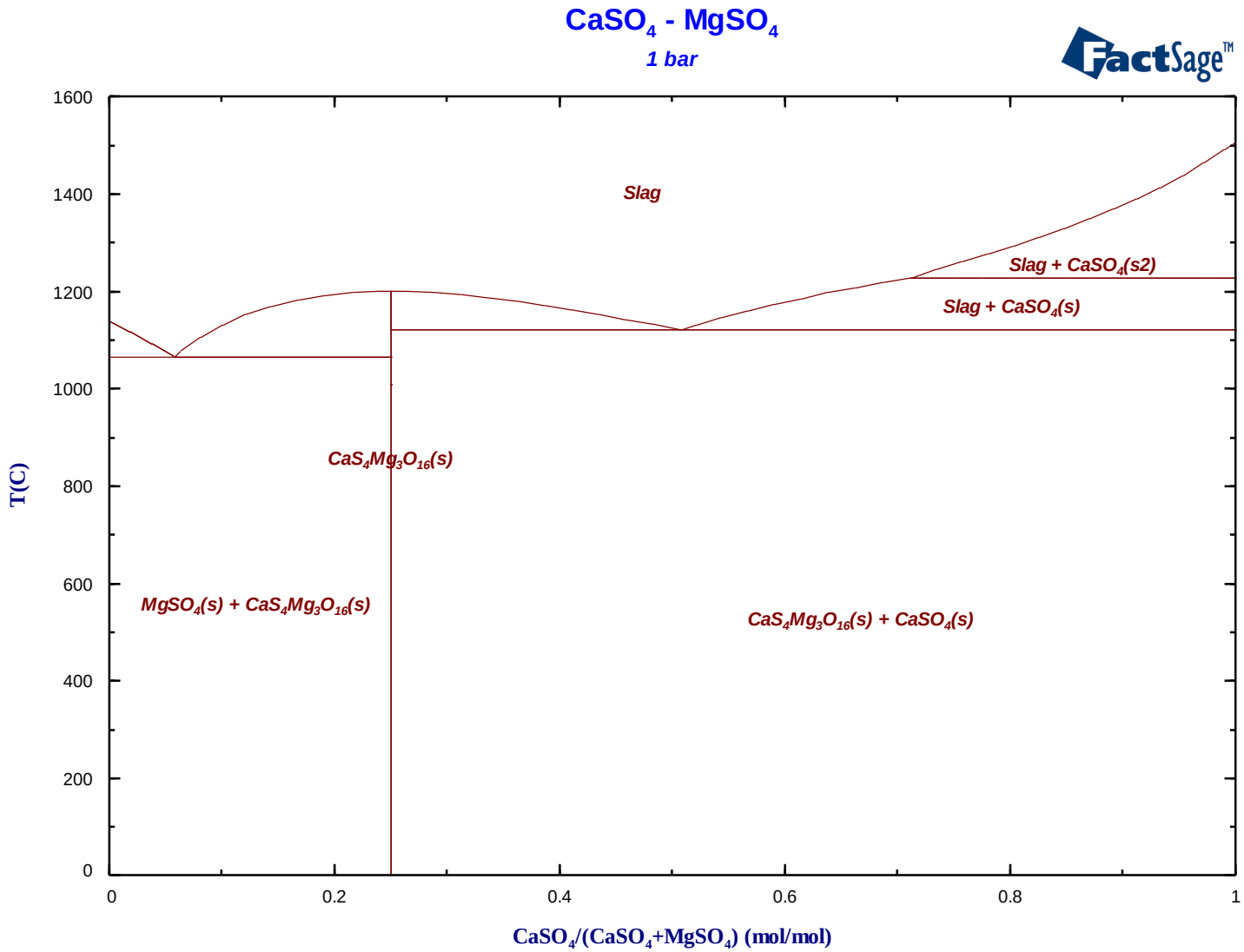

Weight percent
compared with experimental data

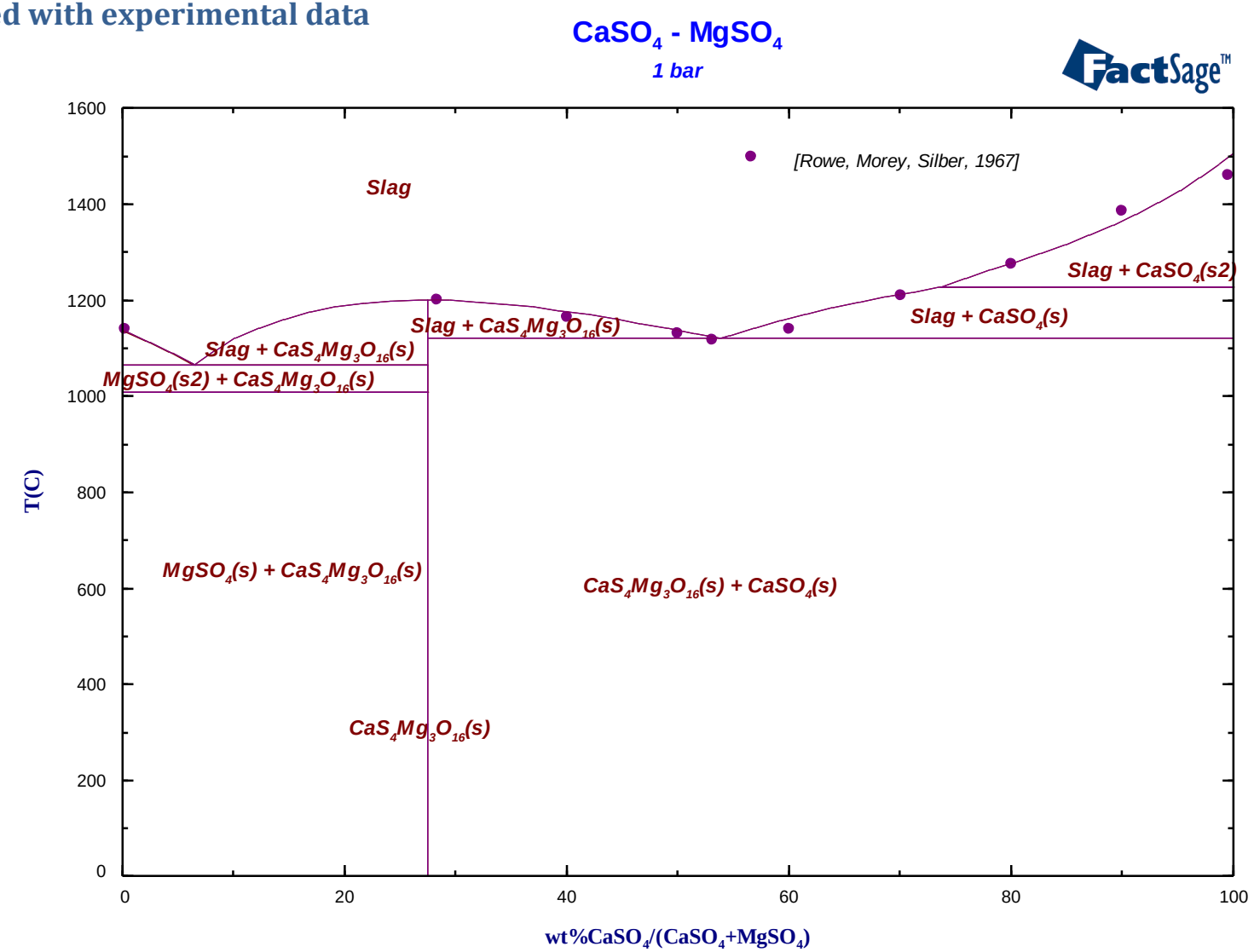

Mole fraction
compared with experimental data

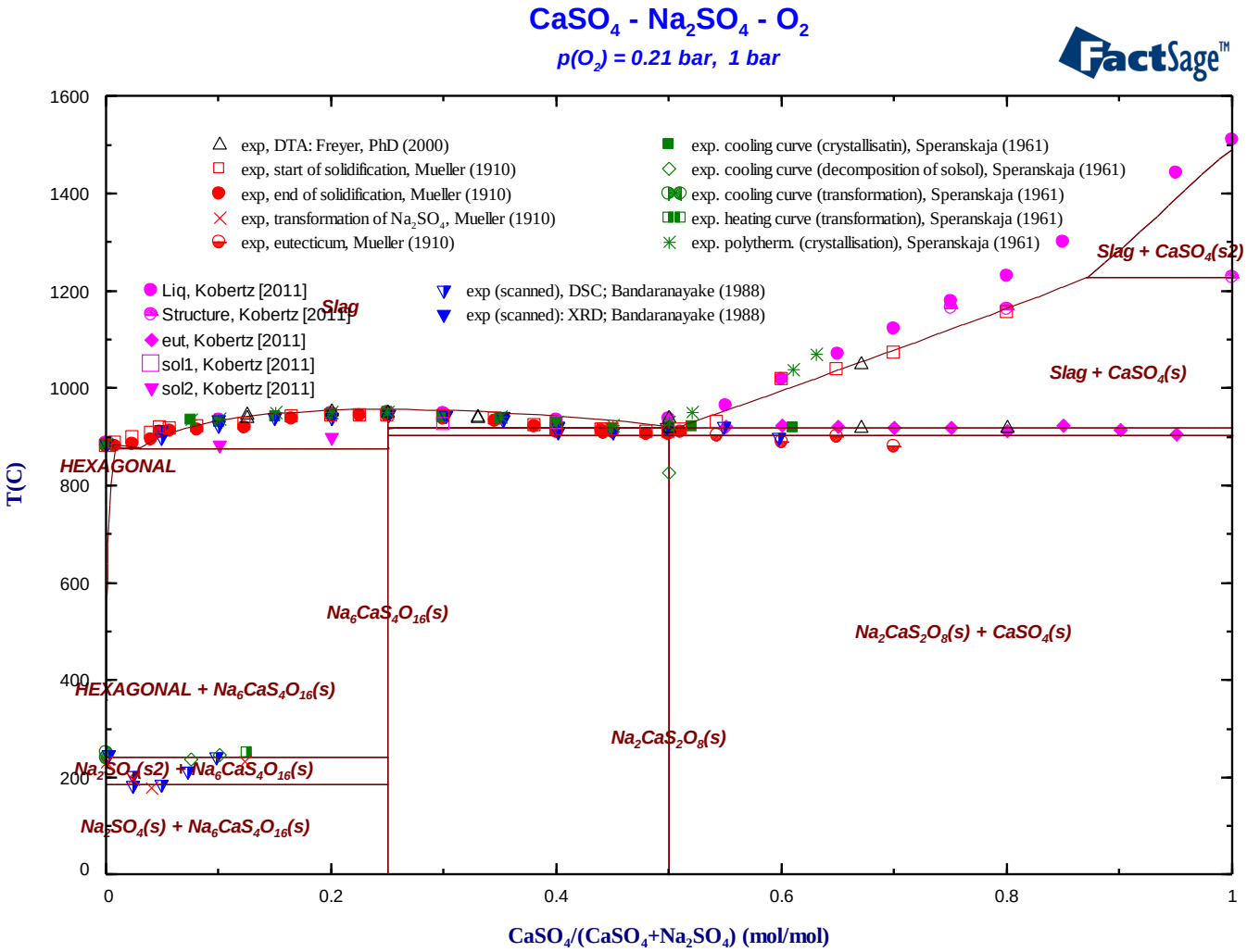

Weight percent

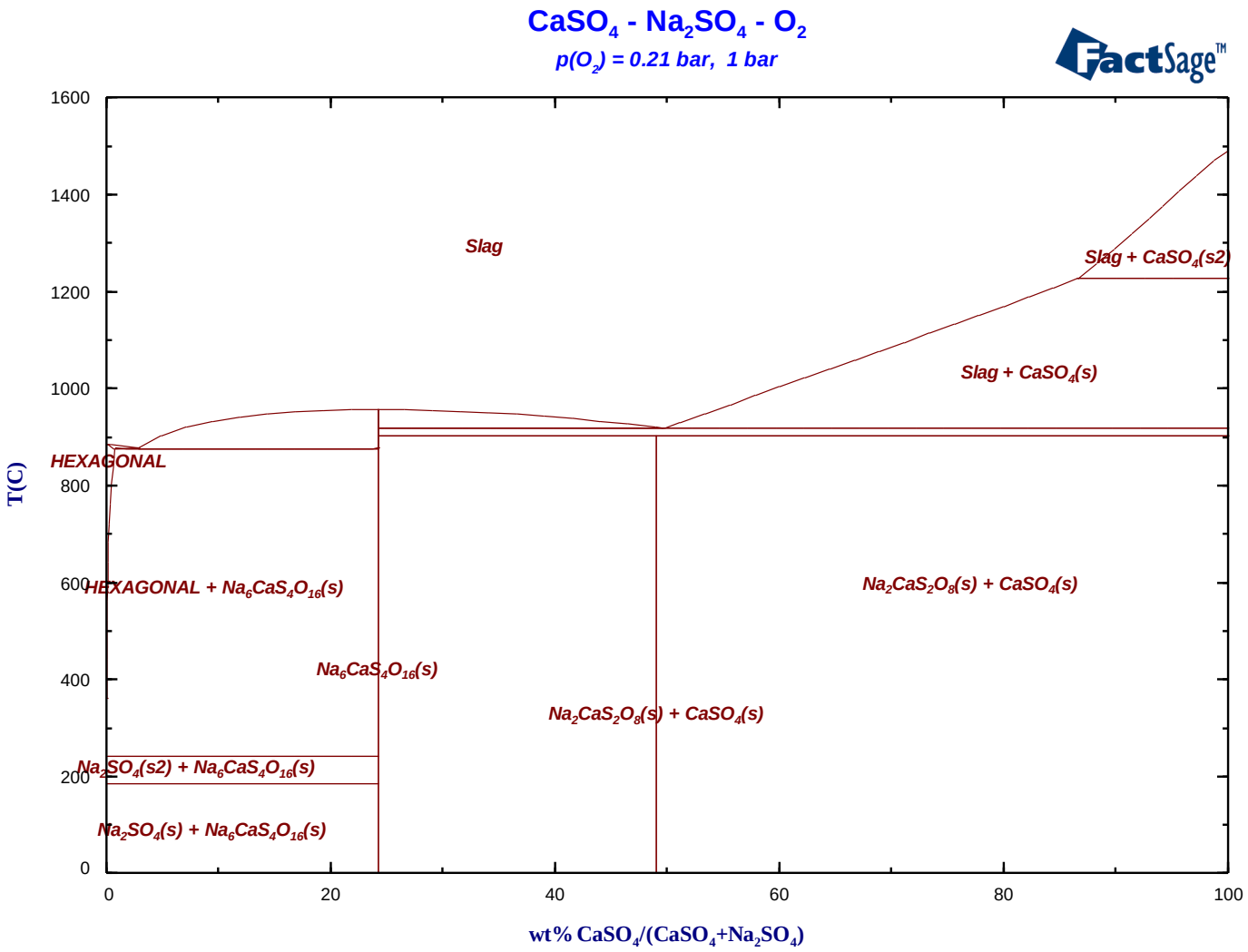

Mole fraction
compared with experimental data

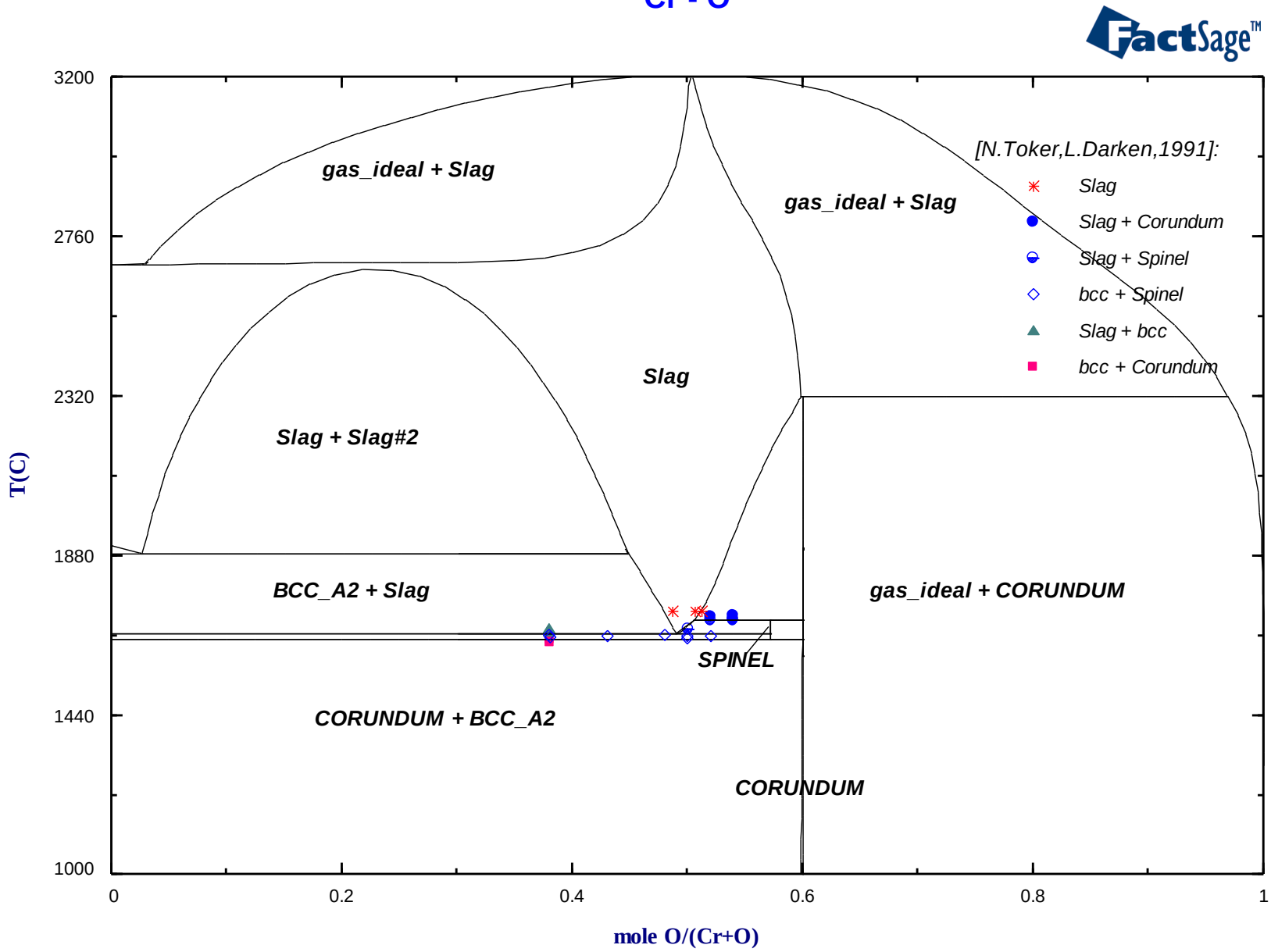

Weight percent

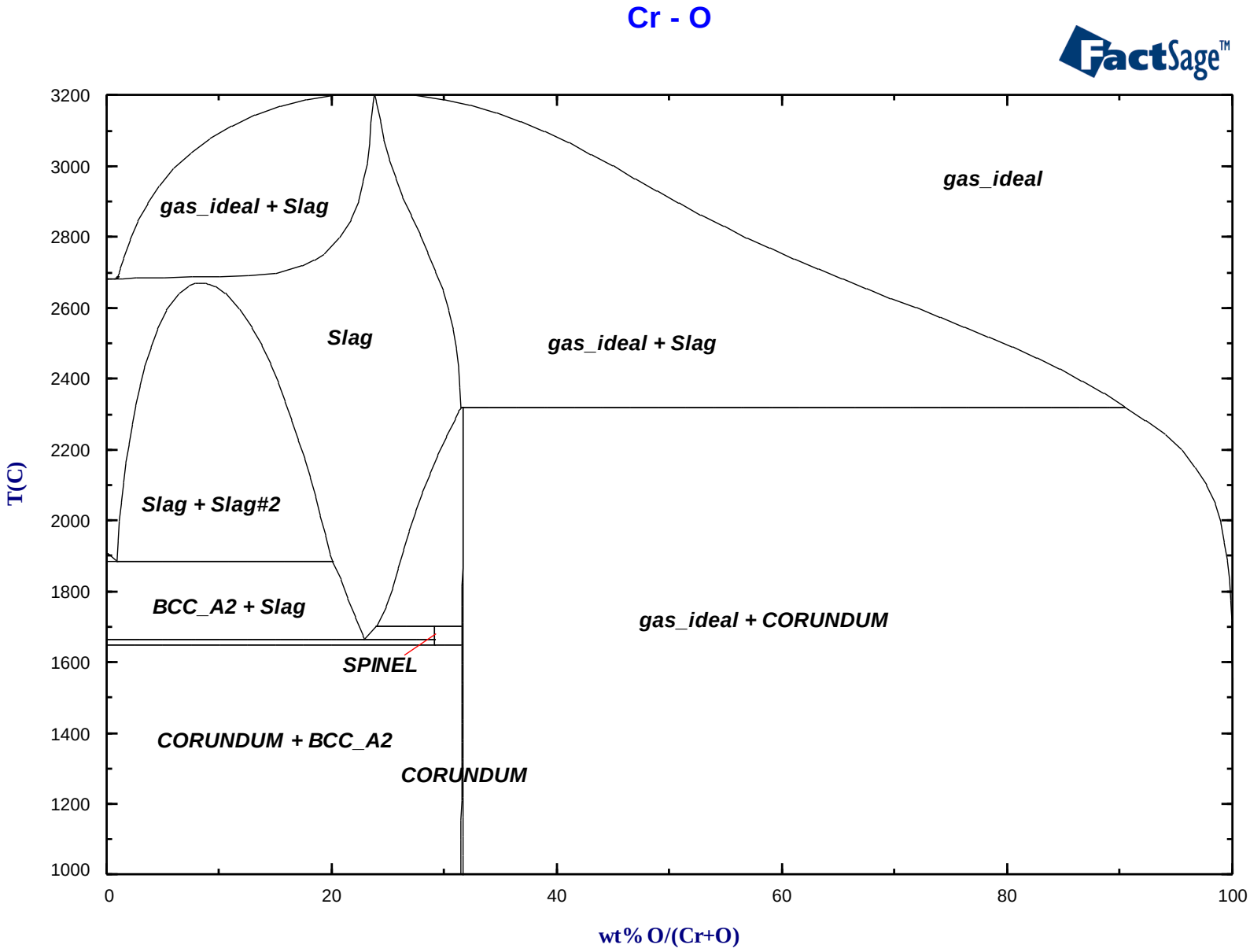

Mole fraction with isobars

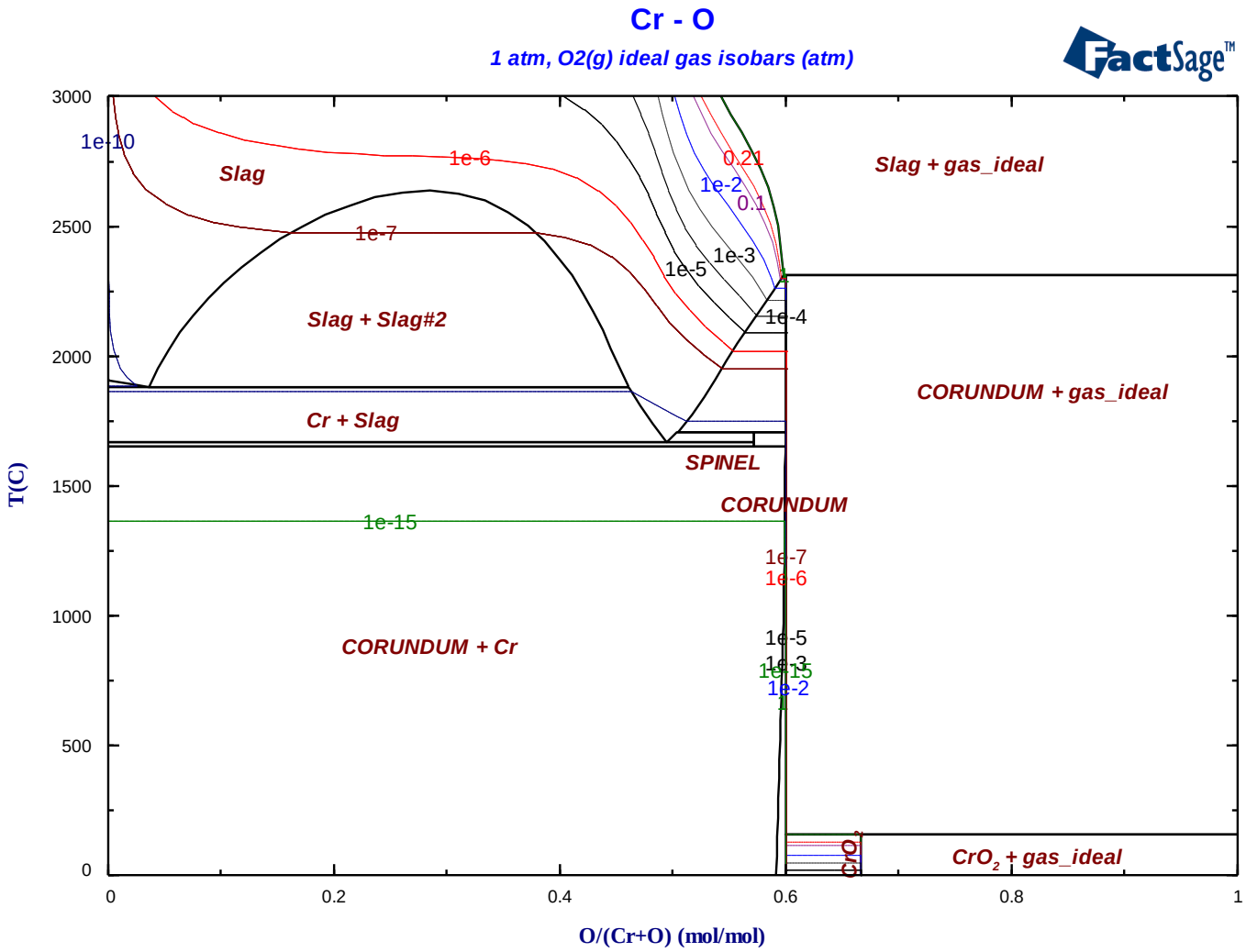

Cr-O2,
Temperature vx. log P(O2) diagram

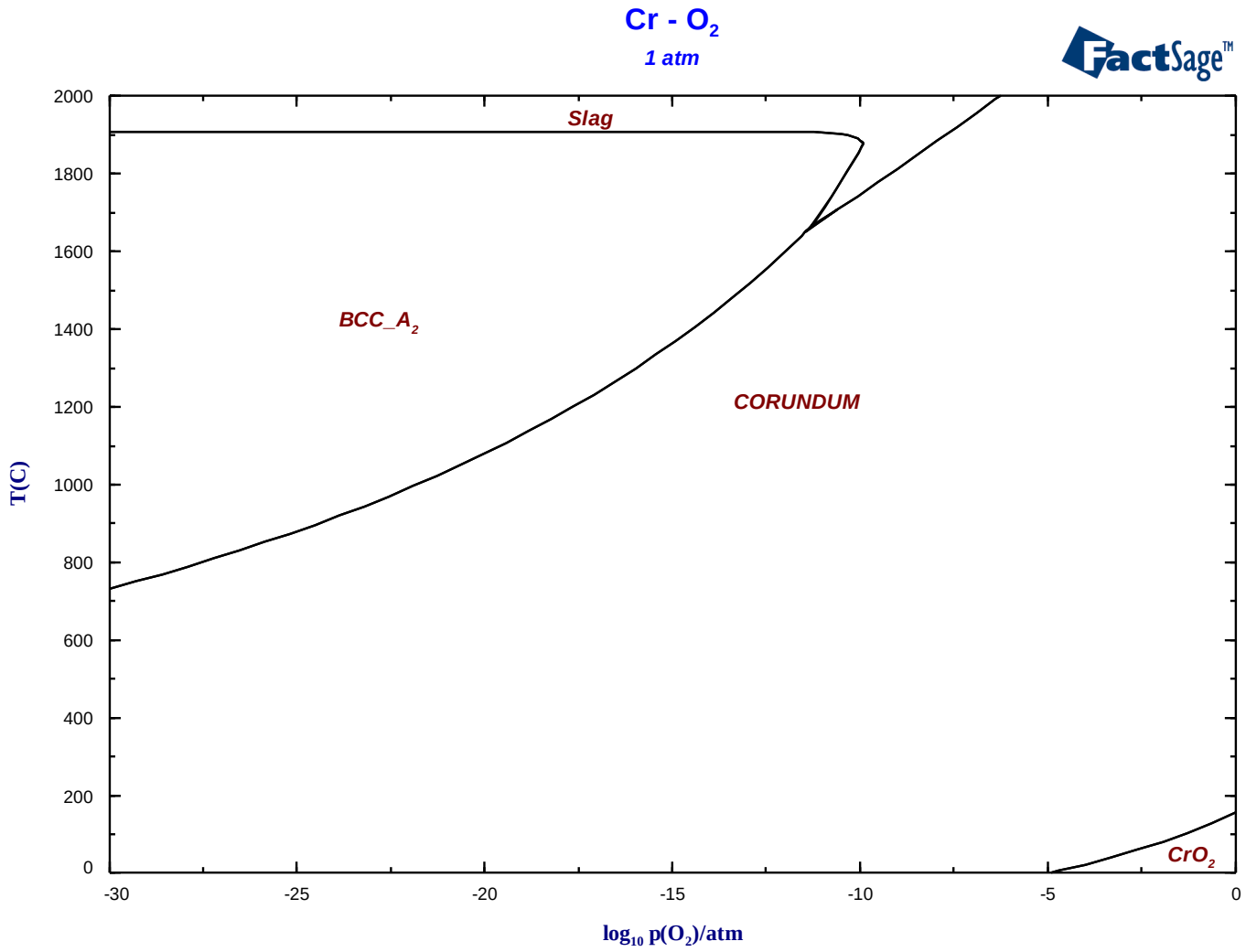

Mole fraction
compared with experimental data

Fe_2O_3 - Cr_2O_3 - O_2

$p(O_2)$ = 0.21 atm

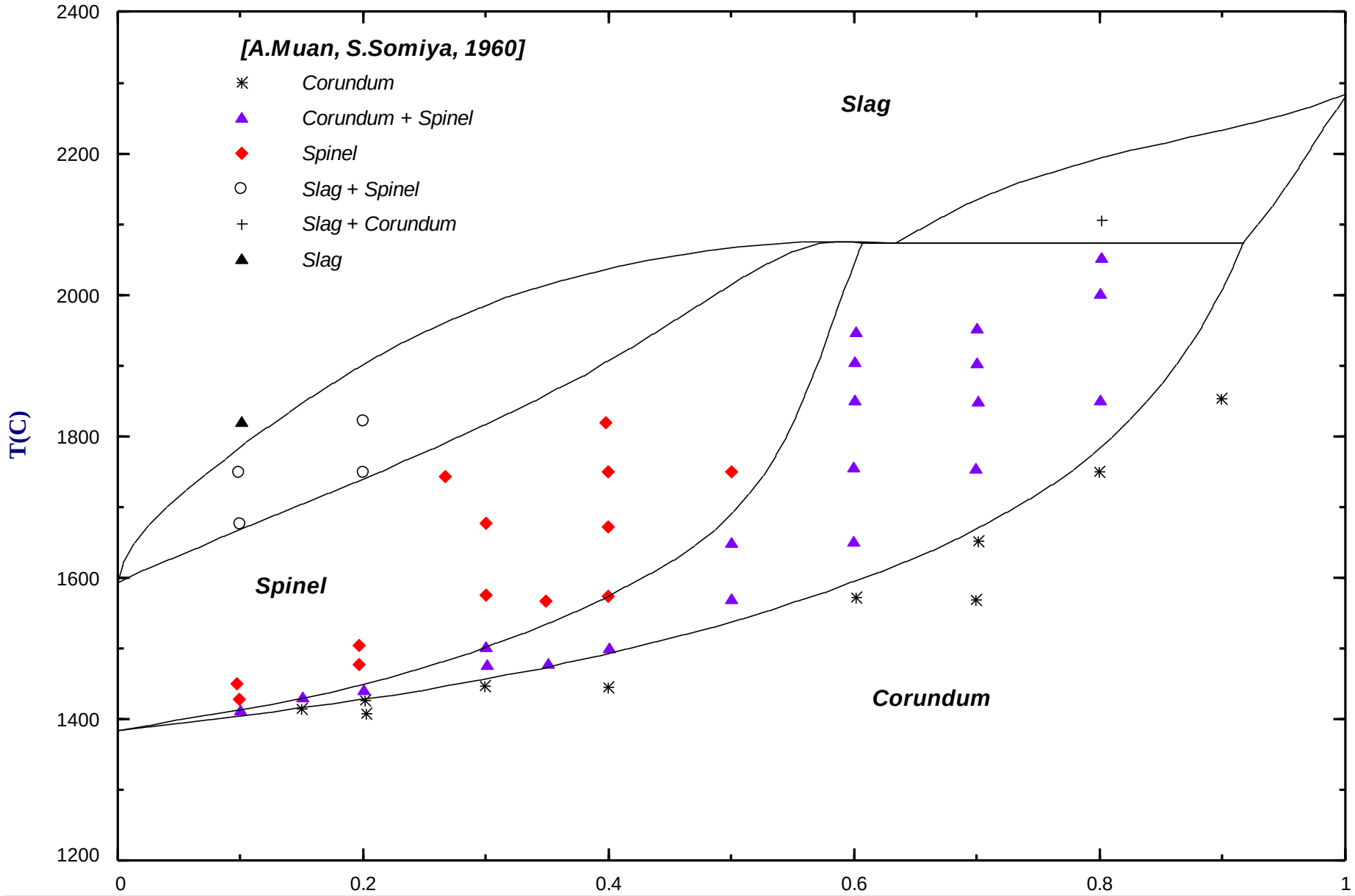

Weight percent

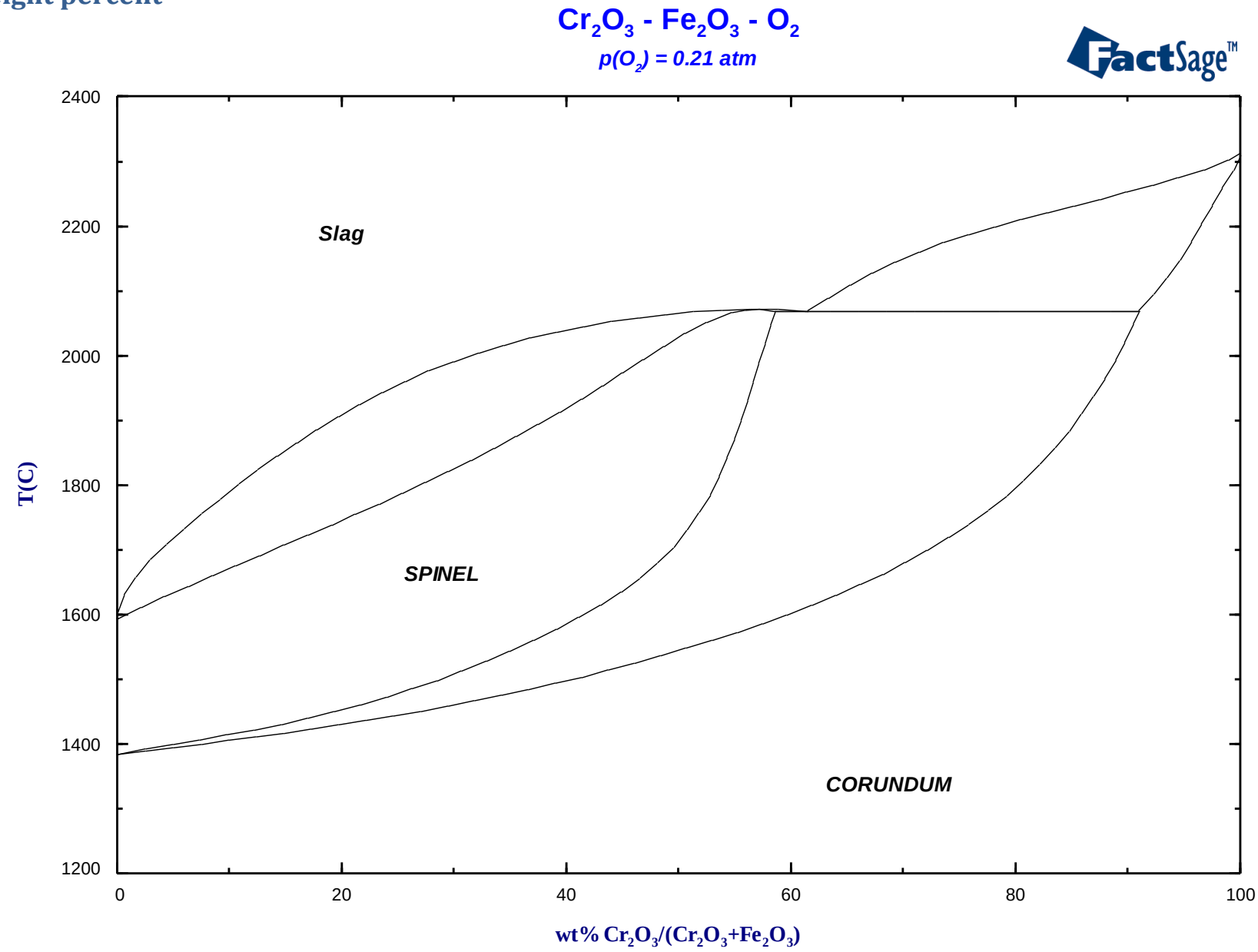

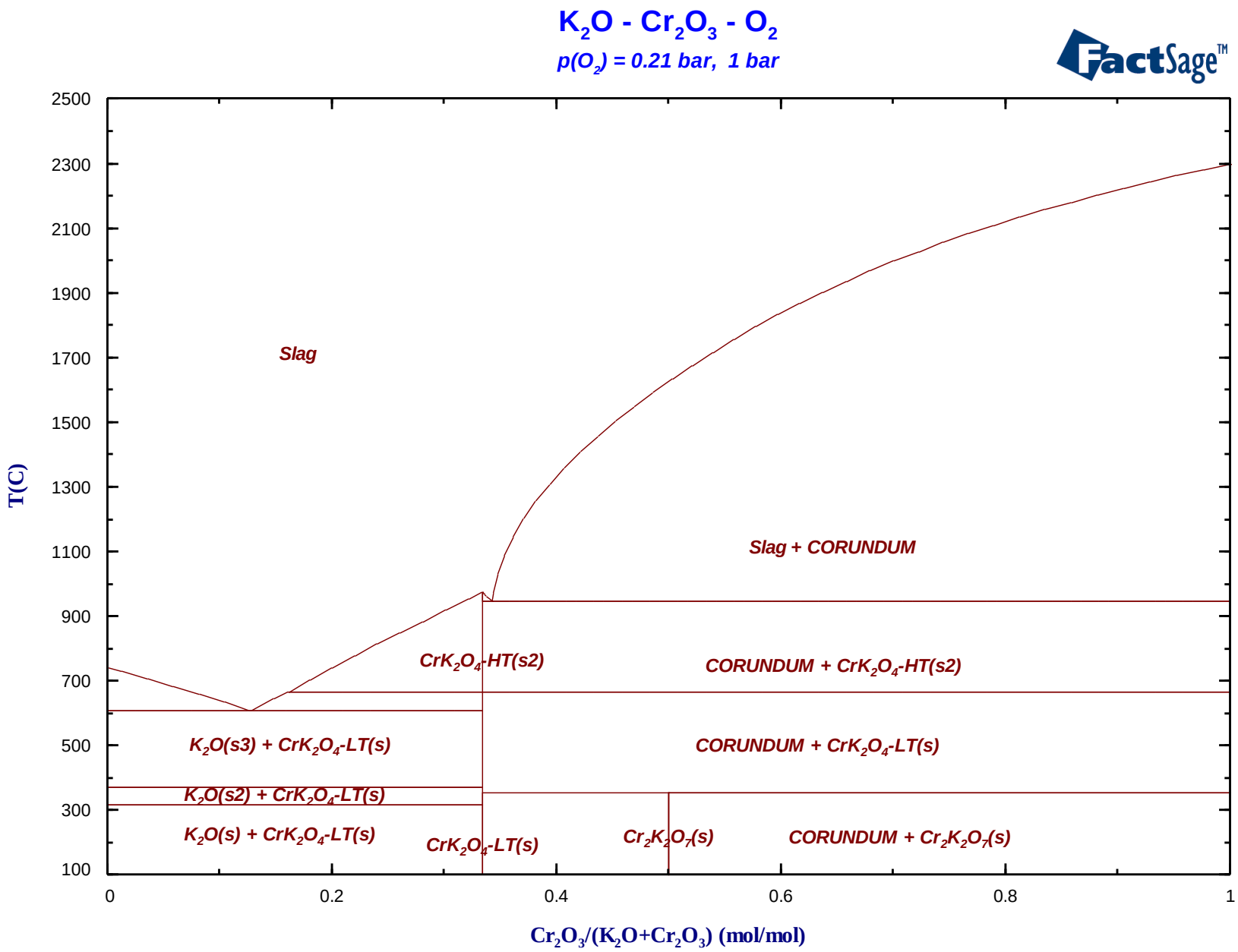
K2O - Cr2O3 - O2
p(O2) = 0.21 bar, 1 bar
FactSage™
T(C)
2500
2300
2100
1900
1700
1500
1300
1100
900
700
500
300
100
0
0.2
0.4
0.6
0.8
1
Cr2O3/(K2O+Cr2O3) (mol/mol)
Slag
Slag + CORUNDUM
CrK2O4-HT(s2)
CORUNDUM + CrK2O4-HT(s2)
K2O(s3) + CrK2O4-LT(s)
CORUNDUM + CrK2O4-LT(s)
K2O(s2) + CrK2O4-LT(s)
K2O(s) + CrK2O4-LT(s)
CrK2O4-LT(s)
Cr2K2O7(s)
CORUNDUM + Cr2K2O7(s)

Weight percent

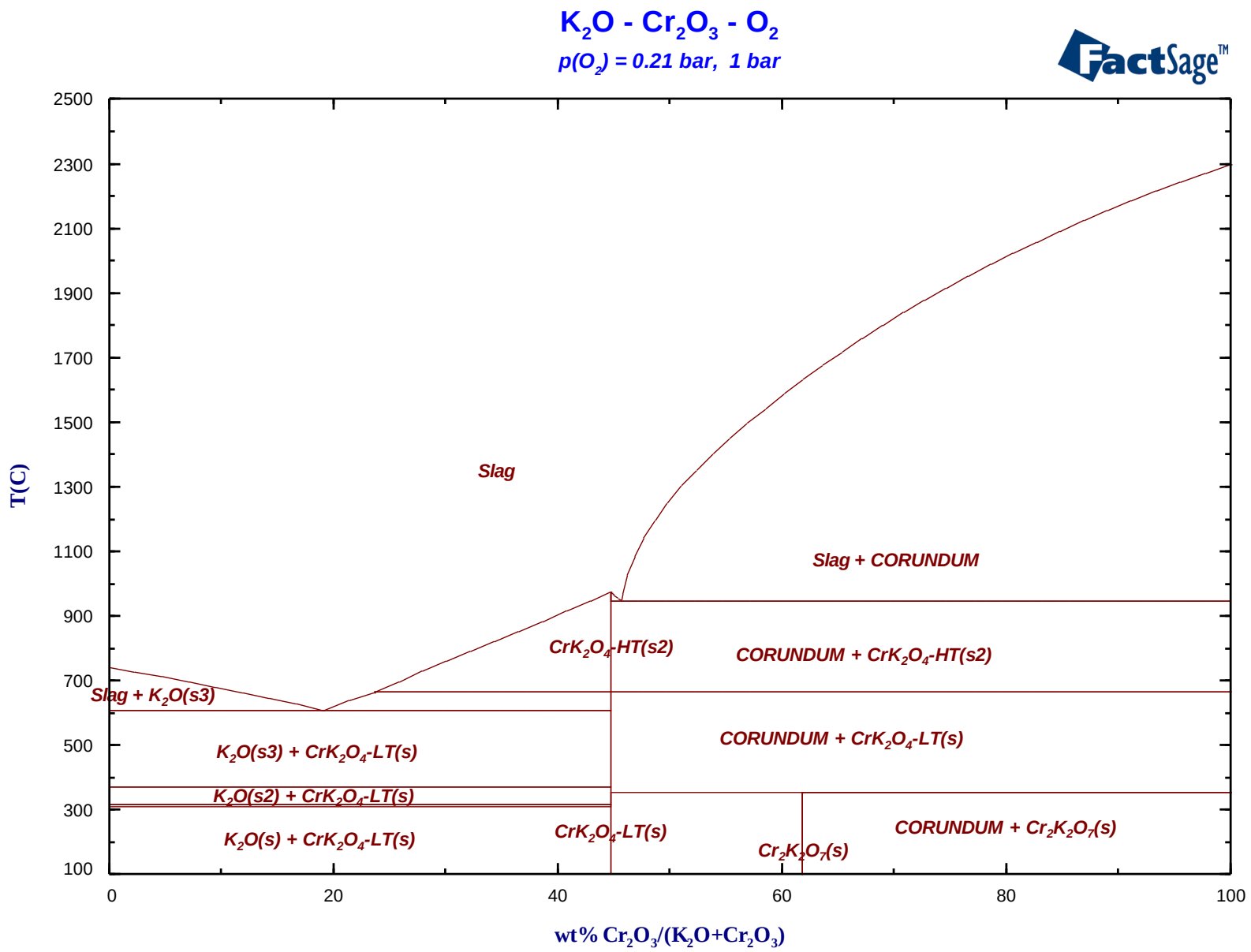

Mole fraction

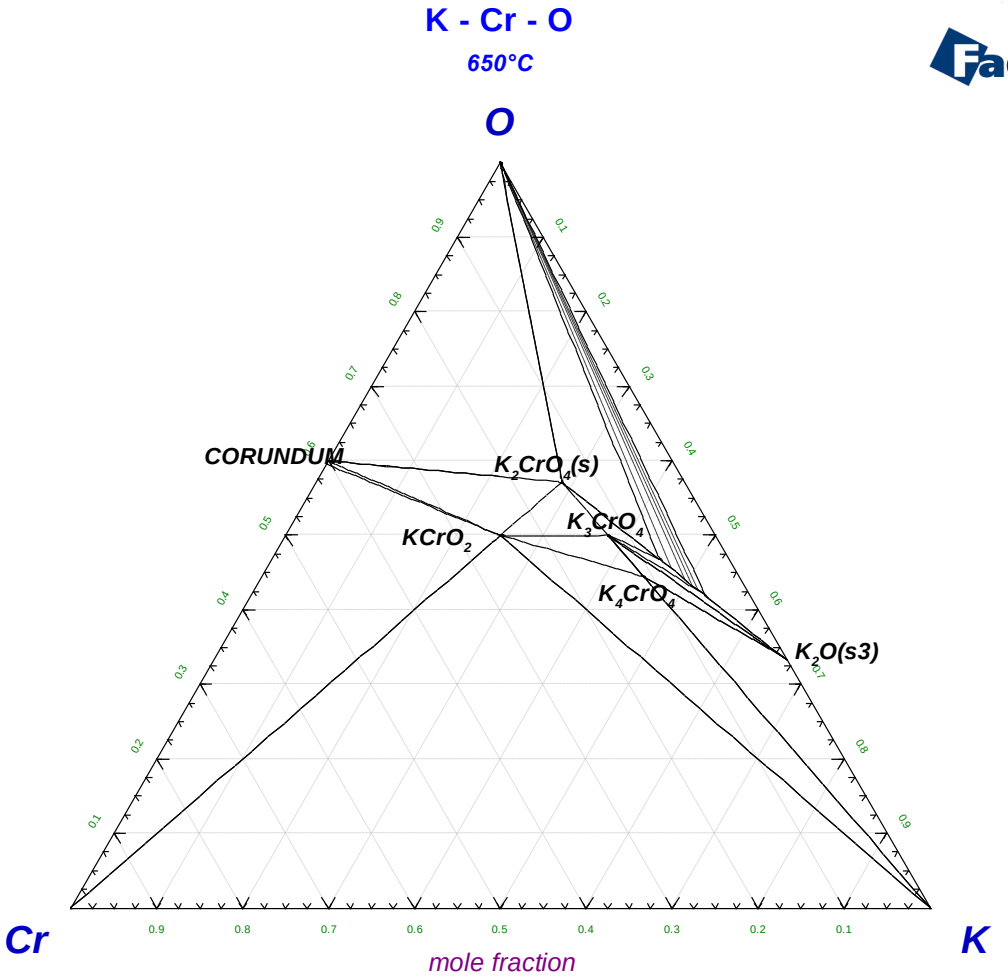

(d)

FactSage™

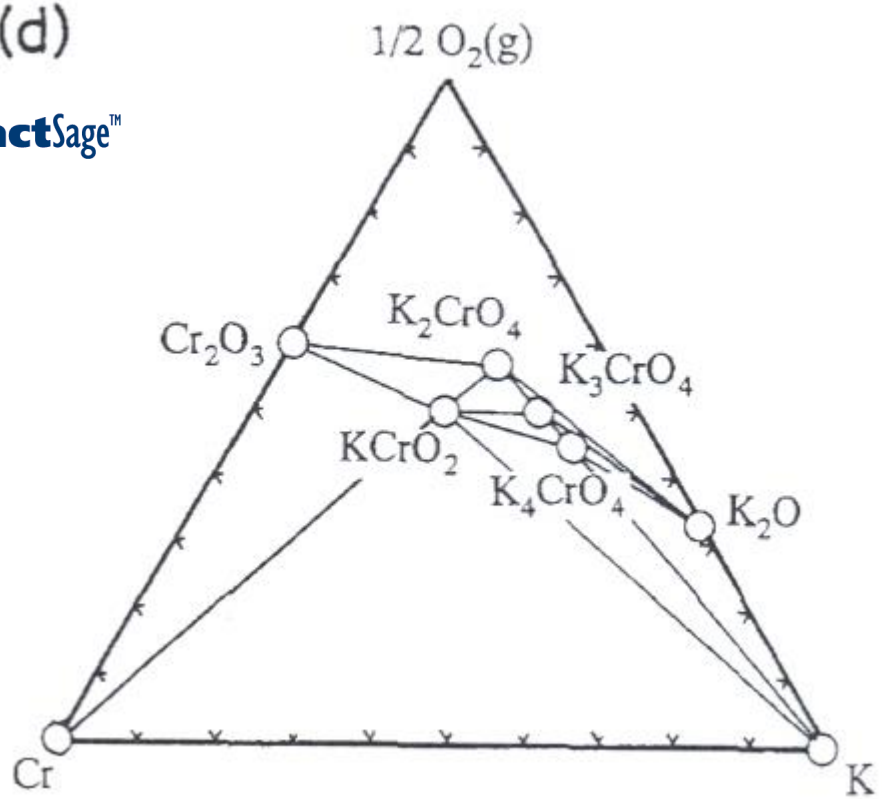

H. Yokokawa, N. Sakai, T. Kawada, M. Dokiya, J. Electrochem. Soc., Vol. 140, No. 12, (1993), pp. 3565-3577.

Mole fraction

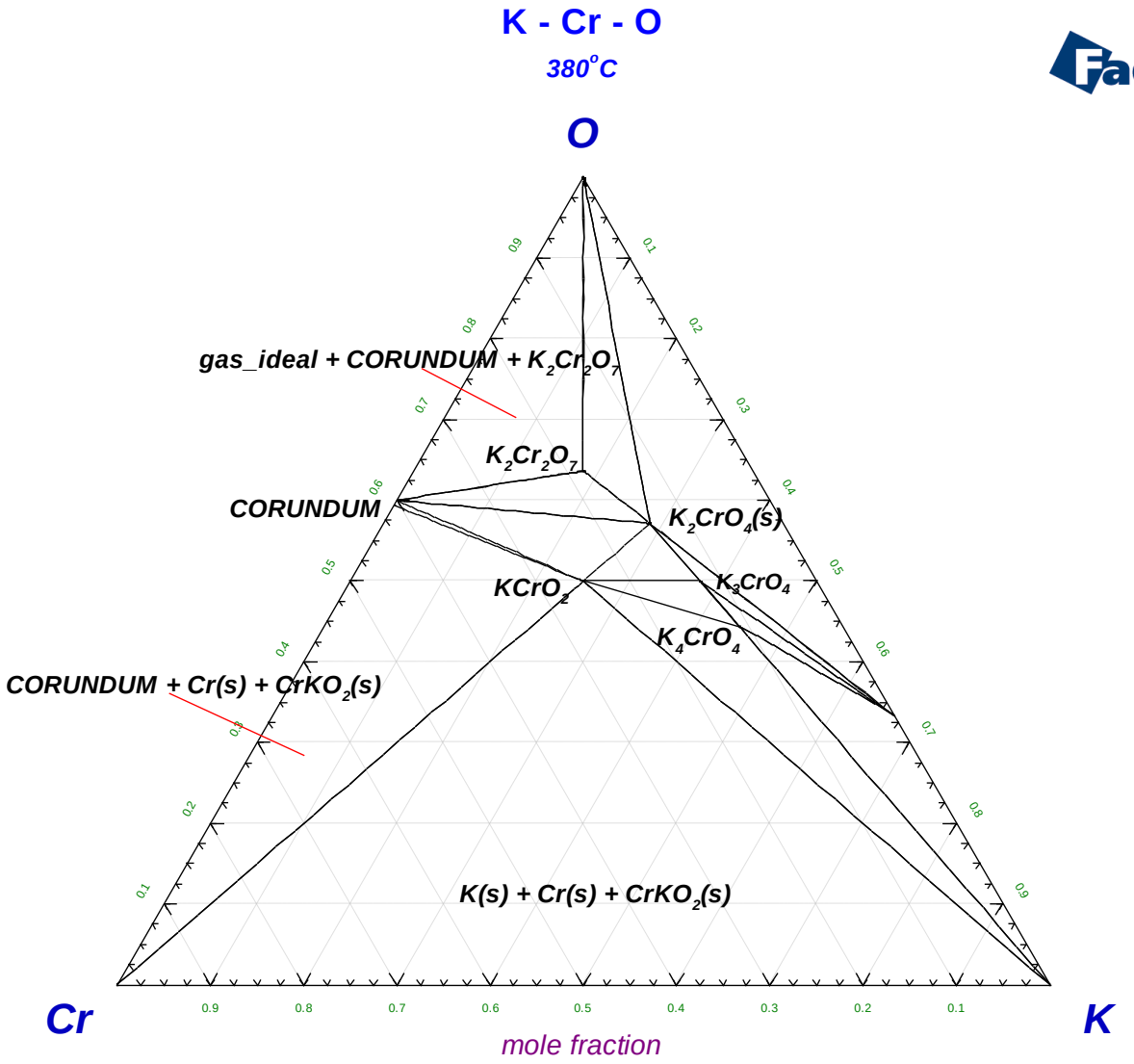

Mole fraction
Isopleth K2Cr2O7-K2CrO4

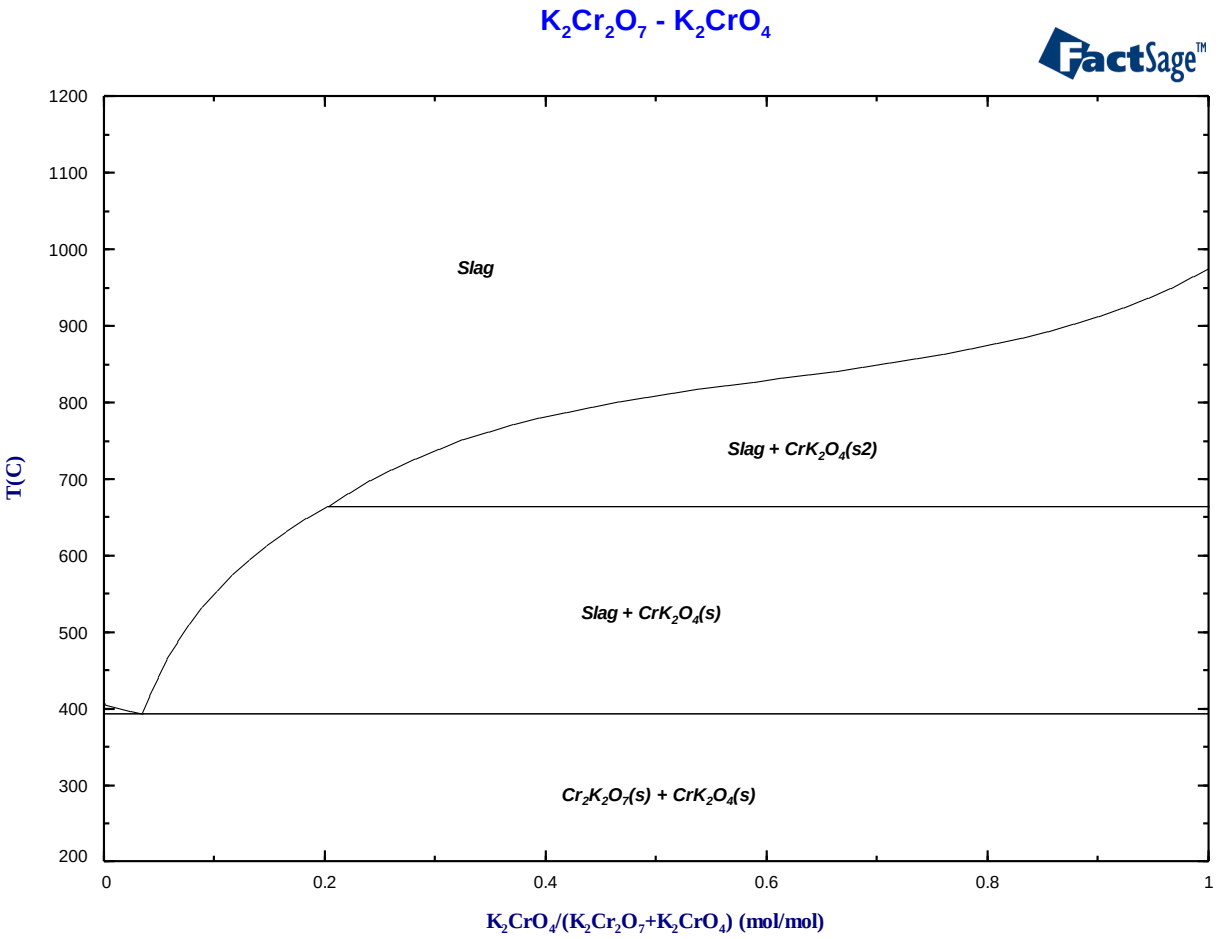

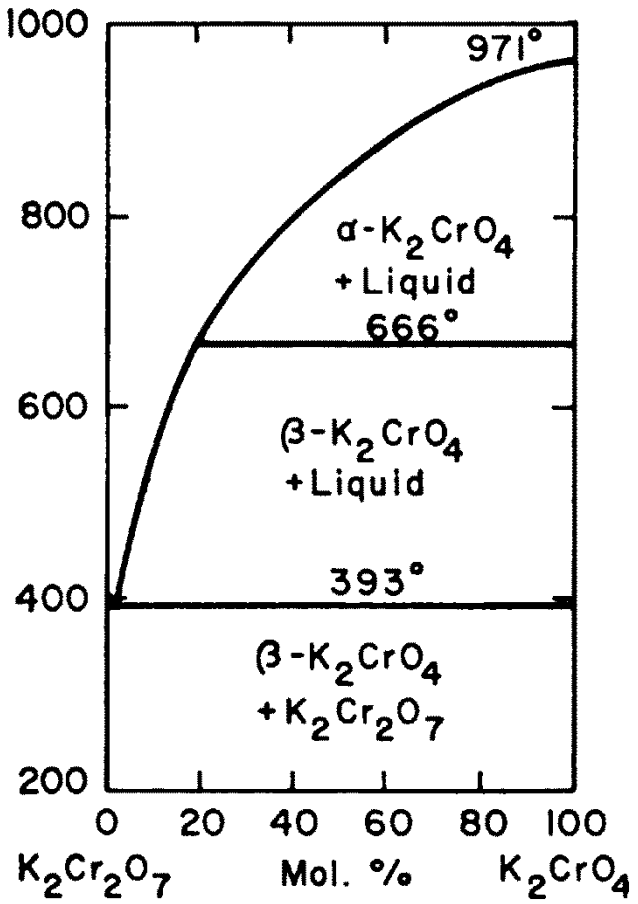

E. Groschuff, Z. Anorg. Chem., 58 [1], (1908), pp.102-112.

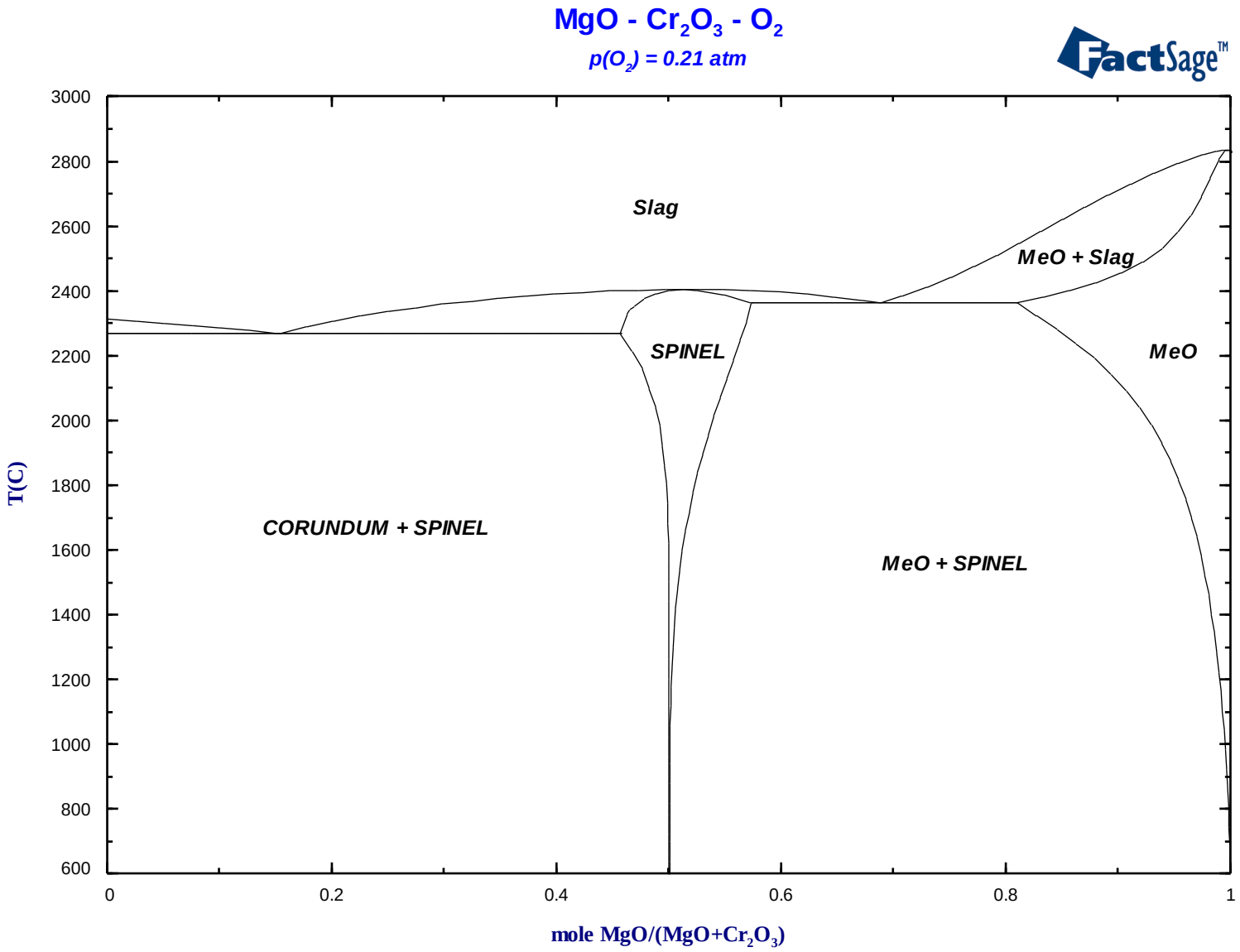
MgO - Cr2O3 - O2
p(O2) = 0.21 atm
FactSage™
Slag
MeO + Slag
SPINEL
MeO
CORUNDUM + SPINEL
MeO + SPINEL
T(C)
3000
2800
2600
2400
2200
2000
1800
1600
1400
1200
1000
800
600
0
0.2
0.4
0.6
0.8
1
mole MgO/(MgO+Cr2O3)

Weight percent
compared with experimental data

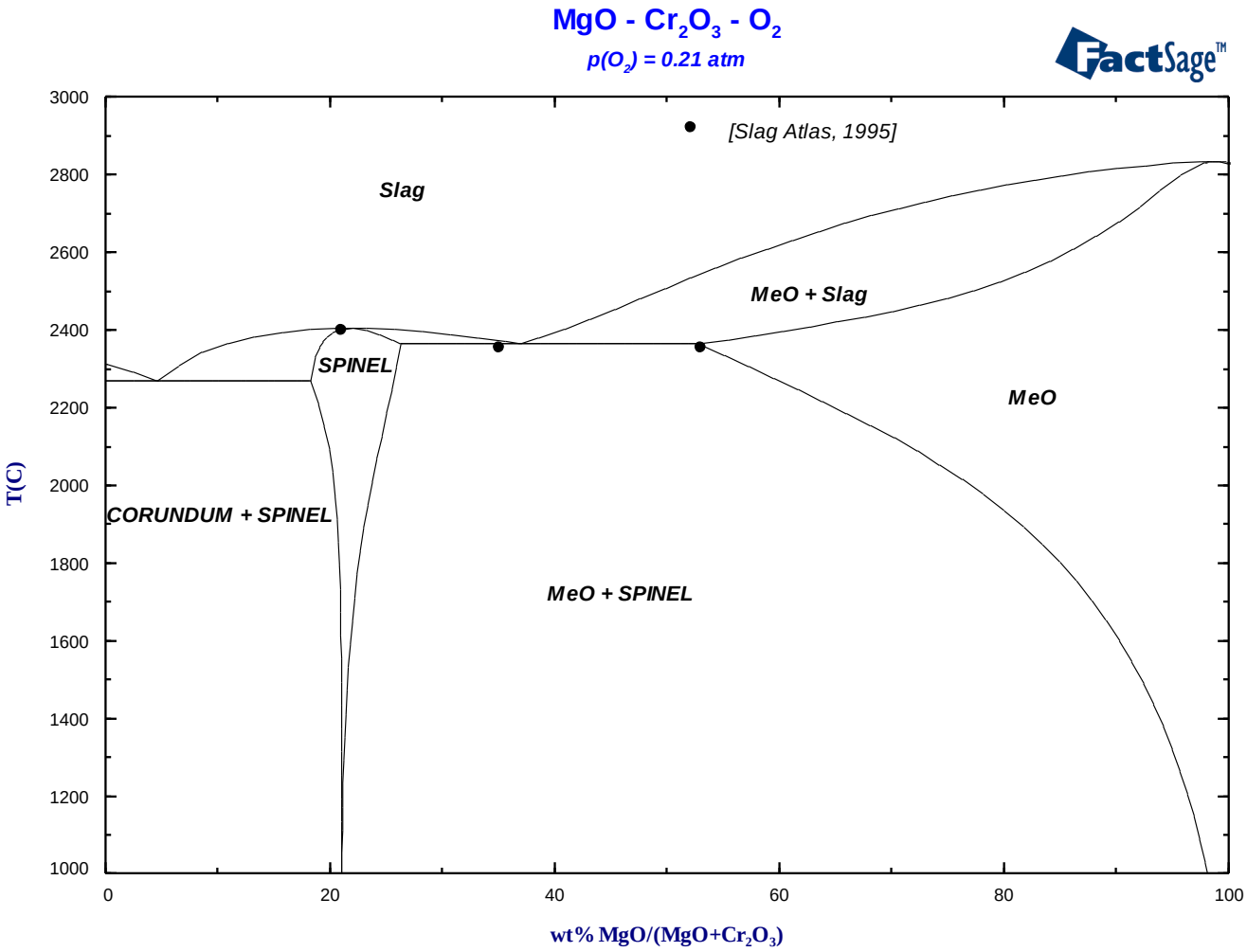

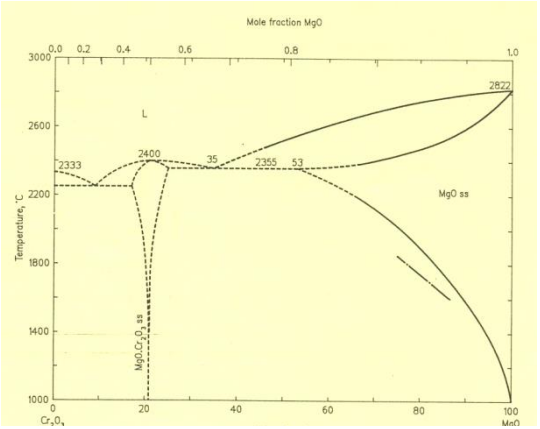

Slag Atlas, 2nd Ed., Verlag Stahl-Eisen, Düsseldorf, 1995., p.68.

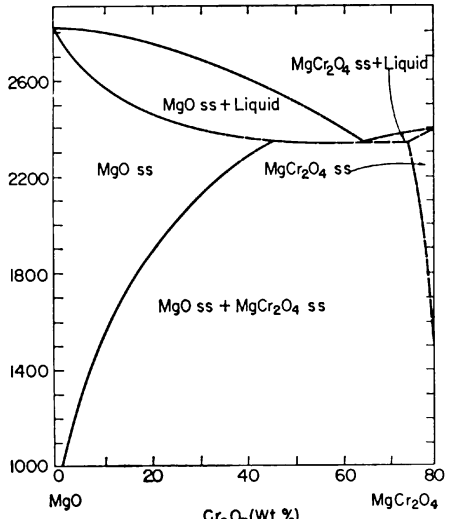

A.M.Alper, R.N. McNally, R.C. Doman, F.G. Keihn, J. Am.Ceram.Soc., 47 (1964), No.4, p.30-33.

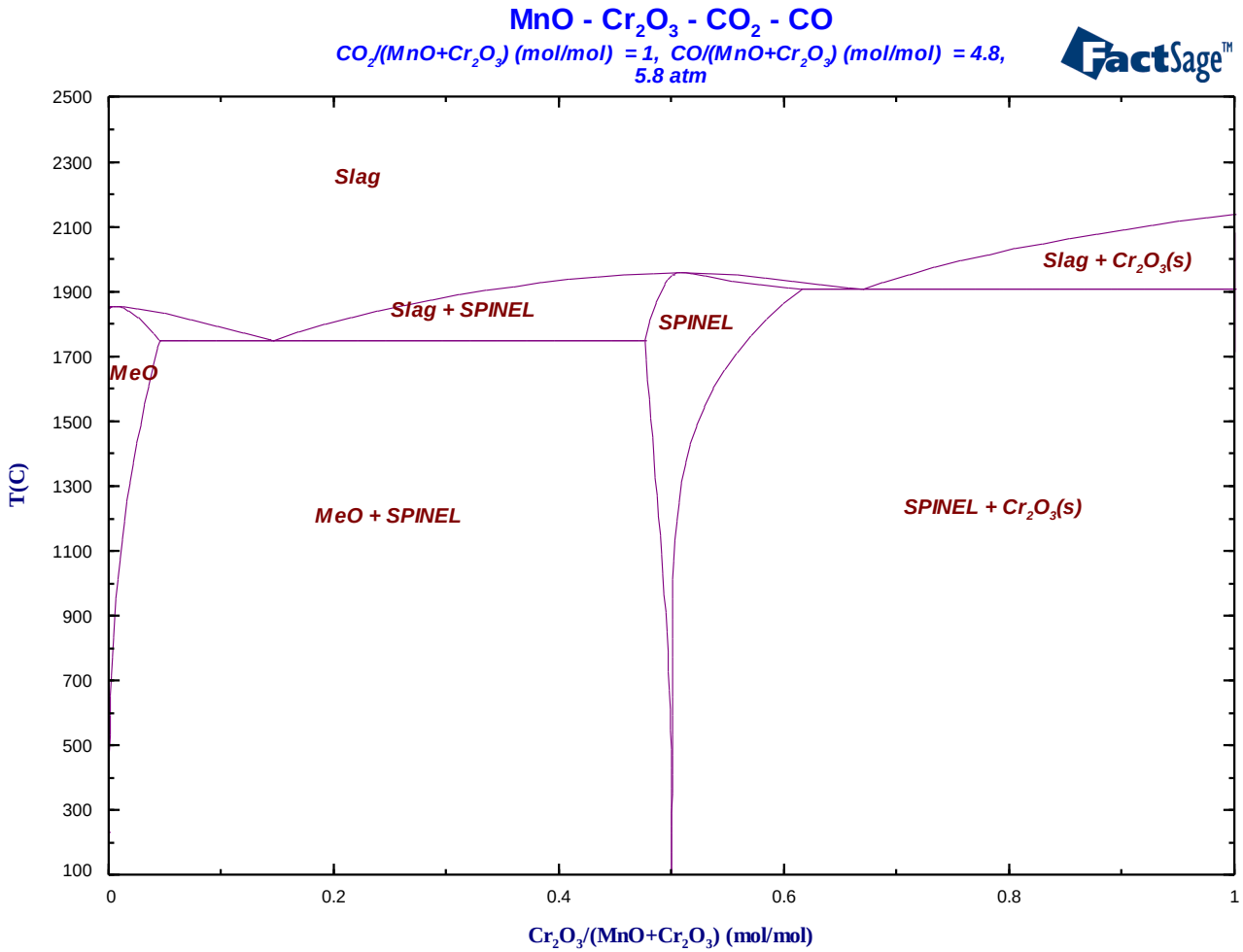
MnO - Cr2O3 - CO2 - CO
CO2/(MnO+Cr2O3) (mol/mol) = 1, CO/(MnO+Cr2O3) (mol/mol) = 4.8, 5.8 atm
FactSage™
Slag
Slag + Cr2O3(s)
Slag + SPINEL
SPINEL
MeO
MeO + SPINEL
SPINEL + Cr2O3(s)
T(C)
2500
2300
2100
1900
1700
1500
1300
1100
900
700
500
300
100
0
0.2
0.4
0.6
0.8
1
Cr2O3/(MnO+Cr2O3) (mol/mol)

Weight percent
compared with experimental data

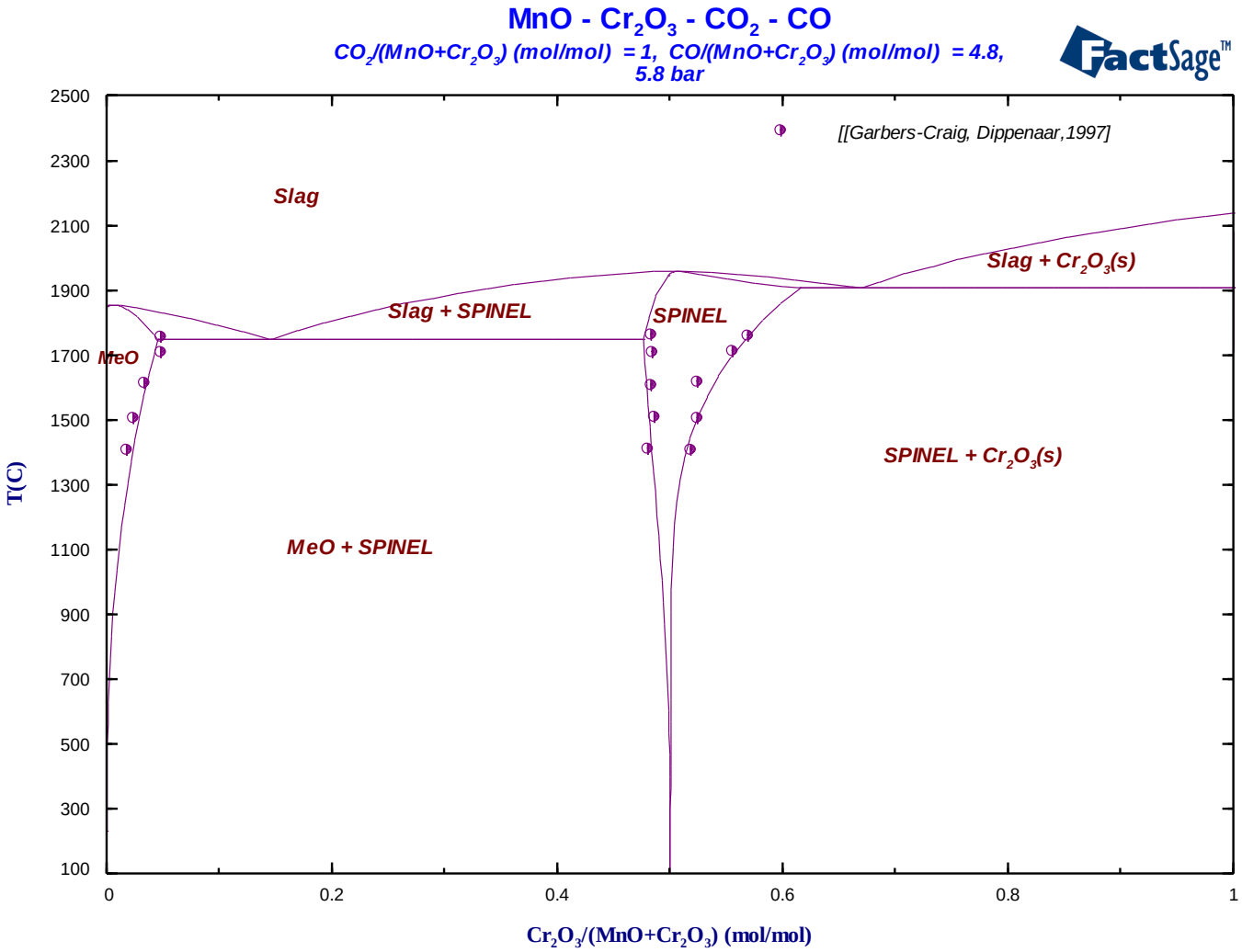

Mole fraction
compared with experimental data

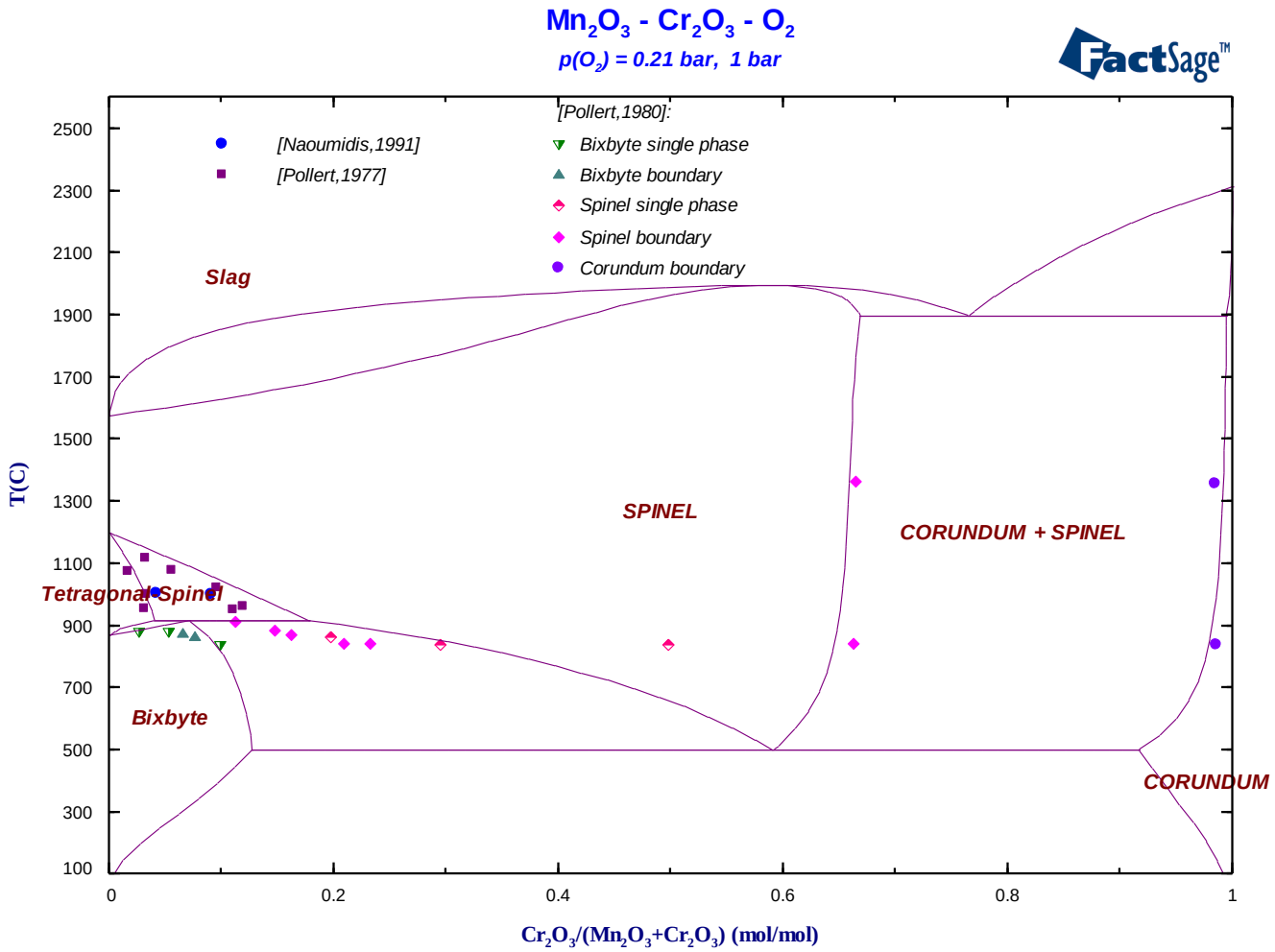

Weight percent

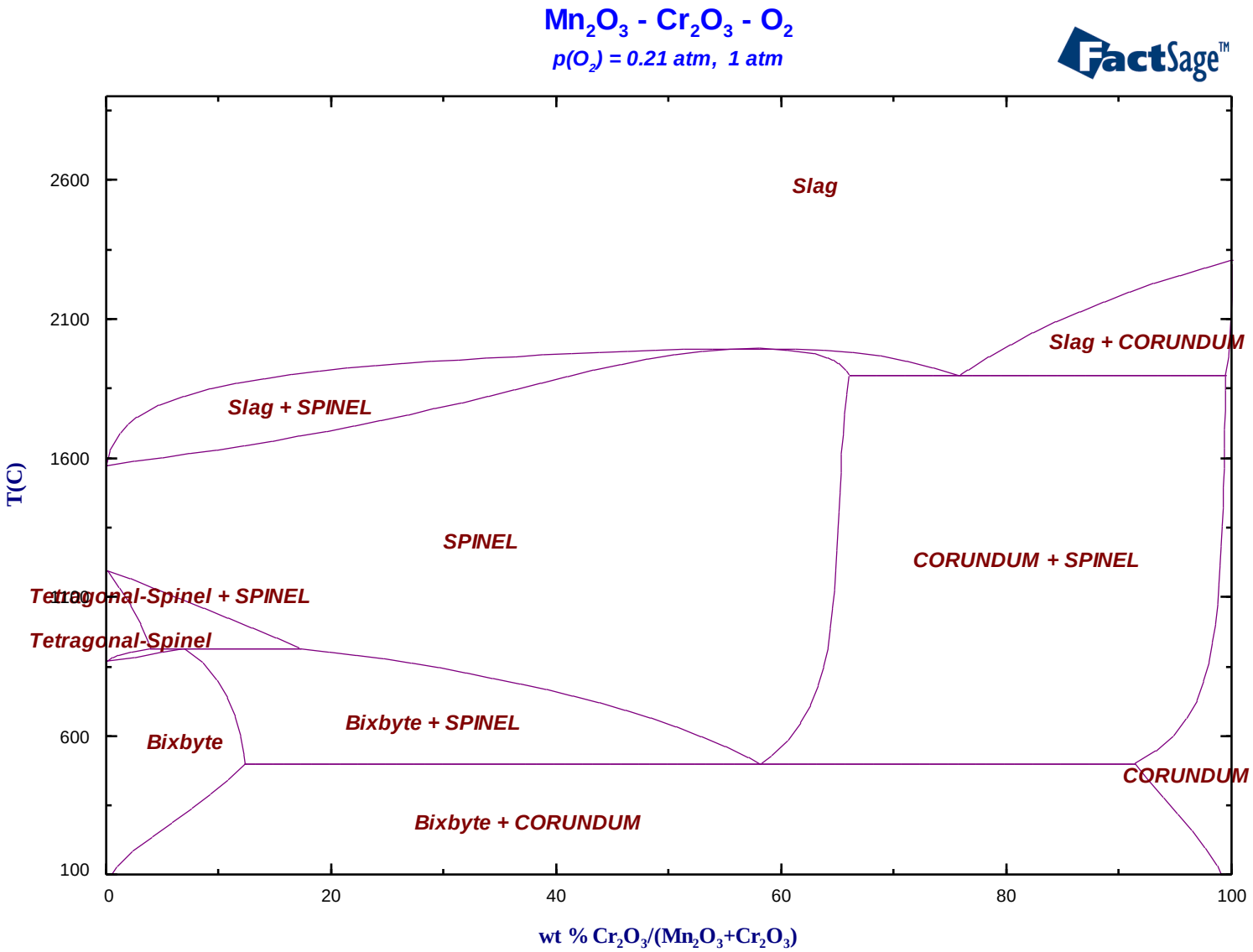

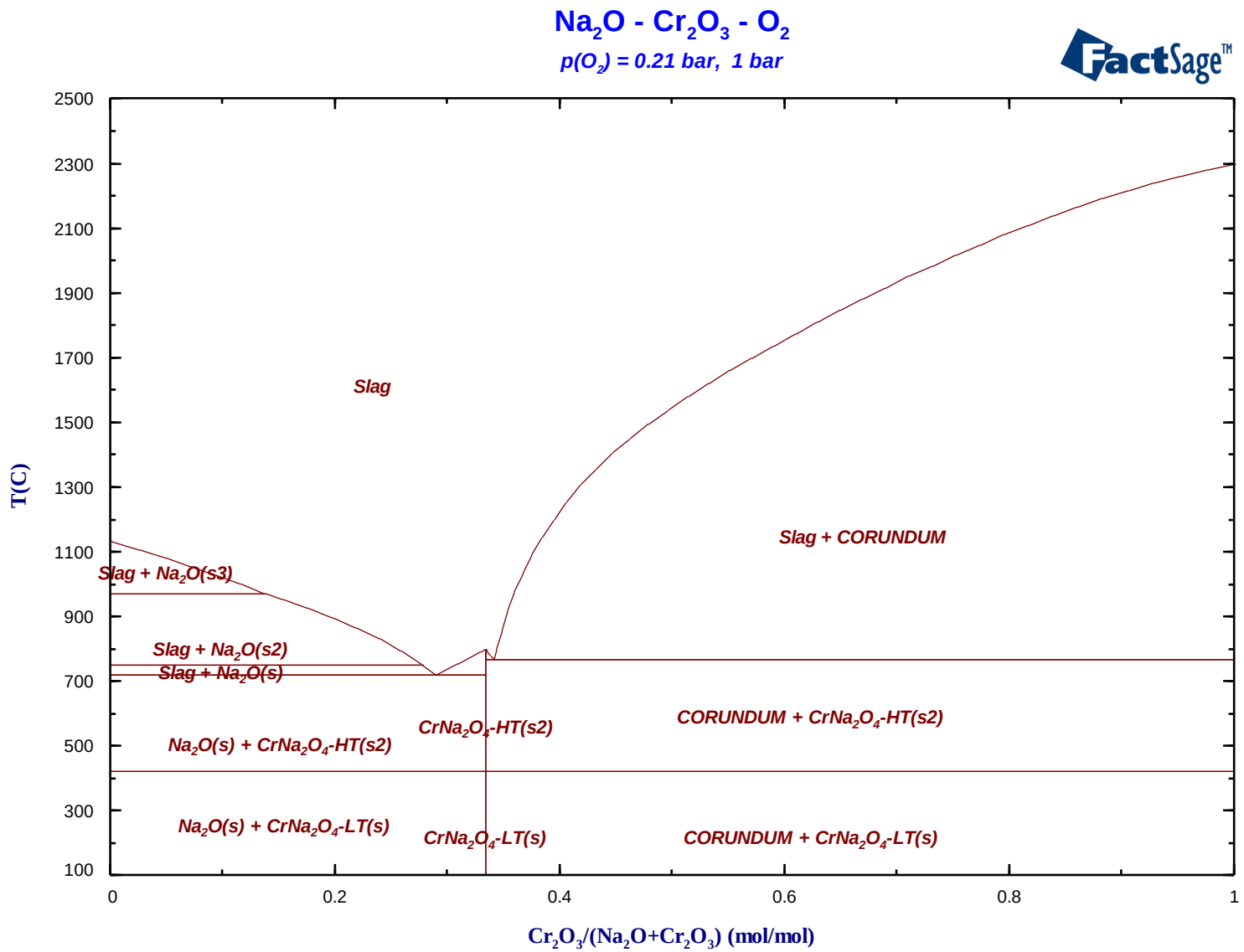
Na2O - Cr2O3 - O2
p(O2) = 0.21 bar, 1 bar
FactSage™
T(C)
2500
2300
2100
1900
1700
1500
1300
1100
900
700
500
300
100
0
0.2
0.4
0.6
0.8
1
Cr2O3/(Na2O+Cr2O3) (mol/mol)
Slag
Slag + CORUNDUM
Slag + Na2O(s3)
Slag + Na2O(s2)
Slag + Na2O(s)
CrNa2O4-HT(s2)
CORUNDUM + CrNa2O4-HT(s2)
Na2O(s) + CrNa2O4-HT(s2)
Na2O(s) + CrNa2O4-LT(s)
CrNa2O4-LT(s)
CORUNDUM + CrNa2O4-LT(s)

Weight percent

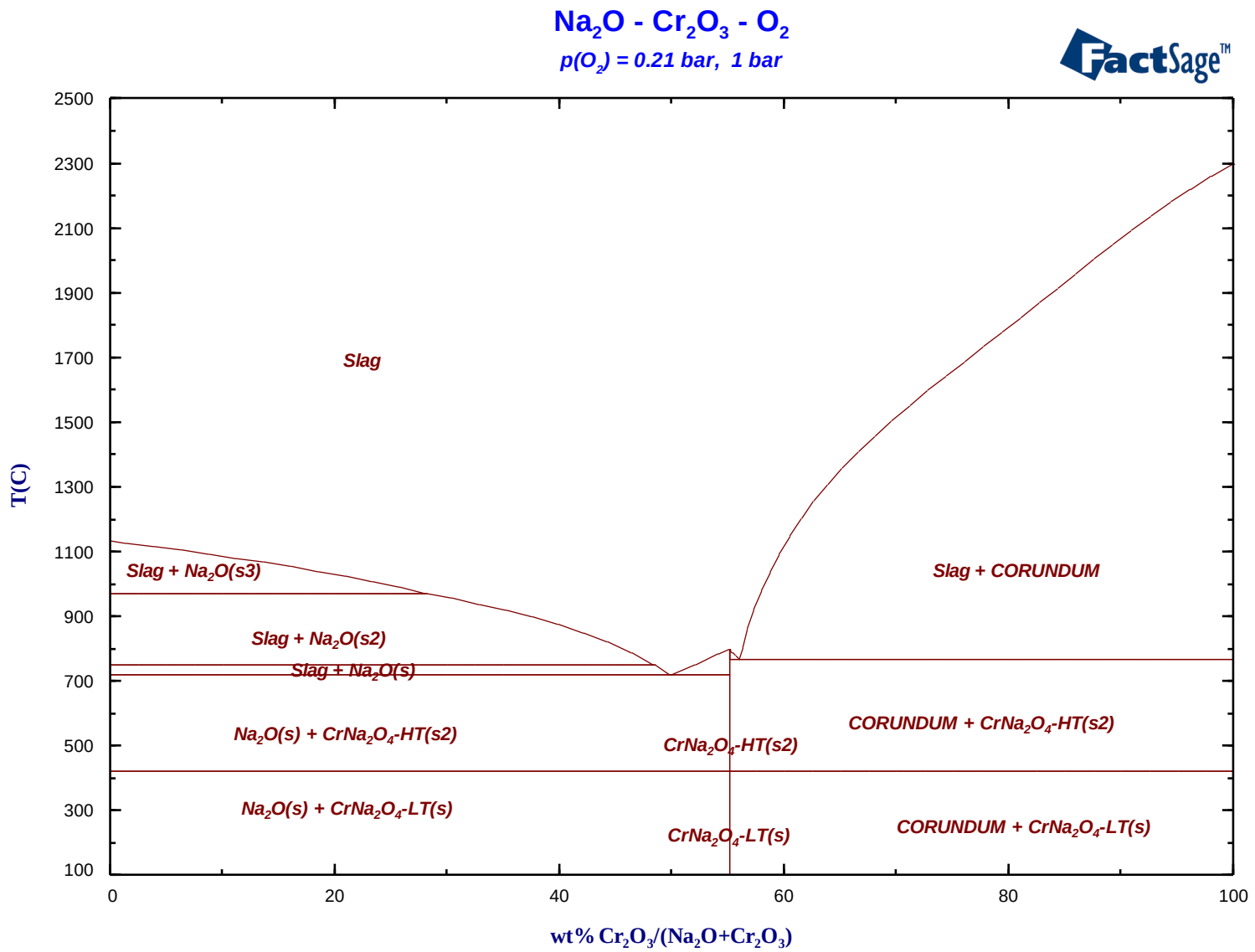

Mole fraction

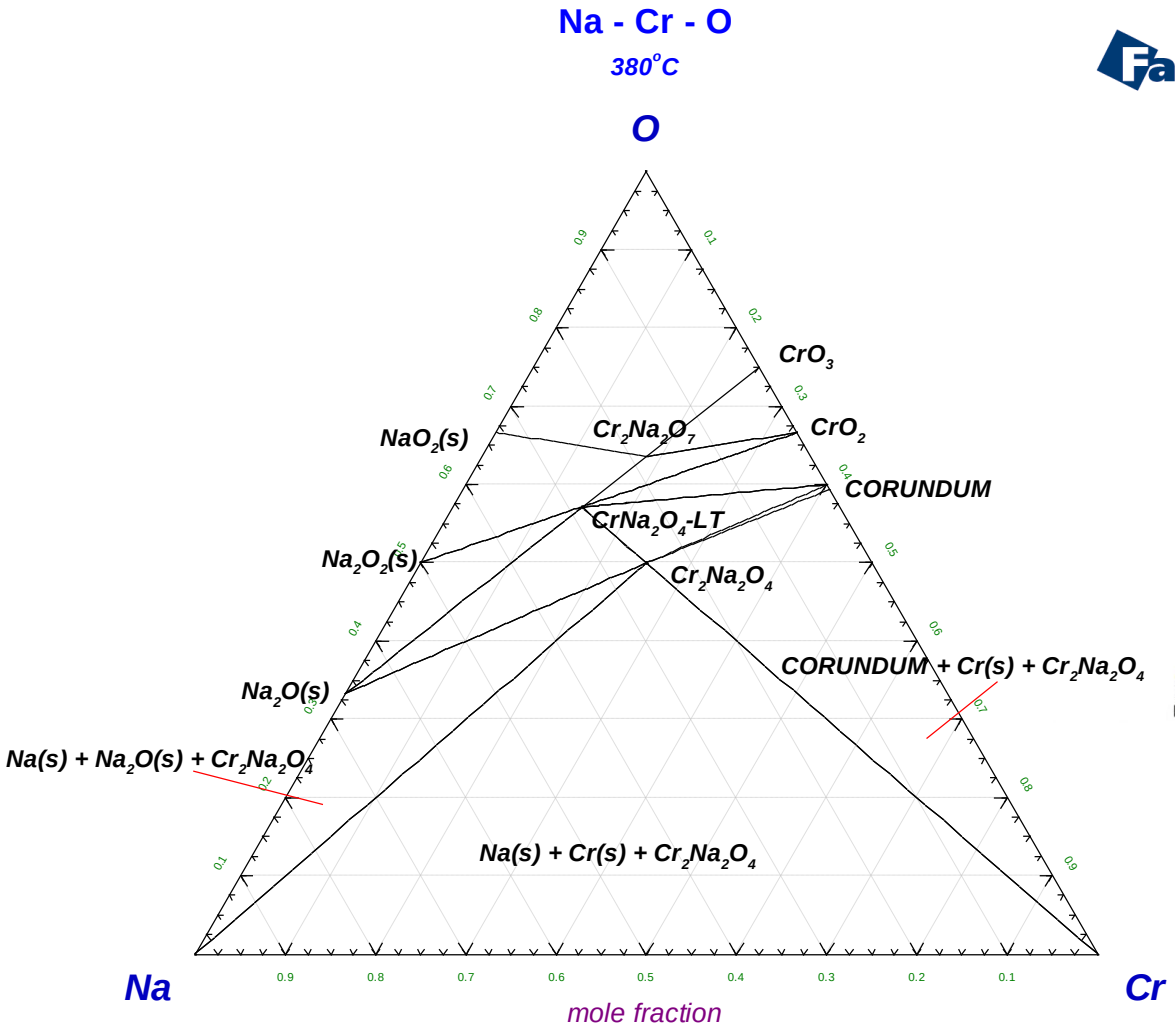

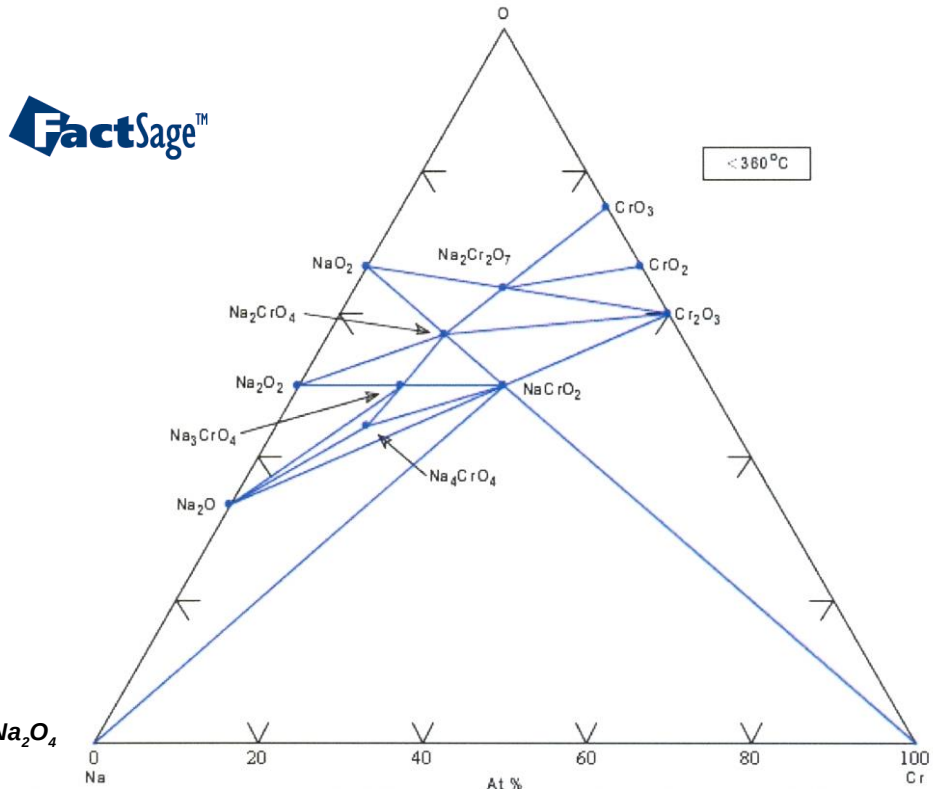

T. B. Lindemer, T. M. Besmann, and C. E. Johnson, J. Nucl. Mater., 100 [1-3] 176-226 (1981).

Mole fraction
compared with experimental data

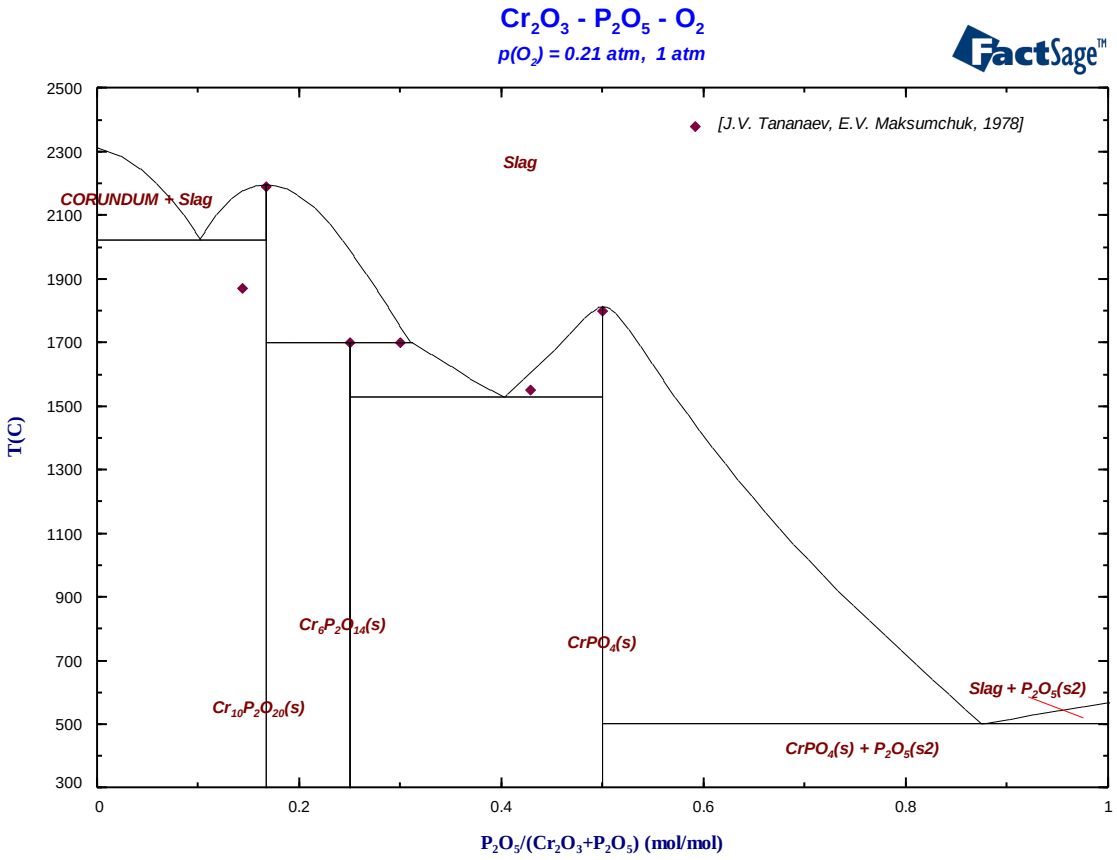

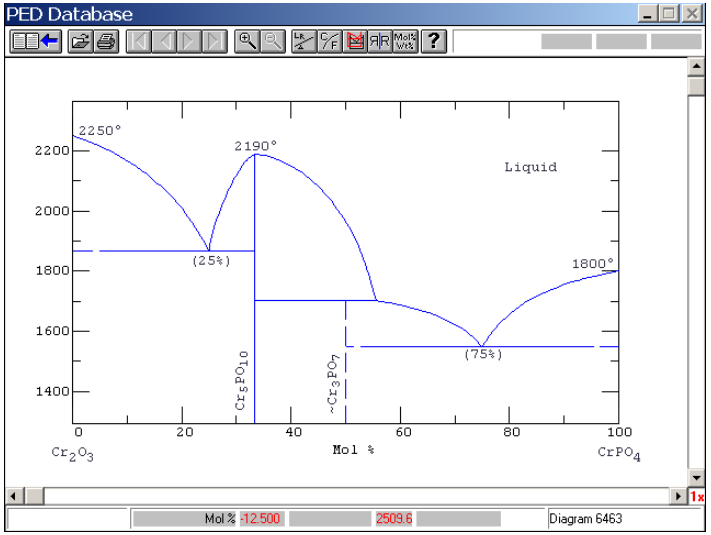

I.V. Tananaev, E.V. Maksimchuk,Y. G. Bushuev, S.A. Shestov, Izv. Akad. Nauk SSSR, Neorg. Mater., 14 [4], (1978), pp.719-722.

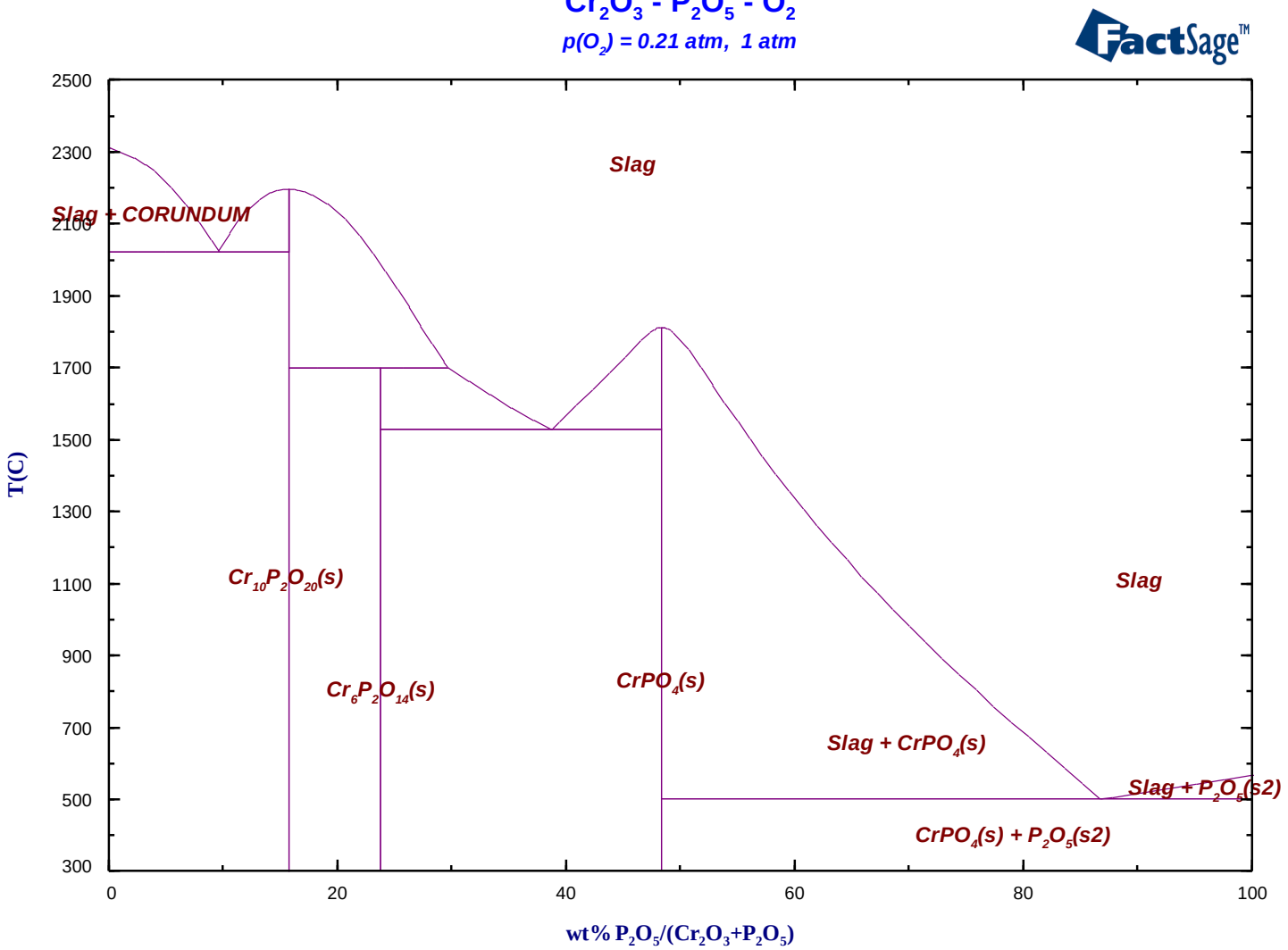
Cr2O3 - P2O5 - O2
p(O2) = 0.21 atm, 1 atm
FactSage™
Slag
Slag + CORUNDUM
Cr10P2O20(s)
Cr6P2O14(s)
CrPO4(s)
Slag
Slag + CrPO4(s)
Slag + P2O5(s2)
CrPO4(s) + P2O5(s2)
T(C)
2500
2300
2100
1900
1700
1500
1300
1100
900
700
500
300
0
20
40
60
80
100
wt% P2O5/(Cr2O3+P2O5)

Mole fraction

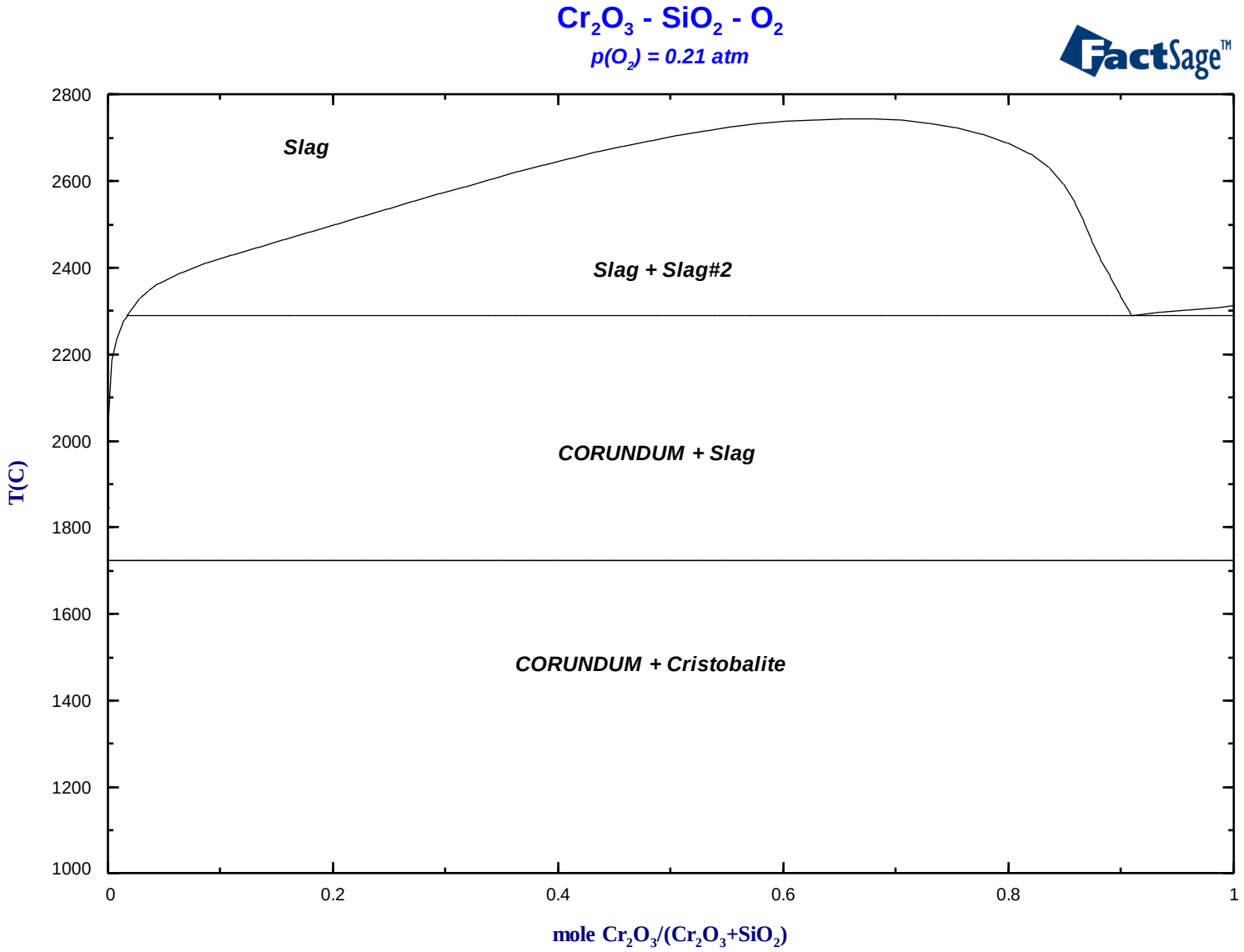

Weight percent

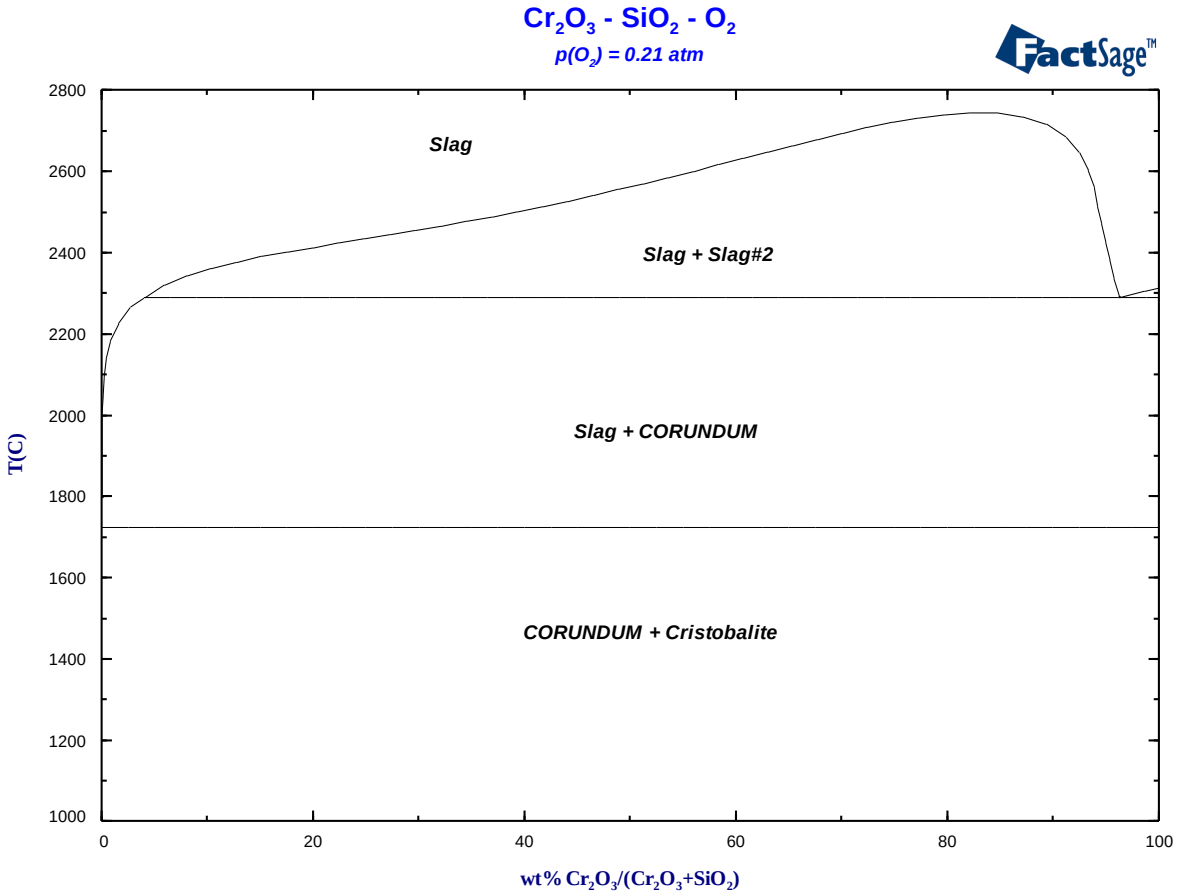

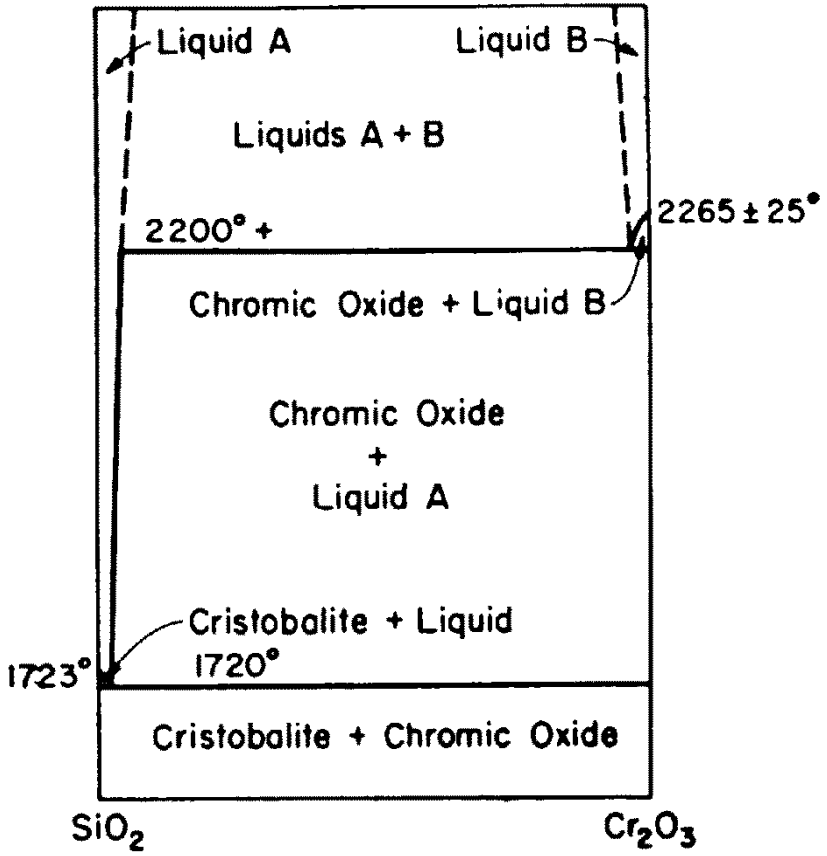

M. L. Keith, J. Am., Ceram. Soc., 37 [10], (1954), pp. 490-496.

Cr2O3-V2O5-O2,

Mole fraction compared with experimental data

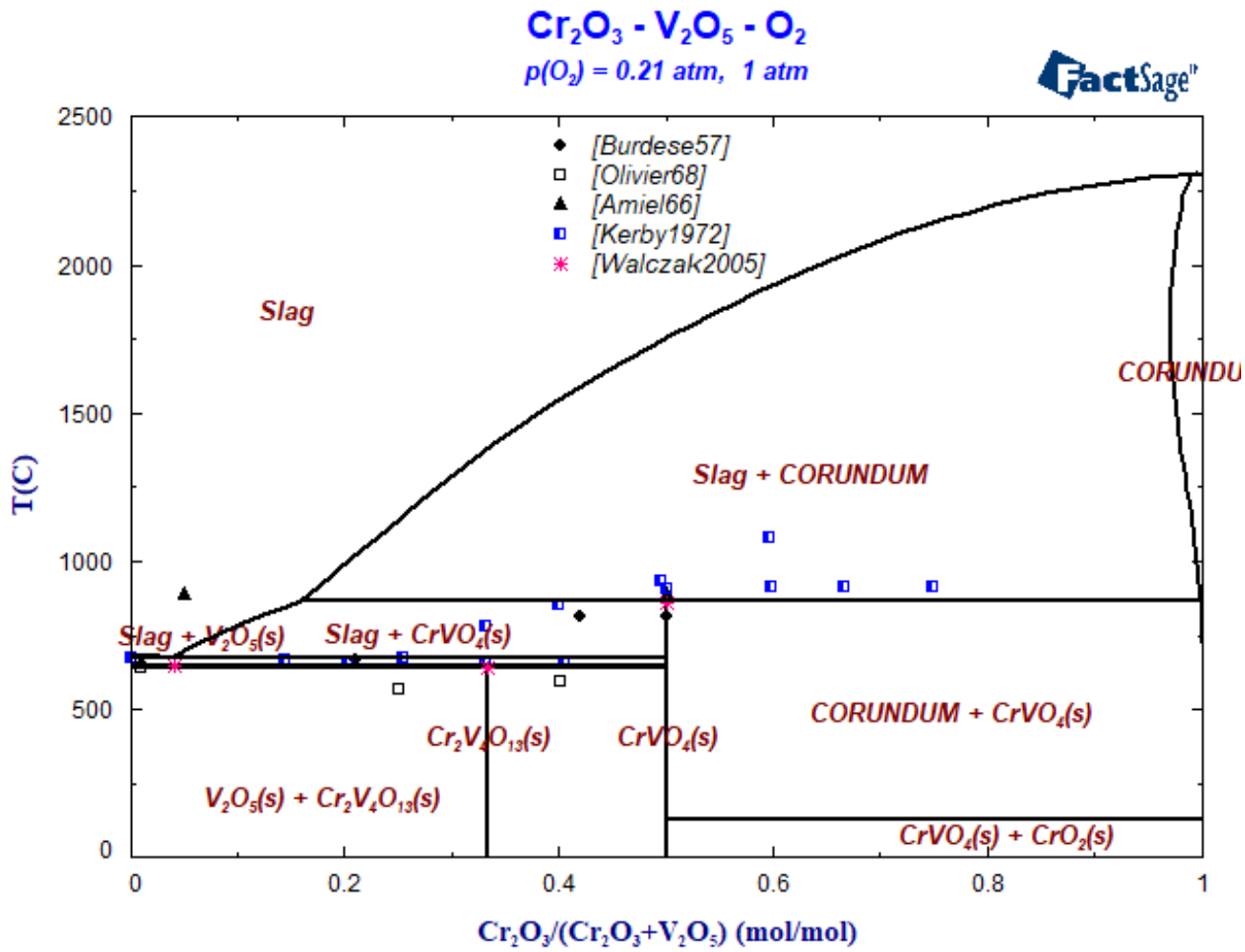

Cr2O3-V2O5-O2,

Weight percent

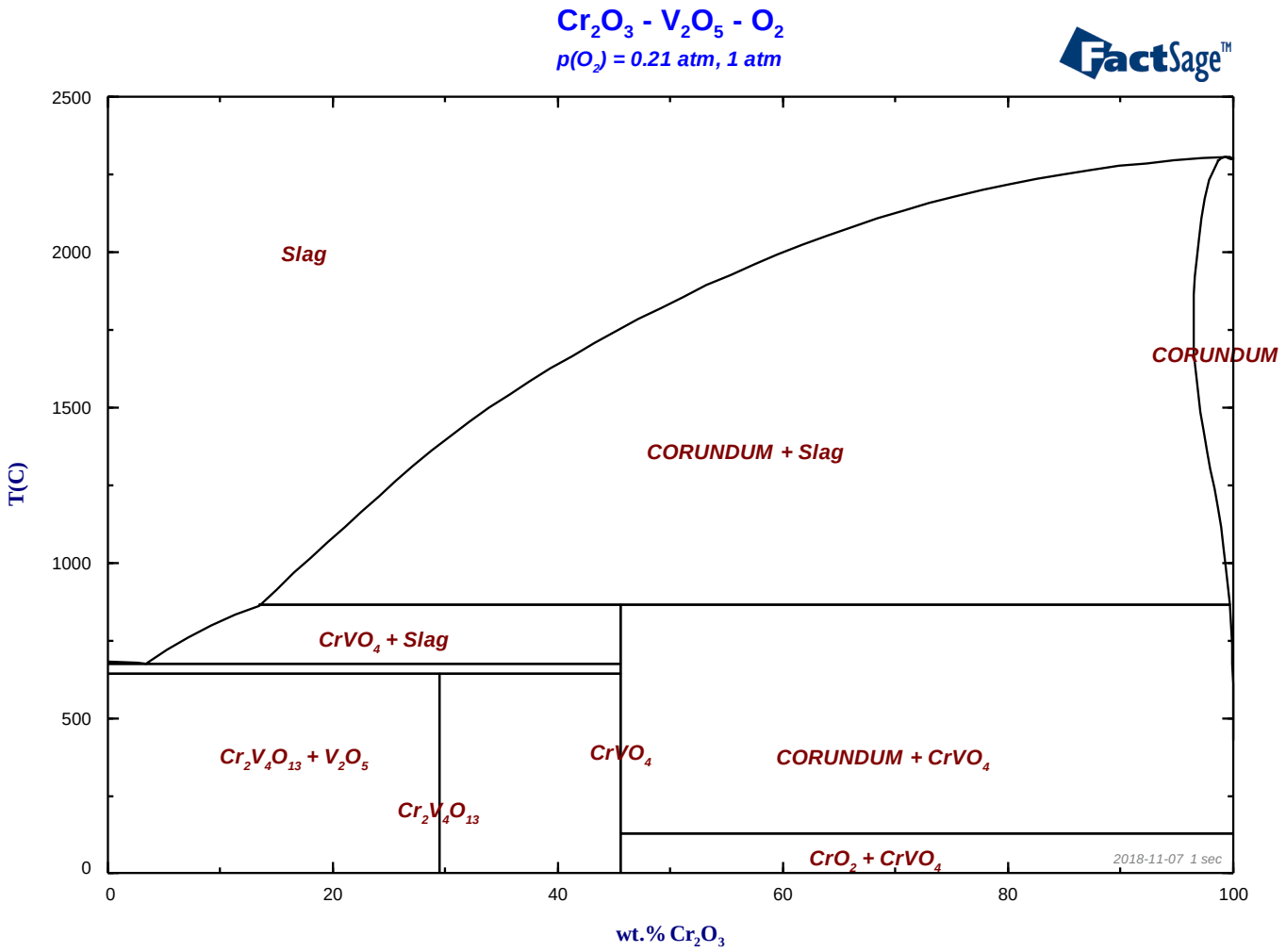

Mole fraction

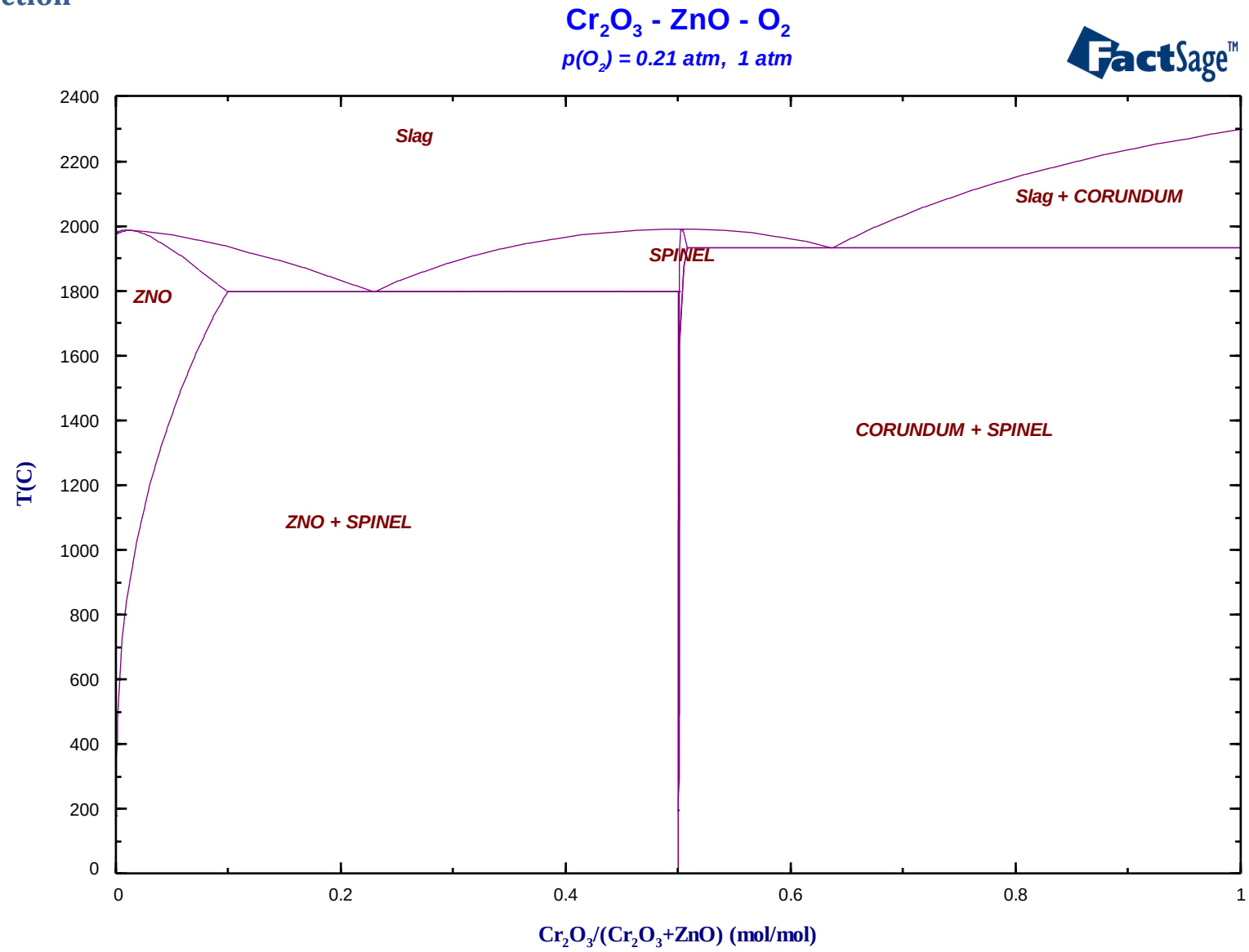

Weight percent

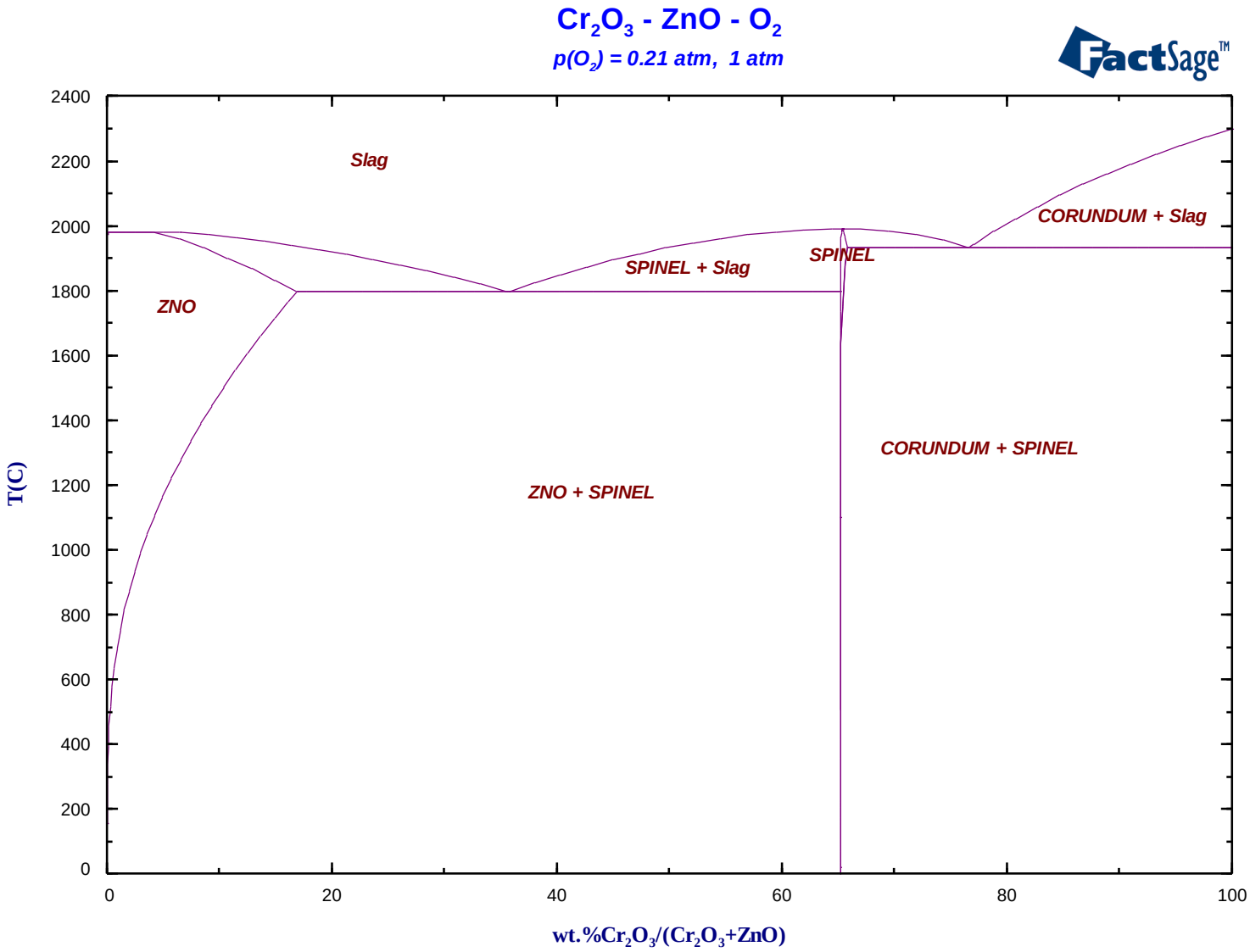

Mole fraction

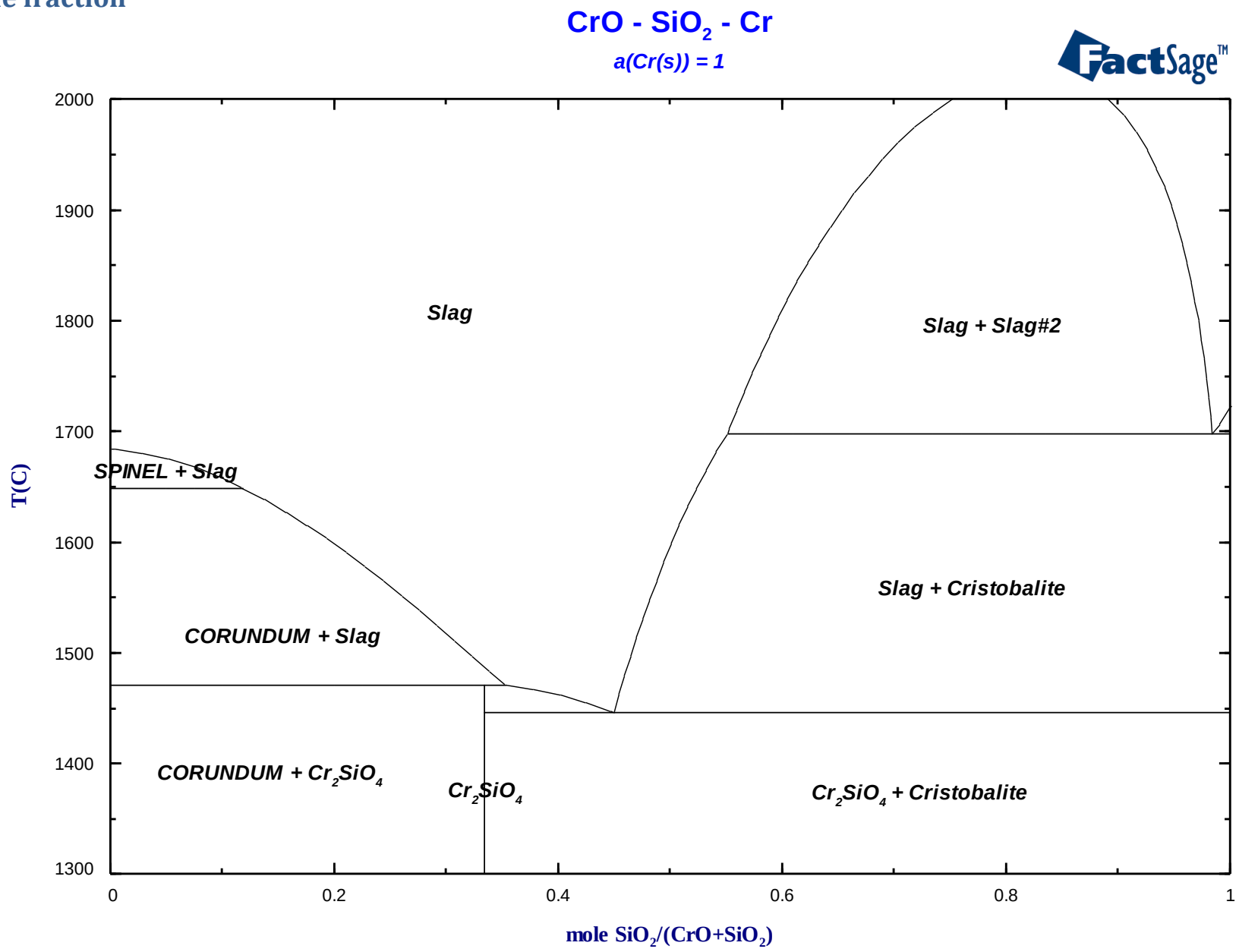

Weight percent
compared with experimental data

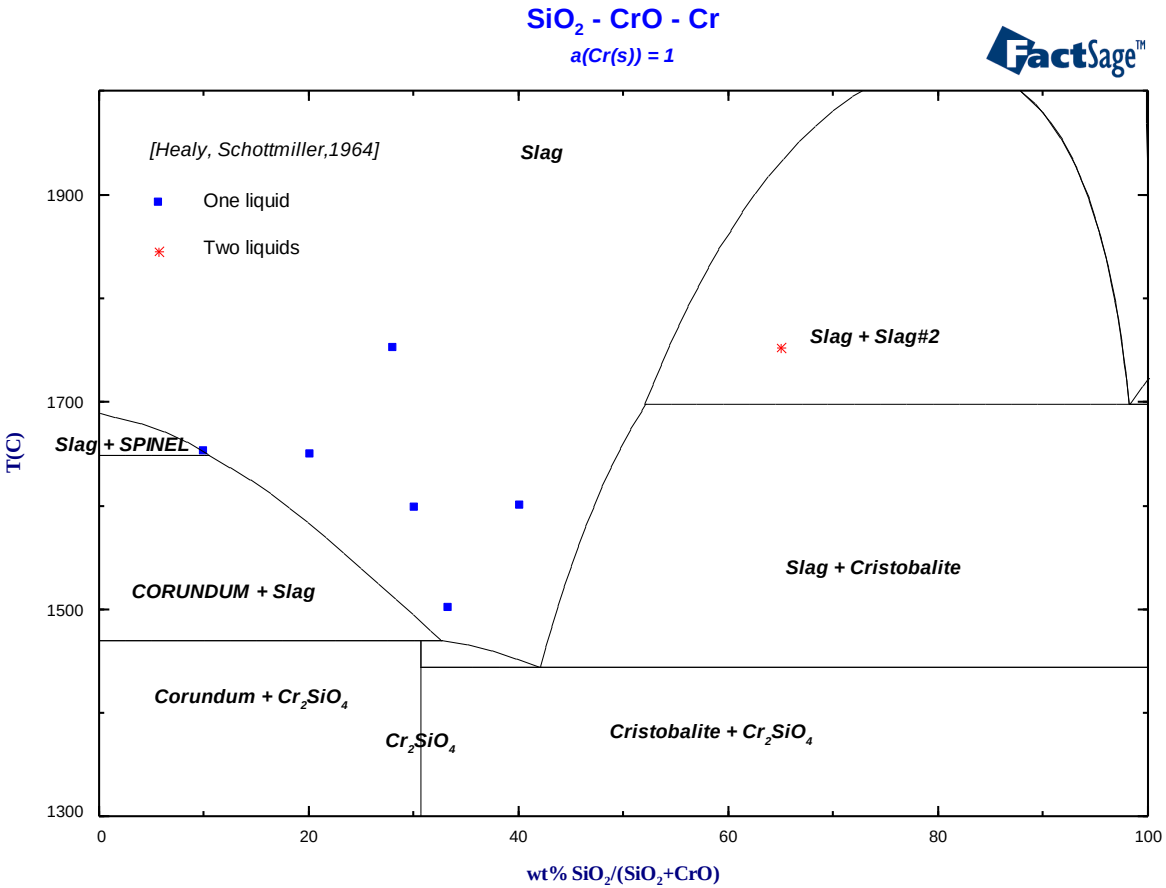

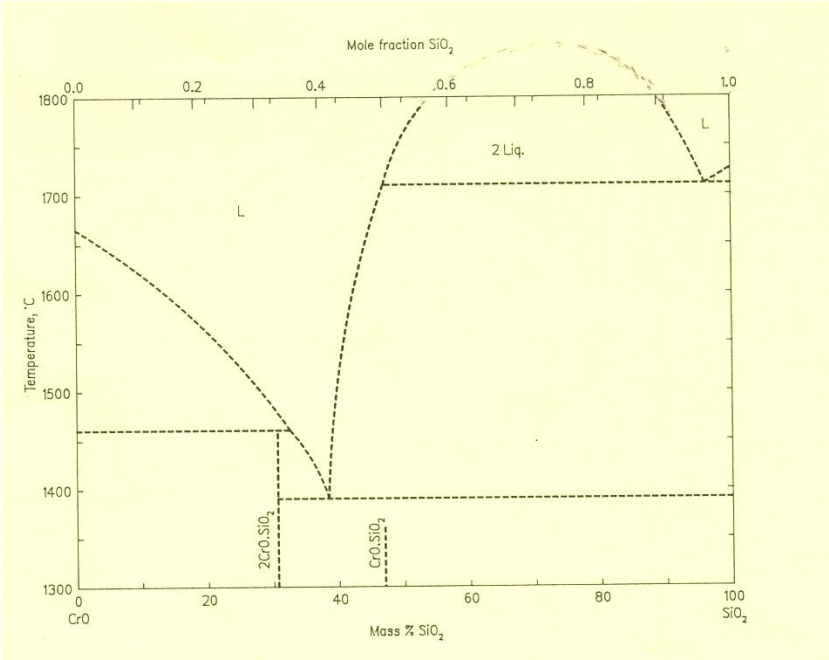

G. W. Healy, J. C. Schottmiller, Trans. Metall. So, AIME 230 (1964), No.2, pp. 420-425.

Mole fraction
compared with experimental data

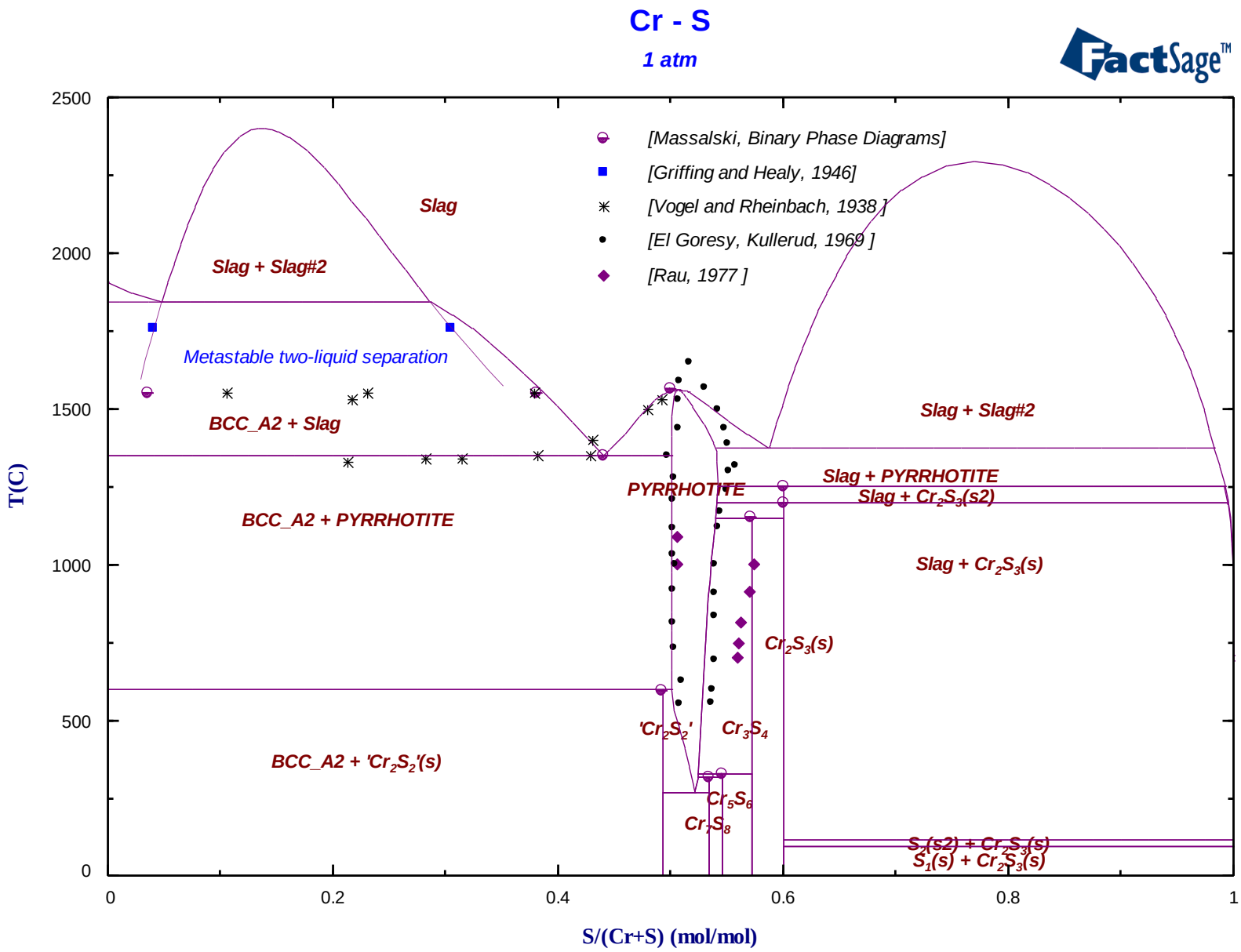

Weight percent

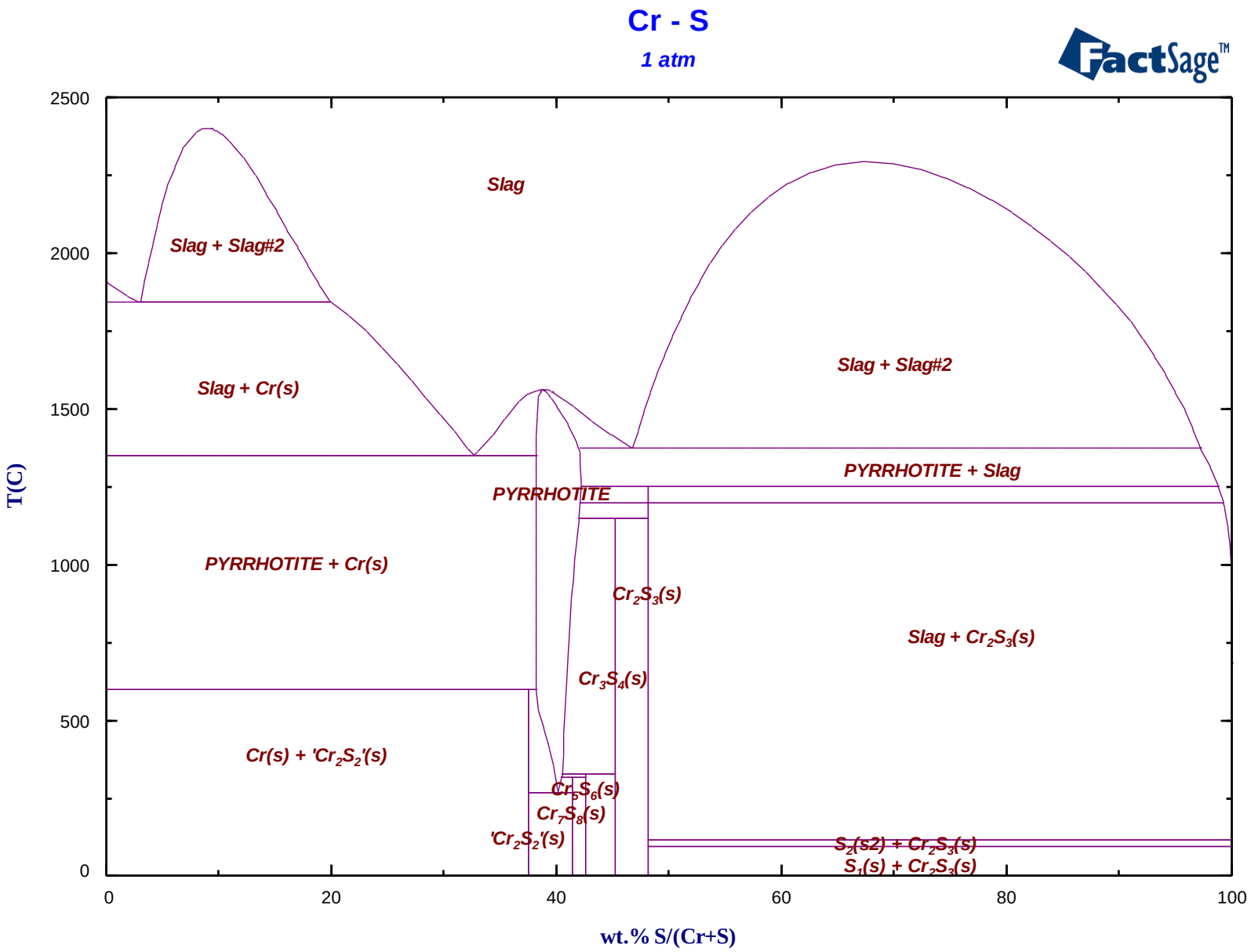

Mole fraction in Kelvin
compared with experimental data

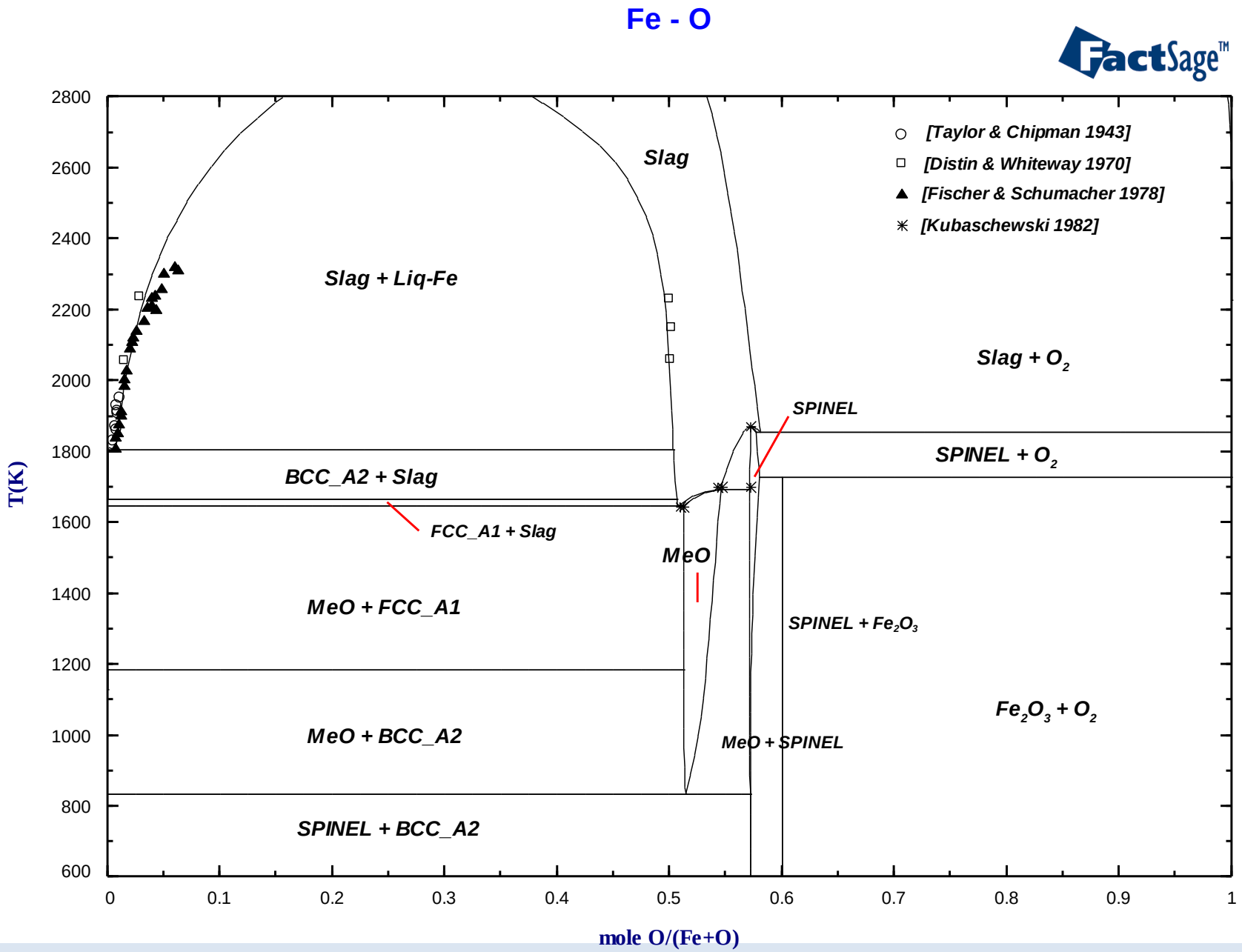

Fe - O

Weight percent in Kelvin

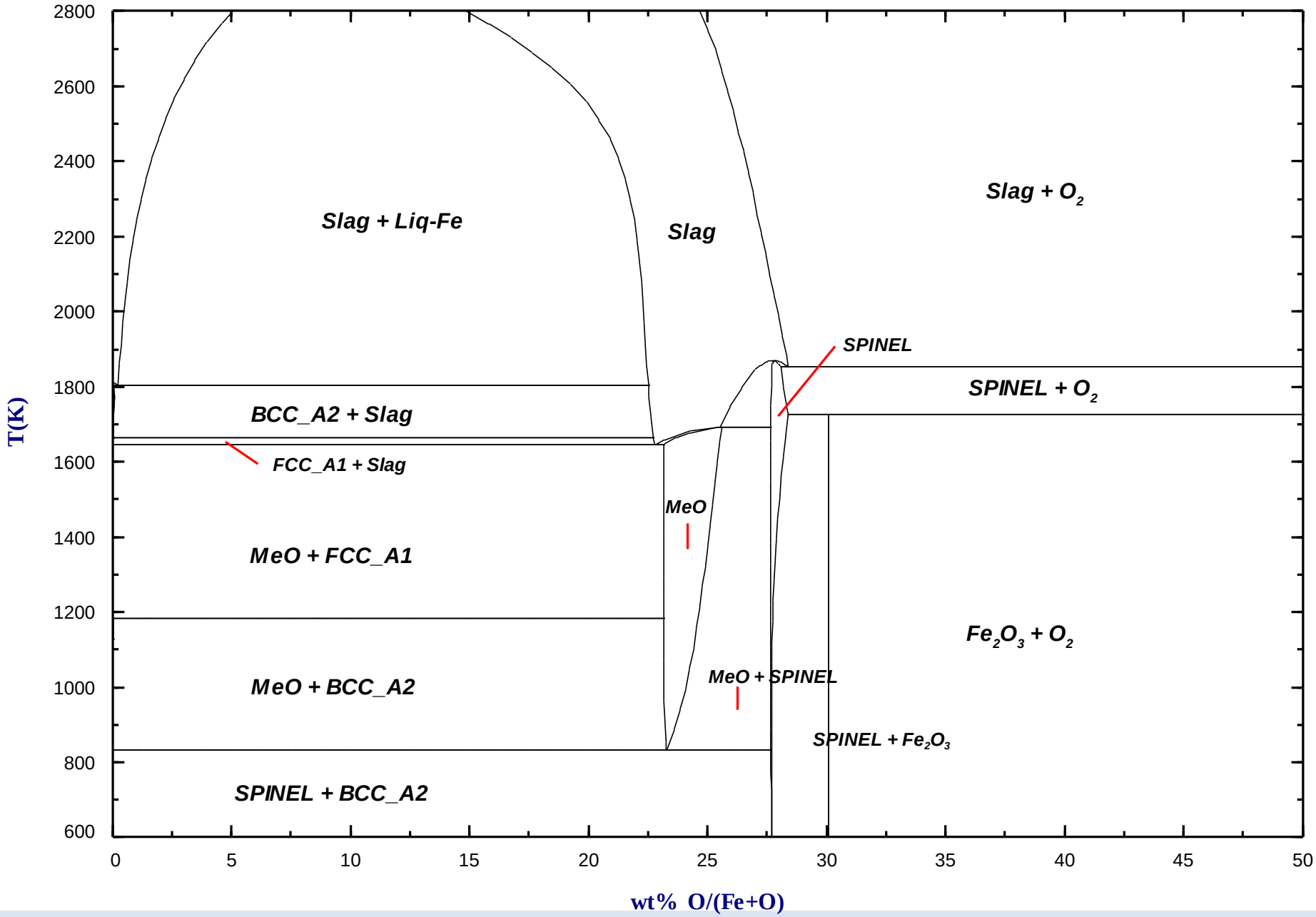

Mole fraction with isobars

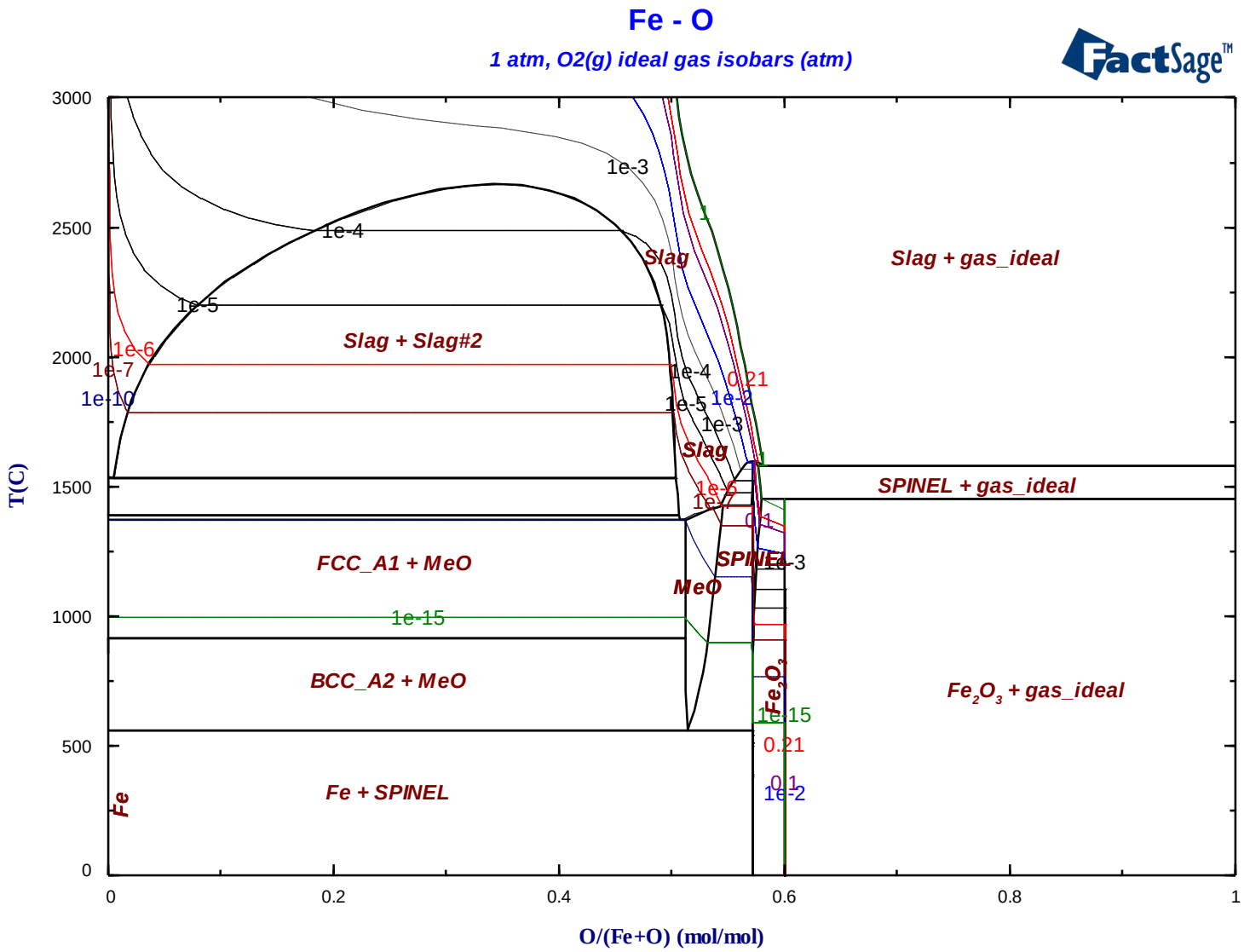

Fe-O2,
Temeprature vs. log P(O2) diagram

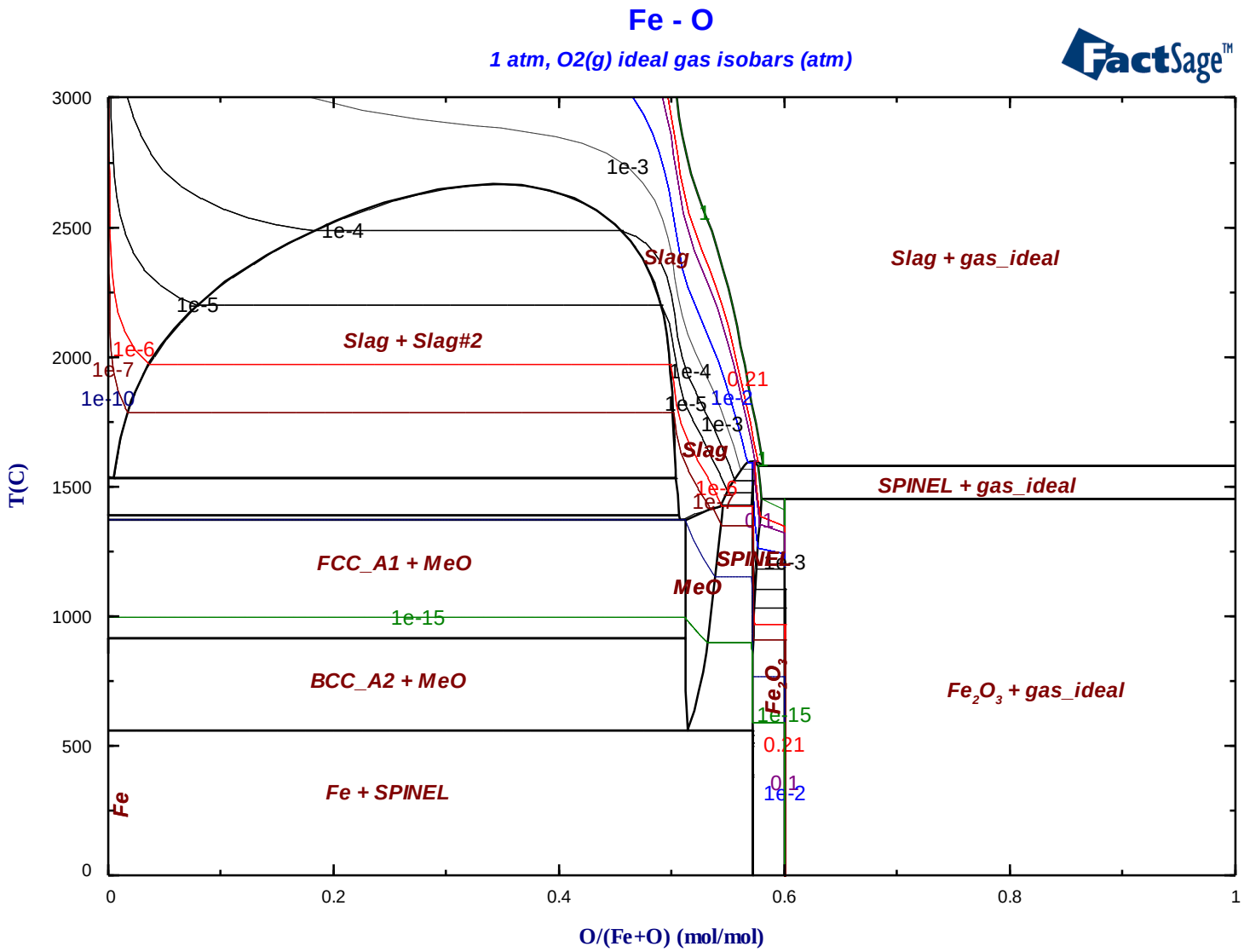

Mole fraction compared with experimental data

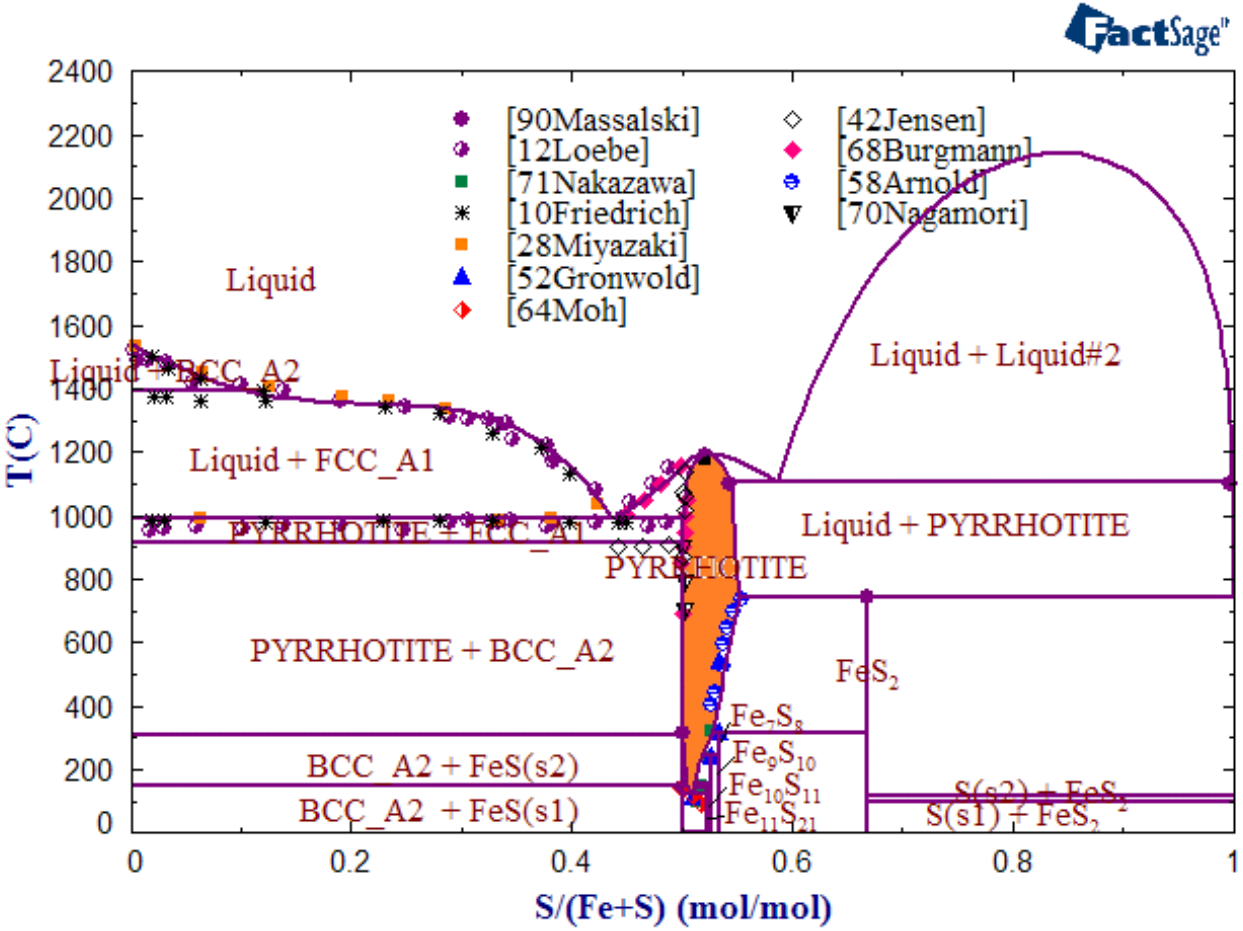

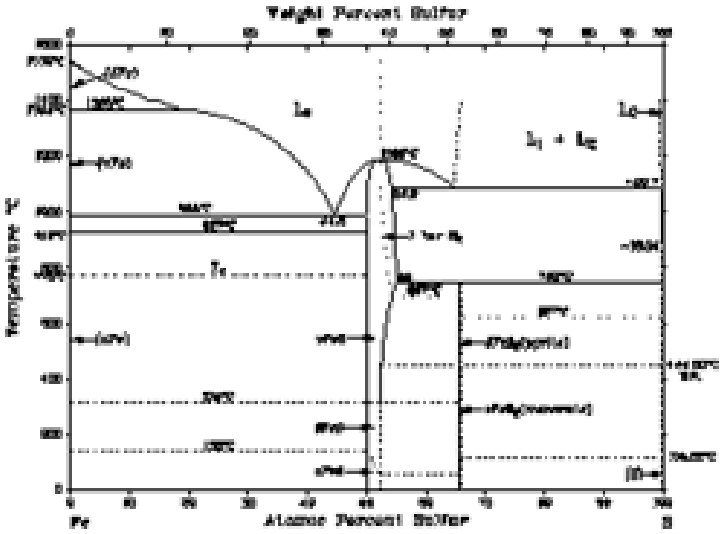

T.B. Massalski, Binary Alloy Phase Diagrams., ASM, 1990.

Weight percent

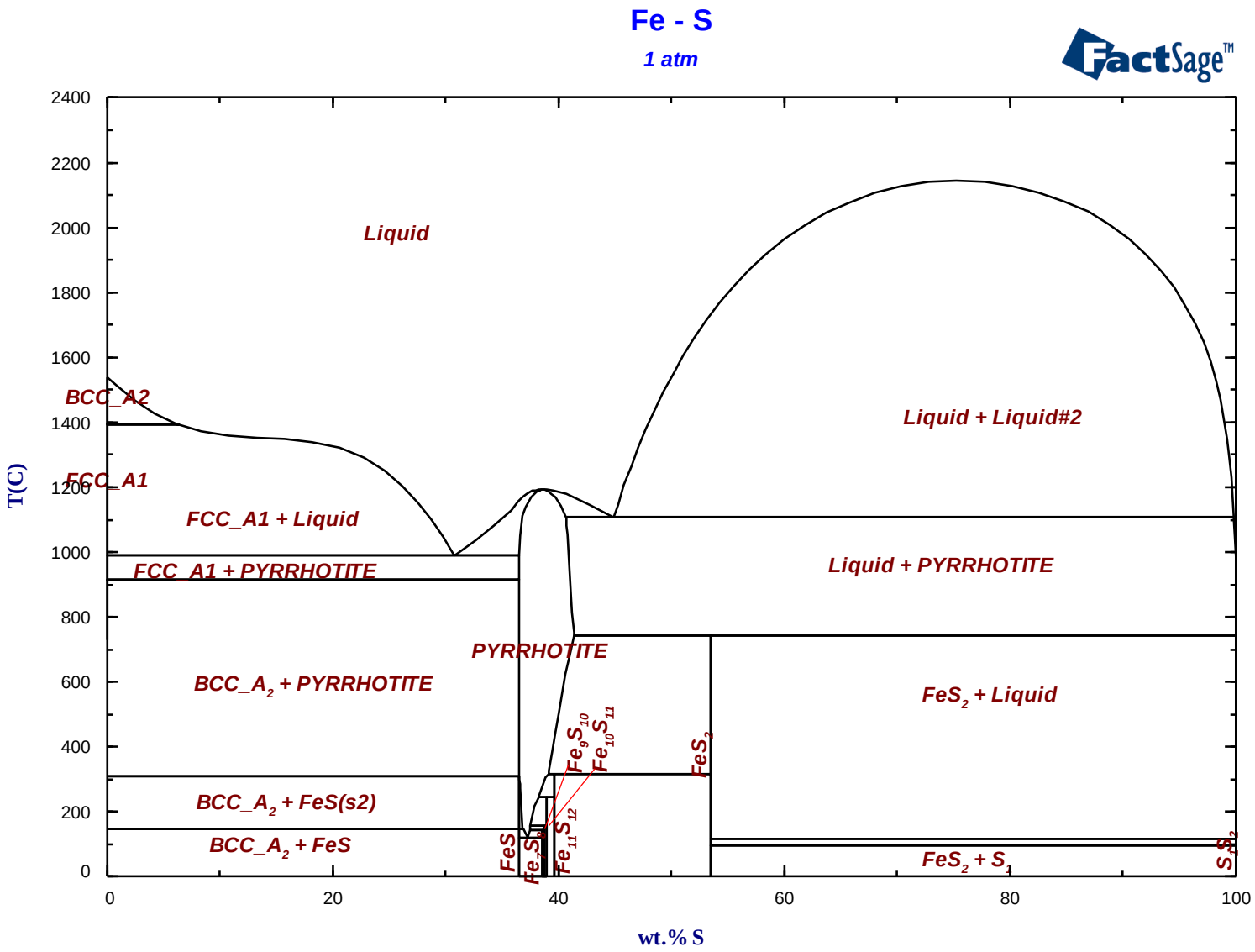

Mole fraction

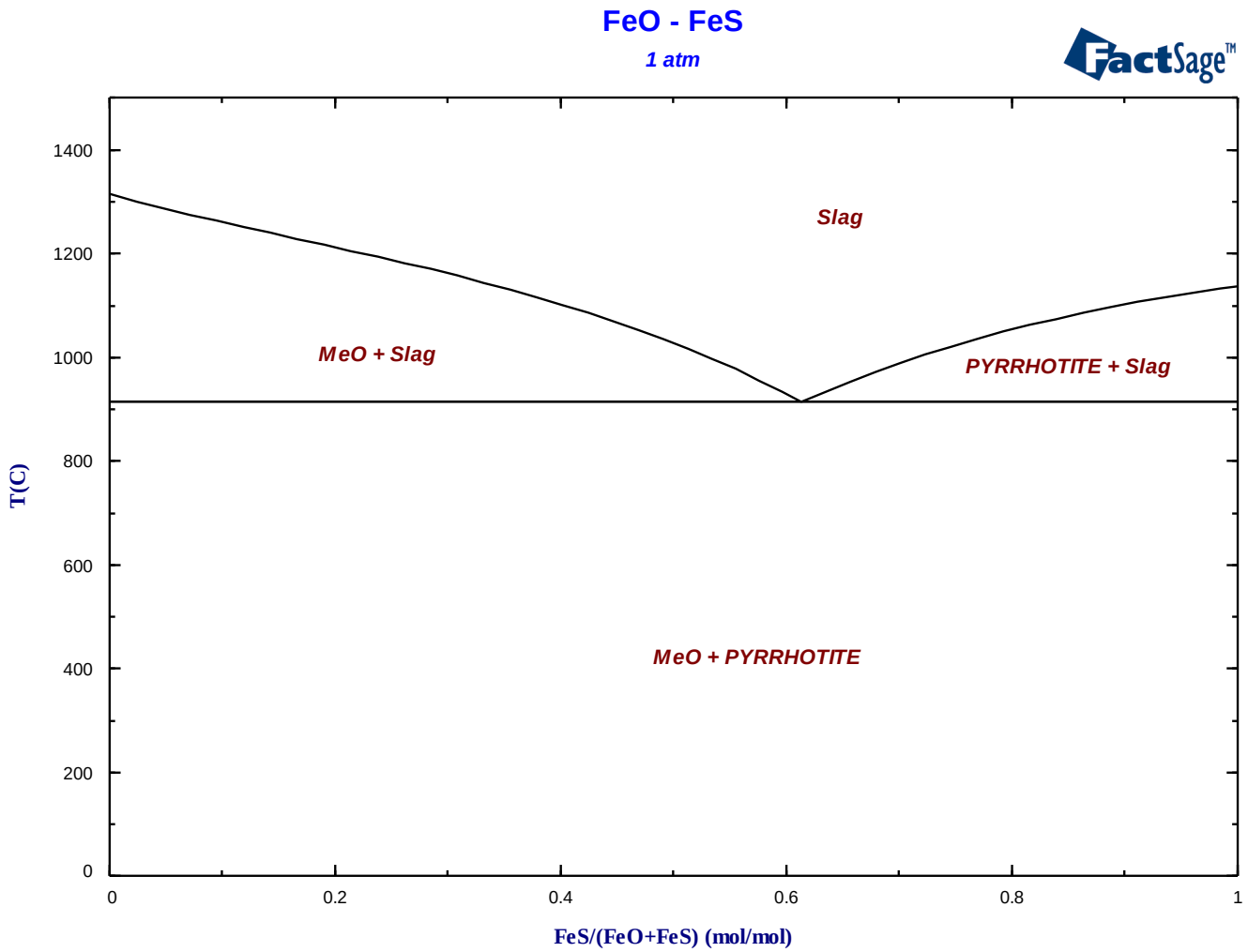

Weight percent

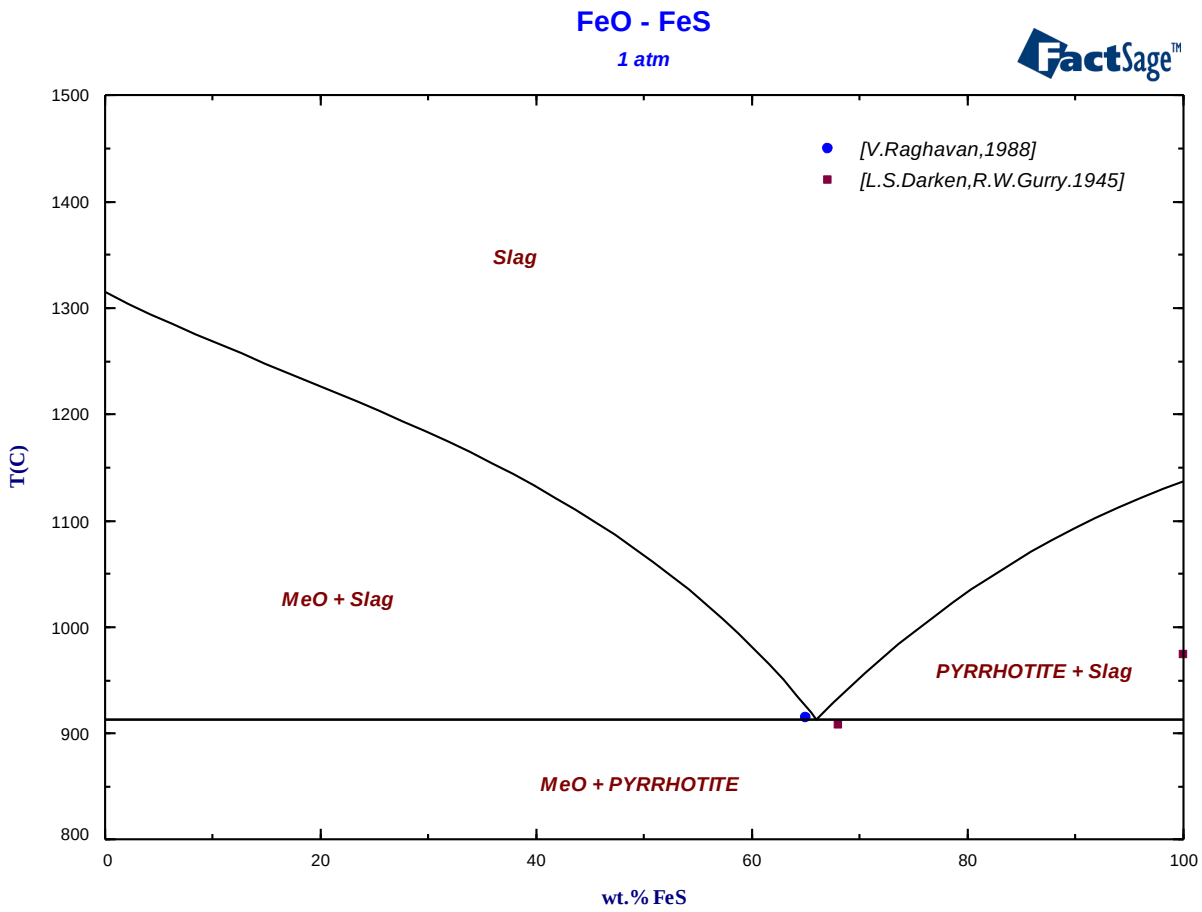

Mole fraction

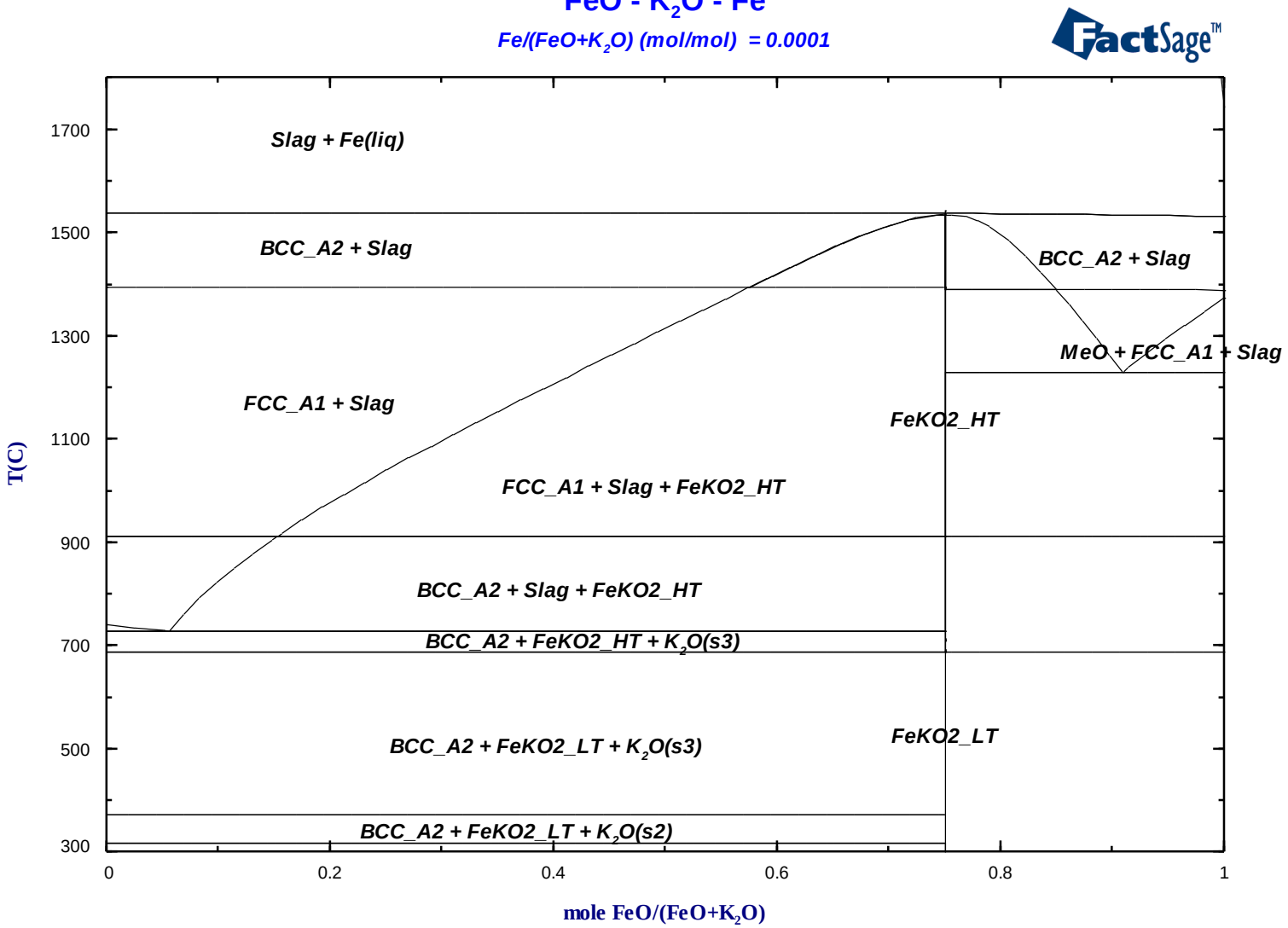

Weight percent

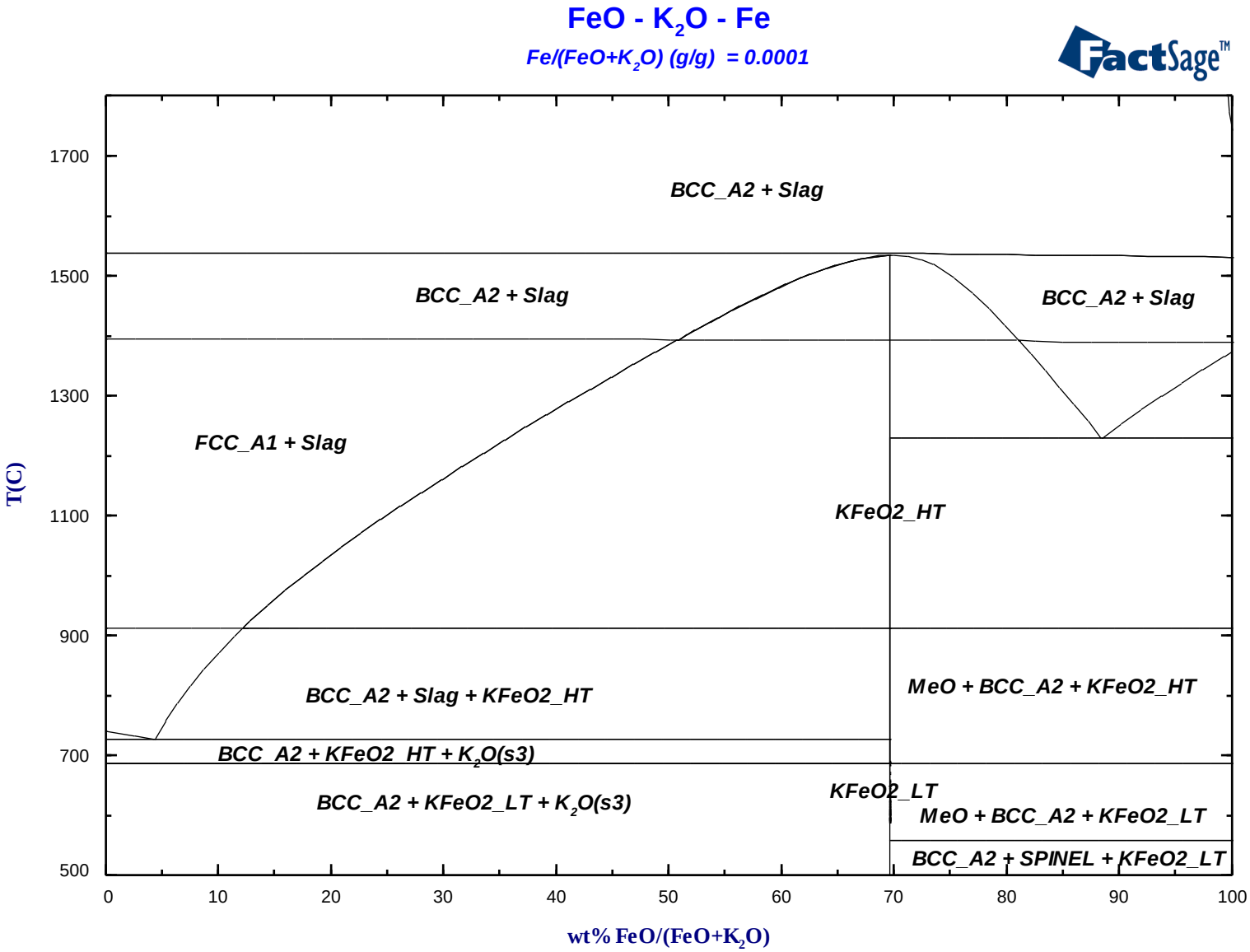

Mole fraction
compared with experimental data

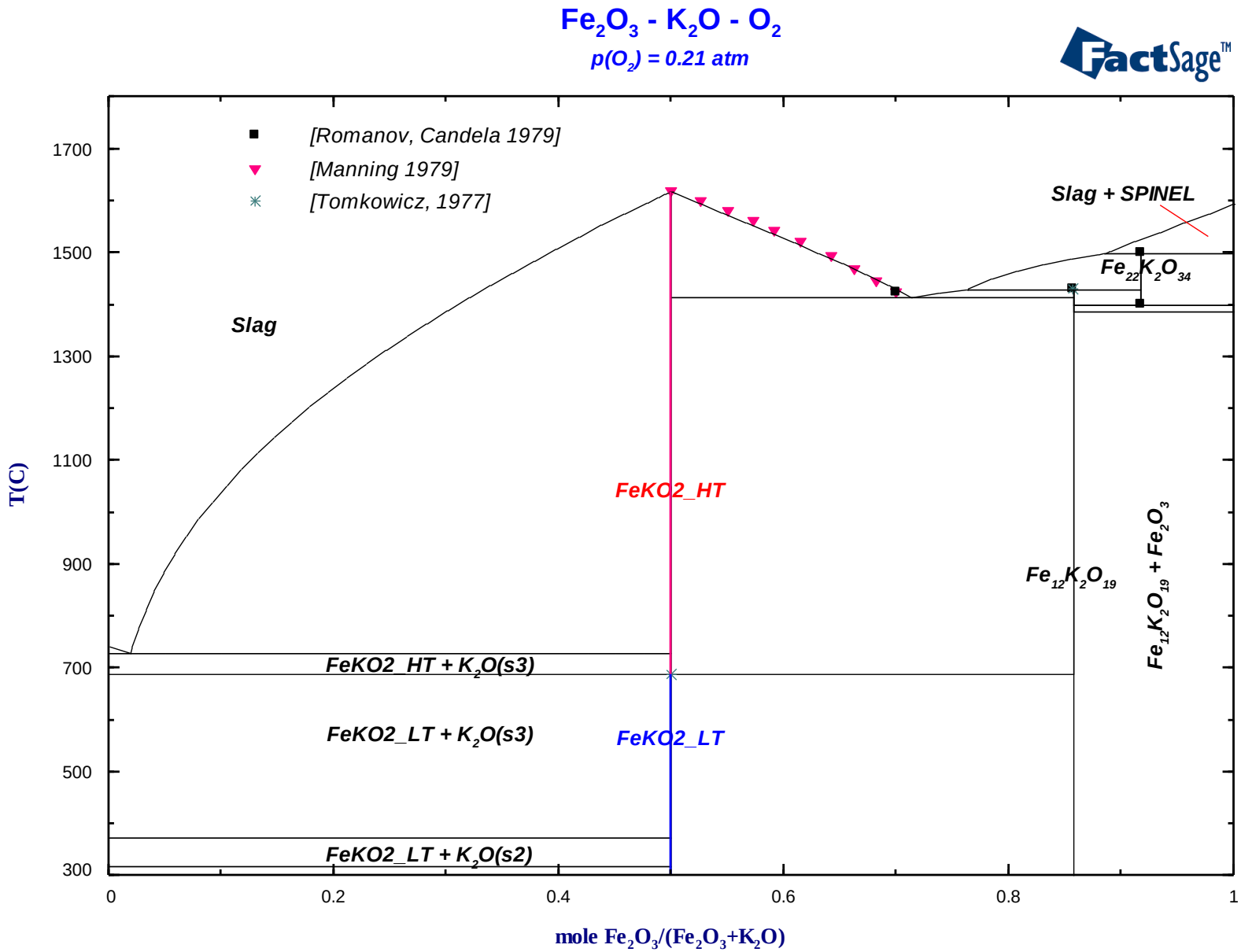

Weight percent

Fe_2O_3 - K_2O - O_2

$p(O_2)$ = 0.21 atm

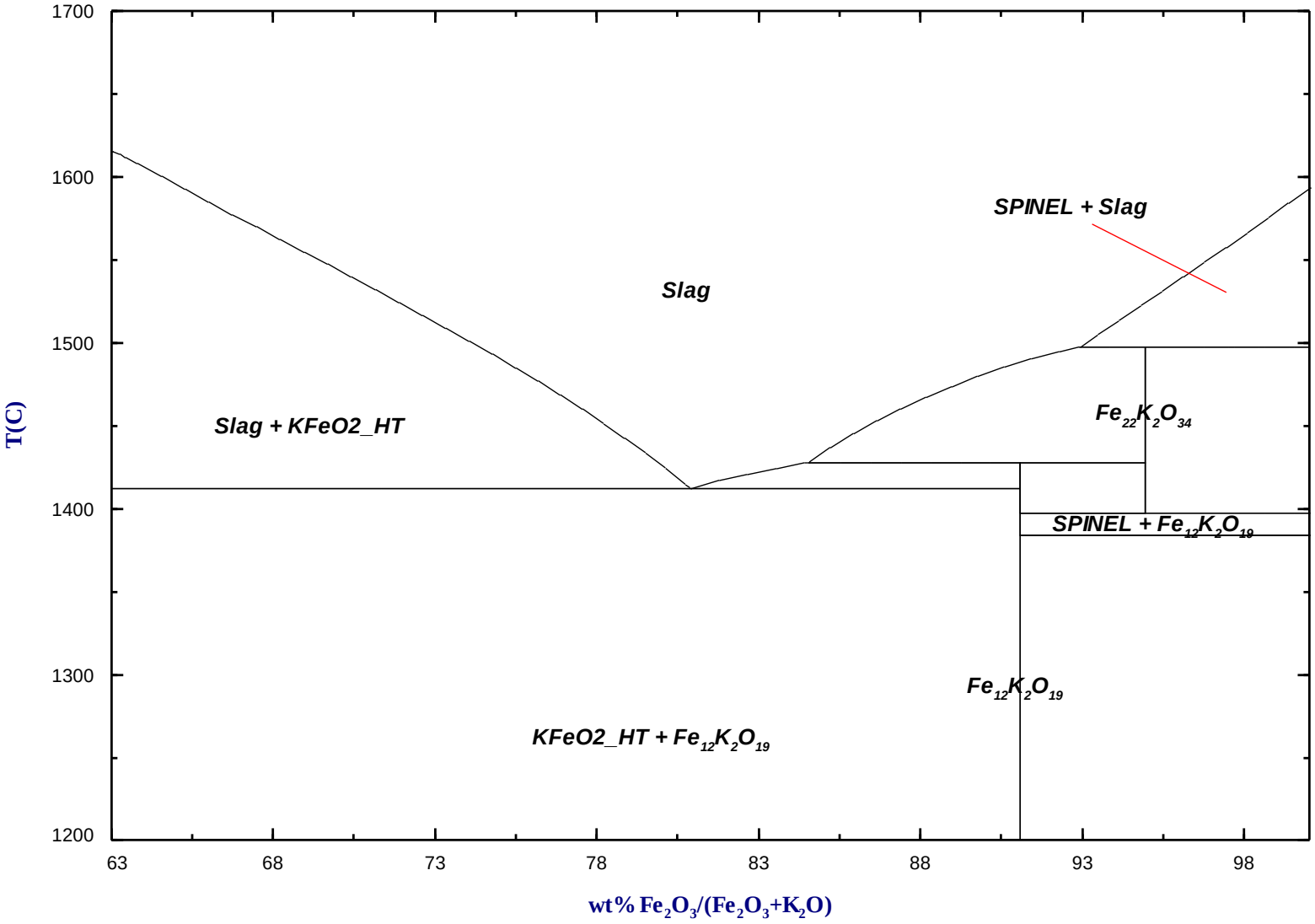

Mole fraction
compared with experimental data

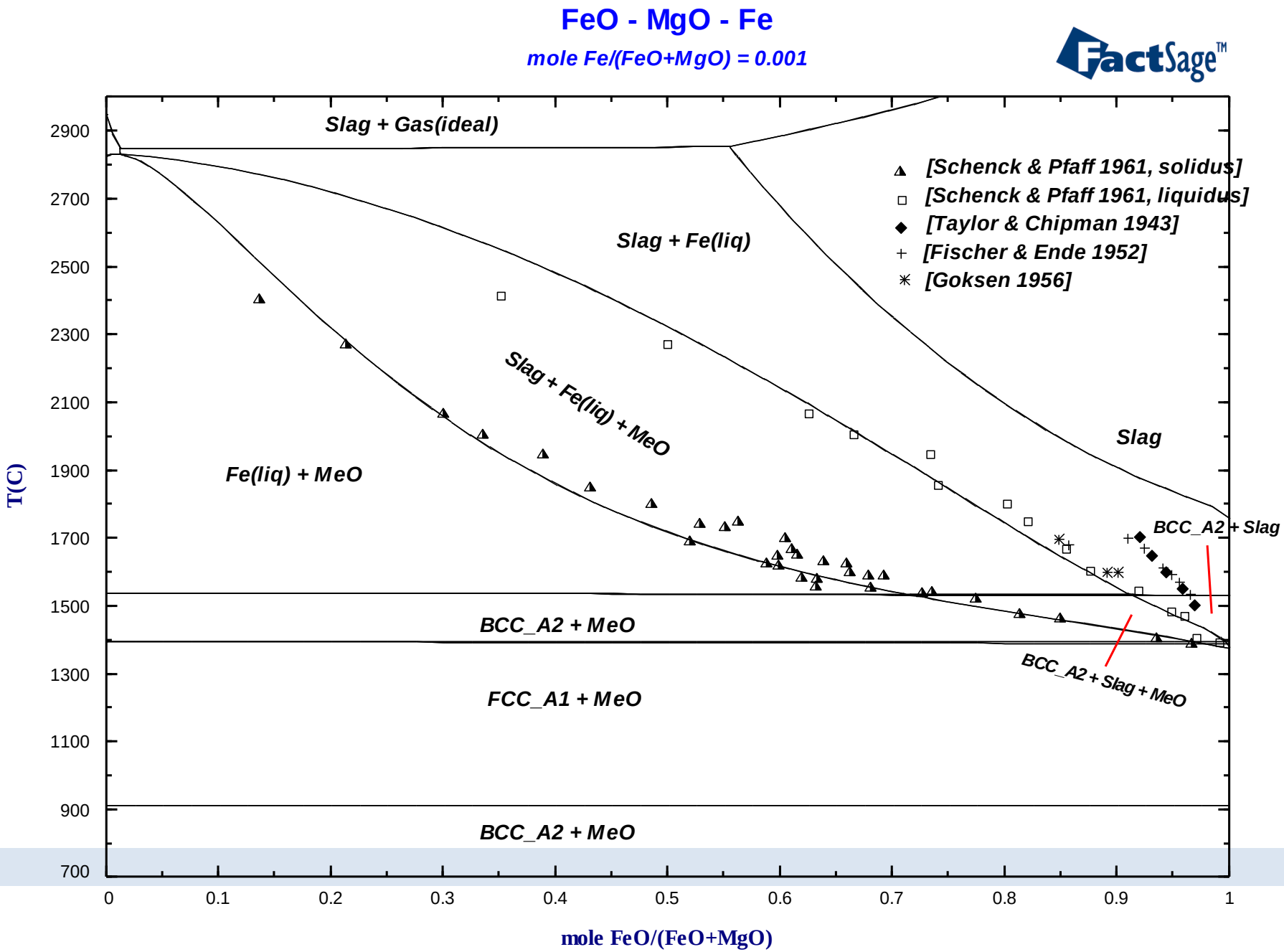

FeO - MgO - Fe

wt% Fe/(FeO+MgO) = 0.001

Weight percent

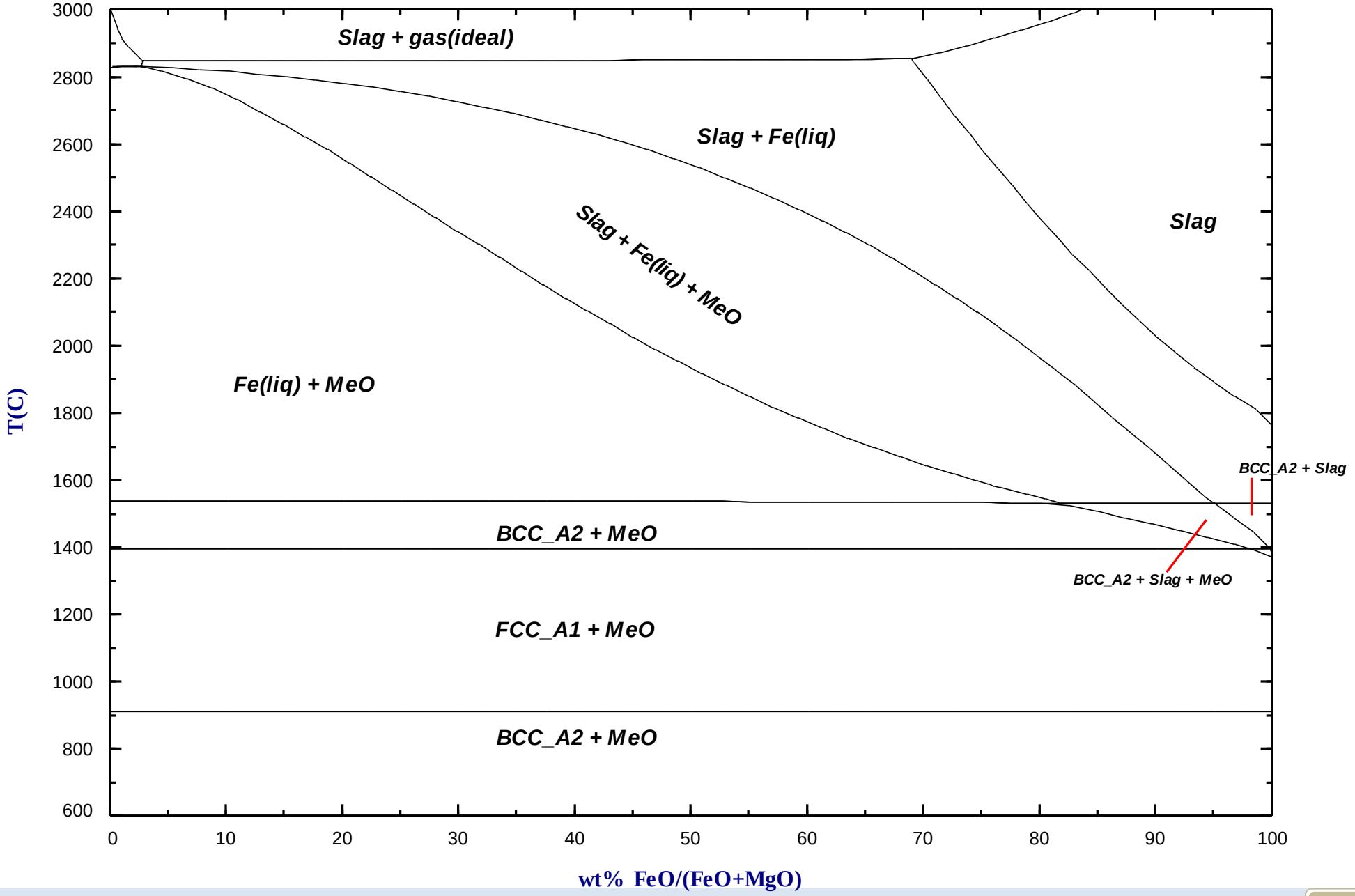

Fe_2O_3 - MgO - O_2

$p(O_2)$ = 0.21 atm

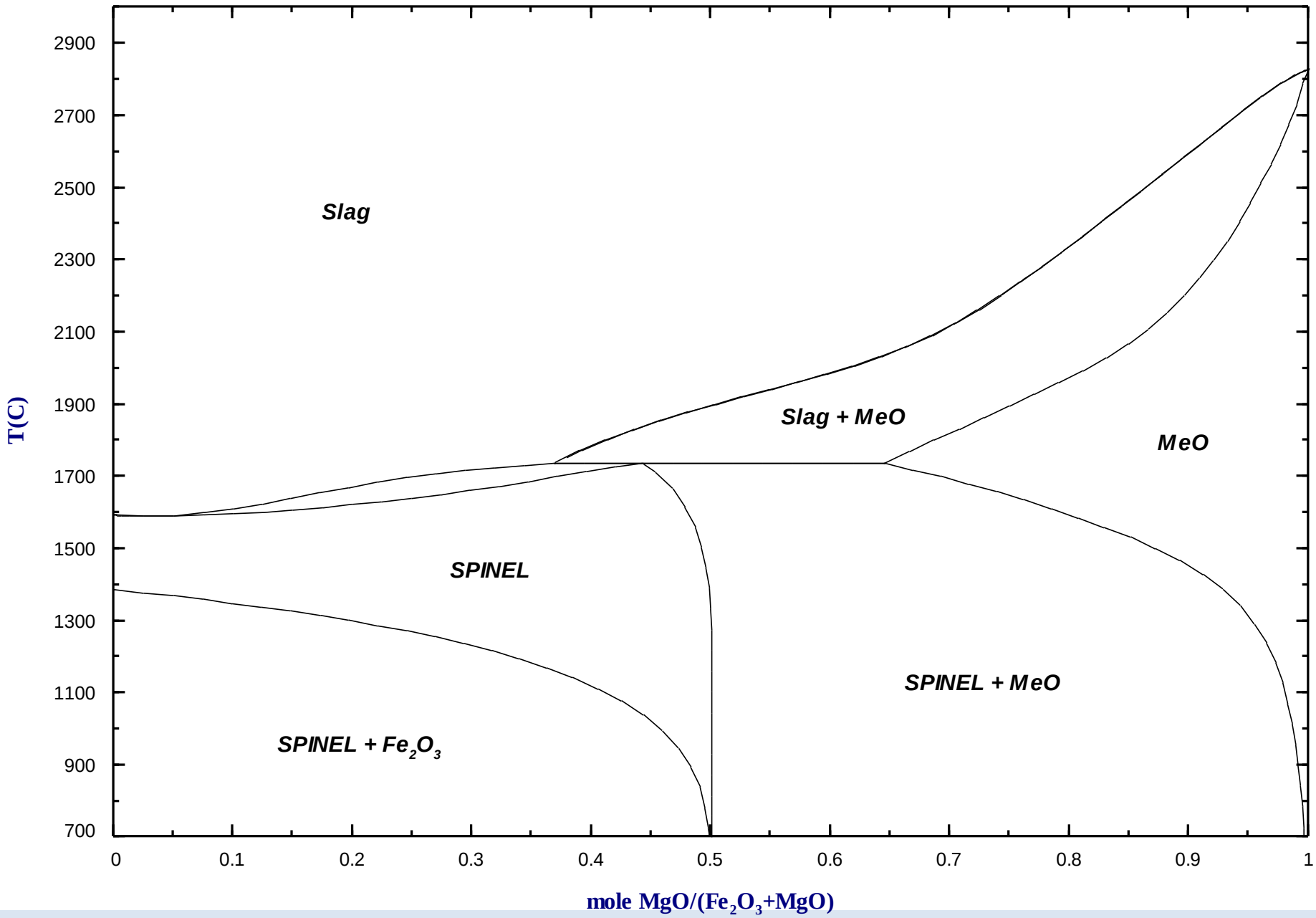

Weight percent
compared with experimental data

Fe_2O_3 - MgO - O_2

$p(O_2)$ = 0.21 atm

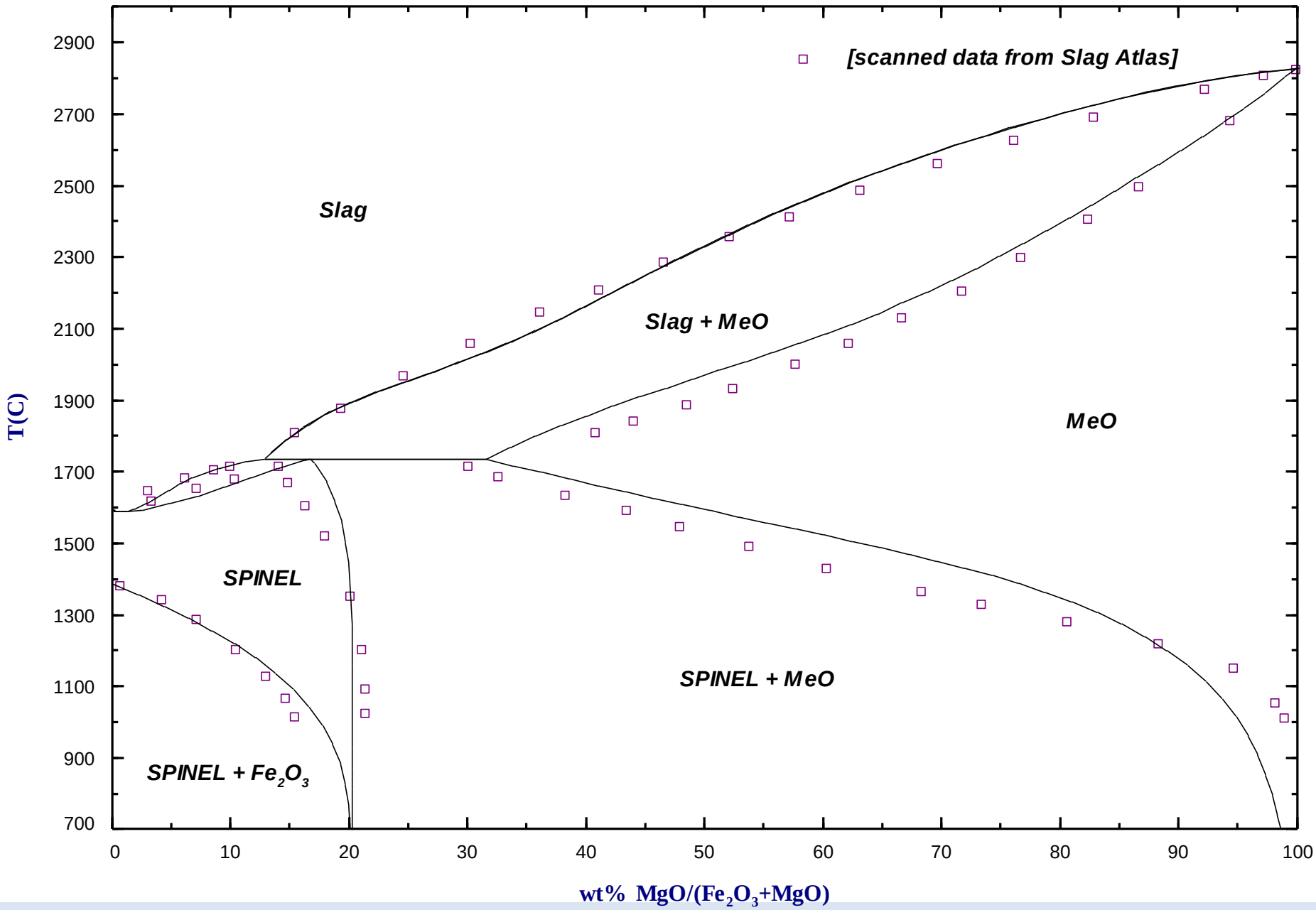

Mole fraction

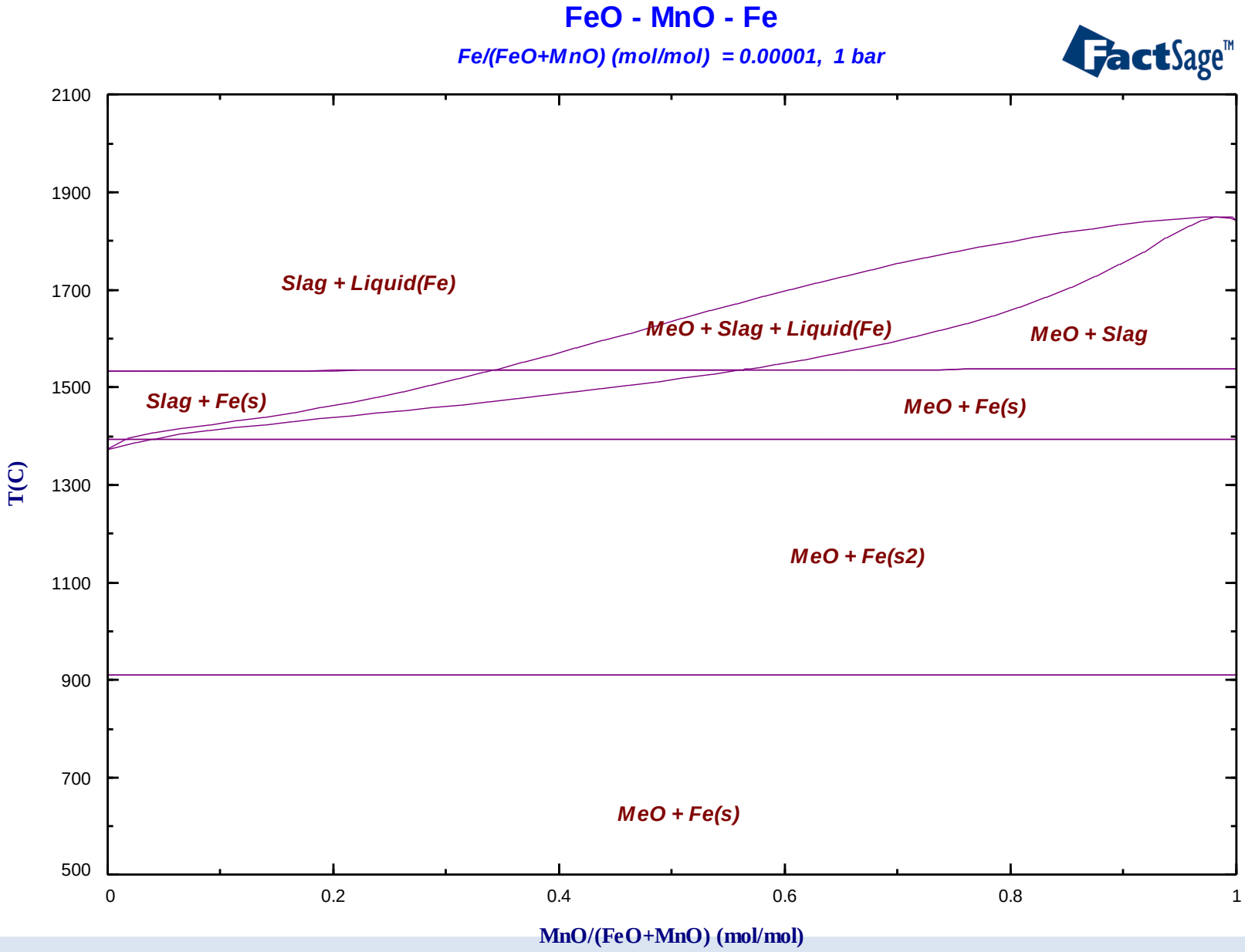

Weight percent
compared with experimental data

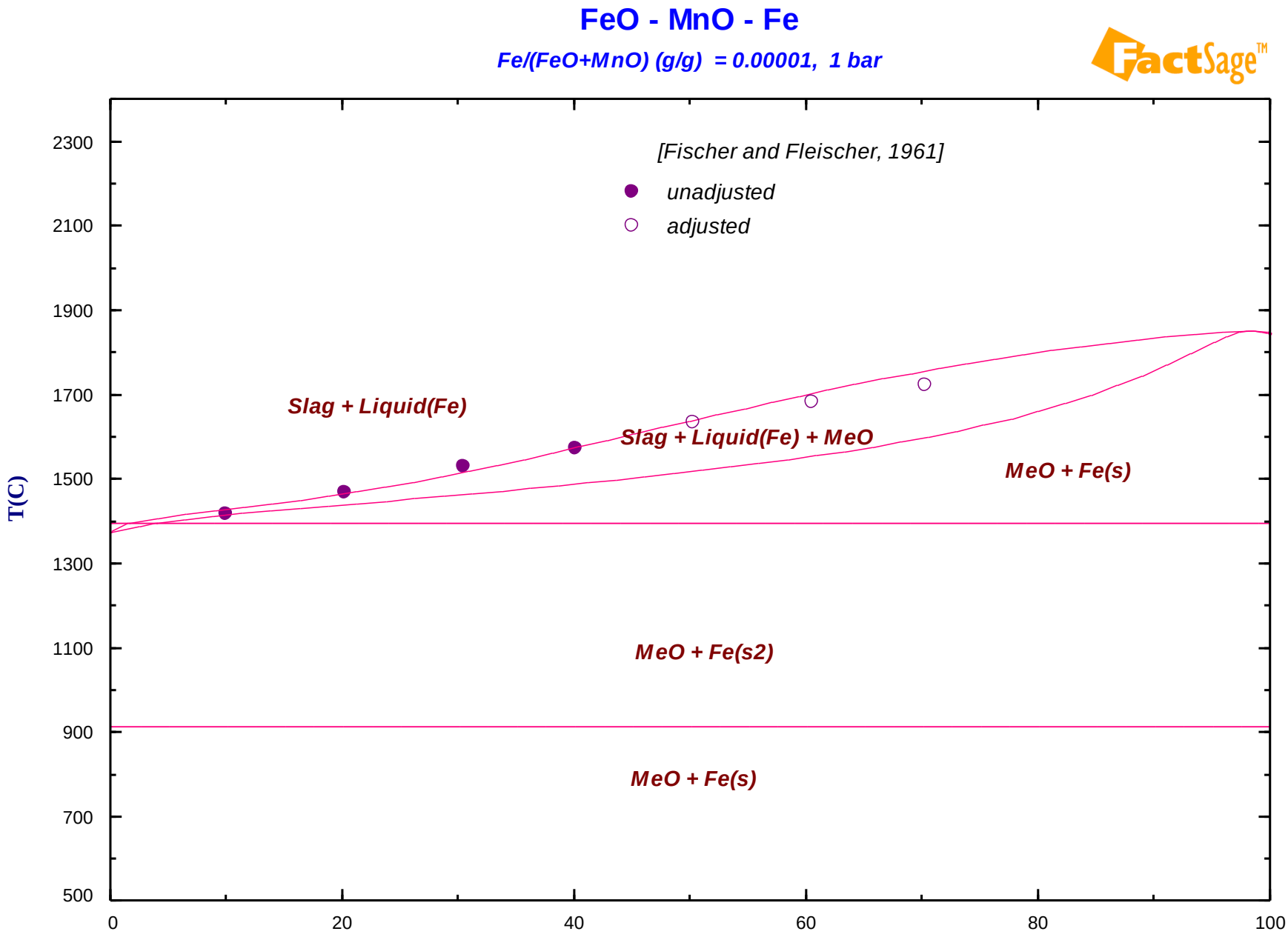

Mole fraction

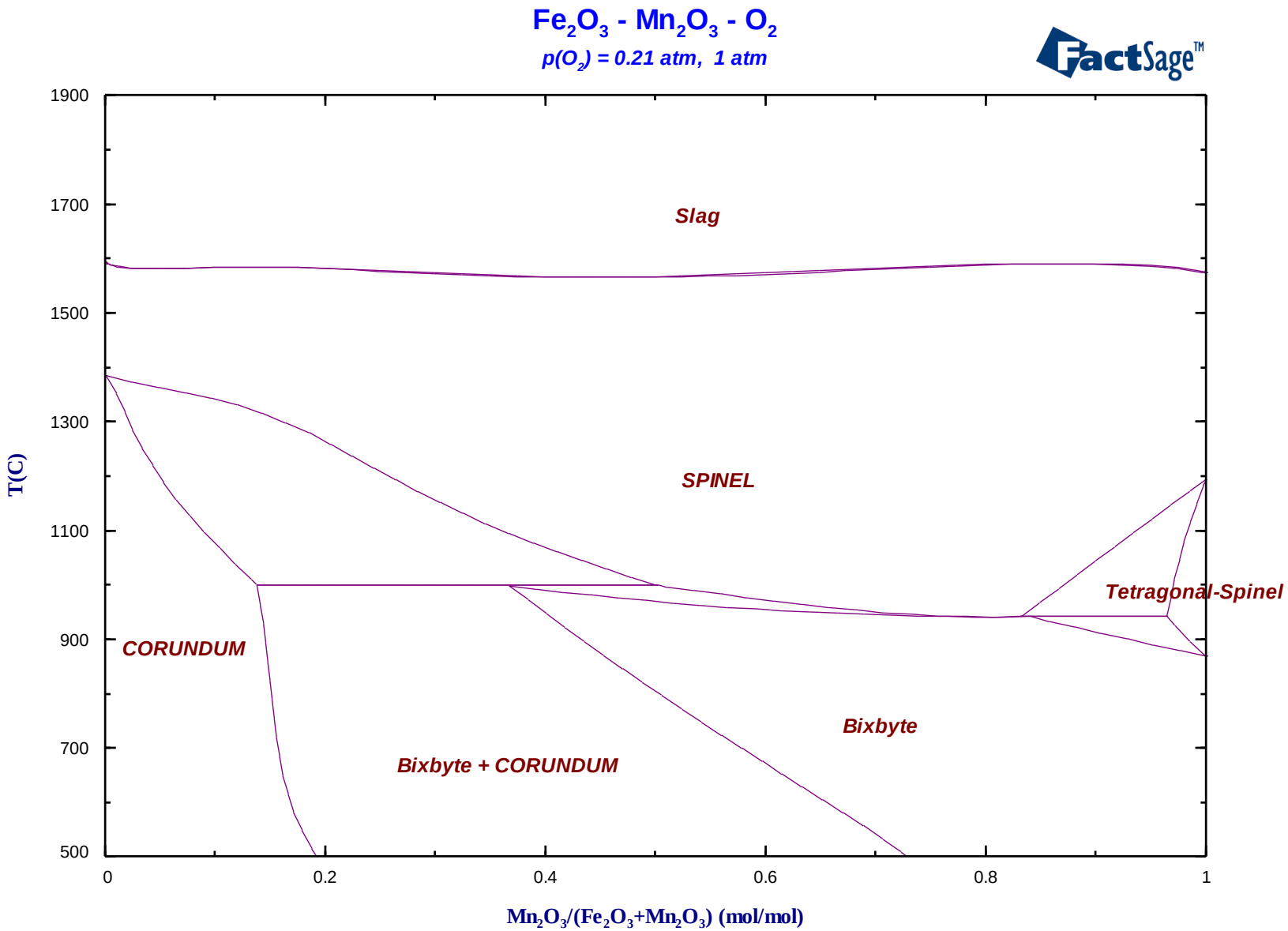

Weight percent
compared with experimental data

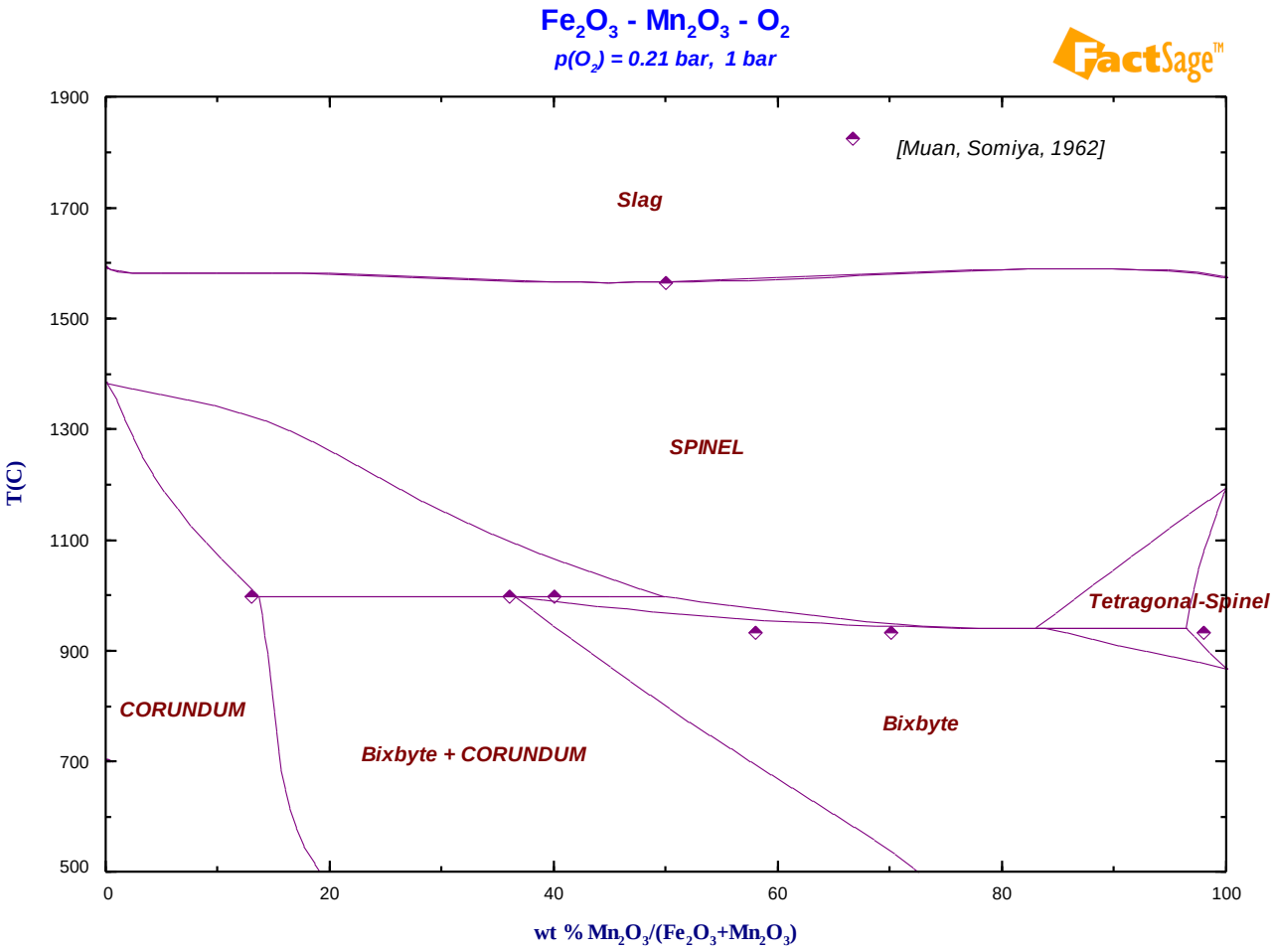

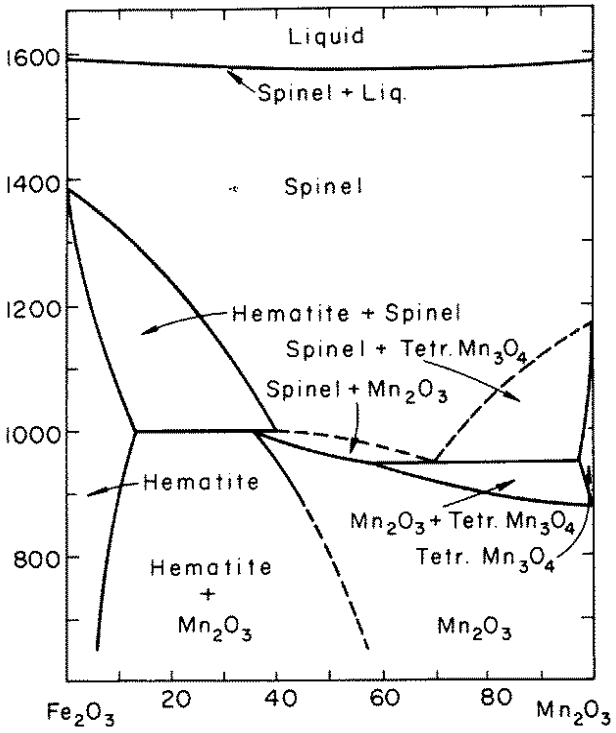

A. Muan, S. Somiya, Am. J. Sci., 260 [3], (1962), pp. 230-240.

Mole fraction

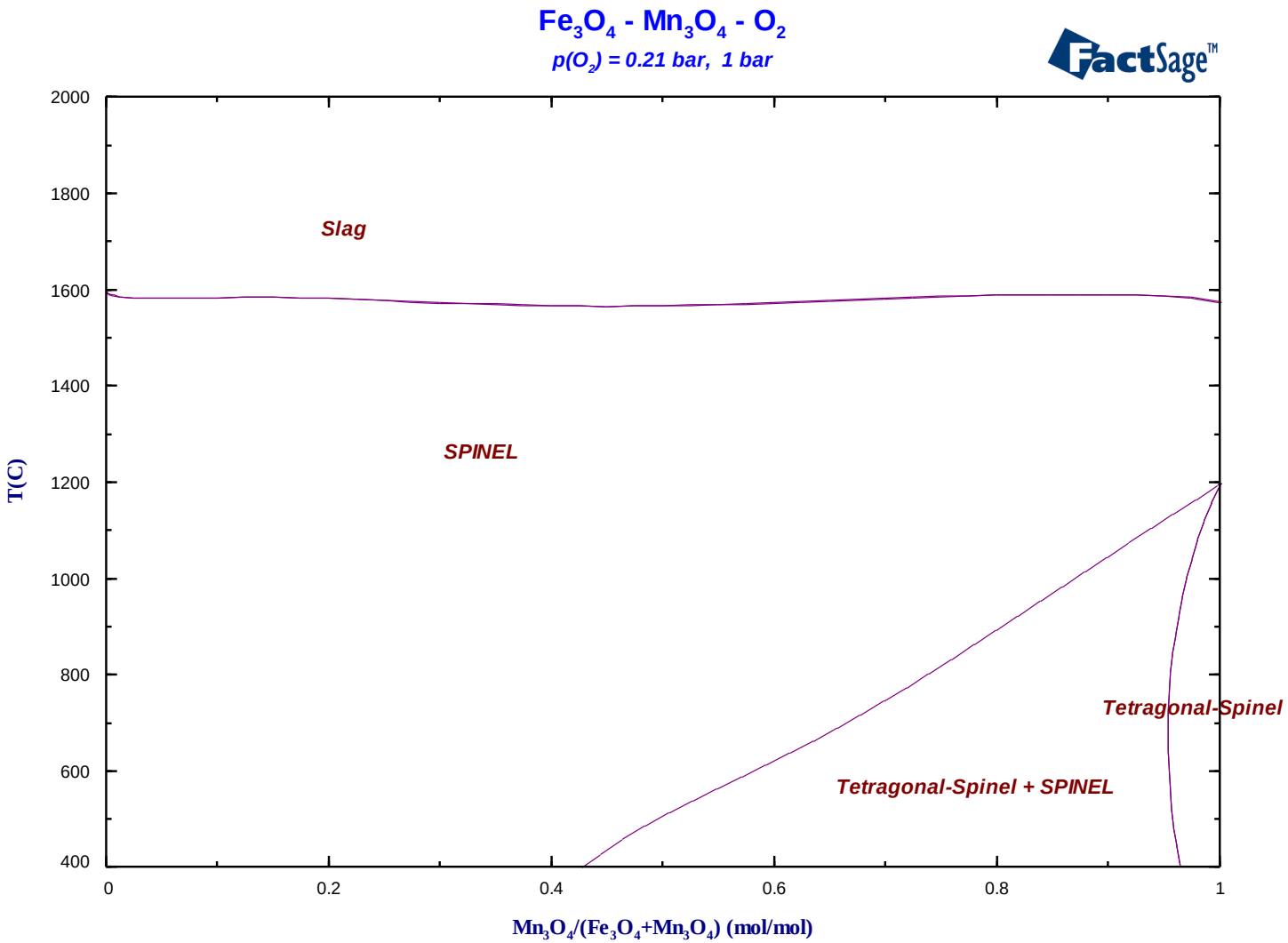

Weight percent

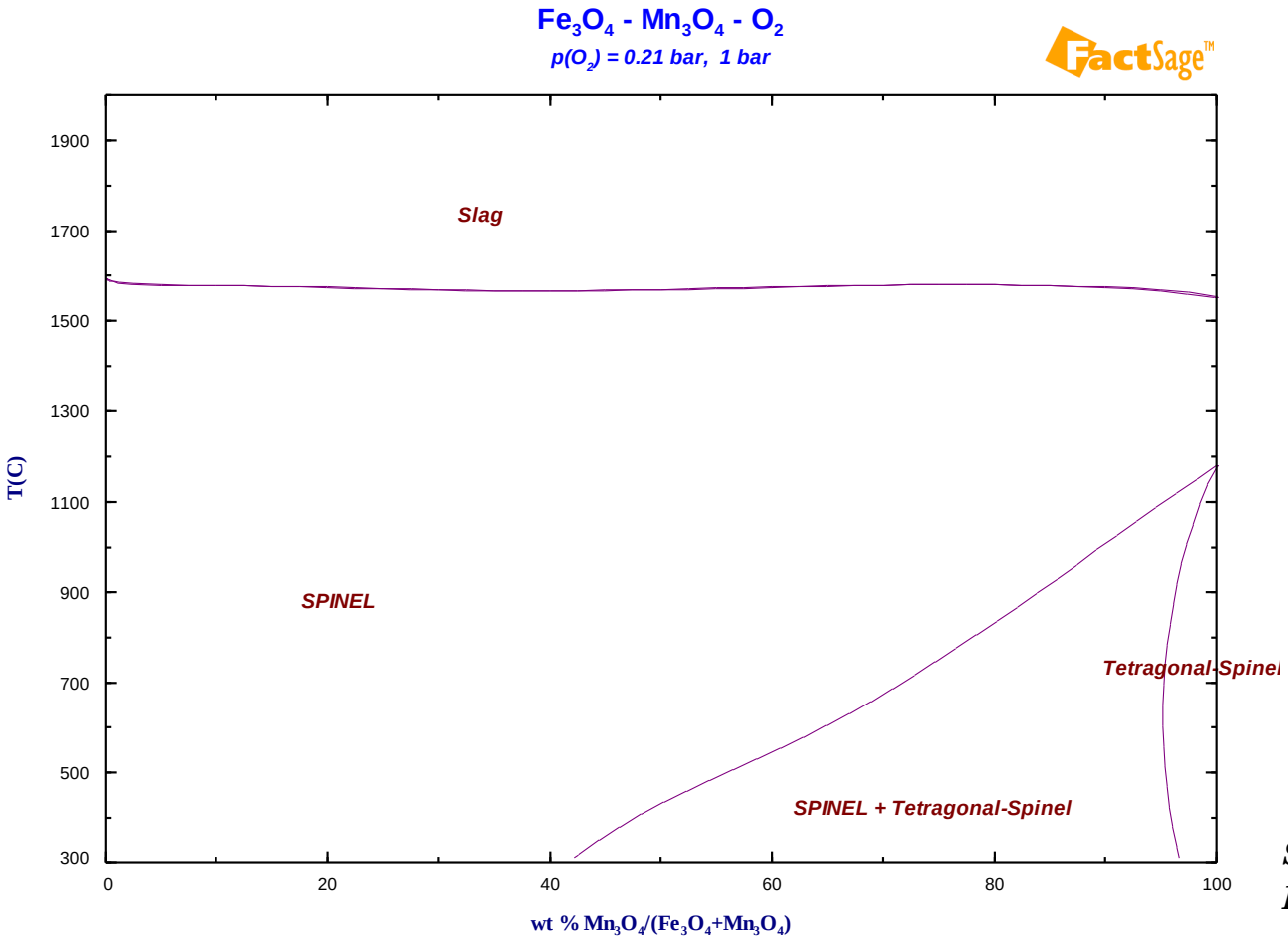

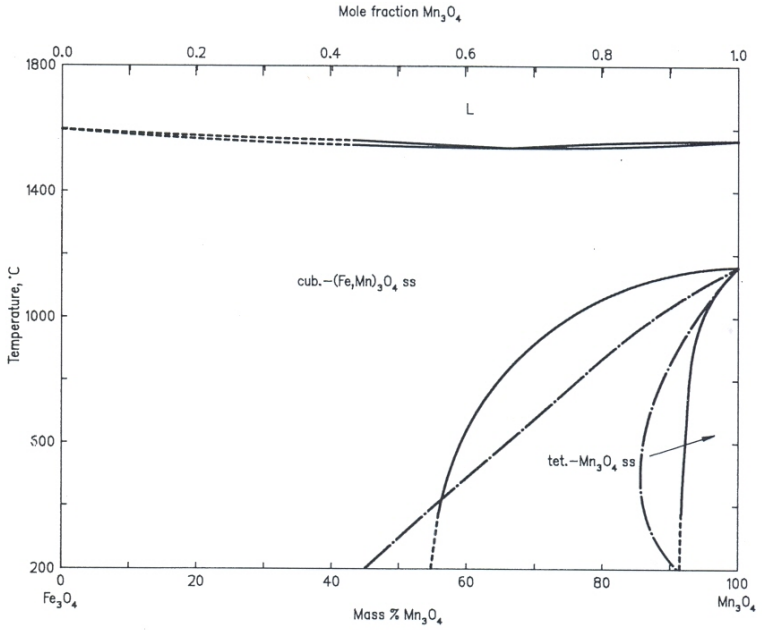

Slag Atlas, 2nd Ed., Verlag Stahl-Eisen, Düsseldorf, 1995., p.673

Mole fraction

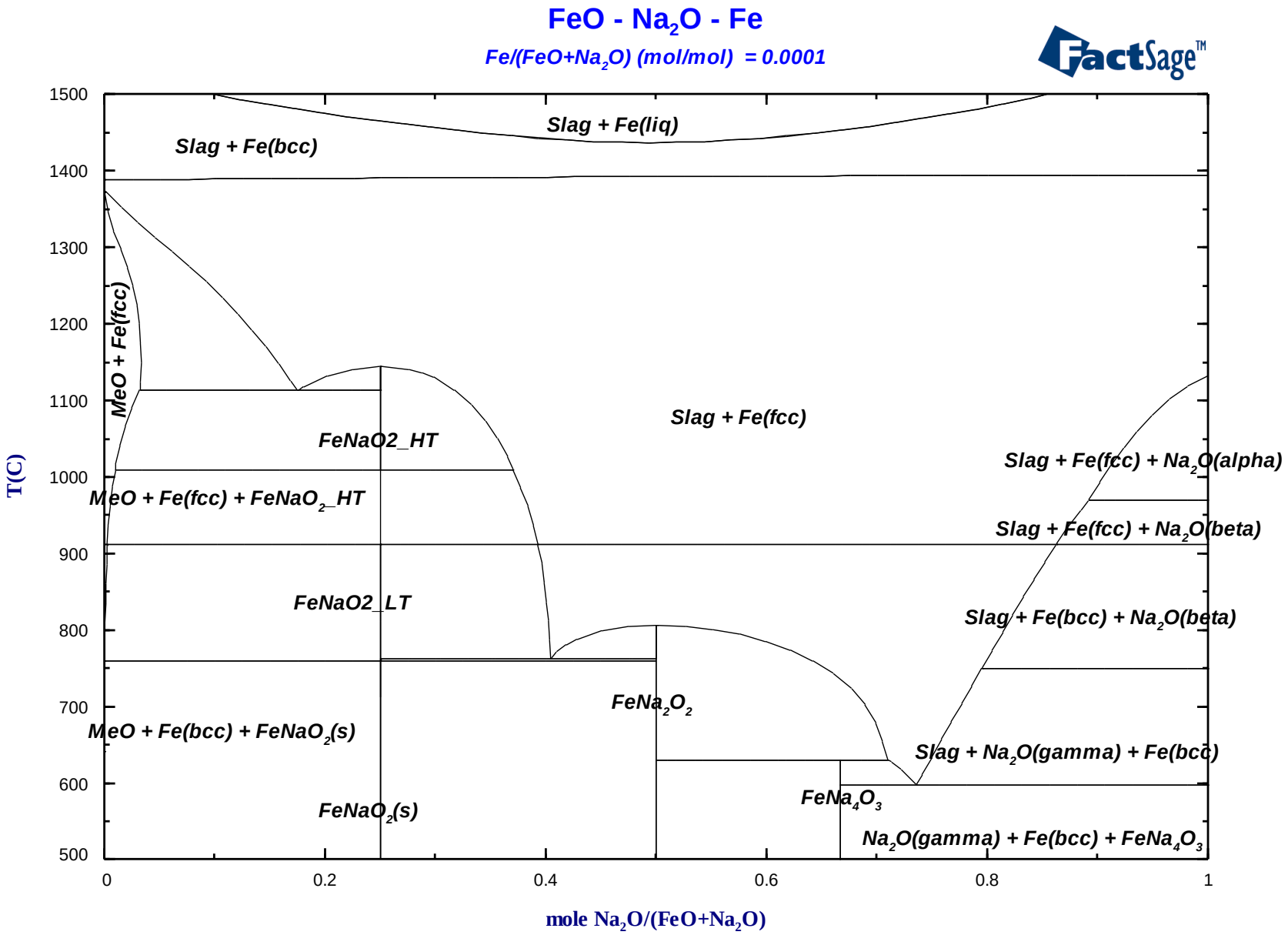

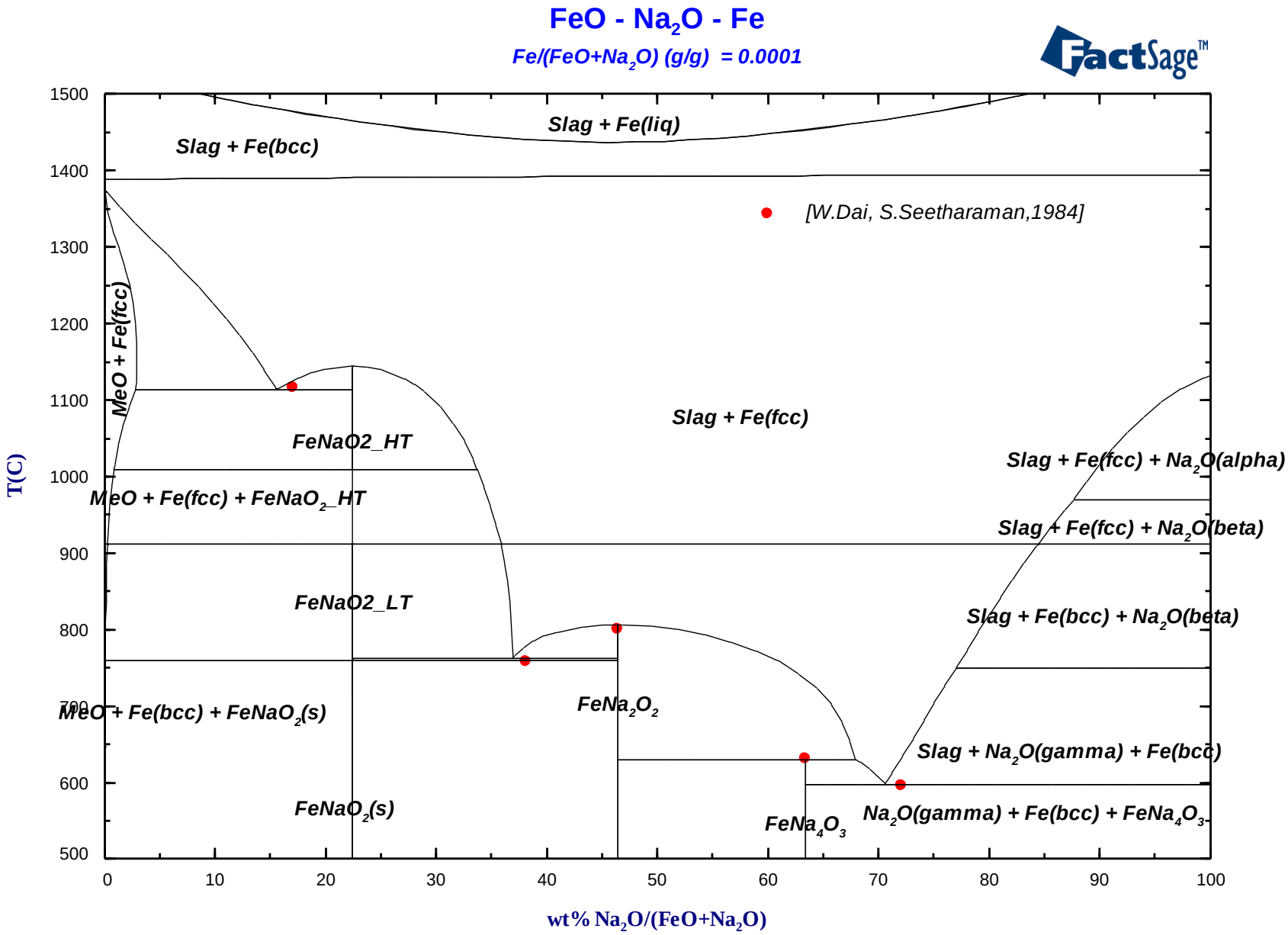
FeO - Na2O - Fe
Fe/(FeO+Na2O) (g/g) = 0.0001
FactSage™
[W.Dai, S.Seetharaman,1984]
Slag + Fe(liq)
Slag + Fe(bcc)
MeO + Fe(fcc)
Slag + Fe(fcc)
FeNaO2_HT
MeO + Fe(fcc) + FeNaO2_HT
Slag + Fe(fcc) + Na2O(alpha)
Slag + Fe(fcc) + Na2O(beta)
FeNaO2_LT
Slag + Fe(bcc) + Na2O(beta)
MeO + Fe(bcc) + FeNaO2(s)
FeNa2O2
Slag + Na2O(gamma) + Fe(bcc)
FeNaO2(s)
FeNa4O3
Na2O(gamma) + Fe(bcc) + FeNa4O3
T(C)
wt% Na2O/(FeO+Na2O)
1500
1400
1300
1200
1100
1000
900
800
700
600
500
0
10
20
30
40
50
60
70
80
90
100

Weight percent
compared with experimental data

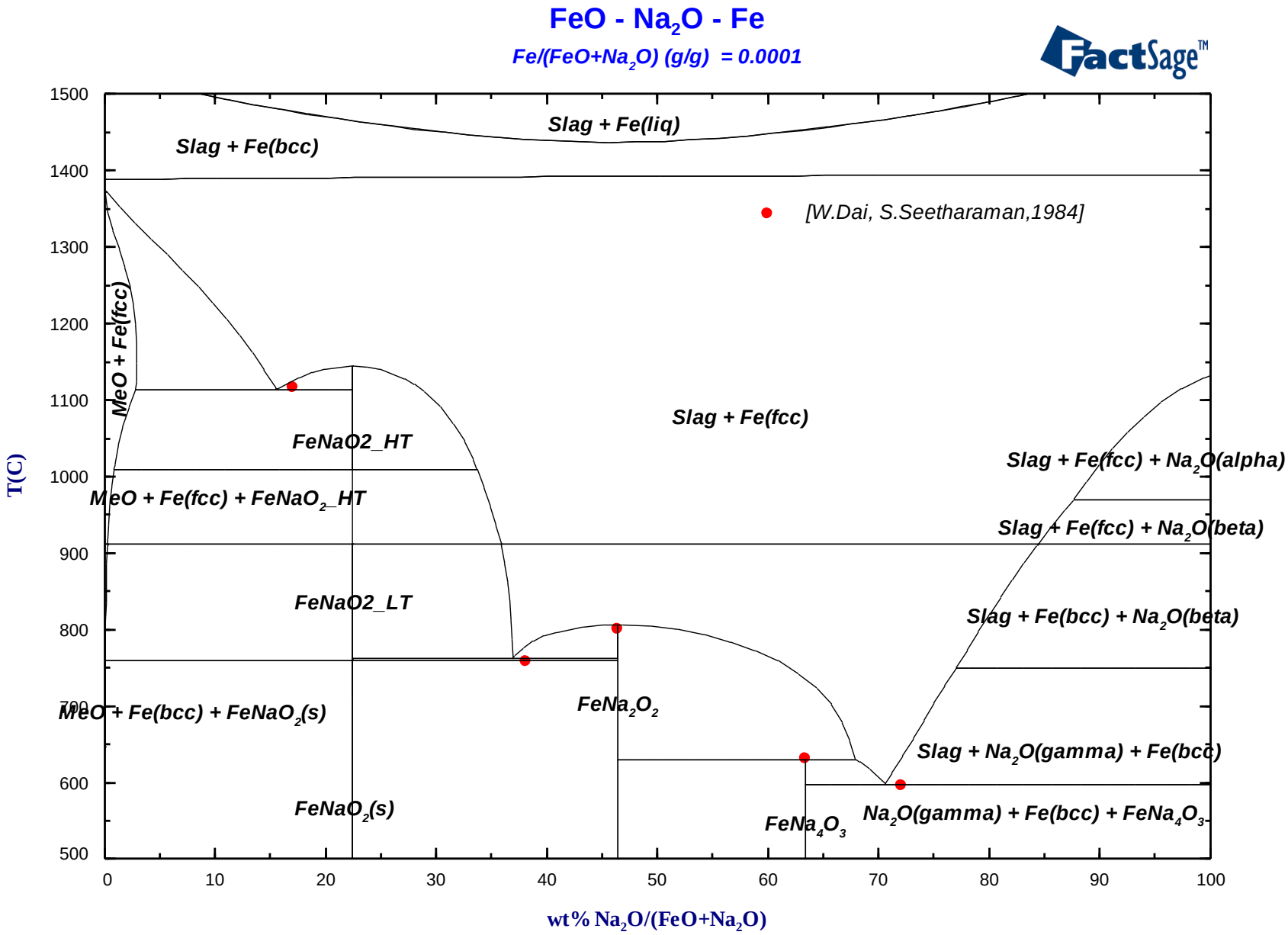

Fe2O3-Na2O-O2,

Mole fraction

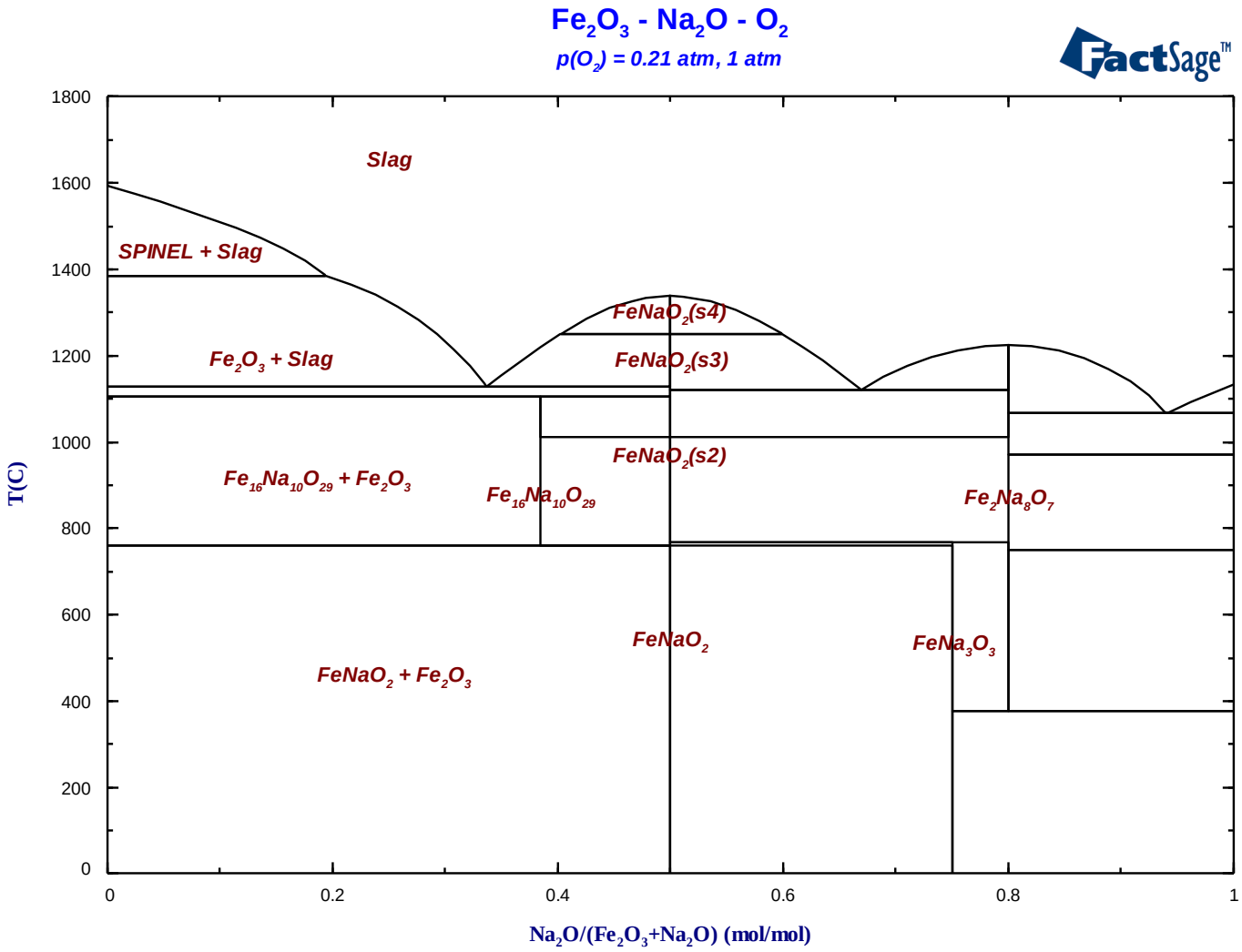

Fe2O3-Na2O-O2,
Weight percent
compared with experimental data

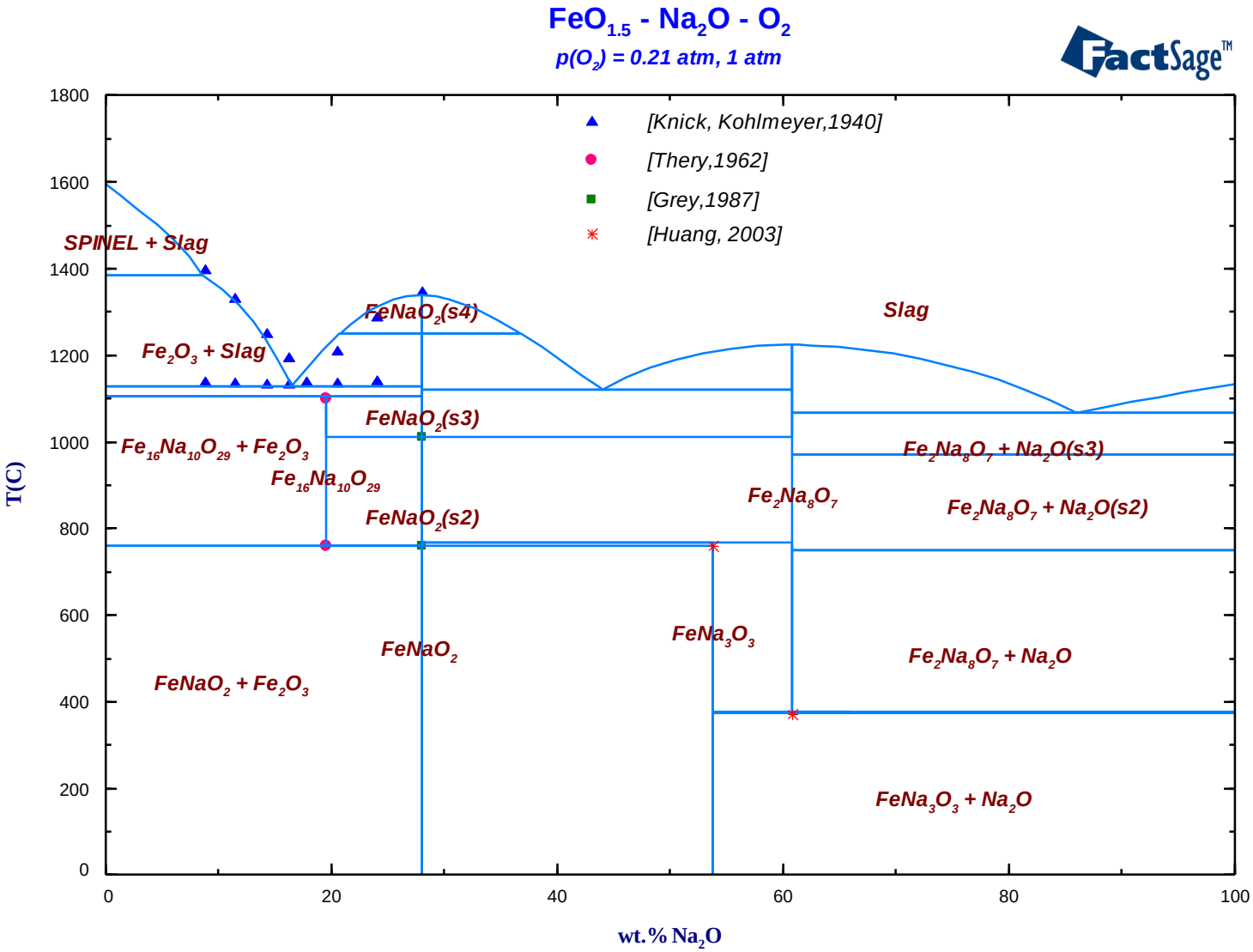

Mole fraction

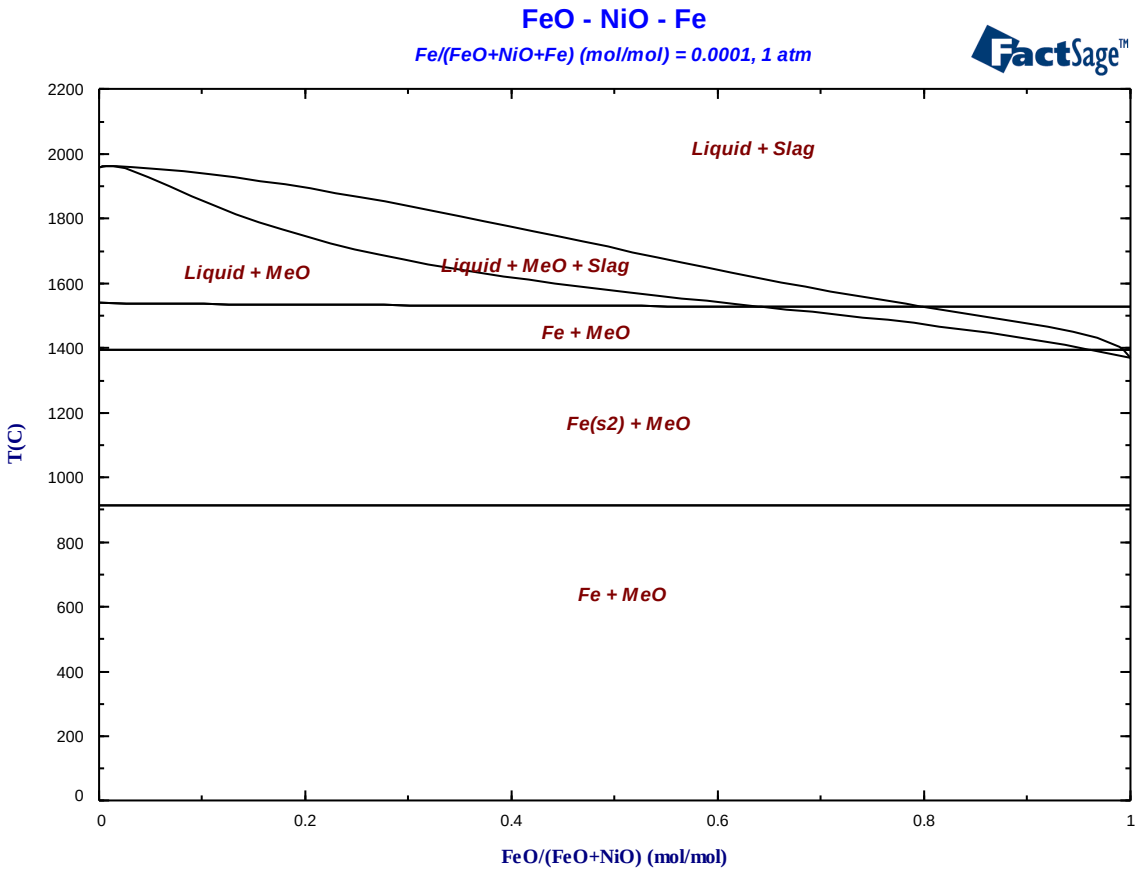

Weight percent compared with experimental data

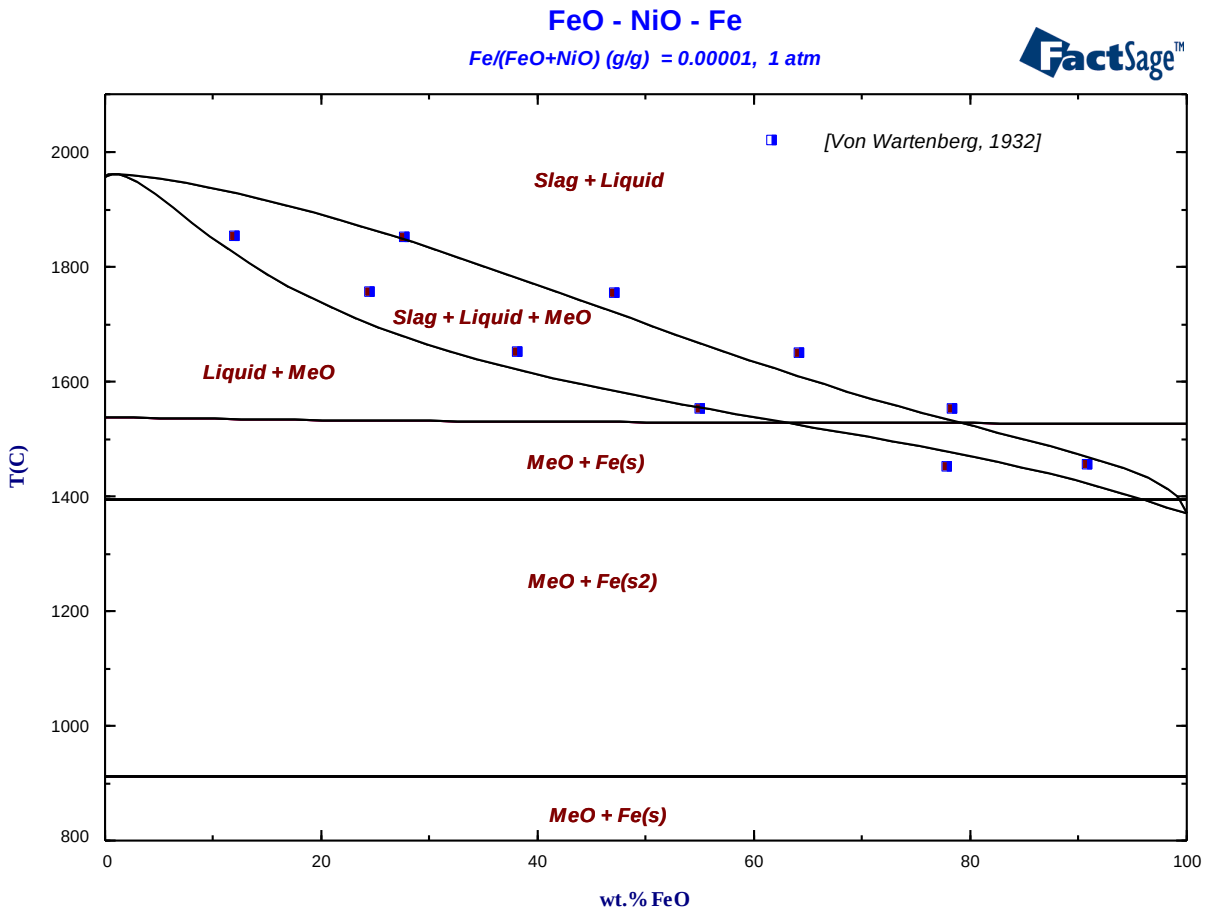

Mole fraction compared with experimental data

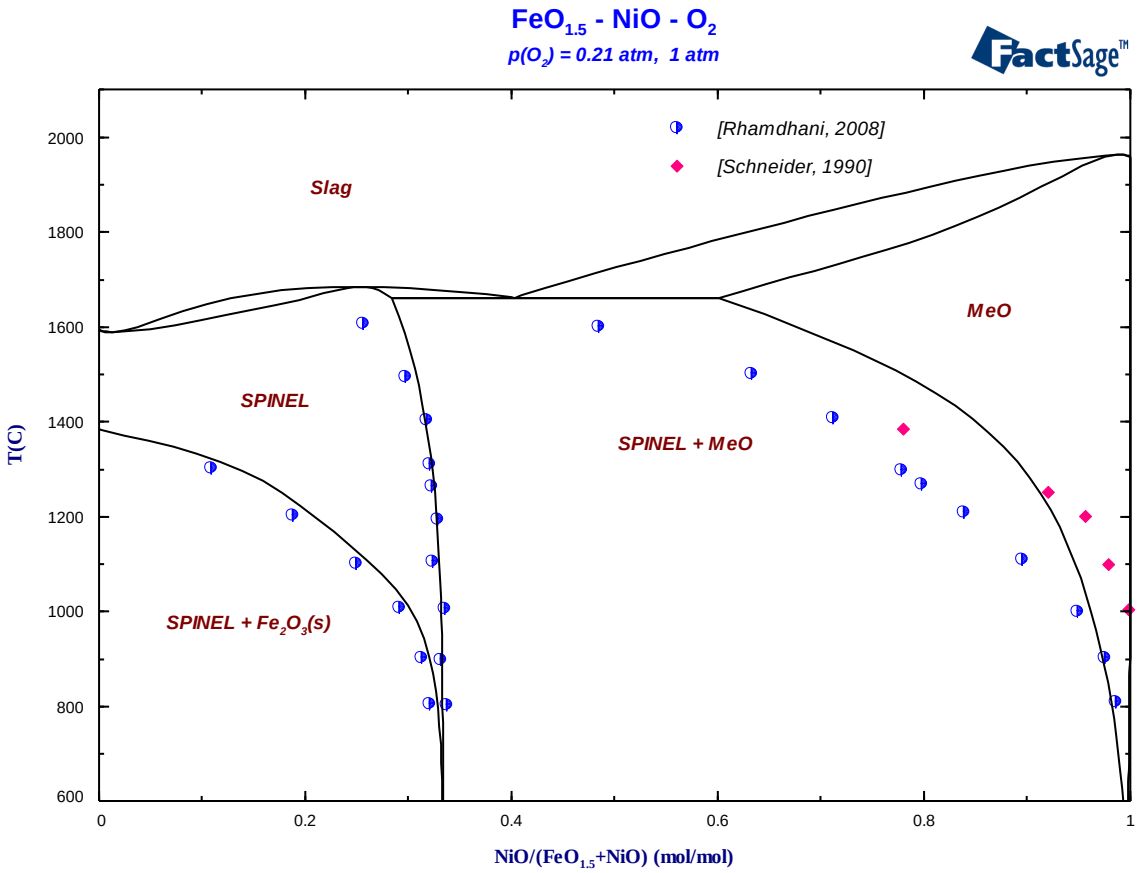

Weight percent

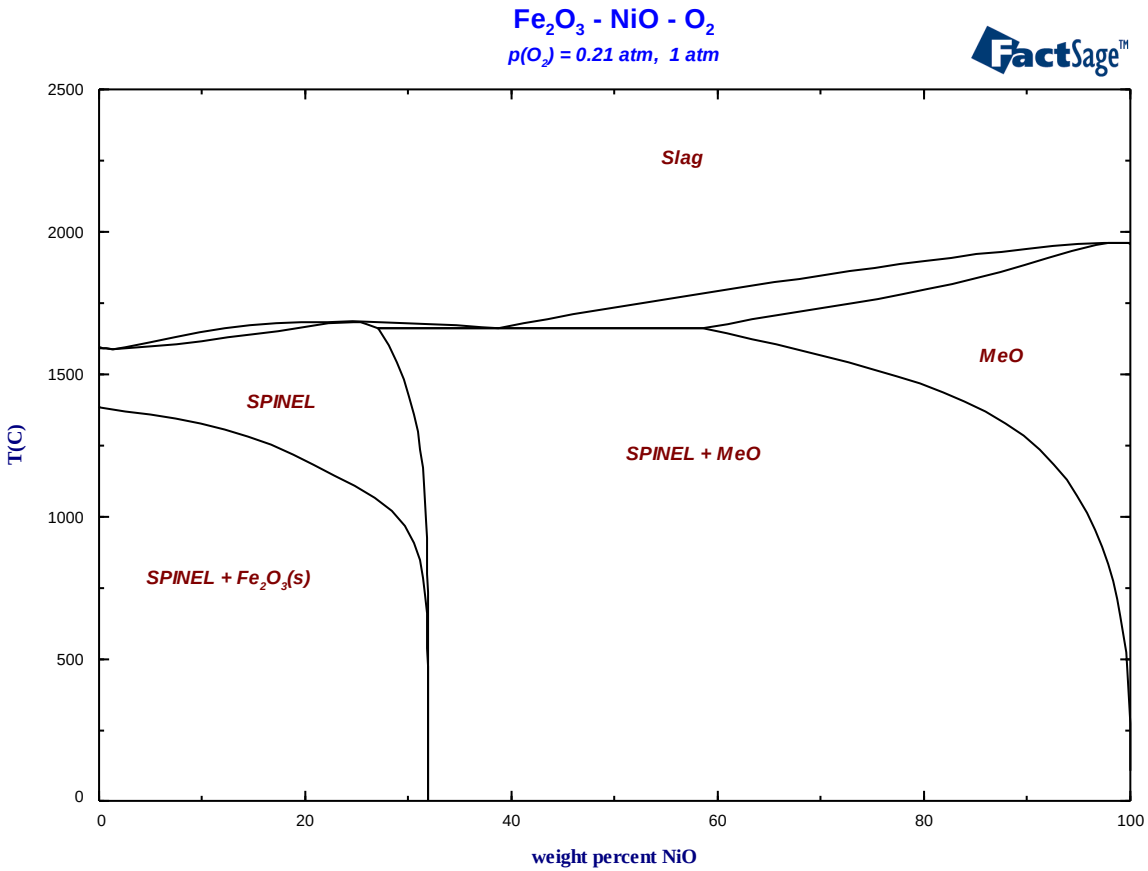

Mole fraction

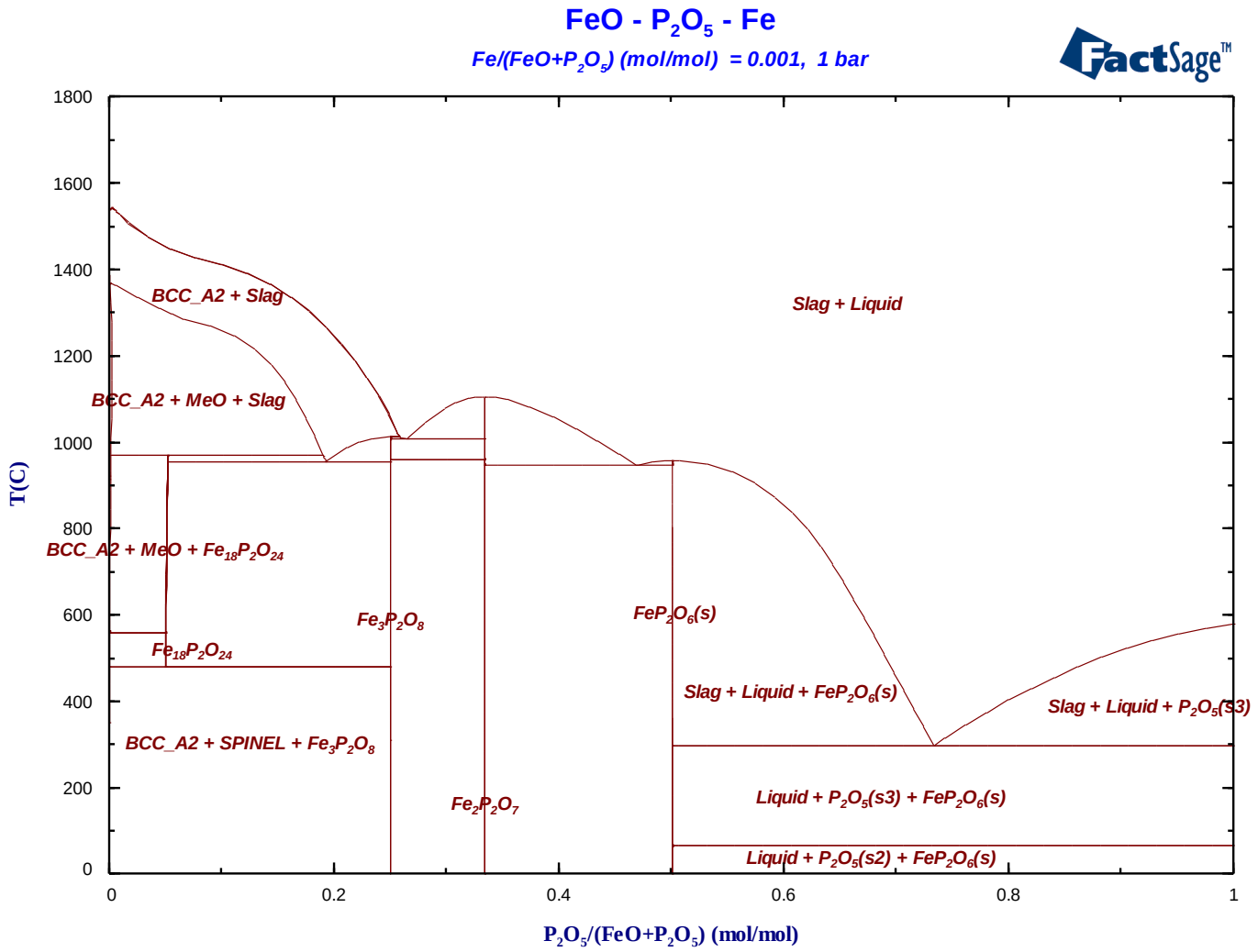

Weight percent
compared with experimental data

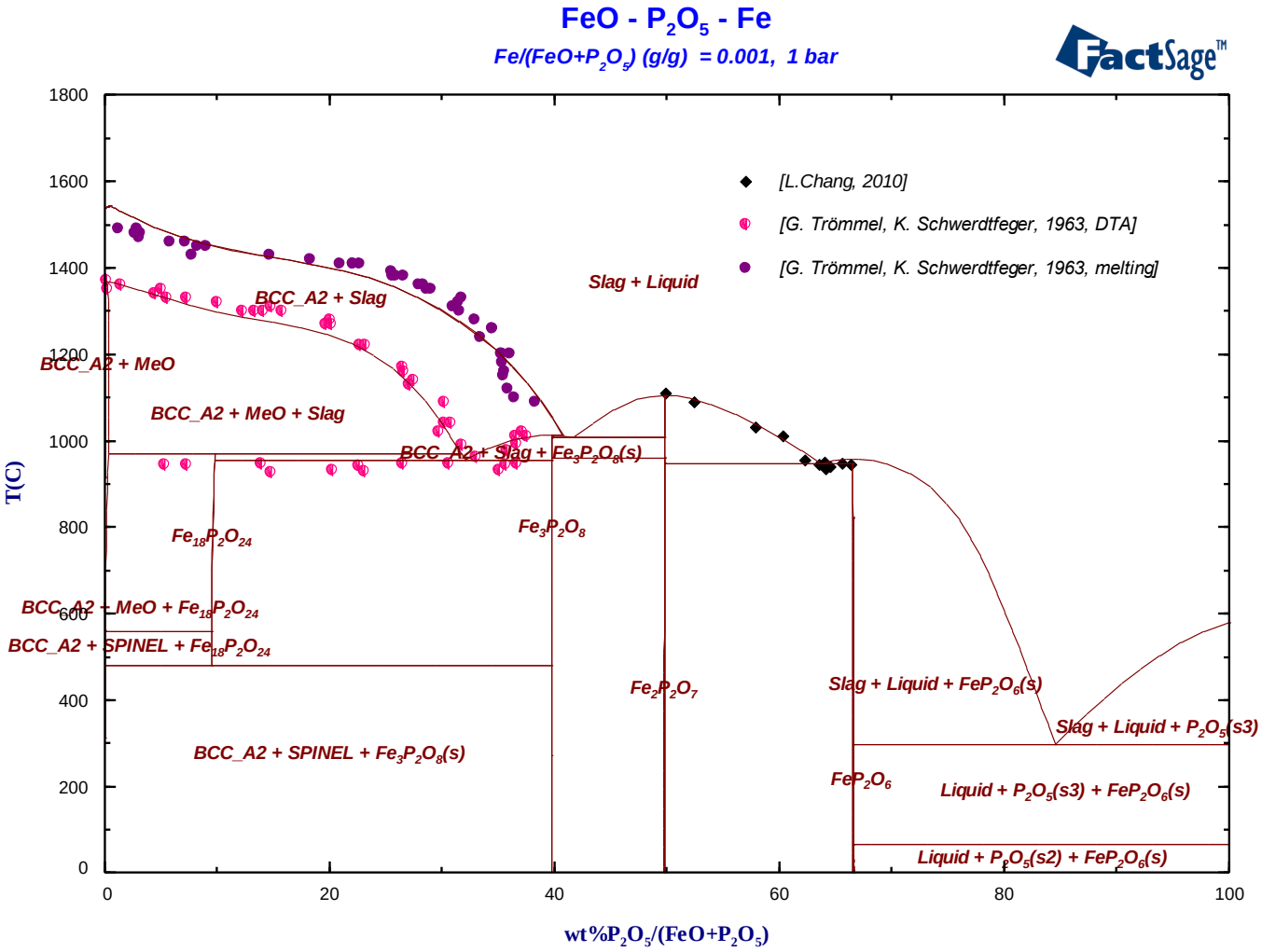

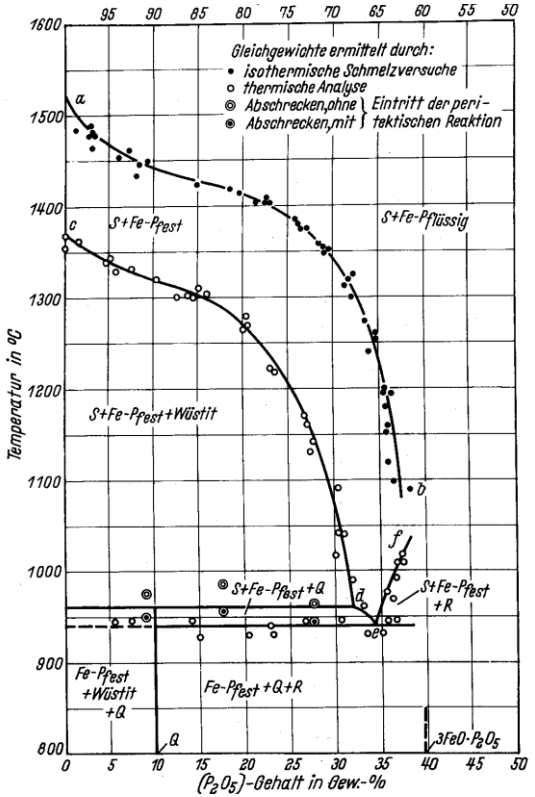

G. Trömmel, K. Schwerdtfeger, Arch. Eisenhütten., 34 [1], (1963), pp-55-59.

Mole fraction

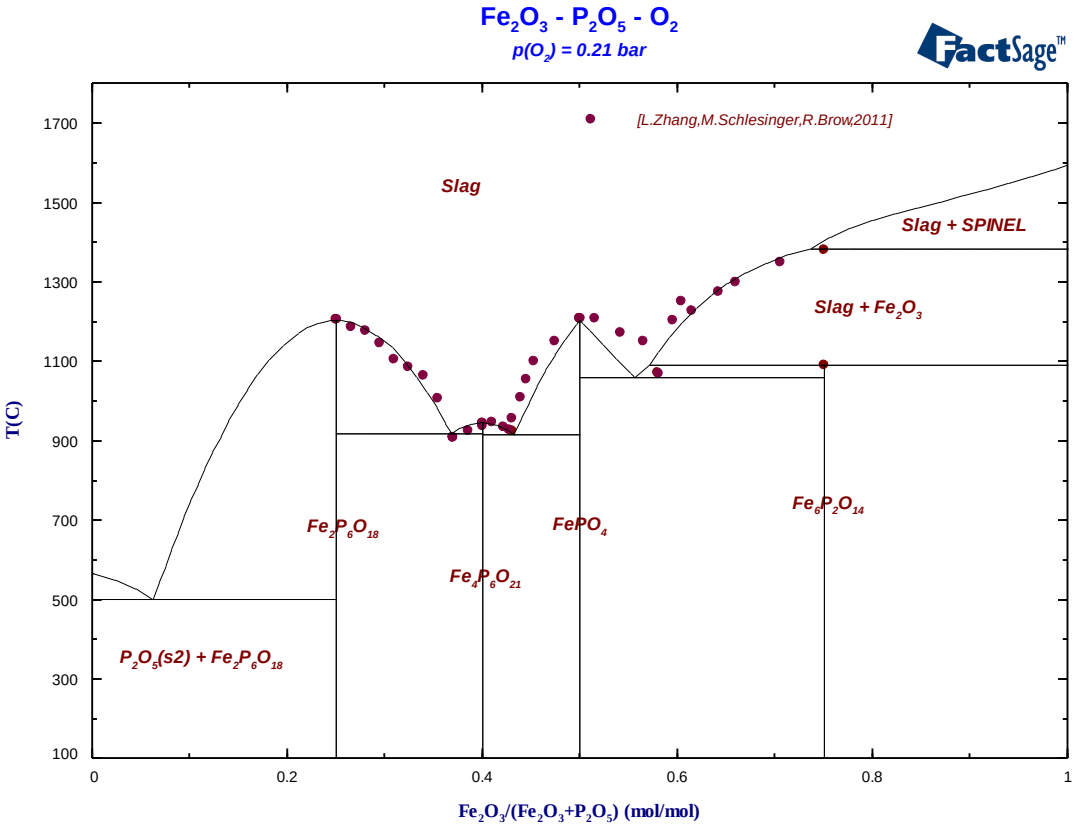

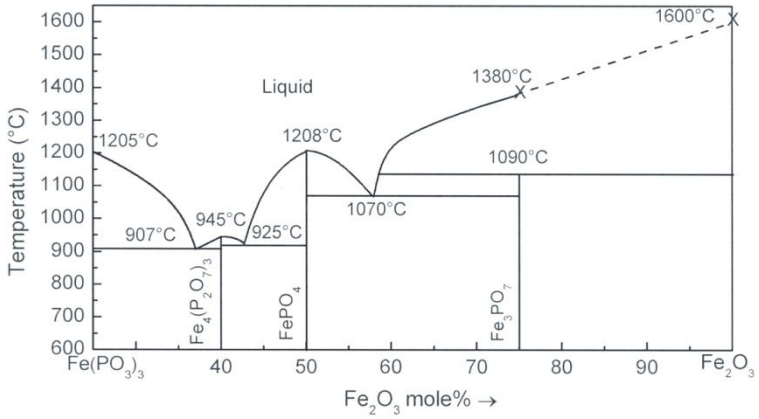

L. Zhang, M. E. Schlesinger, R. K. Brow, (J. Am. Ceram. Society, Vol.94, Issue 5, (2011), pp.1605-

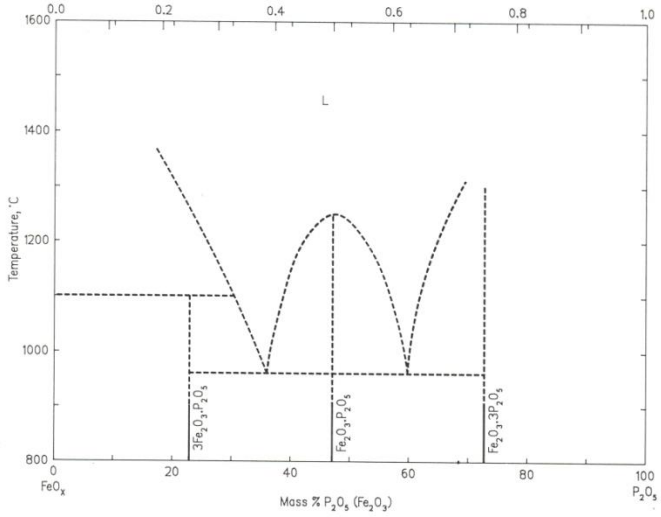

Slag Atlas, 2nd Ed., Verlag Stahl-Eisen, Düsseldorf, 1995., p.68.

Weight percent

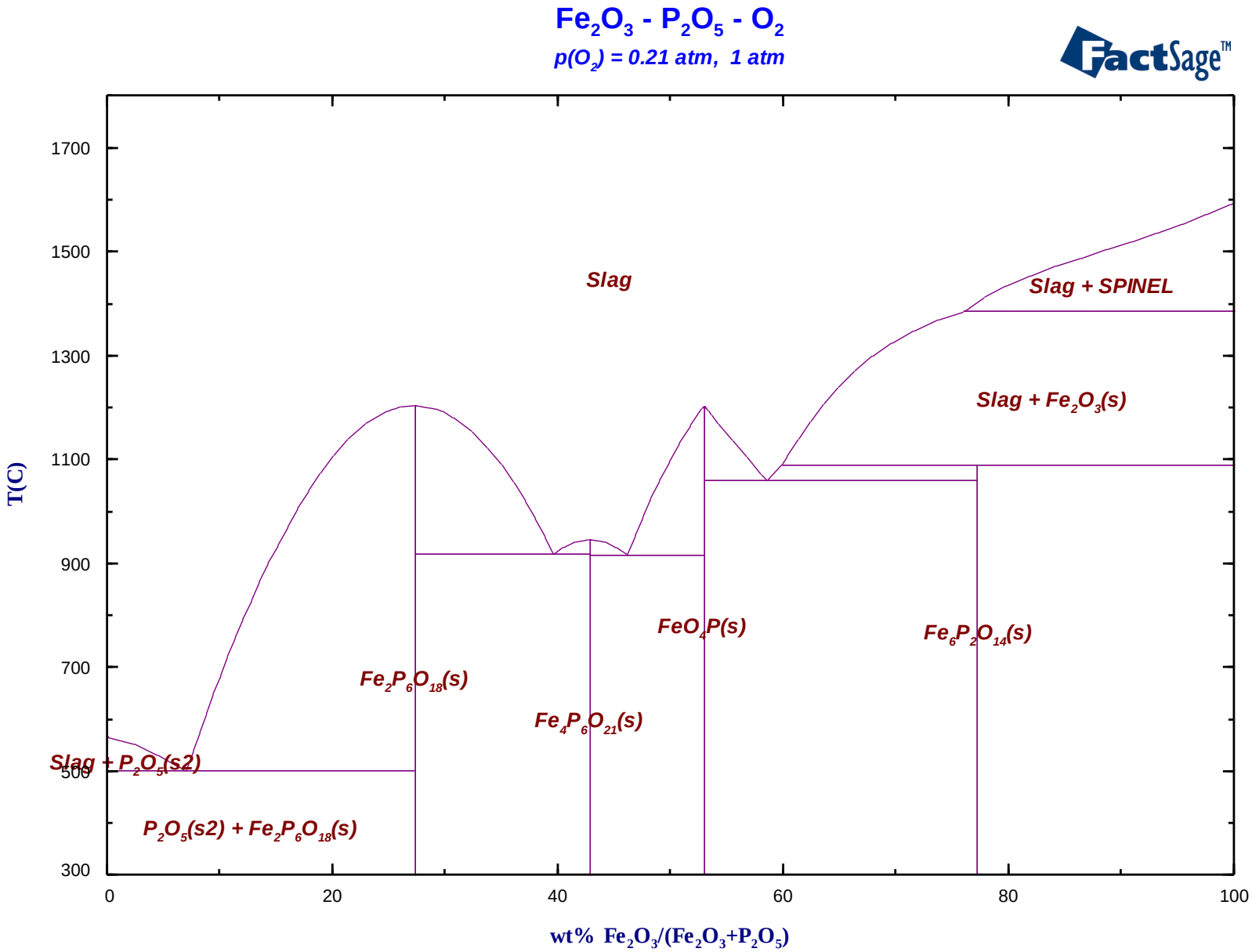

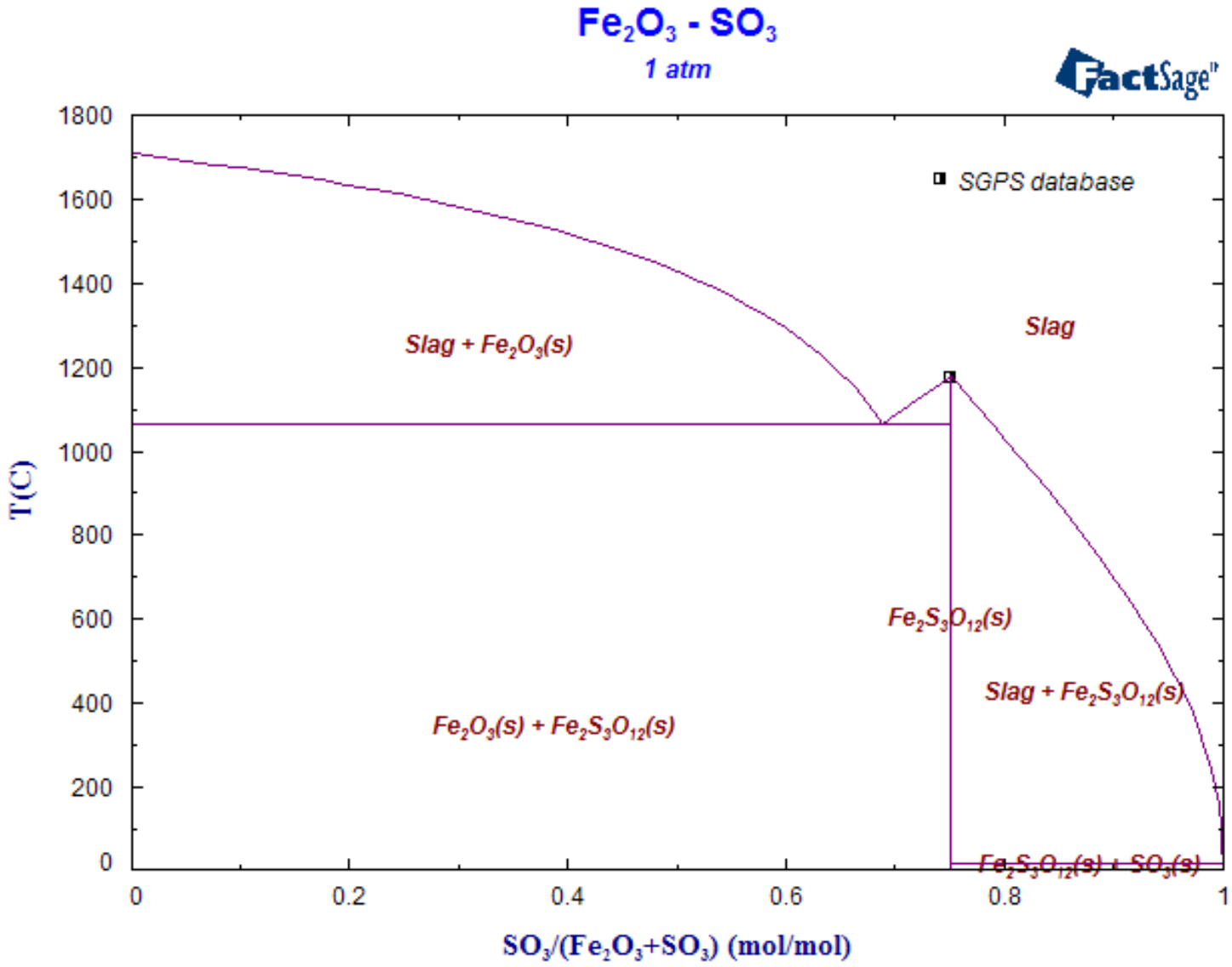
Fe2O3 - SO3
1 atm
FactSage
SGPS database
Slag + Fe2O3(s)
Slag
Fe2S3O12(s)
Slag + Fe2S3O12(s)
Fe2O3(s) + Fe2S3O12(s)
Fe2S3O12(s) + SO3(s)
T(C)
1800
1600
1400
1200
1000
800
600
400
200
0
0
0.2
0.4
0.6
0.8
1
SO3/(Fe2O3+SO3) (mol/mol)

Weight percent

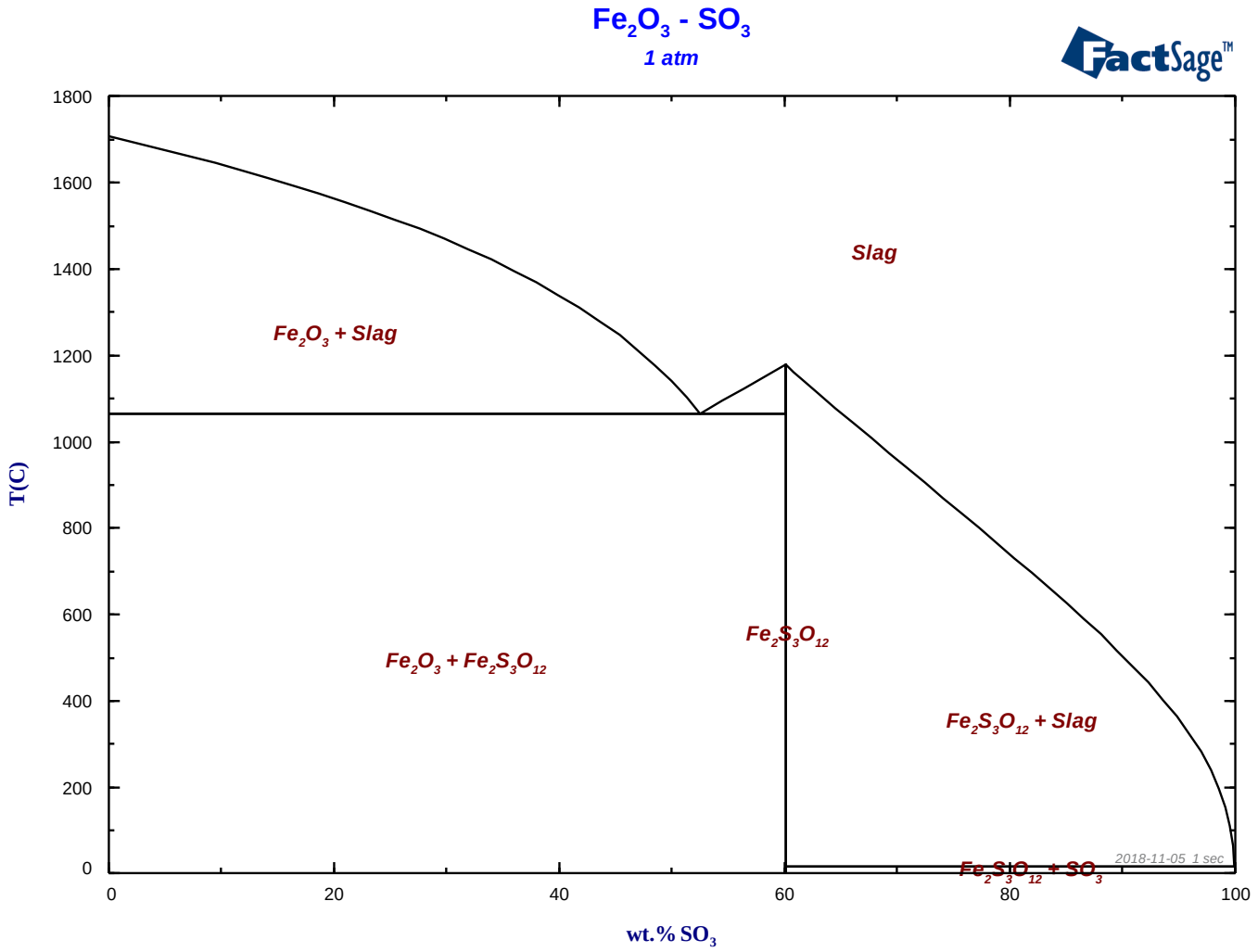

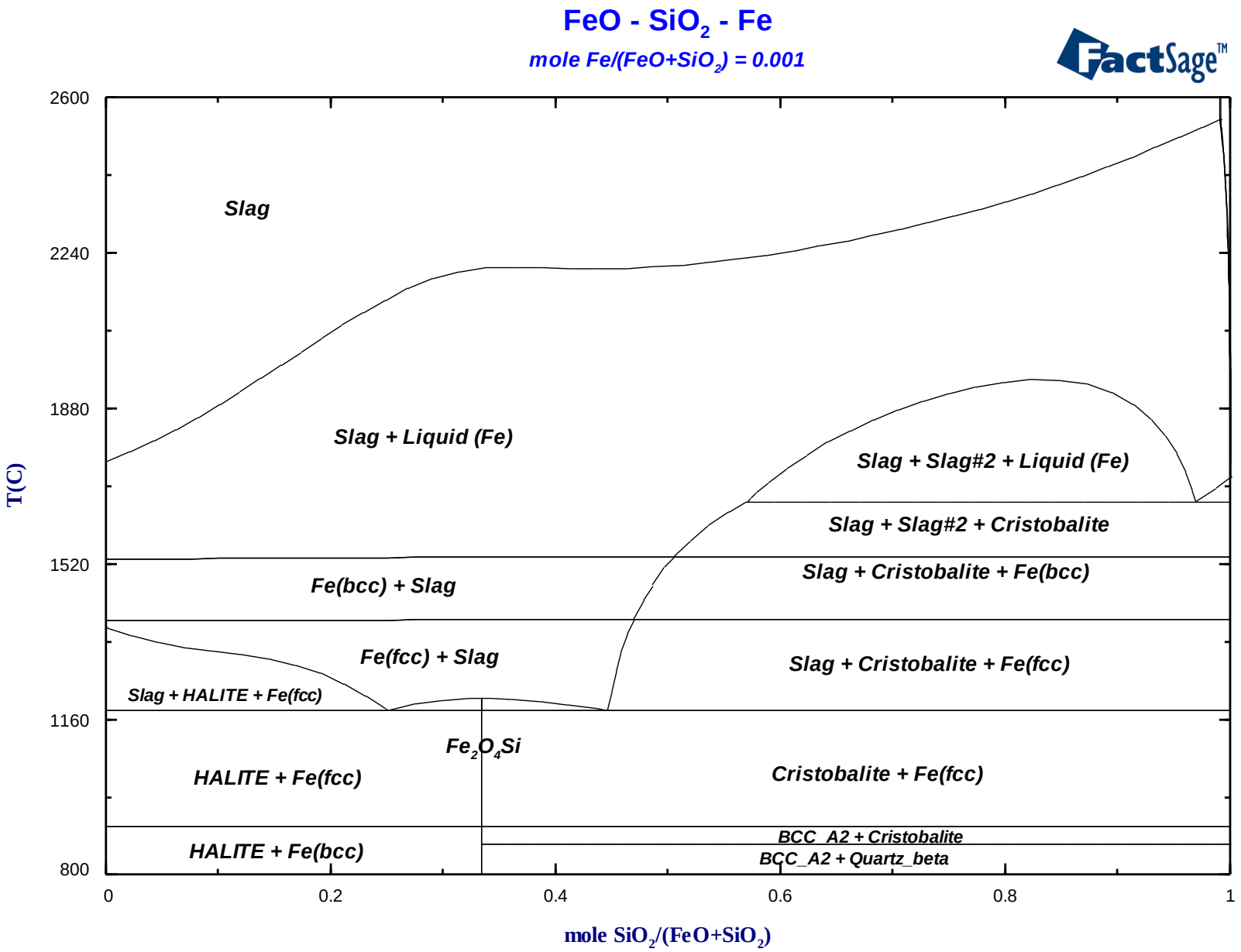
FeO - SiO2 - Fe
mole Fe/(FeO+SiO2) = 0.001
FactSage™
2600
2240
1880
1520
1160
800
T(C)
0
0.2
0.4
0.6
0.8
1
mole SiO2/(FeO+SiO2)
Slag
Slag + Liquid (Fe)
Slag + Slag#2 + Liquid (Fe)
Slag + Slag#2 + Cristobalite
Slag + Cristobalite + Fe(bcc)
Fe(bcc) + Slag
Fe(fcc) + Slag
Slag + Cristobalite + Fe(fcc)
Slag + HALITE + Fe(fcc)
Fe2O4Si
HALITE + Fe(fcc)
Cristobalite + Fe(fcc)
HALITE + Fe(bcc)
BCC_A2 + Cristobalite
BCC_A2 + Quartz_beta

Weight percent
compared with experimental data

FeO - SiO_2 - Fe

wt% Fe/(FeO+SiO_2) = 0.001

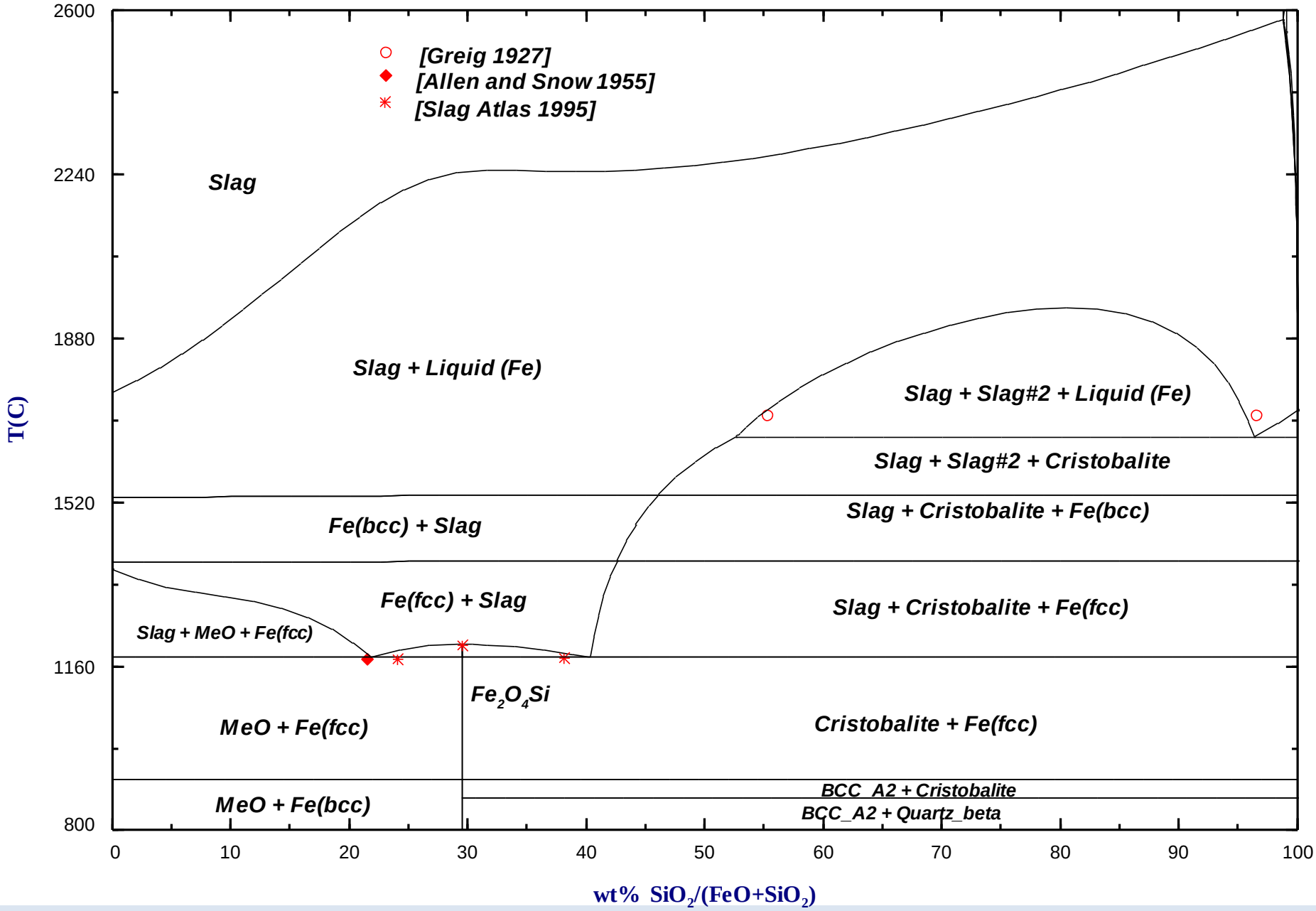

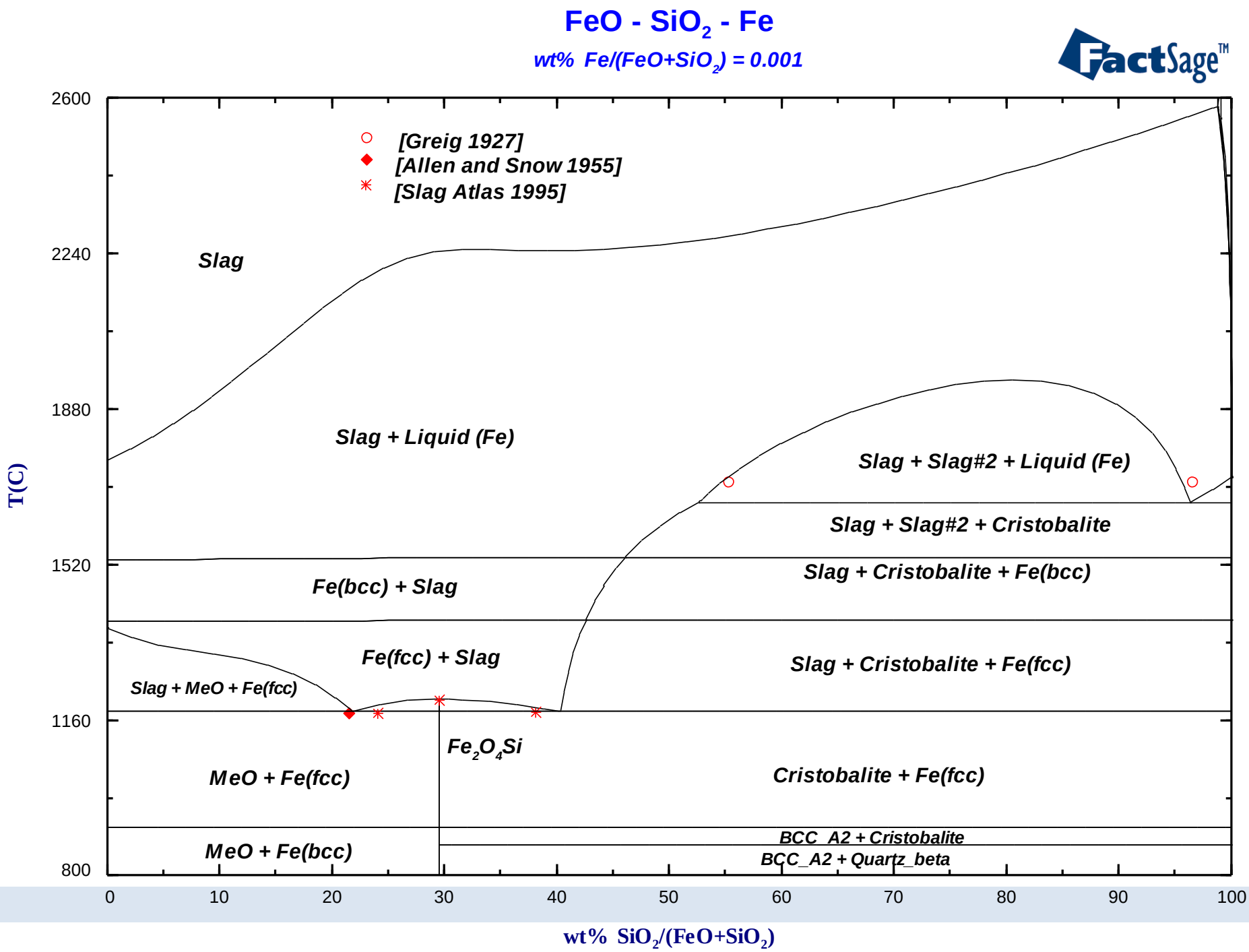
FeO - SiO2 - Fe
wt% Fe/(FeO+SiO2) = 0.001
FactSage™
[Greig 1927]
[Allen and Snow 1955]
[Slag Atlas 1995]
Slag
Slag + Liquid (Fe)
Slag + Slag#2 + Liquid (Fe)
Slag + Slag#2 + Cristobalite
Slag + Cristobalite + Fe(bcc)
Fe(bcc) + Slag
Fe(fcc) + Slag
Slag + Cristobalite + Fe(fcc)
Slag + MeO + Fe(fcc)
Fe2O4Si
MeO + Fe(fcc)
Cristobalite + Fe(fcc)
BCC_A2 + Cristobalite
MeO + Fe(bcc)
BCC_A2 + Quartz_beta
T(C)
2600
2240
1880
1520
1160
800
0
10
20
30
40
50
60
70
80
90
100
wt% SiO2/(FeO+SiO2)

Mole fraction

Fe_2O_3 - SiO_2 - O_2

$p(O_2)$ = 0.21 atm

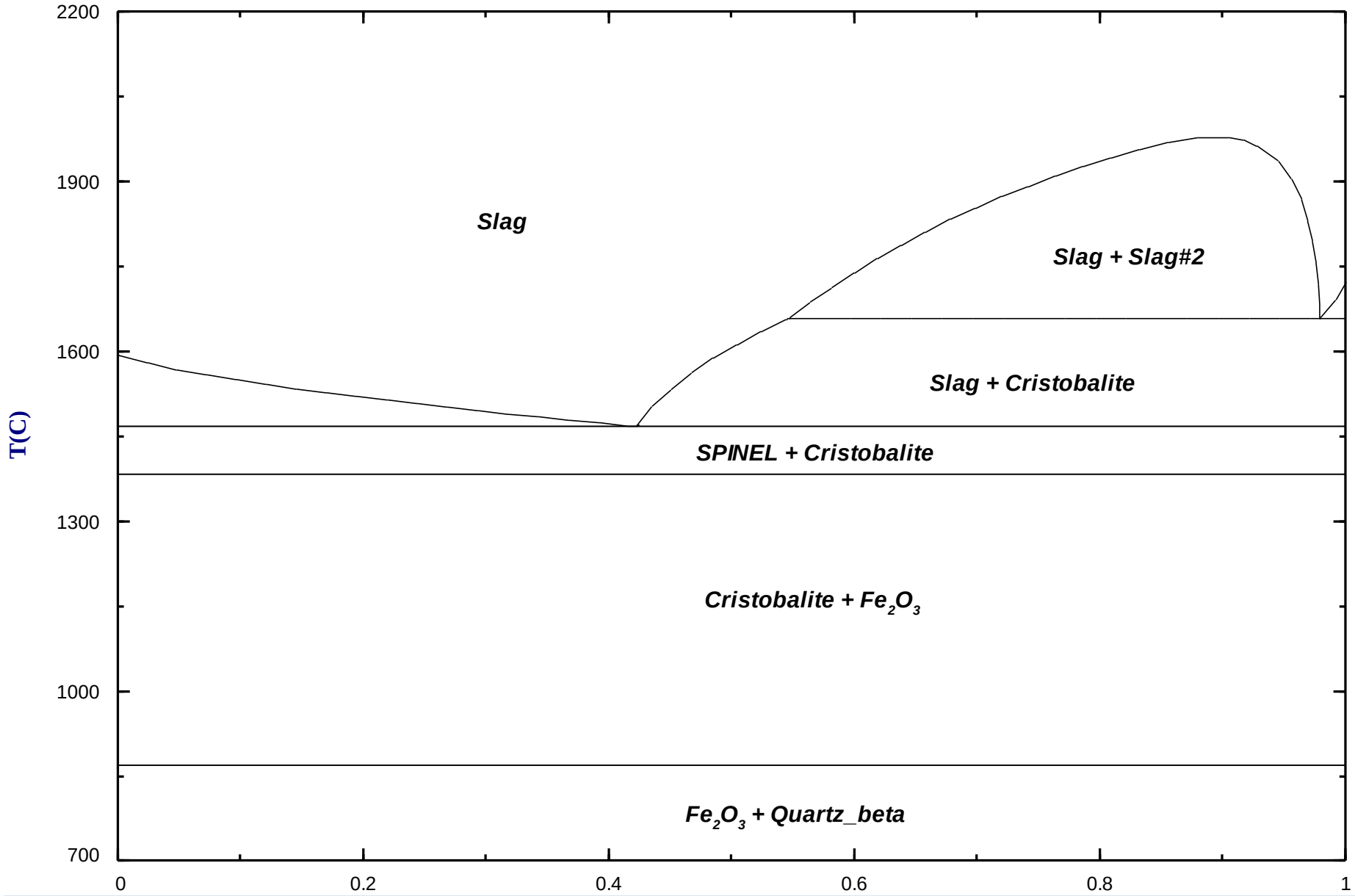

Weight percent
compared with experimental data

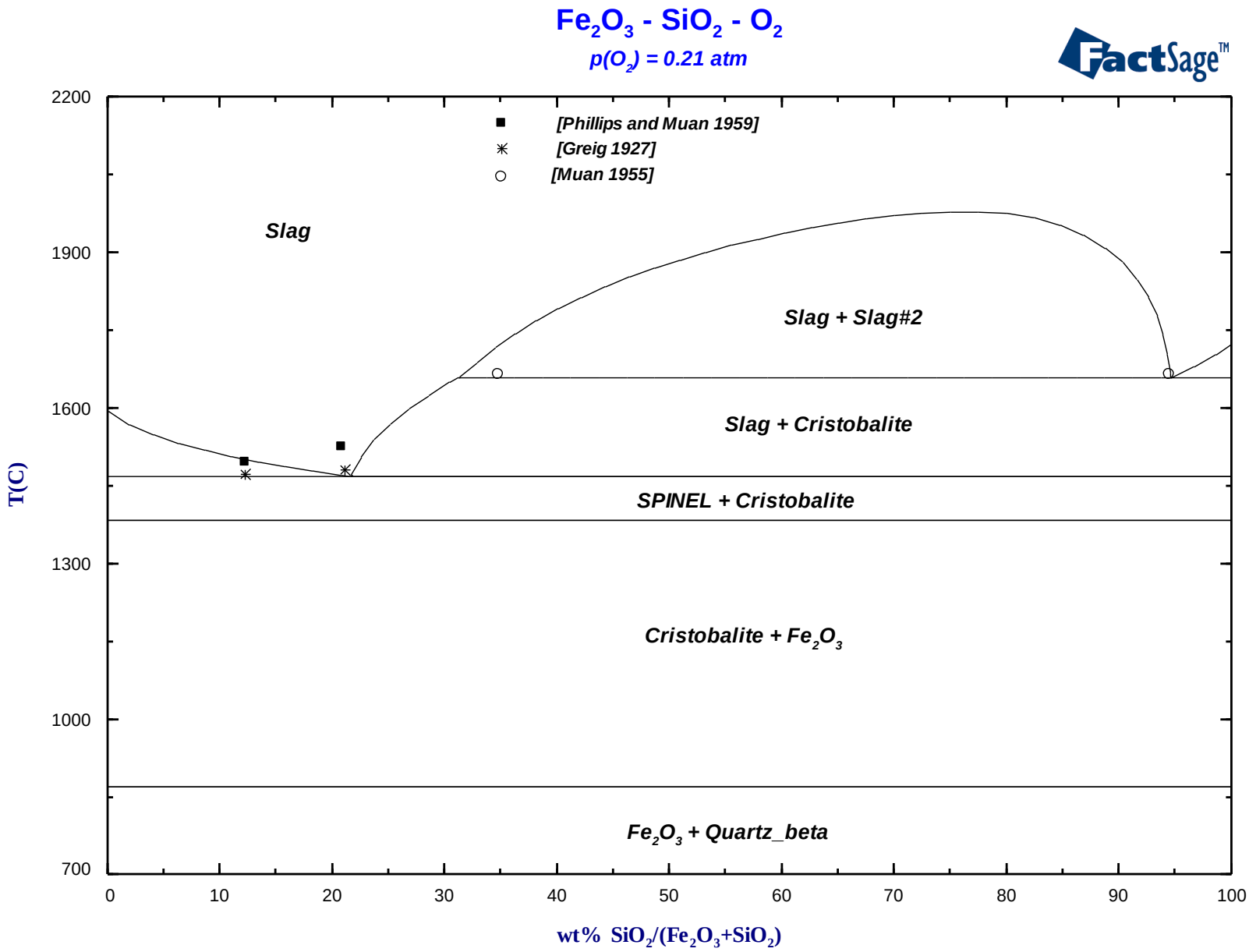

Mole fraction compared with experimental data

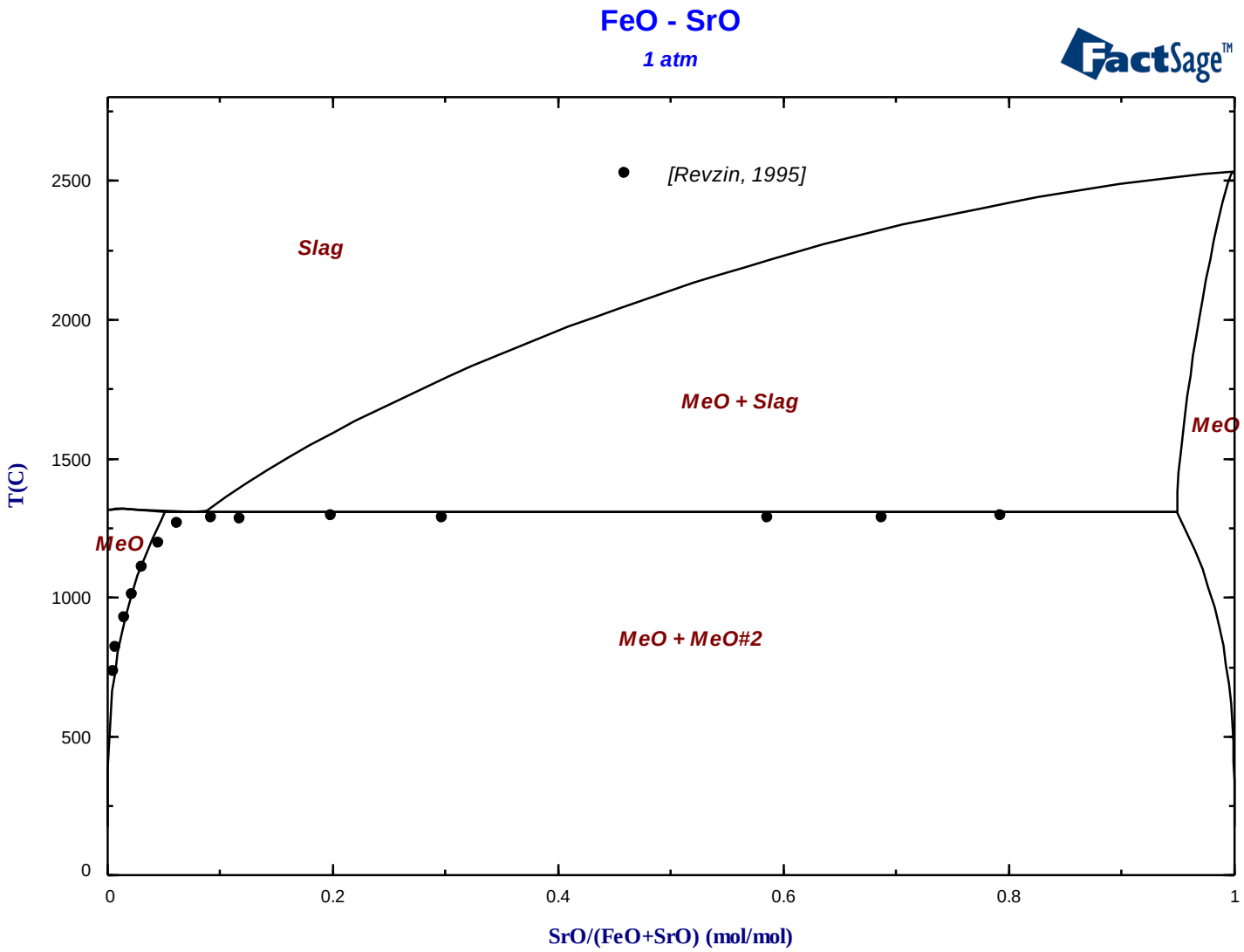

Weight percent

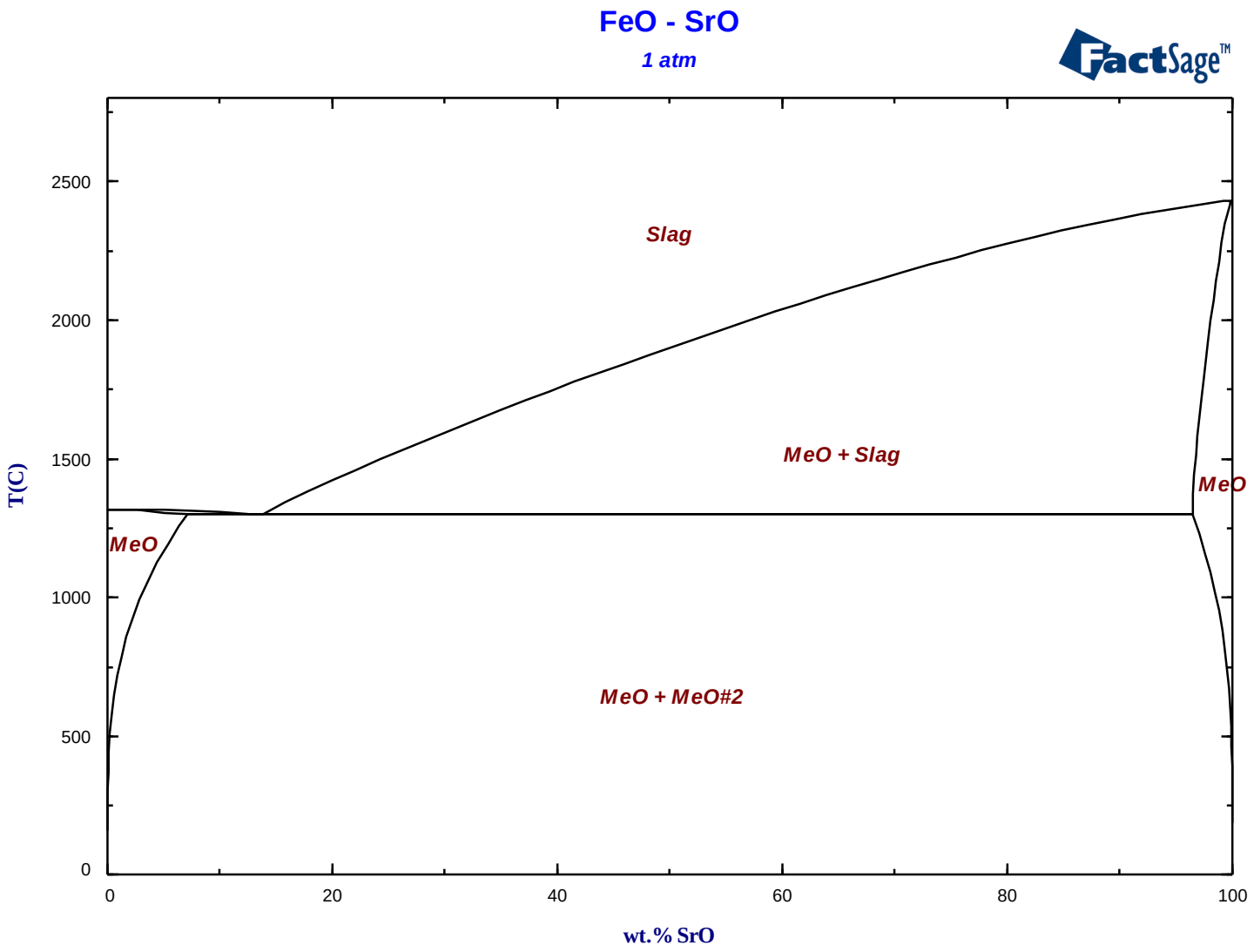

Mole fraction

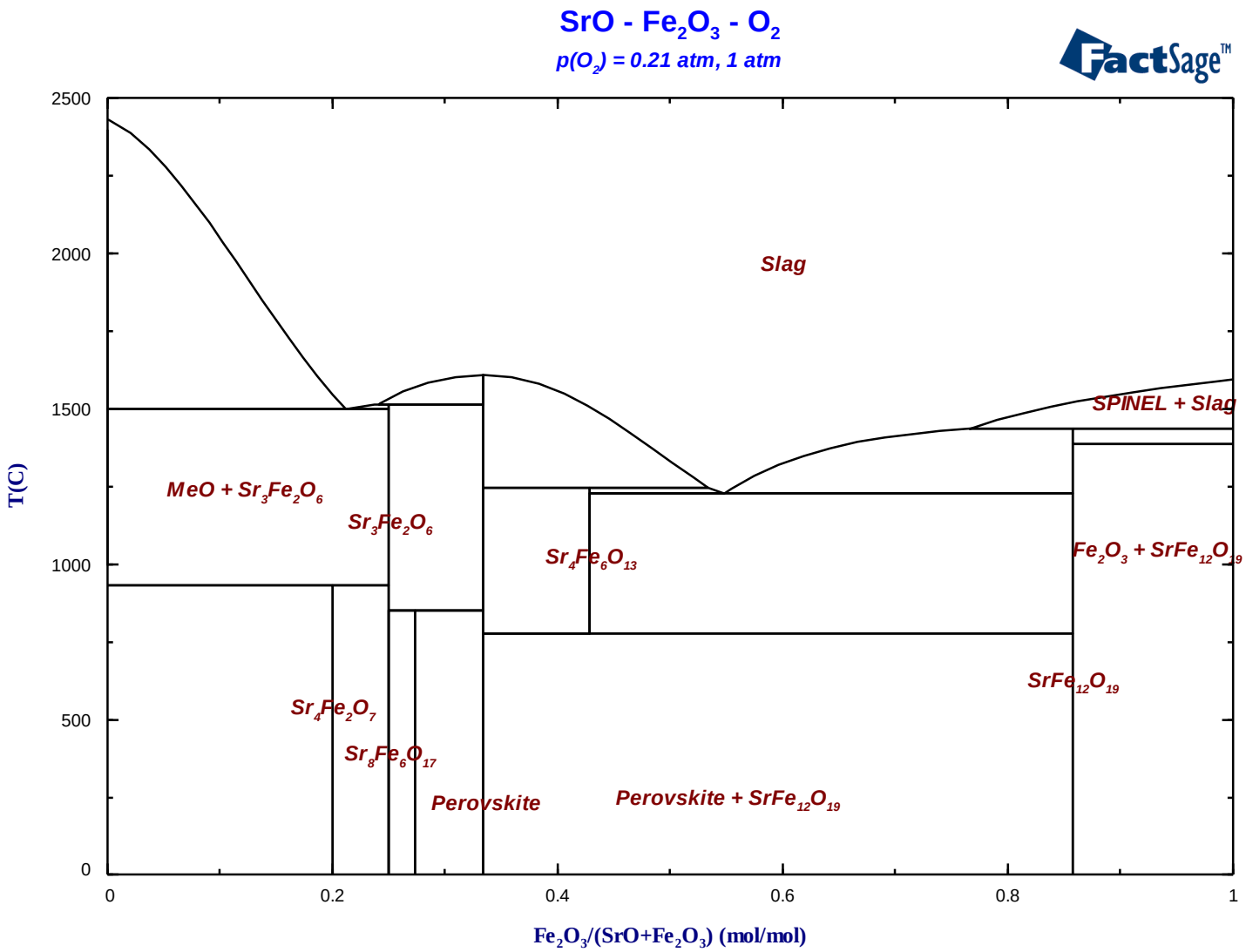

Weight percent compared with experimental data

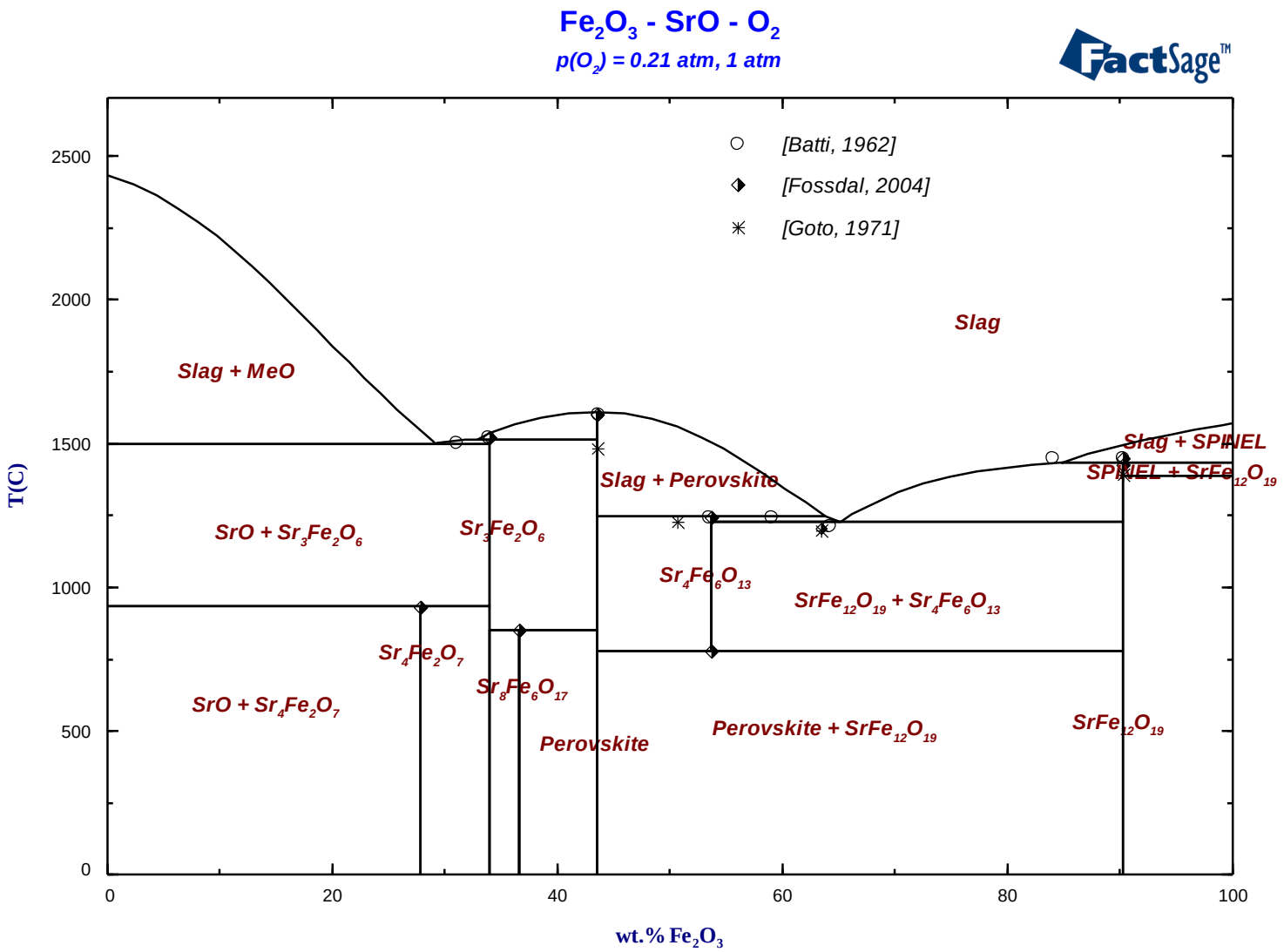

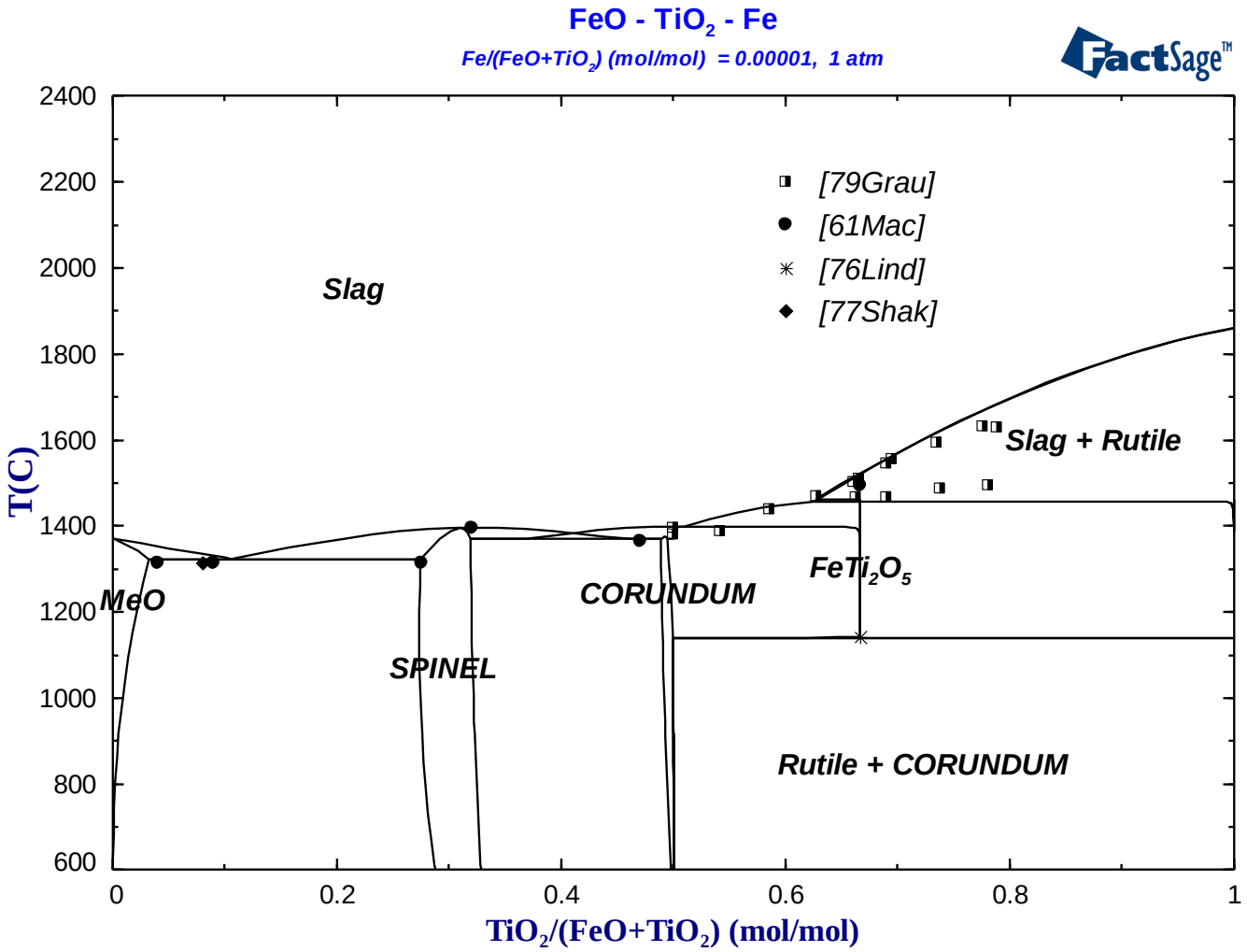
FeO - TiO2 - Fe
Fe/(FeO+TiO2) (mol/mol) = 0.00001, 1 atm
FactSage™
[79Grau]
[61Mac]
[76Lind]
[77Shak]
Slag
Slag + Rutile
MeO
SPINEL
CORUNDUM
FeTi2O5
Rutile + CORUNDUM
T(C)
TiO2/(FeO+TiO2) (mol/mol)
2400
2200
2000
1800
1600
1400
1200
1000
800
600
0
0.2
0.4
0.6
0.8
1

Weight percent

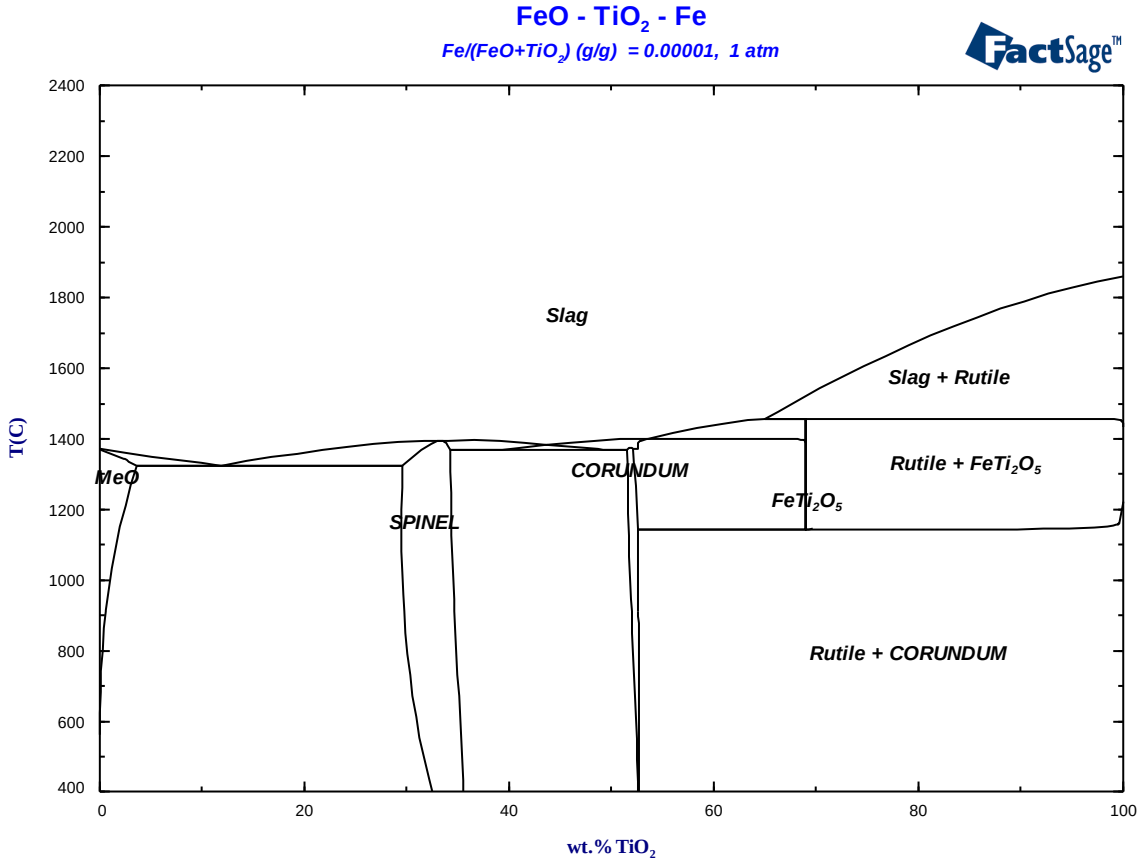

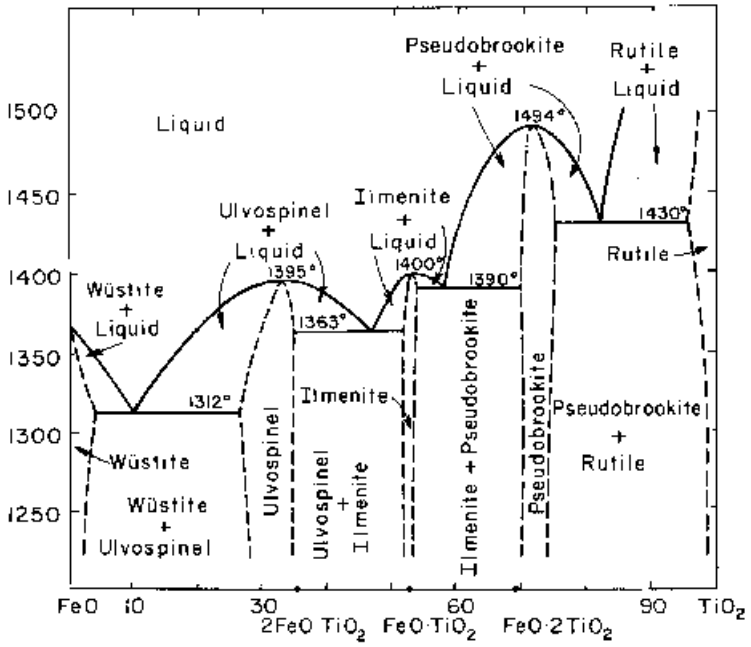

J.B. MacChesney, A. Muan, Am. Mineral, 46 [5-6], (1961), pp. 572-582.

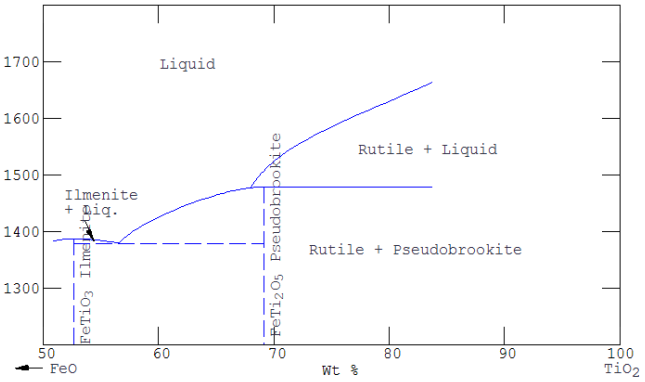

A.E. Grau, Can. Metall. Q., 18 [3], (1979), pp. 313-321.

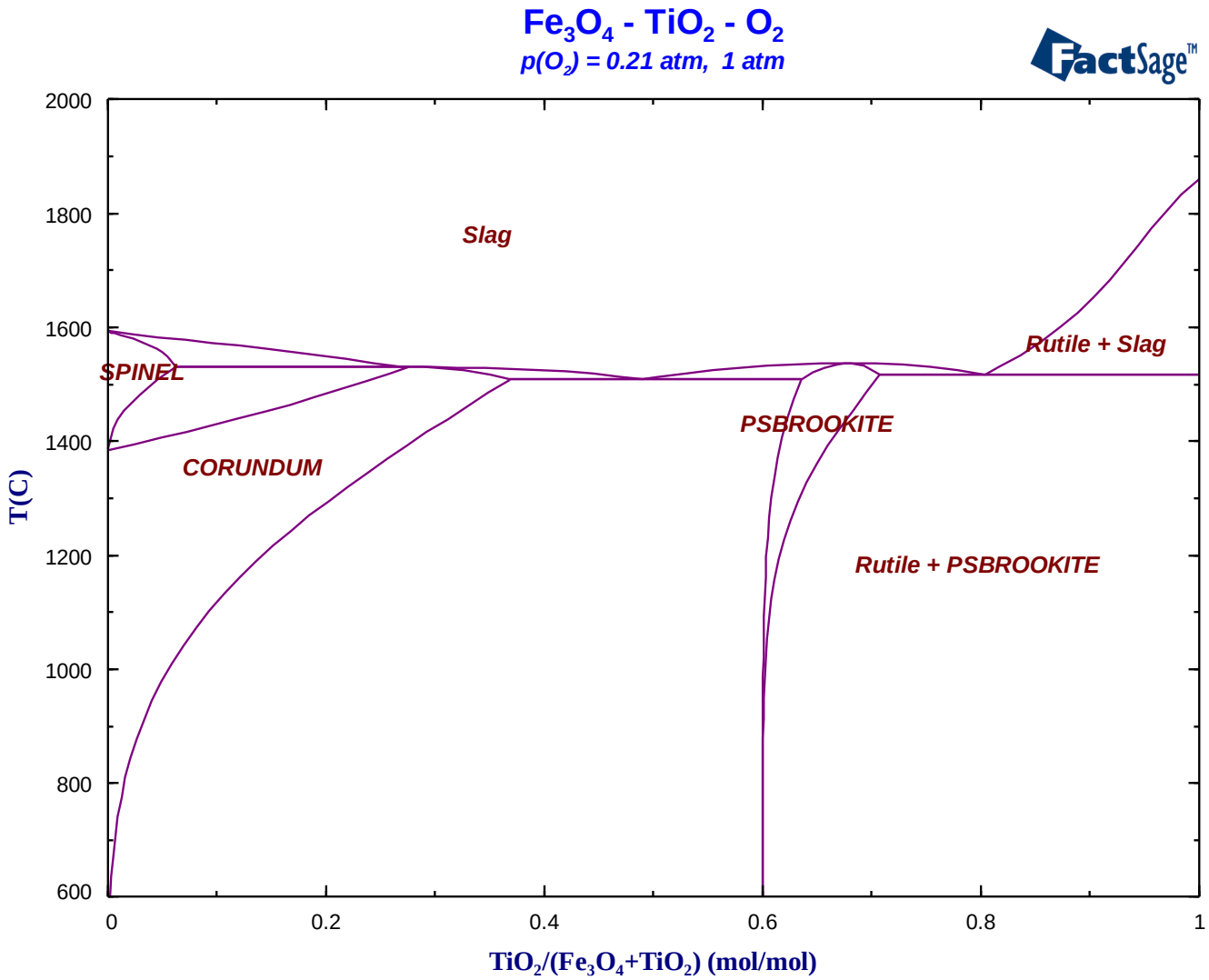
Fe3O4 - TiO2 - O2
p(O2) = 0.21 atm, 1 atm
FactSage™
Slag
SPINEL
CORUNDUM
PSBROOKITE
Rutile + Slag
Rutile + PSBROOKITE
T(C)
2000
1800
1600
1400
1200
1000
800
600
0
0.2
0.4
0.6
0.8
1
TiO2/(Fe3O4+TiO2) (mol/mol)

Weight percent compared with experimental data

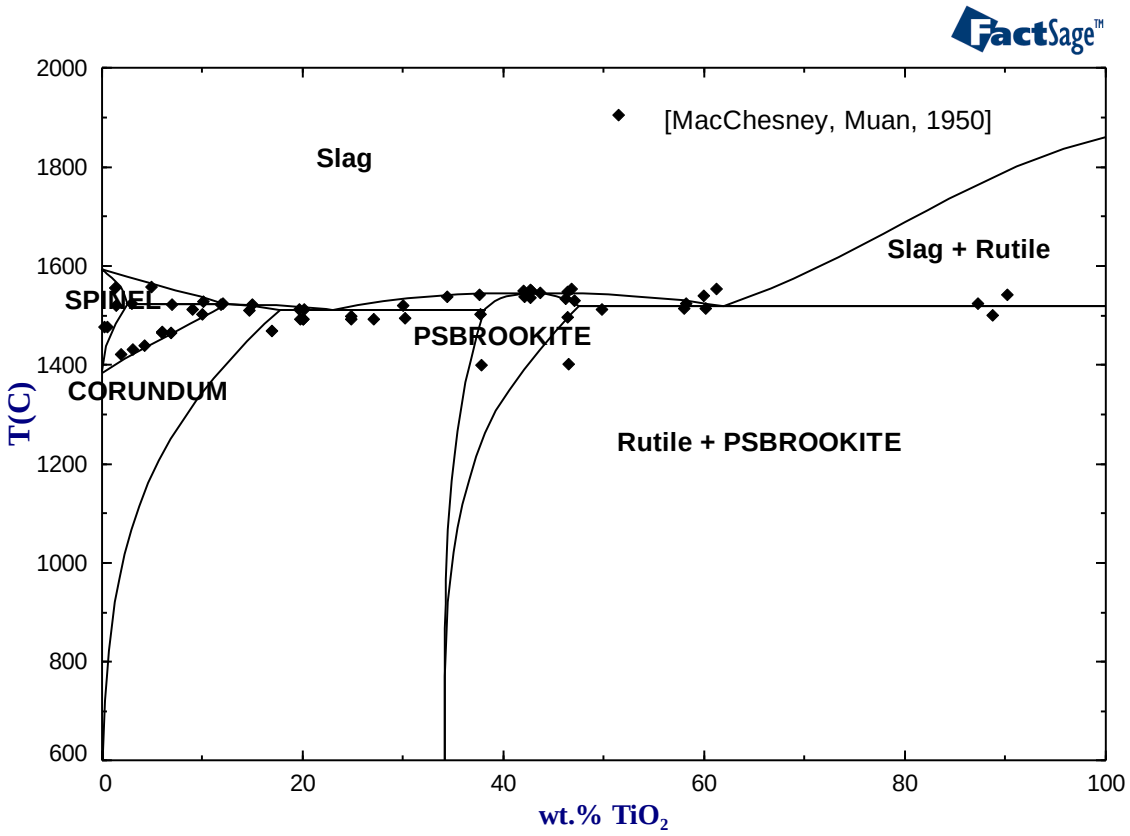

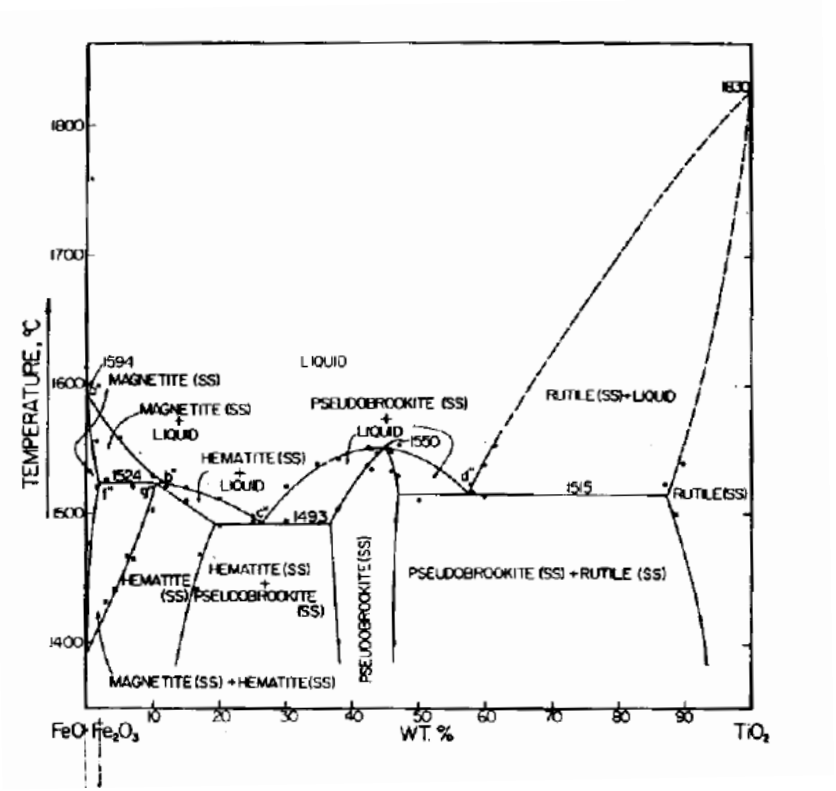

J.B. MacChesney, A. Muan, Am. Mineral, 44 [9-10], (1959), pp. 926-945.

FeO-V2O3-Fe, Mole fraction

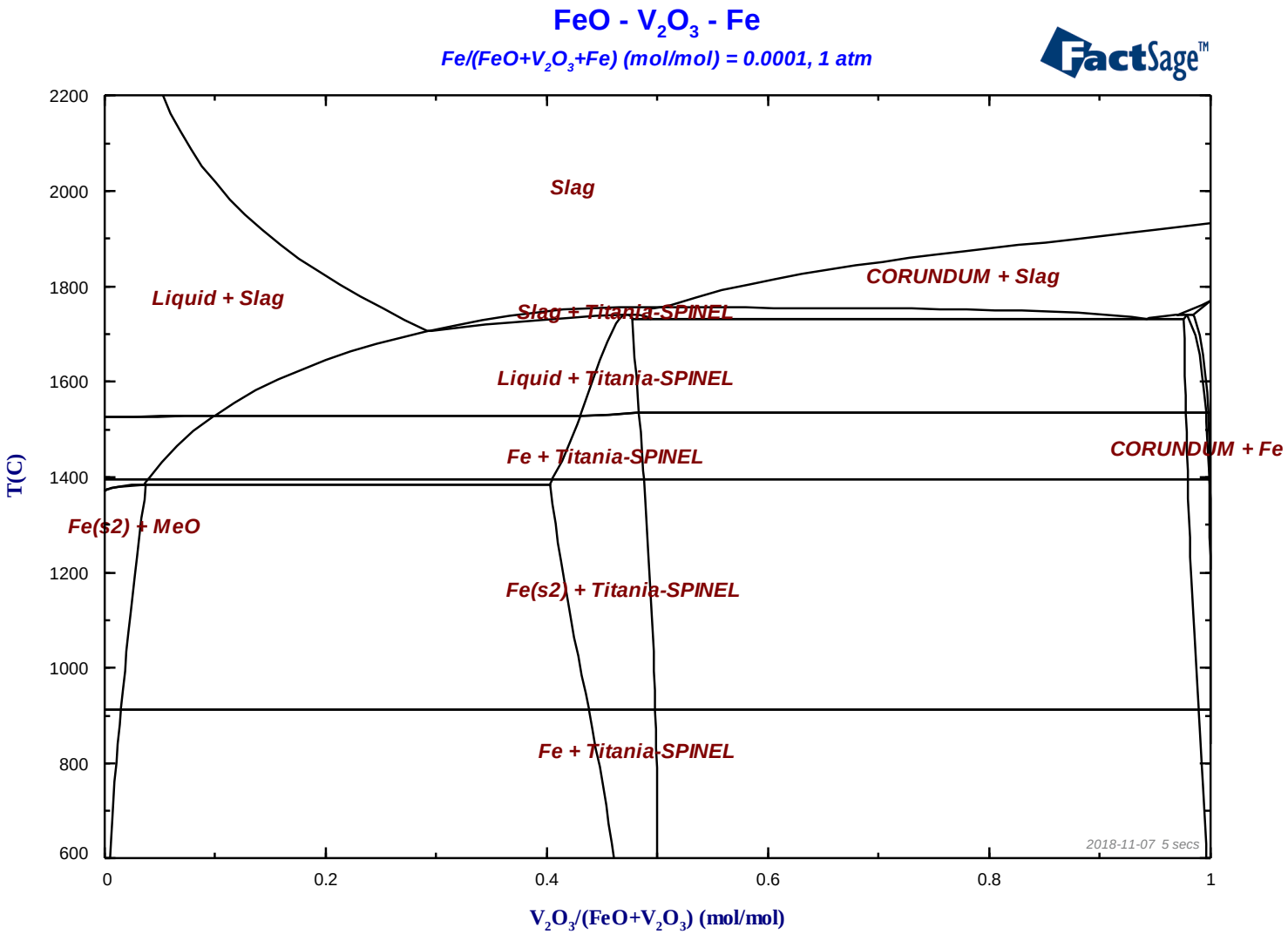

FeO-V2O3-Fe,
Weight percent compared with experimental data

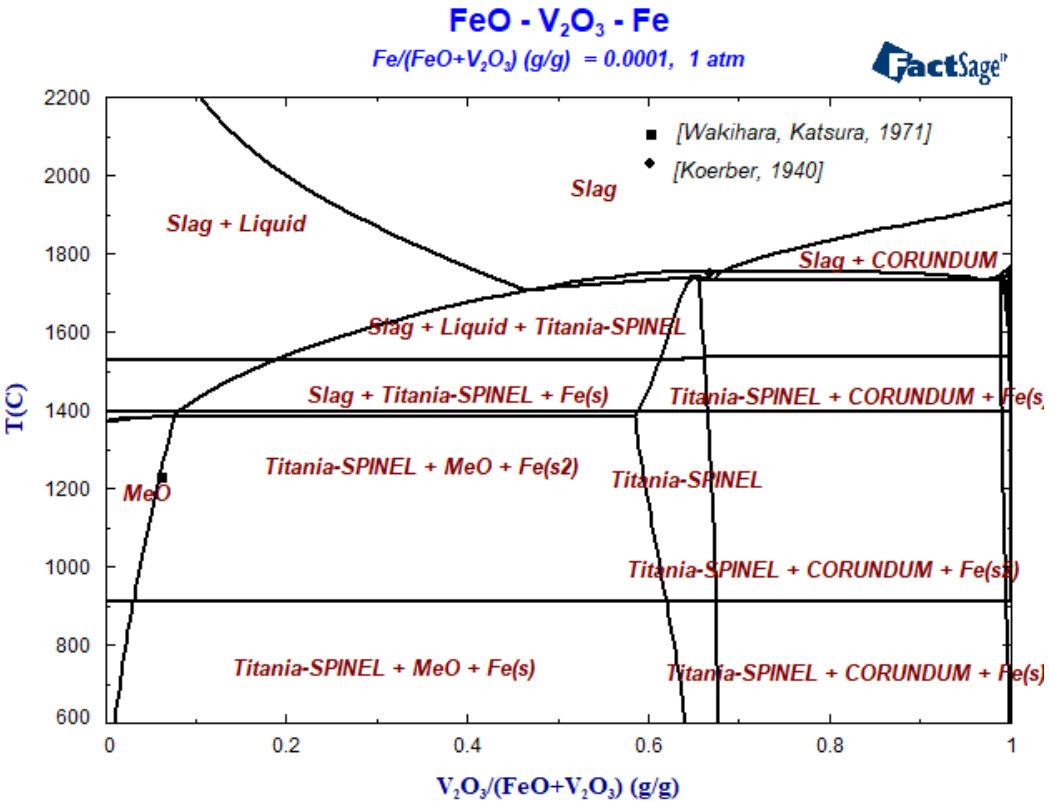

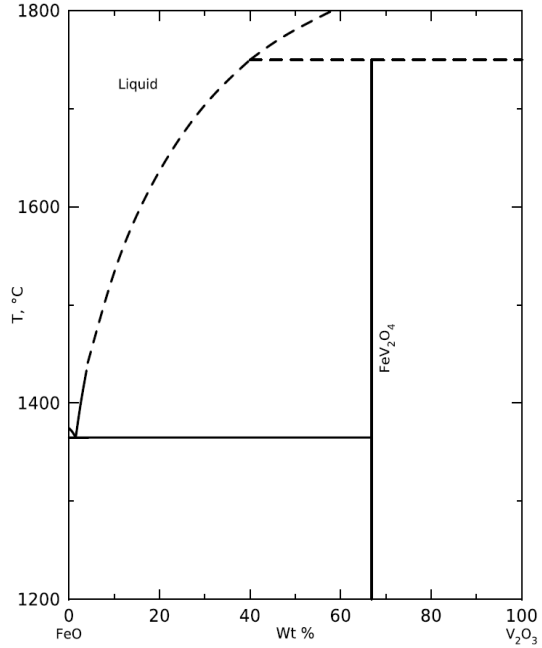

F. Koerber and W. Oelsen, Stahl Eisen, 60 [43] 948-955 (1940).

Fe2O3-V2O5-O2,
Mole fraction compared with experimental data

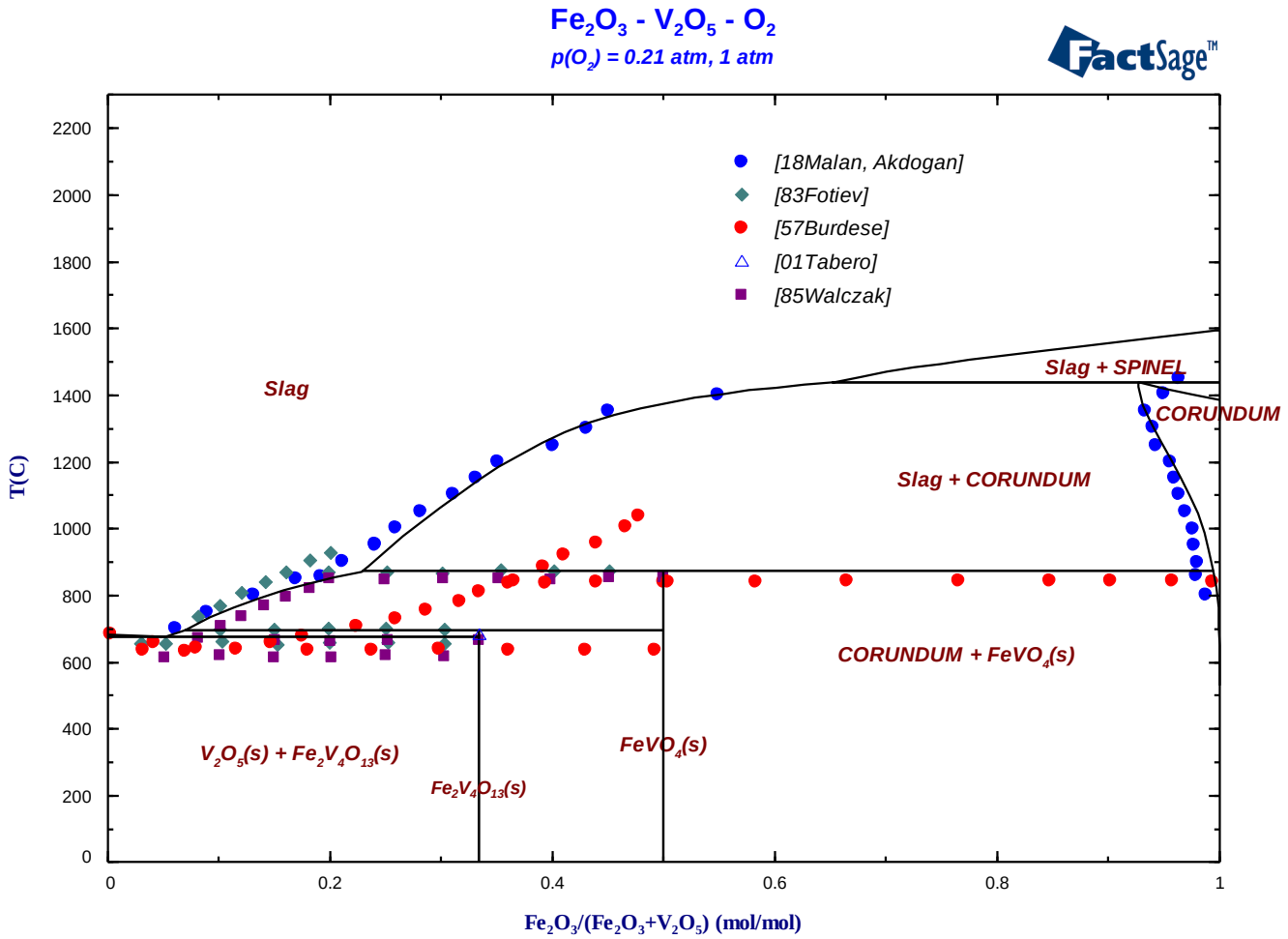

Fe2O3-V2O5-O2,
Weight percent

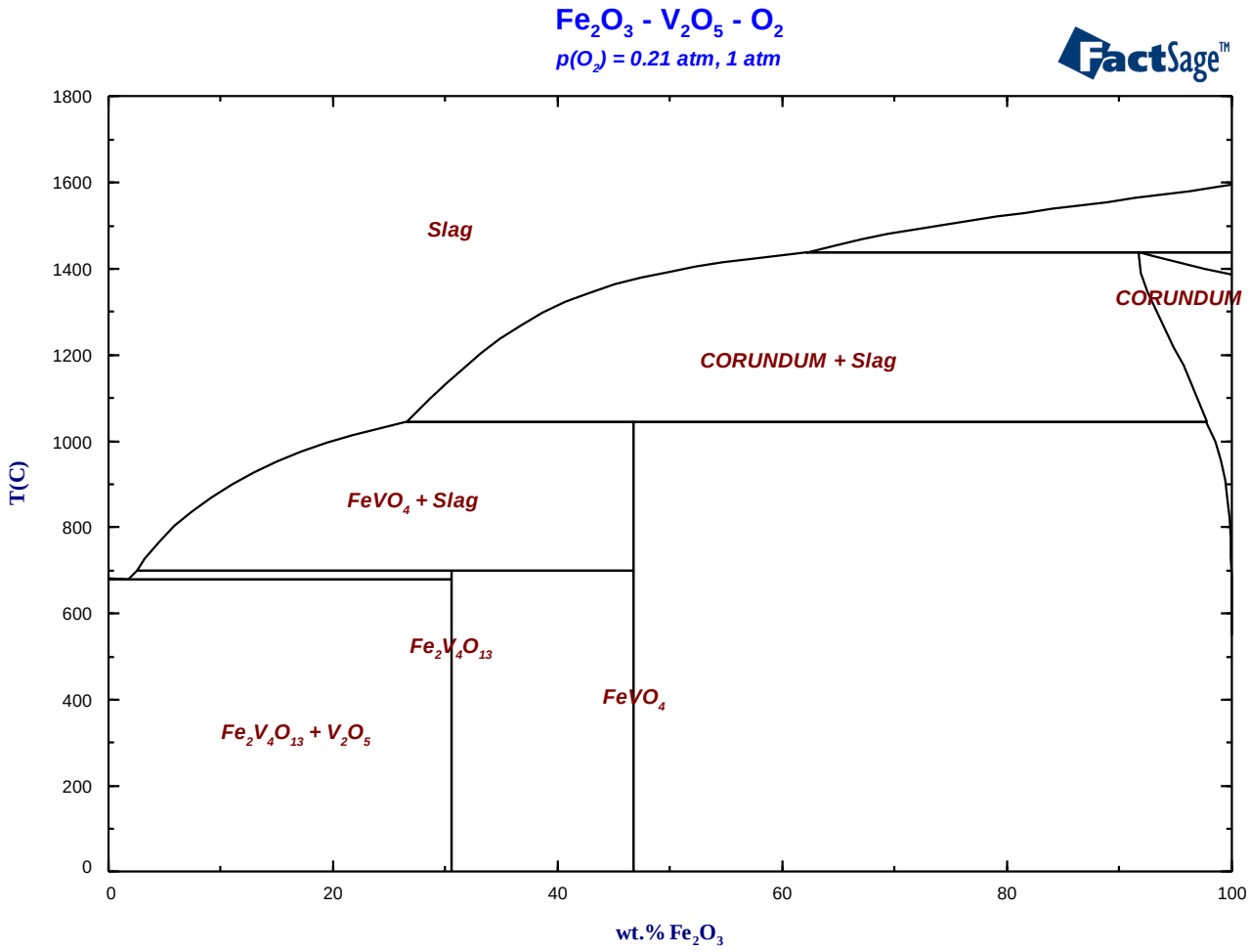

Mole fraction

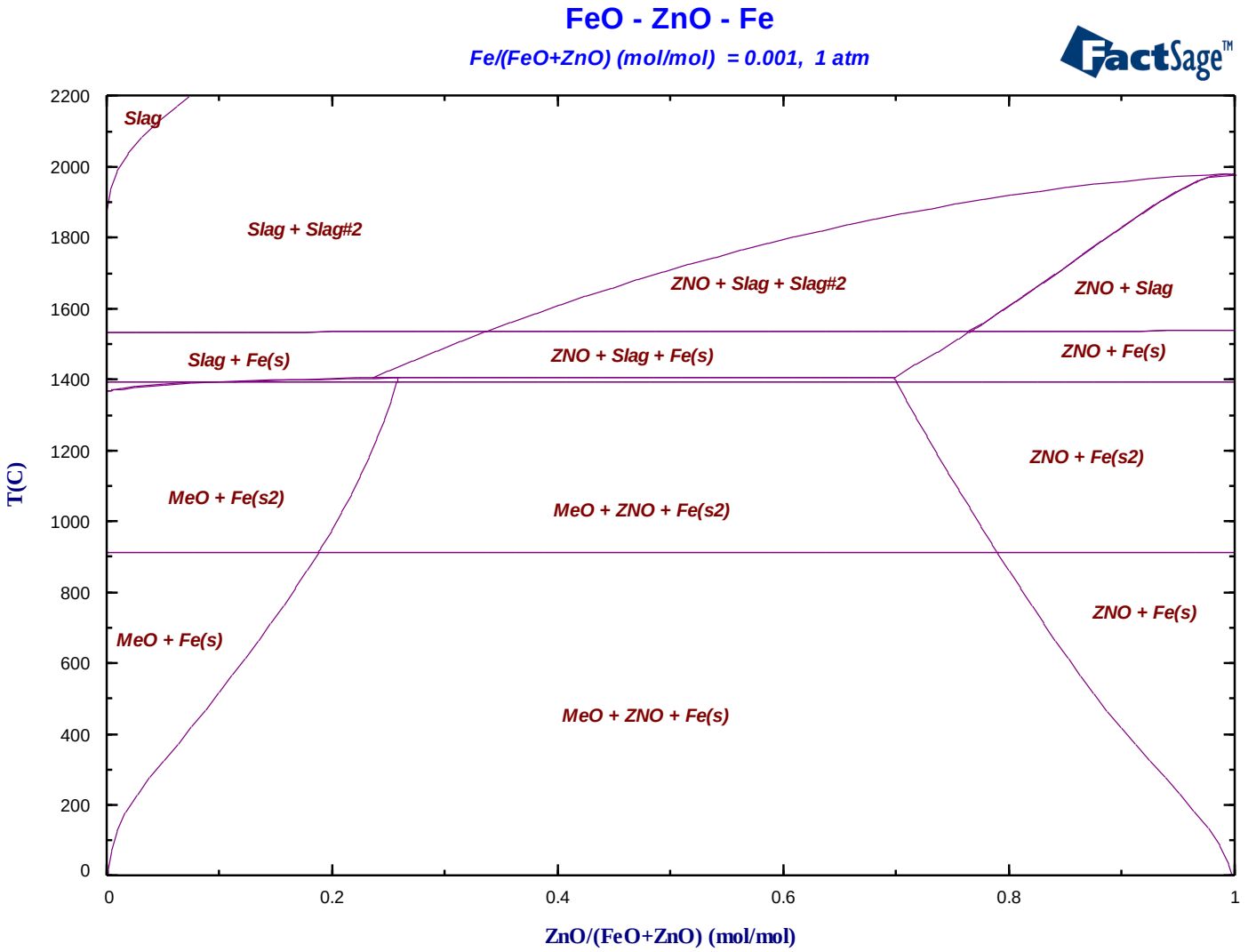

Weight percent
compared with experimental data

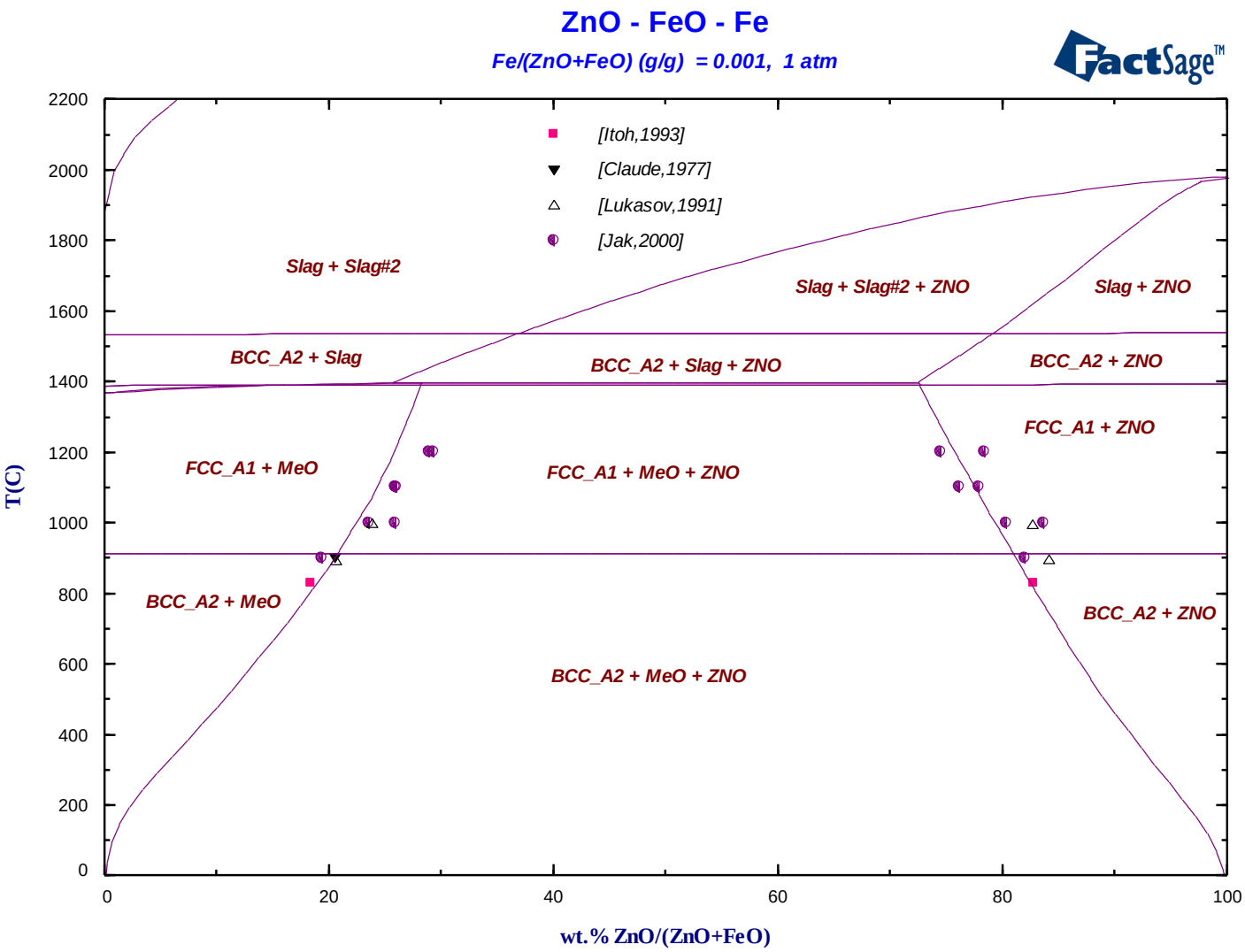

Mole fraction experimental data

$ZnO - FeO_{1.5} - O_2$

$p(O_2)$ = 0.21 atm, 1 atm

compared with FactSage™

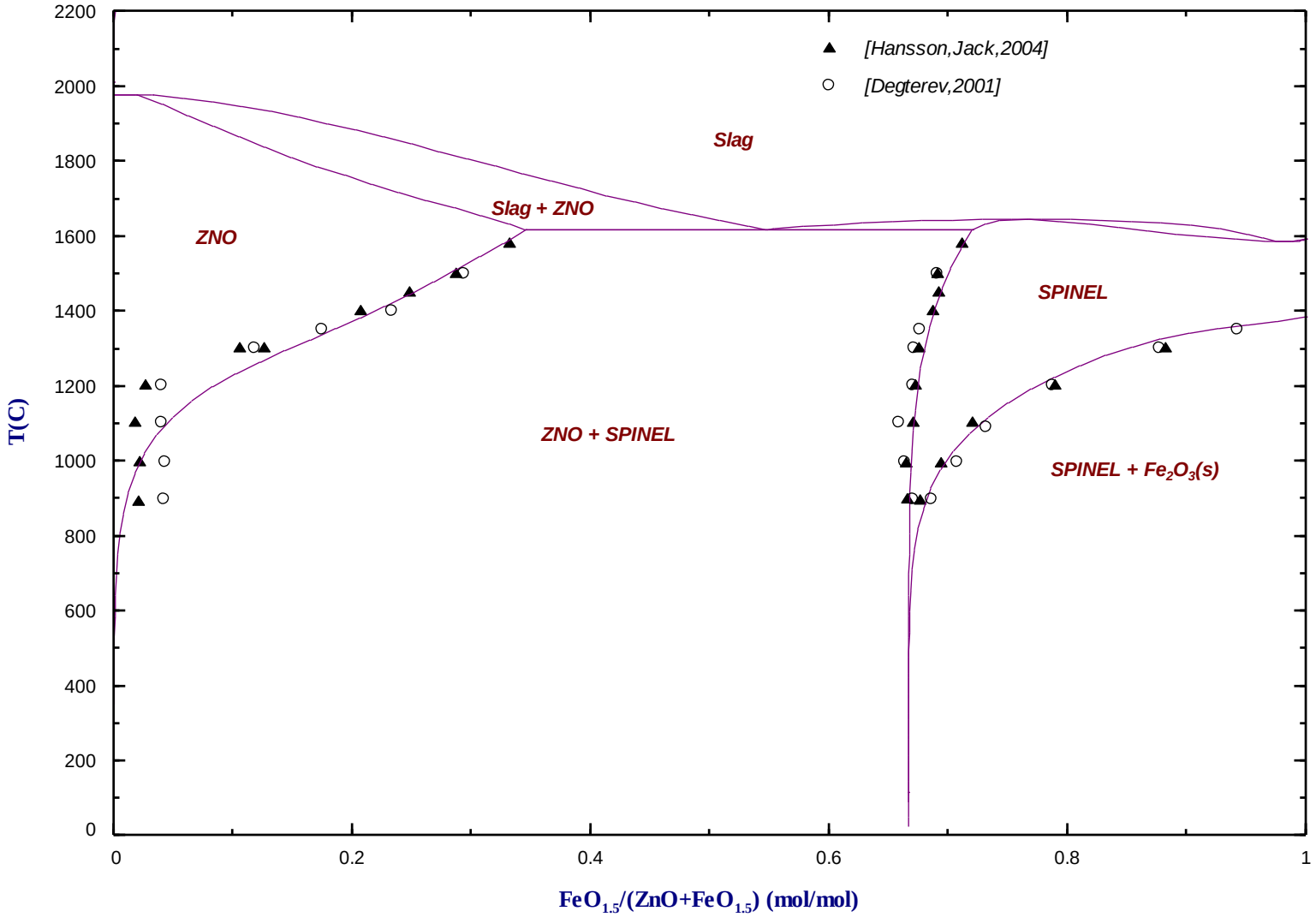

Weight percent

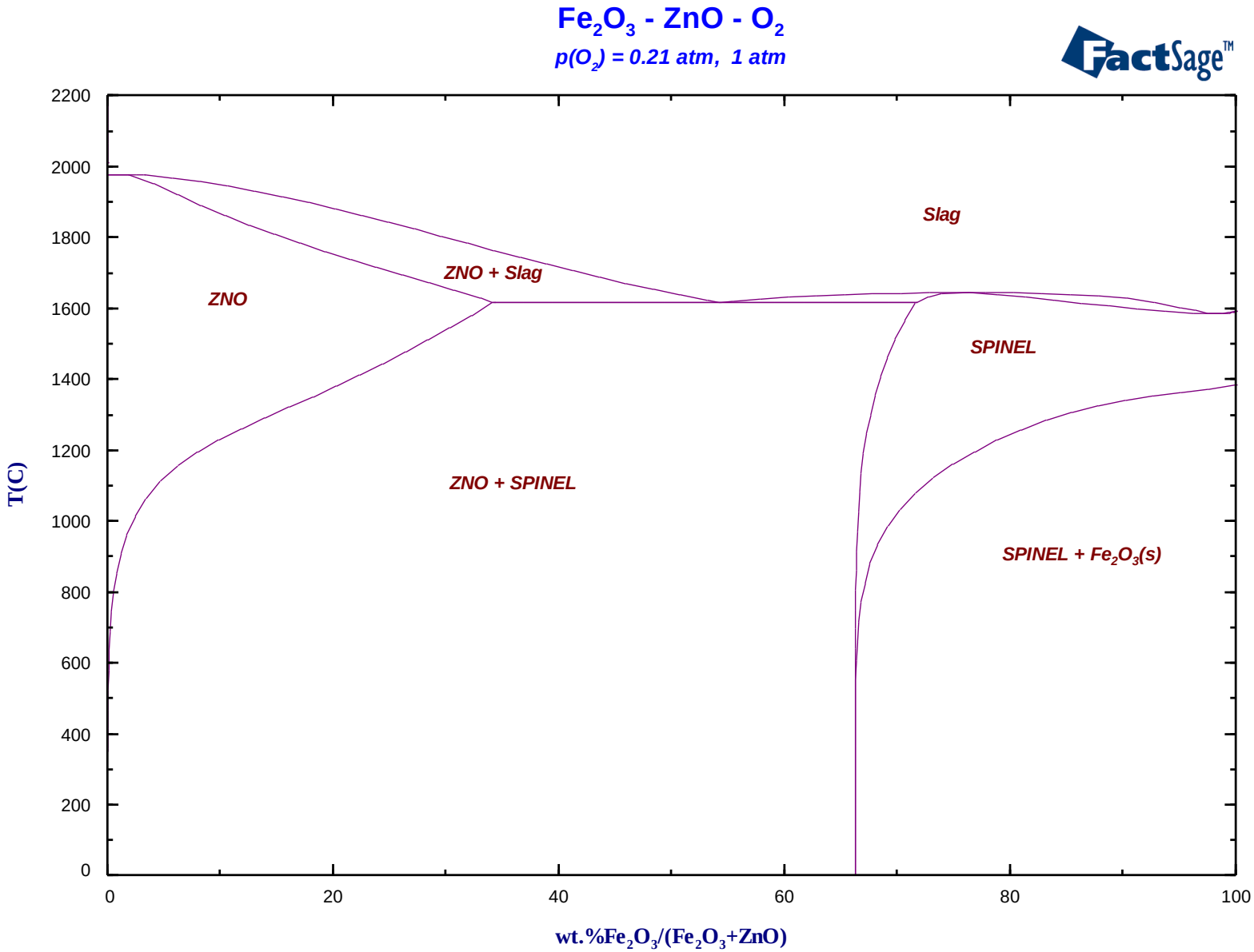

Mole fraction
compared with experimental data

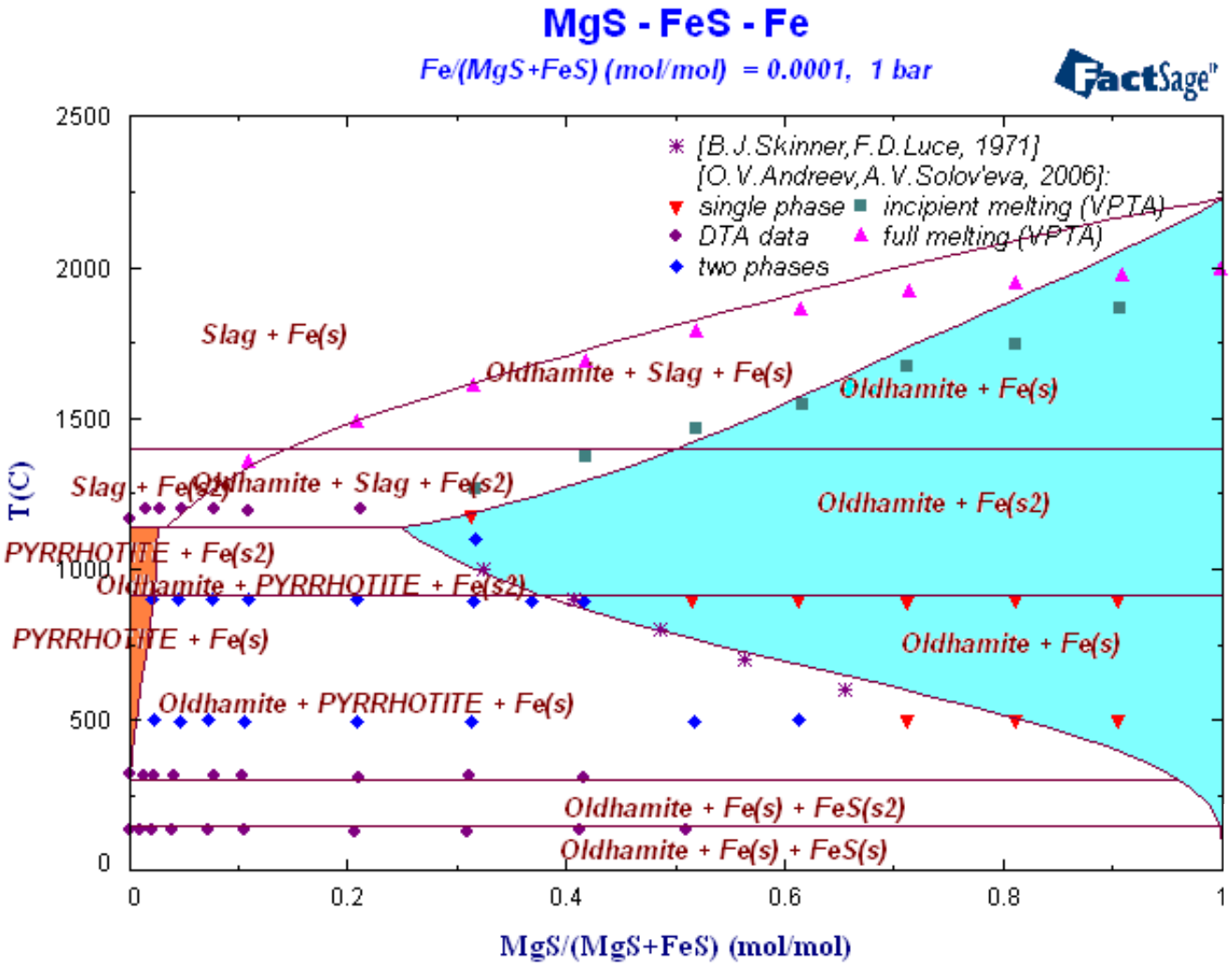

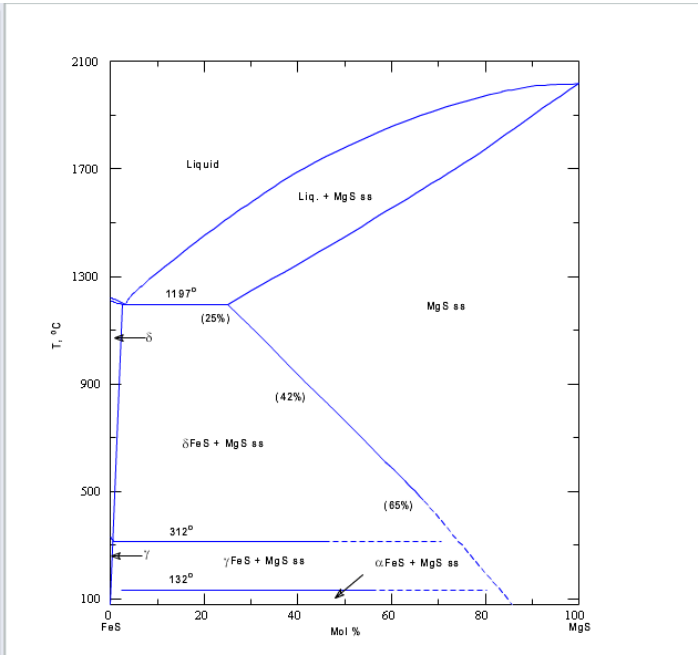

O. V. Andreev, A. V. Solov'eva, and T. M. Burkhanova, Zh. Neorg. Khim., 51 [11] 1938-1941 (2006); Russ. J. Inorg. Chem. (Engl. Transl.), 51 [11] 1826-1828 (2006).

Weight percent

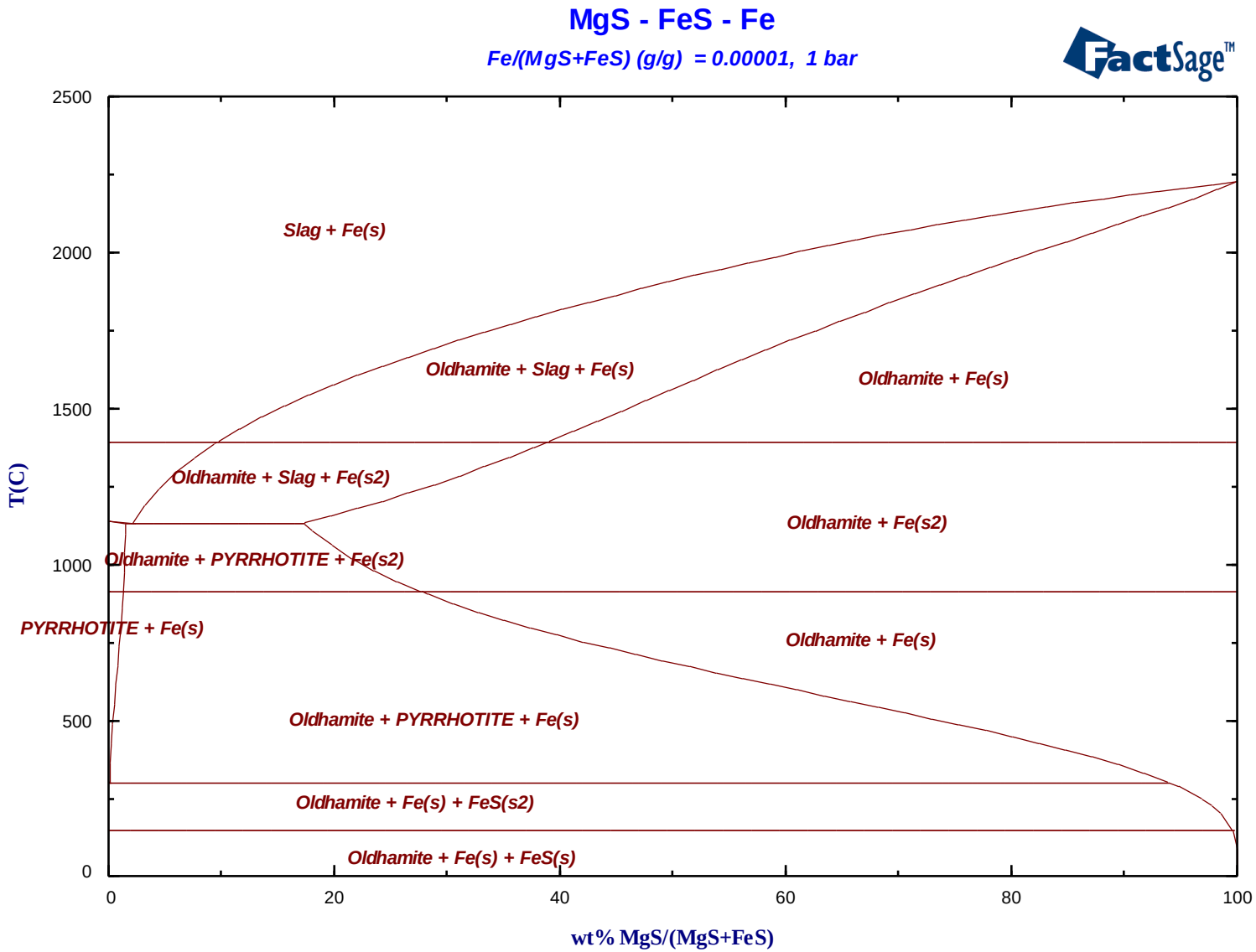

Mole fraction
compared with experimental data

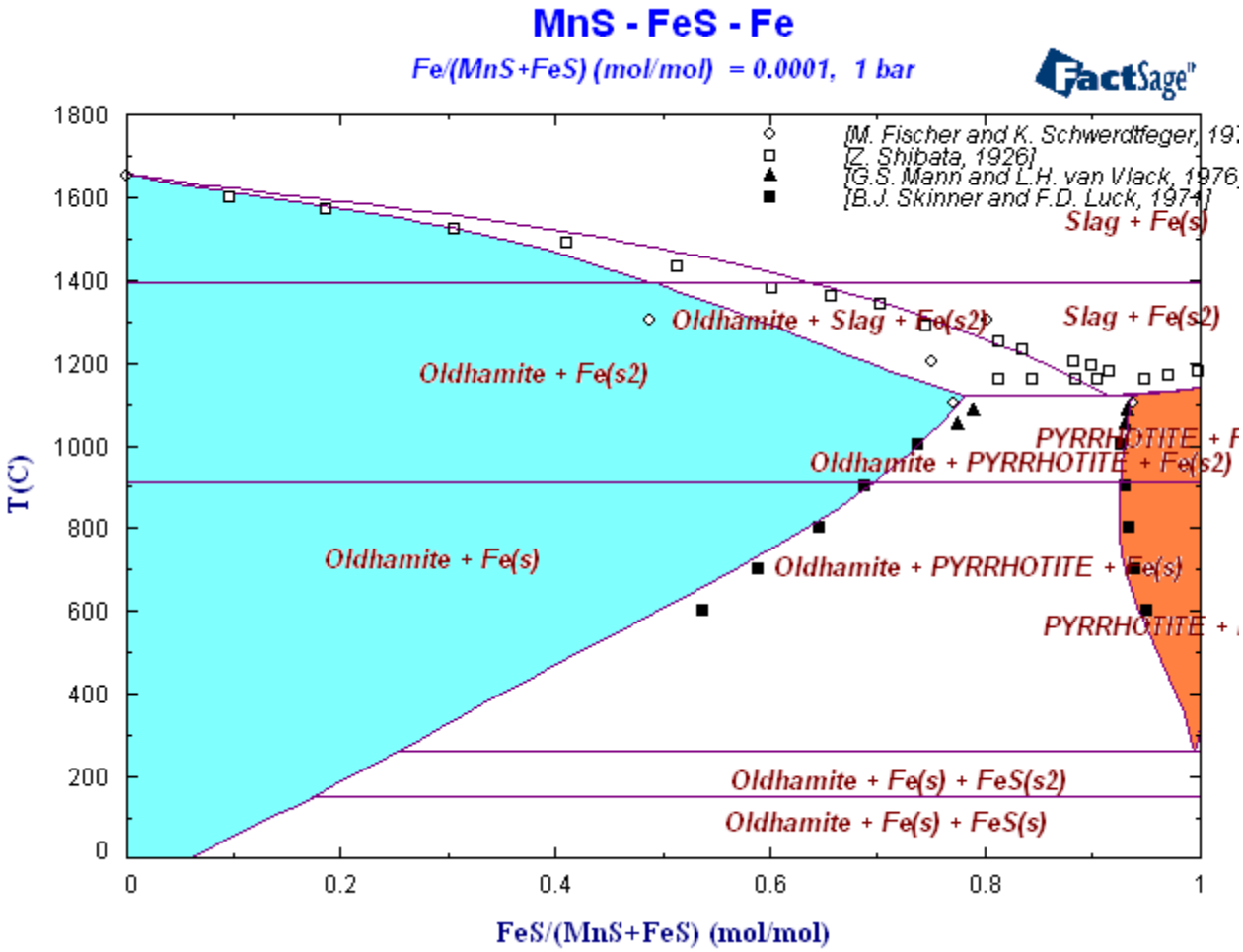

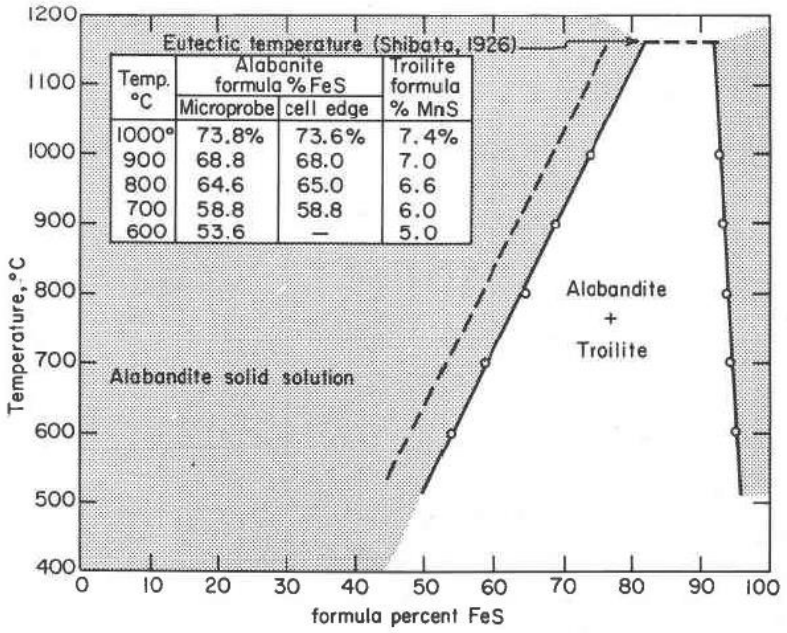

B.J. Skinner, F.D. Luck, Amer. Mineral., Vol.56 (1971), pp. 1269-1296.

Weight percent

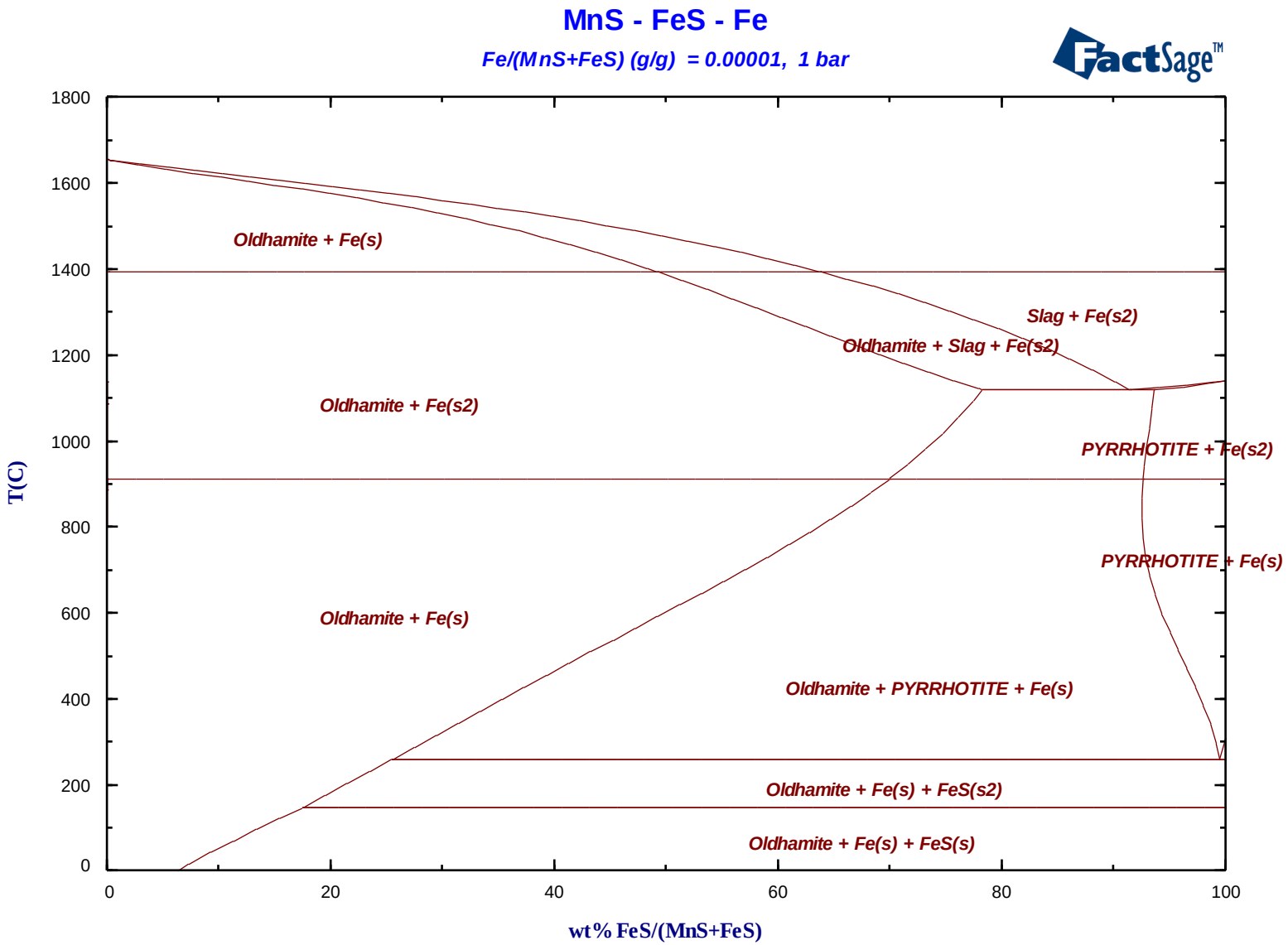

Mole fraction

K_2O - MgO

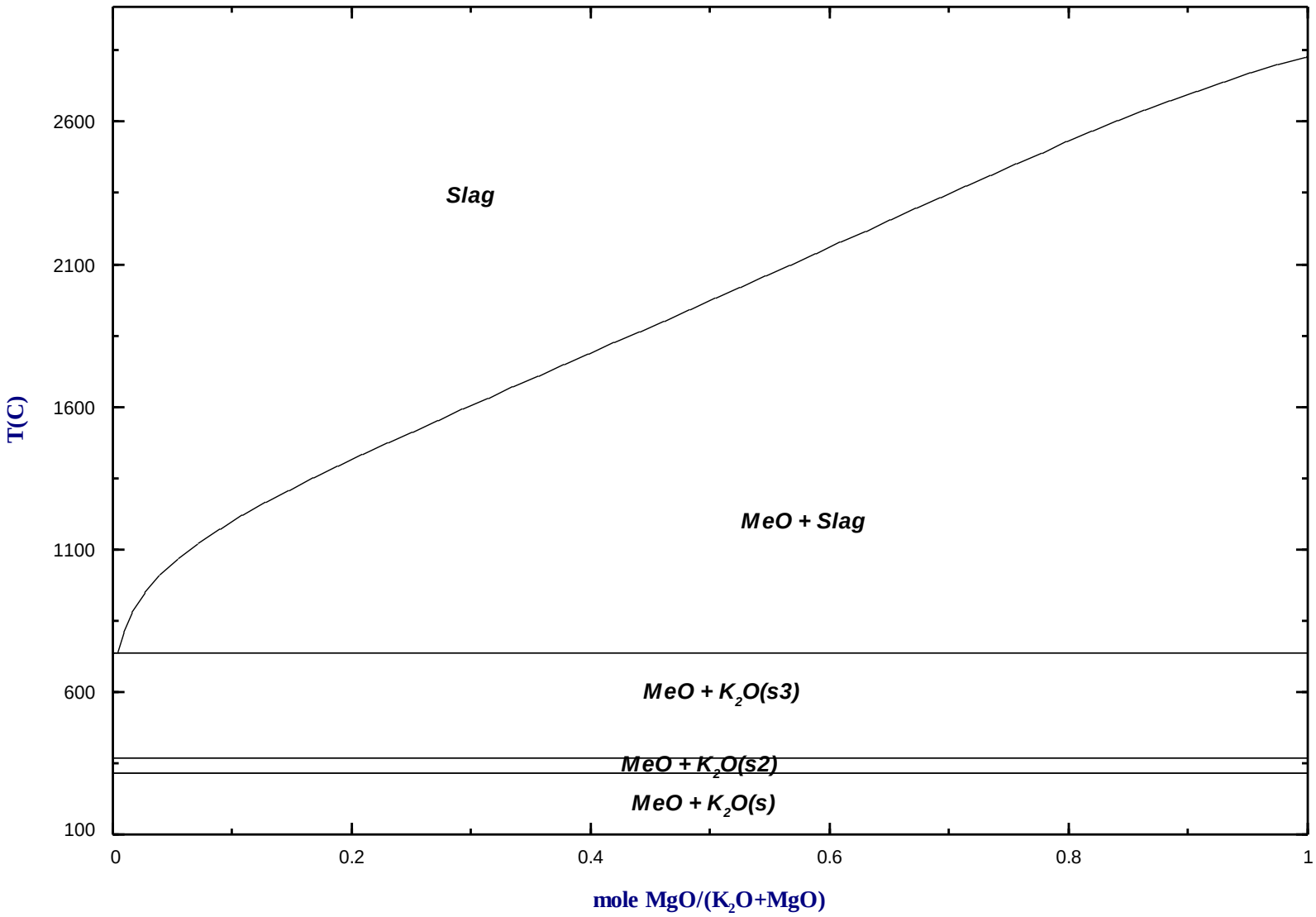

Weight percent

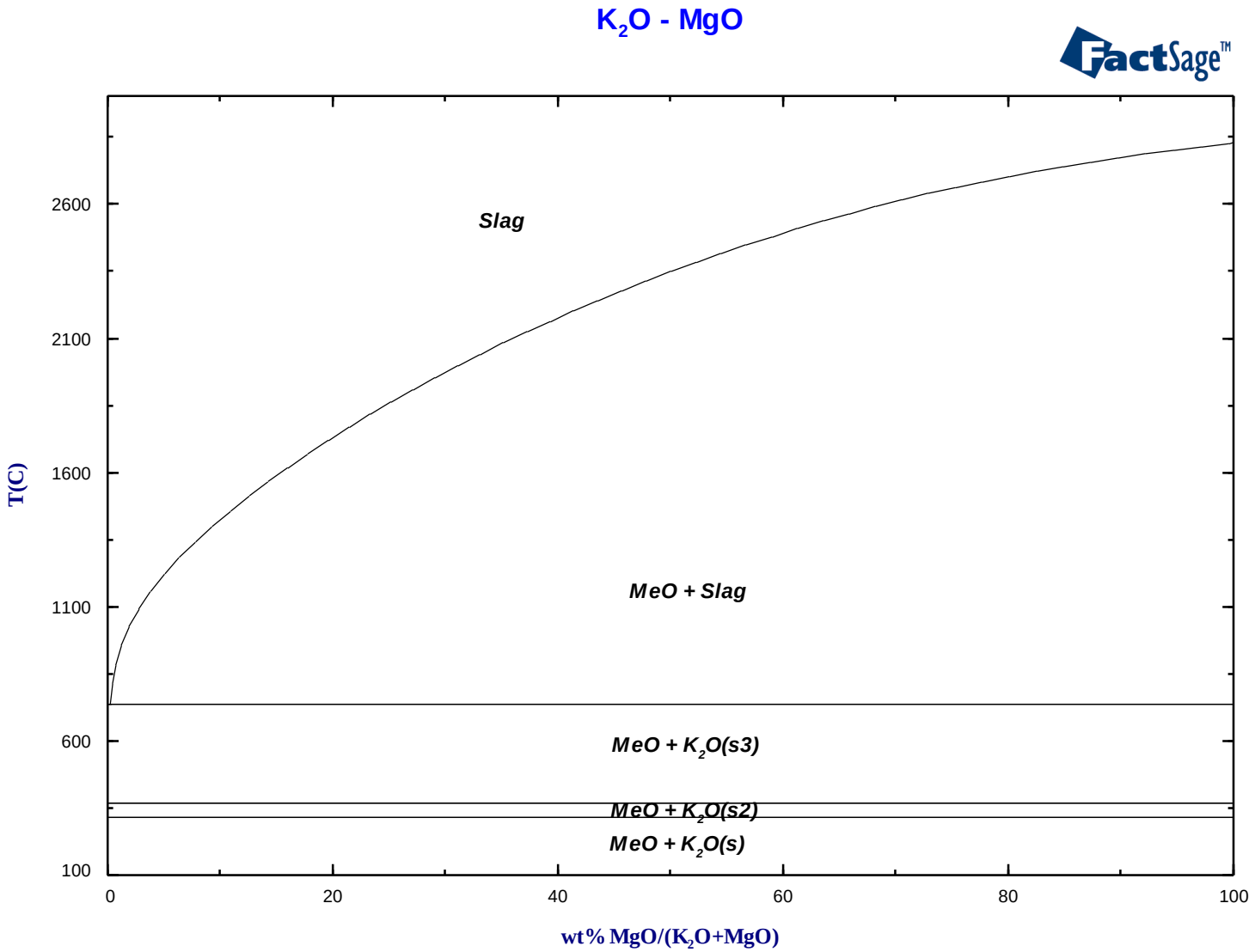

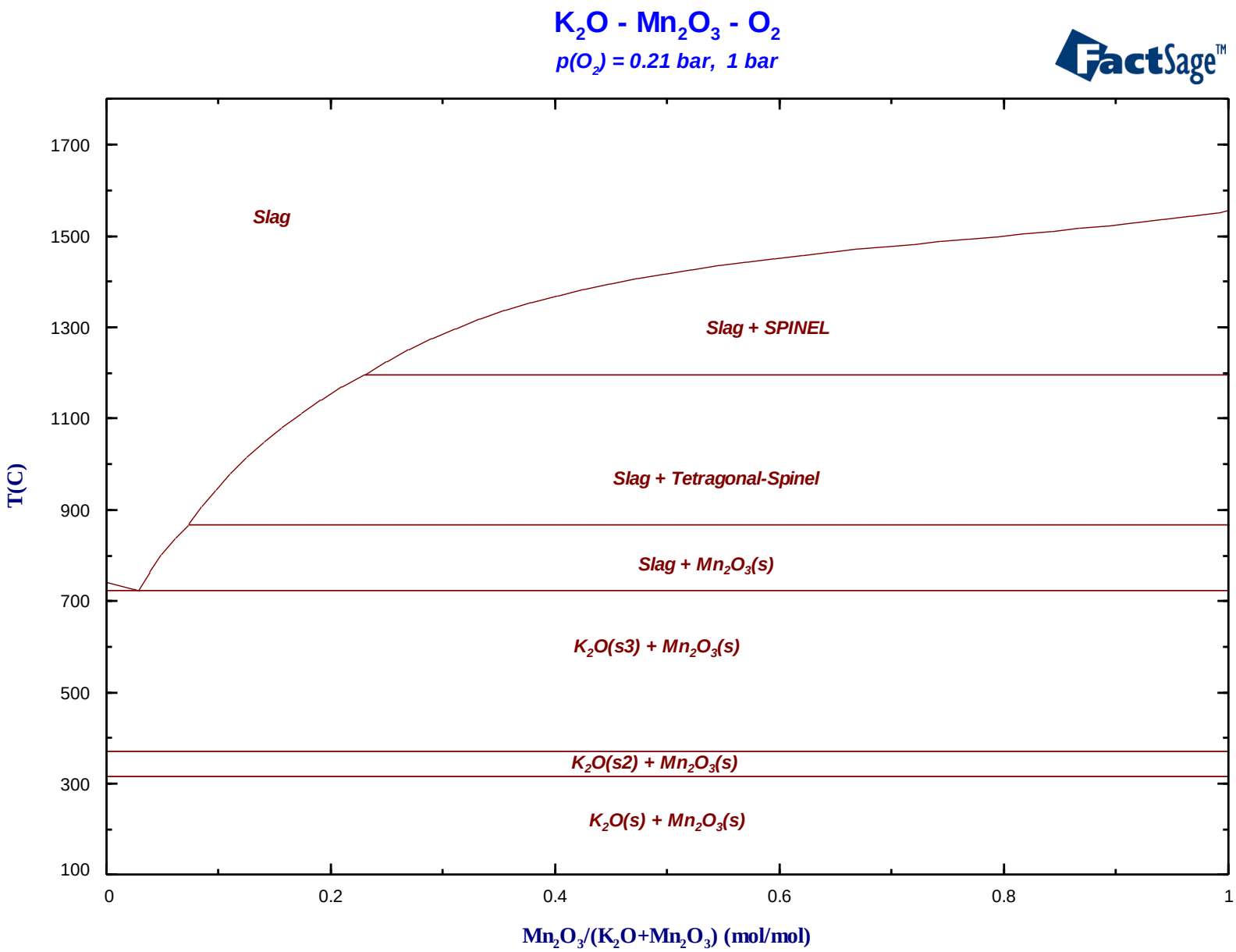
K2O - Mn2O3 - O2
p(O2) = 0.21 bar, 1 bar
FactSage™
Slag
Slag + SPINEL
Slag + Tetragonal-Spinel
Slag + Mn2O3(s)
K2O(s3) + Mn2O3(s)
K2O(s2) + Mn2O3(s)
K2O(s) + Mn2O3(s)
T(C)
1700
1500
1300
1100
900
700
500
300
100
0
0.2
0.4
0.6
0.8
1
Mn2O3/(K2O+Mn2O3) (mol/mol)

Weight percent

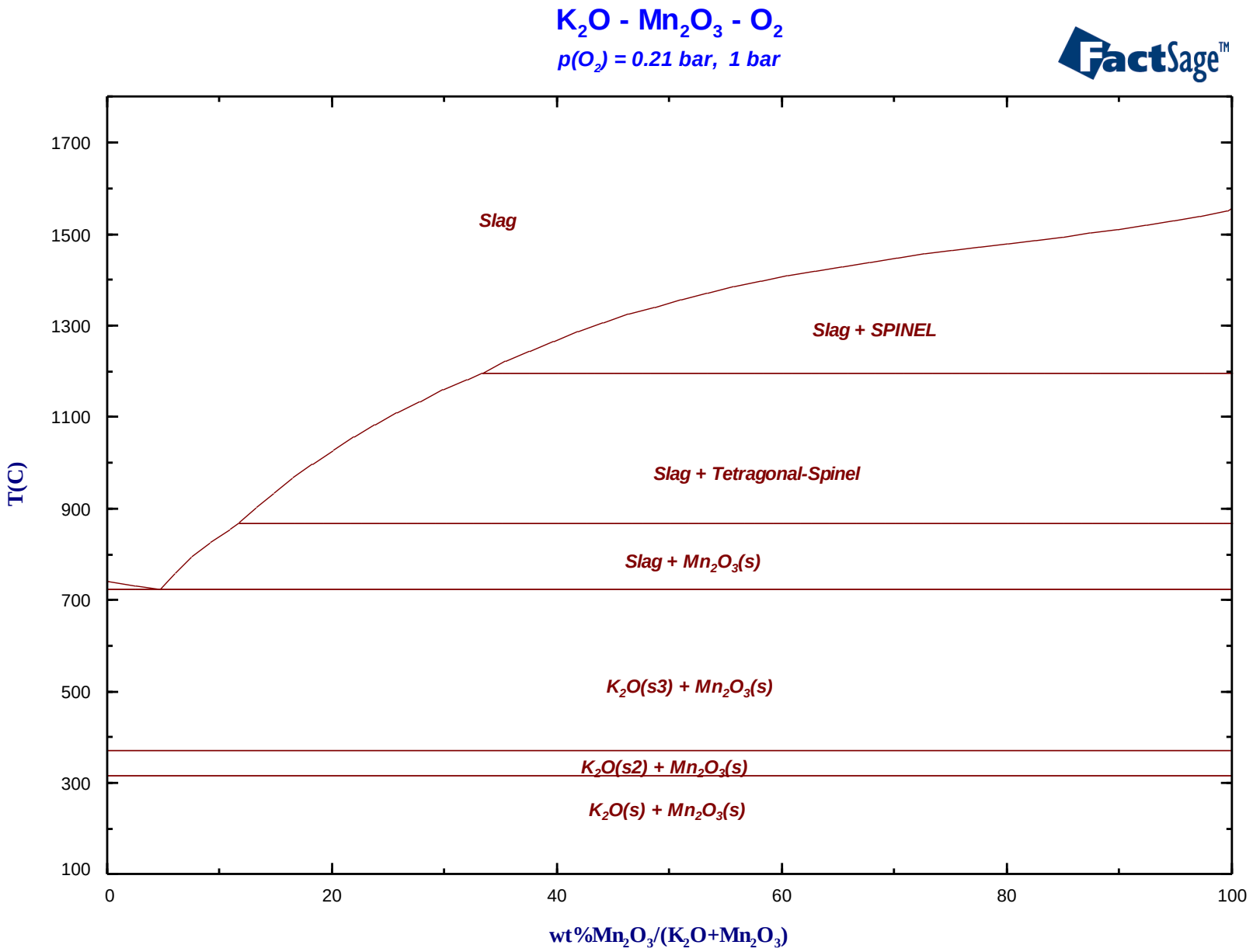

Mole fraction

K_2O - Na_2O

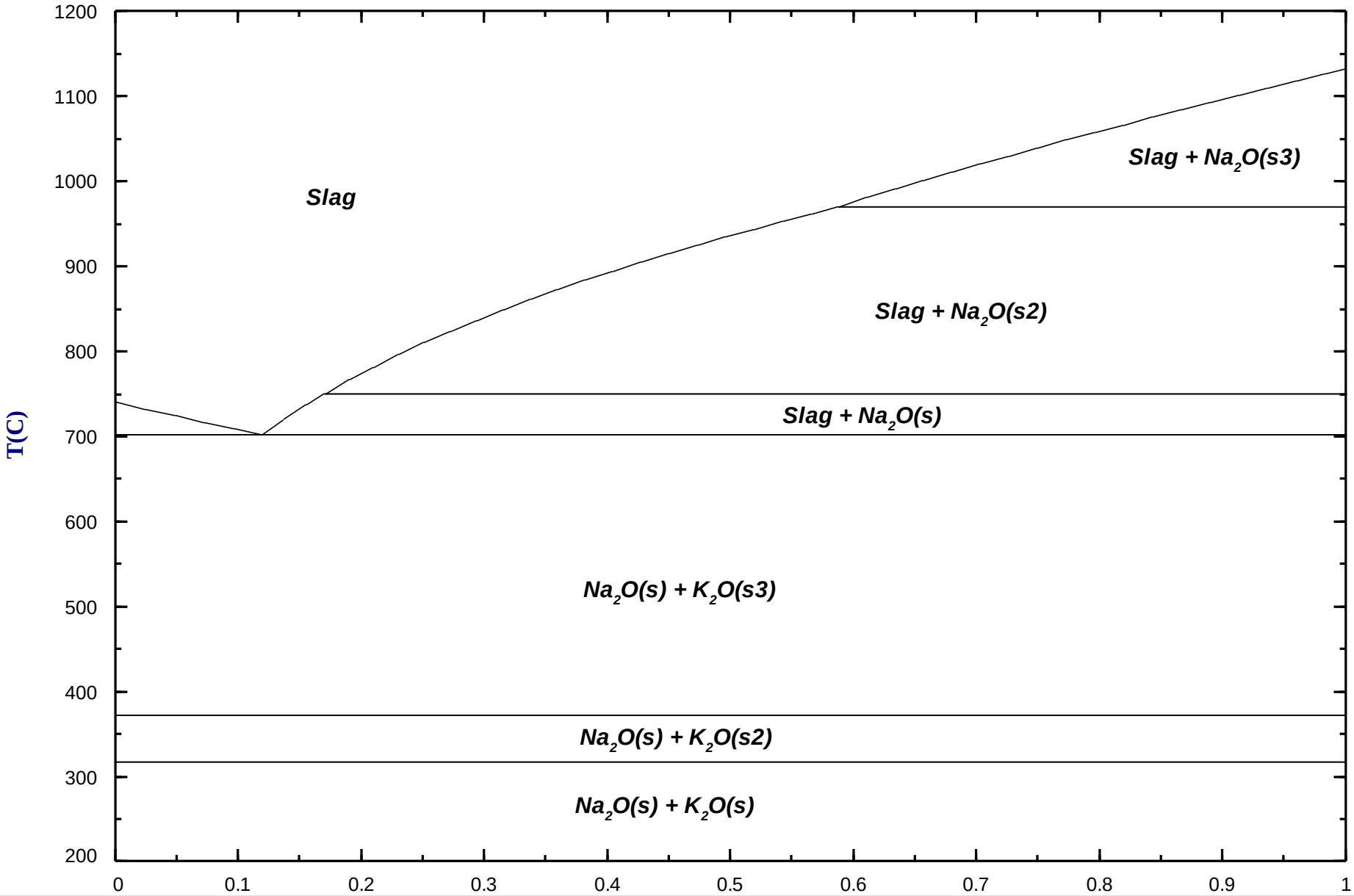

K_2O - Na_2O

Weight percent

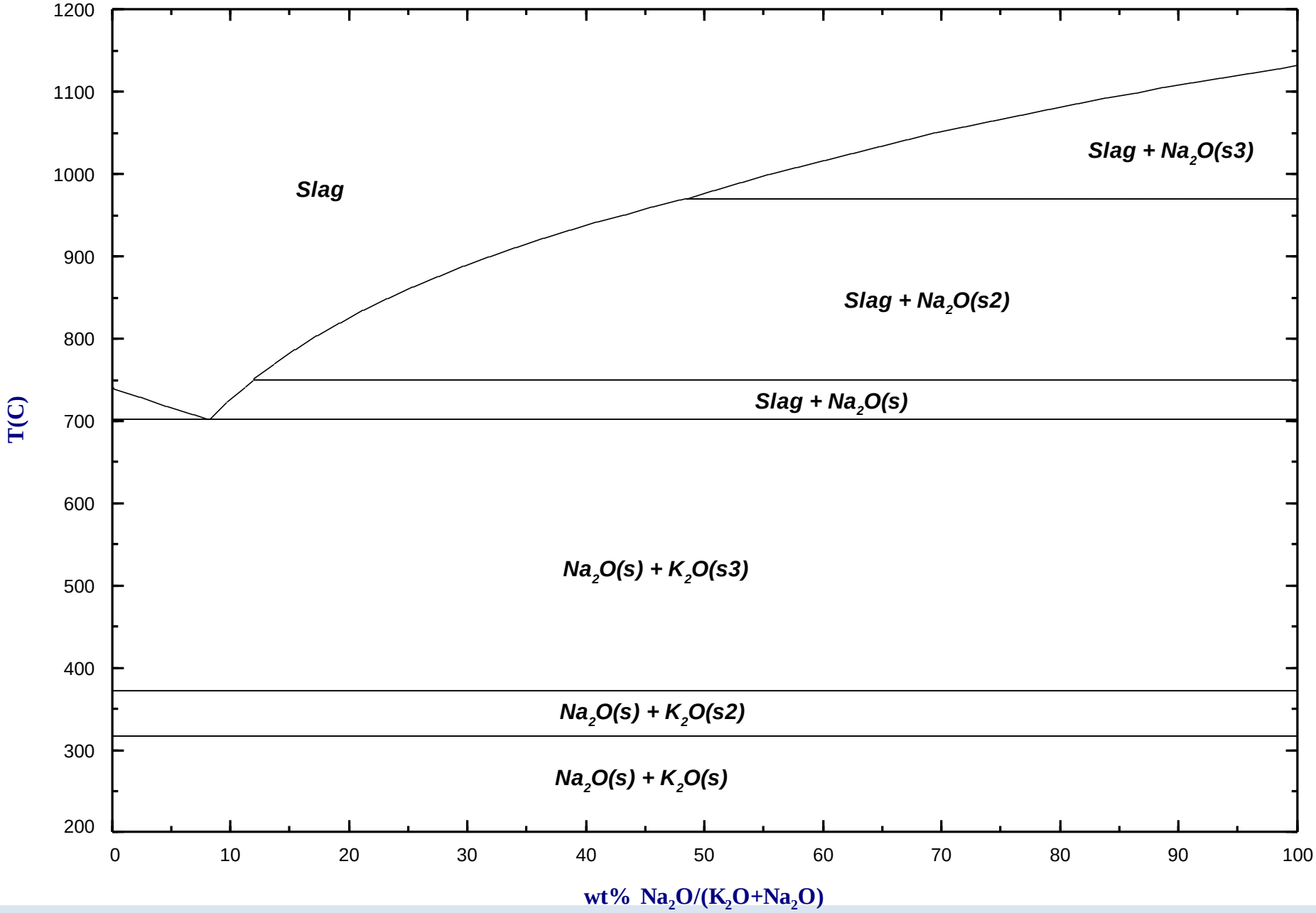

Mole fraction
compared with experimental data

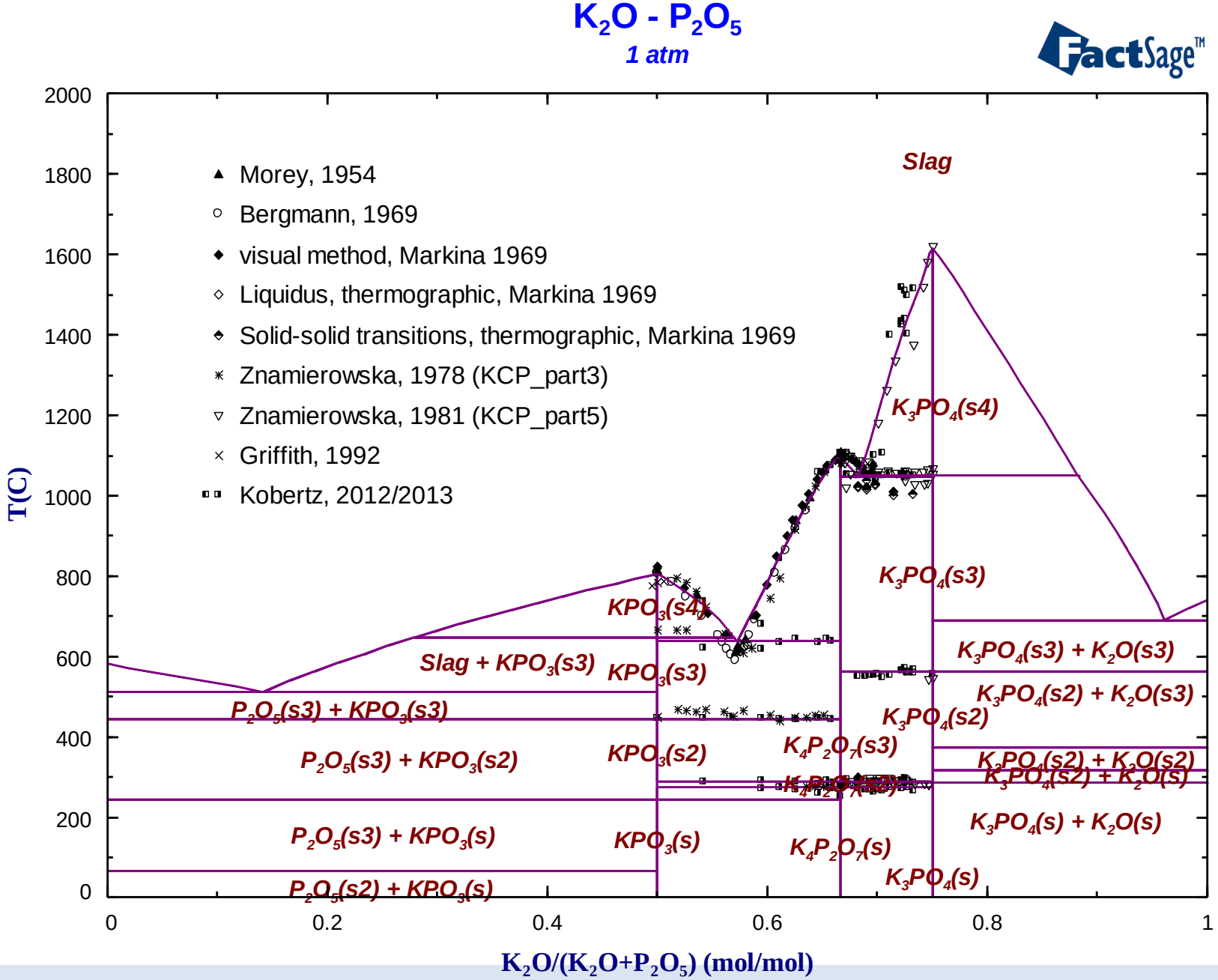

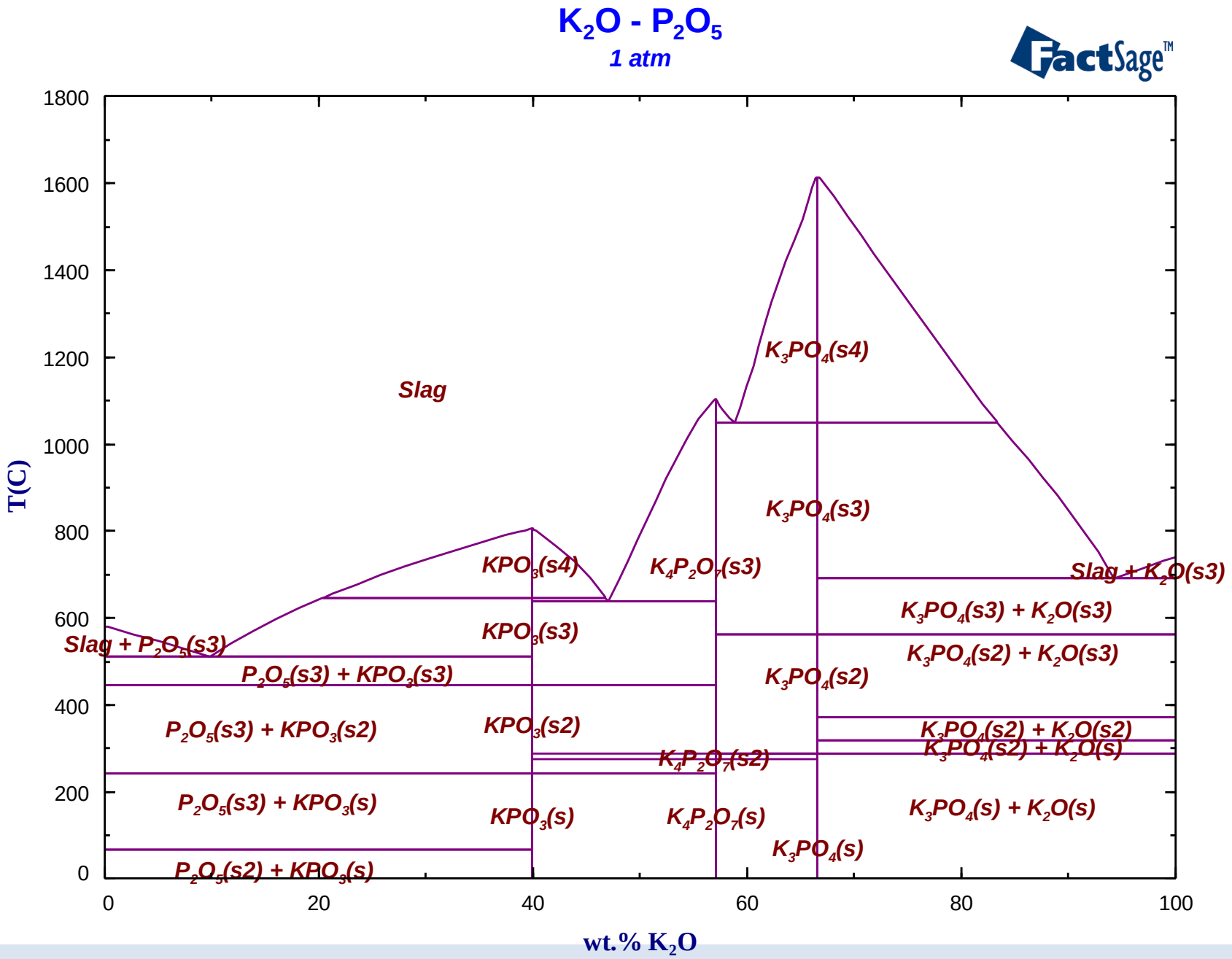
K2O - P2O5
1 atm
FactSage™
T(C)
wt.% K2O
1800
1600
1400
1200
1000
800
600
400
200
0
0
20
40
60
80
100
Slag
K3PO4(s4)
K3PO4(s3)
KPO3(s4)
K4P2O7(s3)
Slag + K2O(s3)
K3PO4(s3) + K2O(s3)
Slag + P2O5(s3)
KPO3(s3)
K3PO4(s2) + K2O(s3)
P2O5(s3) + KPO3(s3)
K3PO4(s2)
P2O5(s3) + KPO3(s2)
KPO3(s2)
K3PO4(s2) + K2O(s2)
K4P2O7(s2)
K3PO4(s2) + K2O(s)
P2O5(s3) + KPO3(s)
KPO3(s)
K4P2O7(s)
K3PO4(s) + K2O(s)
K3PO4(s)
P2O5(s2) + KPO3(s)

Mole fraction
compared with experimental data

K_2O - SiO_2

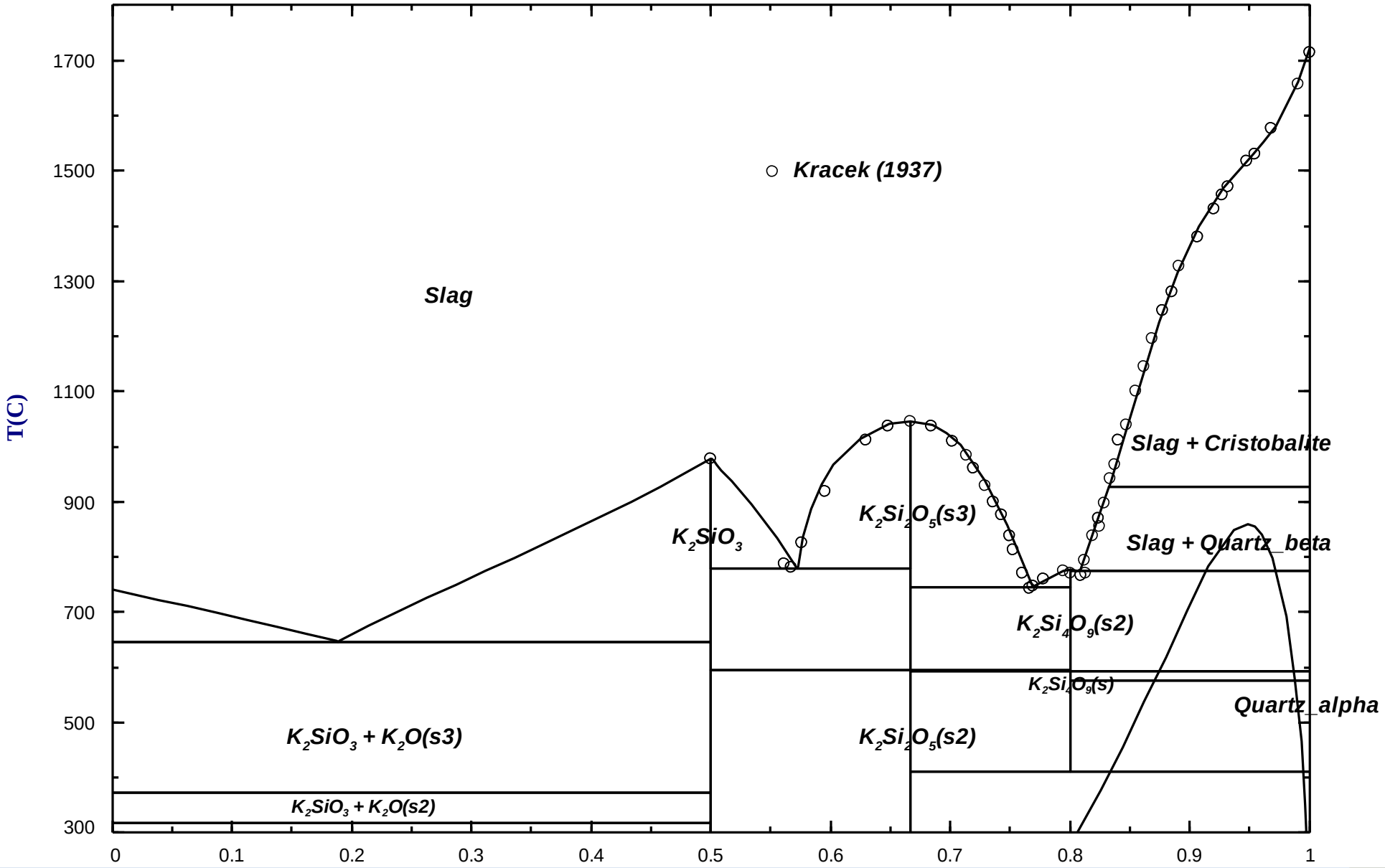

Weight percent

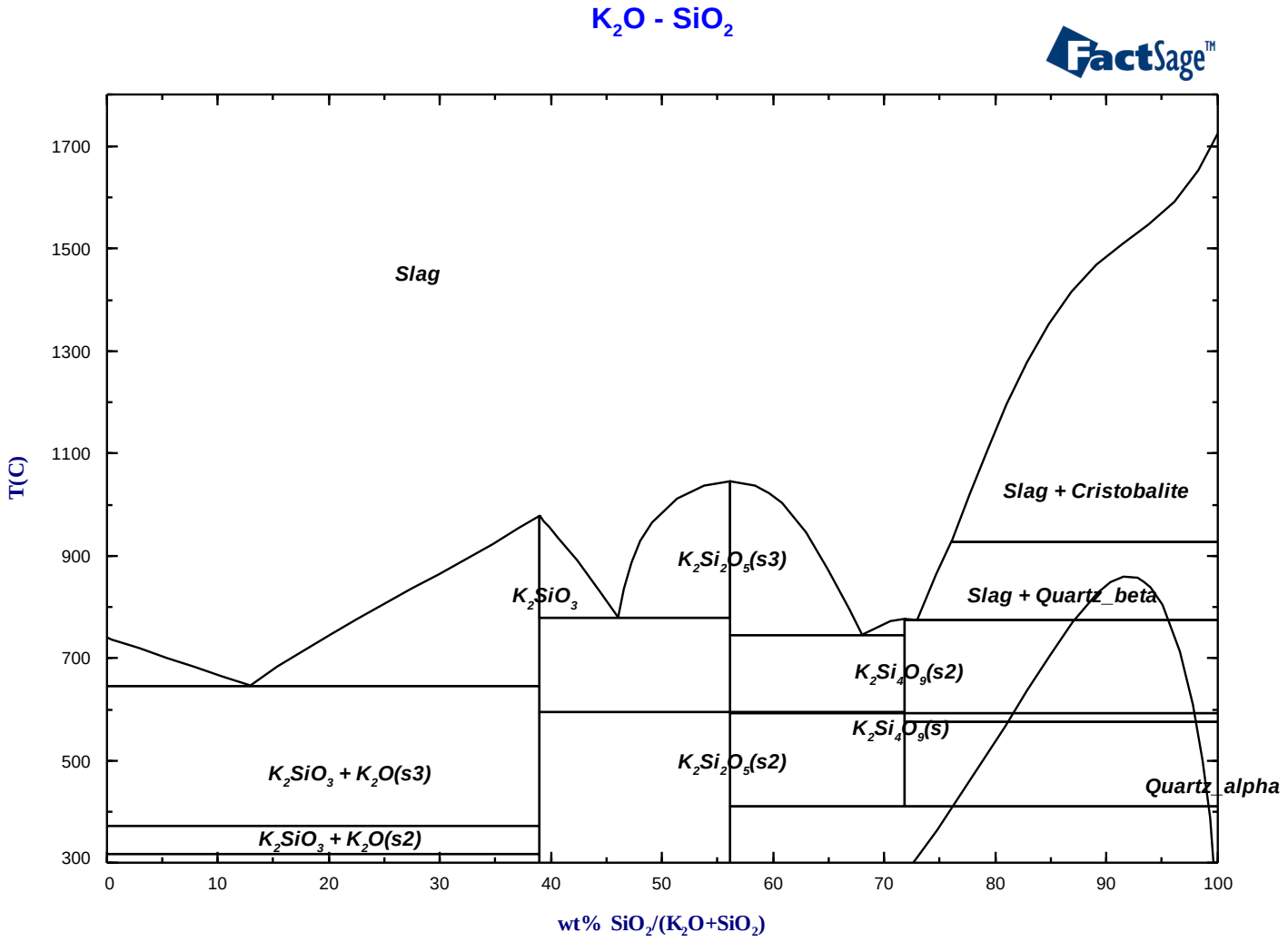

Mole fraction
compared with experimental data

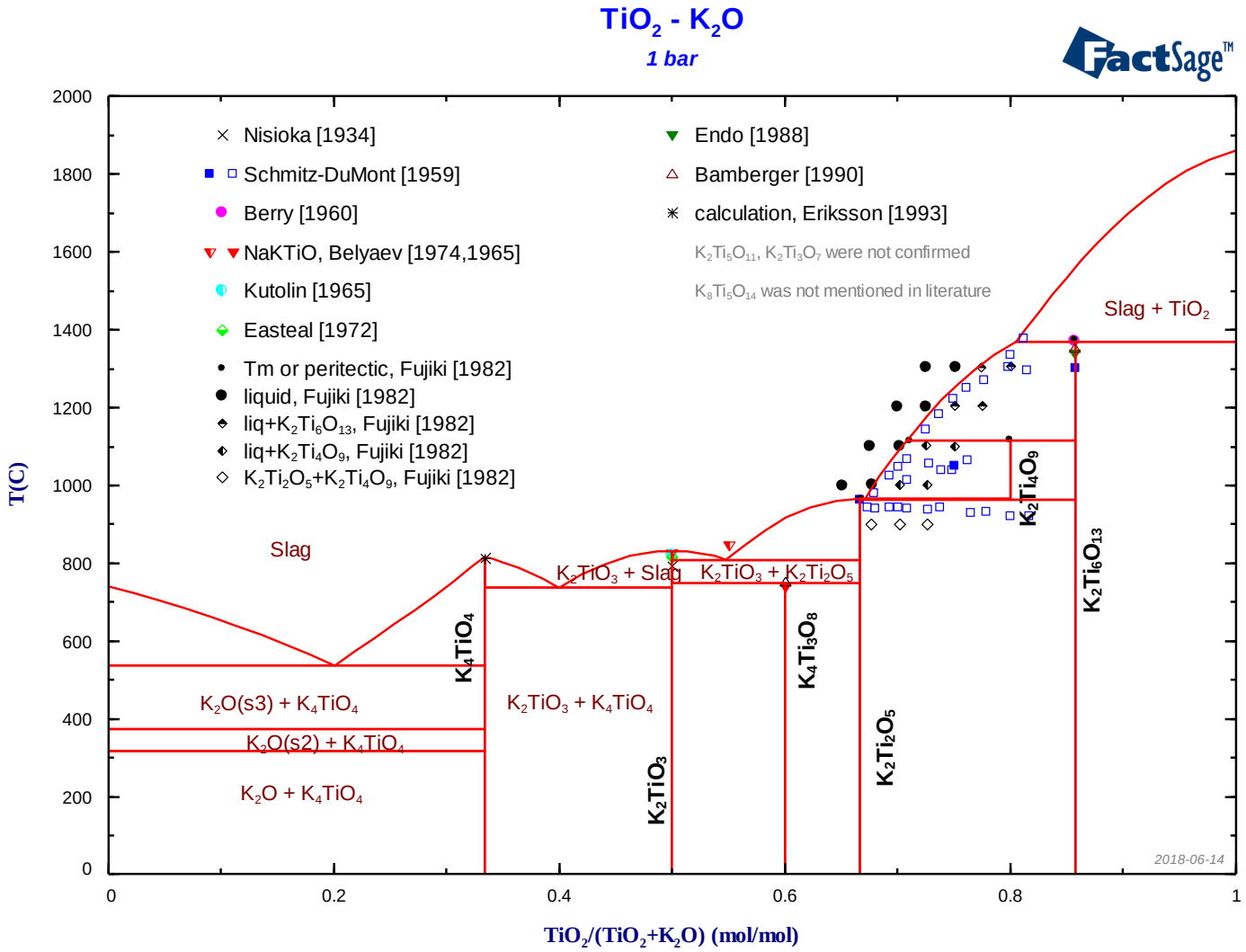

Weight percent

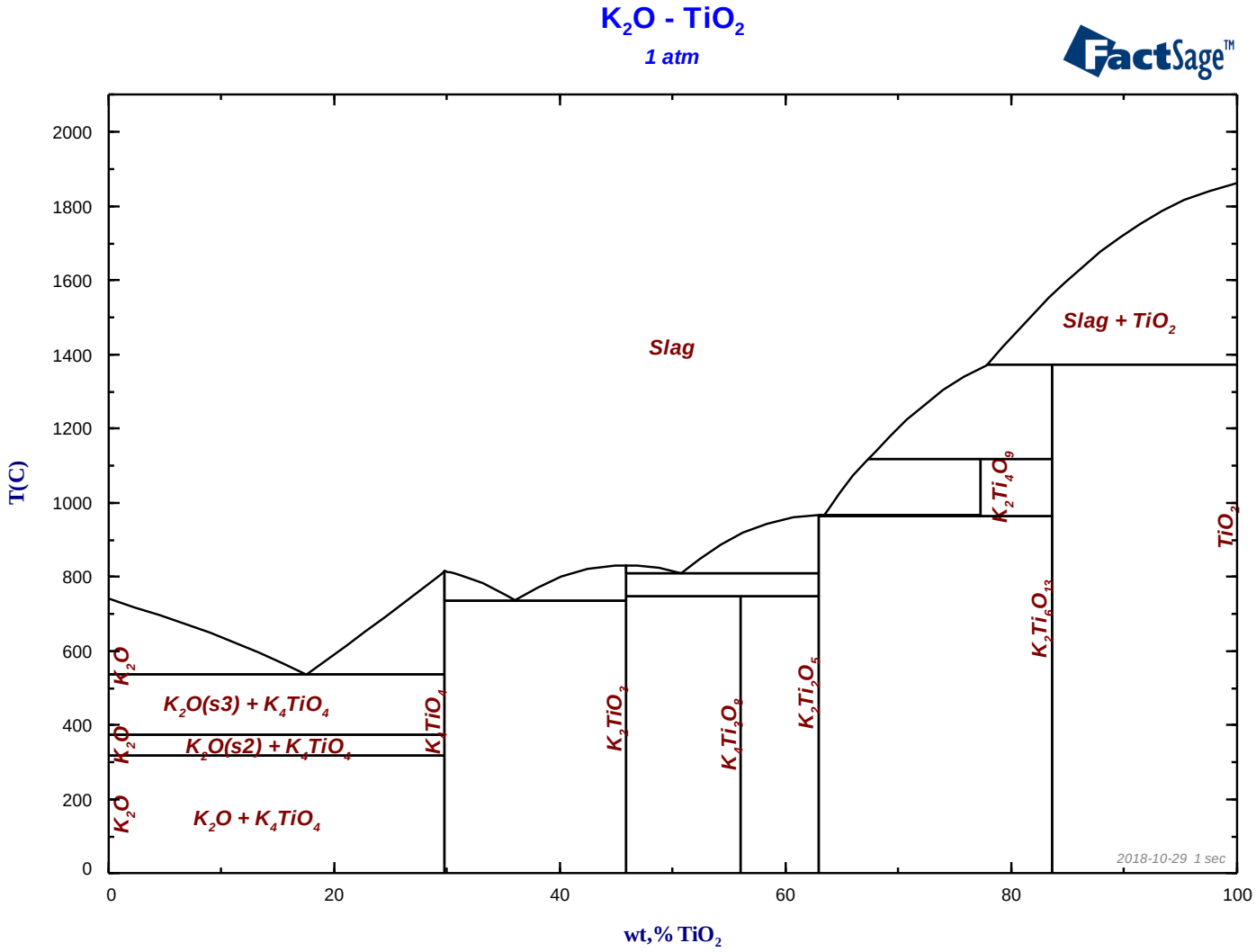

K2O-V2O5,
Mole fraction
compared with experimental data

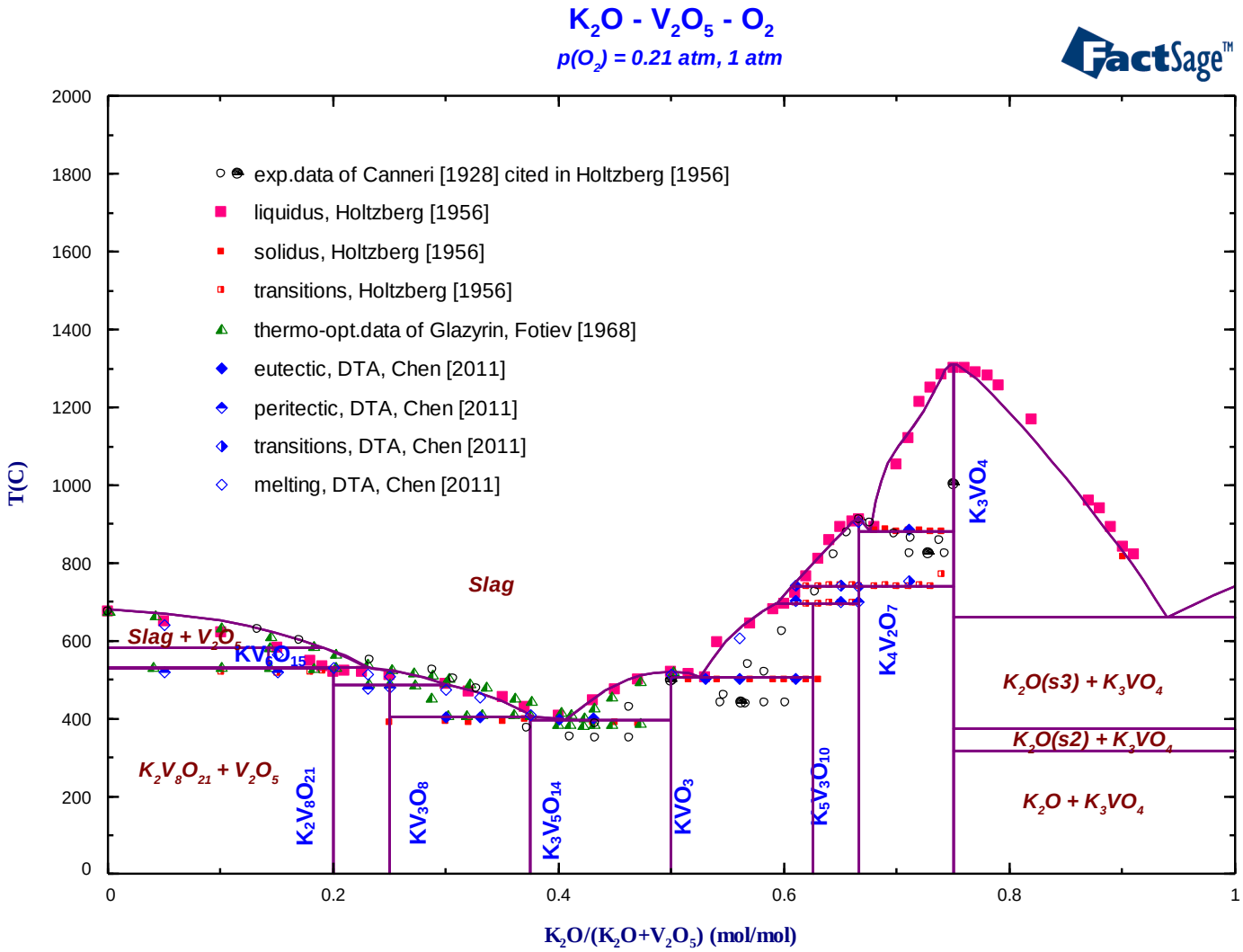

K2O-V2O5,
Weight percent

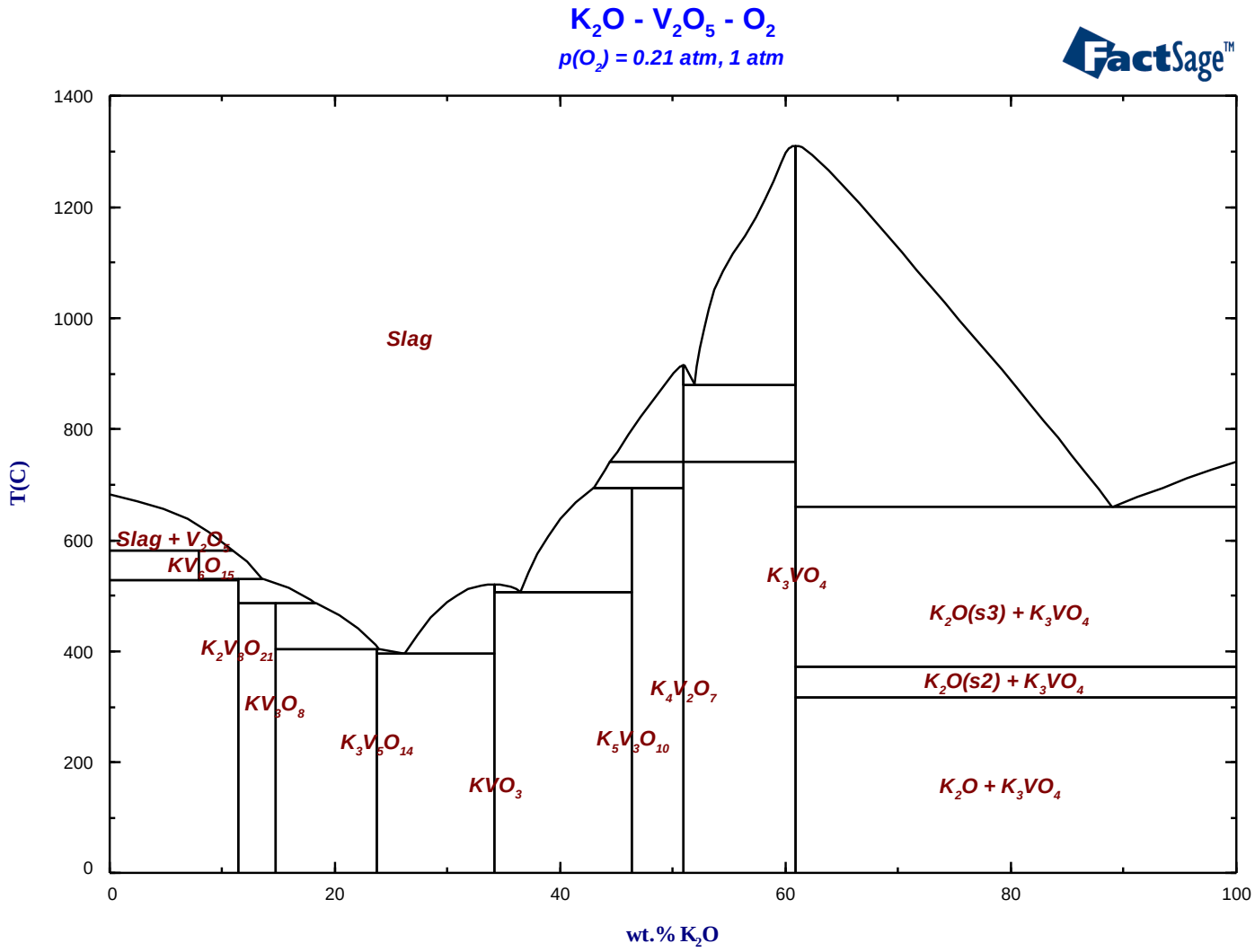

Mole fraction
compared with experimental data

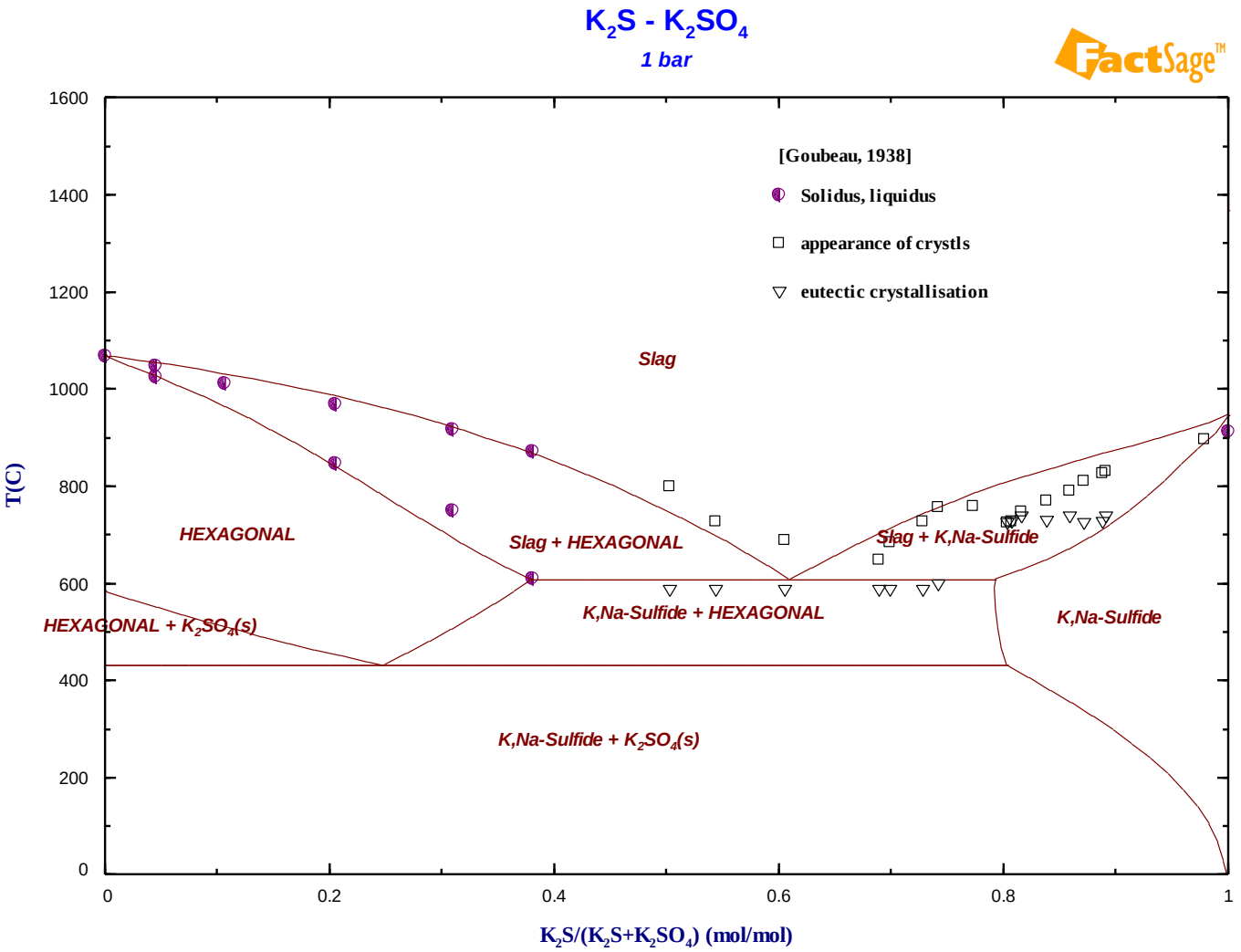

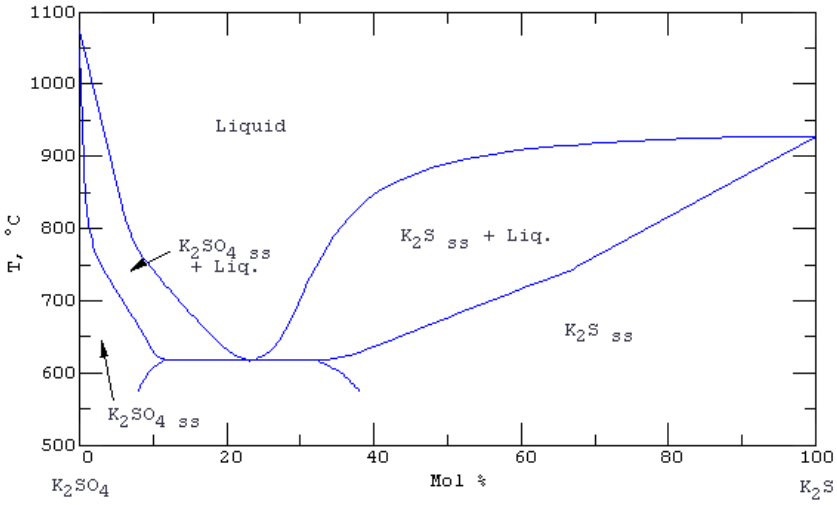

S.W. So, D. Barham, J. Therm. Anal., 20 [2], (1981), pp. 275-280.

Weight percent

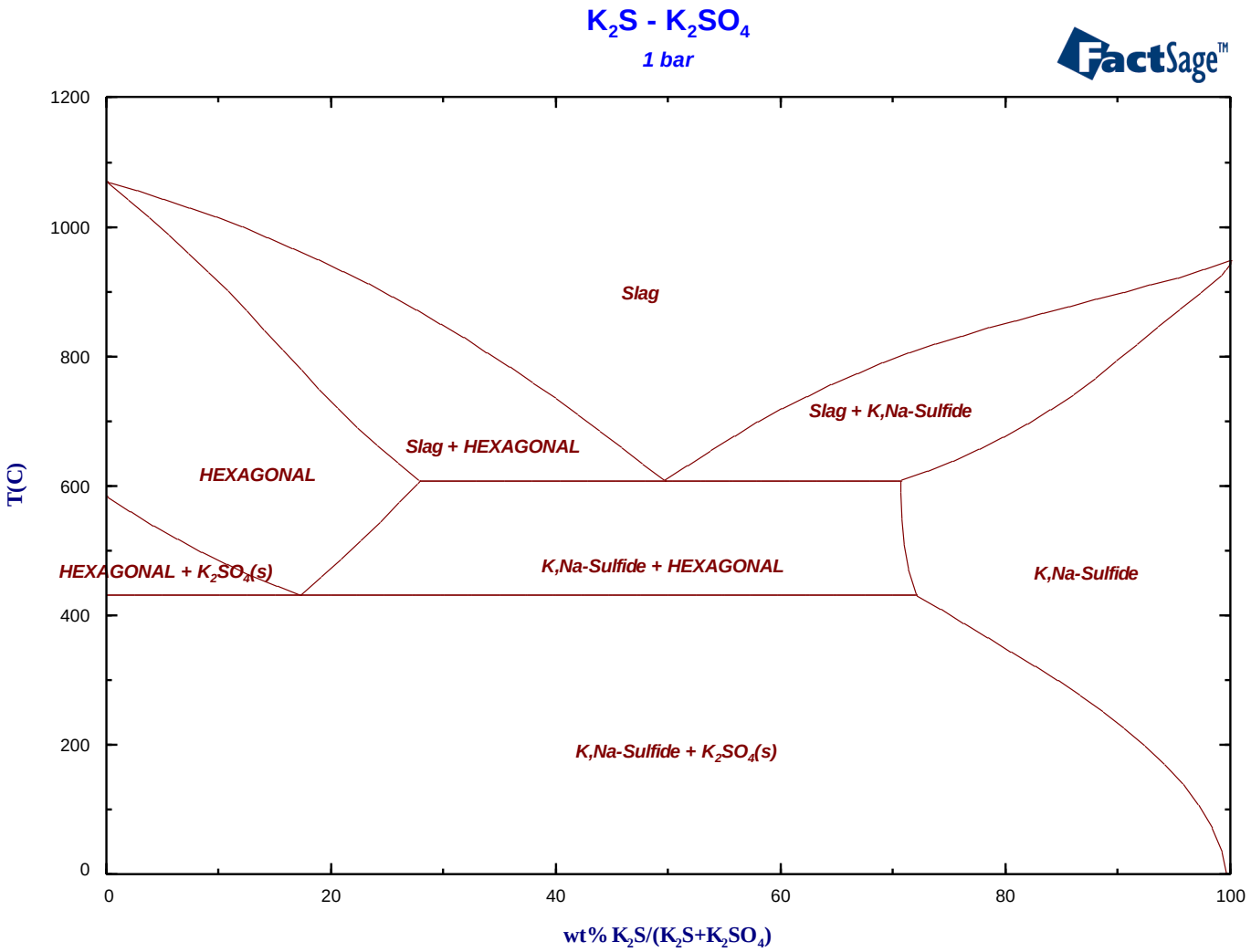

Mole fraction
compared with experimental data

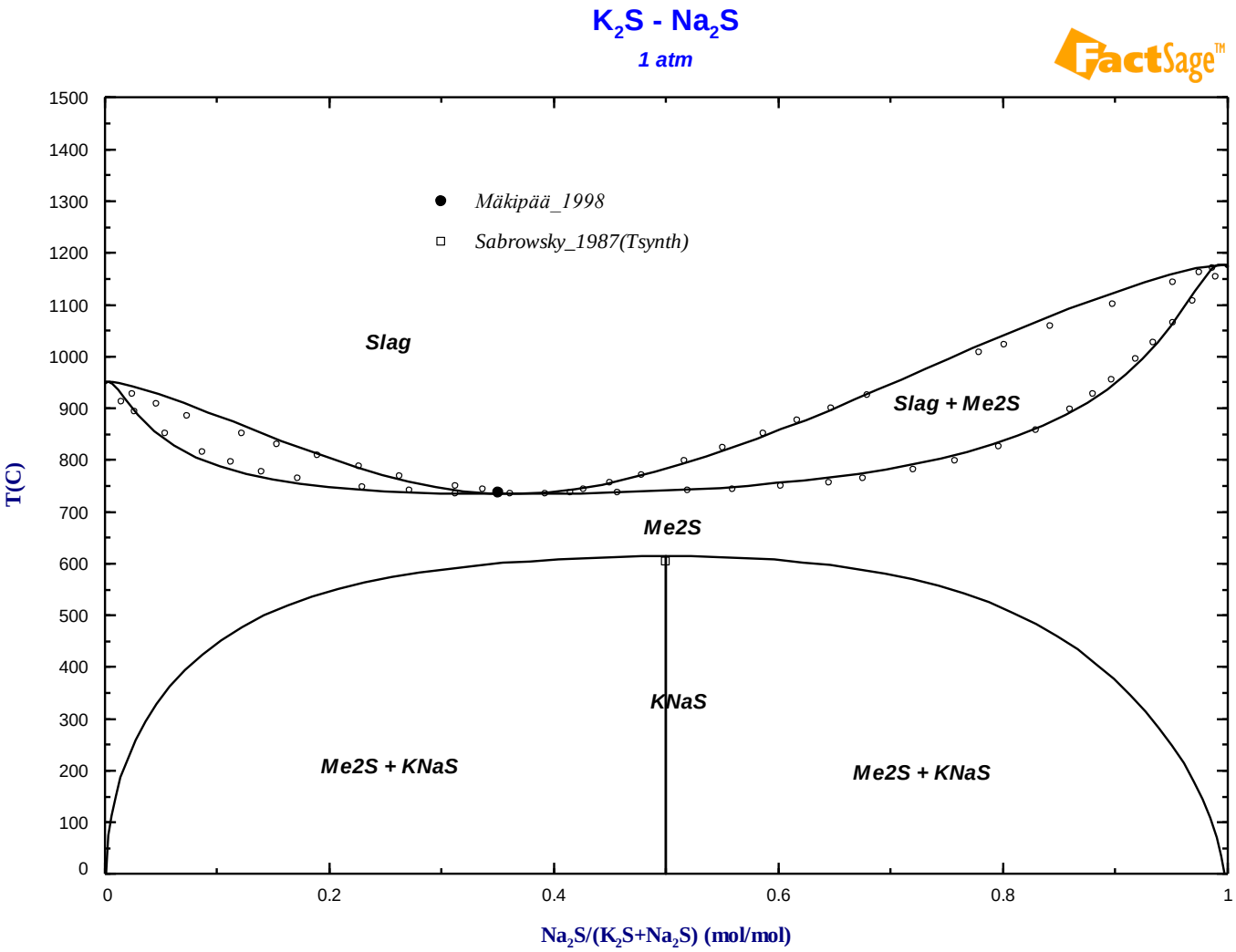

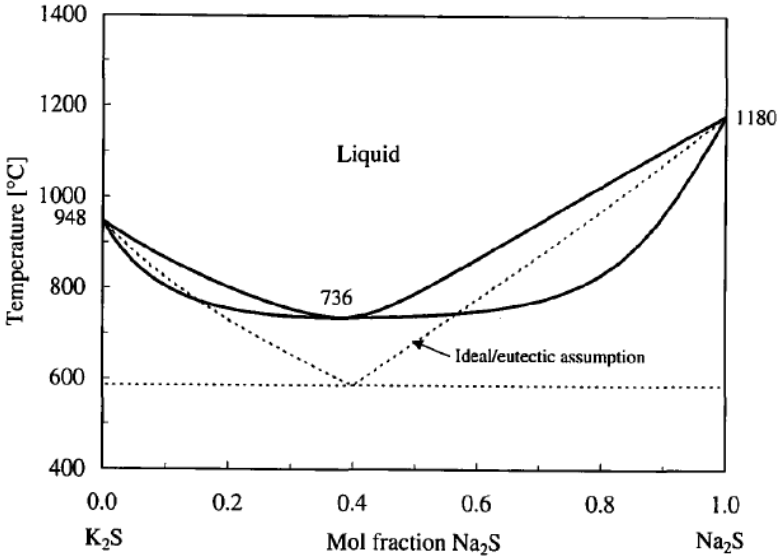

M. Mäkipää, R. Backman, Corrosion of floor tubes in reduced kraft smelts: studies on effects of chlorine and potassium, 9th Internat Symp Corrosion in the Pulp and Paper Industry, 1998; 199-207.

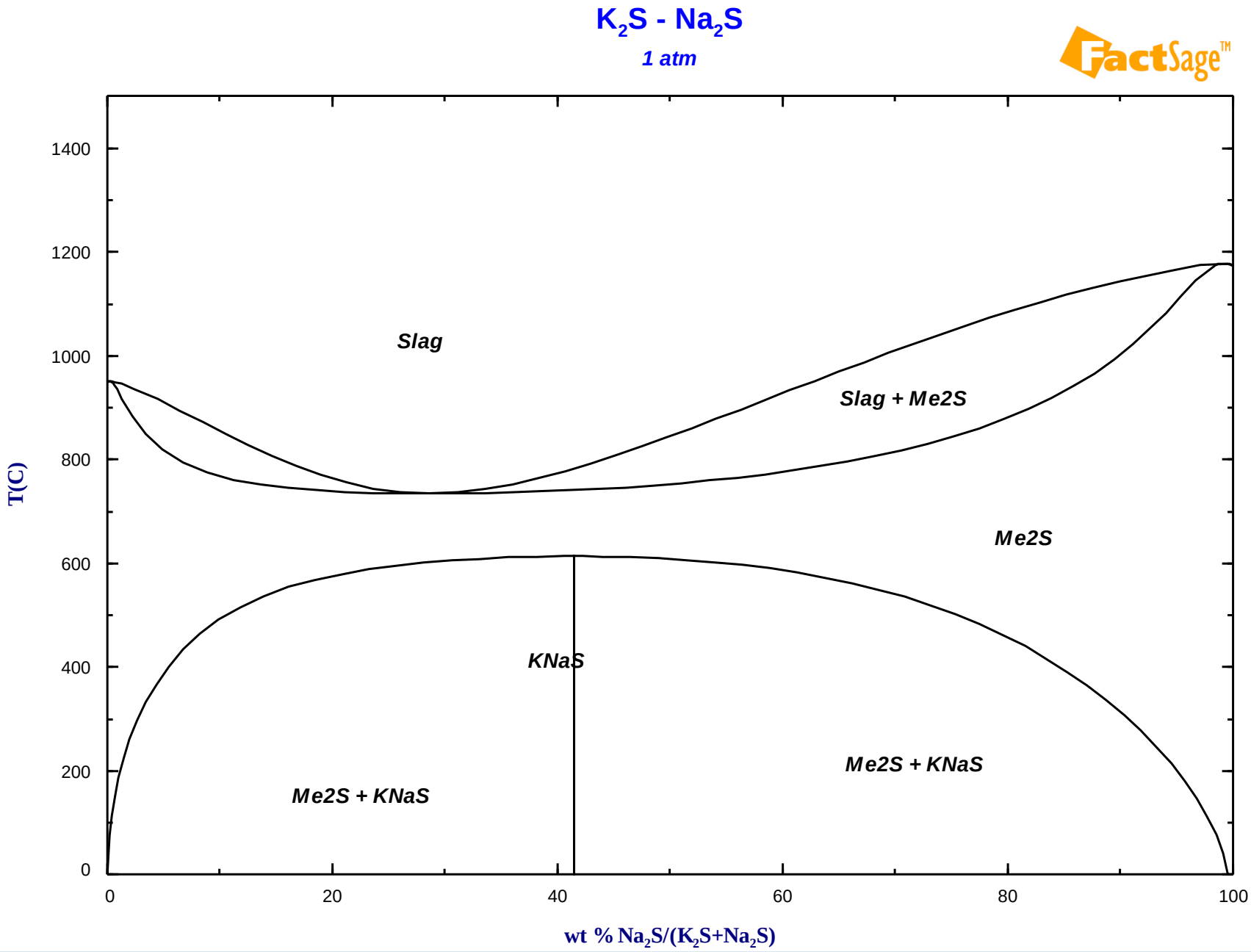
K2S - Na2S
1 atm
FactSage™
1400
1200
1000
800
600
400
200
0
T(C)
Slag
Slag + Me2S
Me2S
KNaS
Me2S + KNaS
Me2S + KNaS
0
20
40
60
80
100
wt % Na2S/(K2S+Na2S)

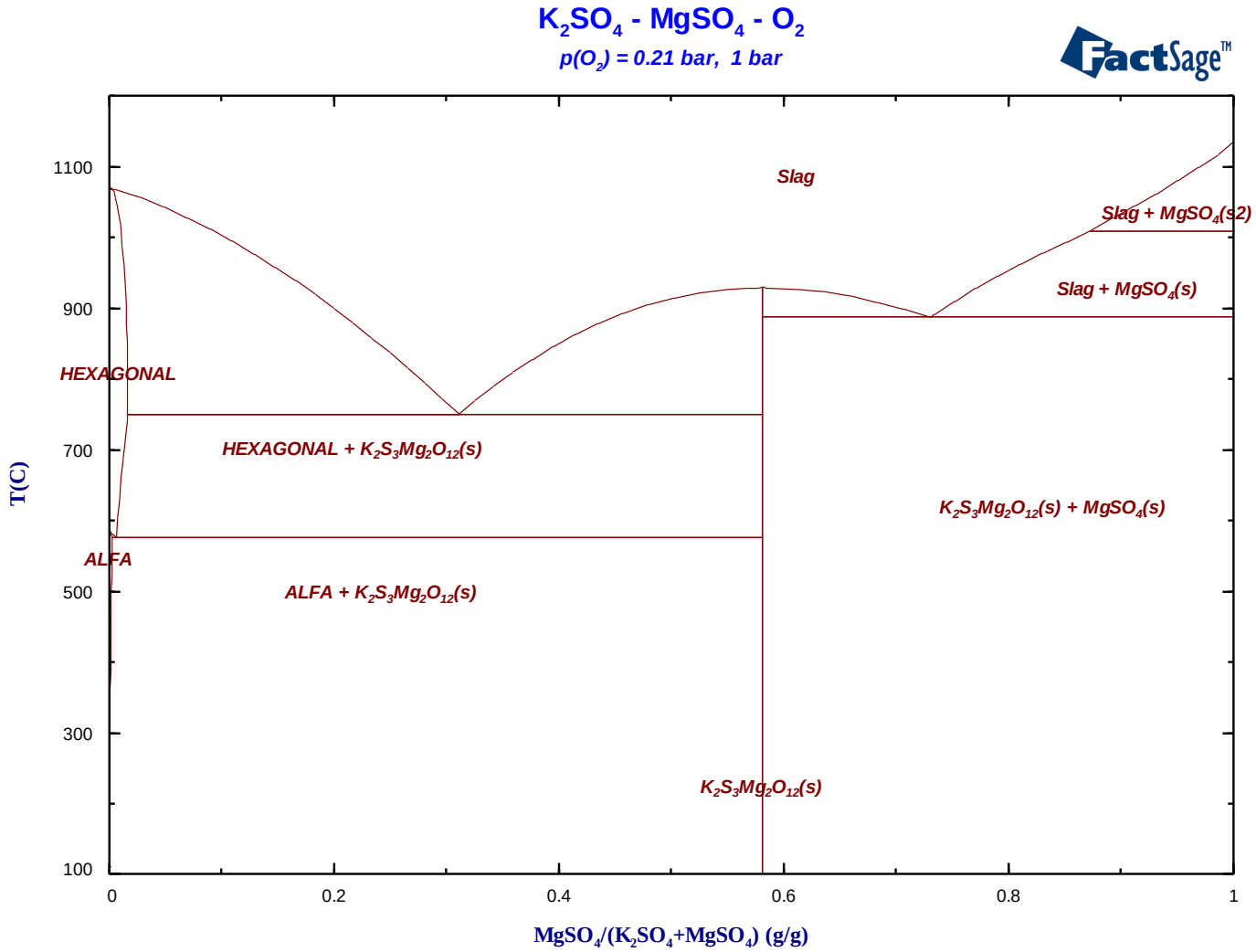
K2SO4 - MgSO4 - O2
p(O2) = 0.21 bar, 1 bar
FactSage™
Slag
Slag + MgSO4(s2)
Slag + MgSO4(s)
HEXAGONAL
HEXAGONAL + K2S3Mg2O12(s)
K2S3Mg2O12(s) + MgSO4(s)
ALFA
ALFA + K2S3Mg2O12(s)
K2S3Mg2O12(s)
T(C)
1100
900
700
500
300
100
0
0.2
0.4
0.6
0.8
1
MgSO4/(K2SO4+MgSO4) (g/g)

Weight percent
compared with experimental data

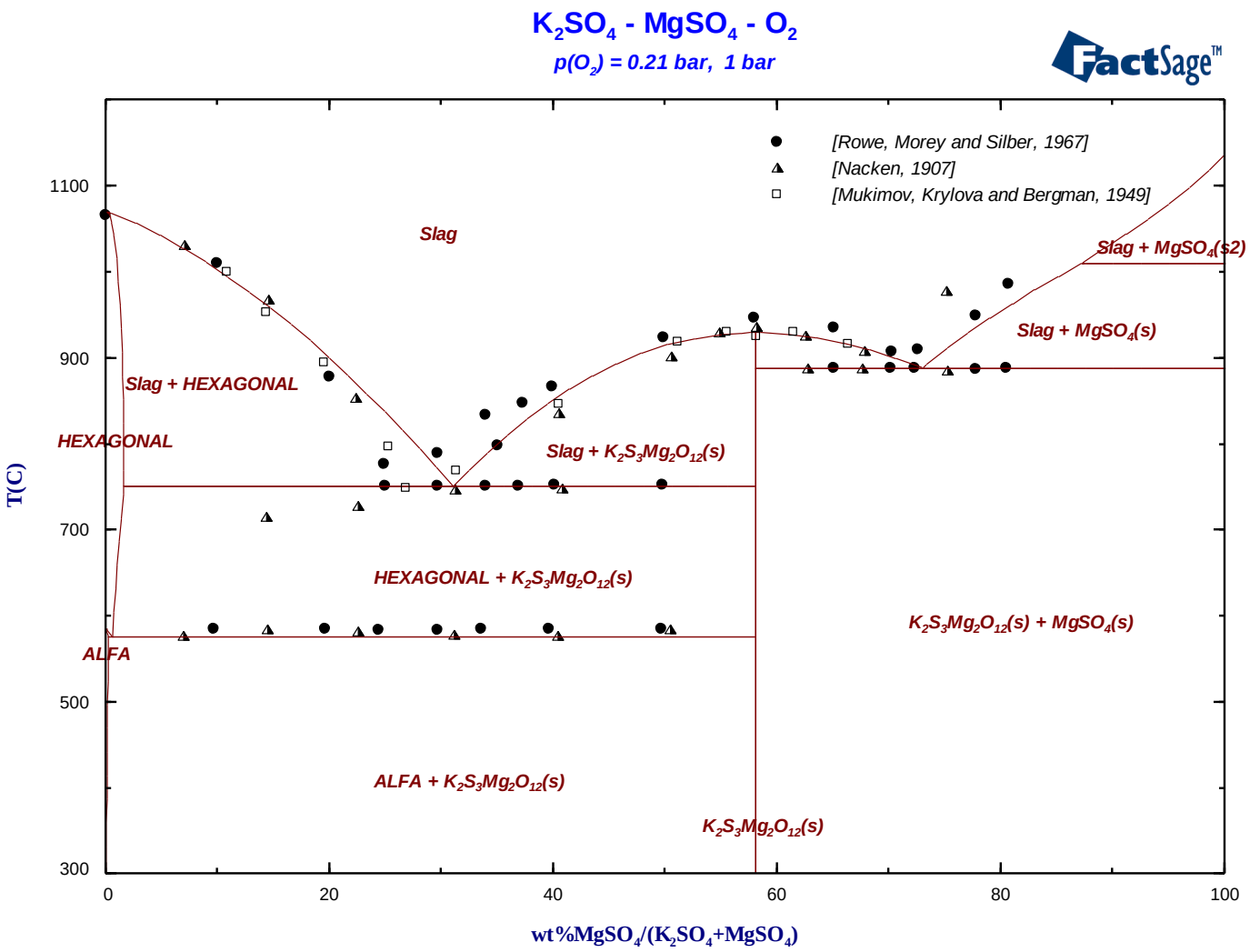

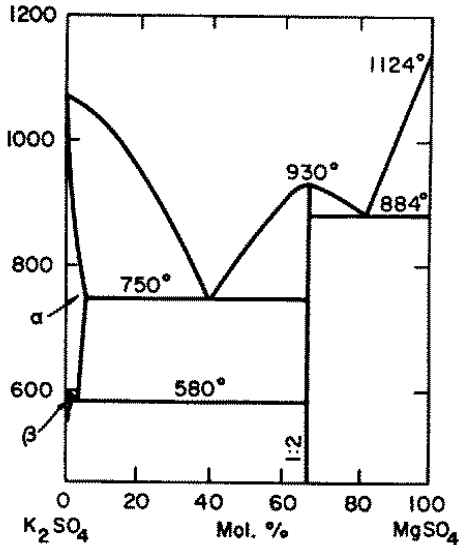

V.A. Efremov, V.M. Zhukovskii, Yu.G. Petrosyan, Z. Anorg. Chem., 81 [3], (1913), pp.102.

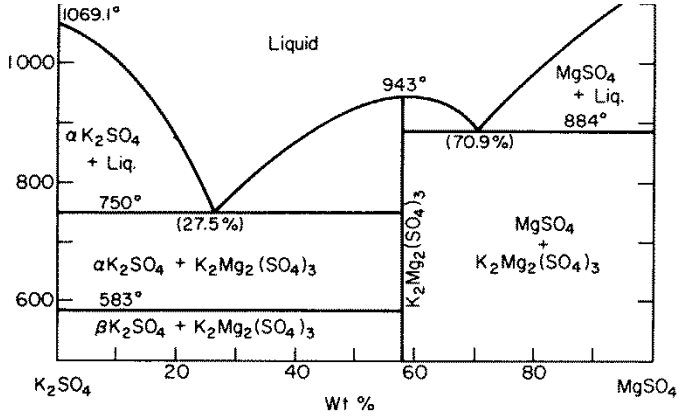

J.J. Rowe, G.W. Morey, C.C. Silber, J. Inorg. Nucl.Chem., 29 [4], (1967), pp.925-942.

Mole fraction
compared with experimental data

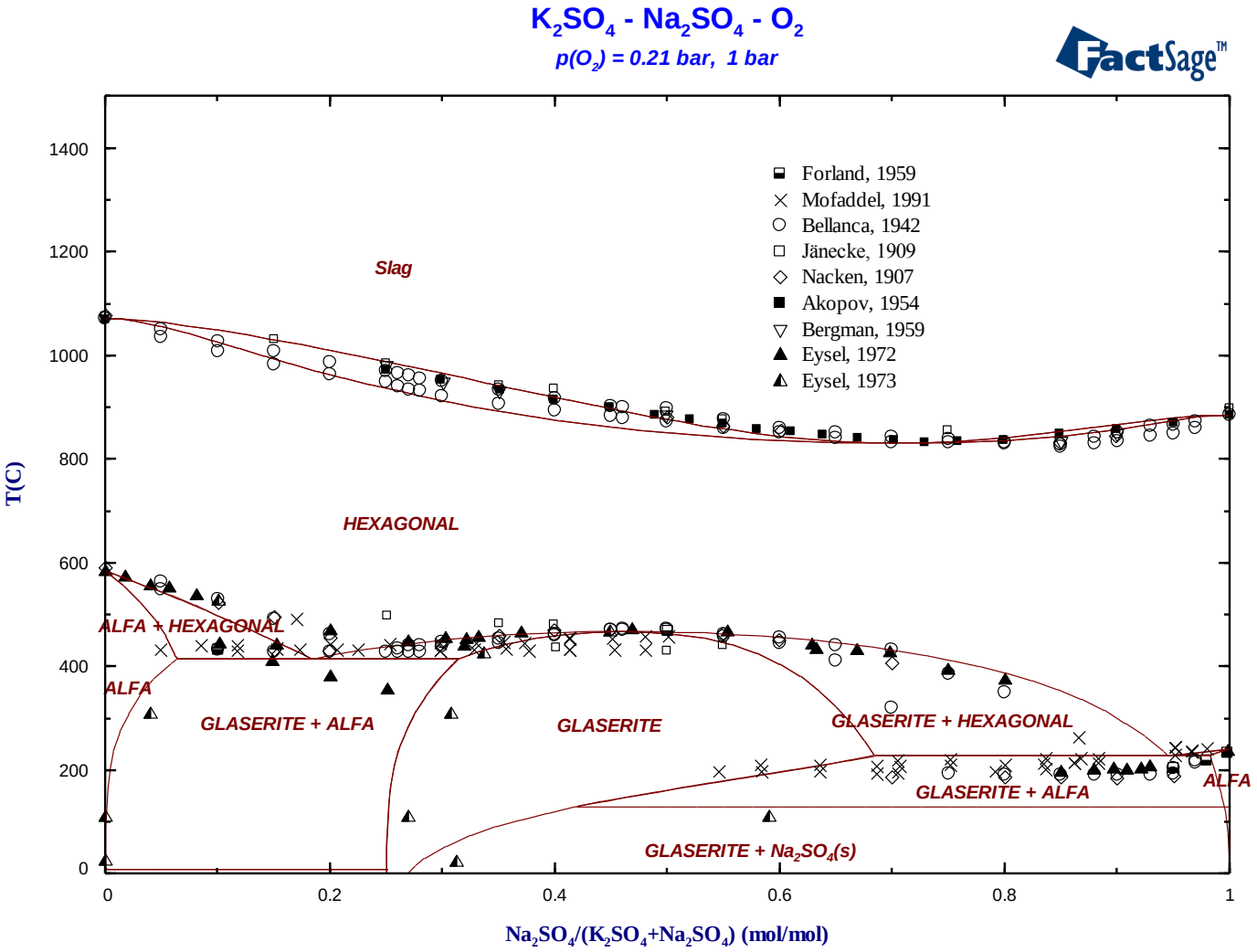

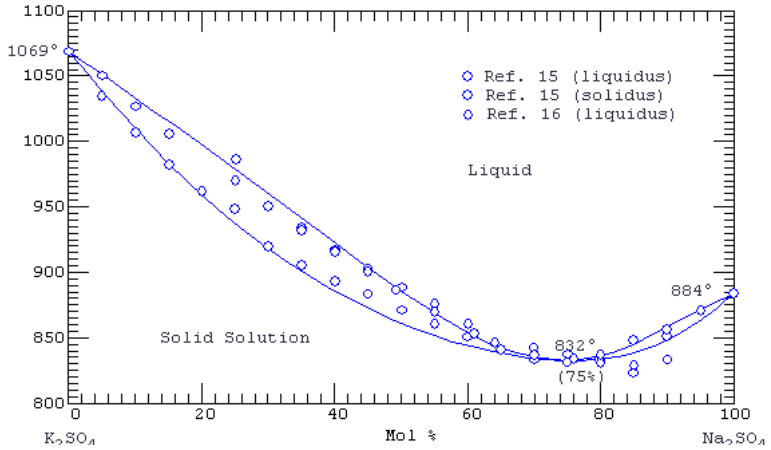

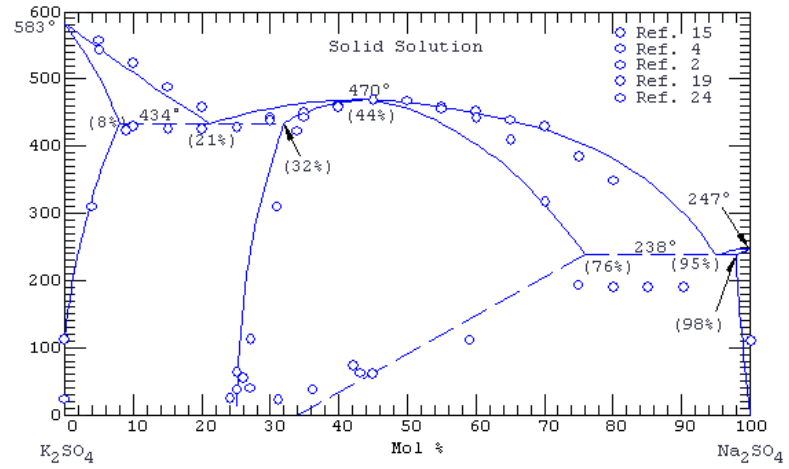

J.M. Sangster, A.D. Pelton, Am. Ceram. Soc., Westerville, Ohio, (1987), pp. 224-231.

Weight percent

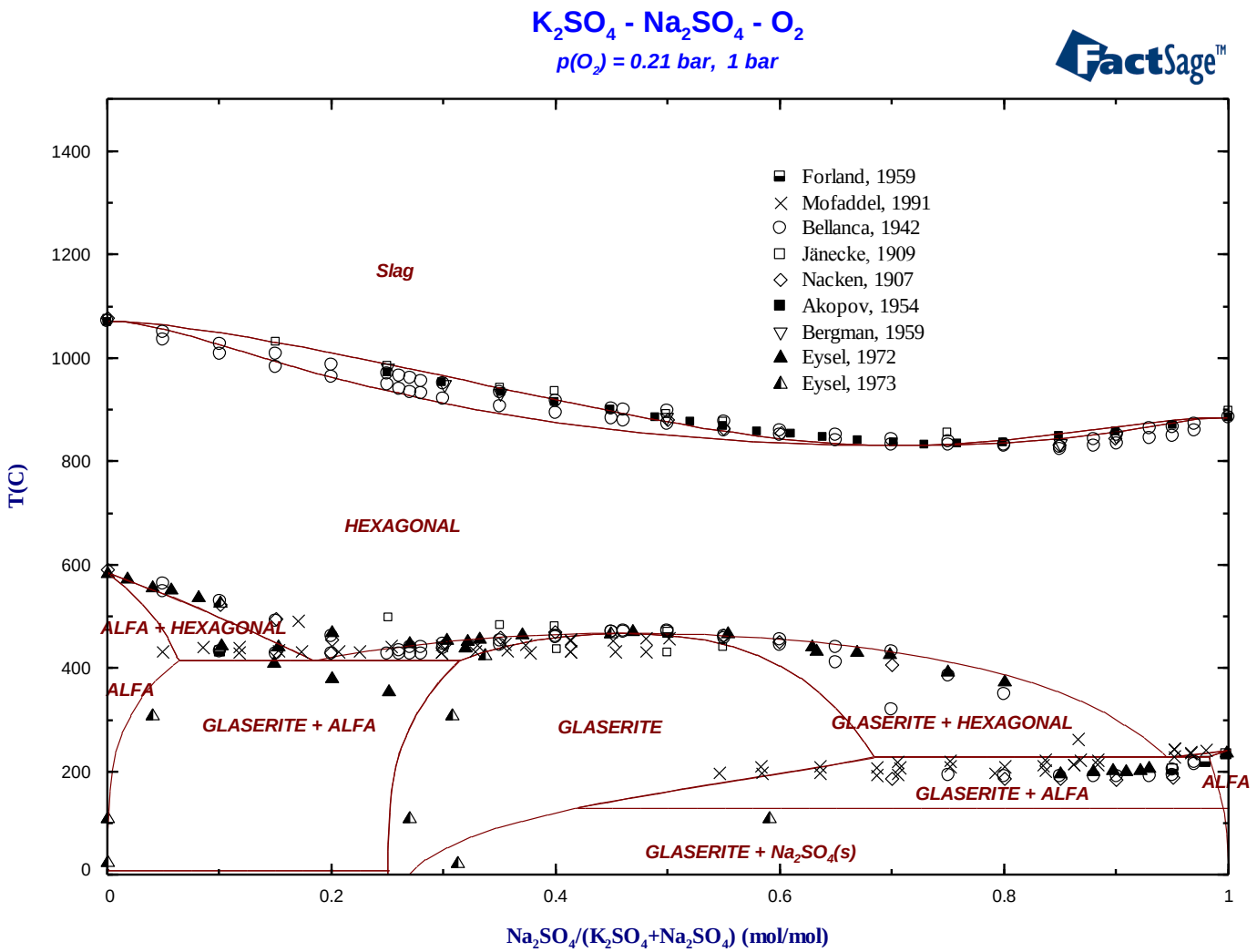

Mole fraction
compared with experimental data

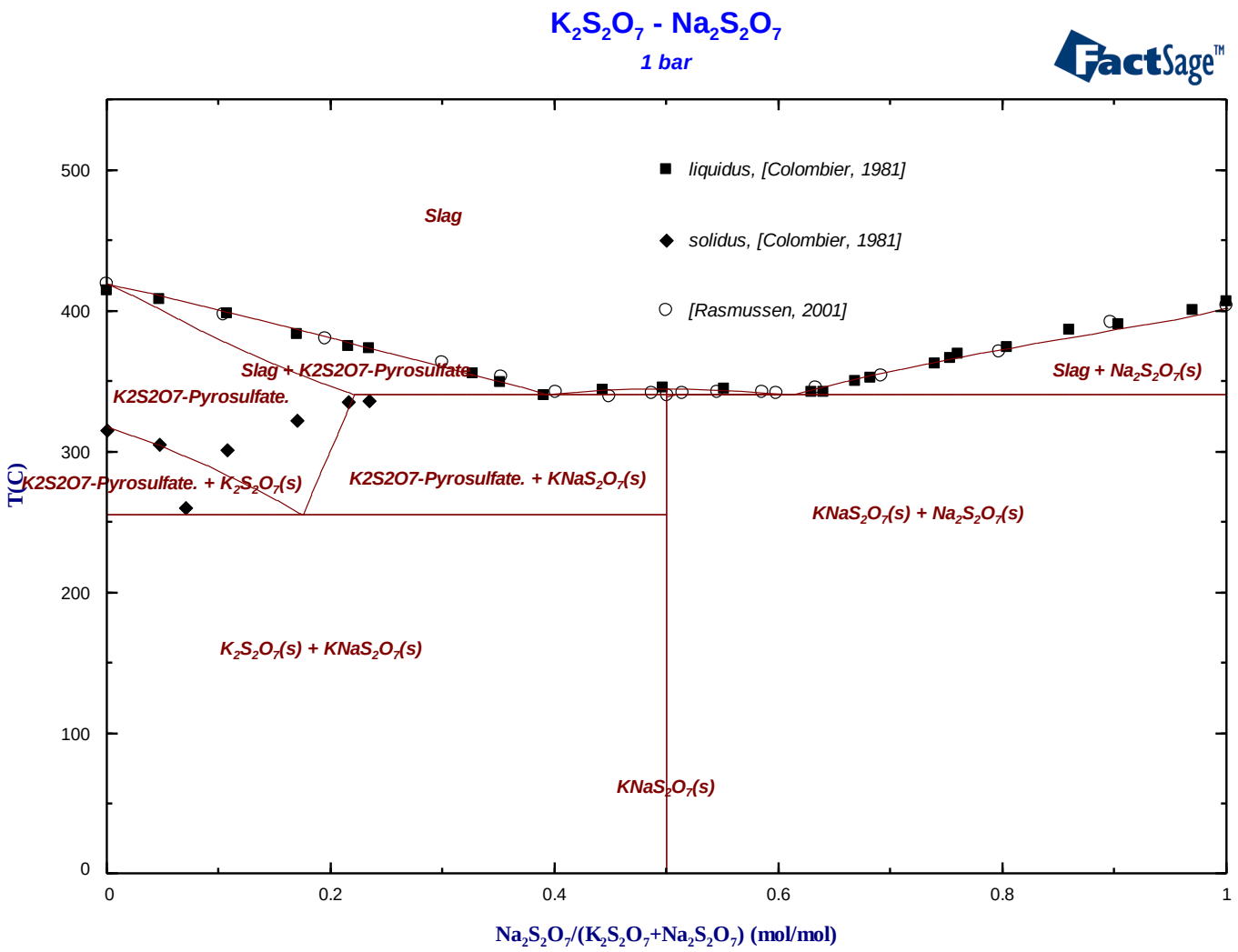

Weight percent

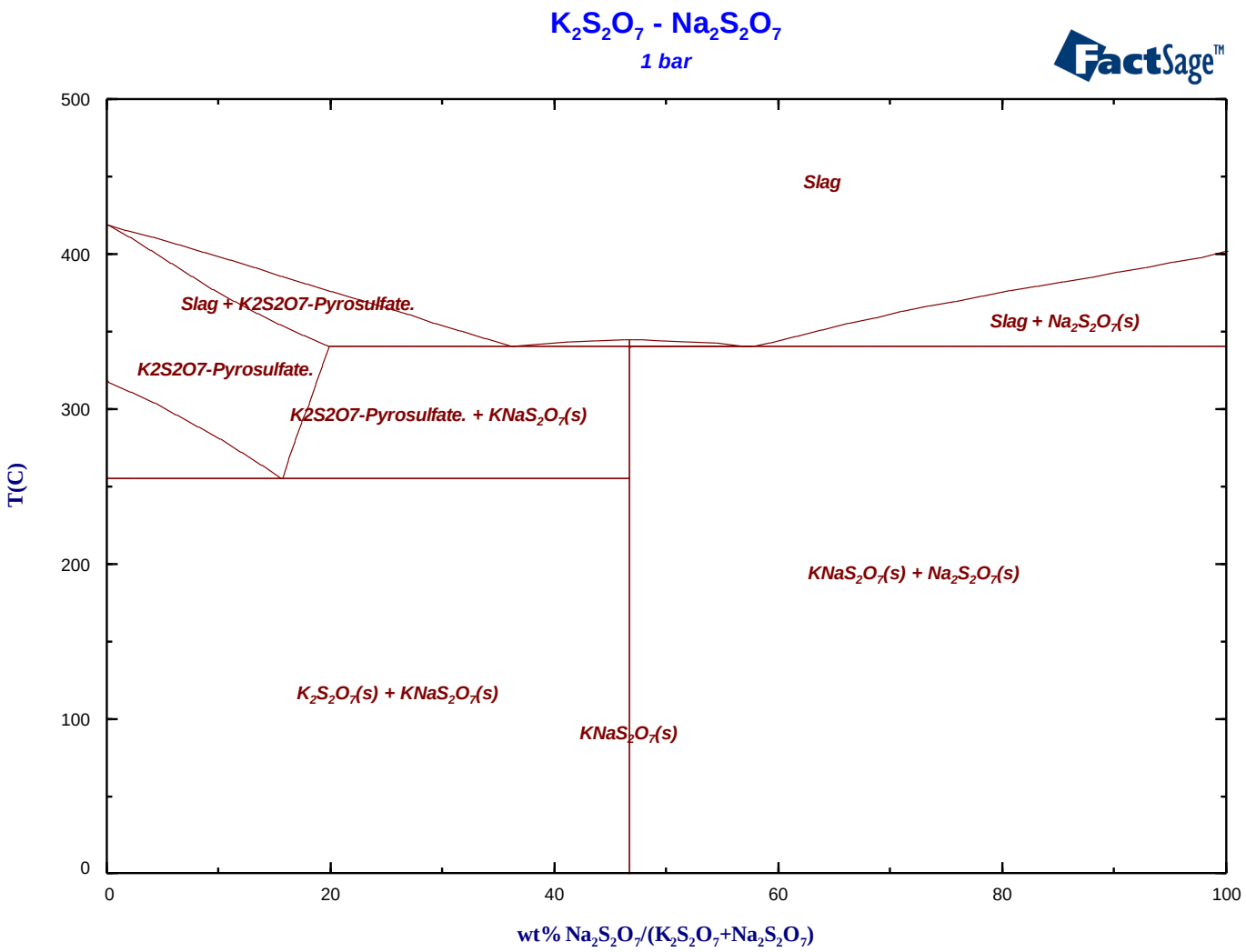

Mg-O,
Mole fraction with isobars

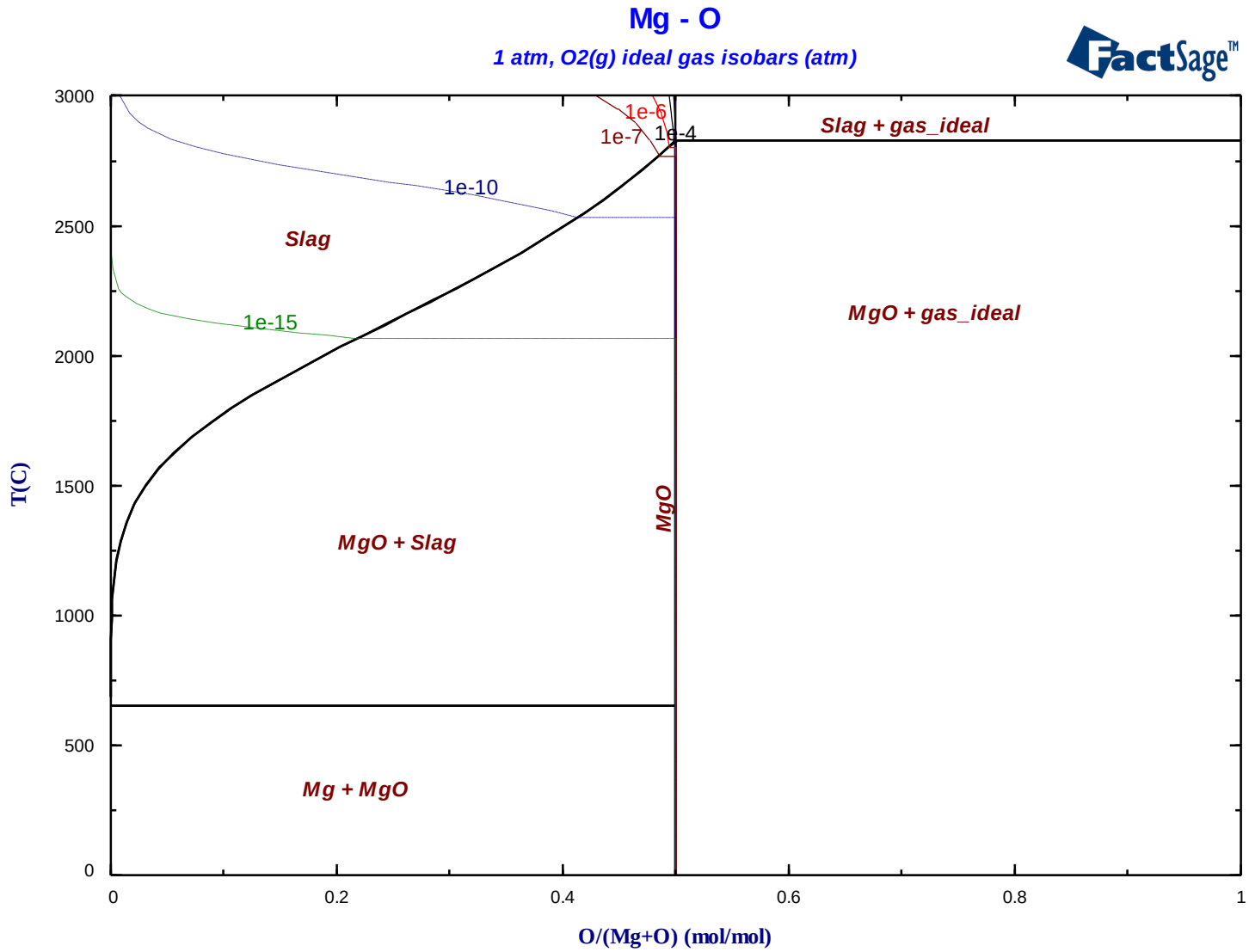

Mg-O,
Temperature vs. log P(O2) diagram

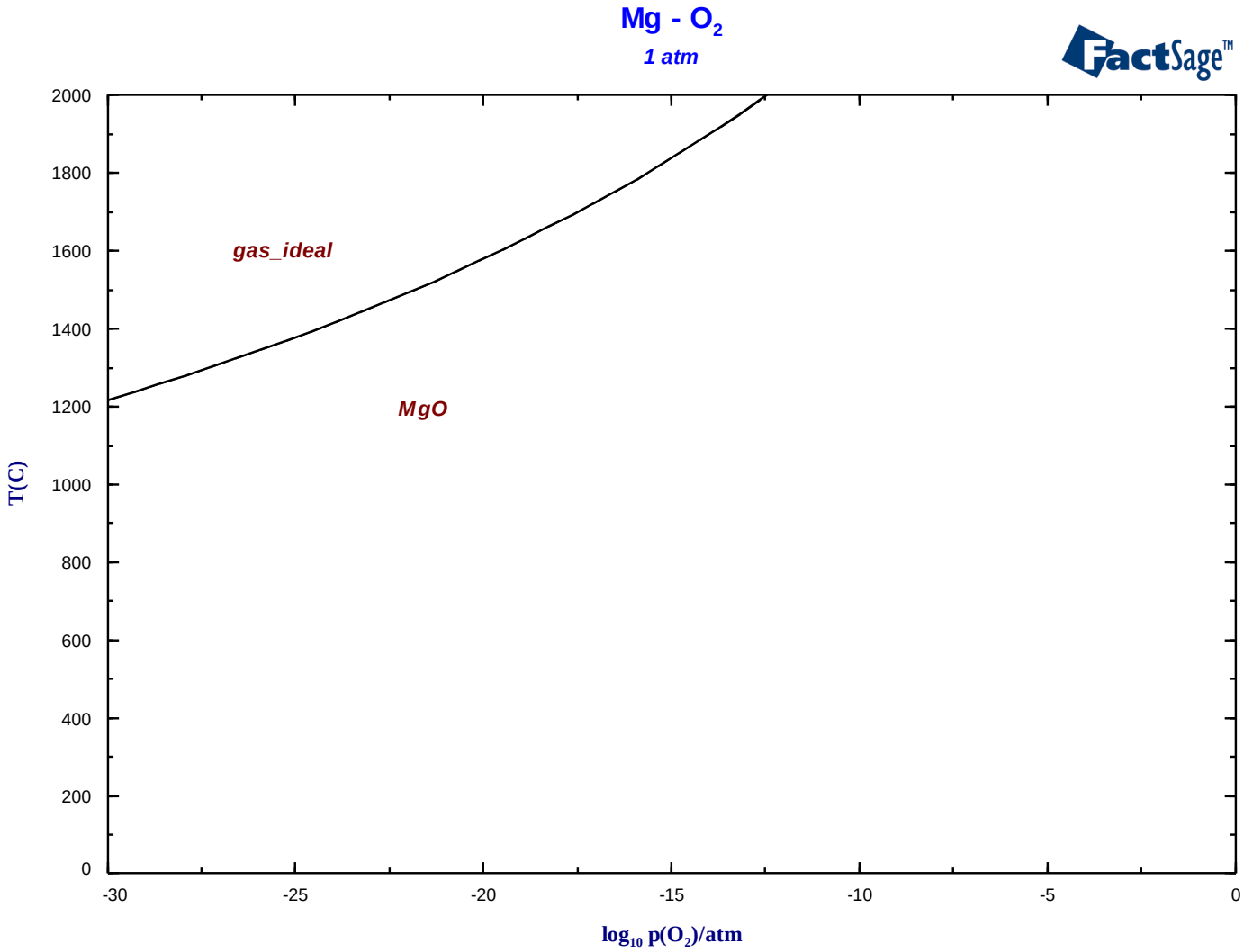

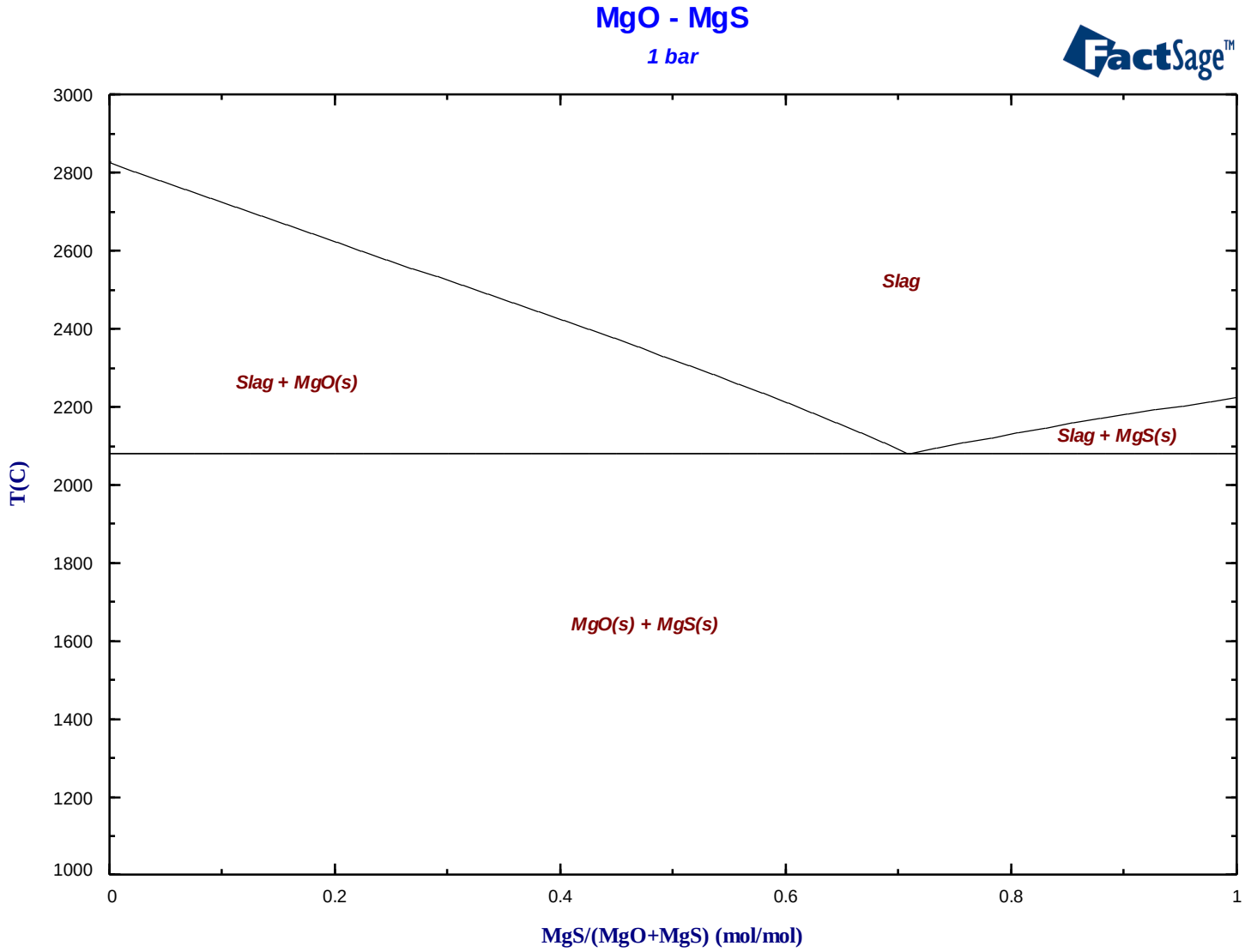
MgO - MgS
1 bar
FactSage™
Slag
Slag + MgO(s)
Slag + MgS(s)
MgO(s) + MgS(s)
T(C)
3000
2800
2600
2400
2200
2000
1800
1600
1400
1200
1000
0
0.2
0.4
0.6
0.8
1
MgS/(MgO+MgS) (mol/mol)

Weight percent

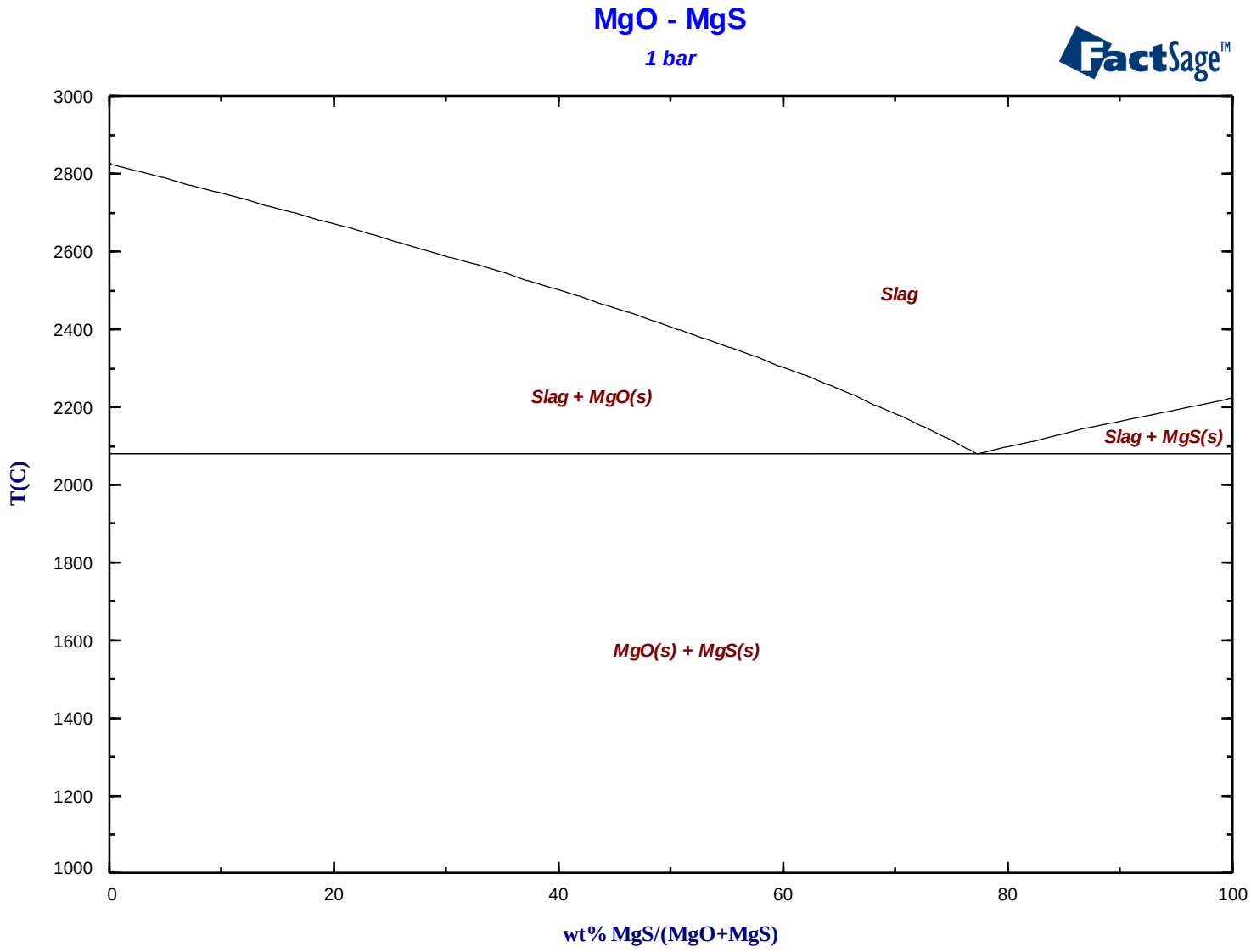

Mole fraction

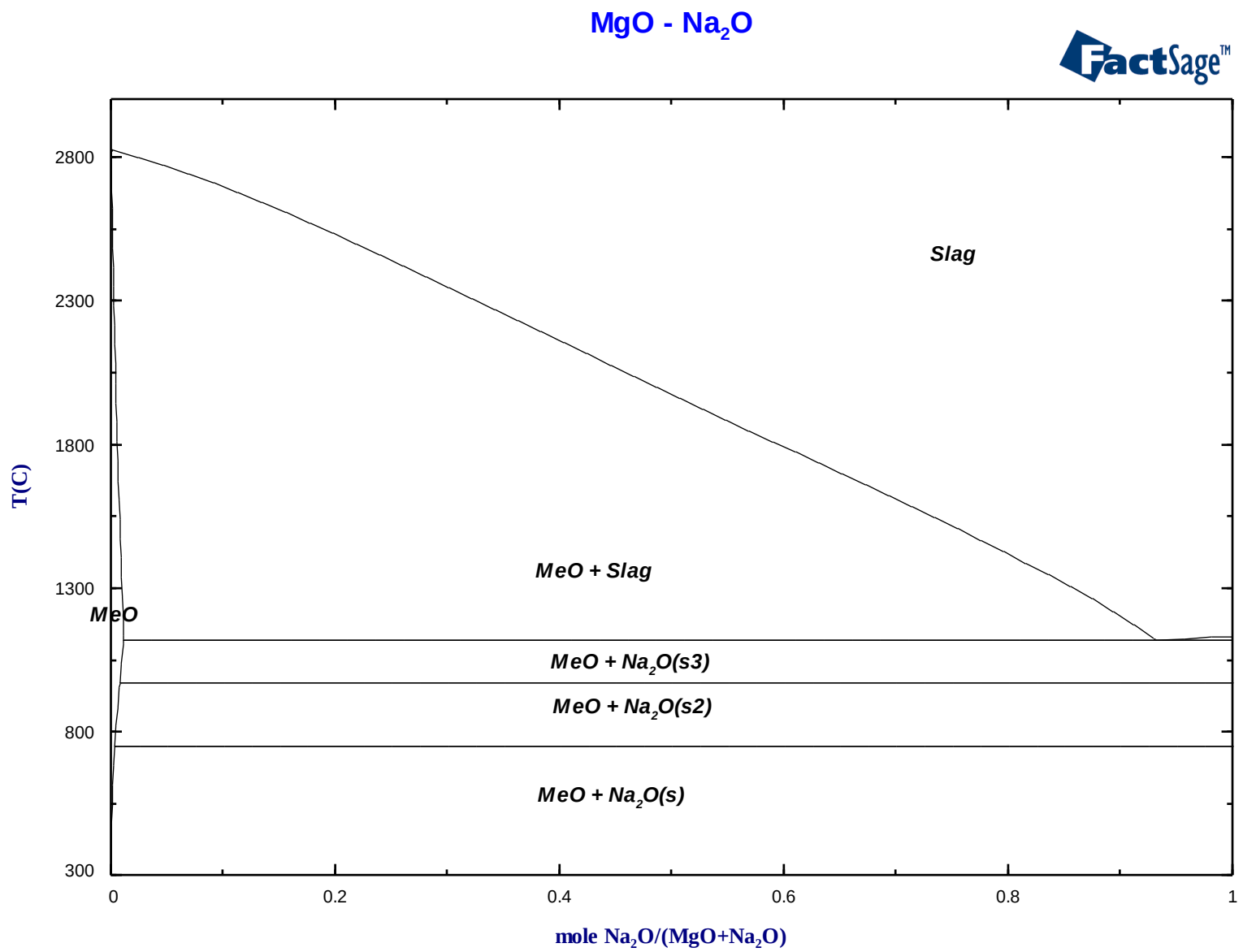

Weight percent

$MgO - Na_2O$

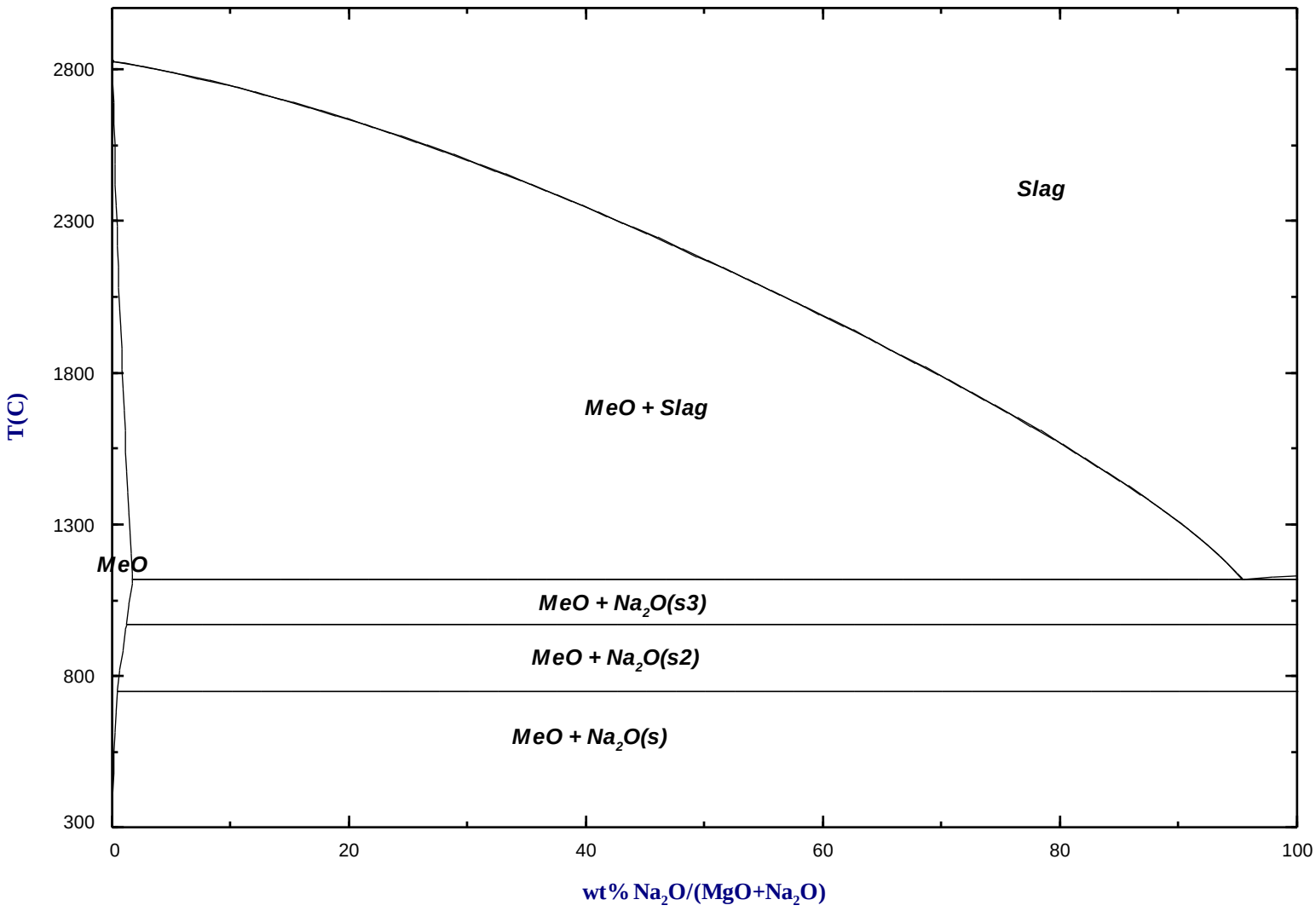

Mole fraction

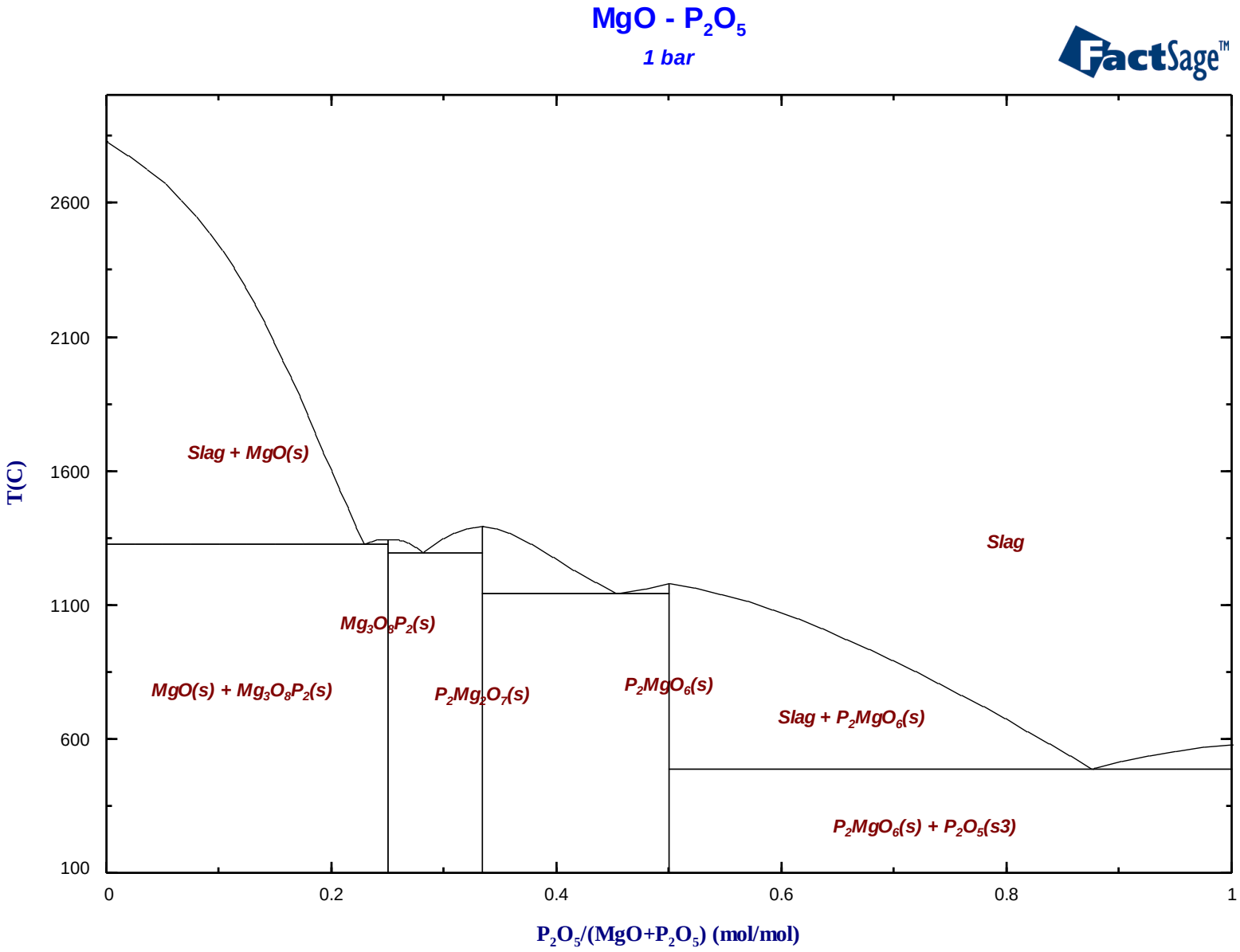

Weight percent

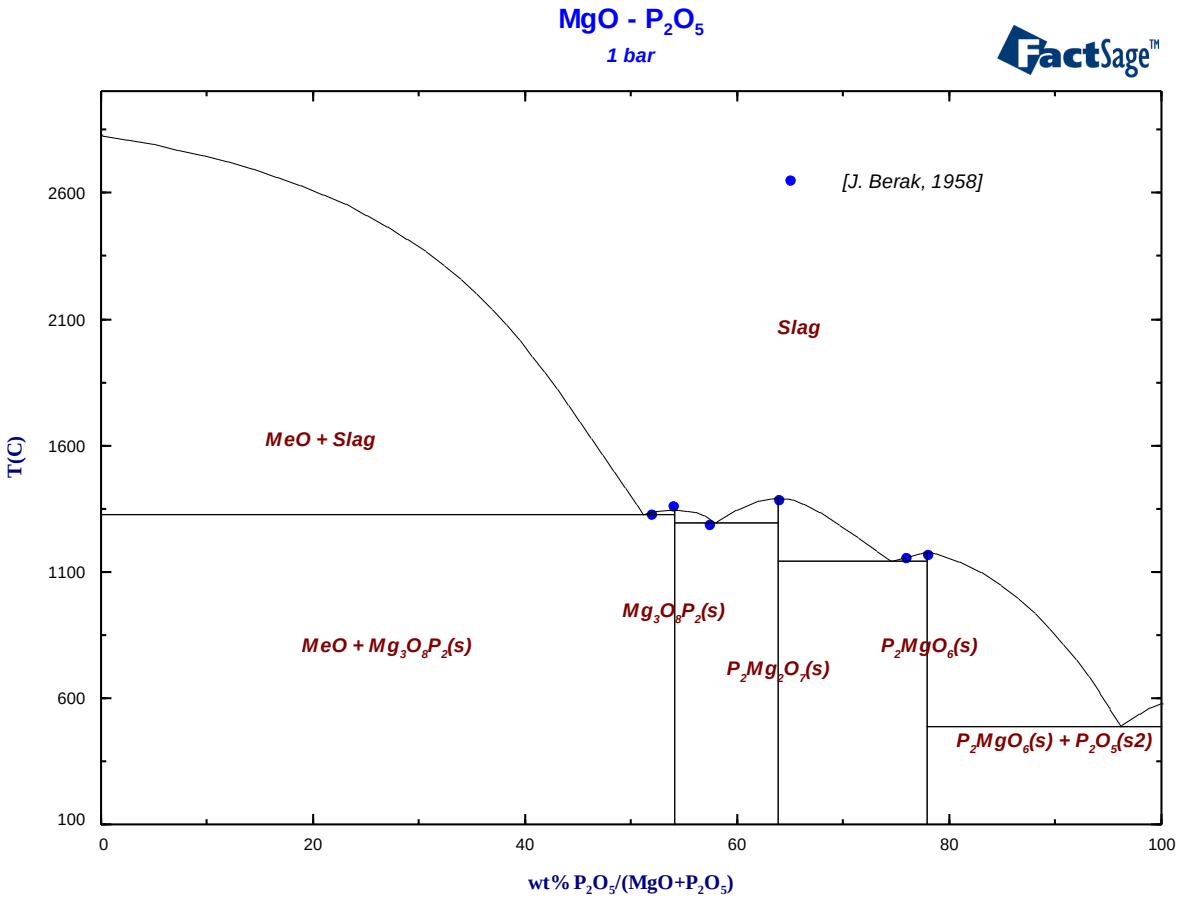

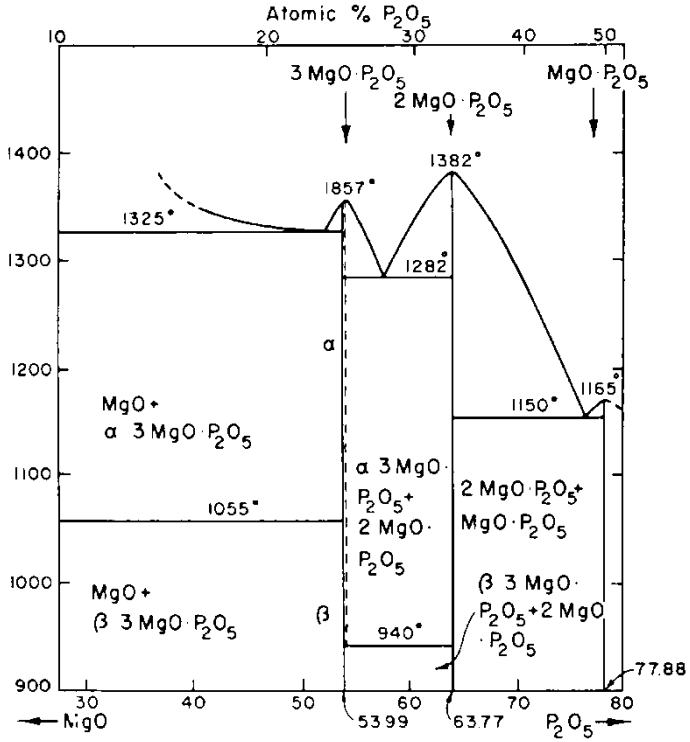

J. Berak, Rocz. Chem., 32 [1], (1958), pp.17-22.

Mole fraction compared with experimental data

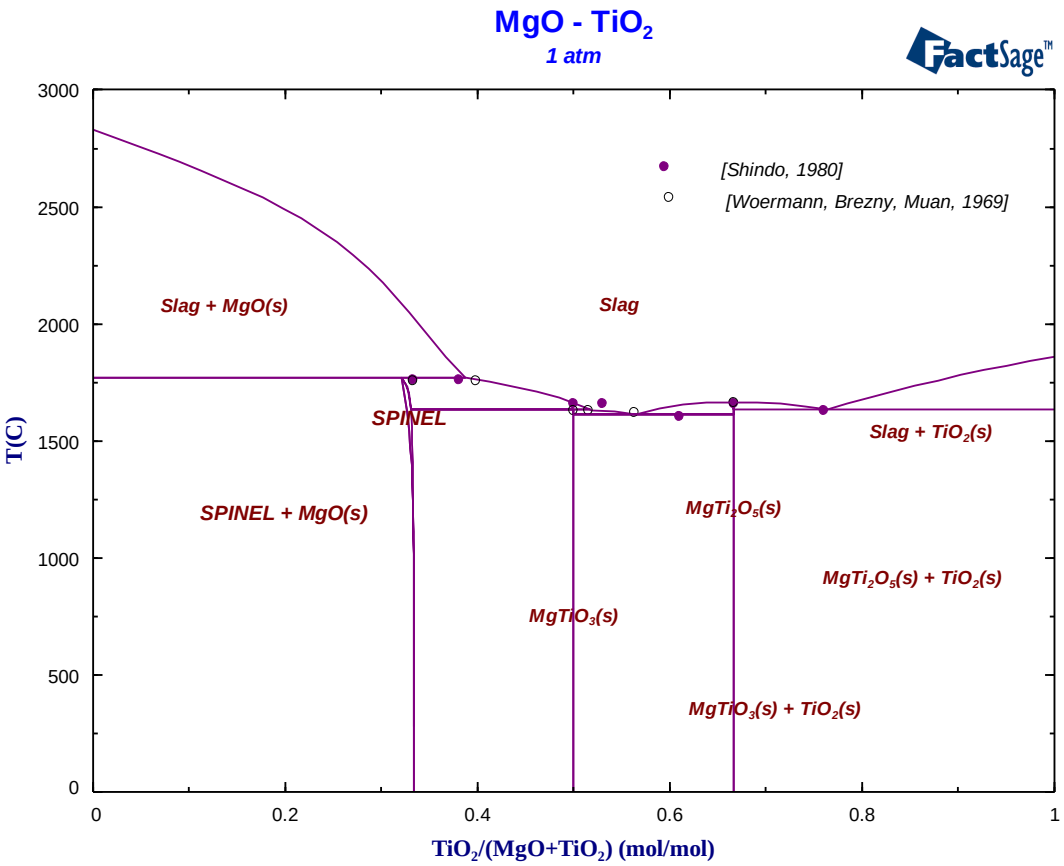

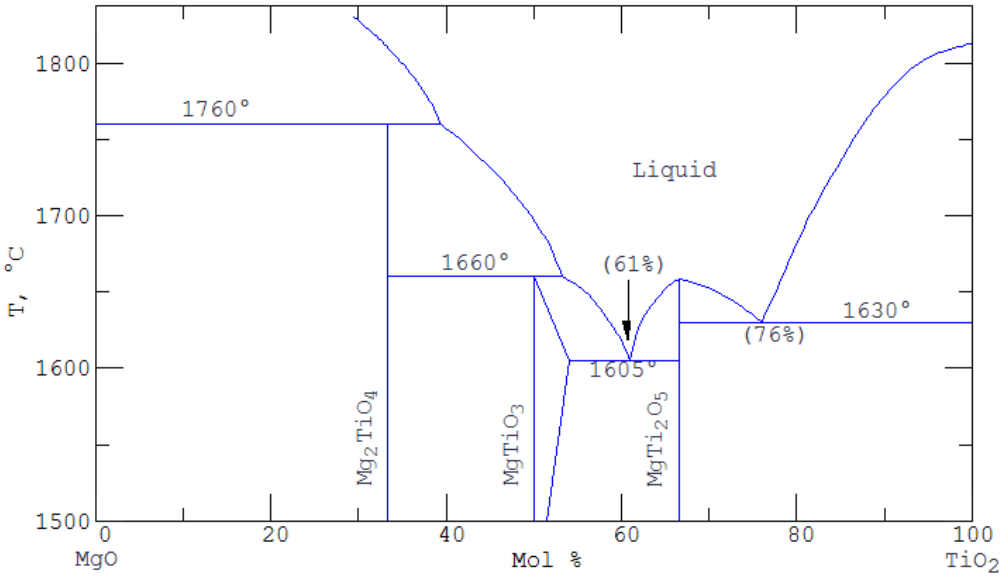

J. Shindo, J. Chryst. Growth, 50 [4], (1980), pp.839-851.

Weight percent

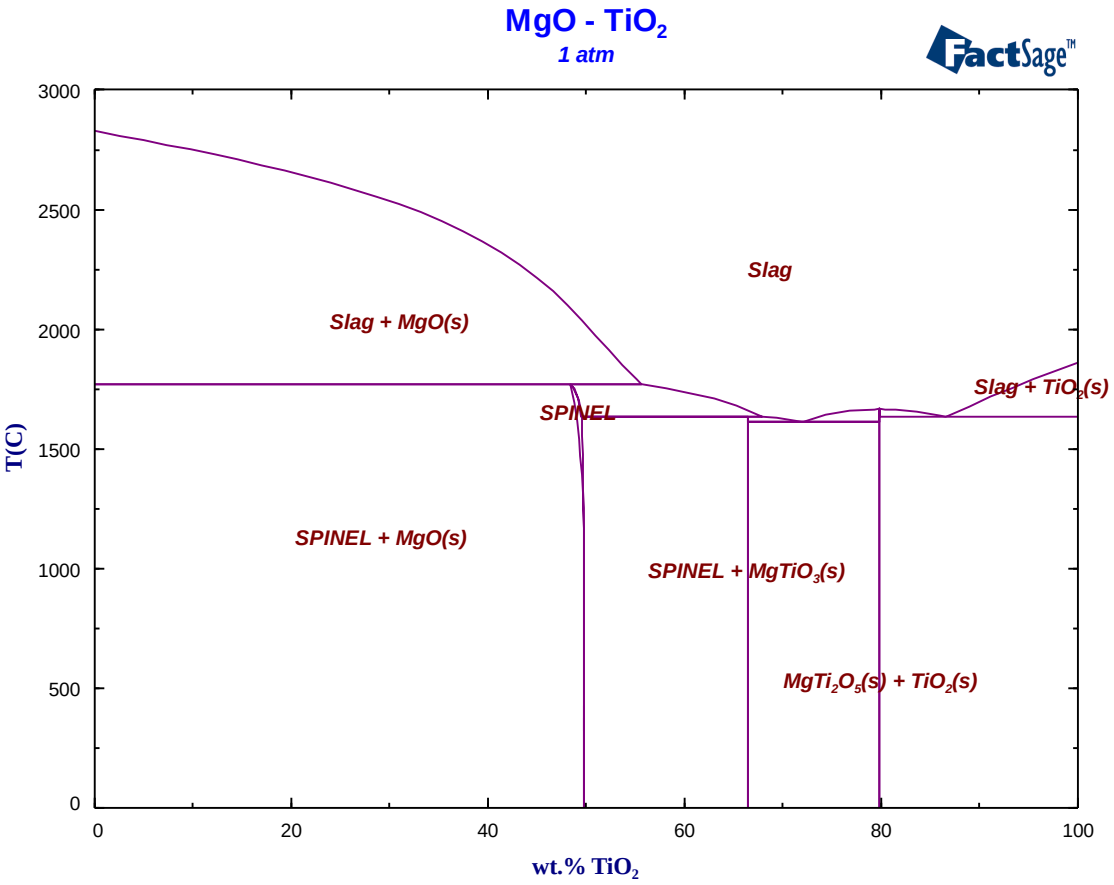

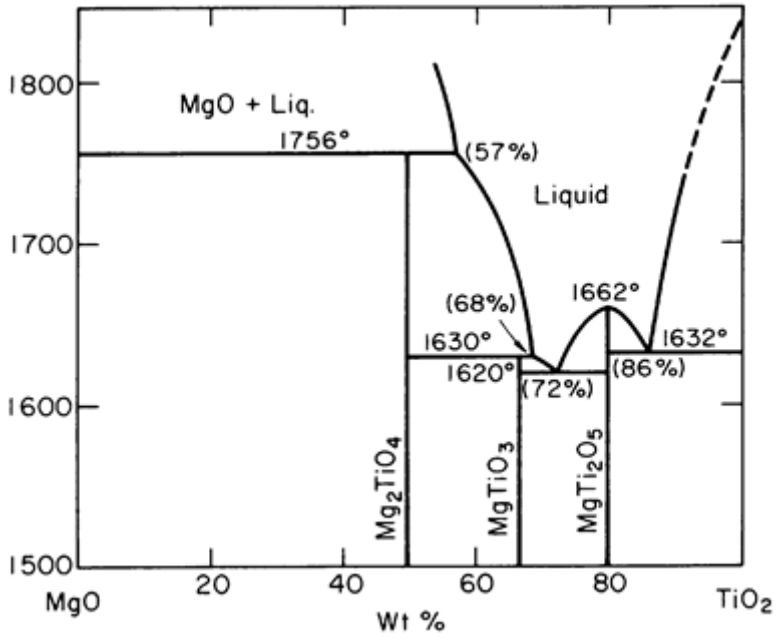

E. Woermann, B. Brezny, A. Muan, Am. J. Sci., 267A, (1969), pp.463-479.

Mole fraction

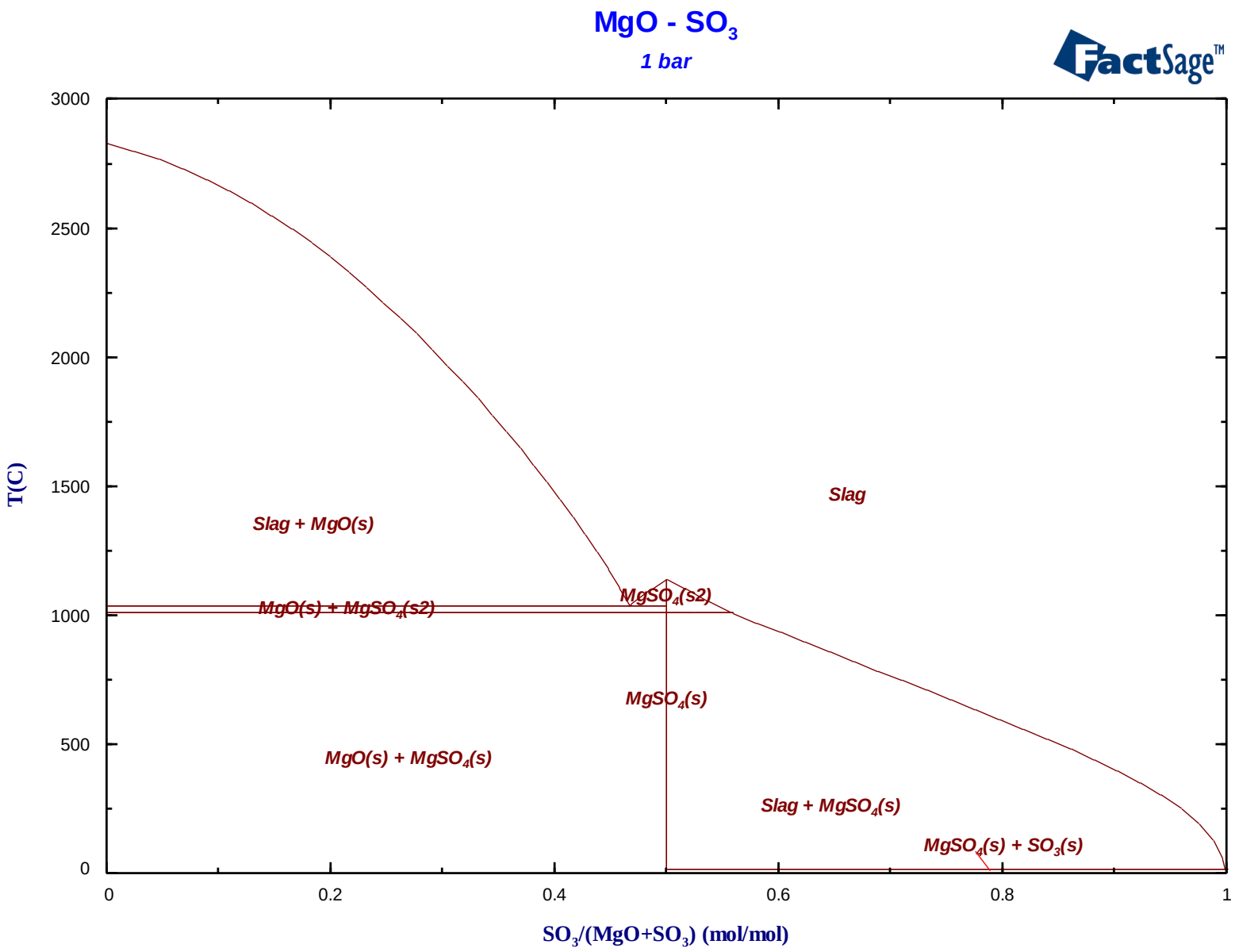

Weight percent

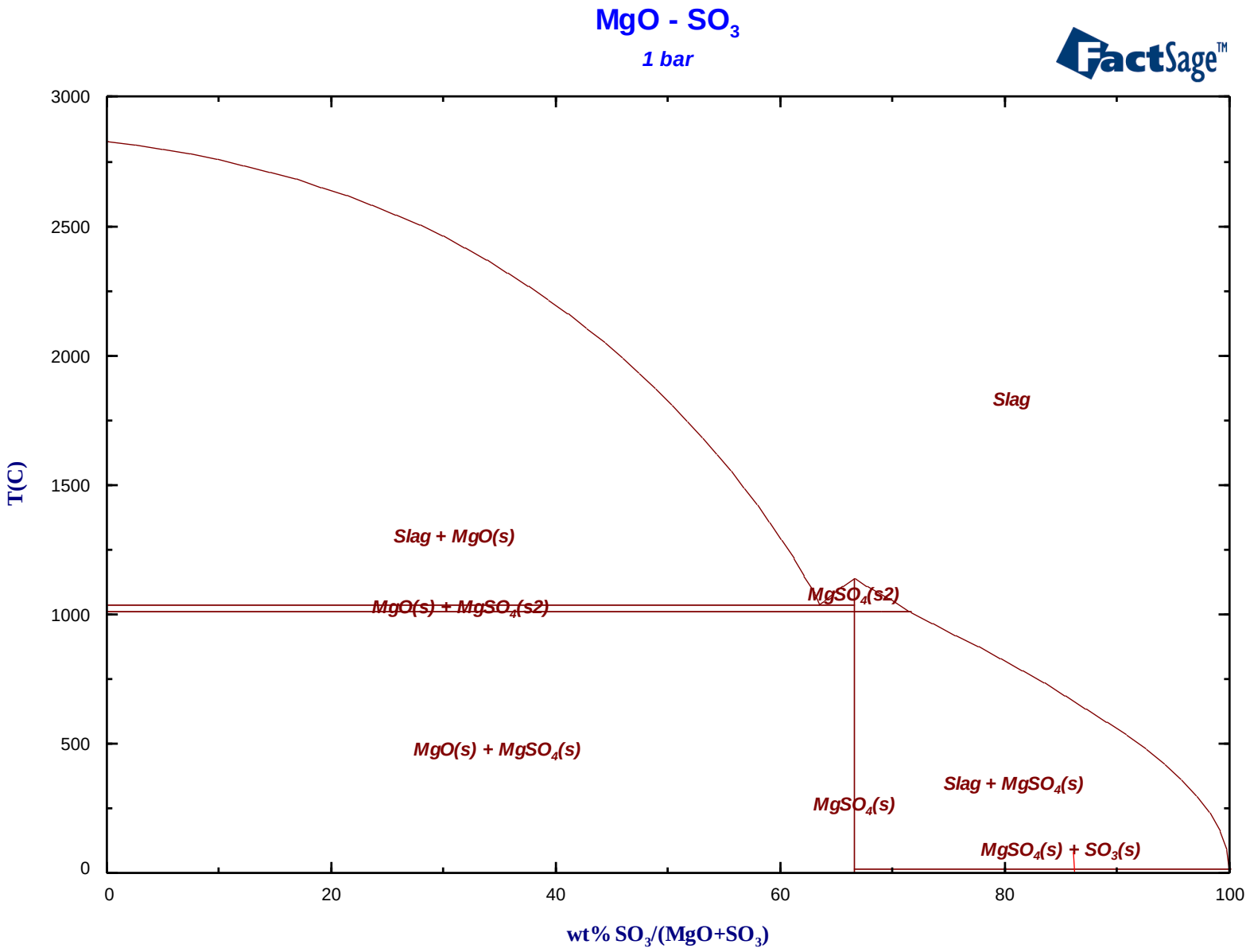

Mole fraction

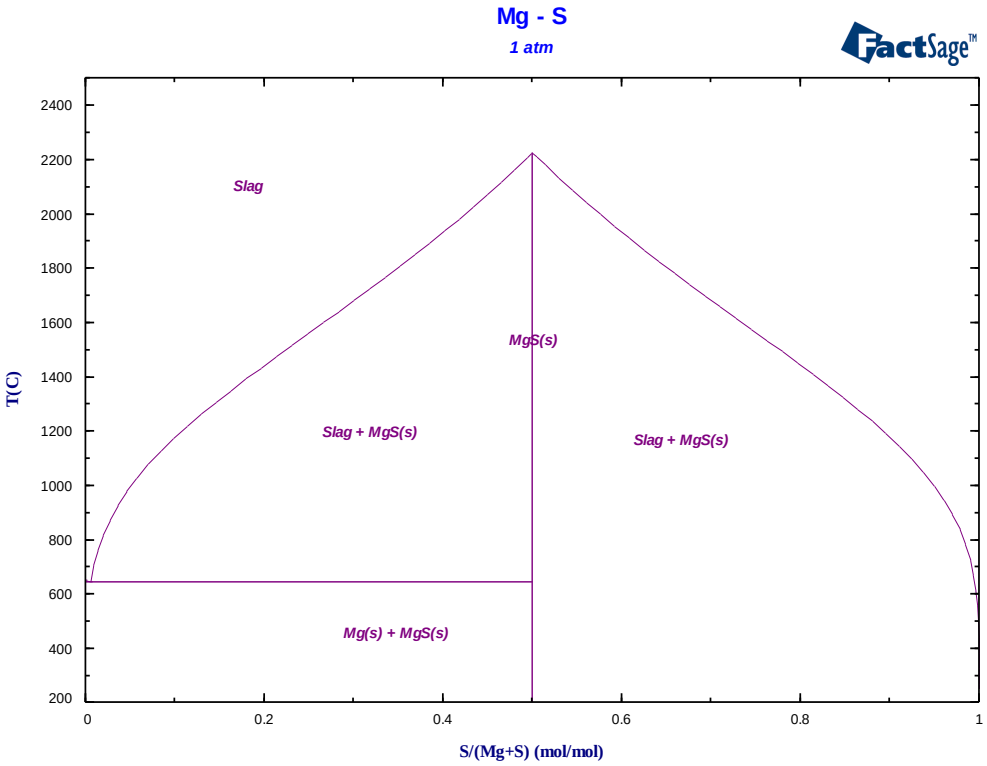

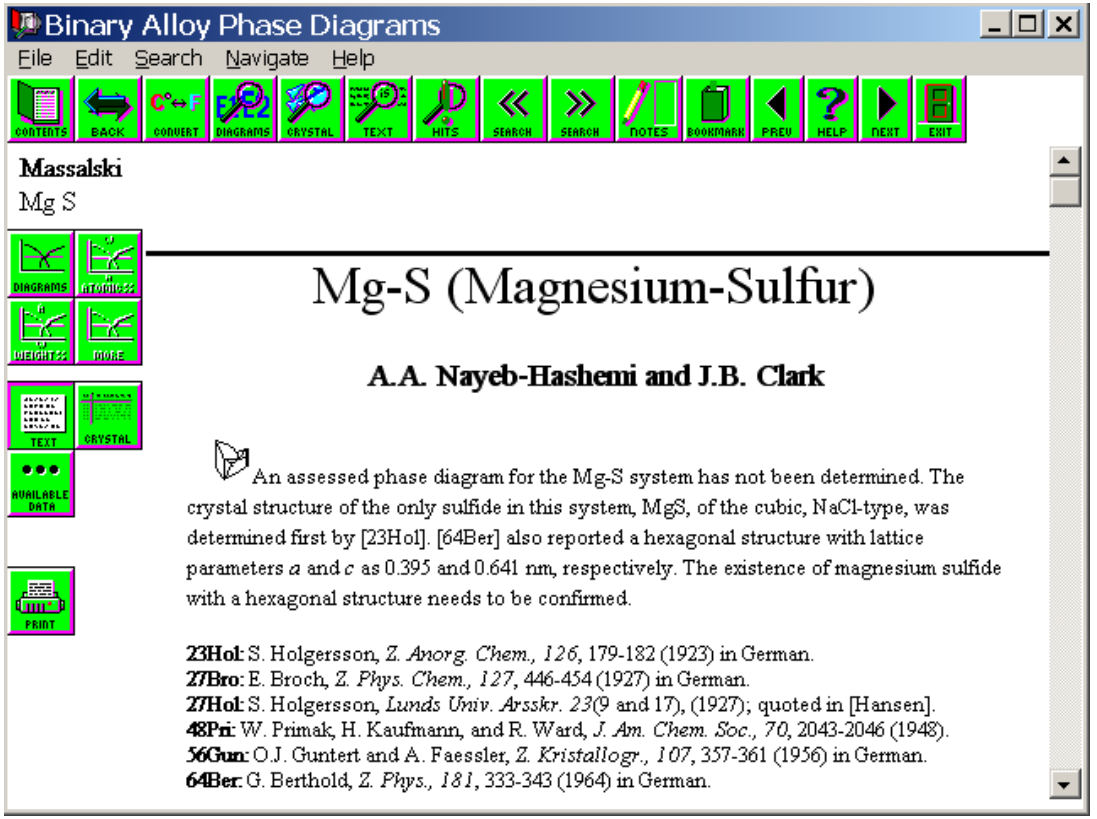

Weight percent

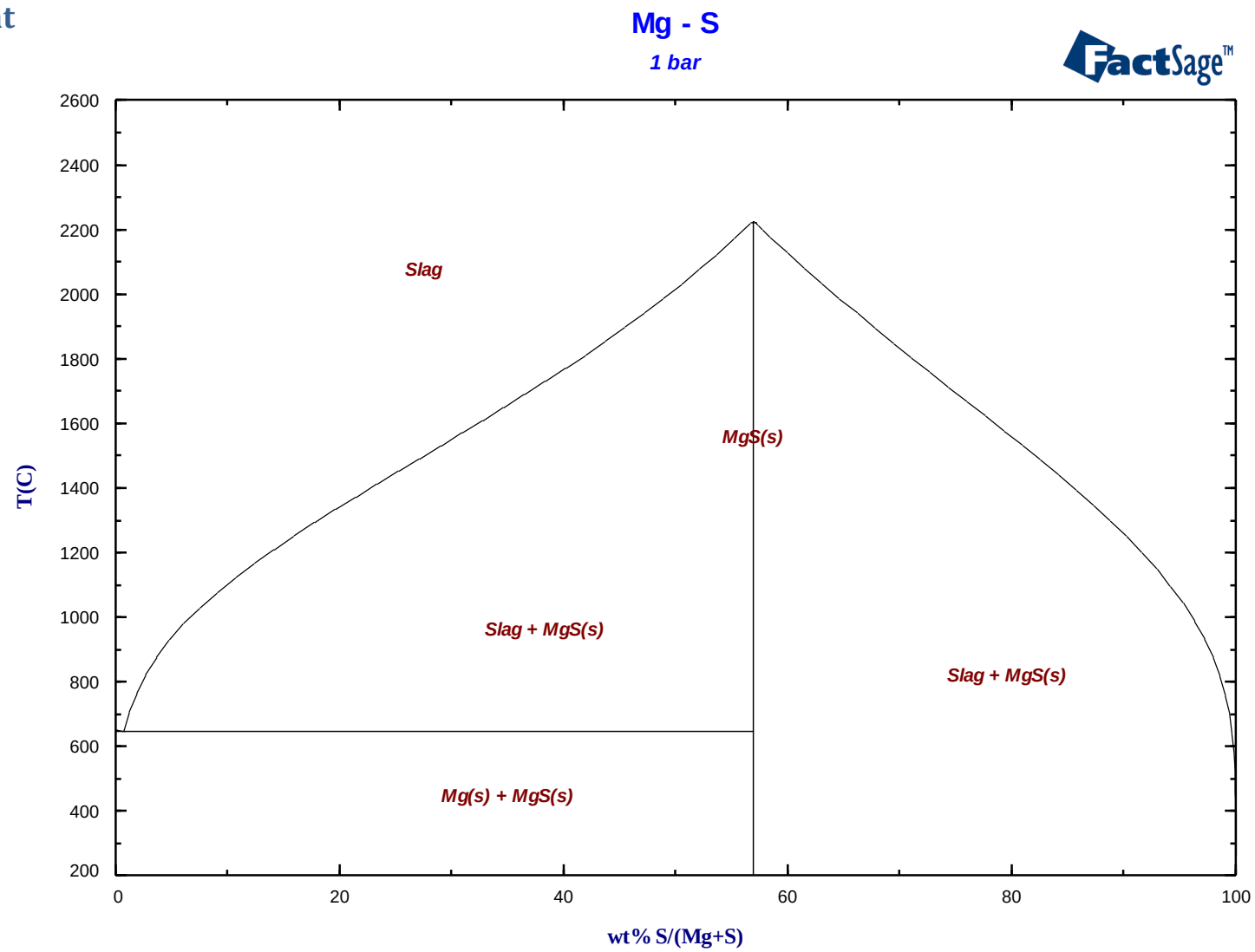

Mole fraction

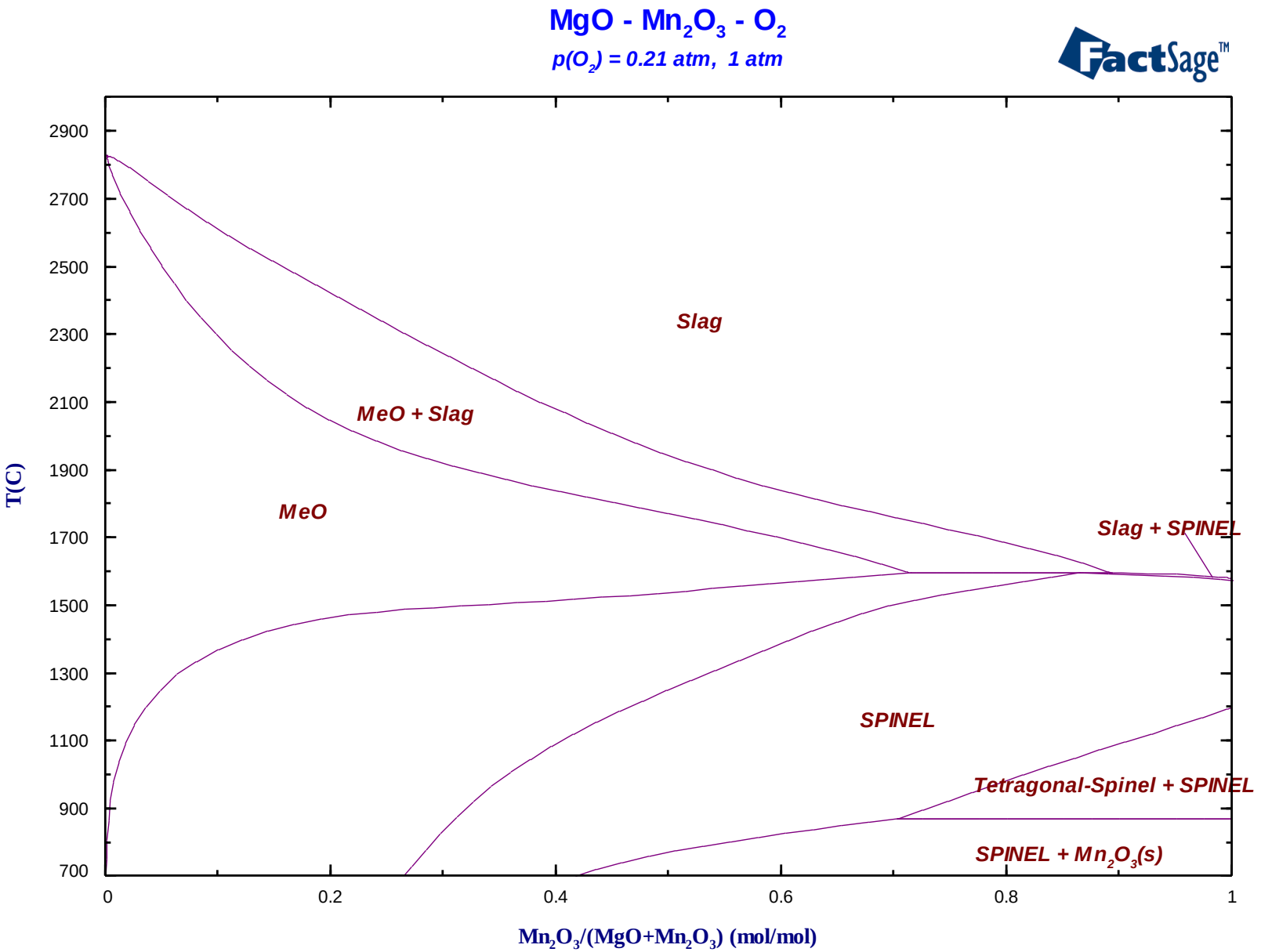

Weight percent
compared with experimental data

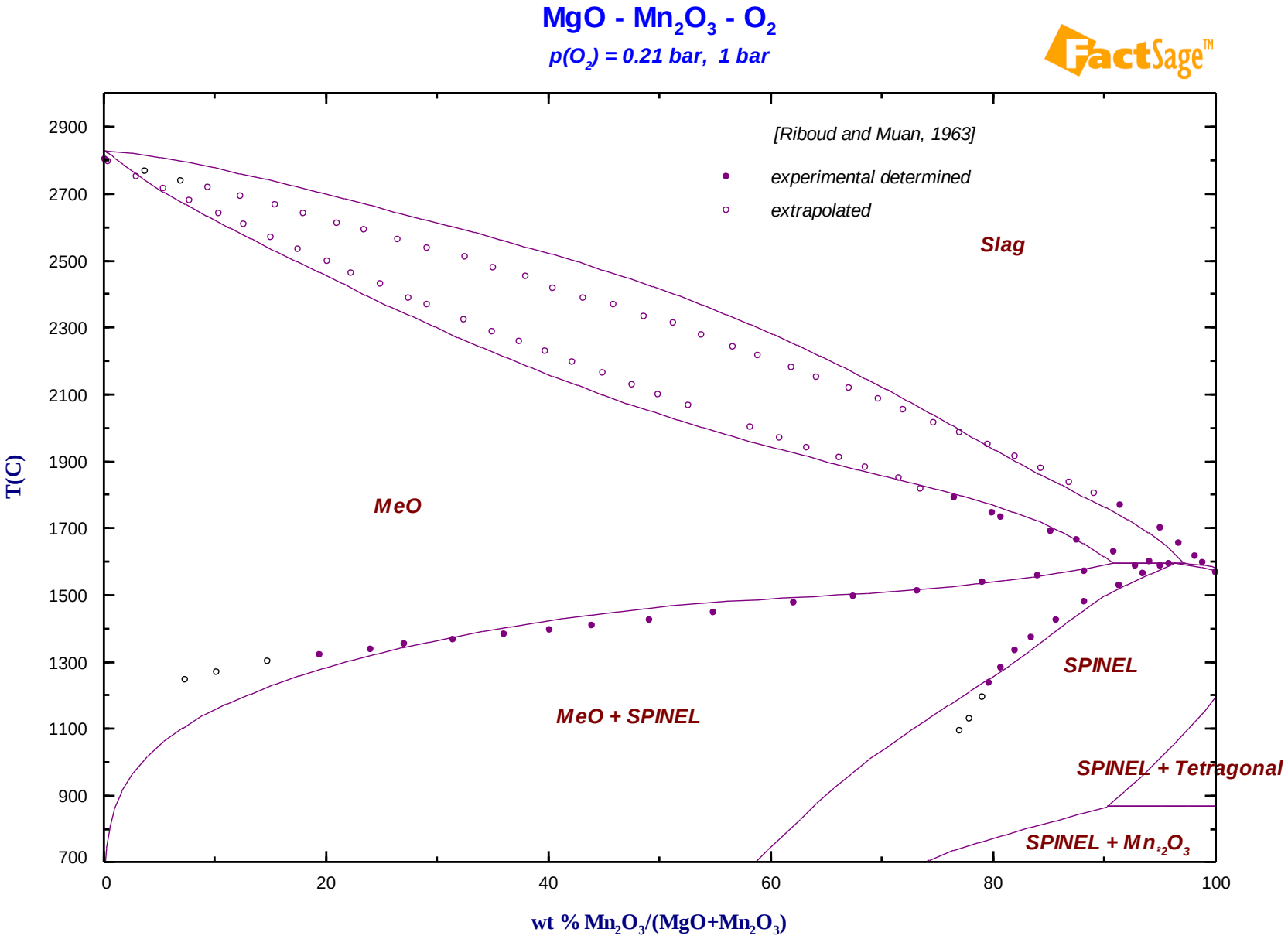

Mole fraction

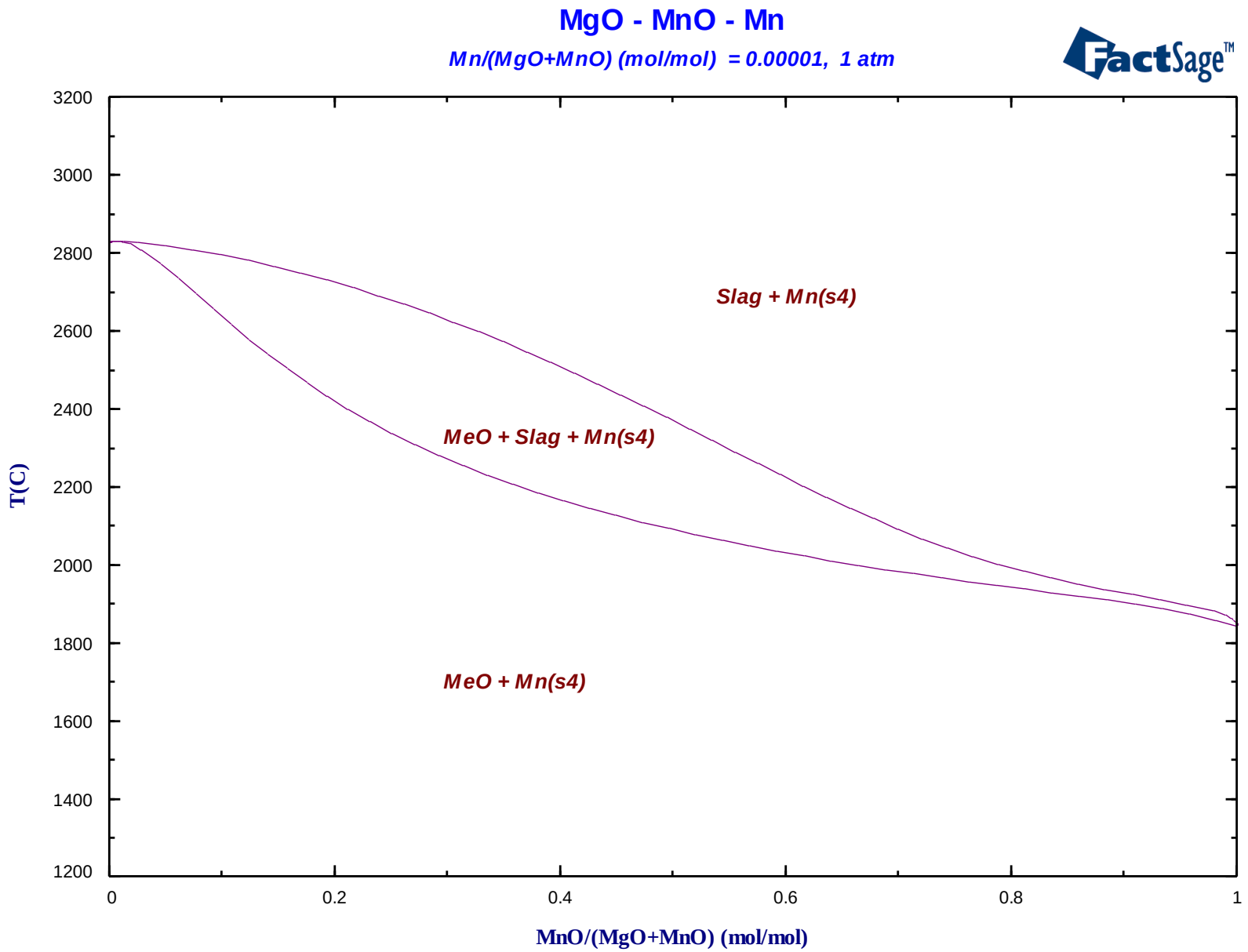

Weight percent
compared with experimental data

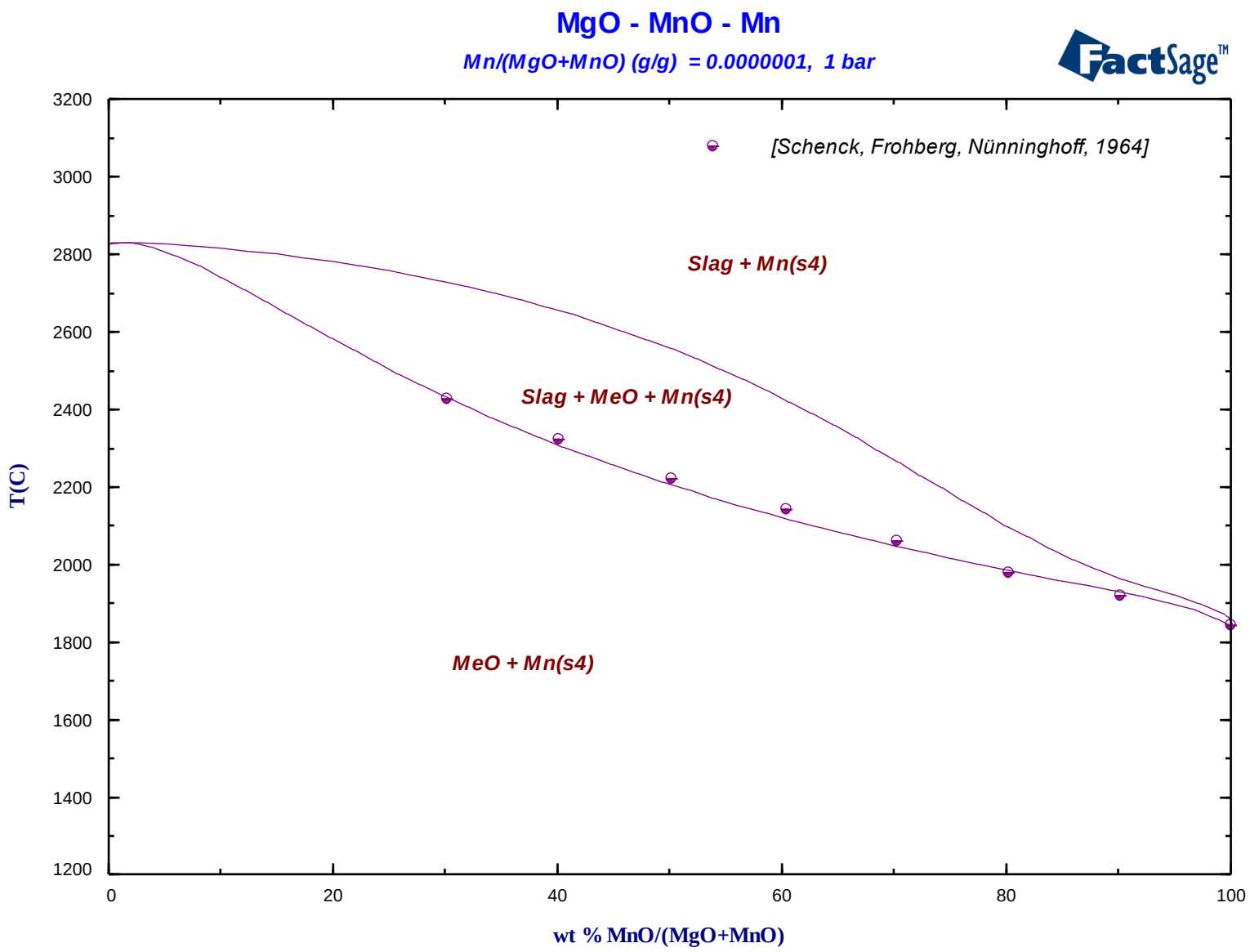

Mole fraction
compared with experimental data

MgO - SiO_2

1 bar

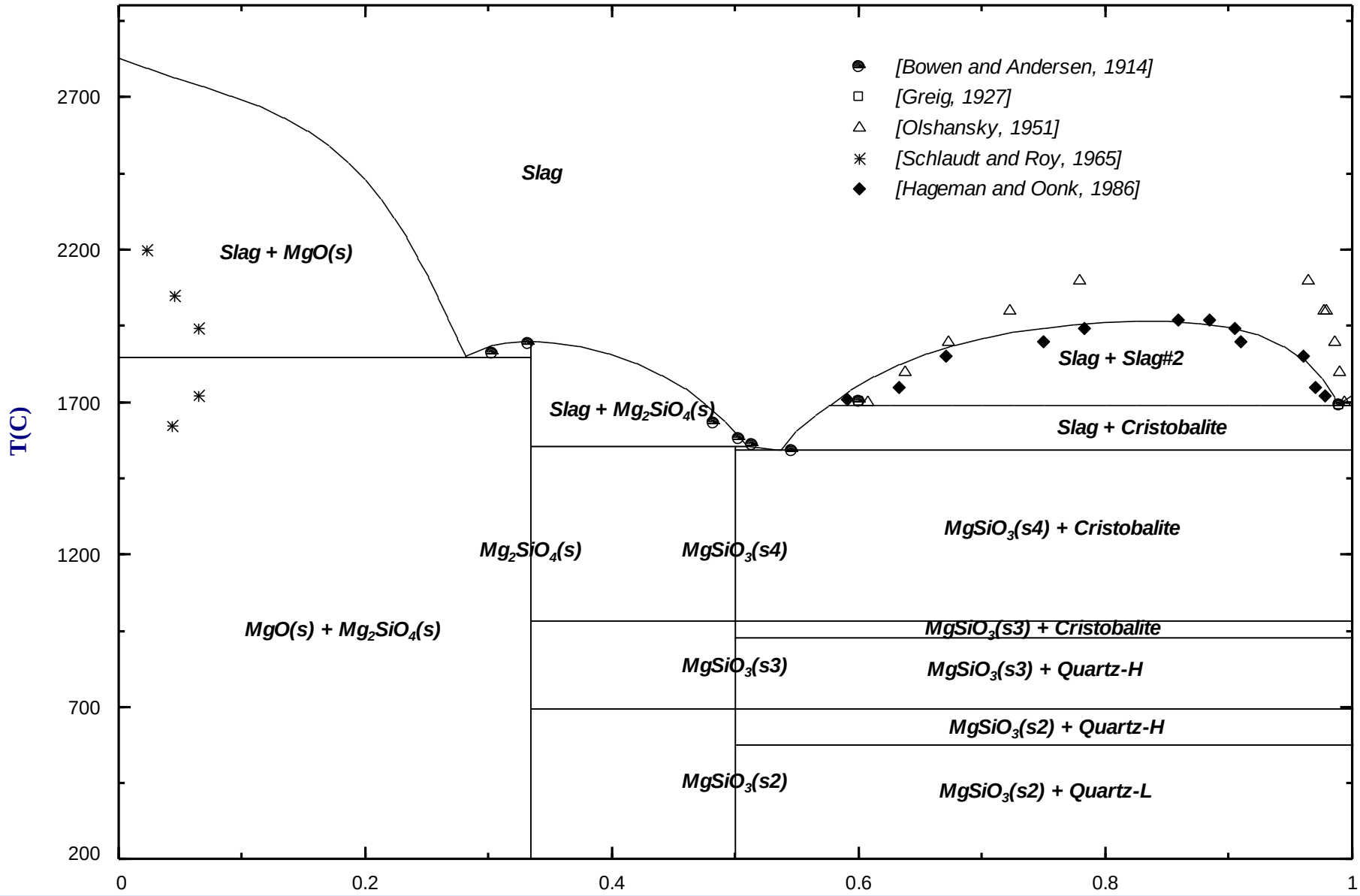

Weight percent
compared with experimental data

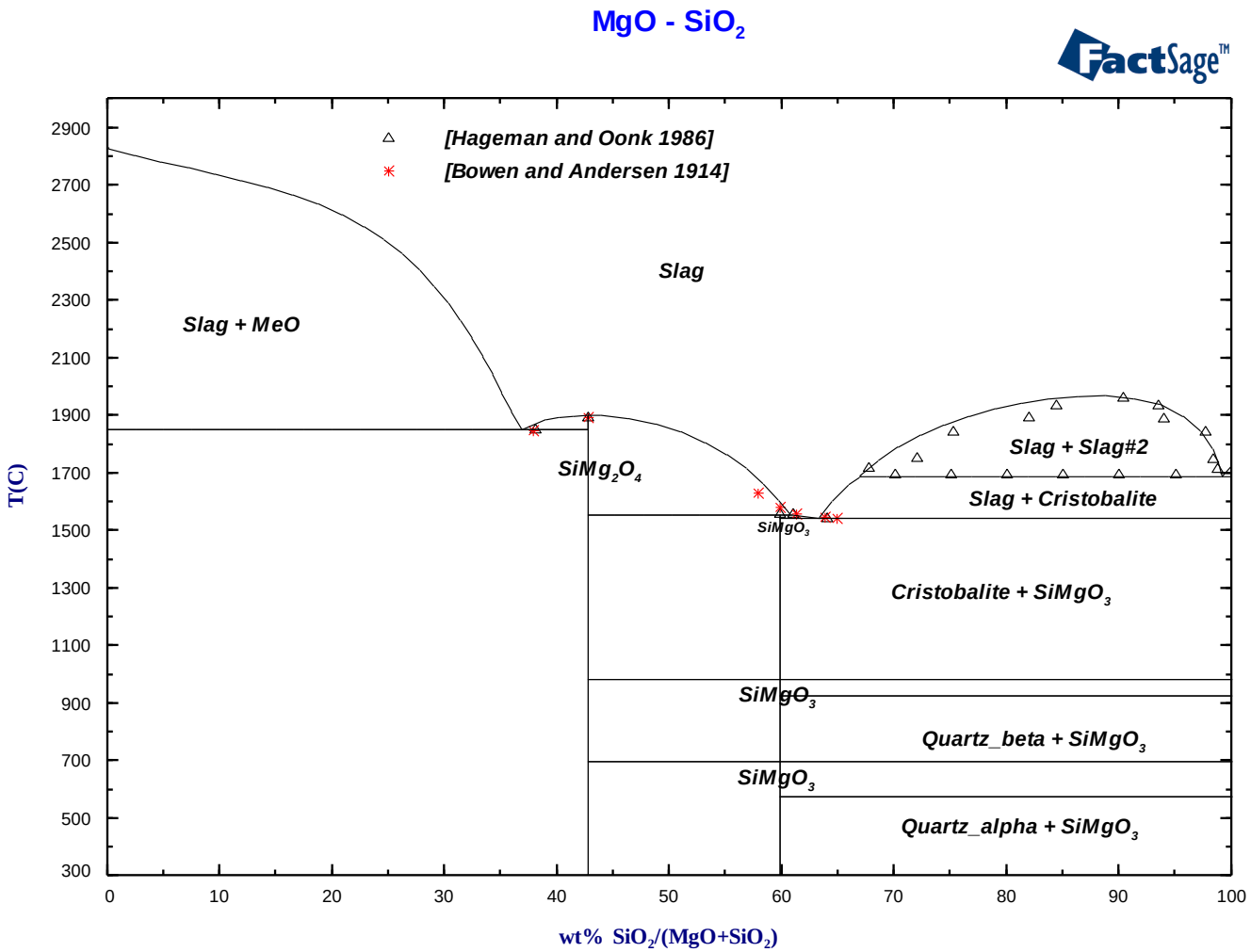

MgO-SrO

Mole fraction compared with experimental data

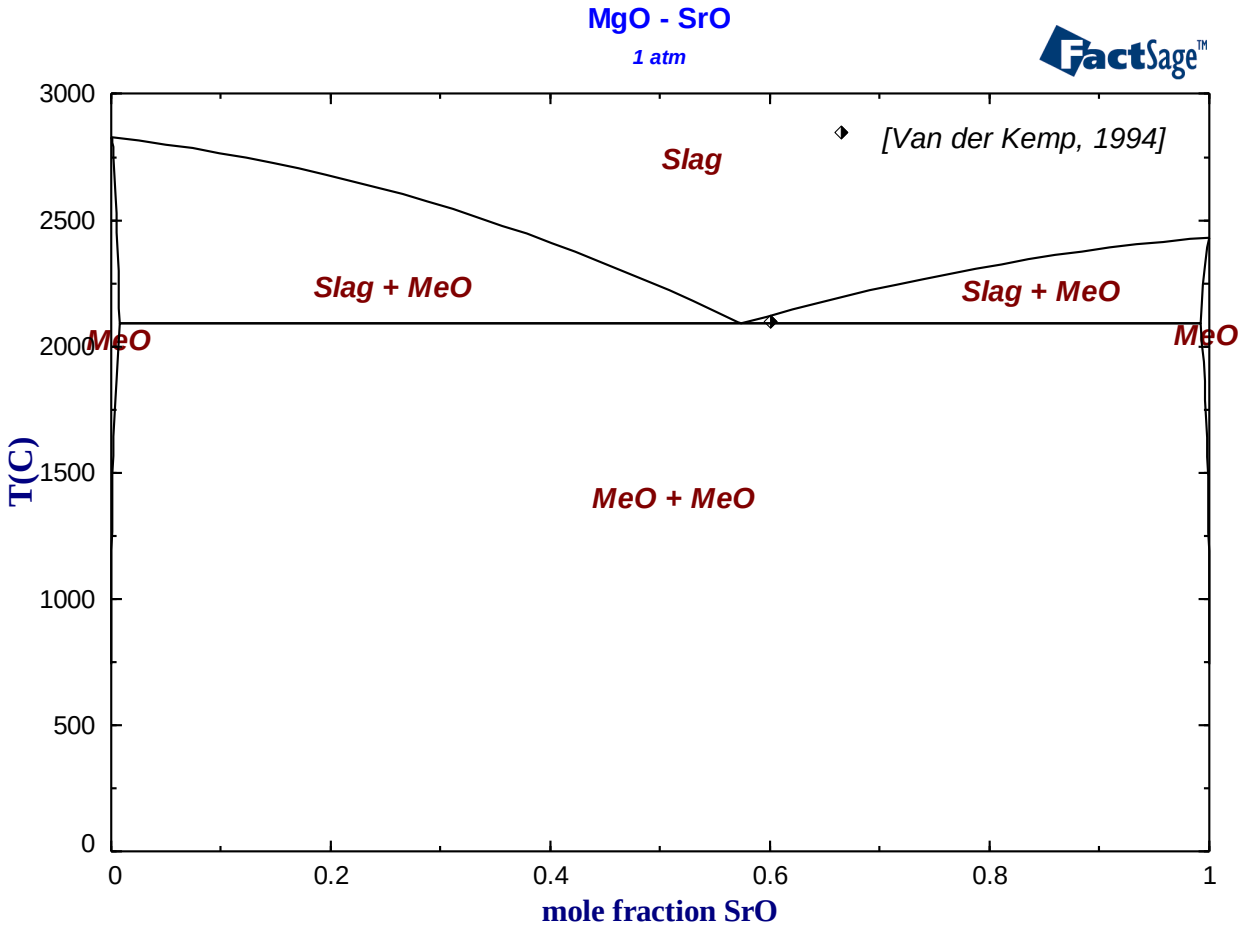

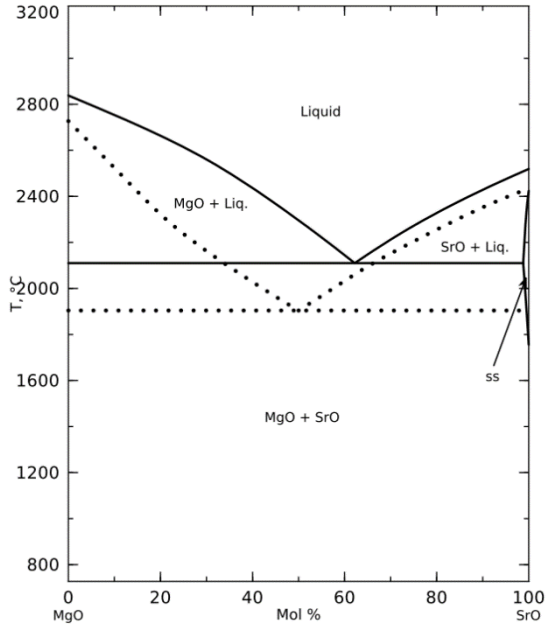

W. J. M. Van der Kemp, J. G. Blok, P. R. Van der Linde, H. A. J. Oonk, A. Schuijff, and M. L. Verdonk, CALPHAD: Comput. Coupling Phase Diagrams Thermochem., 18 [3] 255-267 (1994)

MgO-SrO
Weight percent

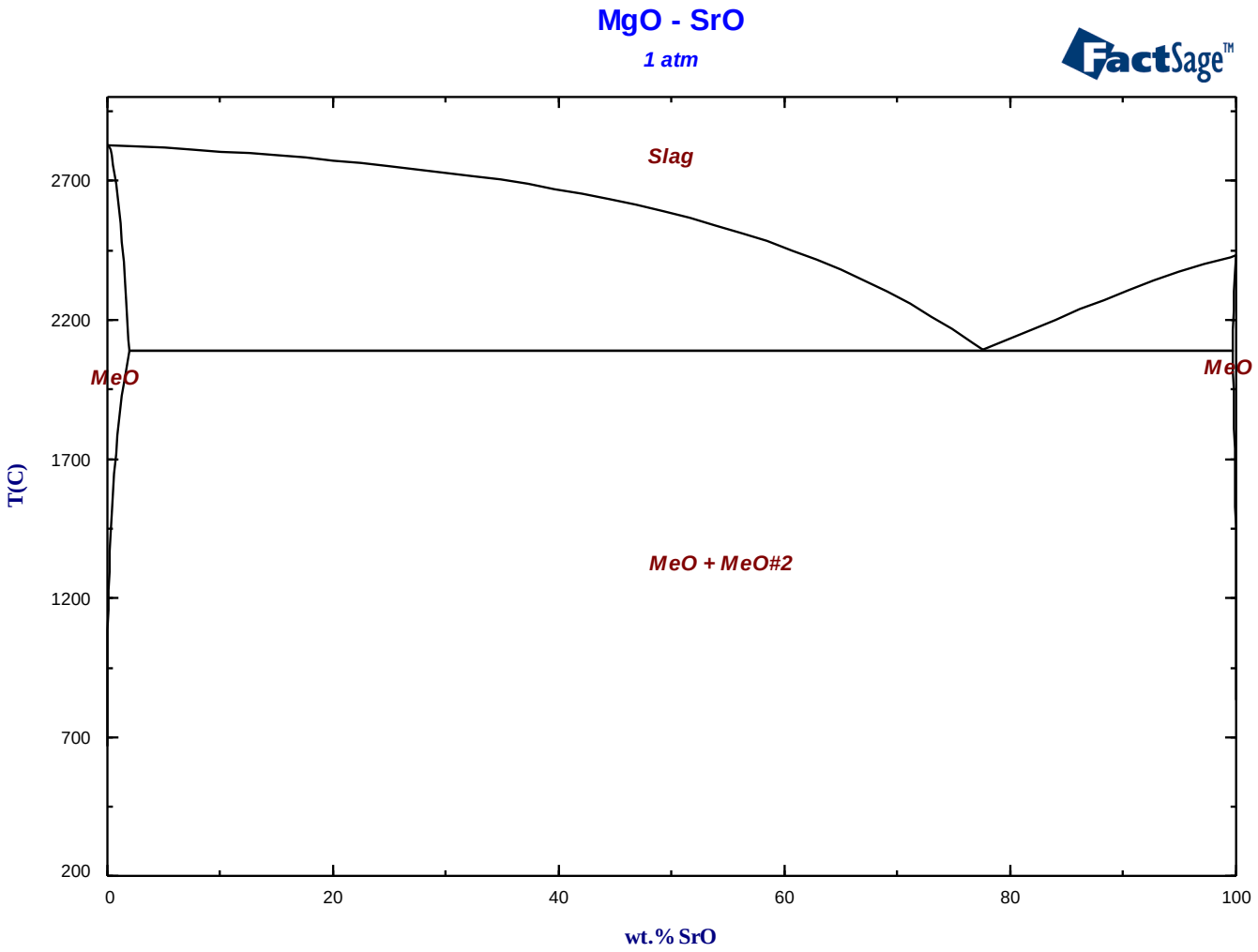

MgO-TiO2, Mole fraction compared with experimental data

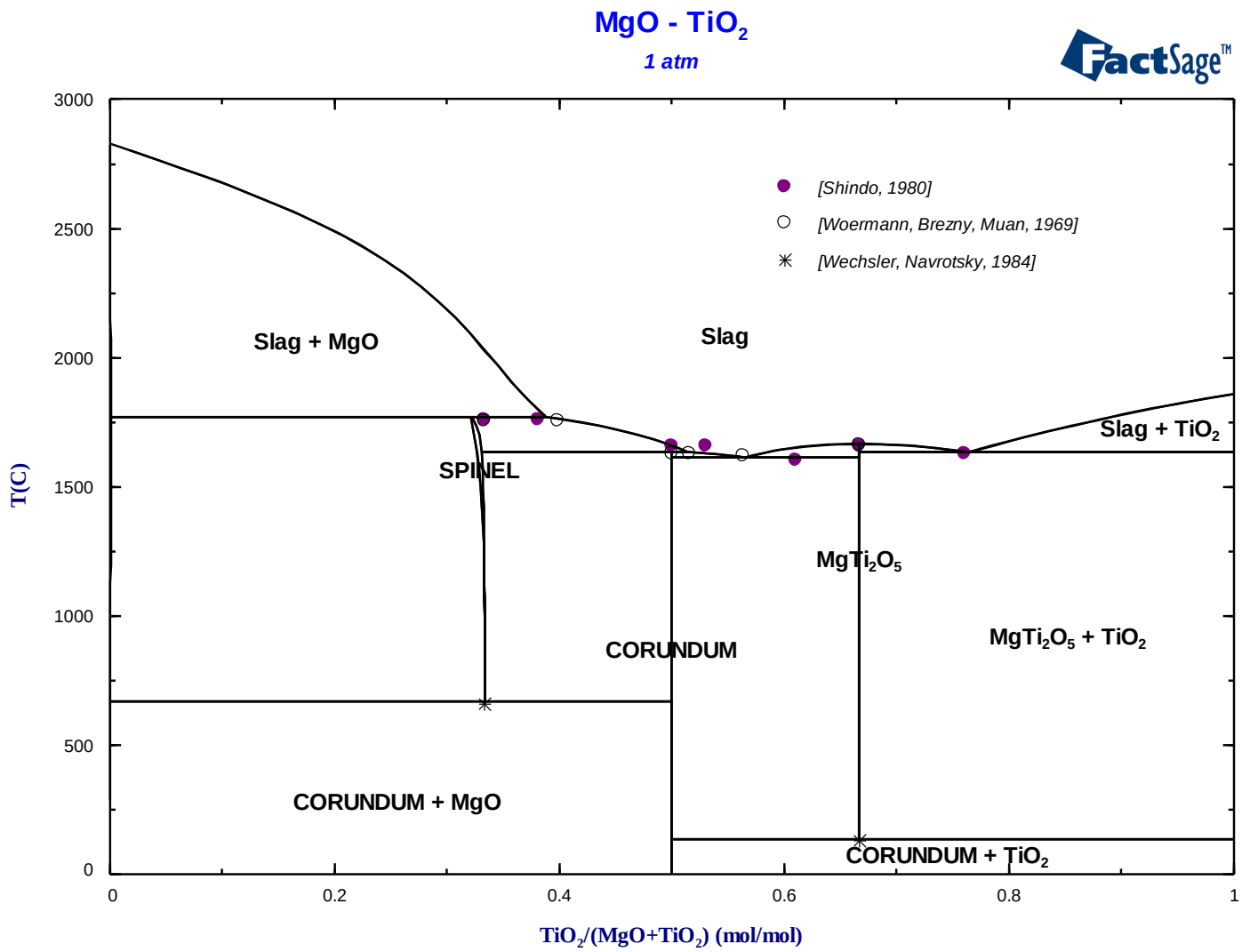

MgO-TiO2, Weight percent

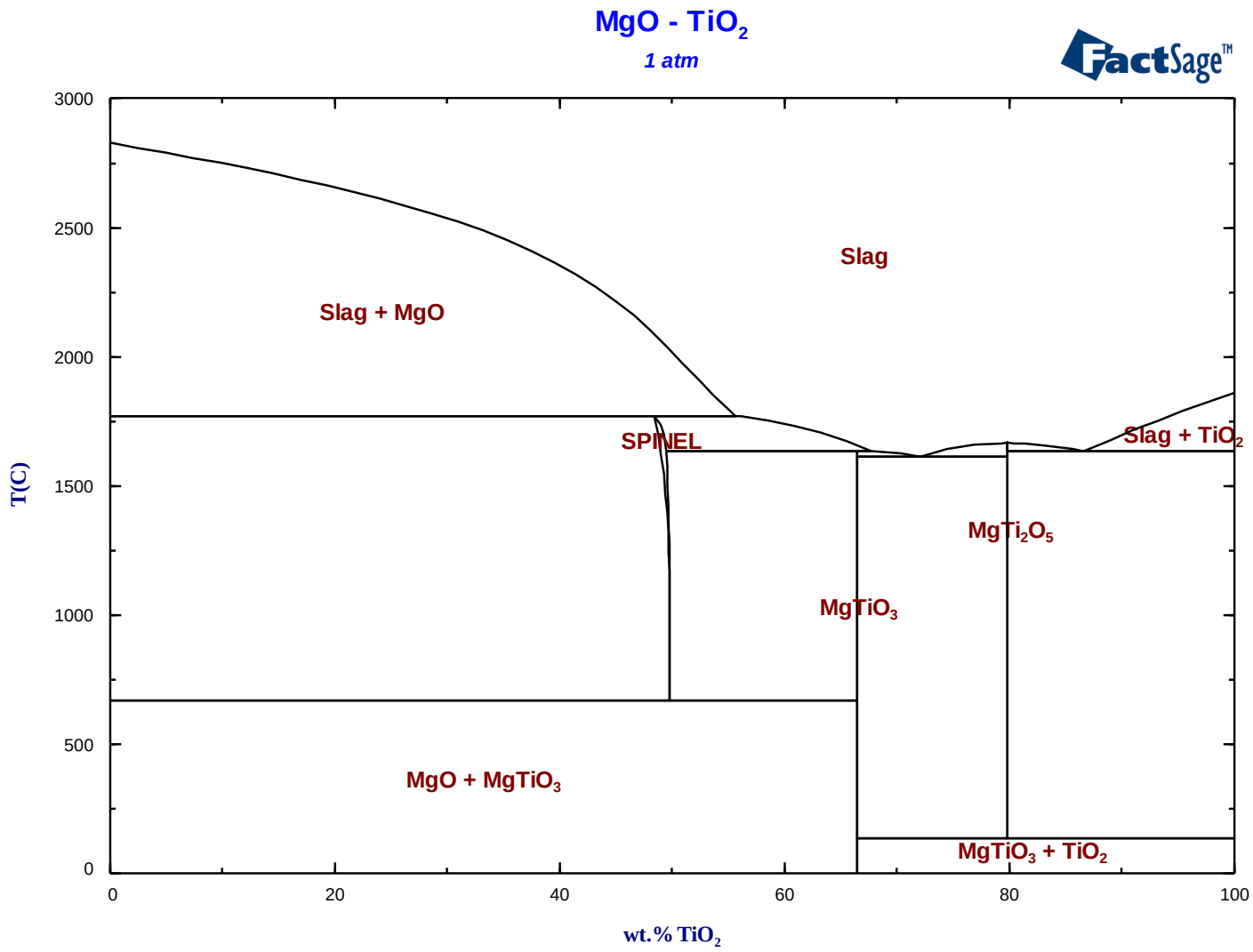

MgO-V2O3,
Mole fraction

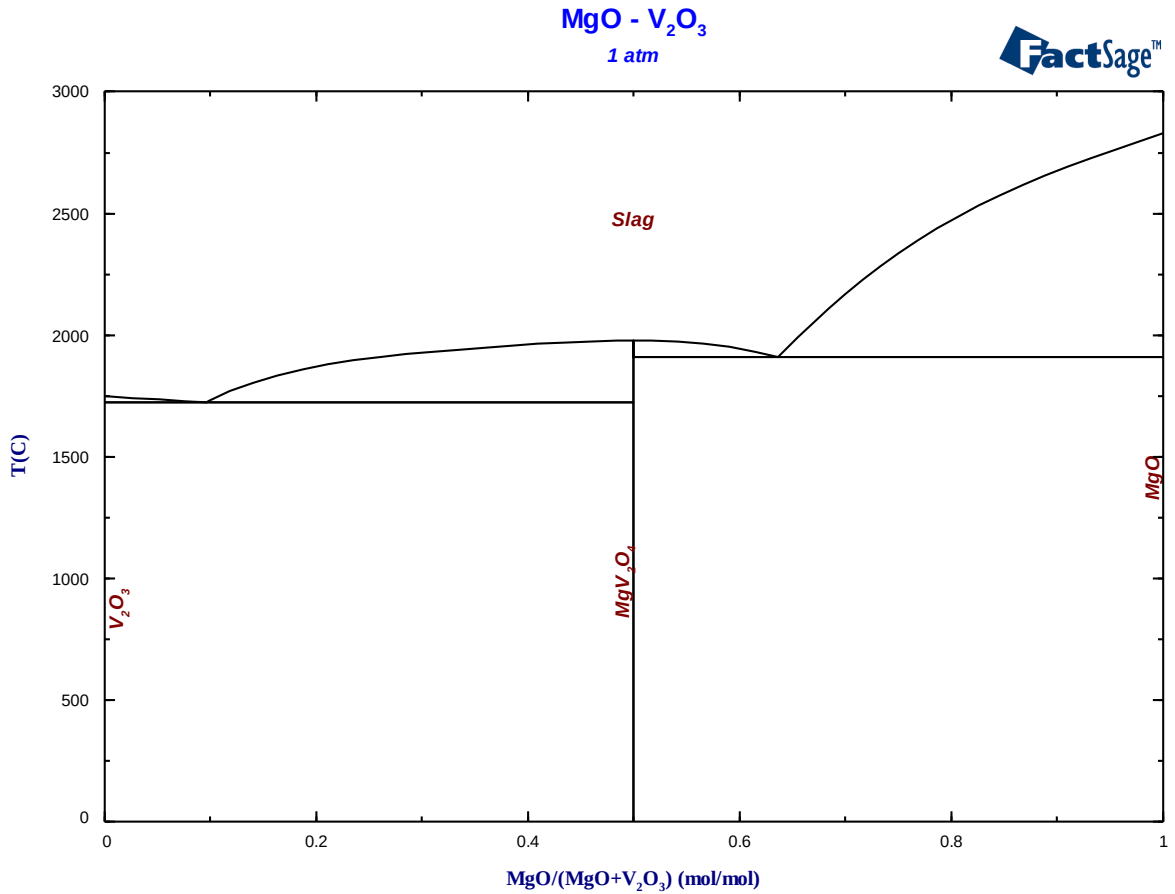

MgO-V2O3,
Weight percent compared with experimental data

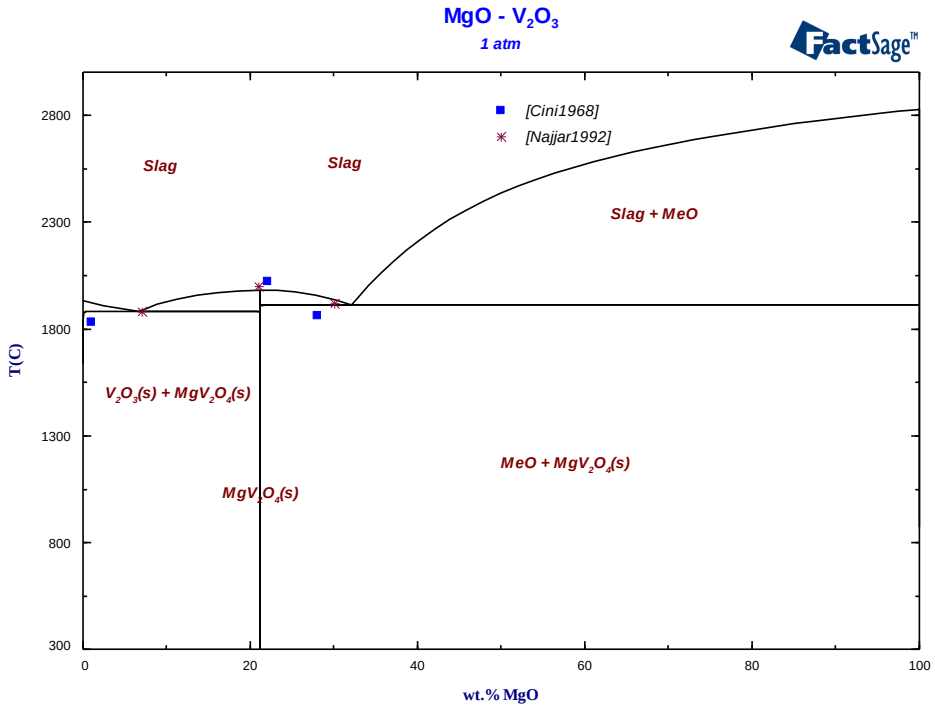

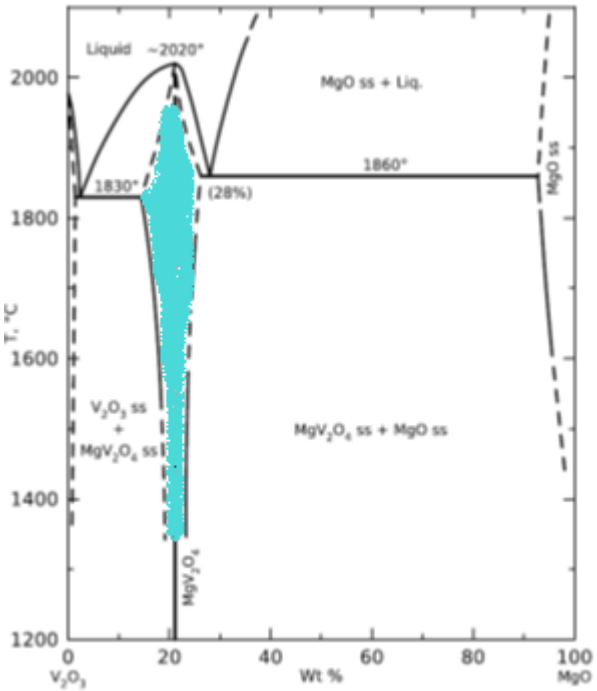

L. Cini, Radex Rundsch., No. 2, 102-112 (1968).

MgO-V2O5-O2,
Mole fraction compared with experimental data

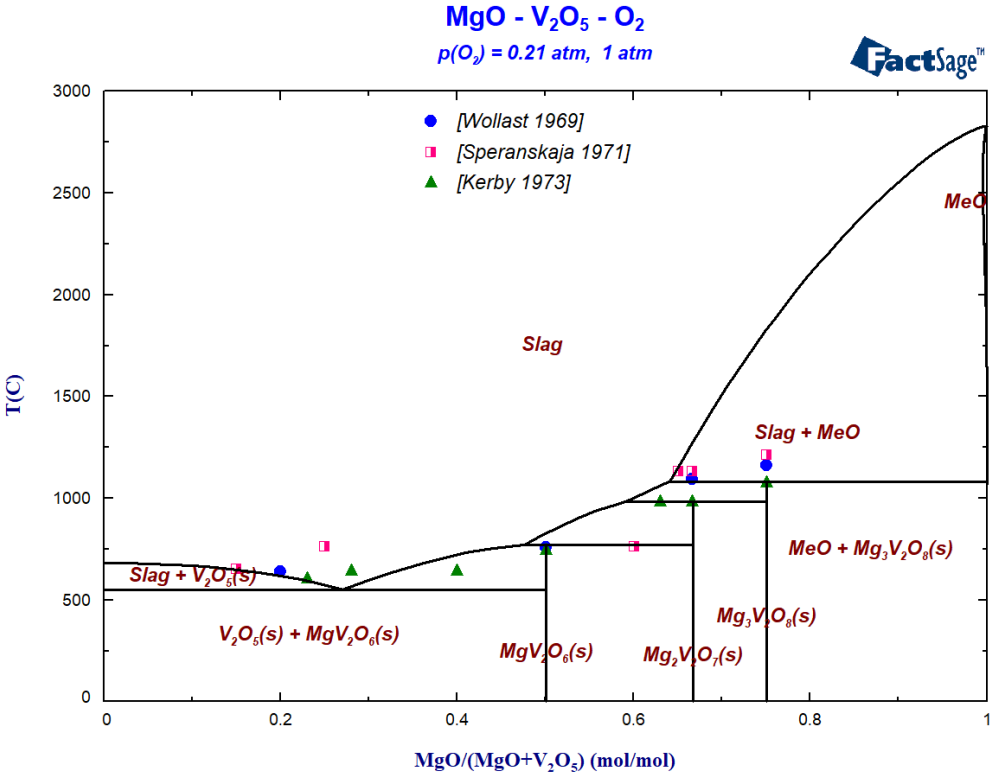

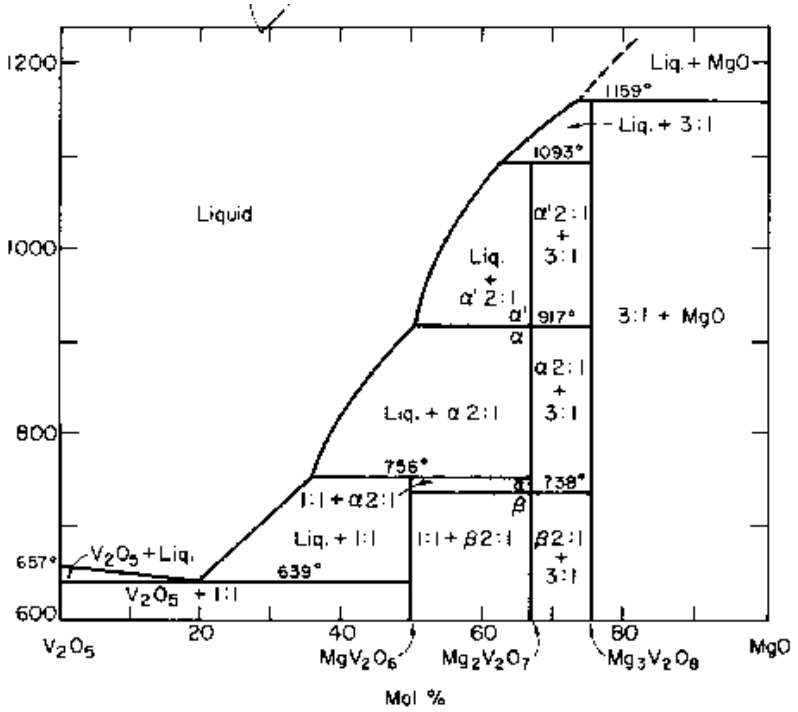

R. Wollast and A. Tazairt, Silic. Ind., 34 [2] 37-45 (1969).

MgO-V2O5-O2,
Weight percent

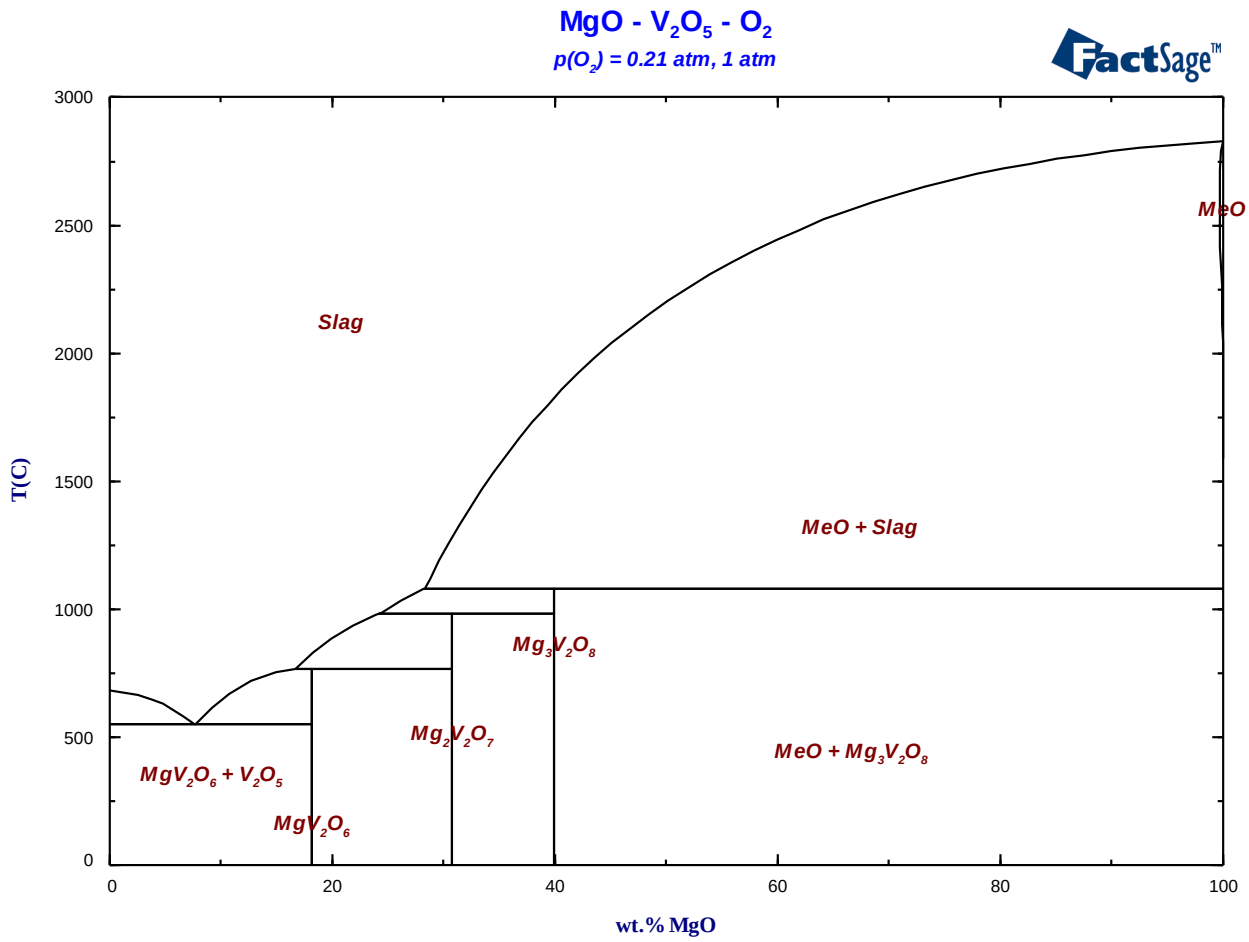

Mole fraction

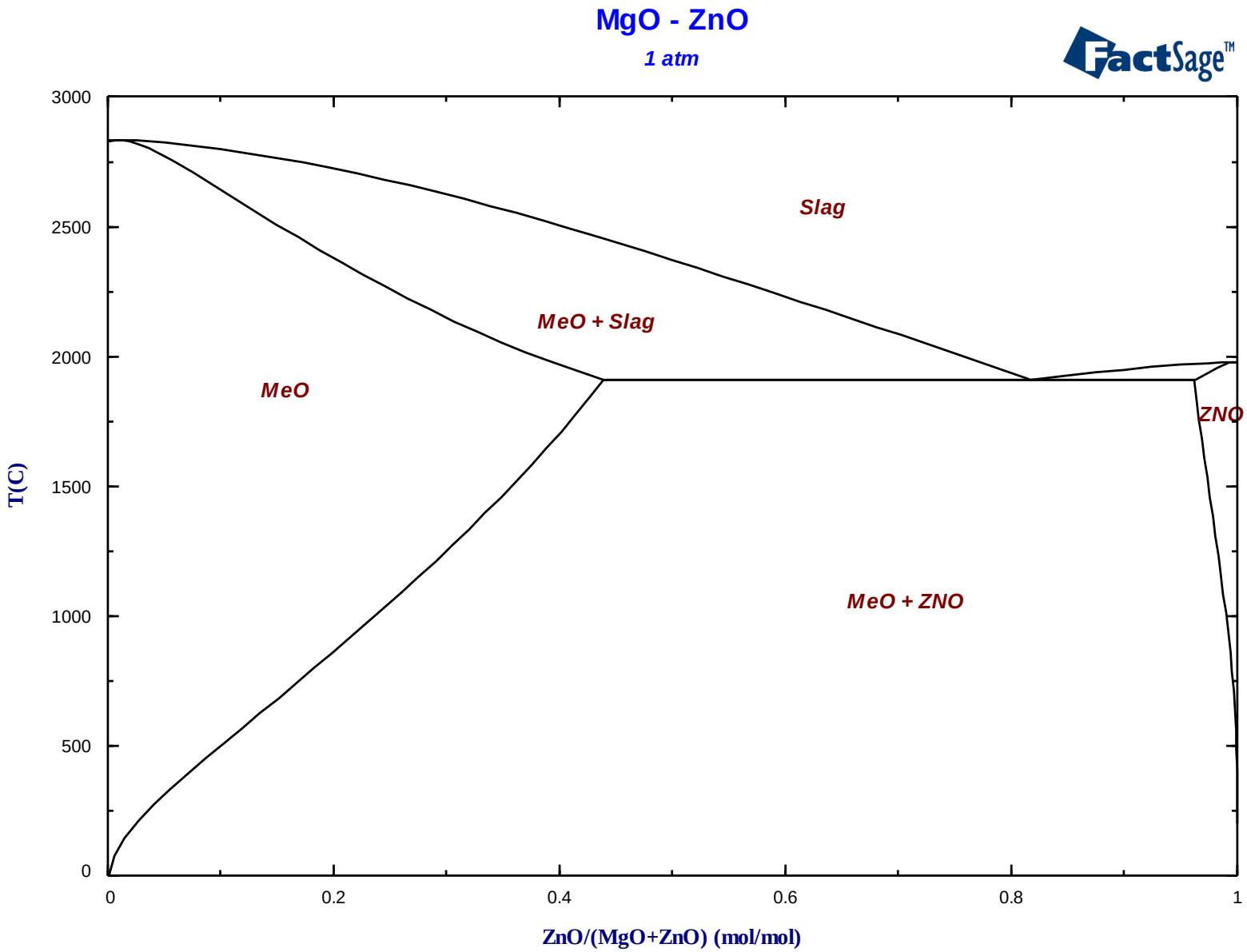

Weight percent

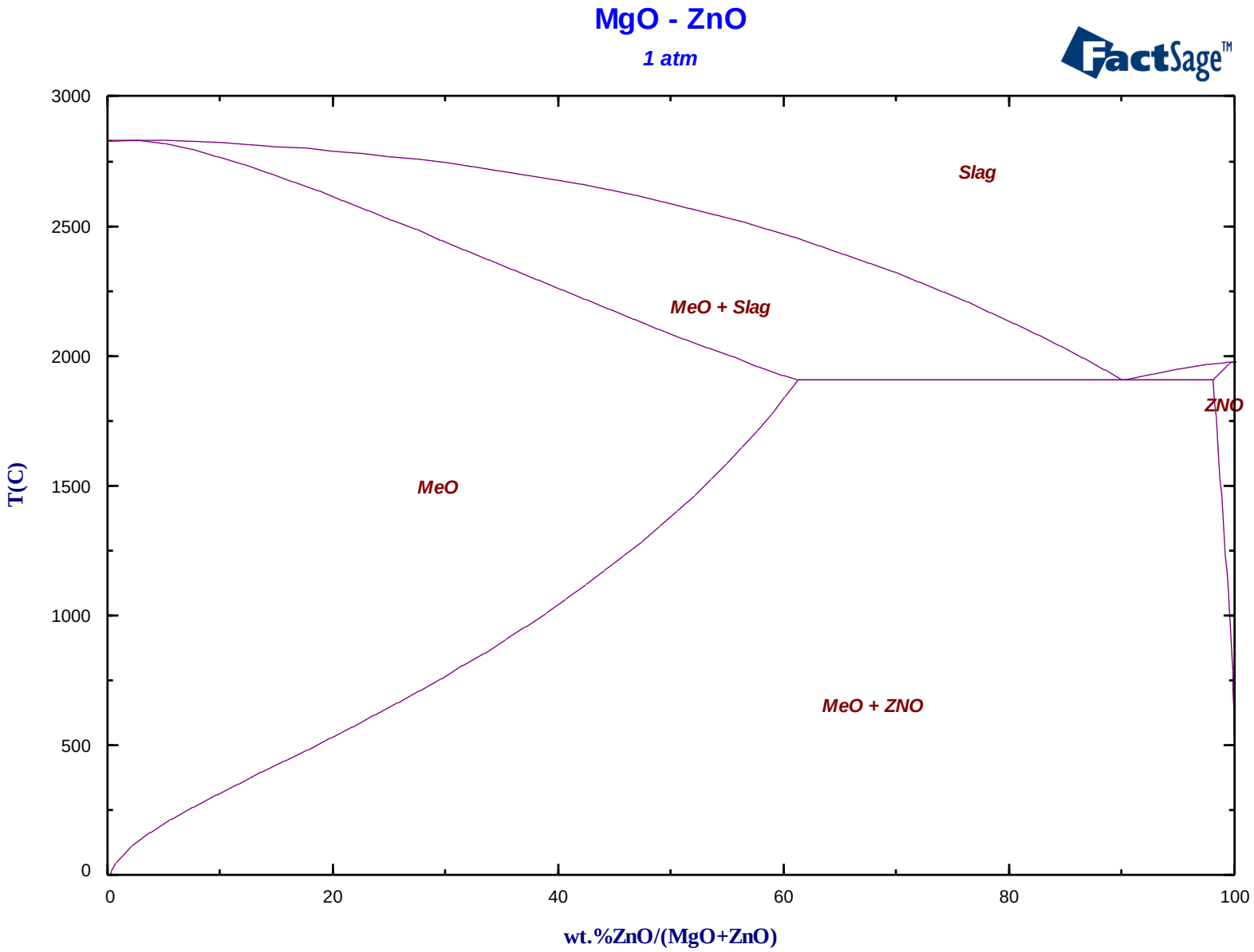

Mole fraction

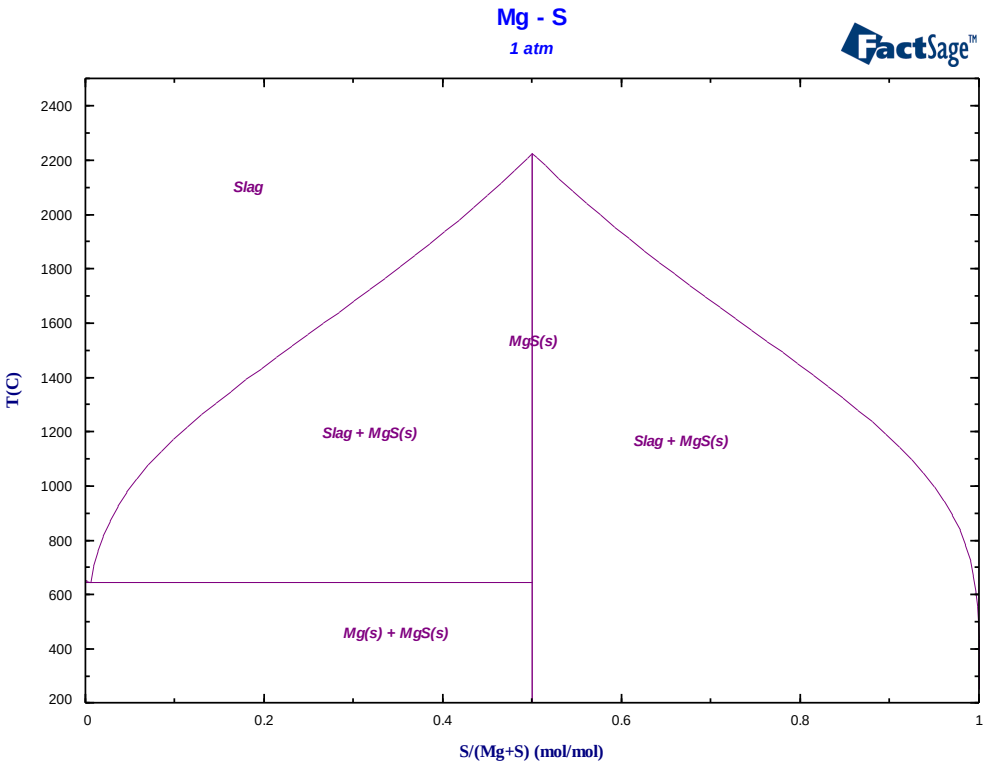

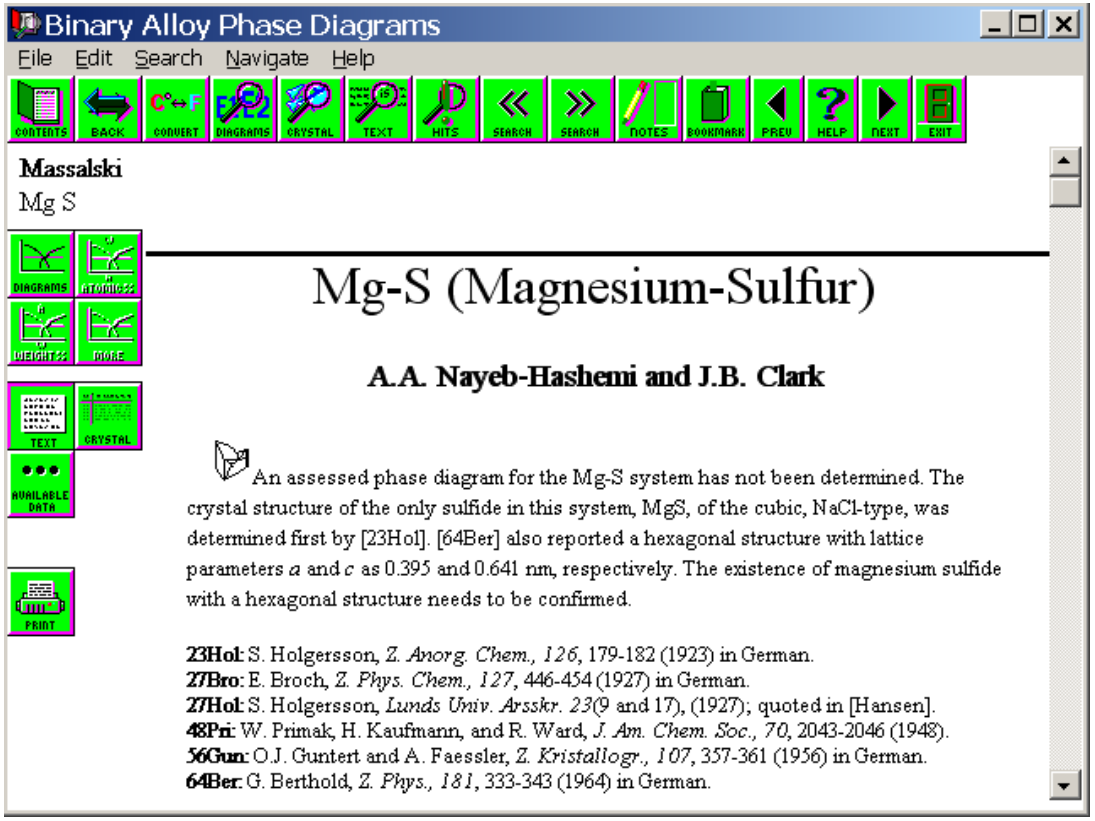

Weight percent

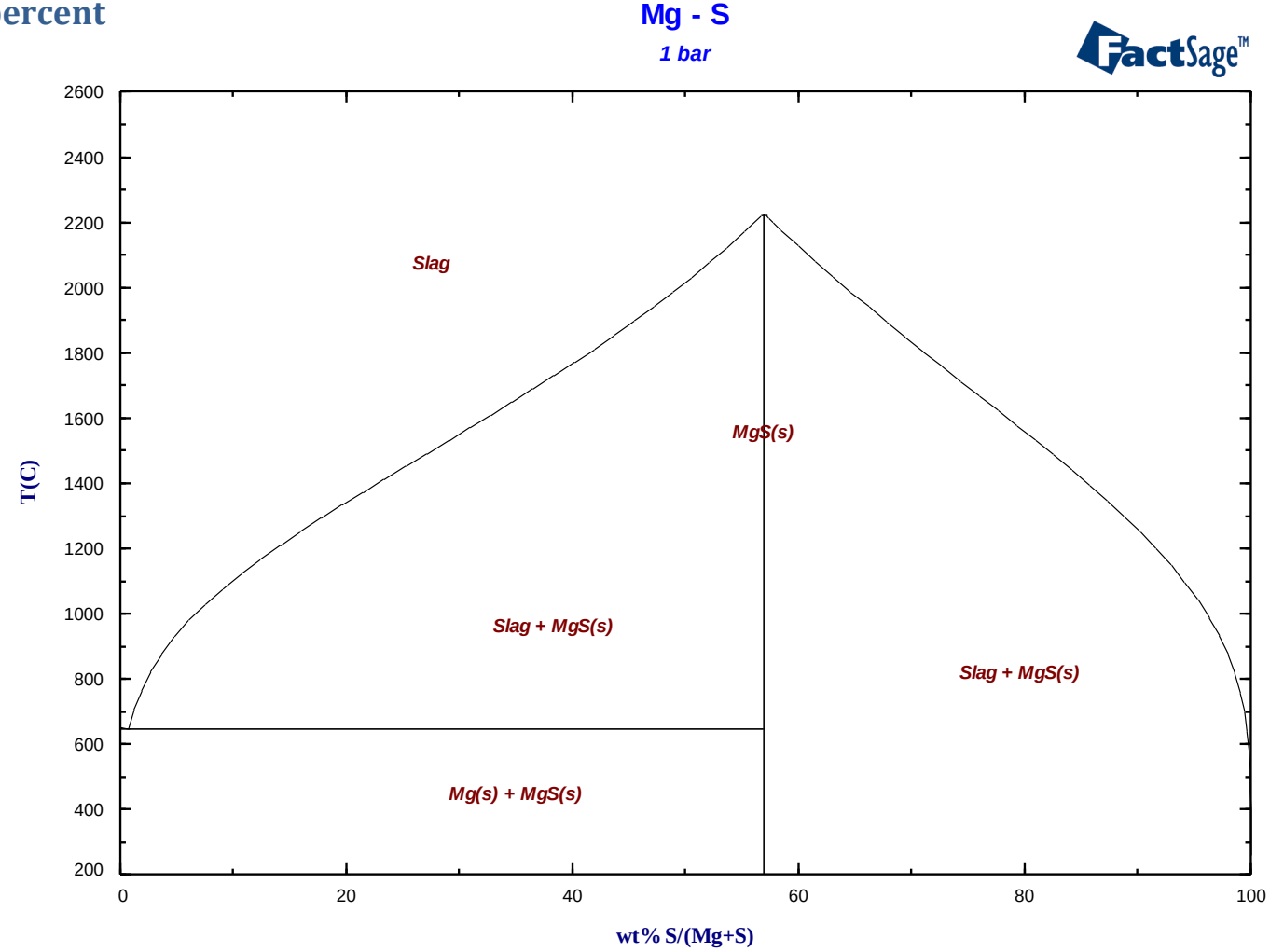

Mole fraction

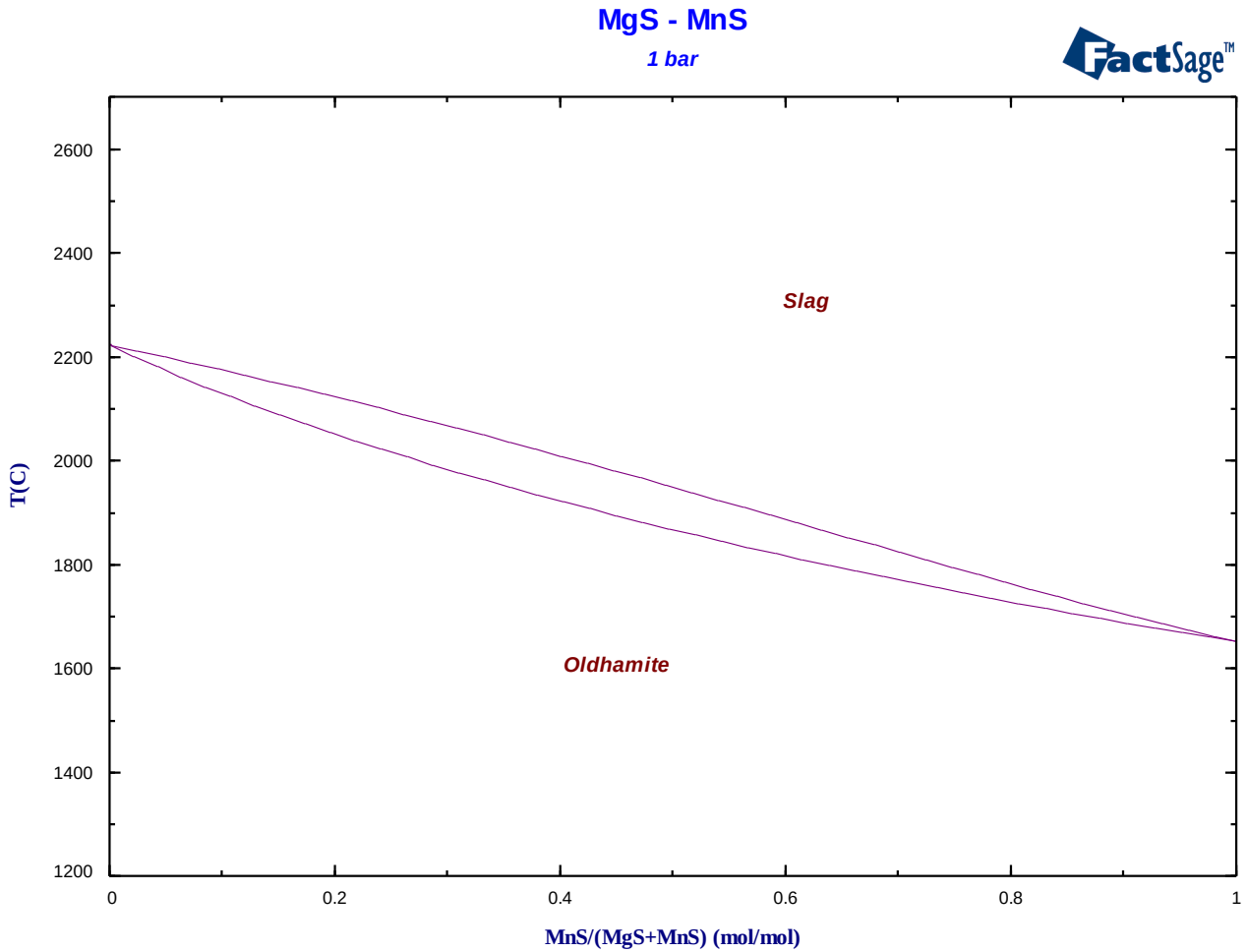

6) *MnS-MgS*

At all temperatures between 600°C and 1000°C, we found that MnS and MgS form a completely miscible solid solution.

B.J. Skinner, F.D. Luck, Amer. Mineral., Vol.56 (1971), pp. 1269-1296.

Weight percent

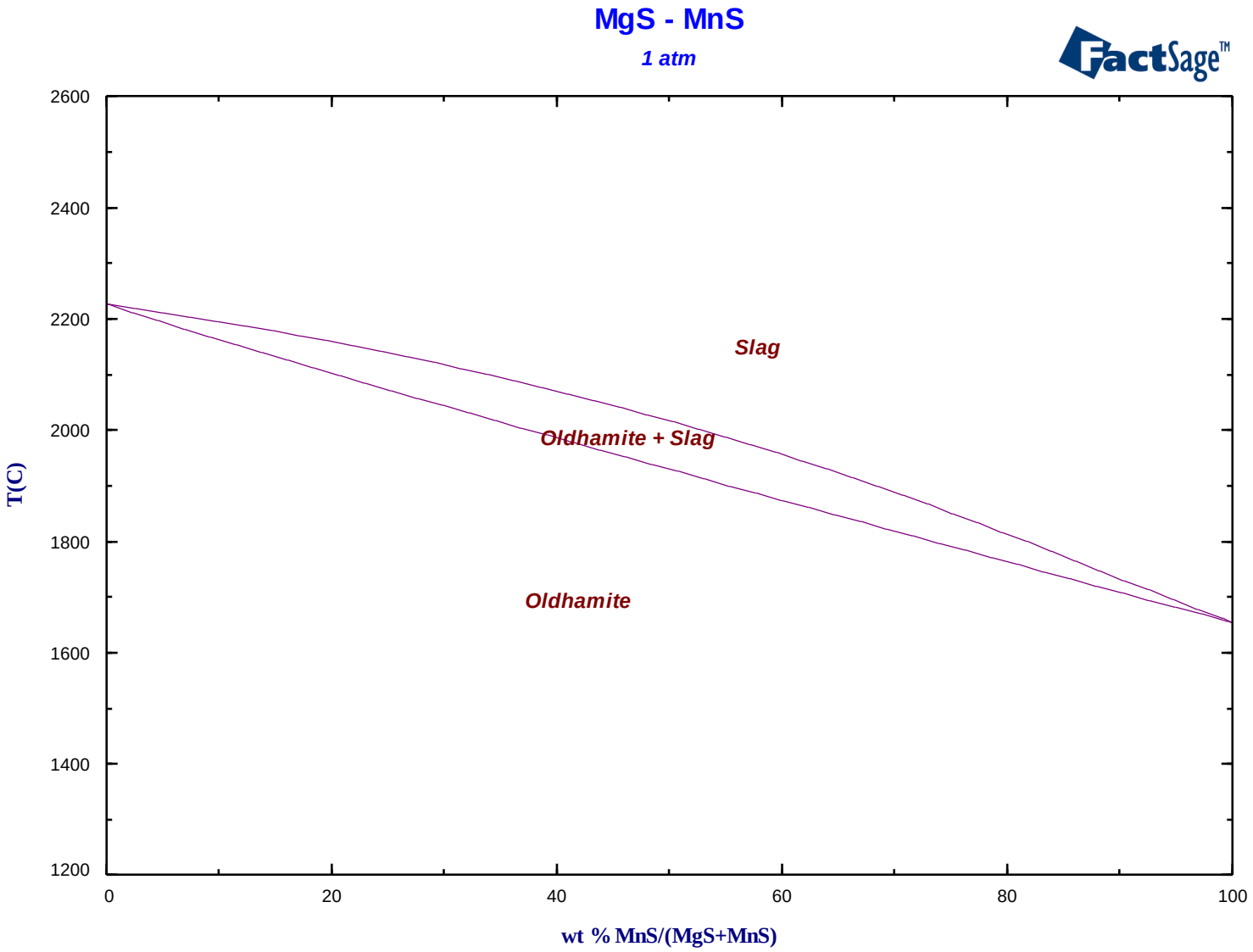

Mole fraction
compared with experimental data

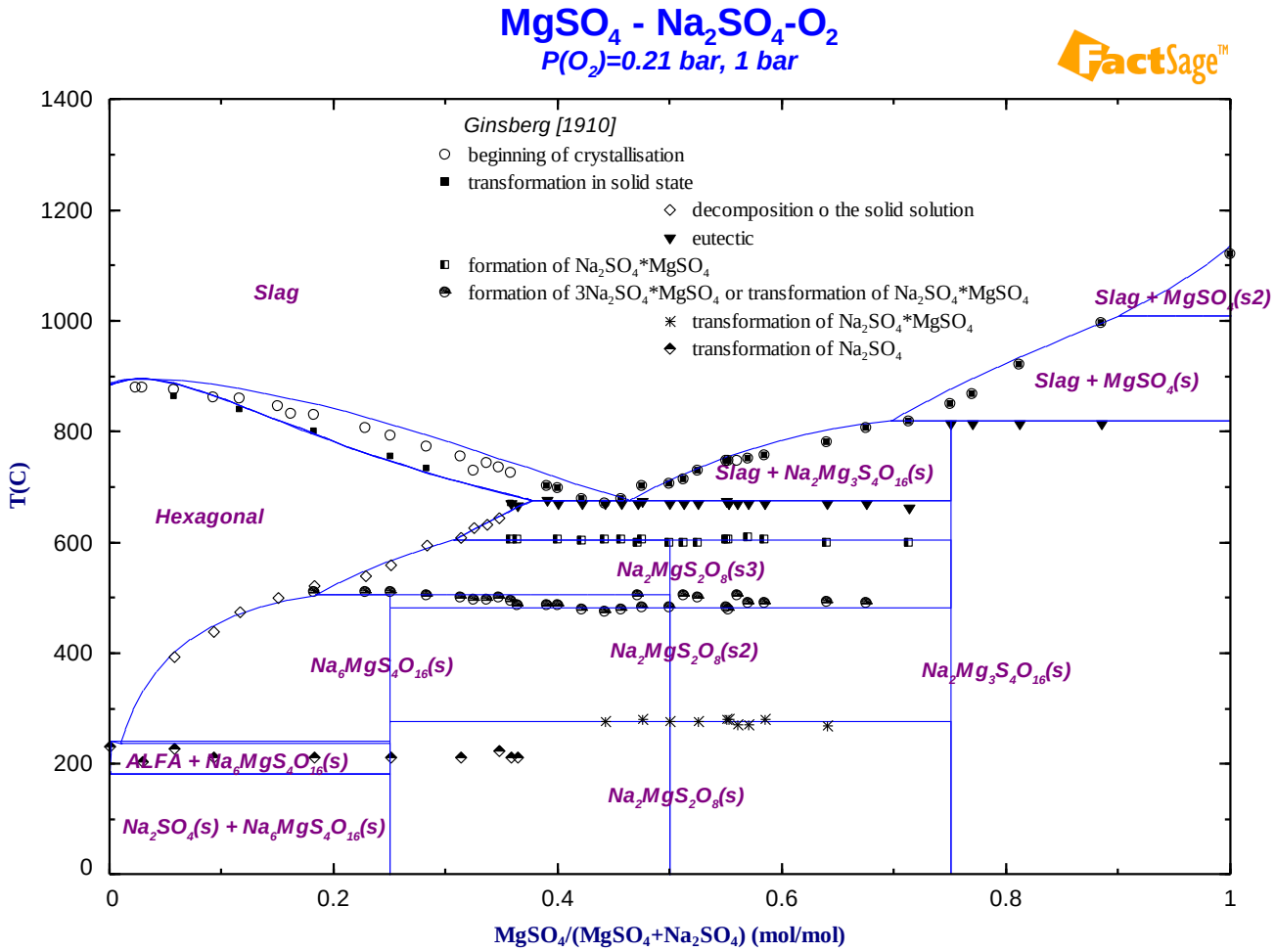

Weight percent

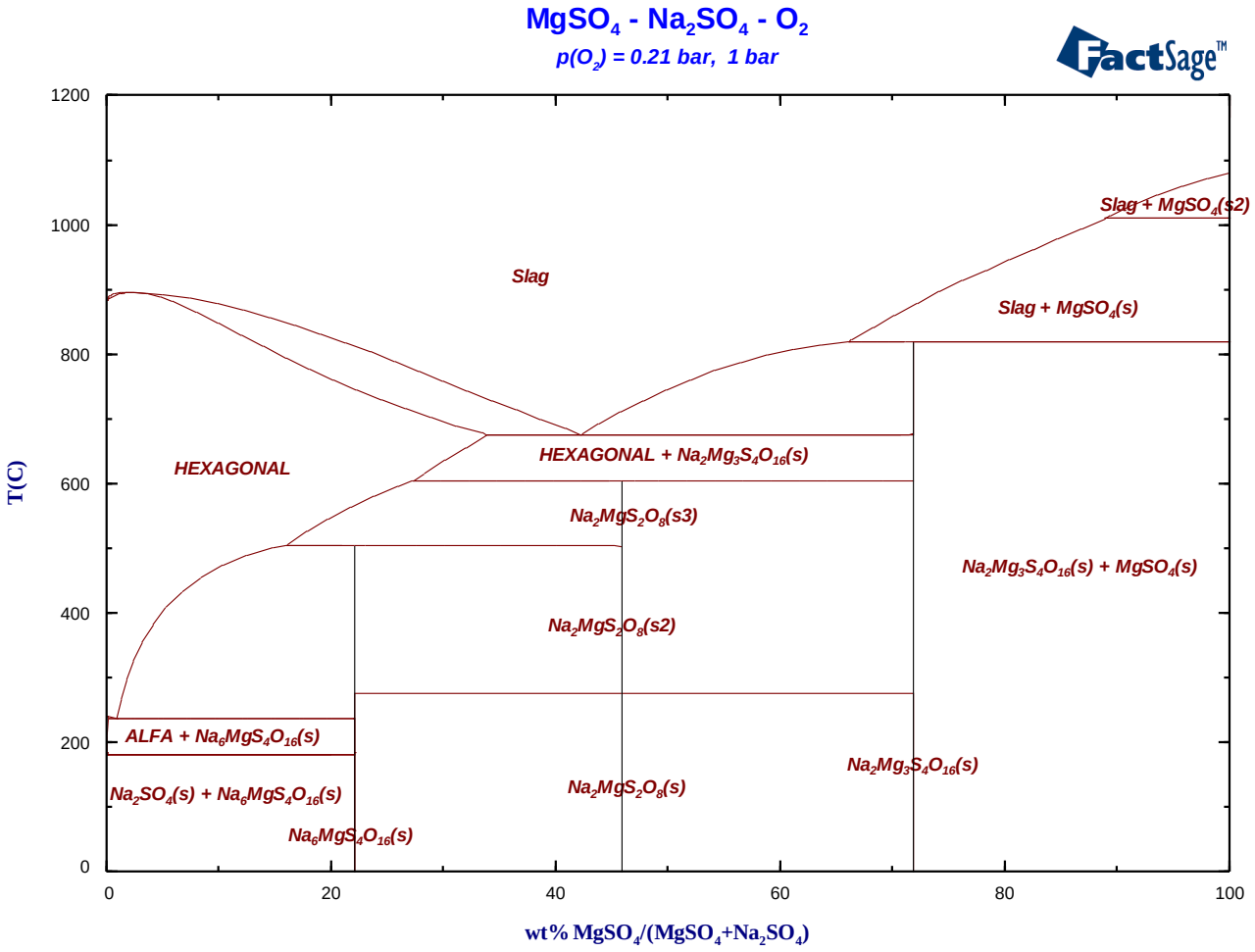

Mole fraction

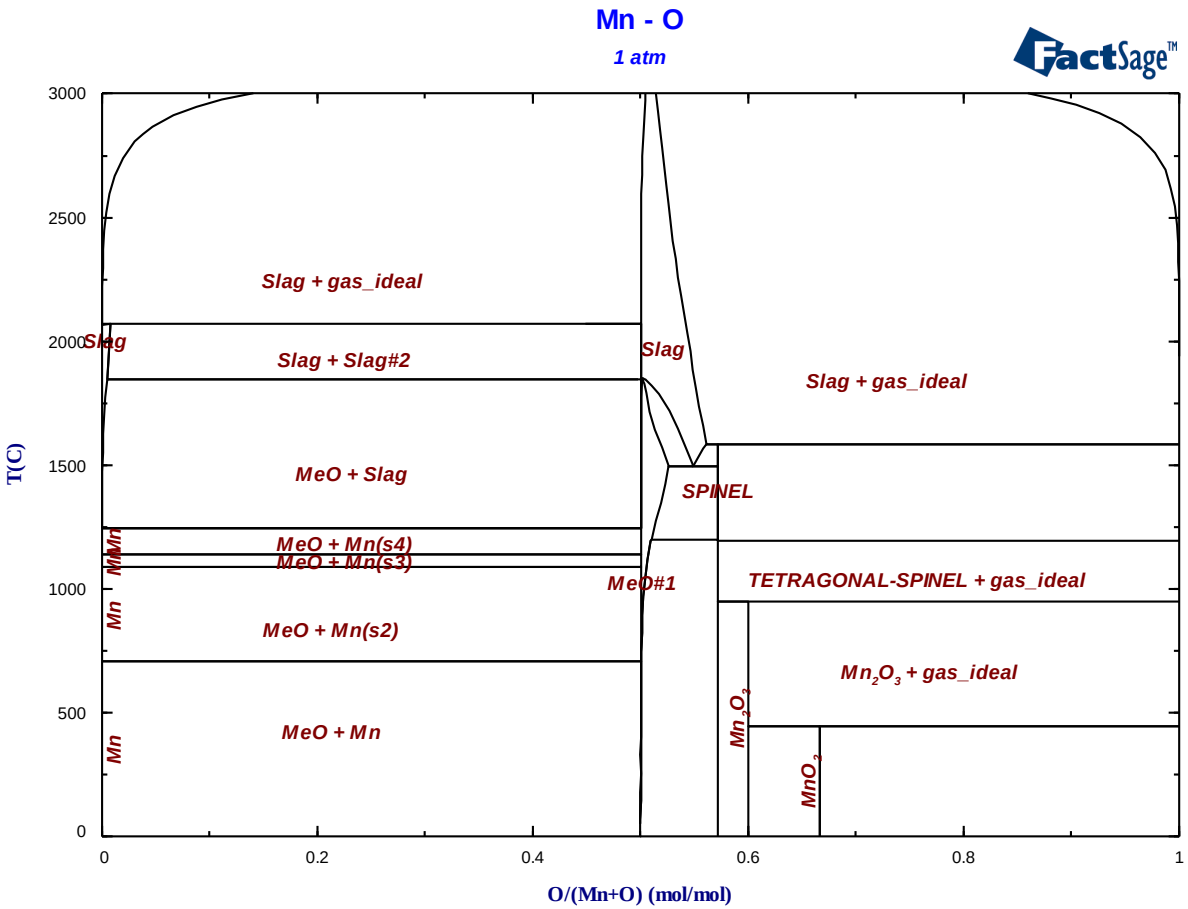

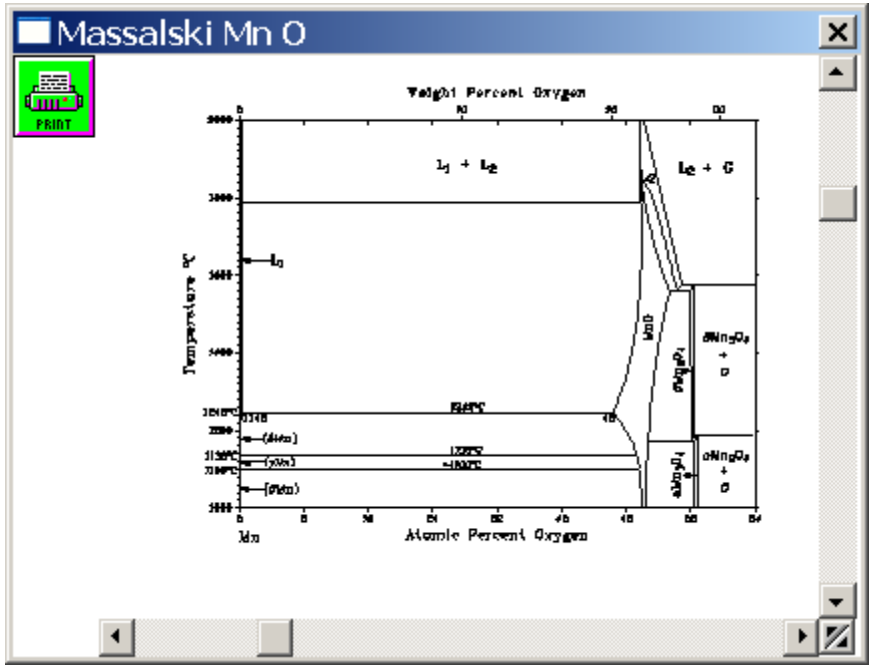

Weight percent

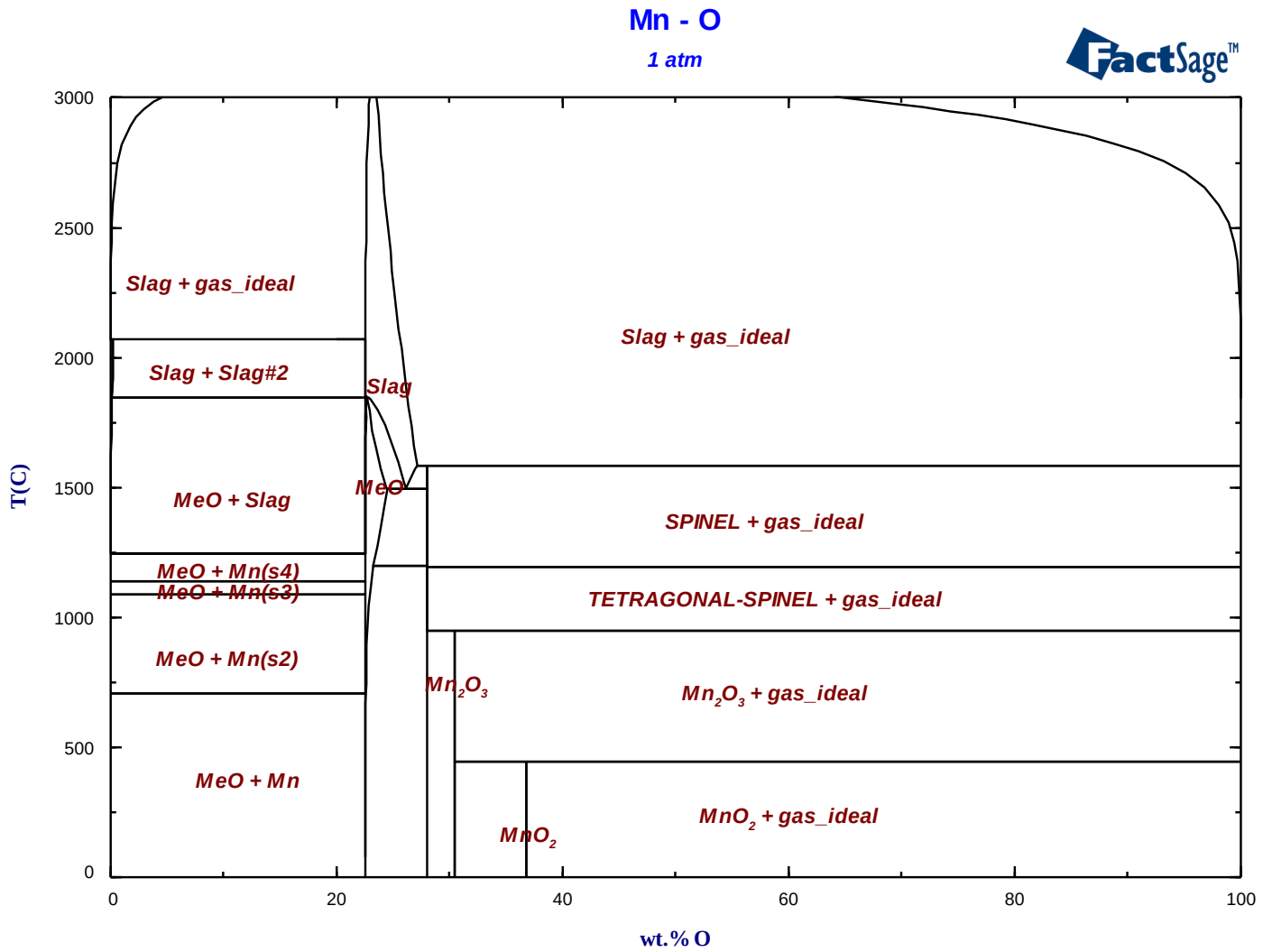

Mn-O,
Mole fraction with isobars

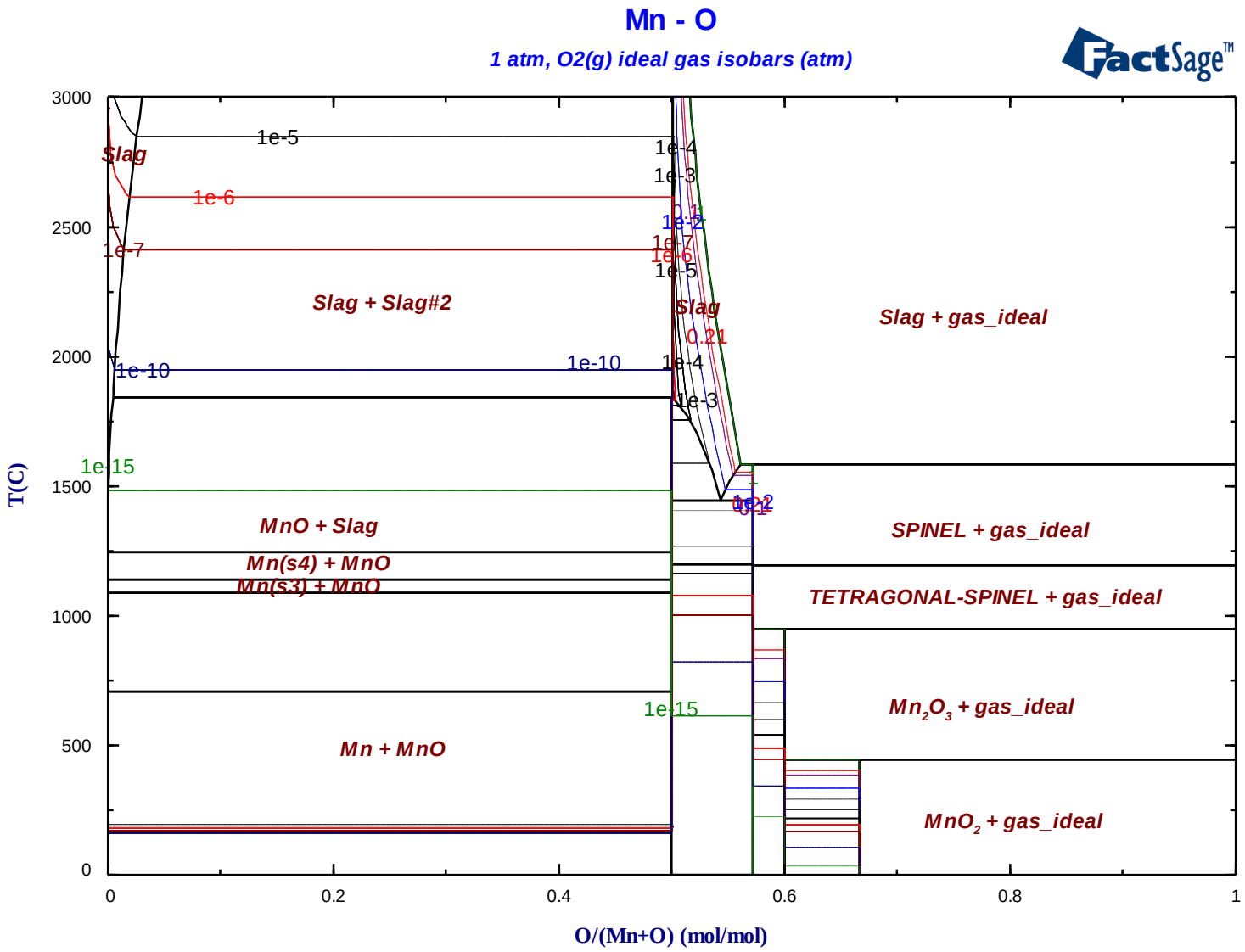

Mn-O2,
Temperature vs. log P(O2) diagram

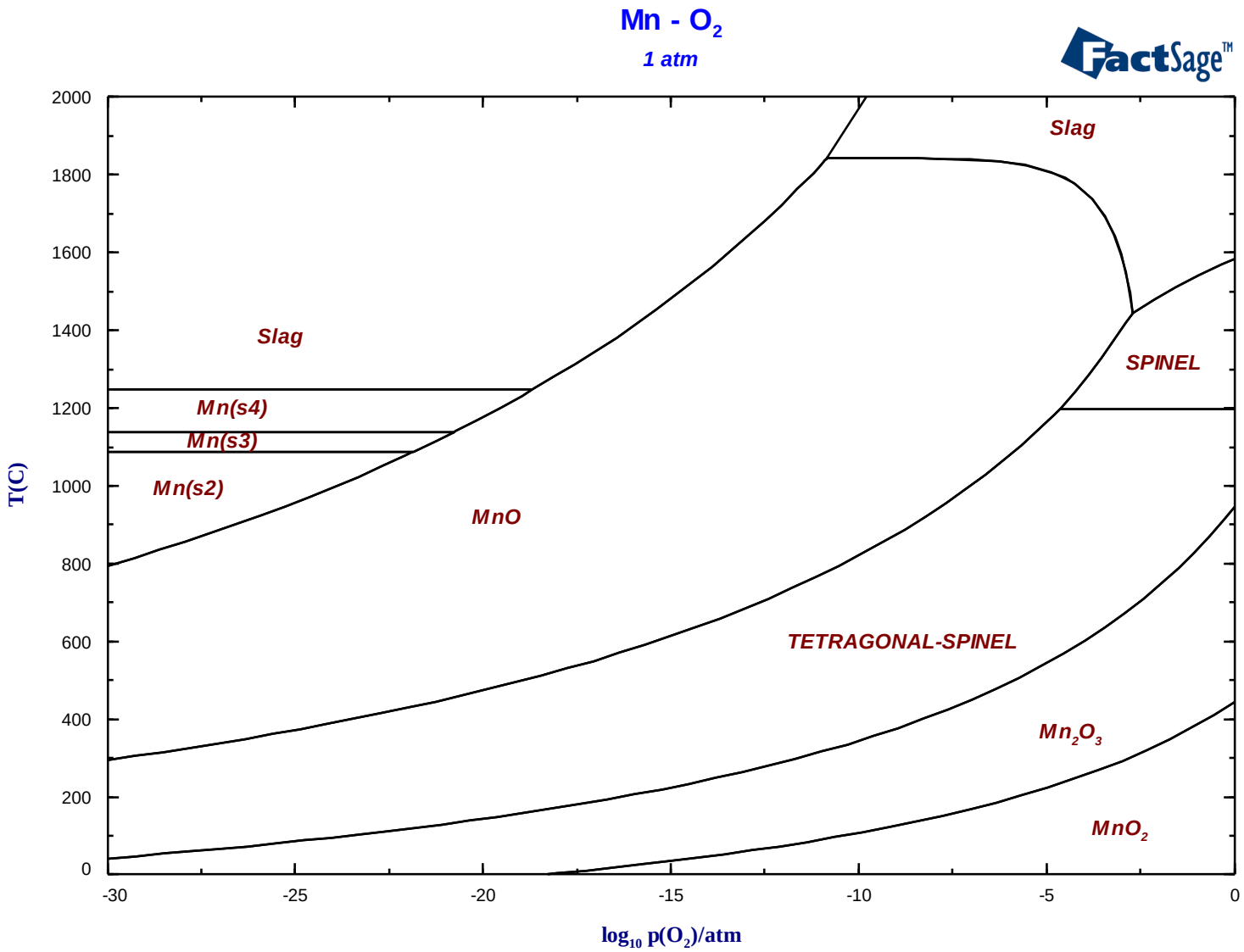

Mole fraction

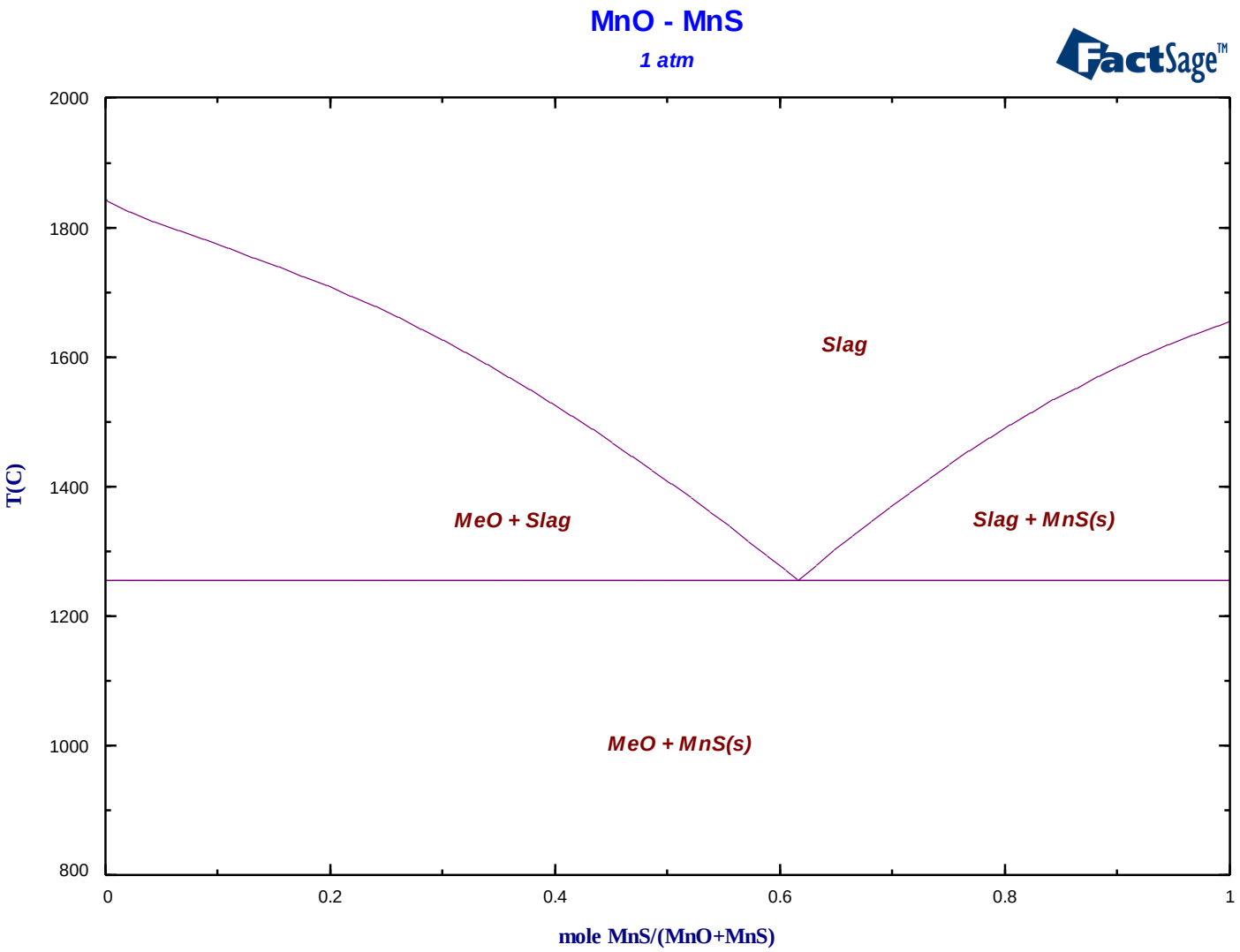

Weight percent compared with experimental data

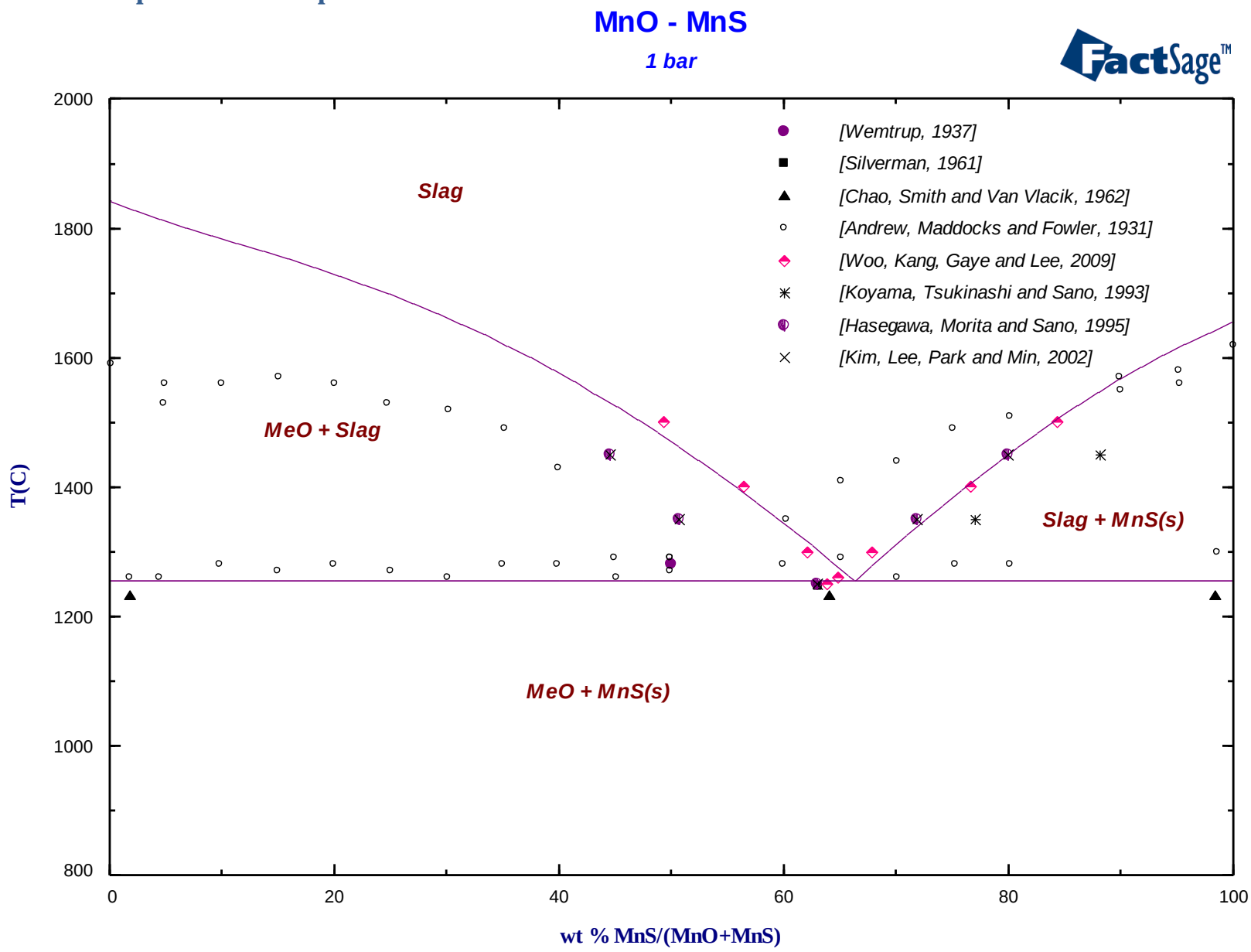

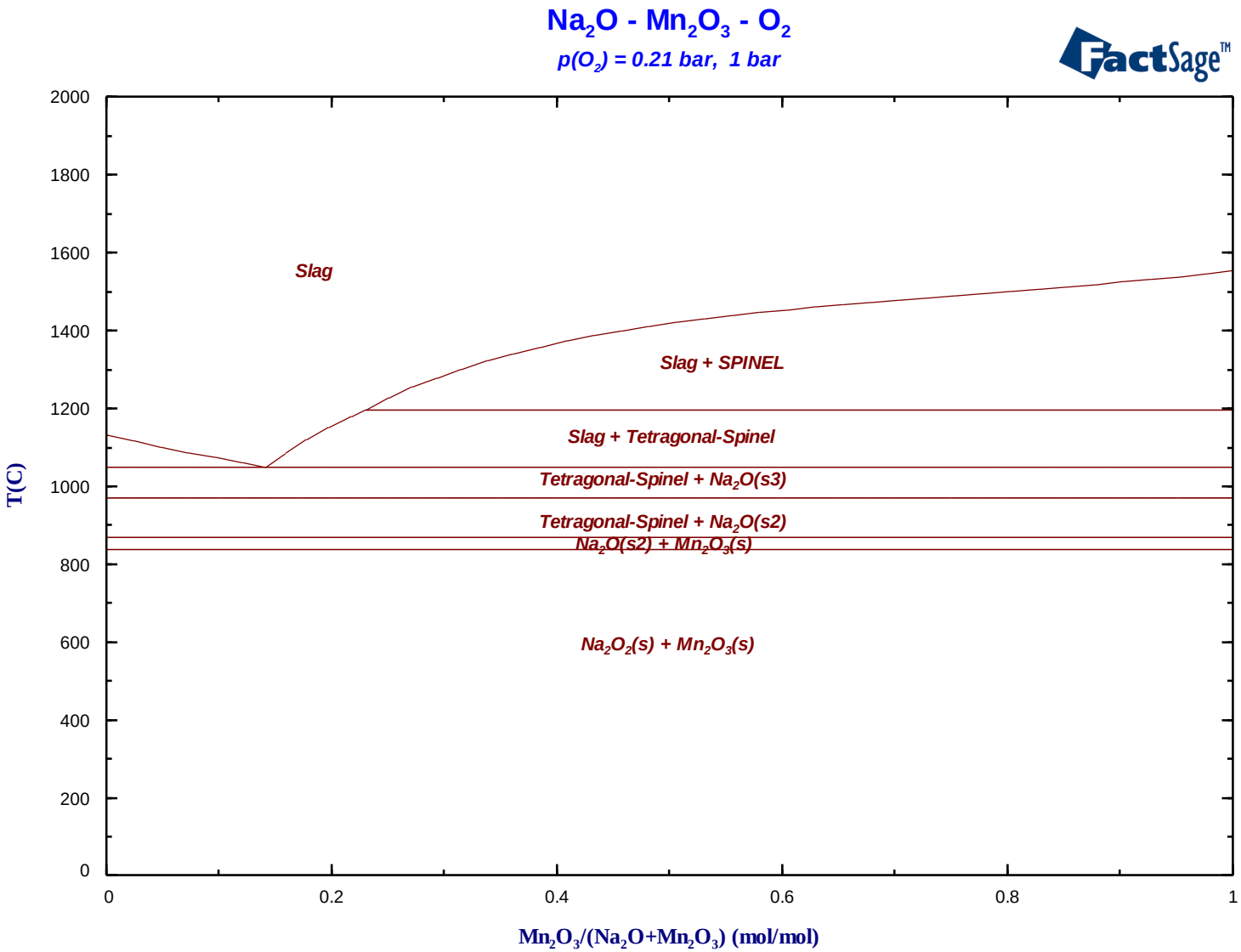
Na2O - Mn2O3 - O2
p(O2) = 0.21 bar, 1 bar
FactSage™
Slag
Slag + SPINEL
Slag + Tetragonal-Spinel
Tetragonal-Spinel + Na2O(s3)
Tetragonal-Spinel + Na2O(s2)
Na2O(s2) + Mn2O3(s)
Na2O2(s) + Mn2O3(s)
T(C)
2000
1800
1600
1400
1200
1000
800
600
400
200
0
0
0.2
0.4
0.6
0.8
1
Mn2O3/(Na2O+Mn2O3) (mol/mol)

Weight percent

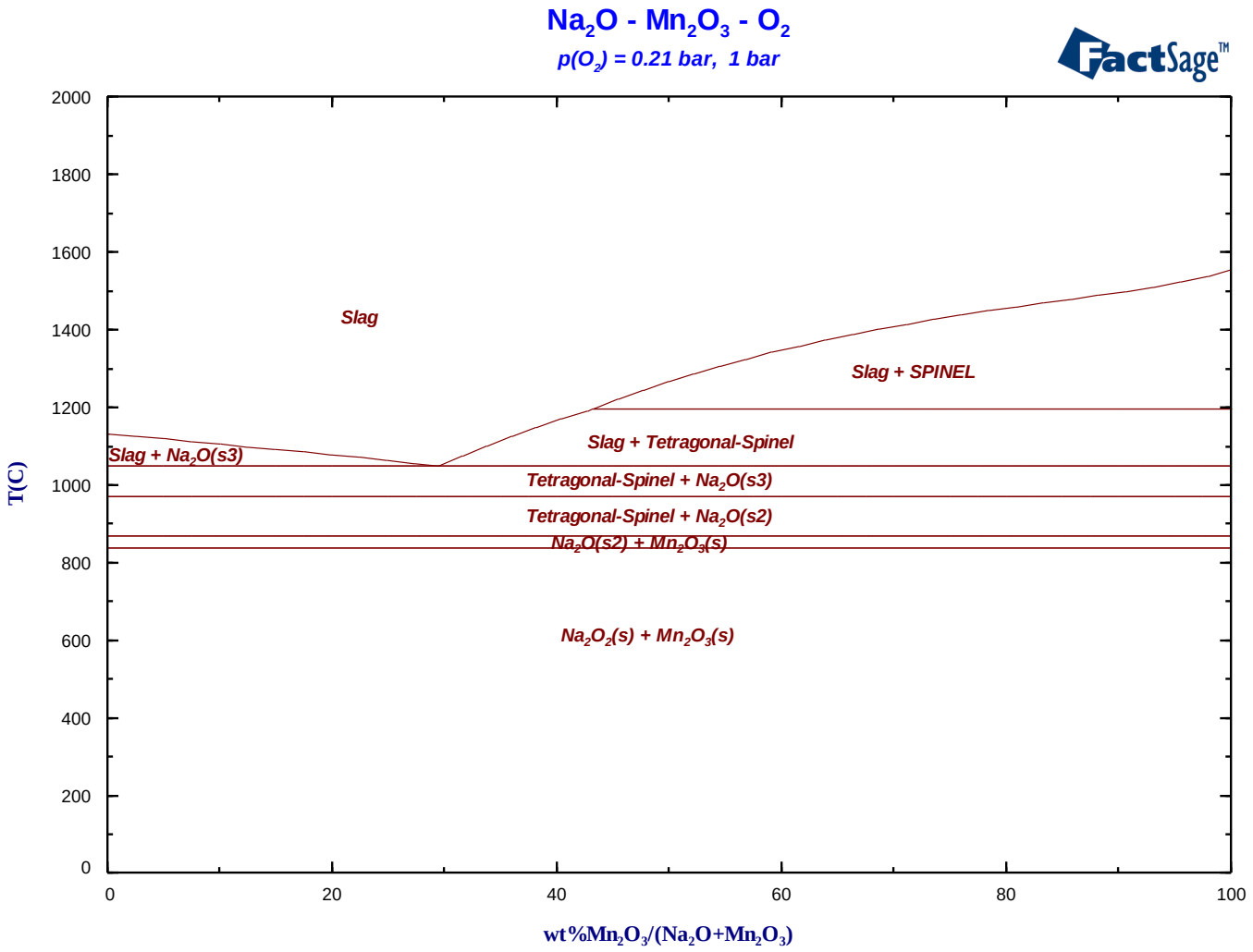

Mole fraction compared with experimental data

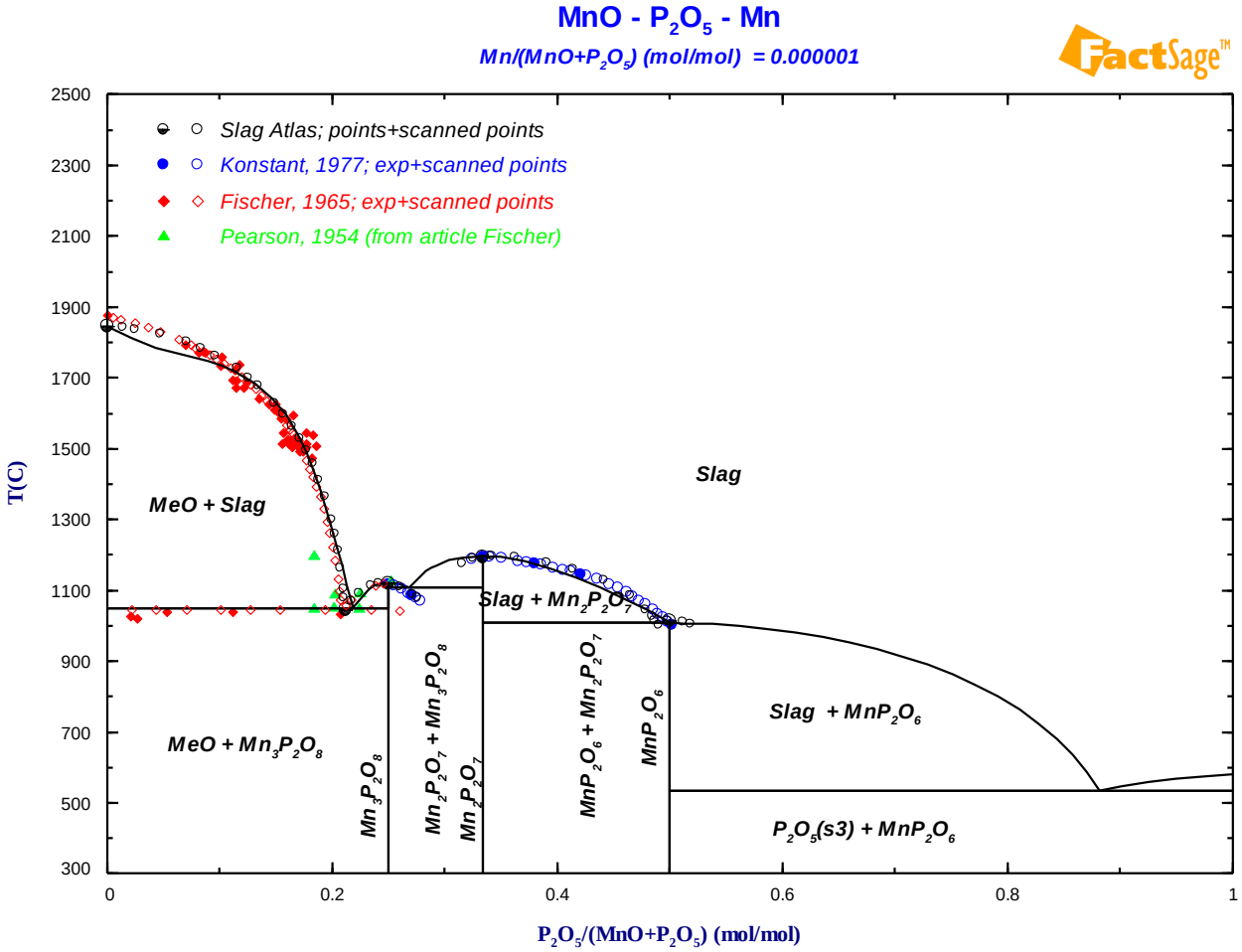

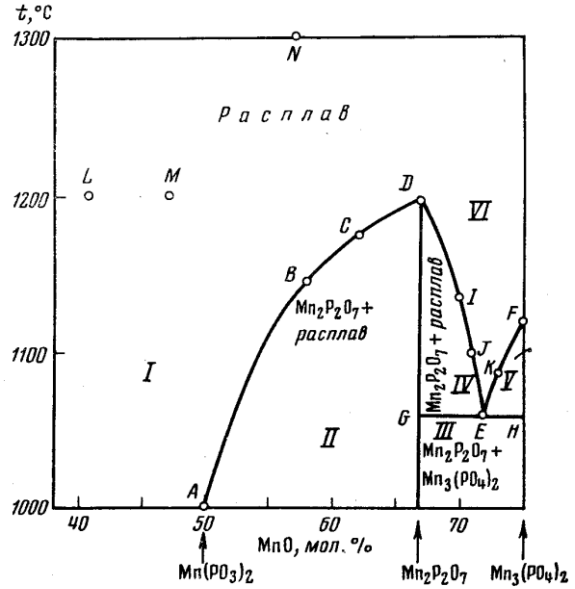

Z.A. Konstant, D. A.I., Manganase phosphate in the system MnO-P₂O₅ (in russian), Neorganicheskije Materiali, 1977; 13: 99-103.

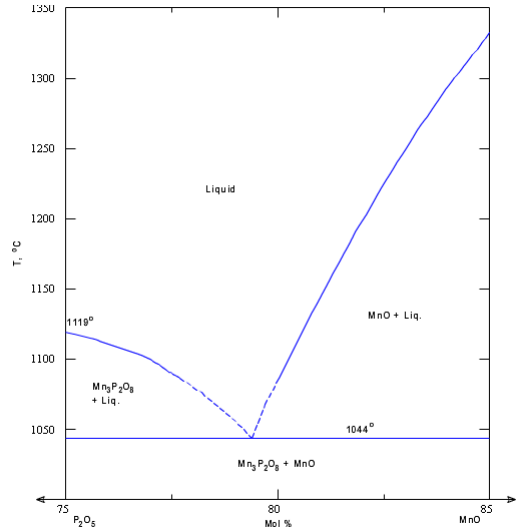

J. Pearson, E.T. Turkdogan, E.M. Fenn, J Iron Steel Inst, 1954; 176: 441-4.

Weight percent

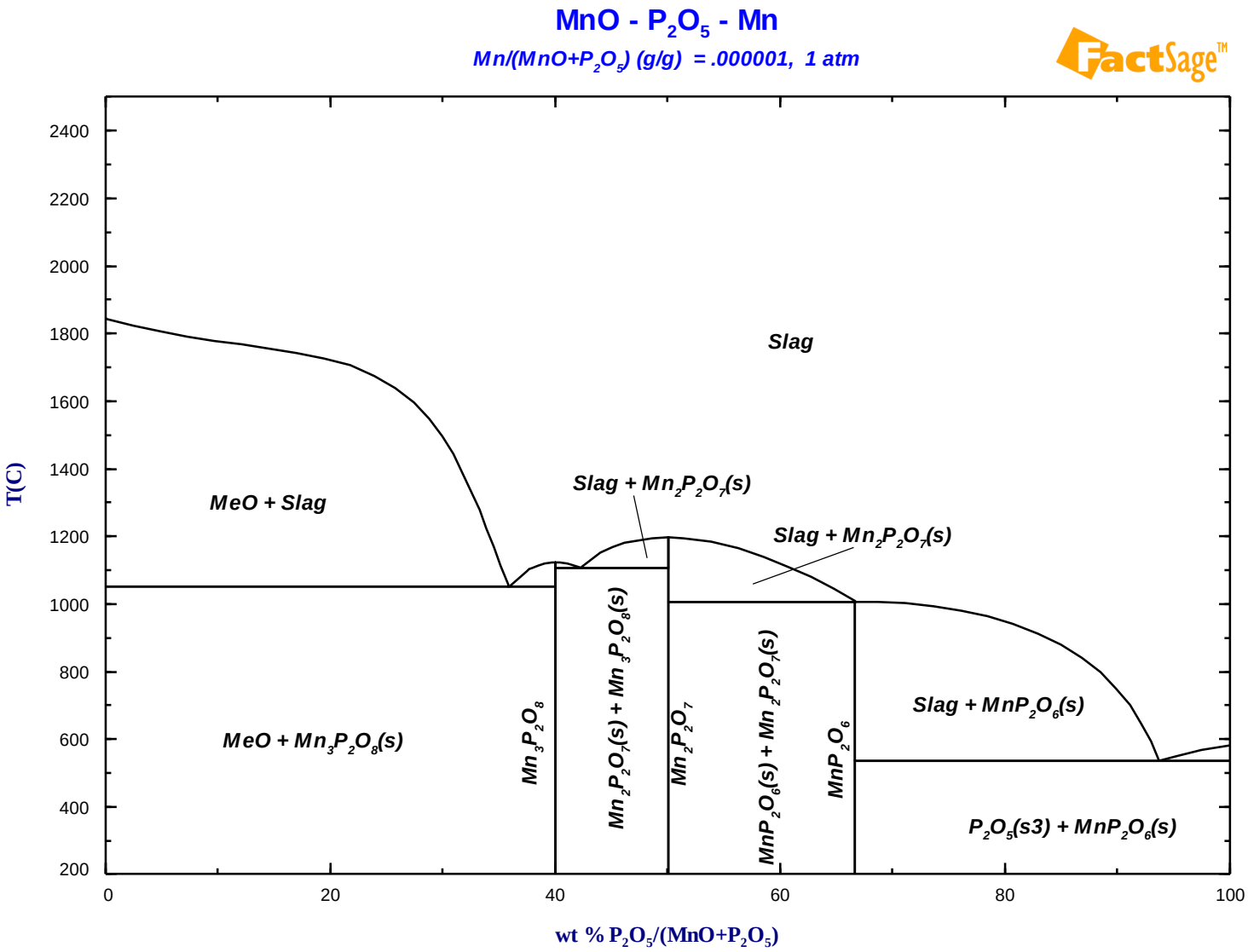

Mole fraction compared with experimental data

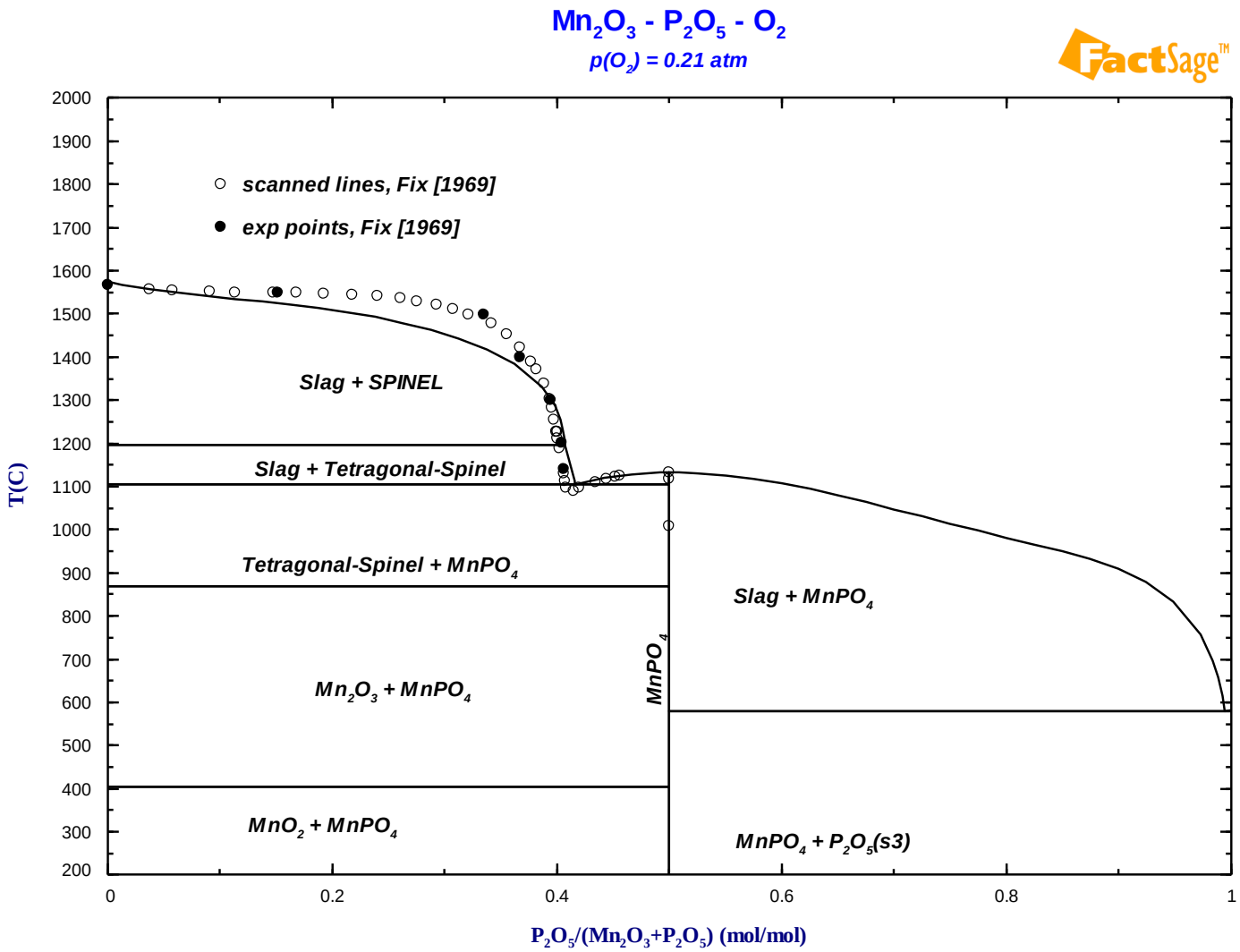

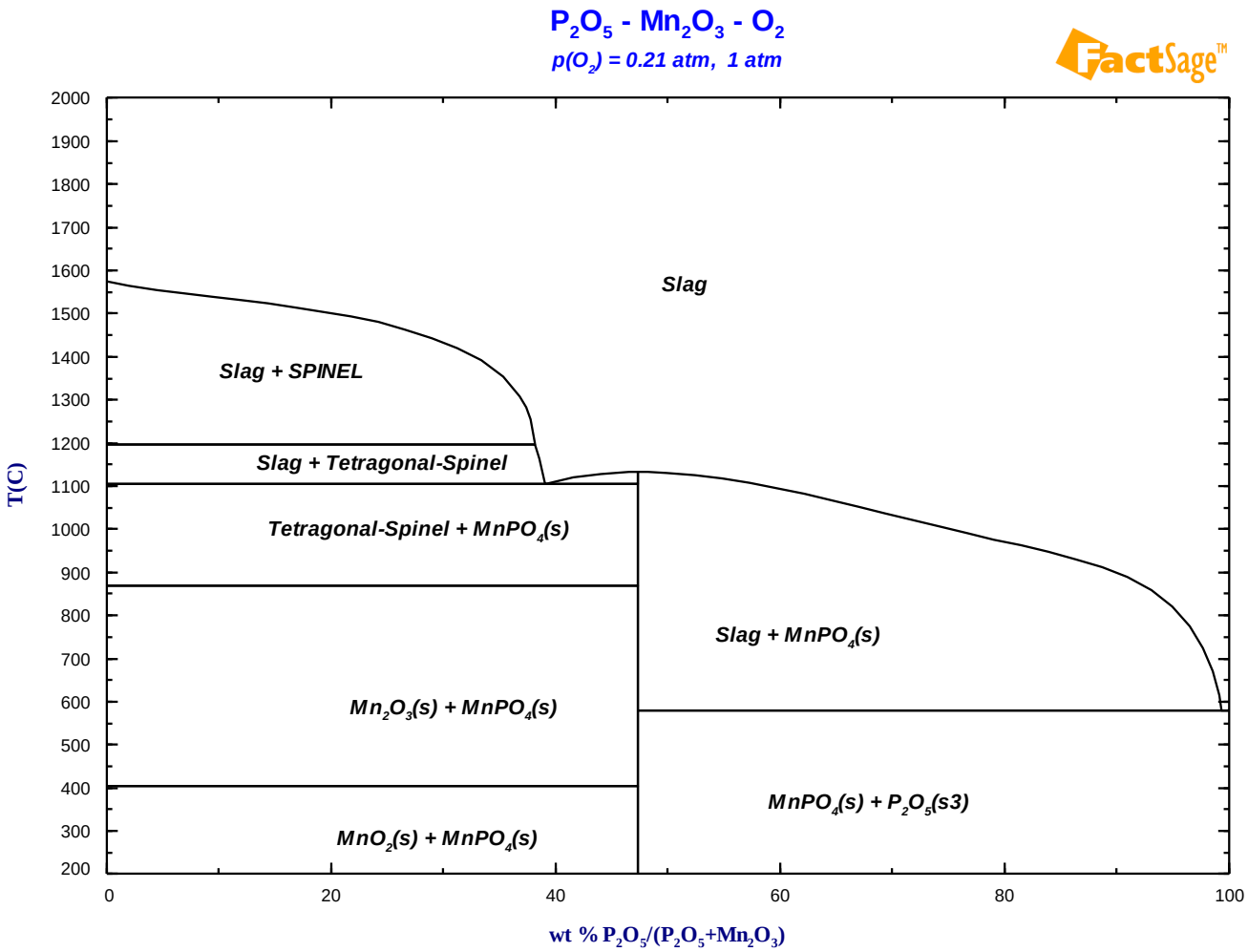

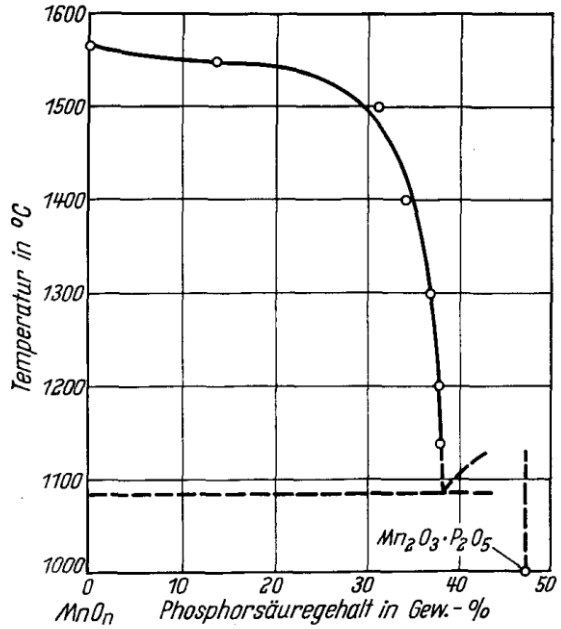

Bild 1. Ausschnitt aus dem Zustandsschaubild MnO_n–P_2O_5 an Luft

W. Fix, H.-E. Wiemer, Das Zustandsschaubild MnO_x-CaO-P_2O_5 an Luft bei Temperaturen von 1510 bis 1610°C, Archiv für das Eisenhüttenwesen, 1969; 40: 215-21.

Mole fraction

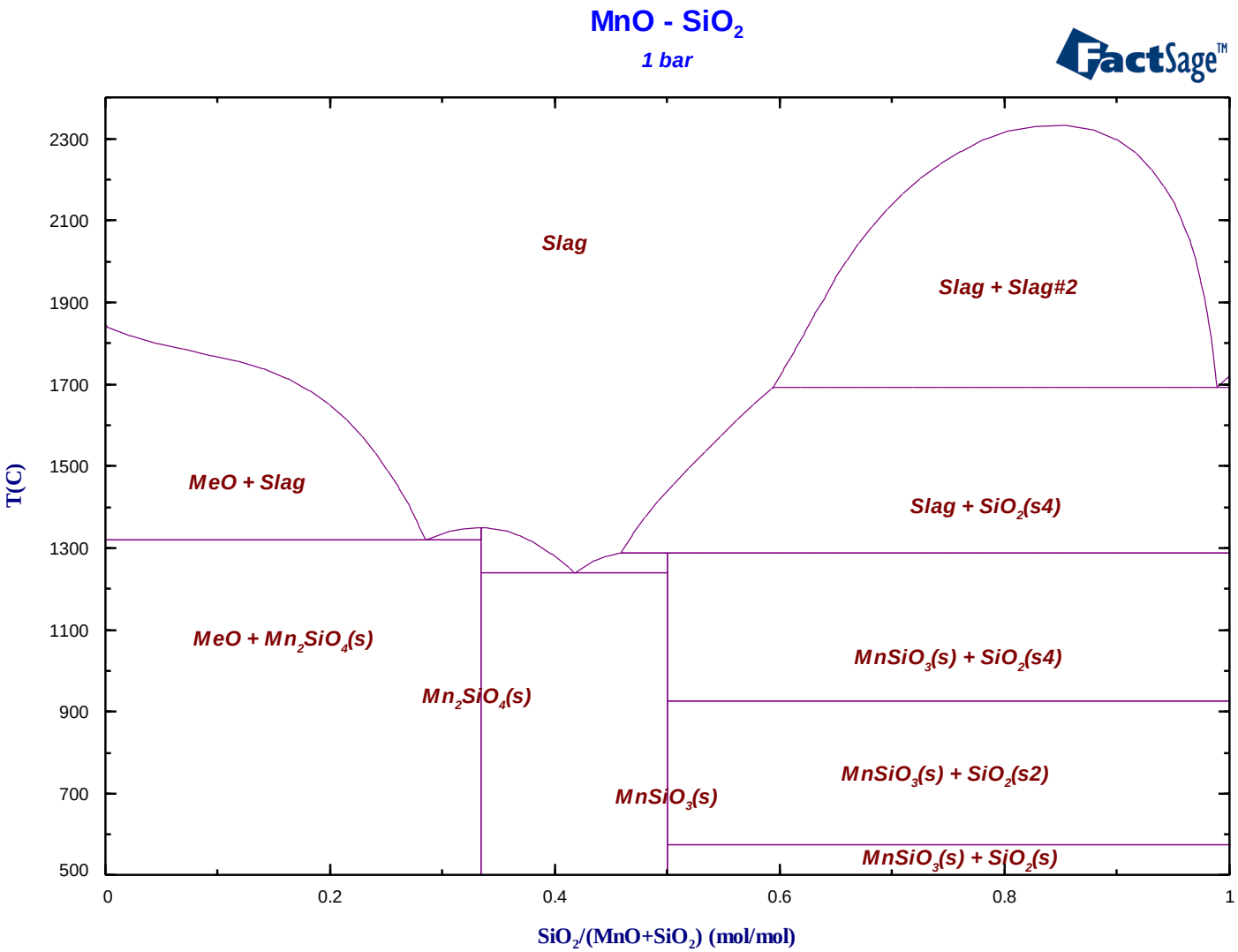

Weight percent compared with experimental data

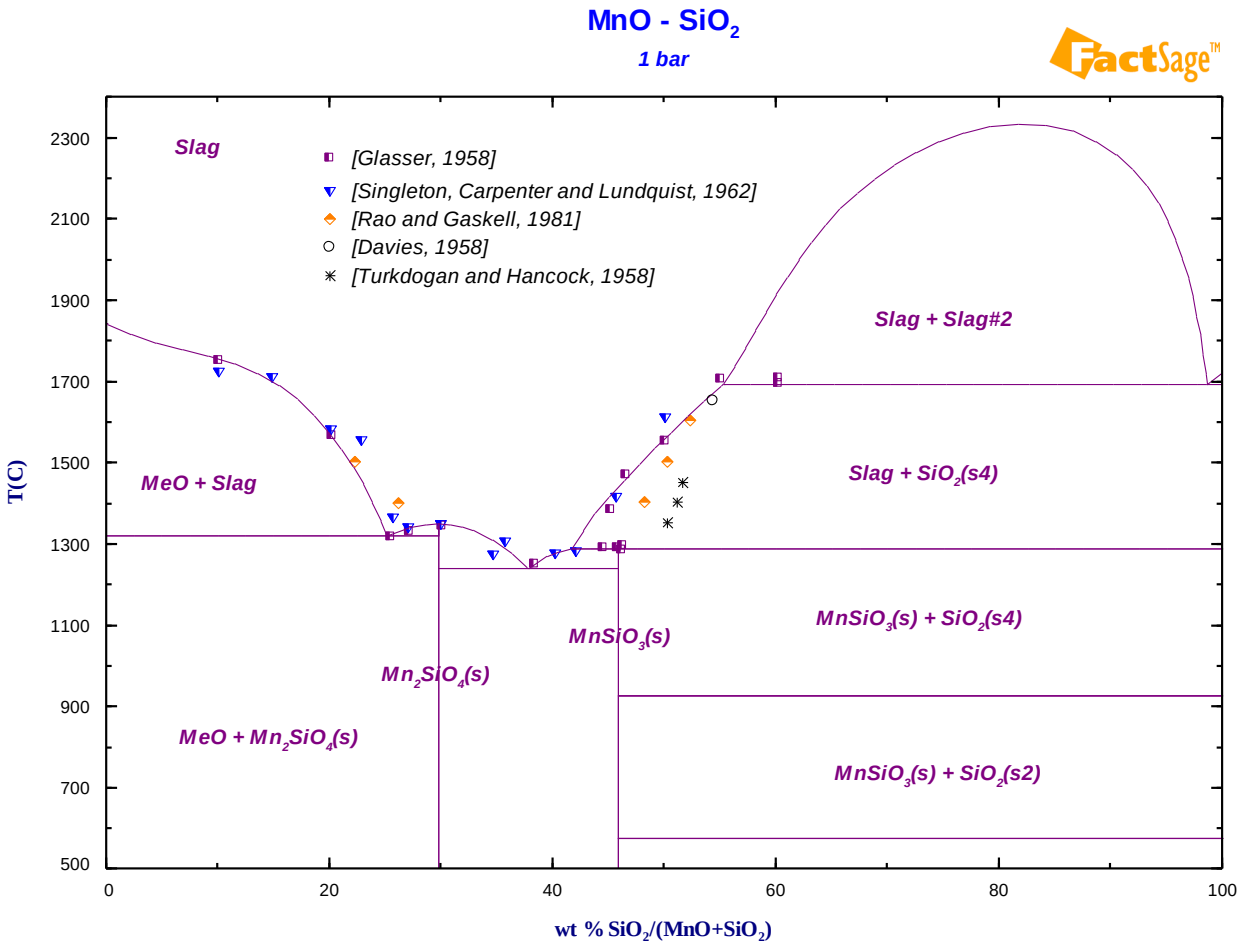

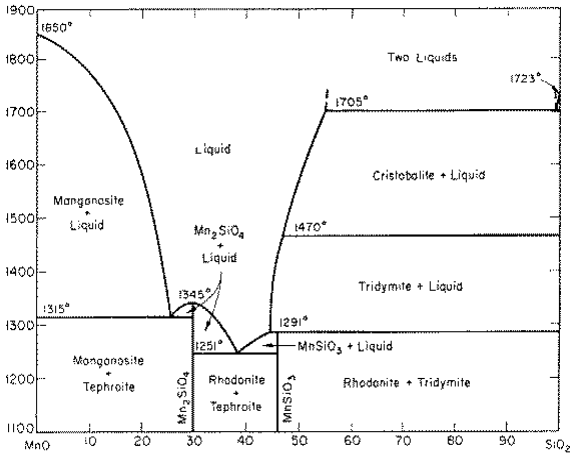

J. White, D.D. Howat, R. Hay, J.R. Tech. Coll. (Glasgow), 3, (1934), pp.231-240.

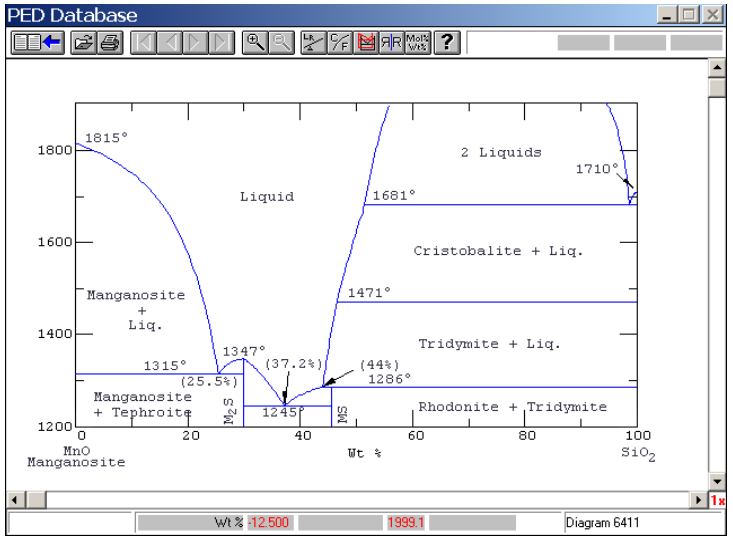

E.L. Singleton, L. Carpenetr, R.V. Lundquist, Rep. Invest.-U.S., Bur. Mines., No. 5938, (1962), pp. 1-31.

Mole fraction compared with experimental data

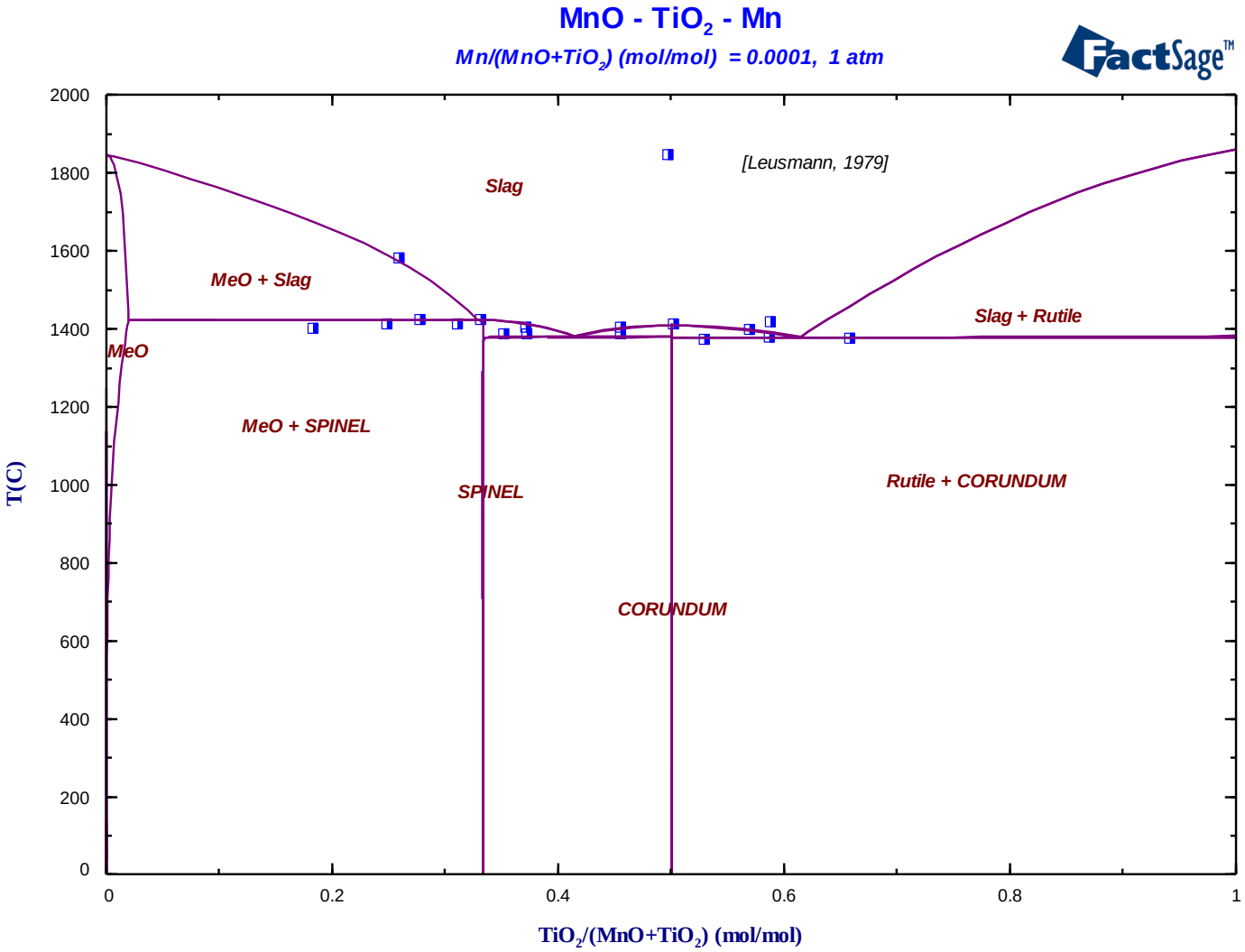

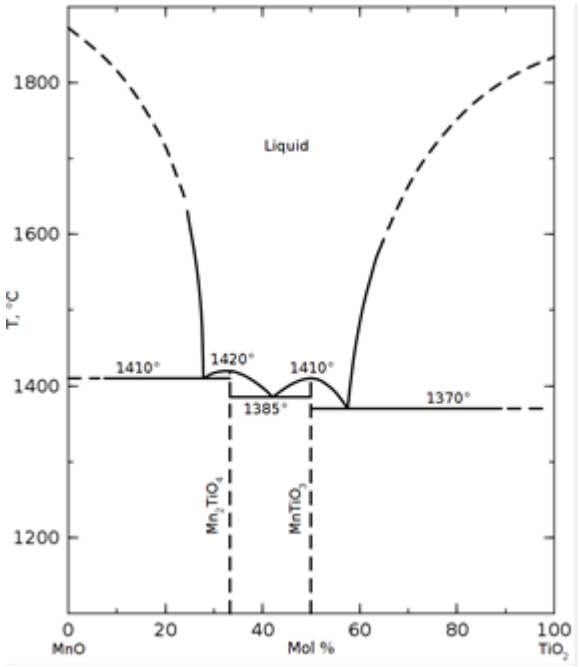

D. Leusmann, Neues Jahrb. Mineral., Monatsh., No. 6, 262-266 (1979).

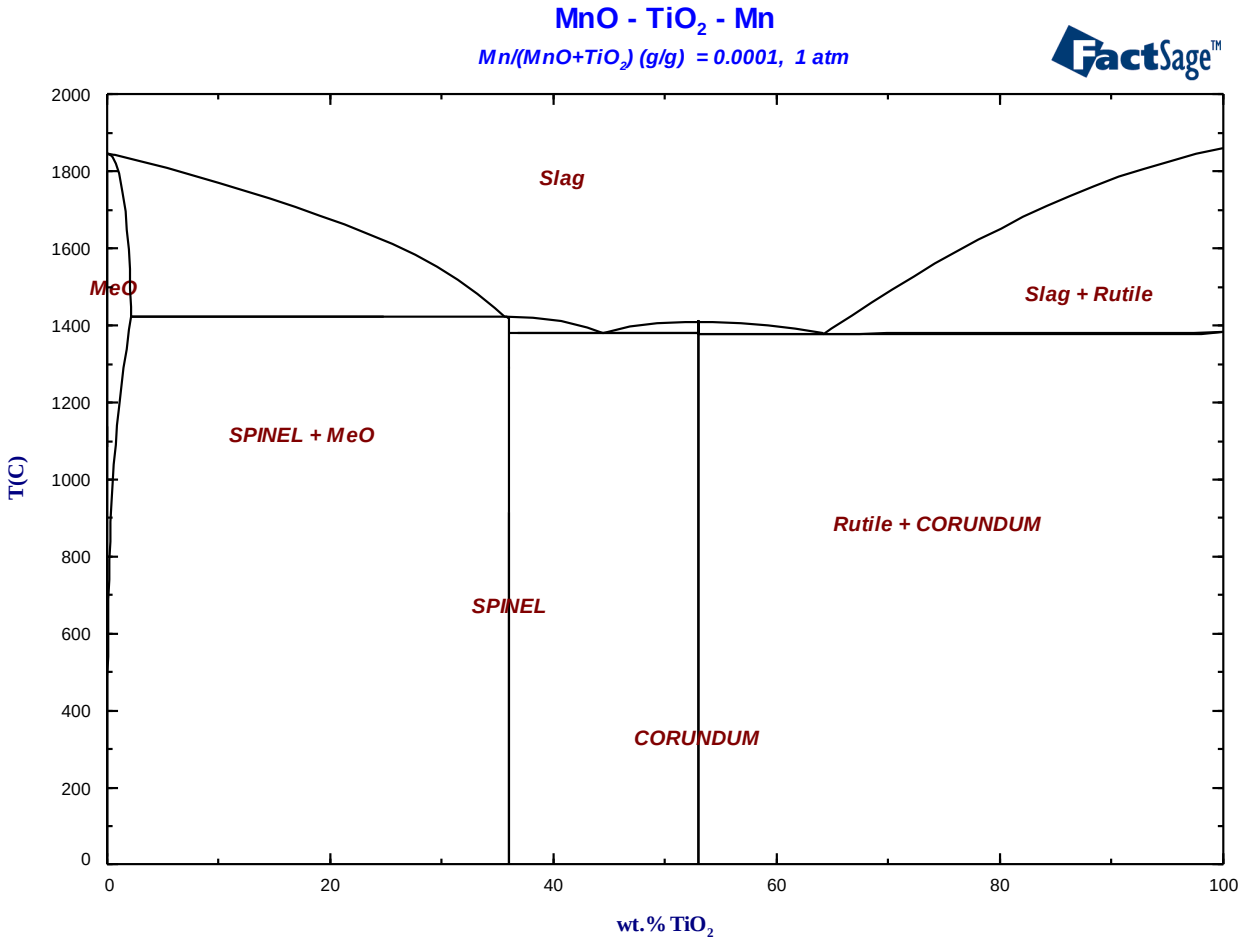
MnO - TiO2 - Mn
Mn/(MnO+TiO2) (g/g) = 0.0001, 1 atm
FactSage™
Slag
MeO
Slag + Rutile
SPINEL + MeO
Rutile + CORUNDUM
SPINEL
CORUNDUM
T(C)
wt.% TiO2
2000
1800
1600
1400
1200
1000
800
600
400
200
0
0
20
40
60
80
100

Mole fraction, P(CO)/P(CO2)=1, compared with experimental data

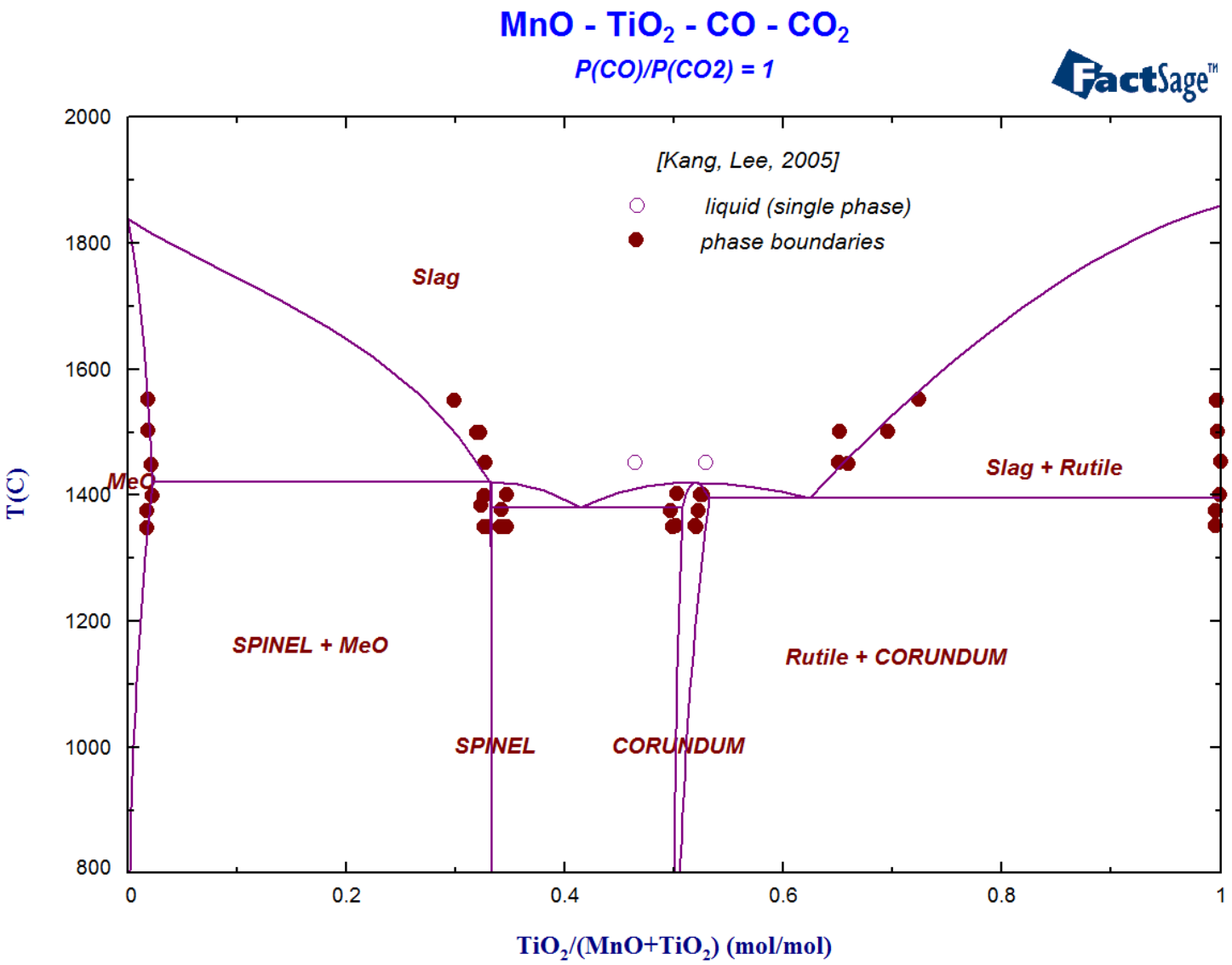

Mole fraction,

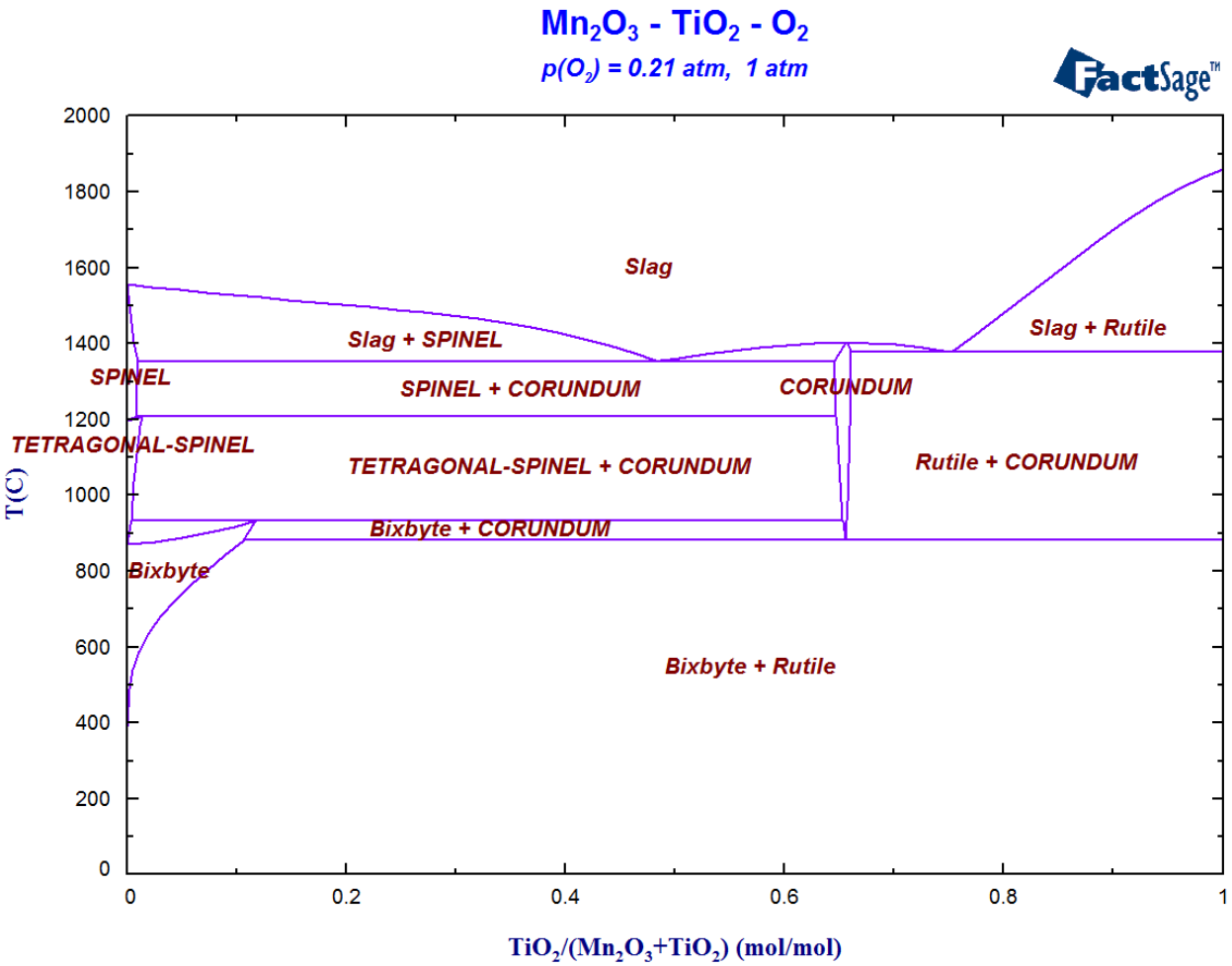

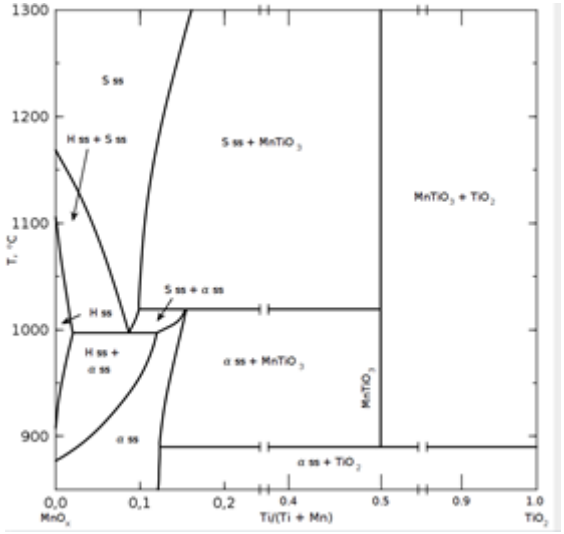

G. I. Chufarov, A. M. Yankin, V. P. Demin, Yu. V. Golikov, and V. F. Balakirev, Zh. Fiz. Khim., 60 [4] 863-866 (1986).

Weight percent,

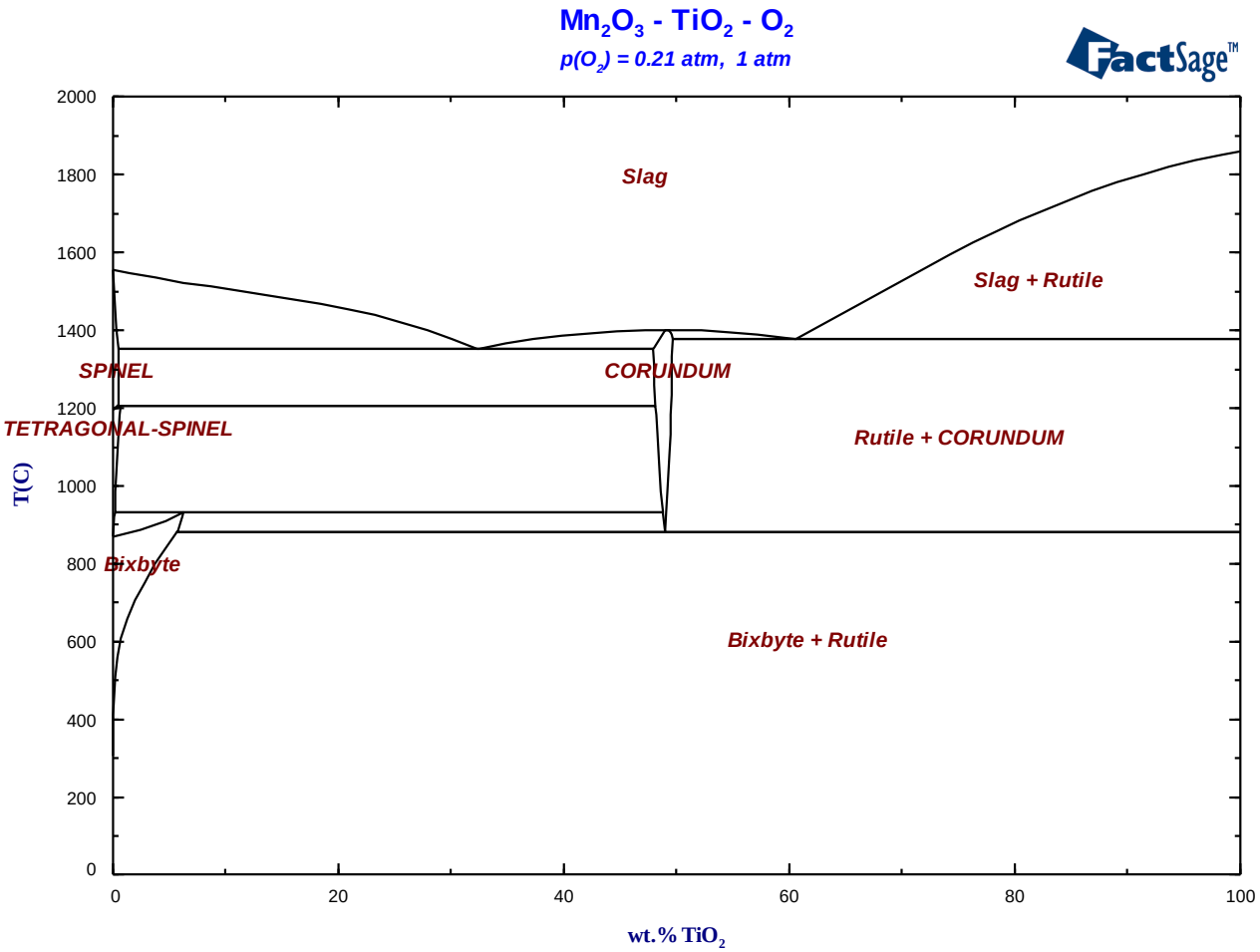

Mole fraction

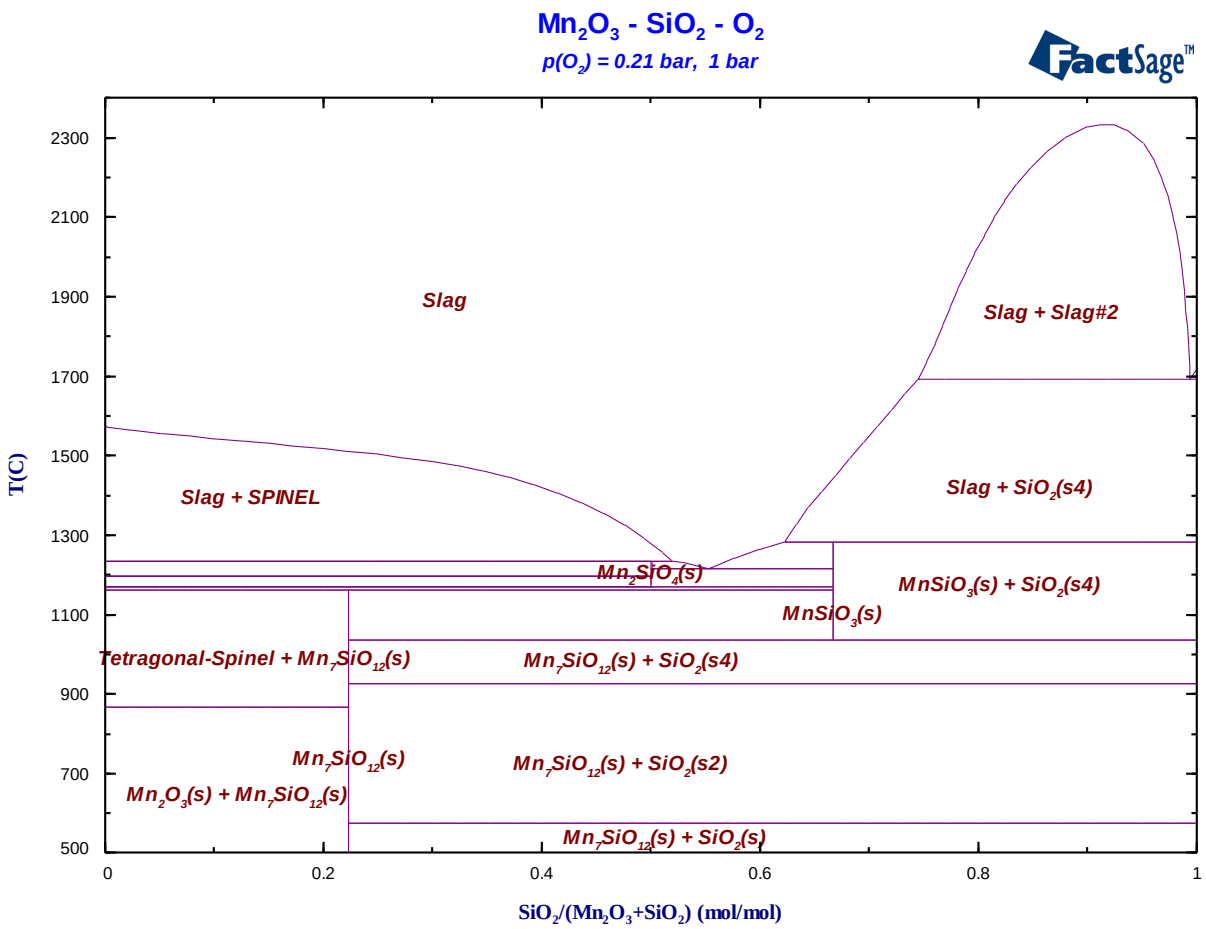

Weight percent compared with experimental data

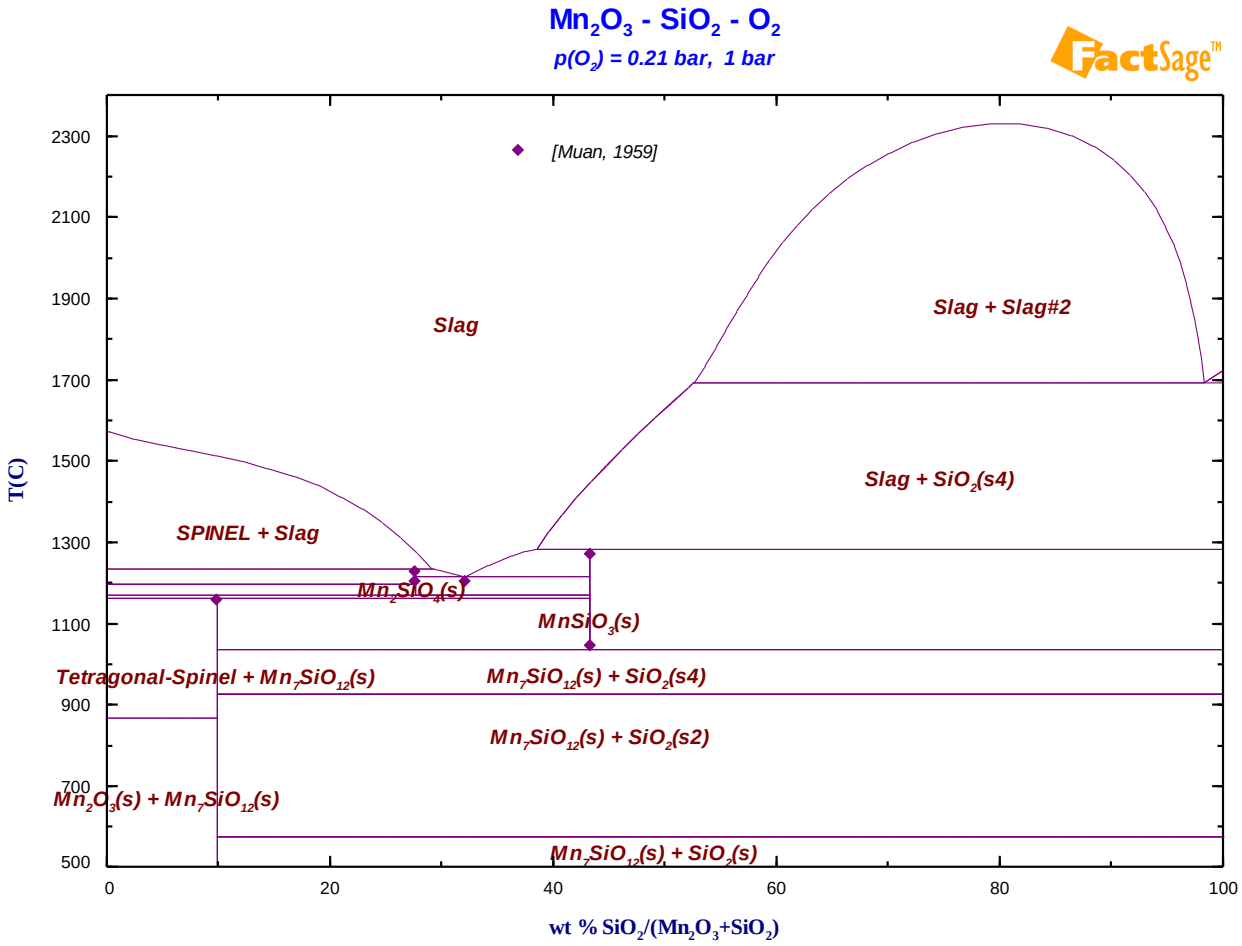

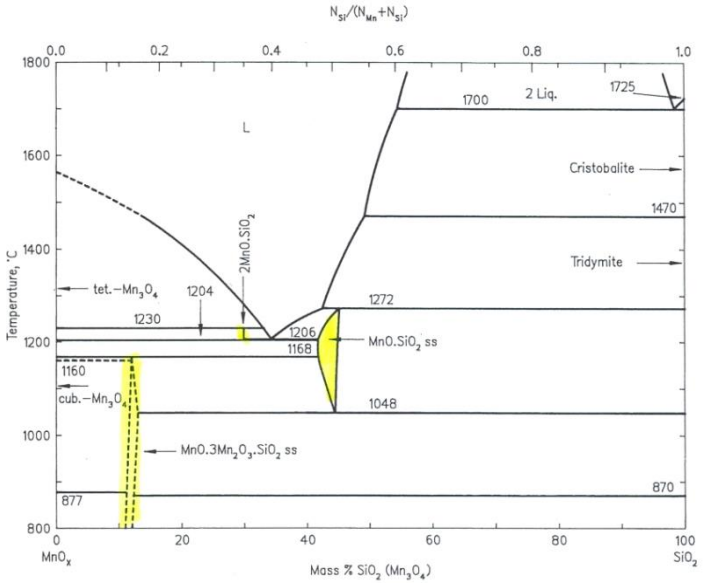

A. Muan, Am. J. Sci., 257 [4], (1959), pp. 297-315.

MnO-V2O5-Mn
Mole fraction
compared with experimental data

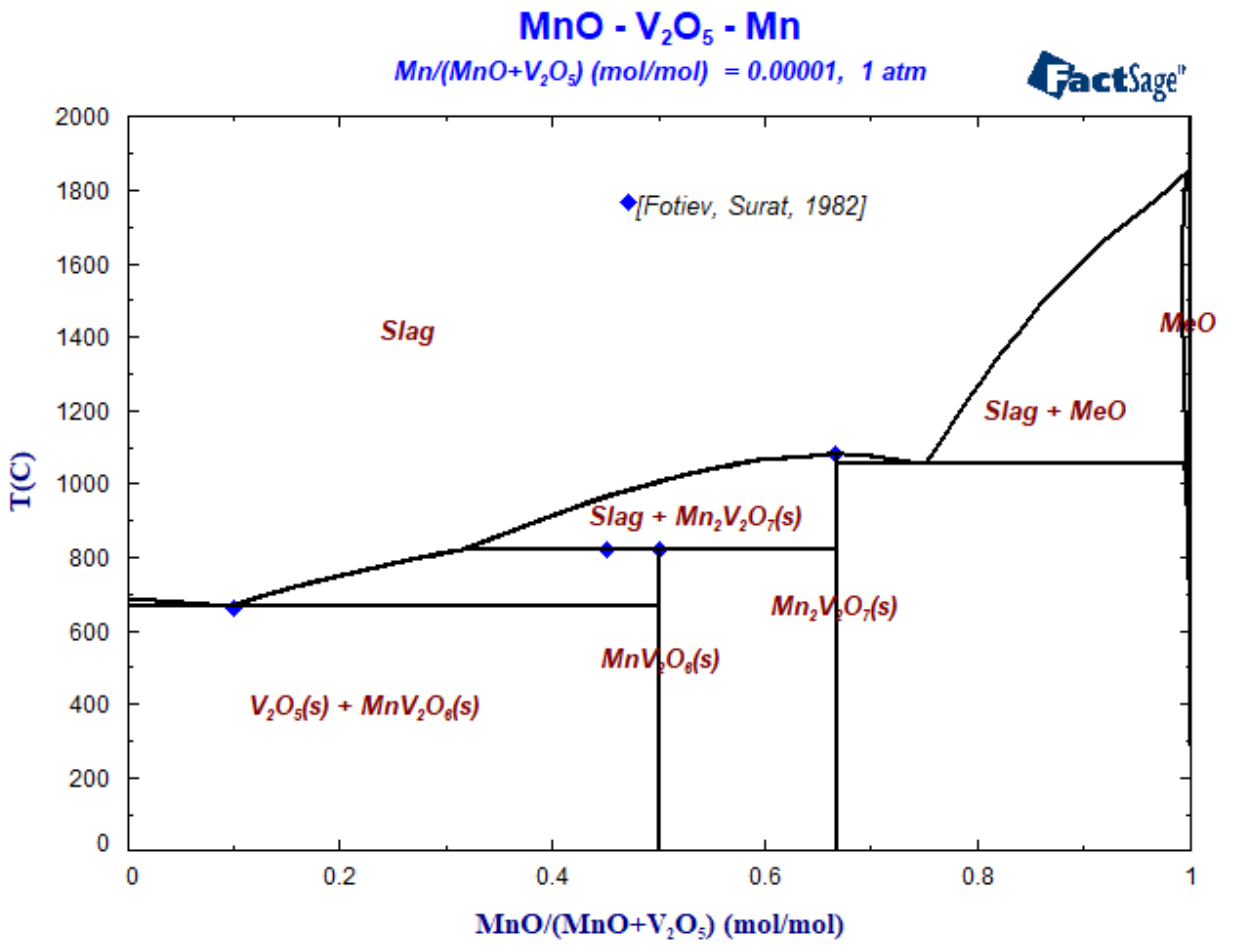

MnO-V2O5-Mn
Weight percent

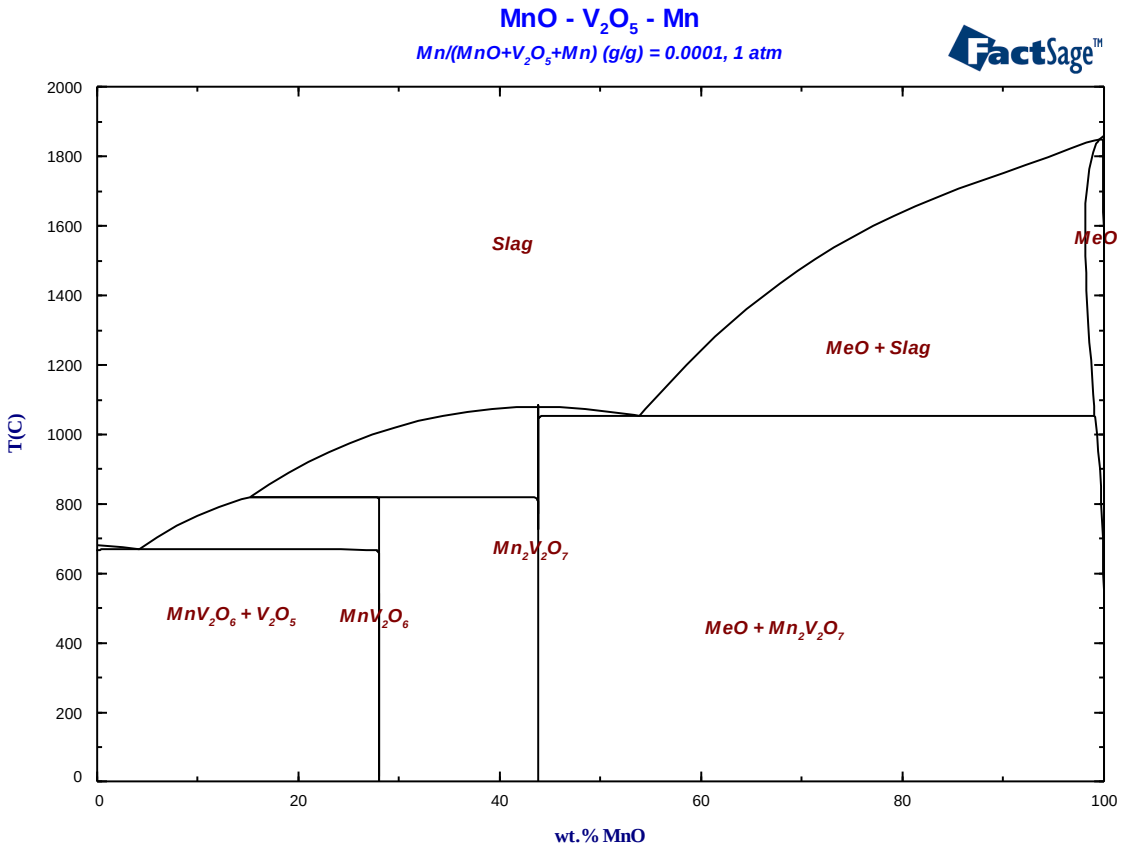

MnO-V2O3, CO/CO2=1

Mole fraction compared with experimental data

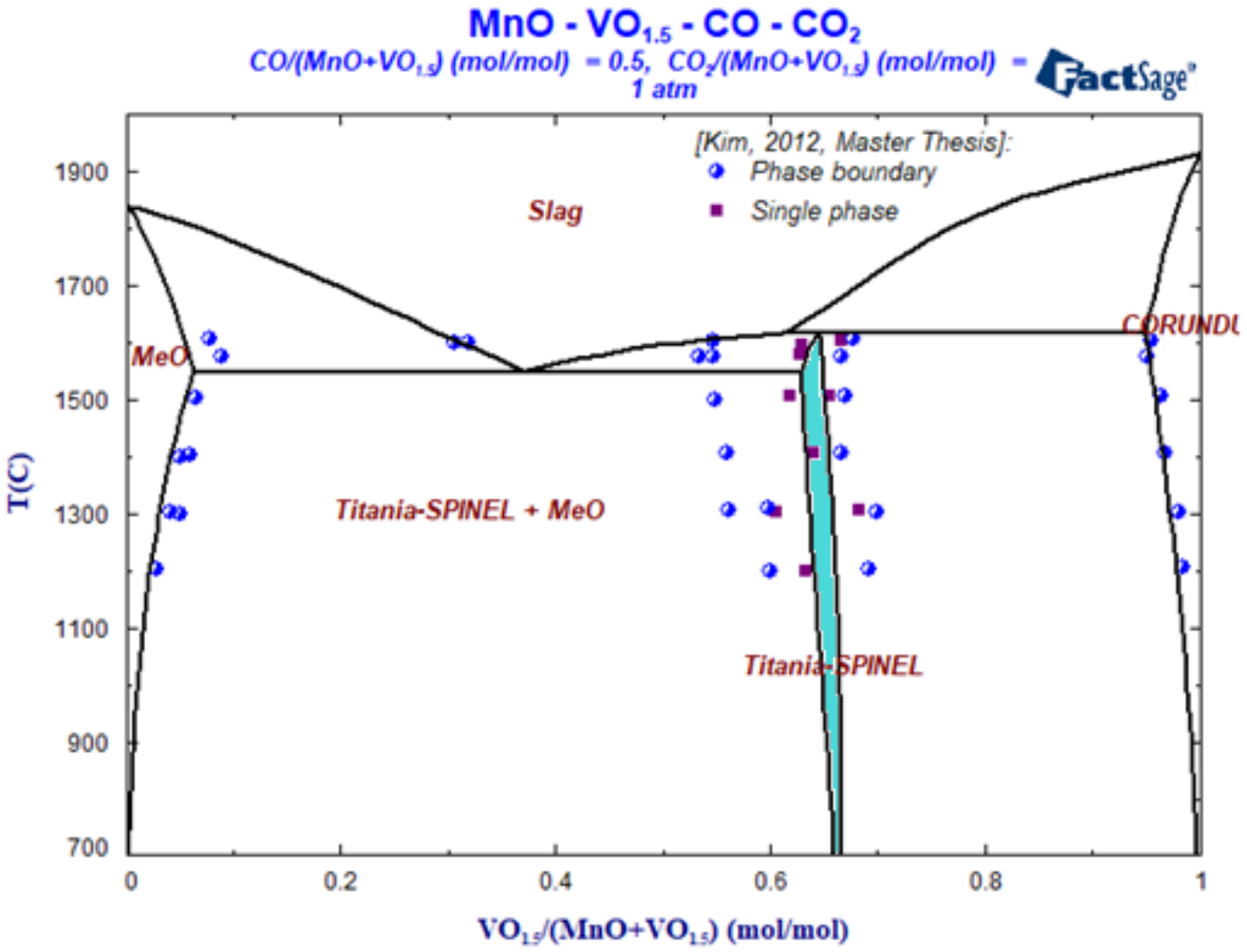

Mole fraction
compared with experimental data

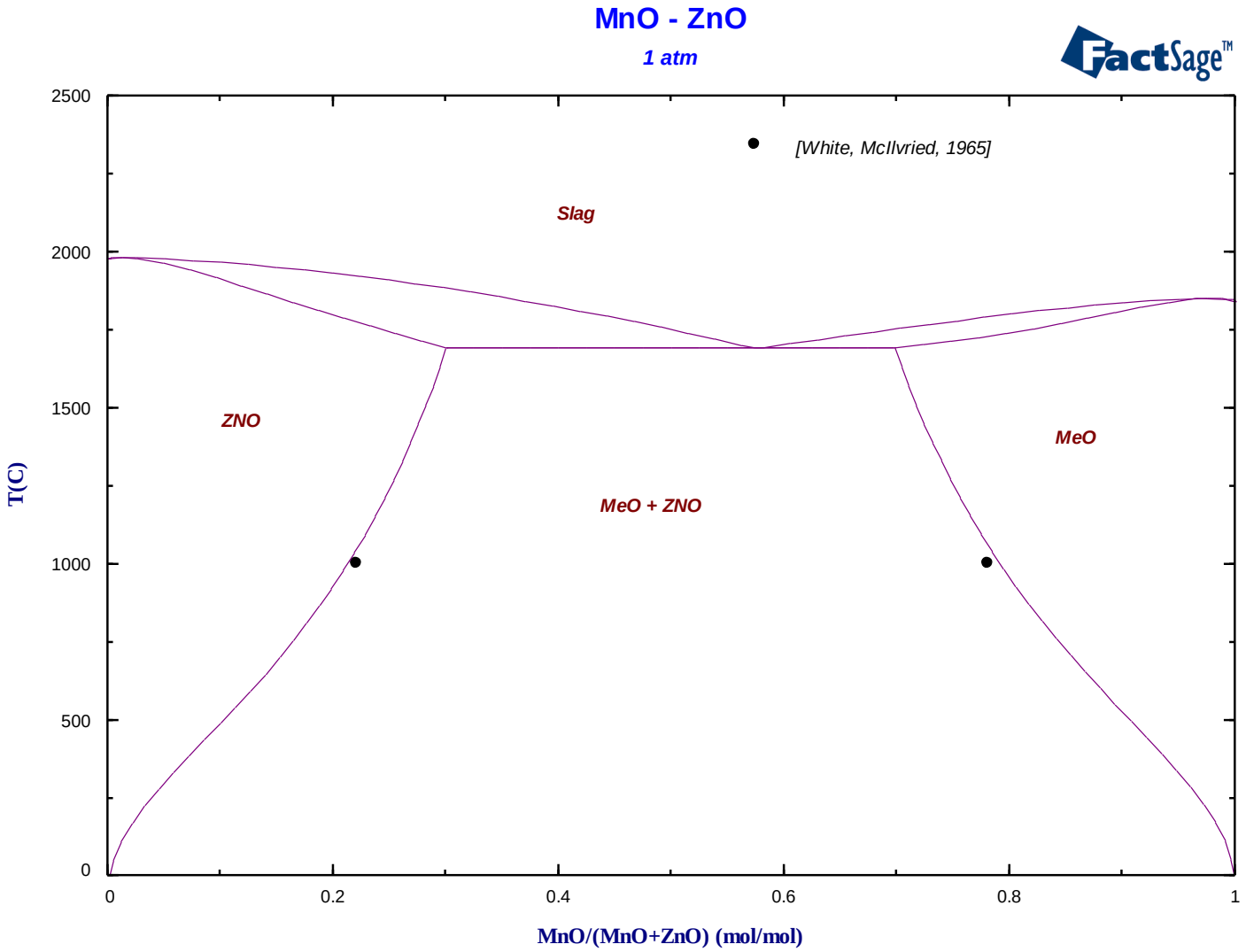

Weight percent

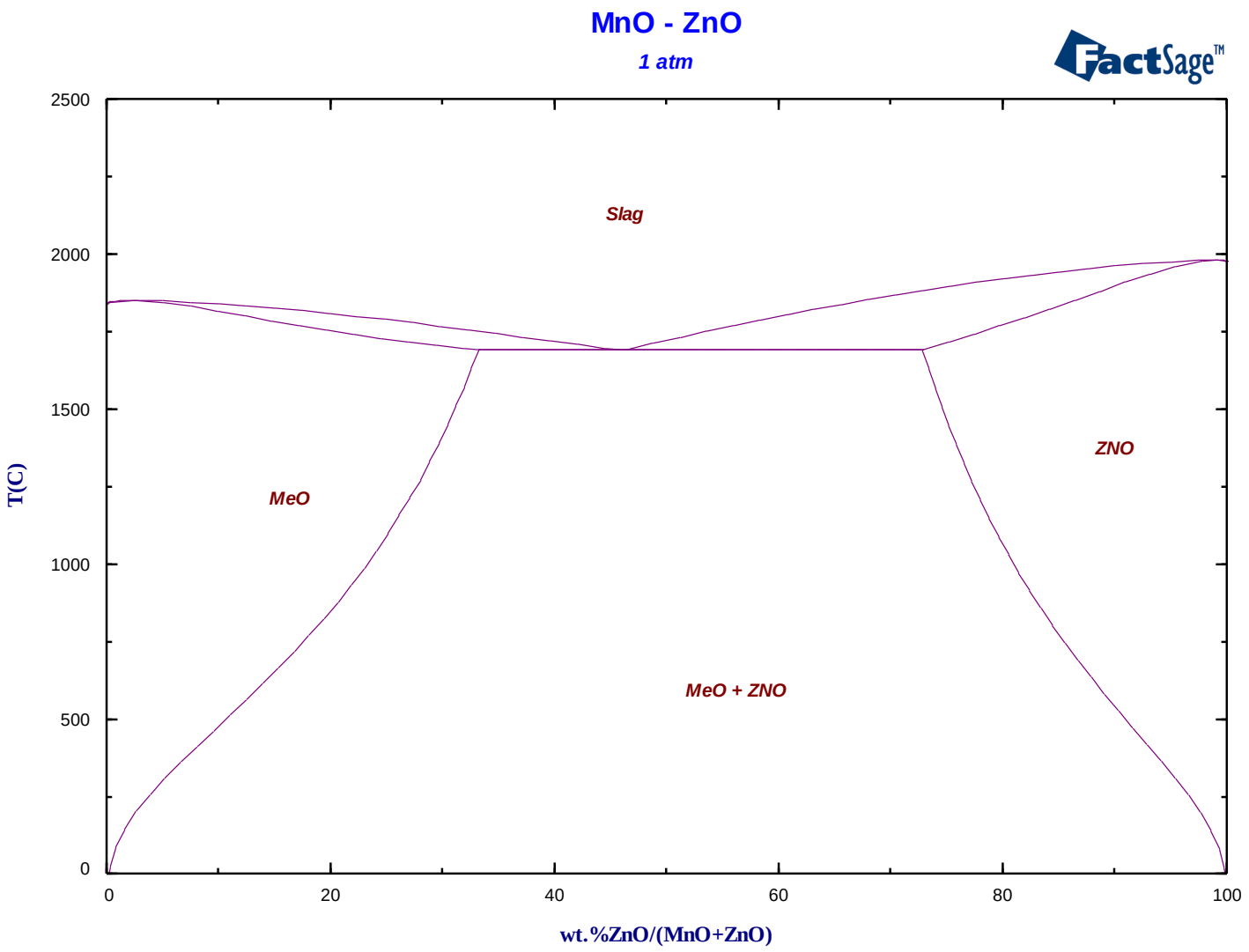

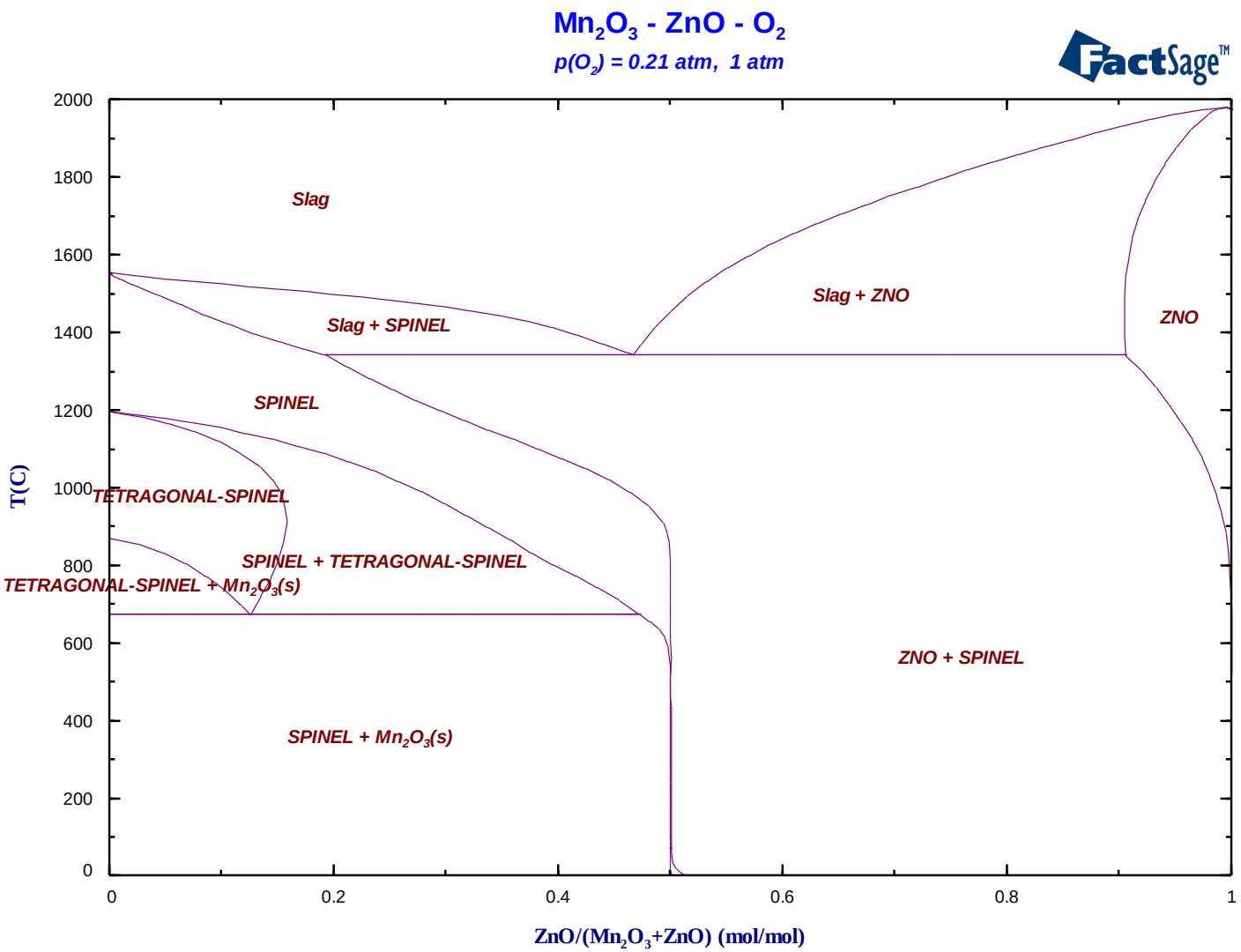
Mn2O3 - ZnO - O2
p(O2) = 0.21 atm, 1 atm
FactSage™
Slag
Slag + SPINEL
Slag + ZNO
ZNO
SPINEL
TETRAGONAL-SPINEL
SPINEL + TETRAGONAL-SPINEL
TETRAGONAL-SPINEL + Mn2O3(s)
ZNO + SPINEL
SPINEL + Mn2O3(s)
T(C)
2000
1800
1600
1400
1200
1000
800
600
400
200
0
0
0.2
0.4
0.6
0.8
1
ZnO/(Mn2O3+ZnO) (mol/mol)

Weight percent

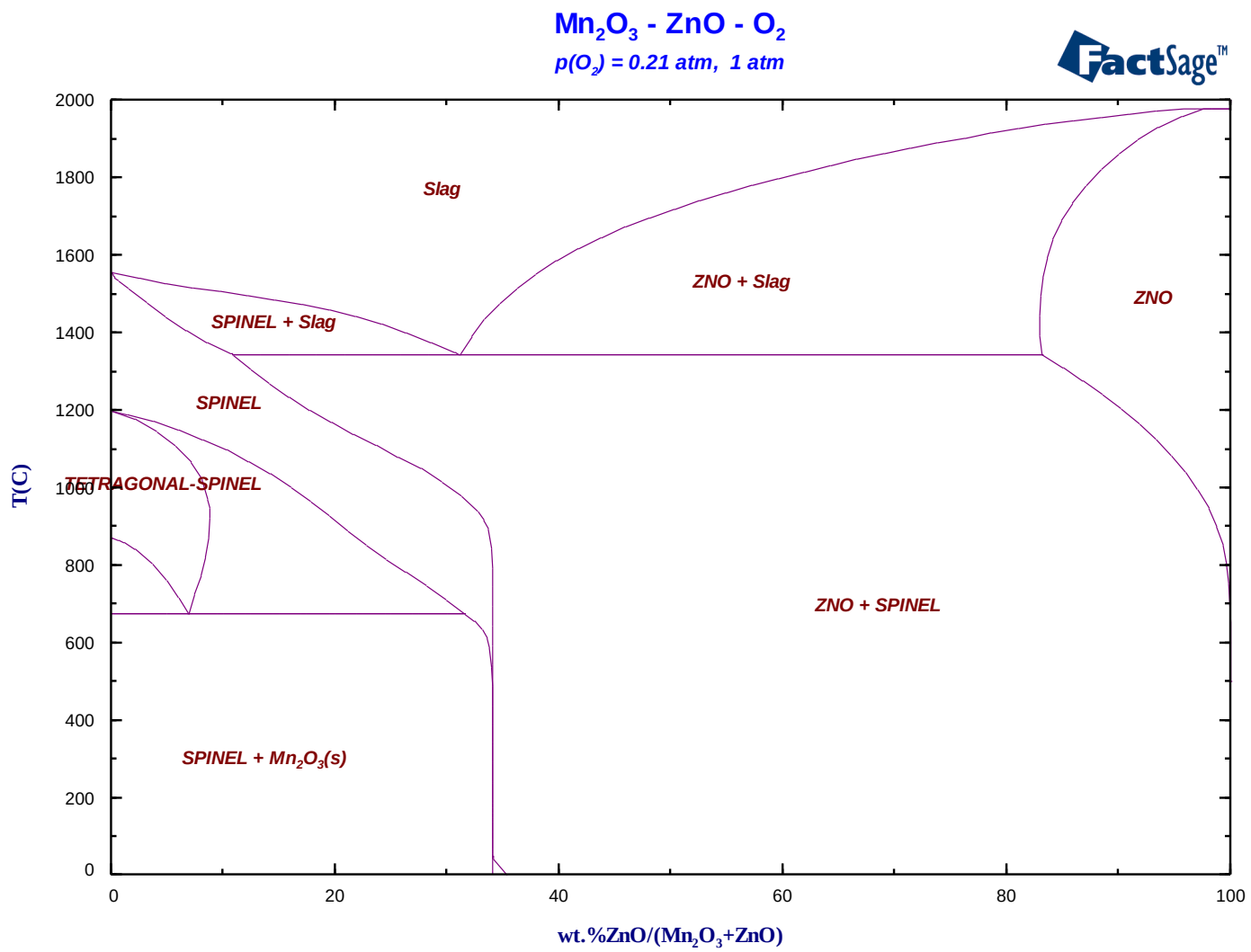

Mole fraction

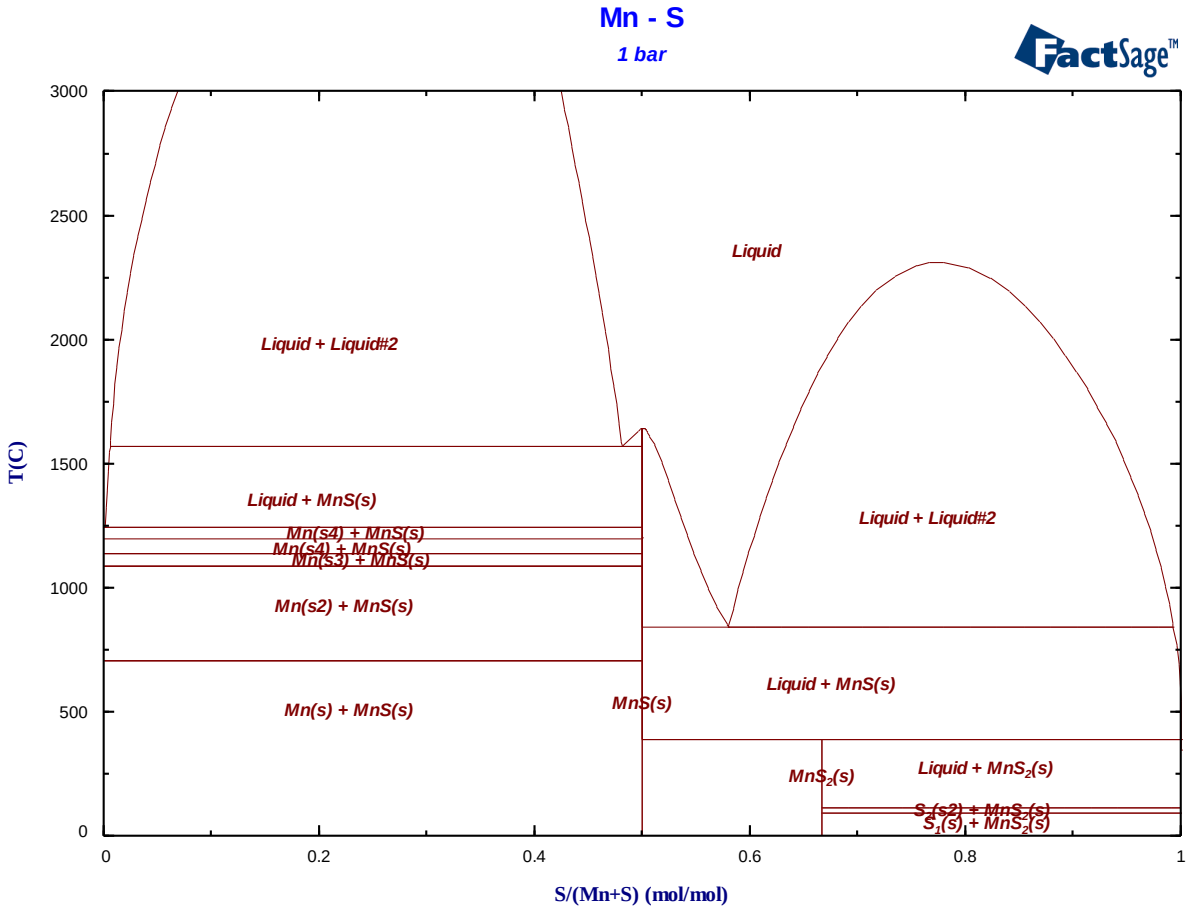

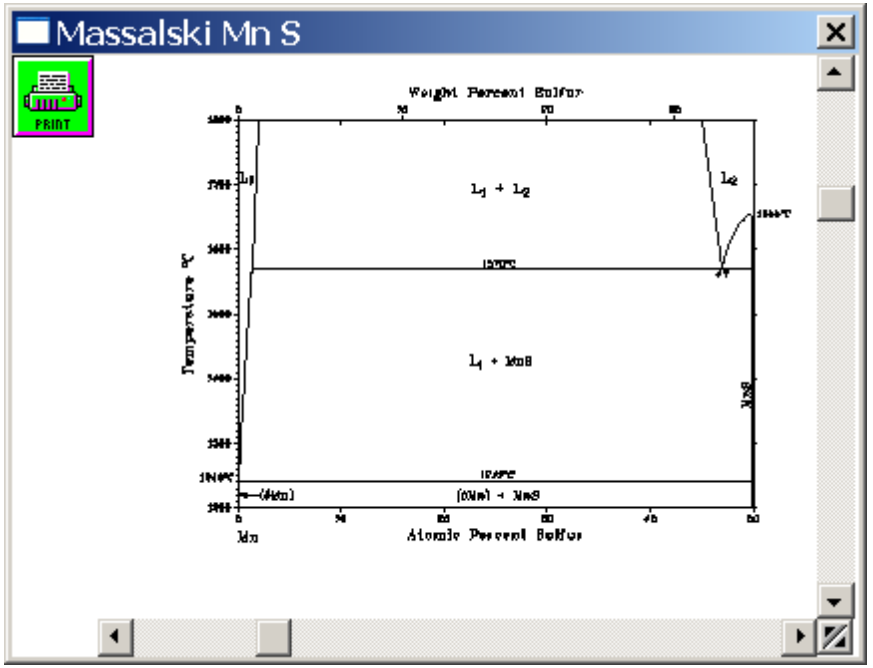

Weight percent

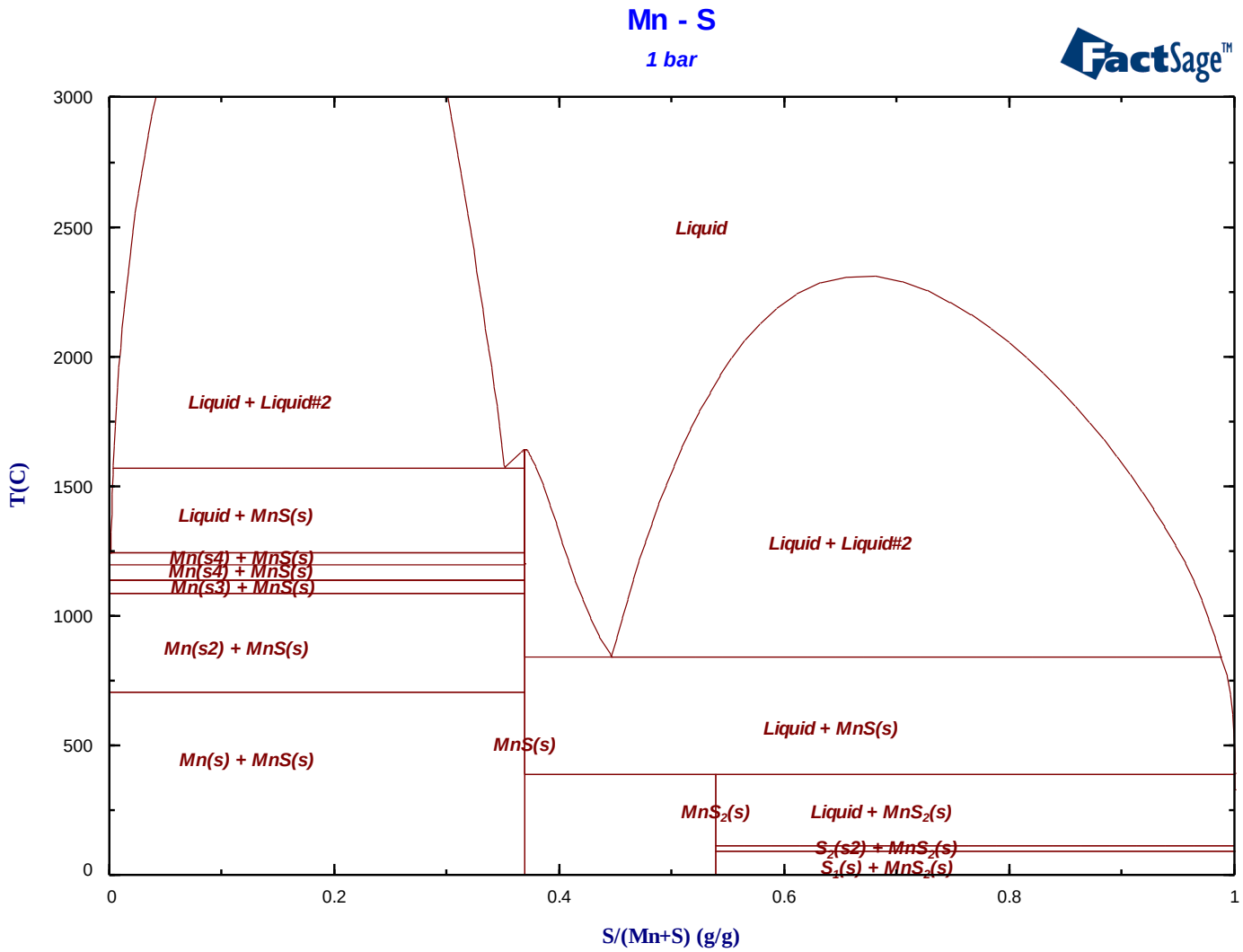

Mole fraction

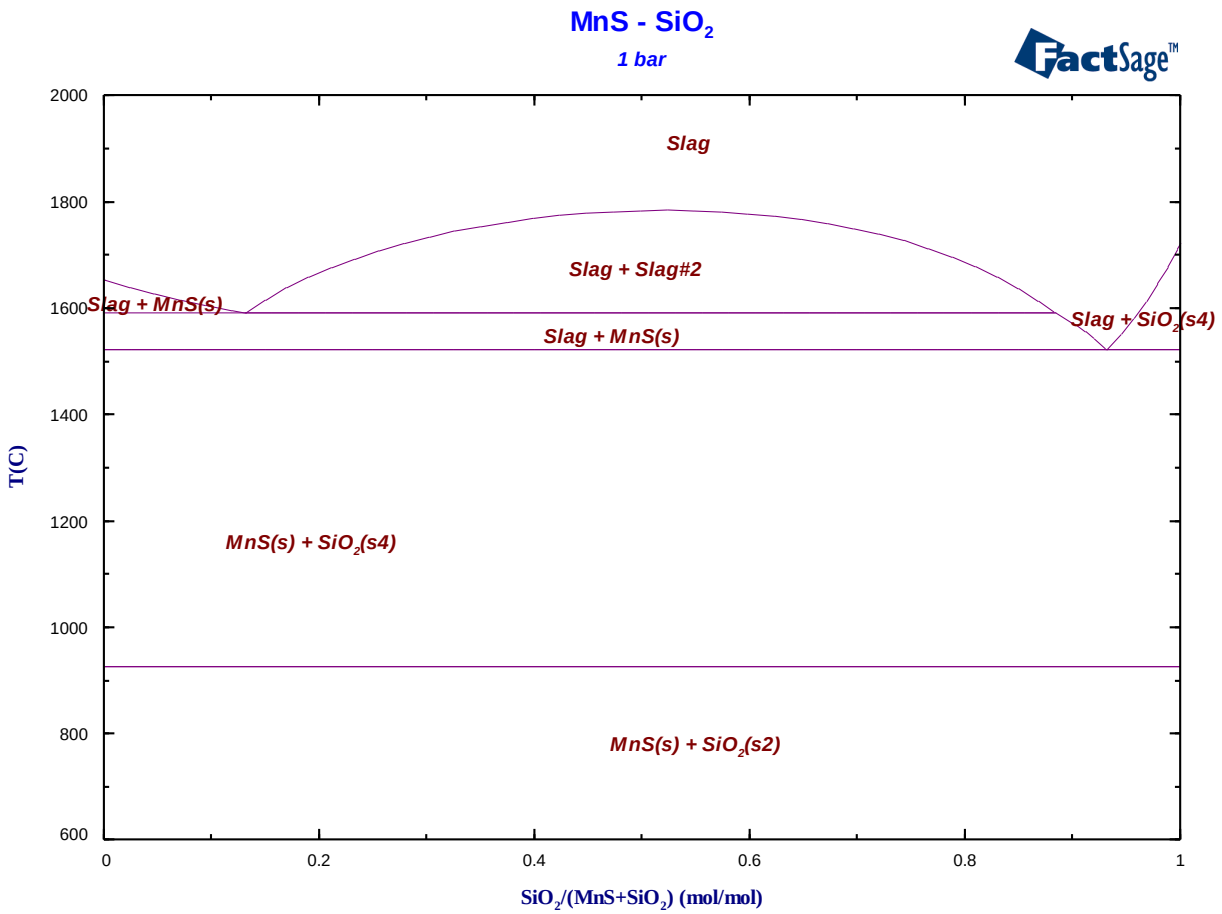

Weight percent

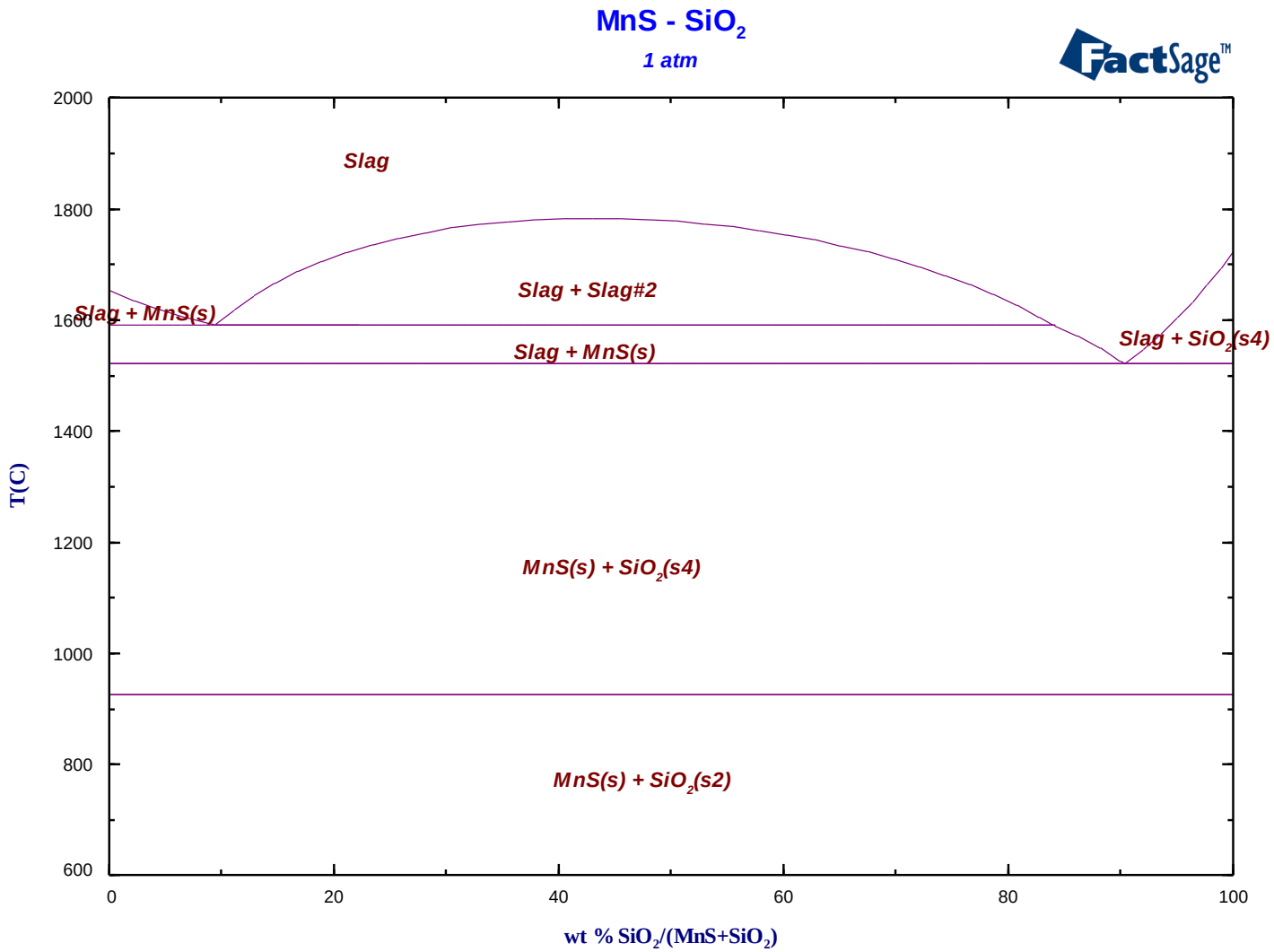

Mole fraction
compared with experimental data

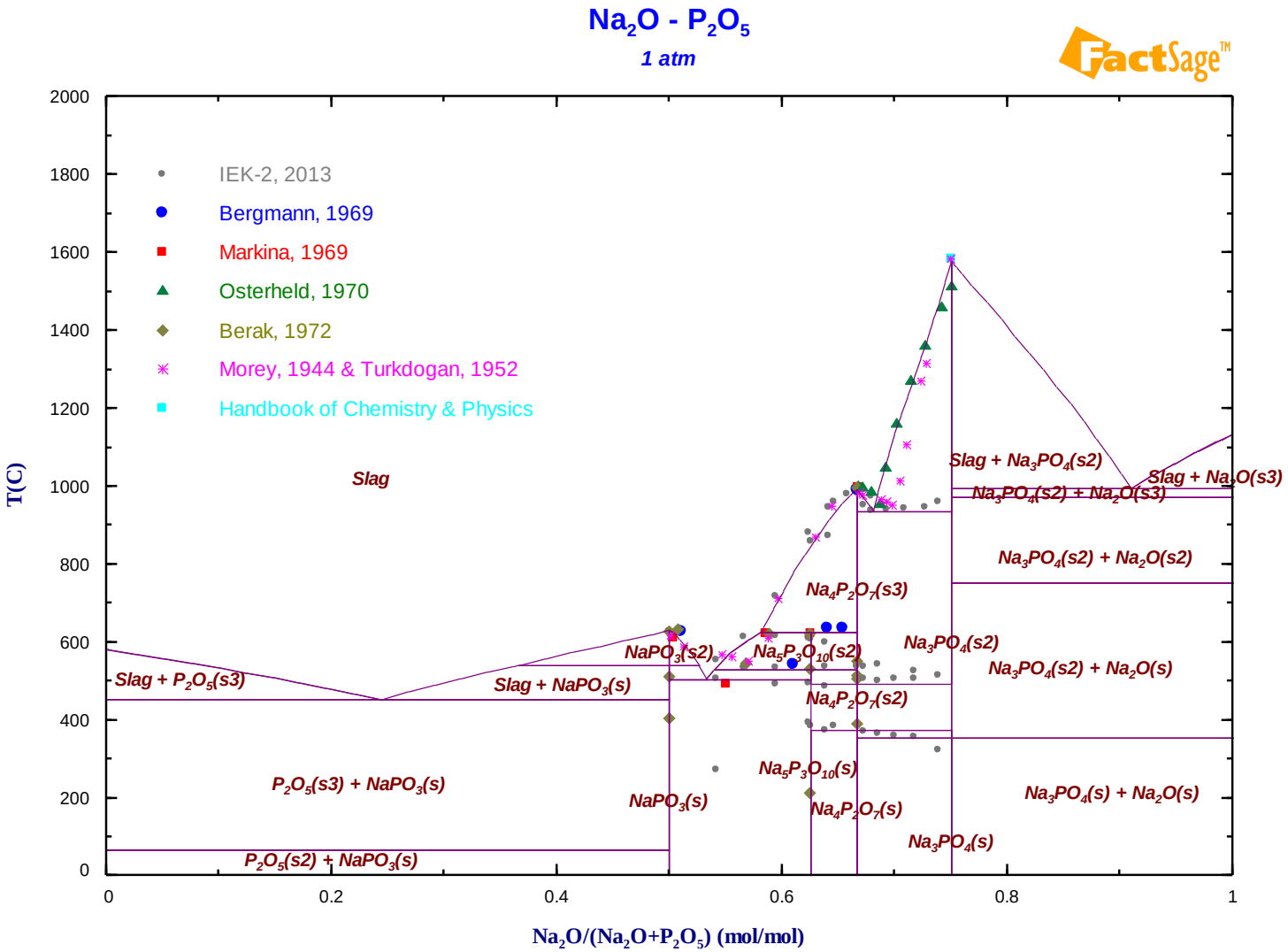

Weight percent

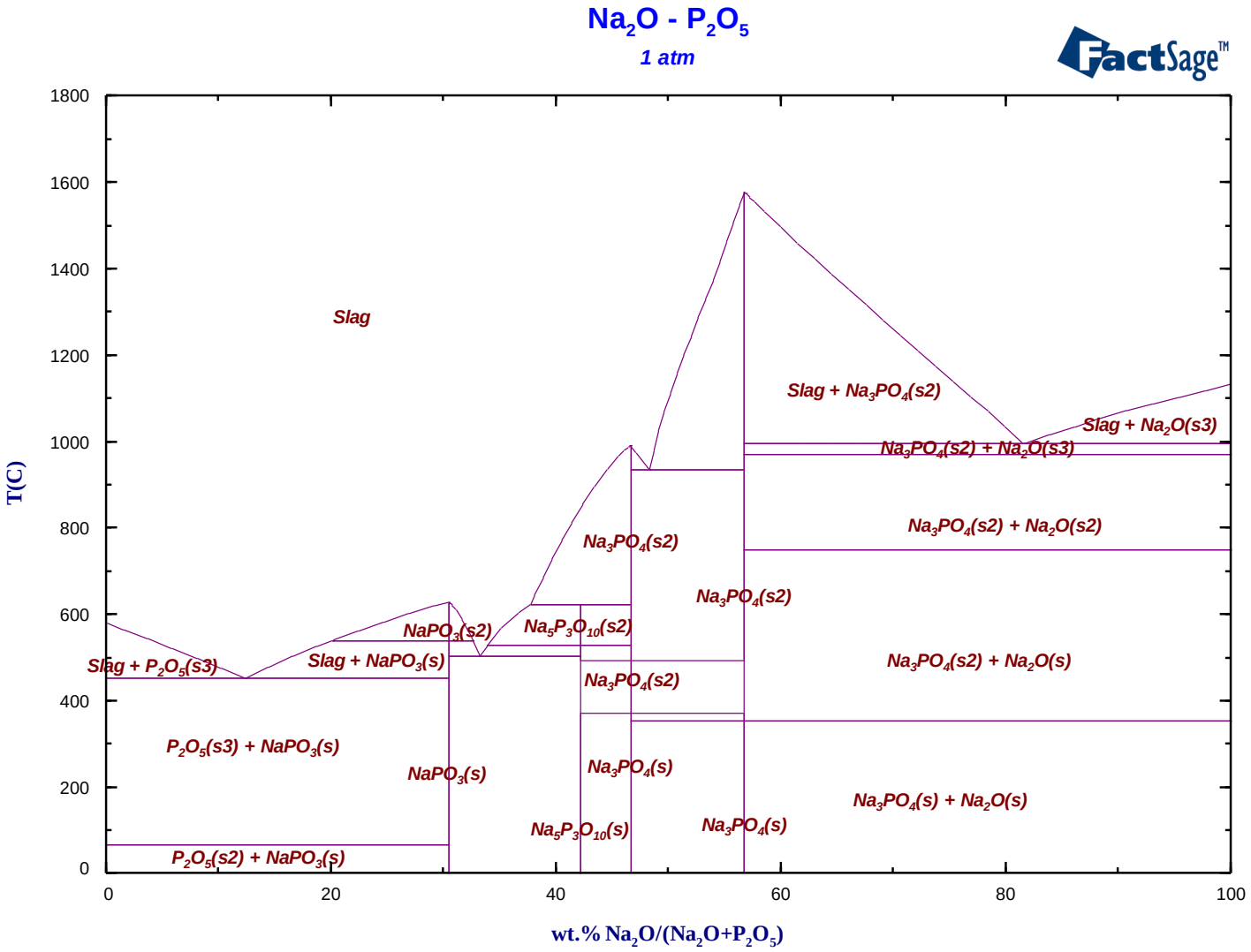

Mole fraction
compared with experimental data

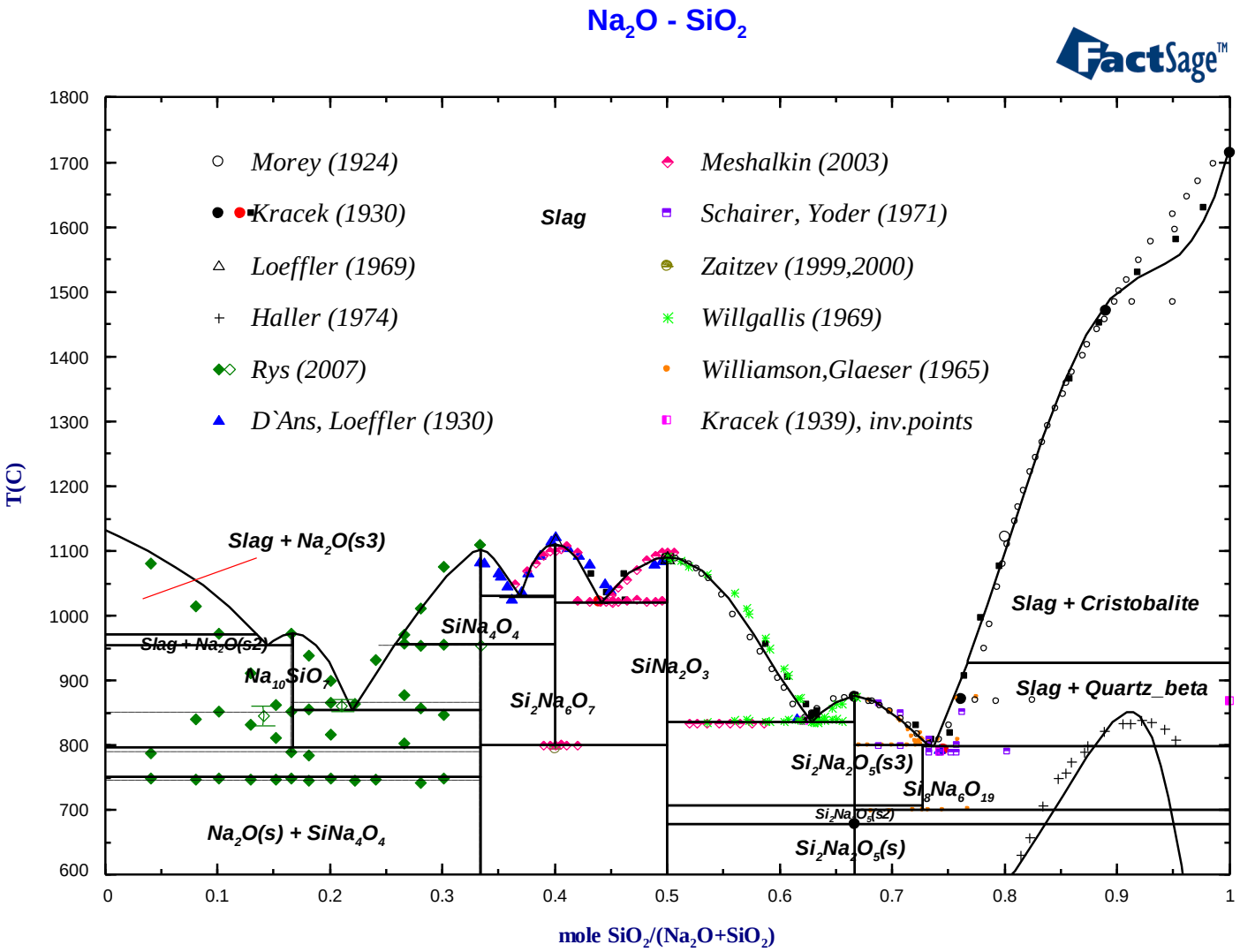

Weight percent

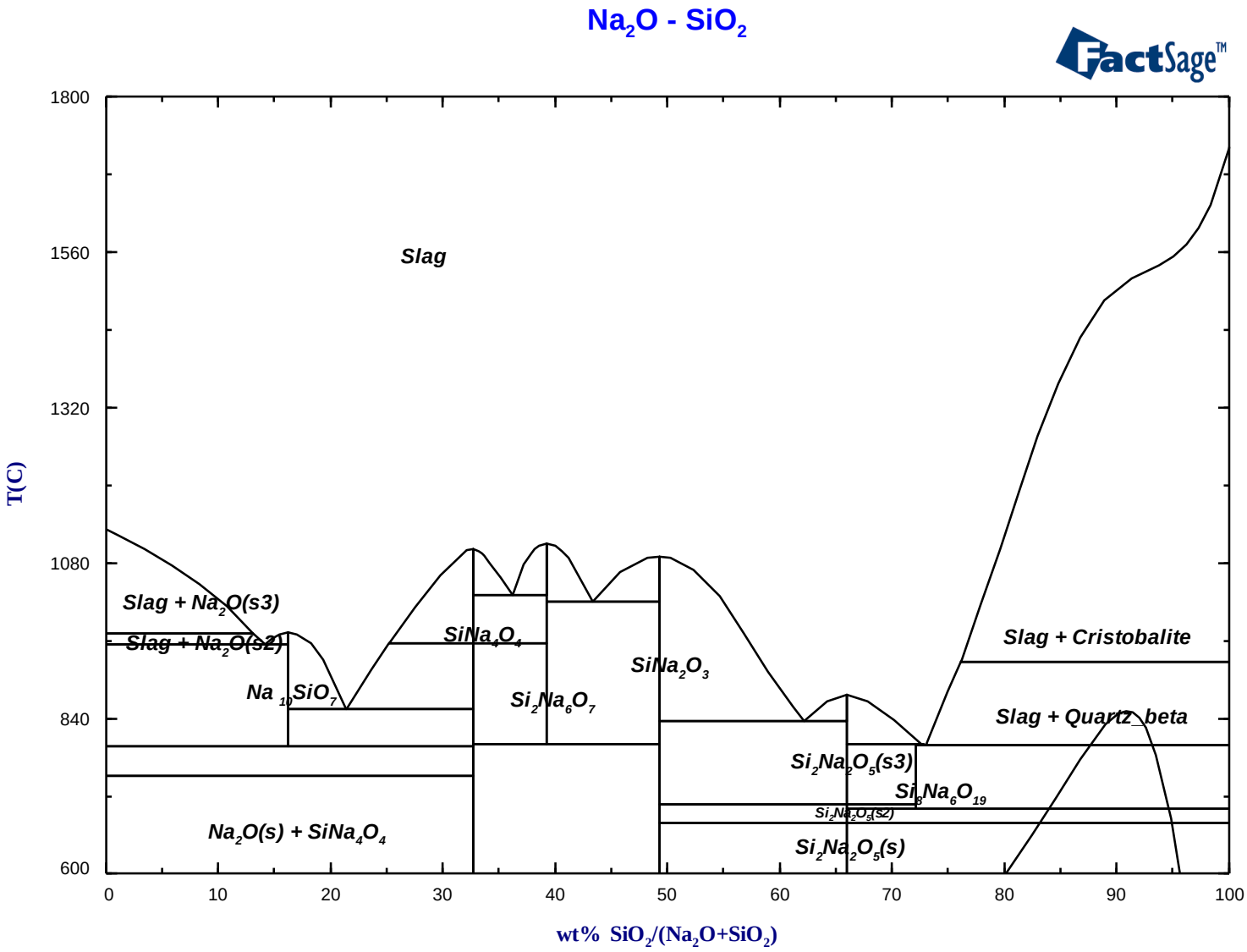

Mole fraction
compared with experimental data

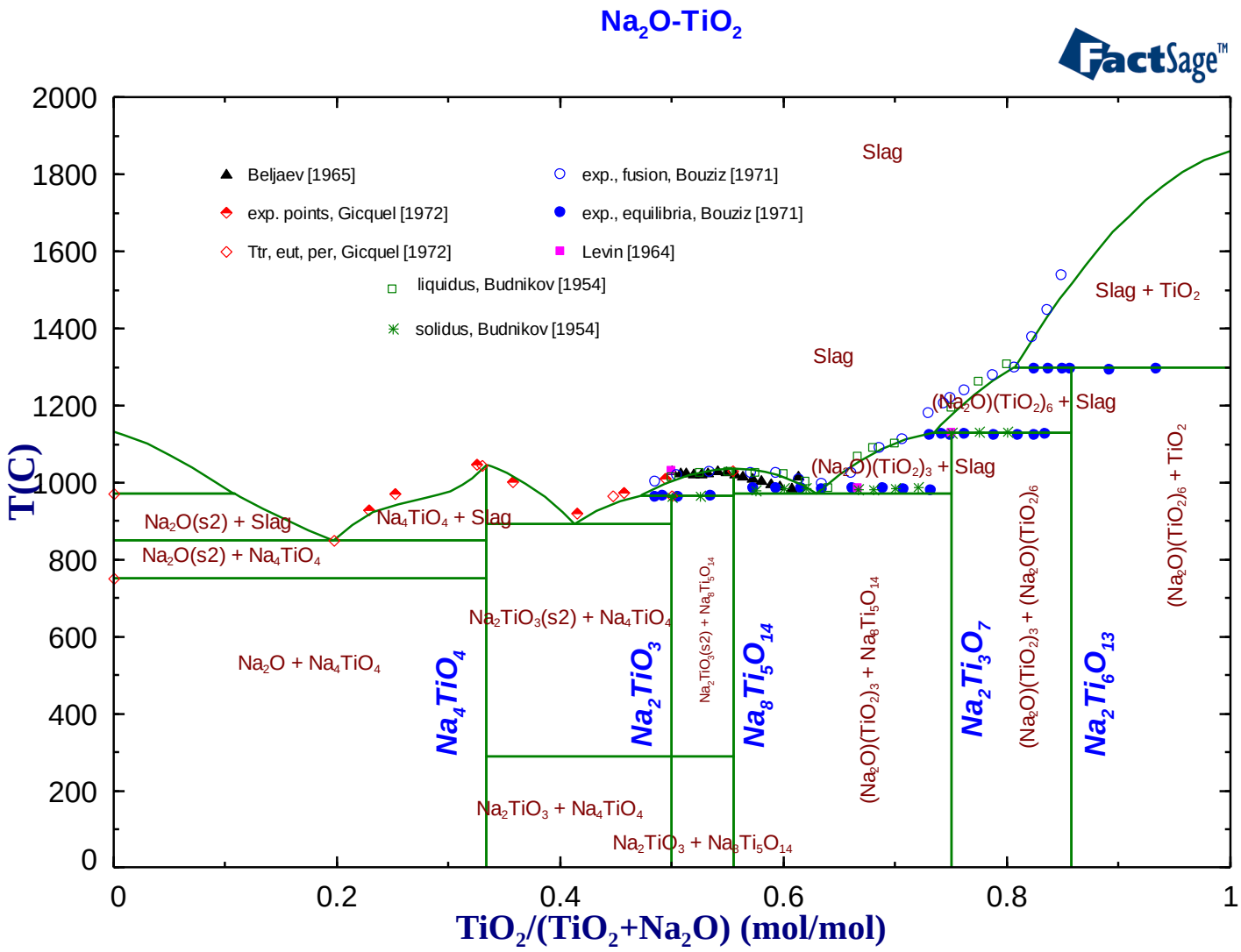

Weight percent

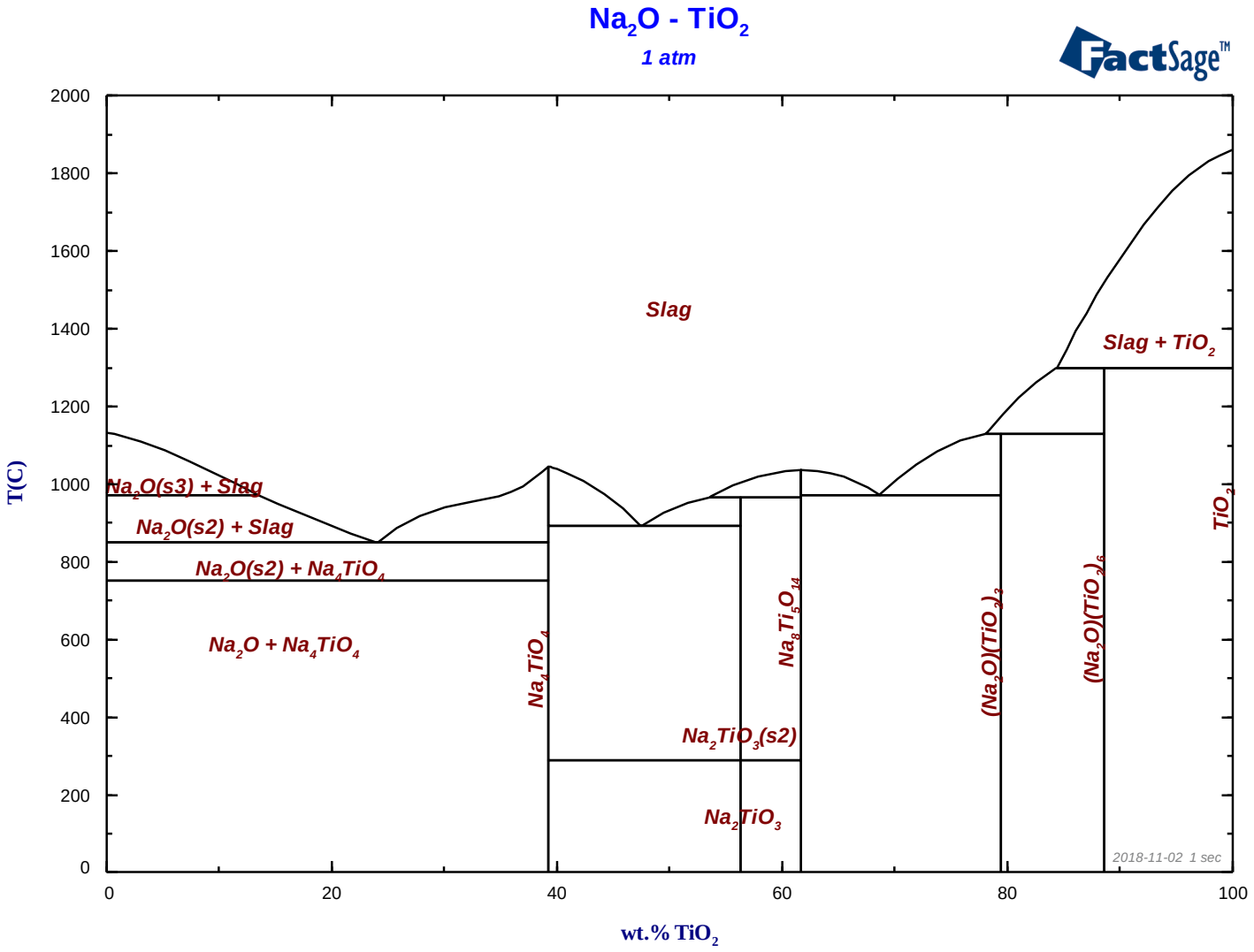

Na2O-V2O5, Mole fraction compared with experimental data

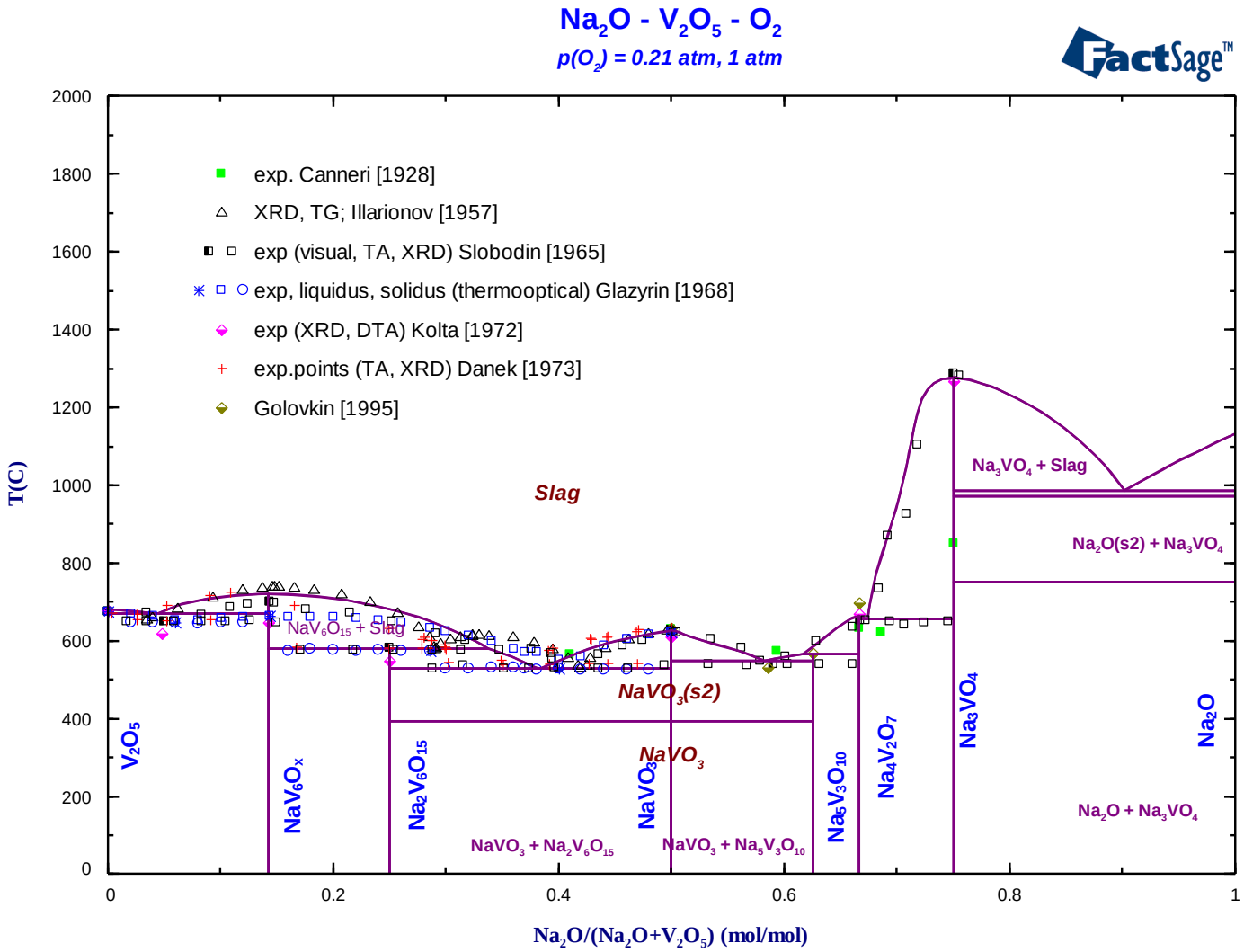

Na2O-V2O5,
Weight percent

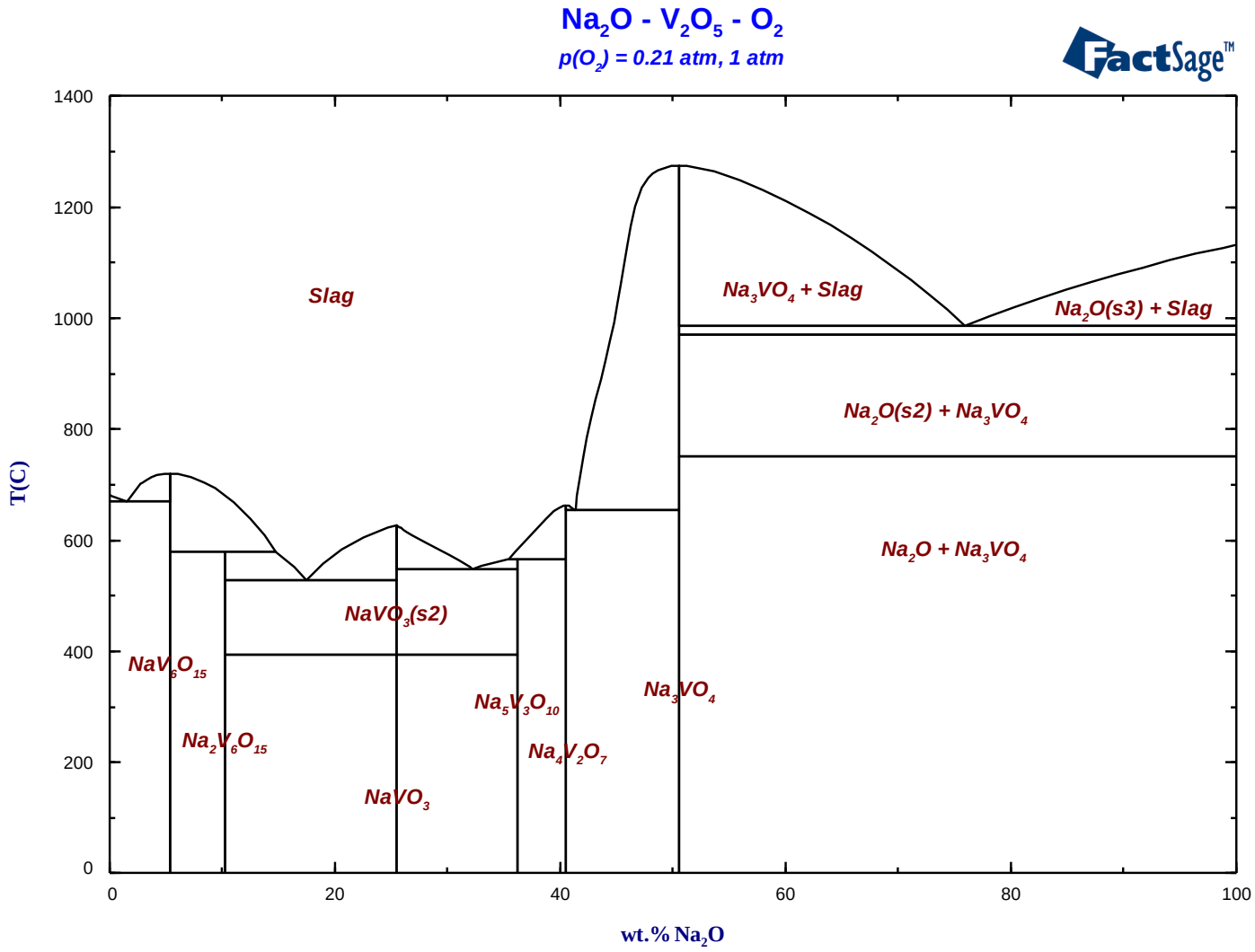

Na2SO4-NiSO4,
Mole fraction
compared with experimental data

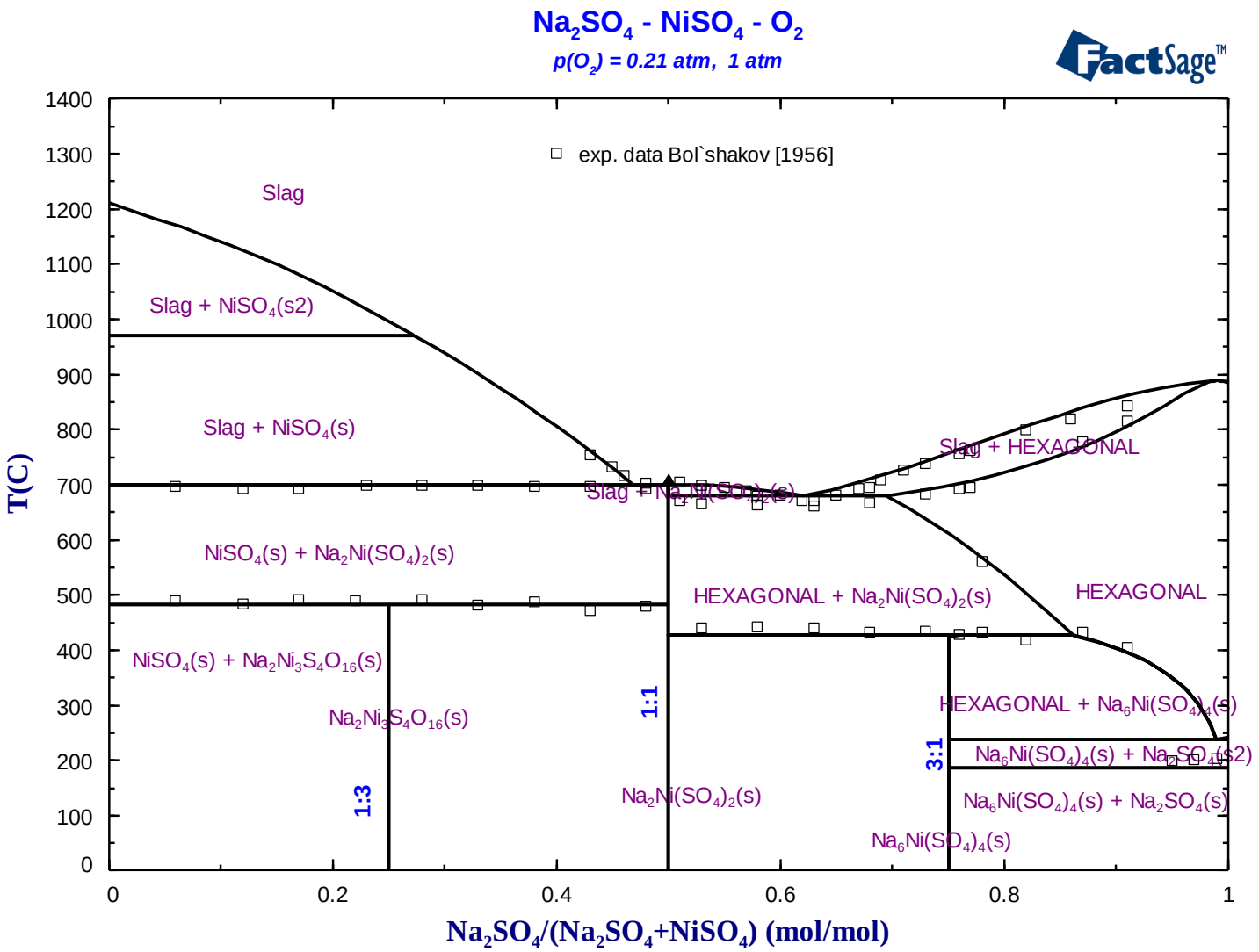

Na2SO4-NiSO4,
Weight percent

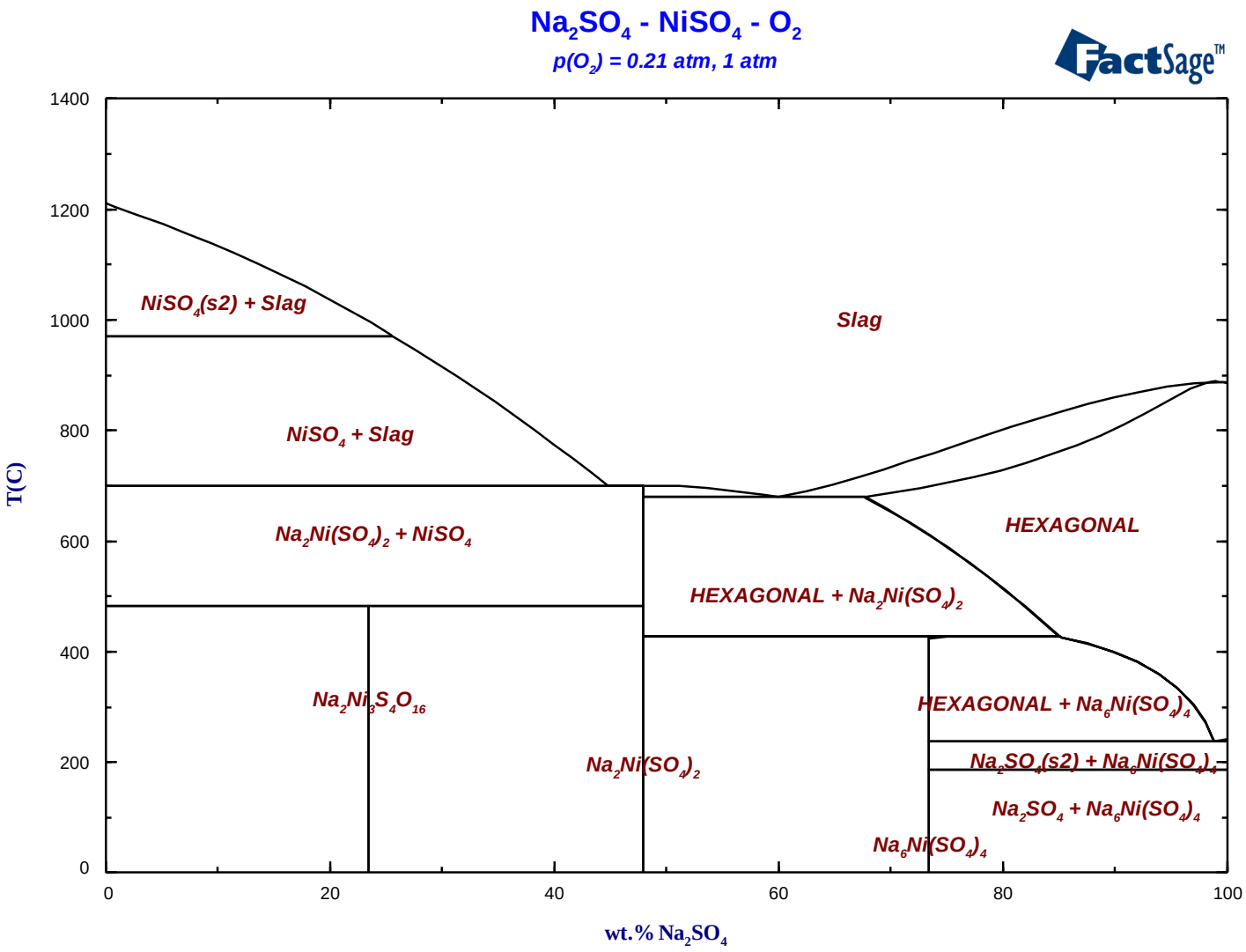

Mole fraction
compared with experimental data

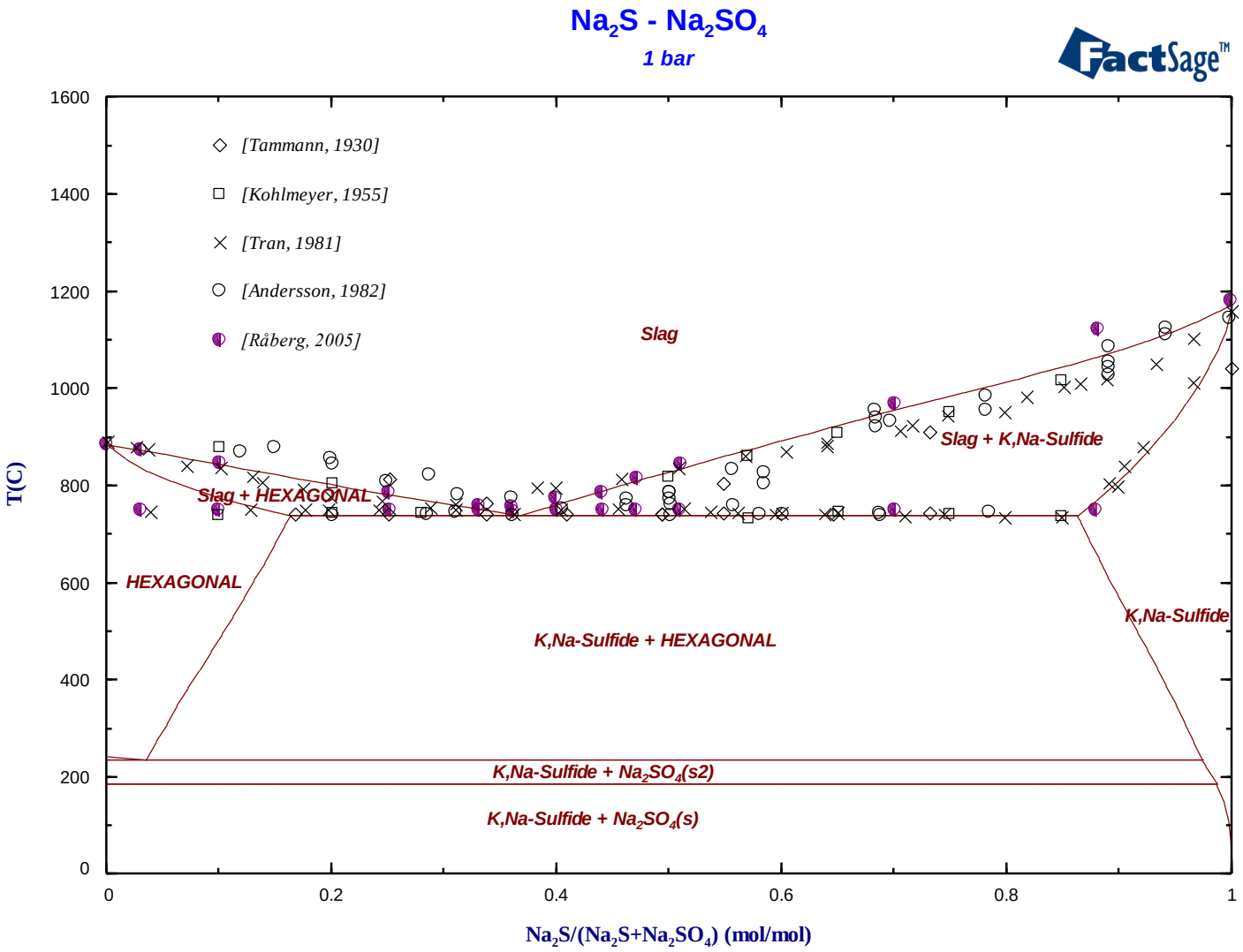

Weight percent

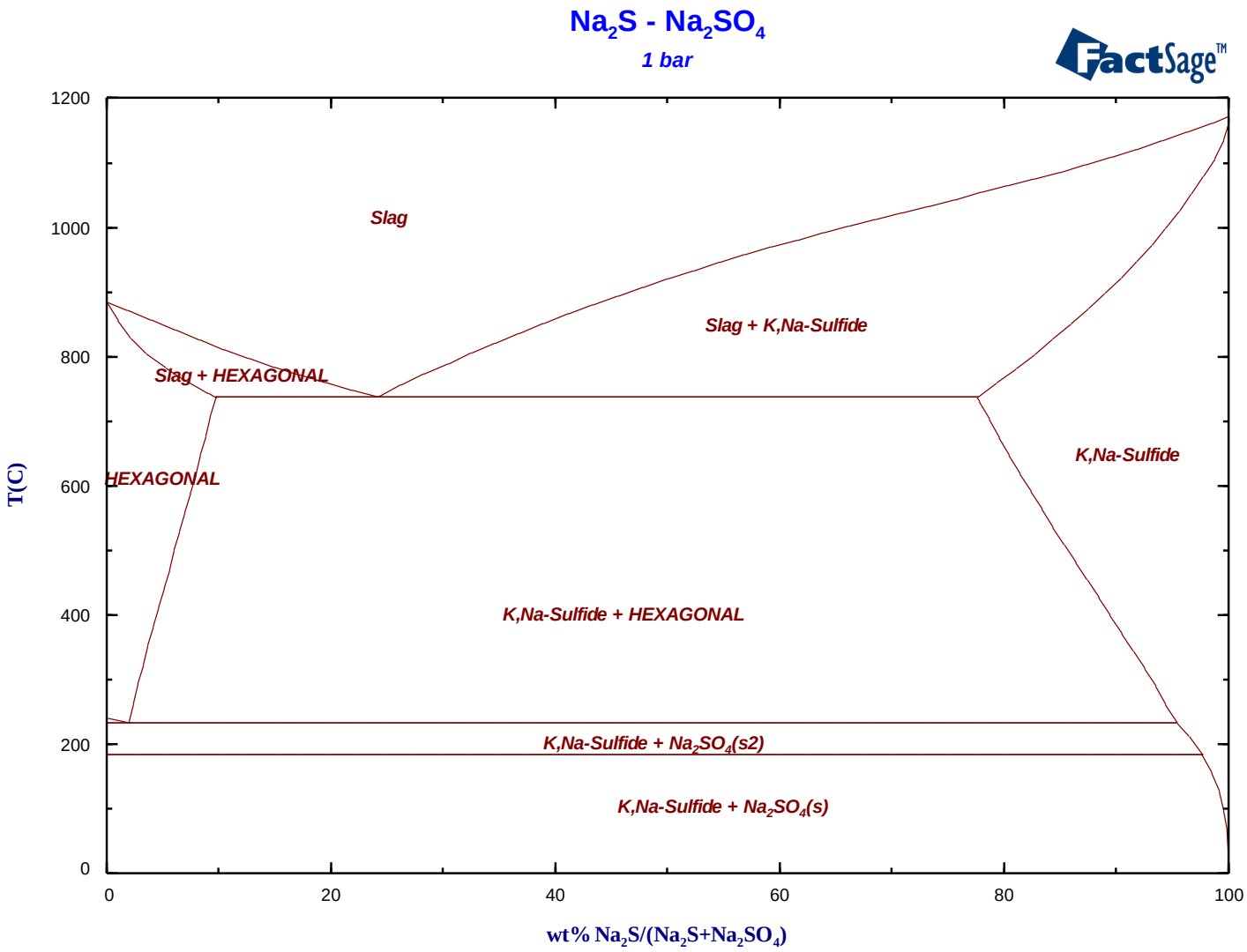

Mole fraction
compared with experimental data

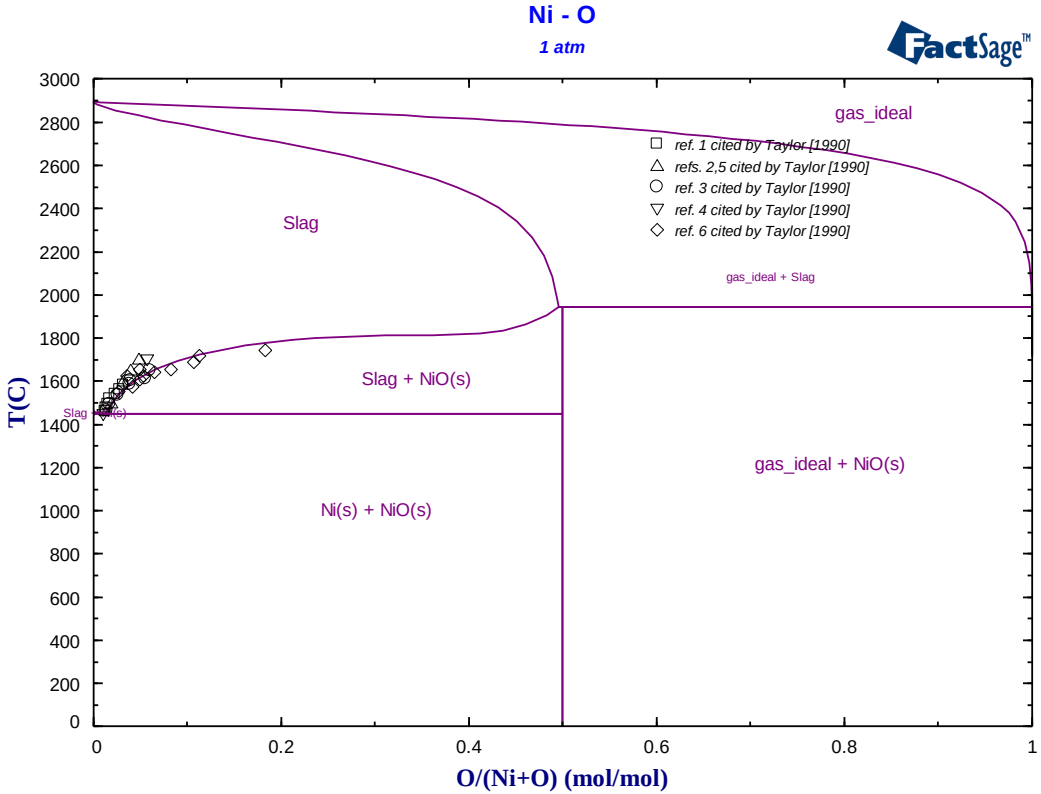

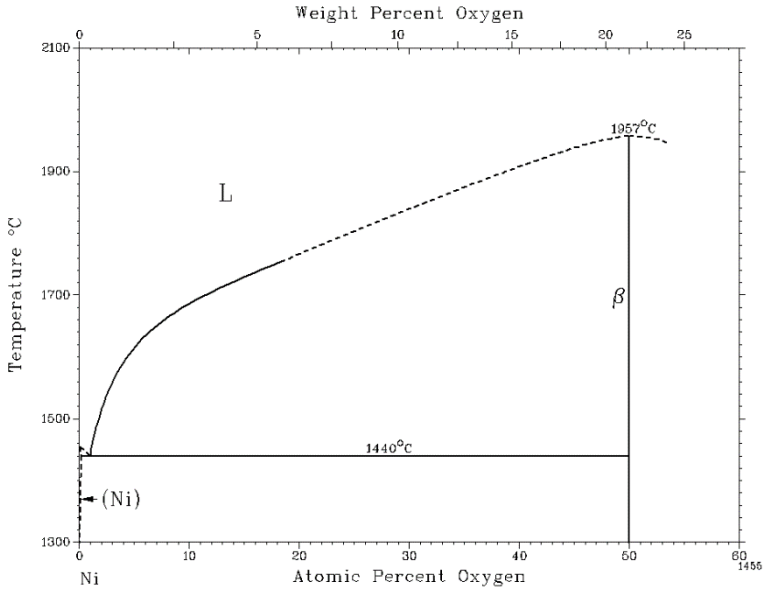

T.B. Massalski (ed), Binary Alloy Phase Diagrams, Second Edition, ASM International, Metals Park, OH 1990.

Weight percent

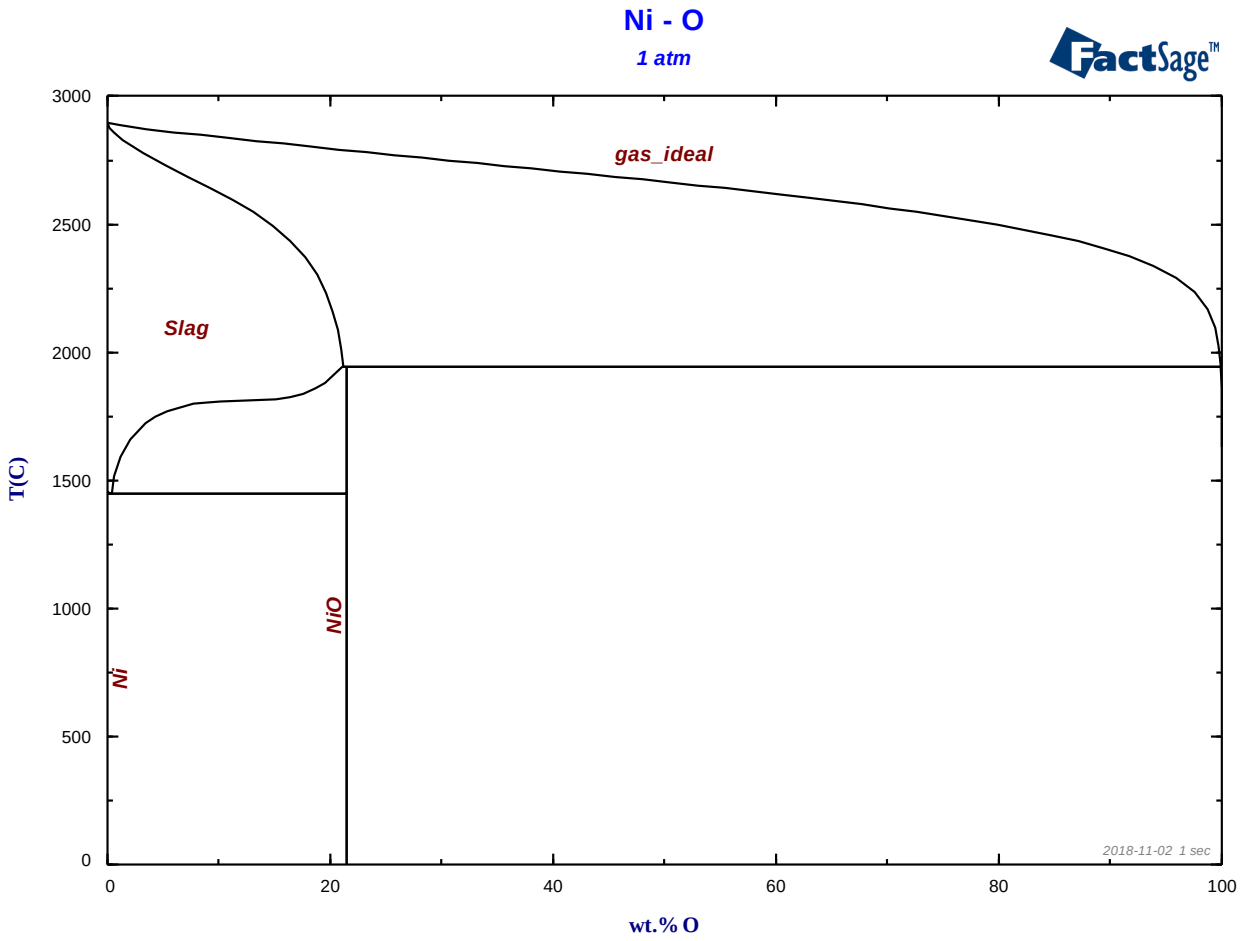

Ni-O,
Mole fraction with isobars

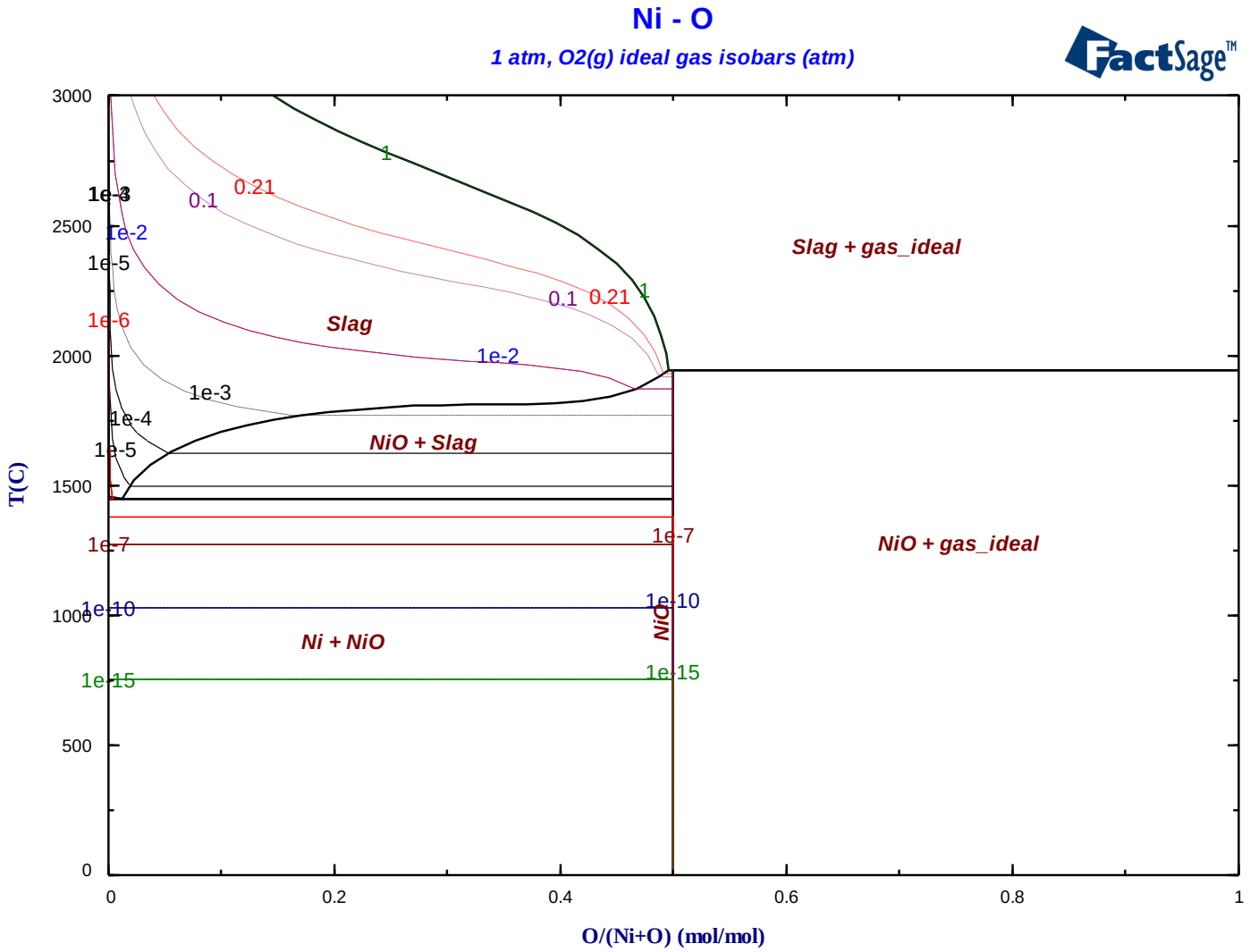

Ni-O,
Temperature vs. log P(O2) diagram

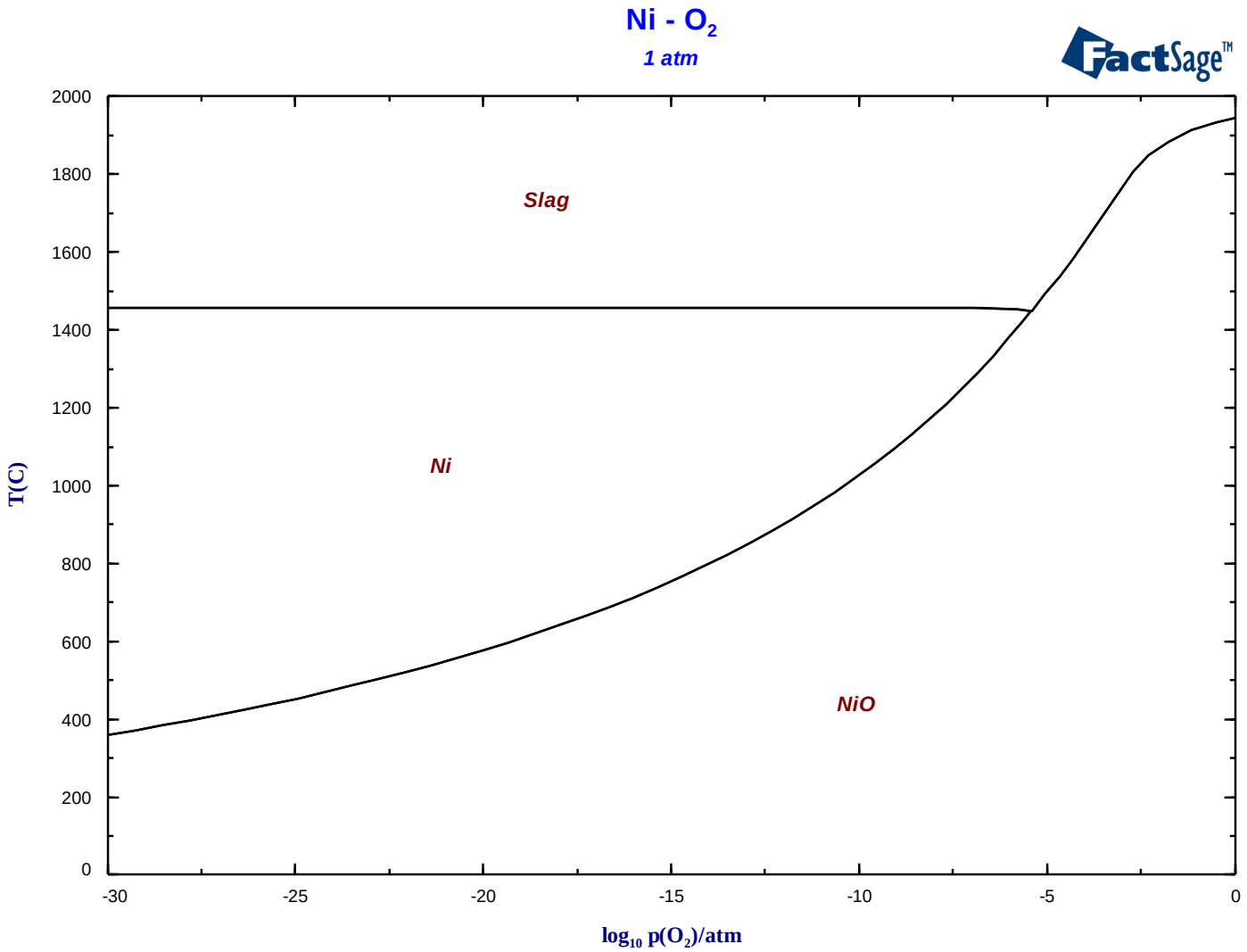

Mole fraction
compared with experimental data

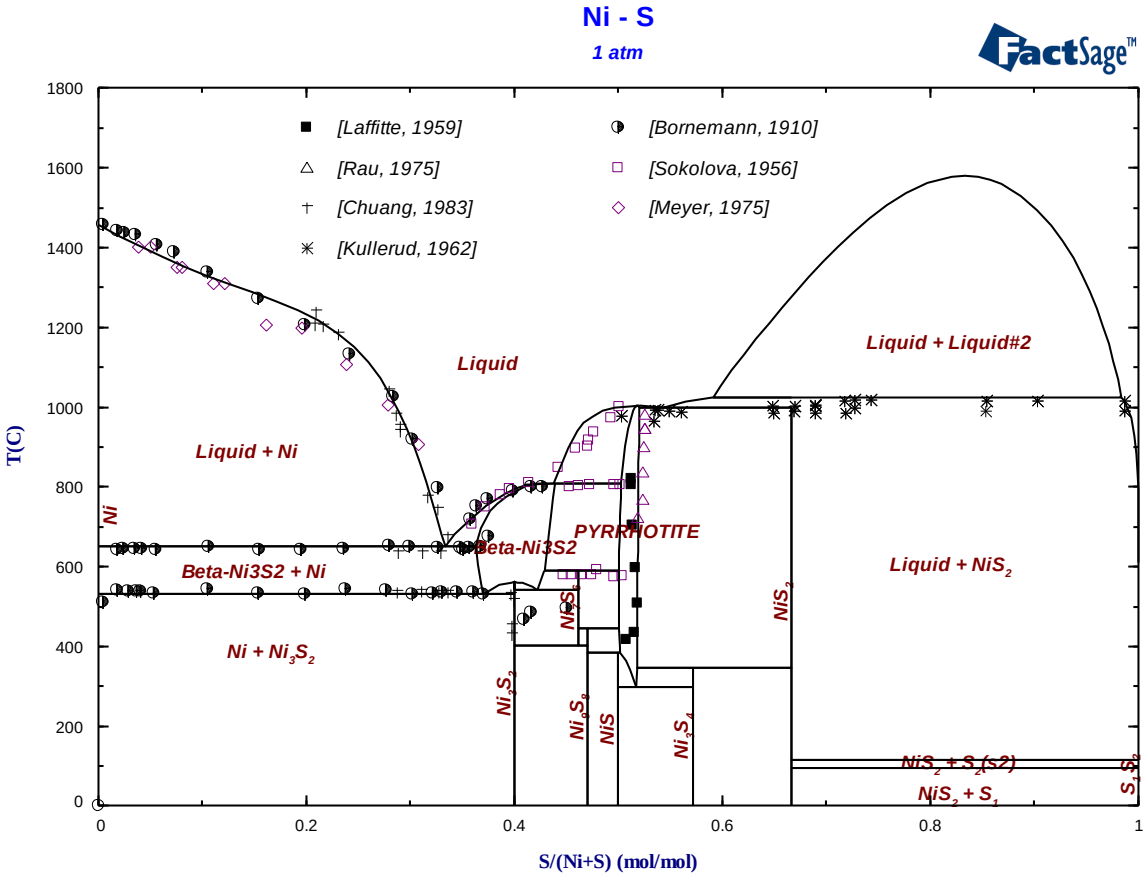

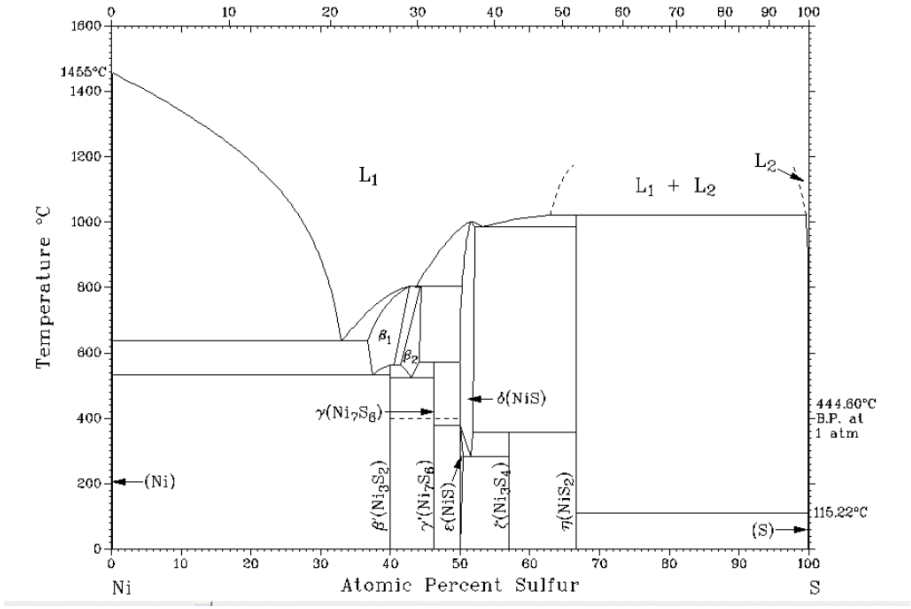

T.B. Massalski (ed), Binary Alloy Phase Diagrams, Second Edition, ASM International, Metals Park, OH 1990.

Ni-S,
Weight percent

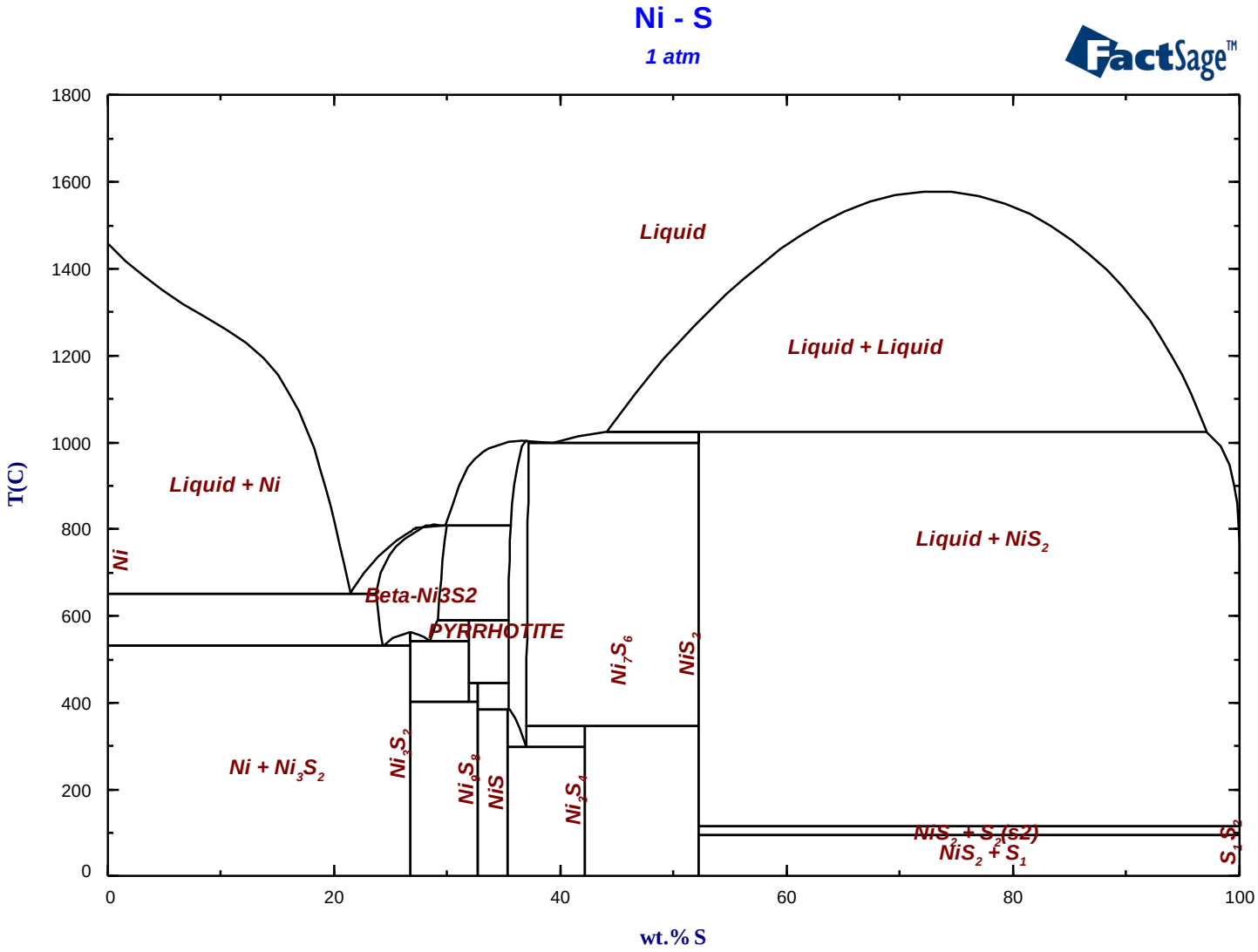

NiO-MgO,
Mole fraction compared with experimental data

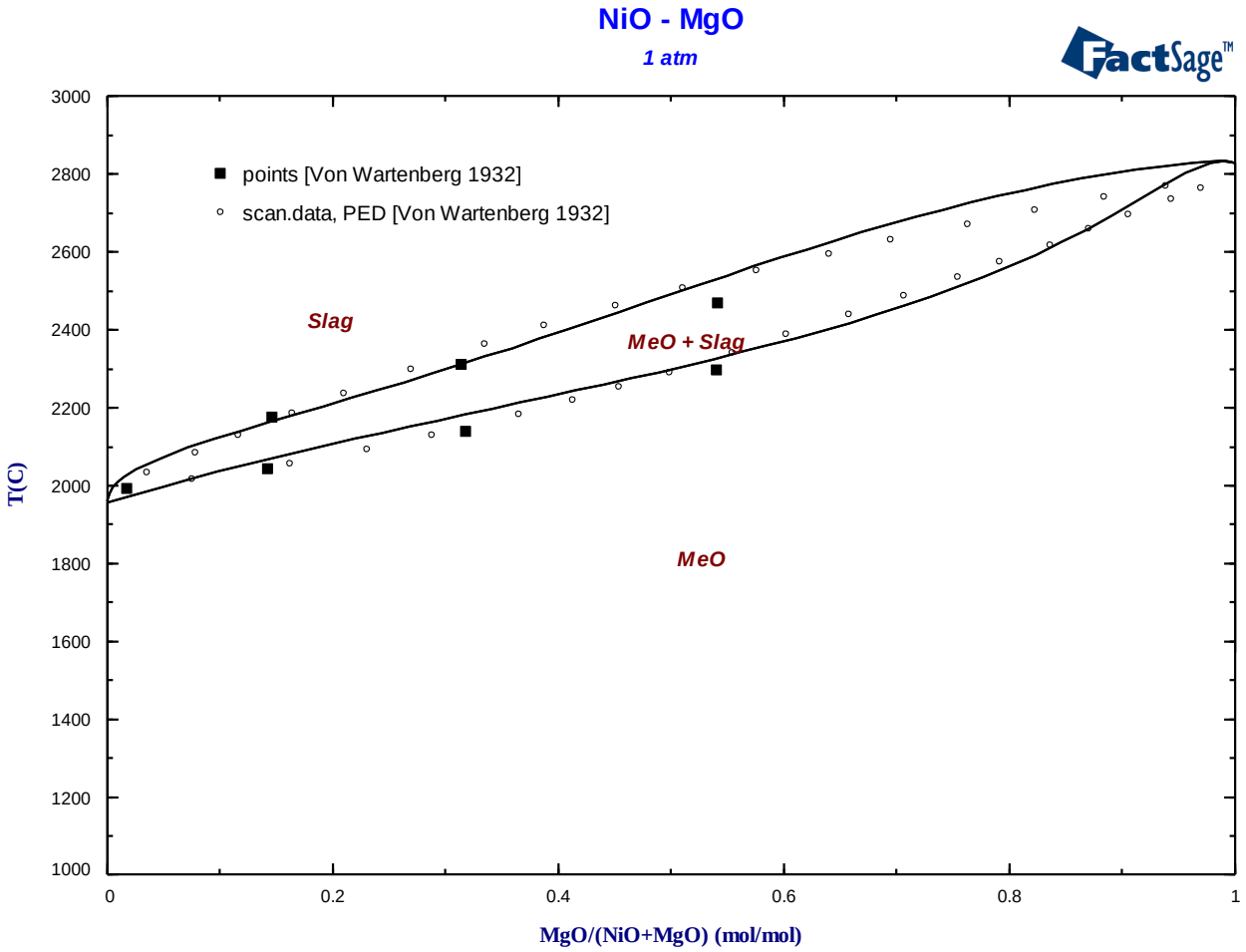

NiO-MgO,
Weight percent

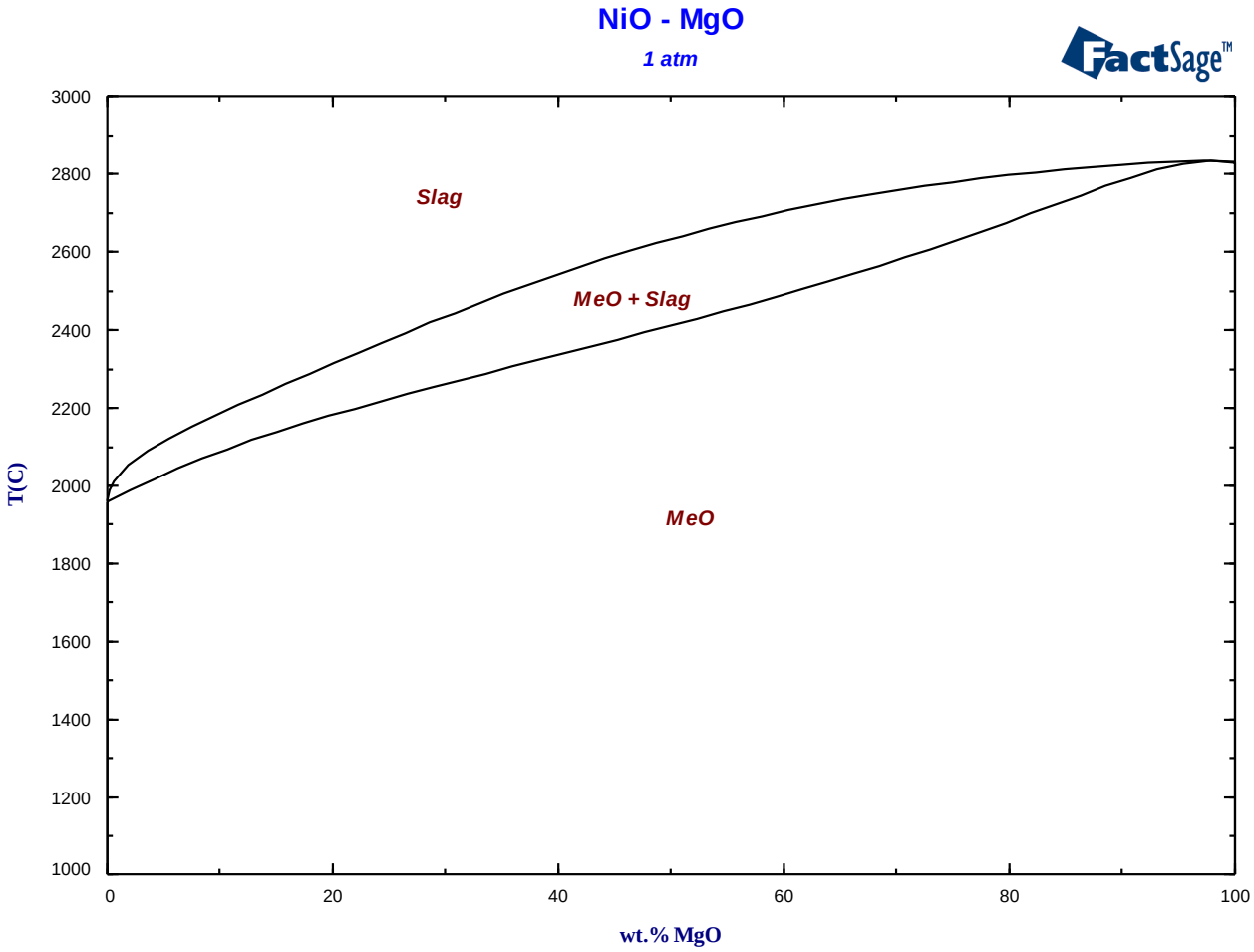

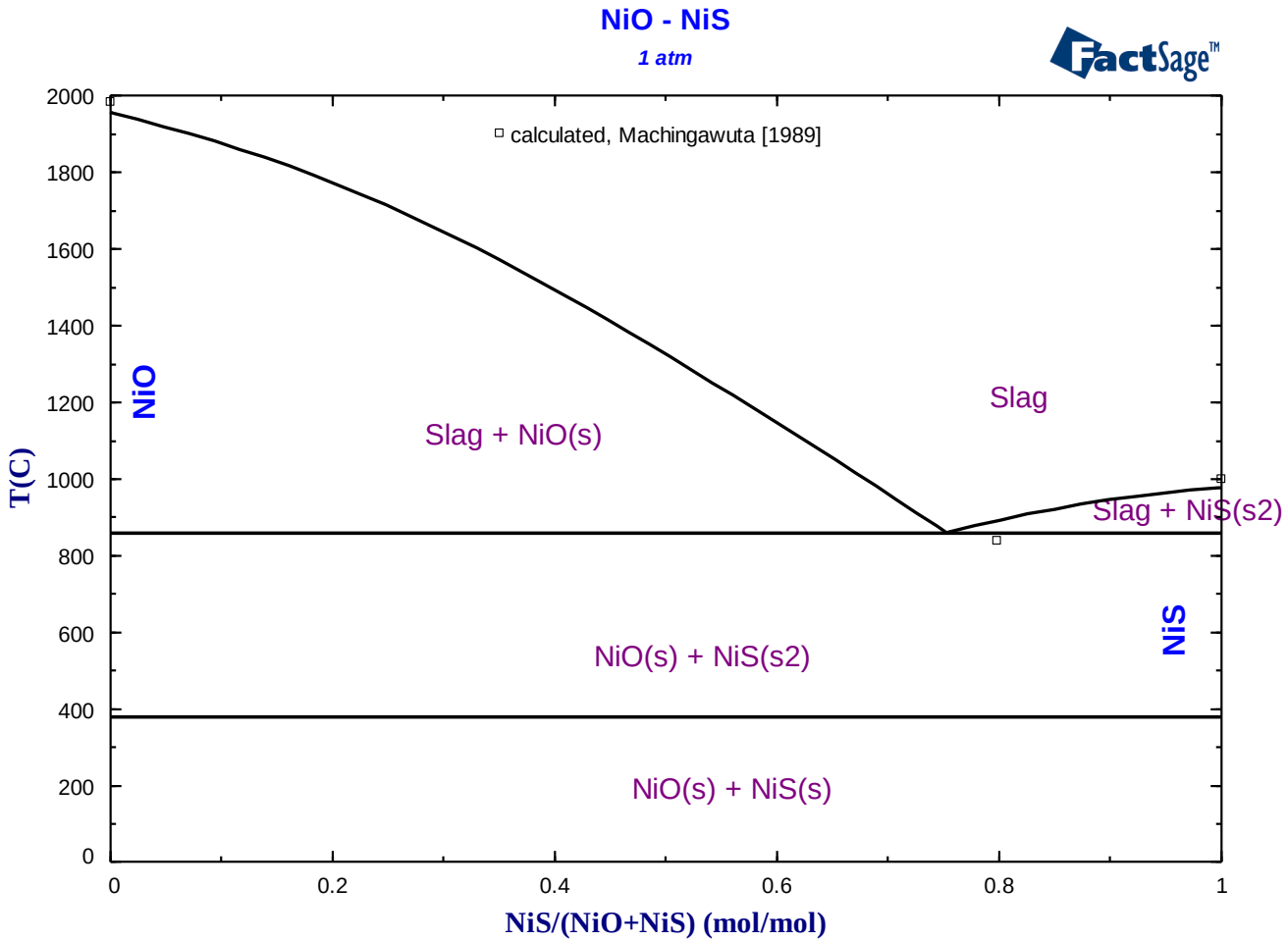
NiO - NiS
1 atm
FactSage™
calculated, Machingawuta [1989]
NiO
Slag
Slag + NiO(s)
Slag + NiS(s2)
NiS
NiO(s) + NiS(s2)
NiO(s) + NiS(s)
T(C)
2000
1800
1600
1400
1200
1000
800
600
400
200
0
0
0.2
0.4
0.6
0.8
1
NiS/(NiO+NiS) (mol/mol)

Weight fraction

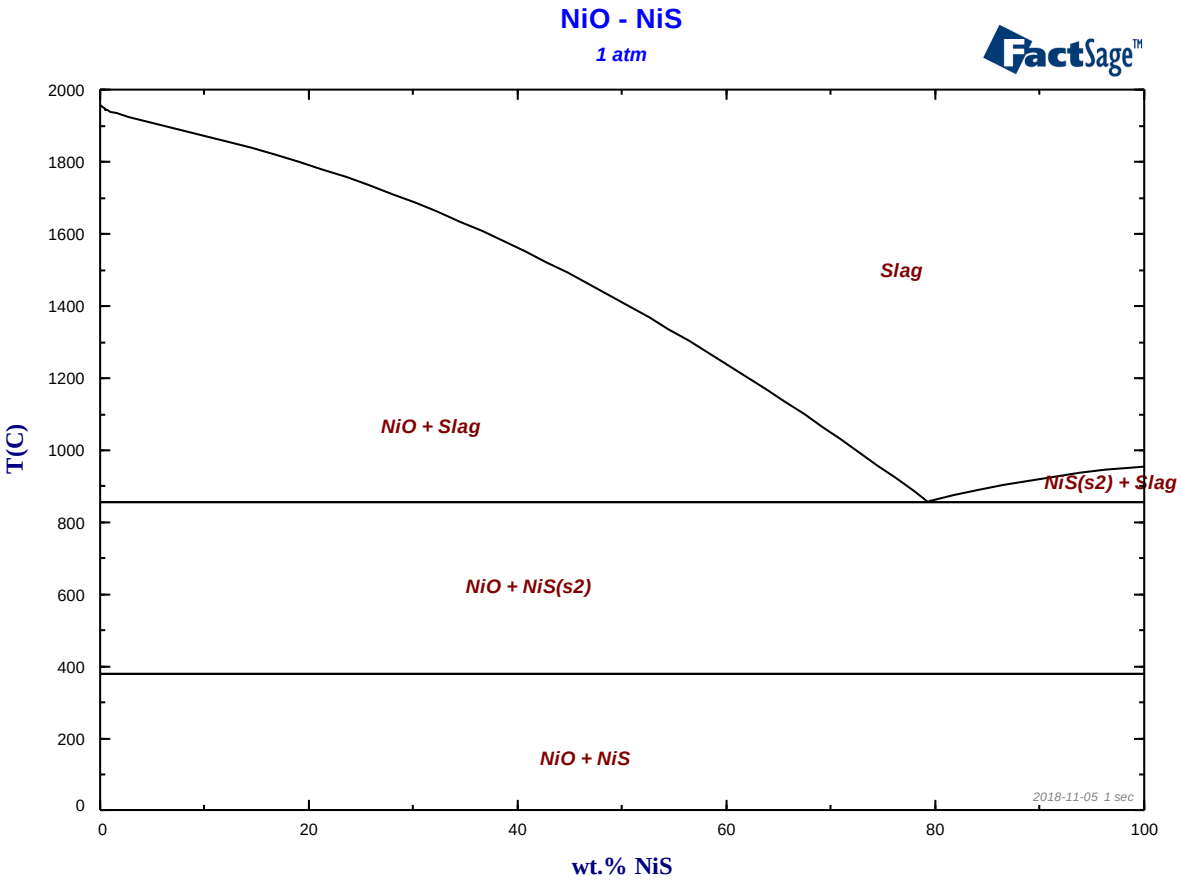

Mole fraction compared with experimental data

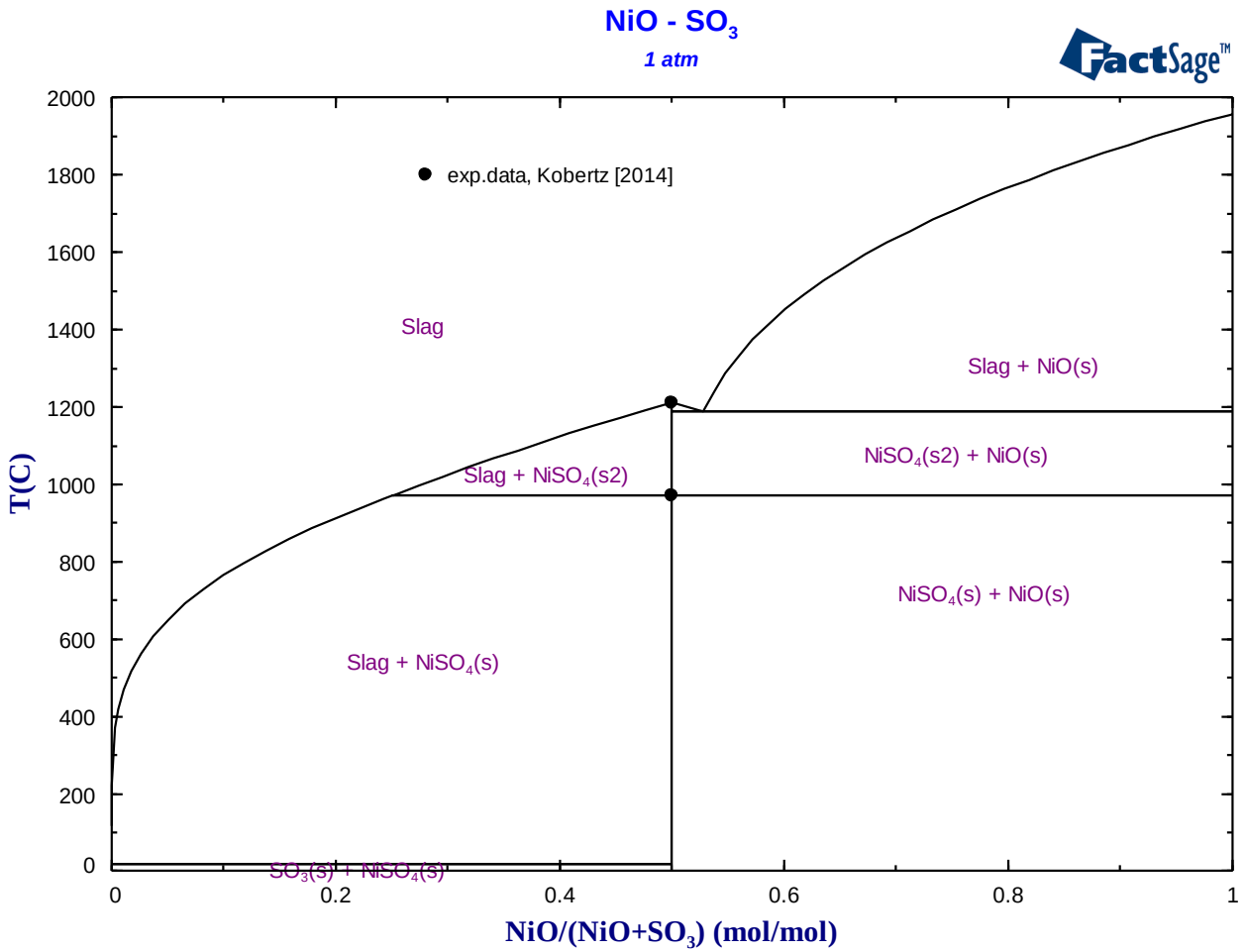

Weight fraction

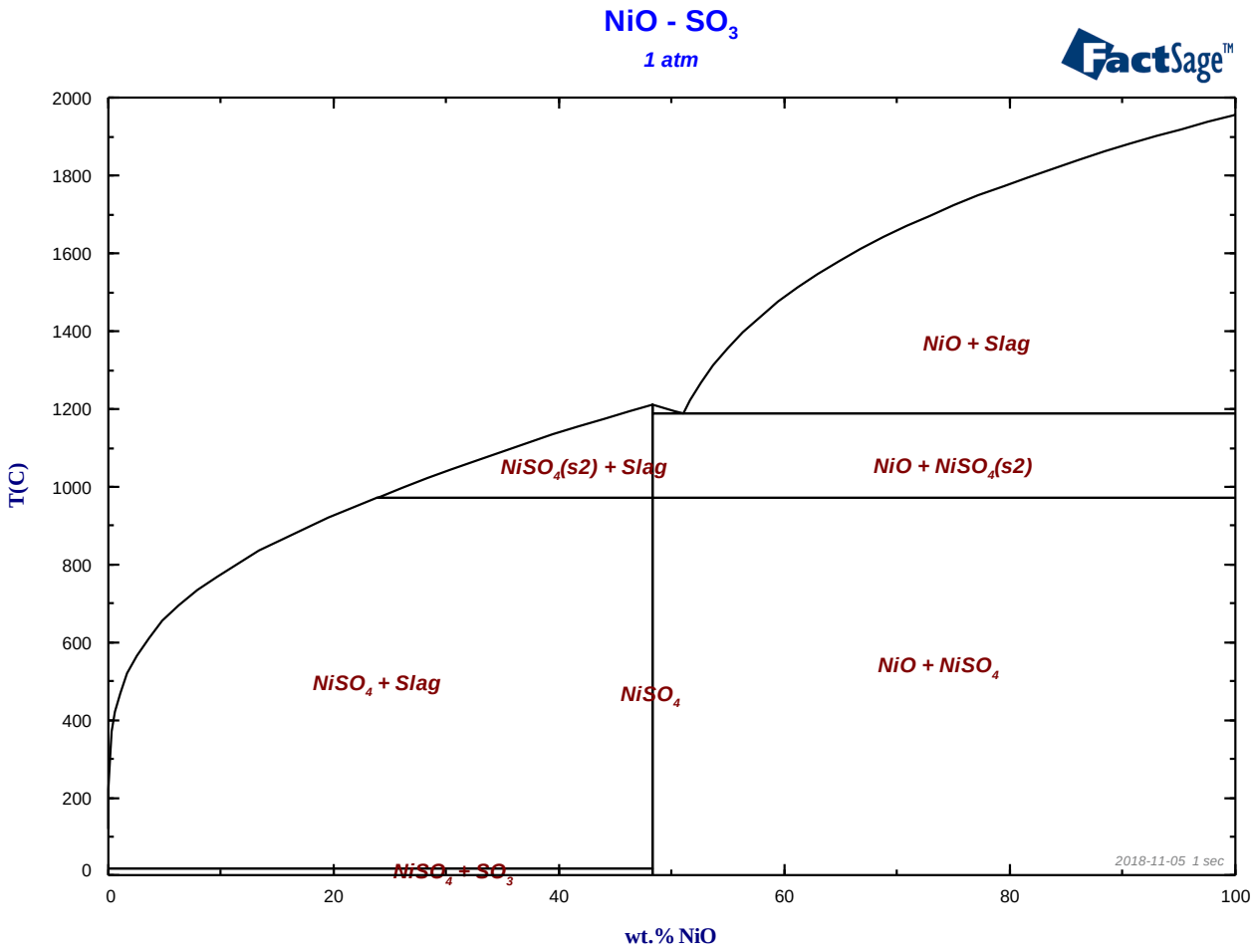

NiO-SrO,
Mole fraction compared with experimental data

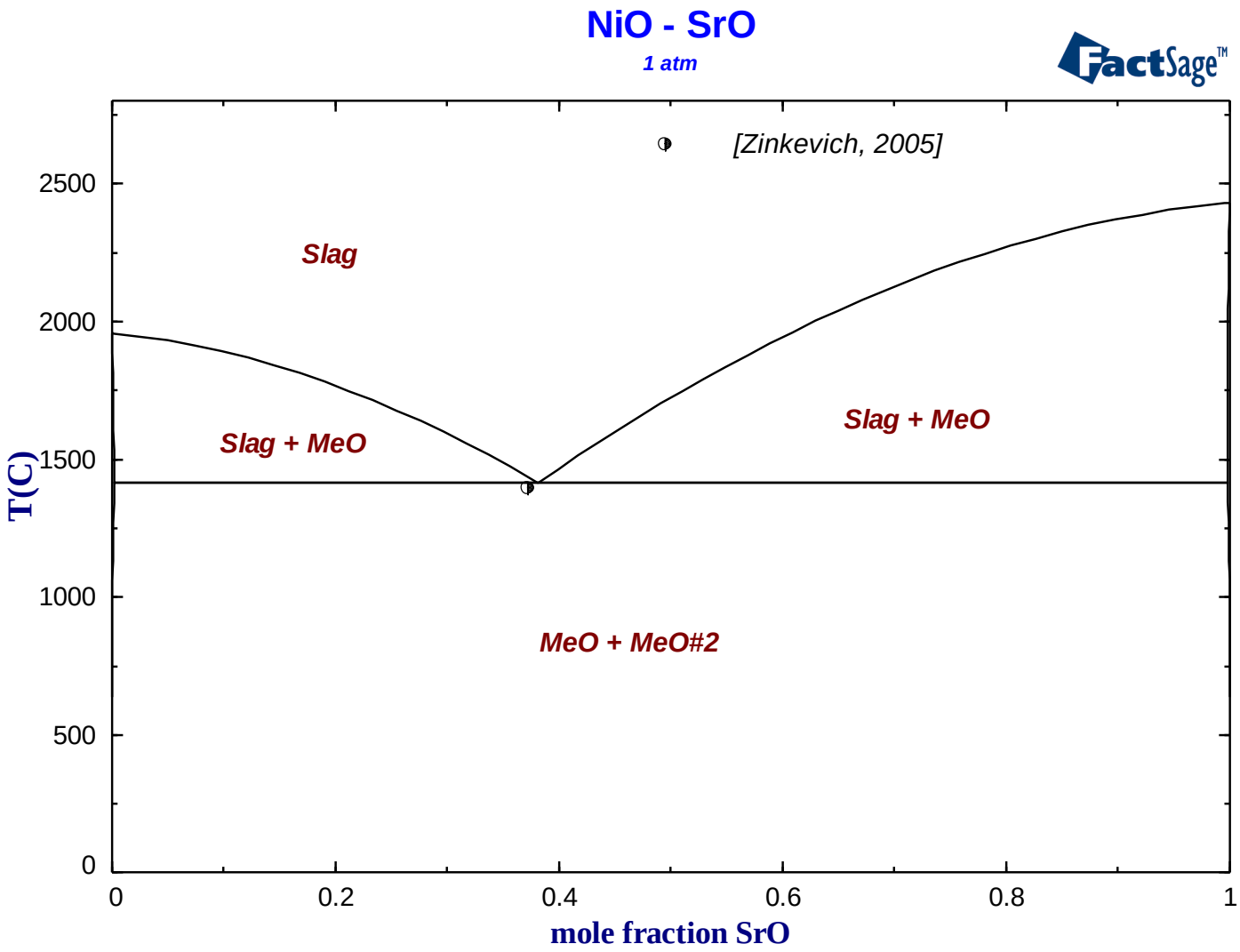

NiO-SrO,
Weight percent

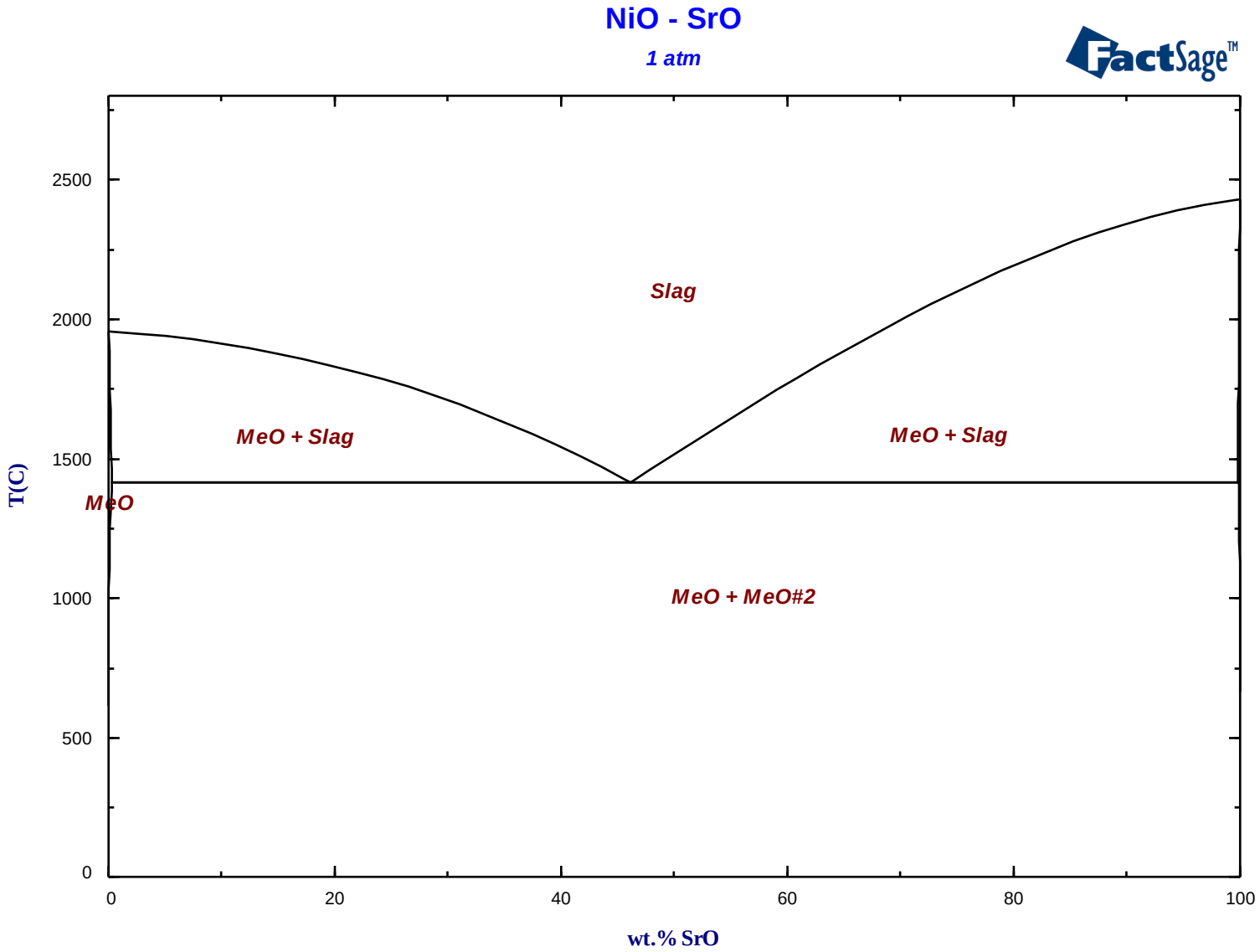

NiO-TiO2,
Mole fraction

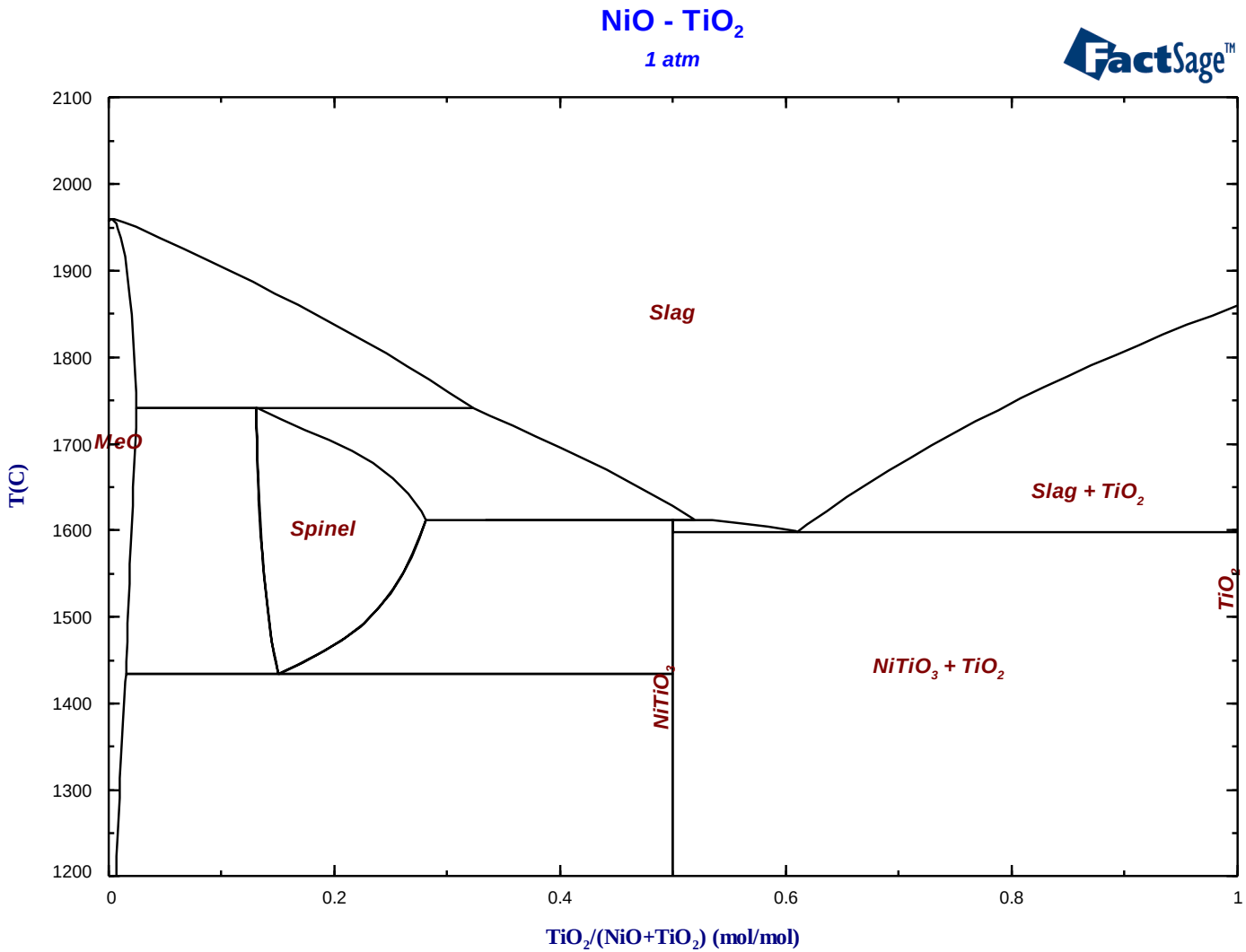

NiO-TiO2,
Weight percent compared with experimental data

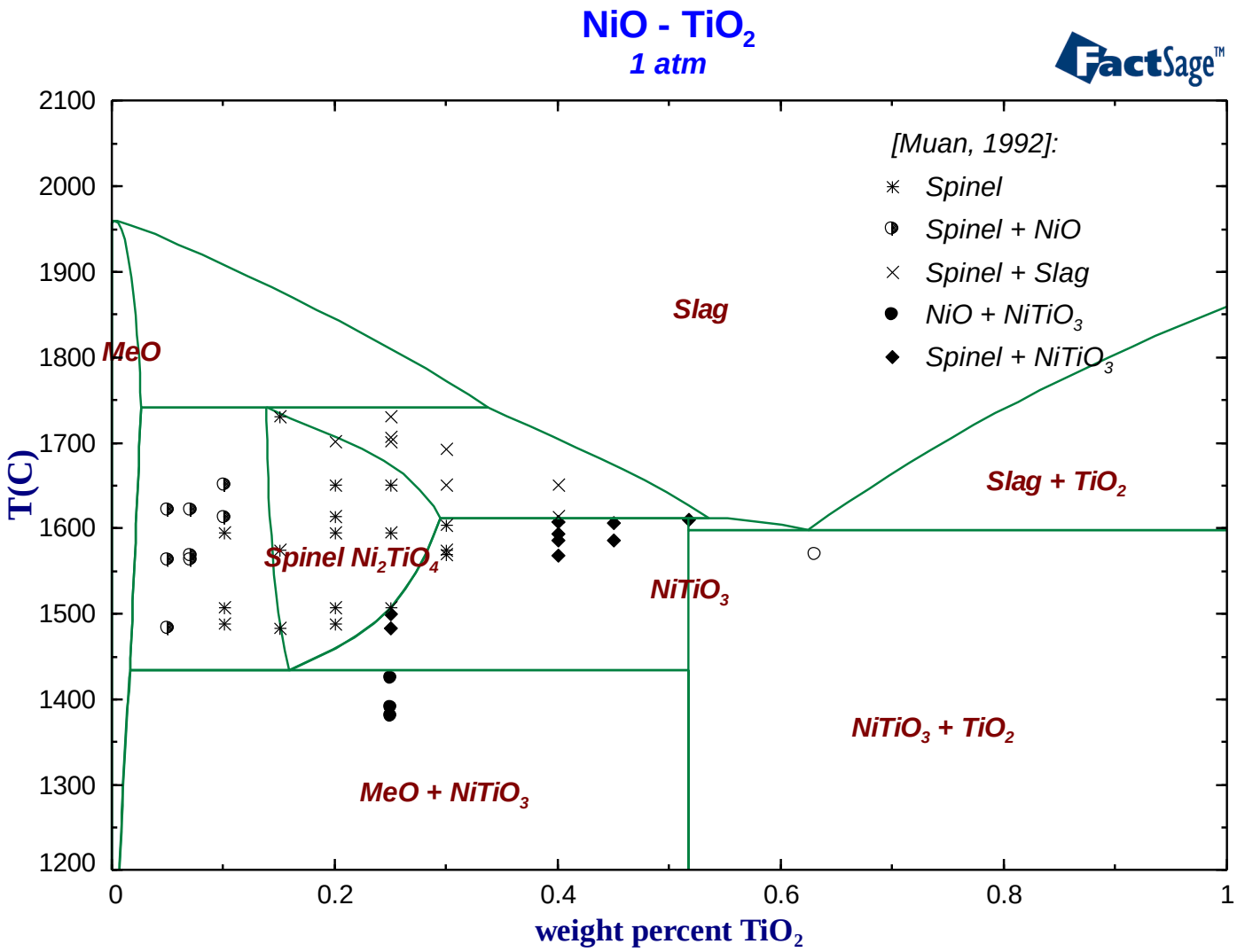

NiO-V2O5-O2,
Mole fraction compared with experimental data

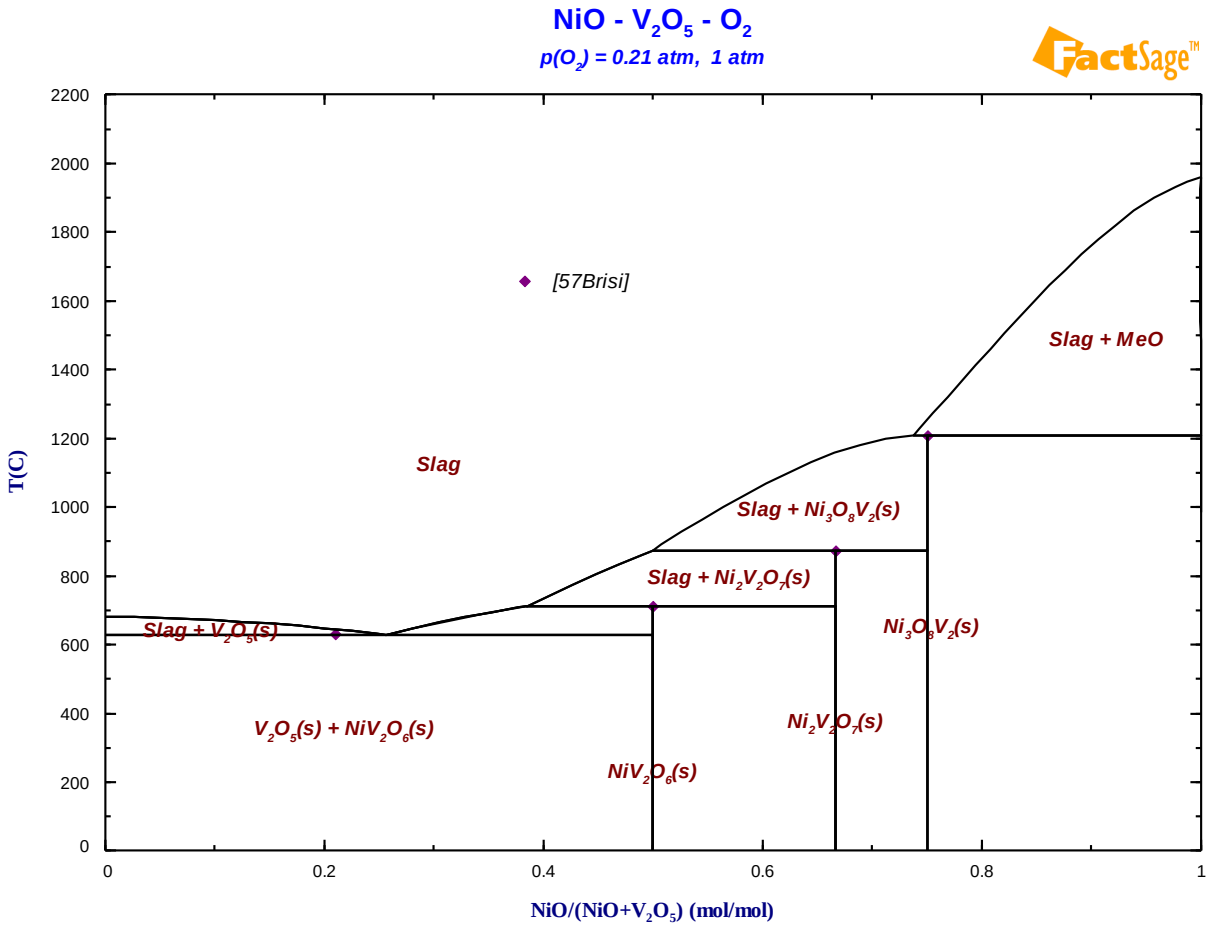

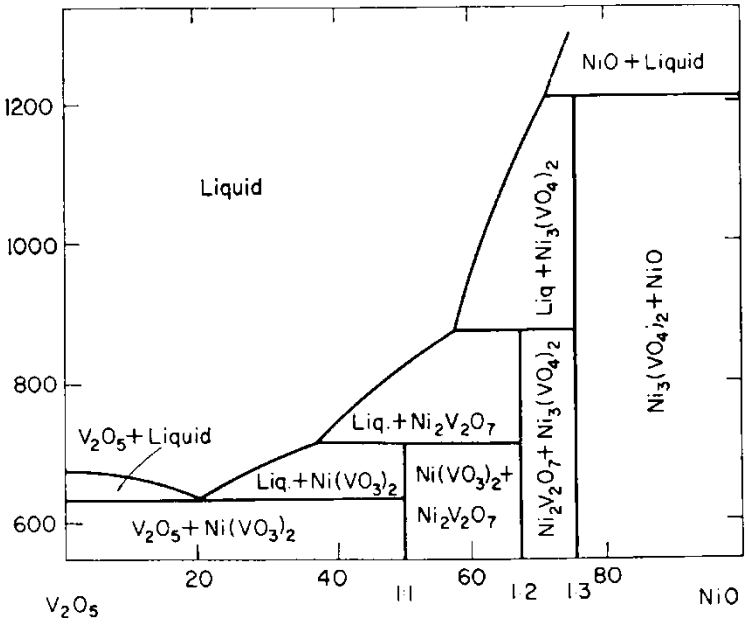

C. Brisi, Ann. Chim. (Rome), 47 [7-8], (1957), pp. 806-816.

NiO-V2O5-o2,
Weight percent

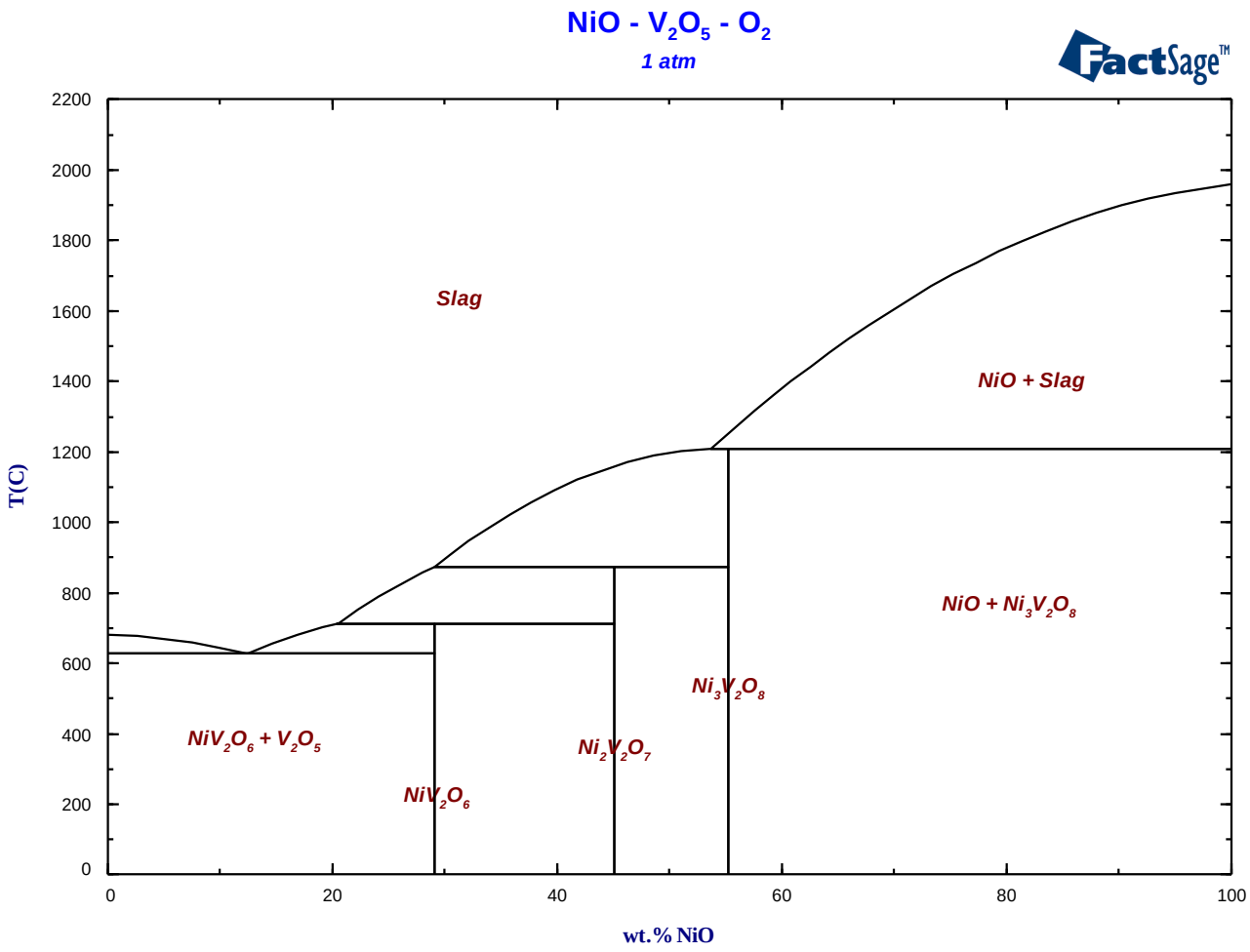

Mole fraction compared with experimental data

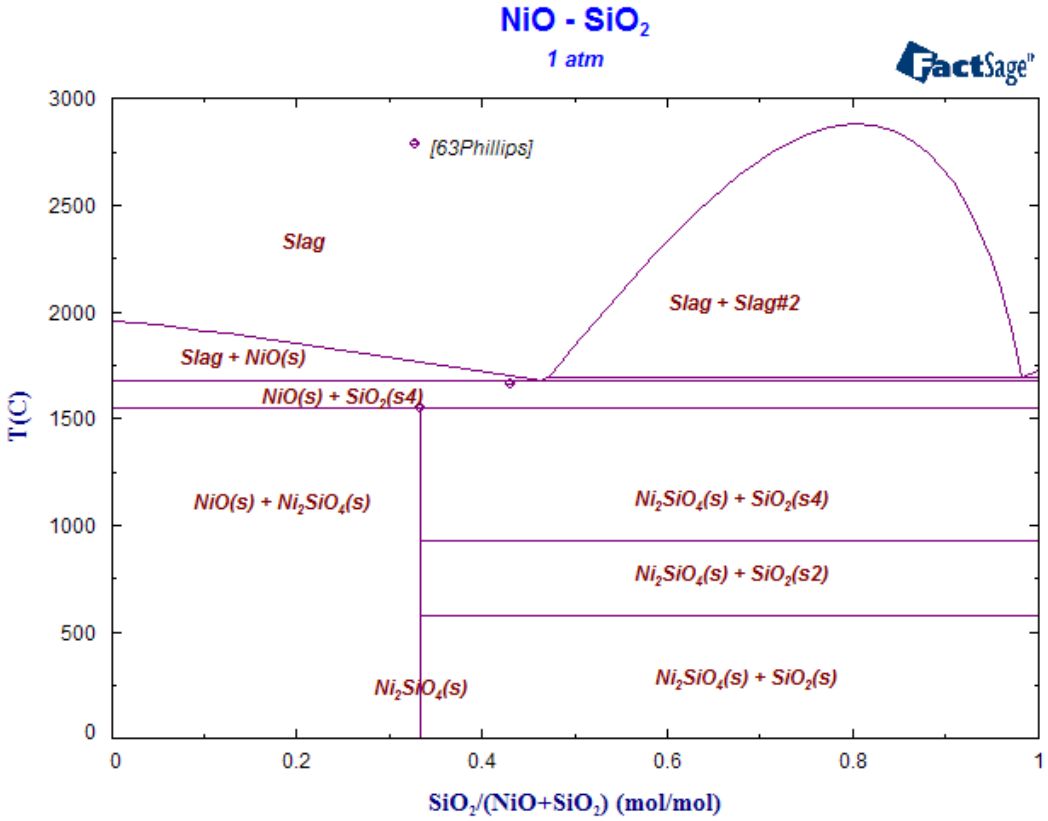

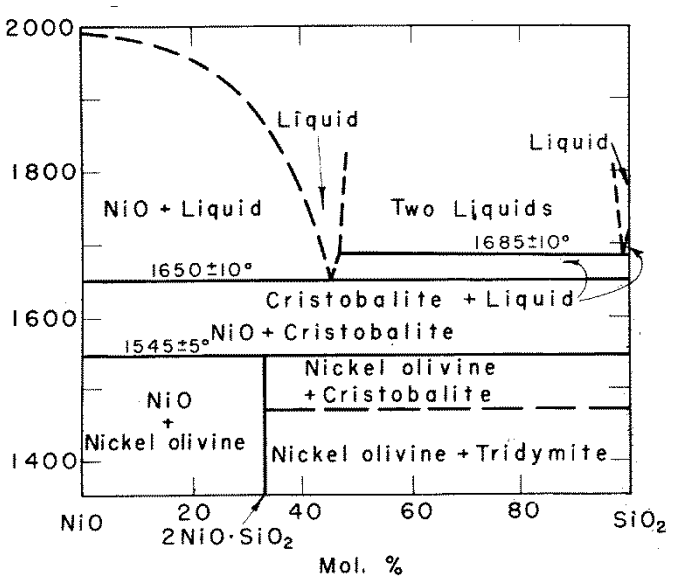

B. Phillips, J.J. Hutta, I. Warshaw, J. Am.Ceram. Soc., 46 [12], (1963), pp.579-583.

Weight percent

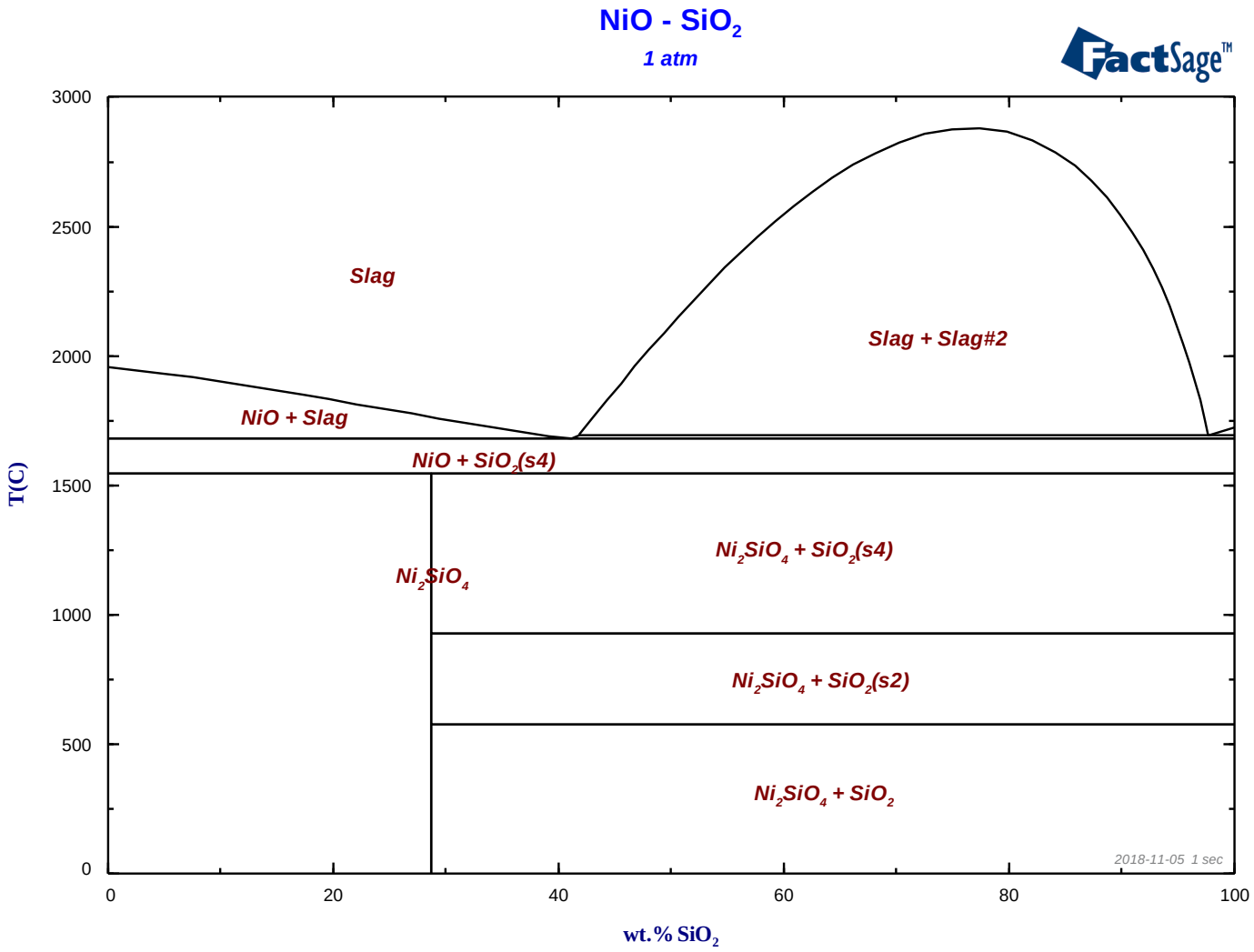

NiO-ZnO,
Mole fraction compared with experimental data

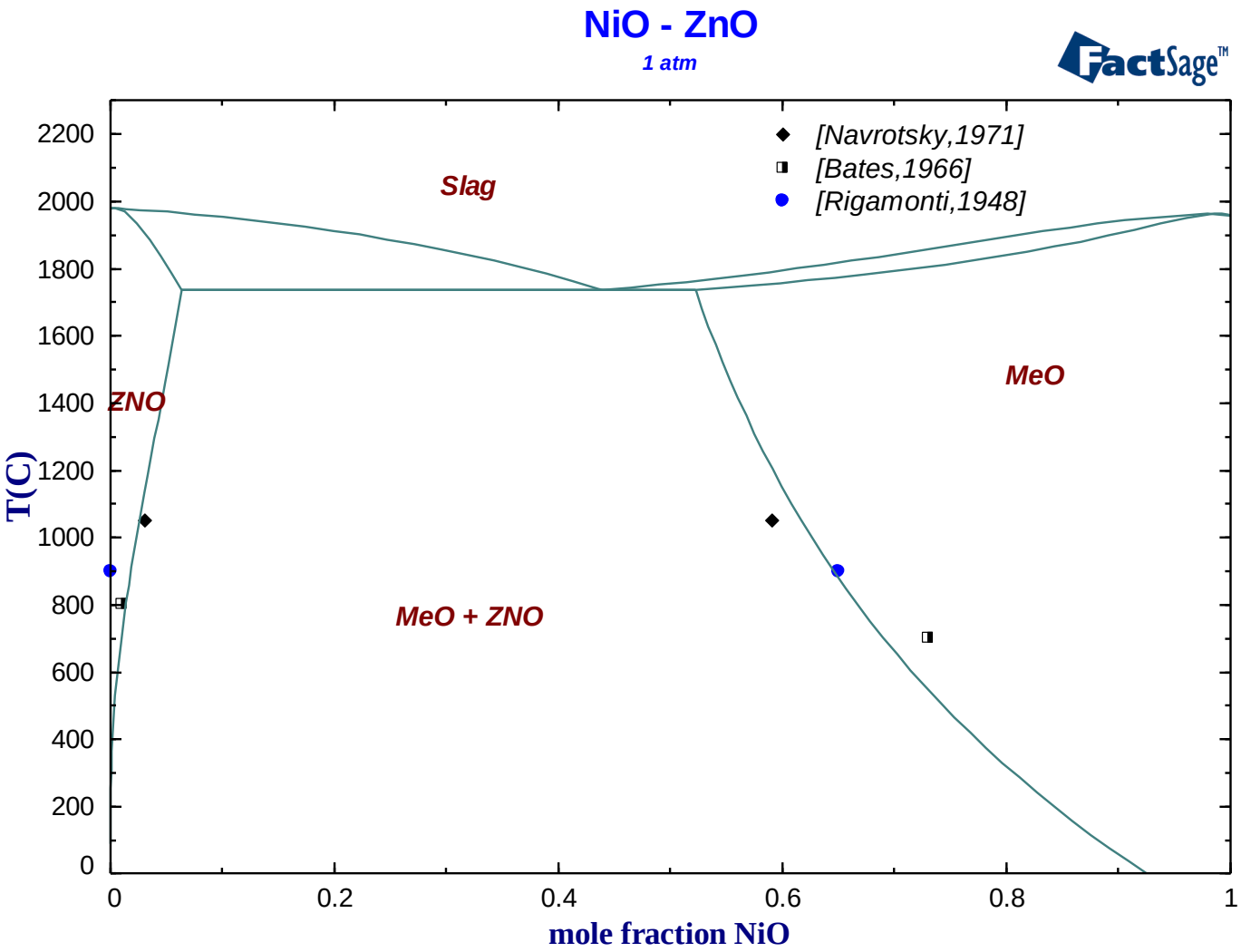

NiO-ZnO,
Weight percent

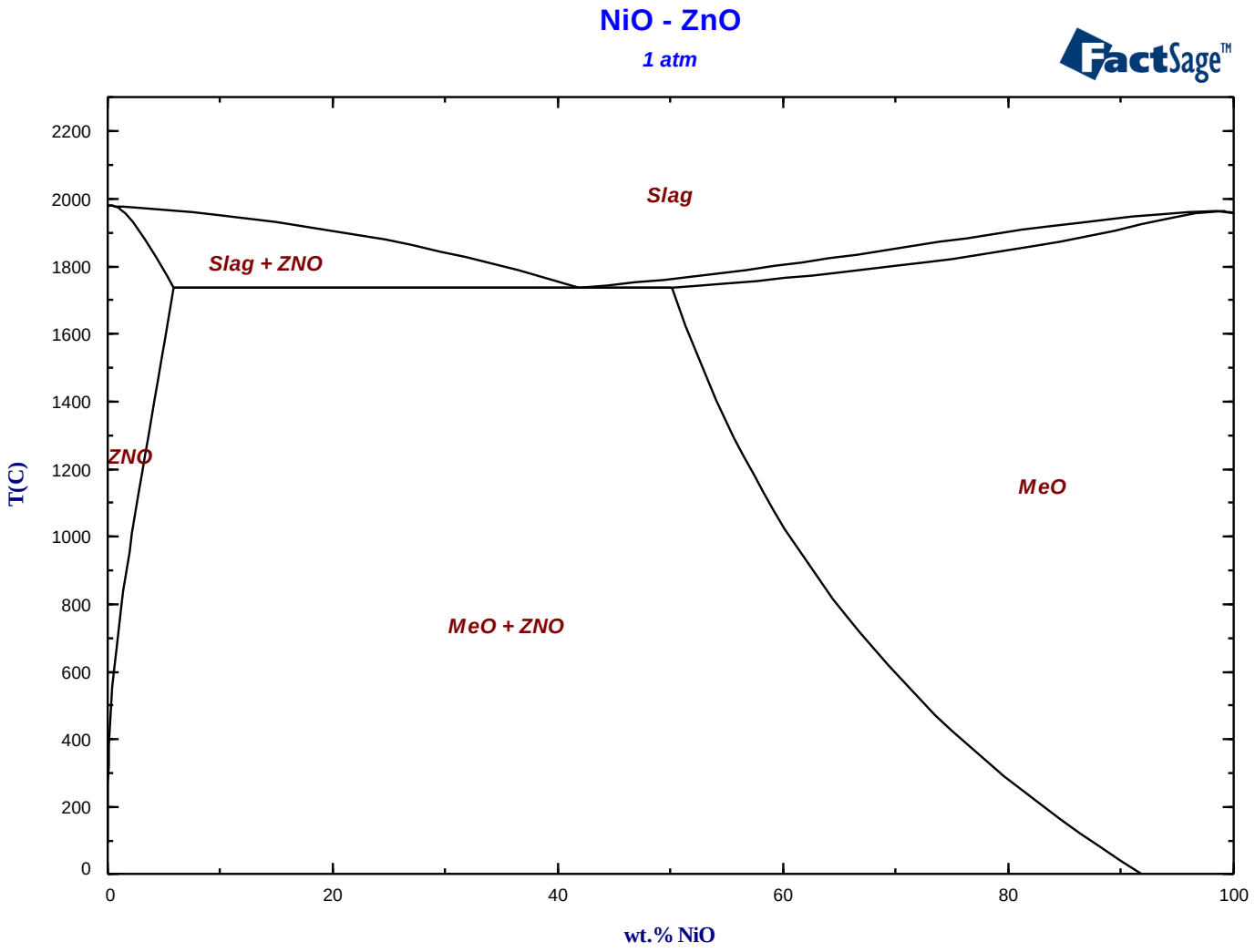

Mole fraction
compared with experimental data

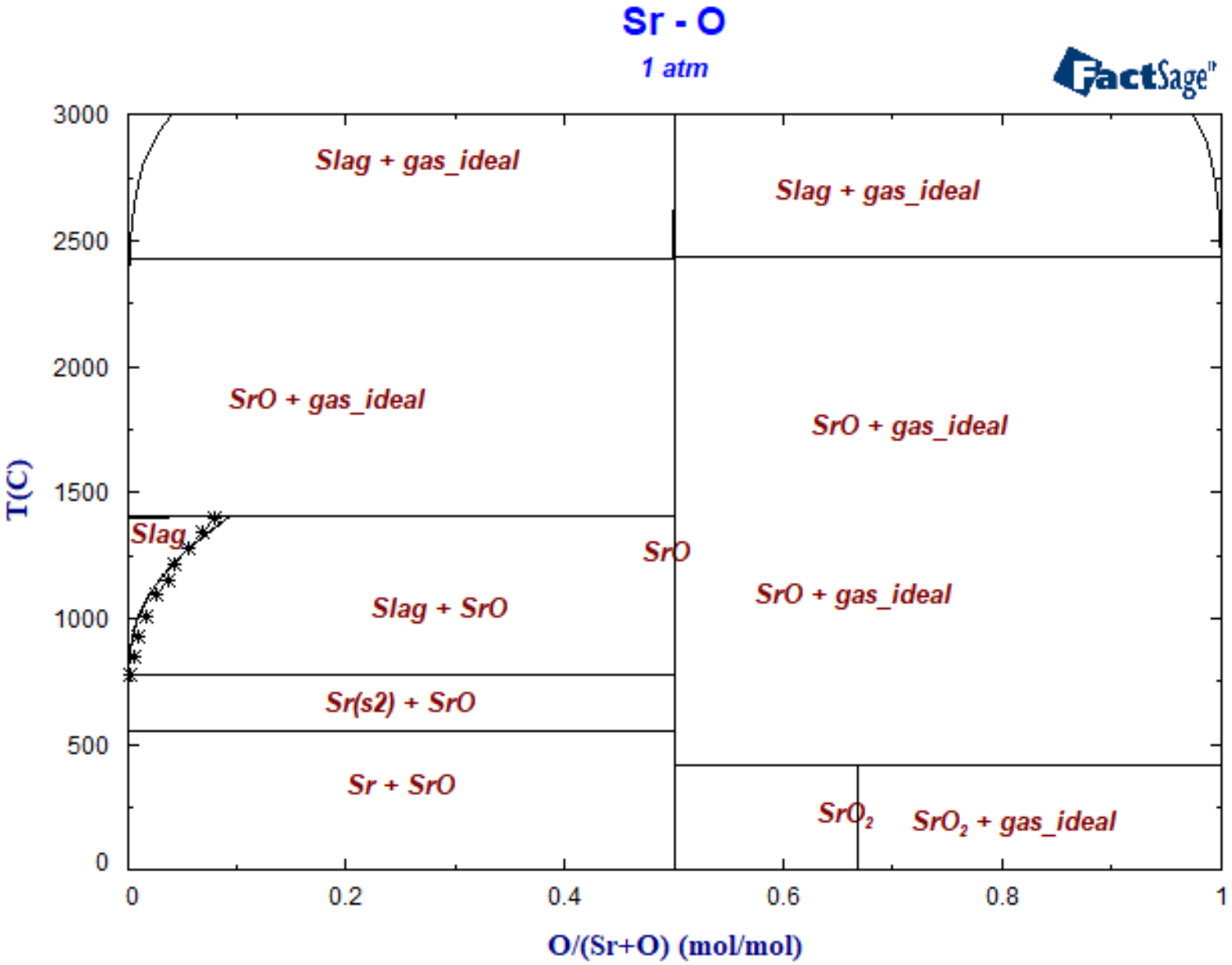

Weight percent

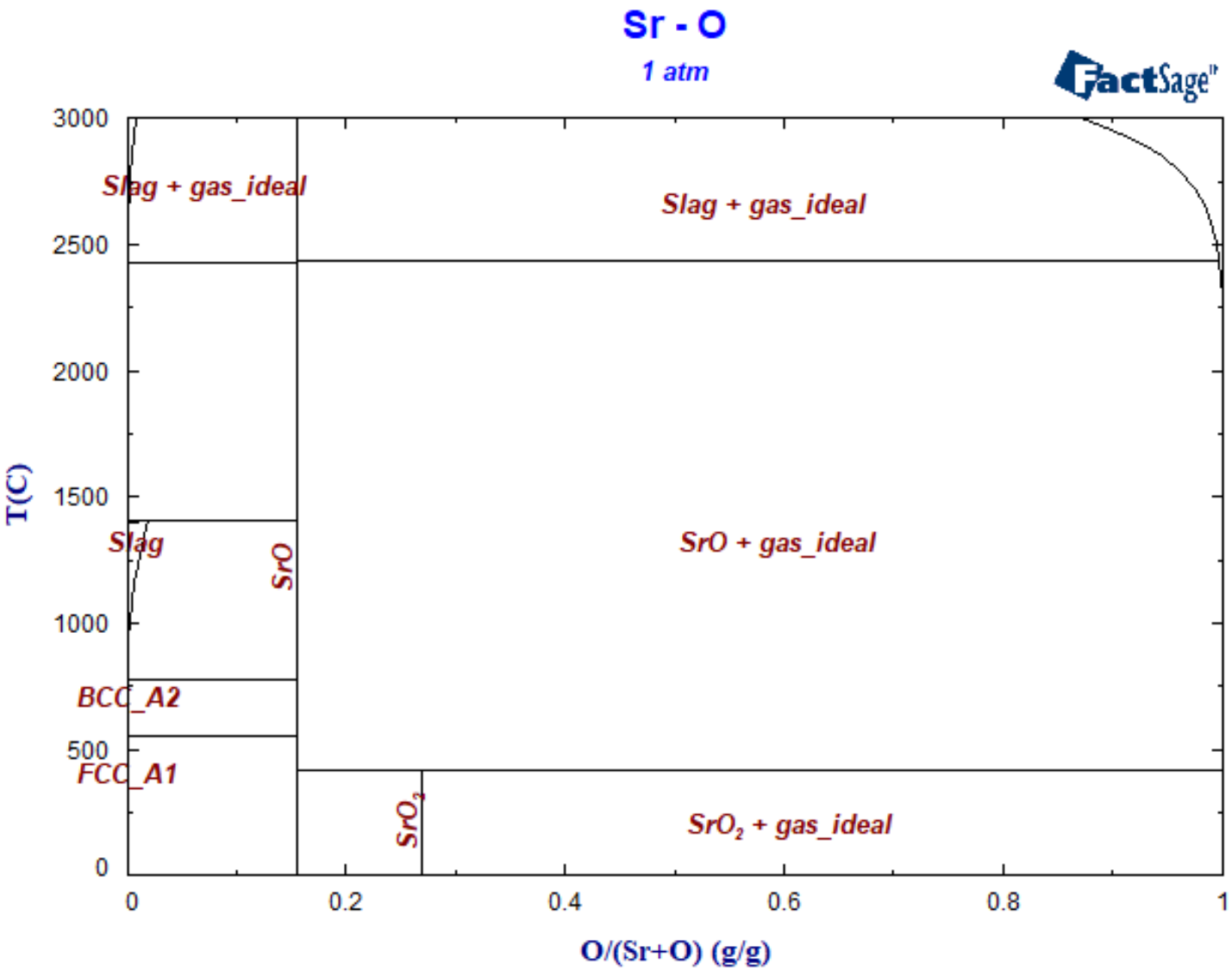

Mole fraction with isobars

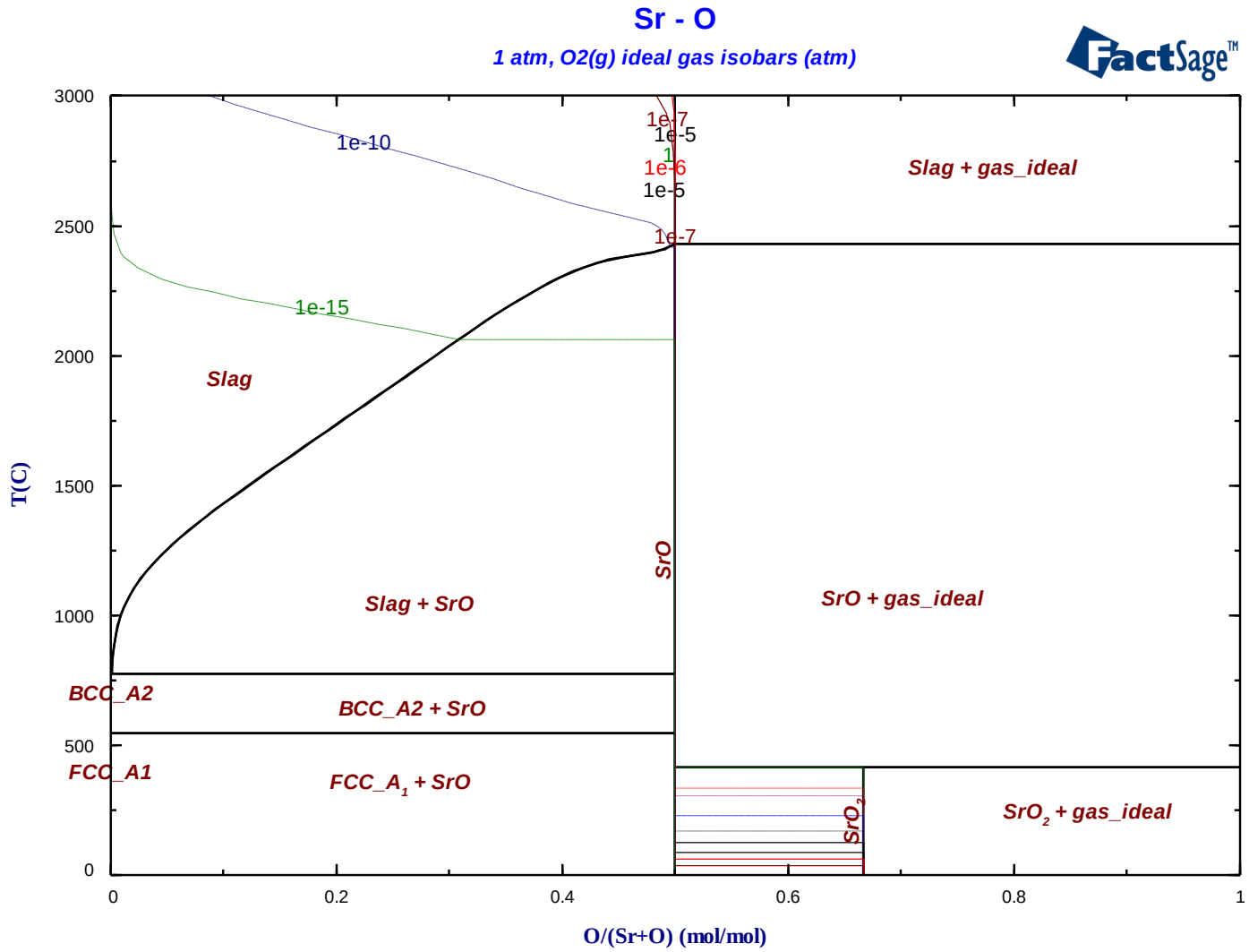

O2-Sr,
Temperature vs. log P(O2) diagram

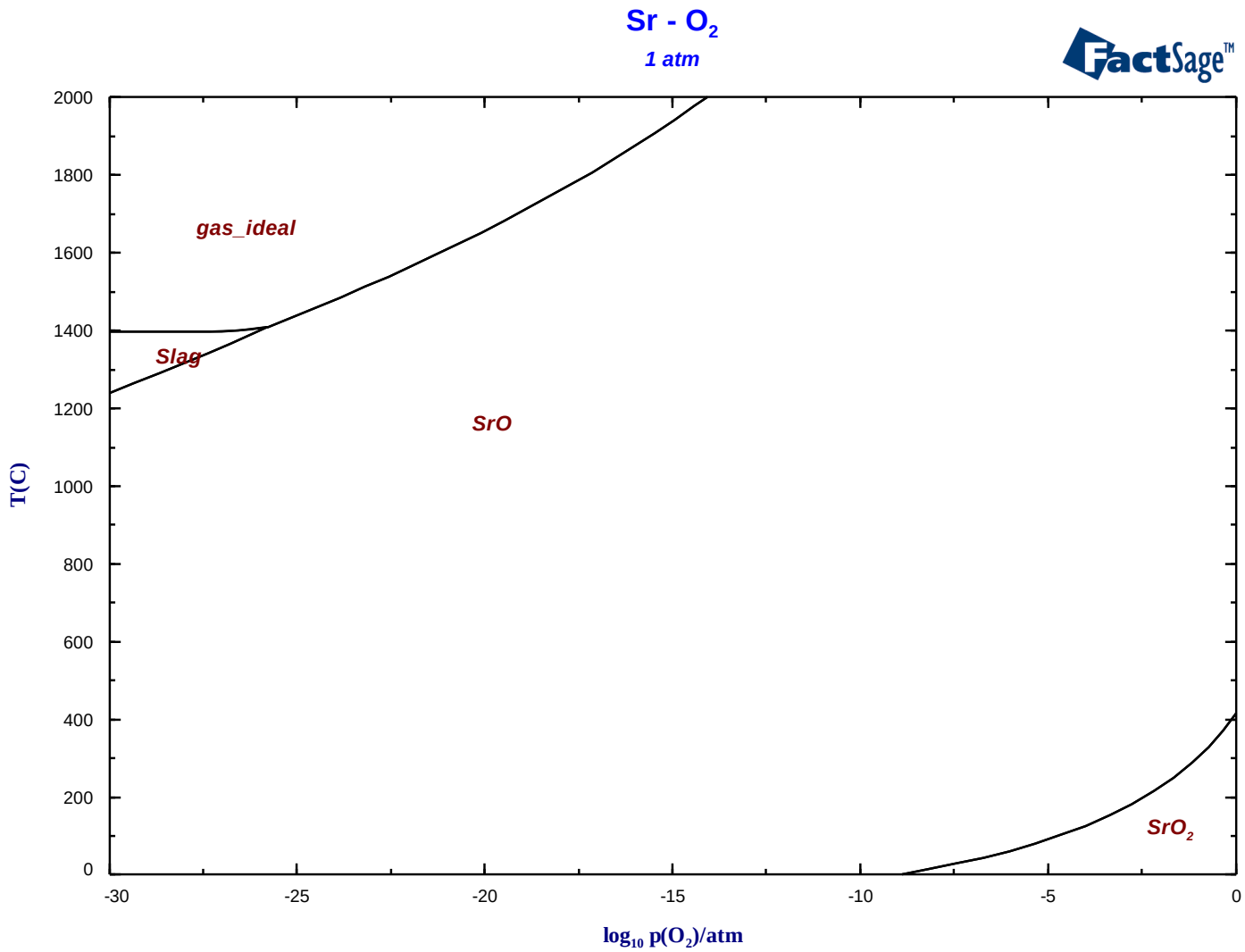

Mole fraction
compared with experimental data

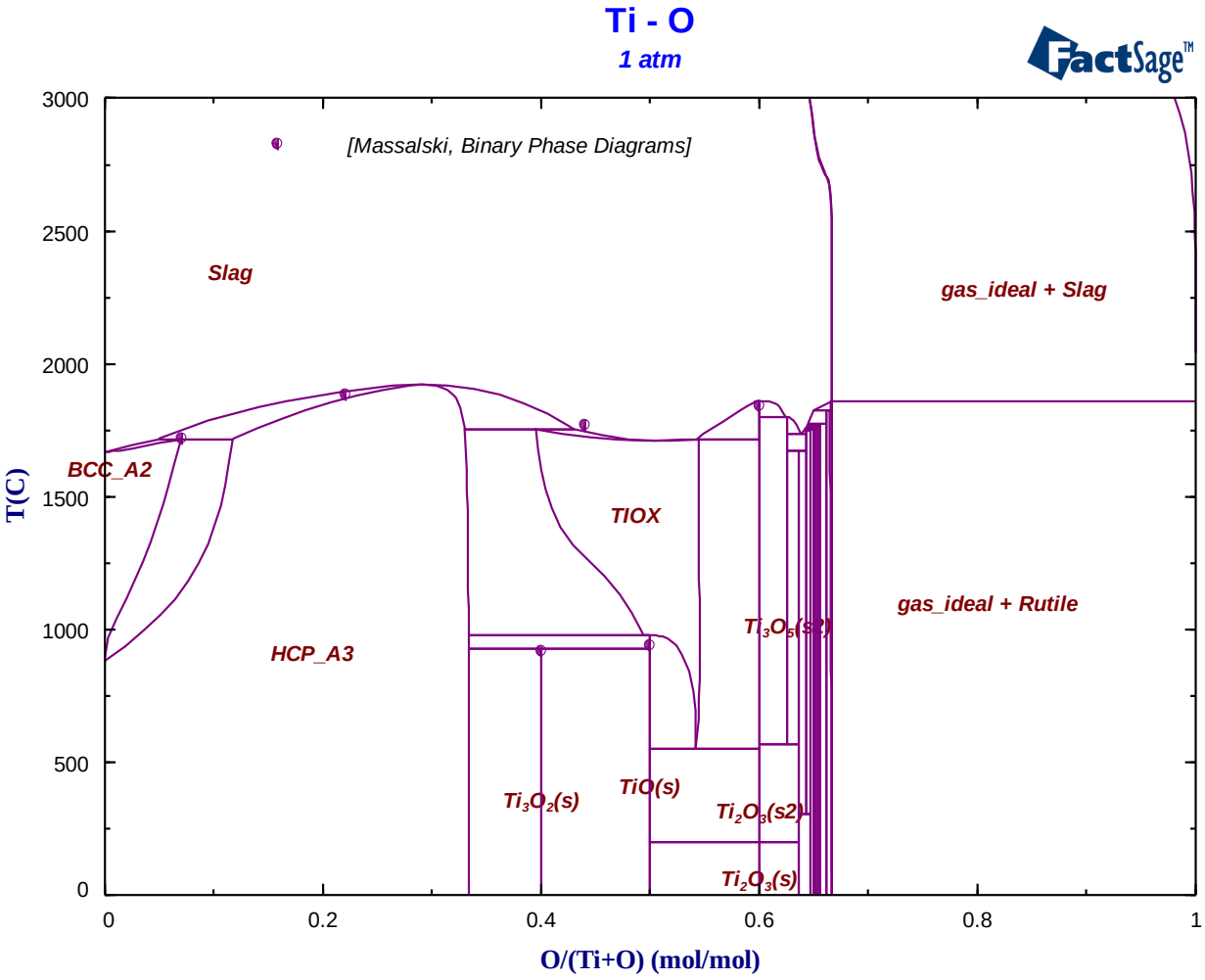

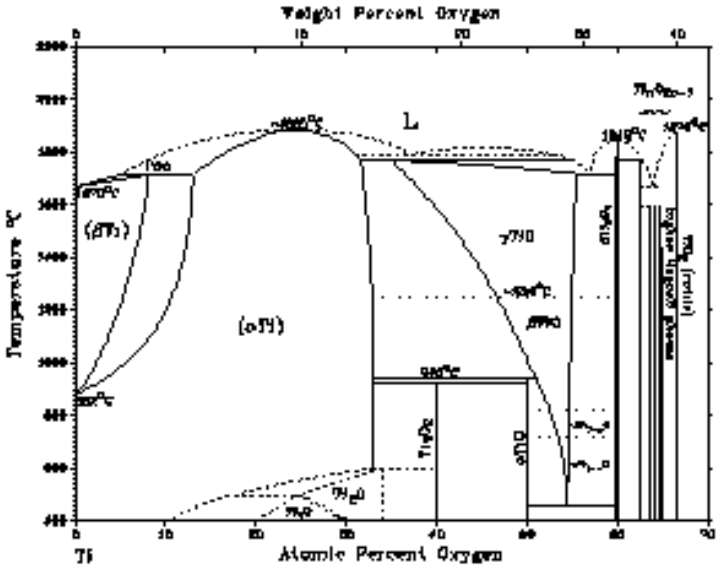

T.B. Massalski (ed), Binary Alloy Phase Diagrams, Second Edition, ASM International, Metals Park, OH 1990.

Weight percent

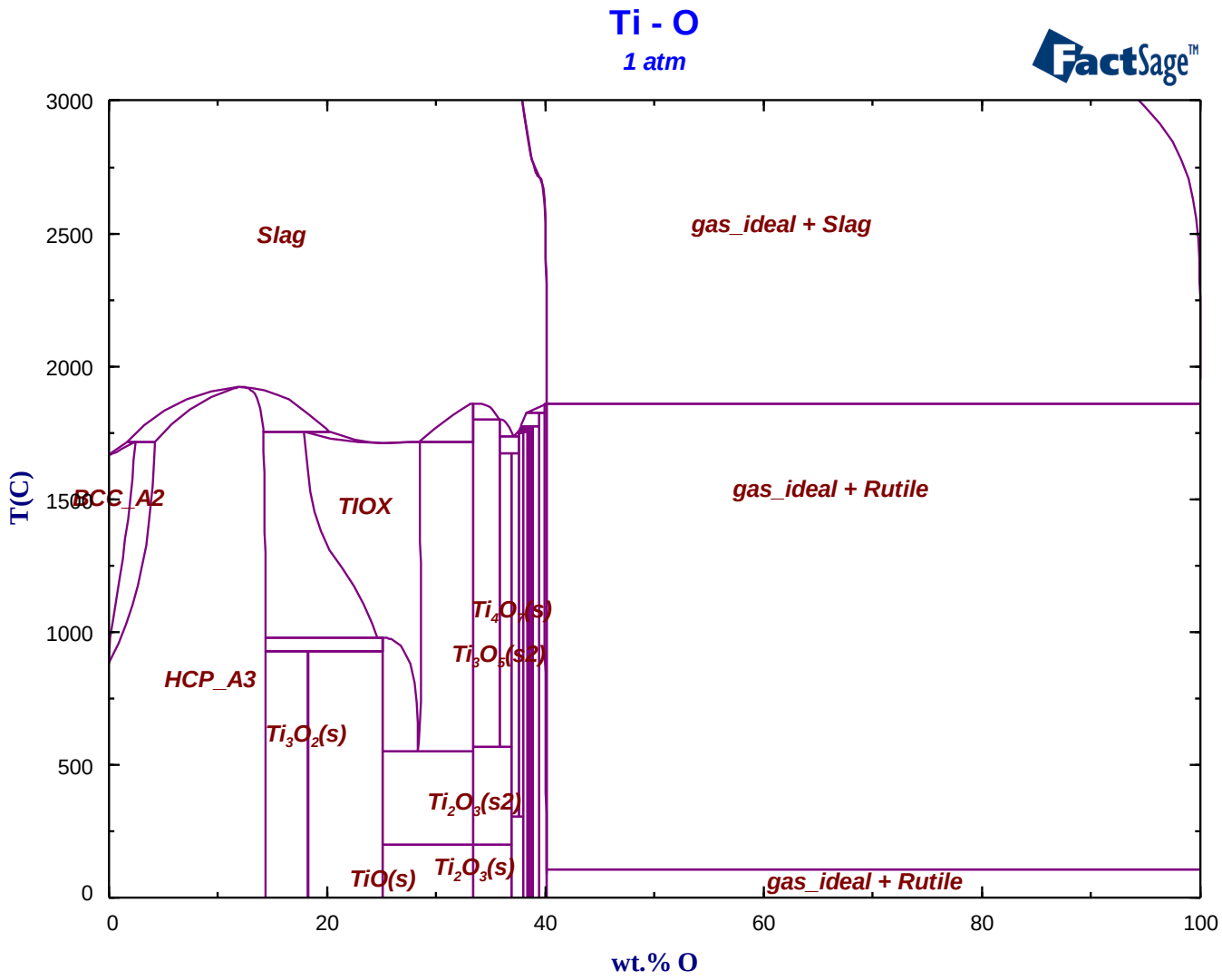

O-Ti,
Mole fraction with isobars

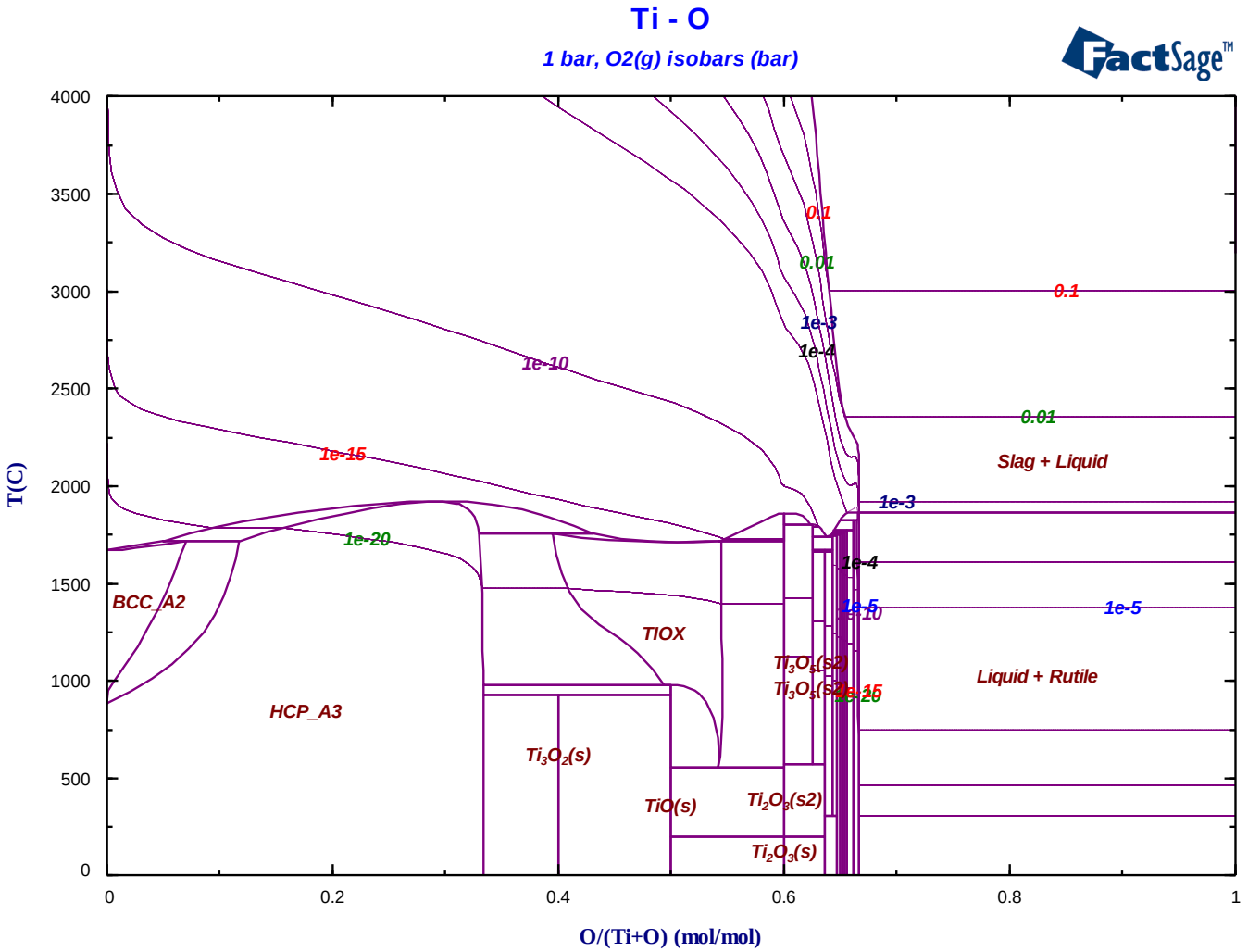

O2-Ti,
Temperature vs. log P(O2) diagram

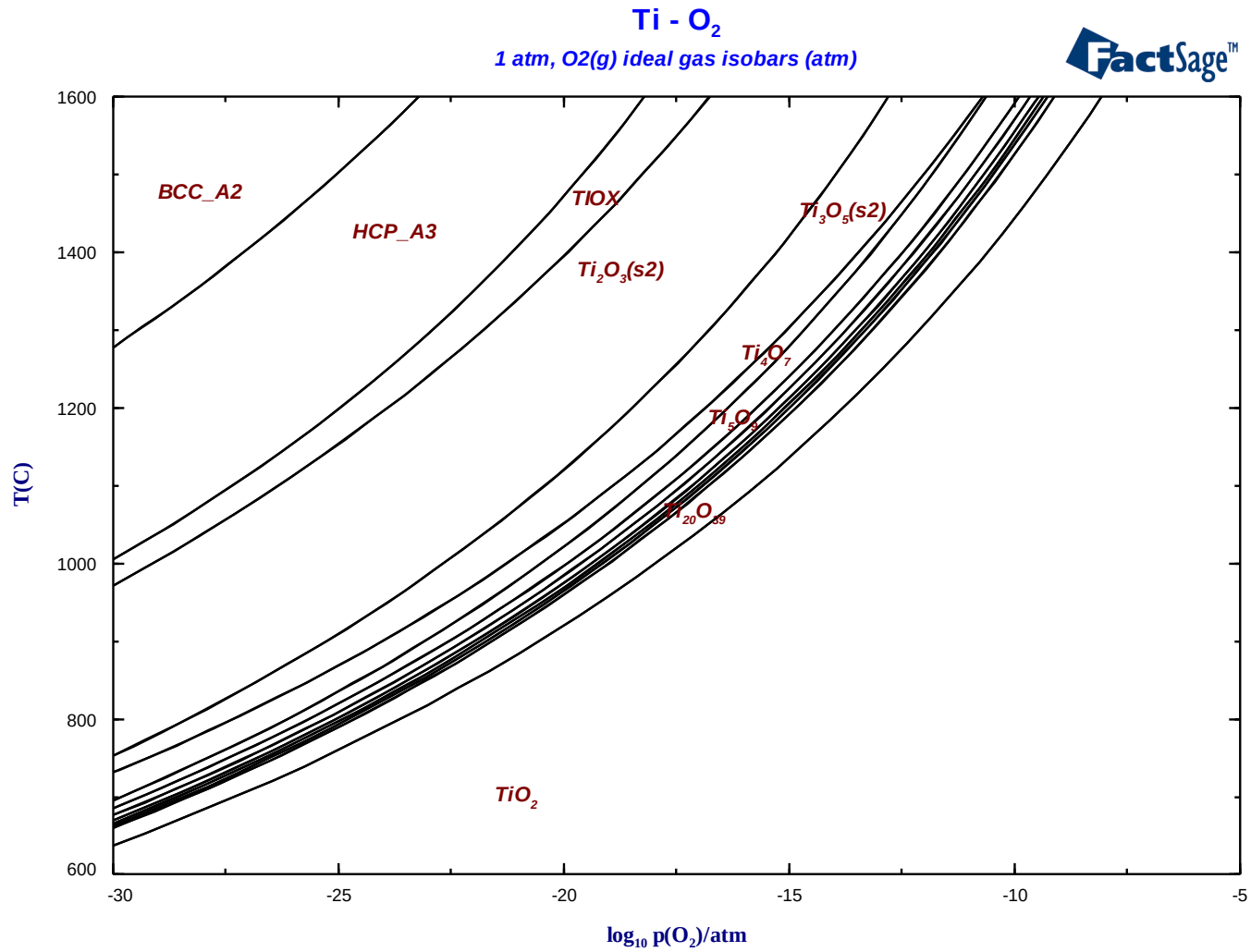

O-V,
Mole fraction

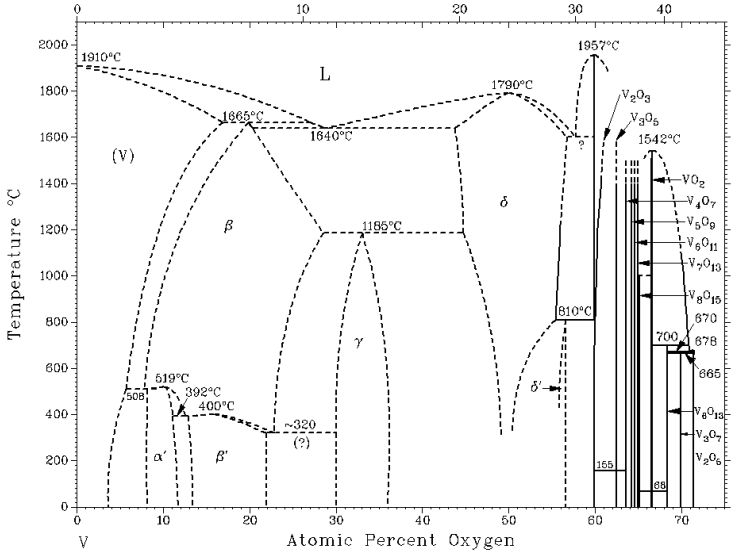

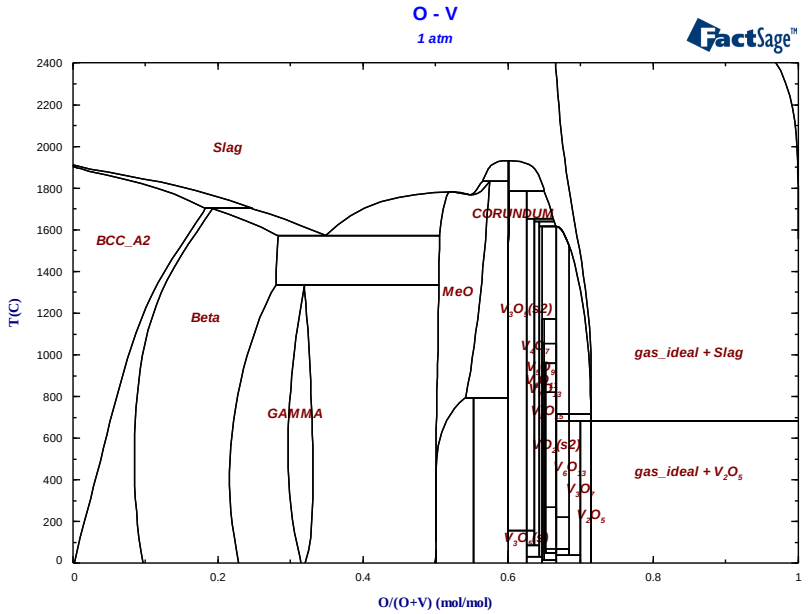

T.B. Massalski (ed), Binary Alloy Phase Diagrams, Second Edition, ASM International, Metals Park, OH 1990.

Phase	Description	Used data
Slag	$(V, V_2O_2, V_2O_3, V_2O_4, V_2O_5)$	Present work
Bcc-A2	$(V, O, VO_3)(Va)_3$	Present work
Beta	(V)(O, Va)	[Yang15]
Gamma	$(V)(O, Va)_{0.5}$	[Yang15]
MeO	$(V^{+2},V^{+3},V)(O^{-2})$	Present work
Corundum	$(V^{+4},V^{+3},Va)_2(O^{-2})_3$	Present work
VO, VO_2, V_2O_3, V_2O_5,	stoichiometric	[Yang15]
V_3O_5, V_3O_7, V_4O_7,	stoichiometric	[Yang15]
V_5O_9, V_6O_{11},	stoichiometric	[Yang15]
V_6O_{13},V_7O_{13},V_8O_{15},	stoichiometric	[Yang15]
$V_{52}O_{64}$	stoichiometric	[Yang15]

O-V,
Weight percent

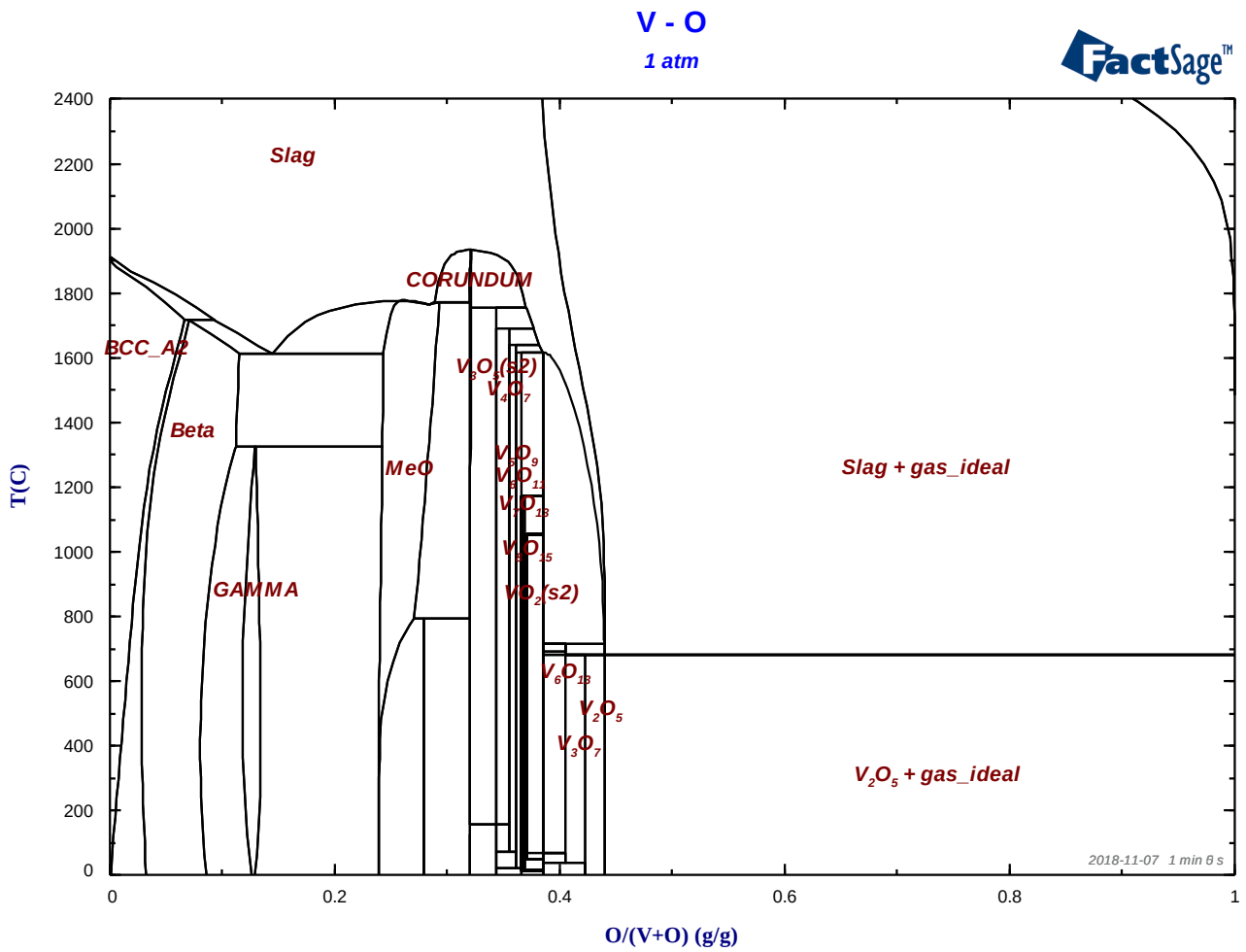

O-V,
Mole fraction with isobars

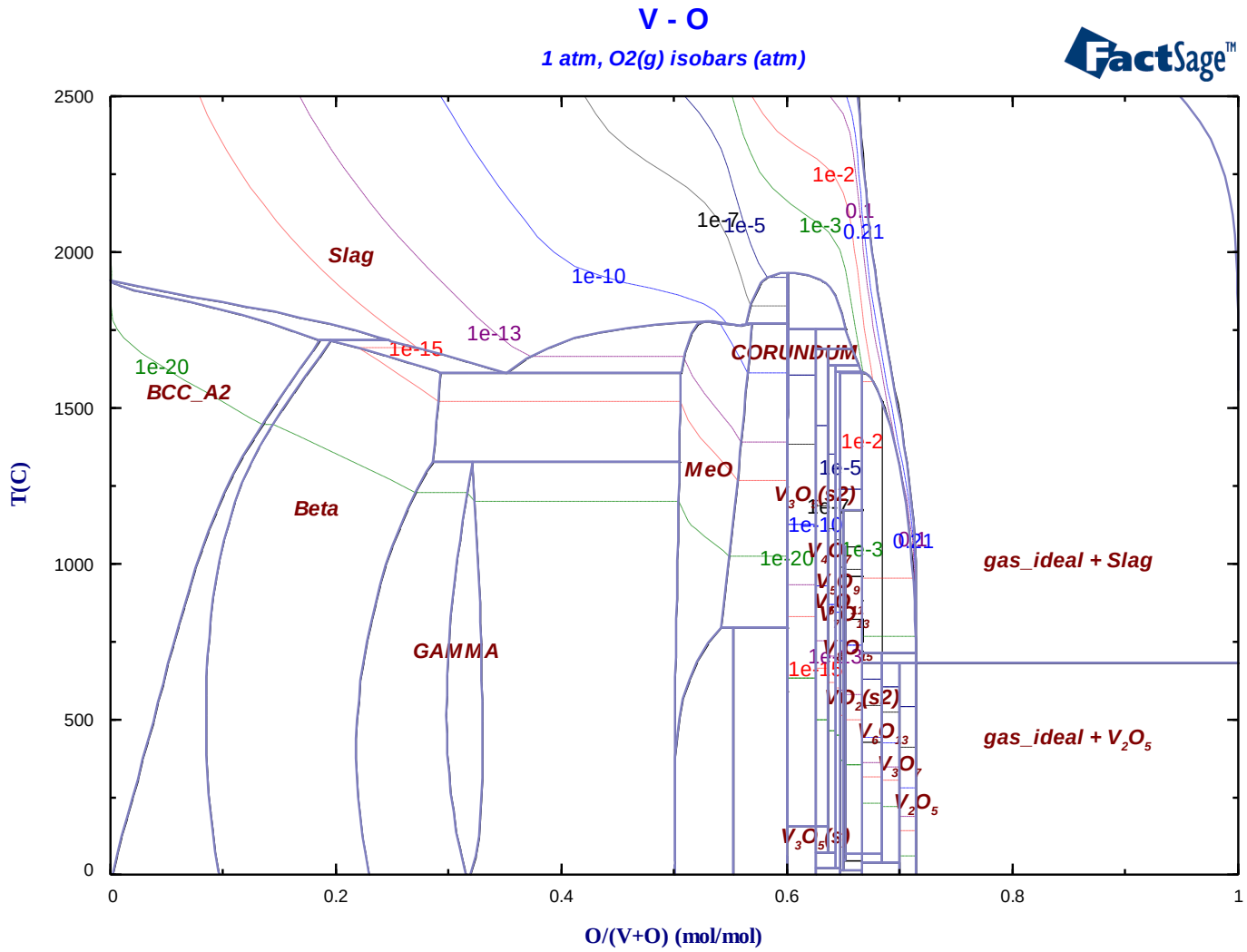

O2-V,
Temperature vs. log P(O2) diagram

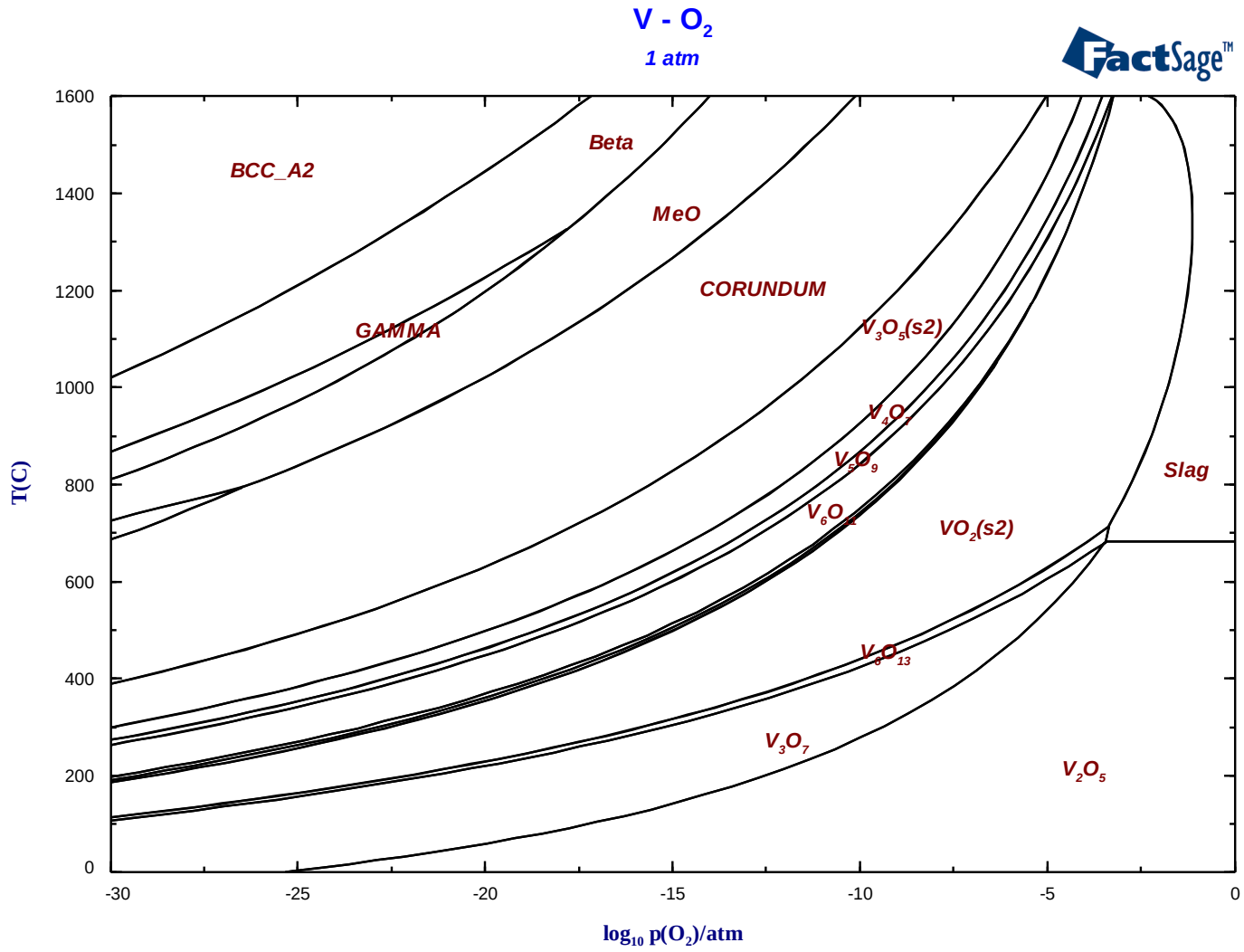

O-Zn,
Mole fraction

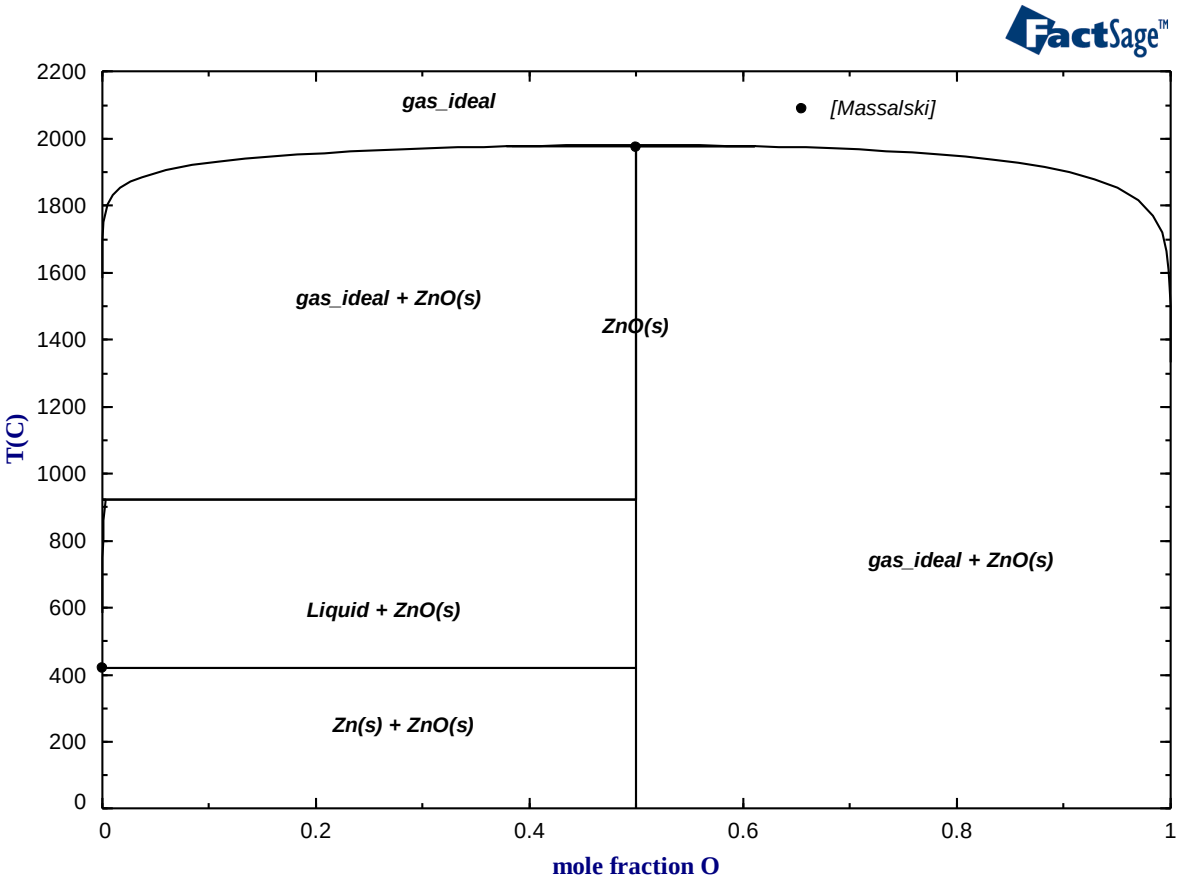

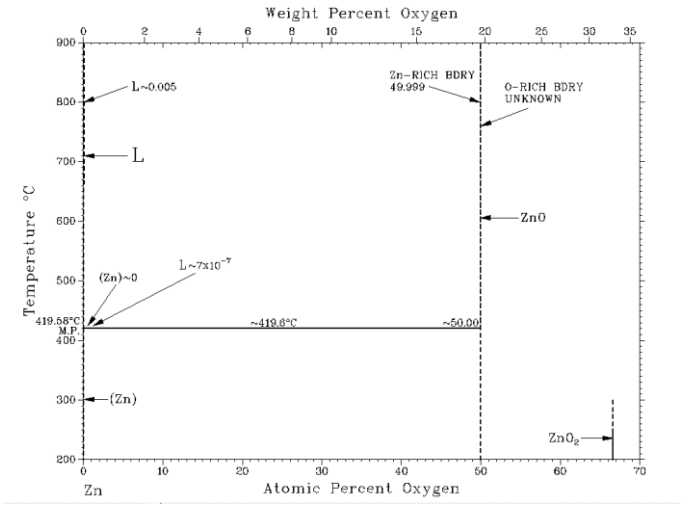

T.B. Massalski (ed), Binary Alloy Phase Diagrams, Second Edition, ASM International, Metals Park, OH 1990.

O-Zn,
Weight percent

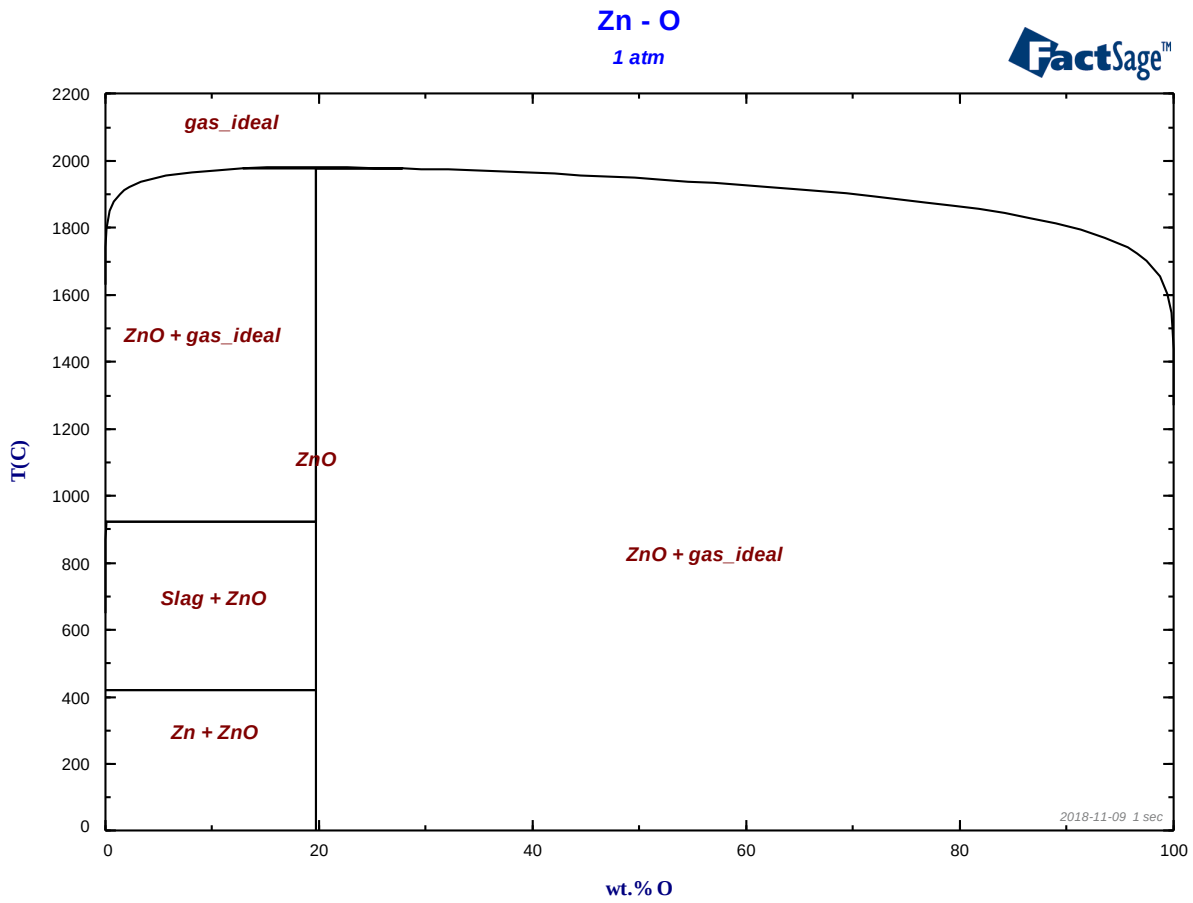

O-Zn,
Mole fraction with isobars

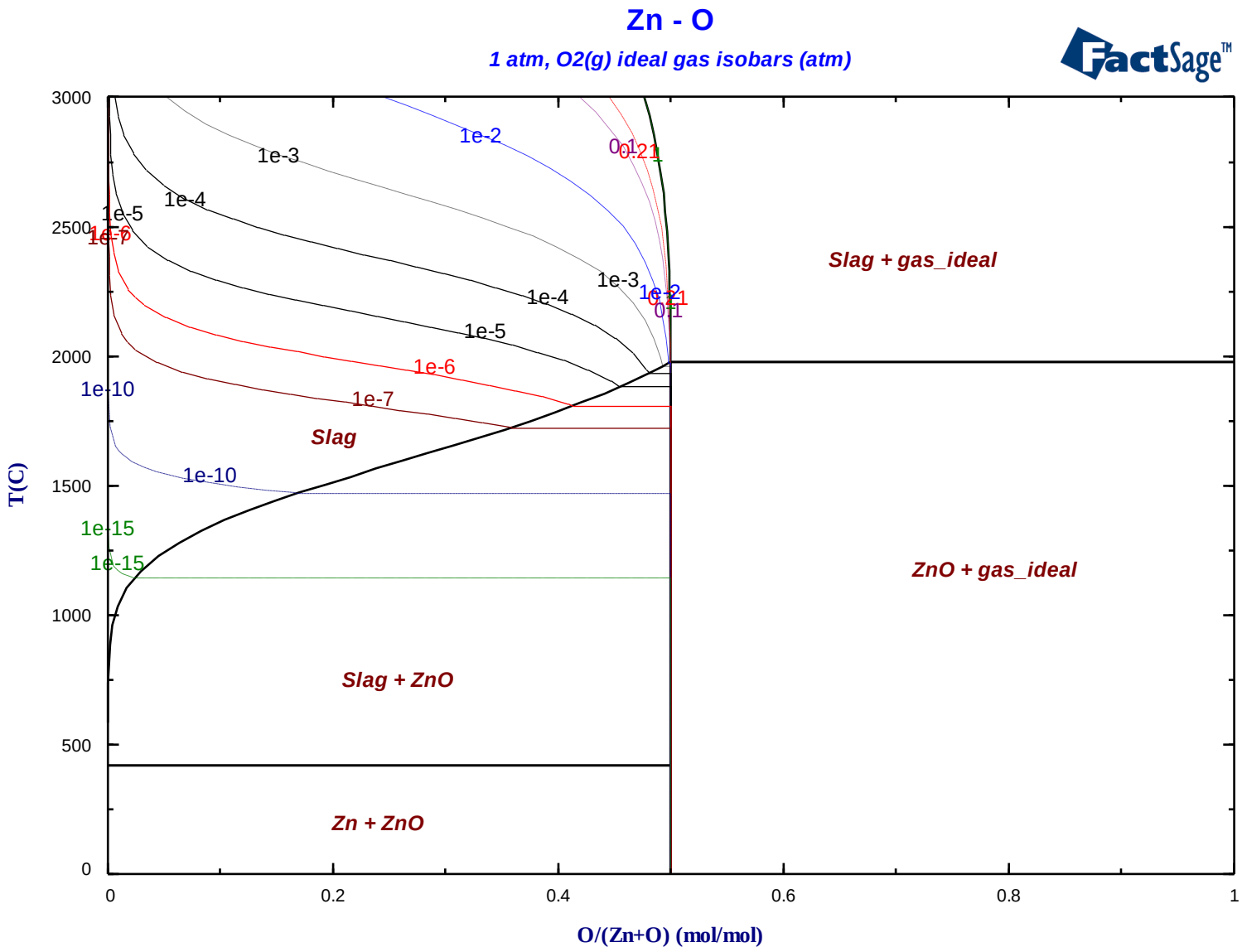

O2-Zn,
Temperature vs. log P(O2) diagram

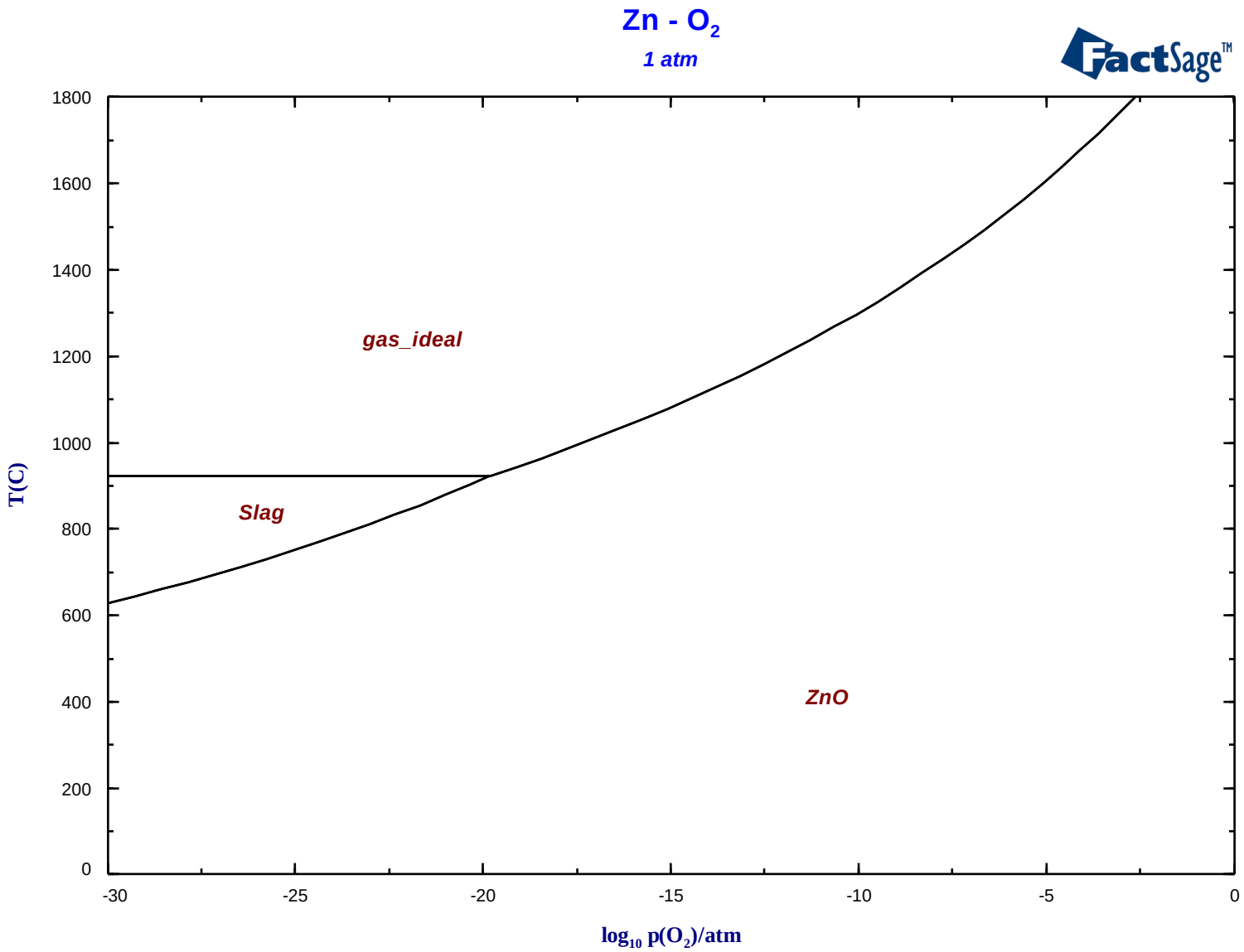

Mole fraction
compared with experimental data

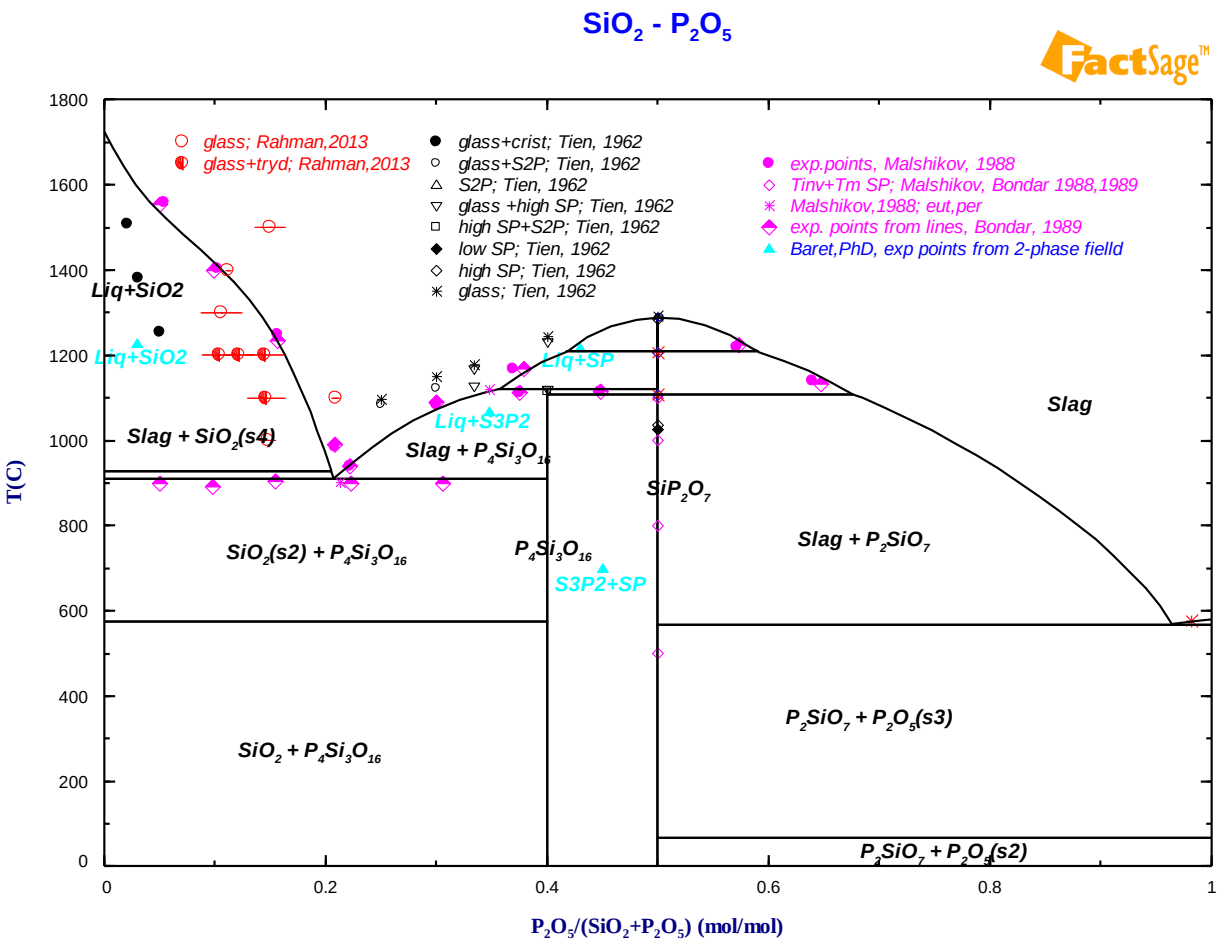

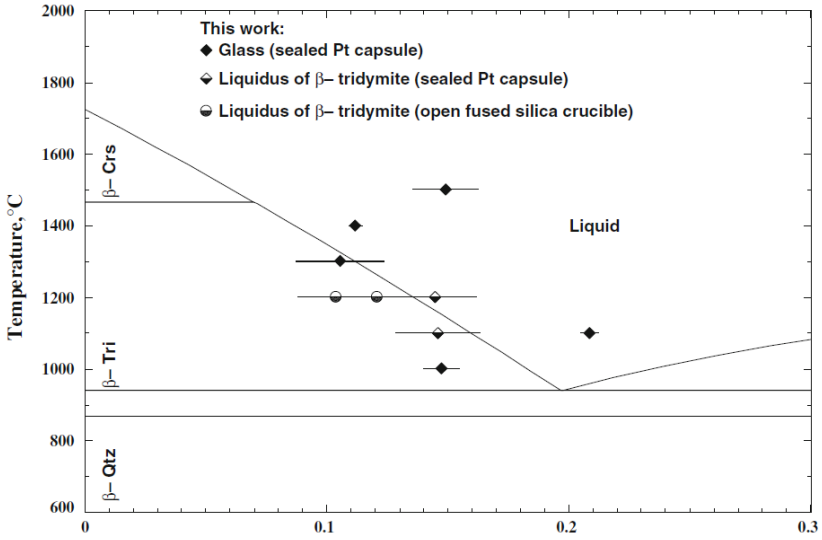

M. Rahman, P. Hudon, I.-H. Jung, Metall Mater Trans B, 2013; 44B: 837-52.

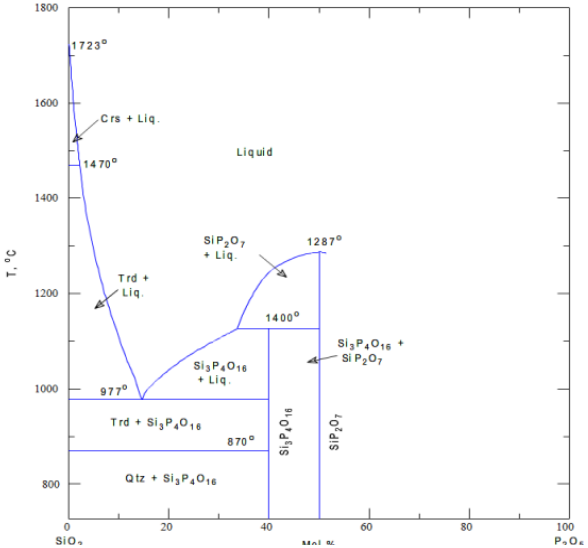

G. Baret, R. Madar, and C. Bernard, J. Electrochem. Soc., 138 [9] 2830-2835 (1991).

Weight percent

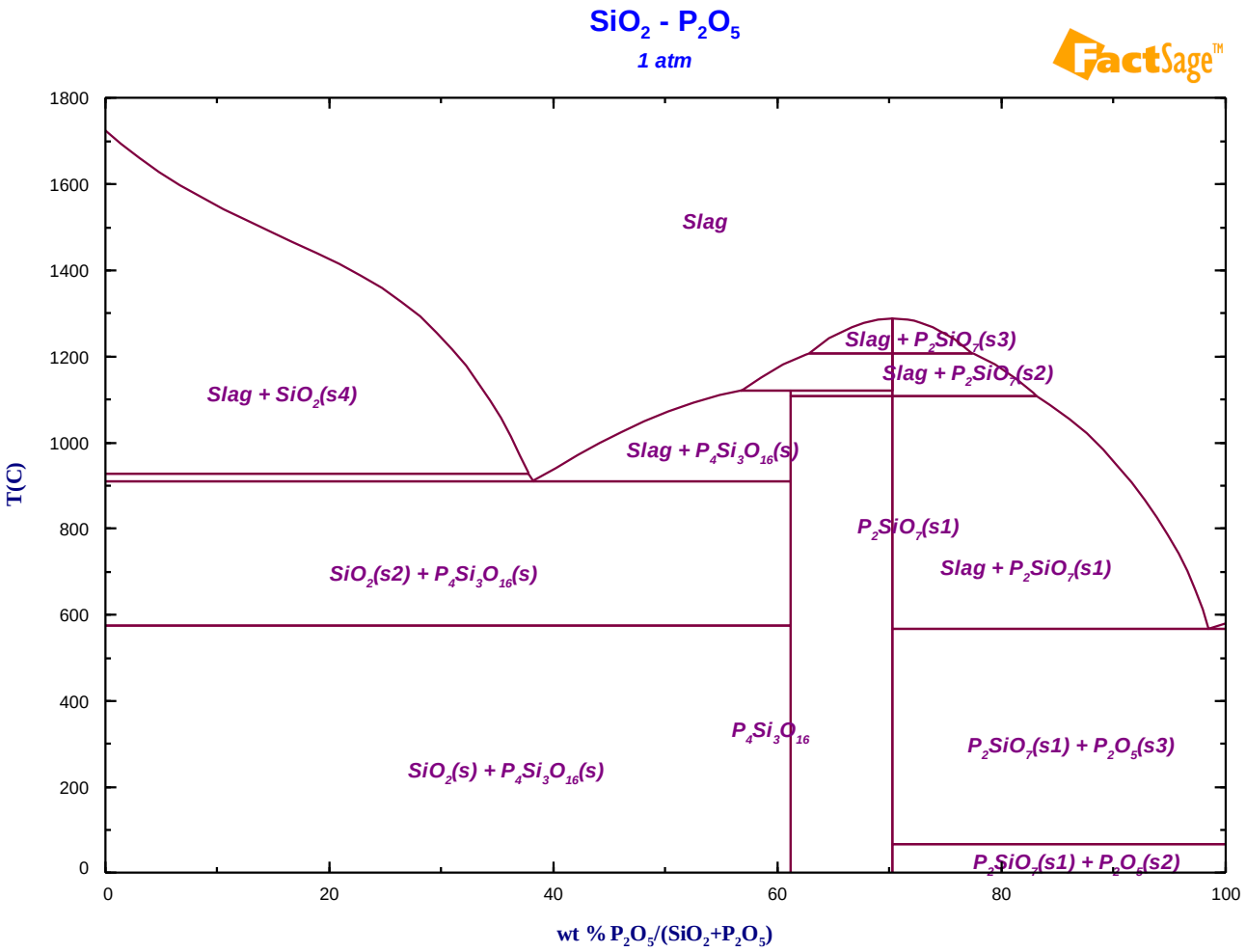

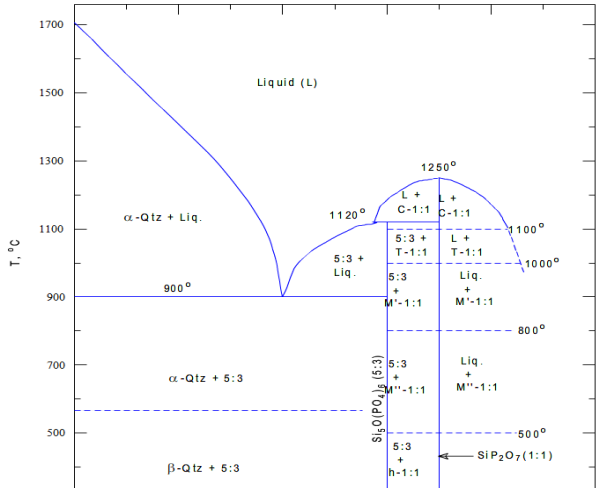

A. E. Mal'shikov and I. A. Bondar, Russ. J. Inorg. Chem. (Engl. Transl.), 33[1] 109-112

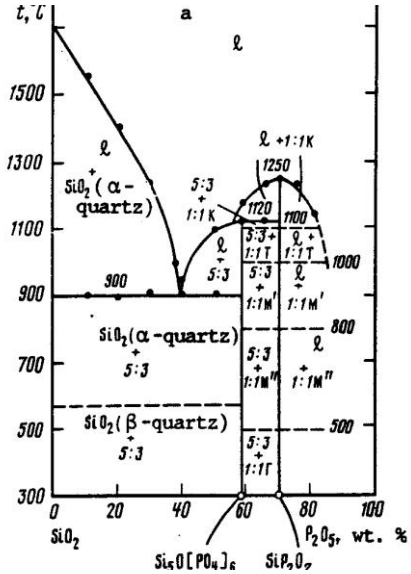

I.A. Bondar', A.E. Mal'shikov, Dokl Phys Chem, 1989; 306: 361-4.

Mole fraction
compared with experimental data

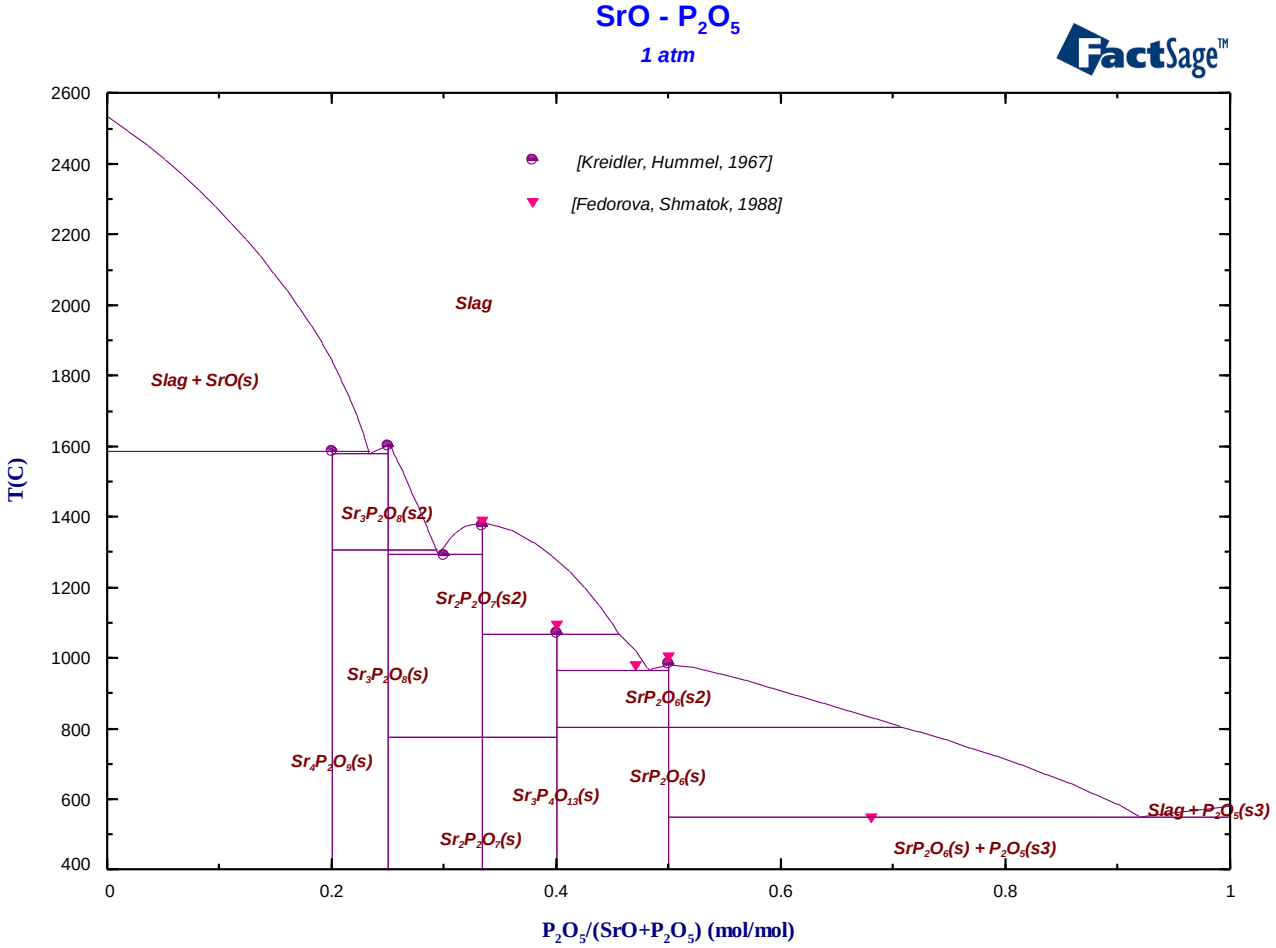

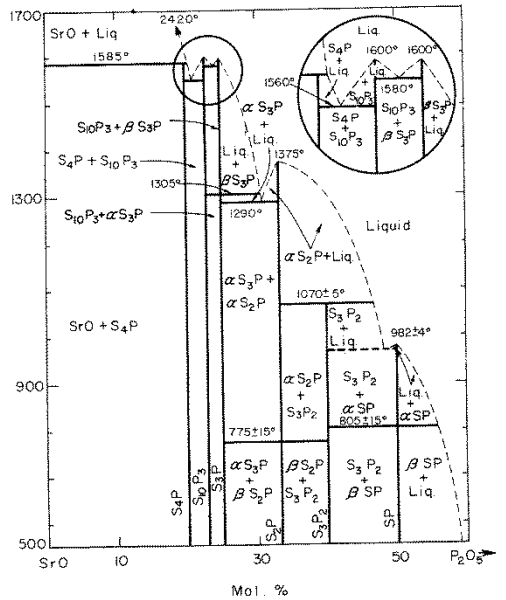

E.R. Kreidler, F.A. Hummel, Inorg. Chem., 6 [5], (1967), pp.884-891.

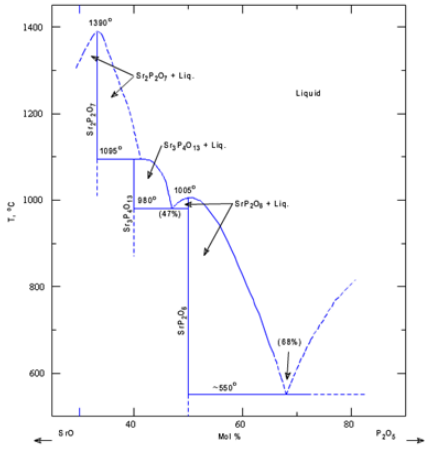

E. N. Fedorova and L. K. Shmatok, Fiz. Khim. Stekla, 14 [4] 636-638 (1988).

Weight percent

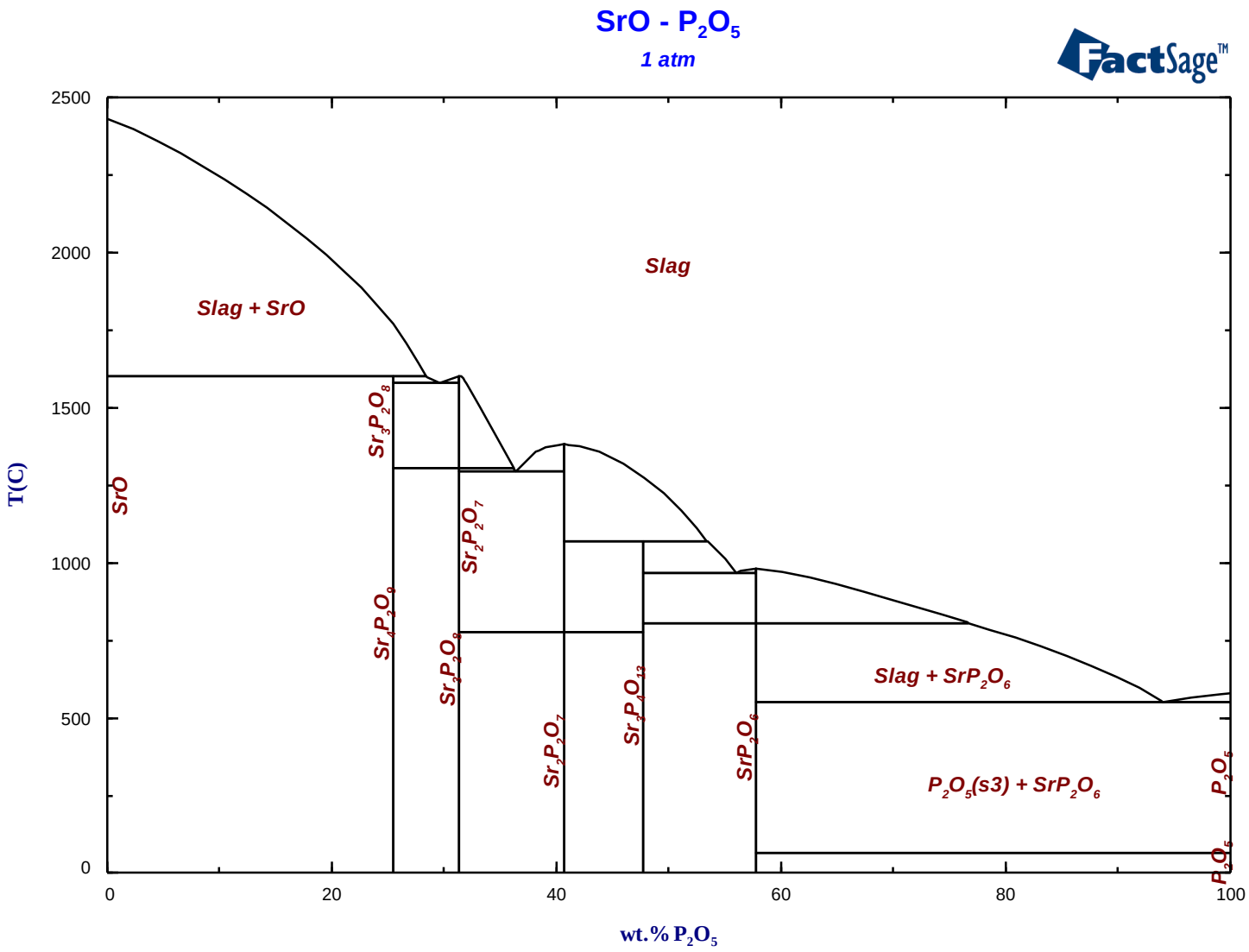

Mole fraction

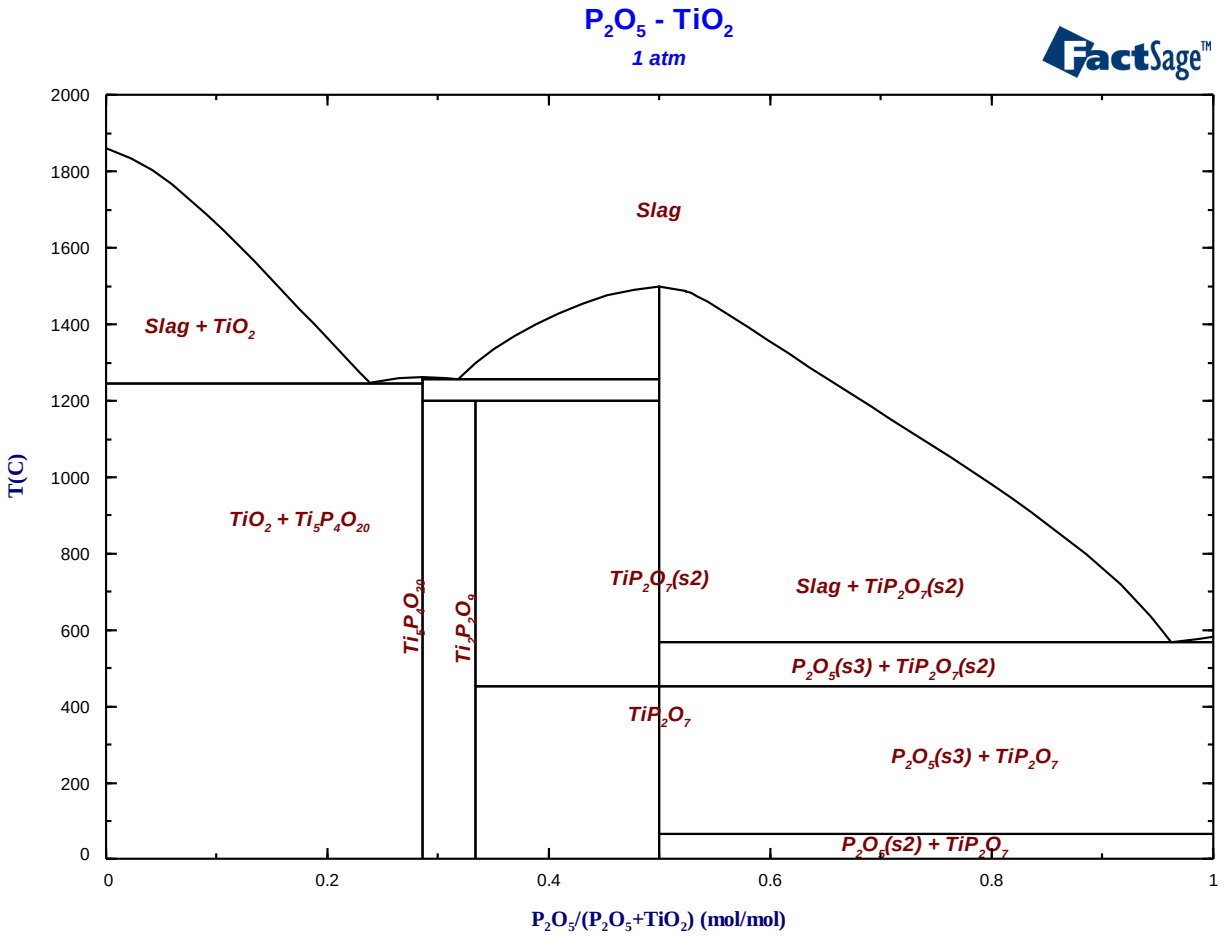

Weight percent
compared with experimental data

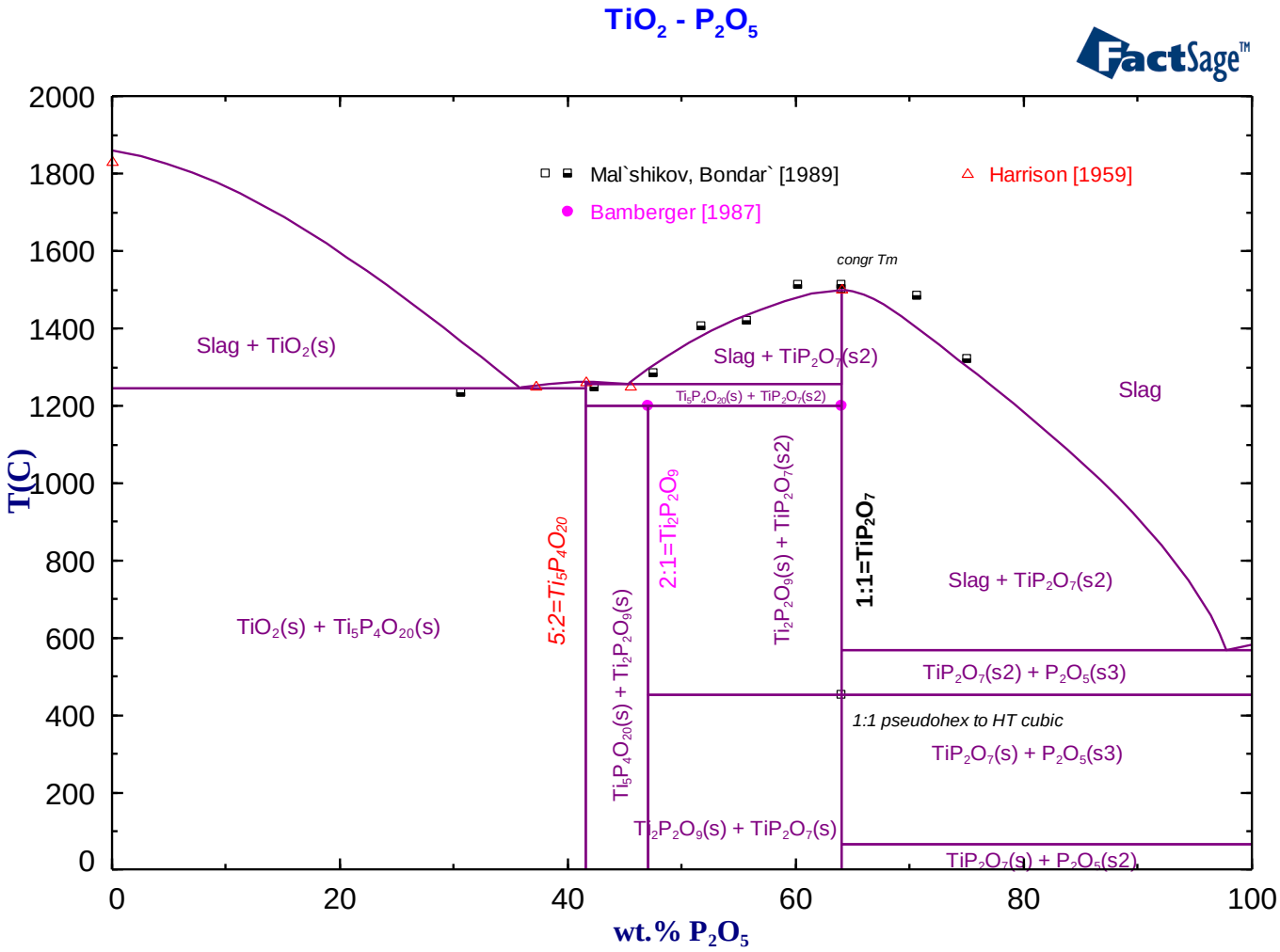

Mole fraction

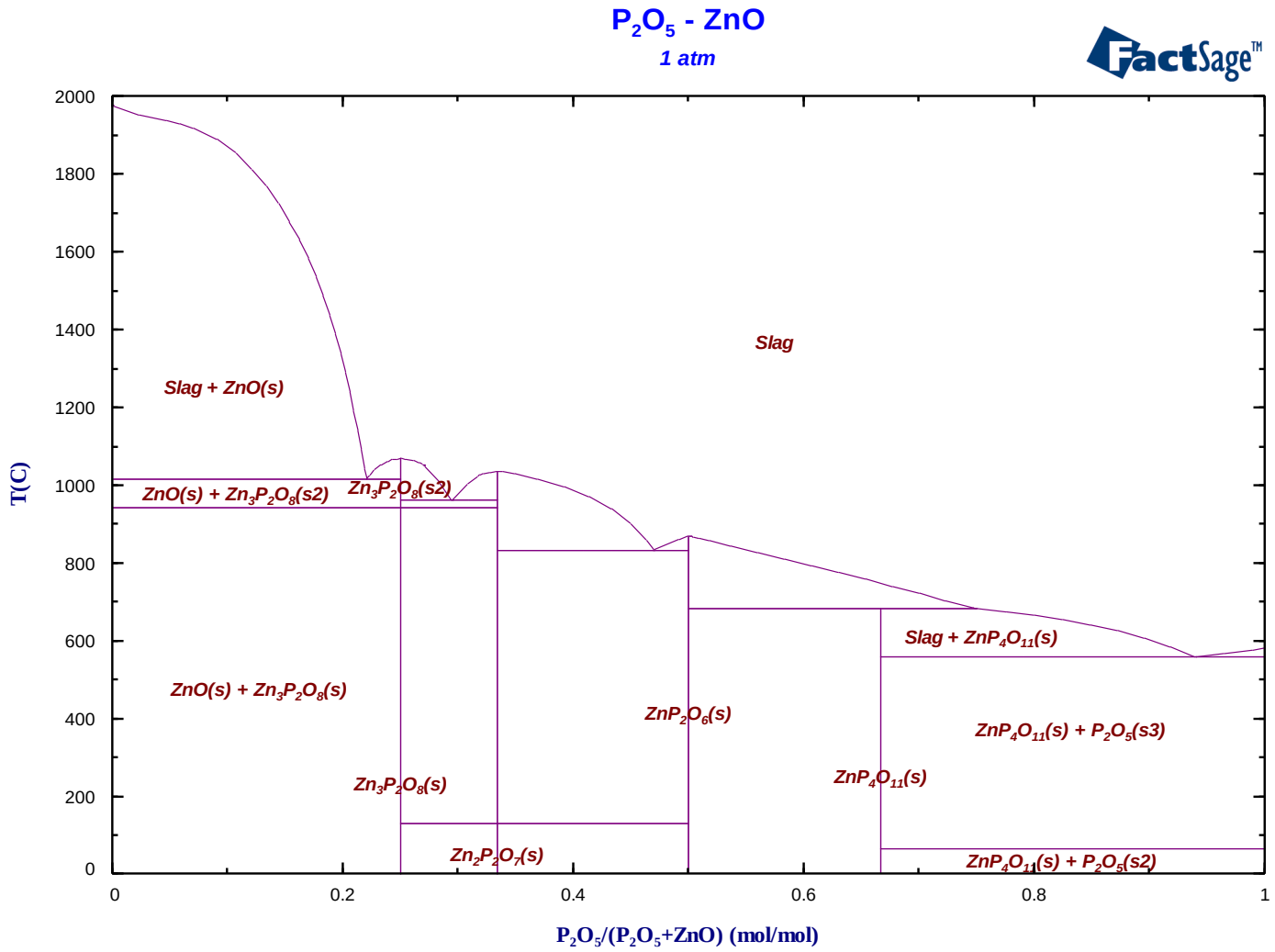

Weight percent
compared with experimental data

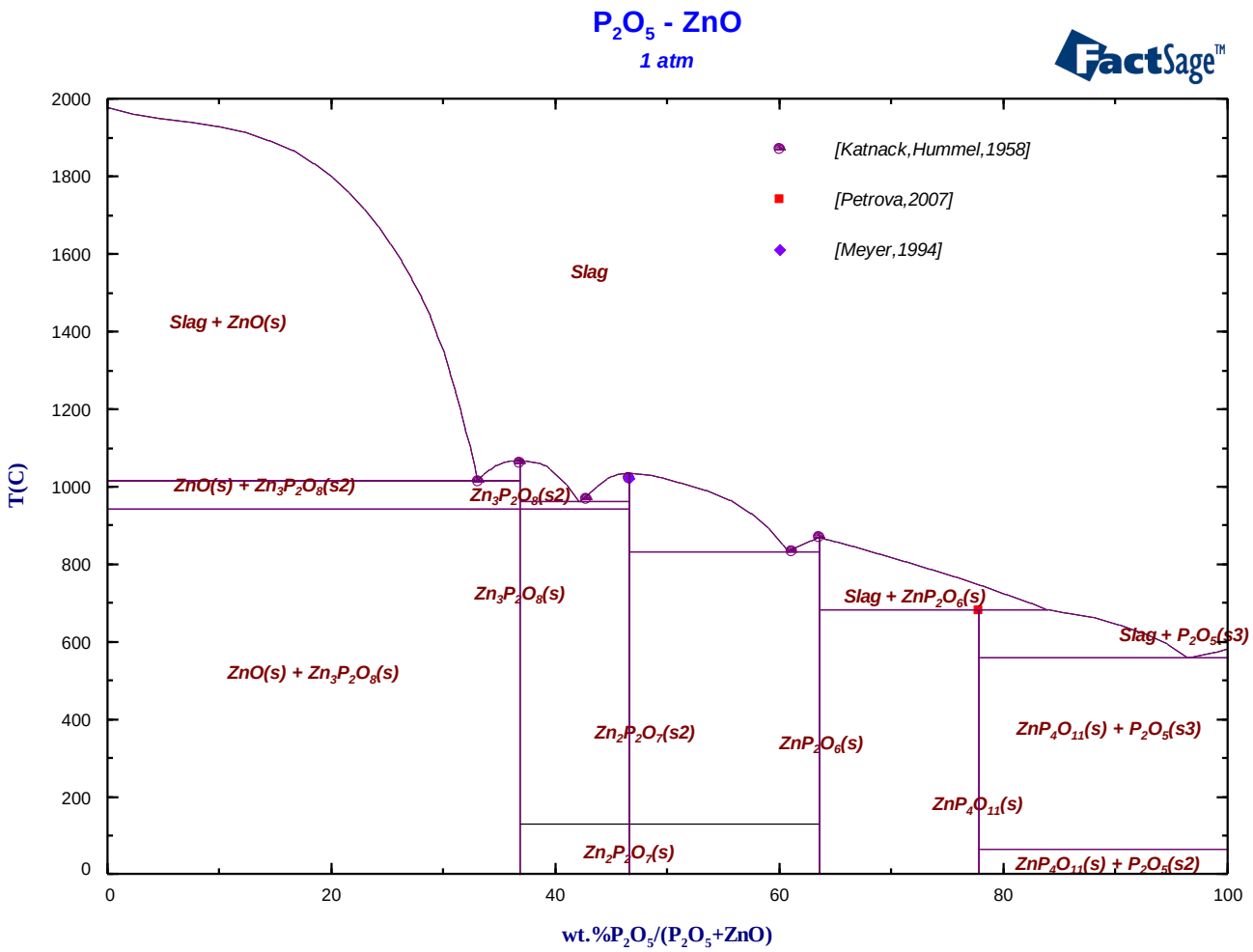

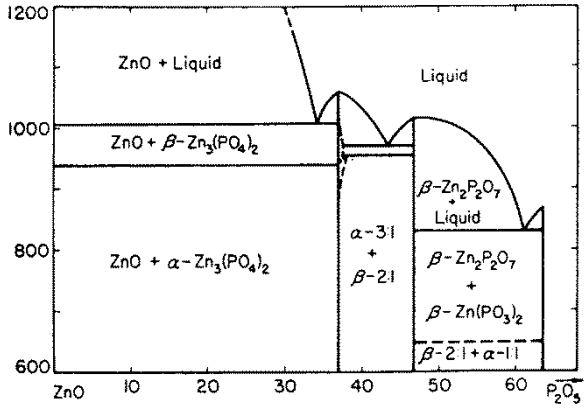

F.L. Katnack, F.A. Hummel, J. Electrochem. Soc., 105 [3], (1958), pp.125-133.

Mole fraction compared with experimental data

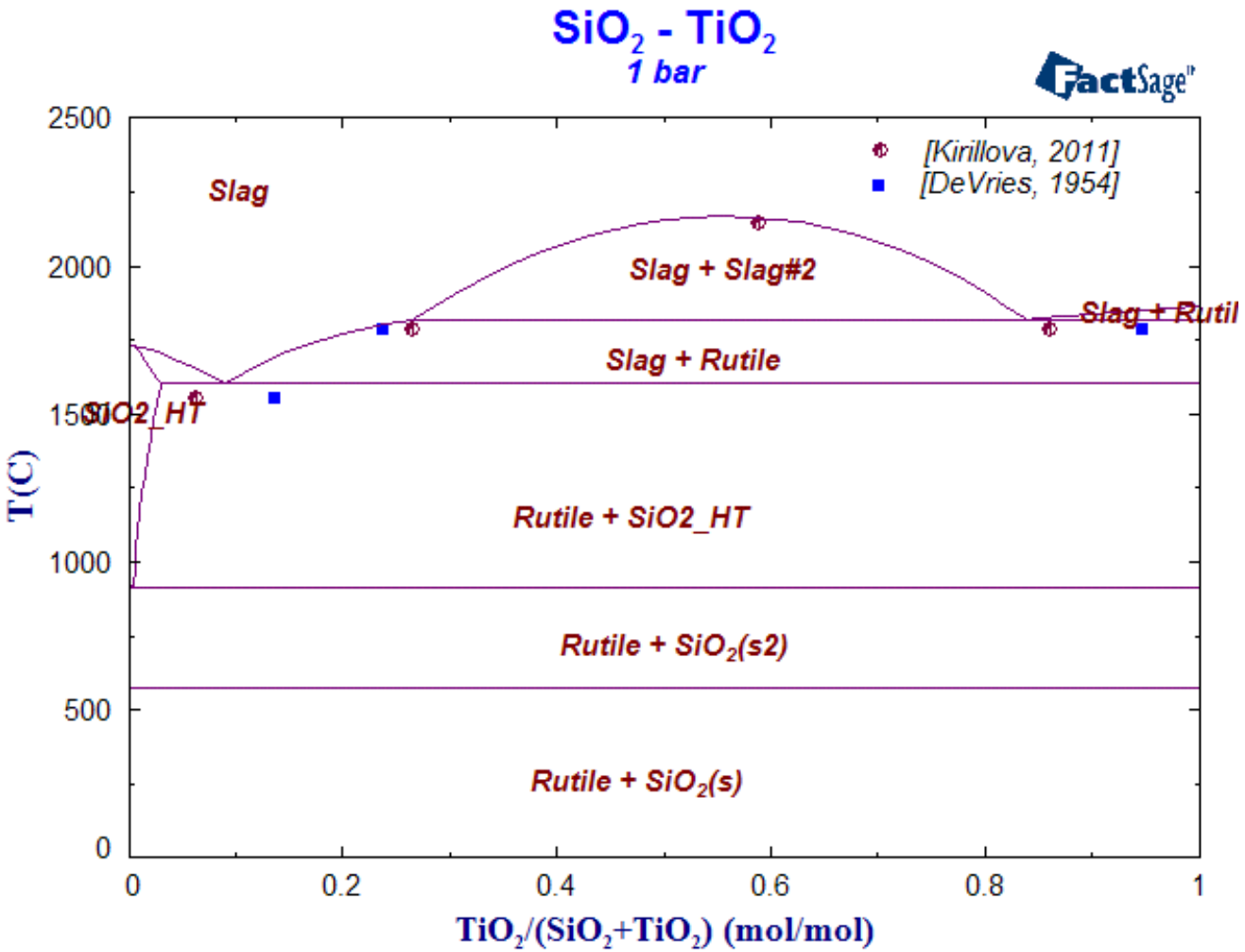

Weight percent

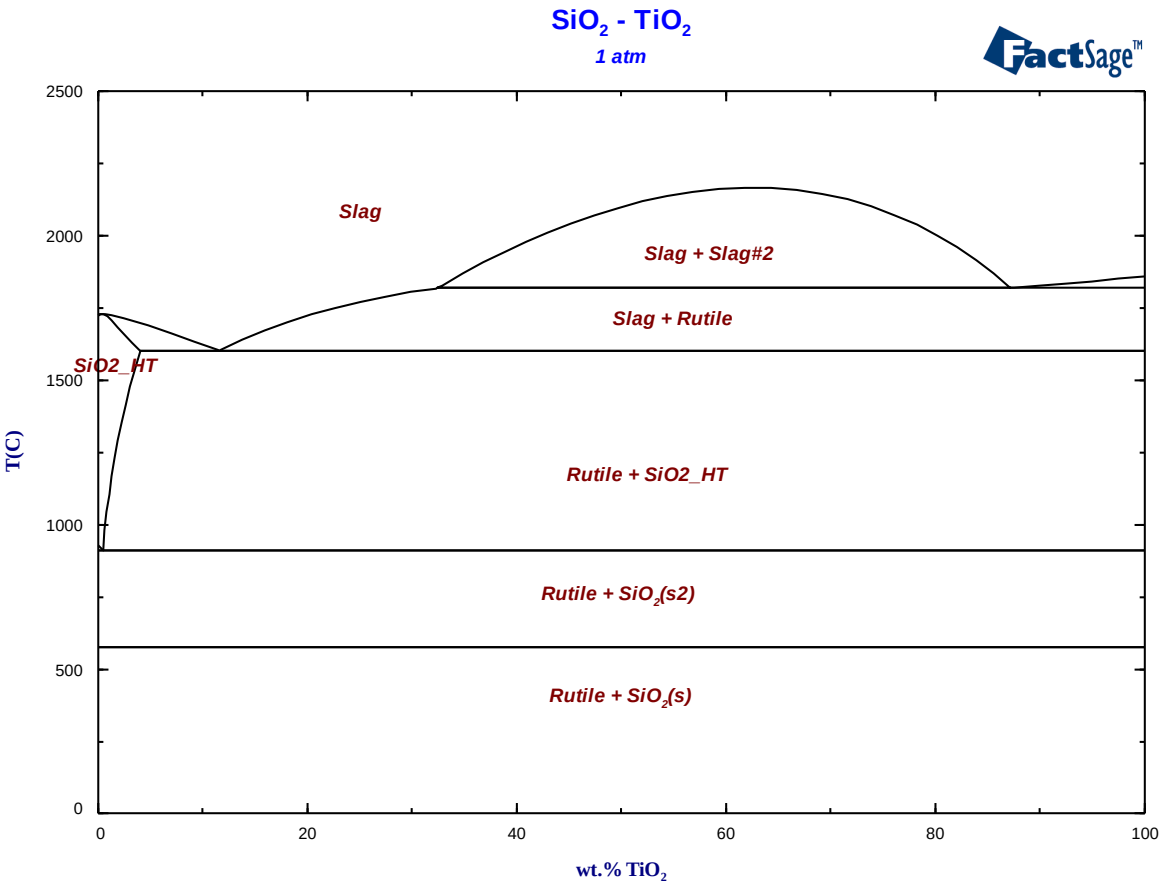

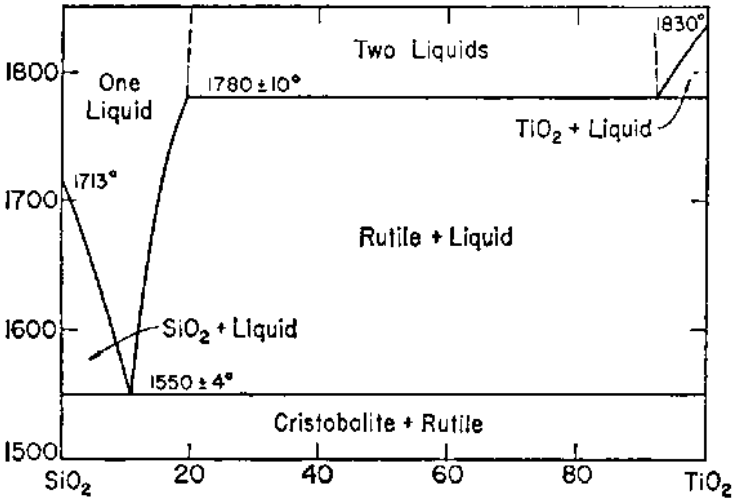

R.C. DeVries, R. Roy, E.F. Osborn, Trans. J. Br. Ceram. Soc., 53 [9], (1954), pp. 525-540.

SiO2-V2O3,
Mole fraction

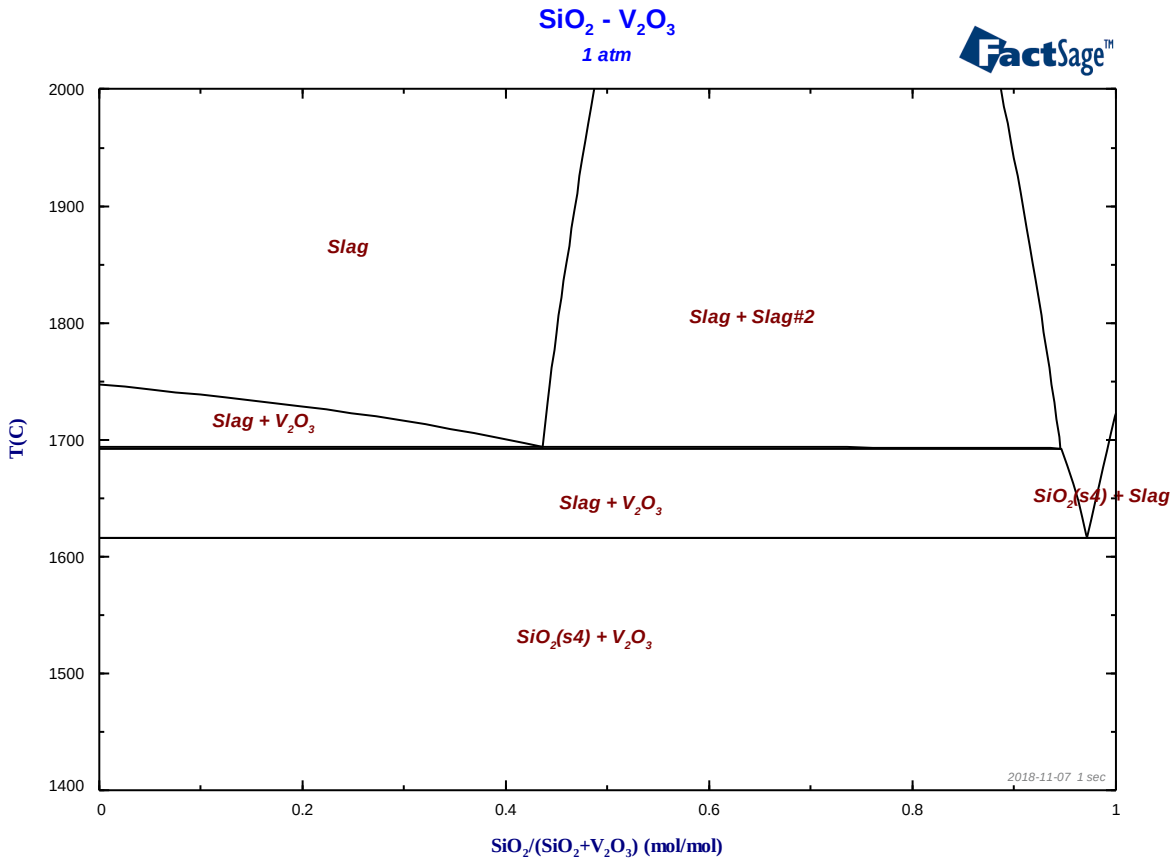

SiO2-V2O3, Weight percent compared with experimental data

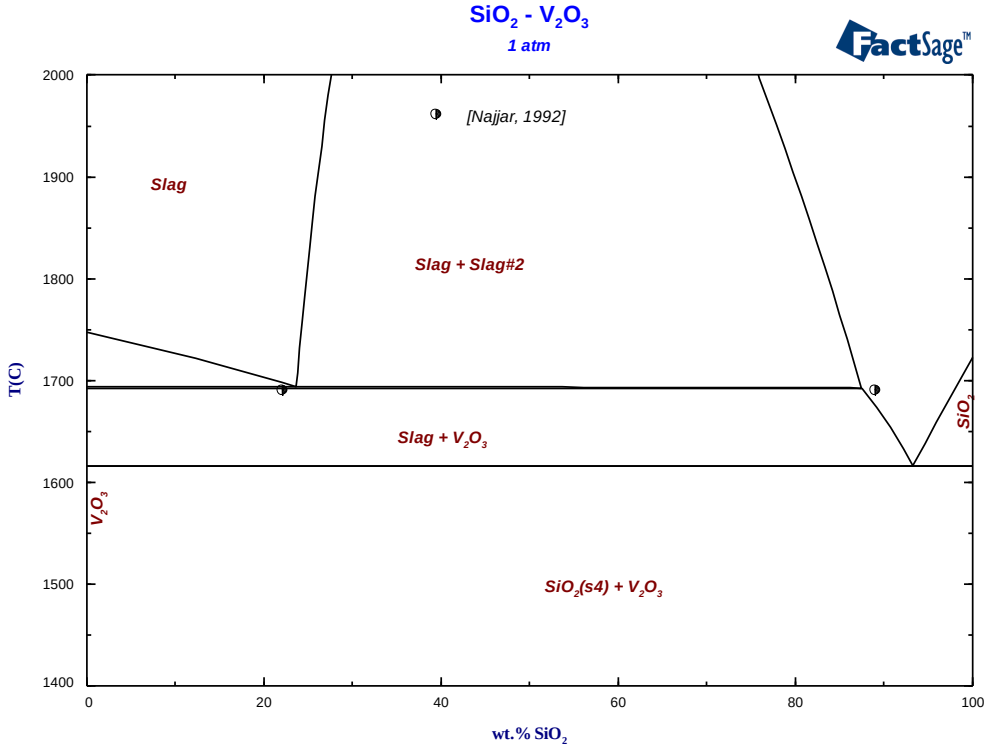

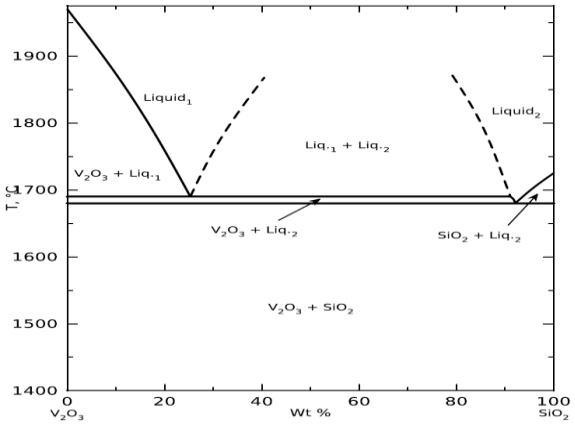

M. S. Najjar, Texaco Inc., White Plains, New York; private communication,

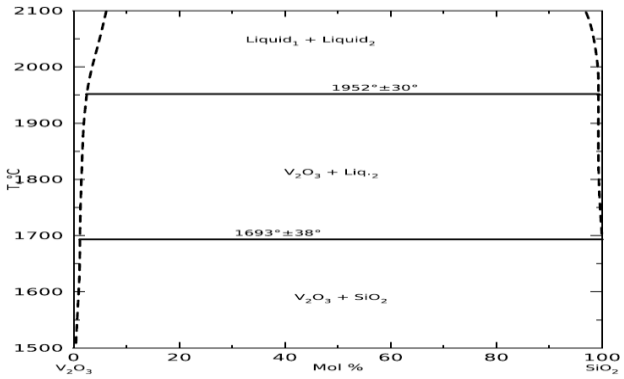

N. N. Lopatko, G. G. Mikhailov, and S. A. Archugov, Neorg. Mater., 32 [1] 71-73 (1996).

SiO2-V2O5-O2, Mole fraction

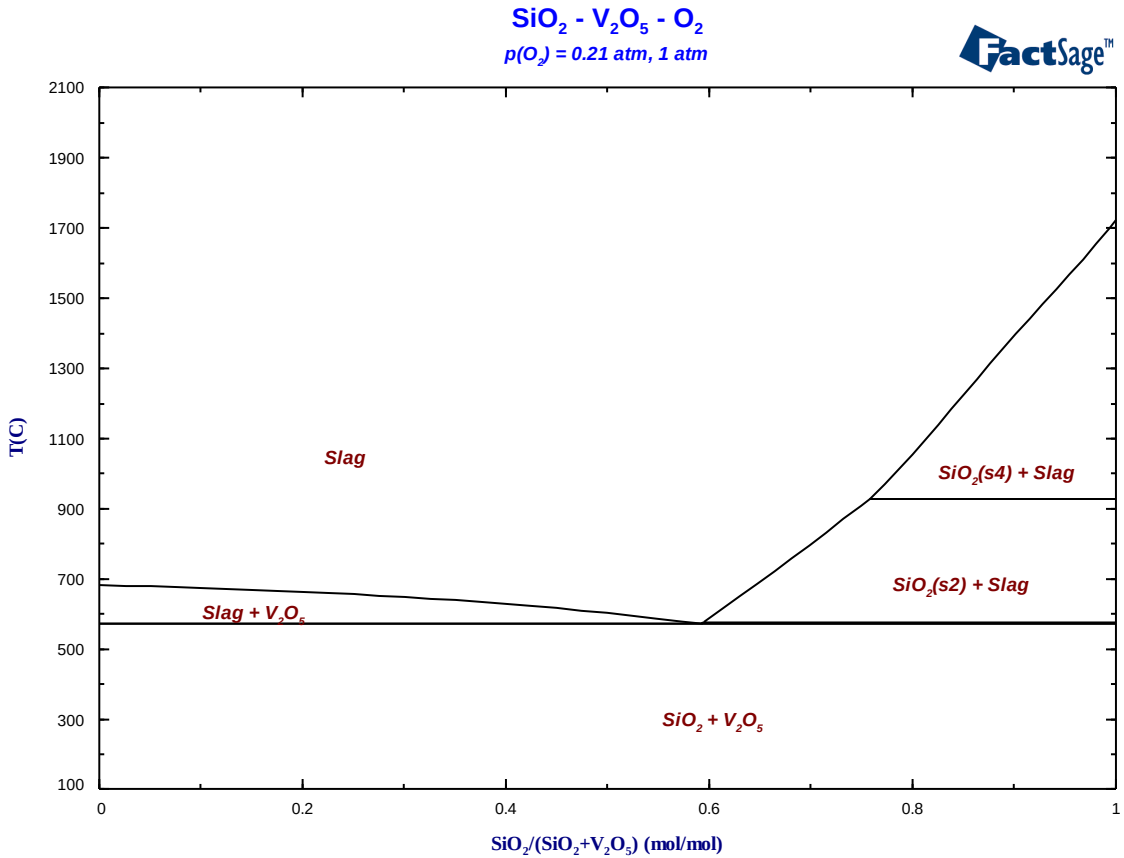

SiO2-V2O5-O2,
Weight percent compared with experimental data

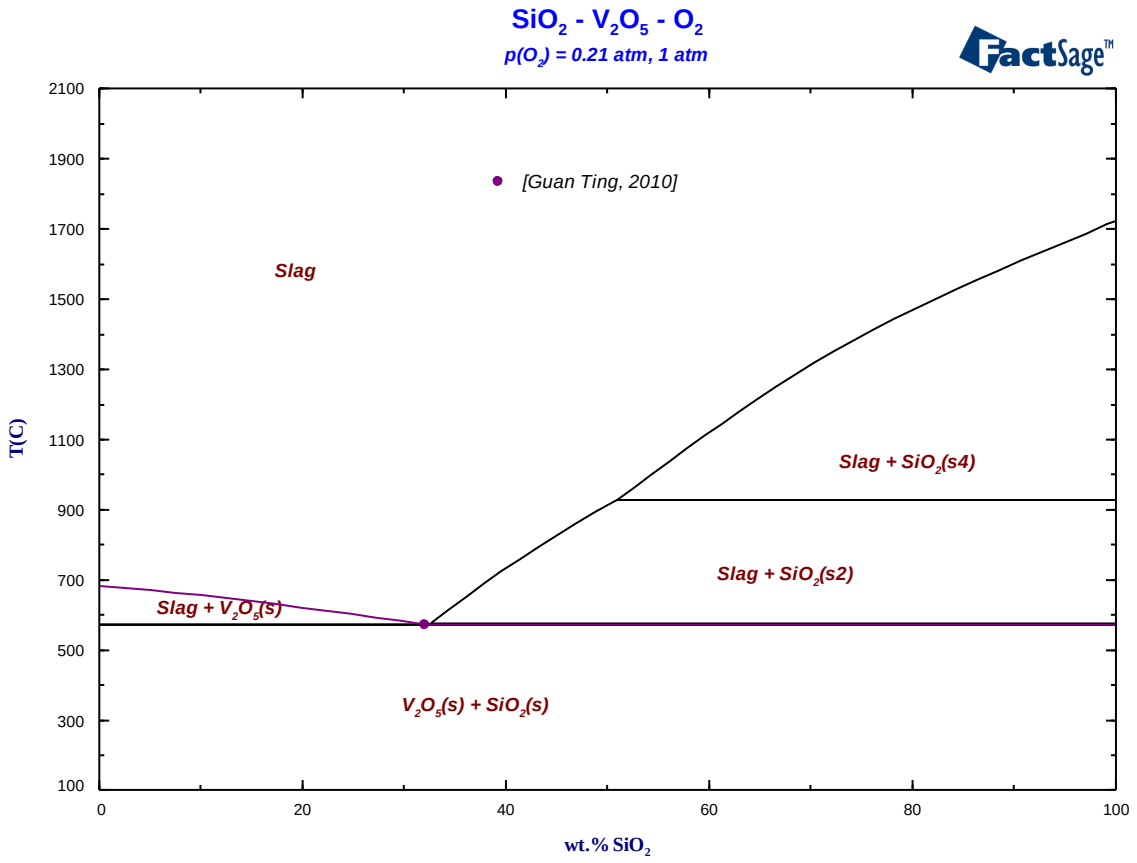

Mole fraction
compared with experimental data

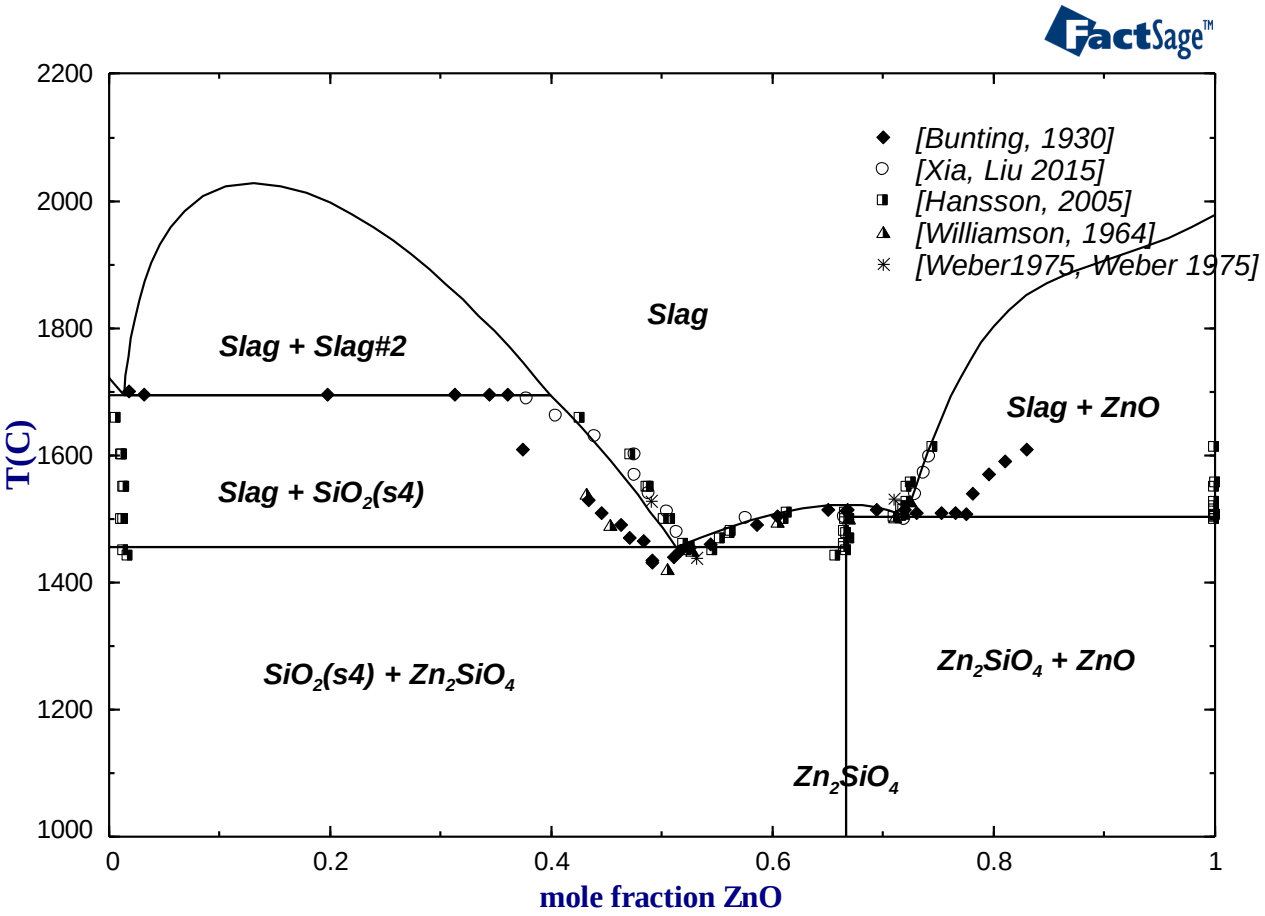

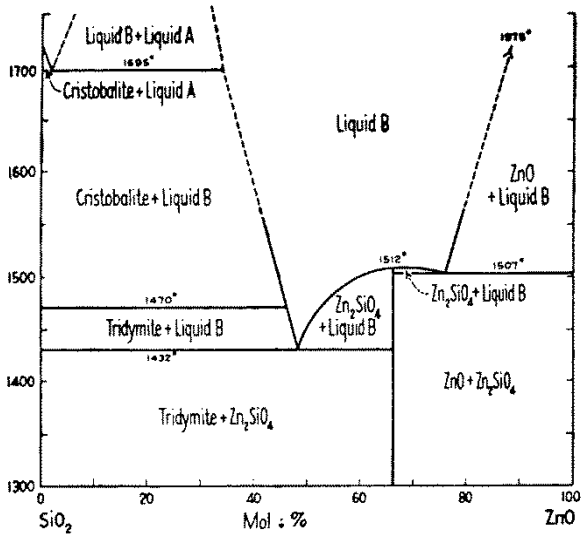

E.Bunting, J. Am. Ceram. Soc., 13 (1930), No.1, pp. 5-10.

Weight percent

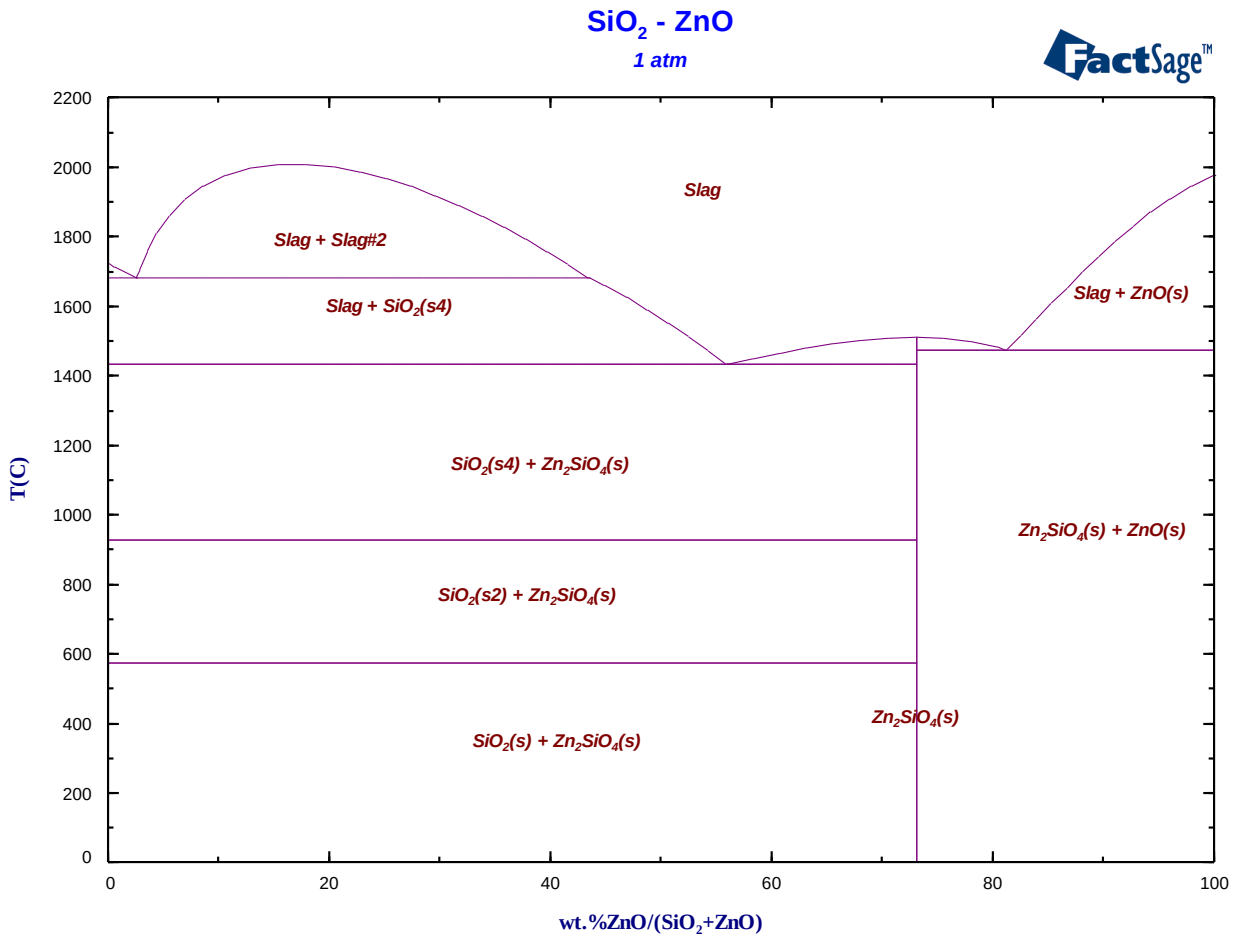

SrO-SiO2,
Mole fraction compared with experimental data

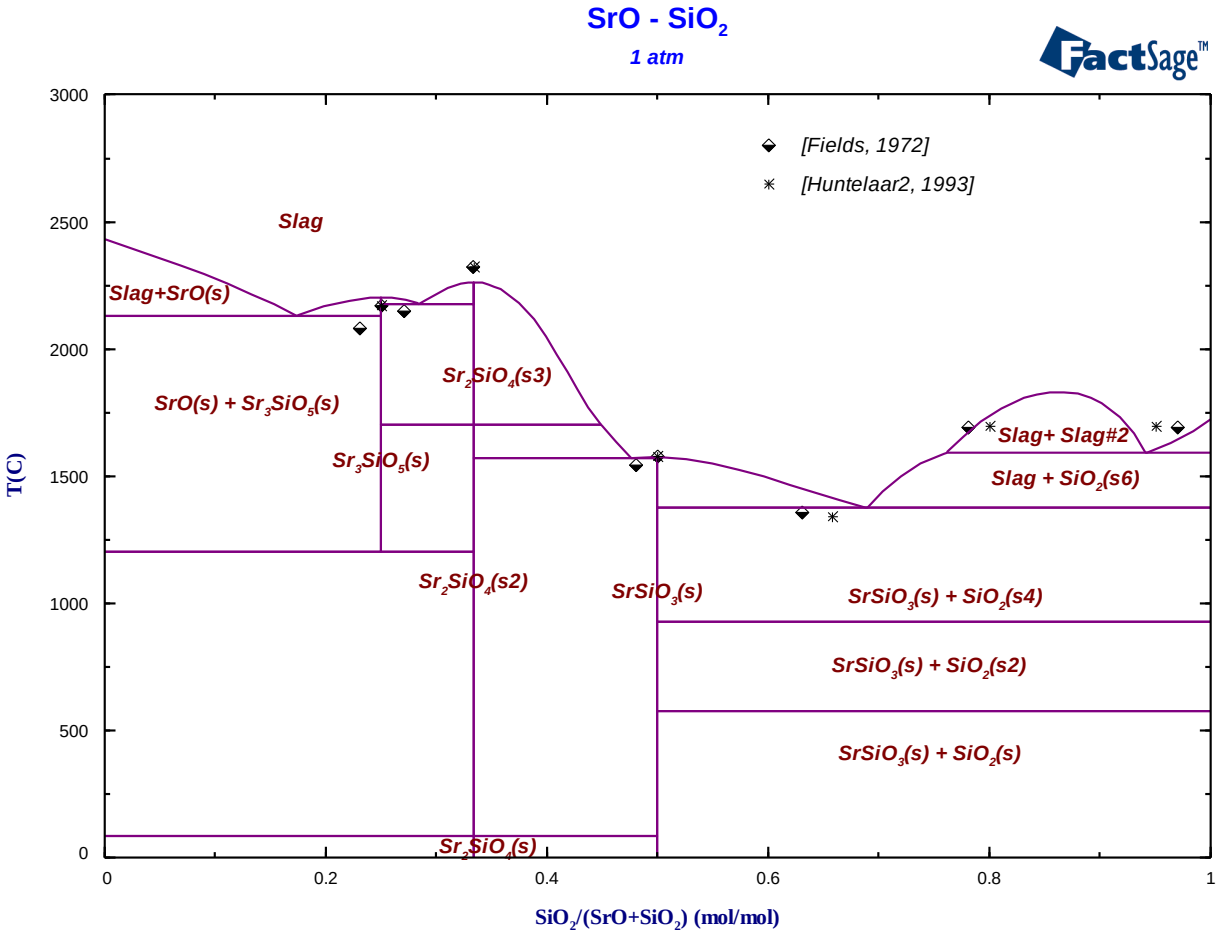

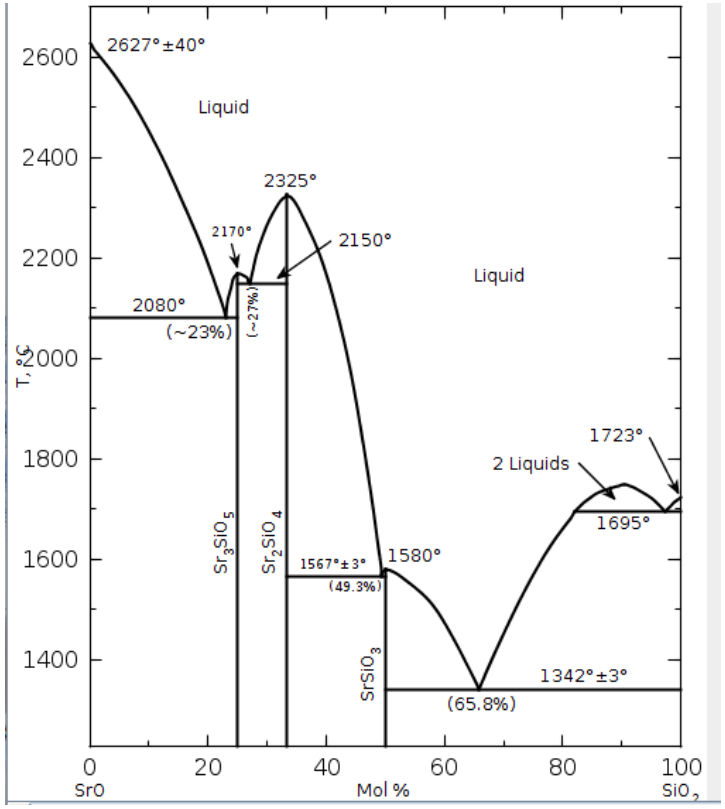

M. E. Huntelaar, E. H. P. Cordfunke, and A. Scheele, J. Alloys Compd., 191 [1] 87-90 (1993).

SrO-SiO2,
Weight percent

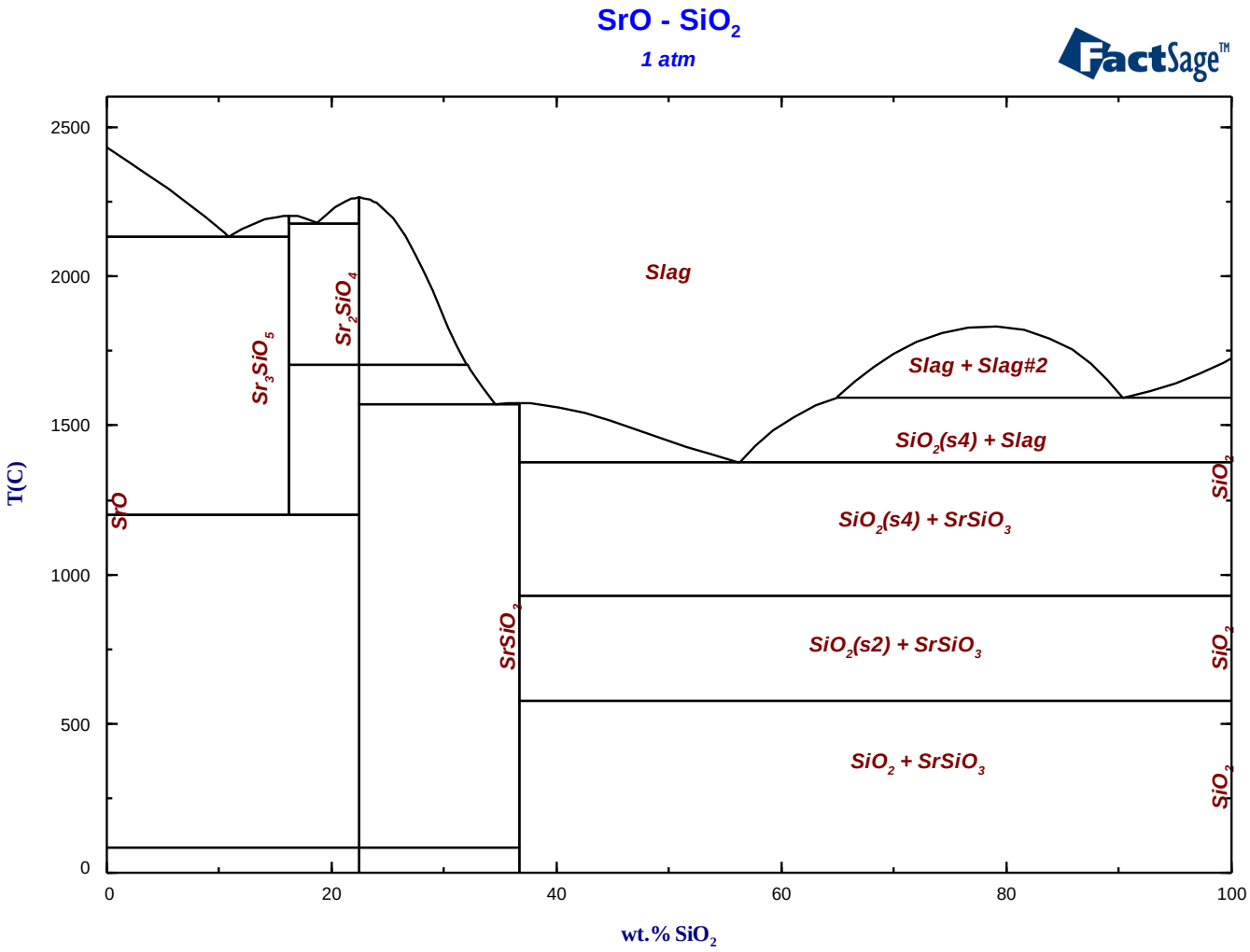

SrO-V2O5-O2,
Mole fraction compared with experimental data

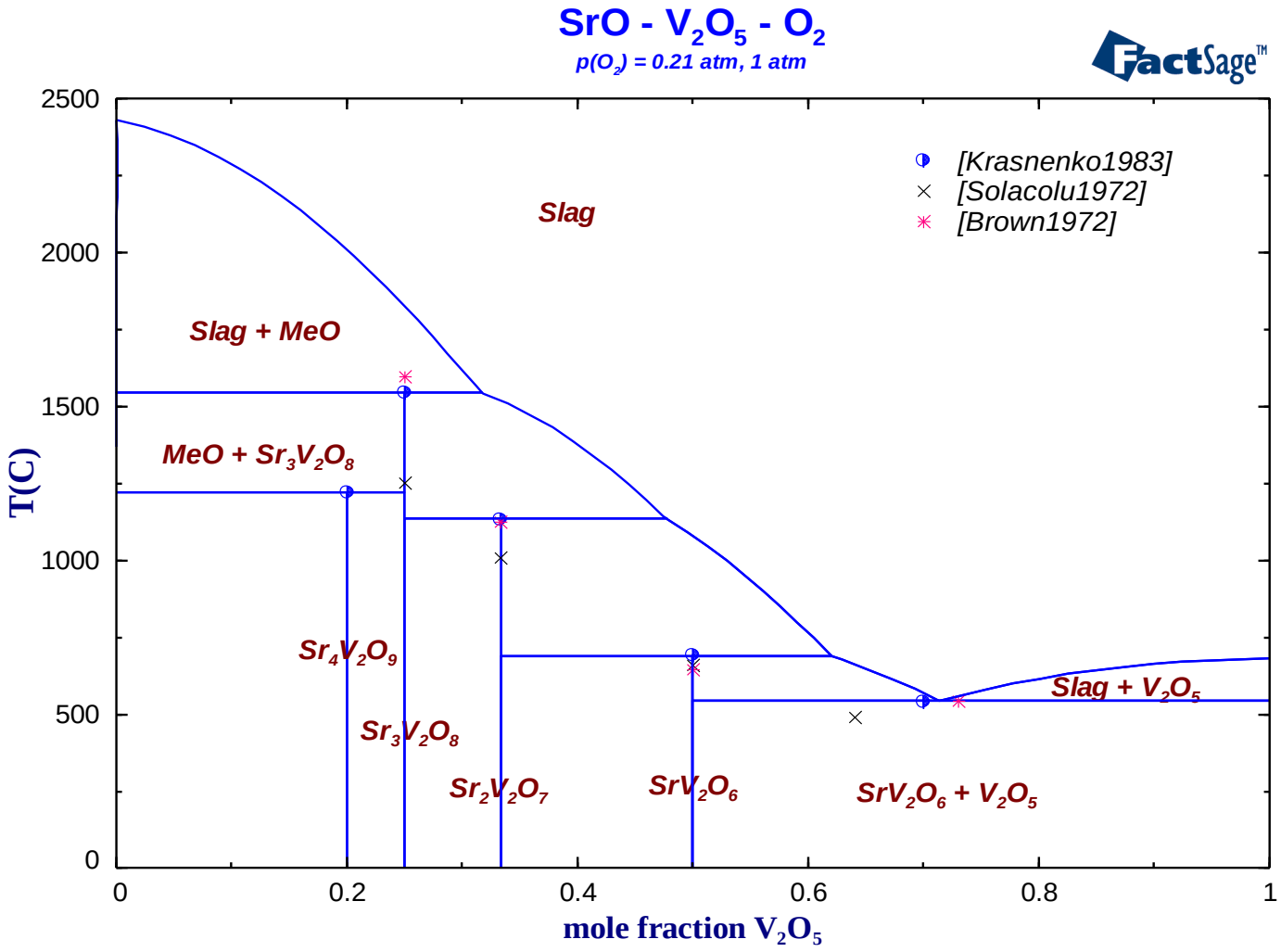

SrO-V2O5-O2,
Weight percent

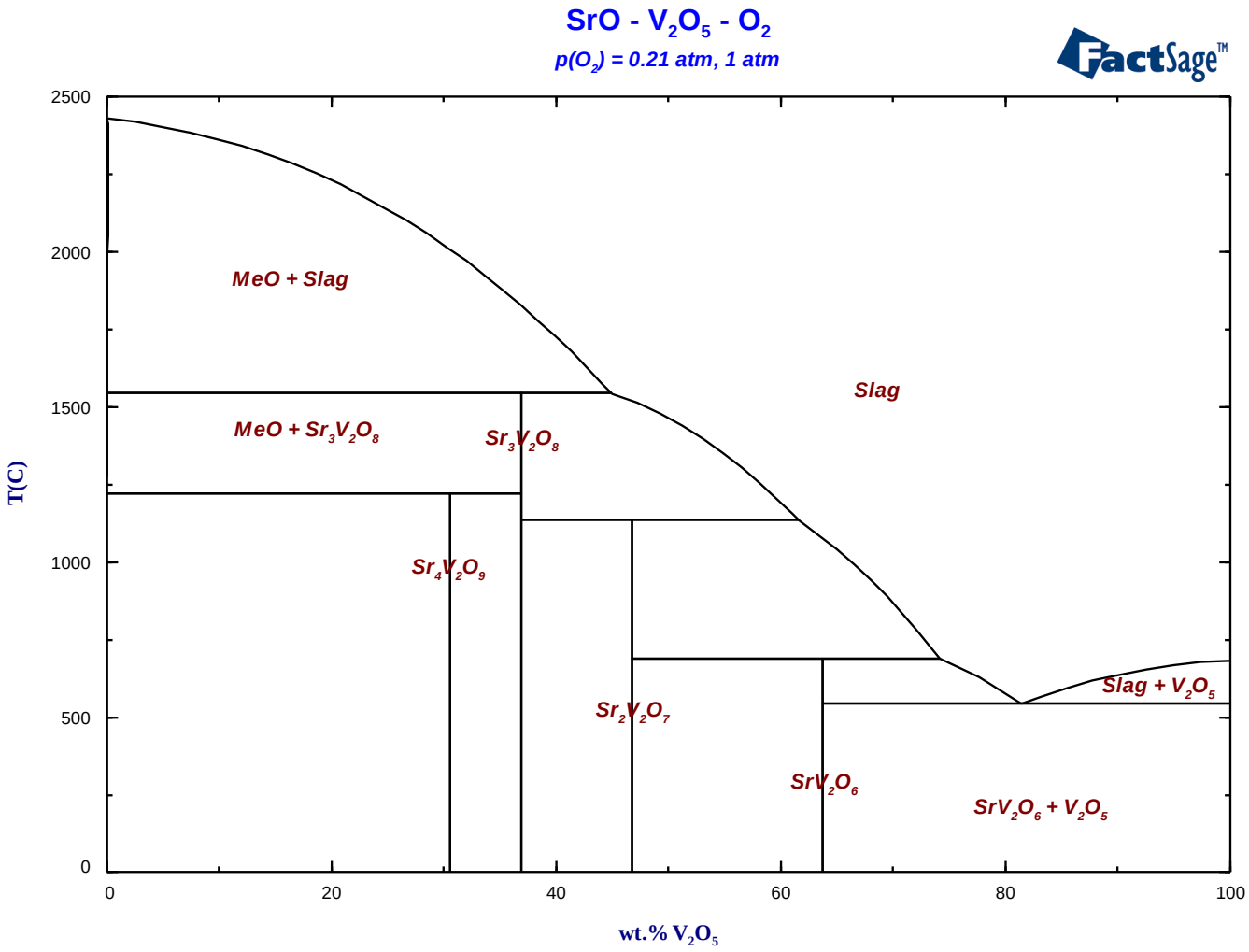

SrO-ZnO,
Mole fraction

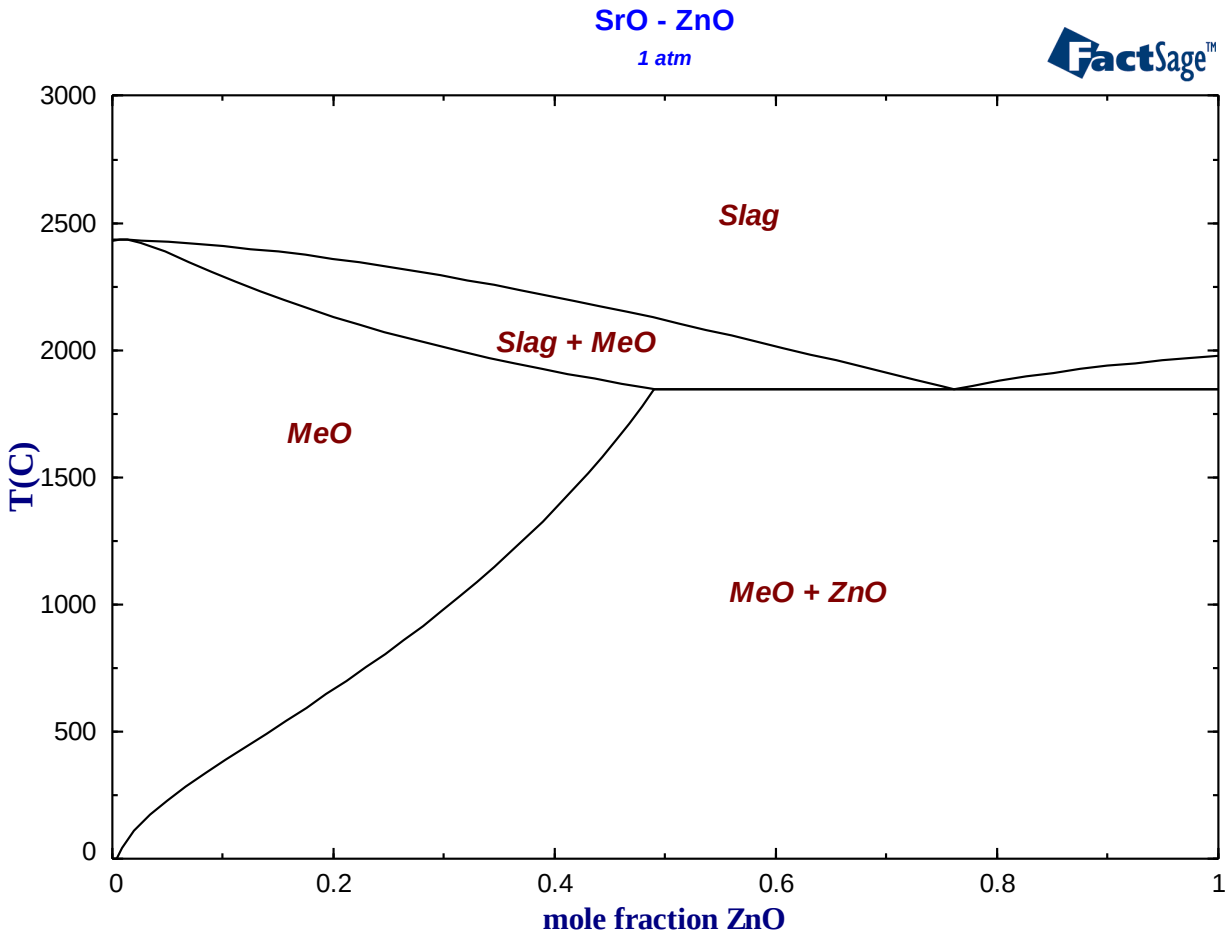

SrO-ZnO,
Weight percent

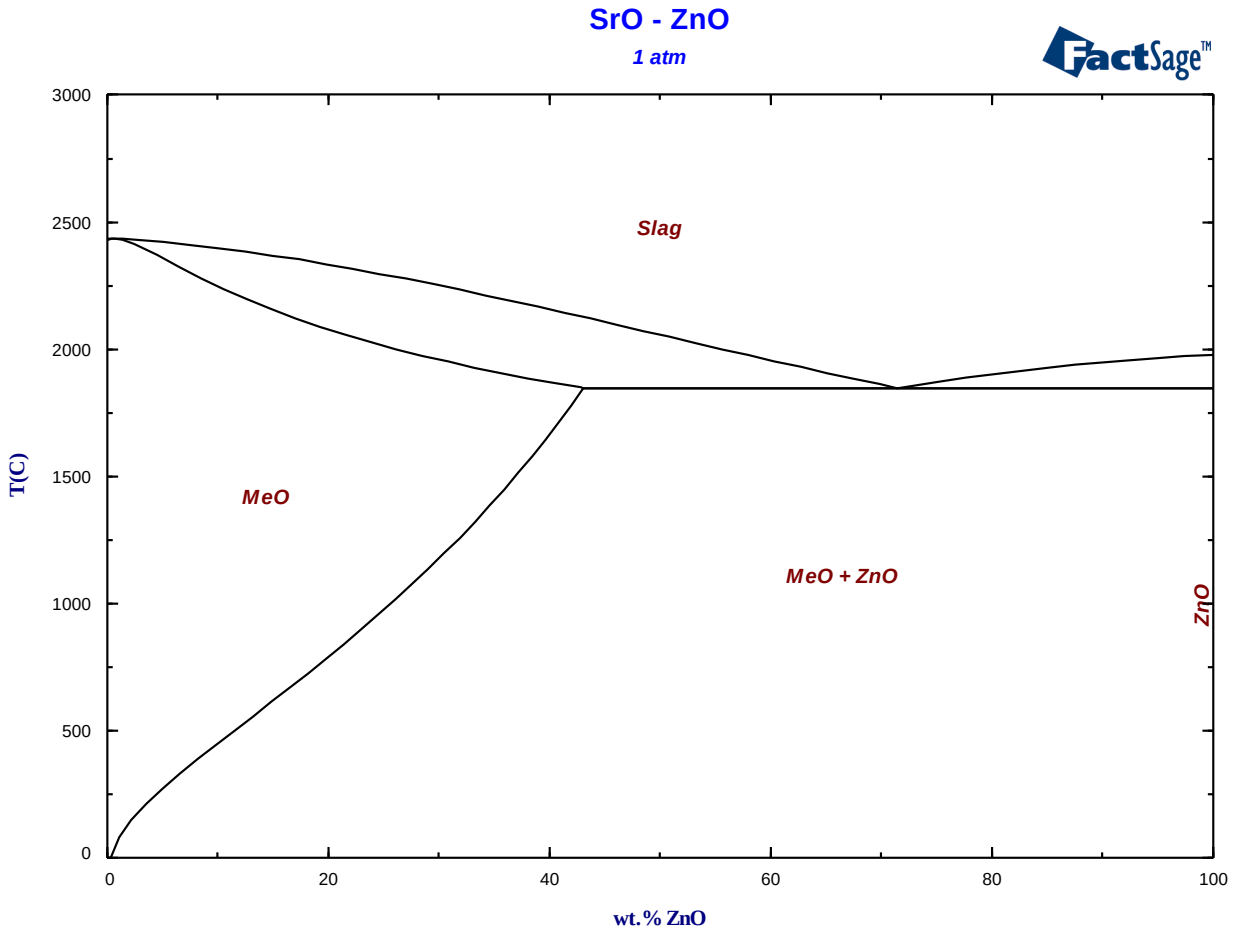

TiO2-VO2,
Mole fraction compared with experimental data

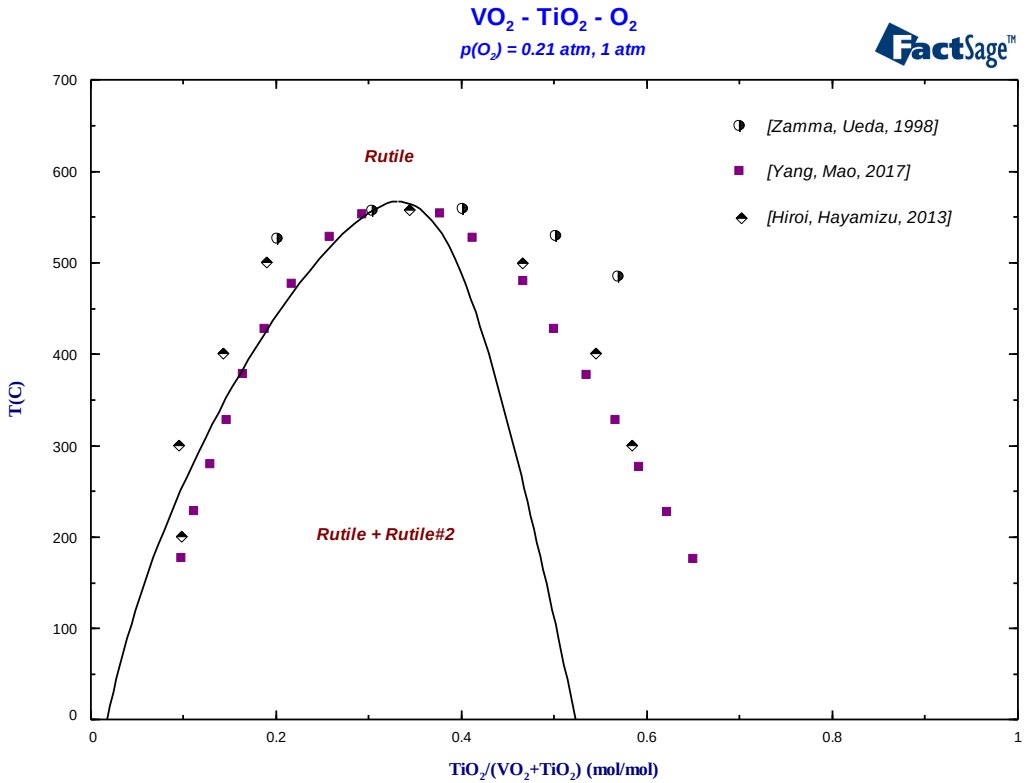

TiO2-VO2,
Weight percent

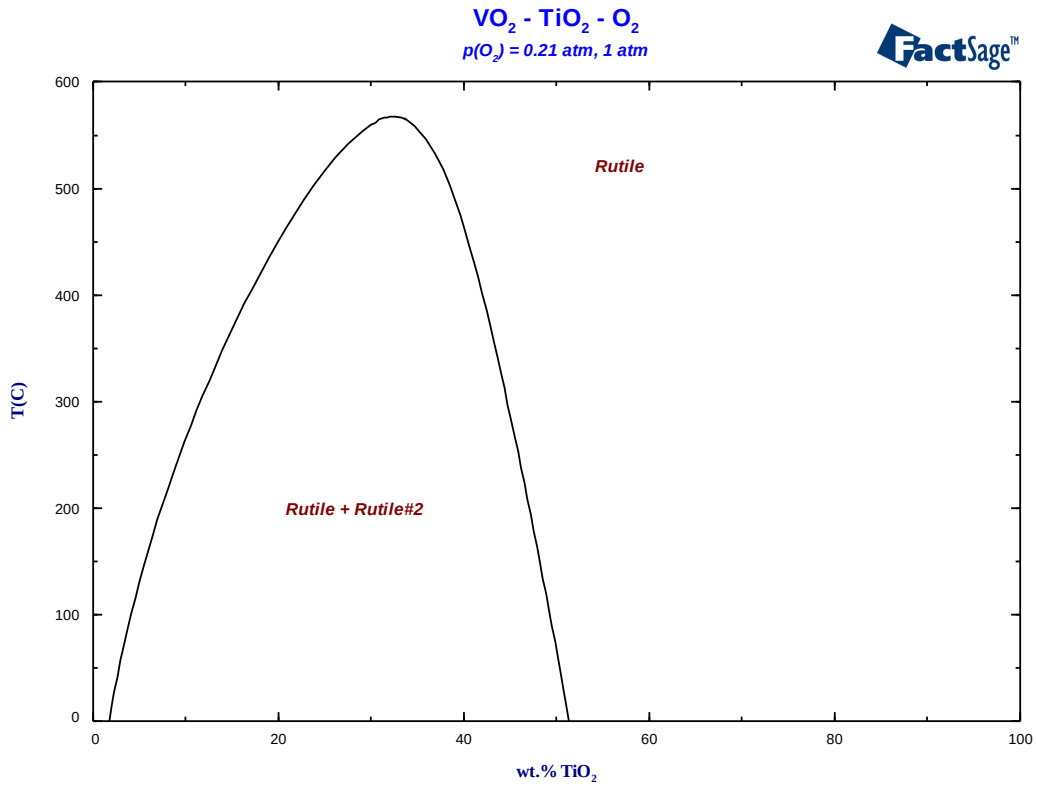

TiO2-V2O3, Mole fraction

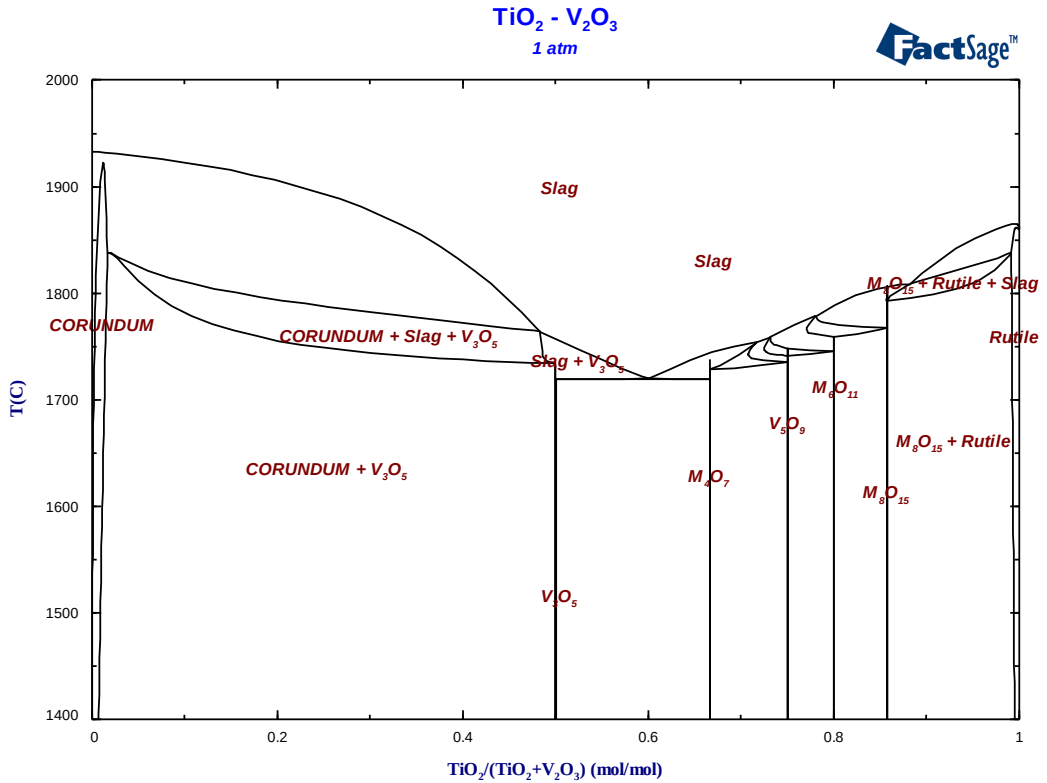

Phase	Description	Used data
Corundum	$(Ti^{+3},V^{+3},V^{+4})_2(Va)_1(O^{-2})_3$	Present work
Pseudobrookite	$(Ti, V)_1(Ti)_1(Ti)_1(O)_5$	Present work
Rutile	$(Ti, V)(O, Va)_2$	[Yang17], present work
V_3O_5	$(Ti, \underline{V})_3(O)_5$	[Yang17]
M_4O_7	$(Ti, V)_4(O)_7$	[Yang17]
V_5O_9	$(Ti, \underline{V})_5(O)_9$	[Yang17]
M_6O_{11}	$(Ti, V)_6(O)_{11}$	[Yang17]
M_8O_{15}	$(Ti, V)_8(O)_{15}$	[Yang17]

TiO2-V2O3,
Wight percent compared with experimental data

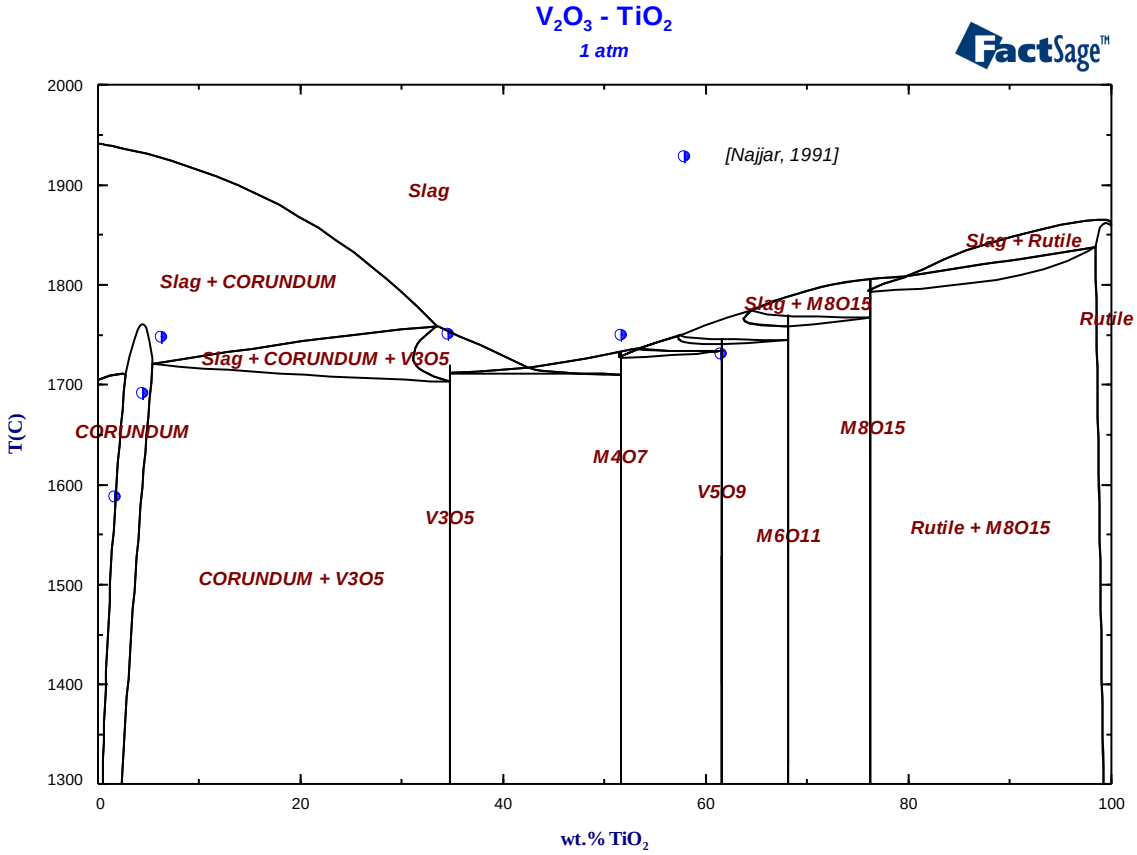

TiO2-V2O5-O2,
Mole fraction compared with experimental data

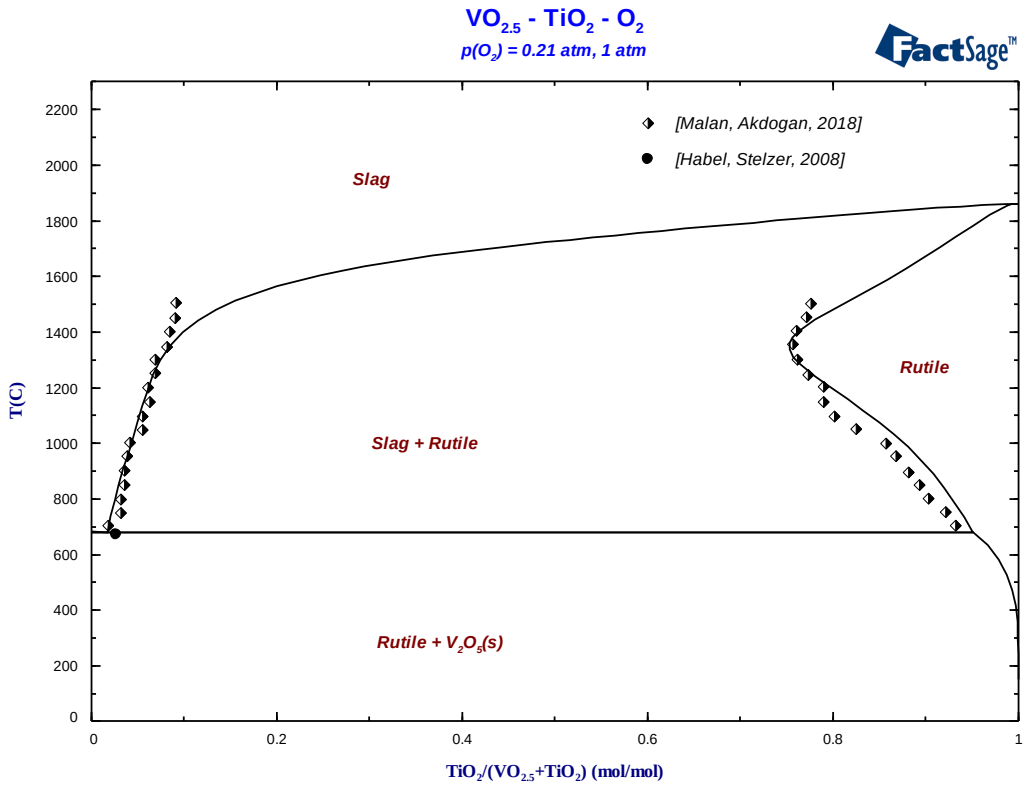

TiO2-V2O5-O2, Weight percent

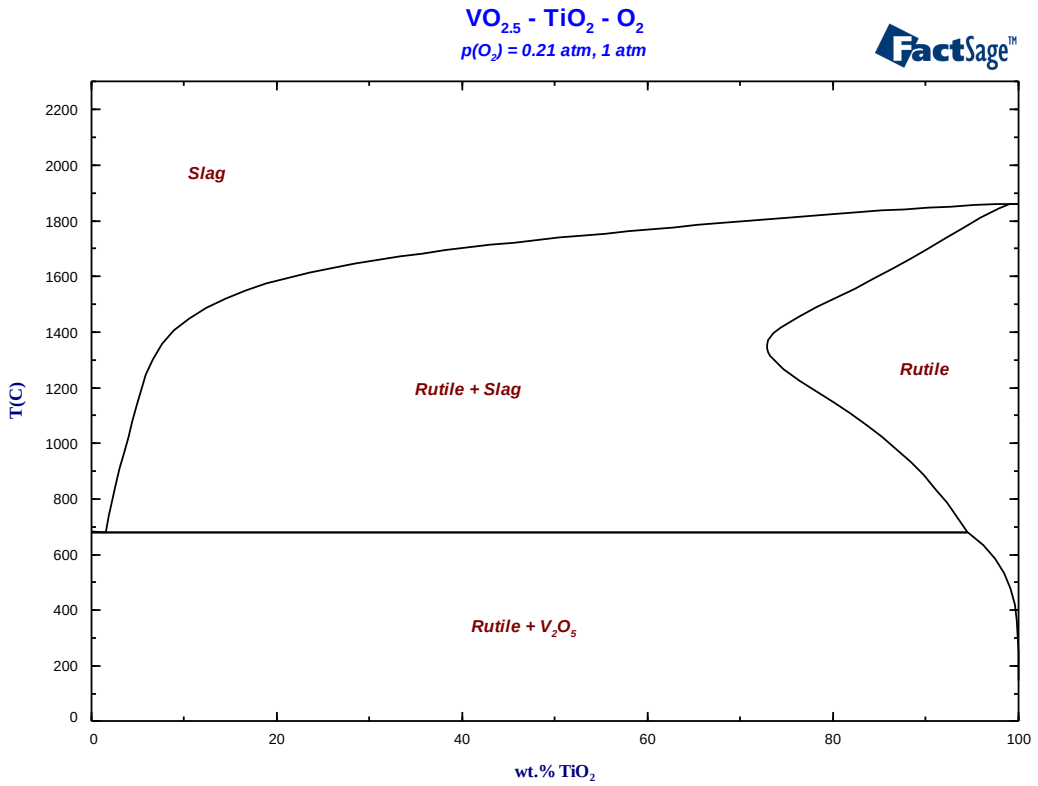

Mole fraction
compared with experimental data

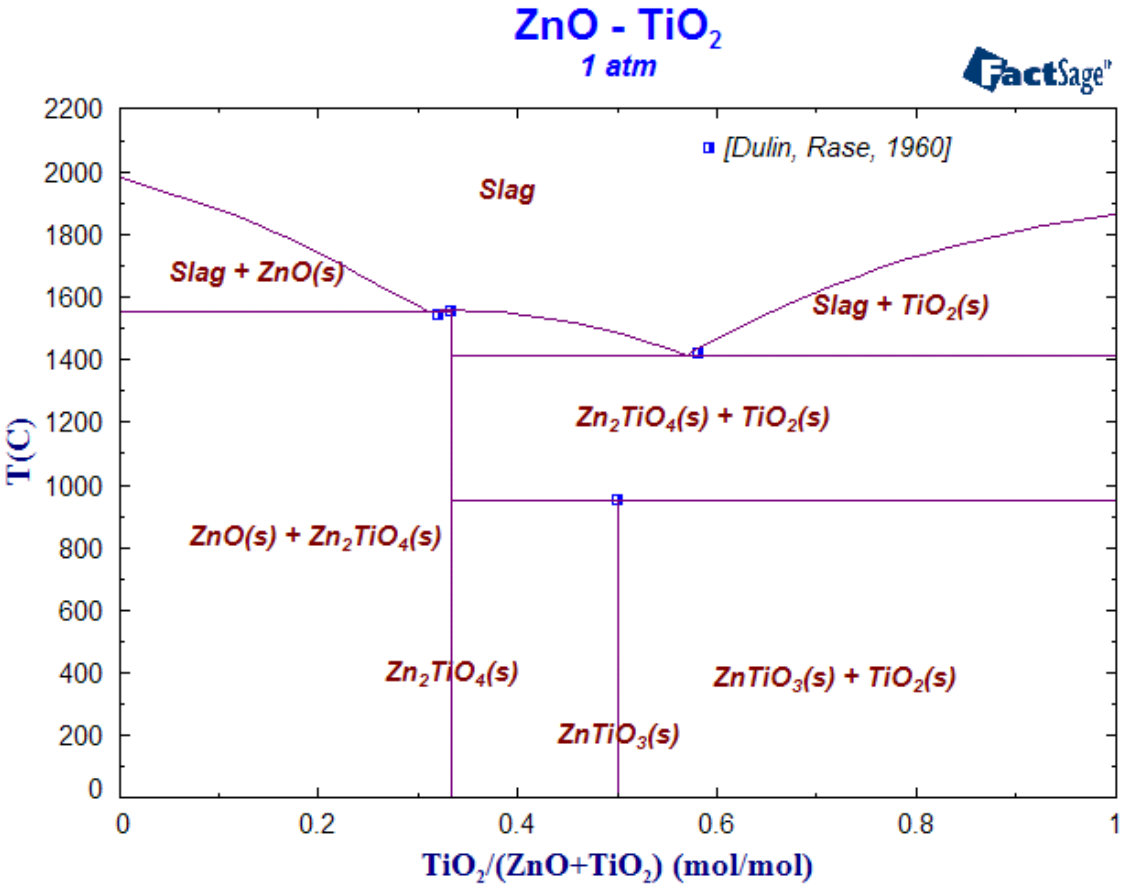

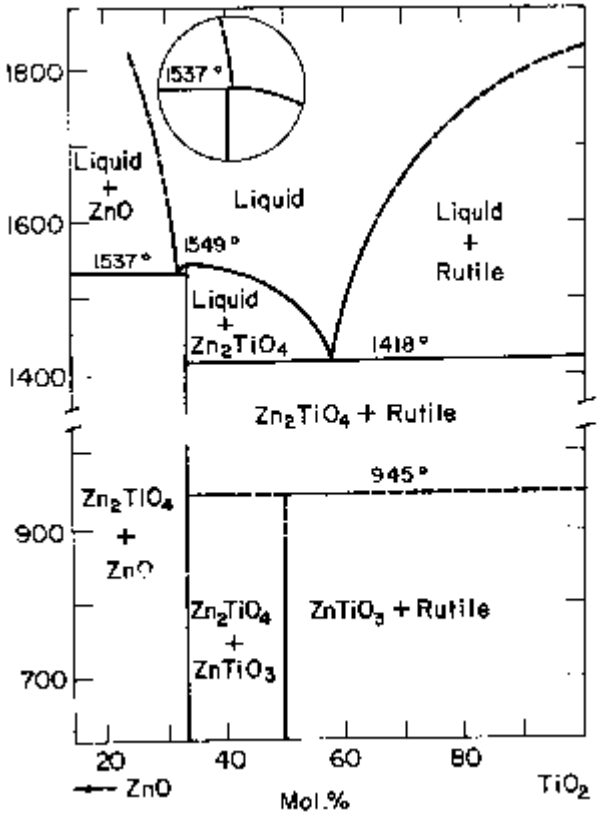

F.H. Dulin, D.E. Rase, J. Am. Chem. Soc., 43 [3], (1960), pp.125-131

Weight percent

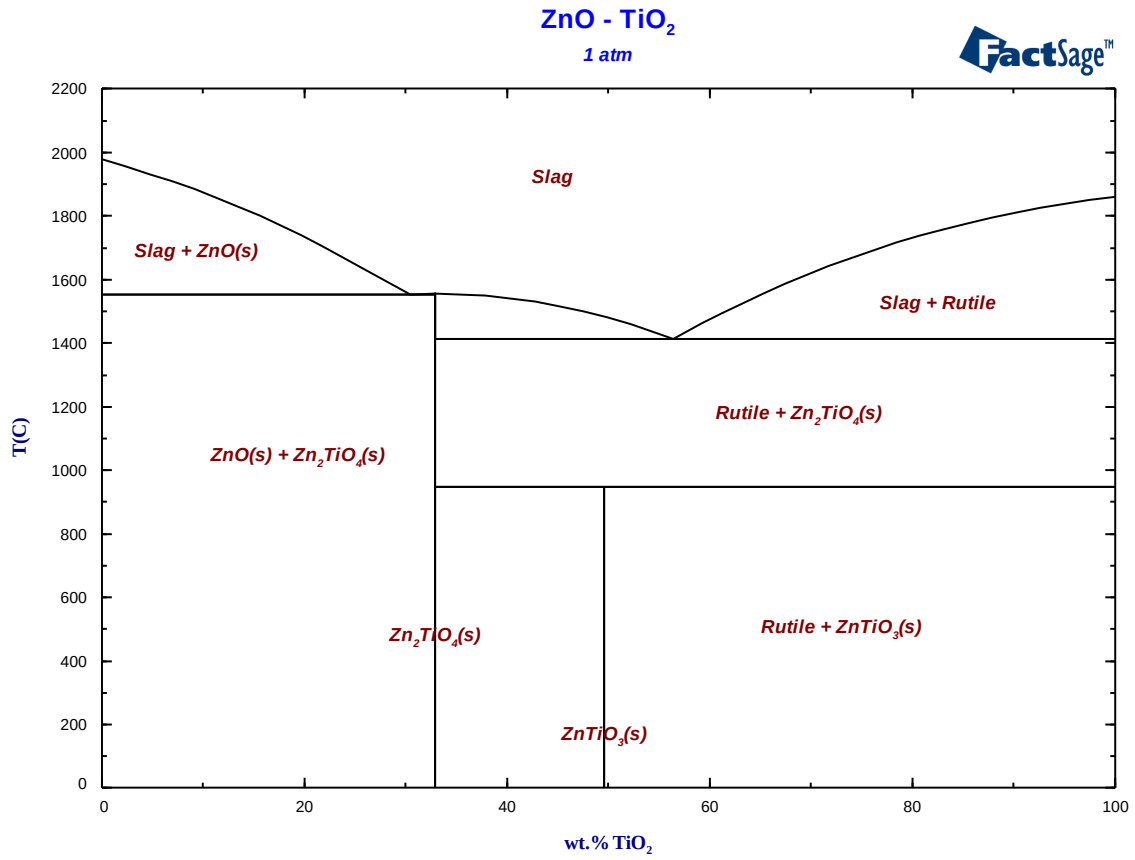

V2O5-ZnO-O2,
Mole fraction
compared with experimental data

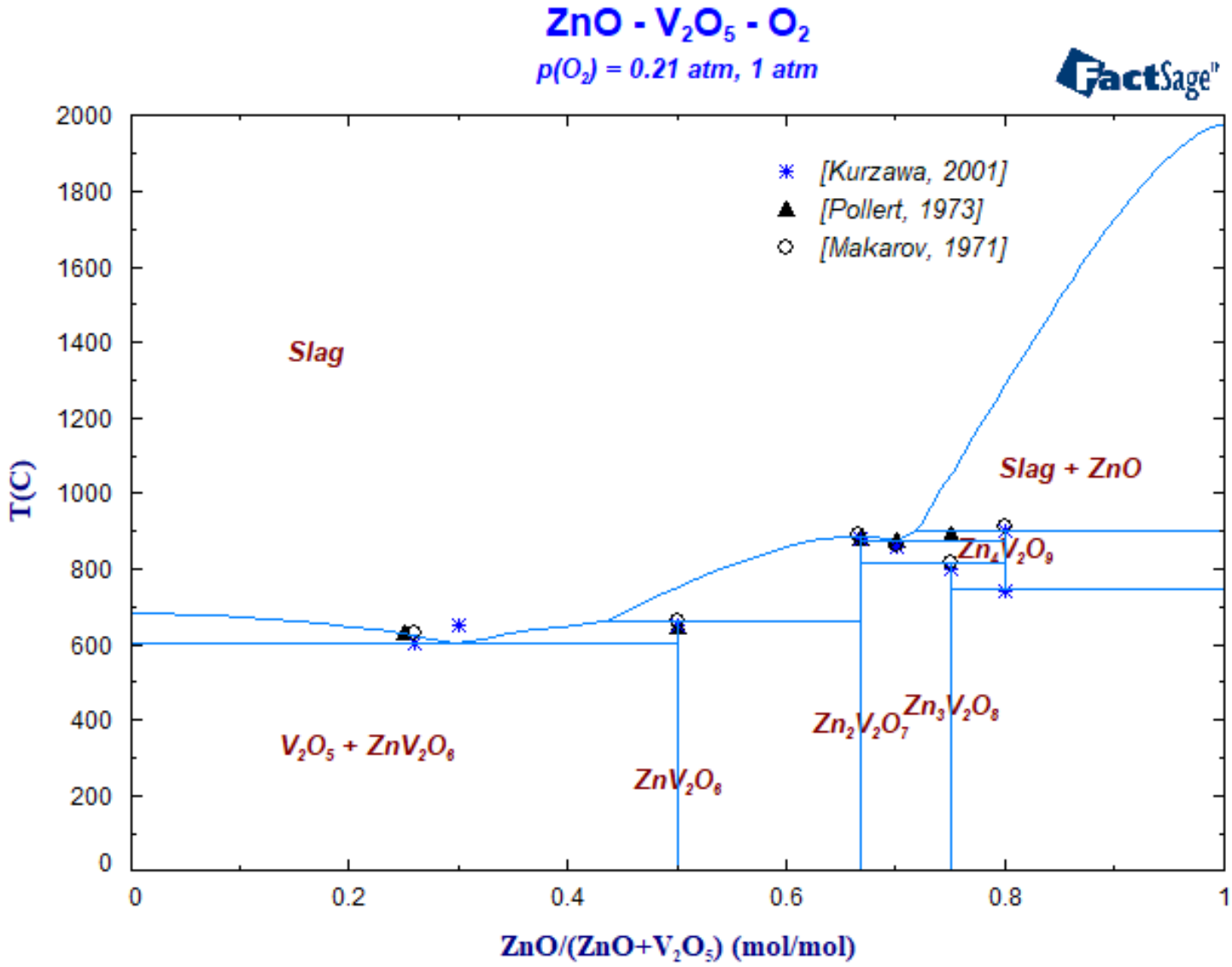

V2O5-ZnO-O2,
Weight percent

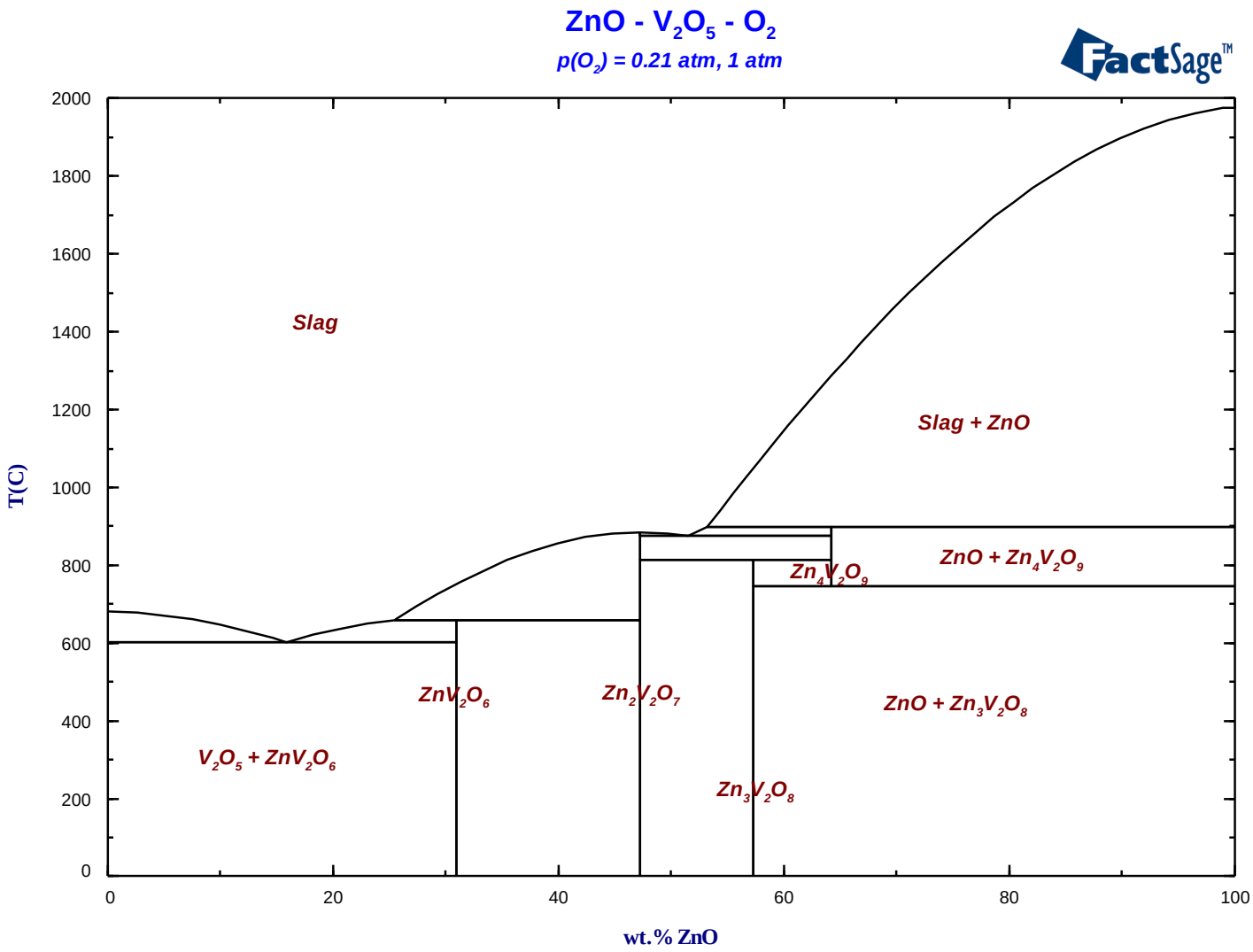

Ternary systems:

Mole fraction 1100°C

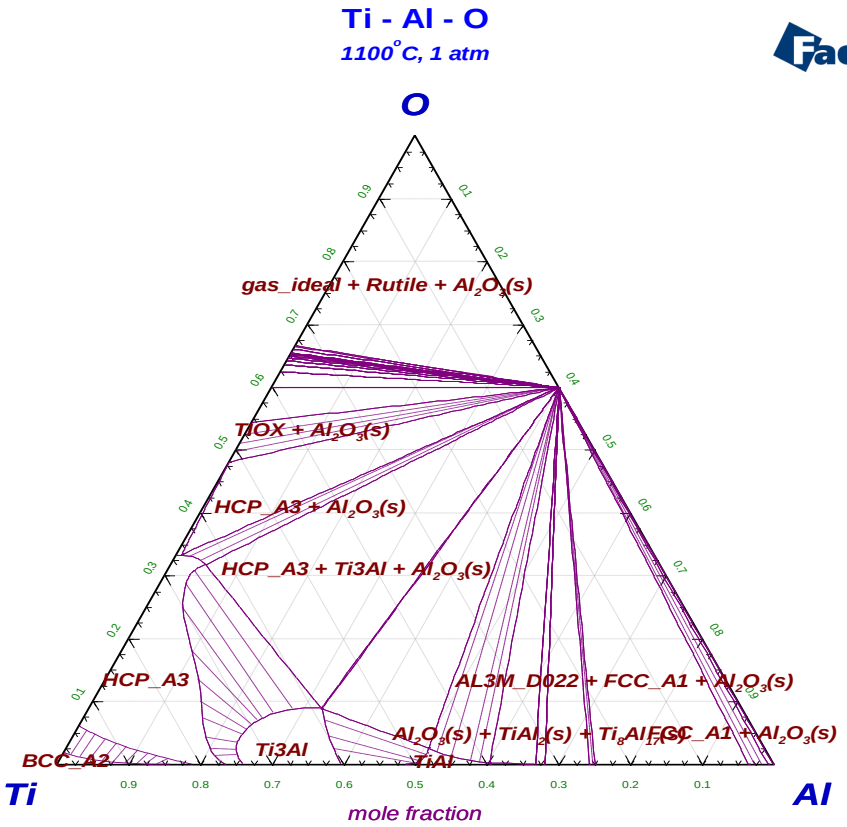

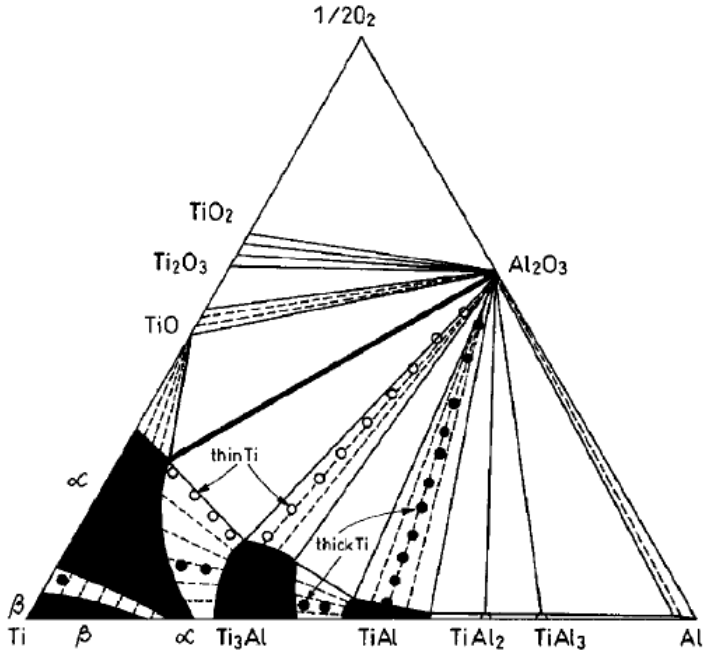

Fig. 7 Experimentally determined isothermal section of the Ti-Al-O system at 1100 °C with diffusion paths indicated [1992Li]

K. Das, P. Choudhury, S. Das. J. Phase Equilib., 23 [6], (2002), pp. 525-536.

Mole fraction 1400°C

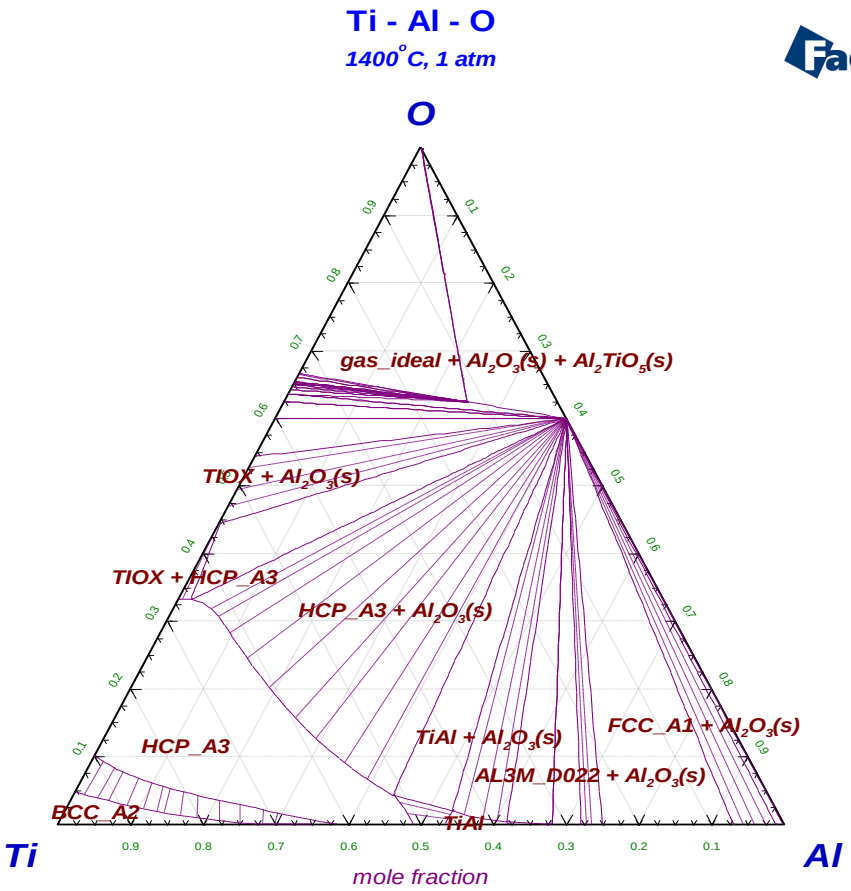

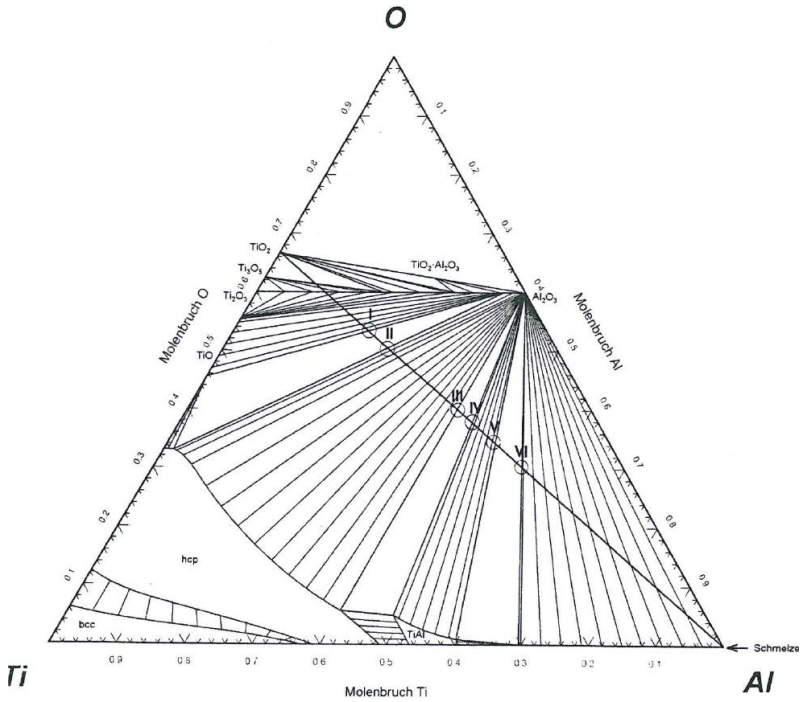

B. Friedrich, J. Hammerschmidt, J.-C. Stoephasius, Erzmetall, 56 [2], (2002), pp. 82-93.

Al2O3-CaF2-CaO,
Mole fraction, 1100°C

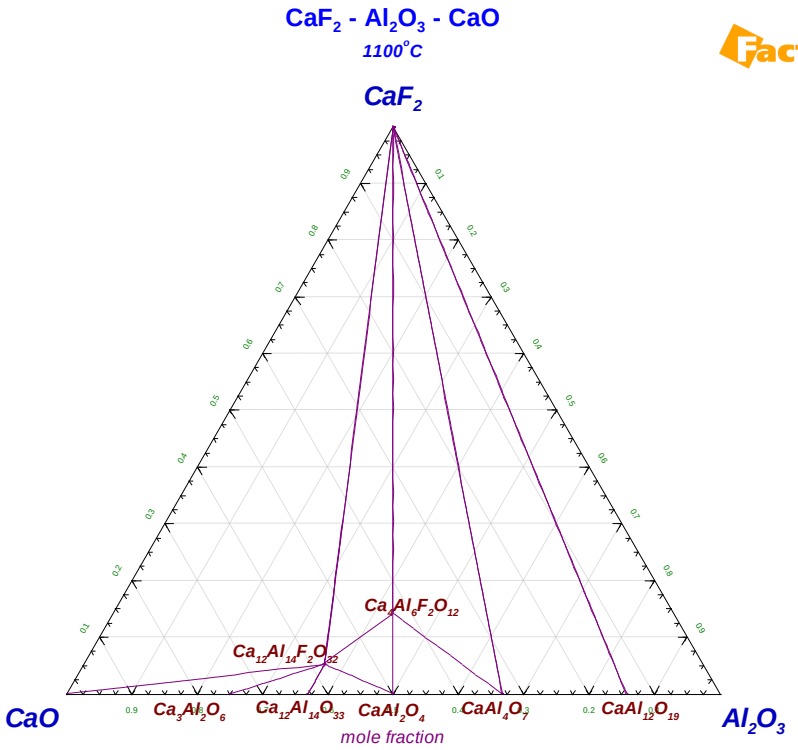

Name	Phase	Description
C3A3F	$3CaO\ 3Al_2O_3\ CaF_2$	$Ca_4Al_6F_2O_{12}$
C11A7F	$11CaO\ 7Al_2O_3\ CaF_2$	$Ca_{12}Al_{14}F_2O_{32}$

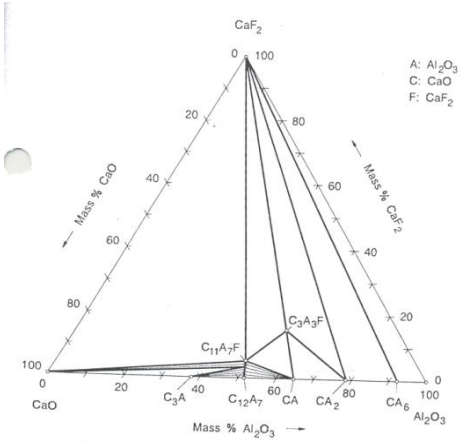

Fig. 3.421. Sub-solidus equilibria in the Al_2O_3-CaF_2-CaO system as determined by Brisi, Rolando [8] and confirmed by Chatterjee, Zhmoidin [1].

Slag Atlas, 2nd Ed., Verlag Stahl-Eisen, Düsseldorf. 1995.

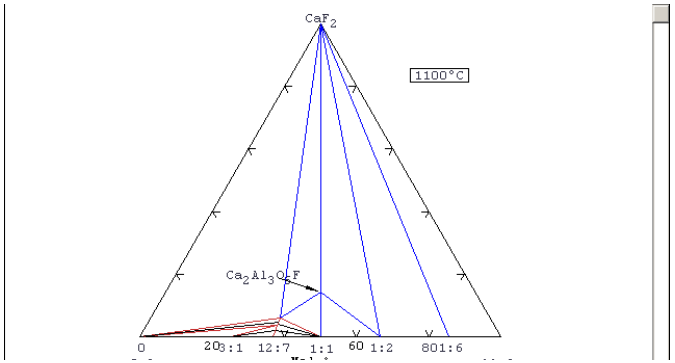

C. Brisi, P. Rolando, Ann. Chim. (Rome), 57 [11], (1967), pp.1304-1315.

Al2O3-CaF2-CaO,

Mole fraction, 1600°C

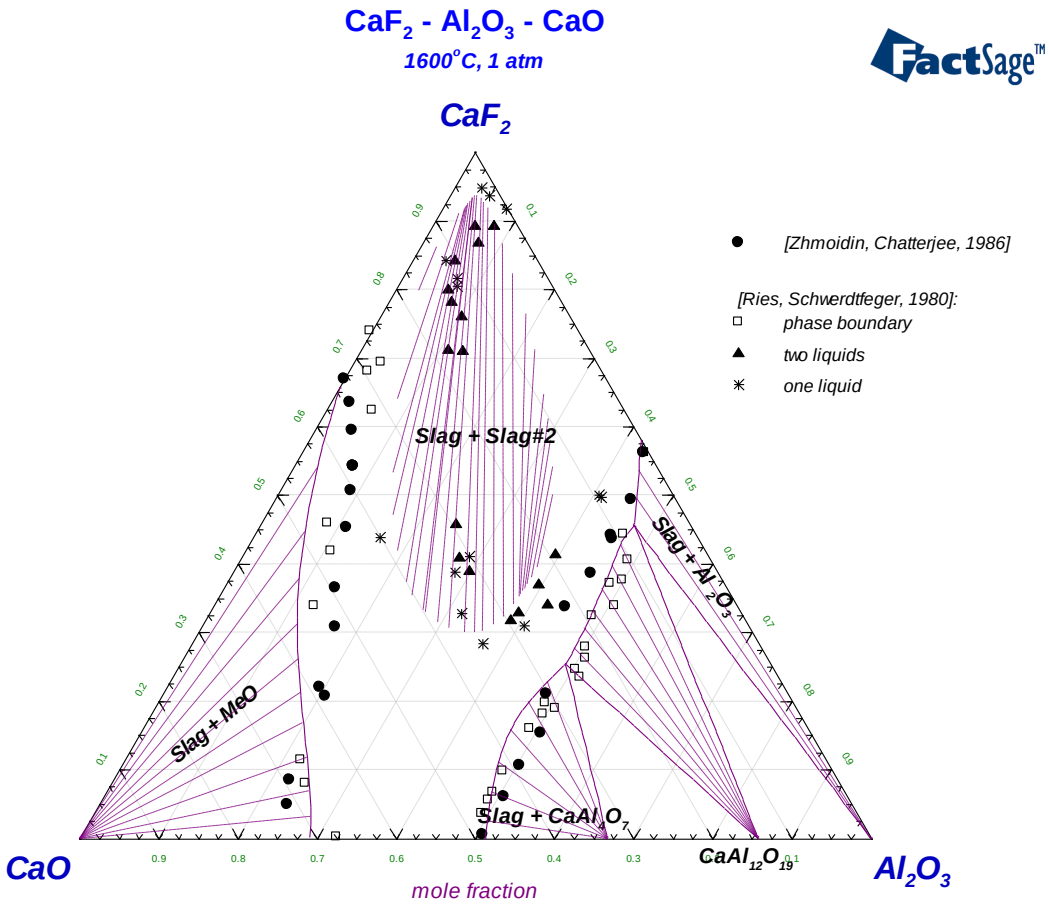

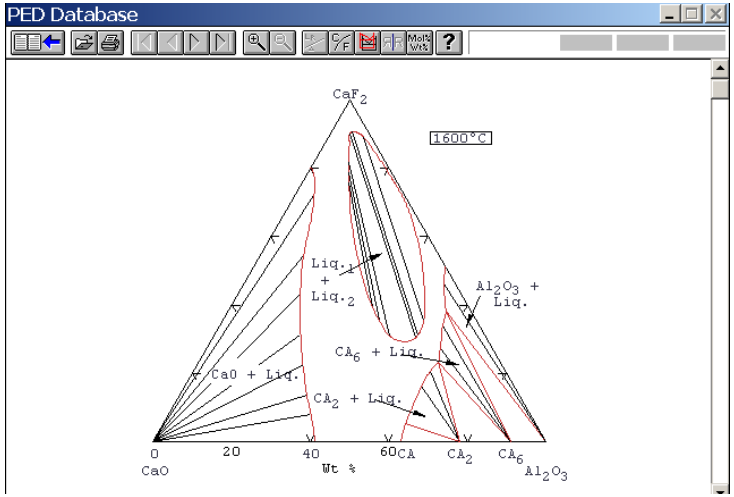

R. Ries, K. Schwerdtfeger, Arch. Eisenhüttenwes., 51, (1980), pp.123-129.

Al2O3-CaF2-CaO,

Mole fraction, 1800°C

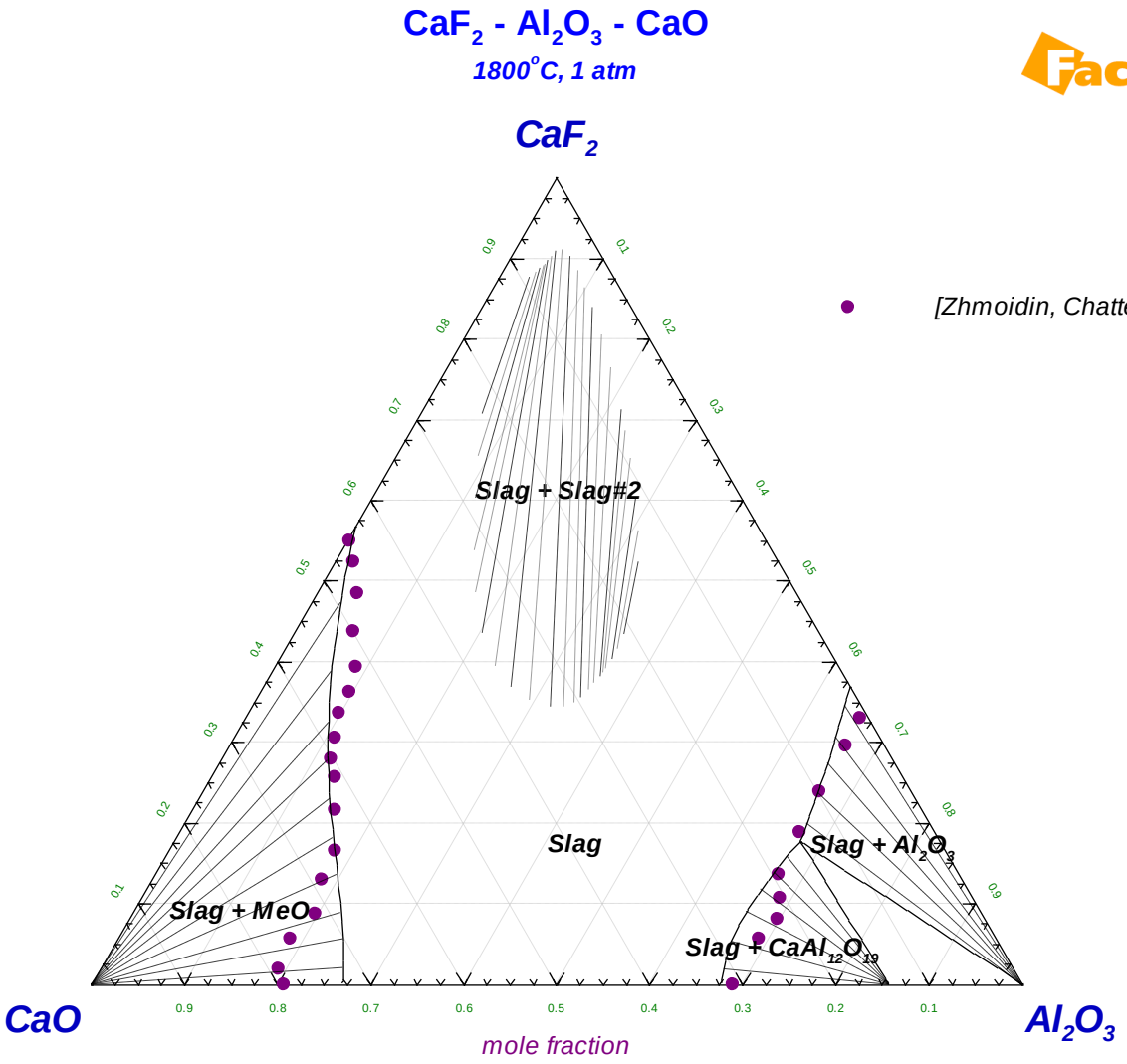

Al2O3-CaF2-CaO,

Weight percent, Isopleth C11A7F-C3A3F

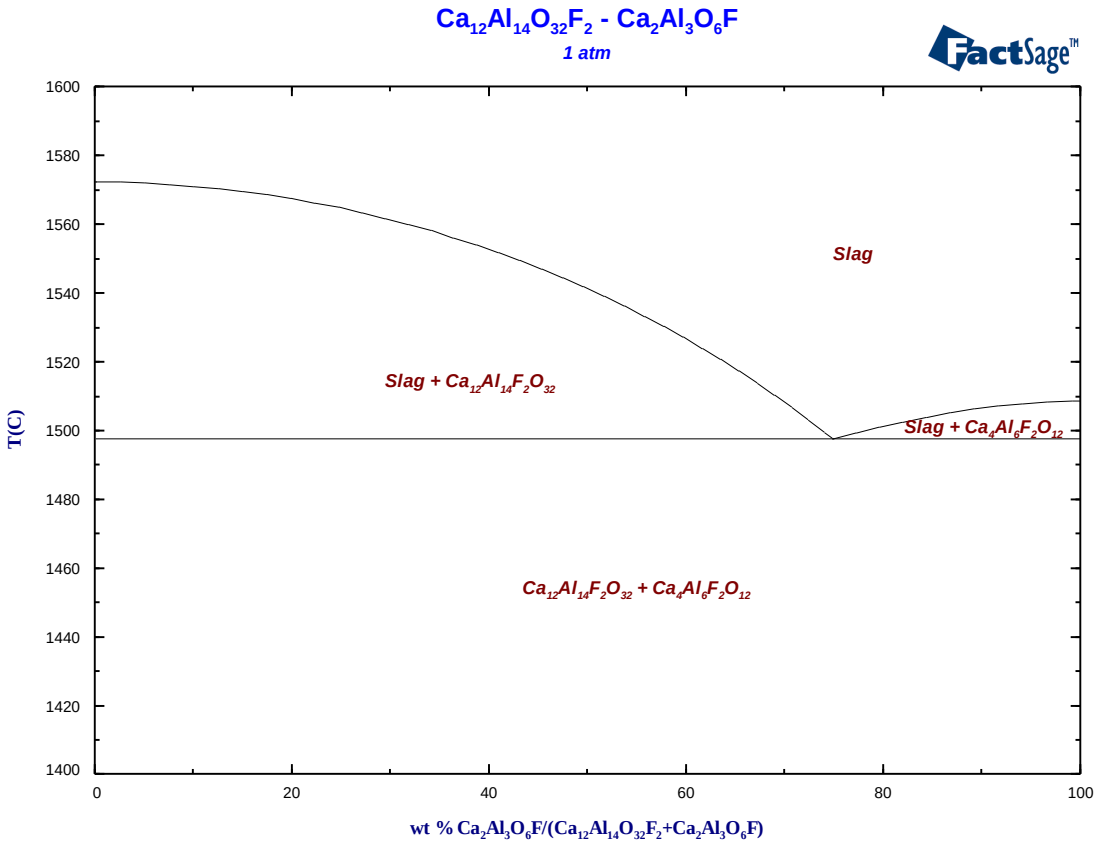

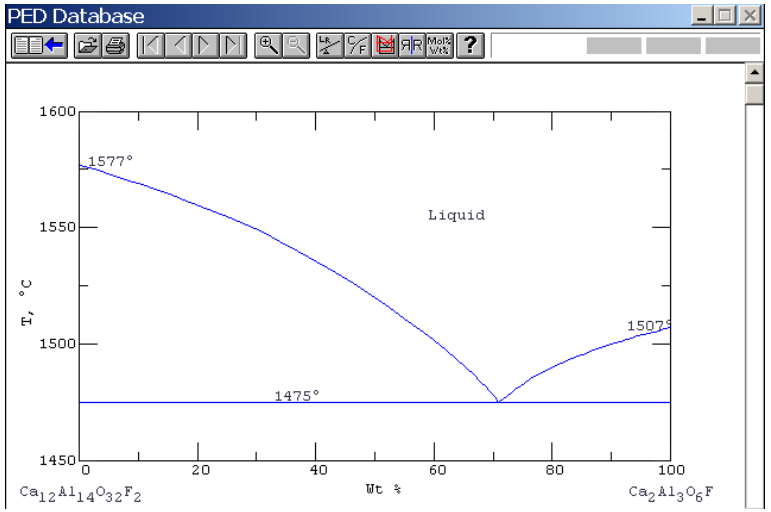

R. Ries, K. Schwerdtfeger, Arch. Eisenhüttenwes., 51, (1980), pp.123-129.

Al2O3-CaF2-CaO,

Weight percent, Isopleth C3A3F-CaAl4O7

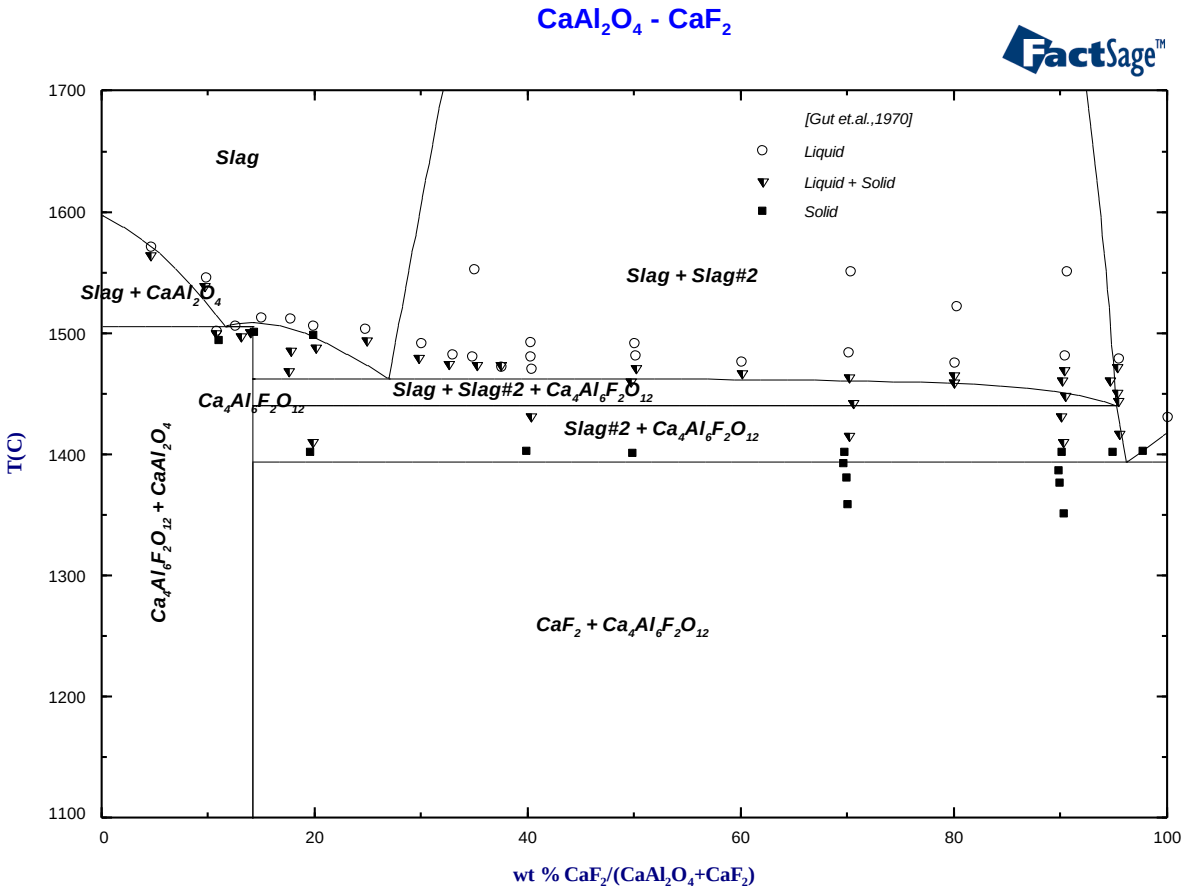

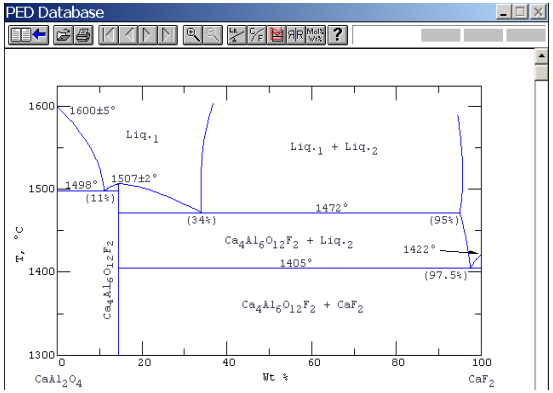

A.K. Chatterjee, G.I. Zhmoidin, Izv. Akad. Nauk SSSR, Neorg. Mater., 8 [5], (1972), pp.886-892.

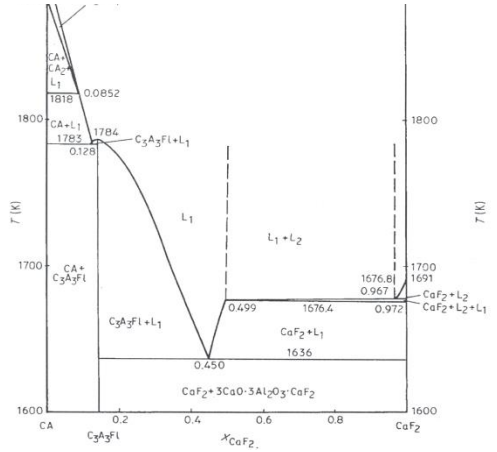

A.I. Zaitsev, N.V. Korolyov, B.M. Mogutnov, Journ. Mater. Scien., 26 (1991), pp.1588-1600.

Al2O3-CaF2-CaO,

Weight percent, Isopleth C3A3F-CaAl4O7

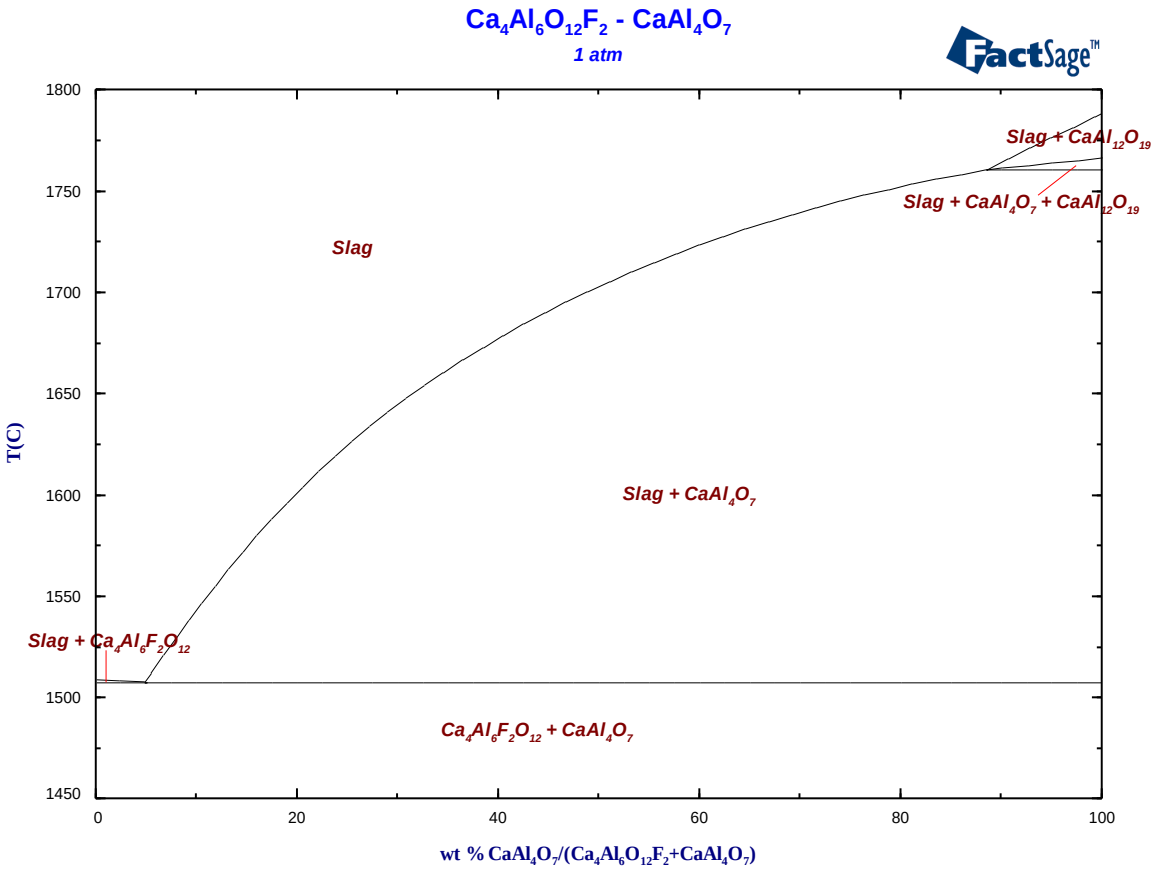

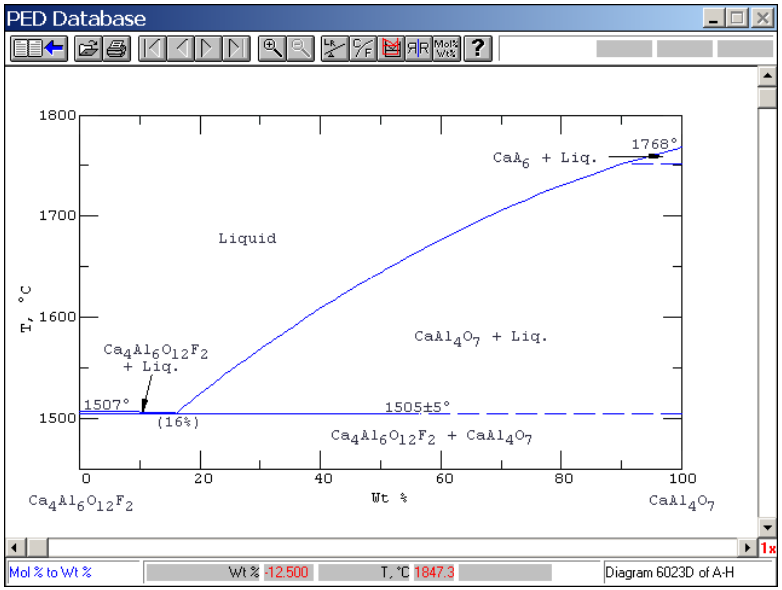

A.K. Chatterjee, G.I. Zhmoidin, Izv. Akad. Nauk SSSR, Neorg. Mater., 8 [5], (1972), pp.886-892.

Mole fraction
Liquidussurface

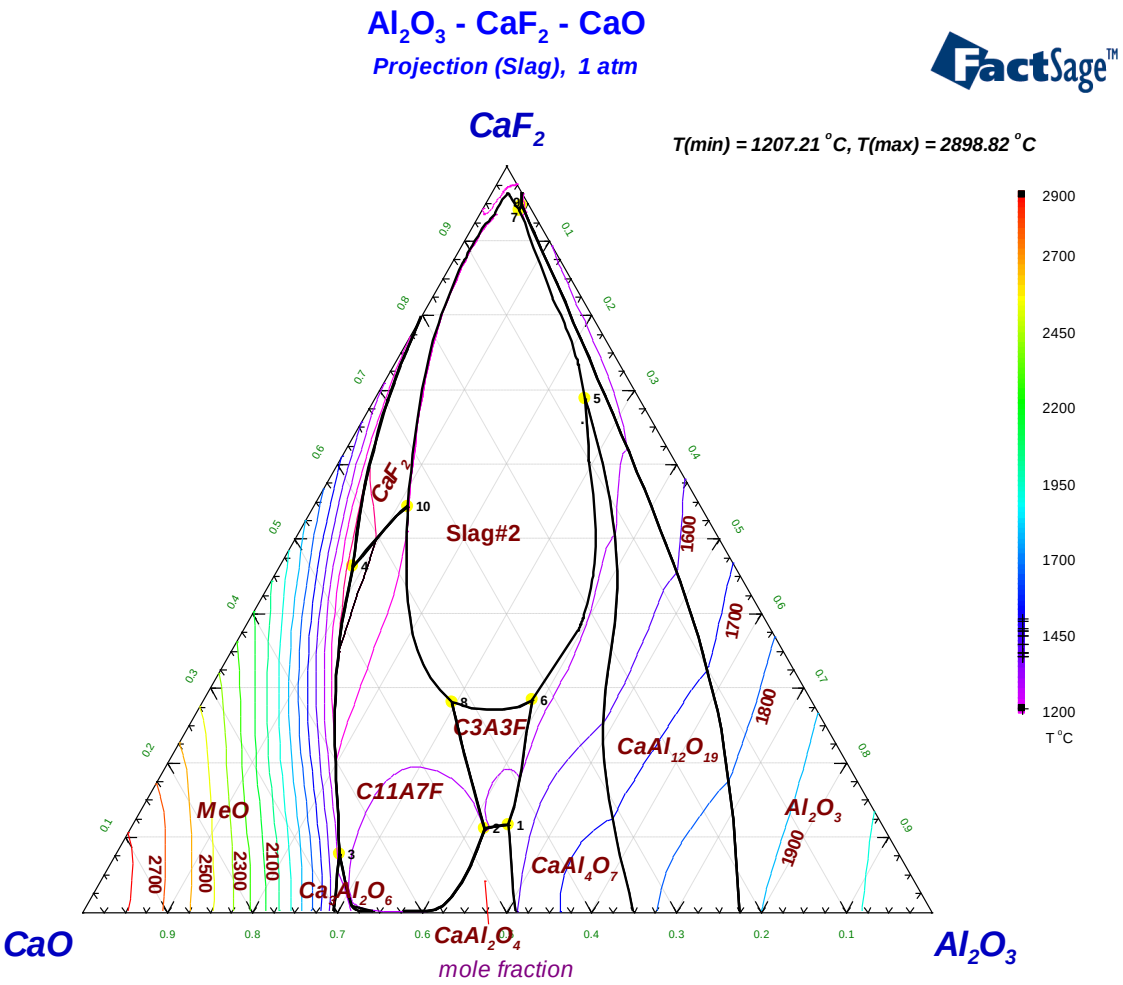

Weight percent
Liquidussurface

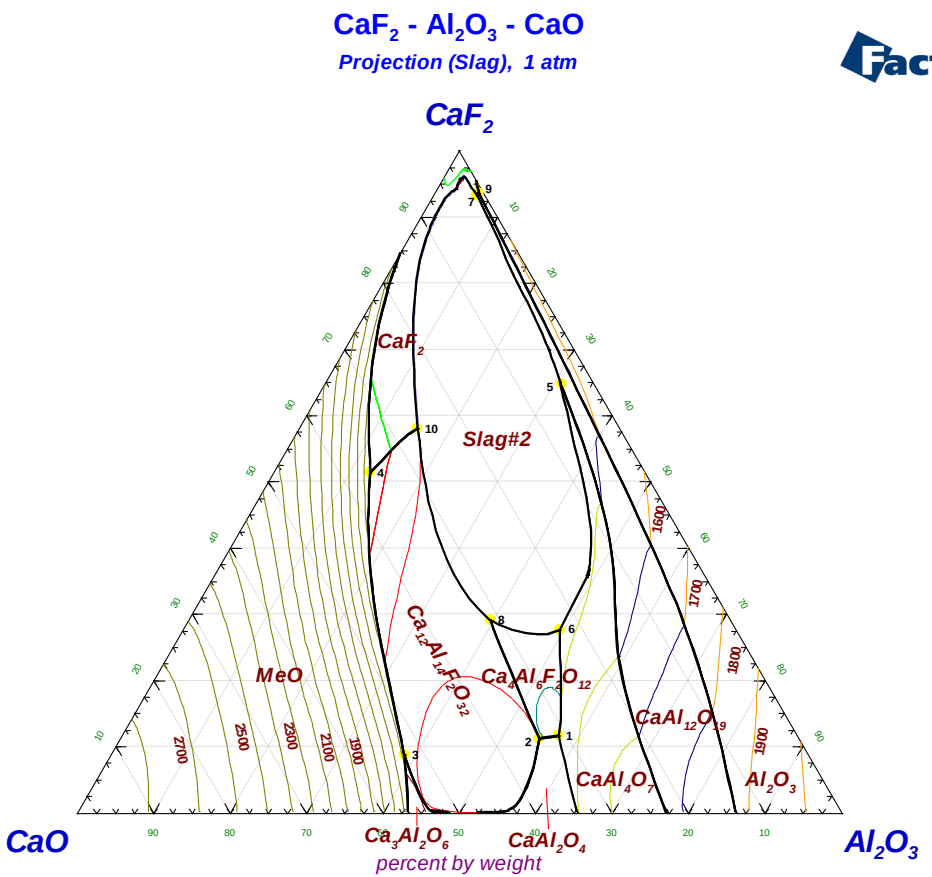

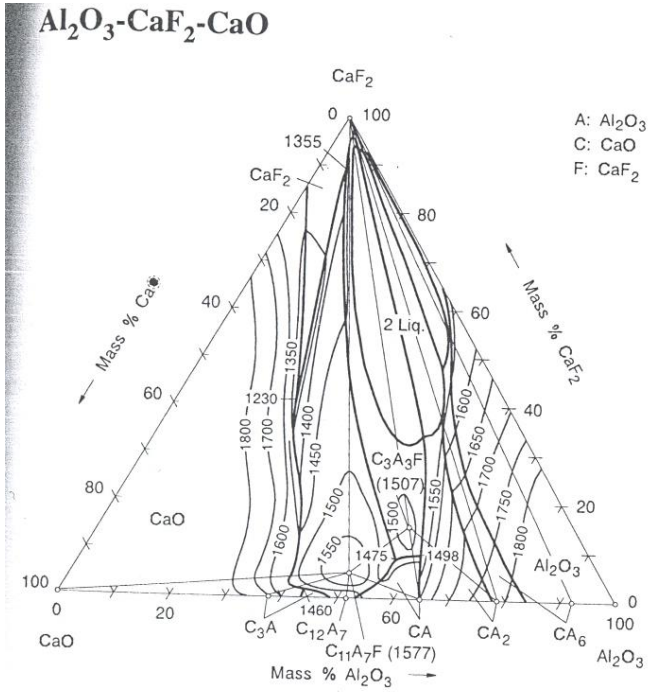

Fig. 3.420. Liquidus surface in the Al_2O_3-CaF_2-CaO system after Chatterjee, Zhmoidin [1] (sealed samples). For liquidus relations in numerous sub-systems, see also Chatterjee, Zhmoidin [2], Smirnov et al. [3] and Zhmoidin, Chatterjee [4].

Slag Atlas, 2nd Ed., Verlag Stahl-Eisen, Düsseldorf, 1995.

Invariant equilibria on the liquidus surface

Intersections with slag	Mole fraction A = CaF2, B = CaO, C = Al2O3				Weight percent A = CaF2, B = CaO, C = Al2O3			
	X(A)	X(B)	X(C)	T(C)	W(A)	W(B)	W(C)	T(C)
1: Ca4Al6F2O12 / CaAl2O4 / CaAl4O7	1: 0.11717	0.43892	0.44390	1506.26	1: 11.577	31.147	57.276	1505.52
2: Ca12Al14F2O32 / Ca4Al6F2O12 / CaAl2O4	2: 0.11168	0.47000	0.41832	1497.18	2: 11.218	33.908	54.874	1497.16
3: Ca12Al14F2O32 / Ca3Al2O6 / MeO	3: 0.07792	0.65849	0.26359	1471.69	3: 8.705	52.838	38.457	1471.69
4: Ca12Al14F2O32 / CaF2 / MeO	4: 0.46309	0.44949	0.08742	1207.59	4: 51.448	35.868	12.683	1207.27
5: CaAl12O19 / CaAl4O7 / Slag#2	5: 0.68884	0.06304	0.24812	1464.03	5: 65.098	4.279	30.622	1464.03
6: Ca4Al6F2O12 / CaAl4O7 / Slag#2	6: 0.28382	0.32789	0.38829	1450.10	6: 27.652	22.945	49.404	1450.04
7: Al2O3 / CaAl12O19 / CaF2	7: 0.94688	0.00839	0.04473	1382.79	7: 93.628	0.596	5.776	1382.79
8: Ca12Al14F2O32 / Ca4Al6F2O12 / Slag#2	8: 0.28174	0.42396	0.29429	1419.42	8: 29.028	31.374	39.598	1419.42
9: Al2O3 / CaAl12O19 / CaF2_s1(s)	9: 0.95183	0.02687	0.02131	1419.41	9: 95.283	1.932	2.785	1419.42
10: Ca12Al14F2O32 / CaF2 / Slag#2	10: 0.54344	0.34462	0.11194	1392.11	10: 57.988	26.412	15.599	1392.18

Al2O3-CaO-CaS,
Weight percent, 1500°C

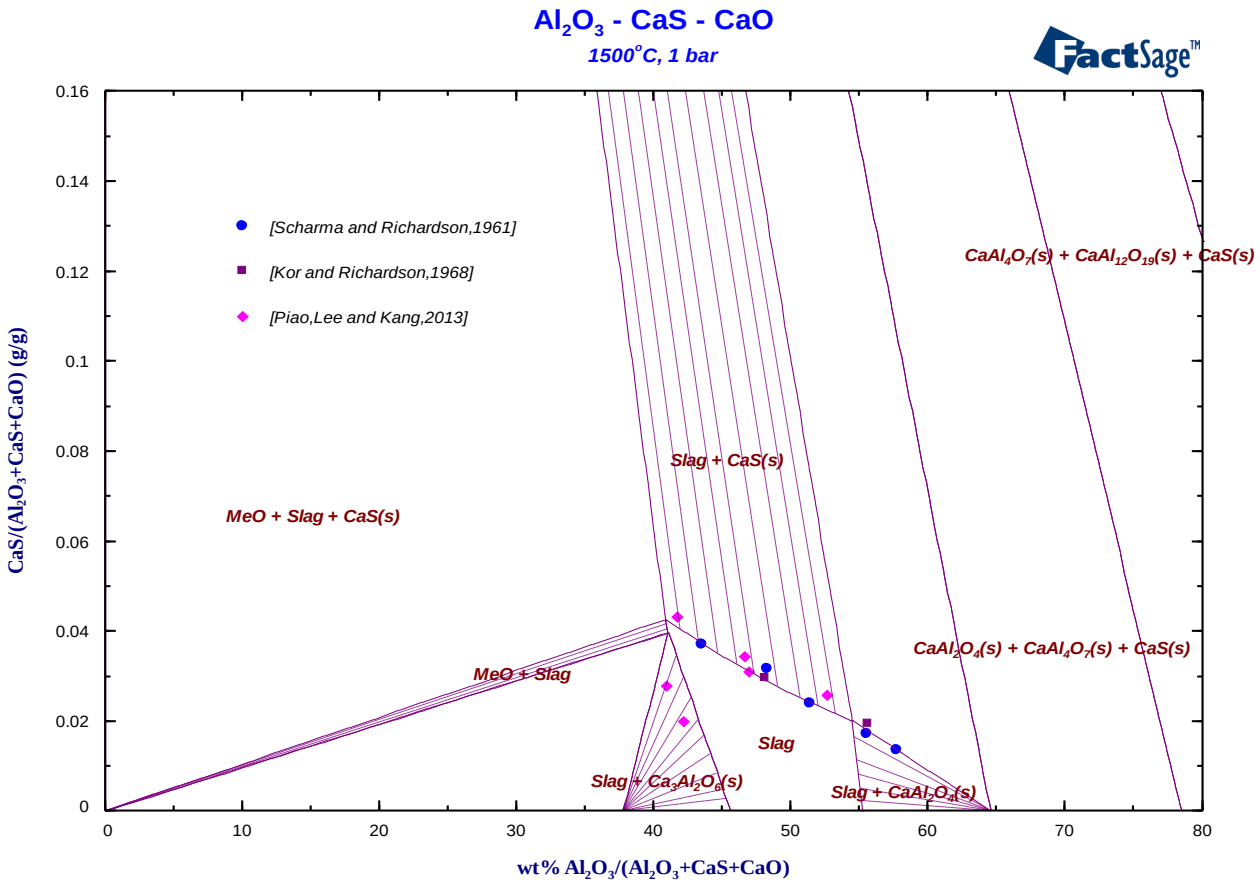

Al2O3-CaO-CaS,
Weight percent, 1550°C

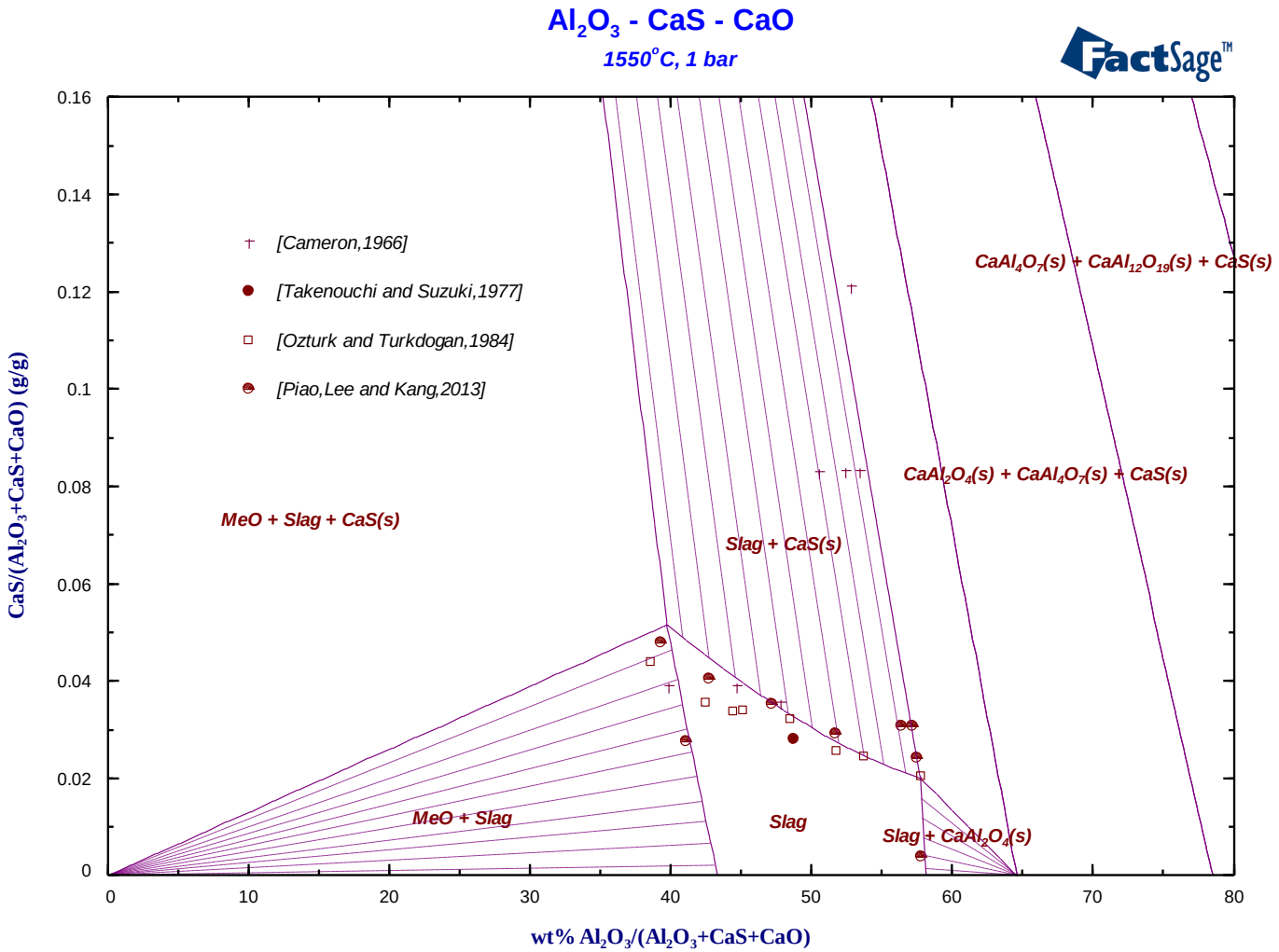

Al2O3-CaO-CaS,
Weight percent, 1600°C

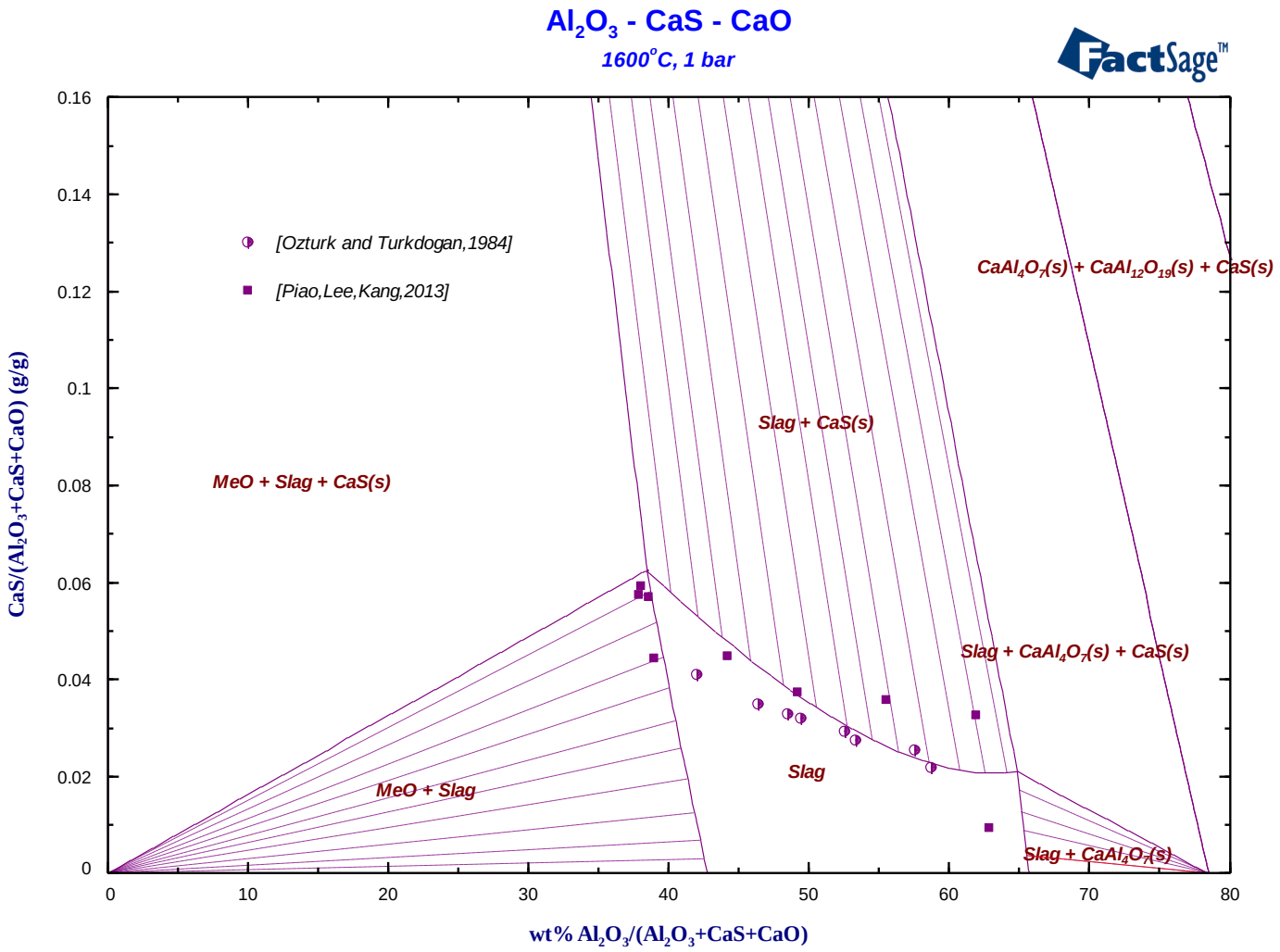

Mole fraction, Liquidussurface

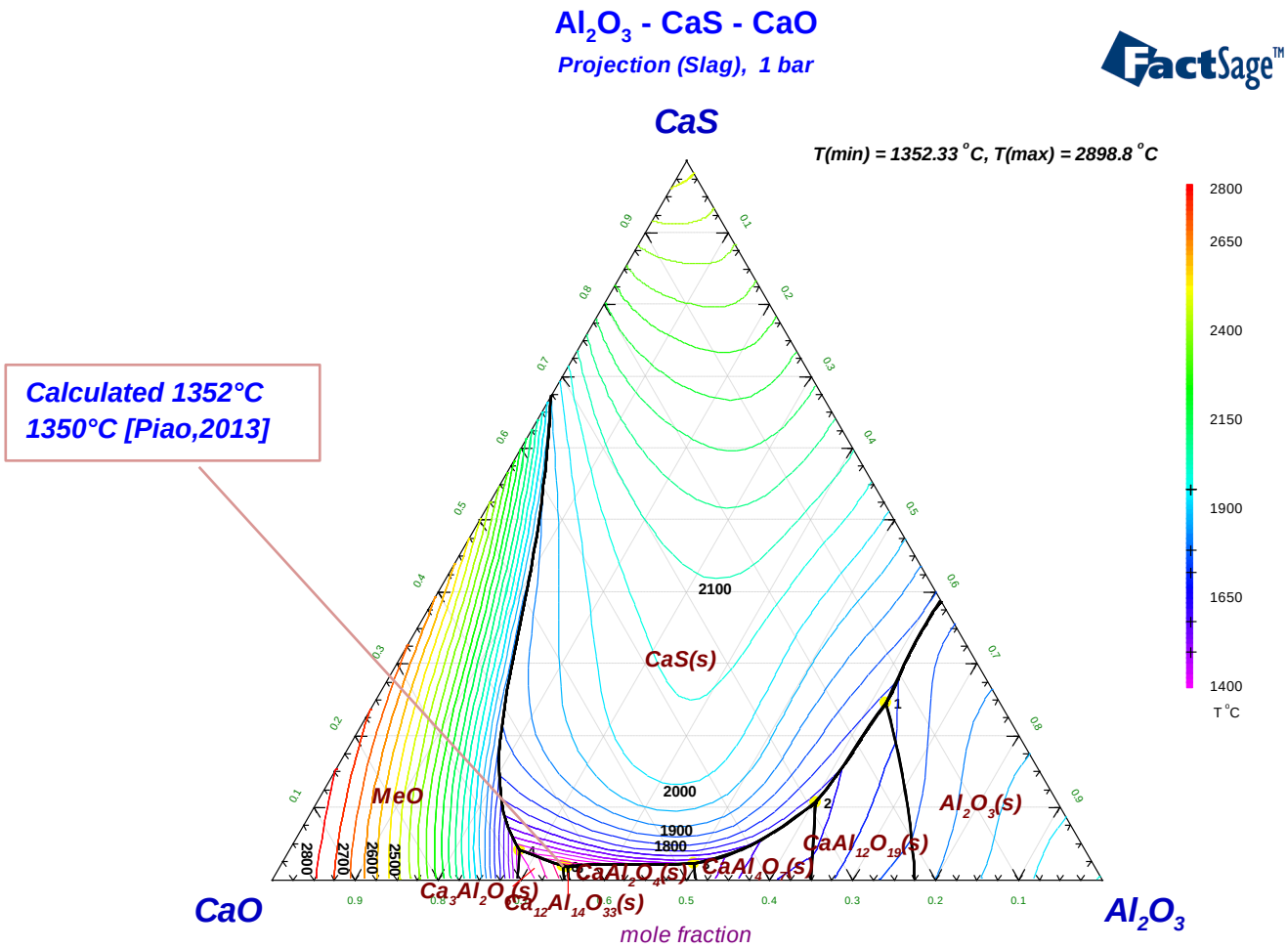

Weight percent, Liquidussurface

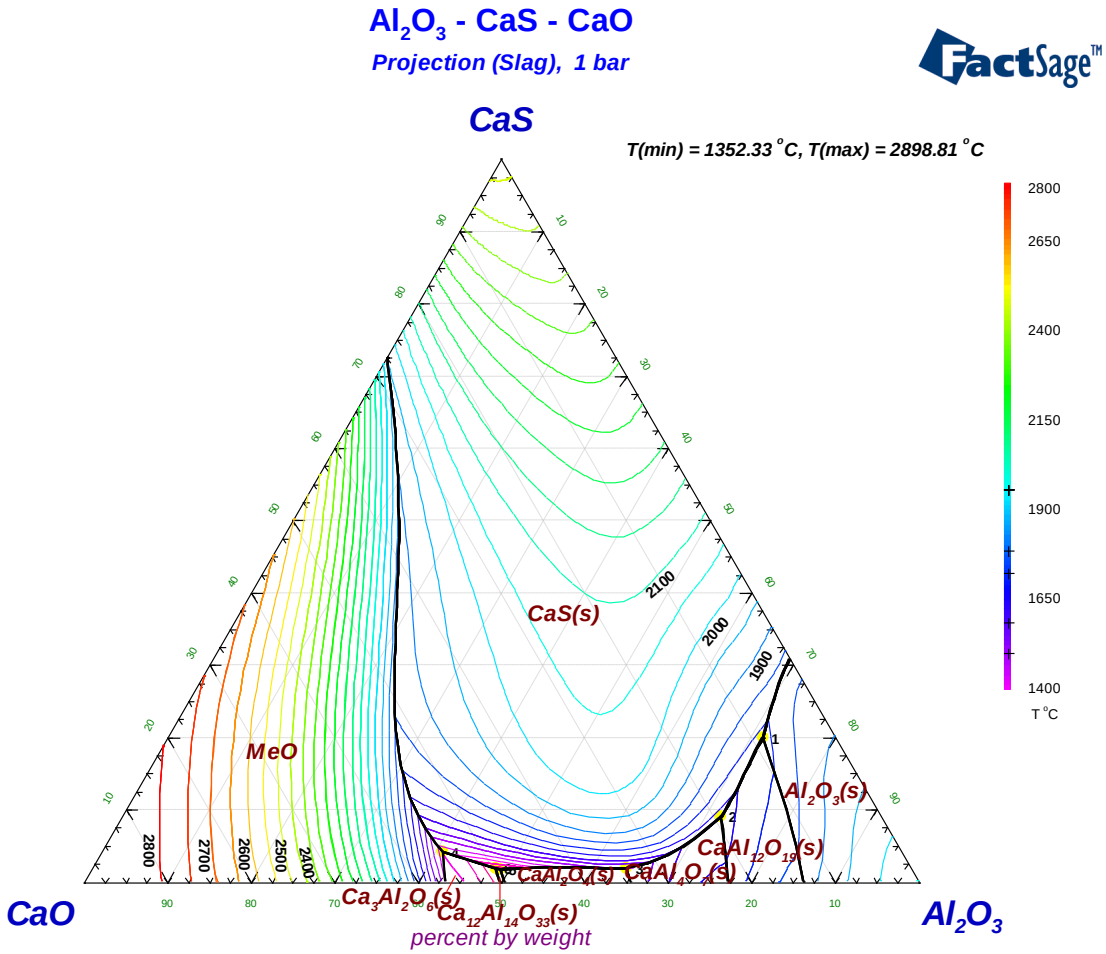

Invariant equilibria on the liquidus surface

Intersections with slag	Mole fraction A = CaS, B = CaO, C = Al2O3				Weight percent A = CaS, B = CaO, C = Al2O3			
	X(A)	X(B)	X(C)	T(C)	W(A)	W(B)	W(C)	T(C)
1: Al2O3(s) / CaAl12O19(s) / CaS(s)	1: 0.24431	0.13697	0.61872	1781.23	1: 19.940	8.689	71.370	1781.23
2: CaAl12O19(s) / CaAl4O7(s) / CaS(s)	2: 0.10698	0.29108	0.60194	1721.60	2: 9.036	19.110	71.854	1721.60
3: CaAl2O4(s) / CaAl4O7(s) / CaS(s)	3: 0.02132	0.47996	0.49872	1582.21	3: 1.939	33.940	64.121	1582.21
4: Ca3Al2O6(s) / CaS(s) / MeO	4: 0.04058	0.68075	0.27866	1497.45	4: 4.212	54.915	40.873	1497.43
5: Ca12Al14O33(s) / CaAl2O4(s) / CaS(s)	5: 0.01767	0.63453	0.34780	1369.73	5: 1.763	49.202	49.035	1355.04
6: Ca12Al14O33(s) / Ca3Al2O6(s) / CaS(s)	6: 0.01811	0.63938	0.34251	1352.33	6: 1.813	49.740	48.447	1352.33

Mole fraction, Liquidussurface

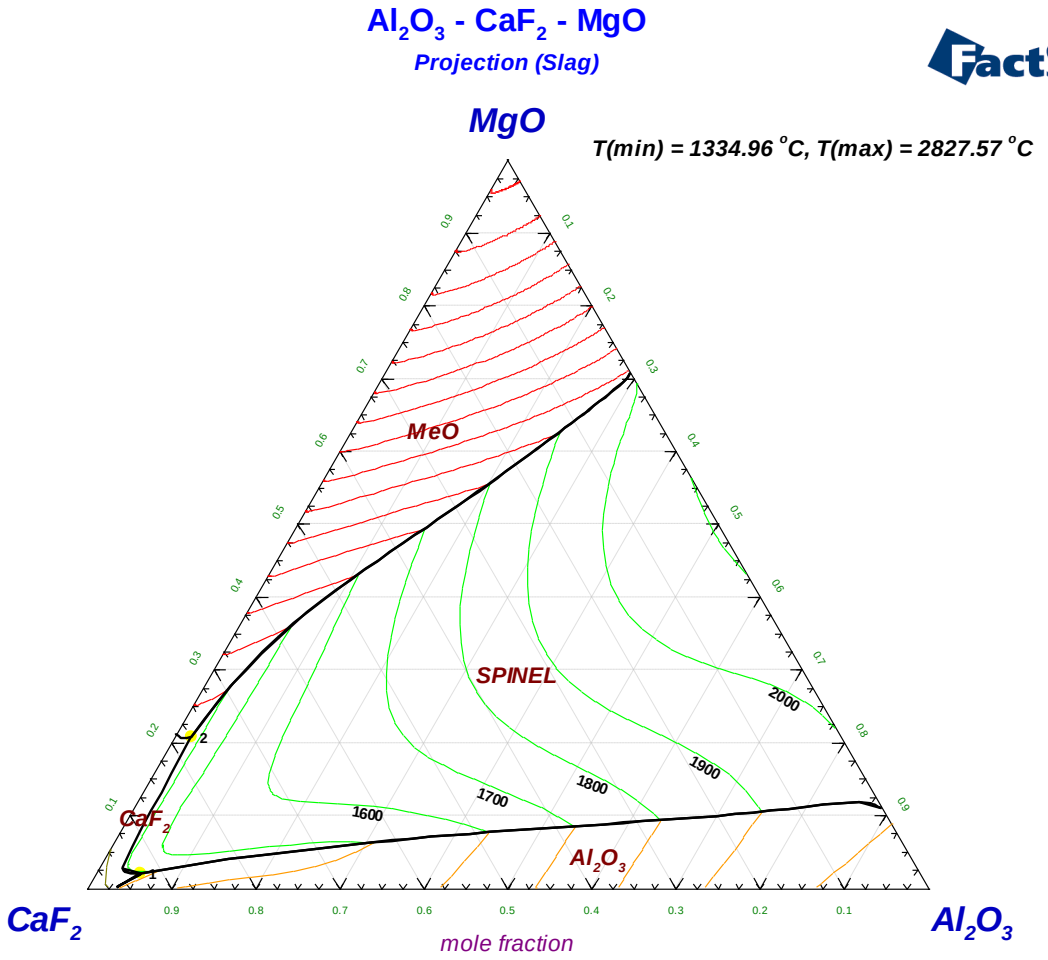

Weight percent, Liquidussurface

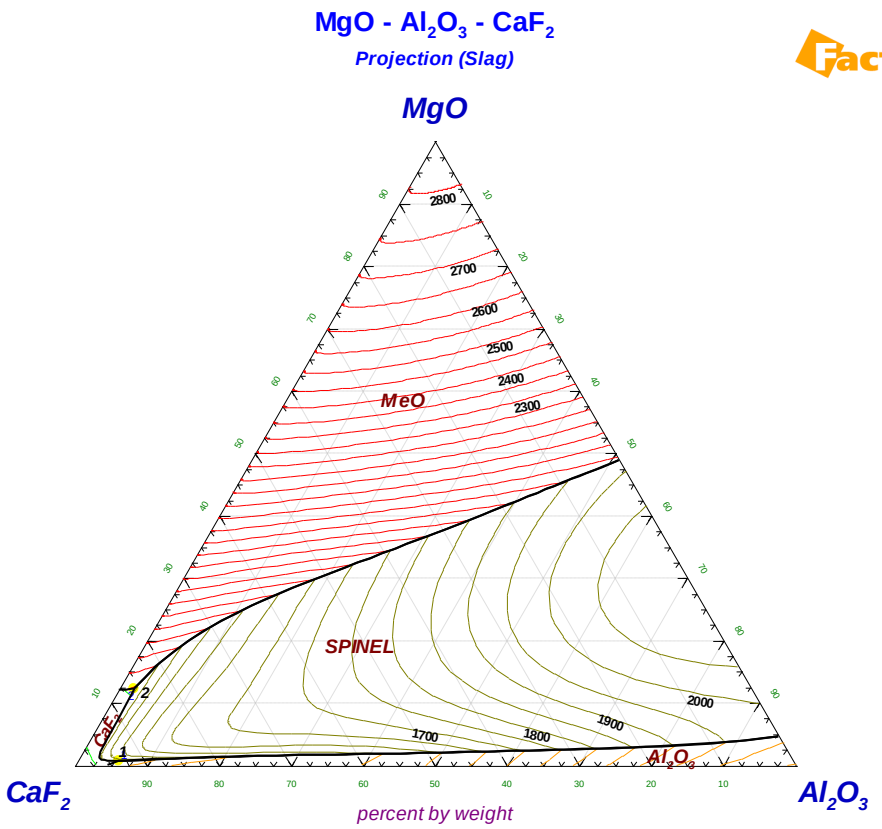

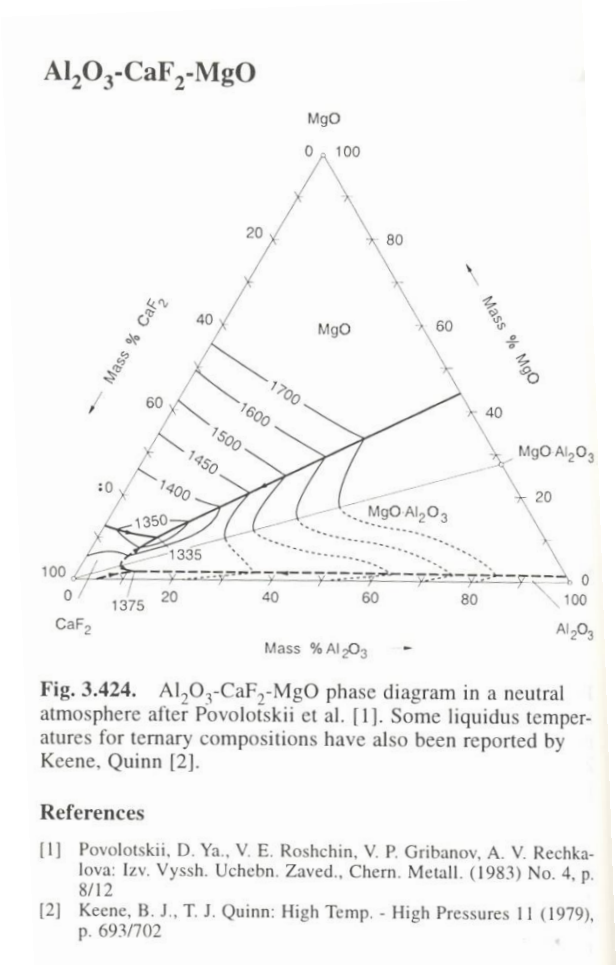

Fig. 3.424. Al_2O_3-CaF_2-MgO phase diagram in a neutral atmosphere after Povolotskii et al. [1]. Some liquidus temperatures for ternary compositions have also been reported by Keene, Quinn [2].

References

[1] Povolotskii, D. Ya., V. E. Roshchin, V. P. Gribanov, A. V. Rechkalova: Izv. Vyssh. Uchebn. Zaved., Chern. Metall. (1983) No. 4, p. 8/12

[2] Keene, B. J., T. J. Quinn: High Temp. - High Pressures 11 (1979), p. 693/702

Slag Atlas, 2nd Ed., Verlag Stahl-Eisen, Düsseldorf, 1995.

Invariant equilibria on the liquidus surface

Intersections with slag	Mole fraction A = MgO, B = CaF2, C = Al2O3				Weight percent A = MgO, B = CaF2, C = Al2O3			
	X(A)	X(B)	X(C)	T(C)	W(A)	W(B)	W(C)	T(C)
1: Al2O3 / CaF2 / SPINEL	1: 0.02010	0.92632	0.05358	1368.36	1: 1.031	92.018	6.951	1368.36
2: CaF2 / MeO / SPINEL	2: 0.20745	0.77272	0.01982	1334.96	2: 11.824	85.317	2.858	1334.96

Weight percent,
Liquidus lines at 1380°C and 1460°C

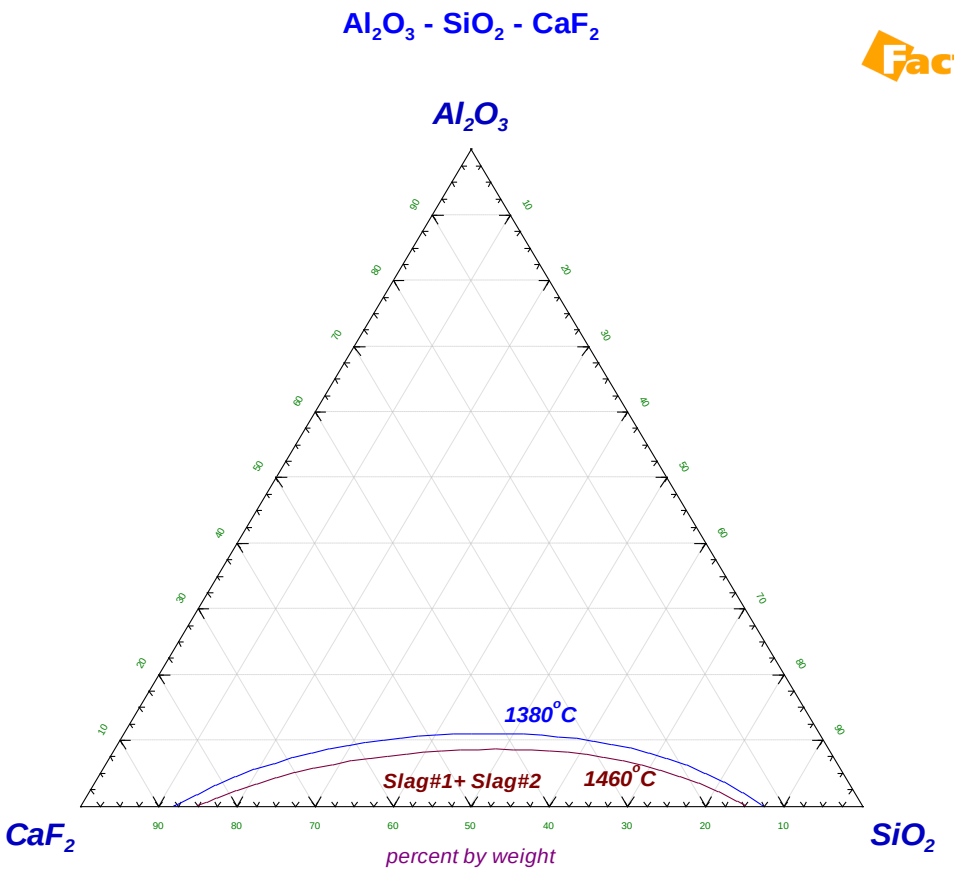

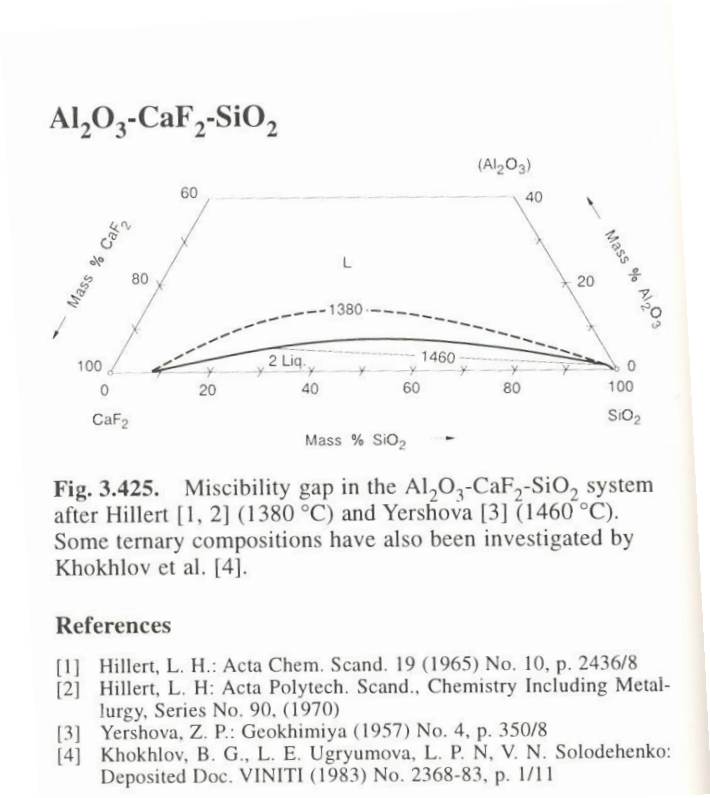

Fig. 3.425. Miscibility gap in the Al_2O_3-CaF_2-SiO_2 system after Hillert [1, 2] (1380 °C) and Yershova [3] (1460 °C). Some ternary compositions have also been investigated by Khokhlov et al. [4].

References

[1] Hillert, L. H.: Acta Chem. Scand. 19 (1965) No. 10, p. 2436/8
[2] Hillert, L. H: Acta Polytech. Scand., Chemistry Including Metallurgy, Series No. 90, (1970)
[3] Yershova, Z. P.: Geokhimiya (1957) No. 4, p. 350/8
[4] Khokhlov, B. G., L. E. Ugryumova, L. P. N, V. N. Solodehenko: Deposited Doc. VINITI (1983) No. 2368-83, p. 1/11

Slag Atlas, 2nd Ed., Verlag Stahl-Eisen, Düsseldorf, 1995.

Al2O3-CaF2-SiO2,

Weight percent 1425°C

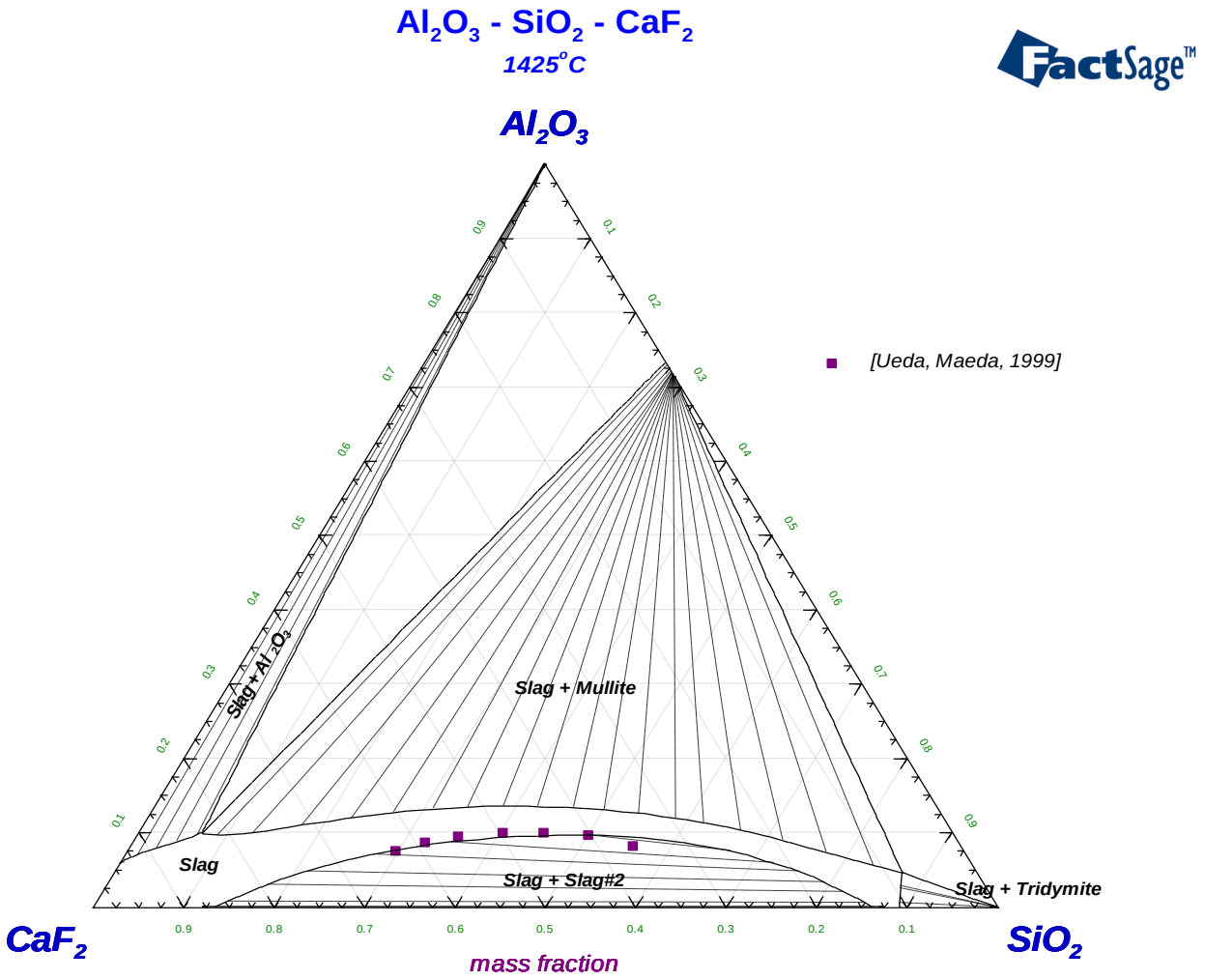

Al2O3-CaF2-SiO2,

Weight percent 1500°C, 1600°C and 1700°C

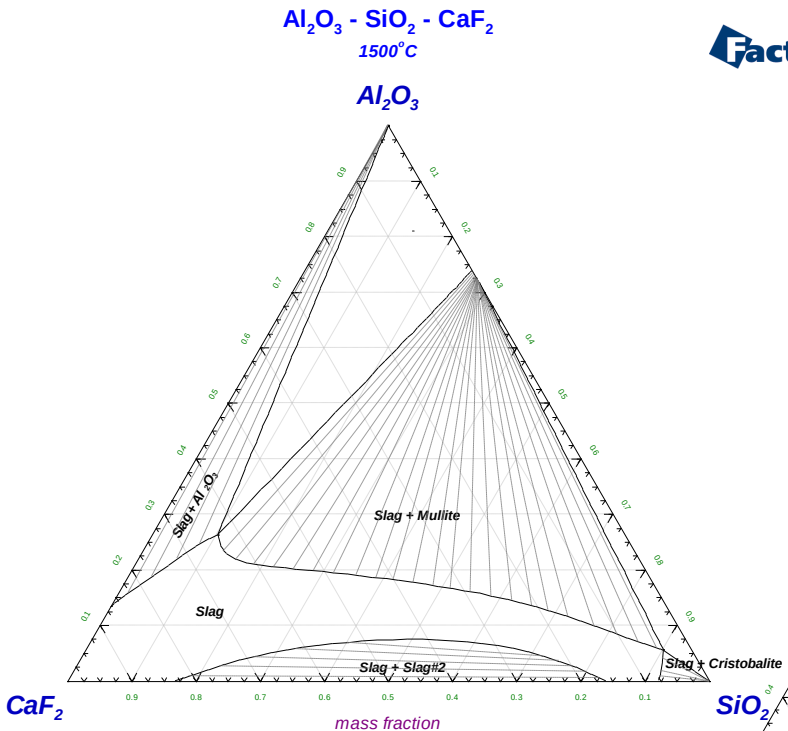

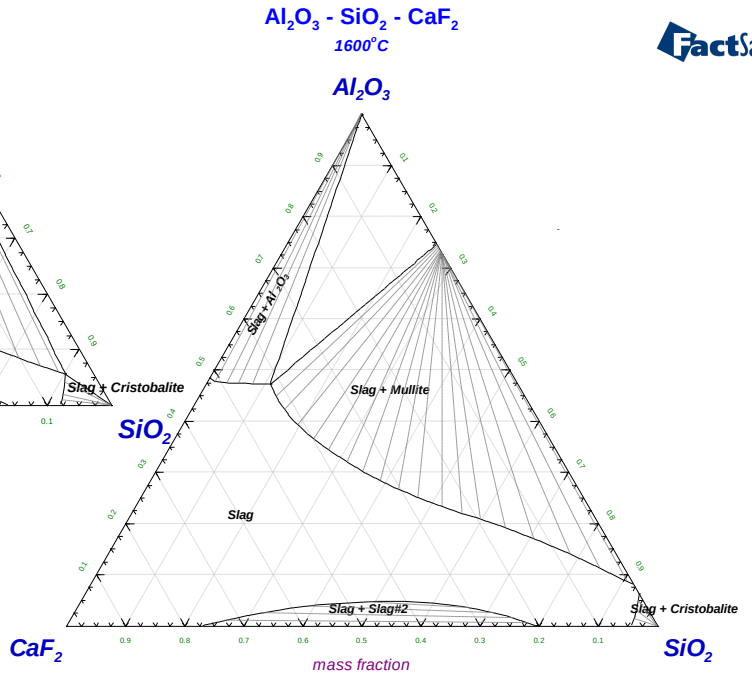

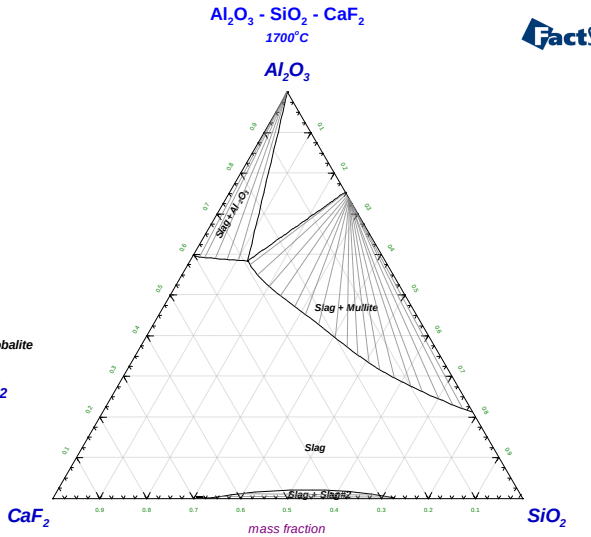

Mole fraction, Liquidussurface

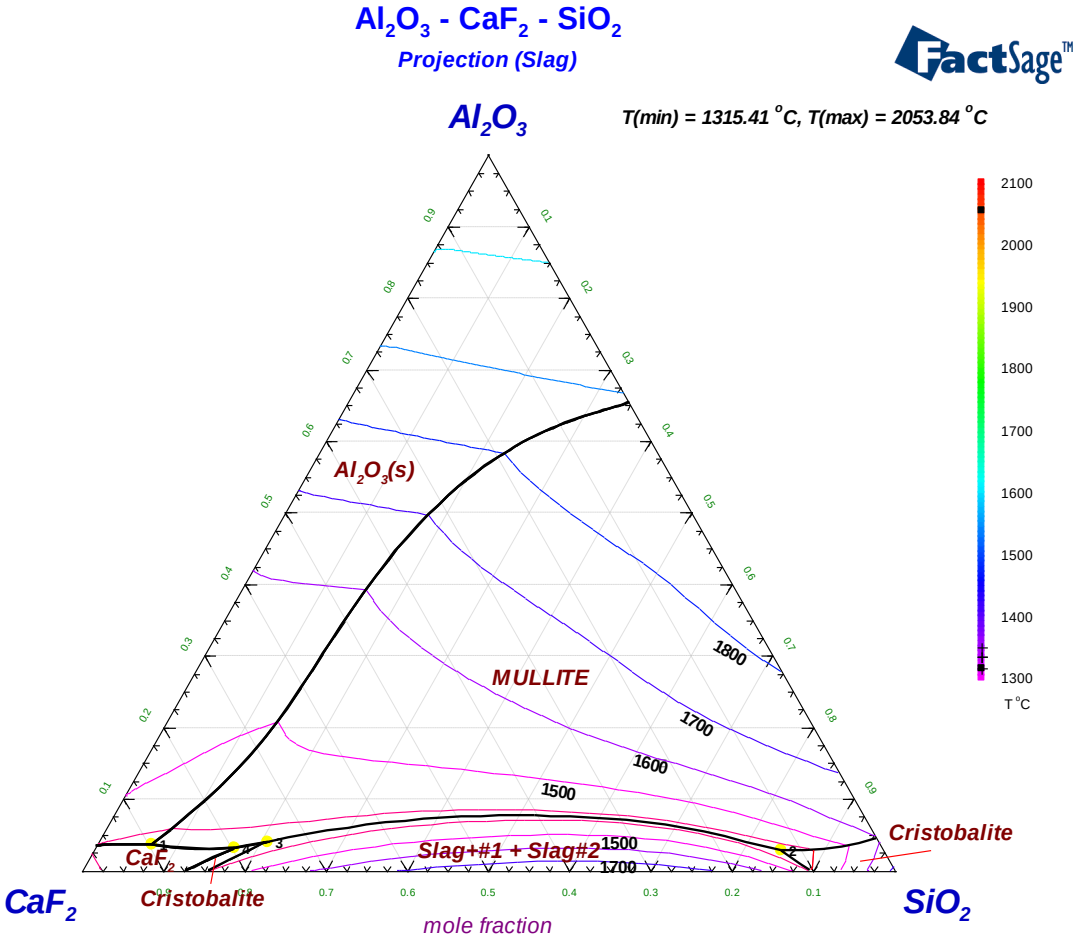

Weight percent, Liquidussurface

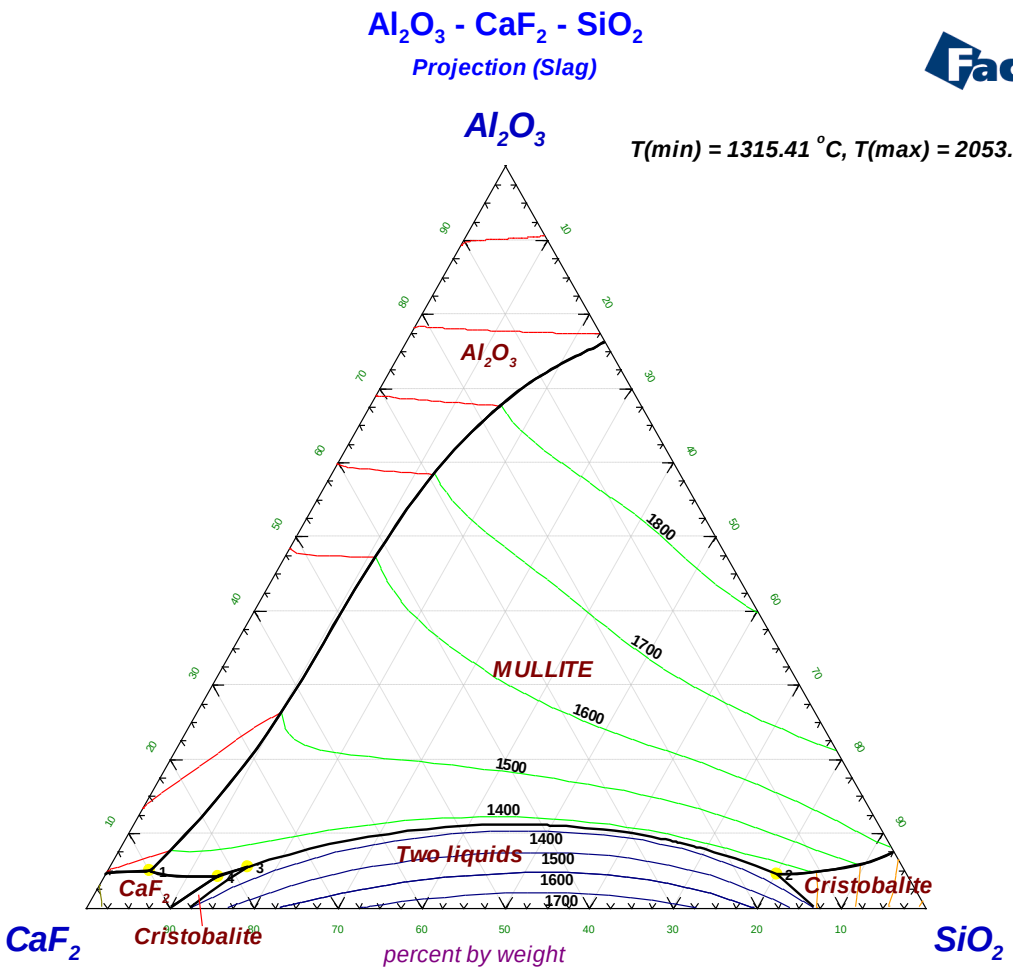

Invariant equilibria on the liquidus surface

Intersections with slag	Mole fraction A = Al2O3, B = CaF2, C = SiO2				Weight percent A = Al2O3, B = CaF2, C = SiO2			
	X(A)	X(B)	X(C)	T(C)	W(A)	W(B)	W(C)	T(C)
1. Al2O3 / CaF2 / MULLITE	1: 0.03733	0.89529	0.06738	1349.38	1. 4.896	89.898	5.207	1349.38
2. MULLITE / Slag#2 / Cristobalite	2: 0.02809	0.12530	0.84661	1334.46	2. 4.509	15.403	80.088	1334.48
3. MULLITE / Cristobalite / Slag#2	3: 0.04019	0.75217	0.20765	1334.46	3. 5.441	77.990	16.569	1334.46
4. CaF2 / MULLITE / Cristobalite	4: 0.03122	0.79700	0.17177	1315.42	4. 4.204	82.168	13.629	1315.41

Al2O3-CaO-Cr2O3,
Mole fraction, Isopleth CaAl2O4-CaCr2O4

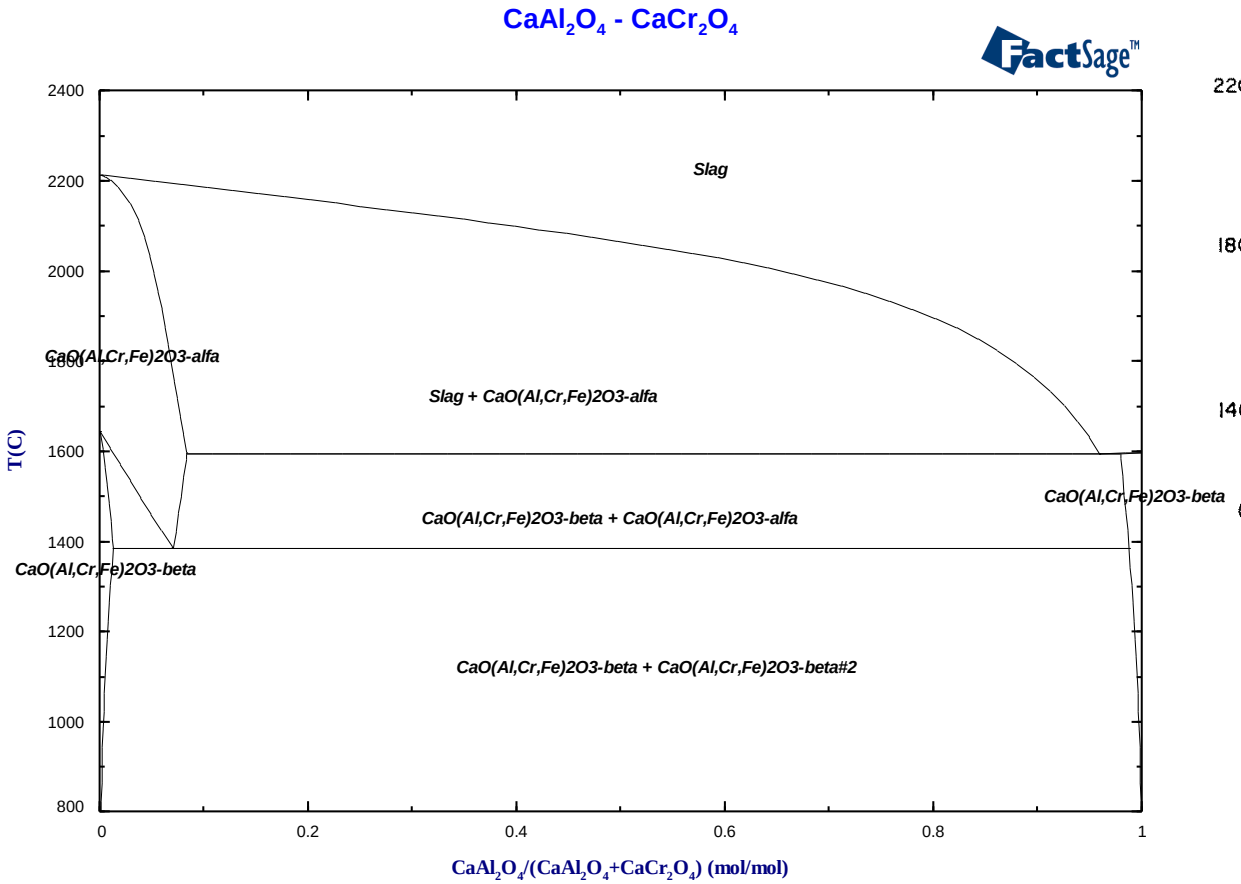

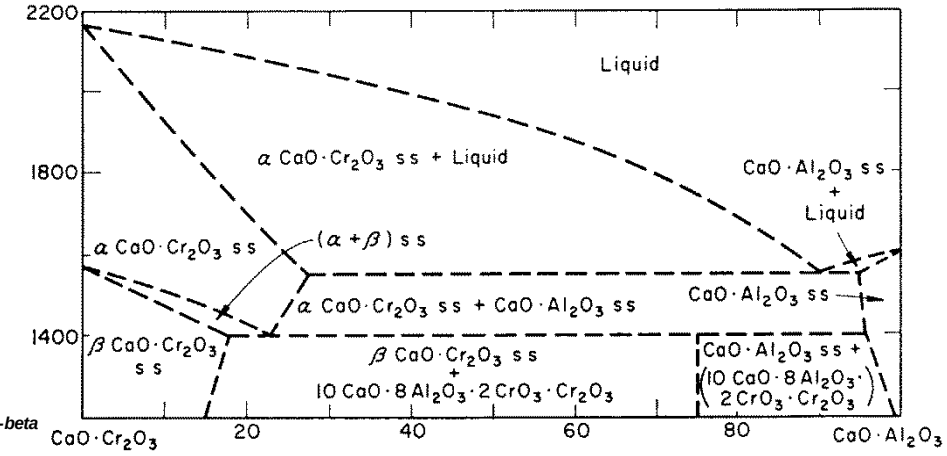

W.F. Ford, W.J. Rees, Trans. Br. Ceram. Soc., 57 [5], (1958), pp. 233-241.

Mole fraction, Liquidussurface

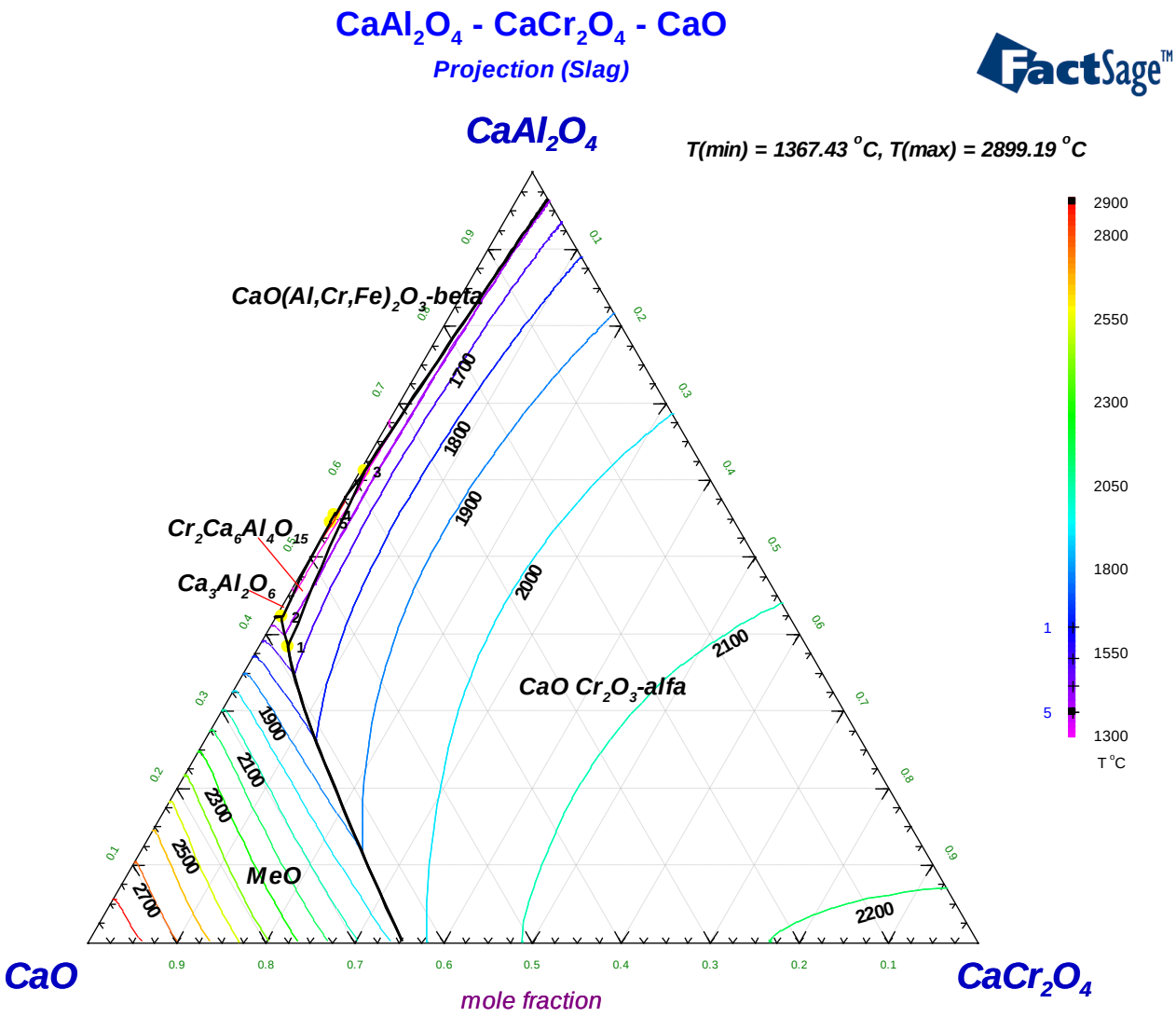

Weight percent, Liquidussurface

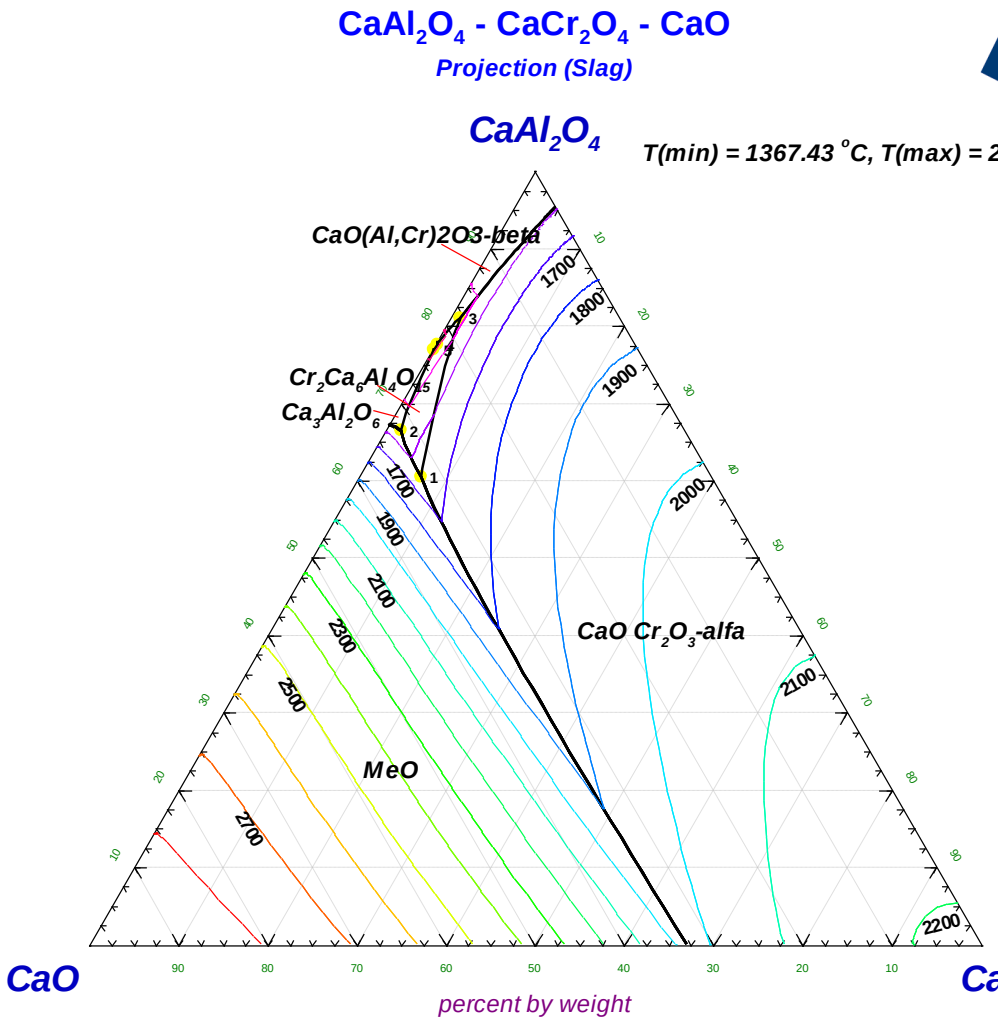

A. Kaiser, B. Sommer, E. Woermann, J. Am. Ceram. Soc., 75 [6], (1992), pp.1463-1471.

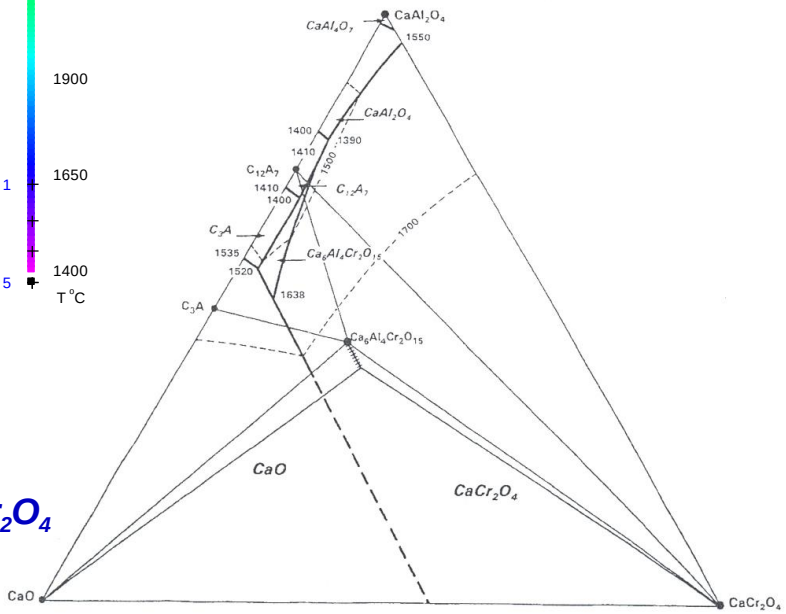

The system $CaO-CaAl_2O_4-"CaCr_2O_4"$; liquidus diagram, $H_2/CO_2 = 1$. For explanation of symbols, see captions of Figs. 1 and 3.

Invariant equilibria on the liquidus surface

Intersections with slag	Mole fraction A = CaAl2O4, B = CaO, C = CaCr2O4				Weight percent A = CaAl2O4, B = CaO, C = CaCr2O4			
	X(A)	X(B)	X(C)	T(C)	W(A)	W(B)	W(C)	T(C)
1: CaO Cr2O3-alfa / Cr2Ca6Al4O15 / MeO	1: 0.38421	0.58226	0.03353	1626.17	1: 60.510	32.538	6.952	1626.17
2: Ca3Al2O6 / Cr2Ca6Al4O15 / MeO	2: 0.42206	0.56991	0.00803	1530.04	2: 66.481	31.853	1.666	1529.92
3: $CaOCr_2O_3$-alfa/ $CaO(Al,Cr)_2O_3$-beta/$Cr_2Ca_6Al_4O_{15}$	3: 0.61156	0.38219	0.00624	1449.05	3: 80.959	17.953	1.088	1449.12
4: Ca12Al14O33 / $CaO(Al,Cr)_2O_3$-beta /$Cr_2Ca_6Al_4O_{15}$	4: 0.55411	0.44475	0.00114	1369.09	4: 77.670	22.121	0.210	1369.09
5: Ca12Al14O33 / Ca3Al2O6 / Cr2Ca6Al4O15	5: 0.54476	0.45421	0.00103	1367.45	5: 77.021	22.787	0.192	1367.43

Al2CaO4-CaCr2O4-CaO-O2, Weight percent 1100°C

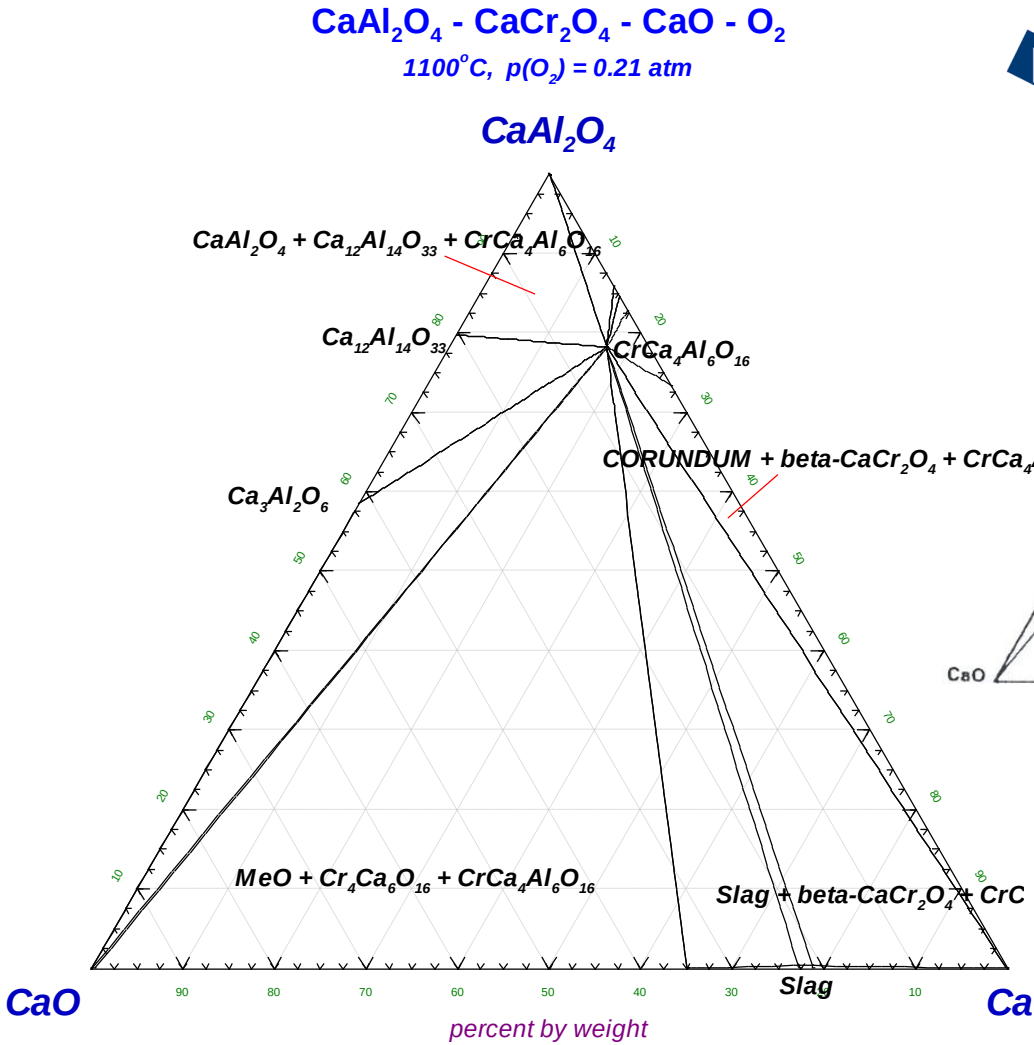

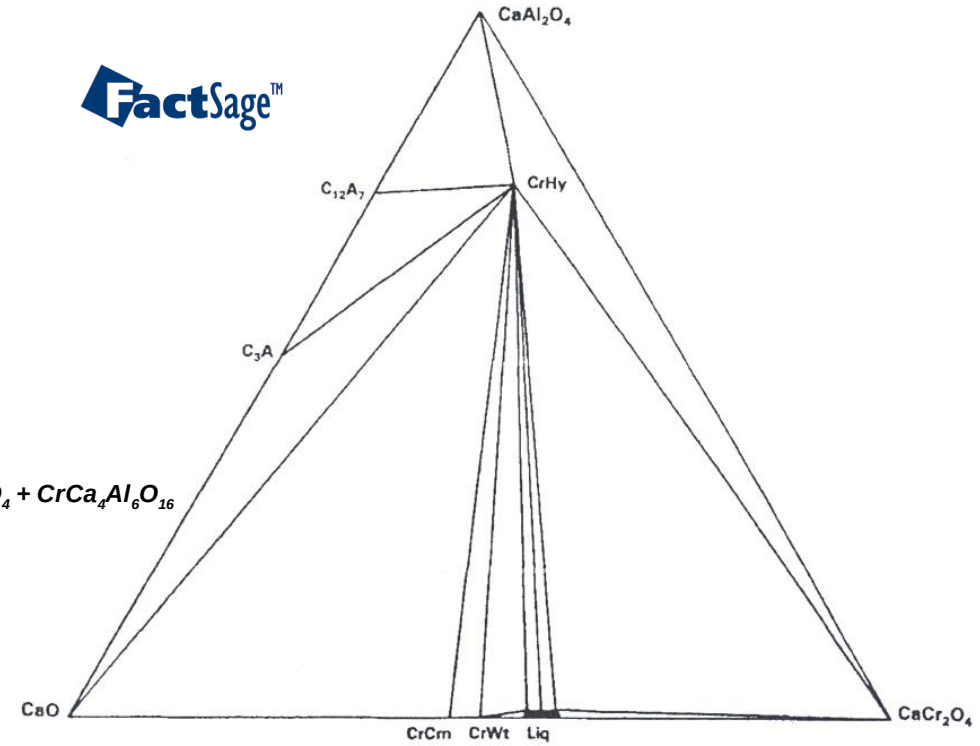

Fig. 4. The system $CaO-CaAl_2O_4-$"$CaCr_2O_4$"; isotherm at 1100°C.

A. Kaiser, B. Sommer, E. Woermann, J. Am. Ceram. Soc., 75 [6], (1992), pp.1463-1471.

Al2CaO4-CaCr2O4-CaO-O2, Weight percent 1300°C

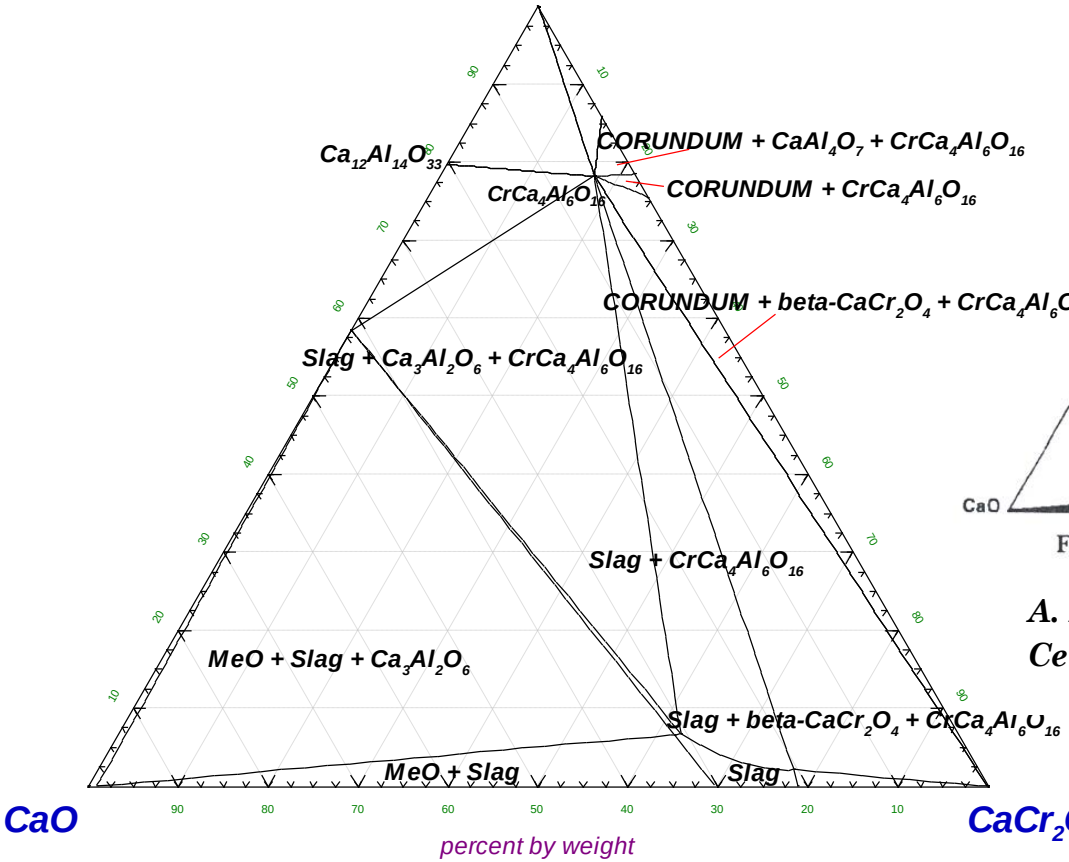

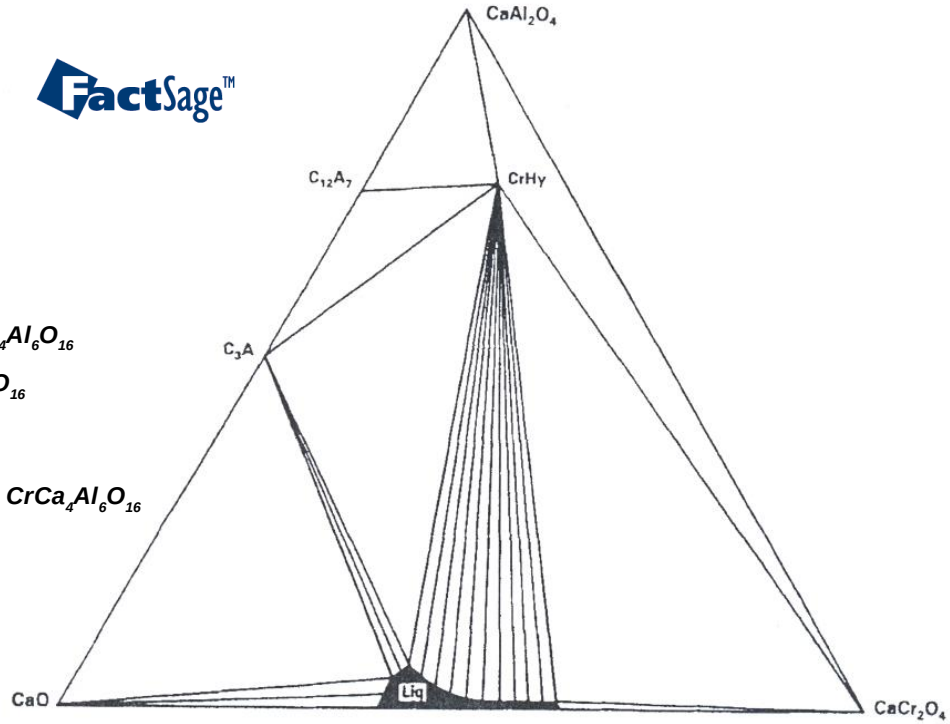

Fig. 5. The system $CaO-CaAl_2O_4-$"$CaCr_2O_4$"; isotherm at 1300°C.

A. Kaiser, B. Sommer, E. Woermann, J. Am. Ceram. Soc., 75 [6], (1992), pp.1463-1471.

Al2O3-CaO-CaCrO4-O2, Weight percent 1300°C

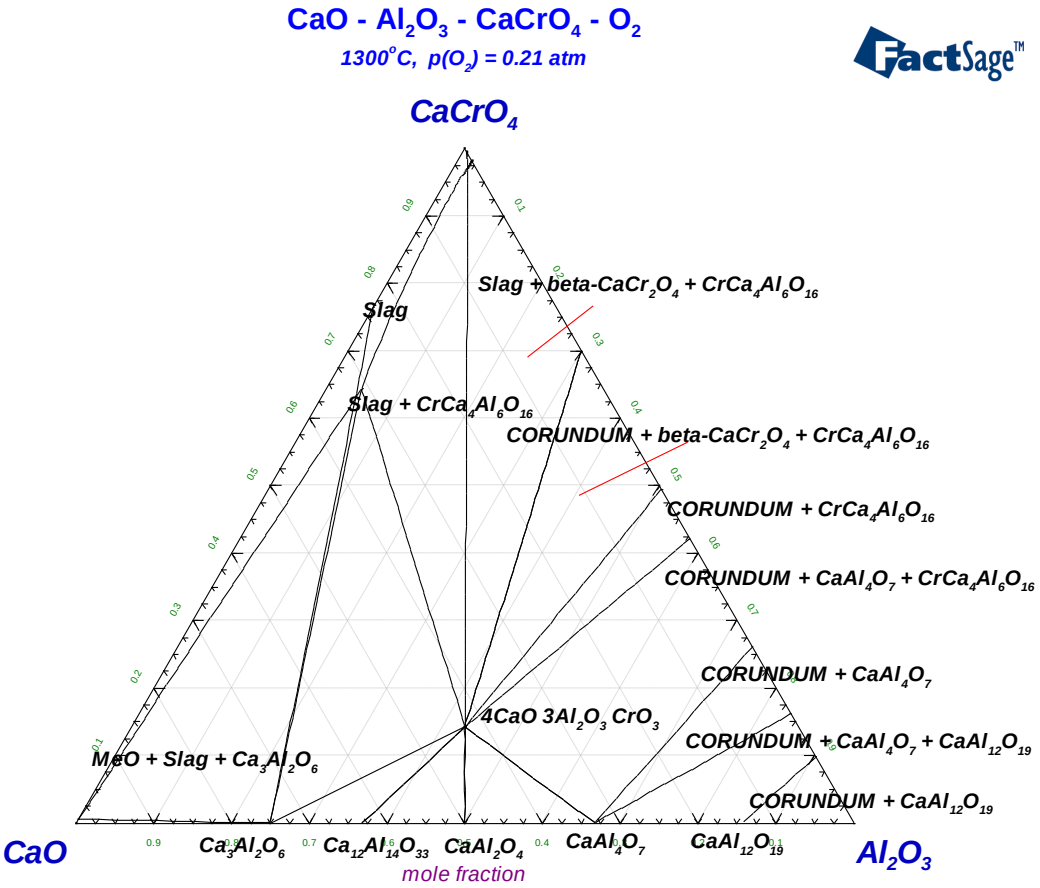

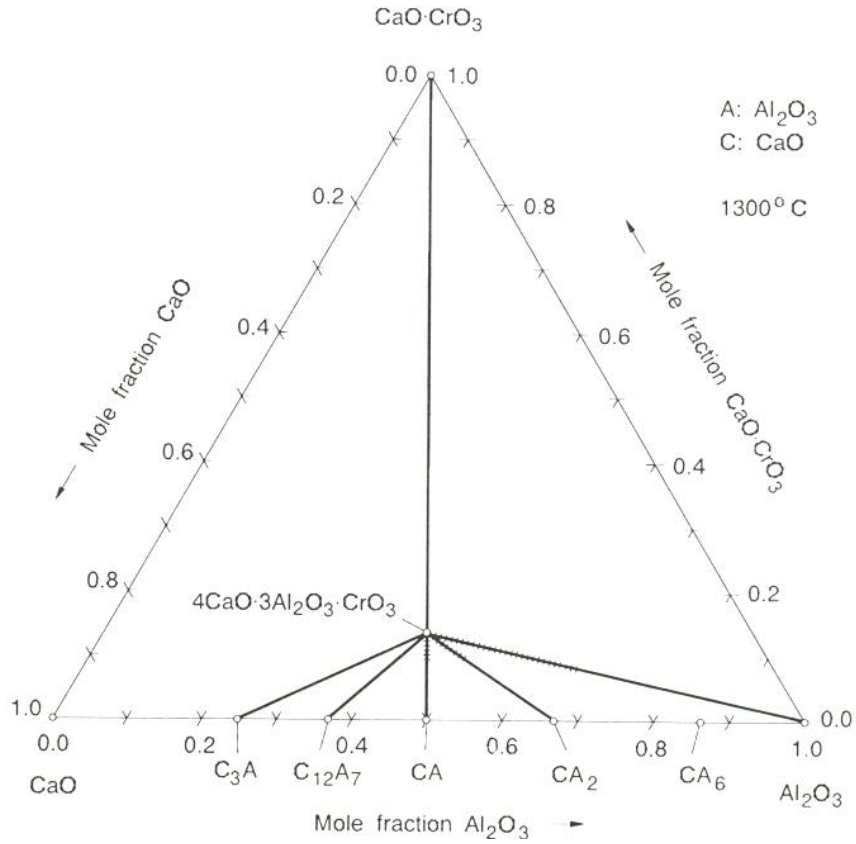

D. Peters, A.F. Hummel, Cem. Concr. Res. 9 (1979), No.2, pp.259-268.

$CaO - Al_2O_3 - CaCrO_4 - O_2$

Projection (Slag), $p(O_2) = 0.21$ atm

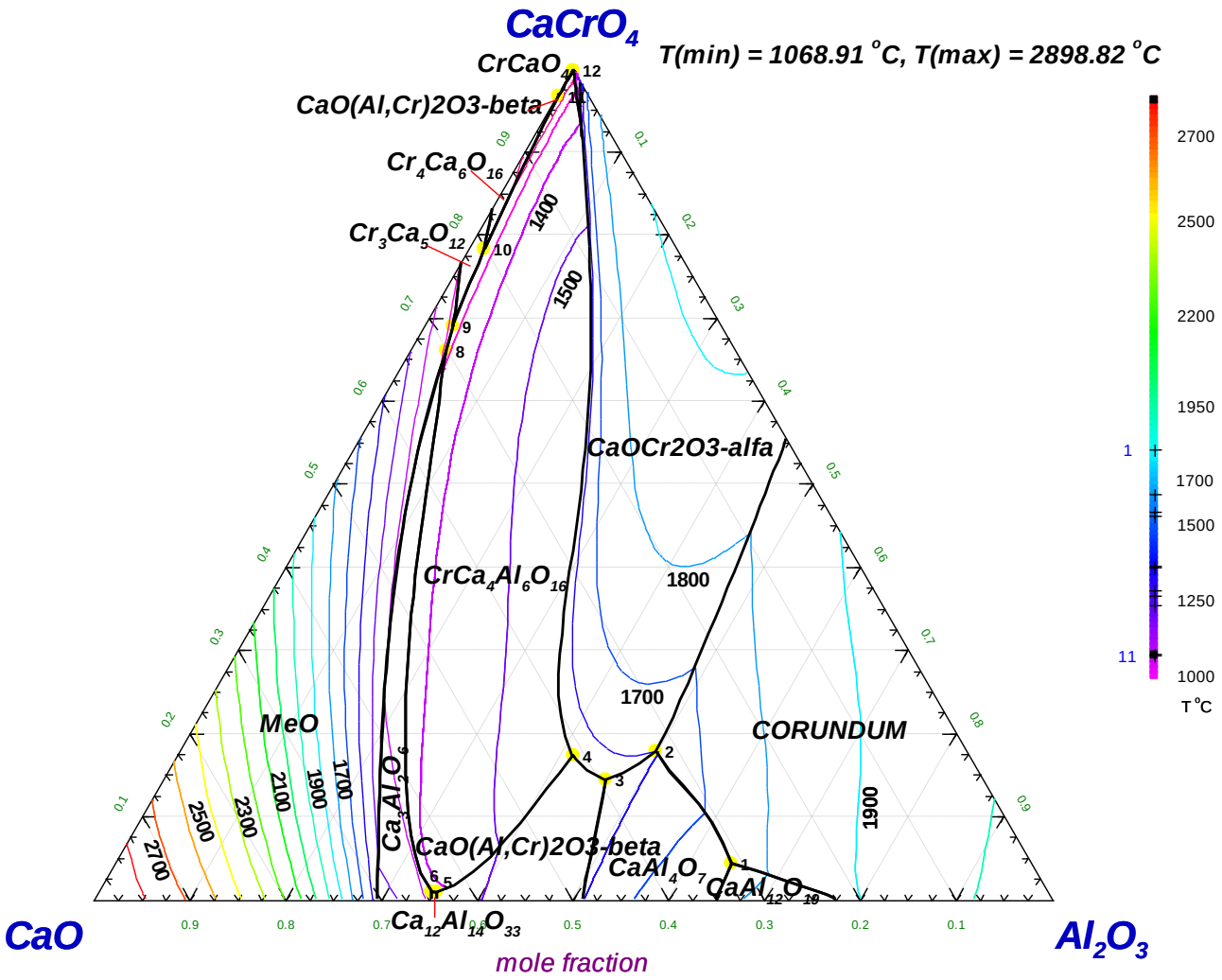

Weight percent, Liquidussurface

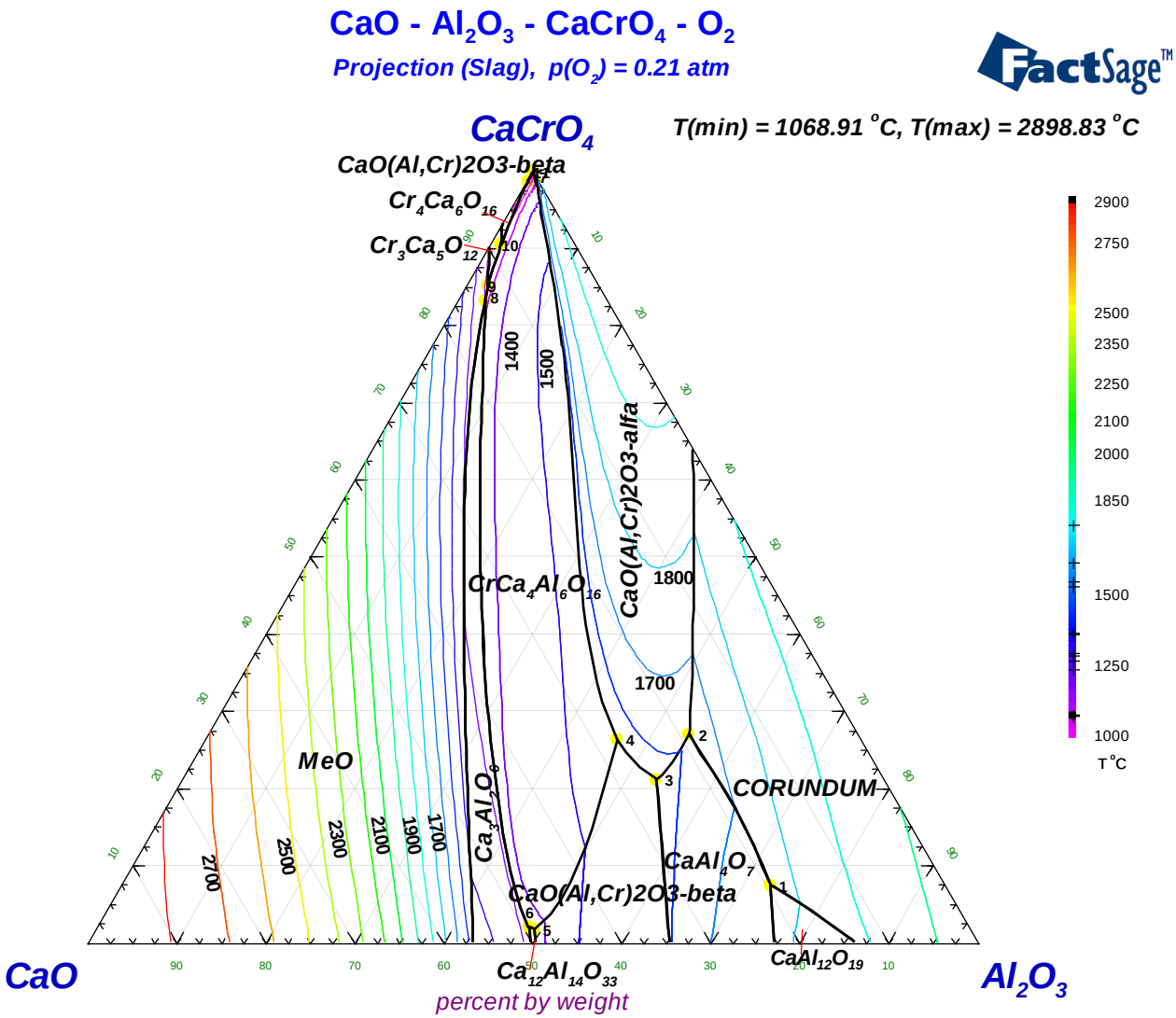

Invariant equilibria on the liquidus surface

Intersections with slag	Mole fraction A = CaCrO4, B = CaO, C = Al2O3				Weight percent A = CaCrO4, B = CaO, C = Al2O3				
		X(A)	X(B)	X(C)	T(C)		W(A)	W(B)	W(C)	T(C)
1: CORANDUM / CaAl12O19 / CaAl4O7	1:	0.04282	0.31255	0.64463	1747.59	1:	7.431	19.488	73.081	1747.59
2: CORANDUM / CaAl4O7 / CaO(Al,Cr)2O3-alfa	2:	0.16630	0.32332	0.51038	1613.12	2:	27.001	18.862	54.137	1613.11
3: CaAl4O7 /CaO Cr_2O_3-alfa/CaO$(Al,Cr,Fe)_2O_3$-beta	3:	0.12175	0.40829	0.46996	1548.14	3:	21.157	25.492	53.352	1548.14
4: CaO Cr2O3-alfa / CaO$(Al,Cr)_2O_3$-beta/CrCa4Al6O16	4:	0.15151	0.43869	0.40980	1528.74	4:	26.265	27.325	46.410	1528.74
5: Ca12Al14O33 / CaO(Al,Cr)2O3-beta / CrCa4Al6O16	5:	0.00831	0.63813	0.35356	1362.92	5:	1.773	48.932	49.294	1362.91
6: Ca12Al14O33 / Ca3Al2O6 / CrCa4Al6O16	6:	0.00947	0.64269	0.34784	1359.73	6:	2.026	49.380	48.594	1359.73
7: CaO Cr2O3-alfa / CaO$(Al,Cr)_2O_3$-beta/CrCa4Al6O16	7:	0.97496	0.00905	0.01599	1290.72	7:	98.615	0.329	1.057	1290.72
8: Ca3Al2O6 / CrCa4Al6O16 / MeO	8:	0.65996	0.30233	0.03771	1280.73	8:	83.200	13.694	3.106	1280.73
9: Cr3Ca5O12(s1) / CrCa4Al6O16 / MeO	9:	0.68999	0.27968	0.03033	1265.10	9:	85.153	12.402	2.446	1265.10
10: Cr3Ca5O12(s1) / Cr4Ca6O16(s1) / CrCa4Al6O16	10:	0.78248	0.20073	0.01679	1234.91	10:	90.400	8.332	1.267	1234.91
11: CaO(Al,Cr)2O3-beta / CrCa4Al6O16 / CrCaO4(s1)	11:	0.99731	0.00054	0.00215	1071.49	11:	99.840	0.019	0.141	1071.49
12: Cr4Ca6O16(s1) / CrCa4Al6O16 / CrCaO4(s1)	12:	0.96581	0.03221	0.00198	1068.92	12:	98.685	1.183	0.132	1068.97

Weight percent 1145 C°

Al_2O_3 - CaO - Fe_2O_3 - O_2

1145°C, $p(O_2)$ = 0.21 atm

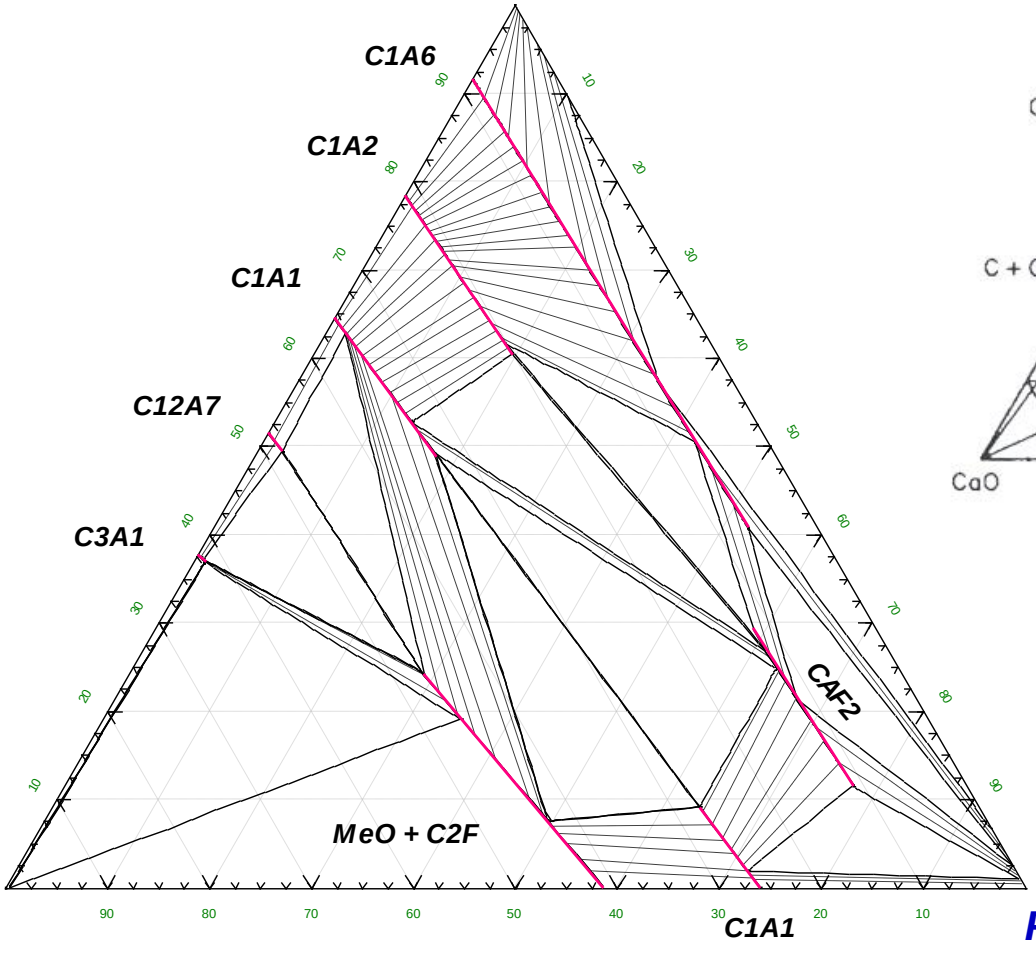

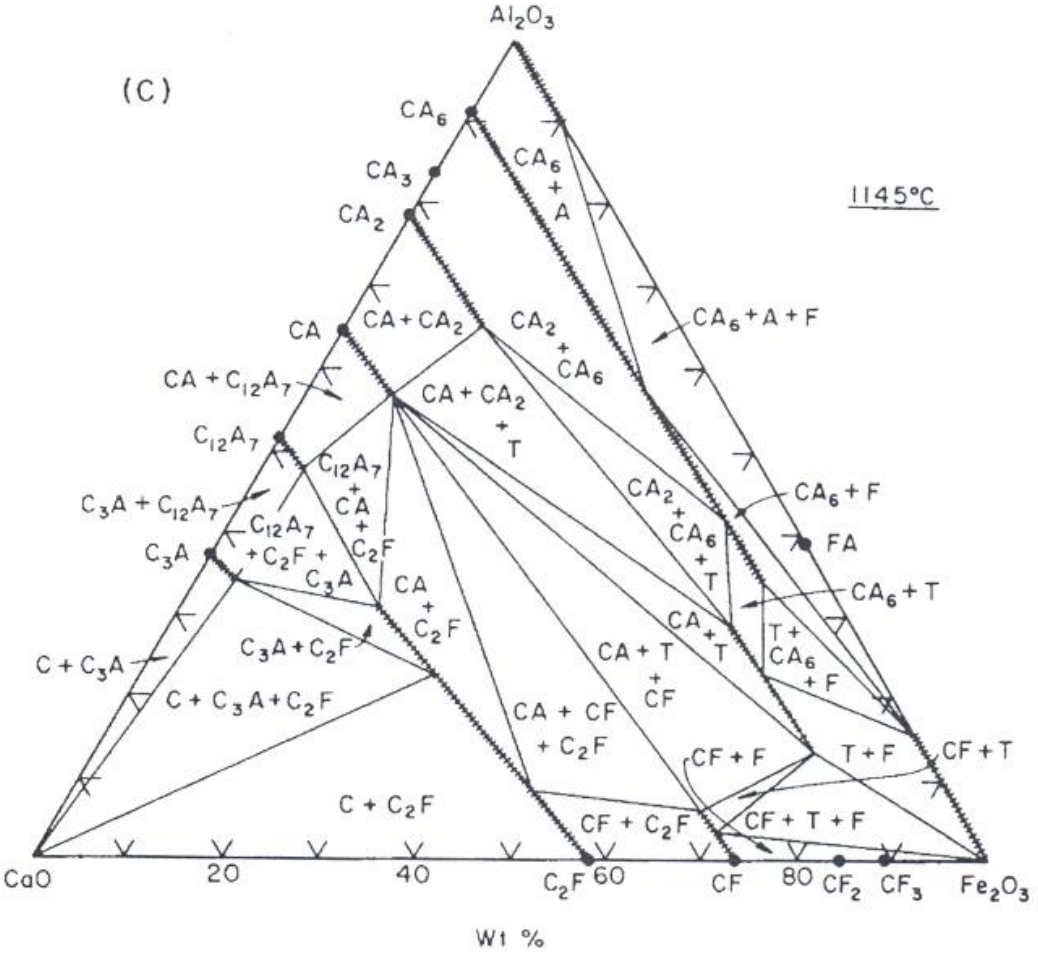

R.R. Dayal, F.P. Glasser, Sci. Ceram., Vol. 3, Edited by G.H. Stewart, Academic Press, New York, (1967), pp.191-214.

Al2O3-CaO-Fe2O3, Weight percent 1330°C

$Al_2O_3 - CaO - Fe_2O_3 - O_2$

1330°C, $p(O_2)$ = 0.21 atm

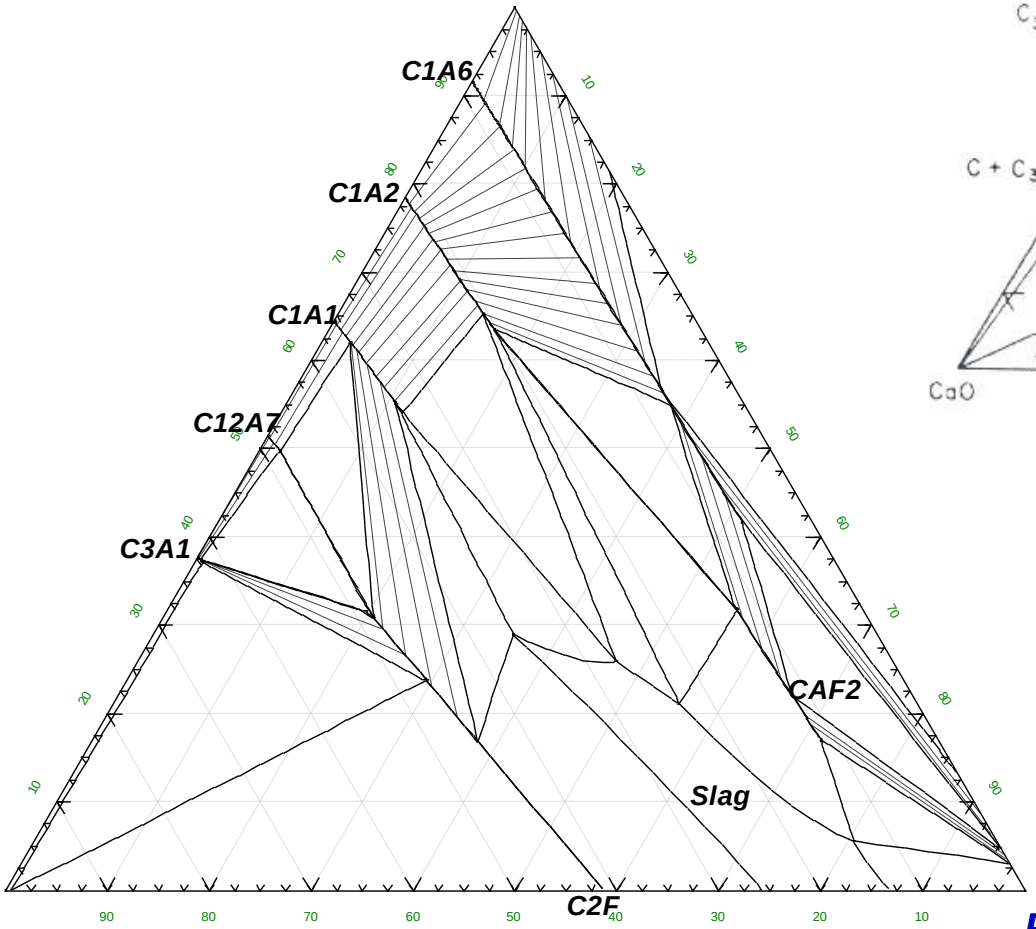

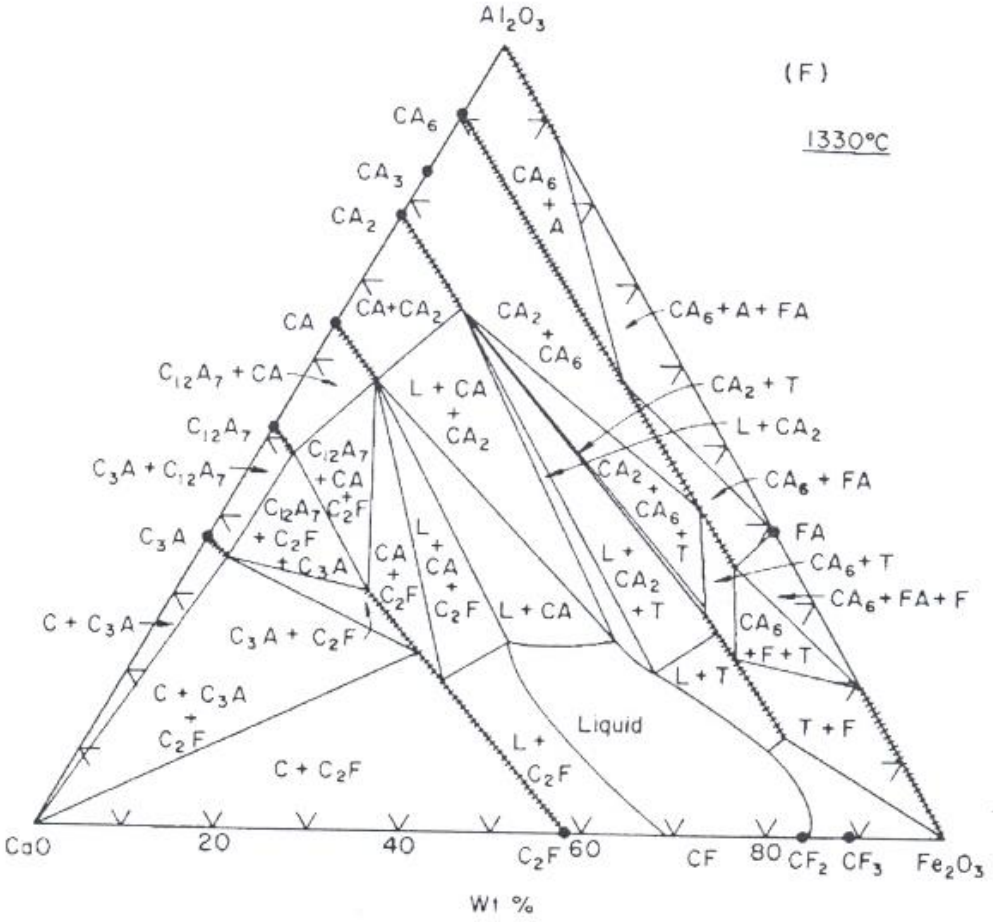

R.R. Dayal, F.P. Glasser, Sci. Ceram., Vol. 3, Edited by G.H. Stewart, Academic Press, New York, (1967), pp.191-214.

Al_2O_3 - CaO - Fe_2O_3 - O_2

Projection (Slag), $p(O_2)$ = 0.21 atm

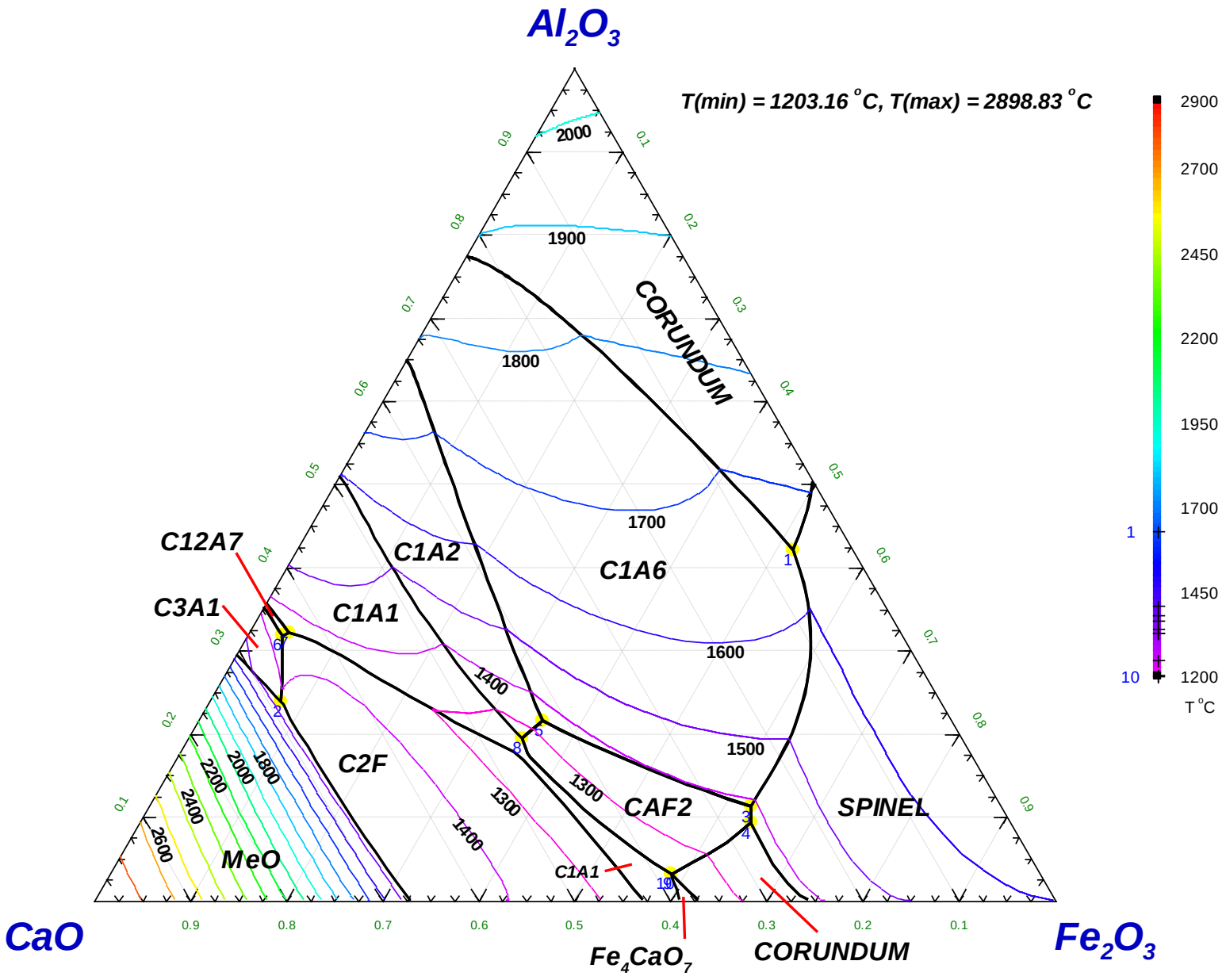

Weight percent
Liquidussurface

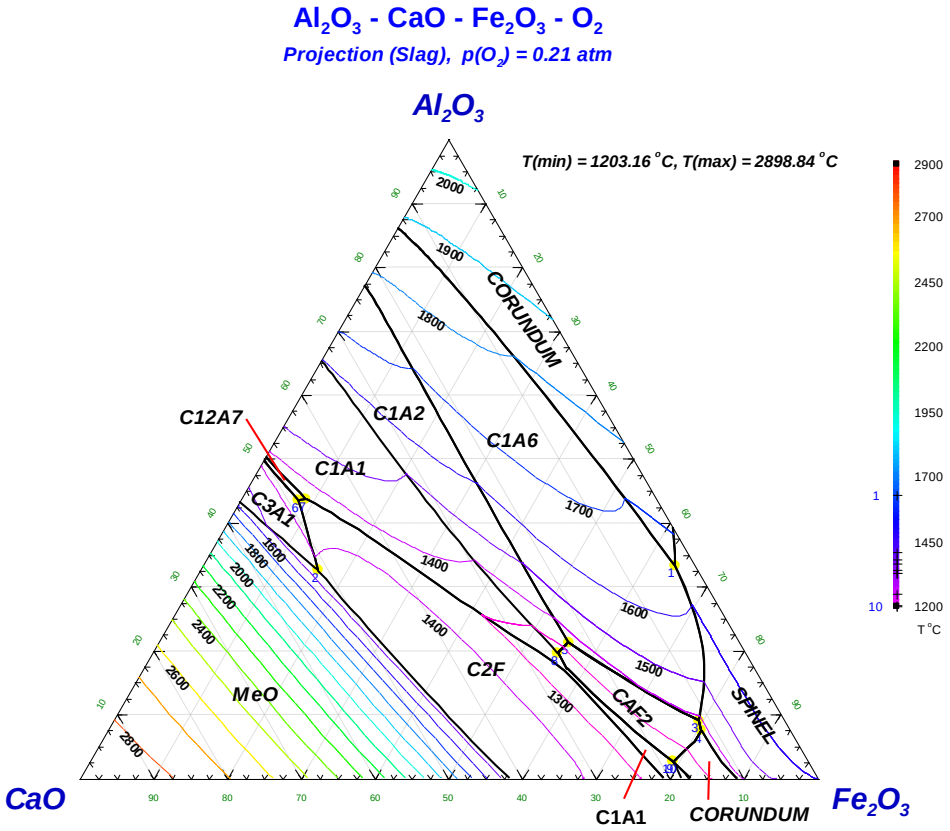

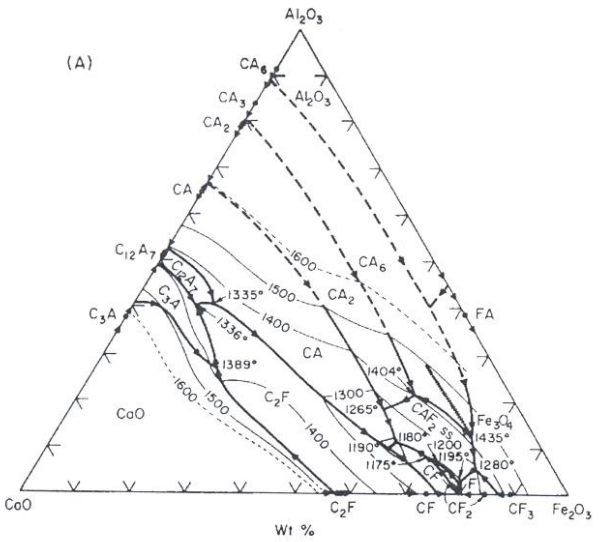

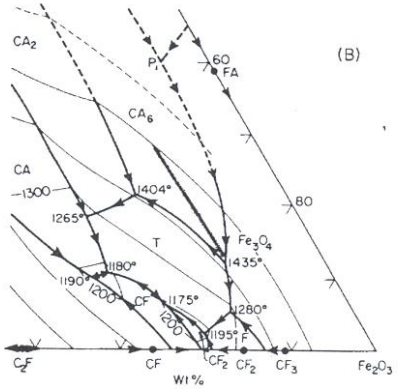

R.R. Dayal, F.P. Glasser, pp.191-214 in „Phase relations in the system CaO-Al2O3-Fe2O3“, Sci. Ceram., Vol. 3, Edited by G.H. Stewart, Academic Press, New York, 1967.

Invariant equilibria on the liquidus surface

Intersections with slag	Mole fraction A = Al2O3, B = CaO, C = Fe2O3				Weight percent A = Al2O3, B = CaO, C = Fe2O3			
	X(A)	X(B)	X(C)	T(C)	W(A)	W(B)	W(C)	T(C)
1: C1A6 / CORANDUM / SPINEL	1: 0.42158	0.06187	0.51655	1628.43	1: 33.336%	2.691%	63.973%	1628.43
2: C2F / C3A1 / MeO	2: 0.23914	0.68577	0.07509	1407.02	2: 32.584%	51.392%	16.024%	1407.01
3: C1A6 / CAF2 / SPINEL	3: 0.1125	0.25993	0.62757	1382.25	3: 9.084%	11.544%	79.372%	1382.25
4: CAF2 / CORANDUM#1 / SPINEL	4: 0.09303	0.26949	0.63749	1365.51	4: 7.504%	11.956%	80.540%	1365.52
5: C1A2 / C1A6 / CAF2	5: 0.2159	0.42508	0.35902	1339.33	5: 21.335%	23.102%	55.564%	1339.33
6: C12A7 / C2F / C3A1	6: 0.31806	0.64507	0.03687	1331.06	6: 43.535%	48.561%	7.904%	1331.06
7: C12A7 / C1A1 / C2F	7: 0.32241	0.6363	0.04129	1330.4	7: 43.744%	47.482%	8.774%	1330.4
8: C1A1 / C1A2 / CAF2	8: 0.19482	0.45724	0.34794	1247.25	8: 19.654%	25.370%	54.976%	1247.25
9: CAF2 / CORANDUM / Fe4CaO7	9: 0.03121	0.38302	0.58576	1203.54	9: 2.692%	18.171%	79.137%	1203.54
10: C1A1 / CAF2 / Fe4CaO7	10: 0.03153	0.38367	0.58481	1203.16	10: 2.721%	18.215%	79.064%	1203.16

Al2O3-CaO-K2O,
Mole fraction 1100°C

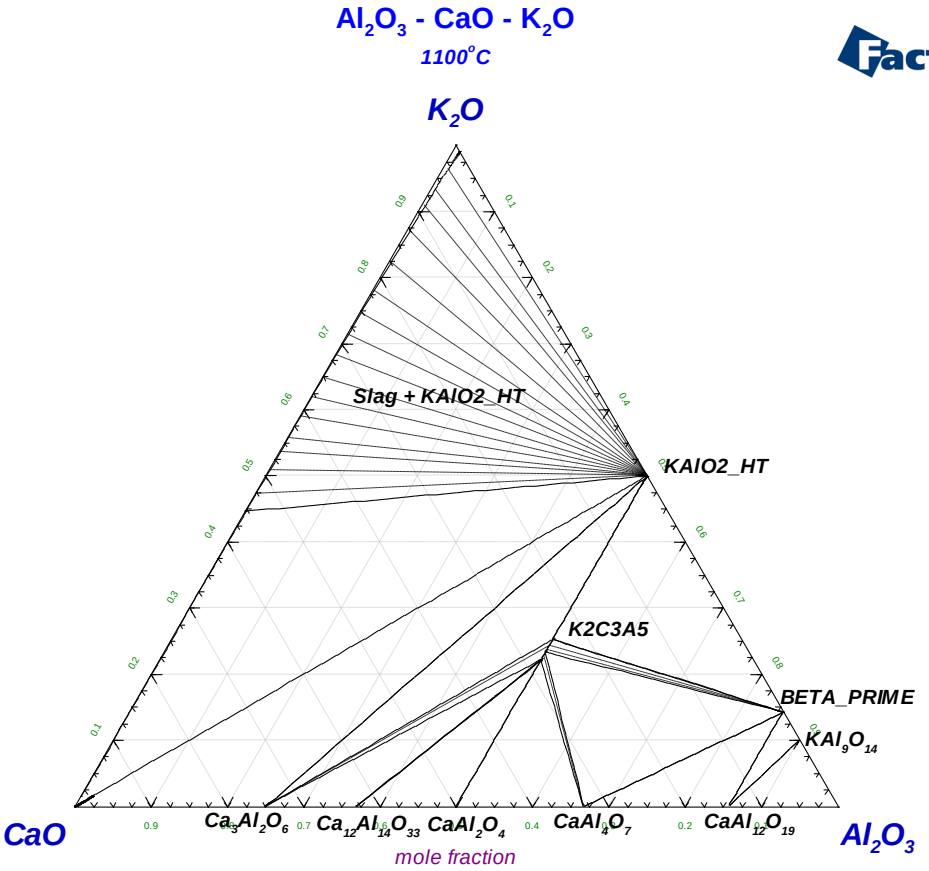

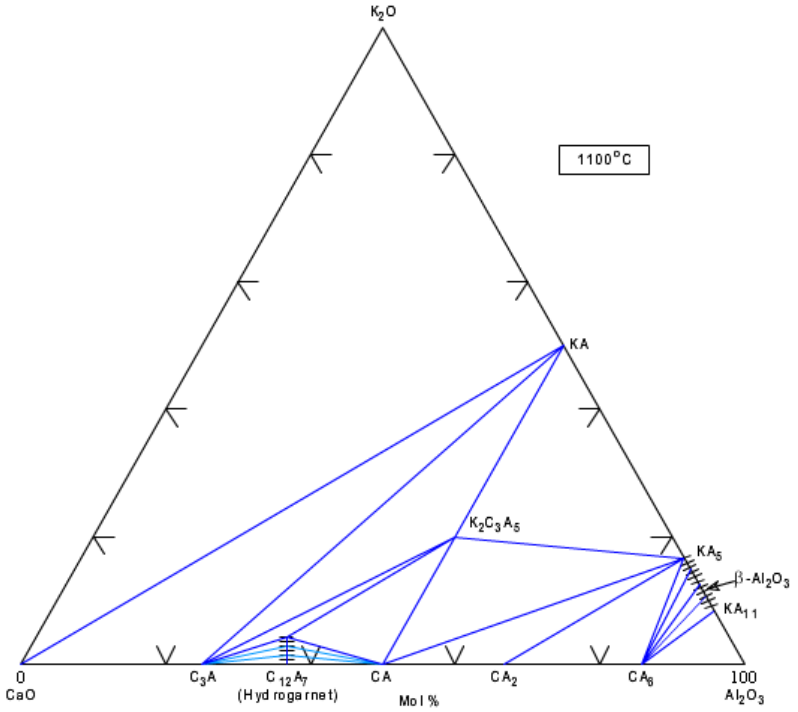

J. A. M. Van Hoek, F. J. J. Van Loo, and R. Metselaar, Mater. Sci. Monogr., 66B (1991), pp. 581-590.

Isopleth KAlO2-CaAl2O4 (proposed calculation)

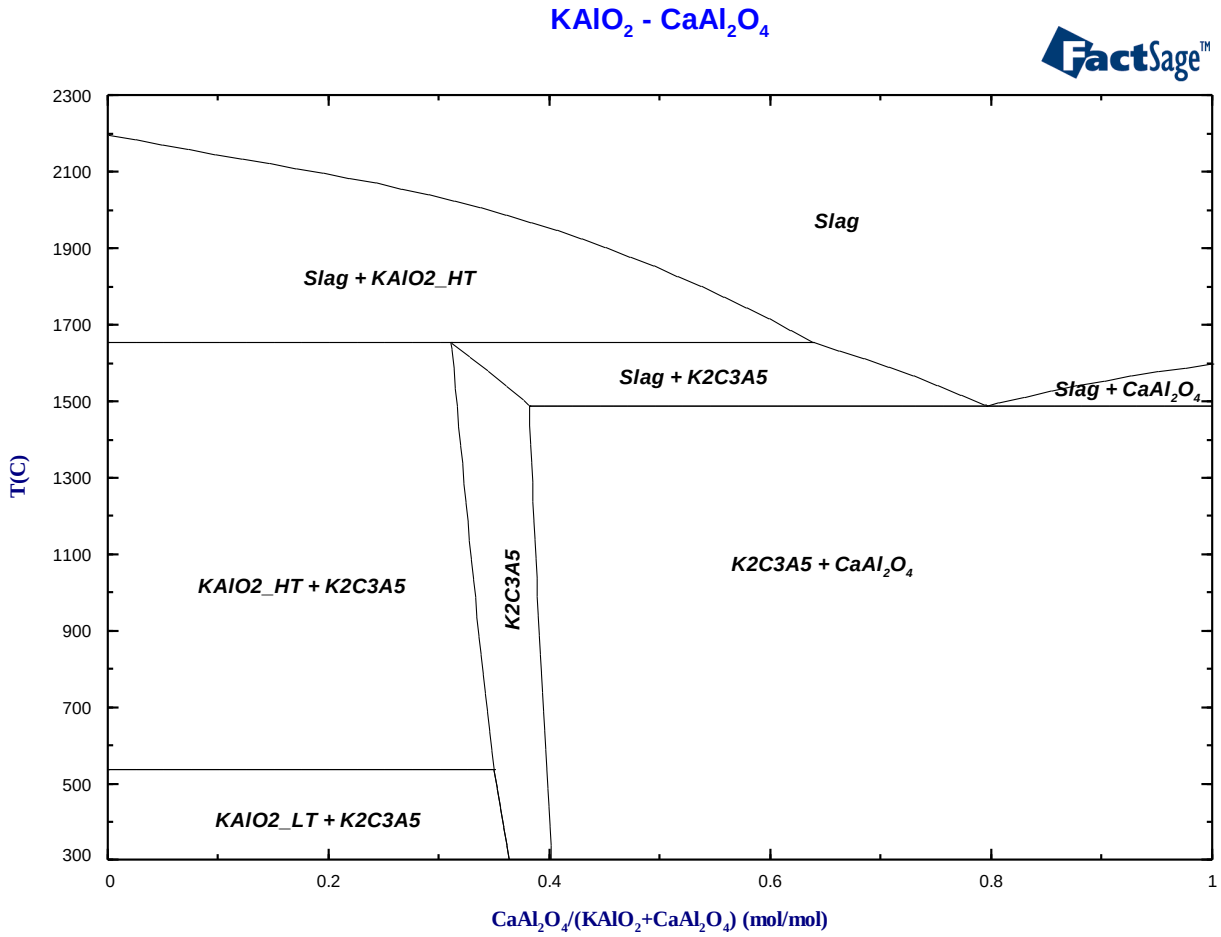

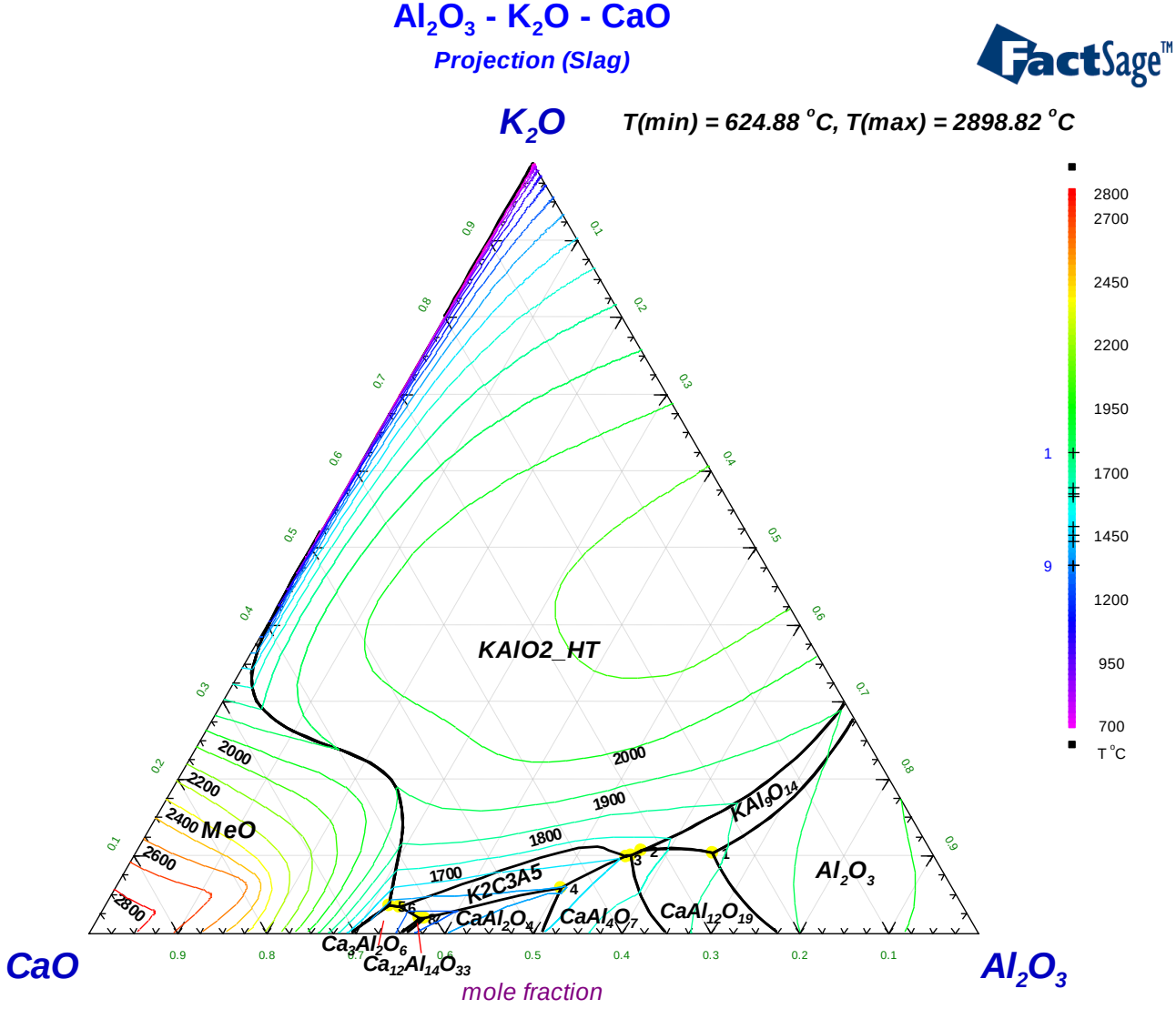
Al2O3 - K2O - CaO
Projection (Slag)
FactSage™
K2O
T(min) = 624.88 °C, T(max) = 2898.82 °C
2800
2700
2450
2200
1950
1700
1450
1200
950
700
T °C
KAlO2_HT
MeO
K2C3A5
KAl9O14
Al2O3
CaAl2O4
CaAl4O7
CaAl12O19
Ca3Al2O6
Ca12Al14O33
2000
2200
2400
2600
2800
1900
1800
1700
CaO
Al2O3
mole fraction

Weight percent
compared with experimental data
Liquidussurface

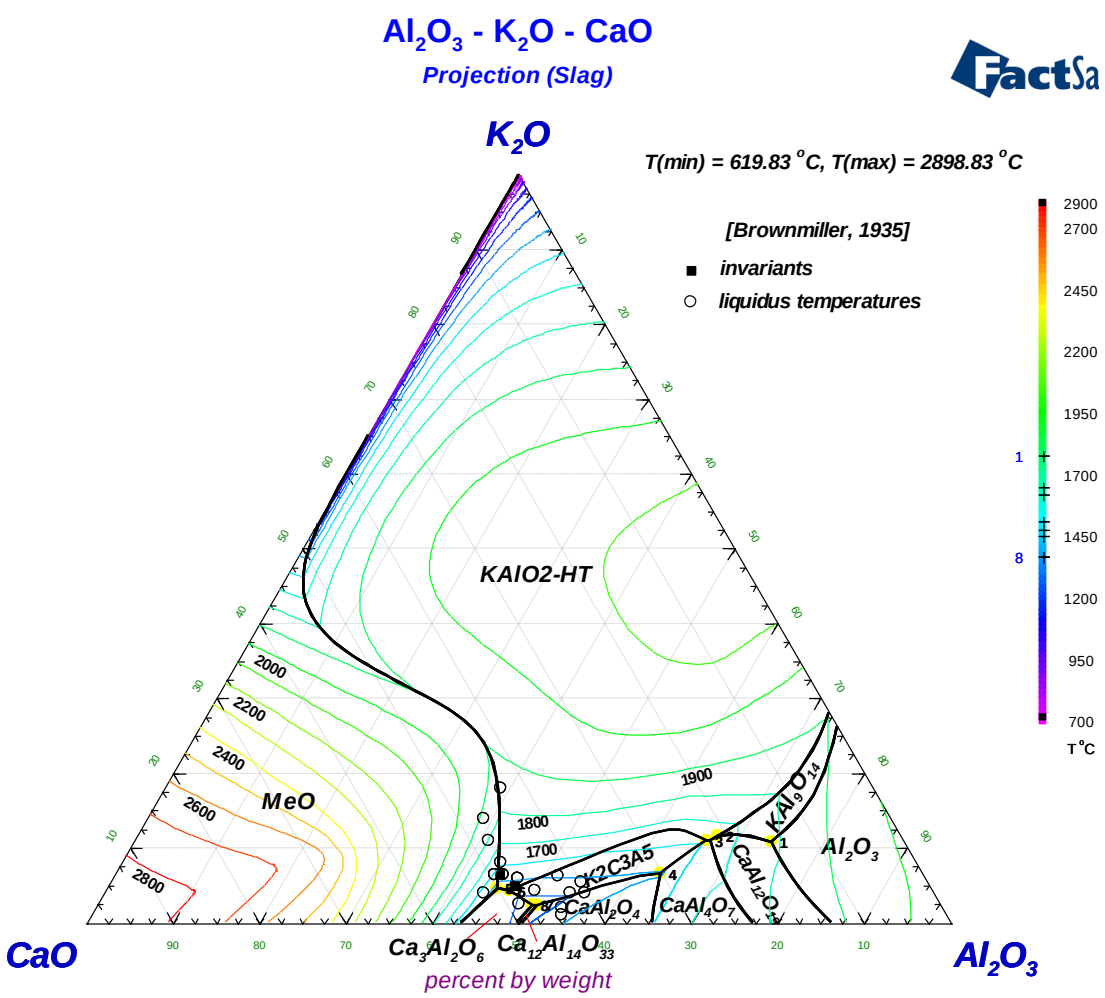

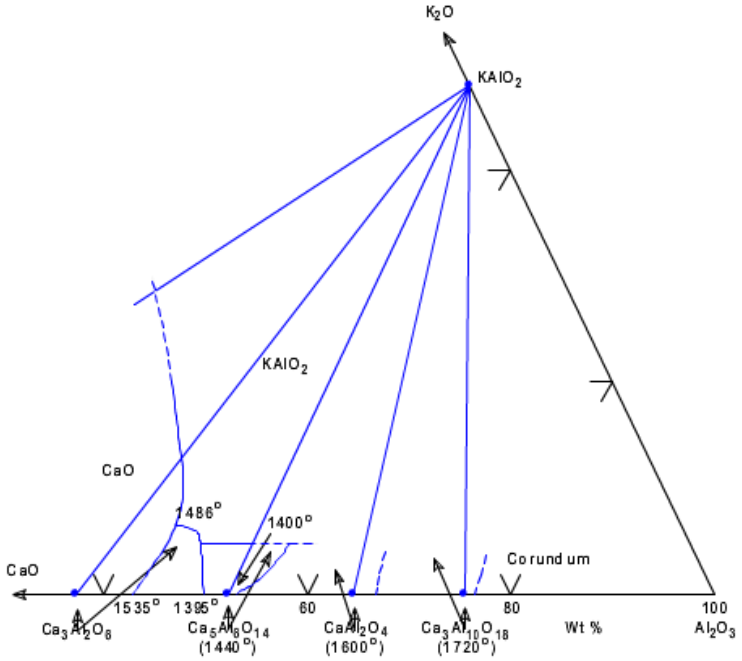

L. T. Brownmiller, Am. J. Sci., 229(29) [171] 260-277 (1935).

Invariant equilibria on the liquidus surface

Intersections with slag	Mole fraction A = K2O, B = CaO, C = Al2O3				Weight percent A = K2O, B = CaO, C = Al2O3				
		X(A)	X(B)	X(C)	T(C)		W(A)	W(B)	W(C)	T(C)
1: Al2O3 / CaAl12O19 / KAl9O14	1:	0.10355	0.24536	0.65109	1779.63	1:	10.850	15.305	73.845	1779.59
2: KAlO2_HT / CaAl12O19 / KAl9O14	2:	0.10619	0.32463	0.56919	1637.27	2:	11.598	21.108	67.294	1637.27
3: K2C3A5 / KAlO2_HT / CaAl4O7	4:	0.09934	0.34581	0.55486	1605.84	3:	10.967	22.728	66.306	1605.83
4: K2C3A5 / CaAl2O4 / CaAl4O7	5:	0.05728	0.43905	0.50367	1488.48	4:	6.631	30.257	63.112	1488.48
5: KAlO2_HT / Ca3Al2O6 / MeO	6:	0.03540	0.64447	0.32013	1450.15	5:	4.624	50.114	45.261	1450.16
6: K2C3A5 / KAlO2_HT / Ca3Al2O6	7:	0.03352	0.63357	0.33291	1424.91	6:	4.348	48.917	46.735	1424.93
7: K2C3A5 / Ca12Al14O33 / CaAl2O4	8:	0.01875	0.61255	0.36870	1334.03	7:	2.396	46.602	51.002	1334.03
8: K2C3A5 / Ca12Al14O33 / Ca3Al2O6	9:	0.01849	0.61799	0.36351	1332.16	8:	2.371	47.175	50.454	1332.16

Al_2O_3 - CaO - MgO

500°C

Al2O3-CaO-MgO,
Mole fraction

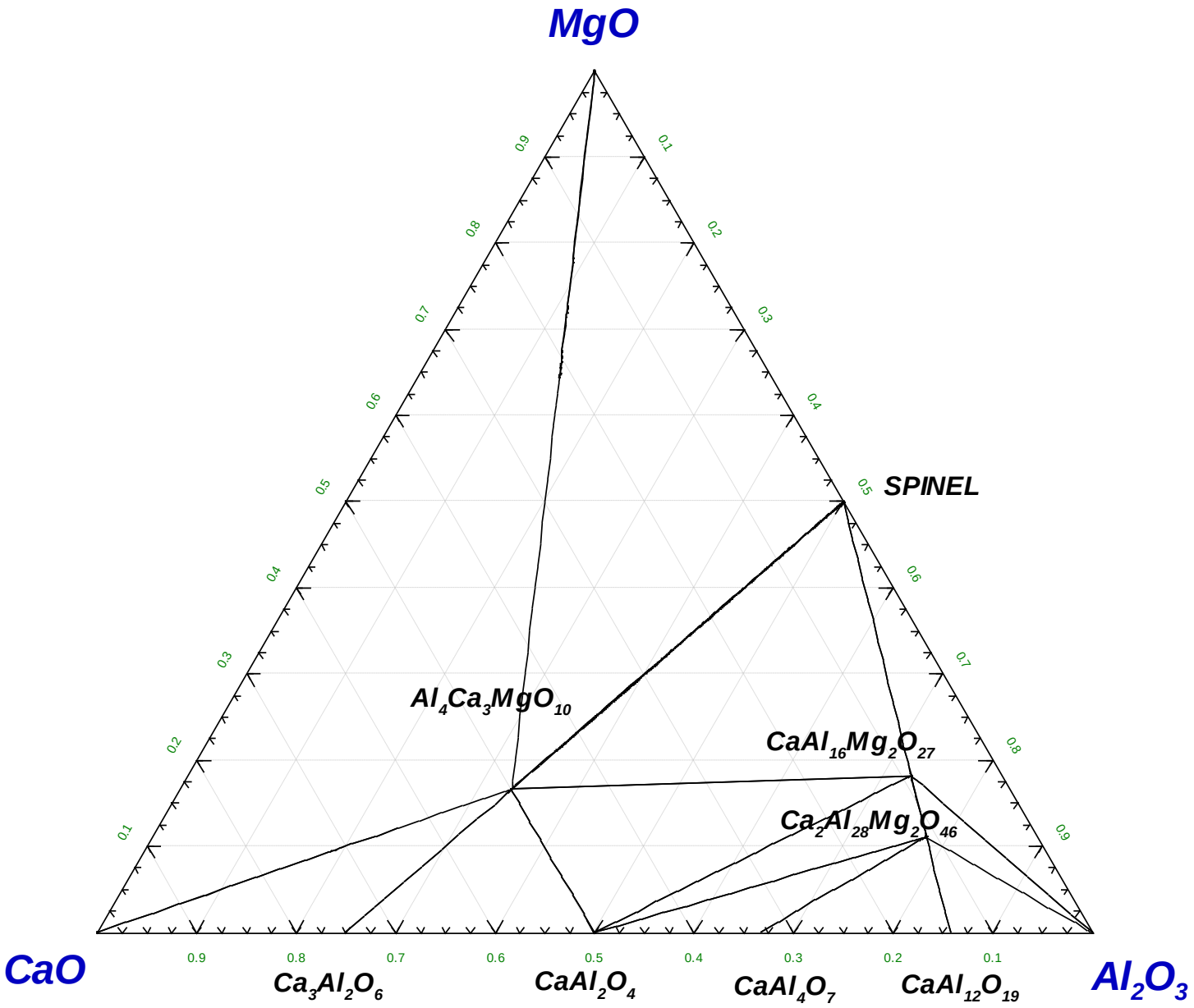

Al_2O_3 - CaO - MgO

1000°C

FactSage™

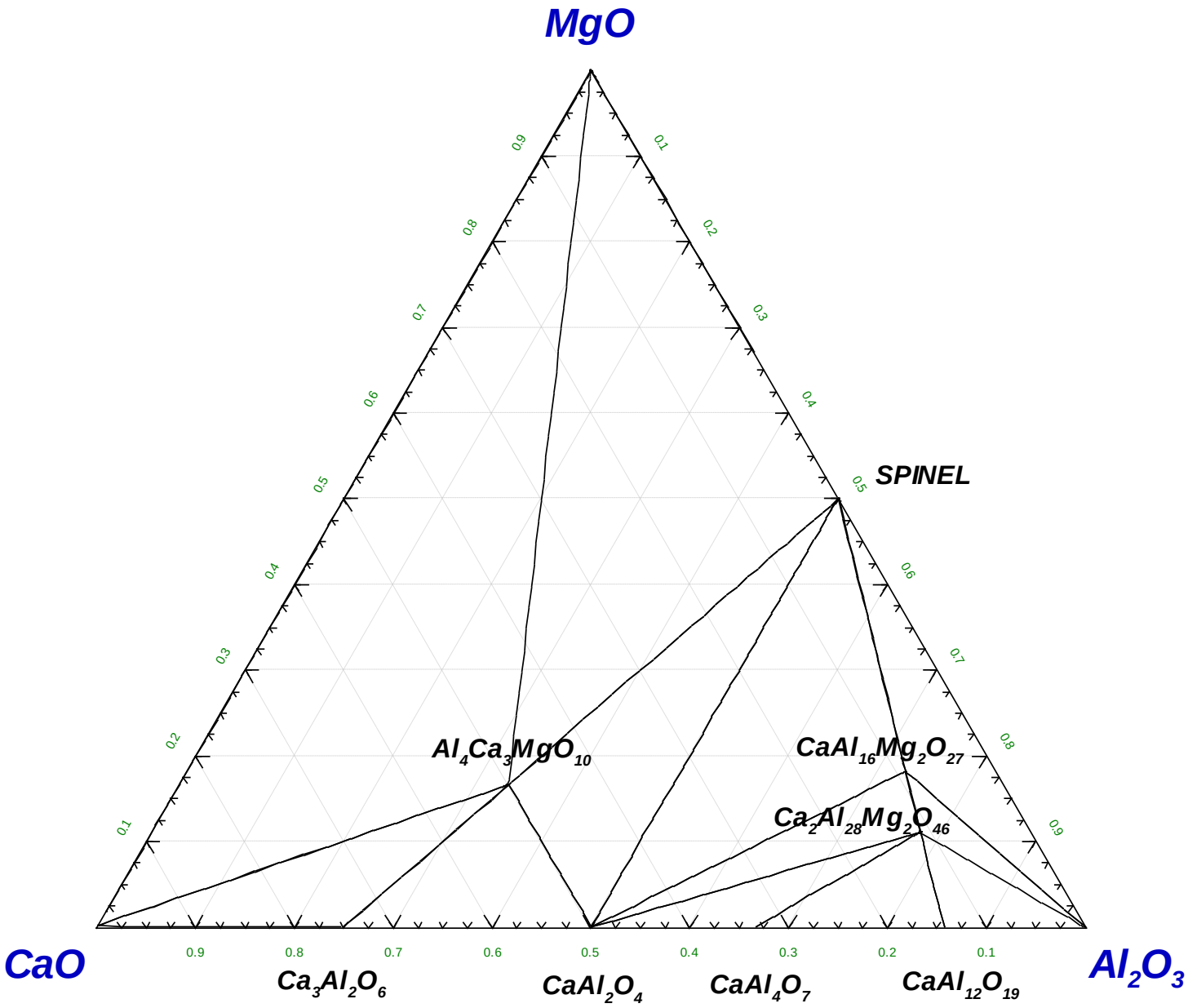

Mole fraction
kurz unterhalb Liquidussurface

Al_2O_3 - CaO - MgO

1320°C

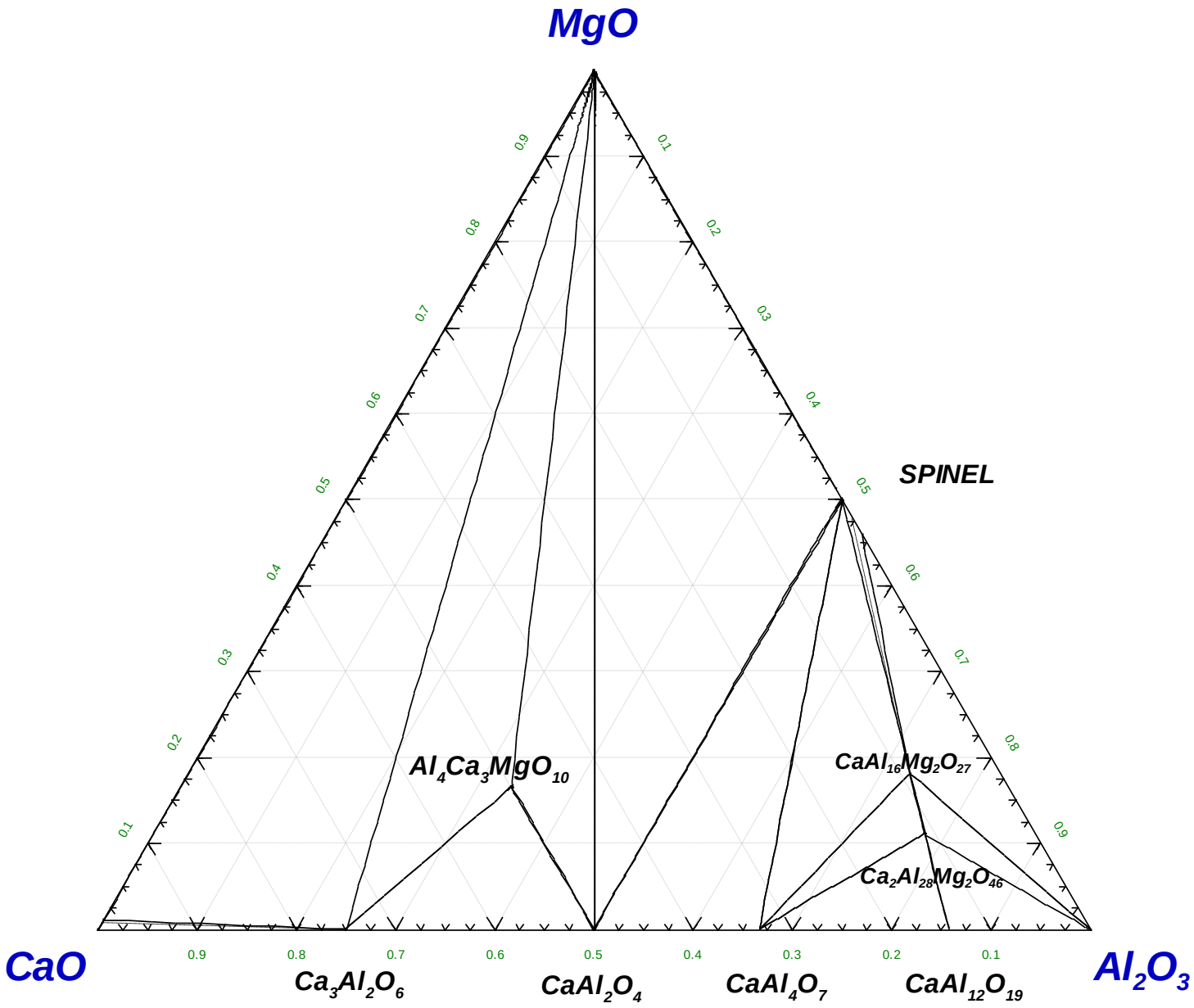

Mole fraction
compared with experimental data

Al_2O_3 - CaO - MgO

1600°C

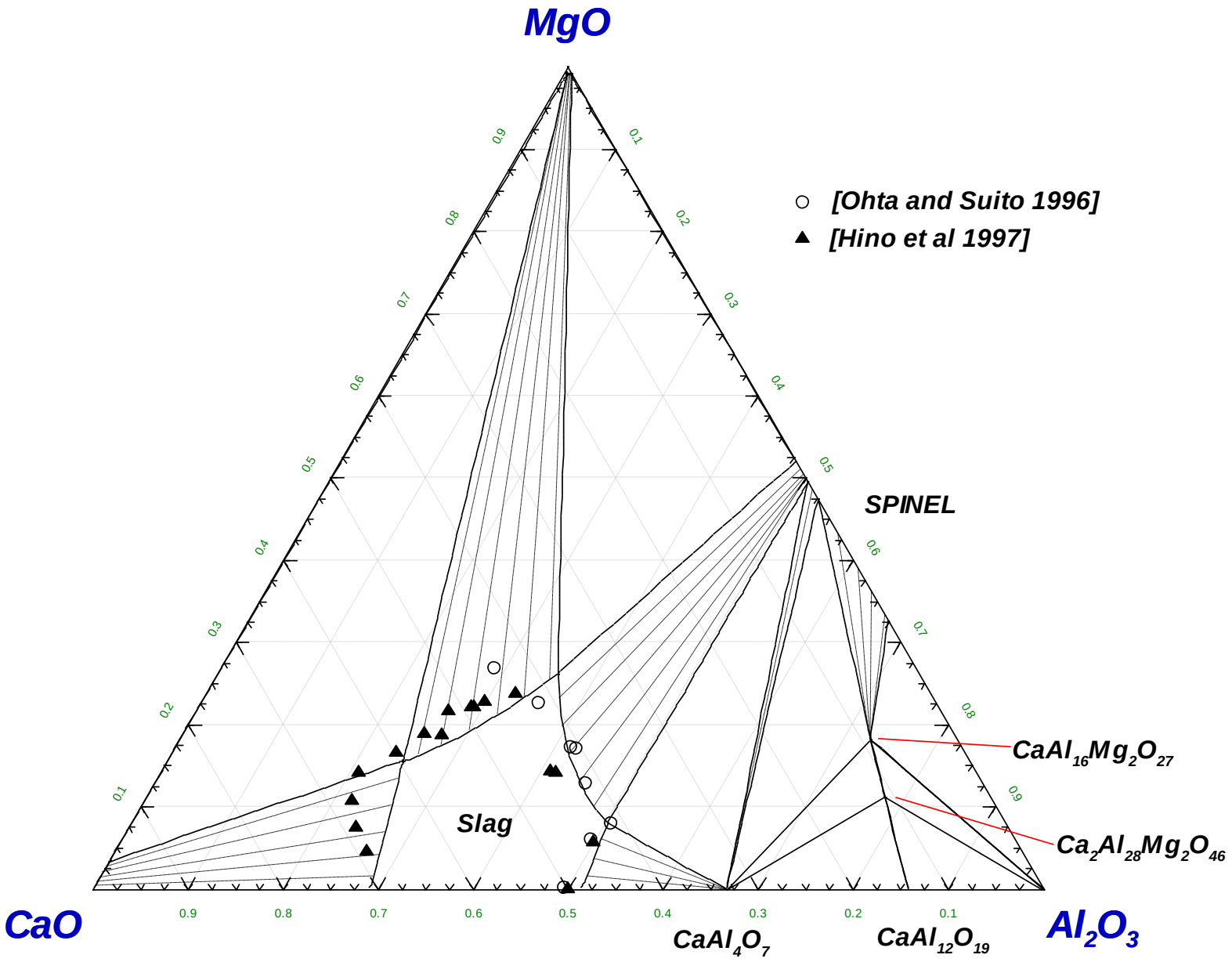

Mole fraction in Kelvin x(Al2O3)=0.5 compared with experimental data

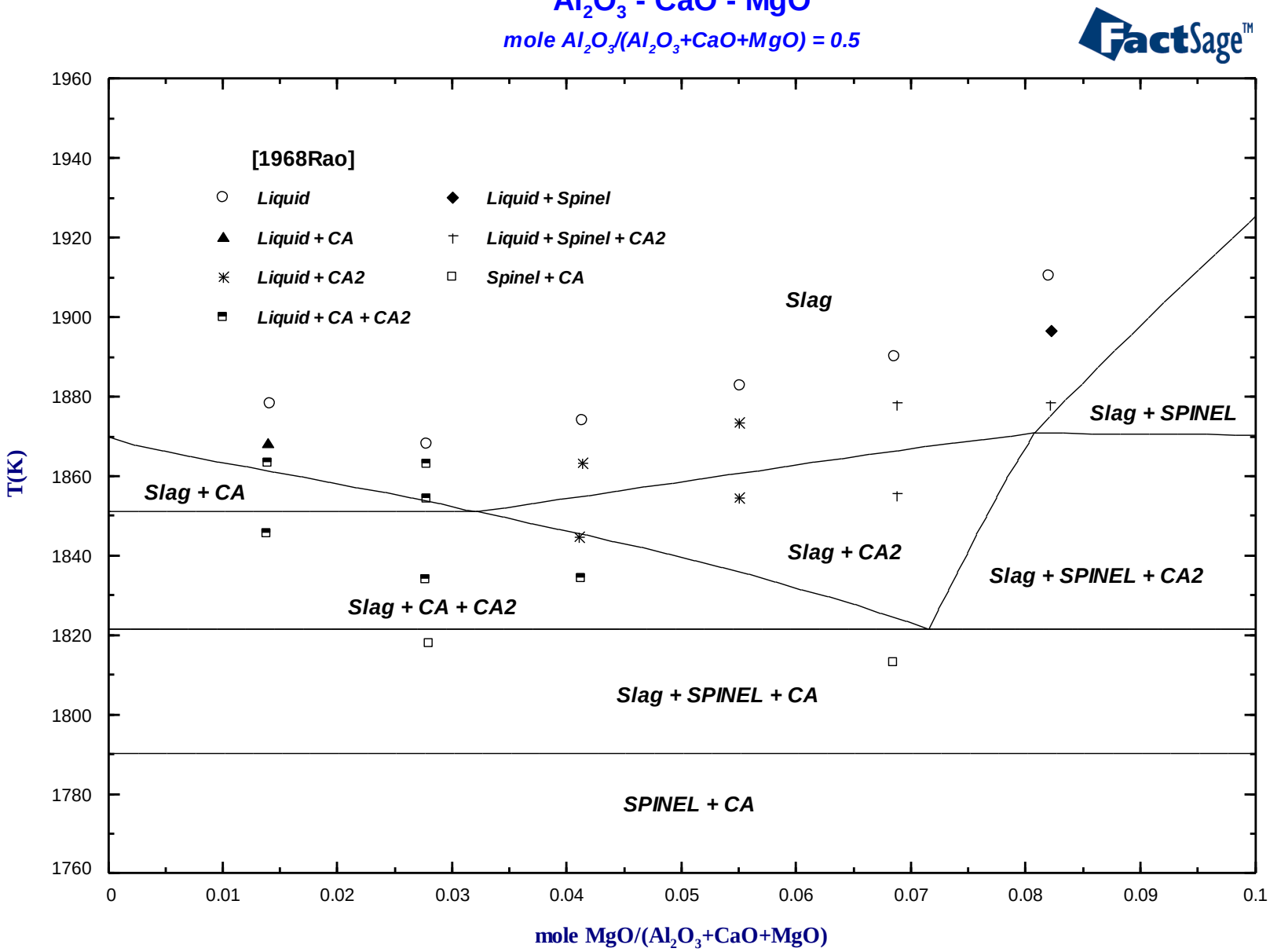

Al_2O_3 - CaO - MgO

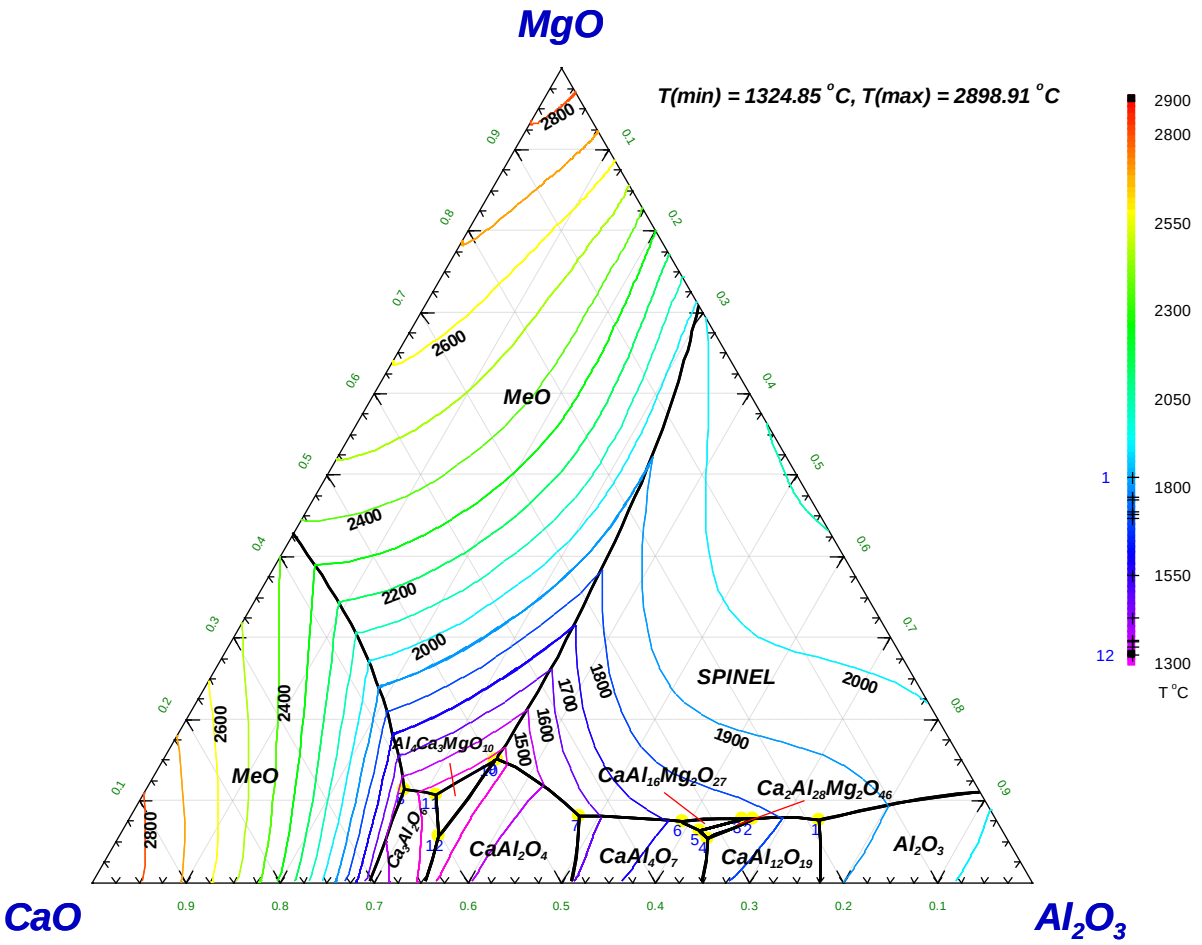

Weight percent
Liquidussurface

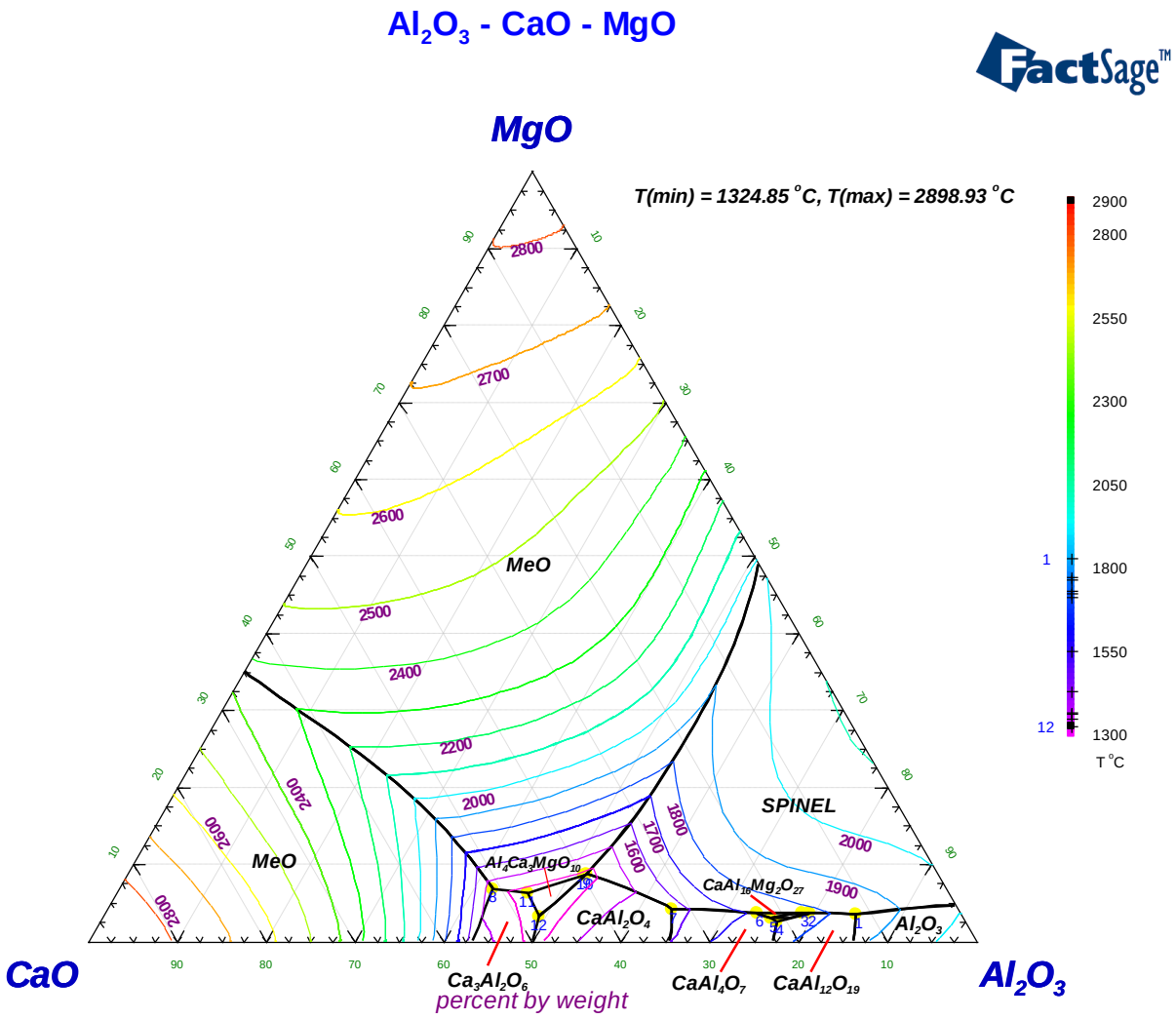

Invariant equilibria on the liquidus surface

Intersections with slag	Mole fraction A = MgO, B = CaO, C = Al2O3				Weight percent A = MgO, B = CaO, C = Al2O3				
		X(A)	X(B)	X(C)	T(C)		W(A)	W(B)	W(C)	T(C)
1: Al2O3 / CaAl12O19 / SPINEL	1:	0.07555	0.18763	0.73682	1827.87	1:	3.433%	11.863%	84.704%	1827.87
2: Ca2Al28Mg2O46 / CaAl12O19 / SPINEL	2:	0.07657	0.25793	0.6655	1772.88	2:	3.613%	16.936%	79.451%	1772.88
3: Ca2Al28Mg2O46 / CaAl16Mg2O27 / SPINEL	3:	0.07694	0.26956	0.65349	1764.58	3:	3.655%	17.816%	78.529%	1764.58
4: Ca2Al28Mg2O46 / CaAl12O19 / CaAl4O7	4:	0.05328	0.31763	0.62909	1731.22	4:	2.553%	21.179%	76.267%	1731.22
5: Ca2Al28Mg2O46 / CaAl16Mg2O27 / CaAl4O7	5:	0.06226	0.32169	0.61605	1723.93	5:	3.010%	21.640%	75.350%	1723.93
6: CaAl16Mg2O27 / CaAl4O7 / SPINEL	6:	0.07375	0.33466	0.59159	1709.75	6:	3.622%	22.870%	73.507%	1709.75
7: CaAl2O4 / CaAl4O7 / SPINEL	7:	0.08027	0.44014	0.47958	1548.46	7:	4.212%	32.131%	63.657%	1548.46
8: Ca3Al2O6 / MEO#1 / MEO#2	8:	0.11323	0.60997	0.2768	1429.61	8:	6.812%	51.059%	42.129%	1429.62
9: CaAl2O4 / MEO#1 / SPINEL	9:	0.15073	0.49357	0.35569	1364.86	9:	8.676%	39.529%	51.795%	1364.86
10: Al4Ca3MgO10 / CaAl2O4 / MEO#1	10:	0.14828	0.49727	0.35445	1362.05	10:	8.537%	39.835%	51.628%	1362.05
11: Al4Ca3MgO10 / Ca3Al2O6 / MEO#1	11:	0.10668	0.58044	0.31288	1345.09	11:	6.254%	47.344%	46.402%	1345.09
12: Al4Ca3MgO10 / Ca3Al2O6 / CaAl2O4	12:	0.05684	0.60158	0.34158	1324.85	12:	3.233%	47.612%	49.155%	1324.85

Mole fraction 1200°C

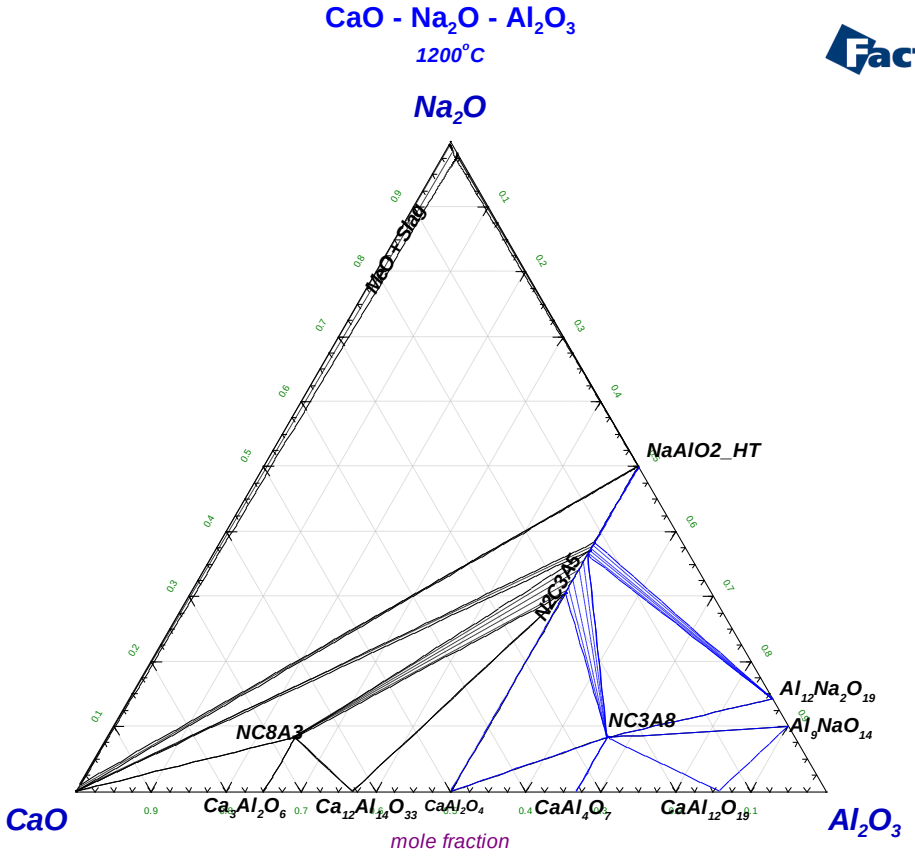

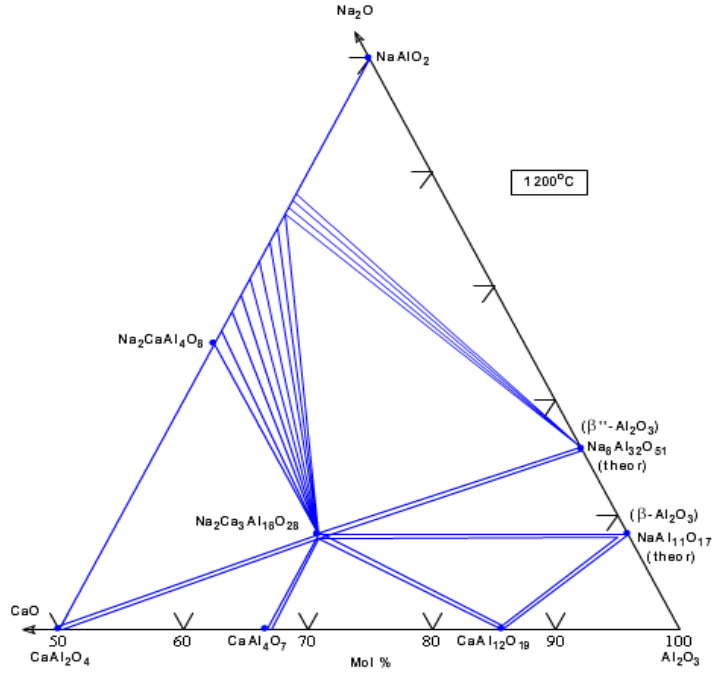

H. Verweij and C. M. P. M. Saris, J. Am. Ceram. Soc., 69 [2] 94-98 (1986).

Al2O3-CaO-Na2O, Mole fraction 1400°C

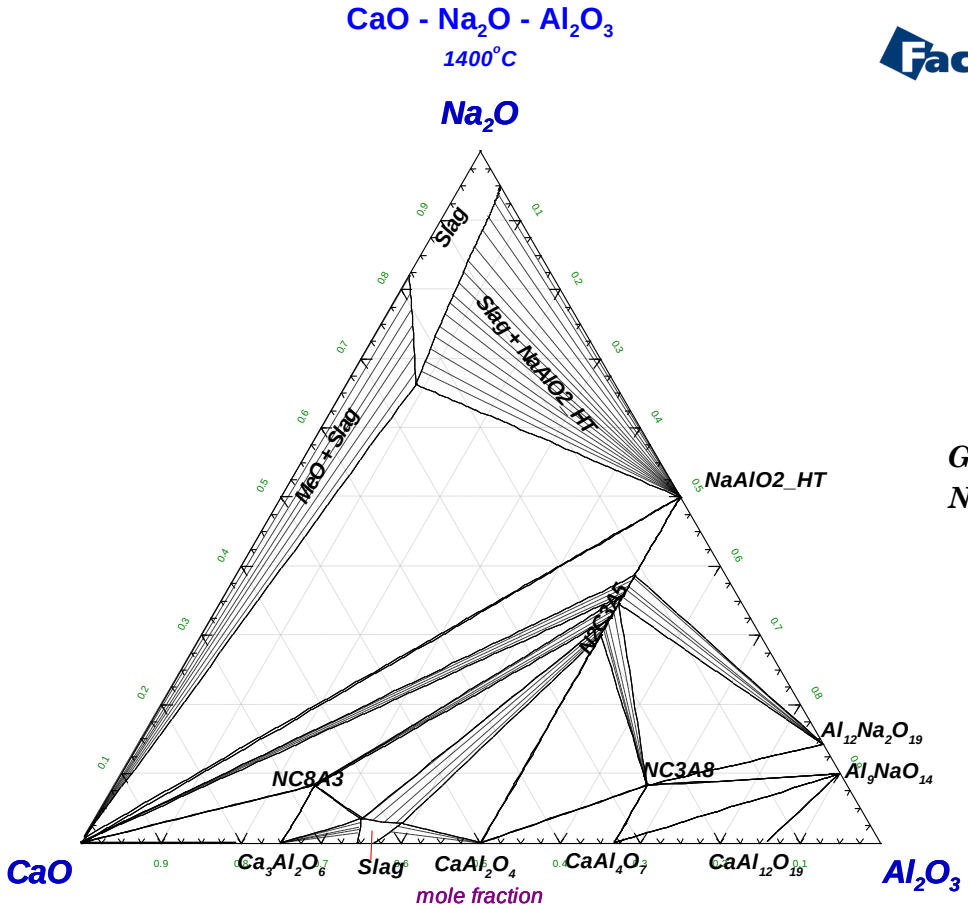

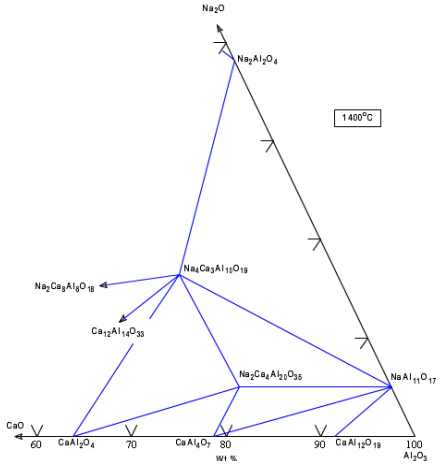

G. I. Zaldat, M. S. Kupriyanova, and A. L. Tubolev, Izv. Akad. Nauk SSSR, Neorg. Mater., 21 [1] 51-53 (1985).

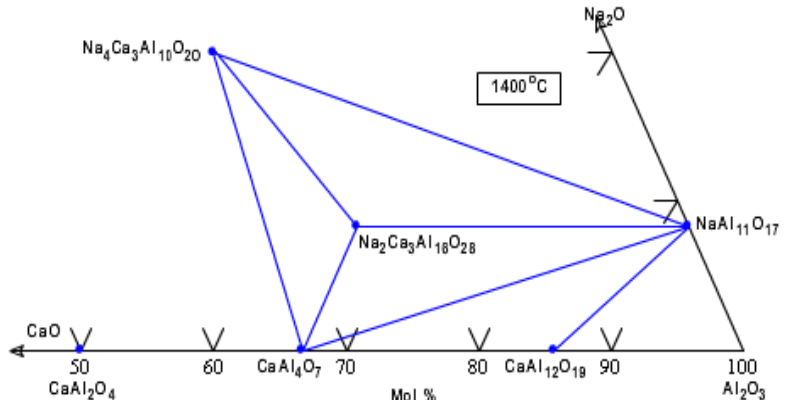

J. D. Hodge, in Proc. - Electrochem. Soc., High Temperature Lamp Chemistry, 1985, Vol. 85-2, pp. 261-270, Edited by E. G. Zubler, The Electrochemical Society, Inc., Pennington, New Jersey, 1985.

Mole fraction
compared with experimental data

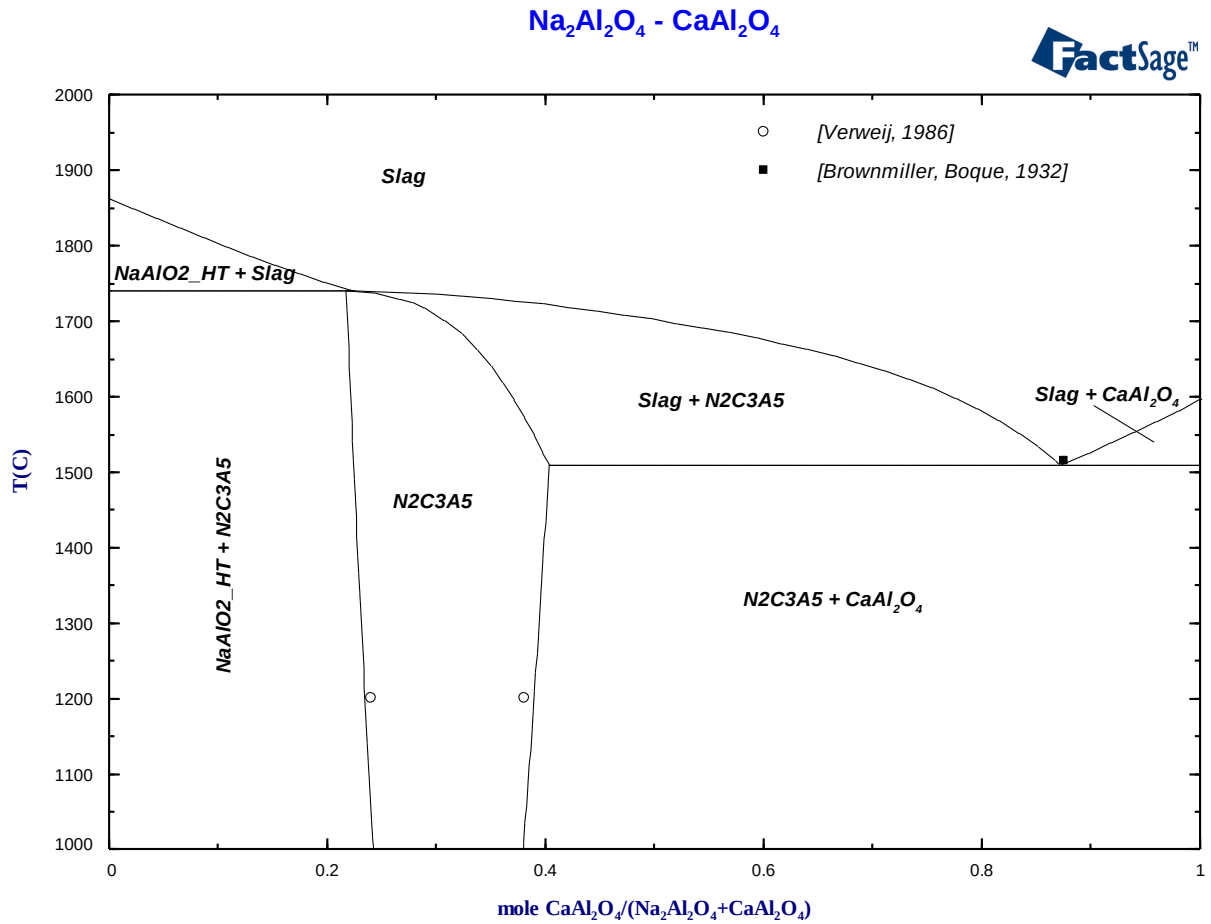

Weight percent
kurz unterhalb Liquidussurface

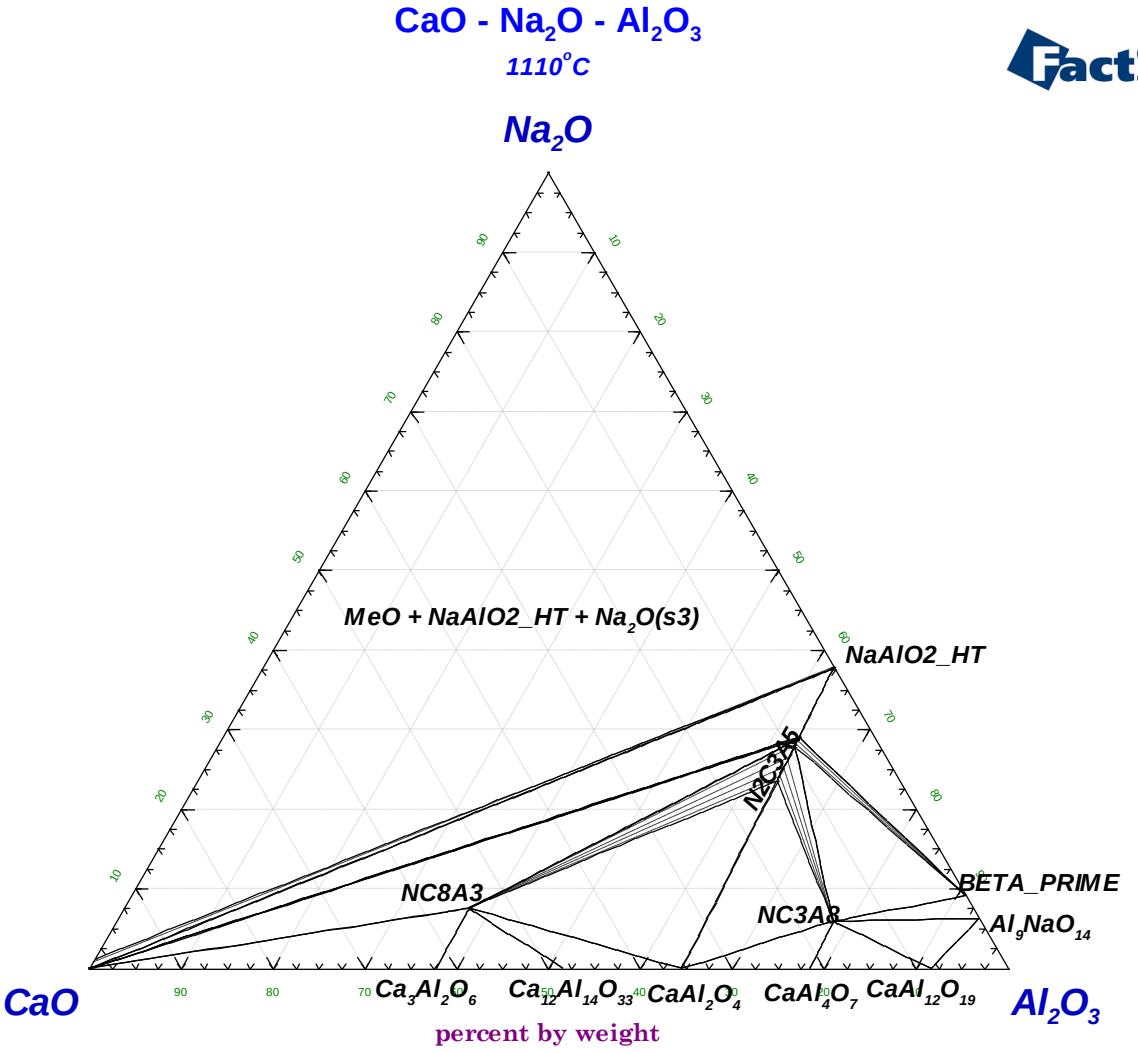

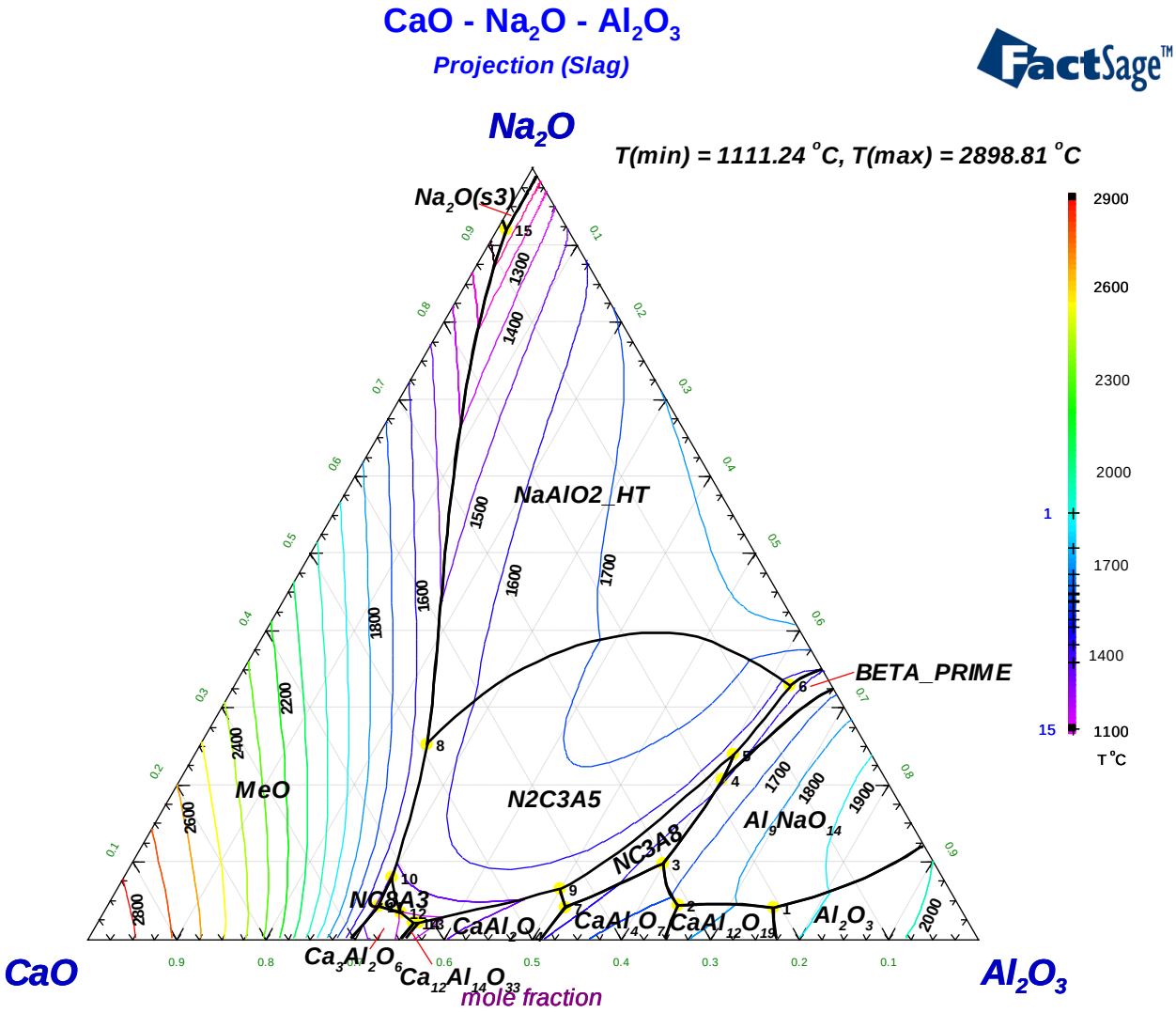
CaO - Na2O - Al2O3
Projection (Slag)
FactSage™
Na2O
T(min) = 1111.24 °C, T(max) = 2898.81 °C
Na2O(s3)
NaAlO2_HT
BETA_PRIME
MeO
N2C3A5
NC3A8
Al9NaO14
NC8A3
CaAl2O4
CaAl4O7
CaAl12O19
Al2O3
Ca3Al2O6
Ca12Al14O33
CaO
Al2O3
mole fraction
T °C
2900
2600
2300
2000
1700
1400
1100

Weight percent
Liquidussurface

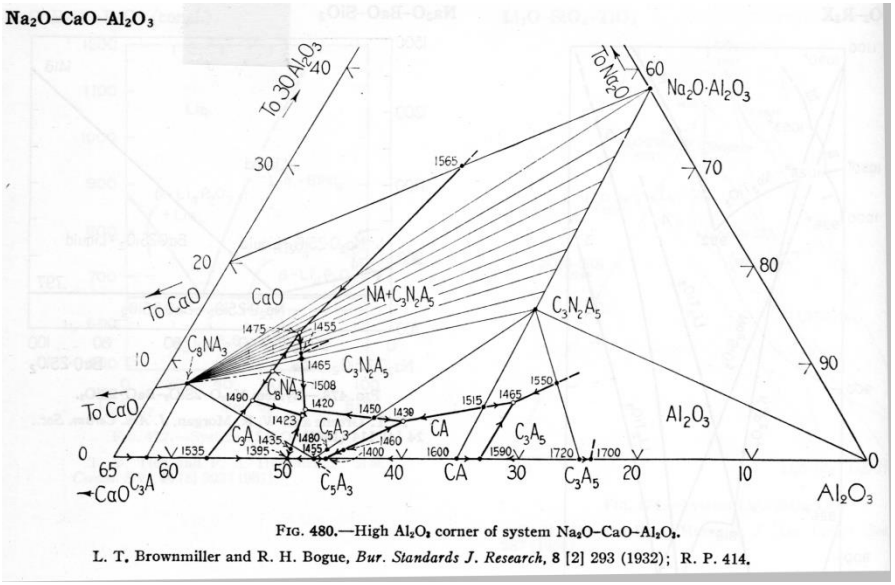

FIG. 480.—High Al_2O_3 corner of system Na_2O–CaO–Al_2O_3.

L. T. Brownmiller and R. H. Bogue, *Bur. Standards J. Research*, 8 [2] 293 (1932); R. P. 414.

$CaO - Na_2O - Al_2O_3$

Projection (Slag)

FactSage™

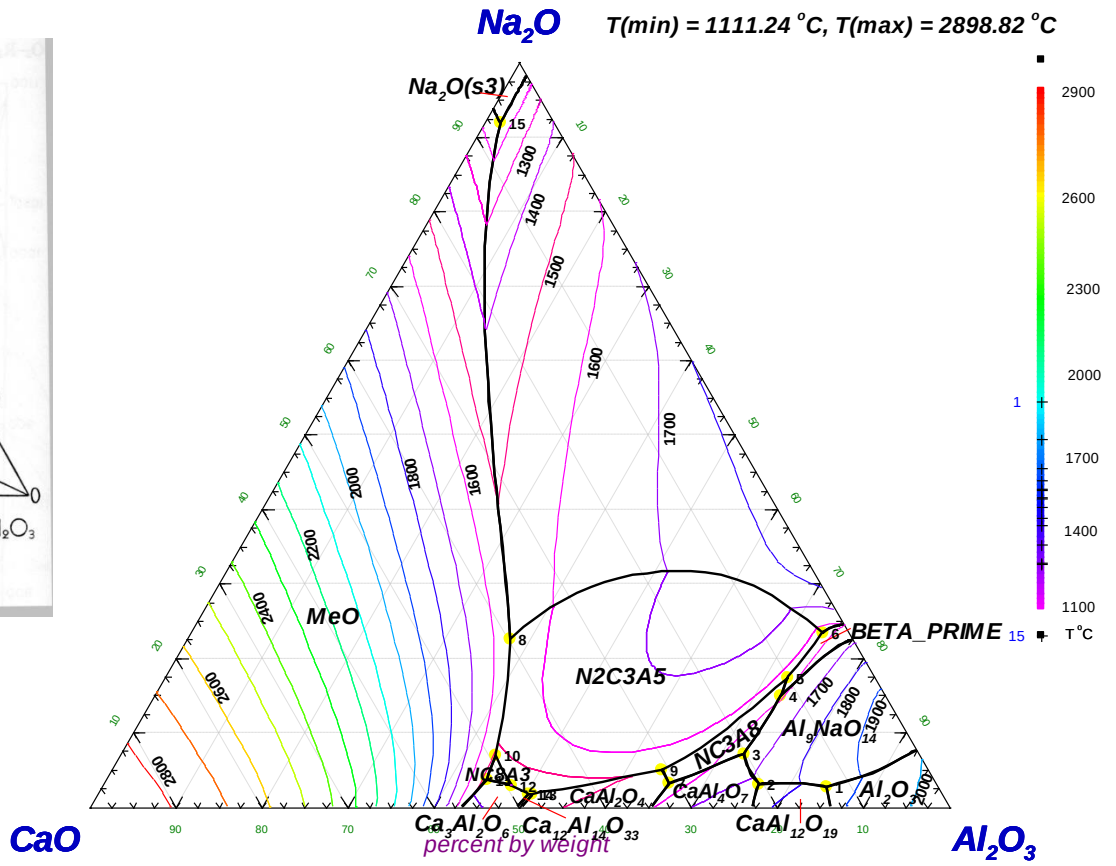

Invariant equilibria on the liquidus surface

Intersections with slag	Mole fraction A = Na2O, B = CaO, C = Al2O3				Weight percent A = Na2O, B = CaO, C = Al2O3			
	X(A)	X(B)	X(C)	T(C)	W(A)	W(B)	W(C)	T(C)
1: Al2O3 / Al9NaO14 / CaAl12O19	1: 0.04008	0.20896	0.75095	1838.57	1: 2.737	12.910	84.353	1838.57
2: Al9NaO14 / CaAl12O19 / CaAl4O7	2: 0.04273	0.31481	0.64247	1718.43	2: 3.086	20.573	76.341	1718.43
3: Al9NaO14 / Ca3Al16Na2O28 / CaAl4O7	3: 0.09709	0.30394	0.59897	1629.53	3: 7.153	20.259	72.589	1629.53
4: Al9NaO14/BETA_PRIME / Ca3Al16Na2O28	4: 0.20582	0.18337	0.61081	1591.94	4: 14.952	12.052	72.996	1591.94
5: N2C3A5 / BETA_PRIME / Ca3Al16Na2O28	5: 0.23811	0.15464	0.60725	1566.19	5: 17.292	10.161	72.547	1566.19
6: N2C3A5 / NaAlO2_HT / BETA_PRIME	6: 0.32787	0.04627	0.62586	1562.66	6: 23.431	2.992	73.578	1562.66
7: Ca3Al16Na2O28 / CaAl2O4 / CaAl4O7	7: 0.04072	0.44244	0.51684	1541.33	7: 3.154	31.001	65.846	1541.32
8: N2C3A5 / NaAlO2_HT / MeO	8: 0.25182	0.49223	0.25595	1535.19	8: 22.519	39.827	37.654	1535.19
9: N2C3A5 / Ca3Al16Na2O28 / CaAl2O4	9: 0.06411	0.43676	0.49913	1509.59	9: 5.007	30.863	64.129	1509.59
10: N2C3A5 / Ca8Al6Na2O18 / MeO	10: 0.07879	0.61861	0.30259	1477.32	10: 6.934	49.257	43.808	1477.32
11: Ca3Al2O6 / Ca8Al6Na2O18 / MeO	11: 0.04173	0.65207	0.30620	1451.31	11: 3.675	51.961	44.364	1451.45
12: N2C3A5 / Ca3Al2O6 / Ca8Al6Na2O18	12: 0.03382	0.63117	0.33501	1393.63	12: 2.925	49.400	47.674	1393.63
13: N2C3A5 / Ca12Al14O33 / CaAl2O4	13: 0.02041	0.61787	0.36171	1334.80	13: 1.738	47.598	50.664	1334.79
14: N2C3A5 / Ca12Al14O33 / Ca3Al2O6	14: 0.02054	0.62282	0.35664	1332.17	14: 1.755	48.132	50.113	1332.16
15: NaAlO2_HT / MeO / Na2O(s3)	15: 0.91919	0.06967	0.01115	1111.24	15: 91.868	6.300	1.833	1111.24

Al2O3-CaO-P2O5,
Weight percent 475°C

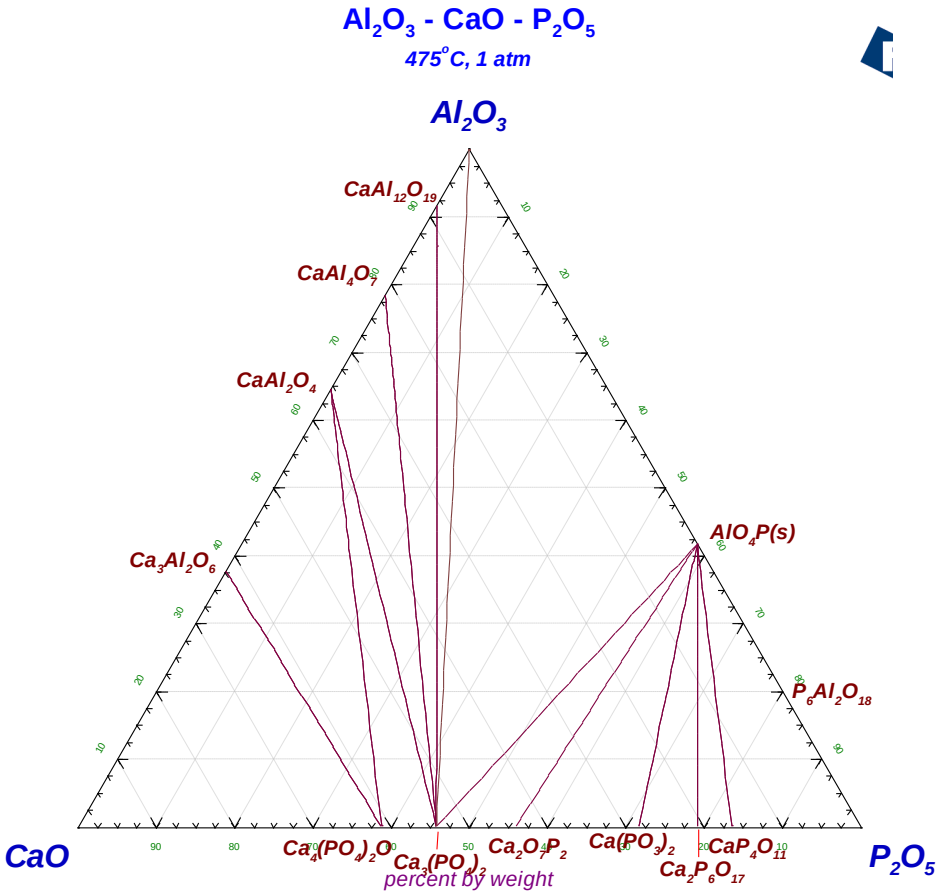

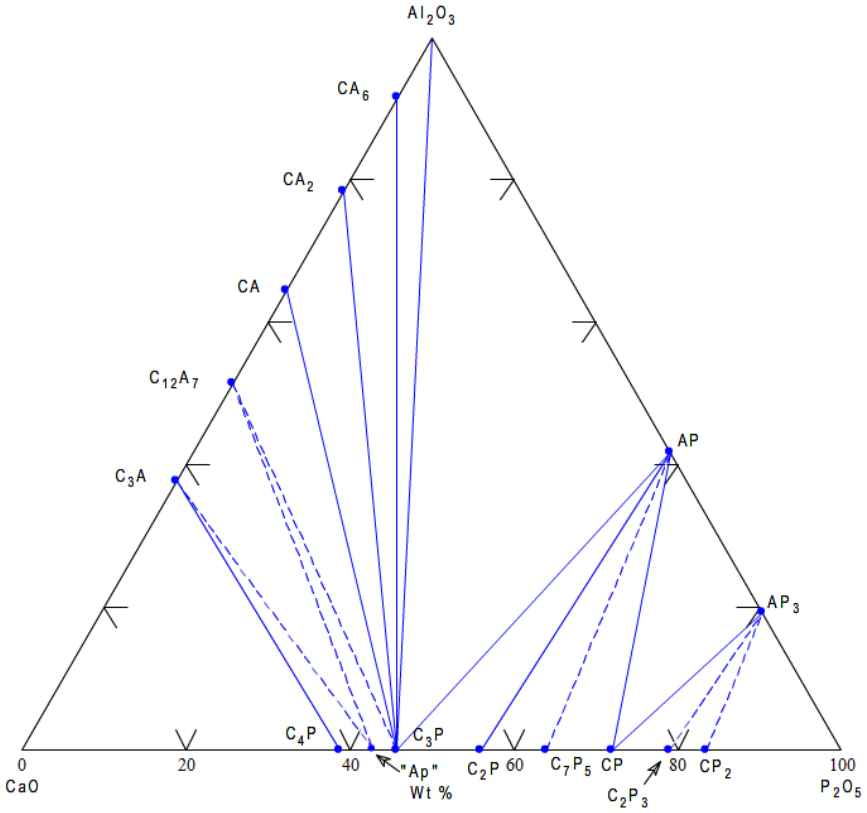

G. R. Boell, A. J. Majumdar, and J. A. Watts, J. Aust. Ceram. Soc., 14 [2] 29-30 (1978).

Weight percent, Isopleth Al2P6O18-Ca2P2O7 compared with experimental data

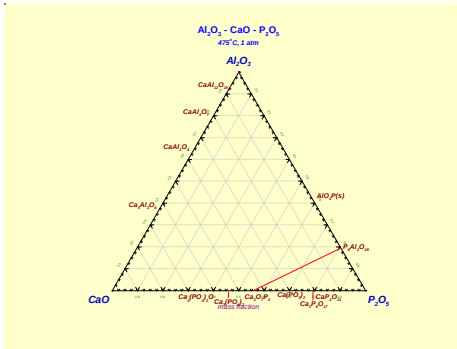

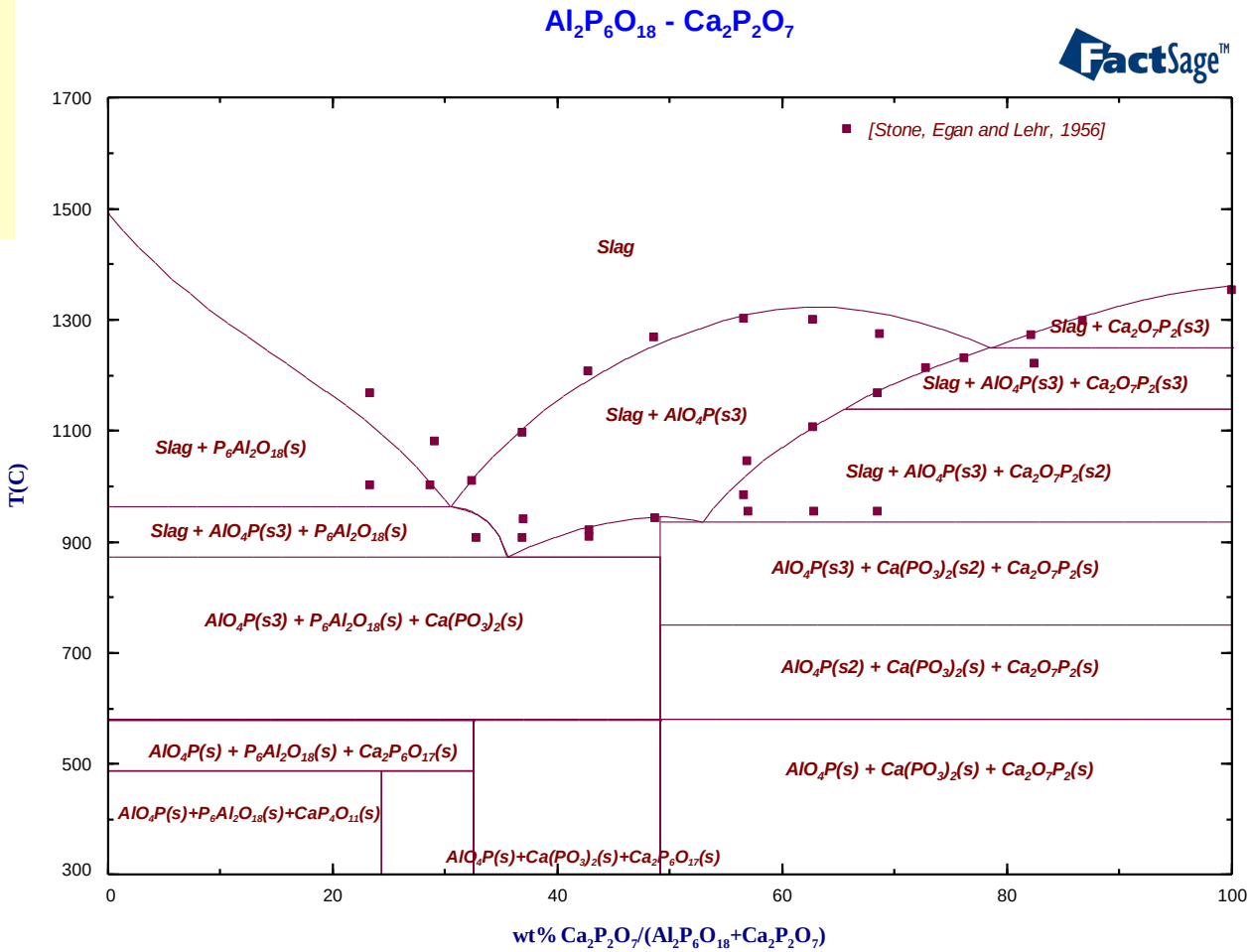

Al2O3-CaO-P2O5,

Weight percent, Isopleth Al2P6O18-CaP2O6

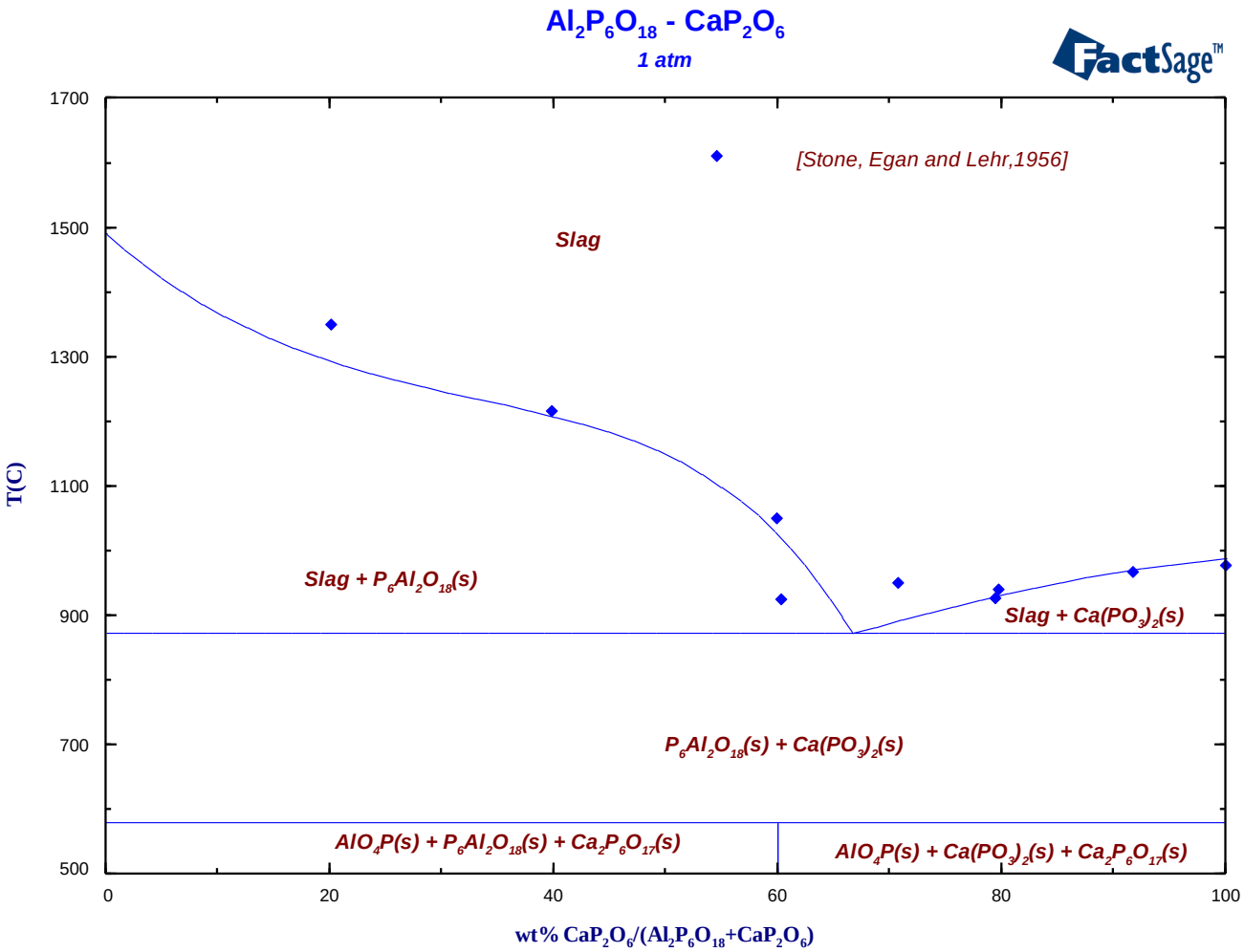

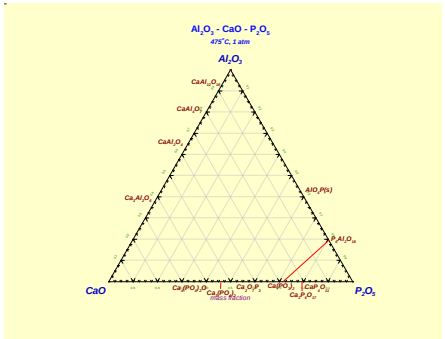

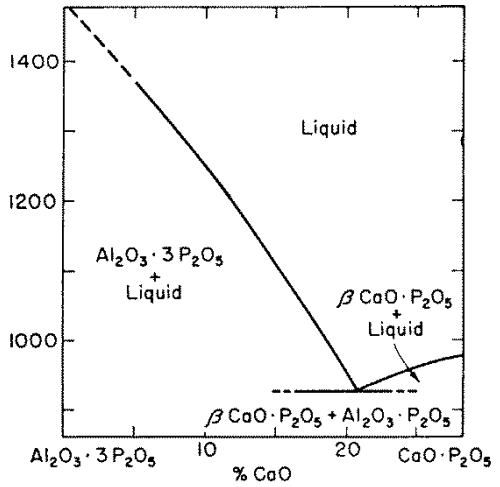

P. E. Stone, E. P. Egan, Jr., and J. R. Lehr, J. Am. Ceram. Soc., 39 [3] , (1956), pp. 89-98 .

Al2O3-CaO-P2O5,

Weight percent, Isopleth Al2P2O8-Ca2P2O7

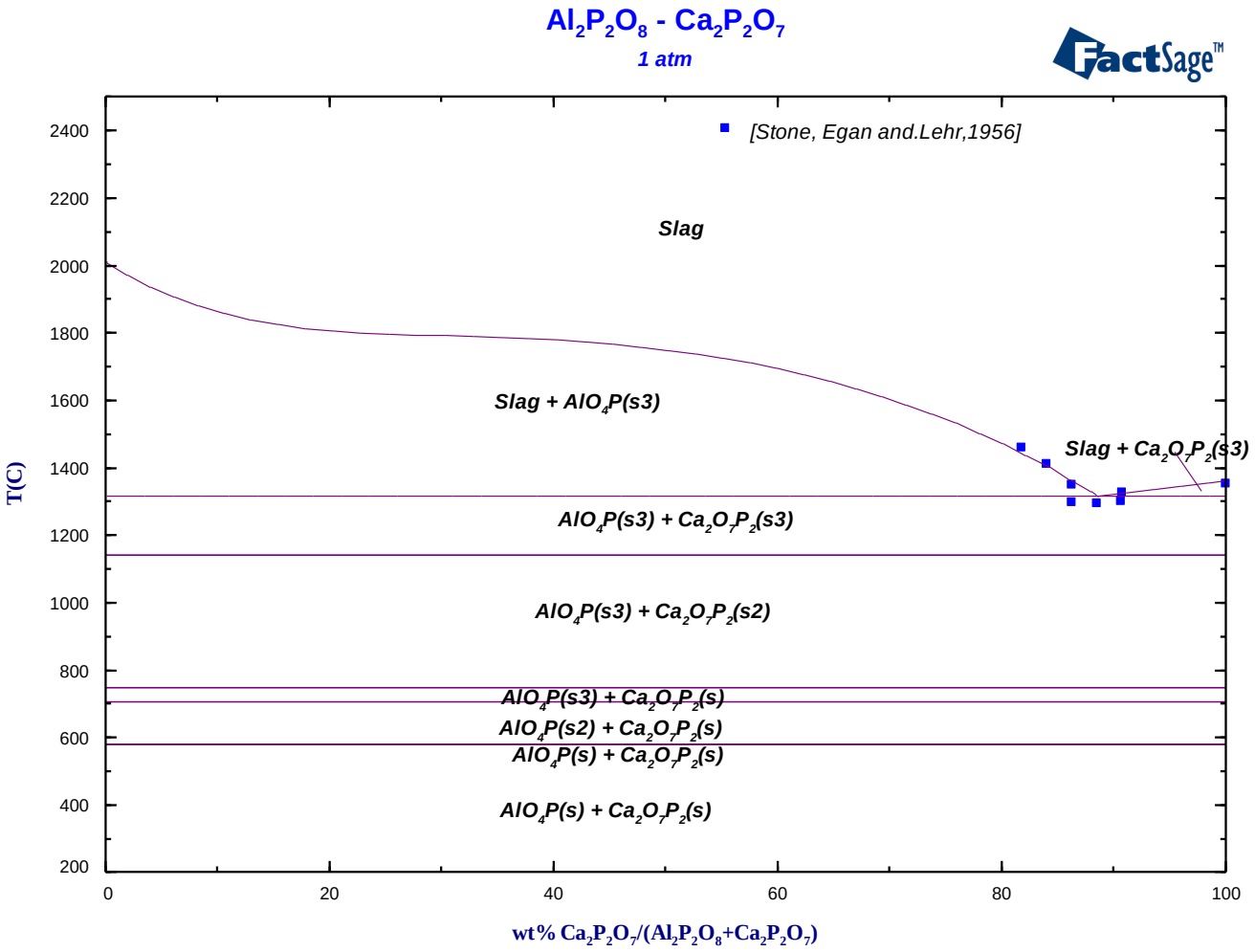

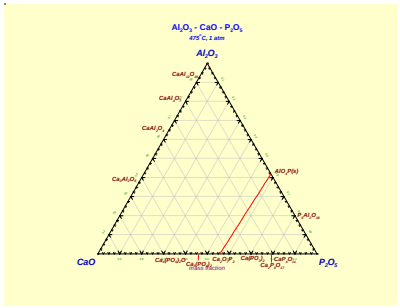

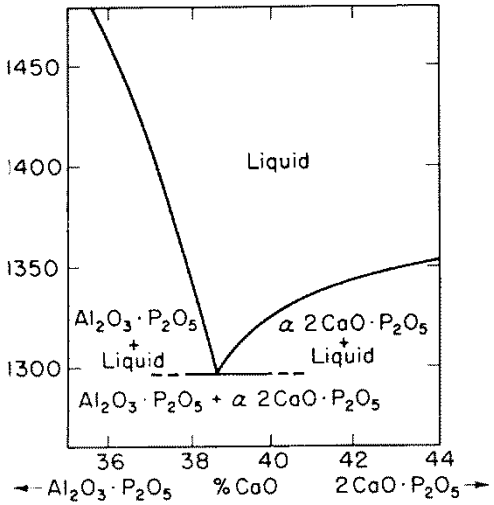

P. E. Stone, E. P. Egan, Jr., and J. R. Lehr, J. Am. Ceram. Soc., 39 [3] , (1956), pp. 89-98 .

Al2O3-CaO-P2O5,

Weight percent, Isopleth Al2P2O8-Ca3P2O8

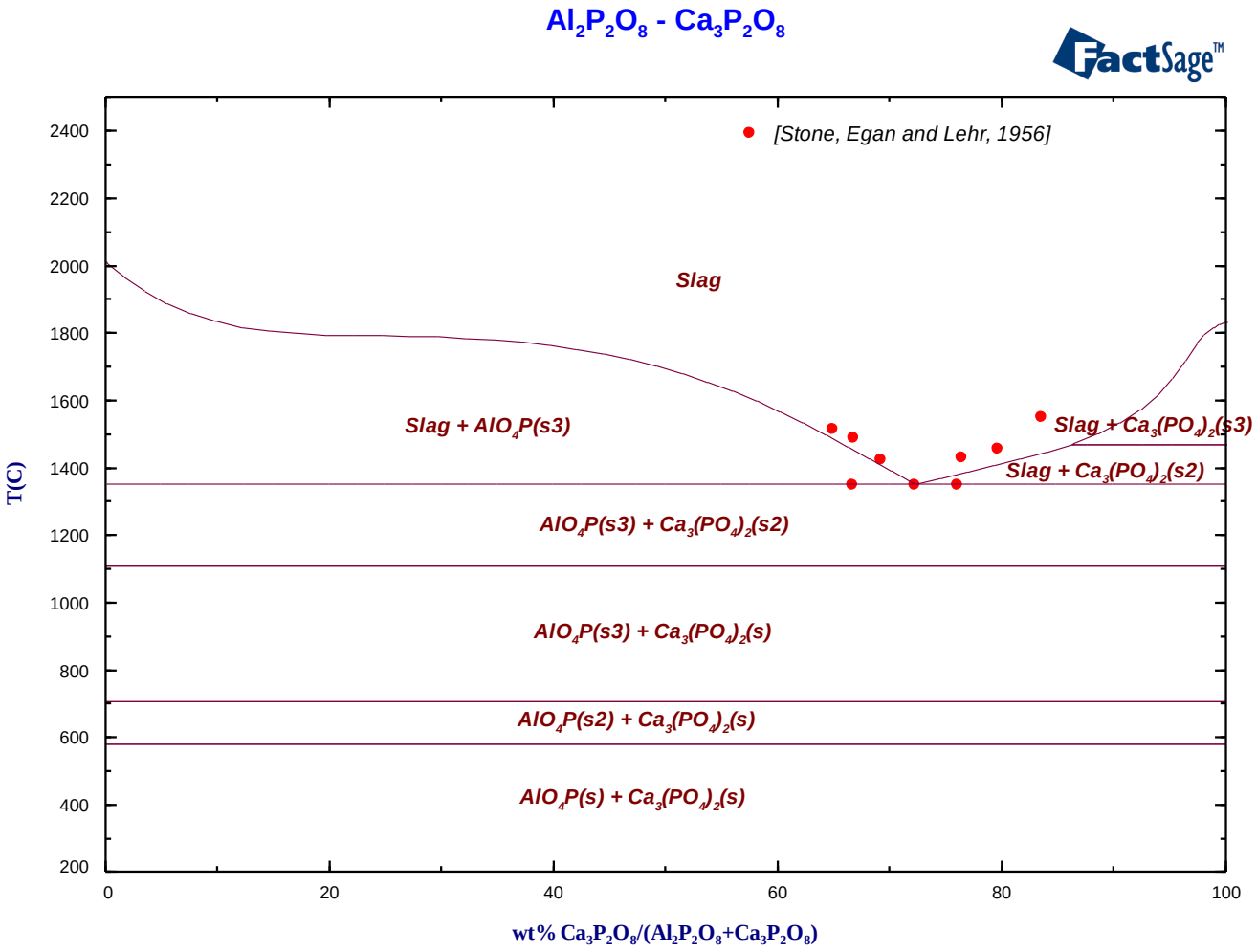

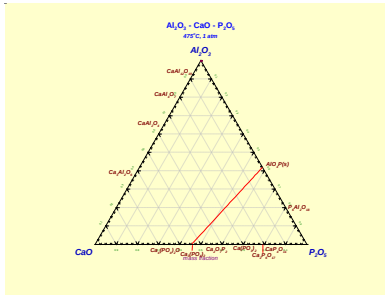

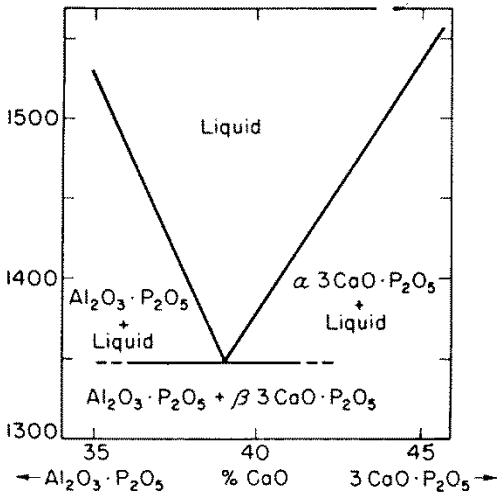

P. E. Stone, E. P. Egan, Jr., and J. R. Lehr, J. Am. Ceram. Soc., 39 [3] , (1956), pp. 89-98 .

Al2O3-CaO-P2O5,

Mole fraction Liquidussurface

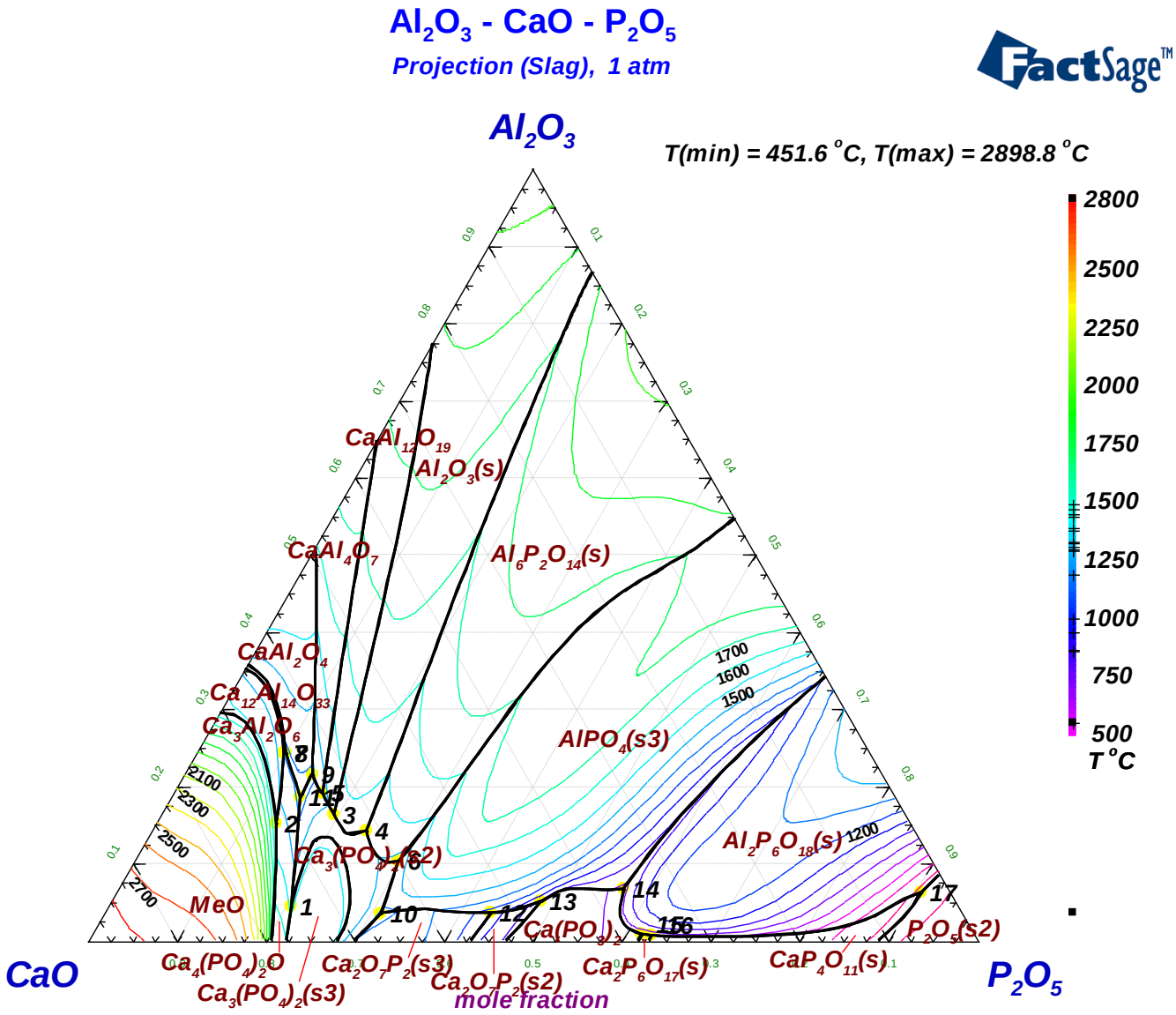

Weight percent
Liquidussurface

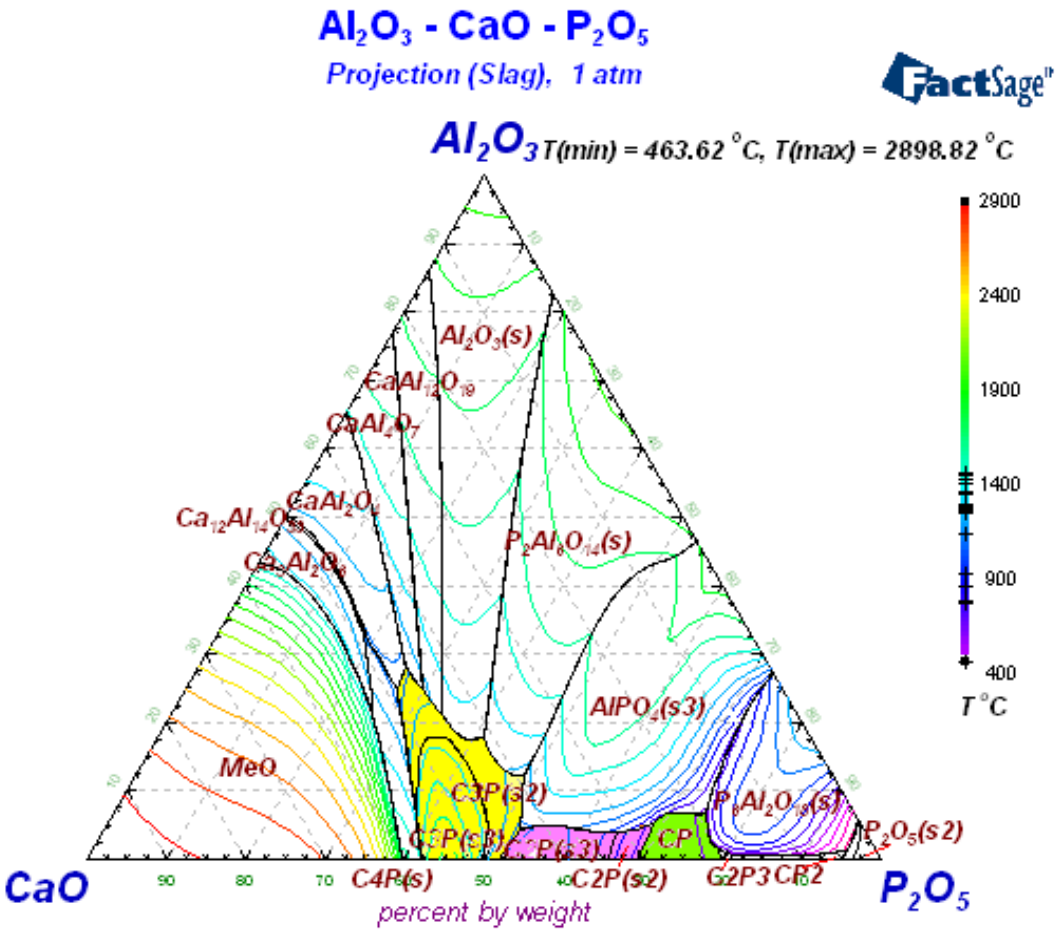

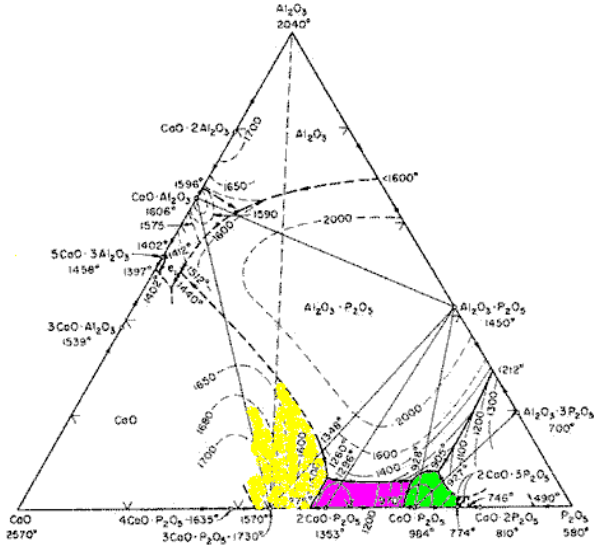

P. E. Stone, E. P. Egan, Jr., and J. R. Lehr, J. Am. Ceram. Soc., 39 [3] , (1956), pp. 89-98 .

Invariant equilibria on the liquidus surface

Intersections with slag	Mole fraction A = Al2O3, B = CaO, C = P2O5				Weight percent A = Al2O3, B = CaO, C = P2O5			
	X(A)	X(B)	X(C)	T(C)	W(A)	W(B)	W(C)	T(C)
1: Ca3(PO4)2(s2) / Ca3(PO4)2(s3) / Ca4(PO4)2O	1: 0.04444	0.74979	0.20577	1469.84	1. 6.715	55.215	38.070	1469.86
2: Ca3Al2O6 / Ca4(PO4)2O / MeO	2: 0.15169	0.71287	0.13544	1450.85	2. 21.095	53.461	25.444	1450.85
3: Al2O3 / Ca3(PO4)2(s2) / CaAl12O19	3: 0.16406	0.64167	0.19427	1428.38	3. 21.110	44.674	34.216	1428.38
4: Al2O3 / Al6P2O14 / Ca3(PO4)2(s2)	4: 0.14256	0.61578	0.24165	1414.59	4. 17.700	41.240	41.060	1414.59
5: Ca3(PO4)2(s2) / CaAl12O19 / CaAl4O7	5: 0.19145	0.64047	0.16808	1364.58	5. 24.847	45.198	29.955	1364.58
6: Al6P2O14 / AlPO4(s3) / Ca3(PO4)2(s2)	6: 0.10324	0.59947	0.29729	1352.01	6. 12.254	38.859	48.887	1352.01
7: Ca12Al14O33 / Ca3Al2O6 / Ca4(PO4)2O	7: 0.24348	0.65776	0.09875	1296.74	7. 33.052	48.656	18.292	1296.74
8: Ca12Al14O33 / Ca4(PO4)2O / CaAl2O4	8: 0.24289	0.65639	0.10072	1289.77	8. 32.890	48.465	18.645	1289.77
9: Ca3(PO4)2(s2) / CaAl2O4 / CaAl4O7	9: 0.21610	0.64030	0.14360	1274.52	9. 28.304	45.786	25.910	1274.52
10: AlPO4(s3) / Ca2O7P2(s3) / Ca3(PO4)2(s2)	10: 0.03579	0.65297	0.31124	1263.12	10. 4.338	43.314	52.348	1263.12
11: Ca3(PO4)2(s2) / Ca4(PO4)2O / CaAl2O4	11: 0.18632	0.66825	0.14542	1257.98	11. 24.822	48.542	26.635	1257.98
12: AlPO4(s3) / Ca2O7P2(s2) / Ca2O7P2(s3)	12: 0.03623	0.52920	0.43457	1139.85	12. 3.887	31.214	64.899	1139.85
13: AlPO4(s3) / Ca(PO3)2(s) / Ca2O7P2(s2)	13: 0.05097	0.46554	0.48349	936.53	13. 5.204	26.121	68.675	936.53
14: Al2P6O18 / AlPO4(s3) / Ca(PO3)2(s)	14: 0.06834	0.36332	0.56834	872.28	14. 6.641	18.765	74.595	872.28
15: Al2P6O18 / Ca(PO3)2(s) / Ca2P6O17	15: 0.00885	0.37302	0.61813	787.04	15. 0.790	19.124	80.086	787.04
16: Al2P6O18 / Ca2P6O17 / CaP4O11	16: 0.00704	0.36282	0.63014	782.43	16. 0.617	18.443	80.941	782.43
17: Al2P6O18 / CaP4O11 / P2O5(s2)	17: 0.06290	0.03225	0.90485	463.62	17. 1.165	3.808	95.027	463.62

Mole fraction

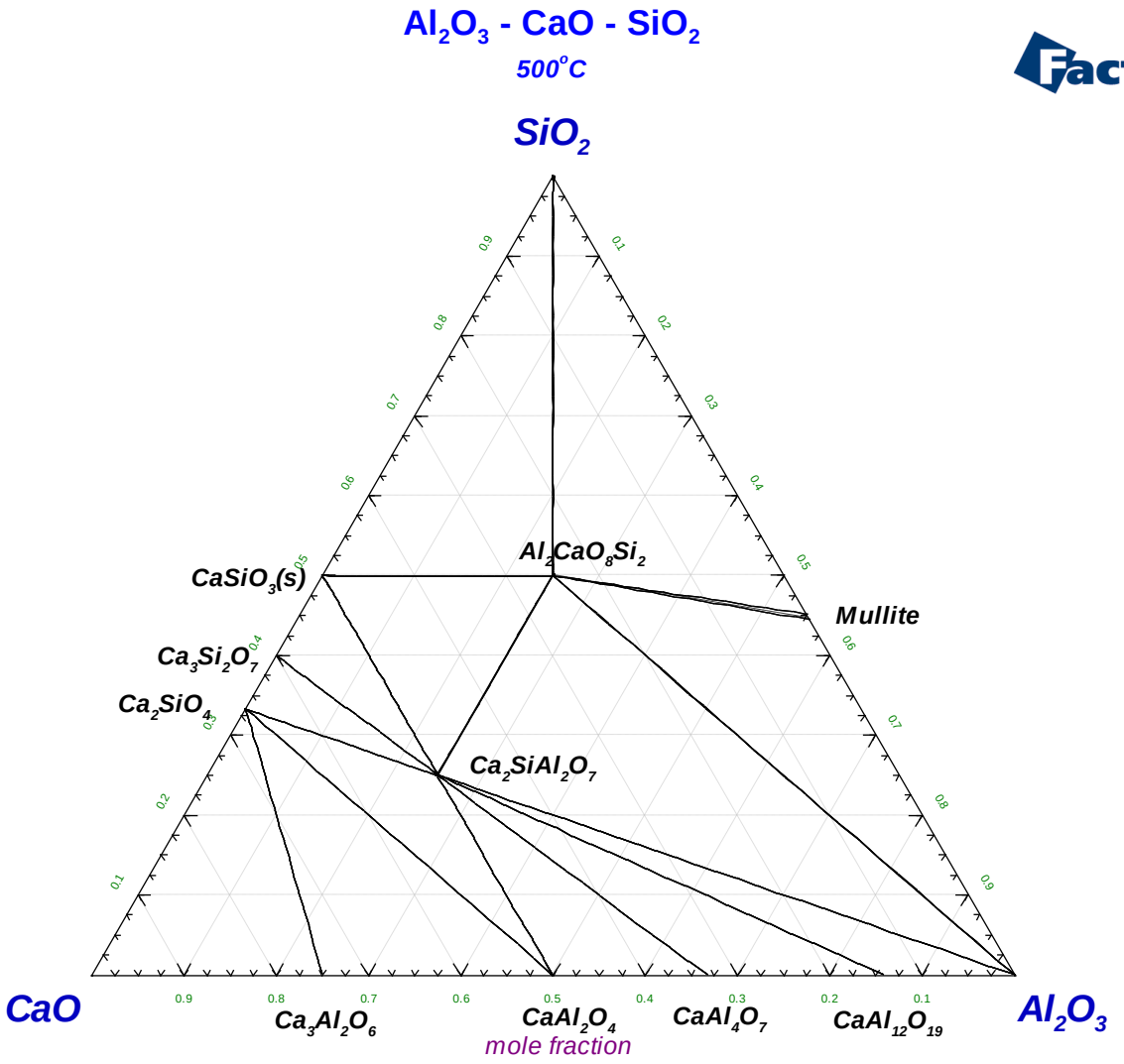

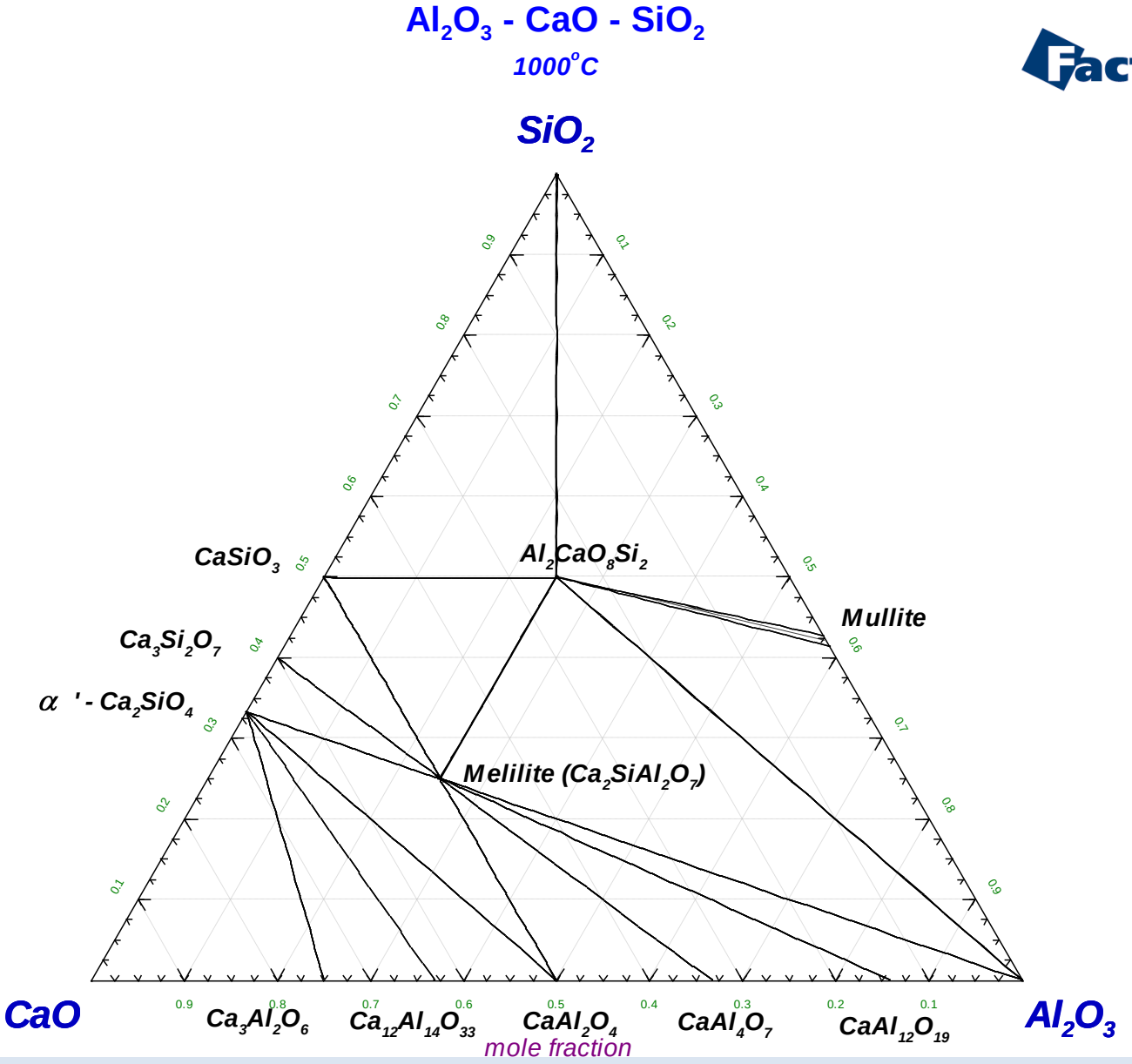
Al2O3 - CaO - SiO2
1000°C
SiO2
CaSiO3
Al2CaO8Si2
Mullite
Ca3Si2O7
α '- Ca2SiO4
Melilite (Ca2SiAl2O7)
CaO
Ca3Al2O6
Ca12Al14O33
CaAl2O4
CaAl4O7
CaAl12O19
Al2O3
mole fraction

Mole fraction
kurz unterhalb Liquidussurface

Al_2O_3 - CaO - SiO_2

1185°C

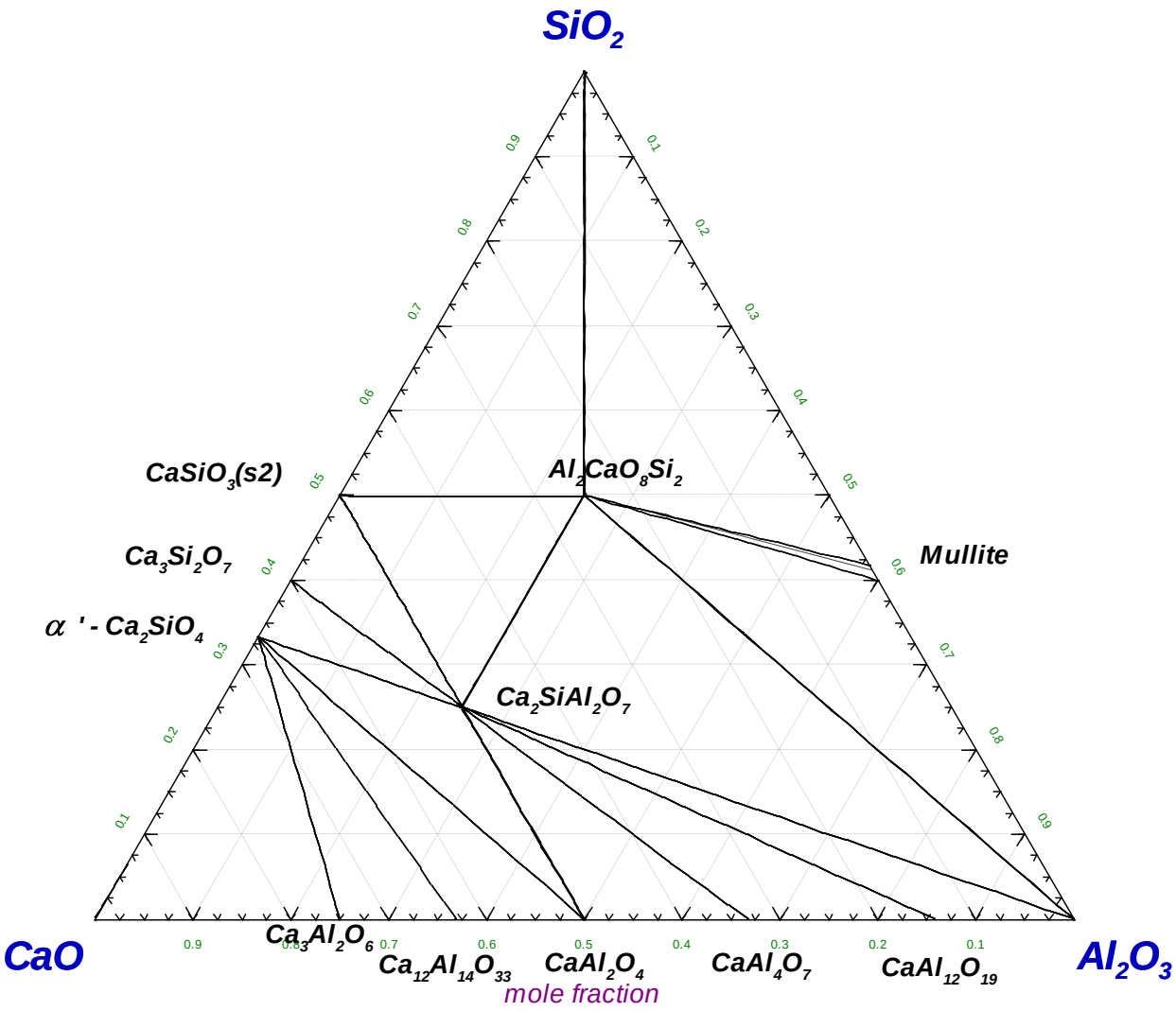

Weight percent
compared with experimental data

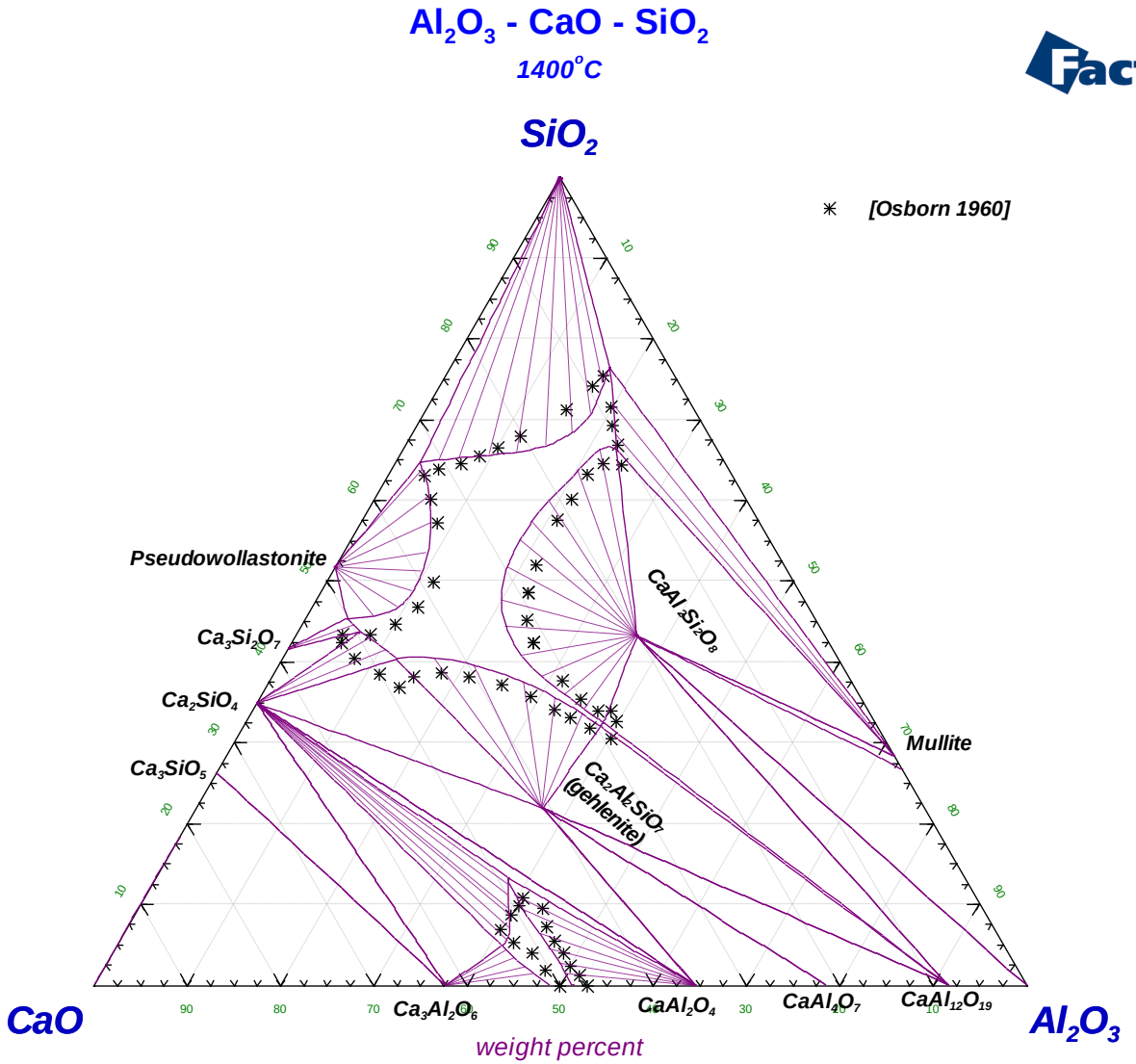

Weight percent
compared with experimental data

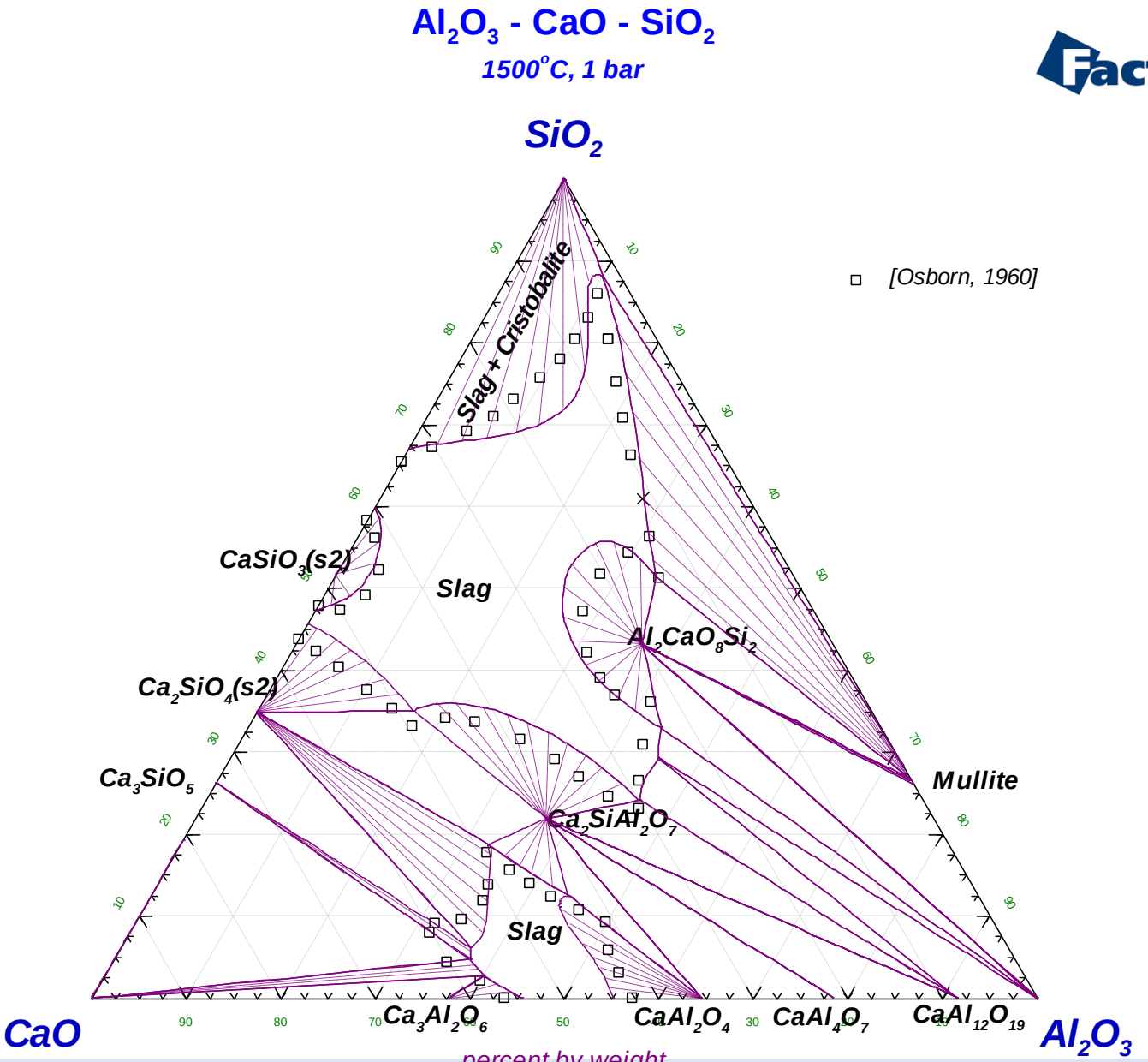

Weight percent
compared with experimental data

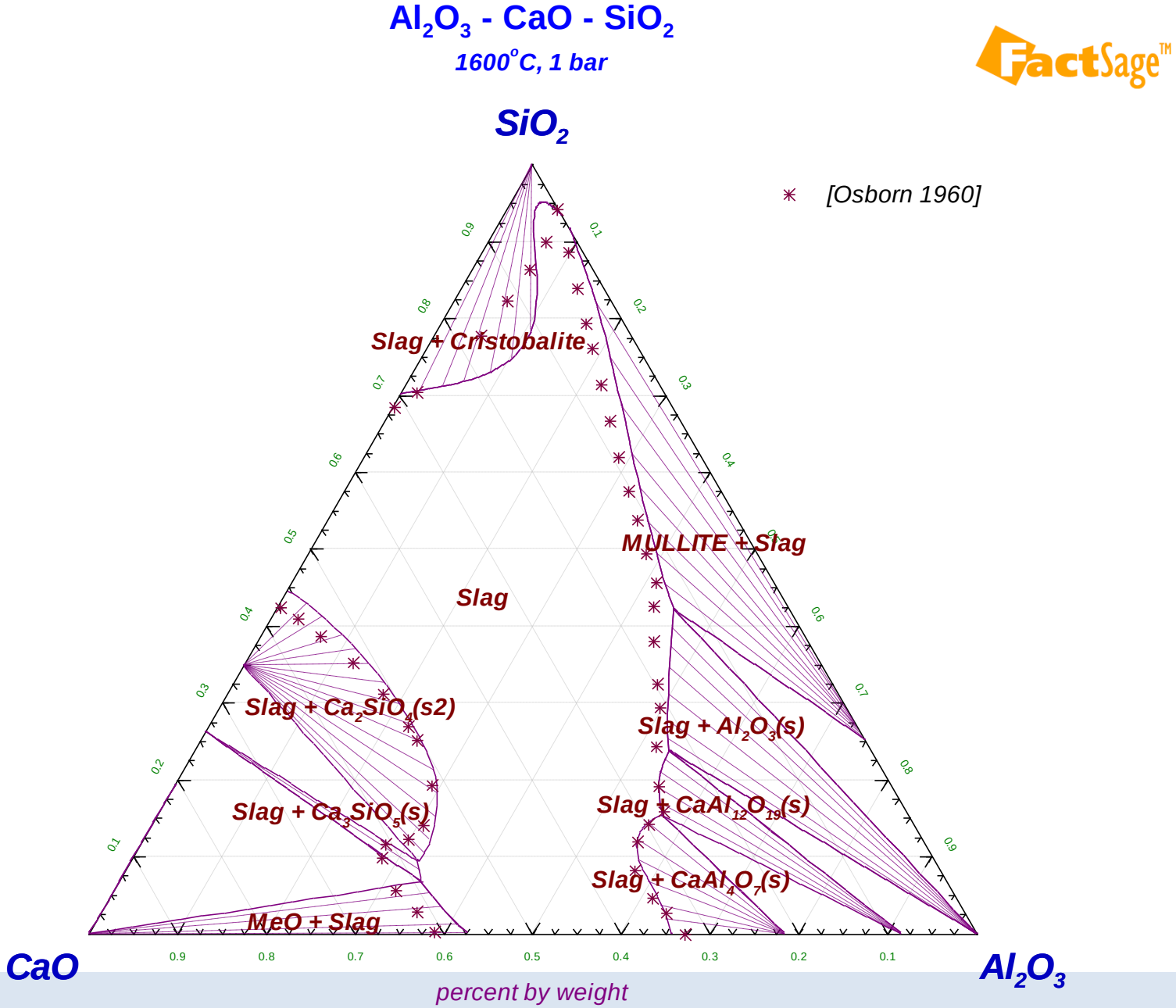

Mole fraction x(Al2O3)=0,25 compared with experimental data

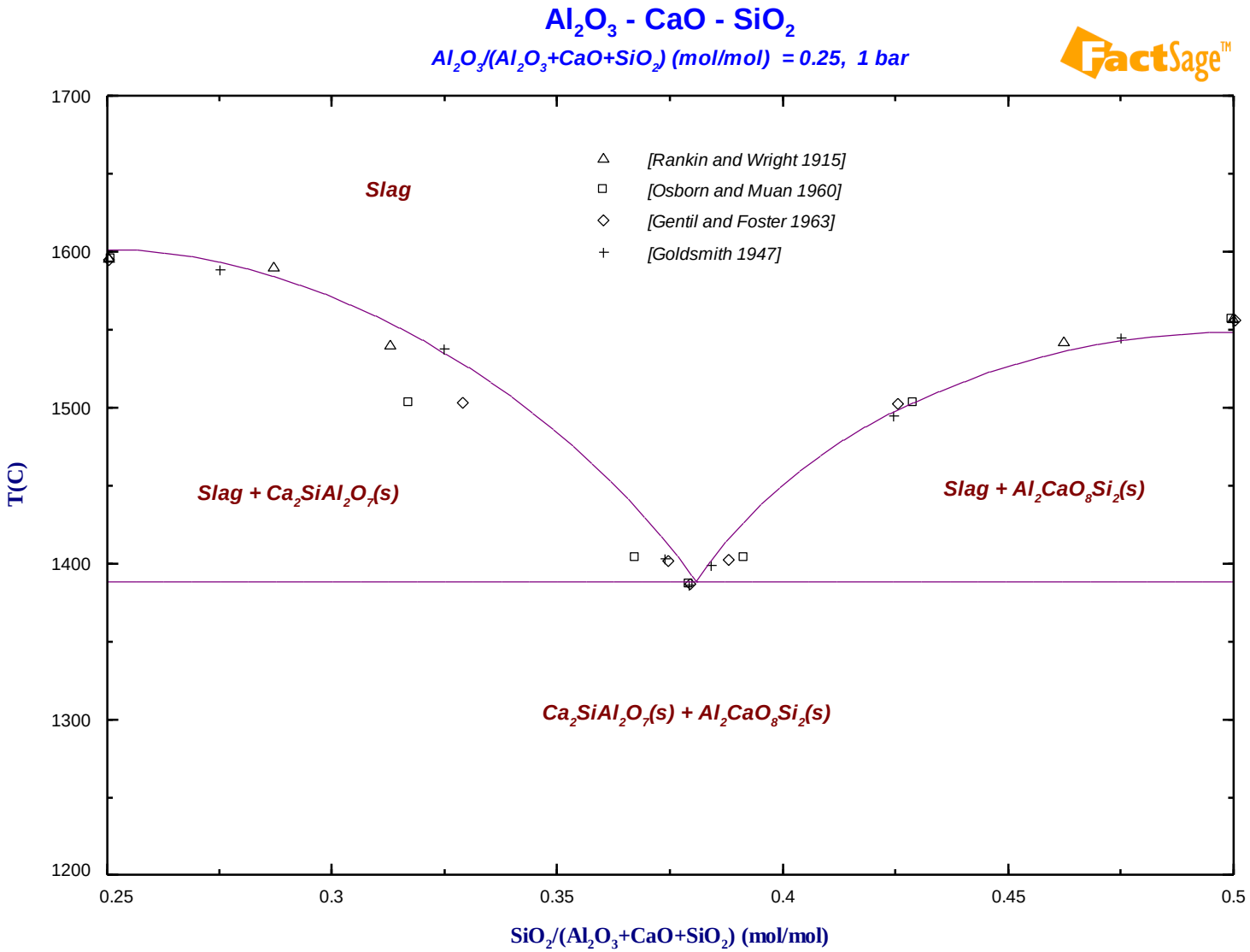

Weight percent
compared with experimental data

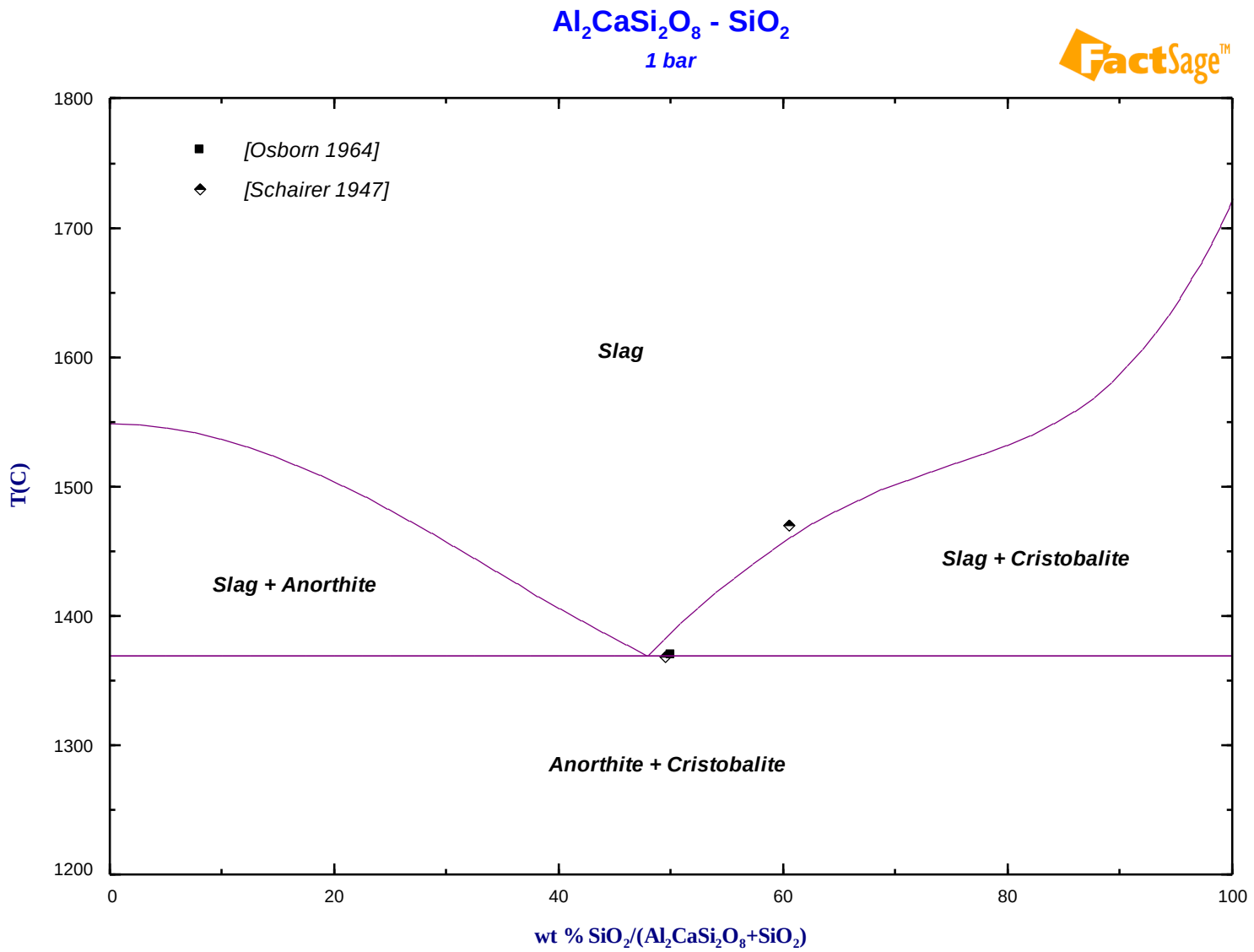

Weight percent Ca2SiO4-Ca12Al14O33 compared with experimental data

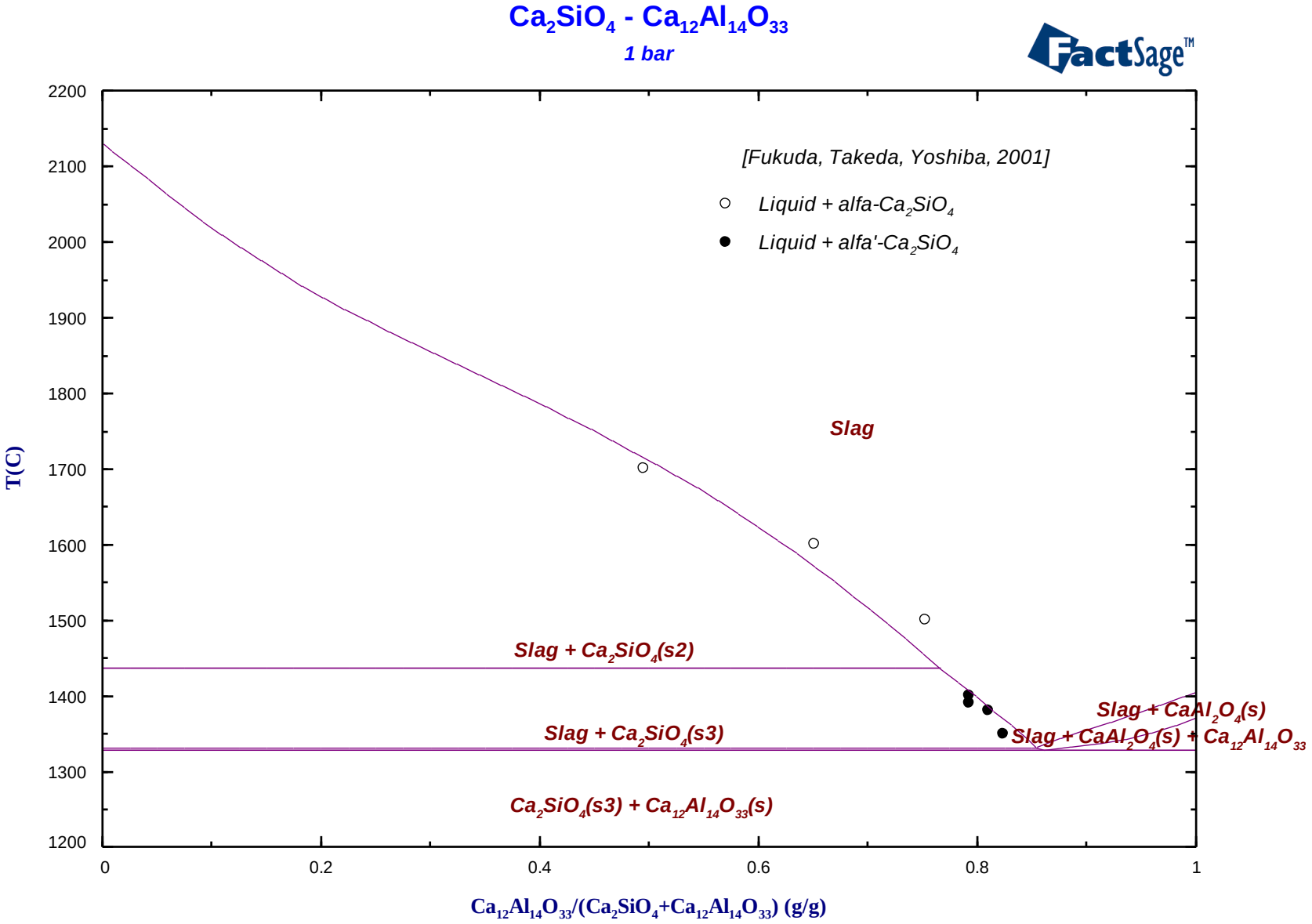

Mole fraction
Liquidussurface

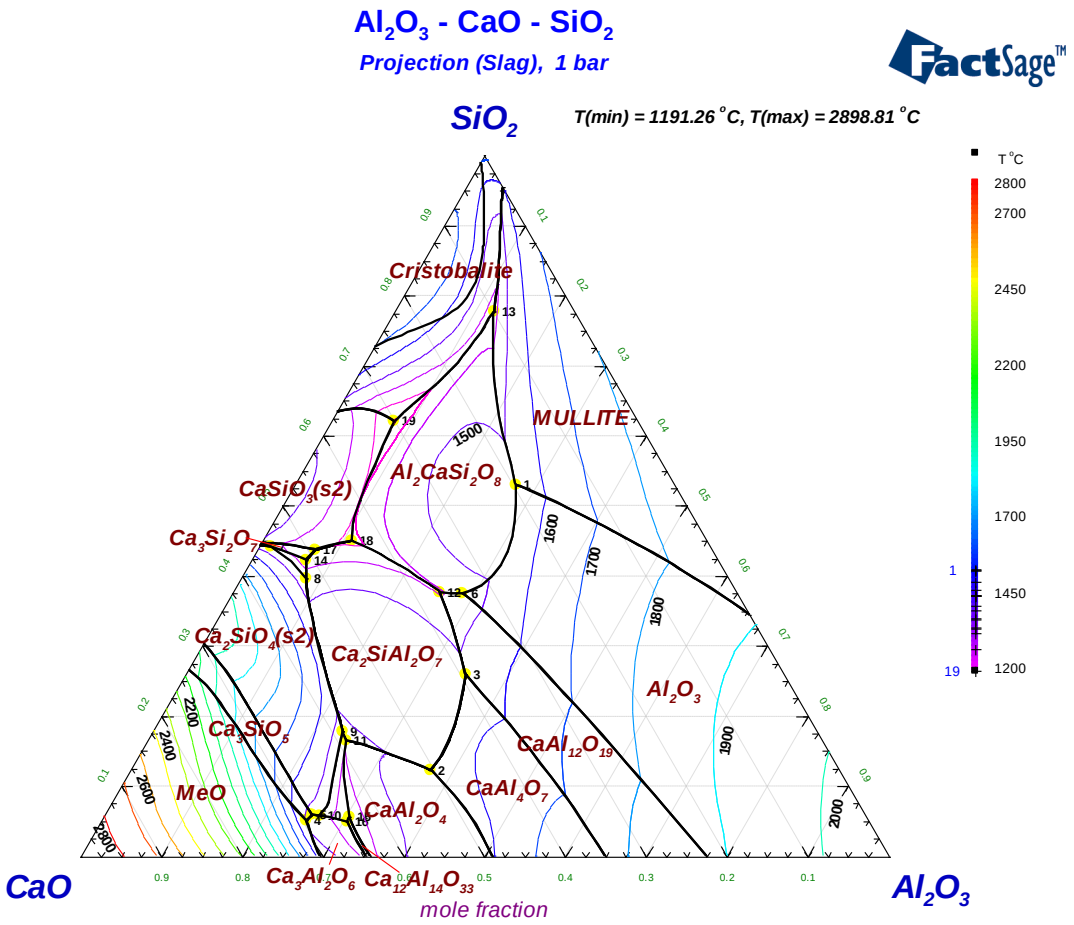

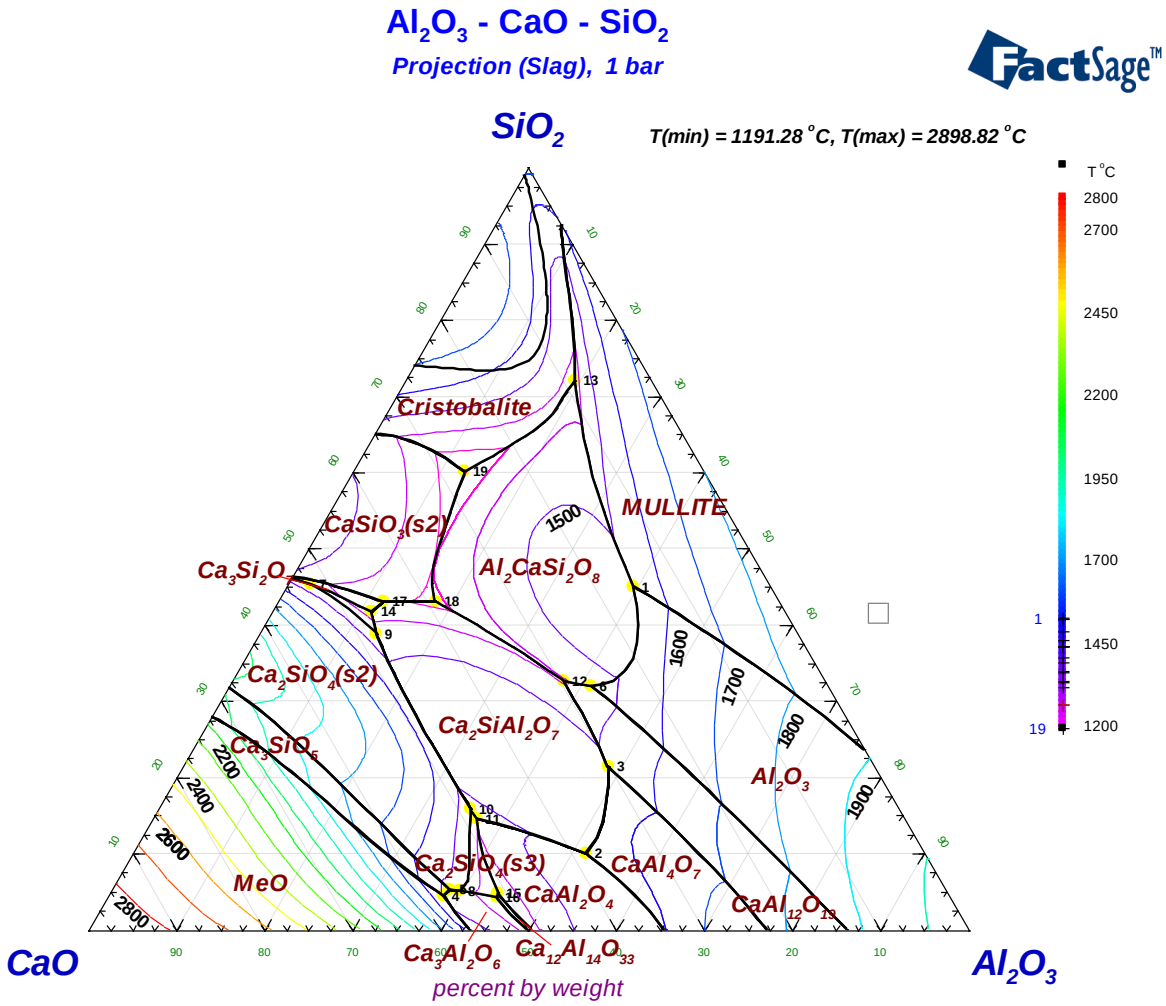
Al2O3 - CaO - SiO2
Projection (Slag), 1 bar
FactSage™
SiO2
T(min) = 1191.28 °C, T(max) = 2898.82 °C
T °C
2800
2700
2450
2200
1950
1700
1450
1200
Cristobalite
MULLITE
CaSiO3(s2)
Ca3Si2O7
Al2CaSi2O8
Ca2SiO4(s2)
Ca2SiAl2O7
Ca3SiO5
Al2O3
Ca2SiO4(s3)
CaAl4O7
MeO
CaAl2O4
CaAl12O19
Ca3Al2O6
Ca12Al14O33
1500
1600
1700
1800
1900
2000
2200
2400
2500
2800
CaO
Al2O3
percent by weight

Invariant equilibria on the liquidus surface

Intersections with slag	Mole fraction A = SiO2, B = CaO, C = Al2O3				Weight percent A = SiO2, B = CaO, C = Al2O3			
	X(A)	X(B)	X(C)	T(C)	W(A)	W(B)	W(C)	T(C)
1: Al2CaSi2O8 / Al2O3 / MULLITE	0.53016	0.19613	0.27371	1522.84	45.017	15.543	39.440	1522.84
2: Ca2SiAl2O7 / CaAl2O4 / CaAl4O7	0.12311	0.50502	0.37187	1520.16	10.046	38.461	51.493	1520.18
3: Ca2SiAl2O7 / CaAl12O19 / CaAl4O7	0.25986	0.39392	0.34621	1518.99	21.387	30.259	48.354	1518.99
4: Ca3Al2O6 / Ca3SiO5 / MeO	0.05097	0.69506	0.25397	1484.01	4.508	57.374	38.117	1483.98
5: Ca2SiO4(s2) / Ca3Al2O6 / Ca3SiO5	0.05915	0.68373	0.25712	1458.08	5.218	56.292	38.489	1457.91
6: Al2CaSi2O8 / Al2O3 / CaAl12O19	0.37610	0.33887	0.28503	1439.36	31.980	26.892	41.128	1439.36
7: Ca2SiO4(s2) / Ca2SiO4(s3) / Ca3Si2O7	0.44186	0.54377	0.01437	1436.73	45.377	52.119	2.505	1436.74
8: Ca2SiAl2O7 / Ca2SiO4(s2) / Ca2SiO4(s3)	0.39705	0.52296	0.07999	1436.73	5.119	55.270	39.610	1436.73
9: Ca2SiAl2O7 / Ca2SiO4(s2) / Ca2SiO4(s3)	0.17838	0.58610	0.23552	1436.73	38.893	47.810	13.297	1436.73
10: Ca2SiO4(s2) / Ca2SiO4(s3) / Ca3Al2O6	0.05839	0.67540	0.26621	1436.73	15.854	48.622	35.524	1436.73
11: Ca2SiAl2O7 / Ca2SiO4(s3) / CaAl2O4	0.16487	0.58942	0.24571	1405.49	14.565	48.599	36.836	1405.49
12: Al2CaO8Si2 / Ca2SiAl2O7 / CaAl12O19	0.37749	0.36681	0.25570	1388.25	32.719	29.672	37.609	1388.23
13: Al2CaSi2O8 / MULLITE / Cristobalite	0.77700	0.10020	0.12279	1364.64	72.018	8.668	19.314	1364.64
14: Ca2SiAl2O7 / Ca2SiO4(s3) / Ca3Si2O7	0.42300	0.50934	0.06766	1360.06	41.749	46.918	11.333	1360.05
15: Ca12Al14O33 / Ca2SiO4(s3) / CaAl2O4	0.05610	0.63973	0.30417	1331.21	4.798	51.060	44.142	1331.21
16: Ca12Al14O33 / Ca2SiO4(s3) / Ca3Al2O6	0.05021	0.64497	0.30482	1330.35	4.294	51.474	44.232	1330.35
17: Ca2SiAl2O7 / Ca3Si2O7 / CaSiO3(s2)	0.43796	0.49015	0.07188	1314.96	43.047	44.964	11.990	1314.96
18: Al2CaSi2O8 / Ca2SiAl2O7 / CaSiO3(s2)	0.45111	0.43833	0.11056	1262.21	43.052	39.042	17.906	1262.21
19: Al2CaSi2O8 / CaSiO3(s2) / Cristobalite	0.62137	0.30113	0.07750	1191.26	60.098	27.182	12.719	1191.37

Mole fraction 1000°C

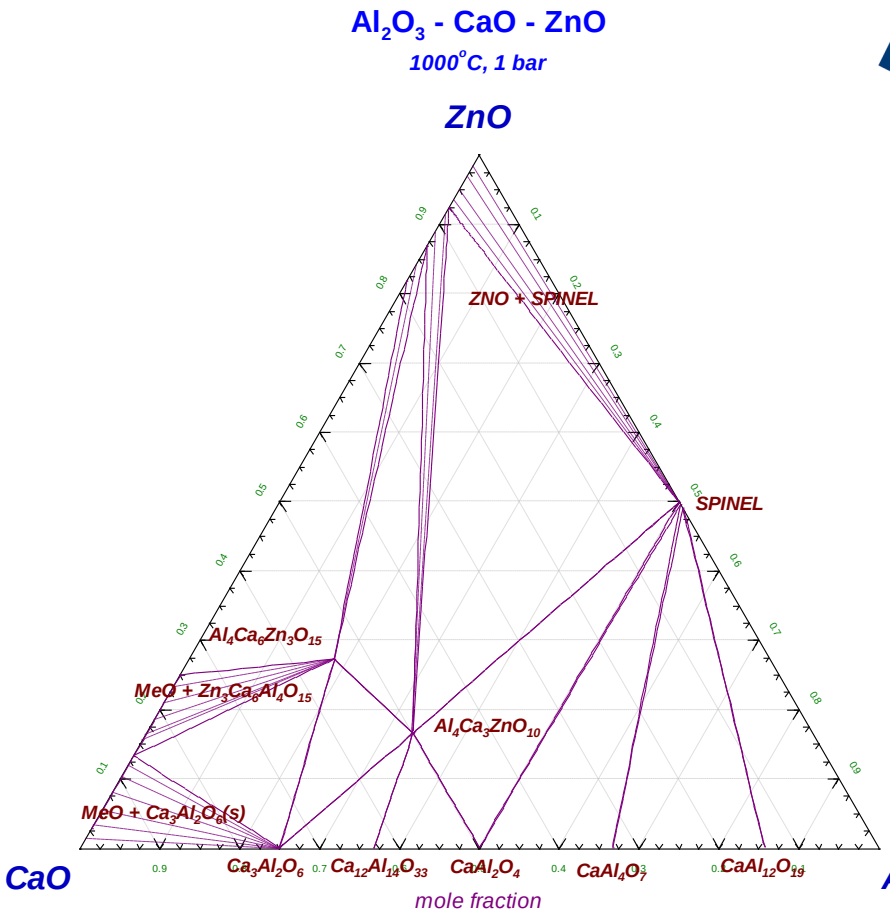

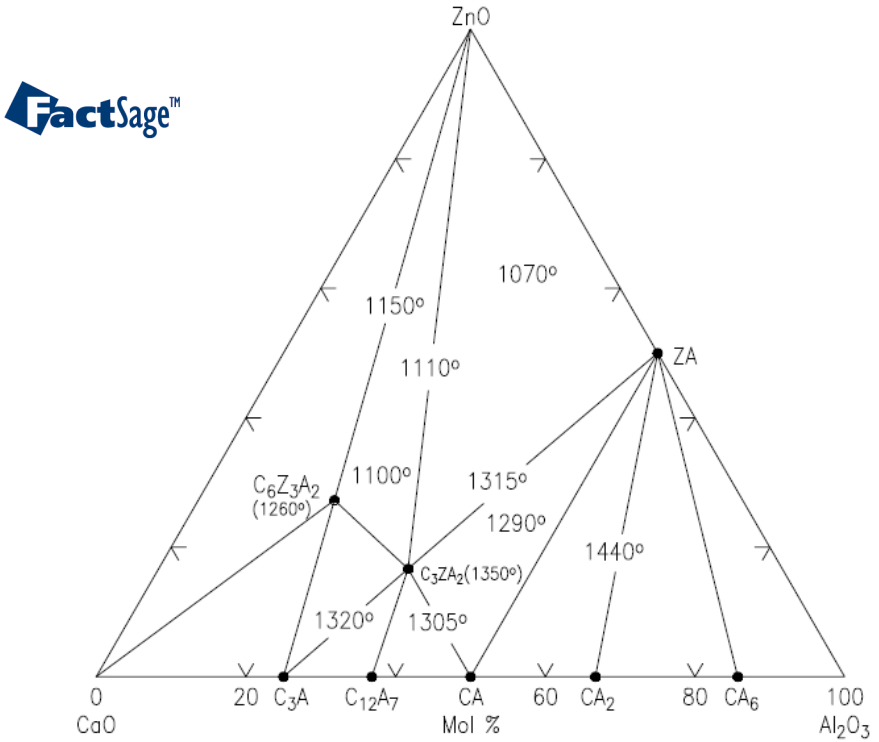

H. Bolio-Arceo, F.P. Glasser, Adv. Cem. Res., 10 [1], (1998), pp. 25-32.

Al_2O_3 - CaO - ZnO

Projection (Slag), 1 atm

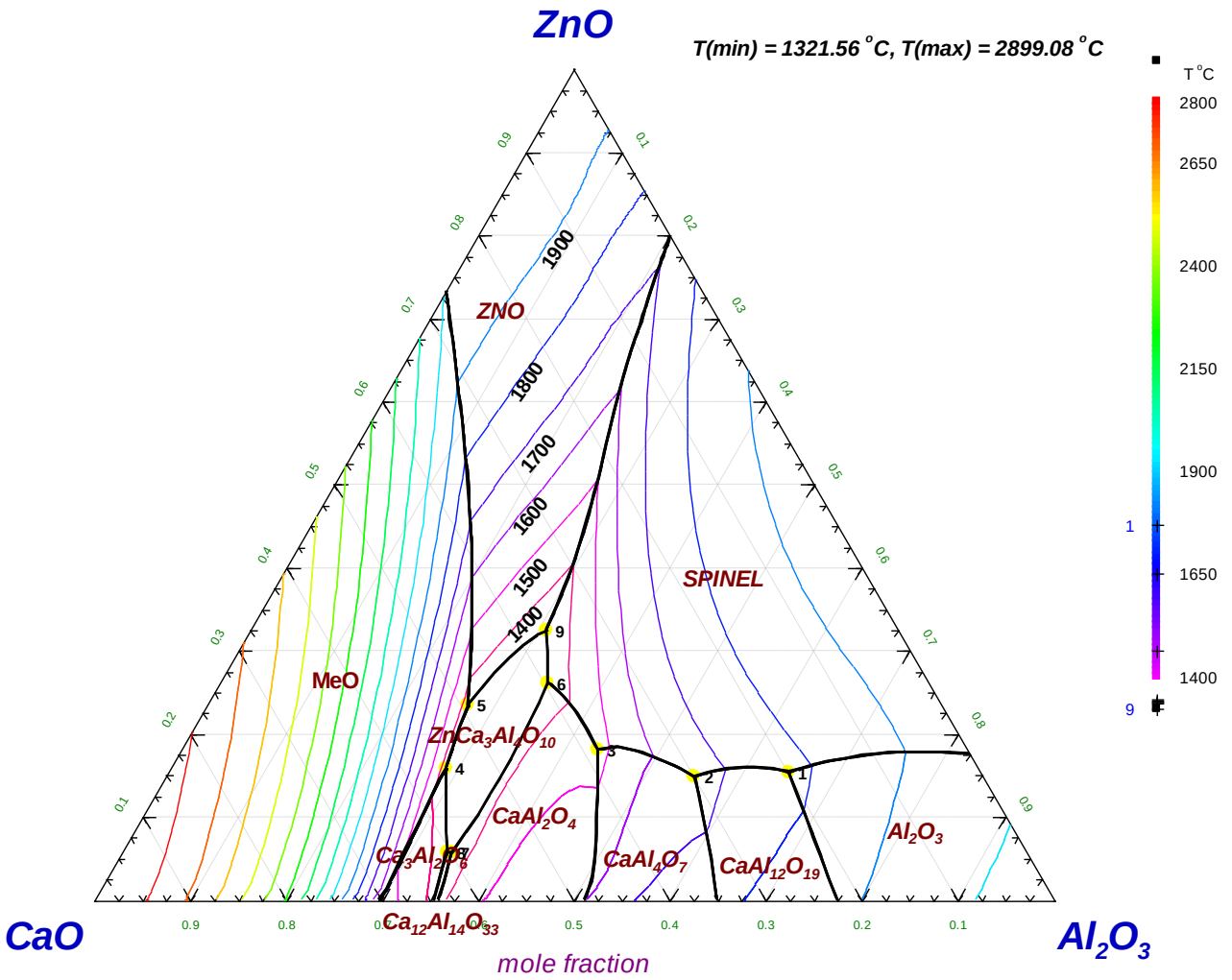

Al_2O_3 - CaO - ZnO

Projection (Slag), 1 atm

FactSage™

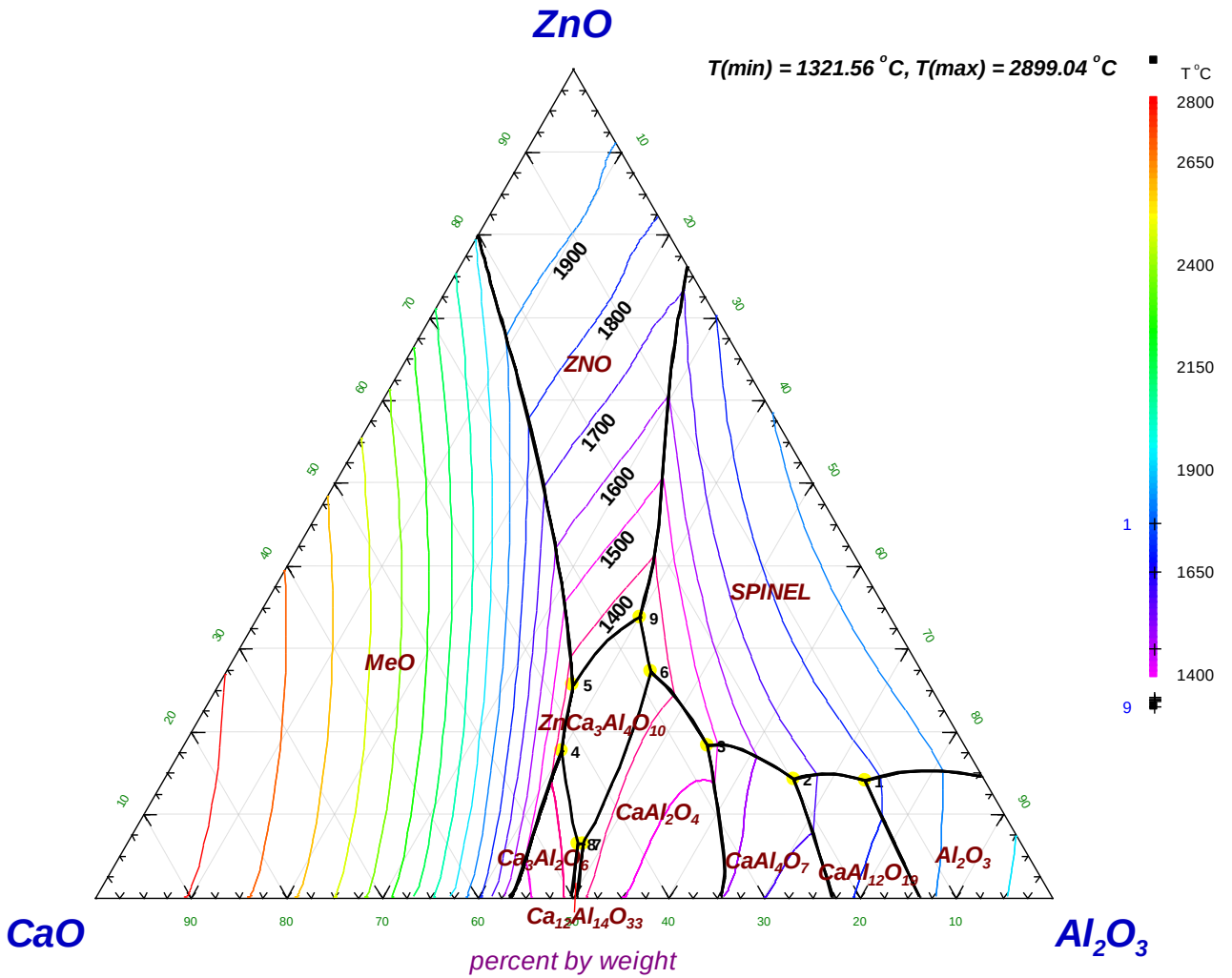

Invariant equilibria on the liquidus surface

Intersections with slag	Mole fraction A = ZnO, B = CaO, C = Al2O3				Weight percent A = ZnO, B = CaO, C = Al2O3				
		X(A)	X(B)	X(C)	T(C)	W(A)	W(B)	W(C)	T(C)
1: Al2O3 / CaAl12O19 / SPINEL	1:	0.15446	0.19876	0.64678	1769.91	14.019	12.431	73.550	1769.88
2: CaAl12O19 / CaAl4O7 / SPINEL	2:	0.14927	0.29983	0.55090	1651.56	14.269	19.750	65.981	1651.56
3: CaAl2O4 / CaAl4O7 / SPINEL	3:	0.18097	0.38510	0.43393	1464.53	18.280	26.804	54.916	1464.53
4: Ca3Al2O6 / MeO / ZnCa3Al4O10	4:	0.15911	0.55398	0.28691	1345.91	17.673	42.400	39.927	1345.91
5: MeO / ZNO / ZnCa3Al4O10	5:	0.23458	0.49392	0.27150	1340.98	25.634	37.193	37.172	1340.99
6: CaAl2O4 / SPINEL / ZnCa3Al4O10	6:	0.26219	0.39593	0.34189	1340.04	27.216	28.320	44.464	1340.09
7: Ca12Al14O33 / CaAl2O4 / ZnCa3Al4O10	7:	0.05804	0.59834	0.34362	1338.04	..6.443	45.767	47.790	1338.04
8: Ca12Al14O33 / Ca3Al2O6 / ZnCa3Al4O10	8:	0.05804	0.60340	0.33856	1335.82	6.463	46.302	47.235	1335.82
9: SPINEL / ZNO / ZnCa3Al4O10	9:	0.32507	0.36656	0.30837	1321.56	33.721	26.202	40.078	1321.56

Al2O3-Cr2O3-Fe2O3,
Weight percent 1250°C

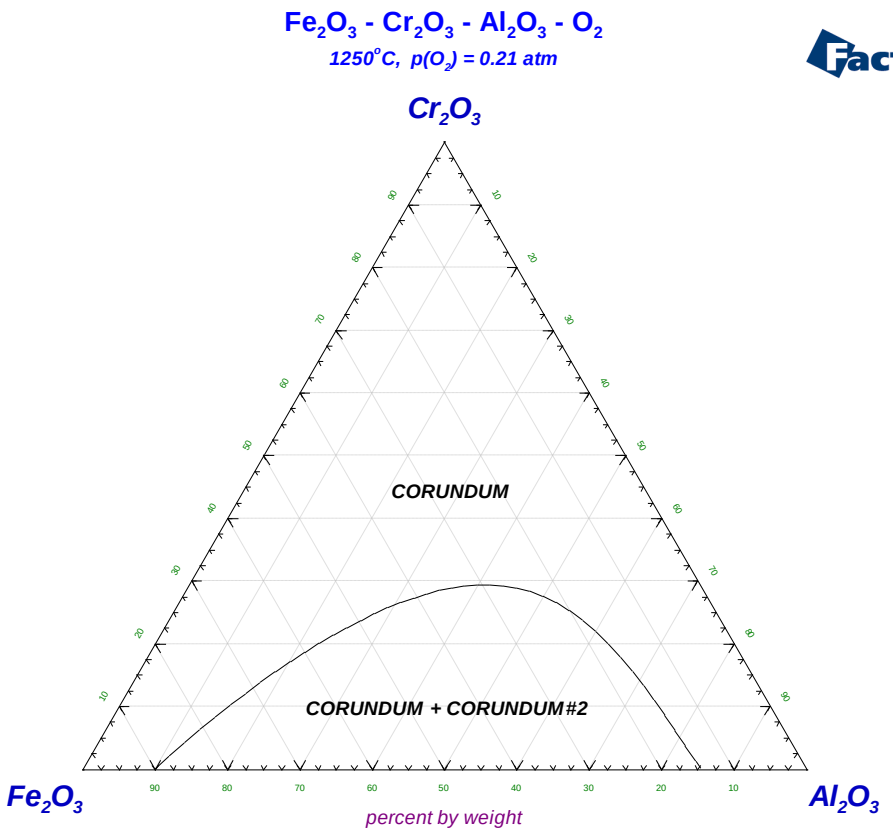

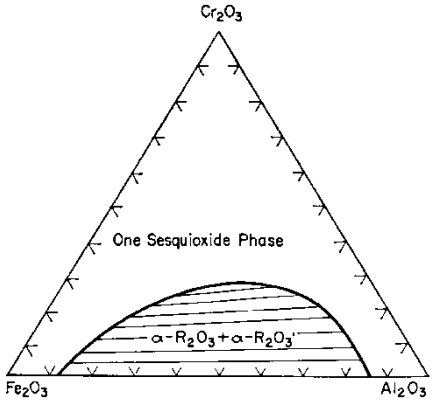

A. Muan and S. Somiya, Journal of Amer. Ceram. Soc., 42 (1959), pp. 603-613.

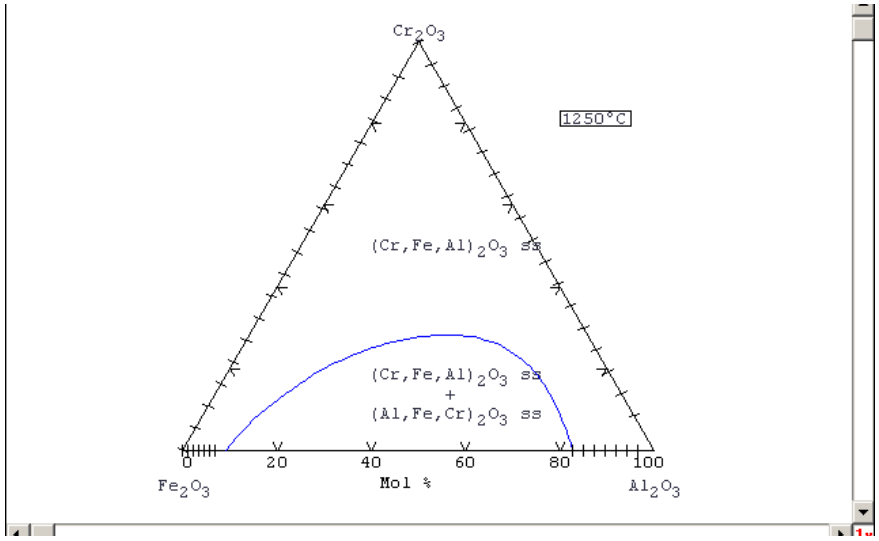

A.A. Fotiev, L.L. Surat, G.A. Korablev, A.I. Treryakov, Zh. Neorg. Khim, N. 26 [1], (1981), pp.242-248.

Al2O3-Cr2O3-Fe2O3, Weight percent 1350°C

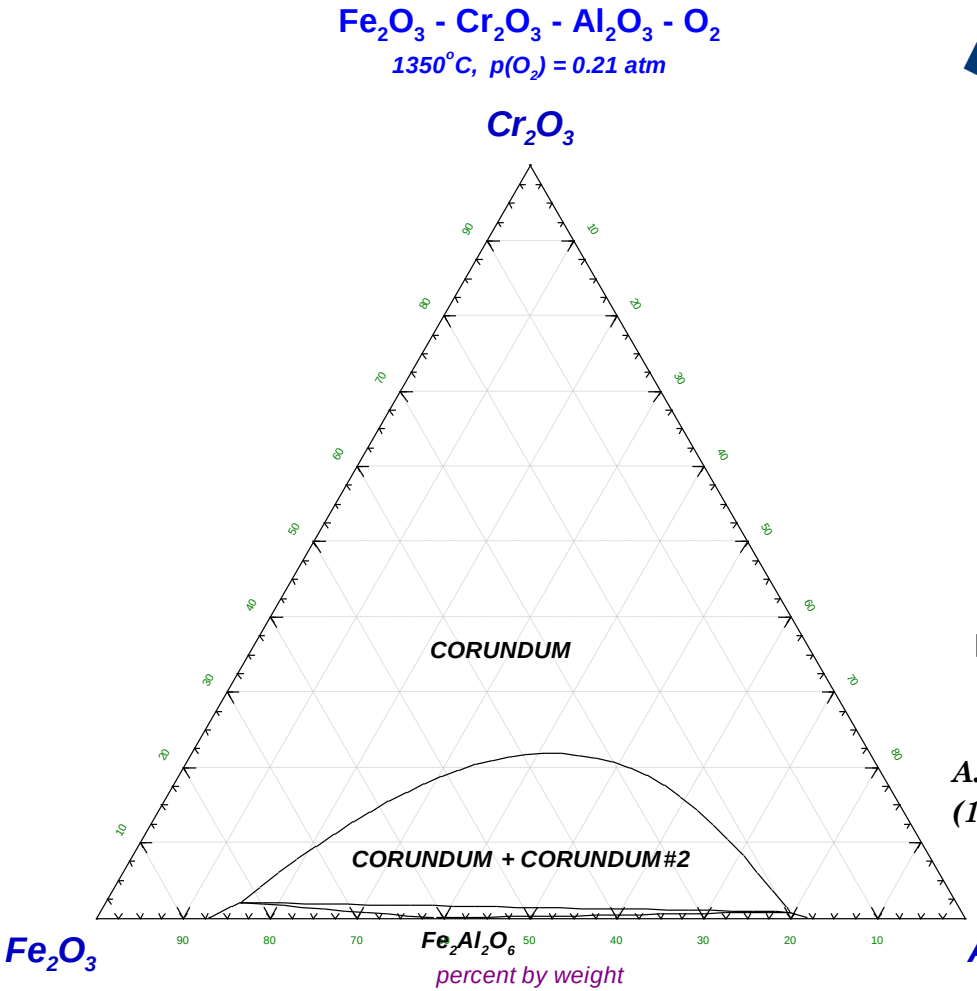

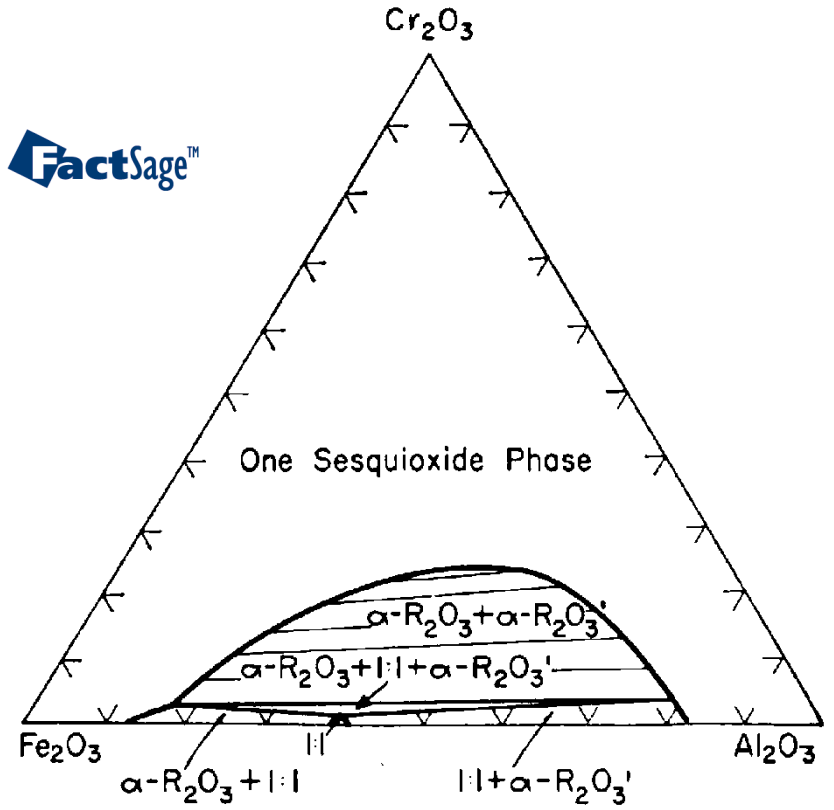

A. Muan and S. Somiya, Journal of Amer. Ceram. Soc., 42 (1959), pp. 603-613.

Al2O3-Cr2O3-Fe2O3, Weight percent 1500°C

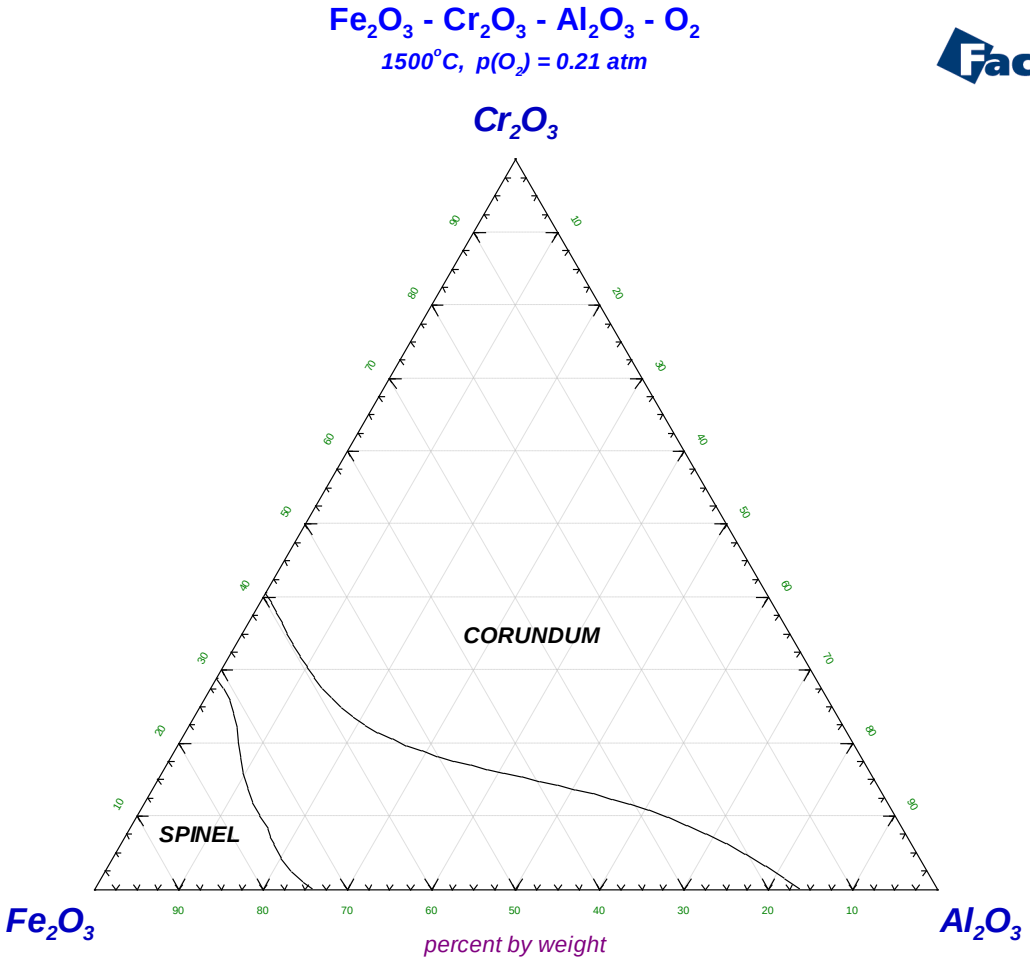

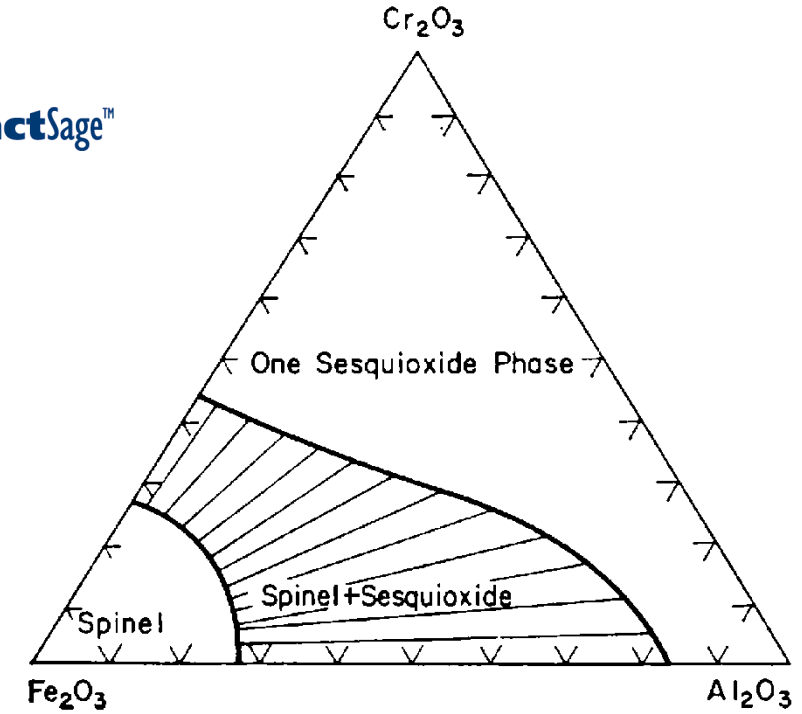

A. Muan and S. Somiya, Journal of Amer. Ceram. Soc., 42 (1959), pp. 603-613.

Al2O3-Cr2O3-MgO, Mole fraction 1700°C

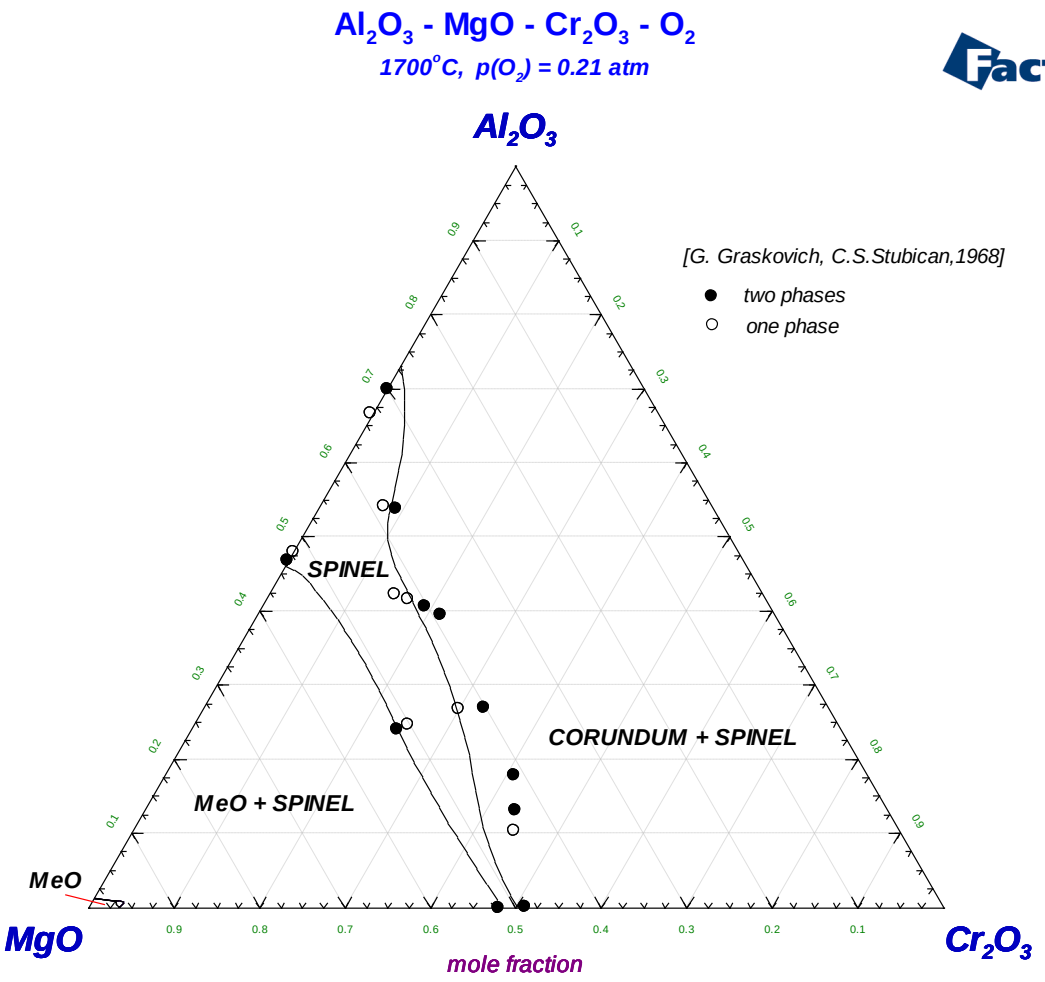

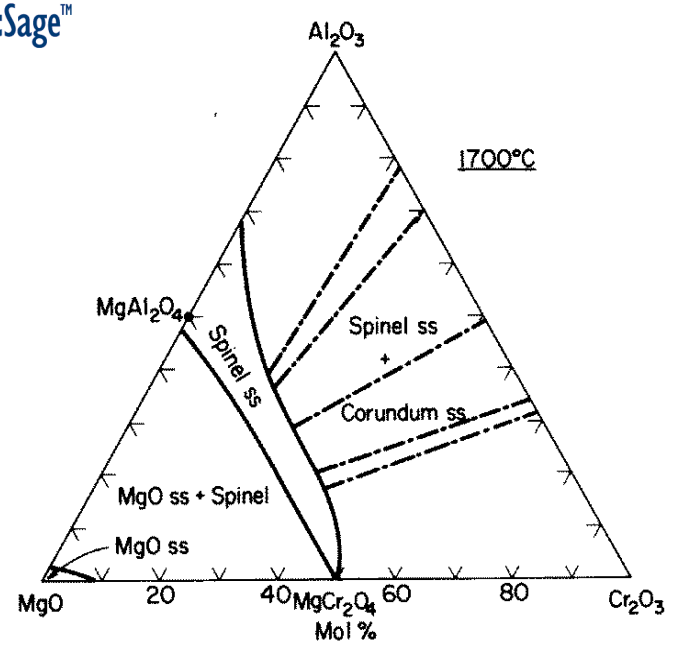

G. Greskovich, C.S. Stubican, J. Am. Ceram. Soc., 51 [1], (1968), pp.42-46.

Al2O3-Cr2O3-SiO2, Weight percent 1550°C

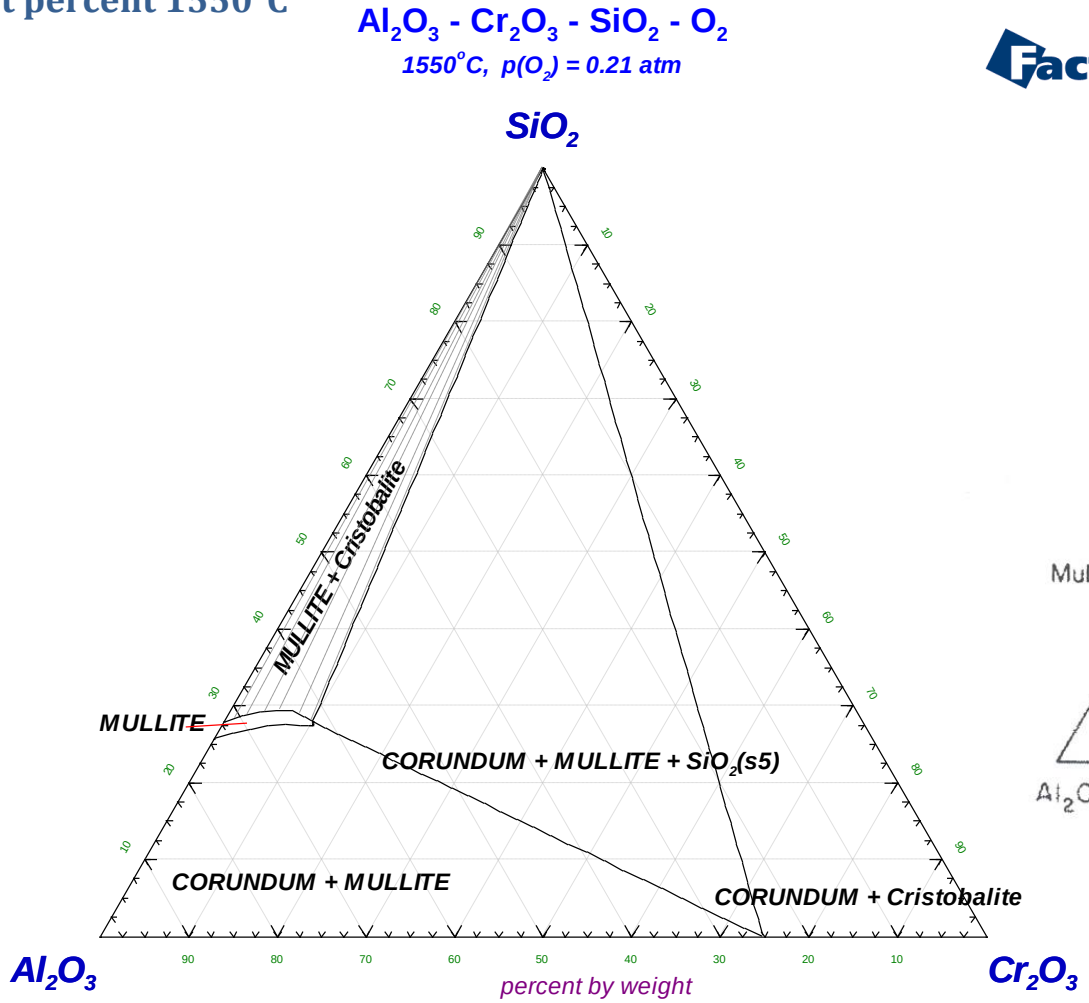

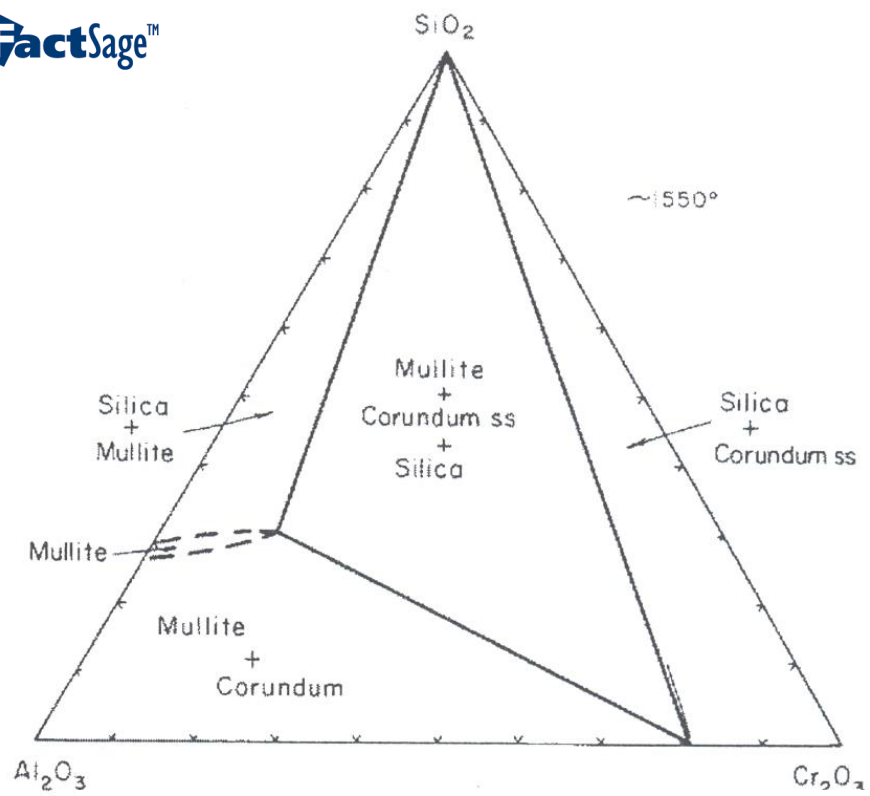

P. L. Roeder, F.P. Glasser, E.F. Osborn, Am. Ceram. Soc. Bull., 43 [4], (1964), p. 303-313.

Al2O3-Cr2O3-SiO2,

Weight percent 1700°C

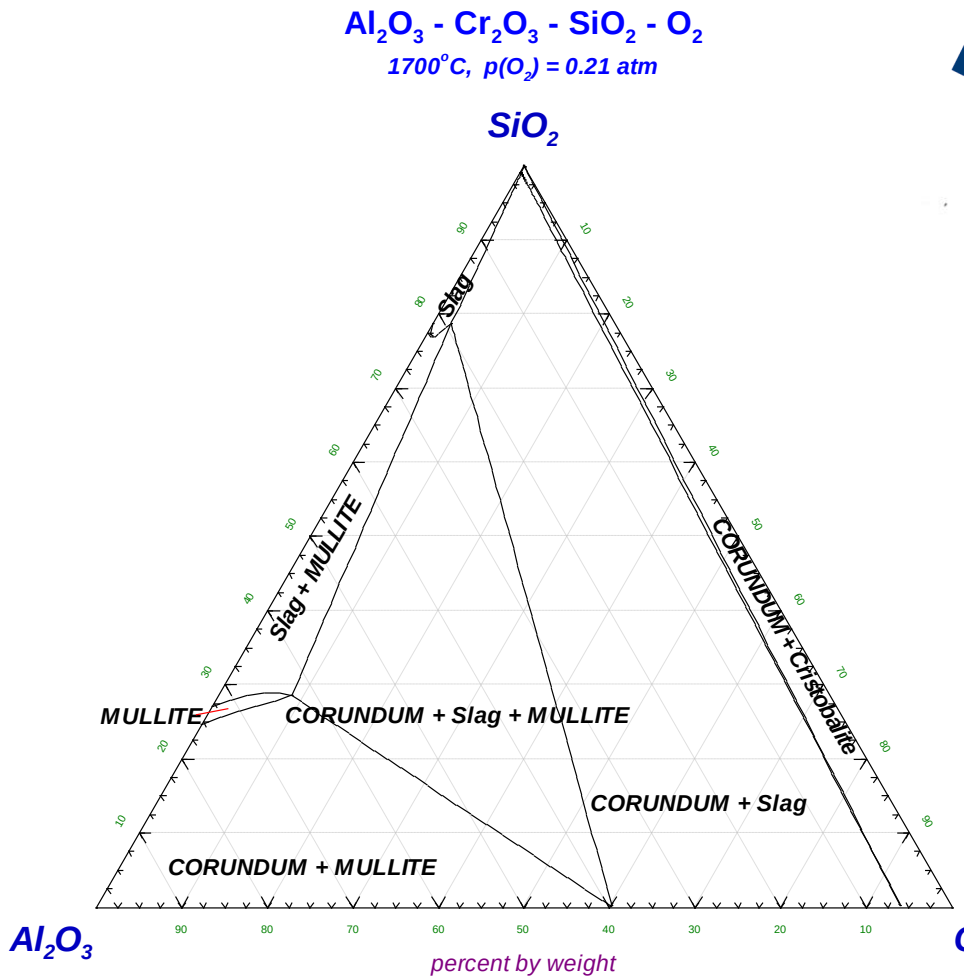

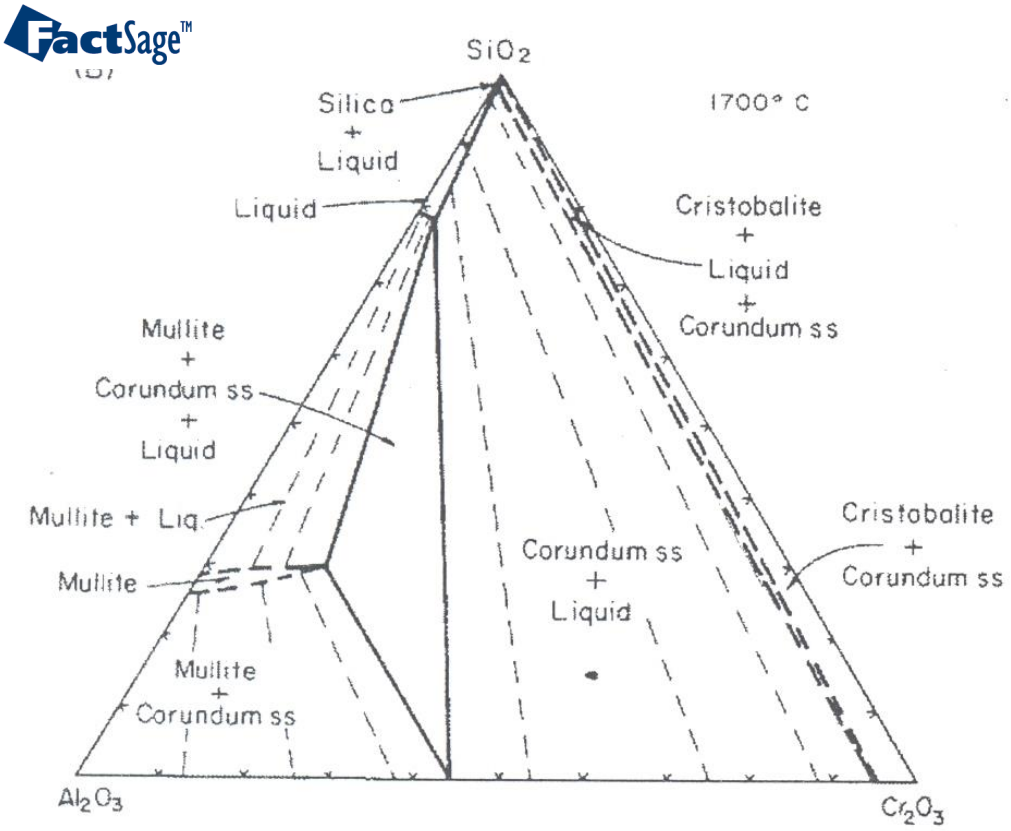

P. L. Roeder, F.P. Glasser, E.F. Osborn, Am. Ceram. Soc. Bull., 43 [4], (1964), p. 303-313.

Al2O3-Cr2O3-SiO2,

Weight percent 1800°C

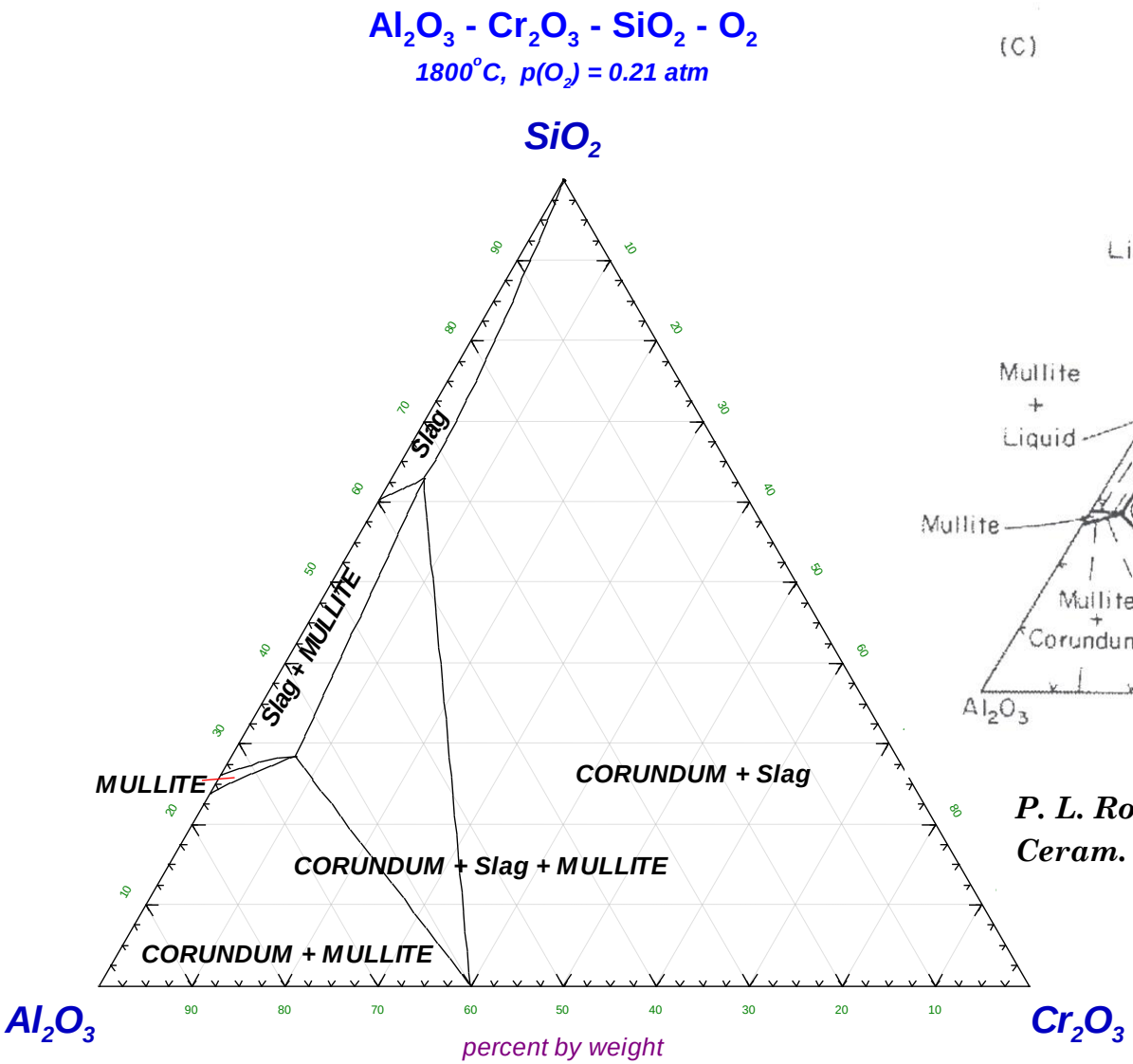

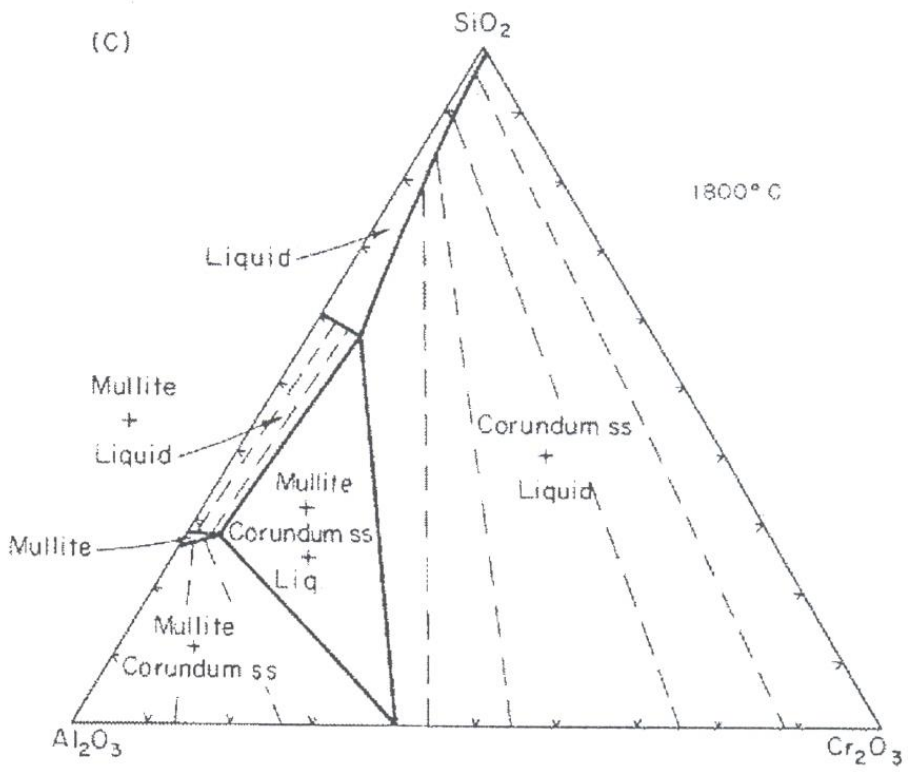

P. L. Roeder, F.P. Glasser, E.F. Osborn, Am. Ceram. Soc. Bull., 43 [4], (1964), pp. 303-313.

Mole fraction
Liquidussurface

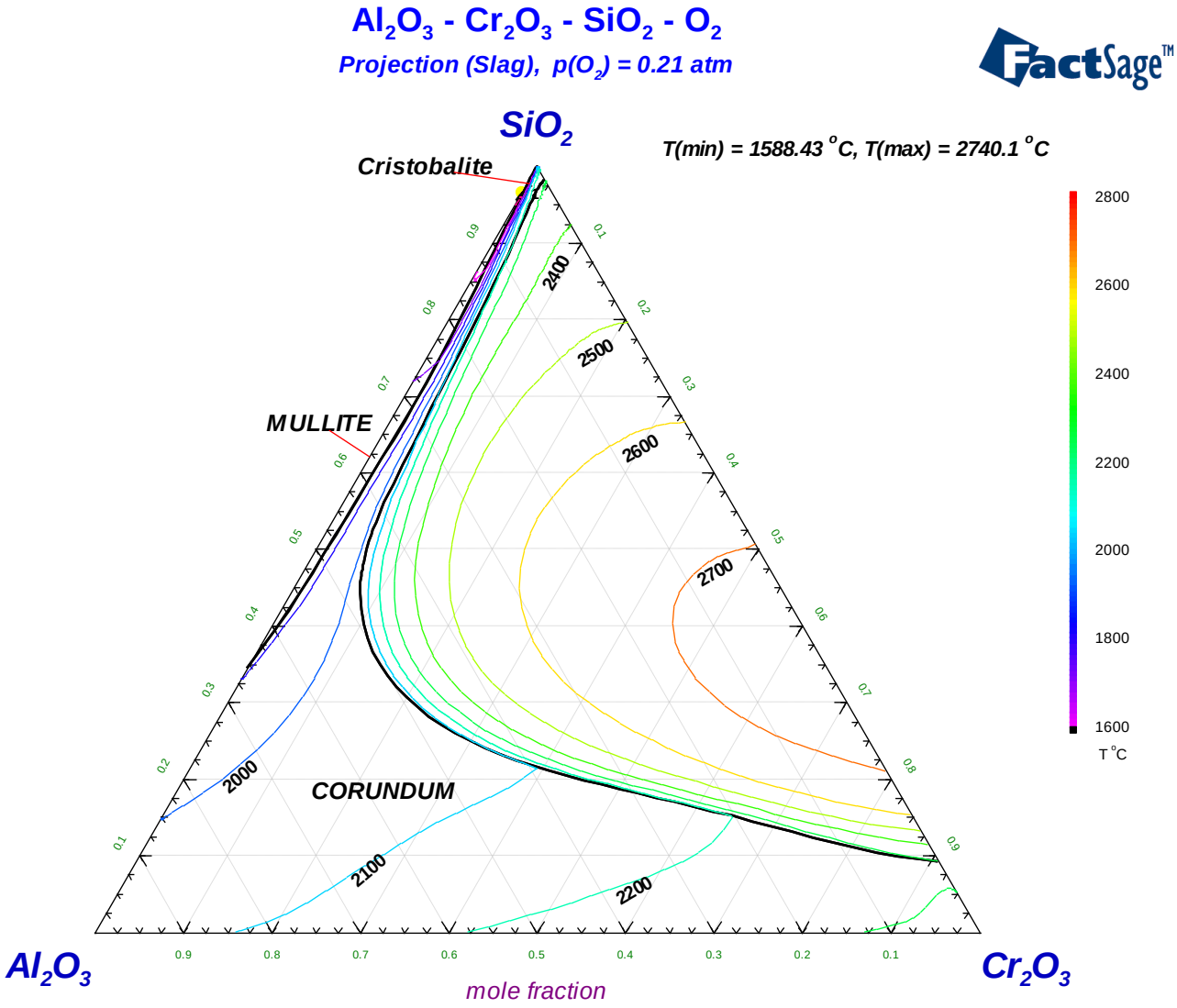

Weight percent
Liquidussurface compared with experimental data

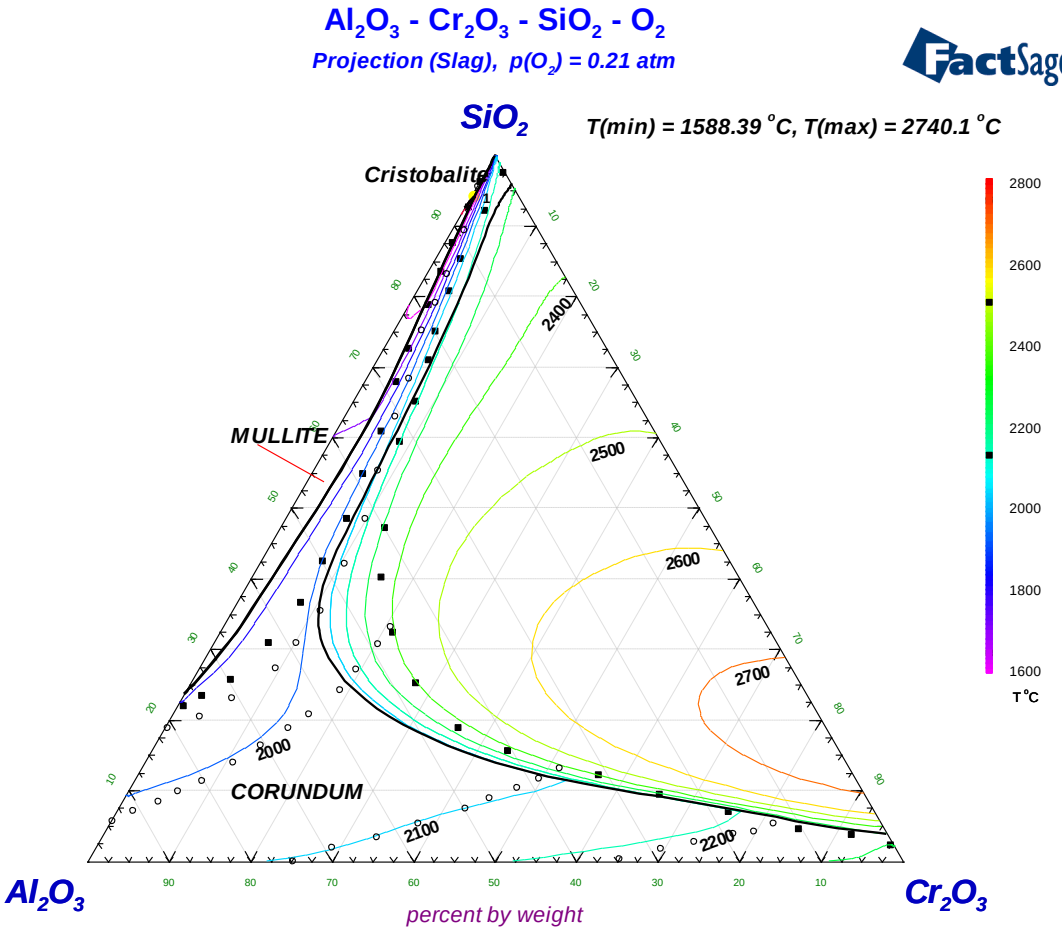

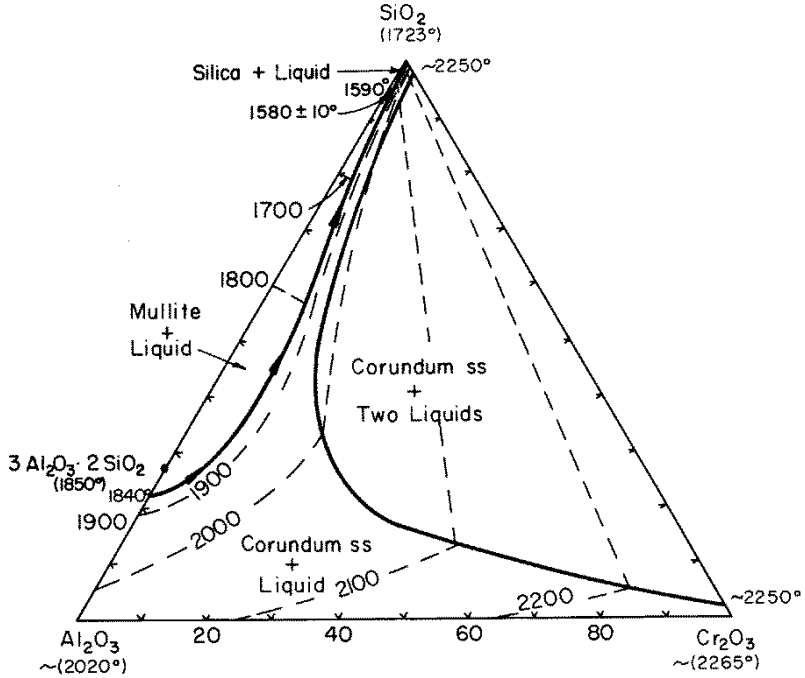

P. L. Roeder, F.P. Glasser, E.F. Osborn, J. Am. Ceram. Soc., 51 [10], (1968), pp. 585-594.

Isopleth FeKO2-AlKO2

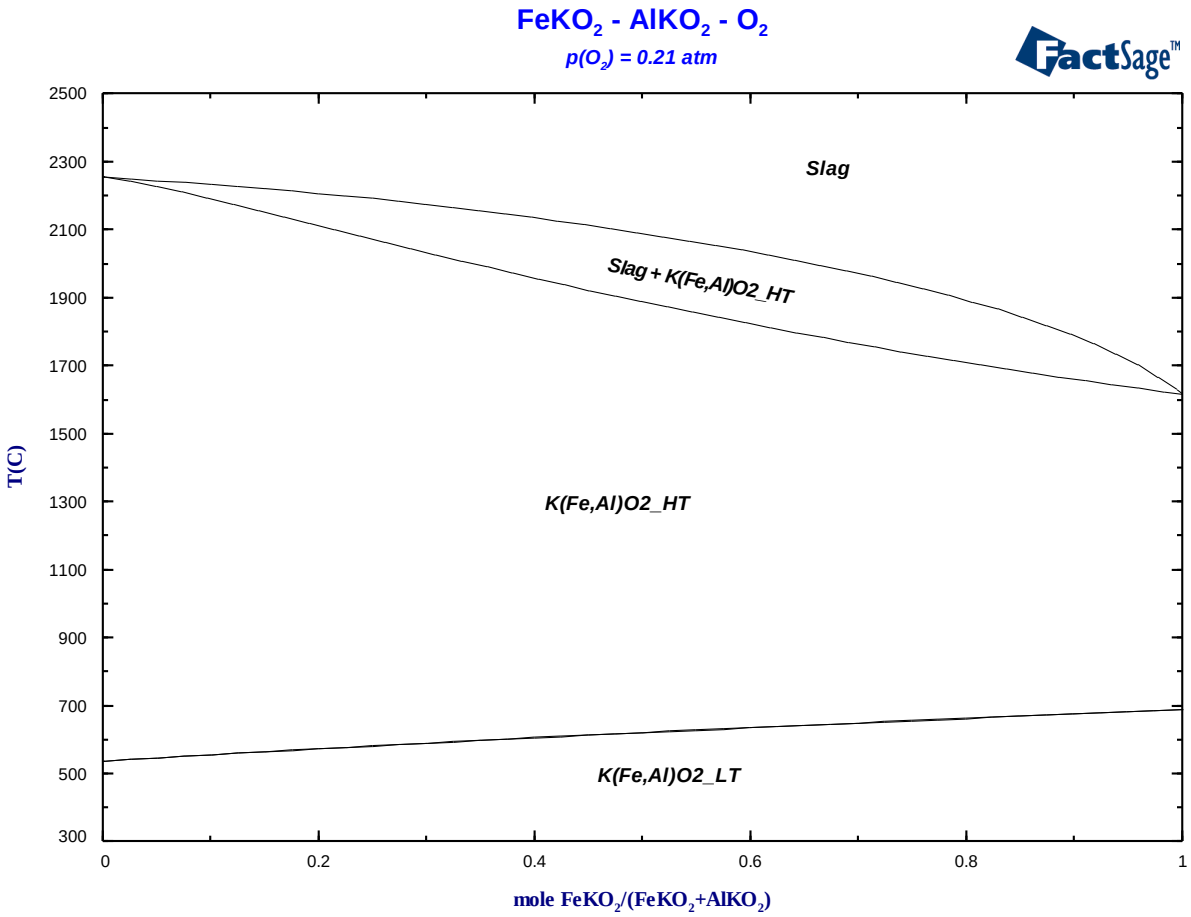

Al2O3-Fe2O3-MgO, Mole fraction 1250°C

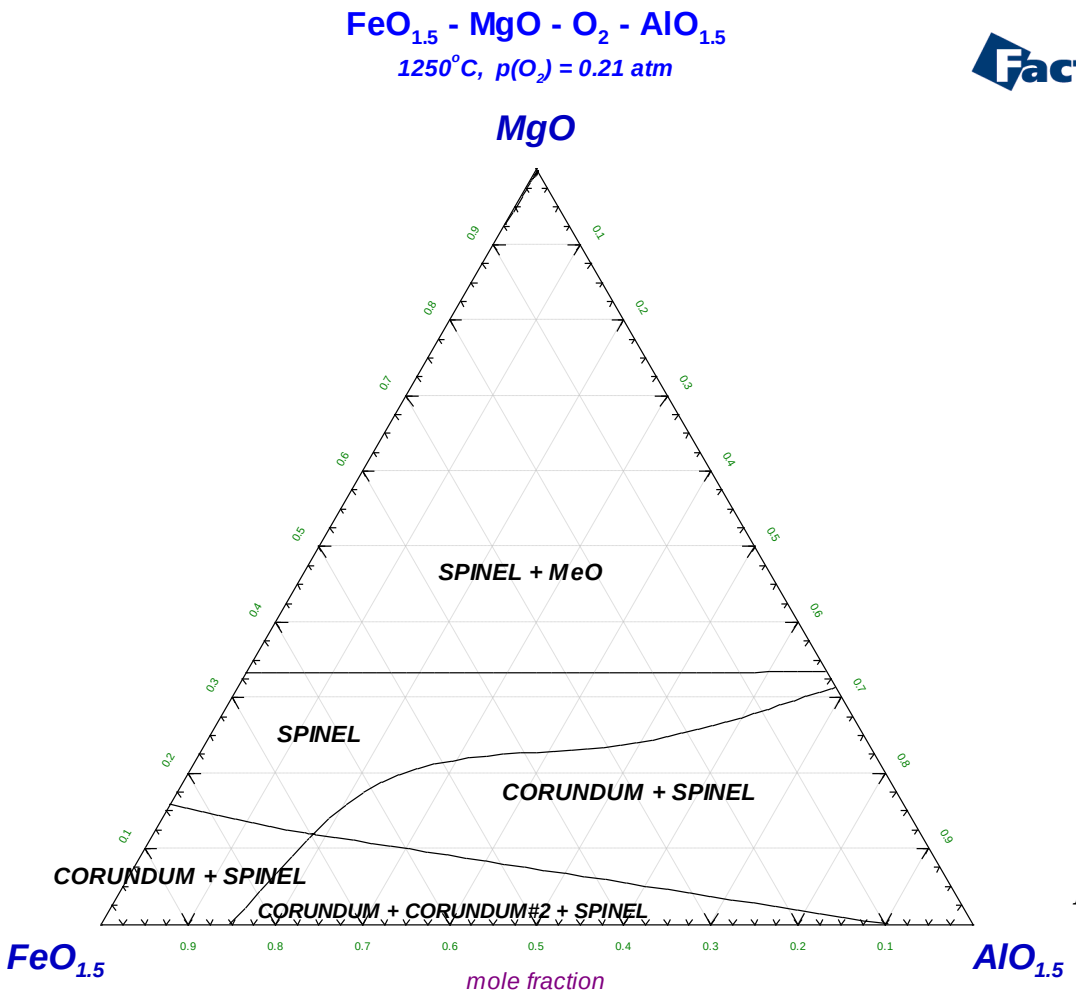

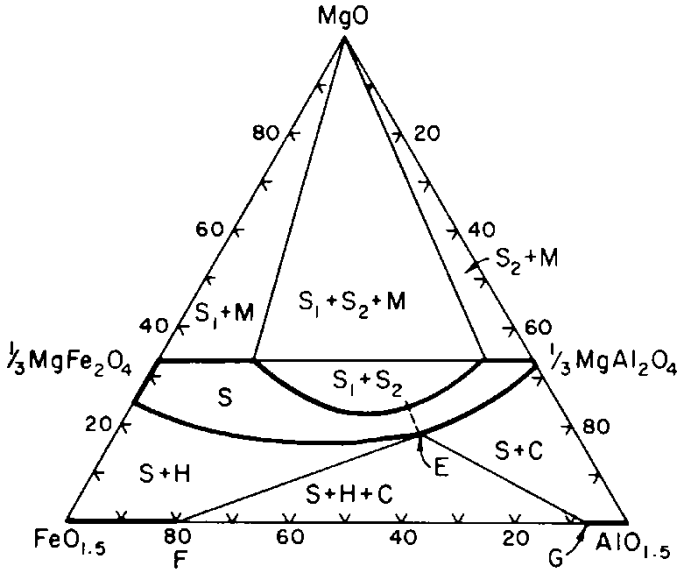

W. Kwestroo, J. Inorg. Nucl. Chem., 9 [1], (1959), pp.65-70.

Al2O3-Fe2O3-MgO, Weight percent 1600°C

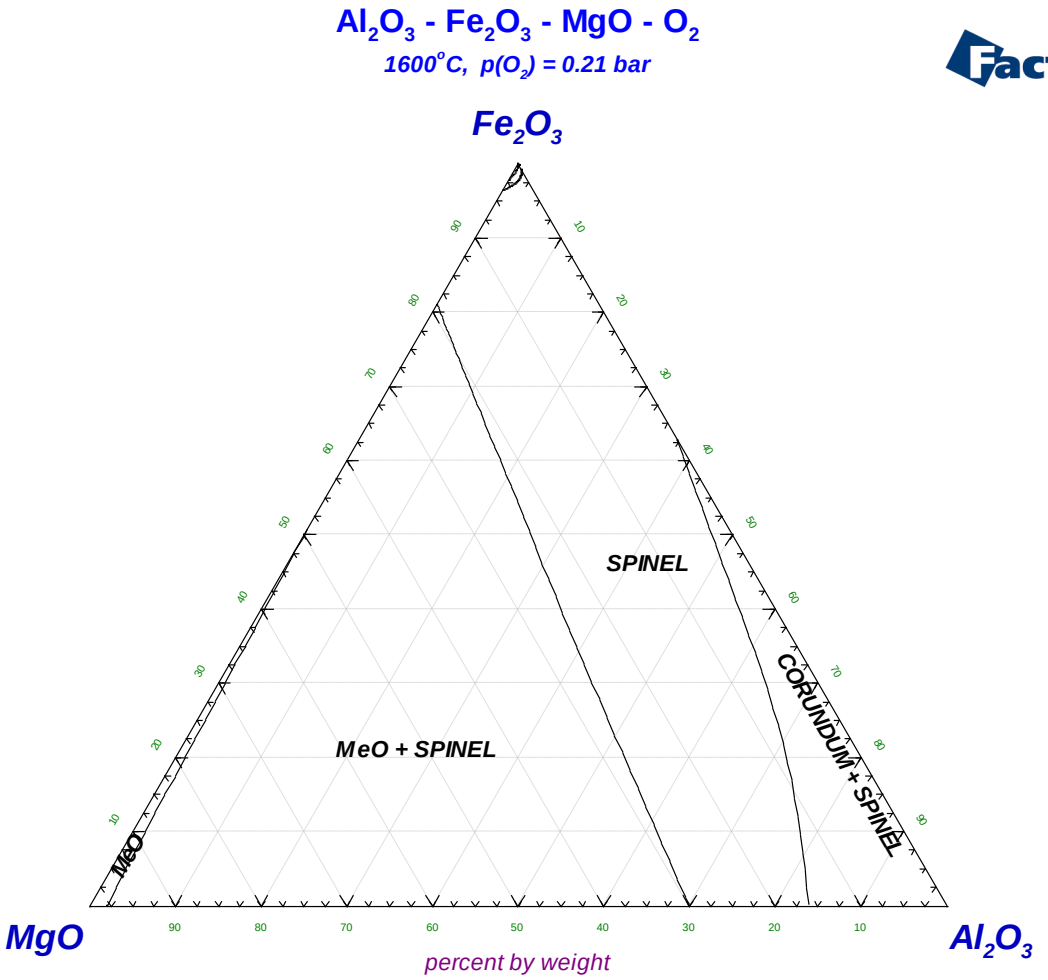

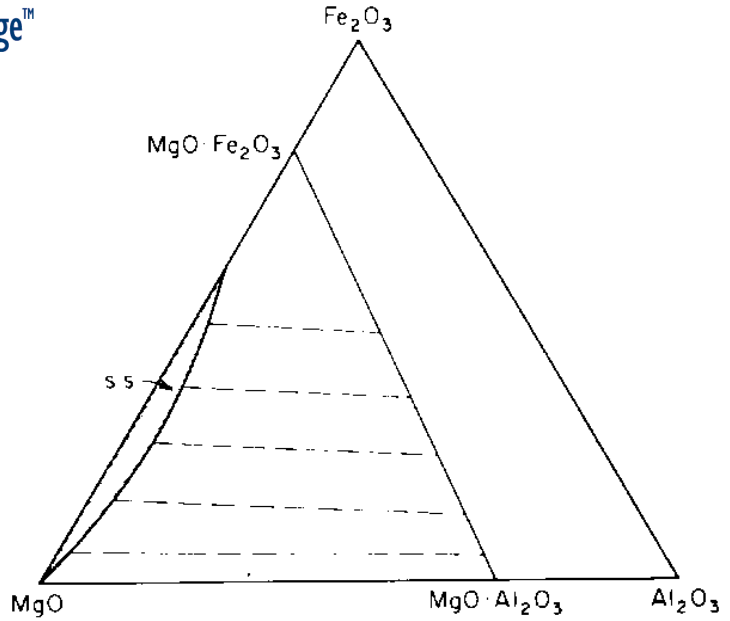

A. Cocco, Radex Randsch., N.6, (1958), pp.282-291.

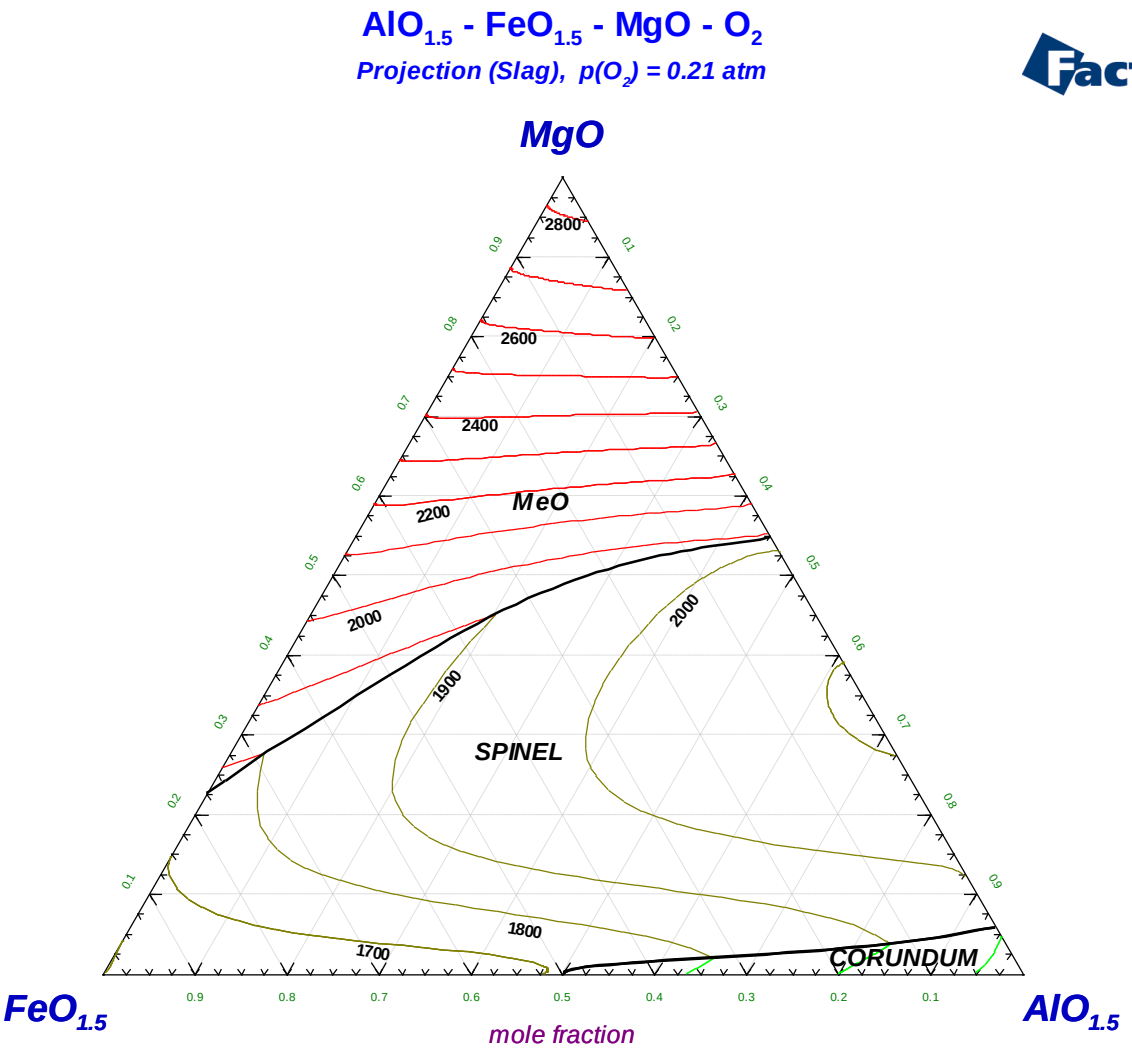
AlO1.5 - FeO1.5 - MgO - O2
Projection (Slag), p(O2) = 0.21 atm
FactSage™
MgO
2800
2600
2400
2200
2000
1900
1800
1700
MeO
SPINEL
CORUNDUM
FeO1.5
AlO1.5
mole fraction

Mole fraction, 700°C

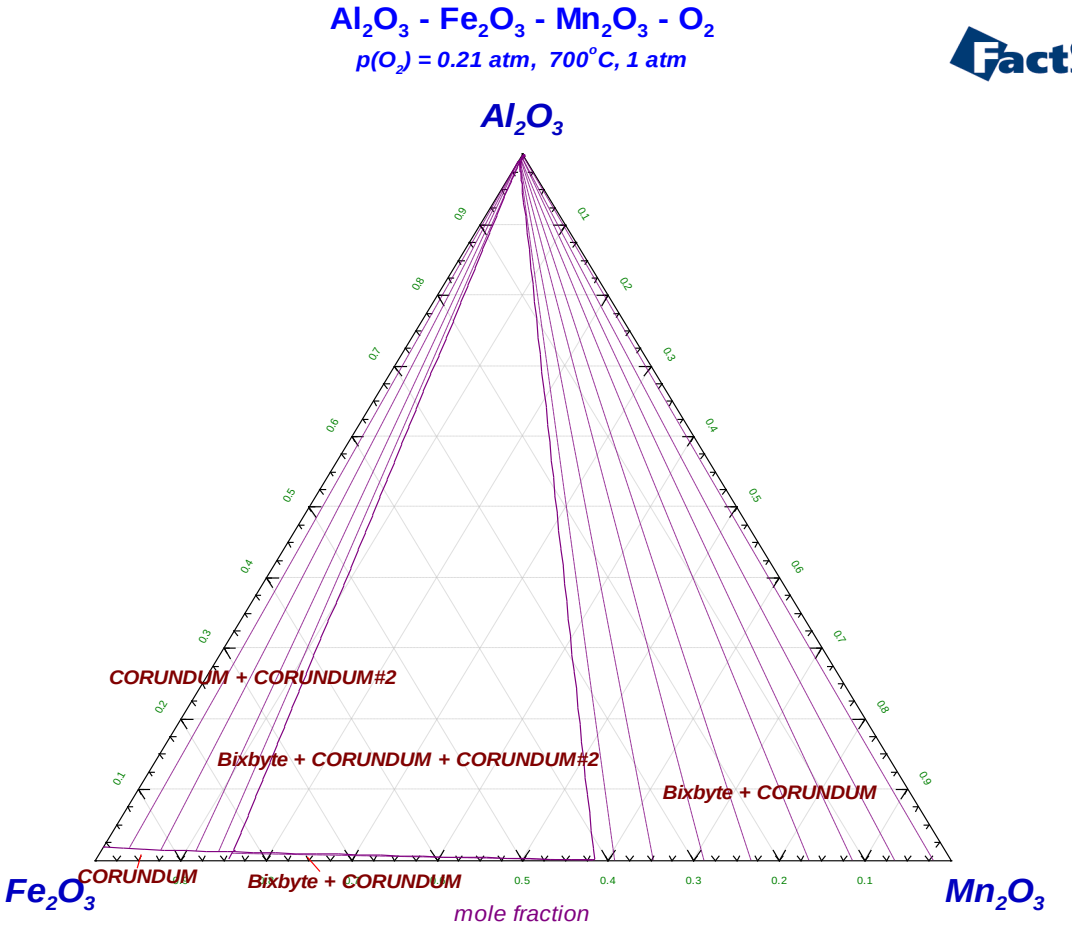

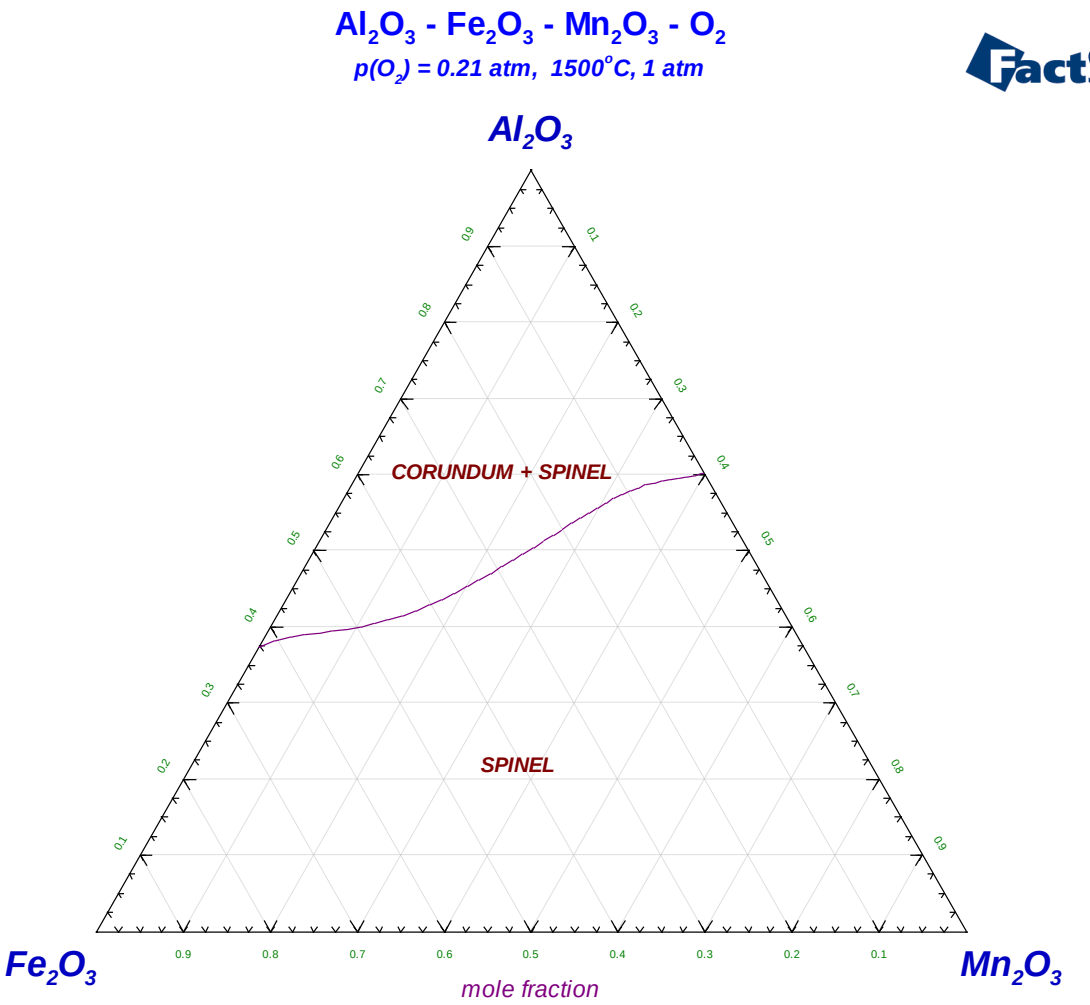
Al2O3 - Fe2O3 - Mn2O3 - O2
p(O2) = 0.21 atm, 1500°C, 1 atm
FactSage™
Al2O3
CORUNDUM + SPINEL
SPINEL
Fe2O3
Mn2O3
mole fraction

Mole fraction, Isopleth Al2FeO4-Al2MnO4

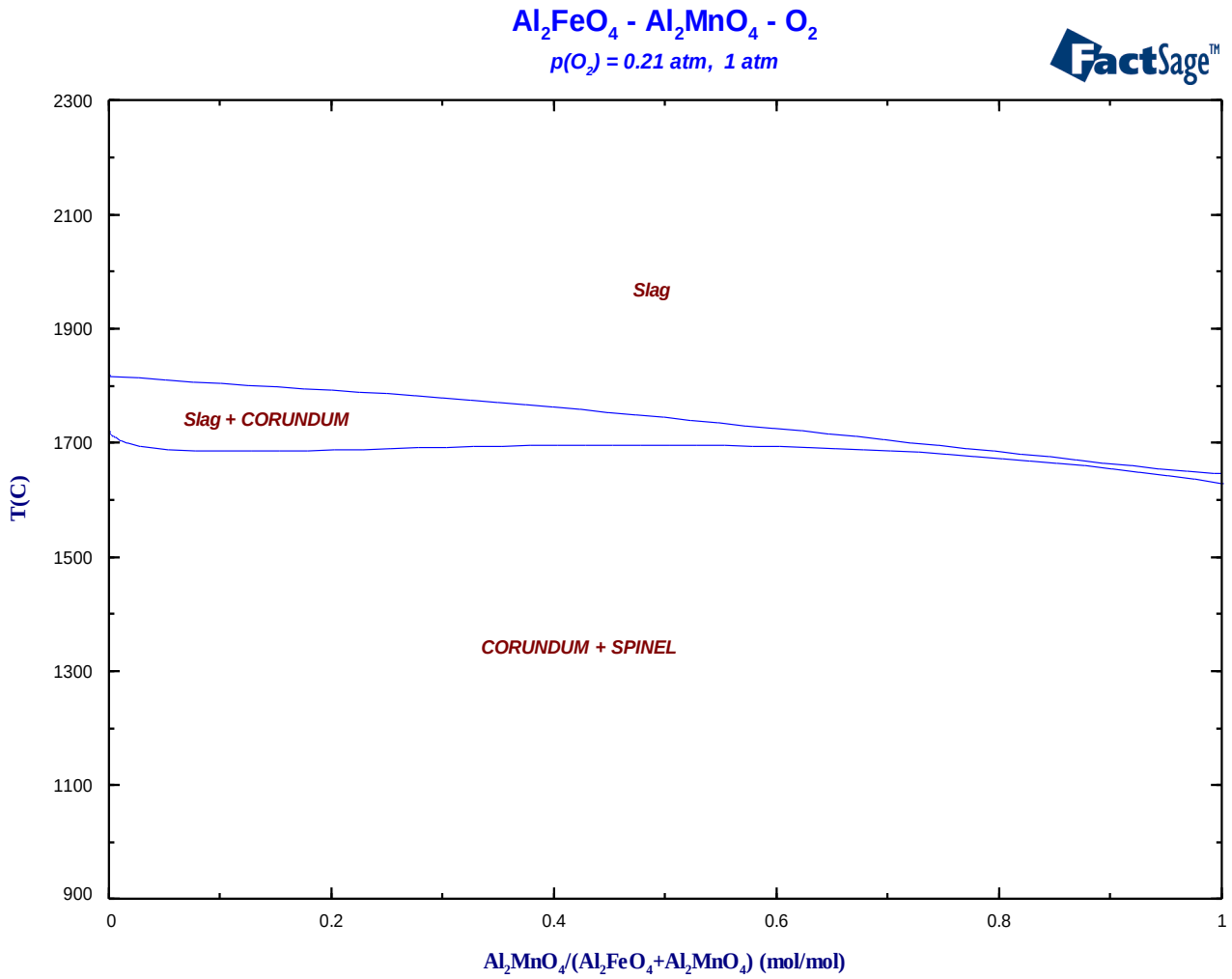

Isopleth FeNaO2-AlNaO2 compared with experimental data

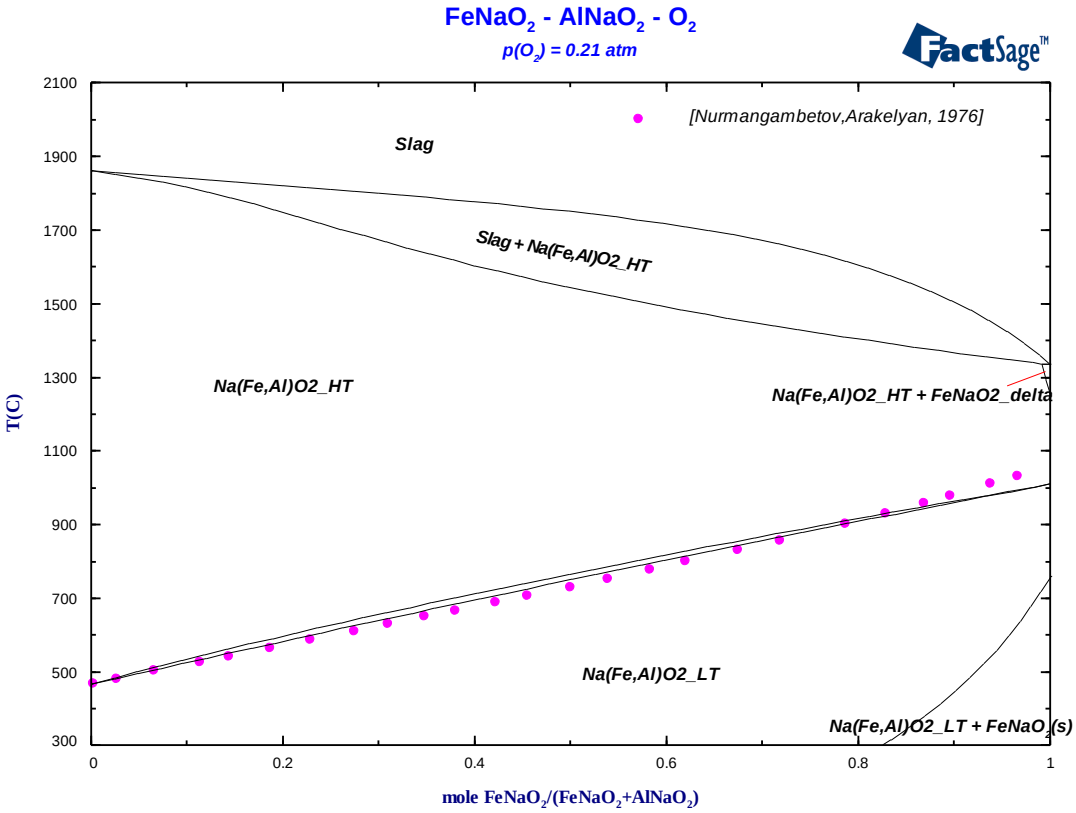

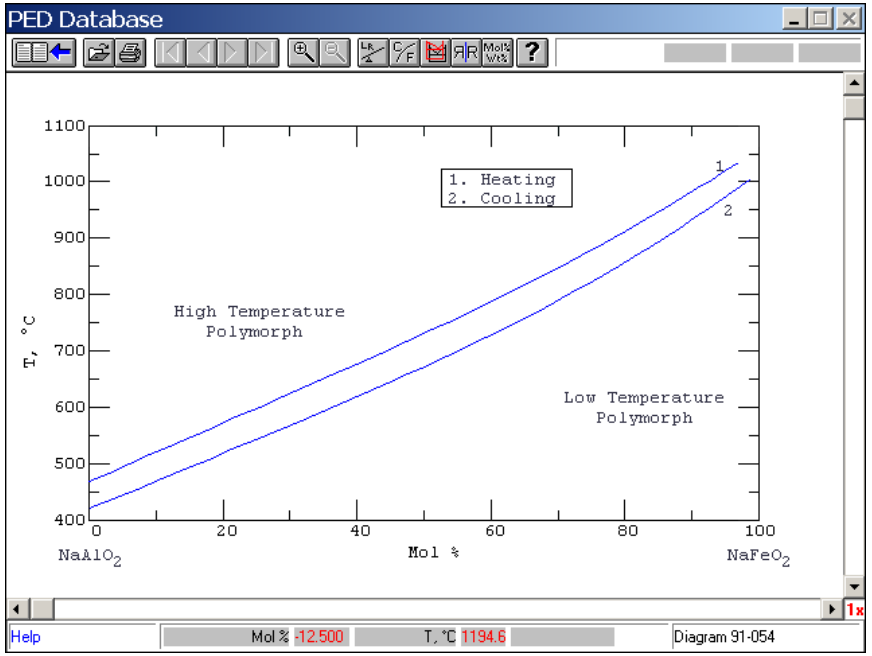

Kh.N. Nurmangambetov, O.I.Arakelyan, S.A.Shcherban, Z.S.Karpenko, M.V.Tsvetkova, Izv. Vyssh.Uchebn,Zaved., Tsvetn. Metall., No.3, (1976), pp.61-65.

Al2O3-Fe2O3-SiO2,
Weight percent 1000°C

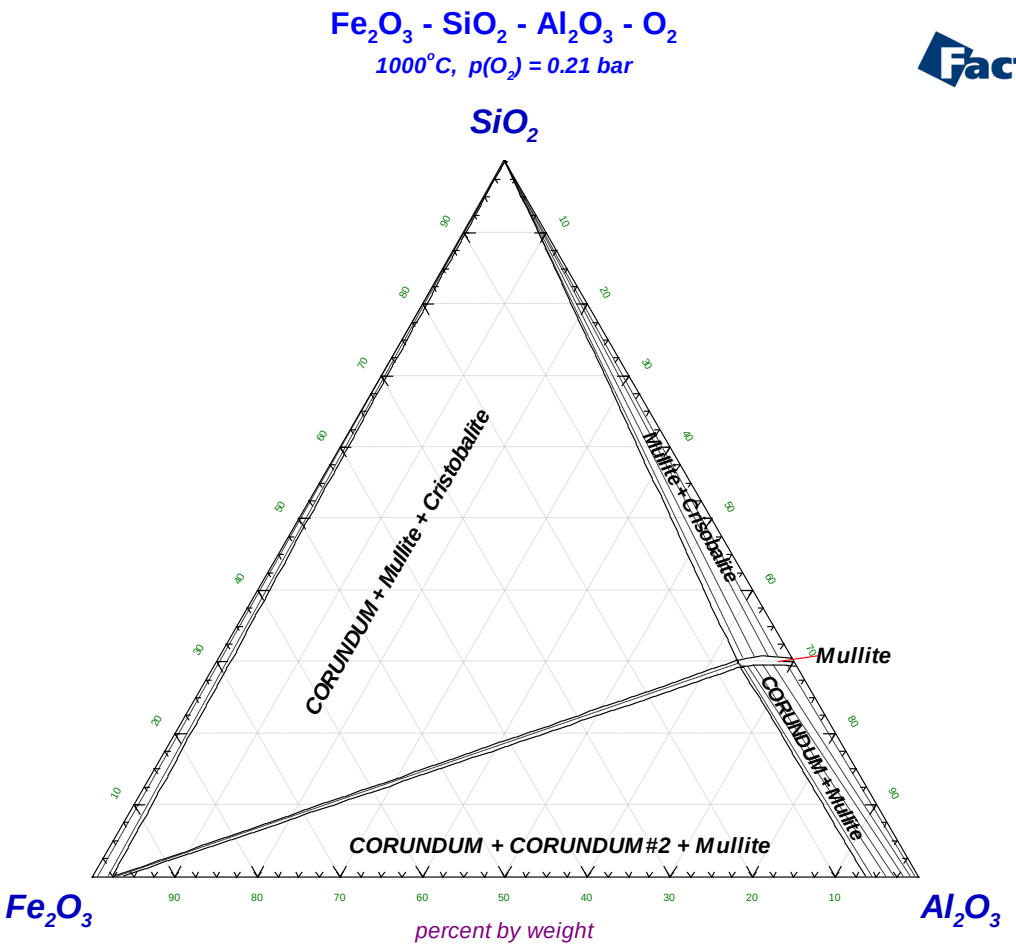

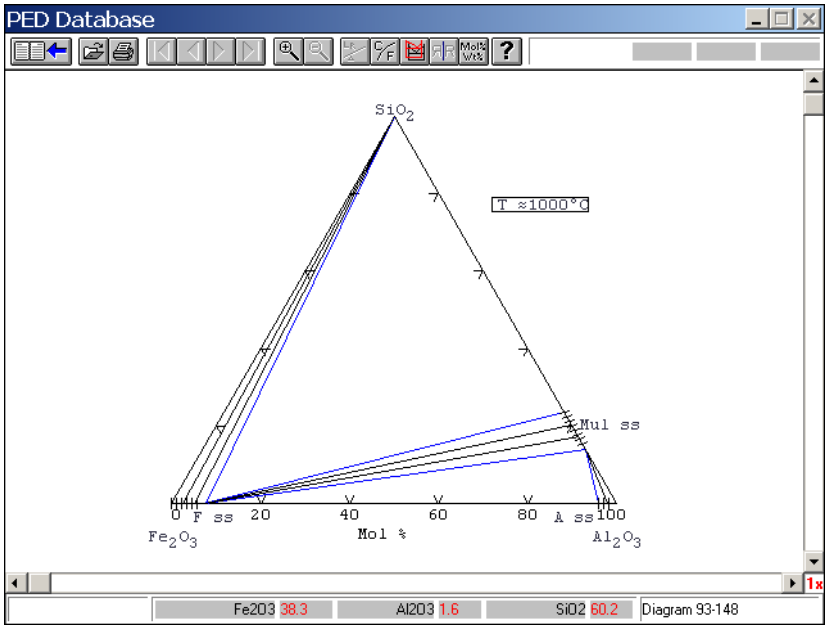

A.A. Fotiev, L.L. Surat, V.G. Dobosh, V.G. Mizin, Zh. Neorg. Khim., 29 [5], (1984), pp.1277-1279.

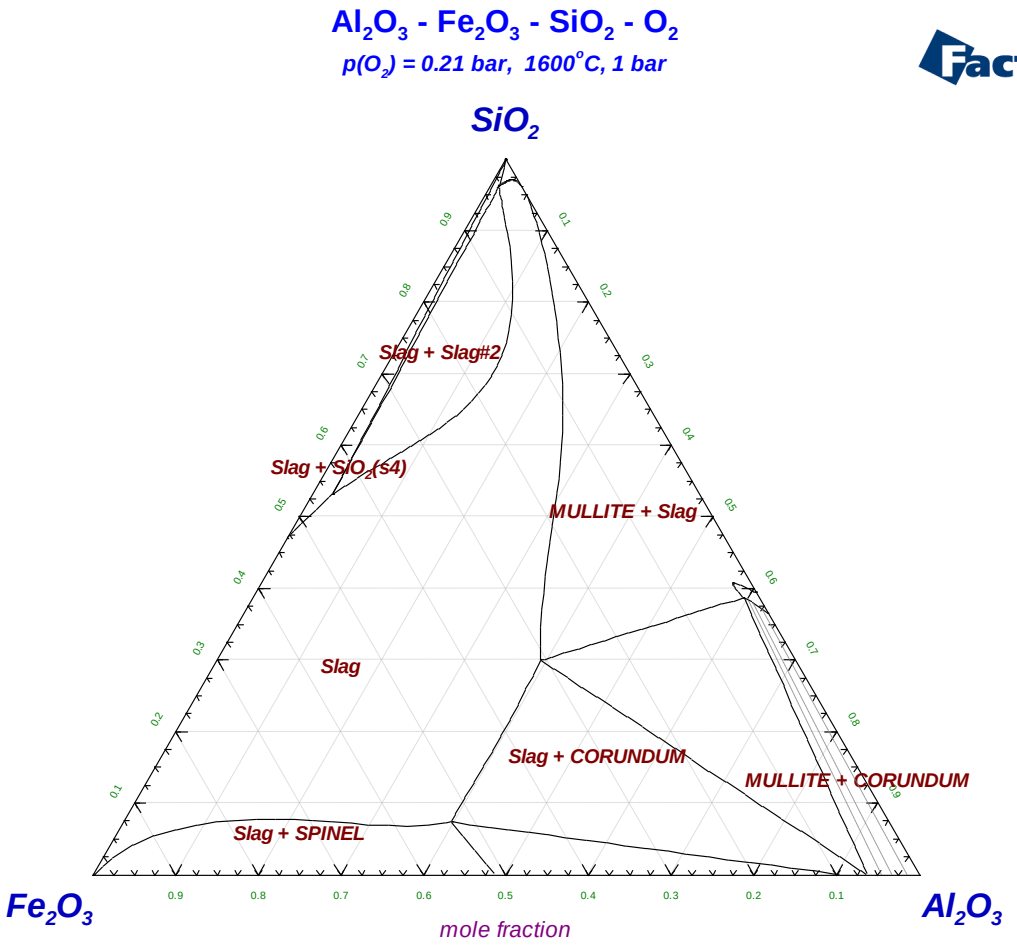
Al2O3 - Fe2O3 - SiO2 - O2
p(O2) = 0.21 bar, 1600°C, 1 bar
FactSage™
SiO2
Slag + Slag#2
Slag + SiO2(S4)
MULLITE + Slag
Slag
Slag + CORUNDUM
MULLITE + CORUNDUM
Slag + SPINEL
Fe2O3
Al2O3
mole fraction

Weight percent
Solidusfläche

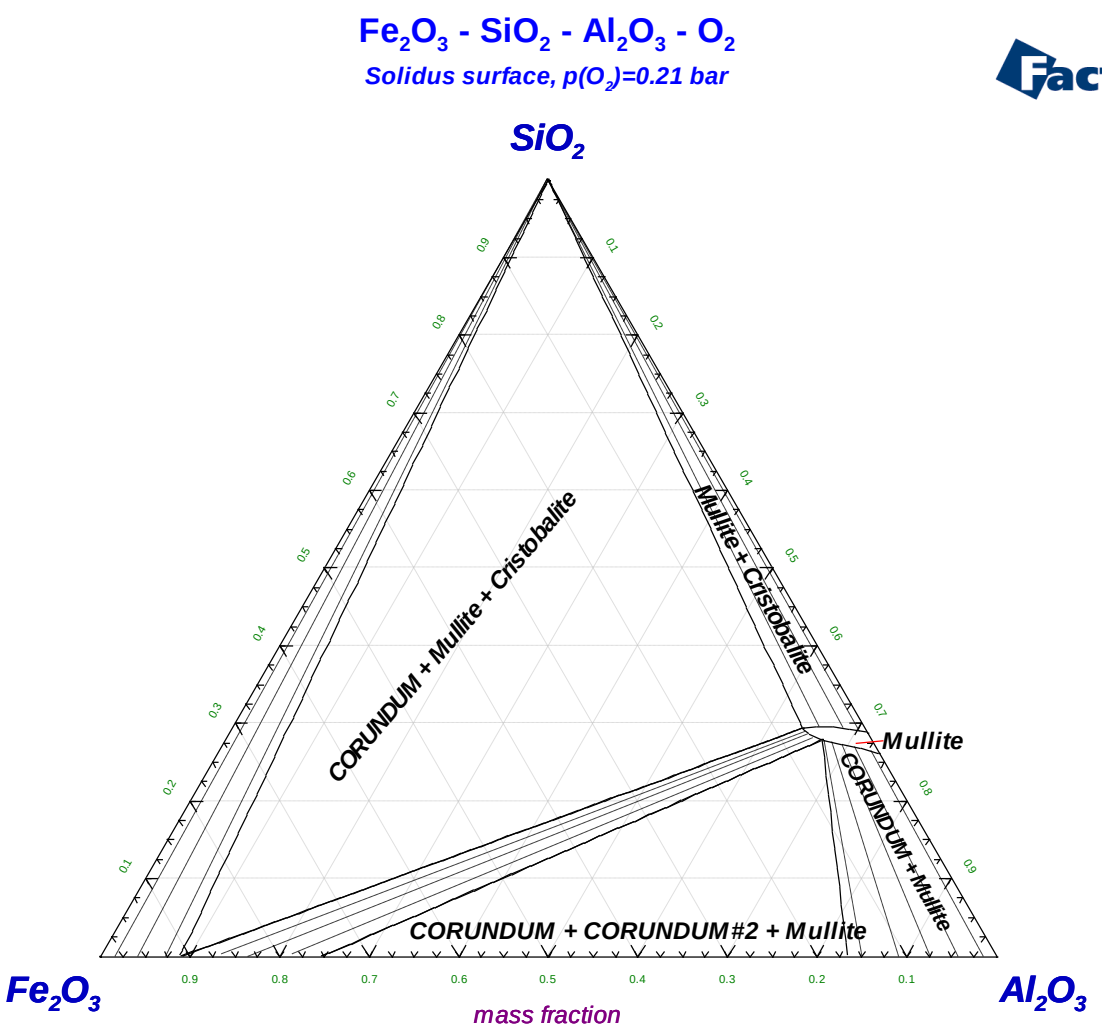

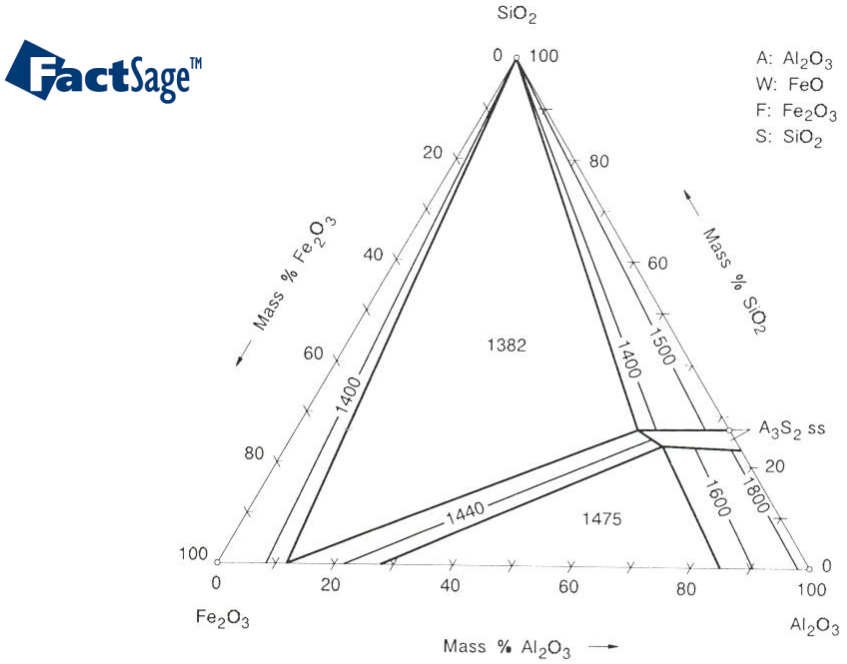

Fig. 3.185. Solidus surface in the system Al_2O_3-FeO_x-SiO_2 in air after Muan [4], as revised by Idink, Woermann [5].

Slag Atlas, 2nd Ed., Verlag Stahl-Eisen, Düsseldorf, 1995.

Al_2O_3 - Fe_2O_3 - SiO_2 - O_2

Projection (Slag), p(O_2) = 0.21 atm, 1 atm

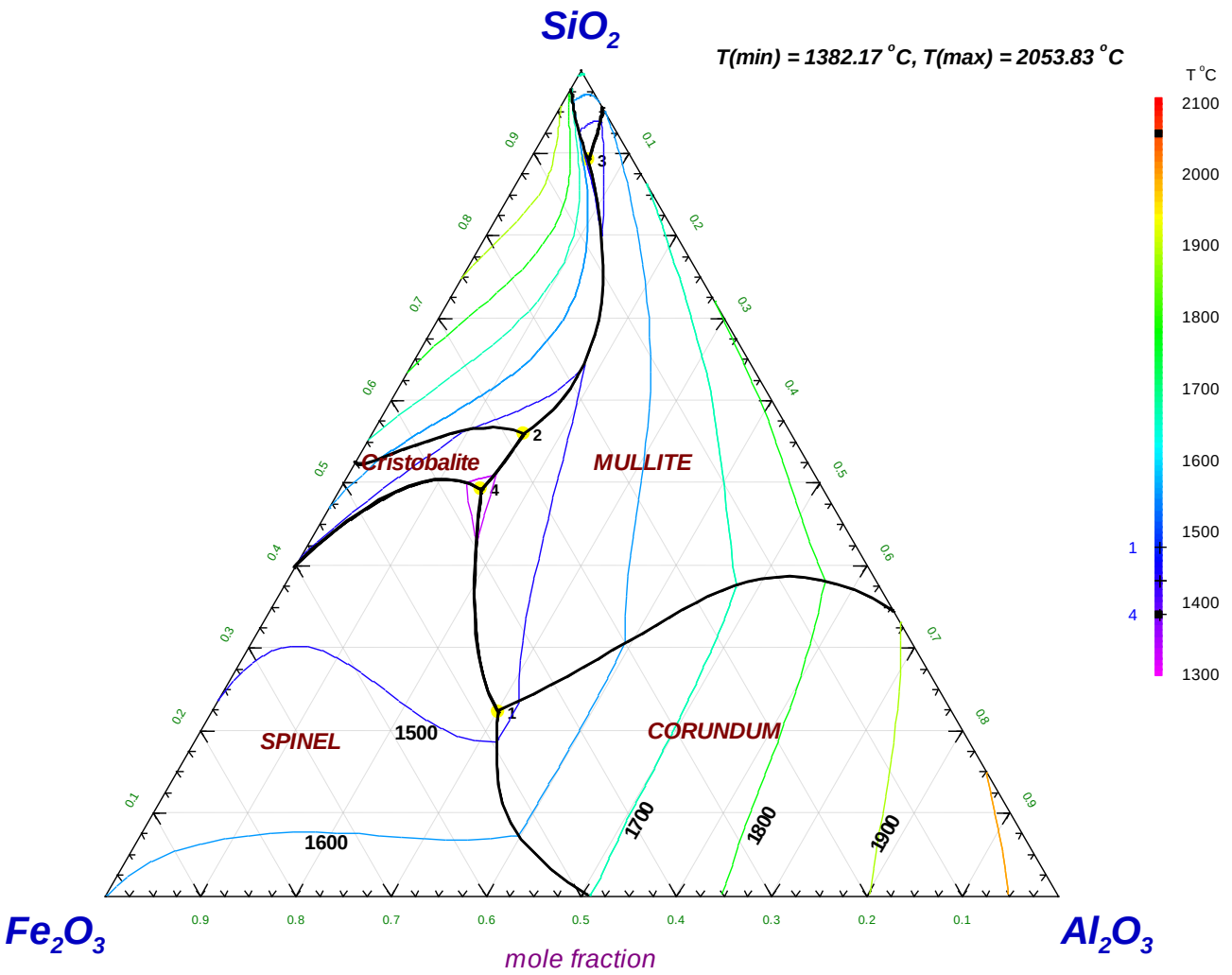

Weight percent
Liquidussurface

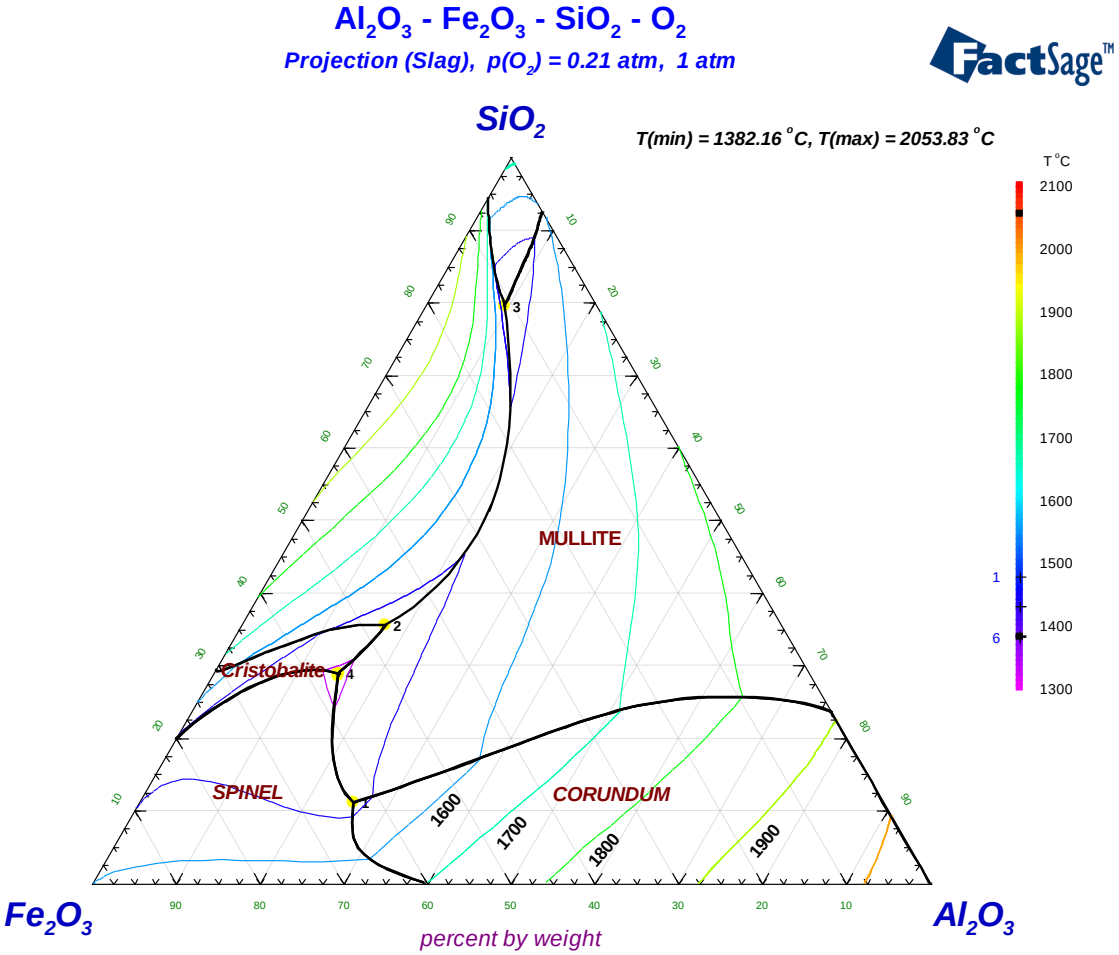

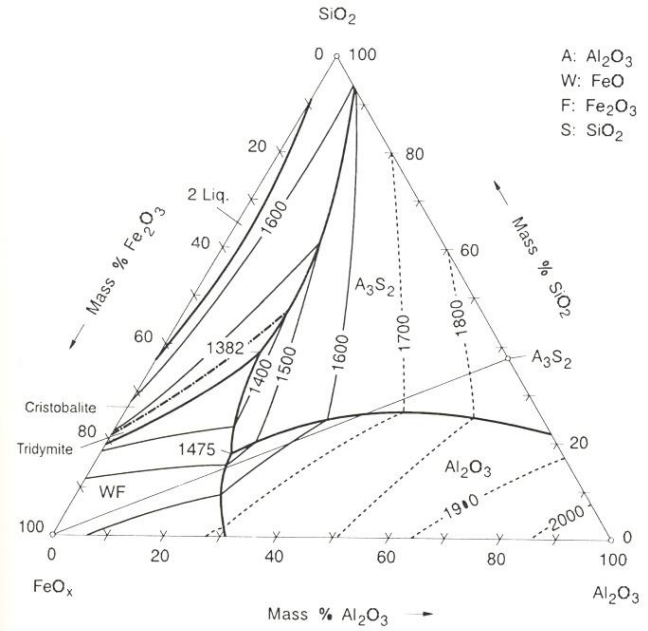

Fig. 3.184. Liquidus surface in the system Al_2O_3-FeO_x-SiO_2 in air after Muan [4], as revised by Idink, Woermann [5].

Slag Atlas, 2nd Ed., Verlag Stahl-Eisen, Düsseldorf, 1995.

Invariant equilibria on the liquidus surface

Intersections with slag	Mole fraction A = SiO2, B = Fe2O3, C = Al2O3				Weight percent A = SiO2, B = Fe2O3, C = Al2O3				
		X(A)	X(B)	X(C)	T(C)		W(A)	W(B)	W(C)	T(C)
1: CORUNDUM / MULLITE / SPINEL	1:	0.22299	0.47567	0.30135	1477.07	1.	11.157	63.255	25.587	1477.07
2: MULLITE / Cristobalite / Slag#2	2:	0.55976	0.28040	0.15985	1430.14	2.	35.512	47.279	17.209	1430.09
3: MULLITE / Cristobalite / Slag#2	3:	0.89153	0.04602	0.06245	1430.08	3.	79.614	10.922	9.464	1430.09
4: CORUNDUM / SPINEL / Cristobalite	4:	0.49217	0.35950	0.14833	1382.83	4.	28.963	56.225	14.812	1382.83

Al2O3-Fe2O3-TiO2, Weight percent 1000°C

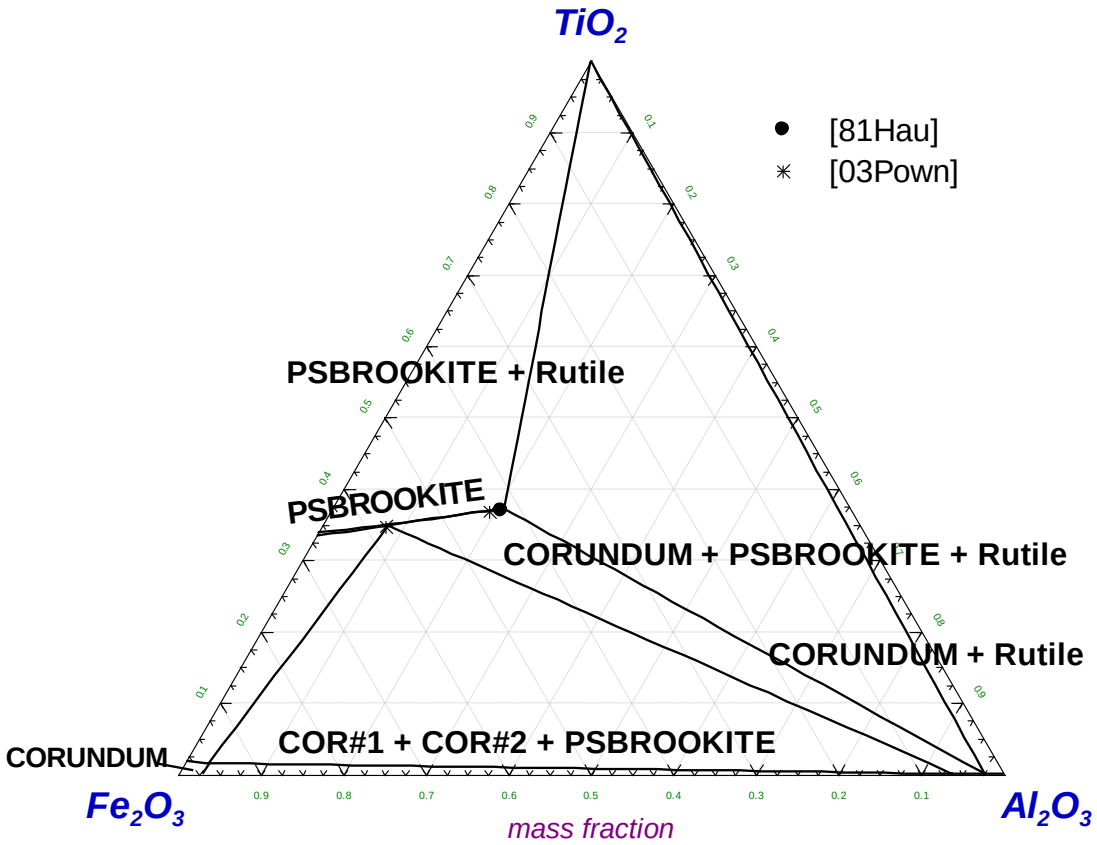

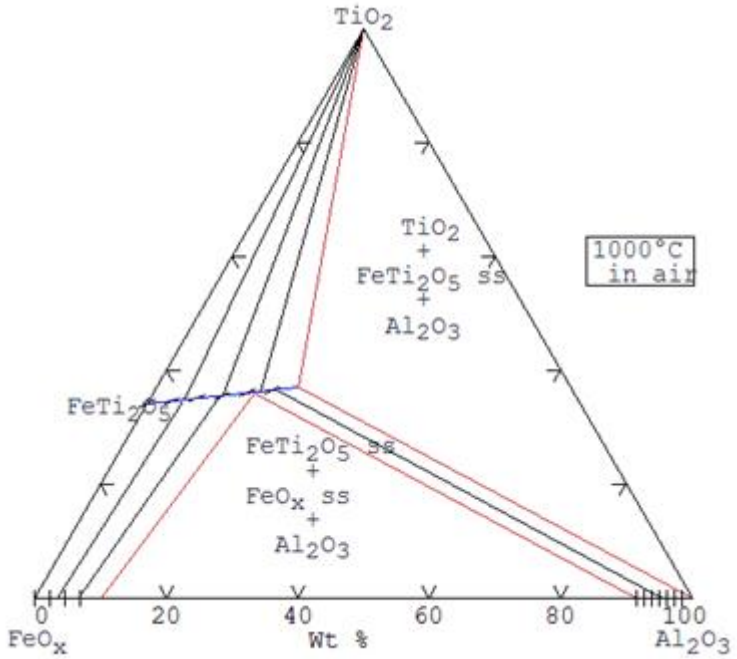

J. Hauck, J. Solid State Chem., 36 [1], (1981), pp. 52-65.

Al2O3-Fe2O3-TiO2, Weight percent 1300°C

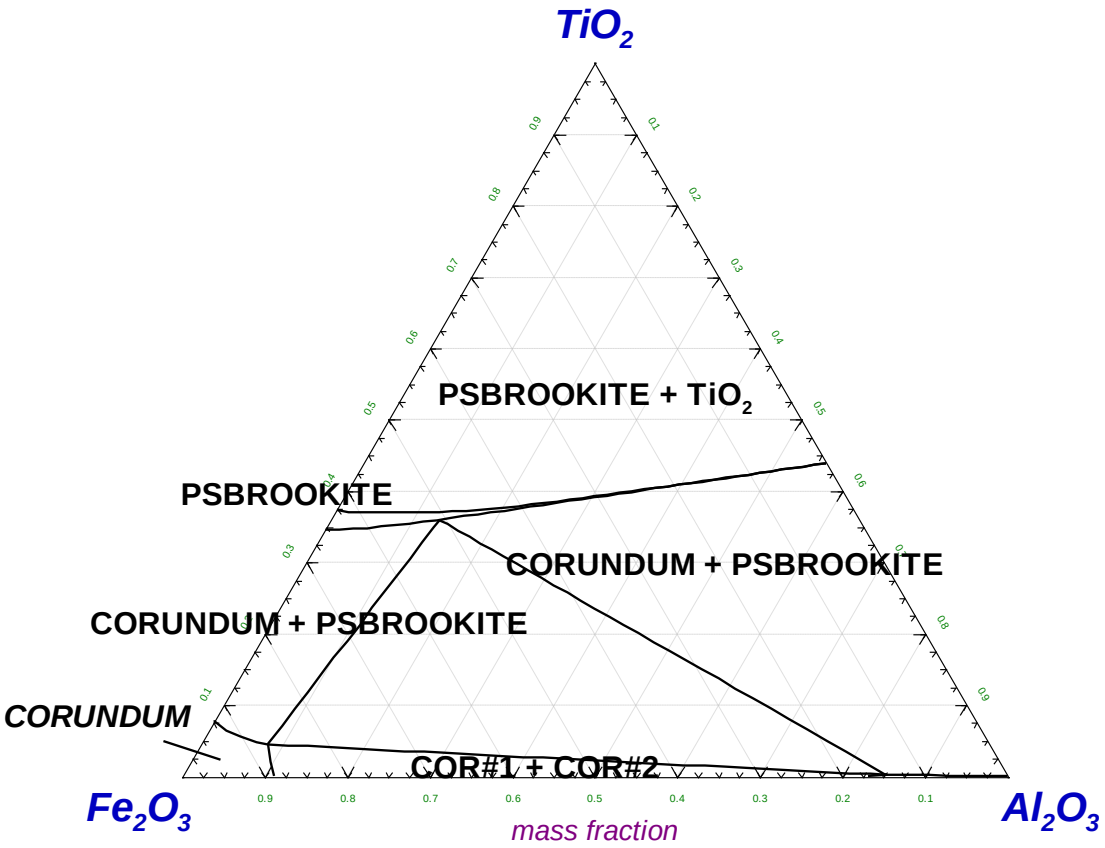

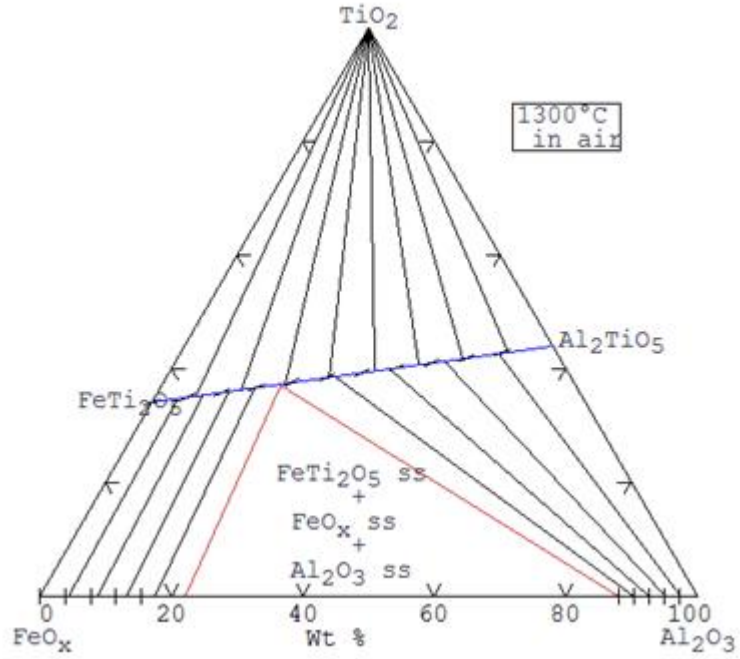

J. Hauck, J. Solid State Chem., 36 [1], (1981), pp. 52-65.

Weight percent, Liquid lines at 1550, 1600 and 1650°C

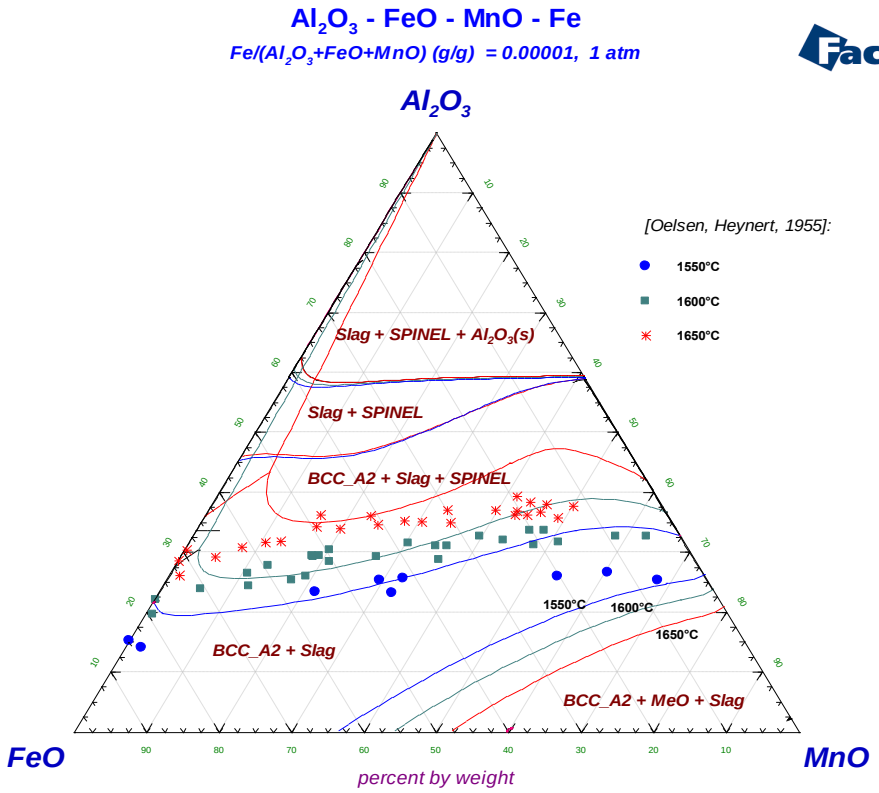

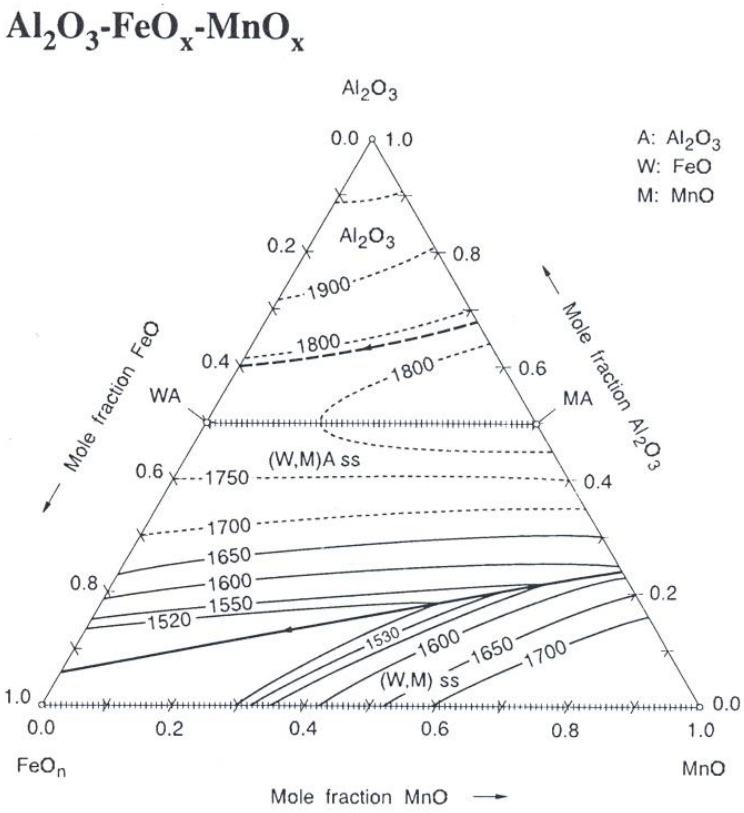

Slag Atlas, 2nd edition, Verlag Stahleisen GmbH, 1995, p. 116.

Al2O3-FeO-SiO2,
Weight percent 1000°C

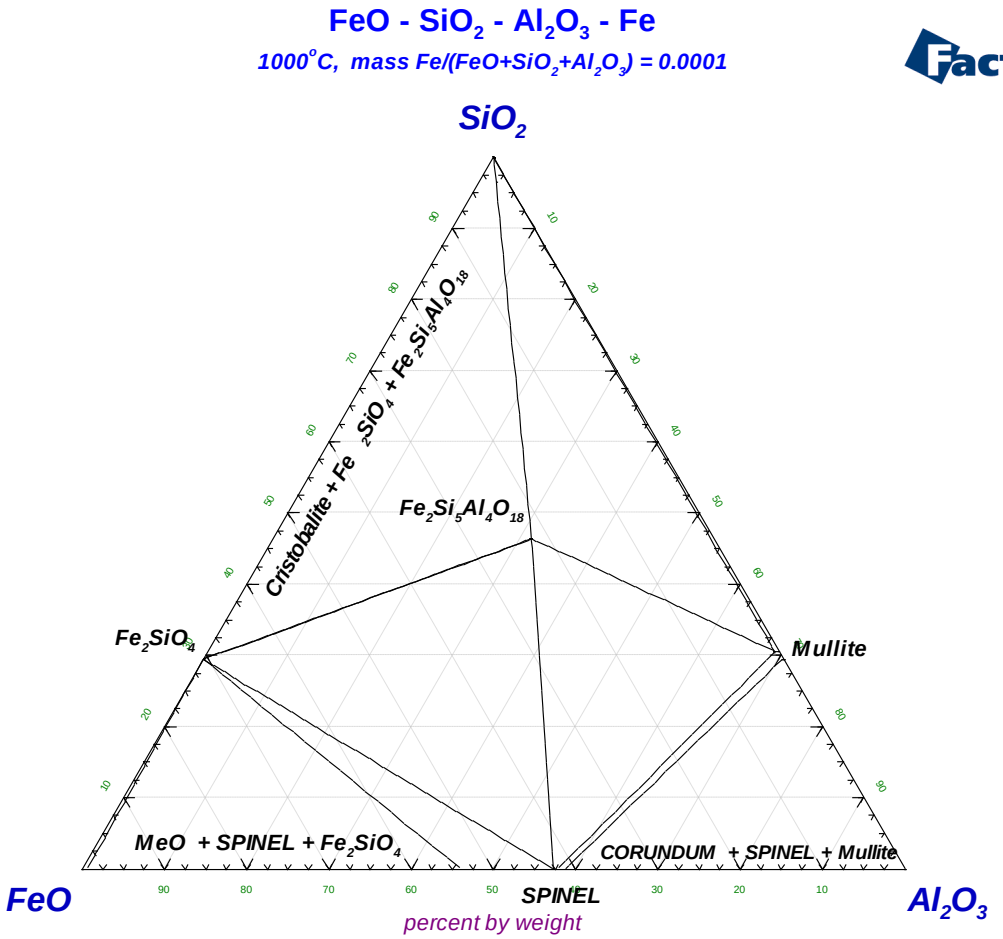

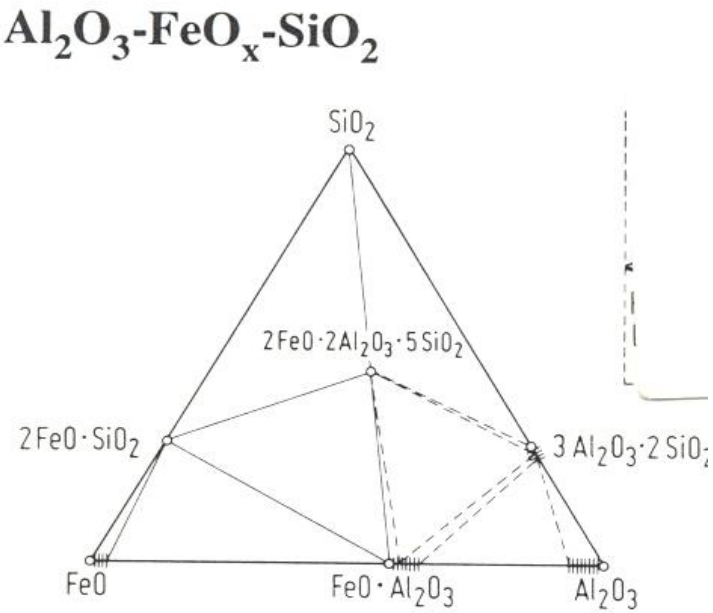

Slag Atlas, 2nd Ed., Verlag Stahl-Eisen, Düsseldorf, 1995.

Al_2O_3 - FeO - SiO_2 - Fe

$Fe/(Al_2O_3+FeO+SiO_2)$ (g/g) = 0.0001, 1700°C, 1 bar

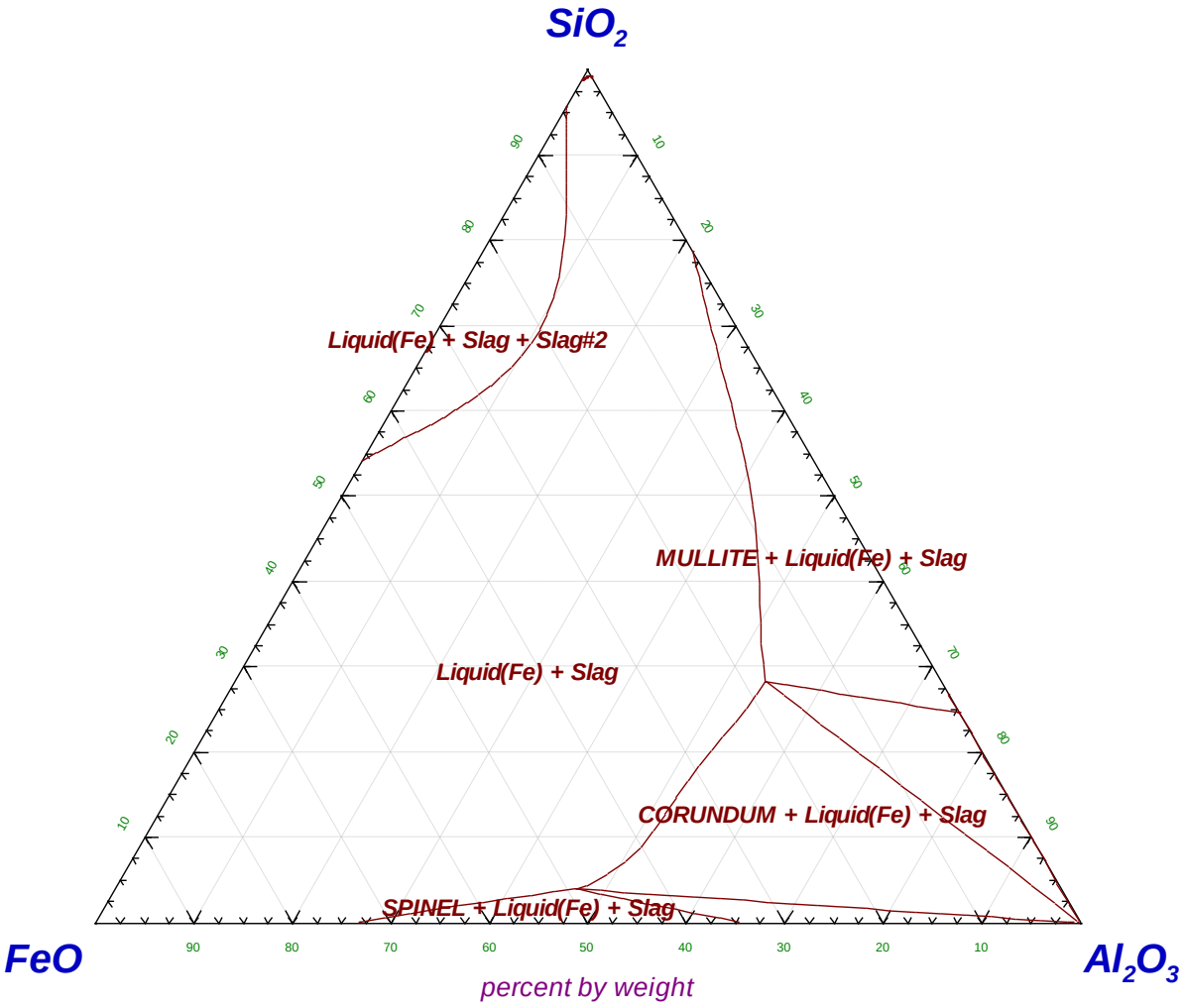

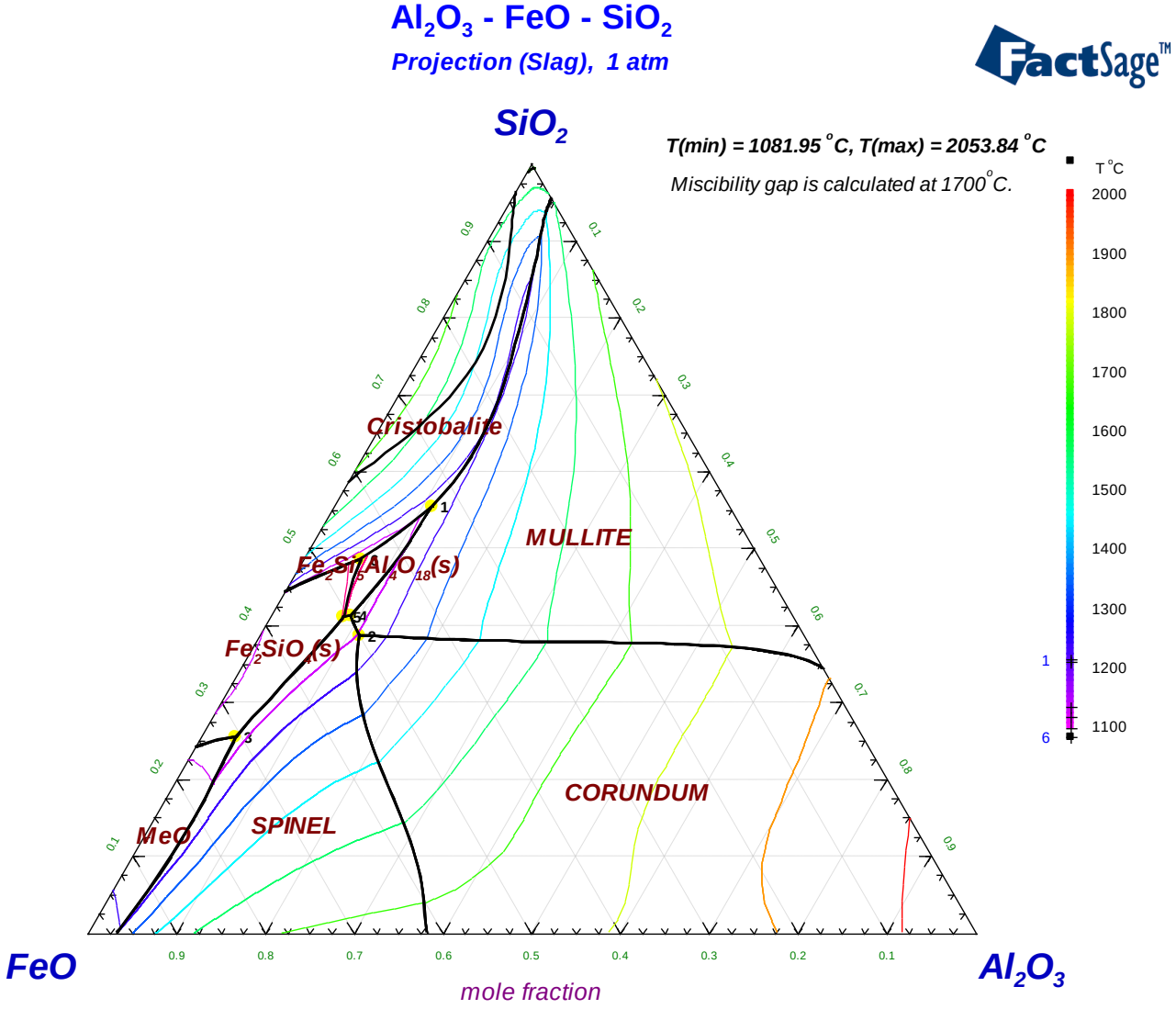
Al2O3 - FeO - SiO2
Projection (Slag), 1 atm
FactSage™
SiO2
T(min) = 1081.95 °C, T(max) = 2053.84 °C
Miscibility gap is calculated at 1700°C.
T °C
2000
1900
1800
1700
1600
1500
1400
1300
1200
1100
Cristobalite
MULLITE
Fe2Si4Al18O38(s)
Fe2SiO4(s)
SPINEL
MeO
CORUNDUM
1
2
3
4
5
6
FeO
Al2O3
mole fraction

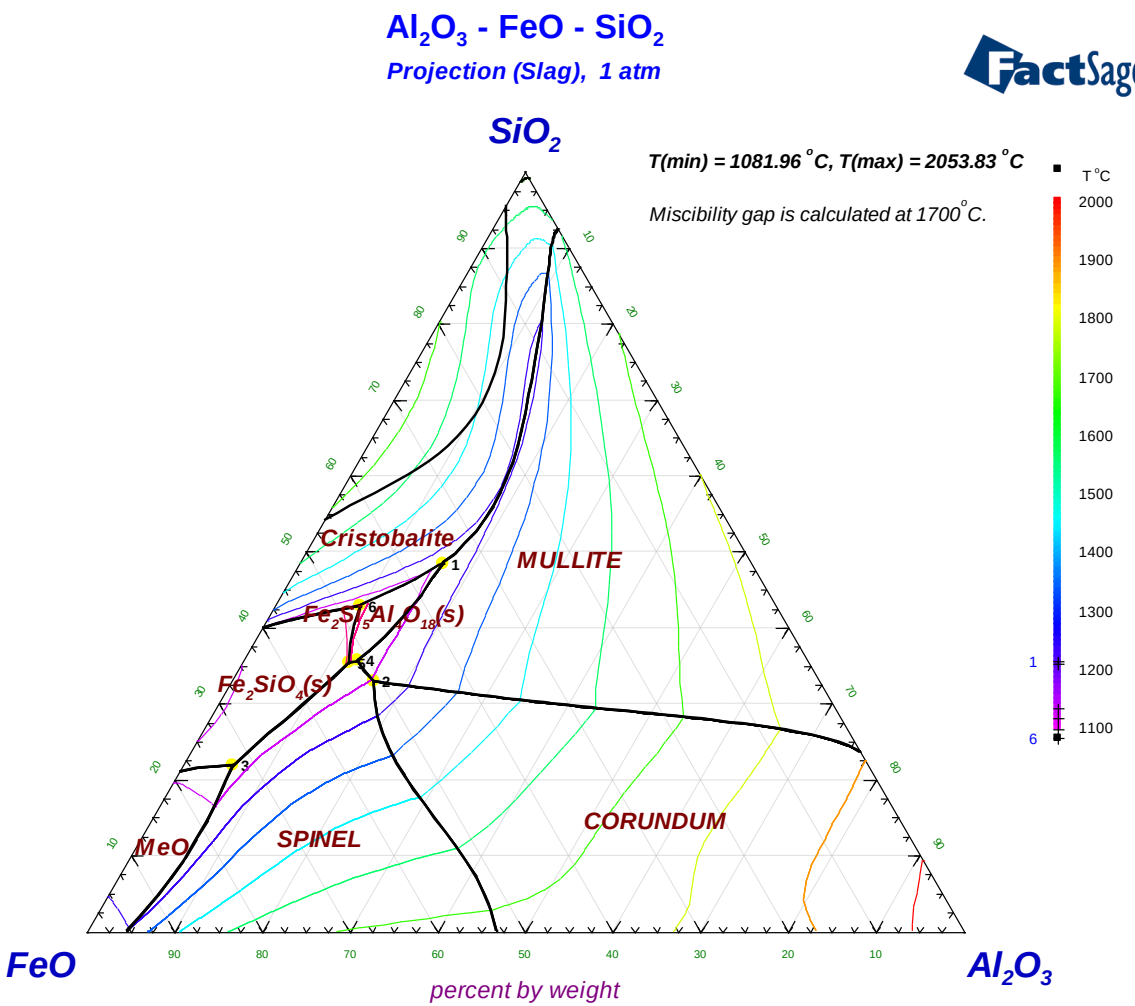

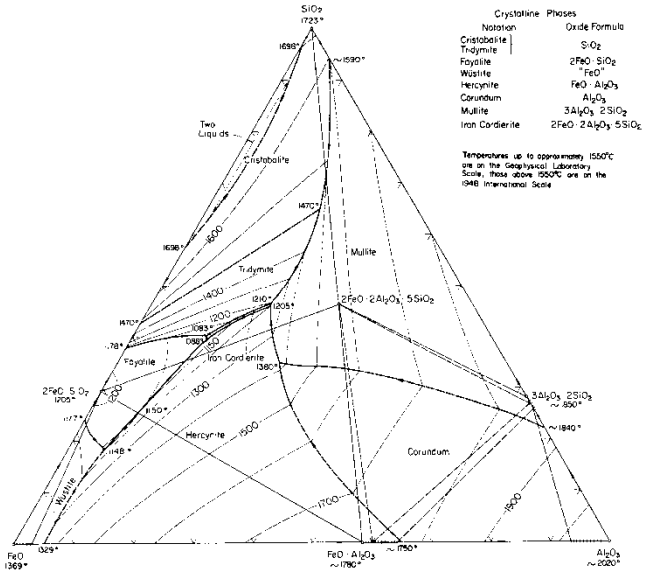

E.F. Osborn, A. Muan: „Phase Equilibrium Diagrams of Oxide Systems“, Plate 9, publ. By American Ceramic Society and the Edward Orton, Jr., Ceramic Foandation, 1960.

Invariant equilibria on the liquidus surface

Intersections with slag	Mole fraction A = SiO2, B = FeO, C = Al2O3				Weight percent A = SiO2, B = FeO, C = Al2O3				
		X(A)	X(B)	X(C)	T(C)		W(A)	W(B)	W(C)	T(C)
1: Fe2Si5Al4O18 / MULLITE / Cristobalite	1:	0.55412	0.33569	0.11019	1213.12	1:	48.050	35.133	16.367	1213.12
2: CORUNDUM / MULLITE / SPINEL	2:	0.38735	0.50009	0.11256	1208.53	2:	32.929	50.834	16.237	1208.54
3: Fe2SiO4(s) / MeO / SPINEL	3:	0.25469	0.70595	0.03937	1131.37	3:	21.850	72.419	5.731	1131.37
4: Fe2Si5Al4O18 / MULLITE / SPINEL	4:	0.41365	0.49720	0.08915	1114.58	4:	35.677	51.275	13.048	1114.58
5: Fe2Si5Al4O18 / Fe2SiO4(s) / SPINEL	5:	0.41056	0.50653	0.08292	1096.96	5:	35.487	52.351	12.162	1096.96
6: Fe2Si5Al4O18 / Fe2SiO4(s) / Cristobalite	6:	0.48676	0.44861	0.06463	1081.97	6:	42.968	47.351	9.681	1081.96

Al2O3-FeO-TiO2,
Weight percent 1000°C

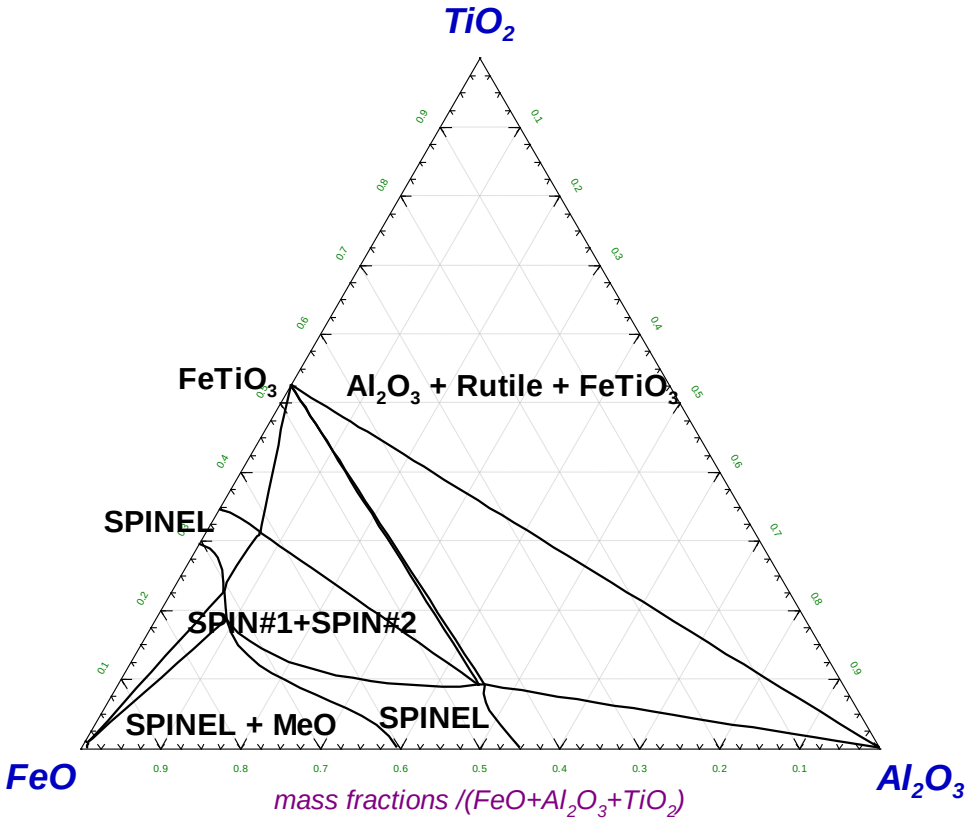

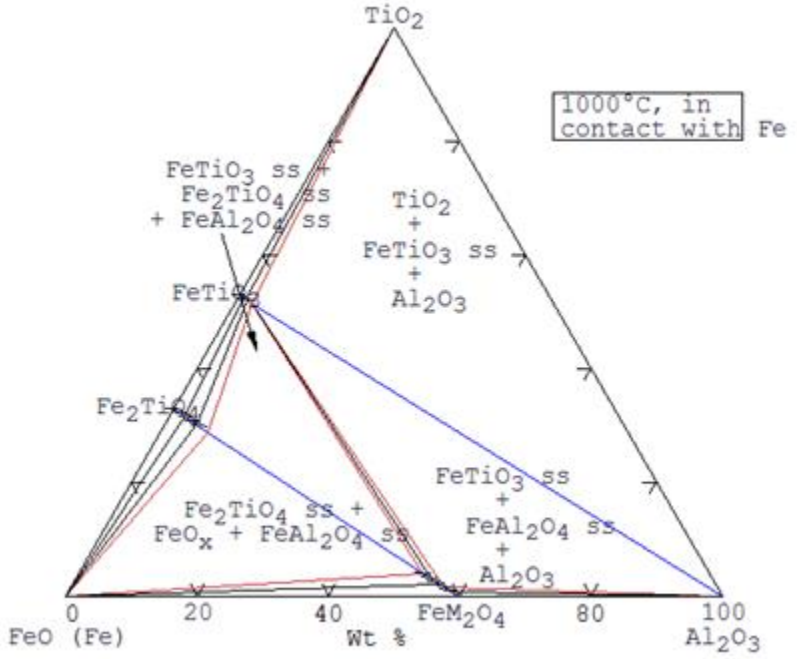

J. Hauck, J. Solid State Chem., 36 [1], (1981), pp. 52-65.

Al2O3-FeO-TiO2, Weight percent 1300°C

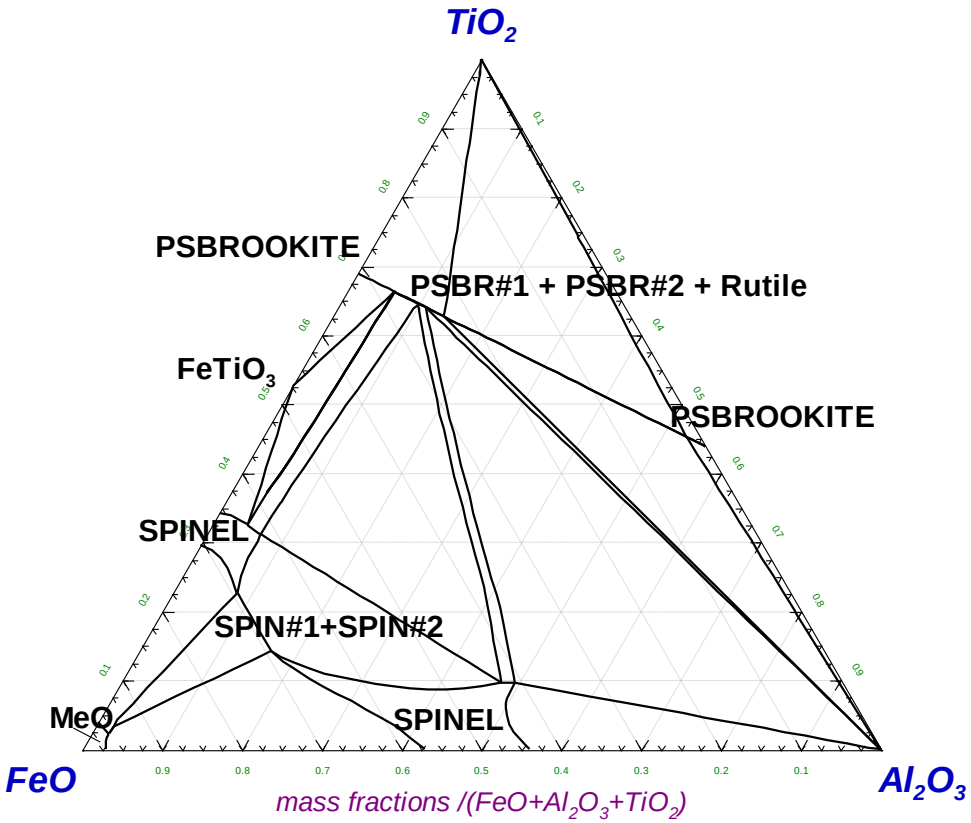

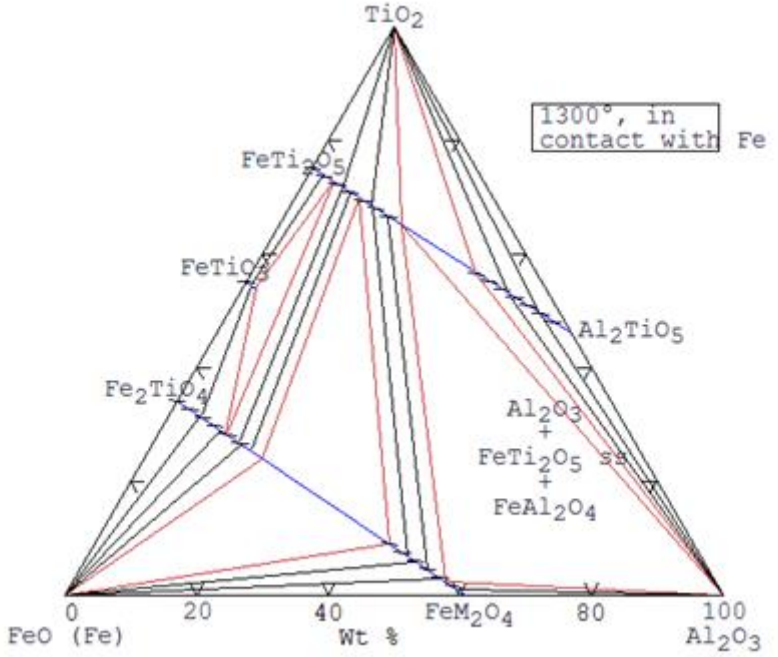

J. Hauck, J. Solid State Chem., 36 [1], (1981), pp. 52-65.

Al2O3-FeO-TiO2,
Mole fraction, Liquidus surface

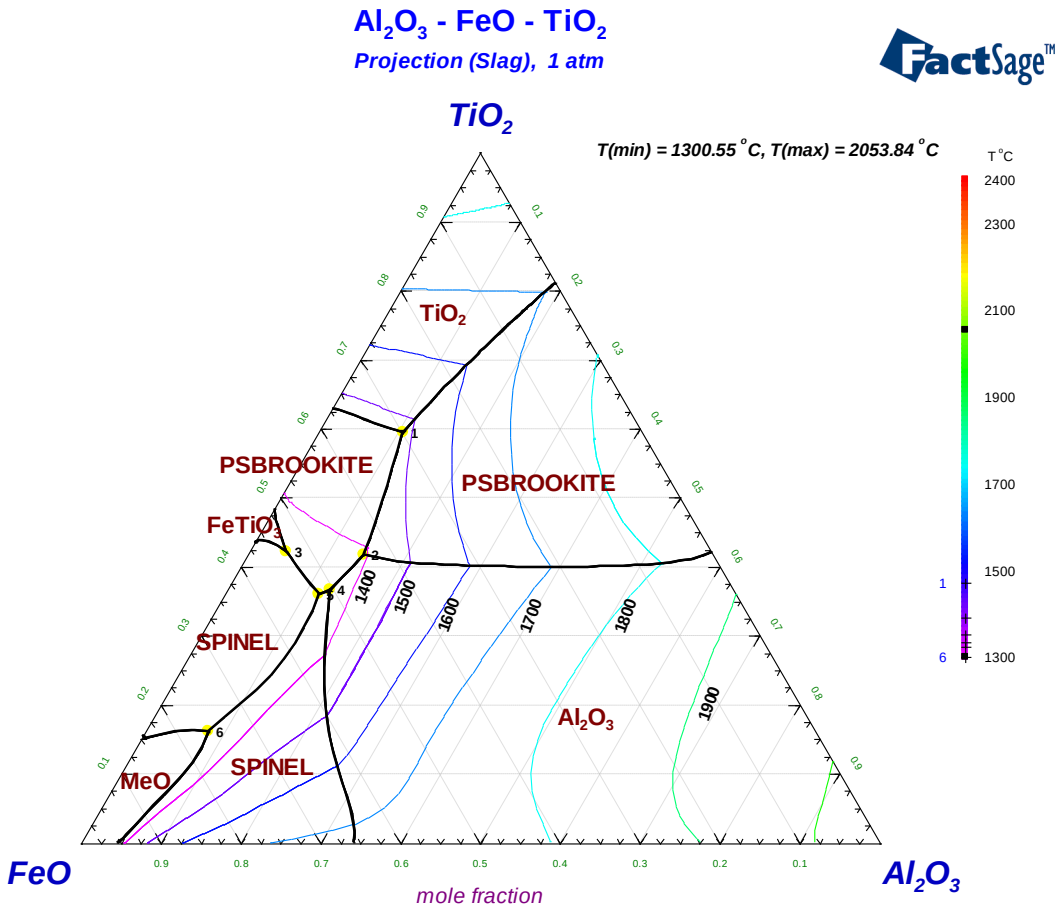

Al2O3-FeO-TiO2,
Weight percent, Liquidus surface

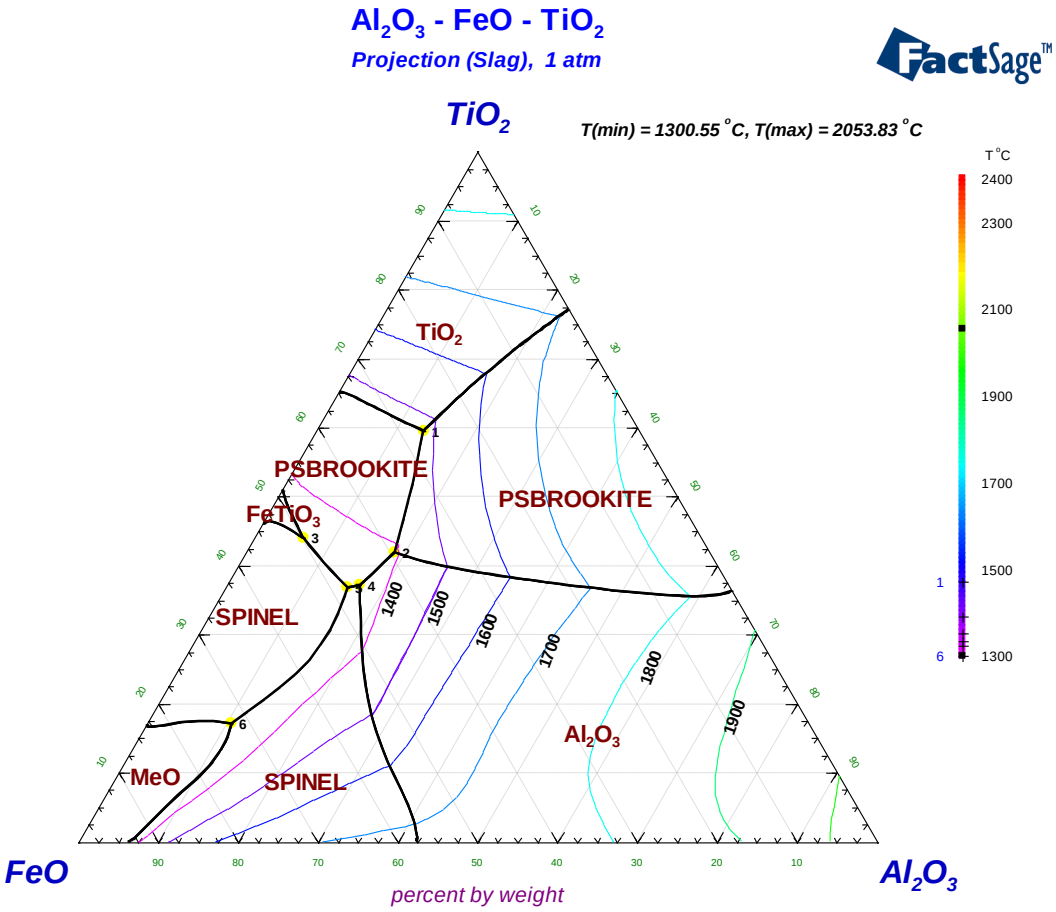

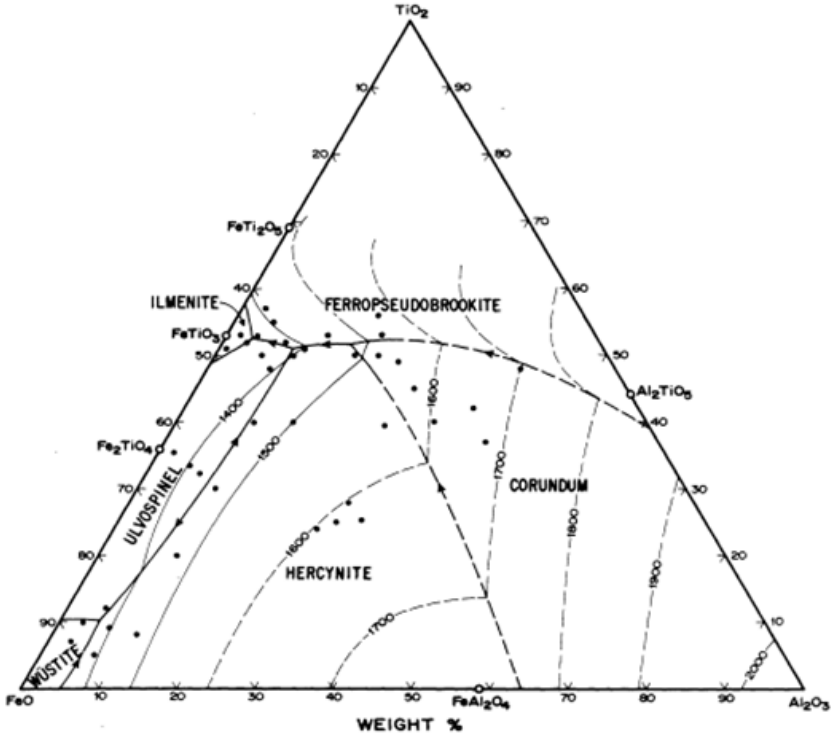

W.A. Scherifels, A. Muan, Proc. Lunar Sci. Conf. 6th (1975), pp.973-985.

Invariant equilibria on the liquidus surface

Intersections with slag	Mole fraction				Weight percent				
	A = TiO2, B = FeO, C = Al2O3				A = TiO2, B = FeO, C = Al2O3				
		X(A)	X(B)	X(C)	T(C)		W(A)	W(B)	W(C)	T(C)
1: PSBROOKITE#1 / PSBROOKITE-#2 / TiO2	1:	0.59524	0.29964	0.10512	1472.17	1:	59.584	26.982	13.433	1472.17
2: Al2O3 / PSBROOKITE-#1/ PSBROOKITE#2	2:	0.41815	0.43669	0.14516	1391.23	2:	41.971	39.429	18.600	1391.22
3: FeTiO3 / PSBROOKITE#1 / SPINEL#1	3:	0.42291	0.53137	0.04572	1351.77	3:	44.087	49.829	6.085	1351.77
4: Al2O3 / PSBROOKITE#1 / SPINEL#1	4:	0.36671	0.50471	0.12859	1335.52	4:	37.233	46.098	16.668	1335.52
5: PSBROOKITE#1 / SPINEL#1 / SPINEL#2	5:	0.36118	0.52154	0.11727	1323.74	5:	36.853	47.871	15.276	1323.74
6: MeO / SPINEL#1 / SPINEL#2	6:	0.16218	0.75957	0.07825	1300.55	6:	17.155	72.277	10.568	1300.55

Al2O3-FeO-V2O3, Mole fraction 600°C

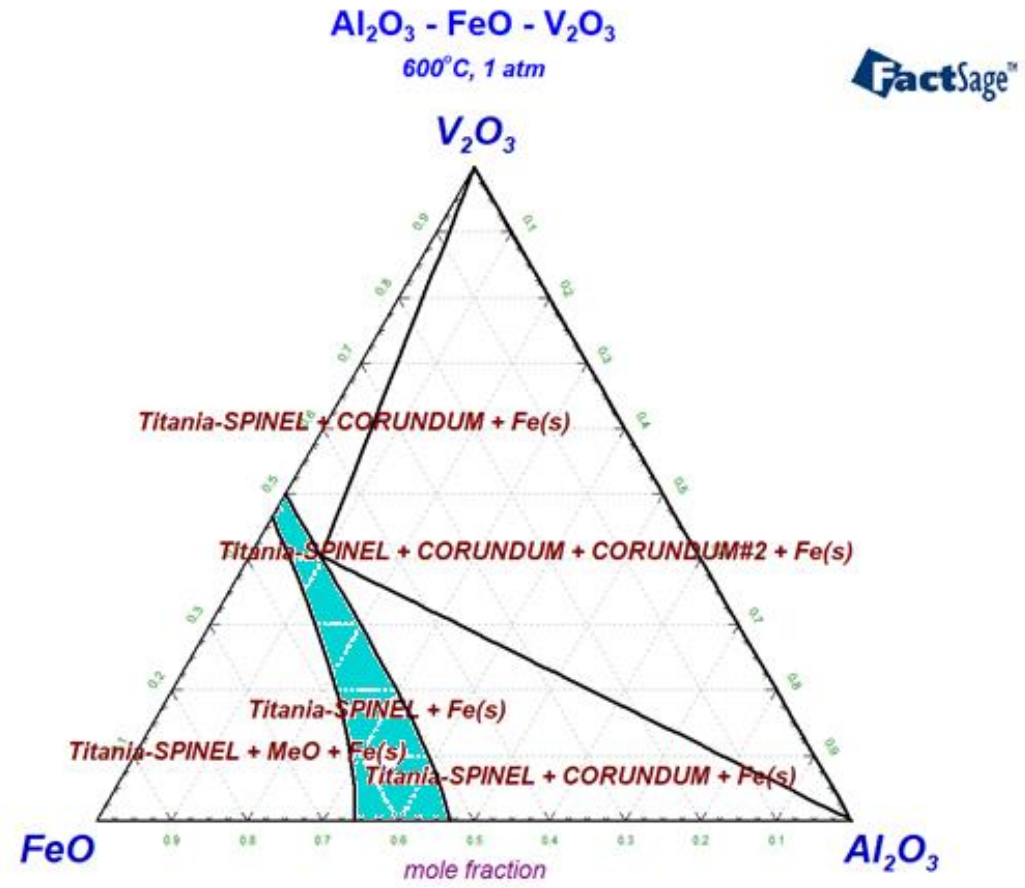

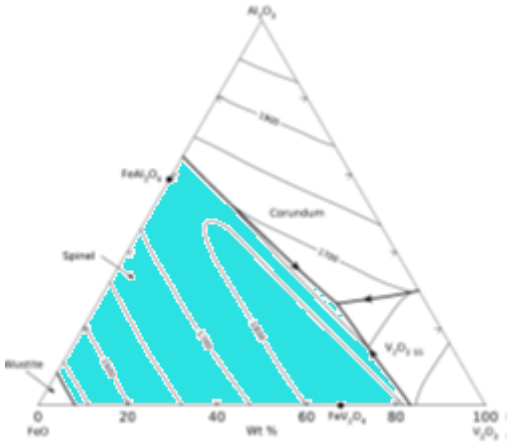

B. Leusmann, N. Jb. Miner. Mh., 12 (1979), pp. 556-559

Al2O3-FeO-V2O3,
Mole fraction 1000°C

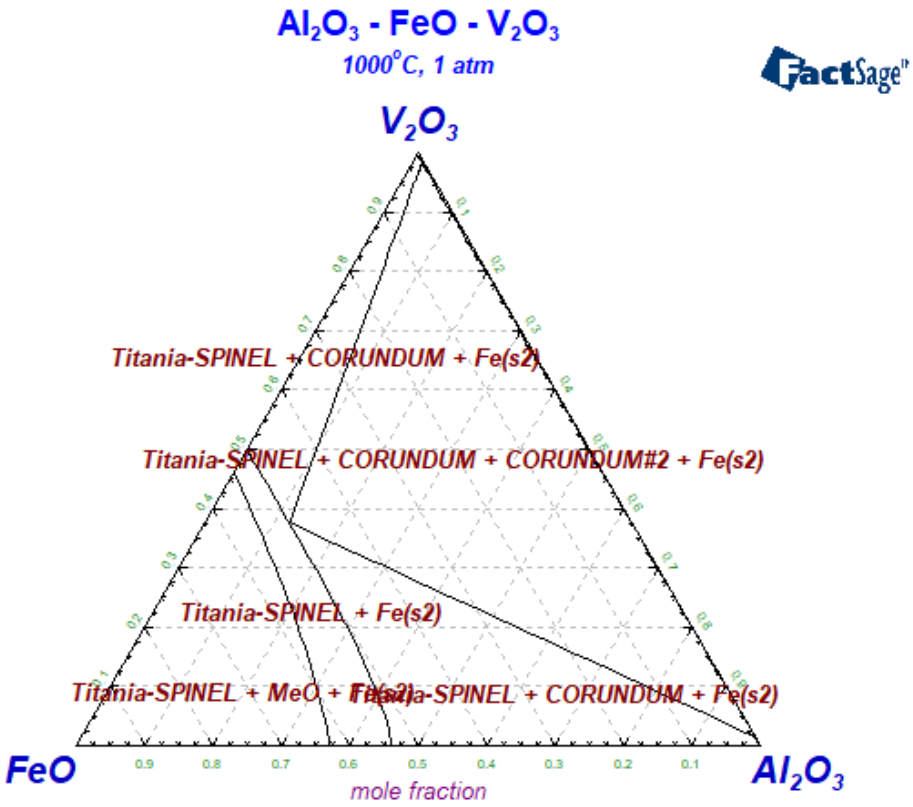

Al2O3-FeO-V2O3, Mole fraction 1500°C

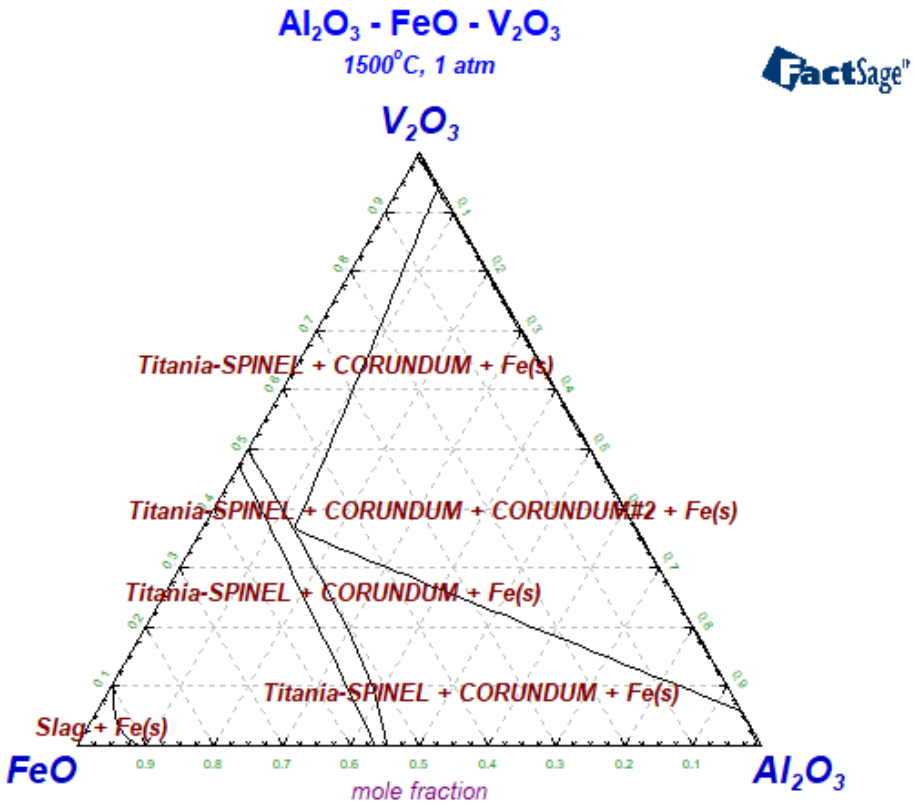

Al2O3-Fe2O3-V2O5,
Mole fraction 600°C

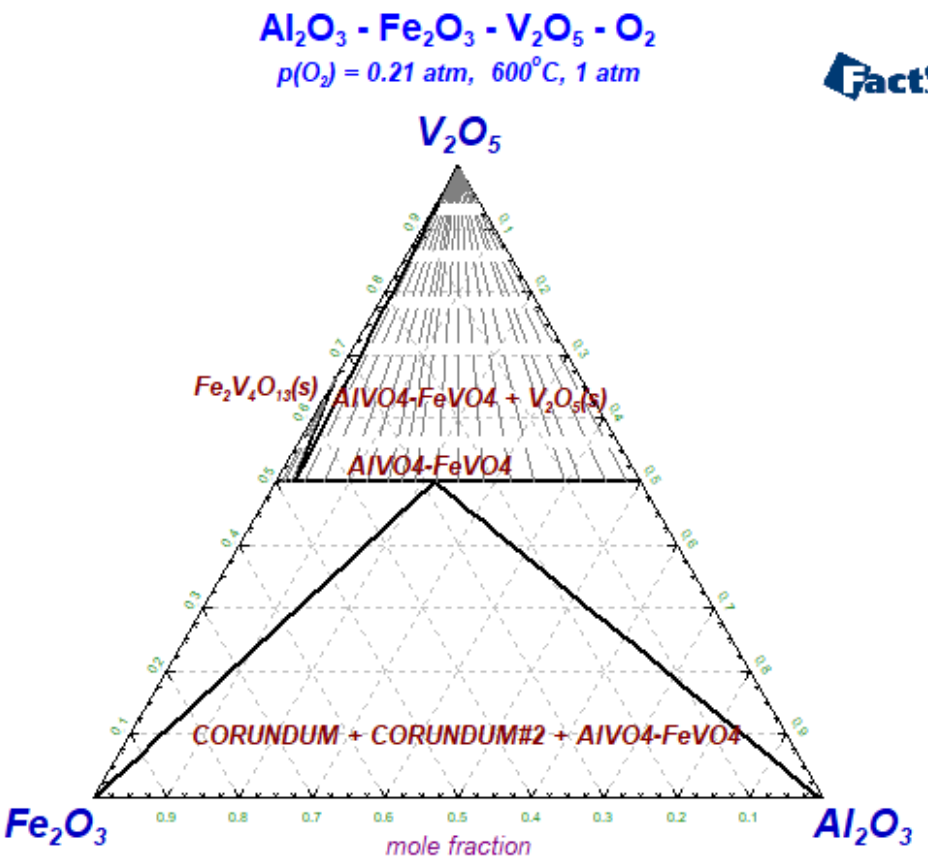

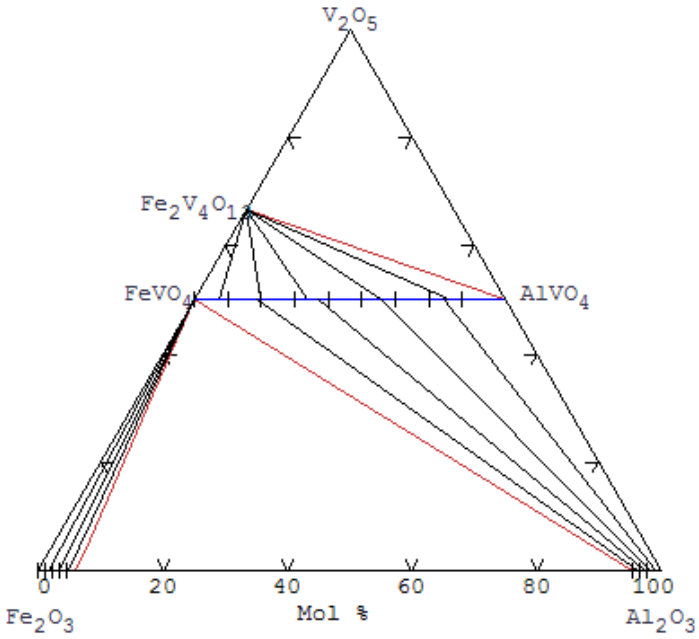

J. A. A.A. Fotiev, L.L. Surat, G.A. Korablev, A.I. Tret'yakov, Zh. Neorg. Khim., 26 [1], (1981), pp. 242-248.

Al2O3-Fe2O3-V2O5,
Mole fraction, Liquidus surface

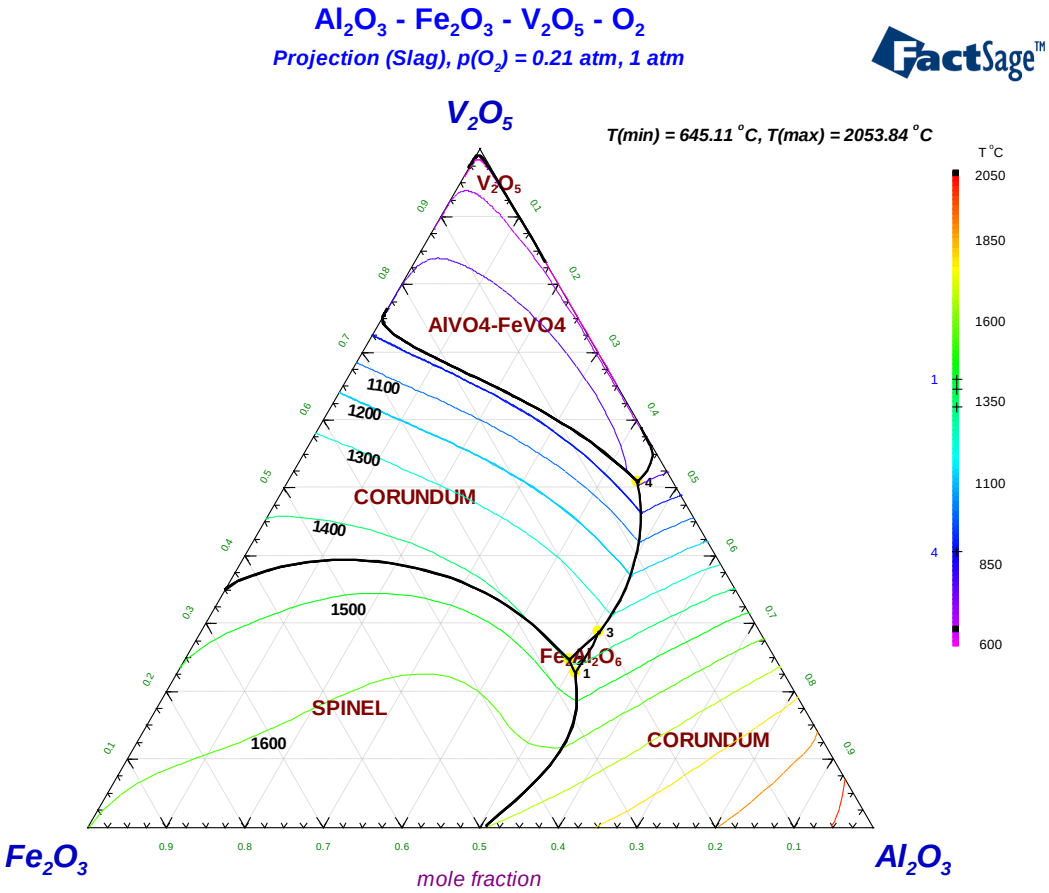

Al2O3-Fe2O3-V2O5,
Weight percent, Liquidus surface

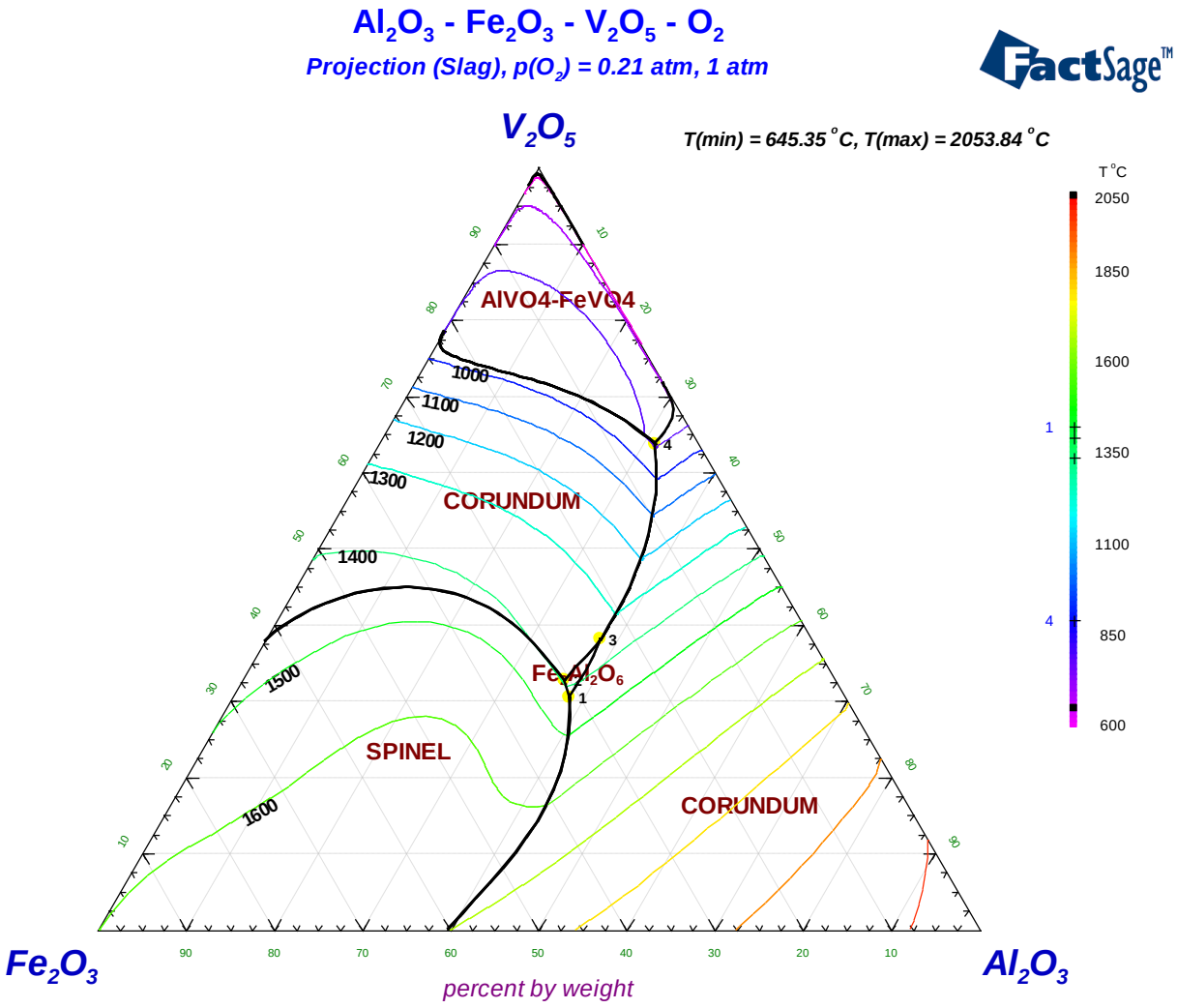

Invariant equilibria on the liquidus surface

Intersections with slag	Mole fraction				Weight percent				
	A = V2O5, B = Fe2O3, C = Al2O3				A = V2O5, B = Fe2O3, C = Al2O3				
		X(A)	X(B)	X(C)	T(C)		W(A)	W(B)	W(C)	T(C)
1. CORUNDUM#1 / Fe2Al2O6 / SPINEL	1:	0.22783	0.26439	0.50778	1417.82	1:	30.597	31.175	38.229	1417.91
2. CORUNDUM#1 / Fe2Al2O6 / SPINEL	2:	0.24692	0.26249	0.49059	1388.31	2:	32.817	30.630	36.553	1388.31
3. CORUNDUM#1 / CORUND#2 /Fe2Al2O6	3:	0.28690	0.20427	0.50883	1334.99	3:	38.173	23.871	37.956	1335.05
4. MeVO4 / CORUNDUM#1 / CORUNDUM#2	4:	0.50959	0.04459	0.44582	887.95	4:	63.805	4.902	31.293	887.91

Al2O3-K2O-MgO,
Mole fraction 1400°C

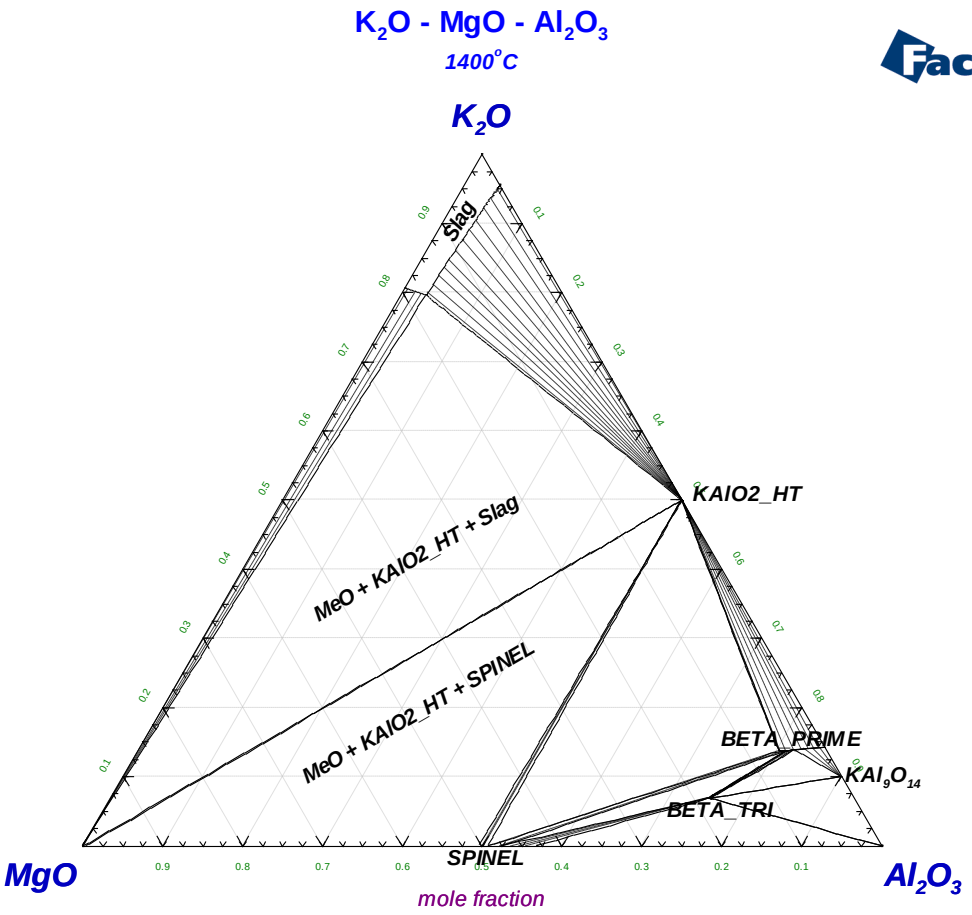

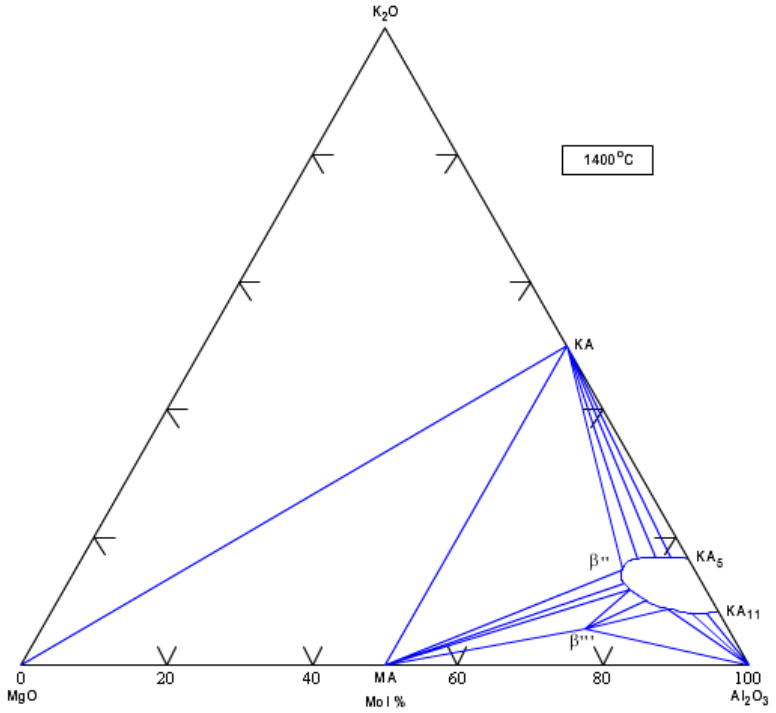

J. A. M. Van Hoek, F. J. J. Van Loo, and R. Metselaar, Key Eng. Mater., 53-55 [Austceram '90] 111-119 (1991).

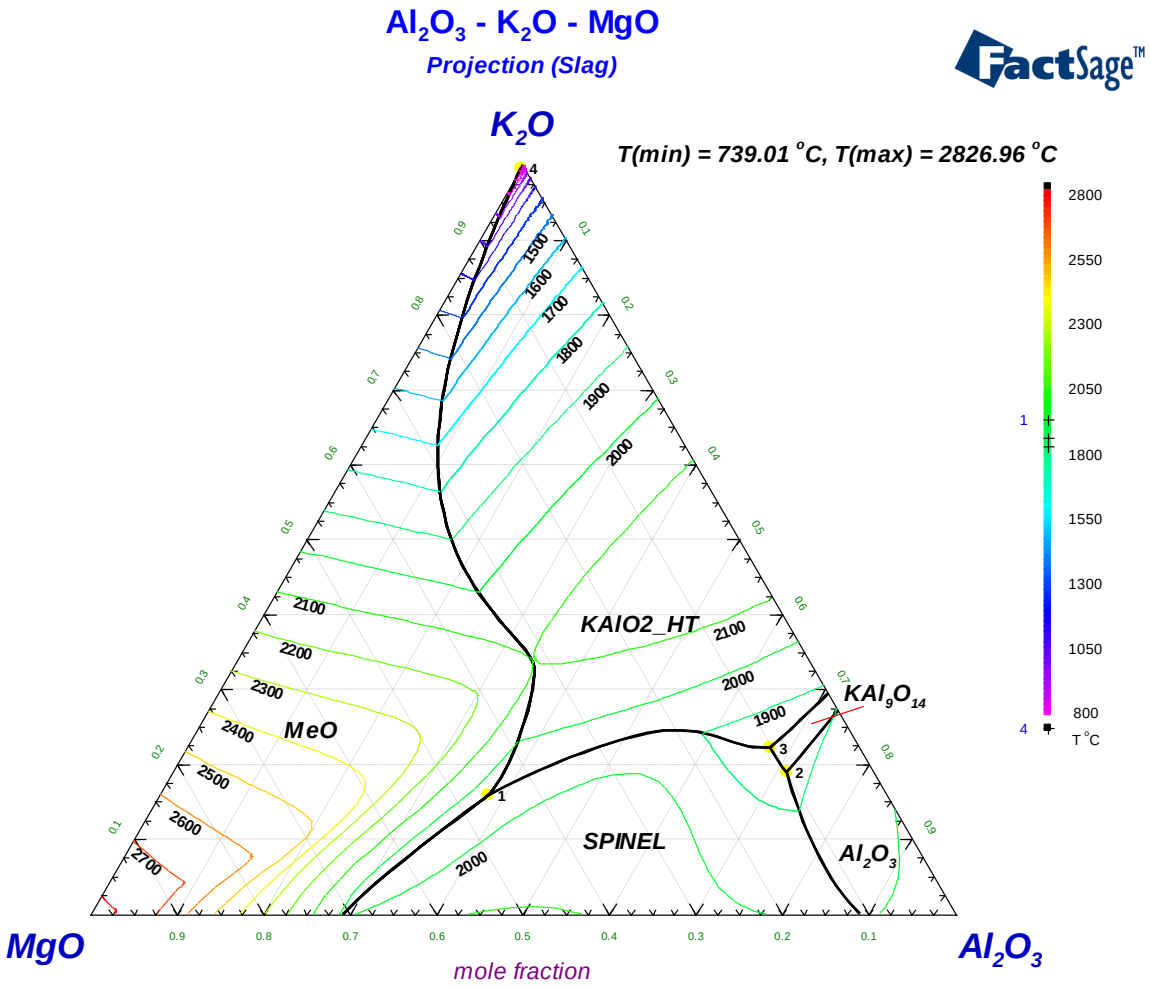
Al2O3 - K2O - MgO
Projection (Slag)
FactSage™
K2O
T(min) = 739.01 °C, T(max) = 2826.96 °C
2800
2550
2300
2050
1800
1550
1300
1050
800
T °C
KAlO2_HT
MeO
SPINEL
KAl9O14
Al2O3
MgO
Al2O3
mole fraction

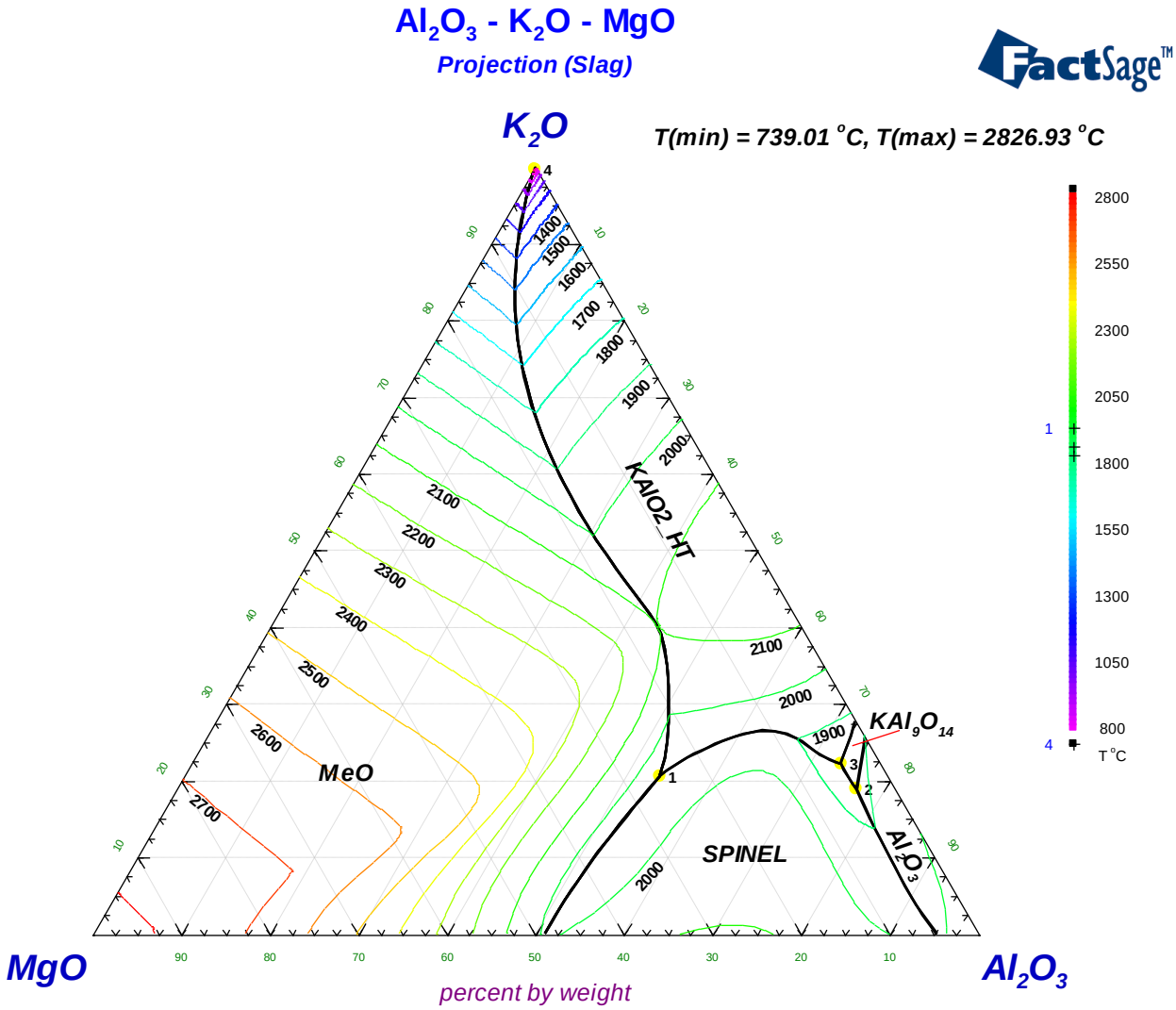
Al2O3 - K2O - MgO
Projection (Slag)
FactSage™
K2O
T(min) = 739.01 °C, T(max) = 2826.93 °C
MgO
Al2O3
percent by weight
KAlO2_HT
MeO
SPINEL
Al2O3
KAl9O14
2800
2550
2300
2050
1800
1550
1300
1050
800
T °C

Invariant equilibria on the liquidus surface

Intersections with slag	Mole fraction A = K2O, B = MgO, C = Al2O3				Weight percent A = K2O, B = MgO, C = Al2O3			
	X(A)	X(B)	X(C)	T(C)	W(A)	W(B)	W(C)	T(C)
1: KAlO2_HT / MeO / SPINEL	1: 0.15875	0.46023	0.38101	1927.44	1: 20.668	25.638	53.694	1927.44
2: Al2O3 / KAl9O14 / SPINEL	2: 0.18928	0.10031	0.71041	1860.24	2: 18.906	4.287	76.807	1860.26
3: KAlO2_HT / KAl9O14 / SPINEL	3: 0.22214	0.10247	0.67539	1826.71	3: 22.279	4.397	73.323	1826.71
4: KAlO2_HT / K2O(s3) / MeO	4: 0.99578	0.00388	0.00034	739.01	4: 99.797	0.166	0.037	739.01

Mole fraction
(proposed calculation)

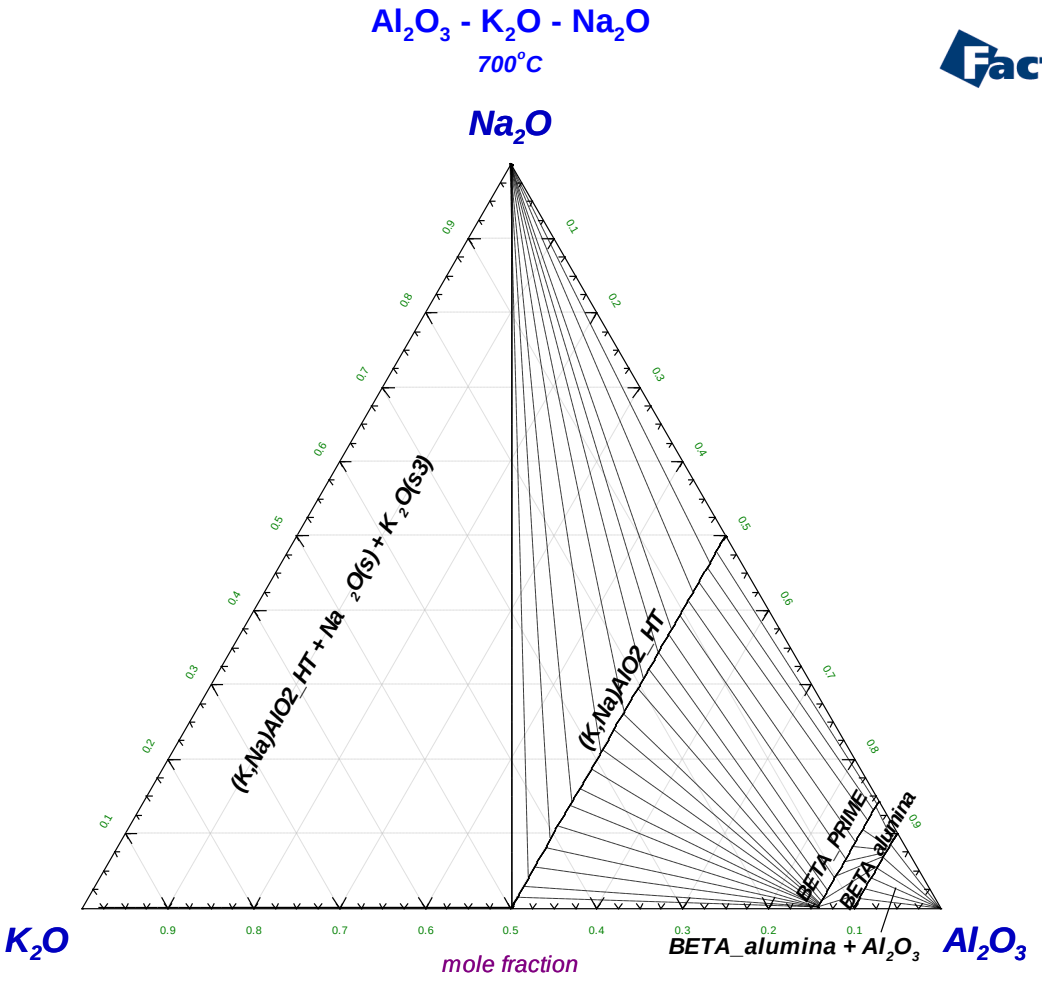

Mole fraction
(proposed calculation)

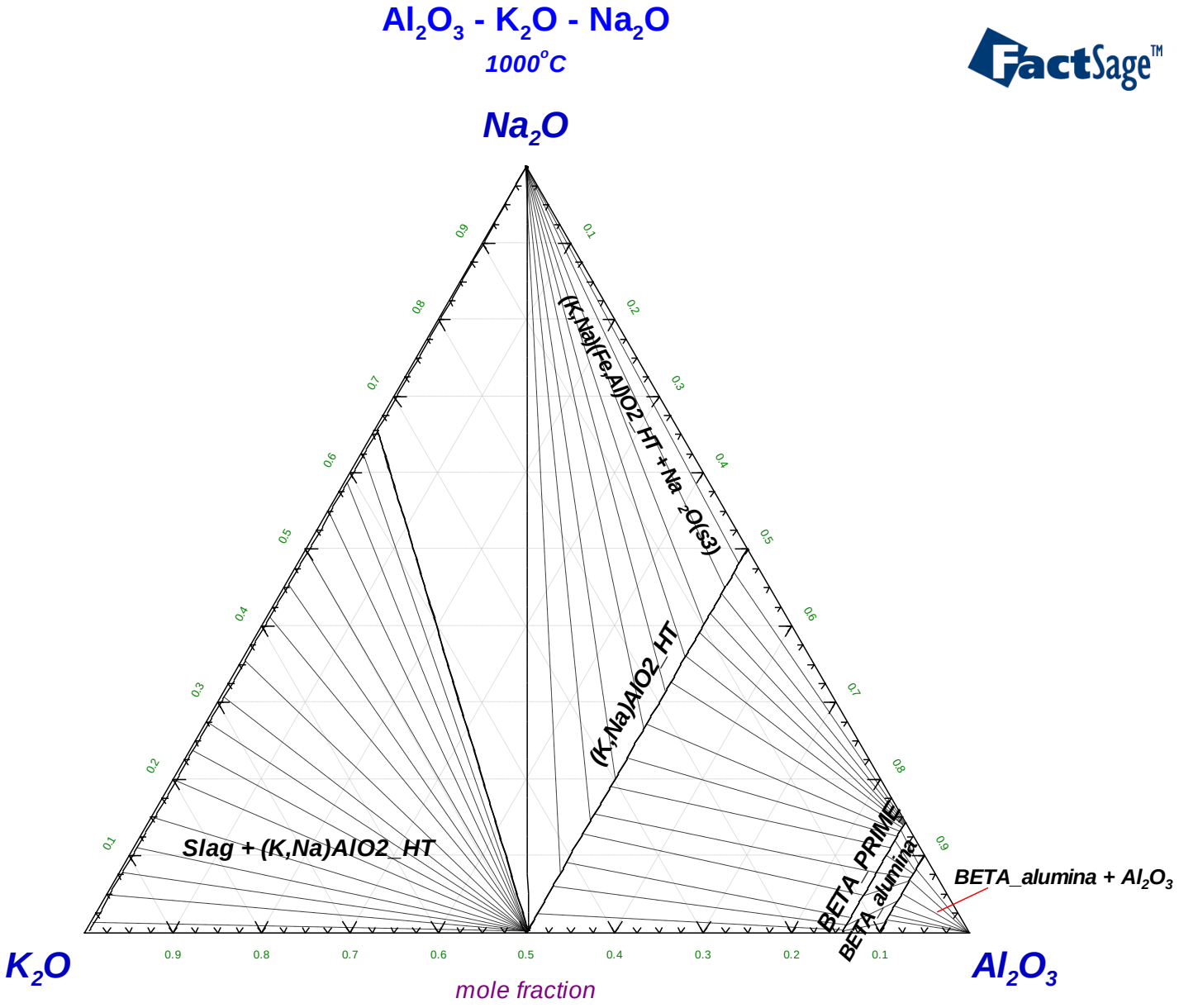

Isopleth AlKO2-AlNaO2 (proposed calculation)

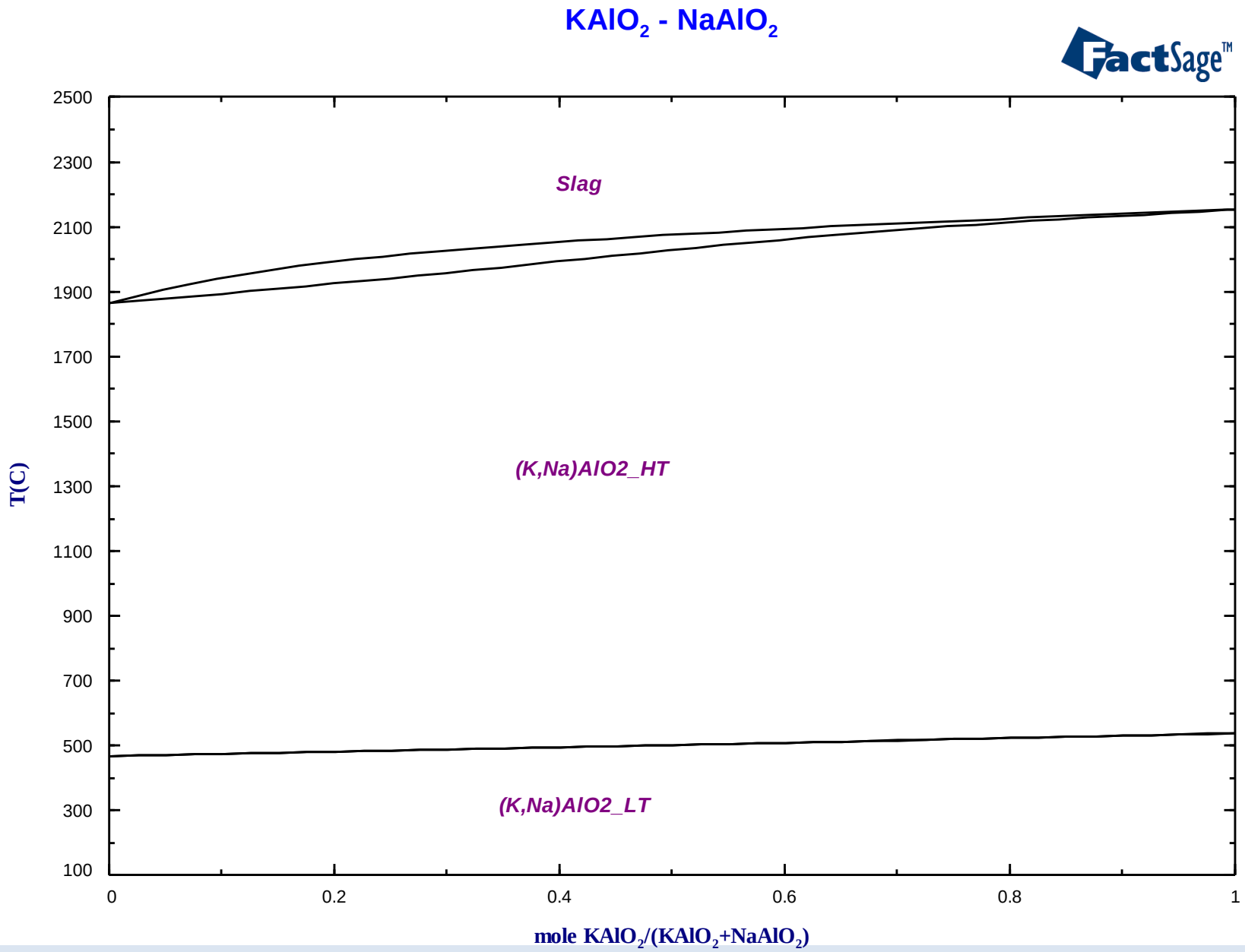

Mole fraction
Liquidussurface
(proposed calculation)

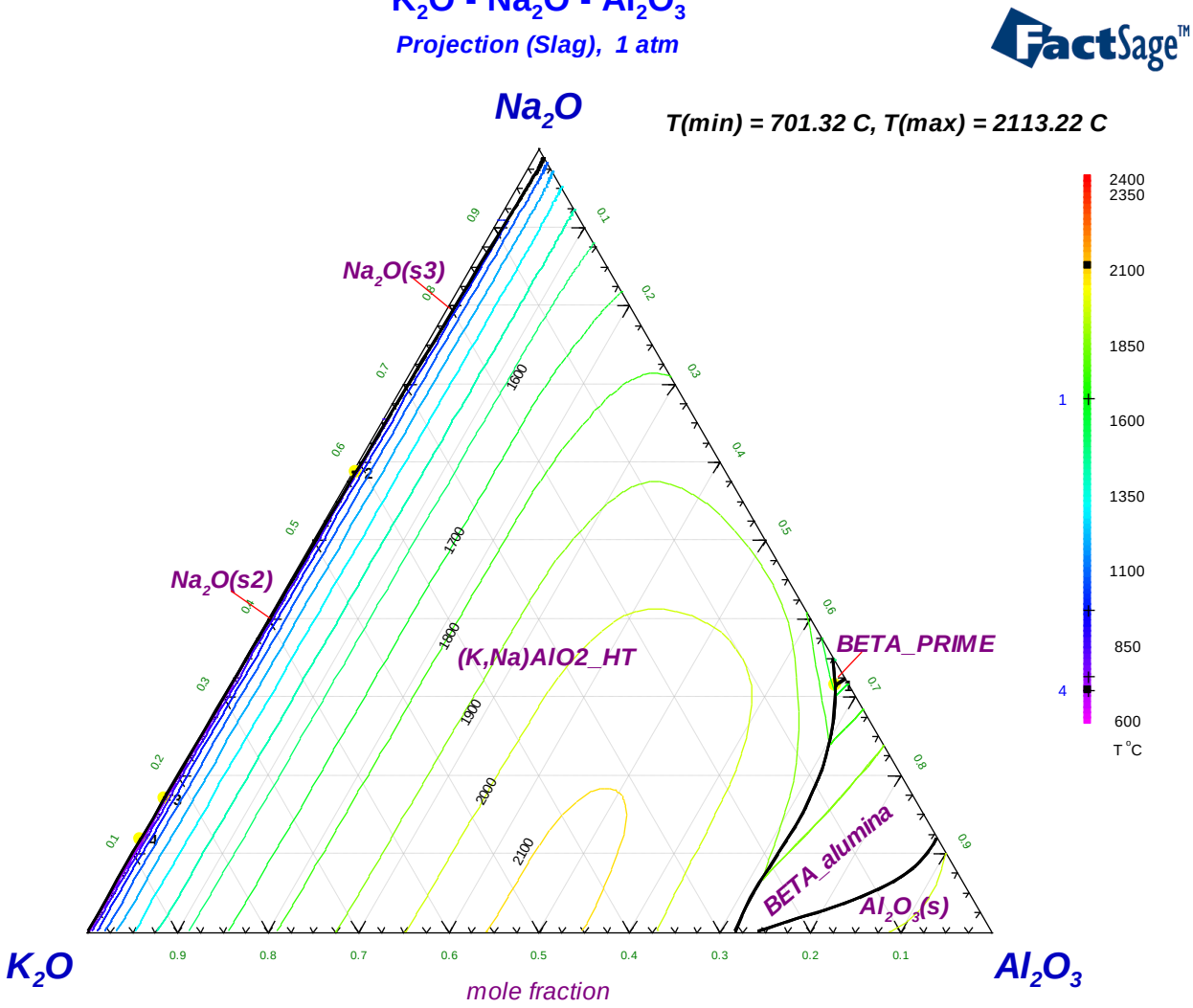

Weight percent
Liquidussurface
(proposed calculation)

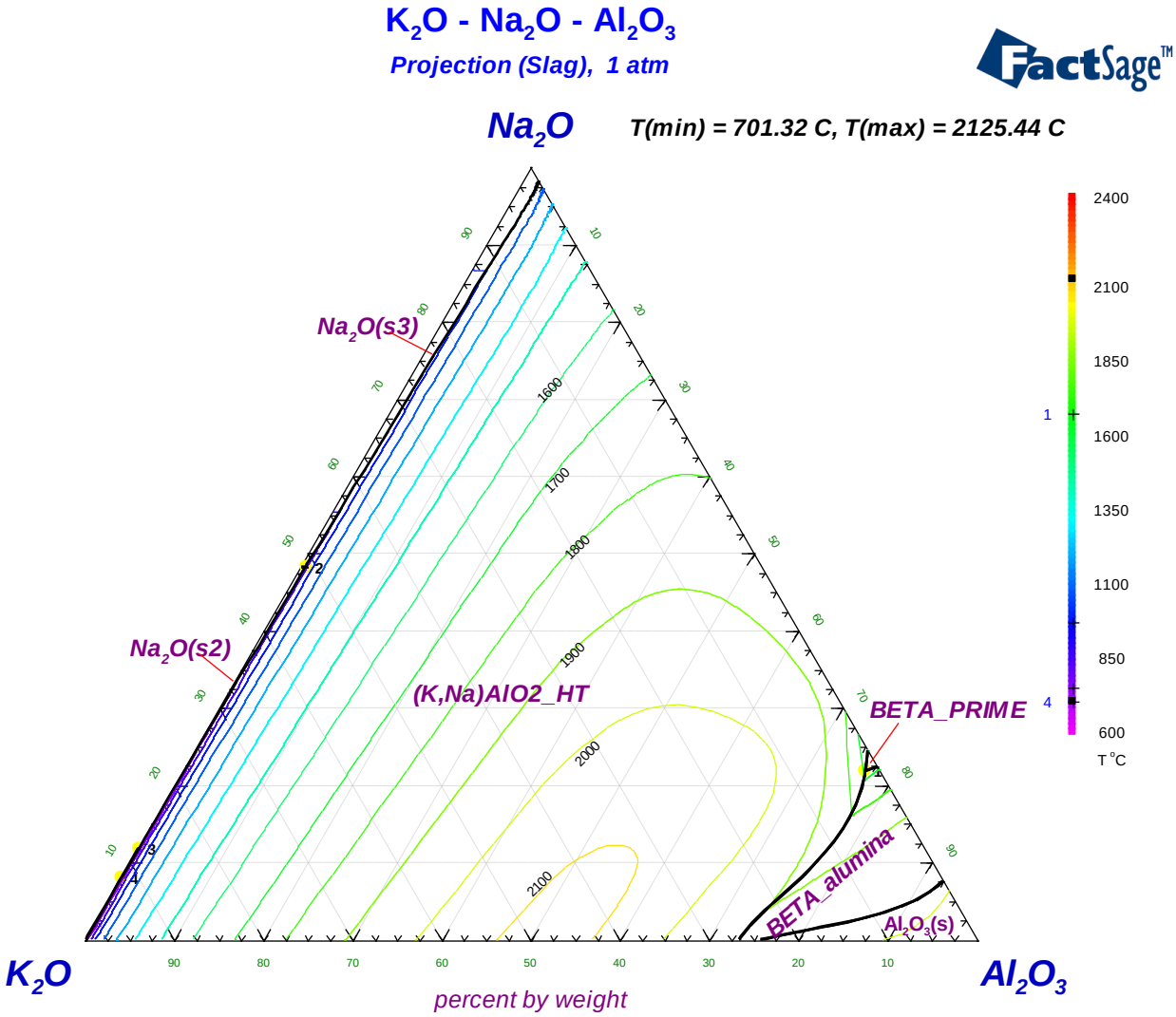

Invariant equilibria on the liquidus surface

Intersections with slag	Mole fraction A = Na2O, B = K2O, C = Al2O3				Weight percent A = Na2O, B = K2O, C = Al2O3			
	X(A)	X(B)	X(C)	T(C)	W(A)	W(B)	W(C)	T(C)
1: (K,Na)AlO2_HT / BETA_PRIME /BETA_alumina	1: 0.31467	0.01467	0.67066	1670.31	1: 21.848	1.548	76.604	1670.29
2: (K,Na)AlO2_HT / Na2O(s2) / Na2O(s3)	2: 0.58745	0.40834	0.00422	970.05	2: 48.351	51.079	0.571	970.05
3: (K,Na)AlO2_HT / Na2O(s) / Na2O(s2)	3: 0.16996	0.82952	0.00052	750.05	3: 11.873	88.068	0.059	750.05
4: (K,Na)AlO2_HT / K2O(s3) / Na2O(s)	4: 0.11848	0.88123	0.00029	701.32	4: 8.125	91.843	0.032	701.32

Mole fraction

Al_2O_3 - K_2O - SiO_2

645°C

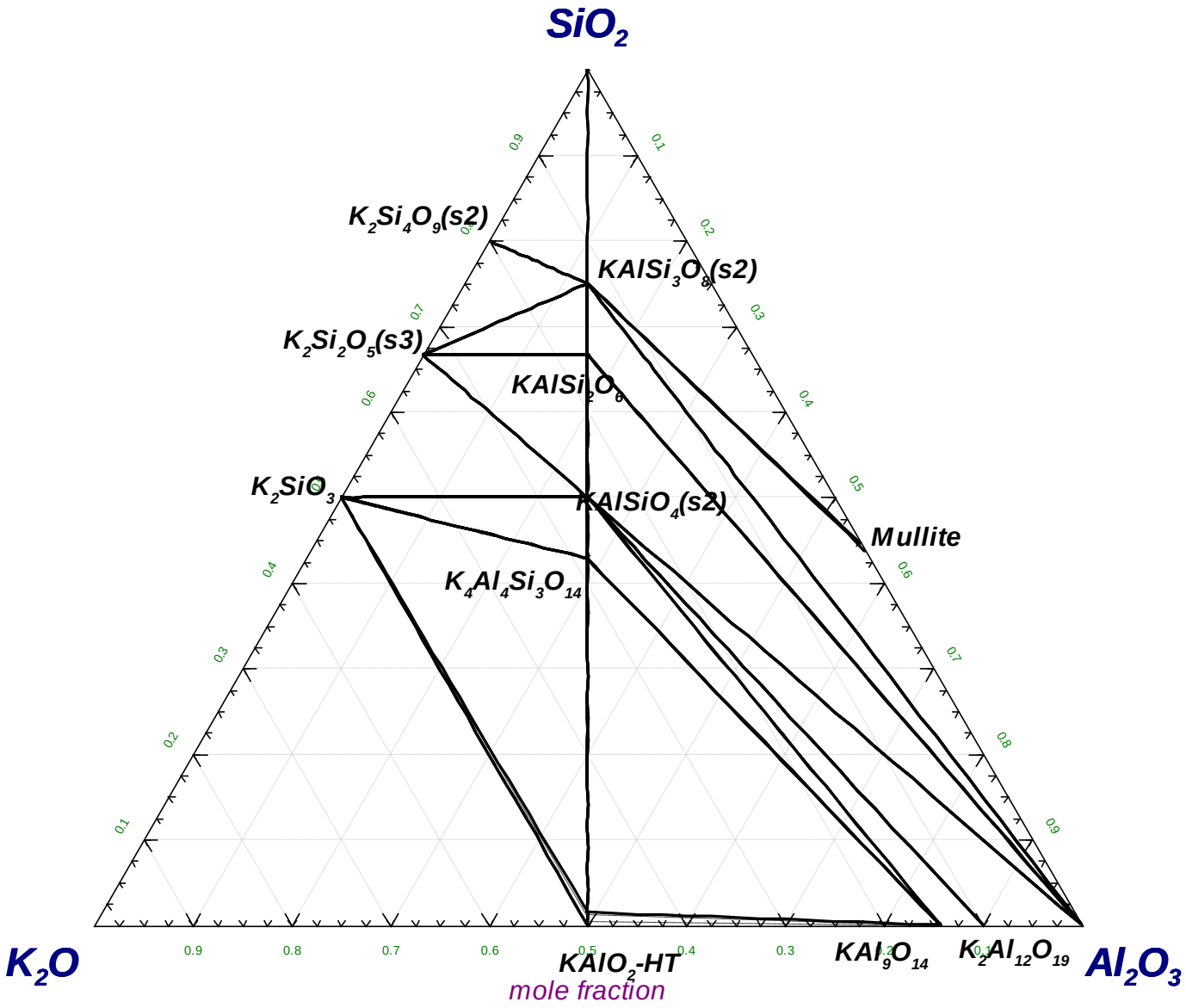

Mole fraction
kurz unterhalb Liquidussurface

Al_2O_3 - K_2O - SiO_2

1000°C

FactSage™

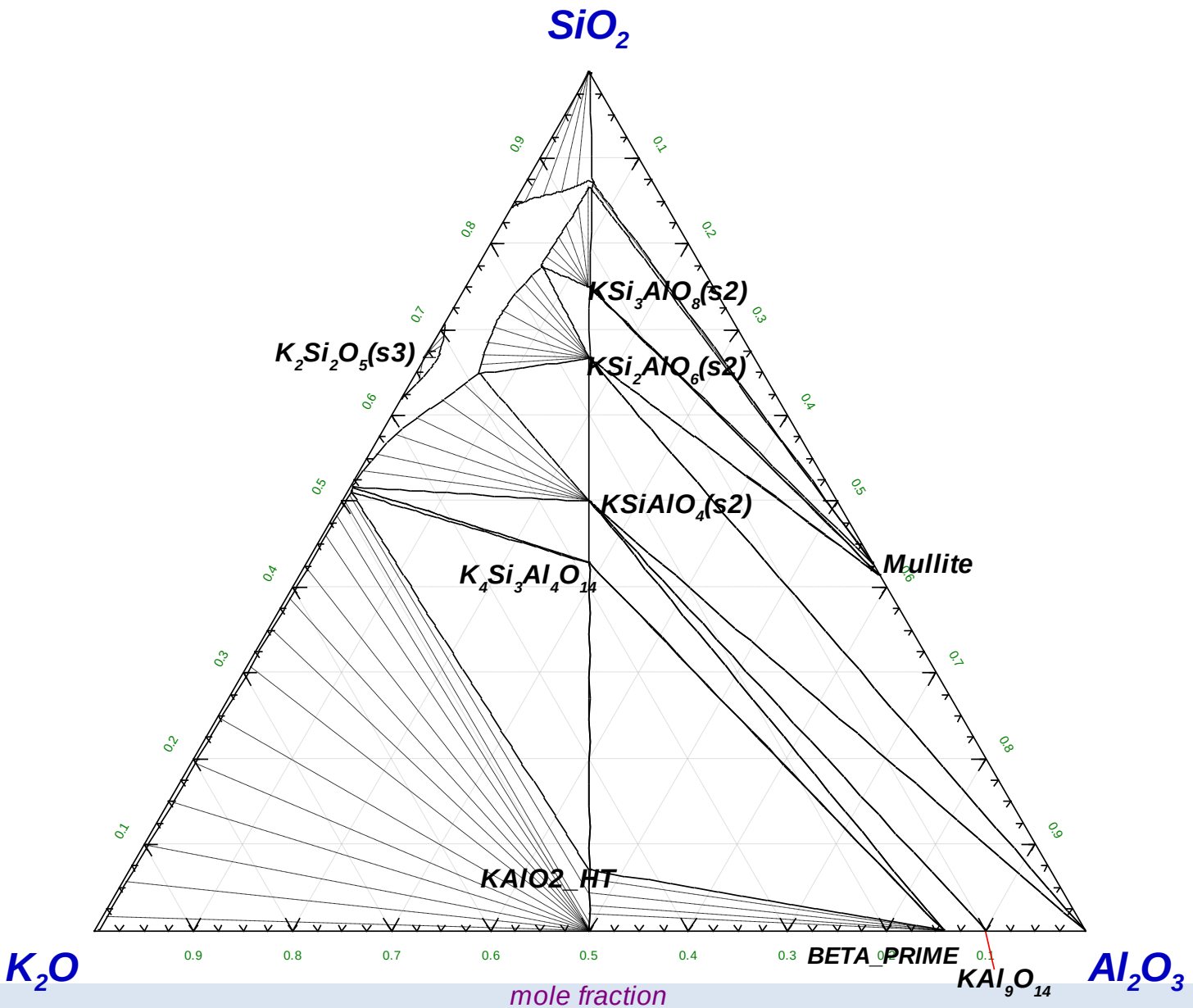

Weight percent
compared with experimental data

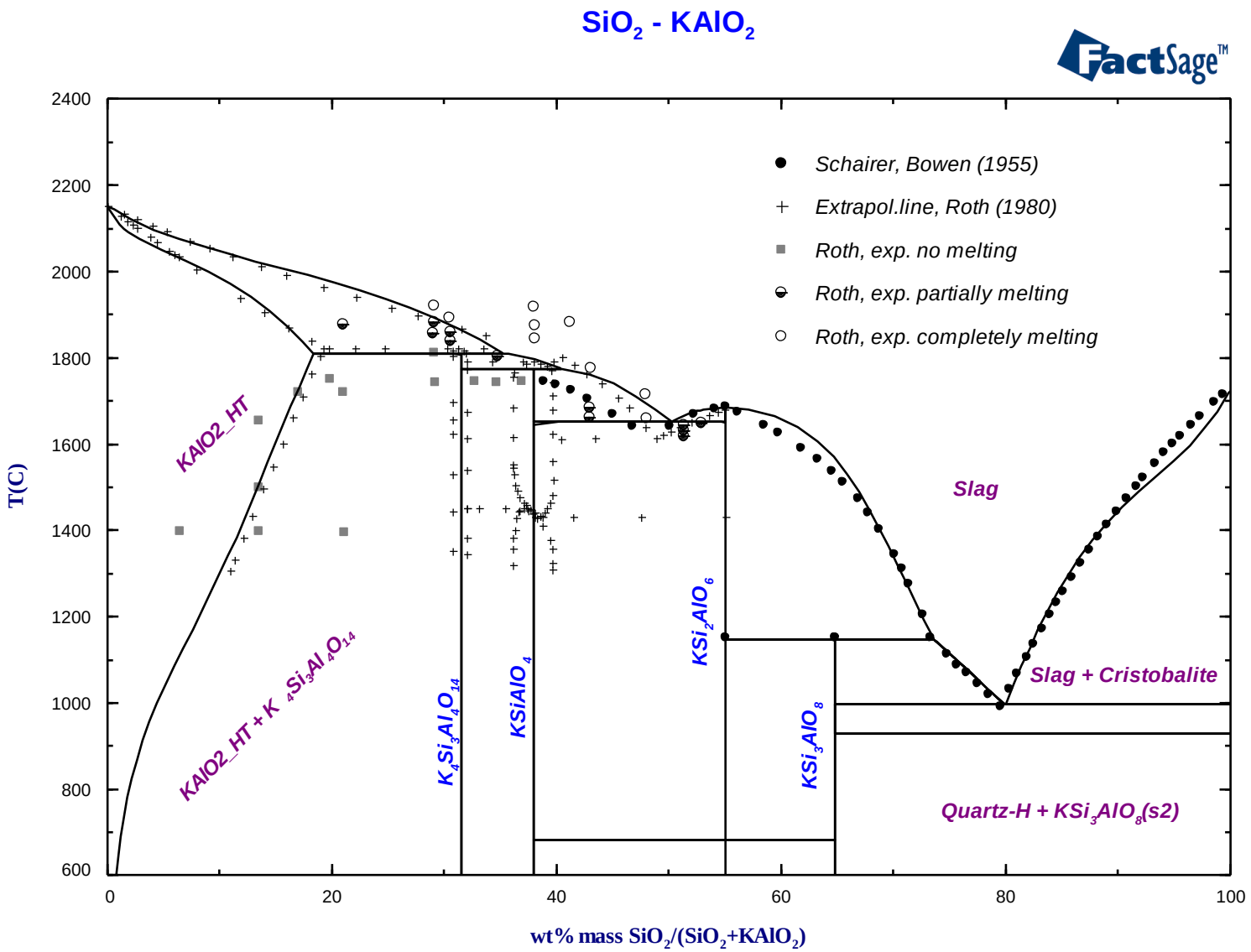

Weight percent
compared with experimental data

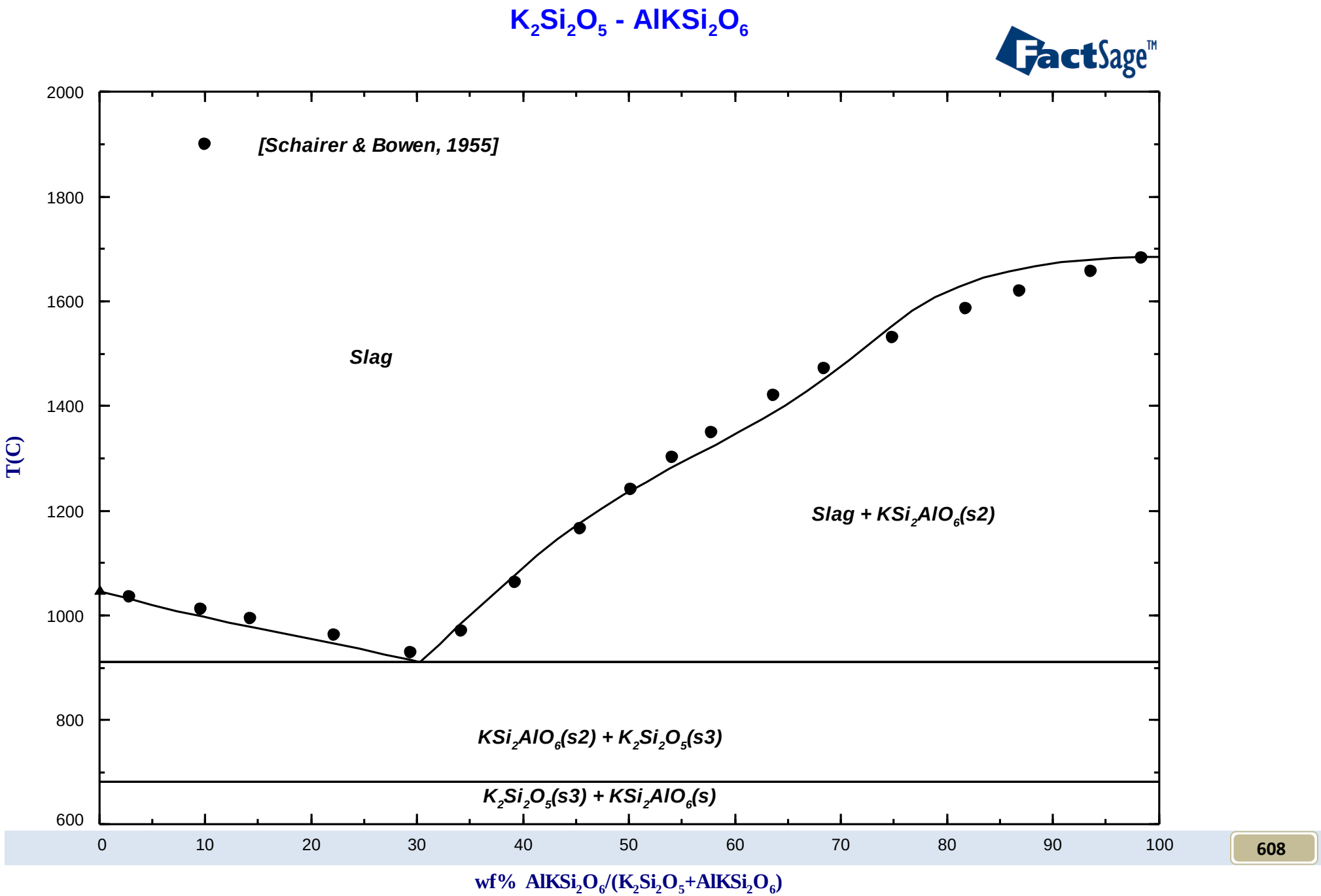

Weight percent K16SiO2-Al6Si2O13 compared with experimental data

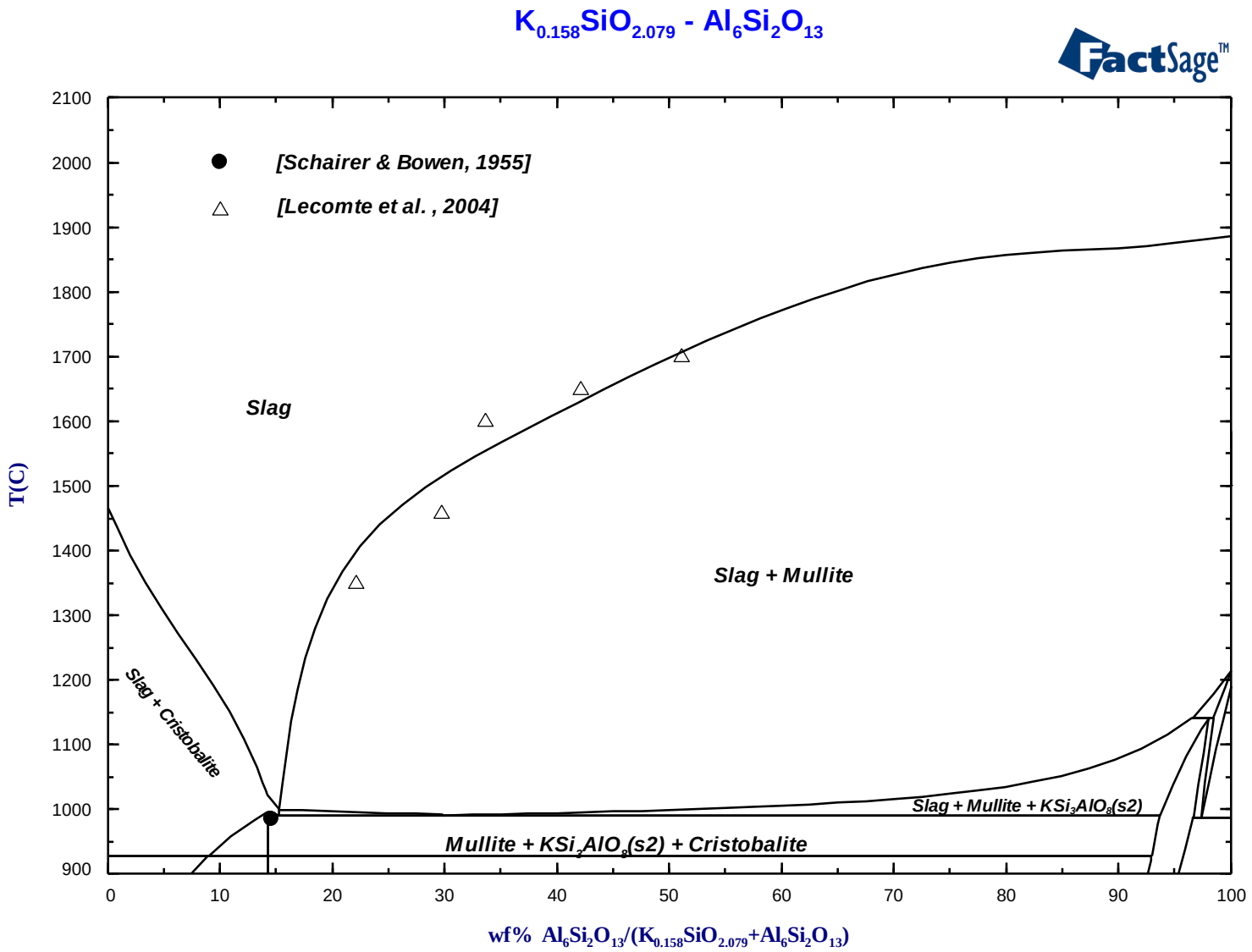

Weight percent KAlSi3O8-K2Si4O9 compared with experimental data

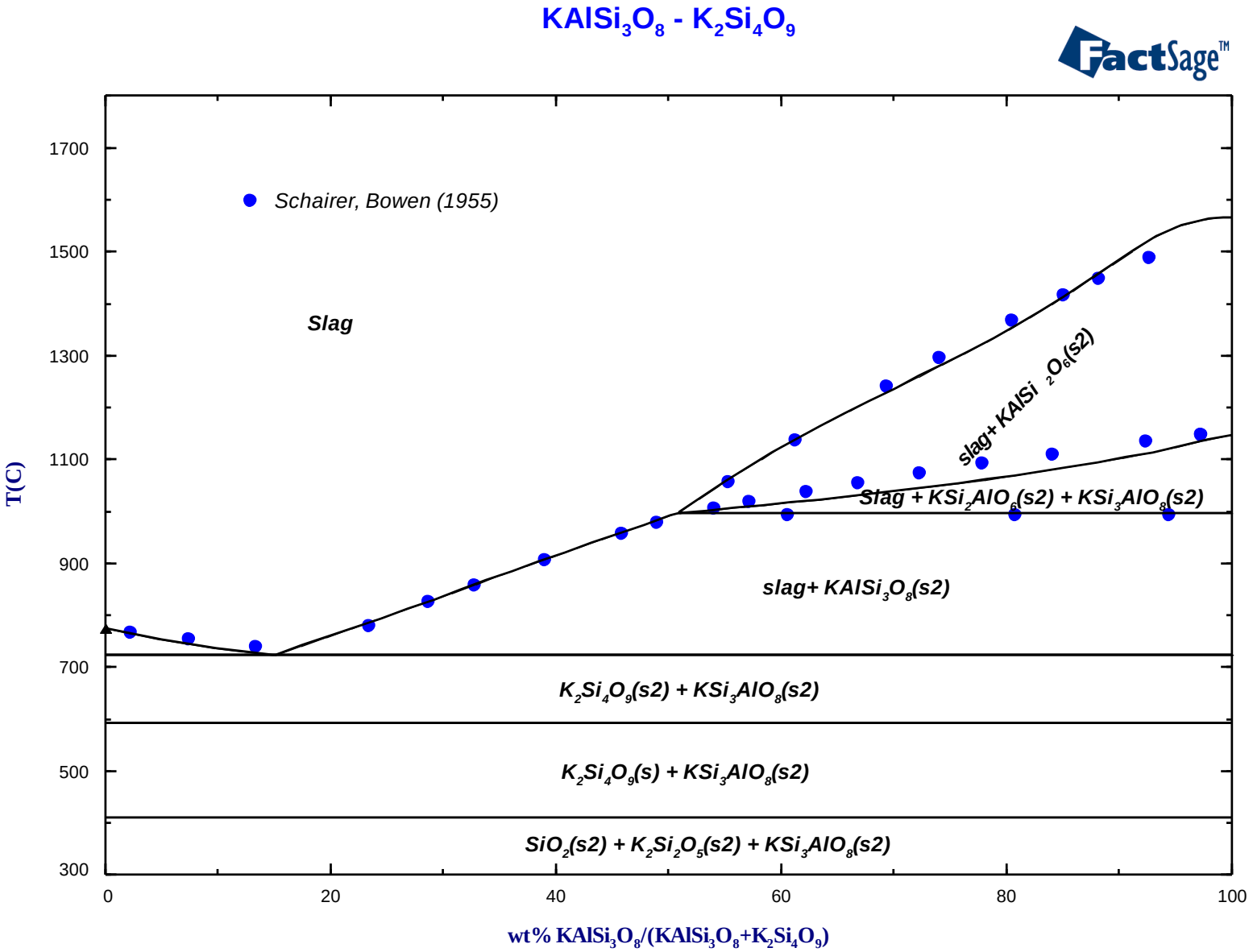

Weight percent KAlSi2O6-Al2O3

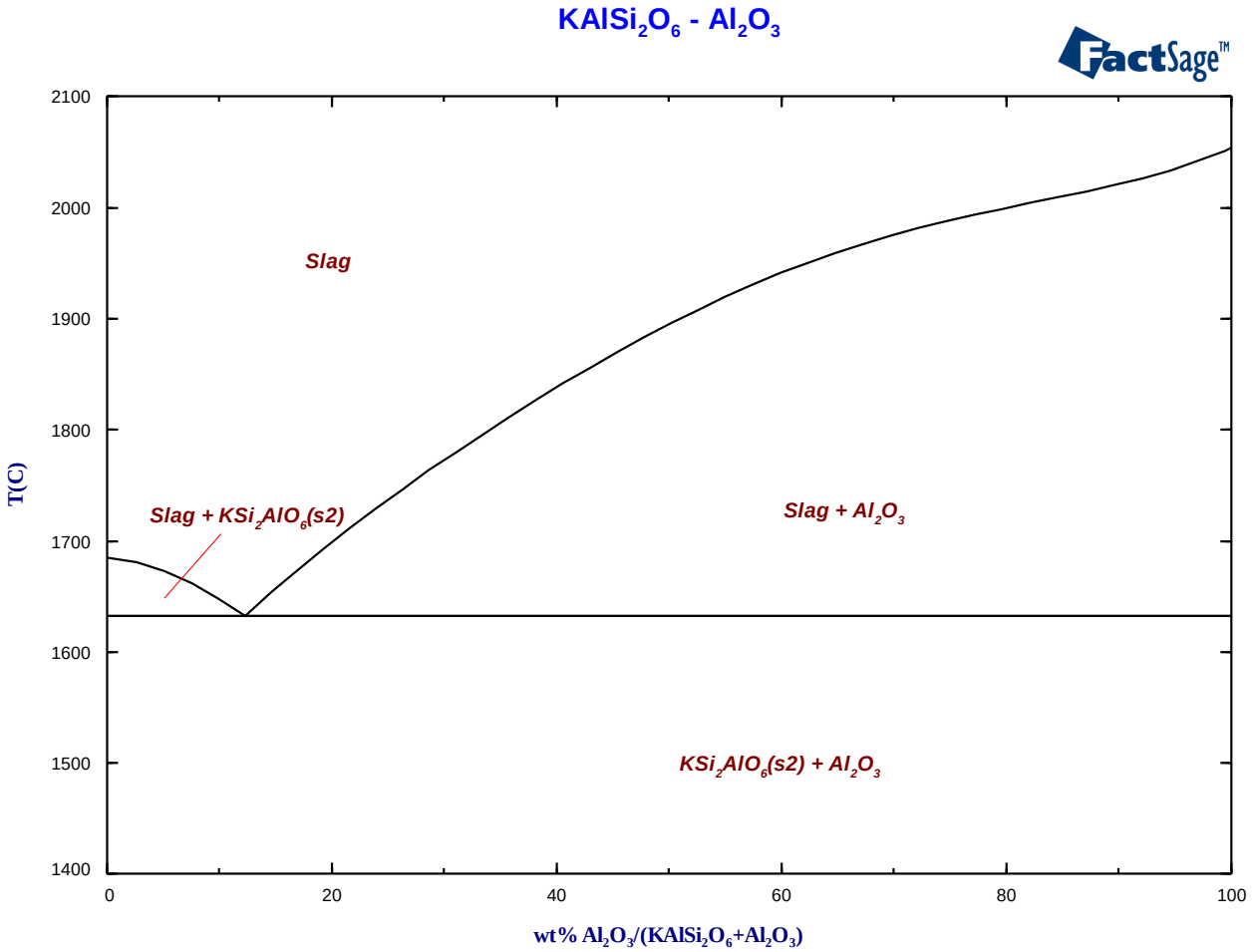

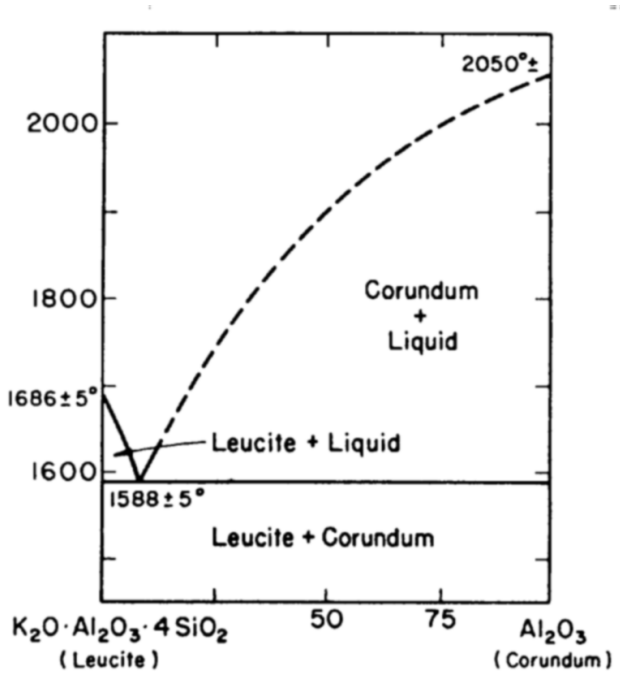

J. F. Schairer, N.L. Bowen, Am. J. Sci., 253 [12], (1955), pp 681-746.

Weight percent KAlSiO4-K2Si2O5

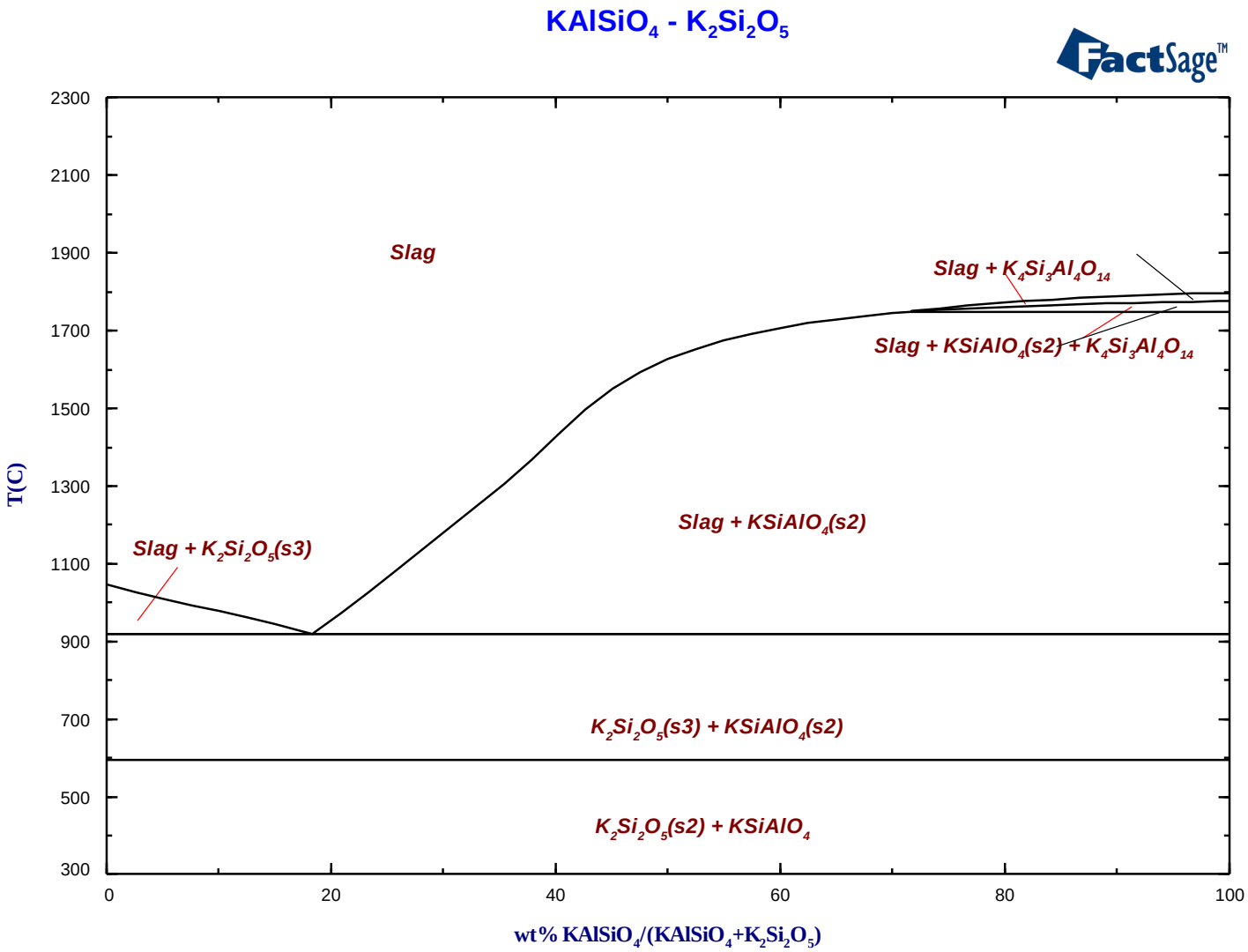

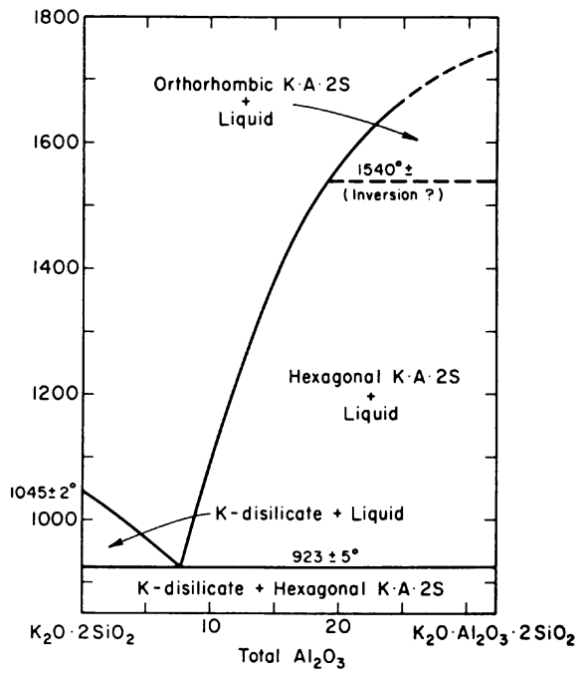

J. F. Schairer, N.L. Bowen, Am. J. Sci., 253 [12], (1955), pp 681-746.

K_2O - Al_2O_3 - SiO_2

Projection (Slag), 1 atm

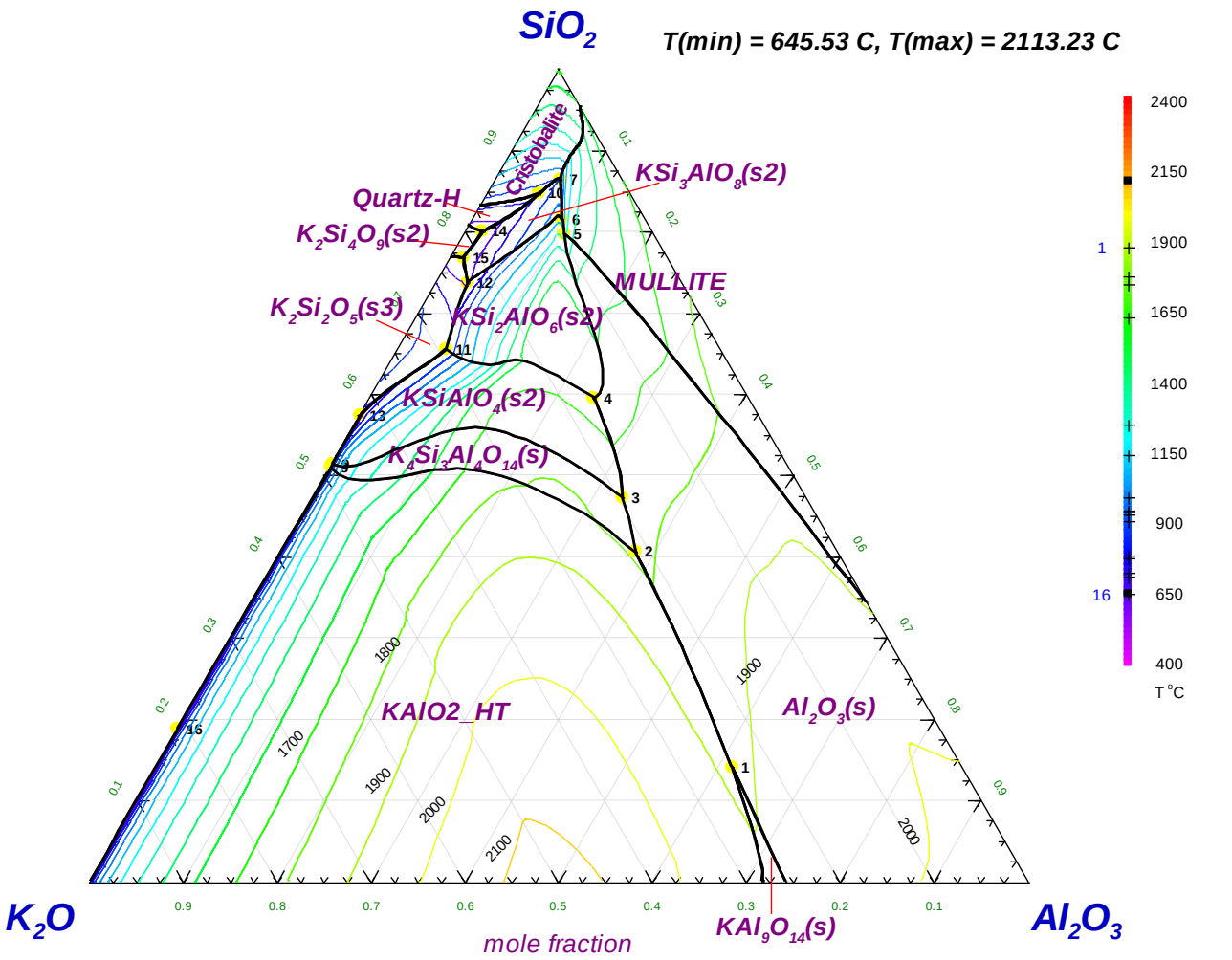

Weight percent
Liquidussurface
compared with experimental data

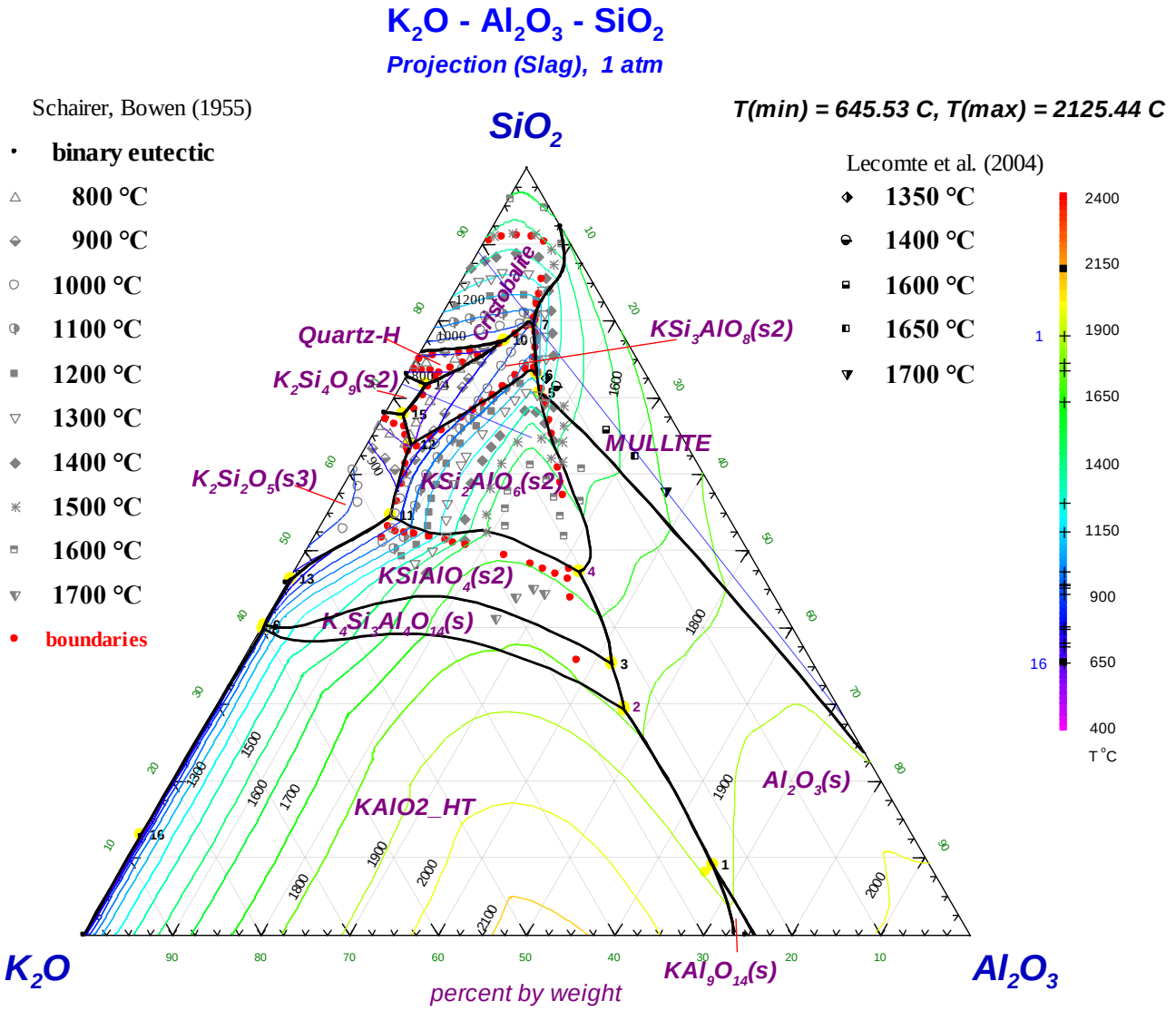

Invariant equilibria on the liquidus surface

Intersections with slag	Mole fraction A = SiO2, B = K2O, C = Al2O3				Weight percent A = SiO2, B = K2O, C = Al2O3			
	X(A)	X(B)	X(C)	T(C)	W(A)	W(B)	W(C)	T(C)
1: KAlO2_HT / Al2O3 / KAl9O14	0.14105	0.24440	0.61455	1878.21	9.001	24.450	66.549	1878.21
2: KAlO2_HT / Al2O3 / K4Si3Al4O14	0.40623	0.21465	0.37912	1774.47	29.308	24.277	46.415	1774.47
3: Al2O3 / K4Si3Al4O14 / KSiAlO4(s2)	0.47271	0.19506	0.33223	1745.79	35.216	22.782	42.002	1745.79
4: Al2O3 / KSi2AlO6(s2) / KSiAlO4(s2)	0.59587	0.16407	0.24006	1627.43	47.274	20.407	32.320	1627.43
5: Al2O3 / KSi2AlO6(s2) / Mullite	0.79740	0.09494	0.10766	1248.86	70.632	13.184	16.184	1248.86
6: KSi2AlO6(s2) / KSi3AlO8(s2) / Mullite	0.81549	0.08804	0.09646	1140.76	72.995	12.354	14.651	1140.76
7: KSi3AlO8(s2) / Mullite / Cristobalite	0.86446	0.06523	0.07031	990.50	79.598	9.416	10.986	990.50
8: KAlO2_HT / K2SiO3 / K4Si3Al4O14	0.50994	0.48728	0.00277	943.82	39.884	59.748	0.368	943.91
9: K2SiO3 / K4Si3Al4O14 / KSiAlO4(s2)	0.51420	0.48369	0.00211	936.46	40.295	59.424	0.281	936.46
10: KSi3AlO8(s2) / Cristobalite / Quartz-H	0.84731	0.09637	0.05633	926.28	77.453	13.810	8.737	926.28
11: K2Si2O5(s3) / KSi2AlO6(s2) / KSiAlO4(s2)	0.65595	0.29192	0.05213	906.12	54.568	38.072	7.359	906.12
12: K2Si2O5(s3) / KSi2AlO6(s2) / KSi3AlO8(s2)	0.73761	0.22816	0.03423	784.22	63.952	31.012	5.037	784.22
13: K2Si2O5(s3) / K2SiO3 / KSiAlO4(s2)	0.57466	0.42314	0.00220	771.36	46.278	53.422	0.301	771.36
14: K2Si4O9(s2) / KSi3AlO8(s2) / Quartz	0.80026	0.18122	0.01851	722.05	71.722	25.462	2.816	722.06
15: K2Si2O5(s3) / K2Si4O9(s2) / KSi3AlO8(s2)	0.76817	0.21697	0.01486	706.83	67.768	30.007	2.225	706.83
16: KAlO2_HT / K2O(s3) / K2SiO3	0.18802	0.81185	0.00013	645.53	12.869	87.115	0.015	645.74

Al2O3-MgO-Na2O, Mole fraction 1500C°

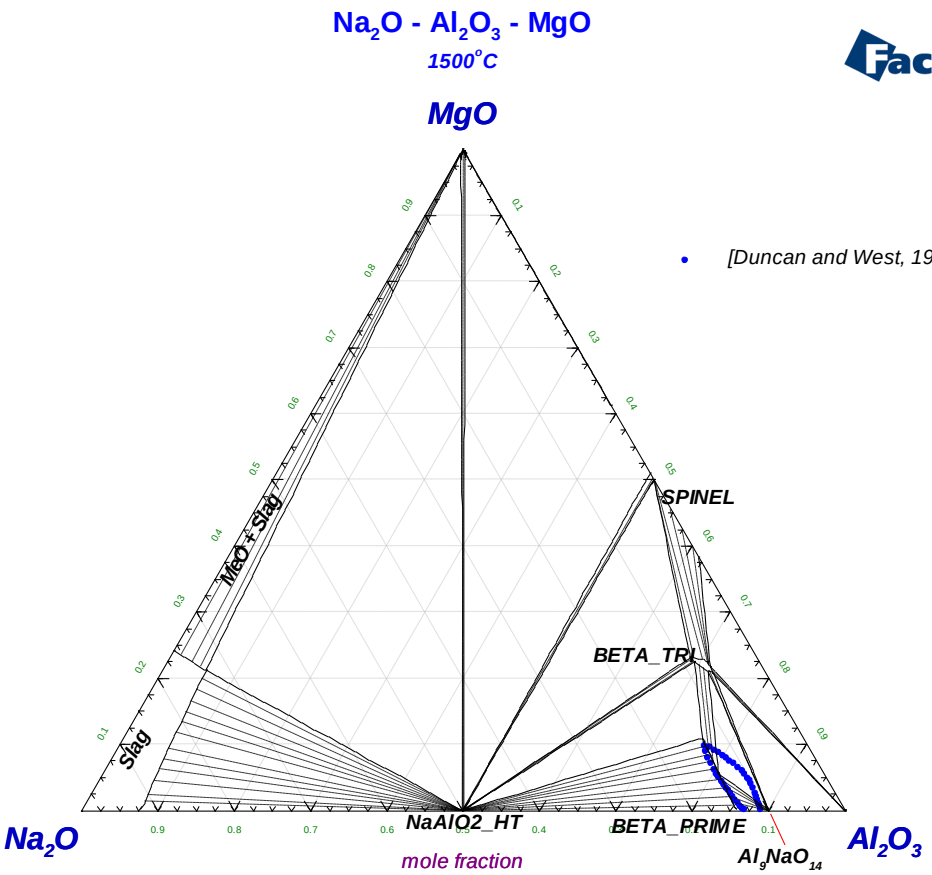

- *[Duncan and West, 1988]*

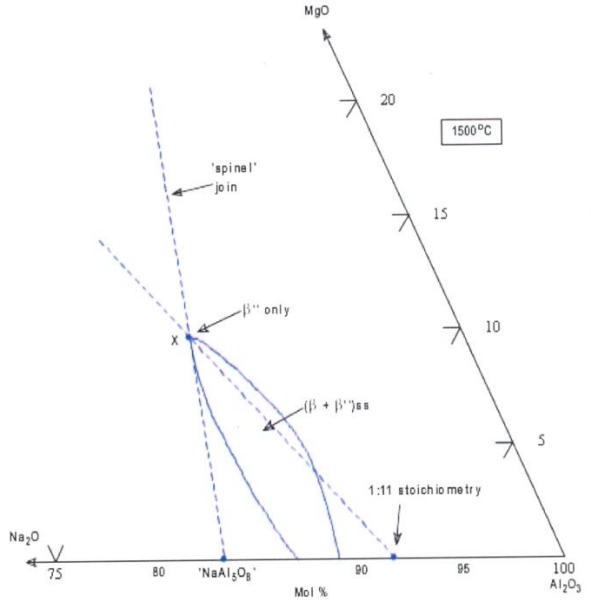

G. K. Duncan and A. R. West, Solid State Ionics, 28-30 [Pt. 1] 338-343 (1988).

Al2O3-MgO-Na2O, Mole fraction 1600C°

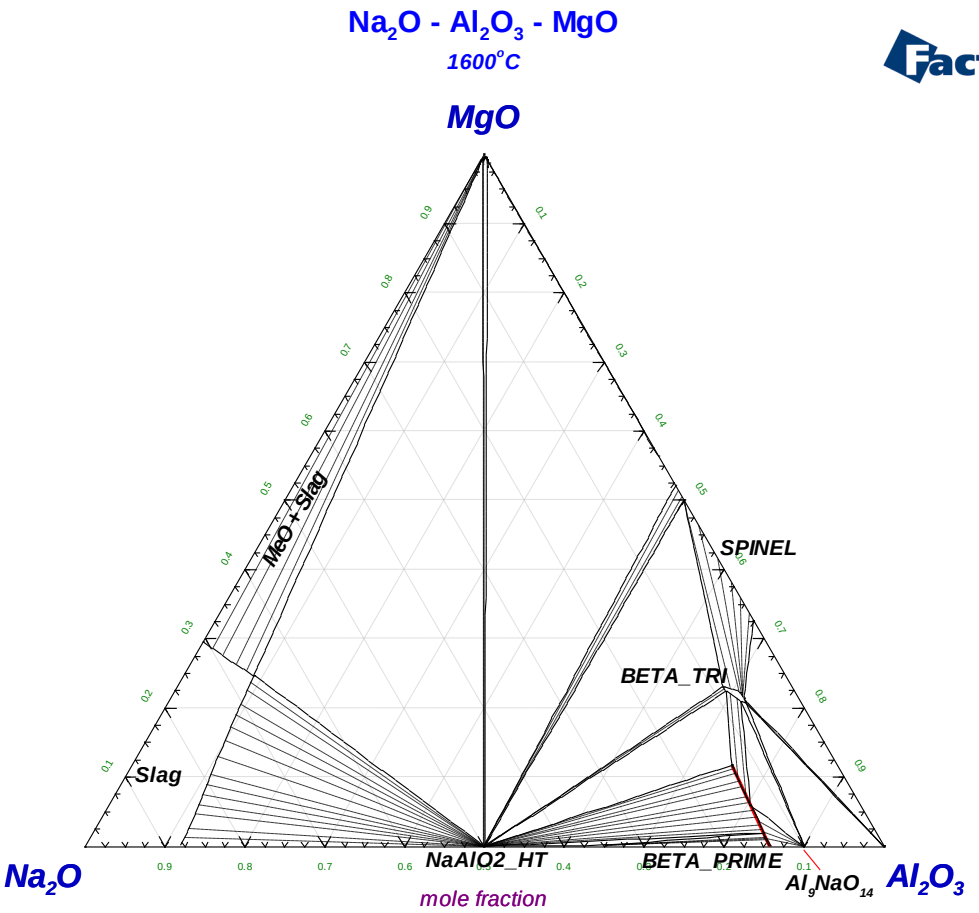

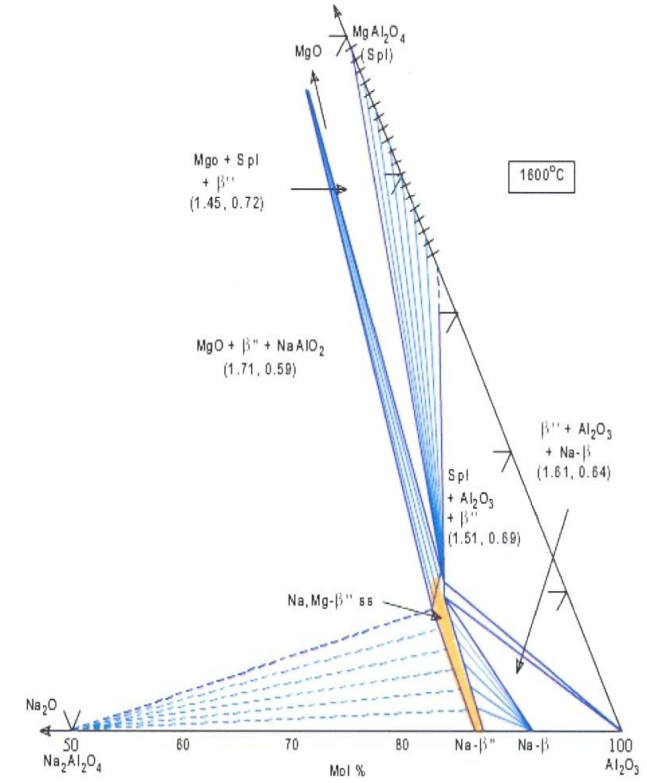

M. Alden, Solid State Ionics, 20 [1] 17-23 (1986).

Mole fraction
compared with experimental data

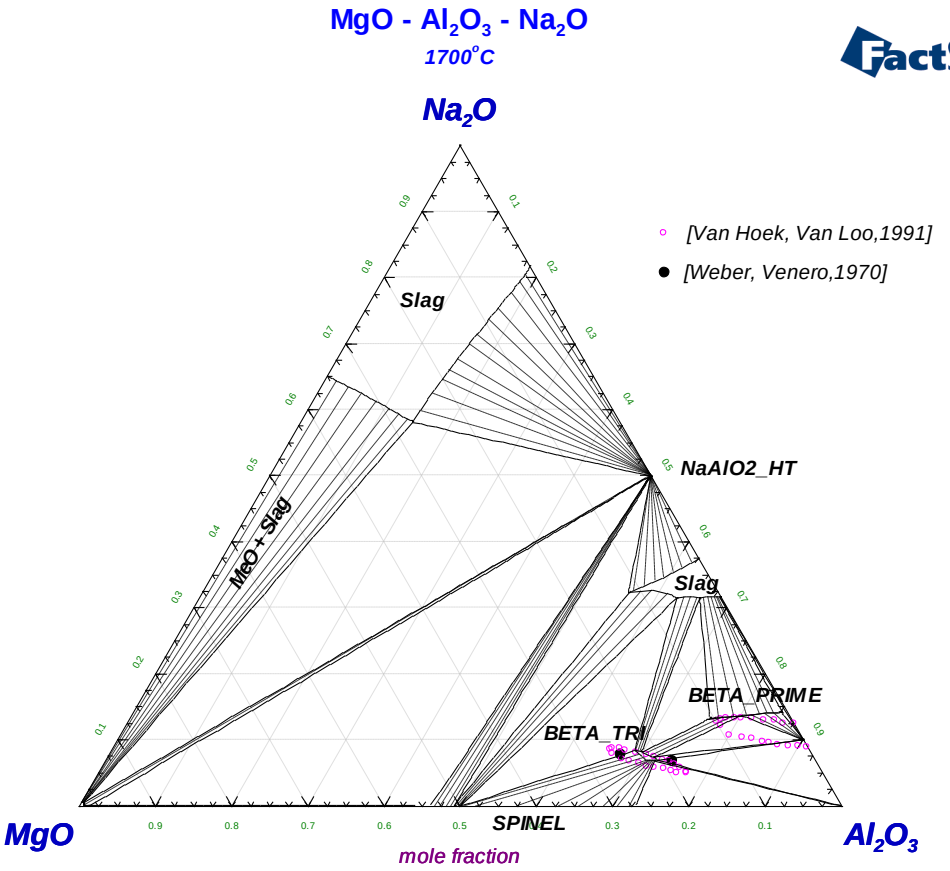

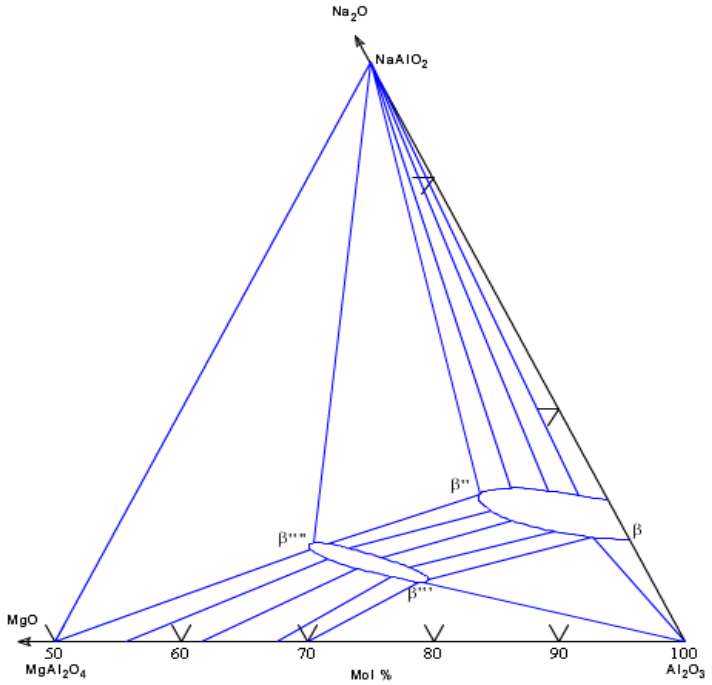

J. A. M. Van Hoek, F. J. J. Van Loo, and R. Metselaar, Key Eng. Mater.,53-55 [Austceram '90]

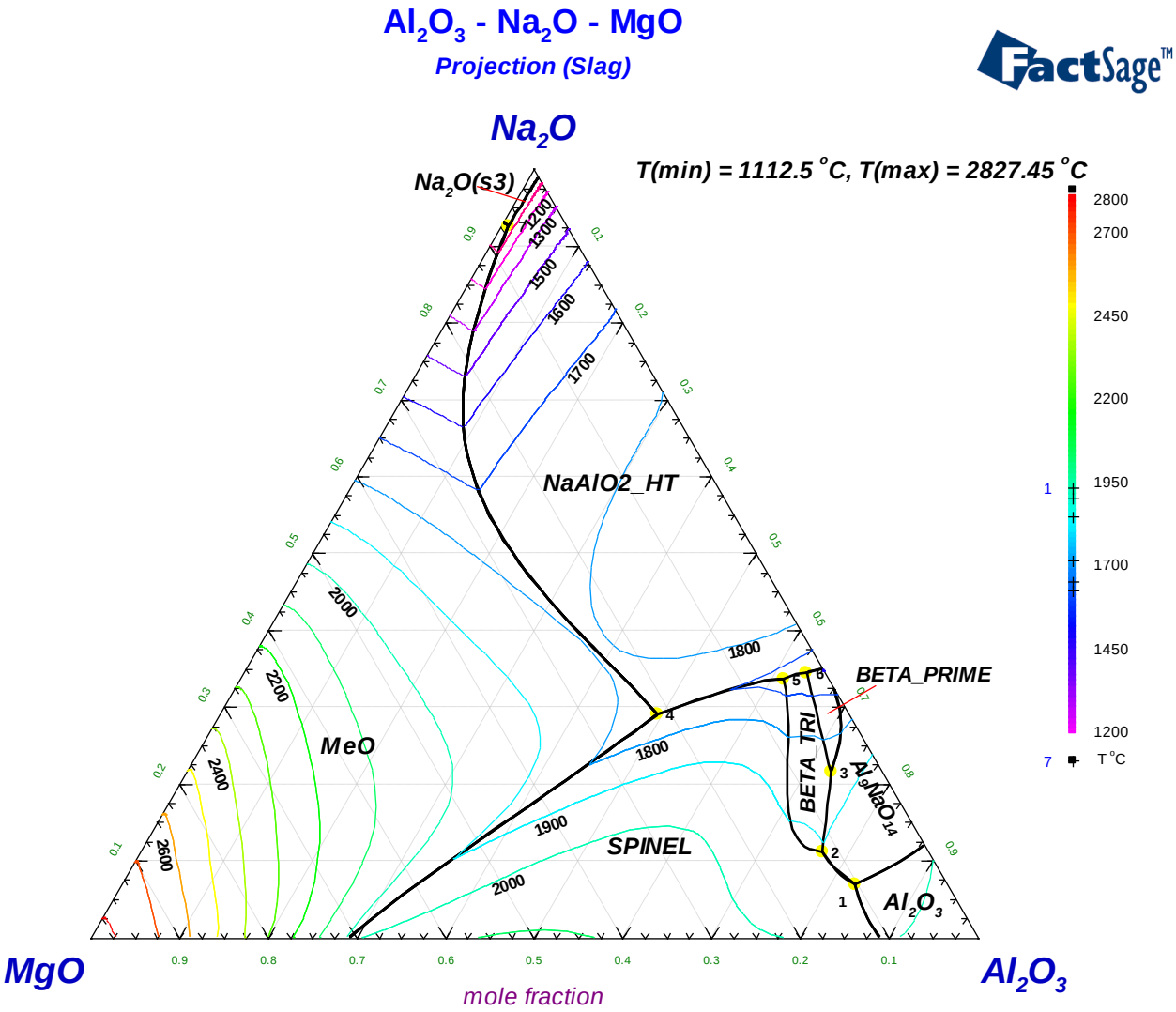
Al2O3 - Na2O - MgO
Projection (Slag)
FactSage™
Na2O
T(min) = 1112.5 °C, T(max) = 2827.45 °C
Na2O(s3)
NaAlO2_HT
MeO
SPINEL
BETA_PRIME
BETA_TRI
Al9NaO14
Al2O3
MgO
mole fraction
T °C
2800
2700
2450
2200
1950
1700
1450
1200

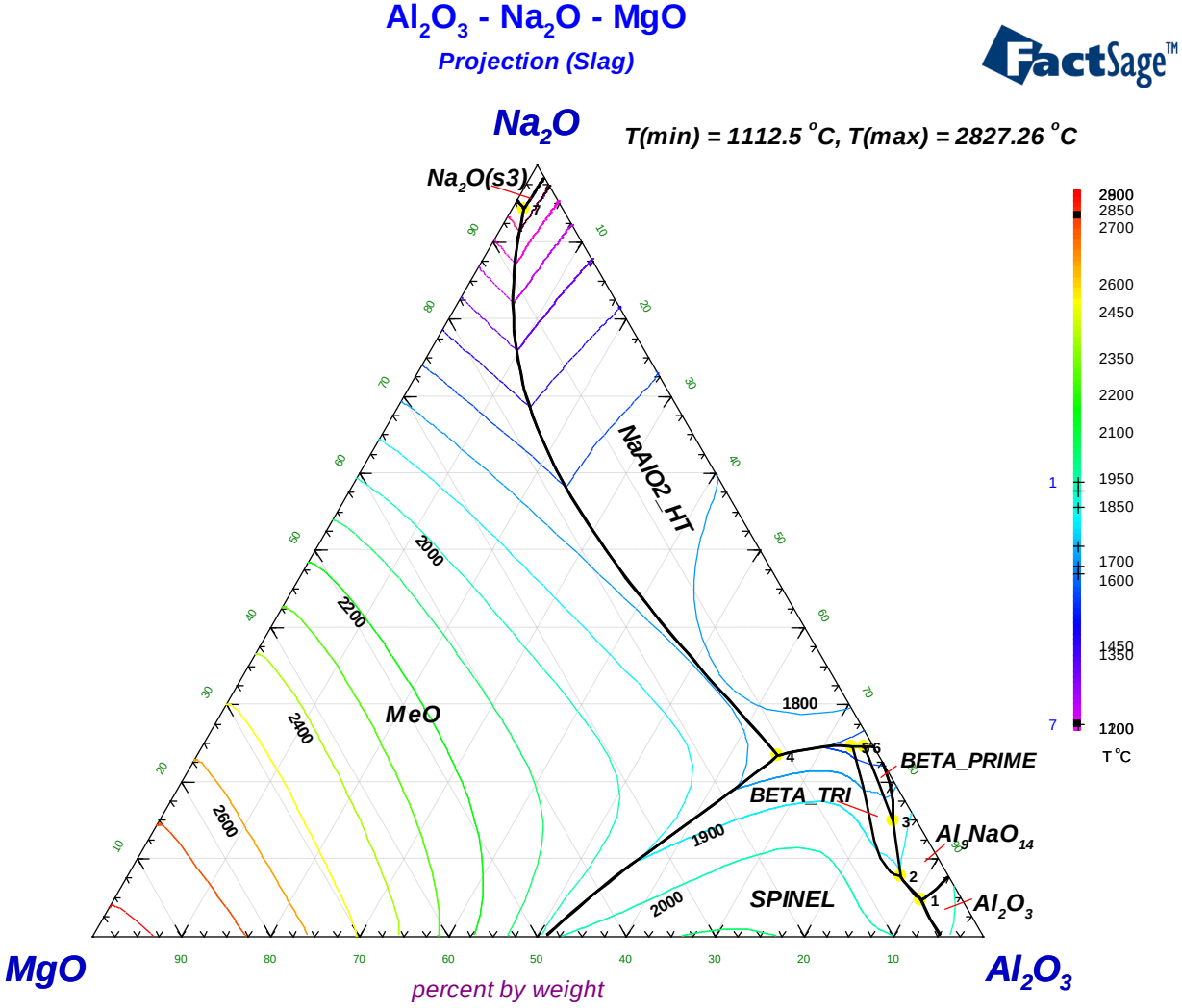
Al2O3 - Na2O - MgO
Projection (Slag)
FactSage™
Na2O
T(min) = 1112.5 °C, T(max) = 2827.26 °C
Na2O(s3)
NaAlO2_HT
MeO
SPINEL
BETA_PRIME
BETA_TRI
Al9NaO14
Al2O3
MgO
percent by weight
T °C
2900
2850
2700
2600
2450
2350
2200
2100
1950
1850
1700
1600
1450
1350
1200
2000
2200
2400
2600
1800
1900
2000

Invariant equilibria on the liquidus surface

Intersections with slag	Mole fraction				Weight percent			
	A = Na2O, B = MgO, C = Al2O3				A = Na2O, B = MgO, C = Al2O3			
	X(A)	X(B)	X(C)	T(C)	W(A)	W(B)	W(C)	T(C)
1: Al2O3 / Al9NaO14 / SPINEL	1: 0.06955	0.10358	0.82687	1929.66	1: 4.646	4.499	90.856	1929.65
2: Al9NaO14 / BETA_TRI / SPINEL	2: 0.11216	0.11863	0.76921	1902.44	2: 7.710	5.303	86.987	1902.42
3: Al9NaO14 / BETA_PRIME / BETA_TRI	3: 0.21624	0.05686	0.72690	1845.13	3: 14.923	2.552	82.525	1845.12
4: NaAlO2_HT / MeO / SPINEL	4: 0.29019	0.21570	0.49411	1714.47	4: 23.340	11.282	65.378	1714.47
5: NaAlO2_HT / BETA_TRI / SPINEL	5: 0.33676	0.04998	0.61327	1648.37	5: 24.436	2.358	73.206	1648.40
6: NaAlO2_HT / BETA_PRIME / BETA_TRI	6: 0.34459	0.02010	0.63531	1623.05	6: 24.564	0.932	74.504	1623.08
7: NaAlO2_HT / MeO / Na2O(s3)	7: 0.92649	0.06510	0.00841	1112.50	7: 94.284	4.308	1.408	1112.50

Al2O3-MgO-P2O5, Mole fraction 1200°C

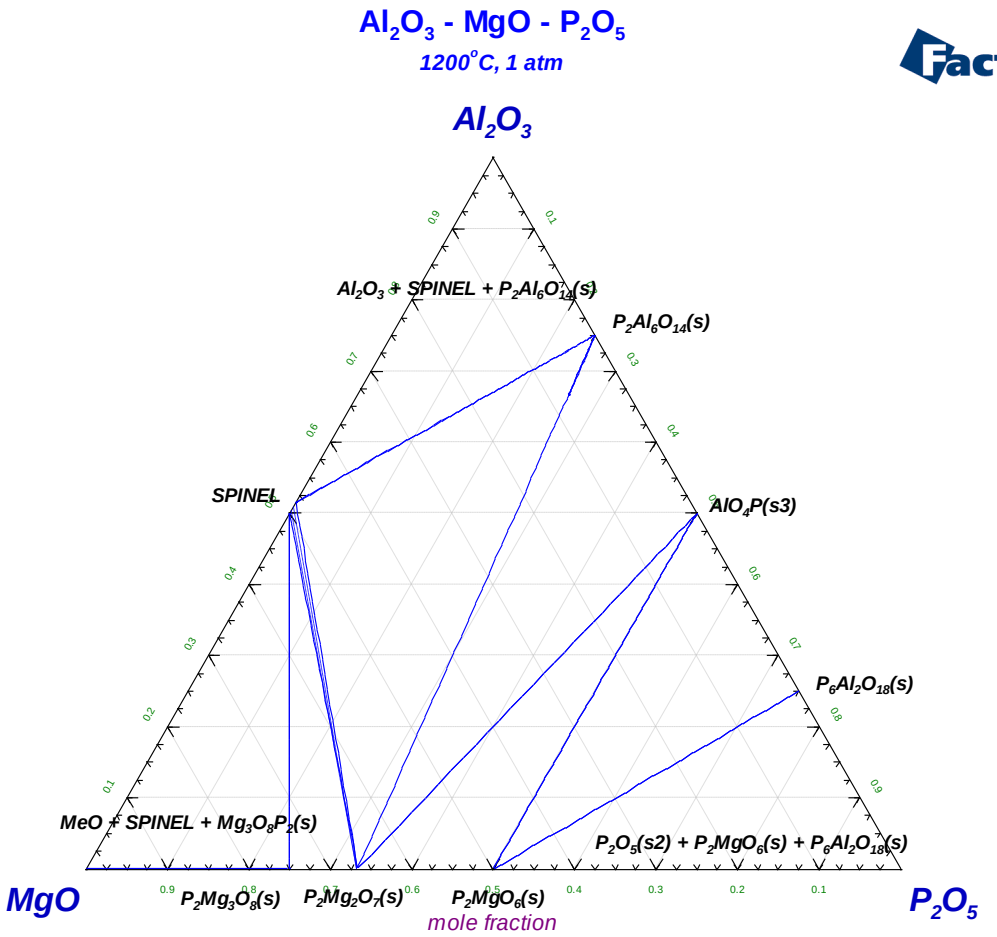

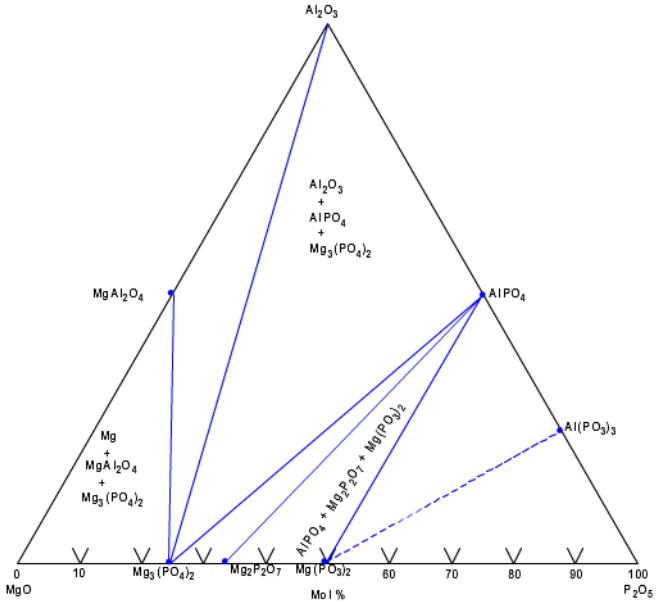

F. J. Gonzalez and J. W. Halloran, J. Am. Ceram. Soc., 63 [9-10] 599-600 (1980).

Al2O3-MgO-P2O5,
Mole fraction, Isopleth Mg(PO3)2-Al(PO3)3

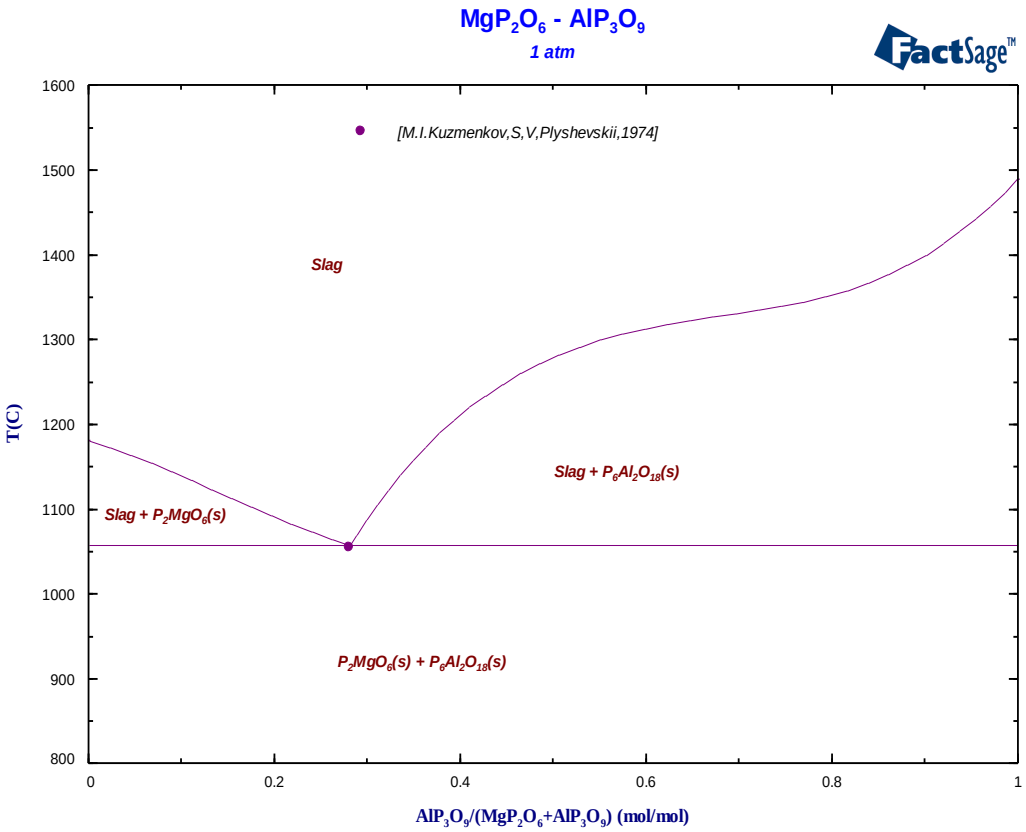

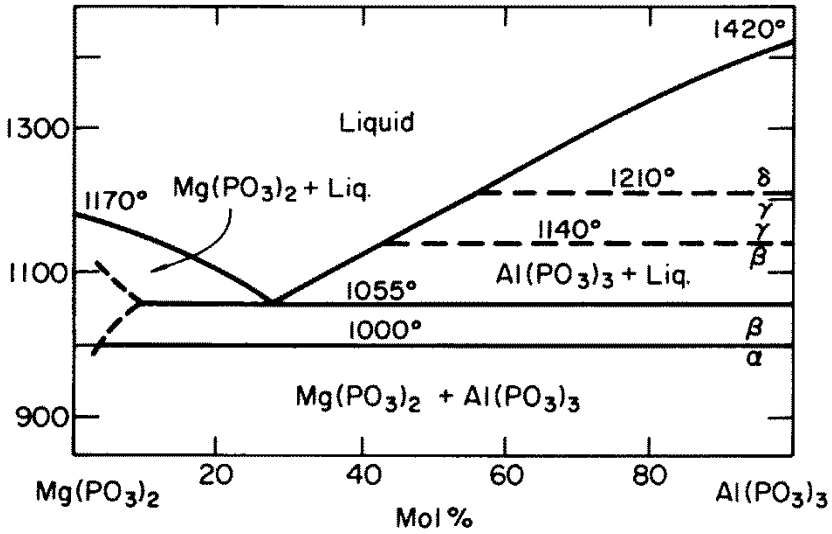

F. J. Gonzalez and J. W. Halloran, J. Am. Ceram. Soc., 63 [9-10] 599-600 (1980).

Mole fraction, Liquidussurface

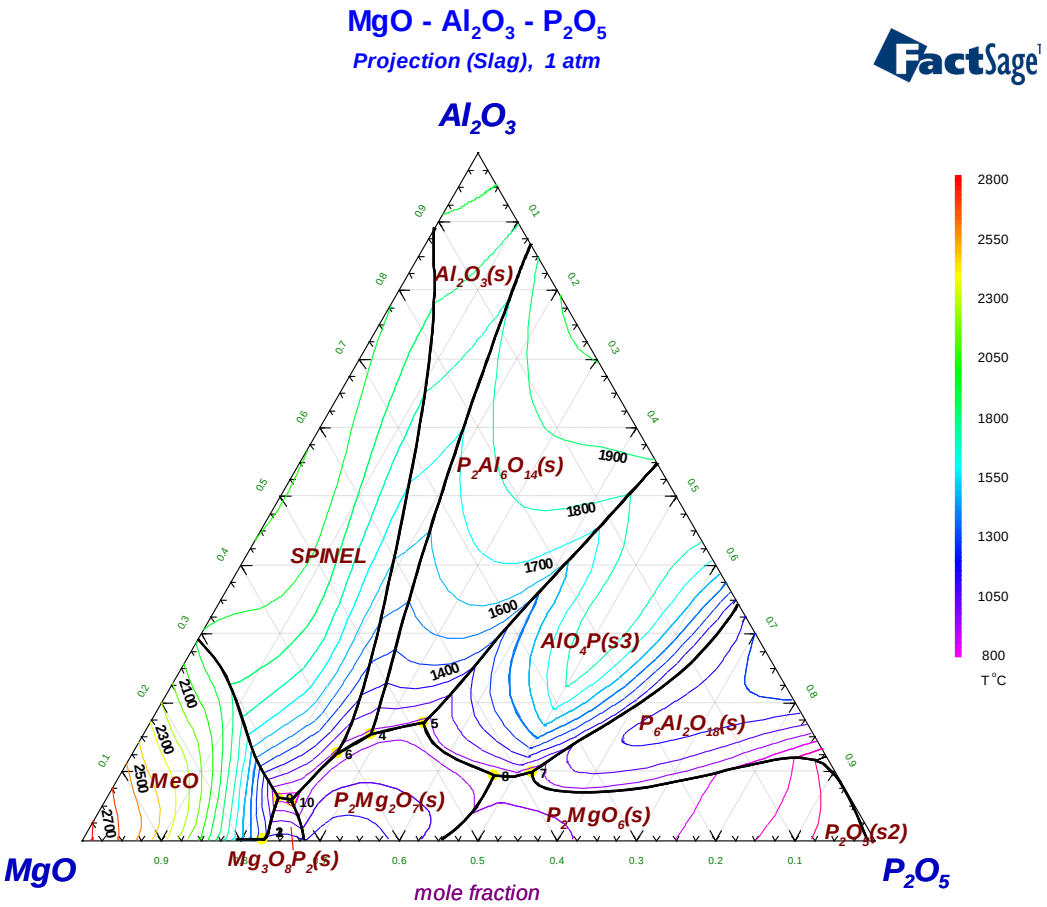

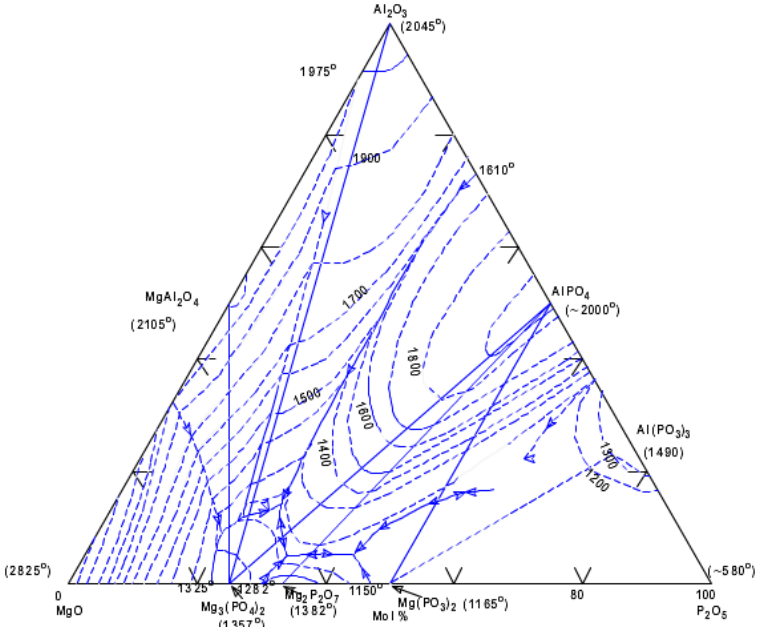

F. J. Gonzalez and J. W. Halloran, J. Am. Ceram. Soc., 63 [9-10] 599-600 (1980).

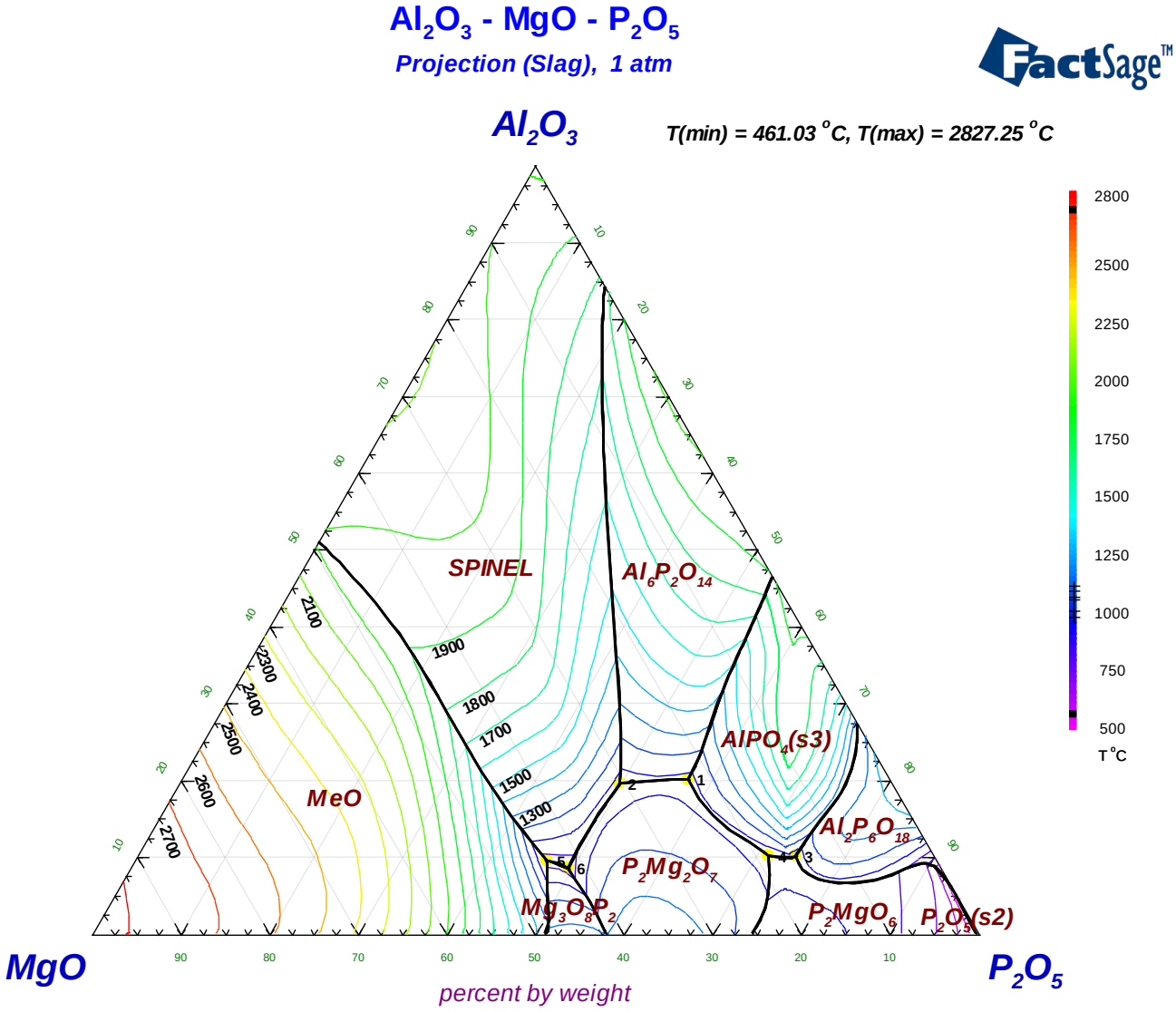
Al2O3 - MgO - P2O5
Projection (Slag), 1 atm
FactSage™
Al2O3
T(min) = 461.03 °C, T(max) = 2827.25 °C
SPINEL
Al6P2O14
AlPO4(s3)
Al2P6O18
P2Mg2O7
Mg3O8P2
P2MgO6
P2O5(s2)
MeO
2100
1900
1800
1700
1500
1300
2300
2400
2500
2600
2700
2800
2500
2250
2000
1750
1500
1250
1000
750
500
T°C
MgO
P2O5
percent by weight

Invariant equilibria on the liquidus surface

Intersections with slag	Mole fraction				Weight percent			
	A = Al2O3, B = MgO, C = P2O5				A = Al2O3, B = MgO, C = P2O5			
	X(A)	X(B)	X(C)	T(C)	W(A)	W(B)	W(C)	T(C)
1: Al6P2O14 / AlPO4(s3) / P2Mg2O7	1: 0.17009	0.48372	0.34619	1066.24	1: 20.171	22.675	57.154	1066.22
2: Al6P2O14 / P2Mg2O7 / SPINEL	2: 0.14716	0.58387	0.26897	1044.20	2: 19.559	30.675	49.767	1044.16
3: Al2P6O18 / AlPO4(s3) / P2MgO6	3: 0.09839	0.38238	0.51924	1010.65	3: 10.118	15.544	74.338	1010.90
4: AlPO4(s3) / P2Mg2O7 / P2MgO6	4: 0.09410	0.43286	0.47304	1002.27	4: 10.187	18.523	71.290	1002.26
5: MeO / Mg3O8P2 / SPINEL	5: 0.06151	0.72072	0.21776	948.18	5: 9.470	43.859	46.671	948.03
6: Mg3O8P2/ P2Mg2O7 / SPINEL	6: 0.05645	0.70688	0.23667	921.57	6: 8.485	41.996	49.519	921.54

Al_2O_3 - MgO - SiO_2

500°C

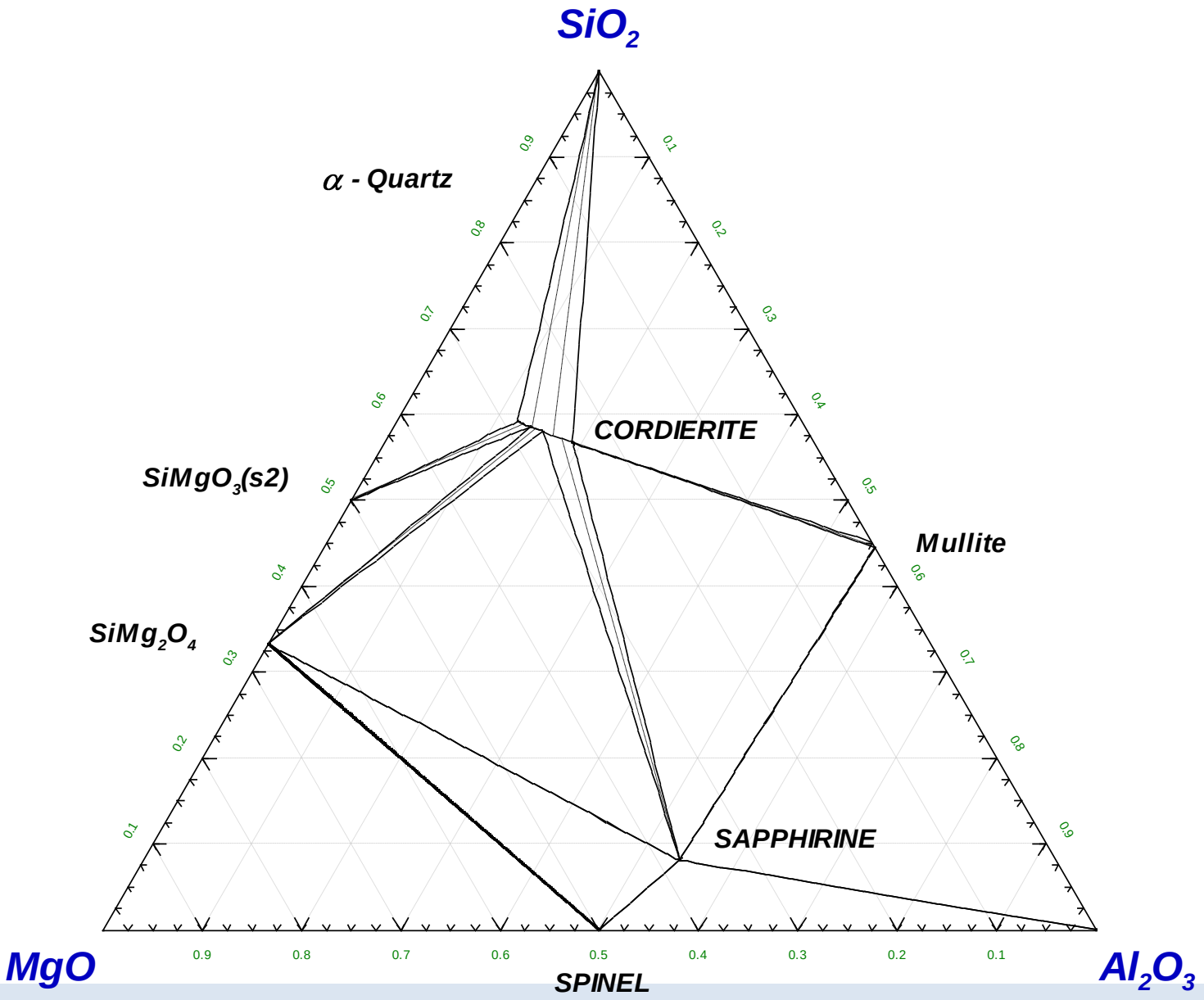

Al_2O_3 - MgO - SiO_2

1000°C

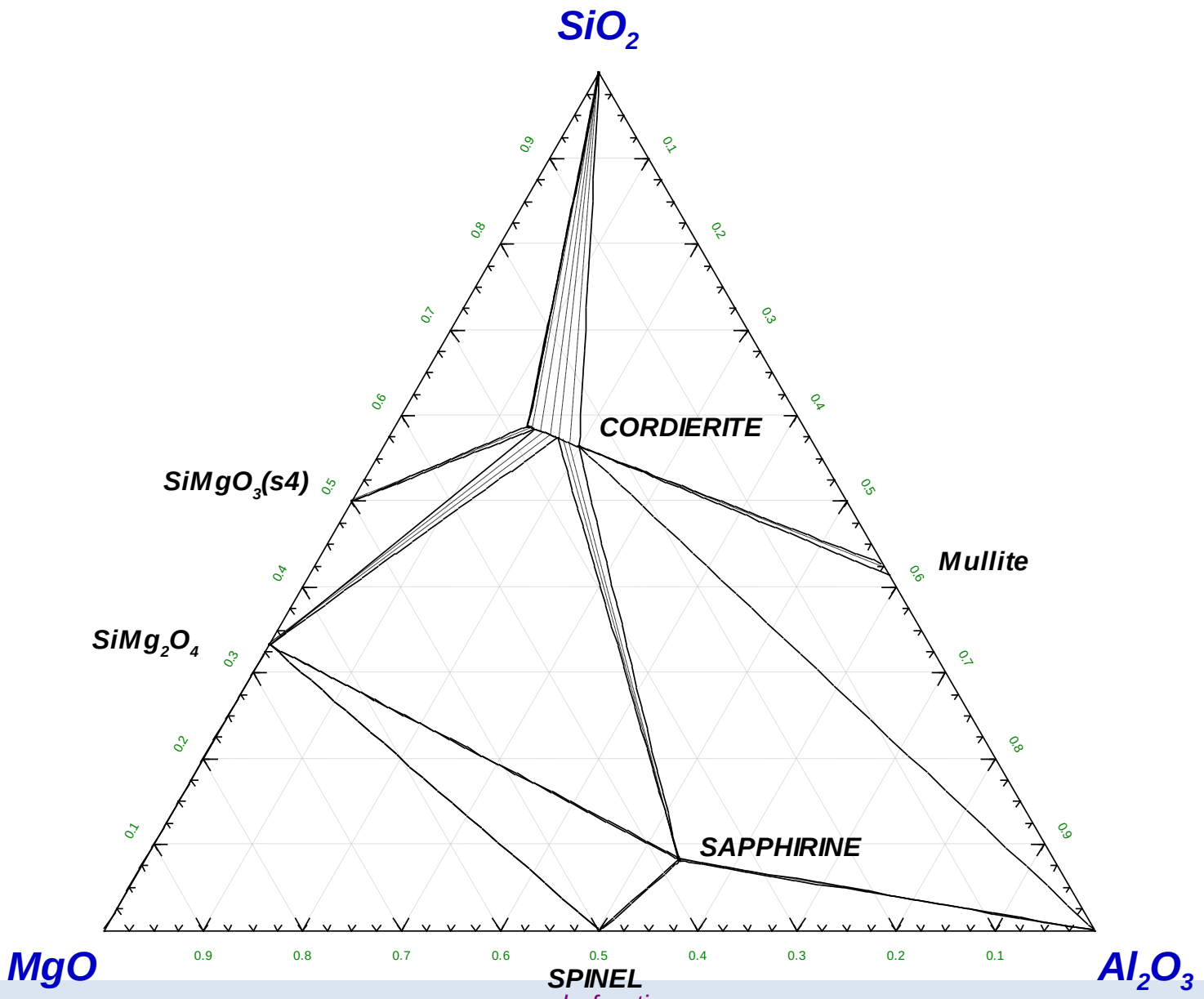

Weight percent
compared with experimental data

Al_2O_3 - MgO - SiO_2

1350°C

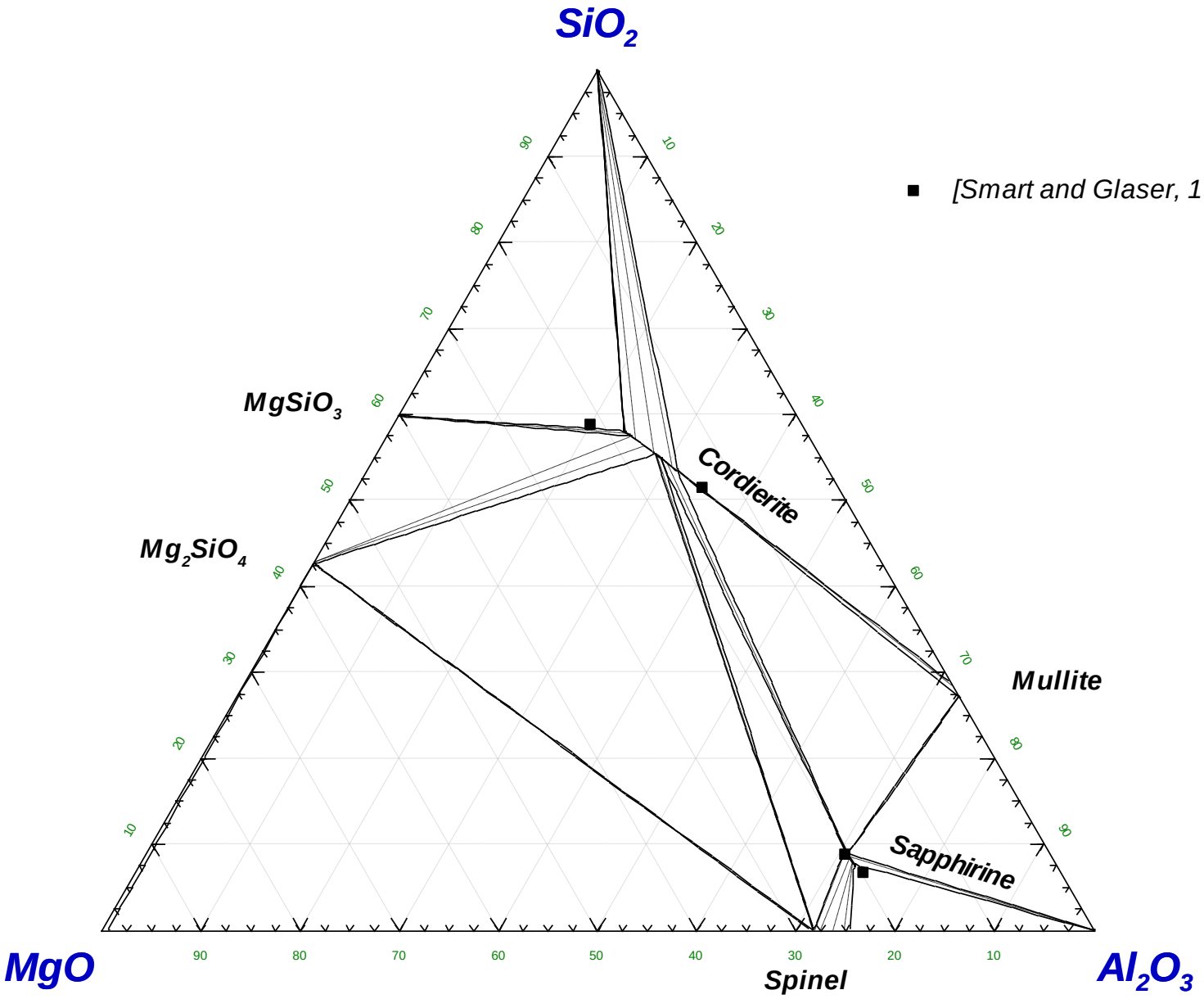

- *[Smart and Glaser, 1981]*

Mole fraction
kurz unterhalb Liquidussurface

Al_2O_3 - MgO - SiO_2

1380°C

FactSage™

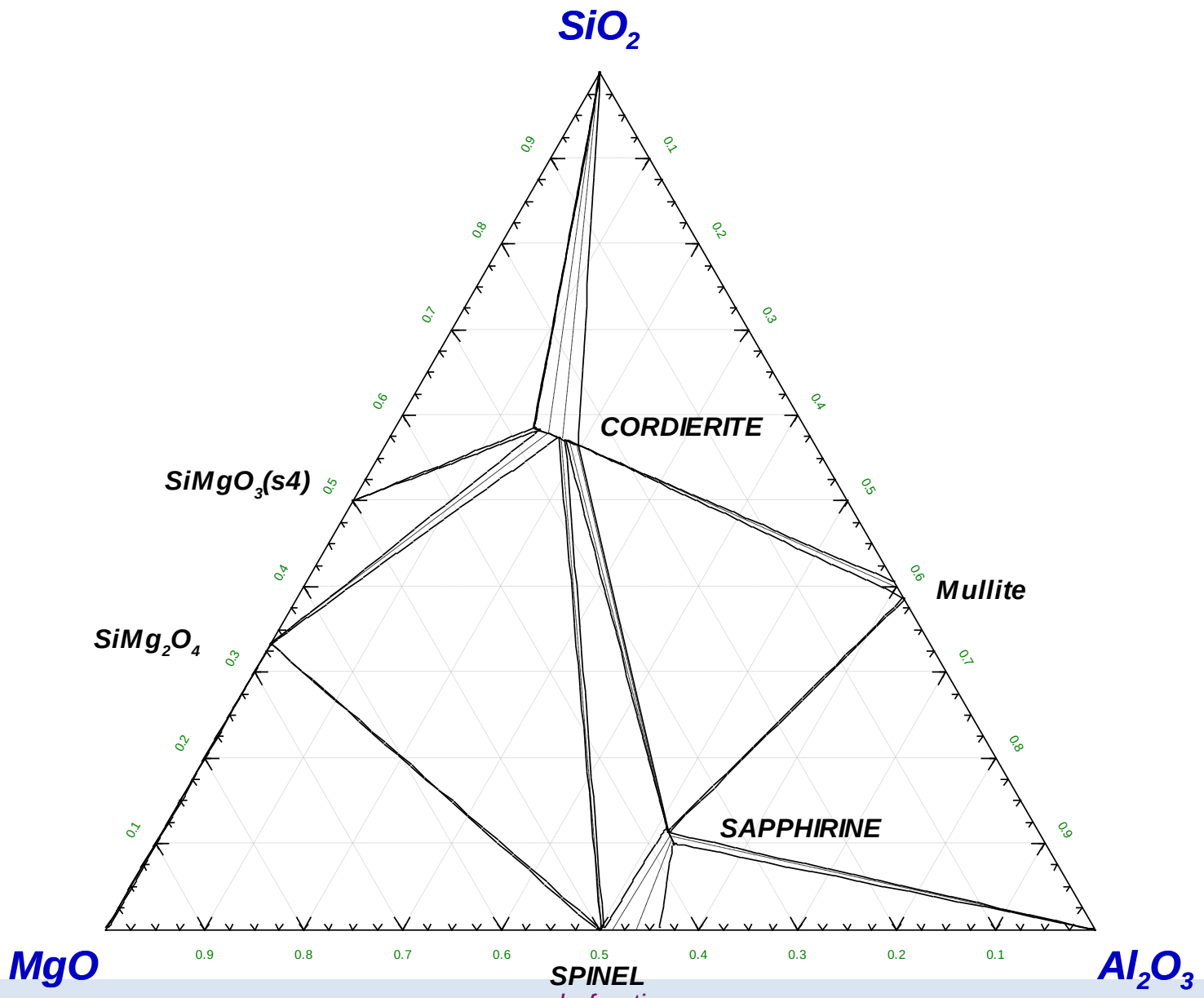

Weight percent
compared with experimental data

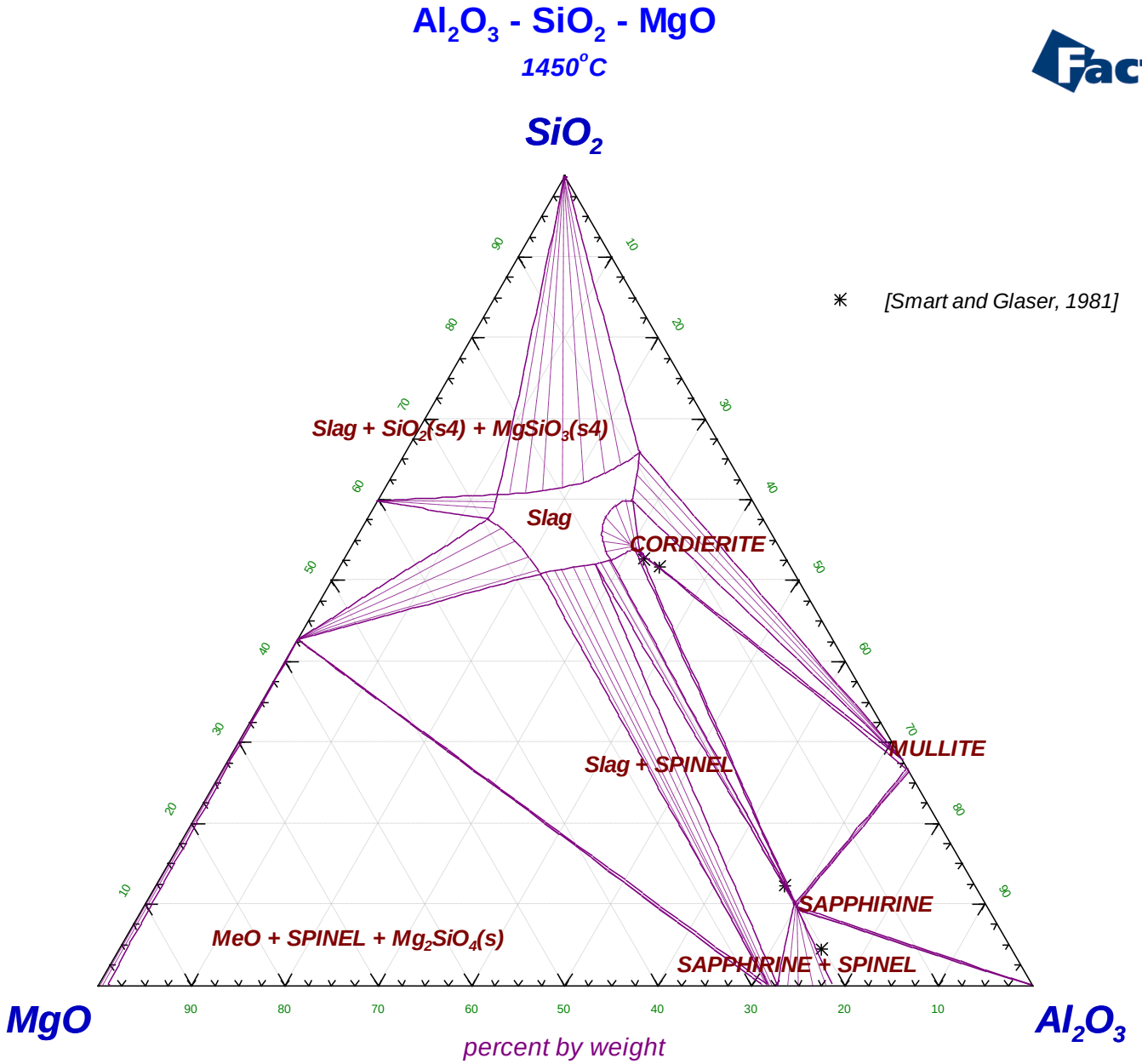

Weight percent compared with experimental data

SiO_2 - $Al_4Mg_2Si_5O_{18}$

1 bar

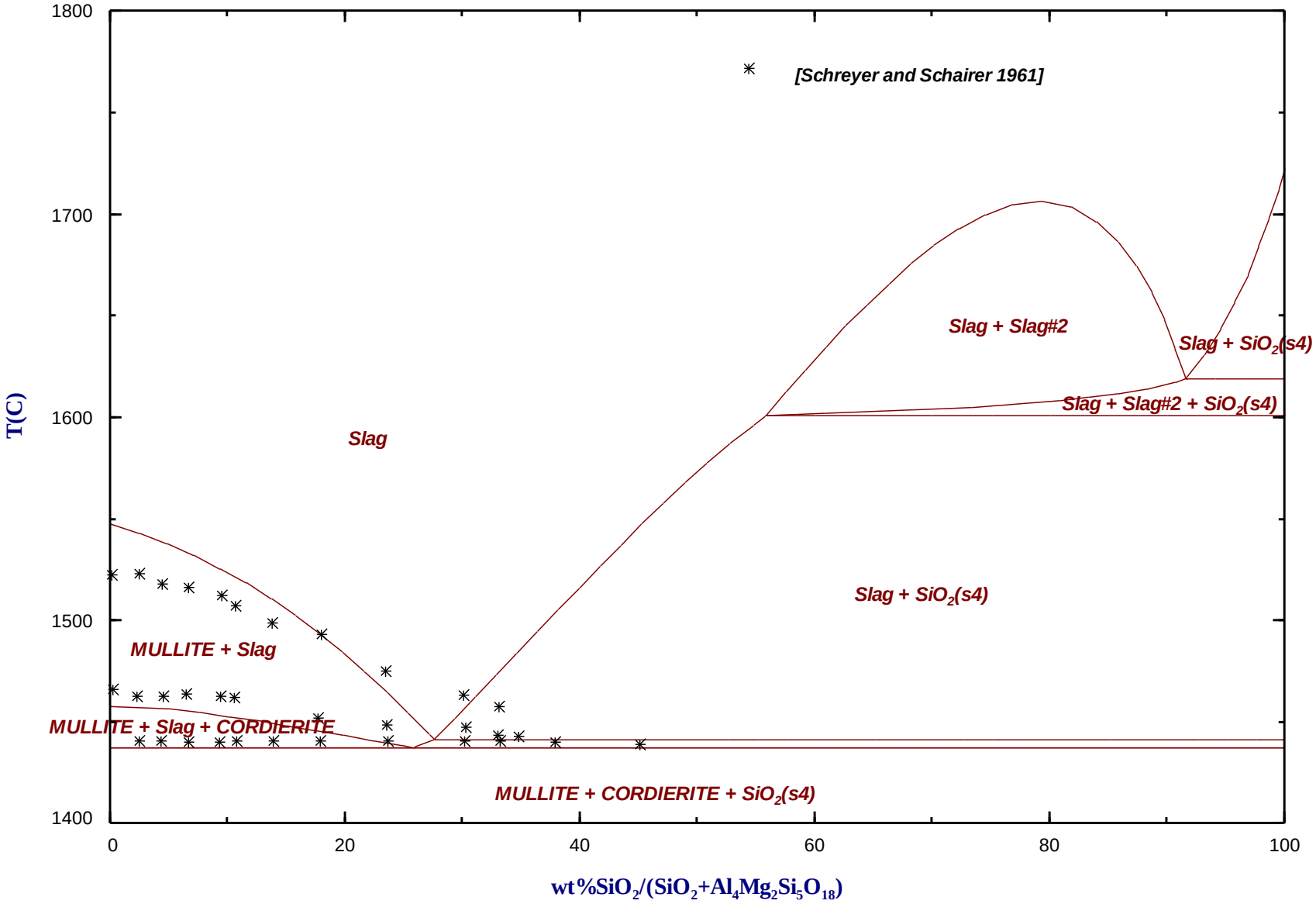

Al_2O_3 - MgO - SiO_2

Projection (Slag), 1 bar

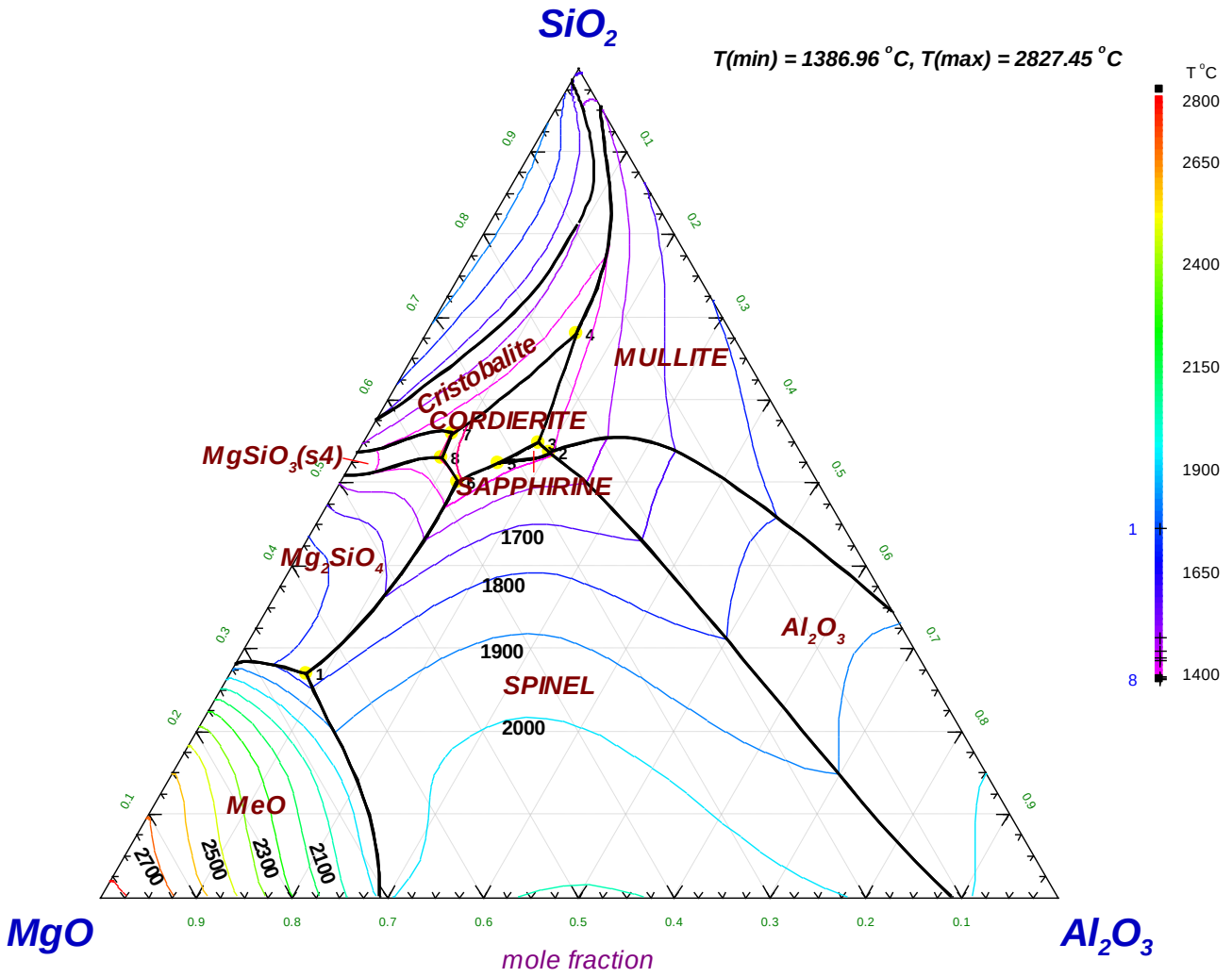

Al_2O_3 - MgO - SiO_2

Projection (Slag), 1 bar

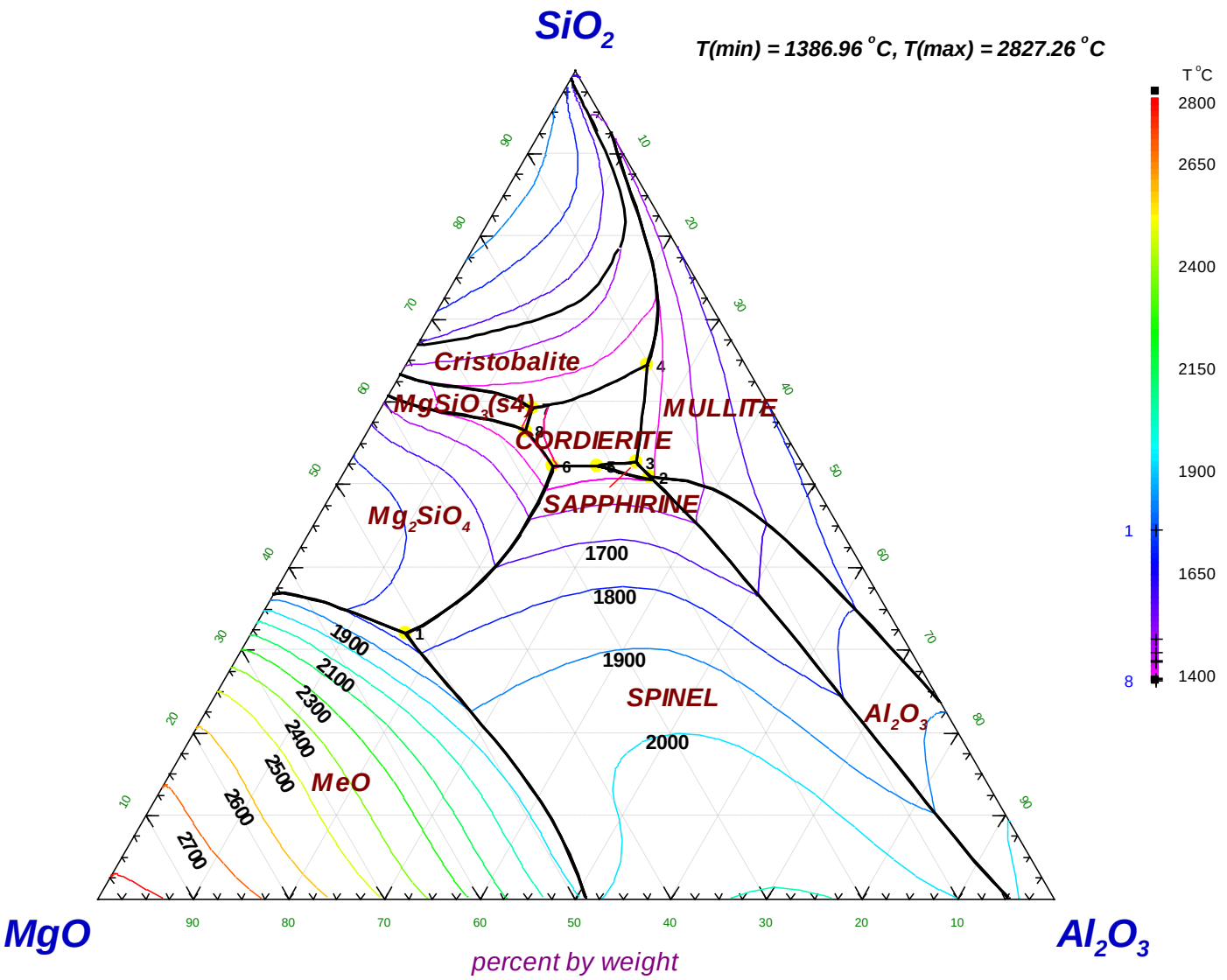

Invariant equilibria on the liquidus surface

Intersections with slag	Mole fraction				Weight percent				
	A = SiO2, B = MgO, C = Al2O3				A = SiO2, B = MgO, C = Al2O3				
		X(A)	X(B)	X(C)	T(C)		W(A)	W(B)	W(C)	T(C)
1: MeO / Mg2SiO4 / SPINEL	1:	0.26930	0.64991	0.08079	1756.15	1:	31.968	51.757	16.275	1756.13
2: Al2O3 / MULLITE / SAPPHIRINE	2:	0.53688	0.26184	0.20129	1491.43	2:	50.298	16.927	32.775	1491.43
3: CORDIERITE / MULLITE / SAPPHIRINE	3:	0.54774	0.26831	0.18396	1455.85	3:	52.392	17.455	30.152	1455.85
4: CORDIERITE / MULLITE / Cristobalite	4:	0.67960	0.16281	0.15758	1437.46	4:	64.065	10.454	25.480	1437.46
5: CORDIERITE / SAPPHIRINE / SPINEL	5:	0.52318	0.32235	0.15447	1433.65	5:	52.194	21.615	26.192	1433.65
6: CORDIERITE / Mg2SiO4 / SPINEL	6:	0.50121	0.37611	0.12268	1395.32	6:	52.194	26.169	21.637	1395.32
7: CORDIERITE / MgSiO3(s4) / Cristobalite	7:	0.55983	0.35135	0.08881	1389.58	7:	59.443	24.637	15.920	1389.58
8: CORDIERITE / Mg2SiO4 / MgSiO3(s4)	8:	0.53043	0.37749	0.09207	1386.96	8:	56.625	26.750	16.626	1386.96

Al2O3-MgO-TiO2,
Weight percent 1000C°

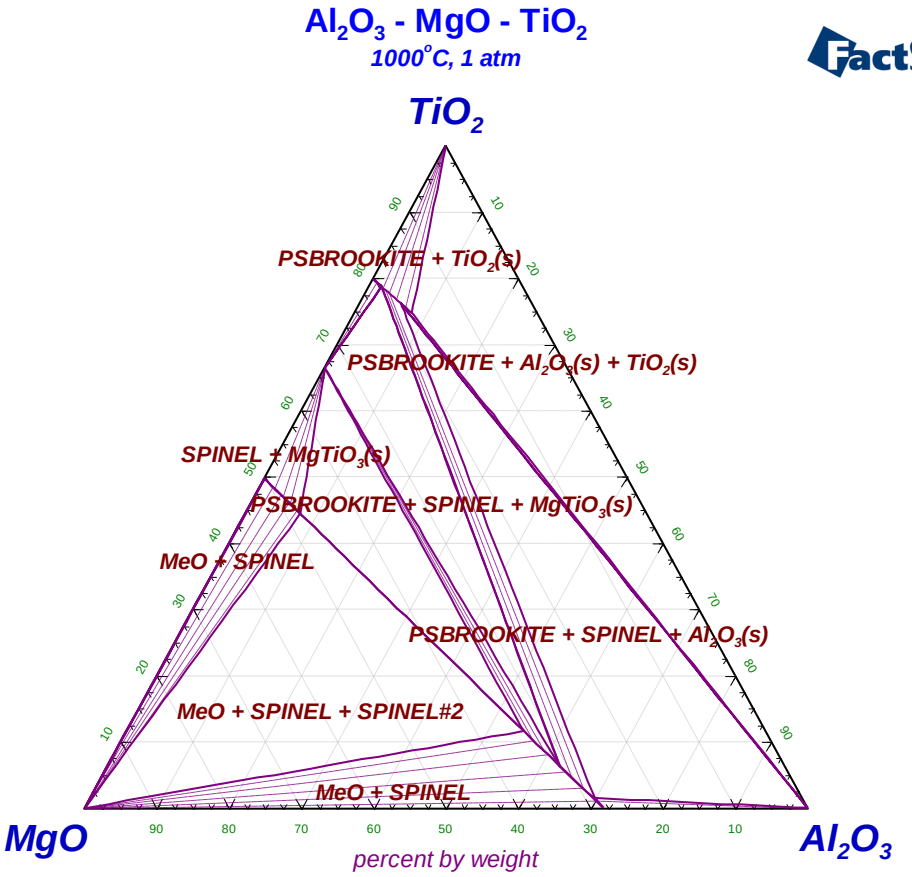

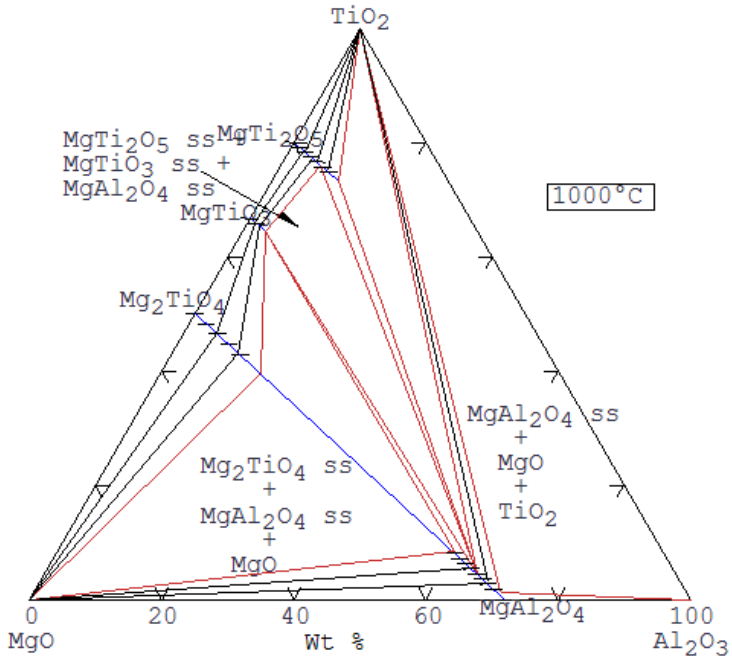

J. Hauck, J. Solid State Chem., 36 [1], (1981), pp. 52-65.

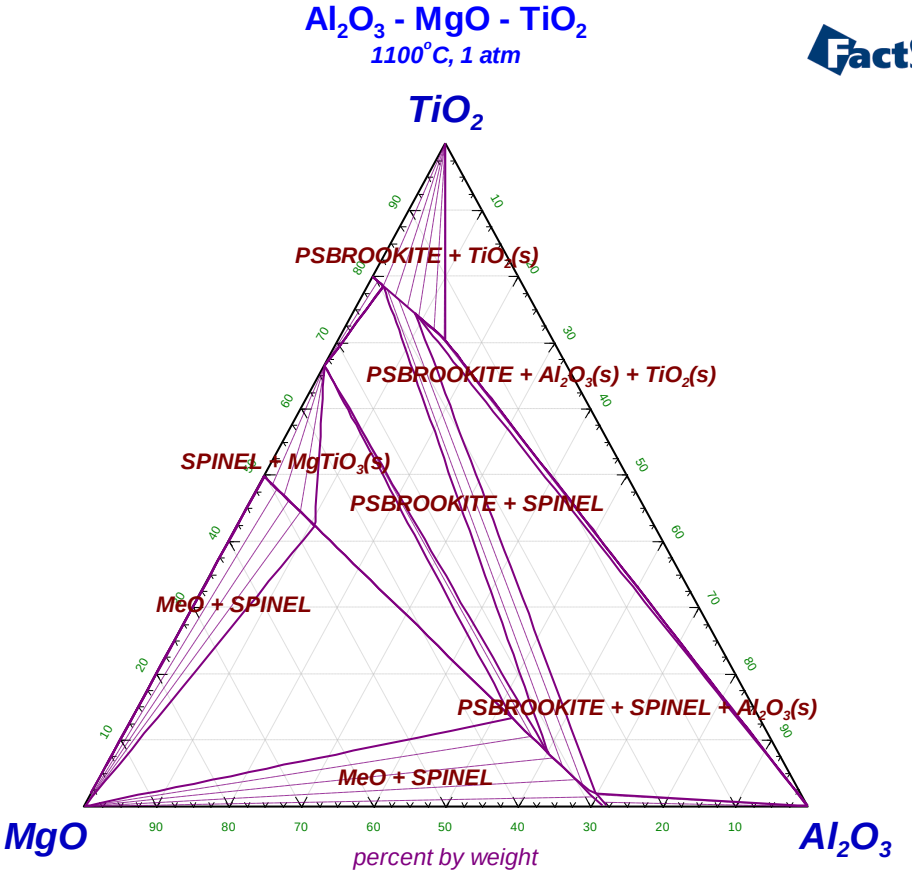

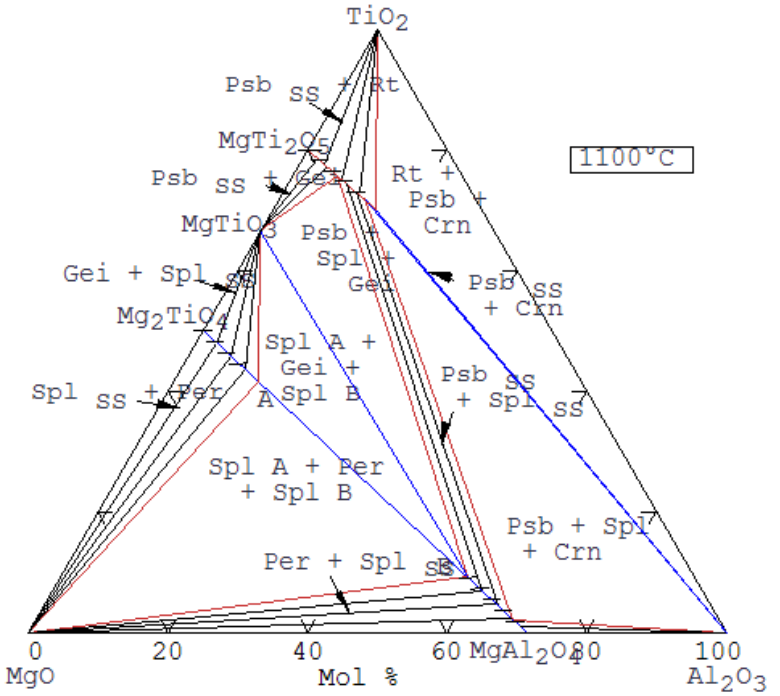

P. Boden, F.P. Glasser, Trans. J. Br. Ceram. Soc., 72[5], (1973), pp. 215-220.

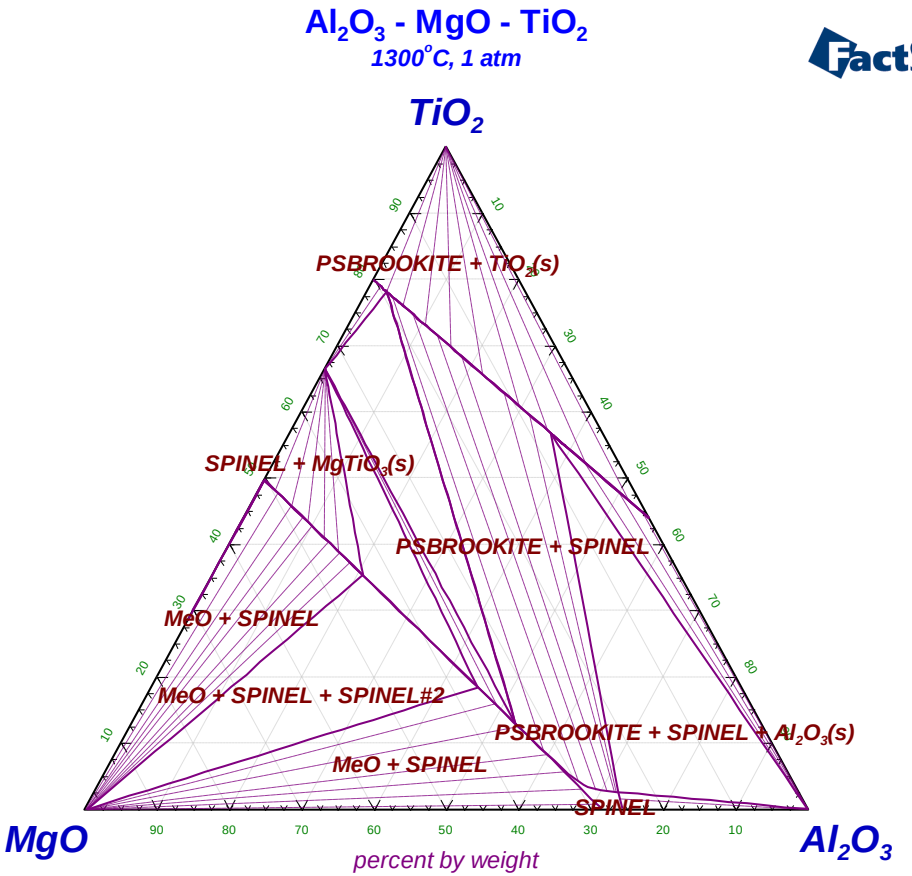

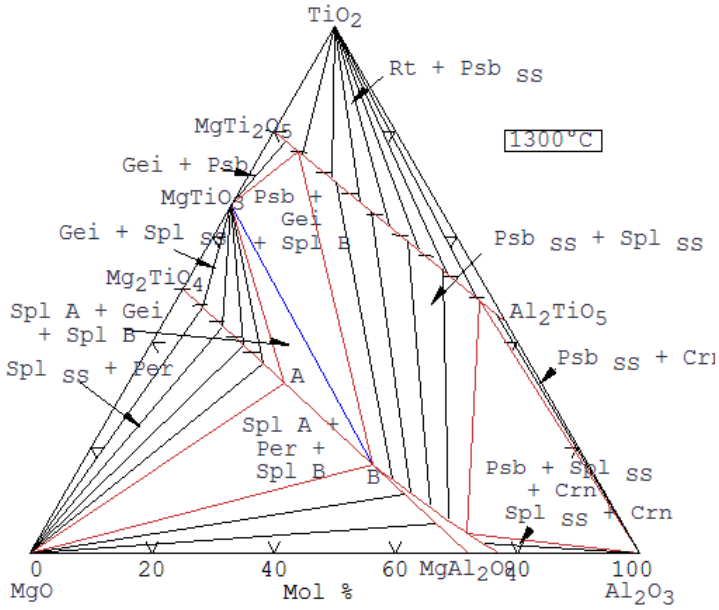

P. Boden, F.P. Glasser, Trans. J. Br. Ceram. Soc., 72[5], (1973), pp. 215-220.

Weight percent 1400C°

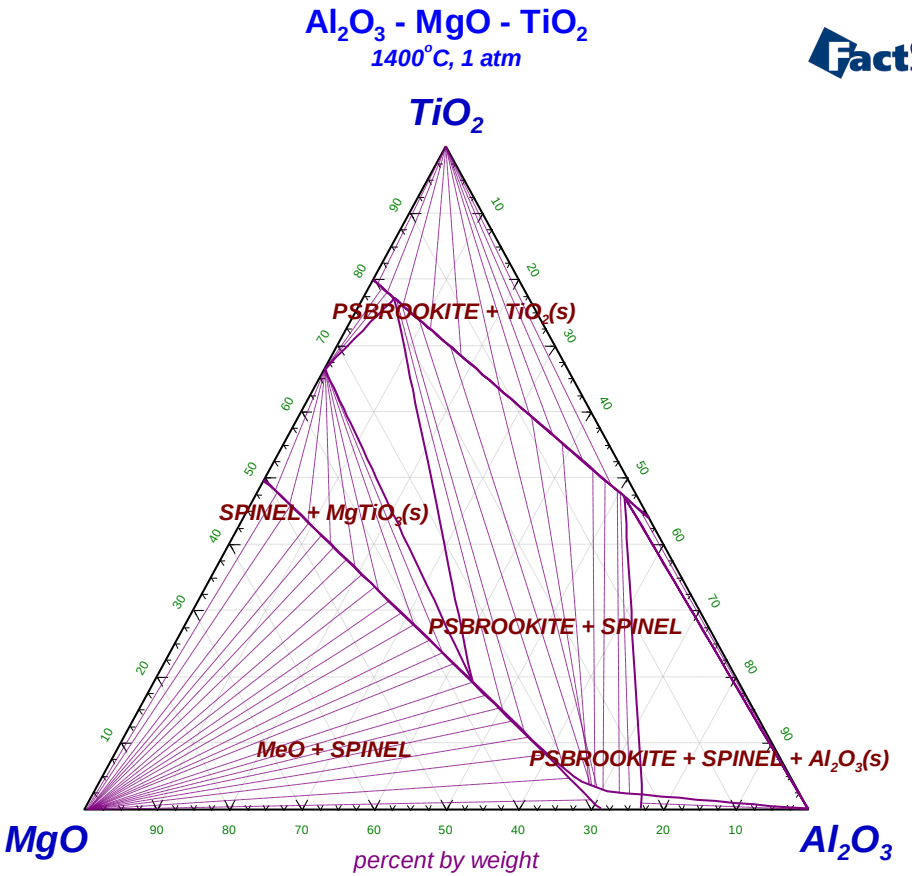

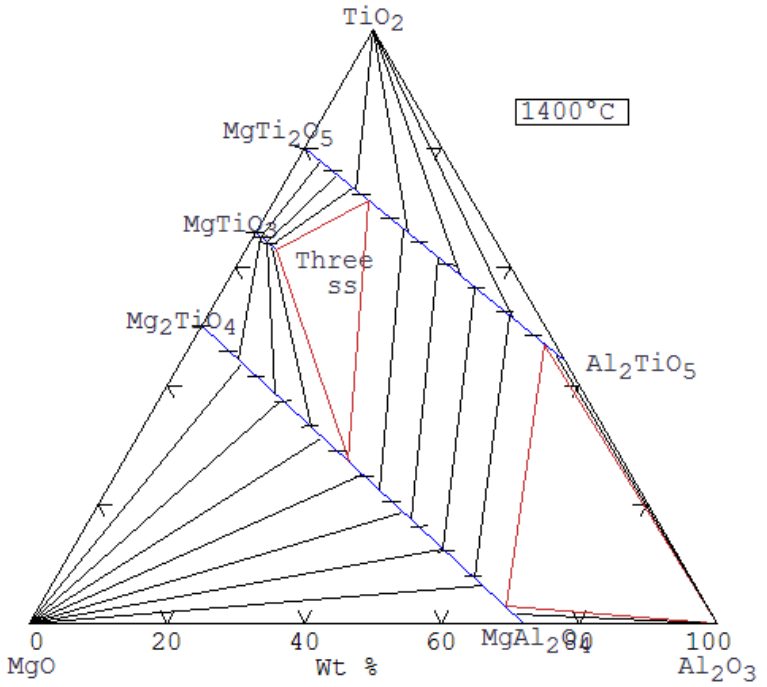

J. Hauck, J. Solid State Chem., 36 [1], (1981), pp. 52-65.

Weight percent 1550C°

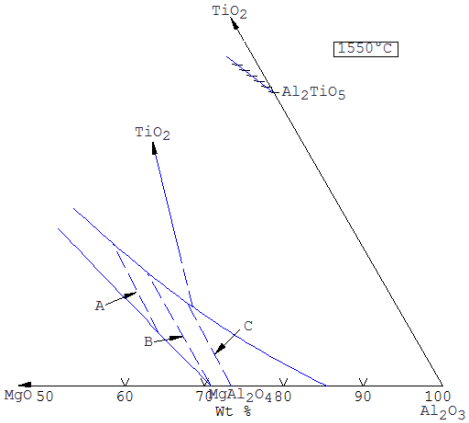

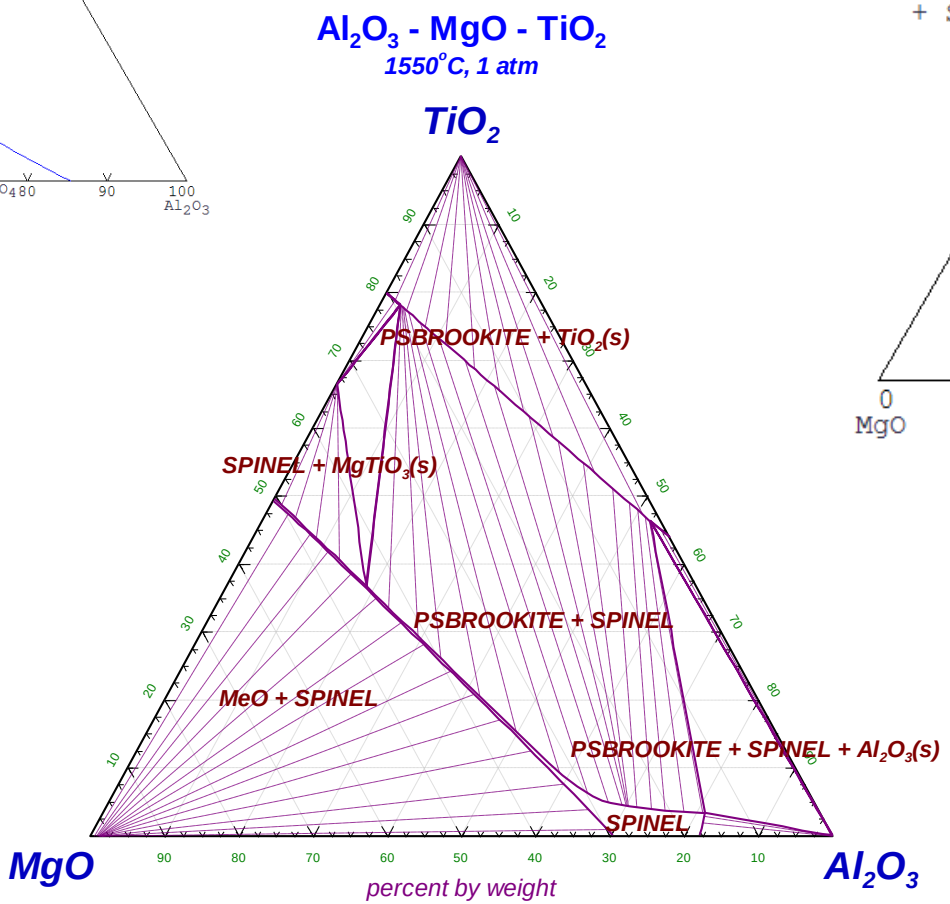

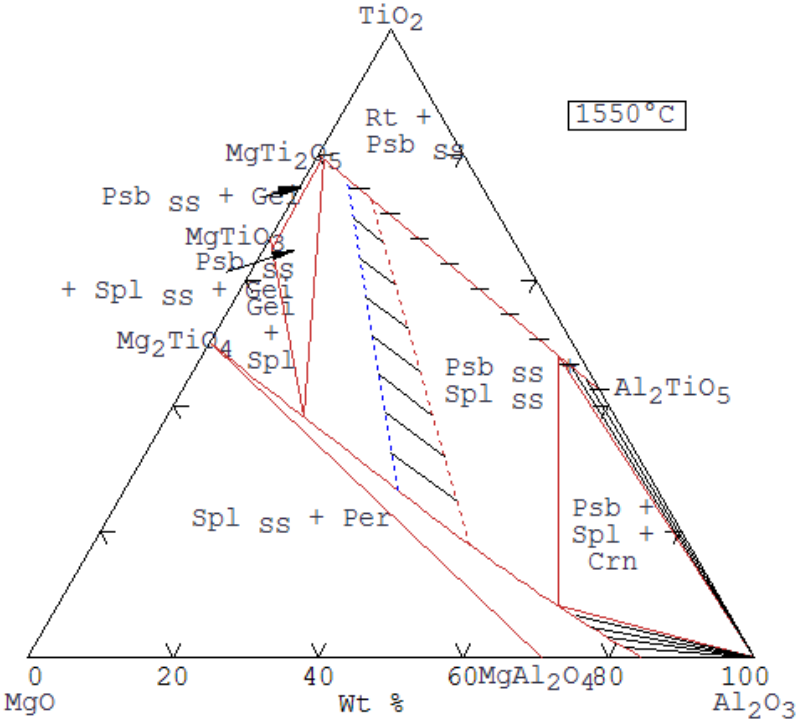

P. Boden, F.P. Glasser, Trans. J. Br. Ceram. Soc., 72[5], (1973), pp. 215-220.

Isopleth Al2MgO4-Mg2TiO4, Mole fraction compared with experimental data

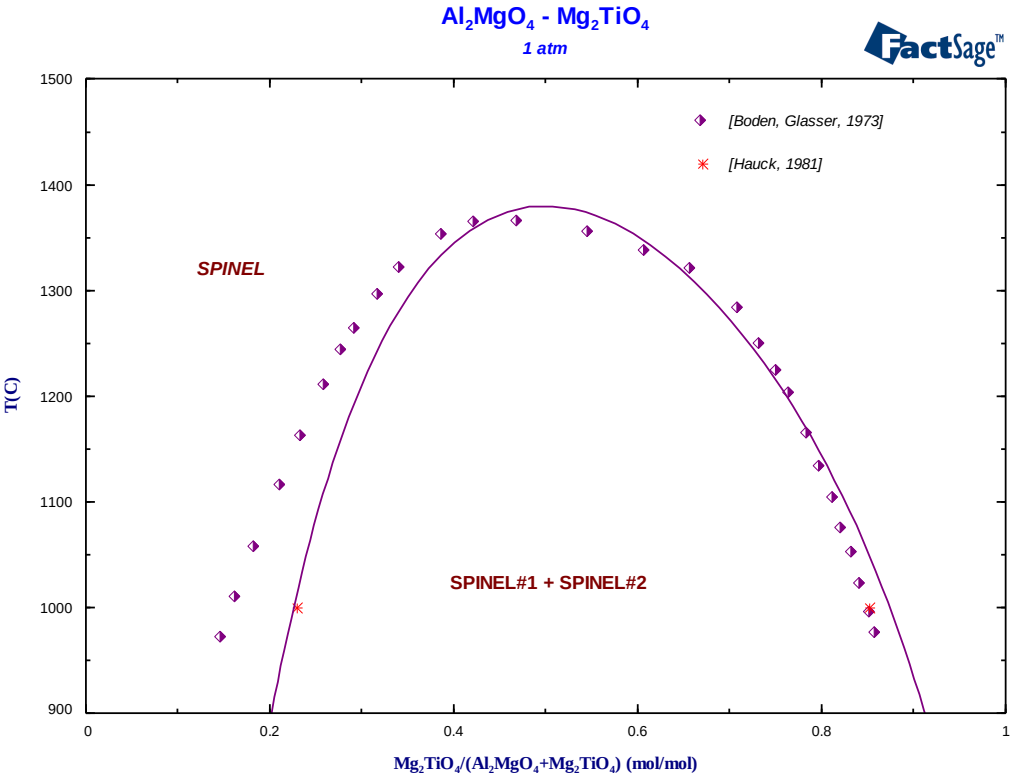

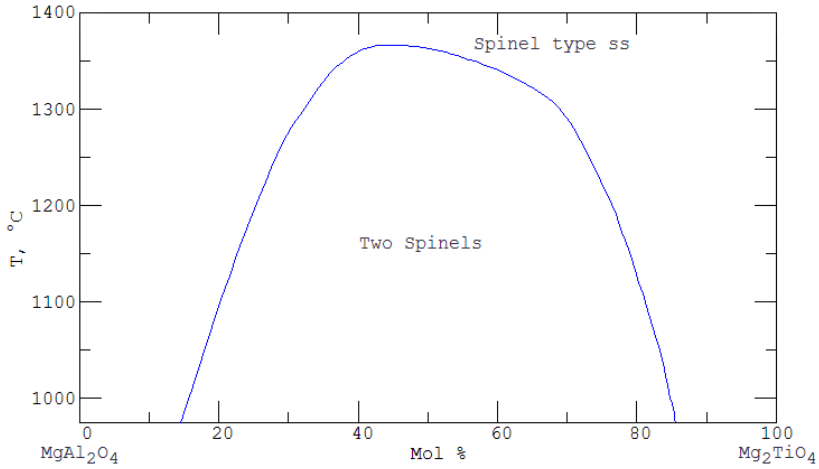

P. Boden, F.P. Glasser, Trans. J. Br. Ceram. Soc., 72[5], (1973), pp. 215-220.

Isopleth Al2TiO5-MgTi2O5, Mole fraction compared with experimental data

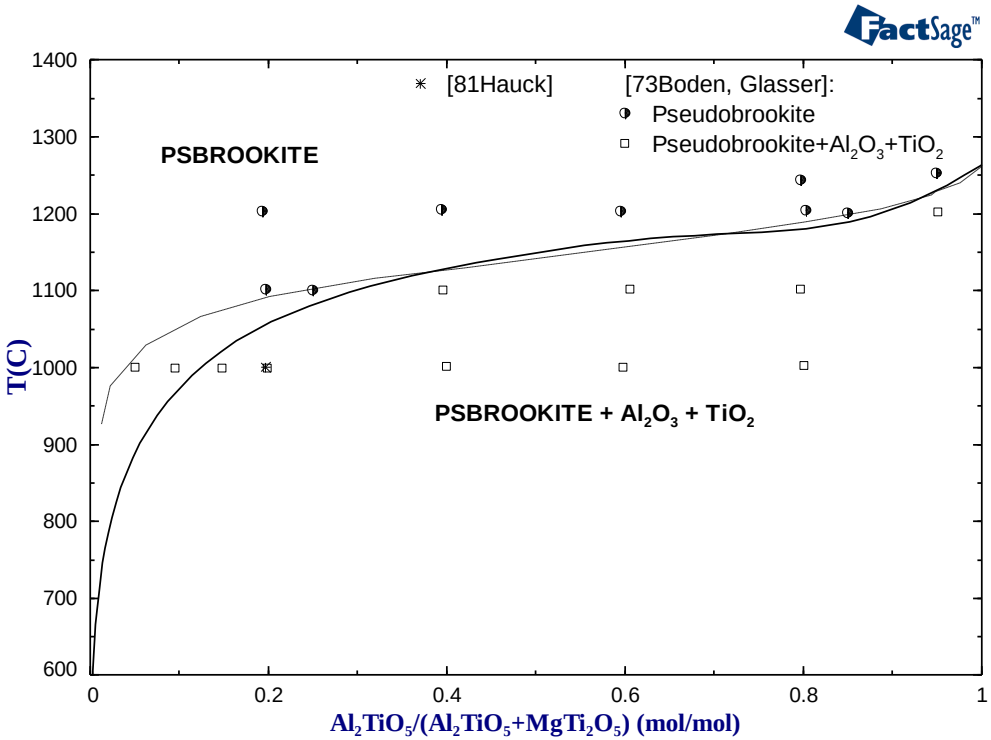

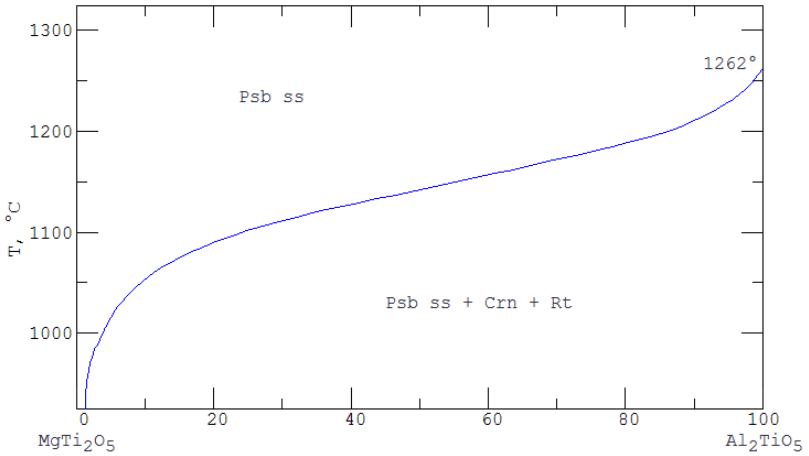

P. Boden, F.P. Glasser, Trans. J. Br. Ceram. Soc., 72[5], (1973), pp. 215-220.

Mole fraction
Liquidussurface

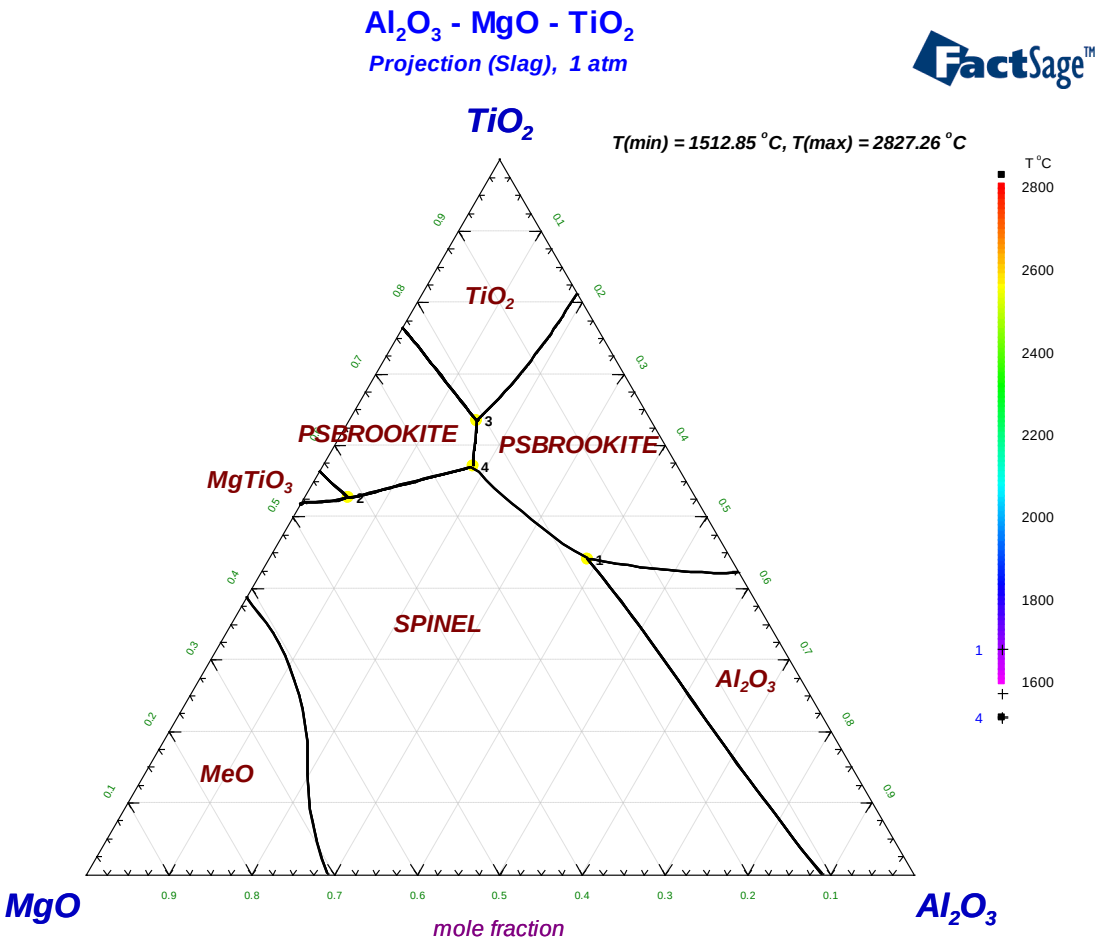

Weight percent
Liquidussurface

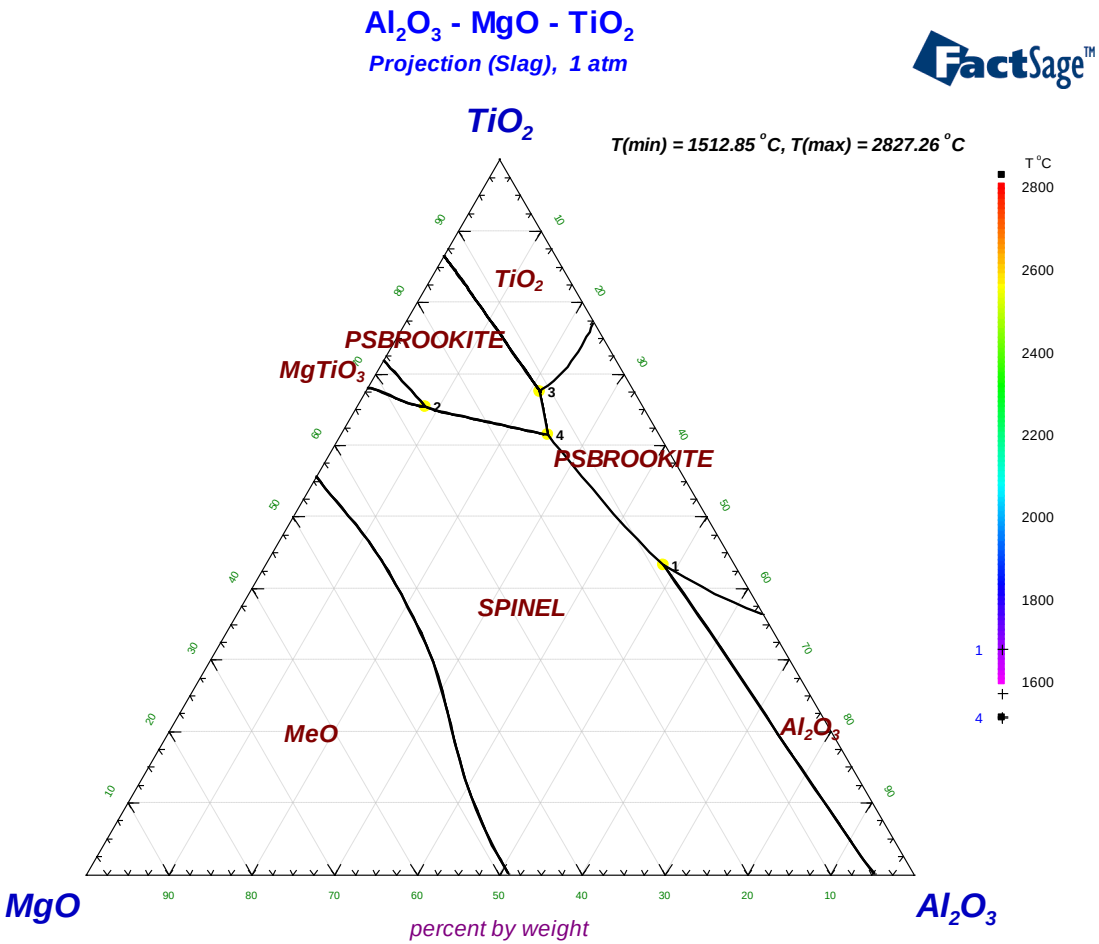

Invariant equilibria on the liquidus surface

Intersections with slag	Mole fraction				Weight percent				
	A = TiO2, B = MgO, C = Al2O3				A = TiO2, B = MgO, C = Al2O3				
		X(A)	X(B)	X(C)	T(C)		W(A)	W(B)	W(C)	T(C)
1: Al2O3 / PSBROOKITE#1 / SPINEL	1:	0.44114	0.17297	0.38590	1679.22	1:	43.203	8.549	48.249	1679.22
2: MgTiO3 / PSBROOKITE#1 / SPINEL	2:	0.52729	0.41980	0.05290	1572.79	2:	65.365	26.262	8.372	1572.79
3: PSBROOKITE#1 / PSBROOKITE#2 / TiO2	3:	0.63434	0.21062	0.15504	1515.44	3:	67.586	11.325	21.089	1515.45
4: PSBROOKITE#1 / PSBRKITE#2 / SPINEL	4:	0.57079	0.24651	0.18270	1512.85	4:	61.479	13.399	25.122	1512.85

Al2O3-MnO-MnS,
Weight percent,

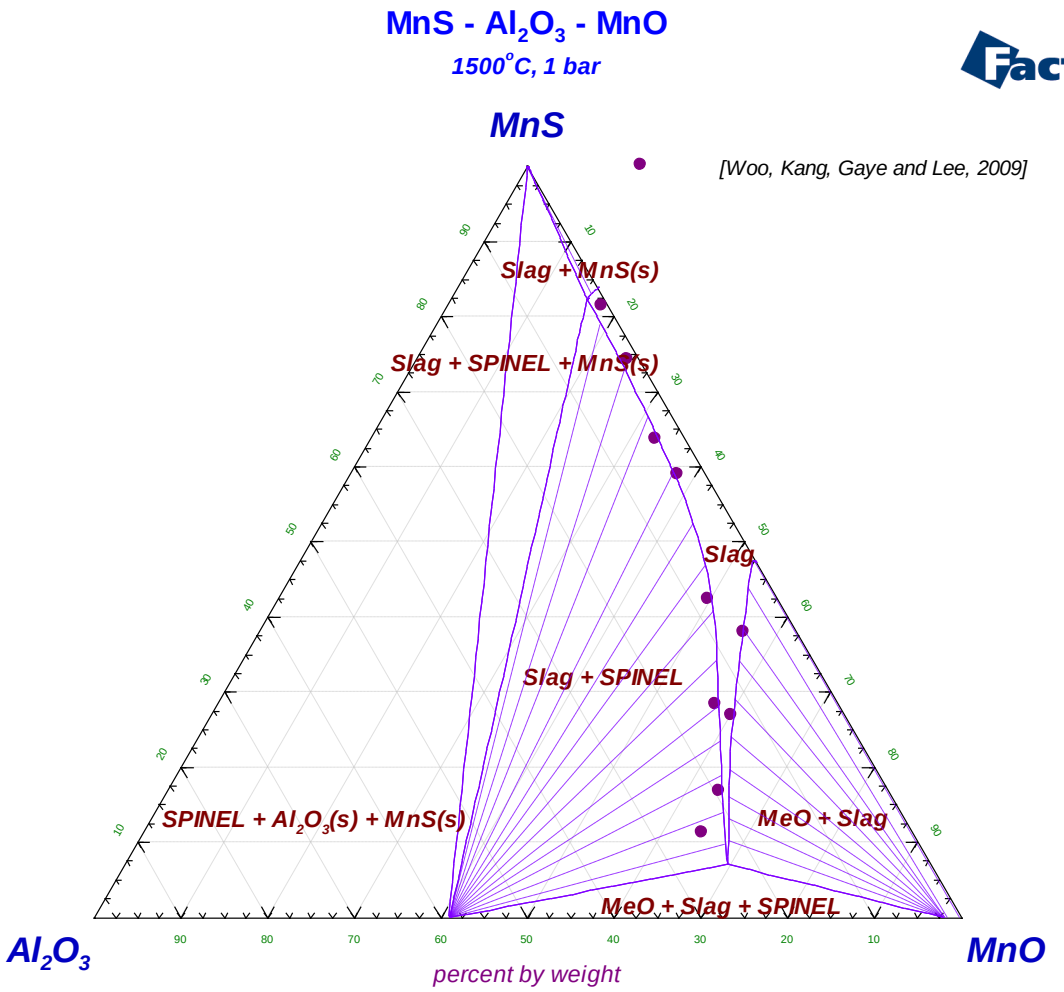

Weight percent,
Co-saturated compositions at various temperatures

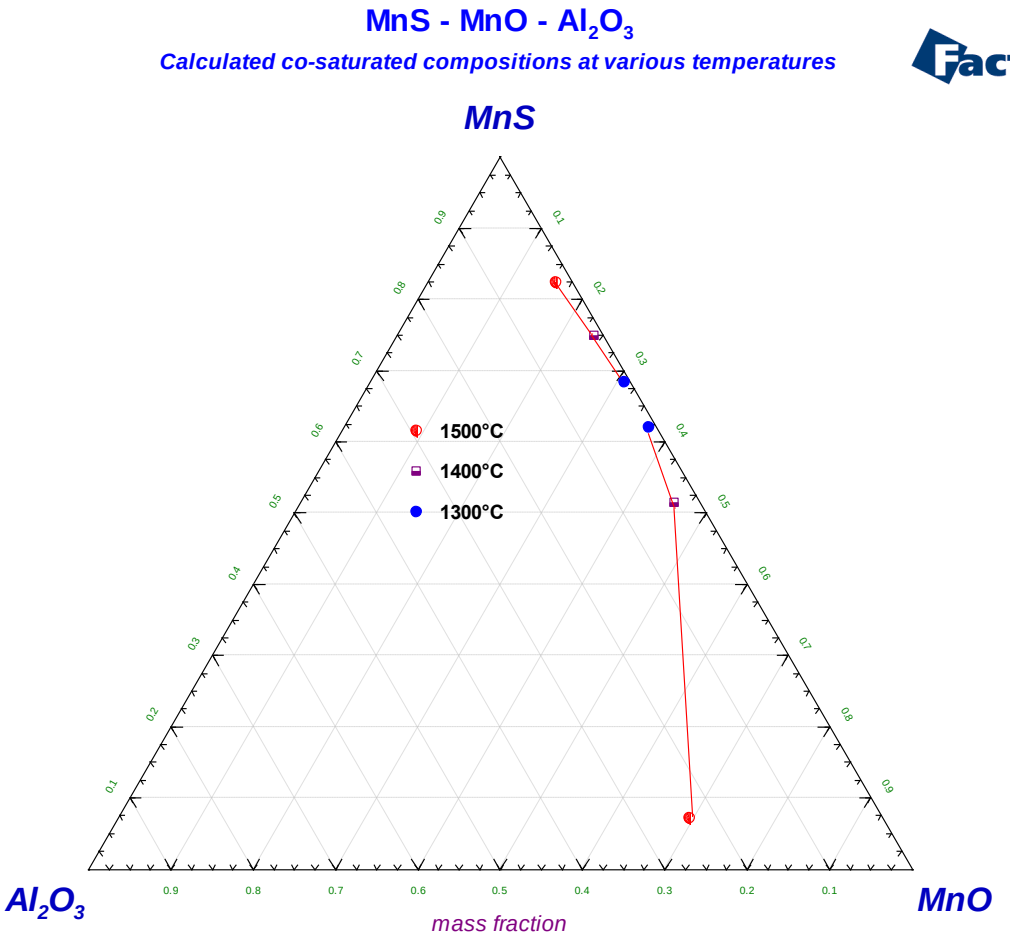

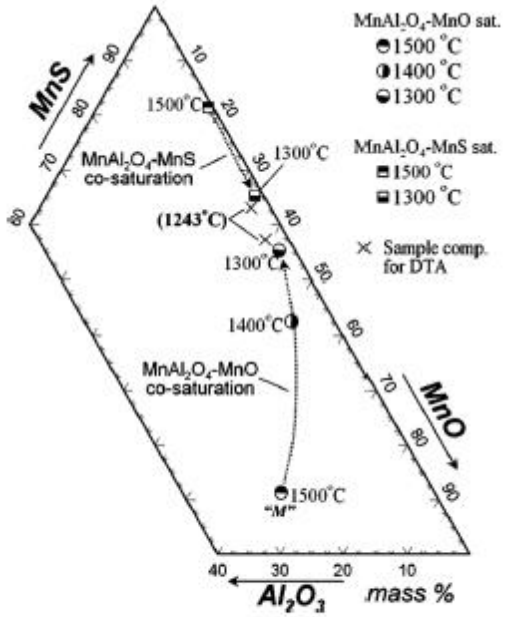

Fig. 10. Co-saturated compositions in the $MnO–Al_2O_3–MnS$ system at various temperatures and sample compositions at which DTA analysis was performed.

D.-H. Woo, Y.-B. Kang, H. Gaye and H.-G. Lee, ISIJ Internat., Vol. 49 (2009), No. 10, pp. 1490-1497.

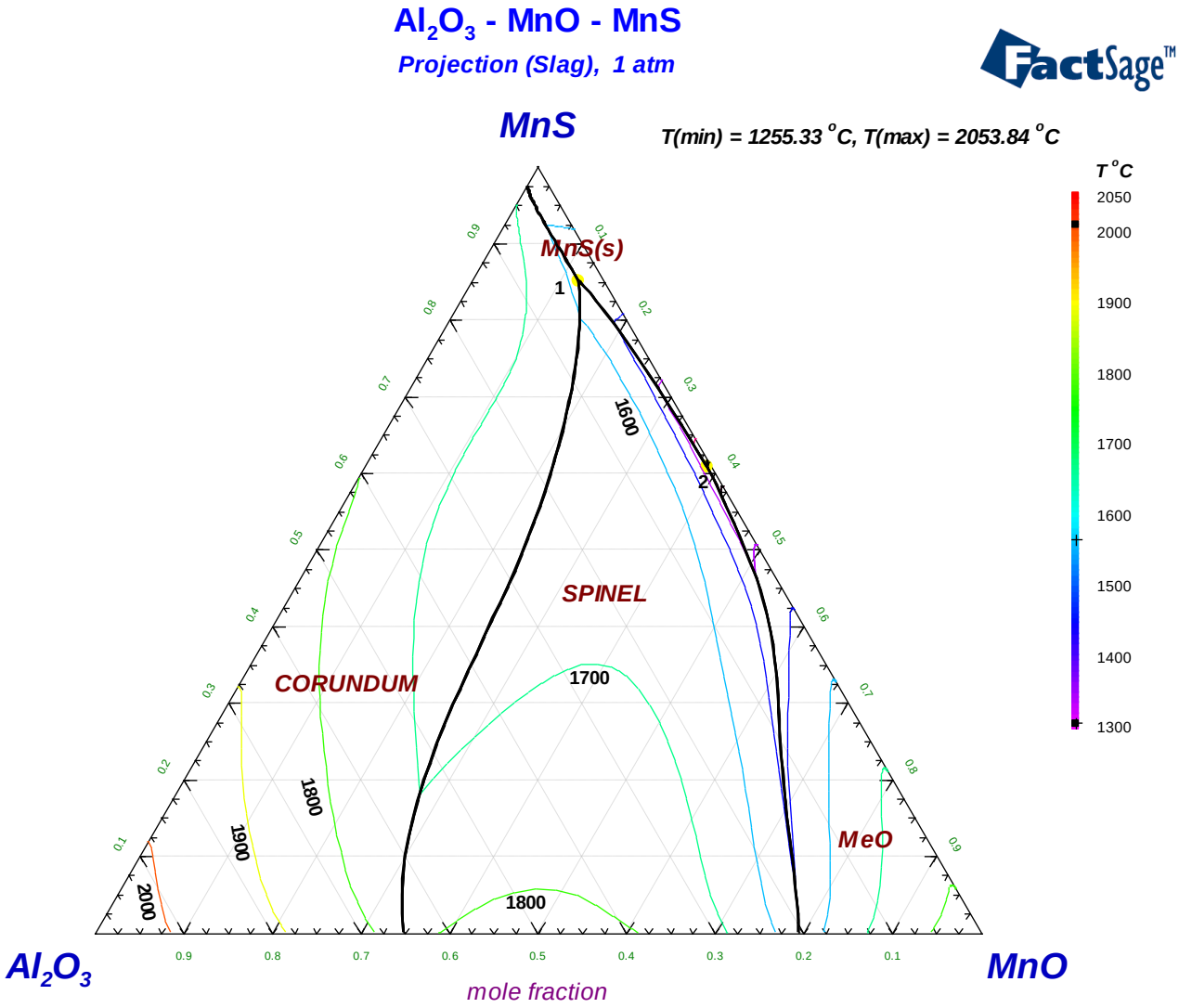
Al2O3 - MnO - MnS
Projection (Slag), 1 atm
FactSage™
MnS
T(min) = 1255.33 °C, T(max) = 2053.84 °C
T °C
2050
2000
1900
1800
1700
1600
1500
1400
1300
MnS(s)
1
1600
2
SPINEL
CORUNDUM
1700
1800
1900
2000
MeO
1800
Al2O3
MnO
mole fraction

Weight percent, Liquidussurface

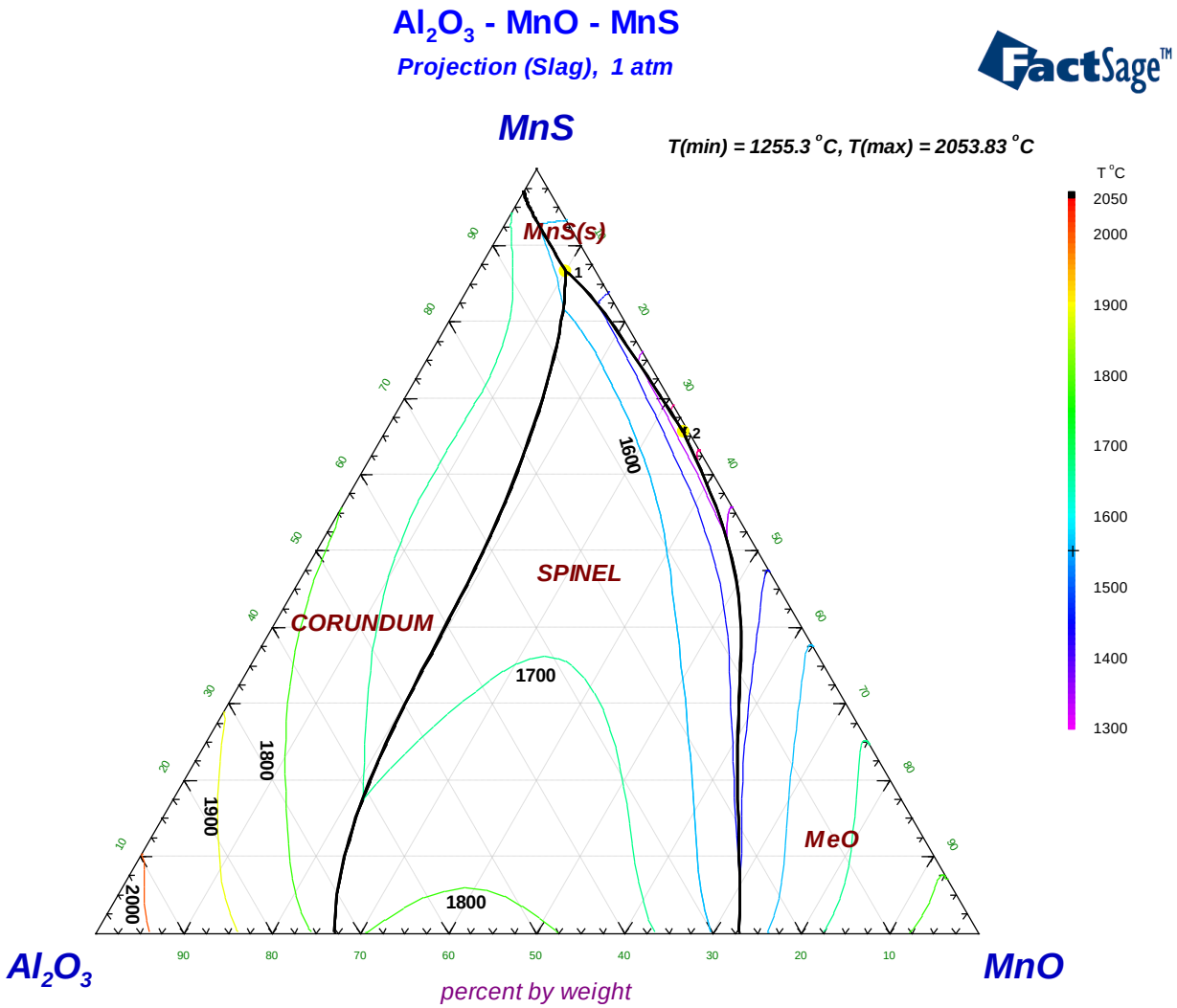

Invariant equilibria on the liquidus surface

Intersections with slag	Mole fraction				Weight percent			
	A = MnS, B = Al2O3, C = MnO				A = MnS, B = Al2O3, C = MnO			
	X(A)	X(B)	X(C)	T(C)	W(A)	W(B)	W(C)	T(C)
1: SPINEL / CORANDUM / MnS(s)	1: 0.85118	0.02860	0.12022	1551.15	1: 86.615	3.411	9.974	1551.15
2: SPINEL / MeO / MnS(s)	2: 0.60909	0.00452	0.38639	1256.39	2: 0.65.534	0.570	33.896	1256.39

Mole fraction 800°C

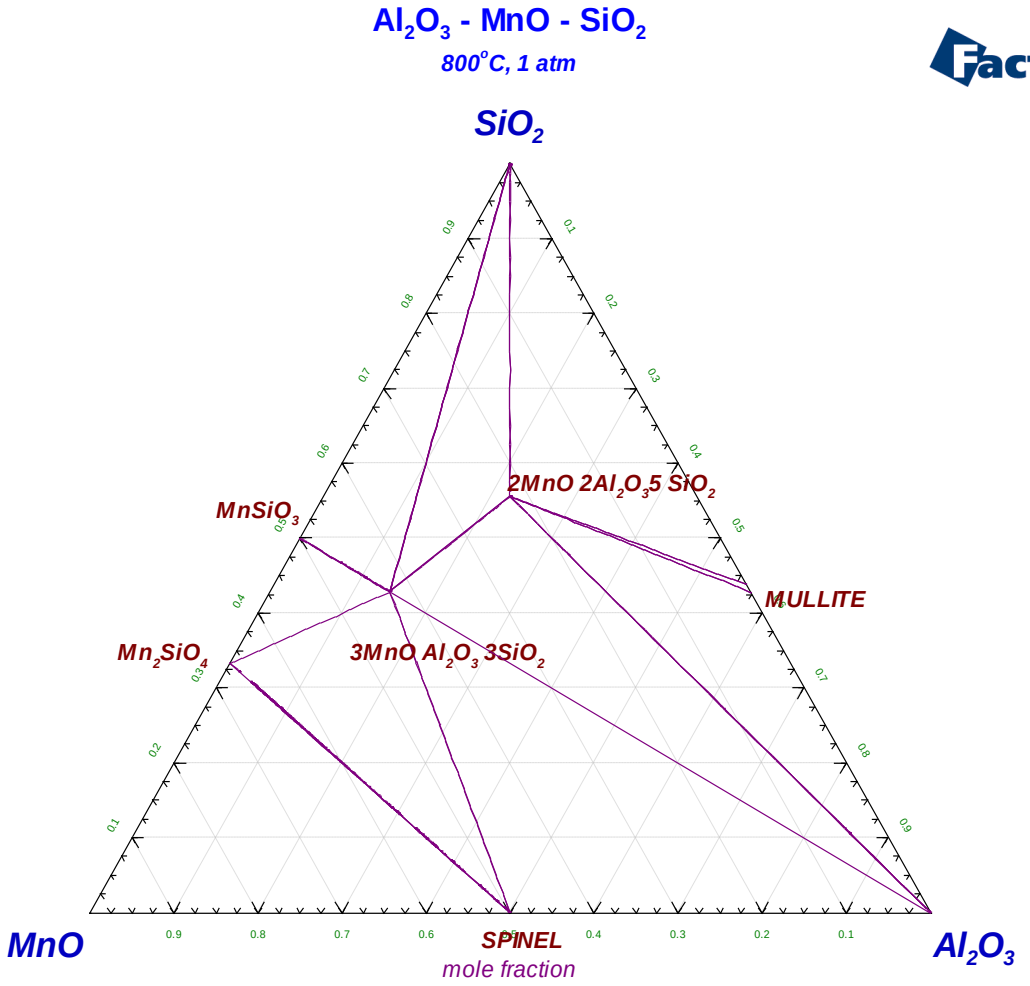

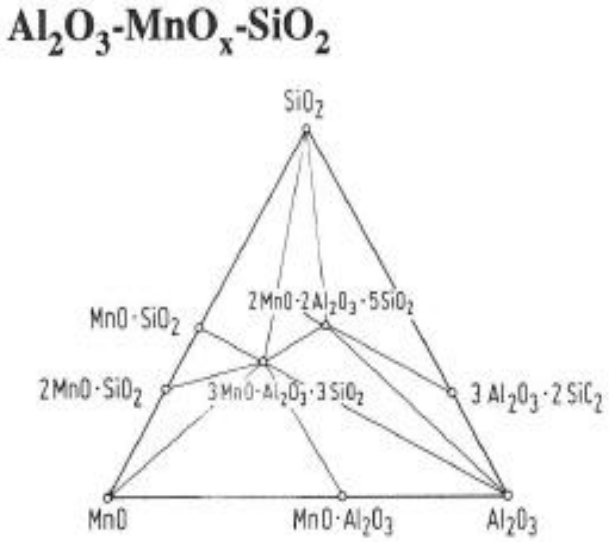

Slag Atlas, 2nd edition, Verlag Stahleisen GmbH,1995, p. 116.

Al2O3-MnO-SiO2, Mole fraction 1550°C

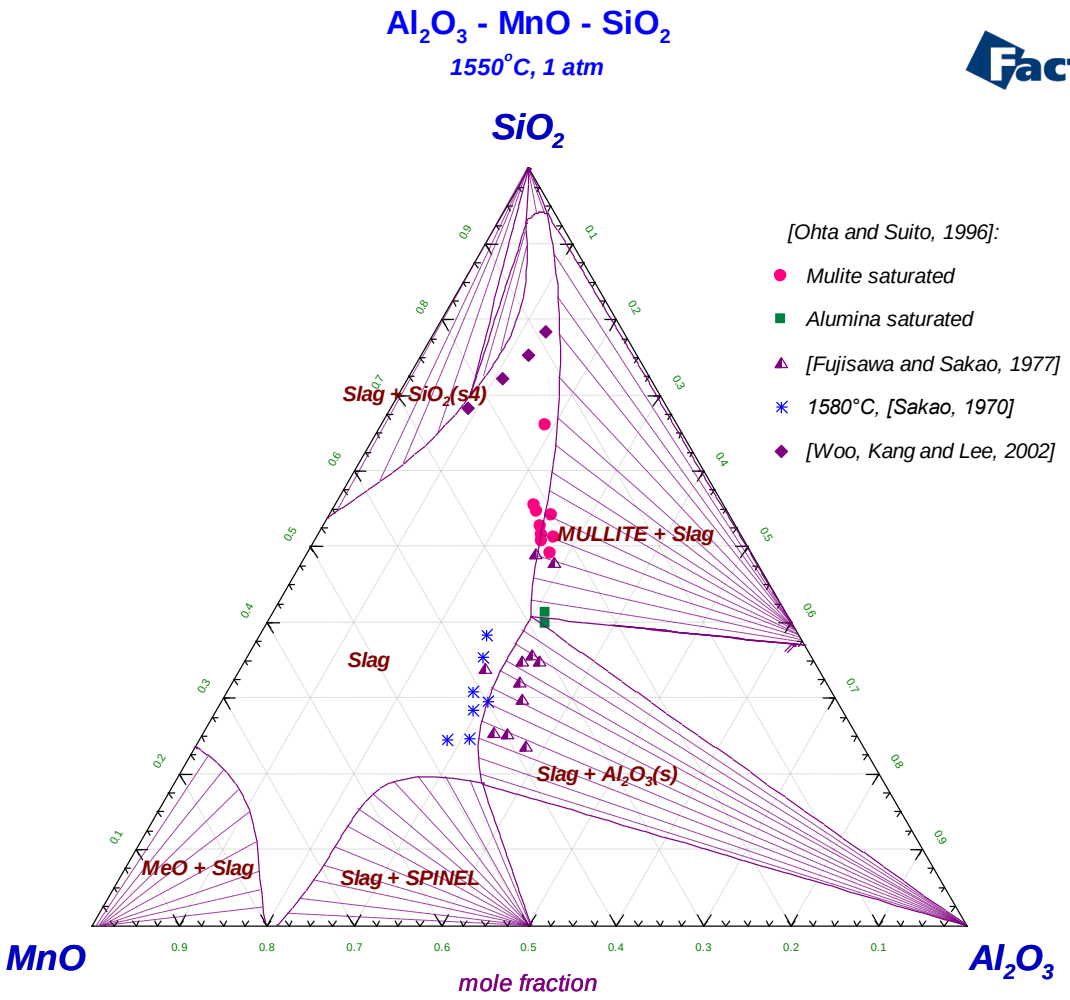

Weight percent, Liquid lines compared with experimental data

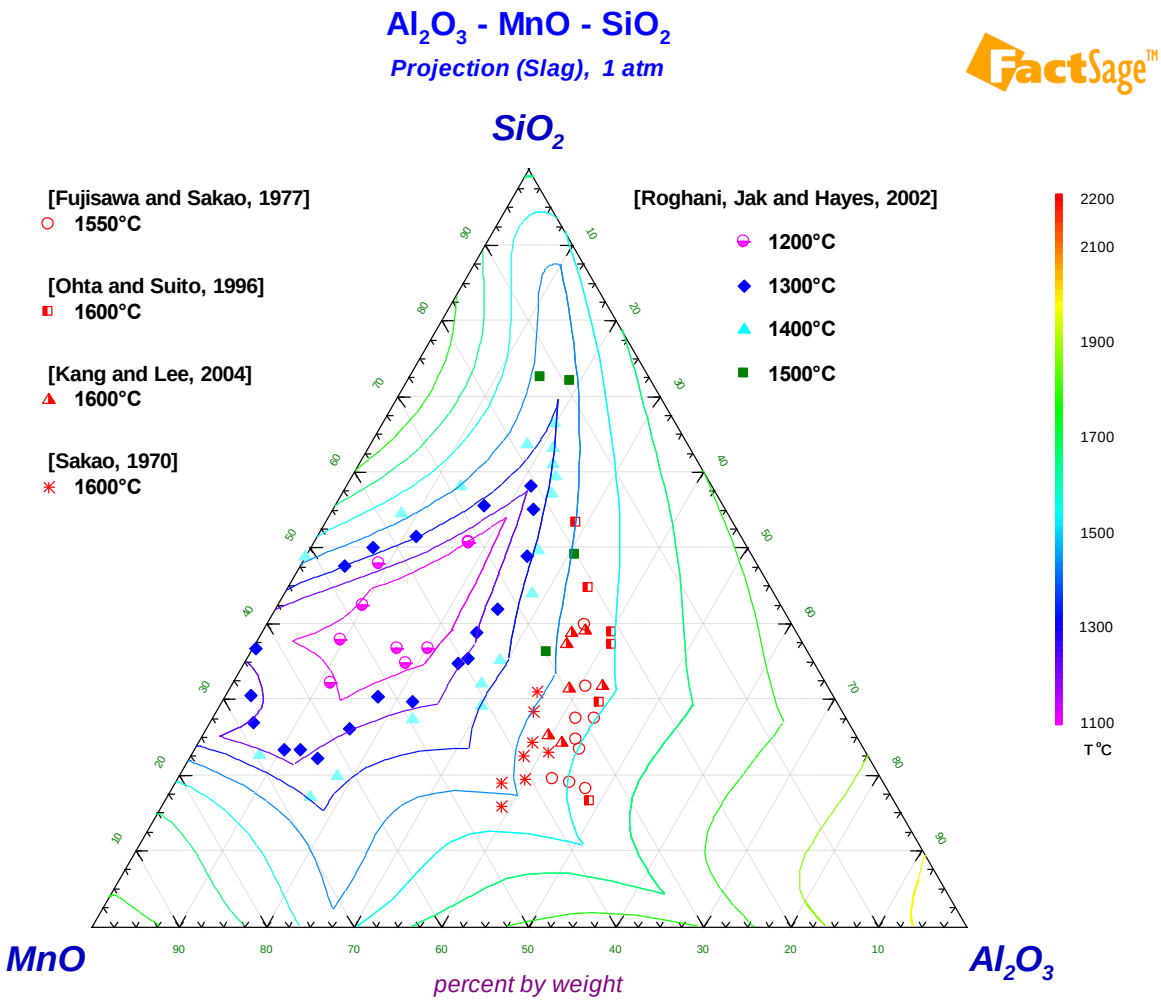

Mole fraction
Liquidussurface

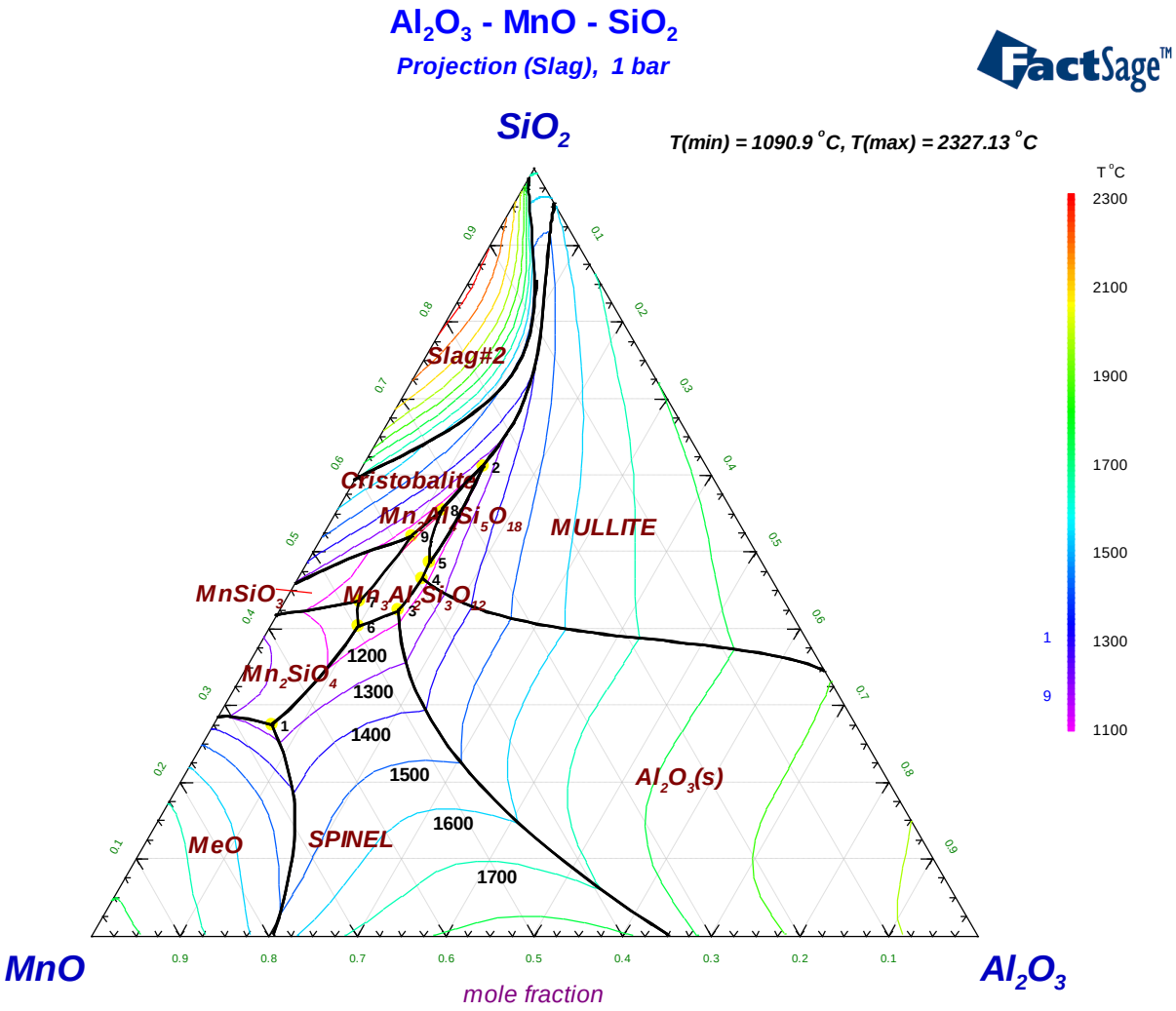

Weight percent
Liquidussurface

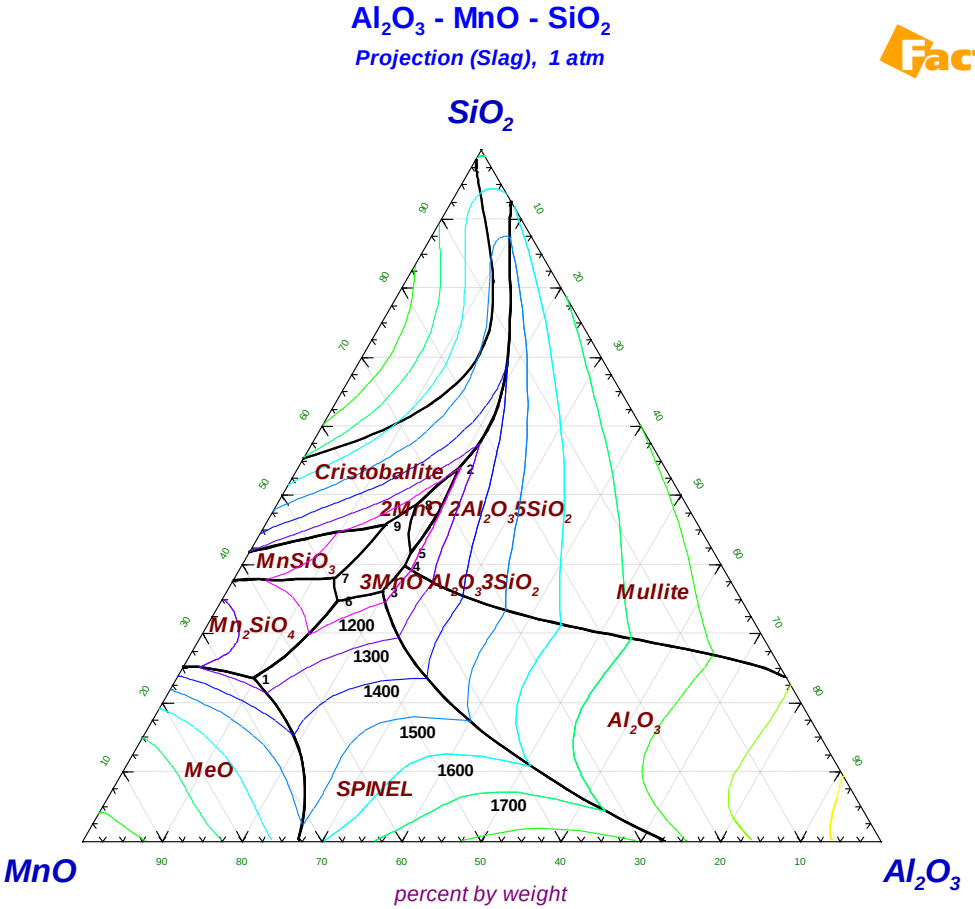

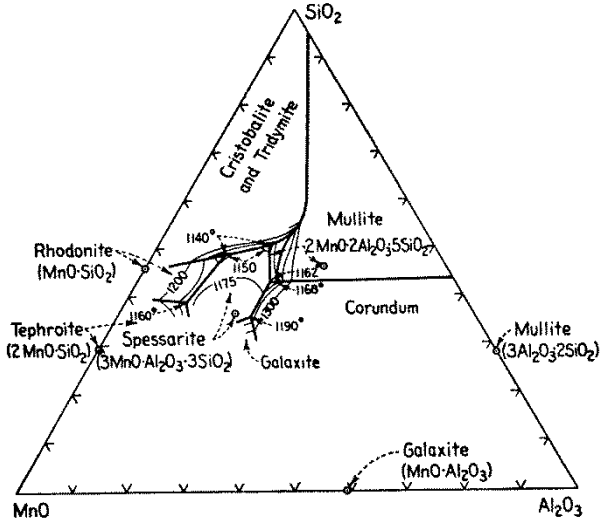

R.B. Snow, J. Amer. Ceram. Soc., 25 [1], (1943), pp.11-20.

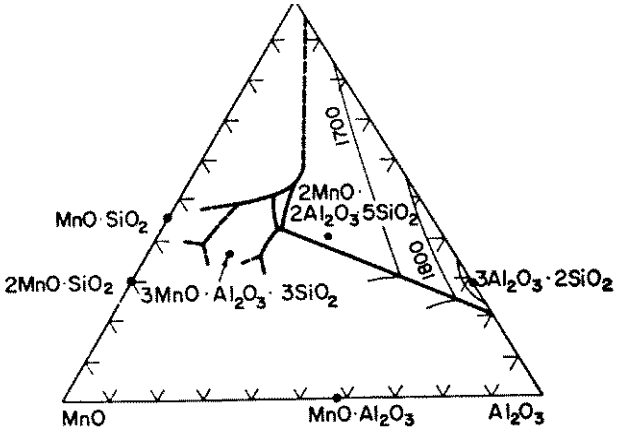

F.Y. Galakhov, Uch. Zap. Kazan. Gos. Univ., No.5, (1957), pp.525-531.

Invariant equilibria on the liquidus surface

Intersections with slag	Mole fraction A = SiO2, B = MnO, C = Al2O3				Weight percent A = SiO2, B = MnO, C = Al2O3			
	X(A)	X(B)	X(C)	T(C)	W(A)	W(B)	W(C)	T(C)
1: MeO / Mn2SiO4(s) / SPINEL	1: 0.27470	0.65867	0.06662	1243.54	1. 23.571	66.727	9.701	1243.54
2: MULLITE / Mn2Al4Si5O18(s) / Cristobalite	2: 0.61217	0.25146	0.13637	1191.89	2. 53.878	25.847	20.275	1191.10
3: Al2O3(s) / Mn3Al2Si3O12(s) / SPINEL	3: 0.42369	0.44064	0.13567	1163.44	3. 36.087	44.305	19.609	1163.43
4: Al2O3(s) / MULLITE / Mn3Al2Si3O12(s)	4: 0.46511	0.39314	0.14176	1155.56	4. 39.769	39.665	20.567	1155.51
5: MULLITE /Mn2Al4Si5O18(s)/Mn3Al2Si3O12	5: 0.48642	0.37413	0.13945	1145.09	5. 41.776	37.903	20.321	1145.02
6: Mn2SiO4(s) / Mn3Al2Si3O12(s) / SPINEL	6: 0.40232	0.49743	0.10025	1128.31	6. 34.691	50.640	14.669	1128.31
7: Mn2SiO4(s) / Mn3Al2Si3O12(s) / MnSiO3(s)	7: 0.43532	0.47953	0.08515	1107.48	7. 37.987	49.403	12.610	1107.48
8: Mn2Al4Si5O18/ Mn3Al2Si3O12 / Cristobalite	8: 0.55535	0.32631	0.11834	1096.18	8. 48.691	33.707	17.602	1095.96
9: Mn3Al2Si3O12(s) / MnSiO3(s) / Cristobalite	9: 0.52098	0.37746	0.10156	1090.90	9. 45.754	39.110	15.136	1090.85

Mole fraction, Liquidussurface

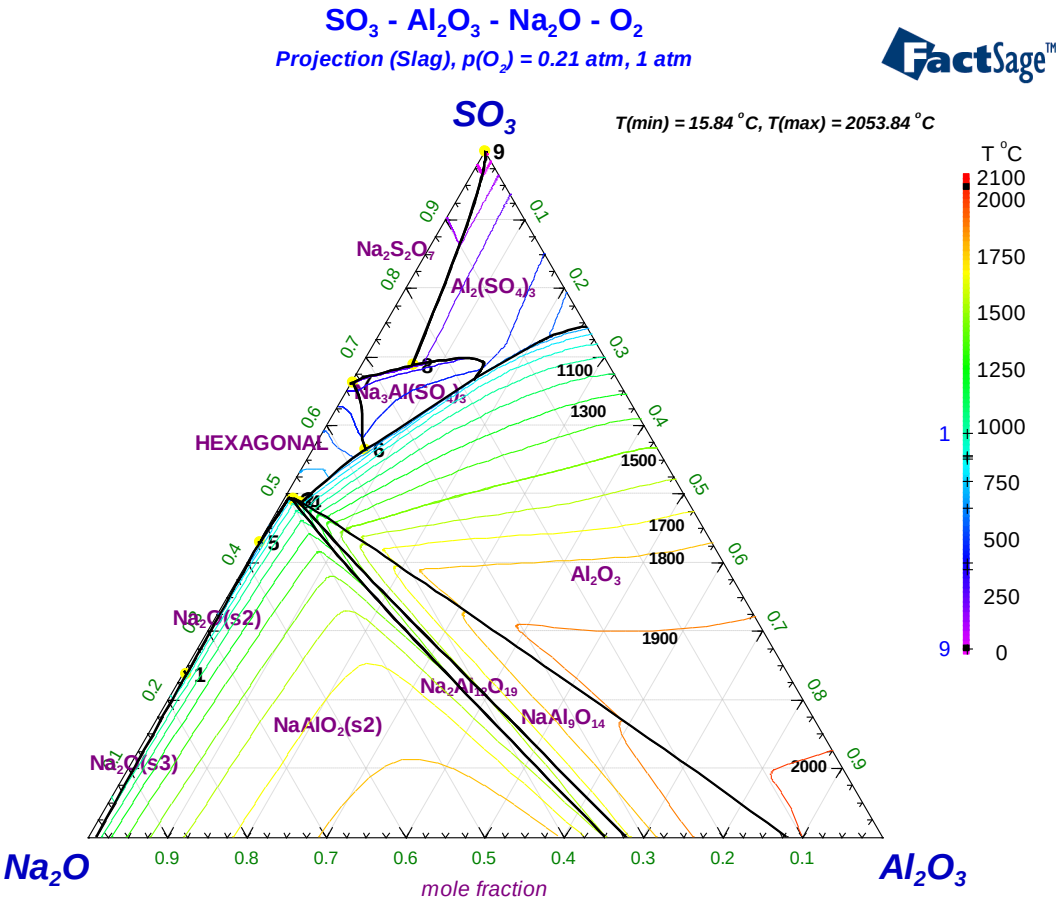

Weight percent, Liquidussurface

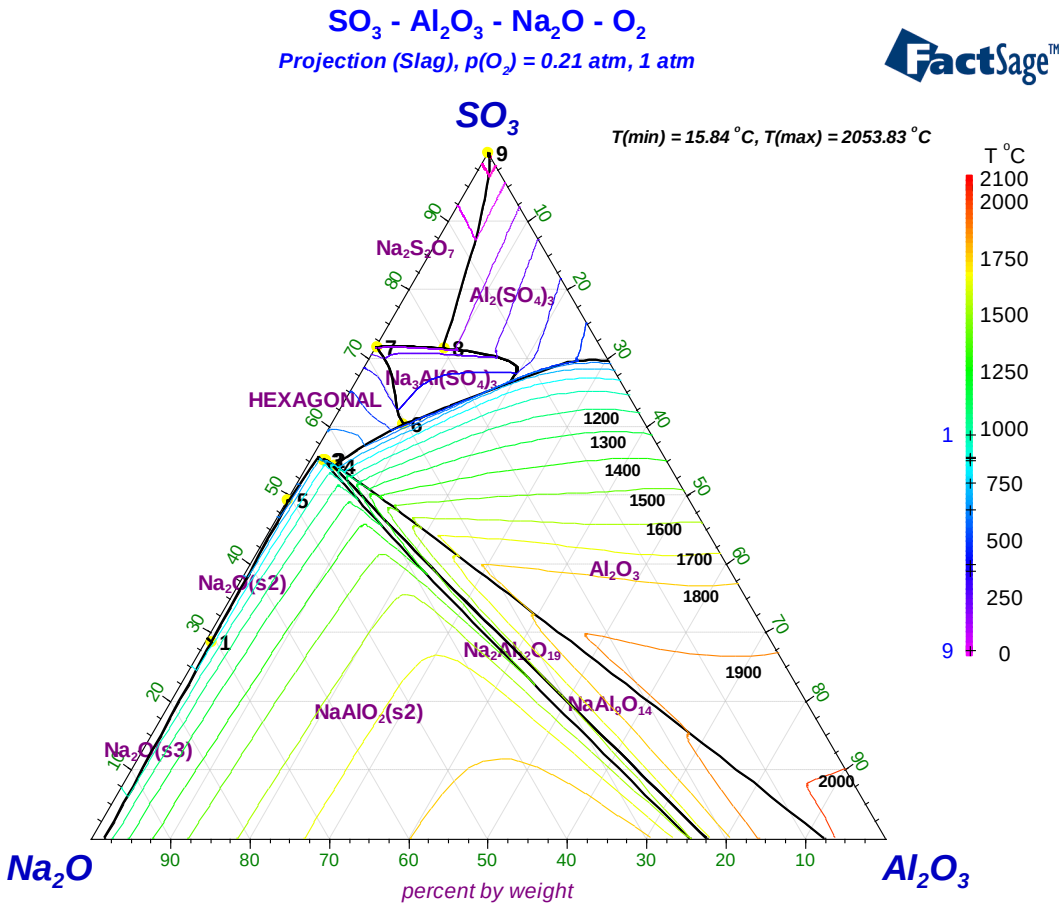

Intersections with slag	Mole fraction				Weight percent			
	A = SO3, B = Na2O, C = Al2O3				A = SO3, B = Na2O, C = Al2O3			
	X(A)	X(B)	X(C)	T(C)	W(A)	W(B)	W(C)	T(C)
1: Na2O(s2) / Na2O(s3) / NaAlO2_HT	1: 0.23775	0.75670	0.00555	970.25	1: 28.624	70.525	0.851	970.05
2. HEXAGONAL / Na2Al12O19 / NaAl9O14	2: 0.49258	0.49367	0.01375	869.36	2: 55.207	42.831	1.963	869.36
3. HEXAGONAL / Na2Al12O19 / NaAlO2_HT	3: 0.49069	0.49672	0.01259	866.27	3: 55.057	43.144	1.799	866.27
4. Al2O3 / HEXAGONAL / NaAl9O14	4: 0.48713	0.48716	0.02571	857.51	4: 54.307	42.043	3.650	857.51
5. Na2O(s2) / Na2SO4(s3) / NaAlO2_HT	5: 0.42893	0.56921	0.00186	756.55	5: 49.193	50.536	0.271	756.55
6. Al2O3 / HEXAGONAL / Na3Al(SO4)3	6: 0.56504	0.36758	0.06737	636.39	6: 60.407	30.421	9.173	636.39
7. HEXAGONAL / Na2S2O7 / Na3Al(SO4)3	7: 0.66179	0.33564	0.00258	394.65	7: 71.553	28.093	0.355	394.70
8. Al2(SO4)3 / Na2S2O7 / Na3Al(SO4)3	8: 0.68748	0.24587	0.06665	365.50	8: 71.412	19.771	8.818	365.50
9. Al2(SO4)3 / Na2S2O7 / SO3	9: 0.99921	0.00017	0.00062	15.84	9: 99.908	0.013	0.079	15.84

Mole fraction kurz unterhalb Liquidussurface

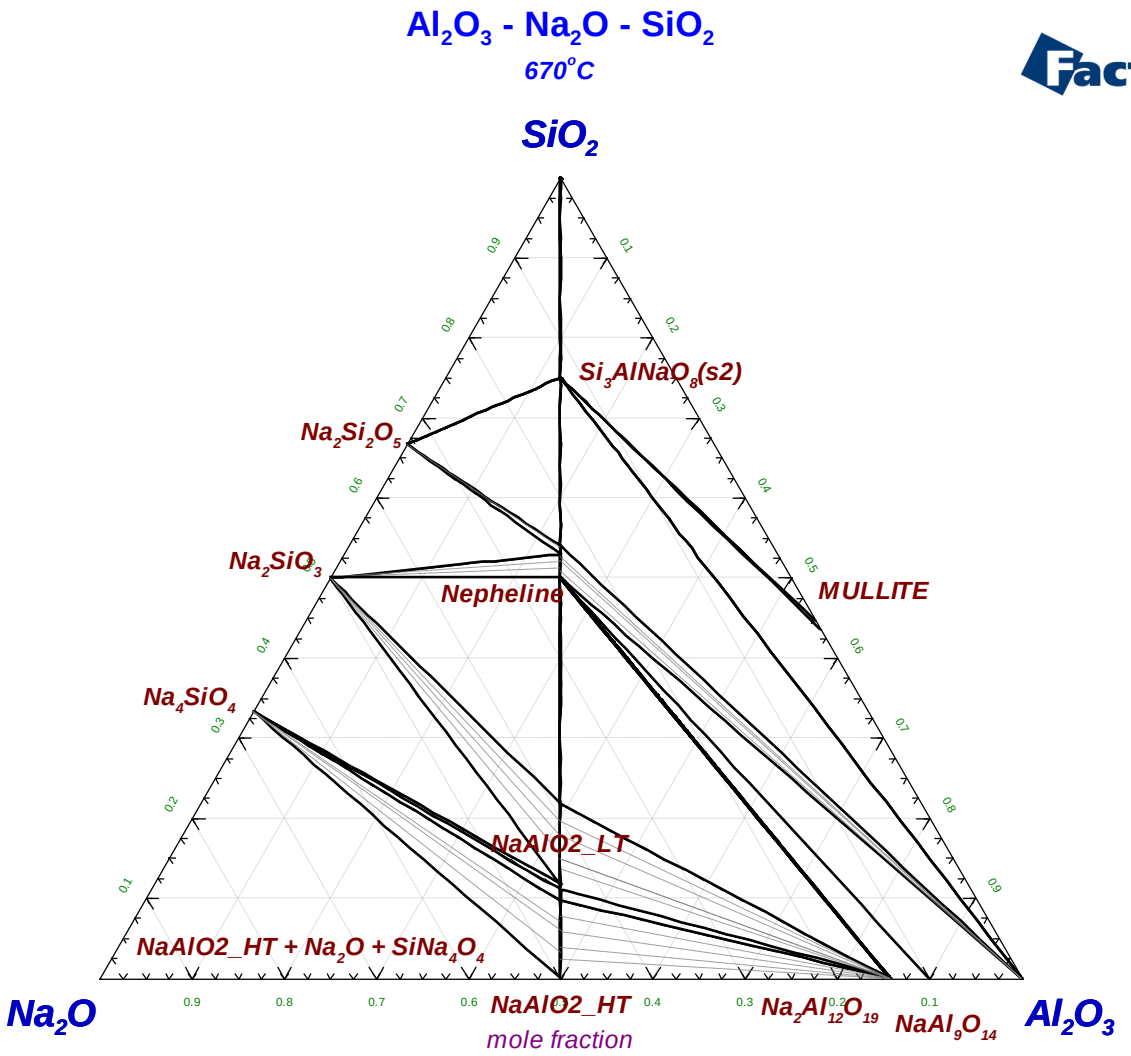

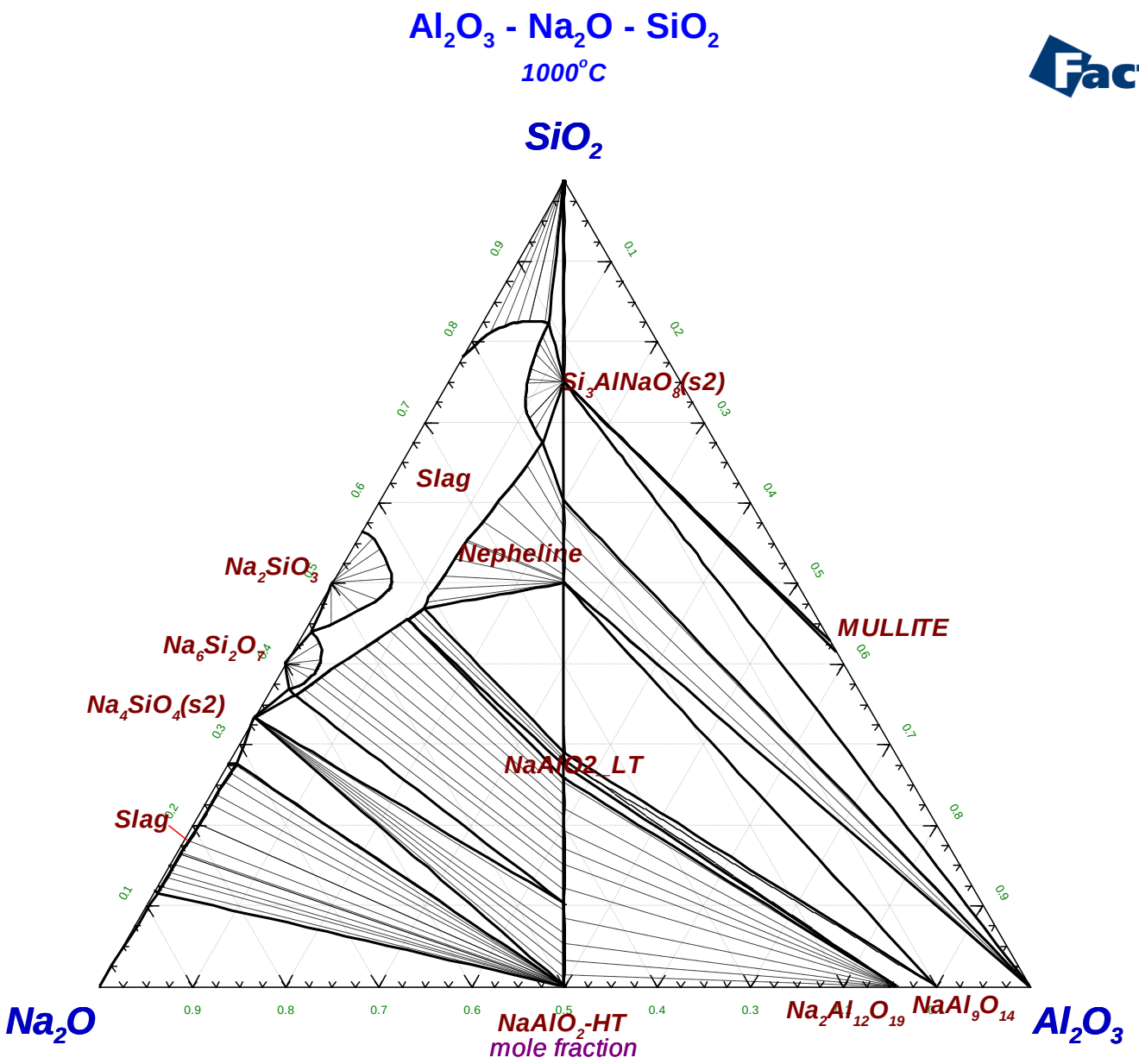
Al2O3 - Na2O - SiO2
1000°C
FactSage™
SiO2
Si3AlNaO8(s2)
Slag
Nepheline
Na2SiO3
Na6Si2O7
Na4SiO4(s2)
MULLITE
NaAlO2_LT
Slag
Na2O
NaAlO2-HT
mole fraction
Na2Al12O19
NaAl9O14
Al2O3

Weight percent in K
compared with experimental data

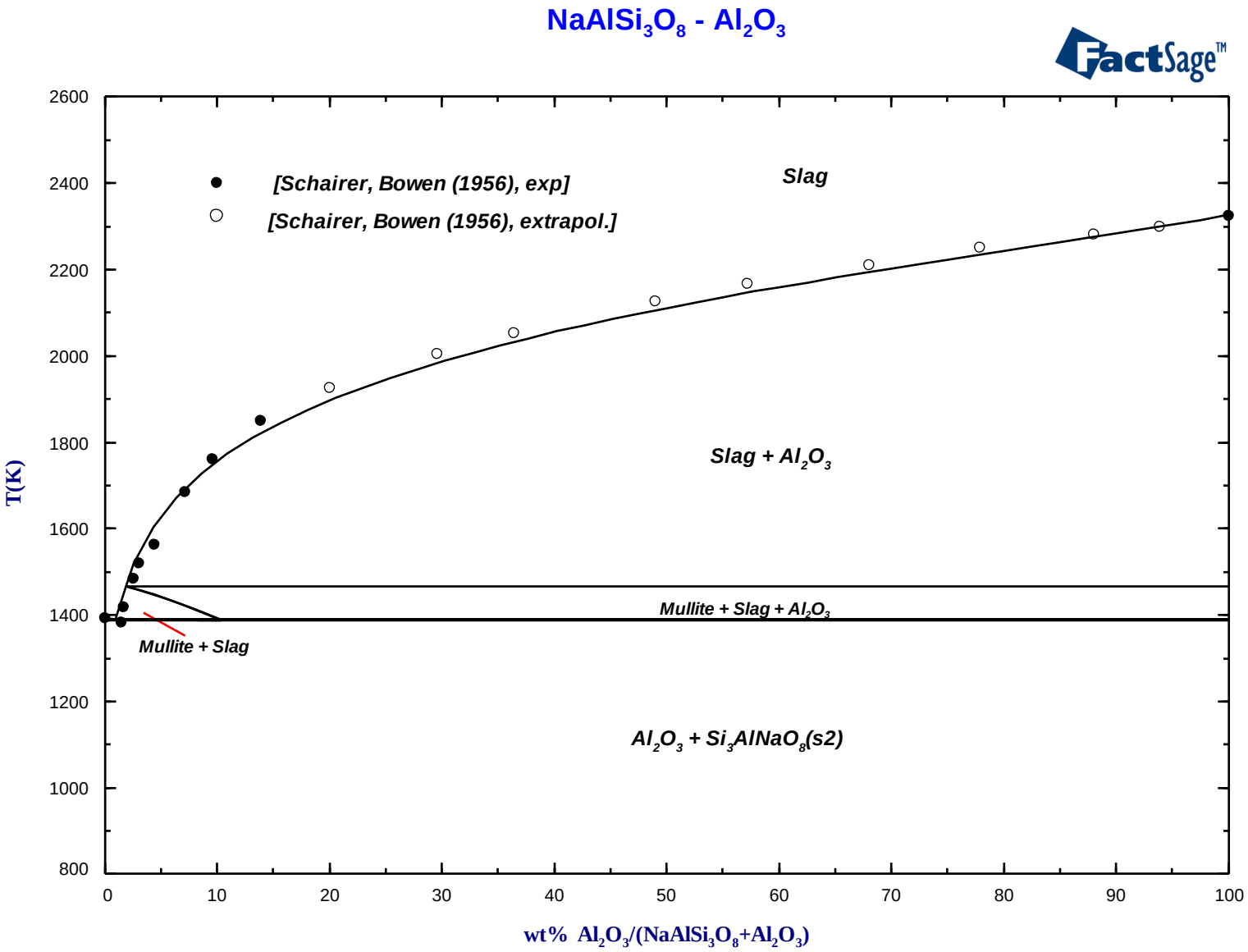

Mole fraction in Kelvin compared with experimental data

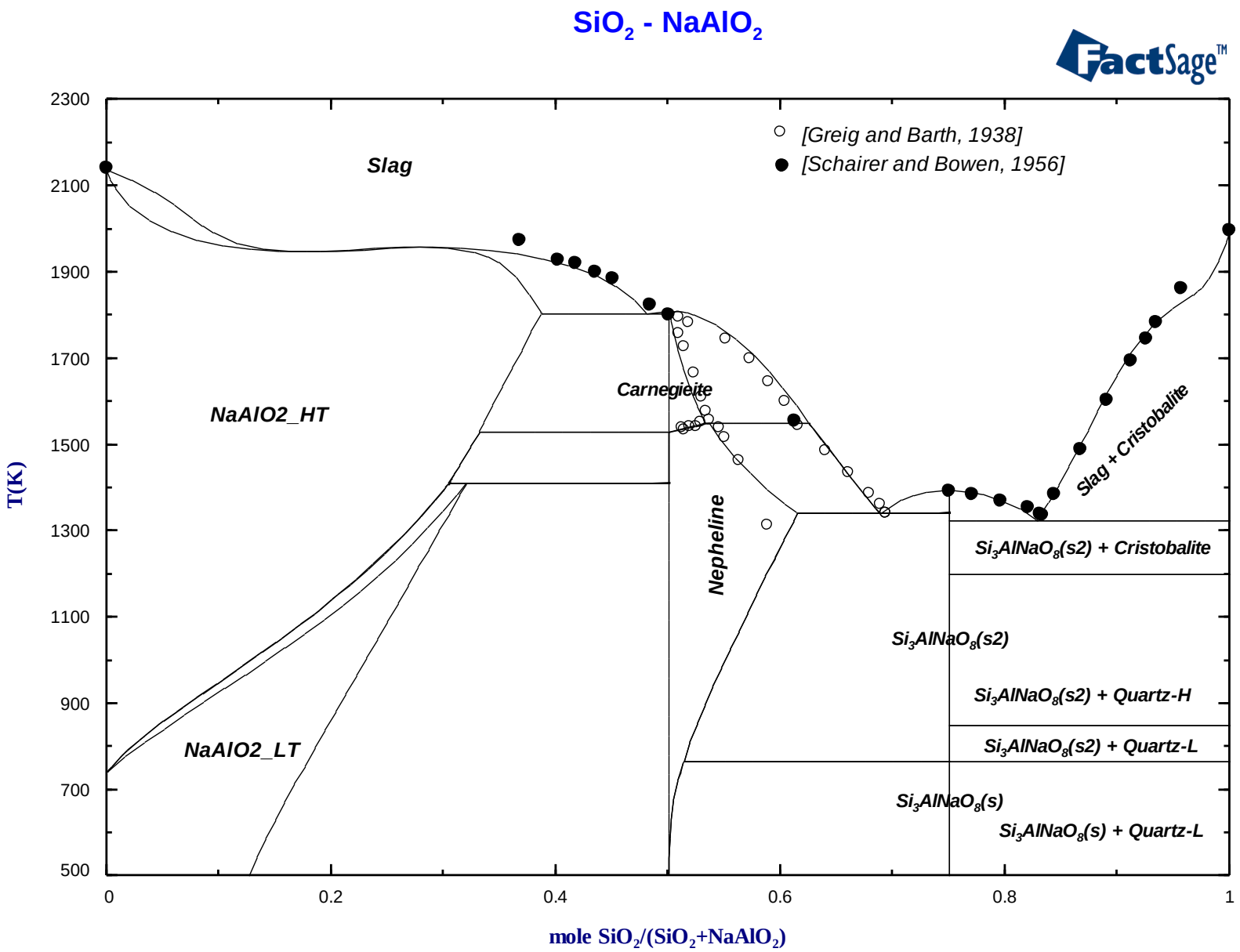

Al2O3-Na2O-SiO2,

Weight percent Na2Si2O5-AlNaSiO4

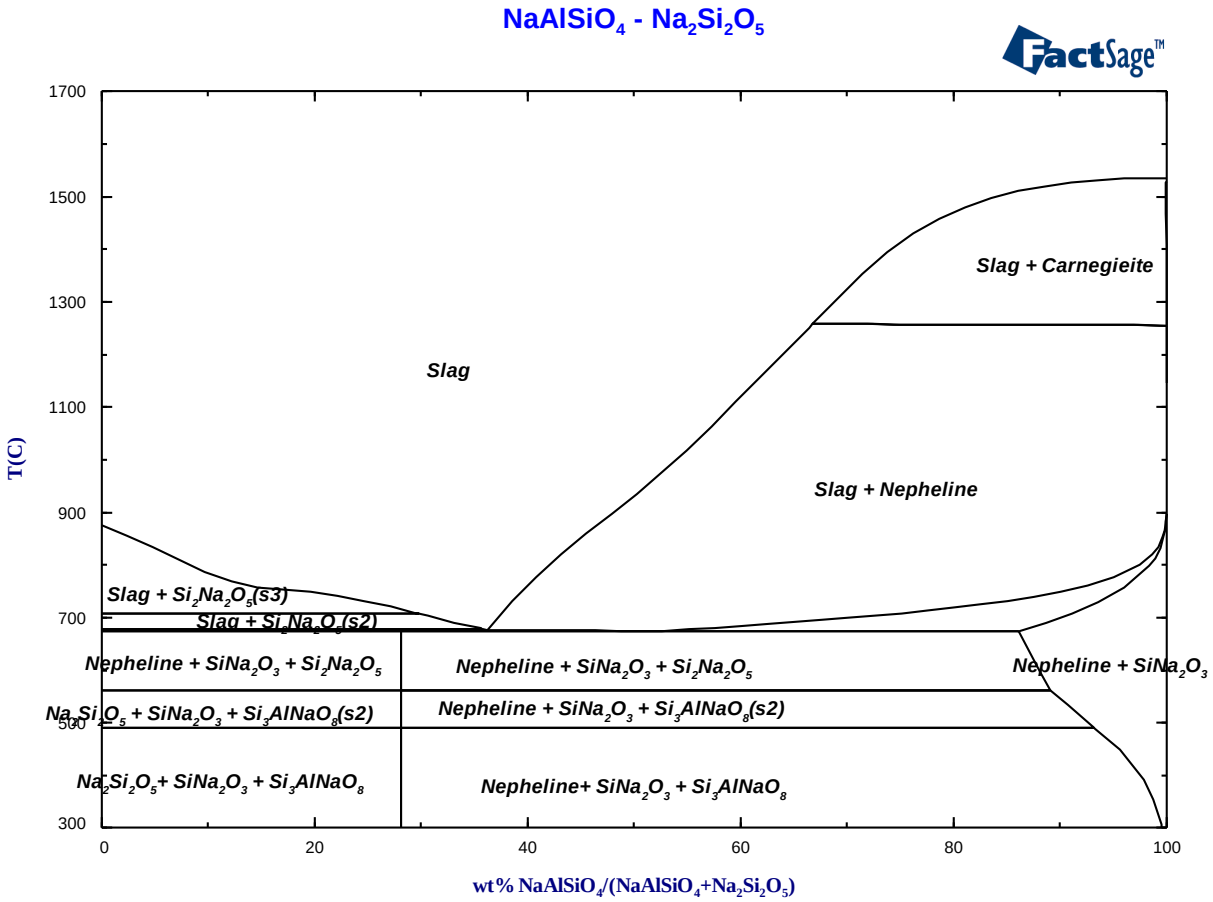

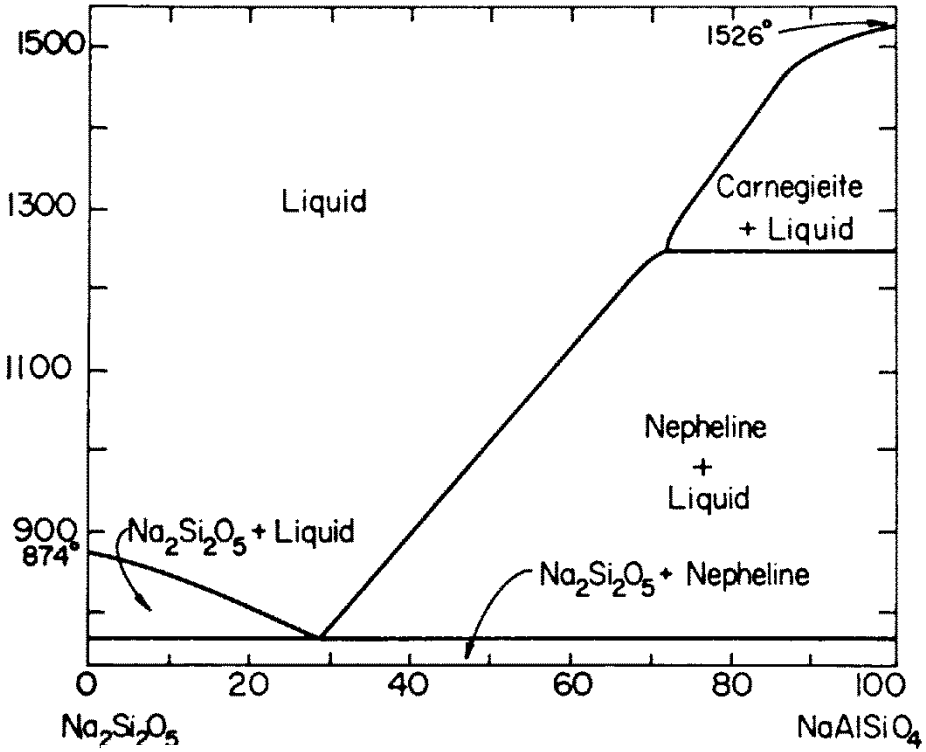

C.E. Tilley, Mineral. Petrogr. Mitt., 43 [6], (1933), pp.406-421.

Al2O3-Na2O-SiO2,

Weight percent Al2O3-AlNaSiO4

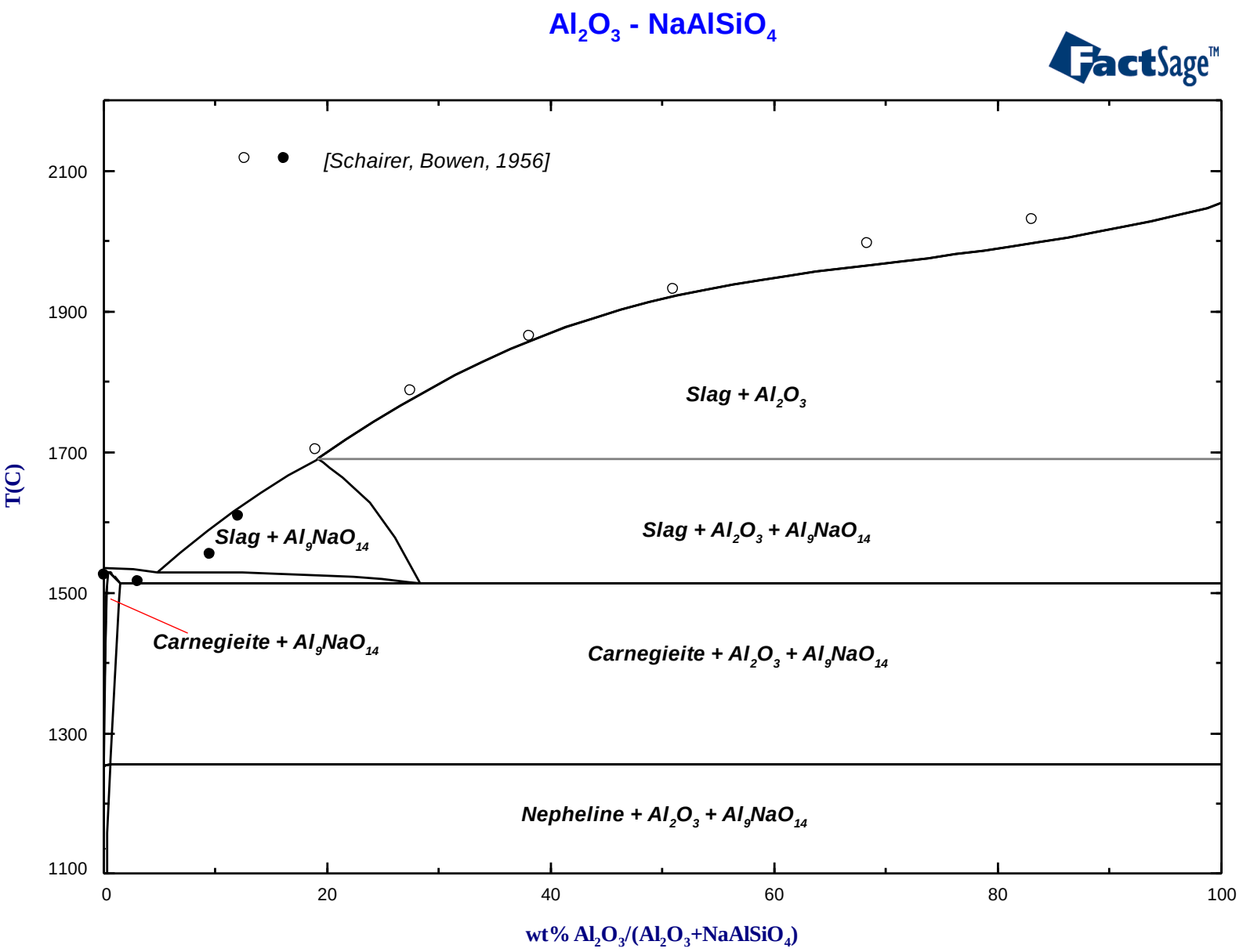

Weight percent Na2SiO3-AlNaSiO4

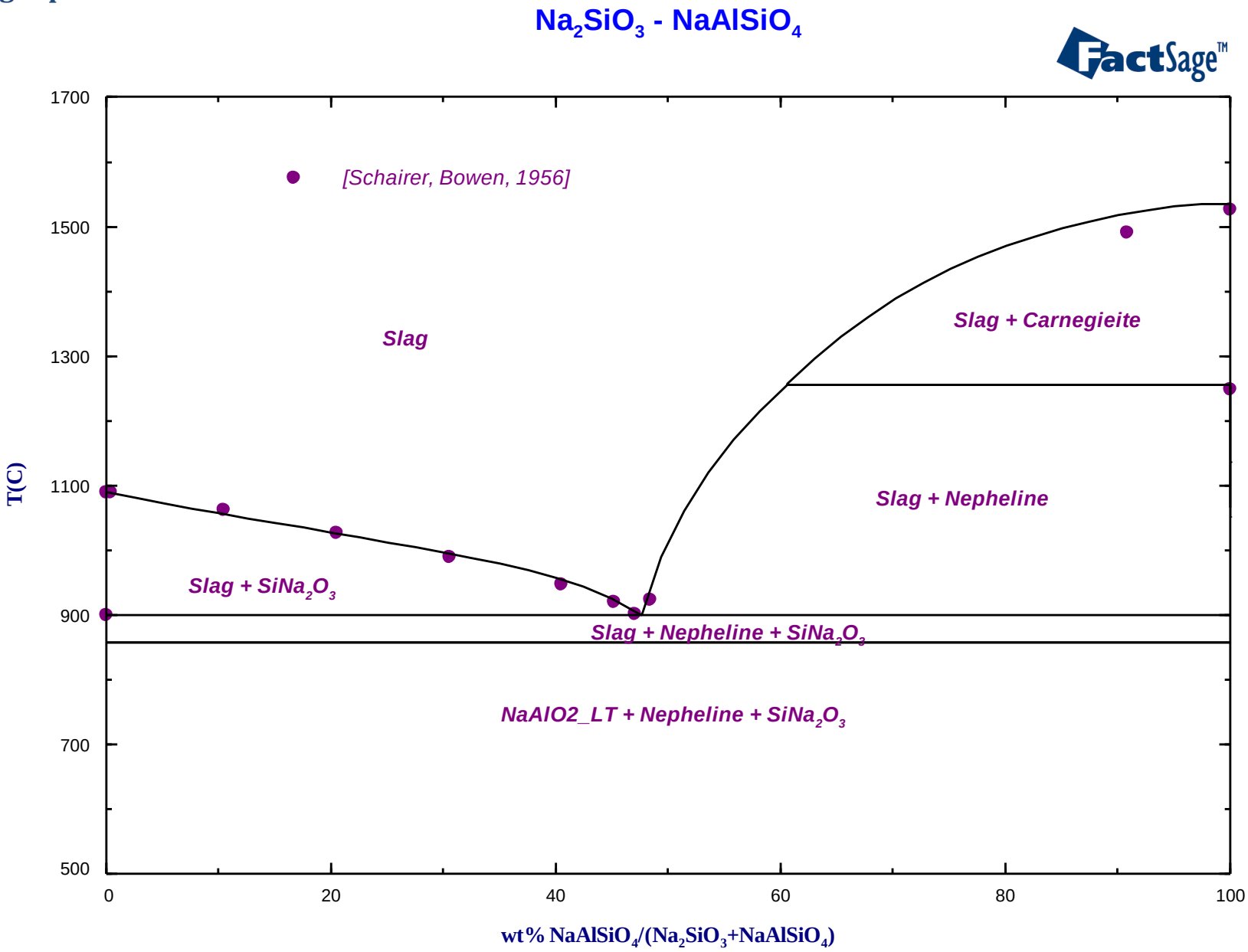

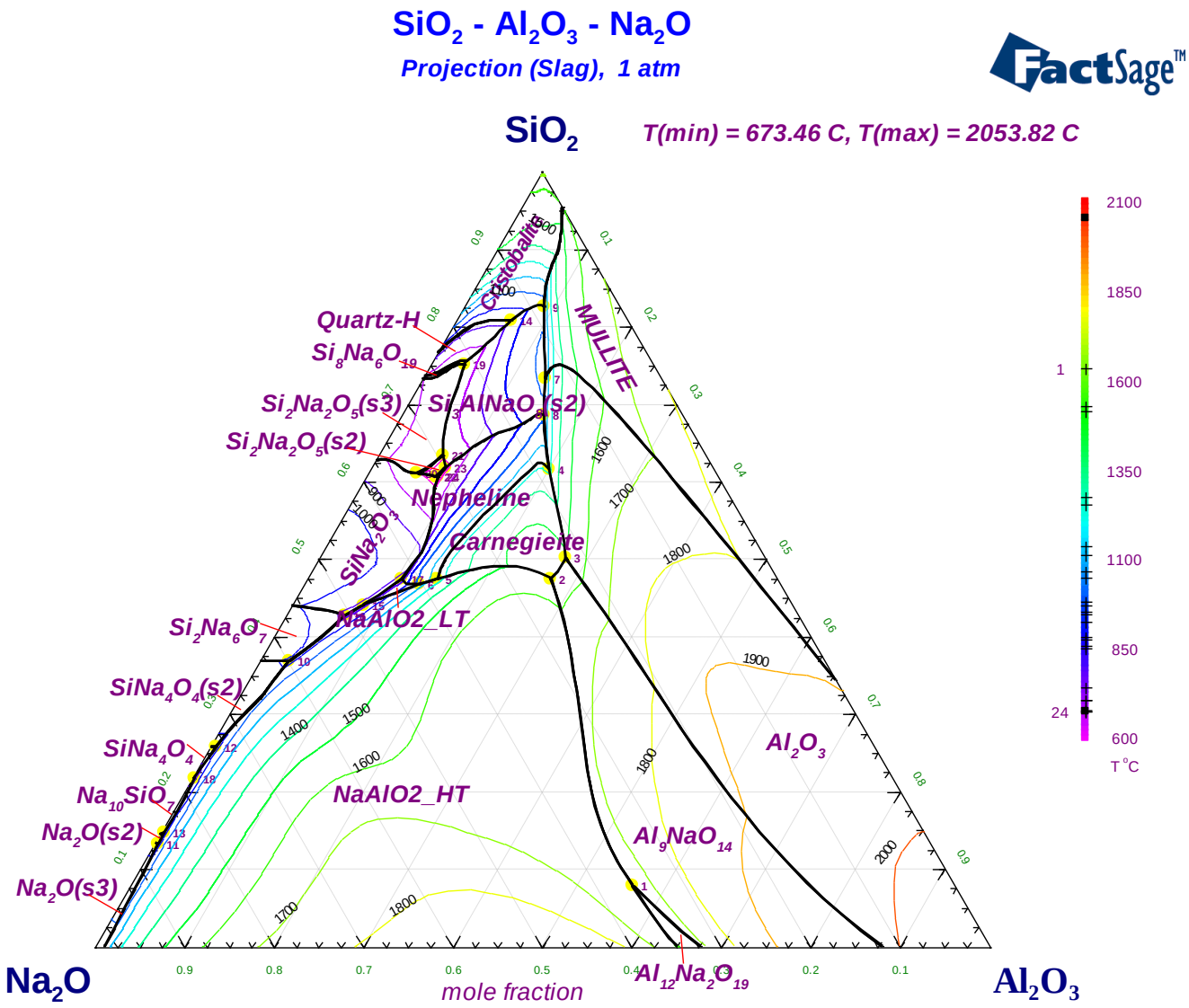
SiO2 - Al2O3 - Na2O
Projection (Slag), 1 atm
FactSage™
SiO2
T(min) = 673.46 C, T(max) = 2053.82 C
Cristobalite
MULLITE
Quartz-H
Si8Na6O19
Si2Na2O5(s3)
Si2AlNaO5(s2)
Si2Na2O5(s2)
Nepheline
Carnegieite
SiNa2O3
NaAlO2_LT
Si2Na6O7
SiNa4O4(s2)
SiNa4O4
Na10SiO7
NaAlO2_HT
Na2O(s2)
Na2O(s3)
Al2O3
Al9NaO14
Al12Na2O19
2100
1850
1600
1350
1100
850
600
T °C
1
24
Na2O
mole fraction
Al2O3

Weight percent
Liquidussurface
compared with experimental data

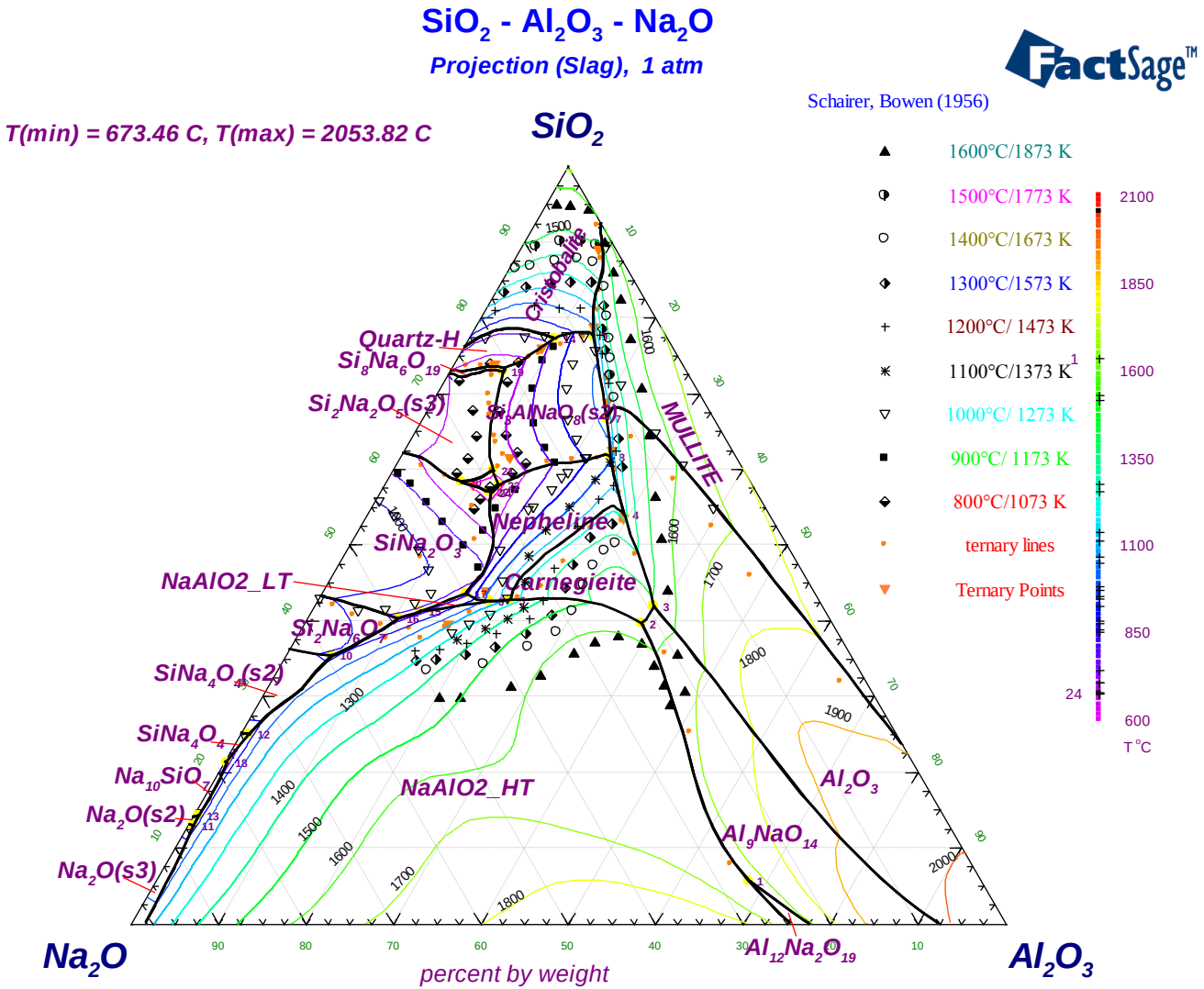

Invariant equilibria on the liquidus surface

Intersections with slag	Mole fraction				Weight percent				
	A = SiO2, B = Na2O, C = Al2O3				A = SiO2, B = Na2O, C = Al2O3				
		X(A)	X(B)	X(C)	T(C)		W(A)	W(B)	W(C)	T(C)
1: NaAlO2_HT / Al12Na2O19 / Al9NaO14	1:	0.07904	0.35961	0.56135	1635.44	1:	5.635	26.448	67.917	1635.44
2: NaAlO2_HT / Al9NaO14 / Carnegieite	2:	0.47531	0.25265	0.27204	1527.43	2:	39.690	21.762	38.548	1527.52
3: Al2O3 / Al9NaO14 / Carnegieite	3:	0.50191	0.22302	0.27507	1513.34	3:	41.870	19.191	38.939	1513.33
4: Al2O3 / Nepheline / Carnegieite	4:	0.61706	0.18390	0.19903	1275.10	4:	53.915	16.575	29.511	1275.10
5: NaAlO2_HT / Nepheline / Carnegieite	5:	0.47506	0.37976	0.14517	1254.27	5:	42.677	35.192	22.131	1254.25
6: NaAlO2_HT / NaAlO2_LT / Nepheline	6:	0.46891	0.40262	0.12847	1135.85	6:	42.542	37.680	19.778	1135.85
7: Al2O3 / MULLITE / Si3AlNaO8(s2)	7:	0.73308	0.13030	0.13662	1113.74	7:	66.684	12.226	21.089	1113.74
8: Al2O3 / Nepheline / Si3AlNaO8(s2)	8:	0.68690	0.15485	0.15824	1065.25	8:	61.596	14.324	24.080	1065.22
9: MULLITE / Si3AlNaO8(s2) / Cristobalite	9:	0.82633	0.08521	0.08846	1048.31	9:	77.638	8.259	14.103	1047.91
10: NaAlO2_HT / Si2Na6O7 / SiNa4O4(s2)	10:	0.36814	0.59931	0.03256	981.91	10:	35.344	59.353	5.304	981.91
11: NaAlO2_HT / Na2O(s2) / Na2O(s3)	11:	0.13261	0.86305	0.00434	970.05	11:	12.872	86.413	0.715	970.10
12: NaAlO2_HT / SiNa4O4(s2) / SiNa4O4(s)	12:	0.25743	0.73623	0.00634	954.75	12:	25.051	73.902	1.047	954.75
13: NaAlO2_HT / Na10SiO7 / Na2O(s2)	13:	0.14709	0.84917	0.00374	947.32	13:	14.289	85.094	0.617	947.32
14: Si3AlNaO8(s2) / Cristobalite / Quartz_H	14:	0.80861	0.13030	0.06108	926.28	14:	77.255	12.842	9.903	926.28
15: NaAlO2_HT / NaAlO2_LT / SiNa2O3	15:	0.44121	0.47948	0.07931	883.04	15:	41.219	46.207	12.574	883.21
16: NaAlO2_HT / Si2Na6O7 / SiNa2O3	16:	0.42716	0.50753	0.06531	877.08	16:	40.240	49.319	10.441	877.07
17: NaAlO2_LT / Nepheline / SiNa2O3	17:	0.47424	0.41964	0.10612	856.75	17:	43.620	39.816	16.564	856.75
18: NaAlO2_HT / Na10SiO7 / SiNa4O4	18:	0.21799	0.77984	0.00217	850.13	18:	21.245	78.397	0.358	850.13
19: Si2Na2O5(s3) / Si3AlNaO8(s2) / Si8Na6O19	19:	0.75226	0.21050	0.03724	740.89	19:	72.852	21.028	6.120	740.90
20: Si2Na2O5(s3) / Si2Na2O5(s2) / SiNa2O3	20:	0.61107	0.33553	0.05341	706.86	20:	58.319	33.032	8.649	706.86
21: Si2Na2O5(s3)/ Si2Na2O5(s2) / Si3AlNaO8(s2)	21:	0.63436	0.29392	0.07173	706.86	21:	59.887	28.622	11.491	706.84
22: Si2Na2O5 / Si2Na2O5(s2) / SiNa2O3	22:	0.60692	0.31578	0.07729	677.84	22:	57.051	30.620	12.329	677.84
23: Nepheline / Si2Na2O5 / Si3AlNaO8(s2)	23:	0.61802	0.29929	0.08269	676.53	23:	57.918	28.932	13.150	676.53
24: Nepheline / Si2Na2O5 / SiNa2O3	24:	0.60592	0.31364	0.08043	673.54	24:	56.843	30.352	12.805	673.46

Al2O3-Na2O-V2O5, Mole fraction 500°C

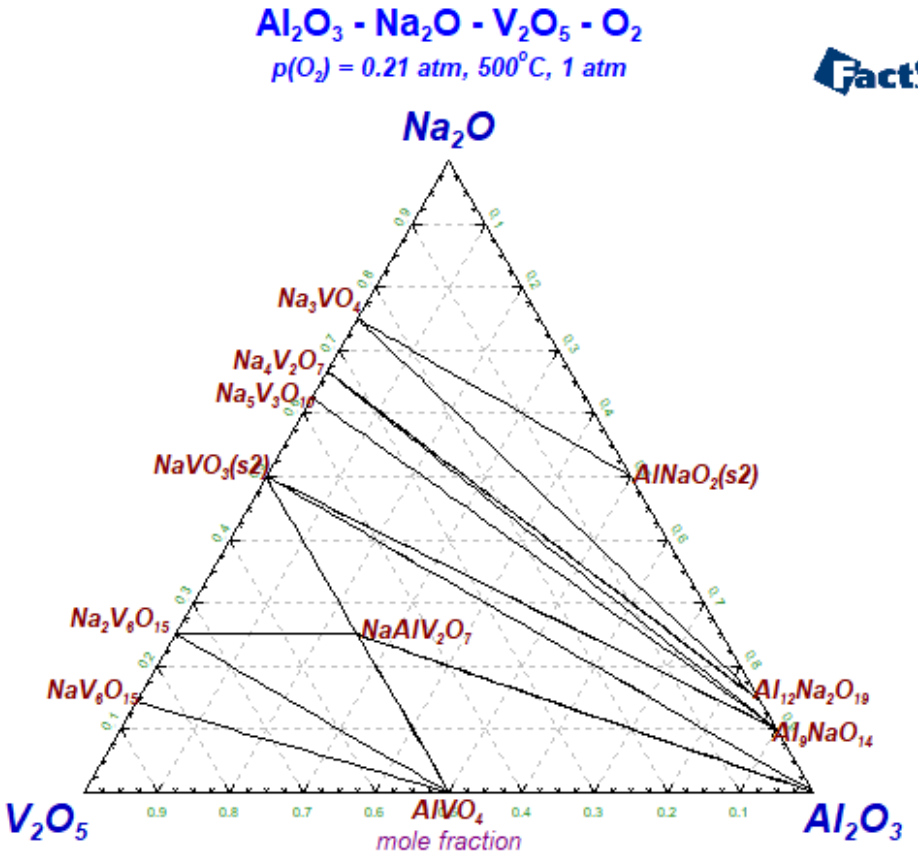

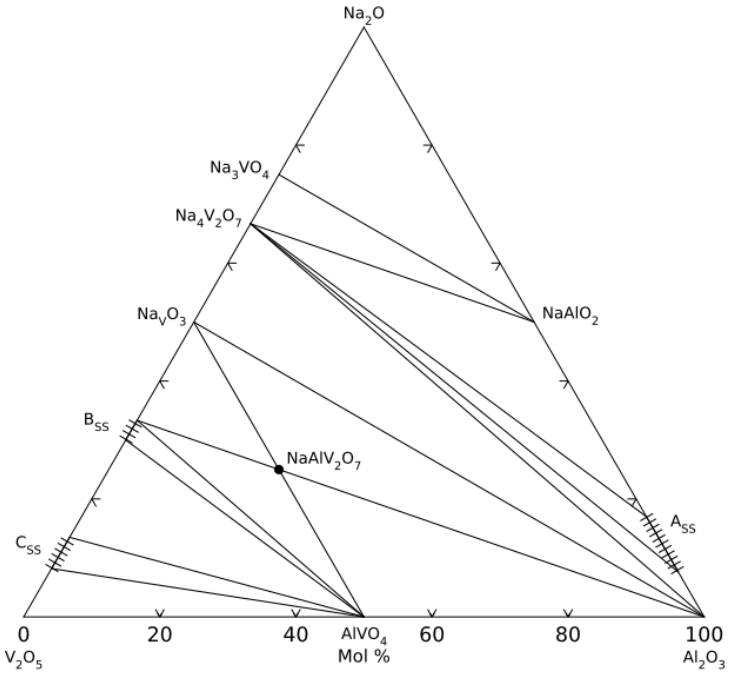

A. A. Fotiev, B. V. Slobodin, L. L. Surat, T. P. Sirina, Zh. Neorg. Khim., 28 [4] 1037-1041

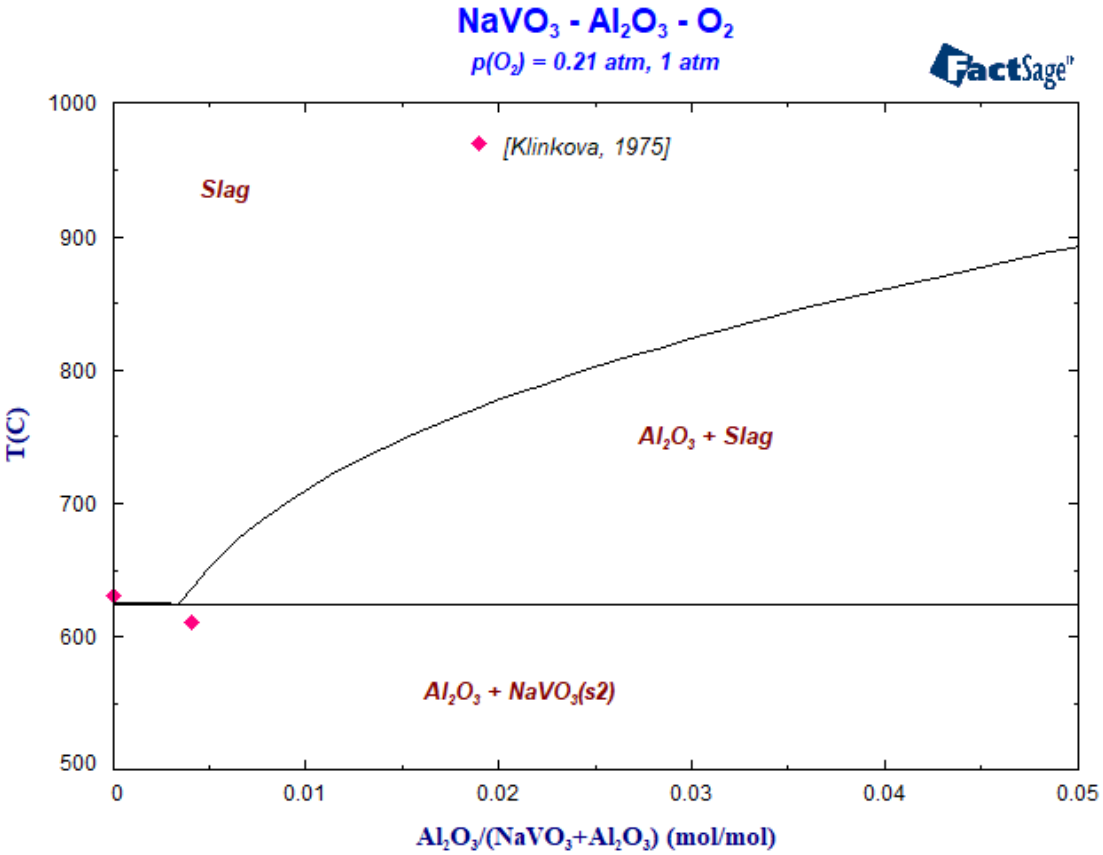

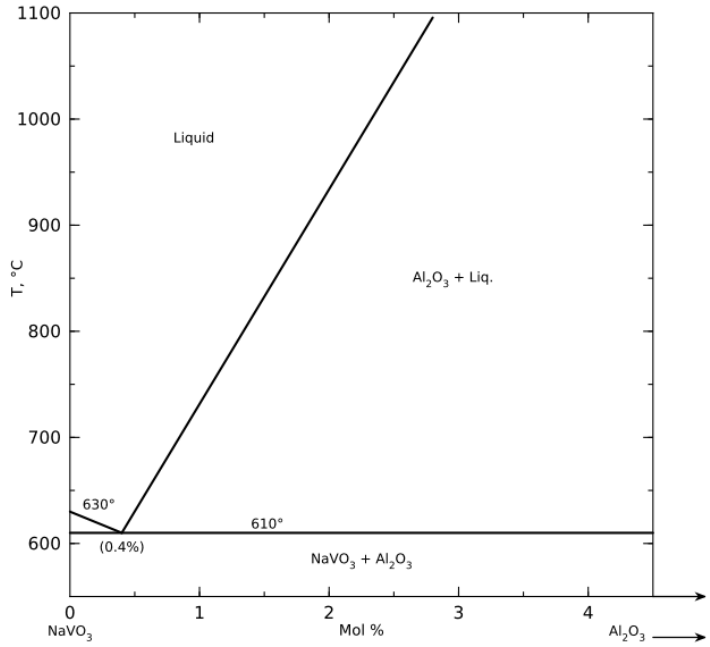

L. A. Klinkova and E. A. Ulkshe, Zh. Neorg. Khim., 20 [2] 481-484 (1975); Russ. J. Inorg.

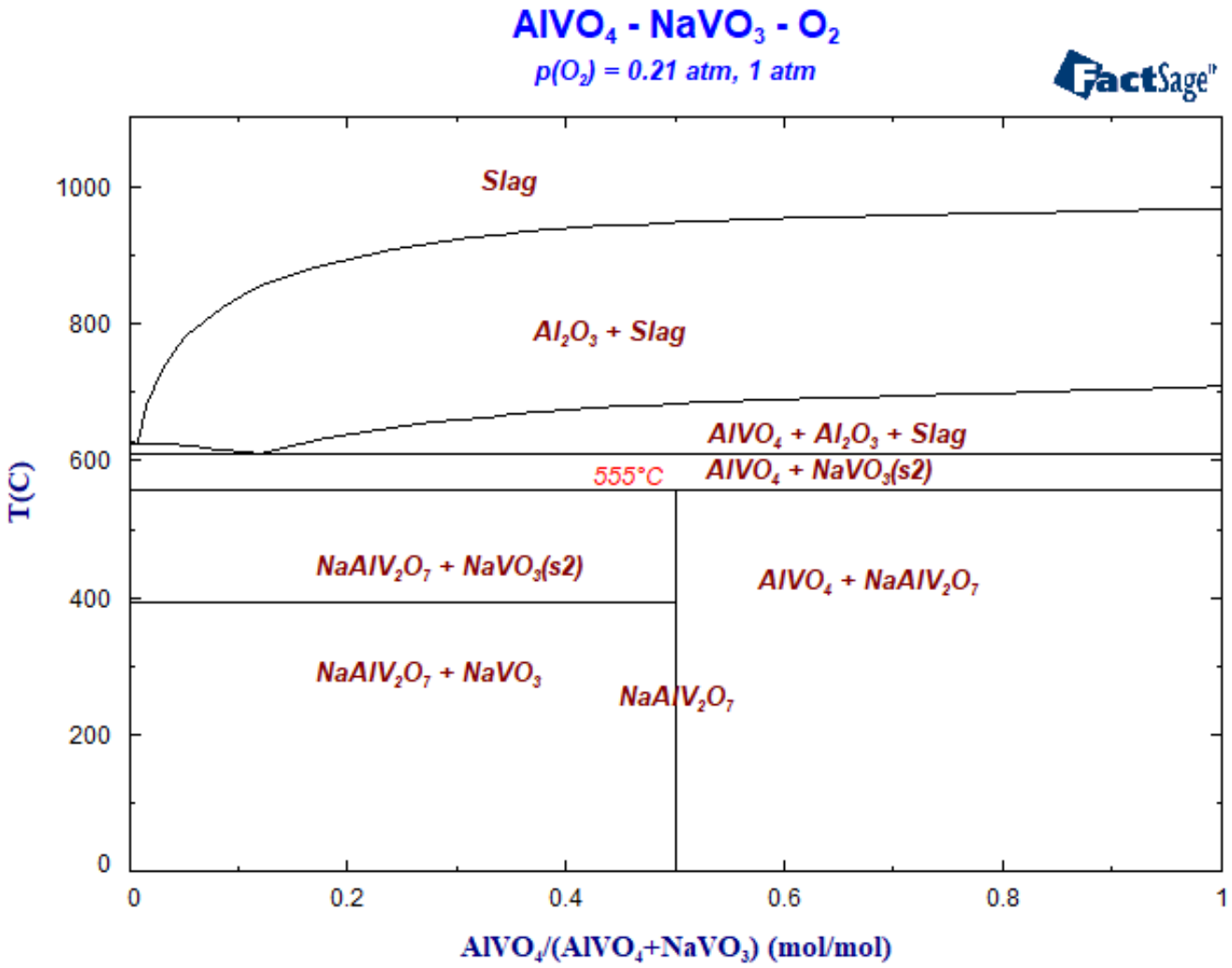

T_m of $NaAlV_2O_7$ is unknown, over 550°C [Fotiev 1983].

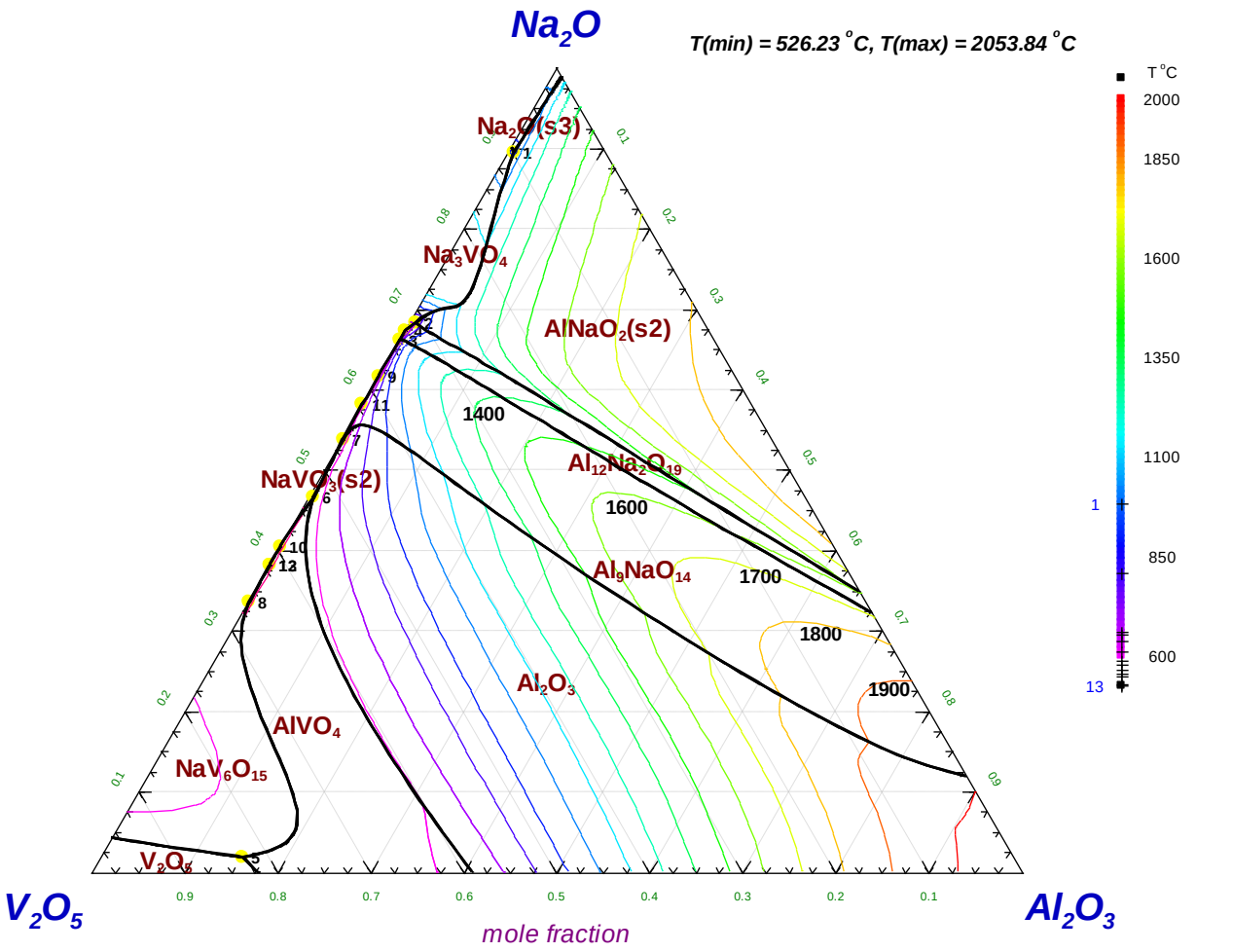
Al2O3 - Na2O - V2O5 - O2
Projection (Slag), p(O2) = 0.21 atm, 1 atm
FactSage™
Na2O
T(min) = 526.23 °C, T(max) = 2053.84 °C
T °C
2000
1850
1600
1350
1100
850
600
1
13
Na2O(s3)
Na3VO4
AlNaO2(s2)
NaVO3(s2)
Al12Na2O19
Al9NaO14
Al2O3
AlVO4
NaV6O15
V2O5
1400
1600
1700
1800
1900
V2O5
Al2O3
mole fraction

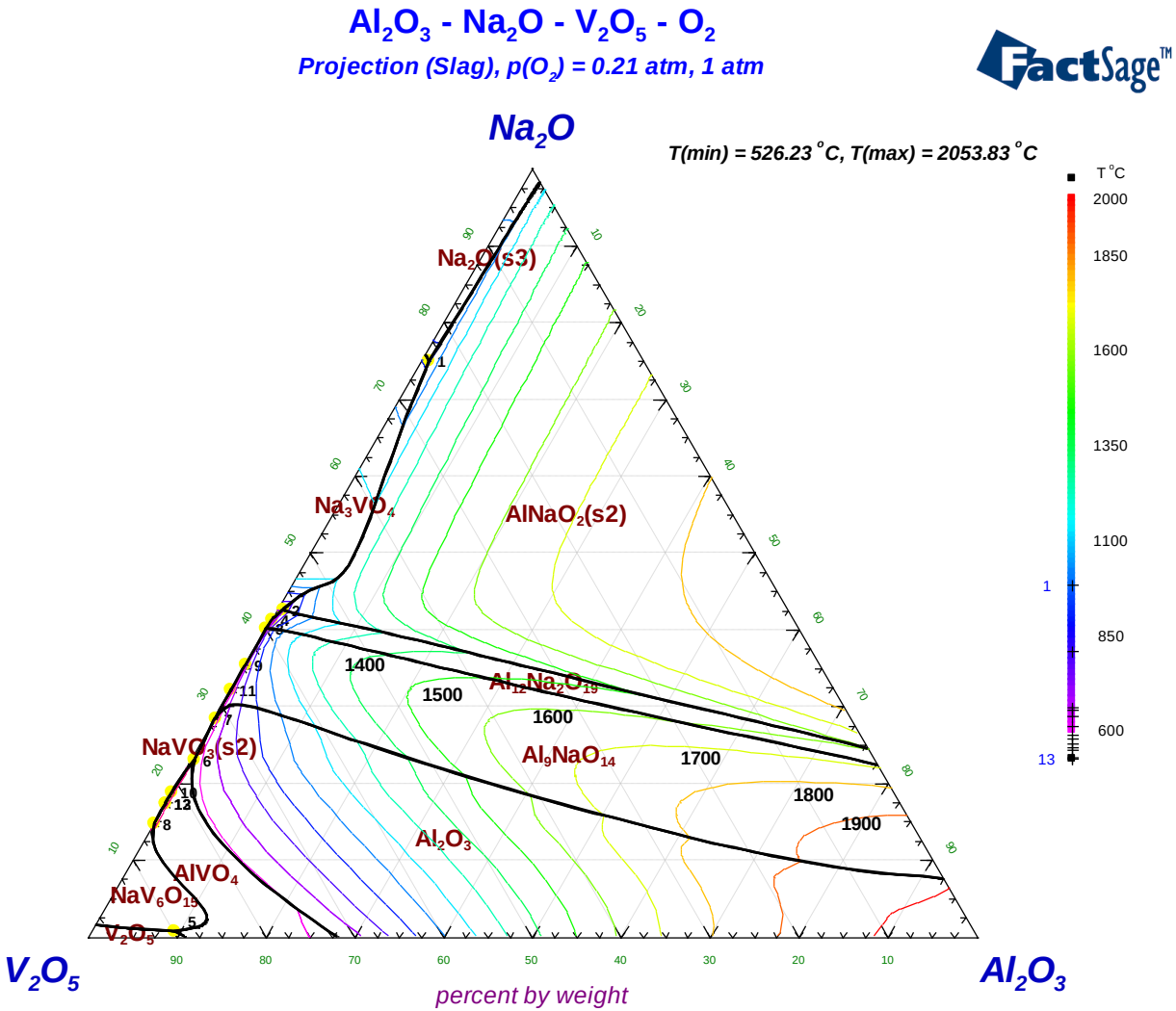
Al2O3 - Na2O - V2O5 - O2
Projection (Slag), p(O2) = 0.21 atm, 1 atm
FactSage™
Na2O
T(min) = 526.23 °C, T(max) = 2053.83 °C
T °C
2000
1850
1600
1350
1100
850
600
Na2O(s3)
Na3VO4
AlNaO2(s2)
Al12Na2O19
Al9NaO14
NaVO3(s2)
Al2O3
AlVO4
NaV6O15
V2O5
1400
1500
1600
1700
1800
1900
V2O5
Al2O3
percent by weight

Invariant equilibria on the liquidus surface

Intersections with slag	Mole fraction A = Na2O, B = V2O5, C = Al2O3				Weight percent A = Na2O, B = V2O5, C = Al2O3			
	X(A)	X(B)	X(C)	T(C)	W(A)	W(B)	W(C)	T(C)
1: AlNaO2(s2) / Na2O(s3) / Na3VO4	1: 0.89537	0.09806	0.00656	981.14	1: 74.993	24.102	0.904	981.14
2: Al12Na2O19 / AlNaO2(s2) / Na3VO4	2: 0.68336	0.31017	0.00647	808.42	2: 42.597	56.739	0.664	809.08
3: Al12Na2O19 / Al9NaO14 / Na4V2O7	3: 0.66268	0.33711	0.00021	659.32	3: 40.107	59.872	0.021	659.34
4: Al12Na2O19 / Na3VO4 / Na4V2O7	4: 0.67385	0.32557	0.00058	652.94	4: 41.335	58.606	0.059	652.75
5: AlVO4 / NaV6O15 / V2O5	5: 0.01911	0.82842	0.15248	637.59	5: 0.707	90.006	9.287	637.59
6: Al2O3 / AlVO4 / NaVO3(s2)	6: 0.46580	0.52852	0.00569	609.78	6: 22.990	76.549	0.462	609.78
7: Al2O3 / Al9NaO14 / NaVO3(s2)	7: 0.53853	0.46039	0.00109	589.08	7: 28.473	71.432	0.095	589.09
8: AlVO4 / Na2V6O15 / NaV6O15	8: 0.33588	0.66259	0.00153	578.13	8: 14.714	85.176	0.110	578.13
9: Al9NaO14 / Na4V2O7 / Na5V3O10	9: 0.61654	0.38338	0.00008	564.36	9: 35.398	64.594	0.008	564.38
10: AlVO4 / NaAlV2O7 / NaVO3(s2)	10: 0.40504	0.59458	0.00038	555.01	10: 18.835	81.136	0.029	555.01
11: Al9NaO14 / Na5V3O10 / NaVO3(s2)	11: 0.58186	0.41797	0.00017	546.70	11: 32.170	67.815	0.015	546.70
12: AlVO4 / Na2V6O15 / NaAlV2O7	12: 0.38161	0.61828	0.00010	527.46	12: 17.376	82.616	0.008	527.45
13: Na2V6O15 / NaAlV2O7 / NaVO3(s2)	13: 0.38243	0.61748	0.00009	526.23	13: 17.426	82.567	0.007	526.23

Mole fraction, Isopleth NiAl2O4-SiO2

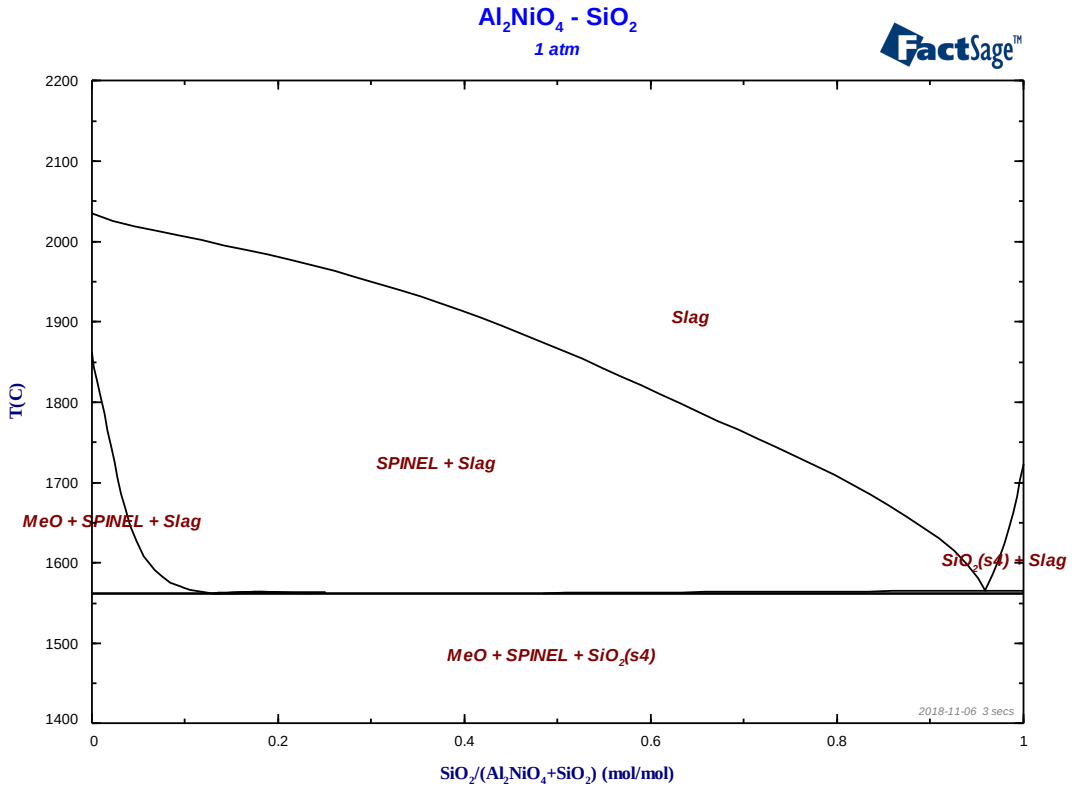

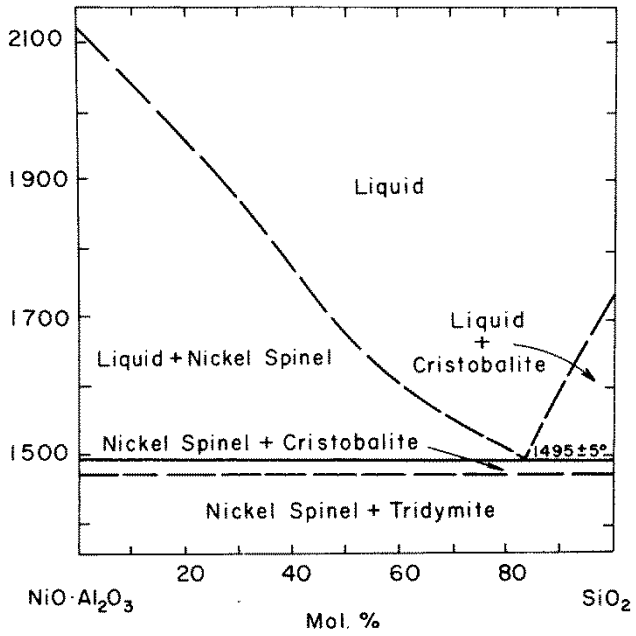

B. Phillips, J.J. Hutta, I. Warshaw, J. Am.Ceram. Soc., 46 [12], (1963), pp.579-583.

Mole fraction, Isopleth NiAl2O4-Ni2SiO4

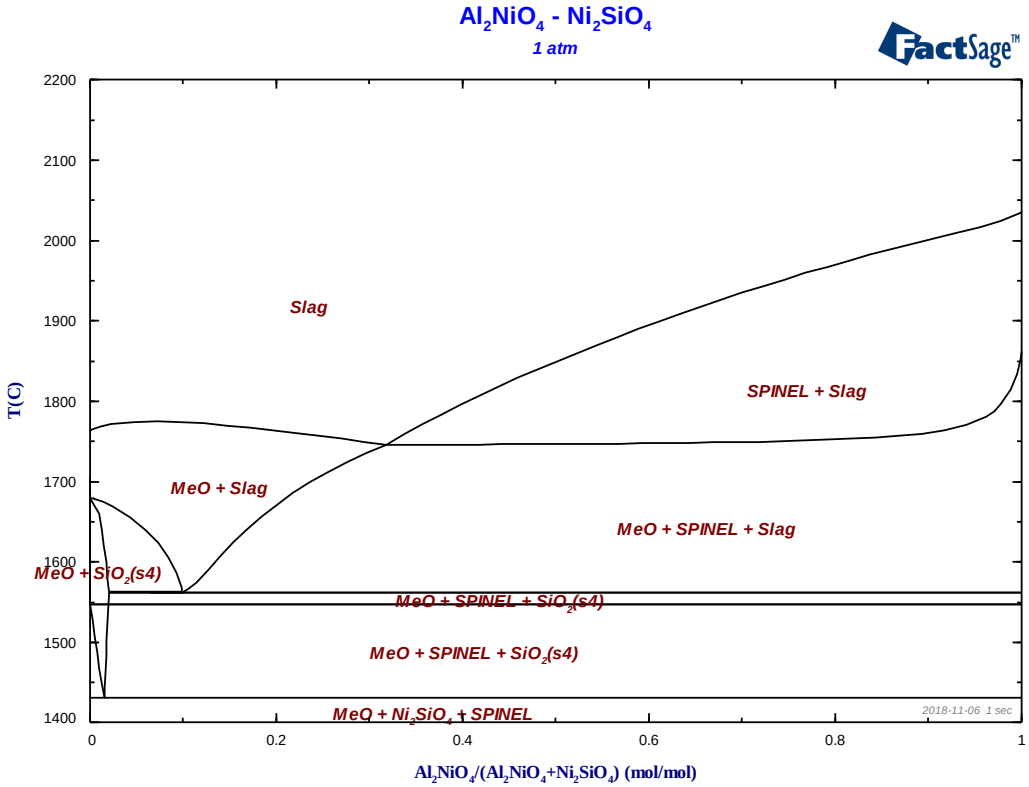

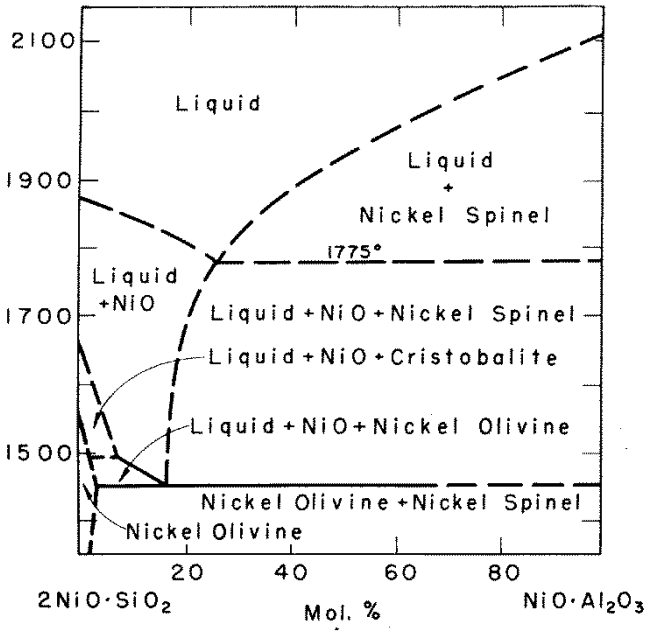

B. Phillips, J.J. Hutta, I. Warshaw, J. Am.Ceram. Soc., 46 [12], (1963), pp.579-583.

Mole fraction, Liquidus surface

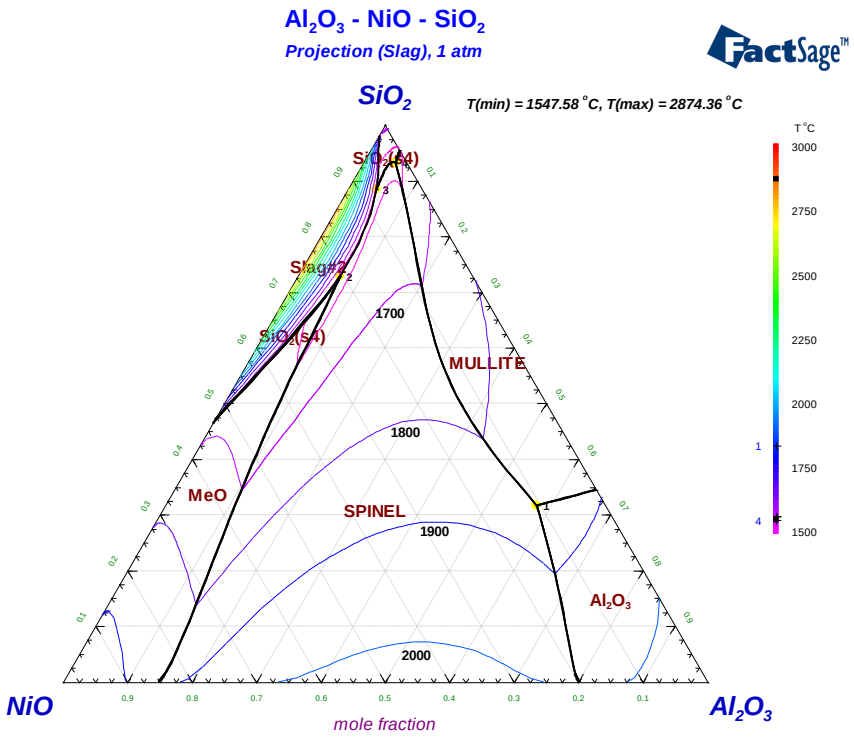

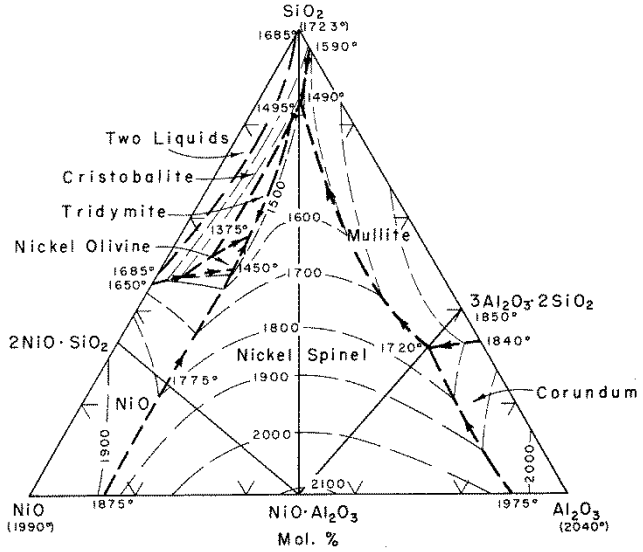

B. Phillips, J.J. Hutta, I. Warshaw, J. Am.Ceram. Soc., 46 [12], (1963), pp.579-583.

Weight percent, Liquidus surface

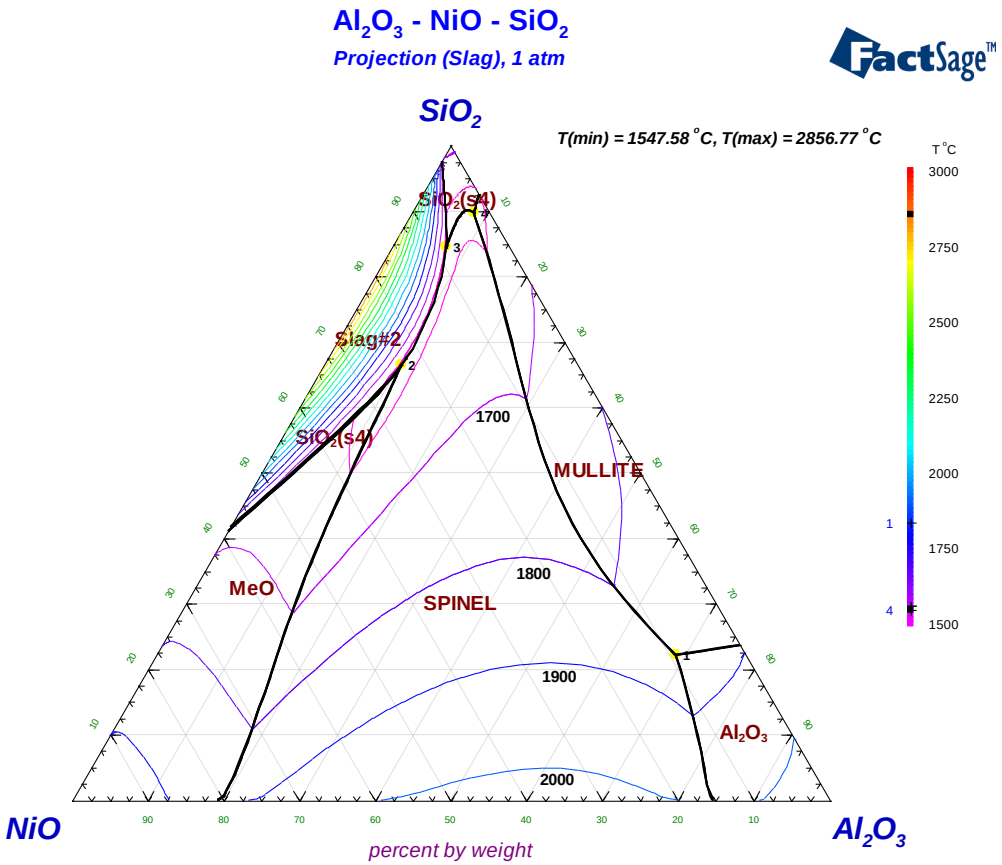

Invariant equilibria on the liquidus surface

Intersections with slag	Mole fraction				Weight percent			
	A = SiO2, B = NiO, C = Al2O3				A = SiO2, B = NiO, C = Al2O3			
	X(A)	X(B)	X(C)	T(C)	W(A)	W(B)	W(C)	T(C)
1 Al2O3 / MULLITE / SPINEL	1: 0.31666	0.10609	0.57726	1837.07	1: 22.173	9.234	68.593	1837.07
2. MeO / SiO2(s4) / Slag#2	2: 0.72872	0.20527	0.06601	1562.08	2: 66.495	23.285	10.221	1562.08
3. MeO / SiO2(s4) / Slag#2	3: 0.88580	0.07008	0.04411	1562.07	3: 84.541	8.315	7.144	1562.08
4. MULLITE / SPINEL / SiO2(s4)	4: 0.93279	0.01723	0.04998	1547.60	4: 89.776	2.061	8.163	1547.59

Al2O3-P2O5-SiO2,
Mole fraction, Isopleth AlPO4-SiO2
compared with experimental data

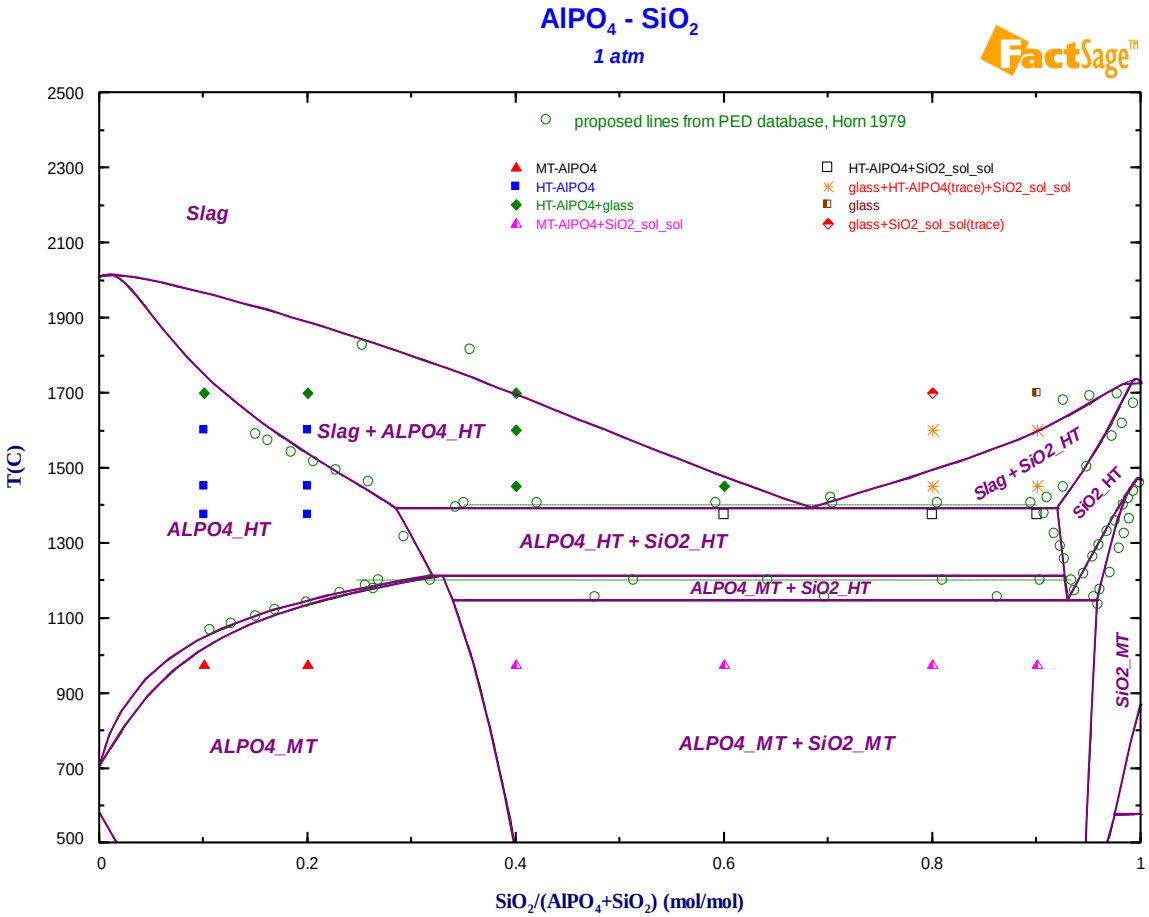

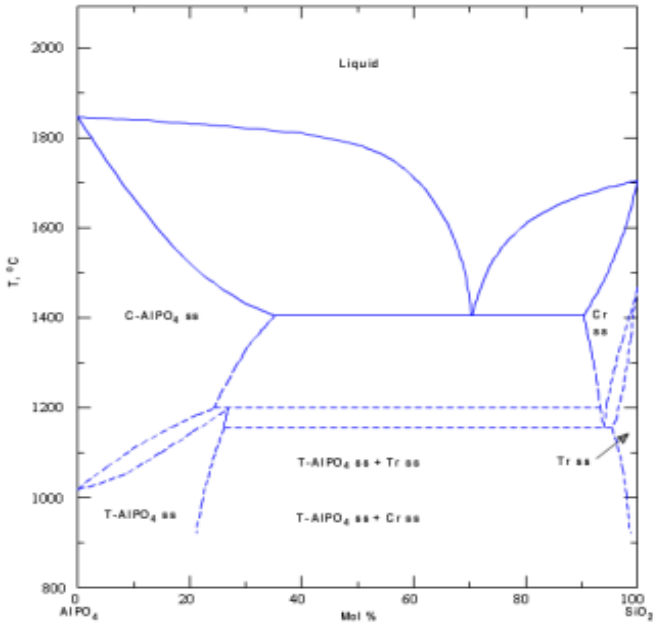

C.E. Tilley, Mineral. Petrogr. Mitt., 43 [6], (1933), pp.406-421.

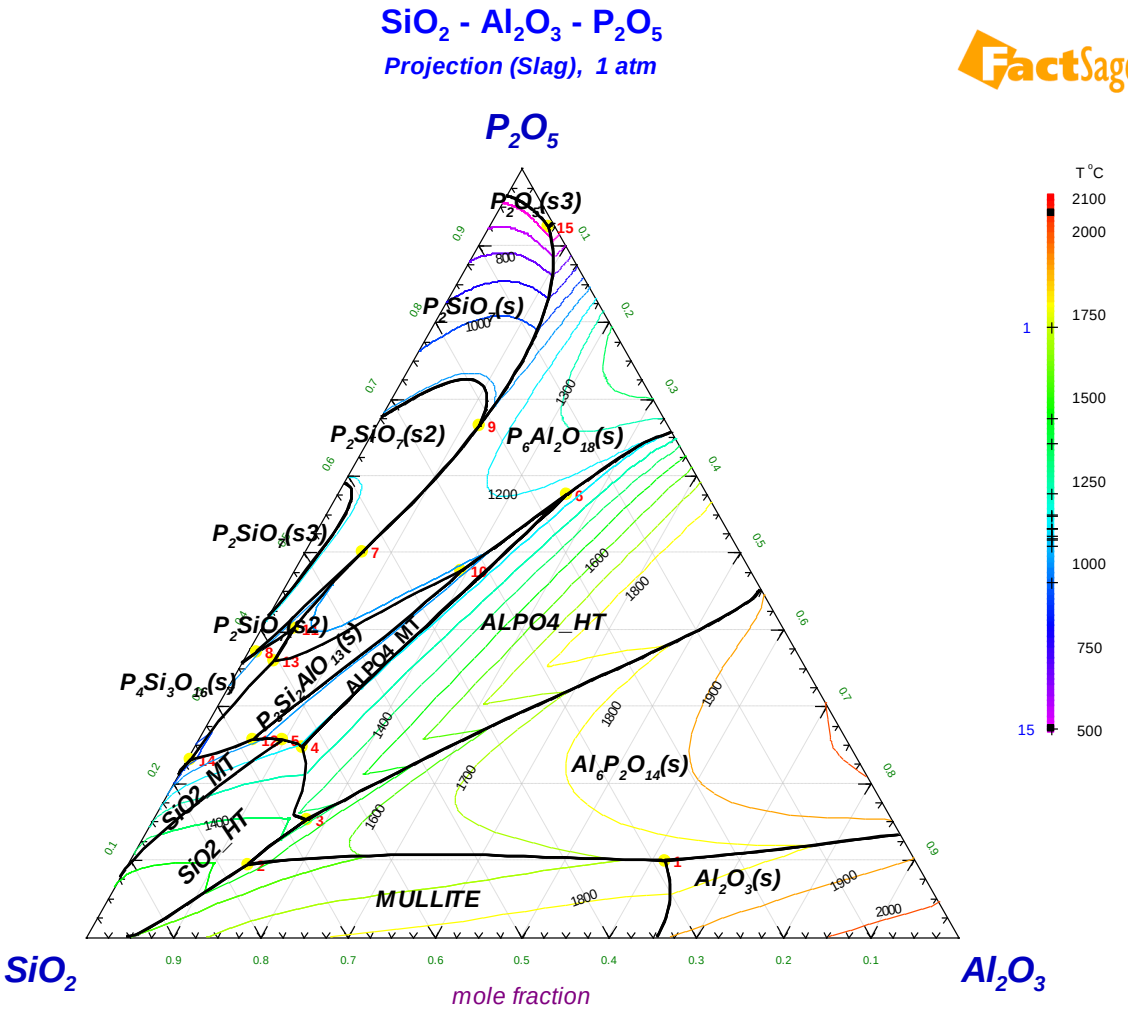
SiO2 - Al2O3 - P2O5
Projection (Slag), 1 atm
FactSage™
P2O5
T °C
2100
2000
1750
1500
1250
1000
750
500
P2O5(s3)
P2SiO7(s)
P2SiO7(s2)
P6Al2O18(s)
P2SiO4(s3)
P2SiO4(s2)
P4Si3O16(s)
P4Si2AlO13(s)
ALPO4_MT
ALPO4_HT
SiO2_MT
SiO2_HT
Al6P2O14(s)
Al2O3(s)
MULLITE
SiO2
Al2O3
mole fraction

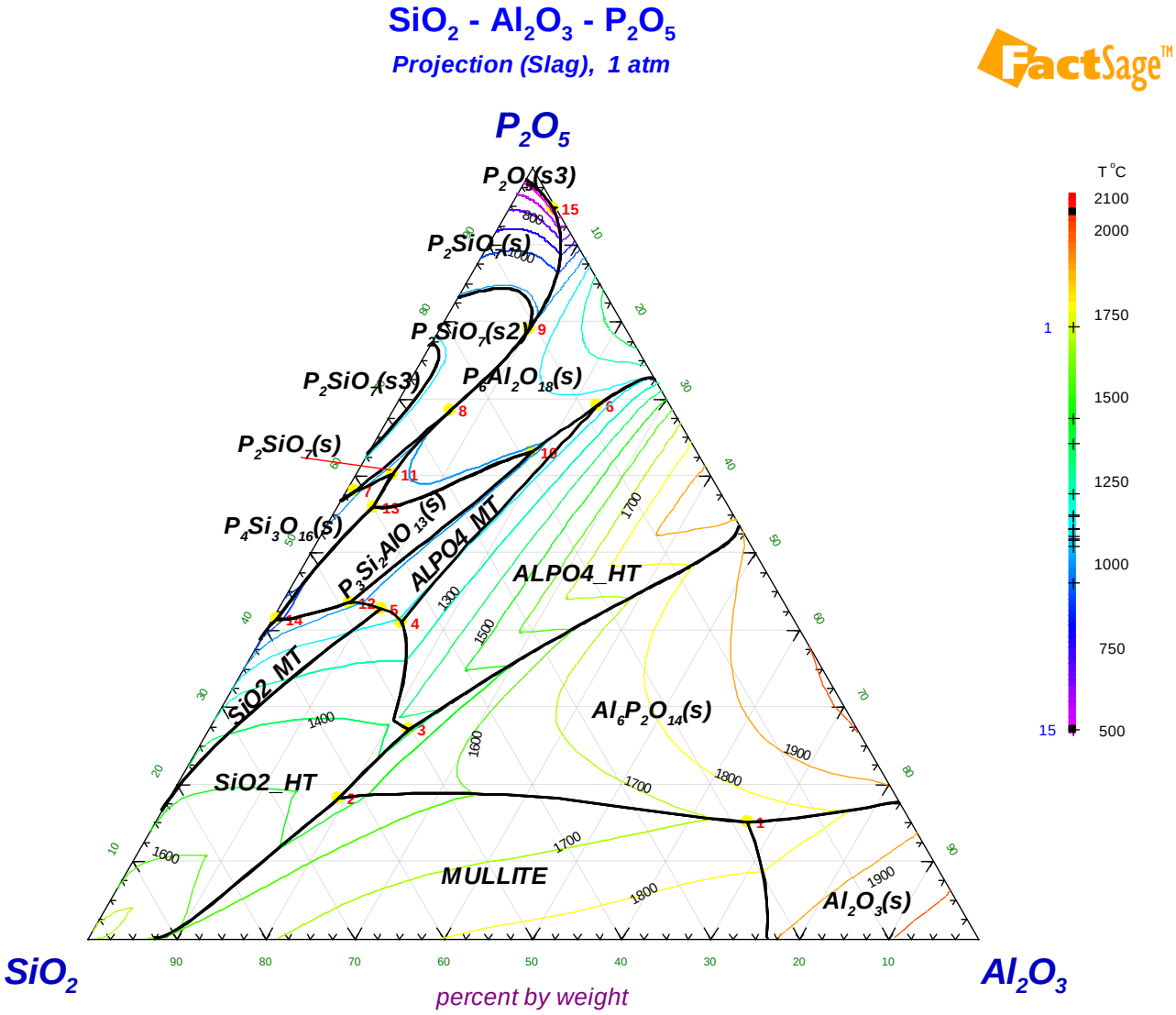
SiO2 - Al2O3 - P2O5
Projection (Slag), 1 atm
FactSage™
P2O5
P2O(s3)
P2SiO4(s)
P2Si2O7(s2)
P2SiO4(s3)
P6Al2O18(s)
P2SiO7(s)
P4Si3O16(s)
P3Si2AlO13(s)
ALPO4_MT
ALPO4_HT
SiO2_MT
SiO2_HT
Al6P2O14(s)
MULLITE
Al2O3(s)
T °C
2100
2000
1750
1500
1250
1000
750
500
SiO2
Al2O3
percent by weight

Invariant equilibria on the liquidus surface

Intersections with slag	Mole fraction A = P2O5, B = SiO2, C = Al2O3				Weight percent A = P2O5, B = SiO2, C = Al2O3			
	X(A)	X(B)	X(C)	T(C)	W(A)	W(B)	W(C)	T(C)
1: Al2O3 / Al6P2O14 / MULLITE	1: 0.09930	0.28633	0.61437	1713.71	1: 15.005	18.313	66.682	1713.71
2: Al6P2O14 / MULLITE / SiO2_HT	2: 0.09426	0.76757	0.13818	1438.99	2: 18.182	62.673	19.146	1438.99
3: ALPO4_HT / Al6P2O14 / SiO2_HT	3: 0.15263	0.67025	0.17713	1363.07	3: 27.082	50.342	22.576	1363.07
4: ALPO4_HT / ALPO4_MT / SiO2_HT	4: 0.24719	0.62871	0.12409	1212.35	4: 41.031	44.174	14.796	1211.90
5: ALPO4_MT / SiO2_HT / SiO2_MT	5: 0.25660	0.64630	0.09709	1147.36	5: 42.773	45.602	11.626	1147.35
6: ALPO4_HT / ALPO4_MT / P6Al2O18	6: 0.57563	0.16021	0.26416	1145.80	6: 69.087	8.139	22.774	1145.80
7: P2SiO7(s1) / P2SiO7(s2) / P6Al2O18	7: 0.50067	0.43266	0.06666	1106.85	7: 57.986	40.930	1.084	1106.85
8: P2SiO7(s1) / P2SiO7(s2) / P4Si3O16	8: 0.37126	0.61908	0.00966	1106.85	8: 68.426	25.029	6.545	1106.85
9: P2SiO7(s1) / P2SiO7(s2) / P6Al2O18	9: 0.66526	0.21631	0.11843	1106.85	9: 79.020	10.876	10.104	1106.85
10: ALPO4_MT / P3Si2AlO13 / P6Al2O18	10: 0.47613	0.33117	0.19270	1083.41	10: 63.086	18.574	18.340	1083.41
11: P2SiO7(s1) / P4Si3O16 / P6Al2O18	11: 0.40127	0.56064	0.03809	1076.64	11: 60.256	35.636	4.109	1076.64
12: ALPO4_MT / P3Si2AlO13 / SiO2_MT	12: 0.25710	0.68001	0.06289	1074.50	12: 43.568	48.777	7.655	1074.50
13: P3Si2AlO13 / P4Si3O16 / P6Al2O18	13: 0.35908	0.60446	0.03646	1053.34	13: 56.007	39.908	4.084	1053.35
14: P3Si2AlO13 / P4Si3O16 / SiO2_MT	14: 0.23087	0.76482	0.00431	945.70	14: 41.396	58.049	0.555	945.63
15: P2O5(s3) / P2SiO7(s1) / P6Al2O18	15: 0.92442	0.00686	0.06872	503.77	15: 94.649	0.297	5.054	503.77

Al2O3-P2O5-ZnO,
Mole fraction, 500°C000°C

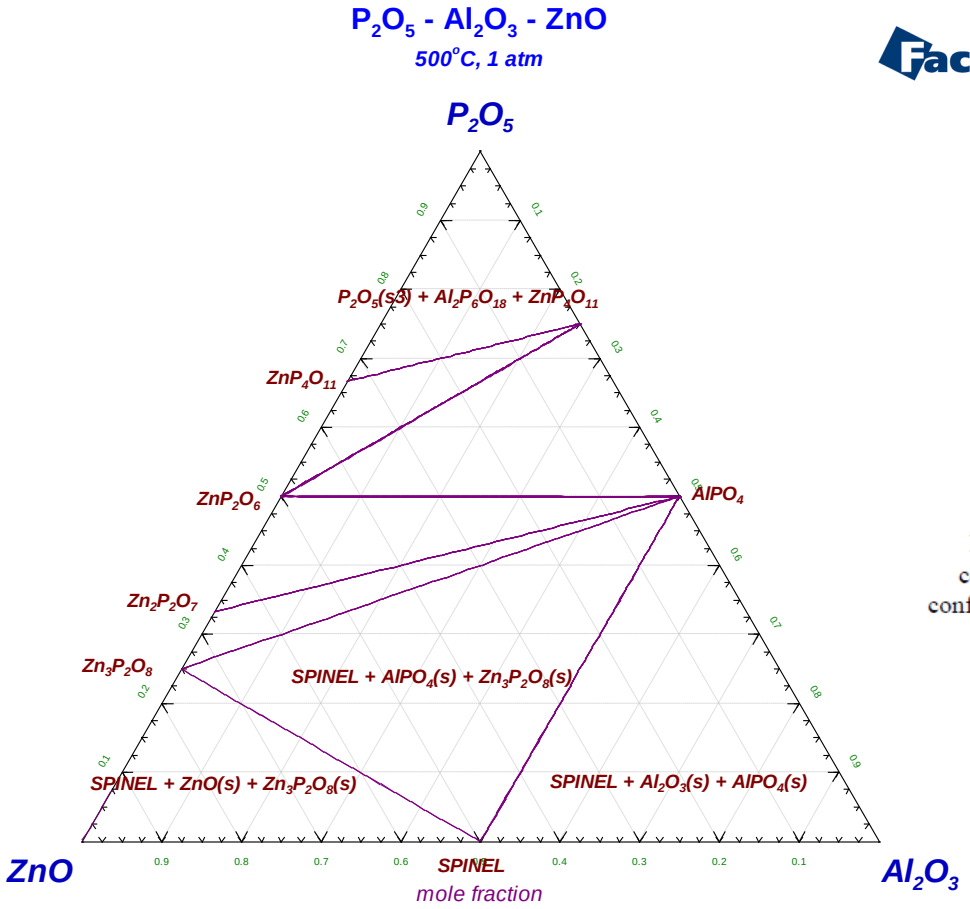

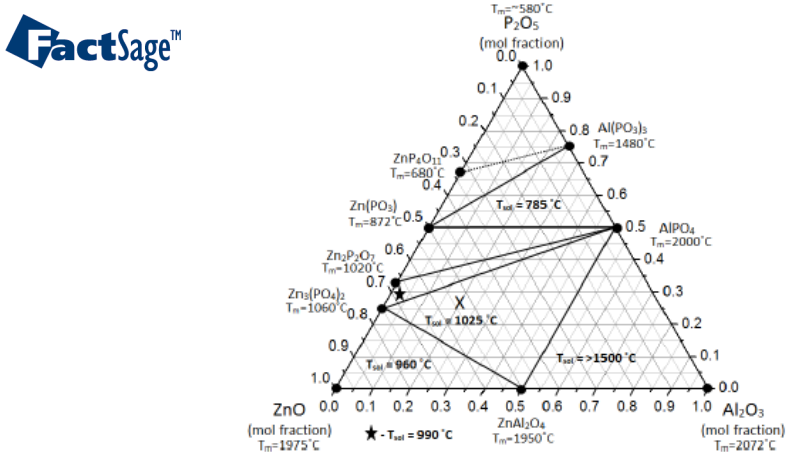

Figure 2: Phase stability diagram for the ZnO-Al_2O_3-P_2O_5 system with reported compound melting temperatures and measured solidus temperatures (solid lines = confirmed; dashed lines = proposed). (The "X" indicates mixture 20 mol% $Zn_2P_2O_7$ 80 mol% Al_2O_3)

Charmayne Elizabeth Smith, Doctoral Dissertation, Missouri University of Science and Technology, 2014.

Al2O3-P2O5-ZnO,
Mole fraction, 1000°C000°C

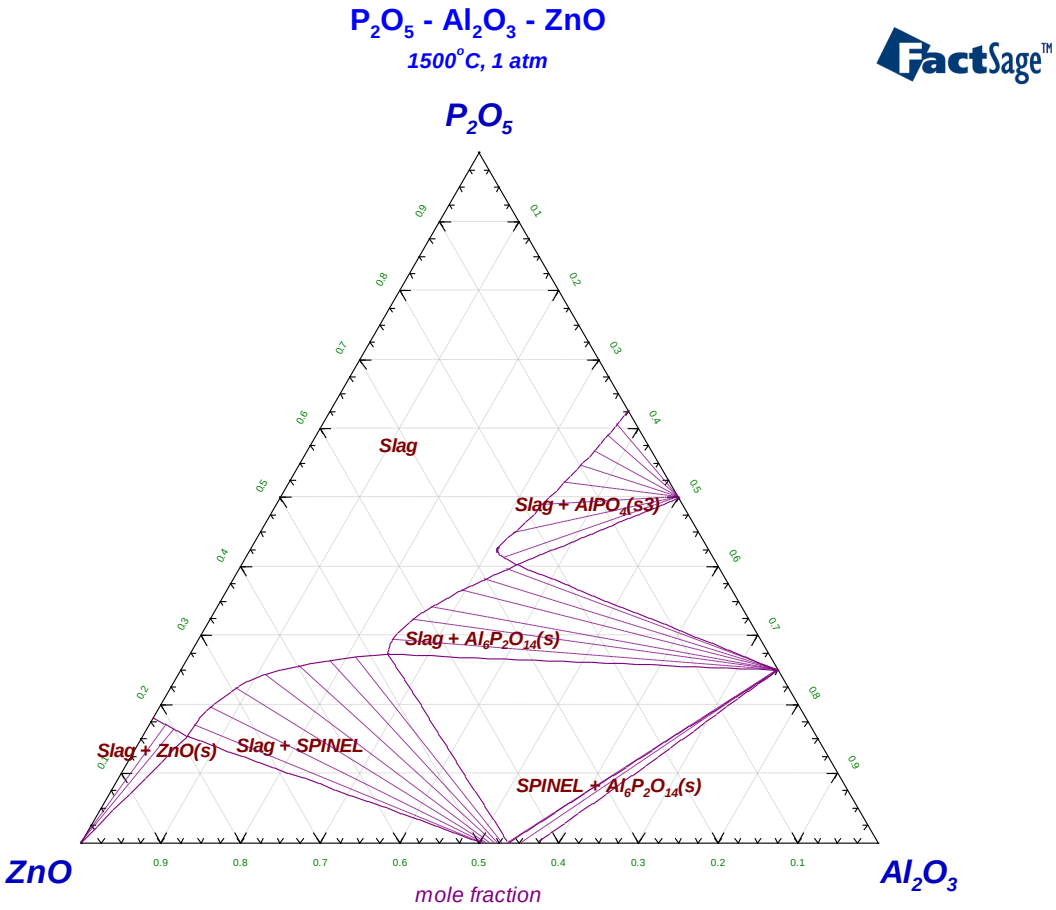

Al_2O_3 - P_2O_5 - ZnO

Projection (Slag), 1 atm

FactSage™

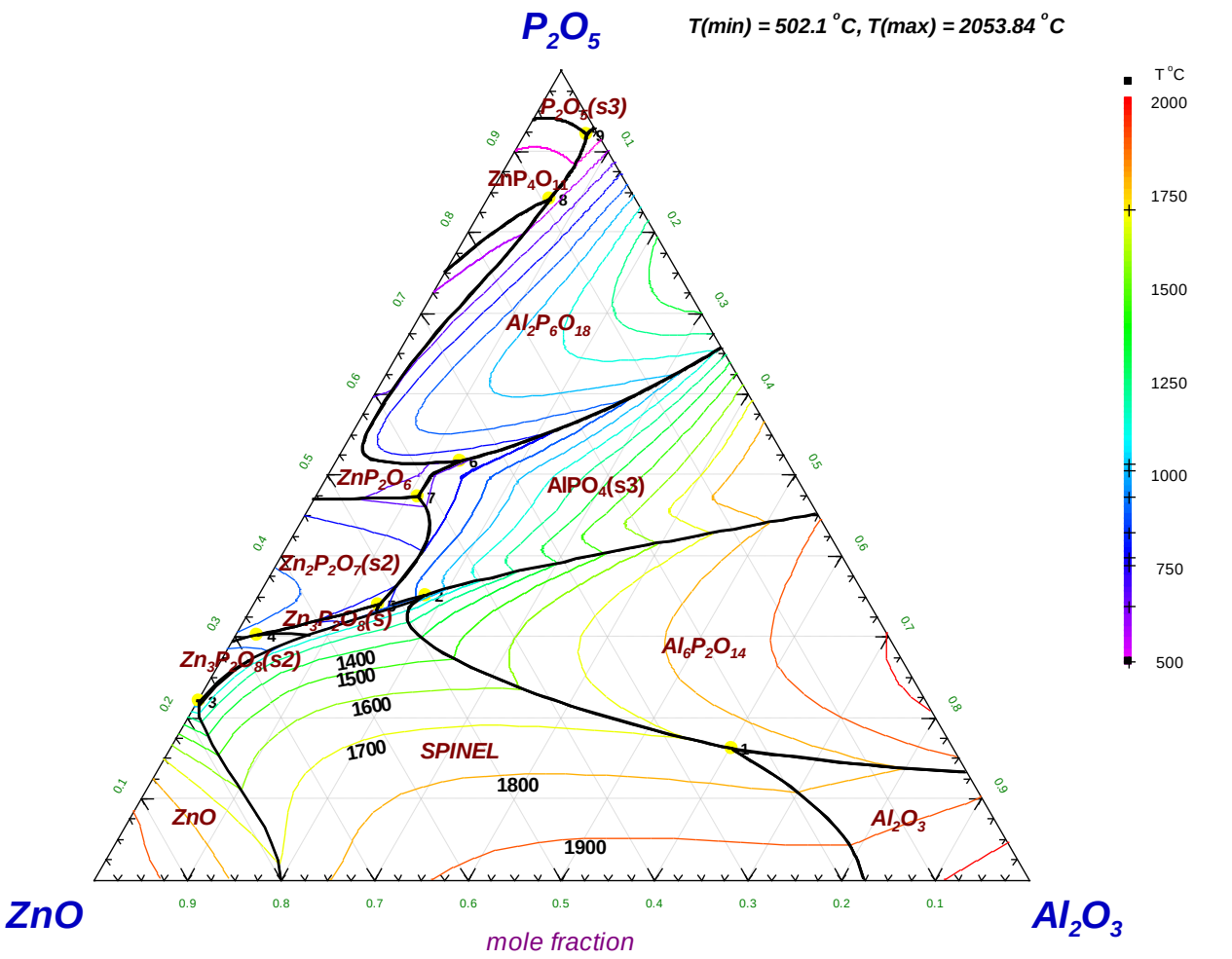

Weight percent, Liquidusfläche

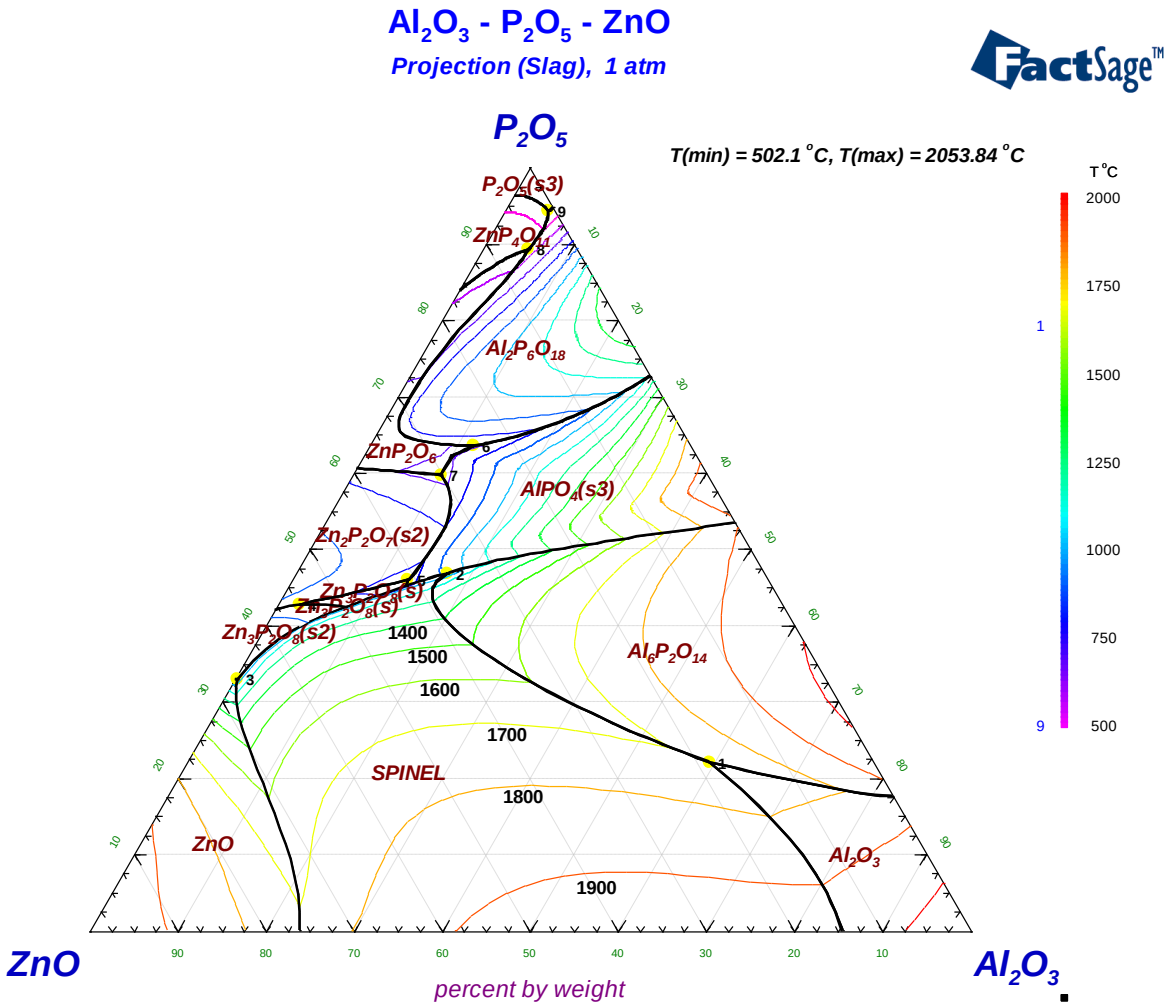

Invariant equilibria on the liquidus surface

Intersections with slag	Mole fraction				Weight percent				
	A = P2O5, B = ZnO, C = Al2O3				A = P2O5, B = ZnO, C = Al2O3				
		X(A)	X(B)	X(C)	T(C)		W(A)	W(B)	W(C)	T(C)
1: Al2O3 / Al6P2O14 / SPINEL	1:	0.16134	0.23631	0.60235	1711.99	1:	22.116	18.572	59.312	1711.99
2: Al6P2O14 / AlPO4_HT(s3) / SPINEL	2:	0.35132	0.46954	0.17914	1030.66	2:	46.893	35.931	17.176	1030.66
3: SPINEL / Zn3P2O8(s2) / ZnO	3:	0.22022	0.77711	0.00267	1012.31	3:	32.983	66.730	0.287	1012.31
4: Zn2P2O7(s2) / Zn3P2O8(s1) / Zn3P2O8(s2)	4:	0.30179	0.67381	0.02439	941.85	4:	42.770	54.747	2.483	941.85
5: AlPO4_HT(s3) / Zn2P2O7(s2) / Zn3P2O8(s1)	5:	0.33904	0.52568	0.13528	847.71	5:	45.965	40.860	13.175	847.71
6: Al2P6O18 / AlPO4_HT(s3) / ZnP2O6	6:	0.51669	0.34973	0.13358	780.18	6:	63.541	24.658	11.800	780.18
7: AlPO4_HT(s3) / Zn2P2O7(s2) / ZnP2O6	7:	0.47283	0.41678	0.11040	758.37	7:	59.770	30.205	10.025	758.38
8: Al2P6O18 / ZnP2O6 / ZnP4O11	8:	0.84063	0.09155	0.06782	649.99	8:	89.254	5.573	5.172	649.99
9: Al2P6O18 / P2O5(s3) / ZnP4O11	9:	0.92069	0.01222	0.06709	502.10	9:	94.344	0.718	4.938	502.10

Al2O3-SiO2-TiO2,

Al2O3-SiO2-TiO2,
Weight fraction, Isopleth section Al2TiO5-SiO2

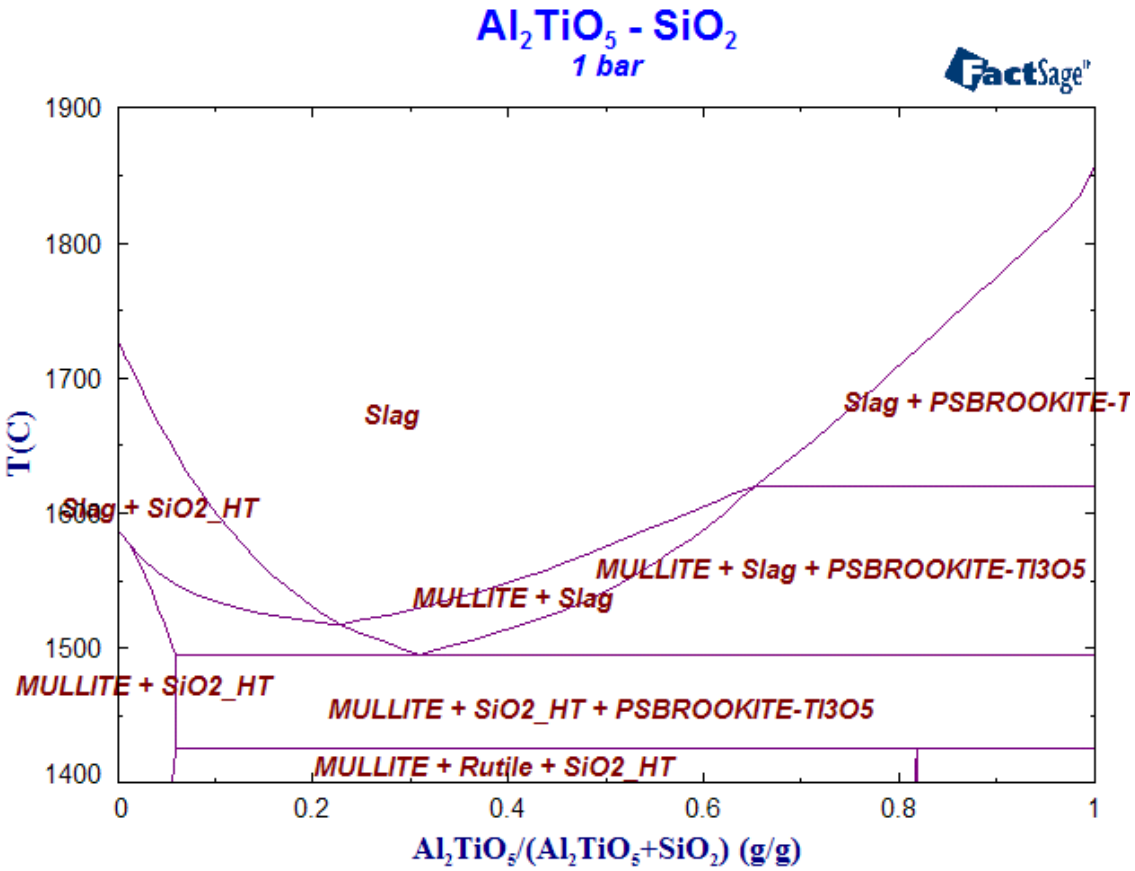

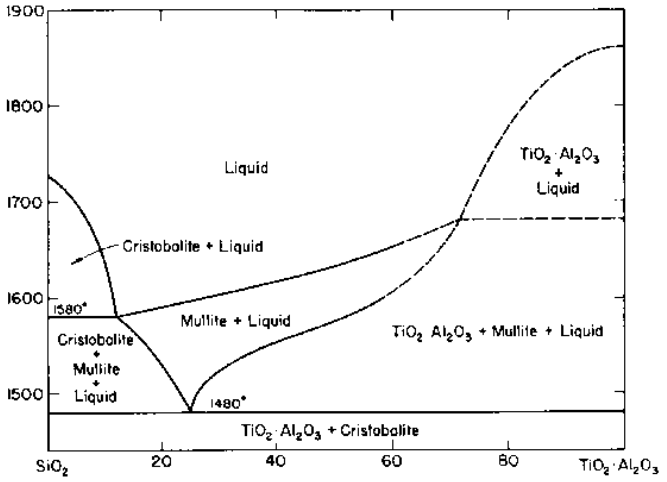

Y.M. Agamawi, J. White, Trans. Br. Ceram. Soc., 51 (1952), pp. 293-325.

Al2O3-SiO2-TiO2, Weight fraction, 1800°C

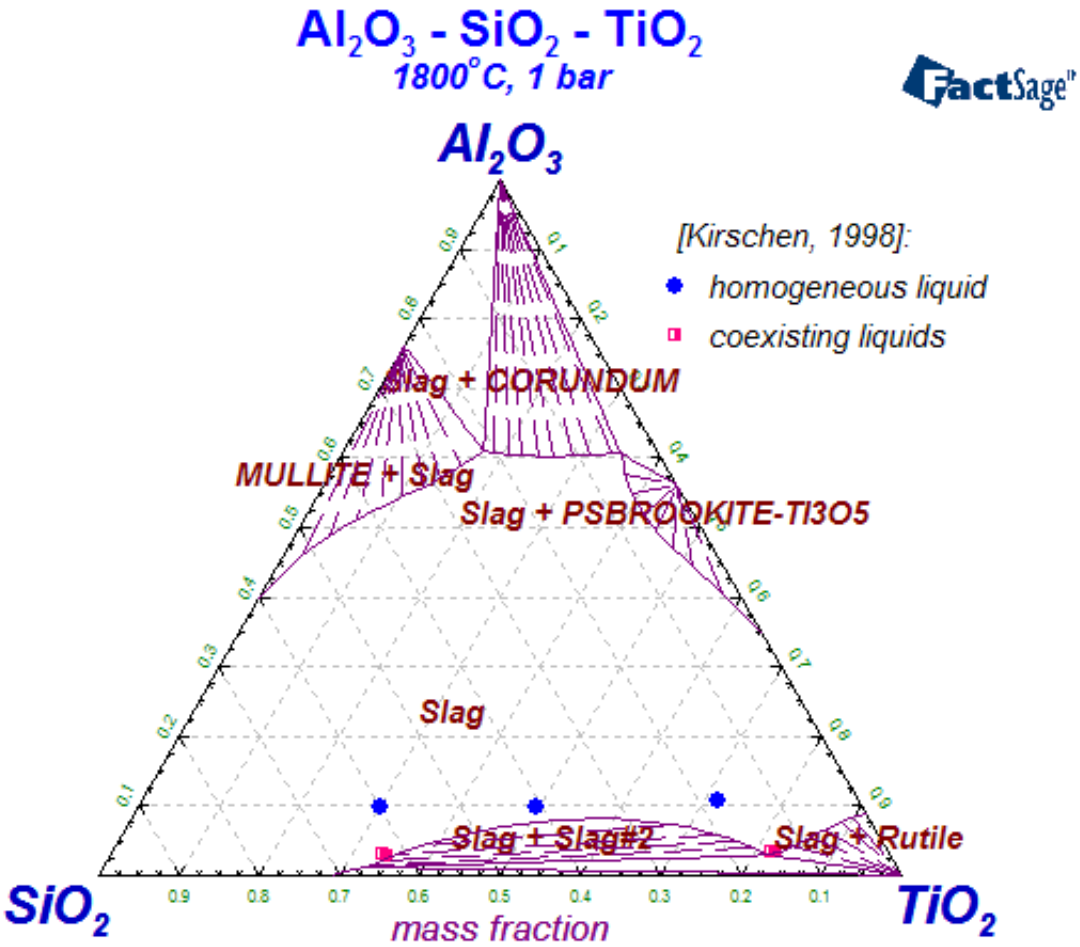

Al2O3-SiO2-TiO2,
Mole fraction, Liquidus surface

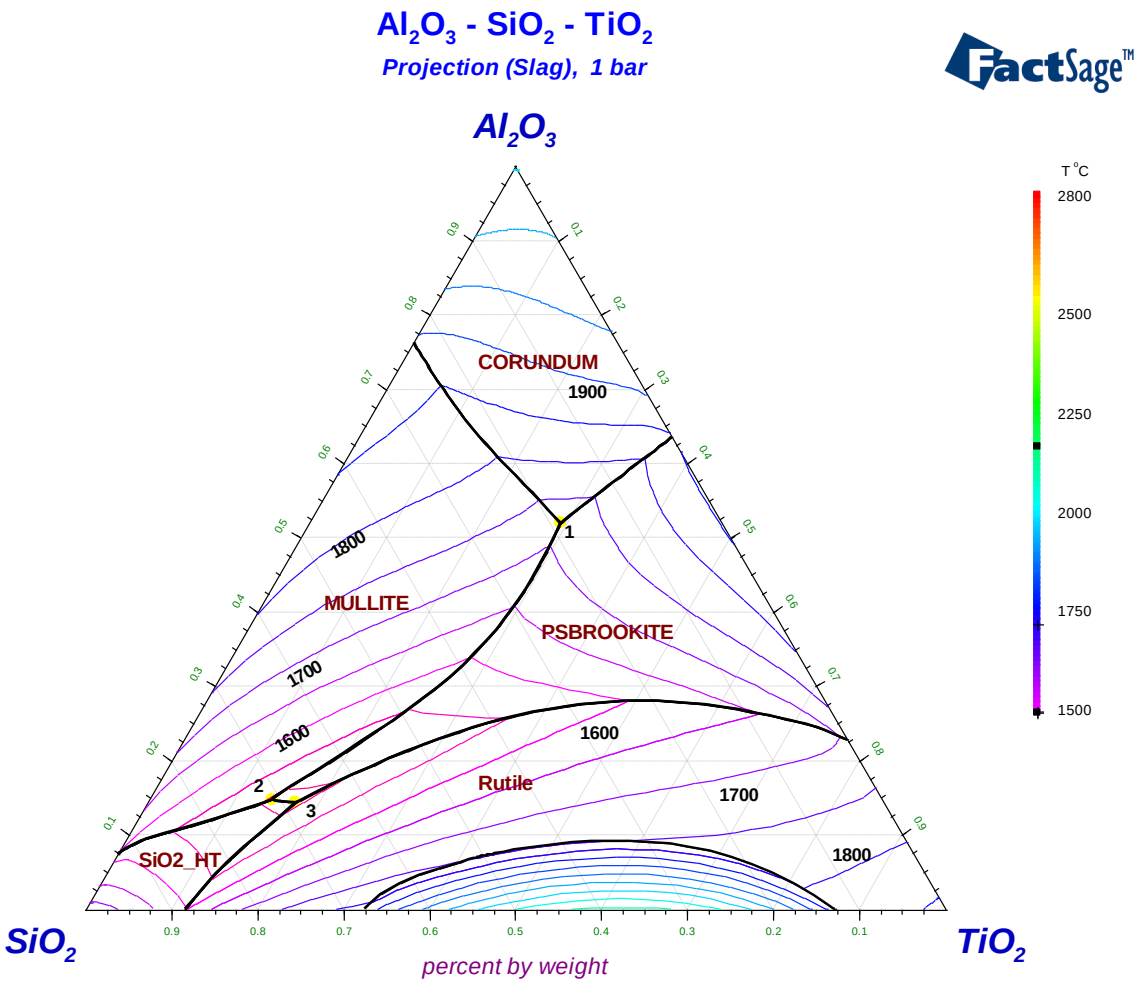

Al2O3-SiO2-TiO2,
Weight percent, Liquidus surface

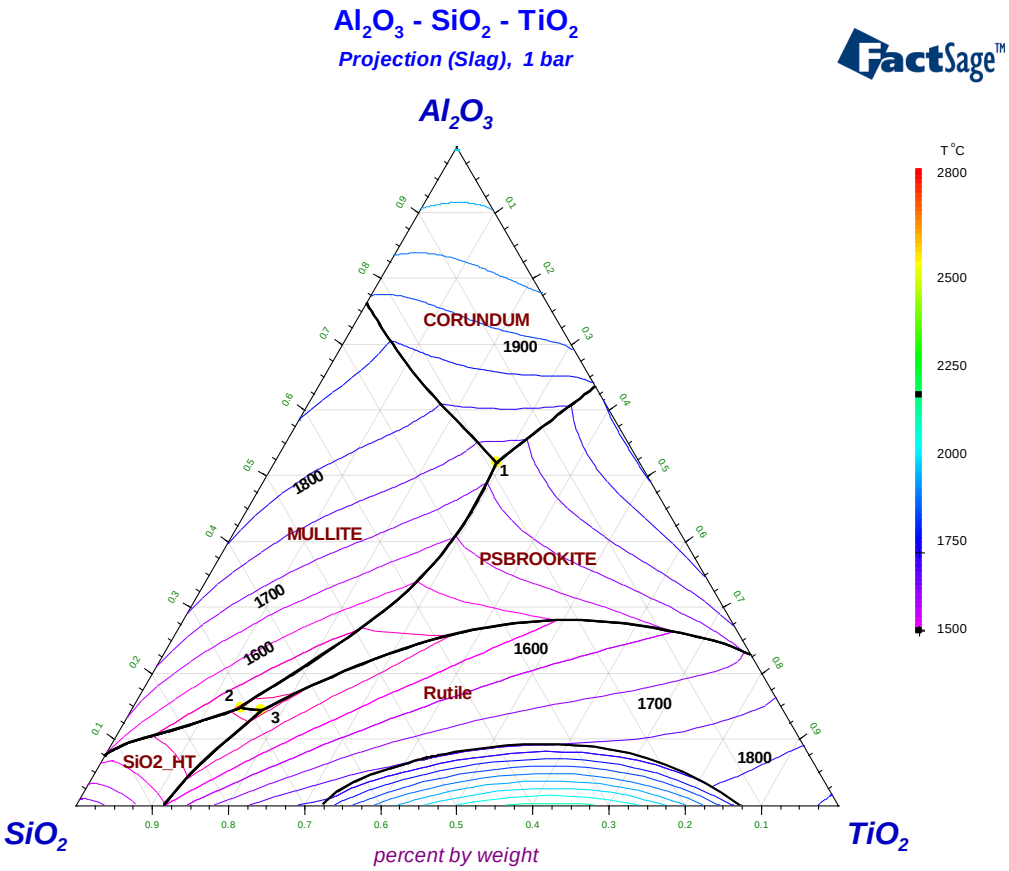

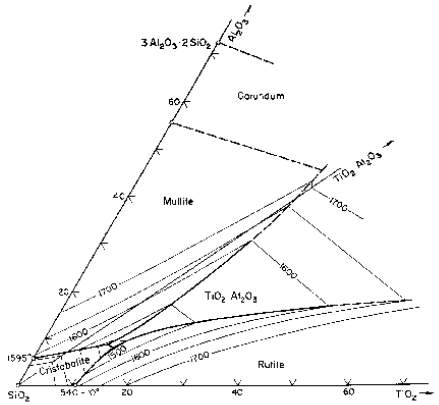

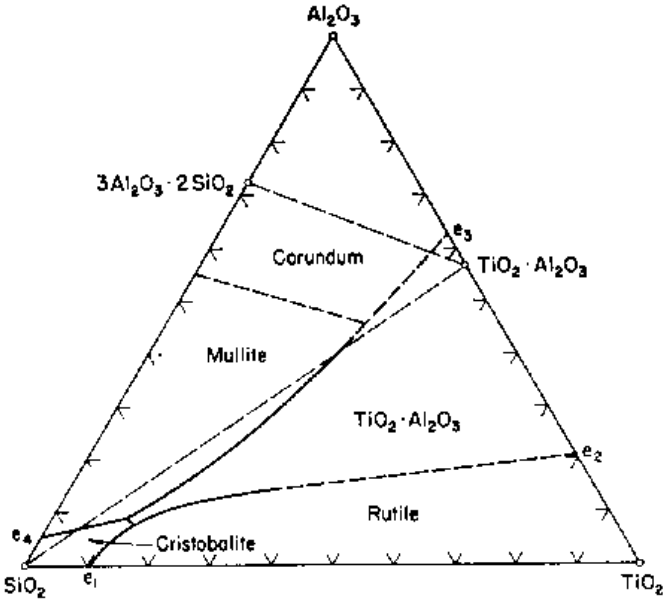

Y.M. Agamawi, J. White, Trans. Br. Ceram. Soc., 51 (1952), pp. 293-325.

Invariant equilibria on the liquidus surface

Intersections with slag	Mole fraction				Weight percent				
	A = P2O5, B = ZnO, C = Al2O3				A = P2O5, B = ZnO, C = Al2O3				
		X(A)	X(B)	X(C)	T(C)		W(A)	W(B)	W(C)	T(C)
1: Al2O3 / Al6P2O14 / SPINEL	1:	0.16134	0.23631	0.60235	1711.99	1:	22.116	18.572	59.312	1711.99
2: Al6P2O14 / AlPO4_HT(s3) / SPINEL	2:	0.35132	0.46954	0.17914	1030.66	2:	46.893	35.931	17.176	1030.66
3: SPINEL / Zn3P2O8(s2) / ZnO	3:	0.22022	0.77711	0.00267	1012.31	3:	32.983	66.730	0.287	1012.31
4: Zn2P2O7(s2) / Zn3P2O8(s1) / Zn3P2O8(s2)	4:	0.30179	0.67381	0.02439	941.85	4:	42.770	54.747	2.483	941.85
5: AlPO4_HT(s3) / Zn2P2O7(s2) / Zn3P2O8(s1)	5:	0.33904	0.52568	0.13528	847.71	5:	45.965	40.860	13.175	847.71
6: Al2P6O18 / AlPO4_HT(s3) / ZnP2O6	6:	0.51669	0.34973	0.13358	780.18	6:	63.541	24.658	11.800	780.18
7: AlPO4_HT(s3) / Zn2P2O7(s2) / ZnP2O6	7:	0.47283	0.41678	0.11040	758.37	7:	59.770	30.205	10.025	758.38
8: Al2P6O18 / ZnP2O6 / ZnP4O11	8:	0.84063	0.09155	0.06782	649.99	8:	89.254	5.573	5.172	649.99
9: Al2P6O18 / P2O5(s3) / ZnP4O11	9:	0.92069	0.01222	0.06709	502.10	9:	94.344	0.718	4.938	502.10

Al2O3-SiO2-V2O5,
Mole fraction, 600°C

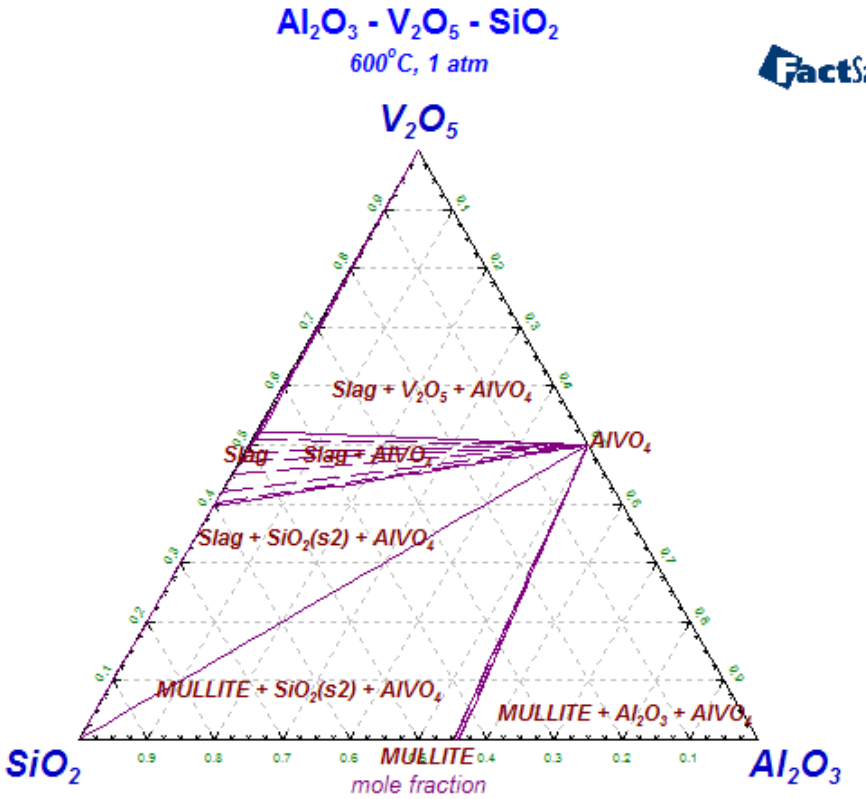

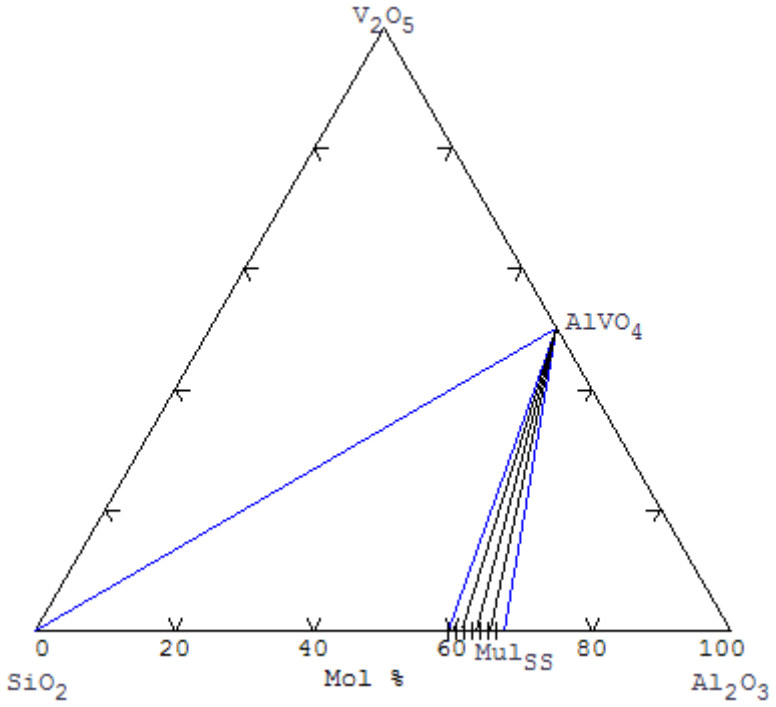

A.A. Fotiev, B.V. Slobodin, L.L. Surat, T.P. Sirina, Zh. Neorg. Khim., 28[4], (1983), pp. 588-591.

Al2O3-SiO2-V2O5, Mole fraction, 1200°C

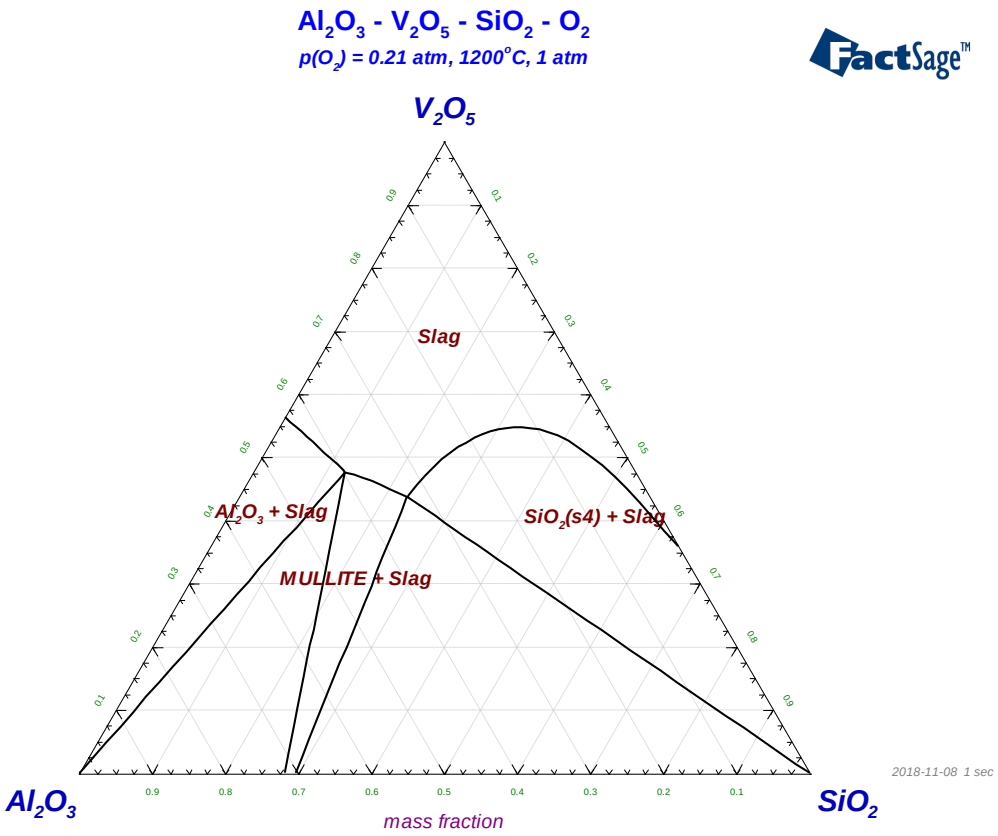

Al2O3-SiO2-V2O5,
Mole fraction, Liquidus surface

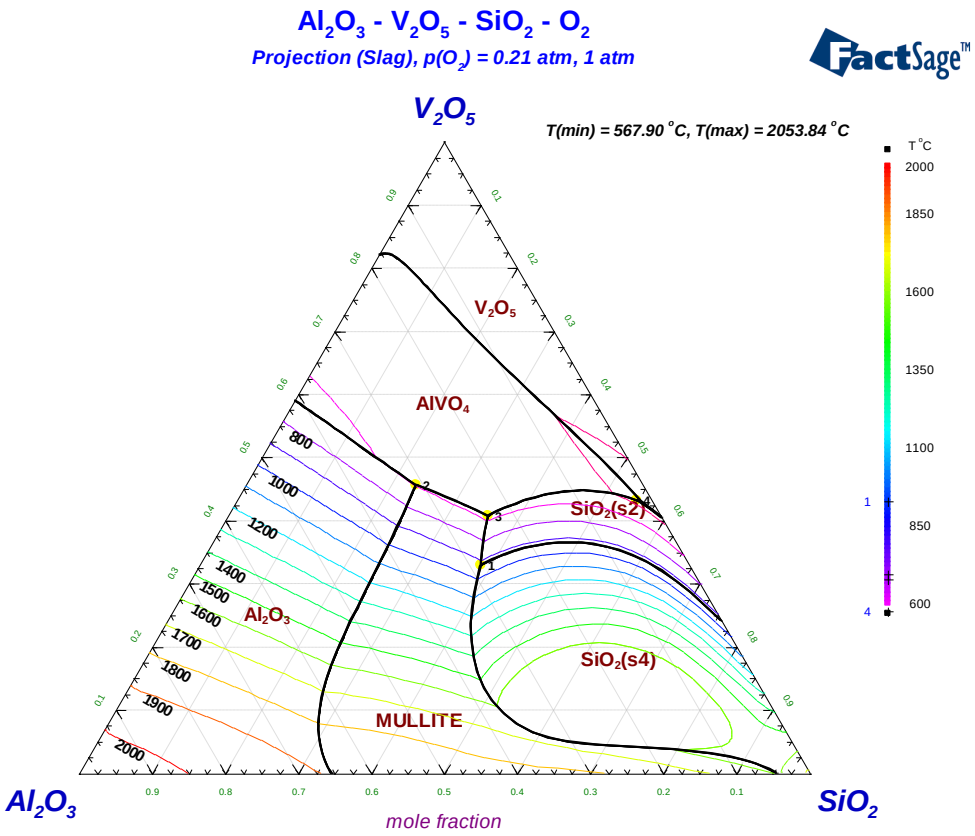

Al2O3-SiO2-V2O5,
Weight percent, Liquidussurface

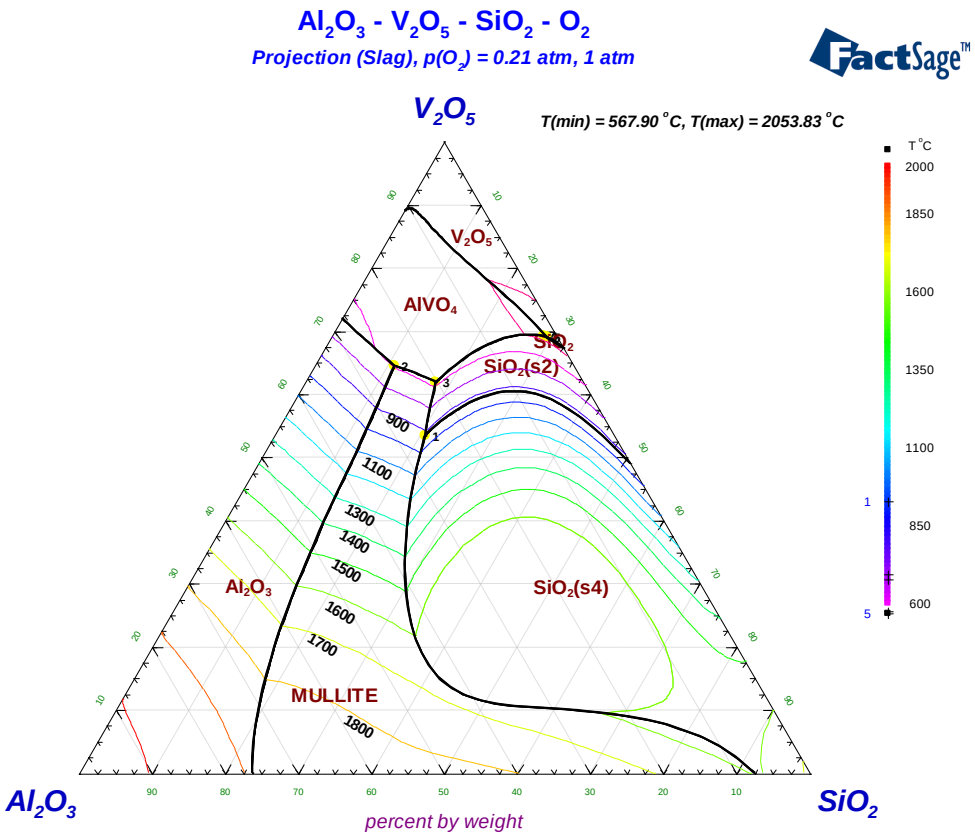

Invariant equilibria on the liquidus surface

Intersections with slag	Mole fraction				Weight percent				
	A = V2O5, B = Al2O3, C = SiO2				A = V2O5, B = Al2O3, C = SiO2				
		X(A)	X(B)	X(C)	T(C)		W(A)	W(B)	W(C)	T(C)
1. MULLITE / SiO2(s4) / SiO2(s2)	1:	0.32976	0.28562	0.38463	926.32	1:	53.451	25.954	20.596	926.28
2. Al2O3 / AlVO4 / MULLITE	2:	0.45721	0.31052	0.23227	693.69	2:	64.576	24.587	10.837	693.69
3. AlVO4 / MULLITE / SiO2(s2)	3:	0.40836	0.23626	0.35537	676.19	3:	62.041	20.123	17.836	676.24
4. AlVO4 / SiO2(s) / SiO2(s2)	4:	0.43271	0.02024	0.54705	574.85	4:	69.258	1.816	28.925	574.85

Al2O3-SiO2-ZnO,
Mole fraction, 500°C

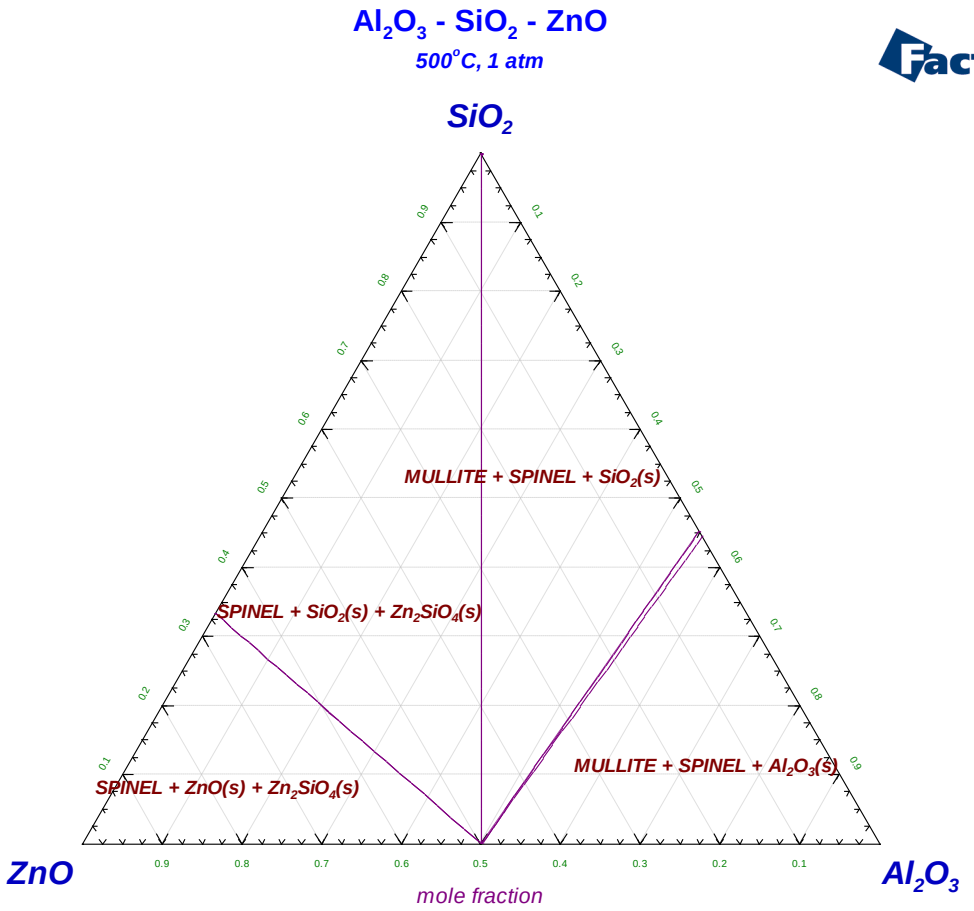

Mole fraction, Liquidussurface

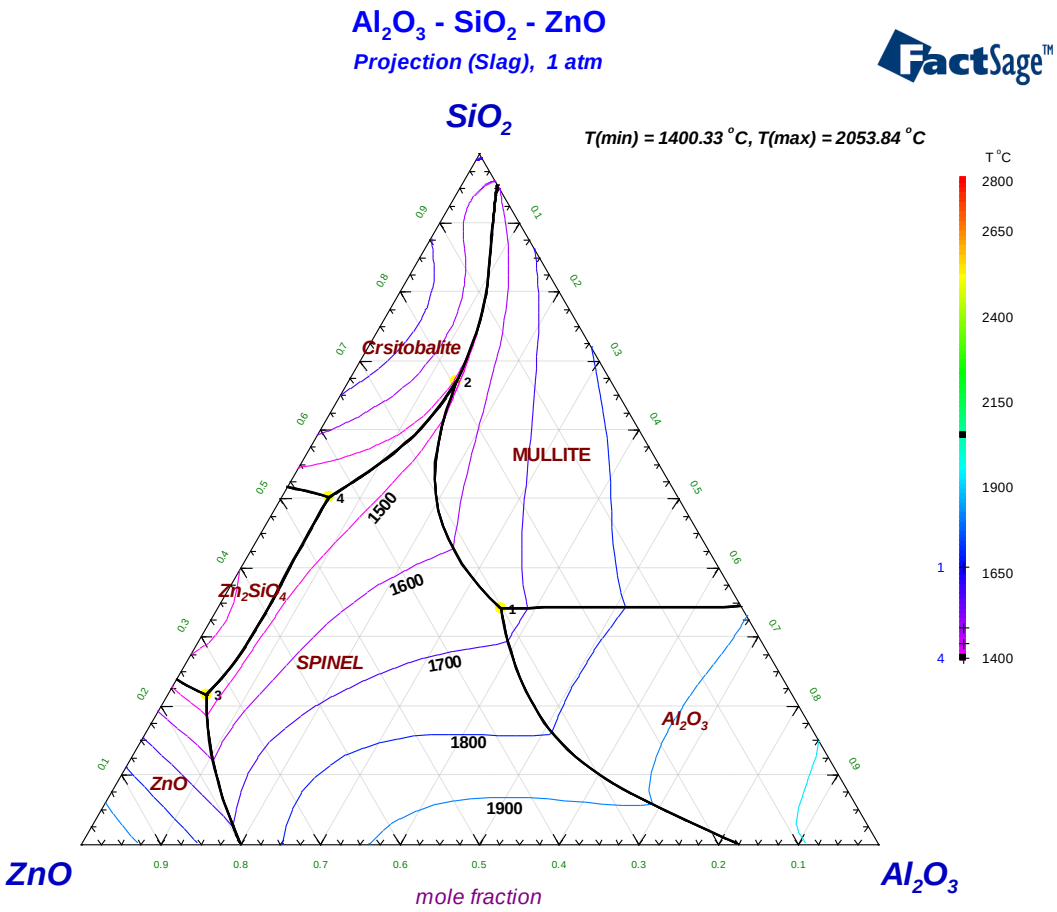

Weight percent,
Liquidussurface compared with experimental data

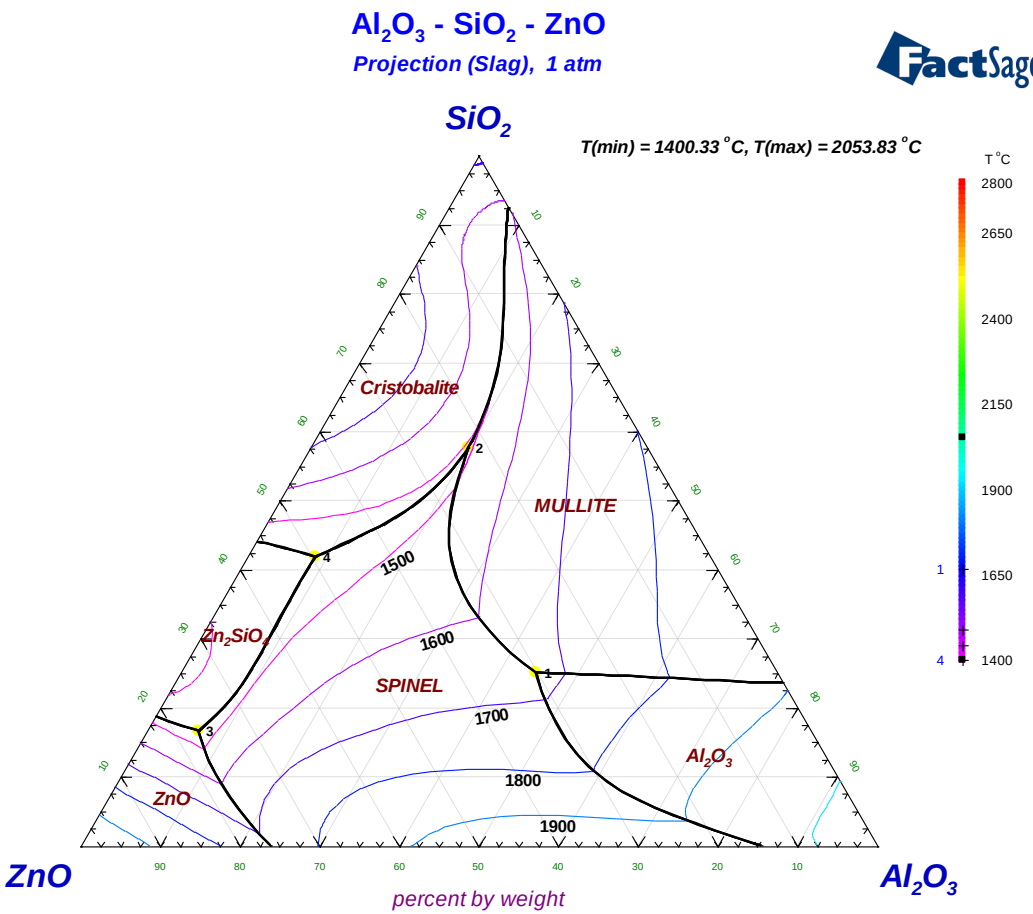

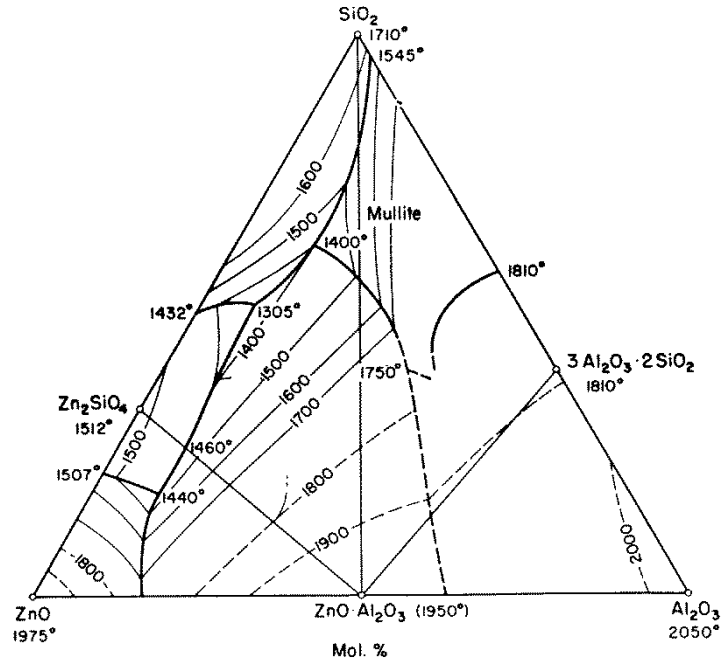

E.N. Bunting, J. Res. Natl. Bur. Stand. (U.S.), 8 [2], (1932), pp. 279-287.

Invariant equilibria on the liquidus surface

Intersections with slag	Mole fraction				Weight percent			
	A = SiO2, B = ZnO, C = Al2O3				A = SiO2, B = ZnO, C = Al2O3			
	X(A)	X(B)	X(C)	T(C)	W(A)	W(B)	W(C)	T(C)
1: Al2O3 / MULLITE / SPINEL	1: 0.34089	0.30263	0.35648	1666.73	1: 25.145	30.234	44.621	1666.76
2: MULLITE / SPINEL / Cristobalite	2: 0.67093	0.19296	0.13611	1489.49	2: 57.677	22.467	19.856	1489.49
3: SPINEL / Zn2SiO4 / ZnO	3: 0.21583	0.73471	0.04946	1442.46	3: 16.668	76.850	6.482	1442.46
4: SPINEL / Cristobalite / Zn2SiO4	4: 0.50218	0.43796	0.05986	1400.33	4: 41.956	49.557	8.487	1400.33

Mole fraction, Liquidussurface

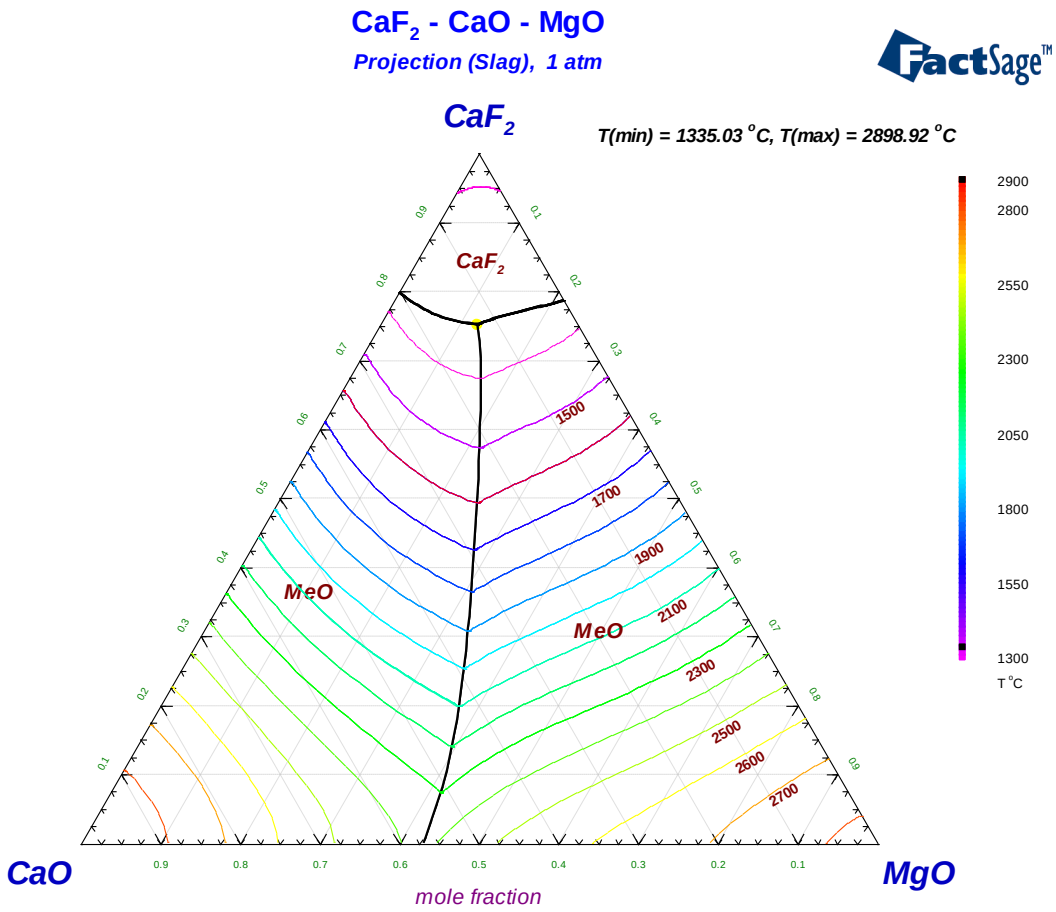

Weight percent, Liquidussurface

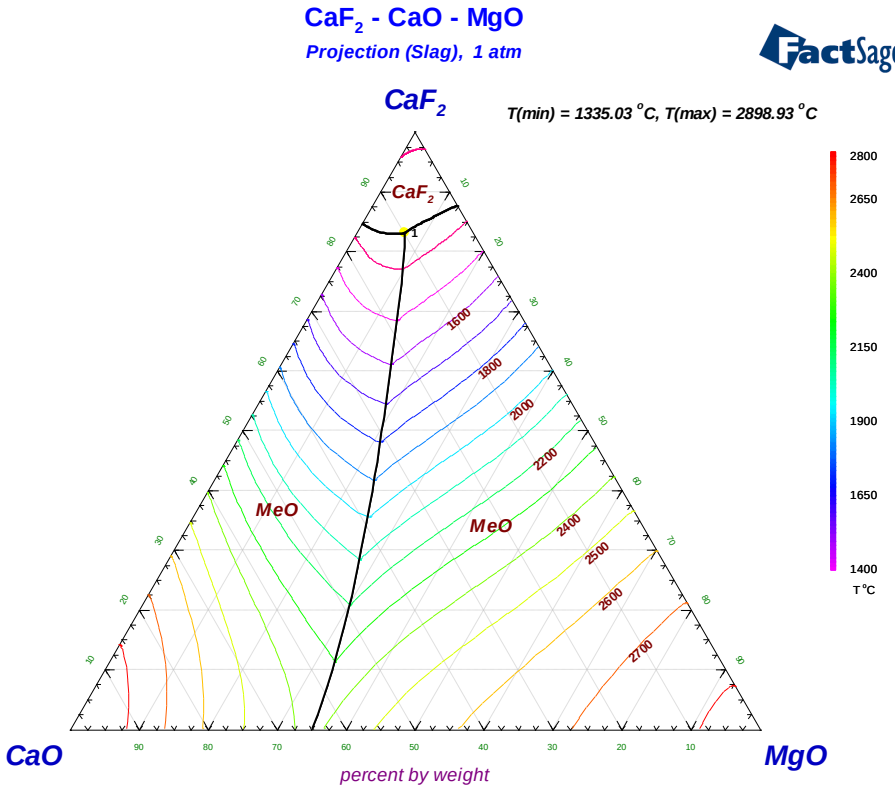

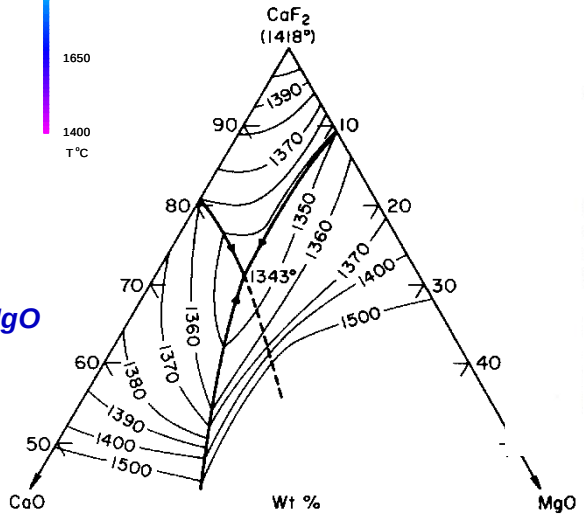

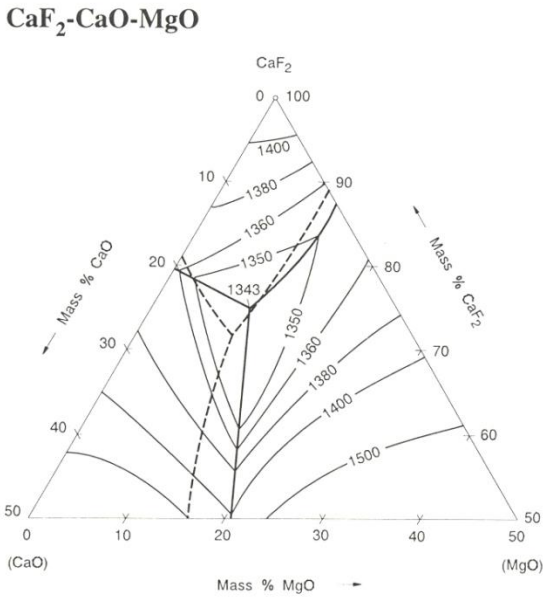

Fig. 3.429. Liquidus surface in the CaF_2-CaO-MgO system after Schlegel [1-3], as determined by DTA. The position of the ternary eutectic, determined by high-temperature microscopy [3], is shown in the figure with dashed lines.

Slag Atlas, 2nd Ed., Verlag Stahl-Eisen, Düsseldorf, 1995.

E. Schlegel, Z. Chem., 5 [8], (1965), p.316.

Invariant equilibria on the liquidus surface

Intersections with slag	Mole fraction				Weight percent			
	A = CaF2, B = CaO, C = MgO				A = CaF2, B = CaO, C = MgO			
	X(A)	X(B)	X(C)	T(C)	W(A)	W(B)	W(C)	T(C)
1: CaF2 / MeO#1 / MeO#2	1: 0.75238	0.12573	0.12189	1335.03	1.0.83080	0.09972	0.06948	1335.03

CaF2-CaO-SiO2, Mole fraction 1060°C

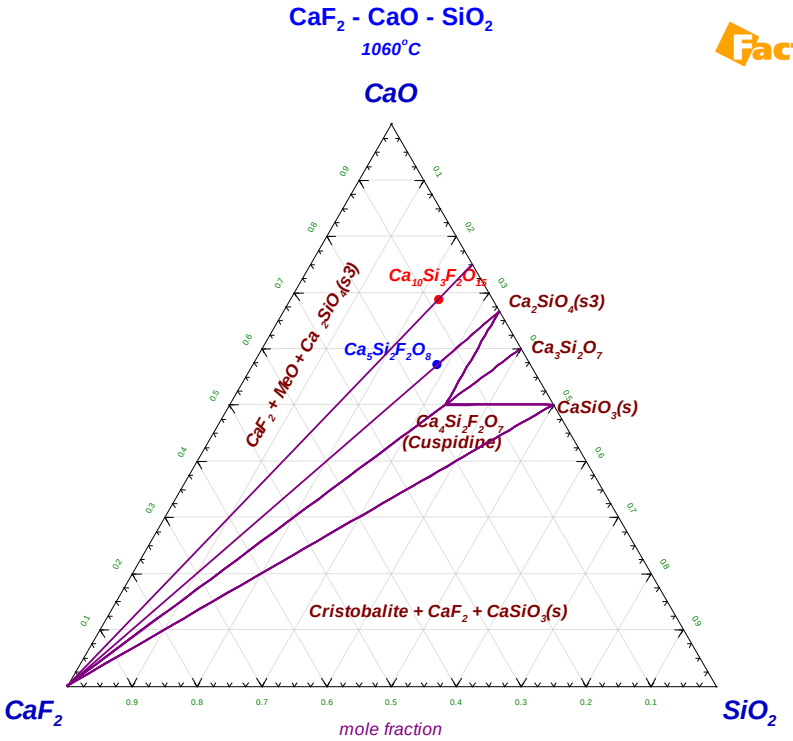

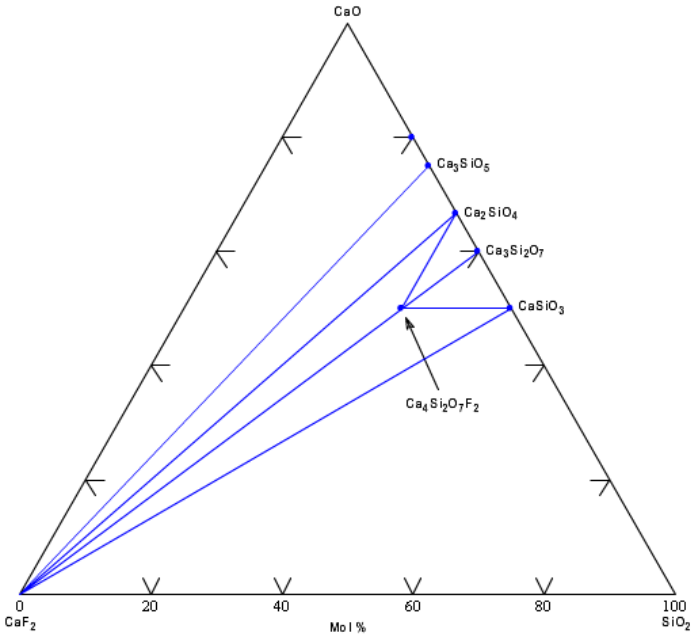

Name	Phase	Used data	Description
C3S2F Cuspidine	3CaO 2SiO2 CaF2	Heat of formation [Fukuyama, Tabata,2003]	Ca4Si2F2O7
C4S2F	4CaO 2SiO2 CaF2		Ca5Si2F2O8
C9S3F	9CaO 3SiO2 CaF2		Ca10Si3F2O15

System CaF_2-CaO-SiO_2; compatibility triangles. C. Brisi, J. Am. Ceram. Soc., 40 [5] 174-178 (1957).

CaF2-CaO-SiO2,

Weight percent, Isopleth Cuspidine-CaF2

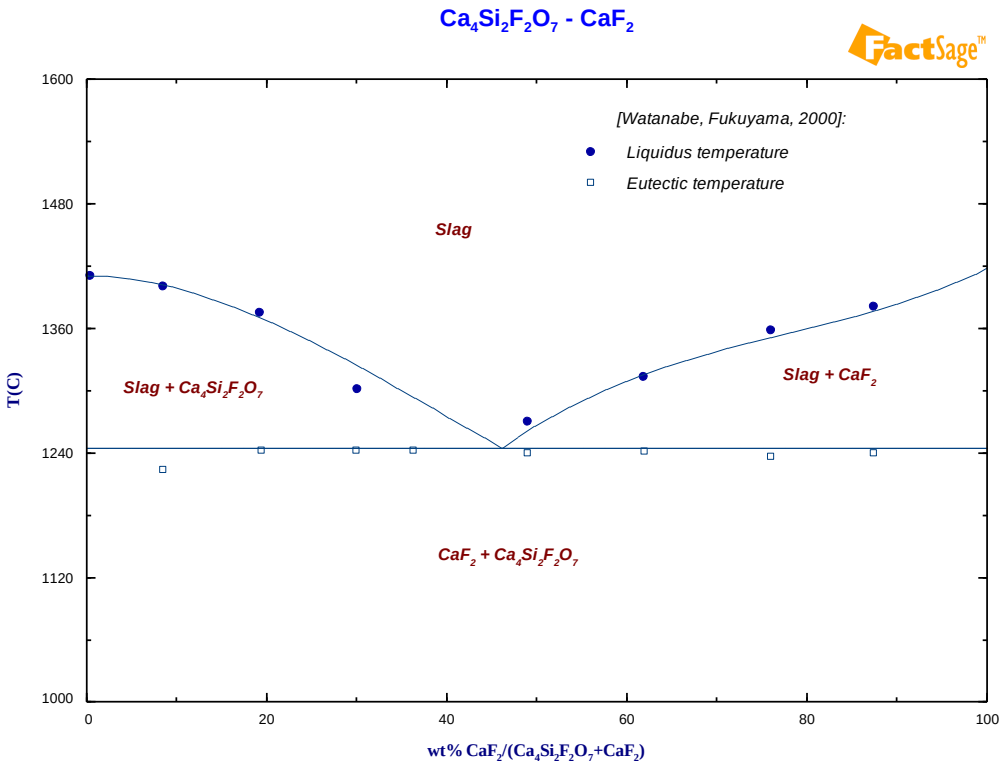

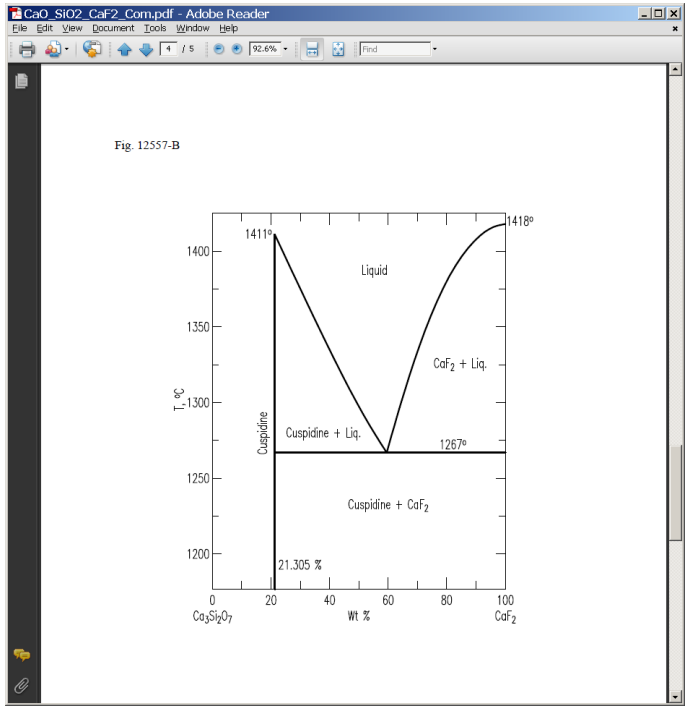

(B) pseudobinary phase diagram for cuspidine-CaF2 system; Cuspidine = Ca4Si2O7F2 - H. Fukuyama, T. Watanabe, M. Susa, and K. Nagata, "Pseudo-binary Phase Diagram of the Cuspidine - CaF2 System - Relating to Mold Flux for Continuous Casting of Steel -"; pp. 61-75 in EPD Congr. 1999, Proc. Sess. Symp., TMS Annual Meeting, San Diego, California, February 28-March 4, 1999. Edited by B. Mishra, Minerals, Metals & Materials Society,

CaF2-CaO-SiO2,

Weight percent, Isopleth CaSiO3-CaF2

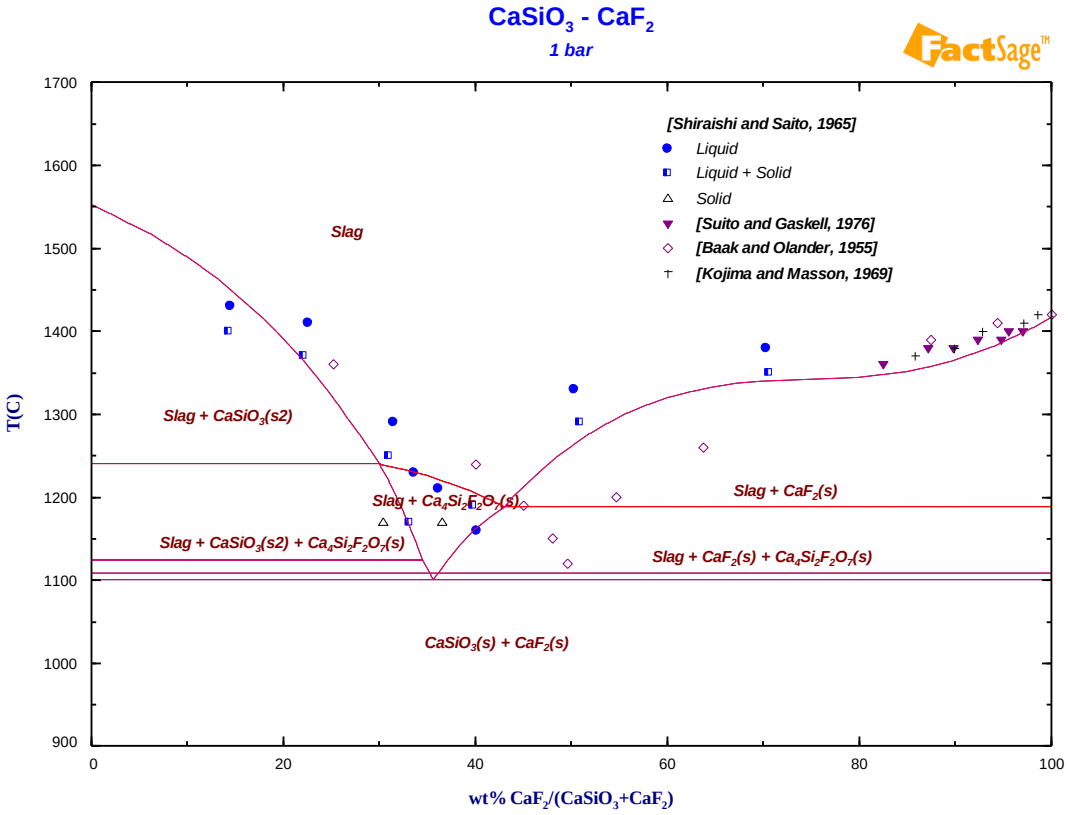

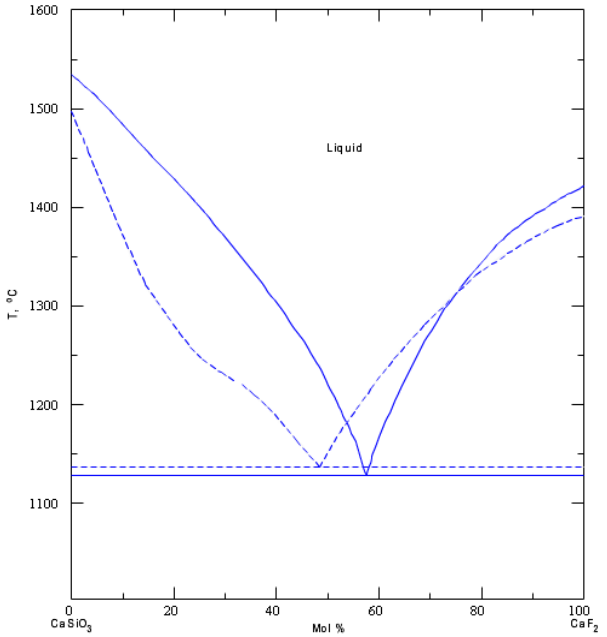

T. Baak and A. Oelander, Acta Chem. Scand., 9 [8] 1350-1354 (1955). Dashed lines after Karandeef. B. Karandeeff, Z. Anorg. Chem., 68 [3] 188-197 (1910)

CaF2-CaO-SiO2,

Weight percent, Isopleth Ca2SiO4-CaF2

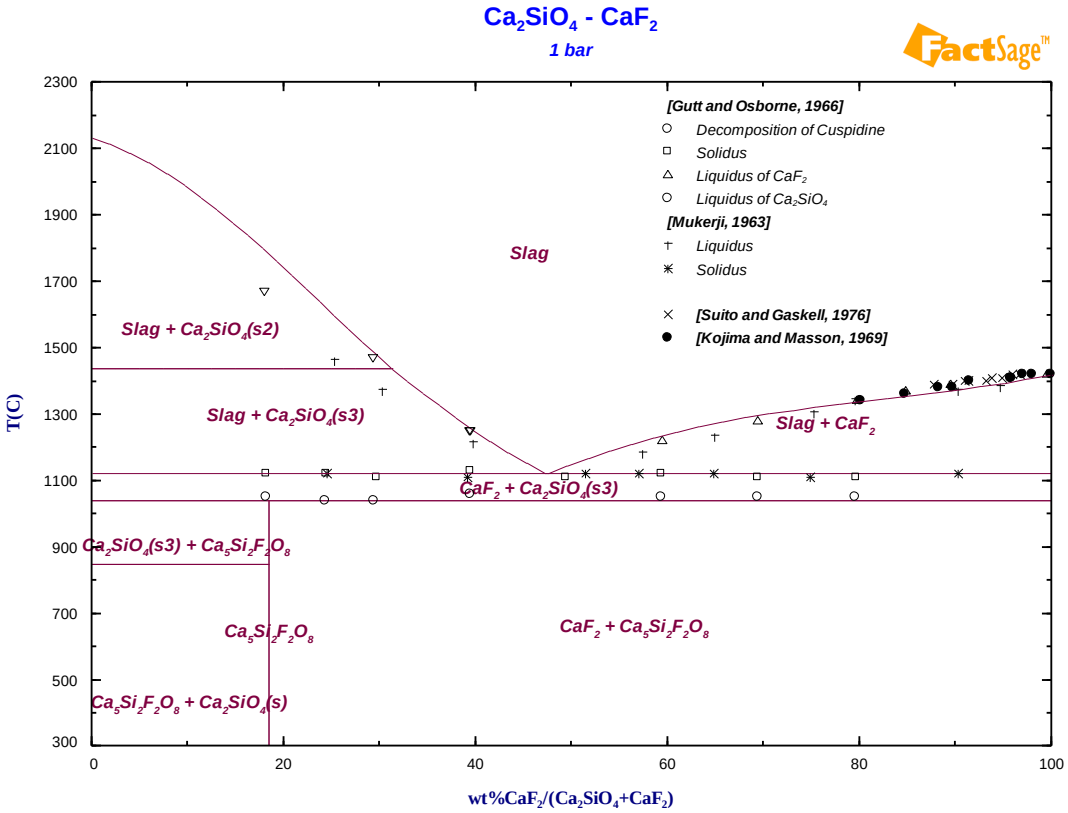

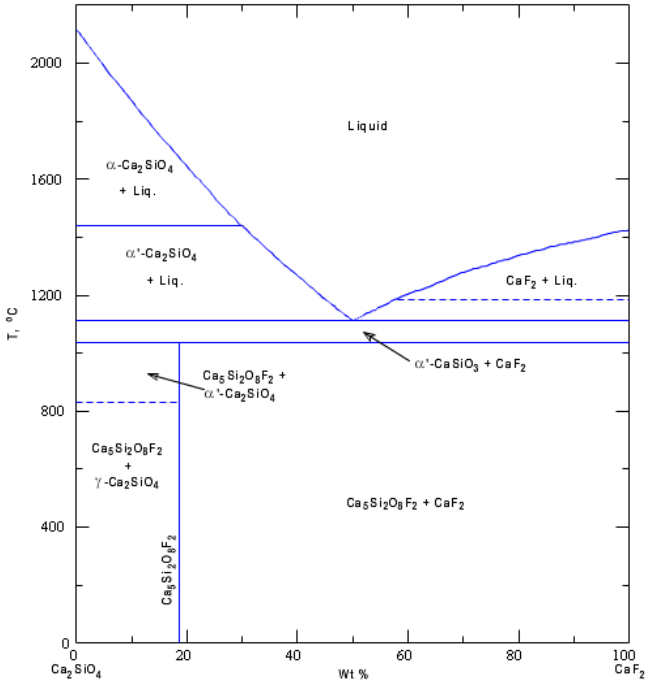

W. H. Gutt and G. J. Osborne, Trans. Br. Ceram. Soc., 65 [9] 521-534 (1966).

CaF2-CaO-SiO2

Weight percent,, Isopleth Ca3SiO5-CaF2

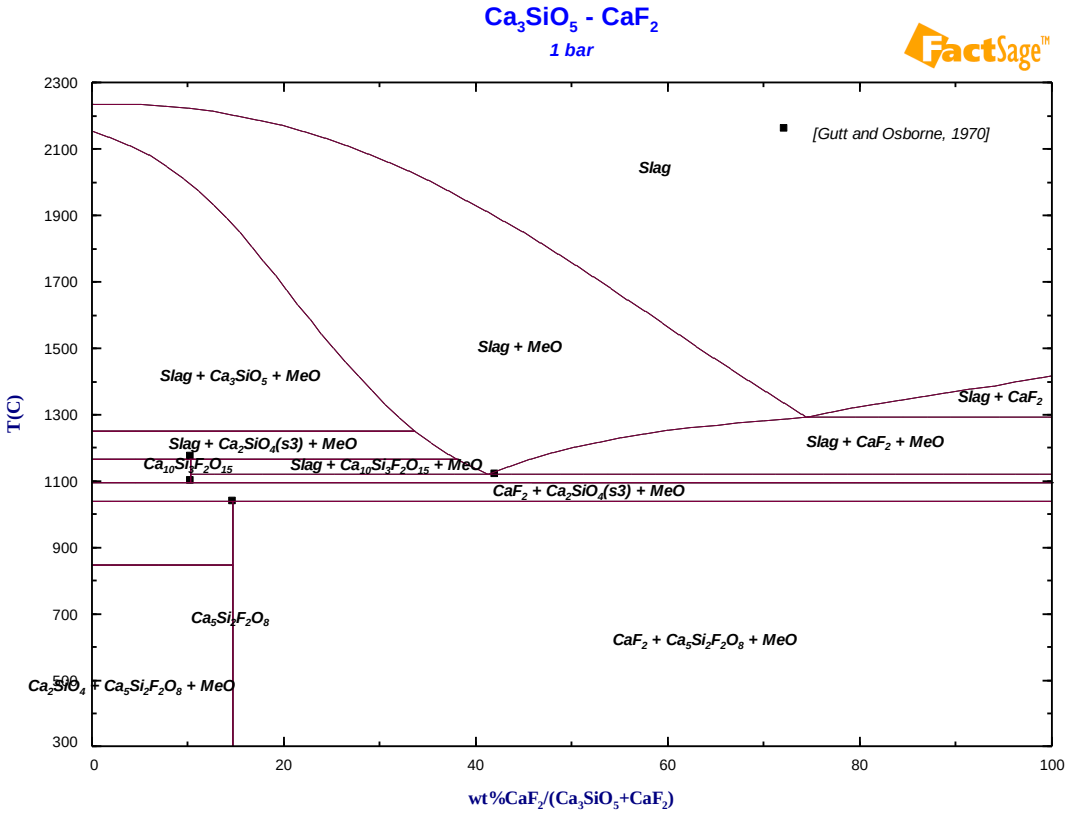

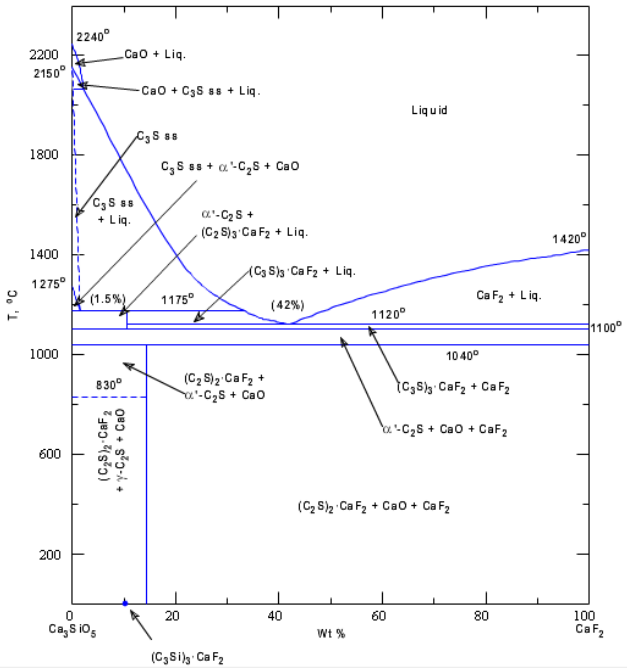

W. H. Gutt and G. J. Osborne, Trans. Br. Ceram. Soc., 65 [9] 521-534 (1966).

Mole fraction, Liquidussurface

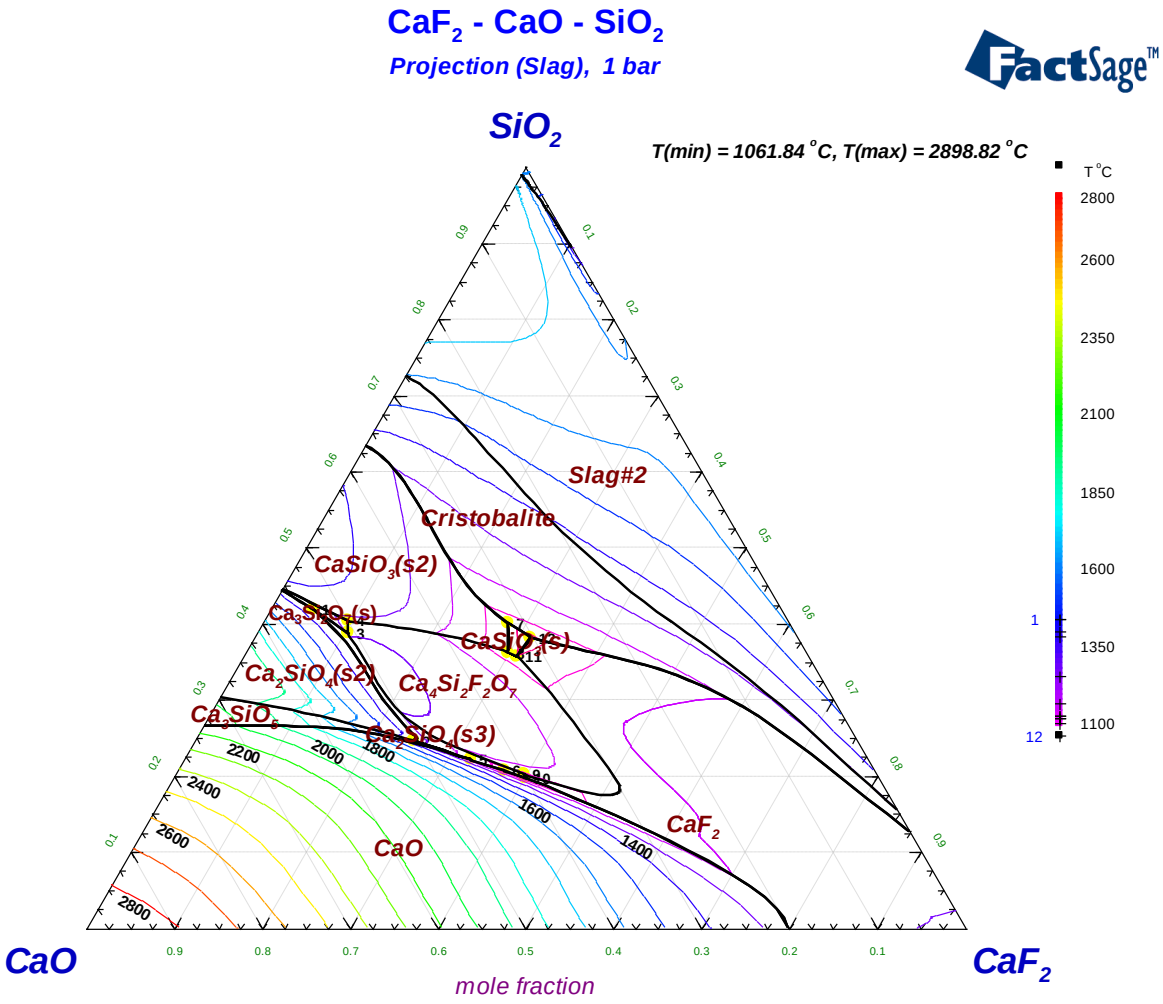

Weight percent, Liquidussurface

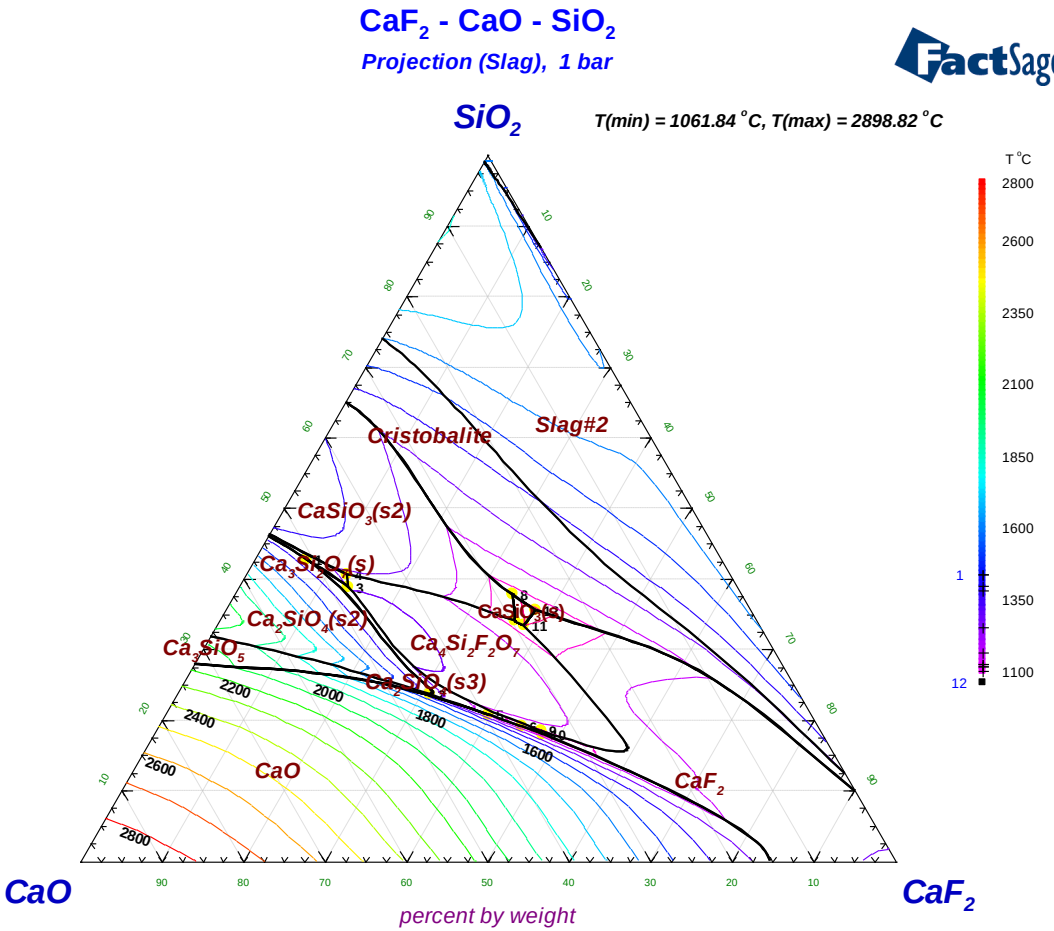

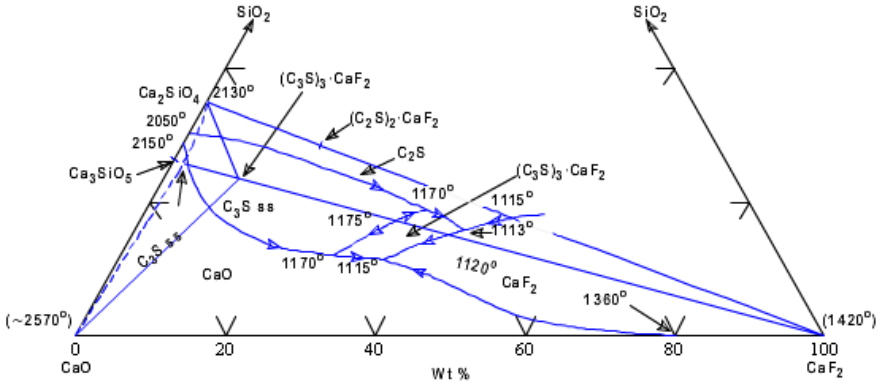

W. H. Gutt and G. J. Osborne, Trans. Br. Ceram. Soc., 69 [3] 125-129 (1970).

Invariant equilibria on the liquidus surface

Intersections with slag	Mole fraction A = SiO2, B = CaO, C = CaF2				Weight percent A = SiO2, B = CaO, C = CaF2			
	X(A)	X(B)	X(C)	T(C)	W(A)	W(B)	W(C)	T(C)
1: Ca2SiO4(s2) / Ca2SiO4(s3) / Ca3Si2O7	1: 0.41903	0.53323	0.04774	1436.73	1: 42.814	50.849	6.337	1436.73
2: Ca2SiO4(s2) / Ca2SiO4(s3) / Ca3SiO5	2: 0.24620	0.50516	0.24865	1436.73	2: 23.655	45.300	31.044	1436.73
3: Ca2SiO4(s3) / Ca3Si2O7 / Ca4Si2F2O7	3: 0.38799	0.50883	0.10319	1396.24	3: 38.917	47.634	13.449	1396.24
4: Ca3Si2O7 / Ca4Si2F2O7 / CaSiO3(s2)	4: 0.40396	0.50079	0.09526	1379.72	4: 40.594	46.968	12.438	1379.72
5: Ca2SiO4(s3) / Ca3SiO5 / CaO	5: 0.22157	0.45206	0.32637	1251.47	5: 20.755	39.520	39.725	1251.53
6: Ca10Si3F2O15 / Ca2SiO4(s3) / CaO	6: 0.20708	0.42144	0.37148	1165.48	6: 19.119	36.315	44.567	1165.48
7: CaSiO3(s2) / CaSiO3 / Cristobalite	7: 0.40134	0.32017	0.27848	1124.14	7: 34.042	29.711	36.247	1124.14
8: Ca4Si2F2O7 / CaSiO3(s2) / CaSiO3(s)	8: 0.36304	0.33949	0.29748	1124.13	8: 37.790	28.137	34.073	1124.13
9: Ca2SiO4(s3) / Ca4Si2F2O7 / CaF2	9: 0.20207	0.40057	0.39736	1118.36	9: 18.500	34.228	47.272	1118.37
10: Ca10Si3F2O15 / Ca2SiO4(s3) / CaF2	10: 0.19763	0.40165	0.40072	1118.32	10: 18.079	34.291	47.631	1118.33
11: Ca4Si2F2O7 / CaF2 / CaSiO3(s)	11: 0.35785	0.33125	0.31090	1100.34	11: 33.412	28.867	37.721	1100.34
12: CaF2 / CaSiO3(s) / Cristobalite	12: 0.38264	0.30355	0.31381	1061.84	12: 35.637	26.386	37.978	1061.84

CaO-CaS-SiO2,
Weight percent 1500°C

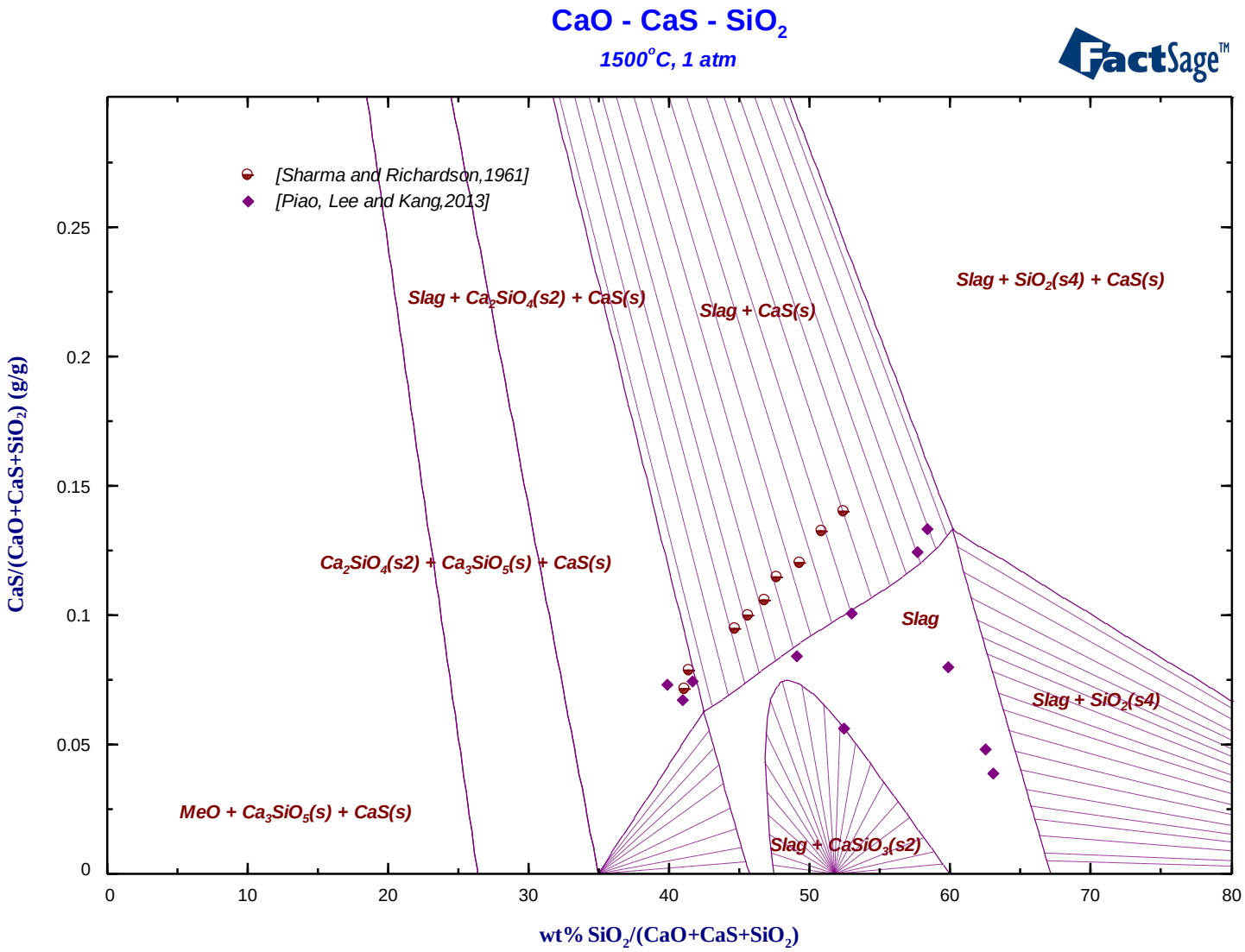

CaO-CaS-SiO2,
Weight percent 1550°C

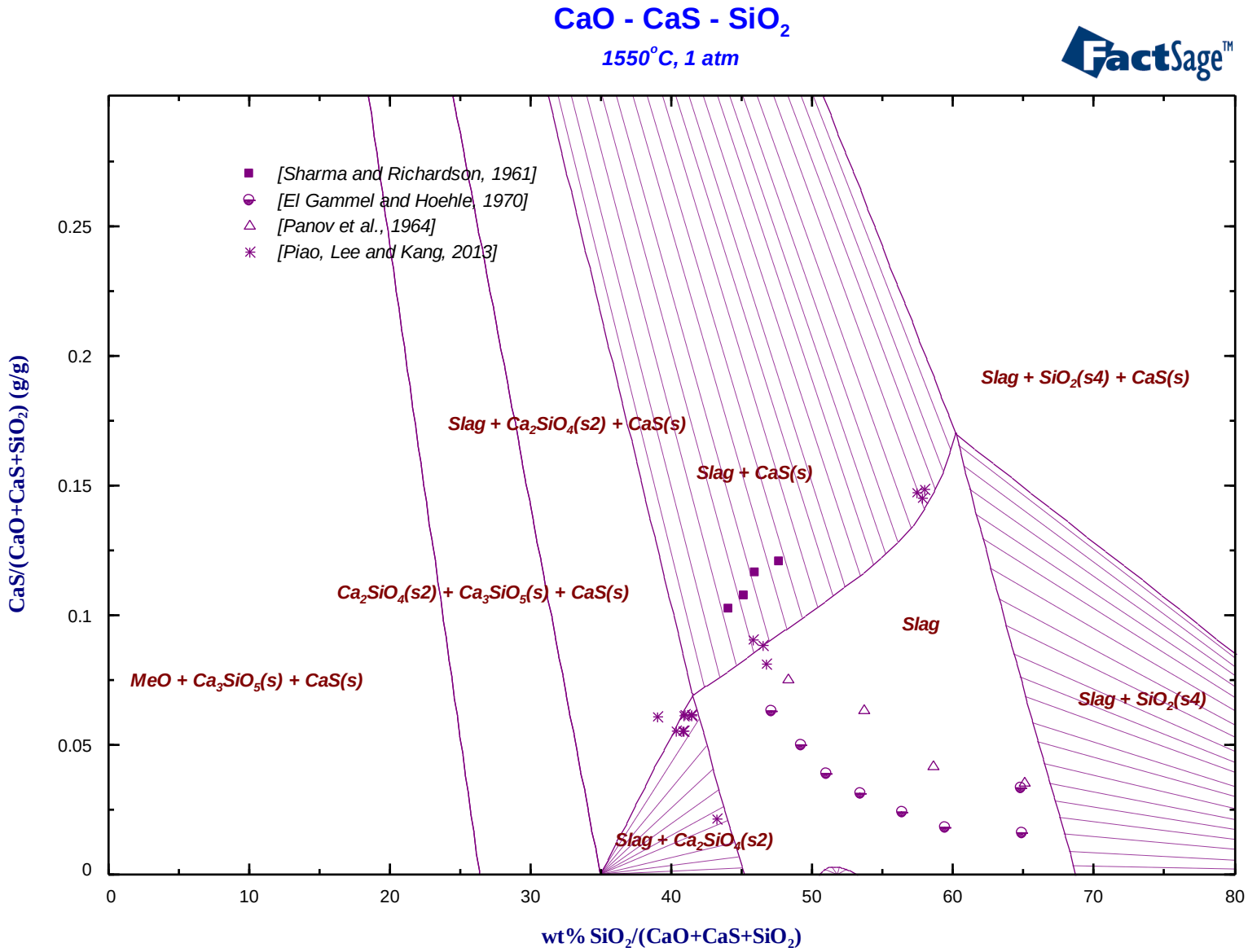

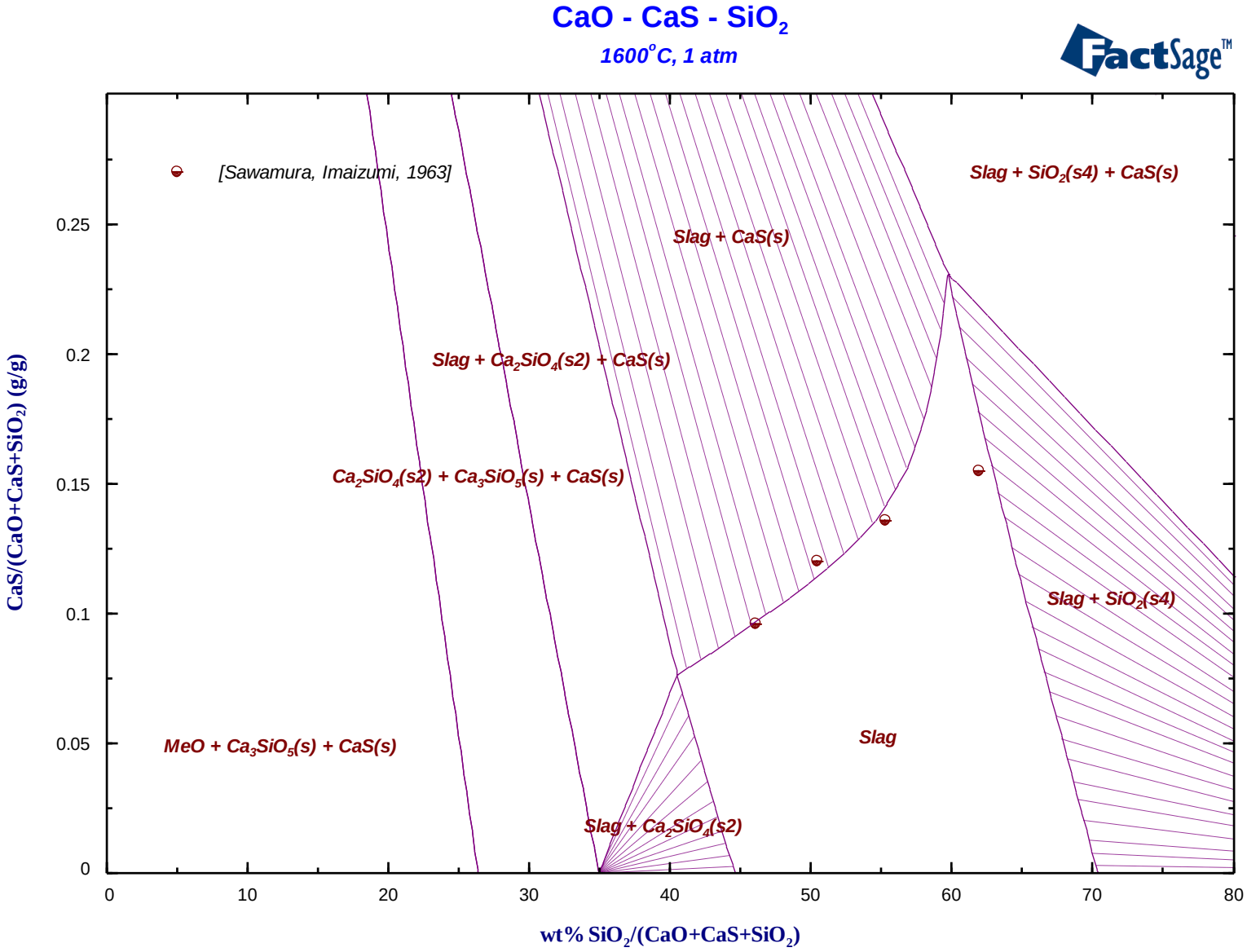
CaO - CaS - SiO2
1600°C, 1 atm
FactSage™
[Sawamura, Imaizumi, 1963]
Slag + SiO2(s4) + CaS(s)
Slag + CaS(s)
Slag + Ca2SiO4(s2) + CaS(s)
Ca2SiO4(s2) + Ca3SiO5(s) + CaS(s)
Slag + SiO2(s4)
MeO + Ca3SiO5(s) + CaS(s)
Slag
Slag + Ca2SiO4(s2)
CaS/(CaO+CaS+SiO2) (g/g)
0
0.05
0.1
0.15
0.2
0.25
0
10
20
30
40
50
60
70
80
wt% SiO2/(CaO+CaS+SiO2)

CaO - CaS - SiO_2

Projection (Slag), 1 bar

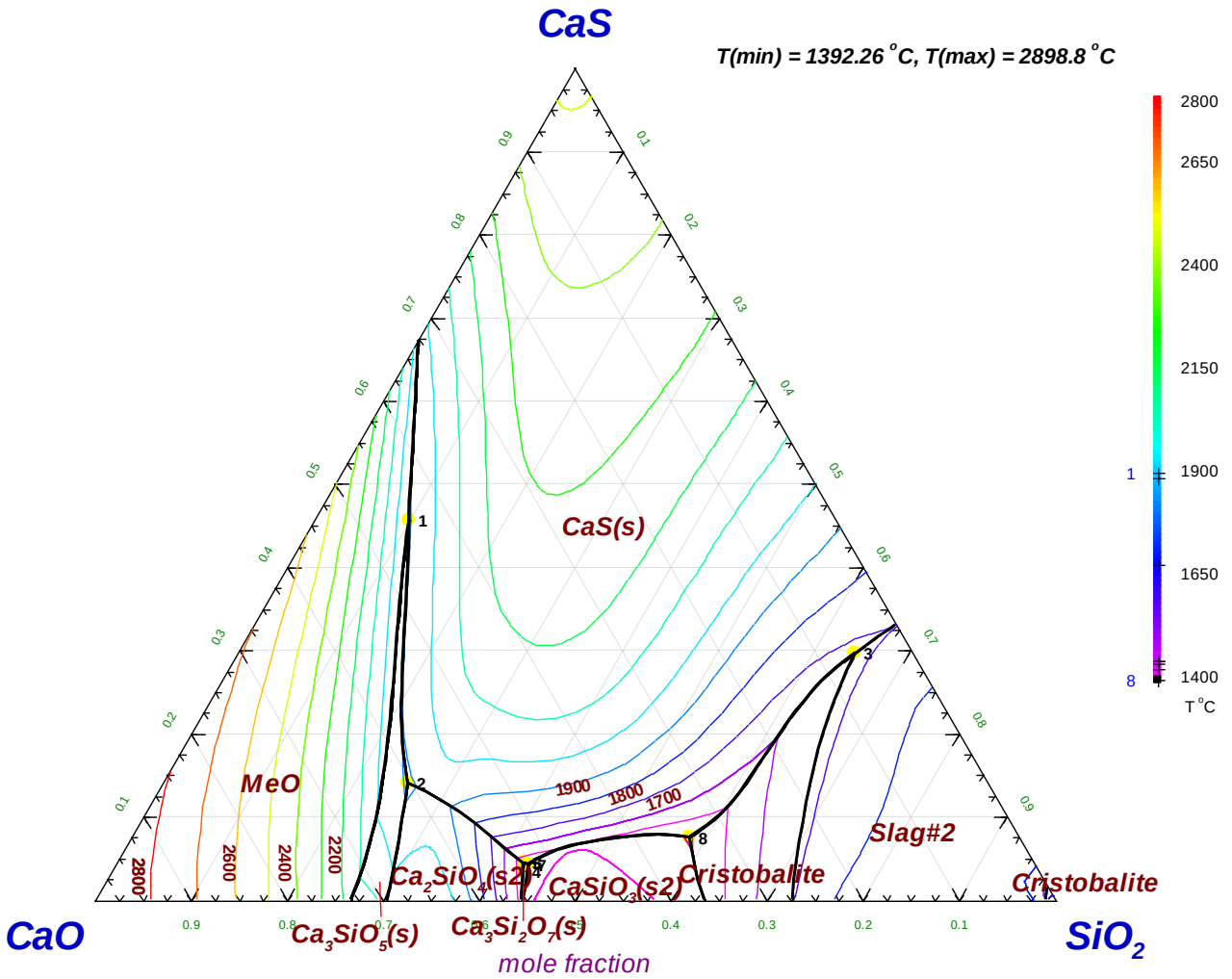

Weight percent, Liquidussurface

CaO - CaS - SiO_2

Projection (Slag), 1 bar

FactSage™

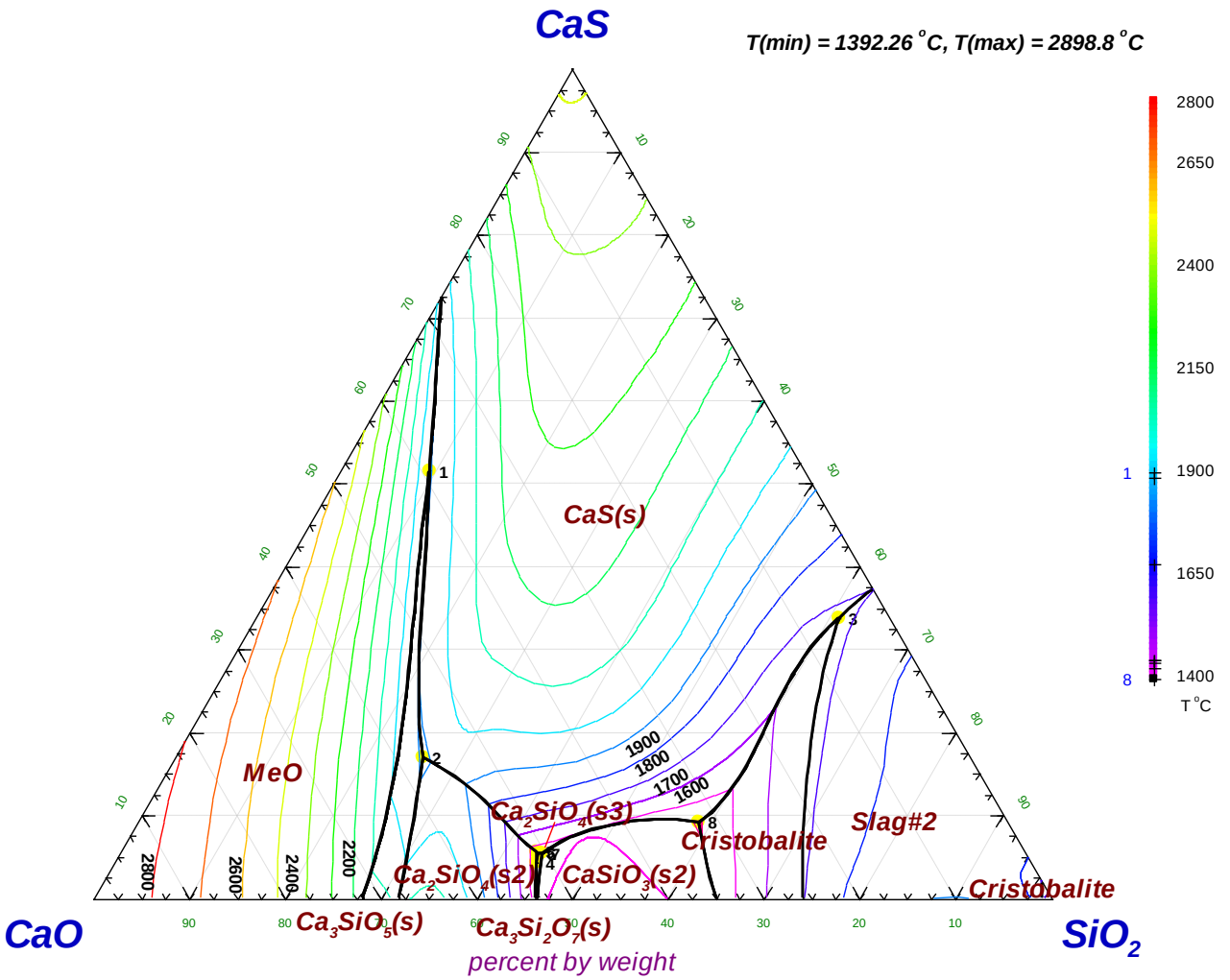

Invariant equilibria on the liquidus surface

Intersections with slag	Mole fraction				Weight percent				
	A = CaS, B = CaO, C = SiO2				A = CaS, B = CaO, C = SiO2				
		X(A)	X(B)	X(C)	T(C)		W(A)	W(B)	W(C)	T(C)
1: Ca3SiO5(s) / CaS(s) / MeO	1:	0.45650	0.44518	0.09832	1894.20	1:	51.615	39.126	9.259	1894.19
2: Ca2SiO4(s2) / Ca3SiO5(s) / CaS(s)	2:	0.14051	0.60451	0.25499	1882.72	2:	17.078	57.111	25.811	1882.72
3: CaS(s) / Cristobalite / Slag#2	3:	0.29675	0.05991	0.64334	1671.99	3:	33.755	5.297	60.947	1671.99
4: Ca2SiO4(s2) / Ca2SiO4(s3) / Ca3Si2O7(s)	4:	0.03518	0.53631	0.42851	1436.73	4:	4.349	51.533	44.118	1436.73
5: Ca2SiO4(s2) / Ca2SiO4(s3) / CaS(s)	5:	0.04493	0.53135	0.42373	1436.73	5:	5.540	50.937	43.523	1436.73
6: Ca2SiO4(s3) / Ca3Si2O7(s) / CaS(s)	6:	0.04439	0.53085	0.42475	1430.84	6:	5.475	50.893	43.631	1430.83
7: Ca3Si2O7(s) / CaS(s) / CaSiO3(s2)	7:	0.04380	0.52629	0.42991	1416.81	7:	5.401	50.447	44.152	1416.80
8: CaS(s) / CaSiO3(s2) / Cristobalite	8:	0.07630	0.34222	0.58148	1392.26	8:	9.230	32.182	58.588	1392.39

CaO-Cr2O3-CrO,
Mole fraction 1000°C

09554

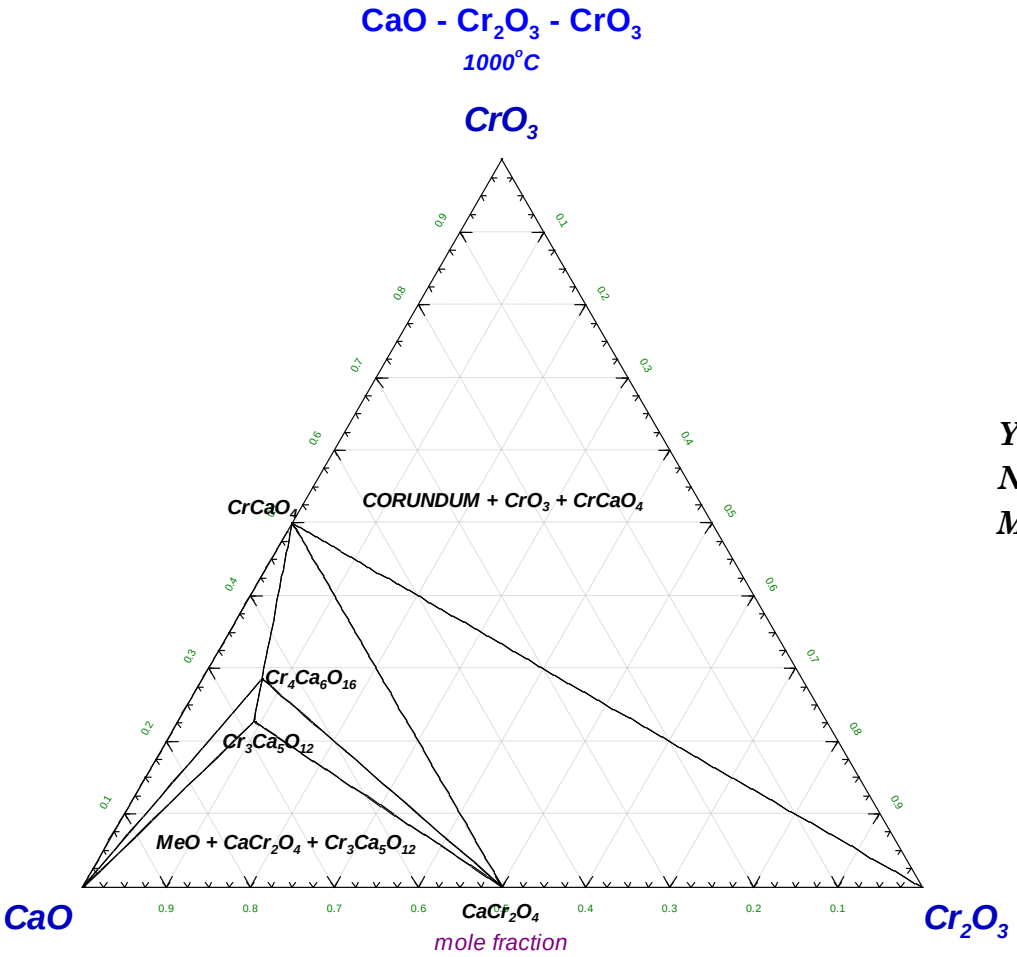

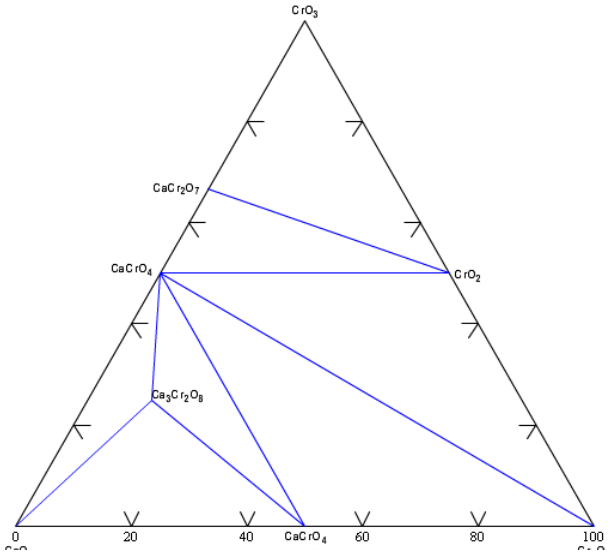

Yu. K. Kisil, N. G. Sharova, and V. A. Ryabin, Izv. Akad. Nauk SSSR, Neorg. Mater., 23 [1] 105-107 (1987); Inorg. Mater. (Engl. Transl.), 23 [1] 88-89 (1987).

Mole fraction CaCr2O4-CaFe2O4-O2

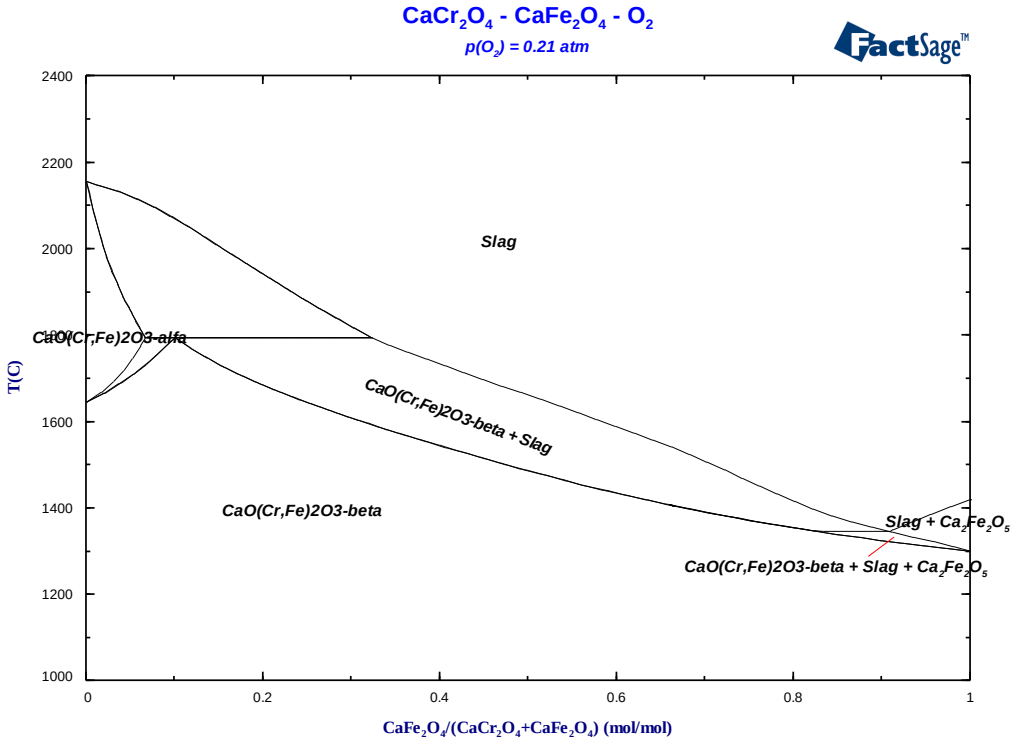

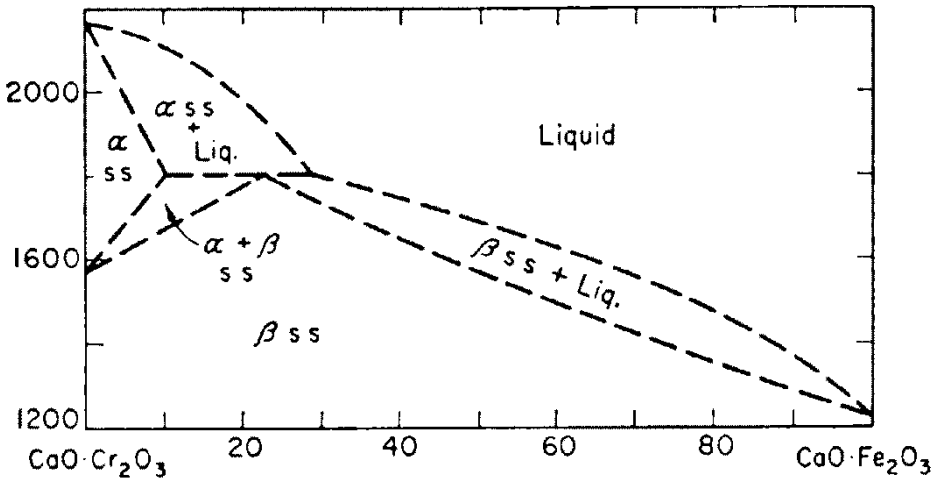

W.F. Ford, W.J. Rees, Trans. Br. Ceram. Soc., 57 [5], (1958), pp.233-241.

Weight percent CaSiO3-Cr2O3 an der Luft

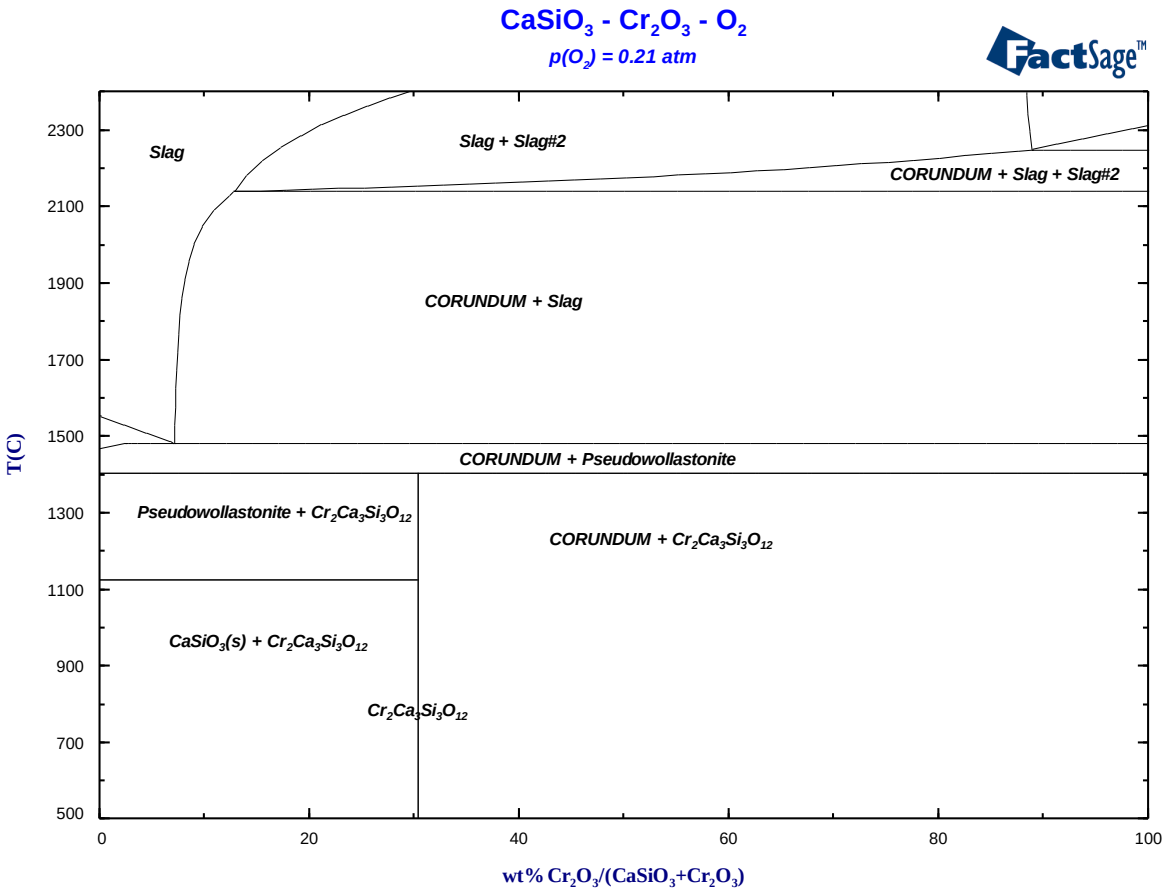

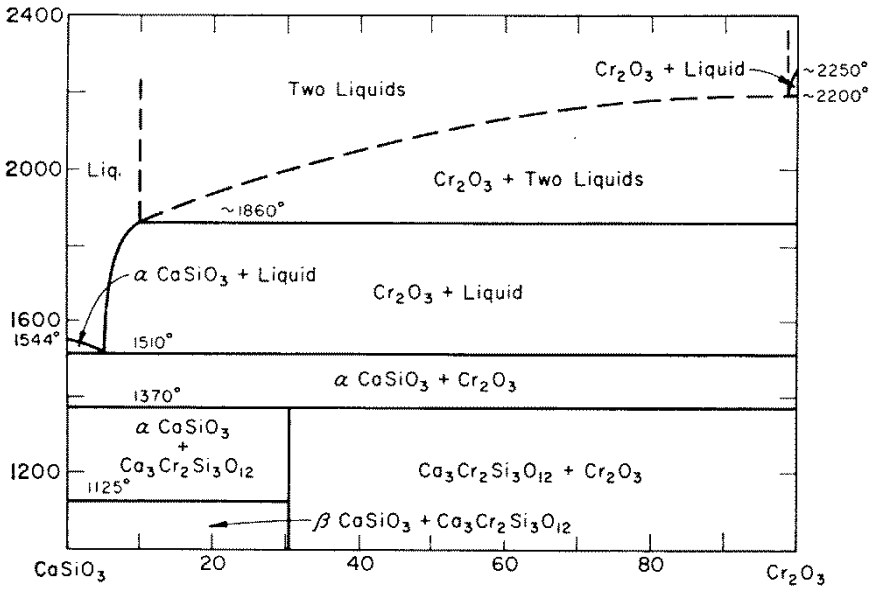

E. P. Glasser, E.F. Osborn, J. Am. Ceram. Soc., 41 [9], (1958), pp. 358-367.

CaO-CrO-SiO2,
Mole fraction 1290°C

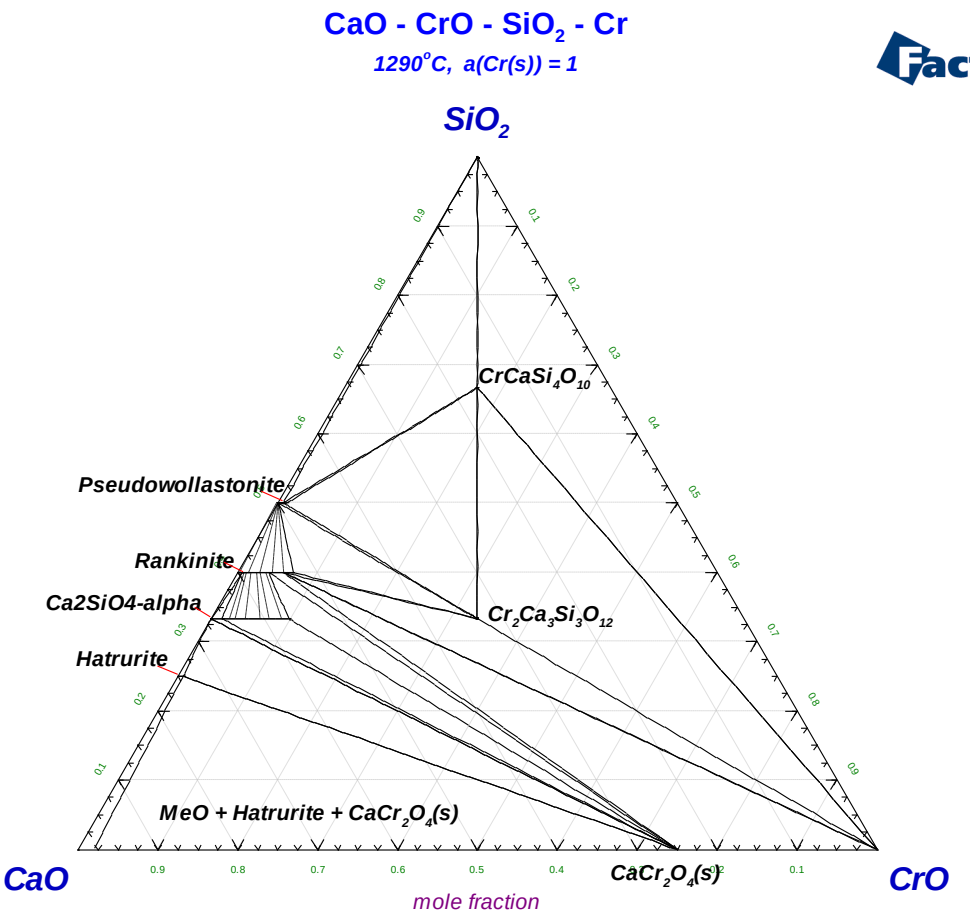

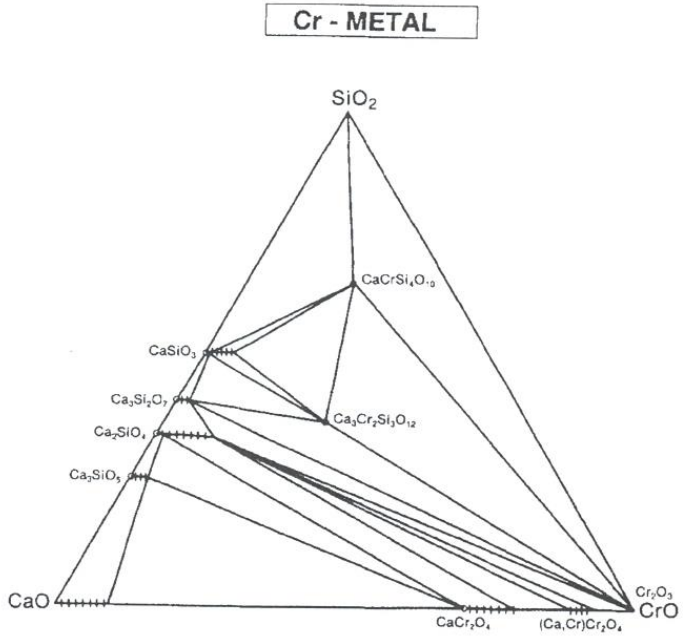

J. P. R. de Villiers, J. Am. Ceram. Soc., 75 [6], (1992), pp. 1333-1341.

Mole fraction
Liquidussurface

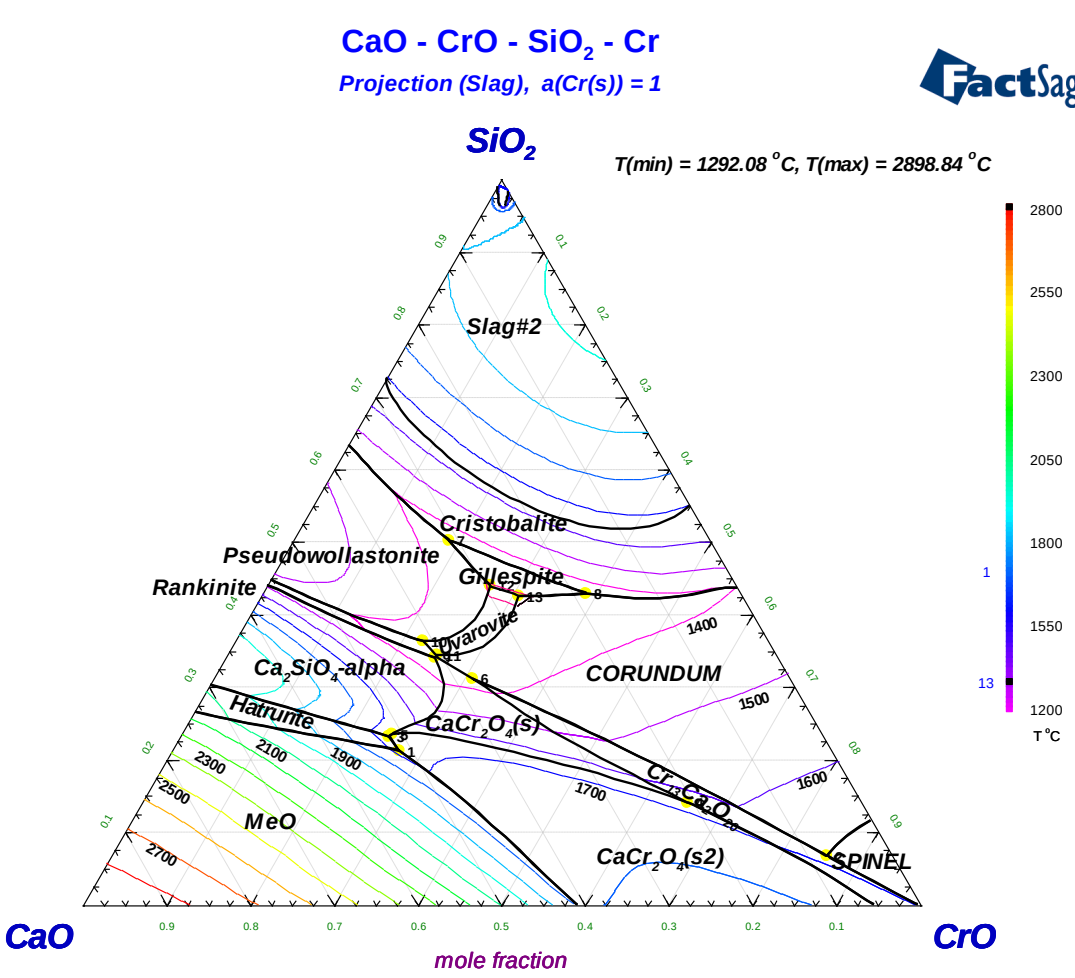

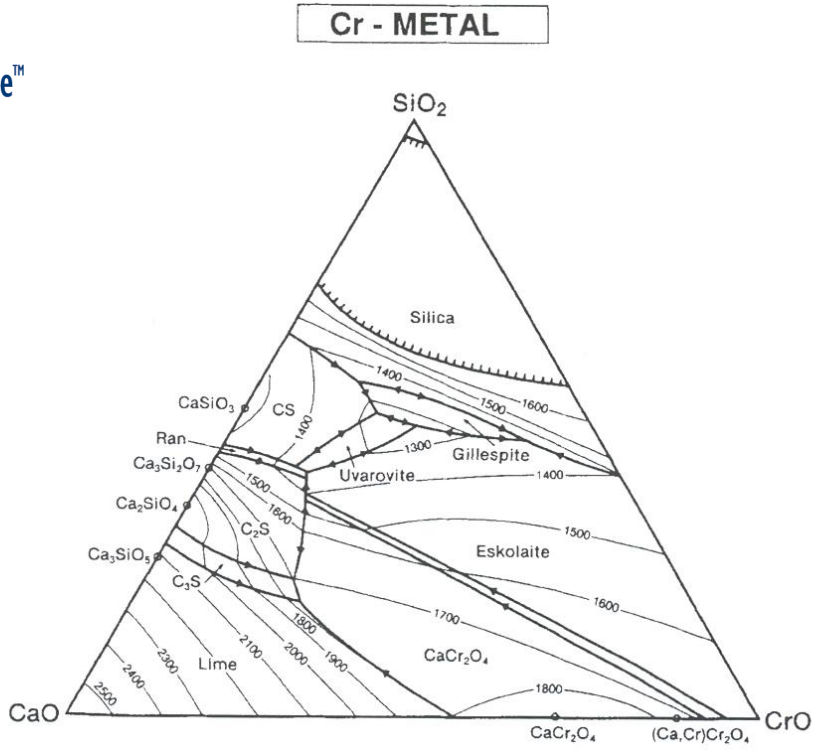

J. P. R. de Villiers, J. Am. Ceram. Soc., 75 [6], (1992), pp. 1333-1341.

Weight percent
Liquidussurface

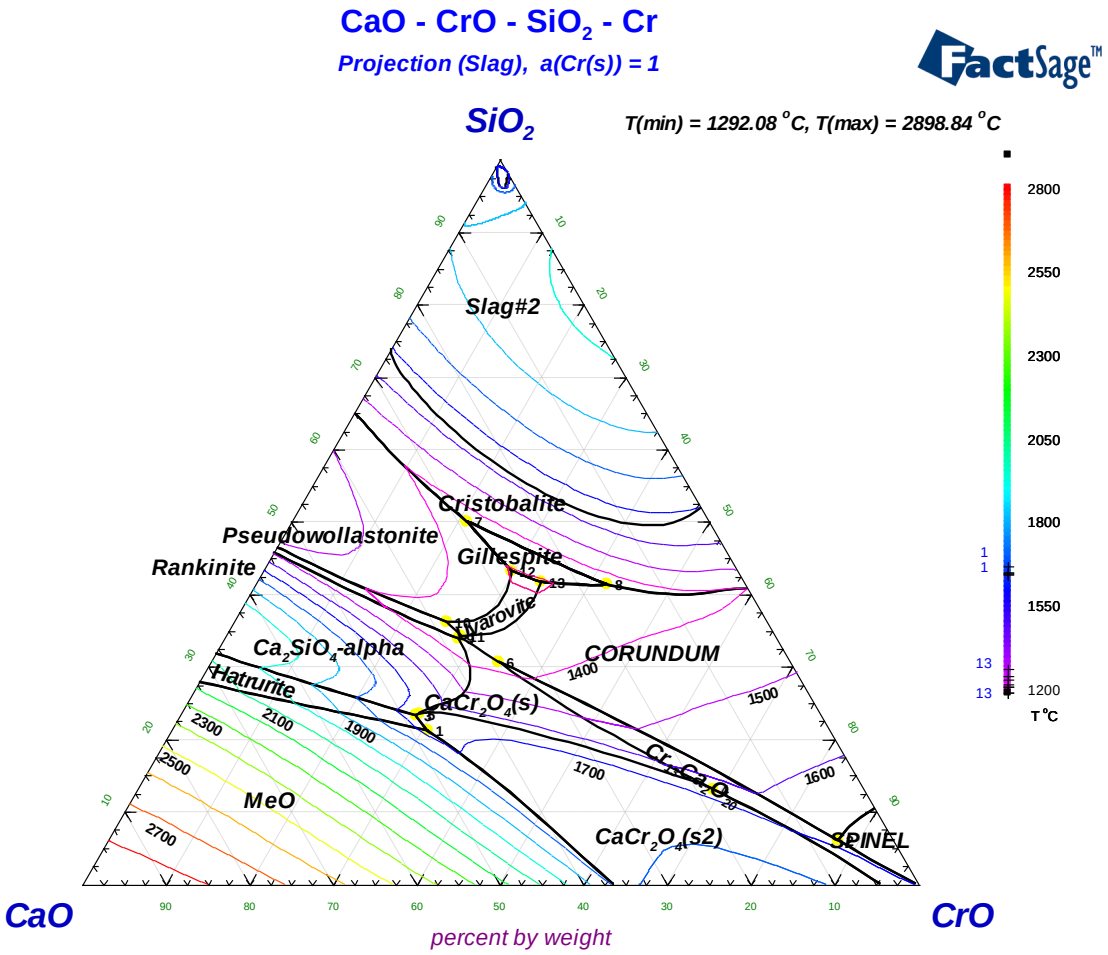

Invariant equilibria on the liquidus surface

Intersections with slag	Mole fraction A = SiO2, B = CaO, C = CrO				Weight percent A = SiO2, B = CaO, C = CrO			
	X(A)	X(B)	X(C)	T(C)	W(A)	W(B)	W(C)	T(C)
1: Hatrurite / CaCr2O4(s2) / MeO	0.21280	0.51626	0.27095	1669.01	21.253	48.123	30.624	1669.01
2: Ca2SiO4-alfa / Hatrurite / CaCr2O4(s2)	0.06777	0.07753	0.85470	1648.85	6.120	6.535	87.346	1648.85
3: CORANDUM / Cr13Ca2O20 / SPINEL	0.23253	0.51835	0.24912	1647.33	23.294	48.464	28.242	1647.33
4: Ca2SiO4-alfa / CaCr2O4(s2) / CaCr2O4(s)	0.14124	0.20663	0.65213	1644.87	13.175	17.988	68.837	1644.87
5: CaCr2O4(s2) / CaCr2O4(s) / Cr13Ca2O20	0.23583	0.51242	0.25175	1644.85	23.607	47.874	28.519	1644.85
6: CORANDUM / CaCr2O4(s) / Cr13Ca2O20	0.31234	0.37853	0.30913	1362.11	30.759	34.791	34.451	1362.11
7: CORANDUM / Gillespite / Cristobalite	0.50300	0.31114	0.18586	1340.39	50.114	28.931	20.955	1340.39
8: Pseudowollastonite / Gillespite / Cristobalite	0.42975	0.18372	0.38652	1327.91	41.376	16.509	42.114	1327.91
9: CORANDUM / CaCr2O4(s) / Rankinite	0.34071	0.40975	0.24954	1314.98	33.884	38.032	28.084	1314.98
10: CORANDUM / Uvarovite / Rankinite	0.36312	0.41094	0.22594	1307.61	36.227	38.264	25.509	1307.61
11: Pseudowollastonite / Uvarovite / Rankinite	0.34552	0.40484	0.24964	1306.56	34.350	37.563	28.086	1306.56
12: CORANDUM / Uvarovite / Gillespite	0.43958	0.29364	0.26678	1292.24	43.286	26.986	29.728	1292.23
13: Pseudowollastonite / Uvarovite / Gillespite	0.42659	0.26624	0.30717	1291.86	41.712	24.297	33.991	1291.86

Weight percent

Liquidus lines at 1200° and 1300°C

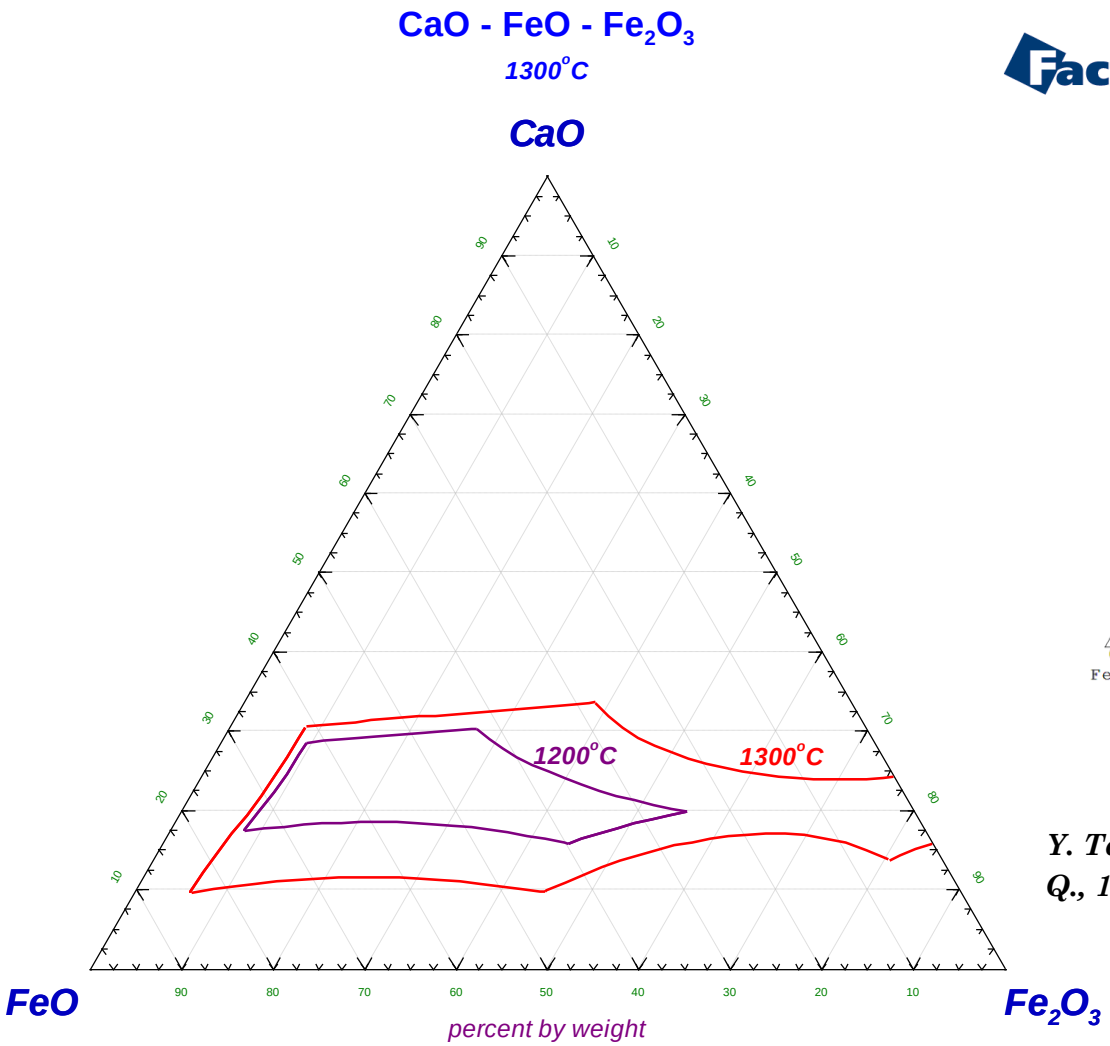

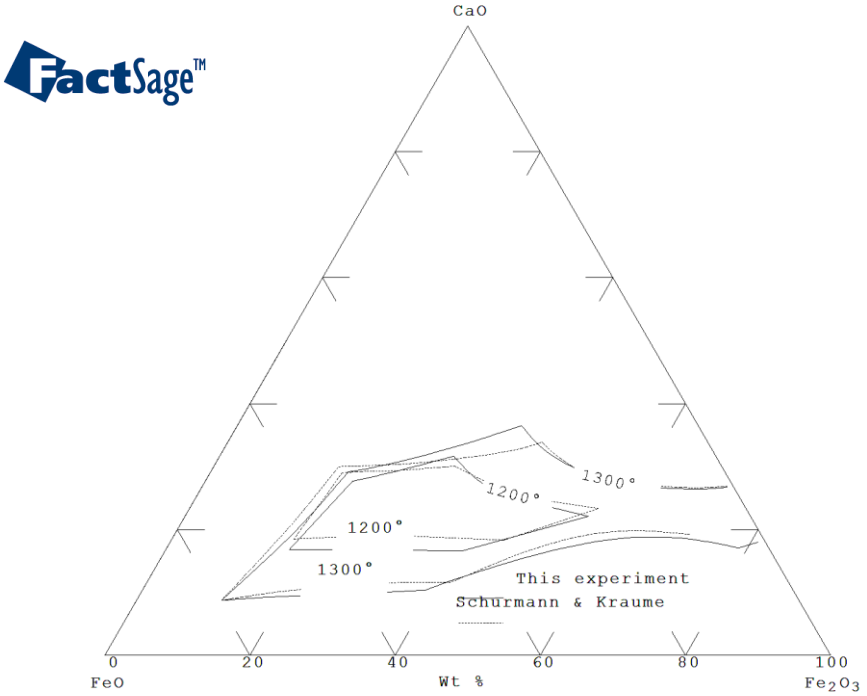

Y. Takeda, S. Nakazawa, A. Yazawa, Can. Metall. Q., 19 [3], (1980), pp.297-305.

CaO-Fe2O3-FeO, Weight percent 1300°C

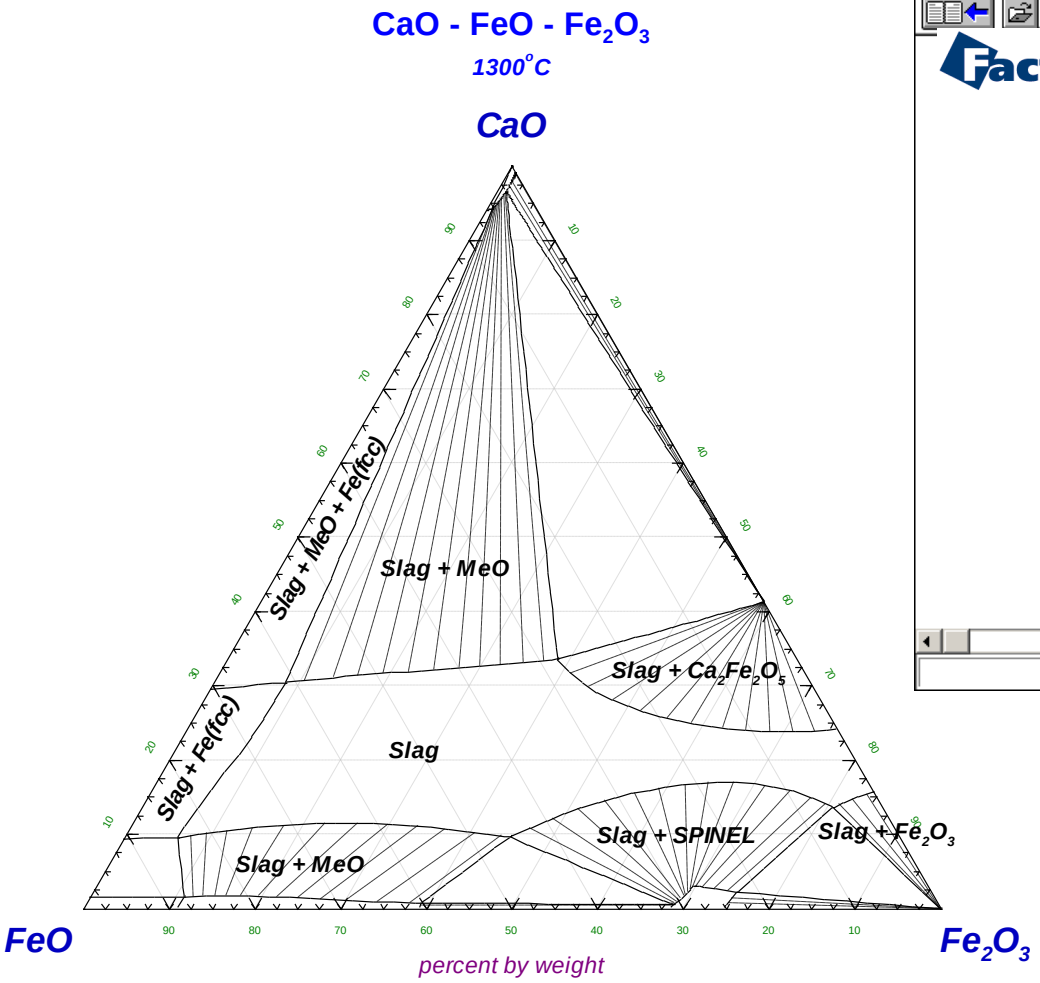

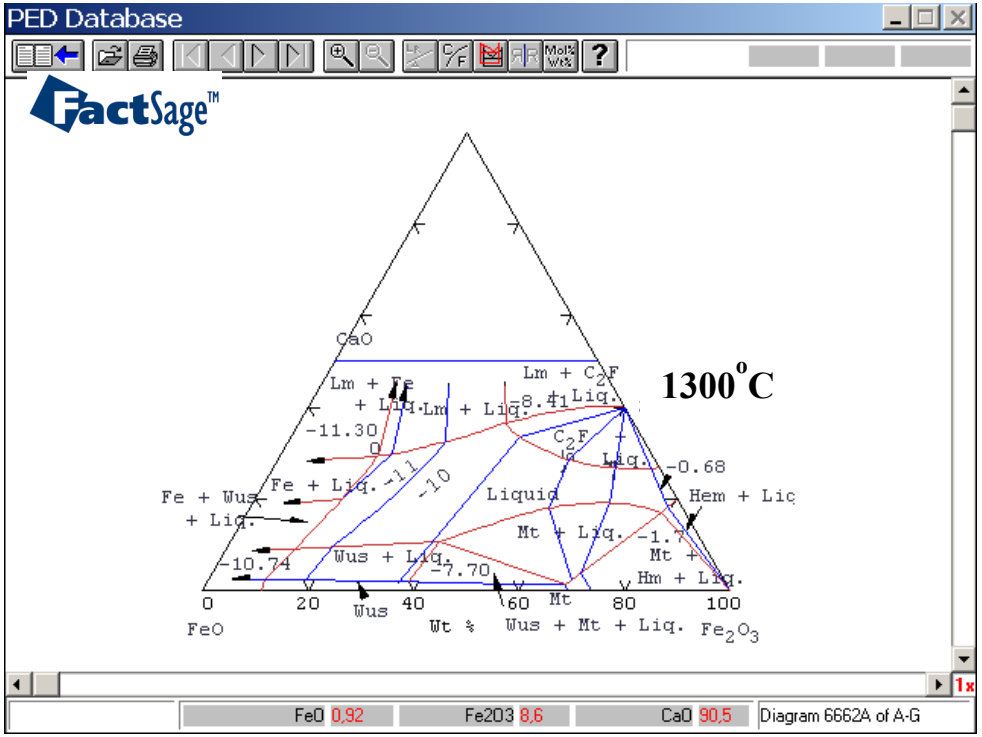

Y. Takeda, S. Nakazawa, A. Yazawa, Can. Metall. Q., 19 [3], (1980), pp.297-305.

CaO-Fe2O3-FeO,
Weight percent 1450°C

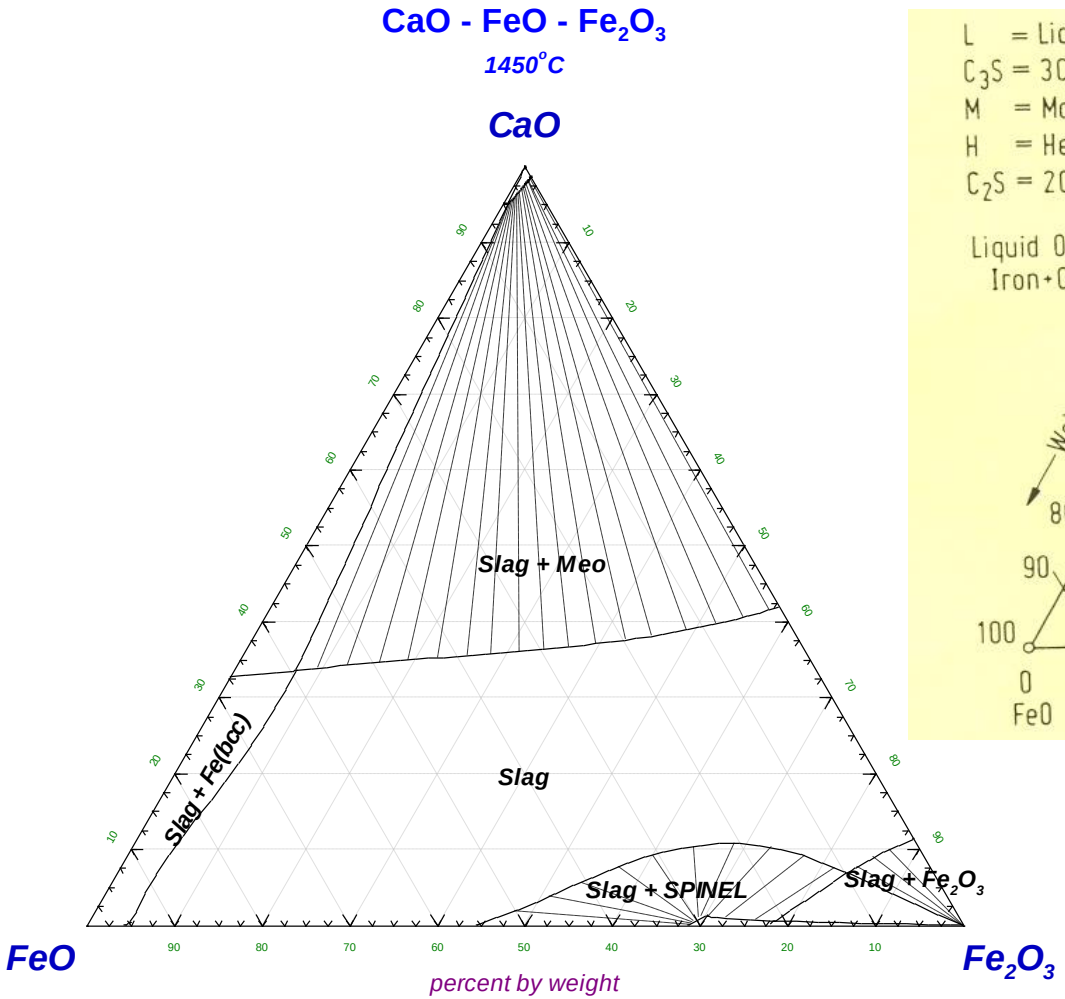

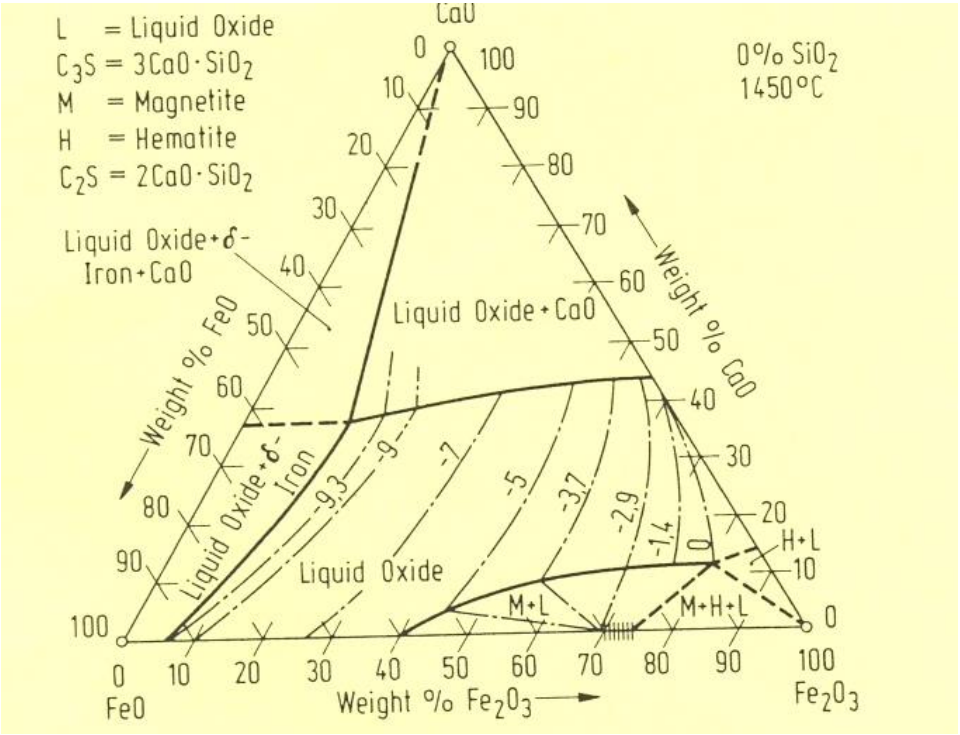

M. Timucin, A.E. Moris, Metall. Trans. I (1970), No.11, pp. 3193-3201.

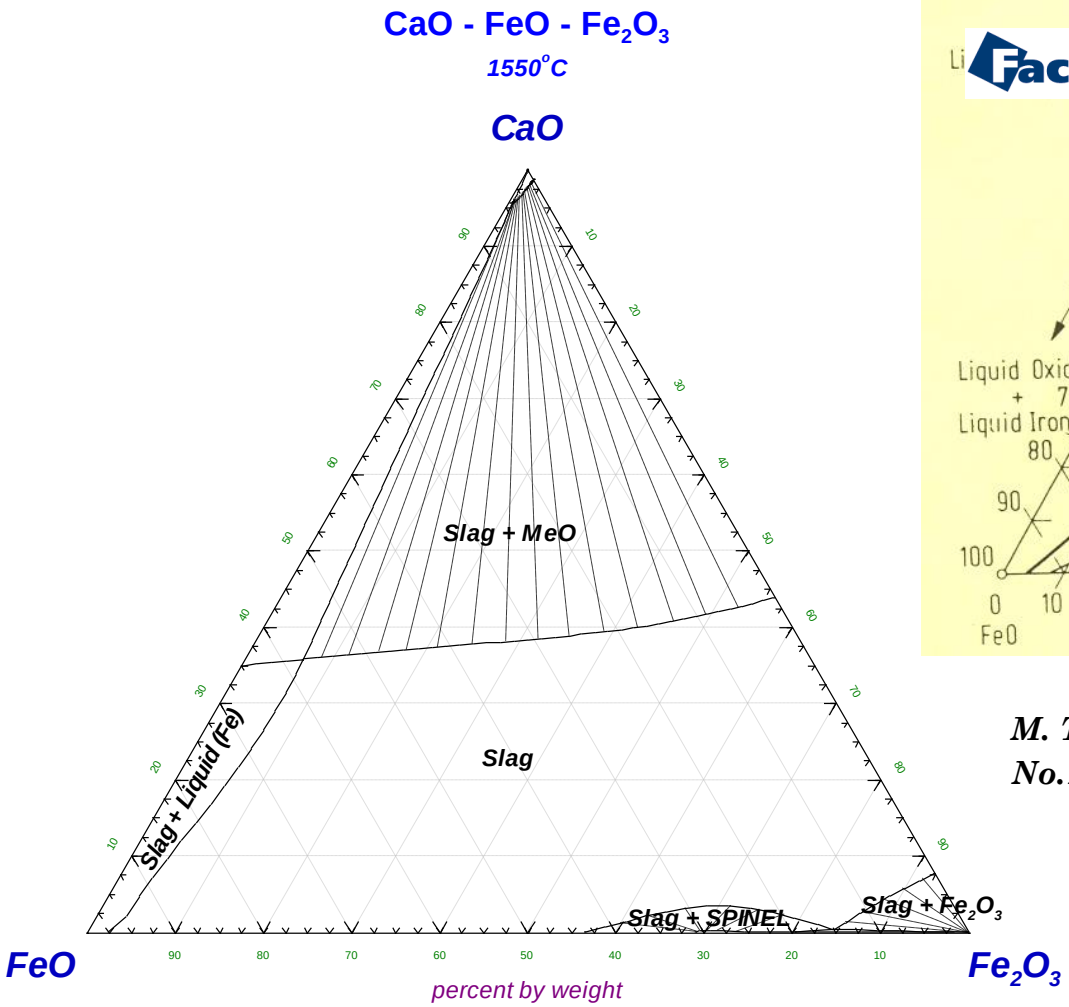

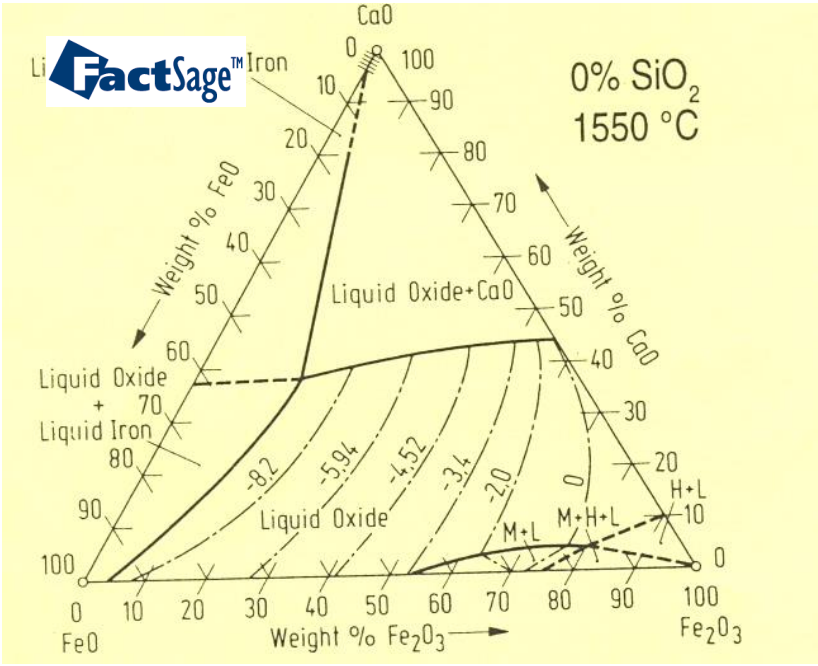

M. Timucin, A.E. Moris, Metall. Trans. I (1970), No.11, pp. 3193-3201.

$CaO - FeO - Fe_2O_3$

Projection (Slag)

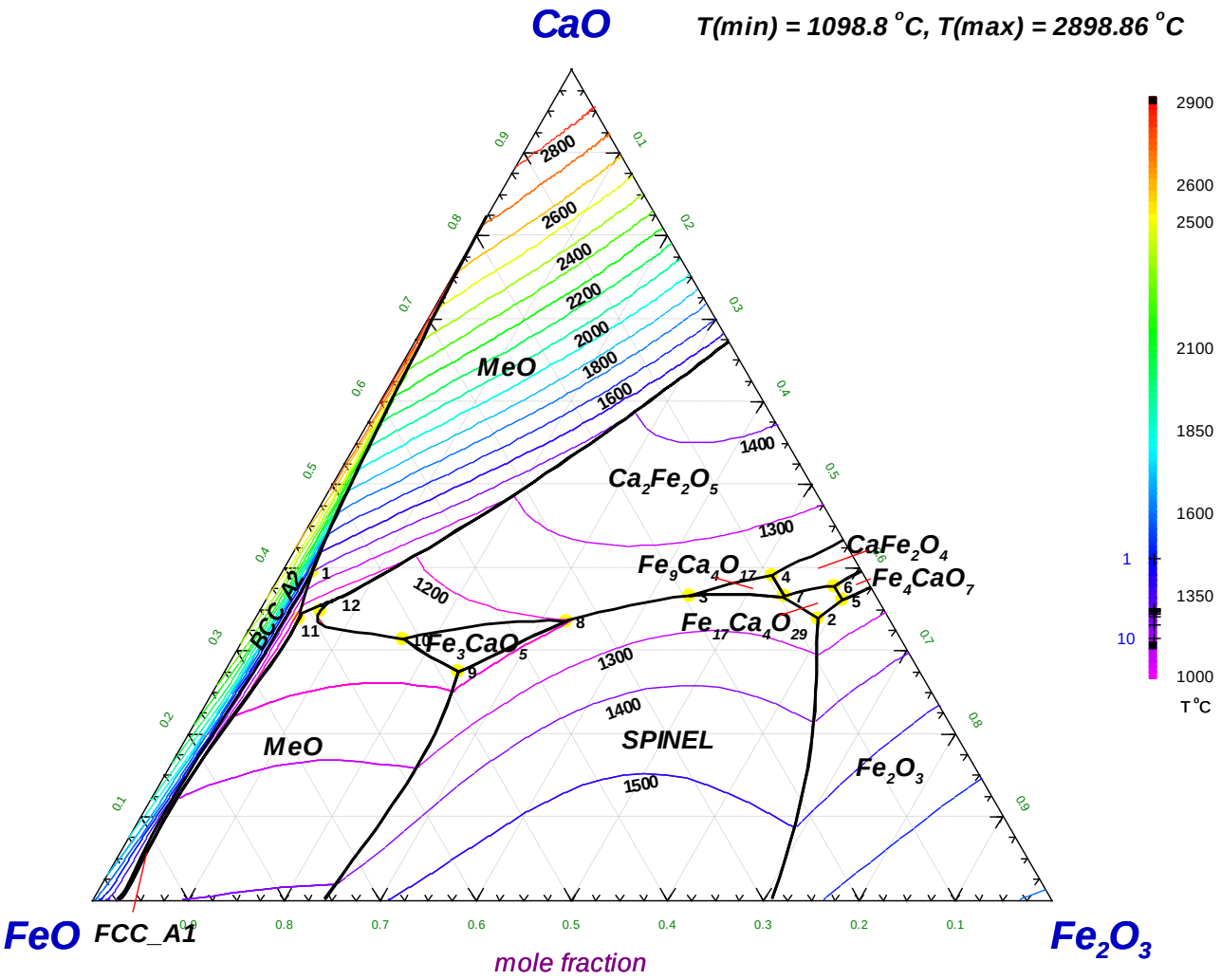

Weight percent
Liquidussurface

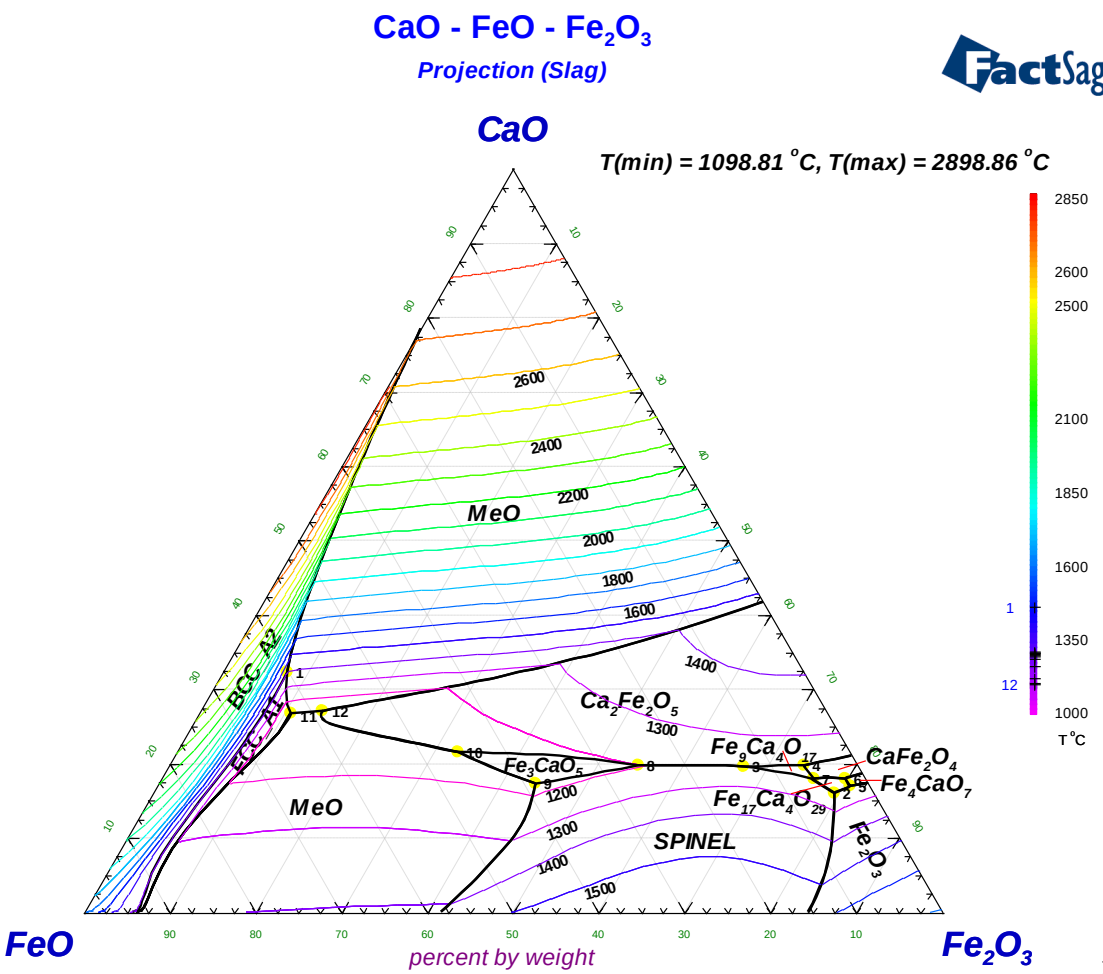

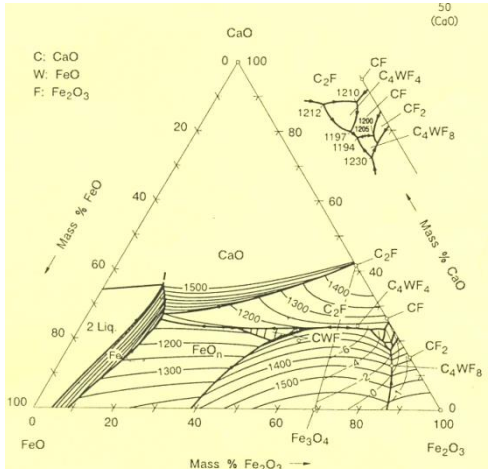

E. Schürmann, G. Kraume, Arch. Eisenhüttenwes., 47 [7], (1976), pp.435-439.

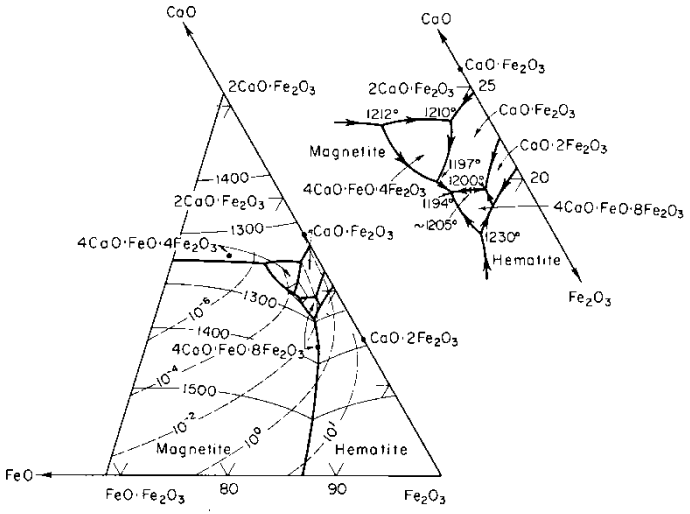

B. Philips, A. Muan, J. Am. Ceram. Soc., 41 [11], (1958), pp.445-454.

Invariant equilibria on the liquidus surface

Intersections with slag	Mole fraction A = CaO, B = FeO, C = Fe2O3				Weight percent A = CaO, B = FeO, C = Fe2O3				
		X(A)	X(B)	X(C)	T(C)		W(A)	W(B)	W(C)	T(C)
1: BCC_A2 / FCC_A1 / MeO	1:	0.39484	0.57296	0.03221	1391.92	1:	32.348	60.138	7.514	1391.92
2: Fe17Ca4O29 / Fe2O3 / SPINEL	2:	0.33854	0.07381	0.58765	1224.51	2:	16.071	4.489	79.440	1224.52
3: Ca2Fe2O5 / Fe9Ca4O17 / SPINEL	3:	0.36595	0.19383	0.44023	1219.06	3:	19.592	13.295	67.114	1219.06
4: Ca2Fe2O5 / CaFe2O4 / Fe9Ca4O17	4:	0.39077	0.09564	0.51358	1218.86	4:	19.778	6.202	74.020	1218.86
5: Fe17Ca4O29 / Fe2O3 / Fe4CaO7	5:	0.36043	0.03701	0.60257	1217.33	5:	16.971	2.232	80.796	1217.33
6: CaFe2O4 / Fe17Ca4O29 / Fe4CaO7	6:	0.37746	0.03704	0.58549	1209.38	6:	18.042	2.268	79.690	1209.38
7: CaFe2O4 / Fe17Ca4O29 / Fe9Ca4O17	7:	0.36518	0.09451	0.54031	1205.53	7:	18.034	5.980	75.986	1205.53
8: Ca2Fe2O5 / Fe3CaO5 / SPINEL	8:	0.33539	0.33777	0.32684	1197.17	8:	19.742	25.473	54.785	1197.17
9: Fe3CaO5 / MeO / SPINEL	9:	0.27427	0.48029	0.24544	1171.44	9:	17.266	38.736	43.998	1171.44
10: Ca2Fe2O5 / Fe3CaO5 / MeO	10:	0.31373	0.51832	0.16795	1127.31	10:	21.547	45.606	32.847	1127.31
11: FCC_A1 / MeO#1 / MeO#2	11:	0.33718	0.61552	0.04730	1109.39	11:	26.752	62.563	10.685	1109.38
12: Ca2Fe2O5 / MeO#1 / MeO#2	12:	0.34774	0.58776	0.06450	1104.16	12:	27.074	58.627	14.299	1104.15

CaO-Fe2O3-MgO, Weight percent 1500°C

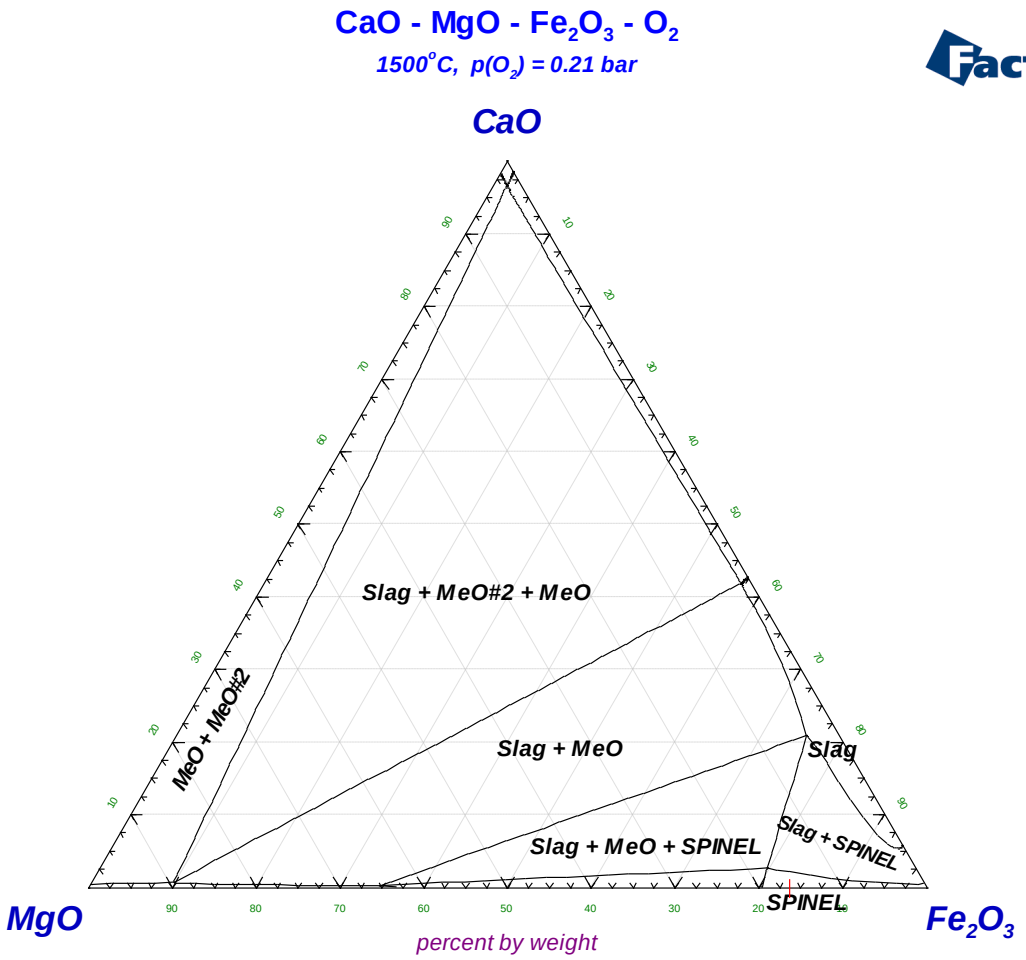

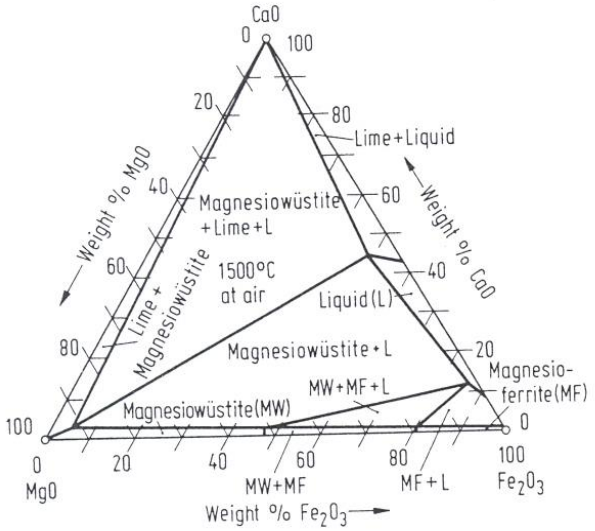

Fig. 3.209. Isothermal section at 1500 °C through the system CaO-FeO_x-MgO in air projected on the CaO-Fe_2O_3-MgO plane after Johnson, Muan [5].

Slag Atlas, 2nd Ed., Verlag Stahl-Eisen, Düsseldorf, 1995.

Weight percent
$P(O_2)=10^{-9}$ bar

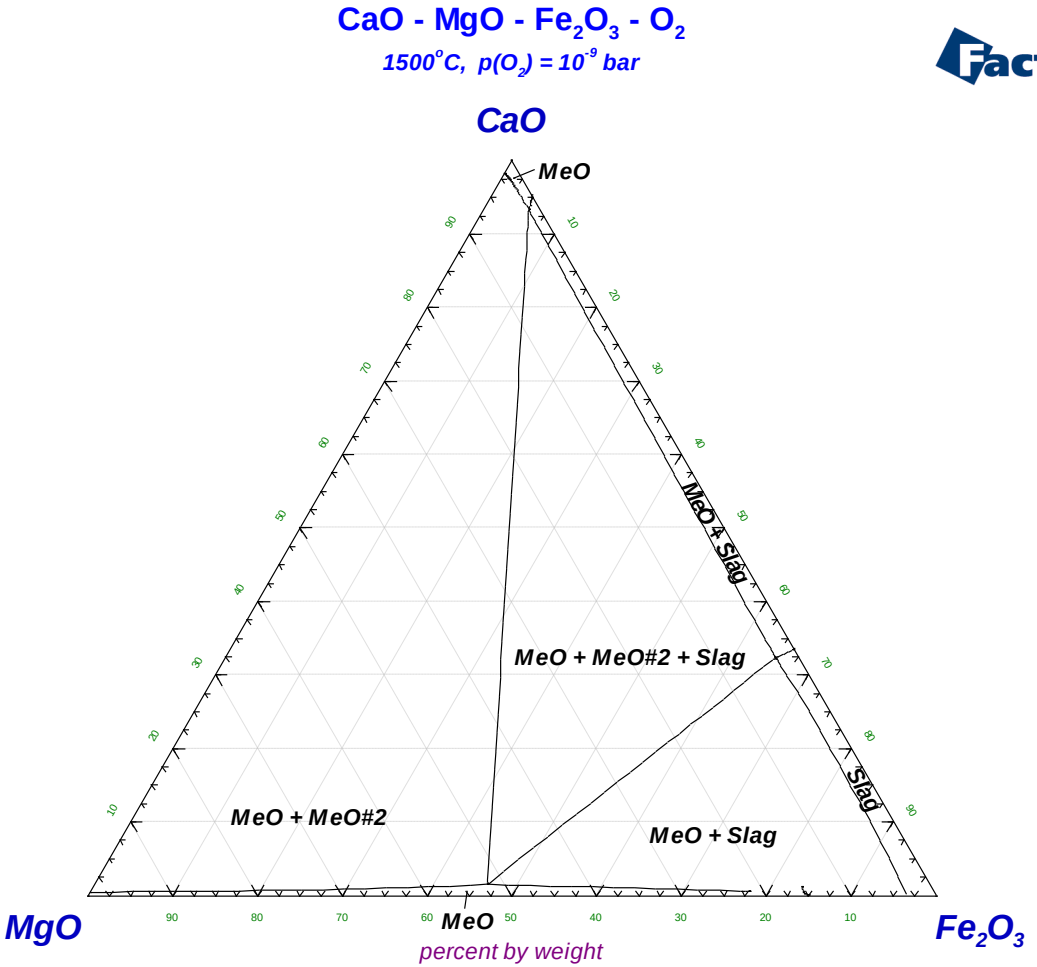

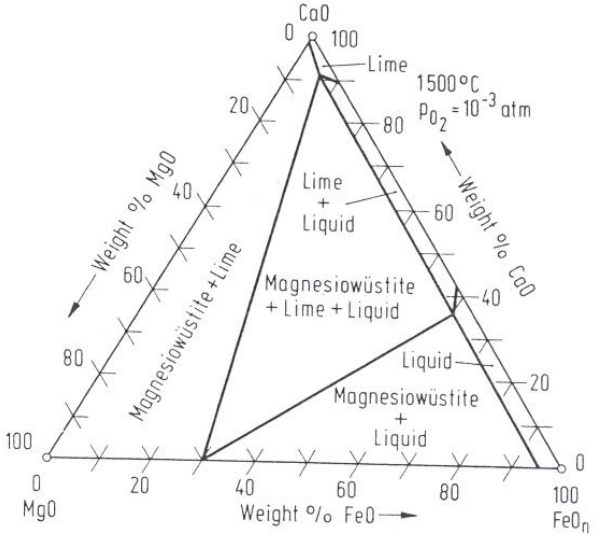

Fig. 3.206. Isothermal section at 1500 °C through the system $CaO\text{-}FeO_n\text{-}MgO$ at oxygen partial pressure of 10^{-9} atm projected on the CaO-FeO-MgO plane after Johnson, Muan [5].

Slag Atlas, 2nd Ed., Verlag Stahl-Eisen, Düsseldorf, 1995.

$CaO - Fe_2O_3 - MgO - O_2$

Projection (Slag), $p(O_2) = 0.21$ atm

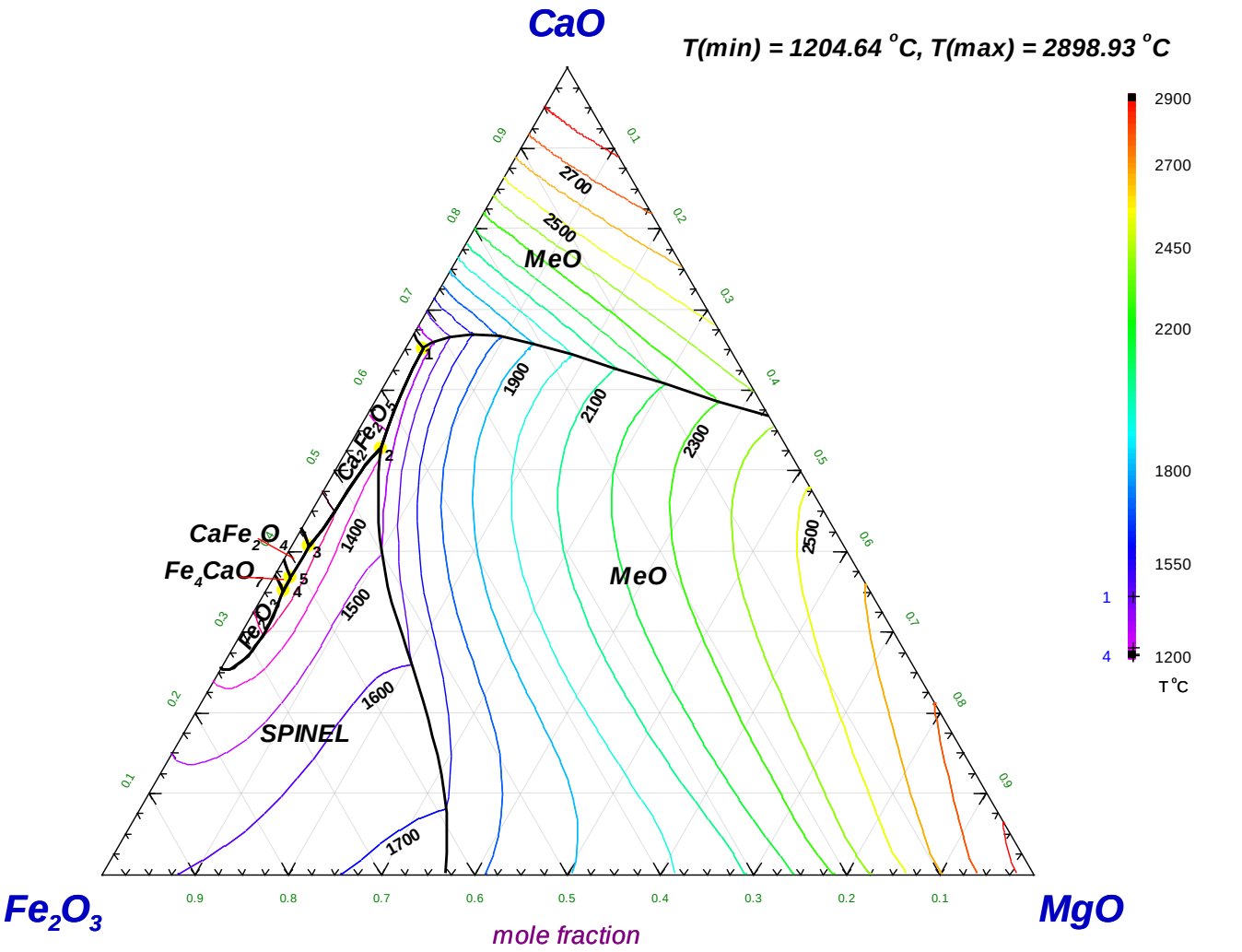

Weight percent
Liquidussurface

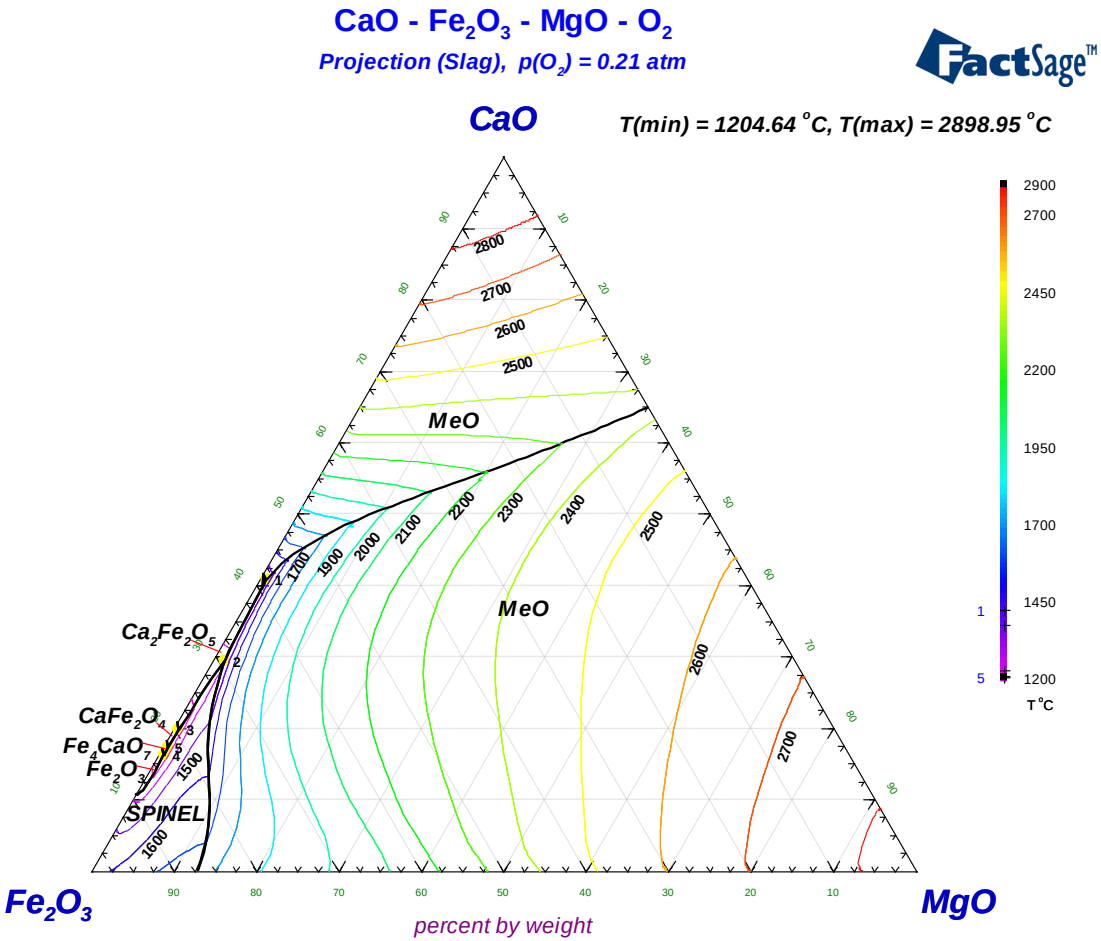

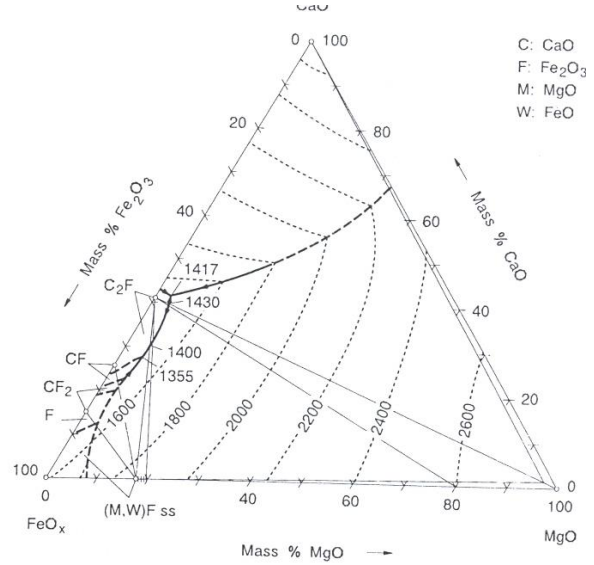

Fig. 3.208. Liquidus surface and compatibility relations in the system CaO-FeO_x-MgO in air, projected on the CaO-Fe_2O_3-MgO plane after Fusenig et al. [6].

Slag Atlas, 2nd Ed., Verlag Stahl-Eisen, Düsseldorf 1995.

Invariant equilibria on the liquidus surface

Intersections with slag	Mole fraction A = CaO, B = Fe2O3, C = MgO				Weight percent A = CaO, B = Fe2O3, C = MgO			
	X(A)	X(B)	X(C)	T(C)	W(A)	W(B)	W(C)	T(C)
1: Ca2Fe2O5 / MeO#1 / MeO#2	1: 0.65110	0.32930	0.0196	1437.05	1: 40.758	58..369	0.873	1437.05
2: Ca2Fe2O5 / MeO#1 / SPINEL	2: 0.52689	0.43652	0.03659	1386.85	2: 29.333	69.203	1.464	1386.85
3: Ca2Fe2O5 / CaFe2O4 / SPINEL	3: 0.40569	0.57383	0.02048	1227.52	3: 19.746	79.537	0.716	1227.52
4: Fe2O3 / Fe4CaO7 / SPINEL	4: 0.35081	0.62940	0.01980	1210.53	4: 16.261	83.079	0.660	1210.53
5: CaFe2O4 / Fe4CaO7 / SPINEL	5: 0.36683	0.61377	0.01941	1204.64	5: 17.234	82.111	0.655	1204.64

CaO-FeO-MgO,
Weight percent 1600°C

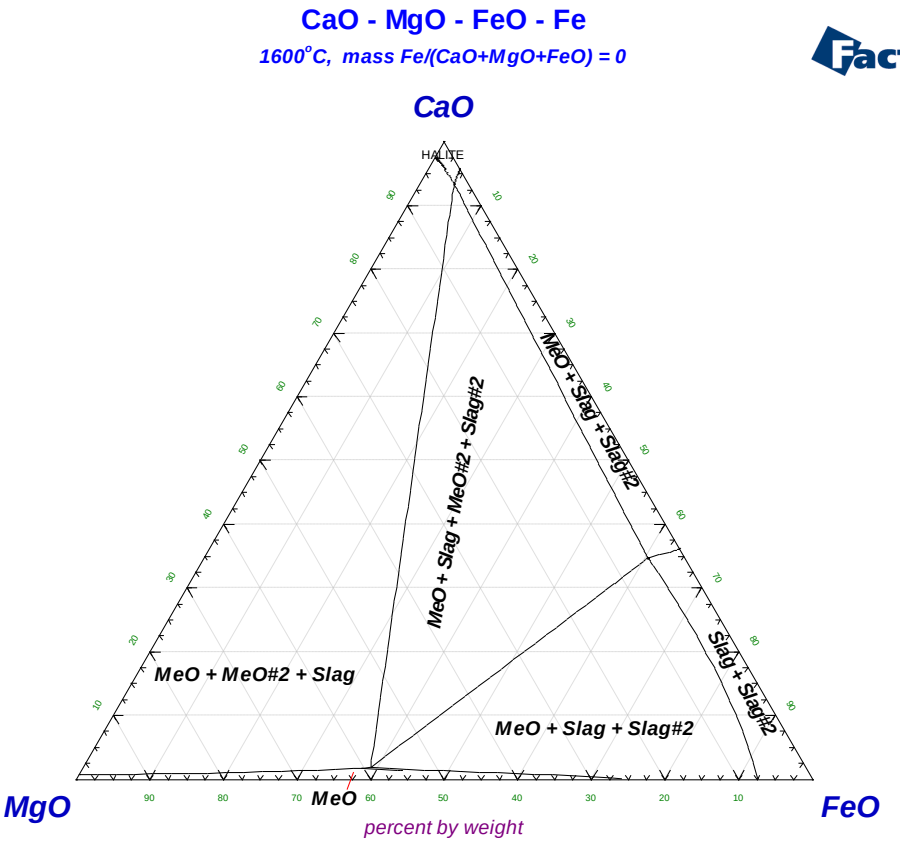

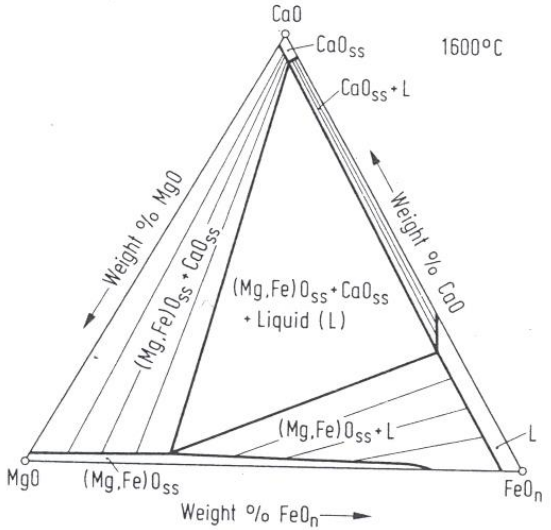

Fig. 3.205. Isothermal section at 1600 °C through the system CaO-FeO$_n$-MgO in contact with metallic iron projected on the CaO-FeO-MgO plane after Trömel et al. [4].

Slag Atlas, 2nd Ed., Verlag Stahl-Eisen, Düsseldorf, 1995.

Weight percent 1150°C

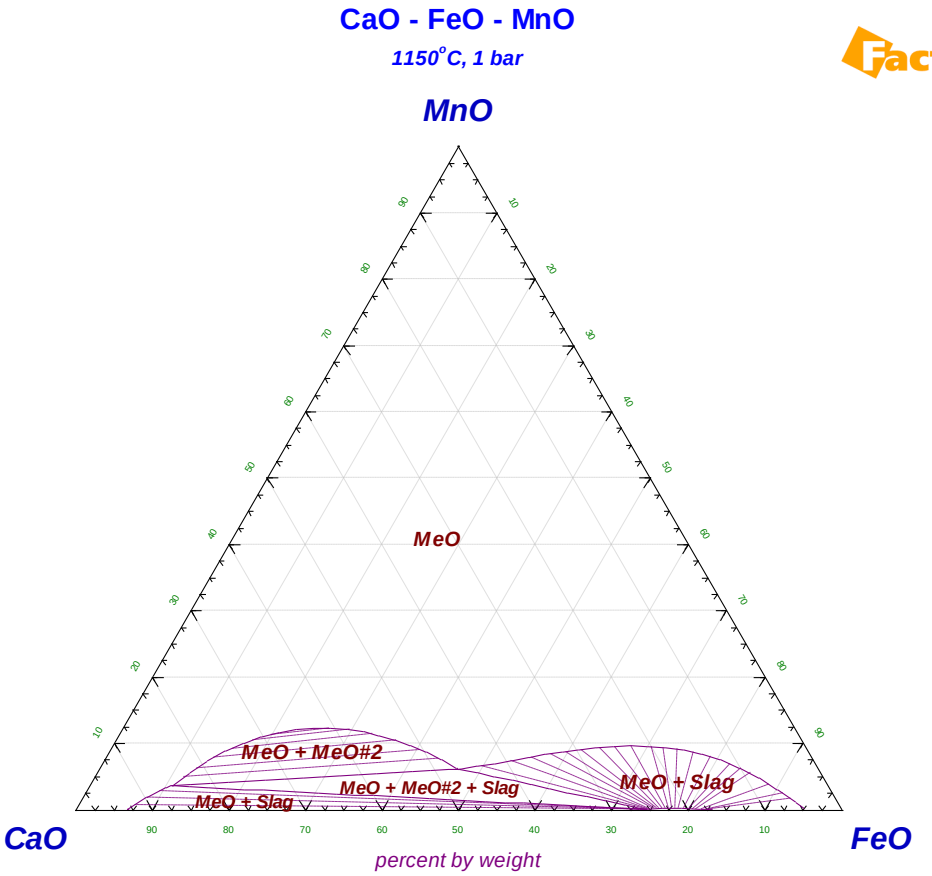

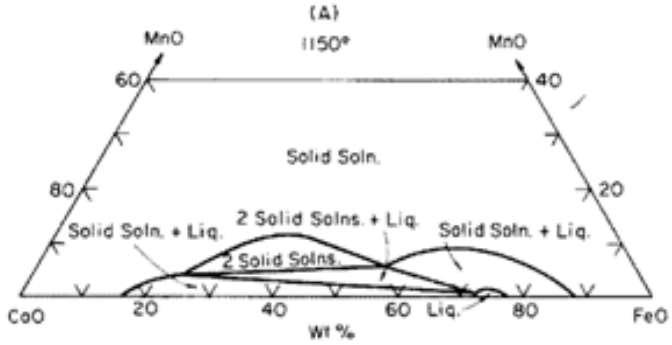

W.A. Fleischer, H.-J. Fischer, Arch. Eisenhüttenwes., 32 [5], (1961), pp. 305-313.

Weight percent 1350°C

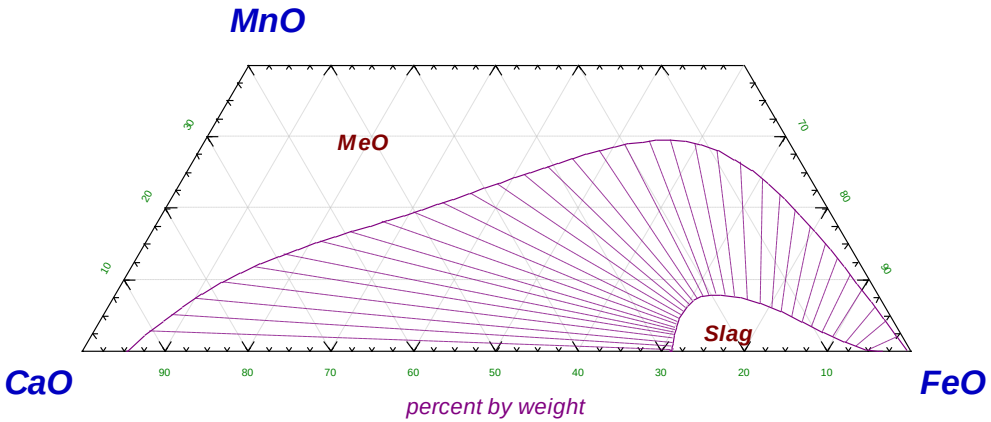

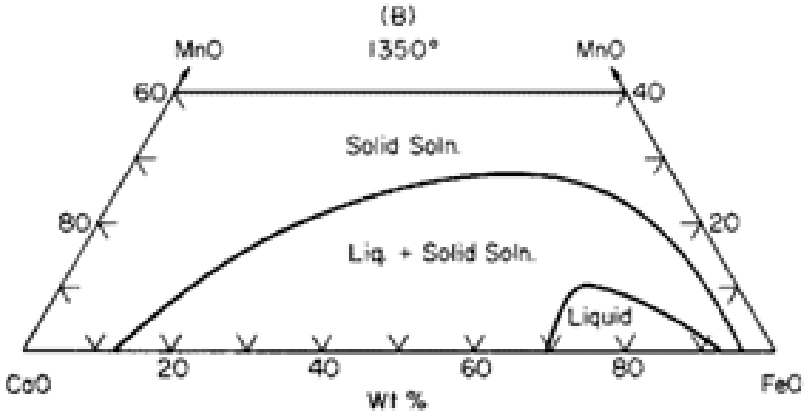

W.A. Fleischer, H.-J. Fischer, Arch. Eisenhüttenwes., 32 [5], (1961), pp. 305-313.

CaO-FeO-MnO, Liquid lines

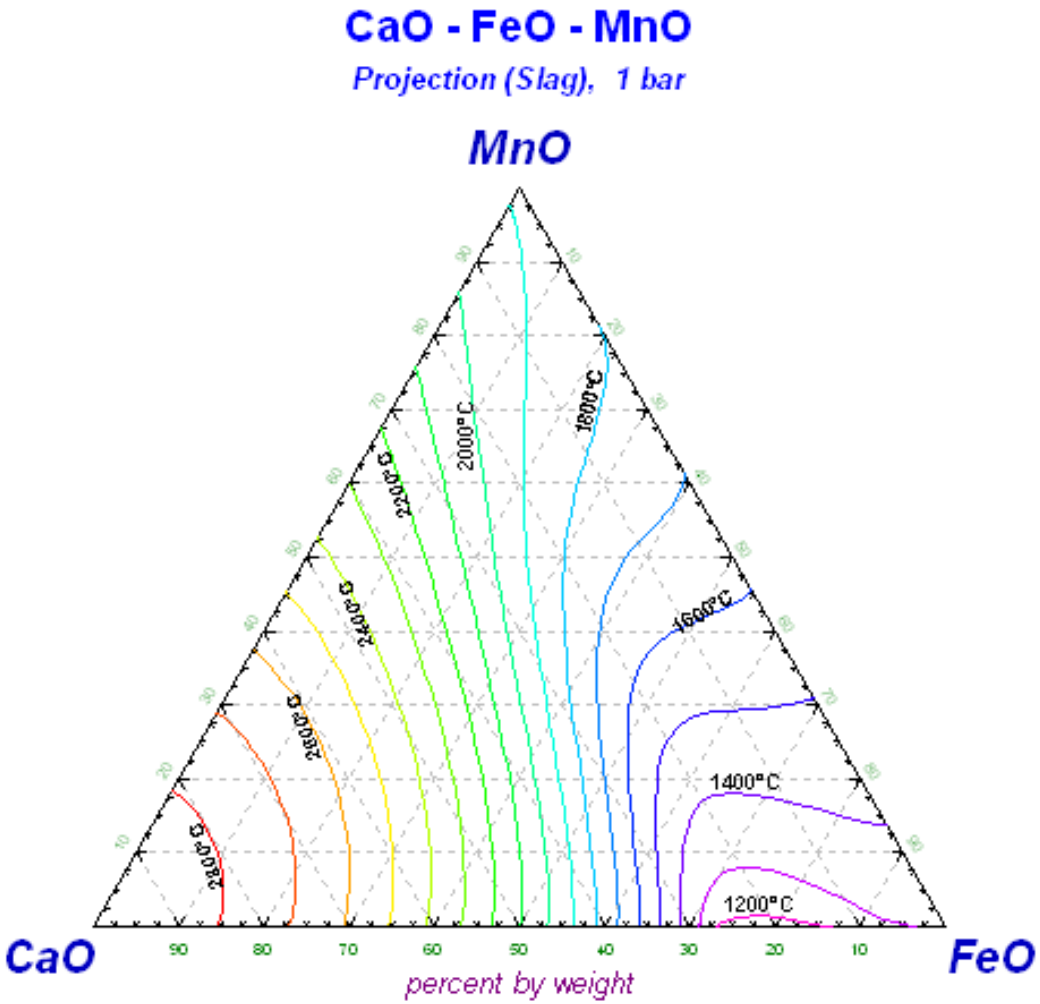

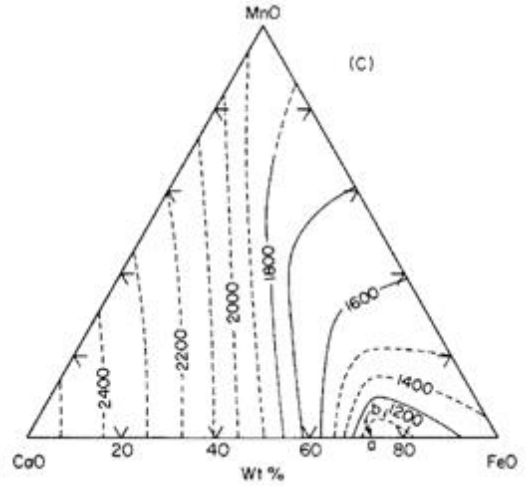

W.A. Fleischer, H.-J. Fischer, Arch. Eisenhüttenwes., 32 [5], (1961), pp. 305-313.

Weight percent, Isothermal section at 1600°C

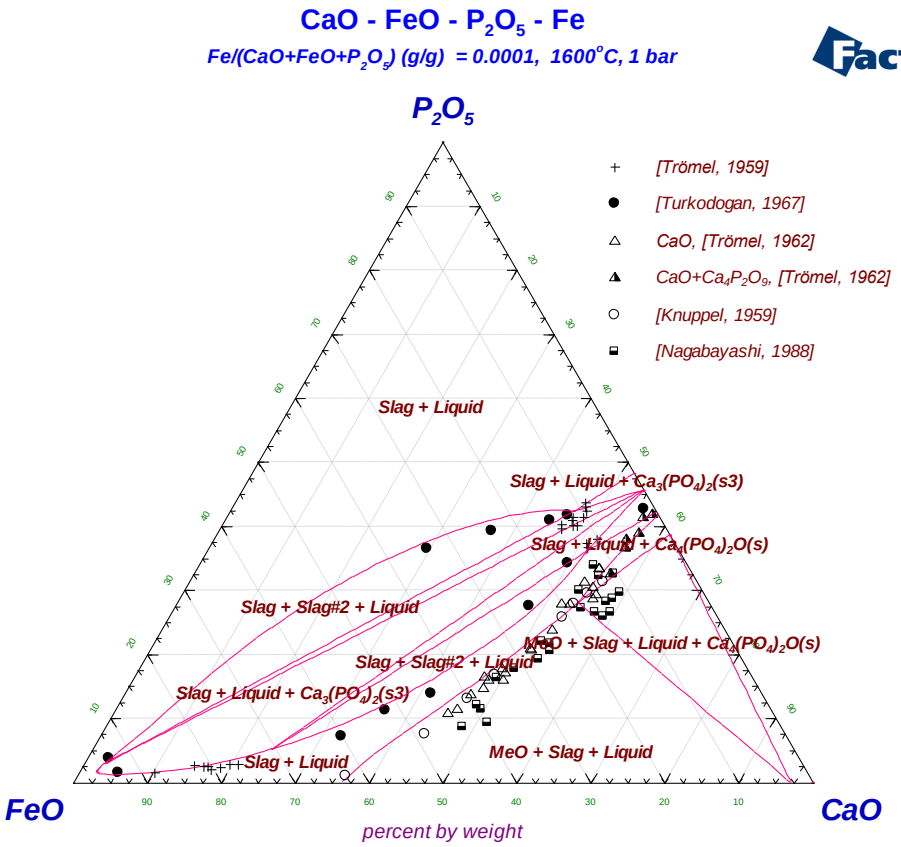

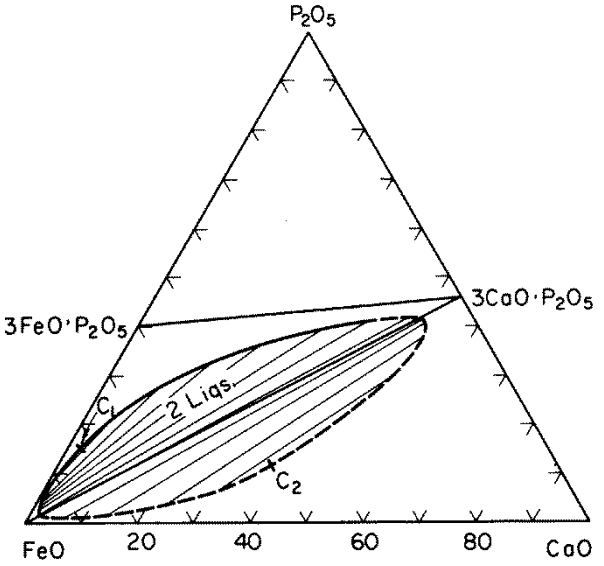

W.Oelsen, H. Maetz, Arch. Eisenhuettenwes., 19, (1948), pp.111-117.

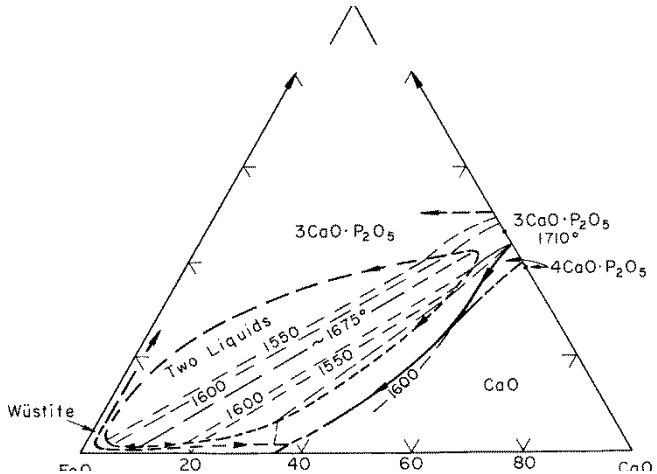

G. Troemel, W. Fix, and H. W. Fritze, Arch. Eisenhuettenwes. 32 [6] 353-359 (1961).

Weight percent, Isopleth section at Ca3P2O8-FeO

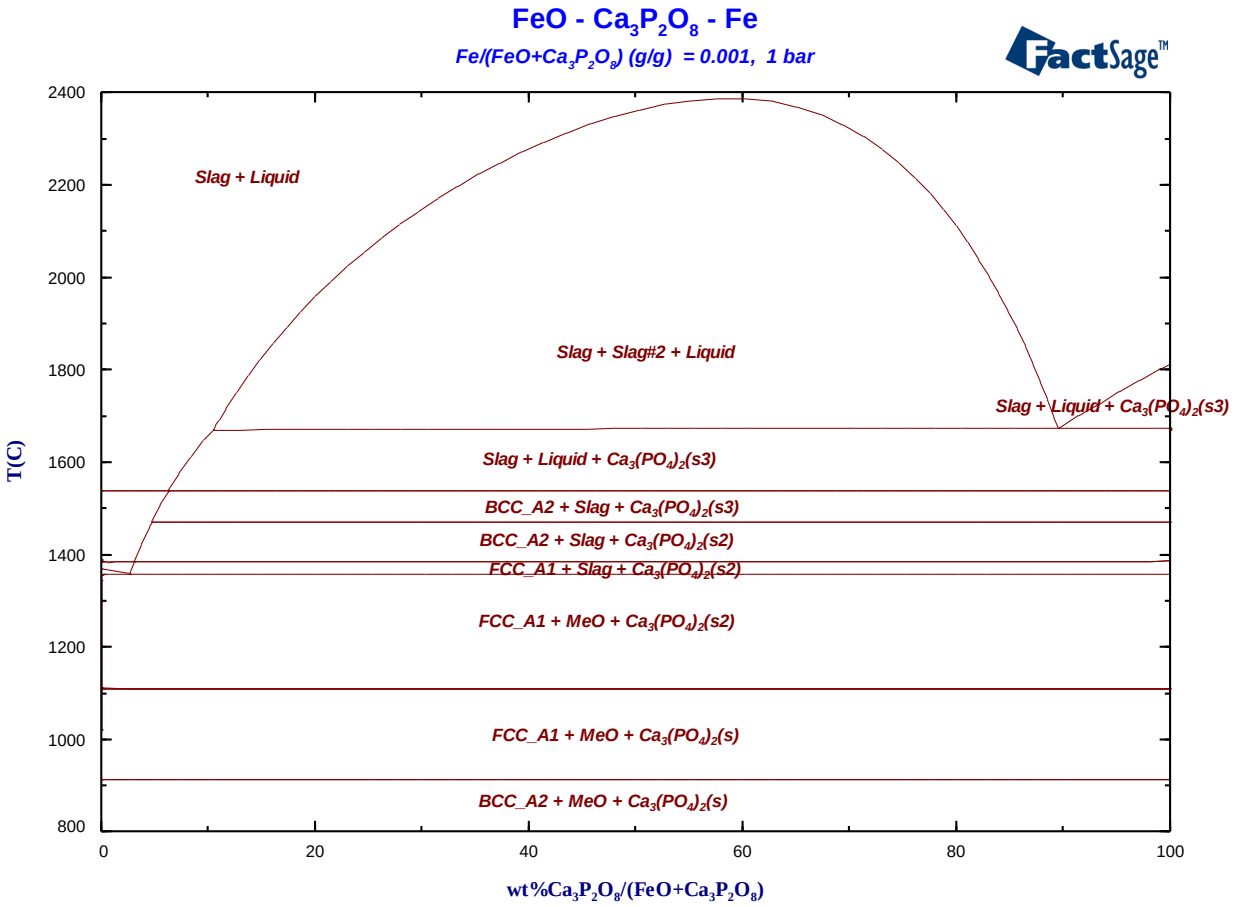

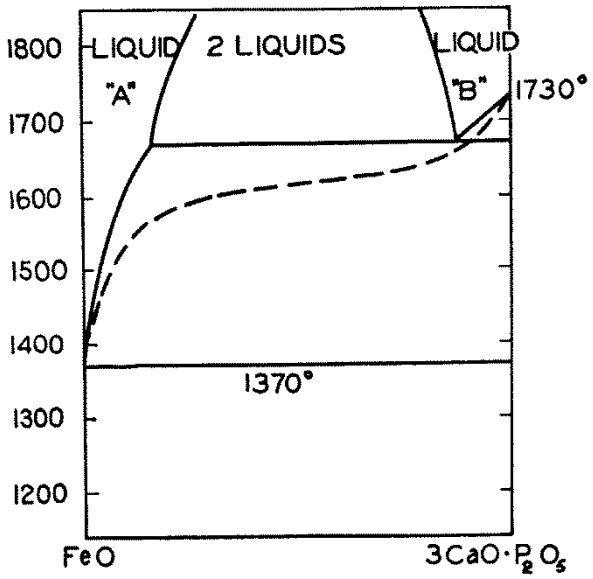

W.Oelsen, H. Maetz, Mitt. Kaiser-Wilhelm Inst. Eisenforsch. Duesseldorf 23 [12] 195-245 (1941).

Weight percent in Kelvin compared with experimental data

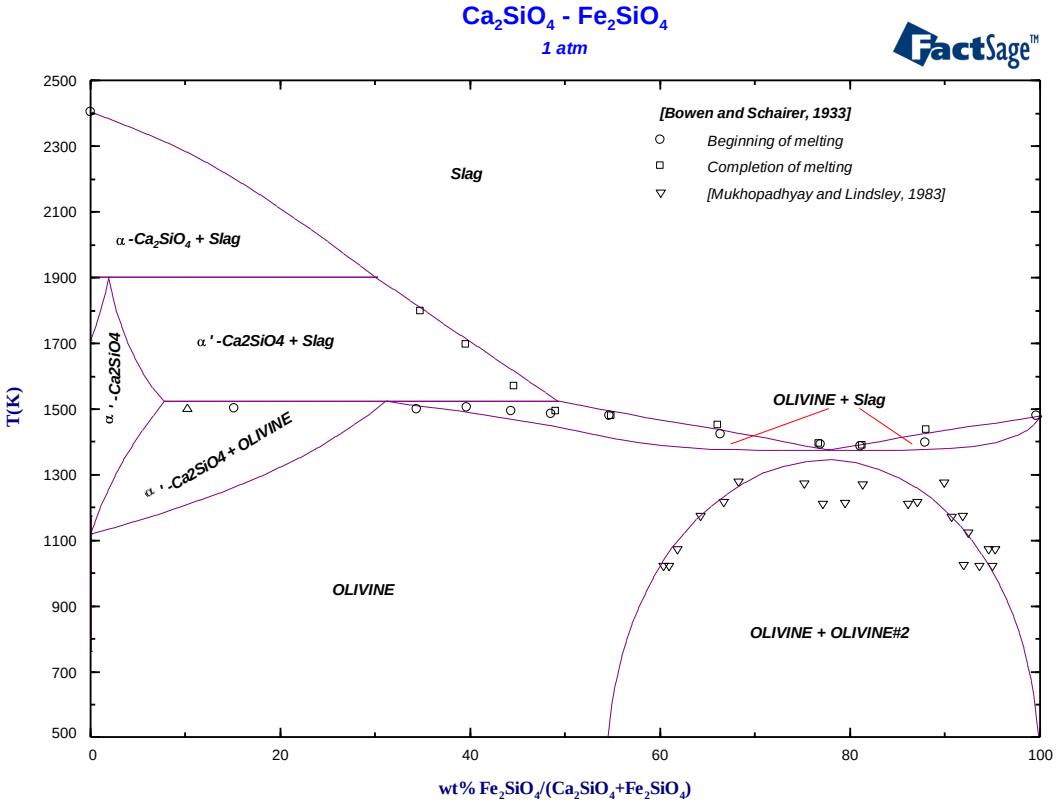

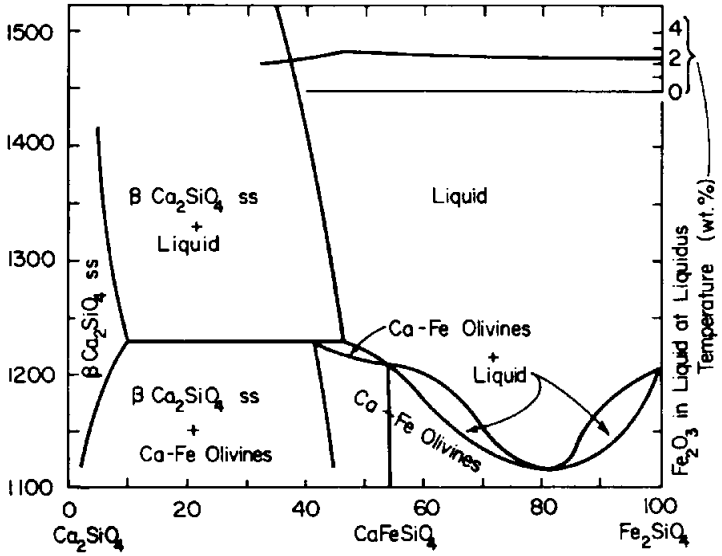

N.L. Bowen,, J.F. Schairer, E. Posnjak, Am. J. Sci., 226 (26),[1953], (1933), pp.193-284.

Weight percent
compared with experimental data

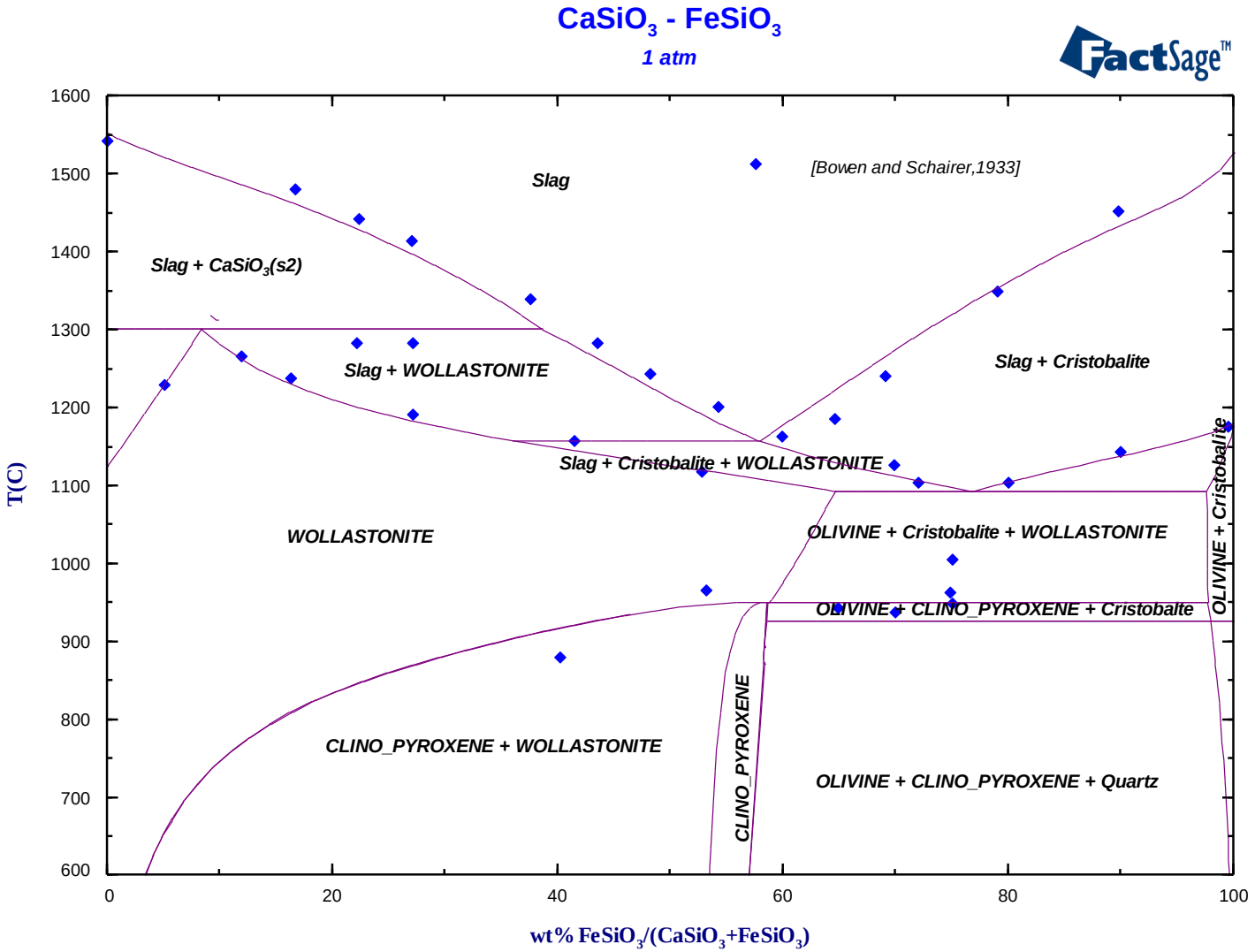

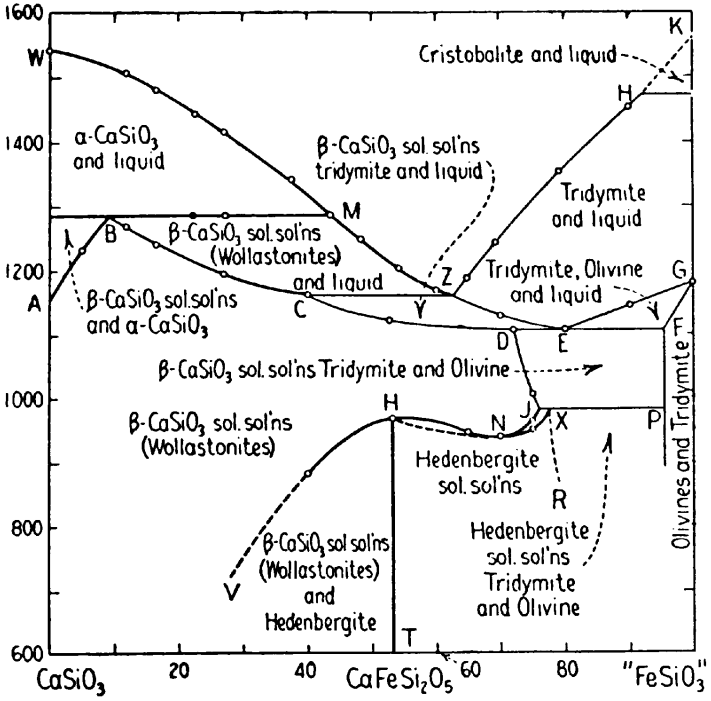

N.L. Bowen,, J.F. Schairer, E. Posnjak, Am. J. Sci., 226 (26),[1953], (1933), pp.193-284.

Weight percent
compared with experimental data

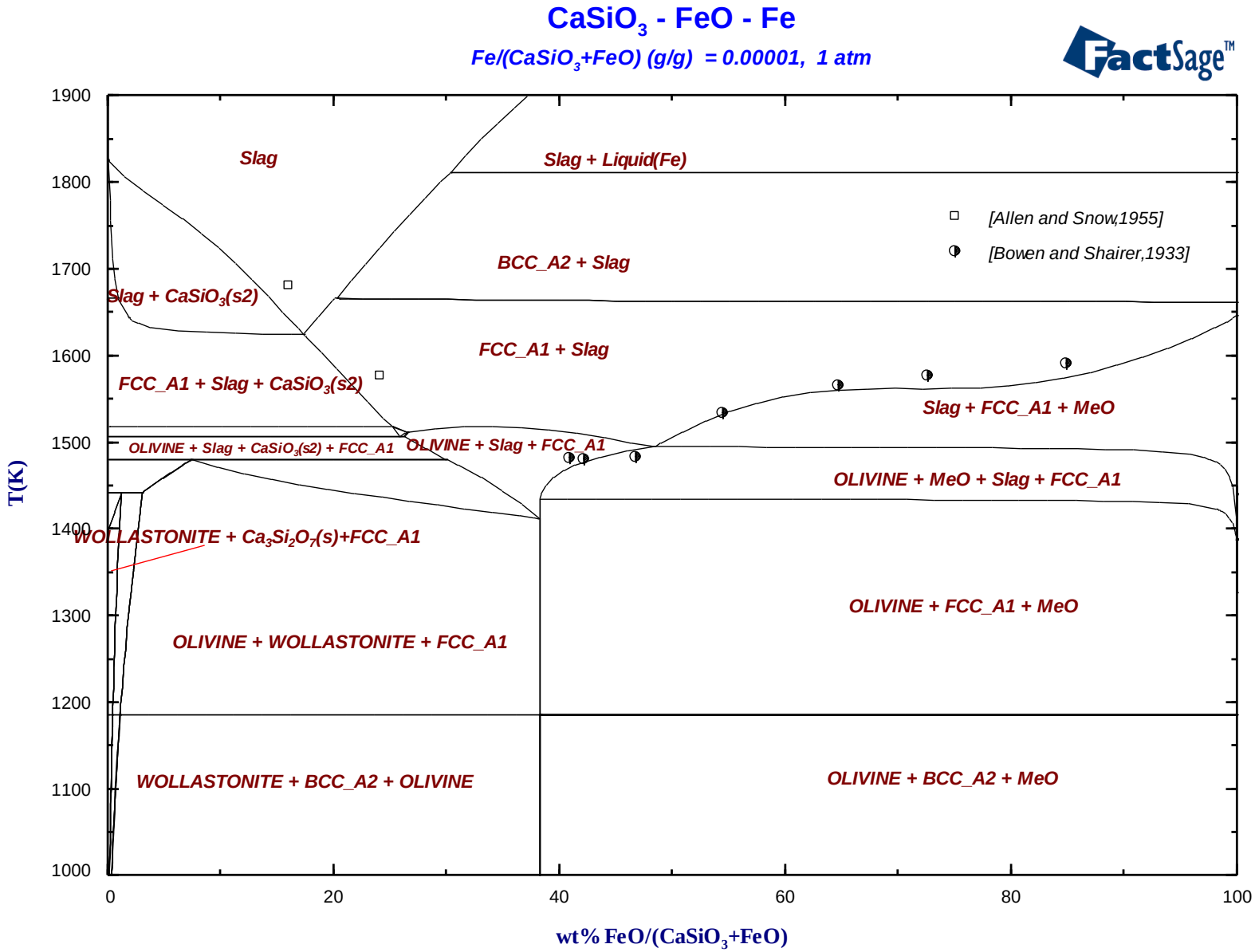

Weight percent
compared with experimental data

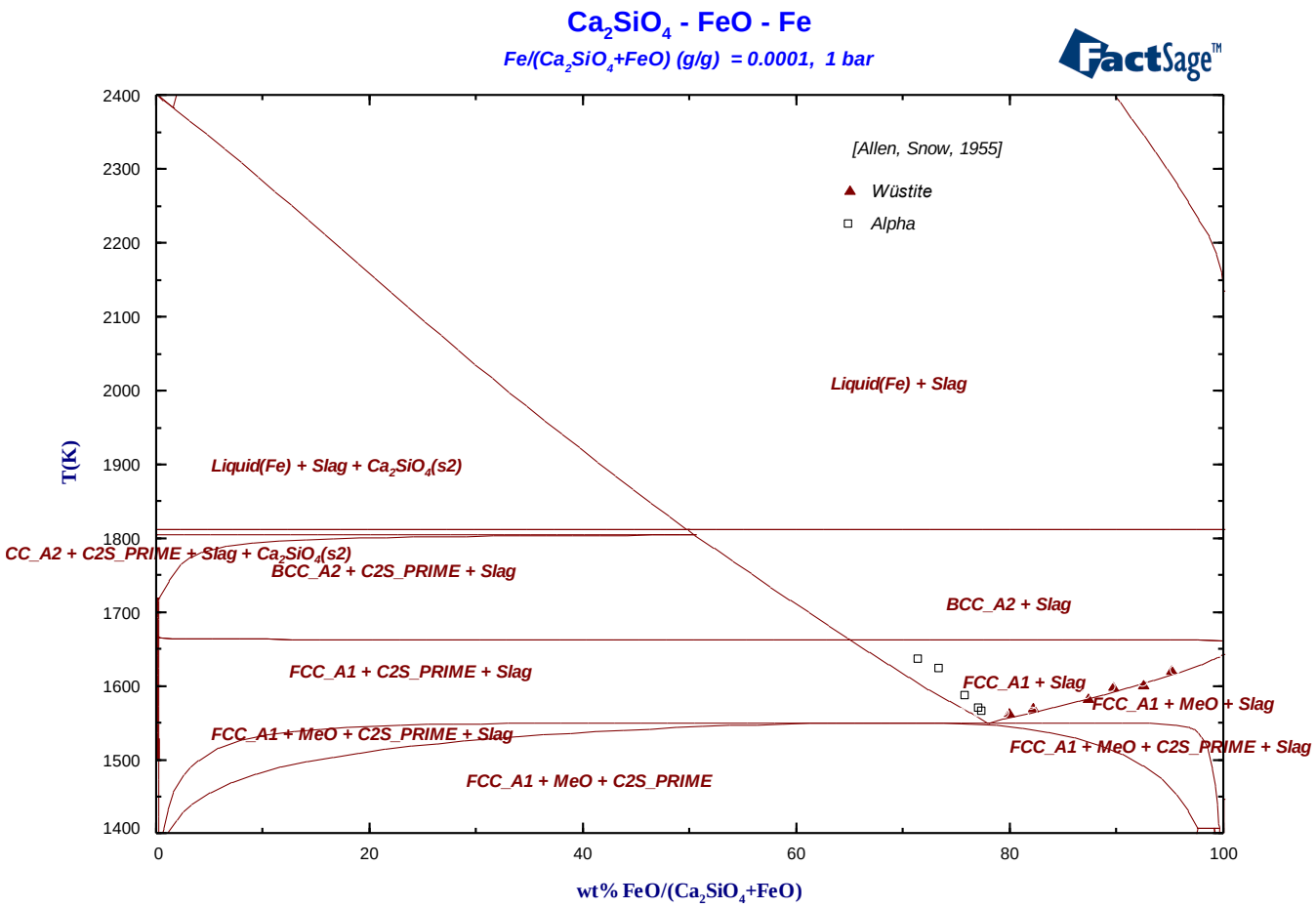

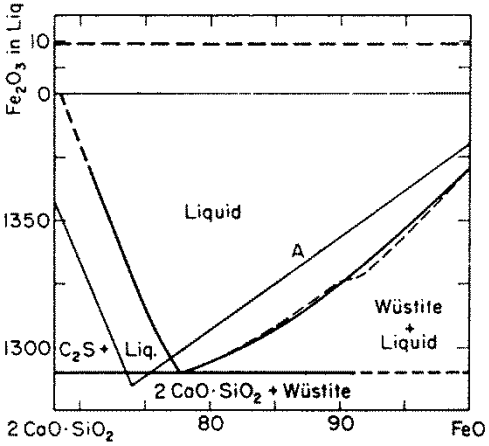

W.C: Allen, R,B, Snow, J. Am. Cer. Soc., vol.38, (1955), pp.264-280.

Weight percent
compared with experimental data

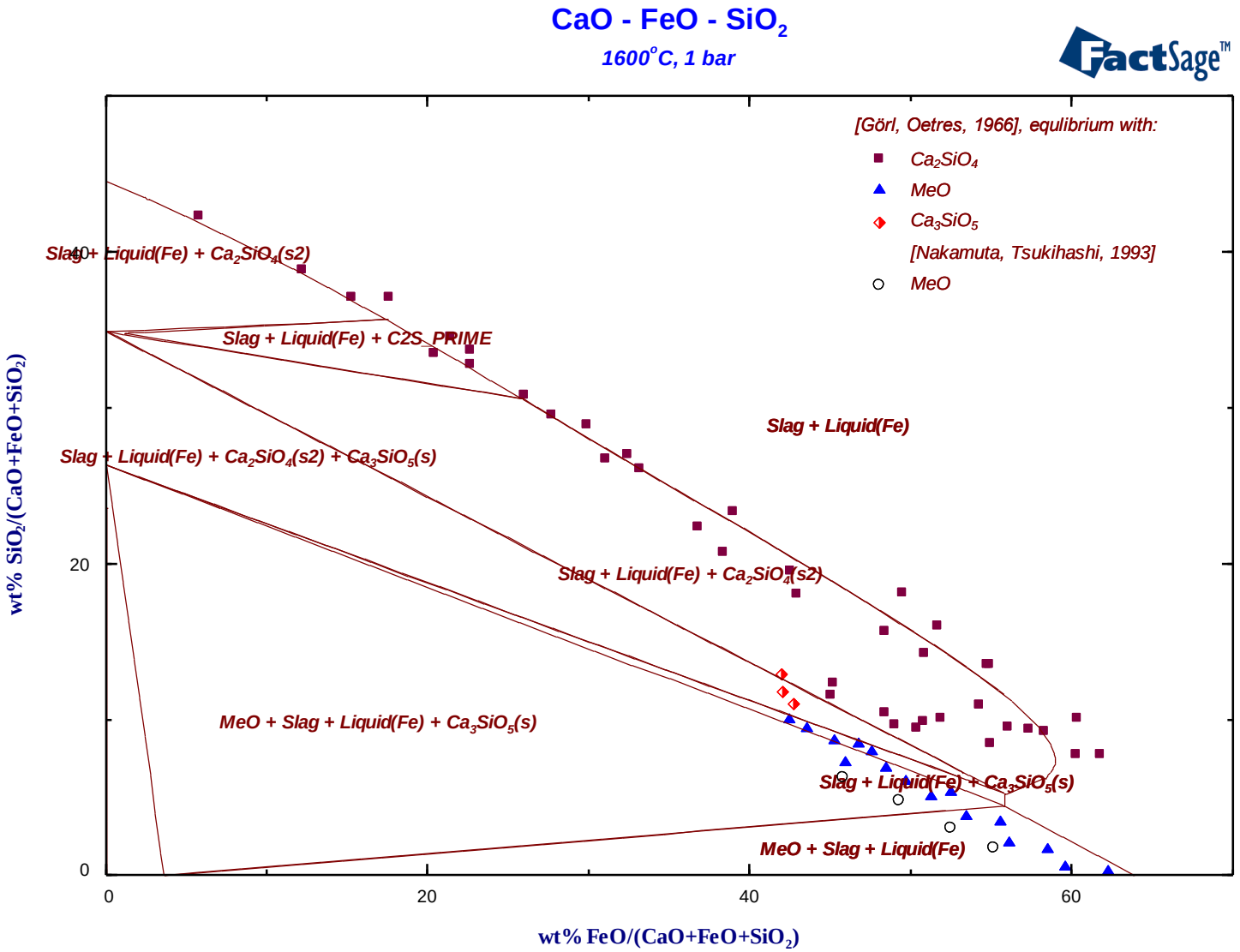

CaO-FeO-SiO2,
Weight percent
Liquiduslines 1200°C, 1300°C, 1400°C, 1650°C

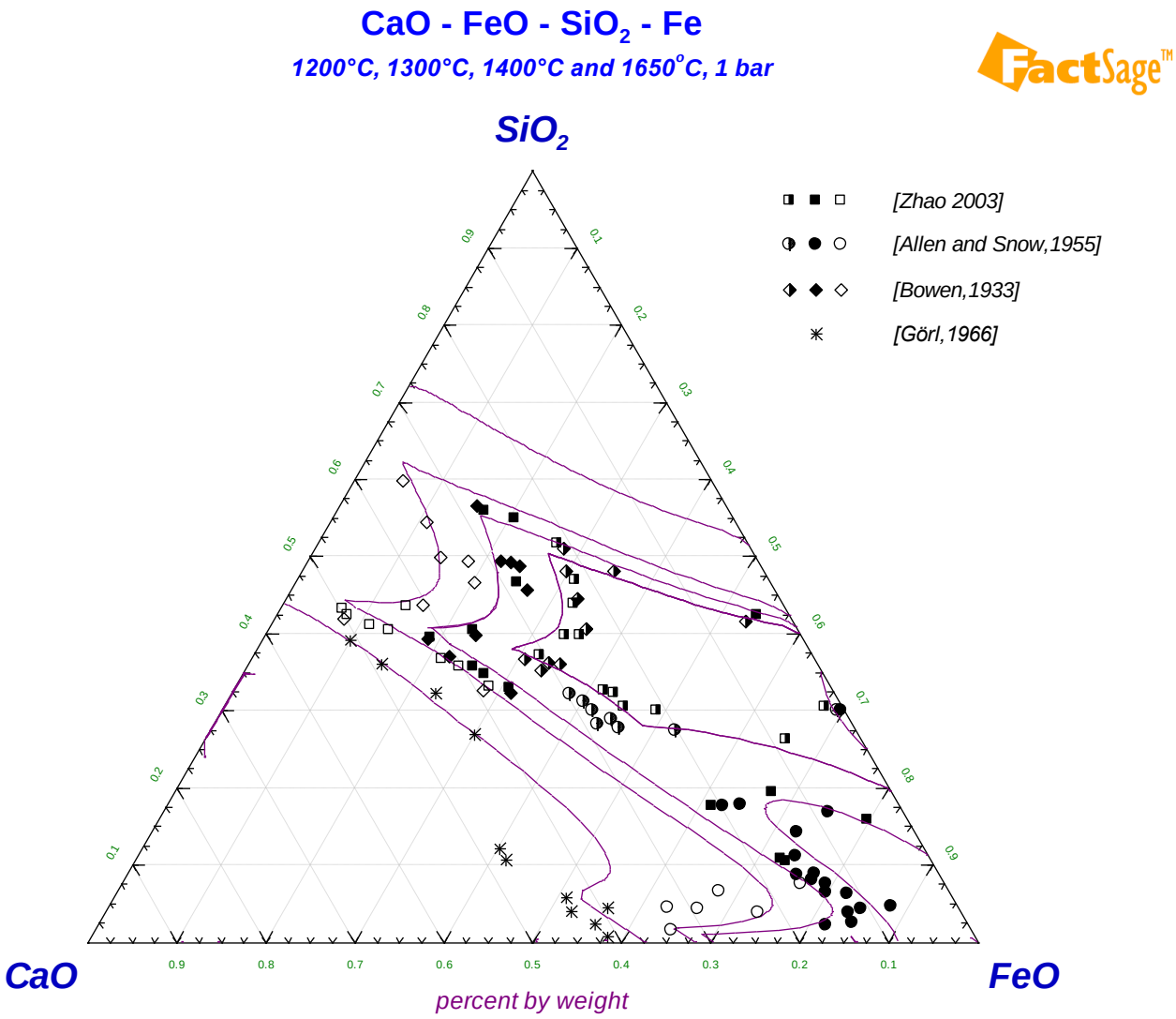

Mole fraction
Liquidussurface

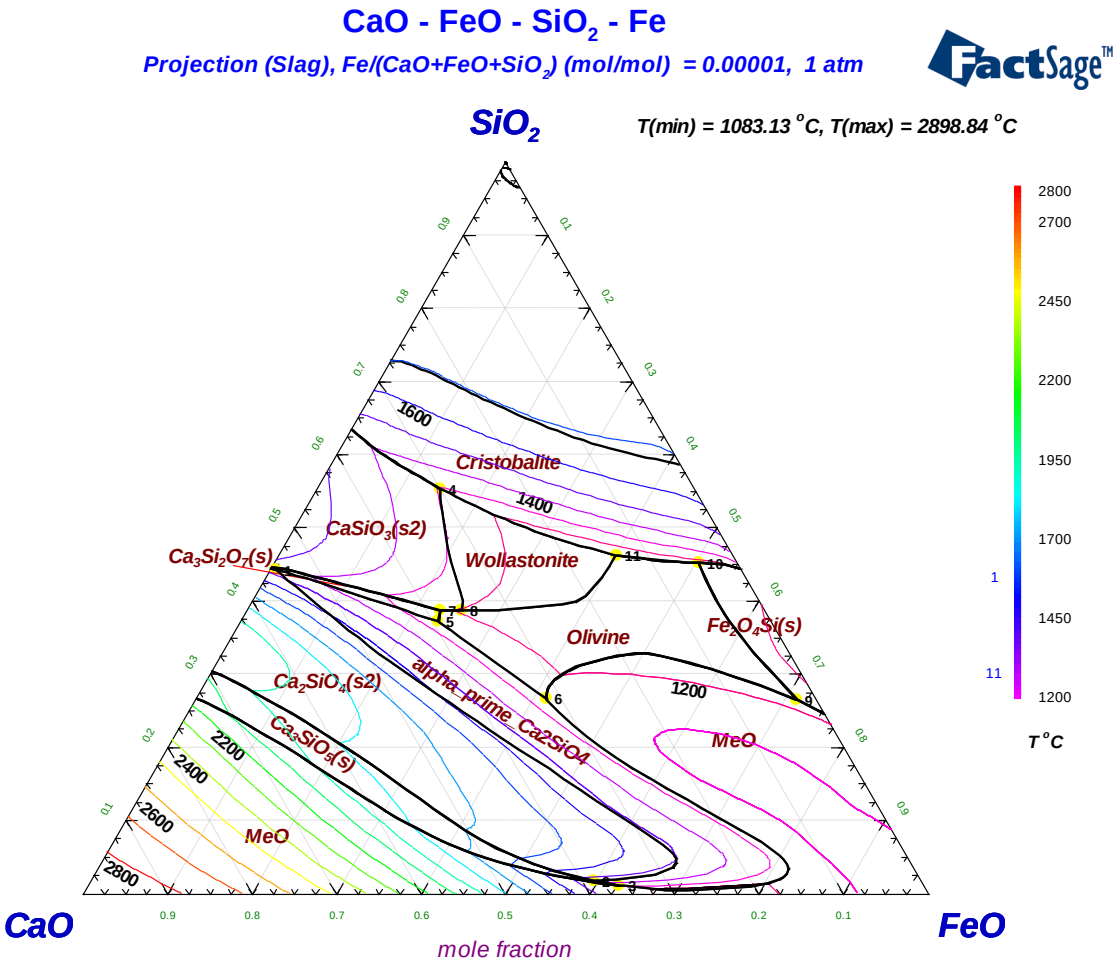

Weight percent,
Liquidussurface compared with experimental data

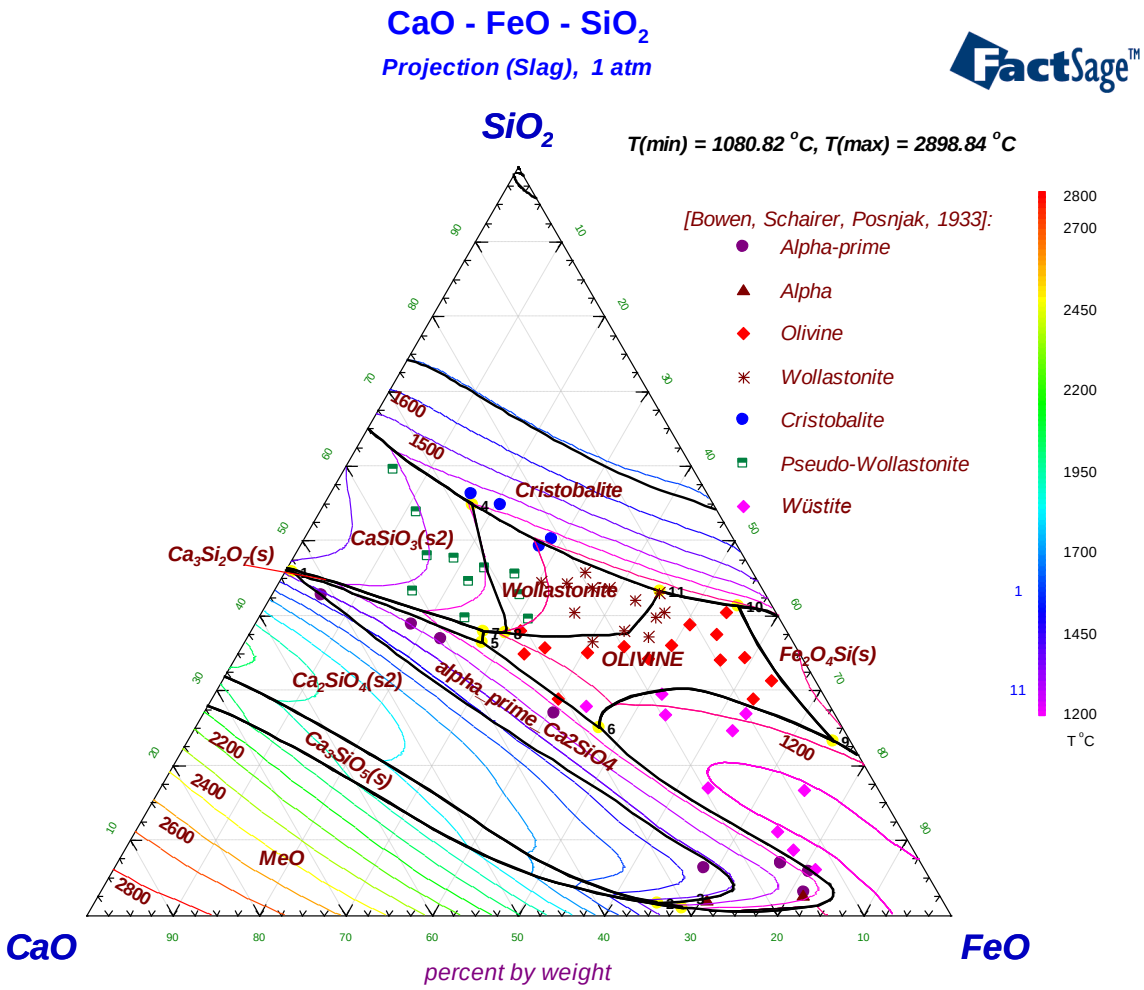

Invariant equilibria on the liquidus surface

Intersections with slag	Mole fraction A = SiO2, B = CaO, C = FeO				Weight percent A = SiO2, B = CaO, C = FeO			
	X(A)	X(B)	X(C)	T(C)	W(A)	W(B)	W(C)	T(C)
1: Ca2SiO4(s2) / Ca3Si2O7 / Ca2SiO4(s)	0.44200	0.55074	0.00726	1453.63	45.818	53.282	0.900	1453.63
2: Ca2SiO4(s2) / Ca3SiO5 / Ca2SiO4(s)	0.01768	0.38654	0.59578	1446.89	1.621	33.072	65.307	1446.87
3: Ca3SiO5 / MeO / Ca2SiO4(s)	0.01072	0.35915	0.63012	1324.28	0.976	30.490	68.534	1324.28
4: CaSiO3(s2) / Cristobalite / Wollastonite	0.55324	0.30080	0.14596	1291.12	54.858	27.837	17.305	1291.12
5: Ca3Si2O7 / OLIVINE / Ca2SiO4(s)	0.37134	0.39363	0.23503	1241.52	36.415	36.026	27.558	1241.52
6: MeO / OLIVINE / Ca2SiO4(s)	0.26565	0.31864	0.41571	1235.49	25.058	28.053	46.889	1235.50
7: Ca3Si2O7 / CaSiO3(s2) / OLIVINE	0.38681	0.38346	0.22974	1212.26	37.945	35.108	26.948	1212.31
8: CaSiO3(s2) / OLIVINE / Wollastonite	0.38652	0.35891	0.25457	1193.46	37.676	32.652	29.672	1193.46
9: Fe2O4Si / Me / OLIVINE	0.26483	0.02241	0.71276	1163.82	23.271	1.838	74.891	1163.83
10: Fe2O4Si / OLIVINE / Cristobalite	0.45140	0.04541	0.50319	1147.05	41.206	3.869	54.925	1147.05
11: OLIVINE / Cristobalite / Wollastonite	0.46202	0.13756	0.40042	1092.45	43.212	12.008	44.780	1092.44

CaO-Fe2O3-SiO2, Weight percent compared with experimental data

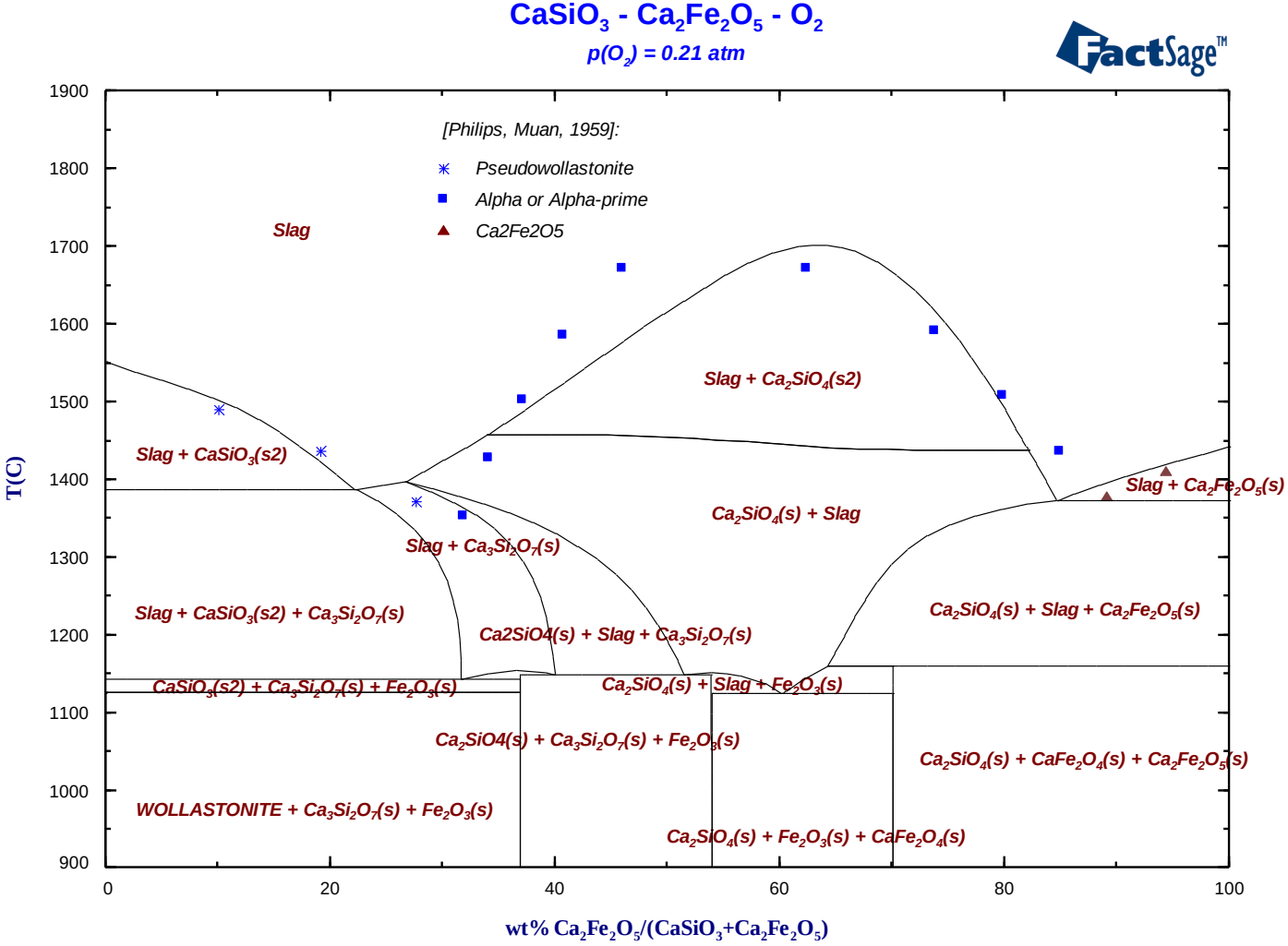

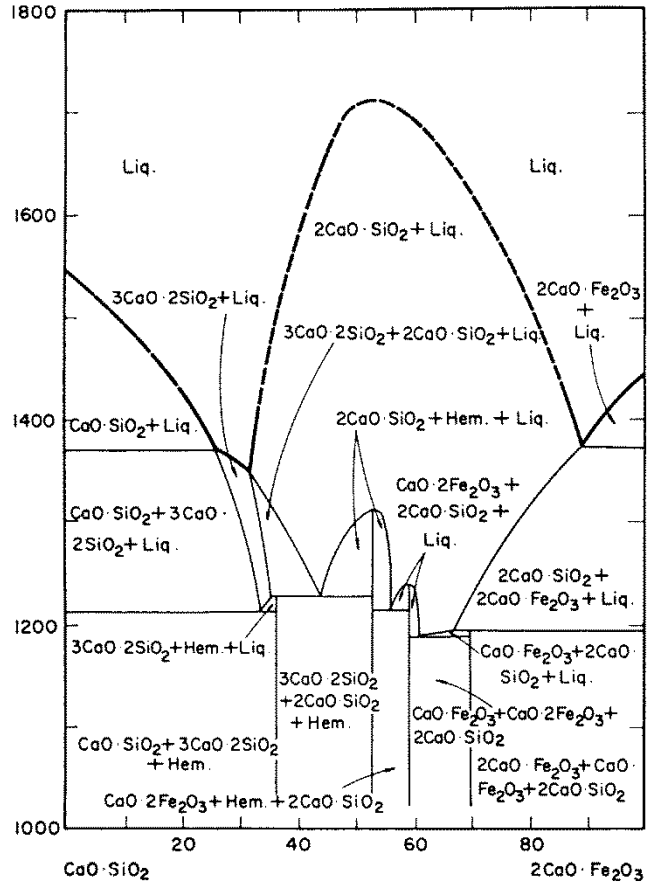

B. Philips, A. Muan, J. Am. Ceram. Soc., 42 [9], (1959), pp.413-423.

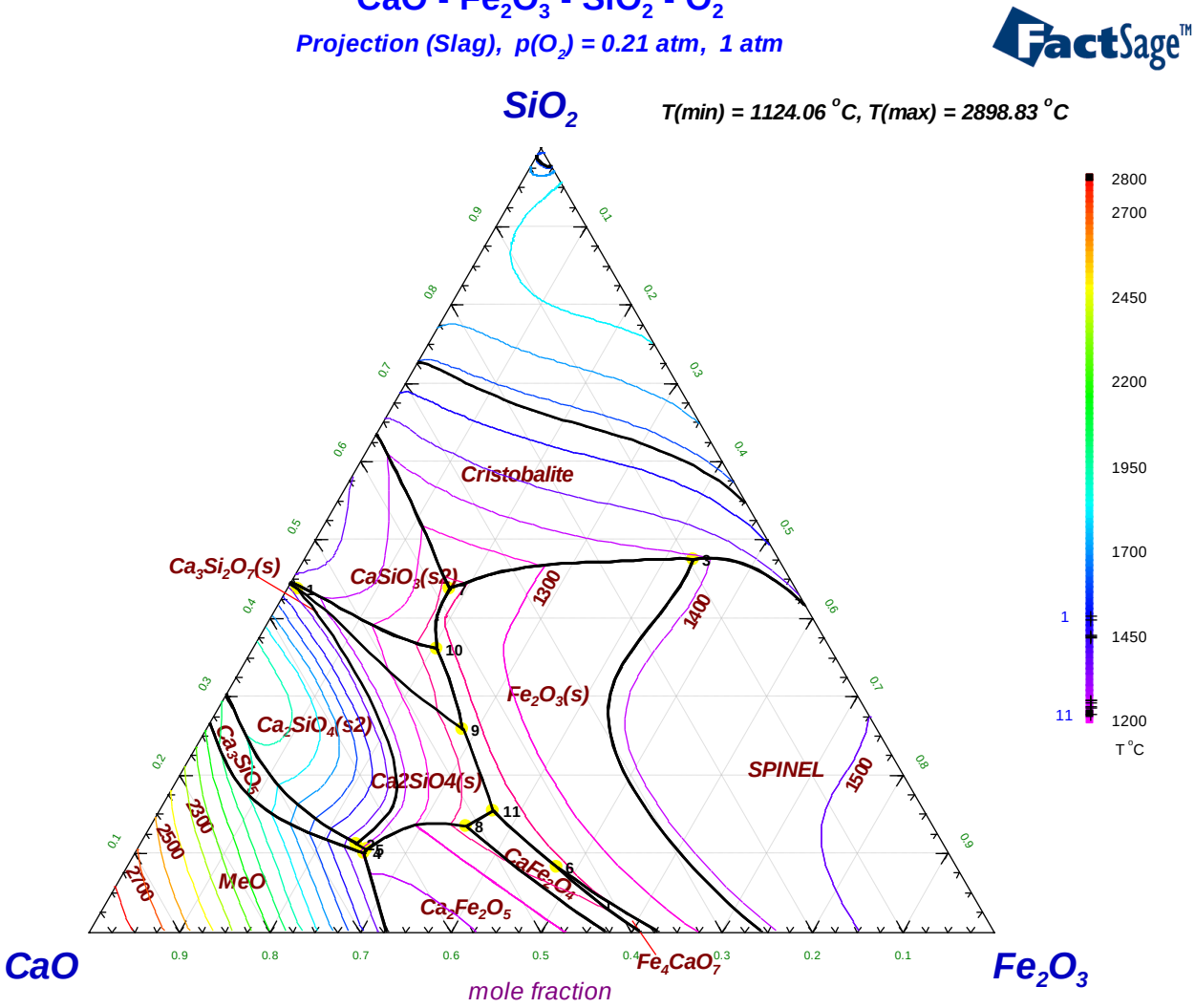
CaO - Fe2O3 - SiO2 - O2
Projection (Slag), p(O2) = 0.21 atm, 1 atm
FactSage™
SiO2
T(min) = 1124.06 °C, T(max) = 2898.83 °C
Cristobalite
Ca3Si2O7(s)
CaSiO3(s2)
Fe2O3(s)
Ca2SiO4(s2)
Ca3SiO5
Ca2SiO4(s)
SPINEL
MeO
CaFe2O4
Ca2Fe2O5
Fe4CaO7
1300
1400
1500
2300
2500
2700
2800
2700
2450
2200
1950
1700
1450
1200
T °C
CaO
Fe2O3
mole fraction

Weight percent,
Liquidussurface compared with experimental data

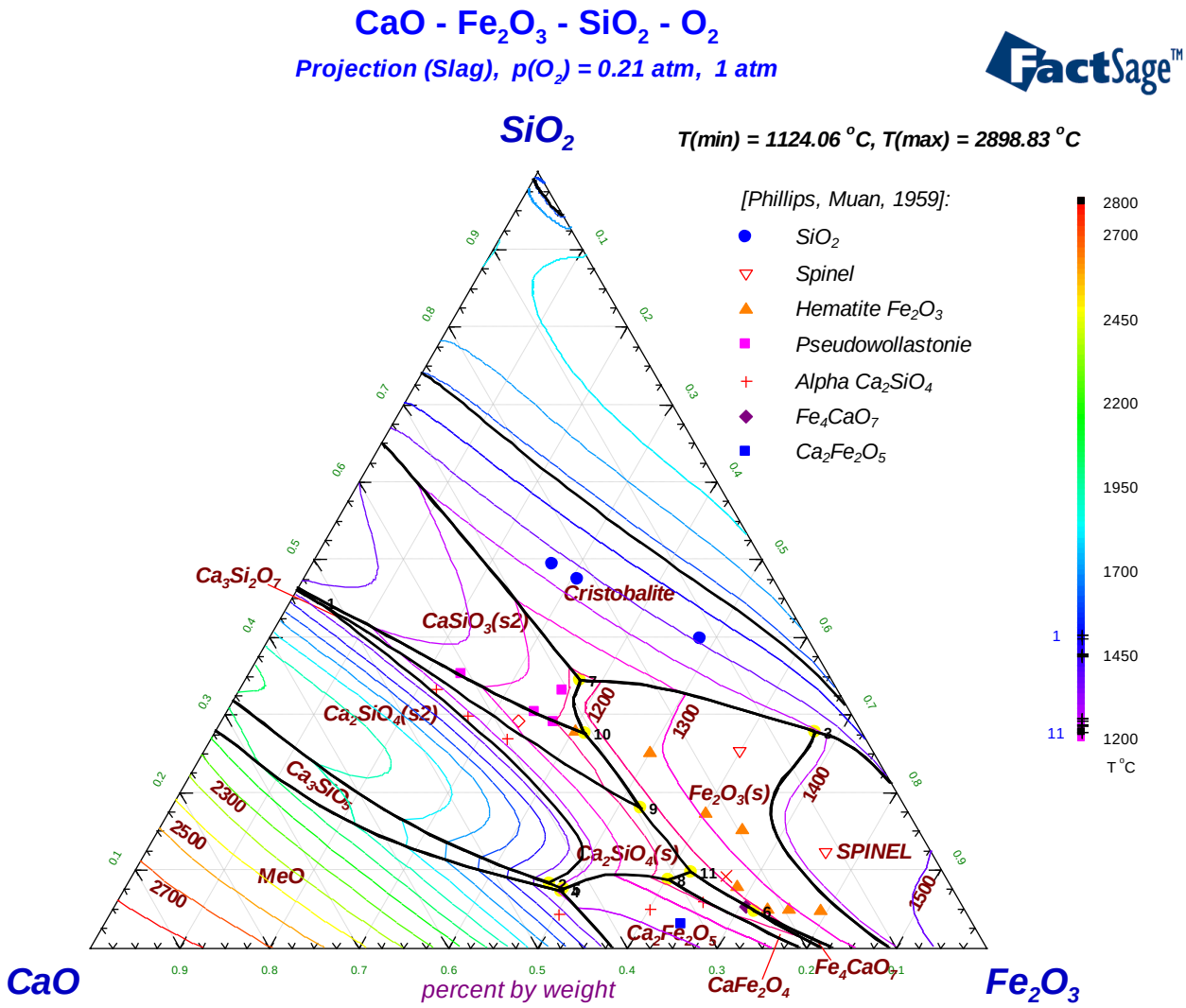

Invariant equilibria on the liquidus surface

Intersections with slag	Mole fraction A = SiO2, B = CaO, C = Fe2O3				Weight percent A = SiO2, B = CaO, C = Fe2O3			
	X(A)	X(B)	X(C)	T(C)	W(A)	W(B)	W(C)	T(C)
1: Ca2SiO4(s2) / Ca3Si2O7 / Ca2SiO4(s)	0.43684	0.55077	0.01239	1446.29	44.403	52.250	3.347	1446.29
2: Ca2SiO4(s2) / Ca3SiO5 / Ca2SiO4(s)	0.11227	0.64722	0.24051	1436.92	8.283	44.562	47.156	1436.92
3: Fe2O3 / SPINEL / Cristobalite	0.47545	0.09376	0.43079	1384.11	27.839	5.124	67.037	1384.11
4: Ca2Fe2O5 / Ca3SiO5 / MeO	0.09961	0.64586	0.25452	1381.65	7.224	43.717	49.059	1381.65
5: Ca2Fe2O5 / Ca3SiO5 / Ca2SiO4(s)	0.10463	0.64092	0.25445	1378.08	7.587	43.375	49.038	1378.08
6: CaSiO3(s2) / Fe2O3 / Cristobalite	0.08271	0.44141	0.47588	1168.83	4.701	23.415	71.884	1168.83
7: CaFe2O4_beta / Fe2O3 / Fe4CaO7	0.43802	0.38216	0.17981	1168.80	34.420	28.028	37.553	1168.80
8: Ca2Fe2O5 / CaFe2O4_beta / Ca2SiO4(s)	0.13460	0.51526	0.35014	1160.07	8.706	31.105	60.189	1160.07
9: Ca3Si2O7 / Fe2O3 / Ca2SiO4(s)	0.25846	0.45703	0.28450	1148.22	17.935	29.598	52.467	1148.21
10: Ca3Si2O7 / CaSiO3(s2) / Fe2O3	0.36137	0.43431	0.20432	1142.56	27.591	30.948	41.461	1142.59
11: CaFe2O4_beta(s) / Fe2O3 / Ca2SiO4(s)	0.15385	0.47534	0.37081	1124.06	9.719	28.025	62.256	1124.06

CaO-Fe2O3-TiO2,
Weight percent CaTiO3-Ca2Fe2O5
compared with experimental data

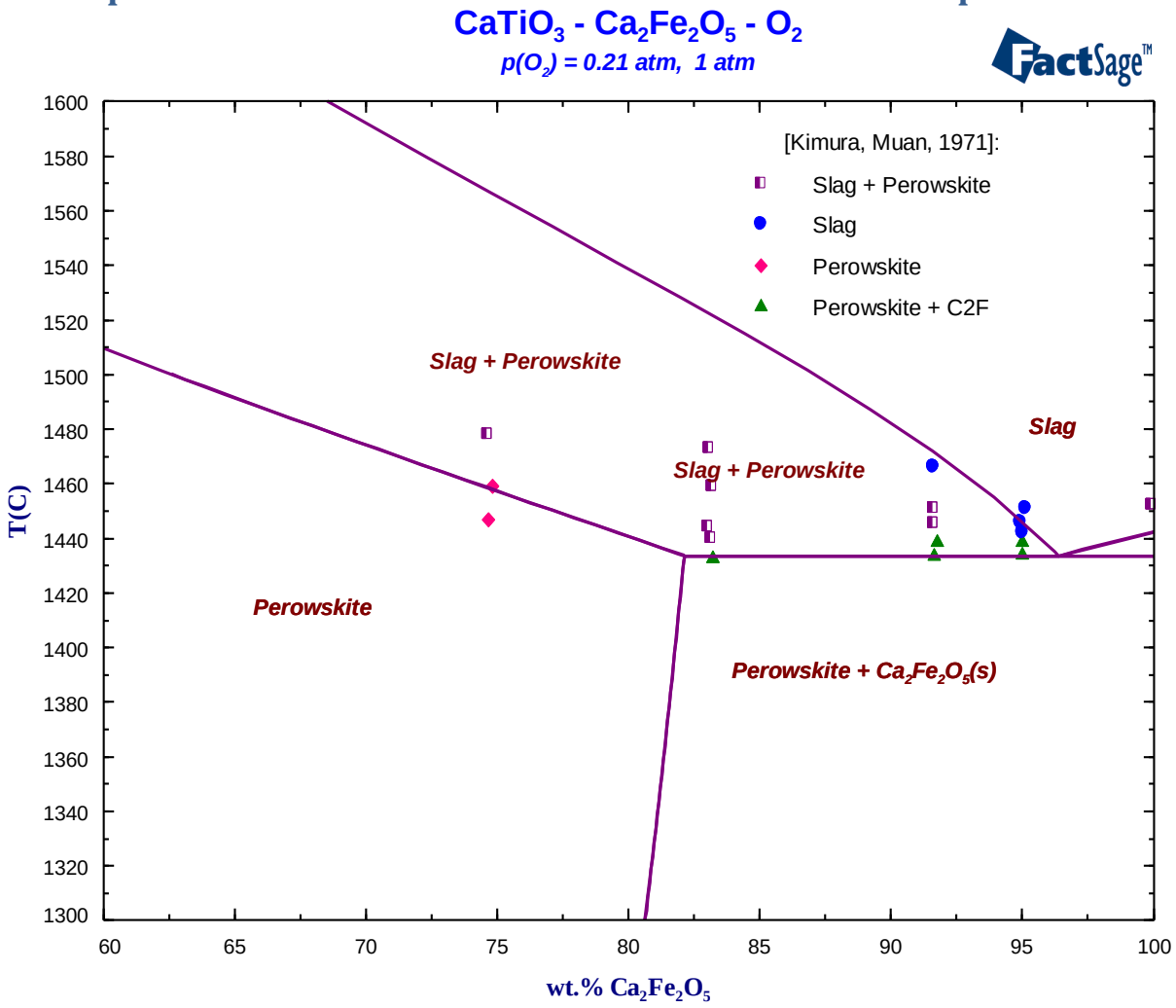

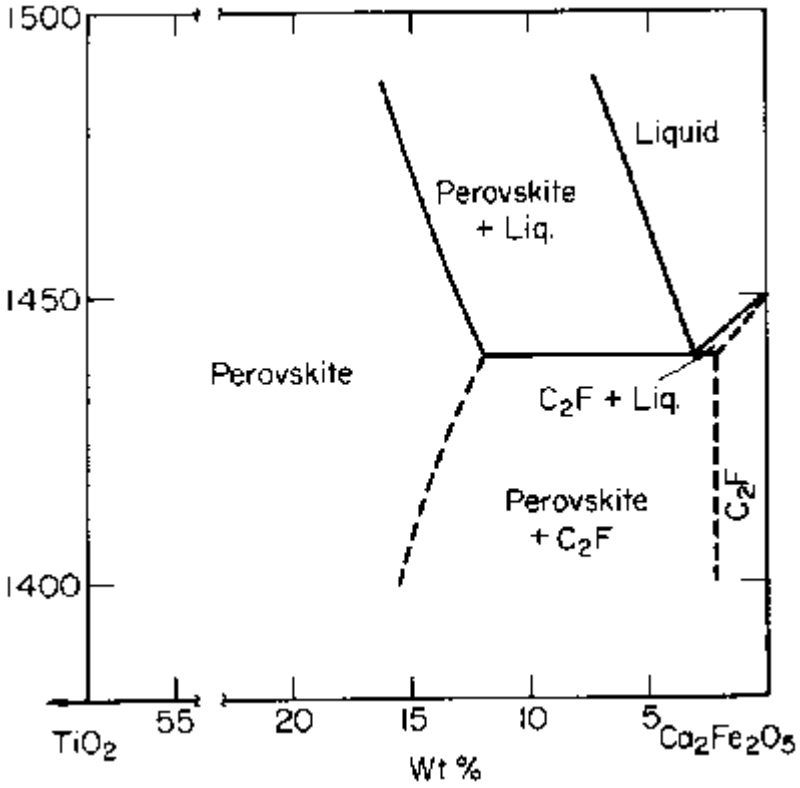

S. Kimura, A. Muan, Am. Mineralogist, 56, [7-8], (1971), pp.1330-1344.

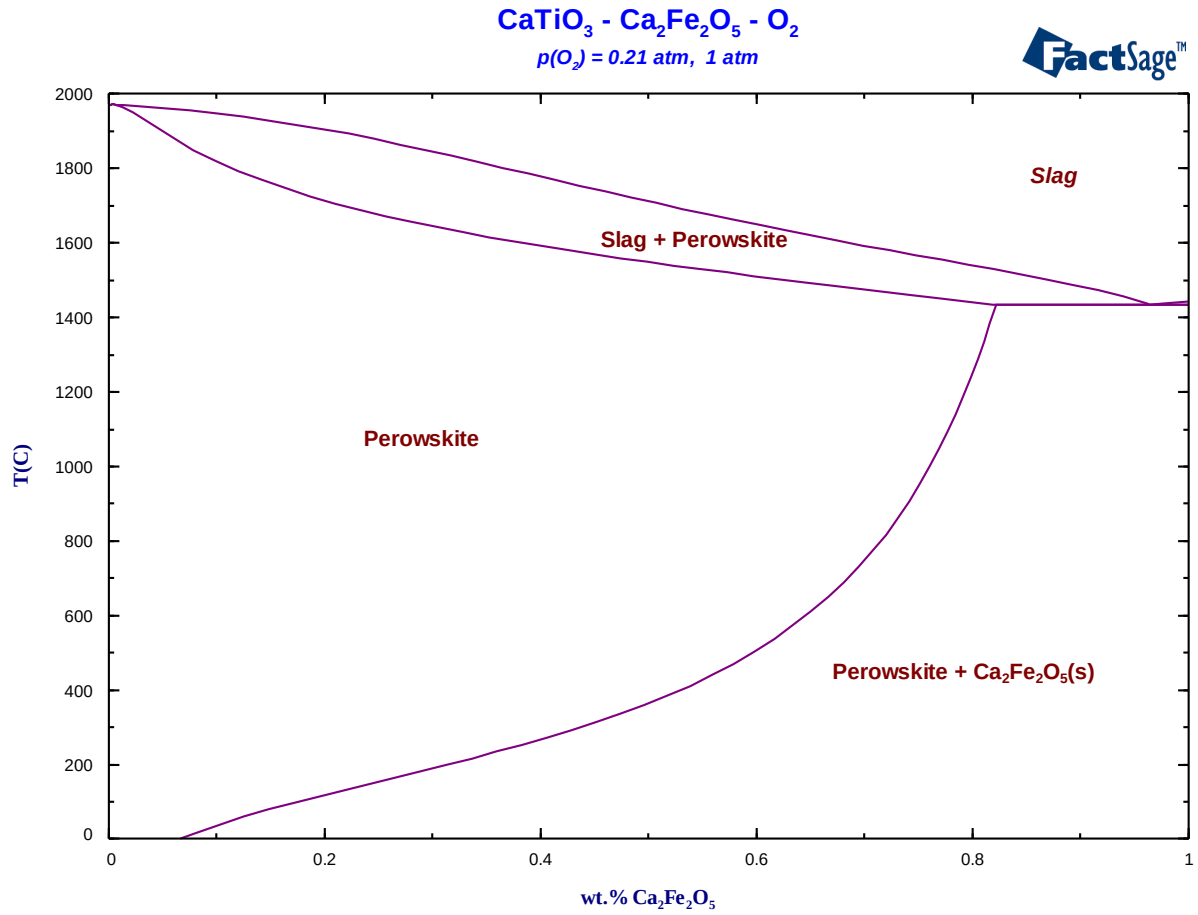
CaTiO3 - Ca2Fe2O5 - O2
p(O2) = 0.21 atm, 1 atm
FactSage™
Slag
Slag + Perowskite
Perowskite
Perowskite + Ca2Fe2O5(s)
T(C)
wt.% Ca2Fe2O5
2000
1800
1600
1400
1200
1000
800
600
400
200
0
0
0.2
0.4
0.6
0.8
1

CaO-Fe2O3-TiO2,
Mole fraction, Liquidus surface

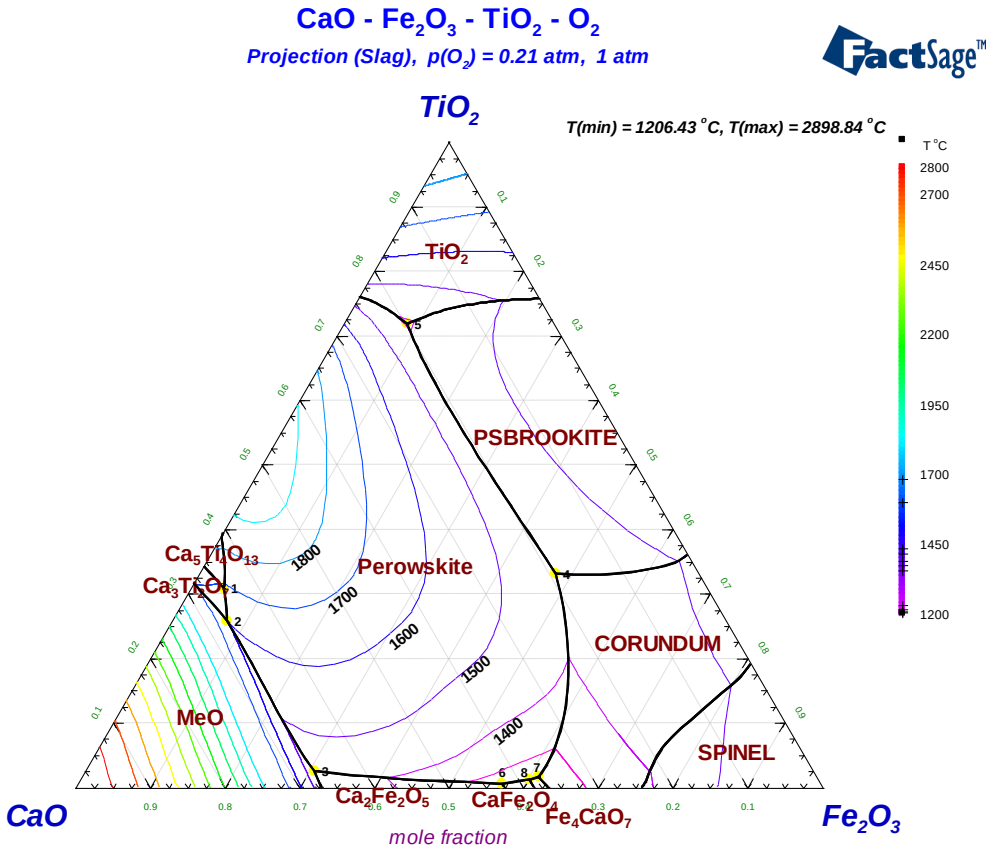

CaO-Fe2O3-TiO2,
Weight percent CaTiO3-Ca2Fe2O5

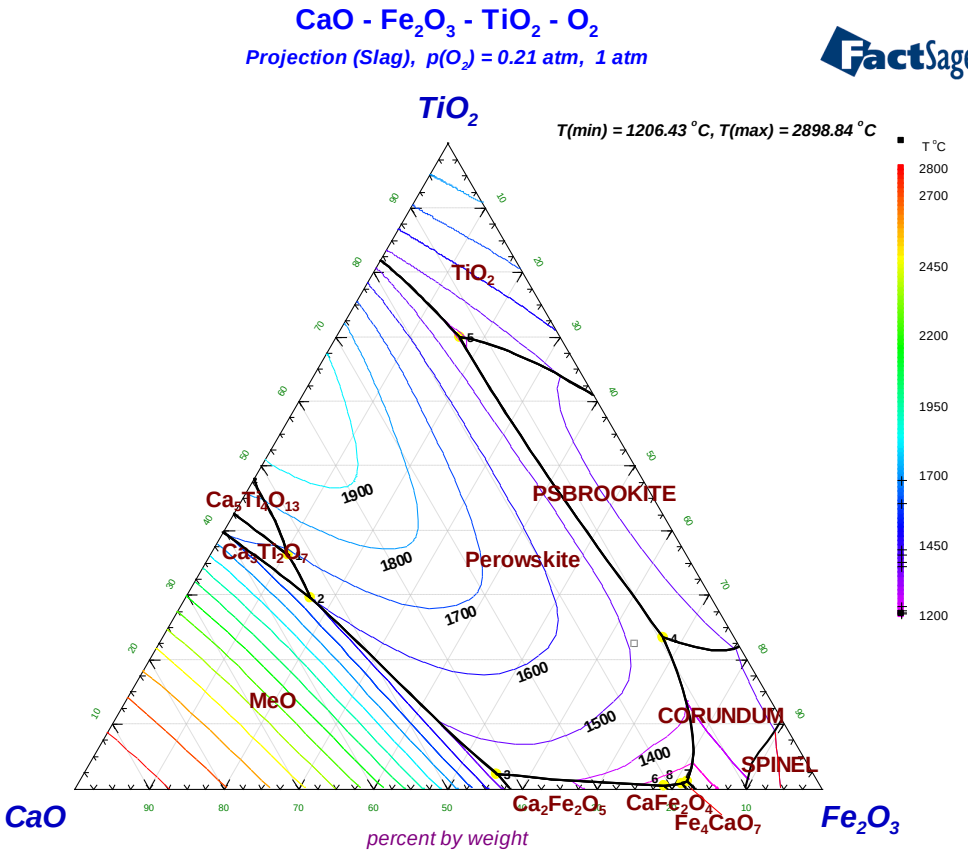

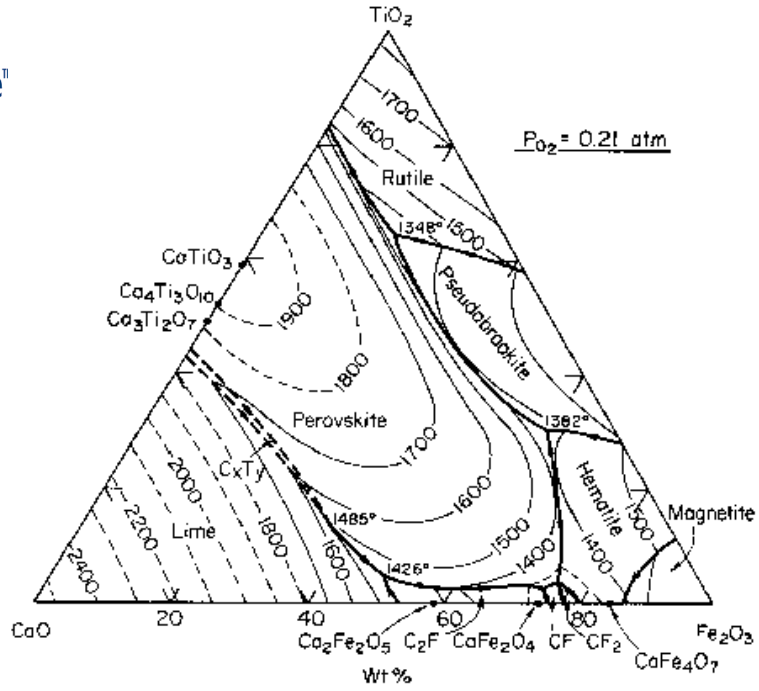

S. Kimura, A. Muan, Am. Mineralogist, 56, [7-8], (1971), pp.1330-1344.

Invariant equilibria on the liquidus surface

Intersections with slag	Mole fraction				Weight percent				
	A = TiO2, B = CaO, C = Fe2O3				A = TiO2, B = CaO, C = Fe2O3				
		X(A)	X(B)	X(C)	T(C)		W(A)	W(B)	W(C)	T(C)
1: Ca3Ti2O7 / Ca5Ti4O13 / Perowskite	1:	0.30835	0.64708	0.04457	1683.94	1:	36.199	53.338	10.463	1683.94
2: Ca3Ti2O7 / MeO#1 / Perowskite	2:	0.25823	0.66809	0.07368	1601.50	2:	29.524	53.632	16.844	1601.50
3: Ca2Fe2O5 / MeO#1 / Perowskite	3:	0.02512	0.66746	0.30742	1433.02	3:	2.266	42.280	55.454	1433.03
4: CORUNDUM / PSBROOKITE / Perowskite	4:	0.33163	0.19114	0.47723	1414.75	4:	23.354	9.451	67.195	1414.75
5: PSBROOKITE / Perowskite / TiO2	5:	0.71854	0.19638	0.08508	1388.05	5:	69.996	13.432	16.572	1388.05
6: Ca2Fe2O5 / CaFe2O4 / Perowskite	6:	0.00017	0.24183	0.75800	1355.27	6:	0.427	20.782	78.791	1231.38
7: CORUNDUM / Fe4CaO7 / Perowskite	7:	0.01640	0.37153	0.61207	1210.11	7:	1.093	17.379	81.529	1210.07
8: CaFe2O4 / Fe4CaO7 / Perowskite	8:	0.01178	0.38608	0.60214	1206.44	8:	0.792	18.232	80.975	1206.43

CaO-Fe2O3-V2O5,
Mole fraction, 600°C

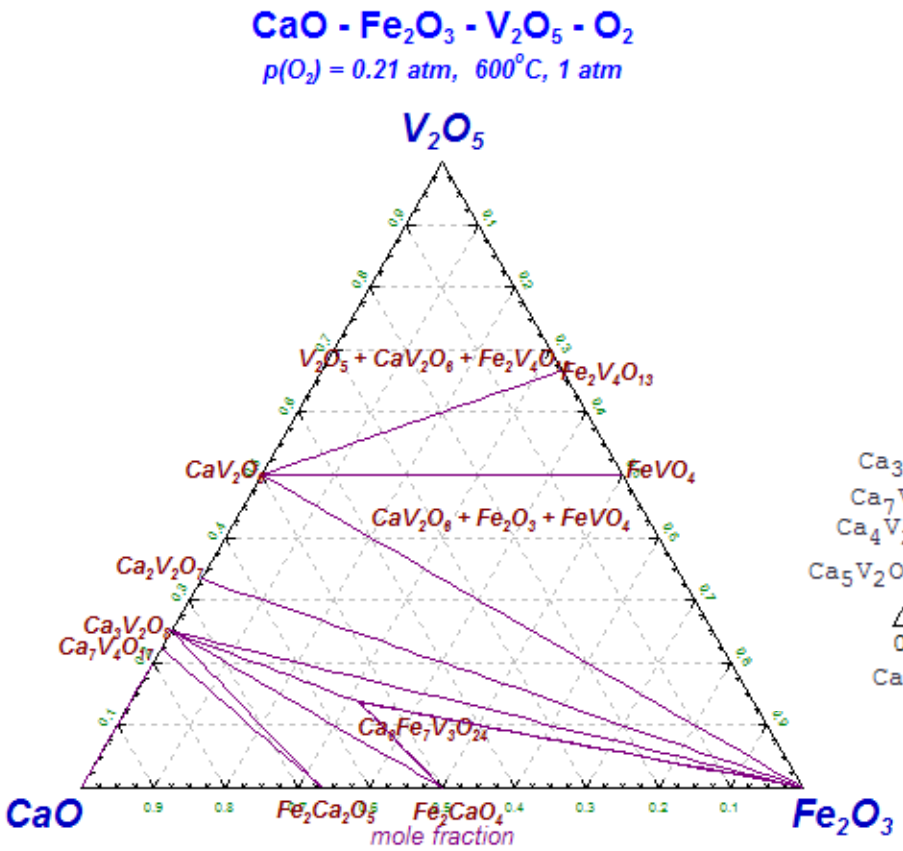

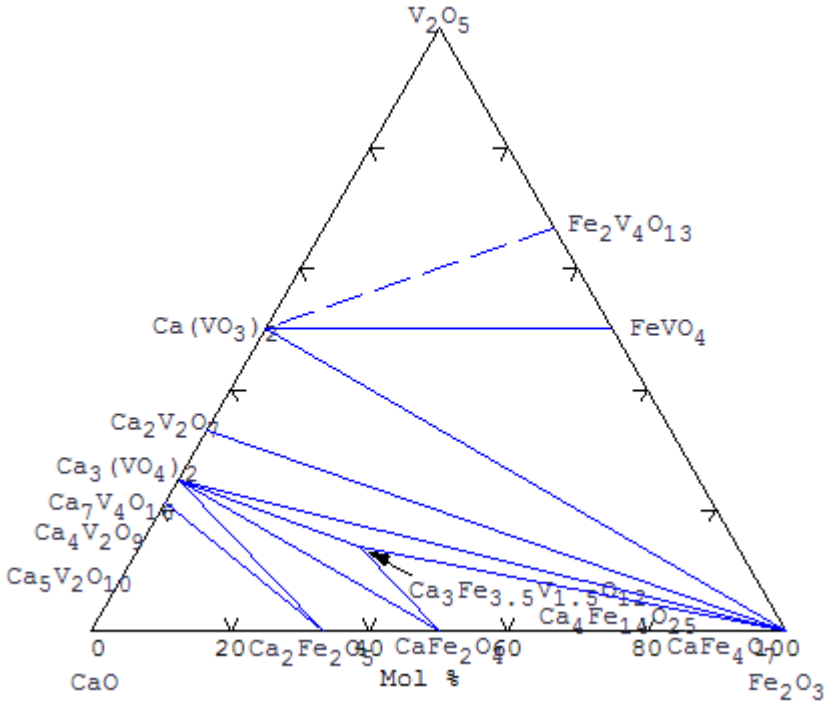

B.V. Slobodin, A.A. Fotiev, S.F. Blinova, Zh. Neorg. Khim., 24 [8], (1979), pp. 2276-2278.

Ternary phases

Phase	Description	Used data
CKP	$CaK_2P_2O_7$	GTT
C2KP3	$CaKP_3O_9$	GTT
C2KP	$CaKPO_4$	GTT
K3P-LT	$(K_2O)_2(P_2O_5)(K_2O,CaO,K_2CaO_2)$	$CaK_4P_2O_8$(s1)-GTT $CaK_6P_2O_9$(s1)-GTT K_3PO_4(s1) IEK-2
K3P-MT	$(K_2O)_2(P_2O_5)(K_2O,CaO,K_2CaO_2)$	$CaK_4P_2O_8$(s2) GTT $CaK_6P_2O_9$(s2) GTT K_3PO_4(s2) IEK-2
	H_{tr} (s1→s2) is proposed to be equal to K_3PO_4	
K3P-HT	$(K_2O)_2(P_2O_5)(K_2O,CaO,K_2CaO_2)$	$CaK_4P_2O_8$(s3) GTT $CaK_6P_2O_9$(s3) GTT K_3PO_4(s3) IEK-2
	H_{tr} (s2→s3) is proposed to be equal to K_3PO_4	

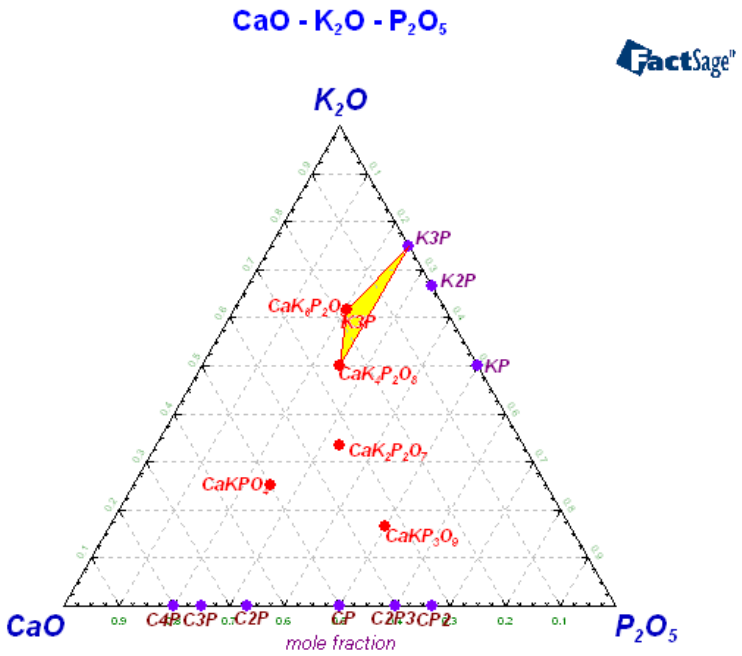

Weight percent, Isopleth CaP2O6-KPO3

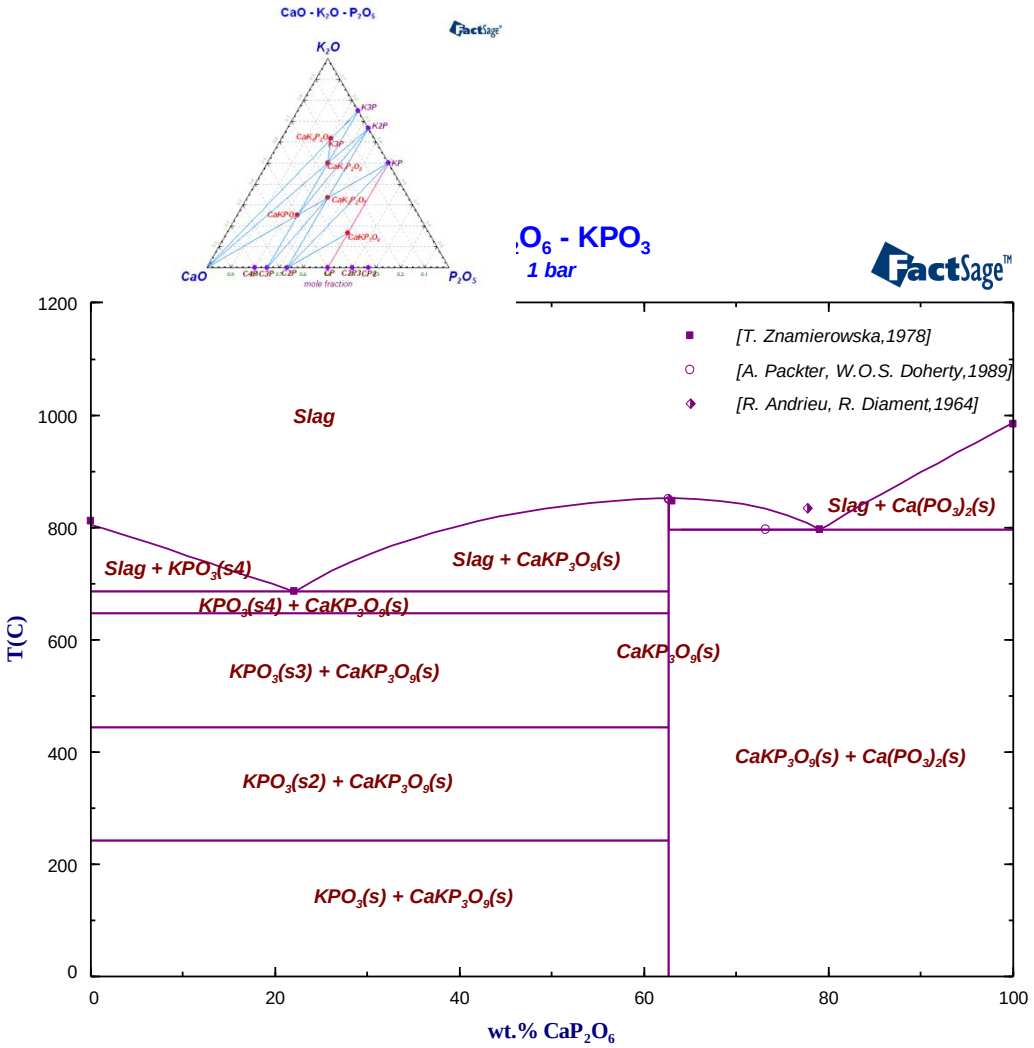

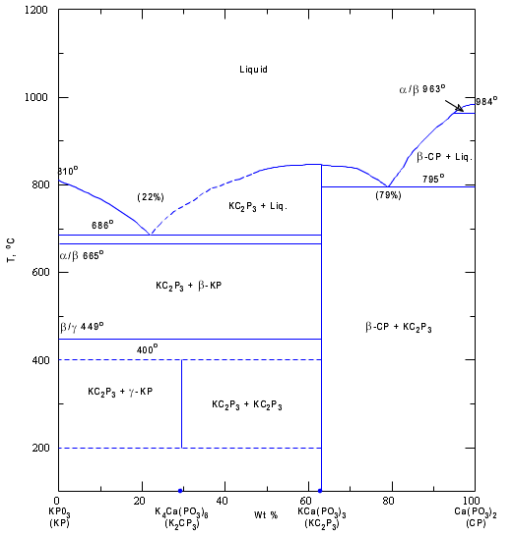

T. Znamierowska-Kubicka, Rocz. Chem., 51 [11] 2089-2098 (1977).

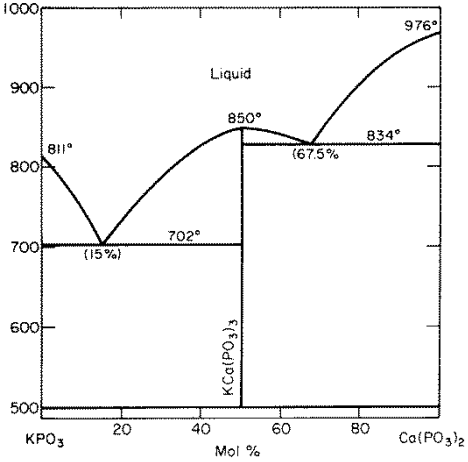

R. Andrieu and R. Diament, C. R. Hebd. Seances Acad. Sci., 259 [25] 4708-4711 (1964).

Weight percent, Isopleth Ca2P2O7-CaKP3O9

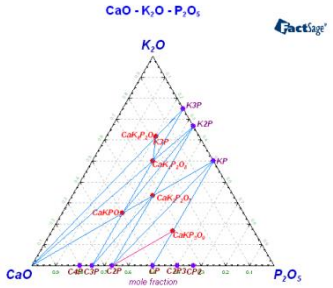

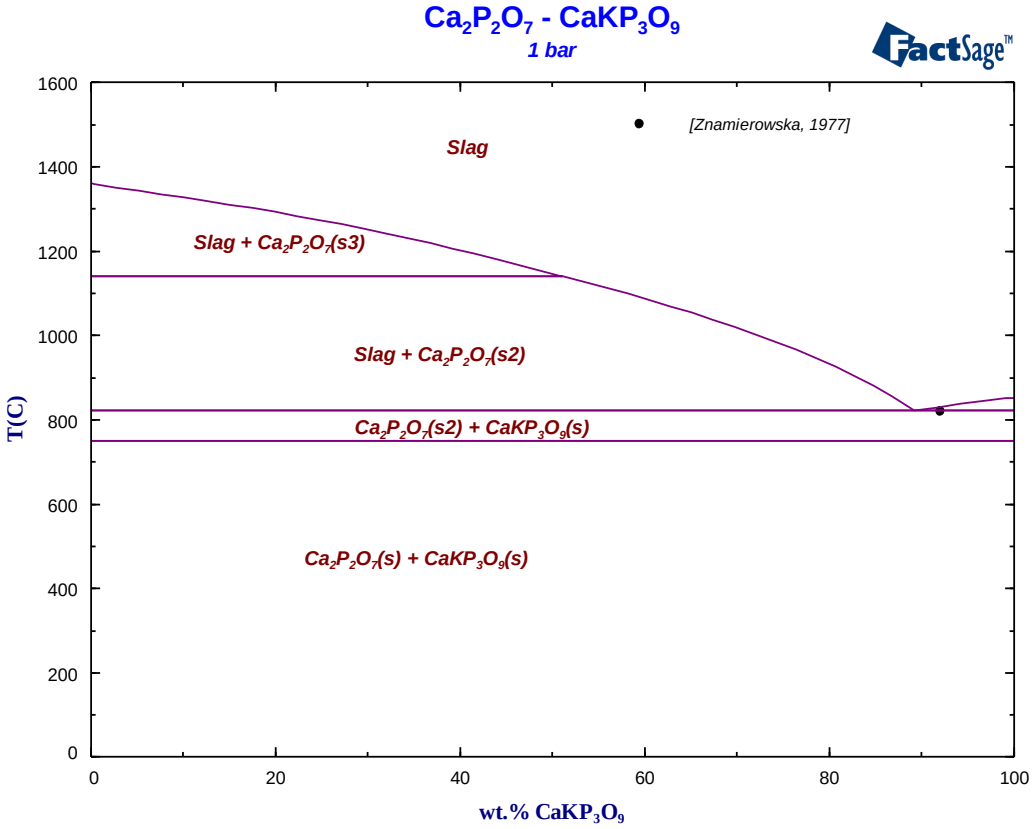

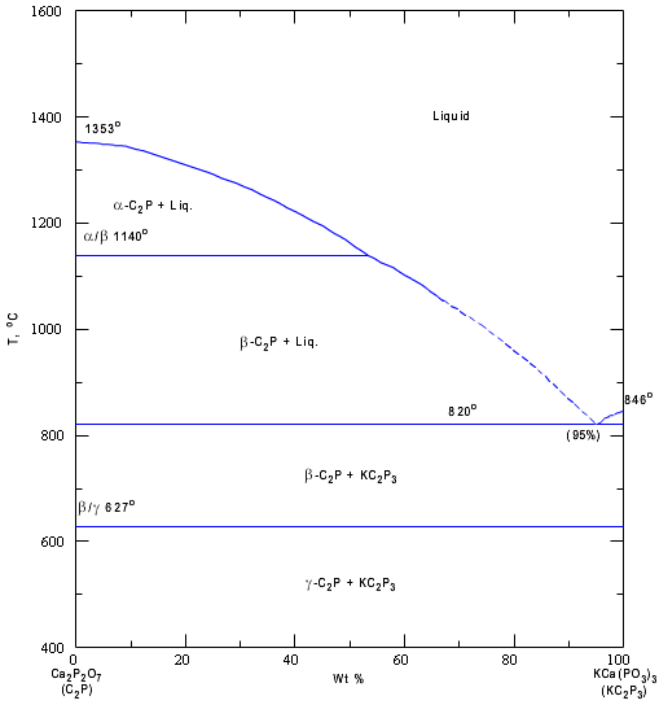

T. Znamierowska-Kubicka, Rocz. Chem., 51 [11] 2089-2098 (1977).

Weight percent, Isopleth Ca2P2O7-K4P2O7

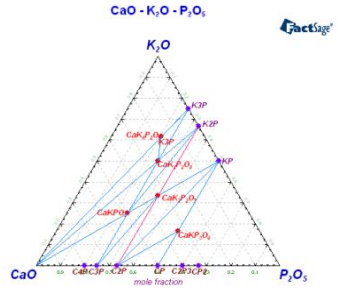

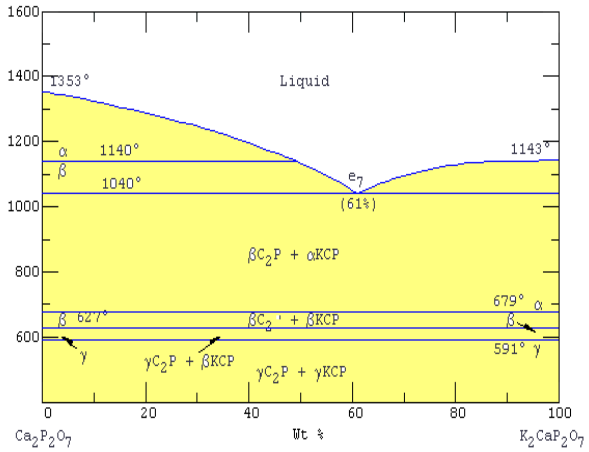

T. Znamierowska, Pol. J. Chem., 52 [6] 1127-1134 (1978).

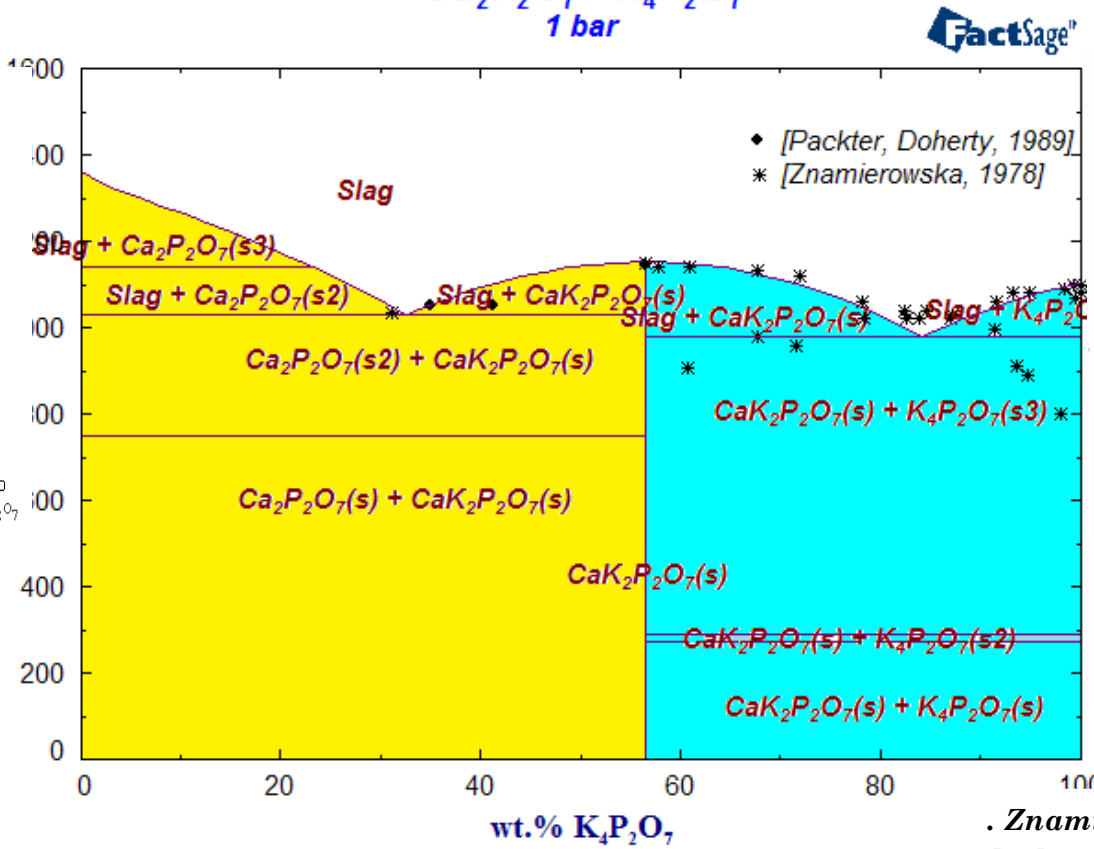

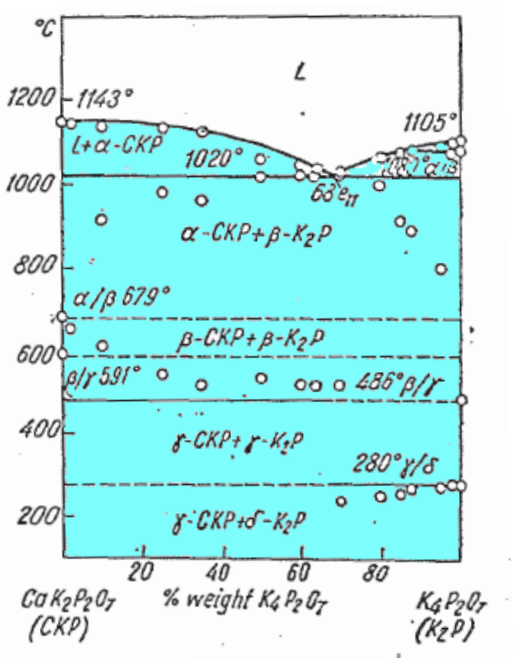

. Znamierowska, Pol. J. Chem., 52 [10] 1889-1895 (1978).

Weight percent, Isopleth K2CaP2O7-KPO3

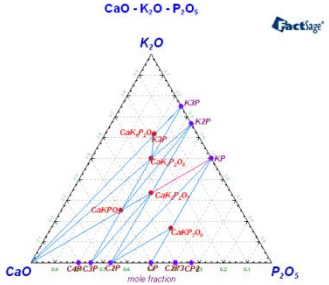

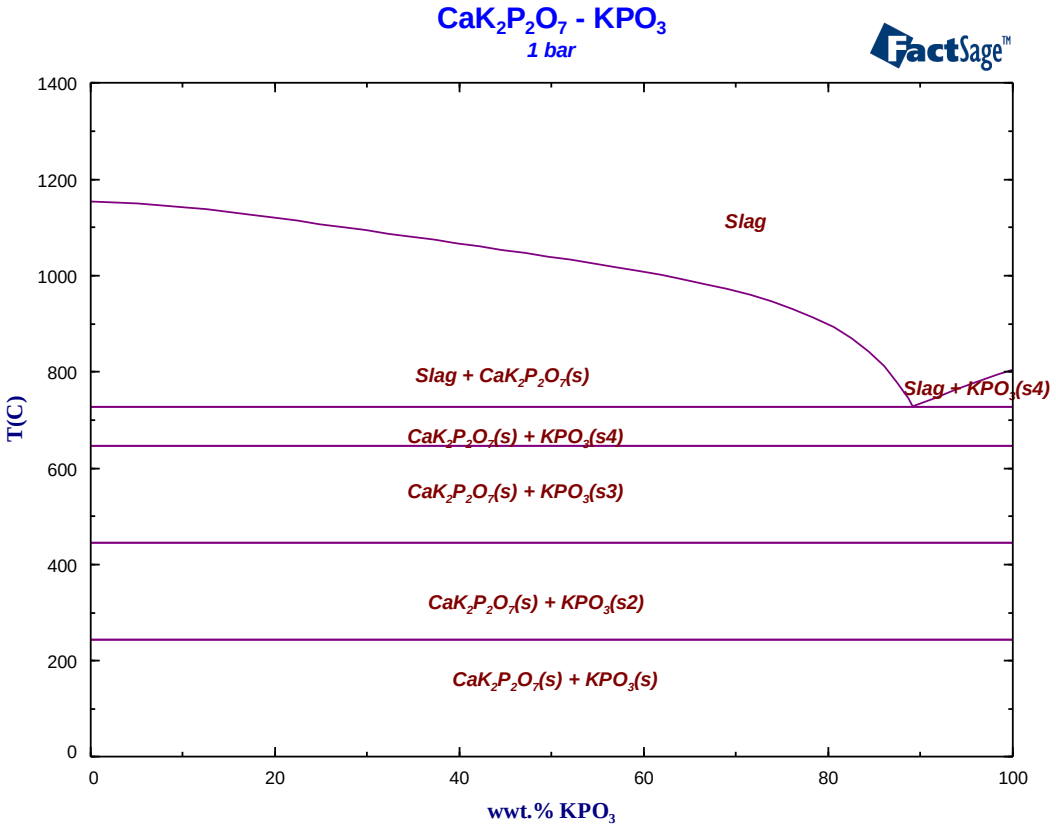

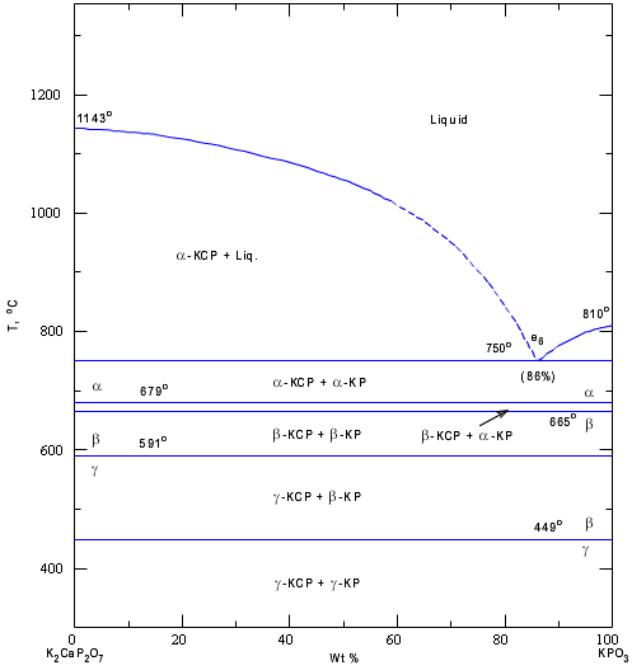

T. Znamierowska, Pol. J. Chem., 52 [6] 1127-1134 (1978).

Weight percent, Isopleth K2CaP2O7-K5P3O10

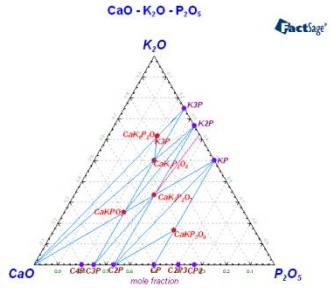

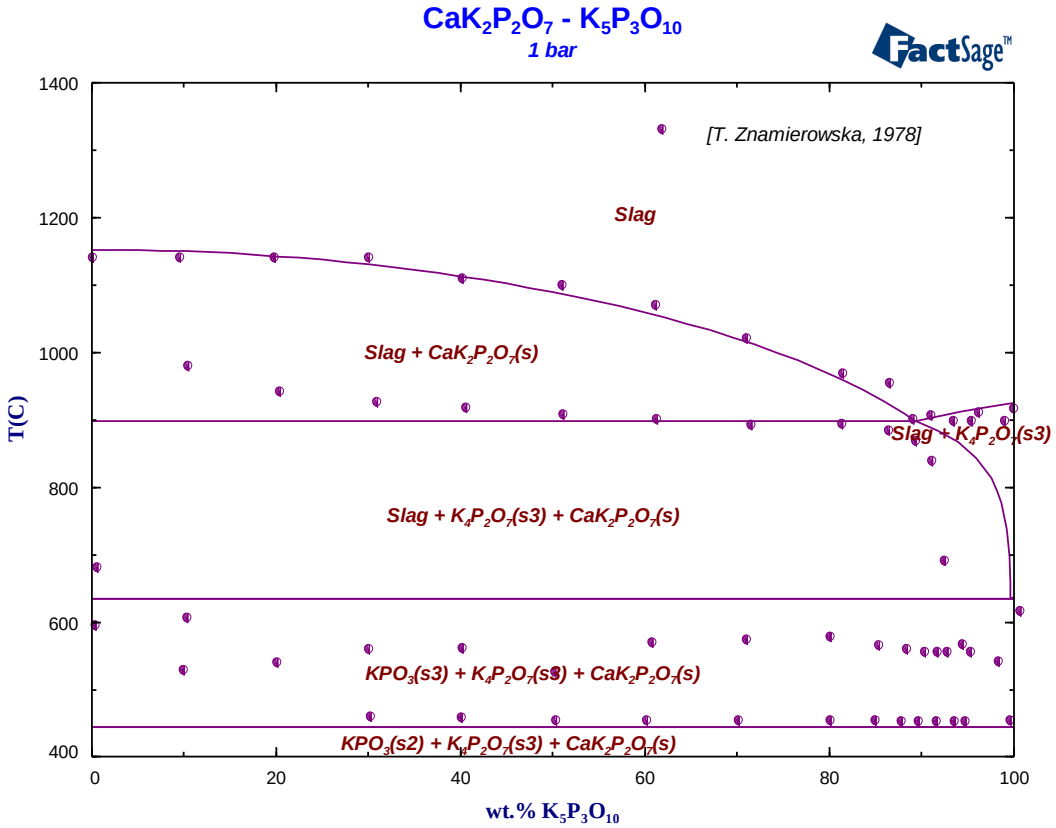

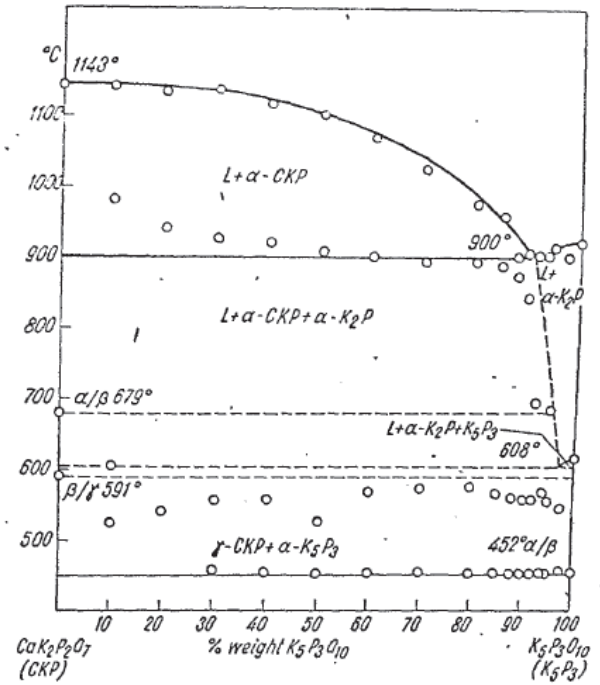

Fig. 5. Phase diagram of $CaK_2P_2O_7$ — $K_5P_3O_{10}$ system

T. Znamierowska, Pol. J. Chem., 52 [10] 1889-1895 (1978).

Weight percent, Isopleth CaKPO4-CaK2P2O7

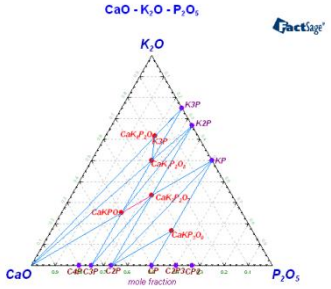

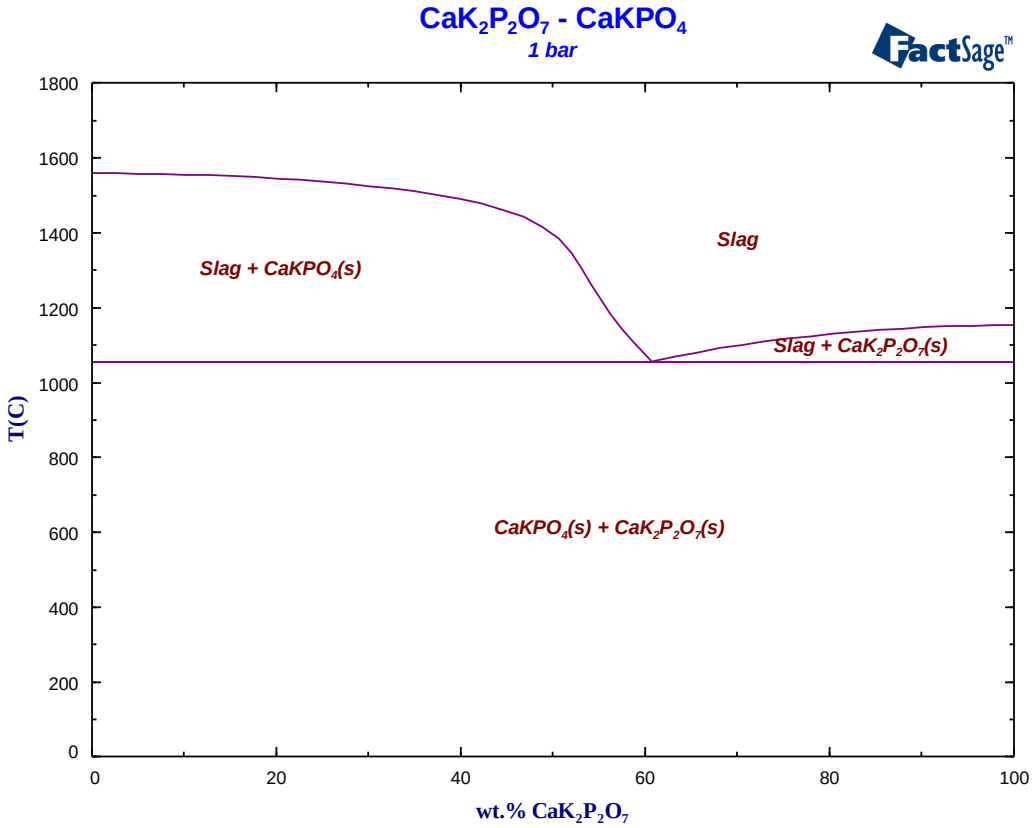

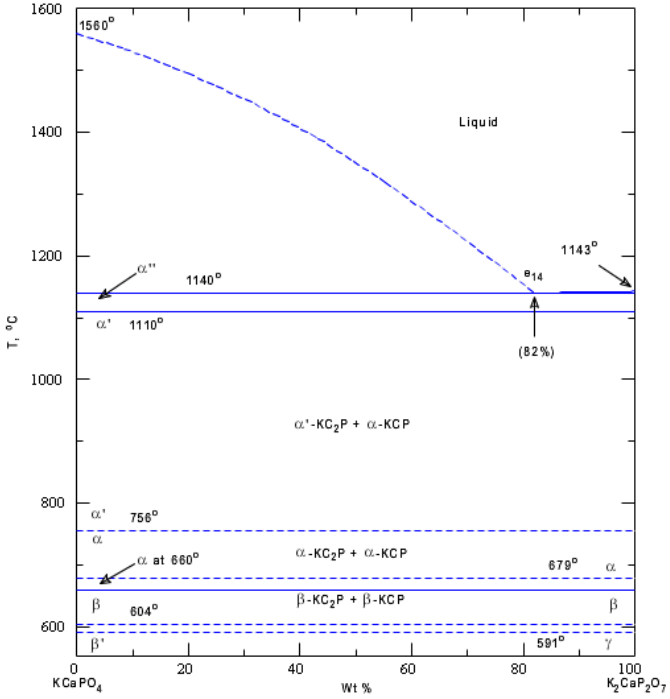

T. Znamierowska, Pol. J. Chem., 53 [7-8] 1415-1423 (1979).

Weight percent, Isopleth CaKPO4-K4P2O7

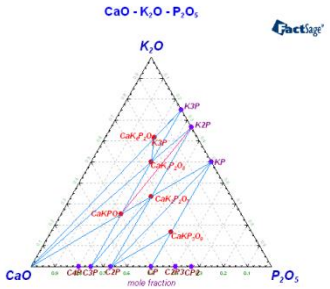

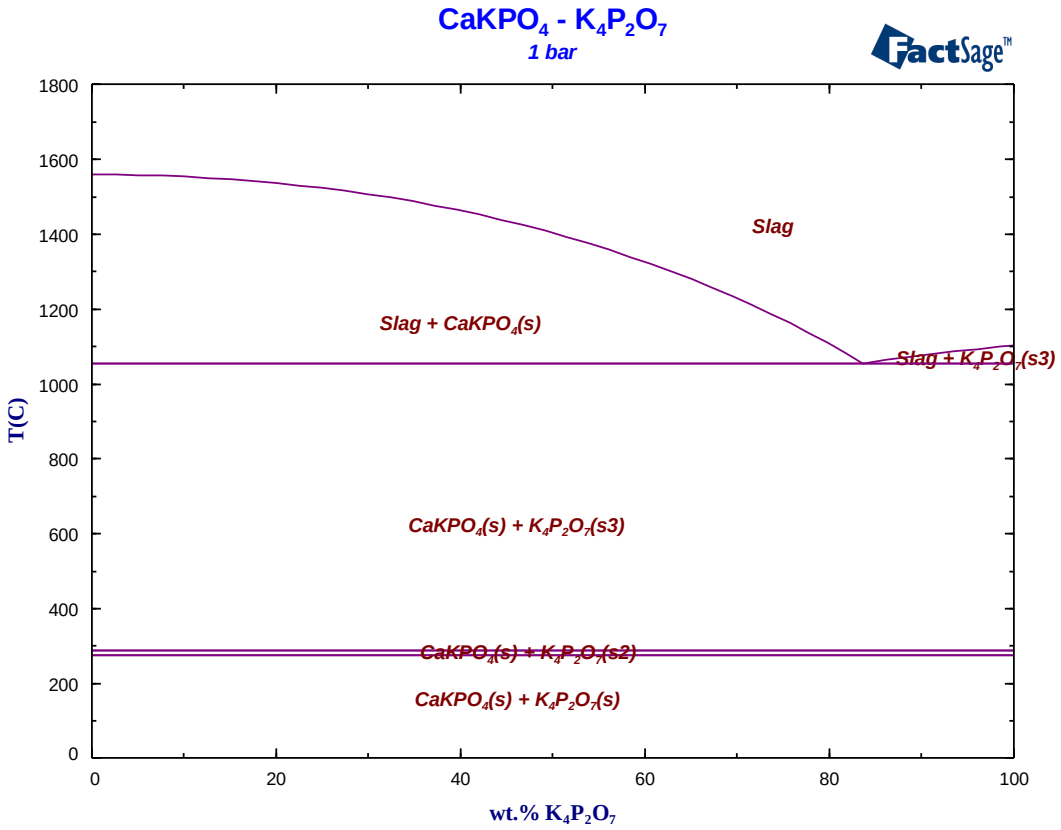

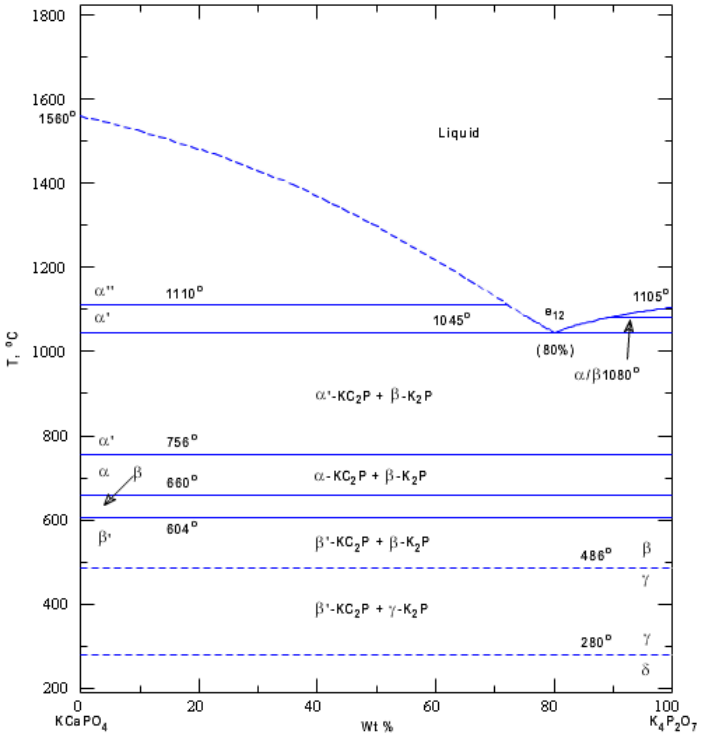

T. Znamierowska, Pol. J. Chem., 53 [7-8] 1415-1423 (1979).

Weight percent, Isopleth CaO-CaKPO4

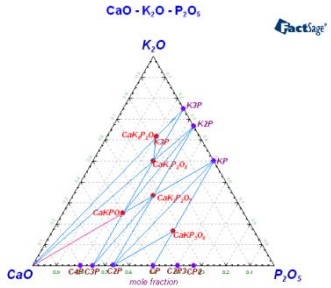

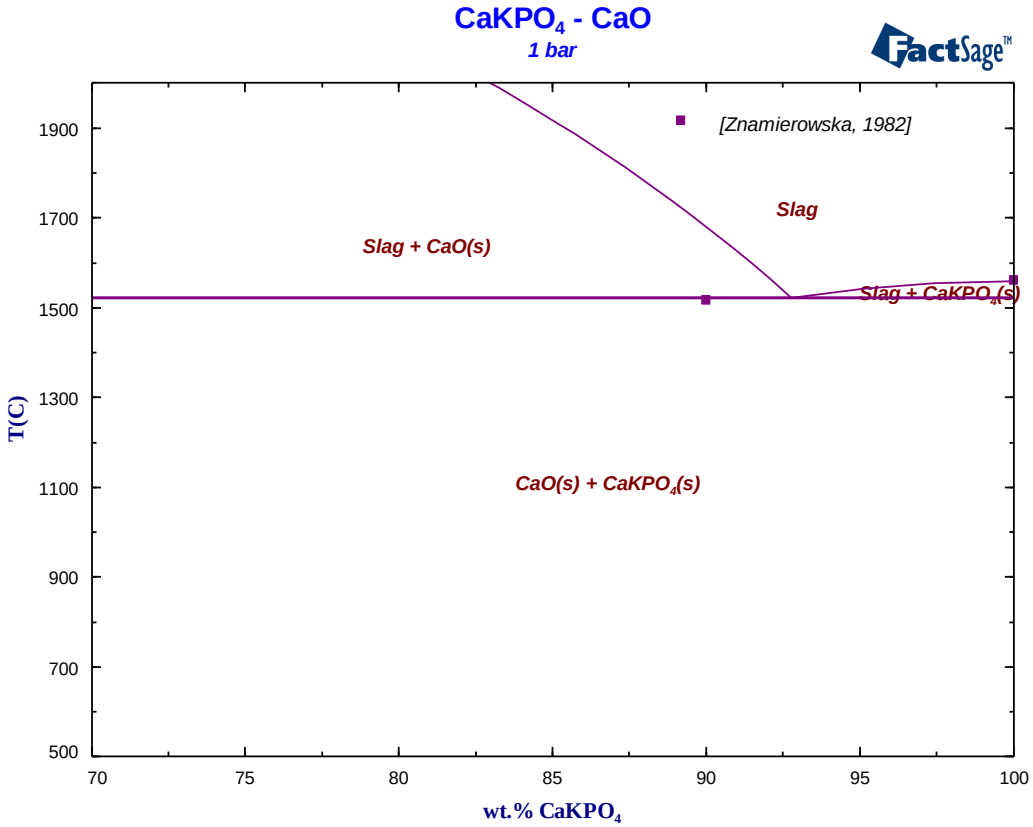

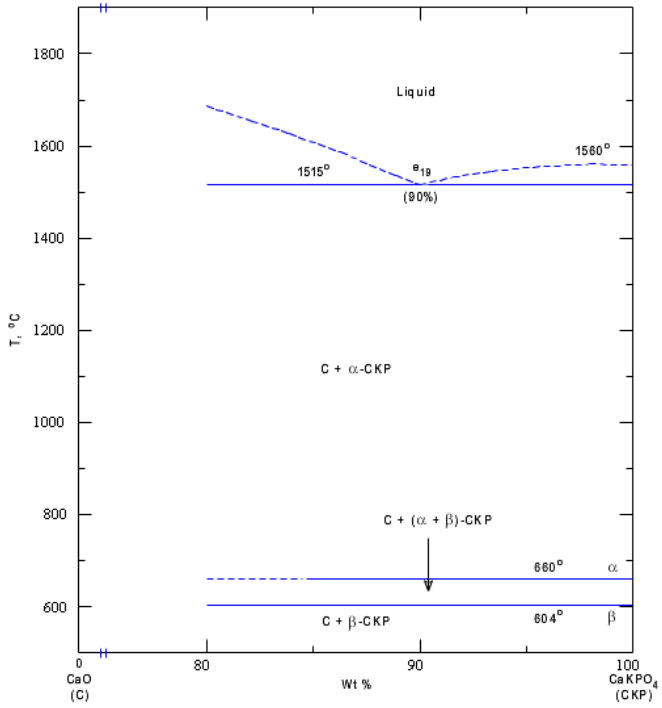

T. Znamierowska, Zesz. Nauk. Politech. Slask., Chem., 709 [100] 15-21 (1982).

Weight percent, Isopleth CaO-K4CaP2O8

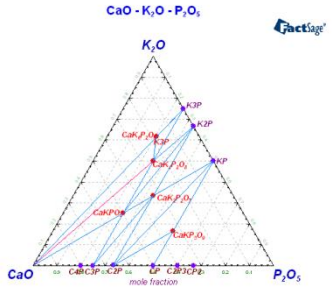

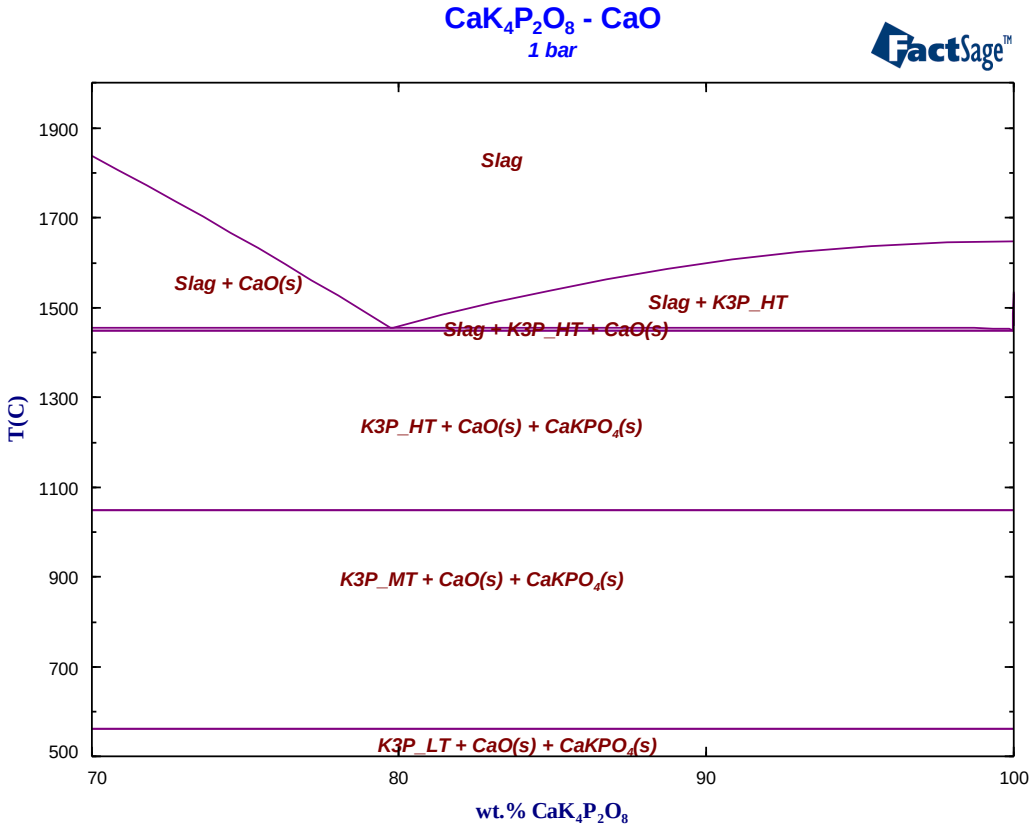

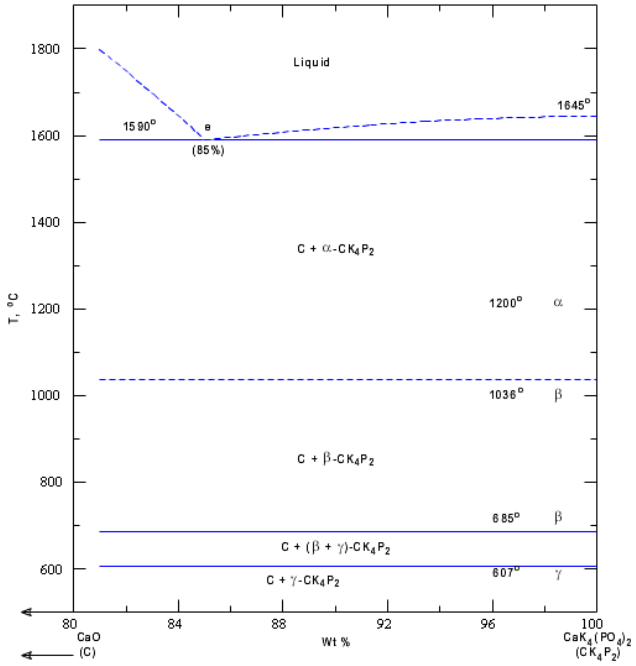

T. Znamierowska, Zesz. Nauk. Politech. Slask., Chem., 709 [100] 15-21 (1982).

Weight percent, Isopleth CaO-K3PO4

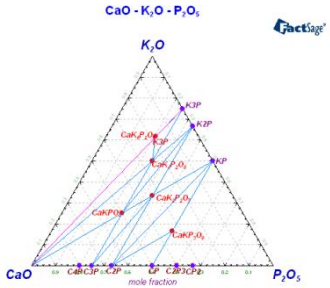

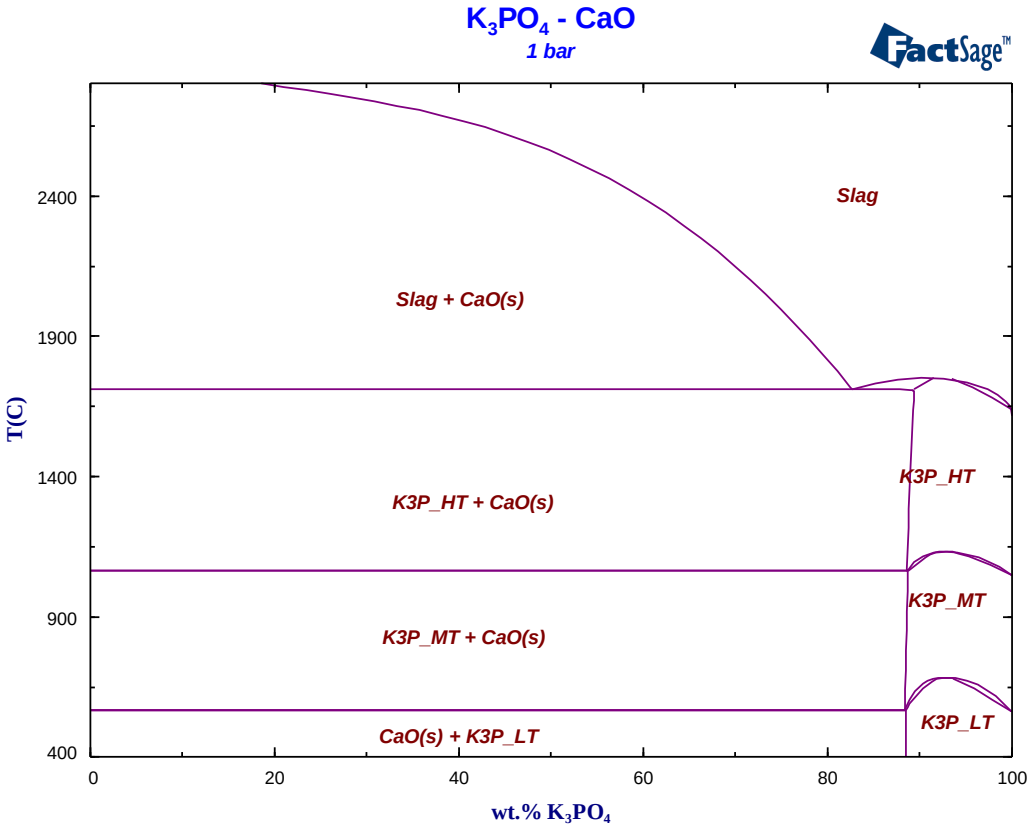

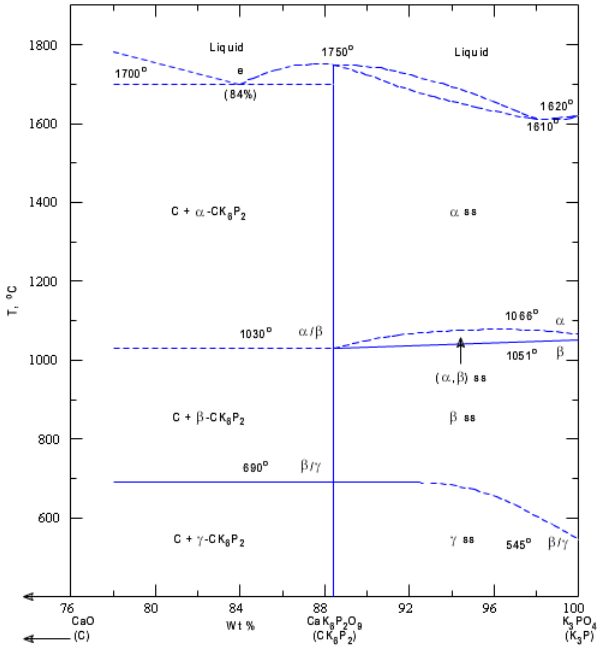

T. Znamierowska, Zesz. Nauk. Politech. Slask., Chem., 709 [100] 15-21 (1982).

Weight percent, 500°C

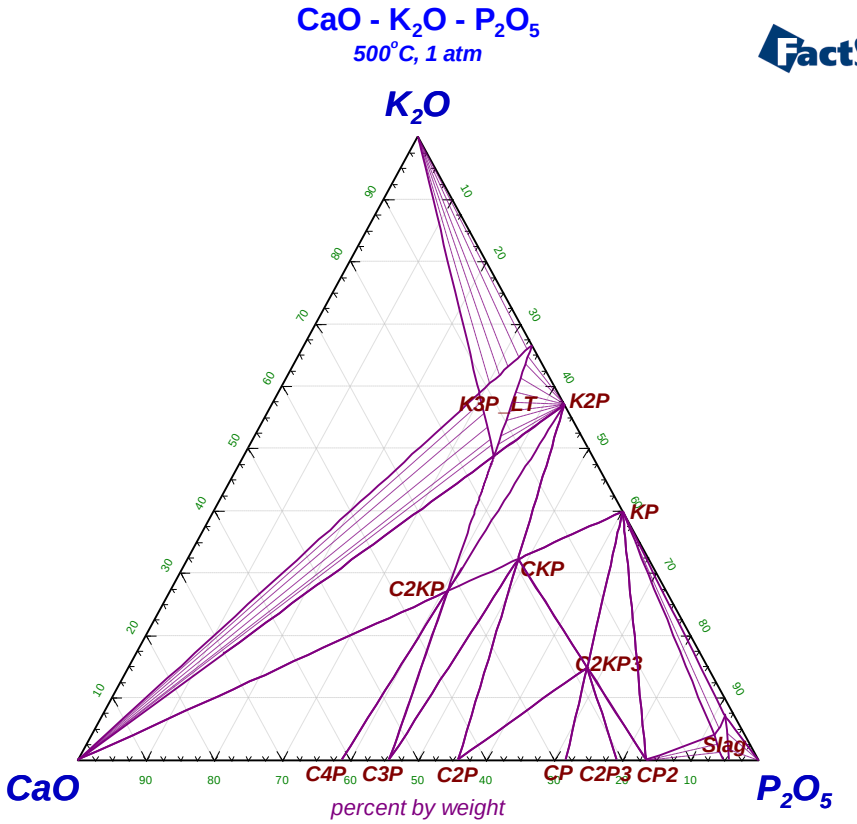

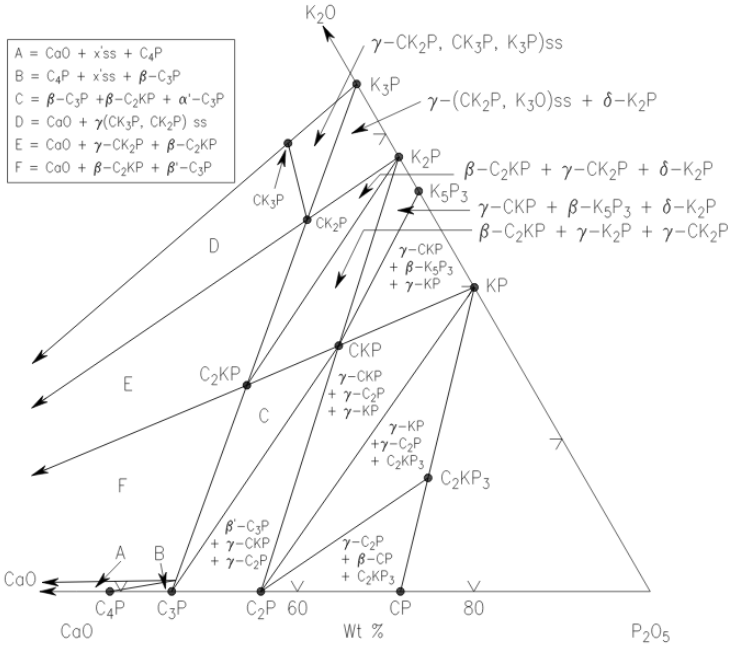

T. Znamierowska, Zesz. Nauk. Politech. Slask., Chem., 709 [100] , p.23-32 (1982).

Mole fraction, 1000°C

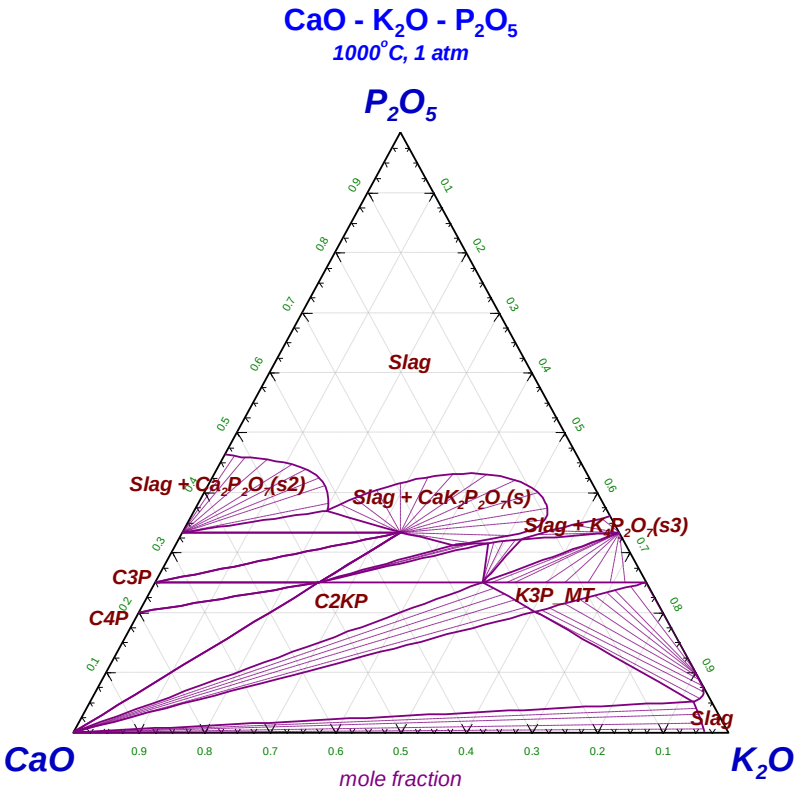

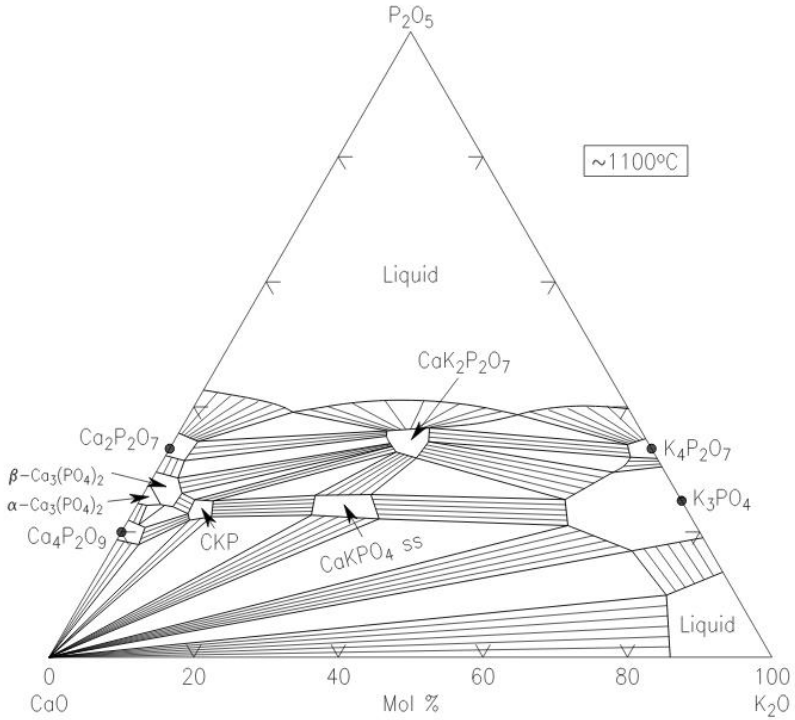

H. H. Franck, M. A. Bredig, and E. Kanert, Z. Anorg. Allg. Chem., 237, p.49-78 (1938).

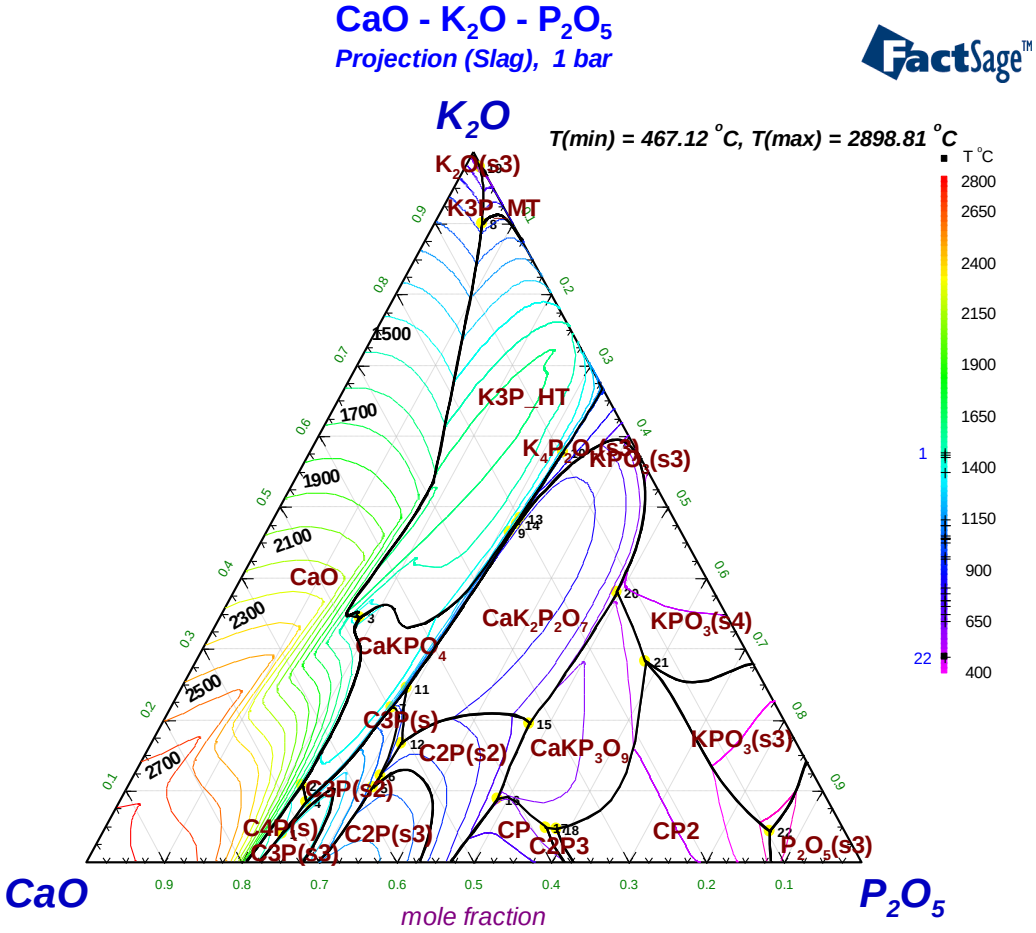
CaO - K2O - P2O5
Projection (Slag), 1 bar
FactSage™
K2O
T(min) = 467.12 °C, T(max) = 2898.81 °C
T °C
2800
2650
2400
2150
1900
1650
1400
1150
900
650
400
K2O(s3)
K3P_MT
K3P_HT
K4P2O7(s3)
KPO3(s3)
CaO
CaK2P2O7
KPO3(s4)
CaKPO4
C3P(s)
C2P(s2)
CaKP3O9
KPO3(s3)
C3P(s2)
C4P(s)
C2P(s3)
C3P(s3)
CP
C2P3
CP2
P2O5(s3)
1500
1700
1900
2100
2300
2500
2700
CaO
P2O5
mole fraction

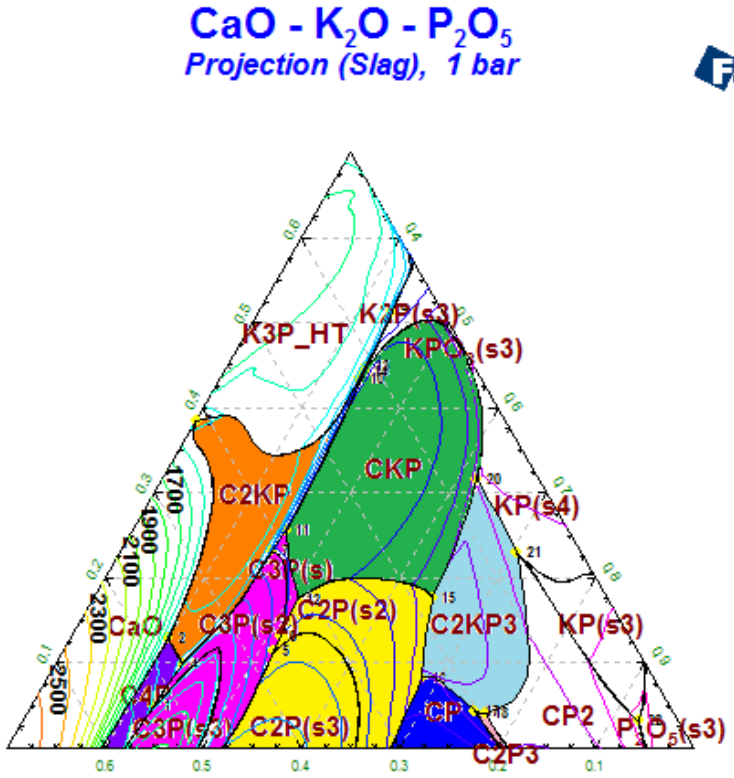

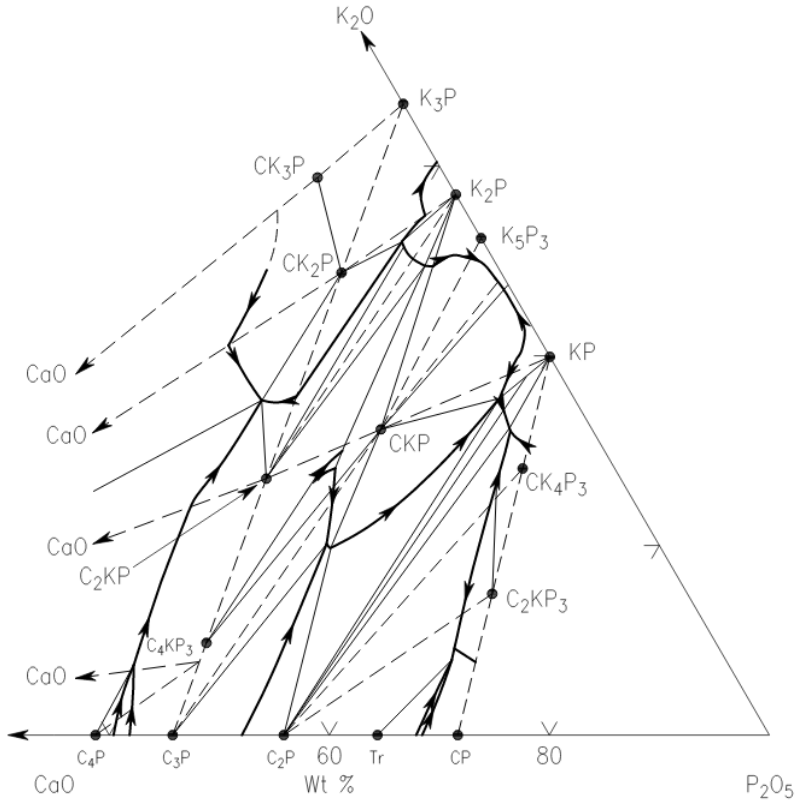

T. Znamierowska, Zesz. Nauk. Politech. Slask., Chem., 709 [100] , p.23-32 (1982).

Invariant equilibria on the liquidus surface

Intersections with slag	Mole fraction A = K2O, B = CaO, C = P2O5				Weight percent A = K2O, B = CaO, C = P2O5			
	X(A)	X(B)	X(C)	T(C)	W(A)	W(B)	W(C)	T(C)
1: Ca3(PO4)2(s2) / Ca3(PO4)2(s3) / C4P	1: 0.03976	0.72781	0.23243	1469.85	1: 4.830	52.628	42.542	1469.85
2: Ca4(PO4)2O / CaKPO4 / CaO	2: 0.10822	0.66763	0.22415	1453.98	2: 12.830	47.123	40.046	1454.00
3: CaKPO4 / CaO / K3P_HT	3: 0.34448	0.47583	0.17969	1446.83	3: 38.338	31.526	30.136	1446.83
4: Ca3(PO4)2(s2) / Ca4(PO4)2O / CaKPO4	4: 0.08431	0.67391	0.24177	1370.87	4: 9.921	47.209	42.870	1370.87
5: Ca2P2O7(s2) / Ca2P2O7(s3) / Ca3(PO4)2(s2)	5: 0.10439	0.57859	0.31702	1139.85	5: 11.267	37.176	51.558	1139.85
6: Ca2P2O7(s2) / Ca3(PO4)2(s2) / Ca3(PO4)2(s)	6: 0.12152	0.55996	0.31851	1110.28	6: 12.999	35.659	51.342	1109.85
7: Ca3(PO4)2(s2) / Ca3(PO4)2(s) / CaKPO4	7: 0.21811	0.49726	0.28463	1110.28	7: 23.129	31.391	45.480	1109.85
8: CaO / K3P_HT / K3P_MT	8: 0.89964	0.03972	0.06064	1062.11	8: 88.664	2.331	9.006	1062.11
9: CaKPO4 / K3P_HT / K3P_MT	9: 0.46483	0.22107	0.31410	1048.15	9: 51.276	5.059	43.665	1048.11
10: K3P_HT / K3P_MT / K4P2O7(s3)	10: 0.57775	0.09575	0.32650	1048.10	10: 43.452	12.303	44.245	1048.10
11: Ca3(PO4)2(s) / CaK2P2O7 / CaKPO4	11: 0.24458	0.46479	0.29063	1043.91	11: 25.497	28.846	45.657	1043.91
12: Ca2P2O7(s2) / Ca3(PO4)2(s) / CaK2P2O7	12: 0.16732	0.50958	0.32310	1025.51	12: 17.473	31.681	50.846	1025.41
13: CaKPO4 / K3P_MT / K4P2O7(s3)	13: 0.48526	0.19745	0.31729	961.10	13: 44.893	10.874	44.233	961.13
14: CaK2P2O7 / CaKPO4 / K4P2O7(s3)	14: 0.47591	0.20700	0.31710	947.69	14: 44.189	11.442	44.368	947.69
15: Ca2P2O7(s2) / CaK2P2O7 / CaKP3O9	15: 0.19514	0.33074	0.47412	808.66	15: 17.636	17.795	64.569	808.66
16: Ca(PO3)2(s) / Ca2P2O7(s2) / CaKP3O9	16: 0.08818	0.42557	0.48625	781.98	16: 8.208	23.584	68.208	781.84
17: Ca(PO3)2(s) / Ca2P6O17 / CaKP3O9	17: 0.04882	0.38266	0.56852	745.52	17: 4.308	20.101	75.592	745.52
18: Ca2P6O17 / CaKP3O9 / CaP4O11	18: 0.04672	0.37033	0.58295	744.42	18: 4.078	19.244	76.678	744.42
19: CaO / K2O(s3) / K3P_MT	19: 0.97885	0.00277	0.01838	715.74	19: 97.090	0.164	2.747	715.74
20: CaK2P2O7 / CaKP3O9 / KPO3(s4)	20: 0.37982	0.12565	0.49453	678.34	20: 31.656	6.234	62.109	678.33
21: CaKP3O9 / KPO3(s3) / KPO3(s4)	21: 0.28308	0.13690	0.58002	645.90	21: 22.855	6.580	70.565	645.90
22: CaP4O11 / KPO3(s3) / P2O5(s3)	22: 0.04325	0.09684	0.85991	467.12	22: 3.096	4.128	92.776	467.13

Ternäre Phasen im $CaO-K_2O-SiO_2$ System

Phase	Beschreibung	Formel
KCS(111)	Stöchiometrisch	K_2CaSiO_4
K_2CS_3 (213)	Stöchiometrisch	$K_4CaSi_3O_9$
K_2CS_6 (216)	Stöchiometrisch	$K_4CaSi_6O_{15}$
K_4CS_{10} (4110)	Stöchiometrisch	$K_8CaSi_{10}O_{25}$
KC_2S_9 (129)	Stöchiometrisch	$K_2Ca_2Si_9O_{21}$
KC_3S_6 (136-HT)	Stöchiometrisch	$K_2Ca_3Si_6O_{16}$ (α, HT)
KC_3S_6 (136-LT)	Stöchiometrisch	$K_2Ca_3Si_6O_{16}$ (β, LT)

CaO-K2O-SiO2,
Weight percent
Isopleth CaSi2O5-K2Si2O5

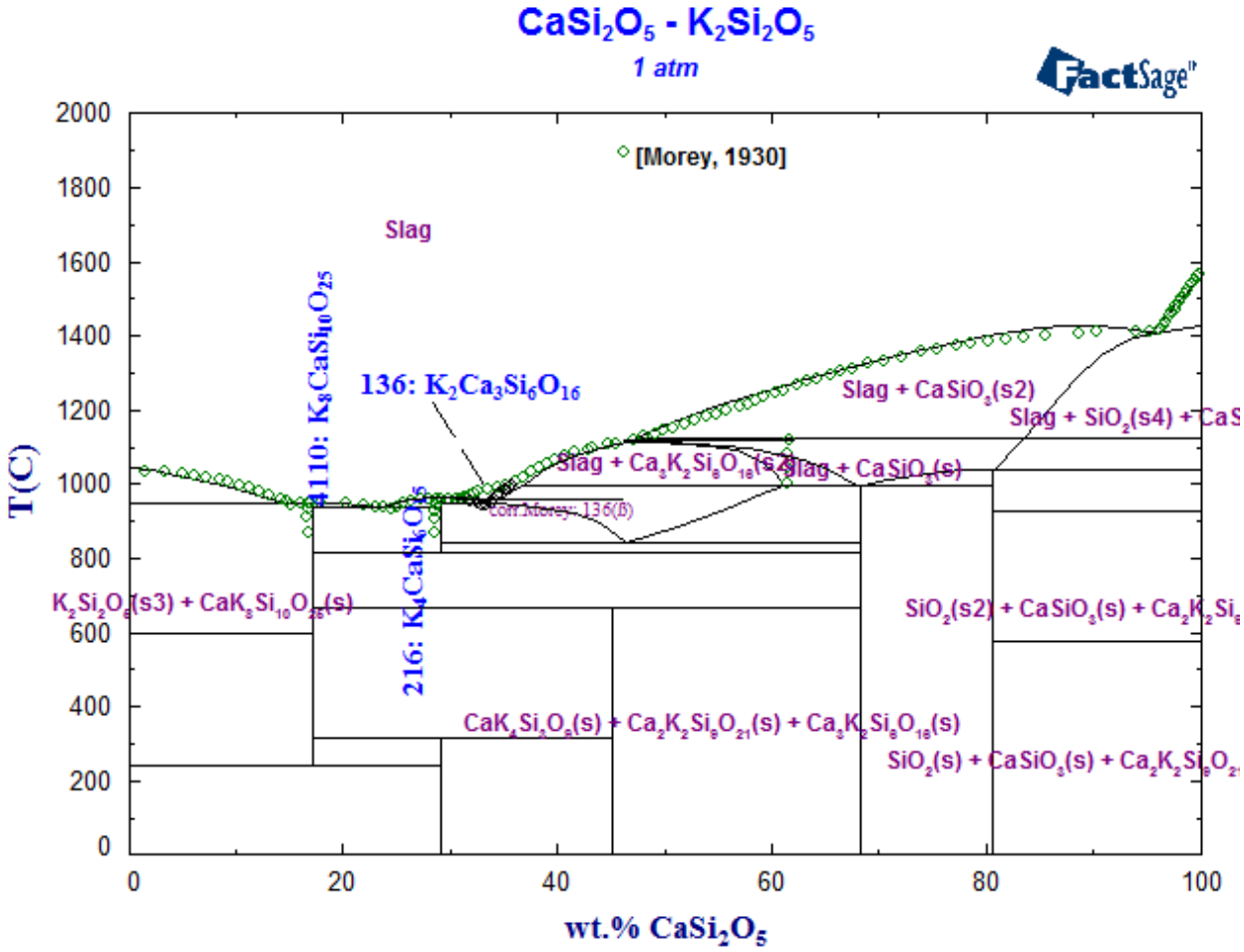

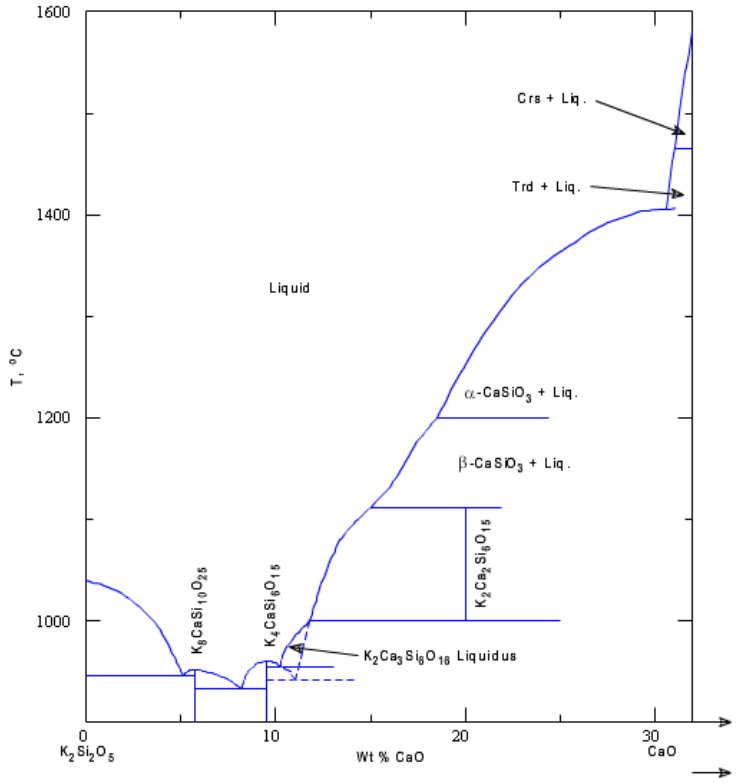

G.W. Morey, F.C. Kracek, N.L. Bowen, The ternary system K_2O-CaO-SiO_2, J. Soc. Glass Technol. 14 (1930) 149-187.

Isopleth CaSiO3-K2Si4O9 compared with experimental data

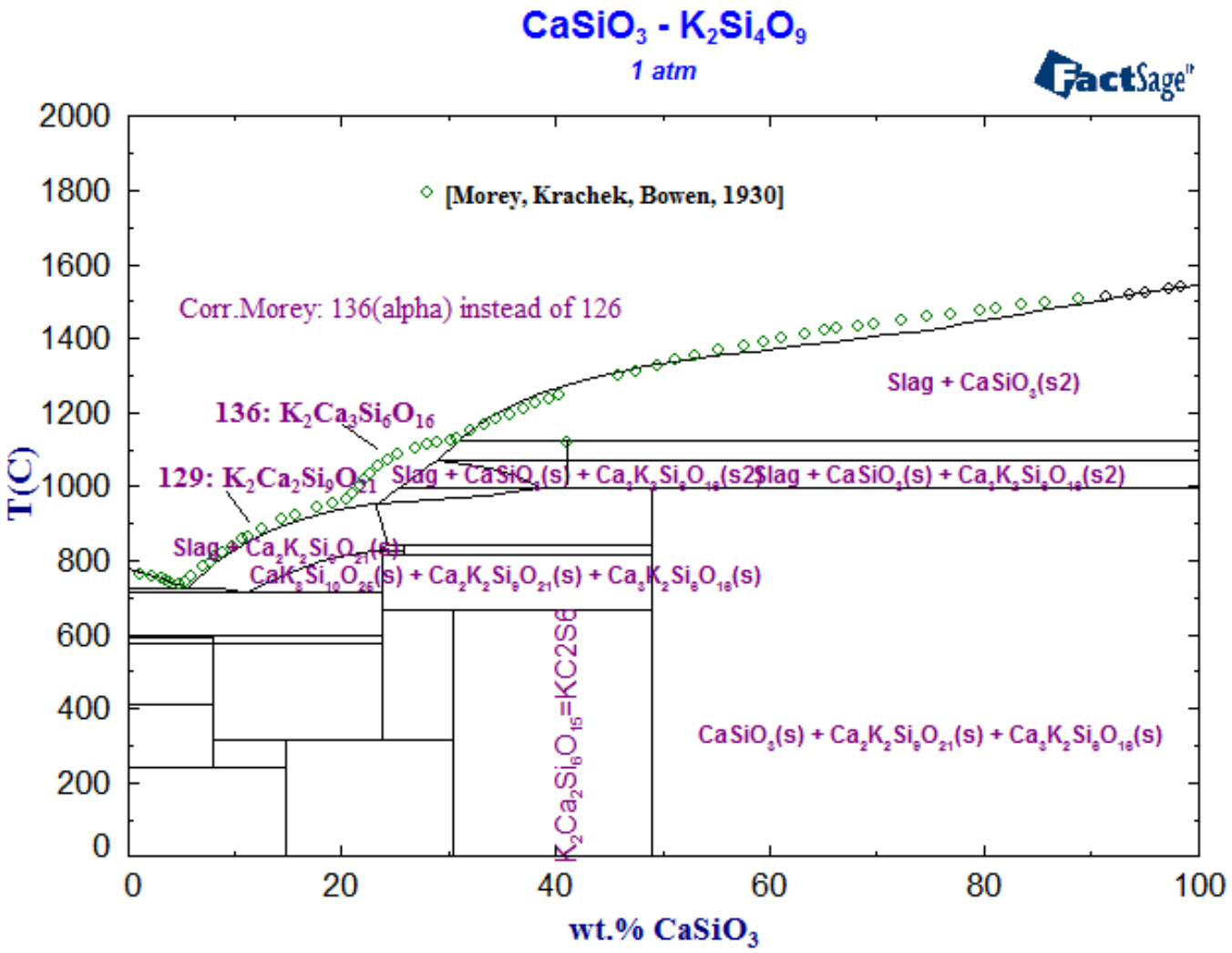

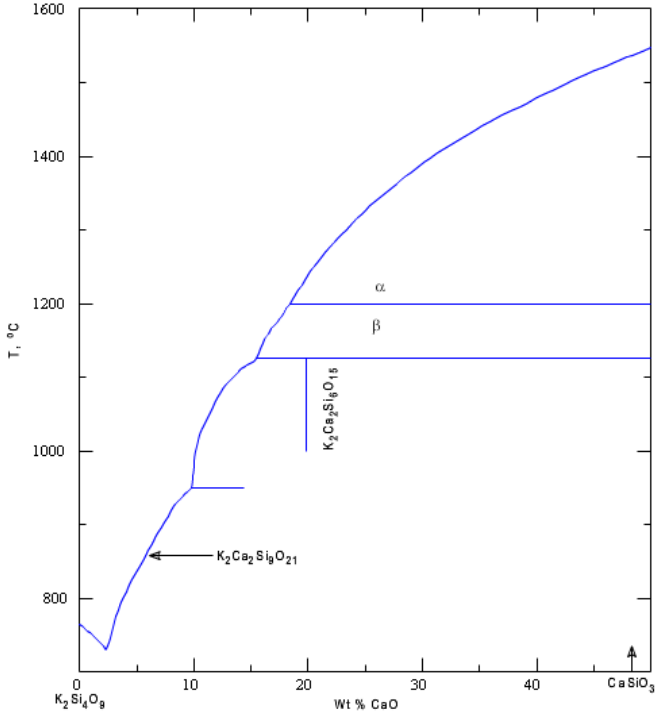

G.W. Morey, F.C. Kracek, N.L. Bowen, The ternary system K_2O-CaO-SiO_2, J. Soc. Glass Technol. 14 (1930) 149-187.

Isopleth K2Si2O5-K2CaSiO4 compared with experimental data

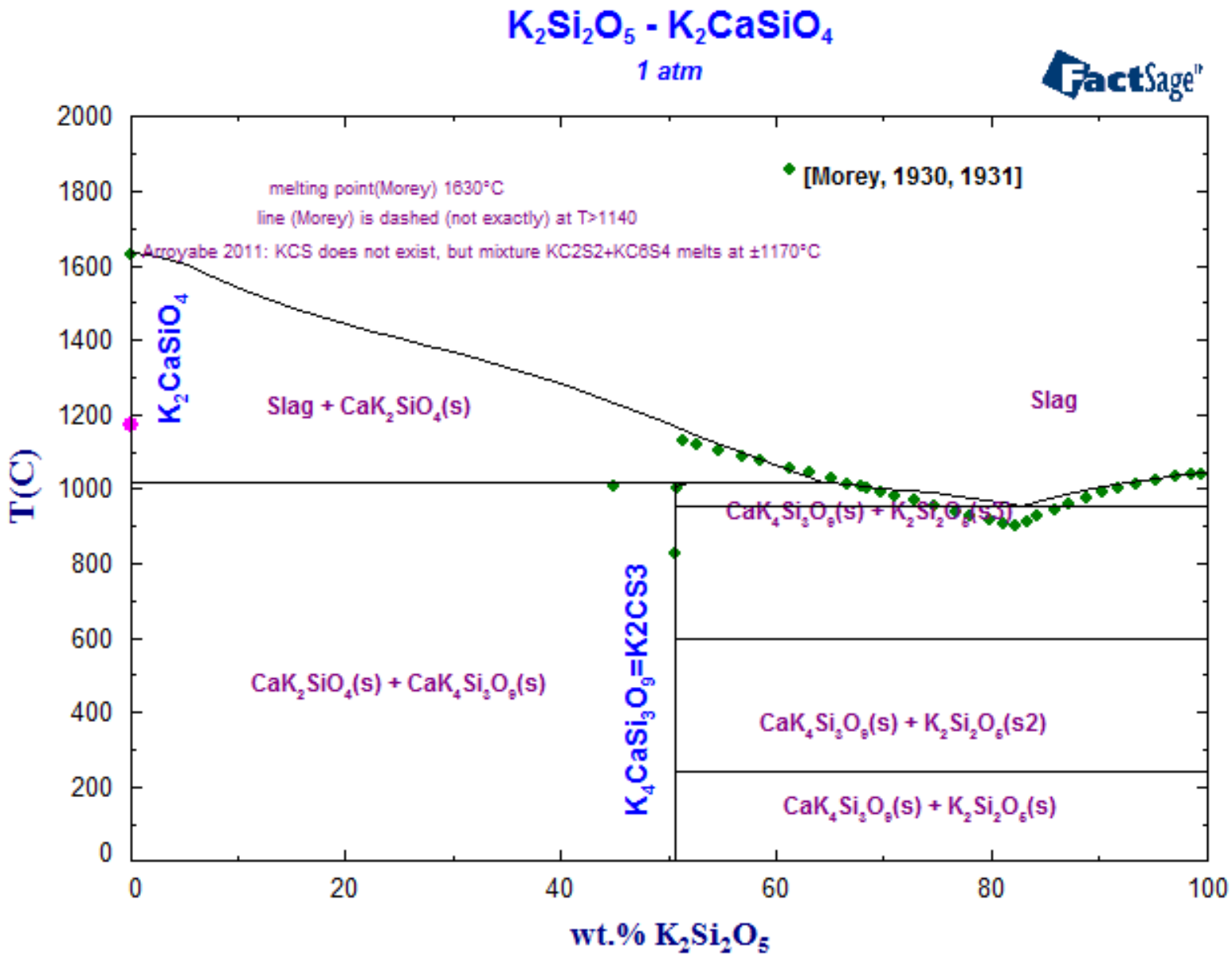

Isopleth CaSiO3-K2SiO3
compared with experimental data

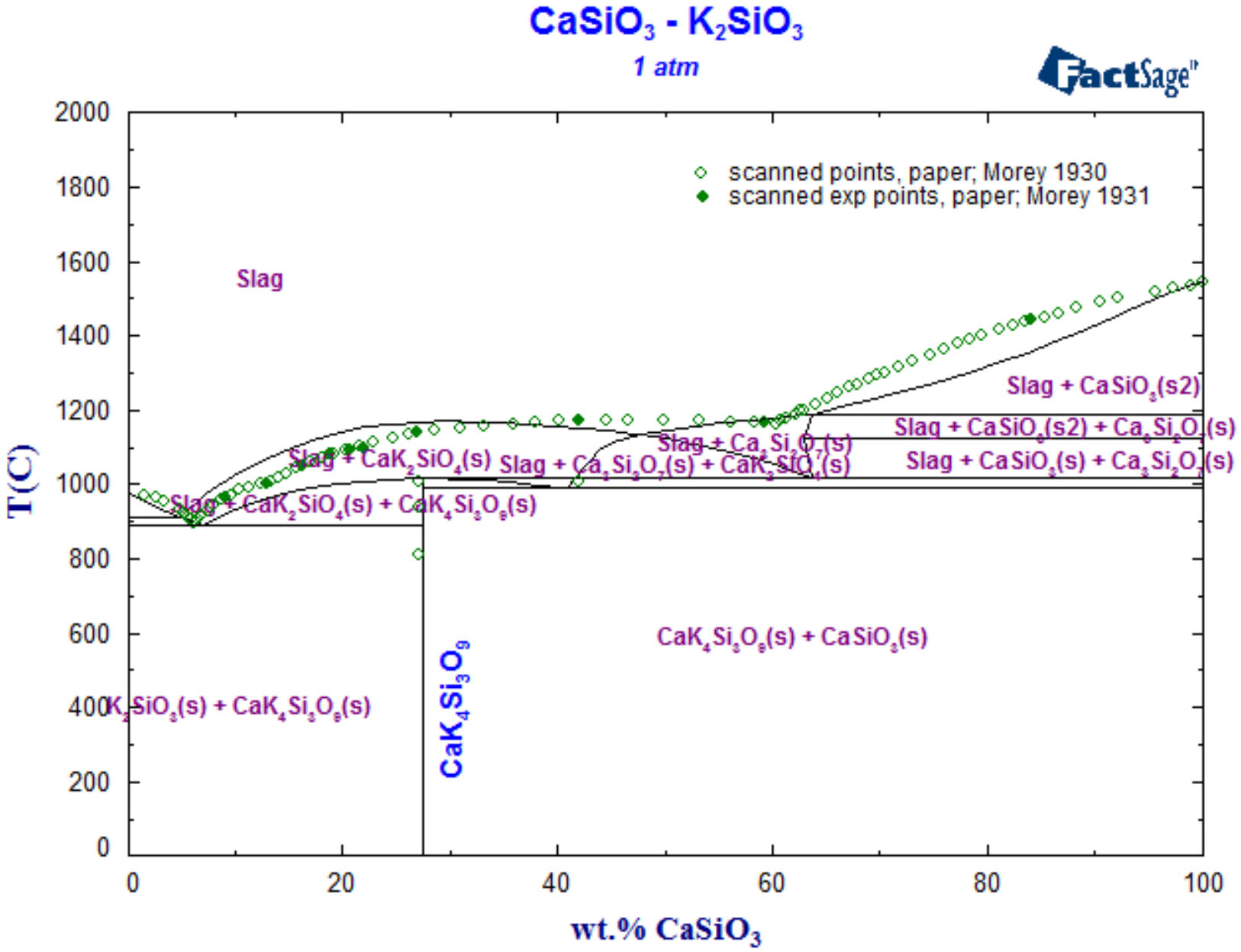

CaO-K2O-SiO2, Mole fraction 300°C

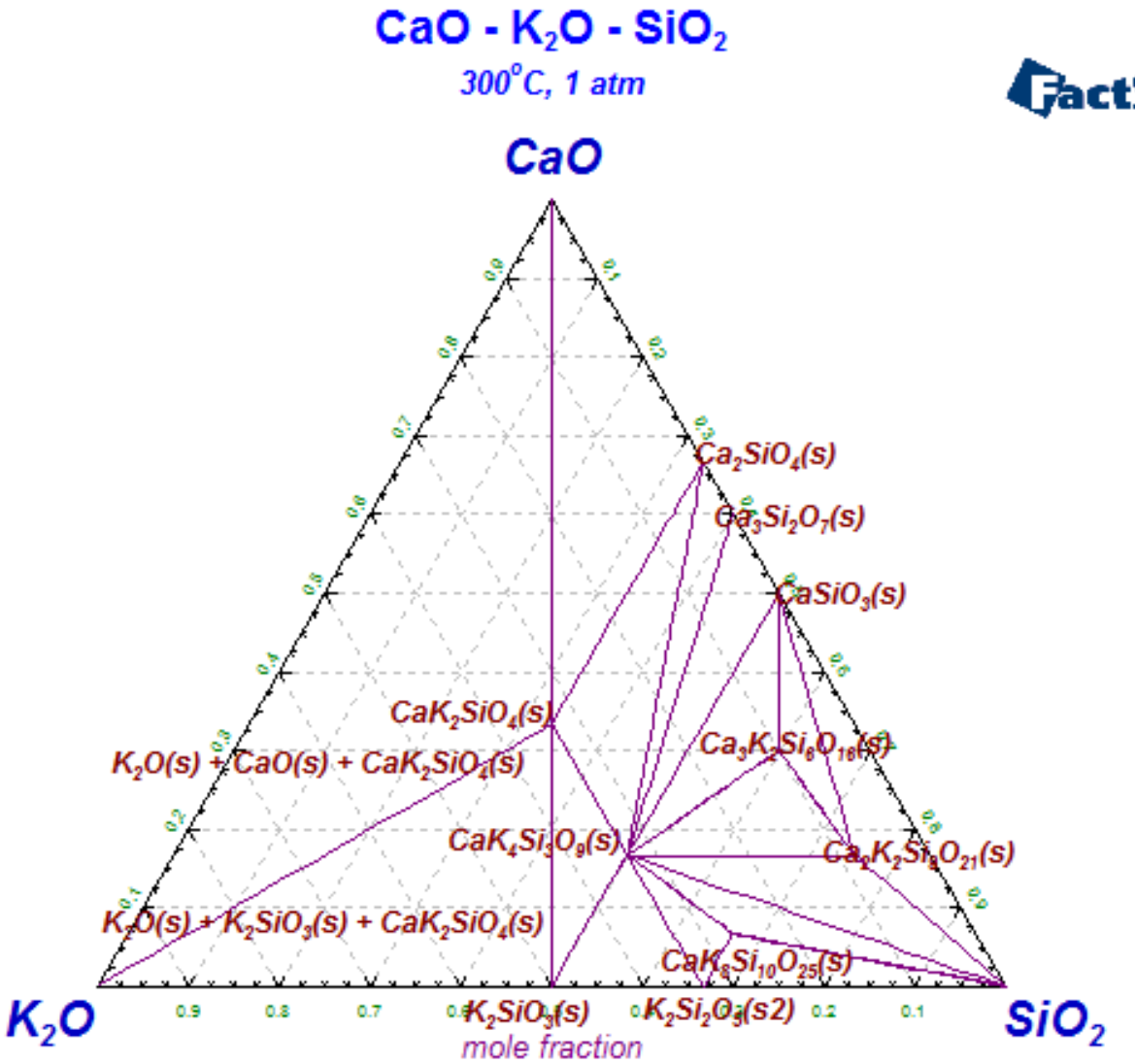

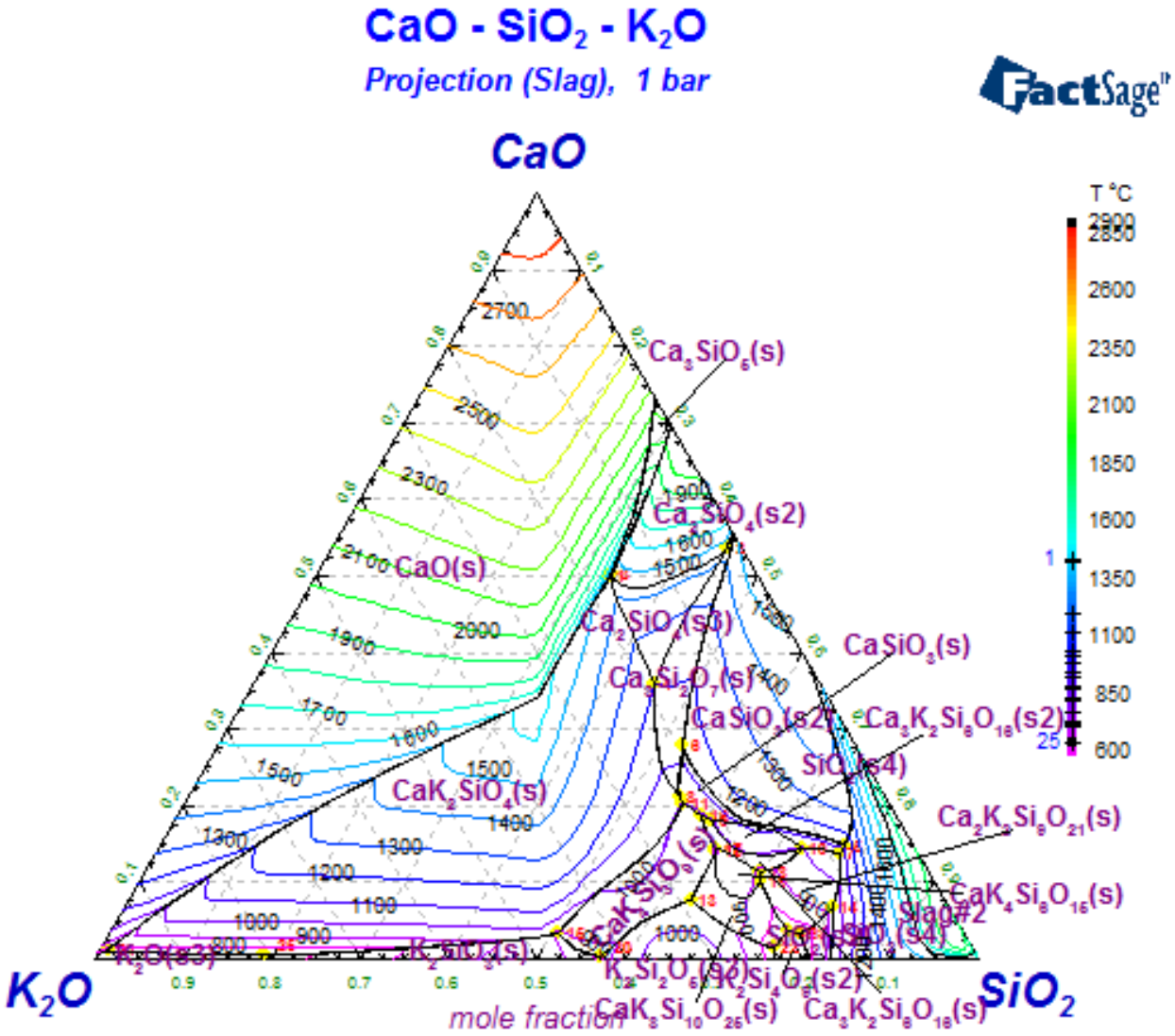
CaO - SiO2 - K2O
Projection (Slag), 1 bar
FactSage
CaO
K2O
SiO2
mole fraction
T °C
Ca3SiO5(s)
Ca2SiO4(s2)
Ca2SiO4(s)
Ca3Si2O7(s)
CaSiO3(s)
CaSiO3(s2)
Ca3K2Si6O18(s2)
SiO2(s4)
Ca2K2Si6O21(s)
CaK4Si6O16(s)
Slag#2
CaK2SiO4(s)
K2O(s3)
K2SiO3(s)
K2Si2O5(s)
K2Si4O9(s2)
CaK6Si10O25(s)
Ca3K2Si6O18(s)

Weight percent
Liquidussurface

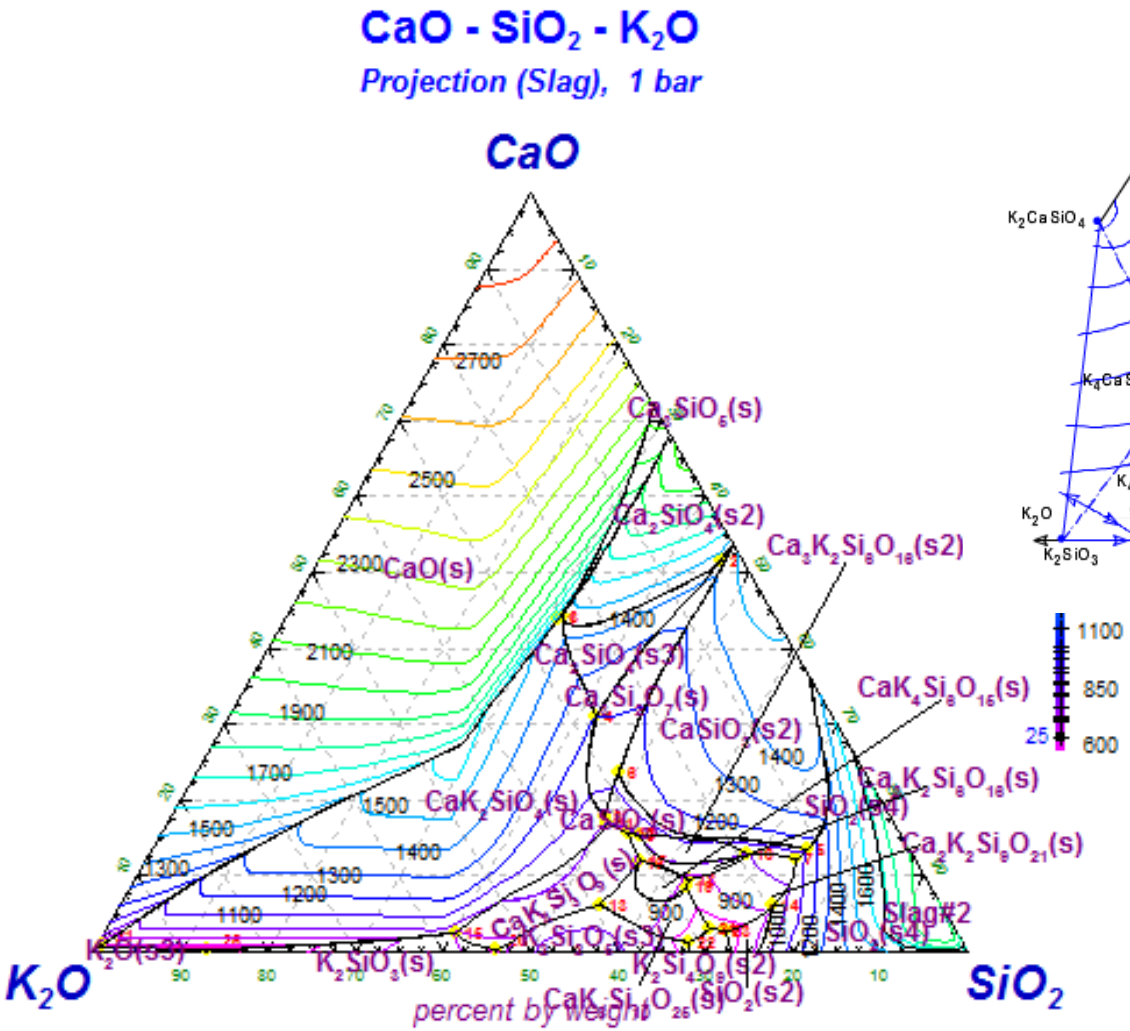

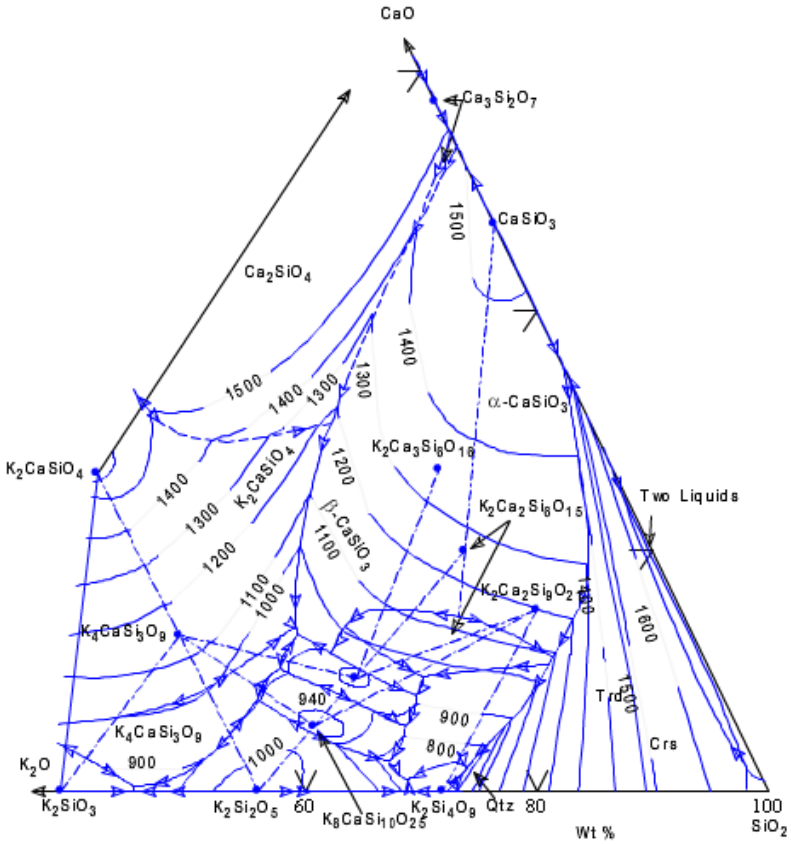

F.C. Kracek, N.L. Bowen, The ternary system O_2, J. Soc. Glass Technol. 14 (1930) 149-187.

Invariant equilibria on the liquidus surface

Intersections with slag	Mole fraction A = CaO, B = K2O, C = SiO2				Weight percent A = CaO, B = K2O, C = SiO2				
		X(A)	X(B)	X(C)	T(C)		W(A)	W(B)	W(C)	T(C)
1: Ca3SiO5(s) / CaK2SiO4(s) / CaO(s)	1:	0.49849	0.16927	0.33224	1440.92	1:	43.773	24.968	31.259	1440.82
2: Ca2SiO4(s2) / Ca2SiO4(s3) / Ca3Si2O7(s)	2:	0.53832	0.01458	0.44710	1436.73	2:	51.669	2.351	45.980	1436.73
3: Ca2SiO4(s3) / Ca3SiO5(s) / CaK2SiO4(s)	3:	0.50279	0.16383	0.33338	1430.70	3:	44.291	24.242	31.466	1430.50
4: Ca2SiO4(s3) / Ca3Si2O7(s) / CaK2SiO4(s)	4:	0.35854	0.18717	0.45430	1198.90	4:	30.917	27.110	41.973	1198.90
5: CaSiO3(s2) / CaSiO3(s) / SiO2(s4)	5:	0.14837	0.07670	0.77494	1124.23	5:	13.396	11.633	74.971	1124.28
6: Ca3Si2O7(s) / CaSiO3(s2) / CaSiO3(s)	6:	0.27754	0.19537	0.52709	1124.13	6:	23.712	28.037	48.251	1124.13
7: Ca2K2Si9O21(s) / CaSiO3(s) / SiO2(s4)	7:	0.13628	0.08964	0.77408	1039.73	7:	12.209	13.489	74.302	1039.73
8: Ca3Si2O7(s) / CaK2SiO4(s) / CaSiO3(s)	8:	0.21285	0.23262	0.55453	1016.54	8:	17.770	32.623	49.607	1016.56
9: Ca3K2Si6O16(s2) /Ca3K2Si6O16/ CaSiO3(s)	9:	0.18151	0.21167	0.60681	993.85	9:	15.289	29.948	54.763	993.99
10: Ca2K2Si9O21 / Ca3K2Si6O16 / CaSiO3(s)	10:	0.14460	0.12792	0.72749	993.62	10:	12.700	18.872	68.429	993.85
11: CaK2SiO4 / CaK4Si3O9 / CaSiO3(s)	11:	0.20190	0.23333	0.56476	988.37	11:	16.840	32.690	50.470	988.37
12: Ca3K2Si6O16 / CaK4Si3O9 / CaSiO3(s)	12:	0.18558	0.21997	0.59445	946.93	12:	15.569	30.998	53.433	946.79
13: CaK4Si3O9 / CaK8Si10O25 / K2Si2O5(s3)	13:	0.07687	0.28704	0.63610	928.84	13:	6.196	38.865	54.938	928.84
14: Ca2K2Si9O21 / SiO2(s4) / SiO2(s2)	14:	0.06814	0.13167	0.80019	926.29	14:	5.942	19.288	74.769	926.29
15: CaK2SiO4 / CaK4Si3O9 / K2SiO3	15:	0.03322	0.45986	0.50693	889.03	15:	2.463	57.268	40.269	889.02
16: CaK4Si3O9 / CaK4Si6O15 / CaK8Si10O25	16:	0.13983	0.22747	0.63270	884.35	16:	11.654	31.845	56.500	884.34
17: Ca3K2Si6O16 / CaK4Si3O9 / CaK4Si6O15	17:	0.14276	0.22521	0.63203	881.00	17:	11.914	31.571	56.515	881.00
18: Ca2K2Si9O21 / Ca3K2Si6O16 /CaK4Si6O15	18:	0.11191	0.19132	0.69677	840.13	18:	9.485	27.239	63.276	838.37
19: Ca2K2Si9O21 / CaK4Si6O15 /CaK8Si10O25	19:	0.10123	0.19602	0.70274	824.81	19:	8.554	27.822	63.623	824.81
20: CaK4Si3O9 / K2Si2O5(s3) / K2SiO3(s)	20:	0.00197	0.42688	0.57116	775.46	20:	0.148	53.874	45.979	775.33
21: CaK2SiO4 / CaO(s) / K2O(s3)	21:	0.01259	0.97819	0.00922	733.34	21:	0.756	98.651	0.593	733.44
22: CaK8Si10O25 / K2Si2O5(s3) / K2Si4O9(s2)	22:	0.01399	0.22545	0.76056	727.23	22:	1.159	31.359	67.482	727.23
23: Ca2K2Si9O21 / K2Si4O9(s2) / SiO2(s2)	23:	0.03178	0.18596	0.78226	725.44	23:	2.688	26.420	70.892	725.44
24: Ca2K2Si9O21 / CaK8Si10O25 /K2Si4O9(s2)	24:	0.03628	0.19791	0.76582	714.21	24:	3.050	27.953	68.996	714.21
25: CaK2SiO4 / K2O(s3) / K2SiO3(s)	25:	0.00405	0.80597	0.18998	643.34	25:	0.259	86.705	13.036	643.34

Mole fraction 1500C°

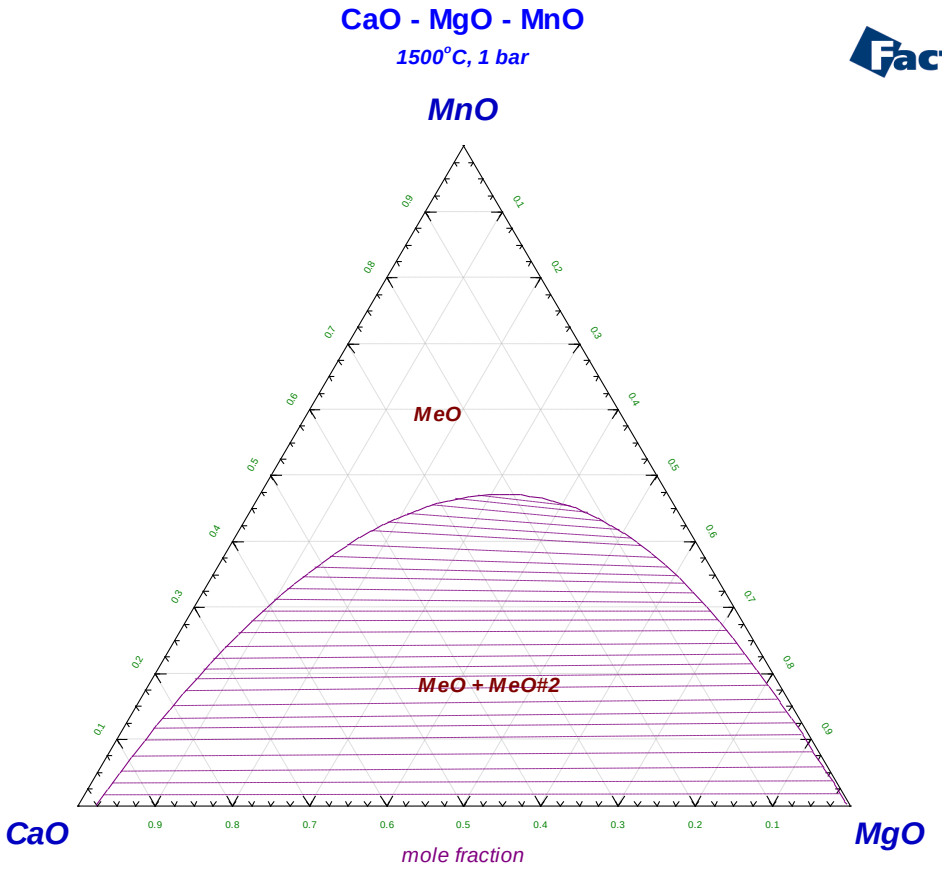

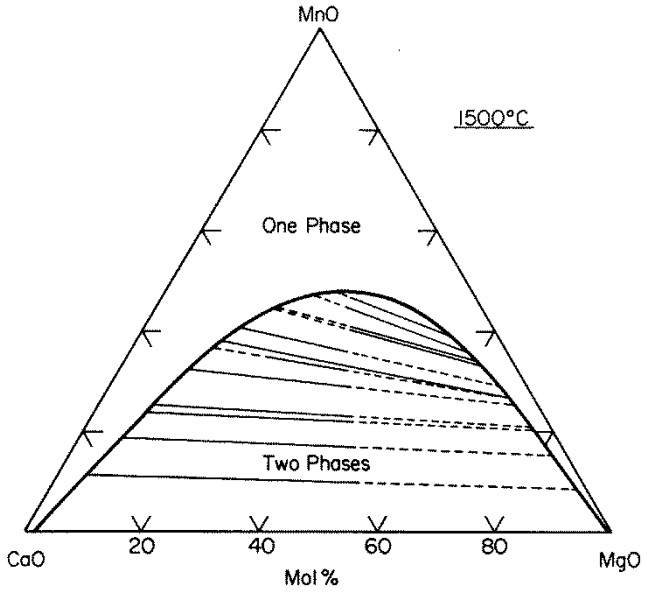

E. Woermann, A. Muan, Mat. Res. Bull. 5 [10], (1970), pp. 779-788.

Mole fraction 1000°C

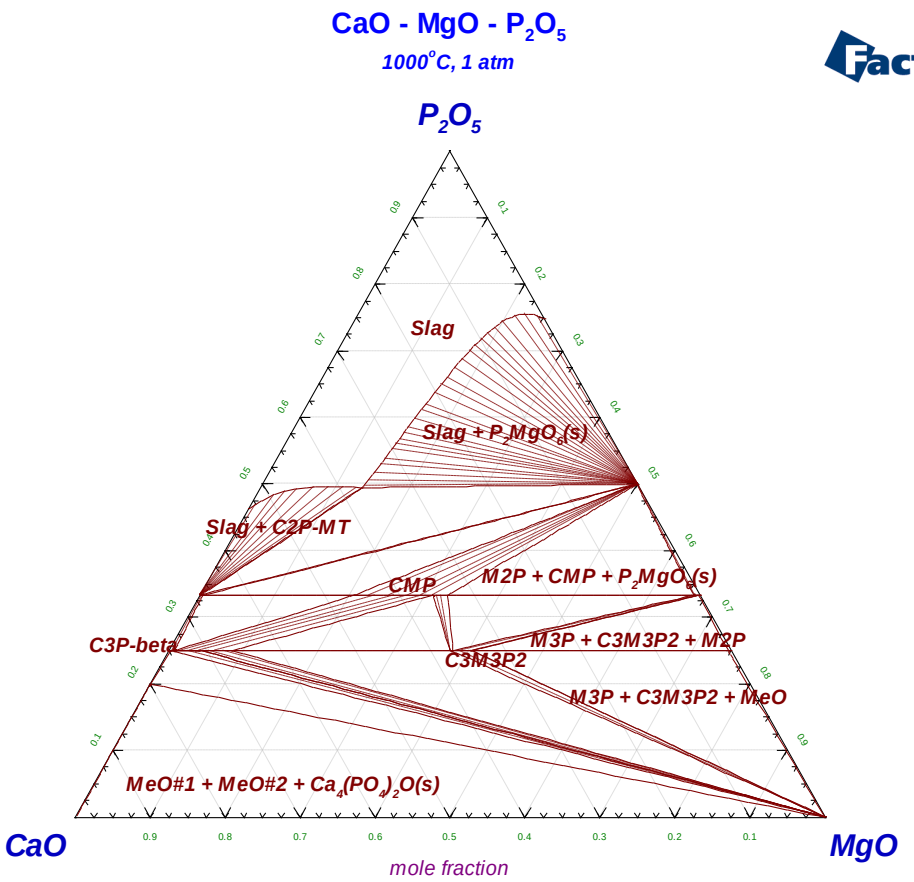

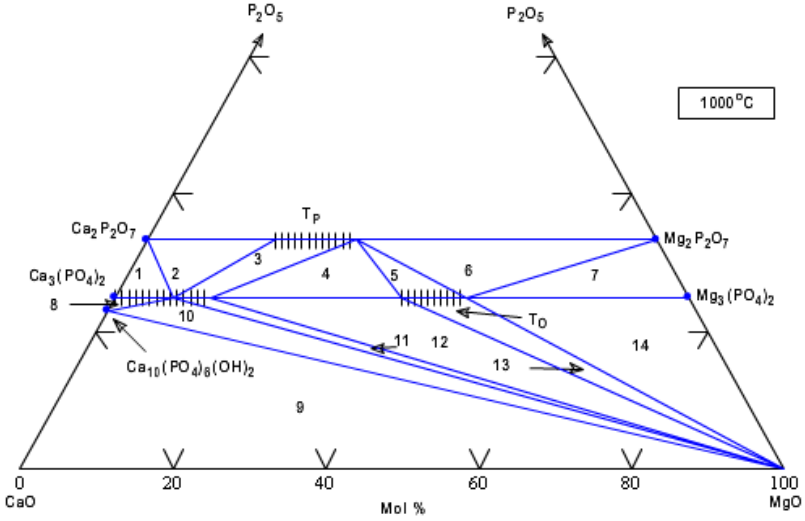

R. A. Terpstra, F. C. M. Driessens, and R. M. H. Verbeeck, Z. Anorg. Allg. Chem., 515, 213-224 (1984).

CaO-MgO-P2O5,

Weight percent, Isopleth Ca3P2O8-Mg3P2O8

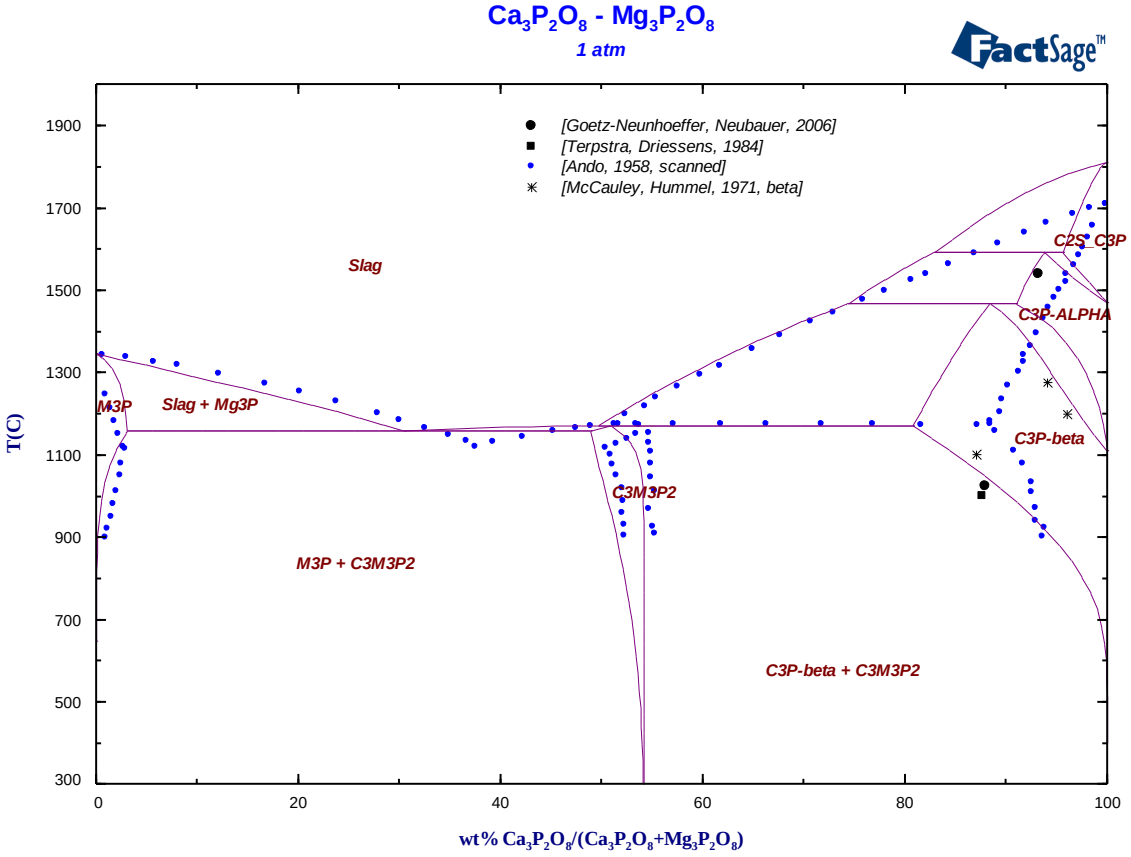

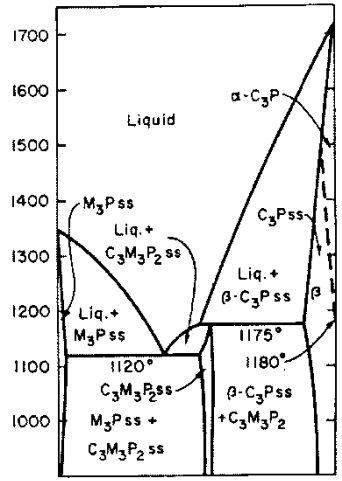

J. Ando, Bull. Chem. Soc. Jpn., 31 [2] 201-205 (1958).

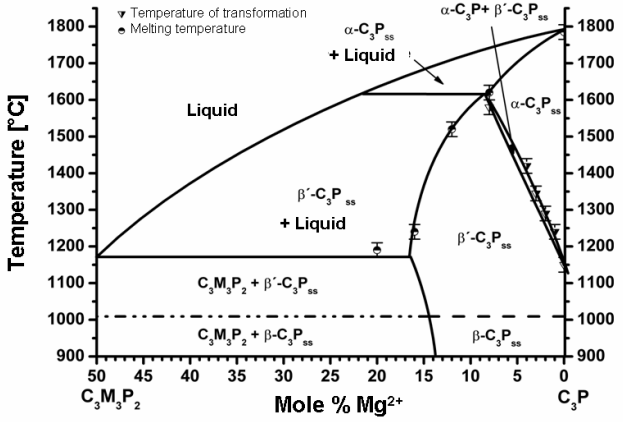

F. Goetz-Neunhoeffer, J, Neubauer, E. Enderle, M. Göbbels, Z. Kristallogr. Suppl. 26 (2007),, 375-380.

$CaO - MgO - SiO_2$

500°C

CaO-MgO-SiO2,
Mole fraction 500C°

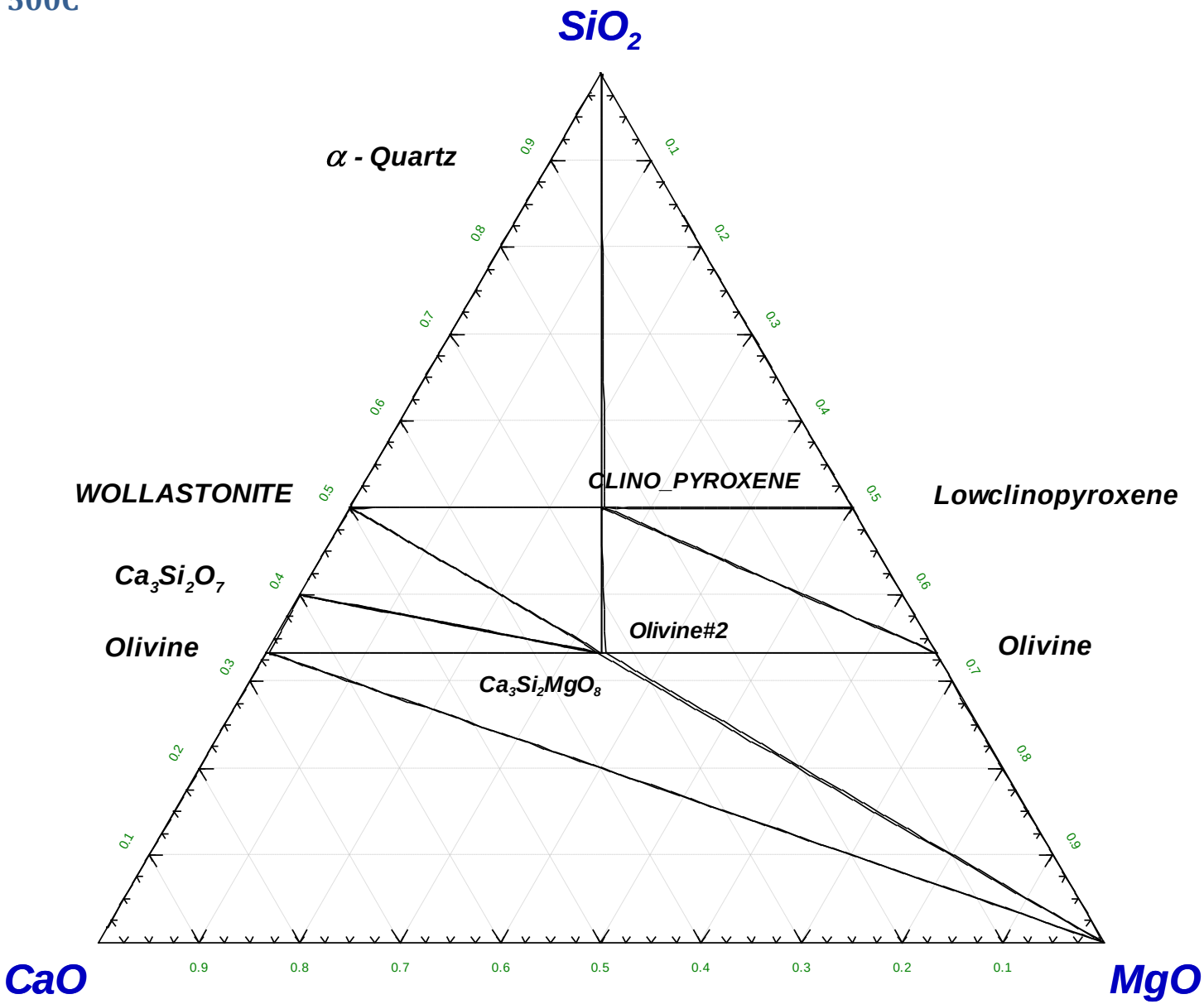

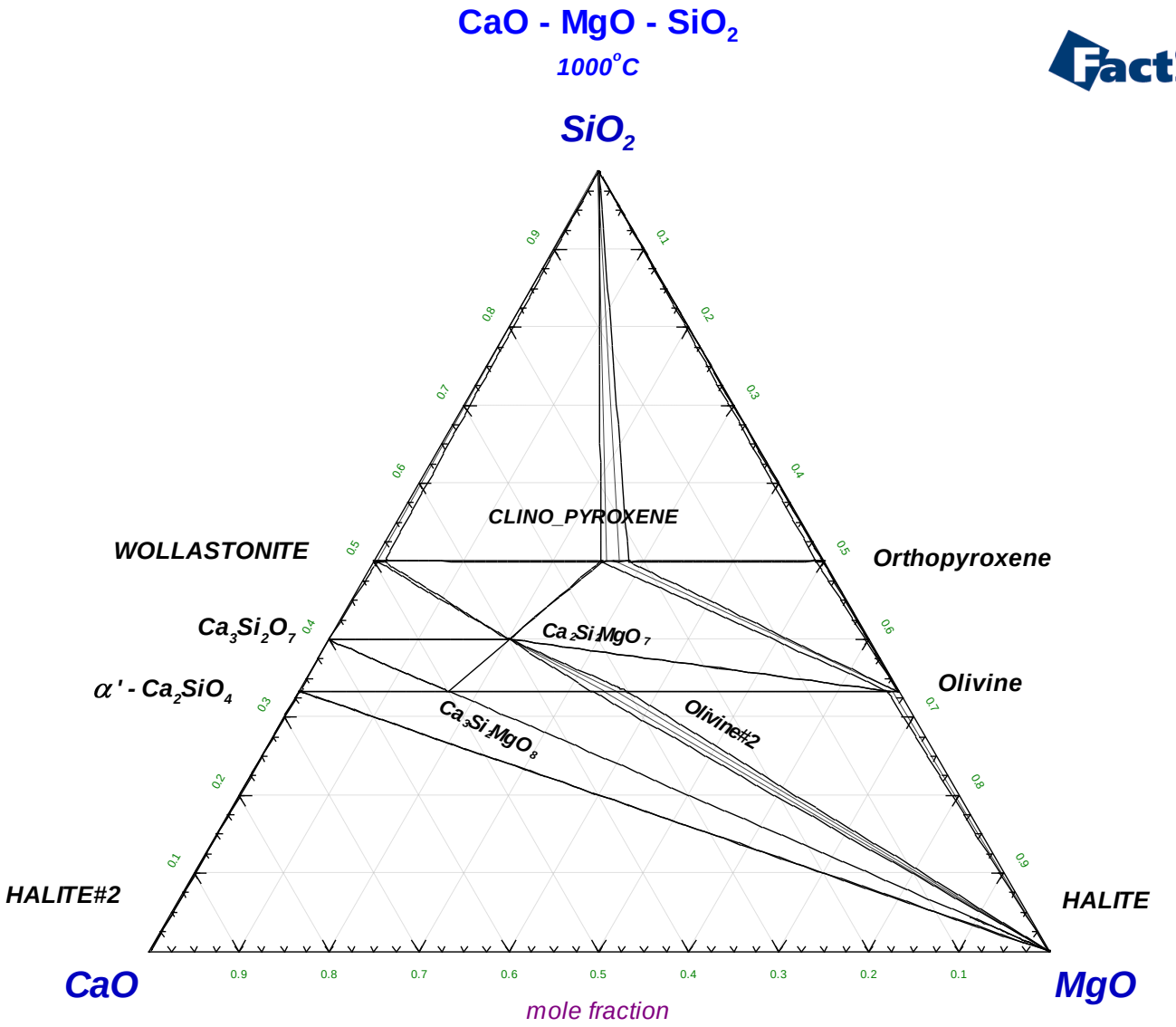
CaO - MgO - SiO2
1000°C
FactSage™
SiO2
CLINO_PYROXENE
WOLLASTONITE
Orthopyroxene
Ca3Si2O7
Ca2SiMgO7
α' - Ca2SiO4
Olivine
Olivine#2
Ca3SiMgO8
HALITE#2
HALITE
CaO
MgO
mole fraction

Mole fraction
kurz unterhalb Liquidussurface

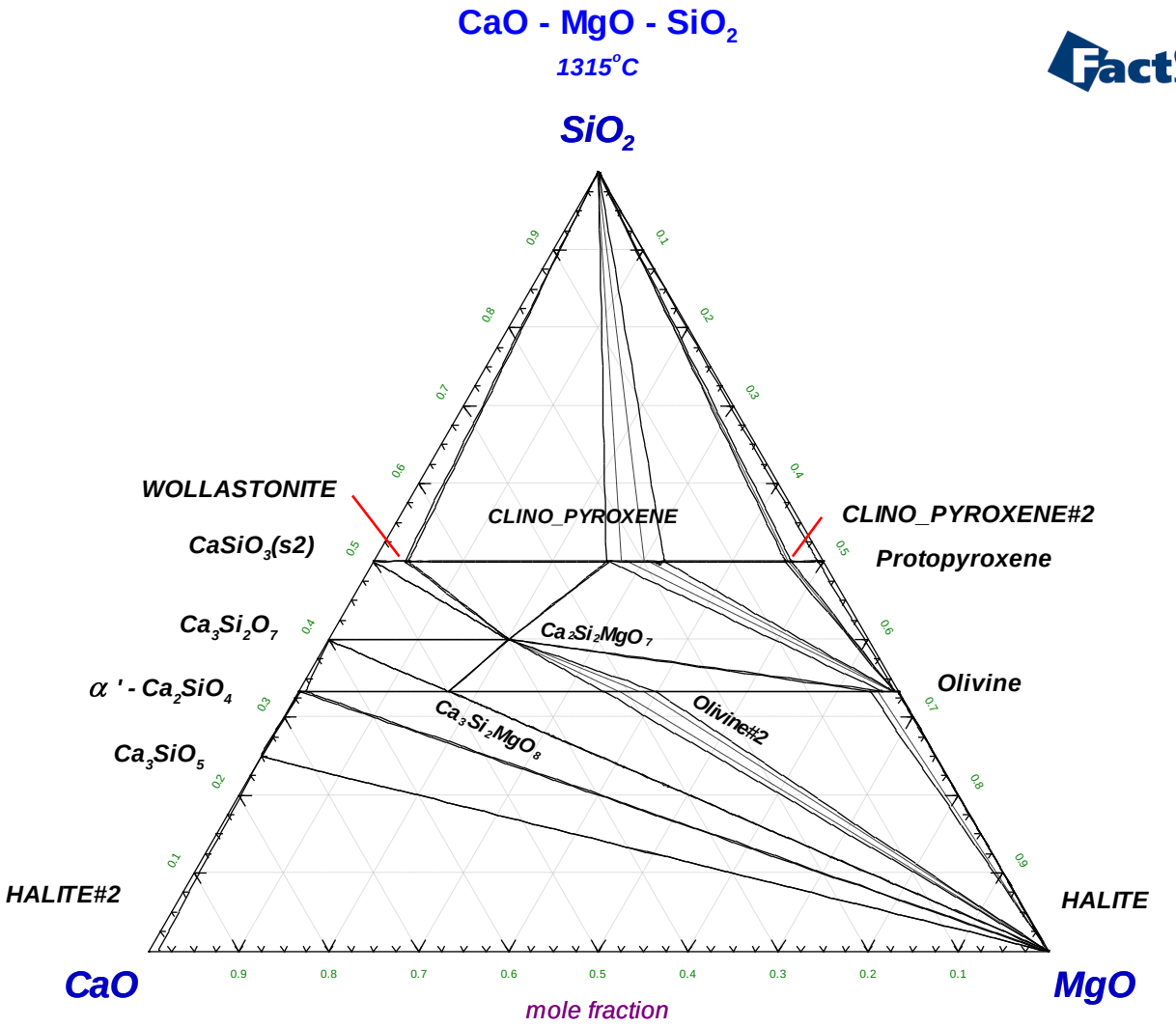

Mole fraction
compared with experimental data

$CaSiO_3$ - $MgSiO_3$

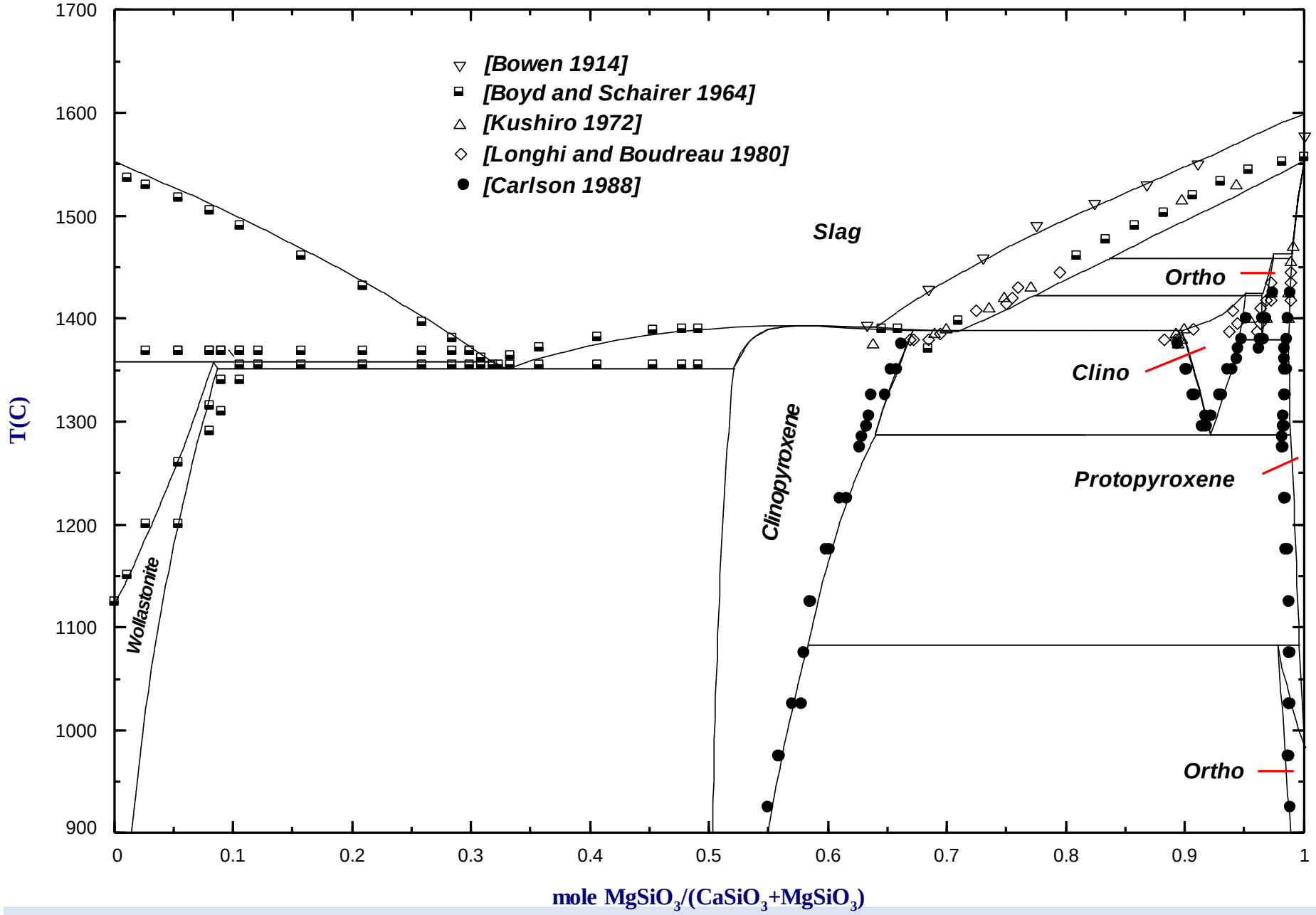

Mole fraction in Kelvin Ca2SiO4-Mg2SiO4 compared with experimental data

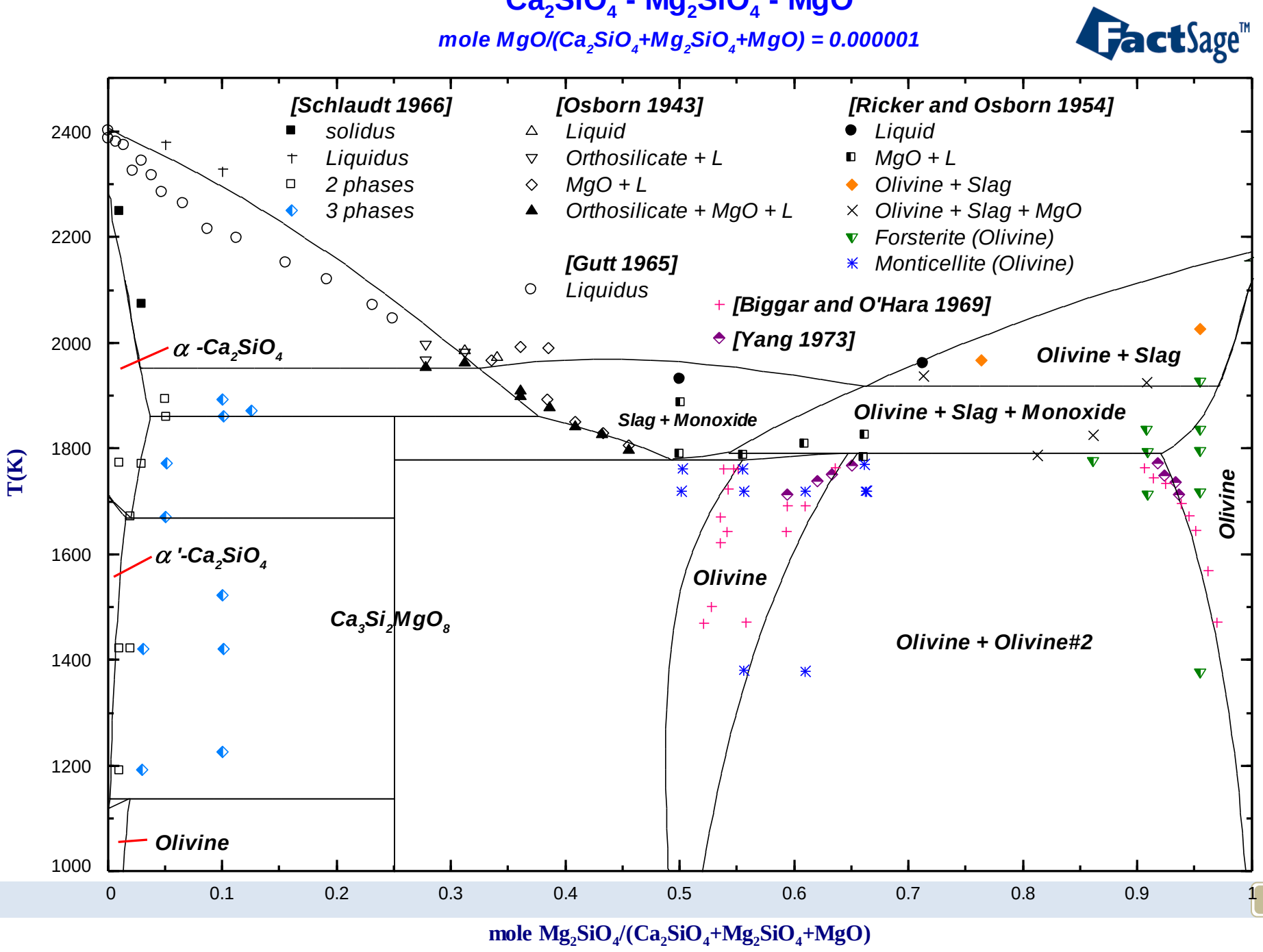

Mole fraction Ca2SiO4-Akermanite compared with experimental data

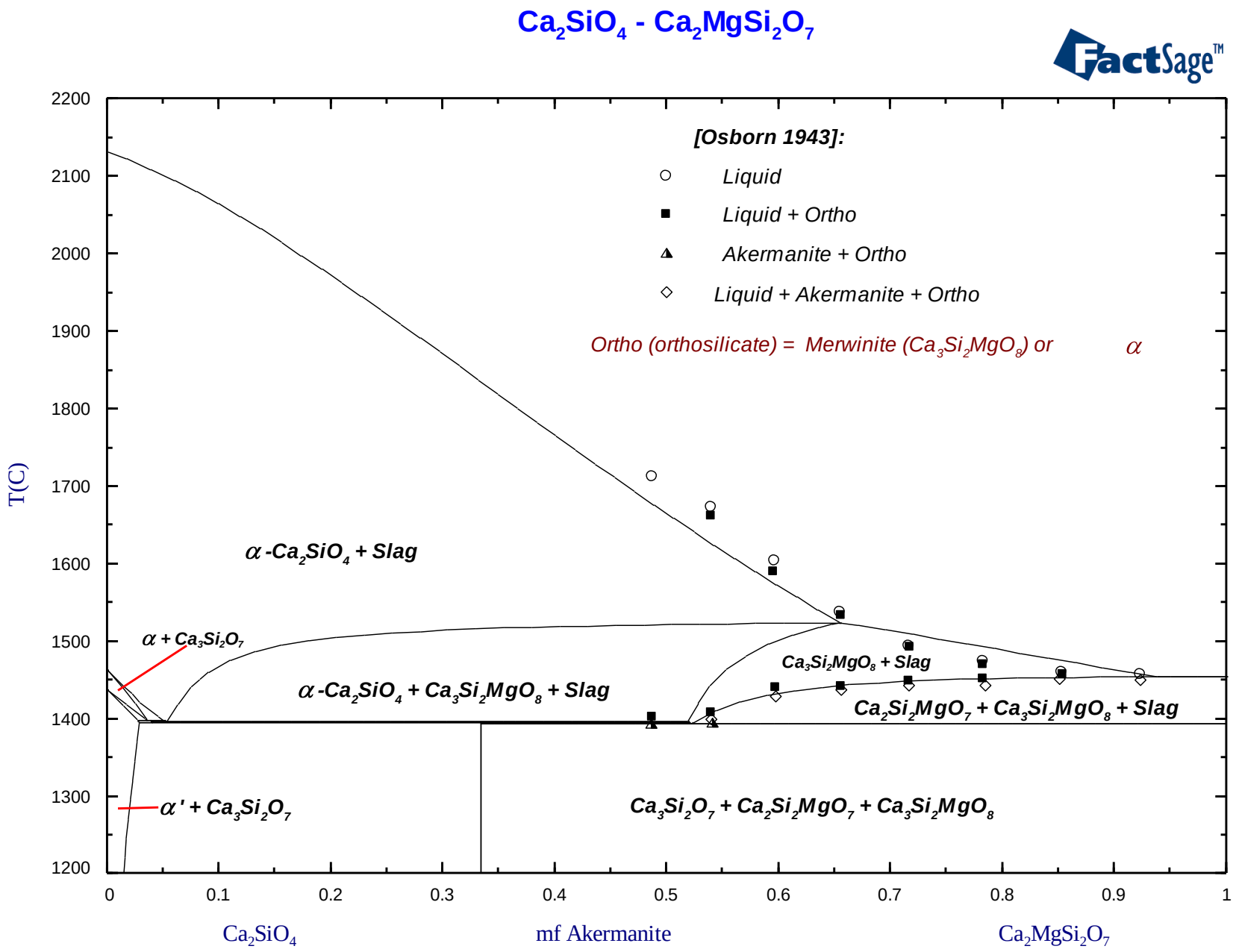

Weight percent CaSiO3-Akermanite compared with experimental data

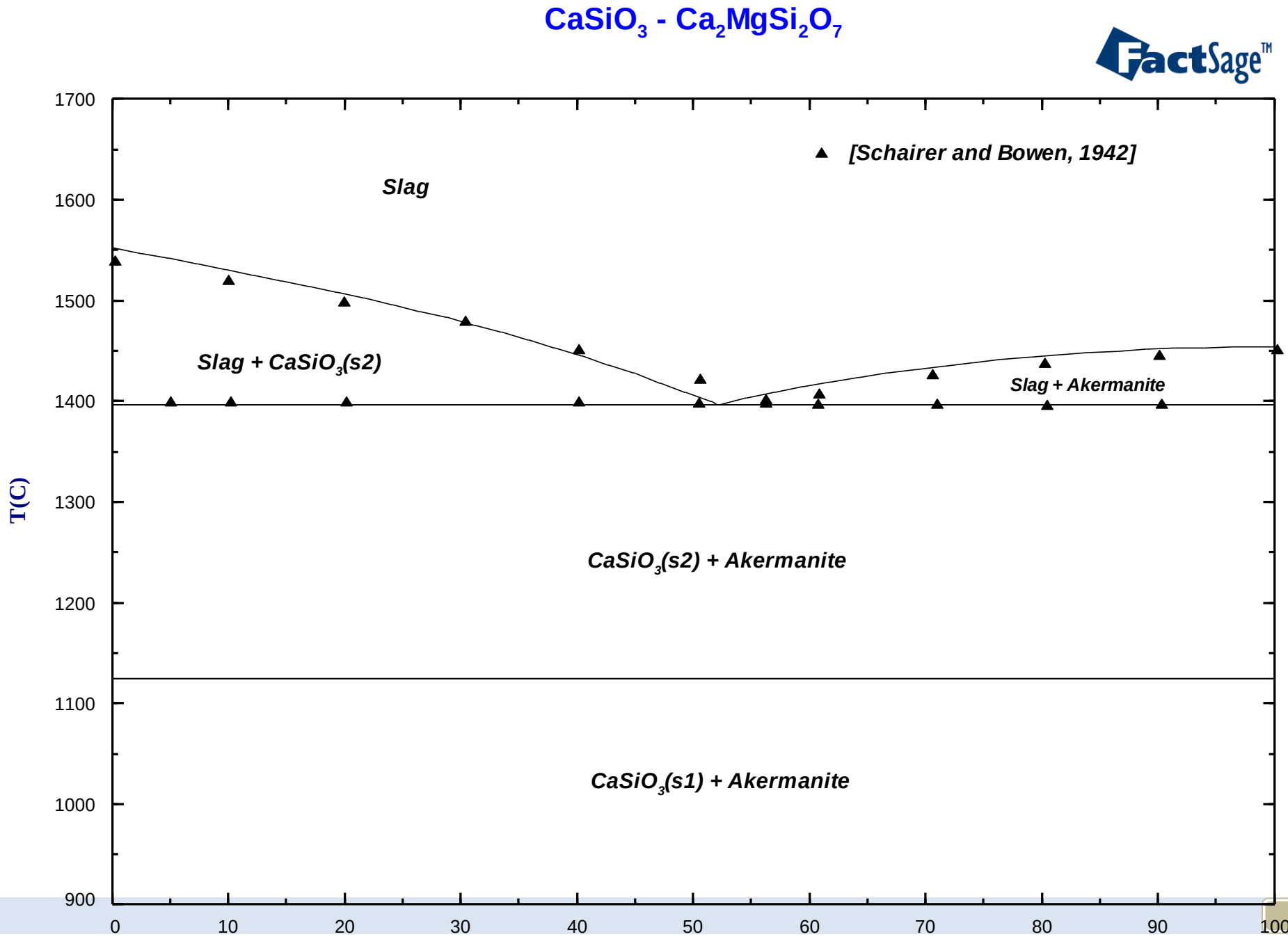

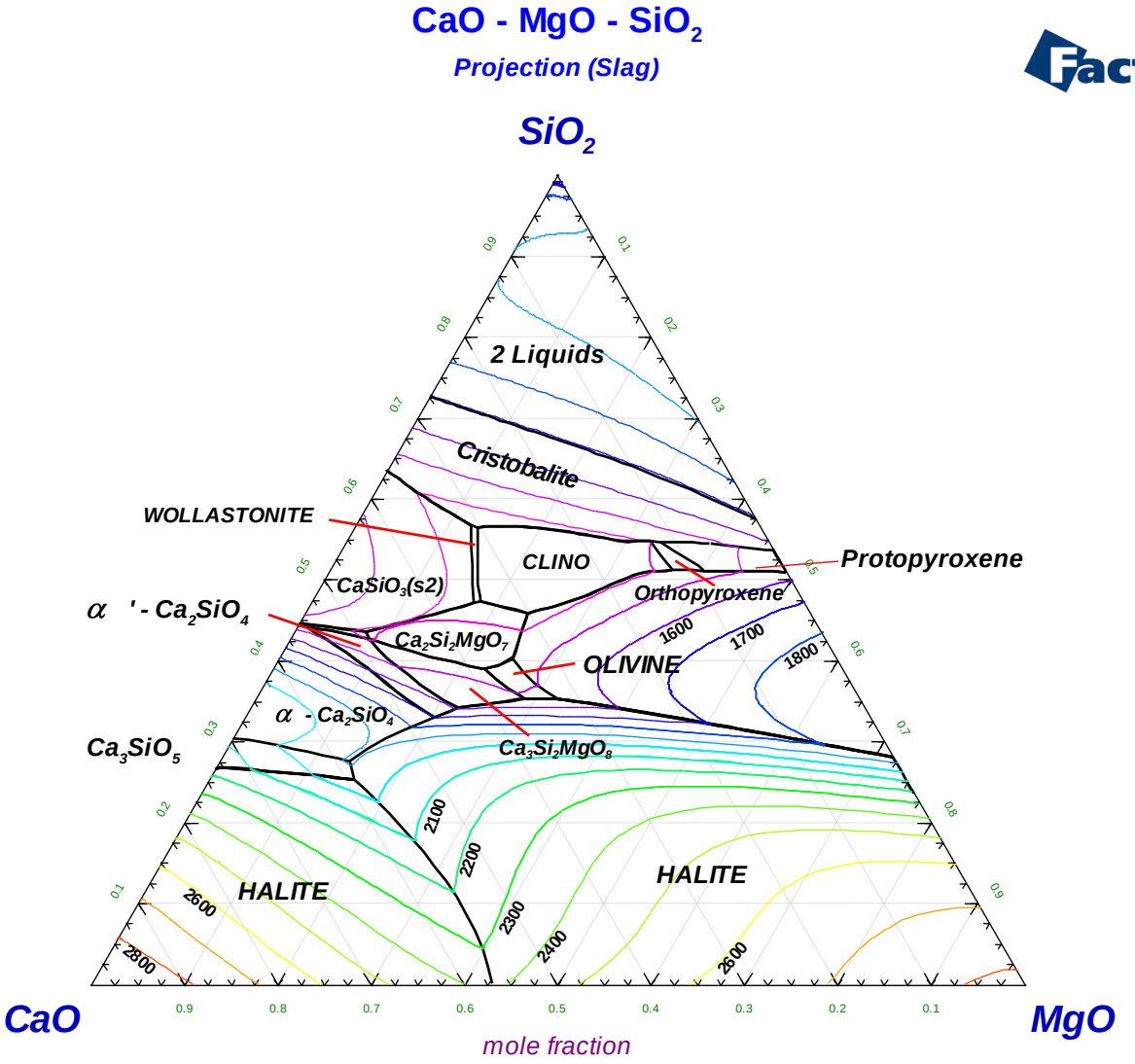
CaO - MgO - SiO2
Projection (Slag)
FactSage™
SiO2
2 Liquids
Cristobalite
WOLLASTONITE
CLINO
Protopyroxene
CaSiO3(s2)
Orthopyroxene
α ' - Ca2SiO4
Ca2Si2MgO7
1600
1700
1800
OLIVINE
α - Ca2SiO4
Ca3SiO5
Ca3Si2MgO8
2100
2200
2300
2400
2600
HALITE
HALITE
2800
CaO
MgO
mole fraction

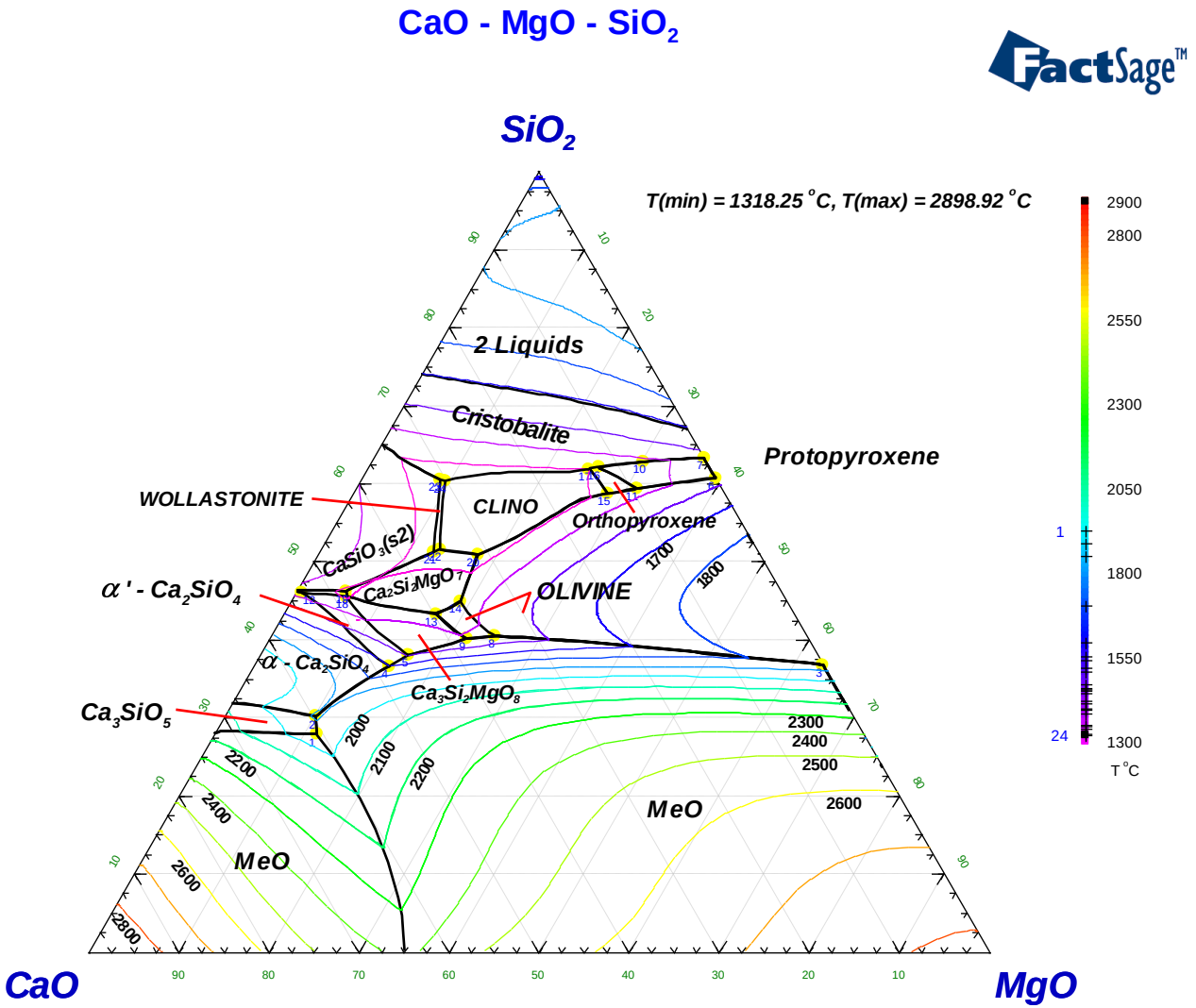
CaO - MgO - SiO2
FactSage™
SiO2
T(min) = 1318.25 °C, T(max) = 2898.92 °C
2 Liquids
Cristobalite
Protopyroxene
WOLLASTONITE
CLINO
Orthopyroxene
CaSiO3(s2)
Ca2Si2MgO7
α ' - Ca2SiO4
OLIVINE
α - Ca2SiO4
Ca3Si2MgO8
Ca3SiO5
MeO
MeO
CaO
MgO
2900
2800
2550
2300
2050
1800
1550
1300
T °C

Invariant equilibria on the liquidus surface

Intersections with slag	Mole fraction A = SiO2, B = CaO, C = MgO				Weight percent A = SiO2, B = CaO, C = MgO				
		X(A)	X(B)	X(C)	T(C)	W(A)	W(B)	W(C)	T(C)
1: Ca3SiO5 / MeO#1 / MeO#2	1:	0.25442	0.59149	0.15409	1924.86	27.996	60.659	11.345	1924.86
2: Ca2SiO4(s2) / Ca3SiO5 / MeO#1	2:	0.27589	0.58505	0.13907	1887.55	30.145	59.662	10.193	1887.56
3: Ca2SiO4(s2) / MeO#1 / α′-Ca2SiO4	3:	0.33028	0.46700	0.20272	1702.33	36.611	48.315	15.074	1702.30
4: Ca3Si2MgO8 / MeO#1 / α′-Ca2SiO4	4:	0.34167	0.43702	0.22131	1594.20	38.048	45.421	16.531	1594.20
5: Ca3Si2MgO8 / MeO#1 / OLIVINE	5:	0.35342	0.35844	0.28814	1506.32	40.105	37.962	21.933	1506.32
6: OLIVINE / Orthopyroxene / Protopyroxene	6:	0.51129	0.08747	0.40123	1458.54	59.309	9.470	31.221	1458.55
7: Ca2SiO4(s2) / Ca3Si2O7 / α′-Ca2SiO4	7:	0.44218	0.54871	0.00911	1455.64	46.041	53.323	0.636	1455.64
8: Ca2Si2MgO7 / Ca3Si2MgO8 / OLIVINE	8:	0.38978	0.38323	0.22699	1450.83	43.322	39.754	16.924	1450.83
9: CLINO_pyroxene/ OLIVINE / Orthopyroxene	9:	0.51149	0.12058	0.36793	1422.77	58.736	12.923	28.341	1422.76
10: Orthopyroxene / Protopyroxene / Cristobalite	10:	0.54736	0.11657	0.33607	1412.37	62.087	12.341	25.572	1412.37
11: CLINO_pyroxene/ Orthopyroxene / Cristobalite	11:	0.54747	0.12712	0.32540	1399.80	61.903	13.416	24.681	1399.80
12: Ca3Si2MgO8 / Ca3Si2O7 / α′-Ca2SiO4	12:	0.42789	0.48967	0.08244	1394.87	45.511	48.608	5.882	1394.87
13: Ca2Si2MgO7 / Ca3Si2O7 / CaSiO3(s2)	13:	0.43564	0.48707	0.07729	1382.81	46.242	48.254	5.504	1382.81
14: CLINO_PYROXENE / Ca2Si2MgO7 / OLIVINE	14:	0.45913	0.30197	0.23890	1350.28	50.946	31.272	17.782	1350.27
15: Ca2Si2MgO7 / CaSiO3(s2) / WOLLASTONITE	15:	0.47119	0.35406	0.17475	1345.80	51.280	35.963	12.758	1345.80
16: CLINO_pyroxene/ Ca2Si2MgO7/WOLLASTONITE	16:	0.47270	0.34601	0.18130	1339.54	51.535	35.207	13.259	1339.54
17: CaSiO3(s2) / Cristobalite / WOLLASTONITE	17:	0.56852	0.30871	0.12277	1325.18	60.545	30.684	8.771	1325.18
18: CLINO_pyroxene/ Cristobalite / WOLLASTONITE	18:	0.56494	0.30314	0.13191	1317.86	60.334	30.216	9.450	1317.86

CaO-MgO-TiO2,

CaO-MgO-TiO2,
Mole fraction, 1300°C

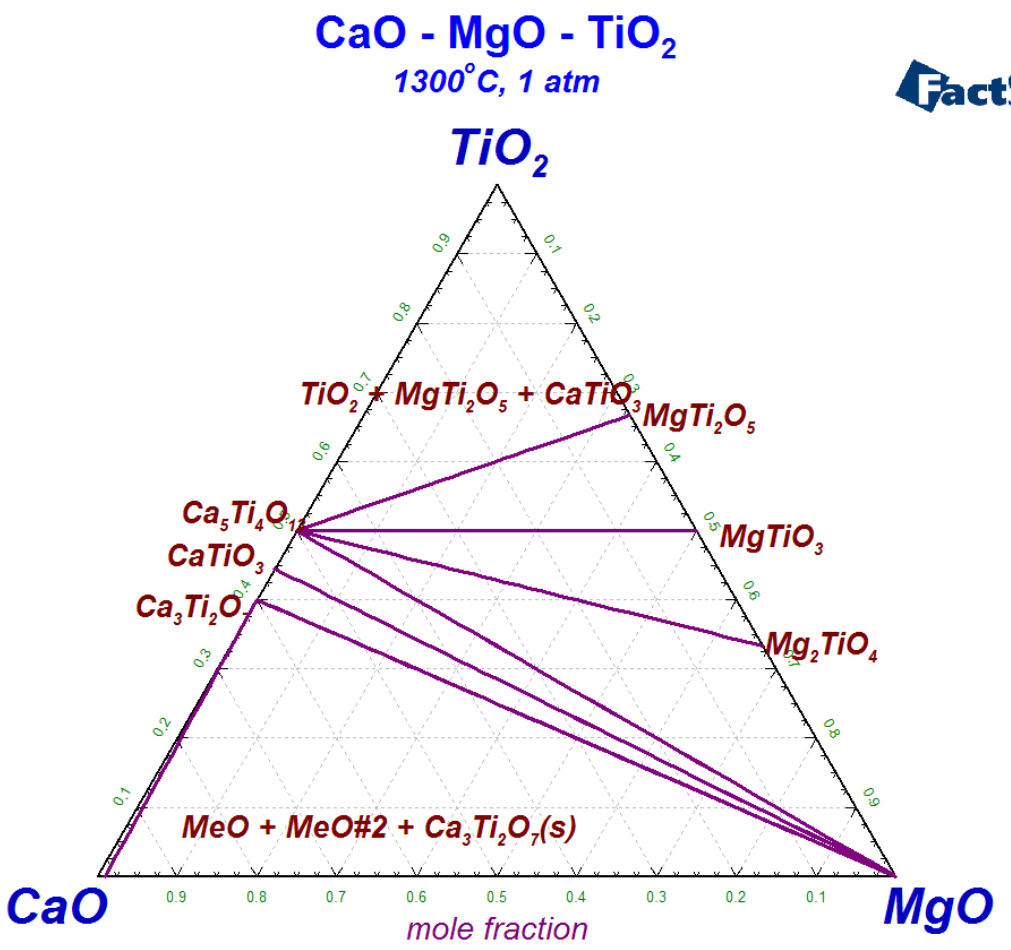

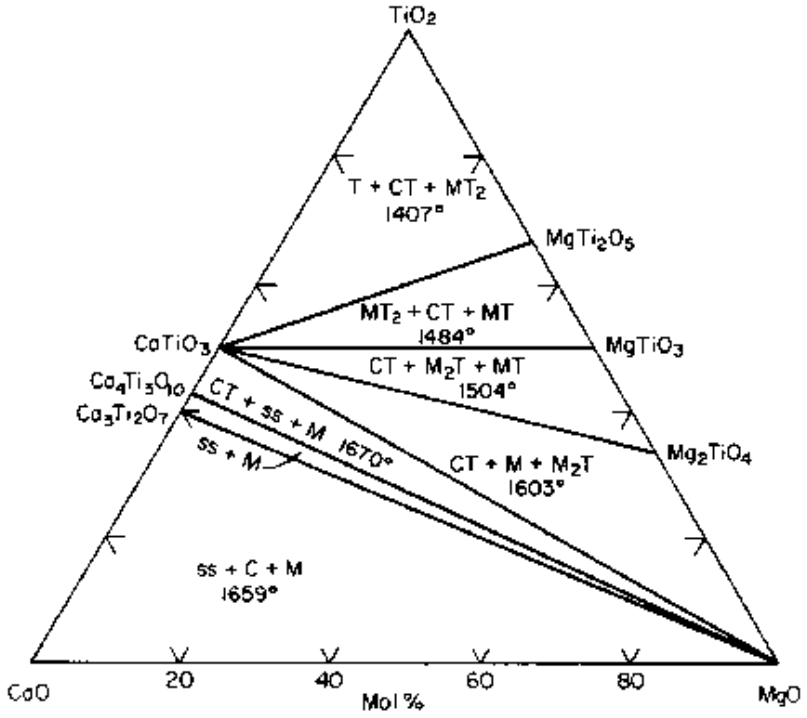

R.L. Schultz, J.Am. Ceram. Soc., 56 [1] (1973), pp. 33-36.

CaO-MgO-TiO2,
Mole fraction, Liquidus surface

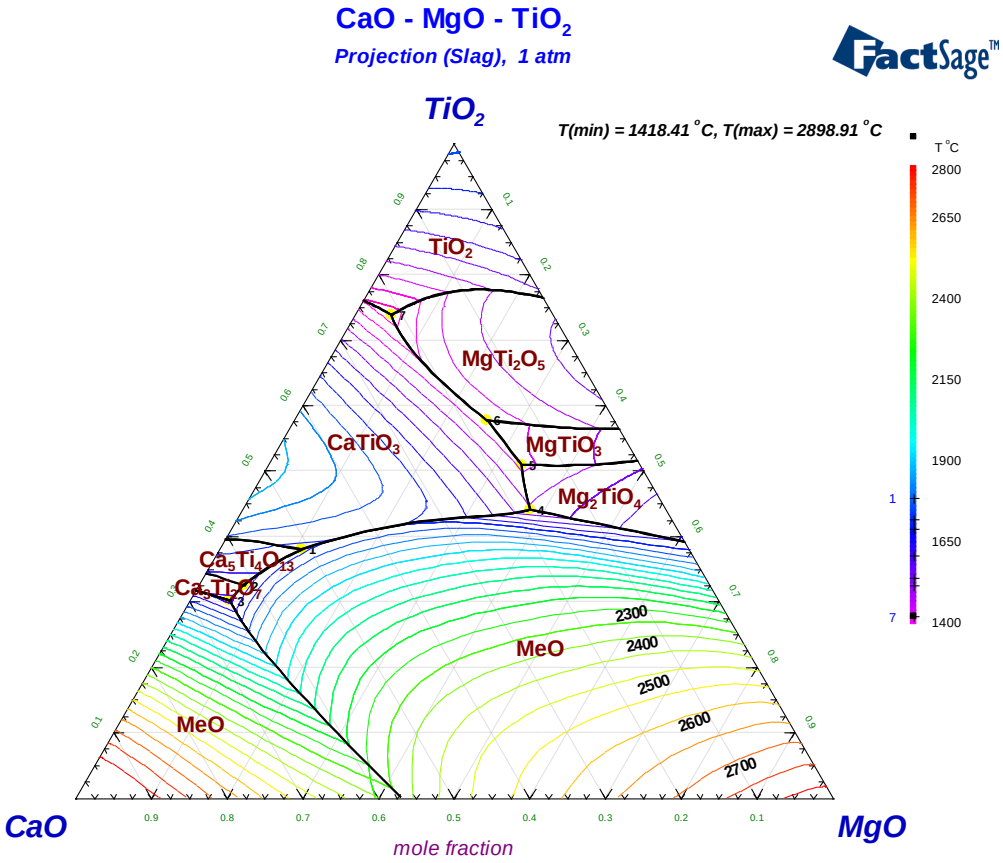

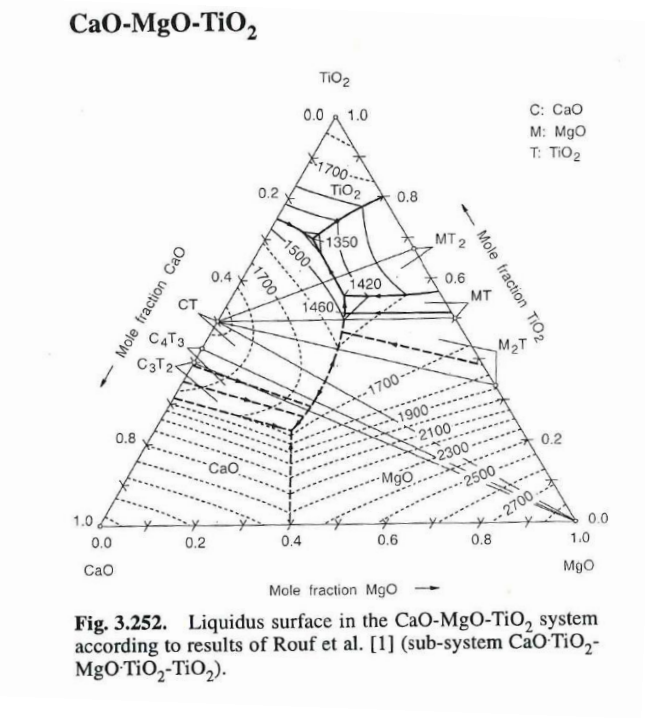

Fig. 3.252. Liquidus surface in the CaO-MgO-TiO_2 system according to results of Rouf et al. [1] (sub-system CaO·TiO_2-MgO·TiO_2-TiO_2).

M.A. Rouf, A.H. Cooper, H.B. Bell, Trans. J. Br. Ceram. Soc., 68 [6], (1969), pp.263-267.

CaO-MgO-TiO2,
Weight percent, Liquidus surface

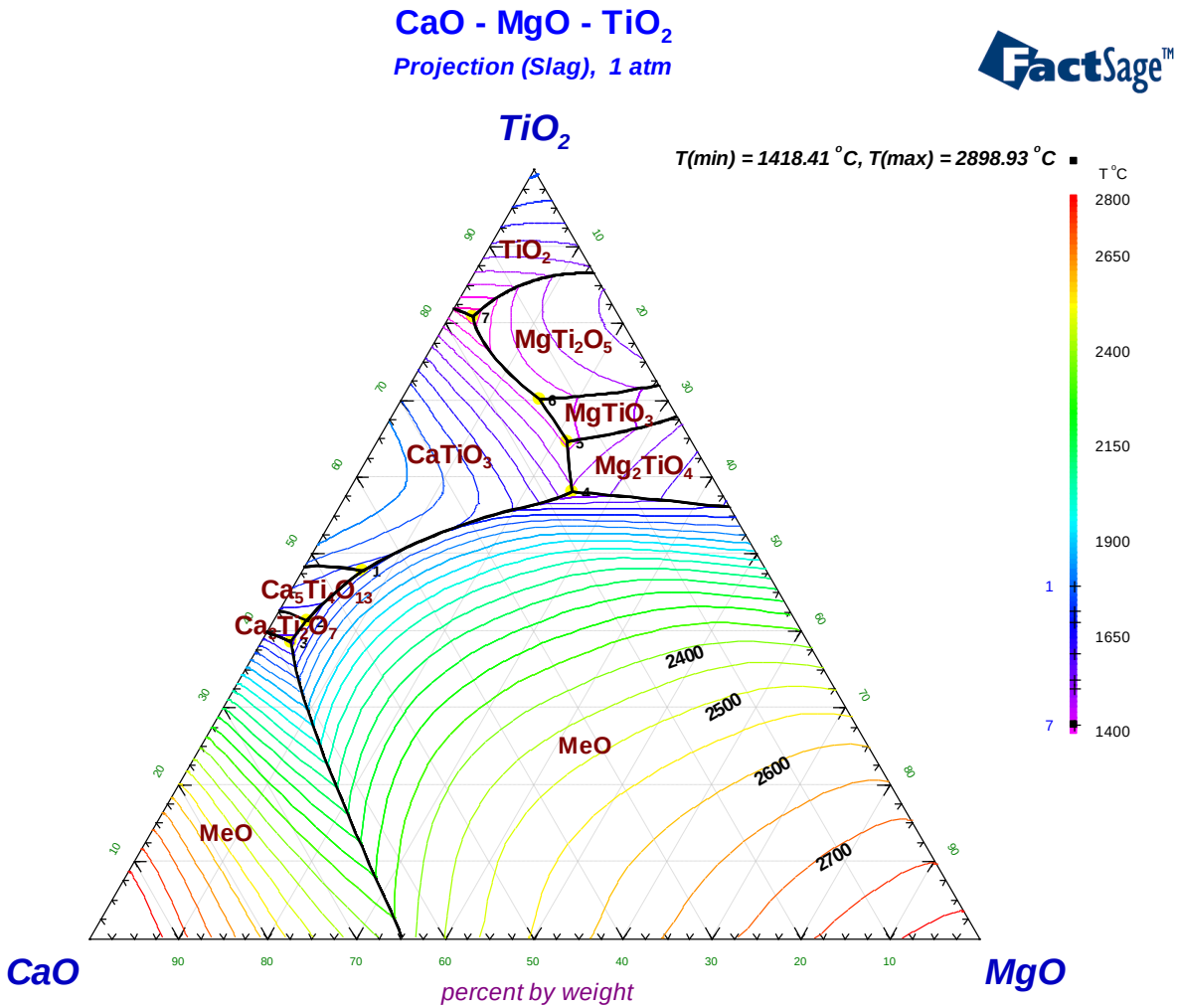

Invariant equilibria on the liquidus surface

Intersections with slag	Mole fraction A = TiO2, B = CaO, C = MgO				Weight percent A = TiO2, B = CaO, C = MgO				
		X(A)	X(B)	X(C)	T(C)		W(A)	W(B)	W(C)	T(C)
1: Ca5Ti4O13 / CaTiO3 / MeO#1	1:	0.37949	0.51204	0.10847	1781.15	1:	47.809	45.295	6.896	1781.15
2: Ca3Ti2O7 / Ca5Ti4O13 / MeO#1	2:	0.32561	0.61511	0.05927	1718.32	2:	41.351	54.850	3.799	1718.32
3: Ca3Ti2O7 / MeO#1 / MeO#2	3:	0.30141	0.64570	0.05289	1687.60	3:	38.570	58.014	3.416	1687.61
4: CaTiO3 / MeO#1 / Mg2TiO4	4:	0.44008	0.17921	0.38071	1606.29	4:	58.055	16.599	25.345	1606.29
5: CaTiO3 / Mg2TiO4 / MgTiO3	5:	0.50904	0.15577	0.33519	1536.80	5:	64.634	13.888	21.478	1536.81
6: CaTiO3 / MgTi2O5 / MgTiO3	6:	0.57755	0.16770	0.25475	1513.84	6:	70.103	14.292	15.605	1513.84
7: CaTiO3 / MgTi2O5 / TiO2	7:	0.73814	0.21371	0.04815	1418.41	7:	80.892	16.445	2.663	1418.41

CaO-MgO-V2O5,

CaO-MgO-V2O5,
Mole fraction, 550°C

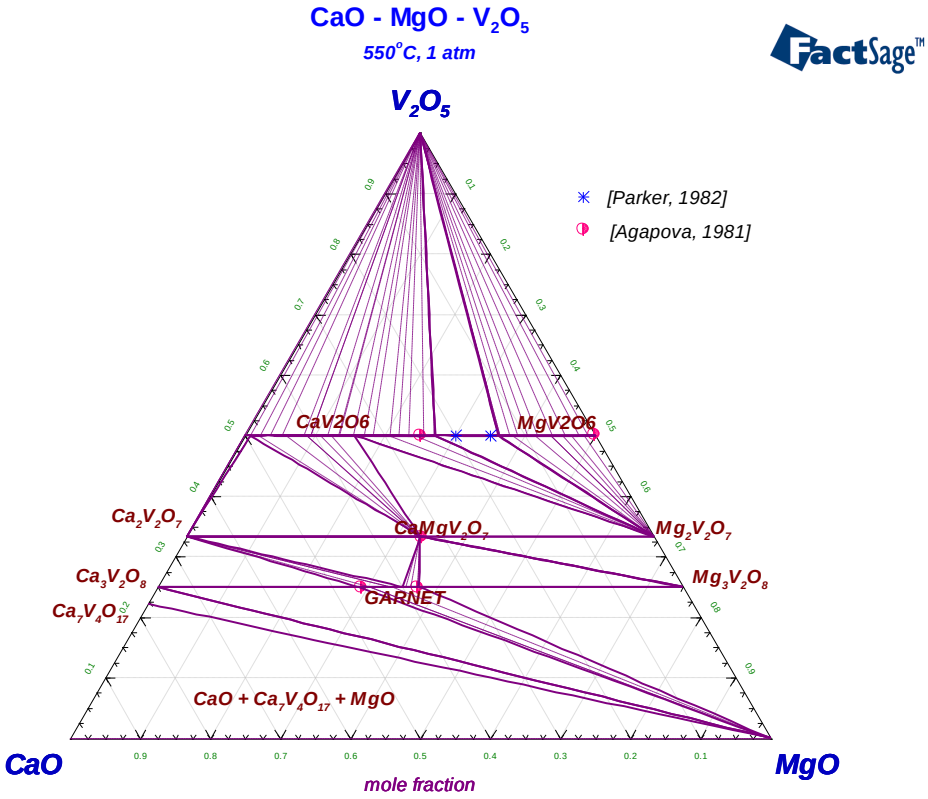

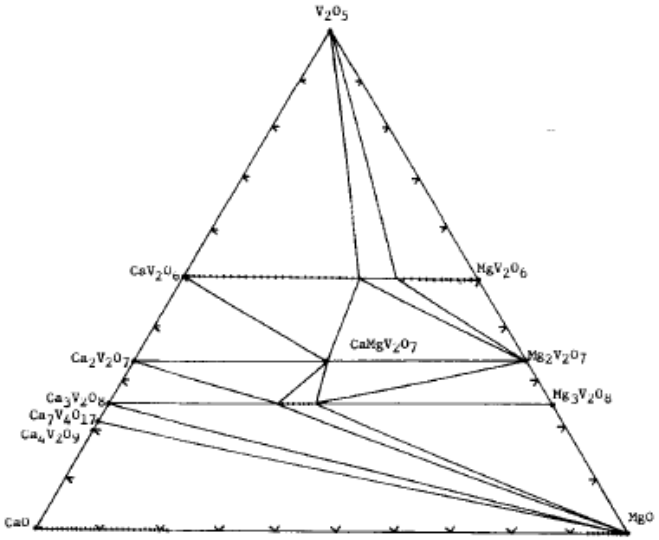

F. J. Parker, R.A. McCauley, Phase Equilib, 7 (1982), pp. 349-351.

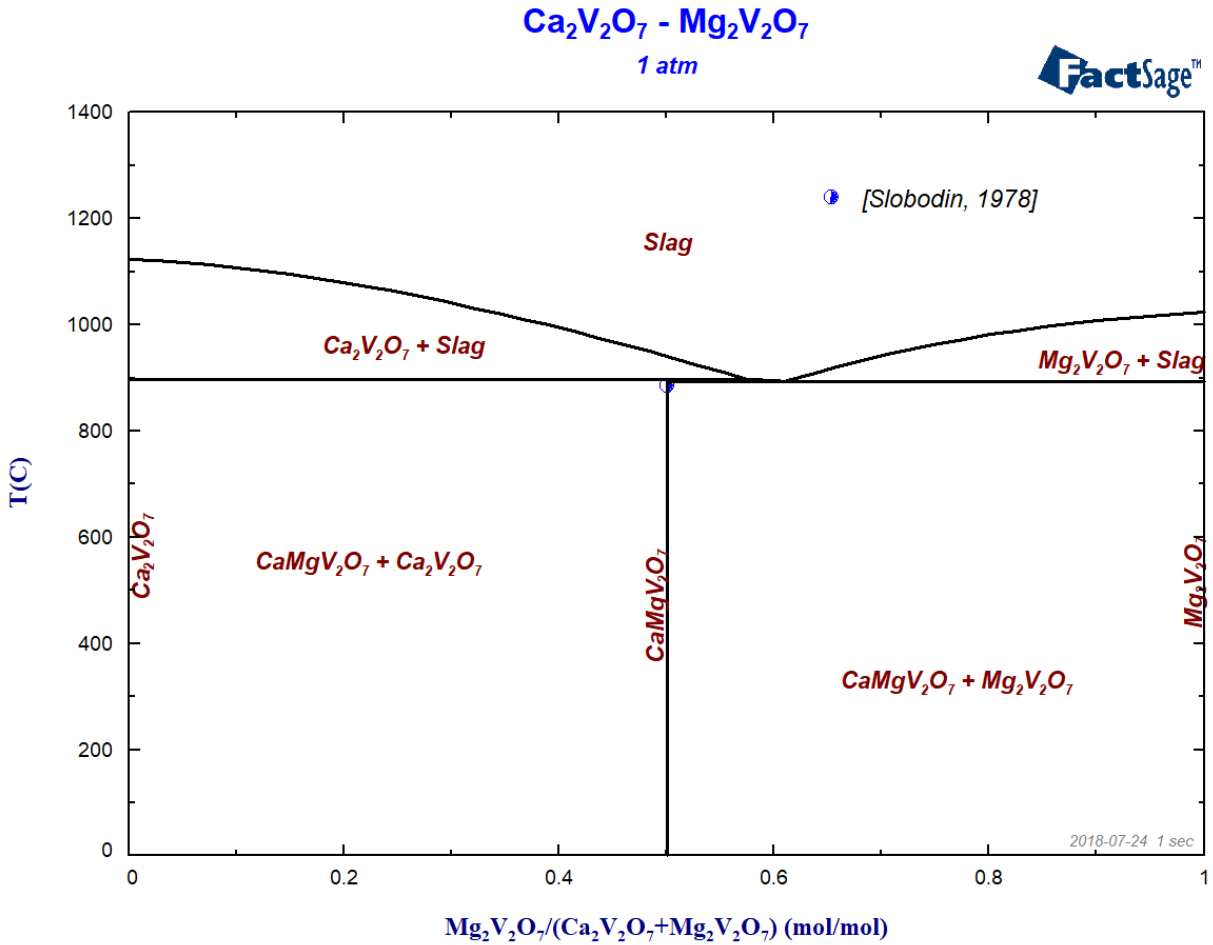
Ca2V2O7 - Mg2V2O7
1 atm
FactSage™
[Slobodin, 1978]
Slag
Ca2V2O7 + Slag
Mg2V2O7 + Slag
CaMgV2O7 + Ca2V2O7
CaMgV2O7 + Mg2V2O7
Ca2V2O7
CaMgV2O7
Mg2V2O7
T(C)
1400
1200
1000
800
600
400
200
0
0
0.2
0.4
0.6
0.8
1
2018-07-24 1 sec
Mg2V2O7/(Ca2V2O7+Mg2V2O7) (mol/mol)

CaO-MgO-V2O5,
Mole fraction, Liquidus surface

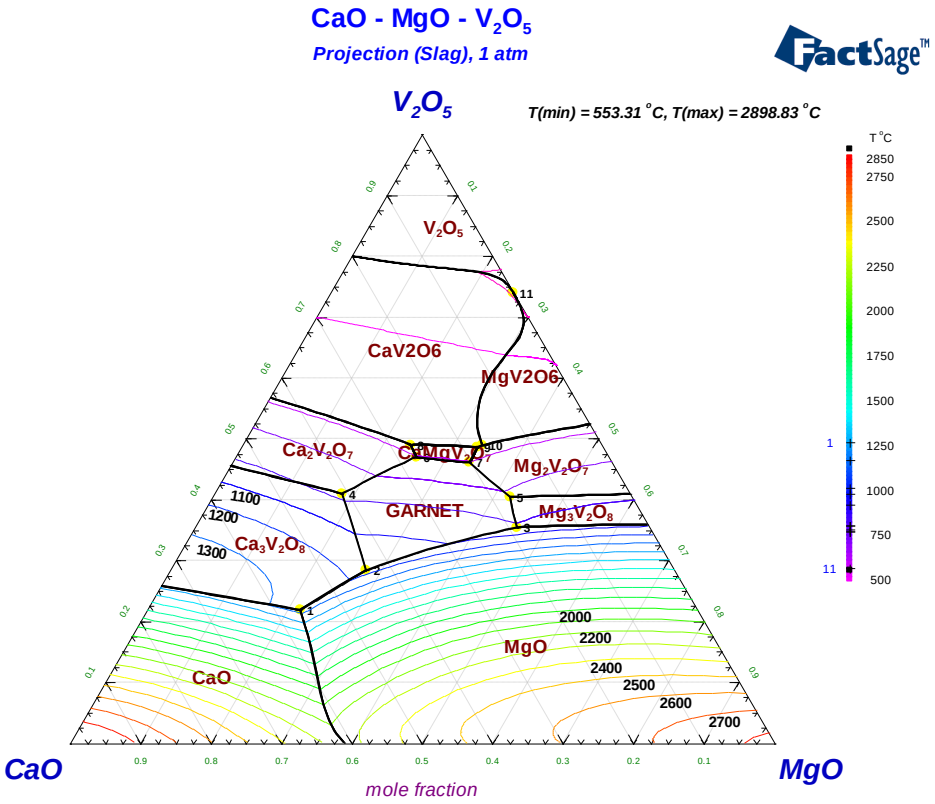

CaO-MgO-V2O5,
Weight percent, Liquidus surface

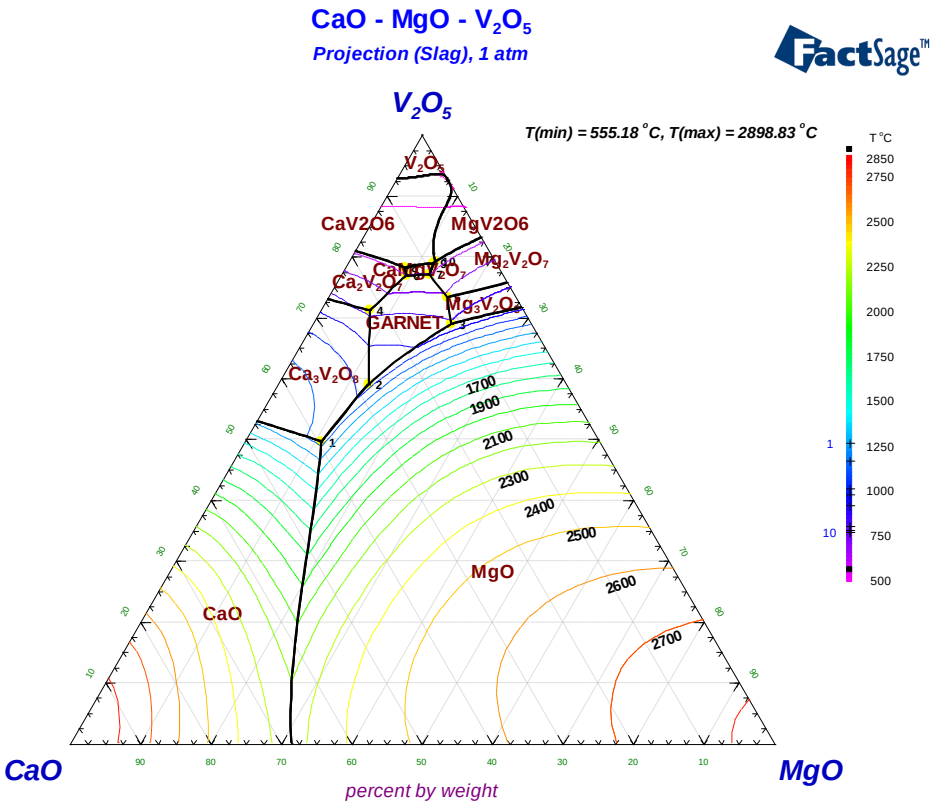

Invariant equilibria on the liquidus surface

Intersections with slag	Mole fraction				Weight percent			
	A = V2O5, B = CaO, C = MgO				A = V2O5, B = CaO, C = MgO			
	X(A)	X(B)	X(C)	T(C)	W(A)	W(B)	W(C)	T(C)
1: Ca3V2O8 / CaO / MgO	1: 0.21897	0.56392	0.21711	1262.81	1: 49.658	39.431	10.911	1262.81
2. Ca3V2O8 / GARNET / MgO	2: 0.28401	0.43707	0.27892	1163.09	2: 59.098	28.041	12.861	1163.09
3. GARNET / Mg3V2O8 / MgO	3: 0.35498	0.18779	0.45723	1011.72	3: 69.036	11.260	19.704	1011.72
4. Ca2V2O7 / Ca3V2O8 / GARNET	4: 0.41020	0.40800	0.18180	975.04	4: 71.181	21.828	6.991	975.03
5. GARNET / Mg2V2O7 / Mg3V2O8	5: 0.40497	0.17273	0.42230	915.02	5: 73.390	9.651	16.959	915.02
6. Ca2V2O7 / CaMgV2O7 / GARNET	6: 0.47054	0.27301	0.25645	802.45	6: 76.943	13.764	9.293	802.45
7. CaMgV2O7 / GARNET / Mg2V2O7	7: 0.46128	0.20181	0.33691	801.96	7: 77.116	10.402	12.481	801.96
8. Ca2V2O7 / CaMgV2O7 / CaV2O6	8: 0.49014	0.27121	0.23865	776.68	8: 78.216	13.344	8.439	776.68
9. CaMgV2O7 / CaV2O6 / Mg2V2O7	9: 0.48611	0.17813	0.33576	766.21	9: 78.986	8.924	12.090	766.20
10. CaV2O6 / Mg2V2O7 / MgV2O6	10: 0.48880	0.17016	0.34105	765.70	10: 79.243	8.505	12.252	765.70

Weight percent, Metasilicate section CaSiO3-MnSiO3

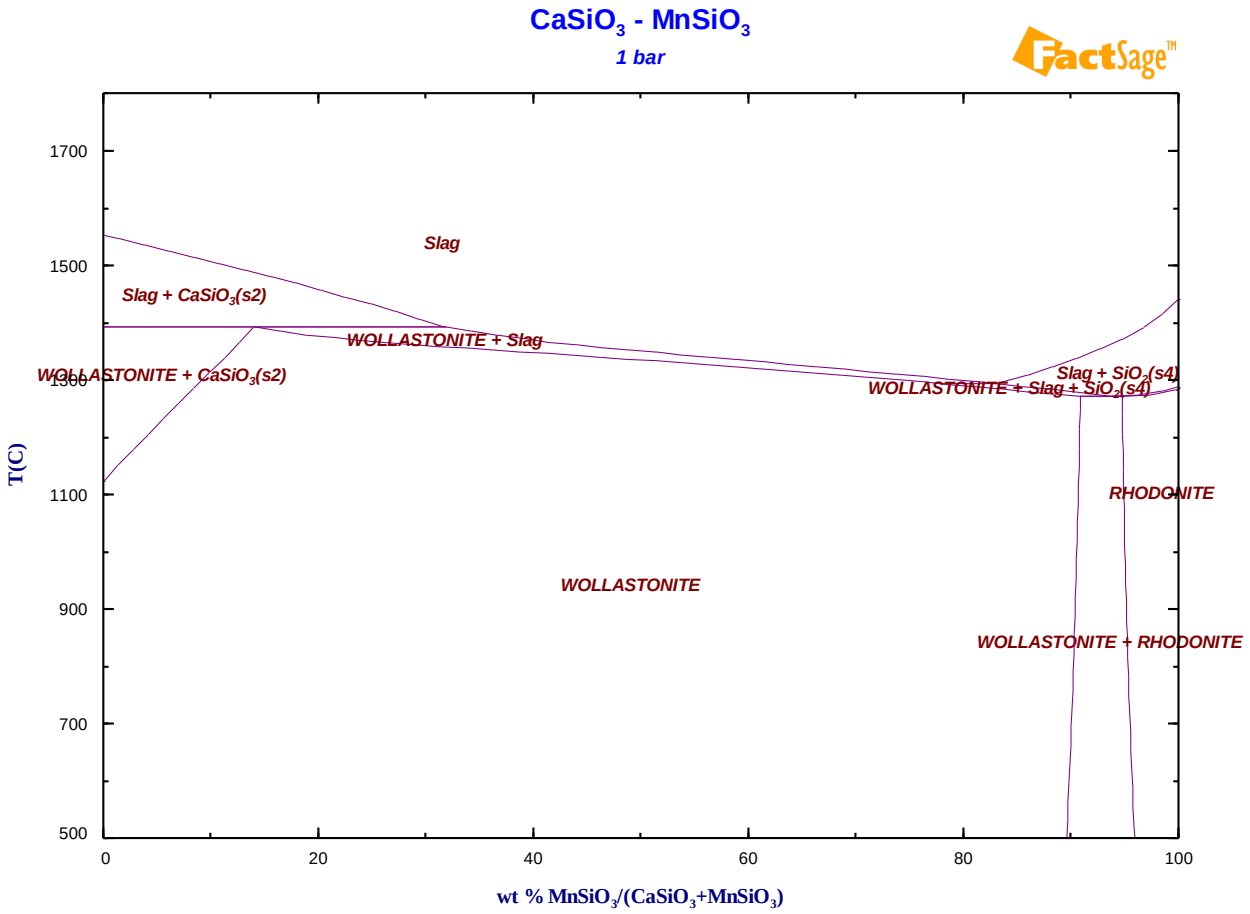

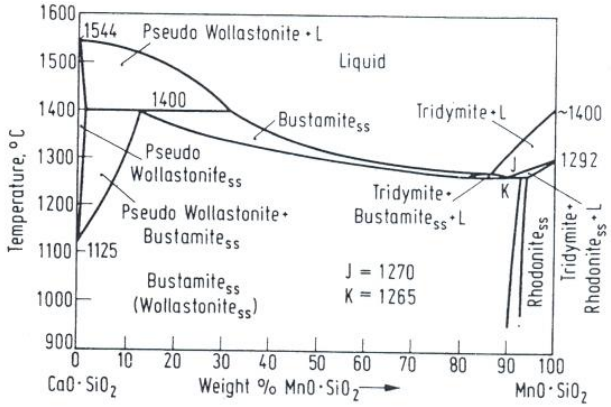

Fig. 3.257. Composition section $CaO{\cdot}SiO_2$-$MnO{\cdot}SiO_2$ after Glasser [1, 2]. Recently, a new ternary solution phase on the $CaO{\cdot}SiO_2$-$MnO{\cdot}SiO_2$ section was reported by Mikirticheva et al. [3].

F.P. Glaser, Am. J. Sci., 259 [1], (1961), pp. 46-59.

Weight percent, Orthosilicate section Ca2SiO4-Mn2SiO4

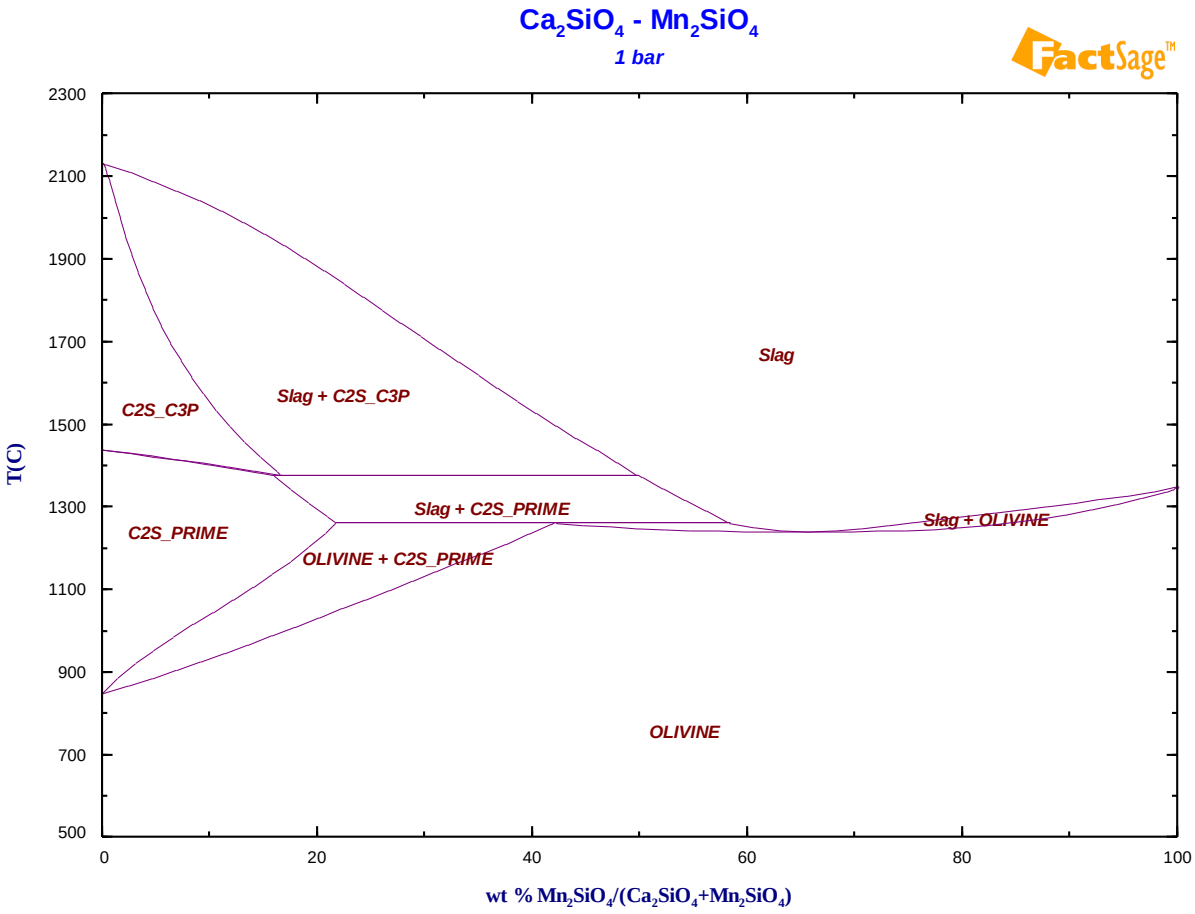

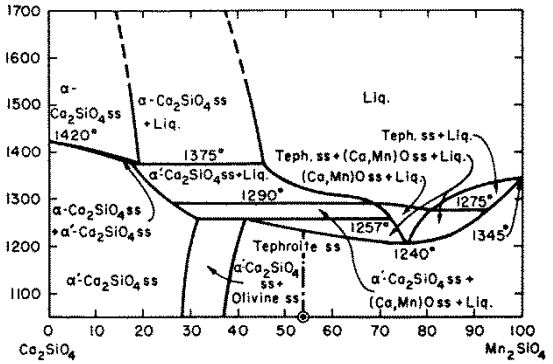

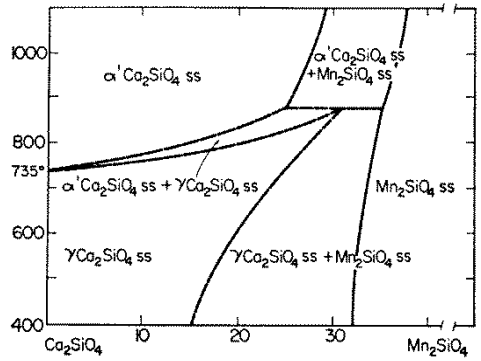

F.P. Glaser, Am. J. Sci., 259 [1], (1961), pp. 46-59.

Mole fraction, Liquidussurface

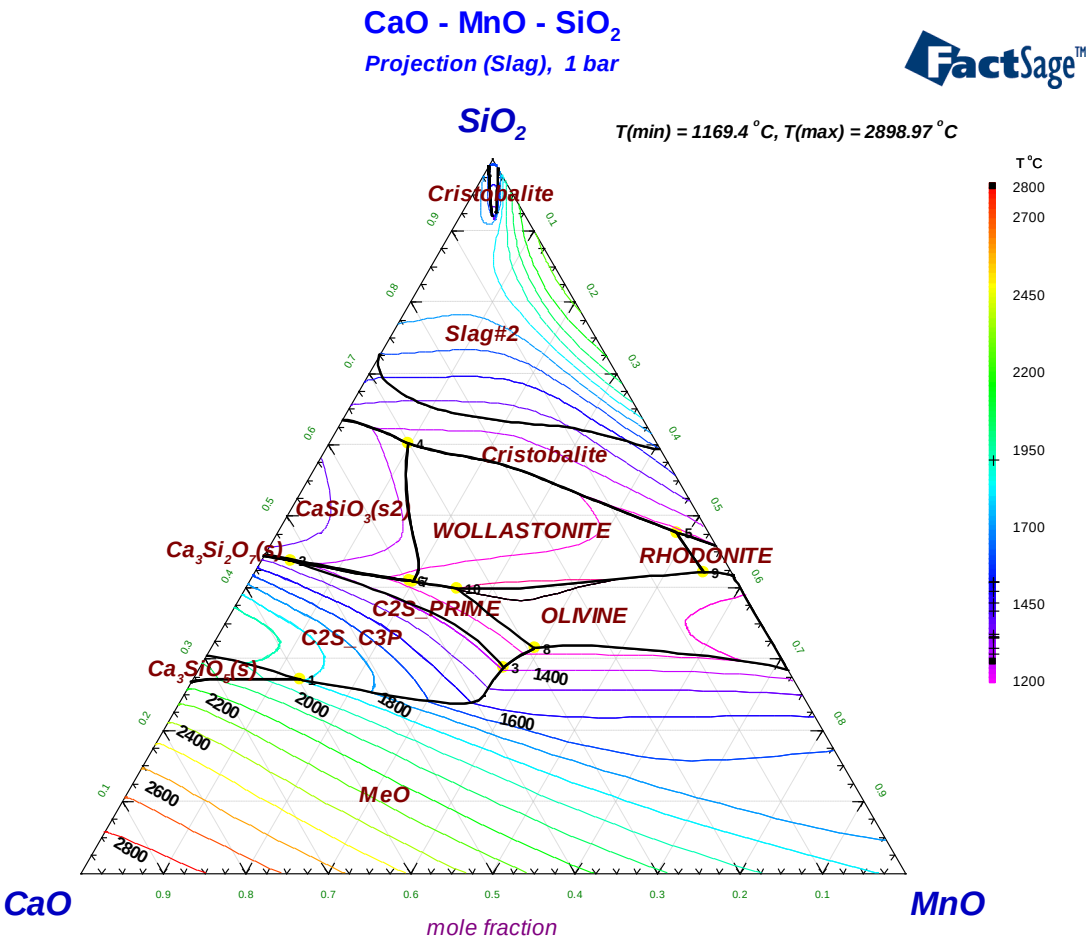

Weight percent, Liquidussurface

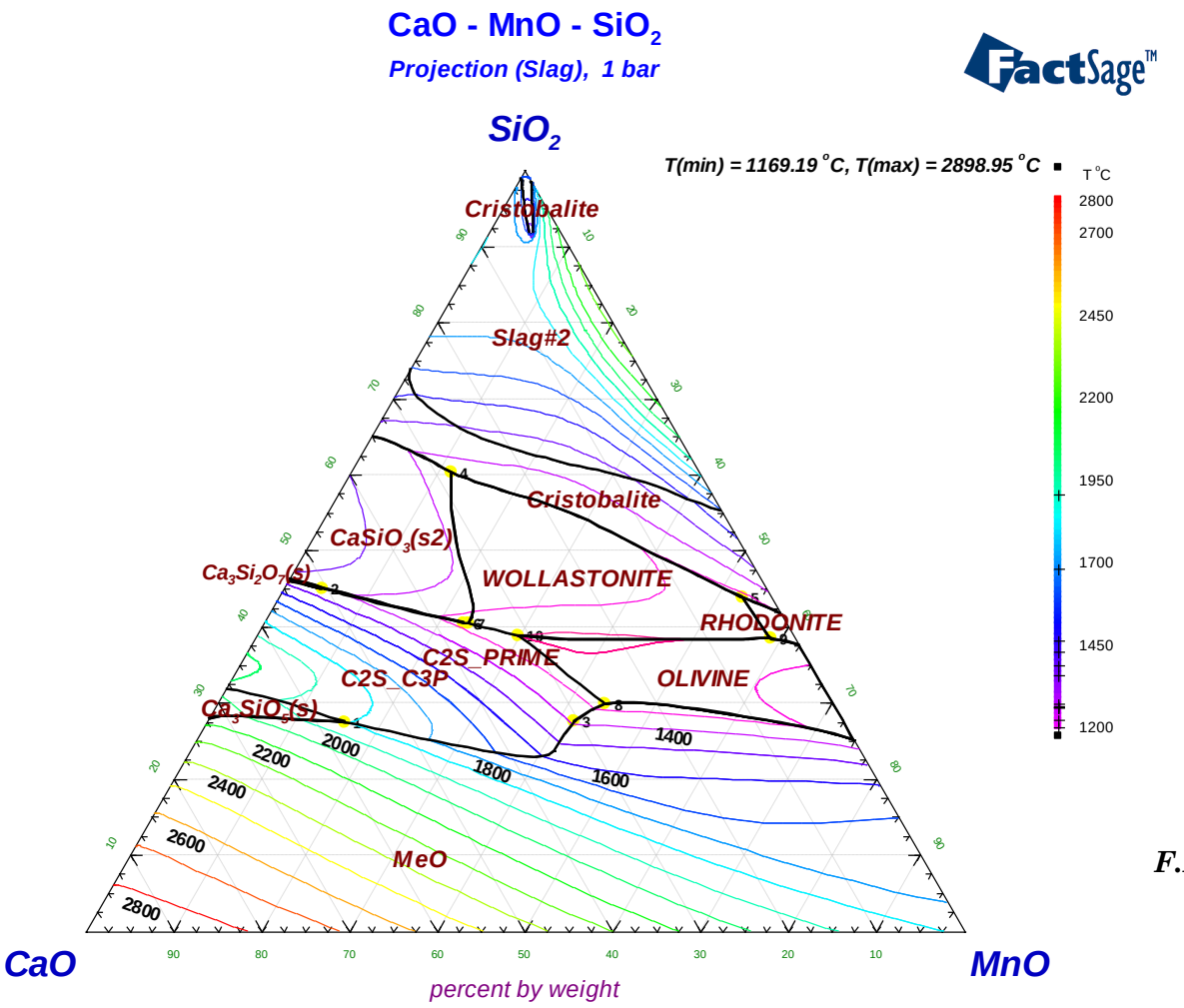

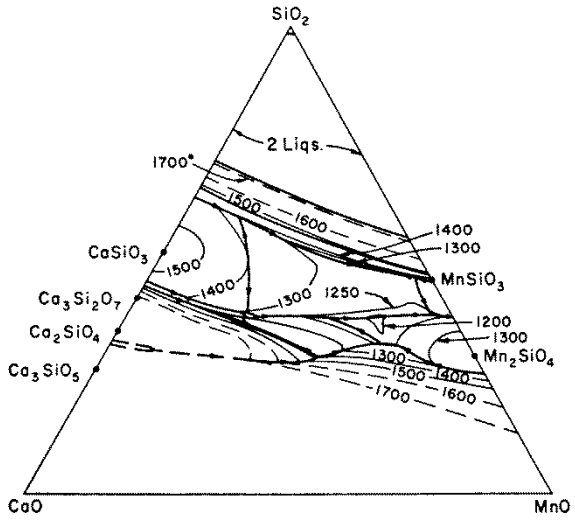

F.P. Glaser, Am. J. Sci., 259 [1], (1961), pp. 46-59.

Invariant equilibria on the liquidus surface

Intersections with slag	Mole fraction A = SiO2, B = CaO, C = MnO				Weight percent A = SiO2, B = CaO, C = MnO			
	X(A)	X(B)	X(C)	T(C)	W(A)	W(B)	W(C)	T(C)
1: C2S_C3P / Ca3SiO5(s) / MeO	1: 0.27068	0.59839	0.13093	1904.47	1: 27.515	0.56.772	15.713	1904.47
2: C2S_C3P / C2S_PRIME / Ca3Si2O7(s)	2: 0.43714	0.52677	0.03609	1427.68	2: 45.001	0.50.612	4.387	1427.68
3: C2S_C3P / C2S_PRIME / MeO	3: 0.28781	0.34234	0.36985	1385.84	3: 27.568	0.30.605	41.826	1385.84
4: CaSiO3(s2) / Cristobalite / WOLLASTONITE	4: 0.60150	0.30210	0.09640	1355.37	4: 60.315	0.28.272	11.413	1355.39
5: RHODONITE / Cristobalite / WOLLASTONITE	5: 0.47700	0.03849	0.48452	1270.42	5: 43.965	0.03.311	52.725	1270.42
6: C2S_PRIME / Ca3Si2O7(s) / CaSiO3(s2)	6: 0.40901	0.39608	0.19490	1262.96	6: 40.545	0.36.645	22.811	1262.96
7: C2S_PRIME / CaSiO3(s2) / WOLLASTONITE	7: 0.40835	0.39211	0.19954	1257.45	7: 40.435	0.36.238	23.327	1257.45
8: C2S_PRIME / MeO / OLIVINE	8: 0.31455	0.29158	0.39387	1256.49	8: 29.909	0.25.876	44.215	1256.48
9: OLIVINE / RHODONITE / WOLLASTONITE	9: 0.42143	0.03307	0.54550	1219.20	9: 38.440	0.02.816	58.744	1219.20
10: C2S_PRIME / OLIVINE / WOLLASTONITE	10: 0.39801	0.34397	0.25802	1198.27	10: 38.881	0.31.361	29.758	1198.27

Ternäre Phasen im $CaO-Na_2O-P_2O_5$ System

Phase	Description	Used data
CNP	$CaNa_2P_2O_7$	GTT
C2NP	$CaNaPO_4$	GTT
CN2P	$CaNa_4P_2O_8$	GTT
CN2P3	$CaNa_4P_6O_{18}$	GTT
N3P-LT	$(Na_2O)_2(P_2O_5)(Na_2O,Na_2CaO_2)$	$CaNa_6P_2O_9$(s1) GTT Na_3PO_4(s1) IEK-2
N3P-MT	$(Na_2O)_2(P_2O_5)(Na_2O,Na_2CaO_2)$	$CaNa_6P_2O_9$(s2) GTT Na_3PO_4(s2) IEK-2
N3P-HT	$(Na_2O)_2(P_2O_5)(Na_2O,Na_2CaO_2)$	$CaNa_6P_2O_9$(s3) GTT Na_3PO_4(s3) IEK-2
	H_{tr} (s1→s2→s3) is proposed to be equal to Na_3PO_4	

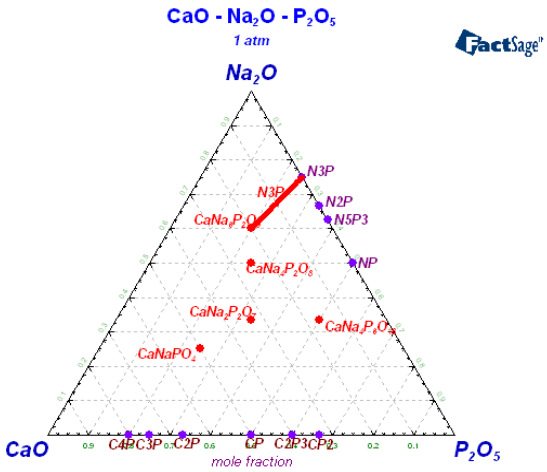

Mole fraction, Isopleth CaP2O6-NaPO3

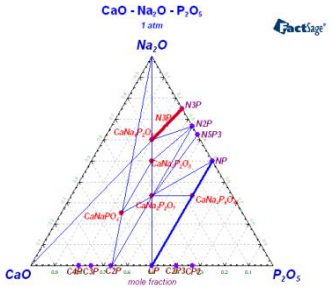

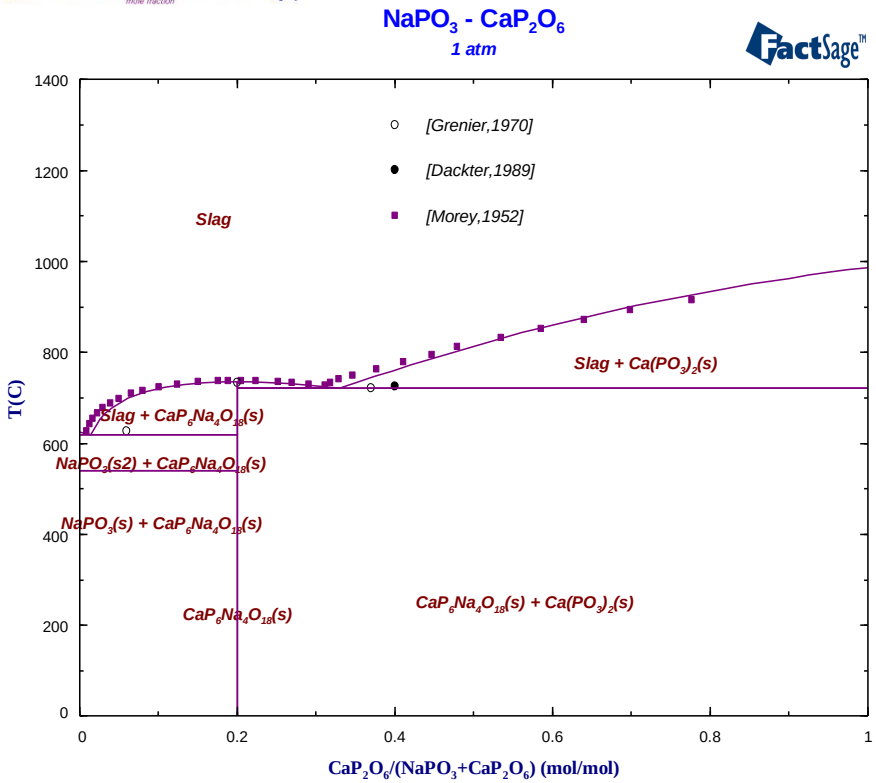

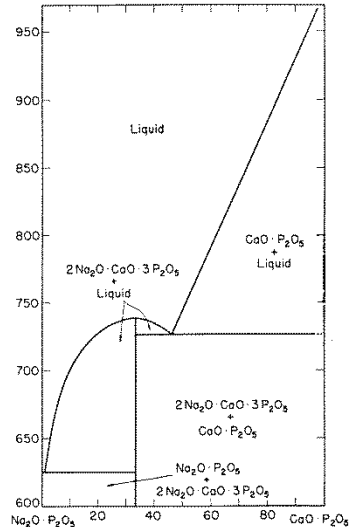

G. W. Morey, J. Am. Chem. Soc., 74 [22] 5783-5784 (1952).

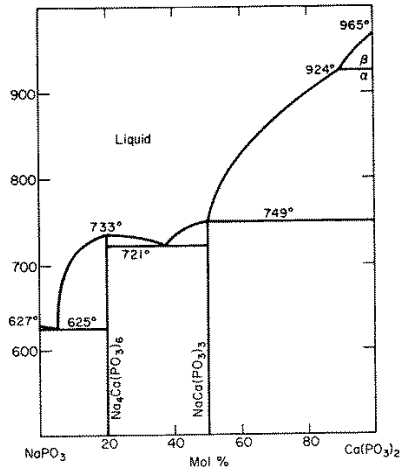

J. C. Grenier, C. Martin, and A. Durif, Bull. Soc. Fr. Mineral. Cristallogr., 93 [1] 52-55 (1970).

Mole fraction, Isopleth CaO-Na3PO4

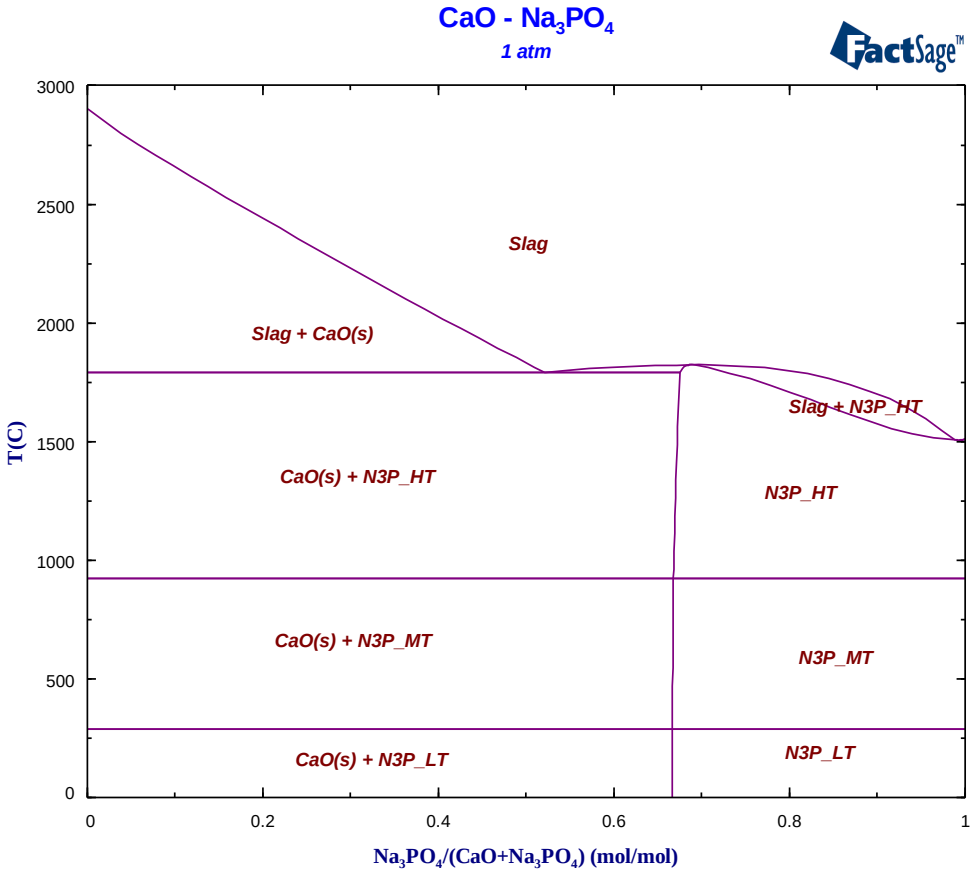

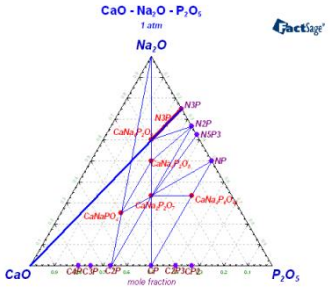

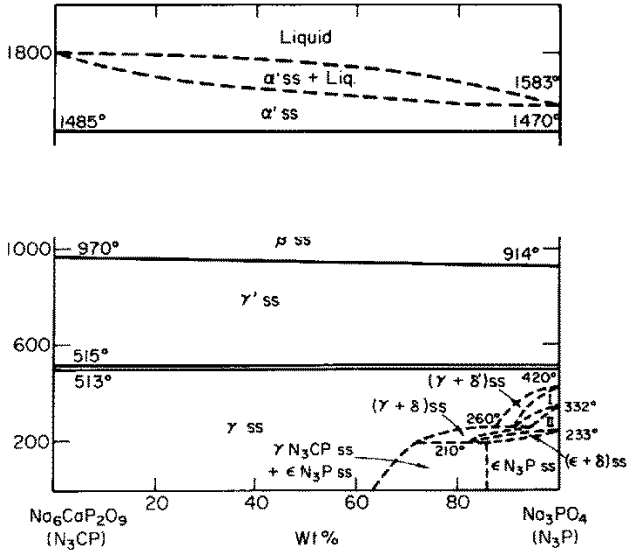

J. Berak and T. Znamierowska, Rocz. Chem., 46 [10] 1697-1708 (1972).

Weight percent, Isopleth Na4CaP2O8-Na4P2O7

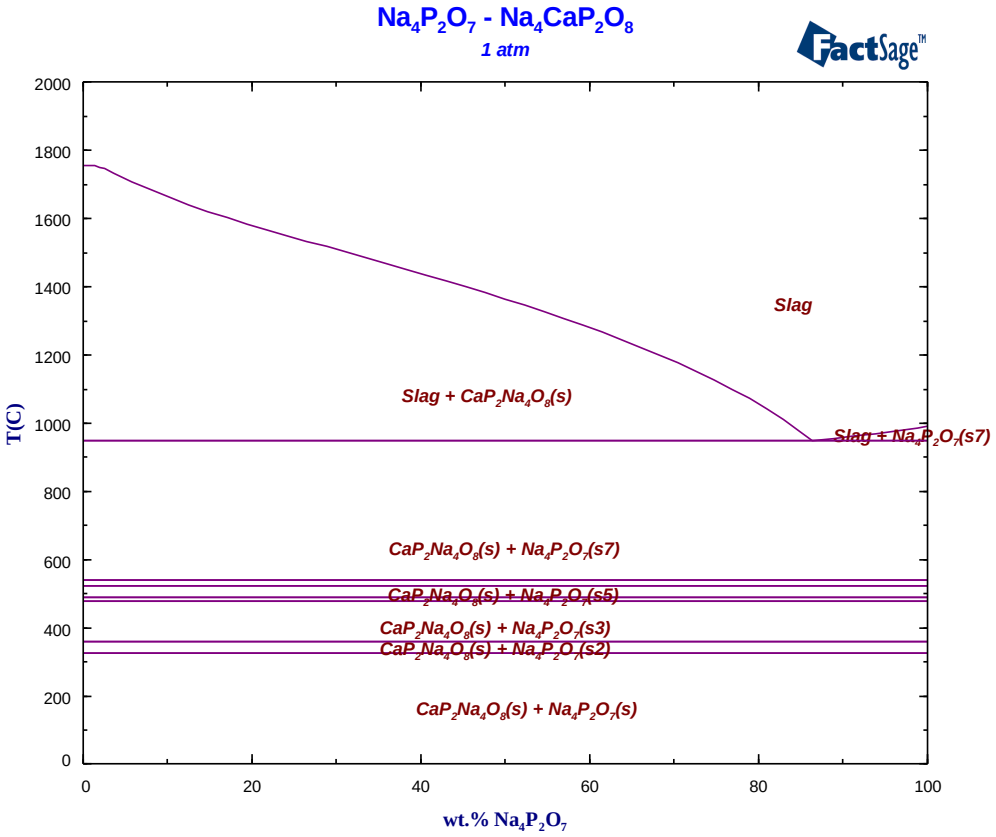

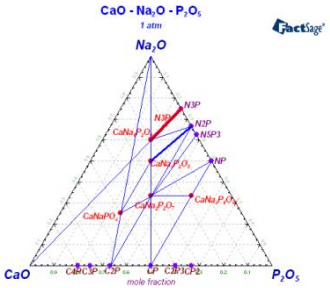

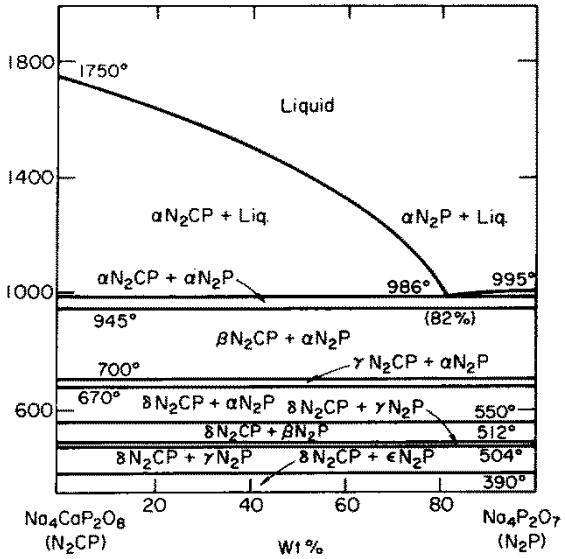

J. Berak and T. Znamierowska, Rocz. Chem., 46 [10] 1697-1708 (1972).

Weight percent, Isopleth NaCaPO4-Na4CaP2O8

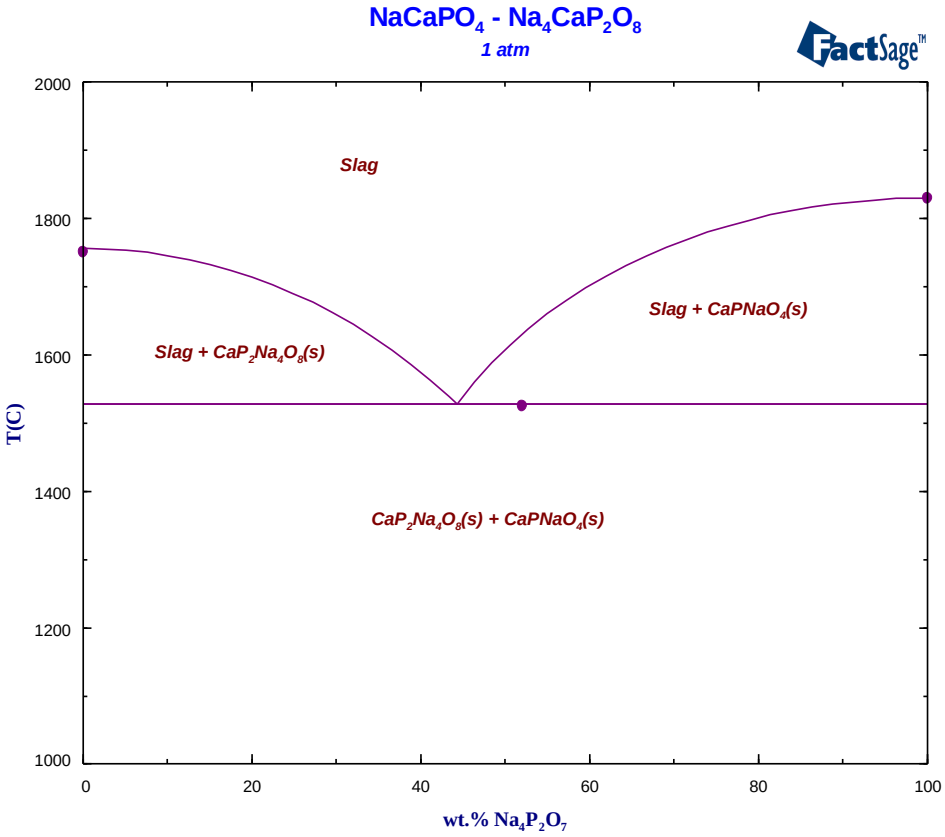

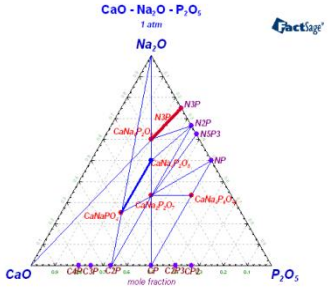

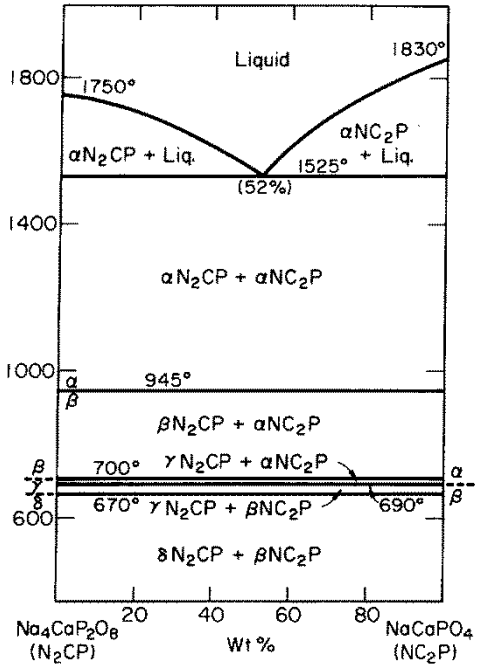

J. Berak and T. Znamierowska, Rocz. Chem., 46 [11] 1921-1929 (1972).

Mole fraction, 300°C

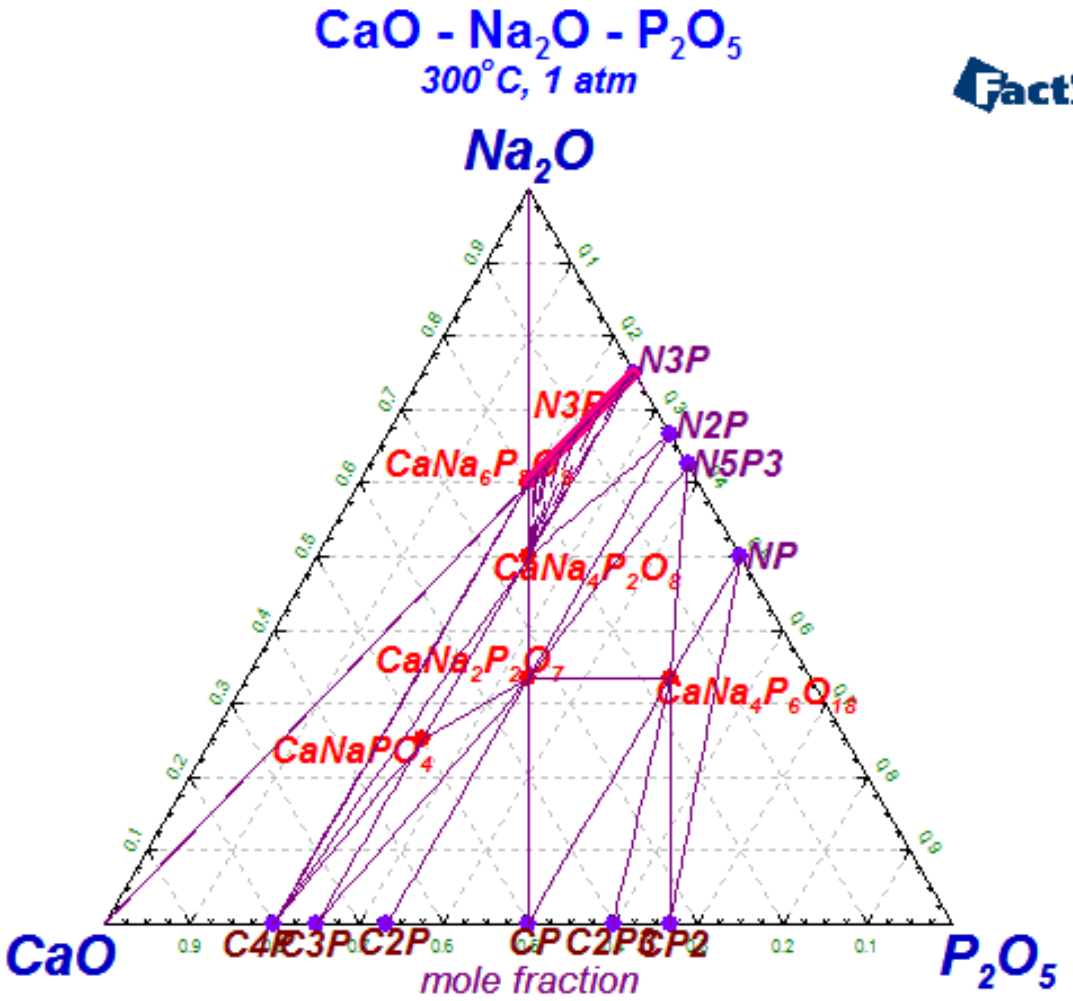

Mole fraction, 1000°C

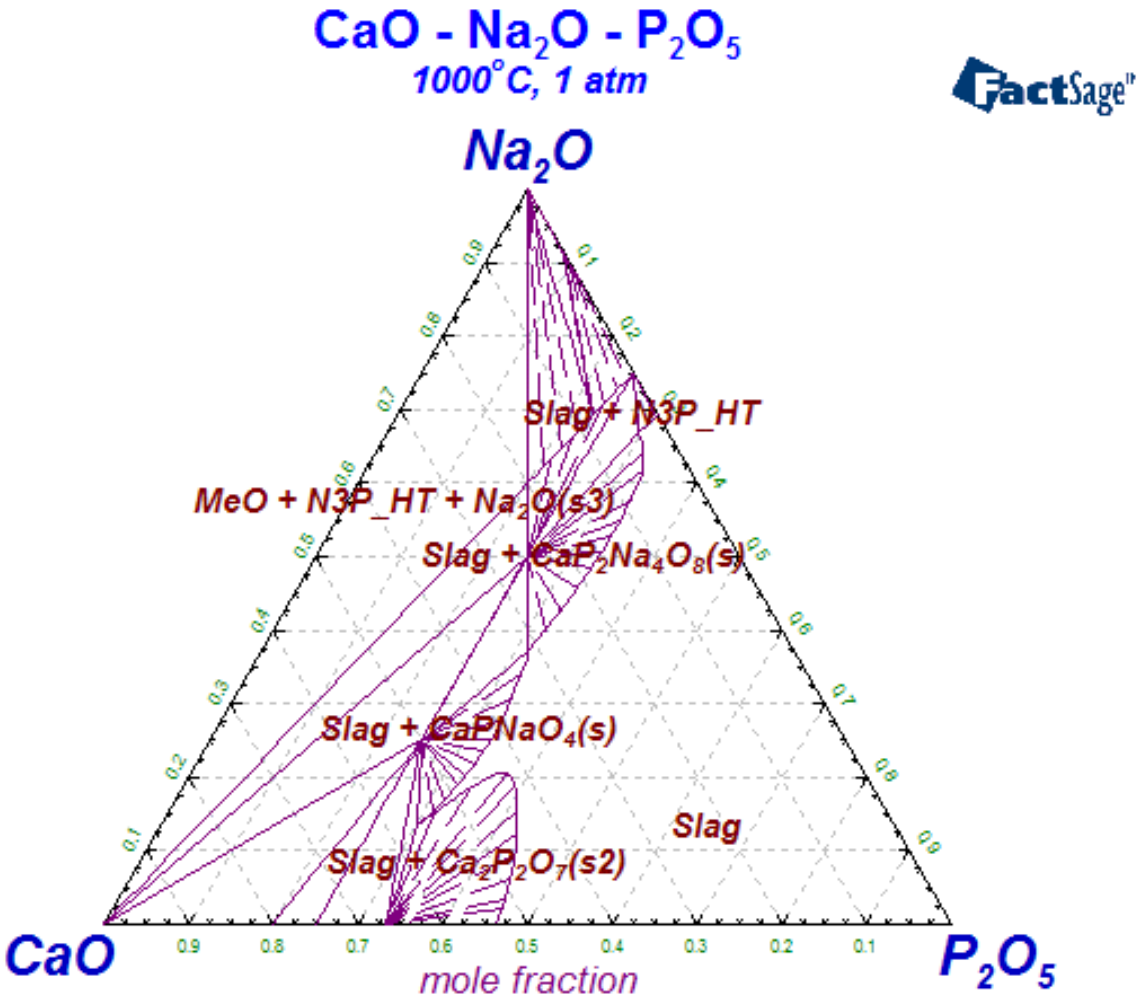

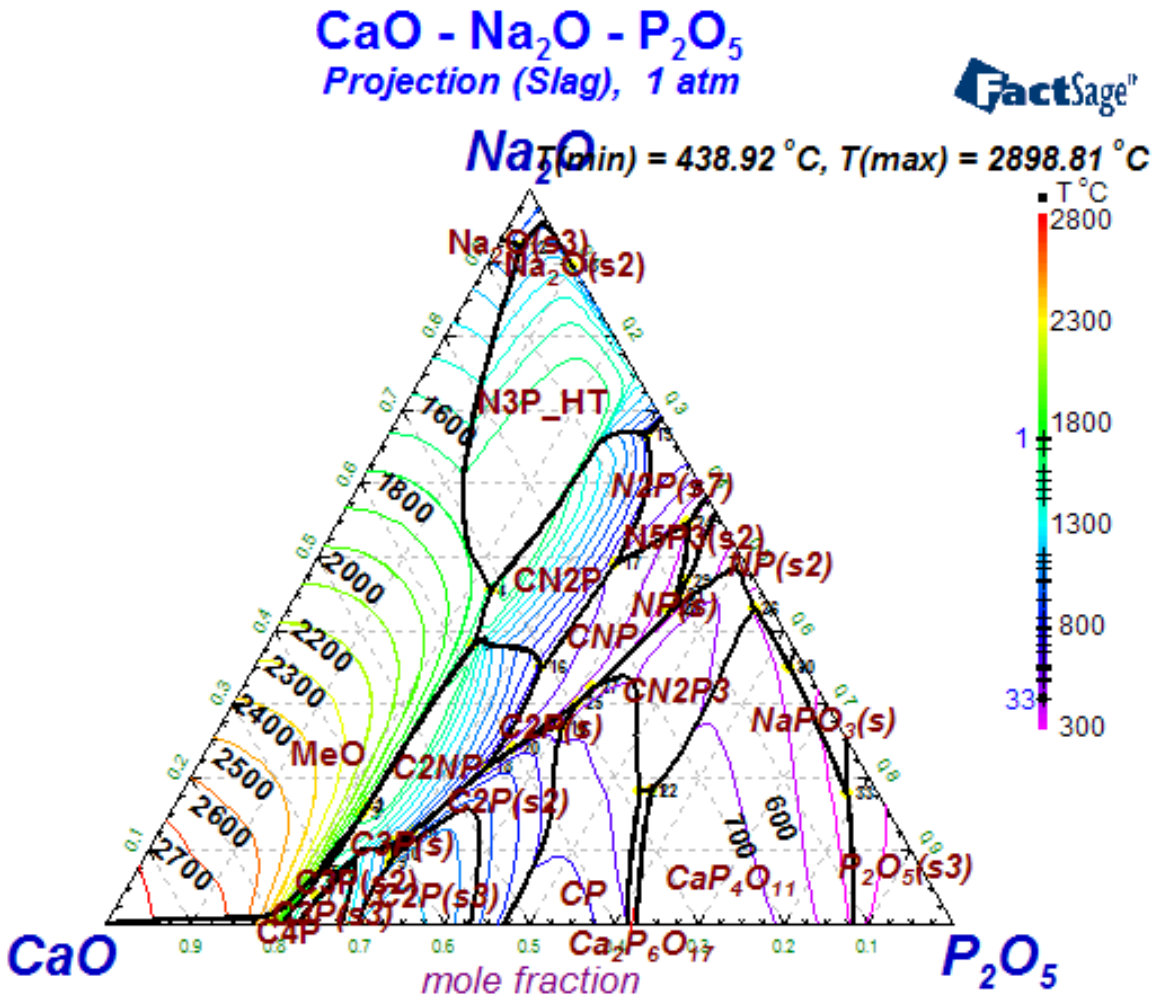
CaO - Na2O - P2O5
Projection (Slag), 1 atm
FactSage
T(min) = 438.92 °C, T(max) = 2898.81 °C
T °C
2800
2300
1800
1300
800
300
1
33
Na2O
CaO
P2O5
mole fraction
Na2O(s3)
Na2O(s2)
N3P_HT
N2P(s7)
N5P3(s2)
NP(s2)
NP(s)
CN2P
CNP
CN2P3
NaPO3(s)
C2P(s)
C2NP
C2P(s2)
C3P(s)
C3P(s2)
C2P(s3)
C4P(s3)
C4P
MeO
CP
CaP4O11
P2O5(s3)
Ca2P6O17
1600
1800
2000
2200
2300
2400
2500
2600
2700
600
700

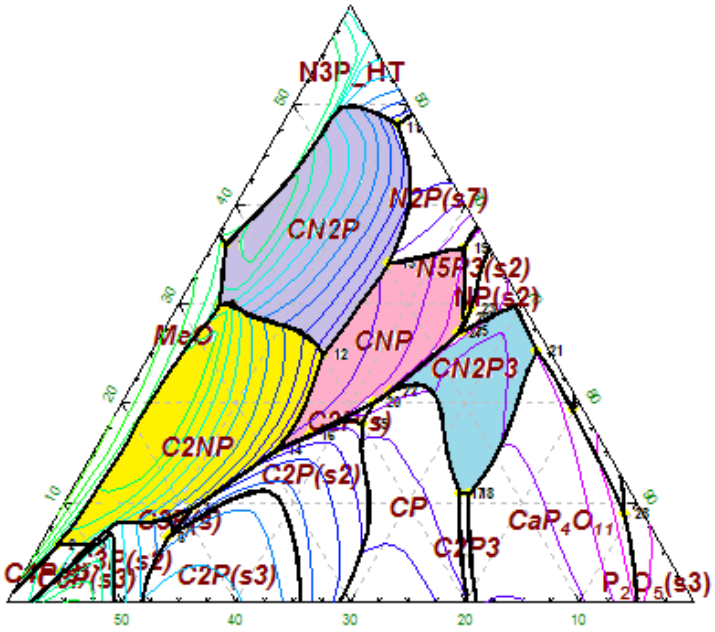

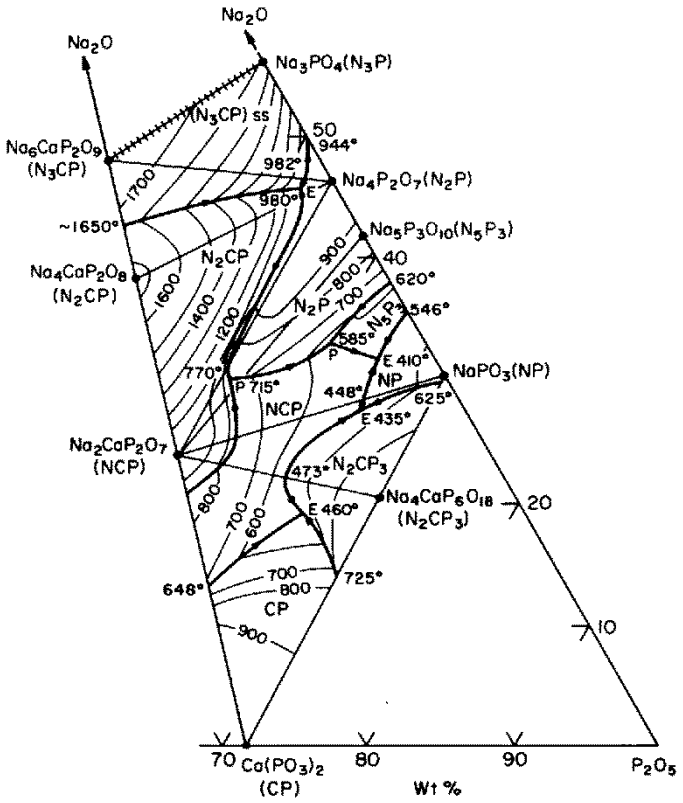

J. Berak, T. Znamierowska, Rocz. Chem. Ann. Soc. Chim. Polonorum, 46(1972), 1697-1708.

Invariant equilibria on the liquidus surface

Intersections with slag	Mole fraction A = Na2O, B = CaO, C = P2O5				Weight percent A = Na2O, B = CaO, C =P2O5			
	X(A)	X(B)	X(C)	T(C)	W(A)	W(B)	W(C)	T(C)
1: CaP2Na4O8 / MeO / N3P_HT	0.45421	0.31892	0.22687	1668.21	35.982	22.859	41.159	1668.21
2: Ca4P2O9 / CaPNaO4 / MeO	0.06961	0.70894	0.22146	1556.21	5.714	52.653	41.633	1556.21
3: CaP2Na4O8 / CaPNaO4 / MeO	0.38047	0.37551	0.24401	1505.46	29.746	26.563	43.691	1505.46
4: Ca3P2O8(s2) / Ca3P2O8(s3) / Ca4P2O9(s)	0.03523	0.73153	0.23324	1469.84	2.861	53.755	43.383	1469.85
5: Ca3P2O8(s2) / Ca4P2O9(s) / CaPNaO4(s)	0.07119	0.68769	0.24113	1422.60	5.715	49.951	44.333	1422.38
6: Ca2P2O7(s2) / Ca2P2O7(s3) / Ca3P2O8(s2)	0.08370	0.62337	0.29292	1139.89	6.348	42.775	50.877	1139.89
7: Ca2P2O7(s2) / Ca3P2O8(s2) / Ca3P2O8(s)	0.09324	0.61279	0.29397	1109.89	7.059	41.973	50.968	1109.85
8: Ca3P2O8(s2) / Ca3P2O8(s) / CaPNaO4(s)	0.10973	0.60386	0.28640	1109.85	8.364	41.643	49.993	1109.22
9: MeO / N3P_HT / Na2O(s3)	0.92202	0.04960	0.02838	1079.78	89.352	4.349	6.300	1079.78
10: Ca2P2O7(s2) / Ca3P2O8(s) / CaPNaO4(s)	0.12407	0.57649	0.29945	1006.32	9.318	39.175	51.507	1006.32
11: CaP2Na4O8(s) / N3P_HT / N3P_MT	0.66708	0.02832	0.30460	922.40	47.981	1.843	50.176	922.41
12: CaP2Na2O7(s) / CaP2Na4O8(s) / CaPNaO4(s)	0.34983	0.31084	0.33933	835.23	24.843	19.972	55.186	835.23
13: CaP2Na2O7(s) / CaP2Na4O8(s) / Na4P2O7(s7)	0.49156	0.15293	0.35551	786.82	34.039	9.582	56.380	786.89
14: Ca2P2O7(s2) / CaP2Na2O7(s) / CaPNaO4(s)	0.21464	0.44358	0.34178	779.80	15.345	28.694	55.961	779.80
15: Ca(PO3)2(s) / Ca2P2O7(s) / Ca2P2O7(s2)	0.26531	0.32987	0.40481	749.85	17.796	20.019	62.185	749.88
16: Ca2P2O7(s) / Ca2P2O7(s2) / CaP2Na2O7(s)	0.23938	0.39837	0.36225	749.85	16.746	25.216	58.038	749.86
17: Ca(PO3)2(s) / Ca2P6O17(s) / CaP6Na4O18(s)	0.18162	0.27772	0.54067	701.97	10.868	15.036	74.096	702.06
18: Ca2P6O17(s) / CaP4O11(s) / CaP6Na4O18(s)	0.18203	0.26564	0.55234	701.70	10.788	14.244	74.968	701.70
19: CaP2Na2O7(s) / Na4P2O7(s7) / Na5P3O10(s2)	0.54496	0.04044	0.41460	602.23	35.593	2.390	62.017	602.26
20: Ca(PO3)2(s) / Ca2P2O7(s) / CaP2Na2O7(s)	0.30025	0.29468	0.40507	598.65	20.089	17.839	62.071	598.65
21: CaP4O11(s) / CaP6Na4O18(s) / NaPO3(s2)	0.43009	0.01999	0.54993	589.27	25.186	1.059	73.755	589.28
22: Ca(PO3)2(s) / CaP2Na2O7(s) / CaP6Na4O18(s)	0.32083	0.26398	0.41519	578.11	21.239	15.812	62.949	578.11
23: Na5P3O10(s2) / NaPO3(s2) / NaPO3(s)	0.43036	0.11390	0.45574	539.41	29.532	4.763	65.705	539.40
24: CaP4O11(s) / NaPO3(s2) / NaPO3(s)	0.46518	0.08291	0.45190	539.40	19.275	0.910	79.815	539.40
25: CaP6Na4O18(s) / NaPO3(s2) / NaPO3(s)	0.34962	0.01824	0.63215	539.40	27.287	6.534	66.179	539.40
26: CaP2Na2O7(s) / Na5P3O10(s2) / NaPO3(s)	0.44789	0.10064	0.45146	532.93	28.476	5.789	65.735	532.92
27: CaP2Na2O7(s) / CaP6Na4O18(s) / NaPO3(s)	0.42501	0.12284	0.45215	529.30	27.042	7.072	65.887	529.30
28: CaP4O11(s) / NaPO3(s) / P2O5(s3)	0.17699	0.03672	0.78629	438.92	8.801	1.652	89.547	438.92

Ternäre Phasen im $CaO-Na_2O-SiO_2$ System

Phase	Beschreibung	Formel
111	Stöchiometrisch	Na_2CaSiO_4
115	Stöchiometrisch	$Na_2CaSi_5O_{12}$
122	Stöchiometrisch	$Na_2Ca_2Si_2O_7$
136	Stöchiometrisch	$Na_2Ca_3Si_6O_{16}$
213	Stöchiometrisch	$Na_4CaSi_3O_9$
NC2S3	Mischphase	$(Na^{1+},Va)_2(Ca^{2+},Va)(CaNa_2Si_3O_9^{2-})$

CaO-Na2O-SiO2,
Weight percent 600°C

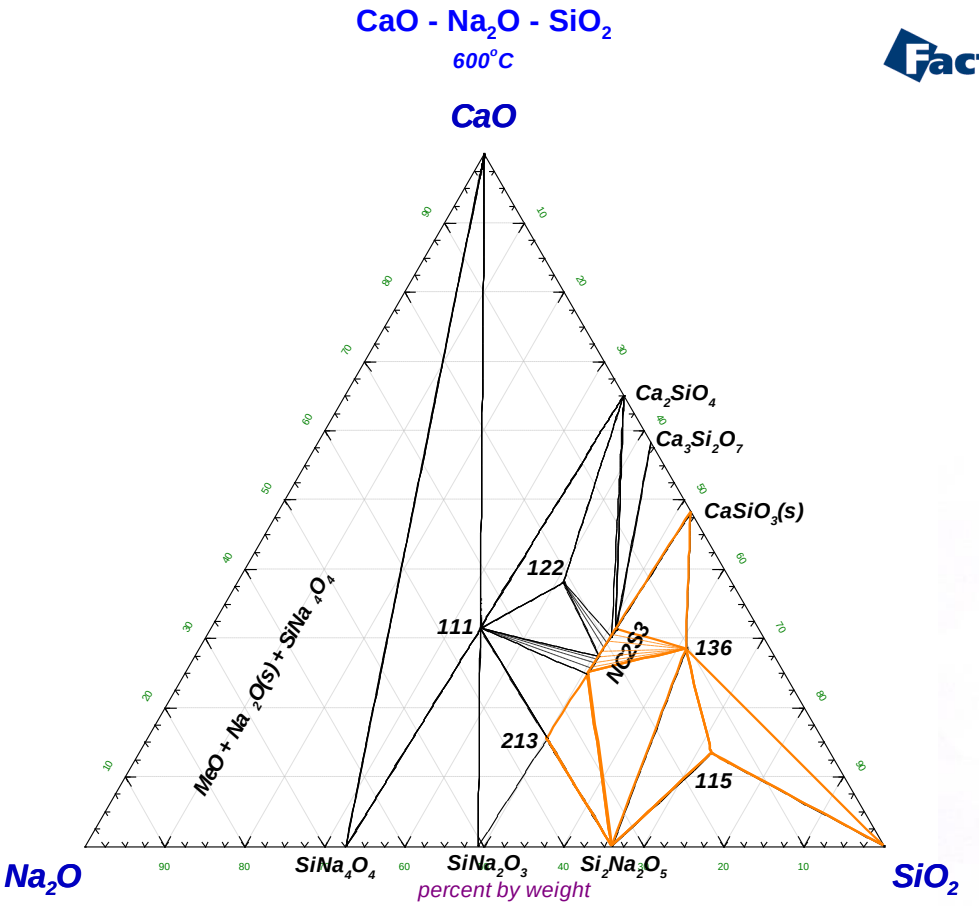

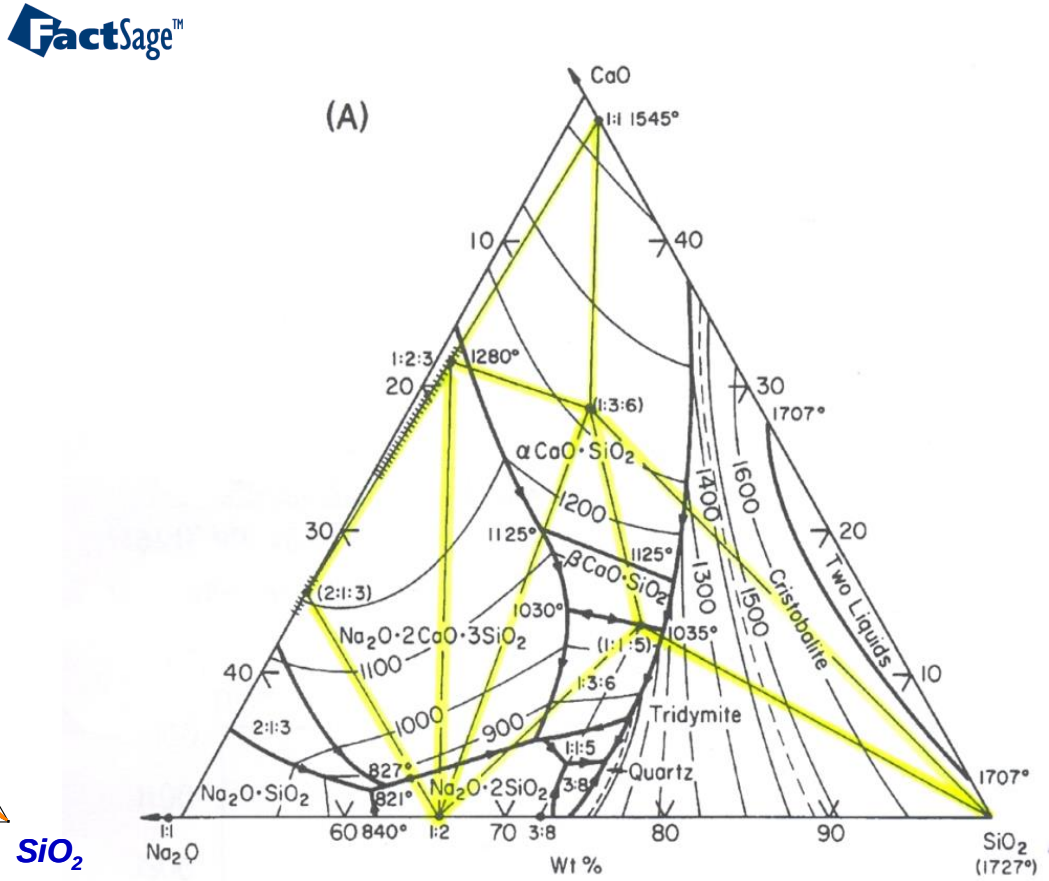

K.A. Shahid, F.P. Glasser, Phys. Chem. Glasses, 12 [2], (1971), pp.50-57.

CaO-Na2O-SiO2, Weight percent 770°C

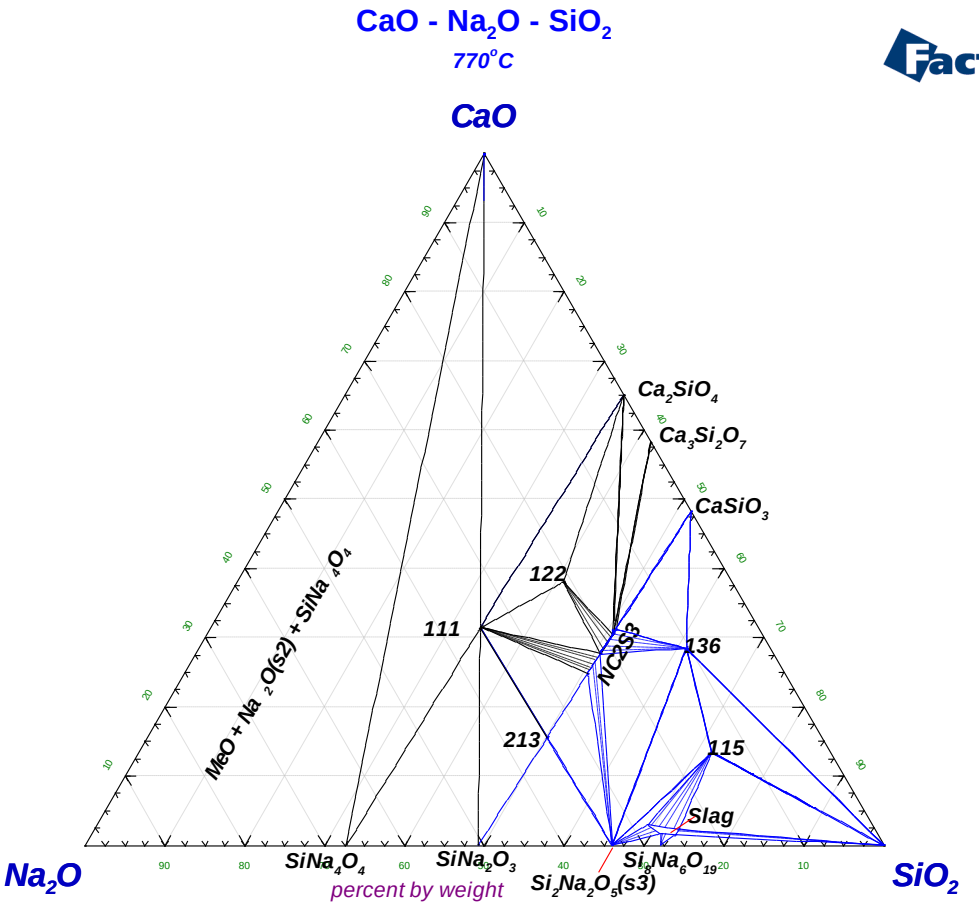

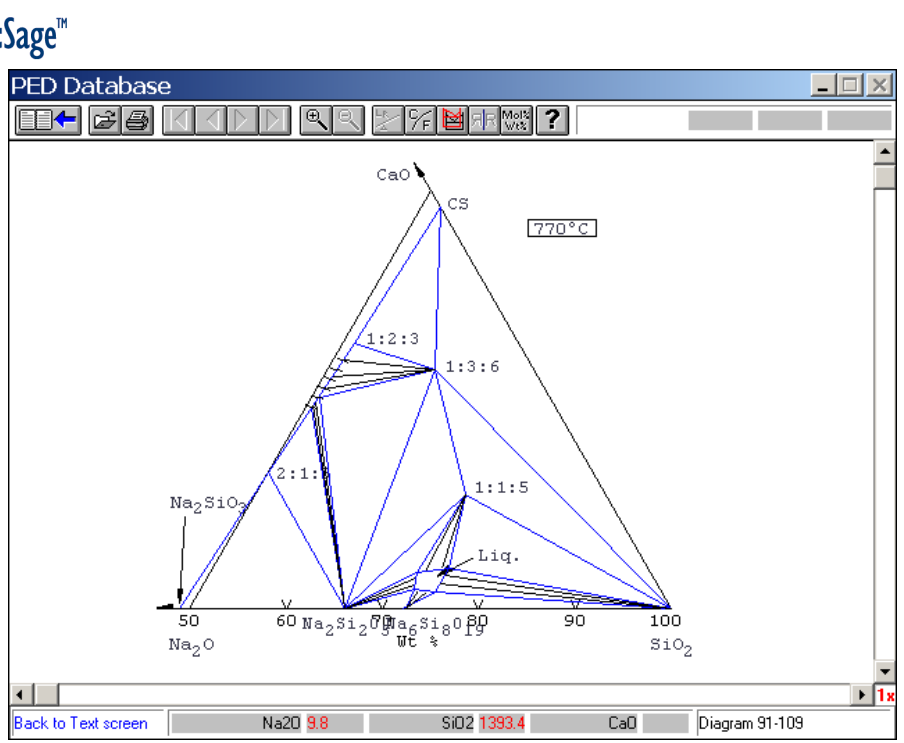

G. K. Moir and F. P. Glasser, Phys. Chem. Glasses, 17 [3] 45-53 (1976).

Orthosilicate isopleth compared with experimental data

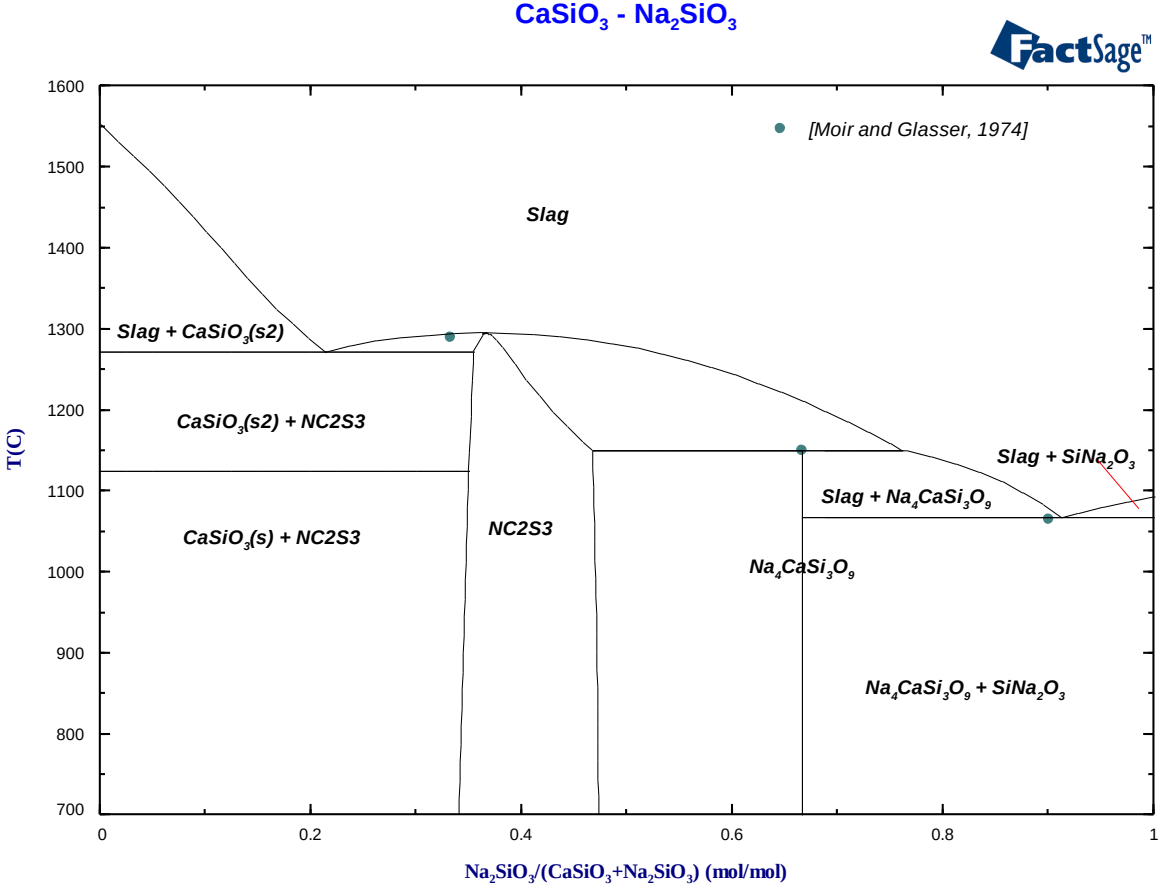

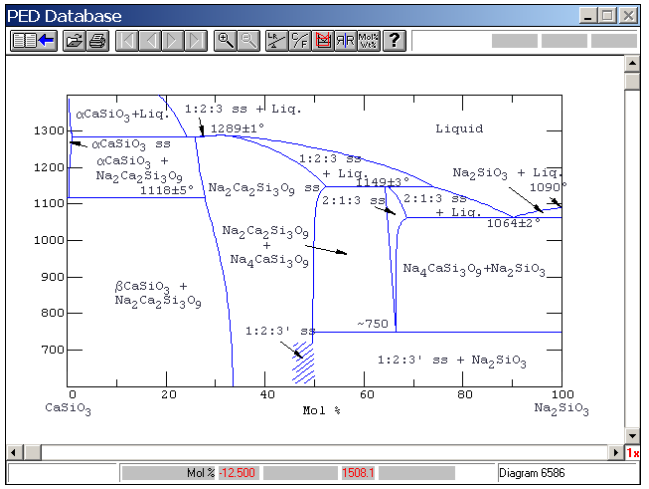

G. K. Moir and F. P. Glasser, Trans. J. Br. Ceram. Soc.,

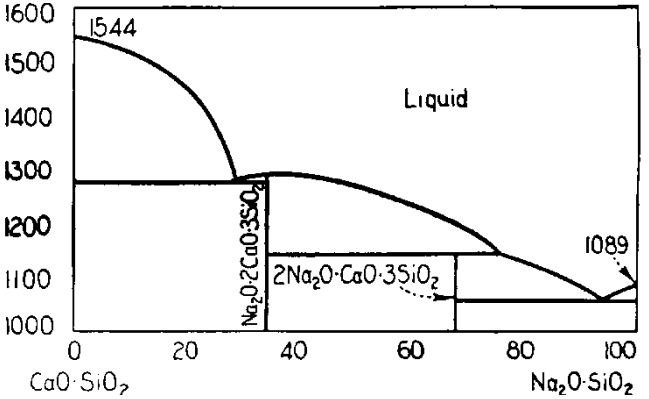

G. W. Morey and N. L. Bowen, J. Soc. Glass Technol., 9, 226-264 (1925).

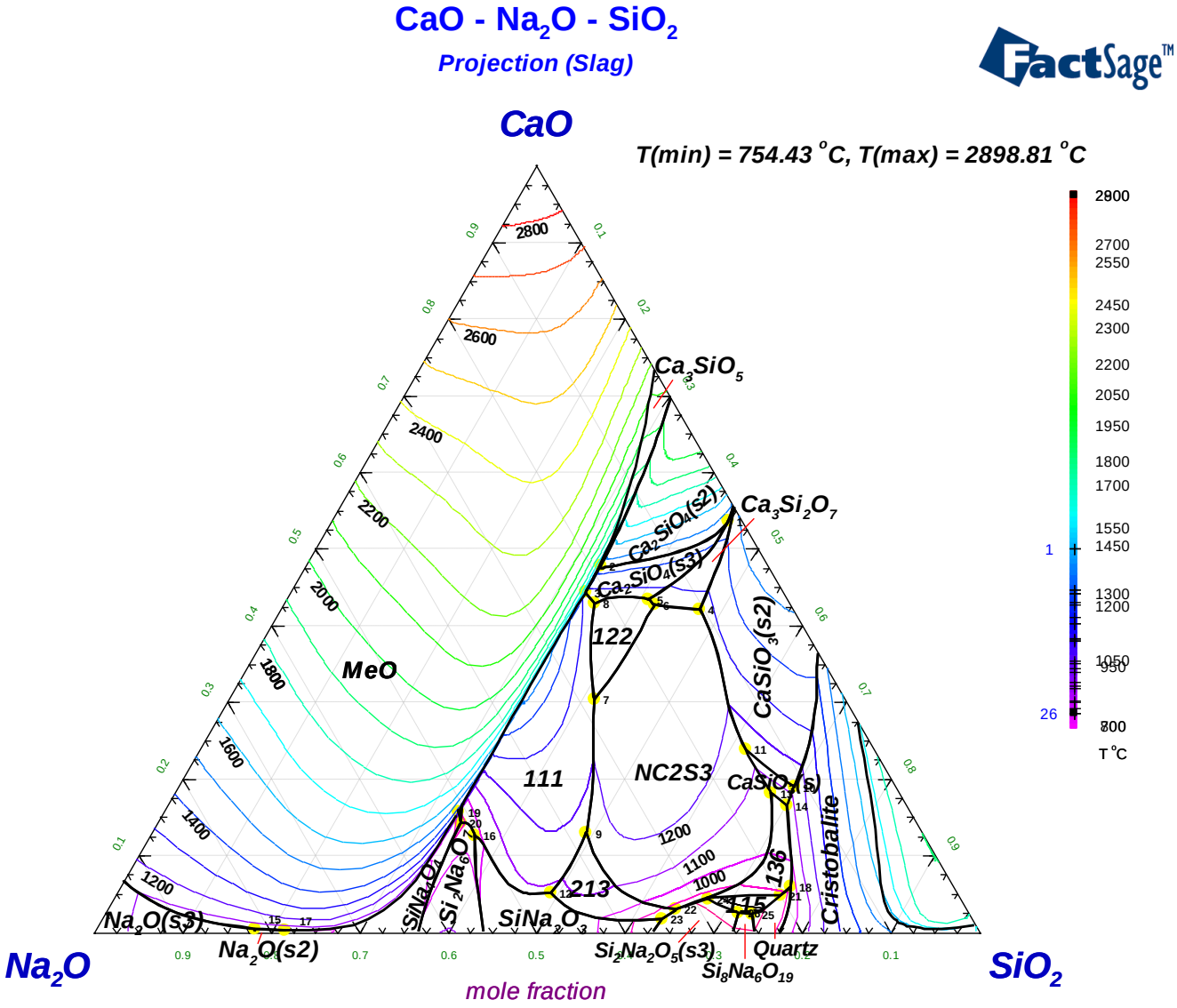
CaO - Na2O - SiO2
Projection (Slag)
FactSage™
CaO
T(min) = 754.43 °C, T(max) = 2898.81 °C
Na2O
SiO2
mole fraction
T °C
Ca3SiO5
Ca3Si2O7
Ca2SiO4(s2)
Ca2SiO4(s3)
CaSiO3(s2)
CaSiO3(s)
MeO
122
111
NC2S3
213
136
115
Cristobalite
Na2O(s3)
Na2O(s2)
Si2Na2O5
Si2Na6O7
SiNa2O3
Si2Na2O5(s3)
Si8Na6O19
Quartz

Weight percent,
Liquidussurface compared with experimental data

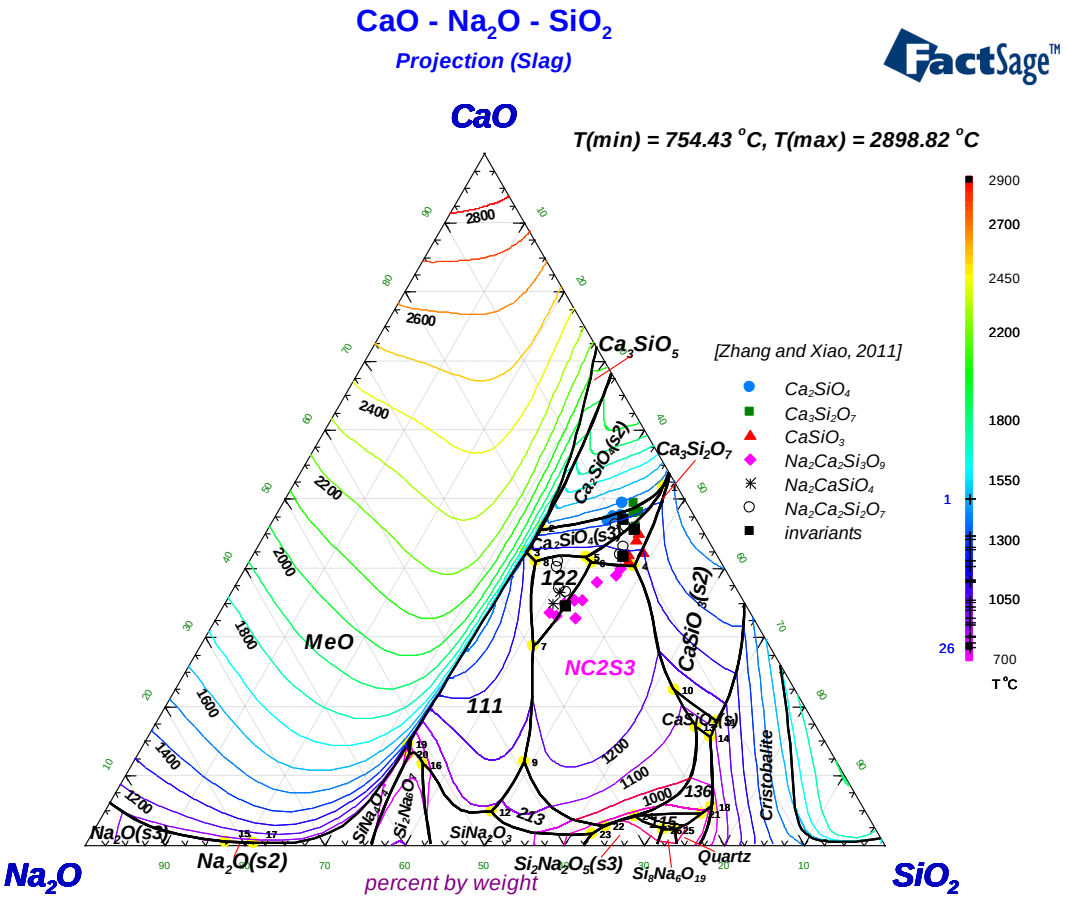

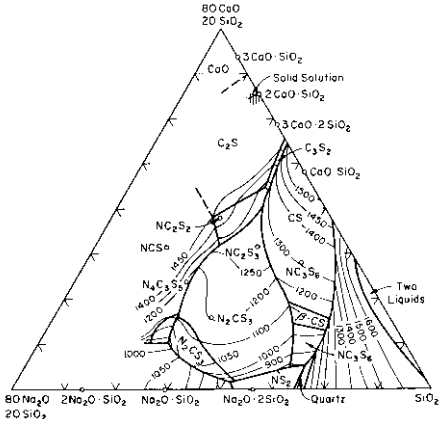

E. R. Segnit, Am. J. Sci., 251 [8] 586-601 (1953).

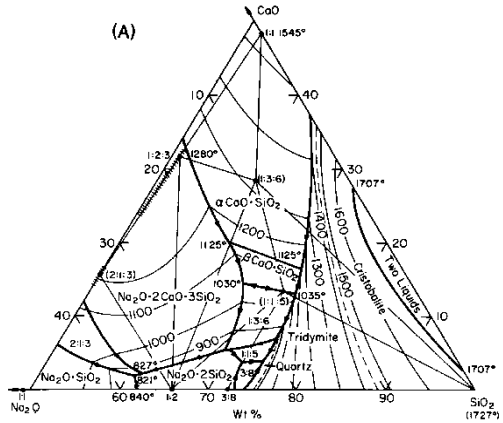

K.A. Shahid, F.P. Glasser, Phys. Chem. Glasses, 12 [2], (1971), pp.50-57.

Invariant equilibria on the liquidus surface

Intersections with slag	Mole fraction A = CaO, B = Na2O, C = SiO2				Weight percent A = CaO, B = Na2O, C = SiO2			
	X(A)	X(B)	X(C)	T(C)	W(A)	W(B)	W(C)	T(C)
1: Ca2SiO4(s2) / Ca2SiO4(s3) / Ca3Si2O7	0.53623	0.01517	0.44860	1436.73	51.877	1.622	46.500	1436.73
2: Ca2SiO4(s2) / Ca2SiO4(s3) / Ca3SiO5	0.47778	0.18892	0.33330	1436.73	45.778	20.006	34.216	1436.73
3: Ca3SiO5 / CaSiNa2O4 / MeO	0.44357	0.22269	0.33374	1267.19	42.354	23.501	34.145	1267.19
4: Ca3Si2O7 / CaSiO3(s2) / NC2S3	0.42136	0.10464	0.47400	1264.36	40.326	11.068	48.606	1264.36
5: Ca2Si2Na2O7 / Ca2SiO4(s3) / Ca3Si2O7	0.43429	0.15633	0.40938	1251.09	41.531	16.523	41.946	1251.10
6: Ca2Si2Na2O7 / Ca3Si2O7 / NC2S3	0.42715	0.15303	0.41981	1248.38	40.833	16.168	42.999	1248.38
7: Ca2Si2Na2O7 / CaSiNa2O4 / NC2S3	0.30413	0.28280	0.41307	1215.96	28.711	29.508	41.782	1215.96
8: Ca2Si2Na2O7 / Ca2SiO4(s3) / CaSiNa2O4	0.42938	0.21913	0.35149	1203.83	40.965	23.106	35.929	1203.83
9: CaSiNa2O4 / NC2S3 / Na4CaSi3O9	0.12899	0.37915	0.49186	1149.07	11.999	38.980	49.022	1149.07
10: CaSiO3(s2) / CaSiO3(s) / Cristobalite	0.18958	0.11433	0.69609	1124.45	22.463	15.050	62.487	1124.14
11: CaSiO3(s2) / CaSiO3(s) / NC2S3	0.23796	0.14425	0.61779	1124.13	17.856	11.901	70.244	1124.13
12: CaSiNa2O4 / Na4CaSi3O9 / SiNa2O3	0.05171	0.45761	0.49068	1065.43	4.774	46.692	48.535	1065.39
13: CaSiO3(s) / NC2S3 / Na2Ca3Si6O16	0.18146	0.14394	0.67460	1059.27	17.065	14.961	67.974	1059.27
14: CaSiO3(s) / Na2Ca3Si6O16 / Cristobalite	0.16476	0.13421	0.70103	1055.21	15.481	13.938	70.580	1055.21
15: MeO / Na2O(s2) / Na2O(s3)	0.00471	0.81632	0.17897	970.05	0.428	82.119	17.453	970.05
16: CaSiNa2O4 / Si2Na6O7 / SiNa2O3	0.12623	0.50643	0.36733	957.78	11.693	51.849	36.458	957.78
17: MeO / Na2O(s2) / SiNa4O4	0.00221	0.78294	0.21485	937.28	0.202	78.828	20.970	937.28
18: Na2Ca3Si6O16 / Cristobalite / Quartz	0.05884	0.18303	0.75813	926.29	5.481	18.845	75.674	926.28
19: CaSiNa2O4 / MeO / SiNa4O4	0.15779	0.50873	0.33348	883.13	14.647	52.188	33.165	885.22
20: CaSiNa2O4 / Si2Na6O7 / SiNa4O4	0.14199	0.51492	0.34309	864.64	13.163	52.758	34.078	864.65
21: Na2Ca3Si6O16 / Na2CaSi5O12 / Quartz	0.04770	0.20087	0.75144	857.44	4.437	20.655	74.907	857.45
22: NC2S3 / Na4CaSi3O9 / Si2Na2O5(s3)	0.02951	0.32739	0.64310	807.32	2.732	33.491	63.777	807.32
23: Na4CaSi3O9 / Si2Na2O5(s3) / SiNa2O3	0.01751	0.34996	0.63253	800.16	1.618	35.747	62.635	800.16
24: Na2Ca3Si6O16 / Na2CaSi5O12 / Si2Na2O5(s3)	0.04391	0.28419	0.67189	772.05	4.074	29.140	66.786	772.05
25: Na2CaSi5O12 / Si8Na6O19 / Quartz	0.02297	0.24441	0.73263	754.81	2.131	25.057	72.813	754.81
26: Na2CaSi5O12 / Si2Na2O5(s3) / Si8Na6O19	0.02446	0.25922	0.71633	754.43	2.268	26.565	71.167	754.43

CaO-NiO-SiO2,

Mole fraction 1340°C

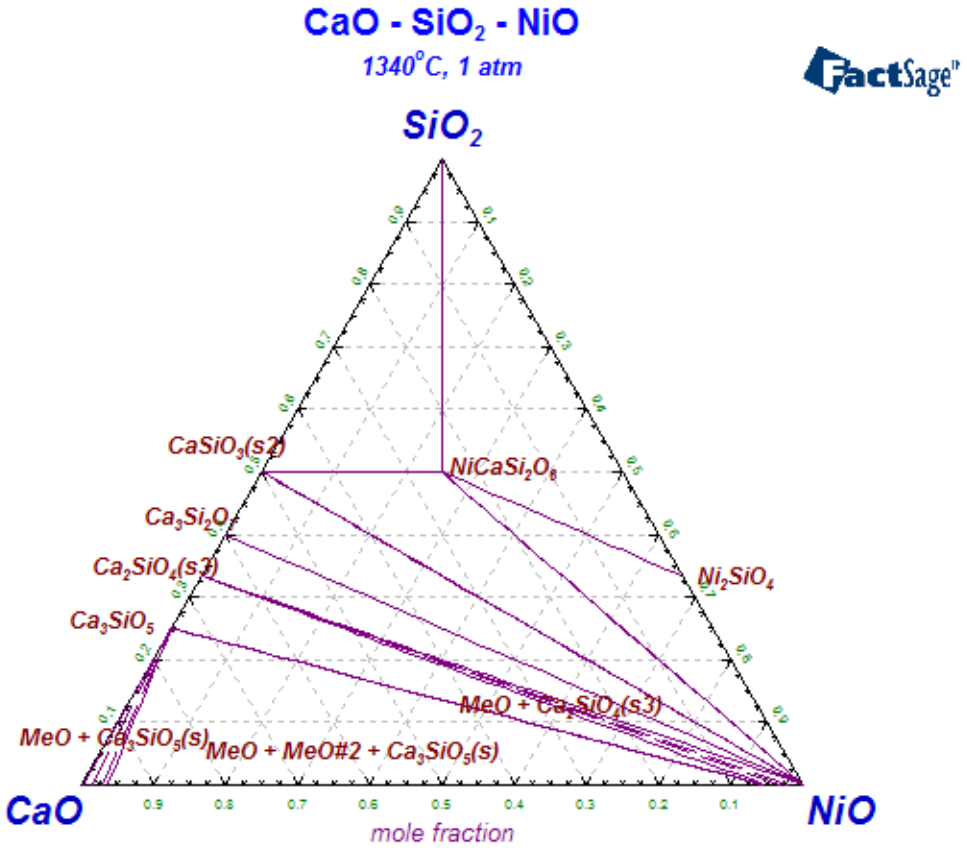

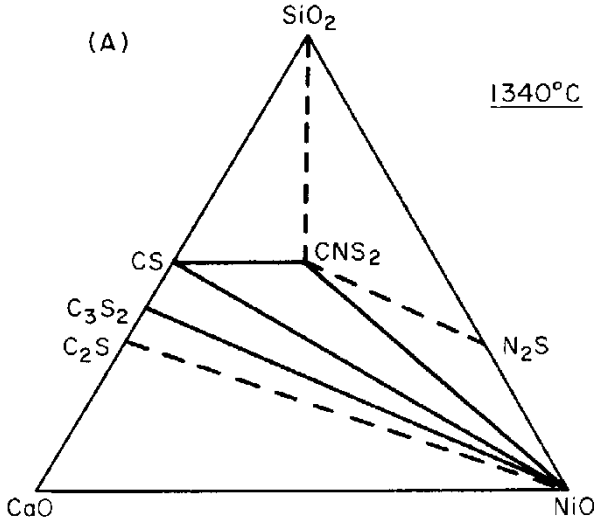

G.M. Biggar, J. Am. Ceram. Soc., 52 [6], (1969), pp. 316-317.

Mole fraction 1390°C

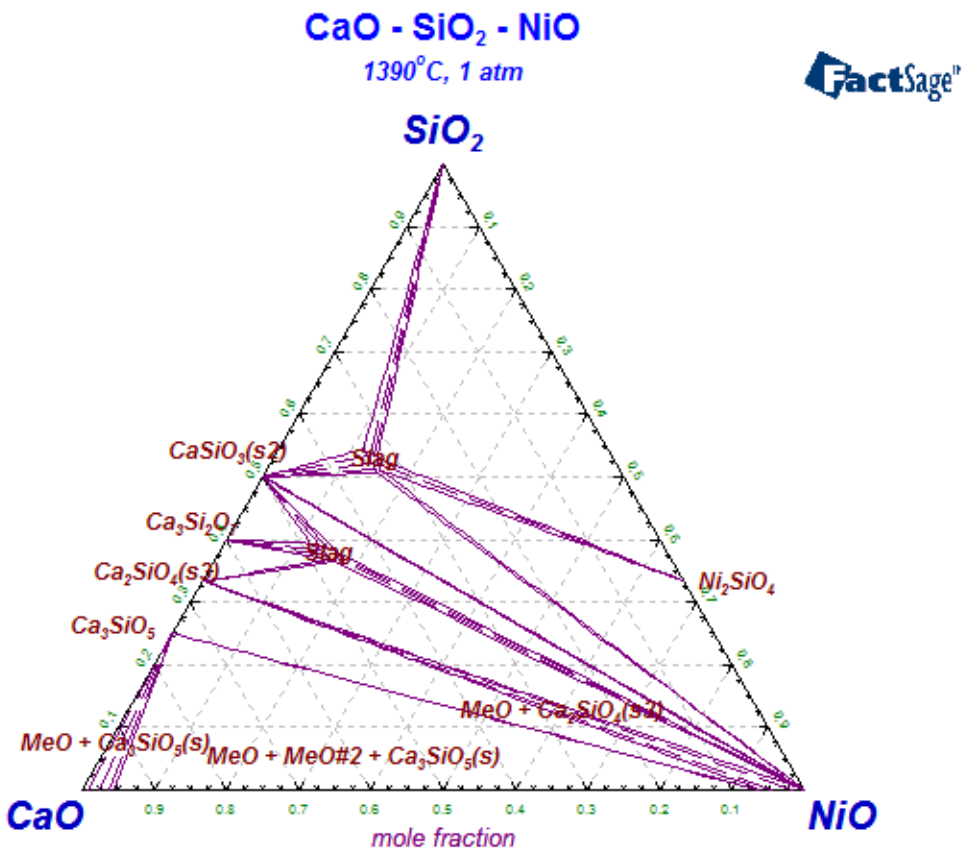

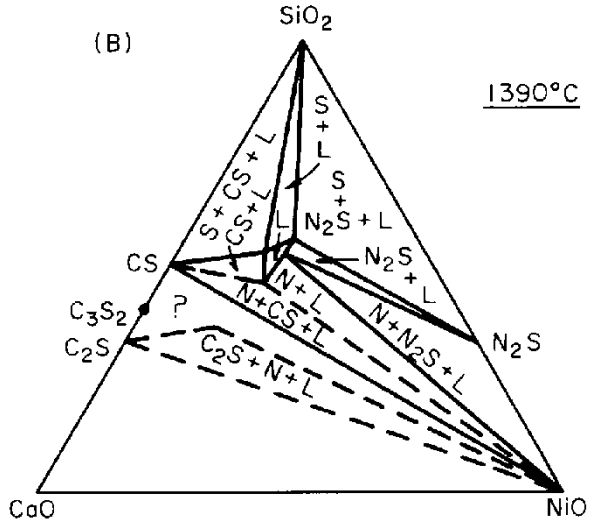

G.M. Biggar, J. Am. Ceram. Soc., 52 [6], (1969), pp. 316-317.

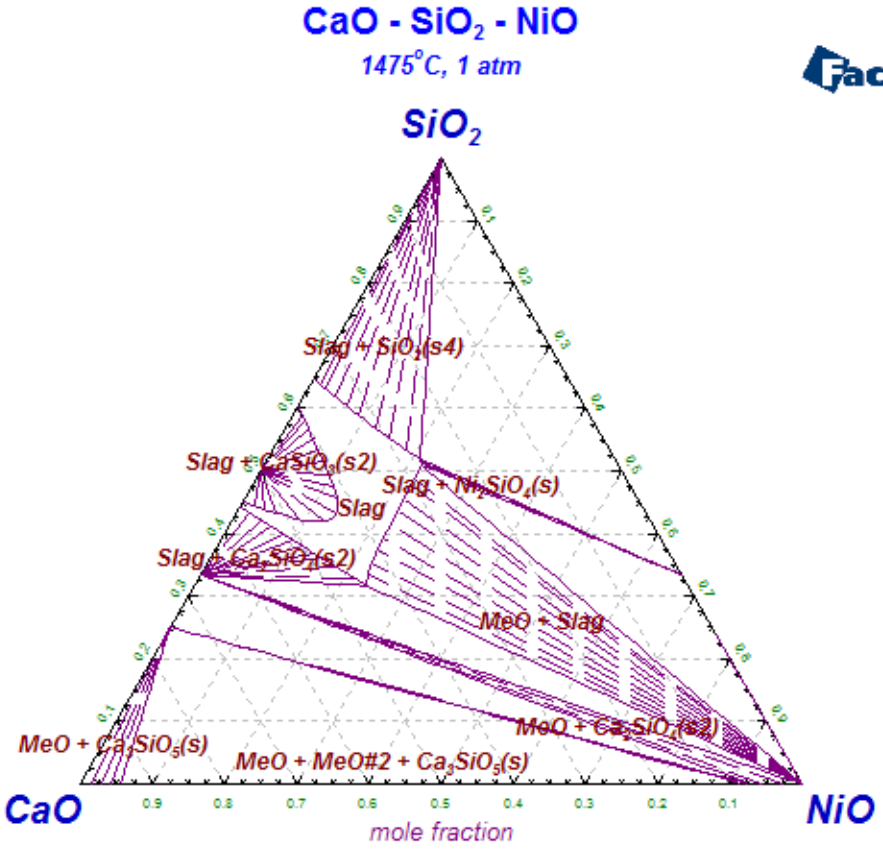

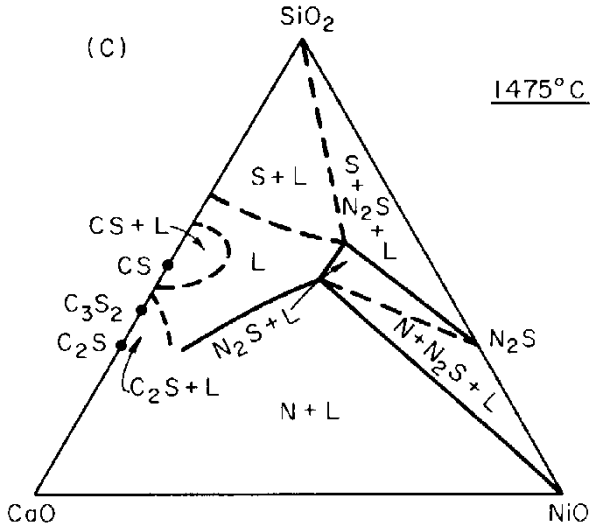

G.M. Biggar, J. Am. Ceram. Soc., 52 [6], (1969), pp. 316-317.

Mole fraction 1550°C

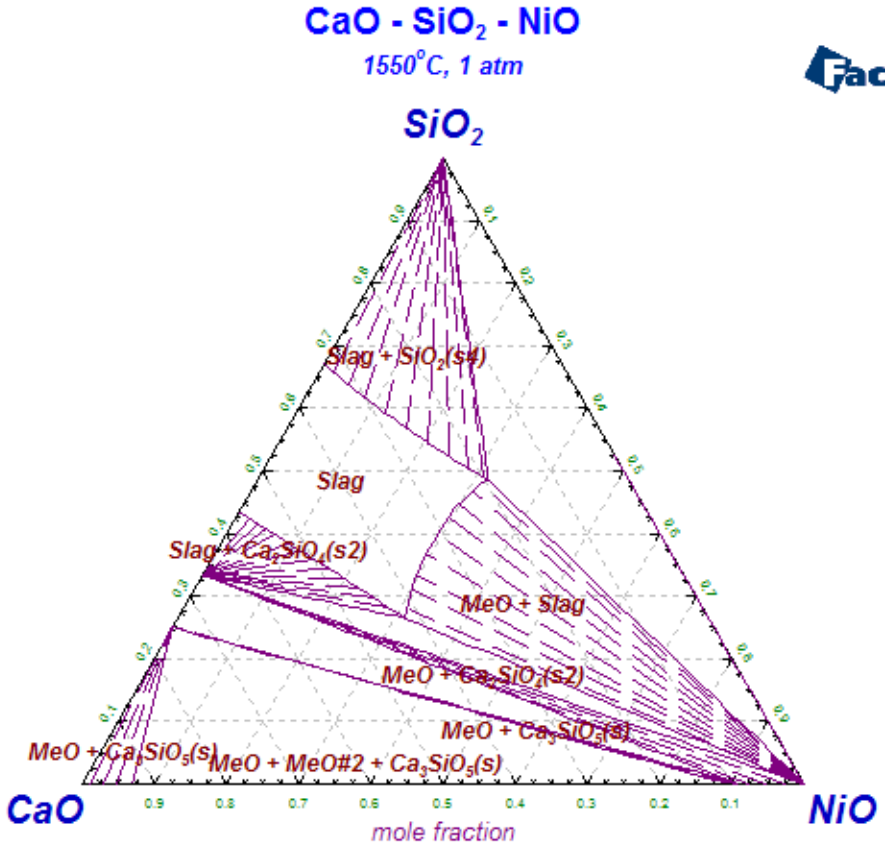

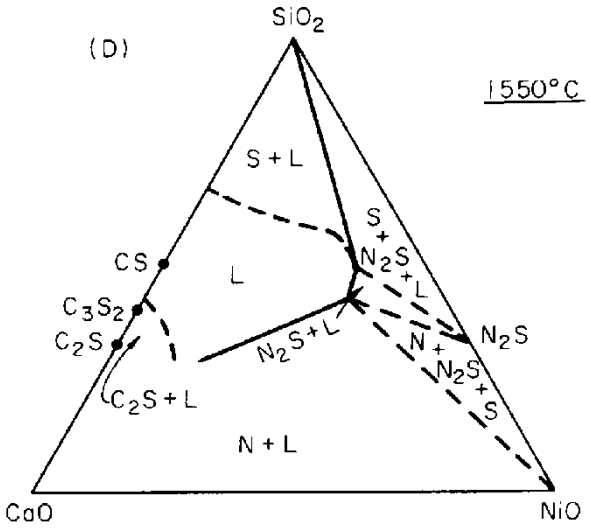

G.M. Biggar, J. Am. Ceram. Soc., 52 [6], (1969), pp. 316-317.

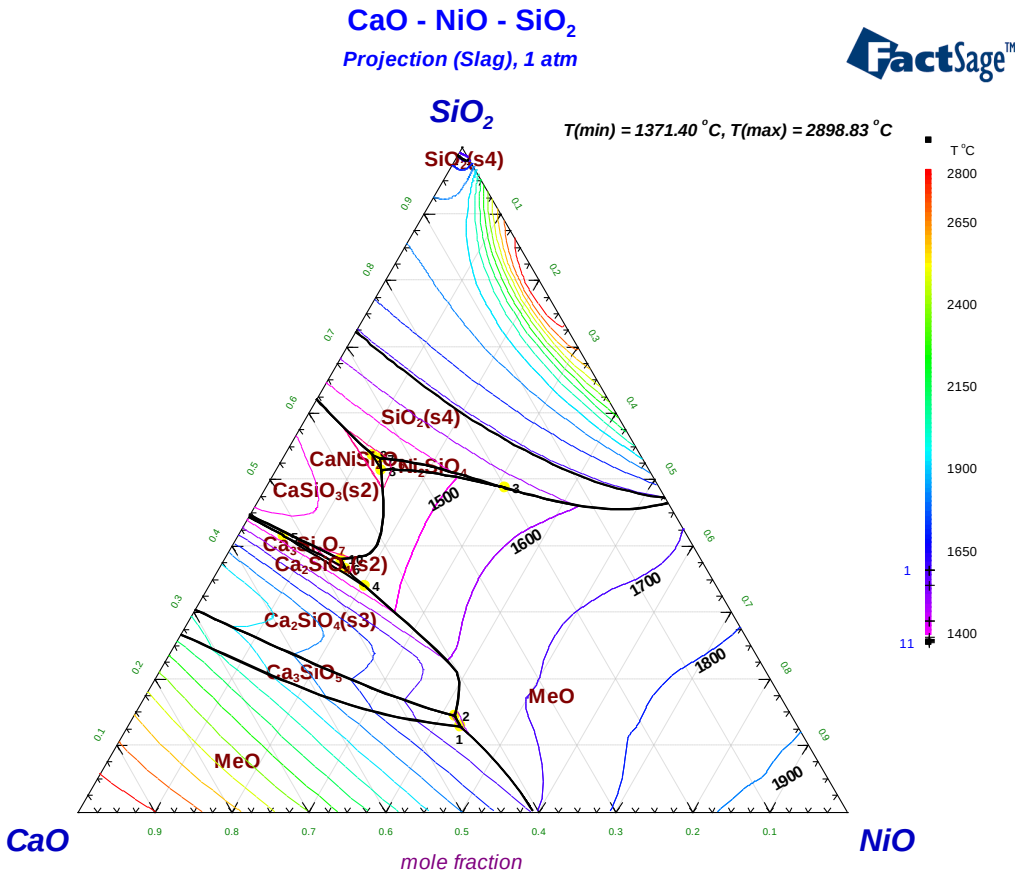
CaO - NiO - SiO2
Projection (Slag), 1 atm
FactSage™
SiO2
T(min) = 1371.40 °C, T(max) = 2898.83 °C
T °C
2800
2650
2400
2150
1900
1650
1400
SiO2(s4)
CaNiSiO4
Ni2SiO4
CaSiO3(s2)
Ca3Si2O7
Ca2SiO4(s2)
Ca2SiO4(s3)
Ca3SiO5
MeO
MeO
1500
1600
1700
1800
1900
CaO
NiO
mole fraction

Weight percent, Liquiudussurface

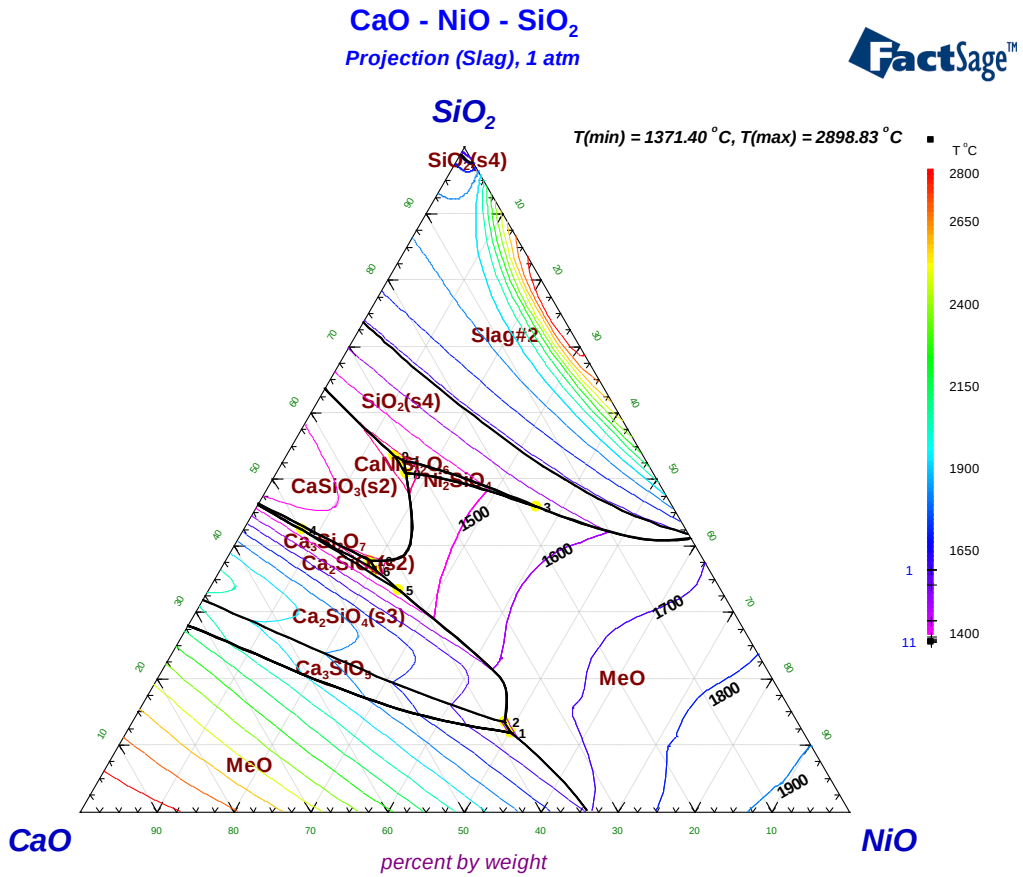

Invariant equilibria on the liquidus surface

Intersections with slag	Mole fraction A = SiO2, B = CaO, C = NiO				Weight percent A = SiO2, B = CaO, C = NiO				
		X(A)	X(B)	X(C)	T(C)		W(A)	W(B)	W(C)	T(C)
1: Ca3SiO5 / MeO#1 / MeO#2	1:	0.12901	0.43797	0.43302	1593.43	1:	12.002	37.986	50.012	1593.43
2: Ca2SiO4(s3) / Ca3SiO5 / MeO#1	2:	0.14353	0.43757	0.41889	1592.33	2:	13.381	38.072	48.546	1592.29
3: MeO#1 / Ni2SiO4 / SiO2(s4)	3:	0.48708	0.20080	0.31211	1546.59	3:	45.843	17.639	36.518	1546.58
4: Ca2SiO4(s3) / Ca2SiO4(s2) / MeO#1	4:	0.33933	0.45712	0.20355	1436.73	4:	42.393	49.972	7.635	1436.73
5: Ca2SiO4(s3) / Ca2SiO4(s2) / Ca3Si2O7	5:	0.41530	0.52453	0.06017	1436.73	5:	33.300	41.868	24.833	1436.73
6: Ca2SiO4(s2) / Ca3Si2O7 / MeO#1	6:	0.36614	0.46849	0.16538	1387.96	6:	36.288	43.336	20.376	1387.96
7: CaNiSi2O6 / Ni2SiO4 / SiO2(s4)	7:	0.53154	0.34059	0.12788	1381.30	7:	52.712	31.523	15.765	1381.30
8: CaNiSi2O6 / CaSiO3(s2) / MeO#1	8:	0.51419	0.34801	0.13780	1378.61	8:	50.895	32.149	16.956	1378.61
9: CaNiSi2O6 / CaSiO3(s2) / SiO2(s4)	9:	0.53741	0.34806	0.11452	1376.08	9:	53.493	32.335	14.171	1376.08
10: Ca3Si2O7 / CaSiO3(s2) / MeO#1	10:	0.37990	0.46765	0.15244	1371.40	10:	37.768	43.392	18.840	1371.40

Mole fraction 600°C

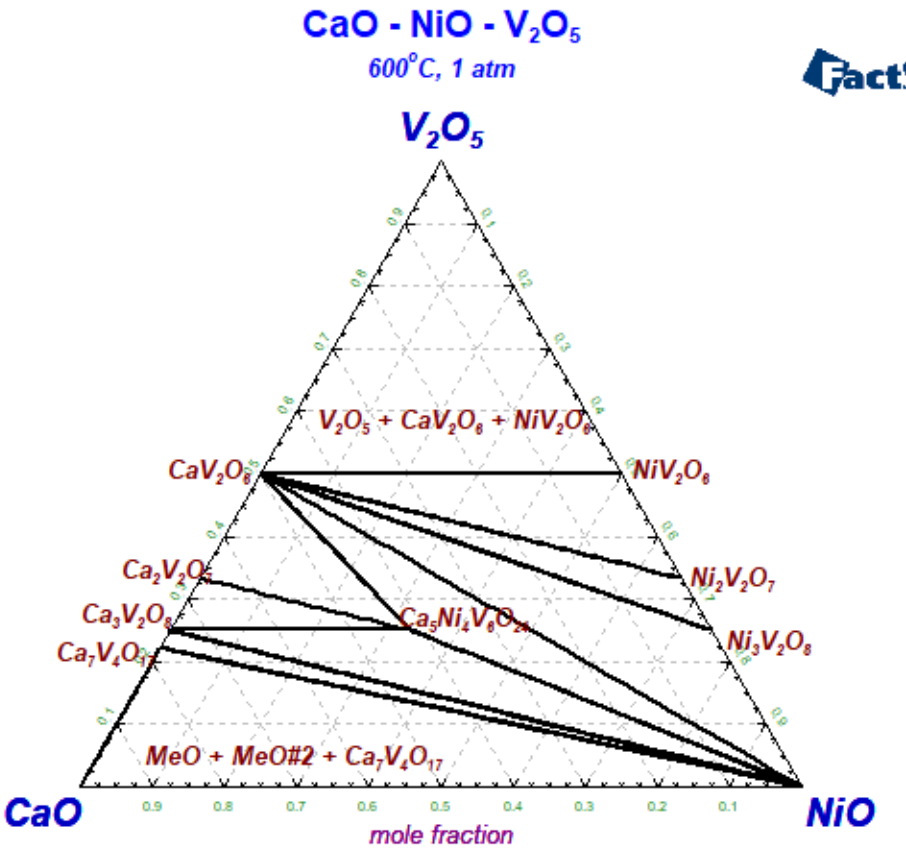

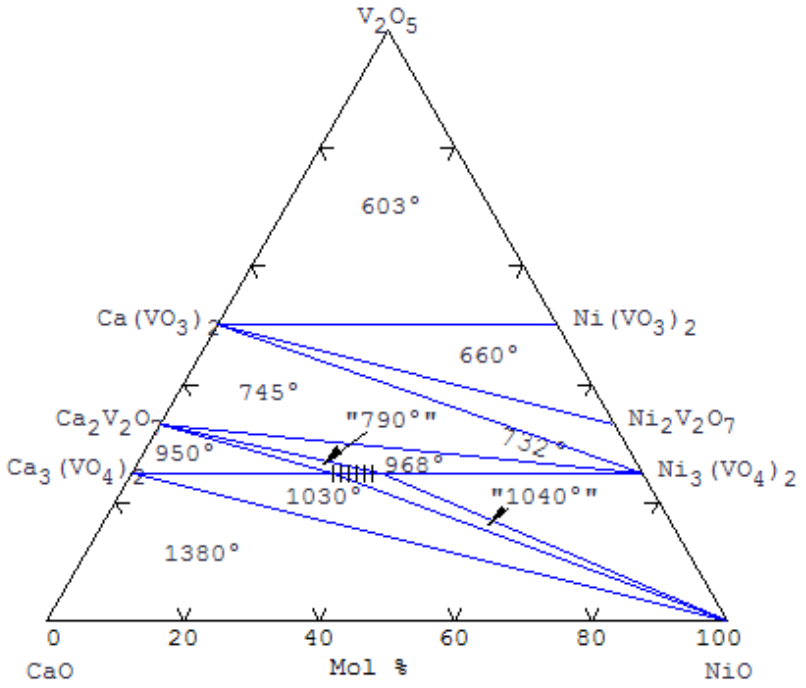

I.A. Arapova, N.P. Tugova, N.G. Sharova, B.V. Slobodin, Zh. Neorg. Khim., 26 [1], (1981), pp.281-282.

CaO-NiO-V2O5,
Mole fraction , Isopleth Ca2V2O7-NiO-O2

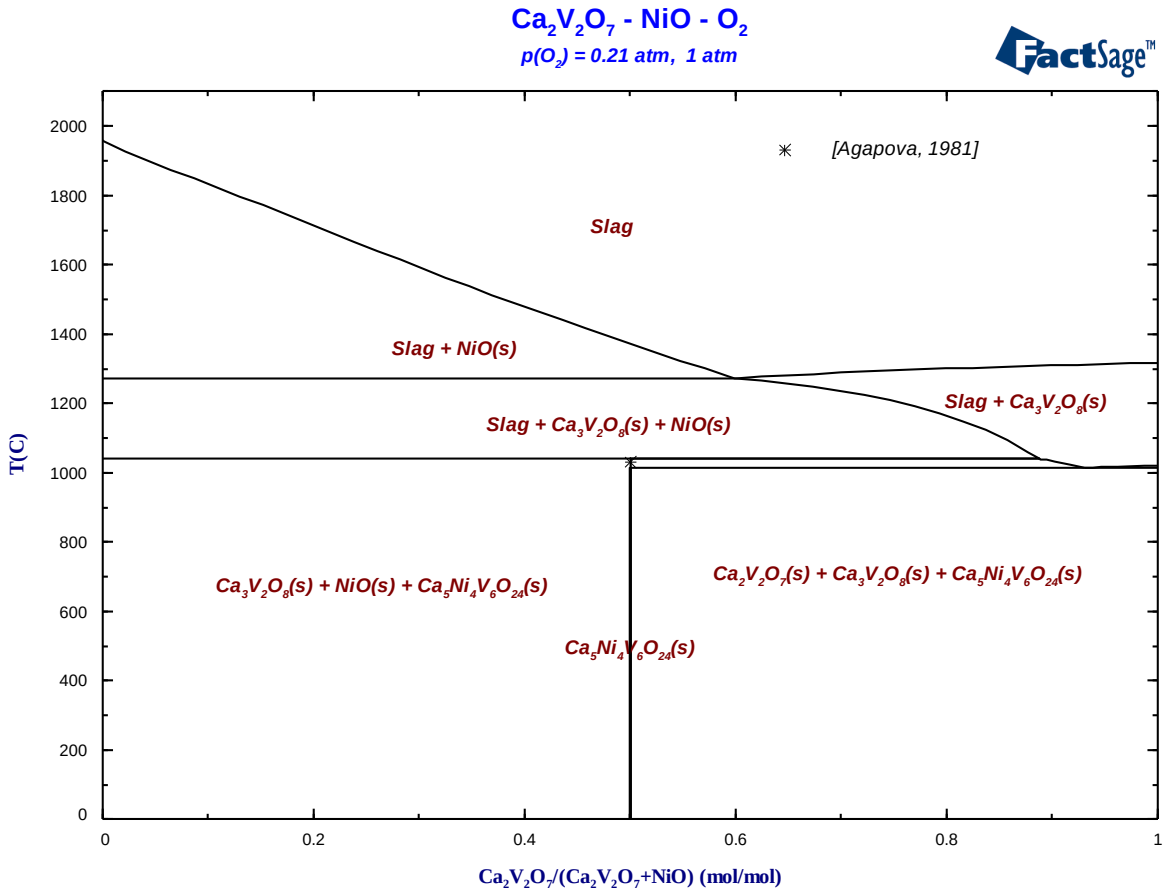

CaO-NiO-V2O5,
Mole fraction , Liquidus surface

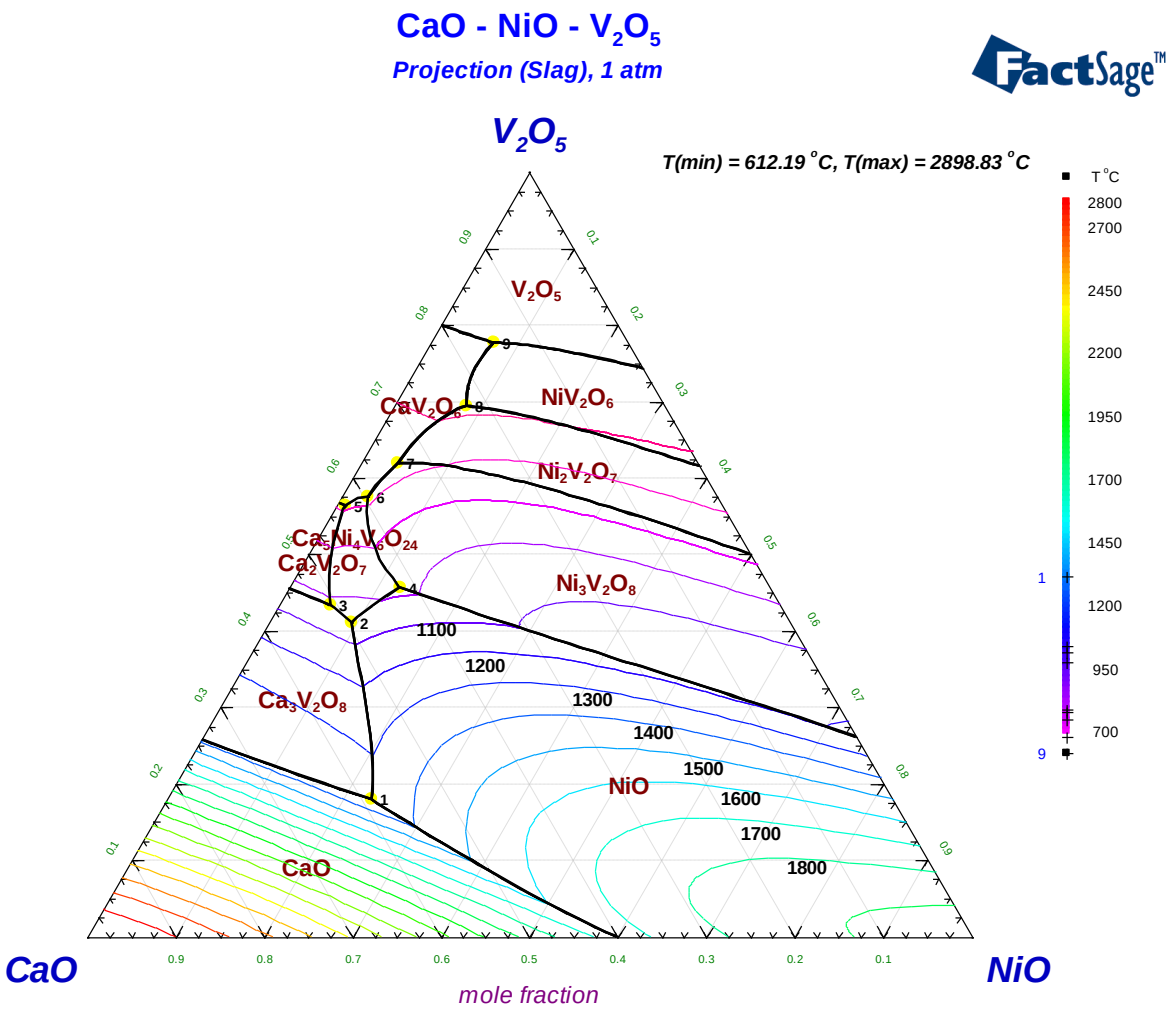

Weight percent , Liquidus surface

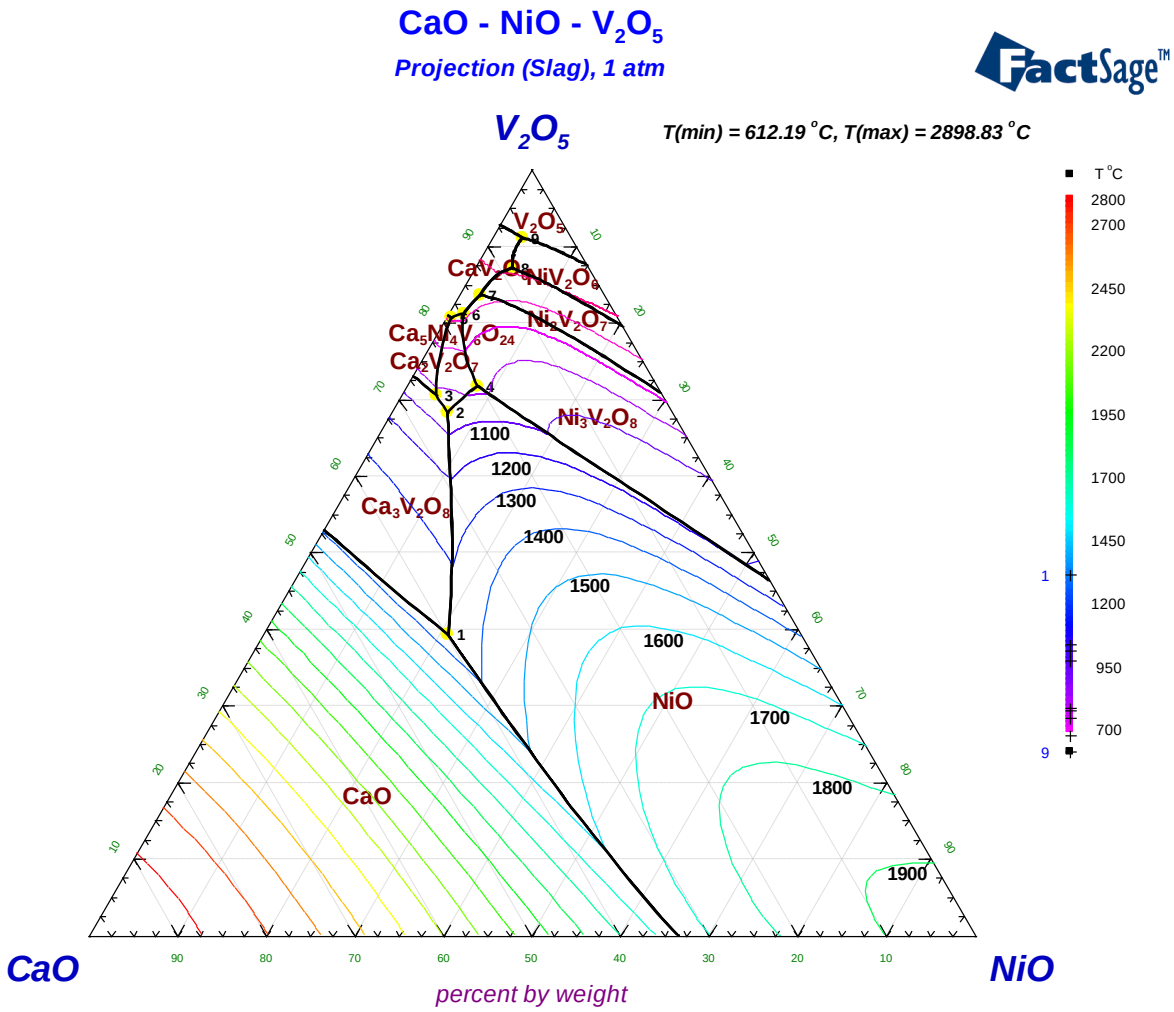

Invariant equilibria on the liquidus surface

Intersections with slag	Mole fraction A = V2O5, B = CaO, C = NiO				Weight percent A = V2O5, B = CaO, C = NiO			
	X(A)	X(B)	X(C)	T(C)	W(A)	W(B)	W(C)	T(C)
1. Ca3V2O8 / CaO / NiO	1: 0.17929	0.58879	0.23192	1312.72	1: 39.313	39.805	20.883	1312.72
2. Ca3V2O8 / Ca5Ni4V6O24 / NiO	2: 0.41099	0.49543	0.09358	1038.57	2: 68.252	25.367	6.382	1038.57
3. Ca2V2O7 / Ca3V2O8 / Ca5Ni4V6O24	3: 0.43340	0.50795	0.05866	1013.54	3: 70.575	25.503	3.923	1013.55
4. Ca5Ni4V6O24 / Ni3V2O8 / NiO	4: 0.45682	0.41818	0.12500	971.48	4: 71.704	20.238	8.058	971.48
5. Ca2V2O7 / Ca5Ni4V6O24 / CaV2O6	5: 0.56458	0.42647	0.00895	784.42	5: 80.684	18.791	0.525	784.43
6. Ca5Ni4V6O24 / CaV2O6 / Ni3V2O8	6: 0.57630	0.39443	0.02927	774.92	6: 81.177	17.130	1.693	774.97
7. CaV2O6 / Ni2V2O7 / Ni3V2O8	7: 0.62013	0.33839	0.04148	746.34	7: 83.632	14.071	2.298	746.33
8. CaV2O6 / Ni2V2O7 / NiV2O6	8: 0.69469	0.22424	0.08107	676.84	8: 87.150	8.674	4.176	676.84
9. CaV2O6 / NiV2O6 / V2O5	9: 0.77707	0.15222	0.07071	612.19	9: 91.094	5.502	3.404	612.19

CaO-P2O5-SiO2, Weight percent

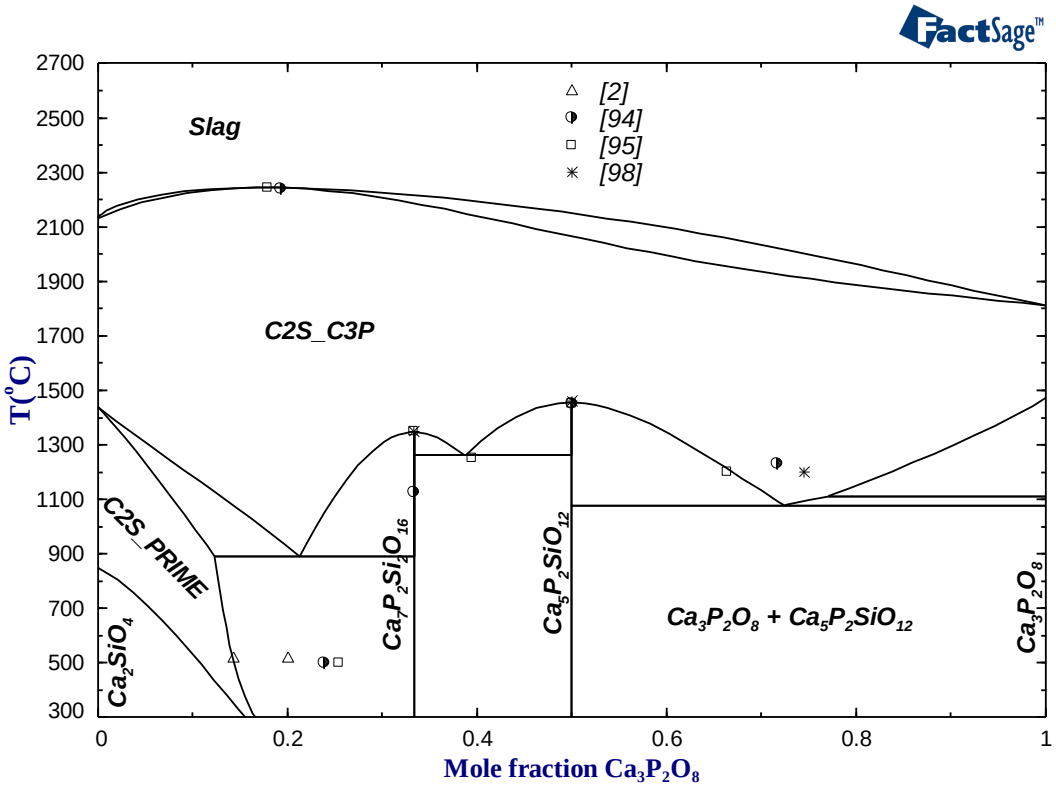

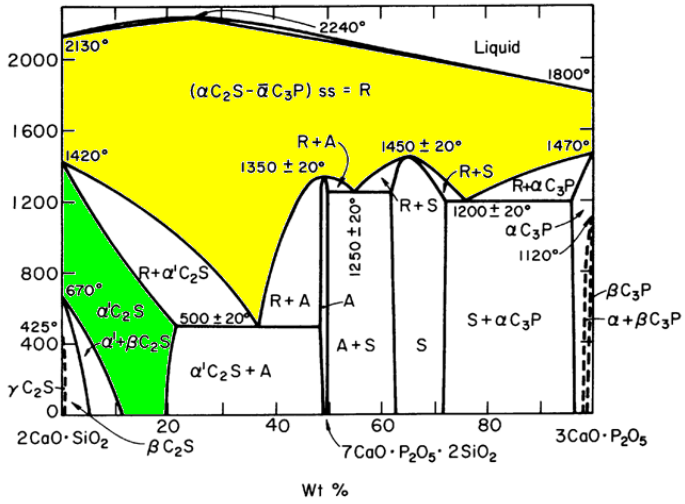

W. Fix, H. Heymann, and R. Heinke, J. Am. Ceram. Soc., 52 [6] 346-347 (1969).

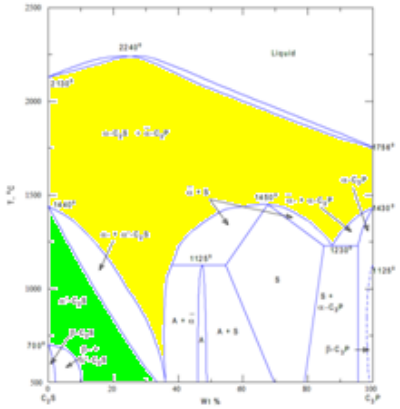

R. W. Nurse, J. H. Welch, W. H. Gutt, J. Chem. Soc.,1077-1083 (1959).

CaO-P2O5-SiO2,

Weight percent, 1000°C

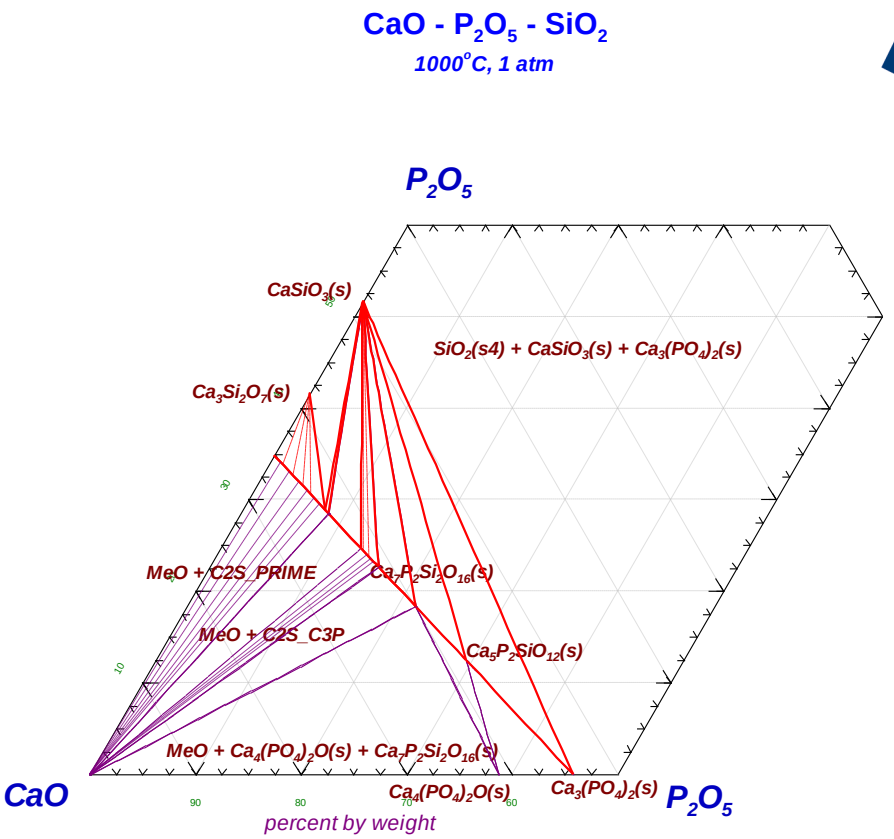

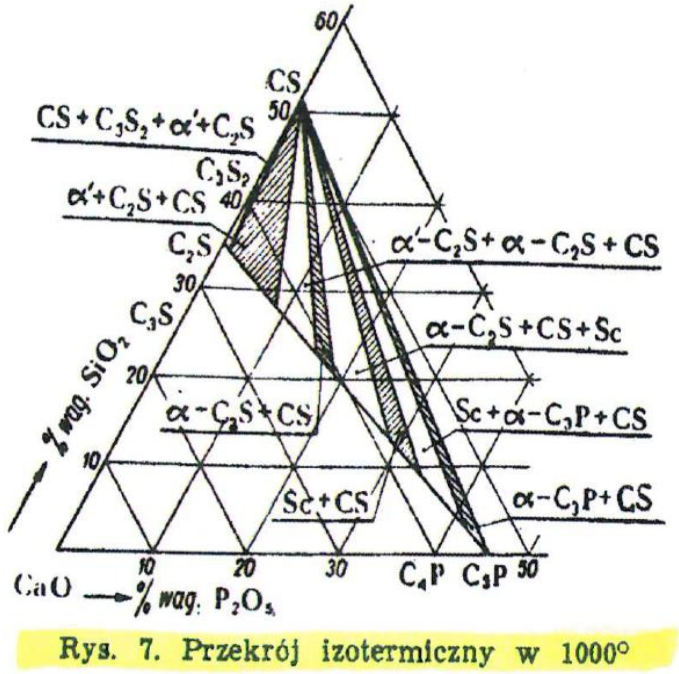

Rys. 7. Przekrój izotermiczny w 1000°

J. Berak and J.Wojciechowska, Rocz. Chem., 30[3] , (1956), pp.757-769 .

CaO-P2O5-SiO2,

Weight percent, 1225°C

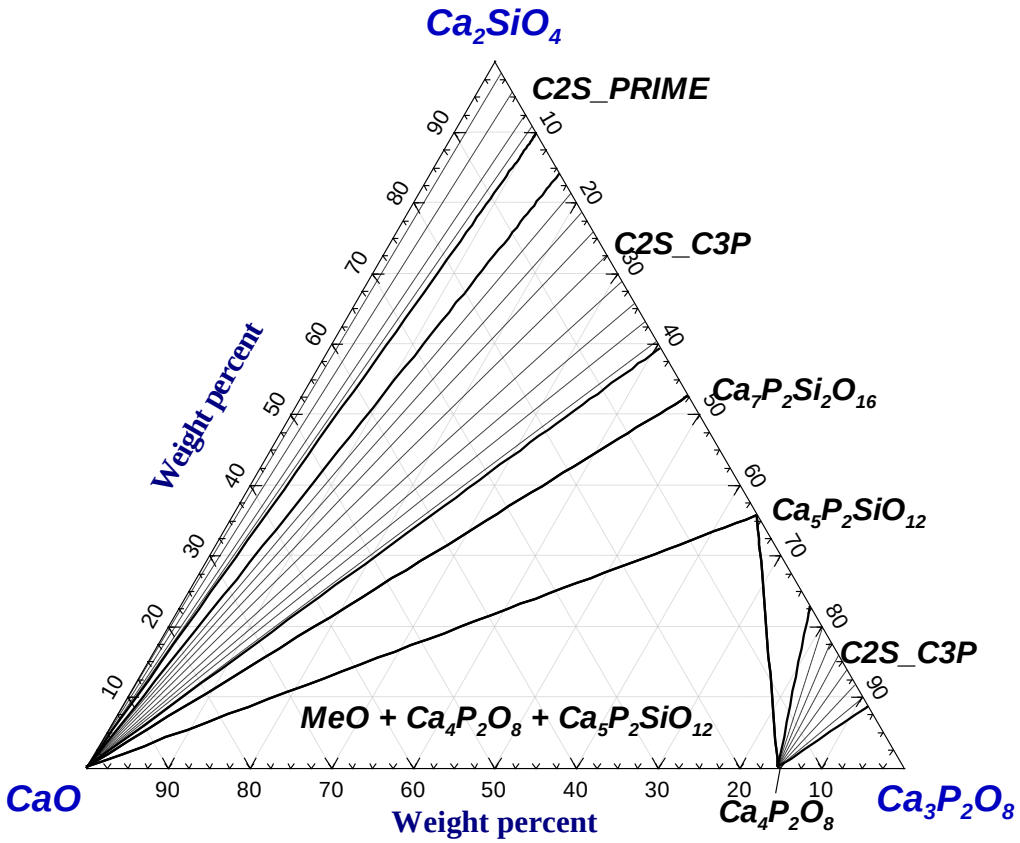

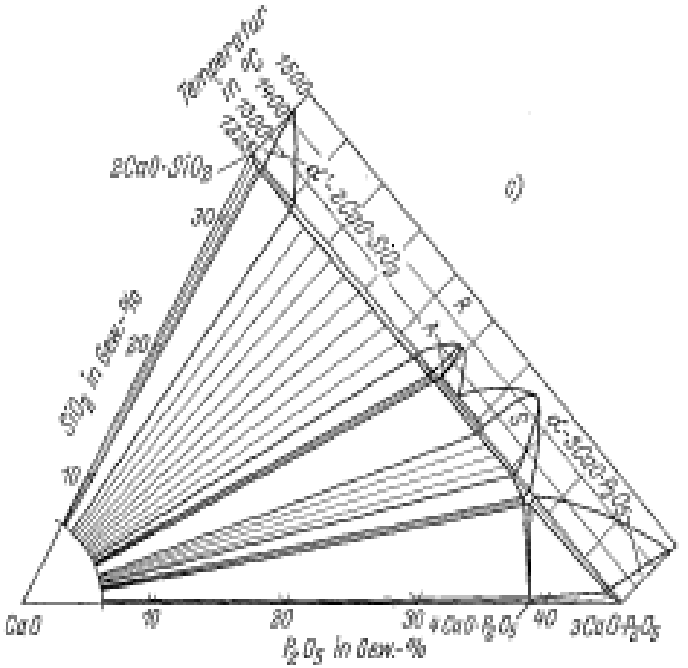

W. Fix, H. Heymann, and R. Heinke, J. Am. Ceram. Soc., 52 [6] 346-347 (1969).

CaO-P2O5-SiO2,

Weight percent, 1600°C

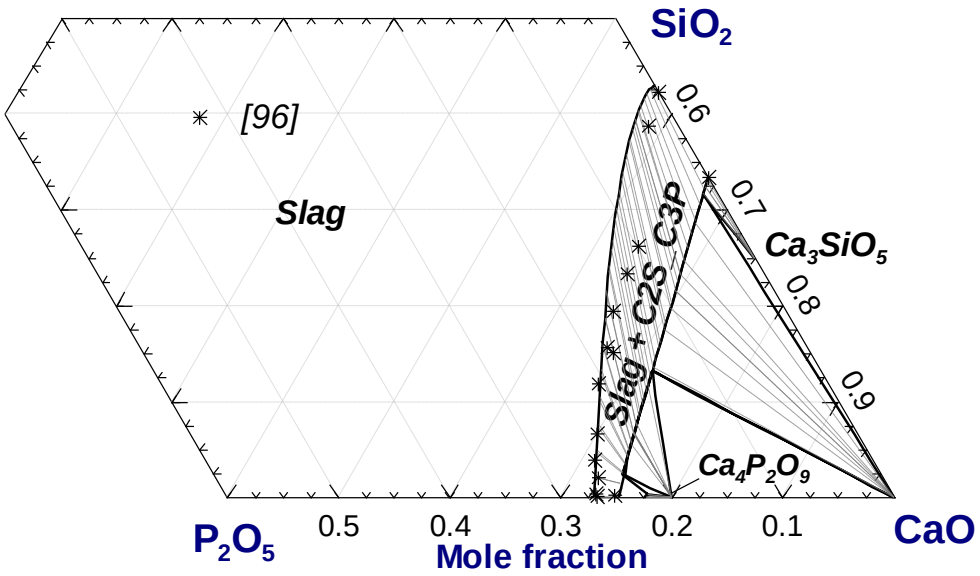

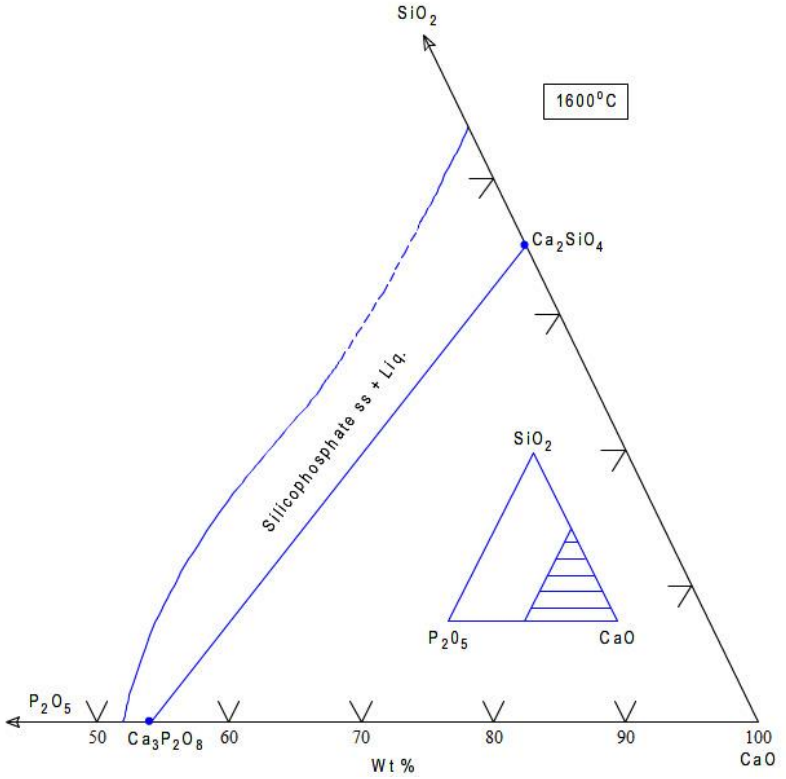

K. Koch ,W. Fix, Arch. Eisenhütenwesen,41[2] , (1970), pp. 111-118.

CaO-P2O5-SiO2,

Weight percent, Isopleth Ca3P2O8-SiO2

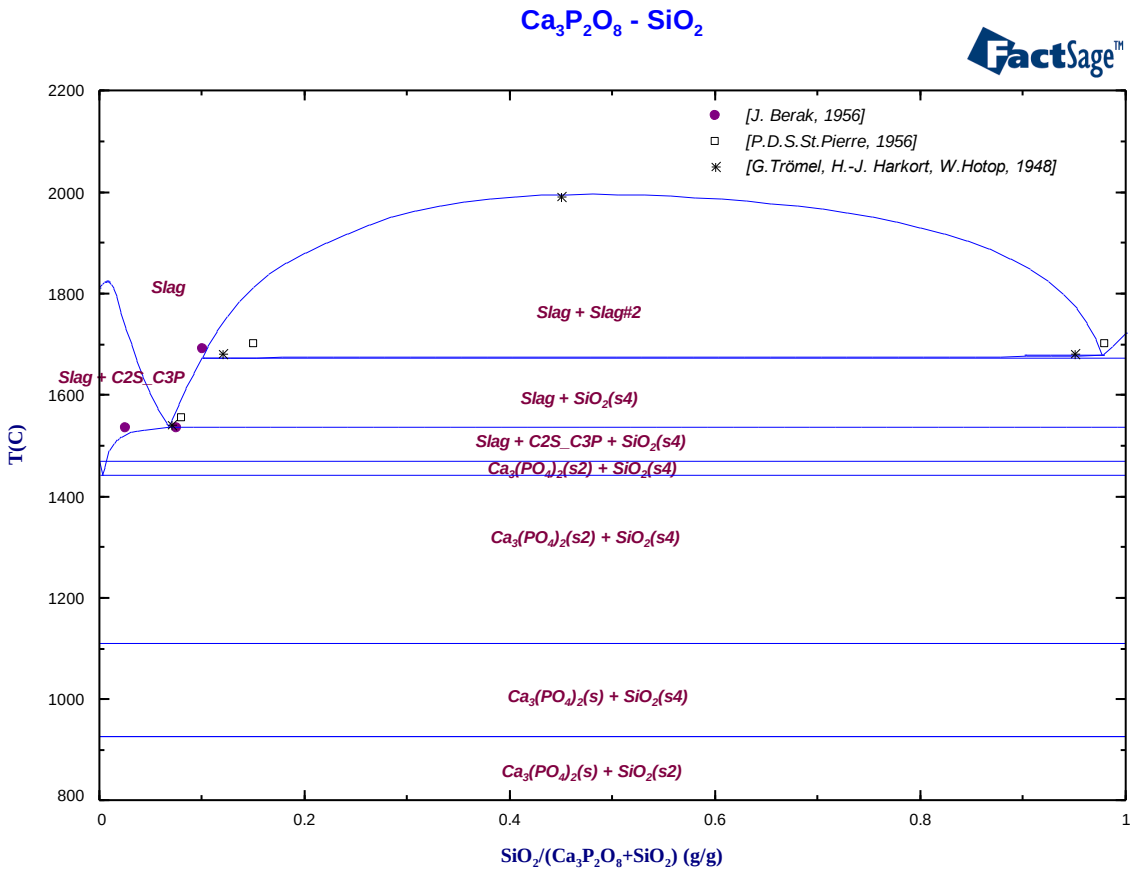

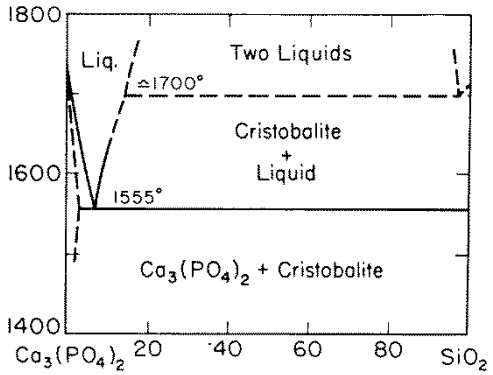

P.D.S. St. Pierre, J. Am. Ceram. Soc., 39[4], (1956), pp. 147-150.

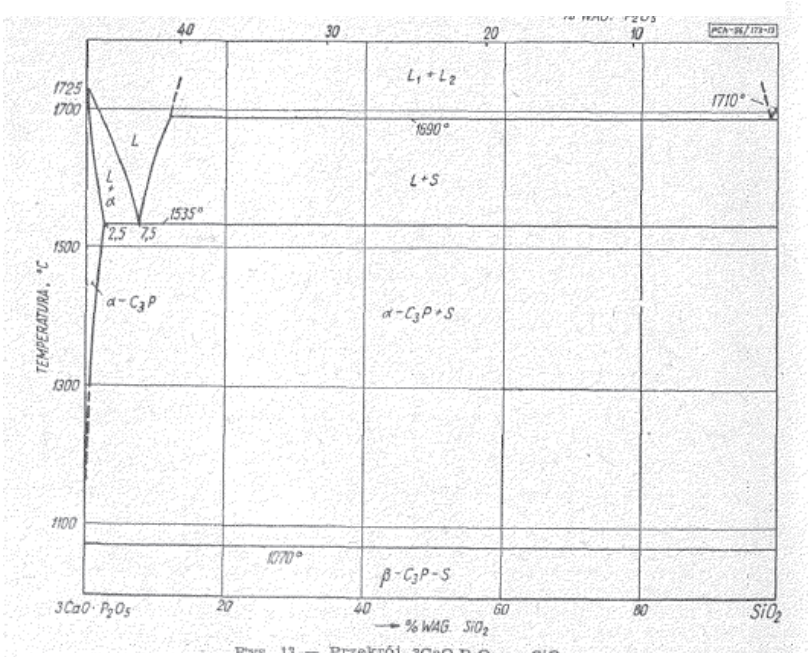

J. Berak, Przem.. Chem., 12 , (1956), pp.478-484 .

Weight percent,
Liquidussurface in CaO-Ecke

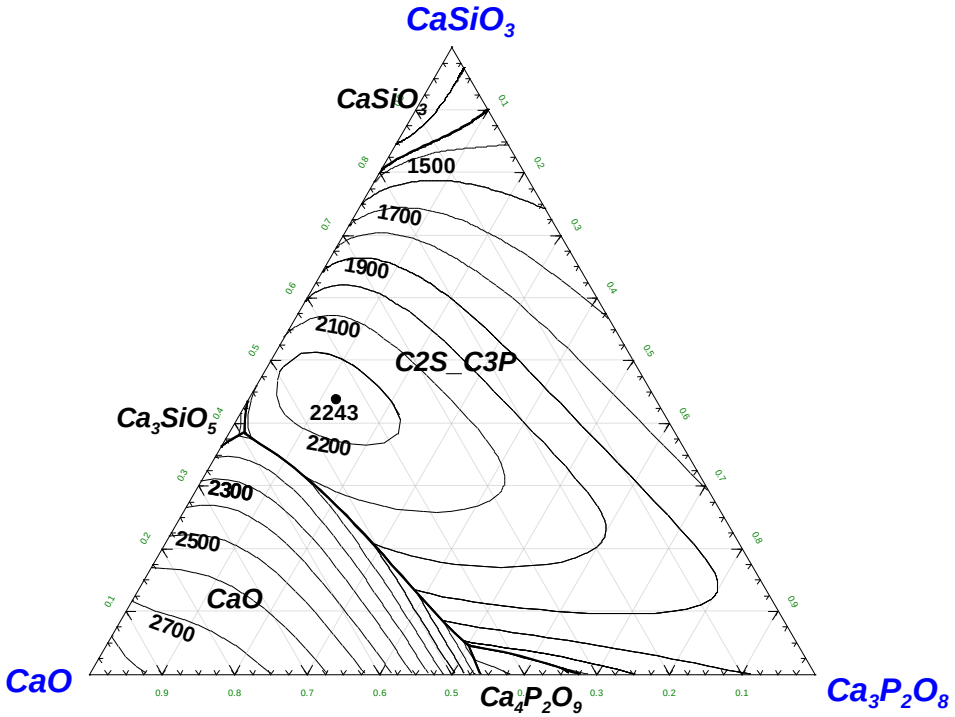

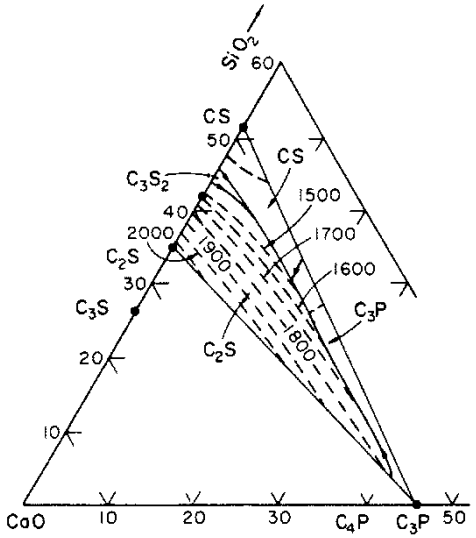

J. Berak and J.Wojciechowska, Rocz. Chem., 30[3] , (1956), pp.757-769 .

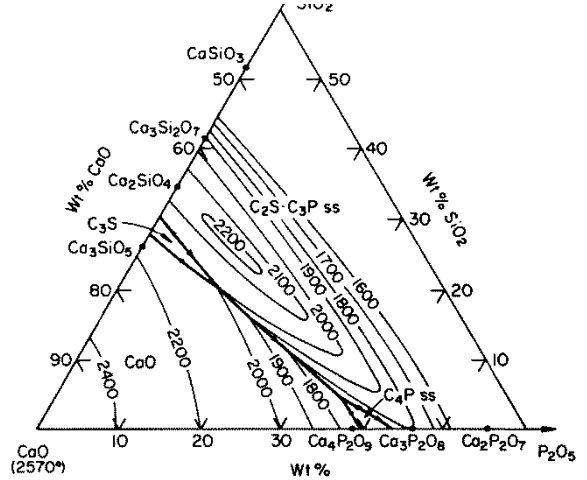

H. Margot-Marette, P. V. Riboud, Mem. Sci. Rev. Metall., 69 [9] 593-604, (1972).

Mole fraction 500°C

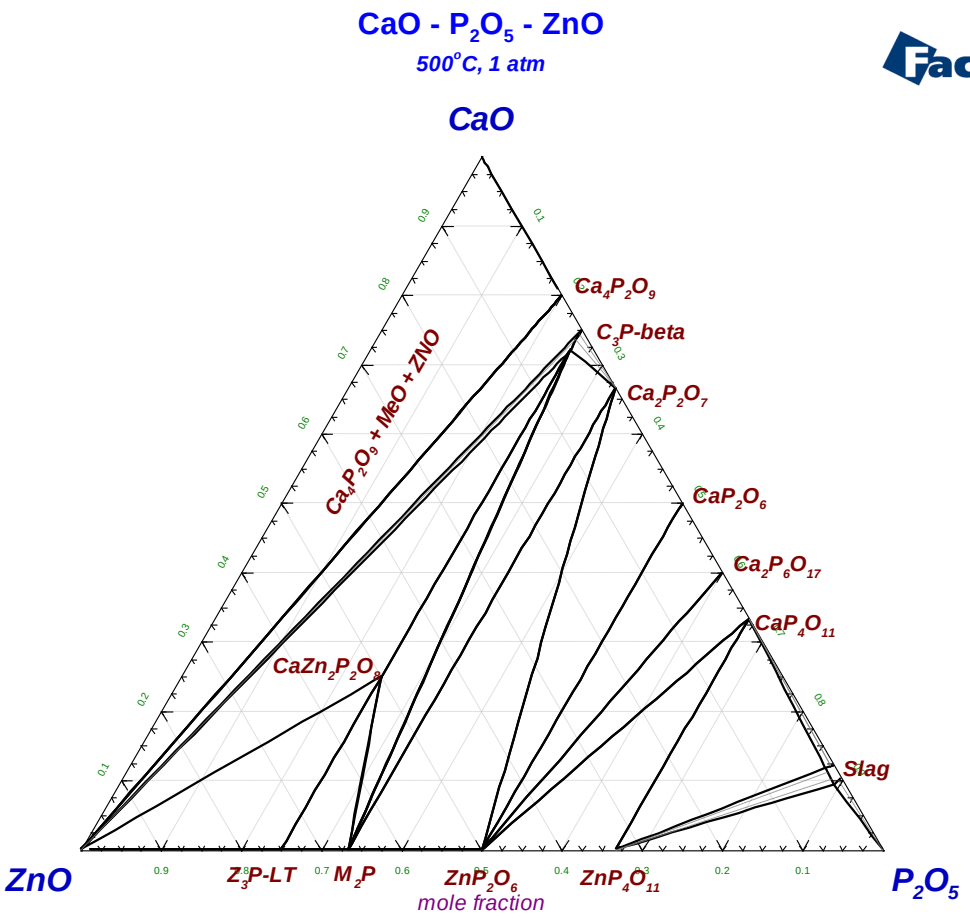

Mole fraction, Isopleth section Ca3P2O8-Zn3P2O8

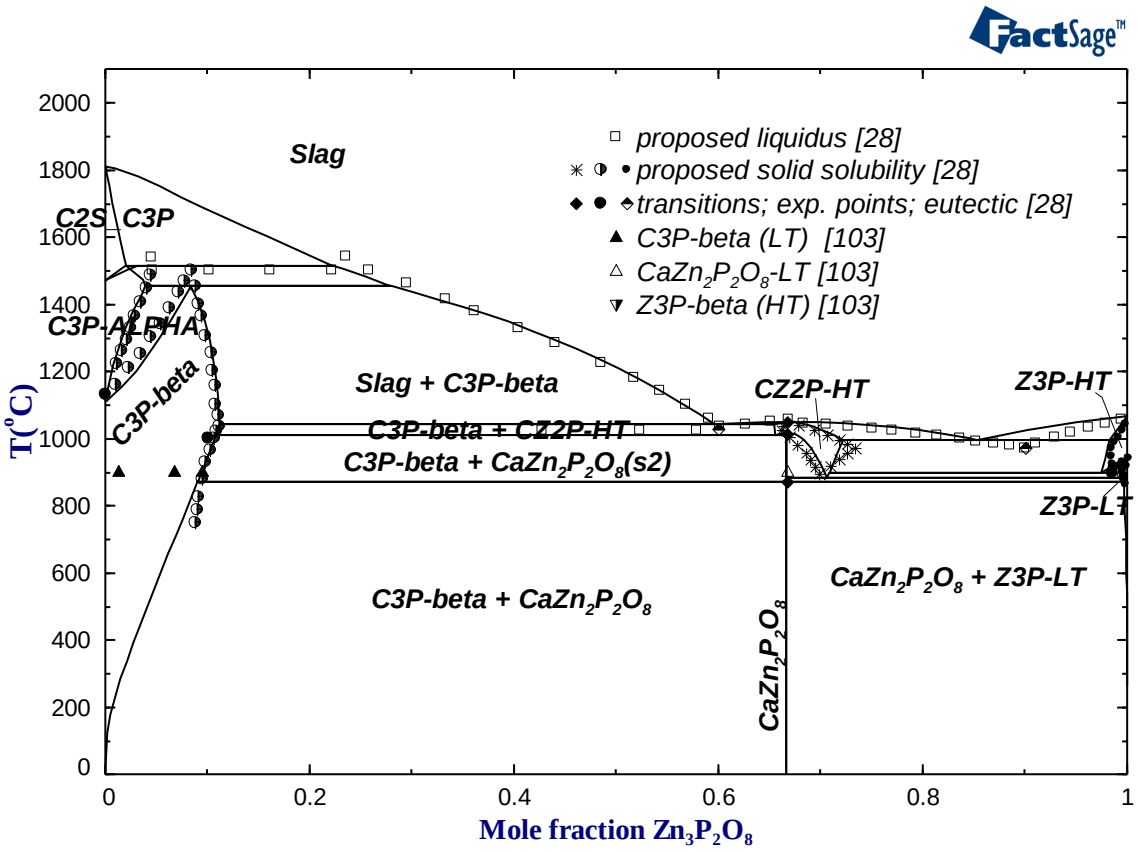

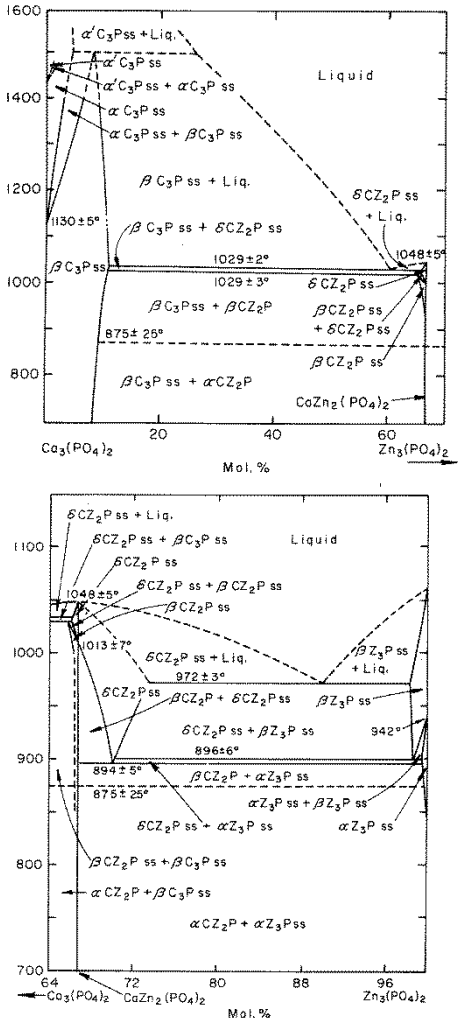

E.R. Kreider, F.A. Hummel, Inorg. Chem., 64[3], (1967), pp. 524-528.

Mole fraction, Isopleth section Ca2P2O7-Zn2P2O7

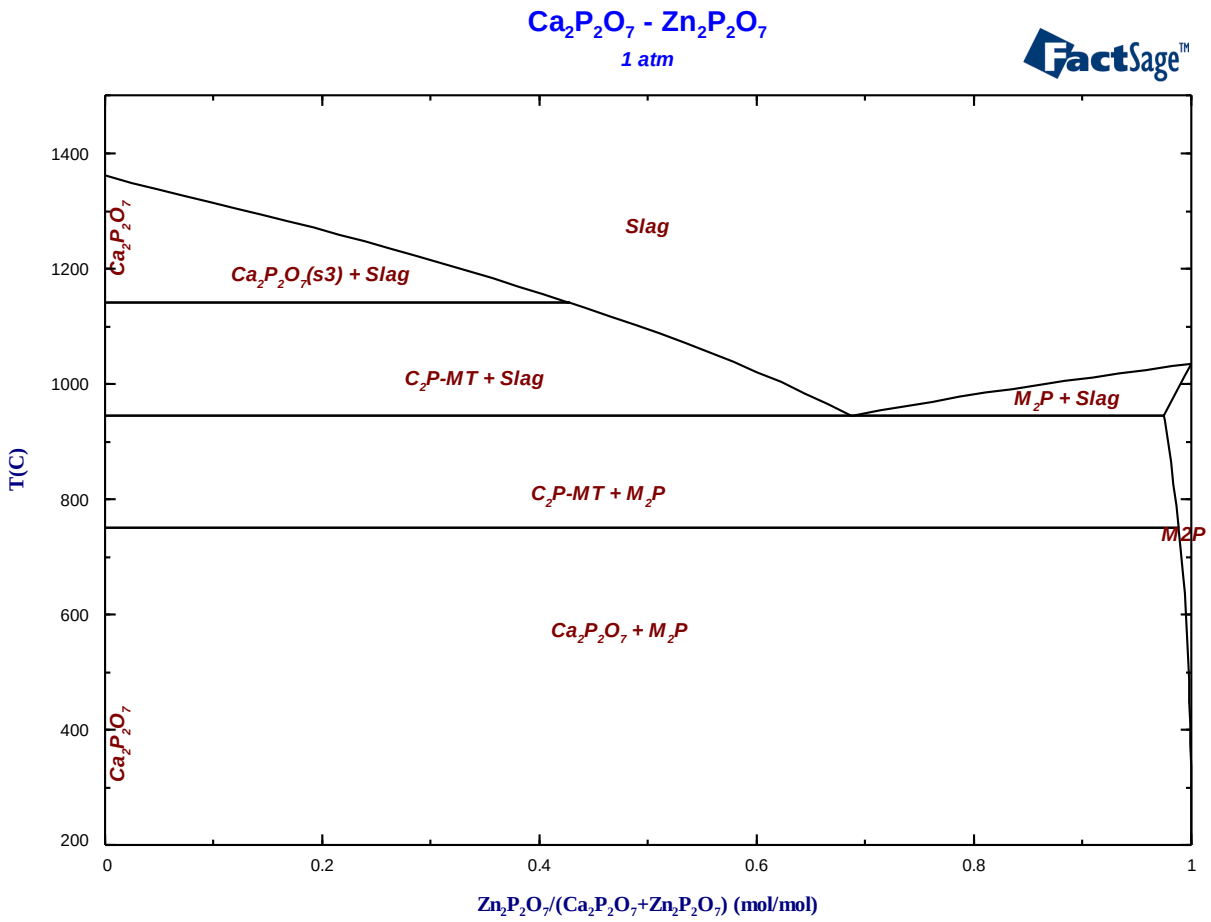

Mole fraction, Liquidussurface

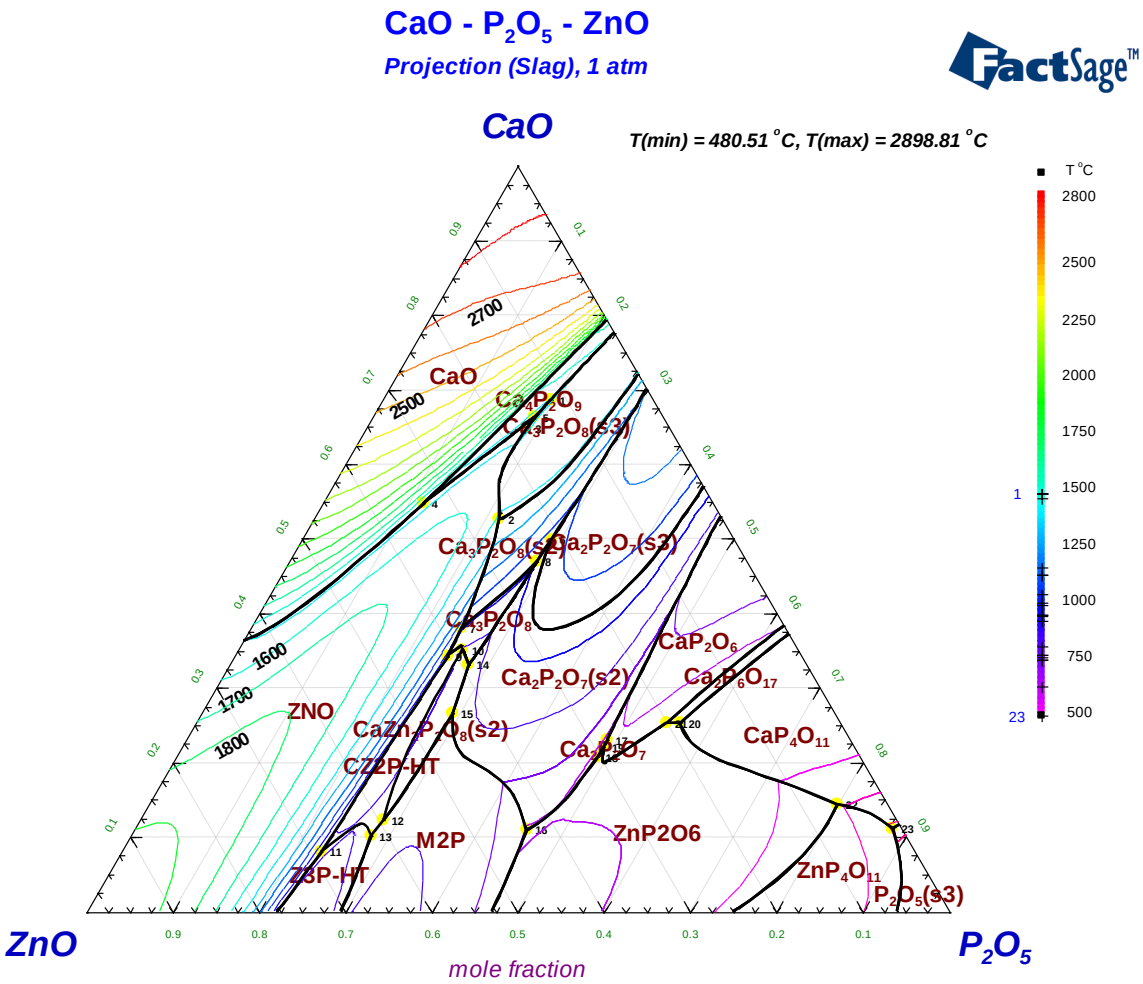

Weight percent, Liquidussurface

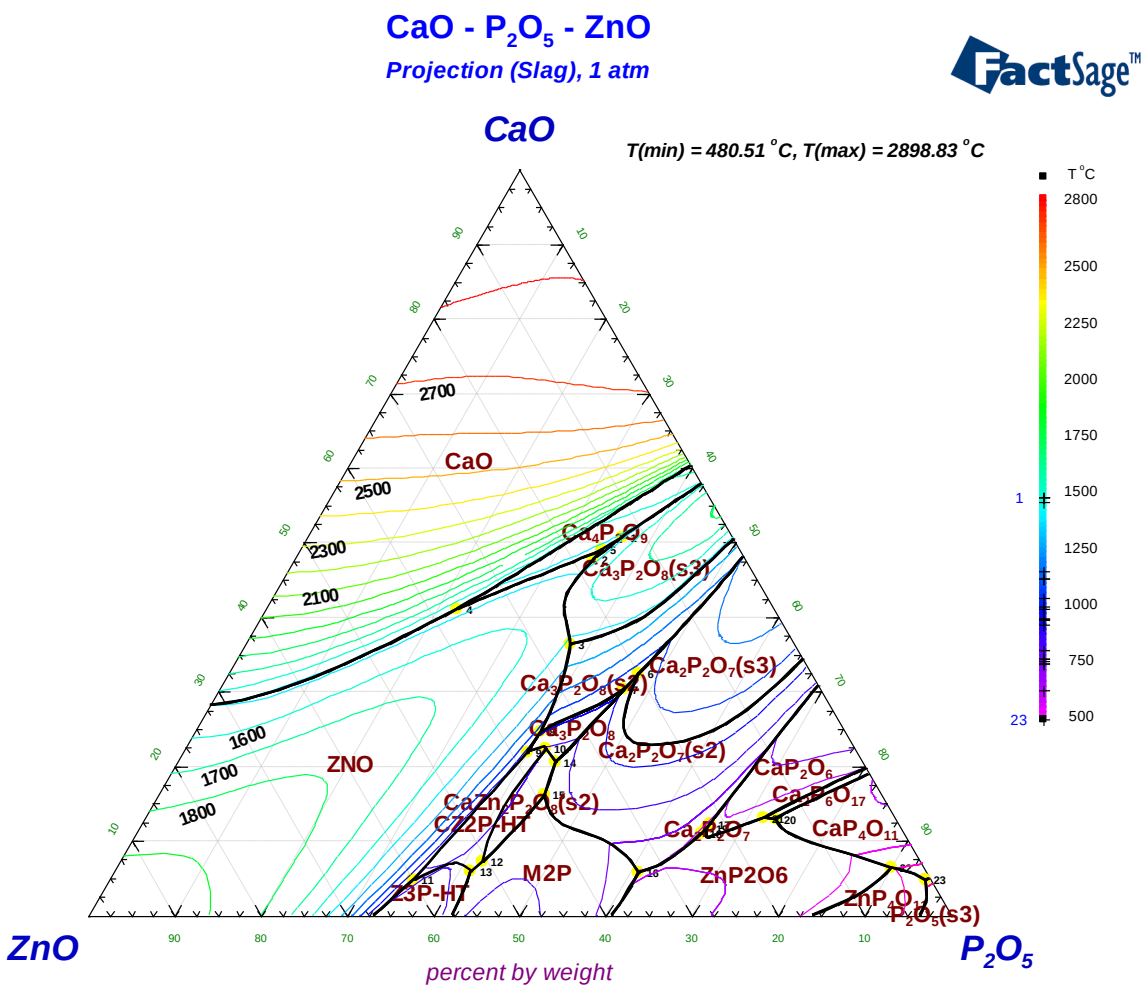

Invariant equilibria on the liquidus surface

Intersections with slag	Mole fraction A = CaO, B = ZnO, C = P2O5				Weight percent A = CaO, B = ZnO, C = P2O5				
	X(A)	X(B)	X(C)	T(C)		W(A)	W(B)	W(C)	T(C)
1. Ca3P2O8(s2) / Ca3P2O8_(s3) / Ca4P2O9	1: 0.68683	0.11828	0.19489	1469.86	1:	50.809	12.698	36.493	1469.85
2. Ca3P2O8(s2) / Ca3P2O8(s3) / ZNO	2: 0.52642	0.25804	0.21554	1469.85	2:	47.757	17.560	4.683	1469.85
3. Ca3P2O8(s2) / Ca3P2O8(s3) / ZNO	3: 0.64923	0.16450	0.18627	1469.85	3:	36.393	25.888	37.719	1469.85
4. Ca4P2O9 / CaO(s) / ZNO	4: 0.54743	0.33582	0.11676	1469.14	4:	41.151	36.634	22.216	1469.14
5. Ca3P2O8(s2) / Ca4P2O9(s) / ZNO	5: 0.66394	0.14863	0.18743	1447.11	5:	49.033	15.929	35.038	1447.09
6. Ca2P2O7(s2) / Ca2P2O7(s3) / Ca3P2O8(s2)	6: 0.49921	0.21150	0.28929	1139.86	6:	32.451	19.951	47.598	1139.85
7. Ca3P2O8(s2) / Ca3P2O8(s) / ZNO	7: 0.38058	0.37491	0.24451	1109.86	7:	30.379	22.697	46.924	1109.85
8. Ca2P2O7(s2) / Ca3P2O8(s2) / Ca3P2O8(s)	8: 0.47058	0.24227	0.28716	1109.85	8:	24.656	35.248	40.097	1109.83
9. CZ2P-HT / Ca3P2O8(s) / ZNO	9: 0.34316	0.41017	0.24666	1021.54	9:	21.959	38.089	39.952	1021.50
10. CZ2P-HT / Ca3P2O8(s) / CaZn2P2O8(s2)	10: 0.35138	0.38792	0.26070	984.49	10:	22.321	35.760	41.919	984.48
11. CZ2P-HT / Z3P-HT / ZNO	11: 0.08031	0.68771	0.23198	973.24	11:	4.822	59.922	35.256	973.25
12. CZ2P-HT / CaZn2P2O8(s2) / M2P	12: 0.12341	0.59385	0.28274	931.23	12:	7.256	50.667	42.077	931.23
13. CZ2P-HT / M2P / Z3P-HT	13: 0.10174	0.61937	0.27889	927.12	13:	5.962	52.671	41.367	927.13
14. Ca2P2O7(s2) / Ca3P2O8(s) / CaZn2P2O8(s2)	14: 0.33064	0.39174	0.27762	923.42	14:	20.641	35.490	43.869	923.42
15. Ca2P2O7(s2) / CaZn2P2O8(s2) / M2P	15: 0.26558	0.44293	0.29149	903.65	15:	16.133	39.046	44.821	903.65
16. Ca2P2O7(s2) / M2P / ZnP2O6	16: 0.10949	0.43537	0.45515	788.08	16:	5.783	33.369	60.848	787.98
17. Ca2P2O7(s) / Ca2P2O7(s2) / CaP2O6(s)	17: 0.23037	0.28101	0.48862	749.85	17:	12.286	21.750	65.964	749.88
18. Ca2P2O7(s) / Ca2P2O7(s2) / ZnP2O6	18: 0.20751	0.30434	0.48815	749.85	18:	11.009	23.433	65.557	749.85
19. Ca2P2O7(s) / CaP2O6_S1(s) / ZnP2O6	19: 0.22043	0.29027	0.48930	740.36	19:	11.724	22.404	65.872	740.36
20. Ca2P6O17(s) / CaP4O11(s) / ZnP2O6	20: 0.25314	0.18534	0.56152	729.02	20:	13.025	13.839	73.136	729.02
21. Ca2P6O17(s) / CaP2O6(s) / ZnP2O6	21: 0.25289	0.20089	0.54622	727.10	21:	13.123	15.128	71.748	727.09
22. CaP4O11(s) / ZnP2O6 / ZnP4O11(s)	22: 0.14346	0.05803	0.79851	607.11	22:	6.379	3.745	89.876	607.11
23. CaP4O11(s) / P2O5(s3) / ZnP4O11(s)	23: 0.11208	0.00927	0.87865	480.52	23:	4.770	0.573	94.657	480.52

CaO-SiO2-V2O3,
Mole fraction 1000°C

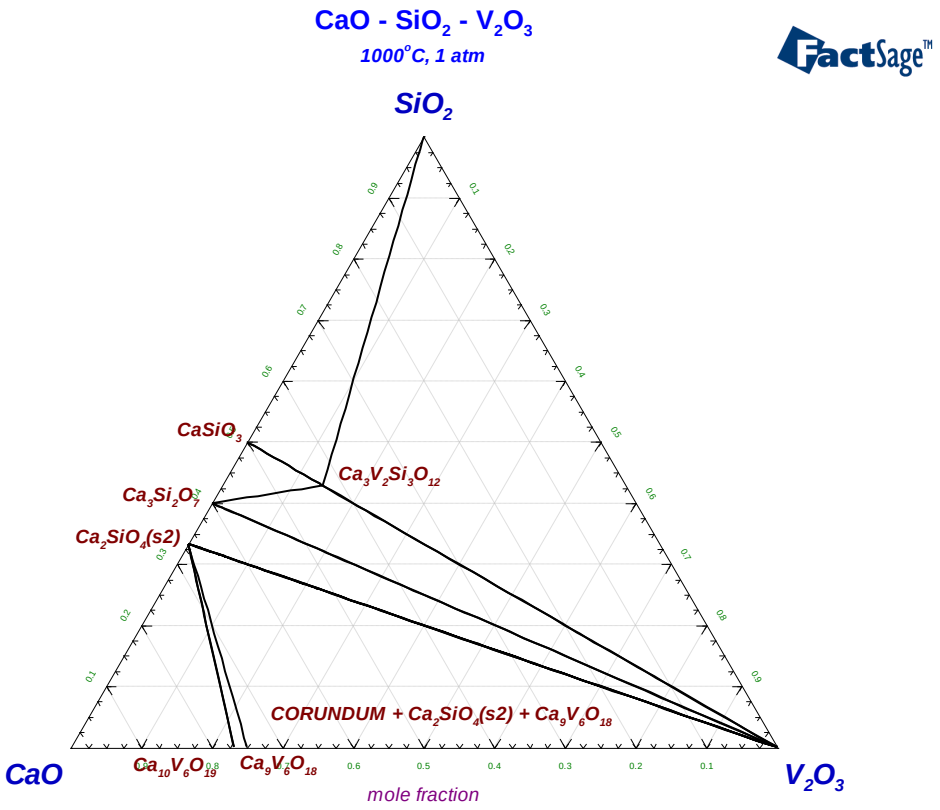

CaO-SiO2-V2O3,
Mole fraction 1500°C

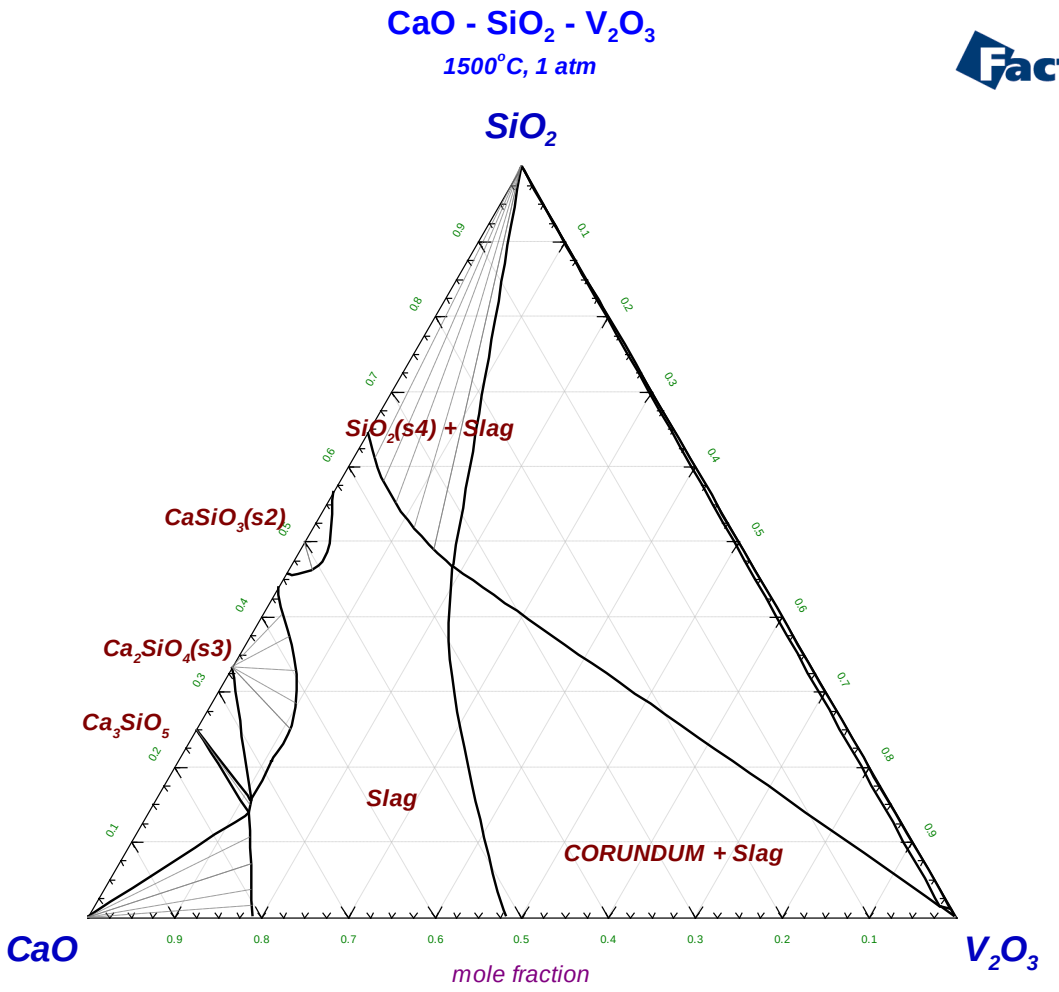

CaO-SiO2-V2O3,
Mole fraction, liquidus surface

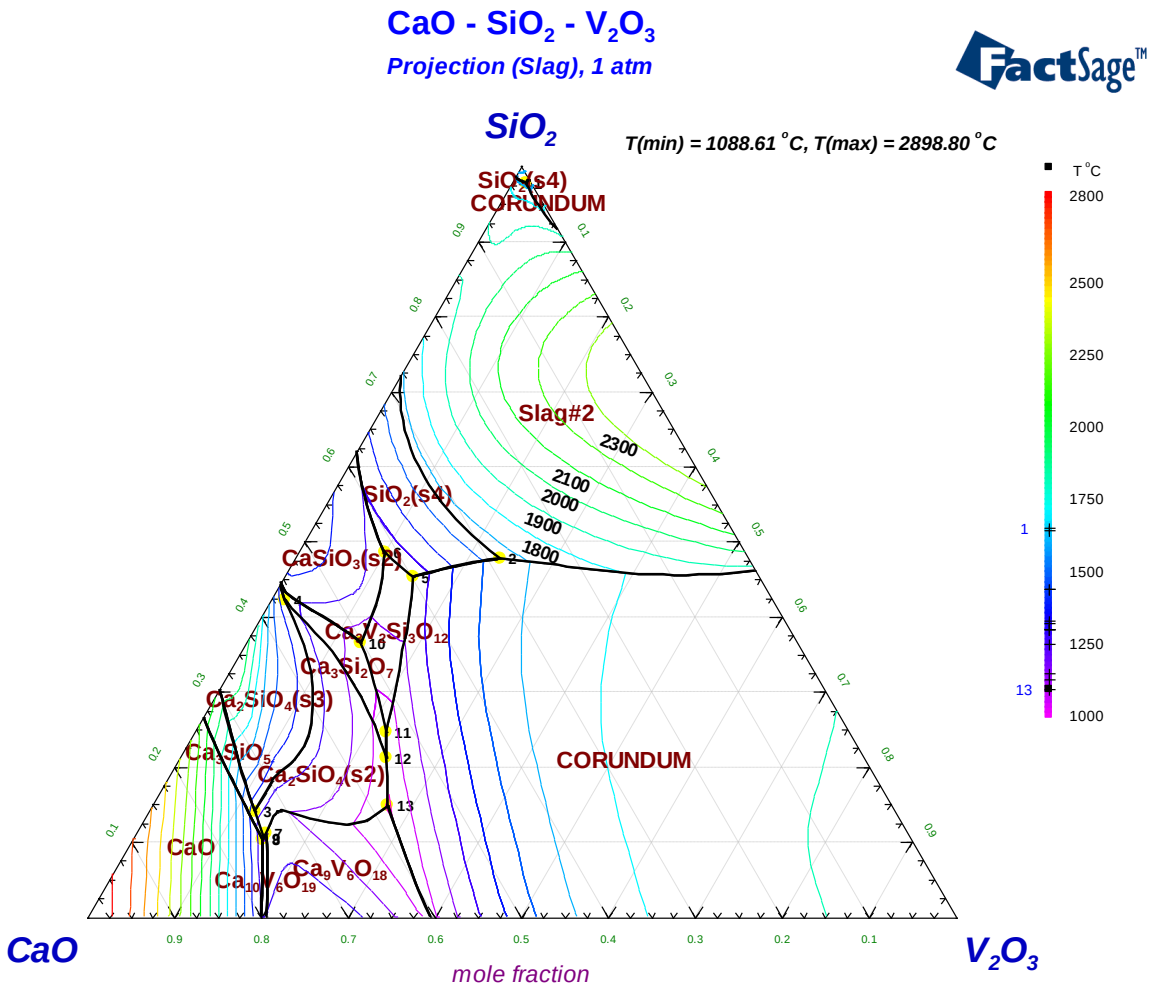

CaO-SiO2-V2O3,
Weight percent, Liquidussurface

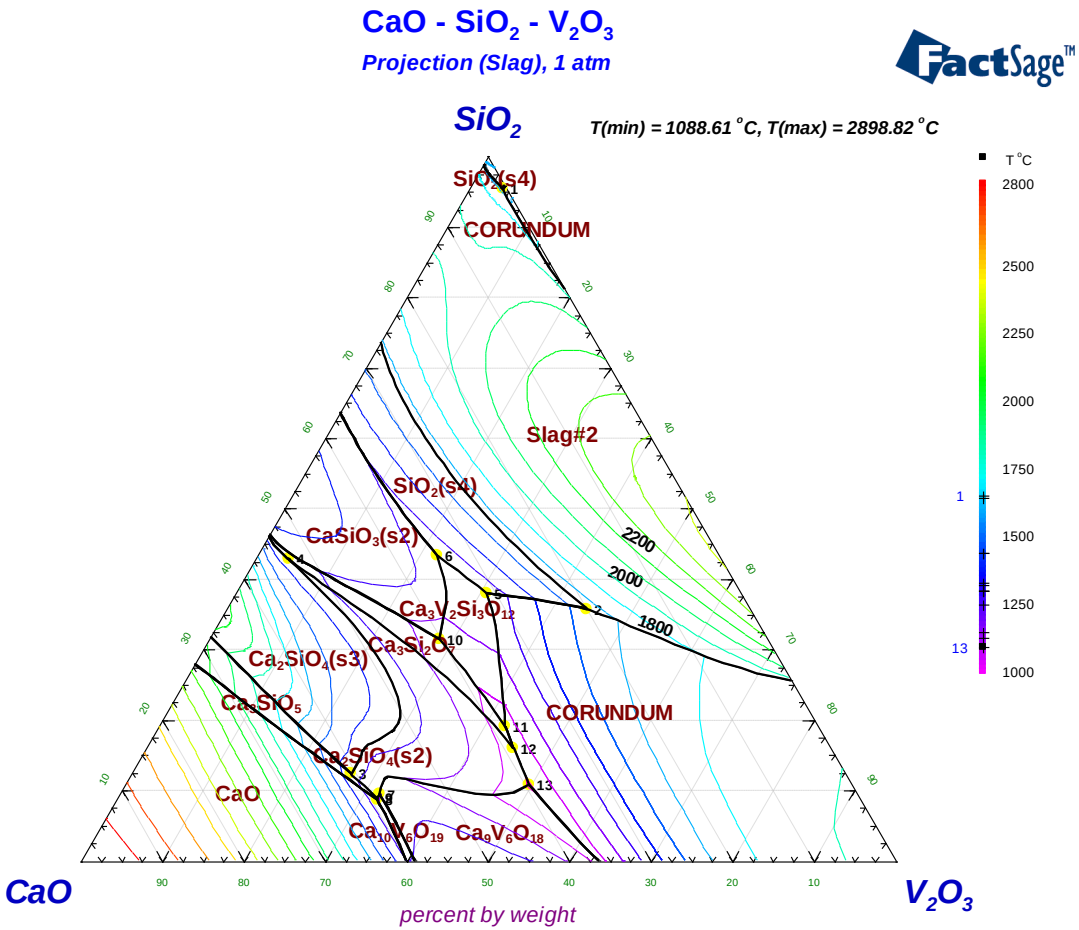

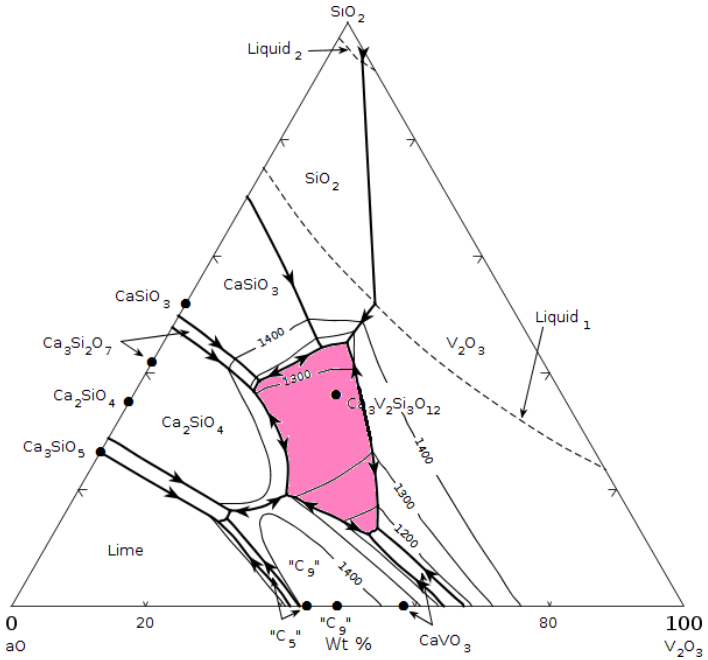

M. S. Najjar and A. Muan, "Vanadium garnet materials", US Patent 4,980,320, December 25, 1990

Invariant equilibria on the liquidus surface

Intersections with slag	Mole fraction A = SiO2, B = CaO, C = V2O3				Weight percent A = SiO2, B =CaO, C = V2O3				
		X(A)	X(B)	X(C)	T(C)		W(A)	W(B)	W(C)	T(C)
1. CORUNDUM / SiO2(s4) / Slag#2	1:	0.97802	0.00563	0.01636	1648.33	1:	97.802	0.563	1.636	1648.33
2. CORUNDUM / SiO2(s4) / Slag#2	2:	0.47852	0.28565	0.23583	1642.28	2:	47.852	28.565	23.583	1642.28
3. Ca2SiO4(s3) / Ca2SiO4(s2) / Ca3SiO5(s)	3:	0.41170	0.55628	0.03203	1417.57	3:	41.170	55.628	3.203	1417.57
4. Ca2SiO4(s3) / Ca2SiO4(s2) / Ca3Si2O7(s)	4:	0.45491	0.39802	0.14707	1325.79	4:	45,491	39.802	14.707	1325.79
5. CORUNDUM / Ca3V2Si3O12 / SiO2(s4)	5:	0.14350	0.70828	0.14822	1325.58	5:	14.350	70.828	14.822	1325.58
6. Ca3V2Si3O12 / CaSiO3(s2) / SiO2(s4)	6:	0.48675	0.41468	0.09858	1318.66	6:	48.675	41.468	9.858	1318.66
7. Ca10V6O19 / Ca2SiO4(s2) / Ca9V6O18	7:	0.10946	0.73790	0.15264	1313.06	7:	10.946	73.790	15.264	1313.06
8. Ca10V6O19 / Ca3SiO5(s) / CaO(s)	8:	0.10015	0.74556	0.15429	1312.31	8:	10.015	74.556	15.429	1312.31
9. Ca10V6O19 / Ca2SiO4(s2) / Ca3SiO5(s)	9:	0.10324	0.74365	0.15312	1311.04	9:	10.324	74.365	15.312	1311.04
10. Ca3Si2O7 / Ca3V2Si3O12 / CaSiO3(s2)	10:	0.37112	0.49951	0.12937	1252.54	10:	37.112	49.951	12.937	1252.54
11. CORUNDUM / Ca3Si2O7 / Ca3V2Si3O12	11:	0.25688	0.52670	0.21642	1156.77	11:	25.688	52.670	21.642	1156.77
12. CORUNDUM / Ca2SiO4(s2) / Ca3Si2O7(s)	12:	0.22753	0.54121	0.23126	1141.02	12:	22.753	54.121	23.126	1141.02
13. CORUNDUM / Ca2SiO4(s2) / Ca9V6O18	13:	0.14804	0.57798	0.27398	1102.06	13:	14.804	57.798	27.398	1102.06

CaO-SiO2-V2O5,
Mole fraction 1500°C

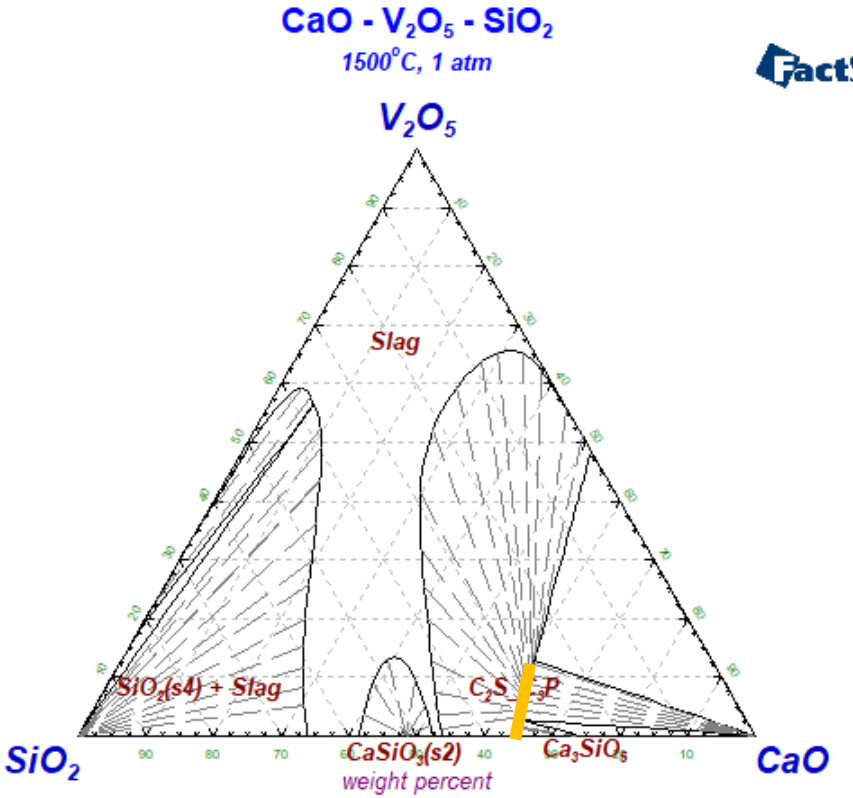

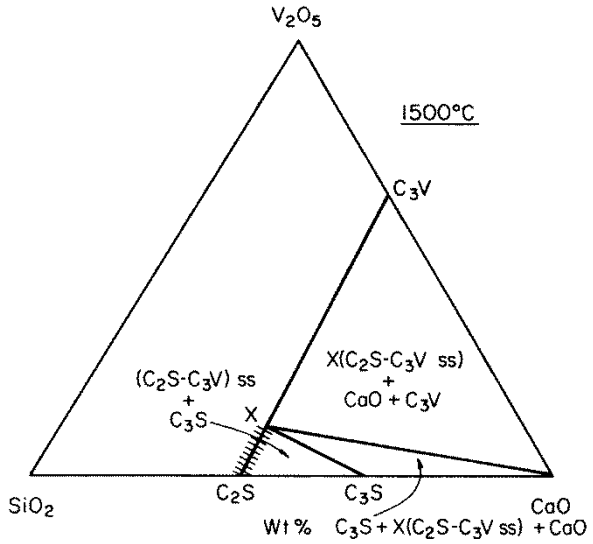

M. Eke, N.H. Brett, Trans. J. Br. Ceram. Soc., 72 [5], (1973), pp. 195-201.

Mole fraction 1000°C

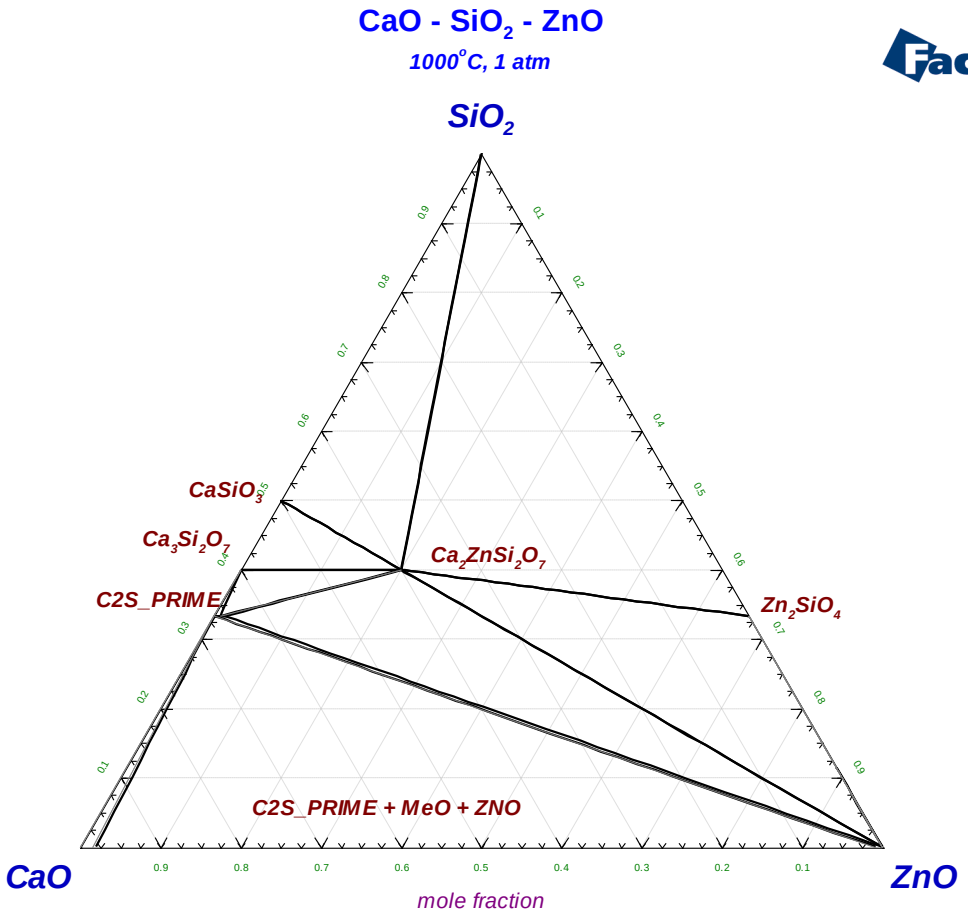

Mole fraction
Isopleth section Ca2SiO4-Zn2SiO4

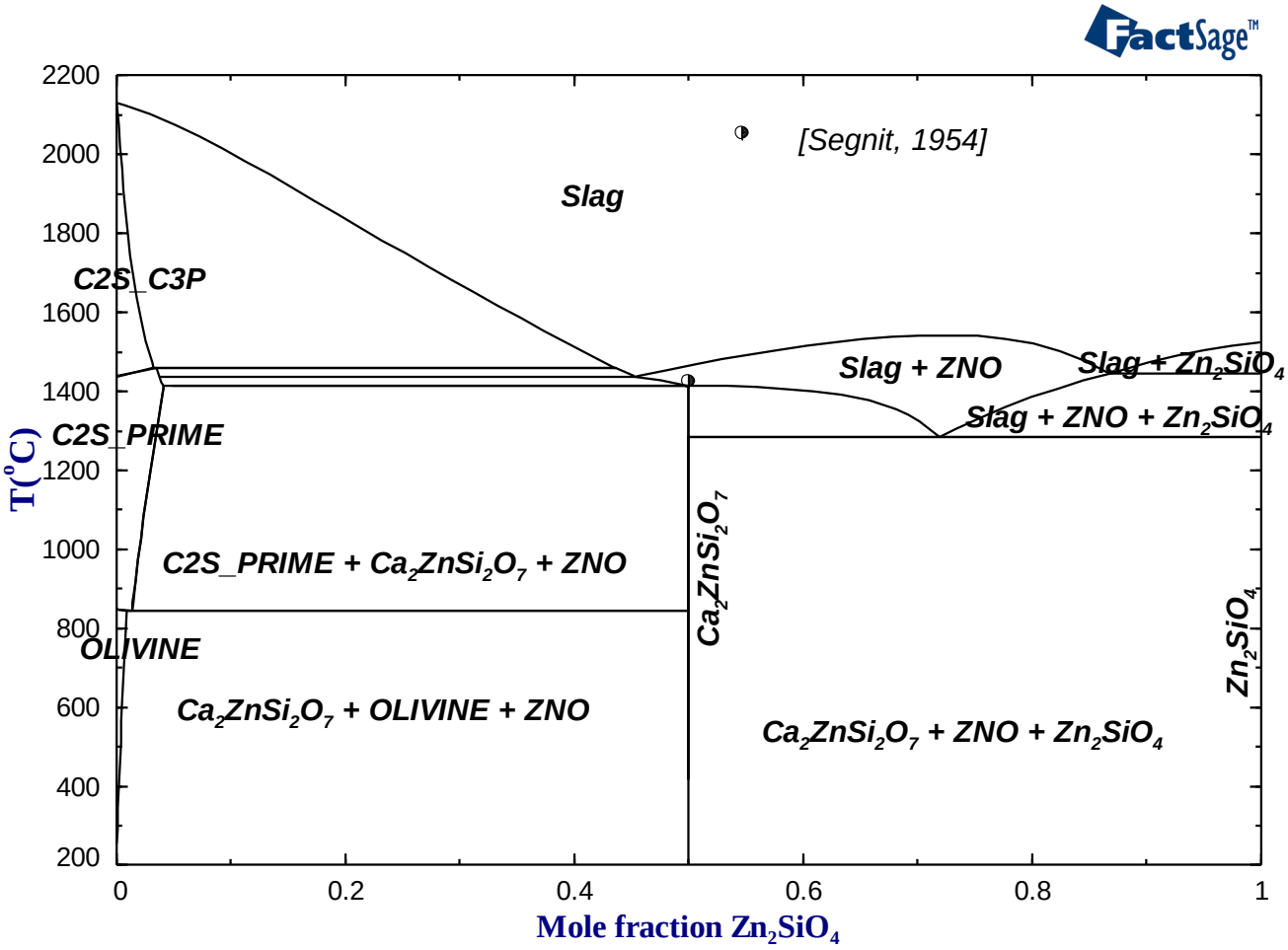

Mole fraction
Isopleth section CaSiO3-ZnO

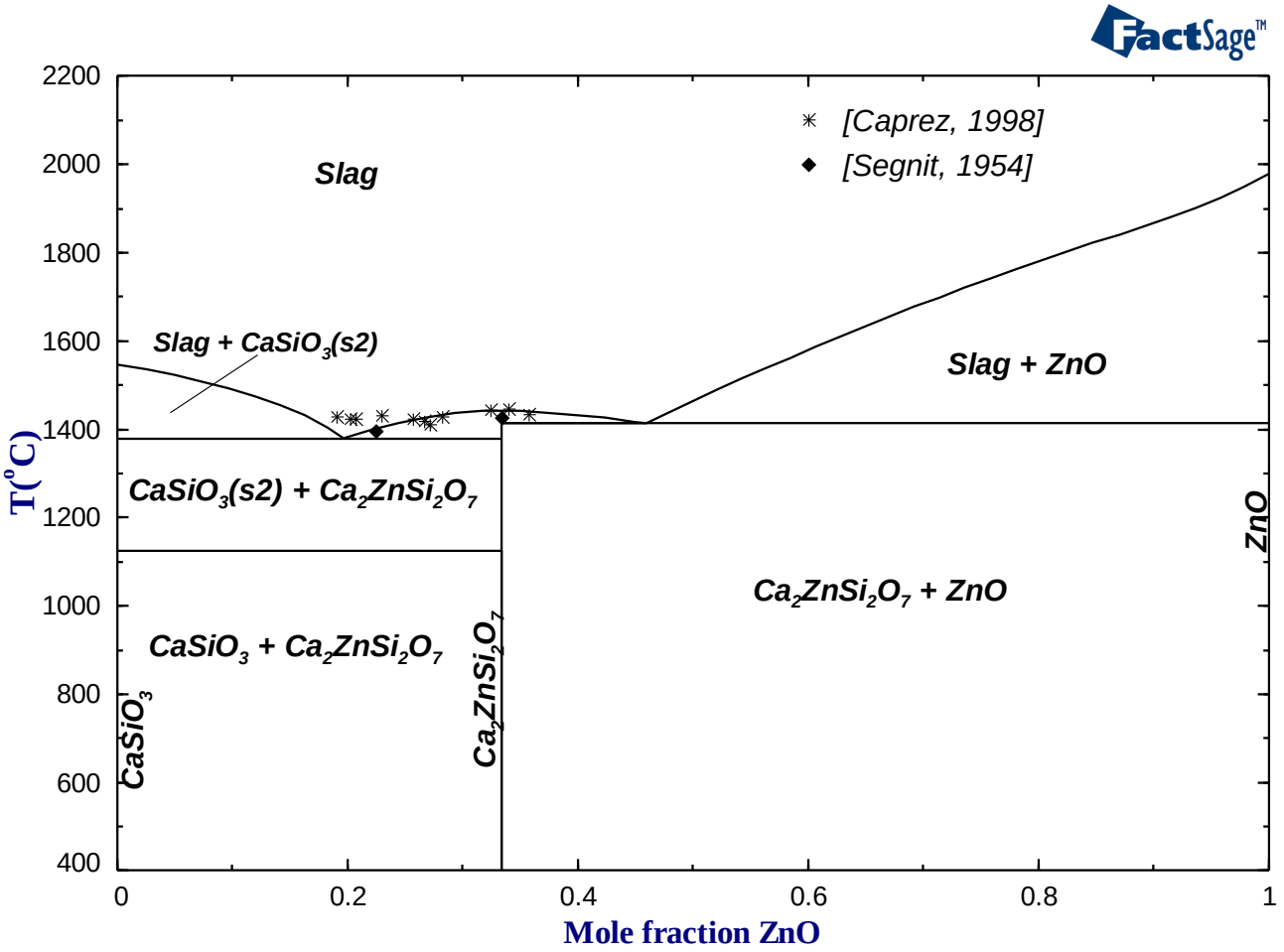

Mole fraction
Liquidussurface

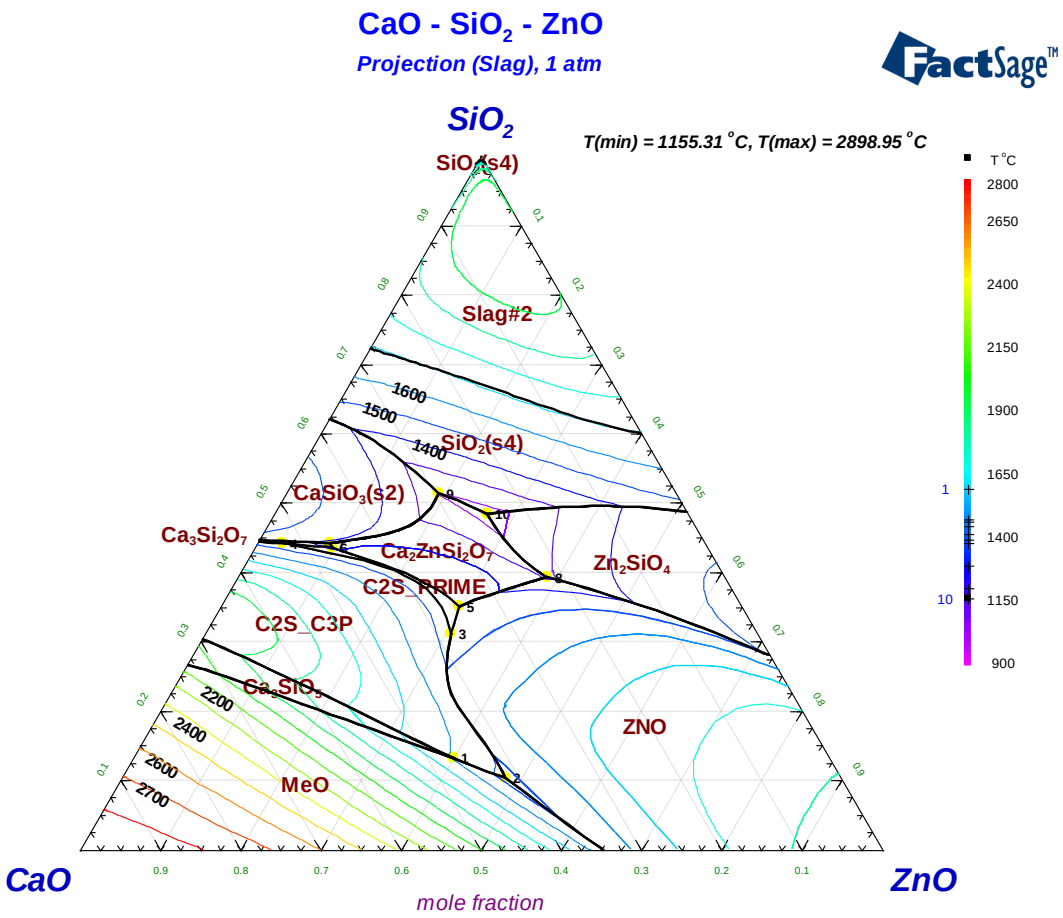

Weight percent
Liquidussurface compared with experimental data

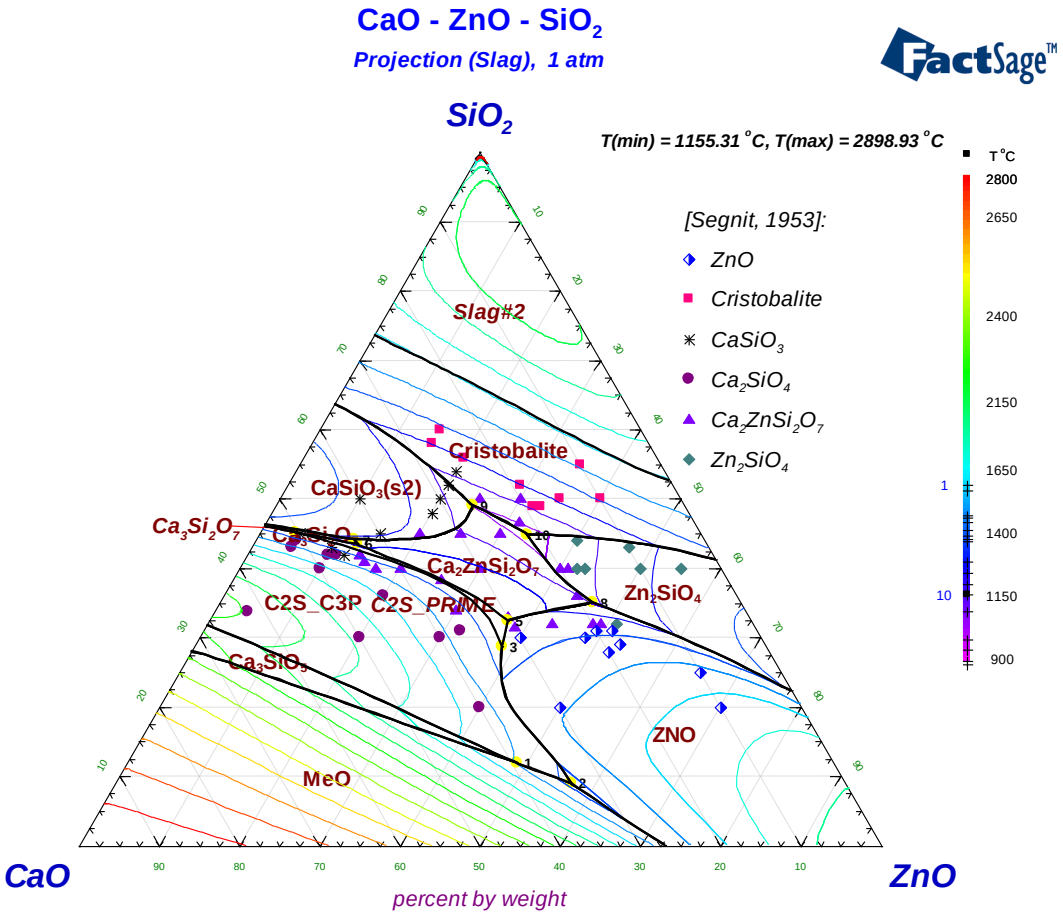

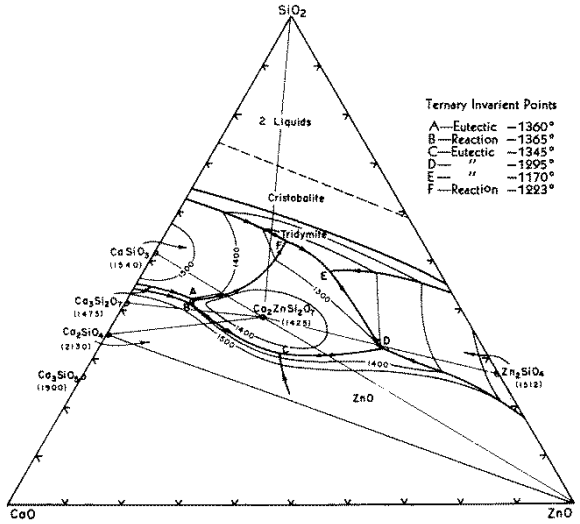

E. R. Segnit, J. Am. Ceram. Soc., 37[6], pp. 273-277 (1954).

Invariant equilibria on the liquidus surface

Intersections with slag	Mole fraction A = SiO2, B = CaO, C = ZnO				Weight percent A = SiO2, B = CaO, C = ZnO				
		X(A)	X(B)	X(C)	T(C)		W(A)	W(B)	W(C)	T(C)
1: C2S_C3P / Ca3SiO5 / MeO	1:	0.13224	0.46891	0.39886	1588.77	1:	11.912	39.423	48.665	1588.77
2: C2S_C3P / MeO / ZNO	2:	0.10277	0.41797	0.47926	1470.14	2:	8.999	34.160	56.841	1470.14
3: C2S_C3P / C2S_PRIME / ZNO	3:	0.31127	0.38169	0.30704	1457.53	3:	28.732	32.882	38.386	1457.54
4: C2S_C3P / C2S_PRIME / Ca3Si2O7	4:	0.44149	0.52716	0.03135	1440.21	4:	45.237	50.413	4.350	1440.20
5: C2S_PRIME / Ca2ZnSi2O7 / ZNO	5:	0.35104	0.35173	0.29723	1412.54	5:	32.447	30.343	37.210	1412.52
6: C2S_PRIME / Ca2ZnSi2O7 / Ca3Si2O7	6:	0.43610	0.46794	0.09596	1388.23	6:	43.488	43.551	12.961	1388.23
7: Ca2ZnSi2O7 / Ca3Si2O7 / CaSiO3(s2)	7:	0.44191	0.46756	0.09053	1375.09	7:	44.151	43.598	12.251	1375.05
8: Ca2ZnSi2O7 / ZNO / Zn2SiO4	8:	0.39347	0.22135	0.38518	1283.39	8:	35.076	18.417	46.507	1283.39
9: Ca2ZnSi2O7 / CaSiO3(s2) / SiO2(s4)	9:	0.51419	0.29591	0.18990	1195.06	9:	49.084	26.363	24.552	1195.06
10: Ca2ZnSi2O7 / SiO2(s4) / Zn2SiO4	10:	0.48417	0.25009	0.26575	1155.31	10:	44.934	21.662	33.404	1155.31

CaS-FeS-MgS,
Mole fraction 700°C

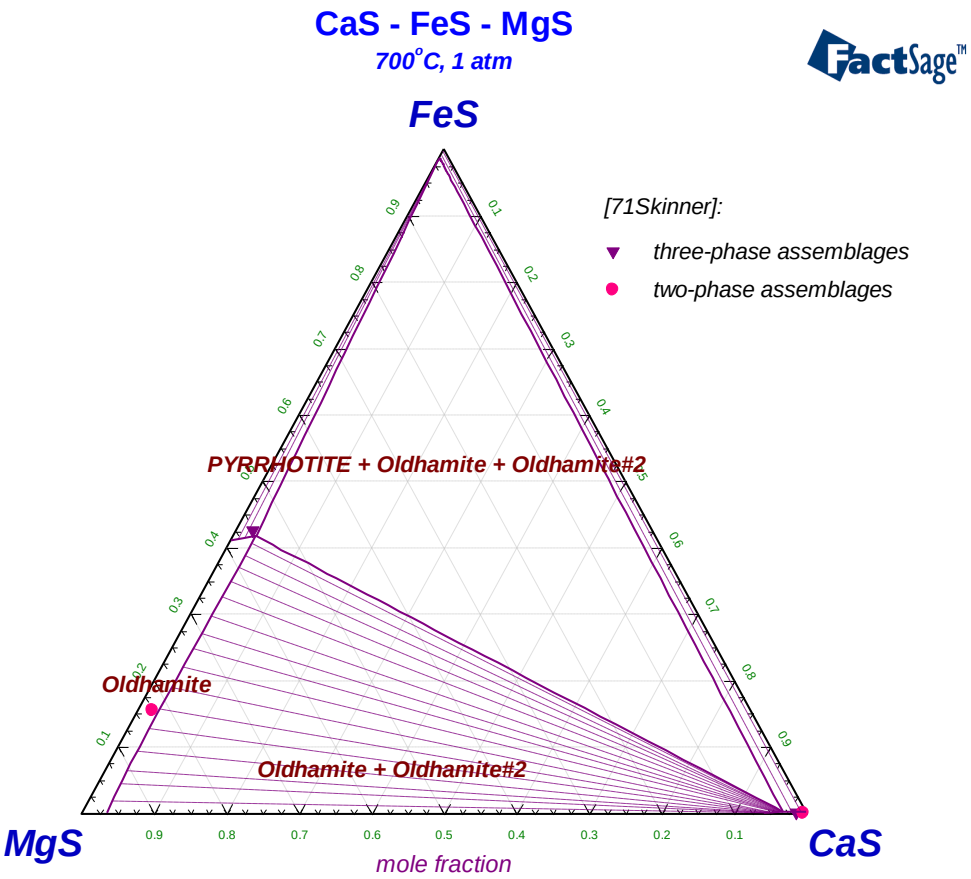

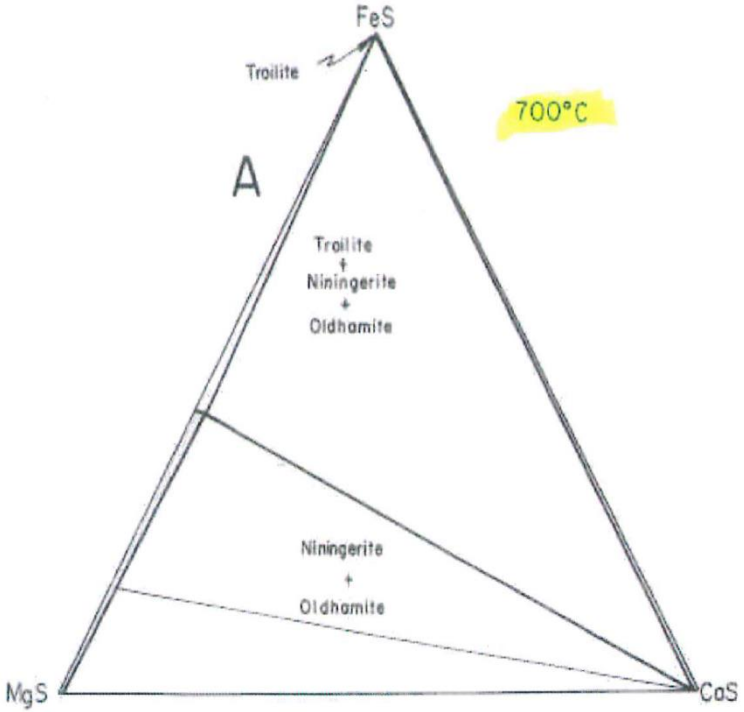

B.J. Skinner, F.D. Luck, Amer. Mineral., Vol.56 (1971), pp. 1269-1296.

CaS-FeS-MgS, Mole fraction 800°C

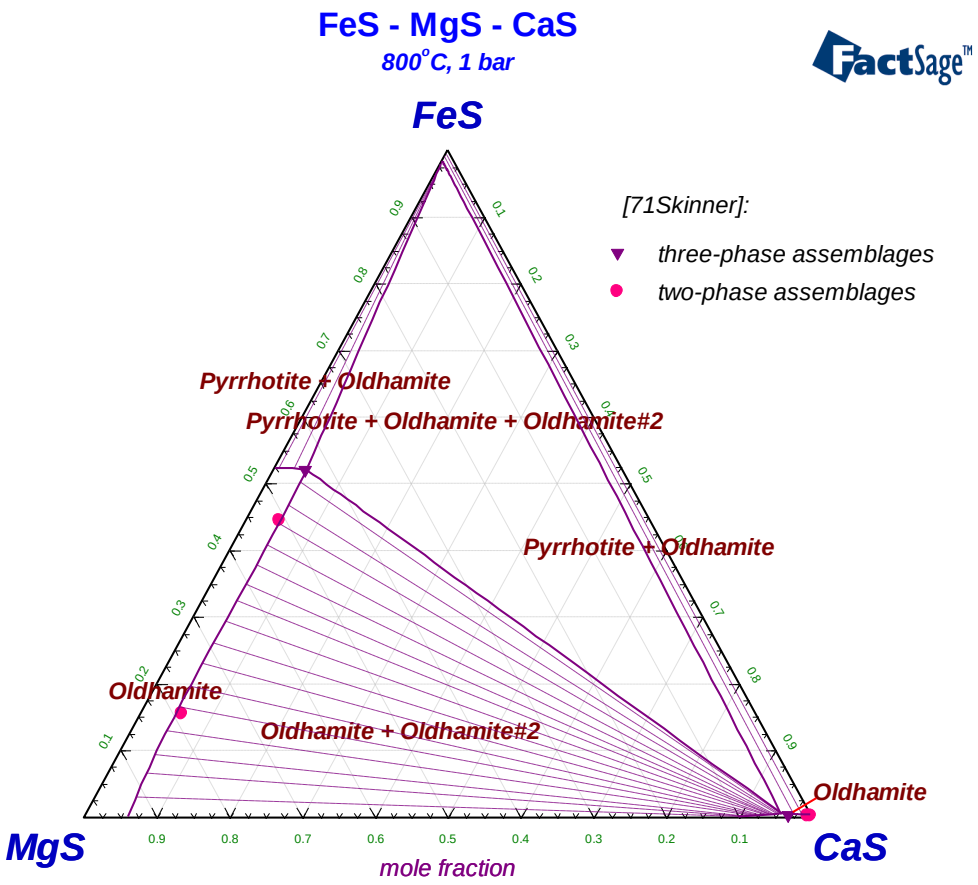

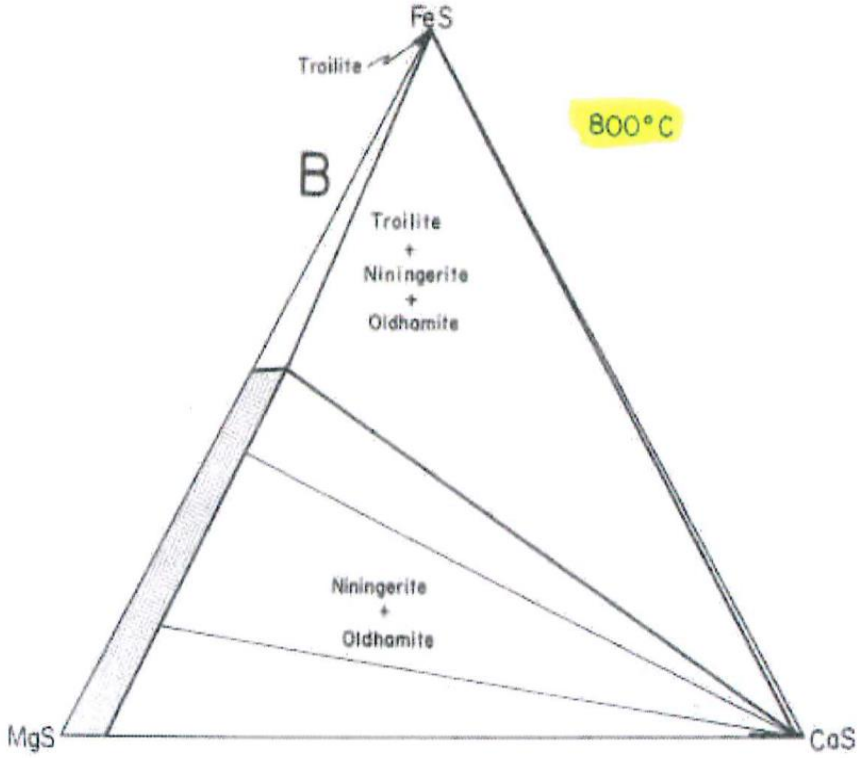

B.J. Skinner, F.D. Luck, Amer. Mineral., Vol.56 (1971), pp. 1269-1296.

CaS-FeS-MgS, Mole fraction 900°C

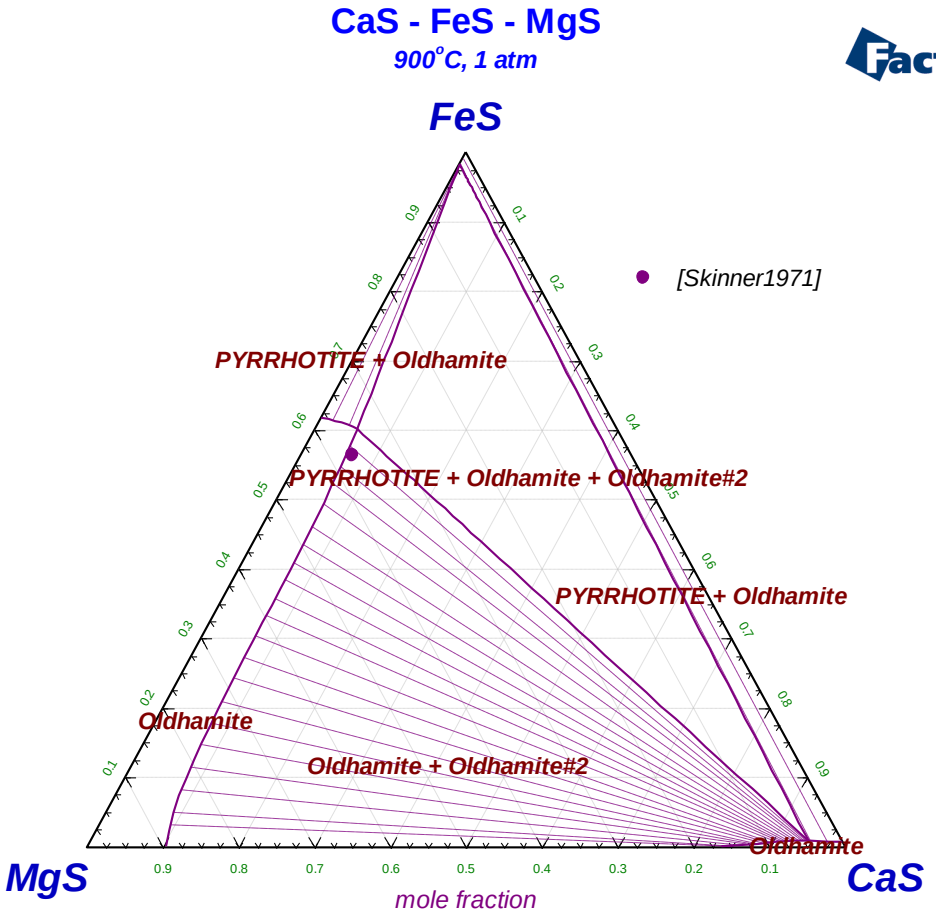

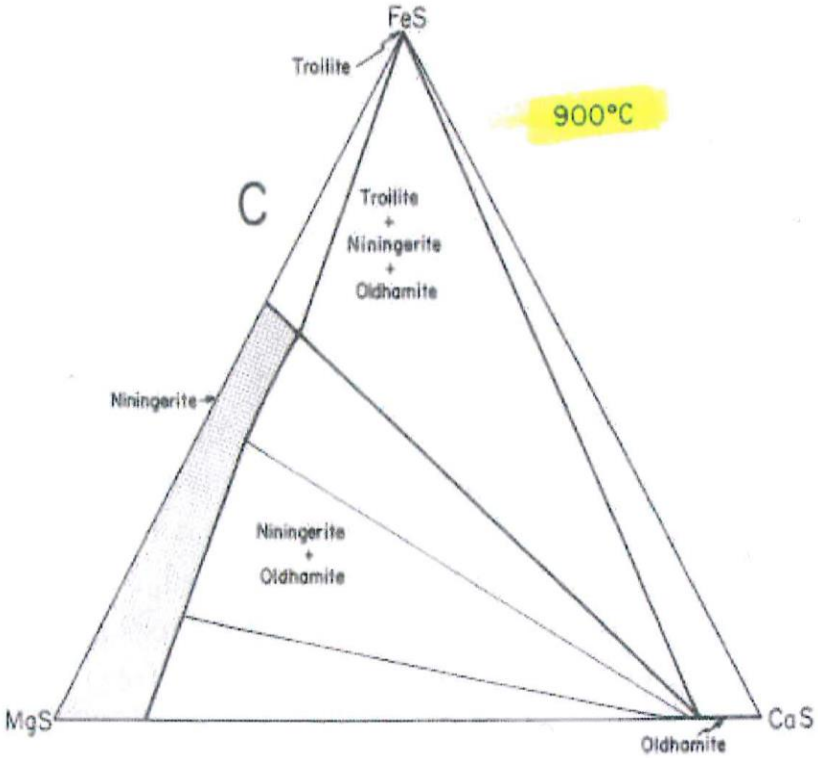

B.J. Skinner, F.D. Luck, Amer. Mineral., Vol.56 (1971), pp. 1269-1296.

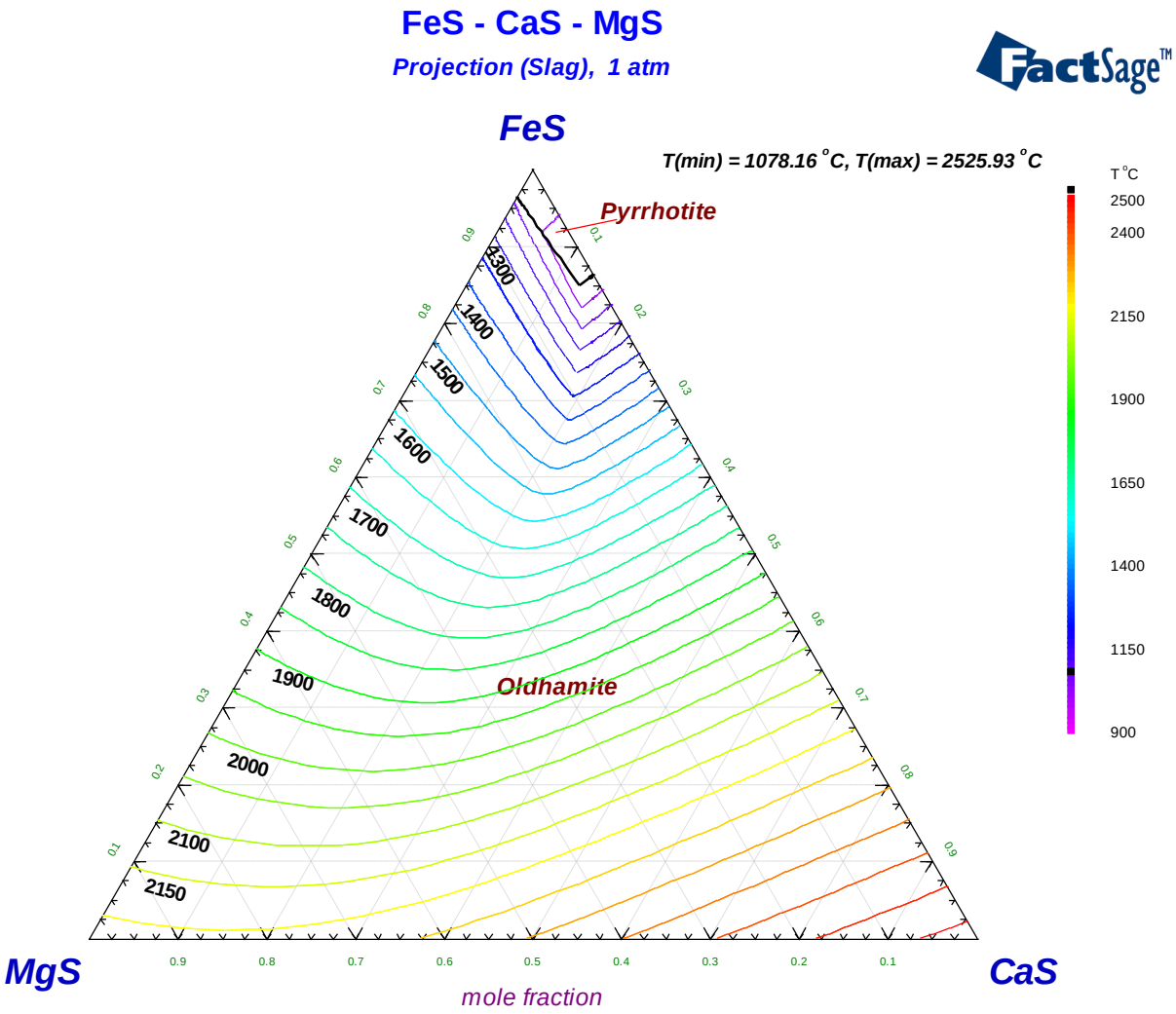
FeS - CaS - MgS
Projection (Slag), 1 atm
FactSage™
FeS
T(min) = 1078.16 °C, T(max) = 2525.93 °C
T °C
2500
2400
2150
1900
1650
1400
1150
900
Pyrrhotite
Oldhamite
1300
1400
1500
1600
1700
1800
1900
2000
2100
2150
MgS
CaS
mole fraction

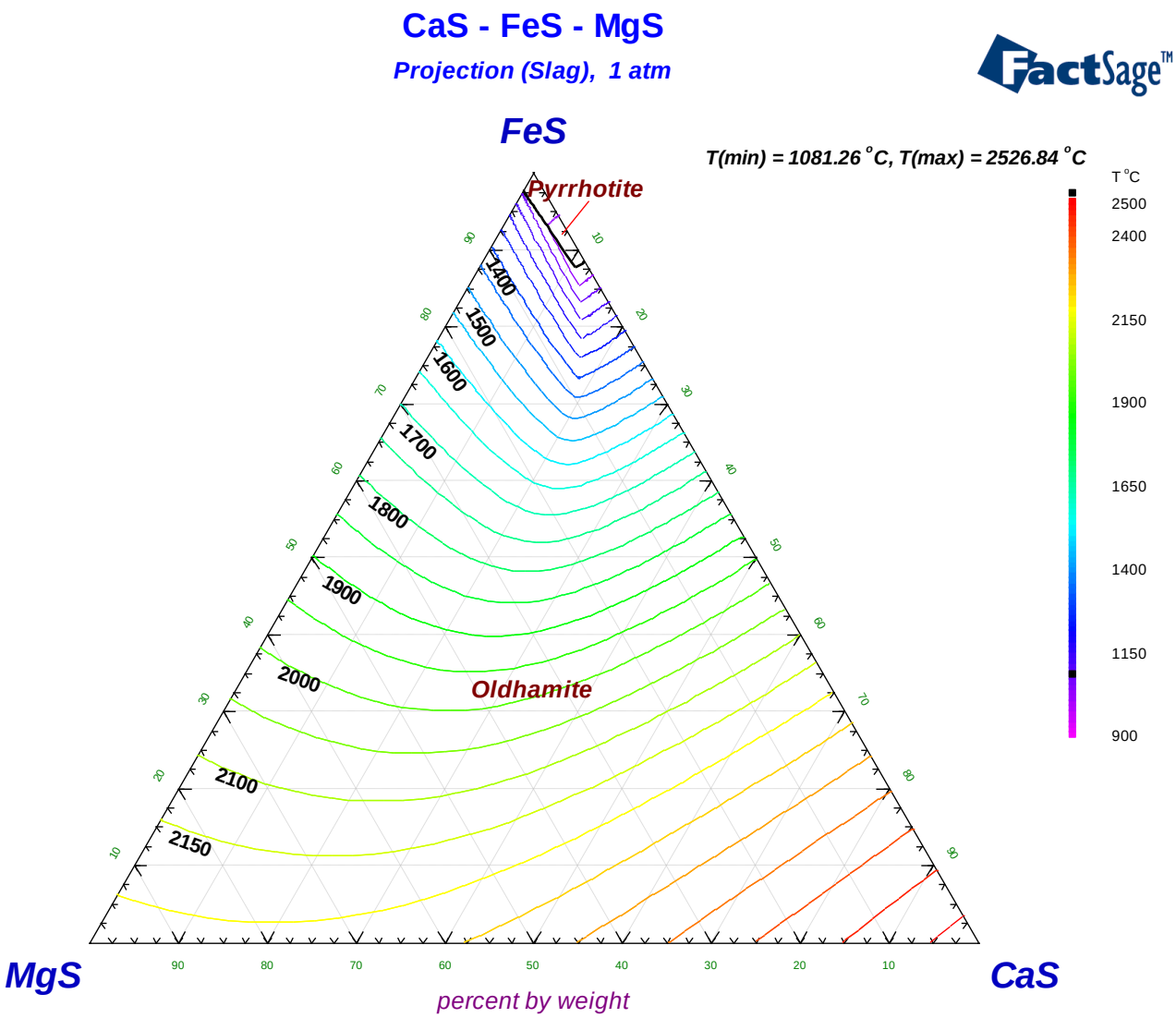
CaS - FeS - MgS
Projection (Slag), 1 atm
FactSage™
FeS
T(min) = 1081.26 °C, T(max) = 2526.84 °C
T °C
2500
2400
2150
1900
1650
1400
1150
900
Pyrrhotite
1400
1500
1600
1700
1800
1900
2000
2100
2150
Oldhamite
MgS
CaS
percent by weight

Invariant equilibria on the liquidus surface

Intersections with slag	Mole fraction				Weight percent			
	A = FeS, B = MgS, C = CaS				A = FeS, B = MgS, C = CaS			
	X(A)	X(B)	X(C)	T(C)	W(A)	W(B)	W(C)	T(C)
Niningerite / Oldhamite / Troilite-HT	0.87924	0.00761	0.11315	1113.77	89.996	0.500	9.504	1113.77

CaS-FeS-MnS,
Mole fraction 700°C

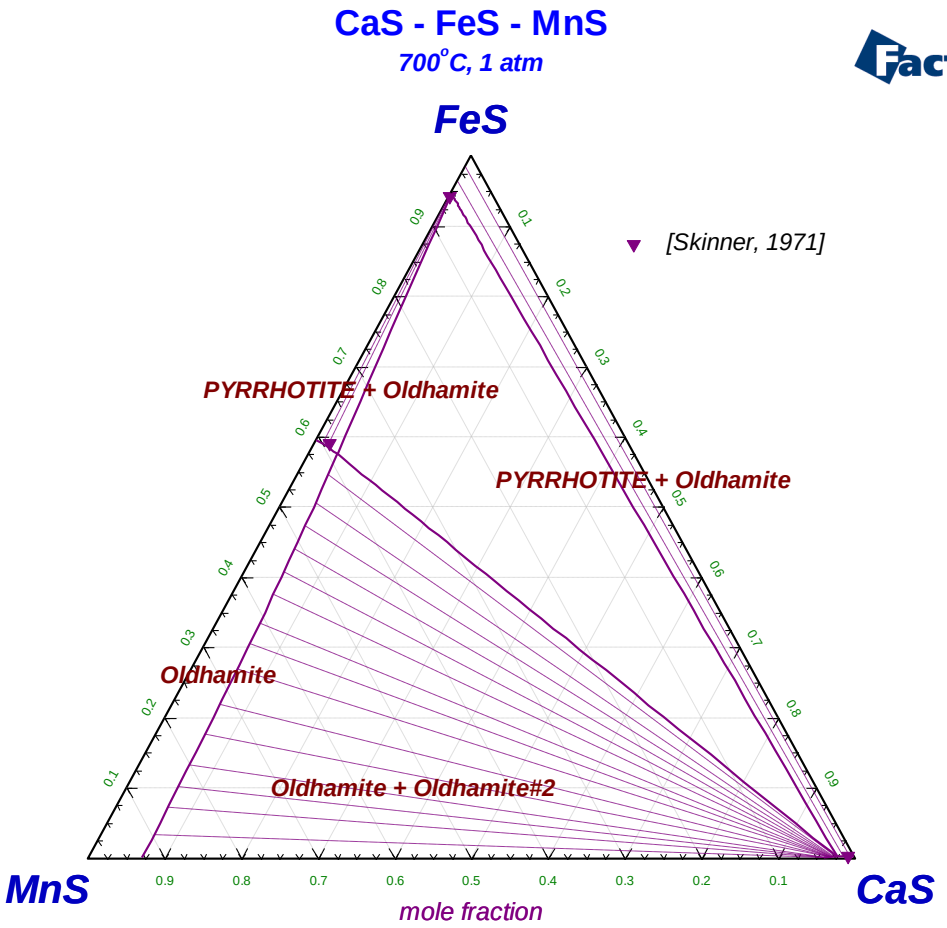

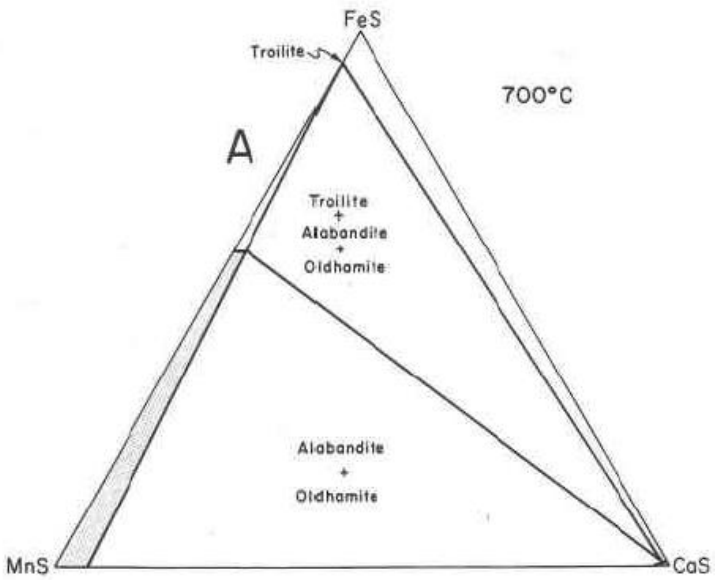

B.J. Skinner, F.D. Luck, Amer. Mineral., Vol.56 (1971), pp. 1269-1296.

CaS-FeS-MnS, Mole fraction 800°C

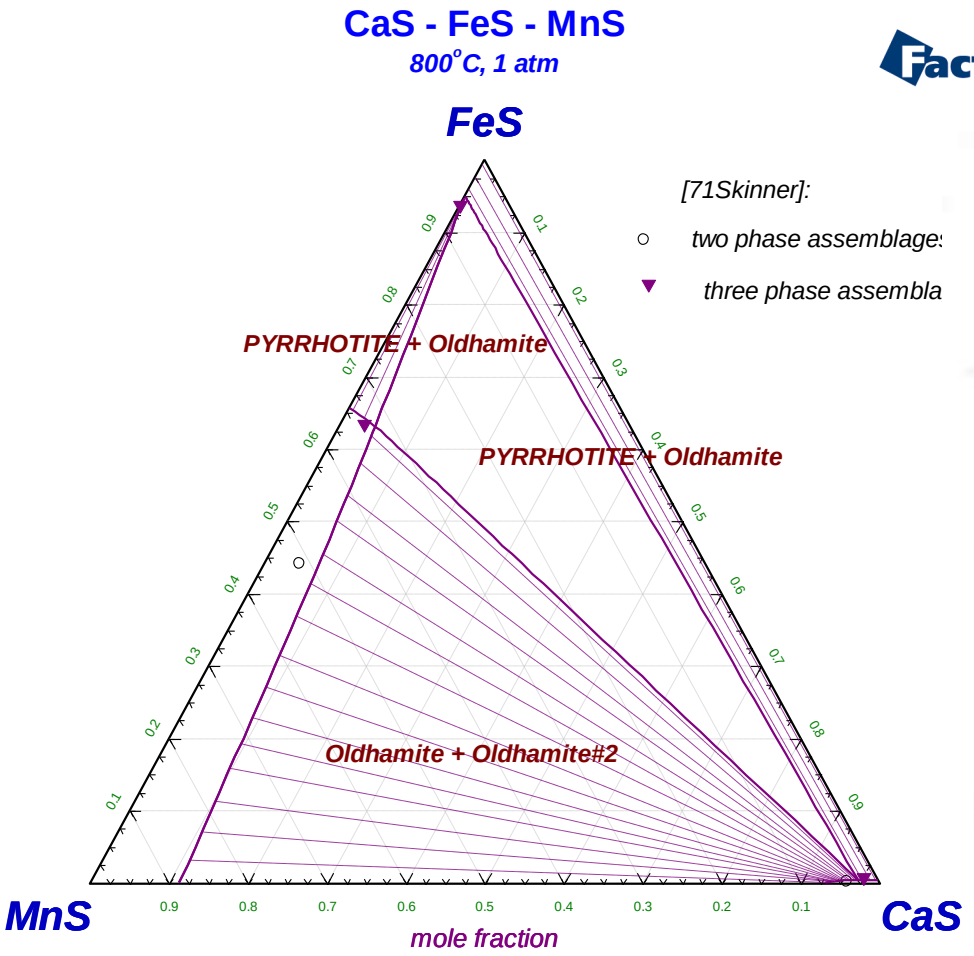

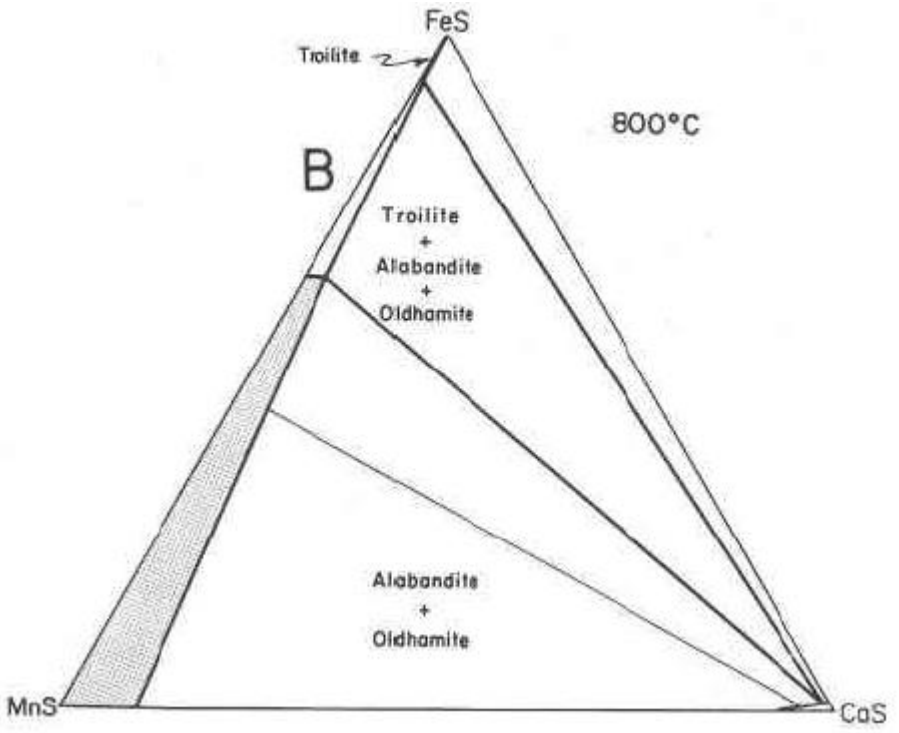

B.J. Skinner, F.D. Luck, Amer. Mineral., Vol.56 (1971), pp. 1269-1296.

CaS-FeS-MnS, Mole fraction 900°C

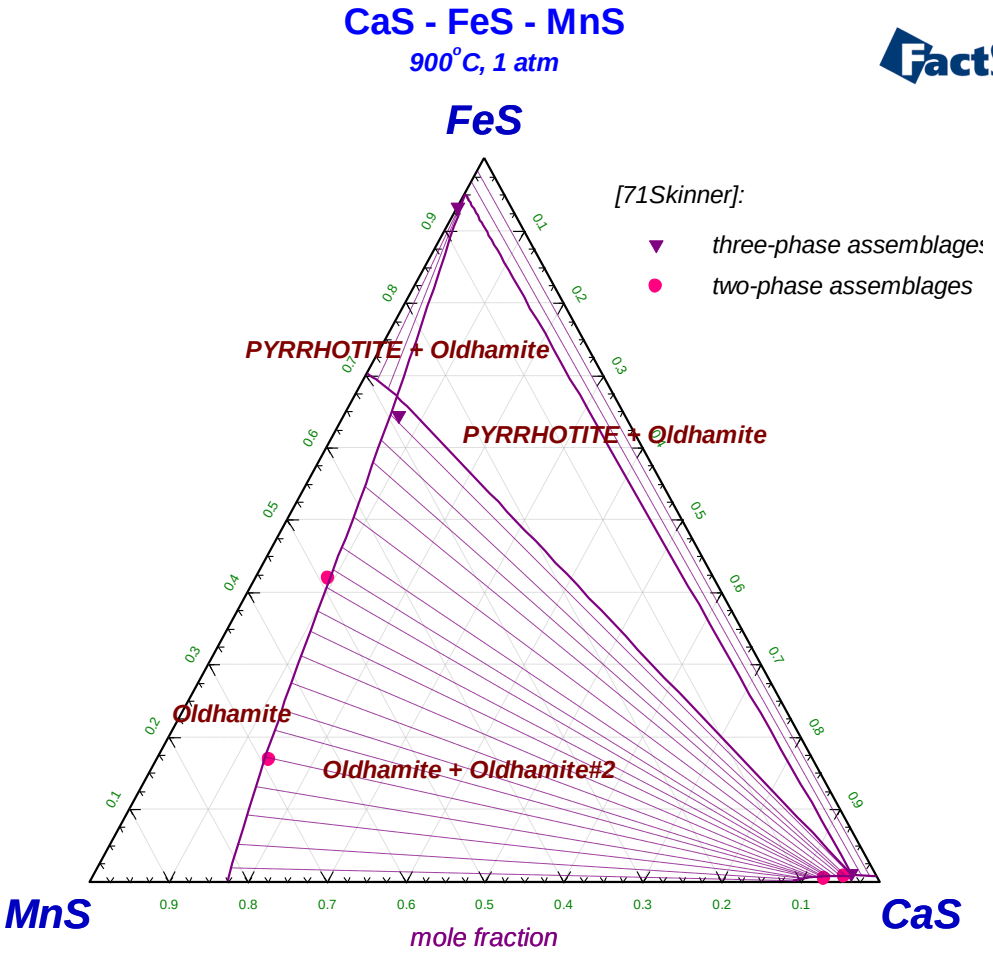

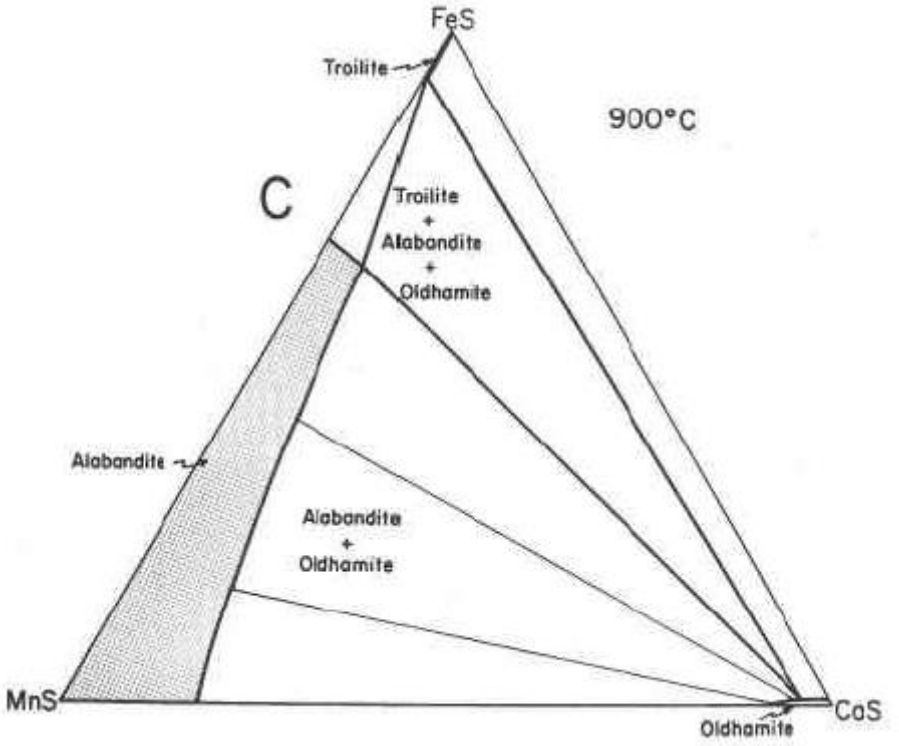

B.J. Skinner, F.D. Luck, Amer. Mineral., Vol.56 (1971), pp. 1269-1296.

Mole fraction, Liquidussurface

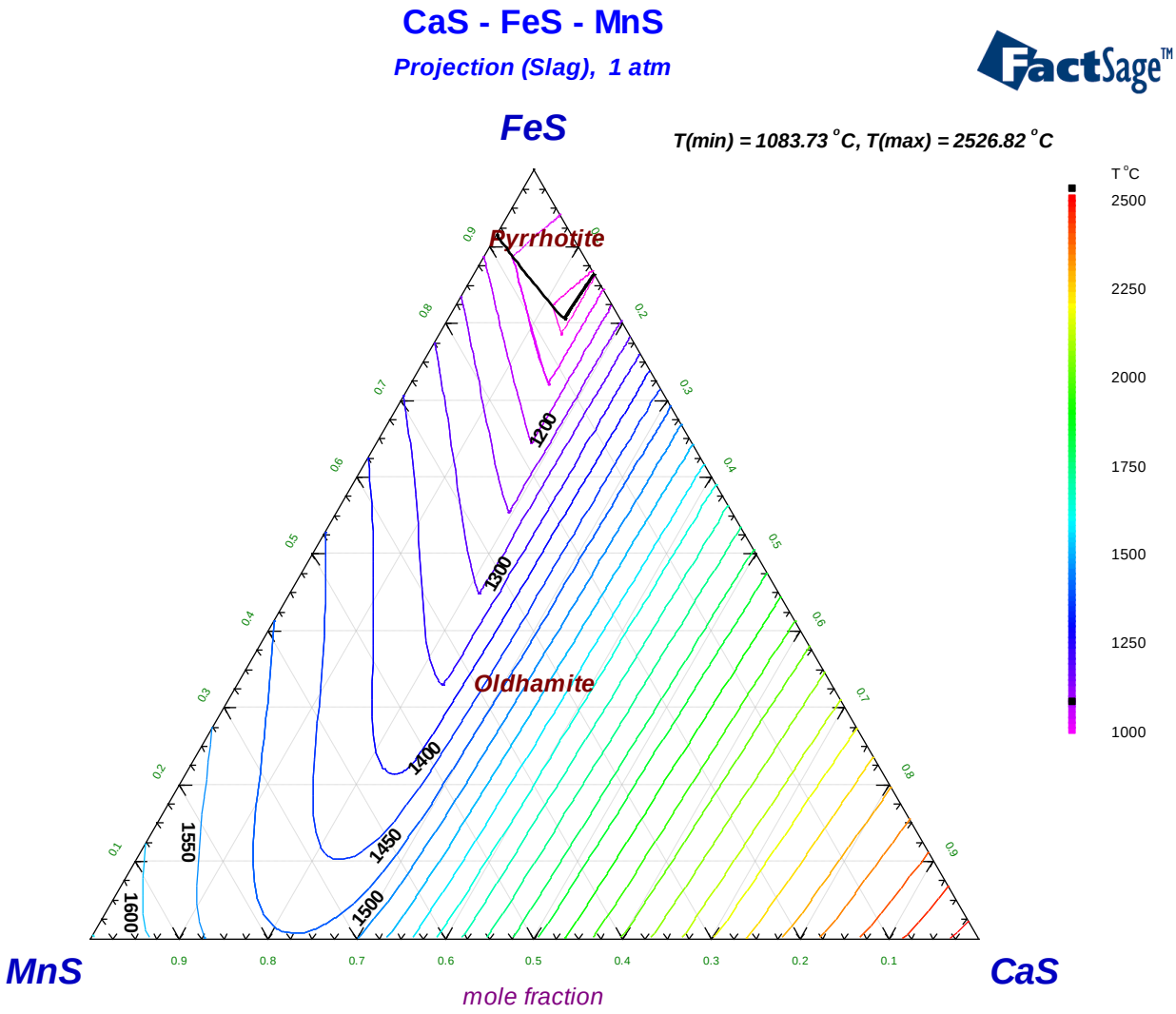

CaS - FeS - MnS

Projection (Slag), 1 atm

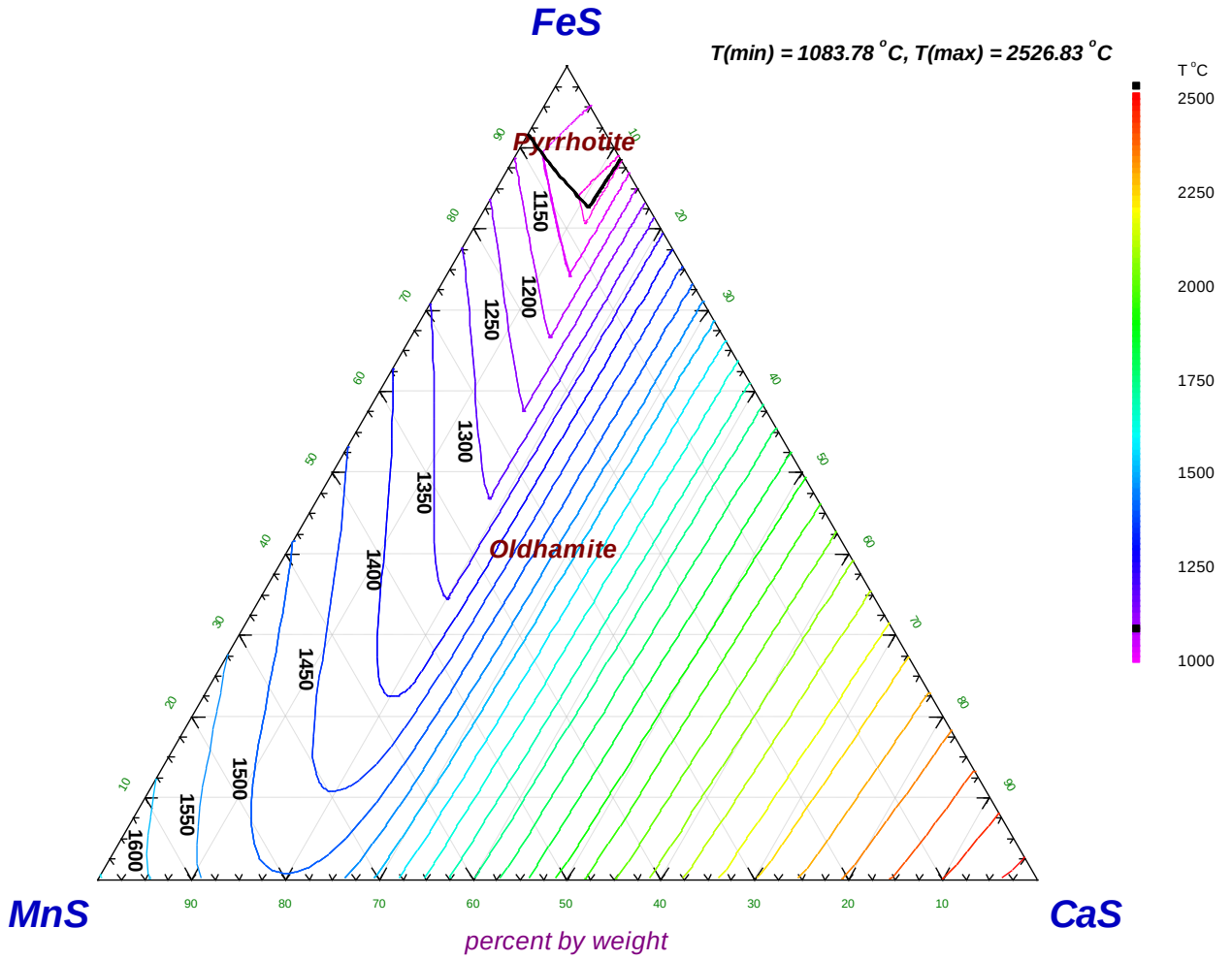

Mole fraction, Isotherms 800°, 900 and 1000°C

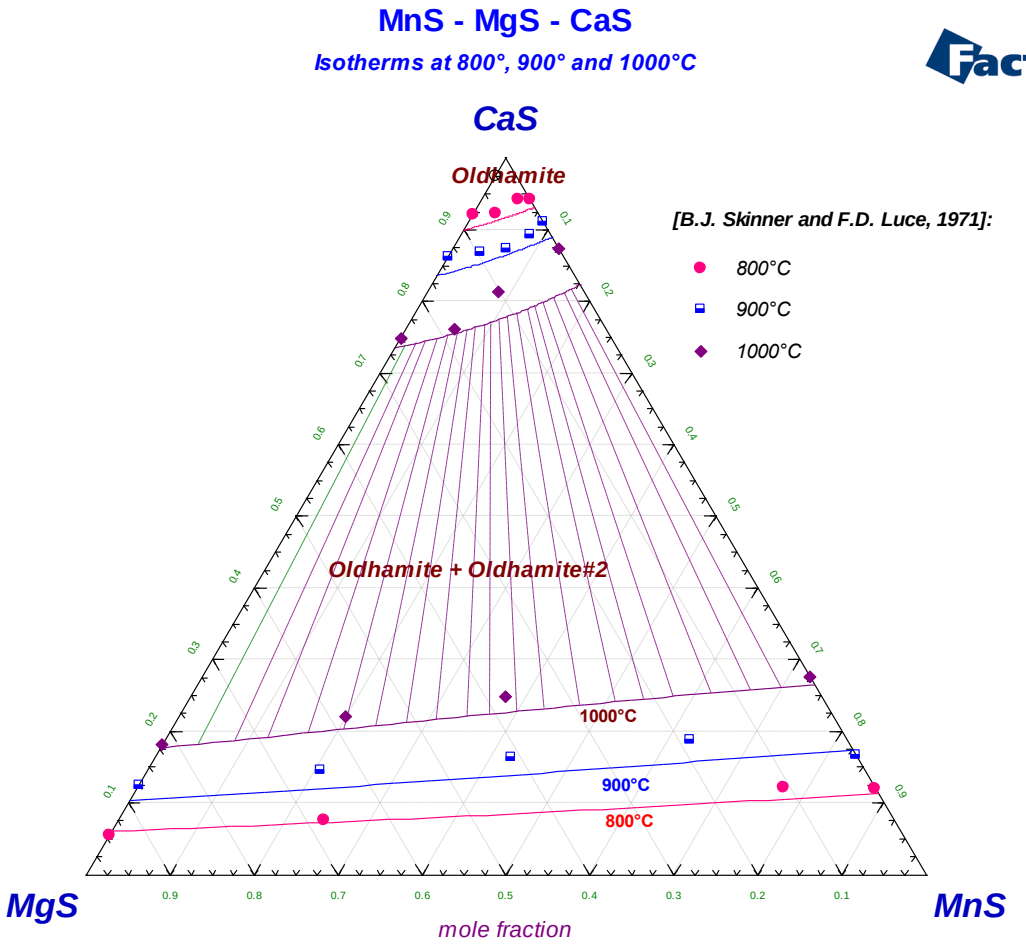

CaS - MgS - MnS

Projection (Slag), 1 atm

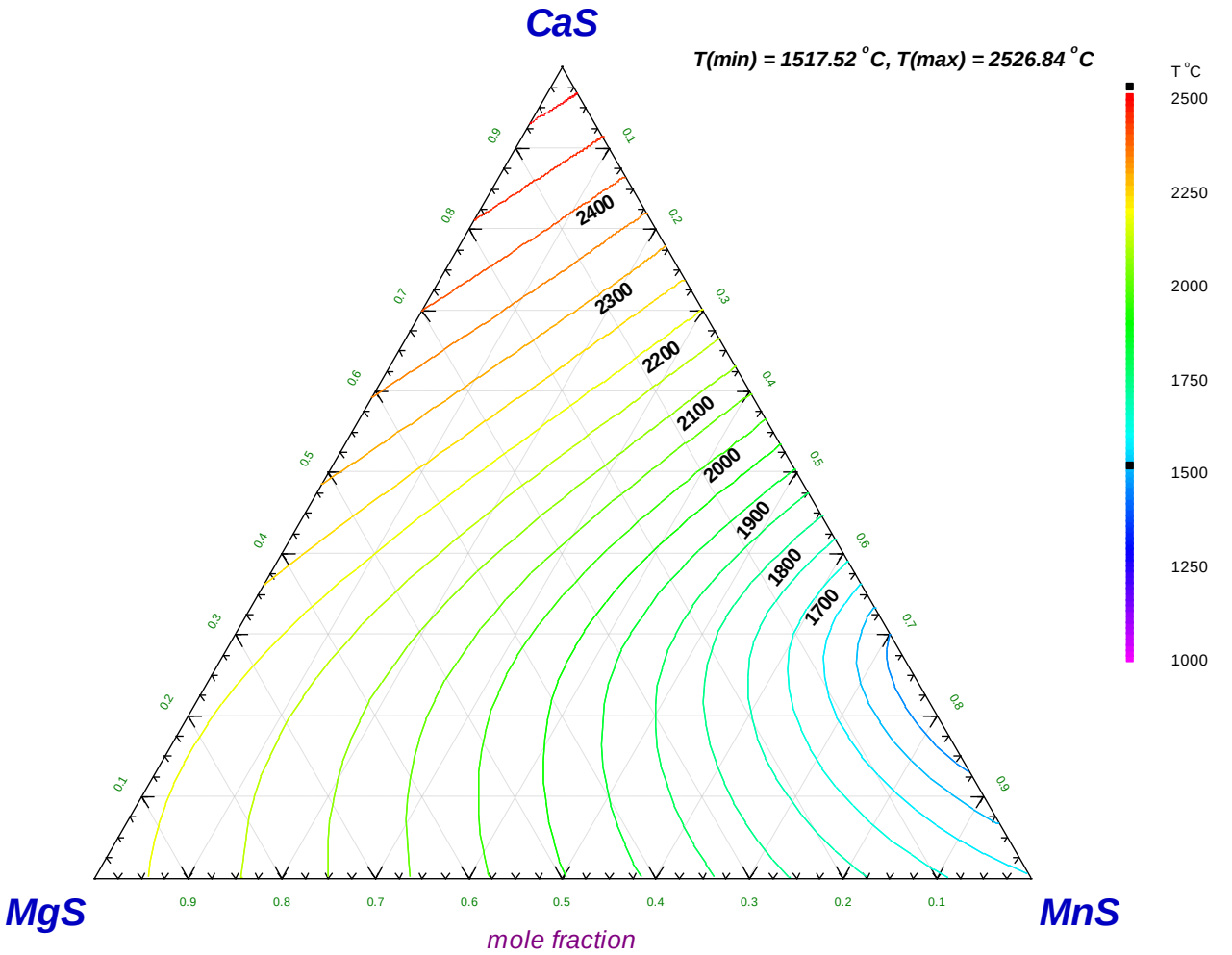

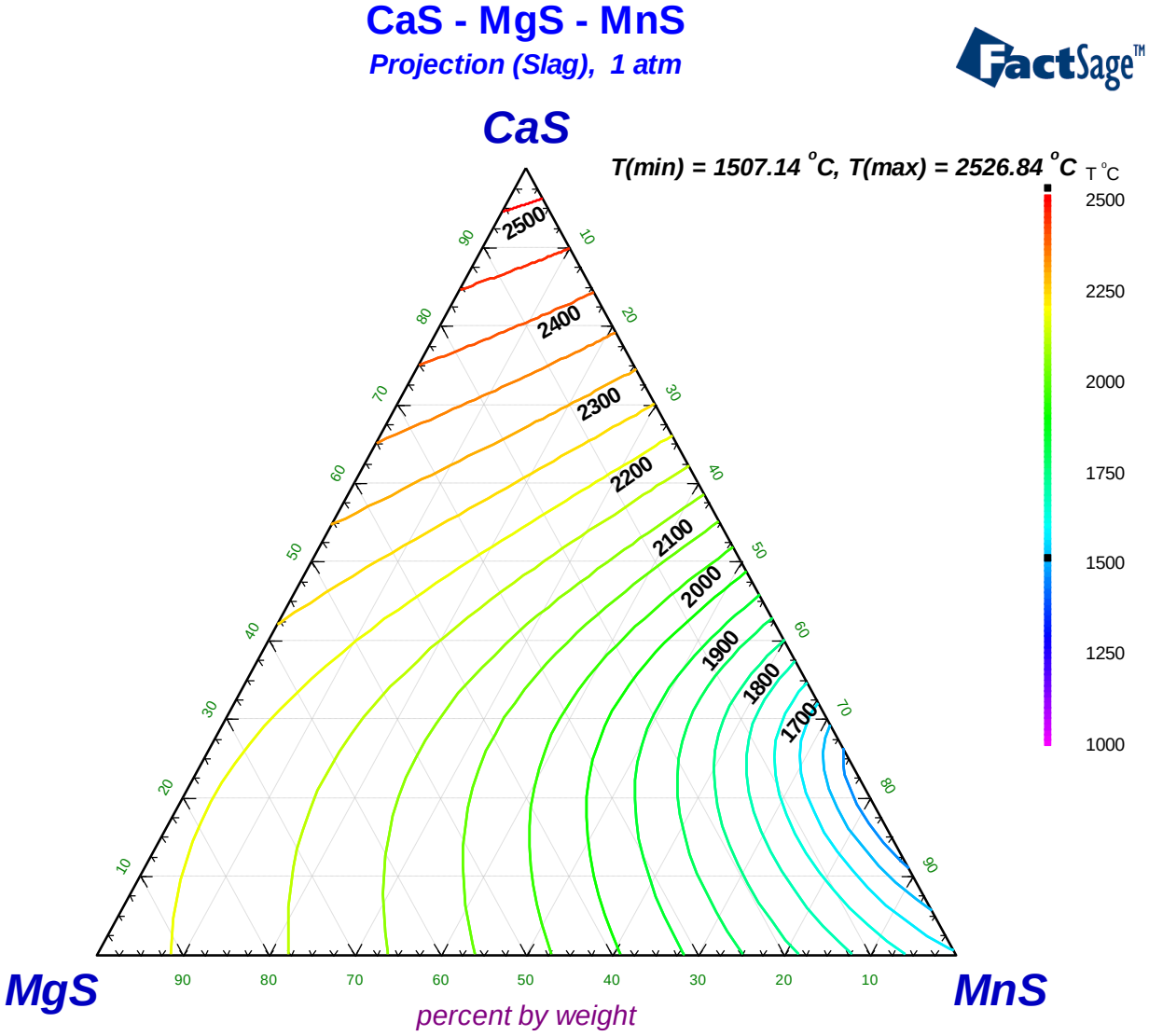
CaS - MgS - MnS
Projection (Slag), 1 atm
FactSage™
CaS
T(min) = 1507.14 °C, T(max) = 2526.84 °C
T °C
2500
2250
2000
1750
1500
1250
1000
2500
2400
2300
2200
2100
2000
1900
1800
1700
MgS
MnS
90 80 70 60 50 40 30 20 10
percent by weight

Weight percent K2SO4-CaMg3S4O16 compared with experimental data

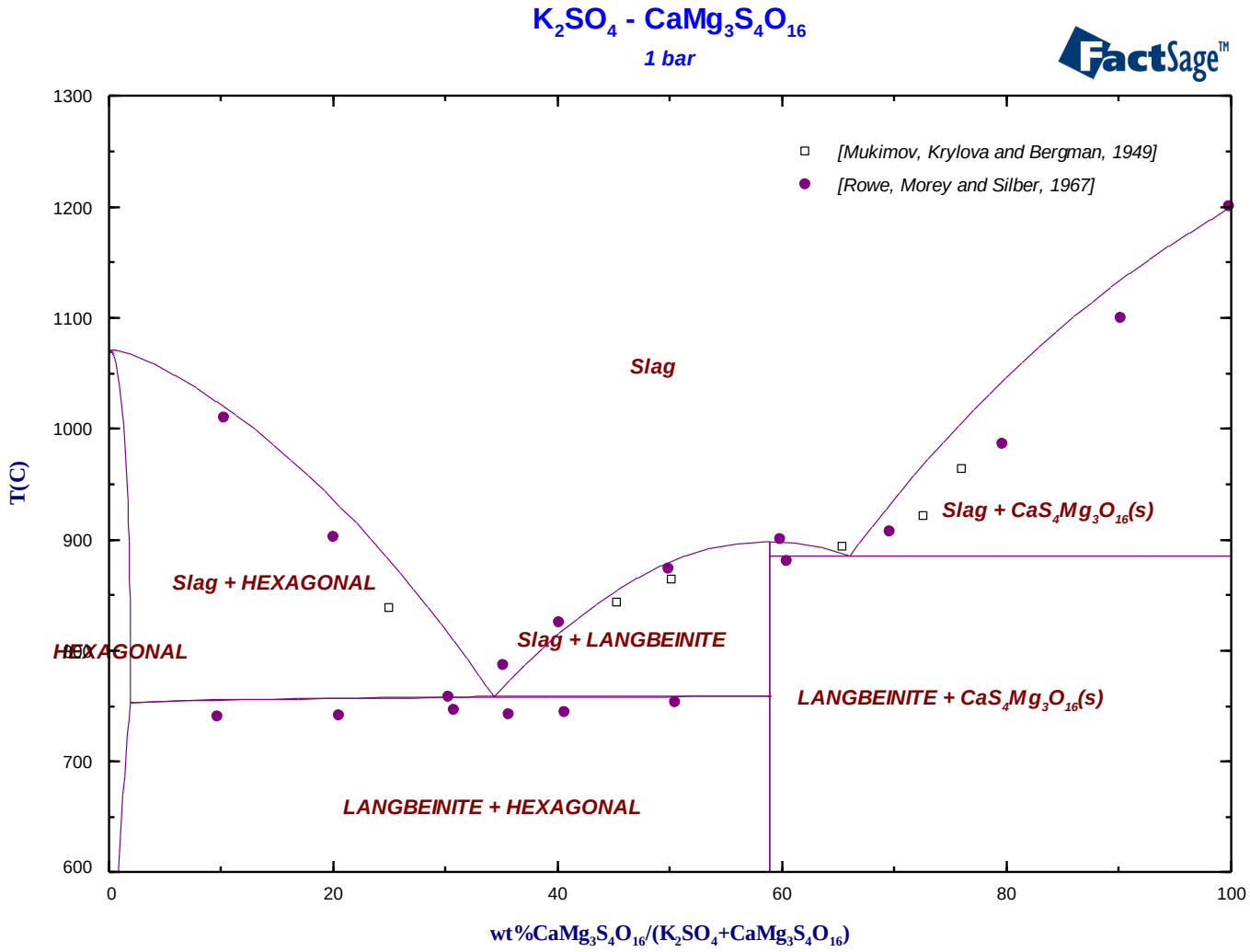

Weight percent K2Mg2S3O12-K2Ca2S3O12

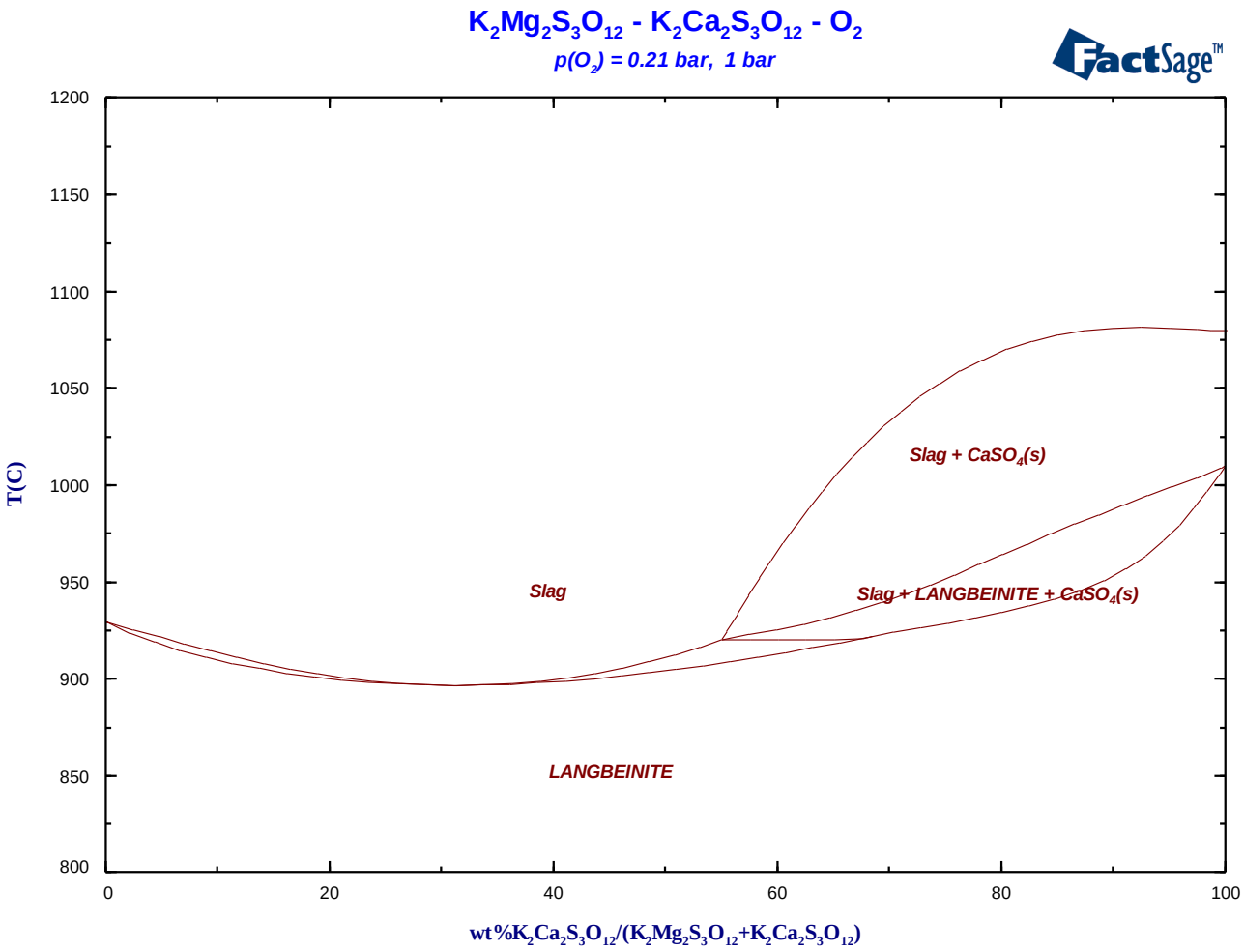

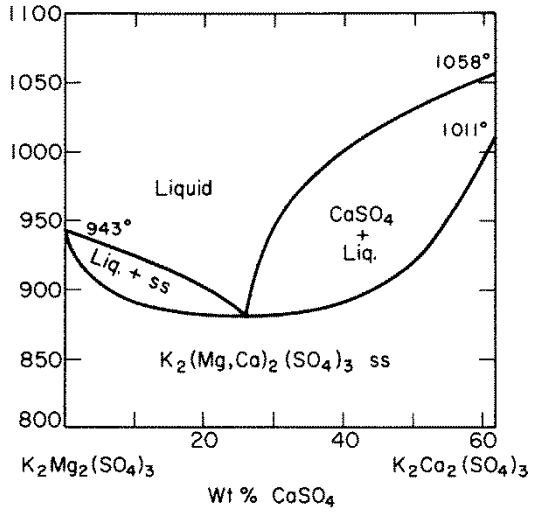

G.W. Morey, J.J. Rowe, R.O. Fournier, J. Inorg Nucl. Chem., 26 [1], (1964), pp. 53-58.

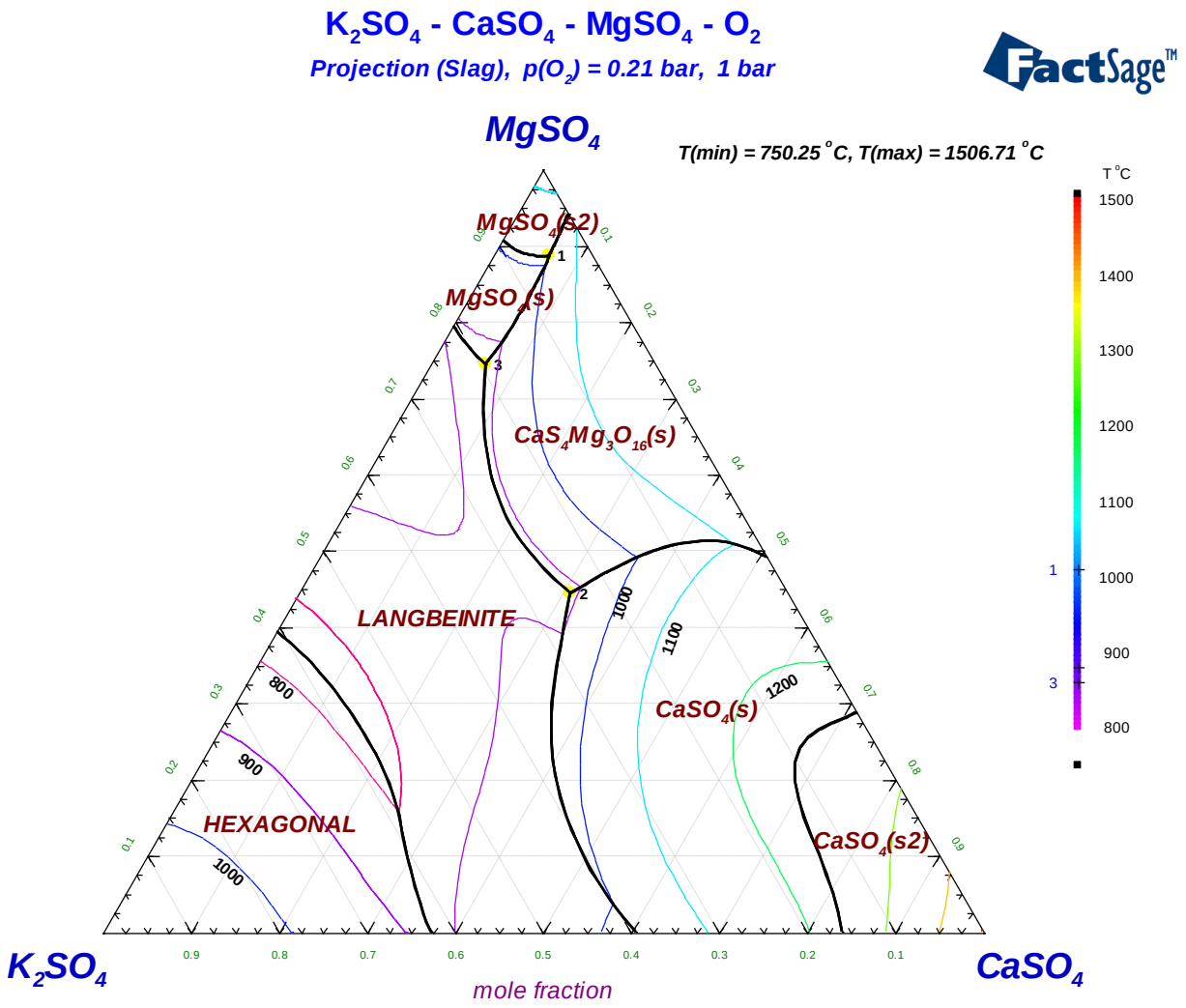
K2SO4 - CaSO4 - MgSO4 - O2
Projection (Slag), p(O2) = 0.21 bar, 1 bar
FactSage™
MgSO4
T(min) = 750.25 °C, T(max) = 1506.71 °C
T °C
1500
1400
1300
1200
1100
1000
900
800
MgSO4(s2)
MgSO4(s)
CaS4Mg3O16(s)
LANGBEINITE
CaSO4(s)
CaSO4(s2)
HEXAGONAL
1
2
3
800
900
1000
1100
1200
K2SO4
CaSO4
mole fraction

Weight percent, Liquidussurface compared with experimental data

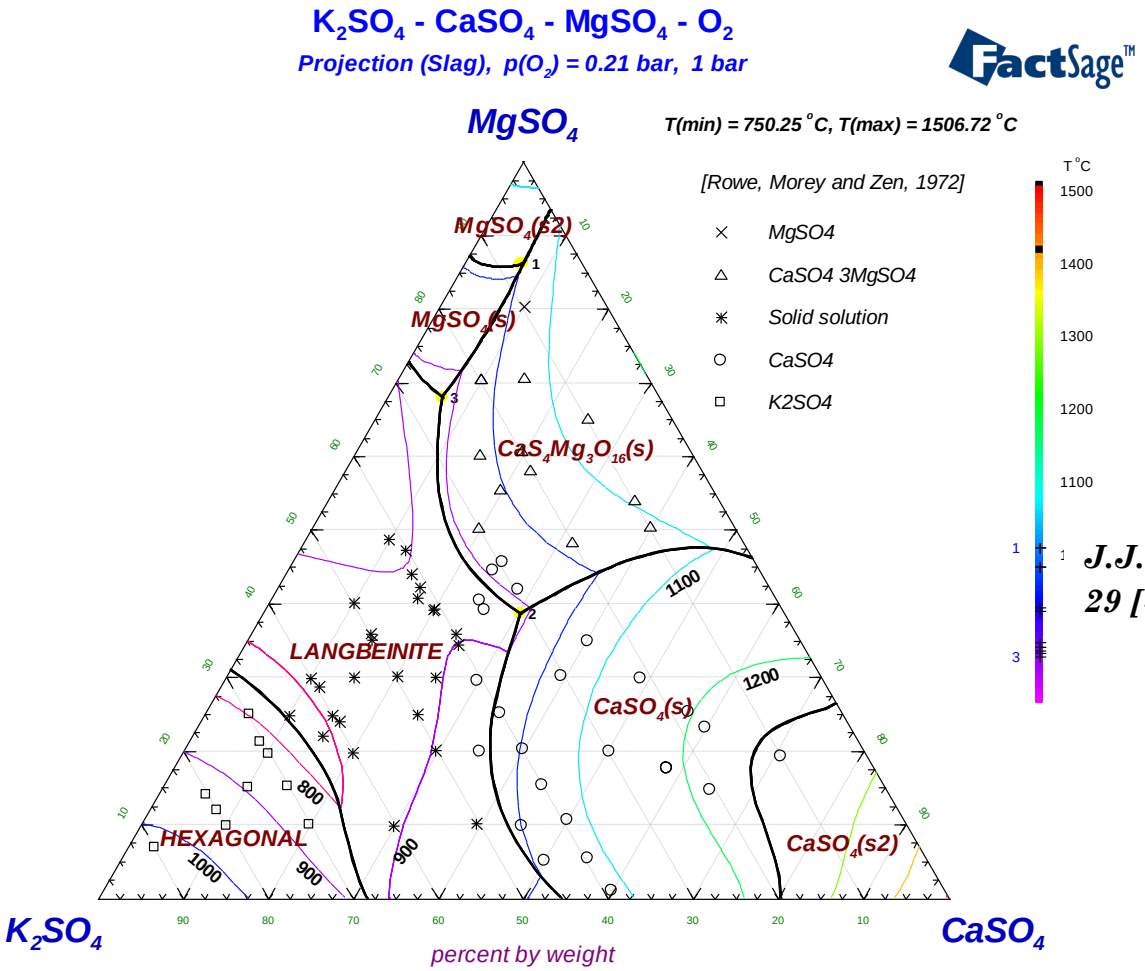

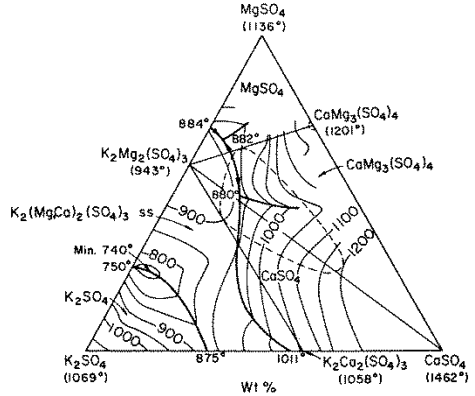

J.J. Rowe, G.W. Morey, J. Inorg. Nucl. Chem., 29 [4], (1967), pp. 925-942.

Invariant equilibria on the liquidus surface

Intersections with slag	Mole fraction A = MgSO4, B = K2SO4, C = CaSO4				Weight percent A = MgSO4, B = K2SO4, C = CaSO4			
	X(A)	X(B)	X(C)	T(C)	W(A)	W(B)	W(C)	T(C)
1: CaS4Mg3O16(s) / MgSO4(s1) / MgSO4(s2)	1: 0.88774	0.04926	0.06300	1009.85	1: 86.163	6.921	6.916	1009.85
2: CaS4Mg3O16(s) / CaSO4(s) / LANGBEINITE	2: 0.44528	0.24643	0.30830	879.95	2: 38.695	31.003	30.302	879.95
3: CaS4Mg3O16(s) / LANGBEINITE / MgSO4(s1)	3: 0.74495	0.19289	0.06216	859.13	3: 68.062	25.514	6.424	859.13

Mole fraction 500°C

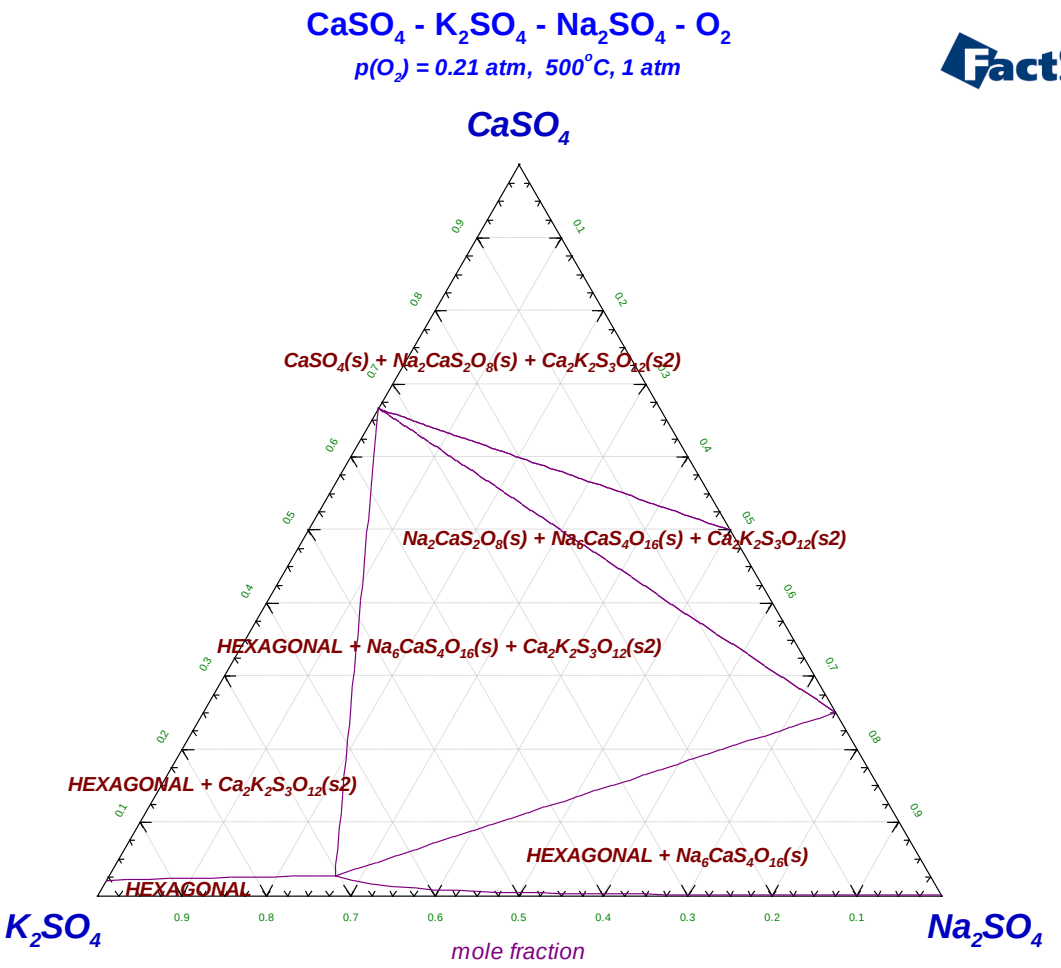

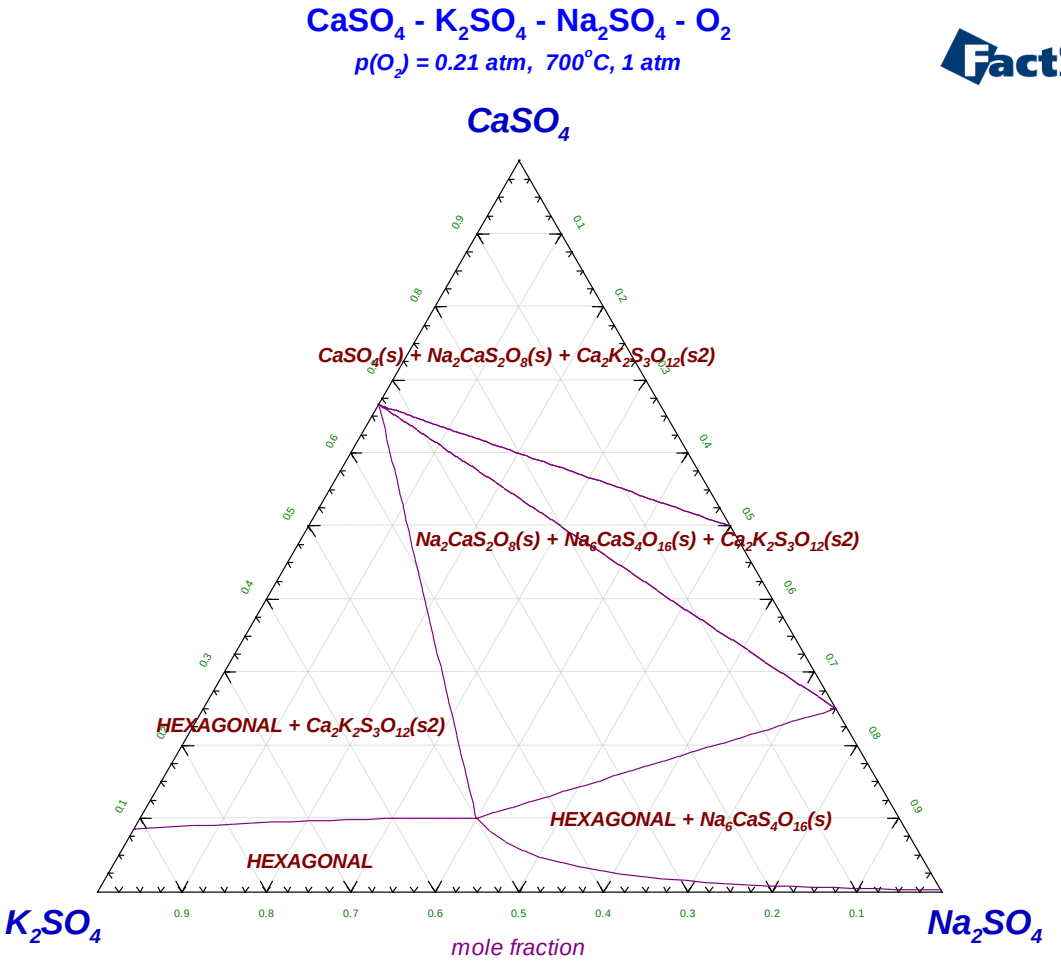
CaSO4 - K2SO4 - Na2SO4 - O2
p(O2) = 0.21 atm, 700°C, 1 atm
FactSage™
CaSO4
CaSO4(s) + Na2CaS2O8(s) + Ca2K2S3O12(s2)
Na2CaS2O8(s) + Na6CaS4O16(s) + Ca2K2S3O12(s2)
HEXAGONAL + Ca2K2S3O12(s2)
HEXAGONAL + Na6CaS4O16(s)
HEXAGONAL
K2SO4
Na2SO4
mole fraction

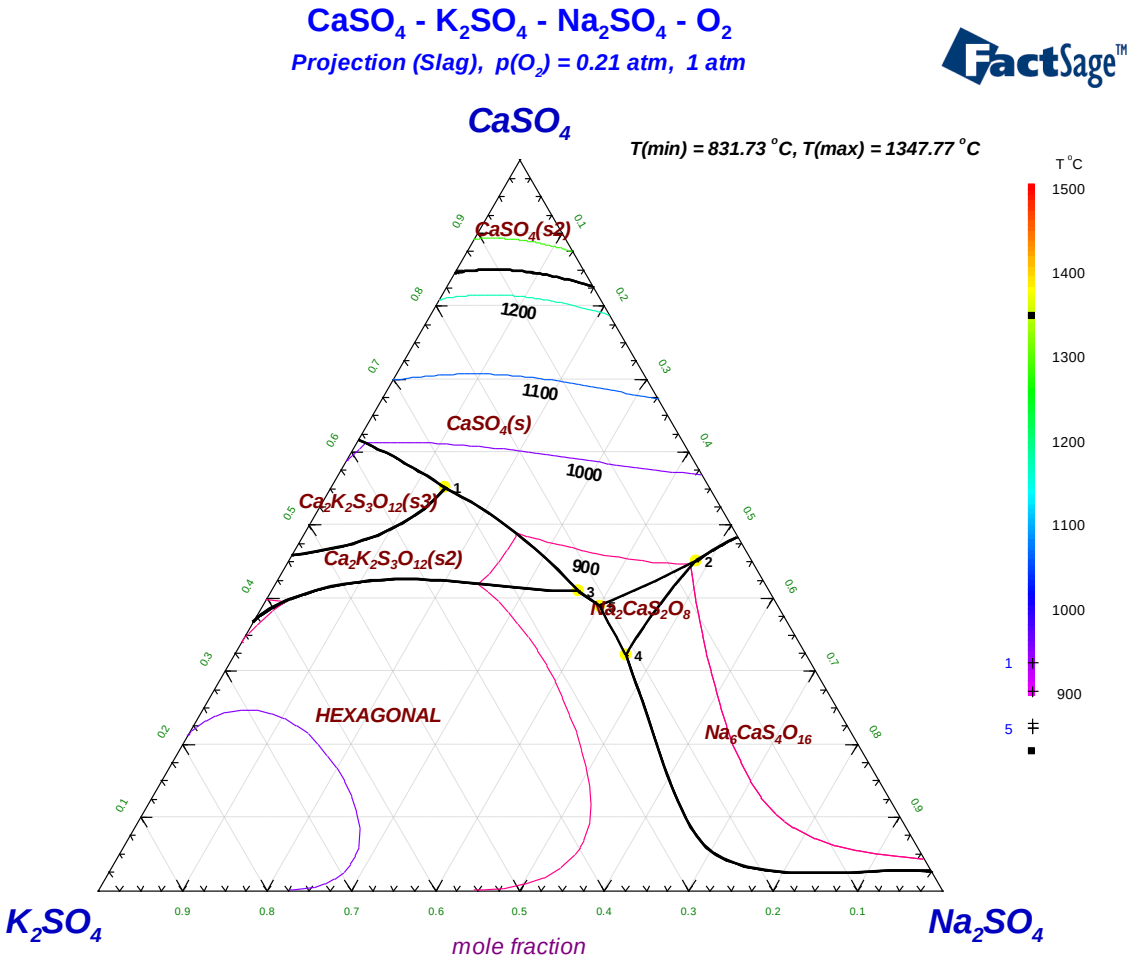
CaSO4 - K2SO4 - Na2SO4 - O2
Projection (Slag), p(O2) = 0.21 atm, 1 atm
FactSage™
CaSO4
T(min) = 831.73 °C, T(max) = 1347.77 °C
T °C
1500
1400
1300
1200
1100
1000
900
CaSO4(s2)
1200
1100
CaSO4(s)
1000
Ca2K2S3O12(s3)
Ca2K2S3O12(s2)
900
Na2CaS2O8
HEXAGONAL
Na6CaS4O16
1
2
3
4
K2SO4
Na2SO4
mole fraction

Weight percent, Liquidussurface

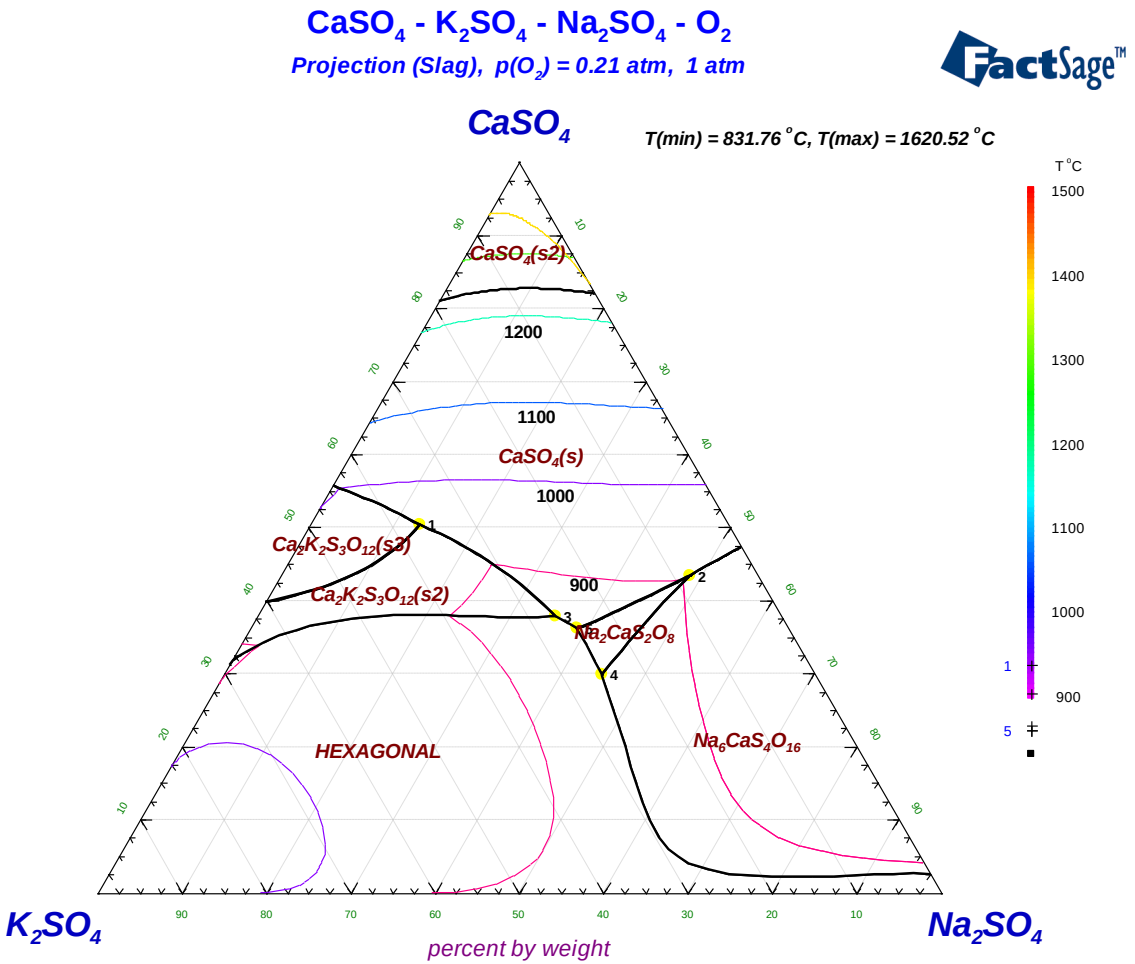

Invariant equilibria on the liquidus surface

Intersections with slag	Mole fraction A = CaSO4, B = K2SO4, C = Na2SO4				Weight percent A = CaSO4, B = K2SO4, C = Na2SO4			
	X(A)	X(B)	X(C)	T(C)	W(A)	W(B)	W(C)	T(C)
1: Ca2K2S3O12(s2) / Ca2K2S3O12(s3) / CaSO4(s)	1: 0.55058	0.31303	0.13638	936.85	1: 50.348	36.640	13.012	936.85
2: CaSO4(s) / Na2CaS2O8 / Na6CaS4O16	2: 0.45104	0.06551	0.48345	902.85	2: 43.399	8.068	48.534	902.85
3: Ca2K2S3O12(s2) / CaSO4(s) / HEXAGONAL	3: 0.40895	0.22566	0.36539	864.74	3: 37.900	26.769	35.331	864.73
4: HEXAGONAL / Na2CaS2O8 / Na6CaS4O16	4: 0.32220	0.21305	0.46475	860.12	4: 29.839	25.255	44.906	860.12
5: CaSO4(s) / HEXAGONAL / Na2CaS2O8	5: 0.38925	0.21063	0.40013	859.23	5: 36.165	25.049	38.787	859.23

Mole fraction 500°C

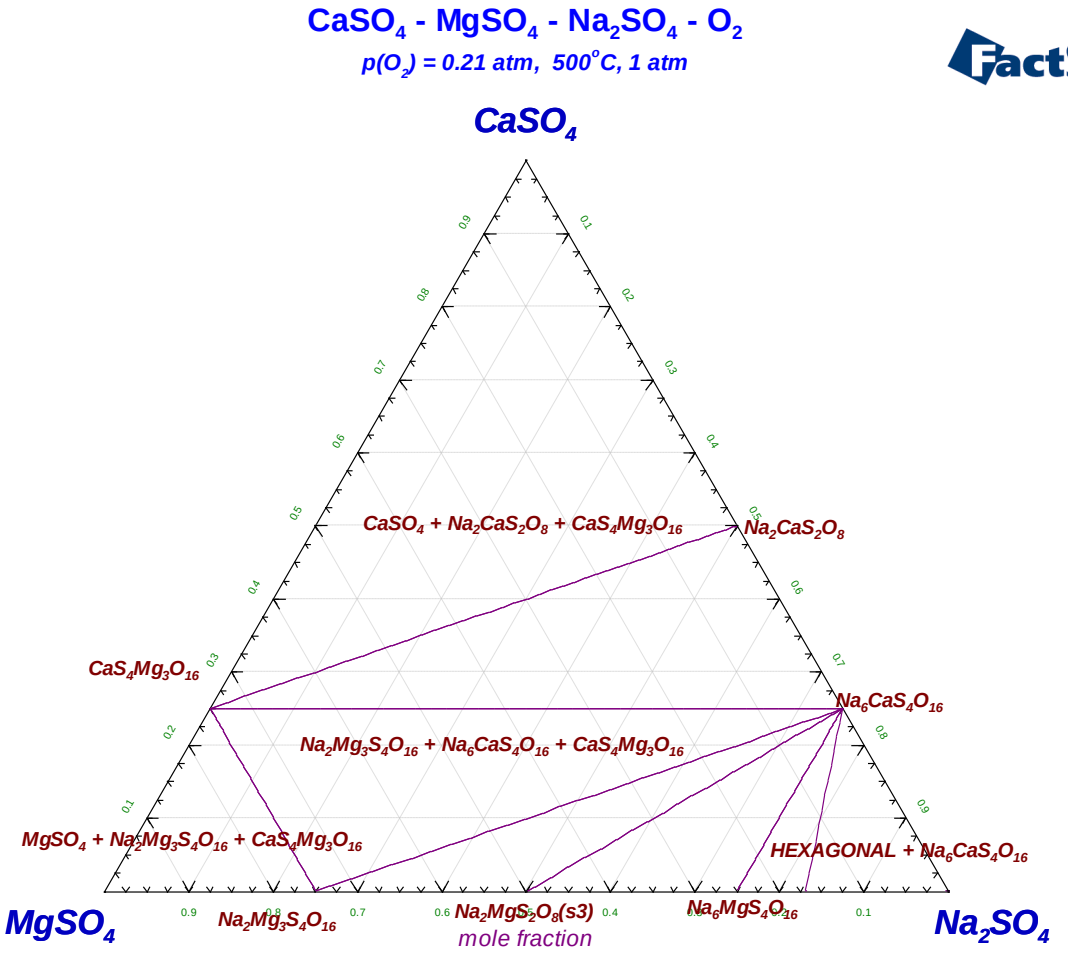

Mole fraction 700°C

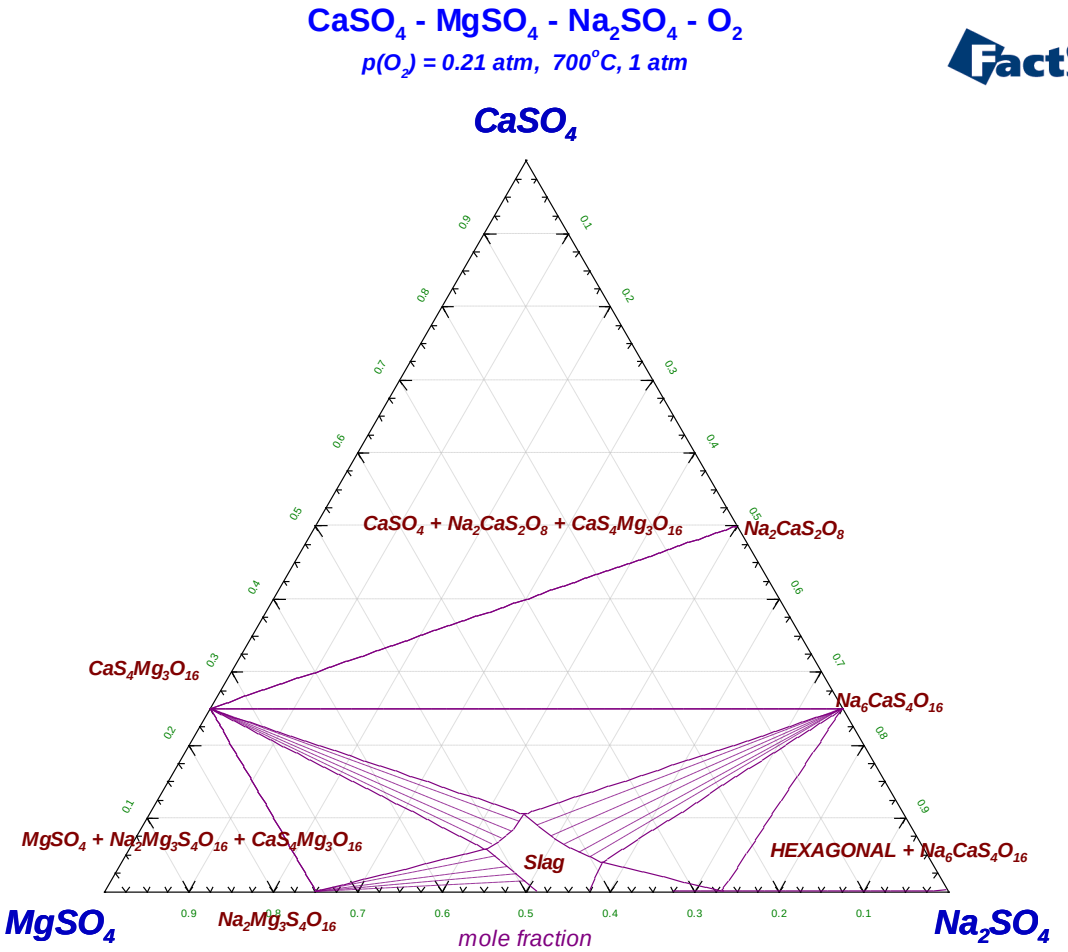

Mole fraction Liqudussurface

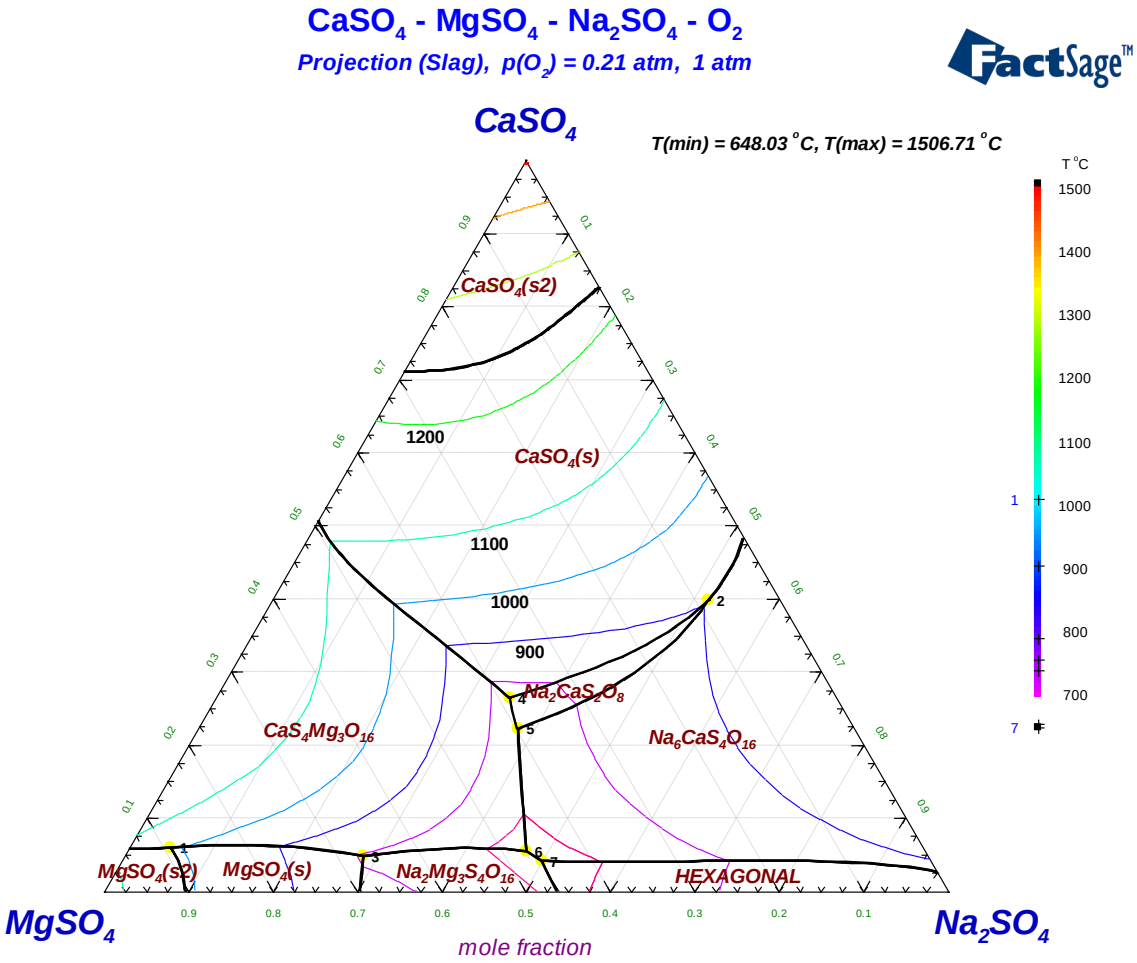

Weight percent, Liqudussurface

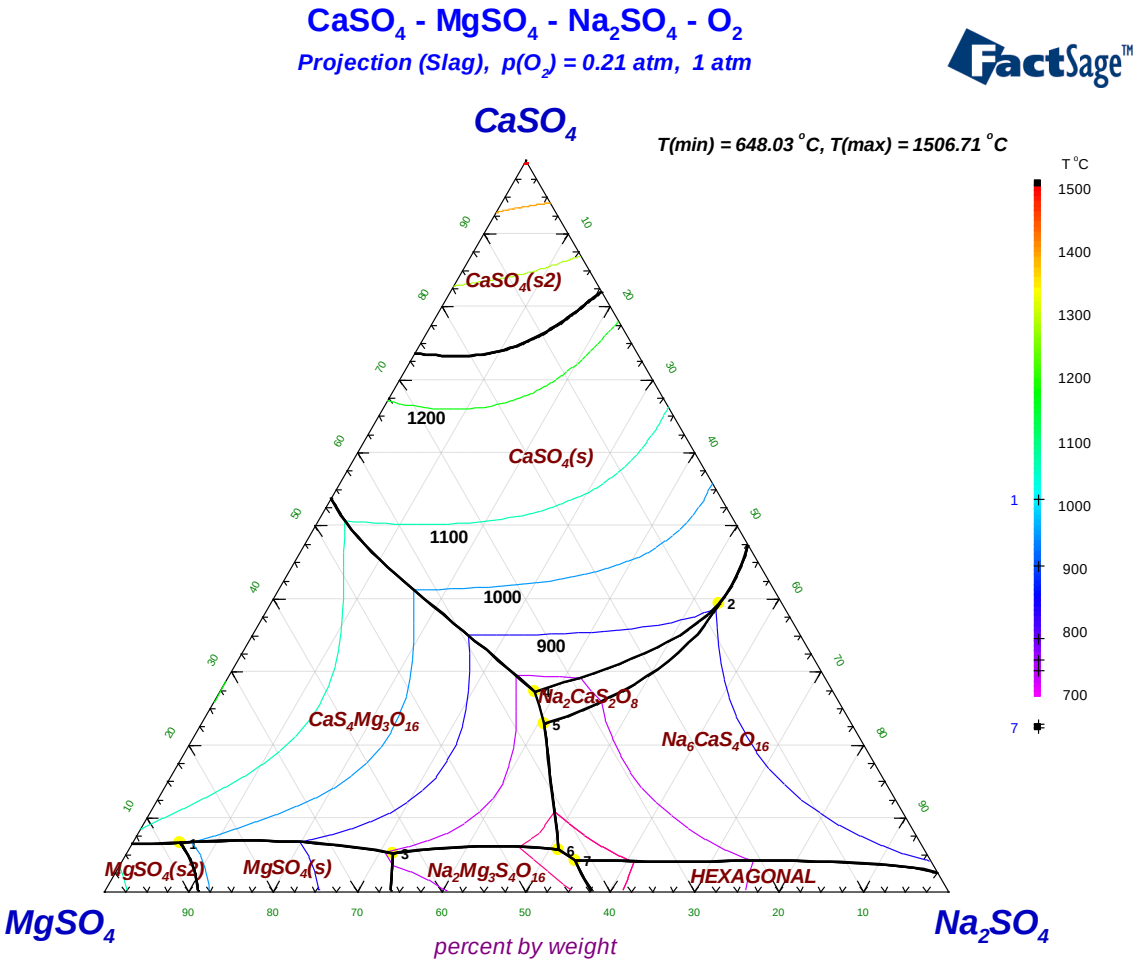

Invariant equilibria on the liquidus surface

Intersections with slag	Mole fraction A = CaSO4, B = MgSO4, C = Na2SO4				Weight percent A = CaSO4, B = MgSO4, C = Na2SO4				
		X(A)	X(B)	X(C)	T(C)		W(A)	W(B)	W(C)	T(C)
1: CaS4Mg3O16 / MgSO4(s) / MgSO4(s2)	1:	0.05918	0.89109	0.04973	1009.85	1:	6.583	87.645	5.772	1009.84
2: CaSO4 / Na2CaS2O8 / Na6CaS4O16	2:	0.39780	0.08512	0.51708	902.85	2:	39.287	7.432	53.281	902.85
3: CaS4Mg3O16 / MgSO4(s) / Na2Mg3S4O16	3:	0.04846	0.66823	0.28331	788.60	3:	5.184	63.198	31.619	788.60
4: CaS4Mg3O16 / CaSO4 / Na2CaS2O8	4:	0.26482	0.38704	0.34814	755.16	4:	27.294	35.269	37.437	755.11
5: CaS4Mg3O16 / Na2CaS2O8 / Na6CaS4O16	5:	0.22165	0.39894	0.37941	737.89	5:	22.845	36.354	40.801	737.88
6: CaS4Mg3O16 / Na2Mg3S4O16 / Na6CaS4O16	6:	0.05464	0.47236	0.47300	653.12	6:	5.658	43.243	51.099	653.12
7: HEXAGONAL / Na2Mg3S4O16 / Na6CaS4O16	7:	0.04100	0.46084	0.49816	648.03	7:	4.235	42.083	53.682	648.03

Mole fraction Cr2FeS4-Cr3S4

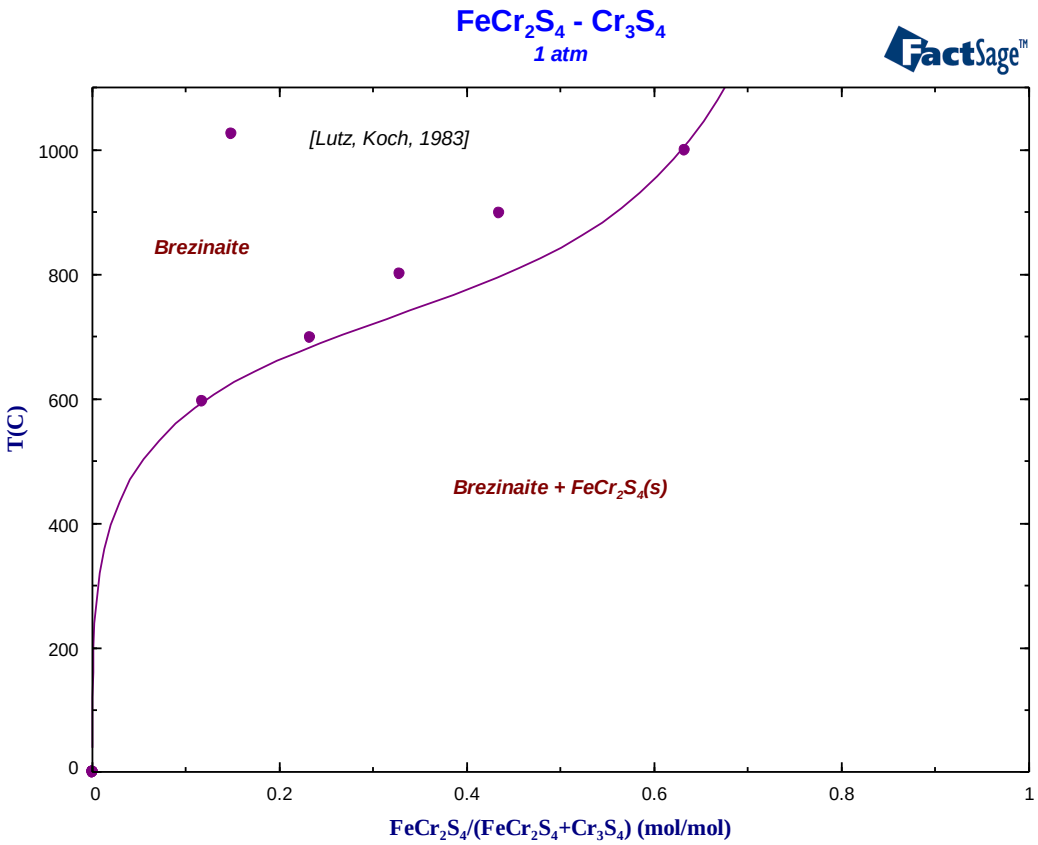

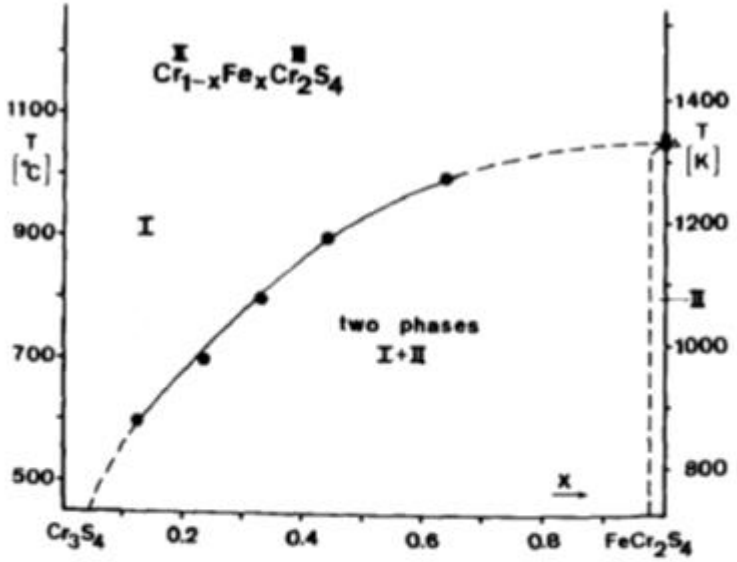

FIG. 2

Phase diagram of the system Cr_3S_4-$FeCr_2S_4$. Cr_3S_4 type I, spinel type, II, phase transition temperature given in ref. (1), ○, (4), □, and (5), △.

H.D. Lutz, U. Koch, H. Siwert, Mat. Res. Bull., 18 (1983), pp.1383-1389.

Weight percent

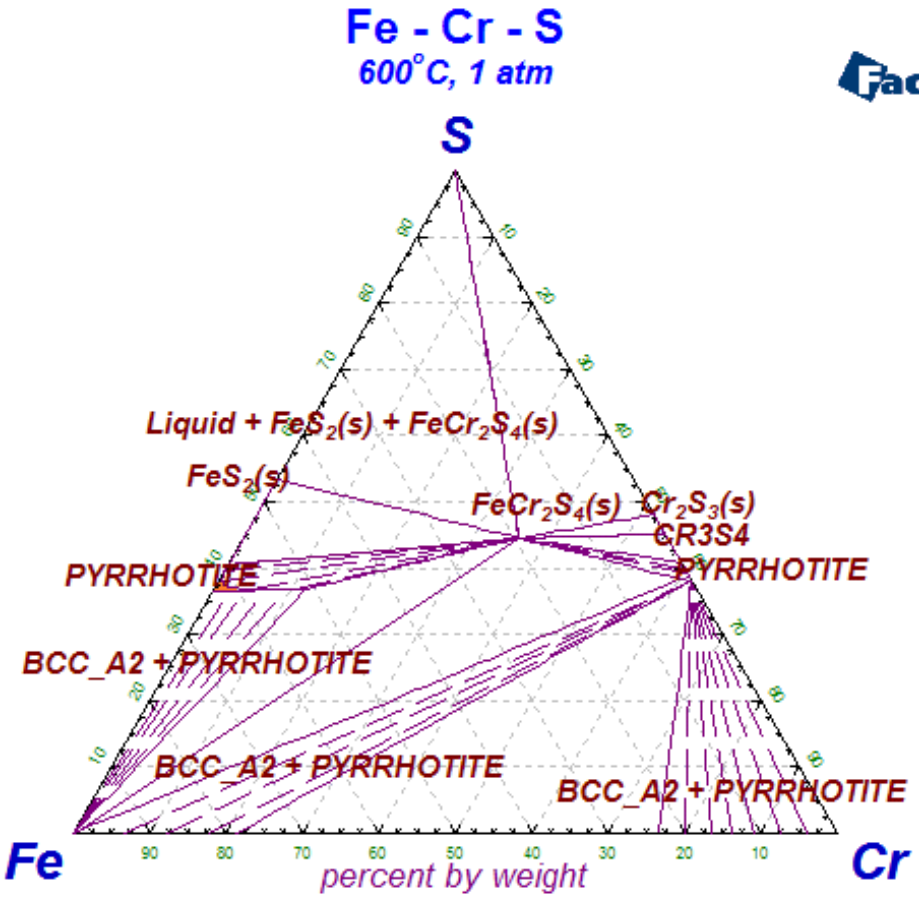

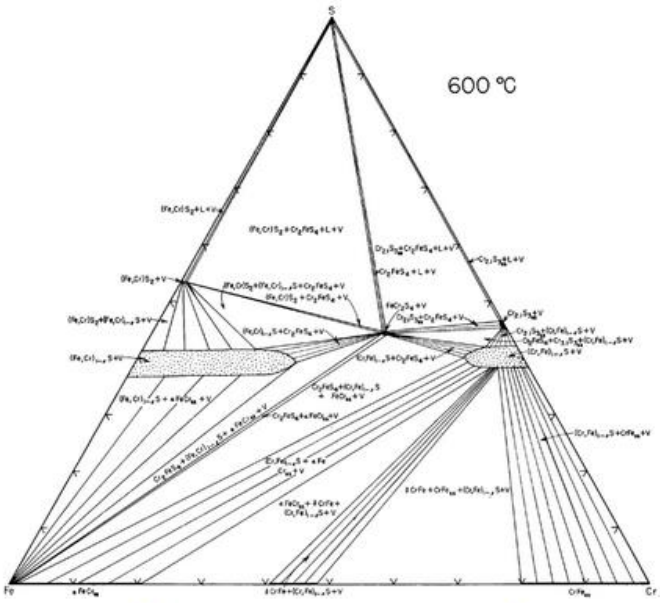

Fig. 7. Phase relations in the Cr-Fe-S system at 600°C. All assemblages are in equilibrium with vapor.

A. El Goresy, G. Kullerud: in Proc. Symp. Meteorite Res., P.M.D. Millman, ed., Reidel, Dordrecht, (1969), pp. 638-656.

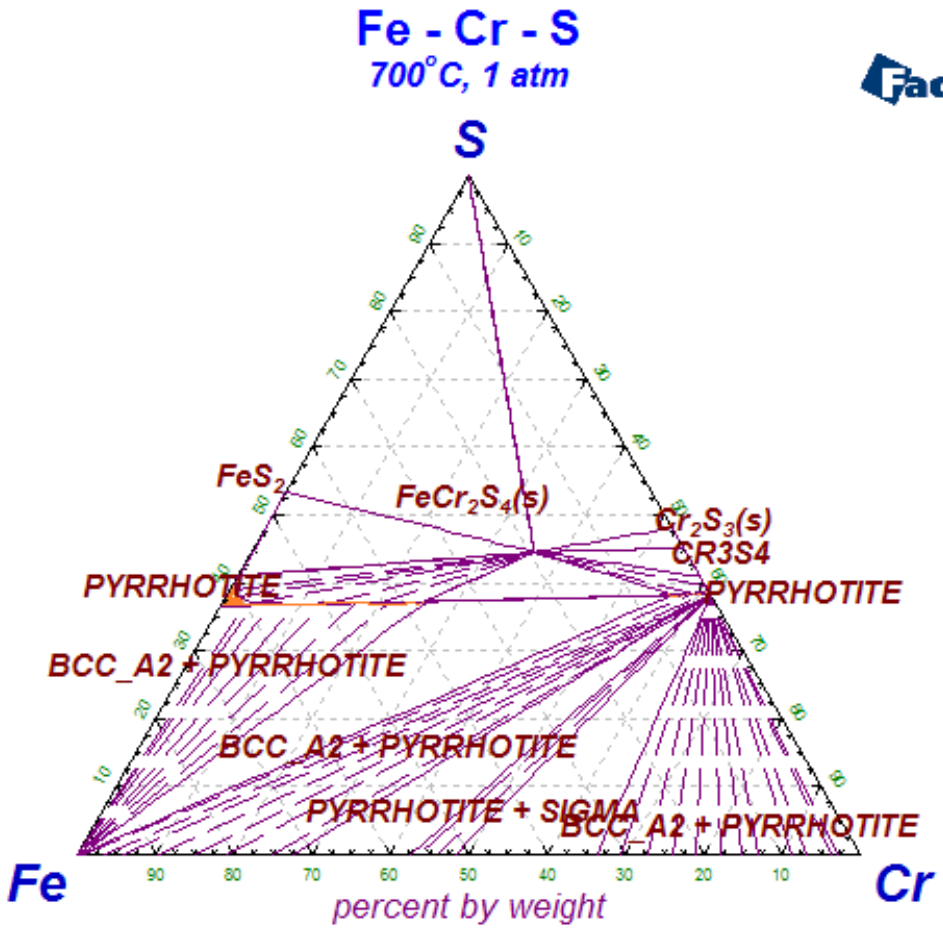

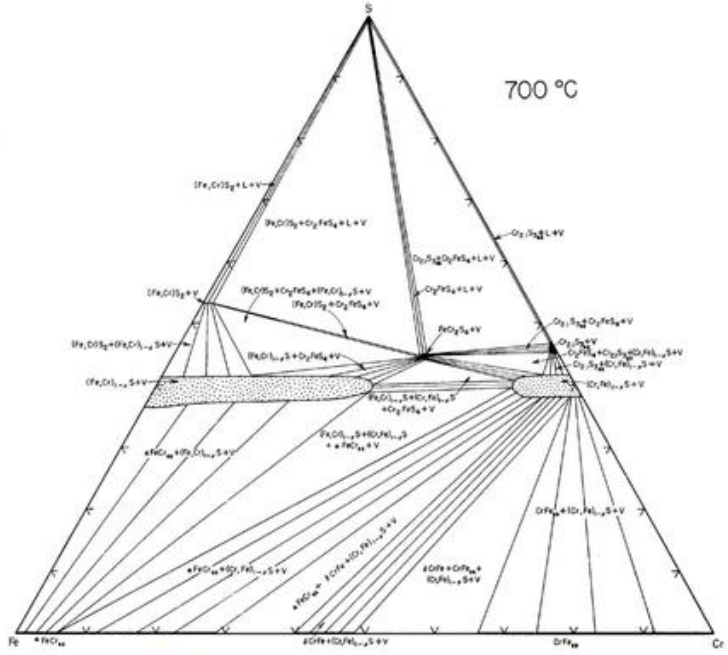

Fig. 6. Phase relations in the Cr-Fe-S system at 700 °C. All assemblages are in equilibrium with vapor.

A. El Goresy, G. Kullerud: in Proc. Symp. Meteorite Res., P.M.D. Millman, ed., Reidel, Dordrecht, (1969), pp. 638-656.

Weight percent 950°C

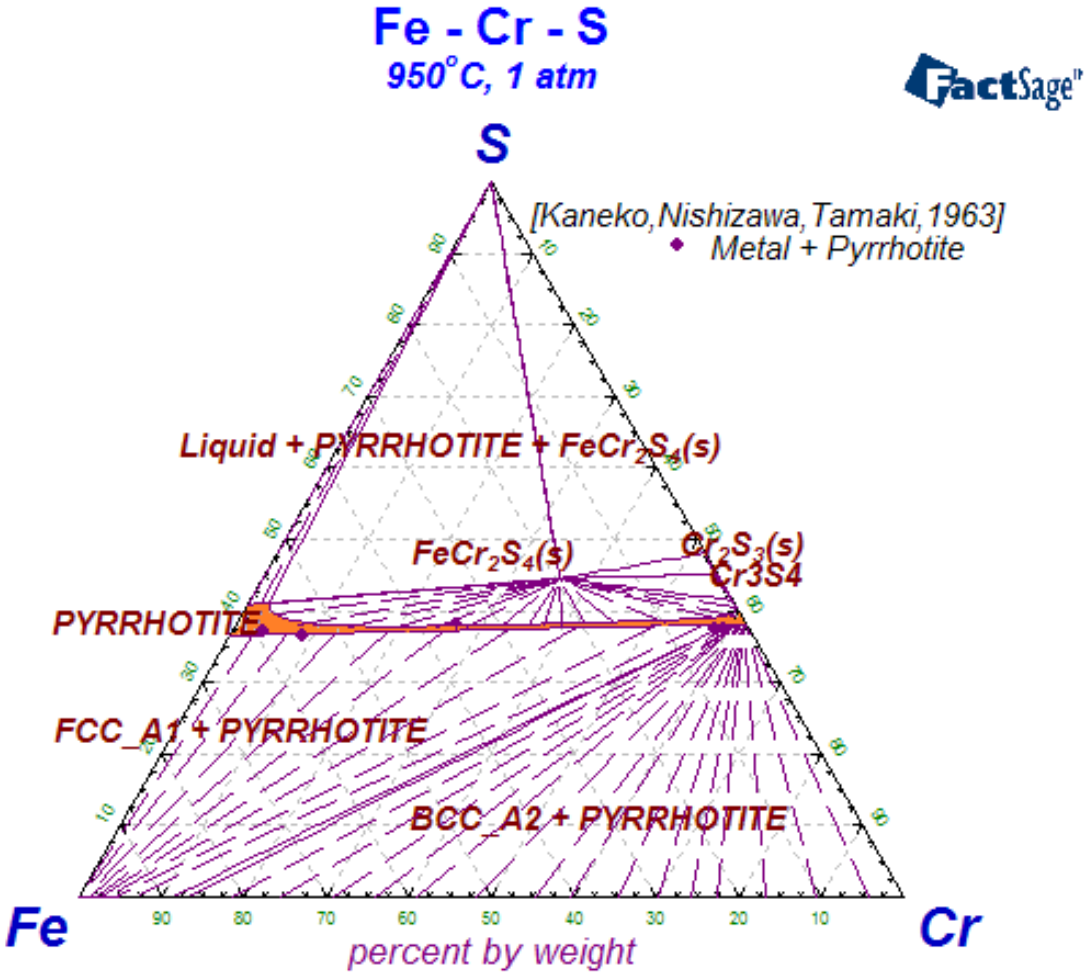

Weight percent 1090°C

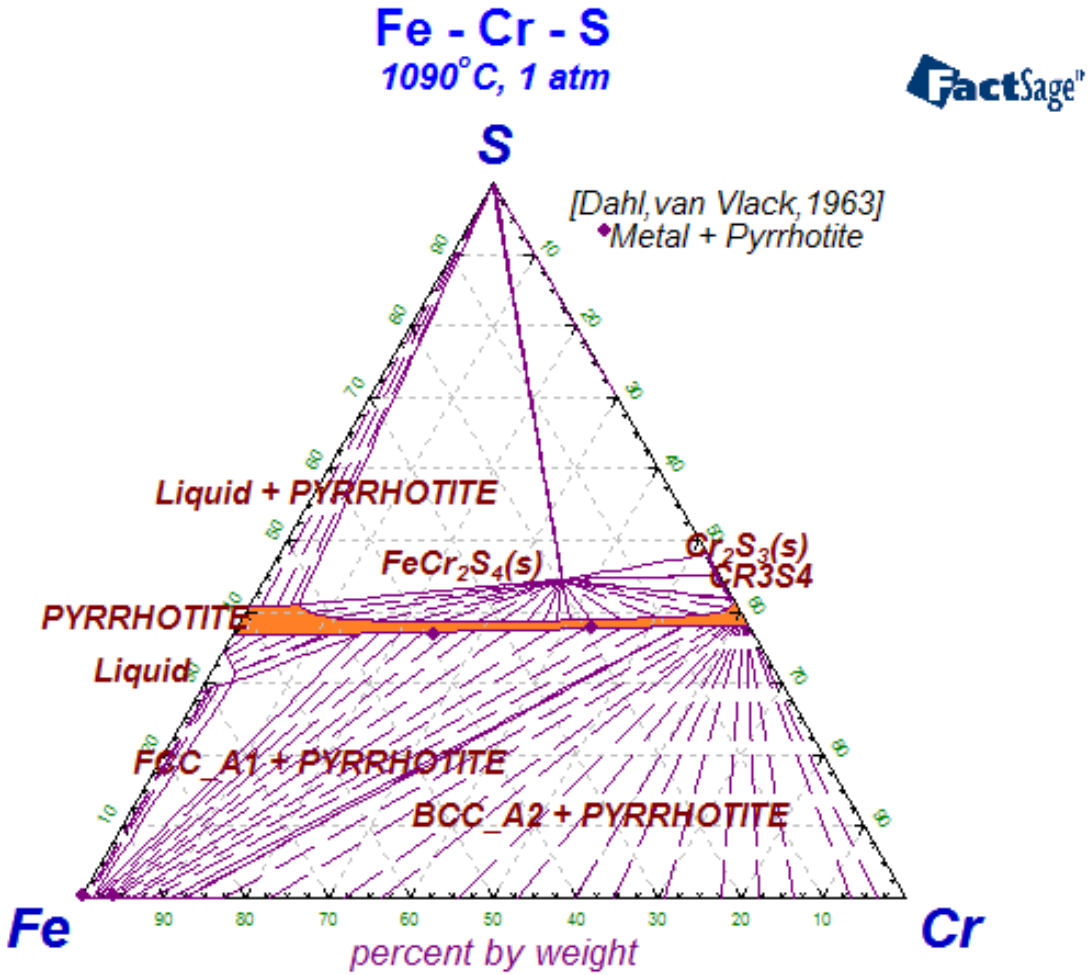

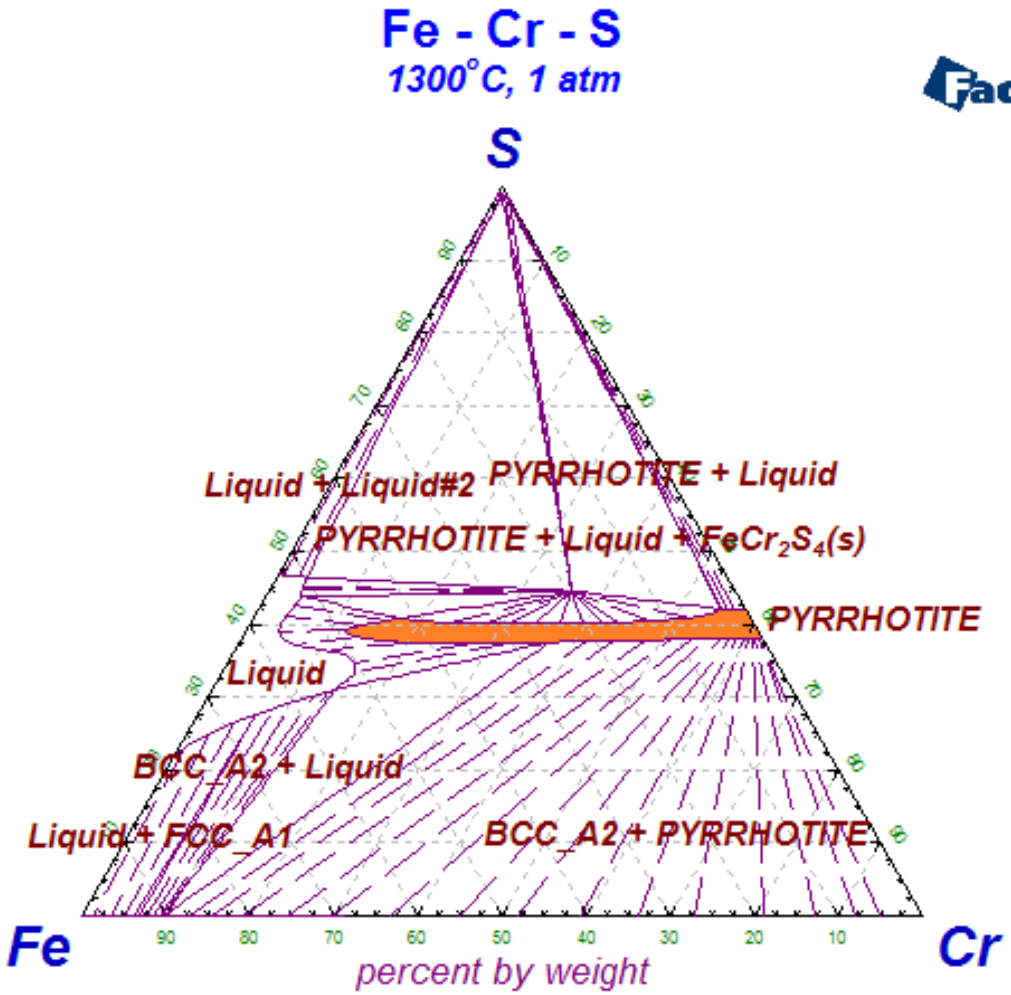
Fe - Cr - S
1300°C, 1 atm
FactSage
S
Liquid + Liquid#2
PYRRHOTITE + Liquid
PYRRHOTITE + Liquid + FeCr2S4(s)
PYRRHOTITE
Liquid
BCC_A2 + Liquid
Liquid + FCC_A1
BCC_A2 + PYRRHOTITE
Fe
Cr
90 80 70 60 50 40 30 20 10
percent by weight

Cr-Fe-S,
Weight percent, isopleth section at ~50 mol% S

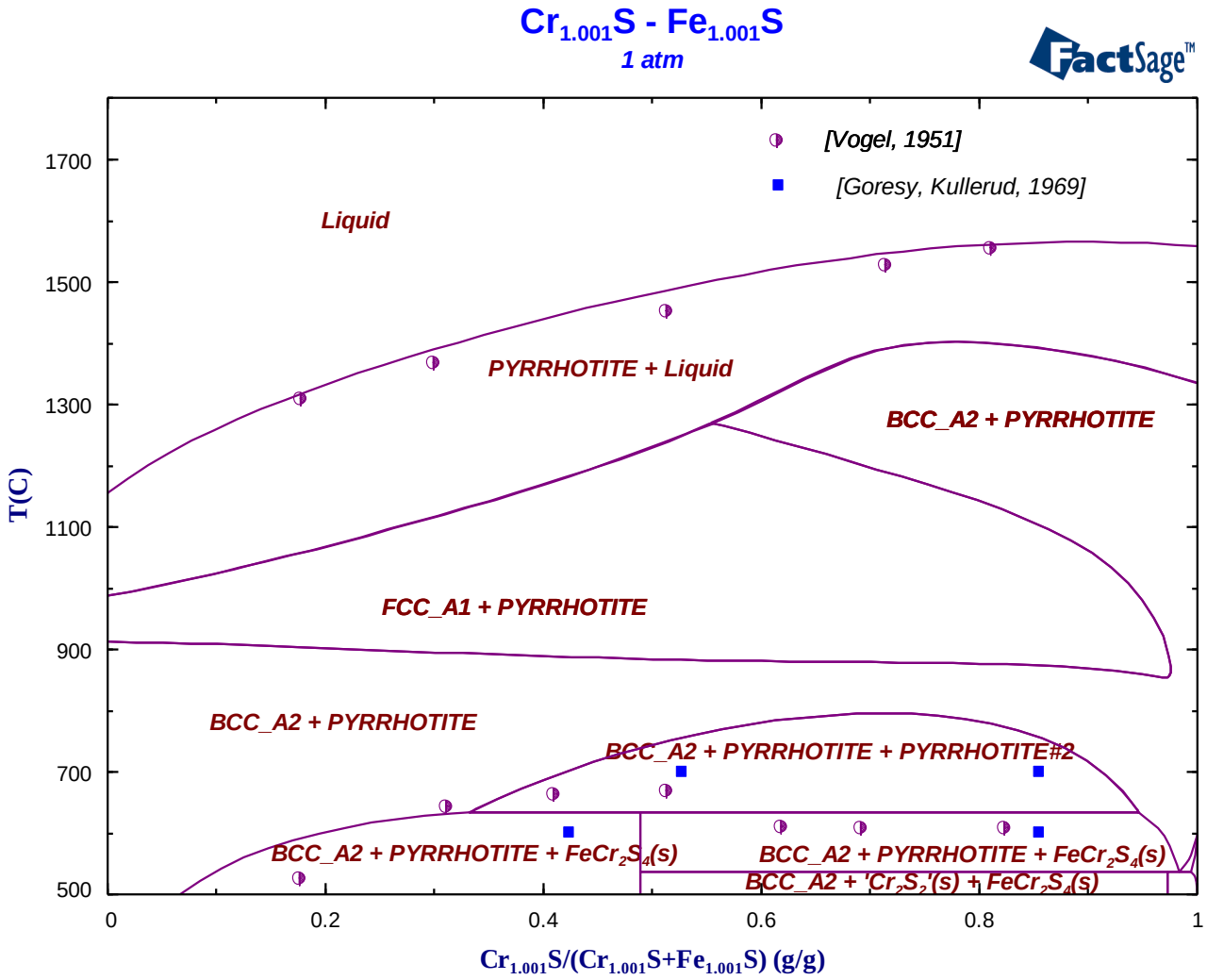

Cr-Mn-S,
Mole fraction Cr2MnS4-Cr3S4

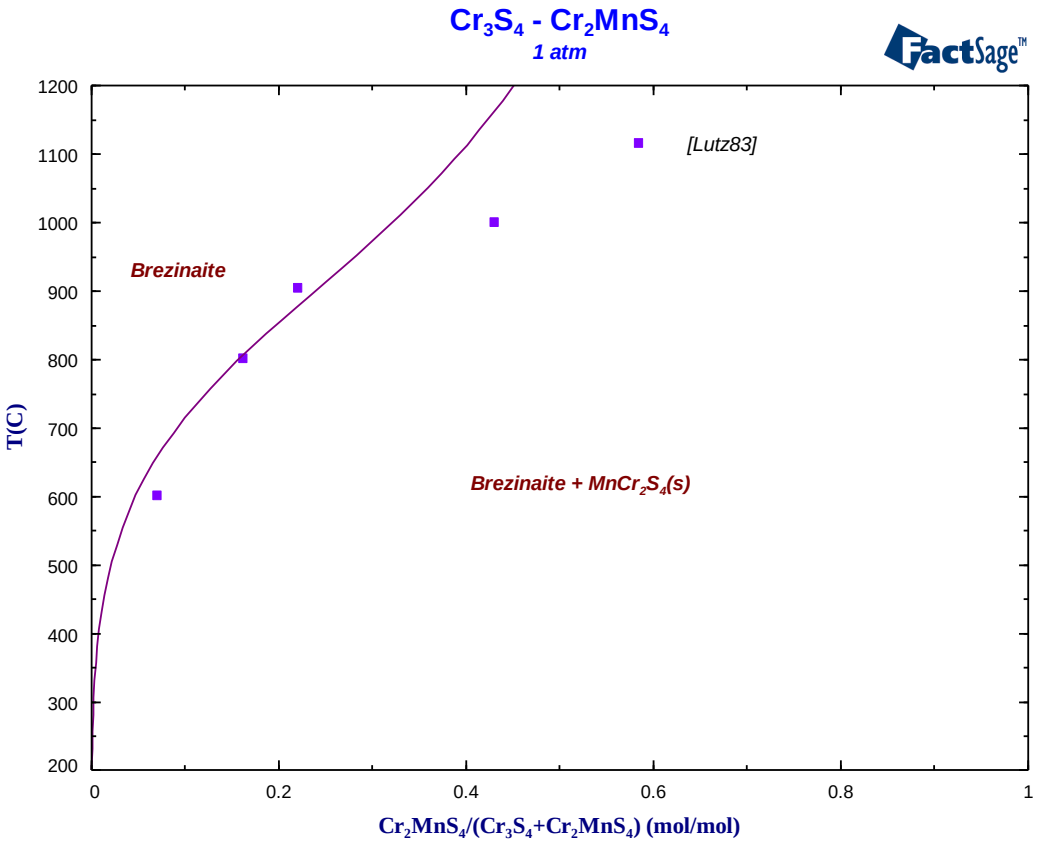

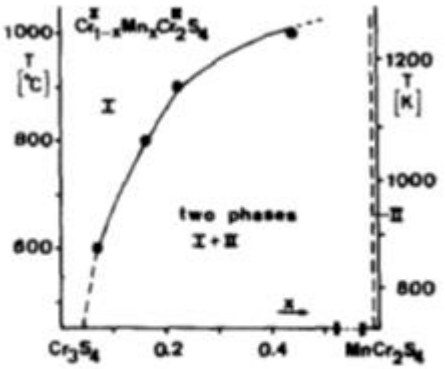

FIG. 1

Phase diagram of the system Cr_3S_4-$MnCr_2S_4$. Fe_3Se_4(Cr_3S_4) type, I, spinel type, II.

H.D. Lutz, U. Koch, H. Siwert, Mat. Res. Bull., 18 (1983), pp.1383-1389.

Mole fraction CrS-MnS

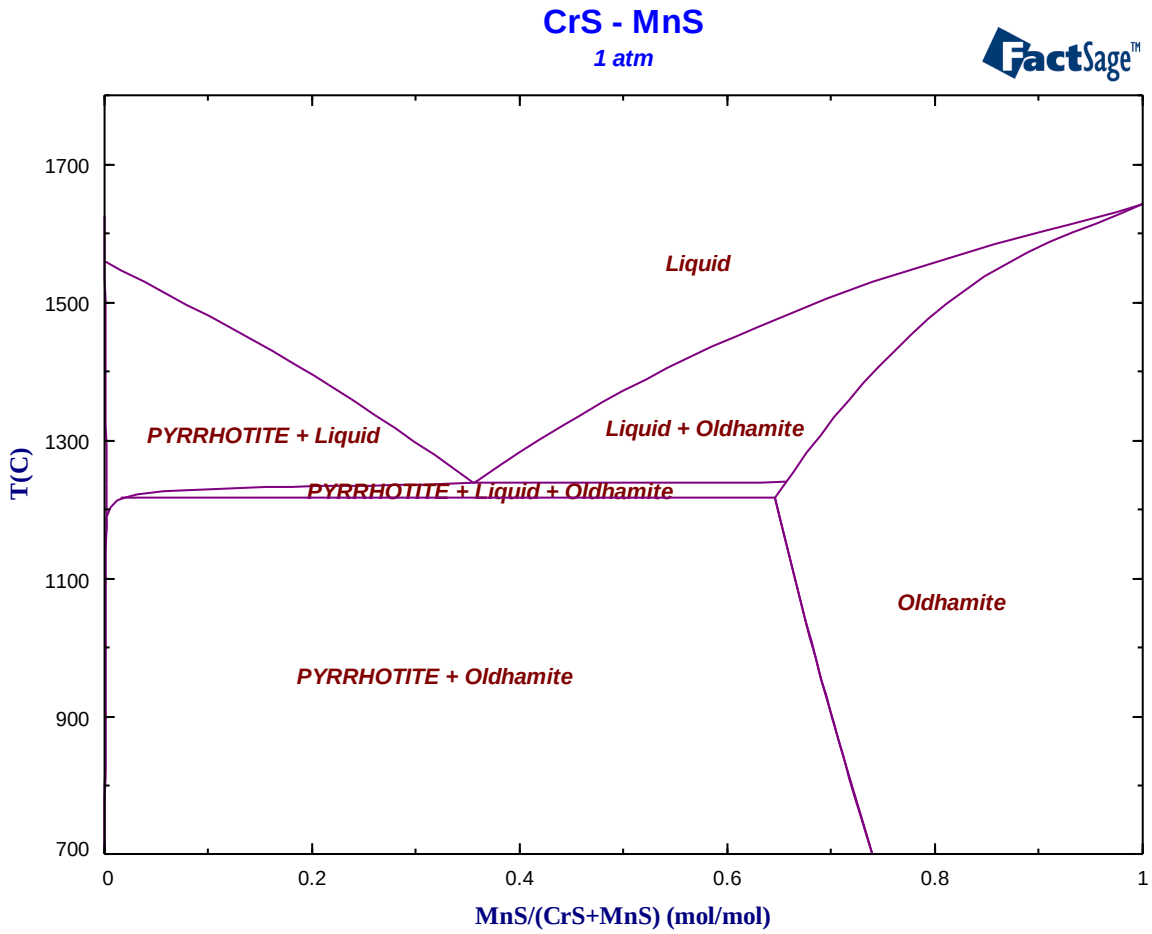

Cr-Mn-S,
Mole fraction 800°C

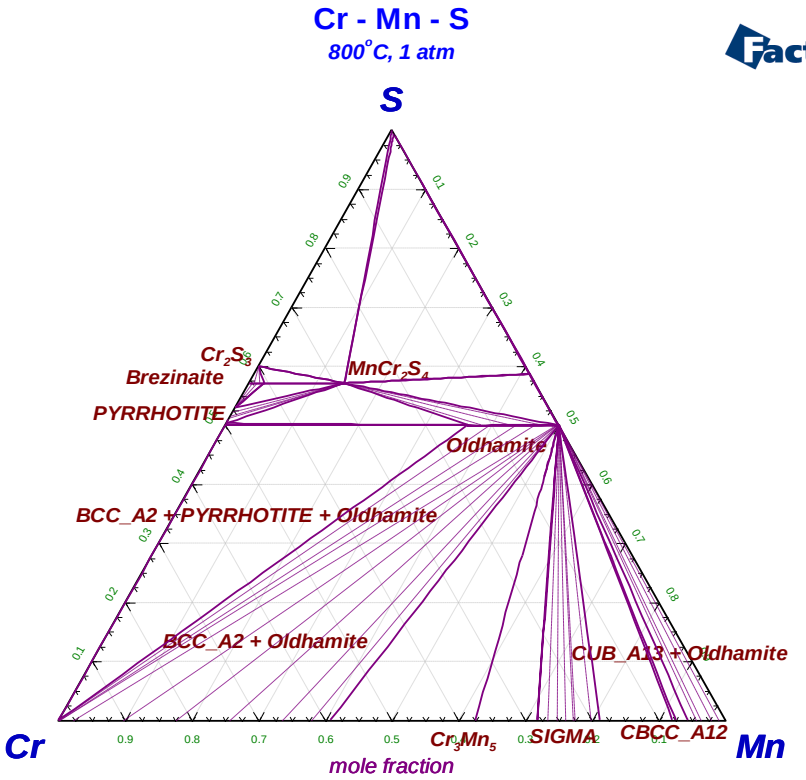

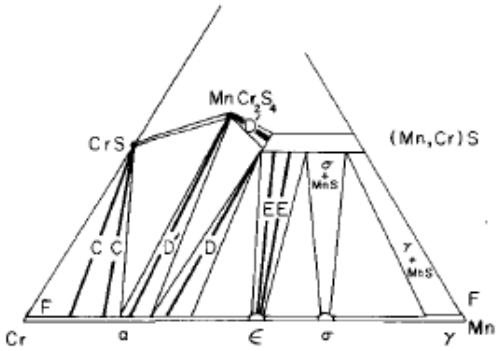

Fig. 8—Schematic representation of portion of Cr-Mn-S phase diagram at 800°C. Postulated tie lines for local equilibrium compositions of phases in contact during reaction are indicated, together with a continuity diagram. Dashed arrows show possible presence of $MnCr_2S_4$ in products.

Shatynski, S.R.; Hirth, J.P.; Rapp, R.A., Metall. Trans. A, 10A (5), 591-598 (1979) (16).

Cr2O3-Fe2O3-FeO, Mole fraction 1300°C

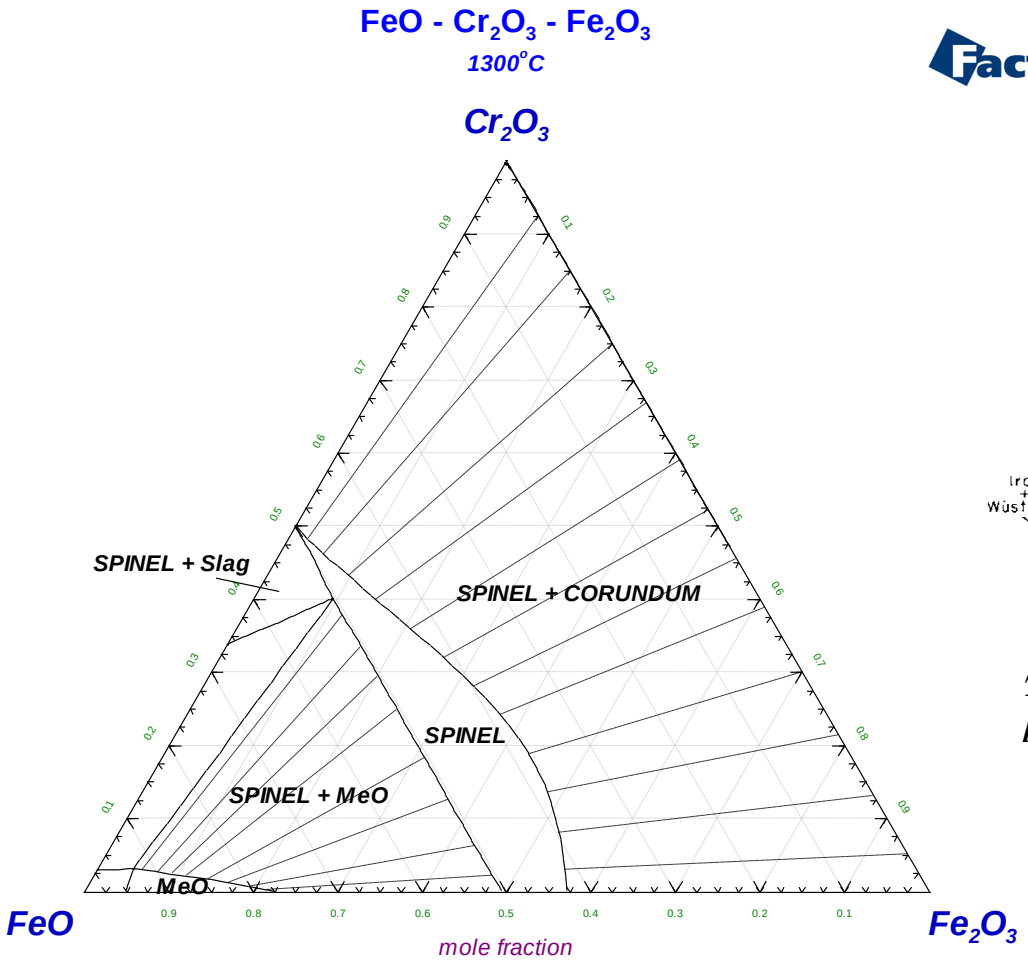

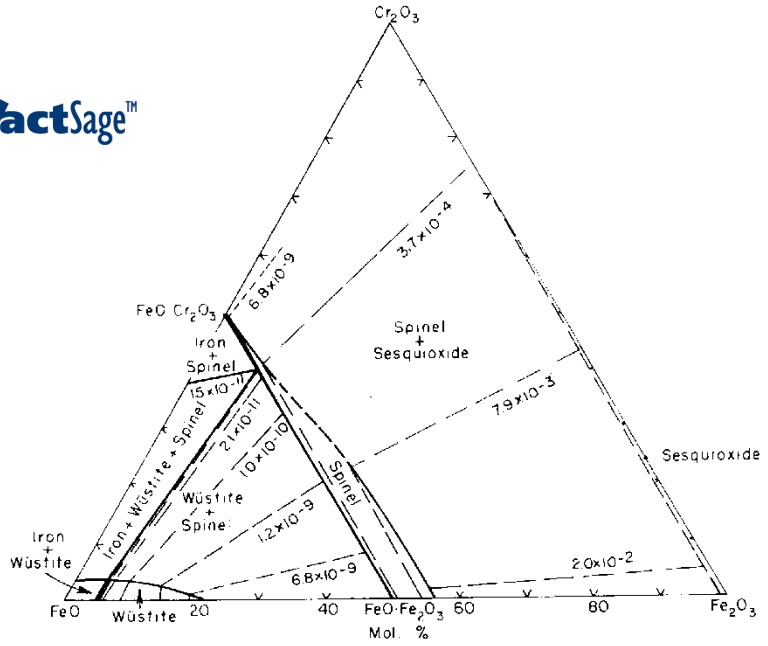

T. Katsura, A. Muan, Trans. Metall. Soc. AIME, 230 [1], (1964), pp.77-84.

Cr2O3-Fe2O3-MgO,
Weight percent 1300°C

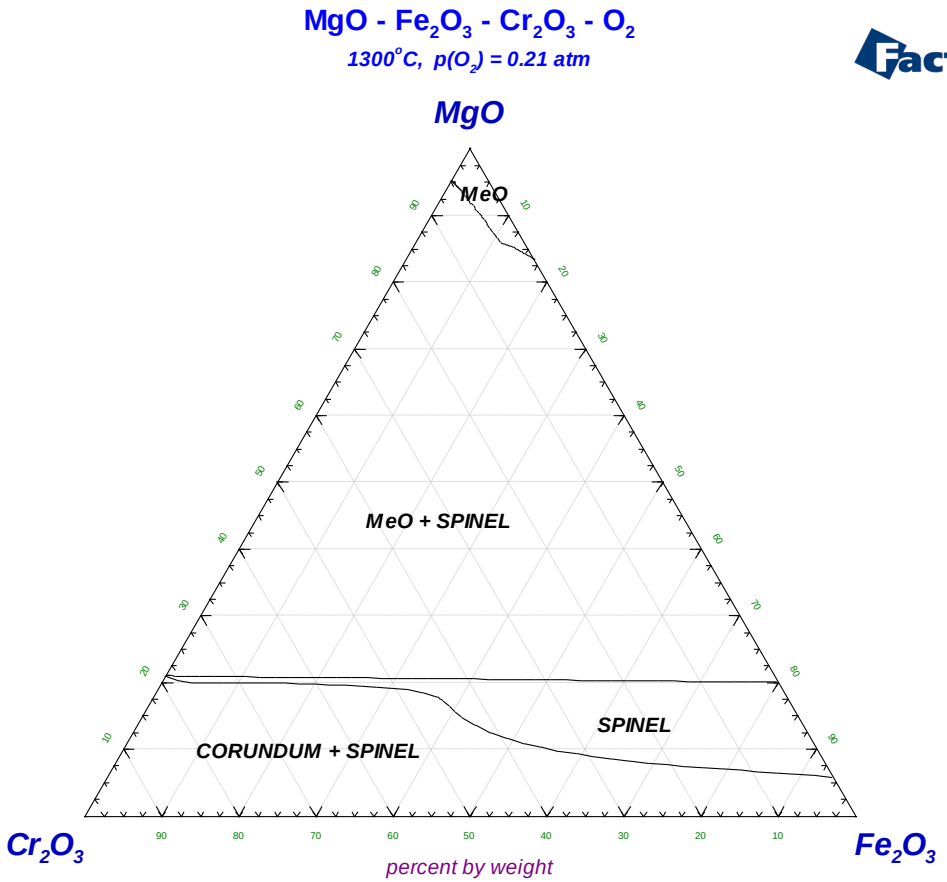

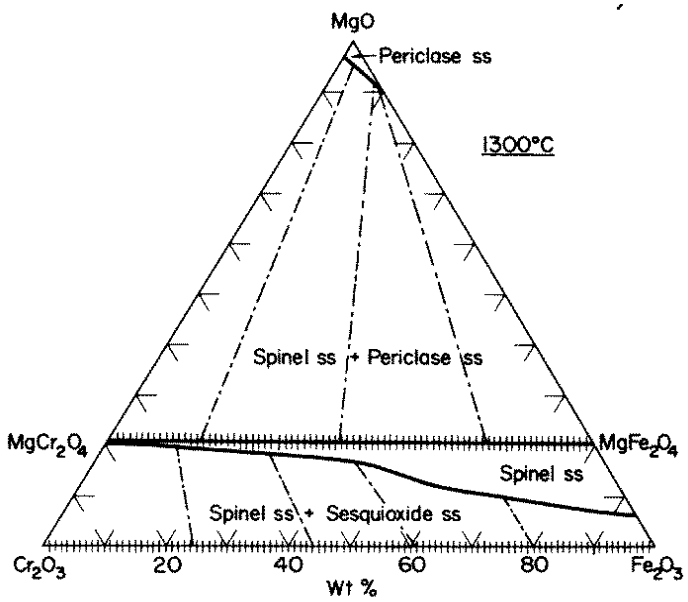

G.C. Ulmer, W.J. Smothers, J. Am. Ceram. Soc., 51 [6], (1968), pp. 315-319.

Cr2O3-Fe2O3-MgO,

Weight percent 1700°C

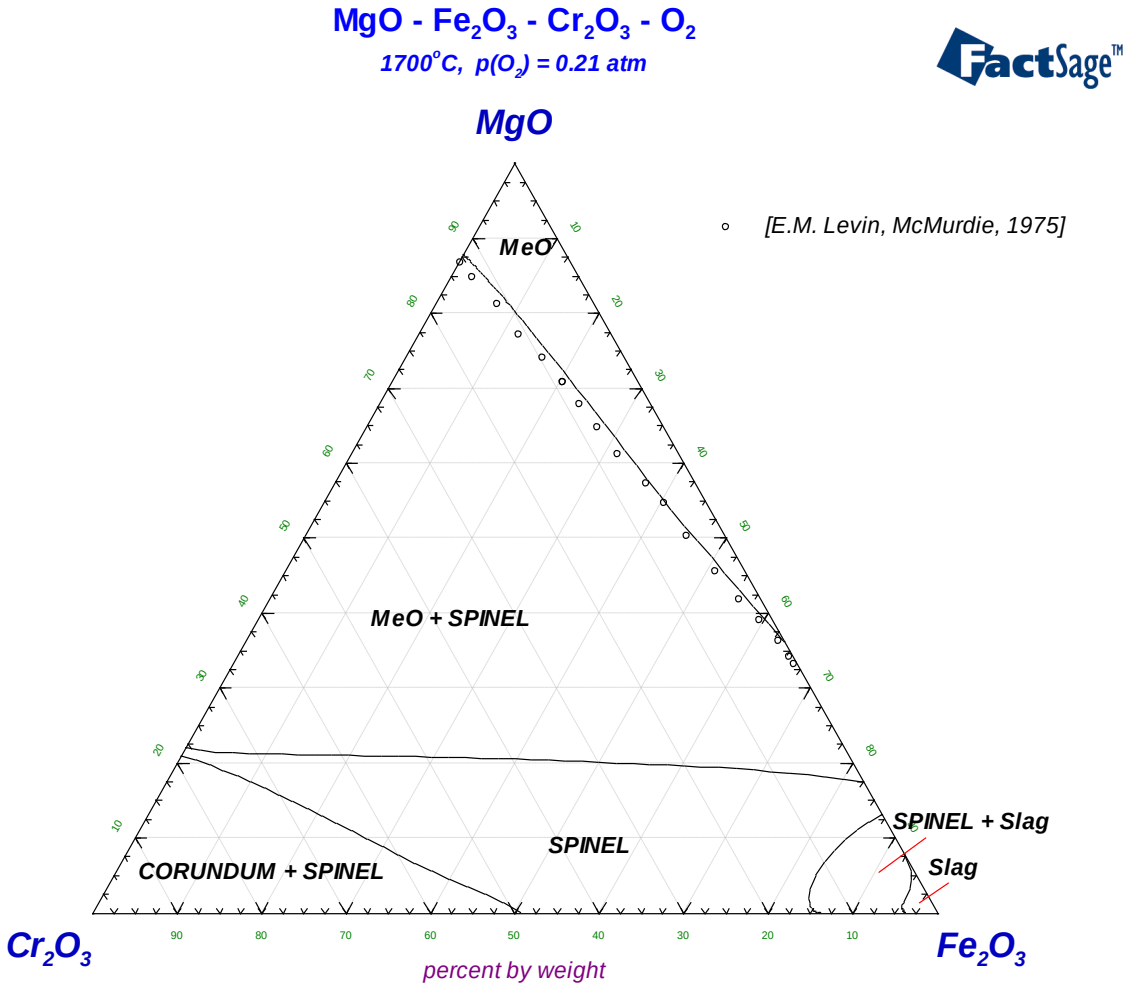

Weight percent
Liquidussurface

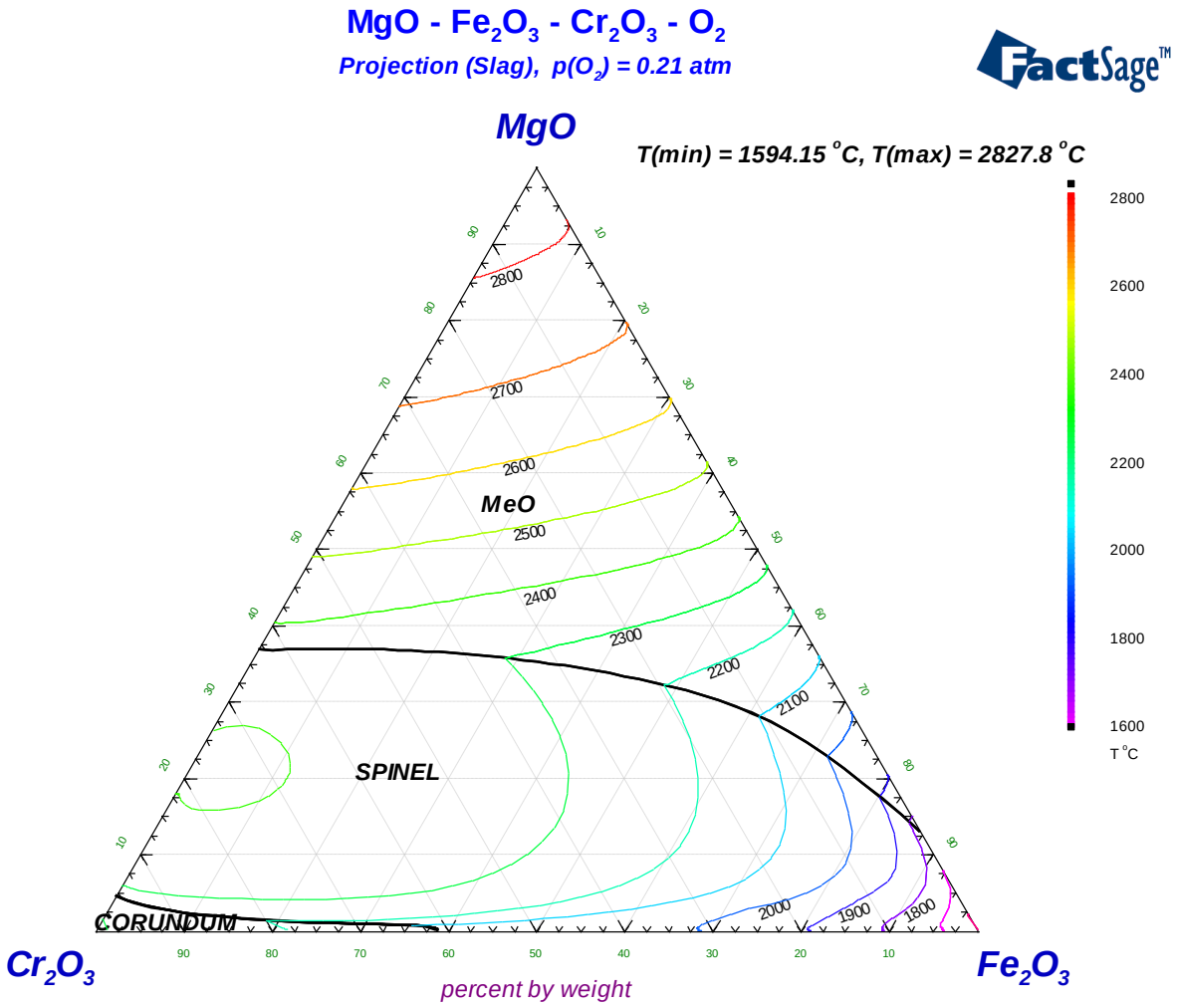

Cr2O3-Fe3O4-SiO2,
Weight percent 1400°C

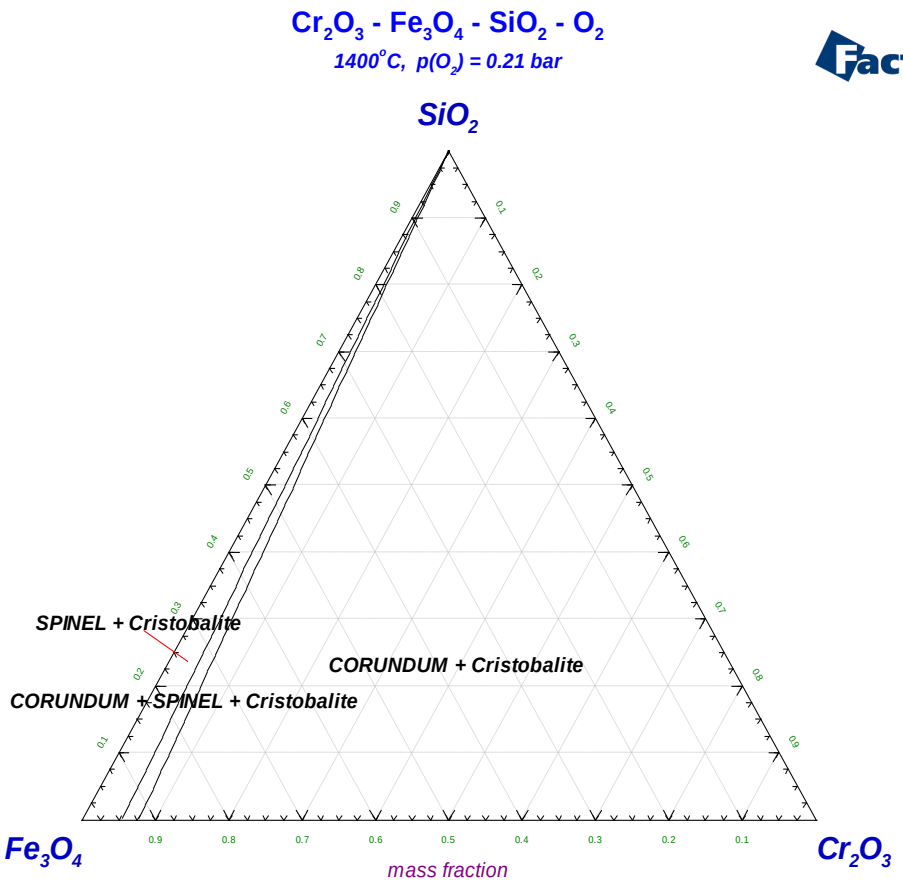

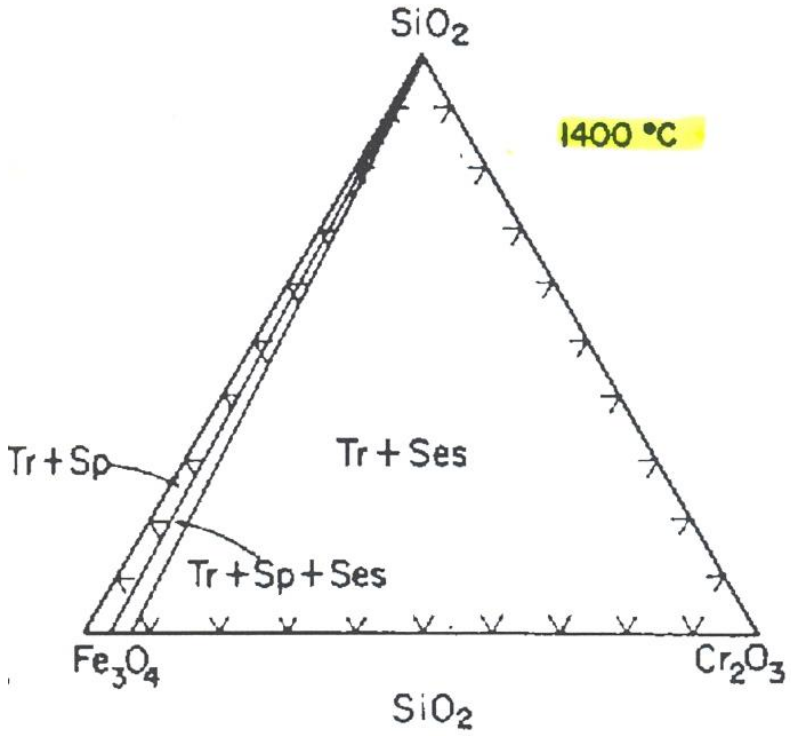

A. Muan and S. Somiya, Journal of Amer. Ceram. Soc., 43(1960), pp. 204-209.

Cr2O3-Fe3O4-SiO2,

Weight percent 1500°C

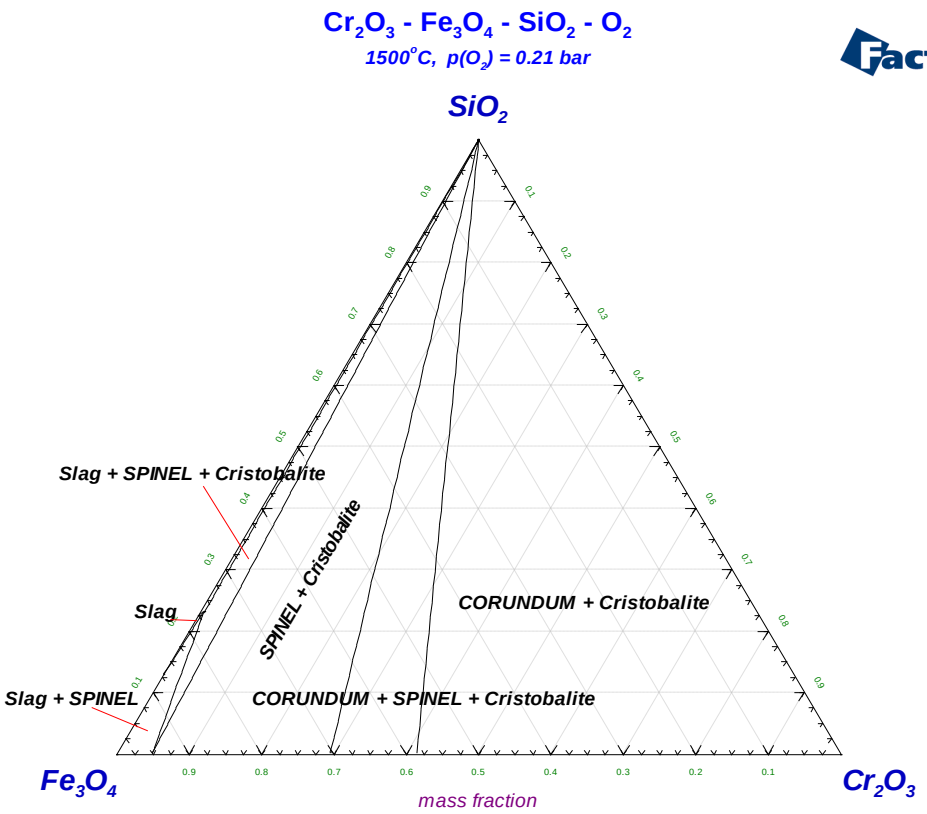

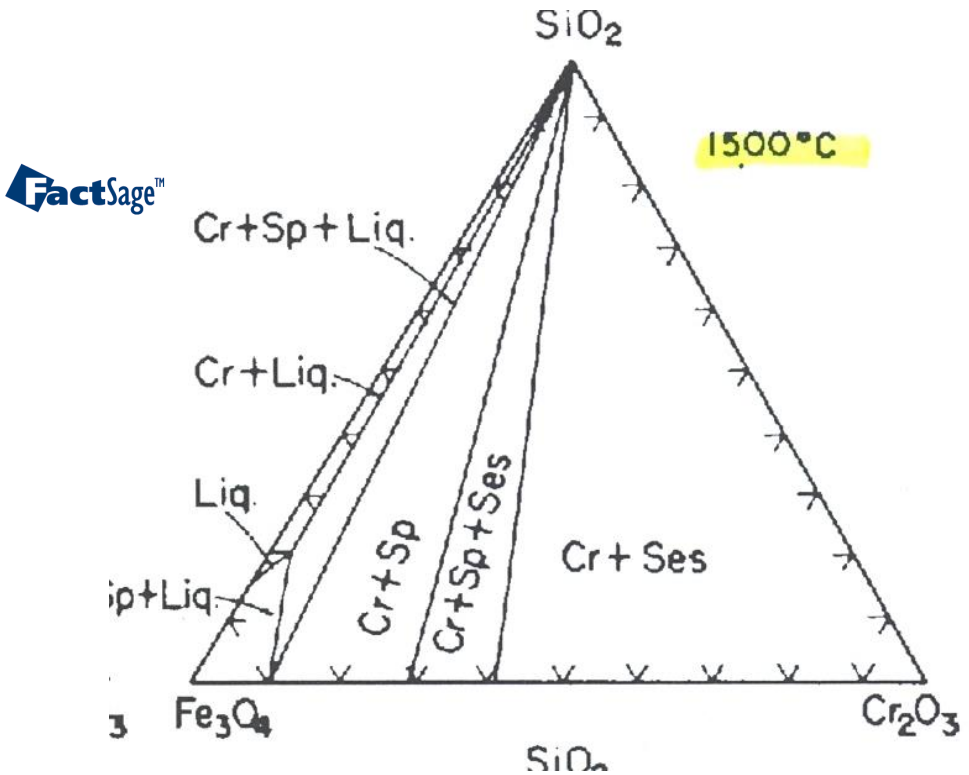

A. Muan and S. Somiya, Journal of Amer. Ceram. Soc., 43(1960), pp. 204-209.

Cr2O3-Fe3O4-SiO2,

Weight percent 1700°C

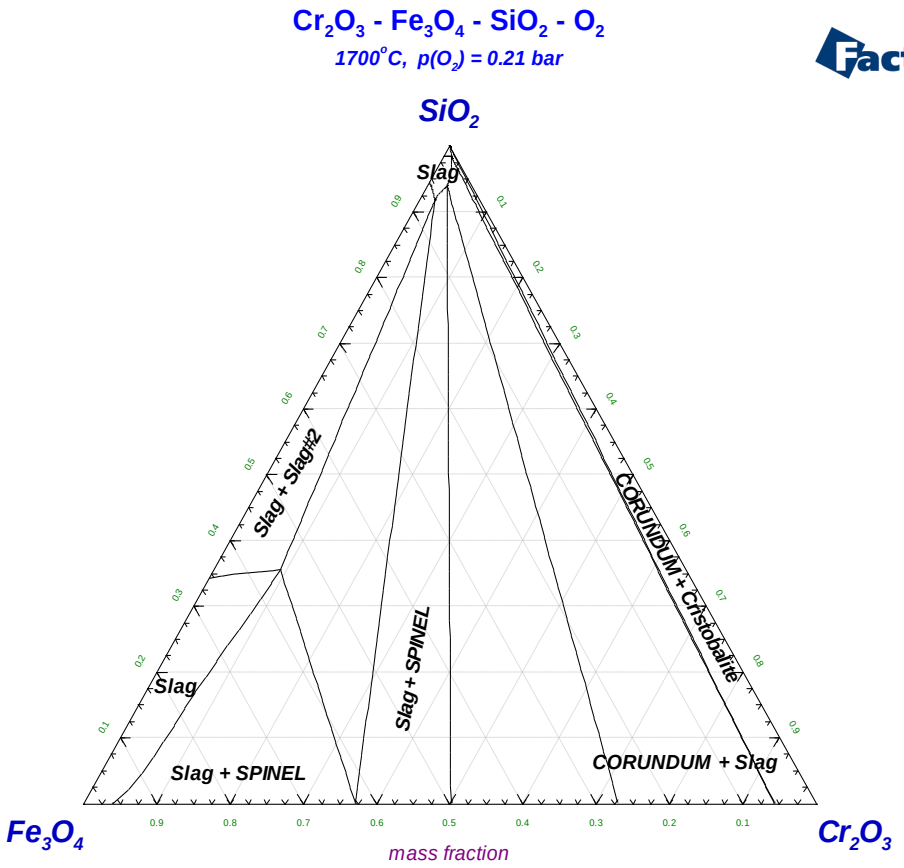

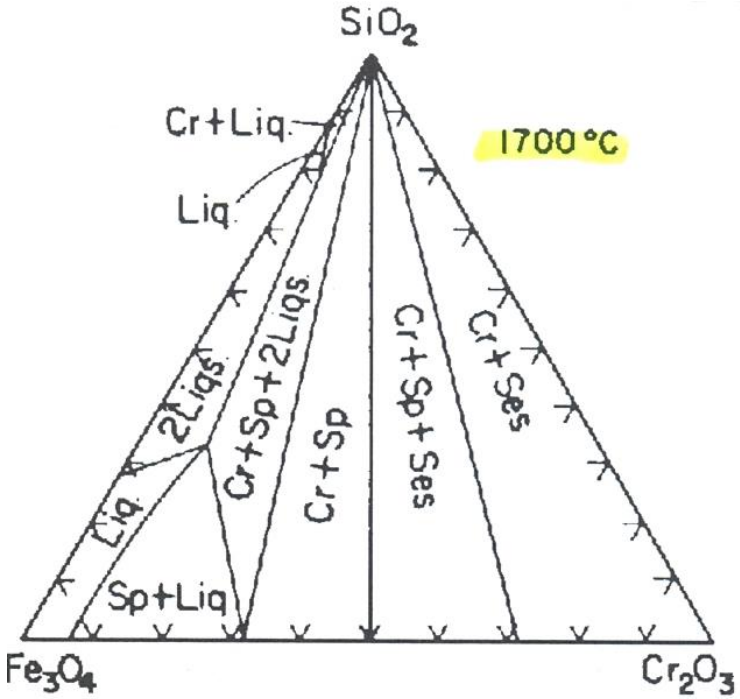

A. Muan and S. Somiya, Journal of Amer. Ceram. Soc., 43(1960), pp. 204-209.

Cr2O3-Fe3O4-SiO2,

Weight percent 1850°C

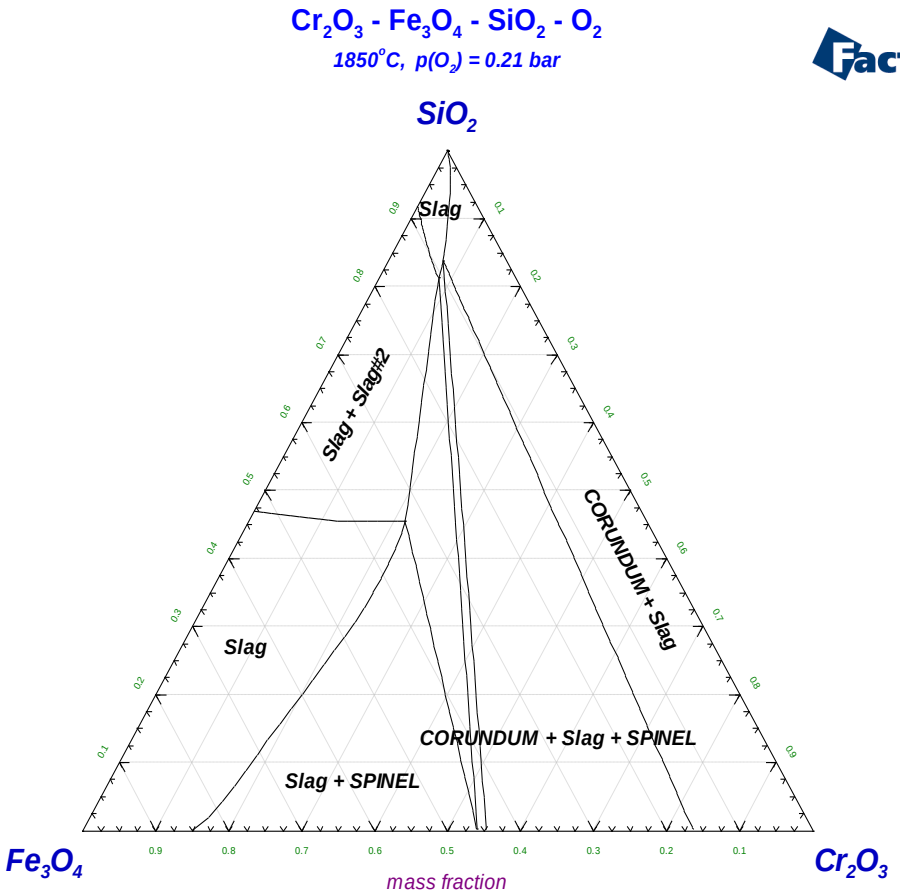

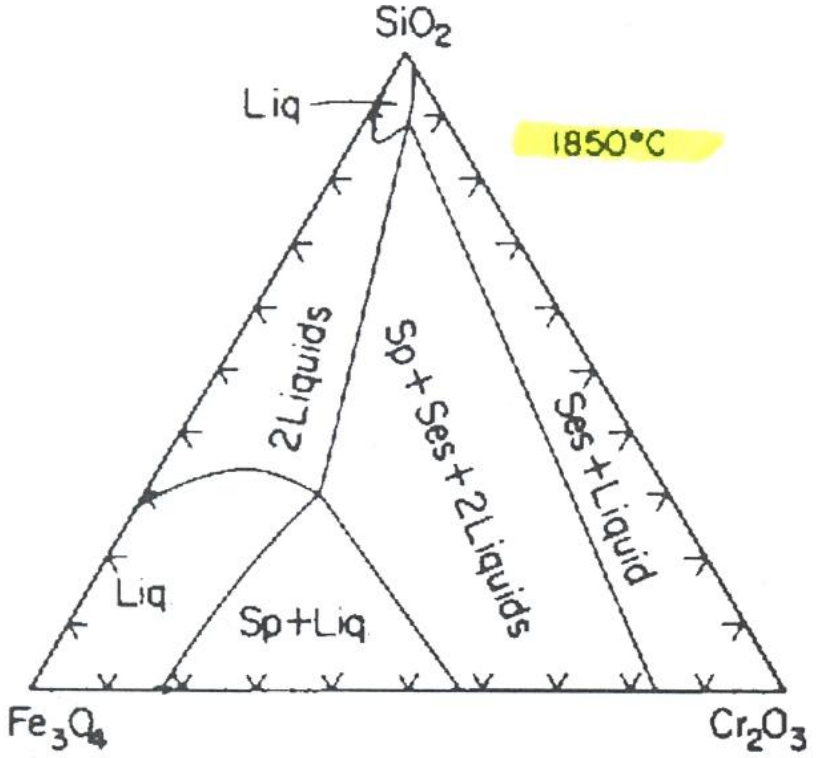

A. Muan and S. Somiya, Journal of Amer. Ceram. Soc., 43(1960), pp. 204-209.

Mole fraction
Isopleth K2CrO4-Na2CrO4

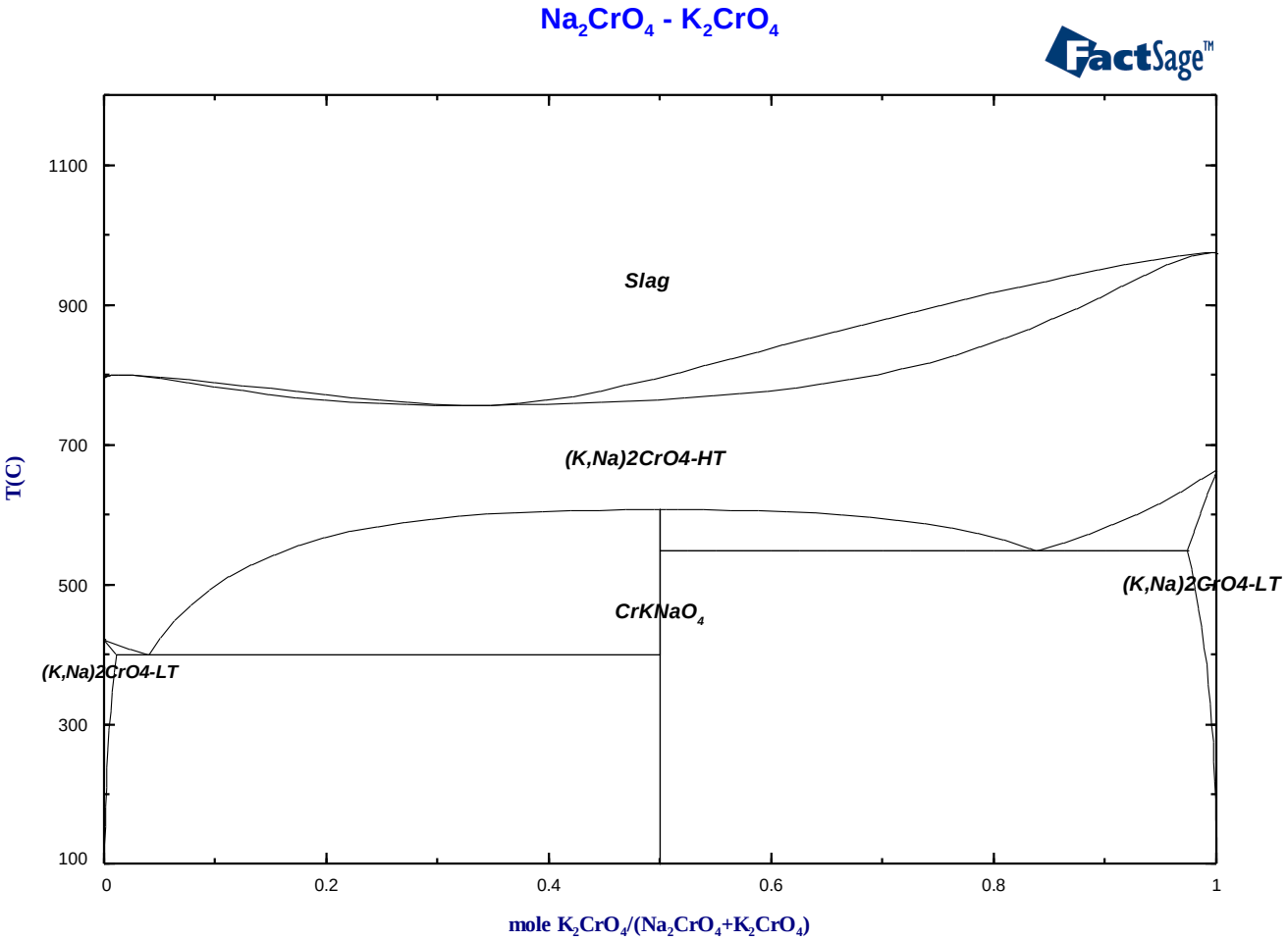

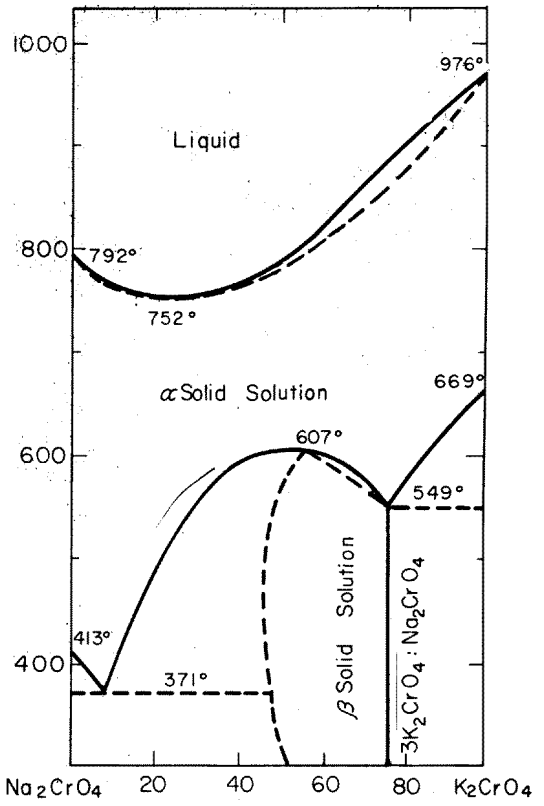

E. P. Dergunov and A. G. Bergman, Izv. Sekt. Fiz.-Khim. Anal., Inst. Obshch. Neorg. Khim., Akad. Nauk SSSR, 21, 184-198 (1952).

Mole fraction
Isopleth K2Cr2O7-Na2Cr2O7

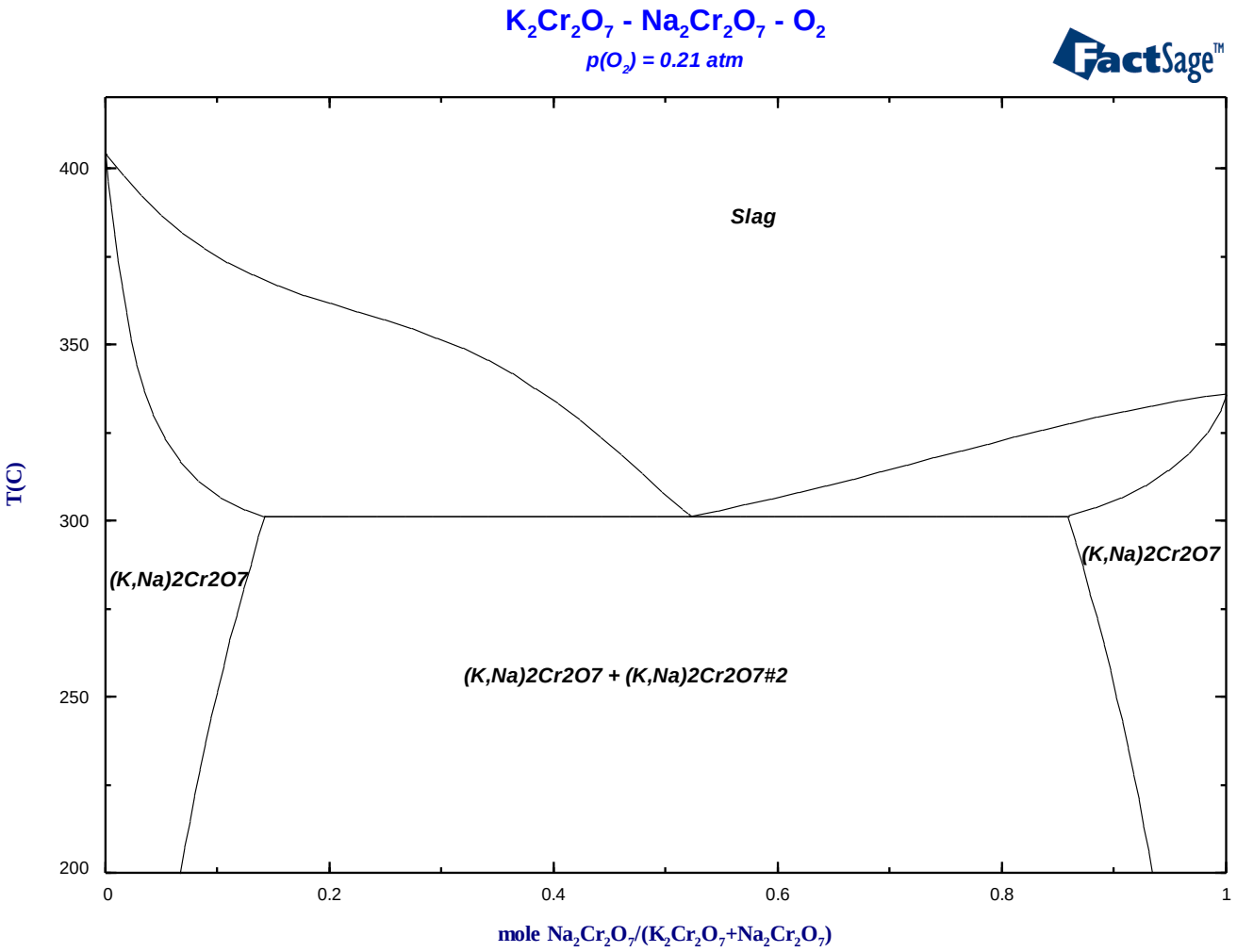

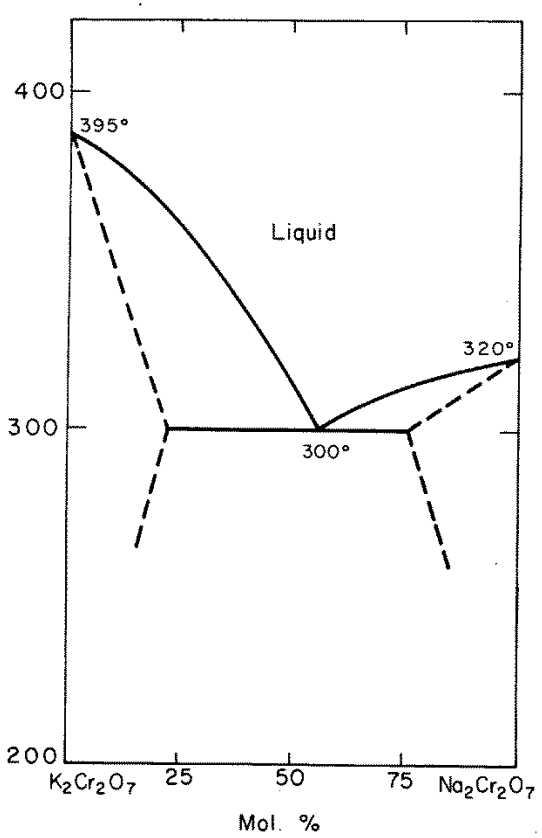

A. P. Palkin and I. M. Bokhovkin, Tr. Voronezh. Gos. Univ., 9 [3] 5-20 (1937).

Cr2O3-MgO-SiO2,
Weight percent 1540°C

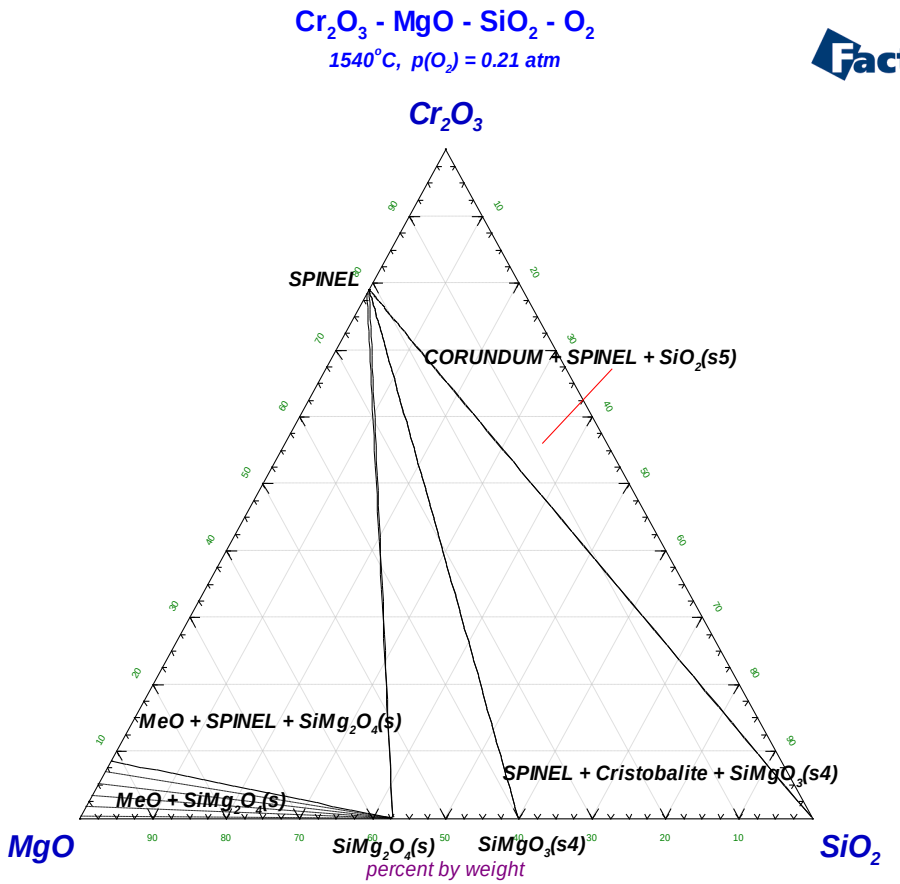

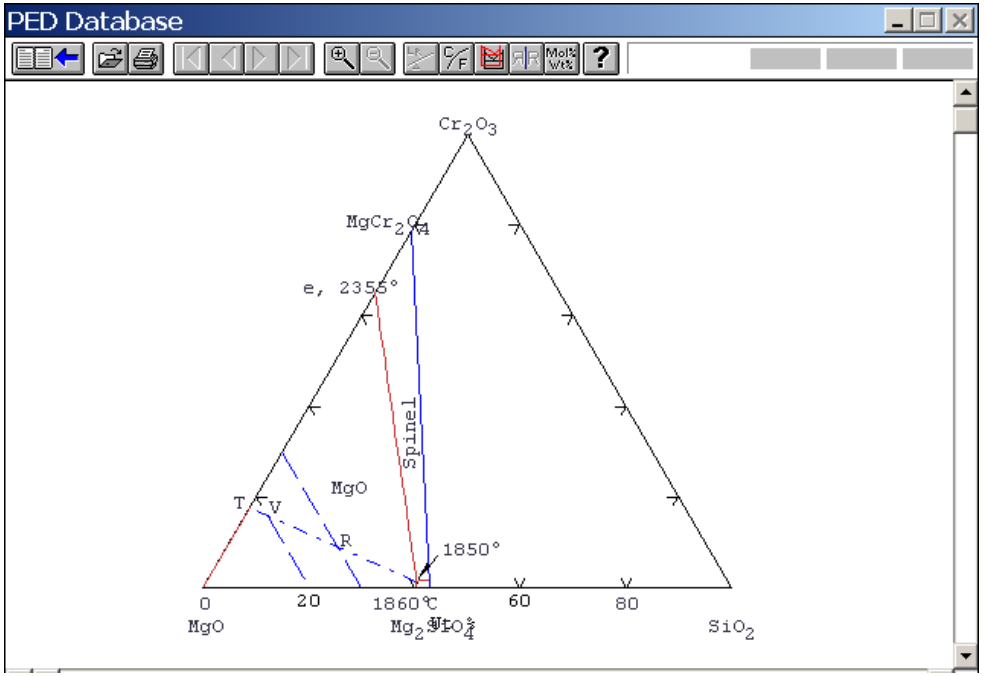

G. E. Goncalves, Thesis, Dept. of Ceramics, University of Sheffield, 1973.

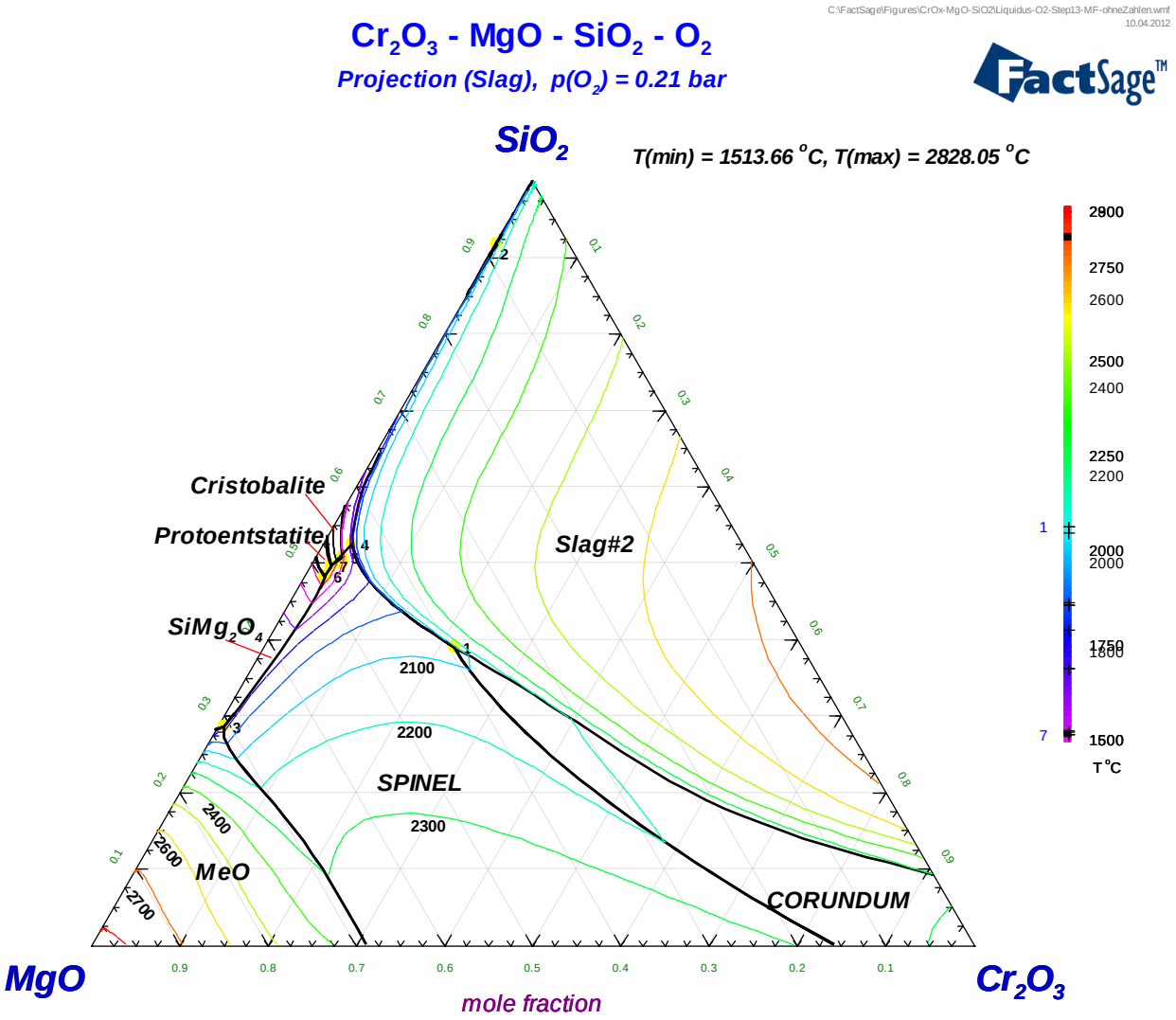
C:\FactSage\Figures\CrOx-MgO-SiO2\Liquidus-O2-Step13-MF-ohneZahlen.wmf
10.04.2012
Cr2O3 - MgO - SiO2 - O2
Projection (Slag), p(O2) = 0.21 bar
FactSage™
SiO2
T(min) = 1513.66 °C, T(max) = 2828.05 °C
Cristobalite
Protoentstatite
SiMg2O4
Slag#2
SPINEL
MeO
CORUNDUM
2100
2200
2300
2400
2600
2700
2900
2750
2600
2500
2400
2250
2200
2000
1750
1600
1500
T °C
MgO
Cr2O3
mole fraction

Weight percent
Liquidussurface

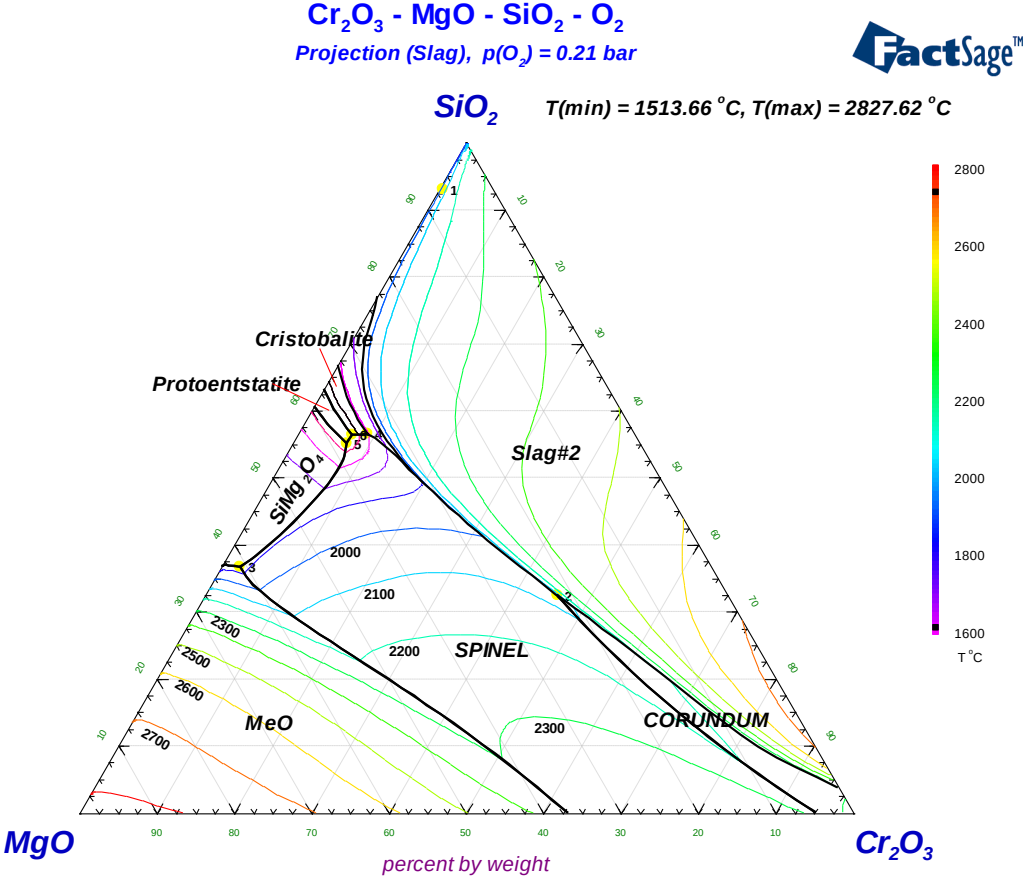

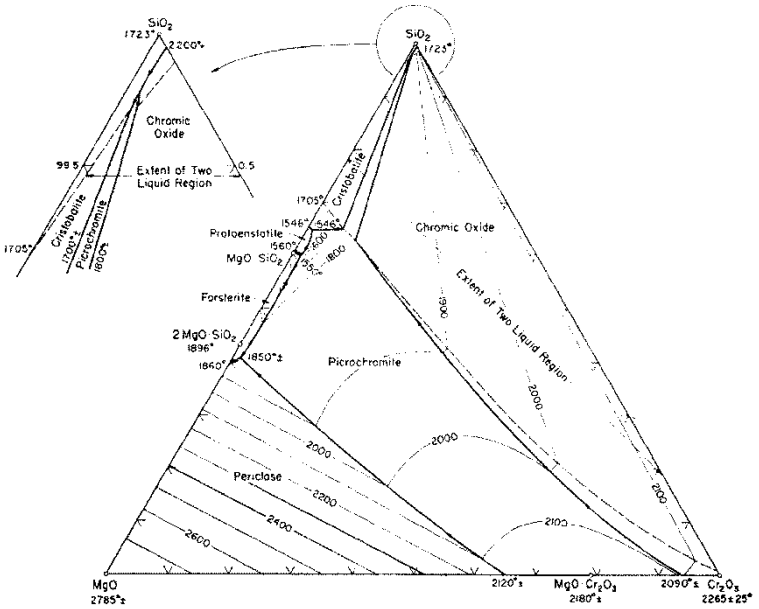

M. L. Keith, J. Am. Cream. Soc., 37 [10], (1954), pp.490-496.

Invariant equilibria on the liquidus surface

Intersections with slag	Mole fraction A = SiO2, B = MgO, C = Cr2O3				Weight percent A = SiO2, B = MgO, C = Cr2O3			
	X(A)	X(B)	X(C)	T(C)	W(A)	W(B)	W(C)	T(C)
1: CORANDUM / SPINEL / Slag#2	1: 0.38985	0.39395	0.21620	2064.98	1: 32.460	22.003	45.537	2064.98
2: CORANDUM / SPINEL / Slag#2	2: 0.90456	0.09361	0.00183	2064.98	2: 93.064	6.460	0.476	2064.98
3: MeO / SPINEL / SiMg2O4	3: 0.28568	0.70682	0.00750	1856.91	3: 36.682	60.880	2.437	1856.91
4: SPINEL / Cristobalite / Slag#2	4: 0.52473	0.44157	0.03370	1789.90	4: 57.906	32.687	9.407	1789.90
5: SPINEL / Cristobalite / Slag#2	5: 0.50671	0.46158	0.03170	1688.77	5: 56.519	34.536	8.945	1688.74
6: Protoentstatite / SPINEL / SiMg2O4	6: 0.48225	0.49383	0.02392	1522.04	6: 55.177	37.901	6.922	1522.03
7: Protoentstatite / SPINEL / Cristobalite	7: 0.49669	0.47912	0.02419	1513.66	7: 56.488	36.552	6.960	1513.66

CrO-MgO-SiO2,
Mole fraction 1300°C

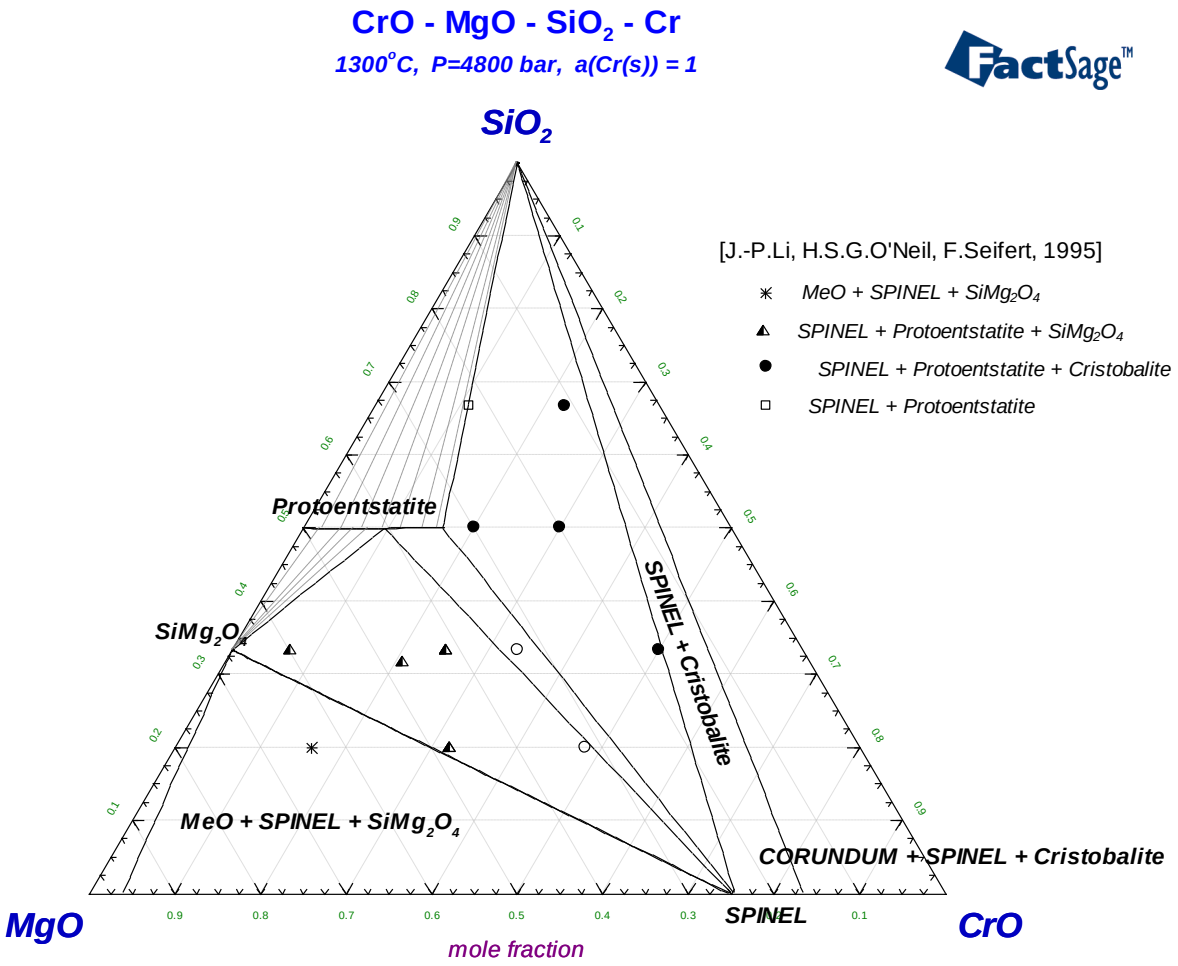

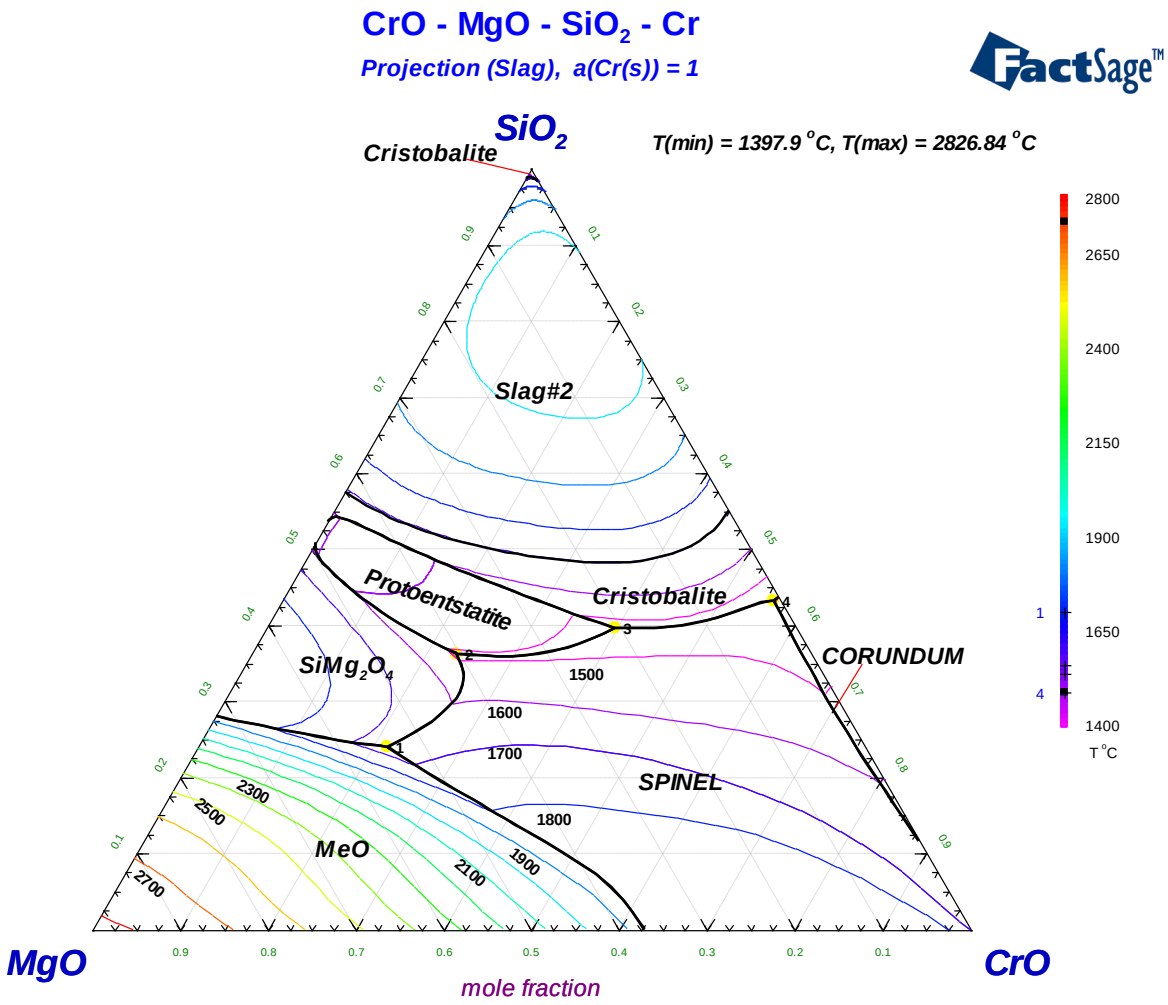
CrO - MgO - SiO2 - Cr
Projection (Slag), a(Cr(s)) = 1
FactSage™
SiO2
T(min) = 1397.9 °C, T(max) = 2826.84 °C
Cristobalite
Slag#2
Protoentstatite
Cristobalite
CORUNDUM
SiMg2O4
SPINEL
MeO
1500
1600
1700
1800
1900
2100
2300
2500
2700
1
2
3
4
2800
2650
2400
2150
1900
1650
1400
T °C
MgO
CrO
mole fraction

Weight percent
Liquidussurface

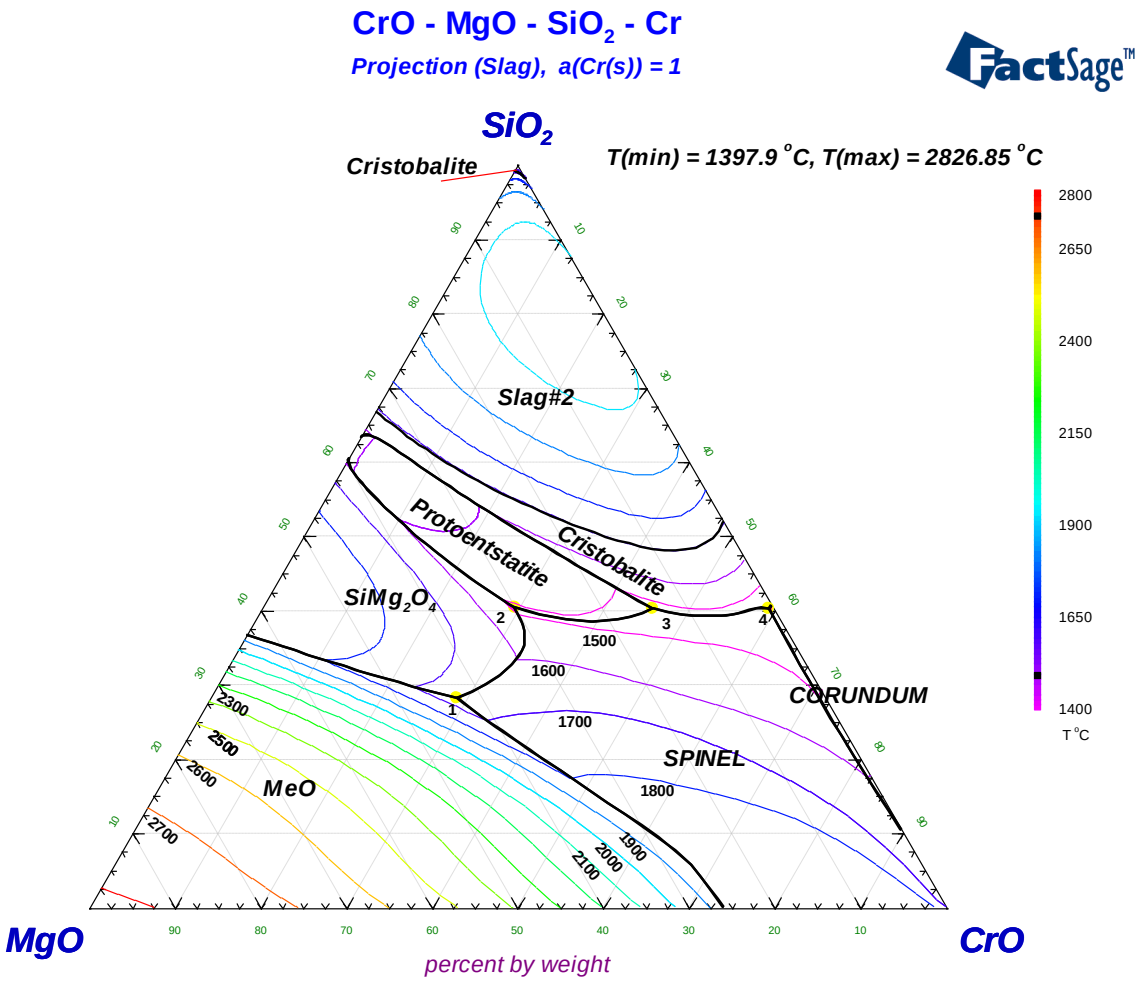

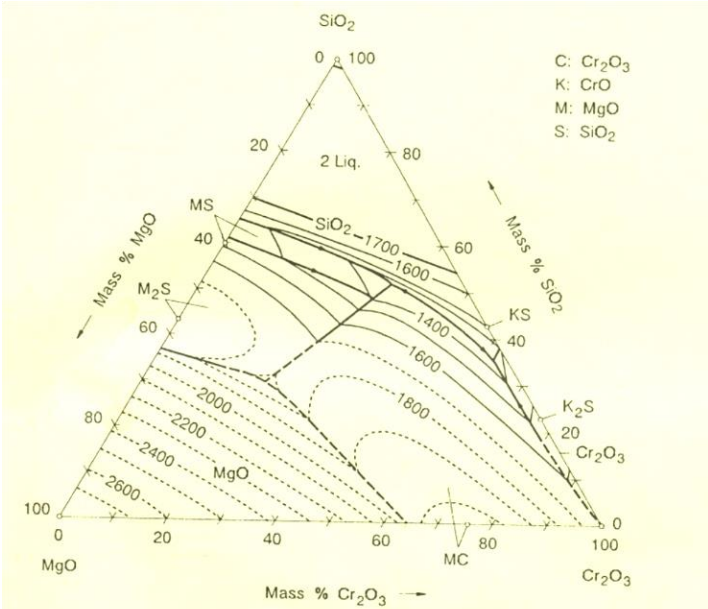

Fig. 3.269. Liquidus surface in the system Cr_2O_3-MgO-SiO_2 in contact with metallic chromium as reported by Muan [6] according to the results of Collins et al. [7].

M. L. Keith, J. Am. Cream. Soc., 37 [10], (1954), pp.490-496.

Invariant equilibria on the liquidus surface

Intersections with slag	Mole fraction A = SiO2, B = MgO, C = CrO				Weight percent A = SiO2, B = MgO, C = CrO			
	X(A)	X(B)	X(C)	T(C)	W(A)	W(B)	W(C)	T(C)
1: MeO / SPINEL / SiMg2O4	0.24040	0.54388	0.21571	1644.09	28.304	42.954	28.741	1644.10
2: Protoentstatite / SPINEL / SiMg2O4	0.36318	0.40371	0.23311	1482.82	40.453	30.163	29.384	1482.81
3: Protoentstatite / SPINEL / Cristobalite	0.39691	0.20635	0.39674	1456.63	40.324	14.063	45.614	1456.63
4: CORANDUM / SPINEL / Cristobalite	0.43165	0.00796	0.56039	1397.90	40.297	0.499	59.204	1397.90

Fe-Mn-S,
Mole fraction 800°C

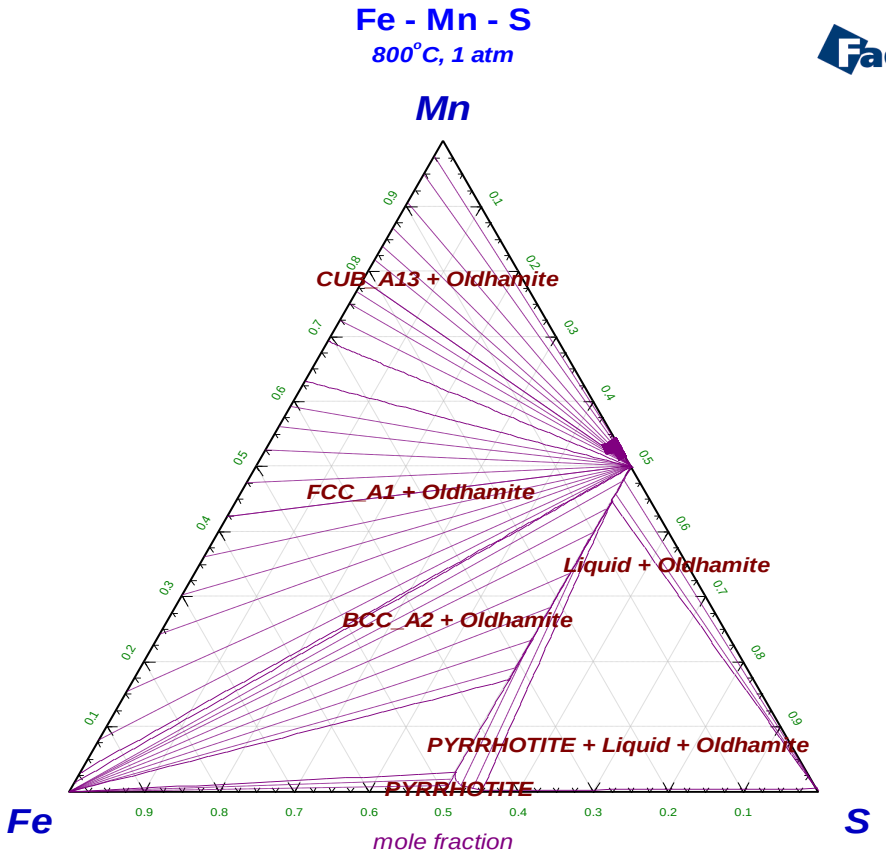

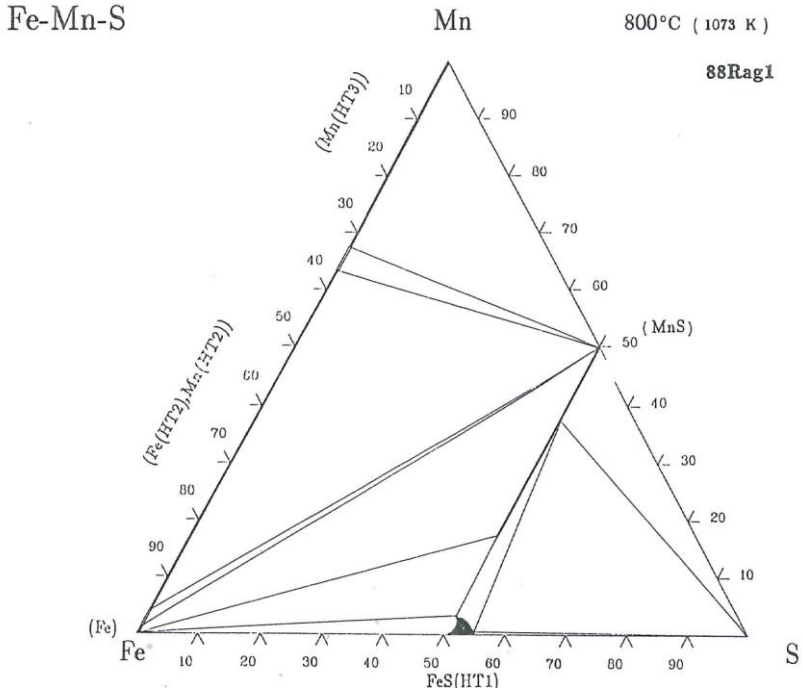

V. Raghavan, D.P. Antia, J. Alloy Phase Diagrams, India, 4[1], (1988), pp. 16-36.

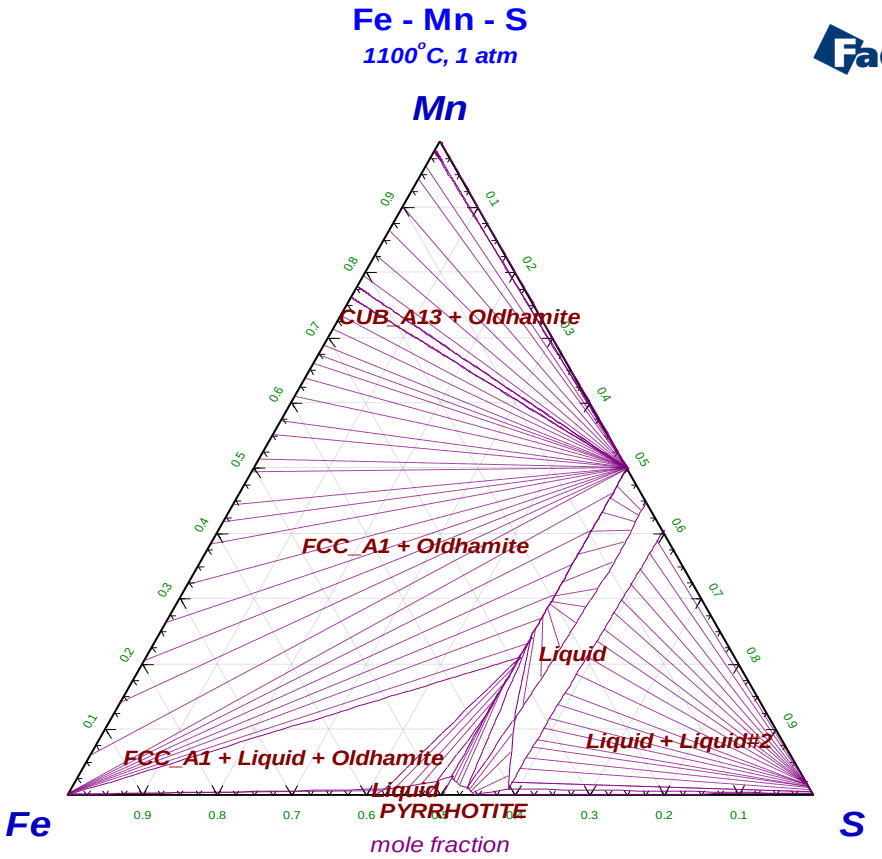

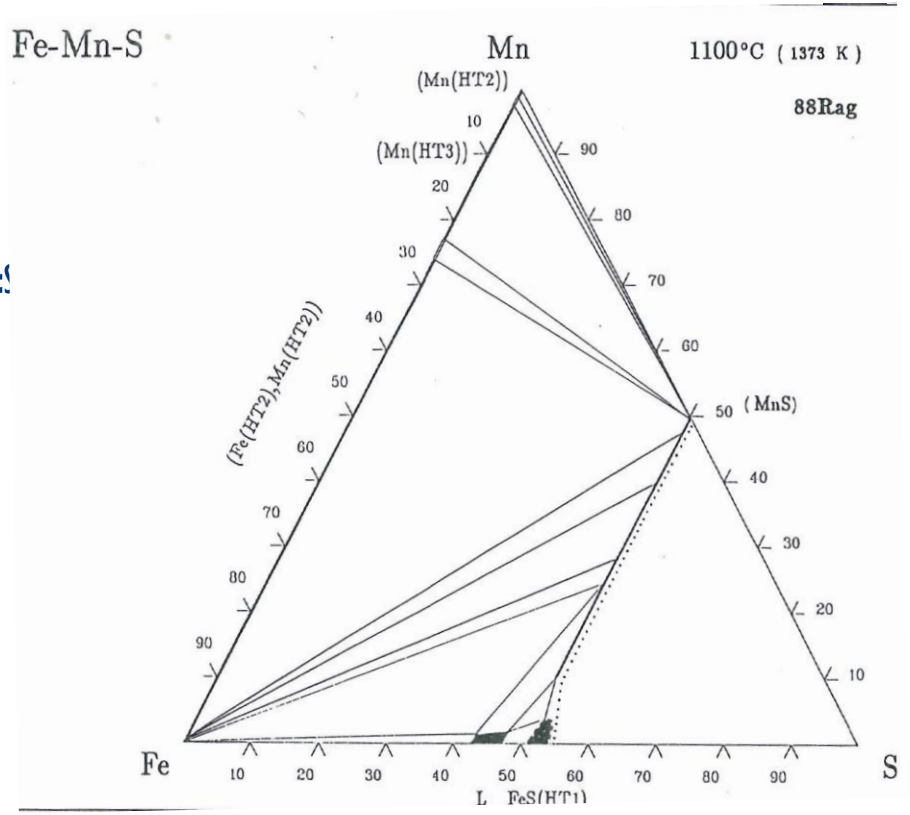

V. Raghavan, Phase Diagrams of Ternary Iron Alloys, The Indian Institute of Metals, Calcutta, India [2], (1988), pp. 154-173.

Weight fraction

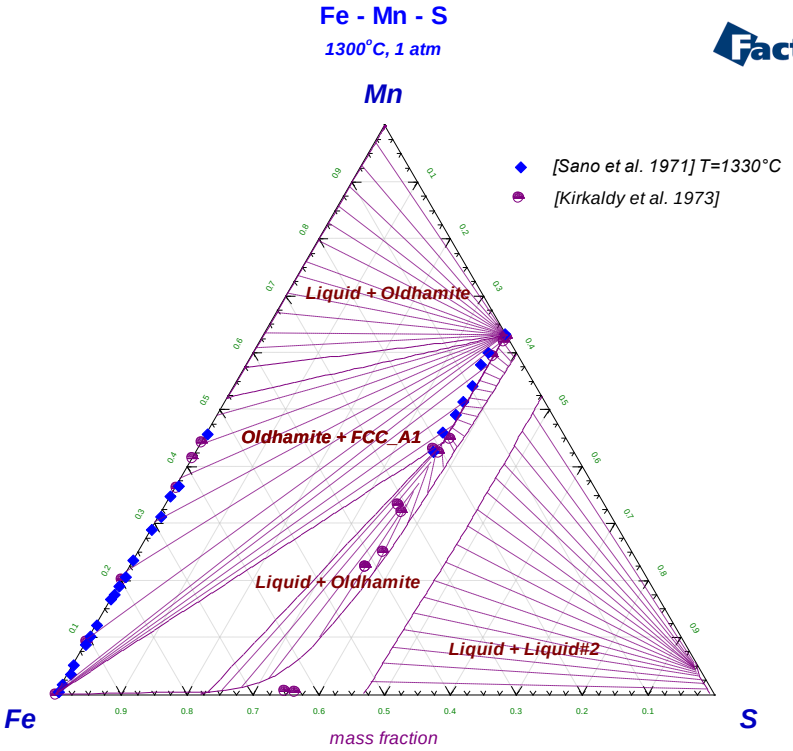

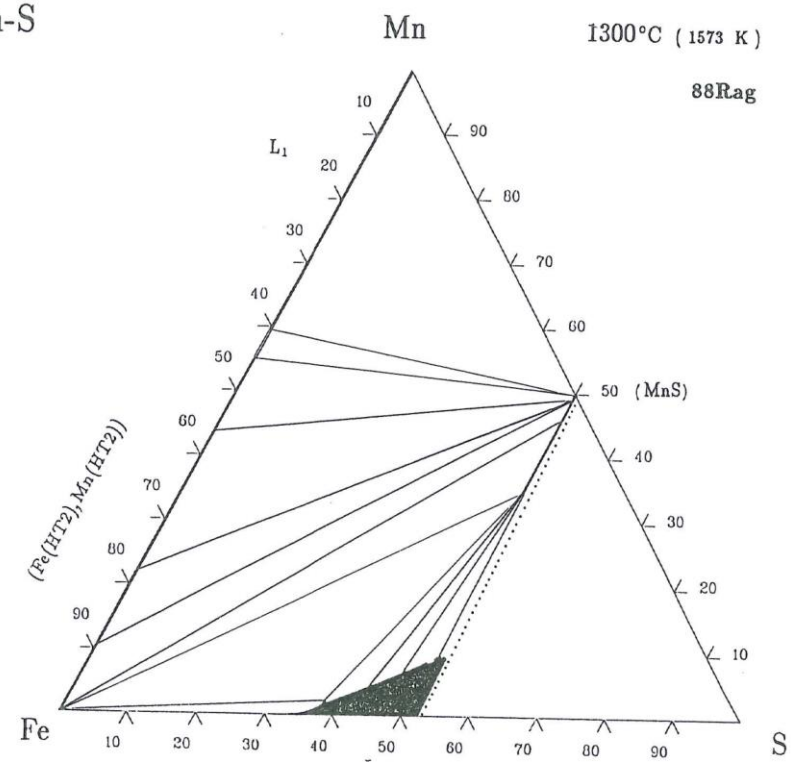

V. Raghavan, Phase Diagrams of Ternary Iron Alloys, The Indian Institute of Metals, Calcutta, India [2], (1988), pp. 154-173.

Weight fraction

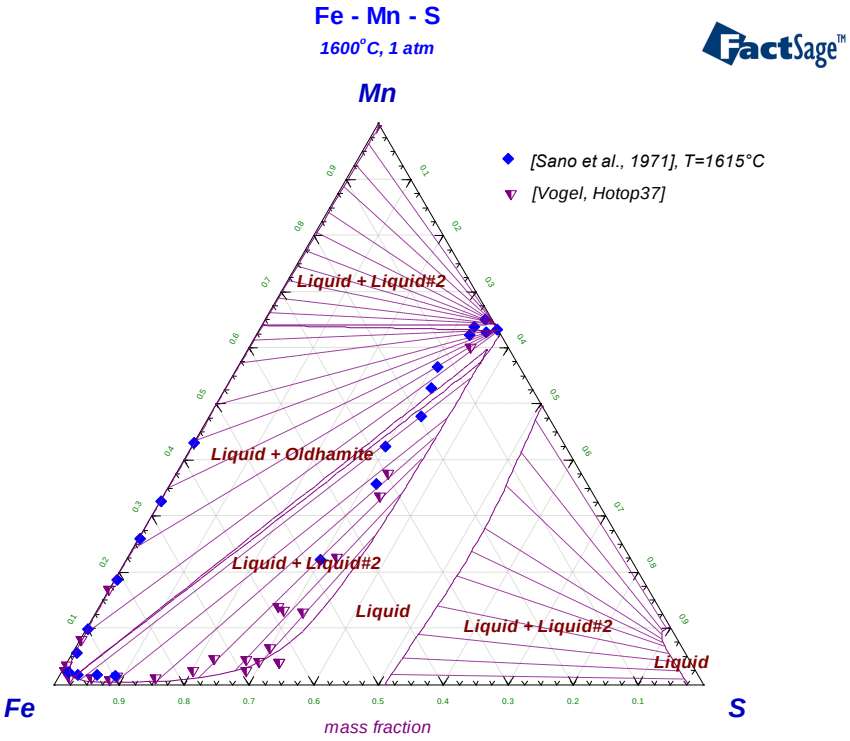

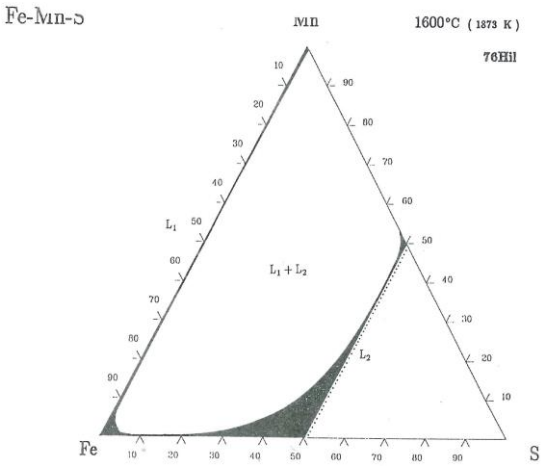

M. Hillert, L.-I. Staffansson, Metallurg. Transact., Section B: Process Metallurgy, 7B, (1976), pp. 203-211.

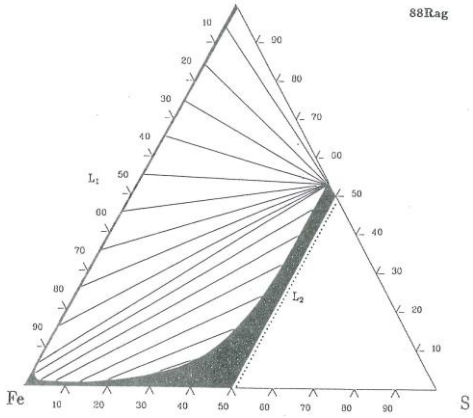

V. Raghavan, Phase Diagrams of Ternary Iron Alloys, The Indian Institute of Metals, Calcutta, India [2], (1988), pp. 154-173.

Weight fraction 1600°C, solubility of Mn and S in Fe-rich liquid

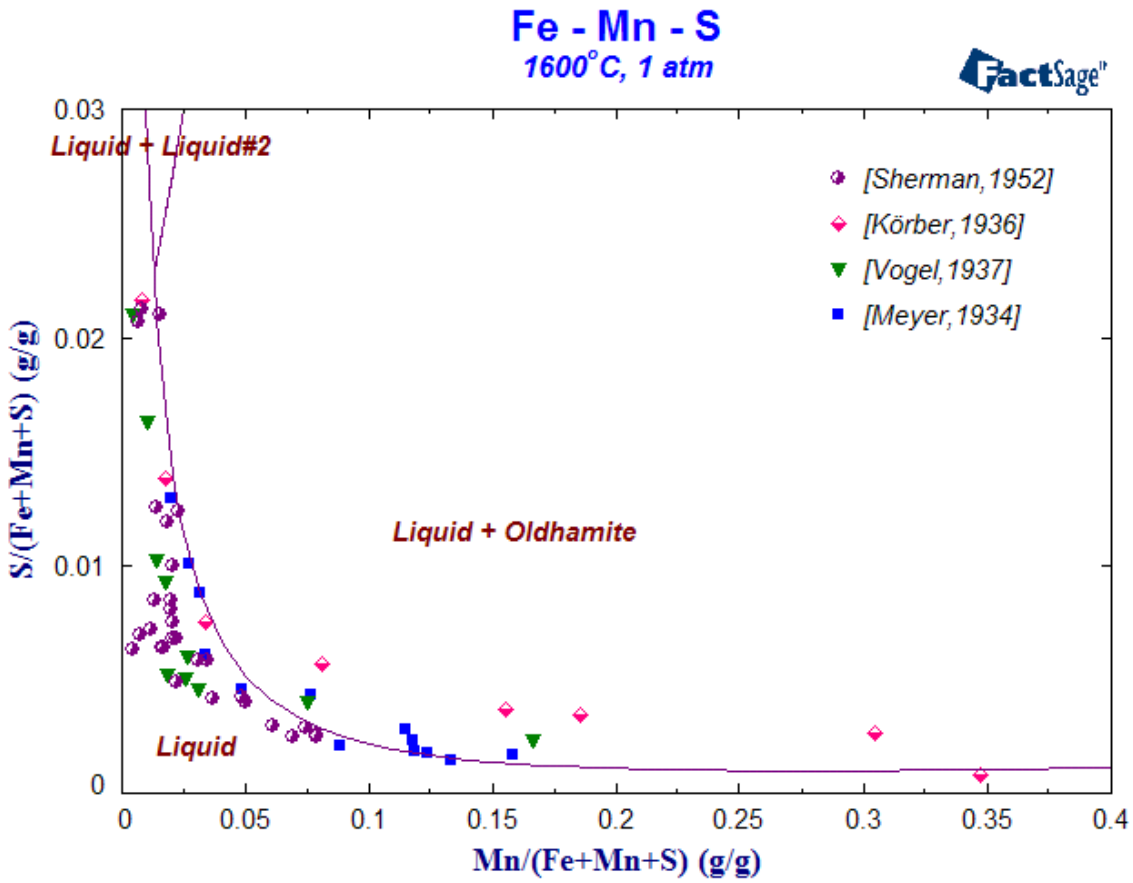

Weight fraction, isopleth section Fe/Mn=97/3

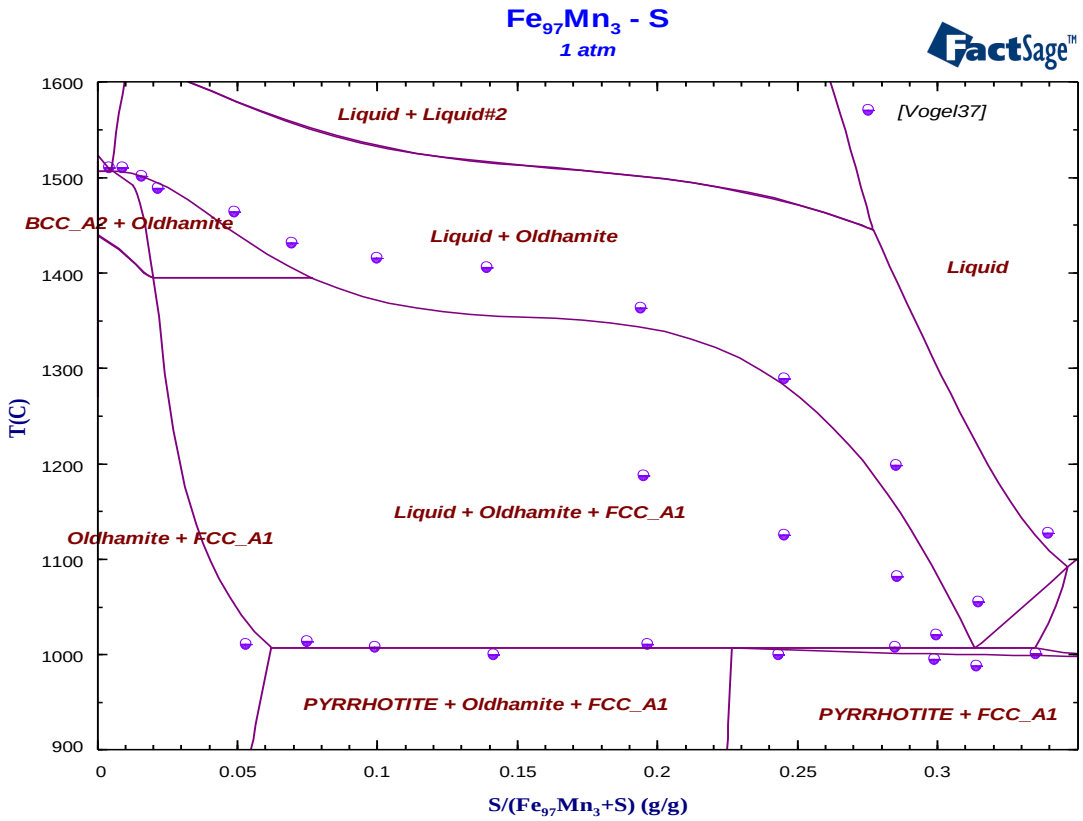

Mole fraction 1100°C, relationship between S potential and Mn fraction

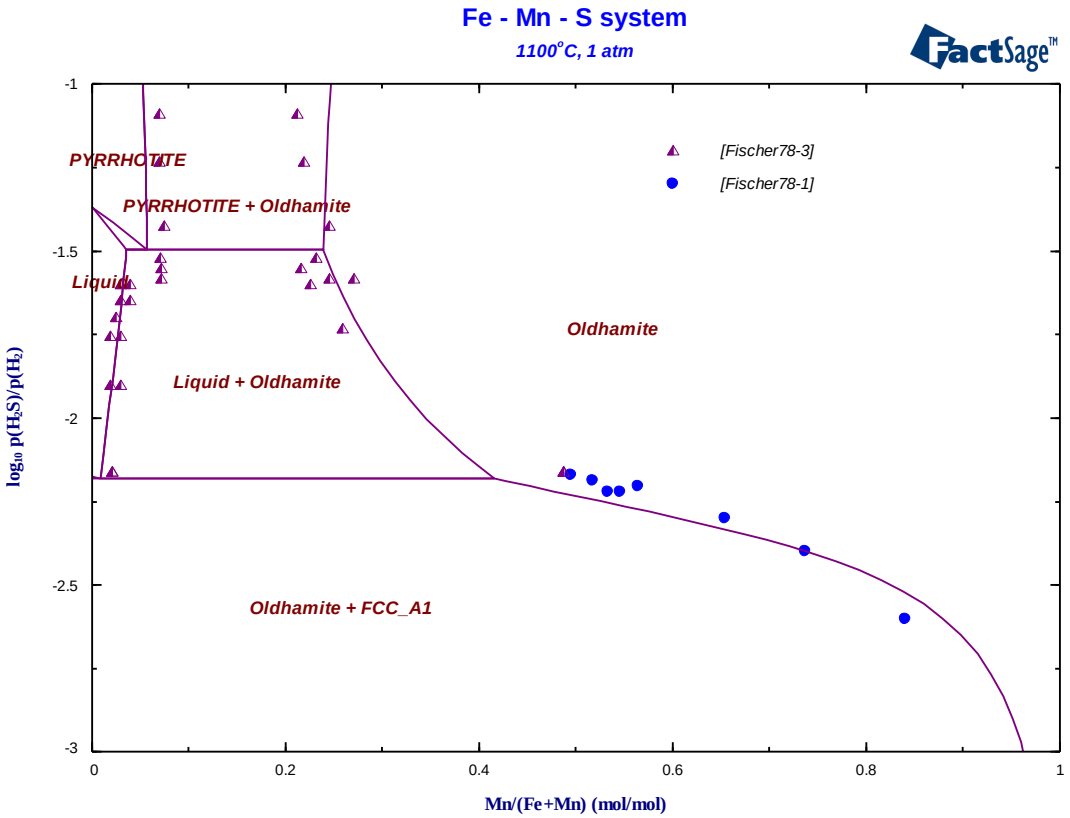

Fe-Ni-S,
Weight percent 550°C

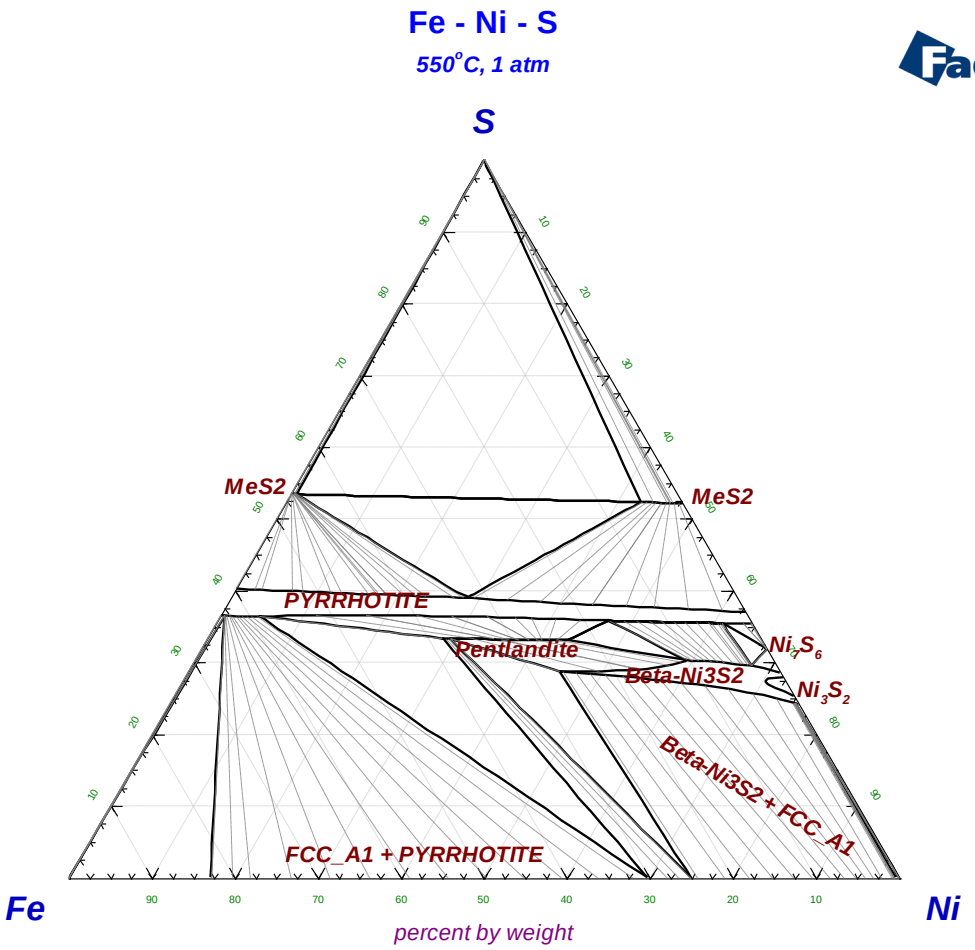

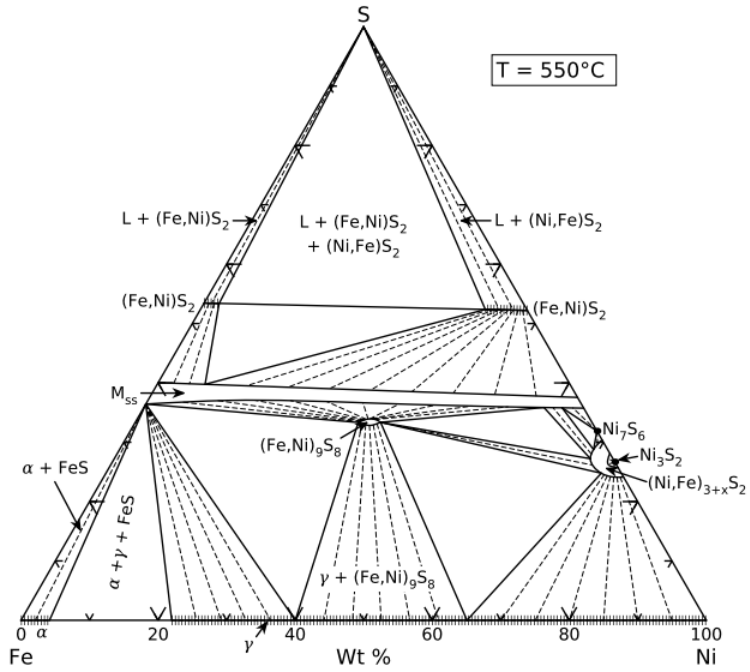

G. Kullerud, R. A. Yund, G. H. Moh, "Phase Relations in the Cu-Fe-S, Cu-Ni-S, and Fe-Ni-S Systems"; pp. 323-343 in Magmat. Ore Deposits, Symp., Stanford University, Stanford, California, November 12-13, 1966. Edited by H. D. B. Wilson, The Economic Geology Publishing Company, Mount Pleasant, Michigan, 1969.

Fe-Ni-S,
Weight percent 650°C

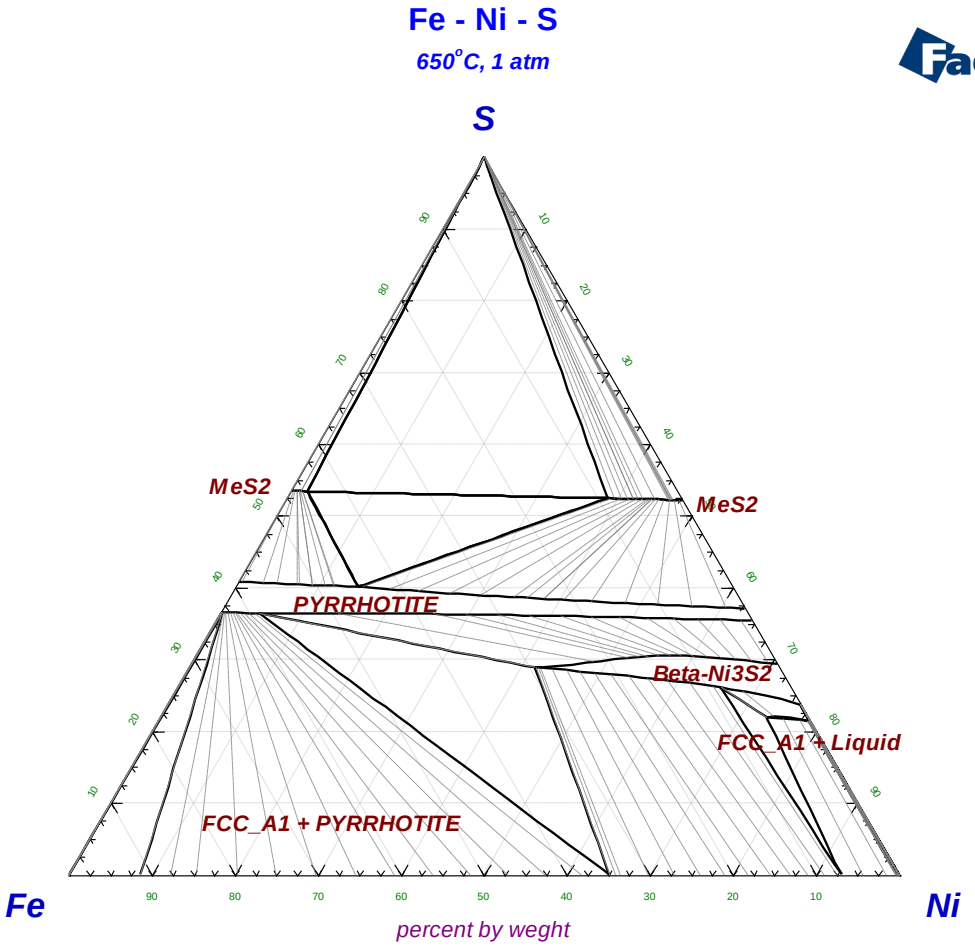

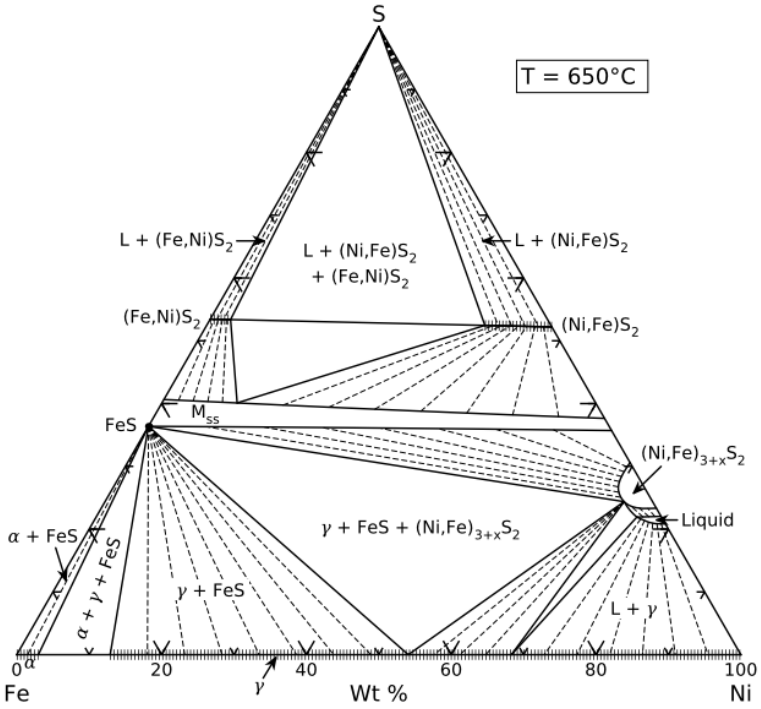

G. Kullerud, R. A. Yund, G. H. Moh, "Phase Relations in the Cu-Fe-S, Cu-Ni-S, and Fe-Ni-S Systems"; pp. 323-343 in Magmat. Ore Deposits, Symp., Stanford University, Stanford, California, November 12-13, 1966. Edited by H. D. B. Wilson, The Economic Geology Publishing Company, Mount Pleasant, Michigan, 1969.

Fe-Ni-S,
Weight percent 900°C

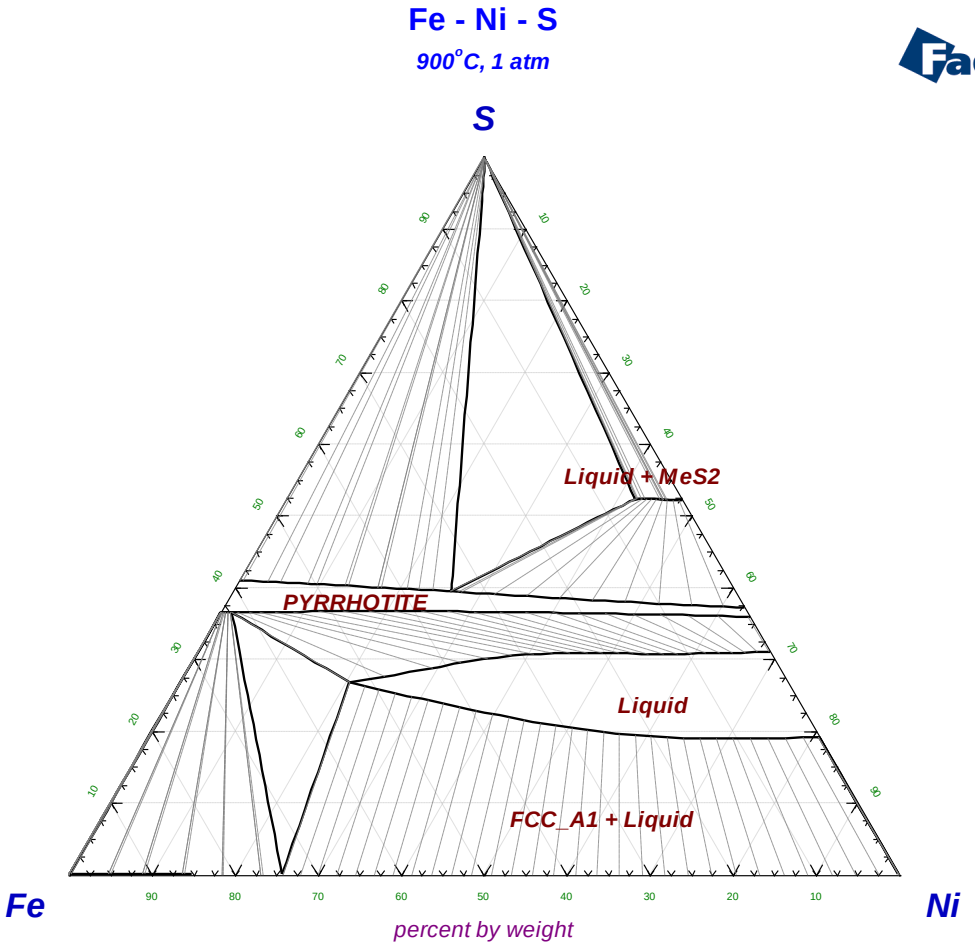

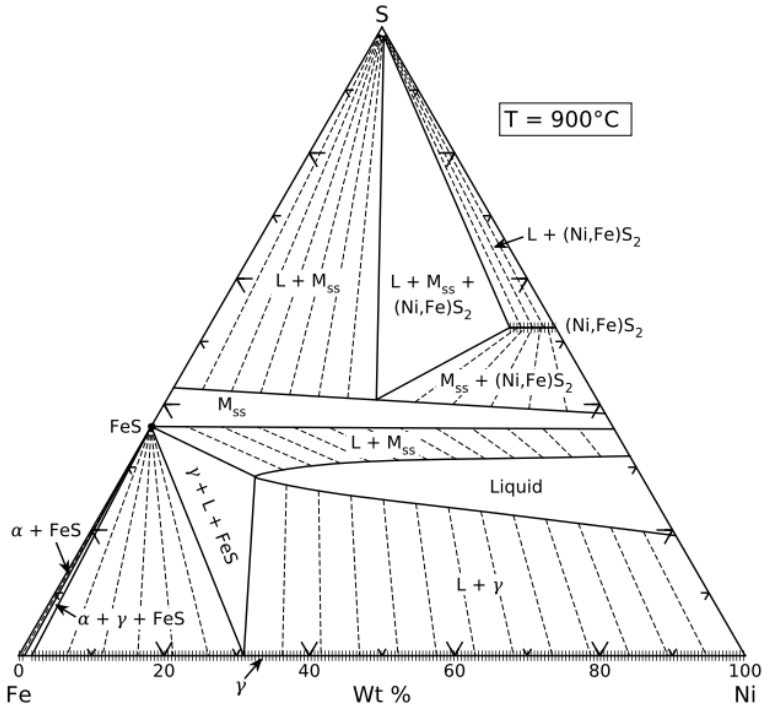

G. Kullerud, R. A. Yund, G. H. Moh, "Phase Relations in the Cu-Fe-S, Cu-Ni-S, and Fe-Ni-S Systems"; pp. 323-343 in Magmat. Ore Deposits, Symp., Stanford University, Stanford, California, November 12-13, 1966. Edited by H. D. B. Wilson, The Economic Geology Publishing Company, Mount Pleasant, Michigan, 1969.

Fe-Ni-S,
Weight percent 1100°C

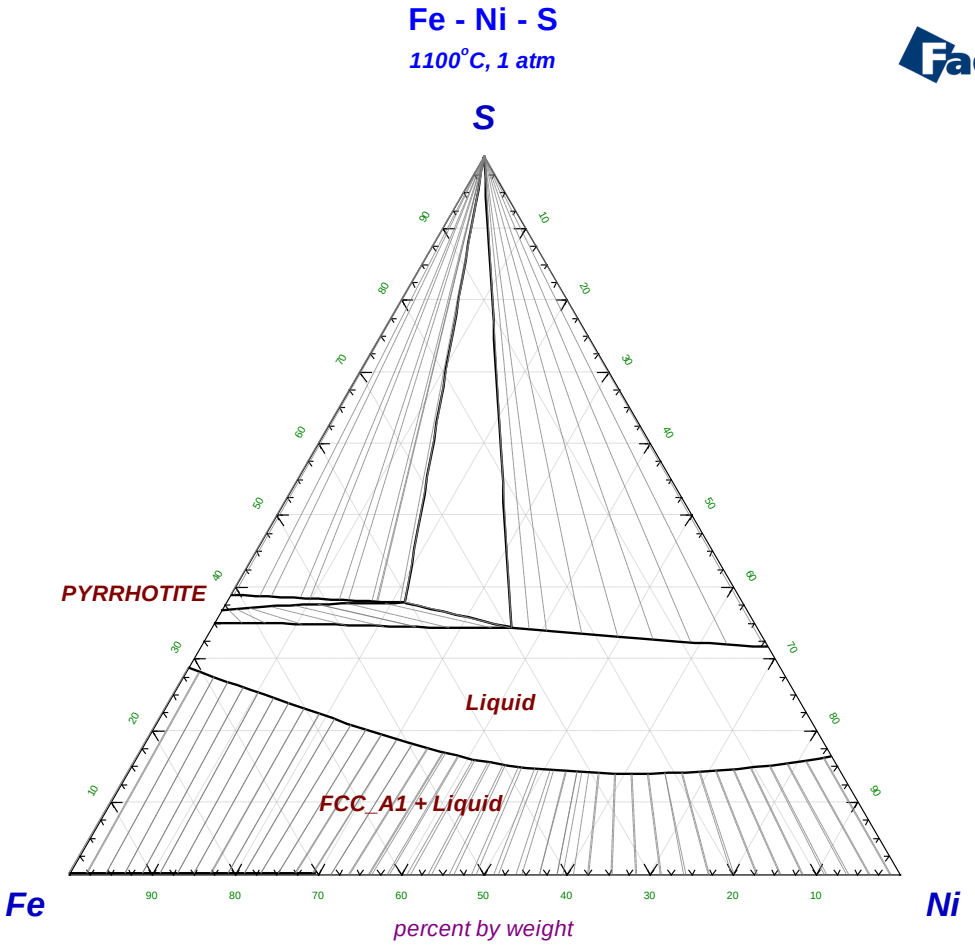

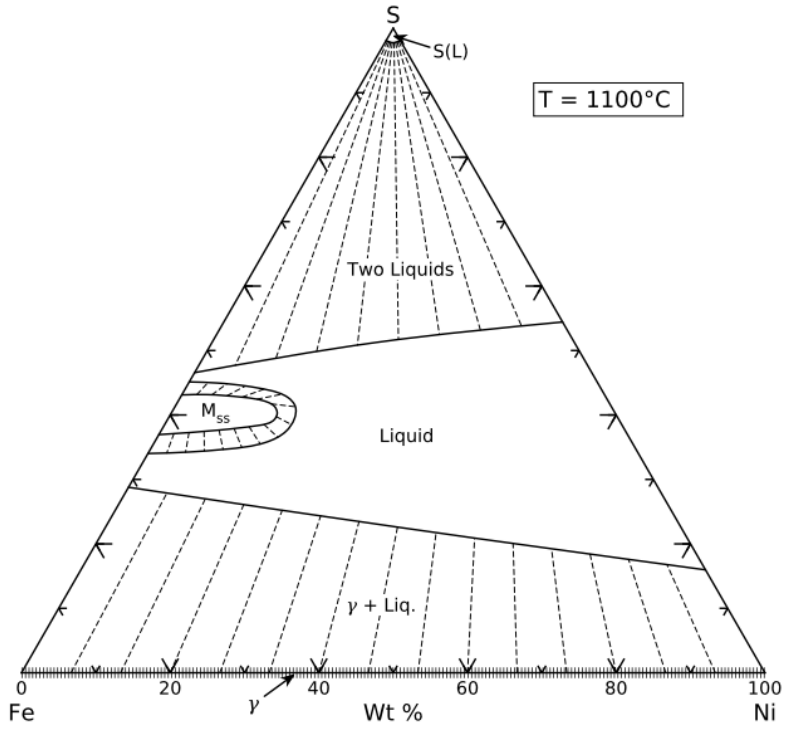

G. Kullerud, R. A. Yund, G. H. Moh, "Phase Relations in the Cu-Fe-S, Cu-Ni-S, and Fe-Ni-S Systems"; pp. 323-343 in Magmat. Ore Deposits, Symp., Stanford University, Stanford, California, November 12-13, 1966. Edited by H. D. B. Wilson, The Economic Geology Publishing Company, Mount Pleasant, Michigan, 1969.

Fe-Ni-S,
Weight percent, Isopleth FeS2-NiS2

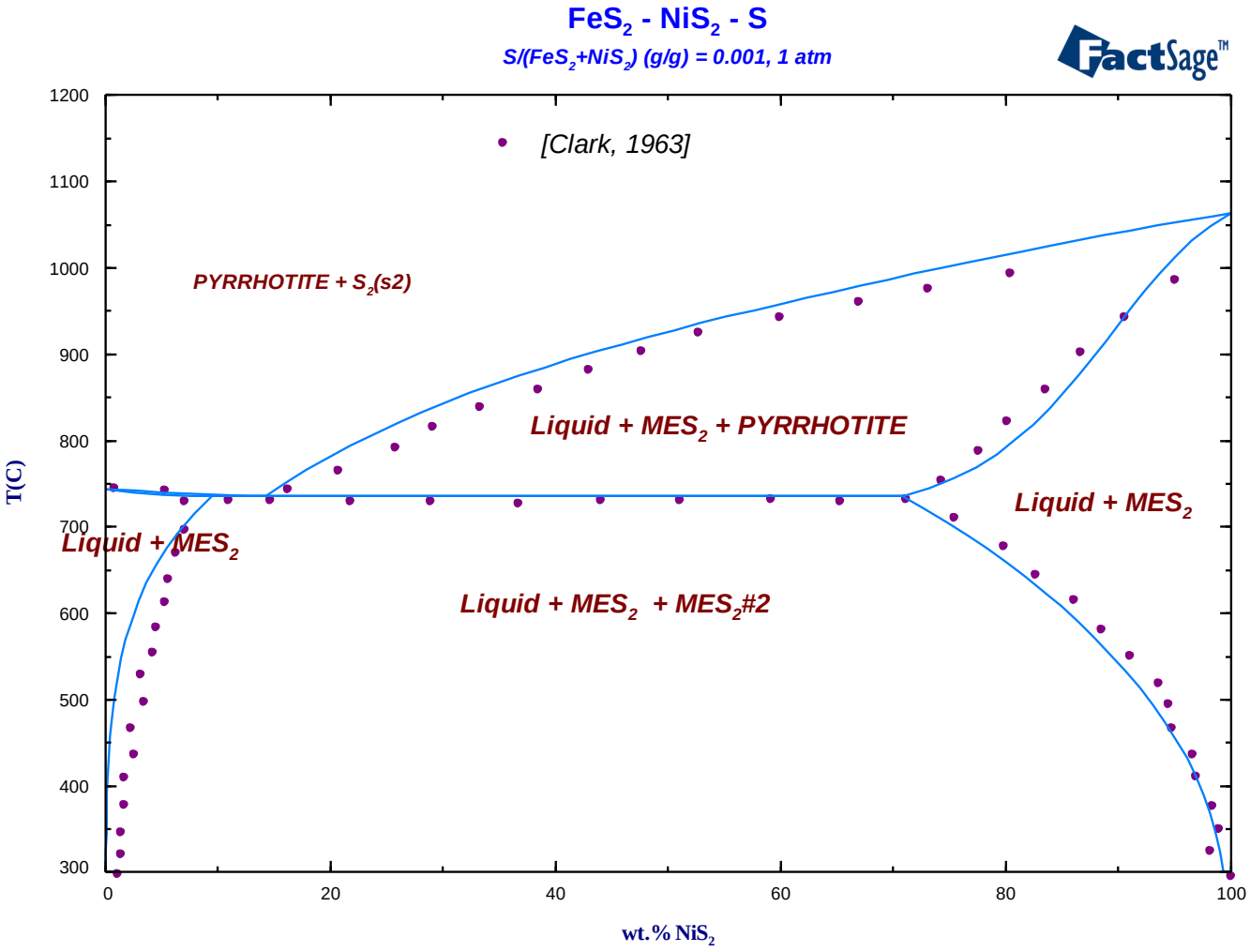

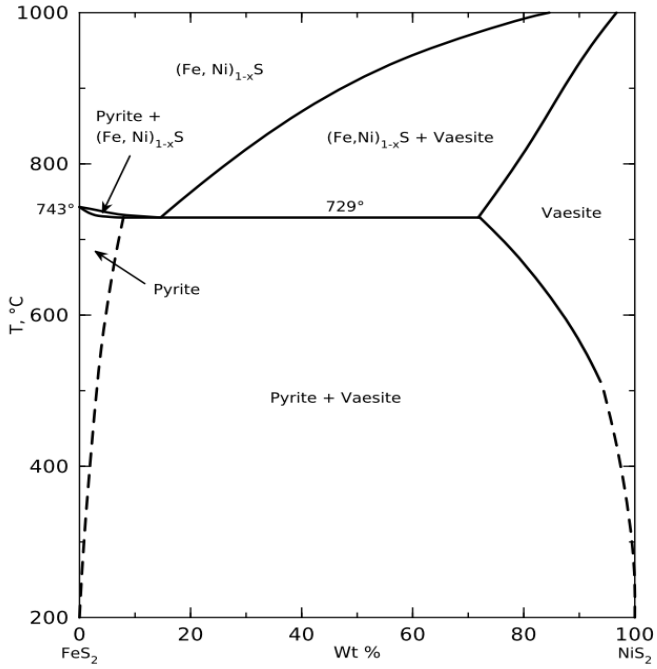

L. A. Clark, Econ. Geol., 58 [6] 853-885 (1963).

Fe-O-S,
Mole fraction, Liquidus lines at 1000°-1500°C

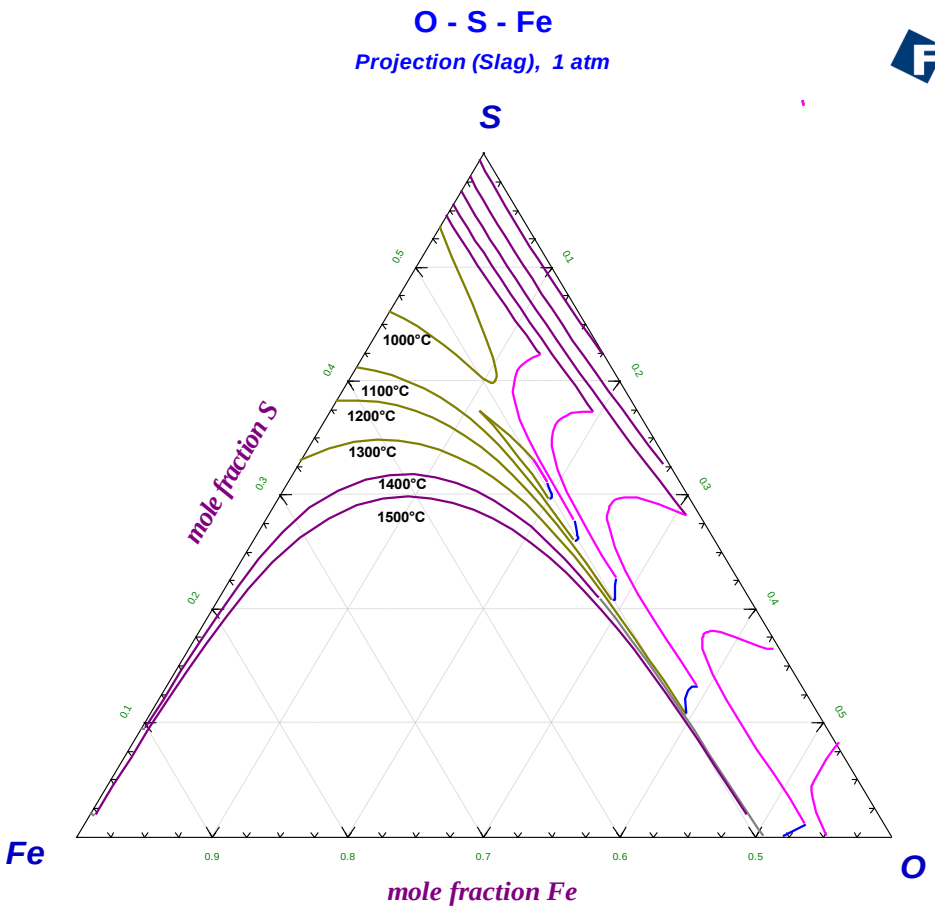

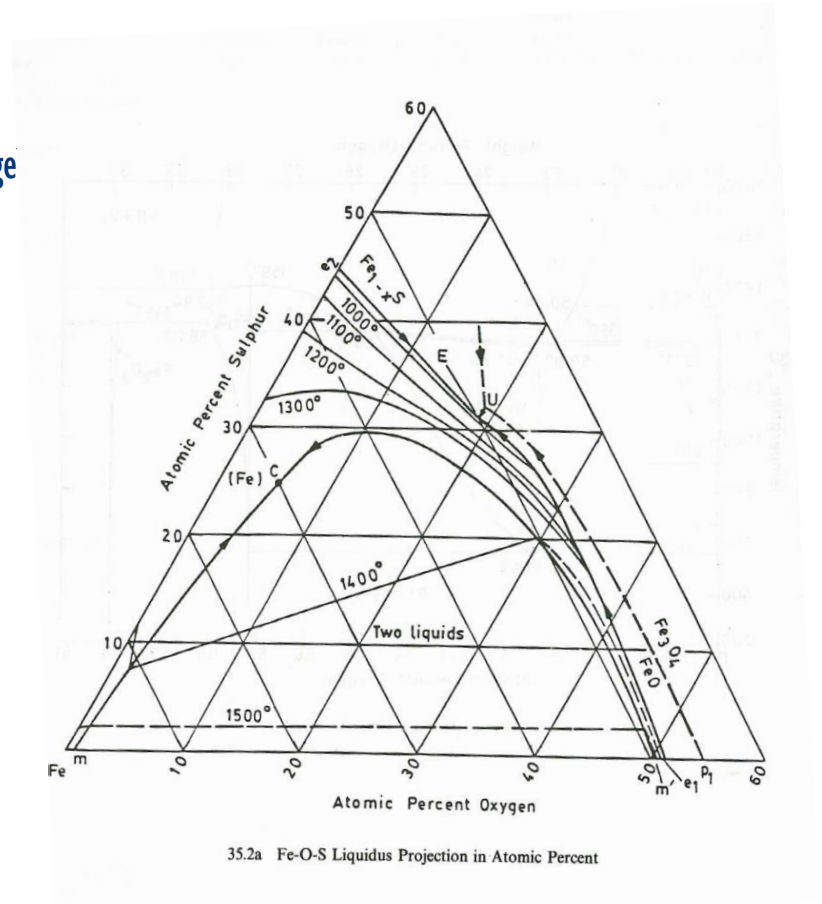

35.2a Fe-O-S Liquidus Projection in Atomic Percent

V. Raghavan, Phase diagrams of Ternary Iron Alloys, Part 2, Ternary systems containing Iron and Sulphur, The Indian Institute of Metals, Calcutta,1988.

Fe-O-S,
Mole fraction, 1324°C

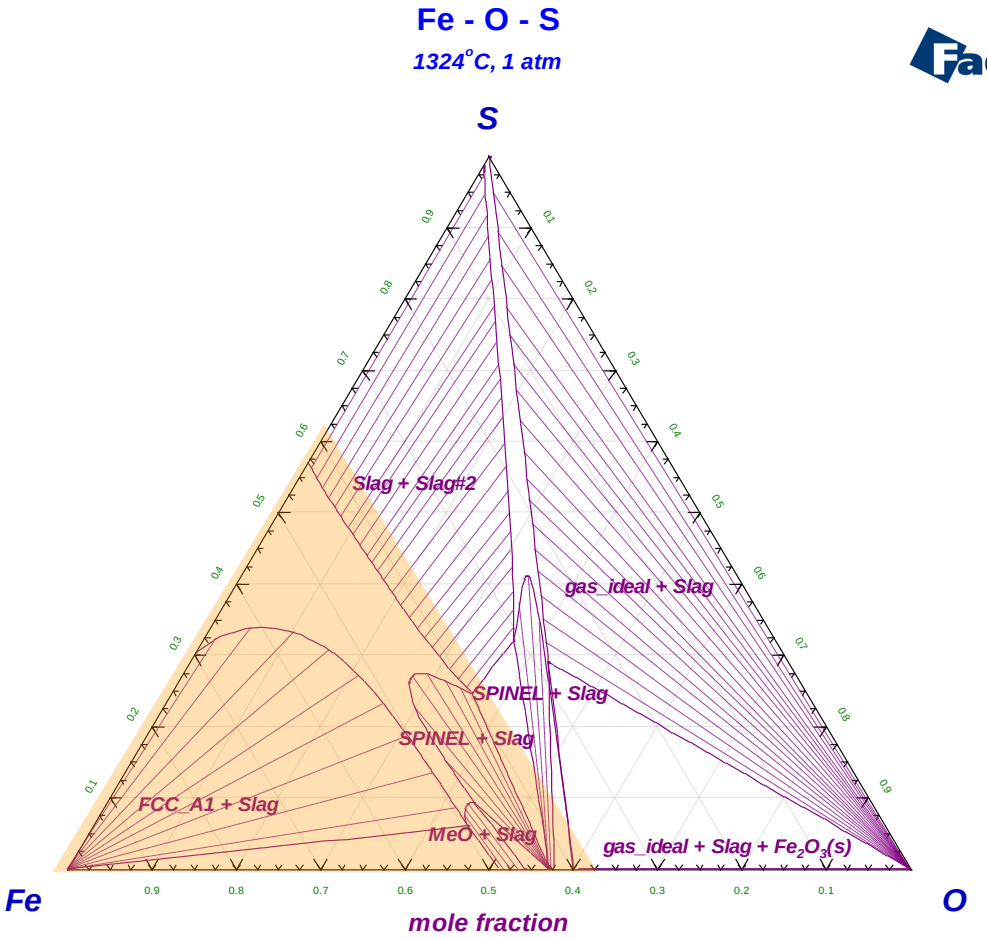

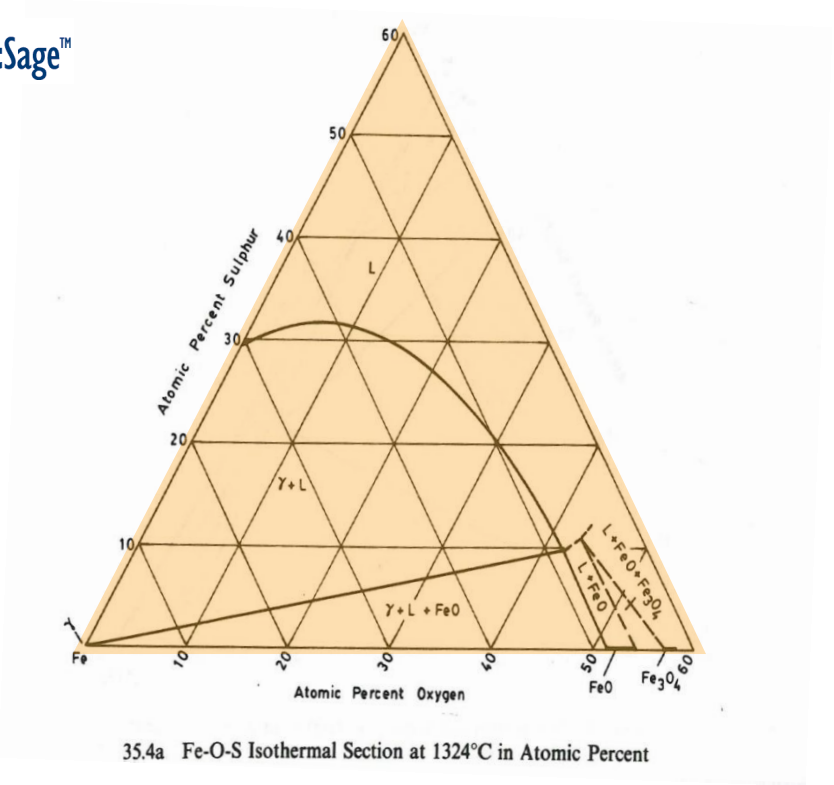

35.4a Fe-O-S Isothermal Section at 1324°C in Atomic Percent

V. Raghavan, Phase diagrams of Ternary Iron Alloys, Part 2, Ternary systems containing Iron and Sulphur, The Indian Institute of Metals, Calcutta,1988.

Fe-O-S,
Mole fraction, 1100°C

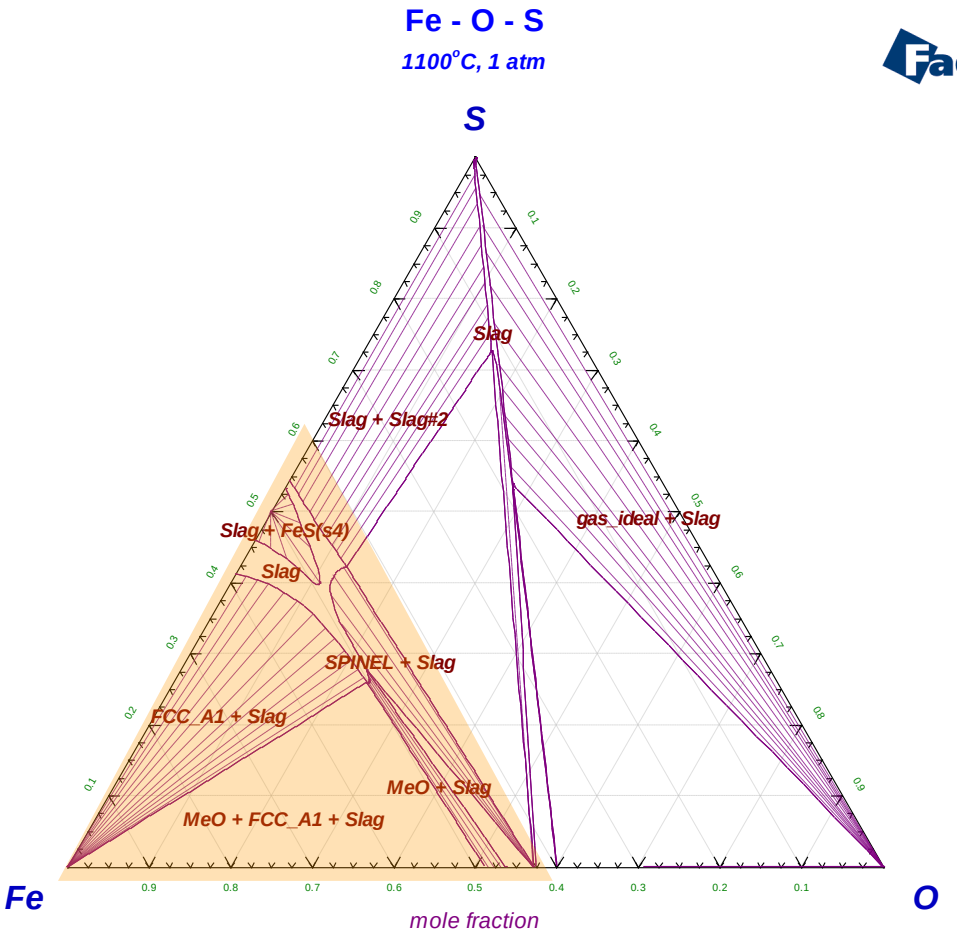

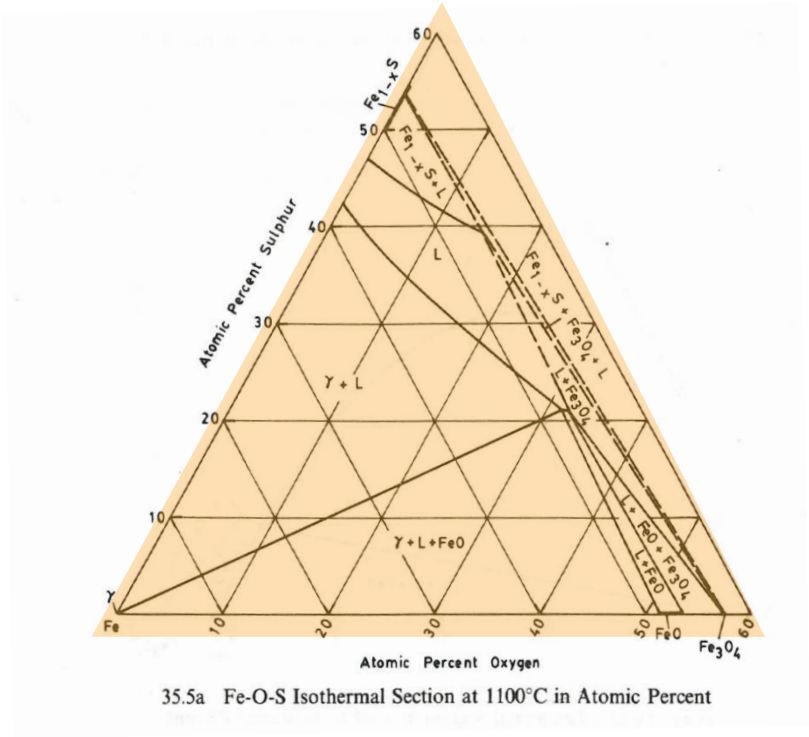

35.5a Fe-O-S Isothermal Section at 1100°C in Atomic Percent

V. Raghavan, Phase diagrams of Ternary Iron Alloys, Part 2, Ternary systems containing Iron and Sulphur, The Indian Institute of Metals, Calcutta,1988.

Fe-O-S,
Mole fraction, 900°C

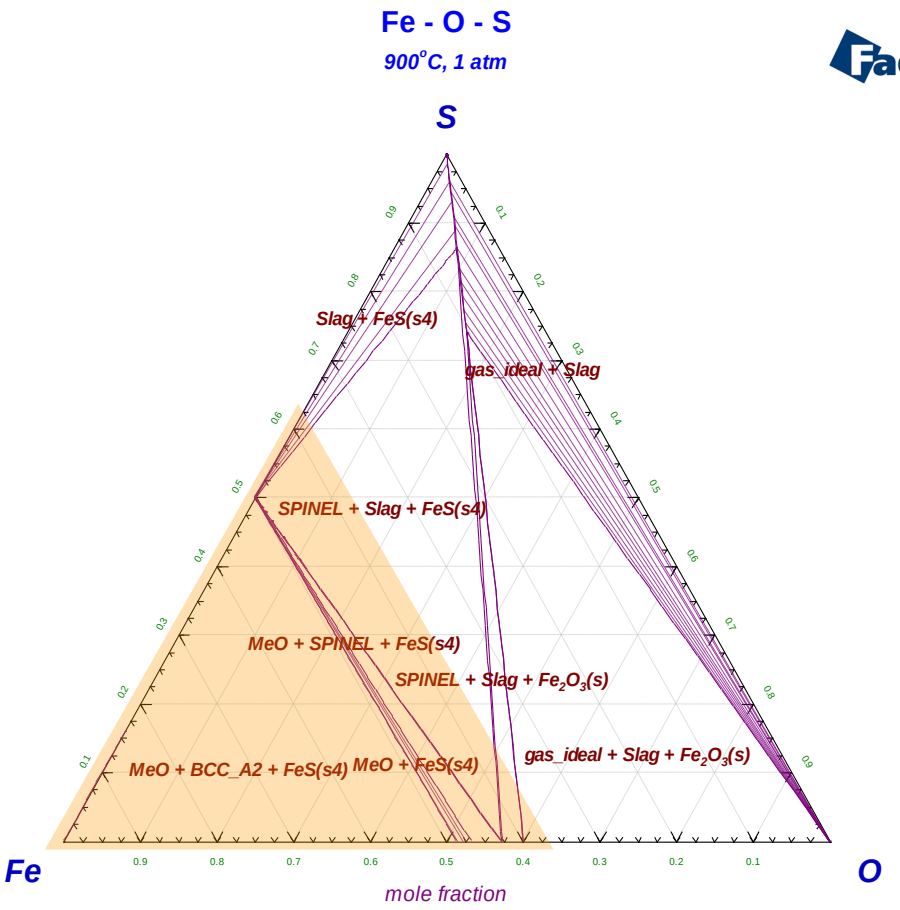

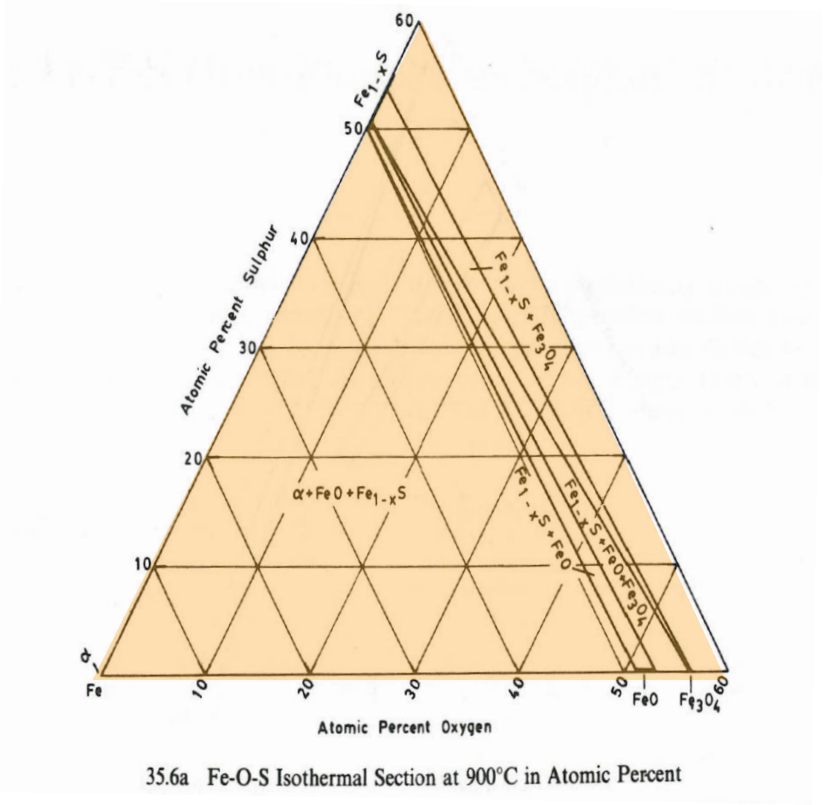

35.6a Fe-O-S Isothermal Section at 900°C in Atomic Percent

V. Raghavan, Phase diagrams of Ternary Iron Alloys, Part 2, Ternary systems containing Iron and Sulphur, The Indian Institute of Metals, Calcutta,1988.

Fe-O-S,
Mole fraction, 550°C

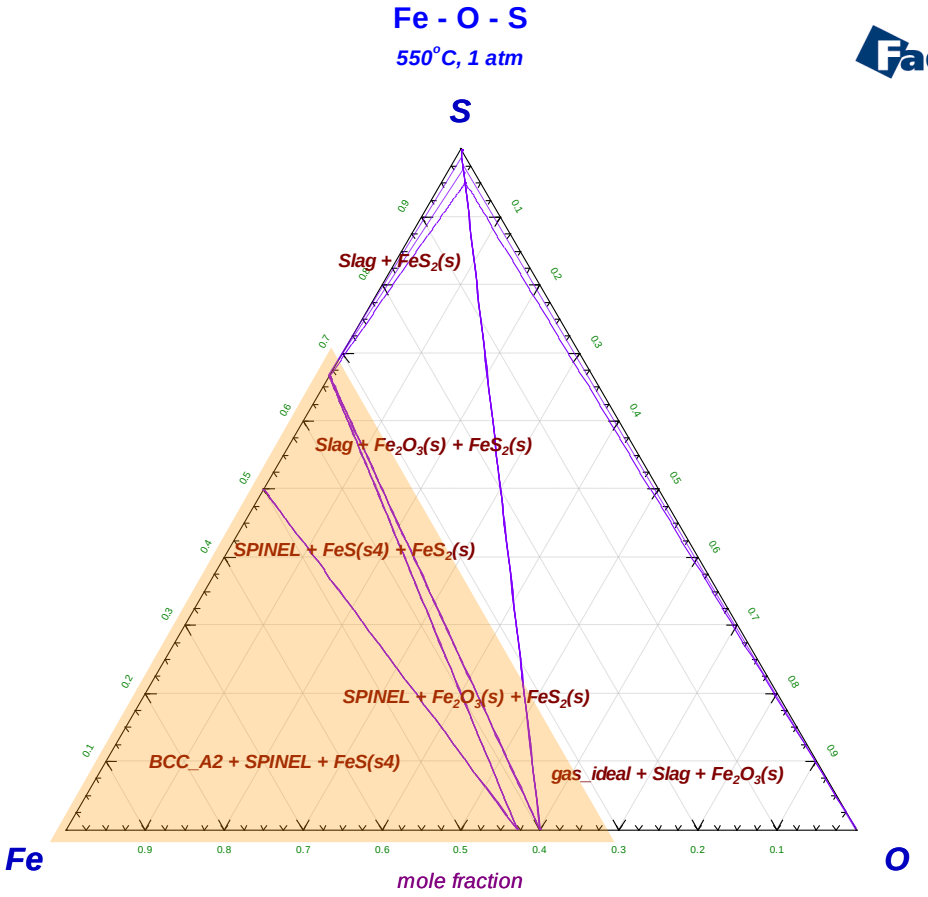

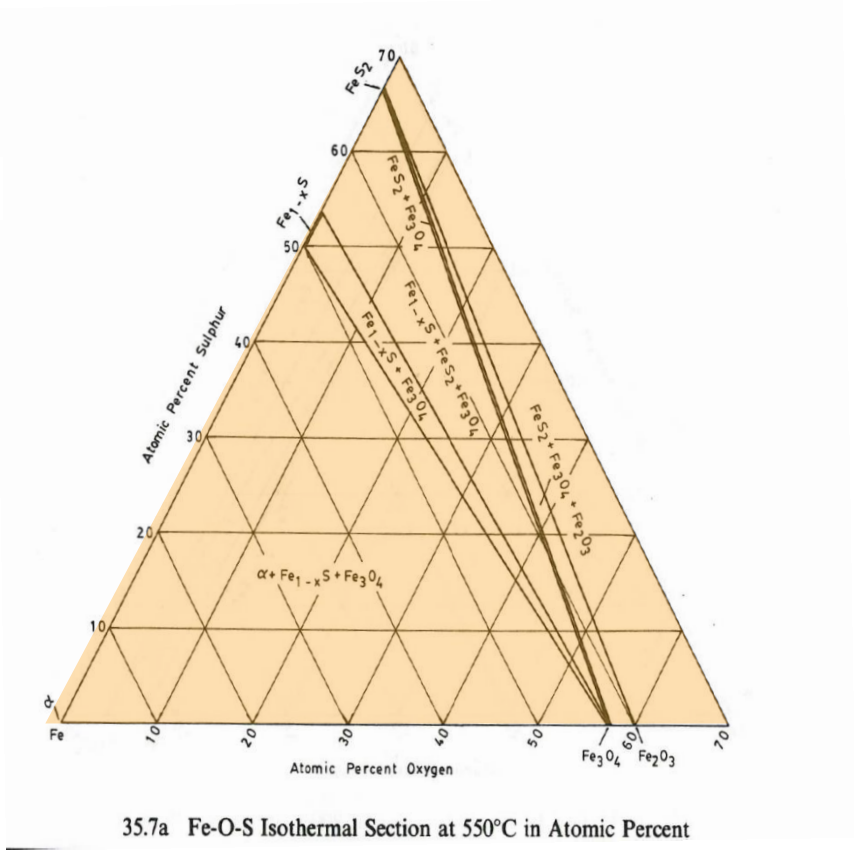

35.7a Fe-O-S Isothermal Section at 550°C in Atomic Percent

V. Raghavan, Phase diagrams of Ternary Iron Alloys, Part 2, Ternary systems containing Iron and Sulphur, The Indian Institute of Metals, Calcutta,1988.

Fe2O3-FeO-MgO,
Weight percent 1300°C

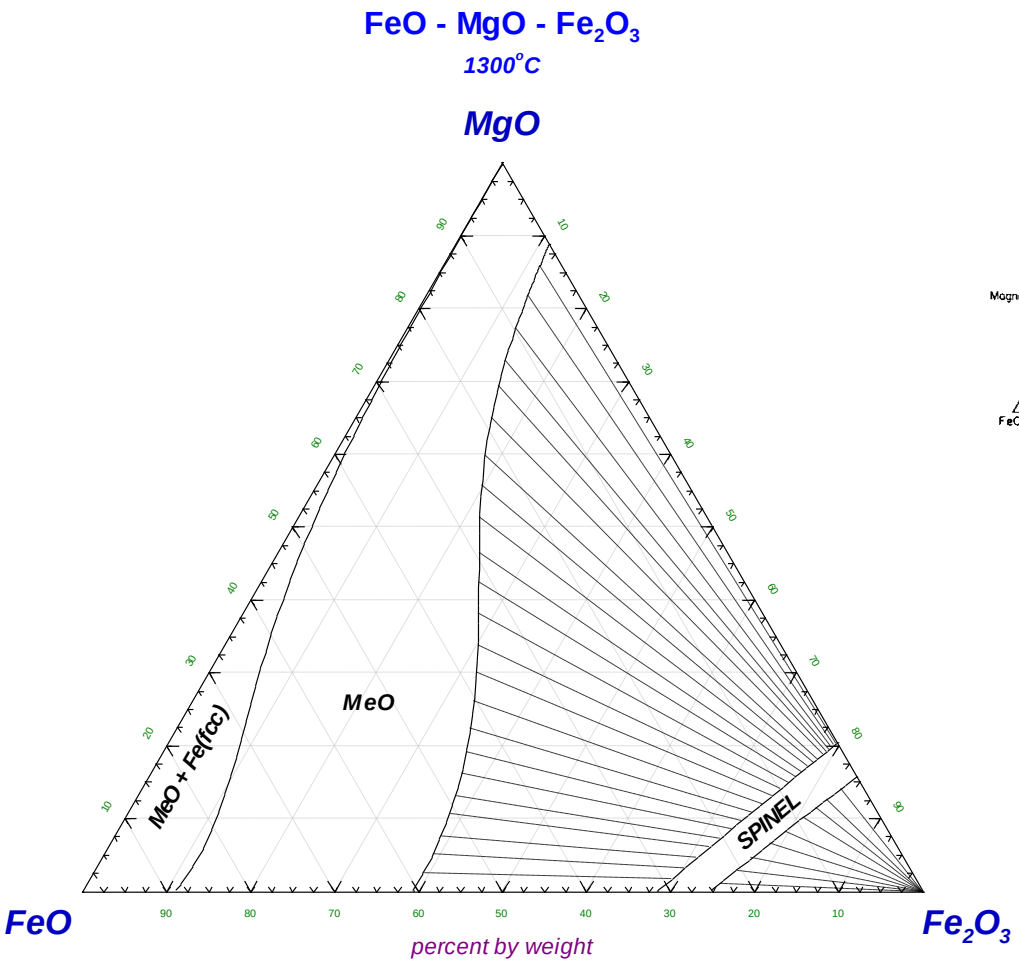

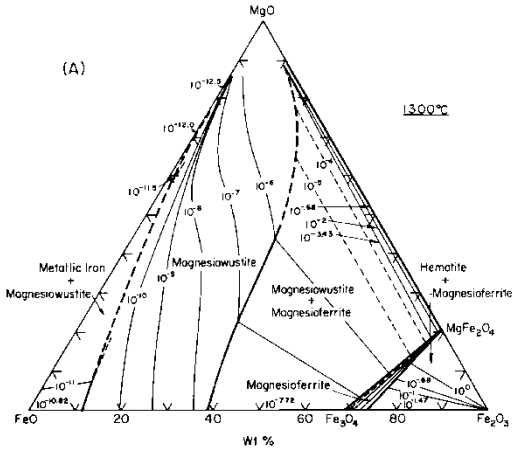

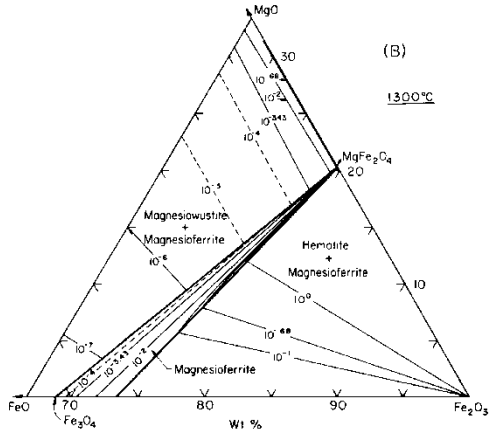

D.H. Speidel, J. Am. Ceram. Soc., 50 [5], (1967), pp. 243-248.

Fe2O3-FeO-MgO,
Weight percent 1400°C

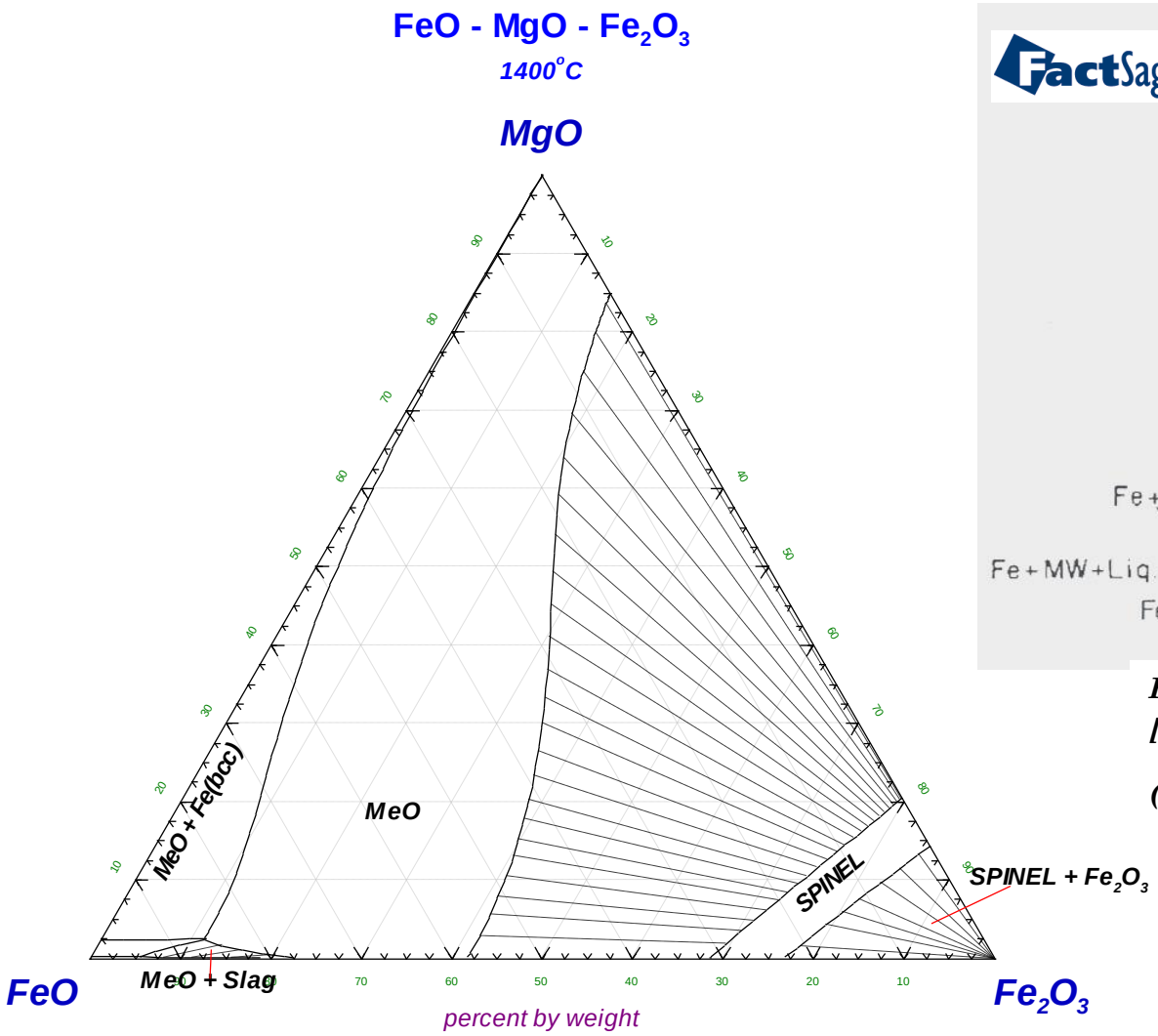

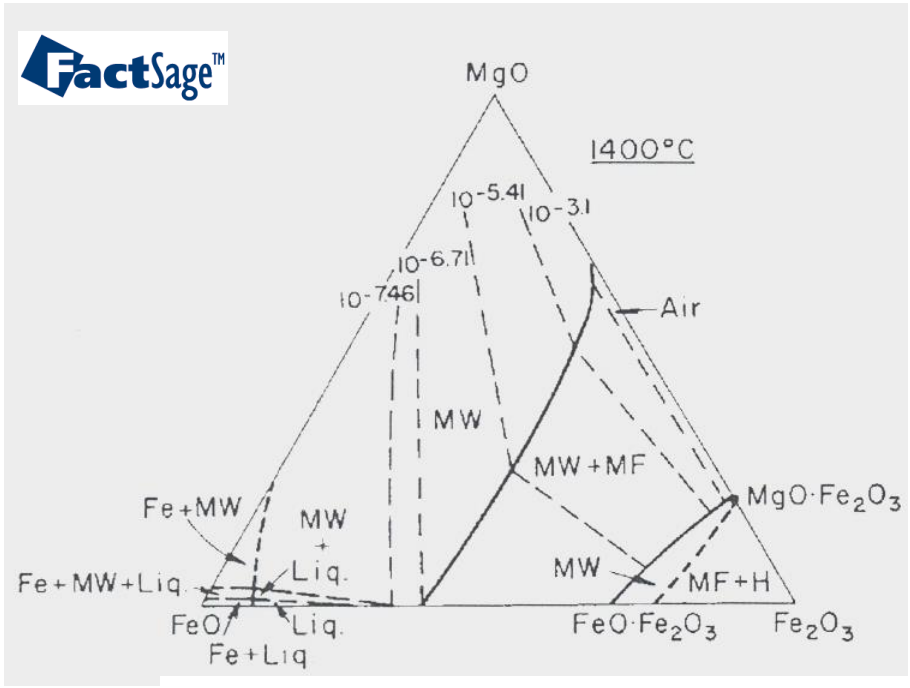

B. Phillips, A. Muan, J. Am. Ceram. Soc., 45 [12],

(1962), pp.588-591.

Fe2O3-FeO-MgO,
Weight percent 1500°C

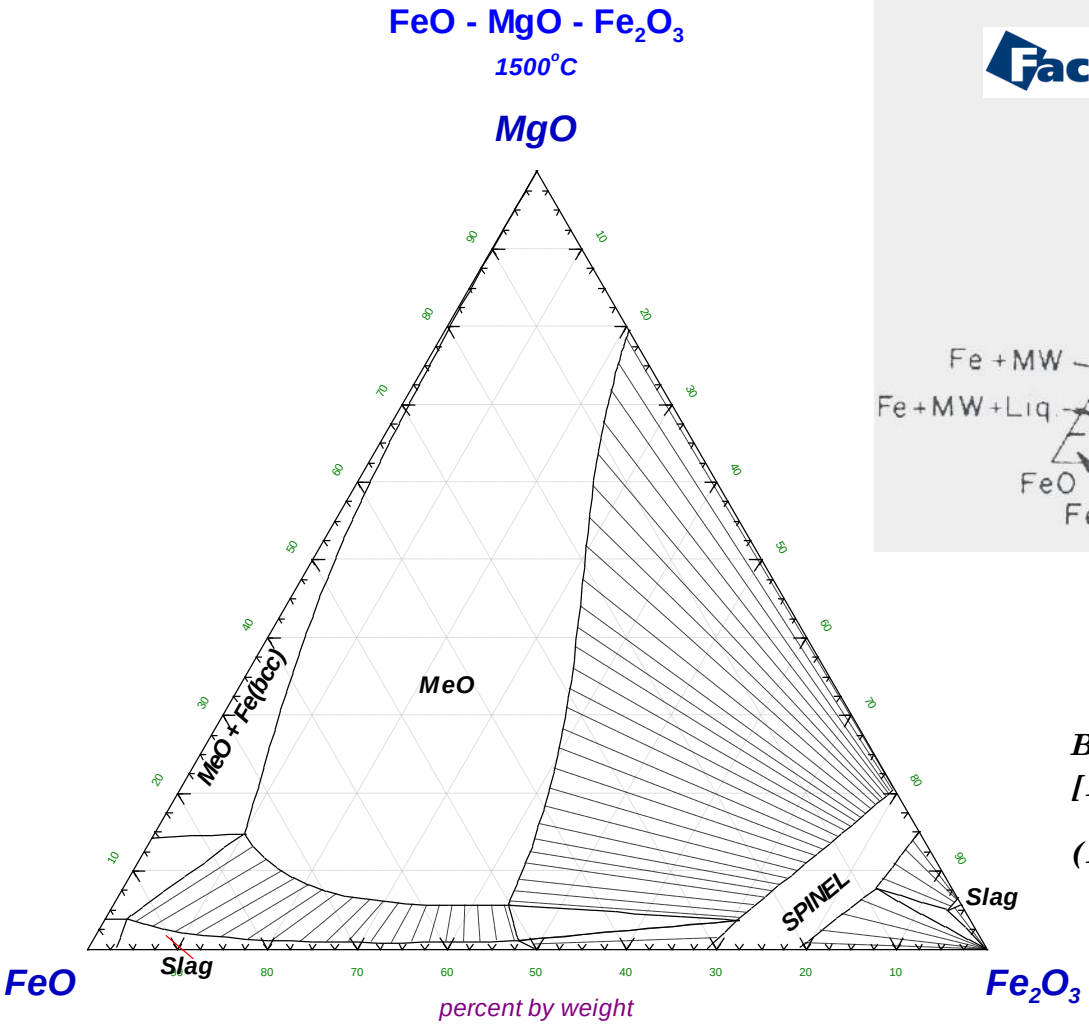

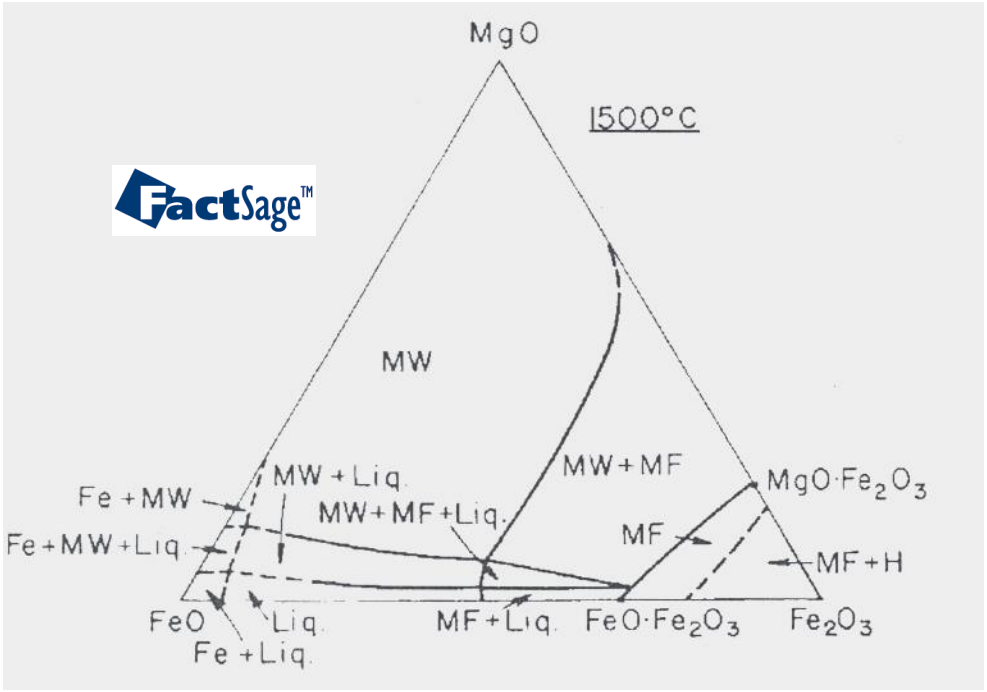

B. Phillips, A. Muan, J. Am. Ceram. Soc., 45 [12],

(1962), pp.588-591.

Fe2O3-FeO-MgO,
Weight percent 1600°C

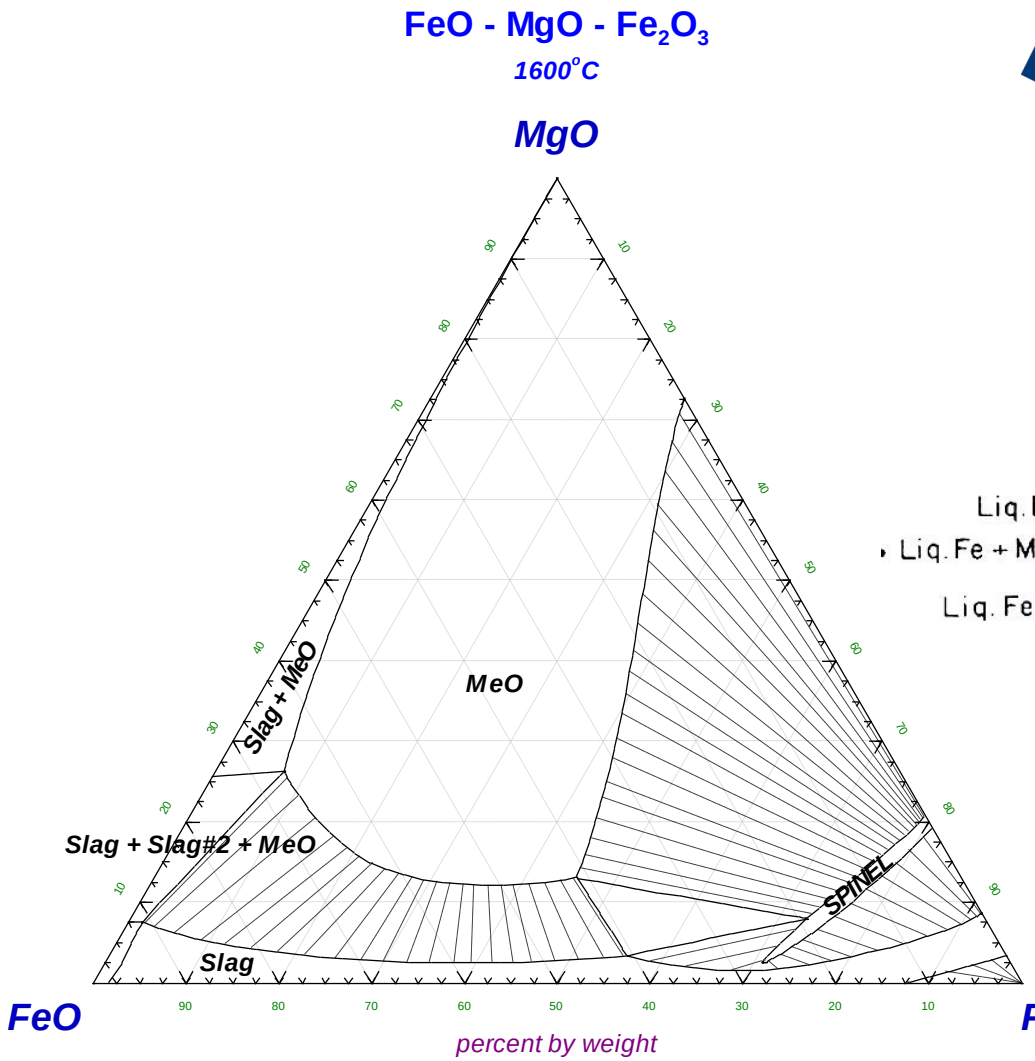

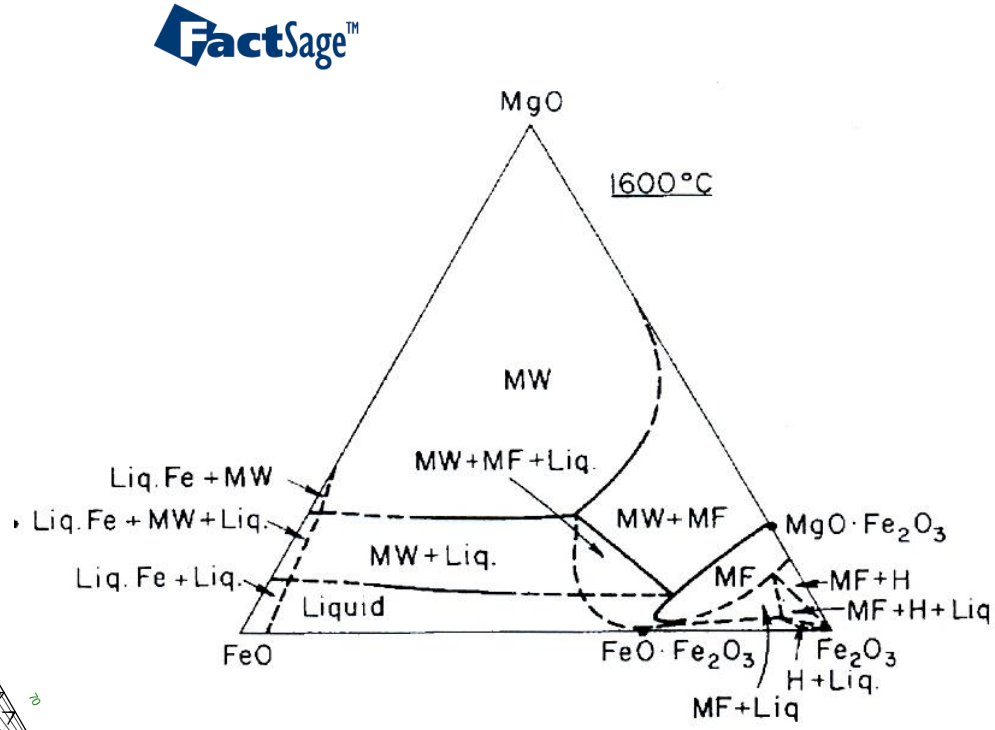

B. Phillips, A. Muan, J. Am. Ceram. Soc., 45 [12], (1962), pp.588-591.

Fe2O3-FeO-P2O5,
Mole fraction 900°C

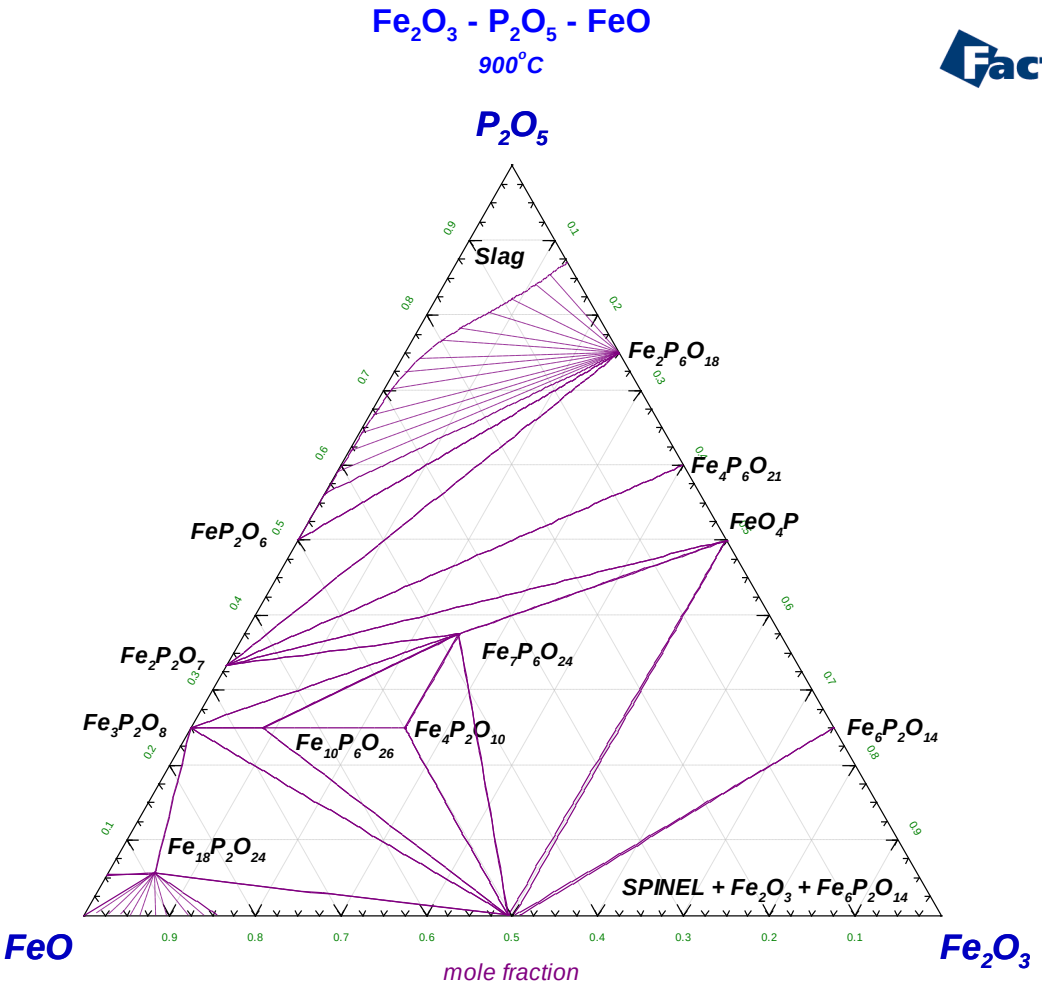

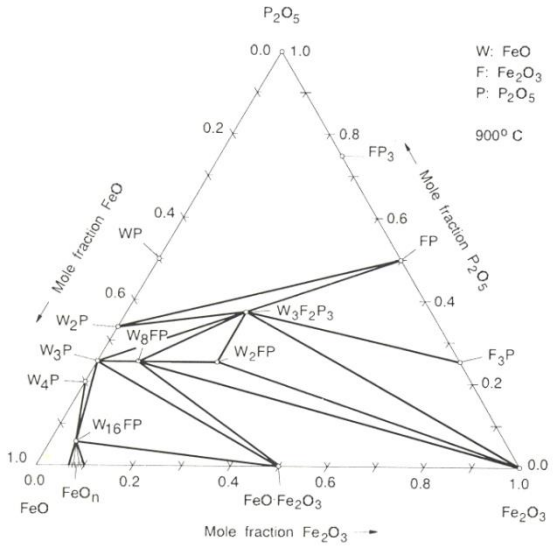

Fig. 3.105. Isothermal section through the FeO-Fe_2O_3-P_2O_5 system at 900 °C after Modaressi et al. [3]. Two ternary phases reported previously by Wentrup [1] have been reformulated. According to Gorgunov et al. [5], $3FeO{\cdot}2Fe_2O_3\,3P_2O_5$ melts at 996 °C. For a discussion of the ternary system Fe-O-P, see Raghavan [6].

Slag Atlas, 2nd Ed., Verlag Stahl-Eisen, Düsseldorf, 1995., p.68. A. Modaressi, J.C. Kaell, B.Malaman, R. Gerardi, C. Gleitze, Mat. Res. Bull. 18 (1983), No. 1, pp.101-109.

Fe2O3-FeO-SiO2,
Weight percent 1200°C

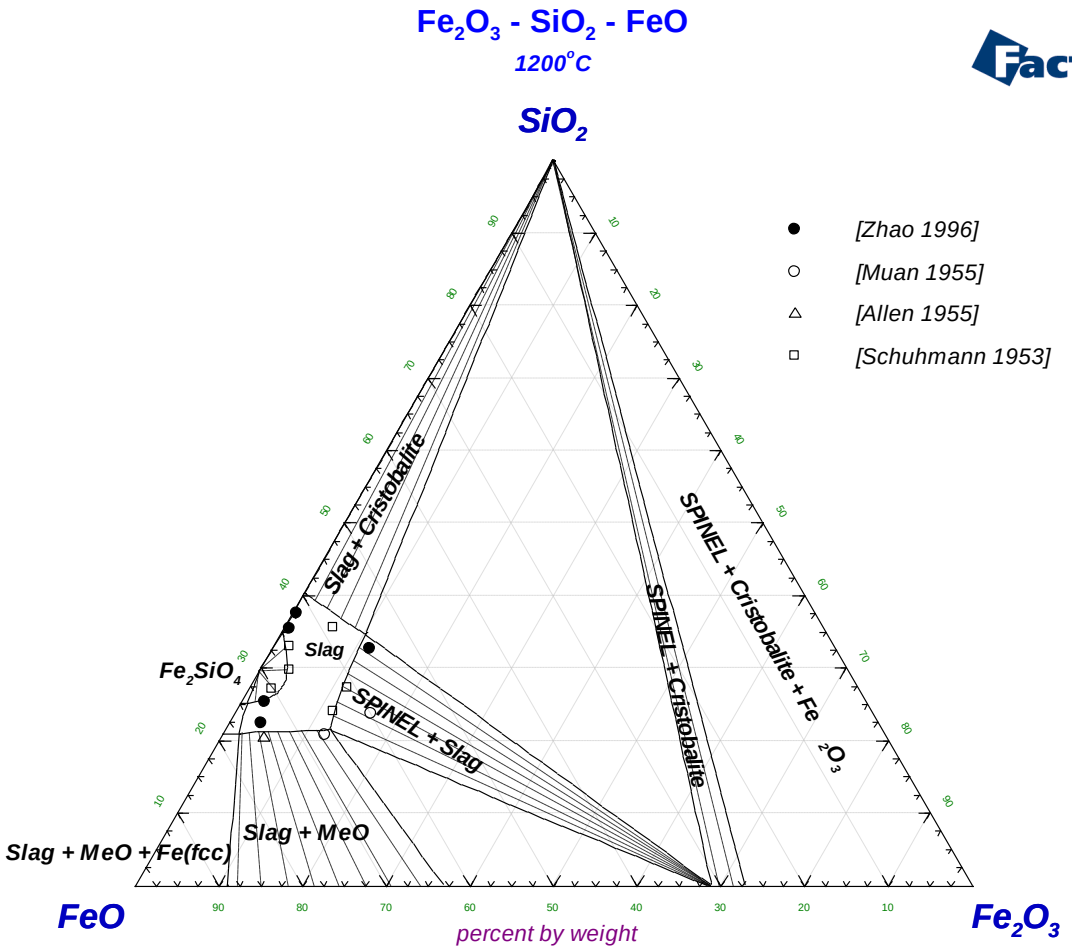

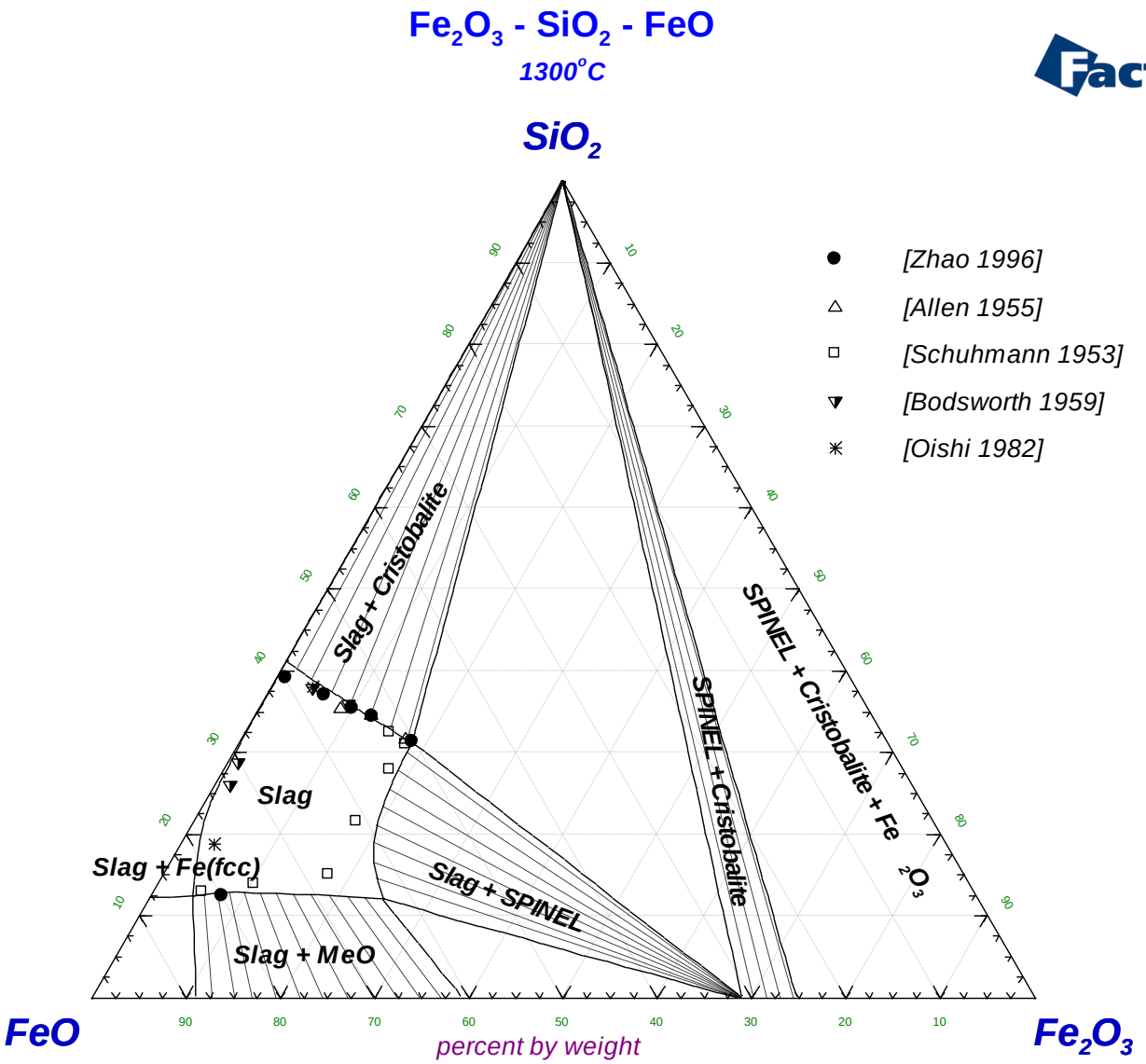
Fe2O3 - SiO2 - FeO
1300°C
SiO2
[Zhao 1996]
[Allen 1955]
[Schuhmann 1953]
[Bodsworth 1959]
[Oishi 1982]
Slag + Cristobalite
SPINEL + Cristobalite + Fe2O3
SPINEL + Cristobalite
Slag
Slag + Fe(fcc)
Slag + SPINEL
Slag + MeO
FeO
Fe2O3
percent by weight

Fe2O3-FeO-SiO2,
Weight percent, Liquidus lines at 1500-1650°C

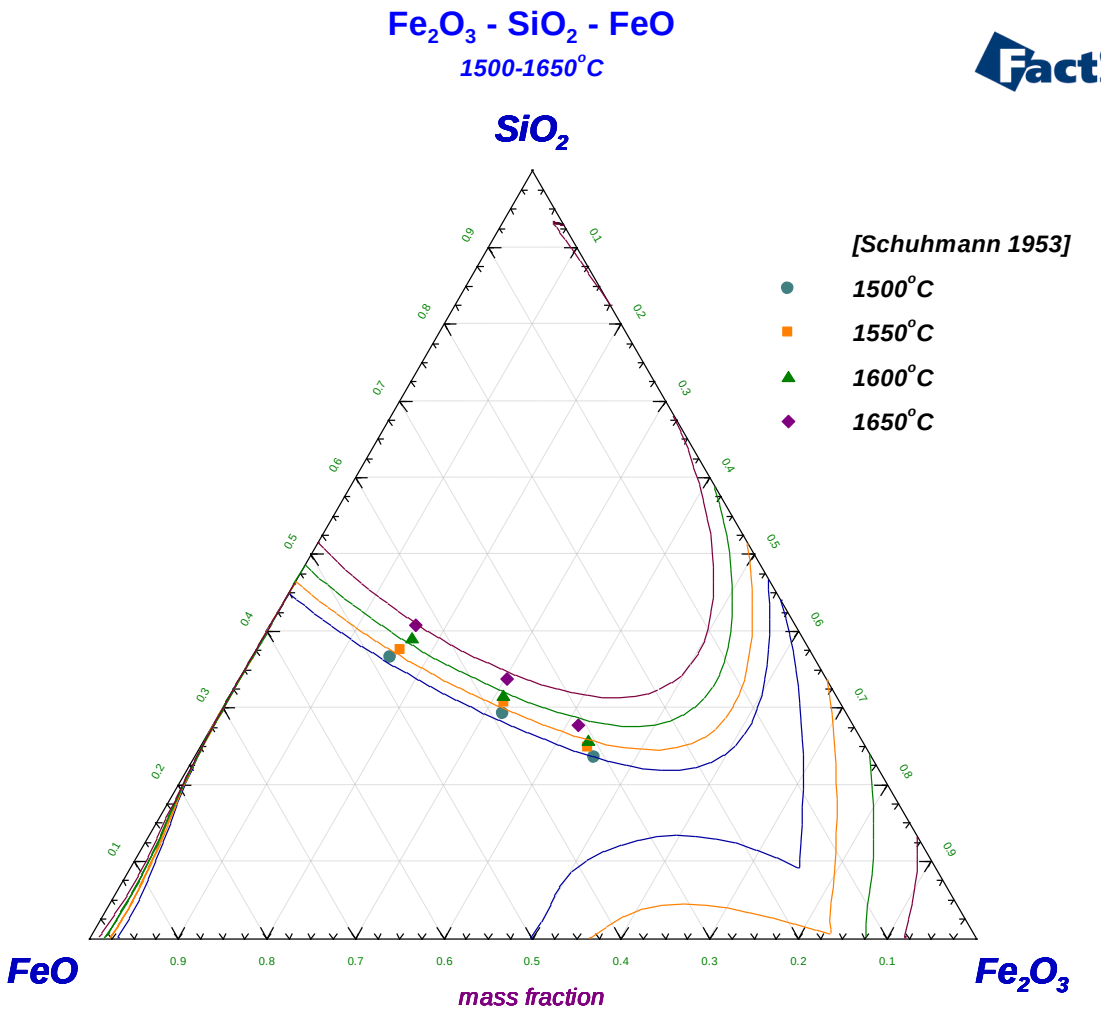

Fe2O3-FeO-SrO,
Mole fraction 1000°C

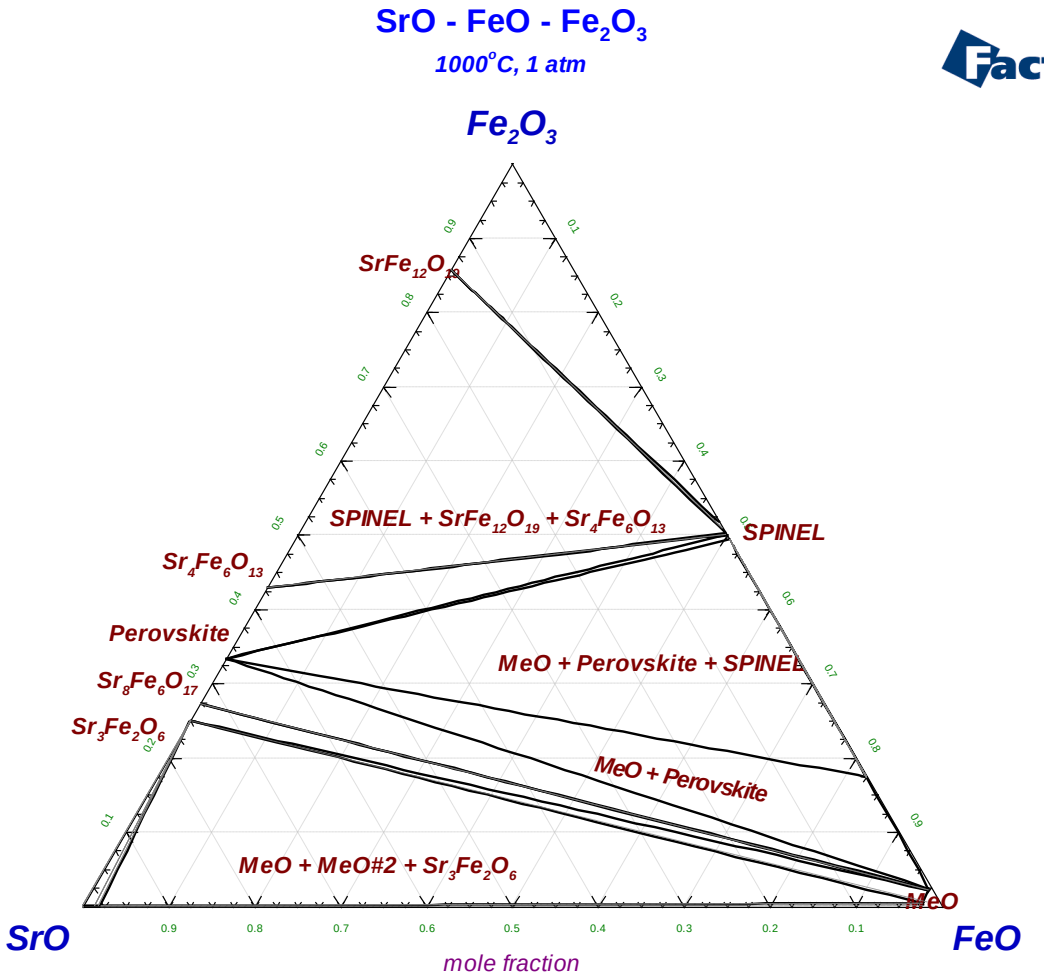

Fe2O3-FeO-SrO,
Mole fraction 1500°C

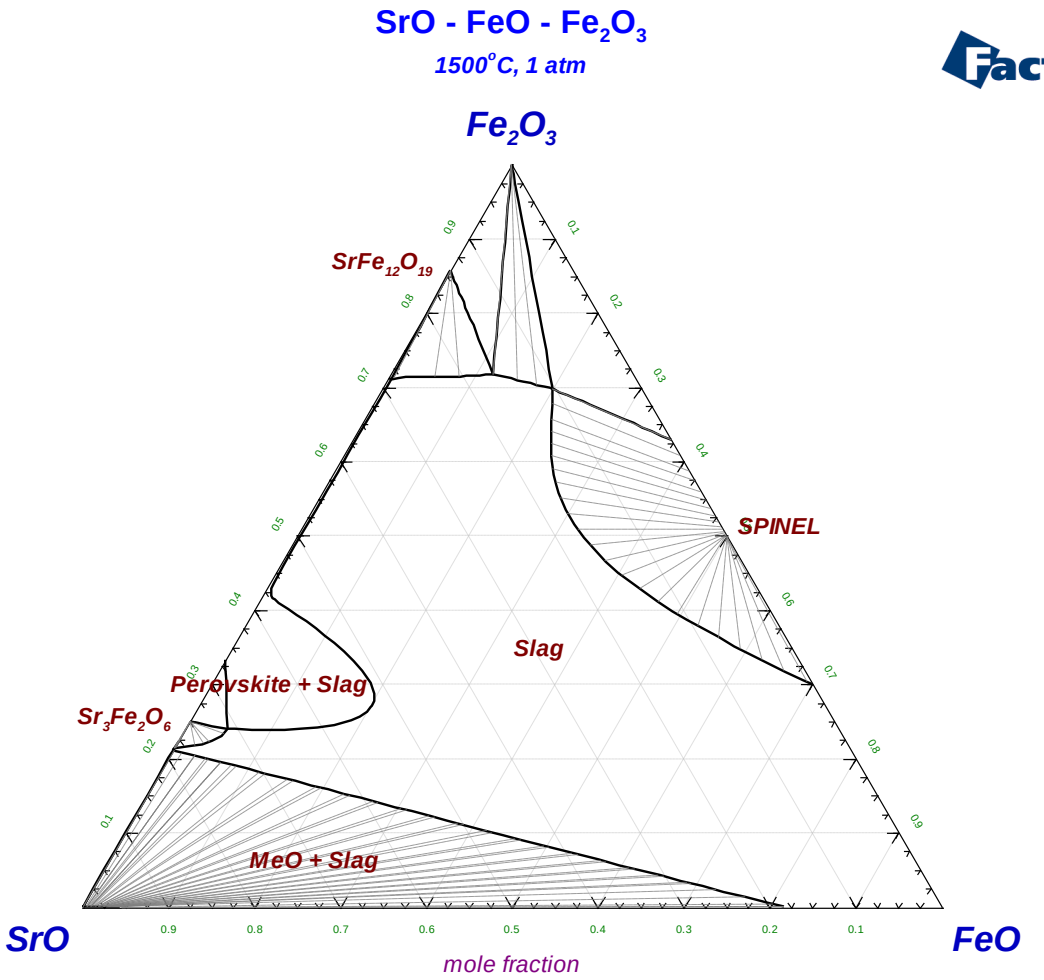

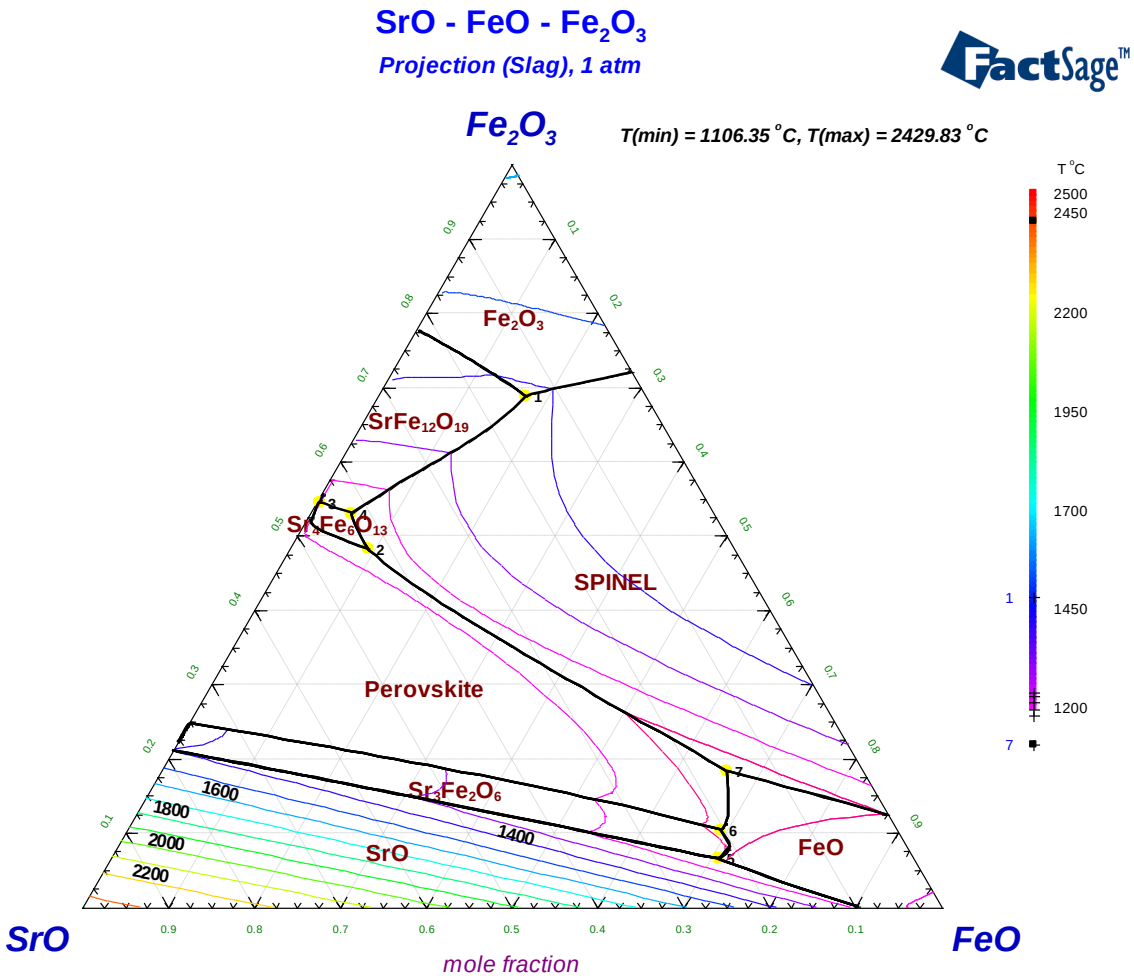
SrO - FeO - Fe2O3
Projection (Slag), 1 atm
FactSage™
Fe2O3
T(min) = 1106.35 °C, T(max) = 2429.83 °C
T °C
2500
2450
2200
1950
1700
1450
1200
Fe2O3
SrFe12O19
SrFe6O13
SPINEL
Perovskite
Sr3Fe2O6
SrO
FeO
1600
1800
2000
2200
1400
SrO
FeO
mole fraction

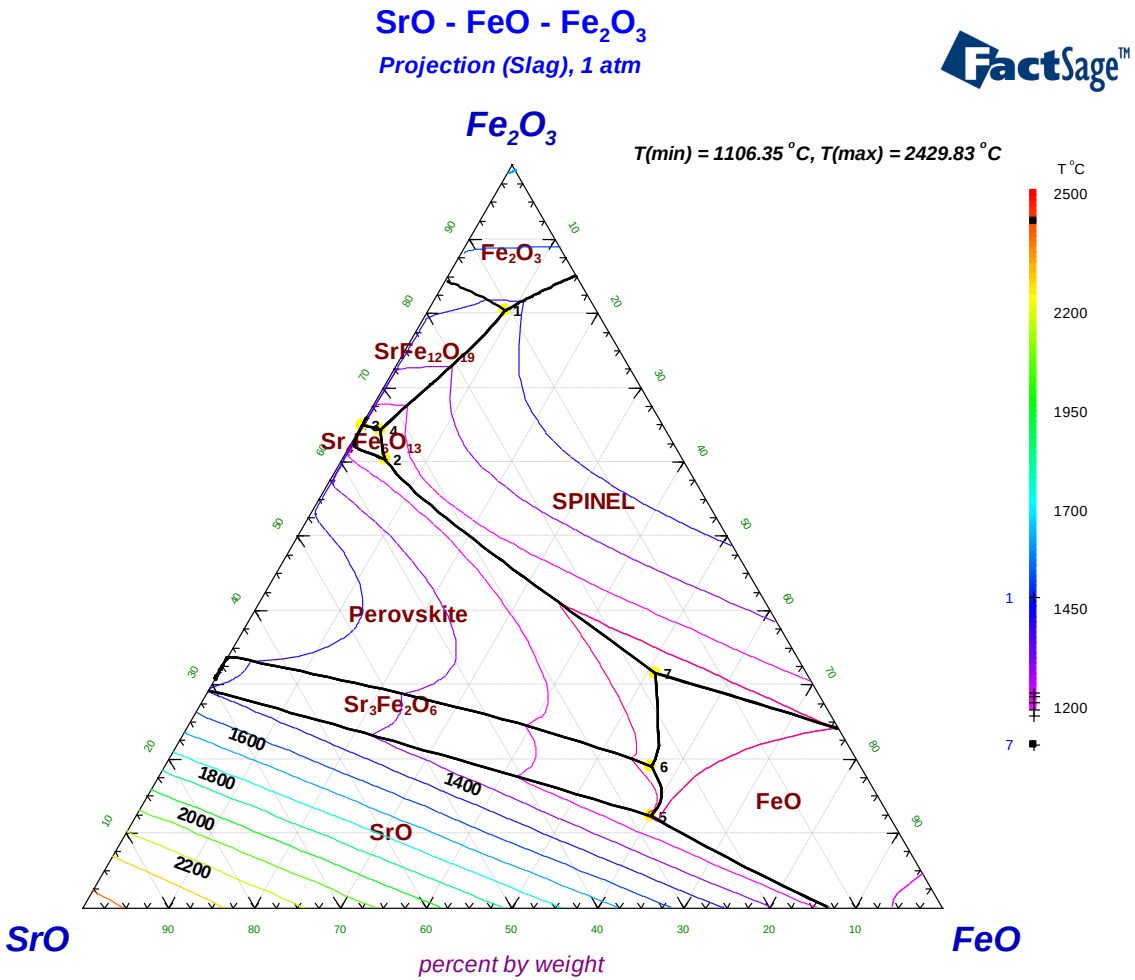
SrO - FeO - Fe2O3
Projection (Slag), 1 atm
FactSage™
Fe2O3
T(min) = 1106.35 °C, T(max) = 2429.83 °C
T °C
2500
2200
1950
1700
1450
1200
Fe2O3
SrFe12O19
Sr3Fe2O6
SPINEL
Perovskite
Sr3Fe2O6
FeO
SrO
1600
1800
2000
2200
1400
SrO
FeO
percent by weight

Invariant equilibria on the liquidus surface

Intersections with slag	Mole fraction A = Fe2O3, B = SrO, C = FeO				Weight percent A = Fe2O3, B = SrO, C = FeO			
	X(A)	X(B)	X(C)	T(C)	W(A)	W(B)	W(C)	T(C)
1: Fe2O3 / SPINEL / SrFe12O19	1: 0.68863	0.13915	0.17222	1477.77	1: 80..409	10.543	9.047	1477.78
2: Perovskite / SPINEL / Sr4Fe6O13	2: 0.48223	0.42640	0.09137	1238.90	2: 60.277	34.585	5.138	1238.90
3: Perovskite / Sr4Fe6O13 / SrFe12O19	3: 0.54511	0.45160	0.00329	1227.22	3: 64.923	34.901	0.176	1227.24
4: SPINEL / Sr4Fe6O13 / SrFe12O19	4: 0.53080	0.42134	0.04786	1213.08	4: 64.282	33.110	2.608	1213.12
5: FeO / Sr3Fe2O6 / SrO	5: 0.06522	0.22670	0.70808	1195.63	5: 12.284	27.709	60.007	1195.65
6: FeO / Perovskite / Sr3Fe2O6	6: 0.10421	0.20499	0.69080	1178.71	6: 19.016	24.272	56.712	1178.71
7: FeO / Perovskite / SPINEL	7: 0.18373	0.15715	0.65912	1106.35	7: 31.556	17.514	50.930	1106.35

Fe2O3-FeO-TiO2,
Mole fraction 1300°C

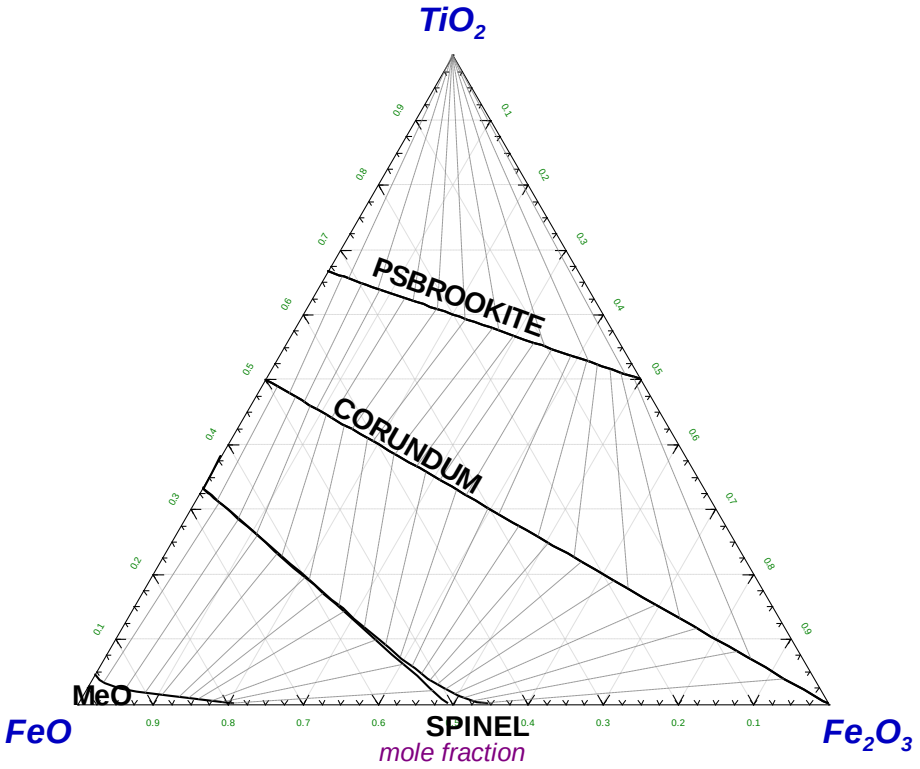

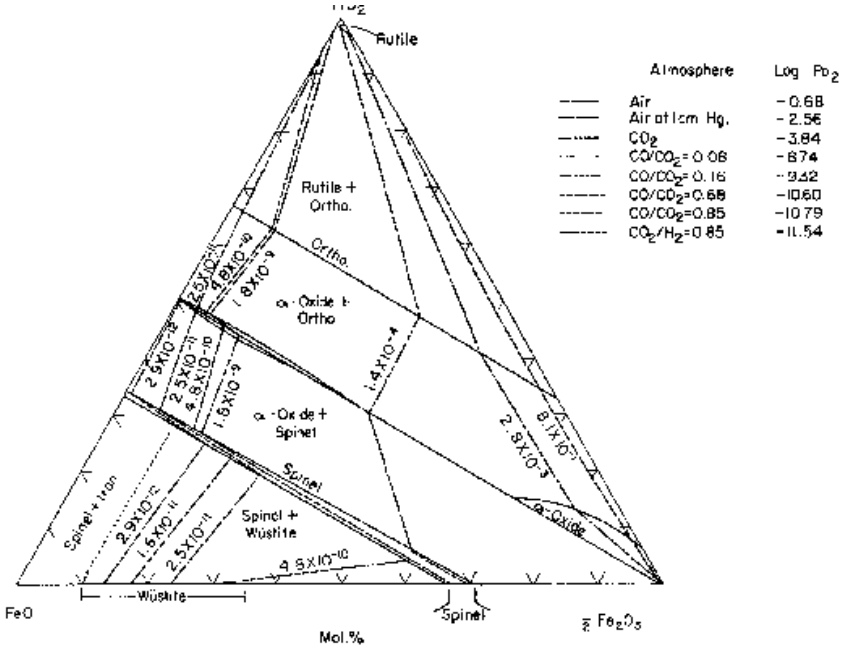

A.H. Webster, N.F.H. Bright, J. Am. Ceram. Soc., 44 [3], (1961), pp.110-116.

Isopleth section FeTi2O5-Fe2TiO5, mole fraction

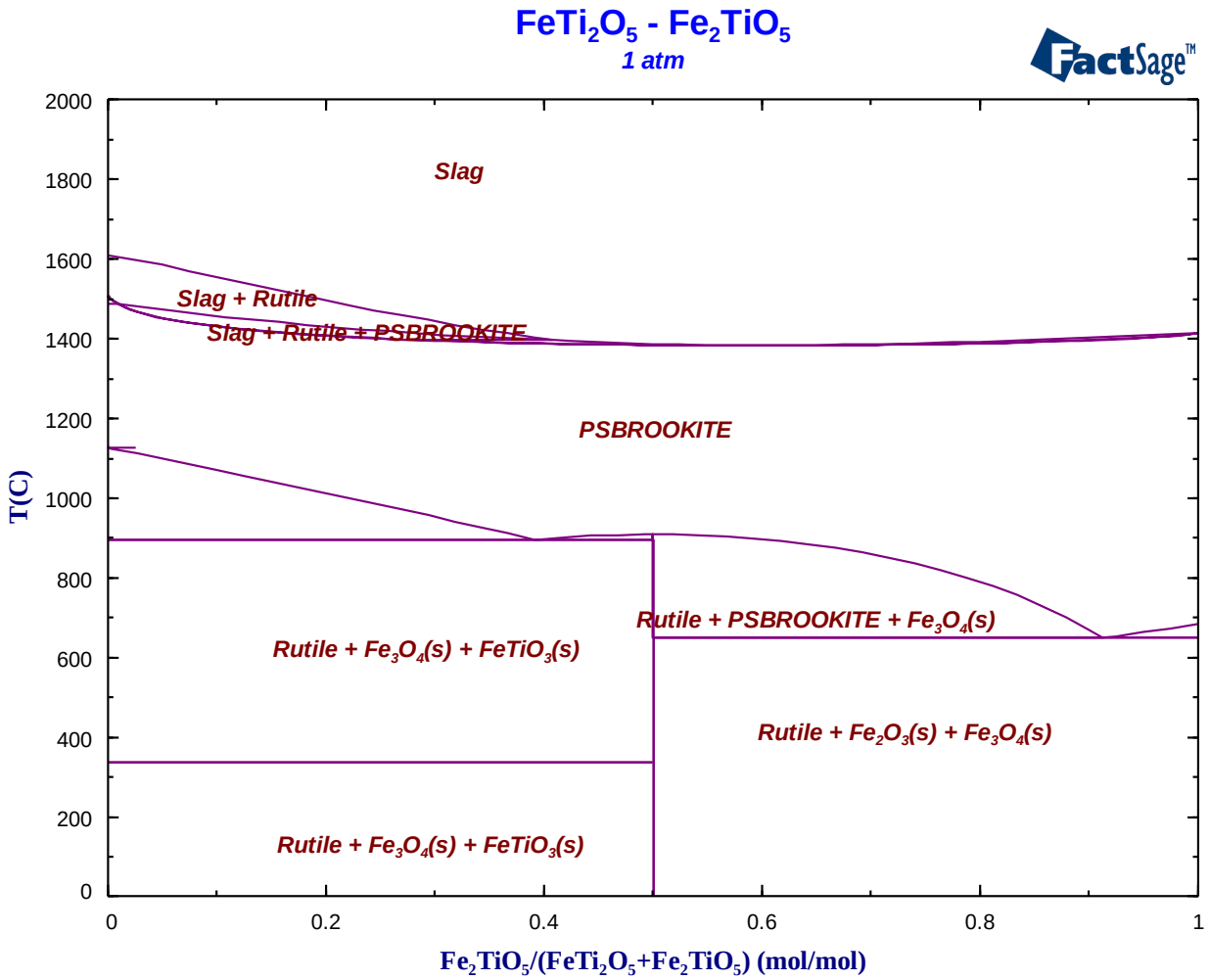

Isopleth section Fe3O4-Fe2TiO4, mole fraction

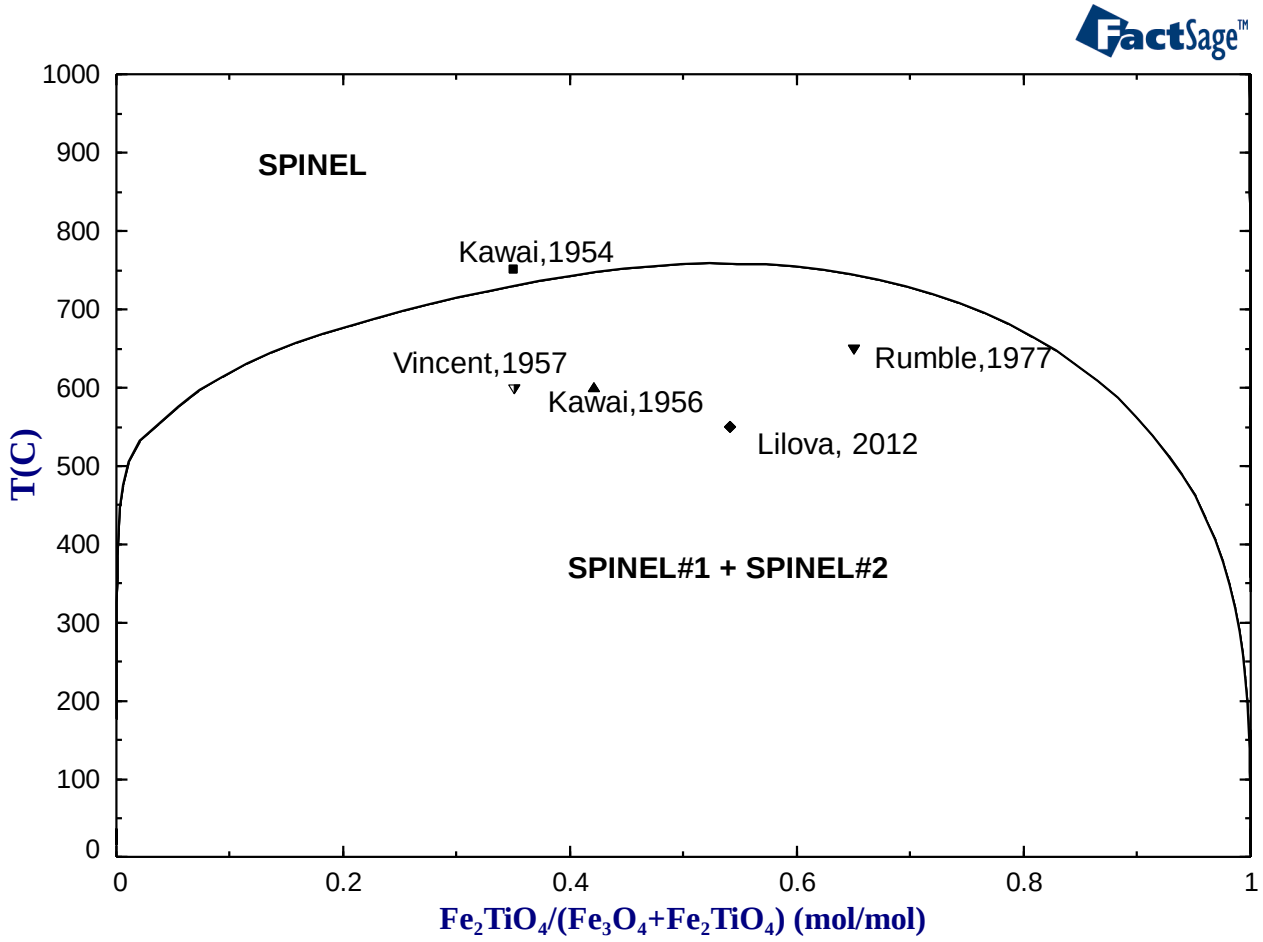

Fe2O3-FeO-V2O3,
Mole fraction 1227°C

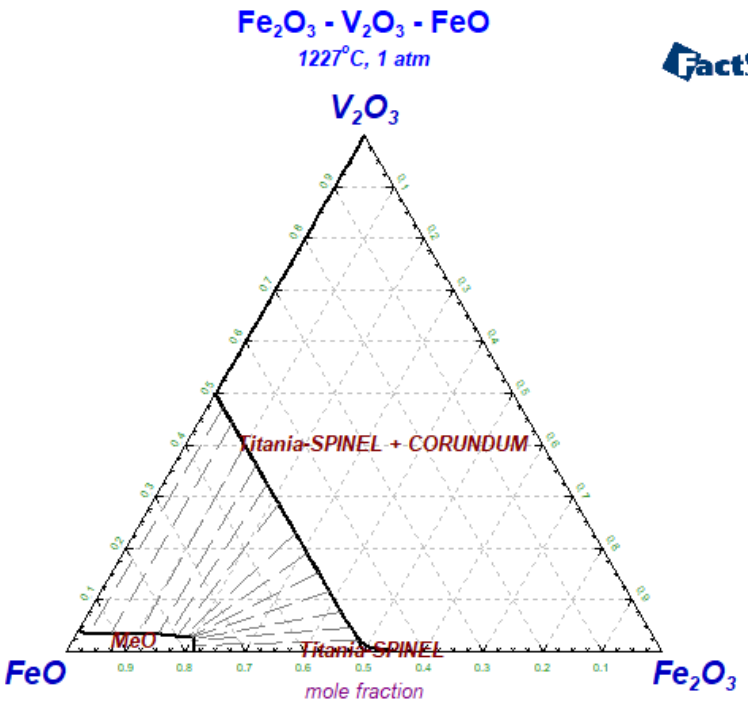

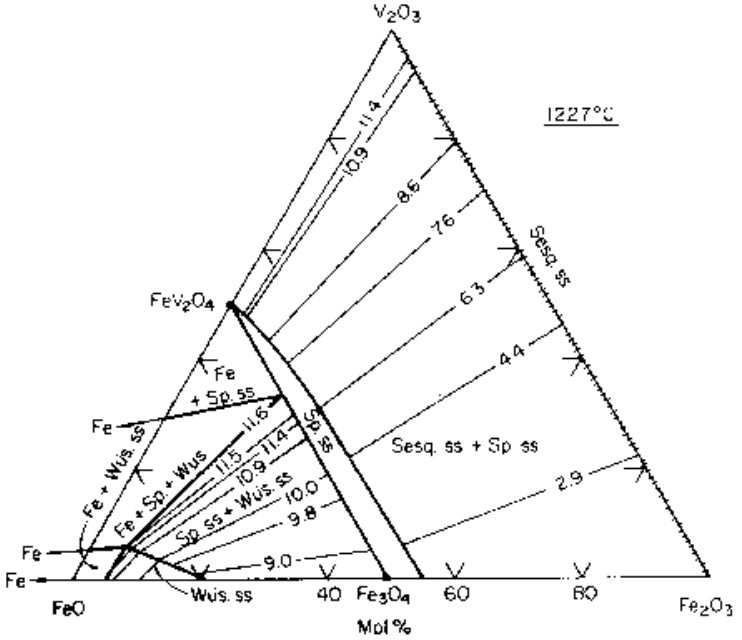

M. Wakihara, T. Katsura, Bull. Chem. Soc. Jpn., 44 [11] (1971, pp. 3043-3046.

Fe2O3-Fe-V2O3,
Mole fraction 1227°C

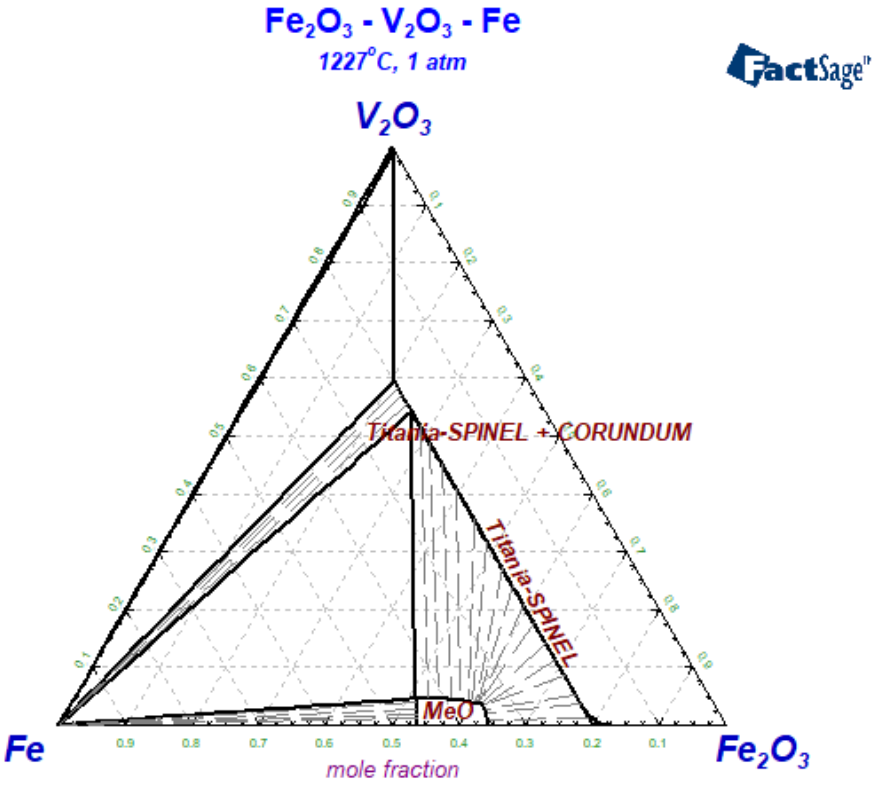

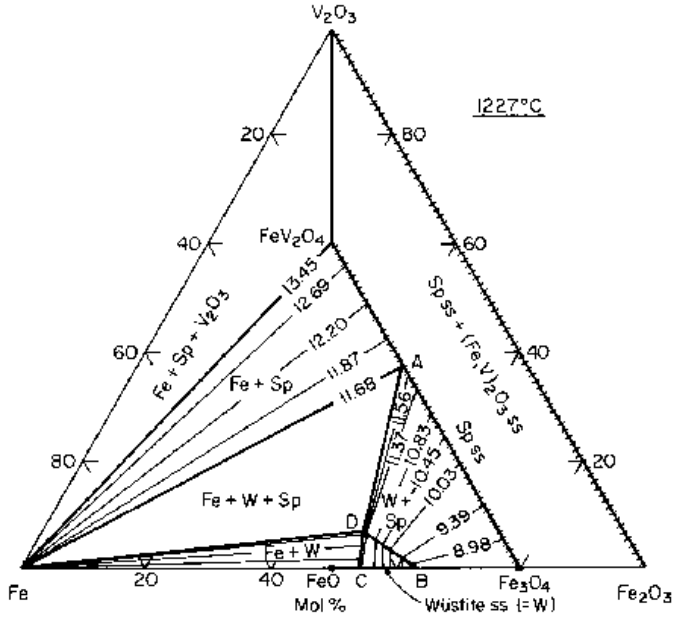

T. Katsura, M. Wakihara, S. Hara, T. Sugihara, BJ. Solid State Chem., 13 [1-2] (1975), pp. 107-113.

Fe2O3-FeO-V2O3,
Mole fraction, Liquidussurface

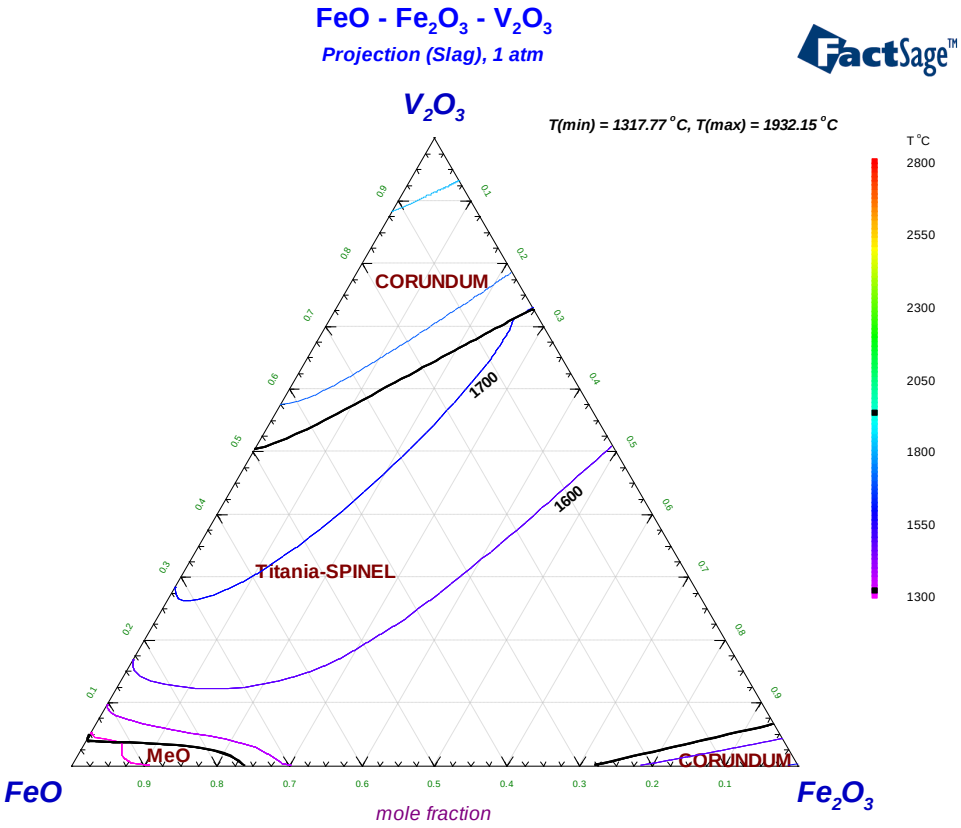

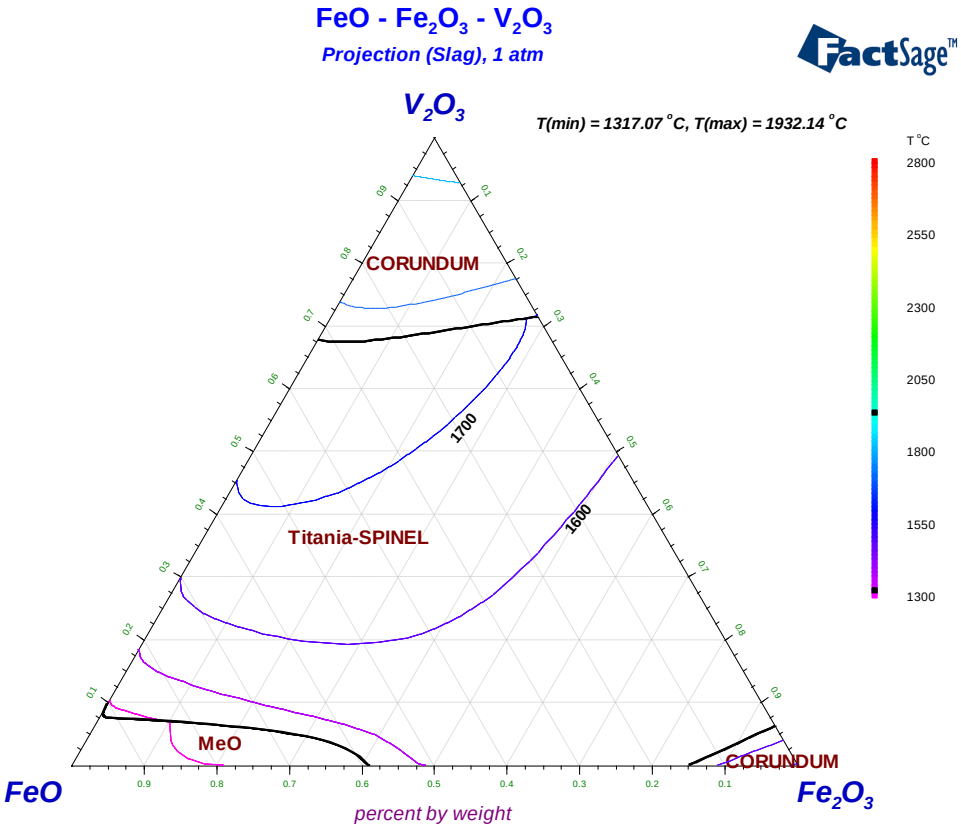
FeO - Fe2O3 - V2O3
Projection (Slag), 1 atm
FactSage™
V2O3
T(min) = 1317.07 °C, T(max) = 1932.14 °C
T °C
2800
2550
2300
2050
1800
1550
1300
CORUNDUM
1700
1600
Titania-SPINEL
MeO
CORUNDUM
FeO
Fe2O3
percent by weight

Fe2O3-K2O-SiO2, Mole fraction 600°C

Ternäre Phasen in Fe_2O_3-K_2O-SiO_2

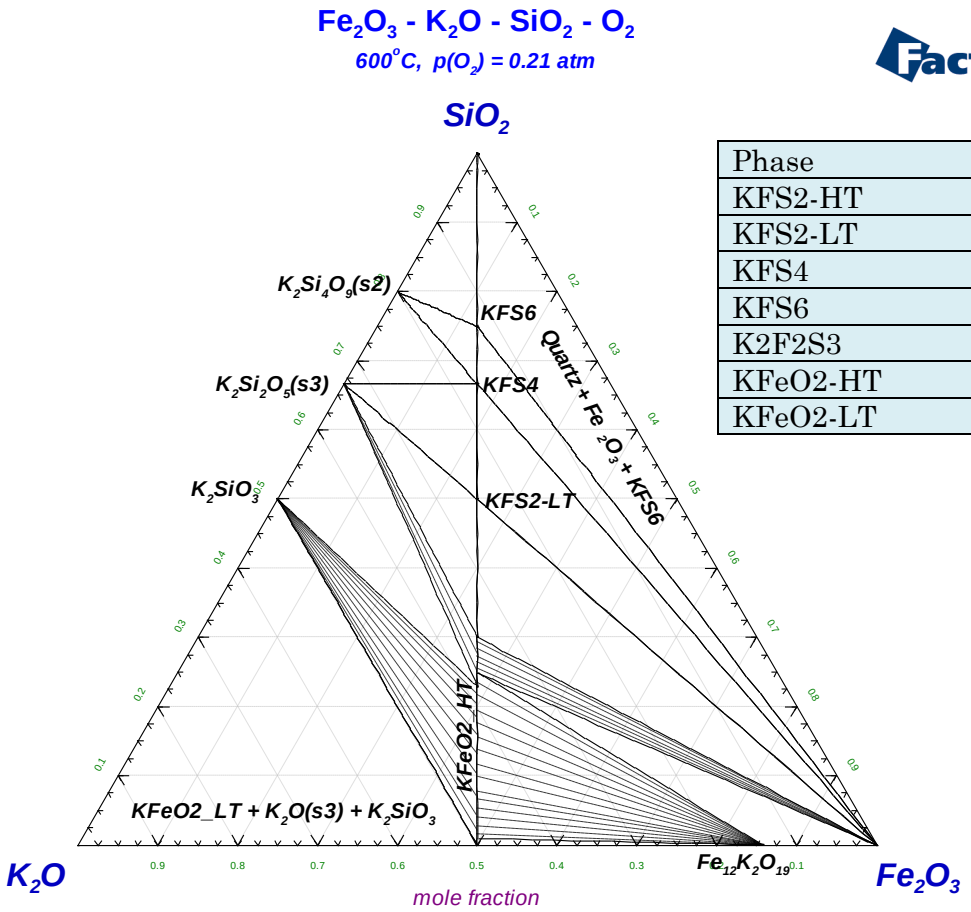

FactSage™

Phase	Beschreibung	Formel
KFS2-HT	Stöchiometrisch	$Fe_2K_2Si_2O_8$
KFS2-LT	Stöchiometrisch	$Fe_2K_2Si_2O_8$
KFS4	Stöchiometrisch	$Fe_2K_2Si_4O_{12}$
KFS6	Stöchiometrisch	$Fe_2K_2Si_6O_{16}$
K2F2S3	Stöchiometrisch	$Fe_4K_4Si_3O_{14}$
KFeO2-HT	Mischphase	$(K^{1+},Va)(Fe^{3+},Si^{4+})(O^{2-})_2$
KFeO2-LT	Mischphase	$(K^{1+},Va)(Fe^{3+},Si^{4+})(O^{2-})_2$

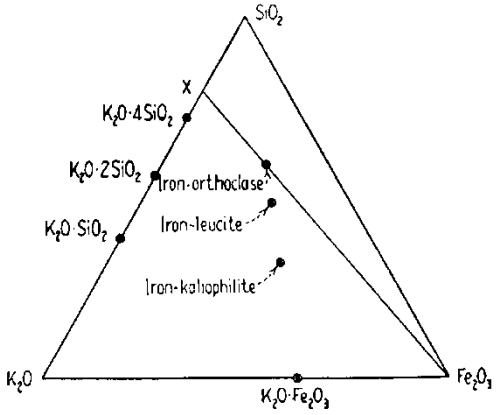

G.T. Faust, Am. Mineral, 21 [12], (1936), pp. 735-763.

Fe2O3-K2O-SiO2, Mole fraction 850°C

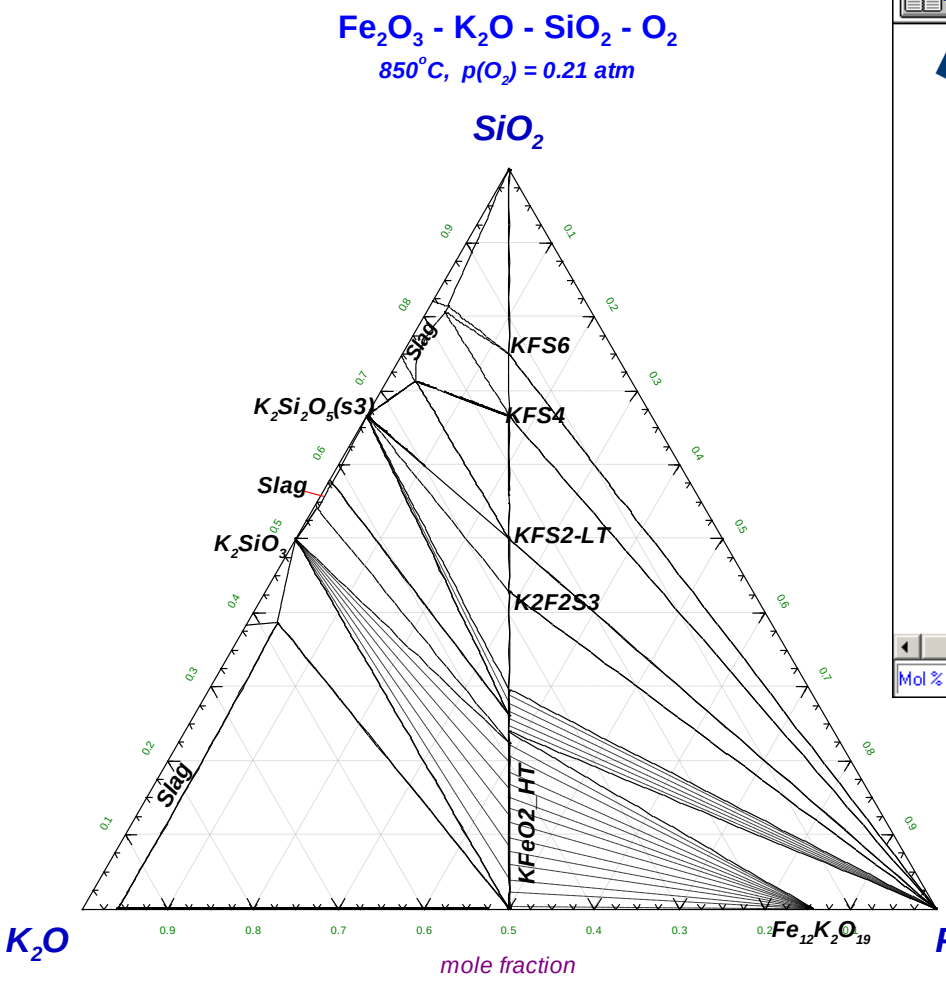

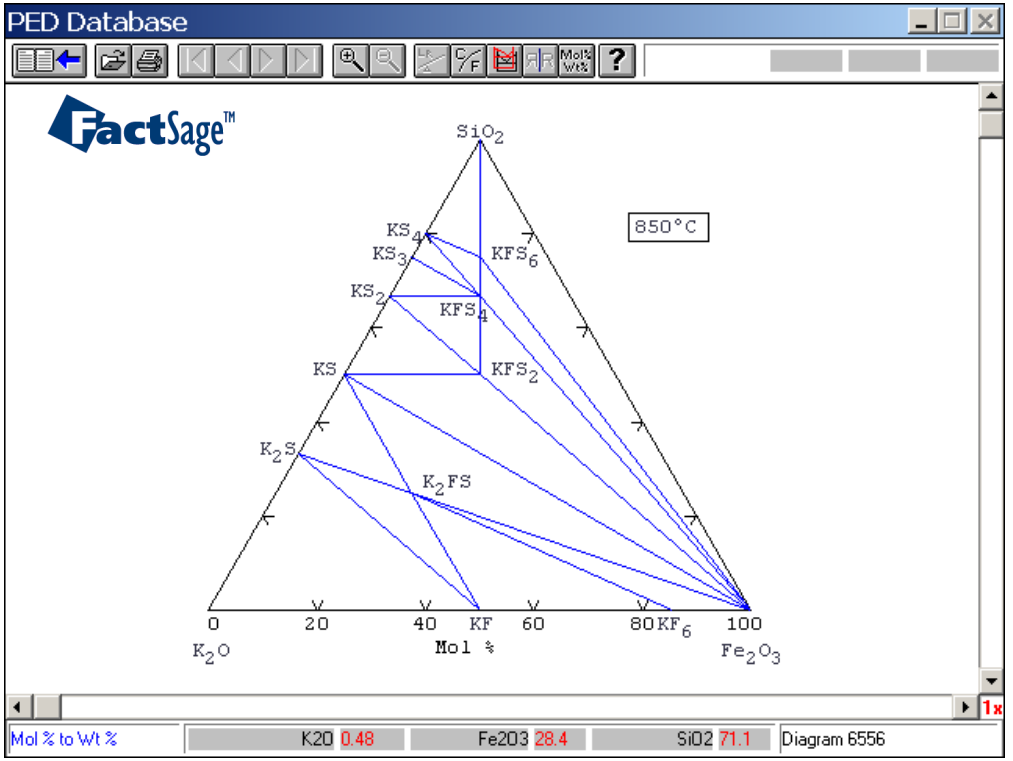

A.P. Protsyuk, G.A. Konechnyi, L.G. Latysheva, Izv. Akad. Nauk SSSR, Neorg. Mater., 15 [1], (1979), pp. 173-174.

Mole fraction,
FeKO2-SiO2 compared with experimental data

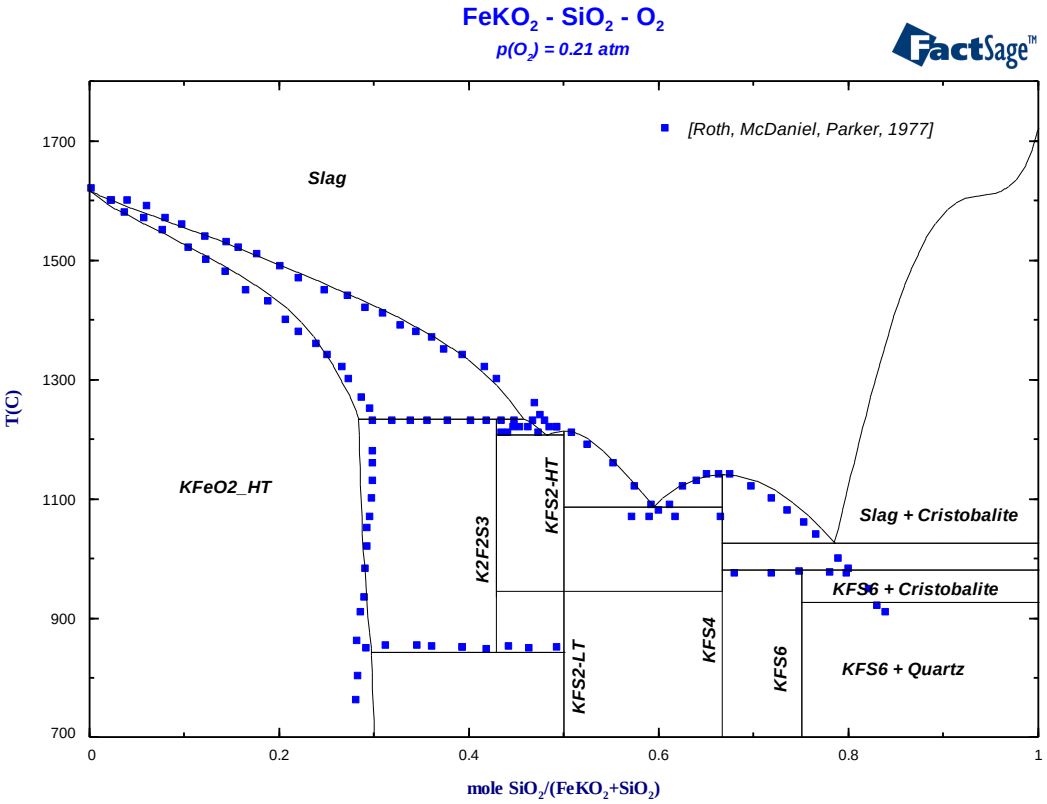

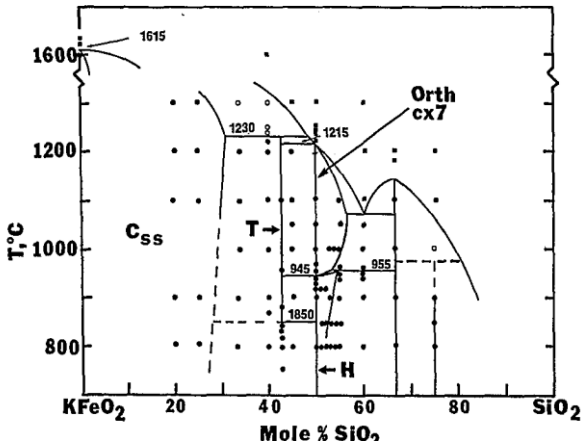

R.S. Roth, Adv. Chem. Ser., No. 186,, (1980), pp. 391-408.

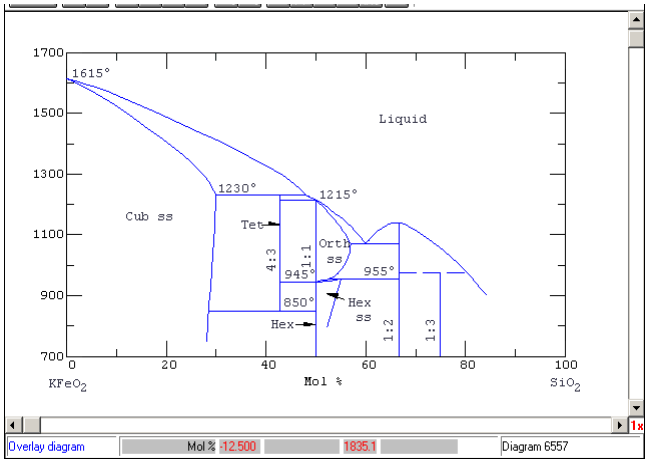

R.S. Roth, C.L. McDaniel, H.S. Parker., Geol. Soc. Am. Abstr., 9 [7], (1977), p. 1149.

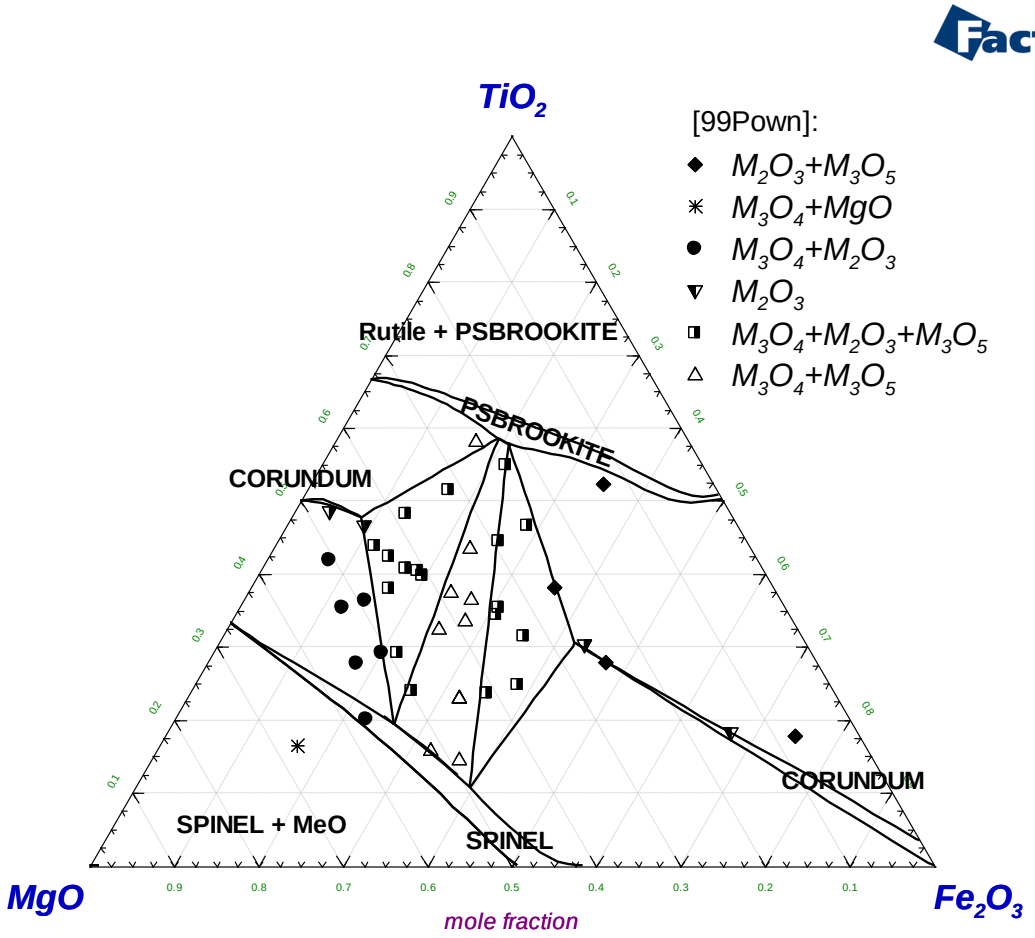
FactSage™
TiO2
[99Pown]:
M2O3+M3O5
M3O4+MgO
M3O4+M2O3
M2O3
M3O4+M2O3+M3O5
M3O4+M3O5
Rutile + PSBROOKITE
PSBROOKITE
CORUNDUM
SPINEL + MeO
SPINEL
CORUNDUM
MgO
Fe2O3
mole fraction

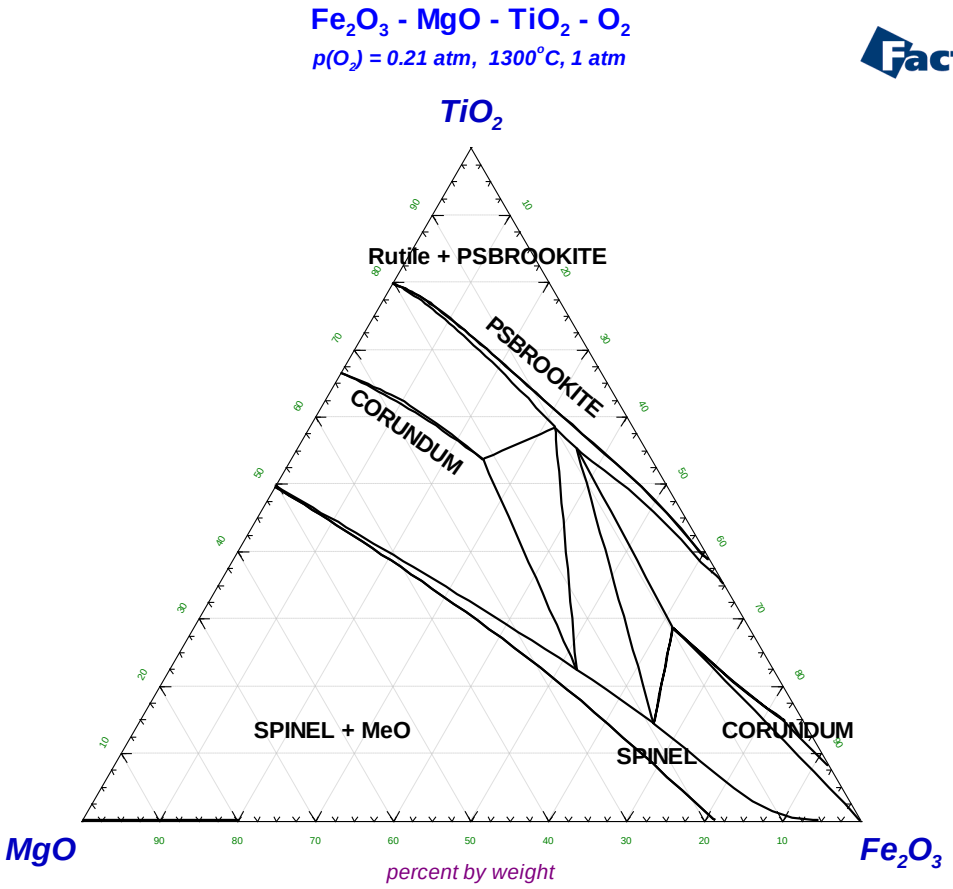

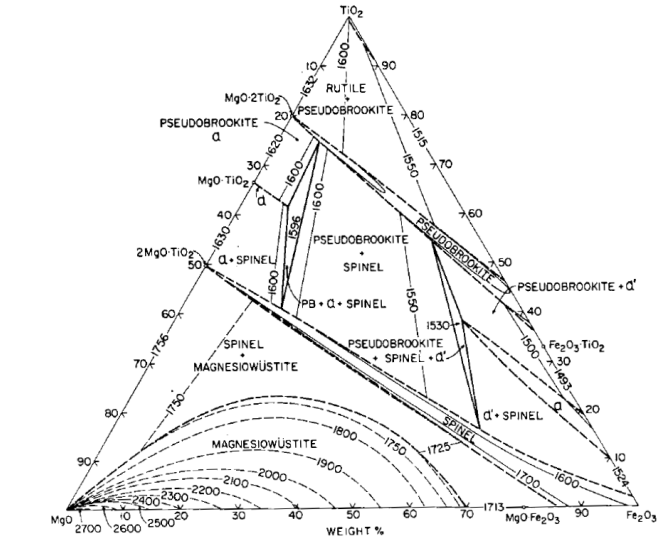

Fig. 7. Approximate 1300°C isothermal section of the system MgO–iron oxide–TiO_2 in air. Abbreviations used have the following meanings: α = geikielite solid solution, α′ = hematite solid solution, PB = pseudobrookite solid solution, S = spinel.

E. Woermann, B. Brezny, A. Muan, Am. J. Sci., 267A (1969), pp. 463-479.

Fe2O3-Mn2O3-SiO2, Mole fraction 1200°C

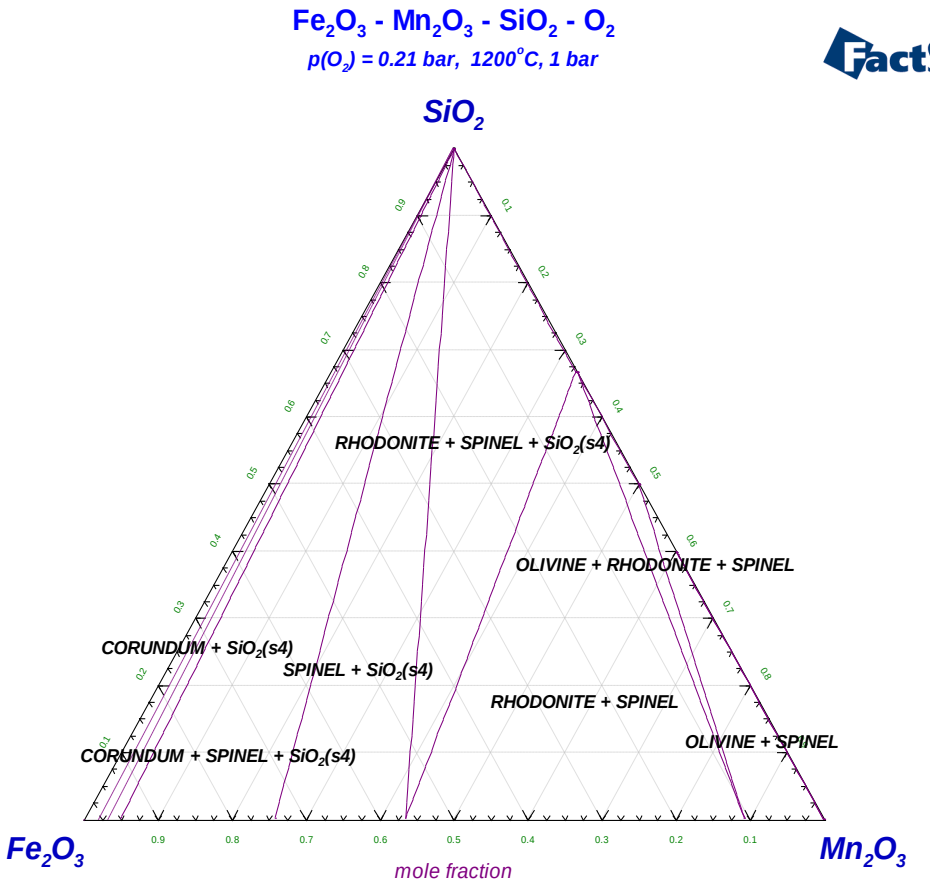

Fe2O3-Mn2O3-SiO2, Mole fraction 1400°C

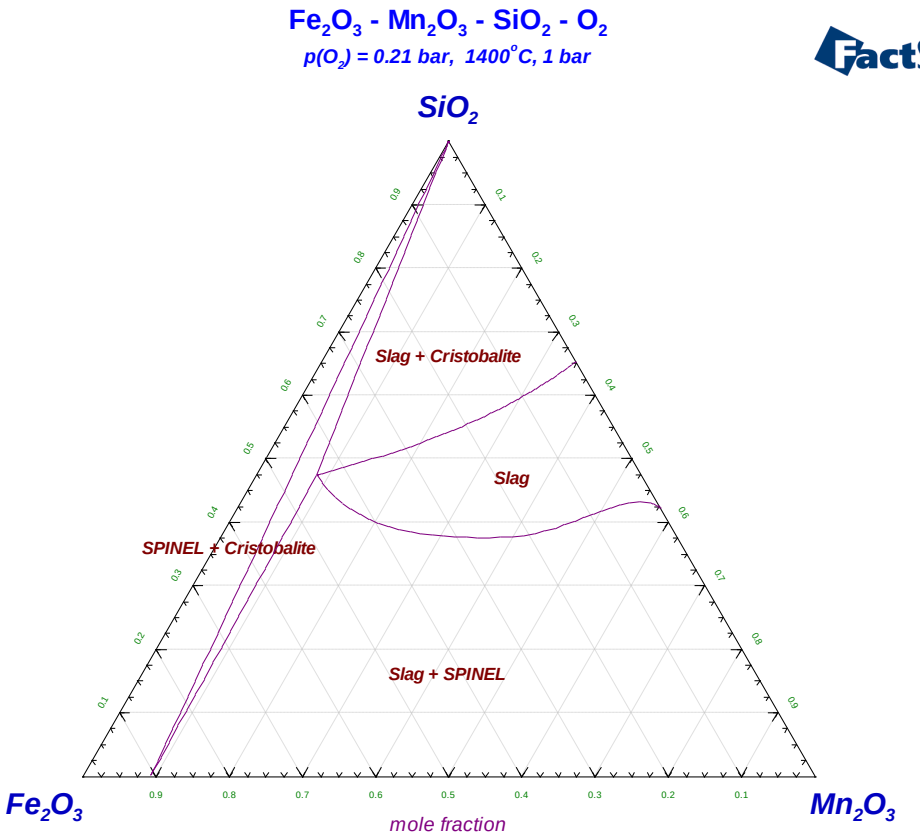

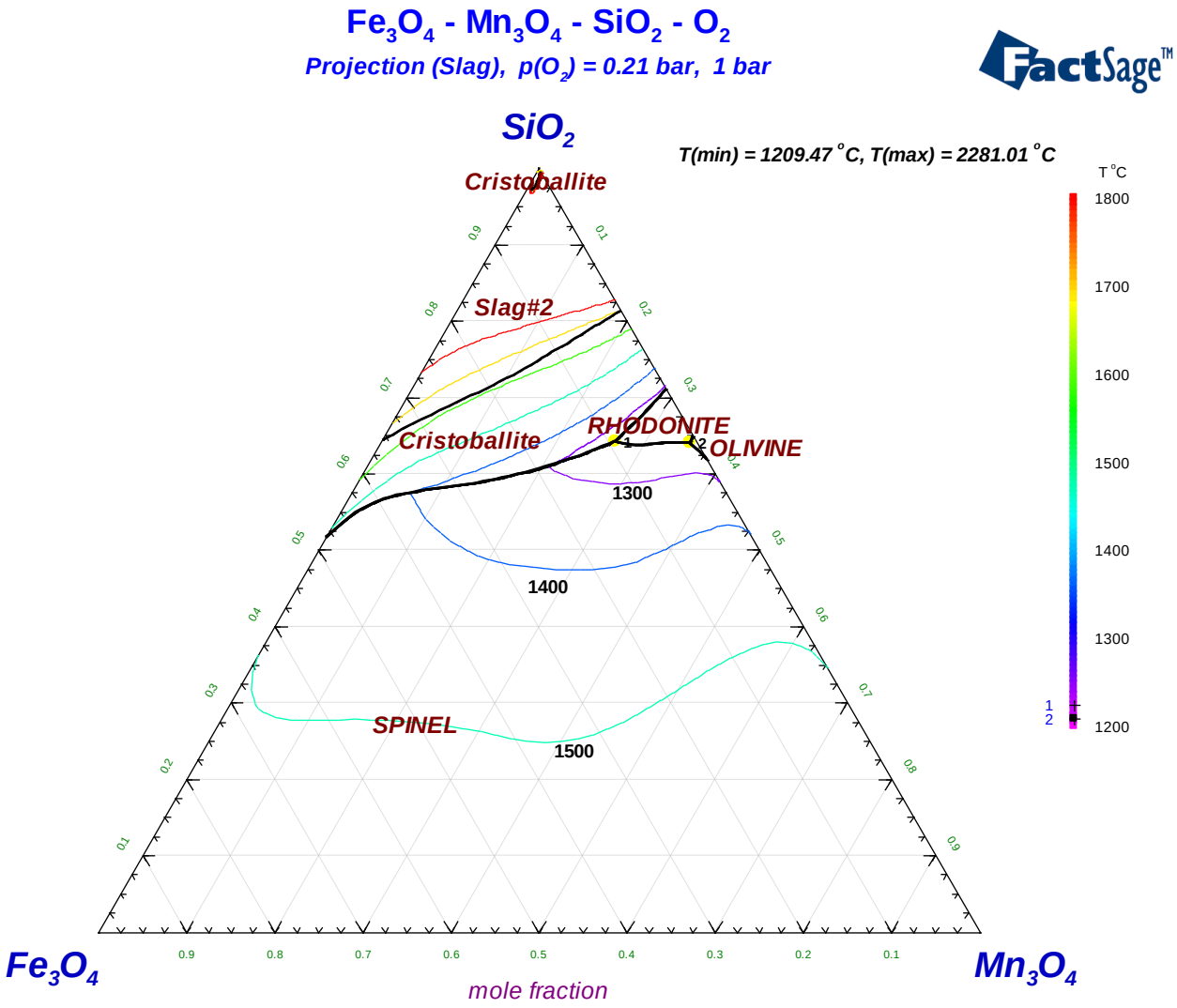
Fe3O4 - Mn3O4 - SiO2 - O2
Projection (Slag), p(O2) = 0.21 bar, 1 bar
FactSage™
SiO2
T(min) = 1209.47 °C, T(max) = 2281.01 °C
T °C
1800
1700
1600
1500
1400
1300
1200
Cristoballite
Slag#2
Cristoballite
RHODONITE
OLIVINE
1
2
1300
1400
SPINEL
1500
Fe3O4
Mn3O4
mole fraction

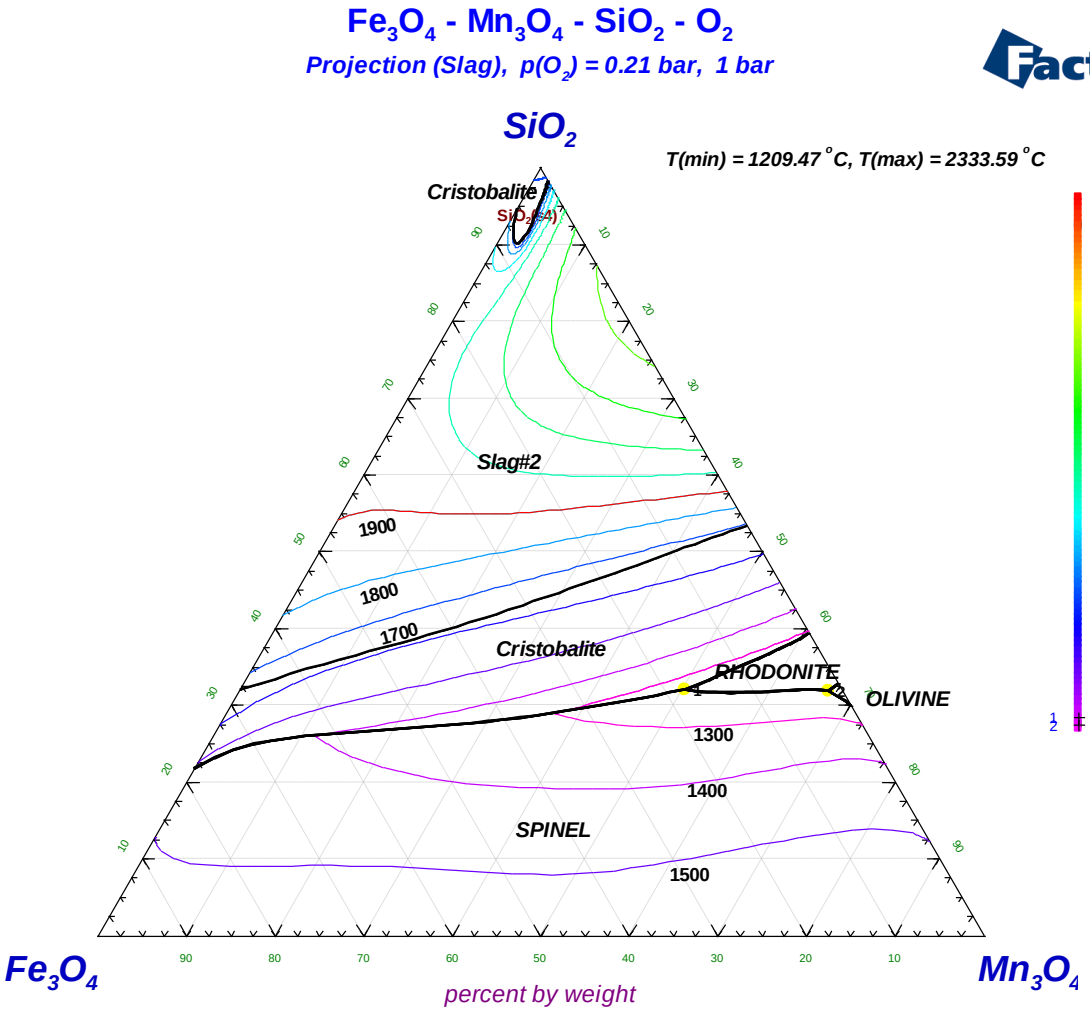

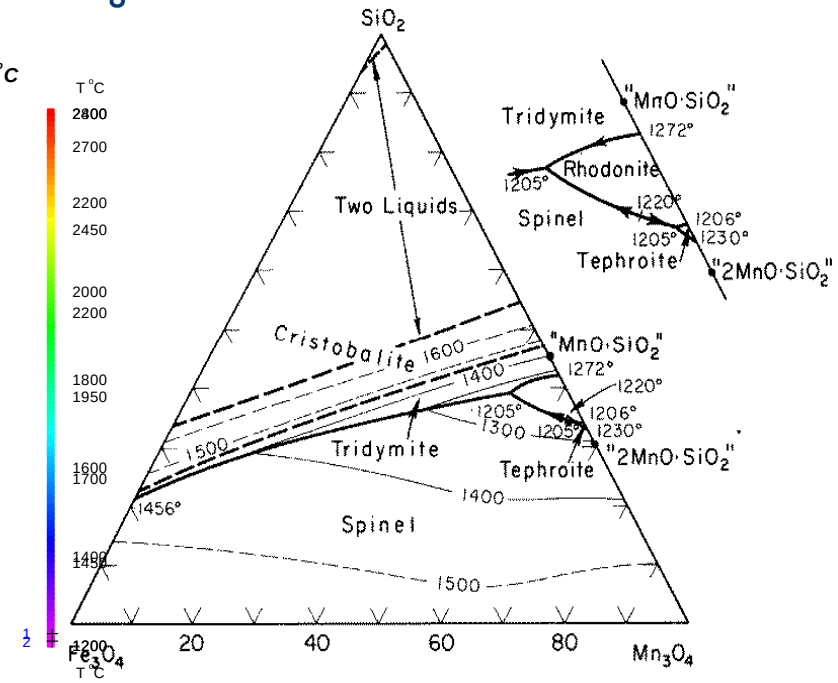

A. Muan and S. Somiya, Am. Mineral., 46 [3-4] 364-378 (1961).

Invariant equilibria on the liquidus surface

Intersections with slag	Mole fraction				Weight percent				
	A = SiO2, B = Fe3O4, C = Mn3O4				A = SiO2, B = Fe3O4, C = Mn3O4				
		X(A)	X(B)	X(C)	T(C)		W(A)	W(B)	W(C)	T(C)
1: RHODONITE / SPINEL / Cristobalite	1:	0.64241	0.09257	0.26502	1225.01	1:	31.987	17.762	50.252	1225.01
2: OLIVINE / RHODONITE / SPINEL	2:	0.64043	0.00830	0.35127	1209.47	2:	31.861	1.590	66.549	1209.47

Fe2O3-Na2O-SiO2, Weight percent 700°C

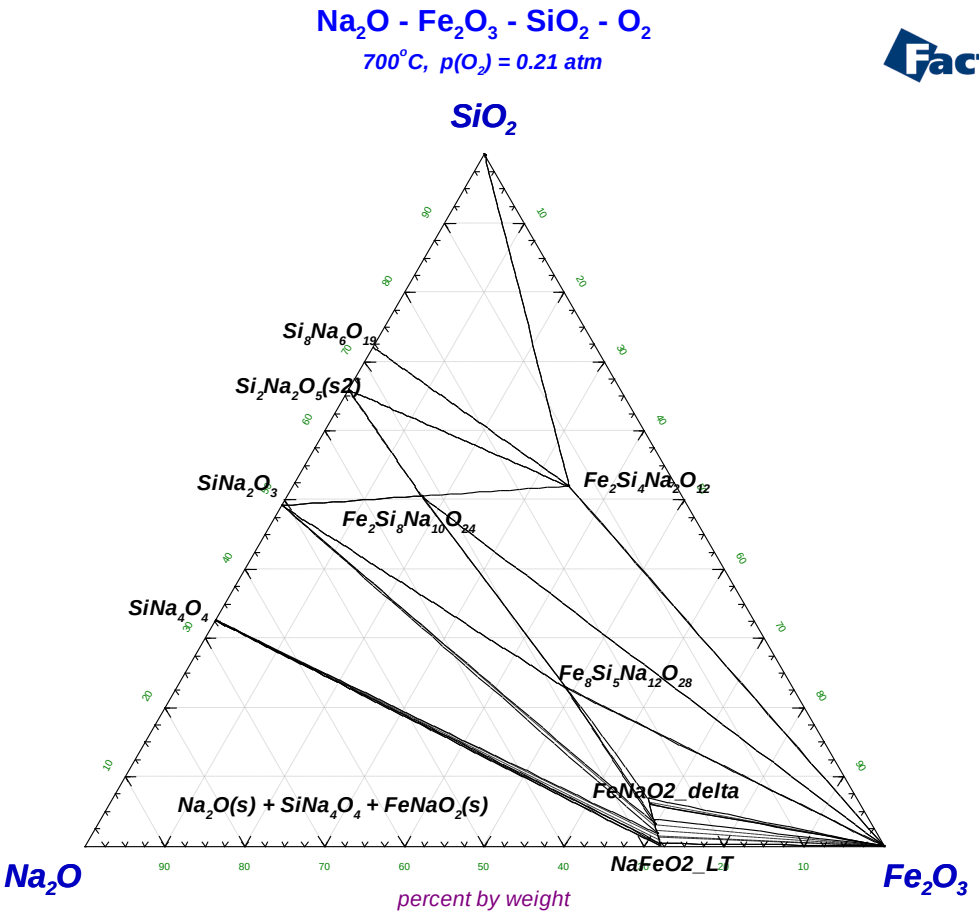

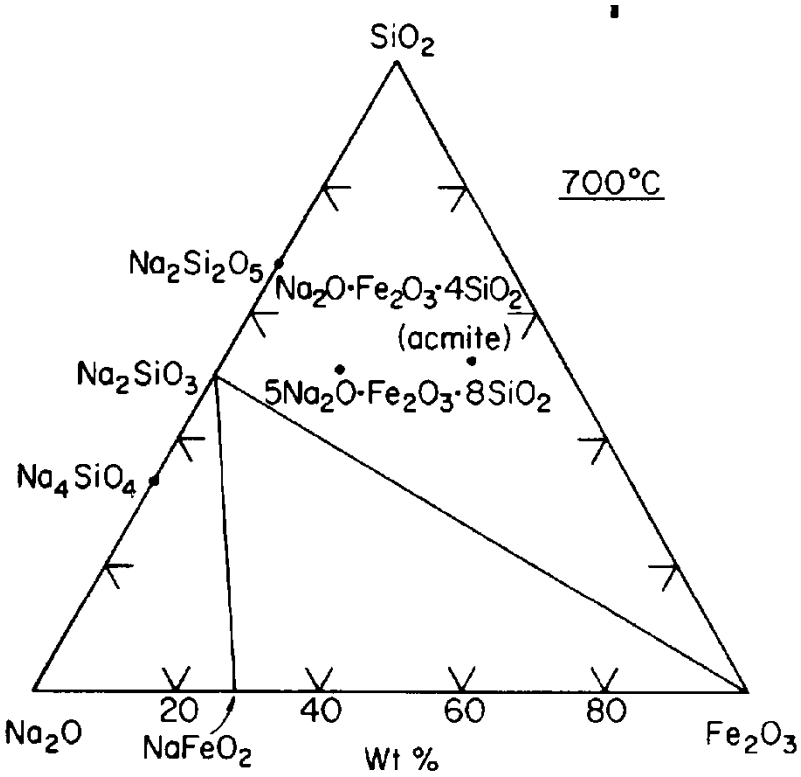

D. W. Collins and L. N. Mulay, J. Am. Ceram. Soc., 53 [2] 74-76 (1970).

Fe2O3-Na2O-SiO2, Weight percent 825°C

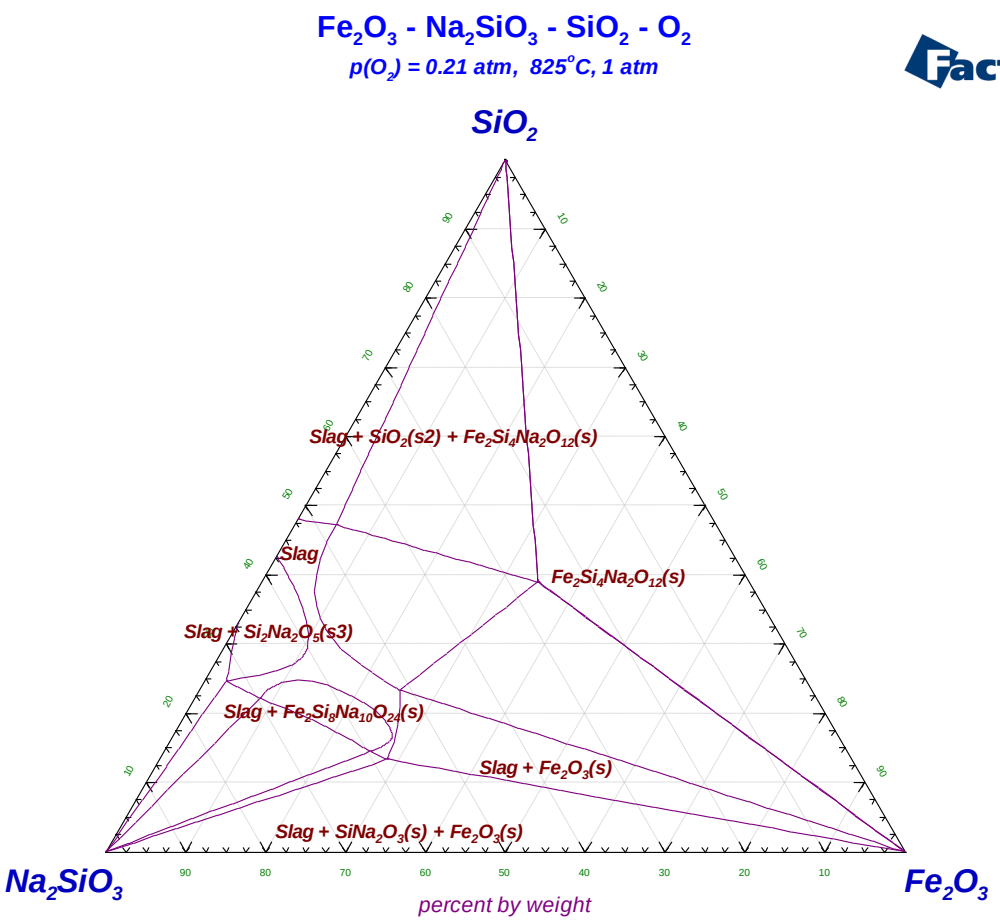

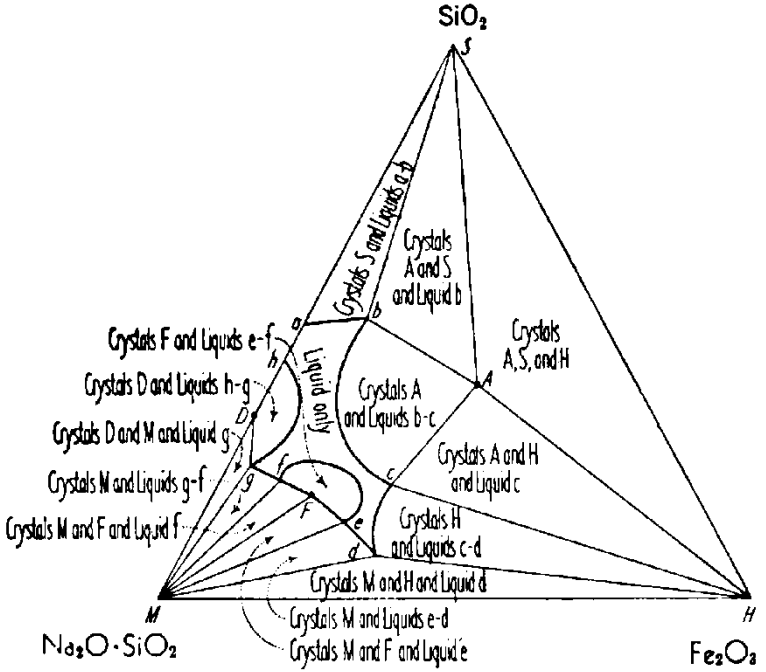

N.L. Bowen, J.F. Schairer, H.W.V. Willems, Am. J. Sci., 220, [20], (1930), pp. 405-455.

Weight percent,
Isopleth Acmite-Na2SiO3

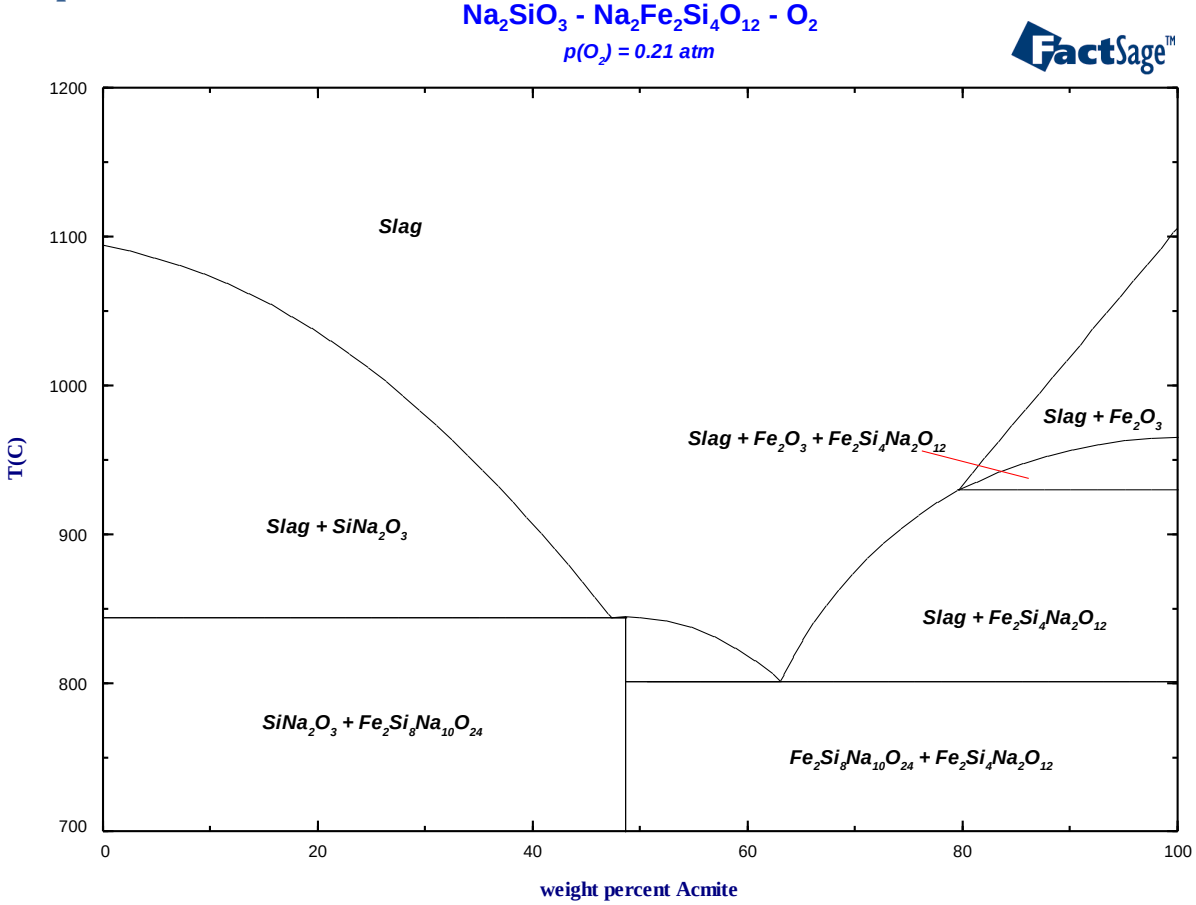

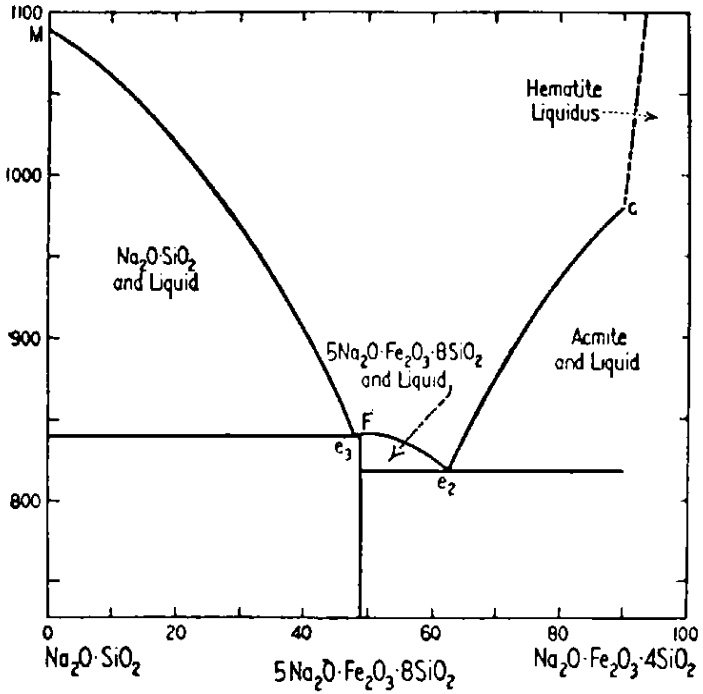

N.L. Bowen, J.F. Schairer, H.W.V. Willems, Am. J. Sci., 220, [20], (1930), pp. 405-455.

Weight percent,
Isopleth Acmite-Na2Si2O5

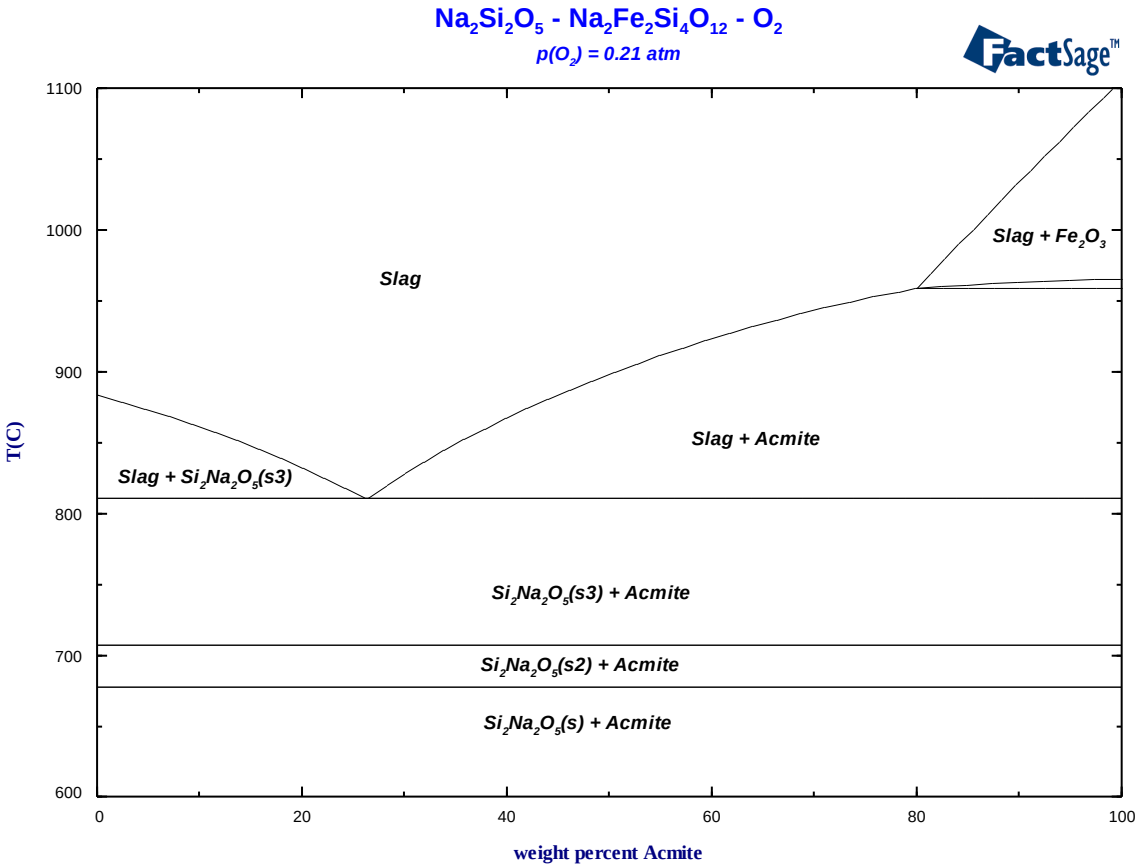

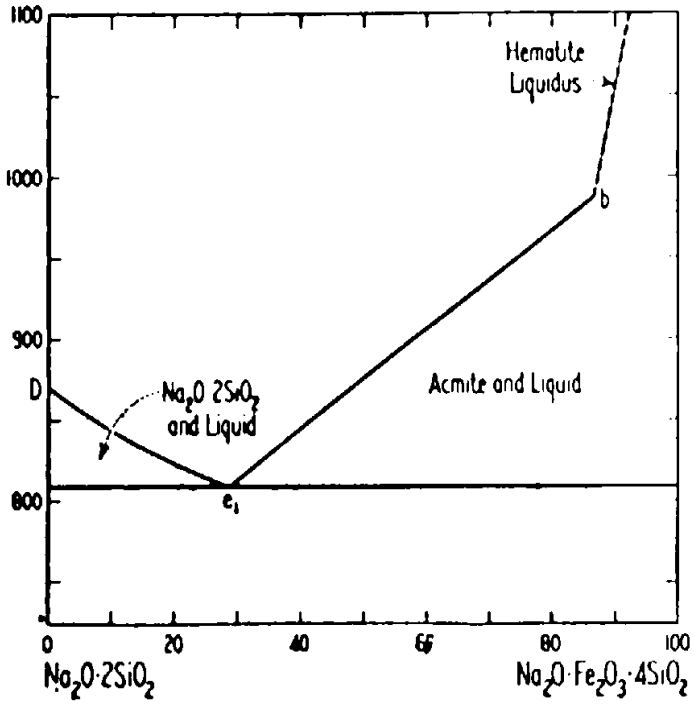

N.L. Bowen, J.F. Schairer, H.W.V. Willems, Am. J. Sci., 220, [20], (1930), pp. 405-455.

Weight percent,
Isopleth Fe2O3-Na2Si2O5

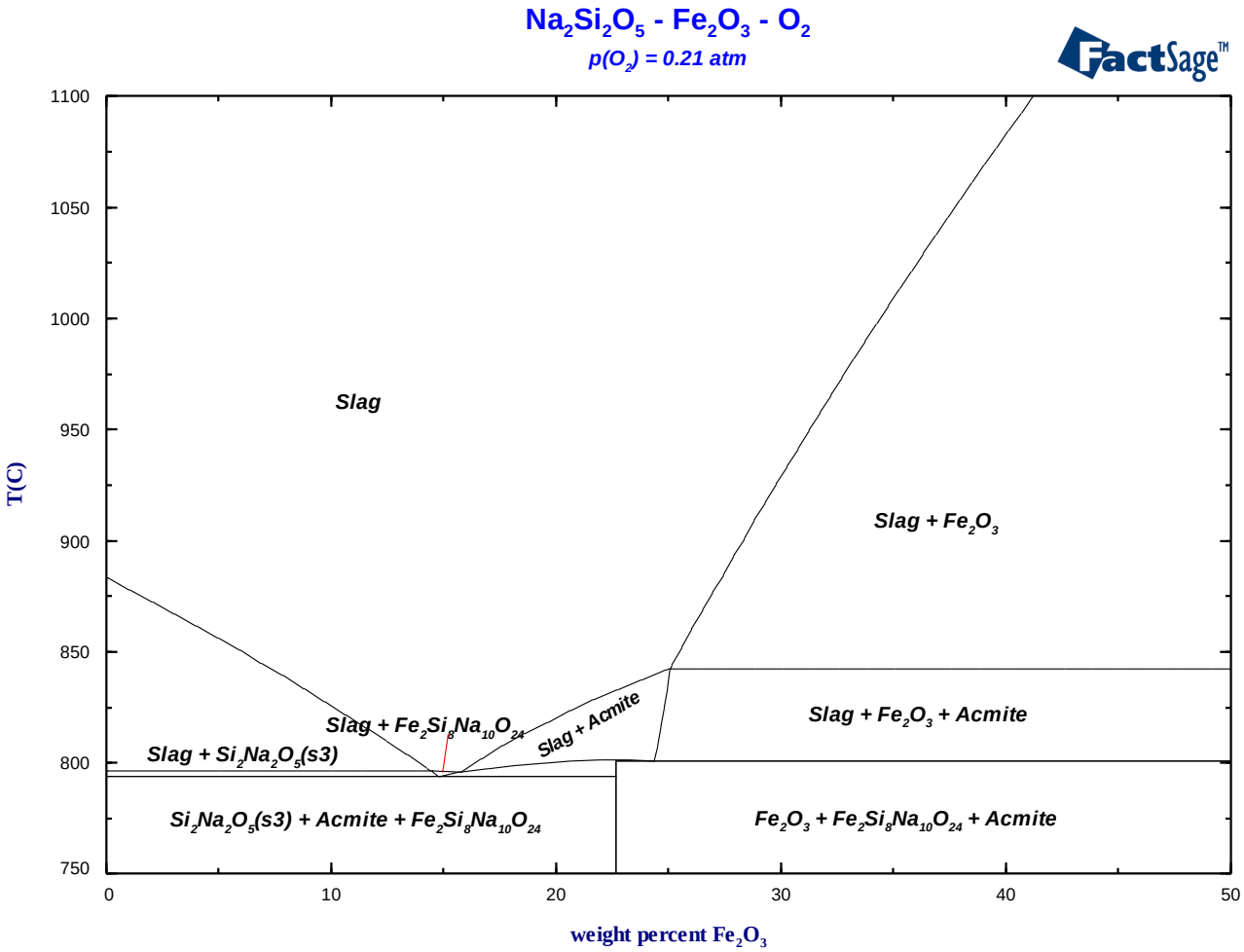

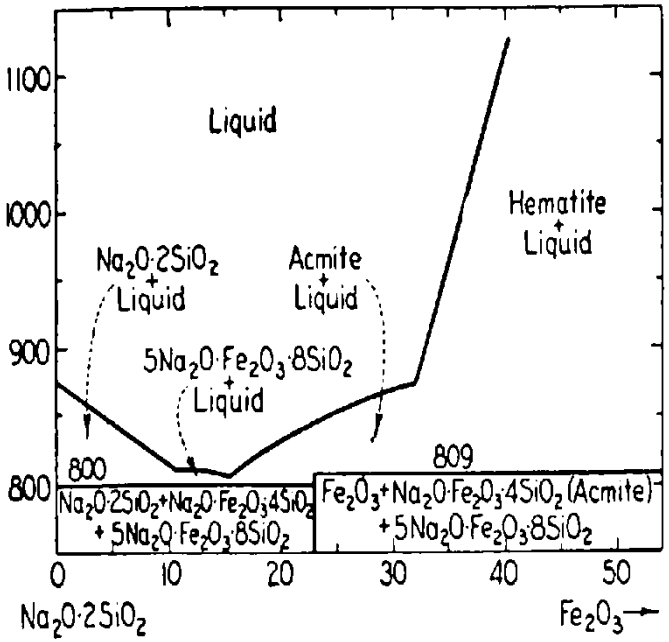

N.L. Bowen, J.F. Schairer, H.W.V. Willems, Am. J. Sci., 220, [20], (1930), pp. 405-455.

Mole fraction,
Isopleth FeNaO2-SiO2

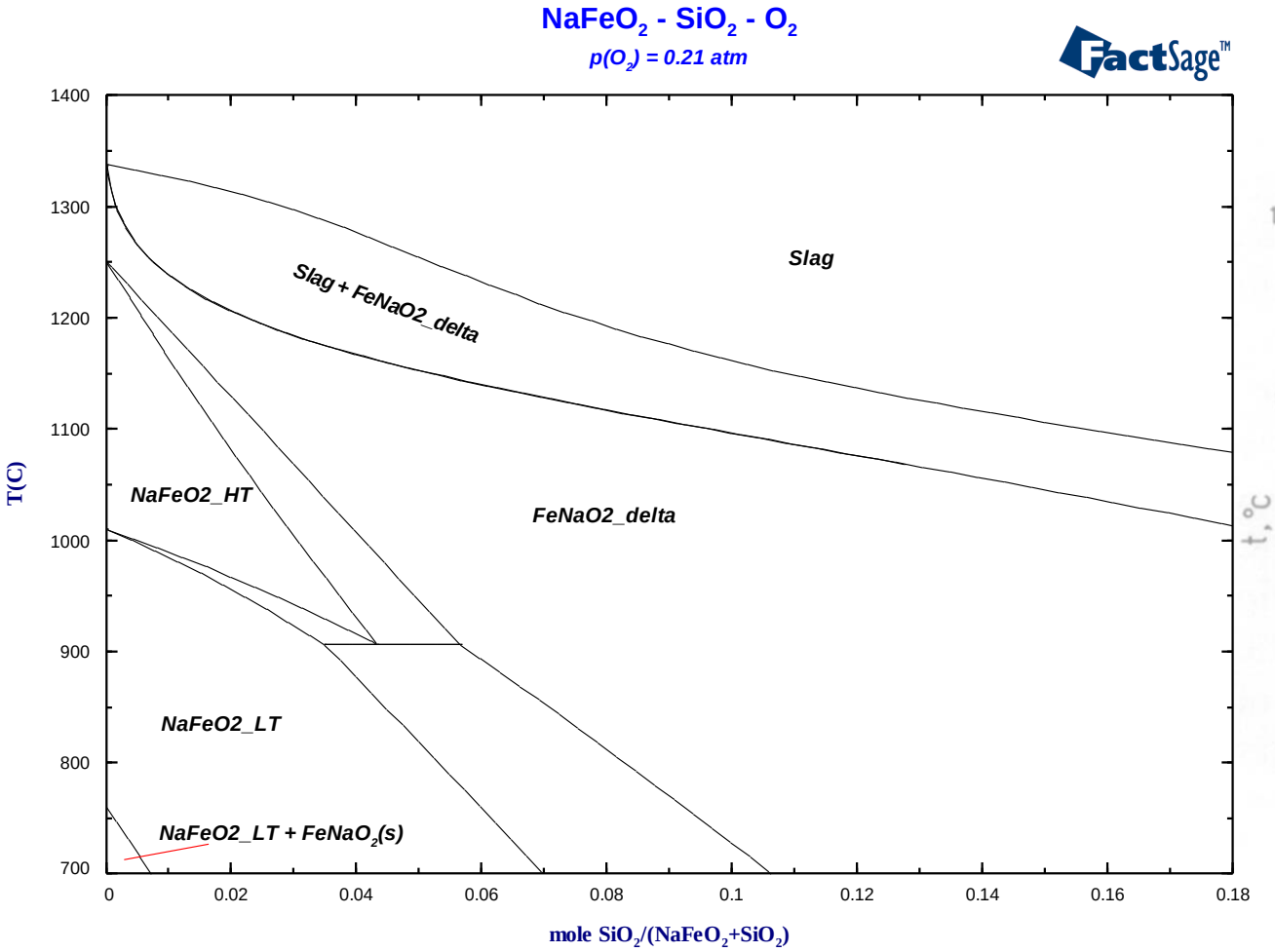

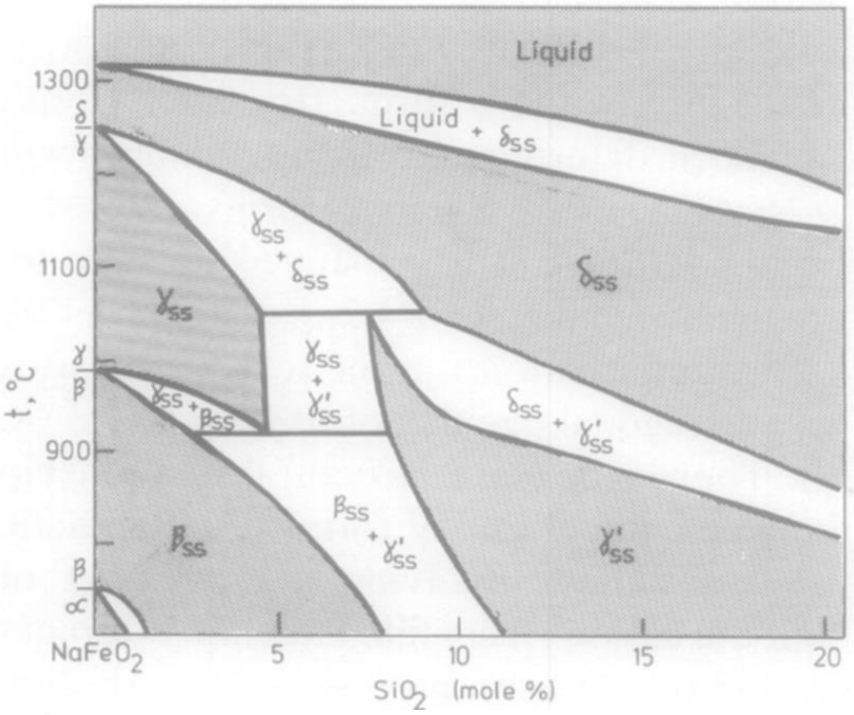

I. E. Grey and C. Li, J. Solid State Chem., 69 [1] 116-125 (1987).

Weight percent,
Isopletale Schnitte mit 5Na2O Fe2O3 8SiO2

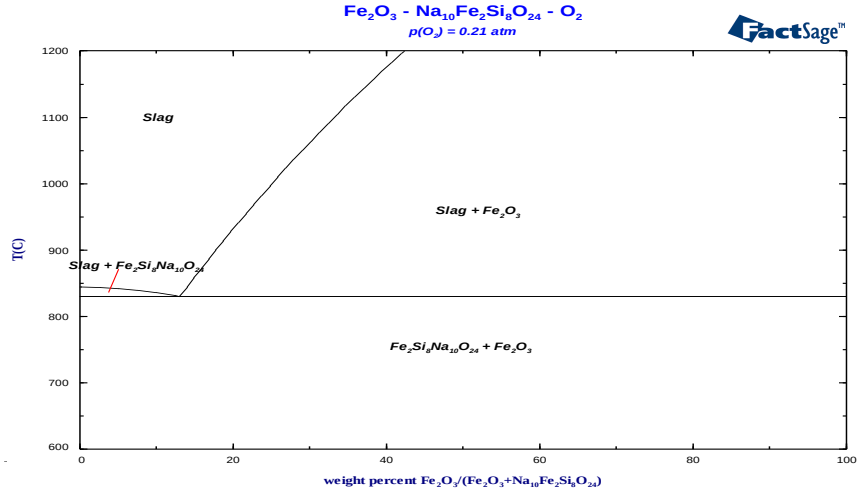

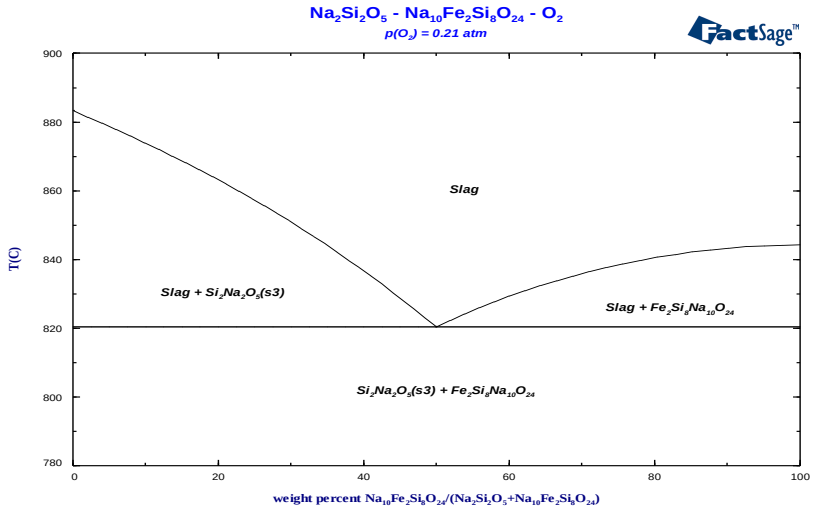

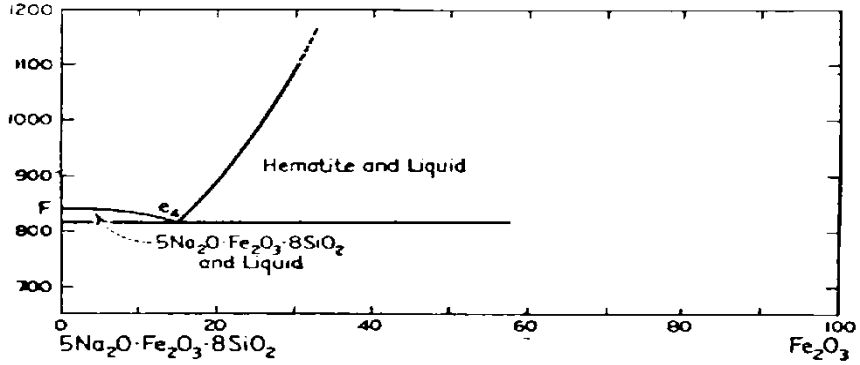

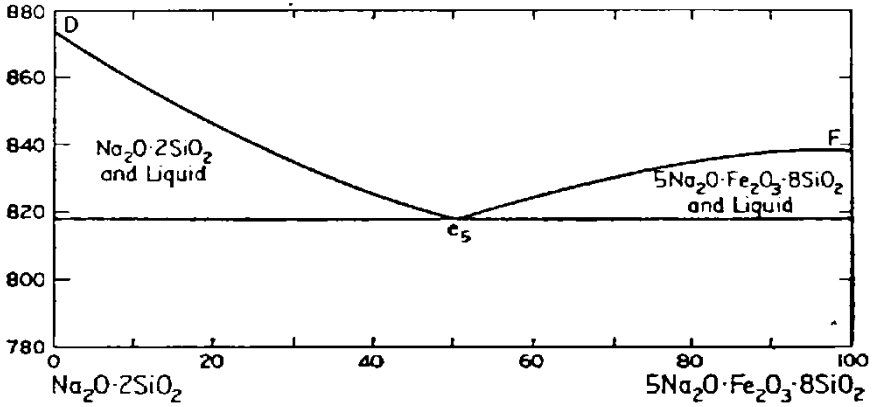

N.L. Bowen, J.F. Schairer, H.W.V. Willems, Am. J. Sci., 220, [20], (1930), pp. 405-455.

Fe_2O_3 - Na_2O - SiO_2 - O_2

Projection (Slag), $p(O_2)$ = 0.21 atm

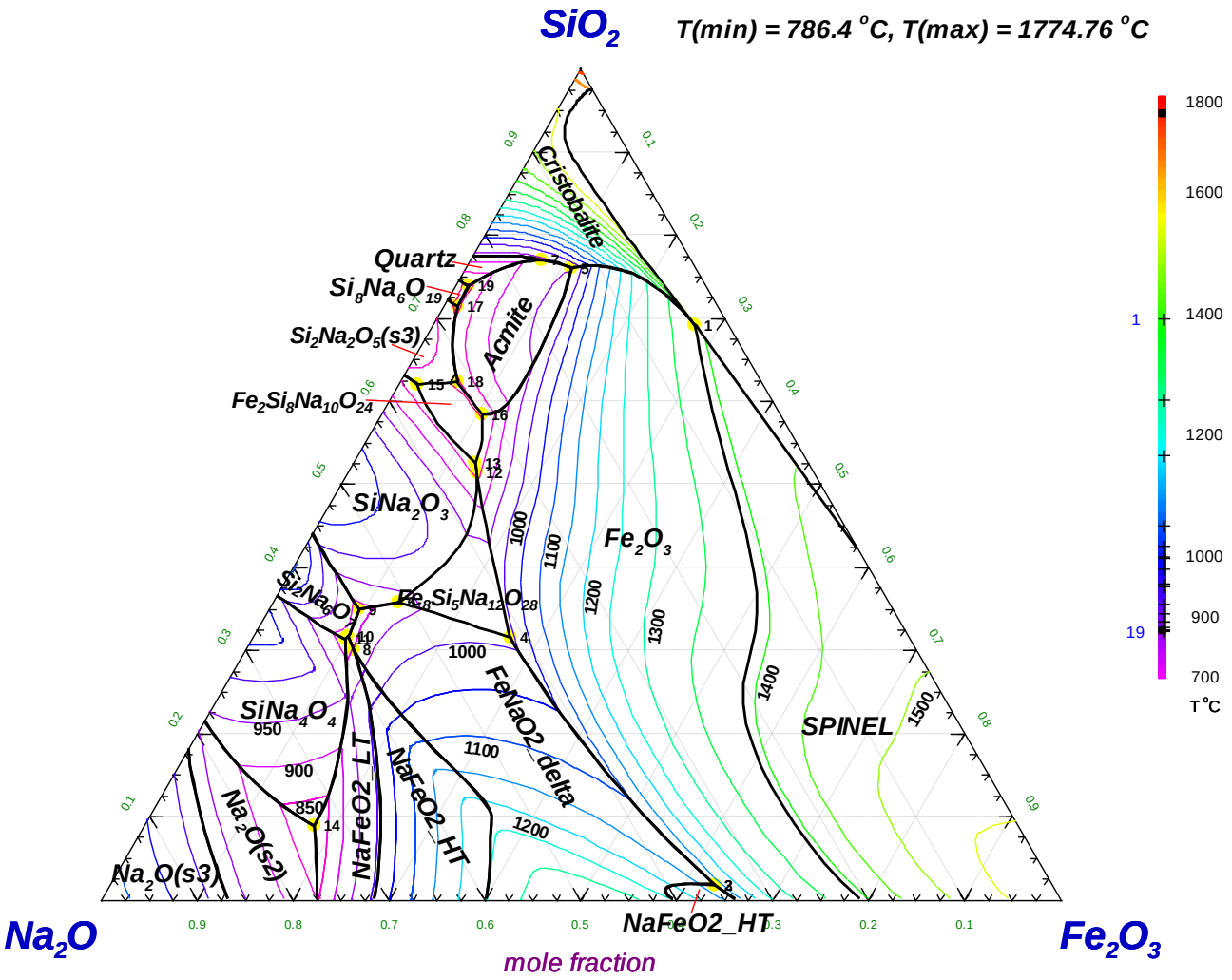

Weight percent, Liquidussurface

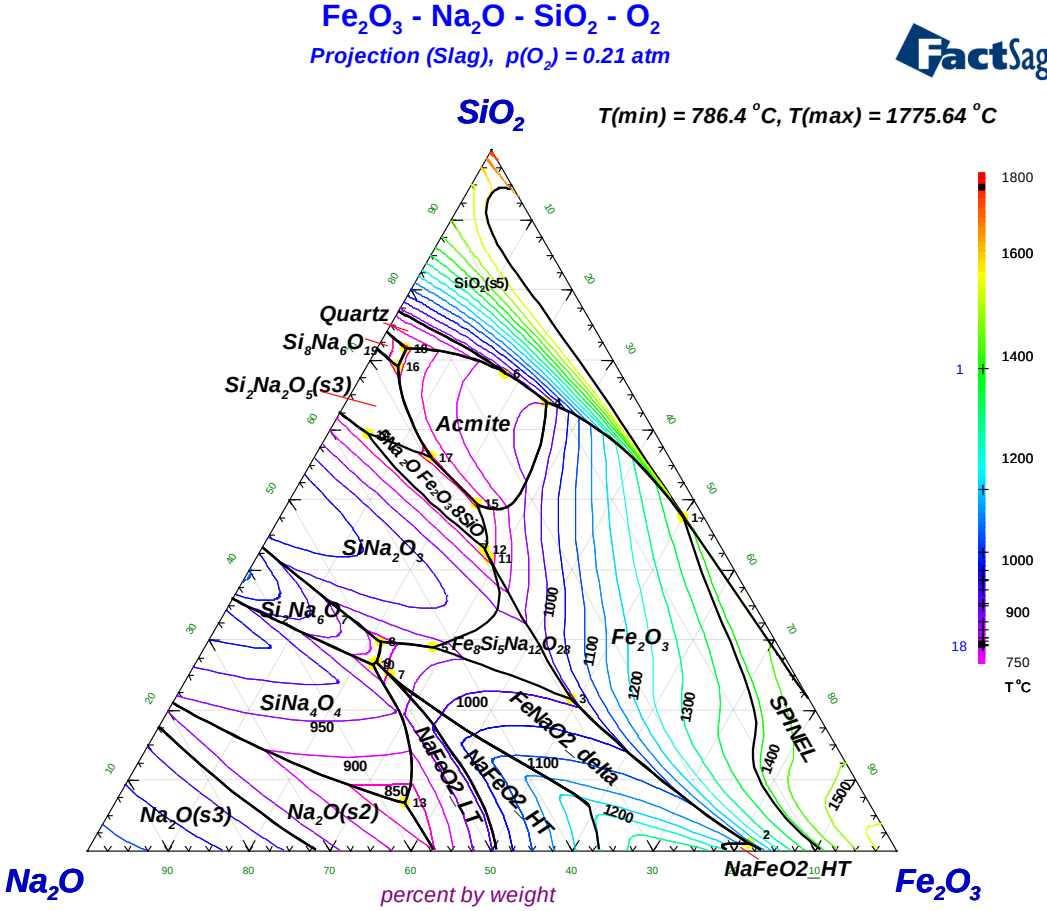

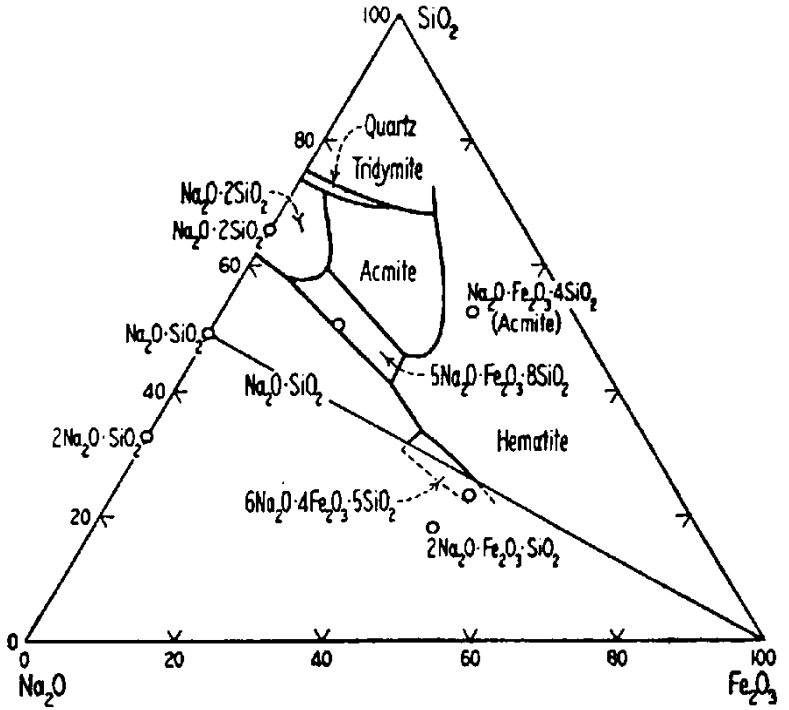

N.L. Bowen, J.F. Schairer, H.W.V. Willems, Am. J. Sci., 220 (20), [20], (1930), pp. 405-455

Weight percent,
Liquidussurface Fe2O3-Na2SiO3-SiO2

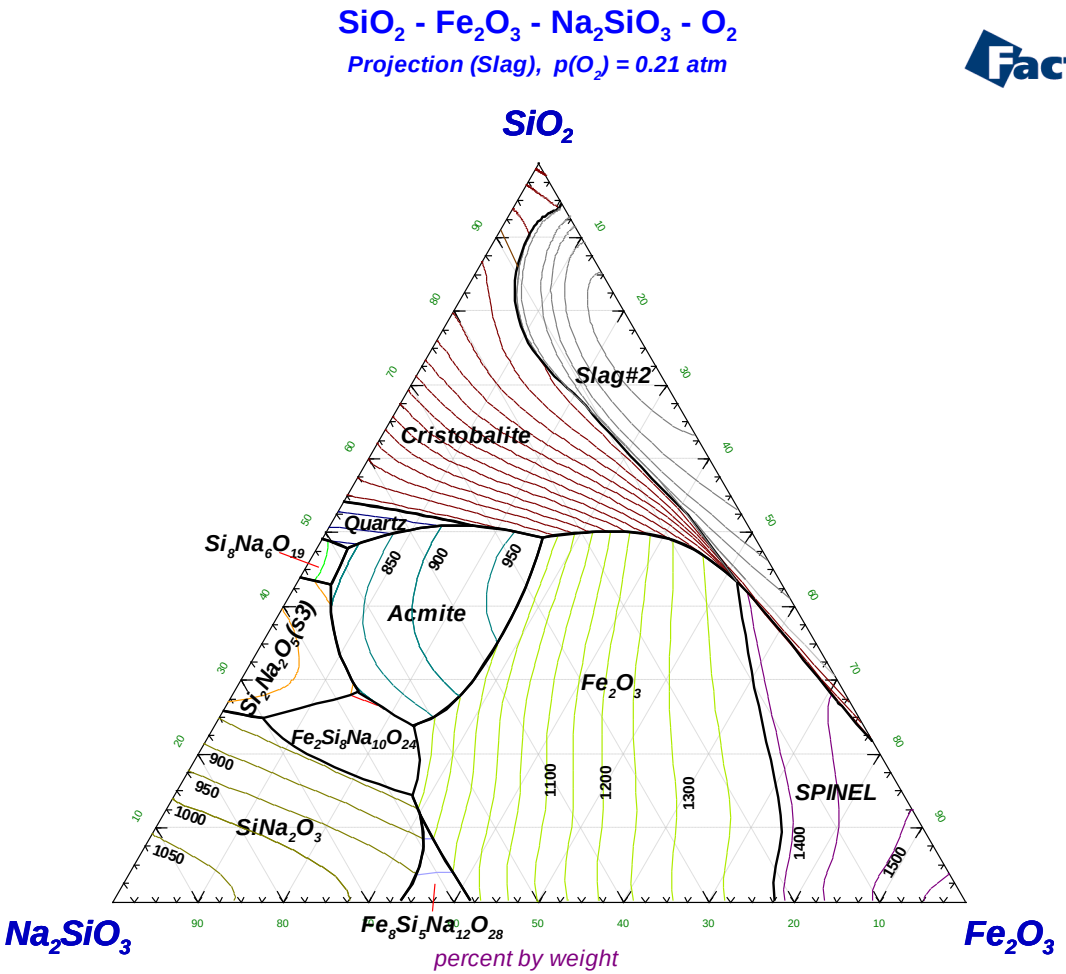

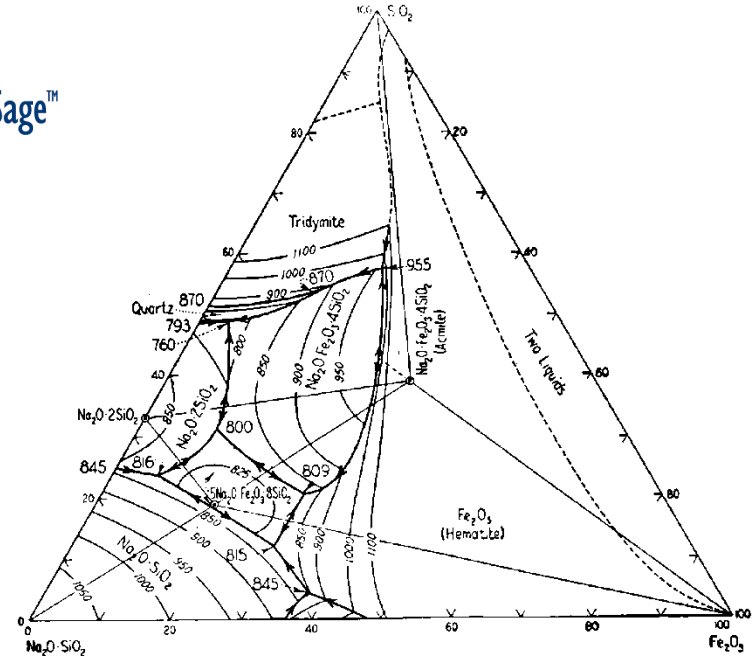

N.L. Bowen, J.F. Schairer, H.W.V. Willems, Am. J. Sci., 220 (20), [20], (1930), pp. 405-455

Invariant equilibria on the liquidus surface

Intersections with slag	Mole fraction A = SiO2, B = Na2O, C = Fe2O3				Weight percent A = SiO2, B = Na2O, C = Fe2O3			
	X(A)	X(B)	X(C)	T(C)	W(A)	W(B)	W(C)	T(C)
1: Fe2O3 / SPINEL / Cristobalite	0.69142	0.03469	0.27389	1384.37	47.516	2.459	50.025	1384.36
2: NaFeO2_HT / Fe2O3 / FeNaO2_delta	0.01782	0.35086	0.63132	1122.80	0.866	17.589	81.544	1122.80
3: Fe2O3 / Fe8Si5Na12O28 / FeNaO2_delta	0.31457	0.41541	0.27002	988.58	21.535	29.335	49.130	988.58
4: Fe2O3 / Acmite / Cristobalite	0.76006	0.12891	0.11103	948.33	63.972	11.192	24.836	948.33
5: Fe8Si5Na12O28 / FeNaO2_delta / SiNa2O3	0.35732	0.51076	0.13192	927.31	28.937	42.668	28.394	927.31
6: Acmite / Cristobalite / Quartz	0.76945	0.15492	0.07563	926.28	68.077	14.139	17.784	926.28
7: NaFeO2_HT / NaFeO2_LT / FeNaO2_delta	0.30108	0.58556	0.11336	906.23	24.957	50.069	24.973	906.23
8: FeNaO2_delta / Si2Na6O7 / SiNa2O3	0.34889	0.55599	0.09512	877.14	29.687	48.802	21.511	877.14
9: NaFeO2_LT / FeNaO2_delta / Si2Na6O7	0.31733	0.58293	0.09974	876.88	26.807	50.798	22.395	876.87
10: NaFeO2_LT / Si2Na6O7 / SiNa4O4	0.31300	0.58875	0.09825	872.51	26.493	51.405	22.102	872.48
11: Fe2O3 / Fe8Si5Na12O28 / SiNa2O3	0.51333	0.35156	0.13511	838.20	41.563	29.362	29.075	838.18
12: Fe2O3 / Fe2Si8Na10O24 / SiNa2O3	0.52549	0.34680	0.12771	819.51	42.980	29.259	27.760	819.52
13: NaFeO2_LT / Na2O(s2) / SiNa4O4	0.08821	0.73342	0.17838	803.70	6.688	57.365	35.947	803.68
14: Fe2Si8Na10O24 / Si2Na2O5(s3) / SiNa2O3	0.62011	0.35935	0.02054	803.36	59.319	35.460	5.221	803.36
15: Fe2O3 / Acmite / Fe2Si8Na10O24	0.58430	0.31063	0.10507	794.51	49.350	27.063	23.586	794.51
16: Acmite / Si2Na2O5(s3) / Si8Na6O19	0.71357	0.27086	0.01557	788.35	68.987	27.012	4.000	788.35
17: Acmite / Fe2Si8Na10O24 / Si2Na2O5(s3)	0.62245	0.31666	0.06089	788.17	56.030	29.403	14.566	788.17
18: Acmite / Si8Na6O19 / Quartz	0.73837	0.24738	0.01425	786.43	71.588	24.741	3.671	786.40

FeO-Na2O-V2O5,
Mole fraction, Subsolidus surface

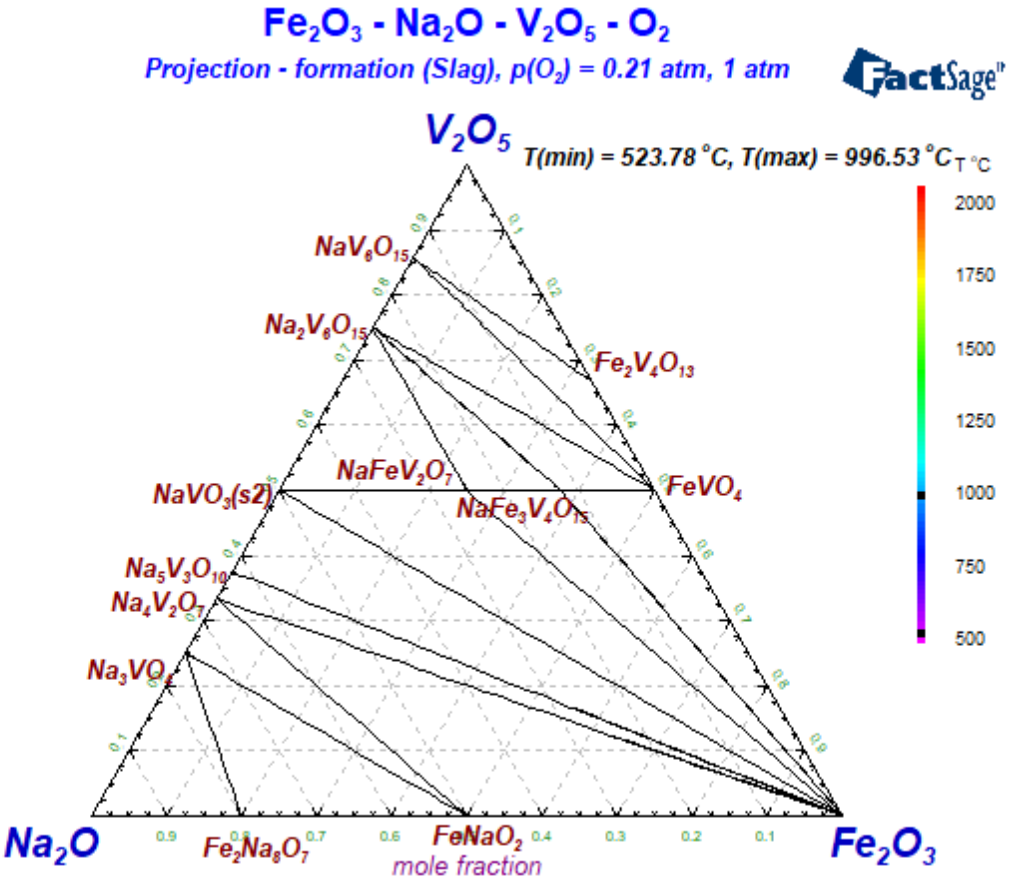

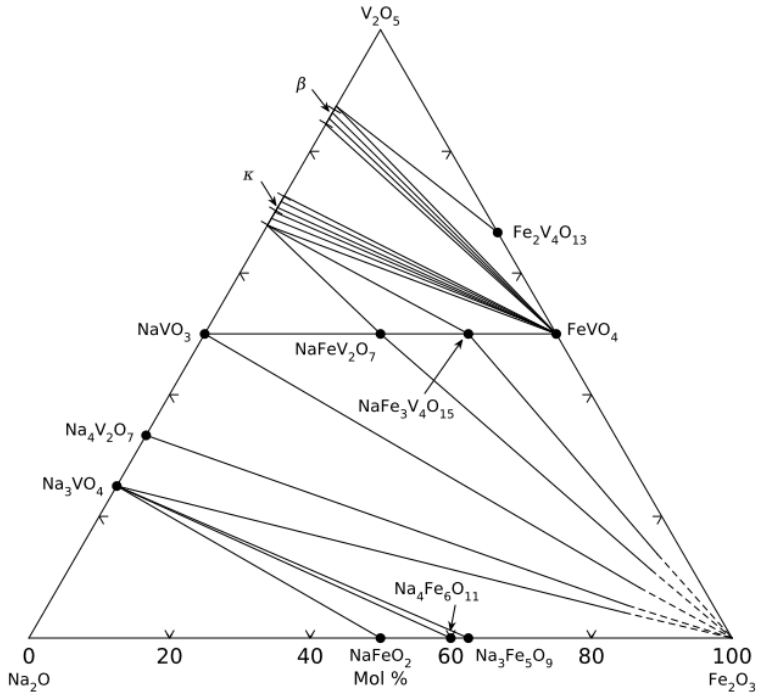

B. V. Slobodin, S. F. Blinova, and A. A. Fotiev, Zh. Neorg. Khim., 23 [10] 2815-2818 (1978).

FeO-Na2O-V2O5,
Mole fraction, Isopleth FeVO4-NaVO3

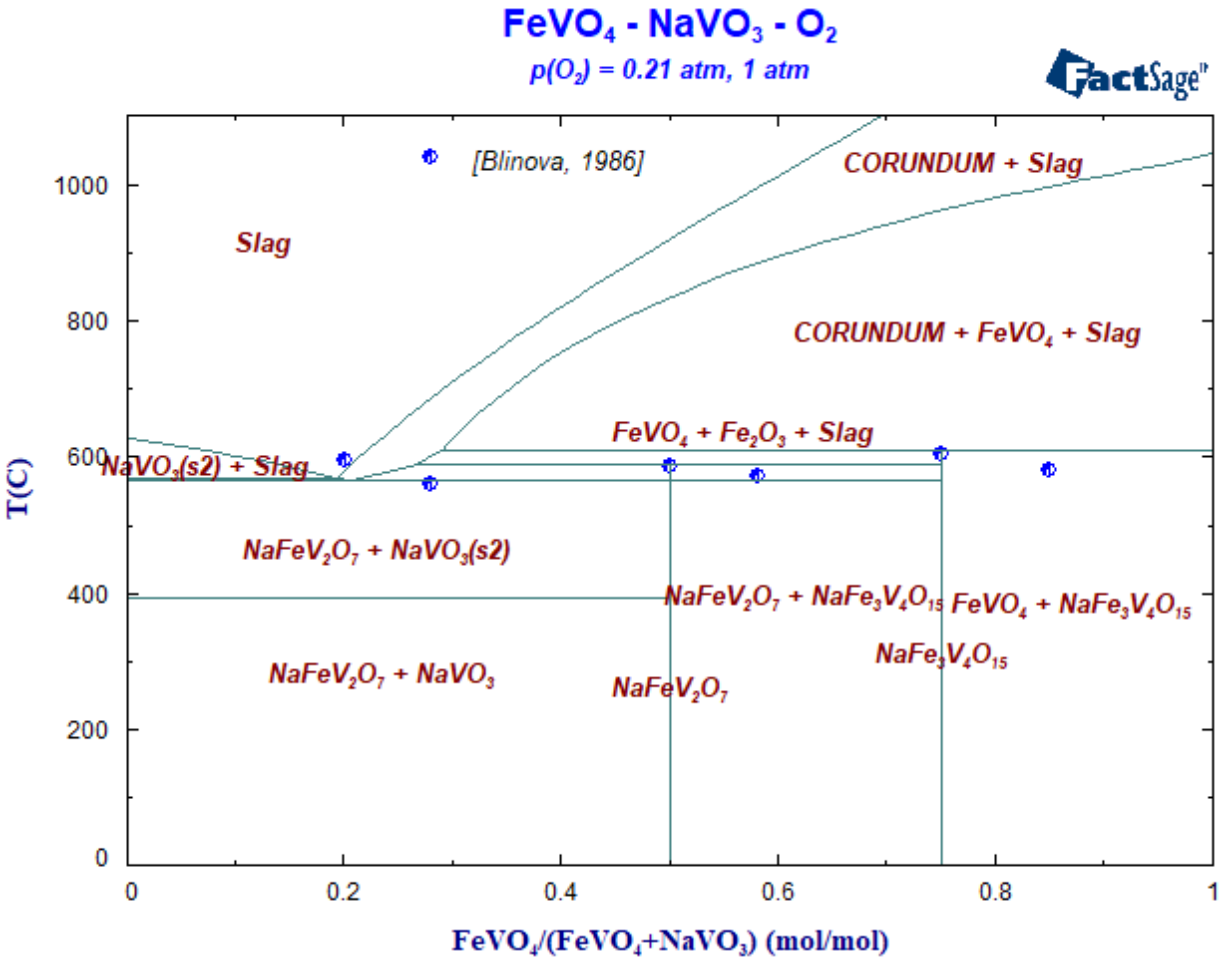

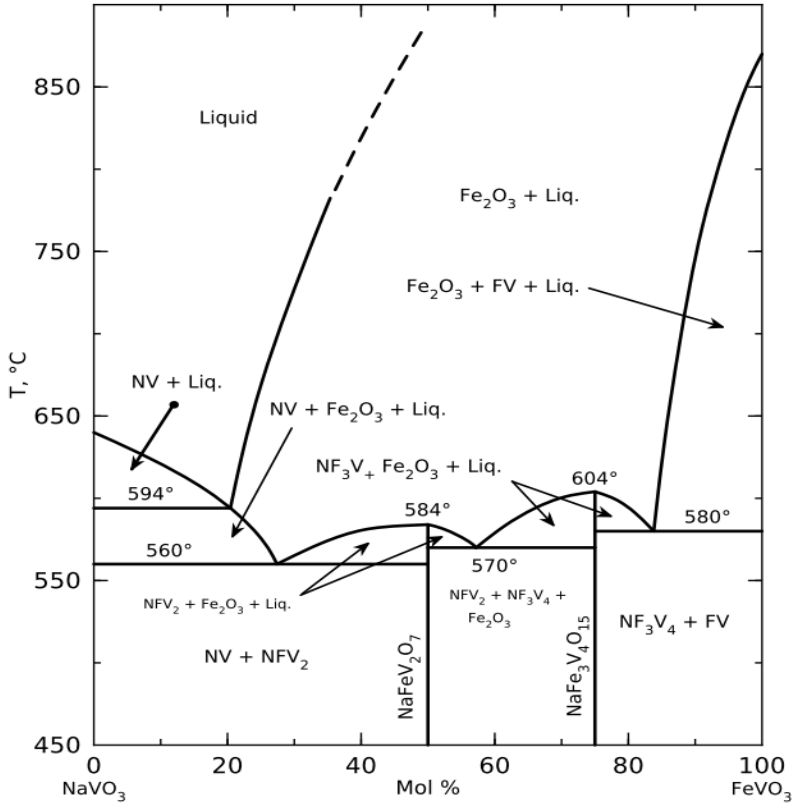

S. F. Blinova, B. V. Slobodin, V. M. Blinov, A. A. Fotiev, Zh. Neorg. Khim., 31 [8] 2093-2095 (1986);

FeO-Na2O-V2O5,
Mole fraction, Liquidus surface

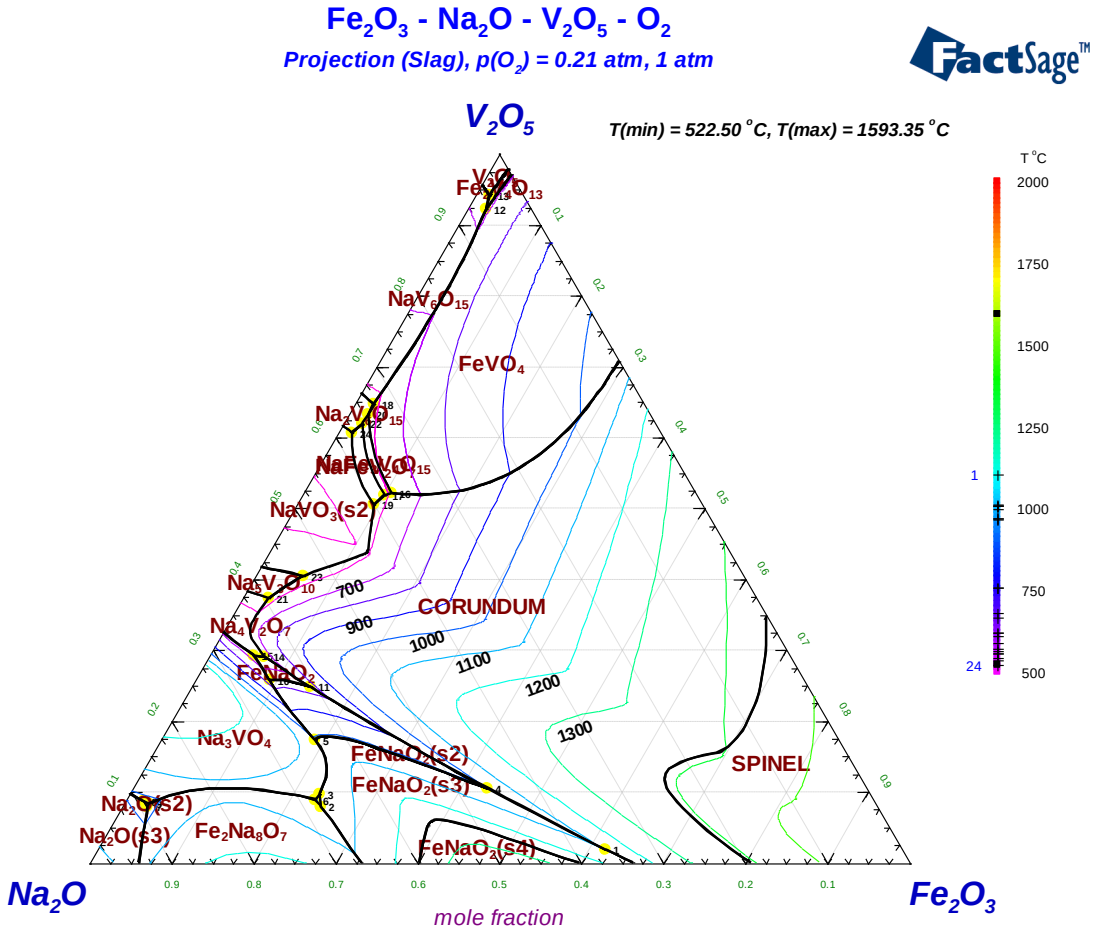

FeO-Na2O-V2O5,
Weight percent, Liquidus surface

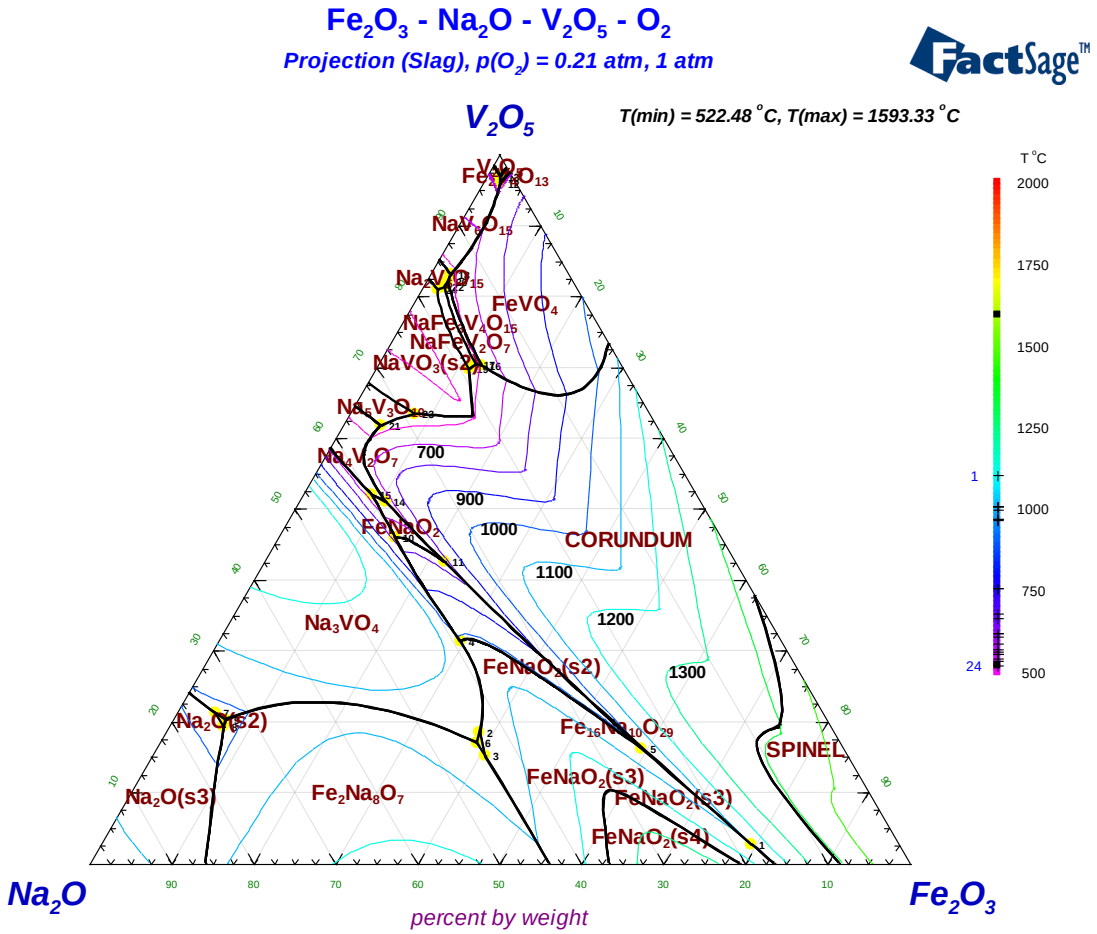

Invariant equilibria on the liquidus surface

Intersections with slag	Mole fraction A = V2O5, B = Na2O, C = Fe2O3				Weight percent A = V2O5, B = Na2O, C = Fe2O3			
	X(A)	X(B)	X(C)	T(C)	W(A)	W(B)	W(C)	T(C)
1: CORUNDUM / Fe16Na10O29 / FeNaO2(s3)	1: 0.01896	0.36092	0.62012	1105.21	1: 2.763	17.919	79.318	1105.22
2: Fe2Na8O7 / FeNaO2(s3) / FeNaO2(s2)	2: 0.07967	0.67805	0.24228	1012.77	2: 18.408	43.210	38.382	1009.87
3: FeNaO2(s3) / FeNaO2(s2) / Na3VO4	3: 0.09743	0.67118	0.23139	1009.87	3: 15.220	44.141	40.639	1009.86
4: Fe16Na10O29 / FeNaO2(s3) / FeNaO2(s2)	4: 0.10426	0.46243	0.43331	1009.85	4: 31.306	39.130	29.564	1009.85
5: FeNaO2(s3) / FeNaO2(s2) / Na3VO4	5: 0.17411	0.63862	0.18727	1009.85	5: 16.233	24.535	59.233	1009.85
6: Fe2Na8O7 / FeNaO2(s2) / Na3VO4	6: 0.08952	0.67984	0.23064	996.53	6: 17.094	44.237	38.668	996.53
7: Fe2Na8O7 / Na2O(s2) / Na2O(s3)	7: 0.07904	0.88959	0.03137	971.74	7: 21.270	74.067	4.663	970.05
8: Na2O(s2) / Na2O(s3) / Na3VO4	8: 0.08720	0.89103	0.02177	970.05	8: 19.291	73.987	6.722	970.05
9: Fe2Na8O7 / Na2O(s2) / Na3VO4	9: 0.08384	0.88607	0.03008	964.82	9: 20.341	73.252	6.408	964.83
10: FeNaO2(s2) / FeNaO2(s) / Na3VO4	10: 0.25754	0.65190	0.09056	759.85	10: 46.056	39.726	14.218	759.85
11: CORUNDUM / Fe16Na10O29 / FeNaO2(s)	11: 0.24800	0.60629	0.14571	759.76	11: 42.572	35.467	21.961	759.76
12: Fe2V4O13 / FeVO4 / NaV6O15	12: 0.92322	0.05469	0.02209	681.08	12: 96.043	1.939	2.018	681.08
13: Fe2V4O13 / NaV6O15 / V2O5	13: 0.94192	0.04163	0.01645	666.14	13: 97.051	1.461	1.488	666.13
14: Fe2O3 / FeNaO2(s) / Na4V2O7	14: 0.29082	0.64121	0.06797	621.24	14: 51.110	38.402	10.488	621.24
15: FeNaO2(s) / Na3VO4 / Na4V2O7	15: 0.29306	0.65322	0.05372	620.35	15: 52.070	39.550	8.380	620.36
16: CORUNDUM / FeVO4 / NaFe3V4O15	16: 0.52230	0.37059	0.10711	609.32	16: 70.332	17.005	12.663	609.32
17: CORUNDUM / NaFe3V4O15 / NaFeV2O7	17: 0.51926	0.38116	0.09958	587.91	17: 70.496	17.634	11.870	587.90
18: FeVO4 / Na2V6O15 / NaV6O15	18: 0.64813	0.32963	0.02223	573.09	18: 83.096	14.401	2.502	573.07
19: CORUNDUM / NaFeV2O7 / NaVO3(s2)	19: 0.50531	0.40098	0.09372	564.49	19: 69.772	18.867	11.361	564.48
20: FeVO4 / Na2V6O15 / NaFe3V4O15	20: 0.63254	0.34377	0.02370	558.98	20: 82.096	15.204	2.700	559.00
21: CORUNDUM / Na4V2O7 / Na5V3O10	21: 0.37354	0.59494	0.03151	558.95	21: 61.850	33.569	4.581	558.95
22: Na2V6O15 / NaFe3V4O15 / NaFeV2O7	22: 0.62004	0.35712	0.02283	544.46	22: 81.393	15.975	2.632	544.44
23: CORUNDUM / Na5V3O10 / NaVO3(s2)	23: 0.40534	0.53722	0.05744	536.58	23: 63.449	28.657	7.894	536.58
24: Na2V6O15 / NaFeV2O7 / NaVO3(s2)	24: 0.60712	0.37650	0.01637	522.50	24: 80.971	17.111	1.917	522.48

Mole fraction 1300°C

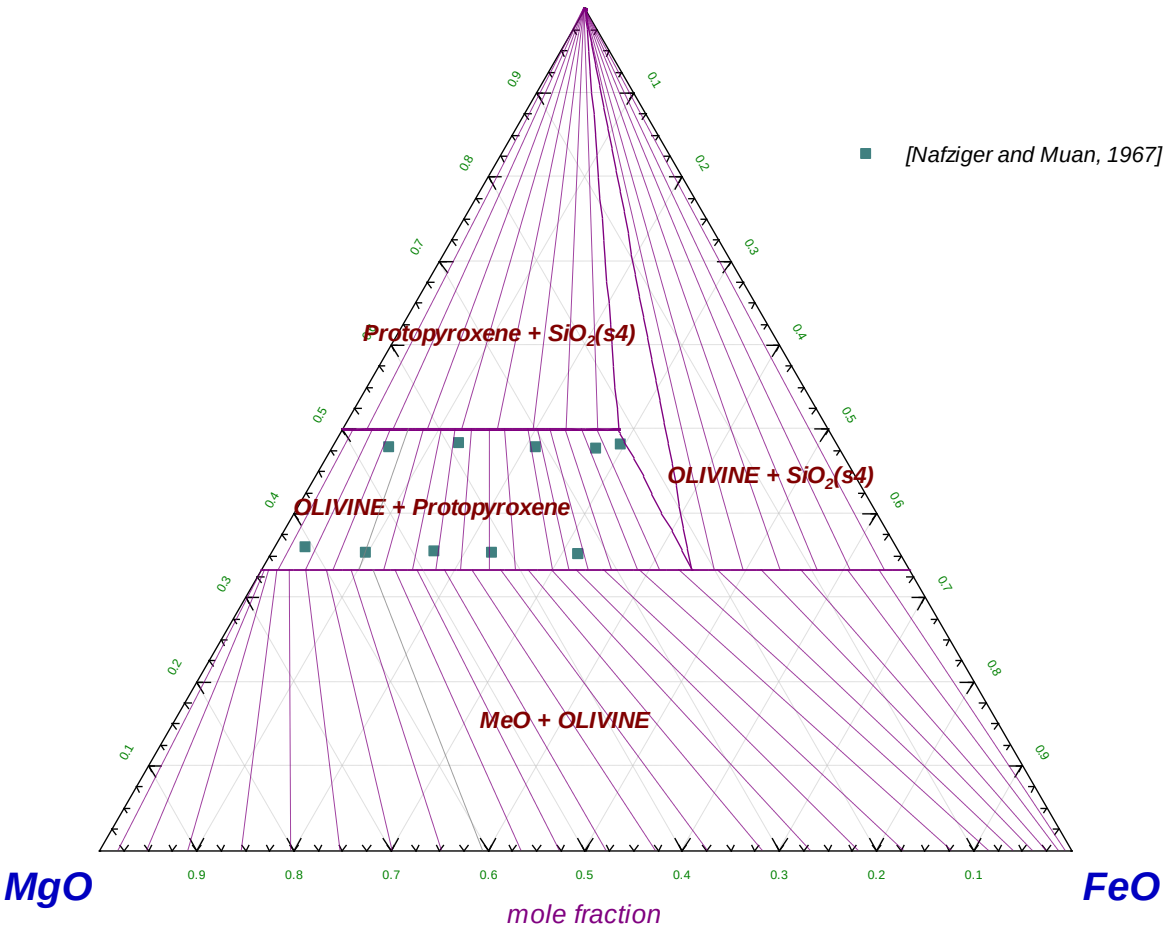

[Nafziger and Muan, 1967]

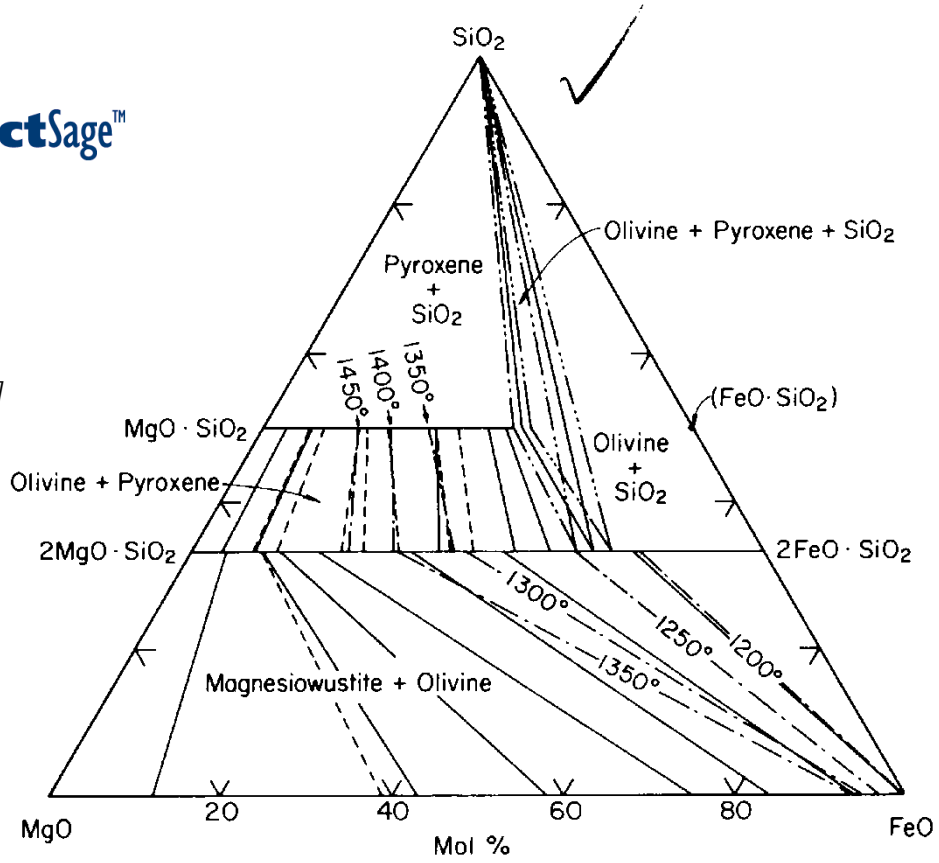

R.H. Nafziger, A. Muan, Am. Mineral., 52, (1967), pp. 1364-1385.

FeO-MgO-SiO2, Weight percent 1450°C

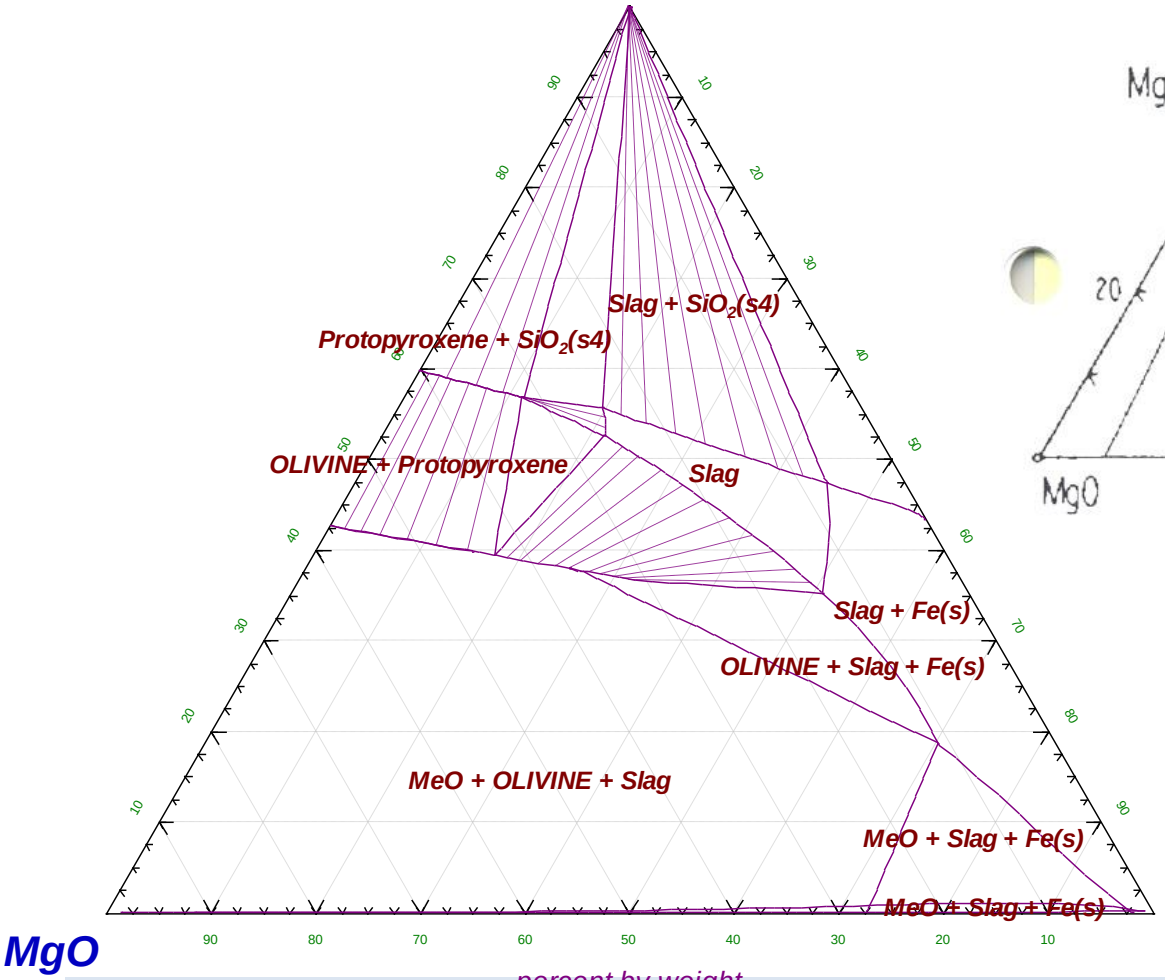

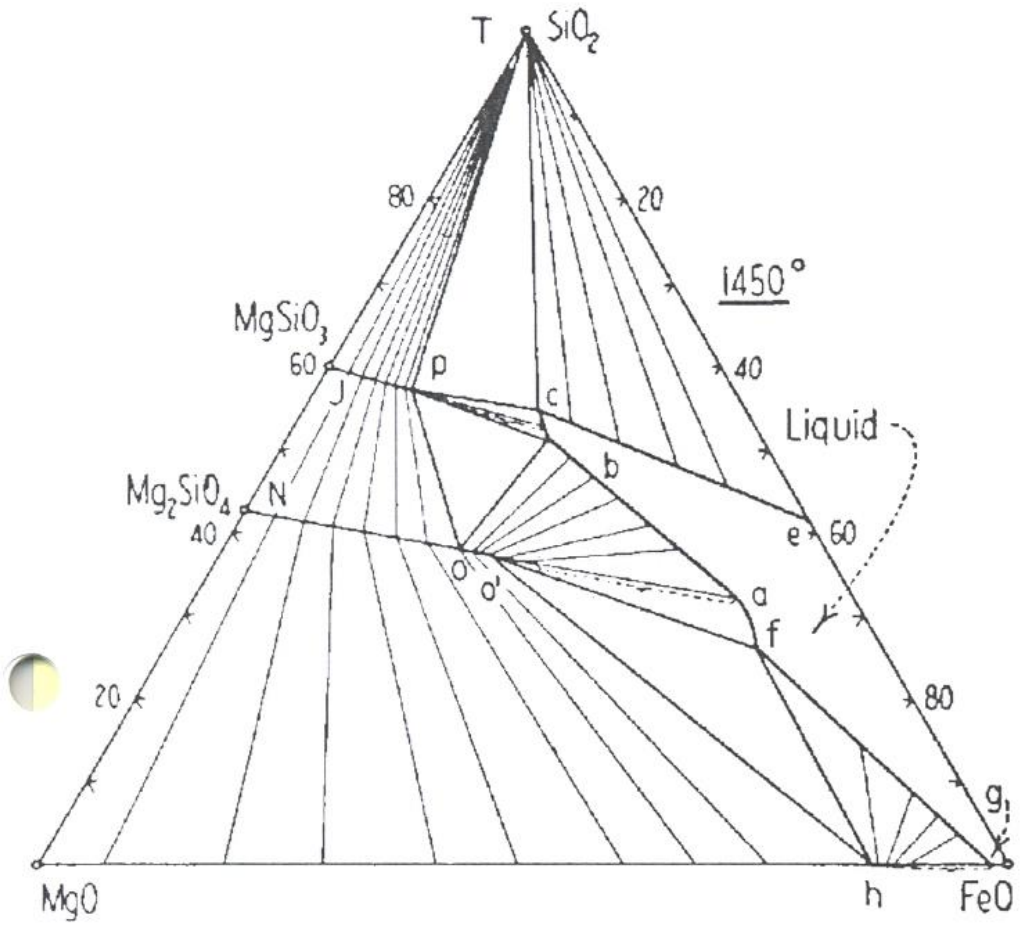

N.L. Bowen, J.F. Schairer, Am. J. Sci., 229 (29) [170], (1935), pp. 151-217.

$FeO - MgO - SiO_2$

1550°C, 1 atm

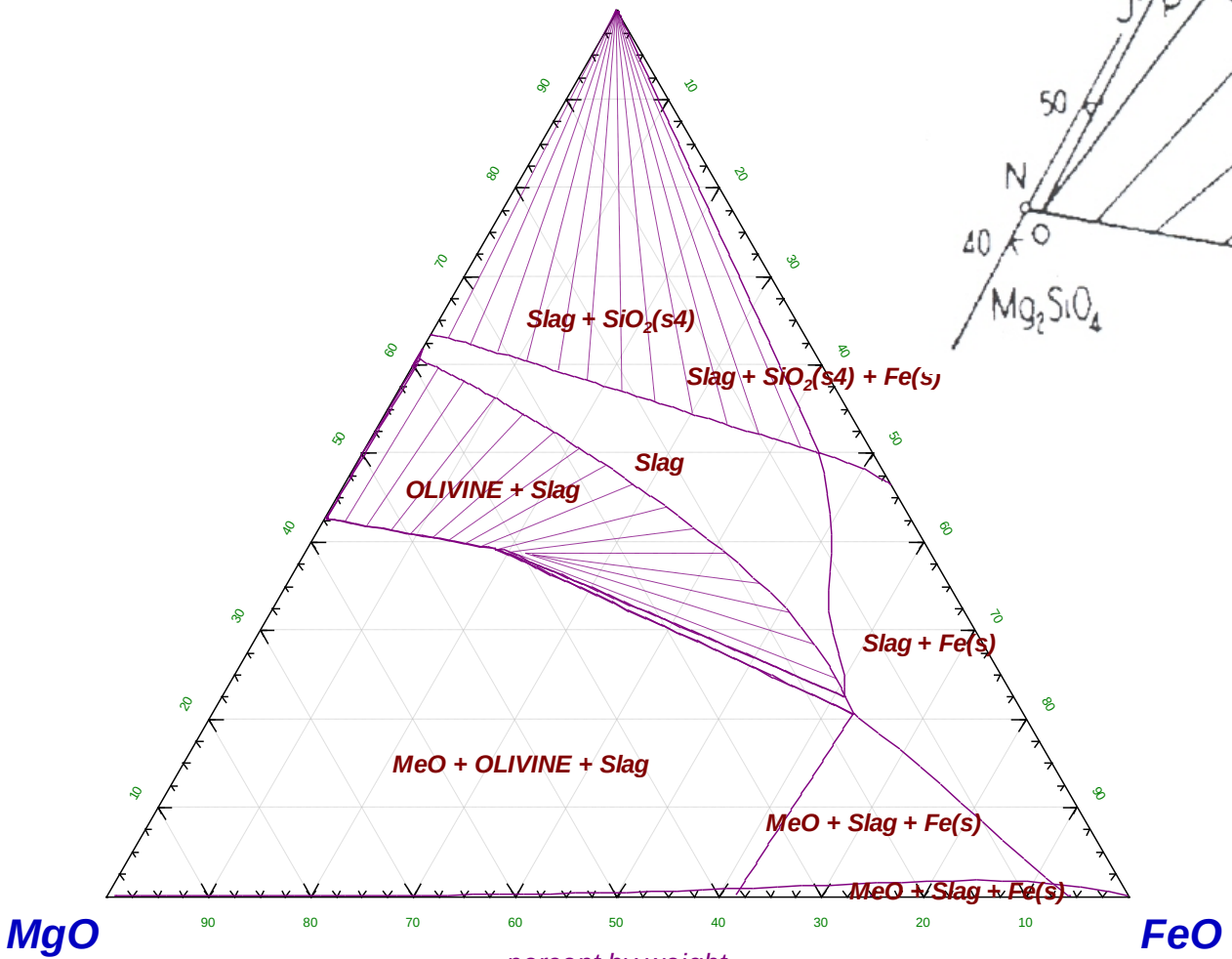

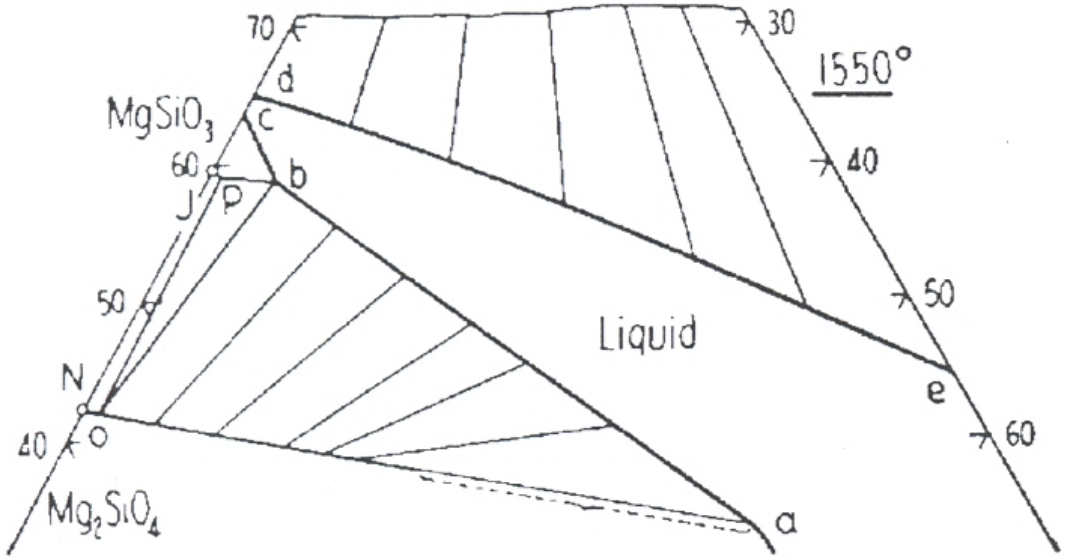

N.L. Bowen, J.F. Schairer, Am. J. Sci., 229 (29) [170], (1935), pp. 151-217.

Mole fraction in Kelvin compared with experimental data

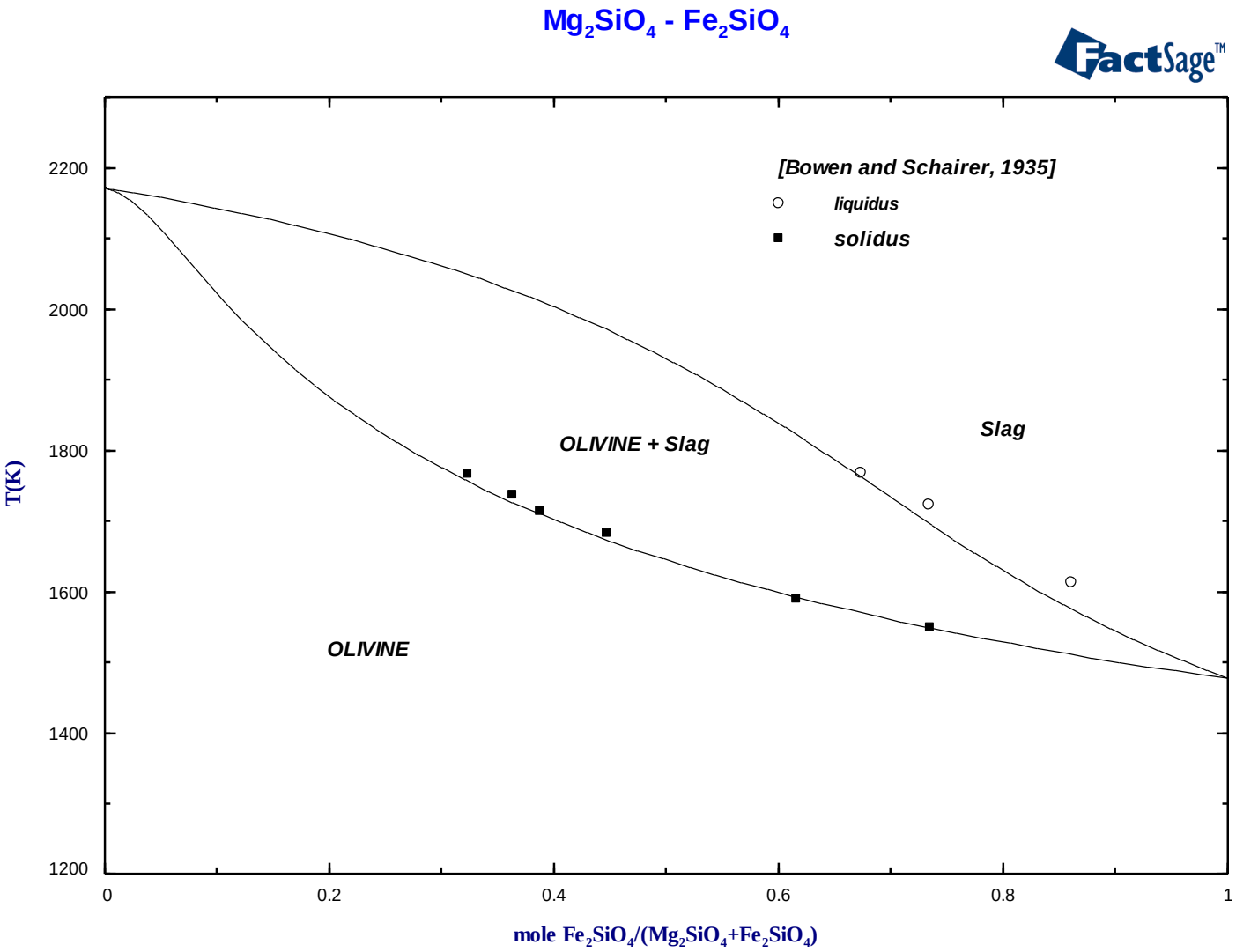

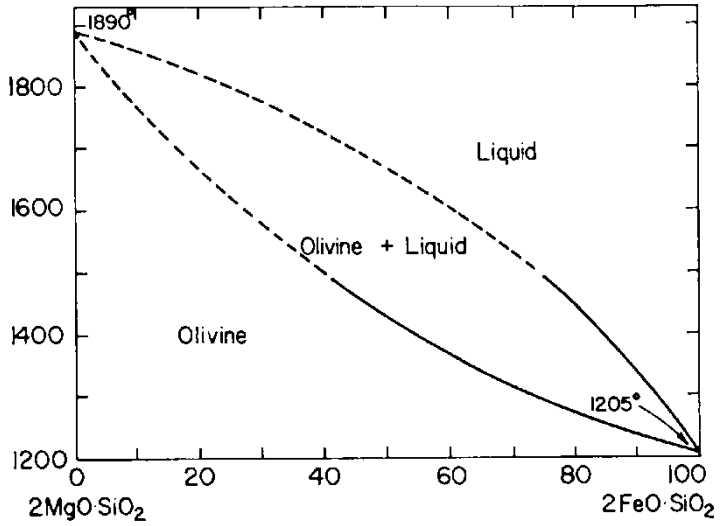

N.L. Bowen, J.F. Schairer, Am. J. Sci.,
229 (29) [170],(1935), pp. 151-217.

Mole fraction in Kelvin MgSiO3-FeSiO3 compared with experimental data

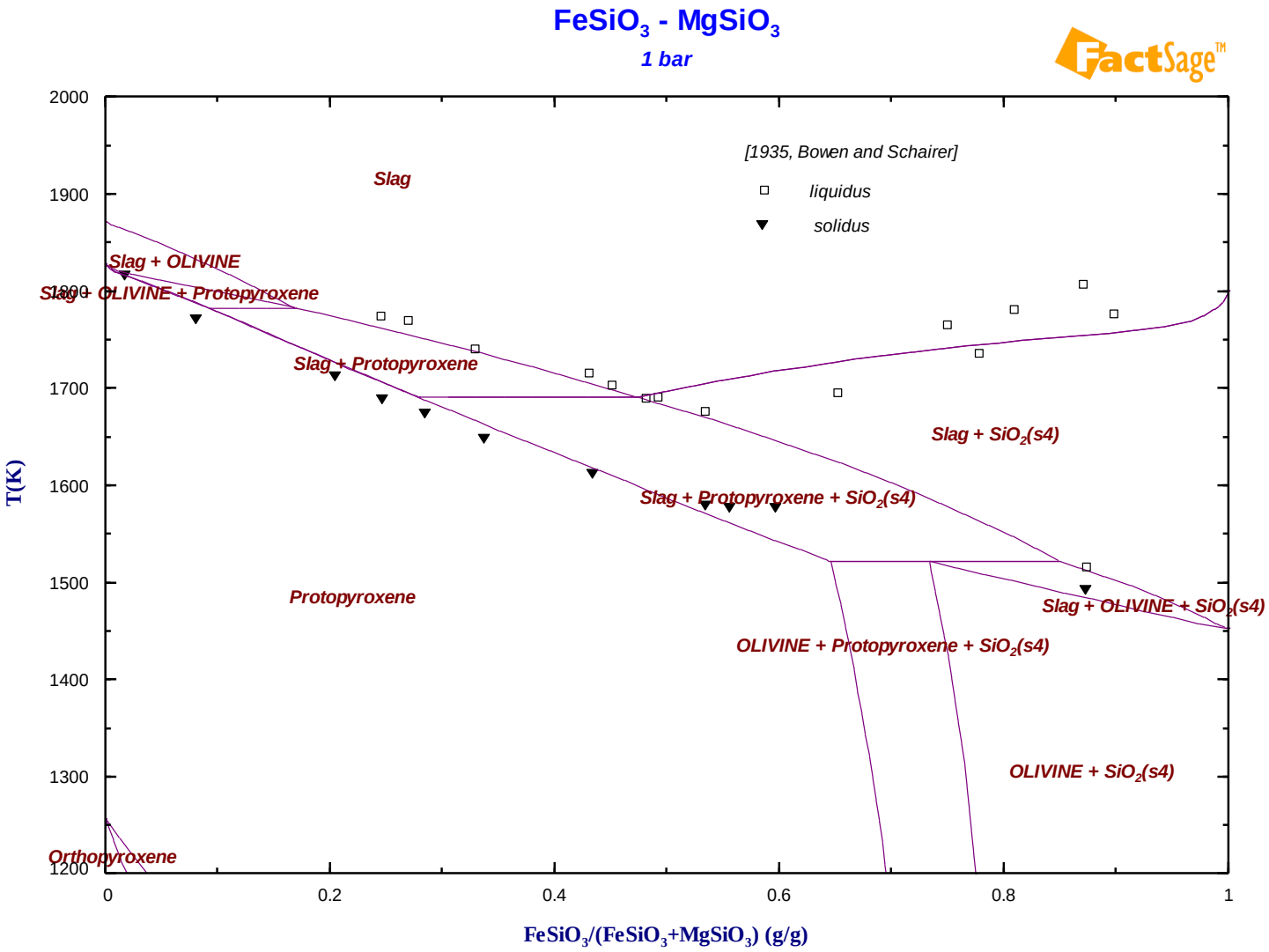

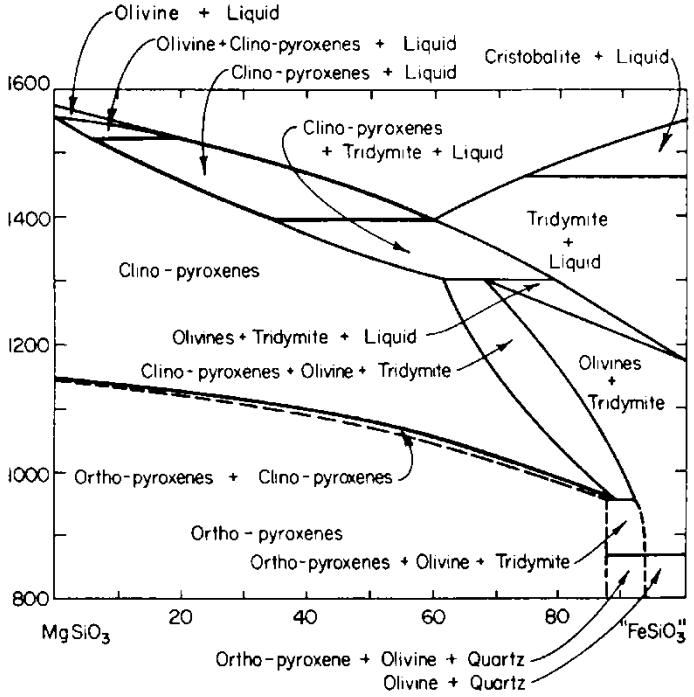

N.L. Bowen, J.F. Schairer, Am. J. Sci., 229 (29) [170], (1935), pp. 151-217.

Mole fraction MgFe2O4-Mg2SiO4-O2

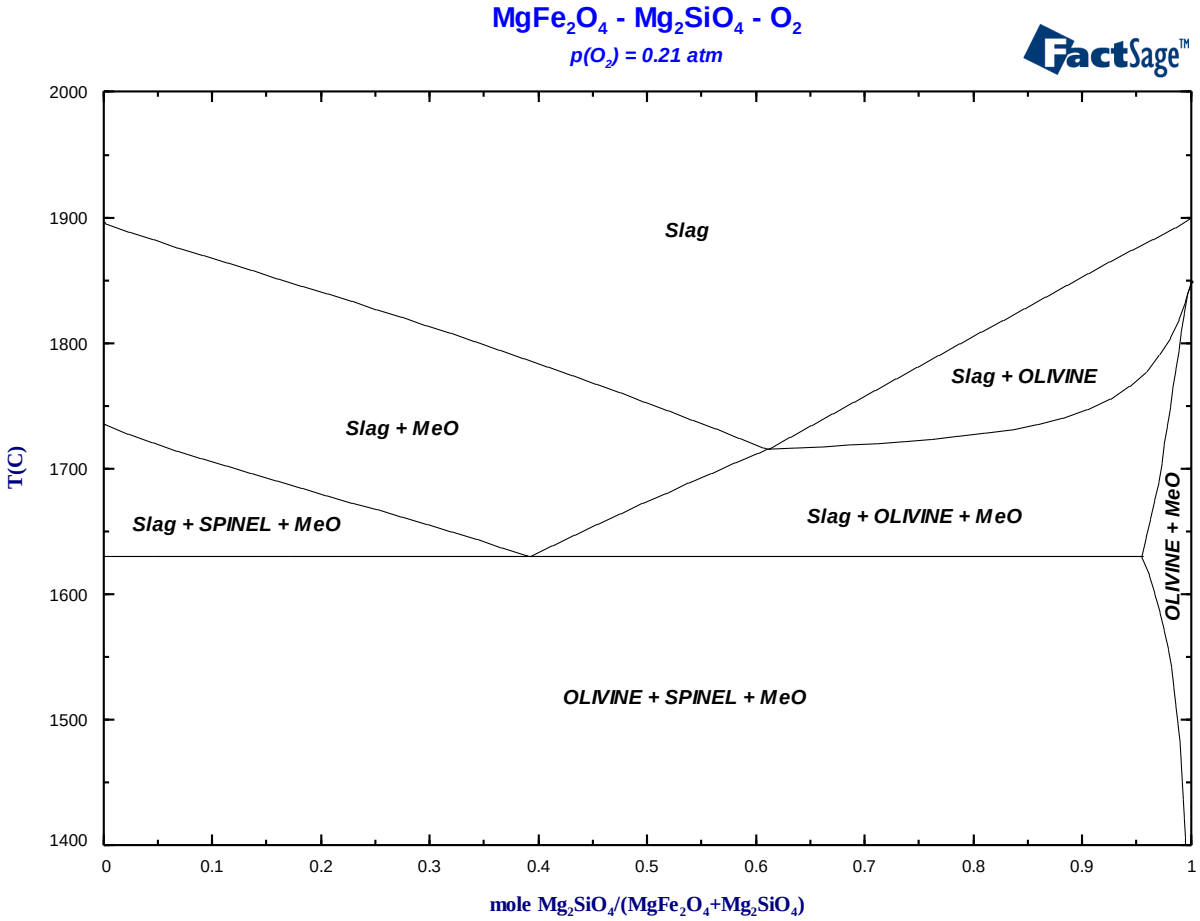

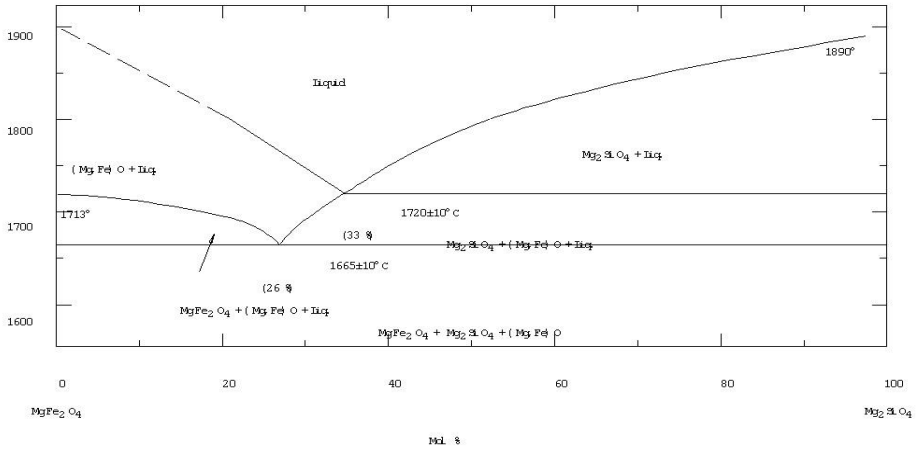

V. Ambruz, J. Havlica, E. Kanclir, Chem. Zwesti, 35 [1], (1981), pp.51-55.

Mole fraction, Liquidussurface

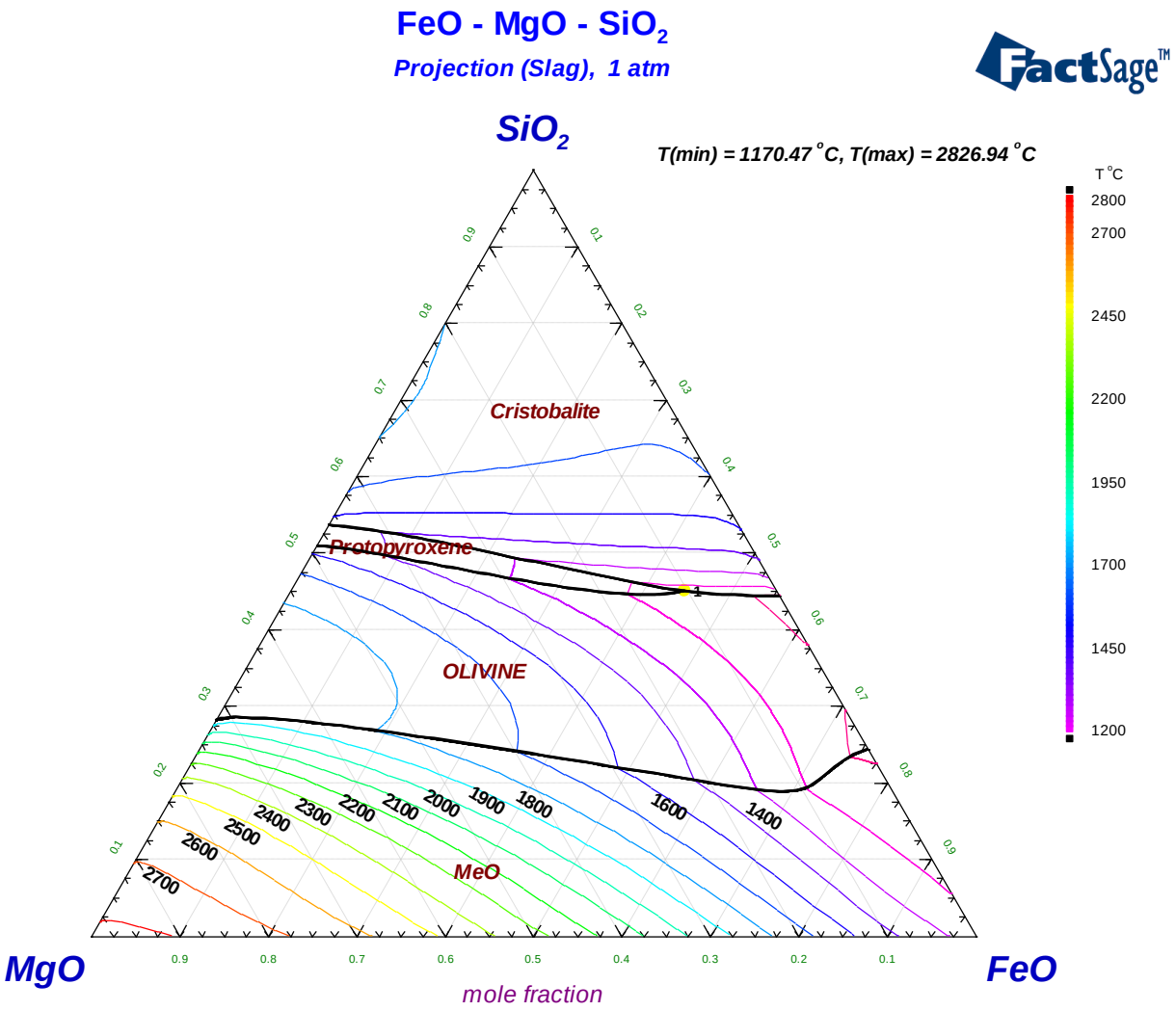

Weight percent,
Liquidussurface compared with experimental data

FeO - MgO - SiO_2

Projection (Slag)

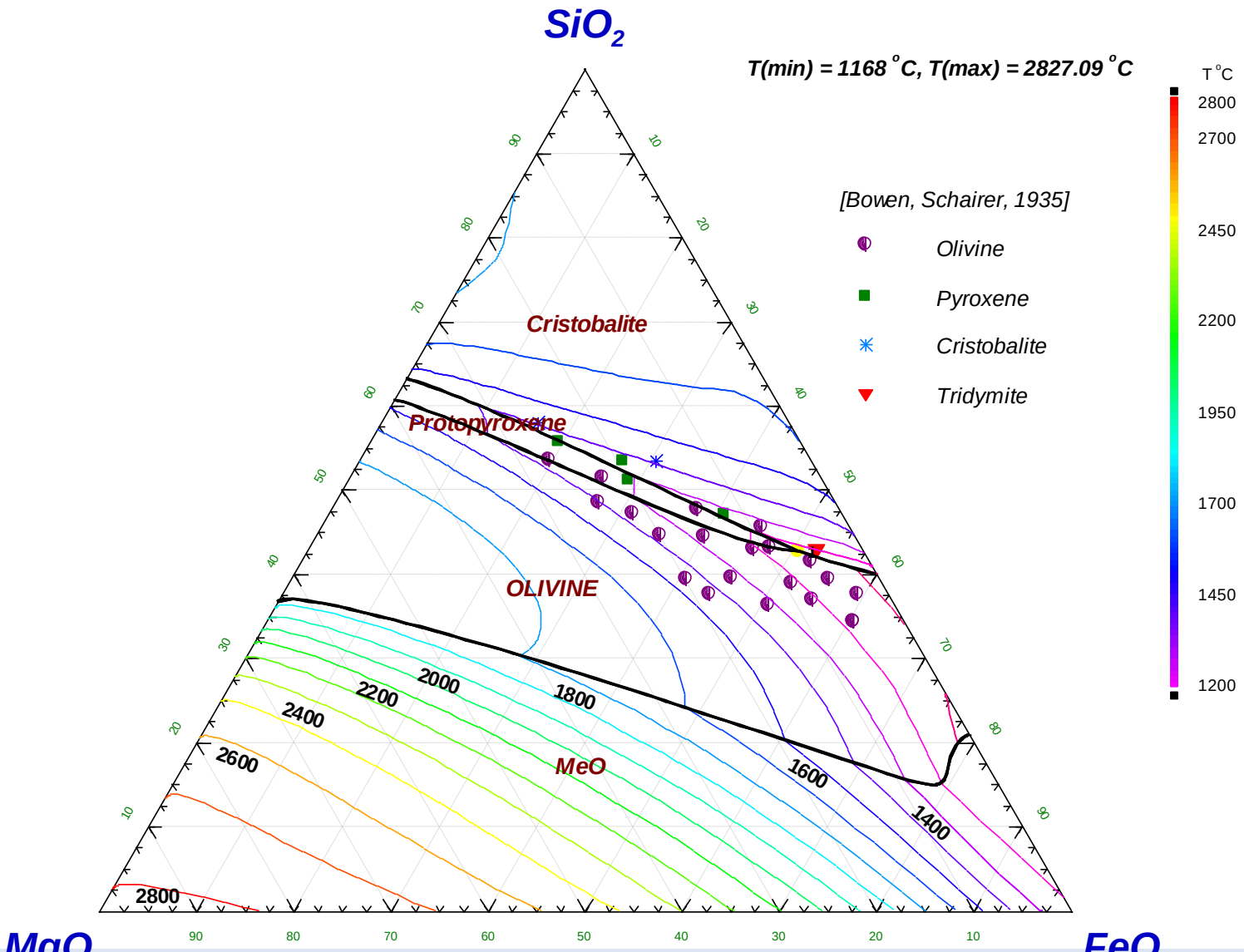

Invariant equilibria on the liquidus surface

Intersections with slag	Mole fraction				Weight percent			
	A = SiO2, B = MgO, C = FeO				A = SiO2, B = MgO, C = FeO			
	X(A)	X(B)	X(C)	T(C)	W(A)	W(B)	W(C)	T(C)
1: PROTOPYROXENE / OLIVINE / Cristobalite	1: 0.44990	0.10418	0.44591	1248.50	1: 42.745	6.623	..50.632	1248.63

FeO-MgO-TiO2,
Mole fraction, 1000°C

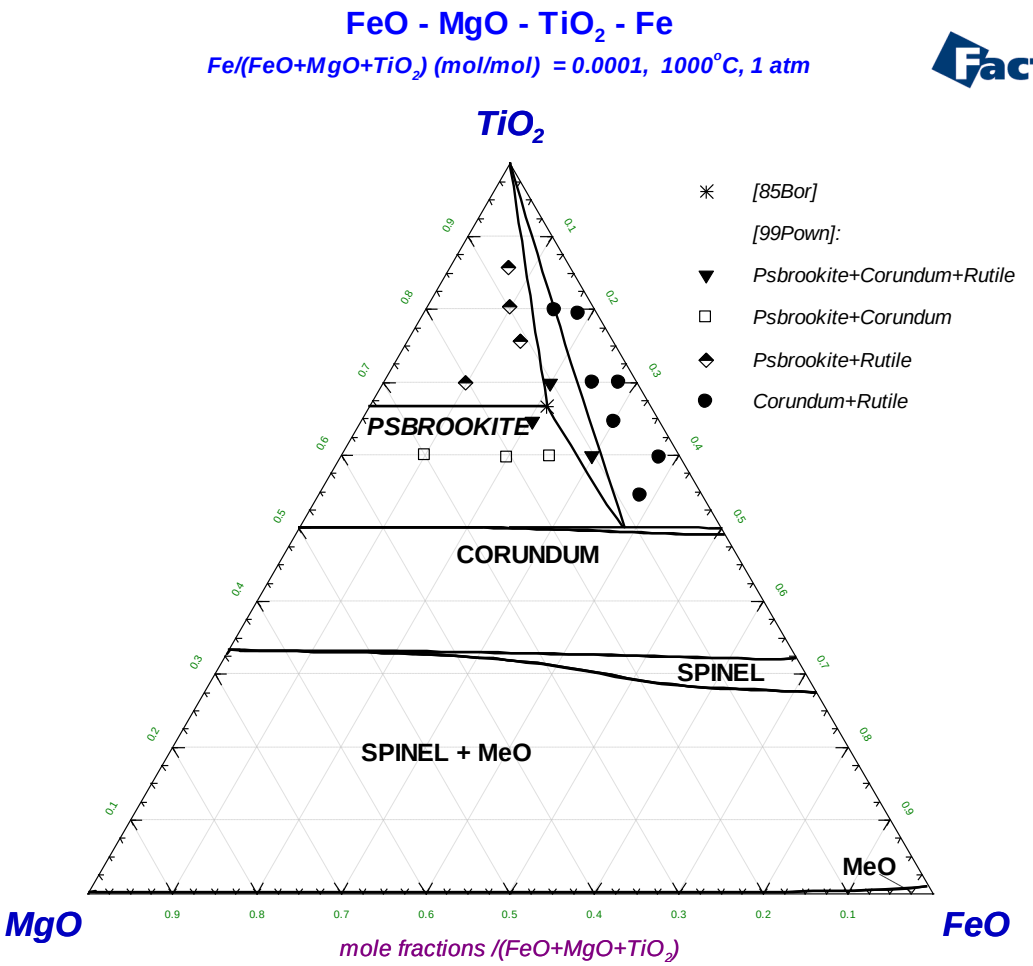

FeO-MgO-TiO2,
Weight percent 1300°C compared with experimental data

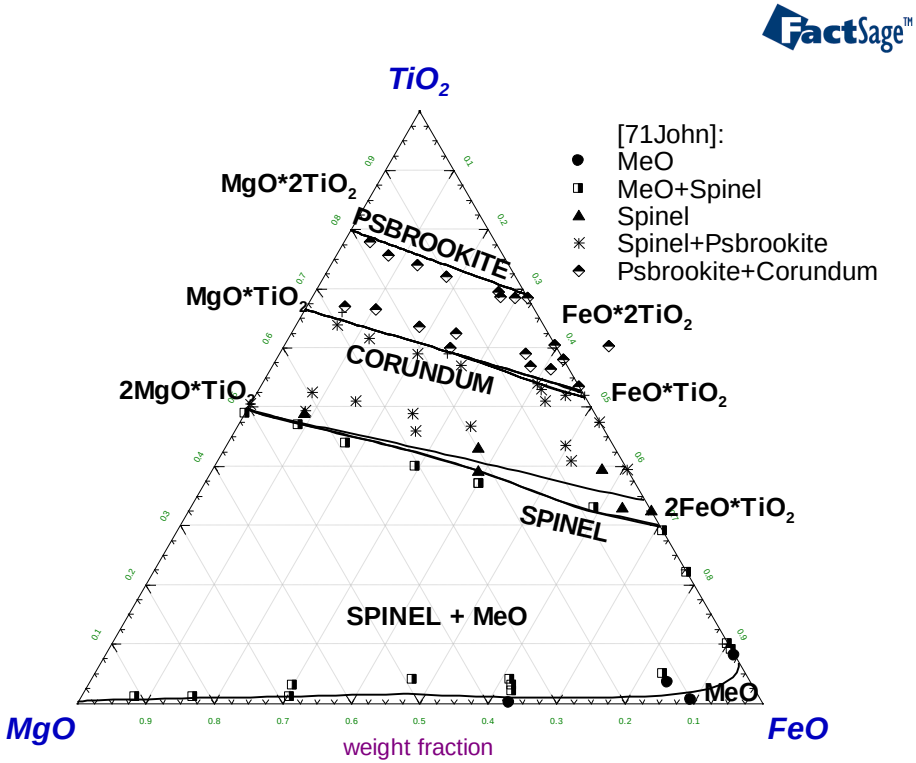

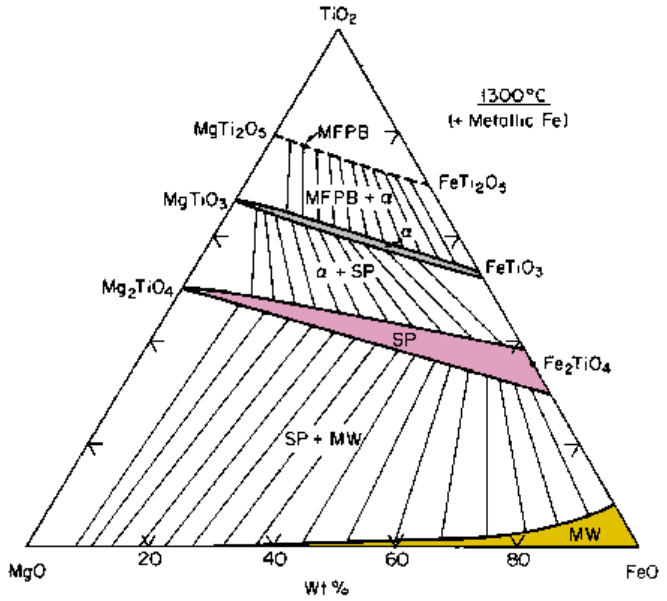

R.E. Johnson, E. Woermann, A. Muan, Am. J. Sci., 271 [3] (1971), pp. 278-292.

FeO-MnO-P2O5,
Weight percent, Part of liquidus surface

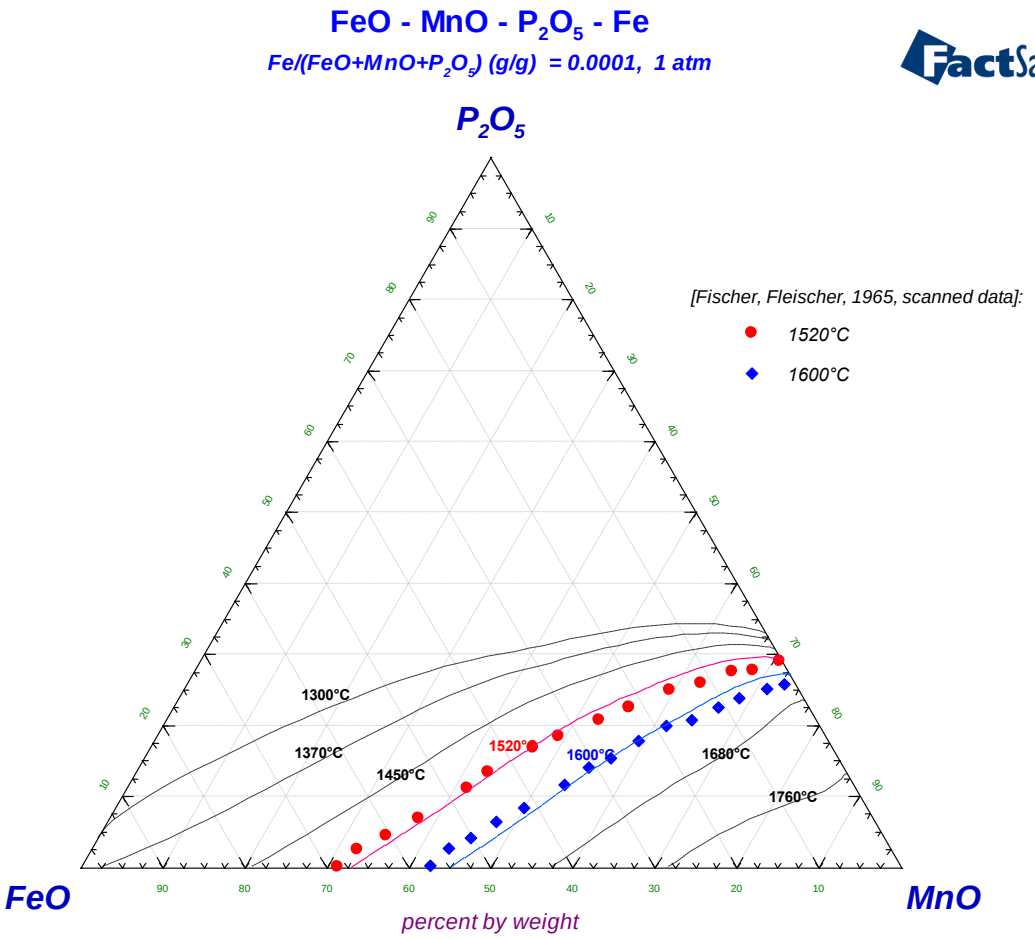

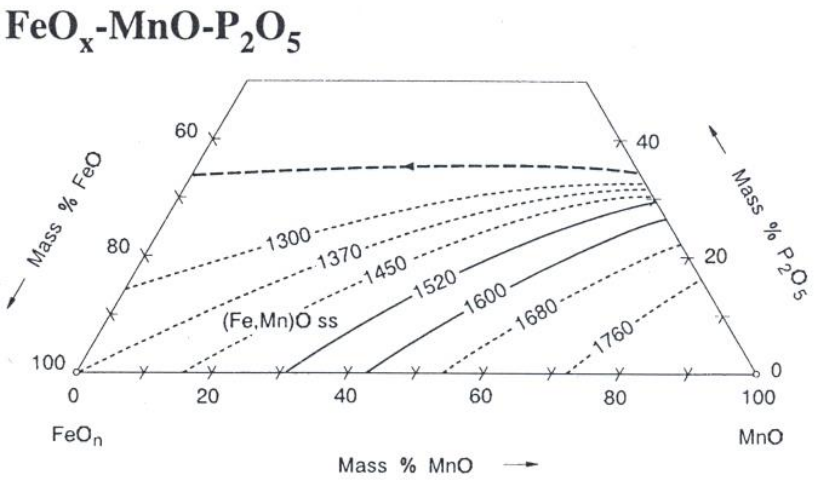

Fig. 3.285. The part of the liquidus surface in the system FeO_n-MnO-P_2O_5 in contact with metallic iron after Fischer, Fleischer [1].

References

[1] Fischer, W. A., H.-J. Fleischer: Arch. Eisenhüttenwes. 36 (1965) No. 11, p. 791/8

Mole fraction, Liquidus surface

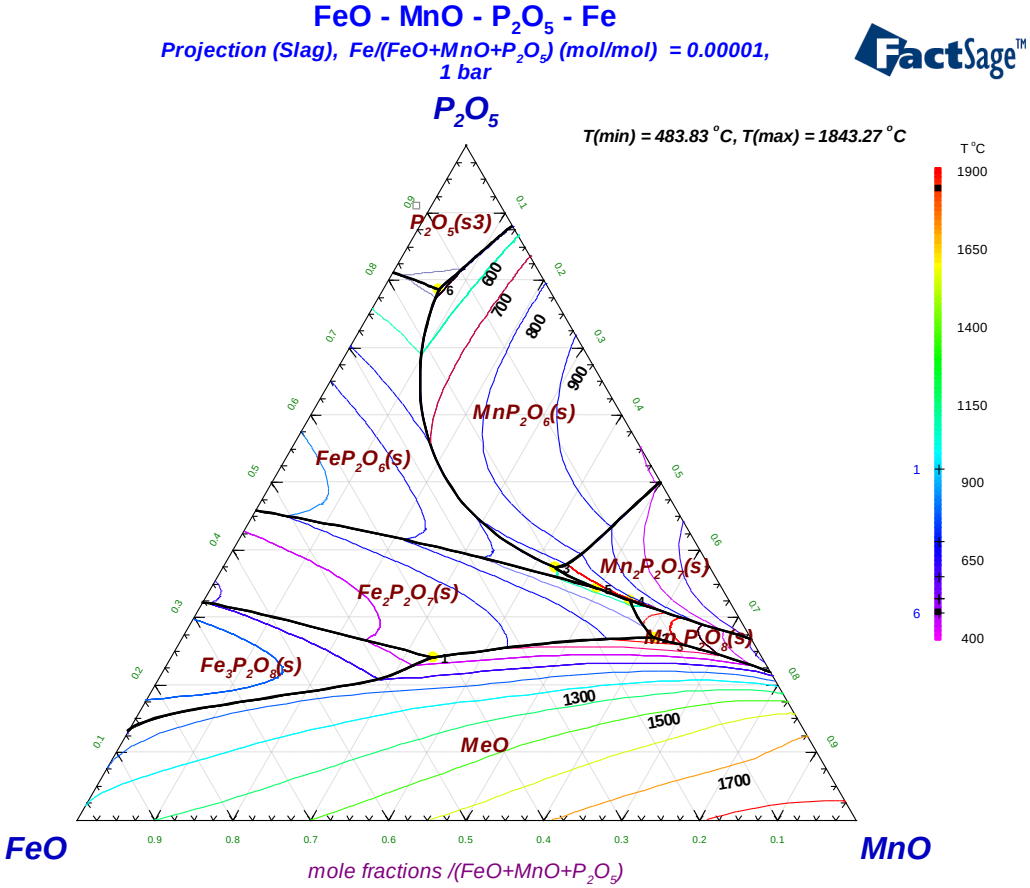

Weight percent, Liquidus surface

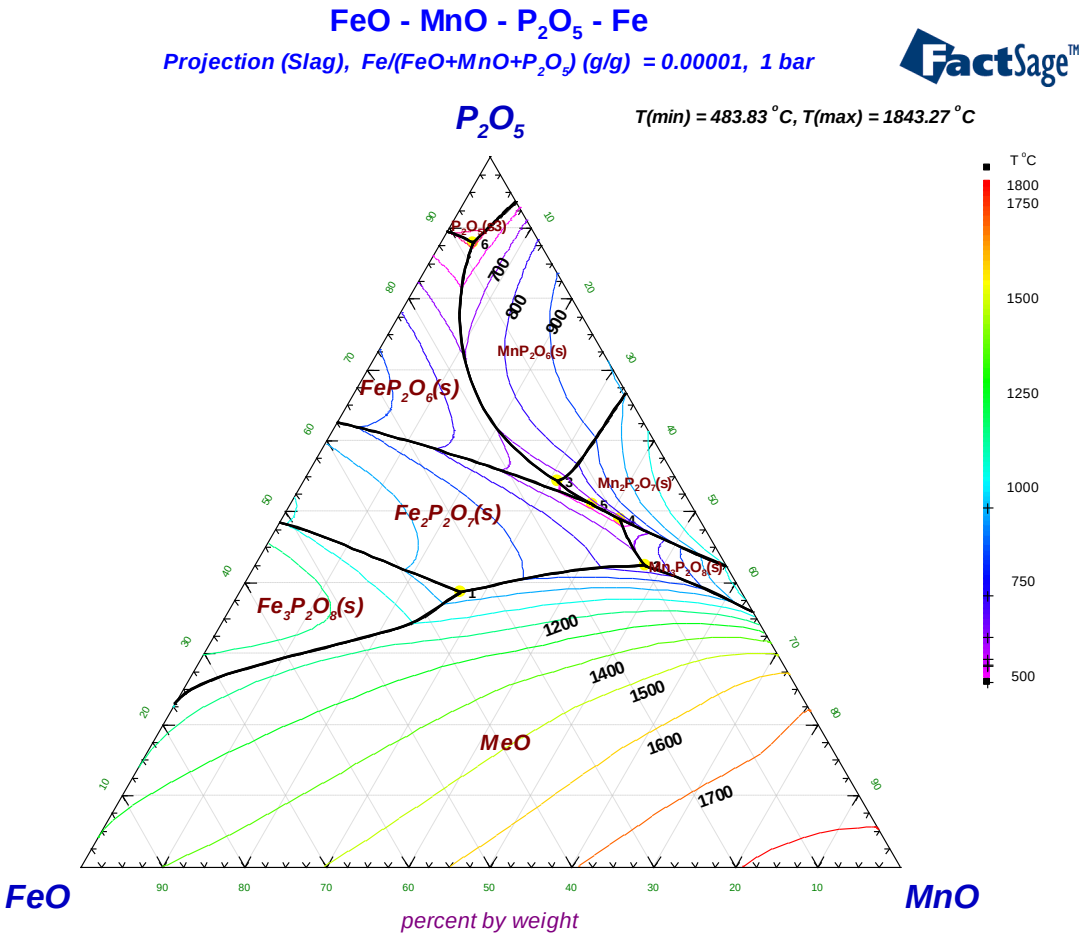

Invariant equilibria on the liquidus surface

Intersections with slag	Mole fraction				Weight percent			
	A = P2O5, B = FeO, C = MnO				A = P2O5, B = FeO, C = MnO			
	X(A)	X(B)	X(C)	T(C)	W(A)	W(B)	W(C)	T(C)
1: Fe2P2O7(s) / Fe3P2O8(s) / MeO	1: 0.24052	0.42177	0.33771	944.32	1: 0.38621	0.34278	0.27101	944.32
2: Fe2P2O7(s) / MeO / Mn3P2O8(s)	2: 0.26907	0.12379	0.60714	712.28	2: 0.42363	0.09864	0.47773	712.28
3: FeP2O6(s) / Mn2P2O7(s) / MnP2O6(s)	3: 0.37300	0.19842	0.42859	600.24	3: 0.54244	0.14604	0.31152	600.25
4: Fe2P2O7(s) / Mn2P2O7(s) / Mn3P2O8(s)	4: 0.32476	0.12658	0.54866	527.15	4: 0.48981	0.09662	0.41357	527.15
5: Fe2P2O7(s) / FeP2O6(s) / Mn2P2O7(s)	5: 0.34292	0.16009	0.49699	526.84	5: 0.51005	0.12050	0.36945	526.84
6: FeP2O6(s) / MnP2O6(s) / P2O5(s3)	6: 0.78540	0.14225	0.07235	483.83	6: 0.87896	0.08057	0.04047	483.83

Weight percent, Isopleth metasilicate section FeSiO3-MnSiO3

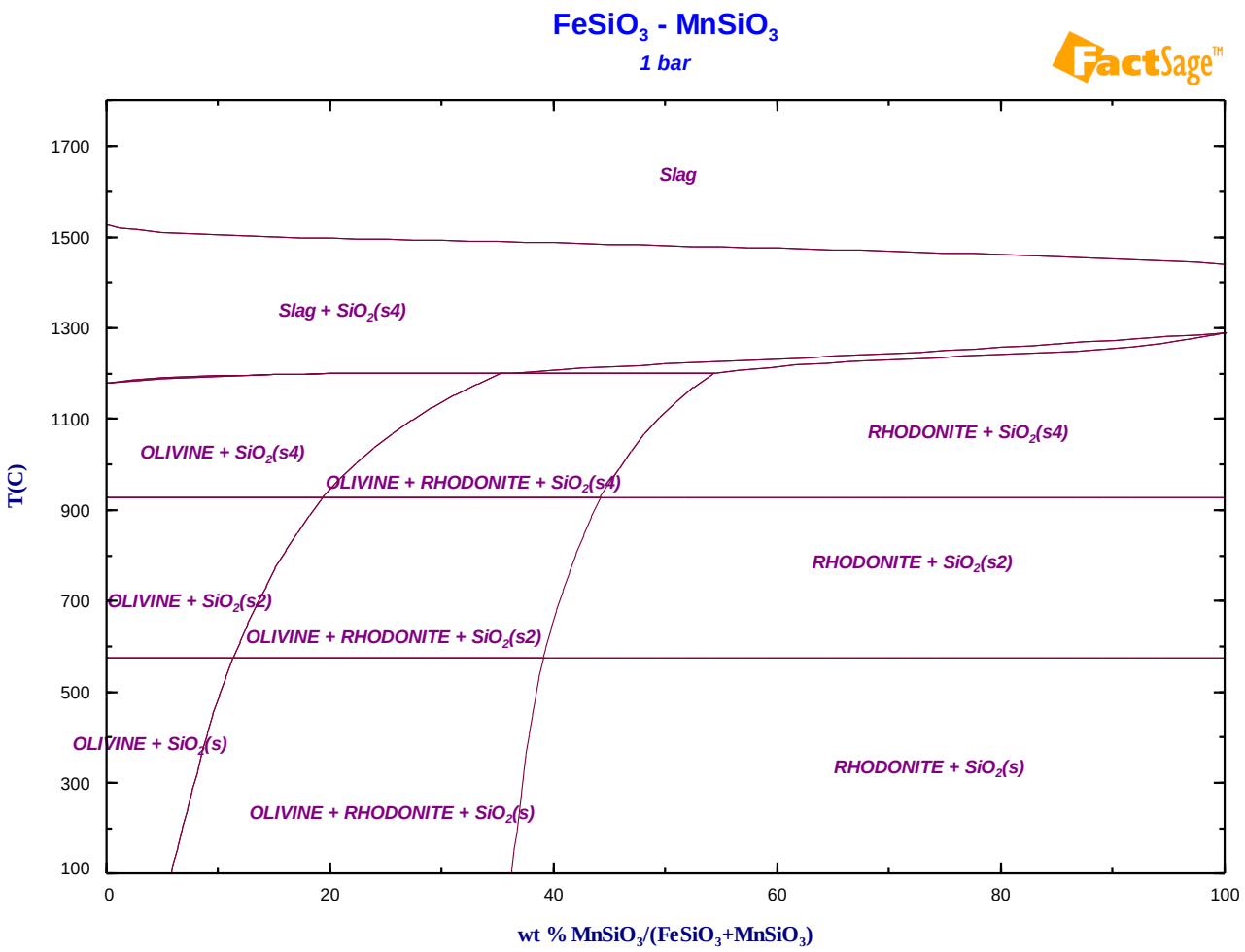

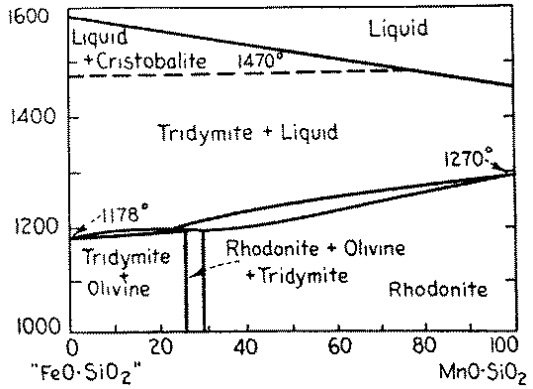

J. White, J. Iron Steel Inst., London, 148 [Pt. 2] 579-712 (1943).

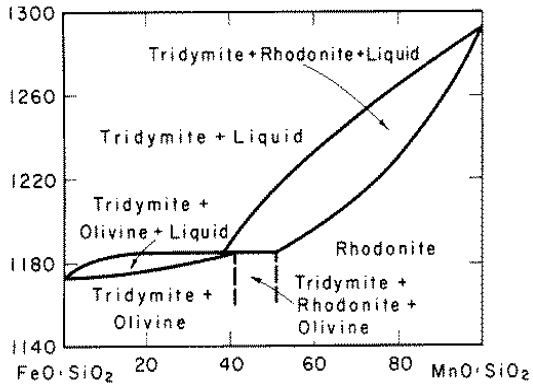

P. V. Riboud and A. Muan, Trans. Metall. Soc. AIME, 224 [1] 27-33 (1962).

Weight percent, Isopleth orthosilicate section Fe2SiO4-Mn2SiO4

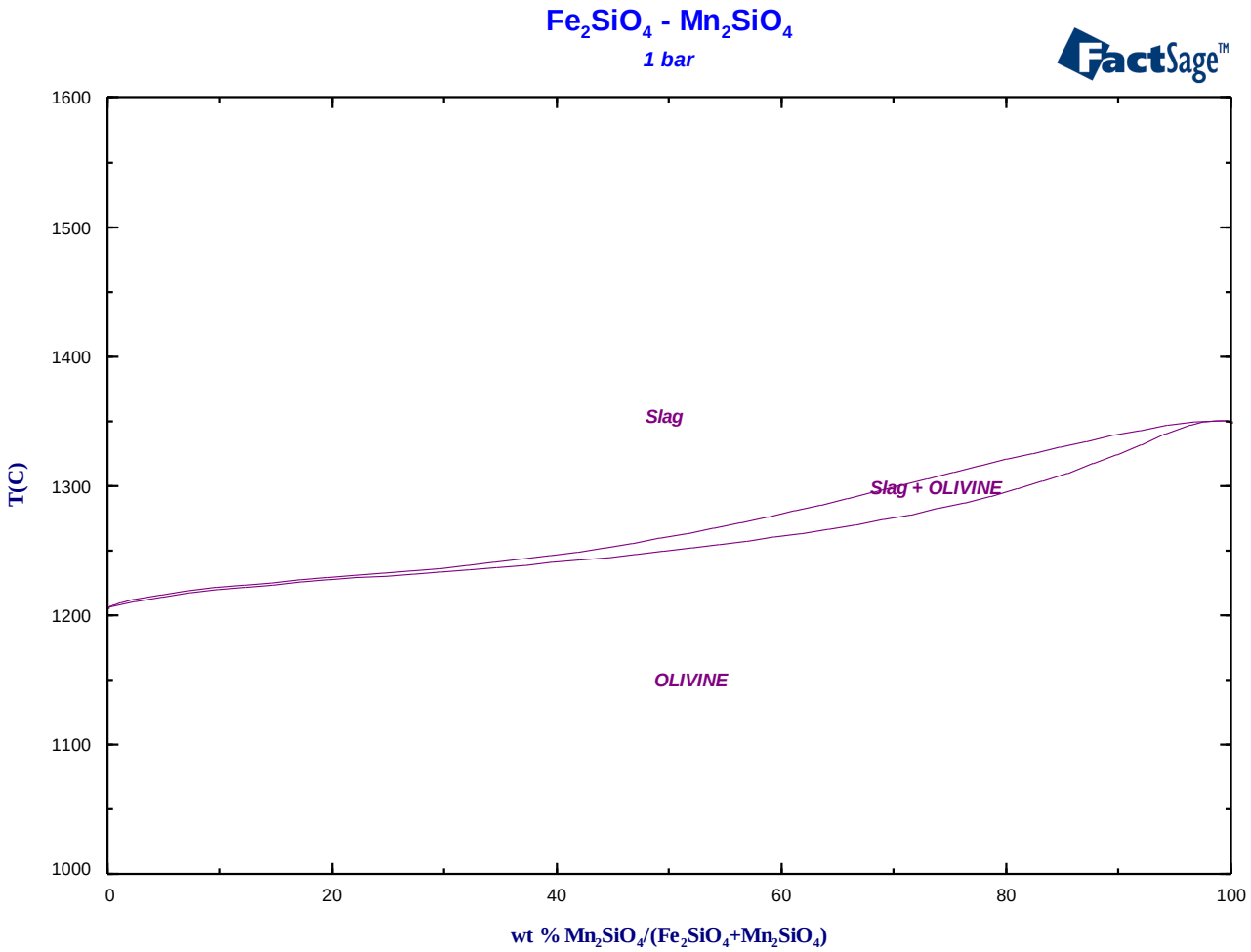

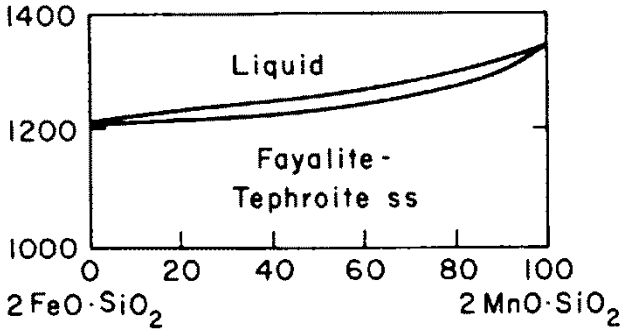

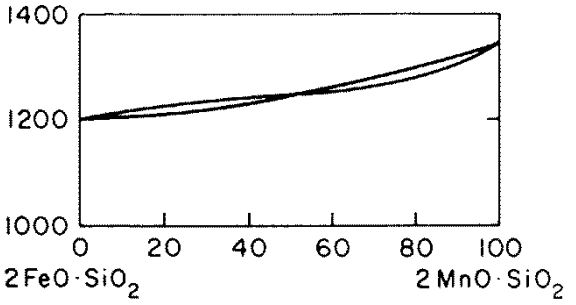

P. T. Carter, A.B. Murad, R. Hay, J. West. Scotl. Iron Steel Inst., 60, (1952), pp. 123-133.

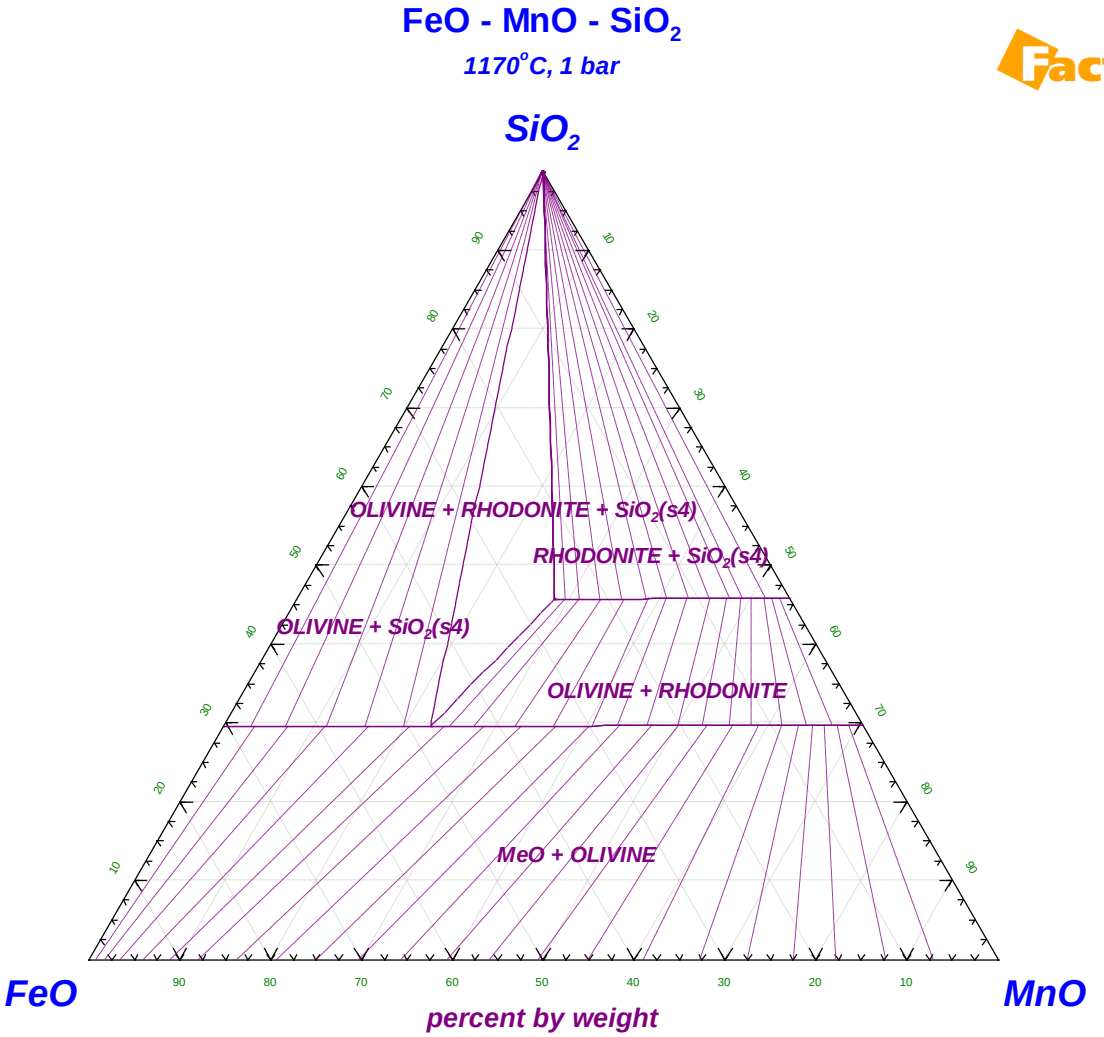

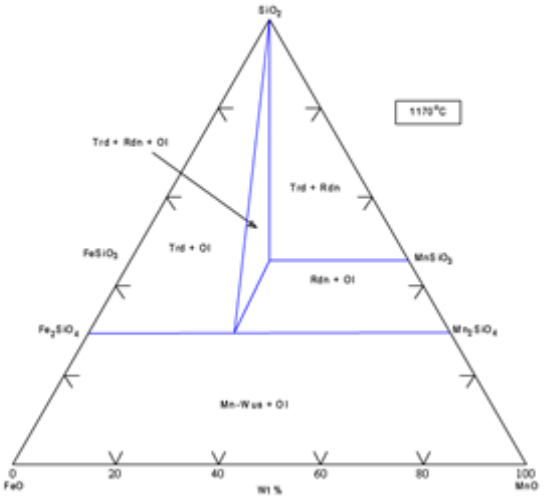

P. V. Riboud and A. Muan, Trans. Metall. Soc. AIME, 224 [1] 27-33 (1962).

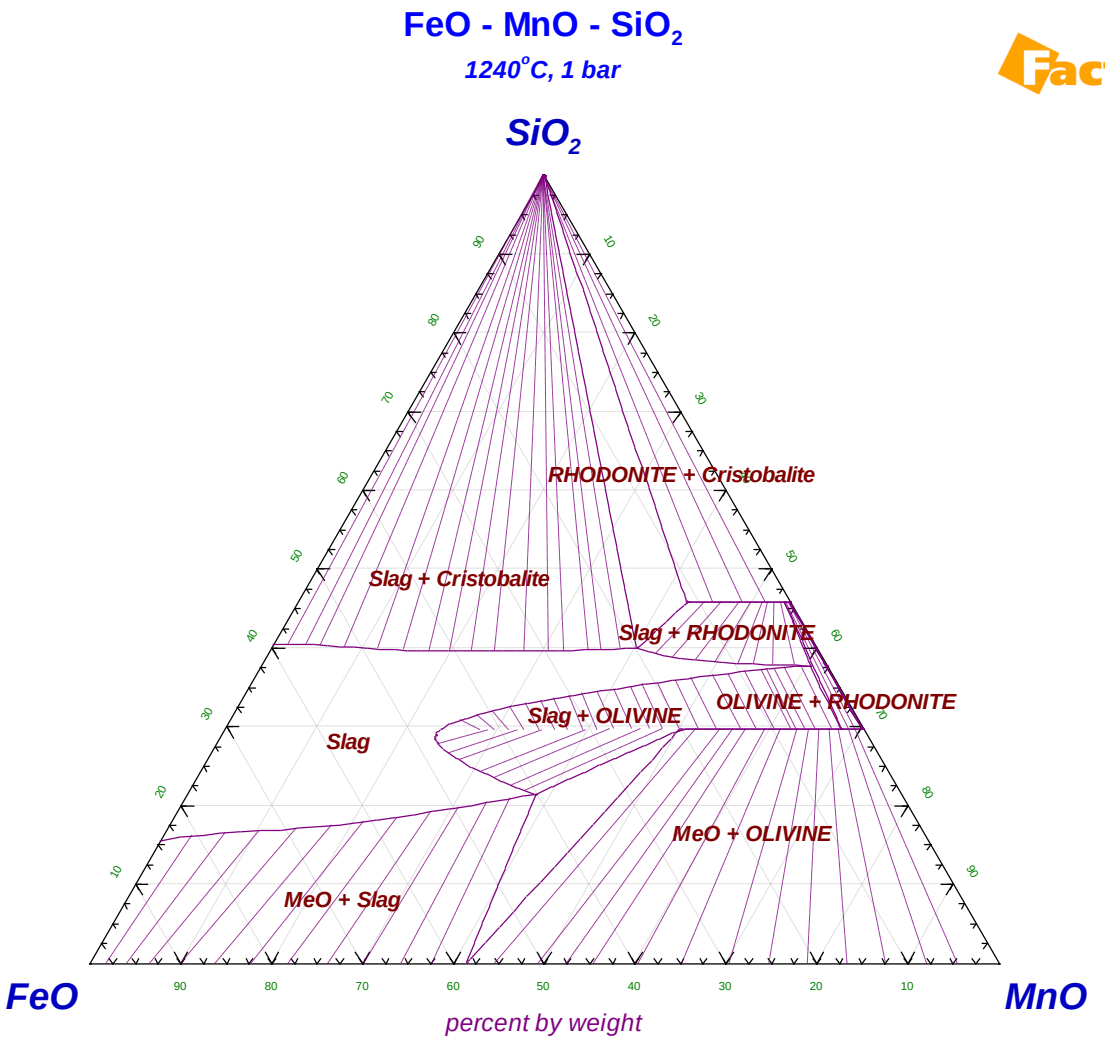

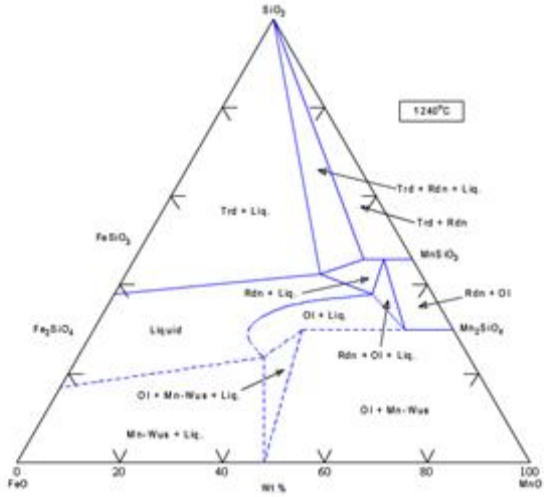

P. V. Riboud and A. Muan, Trans. Metall. Soc. AIME, 224 [1] 27-33 (1962).

FeO - MnO - SiO_2

1300°C, 1 bar

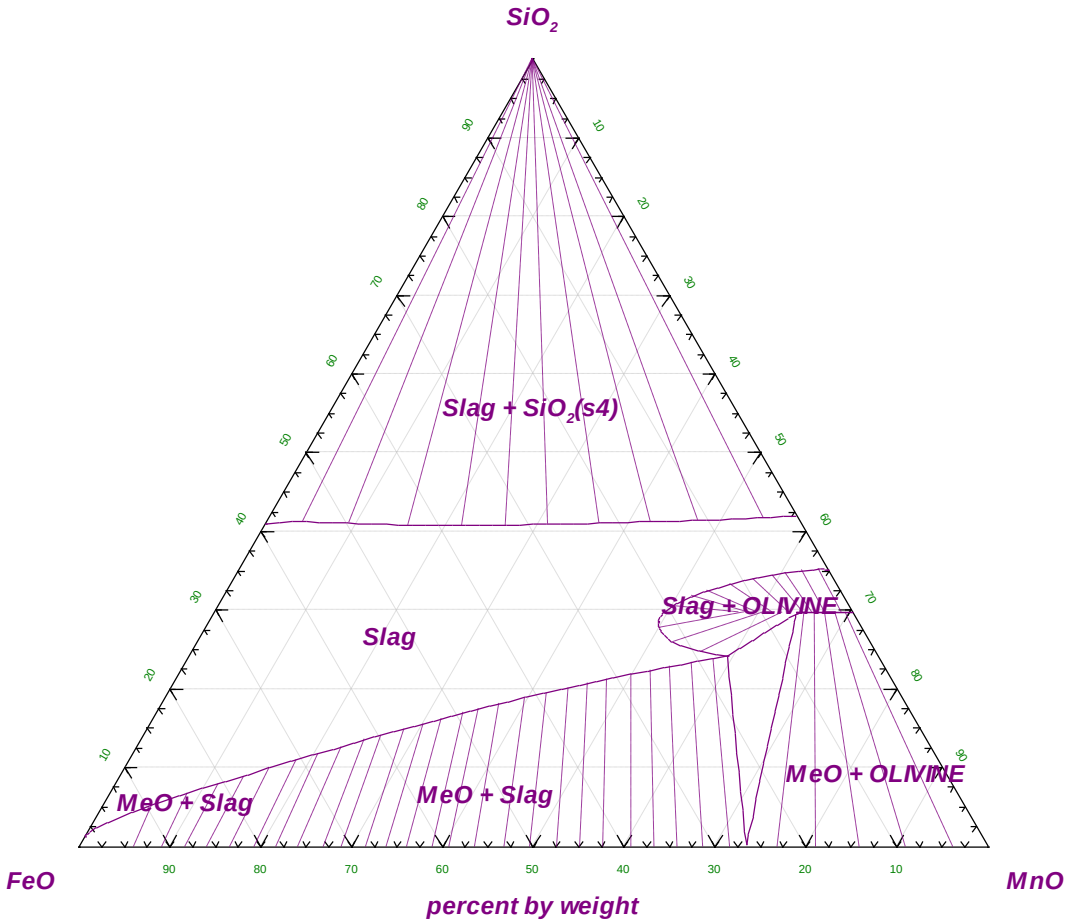

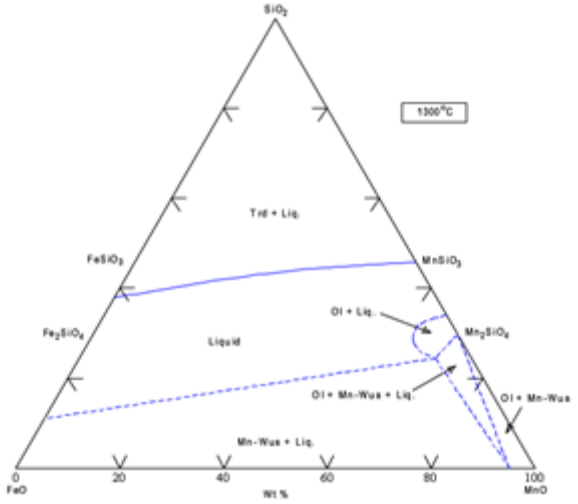

P. V. Riboud and A. Muan, Trans. Metall. Soc. AIME, 224 [1] 27-33 (1962).

Mole fraction, Liquidus surface

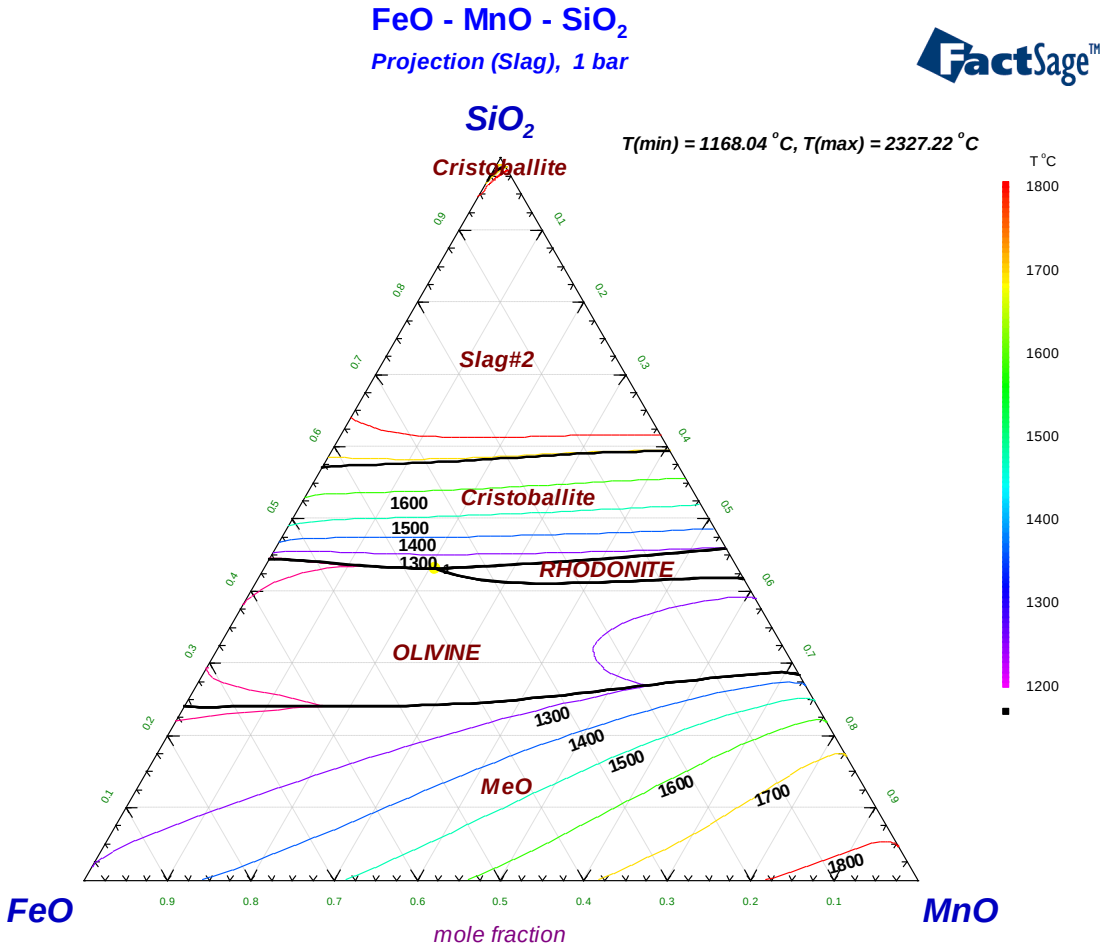

Weight percent, Liquidus surface

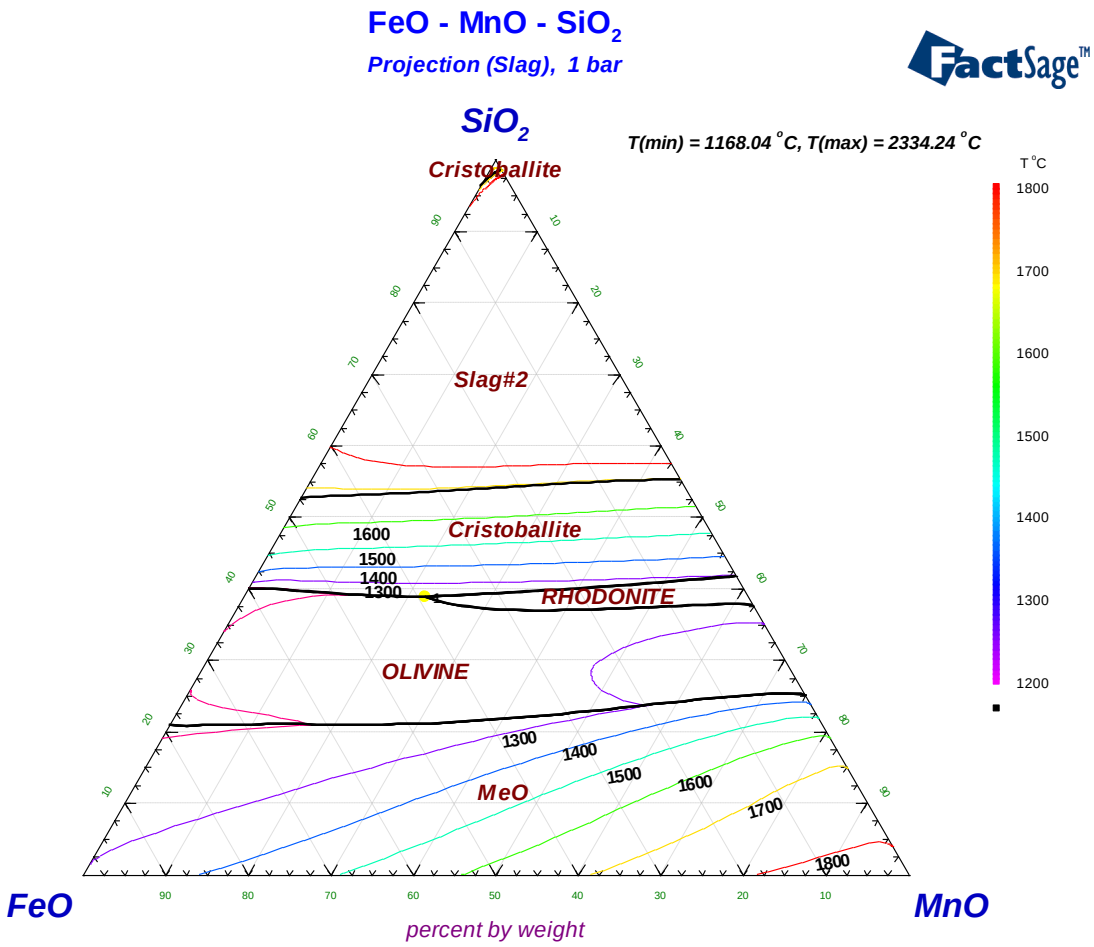

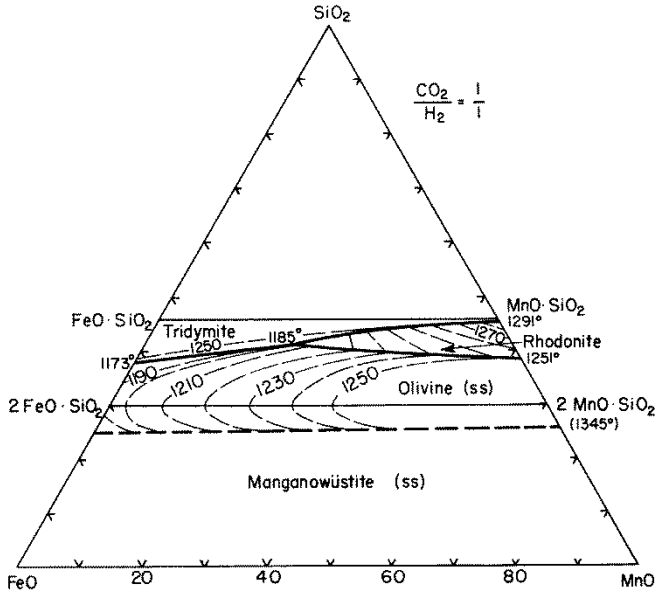

P. V. Riboud and A. Muan, Trans. Metall. Soc. AIME, 224 [1] 27-33 (1962).

Invariant equilibria on the liquidus surface

Intersections with slag	Mole fraction				Weight percent				
	A = SiO2, B = FeO, C = MnO				A = SiO2, B = FeO, C = MnO				
		X(A)	X(B)	X(C)	T(C)		W(A)	W(B)	W(C)	T(C)
1: OLIVINE / RHODONITE / Cristobalite	1:	0.43066	0.36269	0.20665	1200.63	1:	38.857	39.130	22.013	1200.63

Mole fraction 580°C

$FeO - Na_2O - SiO_2 - Fe$

$580^{\circ}C$, $Fe/(FeO+Na_2O+SiO_2)$ (mol/mol) = 0.0001

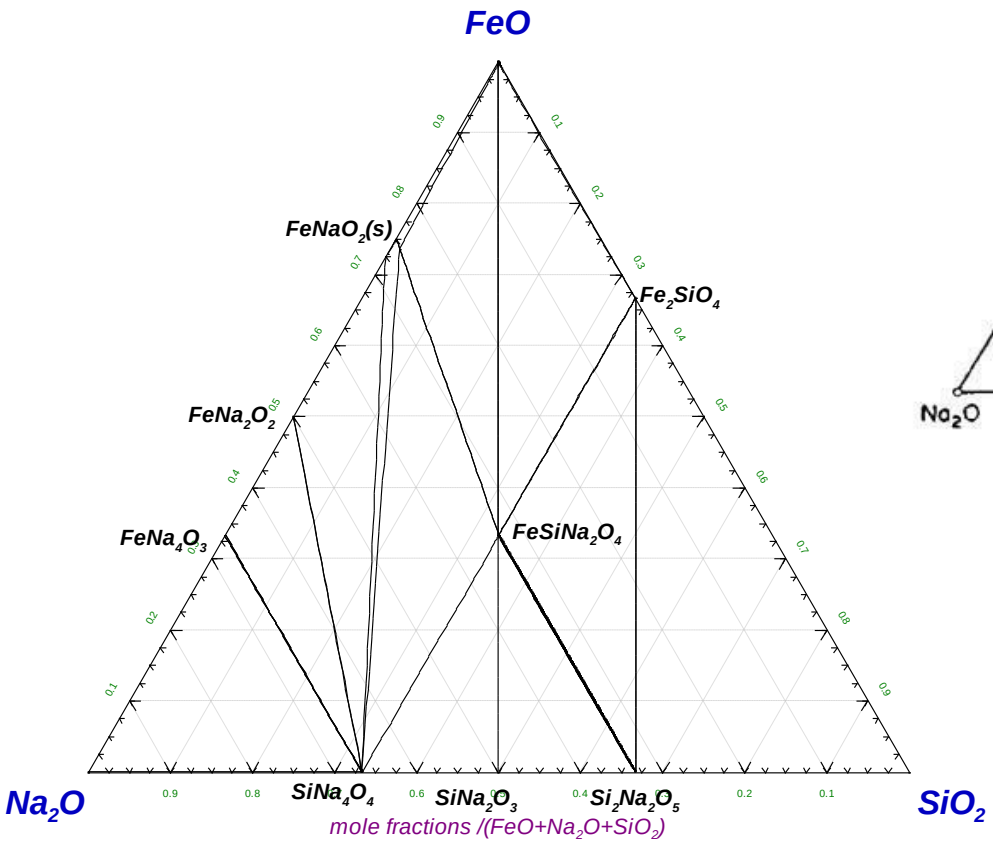

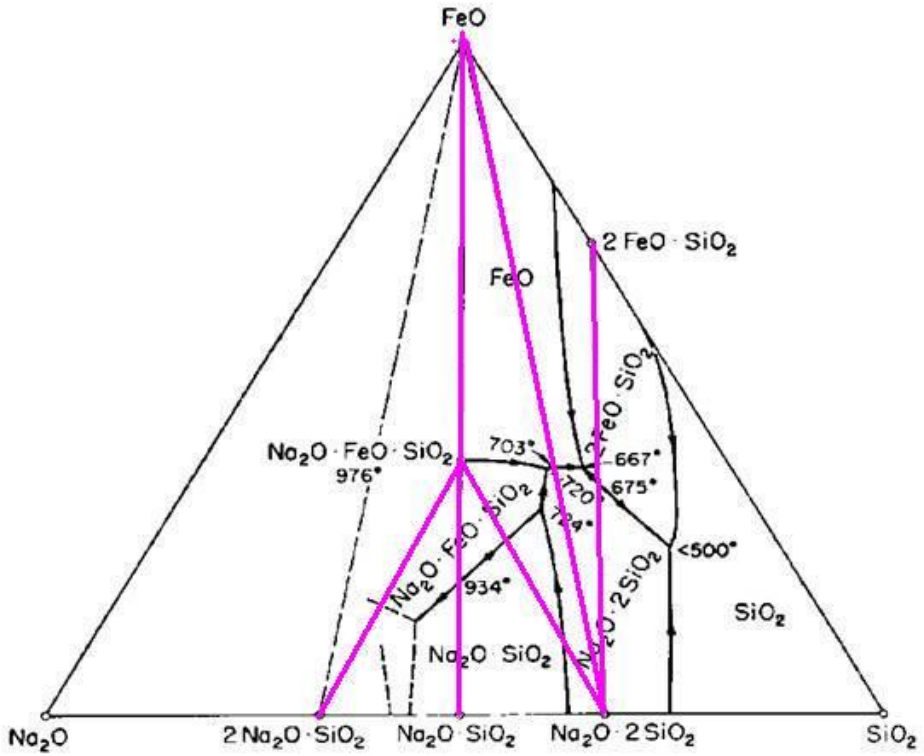

P. T. Carter and M. Ibrahim, J. Soc. Glass Technol., 36 [170] 142-163 (1952).

Mole fraction, Isopleth FeO-Na2SiO3

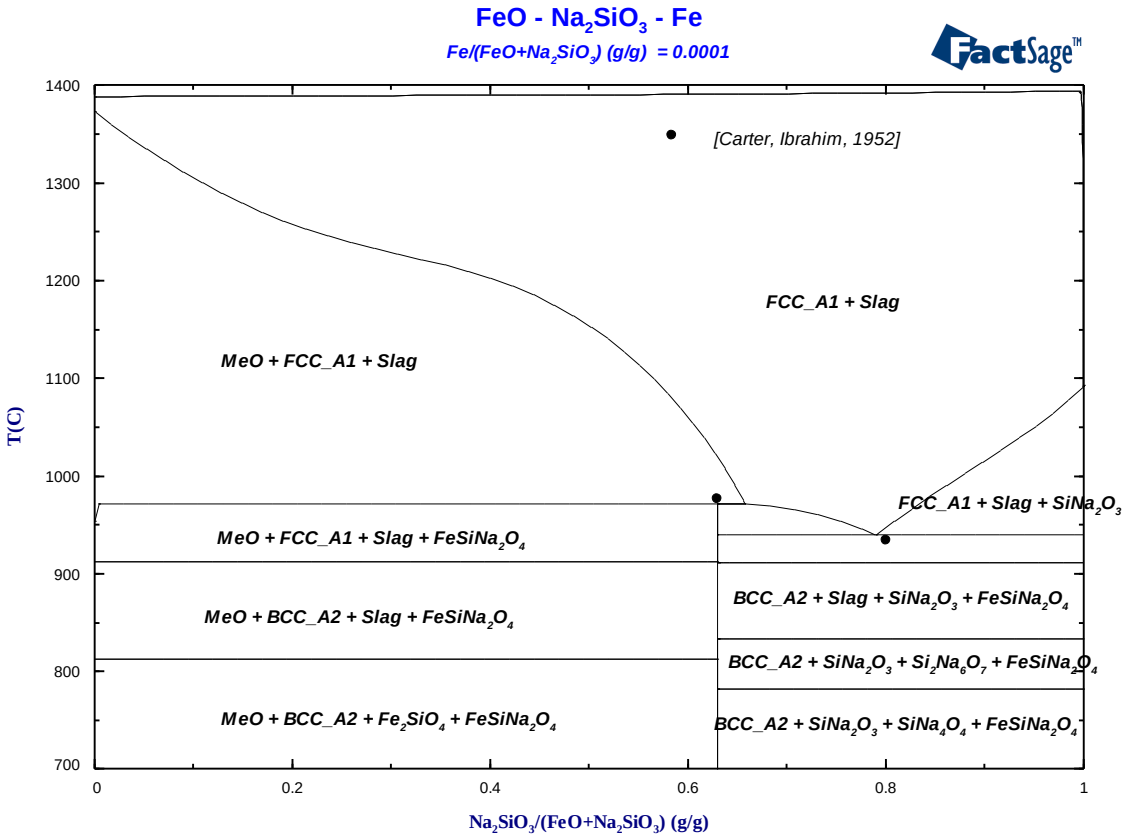

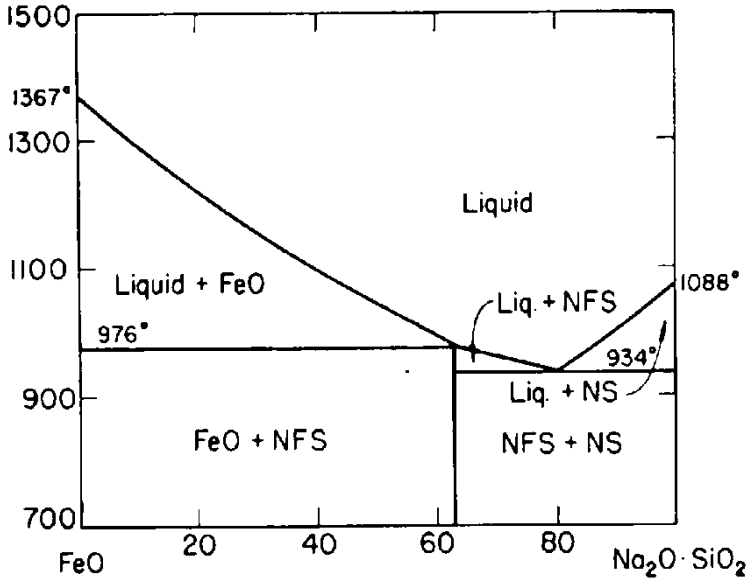

P. T. Carter and M. Ibrahim, J. Soc. Glass Technol., 36 [170] 142-163 (1952).

Mole fraction, Liquidussurface

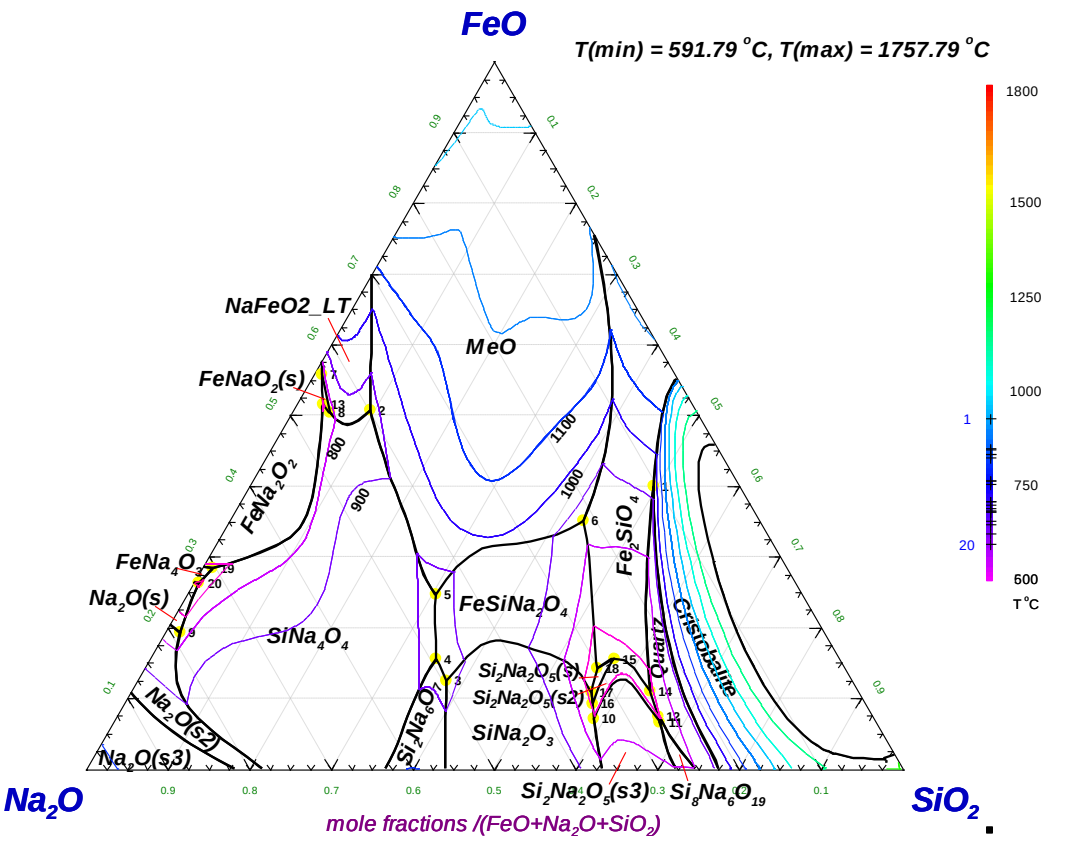

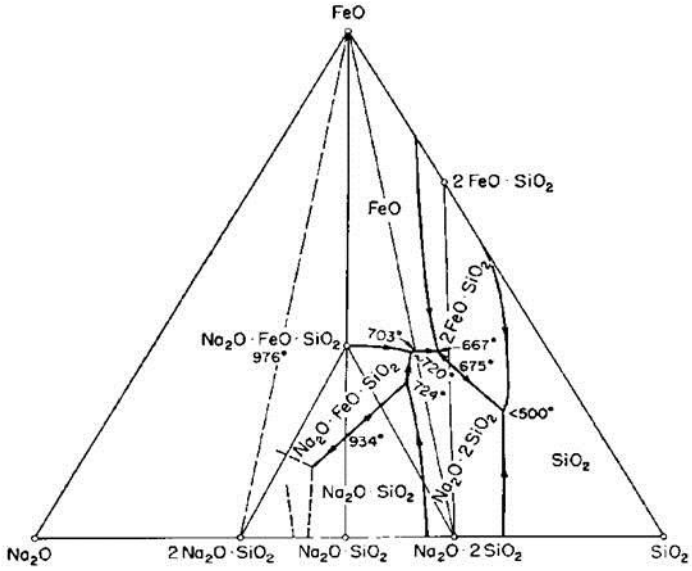

P. T. Carter and M. Ibrahim, J. Soc. Glass Technol., 36 [170] 142-163 (1952).

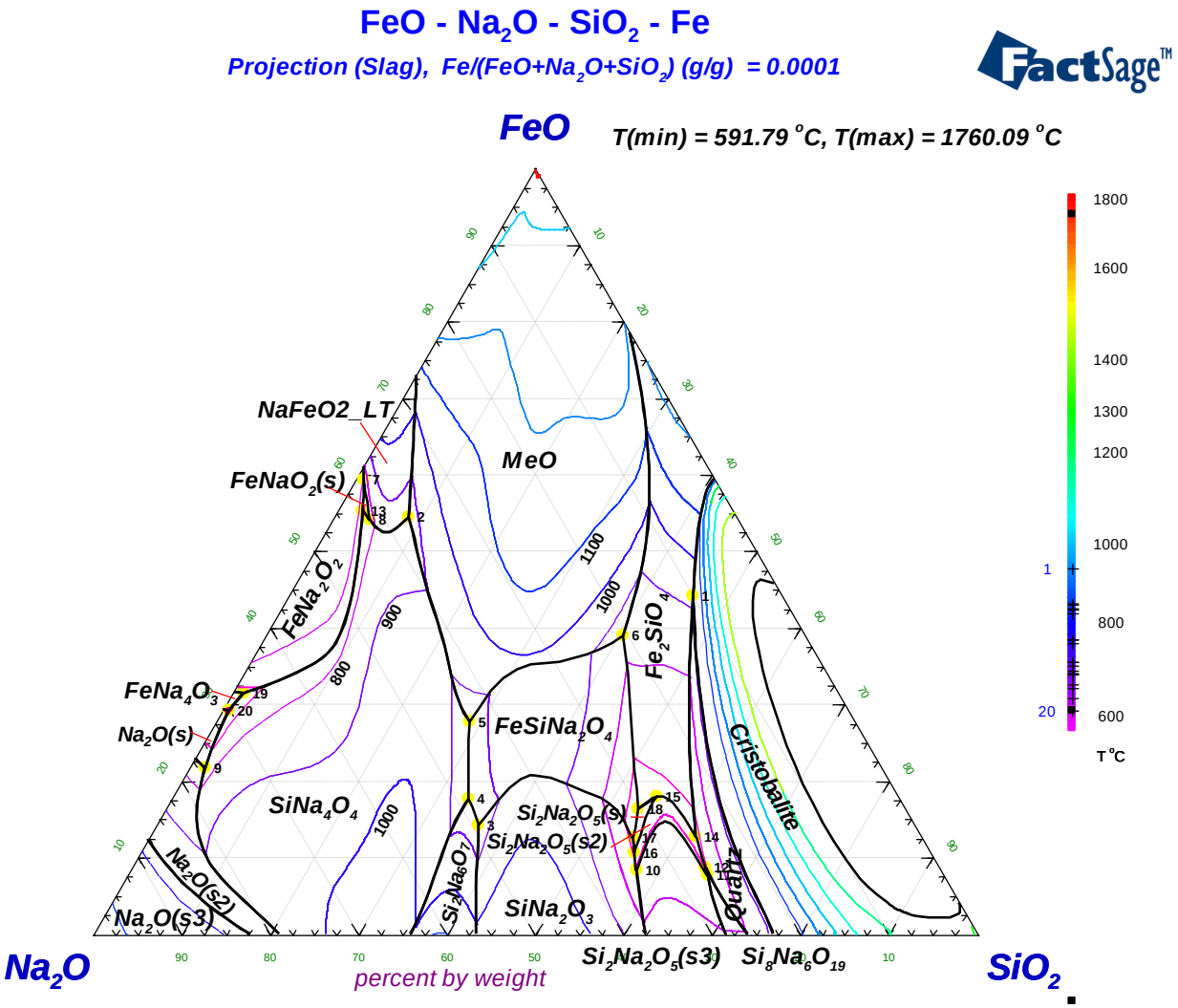
FeO - Na2O - SiO2 - Fe
Projection (Slag), Fe/(FeO+Na2O+SiO2) (g/g) = 0.0001
FactSage™
FeO
T(min) = 591.79 °C, T(max) = 1760.09 °C
NaFeO2_LT
FeNaO2(s)
MeO
FeNa2O2
FeNa4O3
Na2O(s)
SiNa4O4
Na2O(s2)
Na2O(s3)
FeSiNa2O4
Fe2SiO4
Cristobalite
Si2Na2O5(s)
Si2Na2O5(s2)
Si2Na6O7
SiNa2O3
Quartz
Si2Na2O5(s3)
Si8Na6O19
1100
1000
900
800
1000
1800
1600
1400
1300
1200
1000
800
600
T°C
Na2O
SiO2
percent by weight

Invariant equilibria on the liquidus surface

Intersections with slag	Mole fraction A = FeO, B = Na2O, C = SiO2				Weight percent A = FeO, B = Na2O, C = SiO2				
		X(A)	X(B)	X(C)	T(C)		W(A)	W(B)	W(C)	T(C)
1: Fe2SiO4 / Cristobalite / Quartz	1:	0.40027	0.10467	0.49506	926.28	1:	44.248	9.982	45.770	926.30
2: NaFeO2_LT / MeO / SiNa4O4	2:	0.50669	0.39901	0.09430	844.75	2:	54.497	37.021	8.482	844.76
3: FeSiNa2O4 / Si2Na6O7 / SiNa2O3	3:	0.12450	0.49622	0.37929	842.30	3:	14.314	49.217	36.469	842.30
4: FeSiNa2O4 / Si2Na6O7 / SiNa4O4	4:	0.15519	0.49339	0.35142	832.17	4:	17.742	48.659	33.599	832.17
5: FeSiNa2O4 / MeO / SiNa4O4	5:	0.24602	0.44876	0.30522	830.40	5:	27.693	43.576	28.732	830.40
6: Fe2O4Si / FeSiNa2O4 / MeO	6:	0.35046	0.21495	0.43459	821.84	6:	38.973	20.618	40.409	821.89
7: NaFeO2_LT / FeNa2O2 / FeNaO2(s)	7:	0.55758	0.43226	0.01015	759.85	7:	59.381	39.715	0.905	759.87
8: NaFeO2_LT / FeNaO2(s) / SiNa4O4	8:	0.50439	0.44956	0.04605	759.84	8:	54.193	41.670	4.138	759.84
9: Na2O(s) / Na2O(s2) / SiNa4O4	9:	0.19297	0.78835	0.01869	750.05	9:	21.714	76.528	1.759	750.05
10: Si2Na2O5(s2) / Si2Na2O5(s3) / SiNa2O3	10:	0.07122	0.34176	0.58701	706.87	10:	8.311	34.404	57.285	706.87
11: Si2Na2O5(s2) / Si2Na2O5(s3) / Si8Na6O19	11:	0.06595	0.26389	0.67016	706.86	11:	7.721	26.656	65.624	706.86
12: Si2Na2O5(s2) / Si8Na6O19 / Quartz	12:	0.07469	0.26098	0.66433	697.86	12:	8.730	26.320	64.950	697.88
13: FeNa2O2 / FeNaO2(s) / SiNa4O4	13:	0.51606	0.45220	0.03174	687.12	13:	55.329	41.825	2.846	687.13
14: Fe2SiO4 / Si2Na2O5(s2) / Quartz	14:	0.11007	0.25374	0.63619	679.71	14:	12.783	25.423	61.794	679.70
15: Fe2SiO4 / Si2Na2O5(s2) / Si2Na2O5(s)	15:	0.15586	0.27511	0.56902	677.83	15:	17.934	27.308	54.757	677.84
16: Si2Na2O5(s2) / Si2Na2O5(s) / SiNa2O3	16:	0.09169	0.33365	0.57466	677.83	16:	10.660	33.465	55.875	677.83
17: FeSiNa2O4 / Si2Na2O5(s) / SiNa2O3	17:	0.10870	0.32681	0.56450	654.40	17:	12.600	32.679	54.721	654.39
18: Fe2SiO4 / FeSiNa2O4 / Si2Na2O5(s)	18:	0.14234	0.30257	0.55509	643.77	18:	16.406	30.086	53.508	643.77
19: FeNa2O2 / FeNa4O3 / SiNa4O4	19:	0.28422	0.70269	0.01310	620.74	19:	31.532	67.253	1.215	620.63
20: FeNa4O3 / Na2O(s) / SiNa4O4	20:	0.26237	0.73024	0.00739	591.79	20:	29.201	70.112	0.688	591.79

FeO-SiO2-V2O3,
Mole fraction 1100°C

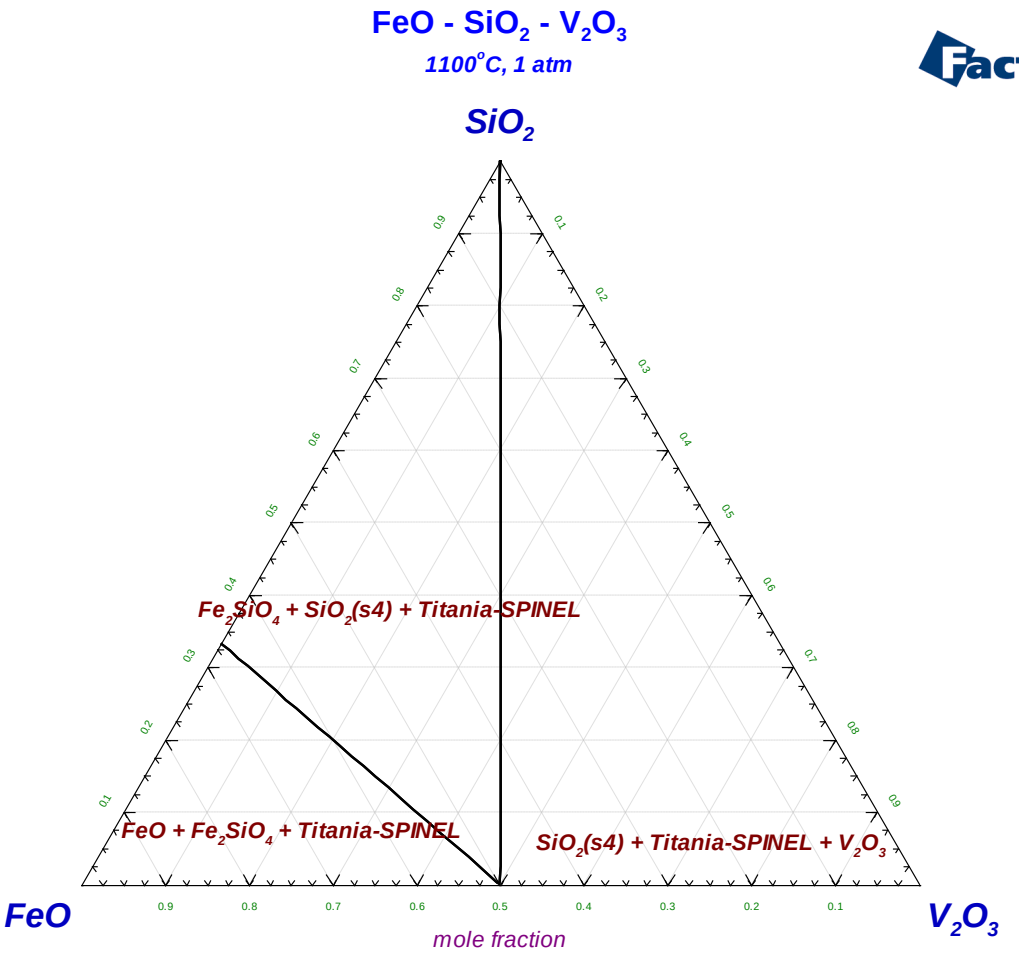

FeO-SiO2-V2O3,
Mole fraction, Liquidussurface

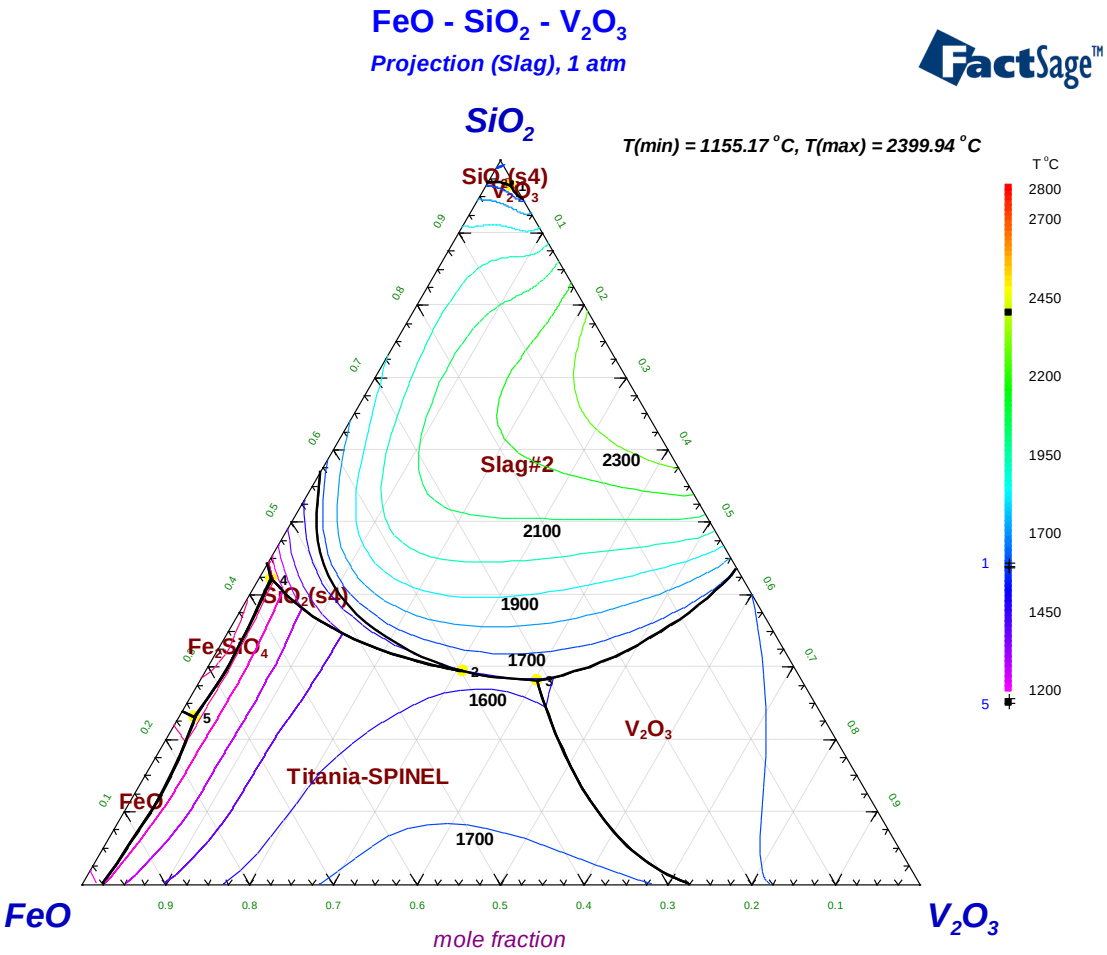

FeO-SiO2-V2O3,
Weight percent, Liquidussurface

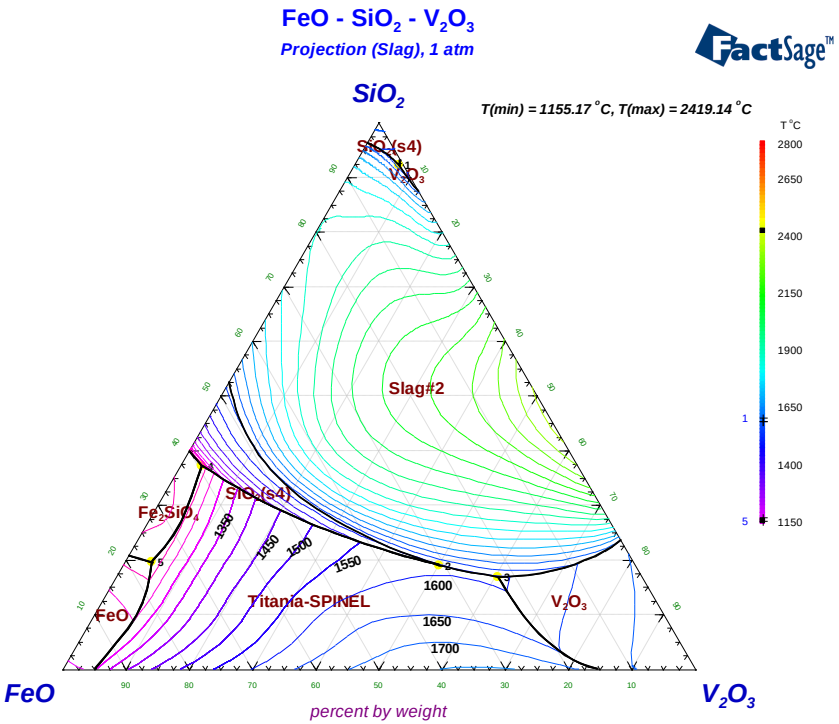

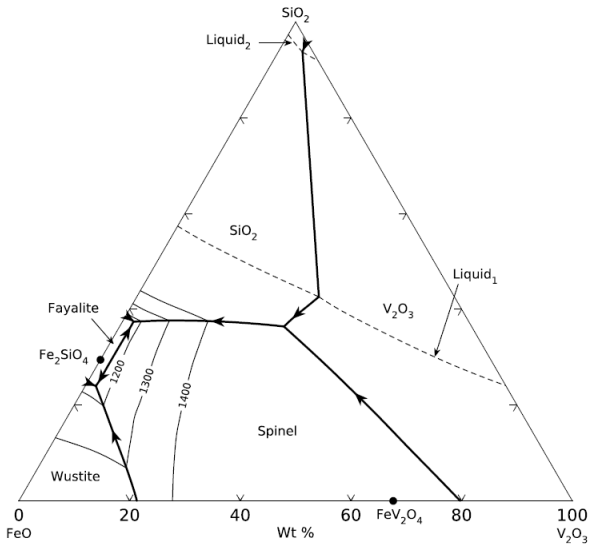

A. Muan and M. S. Najjar, "Composition involving V2O3-FeO-SiO2 and process for making composition", US Patent 5,106,811, April 21, 1992.

Invariant equilibria on the liquidus surface

Intersections with slag	Mole fraction				Weight percent				
	A = SiO2, B = FeO, C = V2O3				A = SiO2, B = FeO, C = V2O3				
		X(A)	X(B)	X(C)	T(C)		W(A)	W(B)	W(C)	T(C)
1: SiO2(s4) / Slag#2 / V2O3	1:	0.96440	0.00593	0.02967	1604.97	1:	92.242	0.678	7.080	1605.00
2. SiO2(s4) / Slag#2 / Titania-SPINEL	2:	0.29327	0.39783	0.30890	1590.87	2:	19.049	30.899	50.052	1590.87
3. Slag#2 / Titania-SPINEL / V2O3	3:	0.28081	0.31574	0.40345	1589.93	3:	16.868	22.678	60.454	1589.93
4. Fe2SiO4 / SiO2(s4) / Titania-SPINEL	4:	0.42179	0.56278	0.01543	1169.45	4:	37.221	59.383	3.396	1169.51
5. Fe2SiO4 / FeO / Titania-SPINEL	5:	0.23042	0.74955	0.02004	1155.18	5:	19.583	76.170	4.248	1155.17

Mole fraction 1085°C

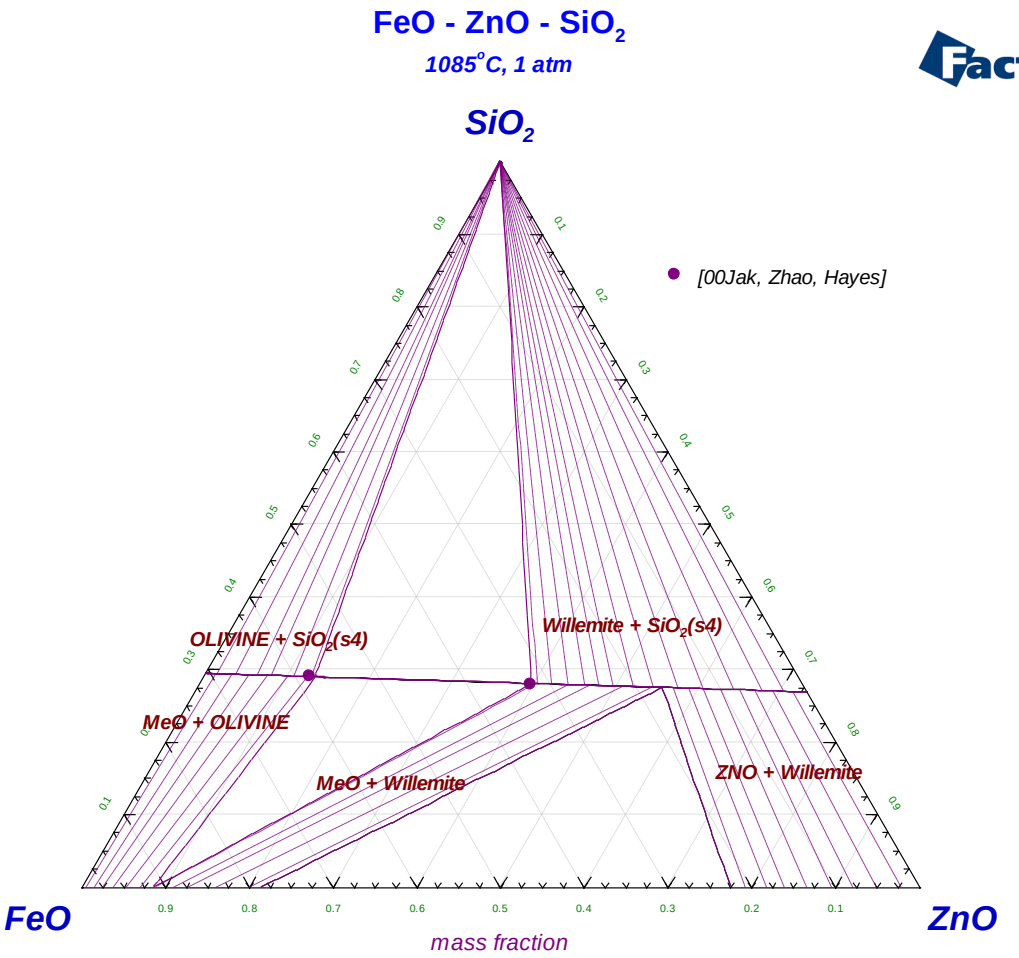

Mole fraction, Isopleth Fe2SiO4-Zn2SiO4-Fe

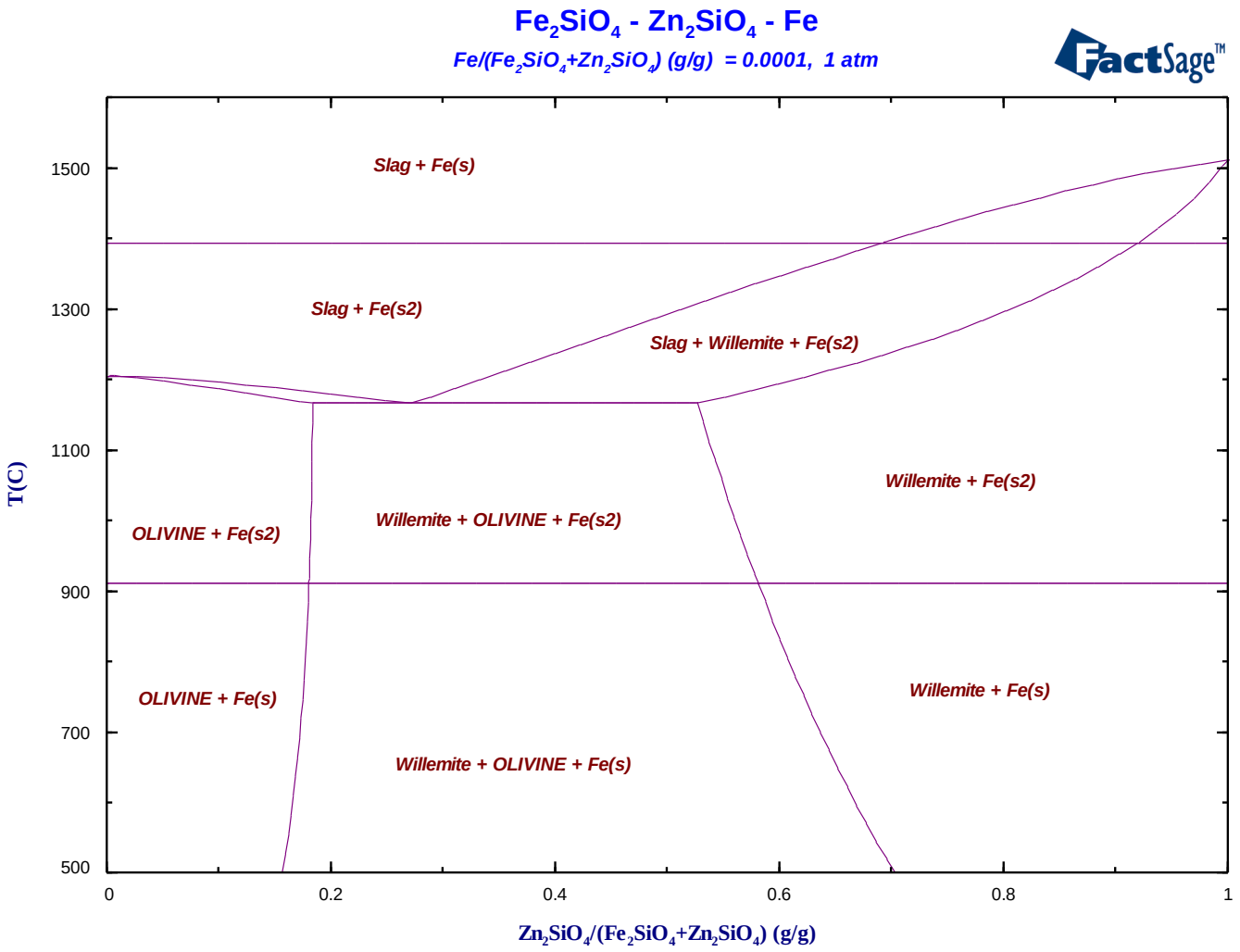

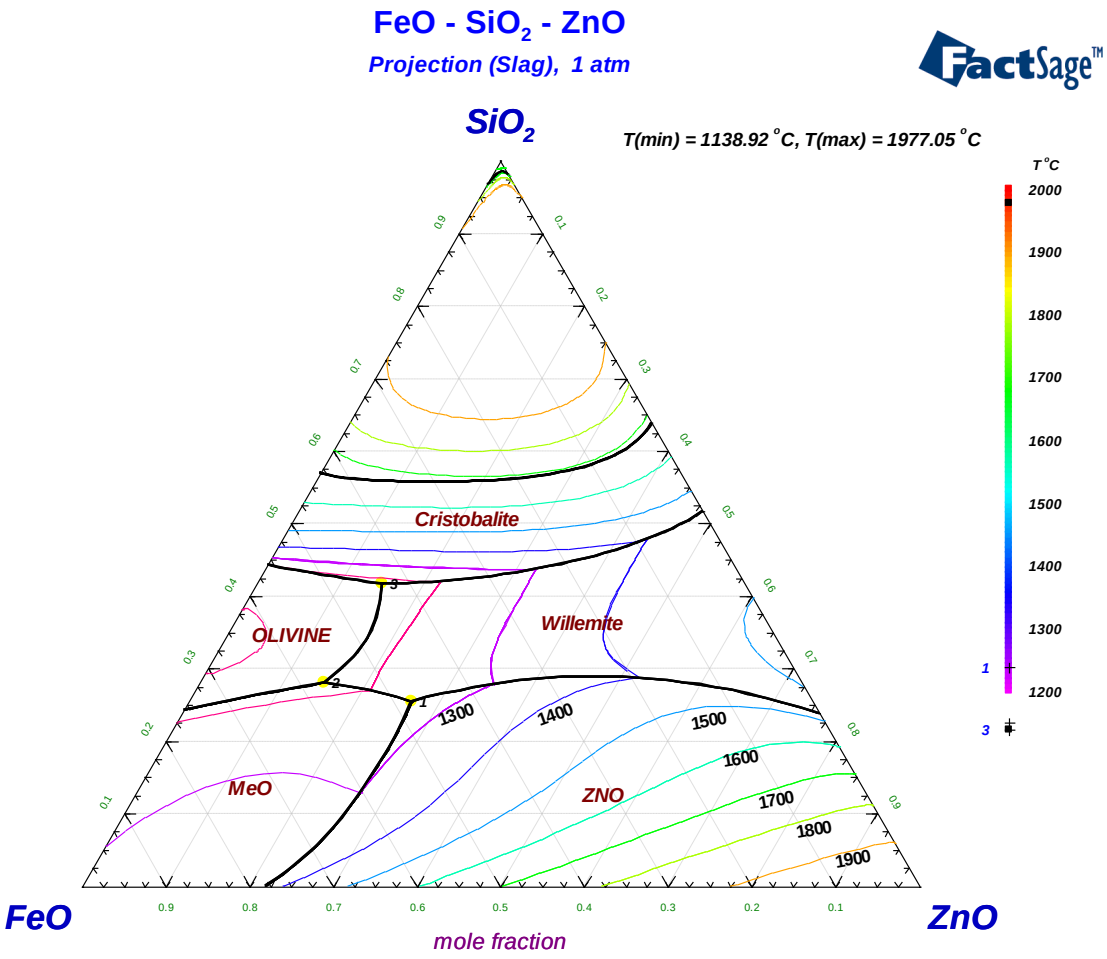
FeO - SiO2 - ZnO
Projection (Slag), 1 atm
FactSage™
SiO2
T(min) = 1138.92 °C, T(max) = 1977.05 °C
T °C
2000
1900
1800
1700
1600
1500
1400
1300
1200
Cristobalite
OLIVINE
Willemite
MeO
ZNO
1
2
3
1300
1400
1500
1600
1700
1800
1900
FeO
ZnO
mole fraction

Weight percent, Liquidussurface compared with experimental data

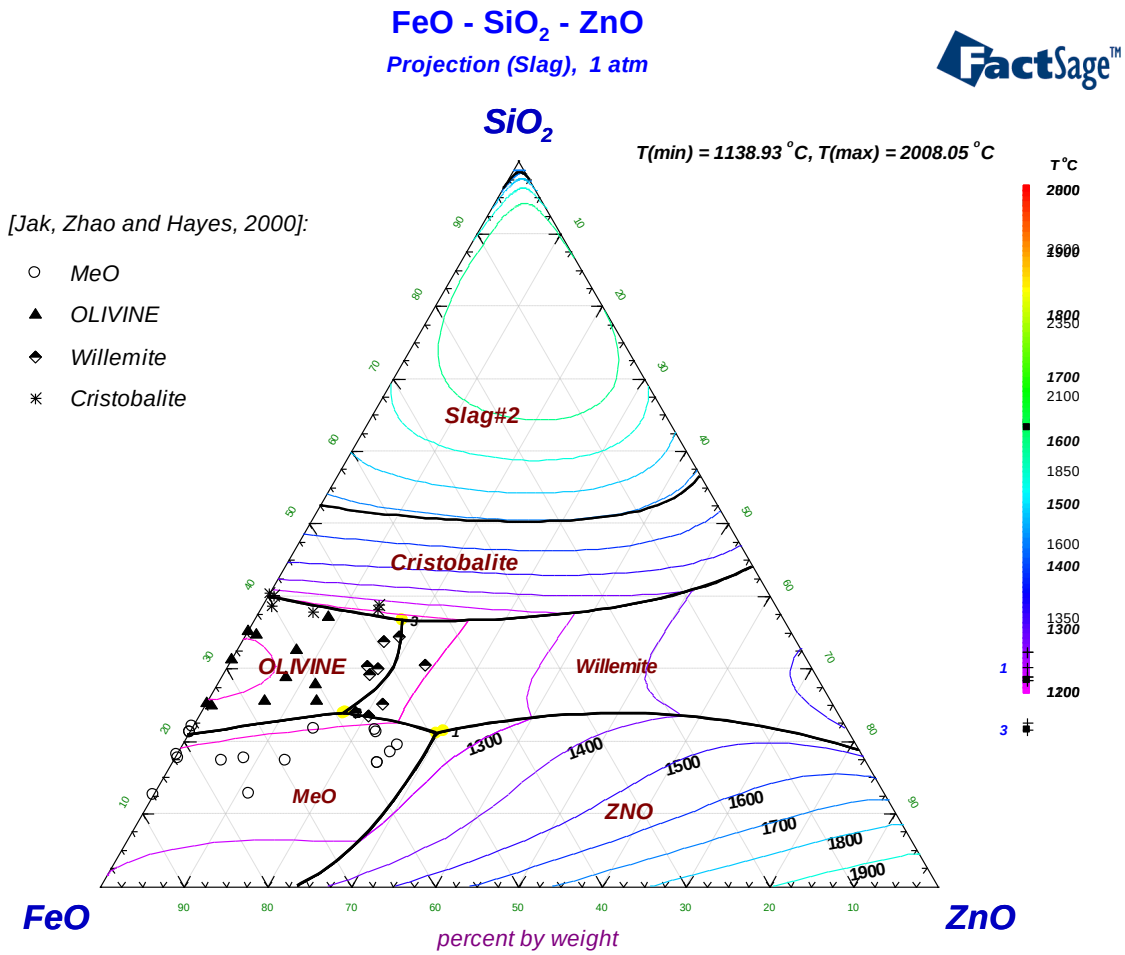

Invariant equilibria on the liquidus surface

Intersections with slag	Mole fraction A = SiO2, B = FeO, C = ZnO				Weight percent A = SiO2, B = FeO, C = ZnO			
	X(A)	X(B)	X(C)	T(C)	W(A)	W(B)	W(C)	T(C)
1: MeO / Willemite / ZNO	1: 0.25479	0.47973	0.26548	1238.15	1: 21.447	48..286	30.267	1238.17
2: MeO / OLIVINE / Willemite	2: 0.28066	0.57088	0.14846	1149.20	2: 24.104	58.626	17.269	1149.20
3: OLIVINE / Cristobalite / Willemite	3: 0.41705	0.43358	0.14937	1139.00	3: 36.654	45.566	17.780	1138.92

FeO-TiO2-Ti2O3,
Mole fraction 1600°C

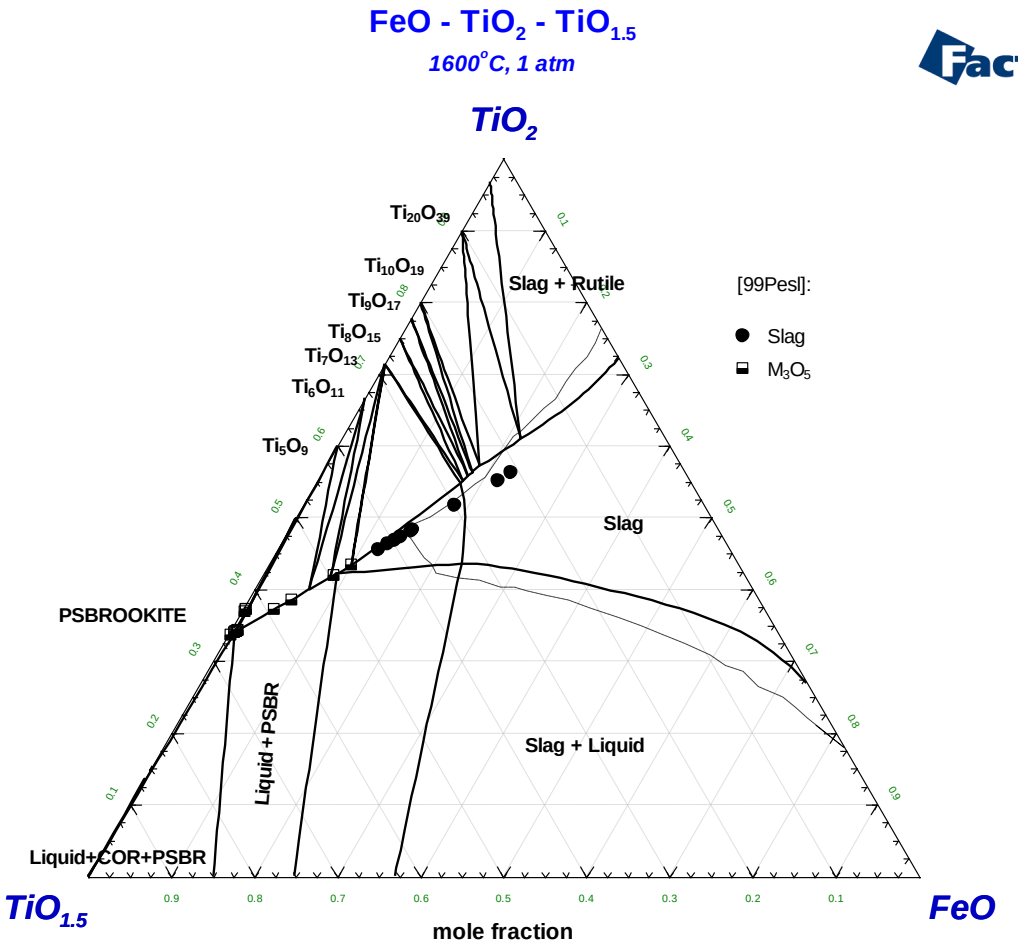

FeO-TiO2-Ti2O3, Mole fraction 1500°C

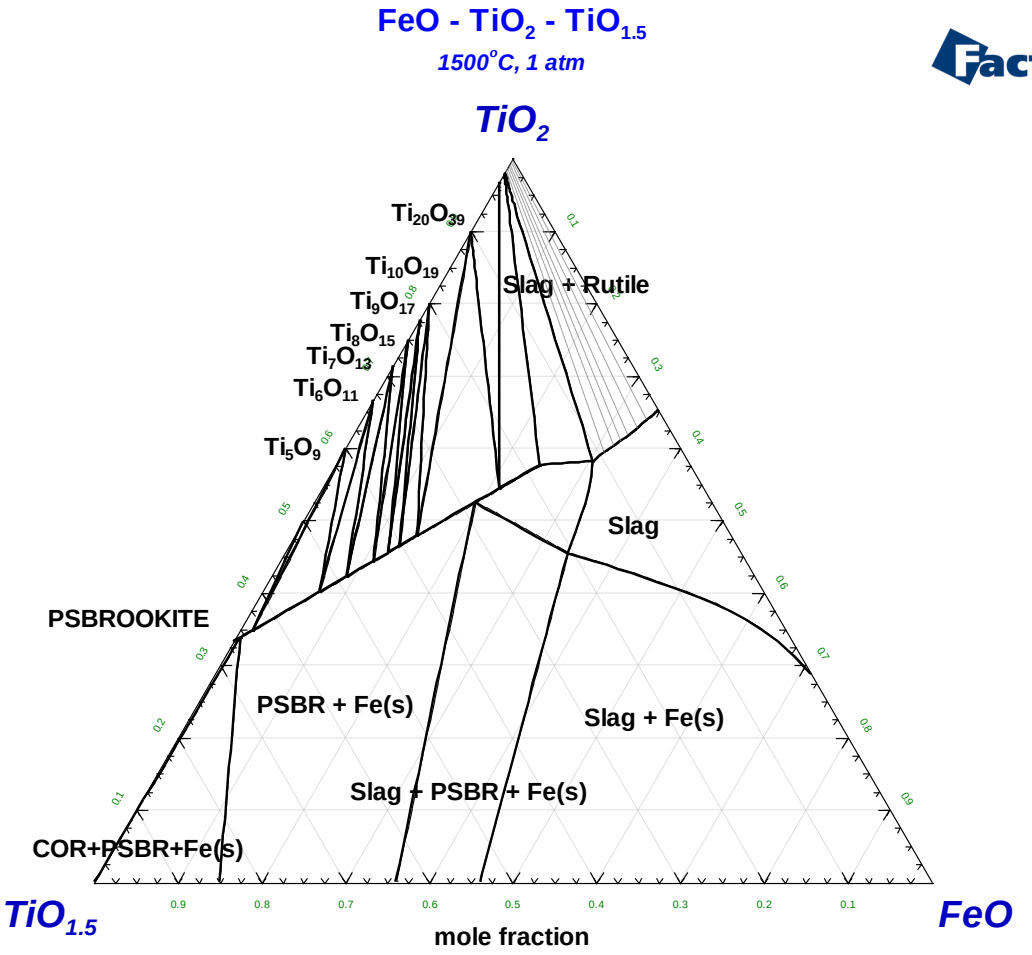

Mole fraction, Isotherms at 600°, 700°, 800°, 900° and 1000°C

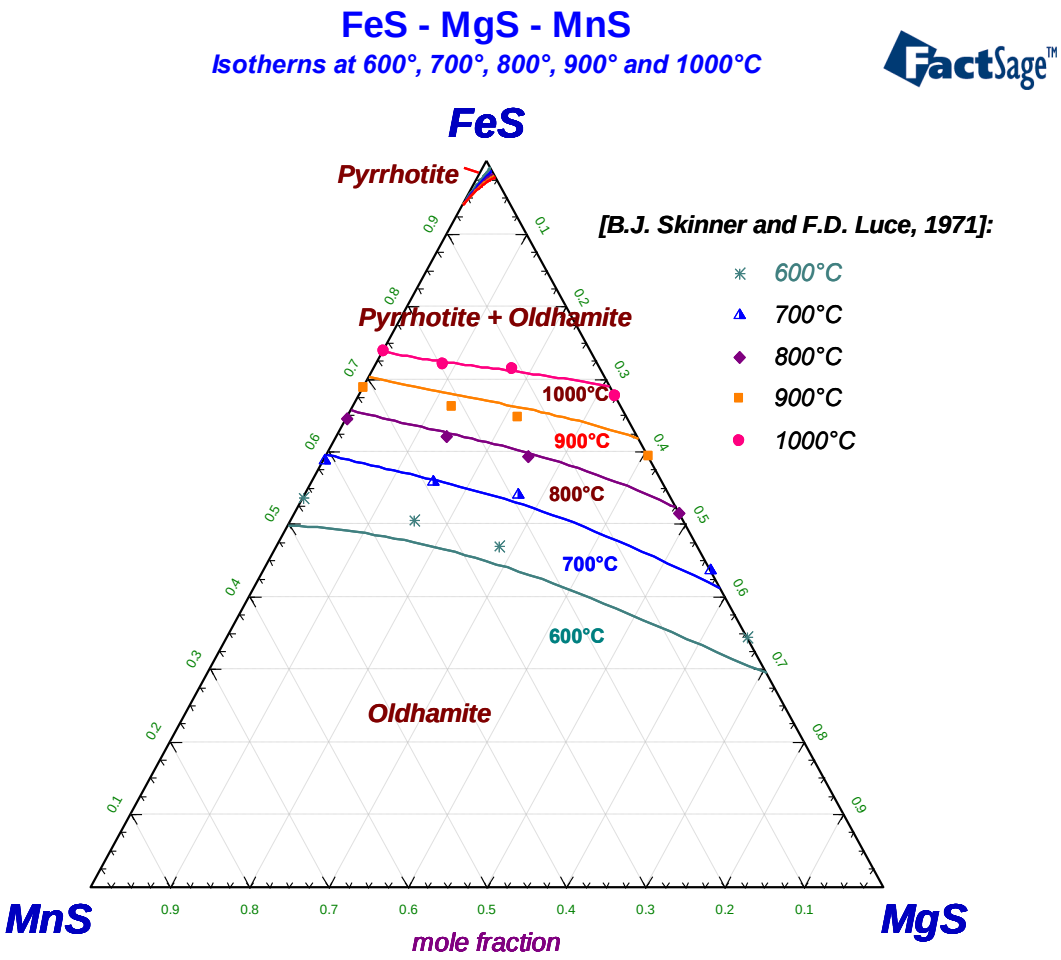

Mole fraction, Liquidussurface

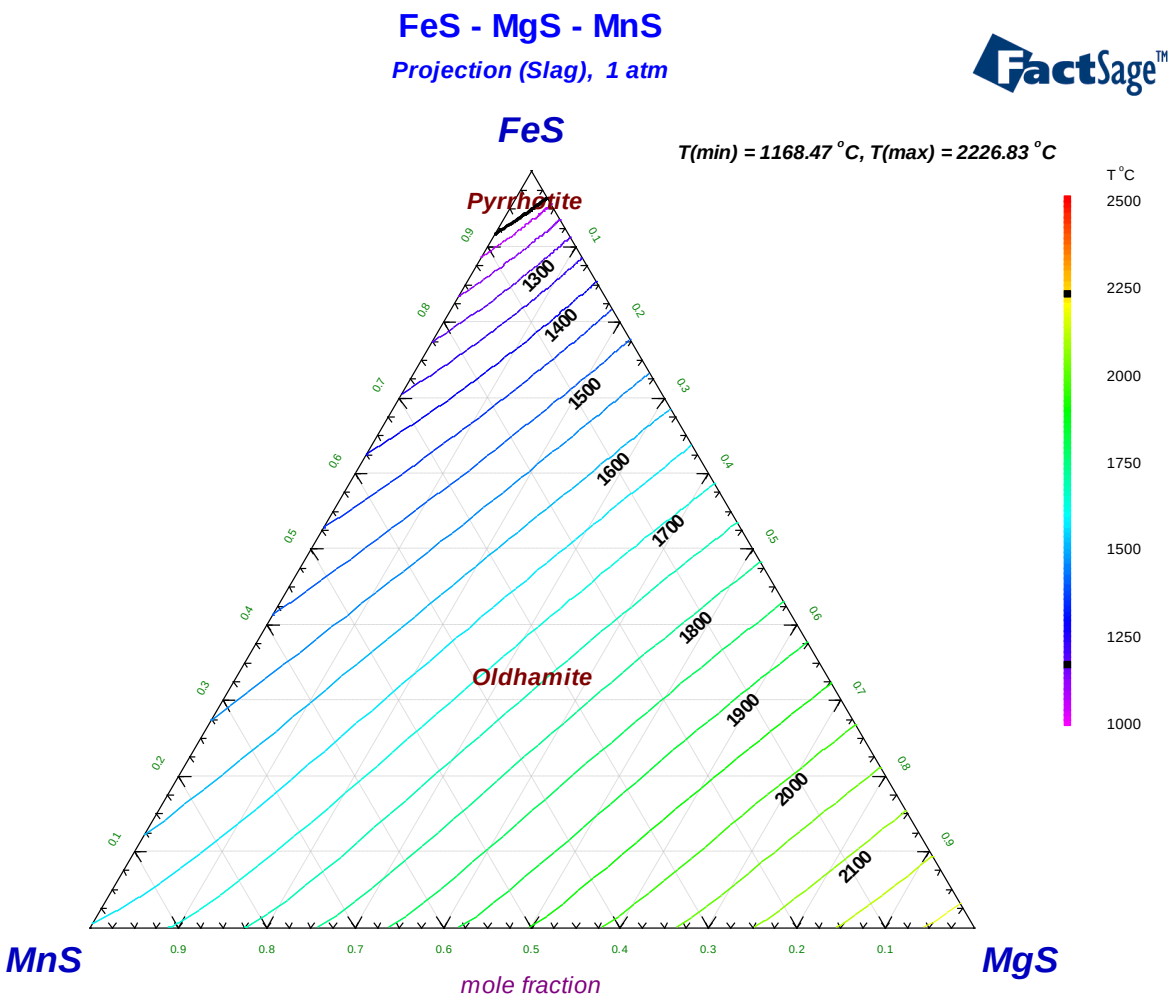

Weight percent, Liquidussurface

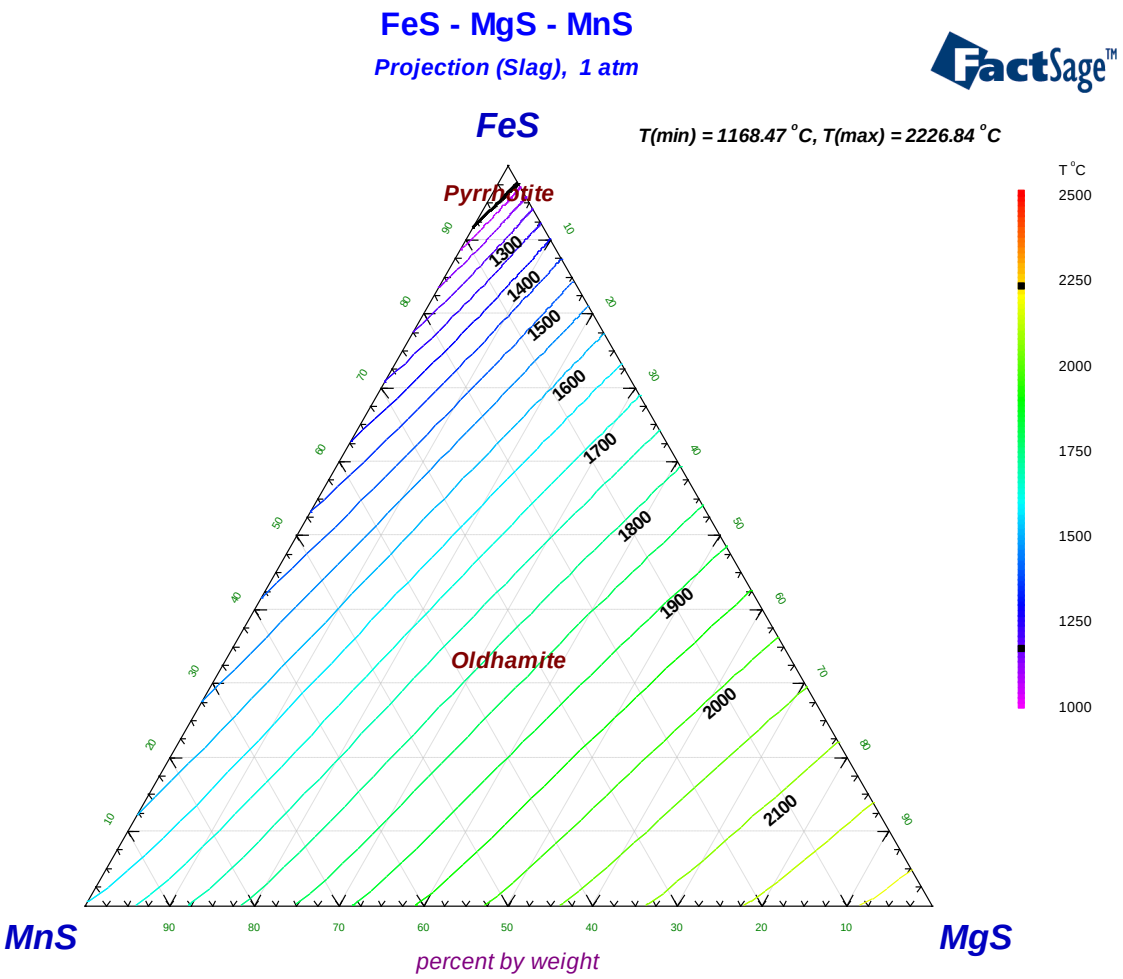

Ternary Phases

Name	*Composition*	*Melting, °C*	*Liquid species*	*Description*
R	$KMgPO_4$	1519, congruent	$KMgPO_4$(liq)	stoichiometric
J	$KMg_4(PO_4)_3$	1148, incongruent	$KMg(PO_3)_3$ (liq)	stoichiometric
W	$K_4Mg_4P_6O_{21}$	790, incongruent		stoichiometric
T1	$K_2MgP_2O_7$	736, incongruent		stoichiometric
T2	$K_4Mg(PO_4)_2$	1377, congruent		K3P-T2-T3 solution
T3	$K_6MgP_2O_9$	1570, incongruent		K3P-T2-T3 solution
B1	$KMg(PO_3)_3$	904, congruent		stoichiometric
B2	$K_2Mg(PO_3)_4$	735, incongruent		stoichiometric

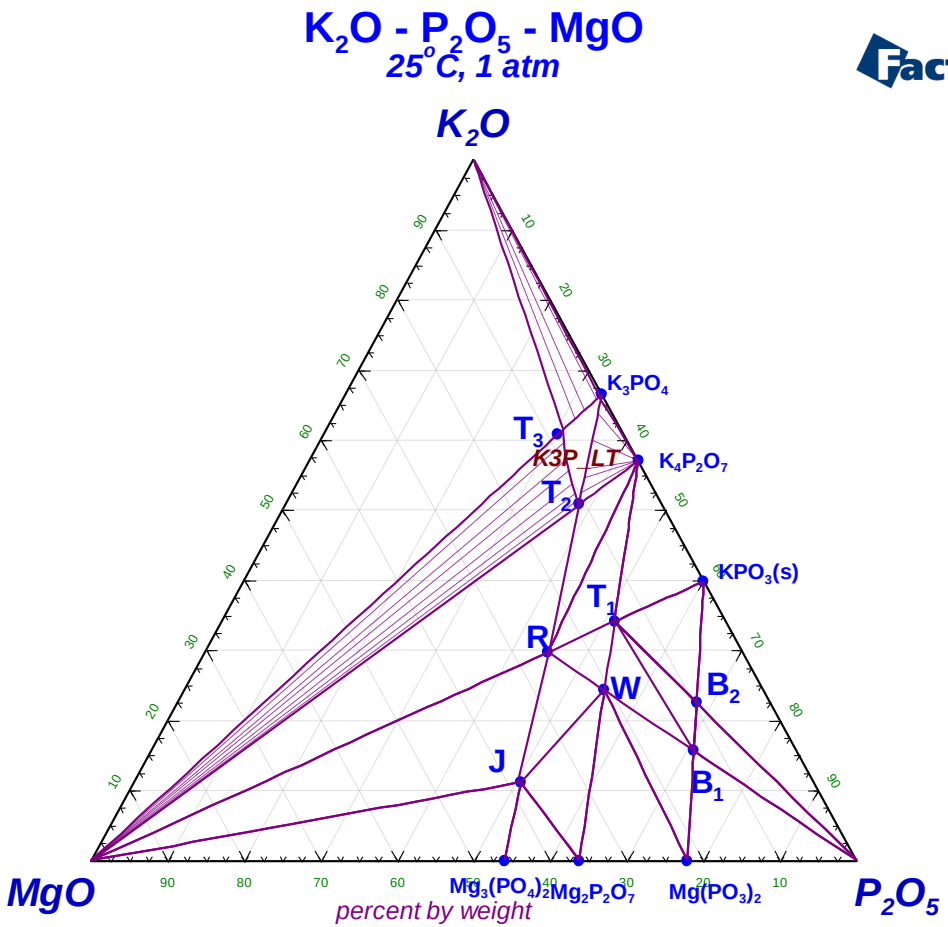

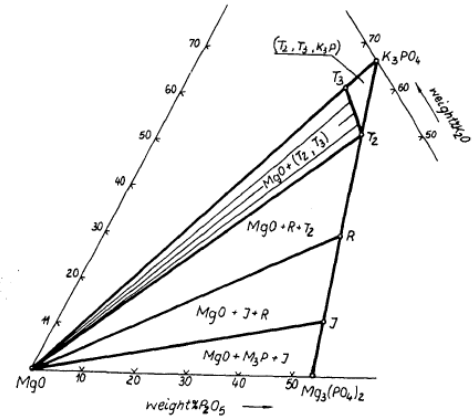

J. Berak and T. Podhajska-Kazmierczak, Pol. J. Chem., 65 [7-8] 1137-1149 (1991).

Weight percent, Isopleth K3PO4-MgO

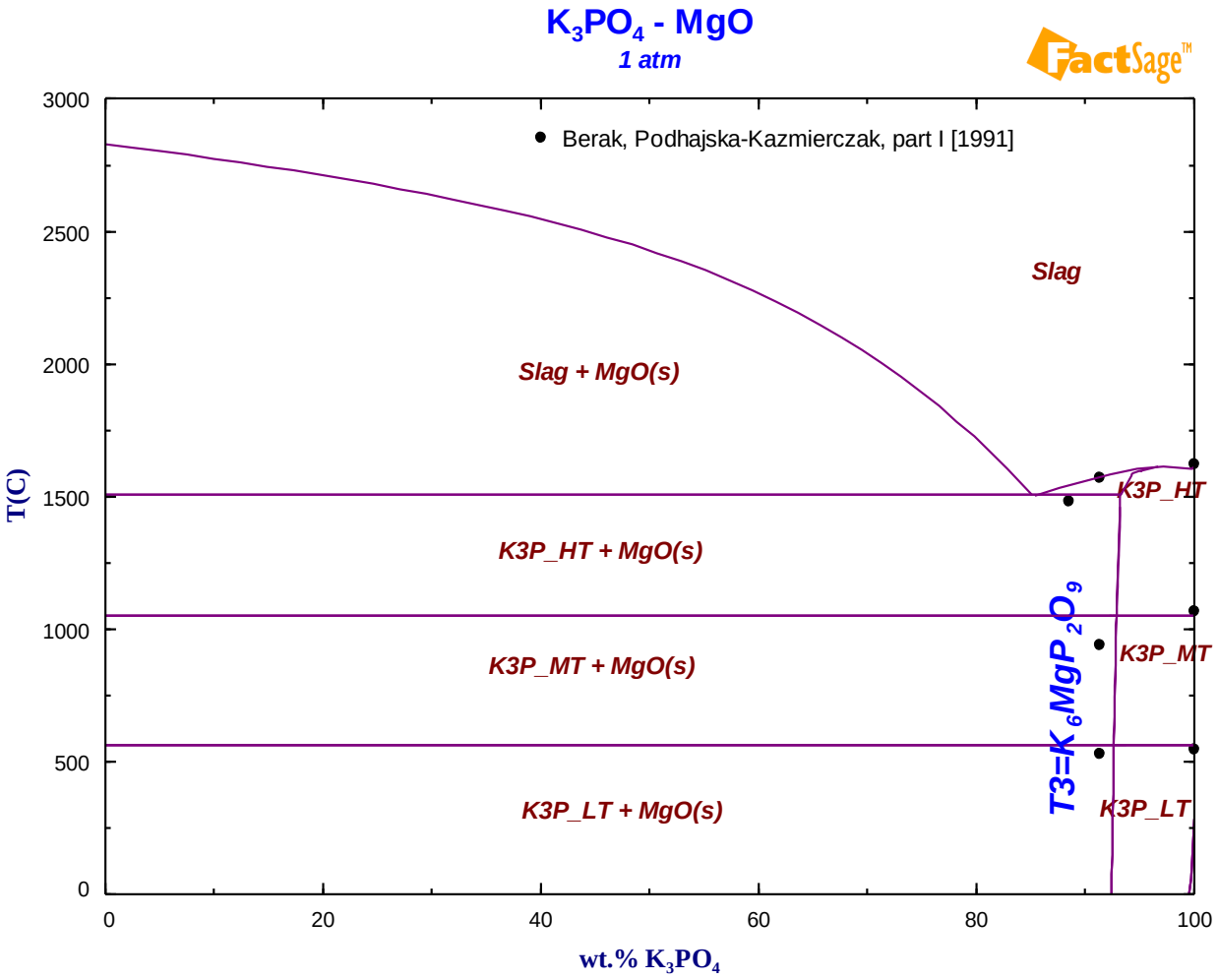

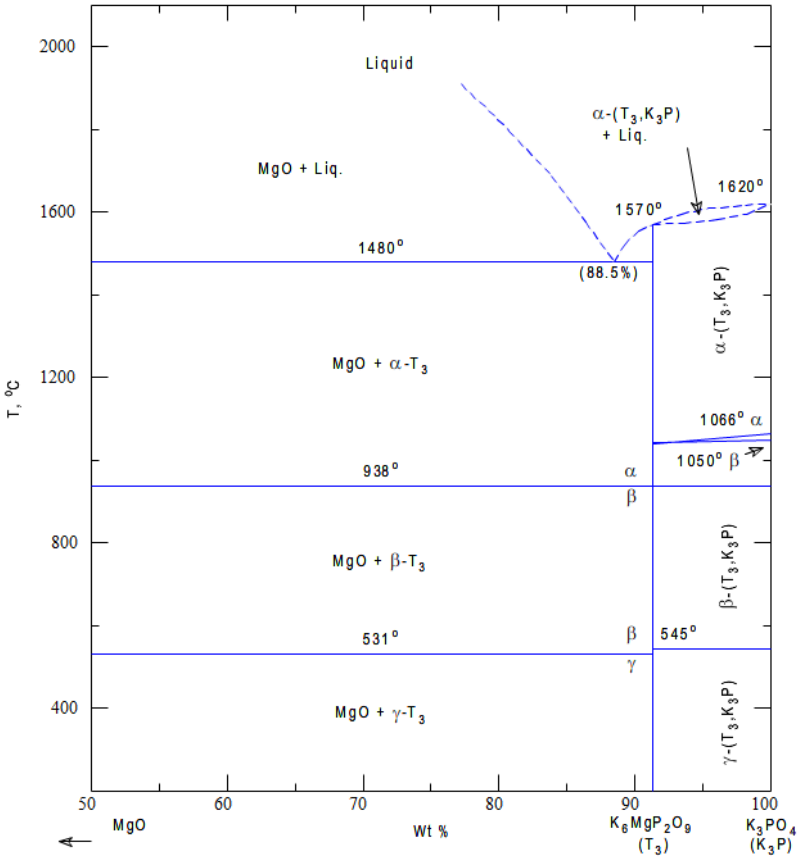

J. Berak and T. Podhajska-Kazmierczak, Pol. J. Chem., 65 [7-8] 1137-1149 (1991)

Weight percent, Isopleth KMgPO4-MgO

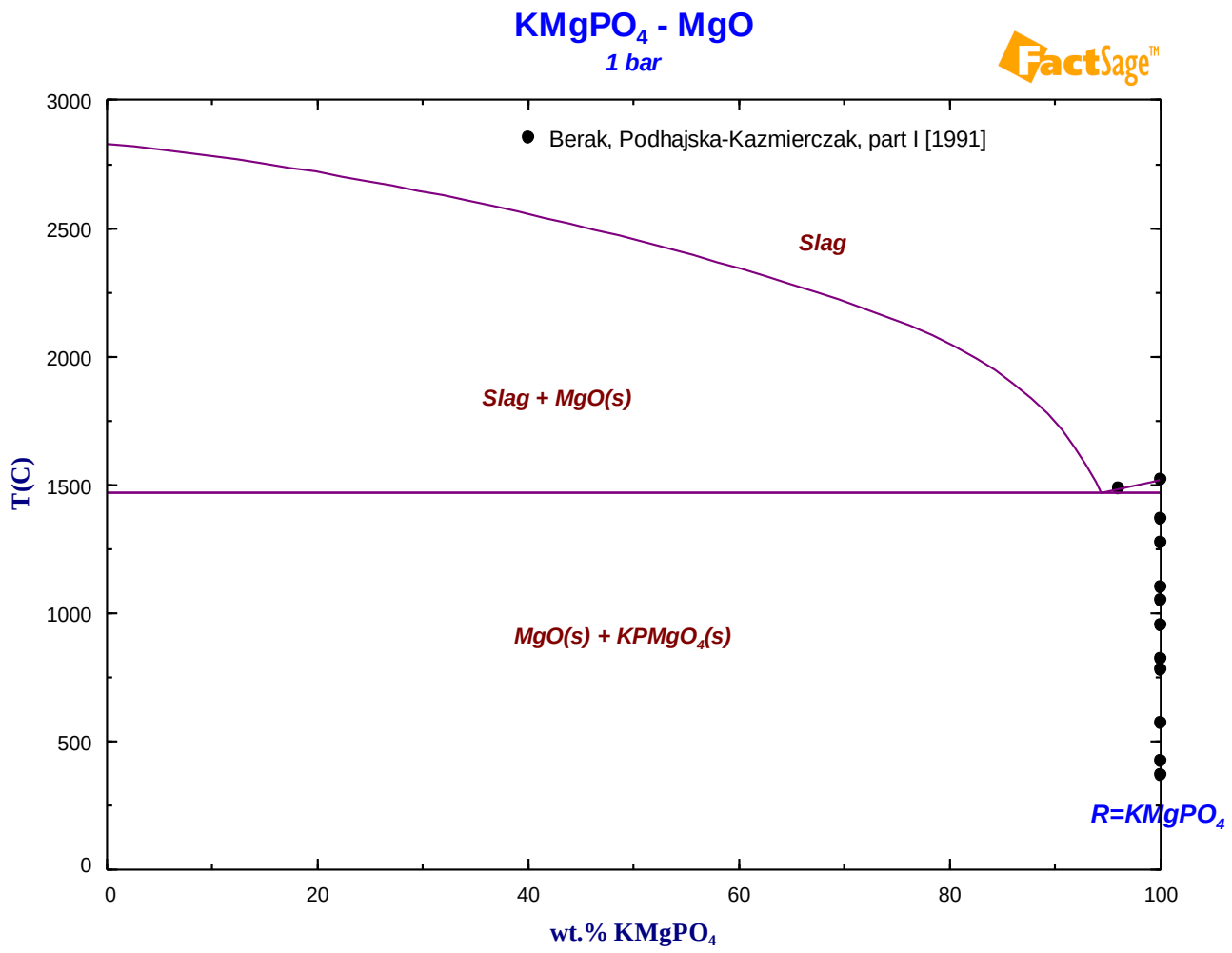

Weight percent, Isopleth KPO3-MgP2O6

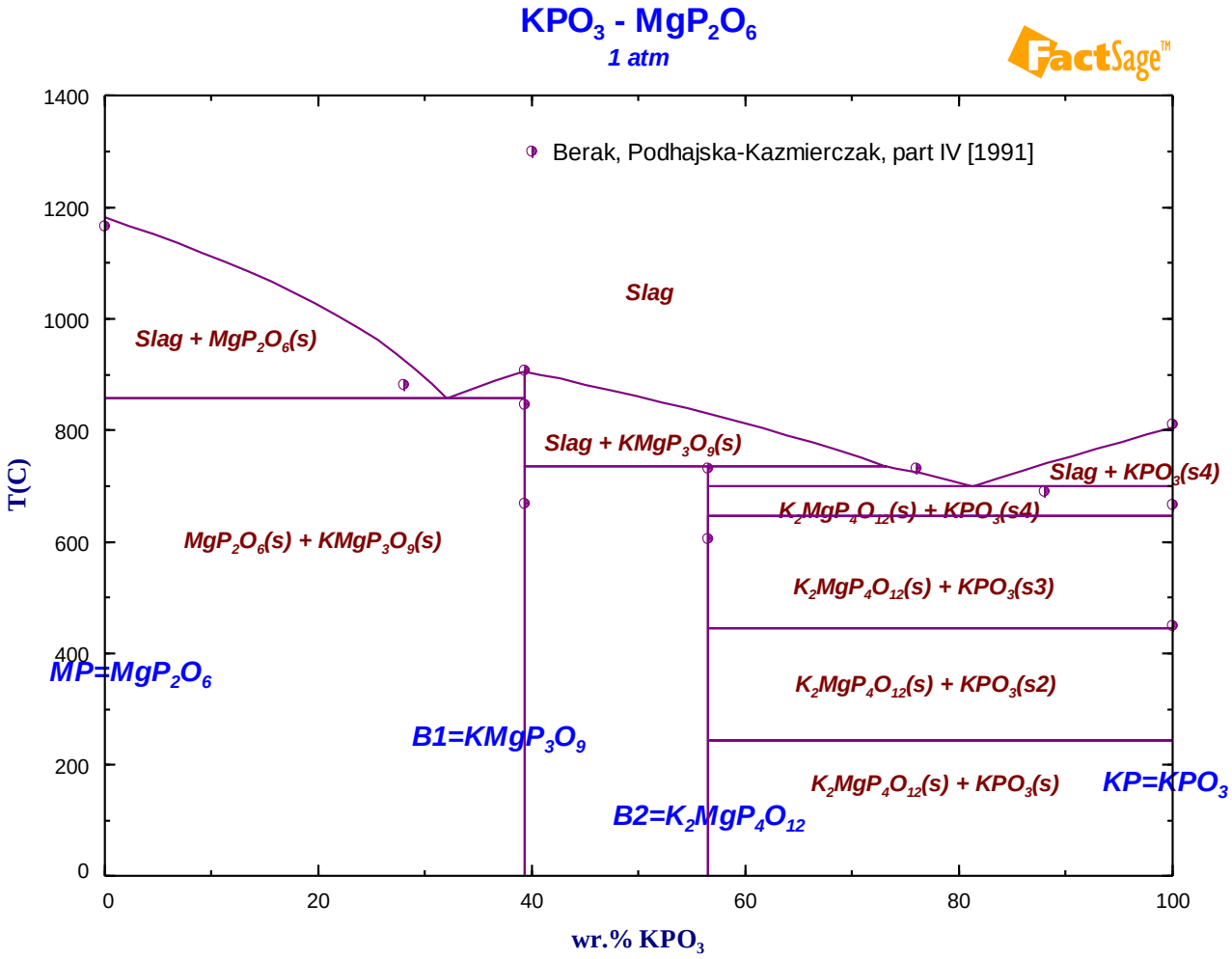

Weight percent, Isopleth K4P2O7-KMgPO4

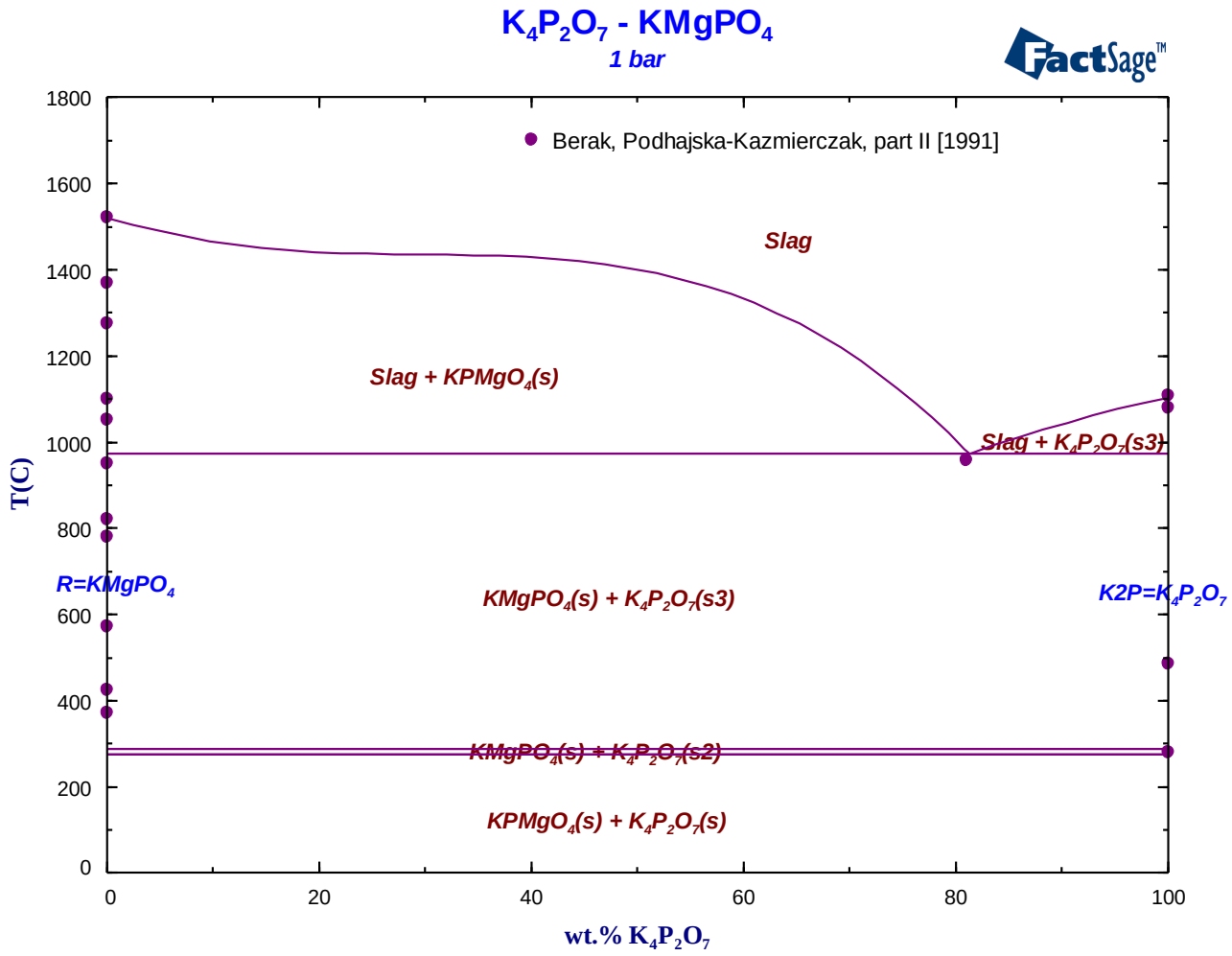

Weight percent, Isopleth K3PO4-KMgPO4

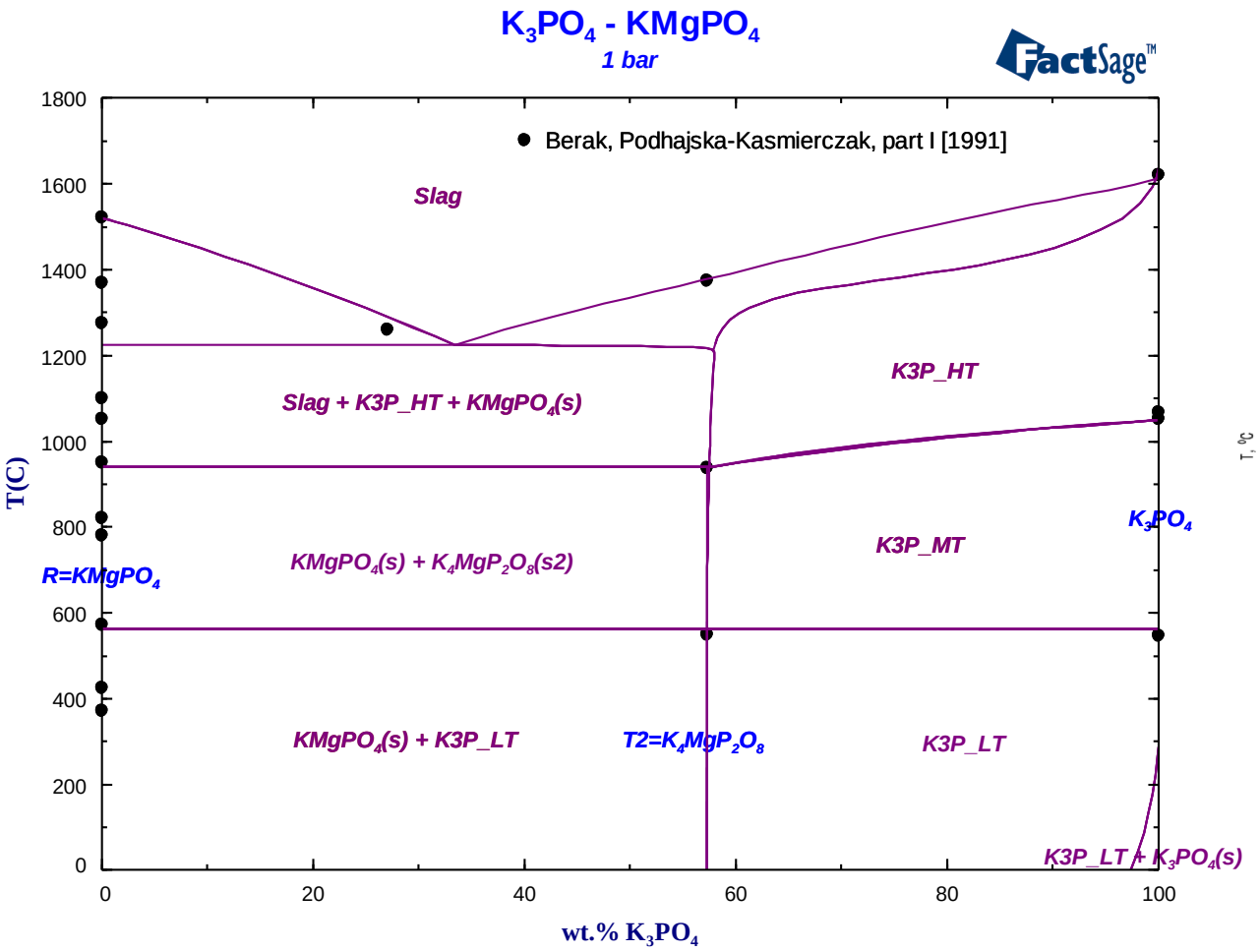

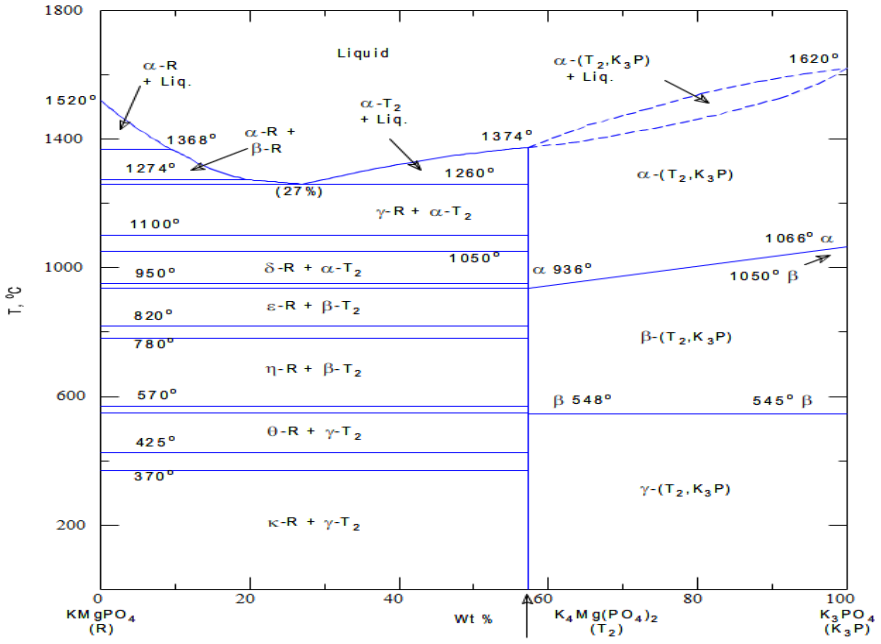

J. Berak and T. Podhajska-Kazmierczak, Pol. J. Chem., 65 [7-8] 1137-1149 (1991)

Weight percent, Isopleth K4P2O7-K4MgP2O8

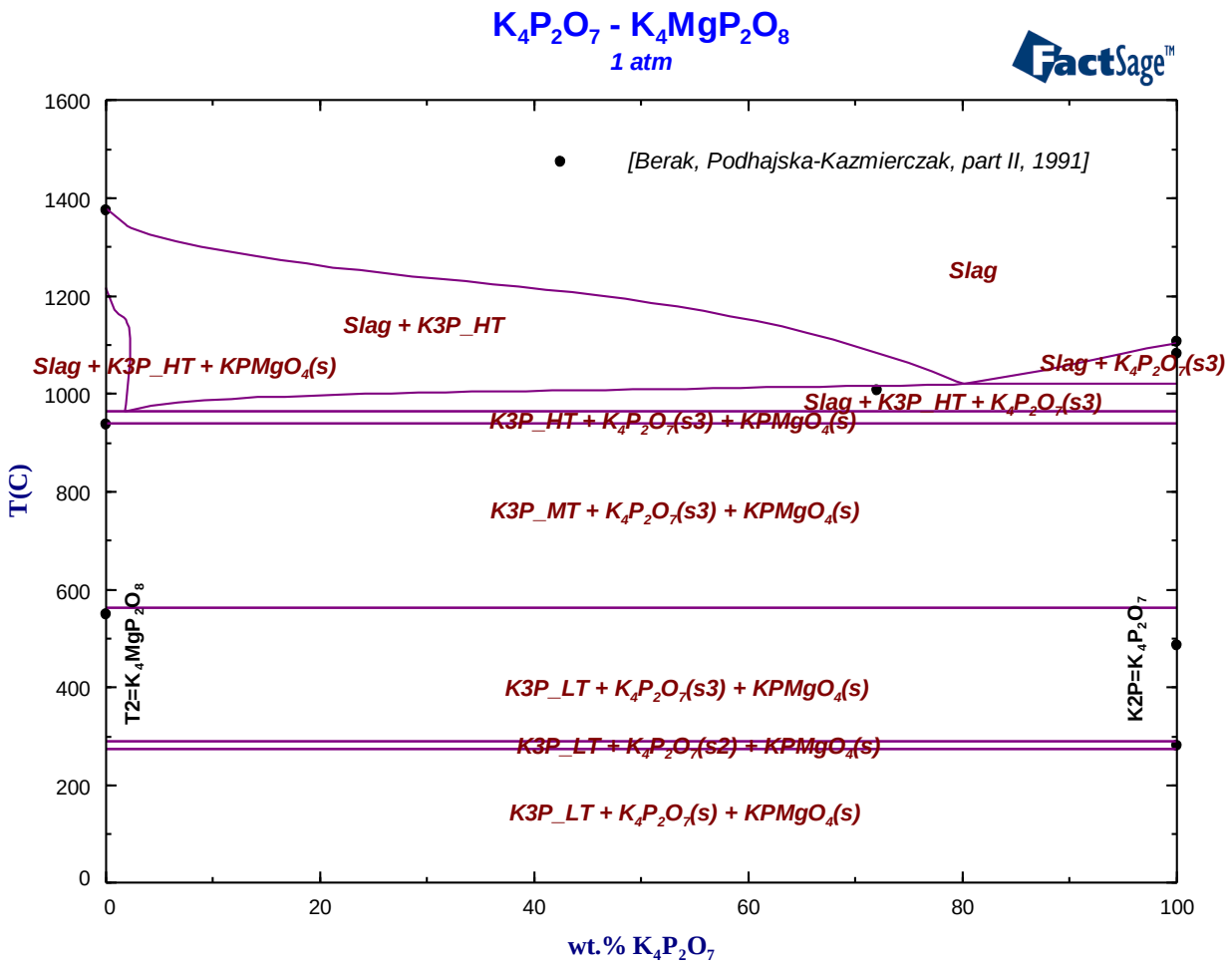

Weight percent, Isopleth KMg4P3O12-MgO

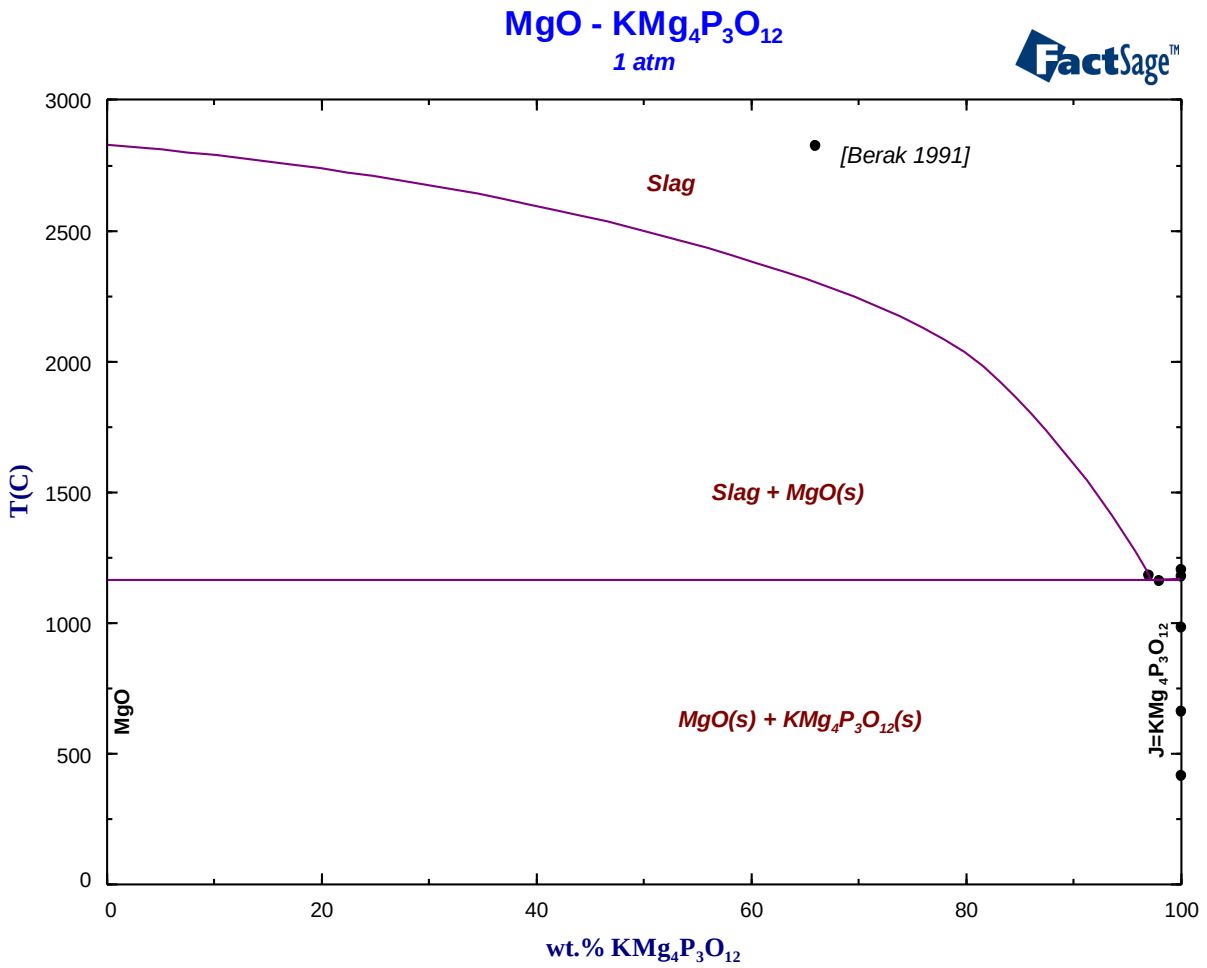

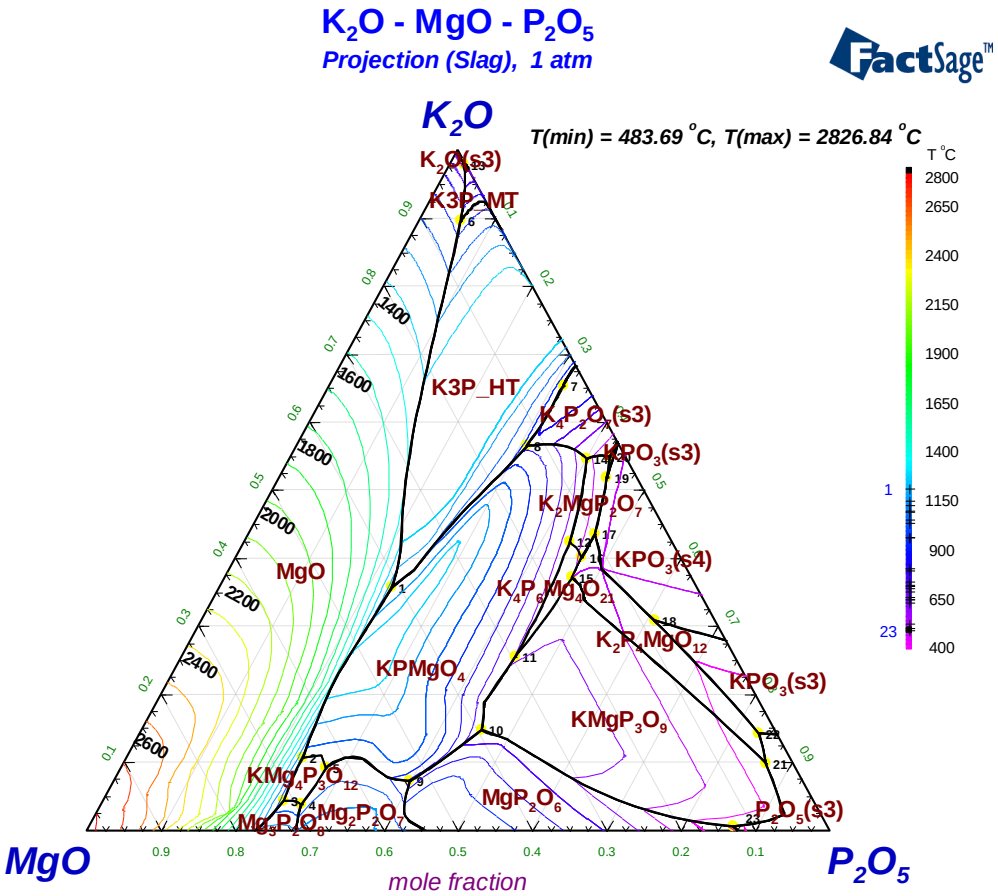
K2O - MgO - P2O5
Projection (Slag), 1 atm
FactSage™
K2O
T(min) = 483.69 °C, T(max) = 2826.84 °C
T °C
2800
2650
2400
2150
1900
1650
1400
1150
900
650
400
K2O(s3)
K3P_MT
K3P_HT
K4P2O7(s3)
KPO3(s3)
K2MgP2O7
KPO3(s4)
K4P6Mg4O21
K2P4MgO12
KPO3(s3)
KPMgO4
KMgP3O9
MgO
KMg4P3O12
Mg2P2O7
MgP2O6
P2O5(s3)
MgO
P2O5
mole fraction

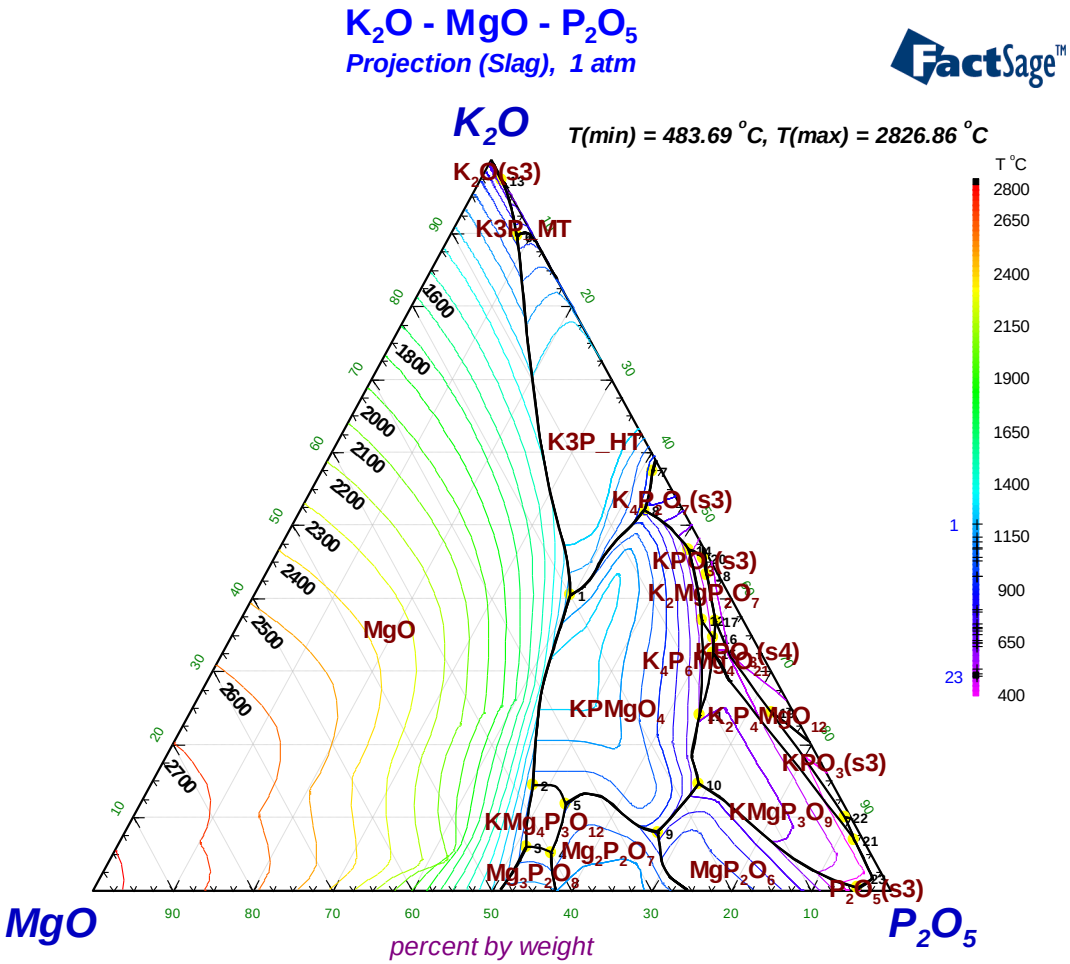

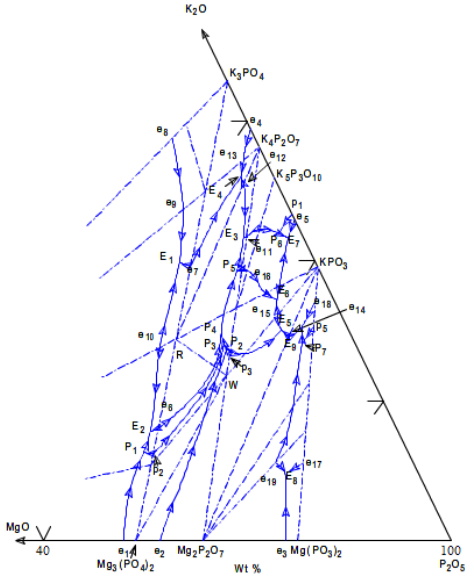

J. Berak and T. Podhajska-Kazmierczak, Pol. J. Chem., 65 [7-8] 1137-1149 (1991)

Invariant equilibria on the liquidus surface

Intersections with slag	Mole fraction A = K2O, B = MgO, C = P2O5				Weight percent A = K2O, B = MgO, C = P2O5			
	X(A)	X(B)	X(C)	T(C)	W(A)	W(B)	W(C)	T(C)
1: K3P_HT / KPMgO4 / MgO	0.35679	0.41127	0.23194	1210.78	40.440	19.945	0.39.614	1210.78
2: KMg4P3O12 / KPMgO4 / MgO	0.10685	0.65568	0.23746	1148.68	14.338	37.646	0.48.016	1148.68
3: KMg4P3O12 / Mg3P2O8 / MgO	0.04241	0.71445	0.24314	1124.97	5.935	42.785	0.51.280	1124.69
4: KMg4P3O12 / Mg2P2O7(s) / Mg3P2O8(s)	0.03834	0.69251	0.26915	1096.11	5.180	40.029	0.54.791	1096.06
5: KMg4P3O12 / KPMgO4 / Mg2P2O7(s)	0.09140	0.63299	0.27562	1090.83	11.754	34.832	0.53.414	1090.73
6: K3P_HT / K3P_MT / MgO	0.89683	0.04818	0.05500	1047.98	89.654	2.061	0.08.285	1047.98
7: K3P_HT / K3P_MT / K4P2O7(s3)	0.65463	0.03125	0.31411	1031.12	57.356	1.172	41.472	1031.12
8: K3P_HT / K4P2O7(s3) / KPMgO4	0.56531	0.12461	0.31008	962.66	52.059	4.910	43.030	962.66
9: KPMgO4 / Mg2P2O7(s) / MgP2O6(s)	0.07172	0.52955	0.39873	961.28	7.977	25.199	66.824	961.26
10: KMgP3O9 / KPMgO4 / MgP2O6(s)	0.14741	0.39433	0.45826	799.95	14.643	16.760	68.596	800.66
11: K4P6Mg4O21 / KMgP3O9 / KPMgO4	0.25437	0.29631	0.44932	790.43	24.038	11.981	63.982	790.42
12: K2MgP2O7 / K4P6Mg4O21 / KPMgO4	0.42353	0.13822	0.43824	733.15	37.052	5.174	57.773	733.15
13: K2O(s3) / K3P_MT / MgO	0.97976	0.00290	0.01734	717.12	97.282	0.123	2.595	717.12
14: K2MgP2O7 / K4P2O7(s3) / KPMgO4	0.54650	0.05448	0.39902	713.57	46.665	1.990	51.344	713.59
15: K2P4MgO12 / K4P6Mg4O21 / KMgP3O9	0.37164	0.16108	0.46728	700.02	32.466	6.021	61.513	700.02
16: K2MgP2O7 / K2P4MgO12 / K4P6Mg4O21	0.40145	0.13285	0.46570	681.43	34.606	4.900	60.494	681.43
17: K2MgP2O7 / K2P4MgO12 / KPO3(s4)	0.43583	0.09782	0.46635	656.32	36.921	3.546	59.533	656.32
18: K2P4MgO12 / KPO3(s3) / KPO3(s4)	0.30835	0.08189	0.60976	645.90	43.241	1.429	55.330	645.92
19: K2MgP2O7 / KPO3(s3) / KPO3(s4)	0.51915	0.04007	0.44078	645.90	24.427	2.776	72.797	645.89
20: K2MgP2O7 / K4P2O7(s3) / KPO3(s3)	0.54892	0.02169	0.42939	625.28	45.544	0.770	53.686	625.24
21: K2P4MgO12 / KMgP3O9 / P2O5(s3)	0.09804	0.03644	0.86553	517.75	6.914	1.100	91.986	517.75
22: K2P4MgO12 / KPO3(s3) / P2O5(s3)	0.14221	0.02405	0.83373	499.22	10.094	0.731	89.175	499.22
23: KMgP3O9 / MgP2O6(s) / P2O5(s3)	0.00531	0.12704	0.86766	483.69	0.388	3.976	95.636	483.73

Ternäre Phasen im K_2O-MgO-SiO_2 System

Phase	Beschreibung	Formel
KMS (111)	Mischphase	$(Mg^{2+},Si^{4+})_1(Si^{4+})_1\ (K^{1+},Va)_2(O^{2-})_4$
KMS_3 (113-LT)	Stöchiometrisch	$K_2MgSi_3O_8$ (s1)
KMS_3 (113-HT)	Stöchiometrisch	$K_2MgSi_3O_8$ (s2)
KMS_5	Stöchiometrisch	$K_2MgSi_5O_{12}$
KM_5S_{12} (Roedderite)	Stöchiometrisch	$K_2Mg_5Si_{12}O_{30}$
$K_2M_2S_5$ (Ortho)	Stöchiometrisch	$K_4Mg_2Si_5O_{14}$
$K_5M_5S_{11}$ (Tetra)	Stöchiometrisch	$K_{10}Mg_5Si_{11}O_{32}$

Weight percent , Isopleth K2SiO3-K2MgSiO4 compared with experimental data

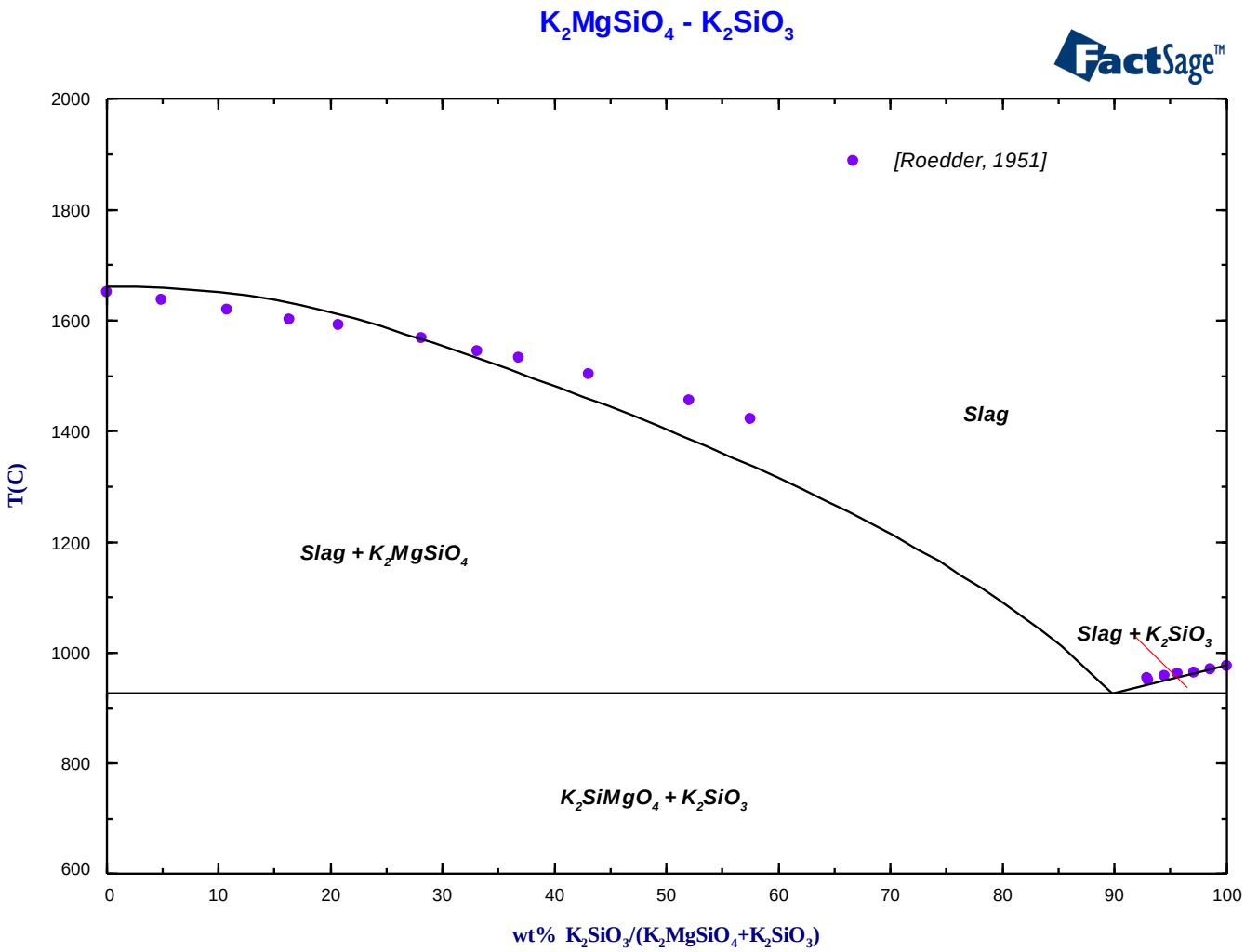

K2O-MgO-SiO2,
Mole fraction, Isopleth 0.5(K2MgSiO4)-SiO2°

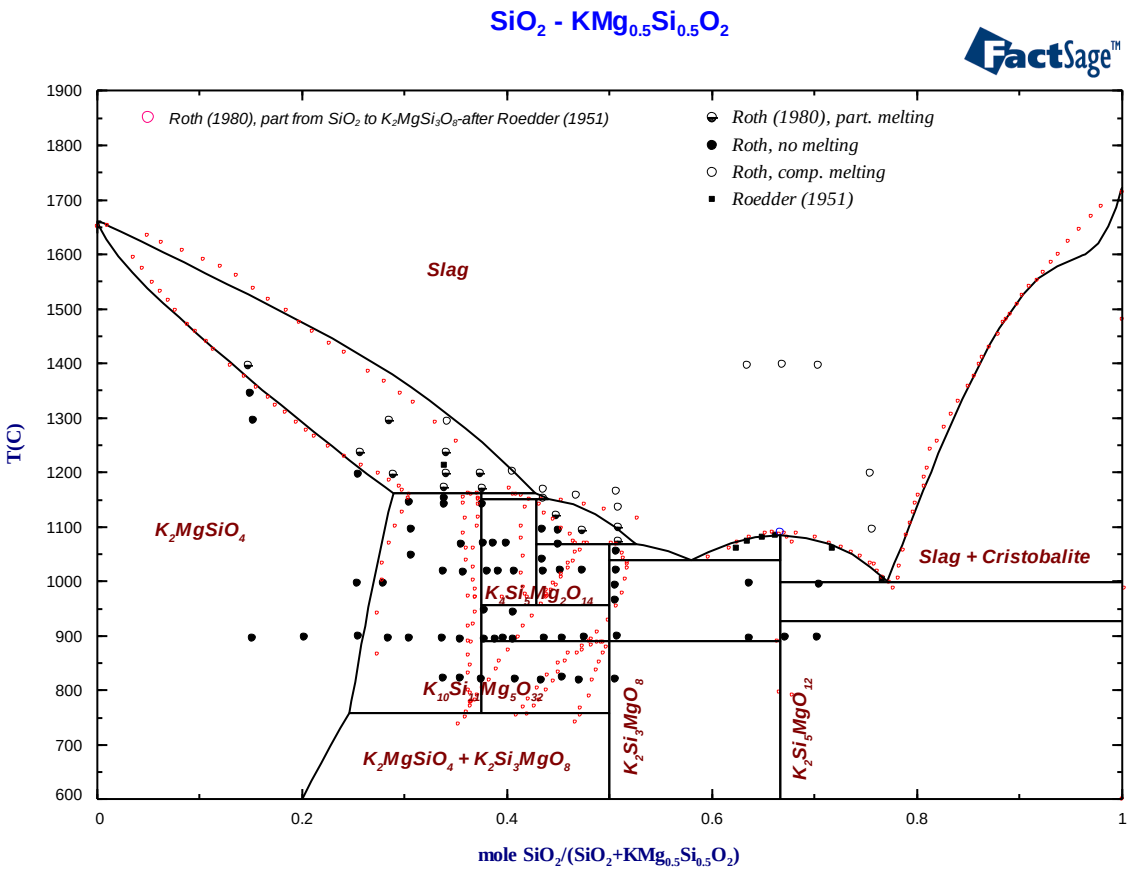

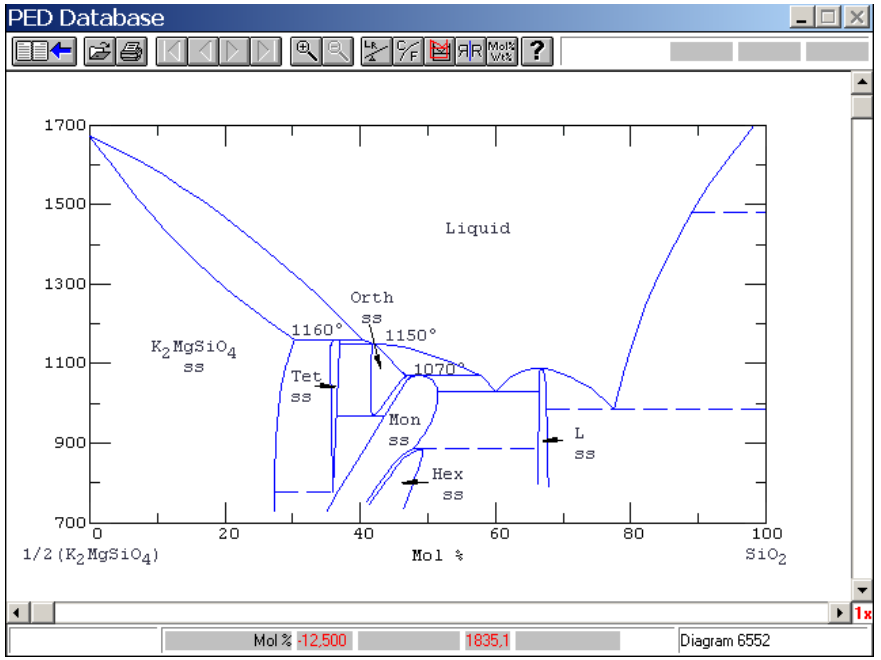

R.S. Roth, Adv. Chem. Ser., No. 186 (1980), pp.391-408.

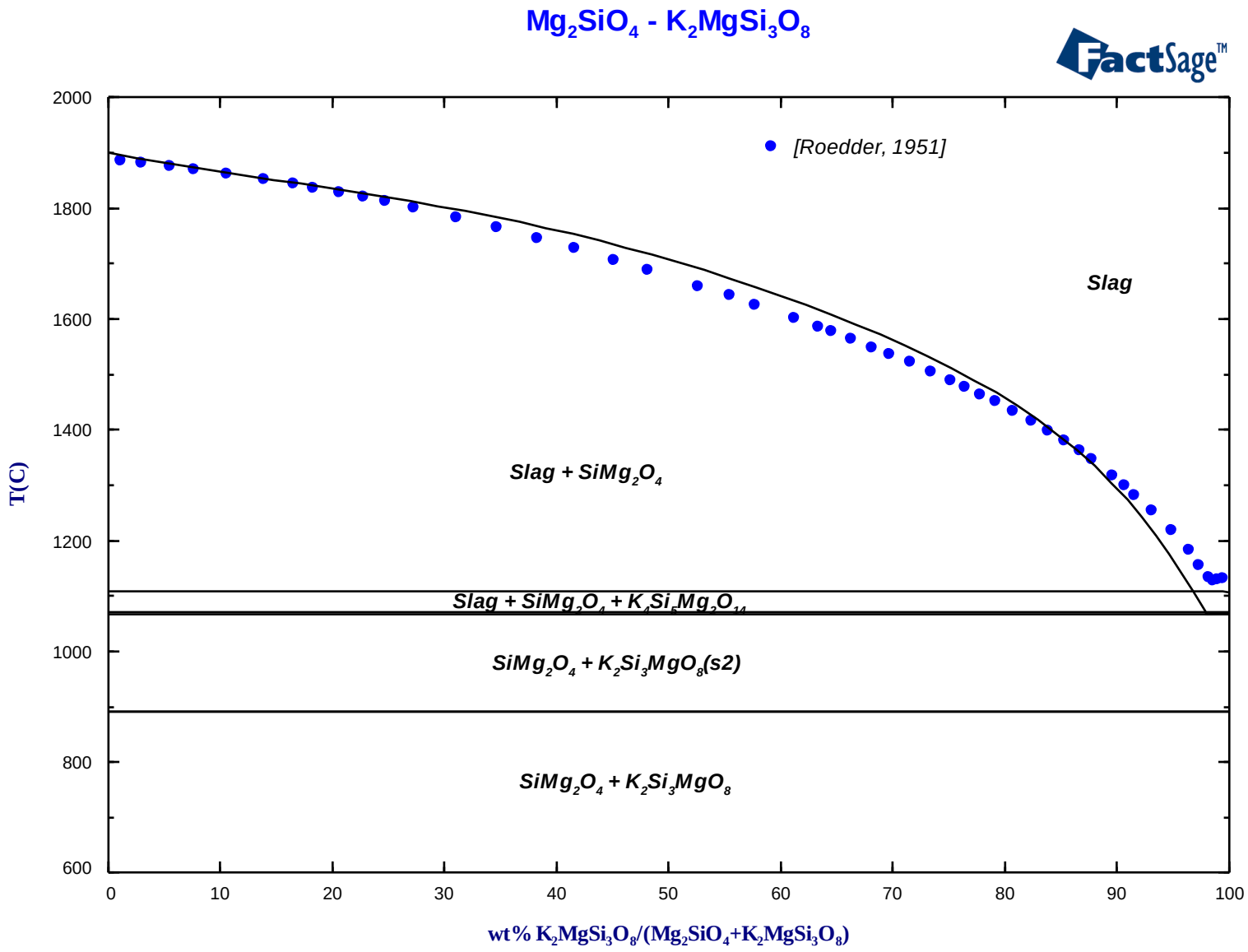
Mg2SiO4 - K2MgSi3O8
FactSage™
[Roedder, 1951]
Slag
Slag + SiMg2O4
Slag + SiMg2O4 + K4Si5Mg2O14
SiMg2O4 + K2Si3MgO8(s2)
SiMg2O4 + K2Si3MgO8
T(C)
2000
1800
1600
1400
1200
1000
800
600
0
10
20
30
40
50
60
70
80
90
100
wt% K2MgSi3O8/(Mg2SiO4+K2MgSi3O8)

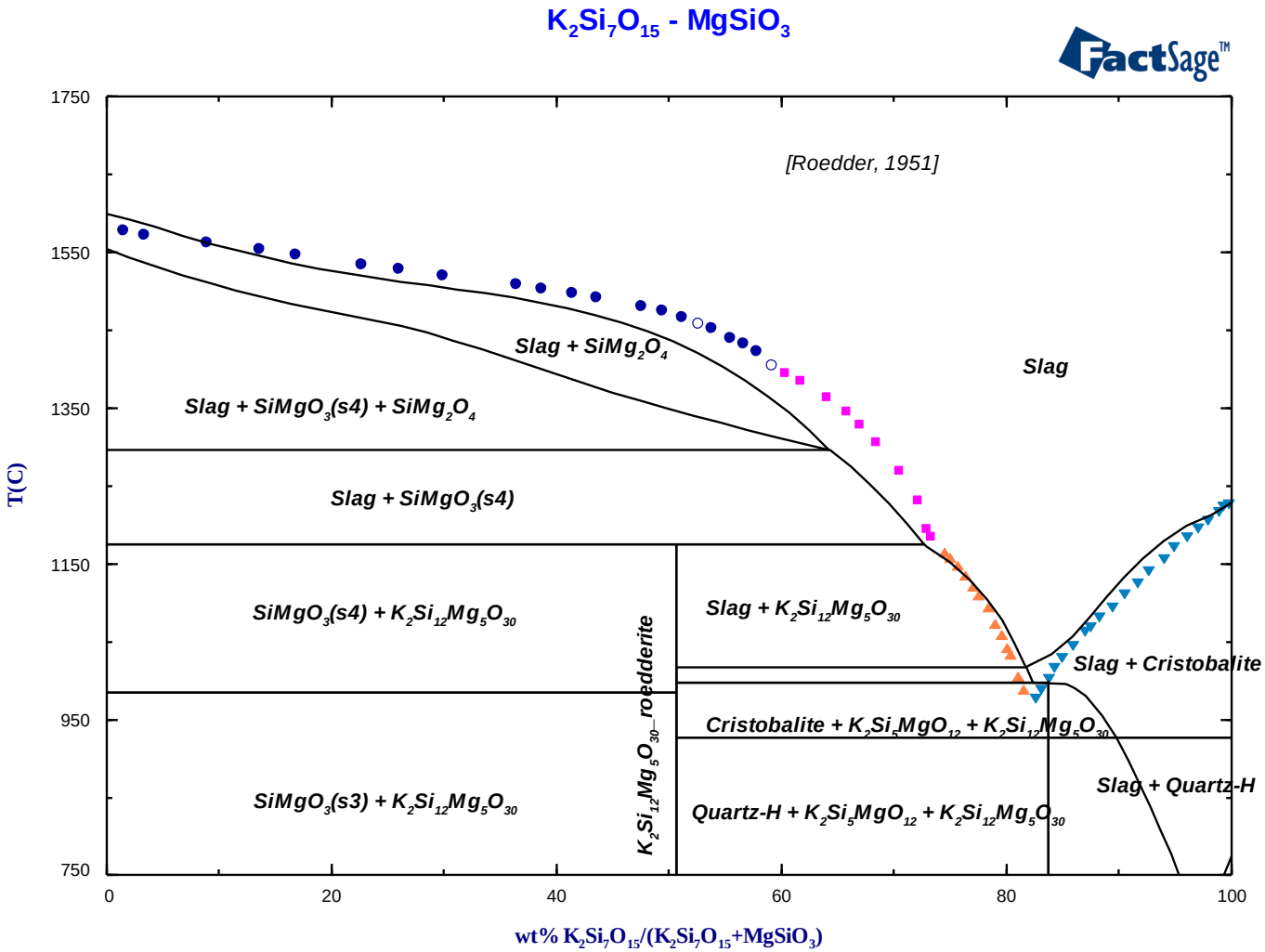
K2Si7O15 - MgSiO3
FactSage™
[Roedder, 1951]
Slag
Slag + SiMg2O4
Slag + SiMgO3(s4) + SiMg2O4
Slag + SiMgO3(s4)
SiMgO3(s4) + K2Si12Mg5O30
Slag + K2Si12Mg5O30
Slag + Cristobalite
Cristobalite + K2Si5MgO12 + K2Si12Mg5O30
Slag + Quartz-H
SiMgO3(s3) + K2Si12Mg5O30
Quartz-H + K2Si5MgO12 + K2Si12Mg5O30
K2Si12Mg5O30_roeddertite
T(C)
1750
1550
1350
1150
950
750
0
20
40
60
80
100
wt% K2Si7O15/(K2Si7O15+MgSiO3)

Weight percent , Isopleth Mg2SiO4-K2MgSi5O12 compared with experimental data°

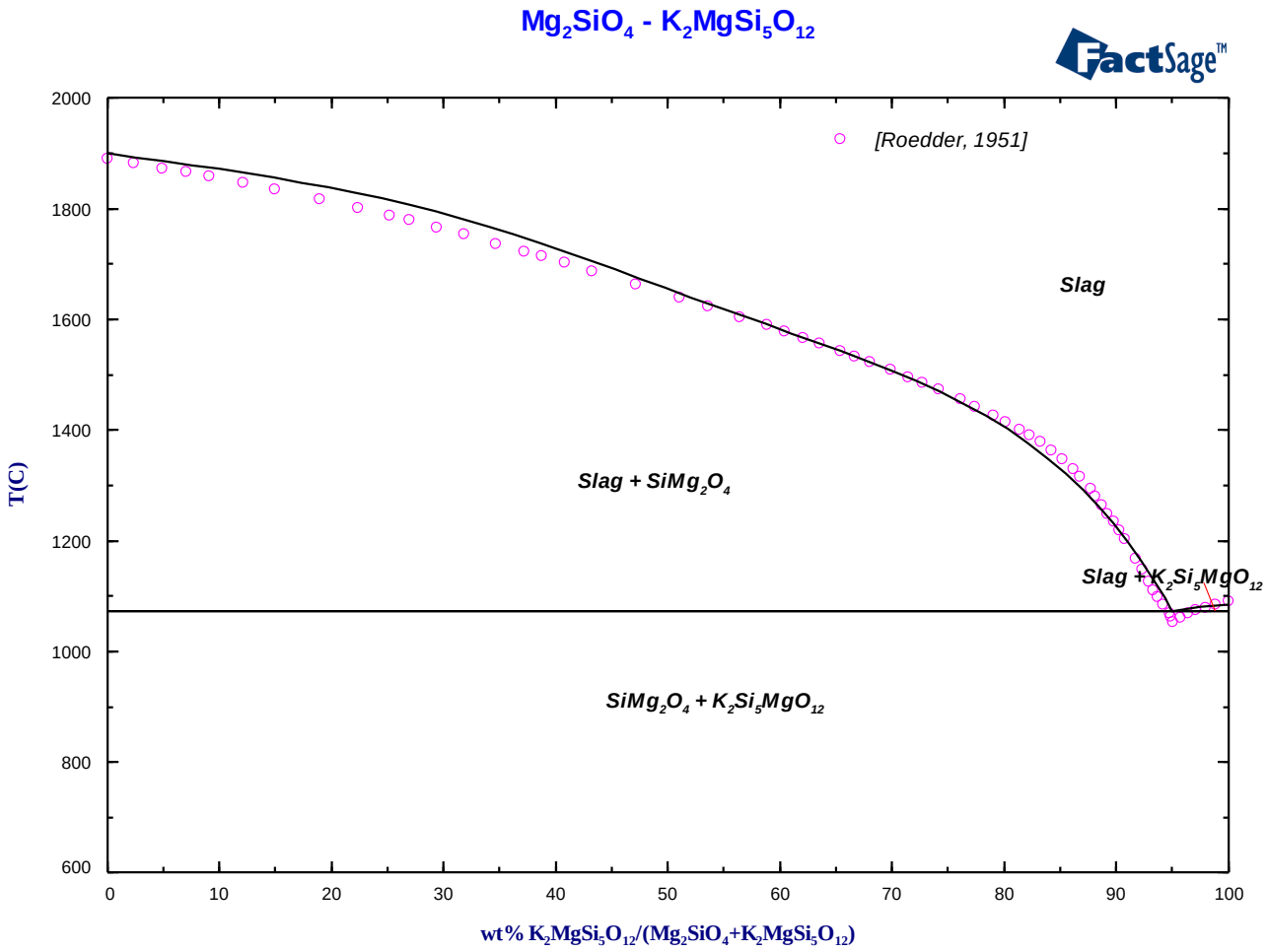

Weight percent
compared with experimental data°

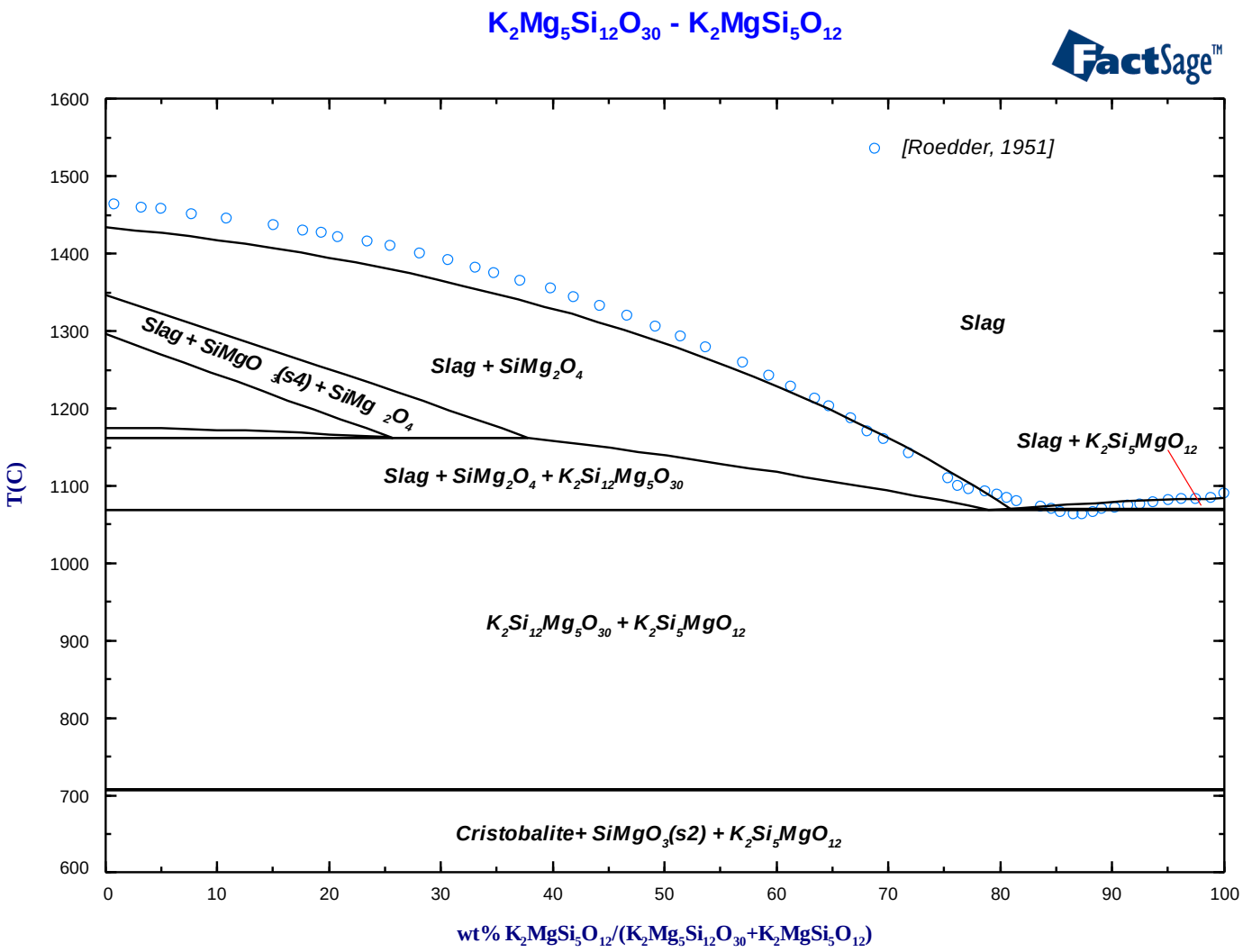

Weight percent
compared with experimental data°

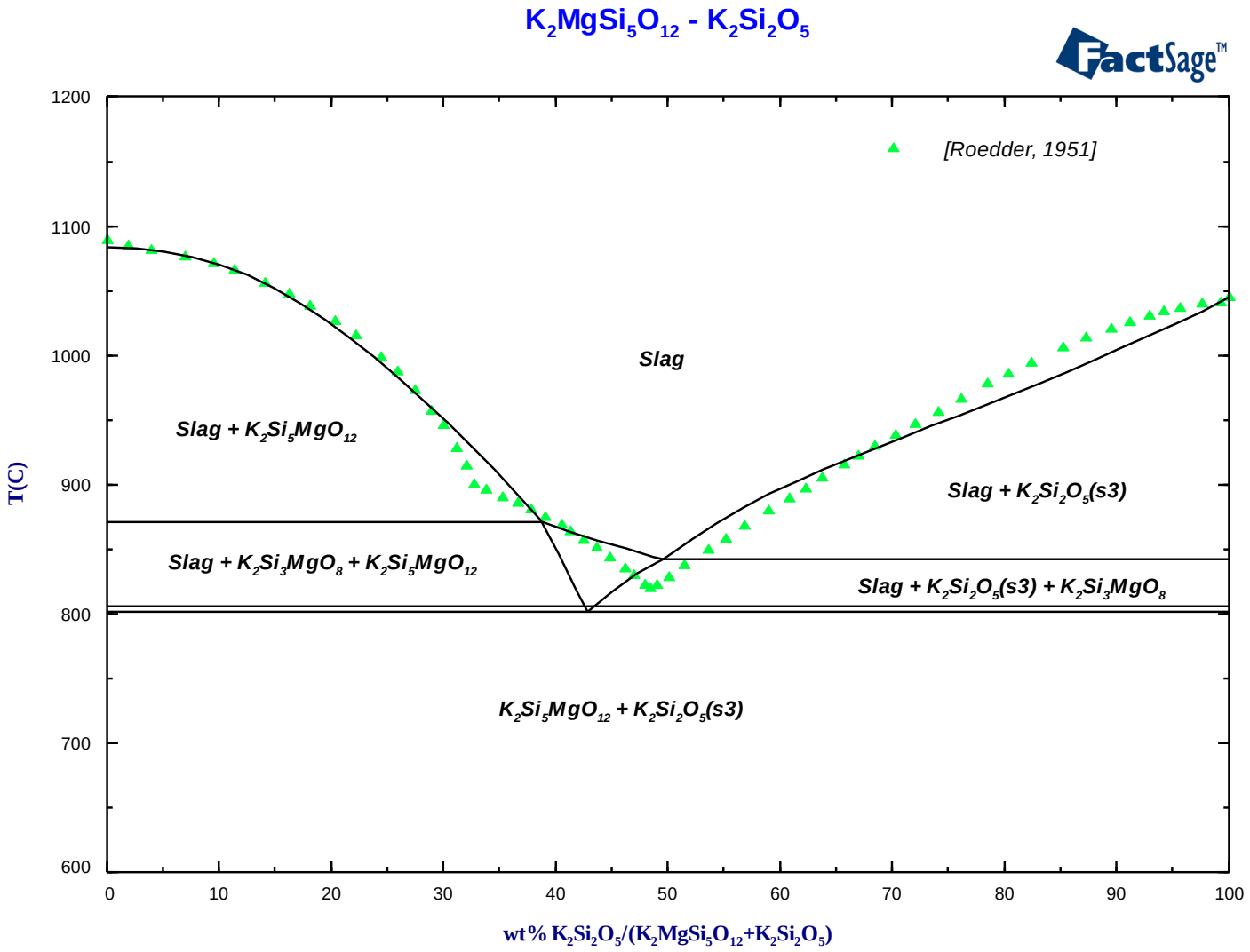

Weight percent , compared with experimental data

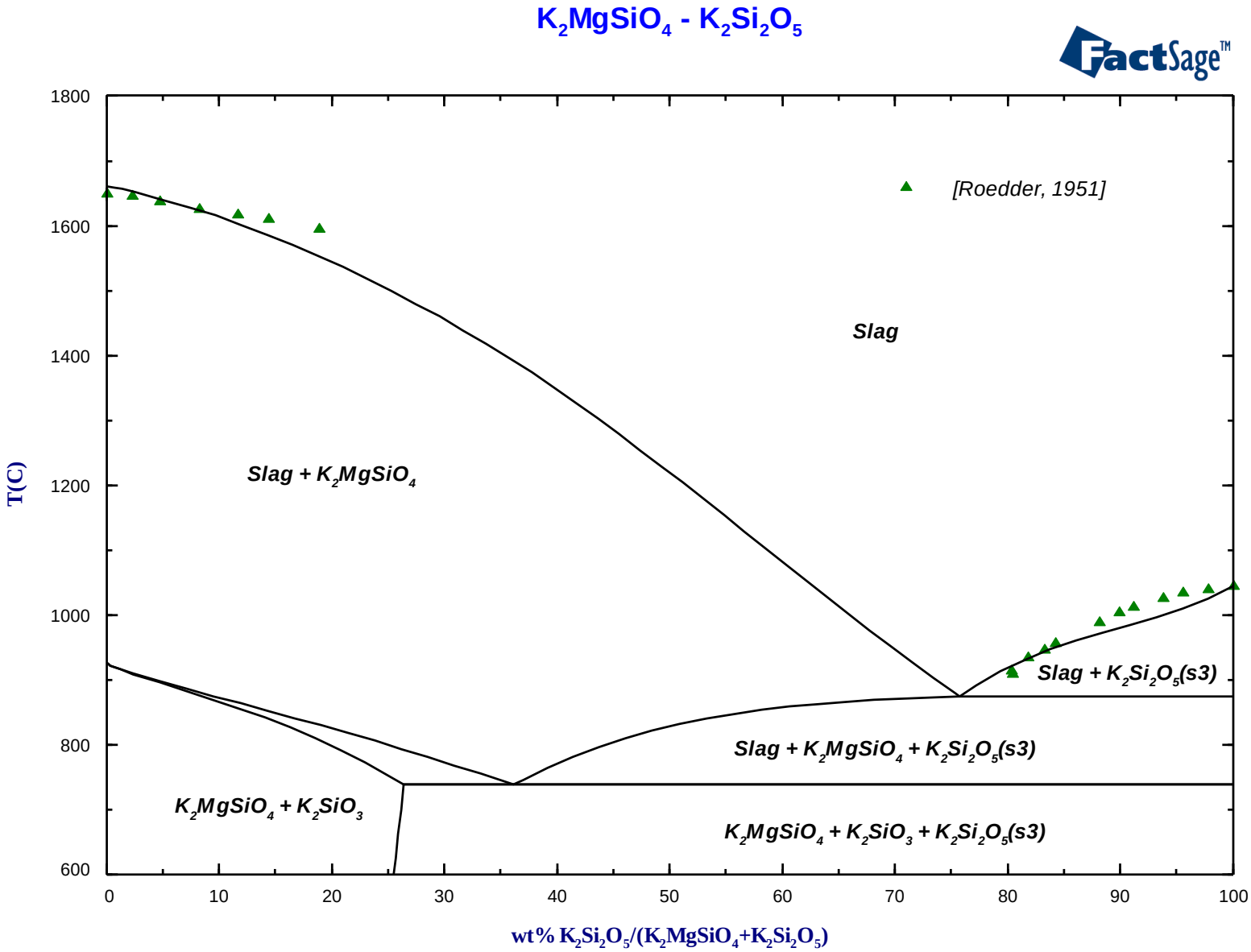

Weight percent
compared with experimental data

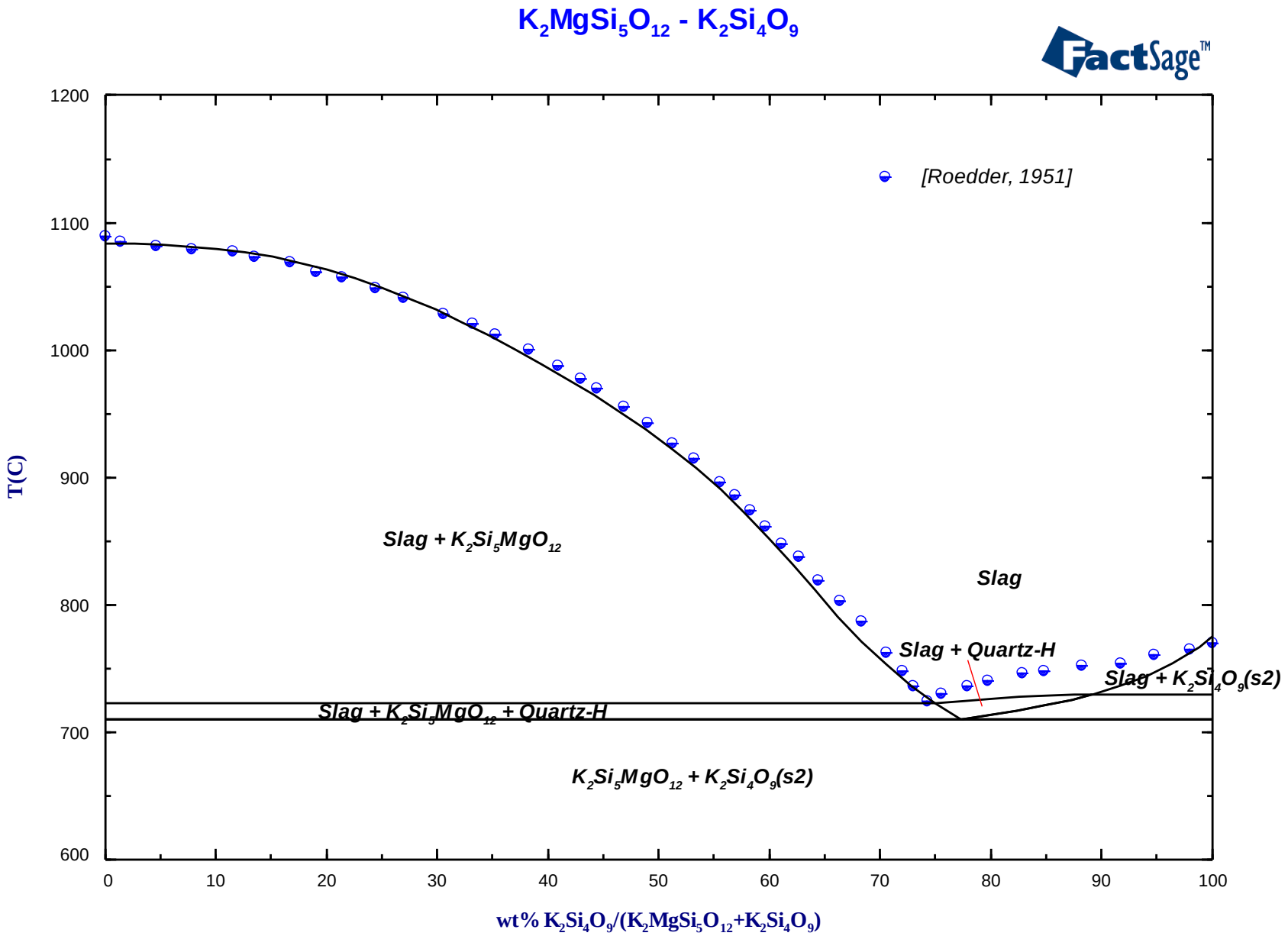

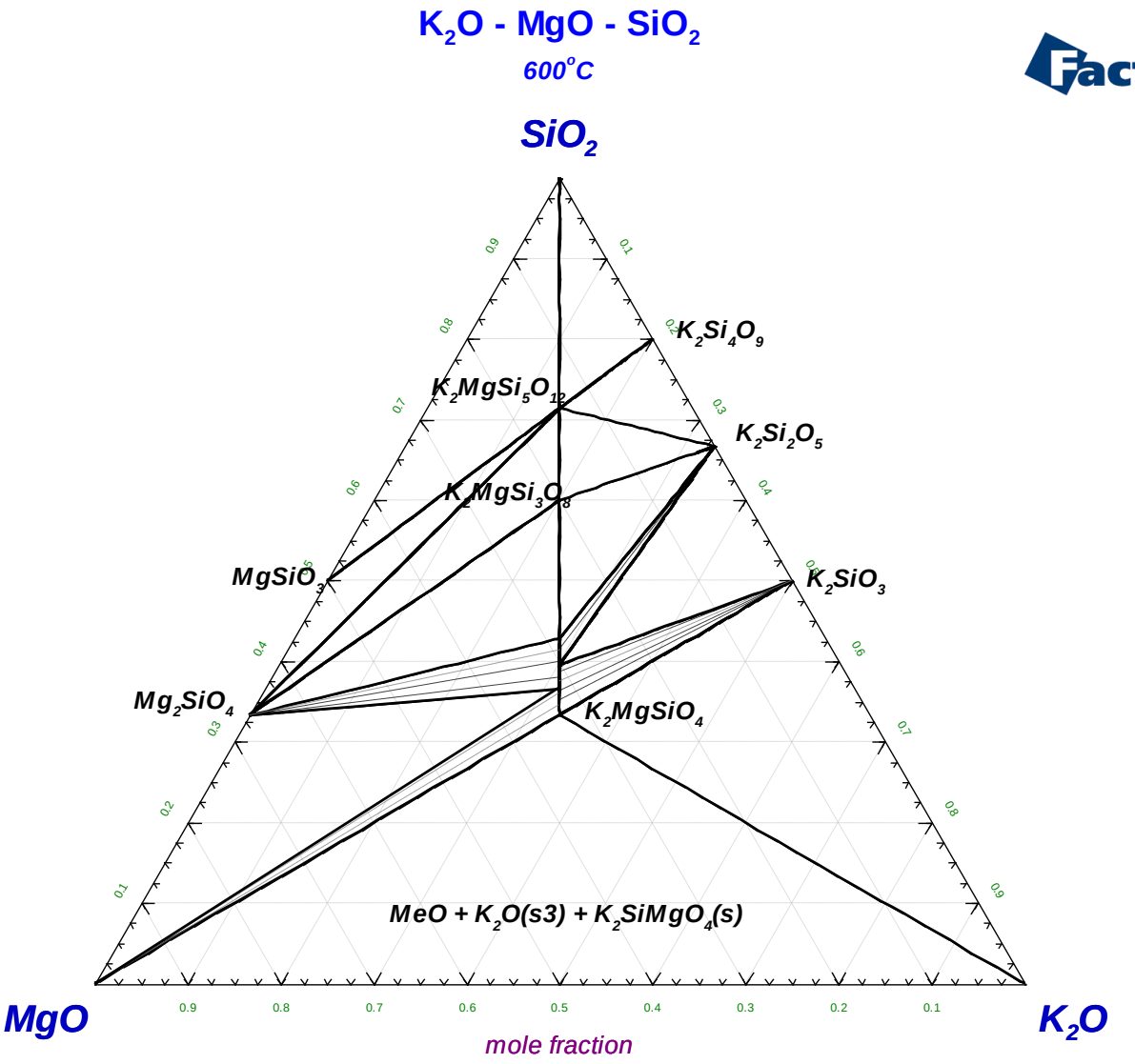
K2O - MgO - SiO2
600°C
FactSage™
SiO2
K2Si4O9
K2MgSi5O12
K2Si2O5
K2MgSi3O8
MgSiO3
K2SiO3
Mg2SiO4
K2MgSiO4
MeO + K2O(s3) + K2SiMgO4(s)
MgO
K2O
mole fraction

K2O-MgO-SiO2,

Mole fraction 1000°C

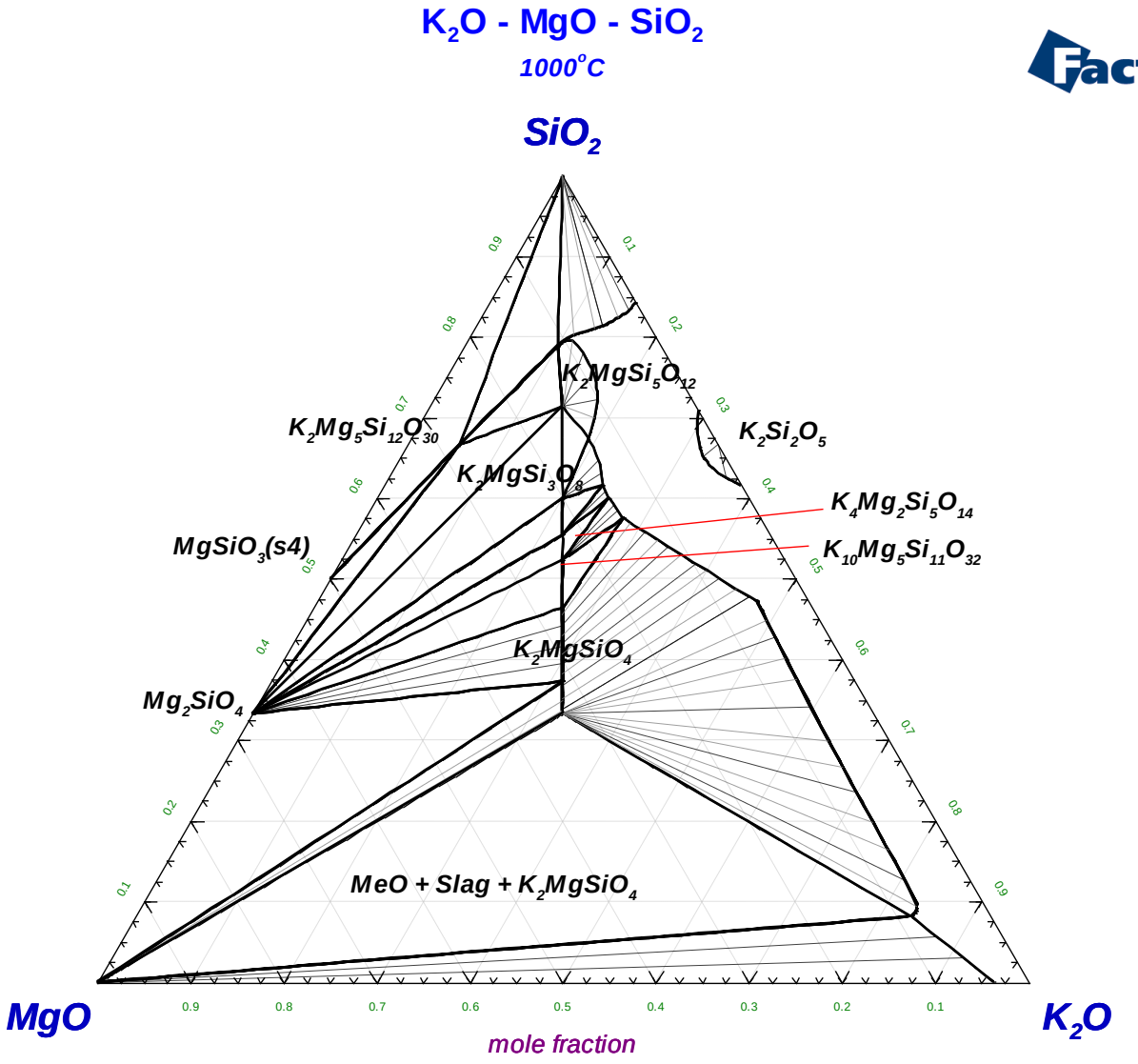

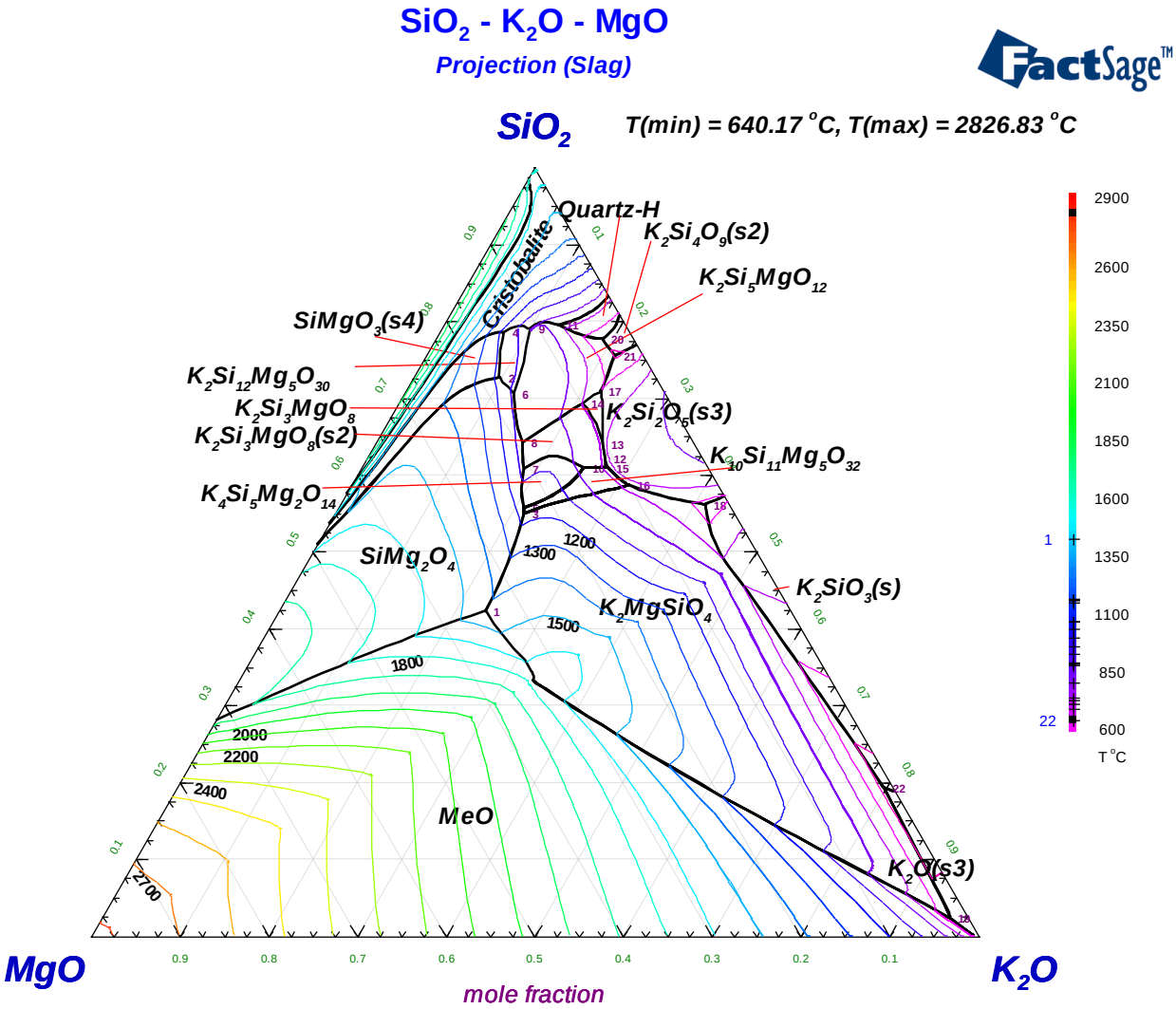
SiO2 - K2O - MgO
Projection (Slag)
FactSage™
SiO2
T(min) = 640.17 °C, T(max) = 2826.83 °C
Quartz-H
Cristobalite
K2Si4O9(s2)
K2Si5MgO12
SiMgO3(s4)
K2Si12Mg5O30
K2Si3MgO8
K2Si3MgO8(s2)
K2Si2O5(s3)
K10Si11Mg5O32
K4Si5Mg2O14
SiMg2O4
K2SiO3(s)
K2MgSiO4
MeO
K2O(s3)
1200
1300
1500
1800
2000
2200
2400
2700
2900
2600
2350
2100
1850
1600
1350
1100
850
600
T °C
MgO
K2O
mole fraction

Weight percent
Liquidussurface

SiO_2 - K_2O - MgO

Projection (Slag)

FactSage™

SiO_2 *T(min) = 640.17 °C, T(max) = 2826.84 °C*

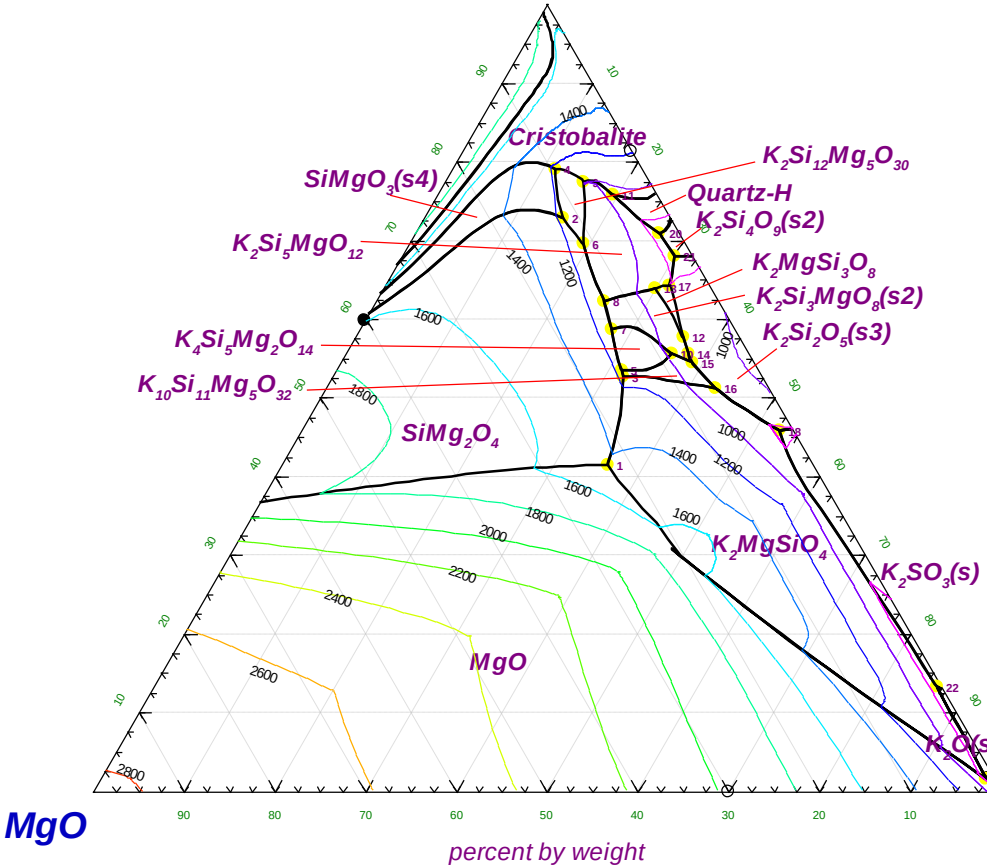

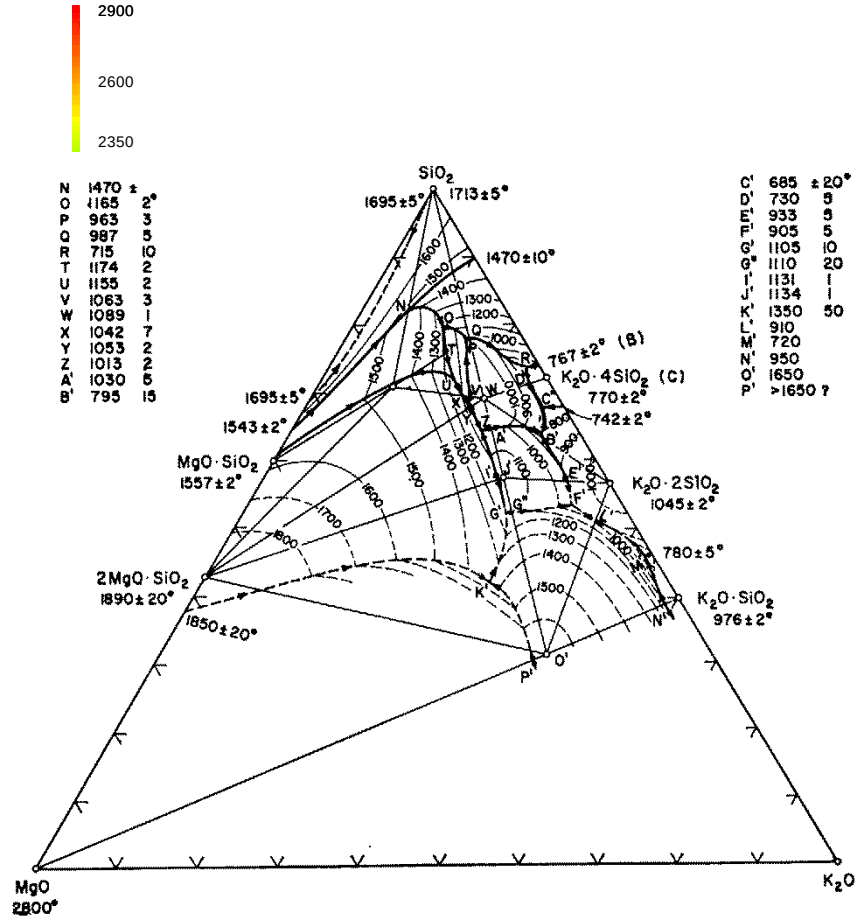

E. W, Roedder, Am. J. Sci., 249 [2], (1951), pp.81-130.

Invariant equilibria on the liquidus surface

Intersections with slag	Mole fraction A = SiO2, B = MgO, C = K2O				Weight percent A = SiO2, B = MgO, C = K2O			
	X(A)	X(B)	X(C)	T(C)	W(A)	W(B)	W(C)	T(C)
1: KMS / MeeO / SiMg2O4	1: 0.42272	0.34388	0.23341	1423.16	1: 41.471	22.630	35.899	1423.17
2: K2Si12Mg5O30 / SiMg2O4 / SiMgO3(s4)	2: 0.72661	0.17618	0.09721	1161.71	2: 72.865	11.851	15.283	1161.71
3: K10Si11Mg5O32 / KMS / SiMg2O4	3: 0.54970	0.23743	0.21287	1158.14	3: 52.719	15.275	32.006	1158.14
4: K2Si12Mg5O30 / SiMgO3(s4) / Cristobalite	4: 0.78610	0.14118	0.07272	1157.64	4: 79.020	9.520	11.460	1157.77
5: K10Si11Mg5O32 / K4Si5Mg2O14 / SiMg2O4	5: 0.55738	0.23370	0.20892	1146.57	5: 53.508	15.049	31.443	1146.57
6: K2Si12Mg5O30 / K2Si5MgO12 / SiMg2O4	6: 0.70614	0.16991	0.12395	1068.88	6: 69.609	11.235	19.156	1068.88
7: K2Si3MgO8(s2) / K4Si5Mg2O14 / SiMg2O4	7: 0.60784	0.20855	0.18361	1065.31	7: 58.695	13.509	27.797	1065.31
8: K2Si3MgO8(s2) / K2Si5MgO12 / SiMg2O4	8: 0.64209	0.19251	0.16540	1034.32	8: 62.306	12.531	25.163	1034.32
9: K2Si12Mg5O30 / K2Si5MgO12 / Cristobalite	9: 0.79010	0.10980	0.10010	996.38	9: 77.409	7.216	15.375	996.37
10: K10Si11Mg5O32/K2Si3MgO8(s2)/ K4Si5Mg2O14	10: 0.60956	0.13916	0.25129	956.34	10: 55.573	8.510	35.916	956.34
11: K2Si5MgO12 / Cristobalite / Quartz_H	11: 0.79498	0.07588	0.12914	926.28	11: 75.833	4.855	19.312	926.28
12: K2Si2O5(s3) / K2Si3MgO8(s2) / K2Si3MgO8	12: 0.62108	0.11006	0.26886	889.85	12: 57.710	6.176	36.113	889.85
13: K2Si2O5(s3) / K2Si3MgO8(s2) / K2Si3MgO8	13: 0.64156	0.10236	0.25608	889.85	13: 63.856	6.097	30.048	889.85
14: K2Si3MgO8(s2) / K2Si3MgO8 / K2Si5MgO12	14: 0.69325	0.09867	0.20808	889.85	14: 55.632	6.613	37.755	889.85
15: K10Si11Mg5O32 / K2Si2O5(s3) / K2Si3MgO8	15: 0.60979	0.11290	0.27731	884.35	15: 54.432	6.760	38.808	884.35
16: K10Si11Mg5O32 / K2Si2O5(s3) / KMS	16: 0.58662	0.10043	0.31296	879.40	16: 51.250	5.885	42.864	879.41
17: K2Si2O5(s3) / K2Si3MgO8 / K2Si5MgO12	17: 0.70855	0.07104	0.22040	801.34	17: 64.312	4.325	31.362	801.30
18: K2Si2O5(s3) / K2SiO3 / KMS	18: 0.56182	0.02621	0.41197	737.96	18: 45.854	1.435	52.712	737.96
19: K2O(s3) / KMS / MeO	19: 0.02360	0.02008	0.95631	724.99	19: 1.536	0.877	97.587	725.01
20: K2Si4O9(s2) / K2Si5MgO12 / Quartz_H	20: 0.77701	0.03460	0.18838	709.70	20: 70.924	2.119	26.958	709.71
21: K2Si2O5(s3) / K2Si4O9(s2) / K2Si5MgO12	21: 0.75555	0.03179	0.21266	687.13	21: 68.051	1.921	30.028	687.12
22: K2O(s3) / K2SiO3 / KMS	22: 0.19260	0.00962	0.79779	640.17	22: 13.285	0.445	86.270	640.17

K2O-Na2O-P2O5,

Mole fraction 400C°

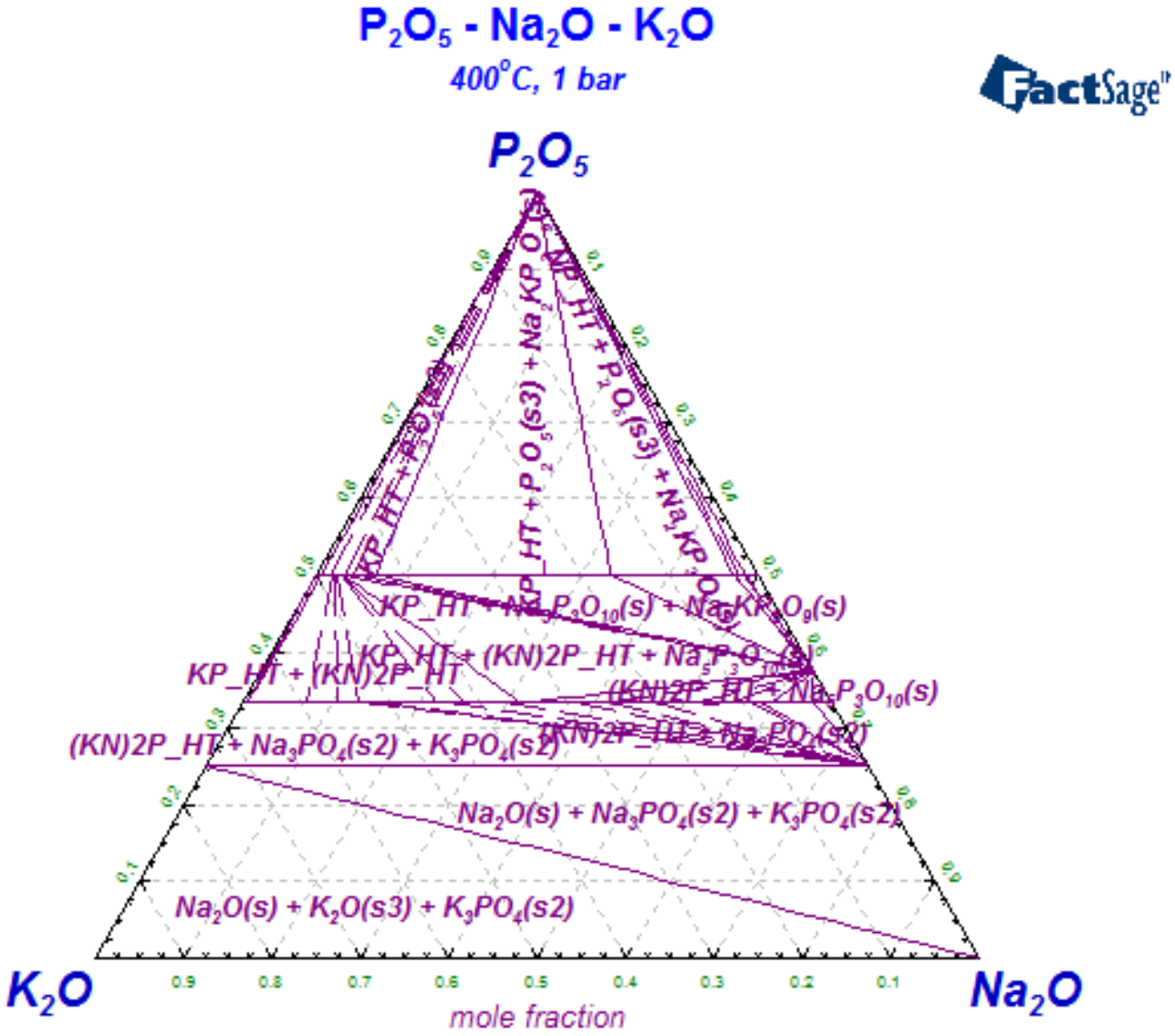

Mole fraction Isopleth KPO3-NaPO3 compared with experimental data

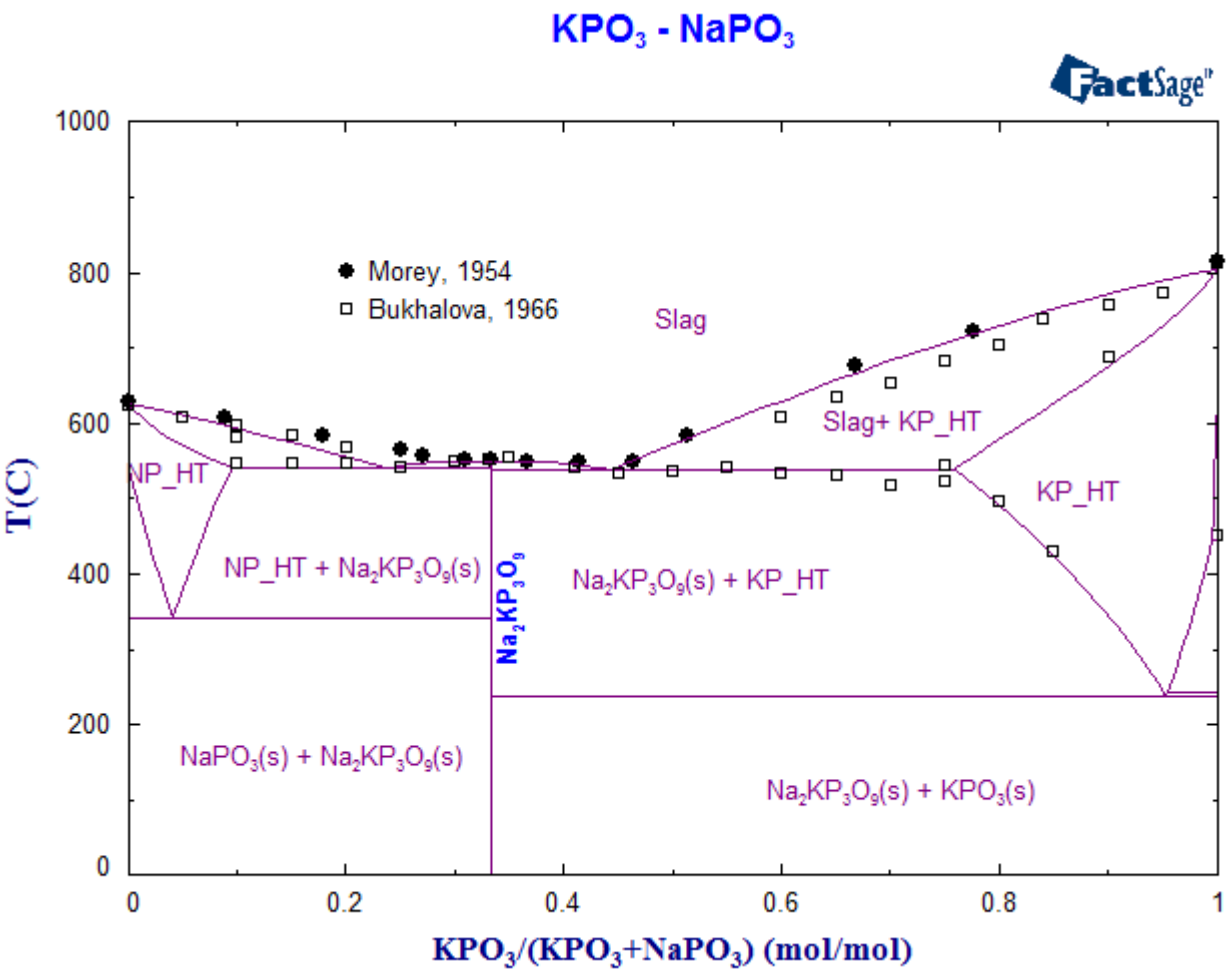

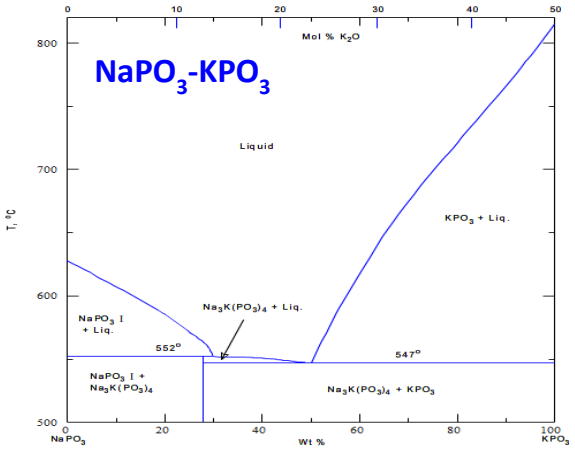

G. W. Morey, J. Am. Chem. Soc., 76 [18] 4724-4726 (1954).

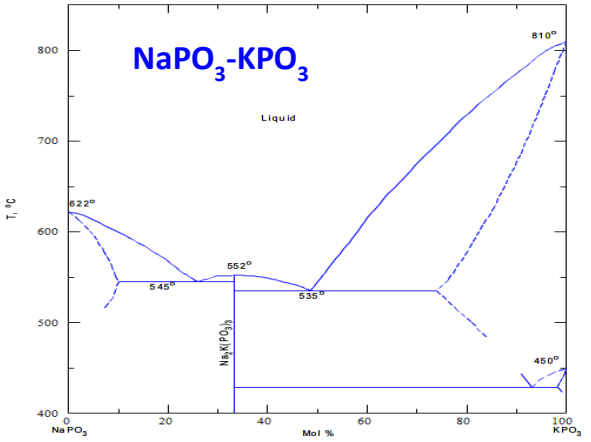

G. A. Bukhalova and I. V. Mardirosova, Zh. Neorg. Khim 11 [4] 920-925 (1966); Russ. J. Inorg. Chem. (Engl.

Mole fraction Isopleth K2P2O7-Na2P2O7 compared with experimental data

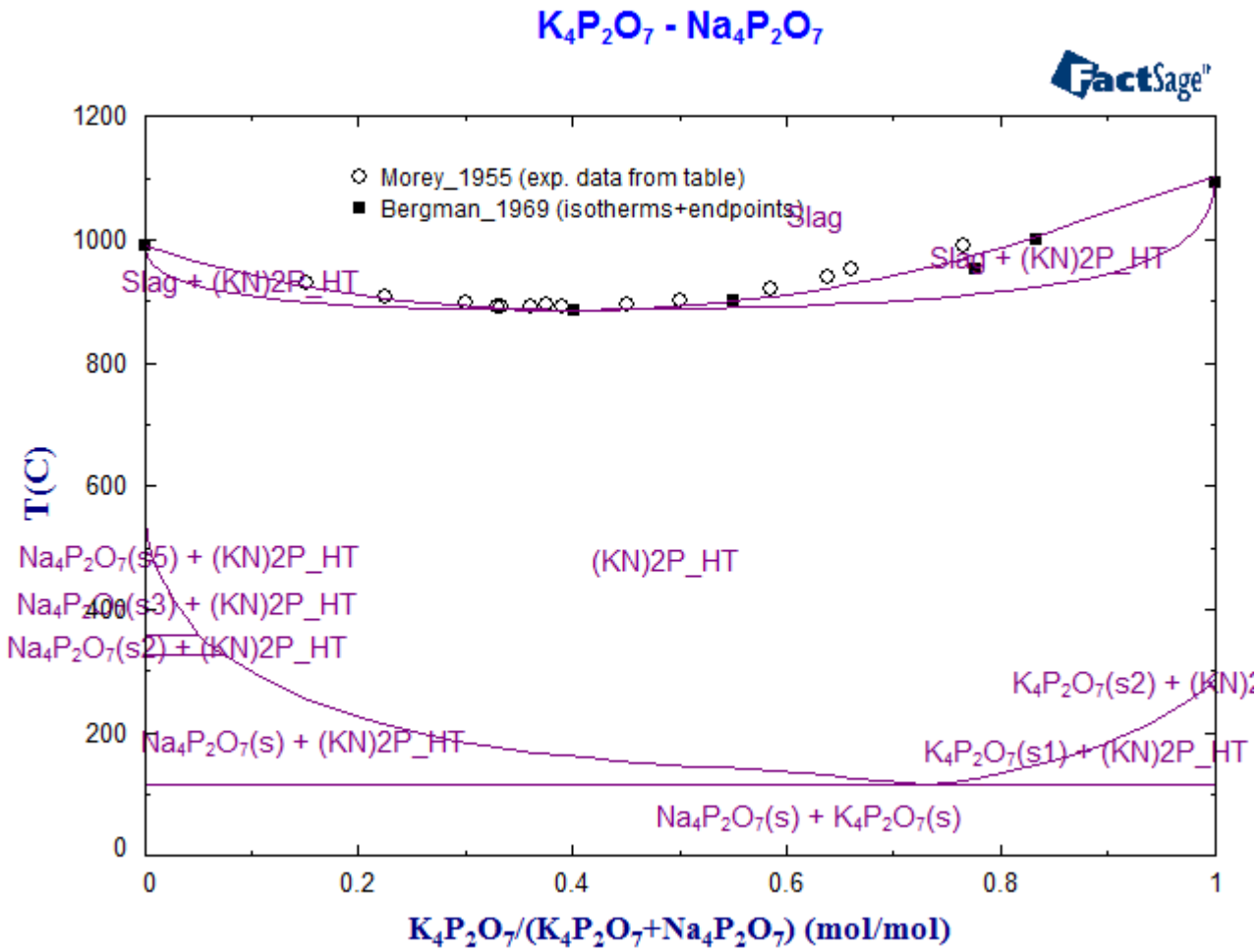

Mole fraction Isopleth K3PO4-Na3PO4 compared with experimental data

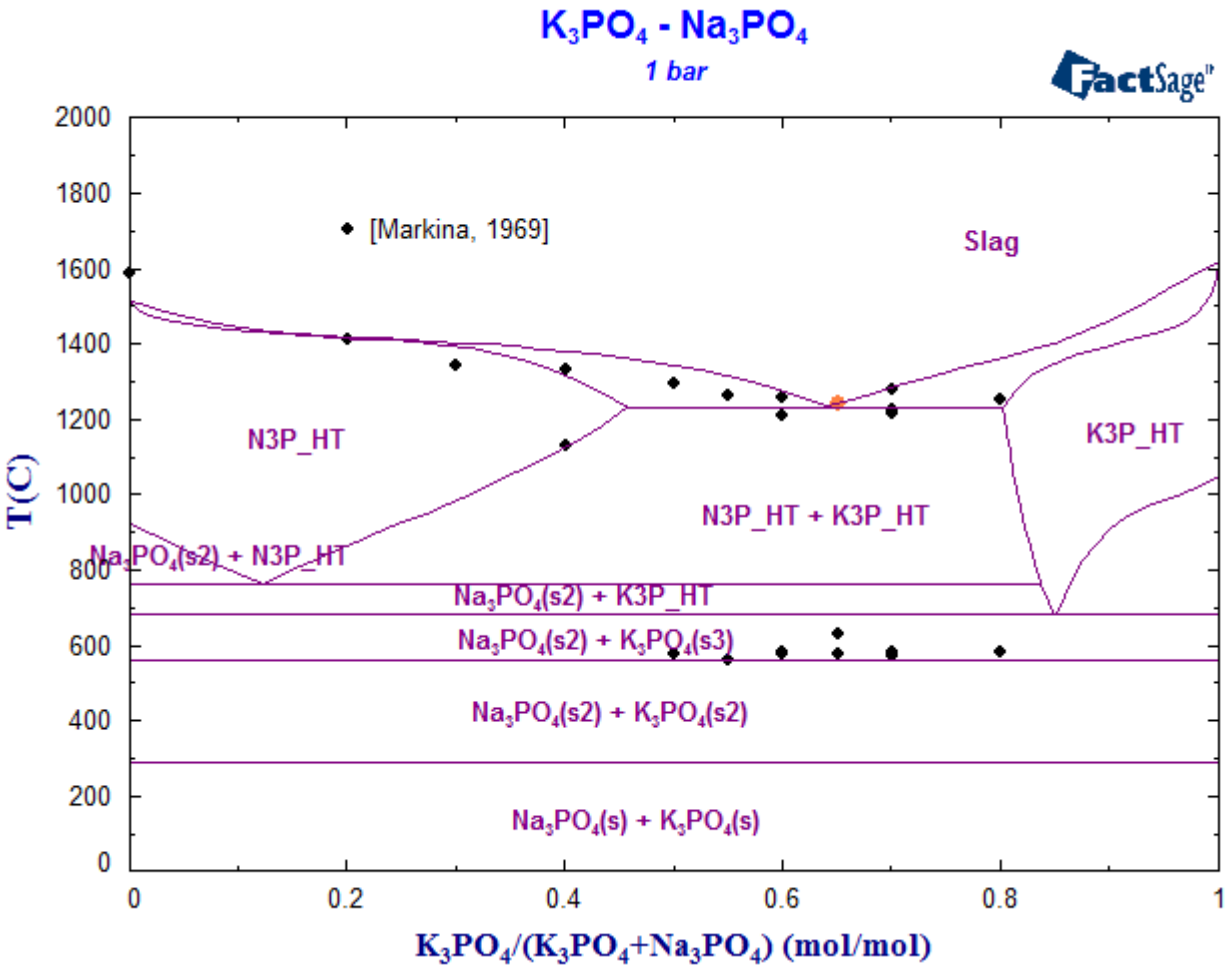

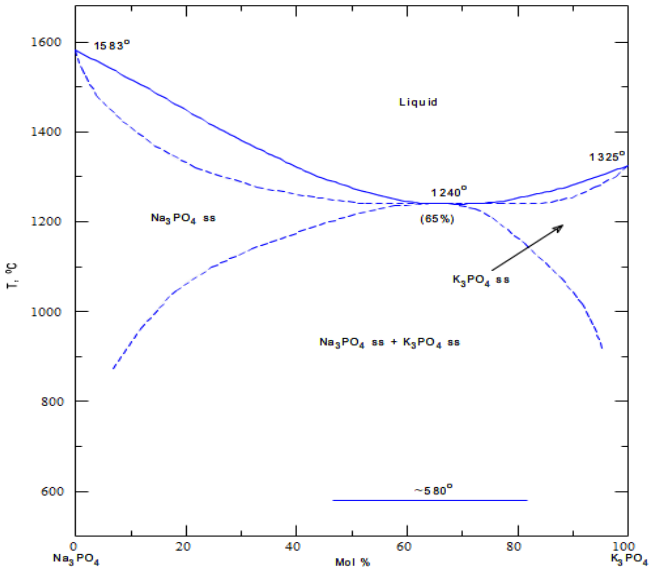

I.B.Markina,N.K. Voskresenskaya, Zh. Neorg. Khim., 14 [8] 2263-2269 (1969); Russ. J. Inorg. Chem. (Engl.

Mole fraction, Subsolidus surface

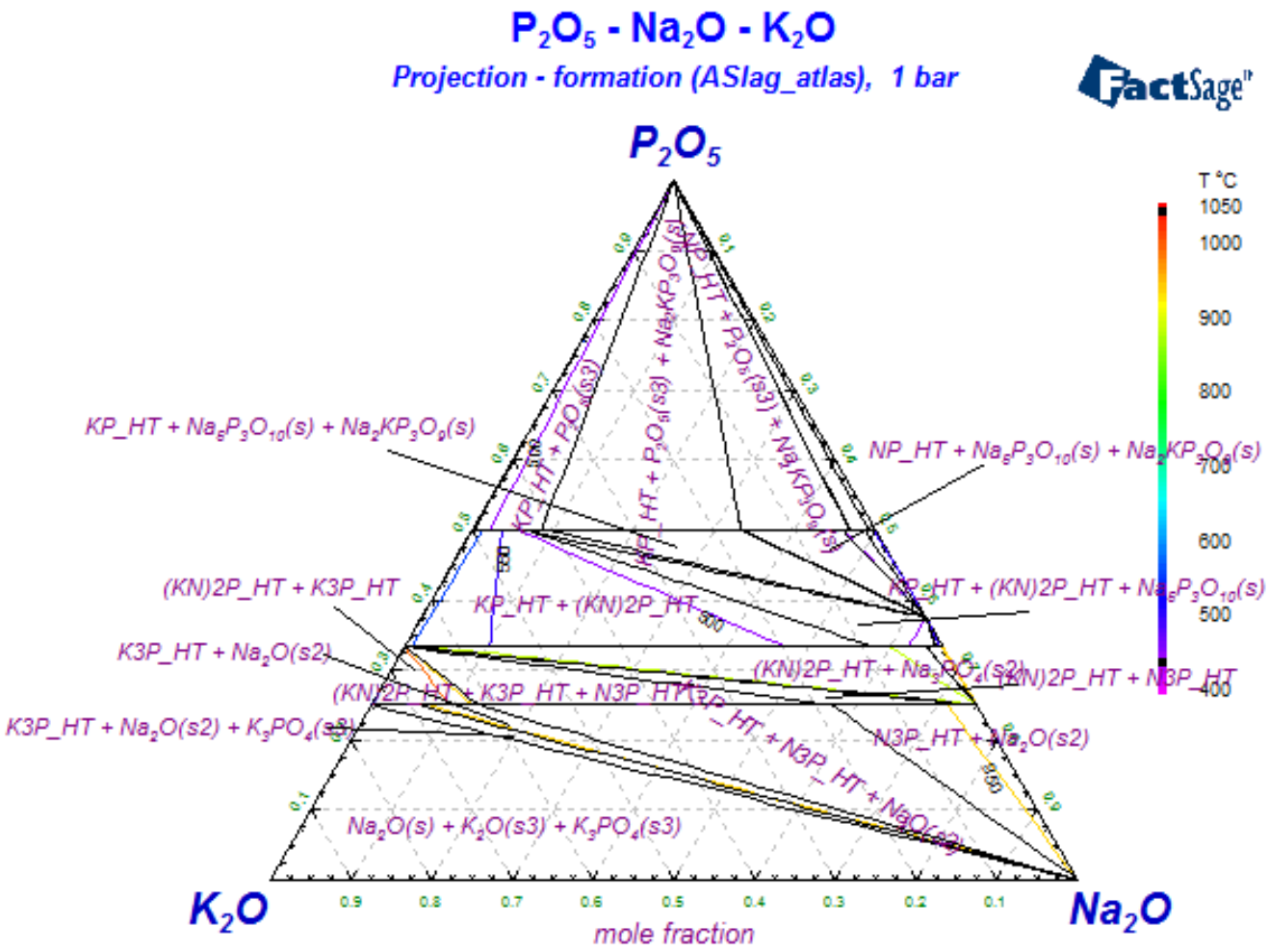

Mole fraction, Reciprocal liquidus surface Na-K-P3O9-PO4

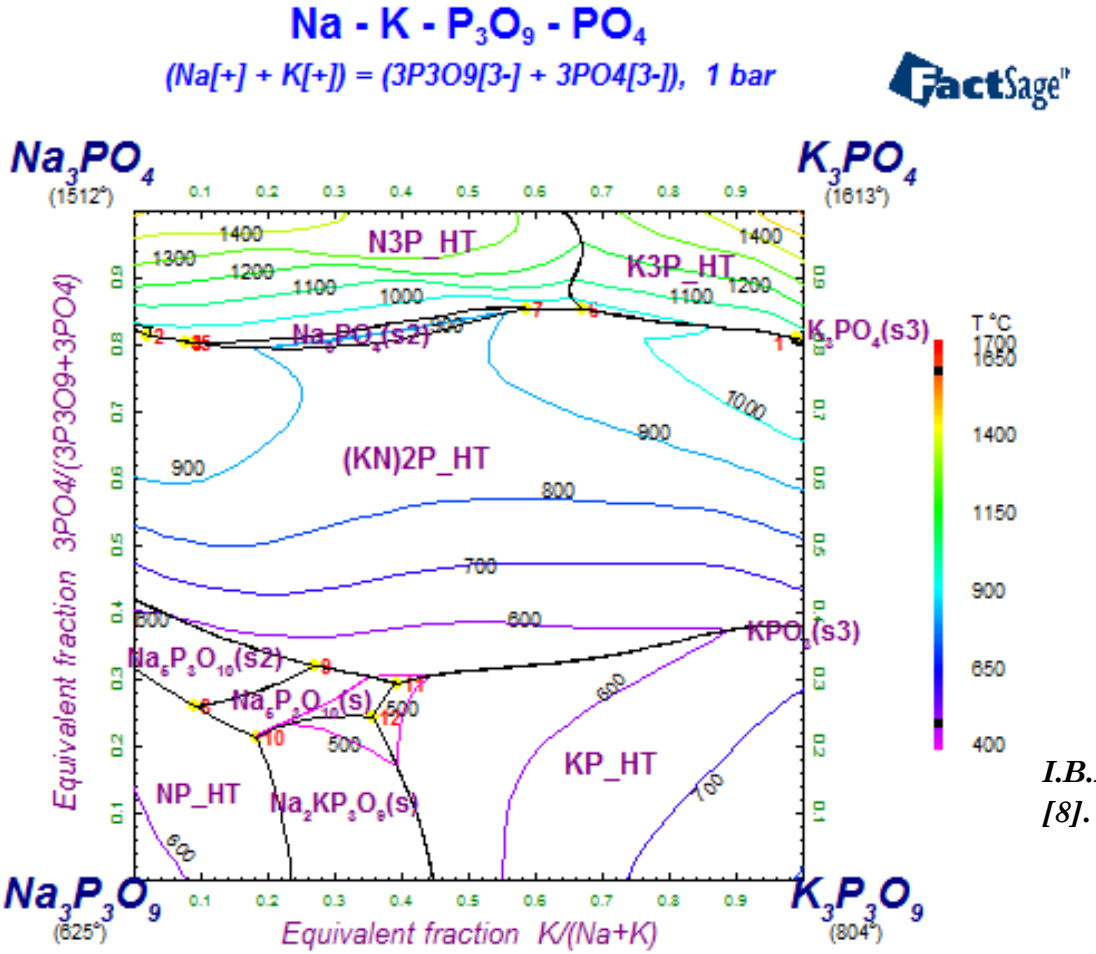

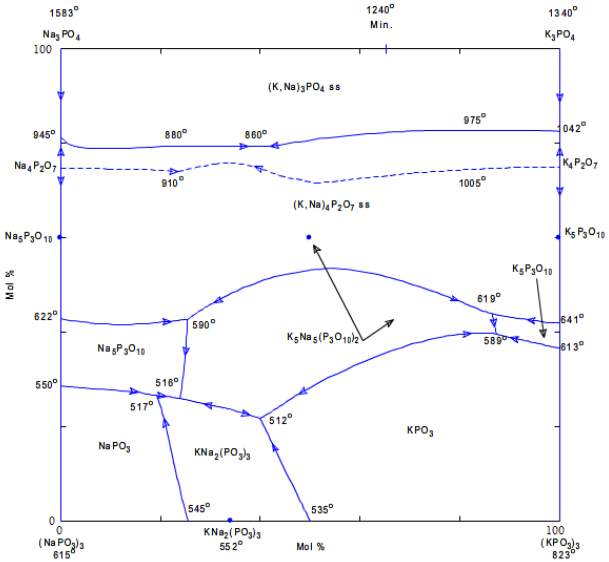

I.B.Markina,N.K. Voskresenskaya, Zh. Neorg. Khim., 14 [8]. Transl.), 14 [8] 1188-1192 (1969) 2263-2269 (1969);

Mole fraction, Liquidus surface

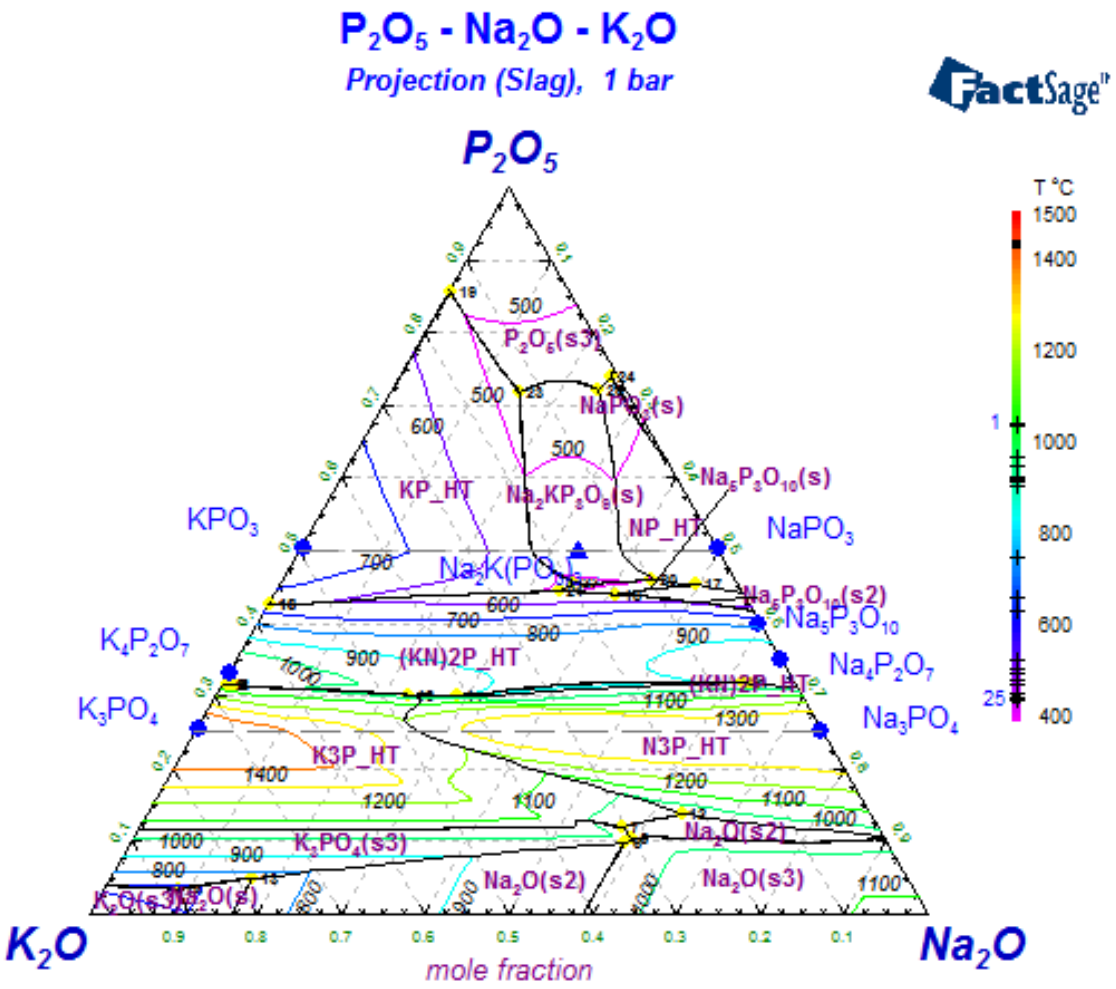

Weight percent, Liquidus surface

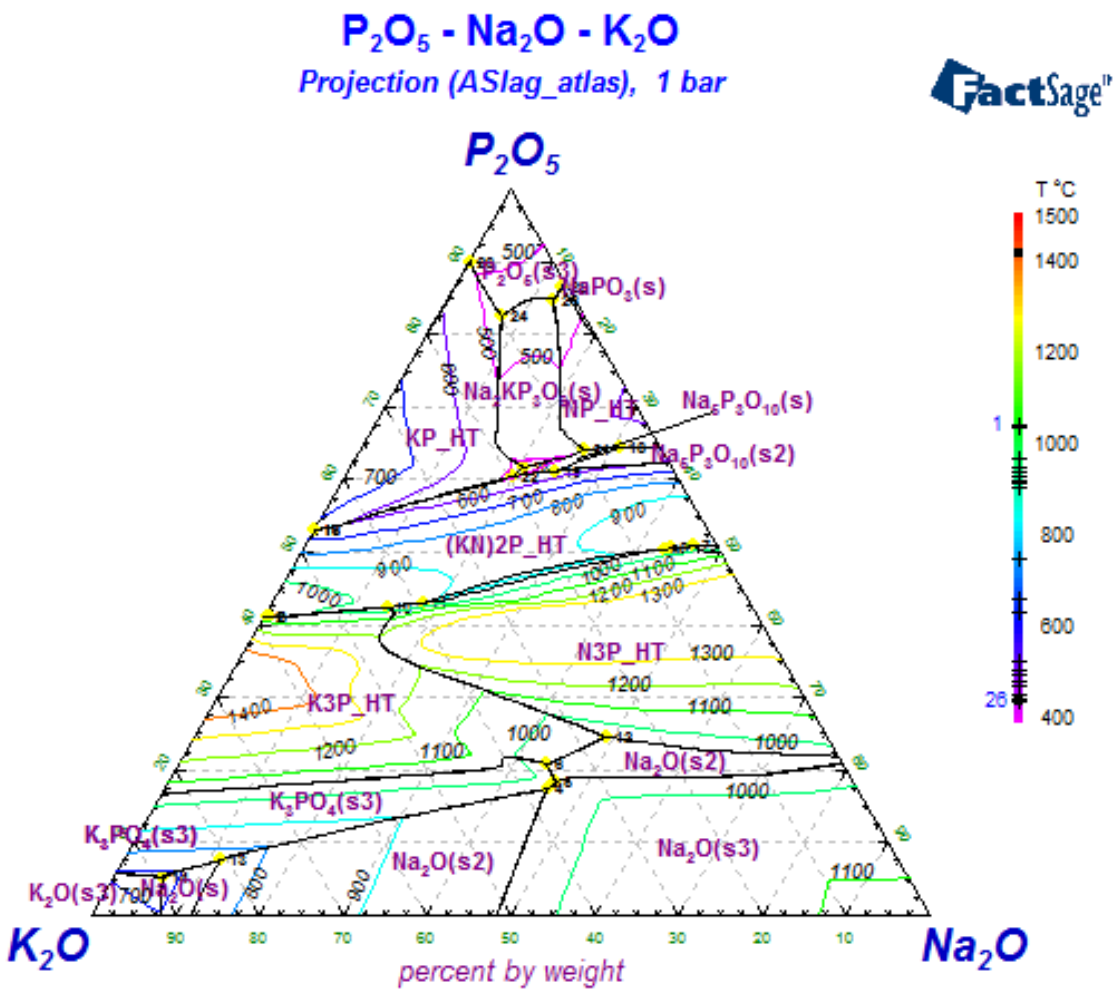

Invariant equilibria on the liquidus surface

Intersections with slag	Mole fraction A = P2O5 B = K2O C = Na2O				Weight percent A = P2O5, B = K2O, C = Na2O				
		X(A)	X(B)	X(C)	T(C)		W(A)	W(B)	W(C)	T(C)
1: (KN)2P_HT / K3P_HT / K4P2O7(s3)	1:	0.31582	0.67679	0.00739	1043.88	1:	41.117	58.551	0.332	1044.72
2: (KN)2P_HT / K3P_HT / K4P2O7(s3)	2:	0.31578	0.67655	0.00767	1043.74	2:	41.113	58.466	0.420	1043.88
3: (KN)2P_HT / K3P_HT / K4P2O7(s3)	3:	0.31509	0.67166	0.01325	1040.77	3:	41.101	58.095	0.804	1040.32
4: (KN)2P_HT / K3P_HT / K4P2O7(s3)	4:	0.31491	0.67033	0.01476	1039.97	4:	17.497	36.858	45.645	970.07
5: K3PO4(s3) / Na2O(s2) / Na2O(s3)	5:	0.10411	0.30109	0.59480	970.05	5:	18.471	35.450	46.079	969.99
6: K3PO4(s3) / Na2O(s2) / Na2O(s3)	6:	0.09853	0.31278	0.58869	970.05	6:	20.768	35.274	43.958	951.29
7: K3PO4(s3) / K3P_HT / Na2O(s2)	7:	0.11895	0.30445	0.57660	951.29	7:	50.804	2.661	46.534	941.66
8: (KN)2P_HT / N3P_HT / Na3PO4(s3)	8:	0.31692	0.05334	0.62974	926.44	8:	50.523	5.634	43.843	930.73
9: (KN)2P_HT / Na3PO4(s3) / Na3PO4(s2)	9:	0.31739	0.06176	0.62085	922.40	9:	50.422	6.511	43.067	922.40
10: (KN)2P_HT / K3P_HT / N3P_HT	10:	0.30165	0.46801	0.23034	919.21	10:	42.318	43.571	14.110	919.21
11: (KN)2P_HT / N3P_HT / Na3PO4(s2)	11:	0.30128	0.41069	0.28802	909.97	11:	43.066	38.957	17.977	909.97
12: K3P_HT / N3P_HT / Na2O(s2)	12:	0.13826	0.22419	0.63755	909.72	12:	24.452	26.313	49.235	909.72
13: K3PO4(s3) / Na2O(s) / Na2O(s2)	13:	0.04923	0.78081	0.16997	750.09	13:	7.672	80.760	11.567	750.05
14: K2O(s3) / K3PO4(s3) / Na2O(s)	14:	0.03469	0.87723	0.08807	664.63	14:	5.294	88.837	5.869	664.60
15: (KN)2P_HT / KPO3(s3) / KP_HT	15:	0.42767	0.57134	0.00098	635.88	15:	52.979	46.968	0.053	636.52
16: (KN)2P_HT / K4P2O7(s3) / KP_HT	16:	0.42767	0.57123	0.00110	635.83	16:	52.980	46.959	0.061	635.82
17: NP_HT / Na5P3O10(s) / Na5P3O10(s2)	17:	0.45260	0.05036	0.49705	528.85	17:	64.377	4.753	30.870	528.85
18: (KN)2P_HT / Na5P3O10(s) / Na5P3O10(s2)	18:	0.43996	0.15194	0.40810	528.85	18:	61.192	14.024	24.784	528.85
19: KPO3(s3) / KP_HT / P2O5(s3)	19:	0.85620	0.14143	0.00237	509.78	19:	90.023	9.868	0.109	509.78
20: NP_HT / Na2KP3O9(s) / Na5P3O10(s)	20:	0.46137	0.09848	0.44015	498.97	20:	64.176	9.090	26.733	498.97
21: (KN)2P_HT / KP_HT / Na5P3O10(s)	21:	0.44542	0.21739	0.33719	483.57	21:	60.443	19.577	19.980	483.57
22: KP_HT / Na2KP3O9(s) / Na5P3O10(s)	22:	0.45552	0.19431	0.35017	473.00	22:	61.777	17.487	20.736	473.00
23: KP_HT / Na2KP3O9(s) / P2O5(s3)	23:	0.71866	0.12863	0.15270	454.07	23:	82.538	9.804	7.658	454.07
24: NP_HT / NaPO3(s) / P2O5(s3)	24:	0.74009	0.00840	0.25151	443.68	24:	86.511	0.651	12.837	443.68
25: NP_HT / Na2KP3O9(s) / P2O5(s3)	25:	0.72082	0.03271	0.24647	439.16	25:	84.788	2.554	12.659	439.16

Na_2O - SiO_2 - K_2O

600°C

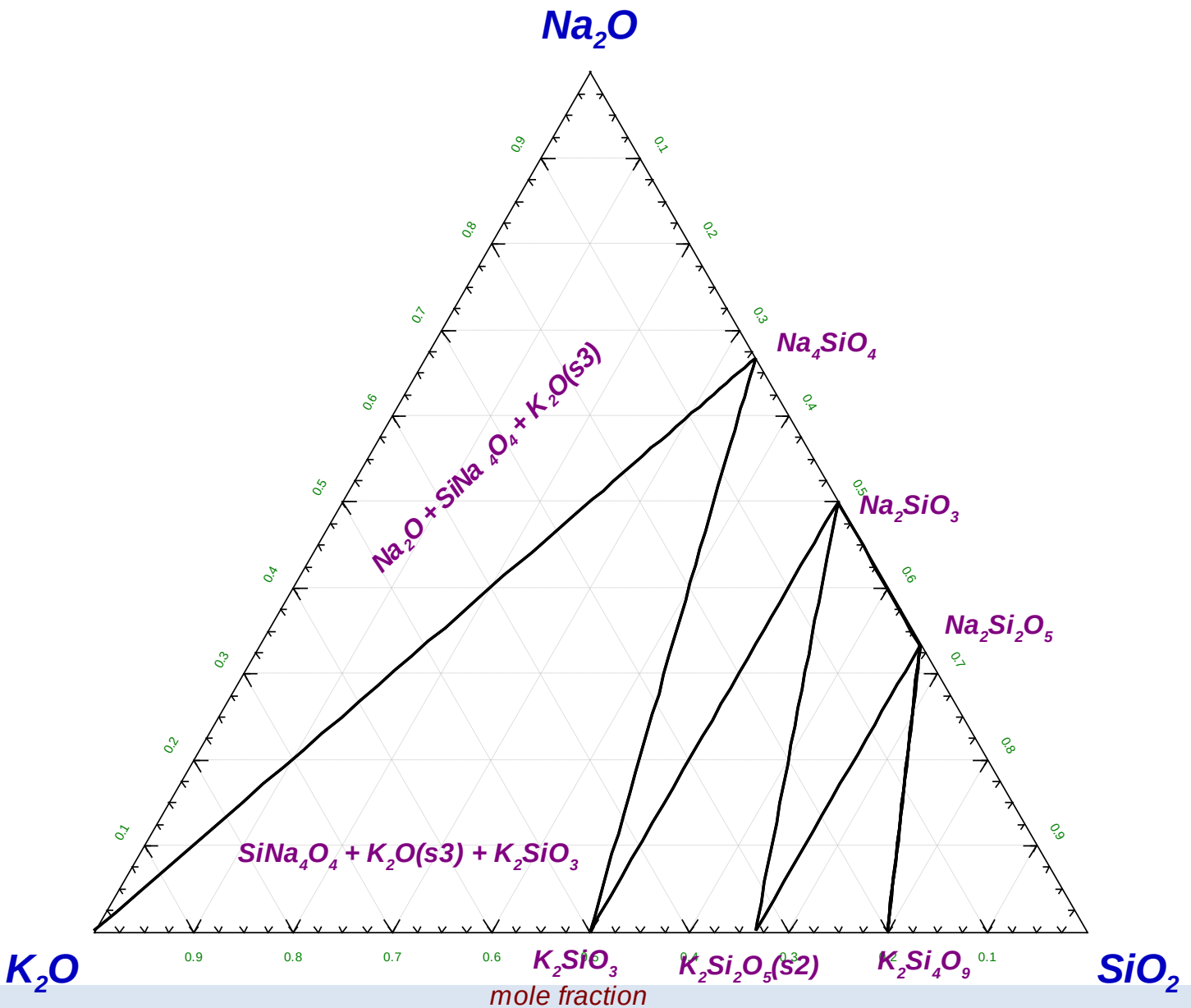

K_2O - Na_2O - SiO_2

800°C

FactSage™

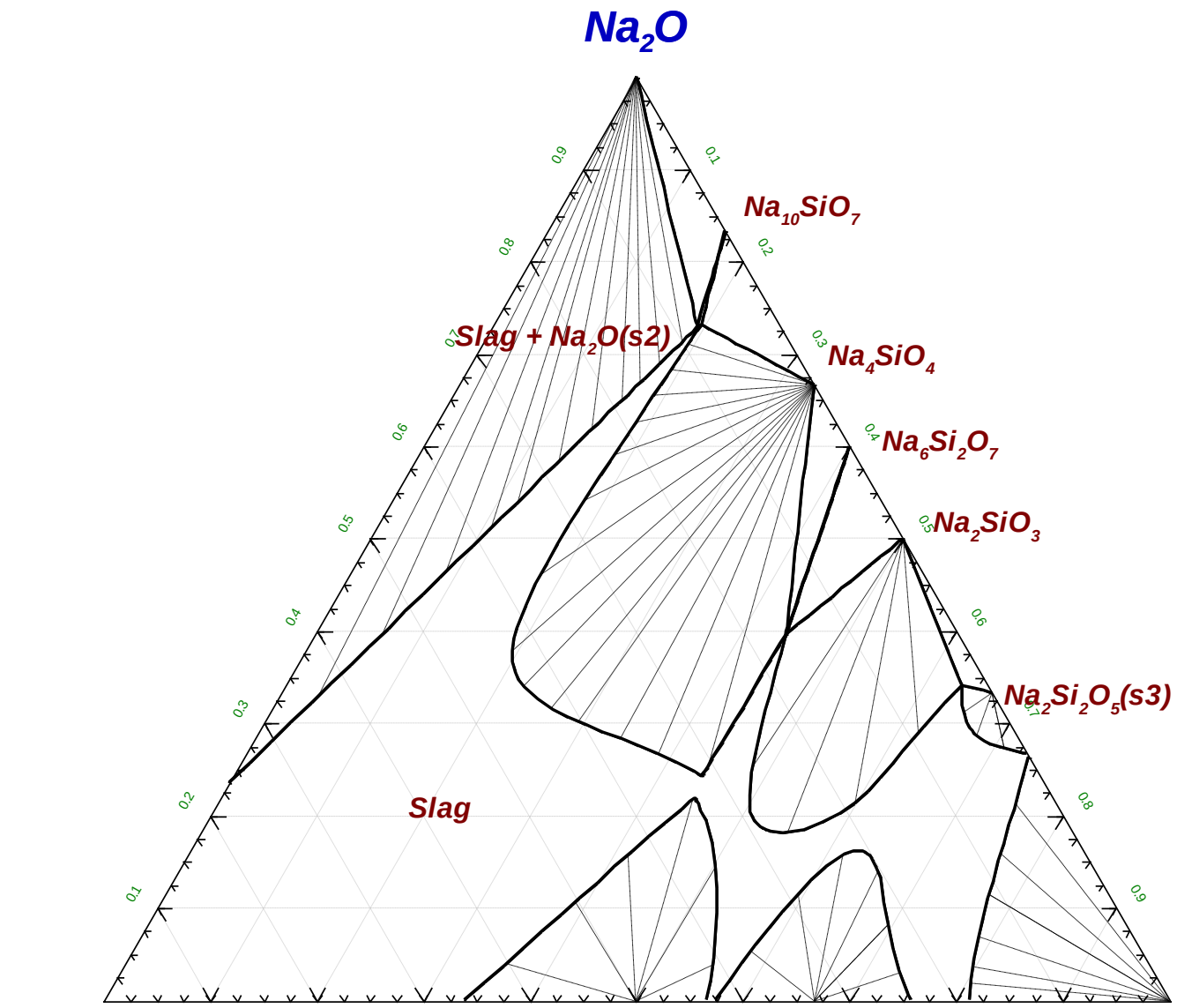

Mole fraction
kurz unterhalb Liquidussurface

K_2O - Na_2O - SiO_2

595°C

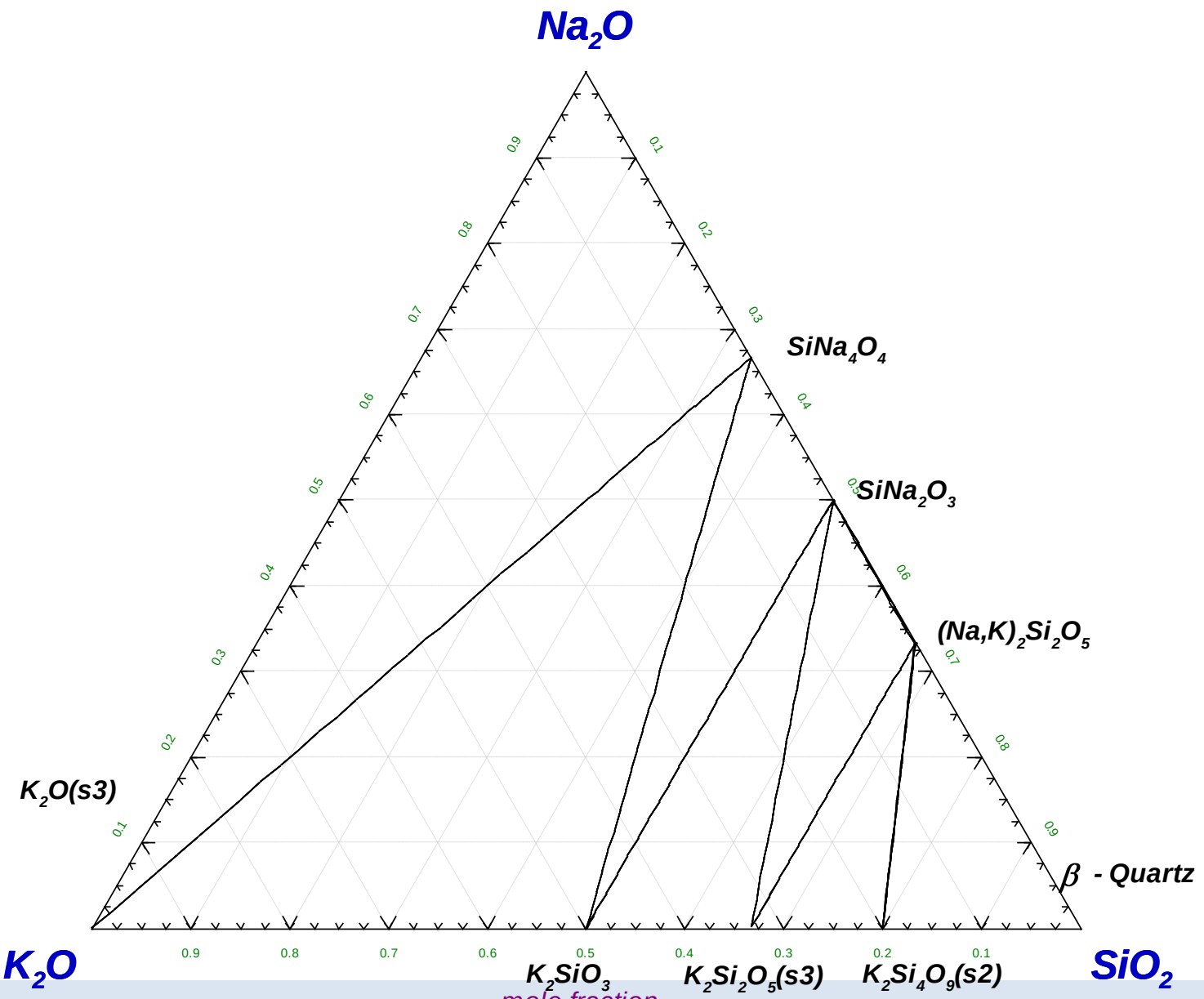

Weight percent
compared with experimental data

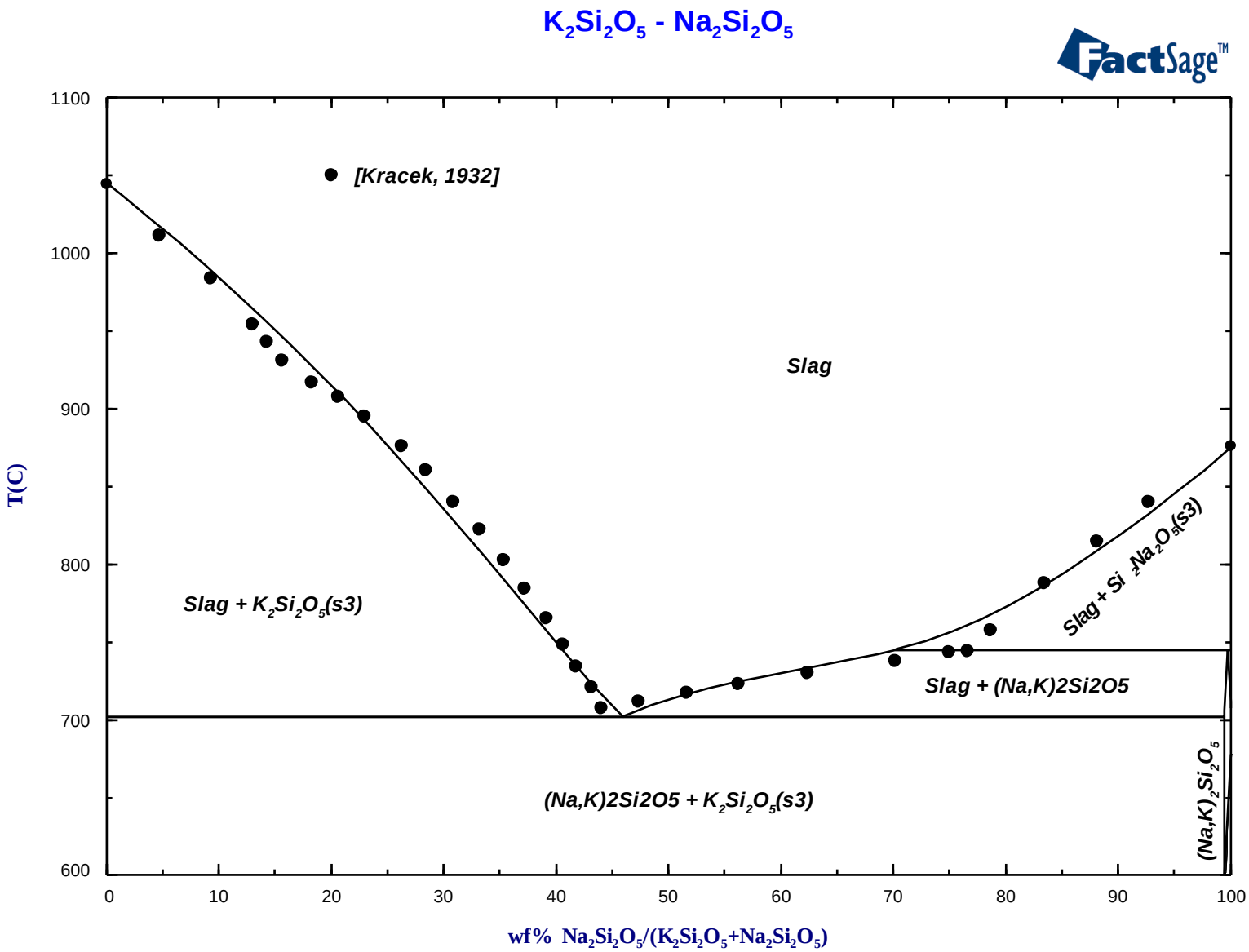

Weight percent
compared with experimental data

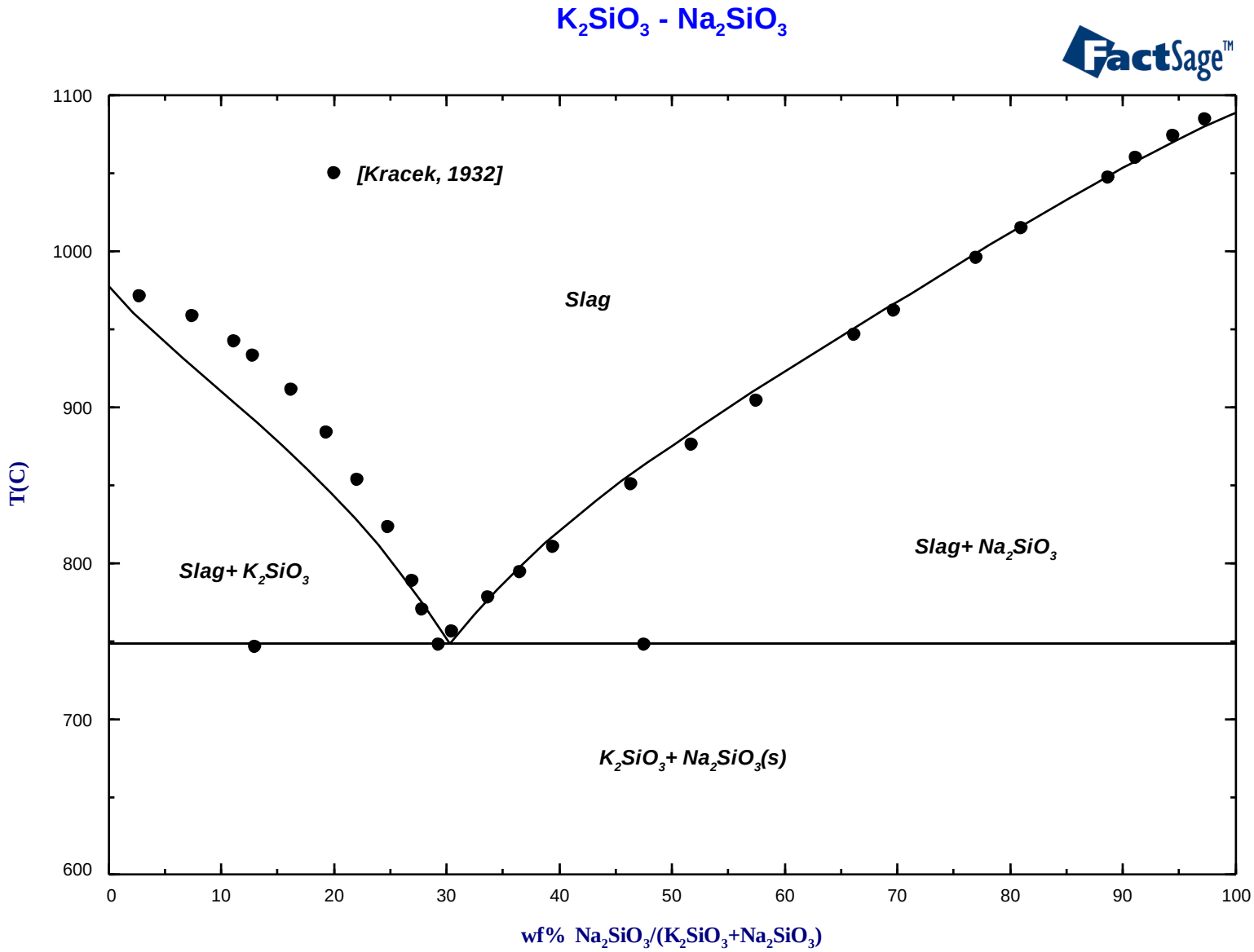

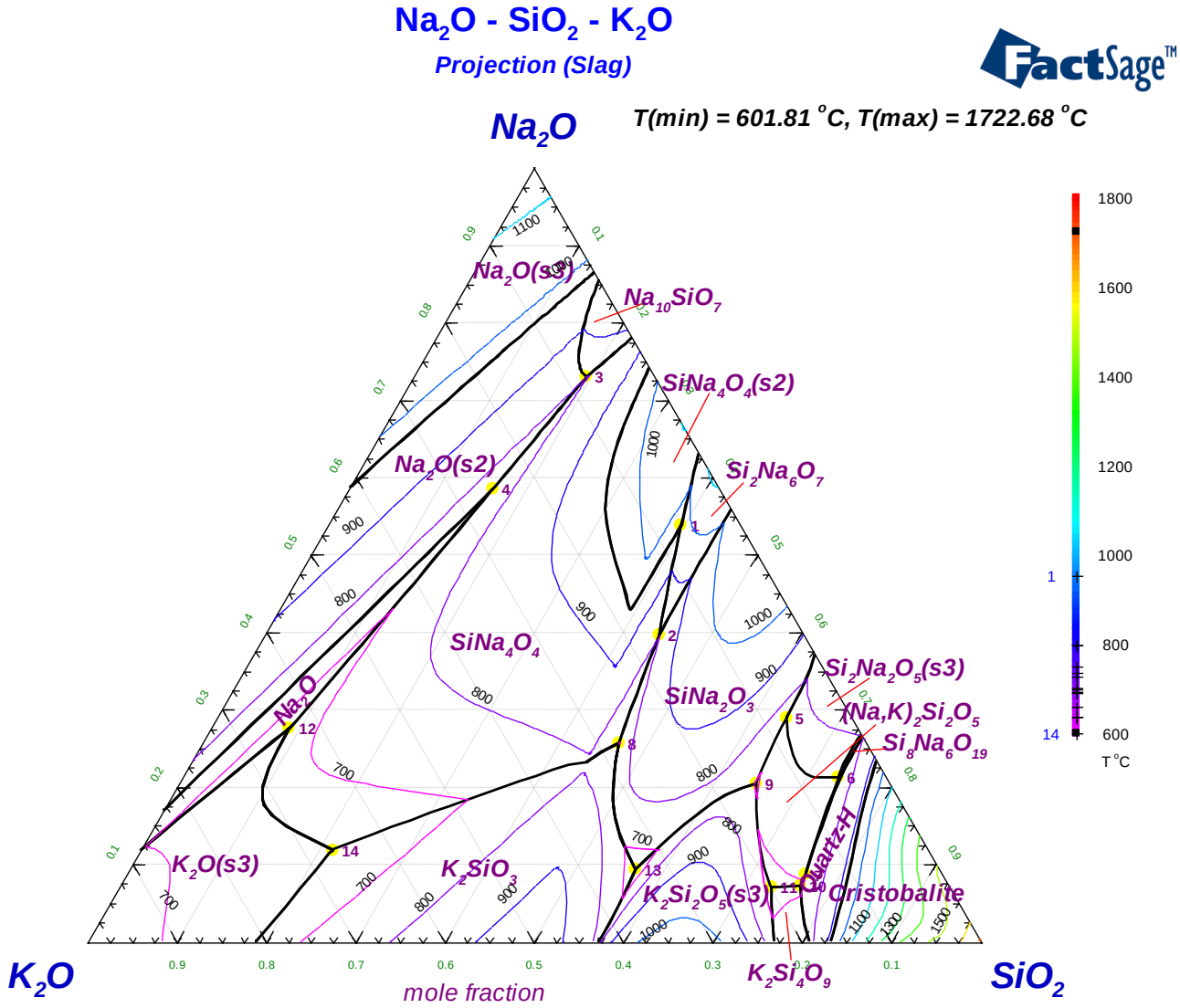
Na2O - SiO2 - K2O
Projection (Slag)
FactSage™
T(min) = 601.81 °C, T(max) = 1722.68 °C
Na2O
K2O
SiO2
mole fraction
Na2O(s3)
Na10SiO7
SiNa4O4(s2)
Si2Na6O7
Na2O(s2)
SiNa4O4
SiNa2O3
Si2Na2O5(s3)
(Na,K)2Si2O5
Si8Na6O19
Na2O
K2O(s3)
K2SiO3
K2Si2O5(s3)
Quartz-H
Cristobalite
K2Si4O9
T °C

Weight percent
Liquidussurface compared with experimental data

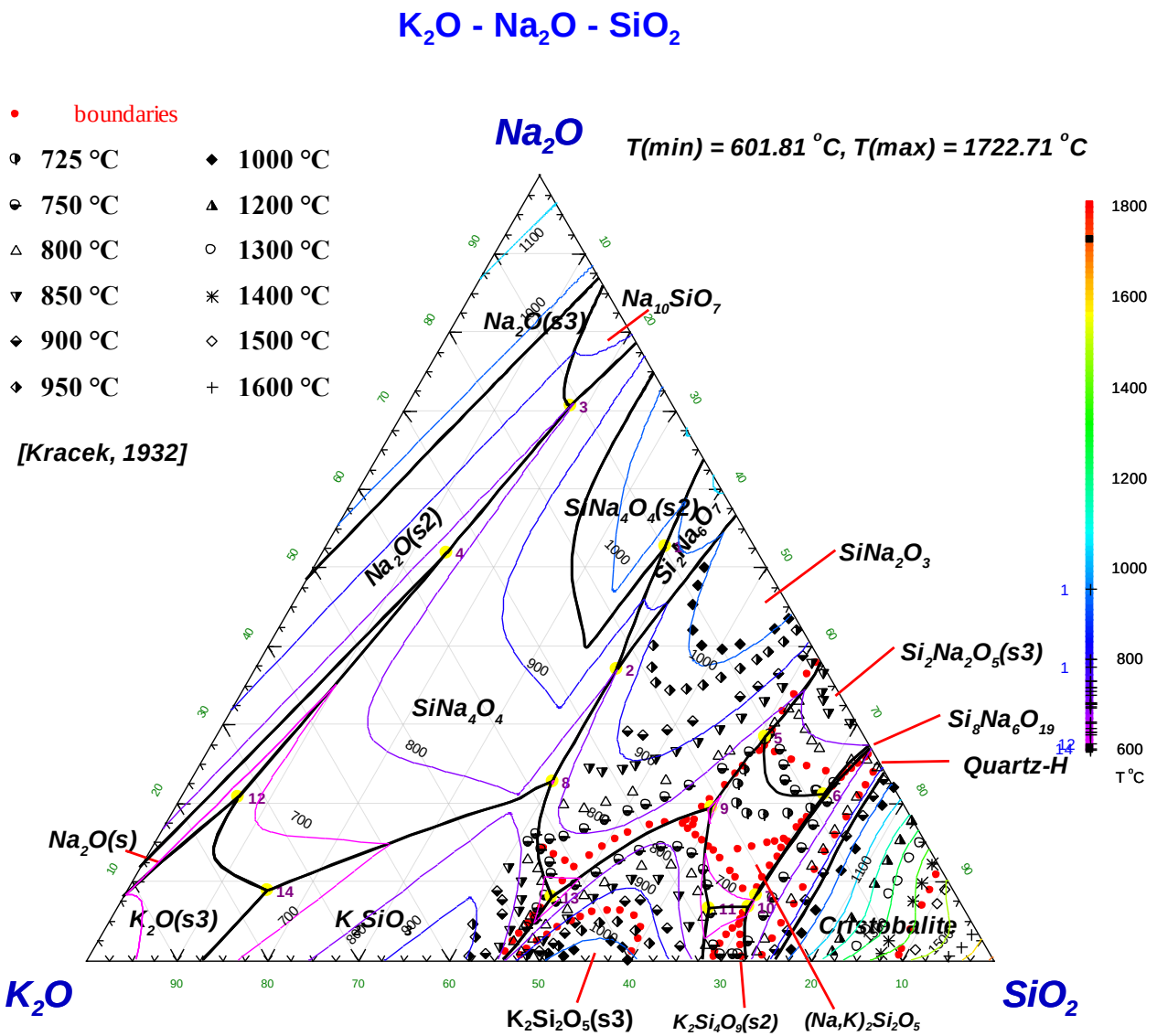

Invariant equilibria on the liquidus surface

Intersections with slag	Mole fraction A = Na2O, B = K2O, C = SiO2				Weight percent A = Na2O, B = K2O, C = SiO2			
	X(A)	X(B)	X(C)	T(C)	W(A)	W(B)	W(C)	T(C)
1: Si2Na6O7 / SiNa4O4(s2) / SiNa4O4	0.53787	0.06599	0.39614	954.75	52.619	9.811	37.569	954.76
2: Si2Na6O7 / SiNa2O3 / SiNa4O4	0.39662	0.16124	0.44215	799.04	37.057	22.895	40.048	799.01
3: Na10SiO7 / Na2O(s2) / SiNa4O4_lt(s)	0.72971	0.07683	0.19346	797.16	70.570	11.292	18.138	797.16
4: Na2O(s) / Na2O(s2) / SiNa4O4	0.58476	0.25397	0.16127	750.05	51.883	34.246	13.871	750.05
5: (Na,K)2Si2O5 / Si2Na2O5(s3) / SiNa2O3	0.28987	0.07234	0.63779	736.68	28.472	10.798	60.730	736.68
6: (Na,K)2Si2O5 / Si2Na2O5(s3) / Si8Na6O19	0.21178	0.05353	0.73469	726.40	21.065	8.092	70.843	726.40
7: (Na,K)2Si2O / Si8Na6O19 / Quartz_H	0.08681	0.15260	0.76059	703.18	8.220	21.961	69.819	703.18
8: K2SiO3 / SiNa2O3 / SiNa4O4	0.25714	0.27650	0.46636	698.69	22.766	37.205	40.028	698.72
9: (Na,K)2Si2O5 / K2Si2O5(s3) / SiNa2O3	0.20501	0.14865	0.64634	694.32	19.386	21.363	59.251	694.32
10: (Na,K)2Si2O5 / K2Si4O9(s2) / Quartz_H	0.07172	0.16511	0.76317	691.83	6.750	23.618	69.632	691.83
11: (Na,K)2Si2O5 / K2Si2O5(s3) / K2Si4O9(s2)	0.07125	0.19872	0.73003	659.22	6.591	27.939	65.470	659.24
12: K2O(s3) / Na2O(s) / SiNa4O4	0.27599	0.63587	0.08814	638.55	20.785	72.780	6.435	638.56
13: K2Si2O5(s3) / K2SiO3 / SiNa2O3	0.09330	0.33999	0.56671	637.13	8.047	44.567	47.386	637.17
14: K2O(s3) / K2SiO3 / SiNa4O4	0.11882	0.66617	0.21501	601.81	8.869	75.573	15.558	601.82

Mole fraction, Isopleth K2TiO3-Na2TiO3 compared with experiments

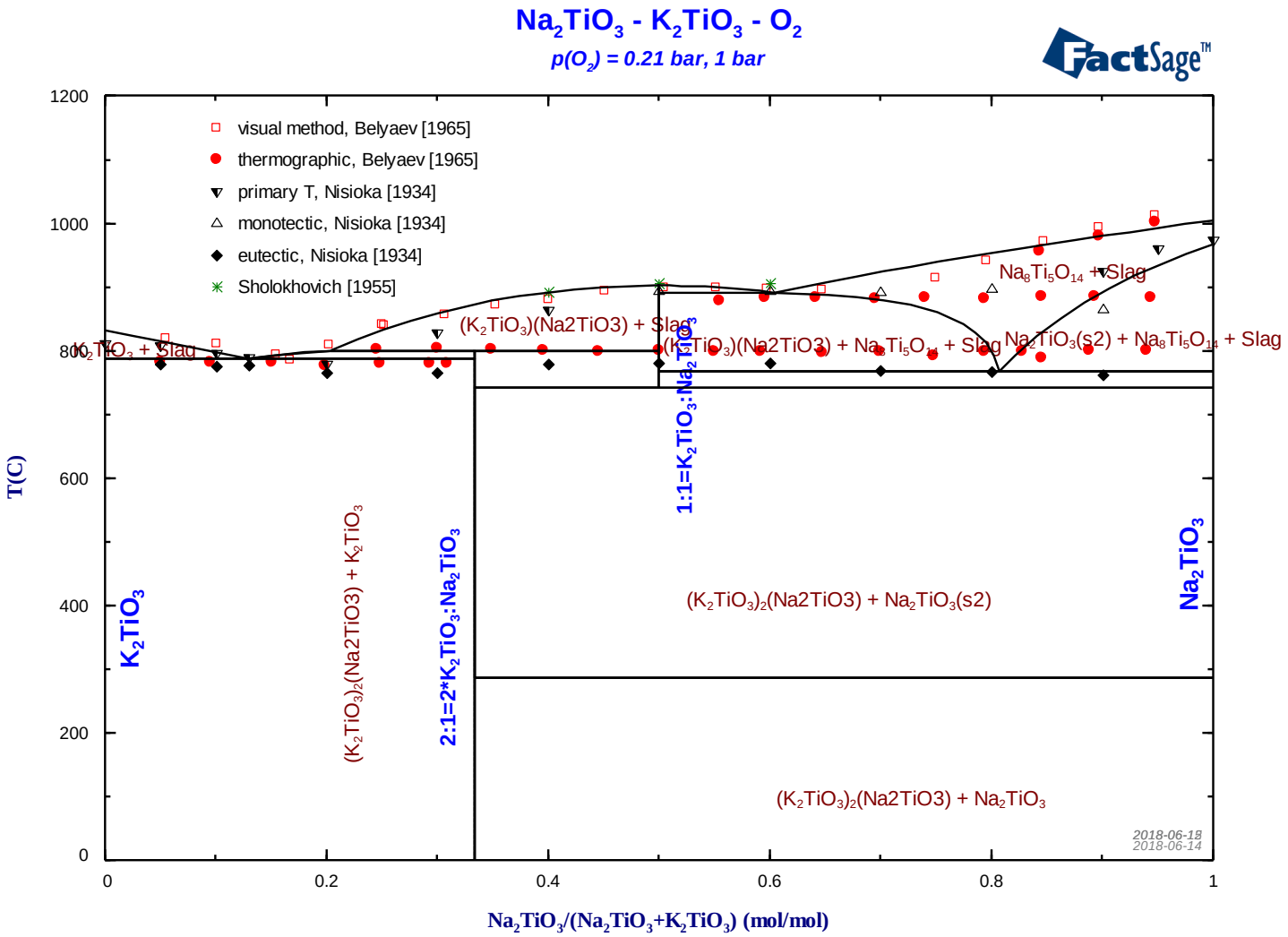

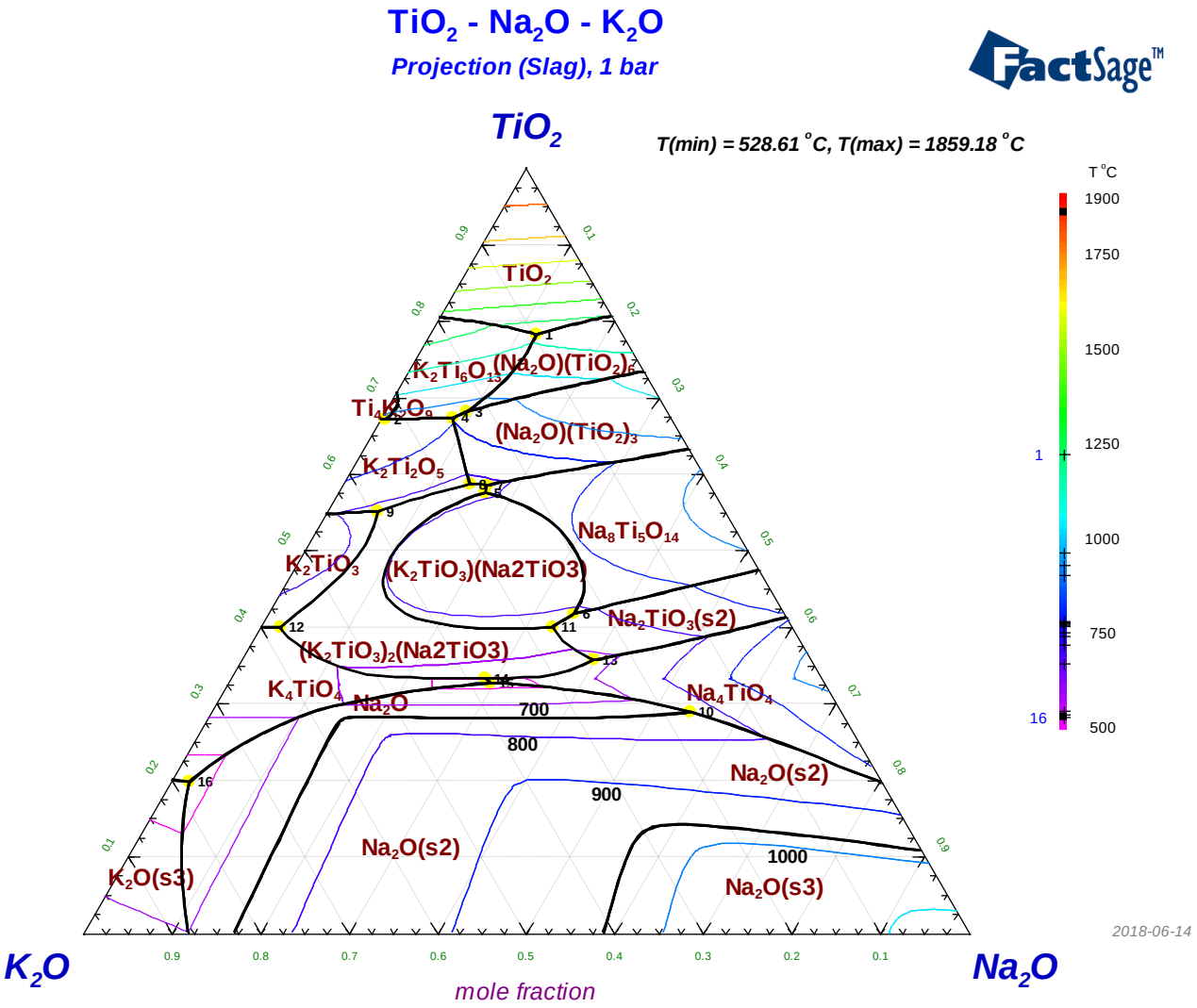
TiO2 - Na2O - K2O
Projection (Slag), 1 bar
FactSage™
TiO2
T(min) = 528.61 °C, T(max) = 1859.18 °C
T °C
1900
1750
1500
1250
1000
750
500
TiO2
K2Ti6O13(Na2O)(TiO2)6
Ti4K2O9
(Na2O)(TiO2)3
K2Ti2O5
Na8Ti5O14
K2TiO3
(K2TiO3)(Na2TiO3)
Na2TiO3(s2)
(K2TiO3)2(Na2TiO3)
K4TiO4
Na2O
Na4TiO4
700
800
900
1000
Na2O(s2)
Na2O(s2)
K2O(s3)
Na2O(s3)
2018-06-14
K2O
Na2O
mole fraction

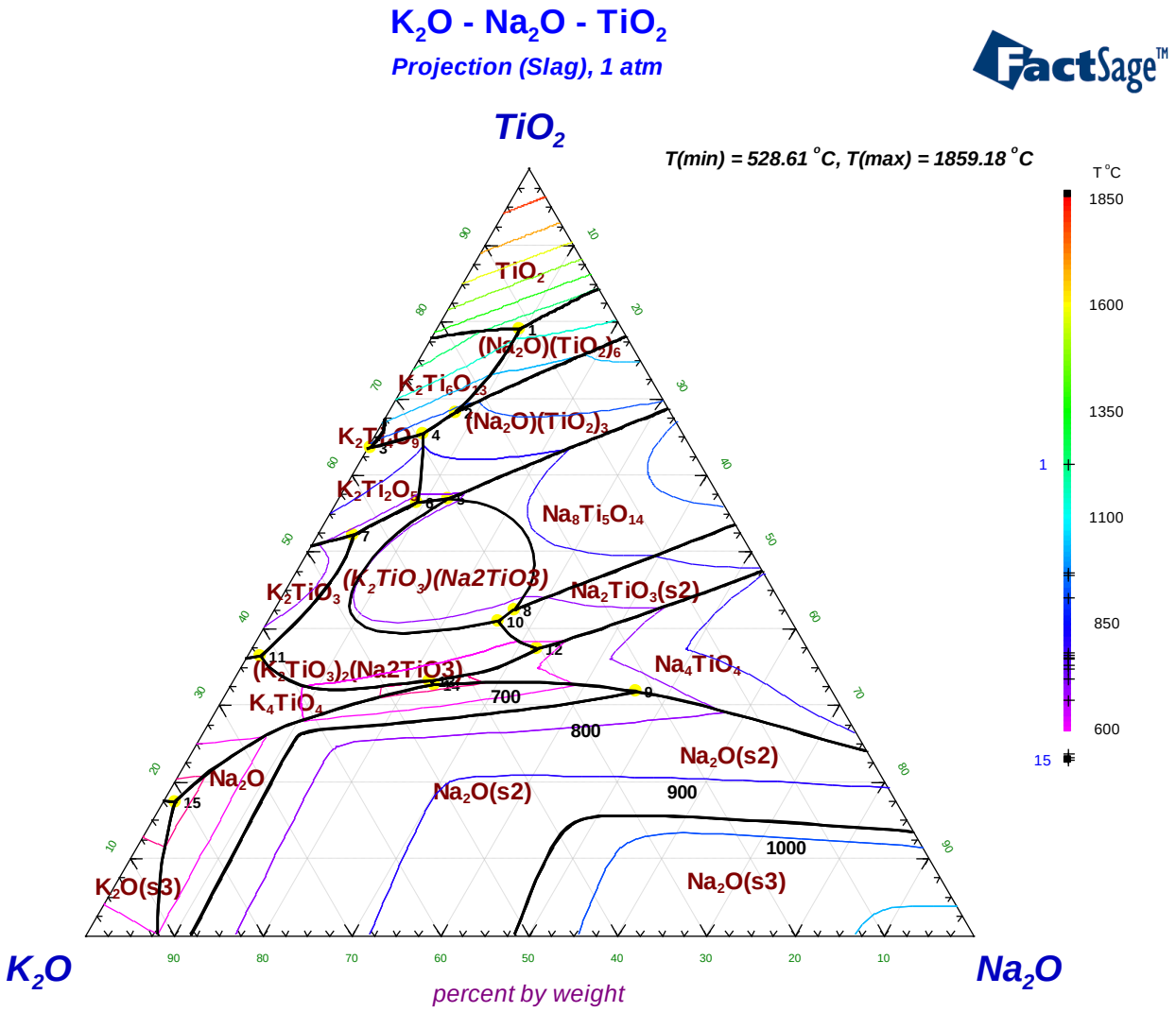
K2O - Na2O - TiO2
Projection (Slag), 1 atm
FactSage™
TiO2
T(min) = 528.61 °C, T(max) = 1859.18 °C
T °C
1850
1600
1350
1100
850
600
(Na2O)(TiO2)6
K2Ti6O13
(Na2O)(TiO2)3
K2Ti4O9
K2Ti2O5
Na8Ti5O14
K2TiO3
(K2TiO3)(Na2TiO3)
Na2TiO3(s2)
(K2TiO3)2(Na2TiO3)
Na4TiO4
K4TiO4
Na2O
Na2O(s2)
K2O(s3)
Na2O(s3)
700
800
900
1000
K2O
Na2O
percent by weight

Invariant equilibria on the liquidus surface

Intersections with slag	Mole fraction A = TiO2, B = K2O, C = Na2O				Weight percent A = TiO2, B = K2O, C = Na2O			
	X(A)	X(B)	X(C)	T(C)	W(A)	W(B)	W(C)	T(C)
1: (Na2O)(TiO2)6 / K2Ti6O13/ TiO2_Rutile	1: 0.78332	0.09651	0.12017	1222.48	1: 79.091	11.493	9.416	1222.48
2: (Na2O)(TiO2)3/ (Na2O)(TiO2)6 / K2Ti6O13	2: 0.69239	0.20791	0.09969	969.20	2: 68.218	24.160	7.623	969.21
3: K2Ti2O5 / K2Ti4O9 / K2Ti6O13	3: 0.67188	0.32323	0.00489	961.97	3: 63.570	36.071	0.359	961.99
4: (Na2O)(TiO2)3 / K2Ti2O5 / K2Ti6O13	4: 0.67304	0.25576	0.07119	909.37	4: 65.347	29.288	5.364	909.37
5:(K2TiO3)2(Na2TiO3) / (Na2O)(TiO2)3 / Na8Ti5O14	5: 0.57479	0.26273	0.16247	780.61	5: 56.868	30.658	12.474	780.61
6:(K2TiO3)2(Na2TiO3) / (Na2O)(TiO2)3 / K2Ti2O5	6: 0.57945	0.29894	0.12161	773.77	6: 56.454	34.351	9.195	773.77
7:(K2TiO3)2(Na2TiO3) / K2Ti2O5 / K2TiO3	7: 0.55170	0.39185	0.05645	769.09	7: 52.162	43.696	4.142	769.07
8:(K2TiO3)(Na2TiO3) / Na2TiO3(s2) / Na8Ti5O14	8: 0.41146	0.25008	0.33846	765.89	8: 42.459	30.437	27.104	765.89
9: Na2O(s) / Na2O(s2) / Na4TiO4	9: 0.28877	0.16965	0.54158	750.07	9: 31.763	22.008	46.229	750.06
10:K2Na2Ti2O6 / (K2TiO3)2(Na2TiO3) /Na2TiO3(s2)	10: 0.40027	0.27277	0.32696	740.50	10: 41.023	32.972	26.005	740.50
11:(K2TiO3)2(Na2TiO3) / K2TiO3 / K4TiO4	11: 0.39921	0.57801	0.02278	718.12	11: 36.338	62.053	1.609	718.12
12:(K2TiO3)2(Na2TiO3) / Na2TiO3(s2) / Na4TiO4	12: 0.35639	0.24628	0.39734	669.47	12: 37.310	30.409	32.281	669.47
13:(K2TiO3)2(Na2TiO3) / K4TiO4 / Na4TiO4	13: 0.33334	0.37923	0.28743	542.45	13: 33.214	44.561	22.225	542.44
14: K4TiO4 / Na2O(s) / Na4TiO4	14: 0.32717	0.37645	0.29638	534.65	14: 32.679	44.348	22.973	534.65
15: K2O(s3) / K4TiO4 / Na2O(s)	15: 0.19726	0.78184	0.02090	528.61	15: 17.370	81.202	1.428	528.61

K2O-Na2O-V2O5
Mole fraction, Isopleth KVO3-NaVO3 compared with experiments

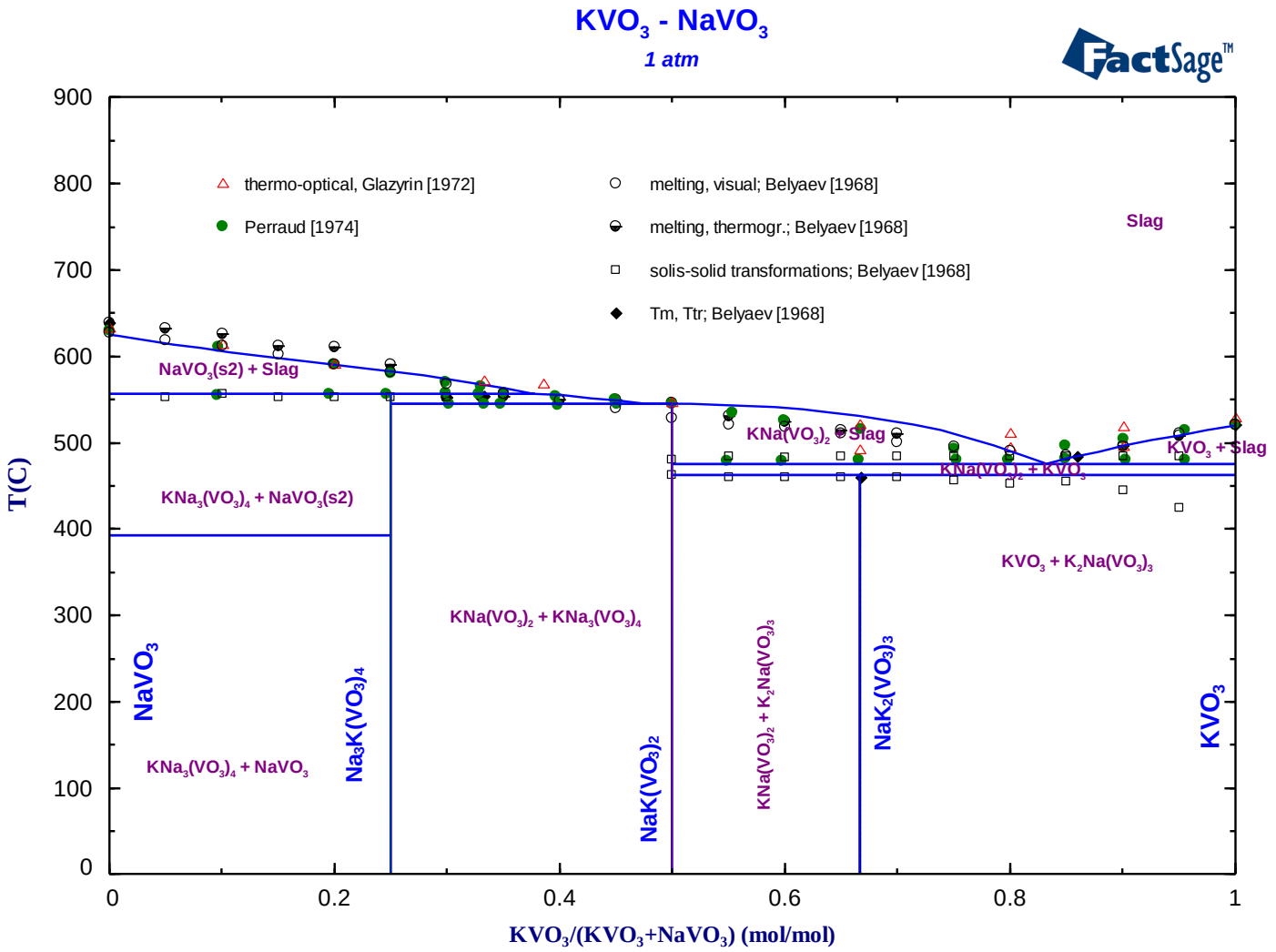

K2O-Na2O-V2O5
Mole fraction, Liquidussurface

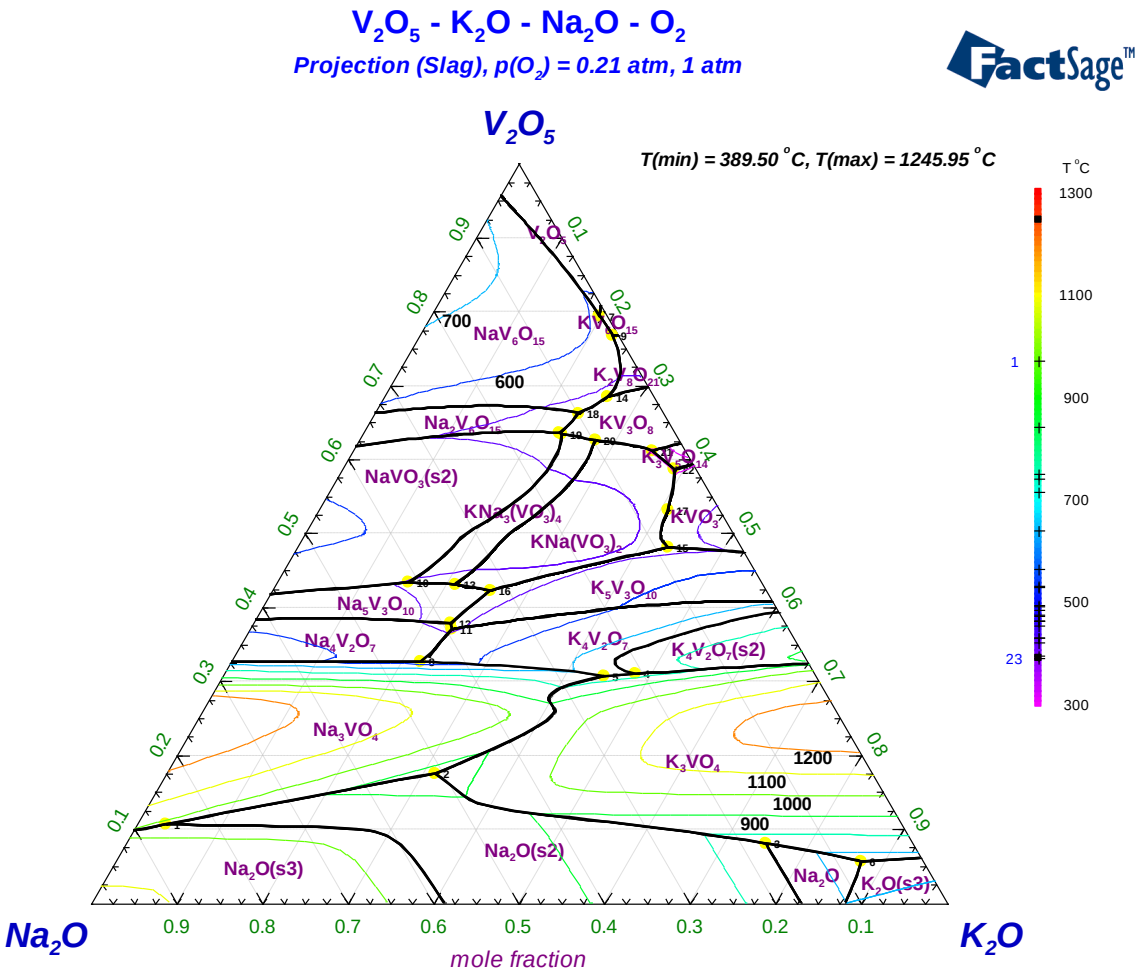

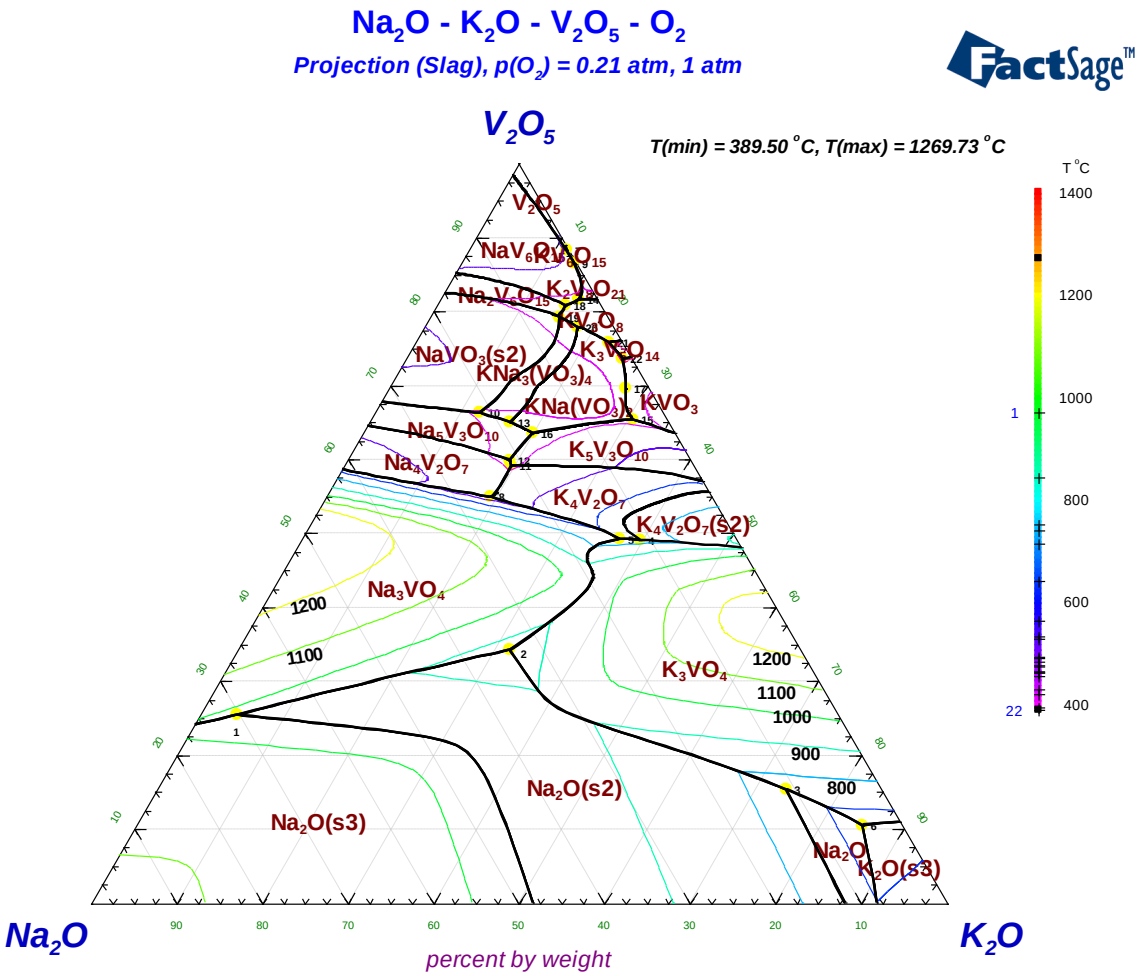
Na2O - K2O - V2O5 - O2
Projection (Slag), p(O2) = 0.21 atm, 1 atm
FactSage™
V2O5
T(min) = 389.50 °C, T(max) = 1269.73 °C
T °C
1400
1200
1000
800
600
400
V2O5
NaV6O15
K2V6O15
Na2V6O15
K2V4O11
V2O3
NaVO3(s2)
K3VO4
KNa3(VO3)4
KNa(VO3)2
KVO3
Na5V3O10
K5V3O10
Na4V2O7
K4V2O7
K4V2O7(s2)
Na3VO4
K3VO4
Na2O(s2)
Na2O(s3)
Na2O
K2O(s3)
1200
1100
1000
900
800
Na2O
K2O
percent by weight

Invariant equilibria on the liquidus surface

Intersections with slag	Mole fraction A = V2O5, B = Na2O, C = K2O				Weight percent A = V2O5, B = Na2O, C = K2O			
	X(A)	X(B)	X(C)	T(C)	W(A)	W(B)	W(C)	T(C)
1: Na2O(s2) / Na2O(s3) / Na3VO4(s)	1: 0.10628	0.85964	0.03408	970.05	1: 25.495	70.271	0.04234	970.05
2. K3VO4(s) / Na2O(s2) / Na3VO4(s)	2: 0.17539	0.51051	0.31410	841.81	2: 34.254	33.975	0.31770	841.76
3. K3VO4(s) / Na2O(s) / Na2O(s2)	3: 0.08094	0.17078	0.74828	750.05	3: 15.369	11.050	0.73581	750.05
4. K3VO4(s) / K4V2O7(s) / K4V2O7(s2)	4: 0.30981	0.20874	0.48144	740.00	4: 49.154	11.286	0.39560	740.02
5. K3VO4(s) / K4V2O7(s) / Na3VO4(s)	5: 0.30654	0.24721	0.44626	714.14	5: 49.291	13.546	0.37163	714.14
6. K2O(s3) / K3VO4(s) / Na2O(s)	6: 0.05634	0.07121	0.87244	639.72	6: 10.582	4.558	0.84860	639.73
7. KV6O15(s) / NaV6O15(s) / V2O5(s)	7: 0.79423	0.00840	0.19737	563.41	7: 88.315	0.318	0.11366	563.41
8. K4V2O7(s) / Na3VO4(s) / Na4V2O7(s)	8: 0.32712	0.45114	0.22174	532.17	8: 54.915	25.807	0.19278	532.17
9. K2V8O21(s) / KV6O15(s) / NaV6O15(s)	9: 0.76814	0.00646	0.22540	528.02	9: 86.592	0.248	0.13159	528.02
10.KNa3(VO3)4(s) / Na5V3O10(s) / NaVO3(s2)	10: 0.43371	0.41196	0.15433	492.48	10: 66.314	21.465	0.12221	492.49
11.K4V2O7(s) / K5V3O10(s) / Na4V2O7(s)	11: 0.37116	0.39221	0.23663	490.60	11: 59.162	21.304	0.19534	490.60
12.K5V3O10(s) / Na4V2O7(s) / Na5V3O10(s)	12: 0.37813	0.39097	0.23090	484.14	12: 59.930	21.116	0.18954	484.14
13.KNa(VO3)2(s) / KNa3(VO3)4(s) / Na5V3O10(s)	13: 0.43118	0.35859	0.21023	475.32	13: 65.108	18.452	0.16441	475.32
14.K2V8O21(s) / KV3O8(s) / NaV6O15(s)	14: 0.68494	0.05397	0.26109	473.23	14: 81.682	2.193	0.16125	473.23
15.K5V3O10(s) / KNa(VO3)2(s) / KVO3(s)	15: 0.48076	0.08531	0.43393	463.37	15: 65.448	3.958	0.30594	463.37
16.K5V3O10(s) / KNa(VO3)2(s) / Na5V3O10(s)	16: 0.42289	0.32219	0.25492	462.33	16: 63.621	16.517	0.19862	462.33
17.K2Na(VO3)3(s) / KNa(VO3)2(s) / KVO3(s)	17: 0.53205	0.06010	0.40784	461.86	17: 69.663	2.681	0.27655	461.86
18.KV3O8(s) / Na2V6O15(s) / NaV6O15(s)	18: 0.66282	0.09933	0.23785	454.55	18: 80.846	4.129	0.15025	454.56
19.KNa3(VO3)4(s) / KV3O8(s) / NaVO3(s2)	19: 0.63473	0.13226	0.23301	429.04	19: 79.294	5.630	0.15076	429.03
20.KNa(VO3)2(s) / KNa3(VO3)4(s) / KV3O8(s)	20: 0.62554	0.09824	0.27622	419.80	20: 77.990	4.174	0.17836	419.80
21.K3V5O14(s) / KNa(VO3)2(s) / KV3O8(s)	21: 0.61176	0.03805	0.35019	394.45	21: 75.893	1.608	0.22499	394.45
22.K2Na(VO3)3(s) / K3V5O14(s) / KNa(VO3)2(s)	22: 0.58709	0.02489	0.38802	389.75	22: 73.706	1.065	0.25229	389.75

K2O-P2O5-ZnO,
Mole fraction, Isopleth KZn4P3O12-ZnO

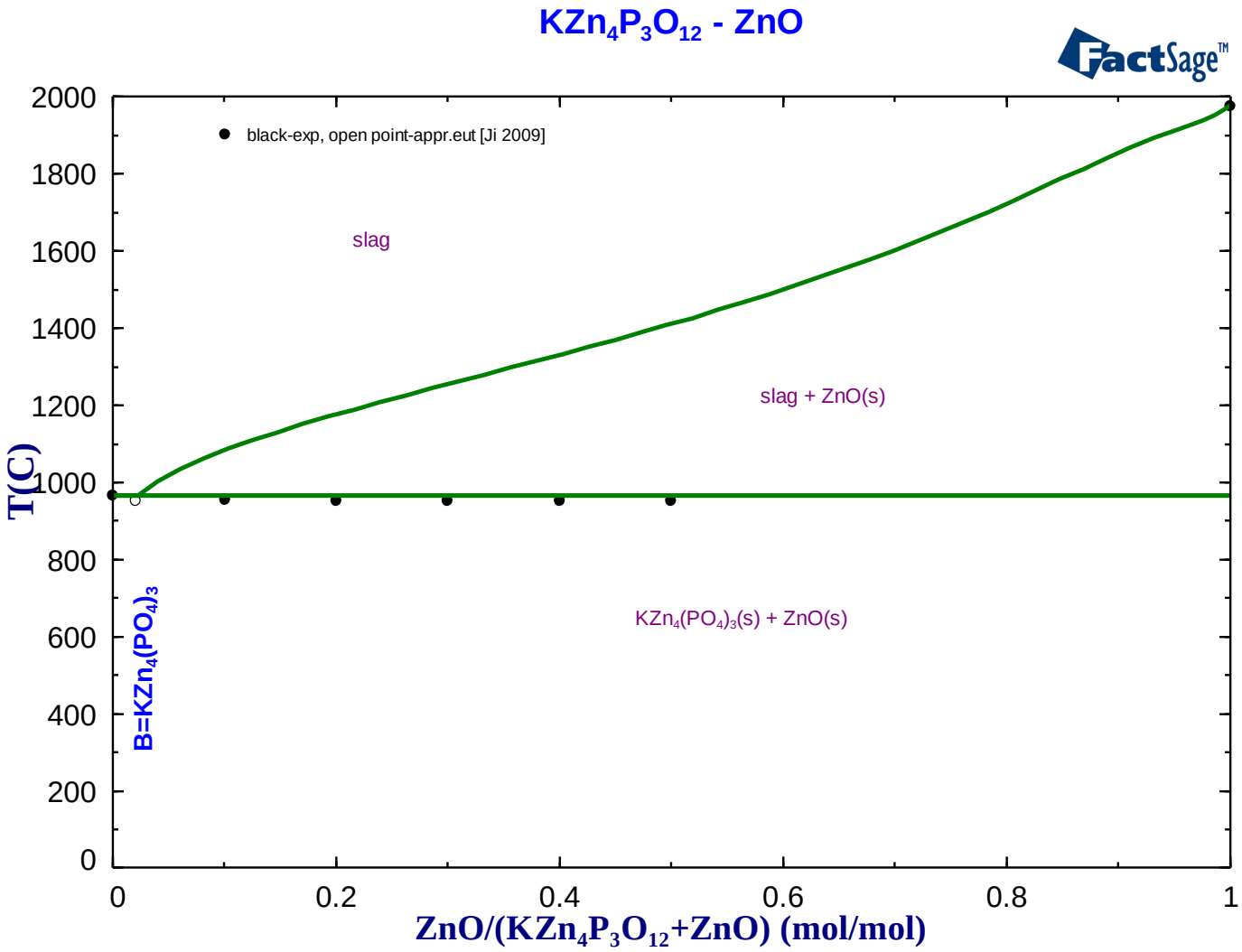

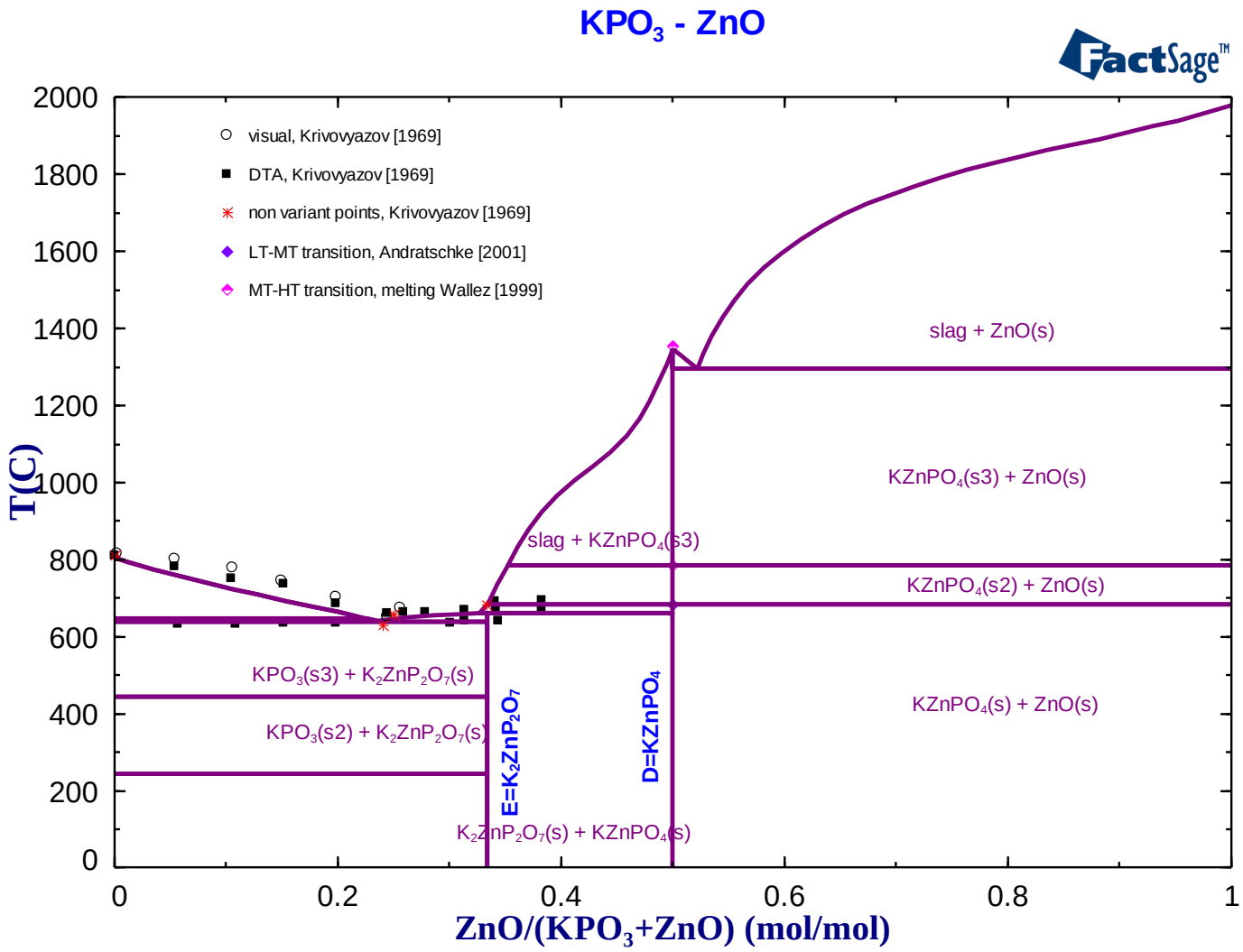
KPO3 - ZnO
FactSage™
visual, Krivovyazov [1969]
DTA, Krivovyazov [1969]
non variant points, Krivovyazov [1969]
LT-MT transition, Andratschke [2001]
MT-HT transition, melting Wallez [1999]
slag + ZnO(s)
KZnPO4(s3) + ZnO(s)
slag + KZnPO4(s3)
KZnPO4(s2) + ZnO(s)
KPO3(s3) + K2ZnP2O7(s)
KPO3(s2) + K2ZnP2O7(s)
E=K2ZnP2O7
D=KZnPO4
KZnPO4(s) + ZnO(s)
K2ZnP2O7(s) + KZnPO4(s)
T(C)
ZnO/(KPO3+ZnO) (mol/mol)
2000
1800
1600
1400
1200
1000
800
600
400
200
0
0
0.2
0.4
0.6
0.8
1

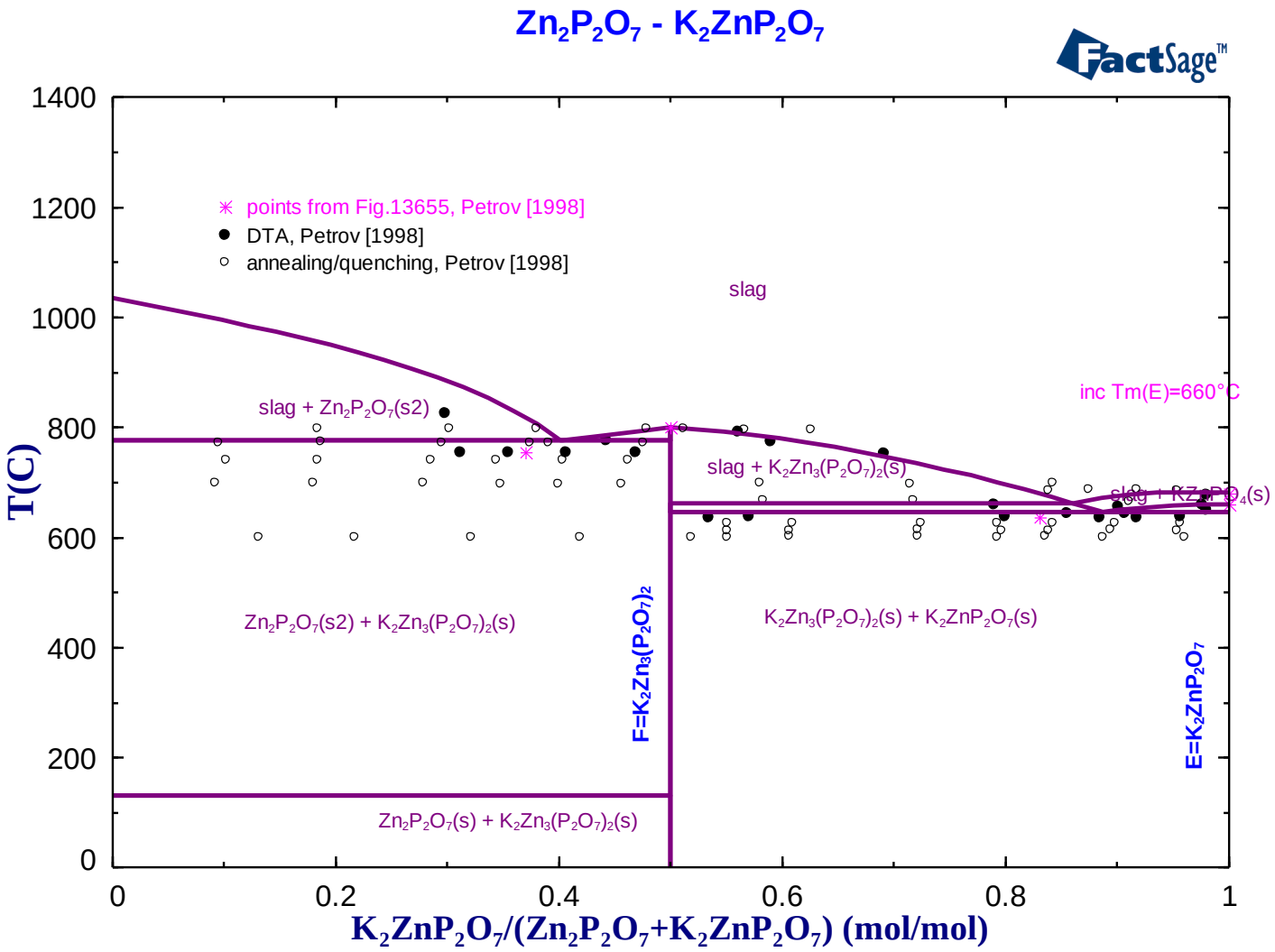
Zn2P2O7 - K2ZnP2O7
FactSage™
points from Fig.13655, Petrov [1998]
DTA, Petrov [1998]
annealing/quenching, Petrov [1998]
slag
inc Tm(E)=660°C
slag + Zn2P2O7(s2)
slag + K2Zn3(P2O7)2(s)
slag + K2ZnP2O7(s)
Zn2P2O7(s2) + K2Zn3(P2O7)2(s)
K2Zn3(P2O7)2(s) + K2ZnP2O7(s)
Zn2P2O7(s) + K2Zn3(P2O7)2(s)
F=K2Zn8(P2O7)2
E=K2ZnP2O7
T(C)
1400
1200
1000
800
600
400
200
0
0
0.2
0.4
0.6
0.8
1
K2ZnP2O7/(Zn2P2O7+K2ZnP2O7) (mol/mol)

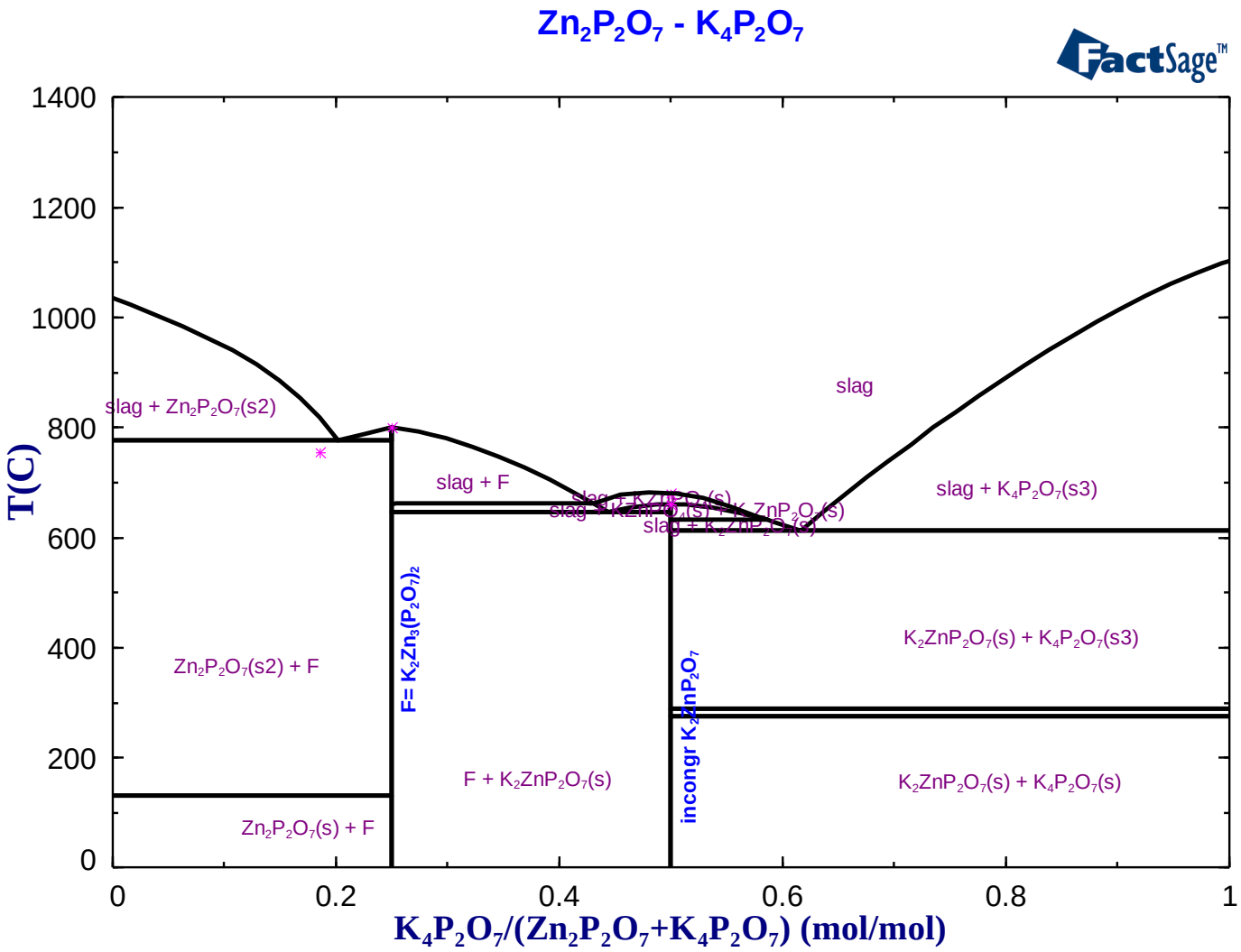
Zn2P2O7 - K4P2O7
FactSage™
T(C)
1400
1200
1000
800
600
400
200
0
0
0.2
0.4
0.6
0.8
1
K4P2O7/(Zn2P2O7+K4P2O7) (mol/mol)
slag + Zn2P2O7(s2)
slag
slag + F
slag + K4P2O7(s3)
Zn2P2O7(s2) + F
F= K2Zn3(P2O7)2
K2ZnP2O7(s) + K4P2O7(s3)
incongr K2ZnP2O7
F + K2ZnP2O7(s)
K2ZnP2O7(s) + K4P2O7(s)
Zn2P2O7(s) + F

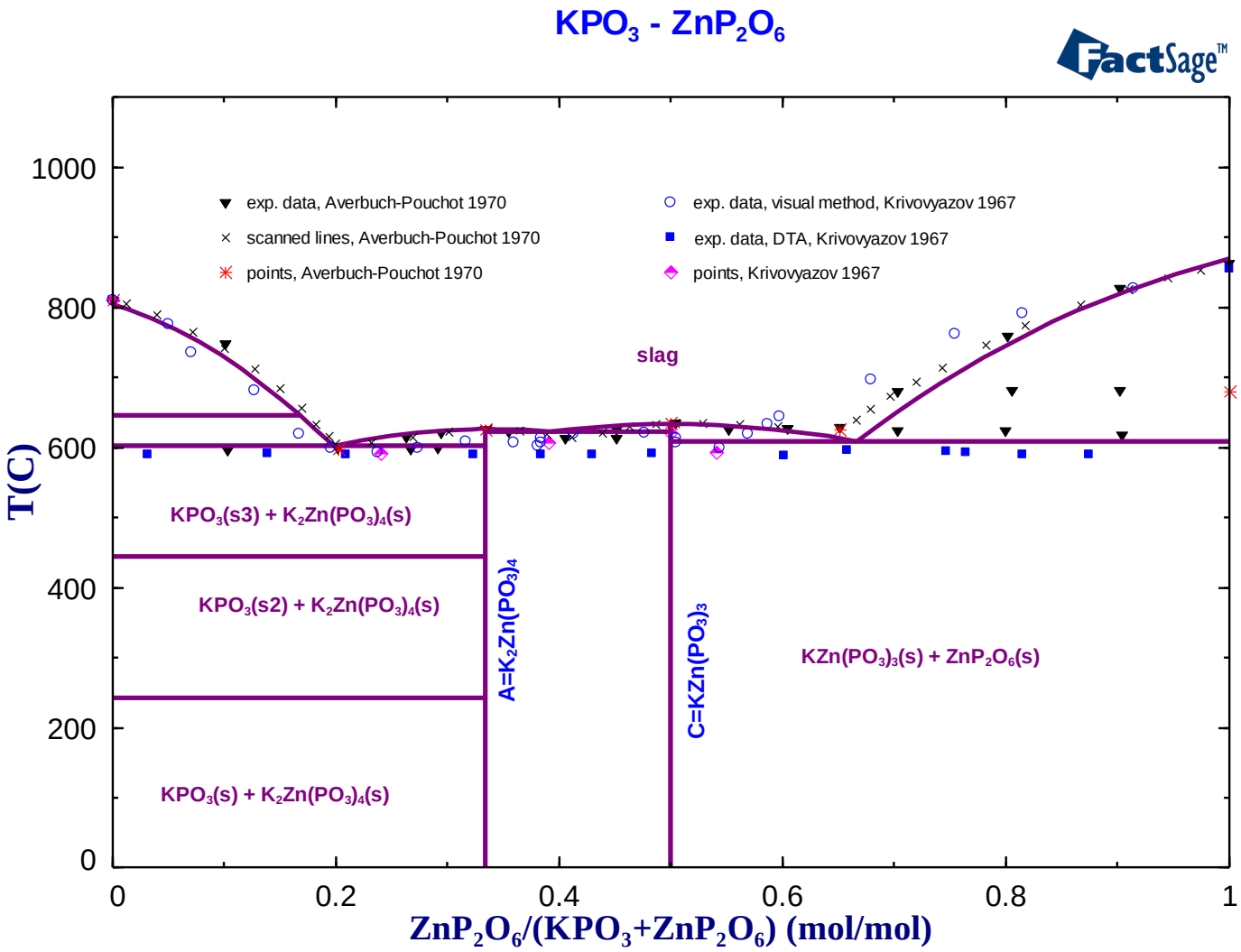
KPO3 - ZnP2O6
FactSage™
exp. data, Averbuch-Pouchot 1970
scanned lines, Averbuch-Pouchot 1970
points, Averbuch-Pouchot 1970
exp. data, visual method, Krivovyazov 1967
exp. data, DTA, Krivovyazov 1967
points, Krivovyazov 1967
slag
KPO3(s3) + K2Zn(PO3)4(s)
KPO3(s2) + K2Zn(PO3)4(s)
KPO3(s) + K2Zn(PO3)4(s)
A=K2Zn(PO3)4
C=KZn(PO3)3
KZn(PO3)3(s) + ZnP2O6(s)
T(C)
1000
800
600
400
200
0
0
0.2
0.4
0.6
0.8
1
ZnP2O6/(KPO3+ZnP2O6) (mol/mol)

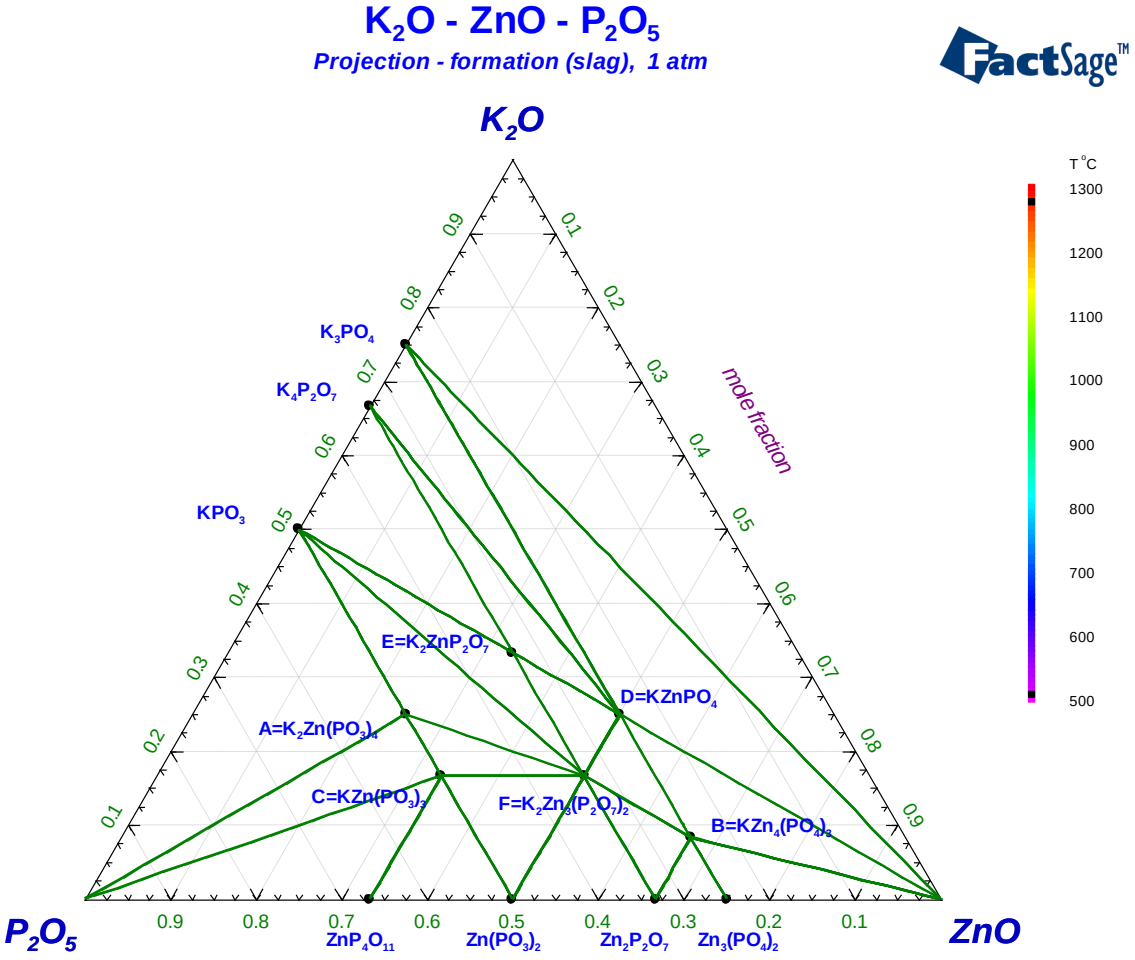
K2O - ZnO - P2O5
Projection - formation (slag), 1 atm
FactSage™
K2O
P2O5
ZnO
mole fraction
T °C
1300
1200
1100
1000
900
800
700
600
500
K3PO4
K4P2O7
KPO3
E=K2ZnP2O7
D=KZnPO4
A=K2Zn(PO3)4
C=KZn(PO3)3
F=K2Zn3(P2O7)2
B=KZn4(PO4)2
ZnP4O11
Zn(PO3)2
Zn2P2O7
Zn3(PO4)2

K2O-P2O5-ZnO,
Mole fraction, Liquidus surface

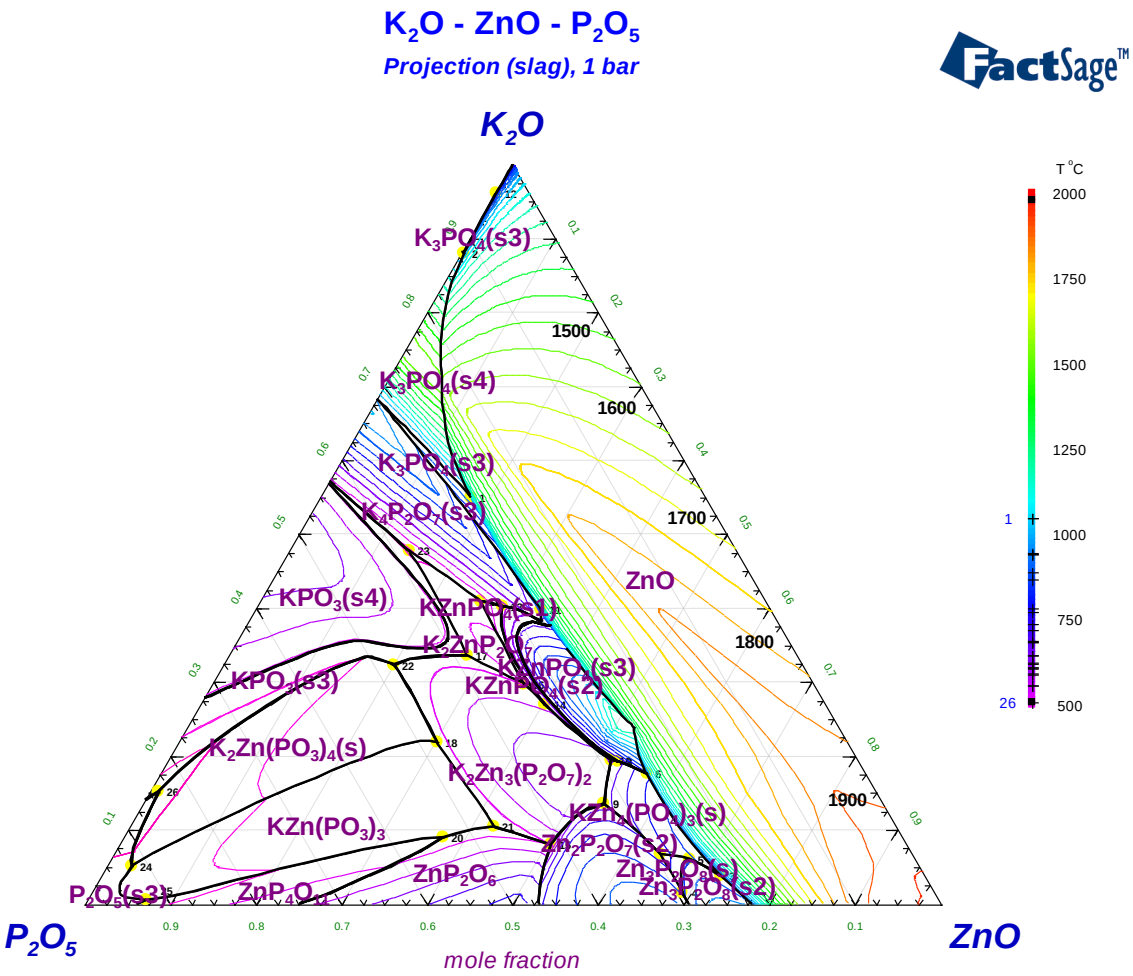

K2O-P2O5-ZnO,
Weight percent, Liquidus surface

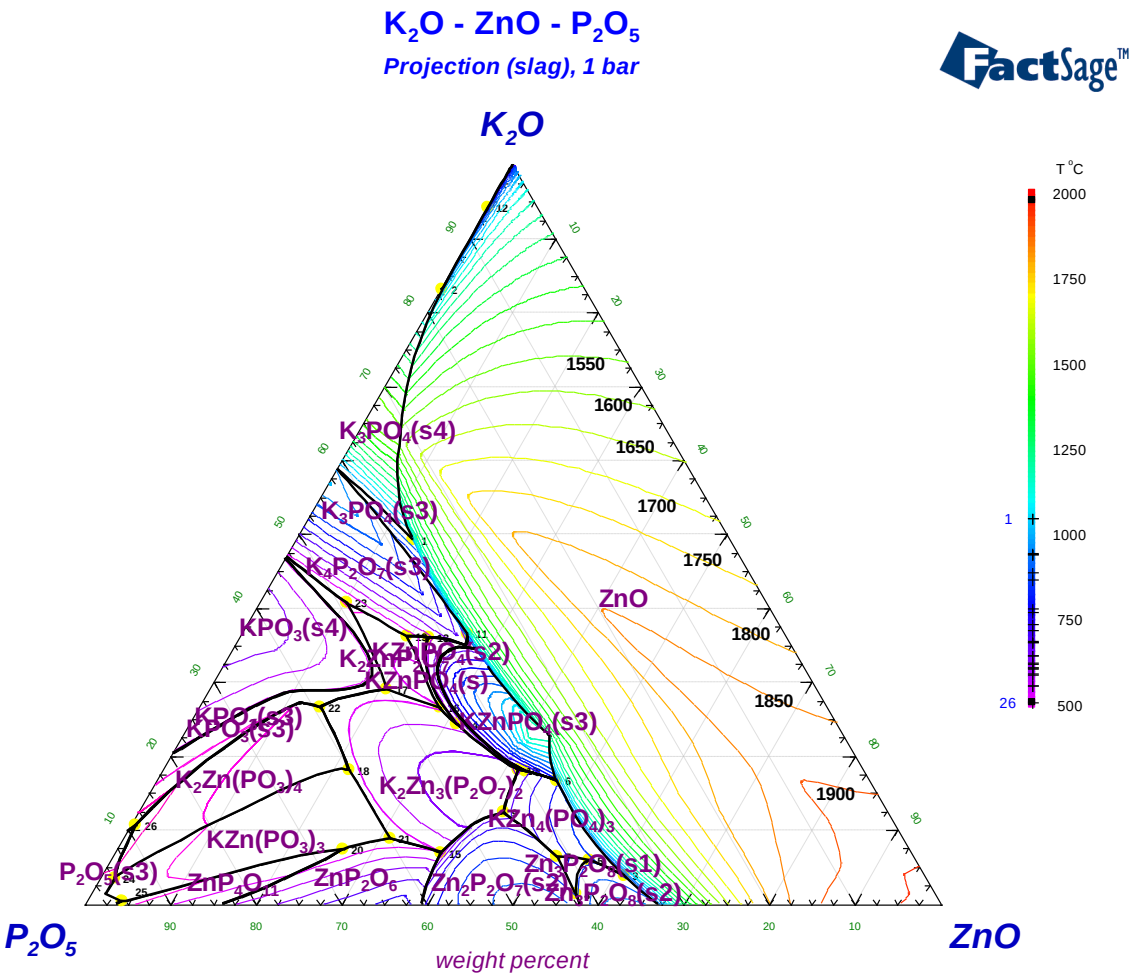

Invariant equilibria on the liquidus surface

Intersections with slag	Mole fraction A = K2O, B = P2O5, C = ZnO				Weight percent A = K2O, B = P2O5, C = ZnO				
		X(A)	X(B)	X(C)	T(C)		W(A)	W(B)	W(C)	T(C)
1: K3PO4(s3) / K3PO4(s4) / ZnO	1:	0.54921	0.27353	0.17726	1048.10	1:	49.277	36.982	13.740	1048.10
2: K3PO4(s3) / K3PO4(s4) / ZnO	2:	0.88024	0.11683	0.00294	1048.10	2:	83.134	16.627	0.240	1048.10
3: KZn4(PO4)3 / Zn3P2O8(s2) / ZnO	3:	0.03835	0.23754	0.72411	946.26	3:	3.753	35.028	61.219	946.26
4: Zn2P2O7(s2) / Zn3P2O8(s) / Zn3P2O8(s2)	4:	0.01541	0.29338	0.69121	941.85	4:	1.462	41.917	56.621	941.85
5: KZn4(PO4)3 / Zn3P2O8(s) / Zn3P2O8(s2)	5:	0.06154	0.26283	0.67563	941.85	5:	5.910	38.035	56.055	941.85
6: KZn4(PO4)3 / KZnPO4_HT(s3) / ZnO	6:	0.17625	0.25494	0.56881	888.98	6:	16.756	36.524	46.720	888.99
7: KZn4(PO4)3 / Zn2P2O7(s2) / Zn3P2O8(s)	7:	0.06794	0.29328	0.63878	867.87	7:	6.399	41.625	51.977	867.87
8: KZn4(PO4)3 / KZnPO4_HT(s3) / KZnPO4_MT(s2)	8:	0.19299	0.28015	0.52686	783.00	8:	18.031	39.442	42.527	783.04
9: K2Zn3(P2O7)2 / KZn4(PO4)3 / Zn2P2O7(s2)	9:	0.13521	0.32513	0.53965	774.25	9:	12.389	44.892	42.719	774.25
10: K2Zn3(P2O7)2 / KZn4(PO4)3 / KZnPO4_MT(s2)	10:	0.19504	0.28742	0.51754	738.95	10:	18.139	40.279	41.582	738.81
11: K3PO4(s3) / K4P2O7_HT(s3) / KZnPO4_MT(s2)	11:	0.39841	0.26823	0.33335	720.10	11:	36.531	37.062	26.407	720.11
12: K2O(s3) / K3PO4(s3) / ZnO	12:	0.96131	0.03864	0.00005	689.43	12:	94.284	5.711	0.004	689.43
13: K4P2O7(s3) / KZnPO4_LT(s) /KZnPO4_MT(s2)	13:	0.40354	0.31039	0.28607	683.50	13:	36.081	41.821	22.098	683.08
14: K2Zn3(P2O7)2 / KZnPO4_LT(s)/KZnPO4_MT(s2)	14:	0.27026	0.32679	0.40294	683.00	14:	24.330	44.331	31.338	683.00
15: K2Zn3(P2O7)2 / Zn2P2O7(s2) / ZnP2O6	15:	0.07985	0.41577	0.50438	646.81	15:	6.992	54.856	38.153	646.81
16: K2Zn3(P2O7)2 / K2ZnP2O7 / KZnPO4_LT(s)	16:	0.29784	0.33731	0.36486	645.69	16:	26.561	45.329	28.110	645.69
17: K2Zn3(P2O7)2 / K2ZnP2O7 / KPO3(s3)	17:	0.33653	0.38509	0.27838	623.47	17:	29.078	50.141	20.781	623.47
18: K2Zn(PO3)4 / K2Zn3(P2O7)2 / KZn(PO3)3	18:	0.21872	0.47918	0.30210	619.36	18:	18.199	60.084	21.717	619.36
19: K2ZnP2O7 / K4P2O7_HT(s3) / KZnPO4_LT(s)	19:	0.41002	0.33280	0.25718	611.64	19:	36.166	44.235	19.598	611.67
20: KZn(PO3)3 / ZnP2O6(s) / ZnP4O11	20:	0.09093	0.53539	0.37367	609.87	20:	7.450	66.100	26.450	609.87
21: K2Zn3(P2O7)2 / KZn(PO3)3 / ZnP2O6(s)	21:	0.10450	0.46919	0.42631	607.68	21:	8.857	59.926	31.217	607.70
22: K2Zn(PO3)4 / K2Zn3(P2O7)2 / KPO3(s3)	22:	0.32398	0.47652	0.19950	593.22	22:	26.678	59.129	14.192	593.21
23: K2ZnP2O7 / K4P2O7_HT(s3) / KPO3(s3)	23:	0.47833	0.38219	0.13947	587.84	23:	40.718	49.025	10.257	587.84
24: K2Zn(PO3)4 / KZn(PO3)3 / P2O5(s3)	24:	0.05167	0.91967	0.02866	557.83	24:	3.533	94.773	1.694	557.83
25: KZn(PO3)3 / P2O5_O'-Phase(s3) / ZnP4O11_S1(s)	25:	0.00513	0.92555	0.06932	555.85	25:	0.352	95.546	4.103	555.85
26: K2Zn(PO3)4_S1(s) / KPO3(s3) / P2O5(s3)	26:	0.15250	0.83760	0.00990	508.00	26:	10.715	88.684	0.601	508.00

Mole fraction, 500°C

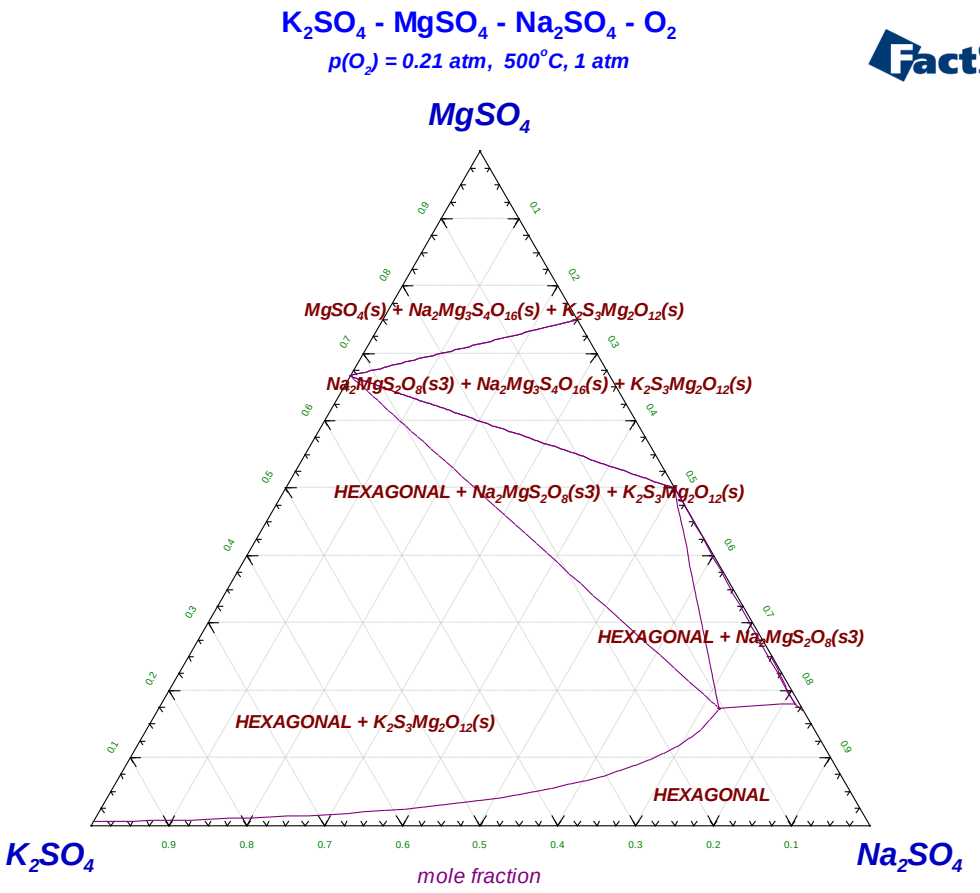

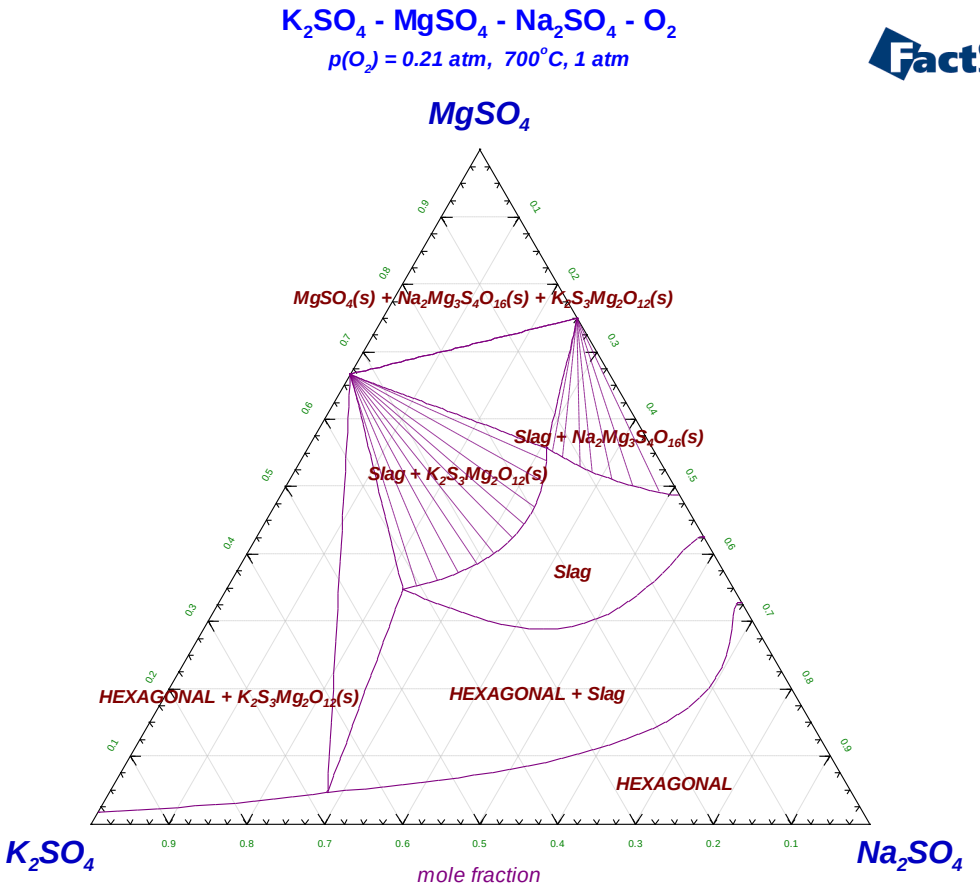
K2SO4 - MgSO4 - Na2SO4 - O2
p(O2) = 0.21 atm, 700°C, 1 atm
FactSage™
MgSO4
MgSO4(s) + Na2Mg3S4O16(s) + K2S3Mg2O12(s)
Slag + Na2Mg3S4O16(s)
Slag + K2S3Mg2O12(s)
Slag
HEXAGONAL + K2S3Mg2O12(s)
HEXAGONAL + Slag
HEXAGONAL
K2SO4
Na2SO4
mole fraction

Mole fraction, Liquidussurface

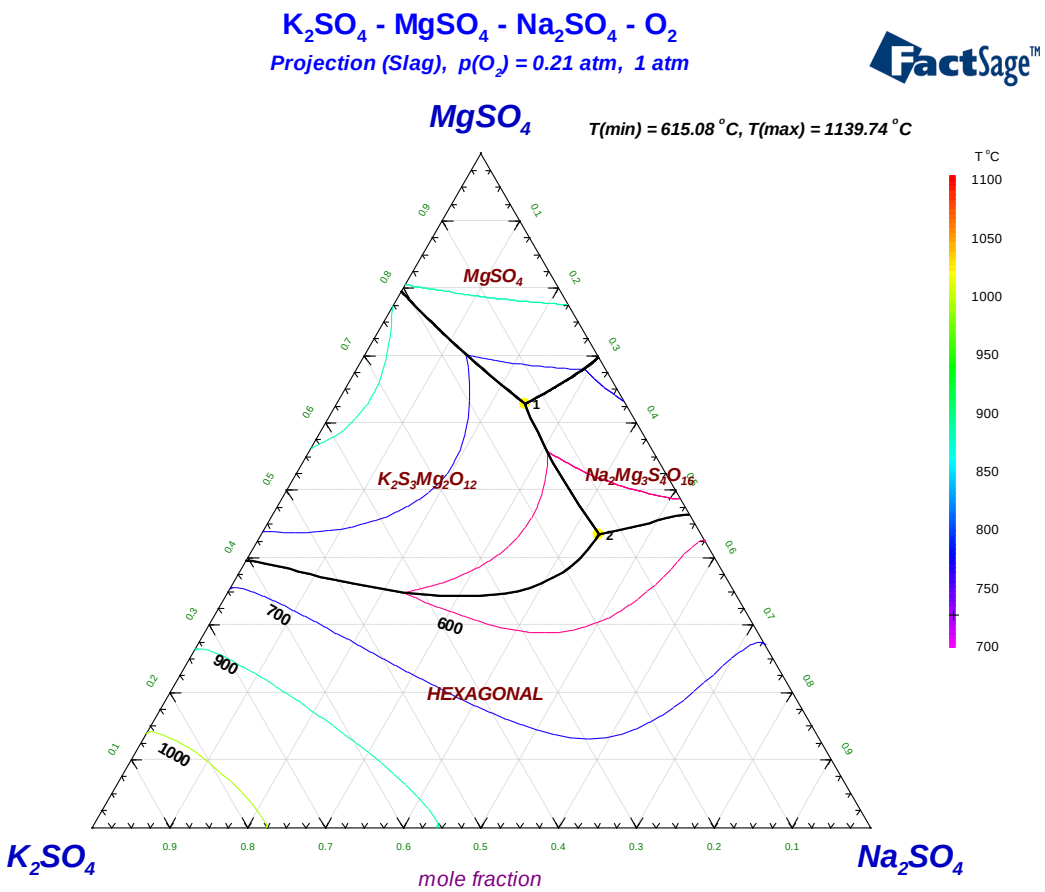

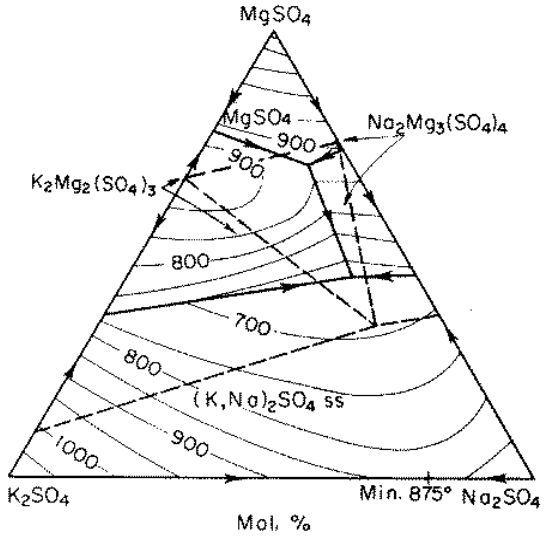

J.J. Rowe, G.W. Morey, J. Inorg. Nucl. Chem., 29 [4], (1967), pp. 925-942.

Weight percent, Liquidussurface

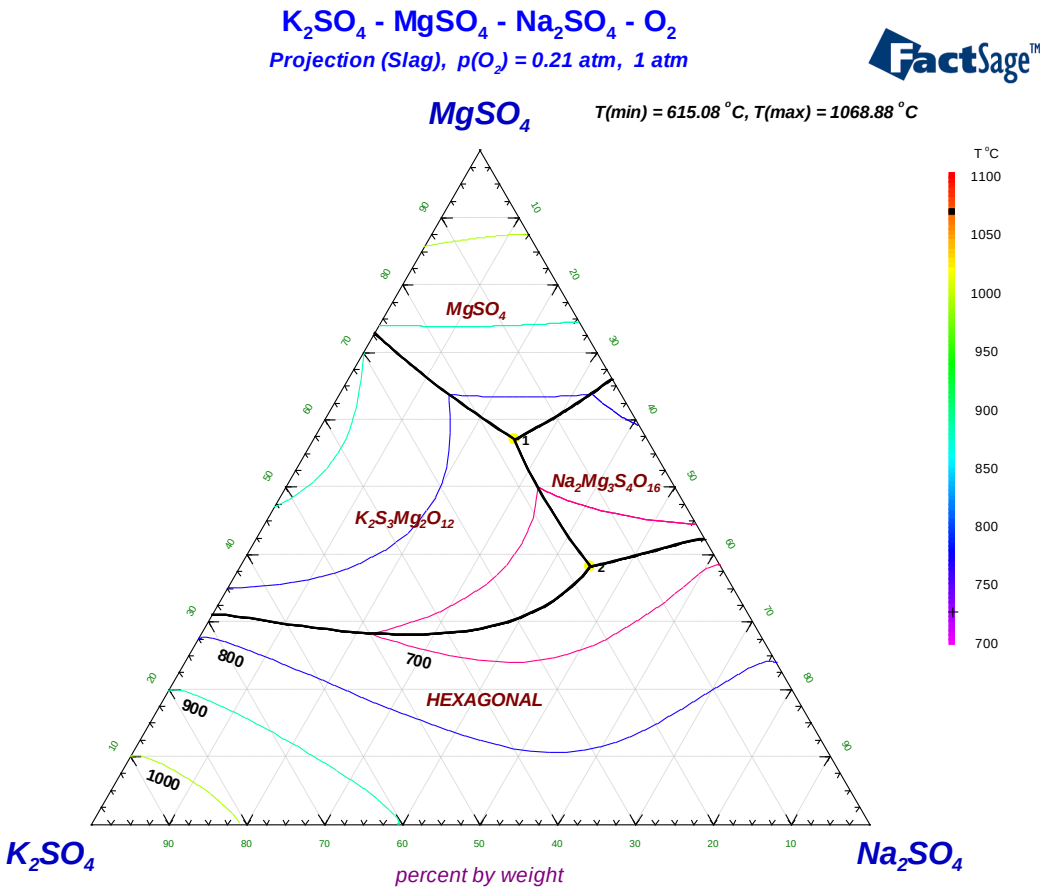

Invariant equilibria on the liquidus surface

Intersections with slag	Mole fraction				Weight percent			
	A = MgSO4, B = K2SO4, C = Na2SO4				A = MgSO4, B = K2SO4, C = Na2SO4			
	X(A)	X(B)	X(C)	T(C)	W(A)	W(B)	W(C)	T(C)
1: K2S3Mg2O12 / MgSO4 / Na2Mg3S4O16	1: 0.62829	0.12938	0.24233	726.30	1: 57.037	17.003	25.960	726.30
2: HEXAGONAL / K2S3Mg2O12 / Na2Mg3S4O16	2: 0.43474	0.13083	0.43443	615.08	2: 38.242	16.661	45.096	615.08

Weight percent, Orthisilicate section Mg2SiO4-Mn2SiO4 compared with experimental data

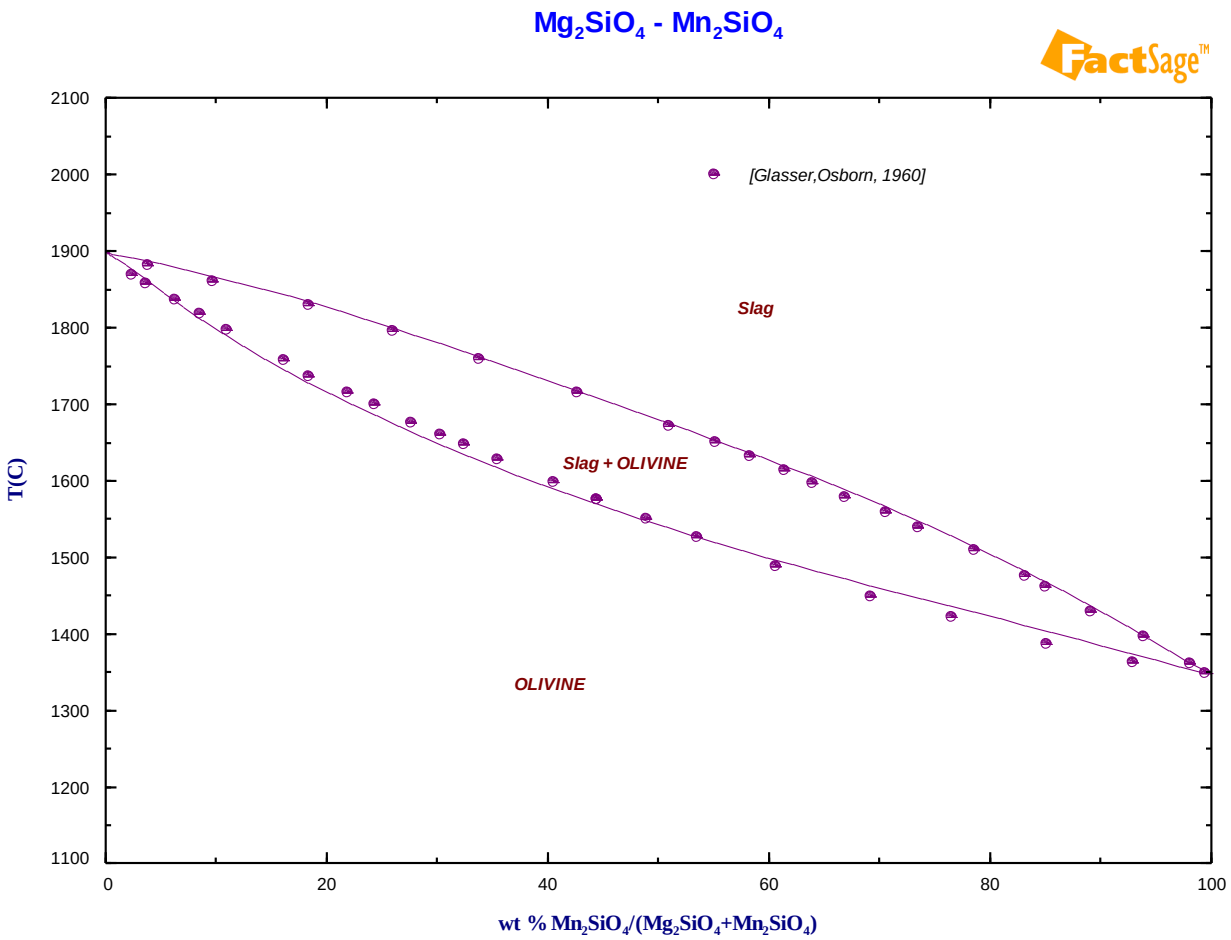

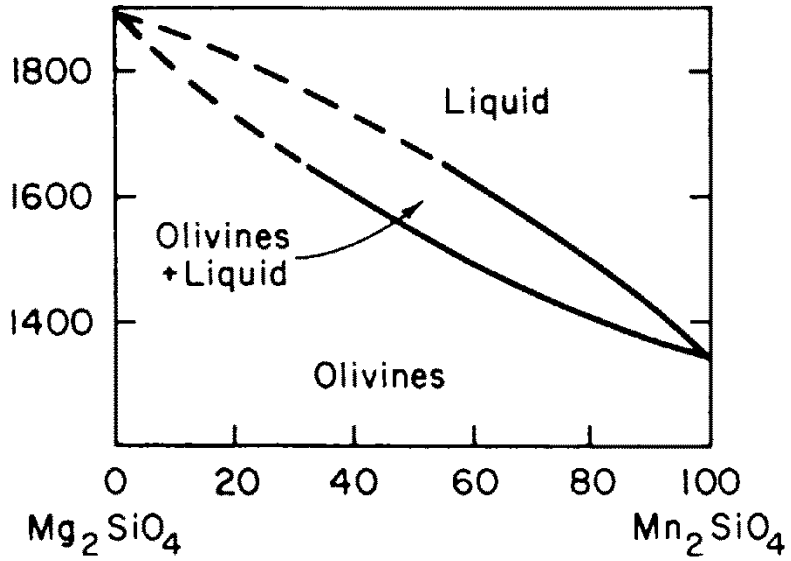

F.P. Glasser, E.F. Osborn, J. Am. Ceram. Soc., 43 [3], (1960), pp. 132-140.

Weight percent, Metasilicate section MgSiO3-MnSiO3 compared with experimental data

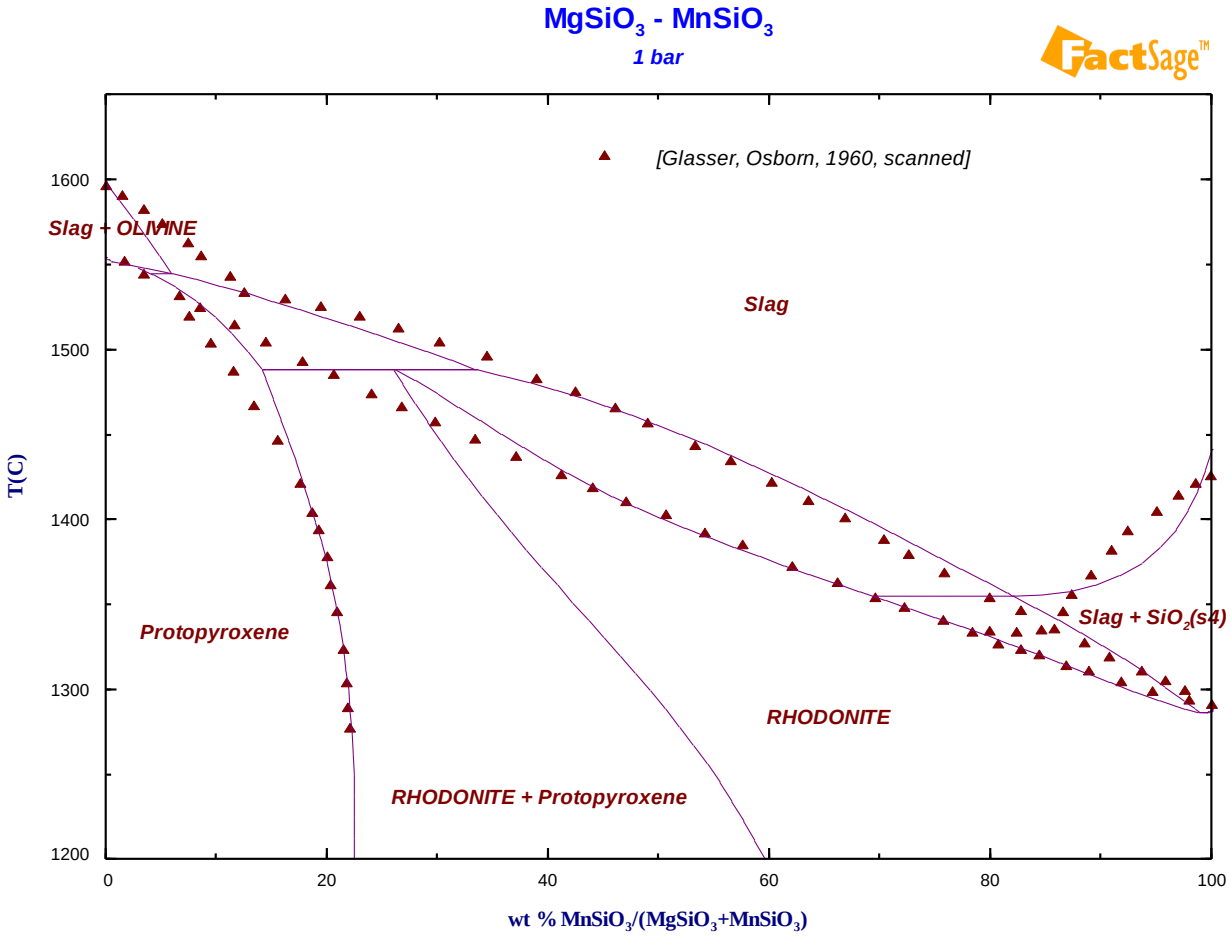

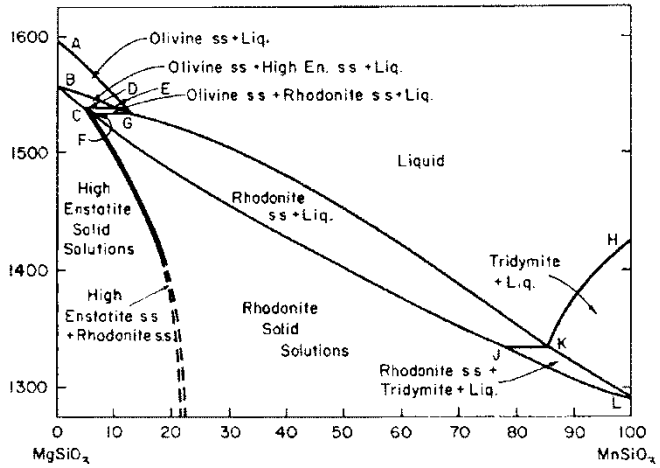

F.P. Glasser, E.F. Osborn, J. Am. Ceram. Soc., 43 [3], (1960), pp. 132-140.

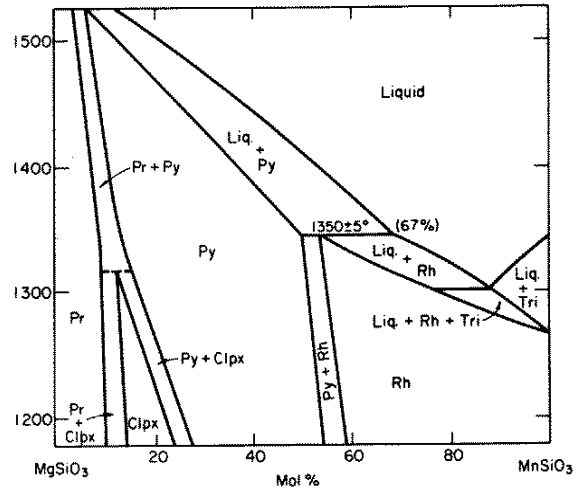

J. Ito, Am. Mineral., 57 [5-6], (1972), pp.865-876.

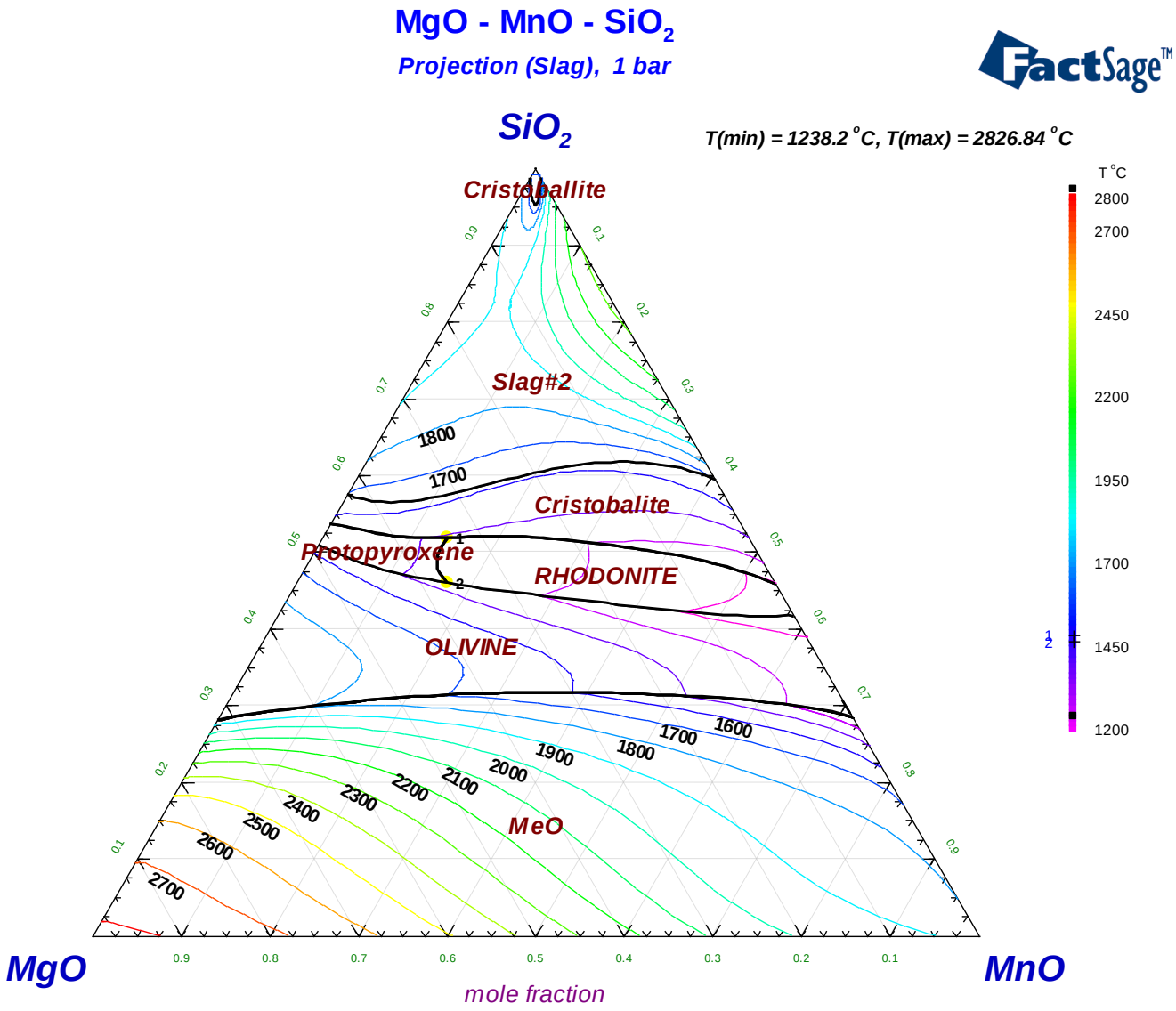
MgO - MnO - SiO2
Projection (Slag), 1 bar
FactSage™
SiO2
T(min) = 1238.2 °C, T(max) = 2826.84 °C
T °C
2800
2700
2450
2200
1950
1700
1450
1200
Cristobalite
Slag#2
1800
1700
Cristobalite
Protopyroxene
RHODONITE
OLIVINE
1700
1600
1900
1800
2000
2100
2200
2300
2400
2500
2600
2700
MeO
MgO
MnO
mole fraction

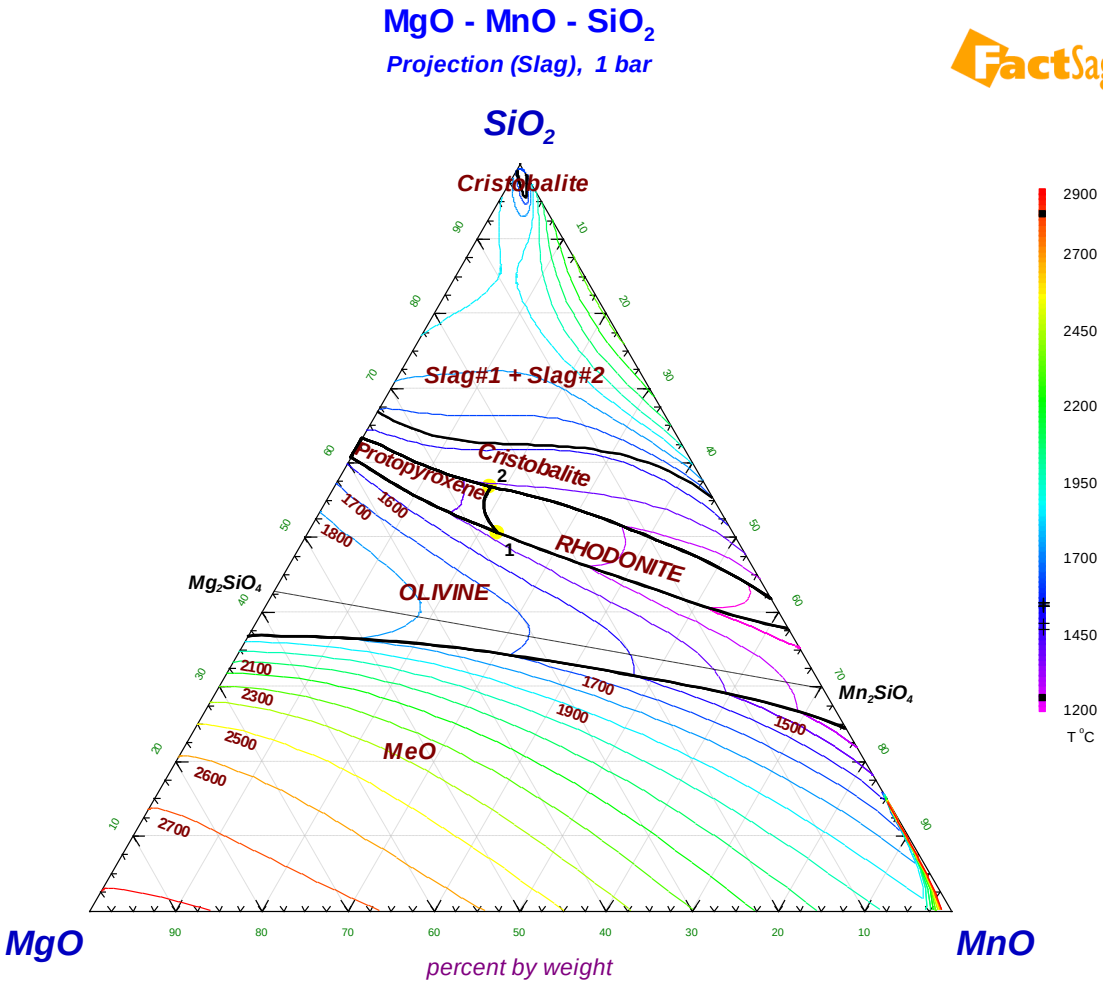

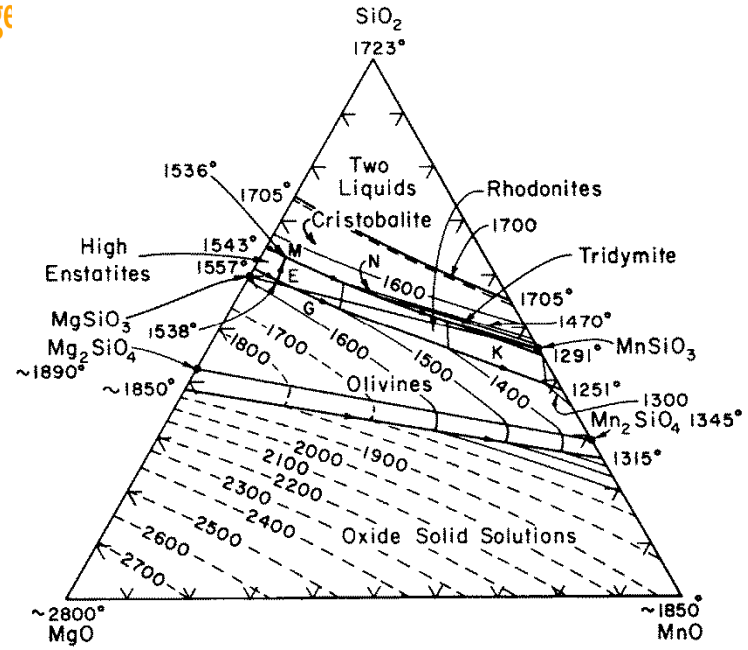

F.P. Glasser, E.F. Osborn, J. Am. Ceram. Soc., 43 [3], (1960), pp. 132-140.

Invariant equilibria on the liquidus surface

Intersections with slag	Mole fraction				Weight percent				
	A = SiO2, B = MgO, C = MnO				A = SiO2, B = MgO, C = MnO				
		X(A)	X(B)	X(C)	T(C)		W(A)	W(B)	W(C)	T(C)
1: Protopyroxene / RHODONITE / Cristobalite	1:	0.51821	0.34089	0.14090	1485.00	1:	56.744	25.040	18.216	1485.00
2: OLIVINE / Protopyroxene / RHODONITE	2:	0.46025	0.36927	0.17048	1464.79	2:	50.620	27.243	22.137	1464.81

MgO-Na2O-P2O5, Ternary phases

Name	Formel	T_m, °C	Liquid species	Description
R	$NaMgPO_4$	968, incongr.		stoichiometric
J	$NaMg_4P_2O_{12}$	1155, incongr.		stoichiometric
T2	$Na_4Mg(PO_4)_2$	1655, congr.	$Na_4Mg(PO_4)_2{\cdot}2/7$	N3P-T2-T3 solution
T3	$Na_6MgP_2O_9$	1665, congr.		N3P-T2-T3 solution
B1	$NaMg(PO_3)_3$	941, incongr.		stoichiometric
B2	$Na_2Mg(PO_3)_4$	916, congr.		stoichiometric
B3	$Na_4Mg(PO_3)_6$	784, incongr.		stoichiometric
F1	$Na_8Mg_6(P_2O_7)_5$	811, congr.	$Na_8Mg_6(P_2O_7)_5{\cdot}1/12$	stoichiometric

Mole fraction, 300°C

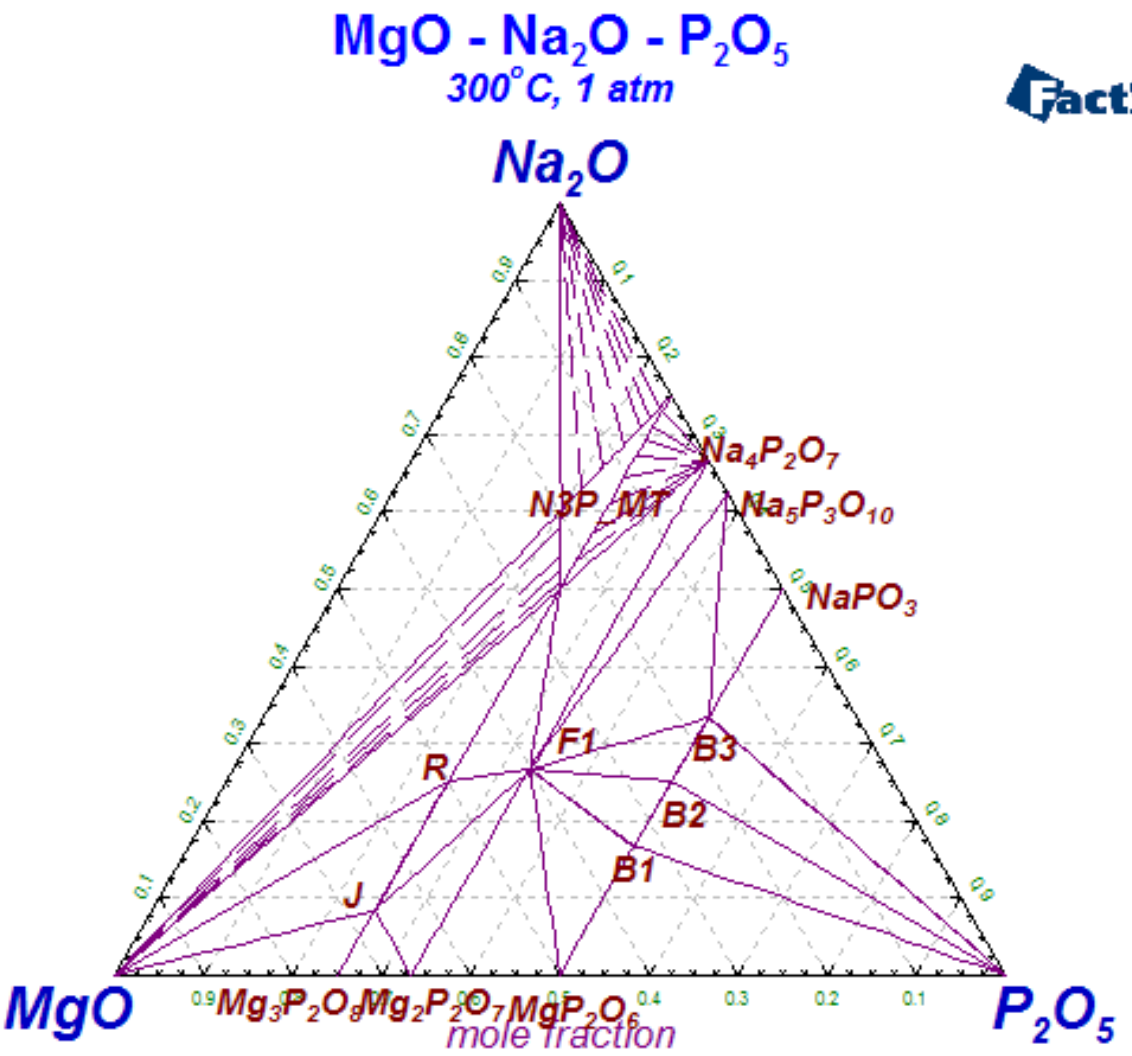

Weight percent, Isopleth NaPO3-Na8Mg6P10O35 compared with experimental data

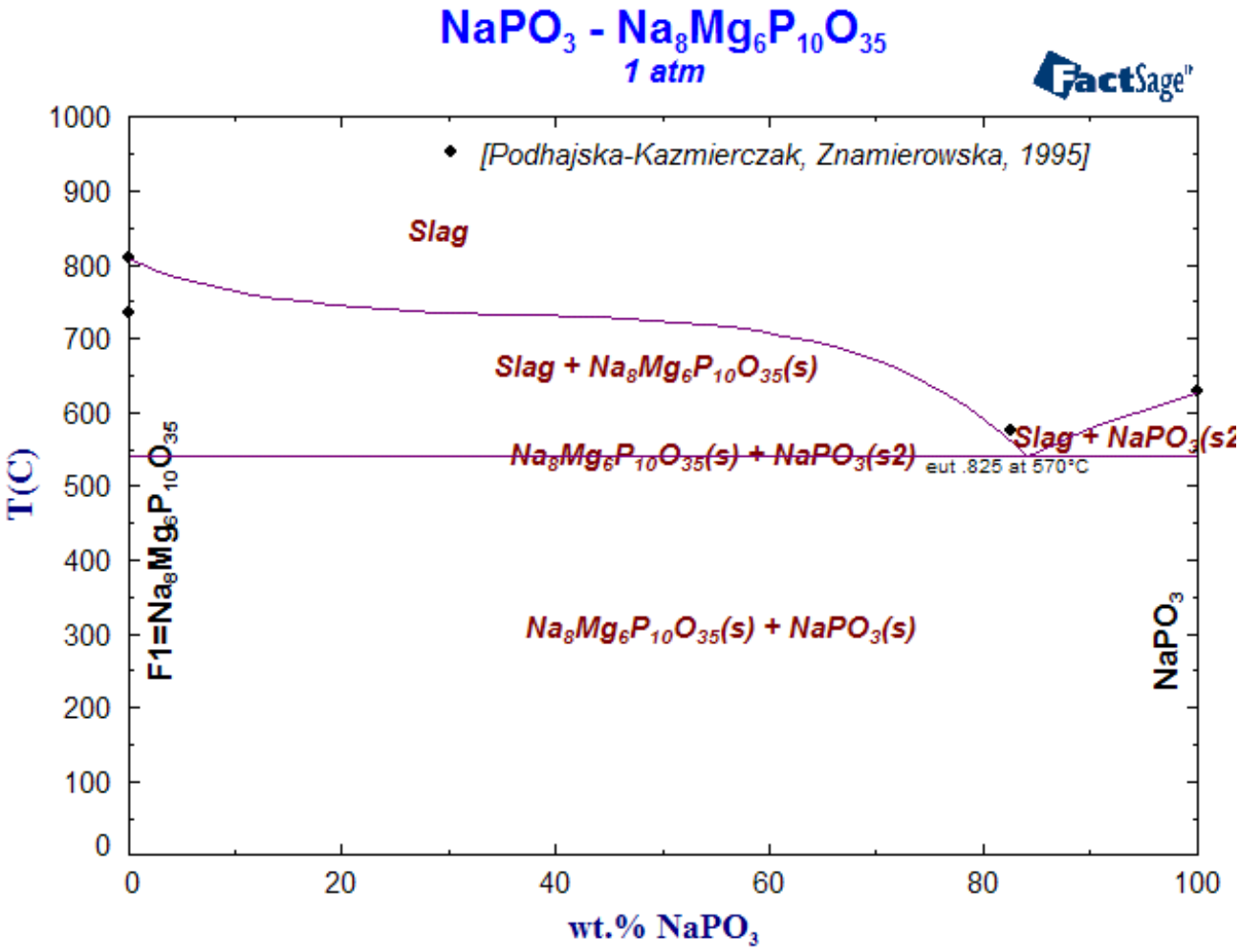

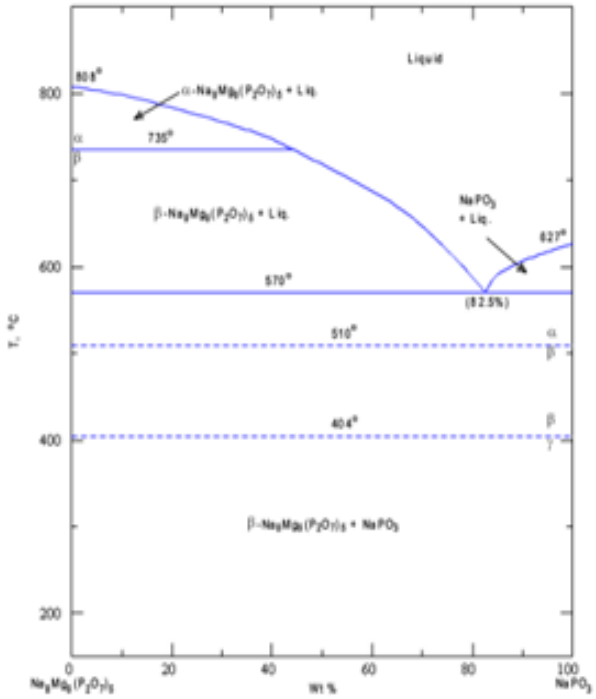

T. Podhajska-Kazmierczak and T. Znamierowska, J. Therm. Anal., 45 [6] 1541-1546 (1995)

Weight percent, Isopleth Na3PO4-Mg3P2O8 compared with experimental data

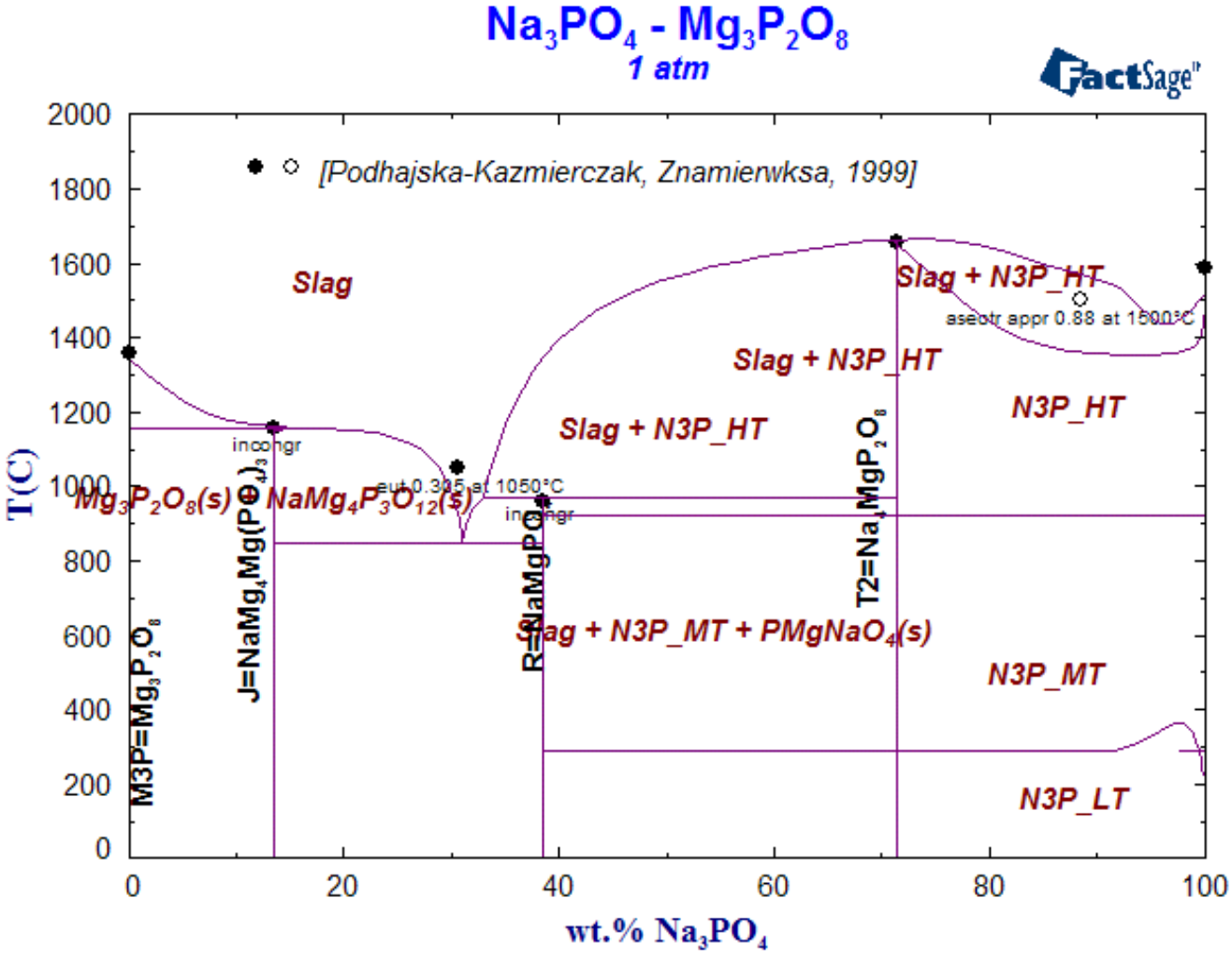

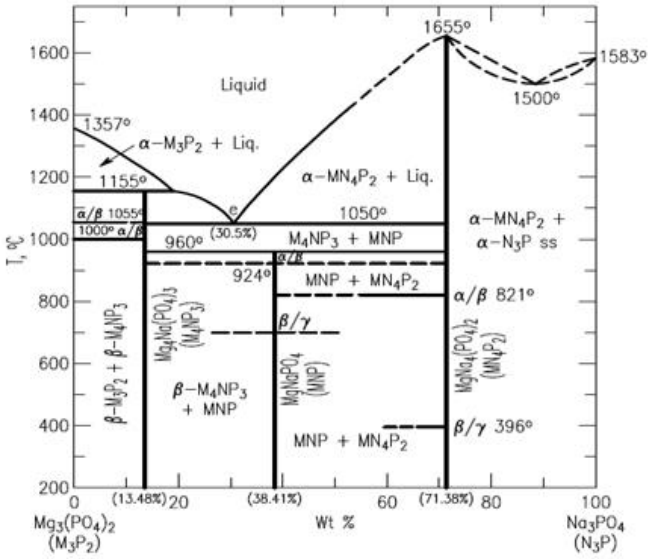

T.Podhajska-Kazmierczak, T.Znamierowska, Pol. J. Chem., 73 [2] 279-286 (1999).

Weight percent, Isopleth MgO-Na3PO4

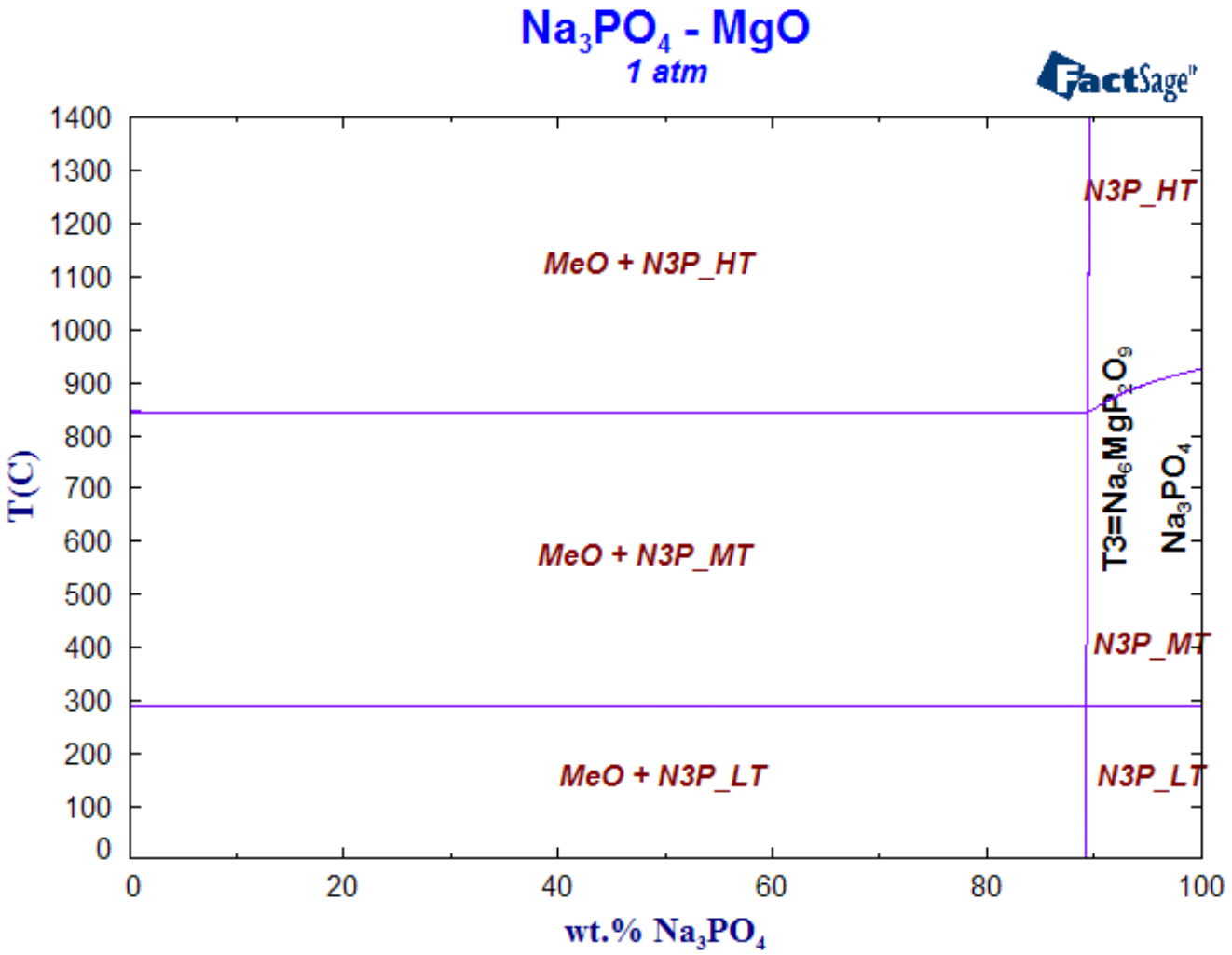

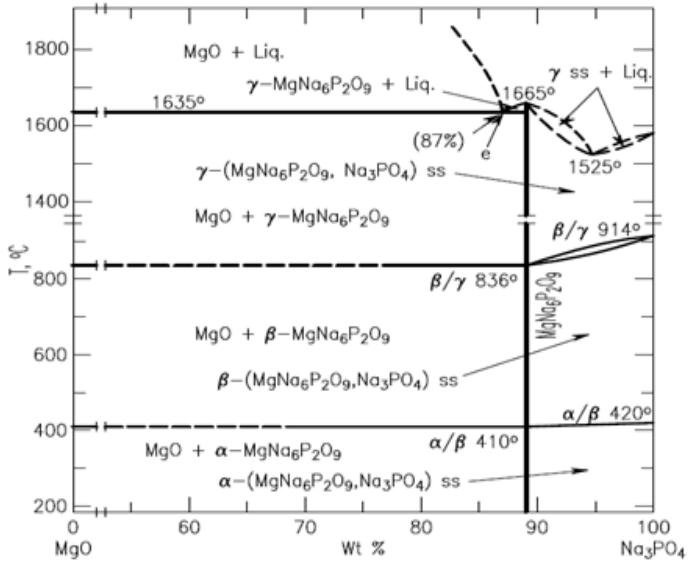

T. Podhajska-Kazmierczak, Pol. J. Chem., 77 [3] 295-301 (2003).

Weight percent, Isopleth MgP2O6-NaPO3 compared with experimental data

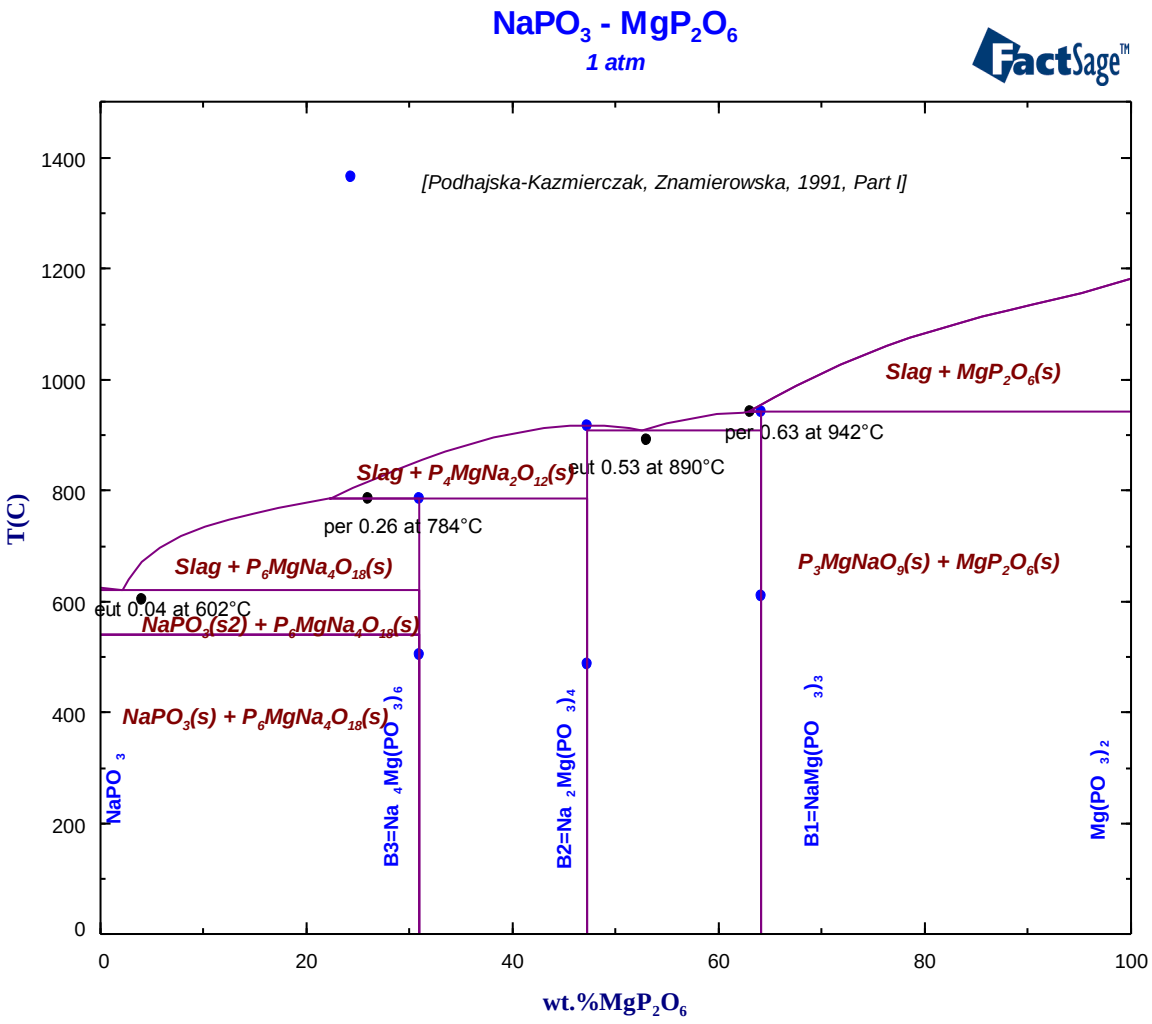

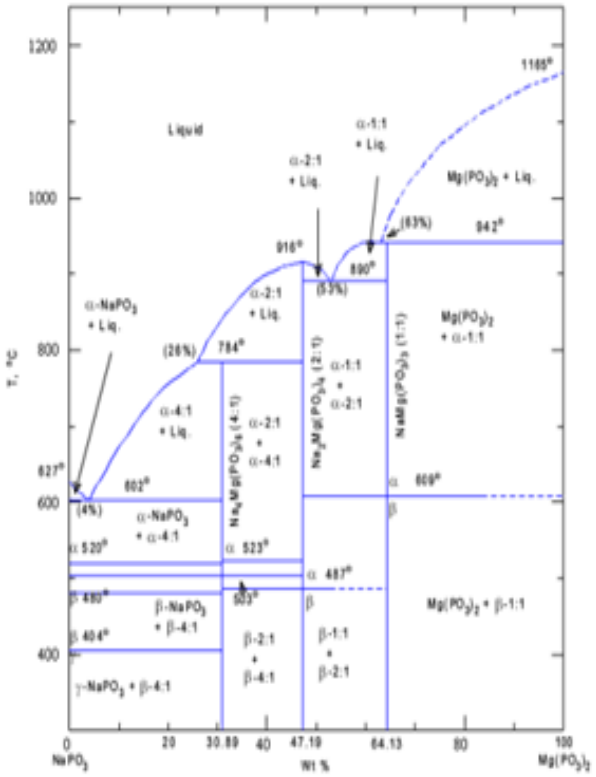

T. Podhajska-Kazmierczak and T. Znamierowska, Pol. J. Chem., 65 [7-8] 1121-1125 (1991).

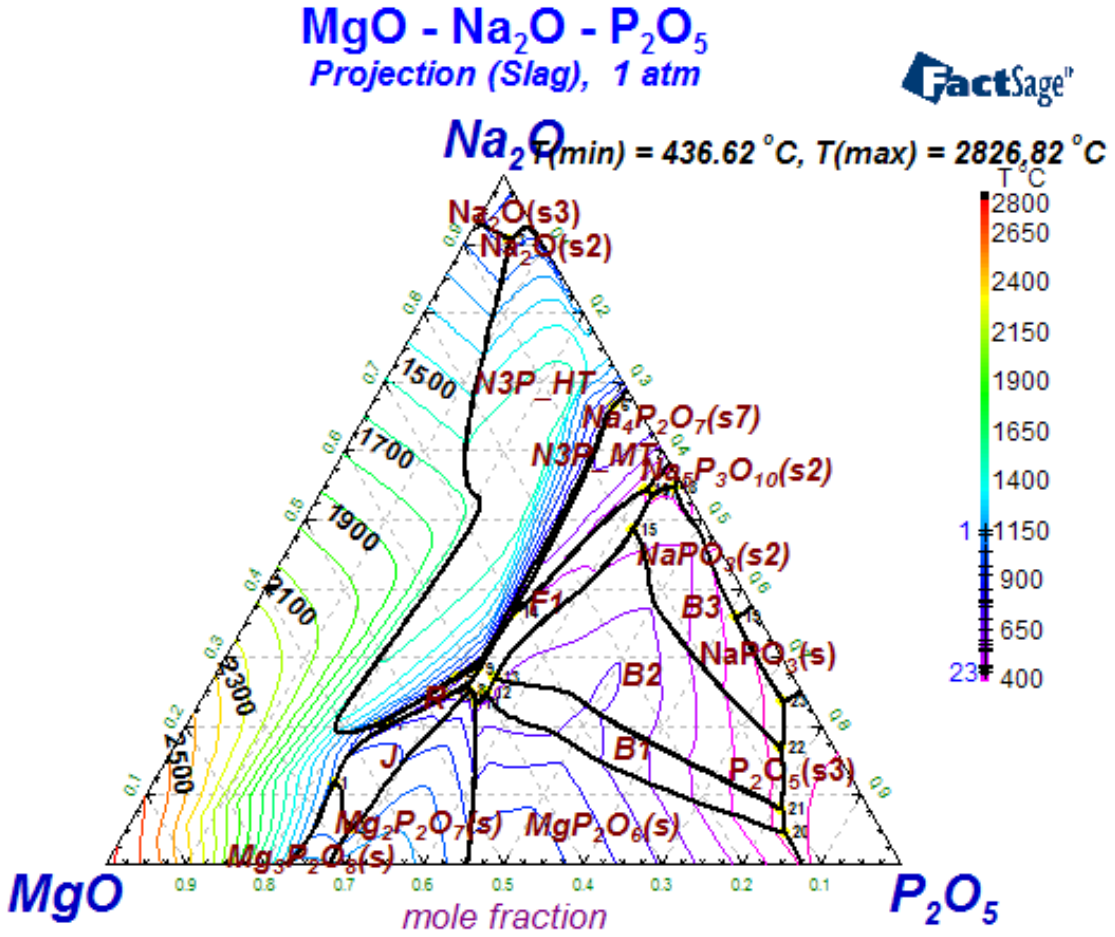
MgO - Na2O - P2O5
Projection (Slag), 1 atm
FactSage
Na2O
T(min) = 436.62 °C, T(max) = 2826.82 °C
T °C
2800
2650
2400
2150
1900
1650
1400
1150
900
650
400
Na2O(s3)
Na2O(s2)
N3P_HT
Na4P2O7(s7)
N3P_MT
Na5P3O10(s2)
NaPO3(s2)
F1
B3
NaPO3(s)
B2
B1
P2O5(s3)
J
Mg2P2O7(s)
MgP2O6(s)
Mg3P2O8(s)
1500
1700
1900
2100
2300
2500
MgO
P2O5
mole fraction

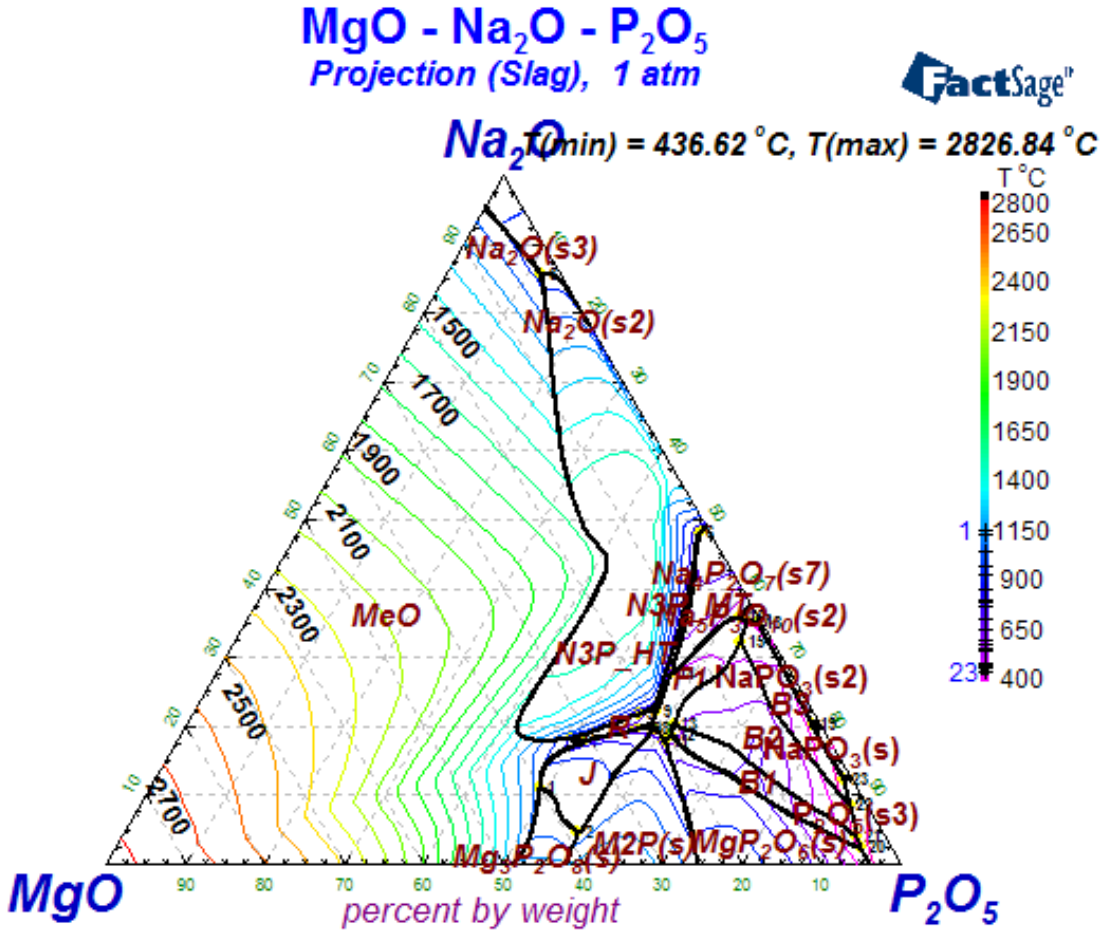
MgO - Na2O - P2O5
Projection (Slag), 1 atm
FactSage
Na2O
T(min) = 436.62 °C, T(max) = 2826.84 °C
T °C
2800
2650
2400
2150
1900
1650
1400
1150
900
650
400
Na2O(s3)
Na2O(s2)
Na4P2O7(s7)
N3P_MT
N3P_HT
NaPO3(s2)
B3
B2
NaPO3(s)
J
B1
P2O5(s3)
M2P(s)
MgP2O6(s)
Mg3P2O8(s)
MeO
1500
1700
1900
2100
2300
2500
2700
MgO
P2O5
percent by weight

Invariant equilibria on the liquidus surface

Intersections with slag	Mole fraction A = Na2O, B = MgO, C = P2O5				Weight percent A = Na2O, B = MgO, C = P2O5				
		X(A)	X(B)	X(C)	T(C)		W(A)	W(B)	W(C)	T(C)
1: MeO / Mg3P2O8(s) / NaMg4P3O12_J	1:	0.11576	0.65616	0.22808	1148.36	1:	10.872	40.072	49.056	1148.36
2: Mg2P2O7(s) / Mg3P2O8(s) / NaMg4P3O12_J	2:	0.05033	0.66713	0.28254	1126.74	2:	4.449	38.350	57.201	1126.74
3: MeO / N3P_HT / Na2O(s3)	3:	0.90573	0.03895	0.05531	1040.27	3:	85.629	2.395	11.976	1040.27
4: MeO / N3P_HT / PMgNaO4_R	4:	0.20469	0.55214	0.24317	967.80	4:	18.265	32.040	49.695	967.80
5: N3P_HT / N3P_MT / PMgNaO4_R	5:	0.27098	0.42308	0.30594	922.40	5:	21.734	22.067	56.199	922.40
6: N3P_HT / N3P_MT / Na4P2O7_S7(s7)	6:	0.66477	0.02929	0.30594	922.38	6:	48.016	1.376	50.609	922.38
7: MeO / NaMg4P3O12_J / PMgNaO4_R	7:	0.20228	0.54231	0.25541	843.66	7:	17.746	30.938	51.316	843.66
8: Mg2P2O7(s) / Na8Mg6P10O35 / NaMg4P3O12_J	8:	0.25182	0.41709	0.33109	793.41	8:	19.654	21.168	59.178	793.37
9: N3P_MT / Na8Mg6P10O35 / PMgNaO4_R	9:	0.28288	0.39004	0.32709	781.71	9:	22.003	19.729	58.268	781.61
10: Na8Mg6P10O35 / NaMg4P3O12_J / PMgNaO4_R	10:	0.24441	0.44744	0.30815	780.81	10:	19.693	23.444	56.863	780.81
11: Mg2P2O7(s) / MgP2O6(s) / Na8Mg6P10O35	11:	0.23325	0.41674	0.35002	768.45	11:	17.861	20.753	61.386	767.97
12: MgP2O6(s) / Na8Mg6P10O35 / P3MgNaO9_B1	12:	0.24684	0.39690	0.35627	761.43	12:	18.688	19.540	61.772	761.36
13:Na8Mg6P10O35/P3MgNaO9_B1/P4MgNa2O12_B2	13:	0.26884	0.37614	0.35502	758.92	13:	20.267	18.439	61.294	758.92
14: N3P_MT / Na4P2O7(s7) / Na8Mg6P10O35	14:	0.36583	0.30422	0.32995	696.79	14:	27.729	14.995	57.276	696.79
15: Na8Mg6P10O35/P4MgNa2O12/P6MgNa4O18_B3	15:	0.48407	0.09554	0.42039	643.32	15:	32.079	4.118	63.8.03	643.36
16: Na4P2O7(s7) / Na5P3O10(s2) / Na8Mg6P10O35	16:	0.54275	0.05054	0.40671	594.82	16:	36.014	2.181	61.805	594.82
17: Na5P3O10(s2)/Na8Mg6P10O35/P6MgNa4O18_B3	17:	0.53638	0.04358	0.42004	573.48	17:	35.133	1.856	63.011	573.48
18: Na5P3O10(s2) / NaPO3(s2) / P6MgNa4O18_B3	18:	0.54629	0.01265	0.44106	549.50	18:	34.915	0.526	64.559	549.53
19: NaPO3(s2) / NaPO3(s) / P6MgNa4O18_B3	19:	0.35779	0.02895	0.61327	539.35	19:	20.087	1.057	78.856	539.40
20: MgP2O6(s) / P2O5(s3) / P3MgNaO9_B1	20:	0.04628	0.12354	0.83018	471.28	20:	2.282	3.962	93.756	471.28
21: P2O5(s3) / P3MgNaO9_B1 / P4MgNa2O12_B2	21:	0.08023	0.11019	0.80958	470.38	21:	4.000	3.572	92.428	470.38
22: P2O5(s3) / P4MgNa2O12_B2 / P6MgNa4O18_B3	22:	0.16699	0.06749	0.76552	457.71	22:	8.502	2.235	89.263	457.71
23: NaPO3(s) / P2O5(s3) / P6MgNa4O18_B3	23:	0.23579	0.03011	0.73409	436.62	23:	12.176	1.011	86.813	436.62

MgO-Na2O-SiO2, Mole fraction 600°C

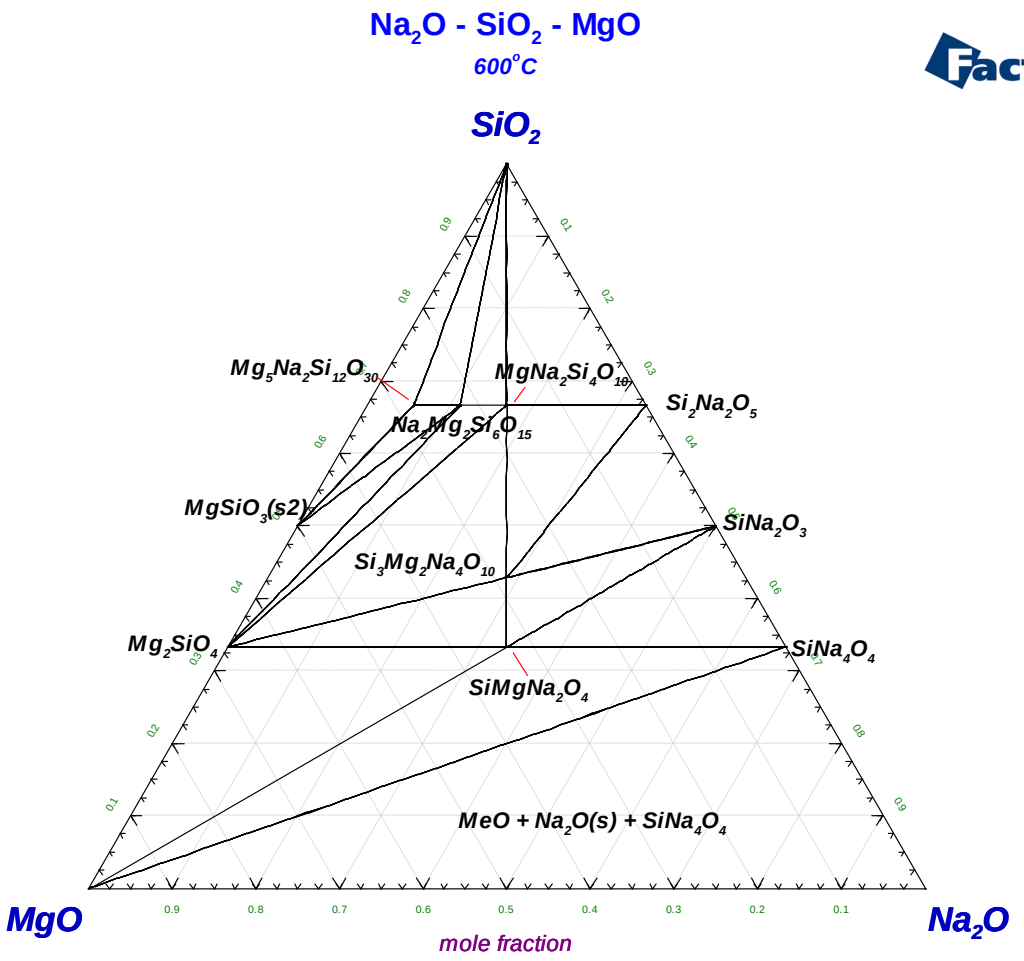

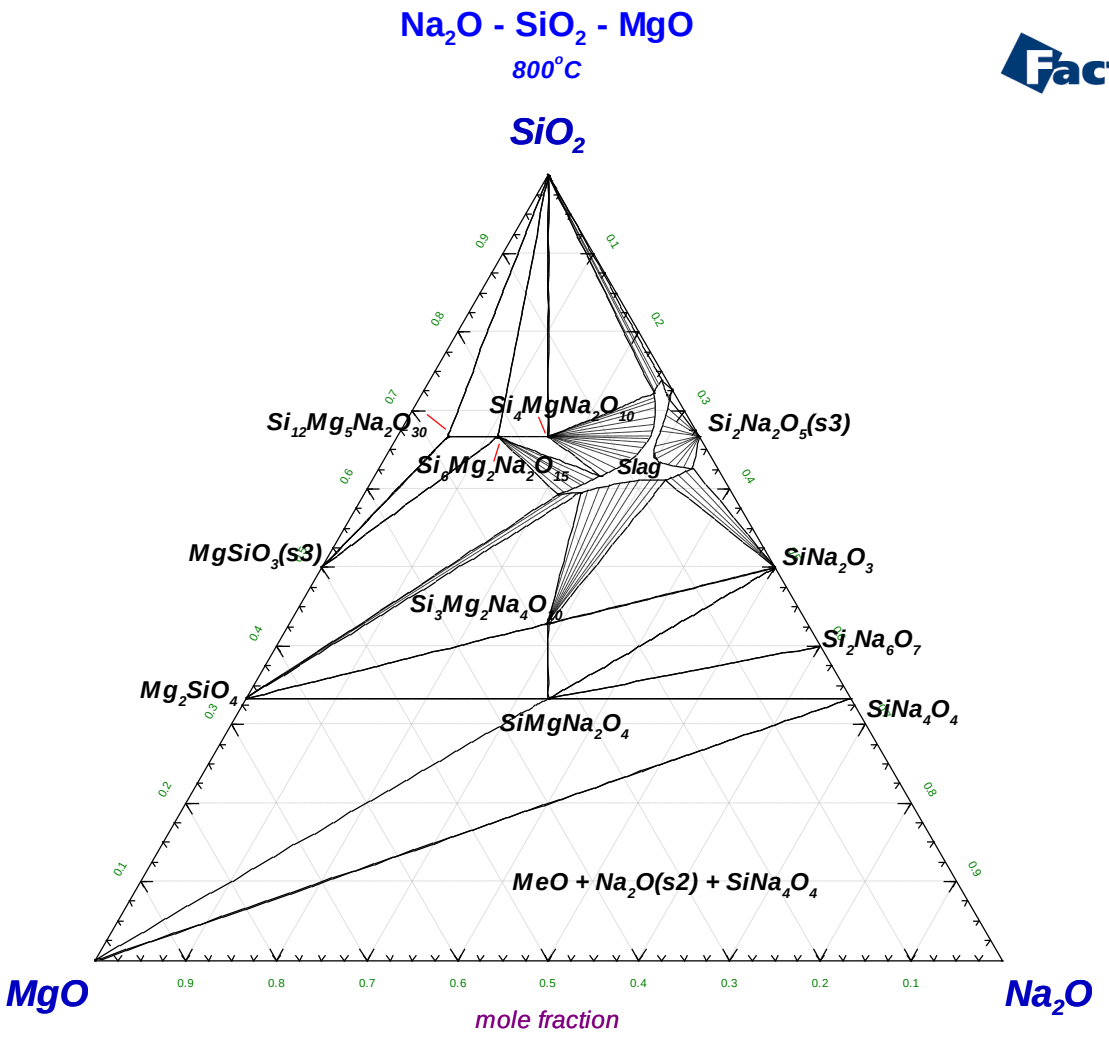
Na2O - SiO2 - MgO
800°C
FactSage™
SiO2
Si12Mg5Na2O30
Si4MgNa2O10
Si2Na2O5(s3)
Si6Mg2Na2O15
Slag
MgSiO3(s3)
SiNa2O3
Si3Mg2Na4O10
Si2Na6O7
Mg2SiO4
SiNa4O4
SiMgNa2O4
MeO + Na2O(s2) + SiNa4O4
MgO
Na2O
mole fraction

Na_2O - SiO_2 - MgO

1200°C

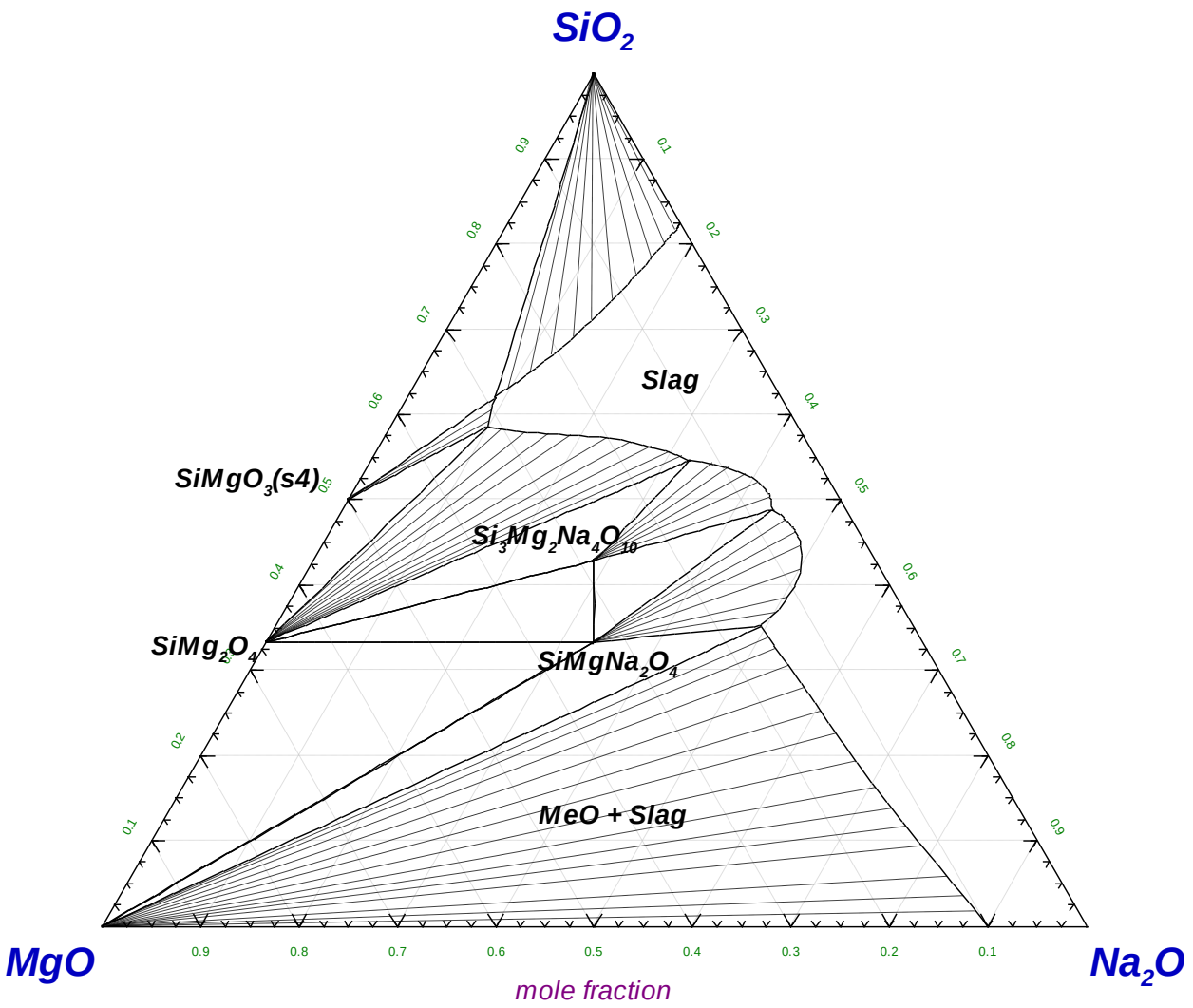

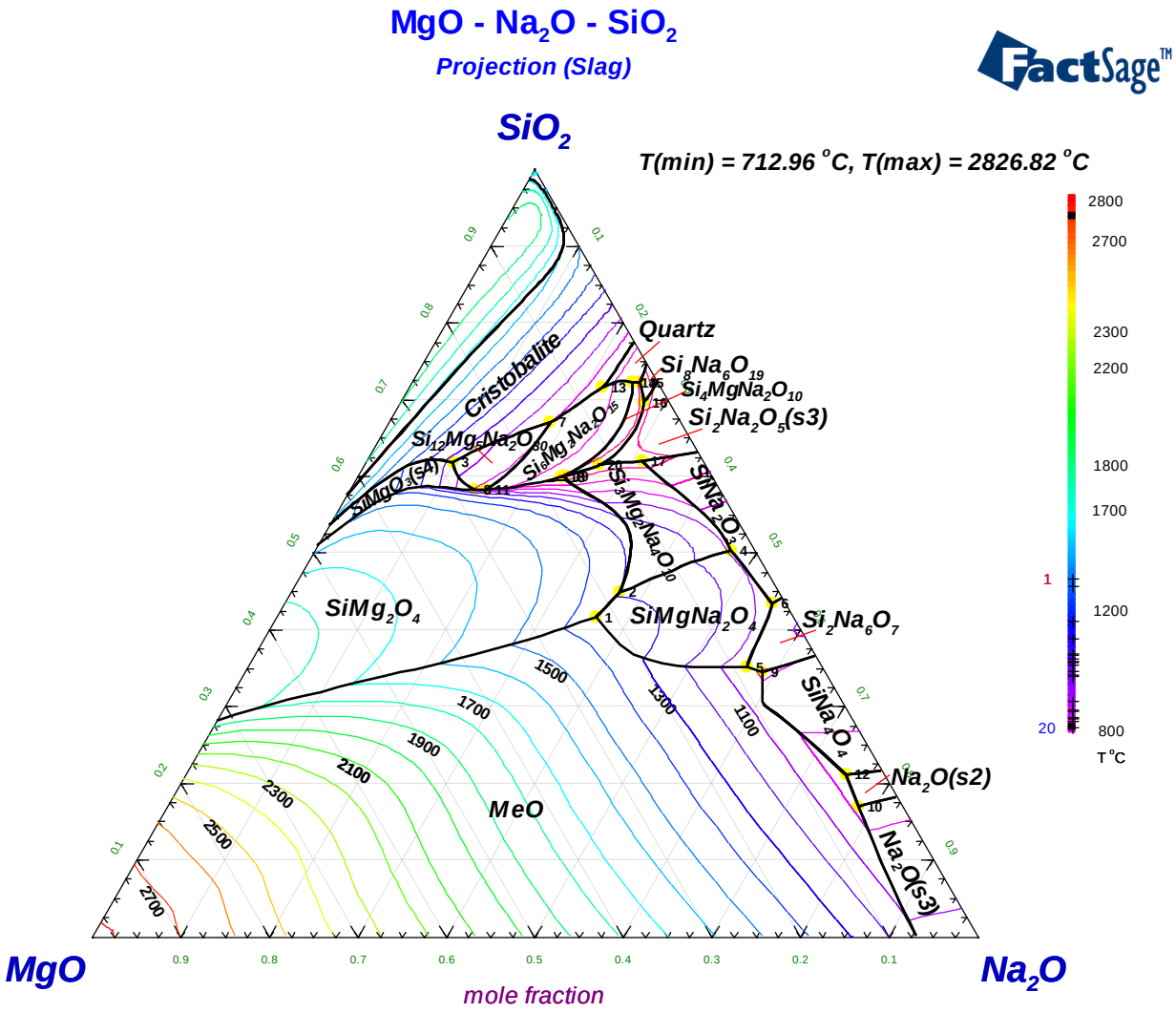
MgO - Na2O - SiO2
Projection (Slag)
FactSage™
SiO2
T(min) = 712.96 °C, T(max) = 2826.82 °C
Quartz
Si8Na6O19
Si4MgNa2O10
Si2Na2O5(s3)
Cristobalite
Si12Mg5Na2O30
Si6Mg1Na2O15
SiMgO3(s4)
Si3Mg2Na4O10
SiNa2O3
SiMg2O4
SiMgNa2O4
Si2Na6O7
SiNa4O4
Na2O(s2)
Na2O(s3)
MeO
1500
1700
1900
2100
2300
2500
2700
1300
1100
2800
2700
2300
2200
1800
1700
1200
800
T°C
MgO
Na2O
mole fraction

Weight percent
Liquidussurface

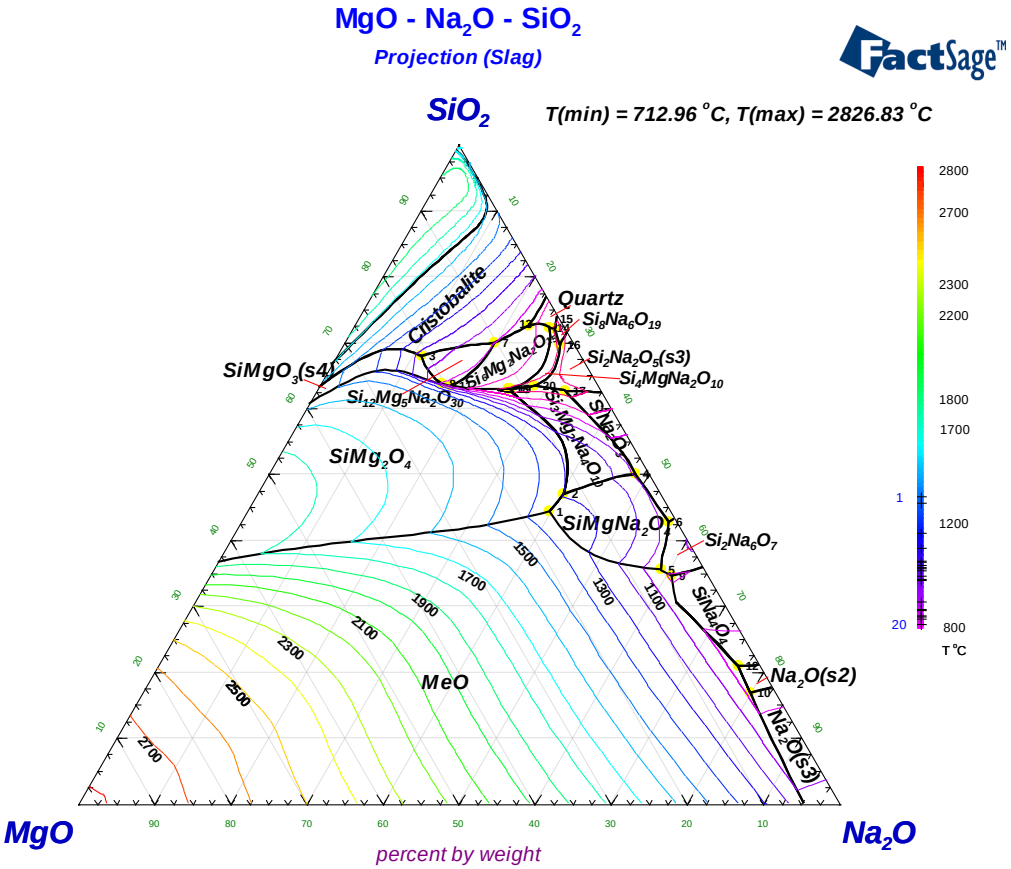

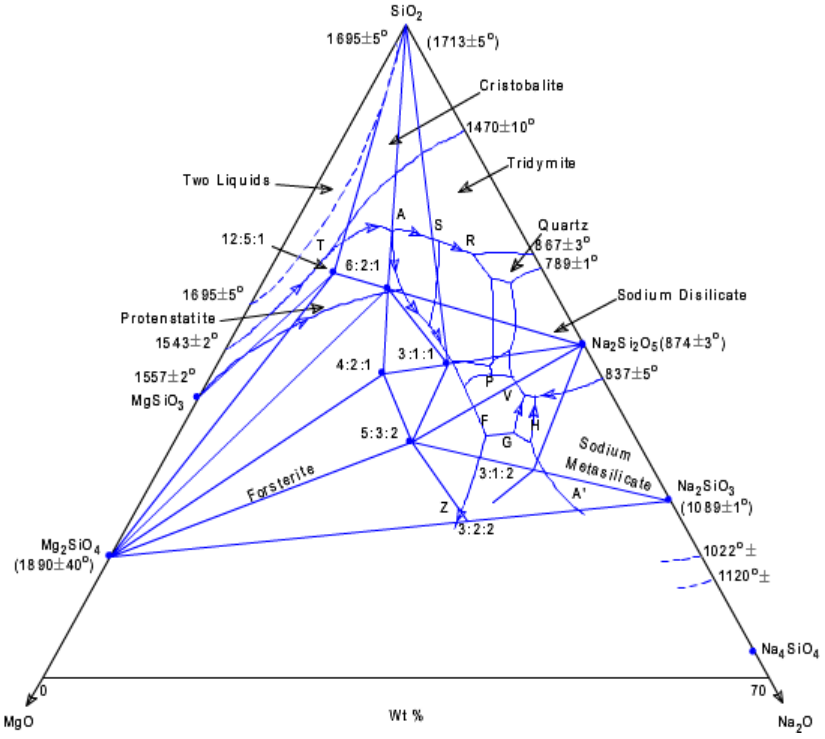

J. F. Schairer, J. Am. Ceram. Soc., 40 [7] 215-235 (1957).

Invariant equilibria on the liquidus surface

Intersections with slag	Mole fraction A = SiO2, B = MgO, C = Na2O				Weight percent A = SiO2, B = MgO, C = Na2O				
		X(A)	X(B)	X(C)	T(C)		W(A)	W(B)	W(C)	T(C)
1: MeO / SiMg2O4 / SiMgNa2O4	1:	0.41659	0.22201	0.36140	1326.64	1:	44.398	15.872	39.730	1326.64
2: Si3Mg2Na4O10 / SiMg2O4 / SiMgNa2O4	2:	0.44814	0.17965	0.37222	1294.45	2:	47.044	12.650	40.306	1294.45
3: Si12Mg5Na2O30 / SiMgO3(s4) / Cristobalite	3:	0.61809	0.28377	0.09815	1153.71	3:	67.946	20.925	11.129	1153.71
4: Si3Mg2Na4O10 / SiMgNa2O4 / SiNa2O3	4:	0.50311	0.02680	0.47010	1078.19	4:	50.010	1.787	48.203	1078.17
5: MeO / Si2Na6O7 / SiMgNa2O4	5:	0.35161	0.08395	0.56445	1017.93	5:	35.510	5.687	58.803	1017.97
6: Si2Na6O7 / SiMgNa2O4 / SiNa2O3	6:	0.43344	0.01490	0.55165	1012.77	6:	42.810	0.987	56.203	1012.77
7: Si12Mg5Na2O30 / Si6Mg2Na2O15 / Cristobalite	7:	0.66963	0.14727	0.18310	995.54	7:	69.951	10.319	19.730	995.54
8: Si12Mg5Na2O30 / SiMg2O4 / SiMgO3(s4)	8:	0.58222	0.27644	0.14134	985.10	8:	63.738	20.301	15.961	985.12
9: MeO / Si2Na6O7 / SiNa4O4	9:	0.34424	0.07041	0.58536	981.48	9:	34.587	4.745	60.668	981.48
10: MeO / Na2O(s2) / Na2O(s3)	10:	0.16922	0.04891	0.78187	970.05	10:	16.779	3.253	79.968	970.05
11: Si12Mg5Na2O30 / Si6Mg2Na2O15 / SiMg2O4	11:	0.58257	0.26292	0.15451	943.31	11:	63.439	19.205	17.355	943.31
12: MeO / Na2O(s2) / SiNa4O4	12:	0.21086	0.04254	0.74659	930.49	12:	20.887	2.827	76.286	930.49
13: Si6Mg2Na2O15 / Cristobalite / Quartz	13:	0.71560	0.06512	0.21927	926.28	13:	72.615	4.433	22.952	926.28
14: Si4MgNa2O10 / Si6Mg2Na2O15 / Quartz	14:	0.72215	0.02781	0.25003	819.99	14:	72.307	1.868	25.825	819.98
15: Si4MgNa2O10 / Si8Na6O19 / Quartz	15:	0.72191	0.01947	0.25862	785.60	15:	72.065	1.304	26.631	785.61
16: Si2Na2O5(s3) / Si4MgNa2O10 / Si8Na6O19	16:	0.69581	0.02838	0.27581	780.07	16:	69.626	1.905	28.470	780.07
17: Si2Na2O5(s3) / Si3Mg2Na4O10 / SiNa2O3	17:	0.61893	0.06874	0.31233	755.11	17:	62.695	4.671	32.635	755.11
18: Si4MgNa2O10 / Si6Mg2Na2O15 / SiMg2O4	18:	0.59848	0.17034	0.23118	748.11	18:	62.918	12.012	25.070	748.11
19: Si3Mg2Na4O10 / Si4MgNa2O10 / SiMg2O4	19:	0.59945	0.16602	0.23453	740.29	19:	62.918	11.689	25.393	740.29
20: Si2Na2O5(s3) / Si3Mg2Na4O10 / Si4MgNa2O10	20:	0.61403	0.11990	0.26607	712.96	20:	63.372	8.301	28.326	712.96

MgO-P2O5-SiO2,
Weight fraction, Isopleth Mg3P2O8-SiO2

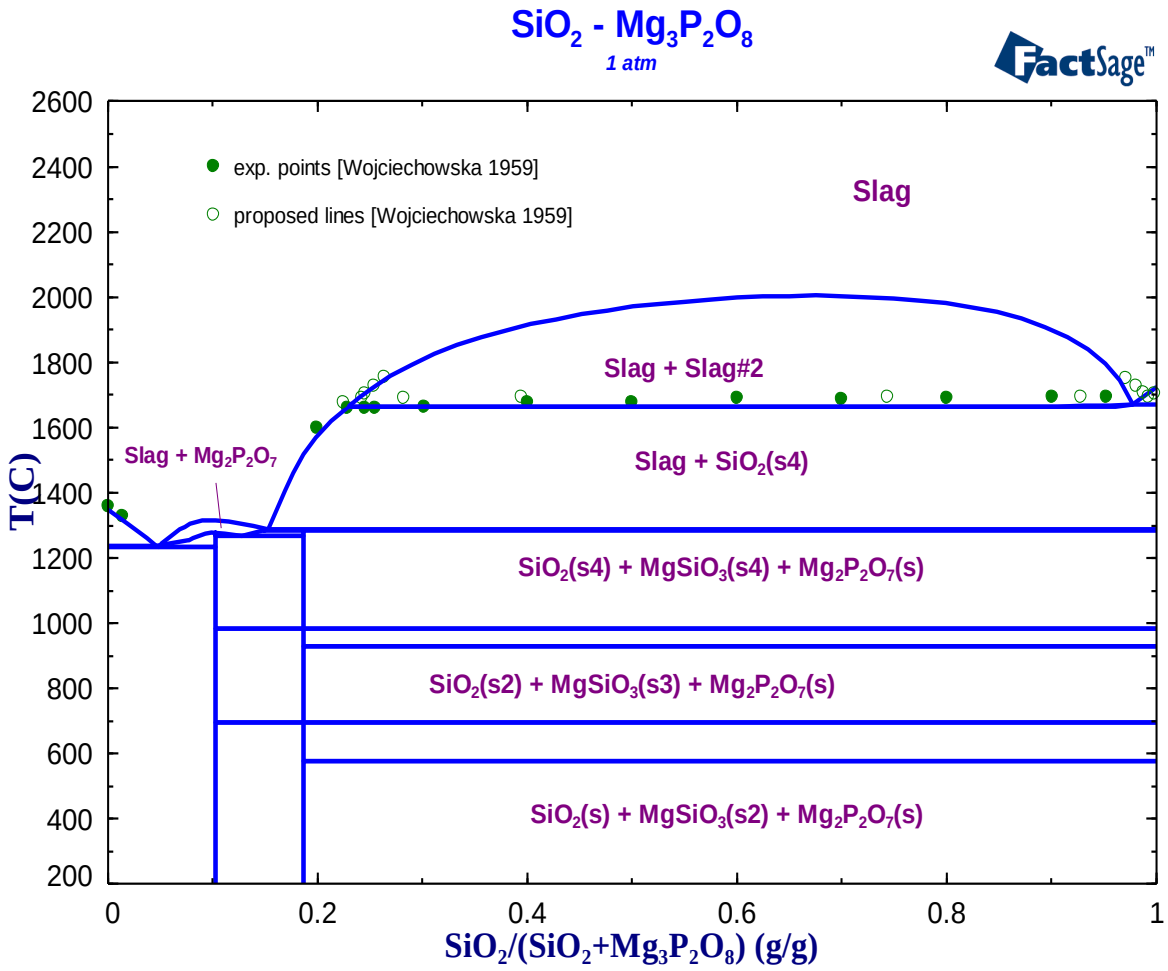

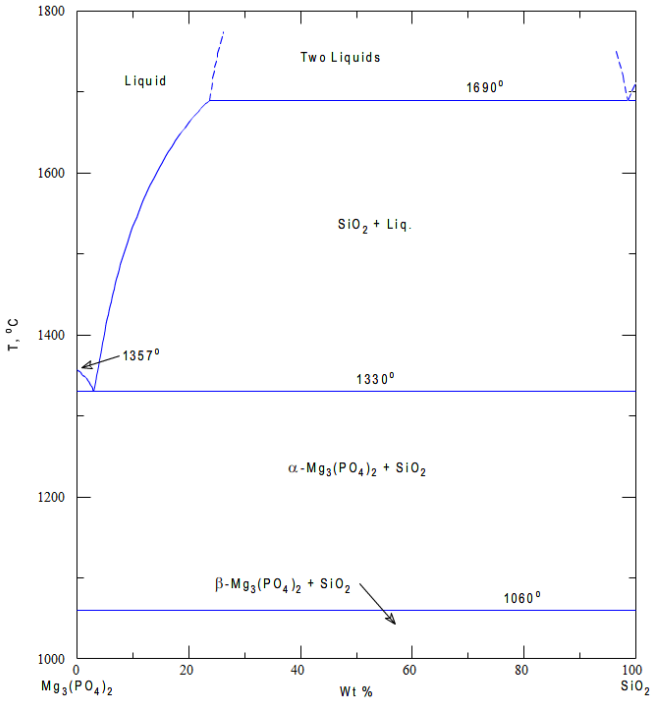

J. Wojciechowska, J. Berak, Rocz. Chem., 33[1] 21-31 (1959).

MgO-P2O5-SiO2,

Gewichtsanteil, Isopleth Mg3P2O8-Mg2SiO4

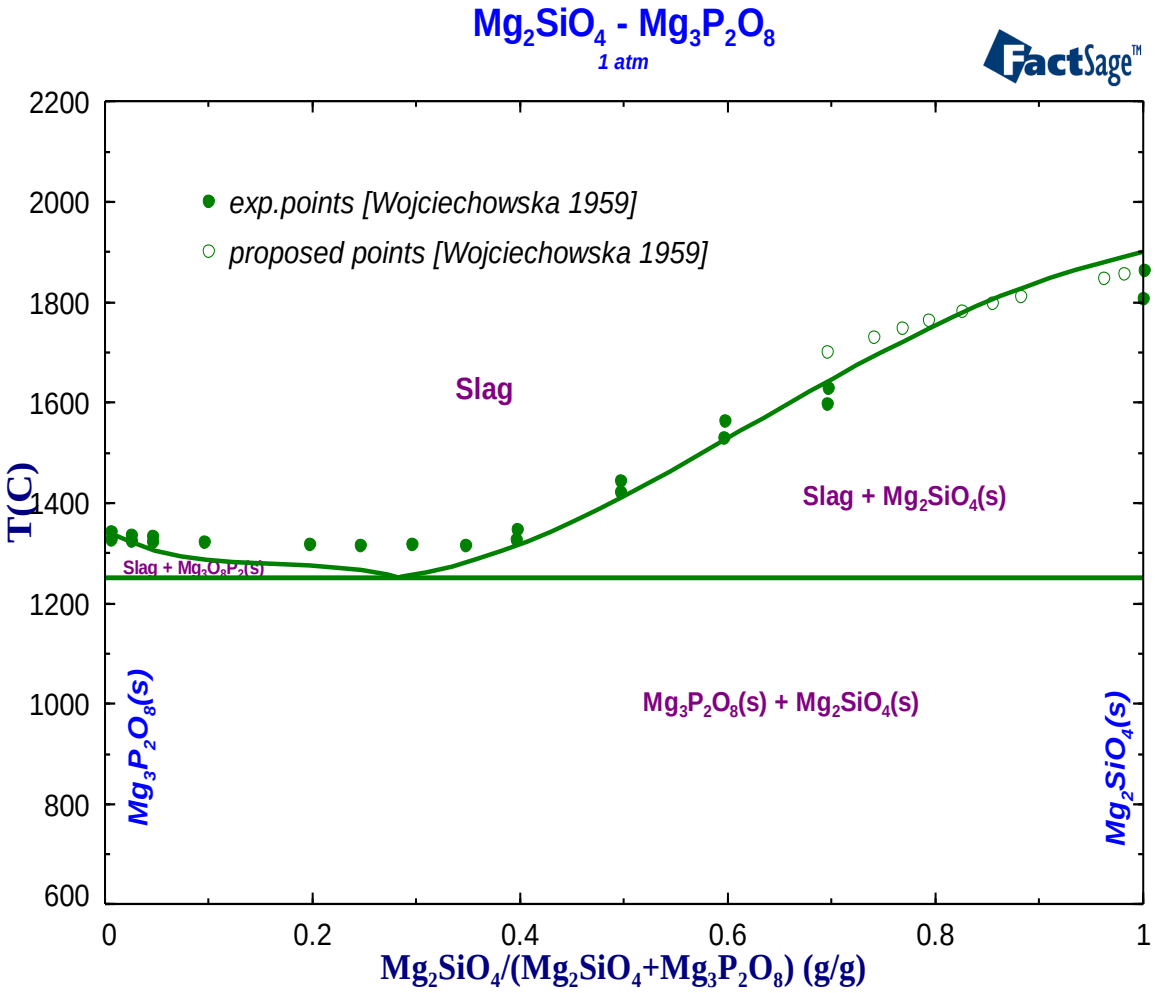

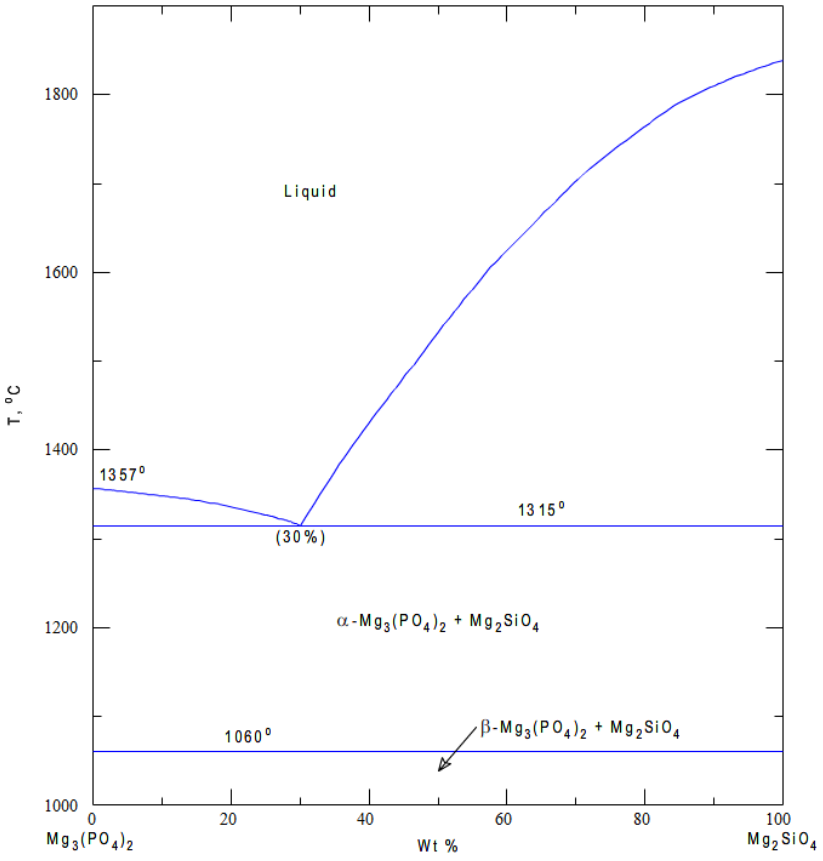

J. Wojciechowska, J. Berak, Rocz. Chem., 33[1] 21-31 (1959).

MgO-P2O5-SiO2,

Gewichtsanteil, Isopleth Mg3P2O8-MgSiO3

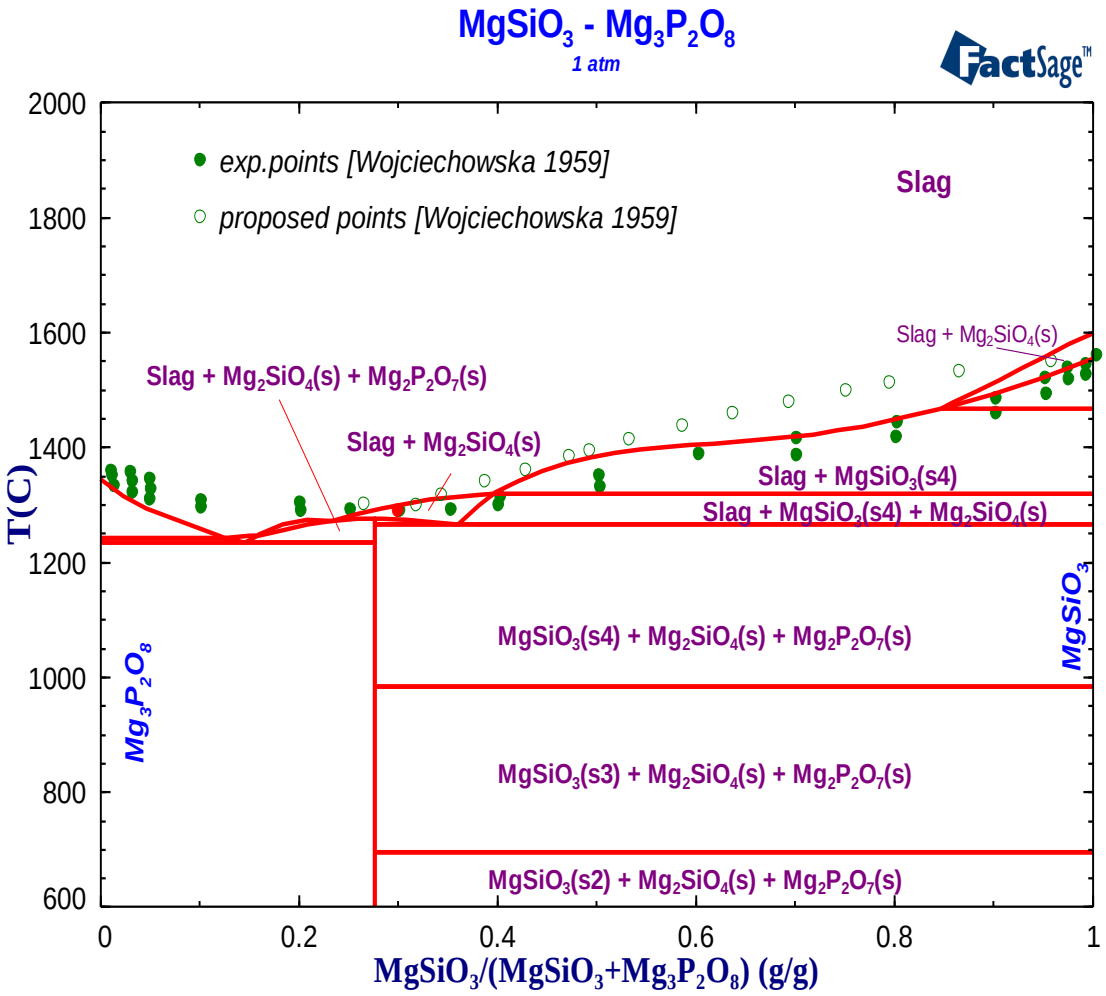

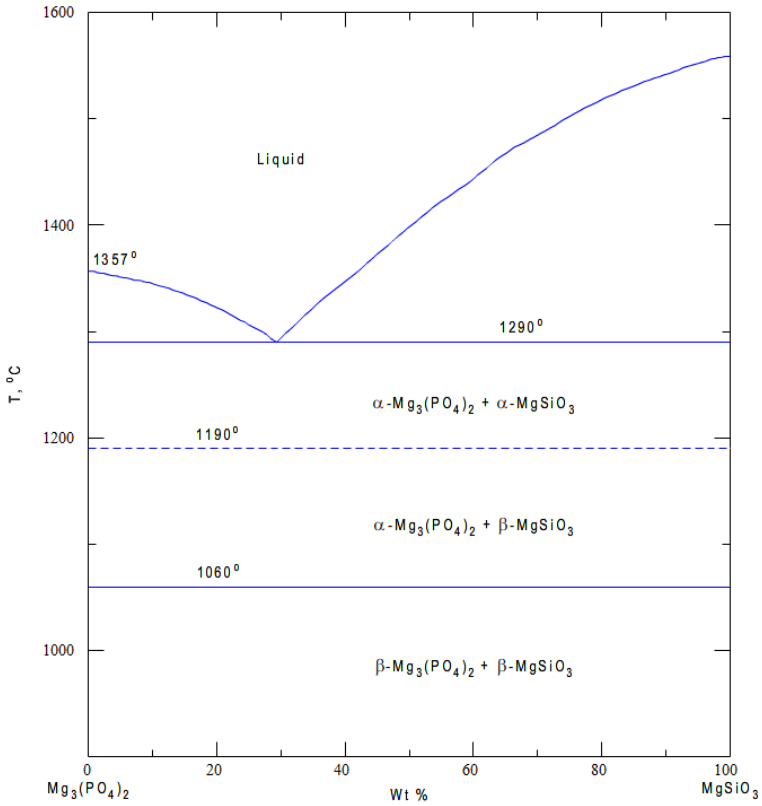

J. Wojciechowska, J. Berak, Rocz. Chem., 33[1] 21-31 (1959).

Mole fraction, Liquidussurface

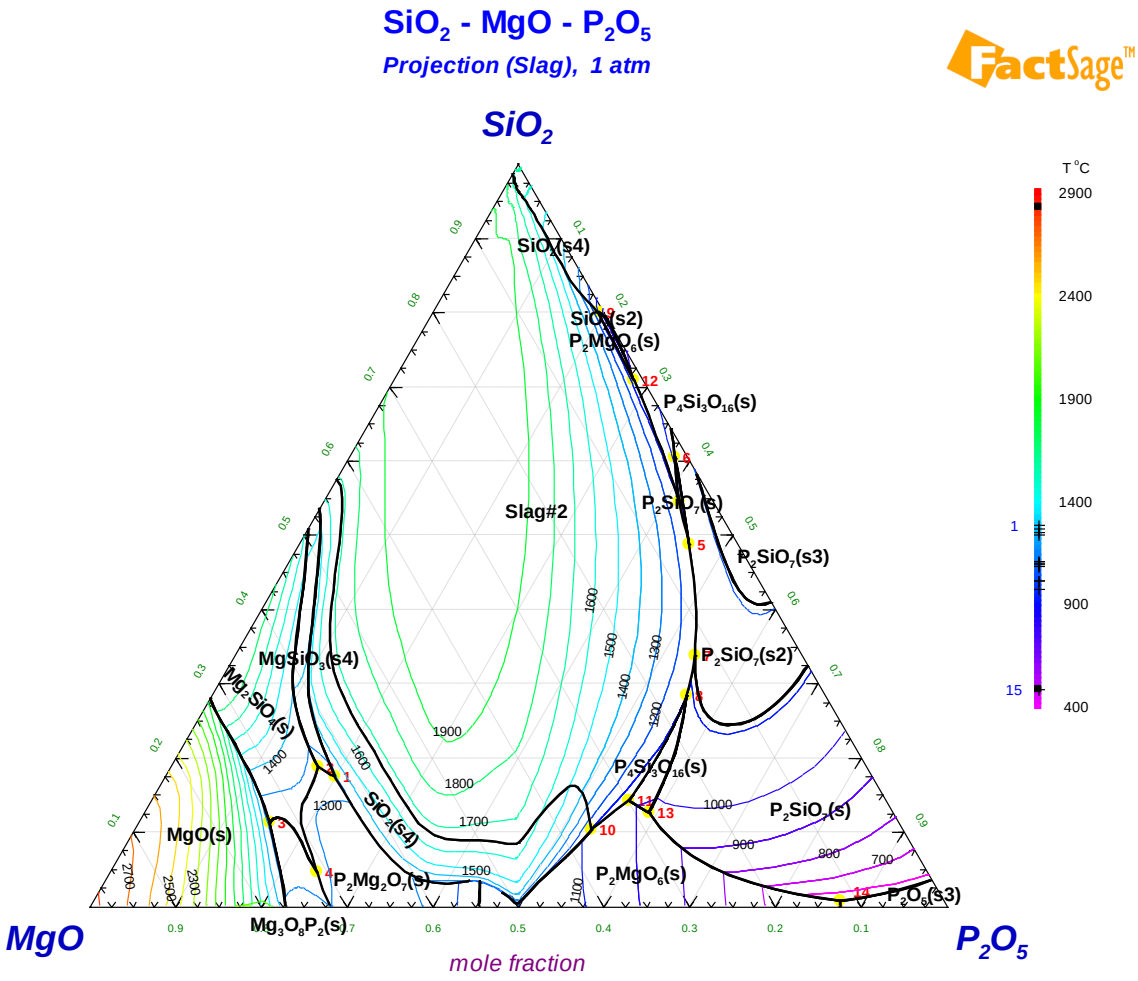

Weight percent, Liquidussurface

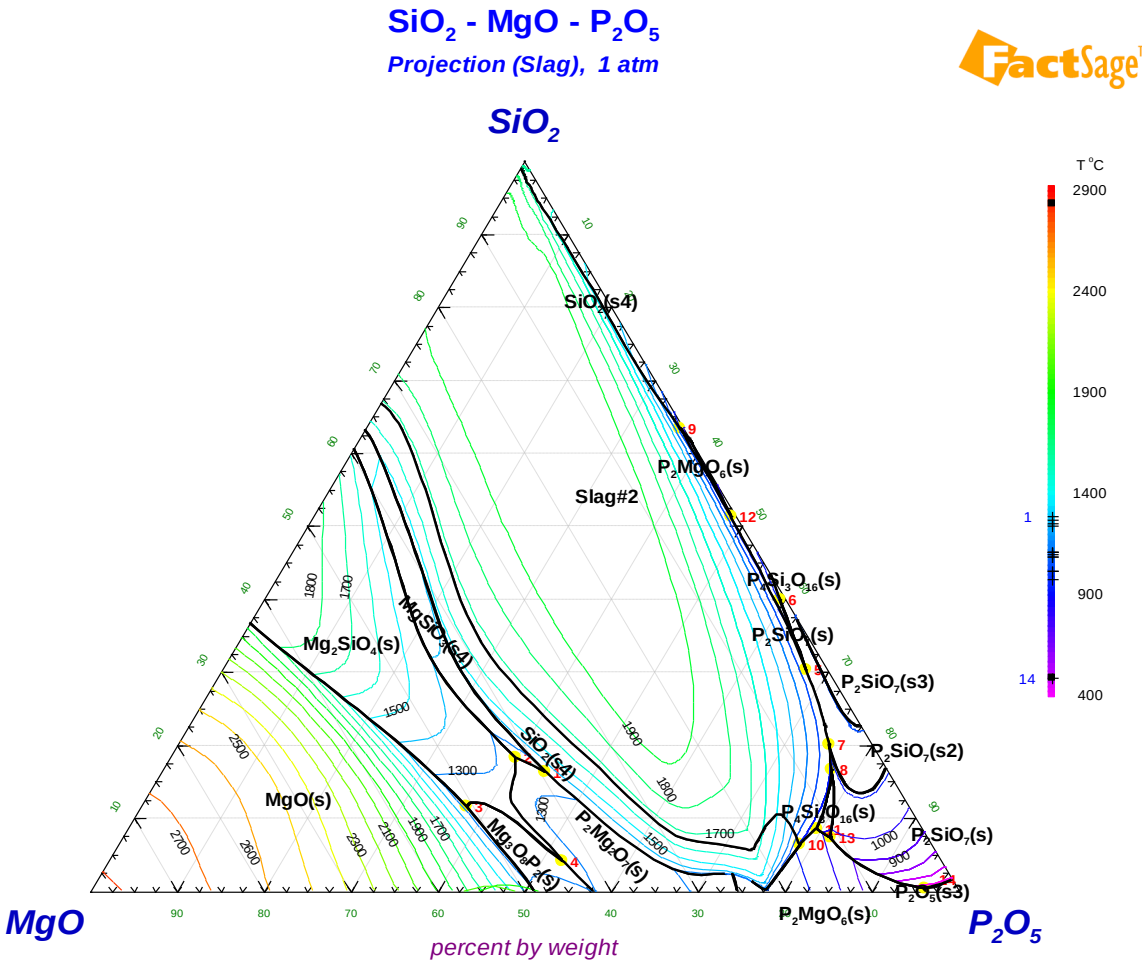

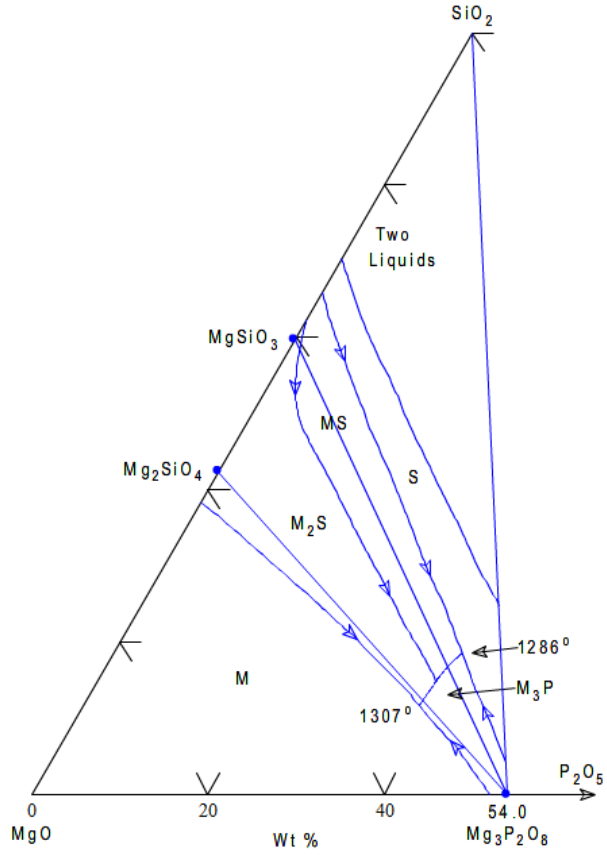

J. Wojciechowska, J. Berak, Rocz. Chem., 33[1] 21-31 (1959).

Invariant equilibria on the liquidus surface

Intersections with slag	Mole fraction A = SiO2, B = MgO, C = P2O5				Weight percent A = SiO2, B = MgO, C = P2O5			
	X(A)	X(B)	X(C)	T(C)	W(A)	W(B)	W(C)	T(C)
1: MgSiO3(s4) / P2Mg2O7 / Cristobalite	1: 0.17445	0.62655	0.19900	1281.75	1: 16.382	39.469	44.149	1281.75
2: Mg2SiO4 / MgSiO3(s4) / P2Mg2O7	2: 0.18815	0.63988	0.17196	1264.97	2: 18.381	41.932	39.687	1264.98
3: Mg2SiO4 / Mg3O8P2 / MgO	3: 0.11252	0.73384	0.15364	1245.53	3: 11.627	50.867	37.507	1245.53
4: Mg2SiO4 / Mg3O8P2 / P2Mg2O7	4: 0.04586	0.71185	0.24229	1233.71	4: 4.185	43.578	52.237	1233.71
5: P2SiO7(s1) / P2SiO7(s2) / Slag#2	5: 0.48737	0.05663	0.45600	1106.85	5: 30.411	2.370	67.219	1106.85
6: P2SiO7(s1) / P2SiO7(s2) / P4Si3O16	6: 0.60507	0.01413	0.38080	1106.85	6: 39.961	0.626	59.413	1106.85
7: P2SiO7(s1) / P2SiO7(s2) / Slag#2	7: 0.33869	0.12436	0.53695	1106.85	7: 20.034	4.934	75.032	1106.85
8: P2SiO7(s1) / Slag#2 / P4Si3O16	8: 0.28385	0.16137	0.55478	1092.72	8: 16.670	6.357	76.972	1092.72
9: P2MgO6 / Cristobalite / Slag#2	9: 0.80058	0.00655	0.19287	1083.00	9: 63.507	0.348	36.144	1083.00
10: P2MgO6 / Cristobalite / Slag#2	10: 0.10297	0.36282	0.53421	1082.99	10: 6.402	15.132	78.466	1082.99
11: P2MgO6 / P4Si3O16 / Slag#2	11: 0.14231	0.29917	0.55852	1013.45	11: 8.560	12.072	79.368	1013.45
12: P2MgO6 / P4Si3O16 / Slag#2	12: 0.70891	0.01020	0.28090	1013.47	12: 51.395	0.496	48.109	1013.45
13: P2MgO6 / P2SiO7(s1) / P4Si3O16	13: 0.12646	0.28388	0.58967	970.70	13: 7.395	11.136	81.468	970.70
14: P2MgO6 / P2O5(s3) / P2SiO7(s1)	14: 0.00736	0.12080	0.87184	486.27	14: 0.343	3.772	95.885	486.28

Mole fraction, 500°C

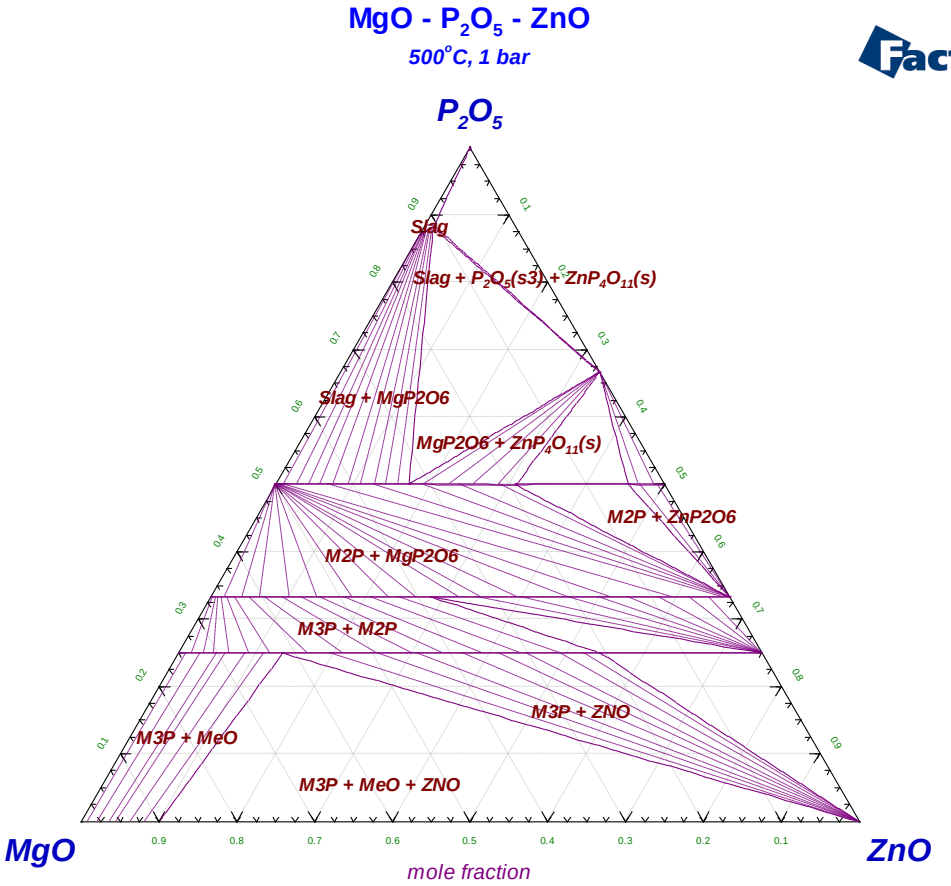

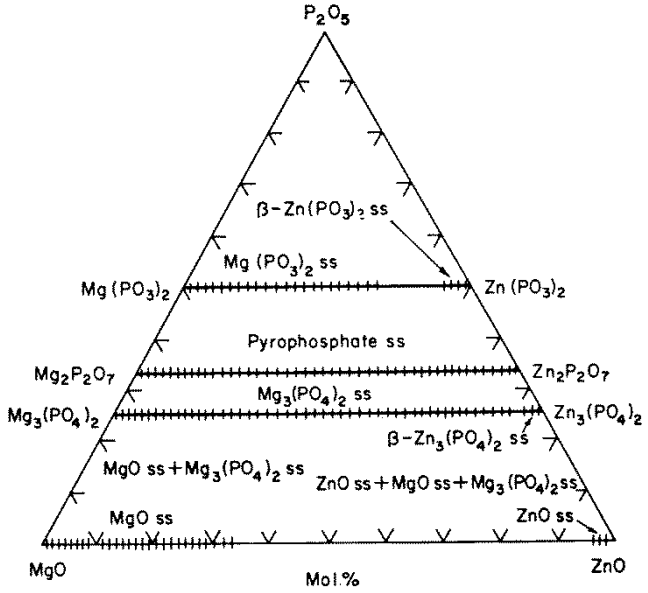

J.F. Sarver, F.L. Katnach, F.A. Hummel, J. Electrochem. Soc., 106 [11], (1959), pp. 960-963.

Mole fraction, Isopleth MgP2O6-ZnP2O6

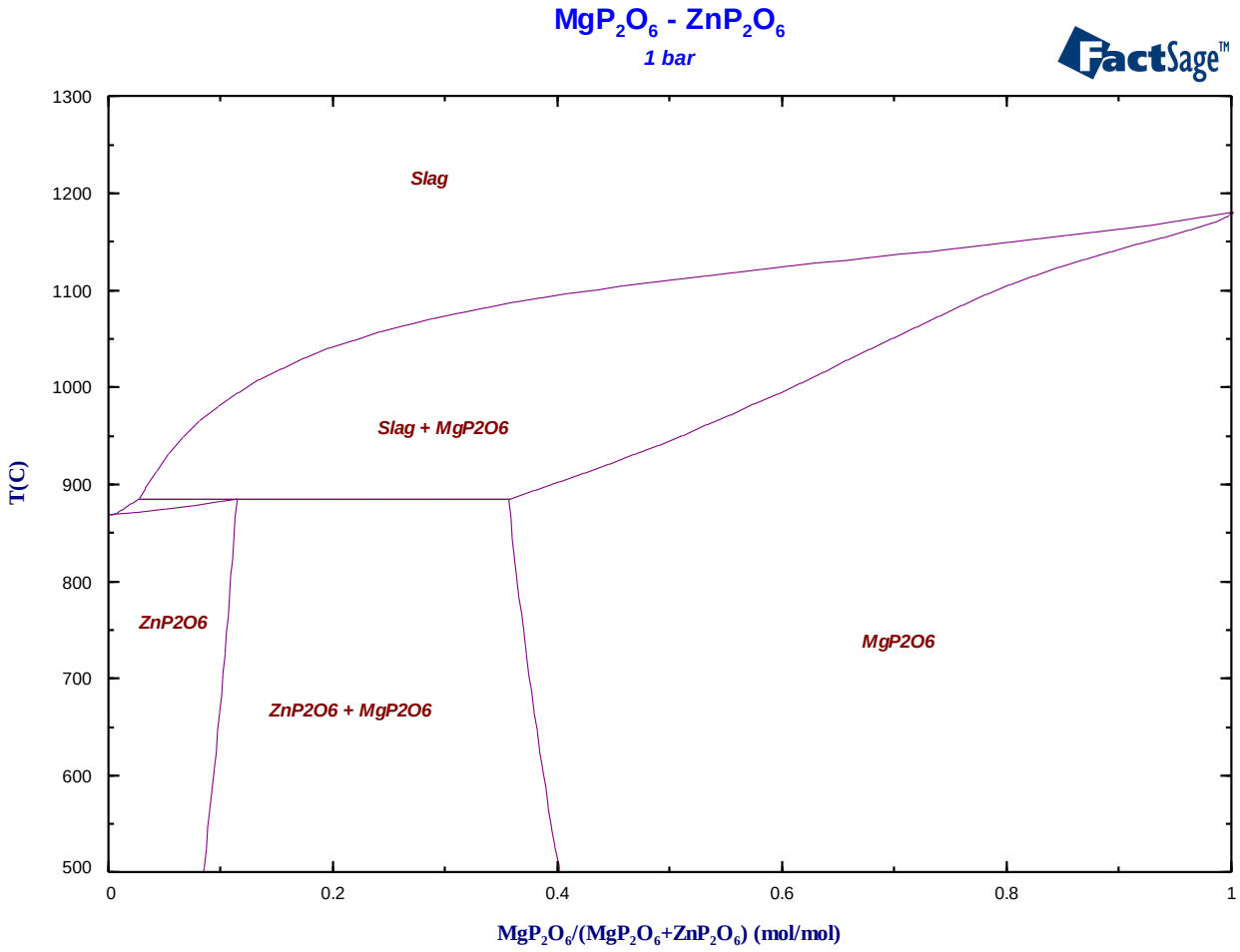

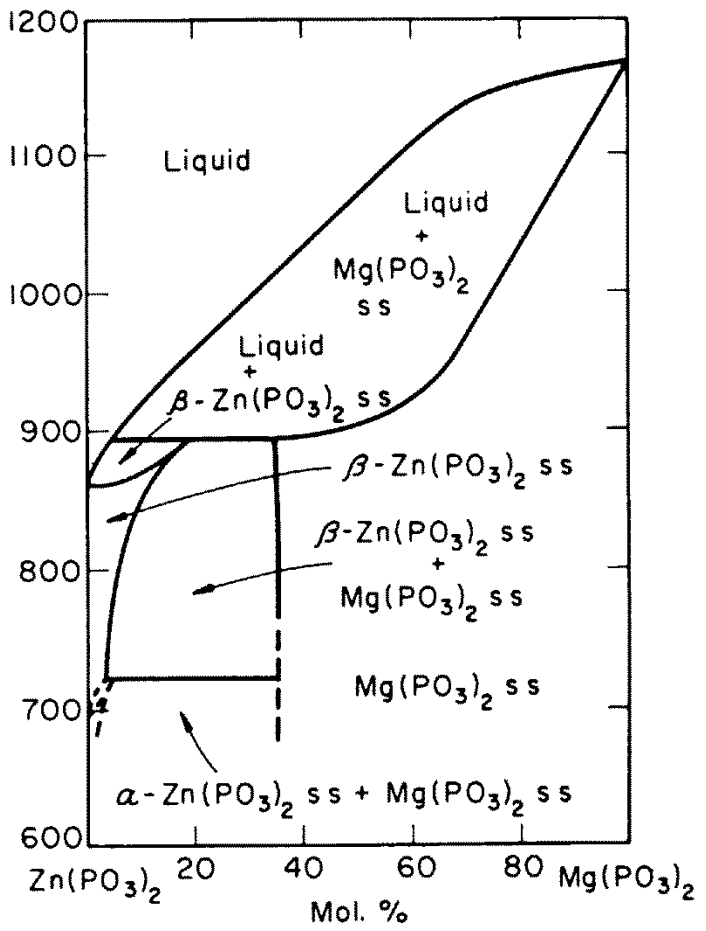

J.F. Sarver, F.A. Hummel, J. Electrochem. Soc., 106 [6], (1959), pp. 500-504.

Mole fraction, Isopleth Mg2P2O7-Zn2P2O7

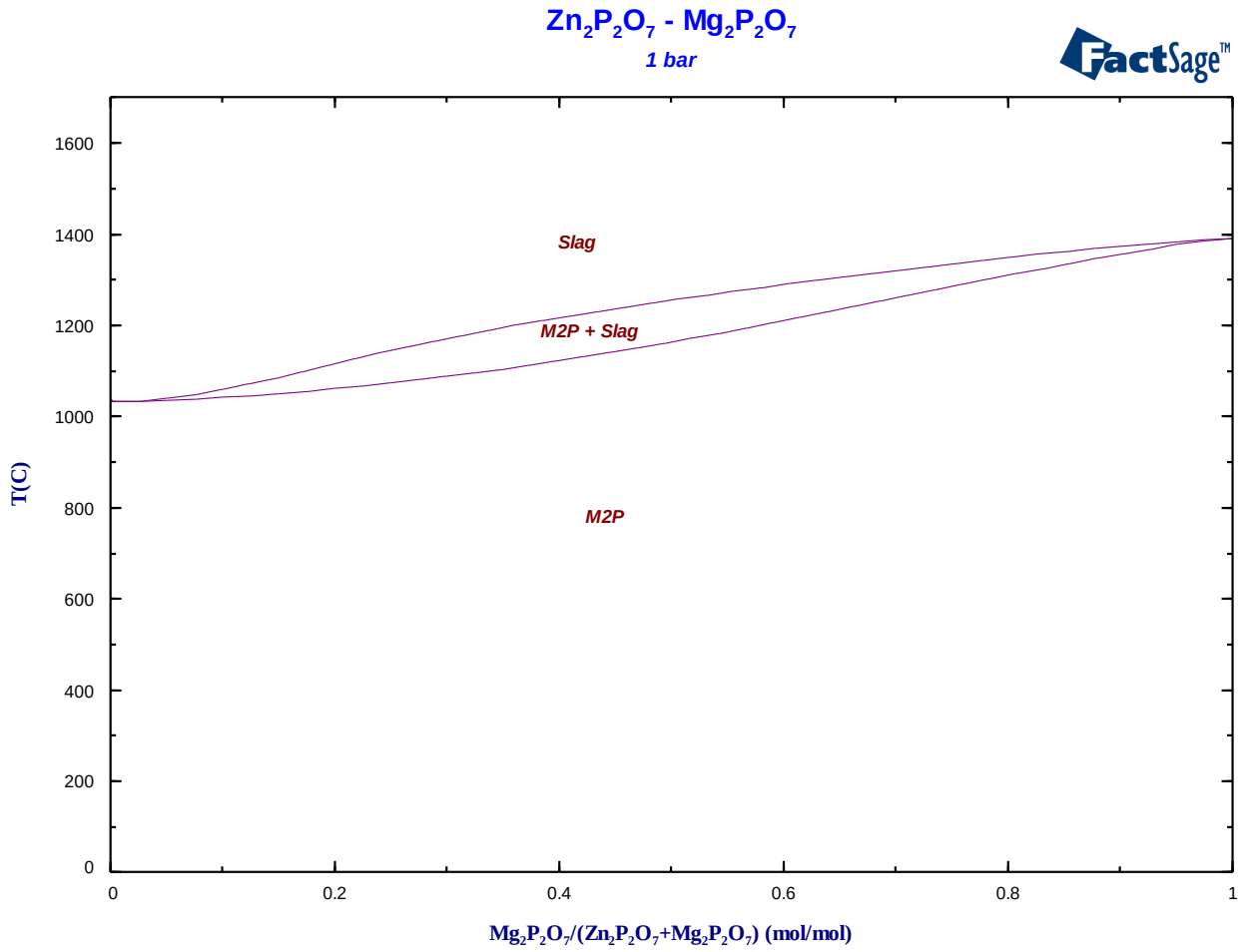

Mole fraction, Isopleth Mg3P2O8-Zn3P2O8

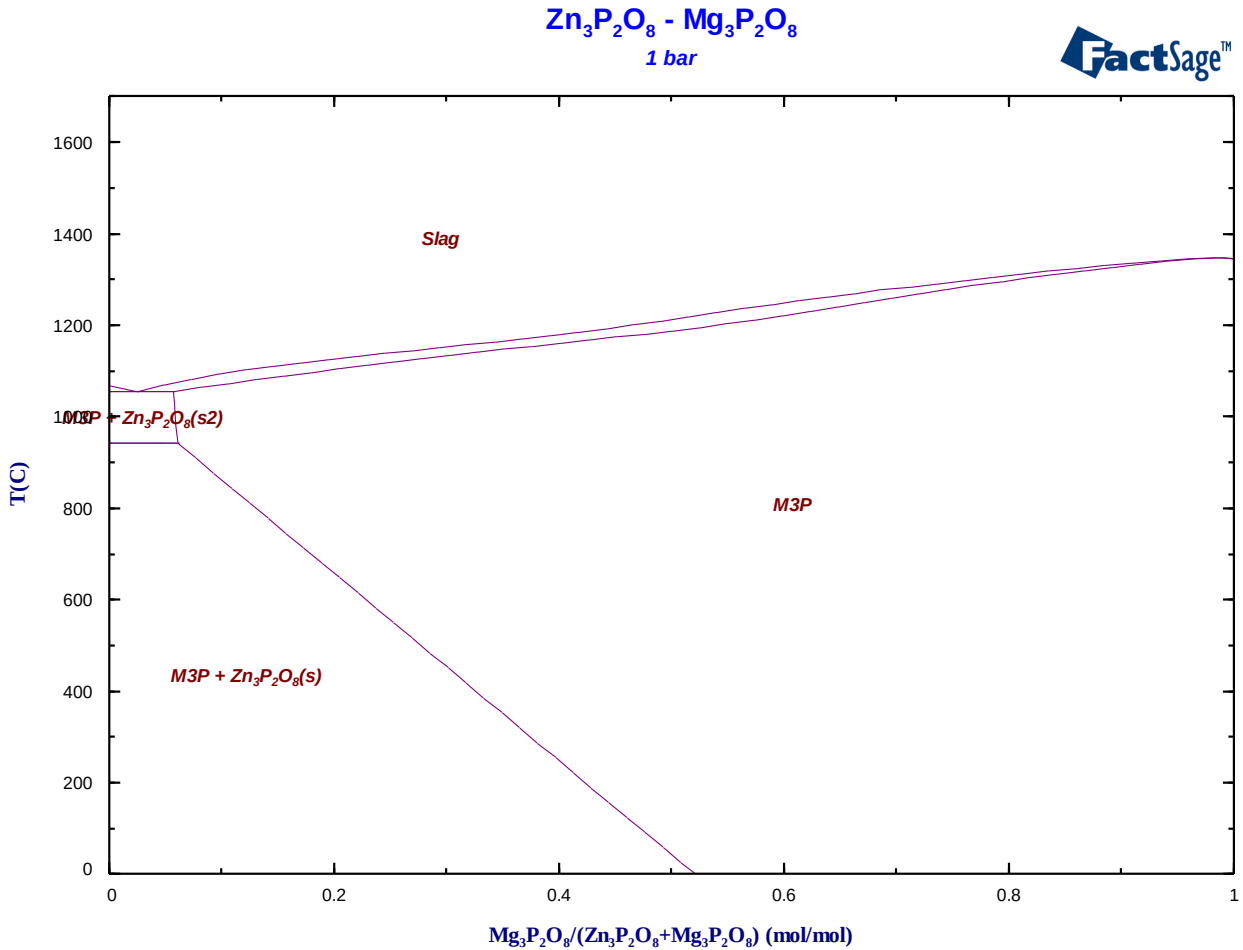

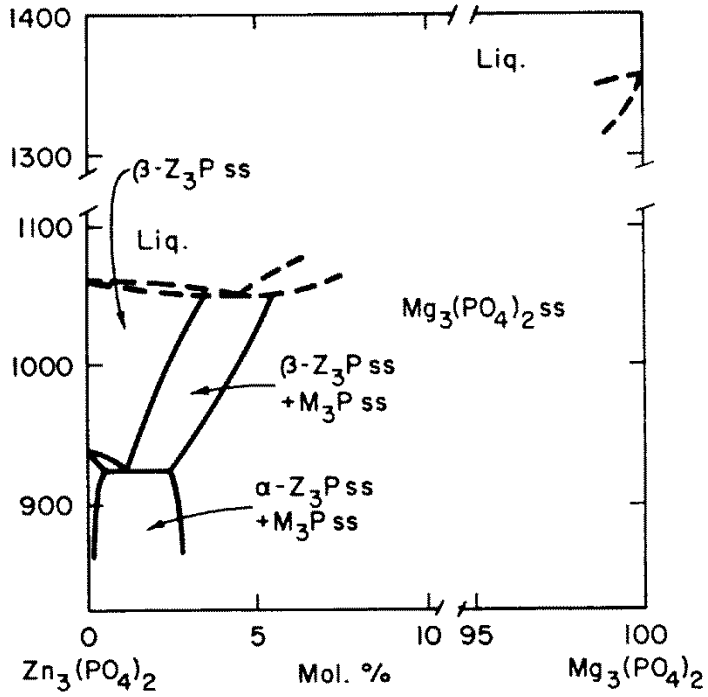

J.F. Sarver, F.L. Katnach, F.A. Hummel, J. Electrochem. Soc., 106 [11], (1959), pp. 960-963.

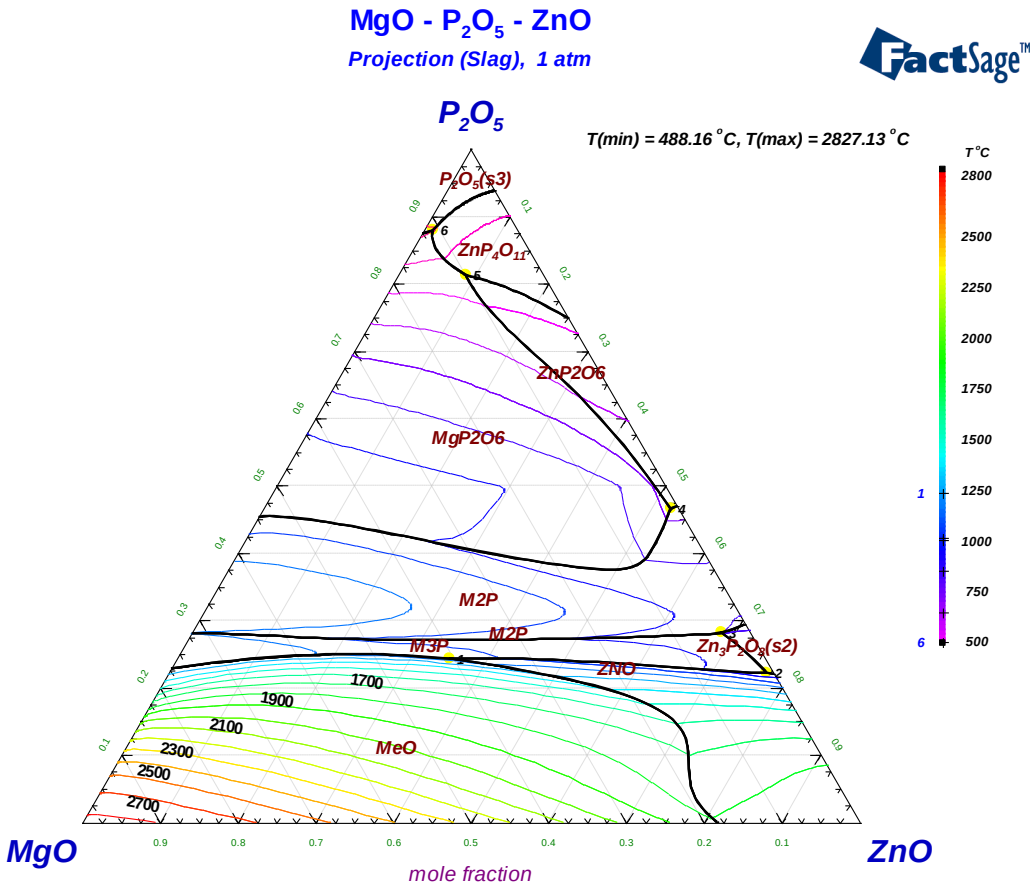
MgO - P2O5 - ZnO
Projection (Slag), 1 atm
FactSage™
P2O5
T(min) = 488.16 °C, T(max) = 2827.13 °C
T °C
2800
2500
2250
2000
1750
1500
1250
1000
750
500
P2O5(s3)
ZnP4O11
ZnP2O6
MgP2O6
M2P
M2P
M3P
Zn3P2O8(s2)
ZnO
MeO
1700
1900
2100
2300
2500
2700
1
2
3
4
5
6
MgO
ZnO
mole fraction

Weight percent, Liquidussurface

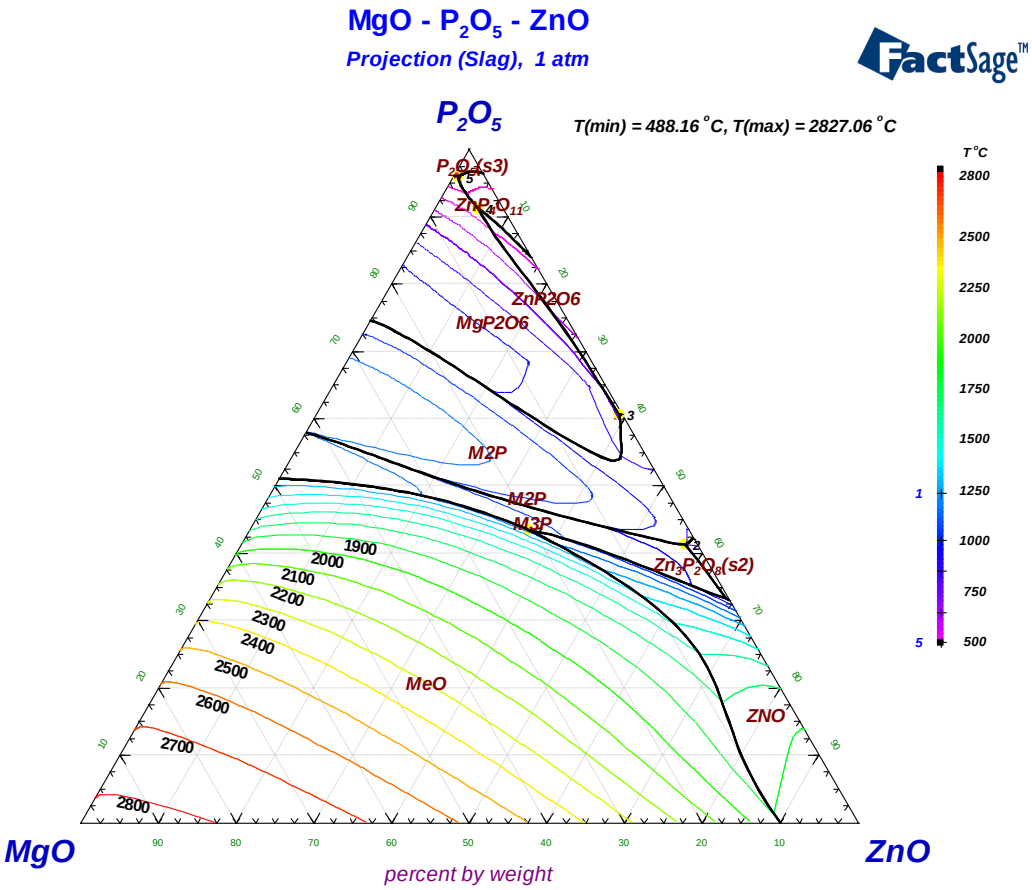

Invariant equilibria on the liquidus surface

Intersections with slag	Mole fraction A = P2O5, B = MgO, C = ZnO				Weight percent A = P2O5, B = MgO, C = ZnO			
	X(A)	X(B)	X(C)	T(C)	W(A)	W(B)	W(C)	T(C)
1: M3P / MeO / ZNO	1: 0.24332	0.40617	0.35051	1229.58	1: 43.481	20.609	35.910	1229.58
2: M2P / M3P / Zn3P2O8_S2(s2)	2: 0.28185	0.03634	0.68181	998.36	2: 41.263	1.510	57.227	998.36
3: M2P / MgP2O6 / ZnP2O6	3: 0.46601	0.01003	0.52396	845.29	3: 60.579	0.370	39.050	845.35
4: MgP2O6 / ZnP2O6 / ZnP4O11_S1(s)	4: 0.81278	0.10001	0.08721	639.68	4: 91.203	3.187	5.611	639.68
5: MgP2O6 / P2O5_O'-Phase(s3) / ZnP4O11_S1(s)	5: 0.87948	0.10960	0.01092	495.12	5: 95.923	3.394	0.683	495.12

MgO-SiO2-TiO2,
Mole fraction, 1400°C

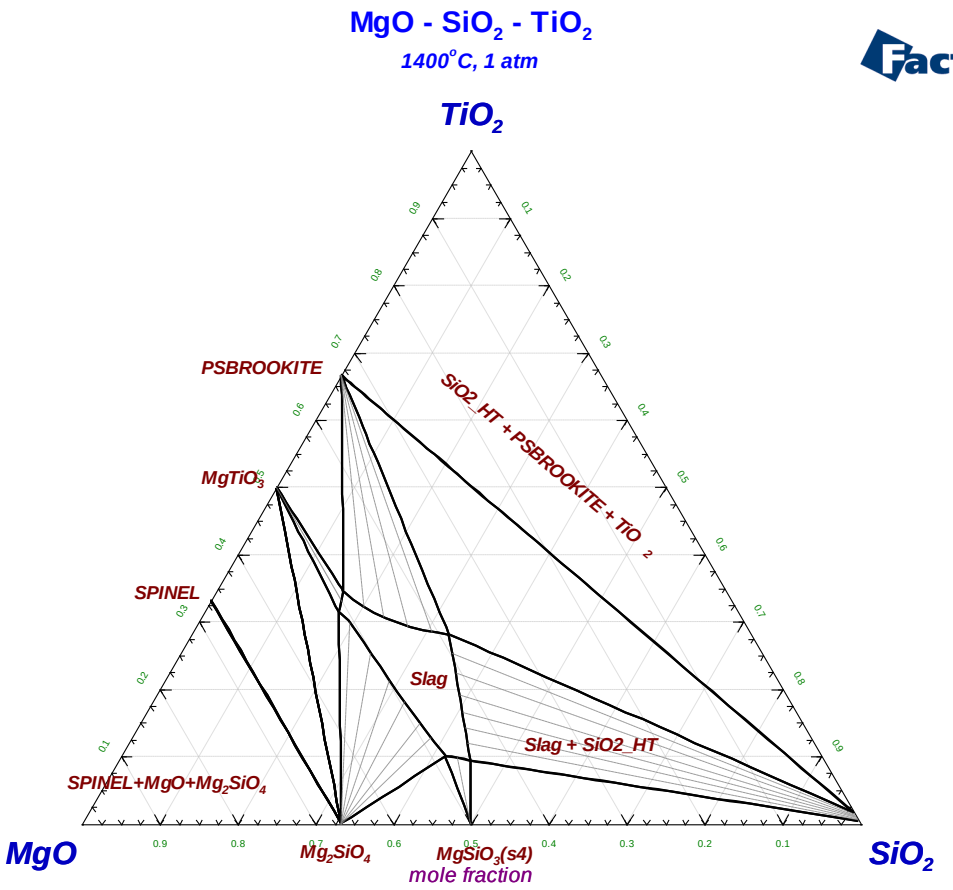

MgO-SiO2-TiO2,
Weight percent, Isopleth section Mg2SiO4-Mg2TiO4

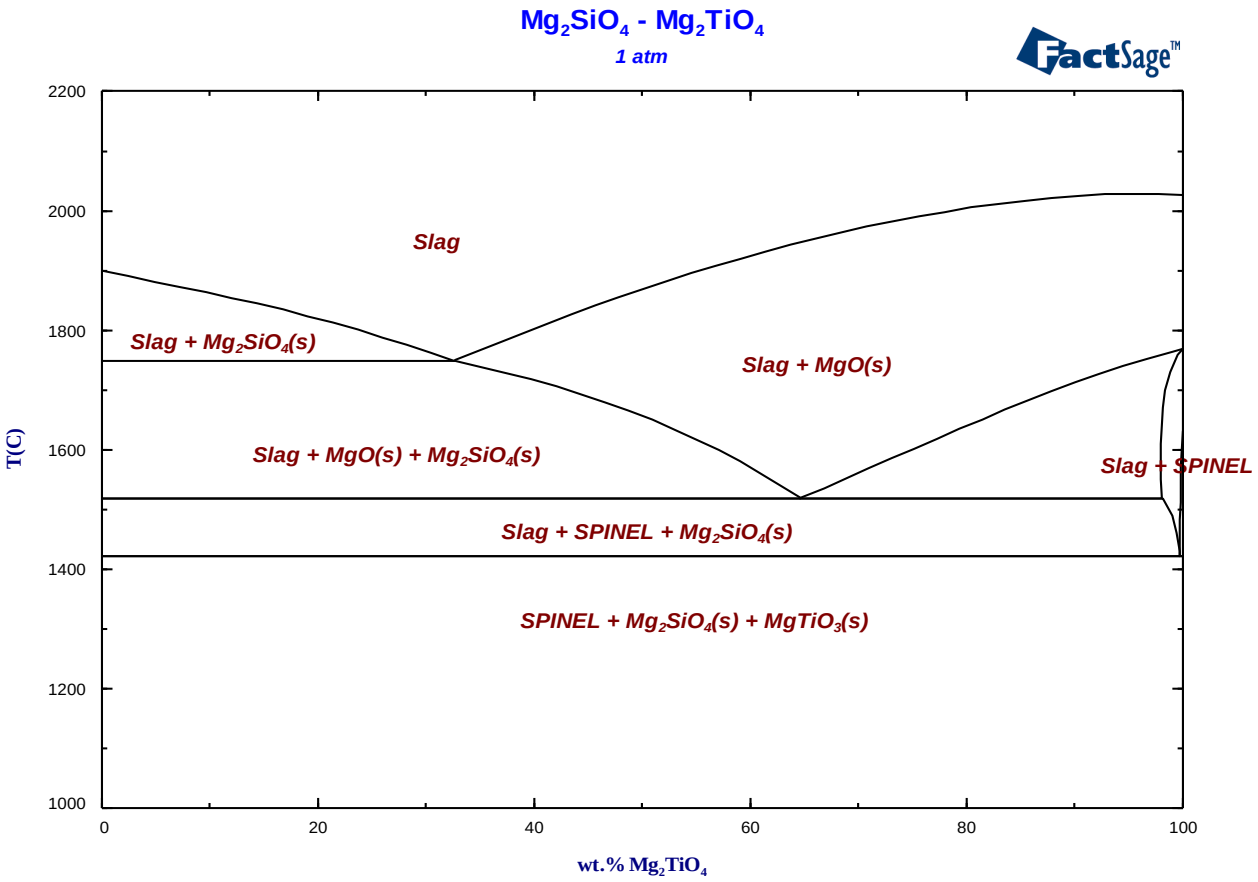

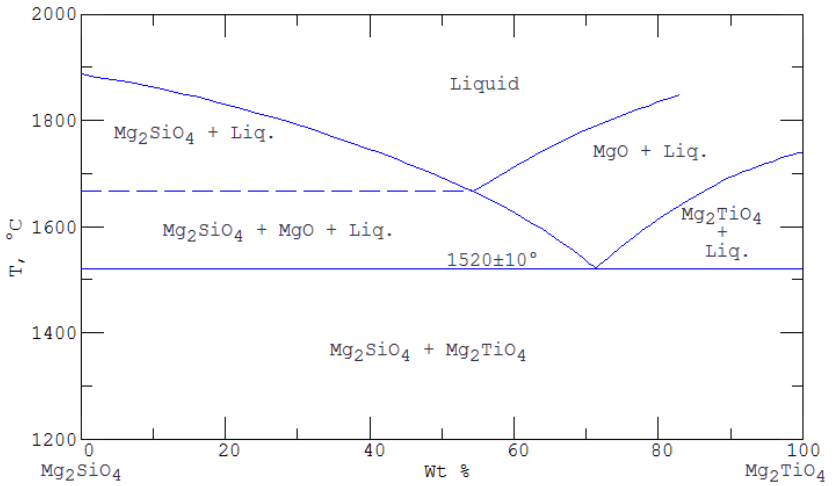

Z. Panek, E. Kanclir, J. Staron, M. Kozlovsky, S. Palco, Silikaty (Prague), 20 [1], (1976), pp. 13-22.

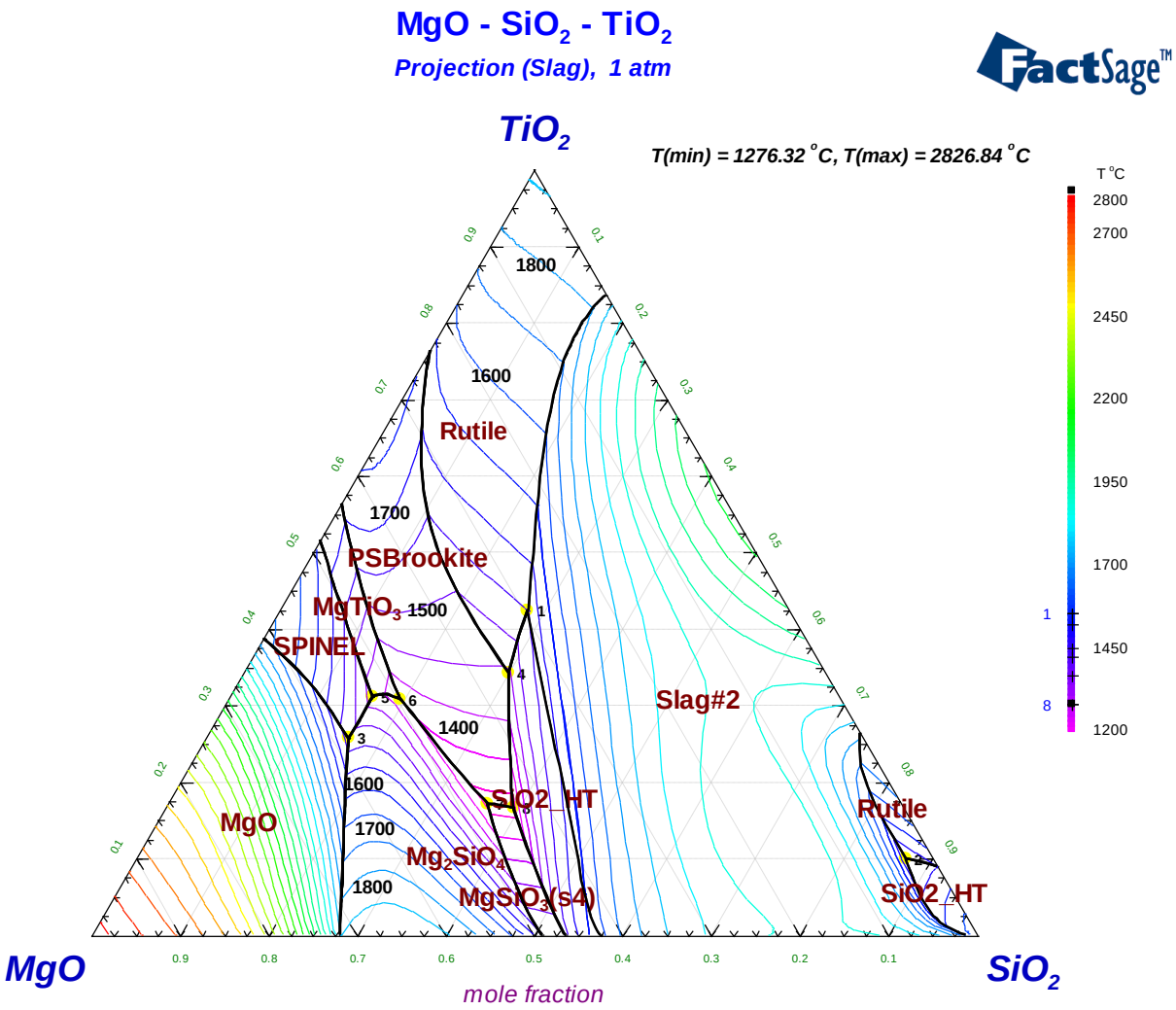
MgO - SiO2 - TiO2
Projection (Slag), 1 atm
FactSage™
TiO2
T(min) = 1276.32 °C, T(max) = 2826.84 °C
T °C
2800
2700
2450
2200
1950
1700
1450
1200
1
8
1800
1600
1700
1500
1400
1600
1700
1800
Rutile
PSBrookite
MgTiO3
SPINEL
MgO
Mg2SiO4
MgSiO3(s4)
SiO2_HT
Slag#2
Rutile
SiO2_HT
1
2
3
4
5
6
7
8
9
MgO
SiO2
mole fraction

MgO-SiO2-TiO2,
Weight percent, Liquidus surface

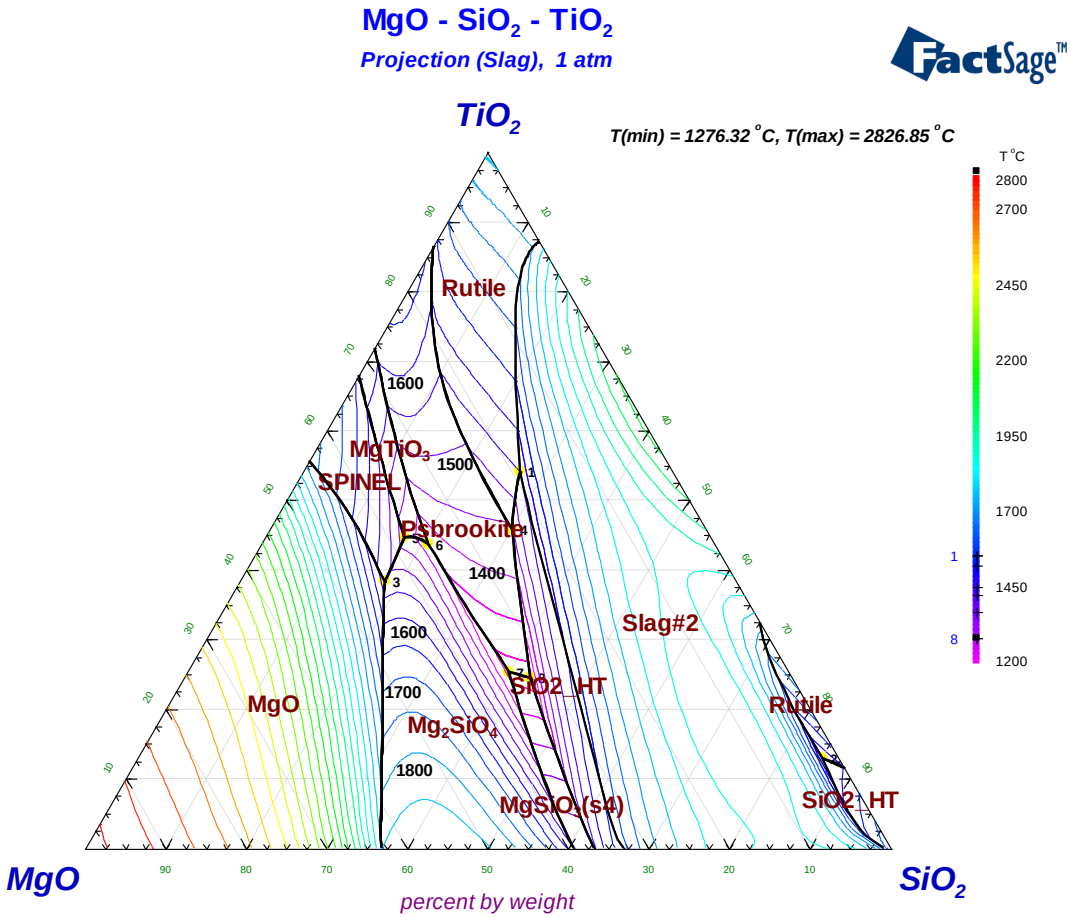

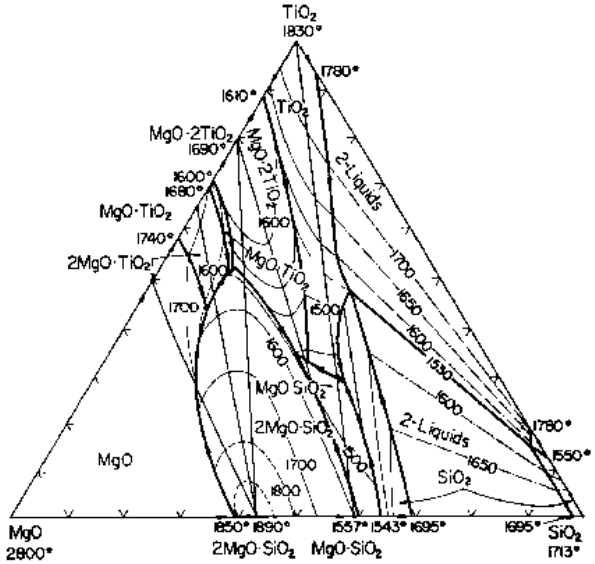

F. Massazza, E. Sirchia, Chim. Ind. (Milan), 40 [6], (1958), pp. 460-467.

Invariant equilibria on the liquidus surface

Intersections with slag	Mole fraction A = TiO2, B = MgO, C = SiO2				Weight percent A = TiO2, B = MgO, C = SiO2			
	X(A)	X(B)	X(C)	T(C)	W(A)	W(B)	W(C)	T(C)
1: Rutile / SiO2_HT / Slag#2	1: 0.42437	0.29491	0.28072	1549.63	1: 54.102	18.974	26.924	1549.61
2: Rutile / SiO2_HT / Slag#2	2: 0.10020	0.03004	0.86975	1549.59	2: 13.019	1.970	85.011	1549.59
3: Mg2SiO4 / MgO / SPINEL	3: 0.25773	0.58126	0.16101	1518.44	3: 38.342	43.638	18.020	1518.44
4: Pseudobrookite / Rutile / SiO2_HT	4: 0.34269	0.35739	0.29992	1443.96	4: 45.773	24.090	30.137	1443.96
5: Mg2SiO4 / MgTiO3 / SPINEL	5: 0.31259	0.52671	0.16070	1420.65	5: 44.701	38.011	17.288	1420.65
6: Mg2SiO4 / Pseudobrookite / MgTiO3_S1(s)	6: 0.30886	0.49682	0.19432	1362.12	6: 43.763	35.524	20.713	1362.12
7: Mg2SiO4 / MgSiO3(s4) / Pseudobrookite	7: 0.17210	0.46698	0.36092	1277.86	7: 25.336	34.692	39.972	1277.86
8: MgSiO3(s4) / Pseudobrookite / SiO2_HT	8: 0.16741	0.44024	0.39235	1276.32	8: 24.448	32.445	43.107	1276.32

MgO-SiO2-V2O5,
Mole fraction, 1450°C

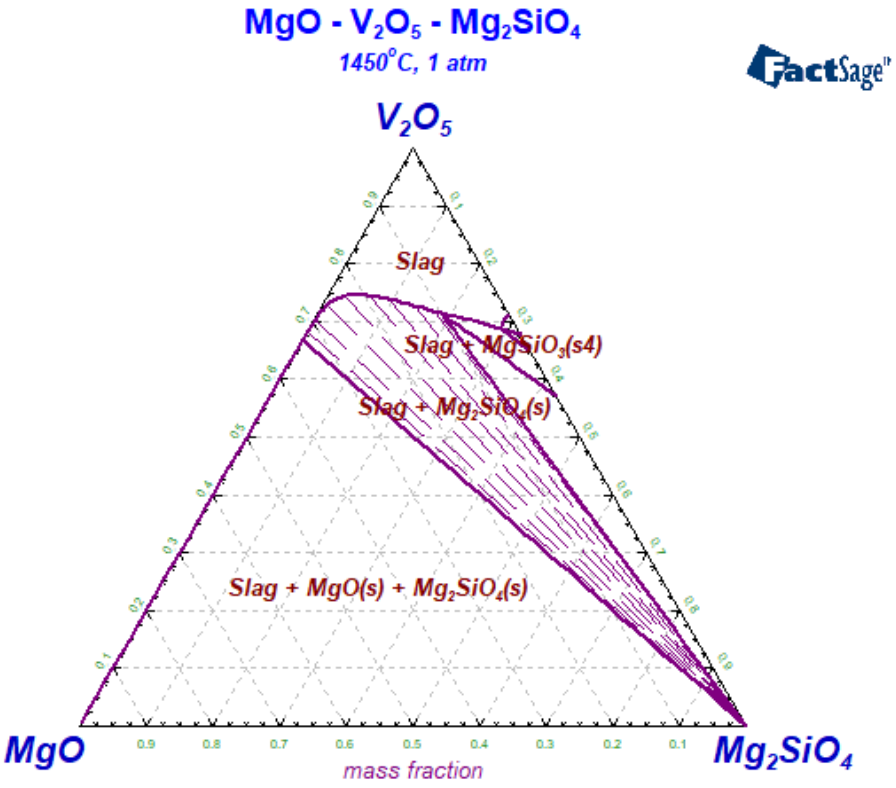

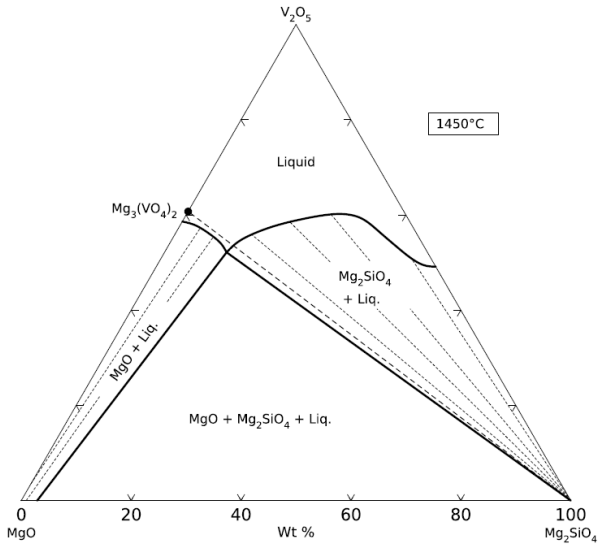

M. Carter and N. H. Brett, Trans. J. Br. Ceram. Soc., 72 [5] 203-207.

MgO-SiO2-V2O5,
Mole fraction, Solidus surface

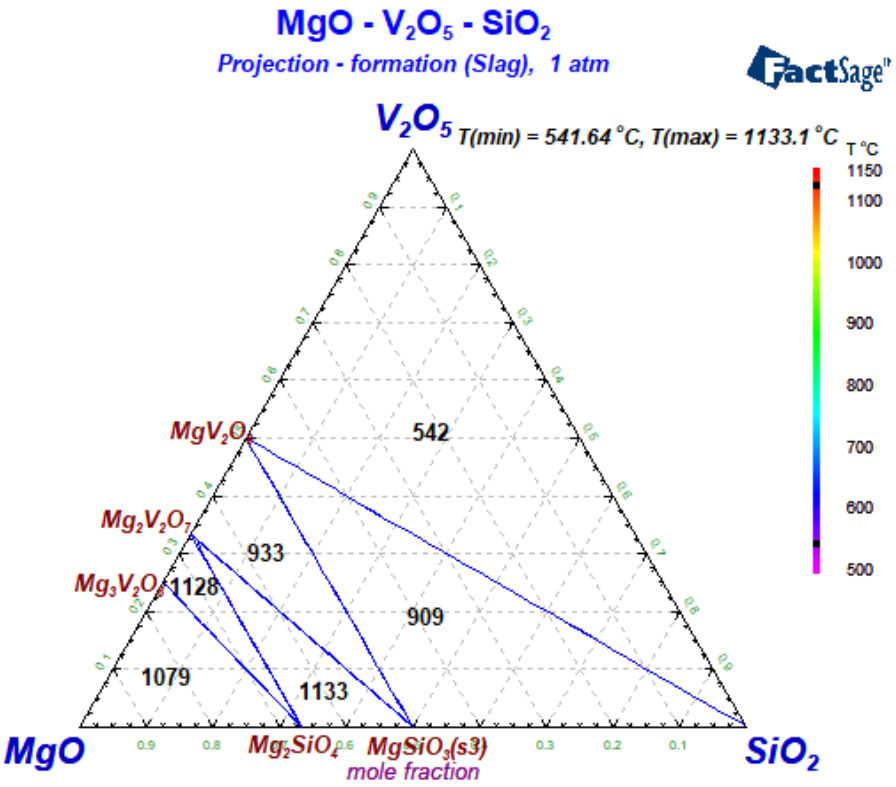

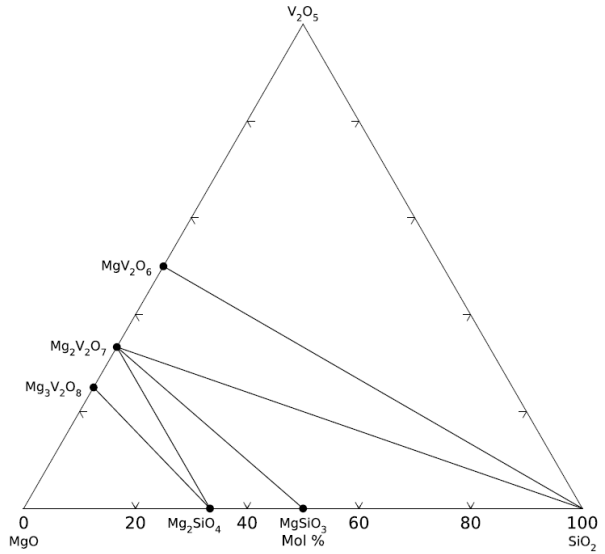

M. J. McGarry and R. A. McCauley, J. Am. Ceram. Soc., 75 [10] 2874-2876 (1992).

MgO-SiO2-V2O3,

MgO-SiO2-V2O3,
Mole fraction, 1400°C

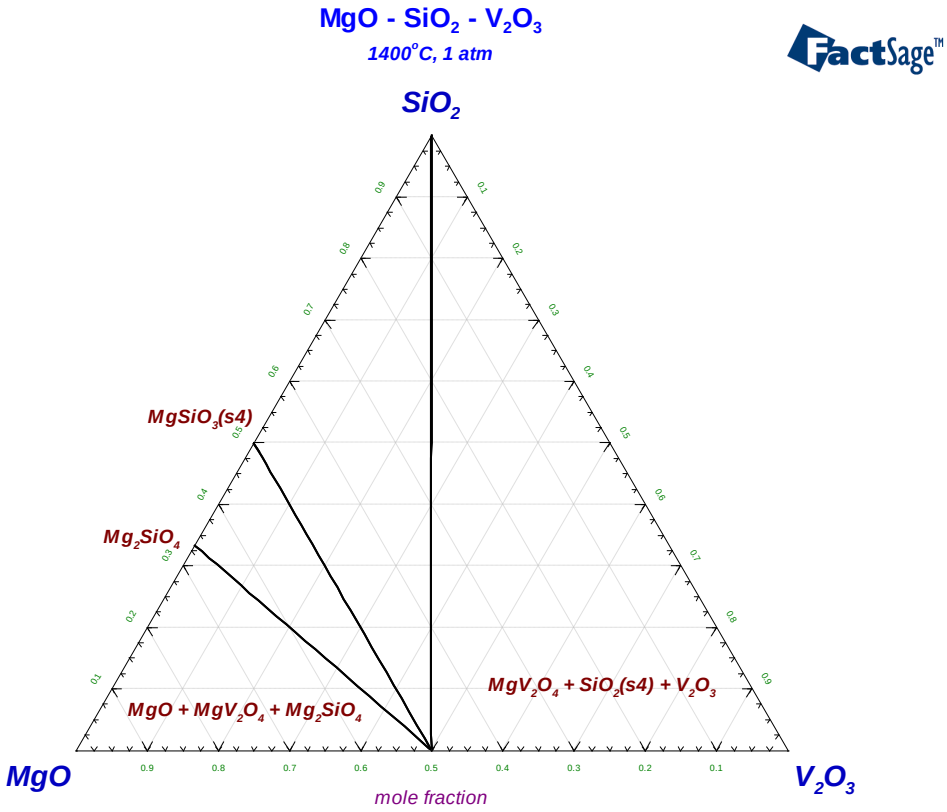

MgO-SiO2-V2O3,
Mole fraction, Liquidus surface

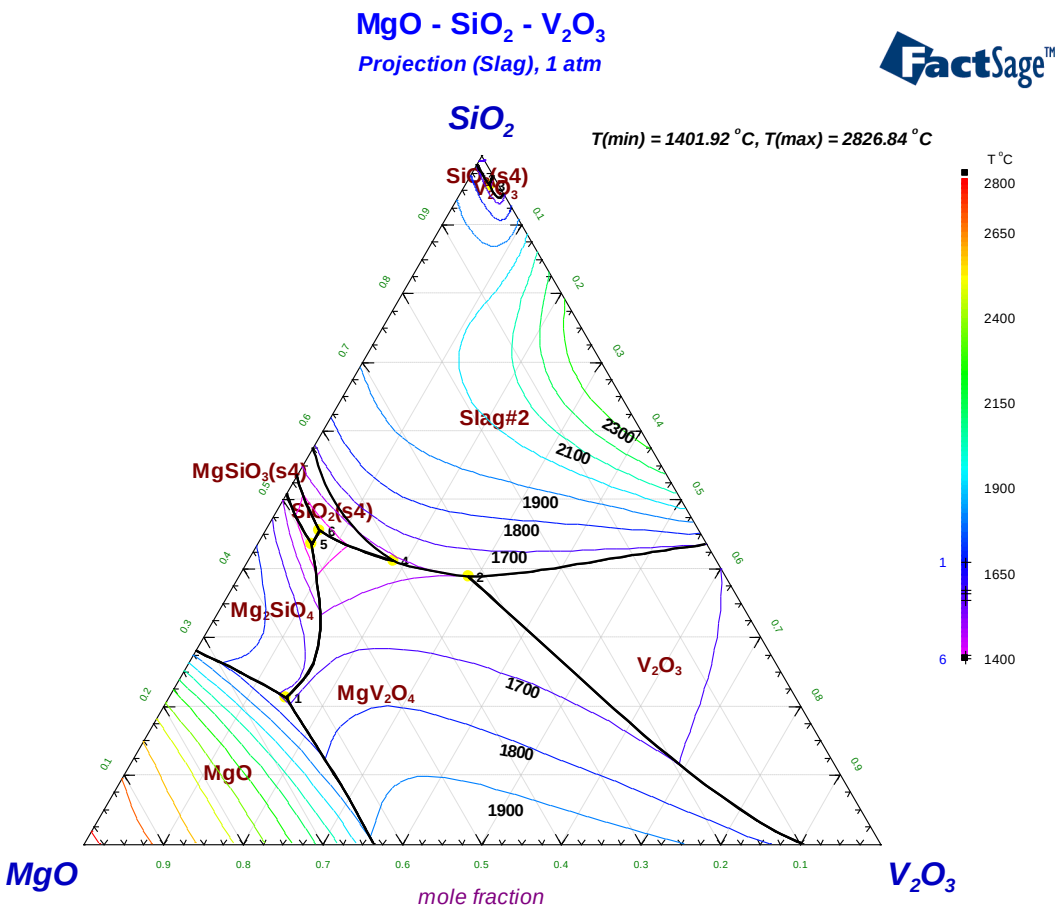

MgO-SiO2-V2O3,
Weight percent, Liquidus surface

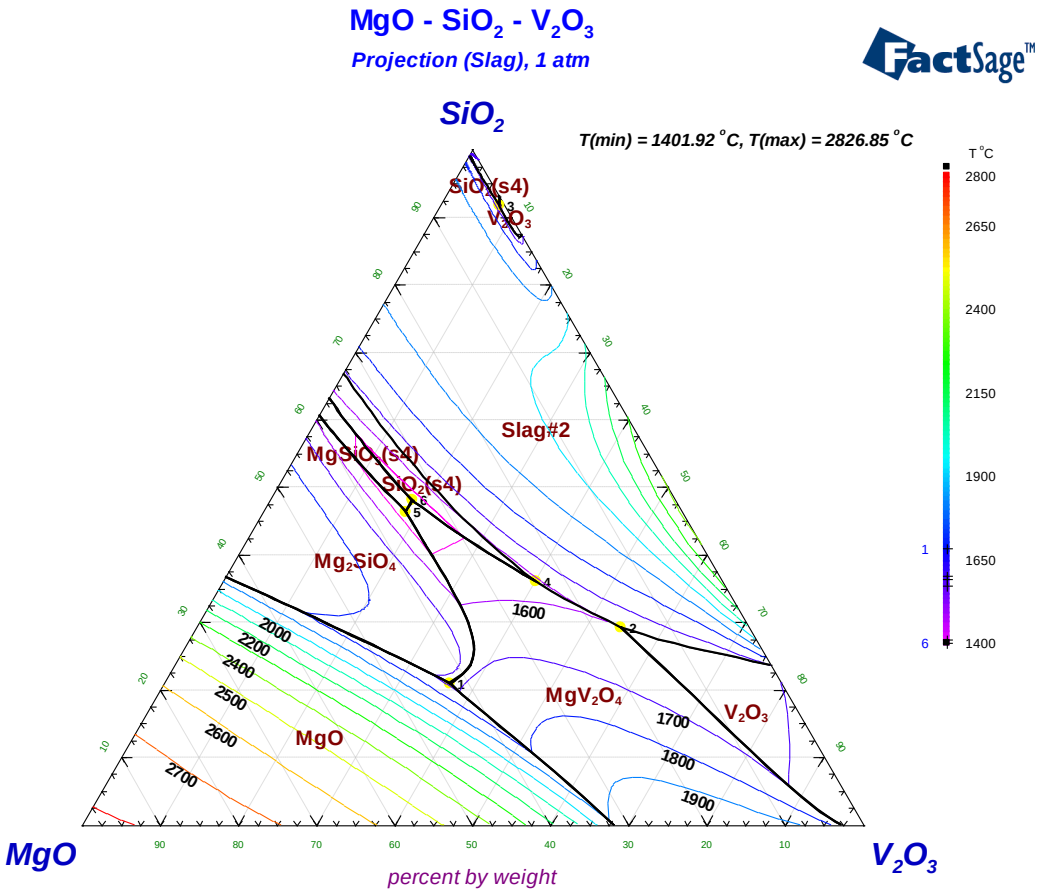

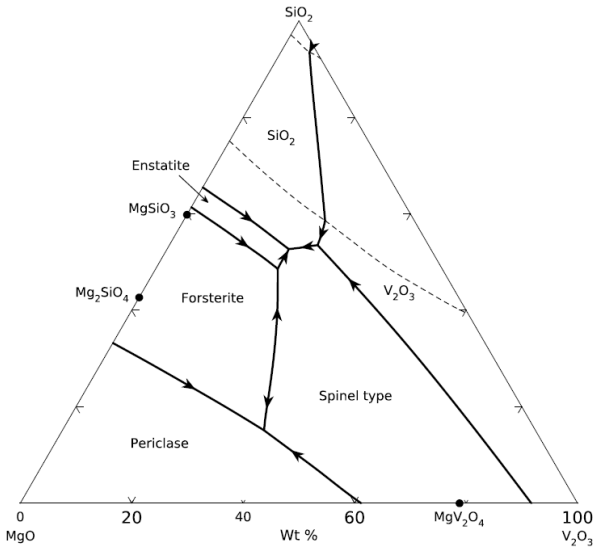

M. S. Najjar and A. Muan, "Ternary composition of V2O3-MgO-SiO2", US Patent 5,094,992, March 10, 1992.

Invariant equilibria on the liquidus surface

Intersections with slag	Mole fraction				Weight percent				
	A = SiO2, B = MgO, C = V2O3				A = TiO2, B = MgO, C = V2O3				
		X(A)	X(B)	X(C)	T(C)		W(A)	W(B)	W(C)	T(C)
1 Mg2SiO4 / MgO / MgV2O4_Spinel	1:	0.21220	0.63959	0.14821	1684.78	1:	20.990	42.438	36.571	1684.78
2. MgV2O4_Spinel / Slag#2 / V2O3	2:	0.38811	0.32267	0.28922	1601.31	2:	29.268	16.323	54.409	1601.31
3. SiO2(s4) / Slag#2 / V2O3	3:	0.95711	0.01125	0.03164	1590.42	3:	91.713	0.723	7.564	1590.43
4. MgV2O4_Spinel / SiO2(s4) / Slag#2	4:	0.41103	0.40533	0.18363	1571.07	4:	36.024	23.829	40.147	1571.07
5. Mg2SiO4 / MgSiO3(s4) / MgV2O4_Spinel	5:	0.43600	0.49521	0.06879	1409.80	5:	46.394	35.348	18.258	1409.80
6. MgSiO3(s4) / MgV2O4_Spinel / SiO2(s4)	6:	0.45511	0.47576	0.06913	1401.92	6:	48.074	33.711	18.215	1401.92

Mole fraction, 1200°C

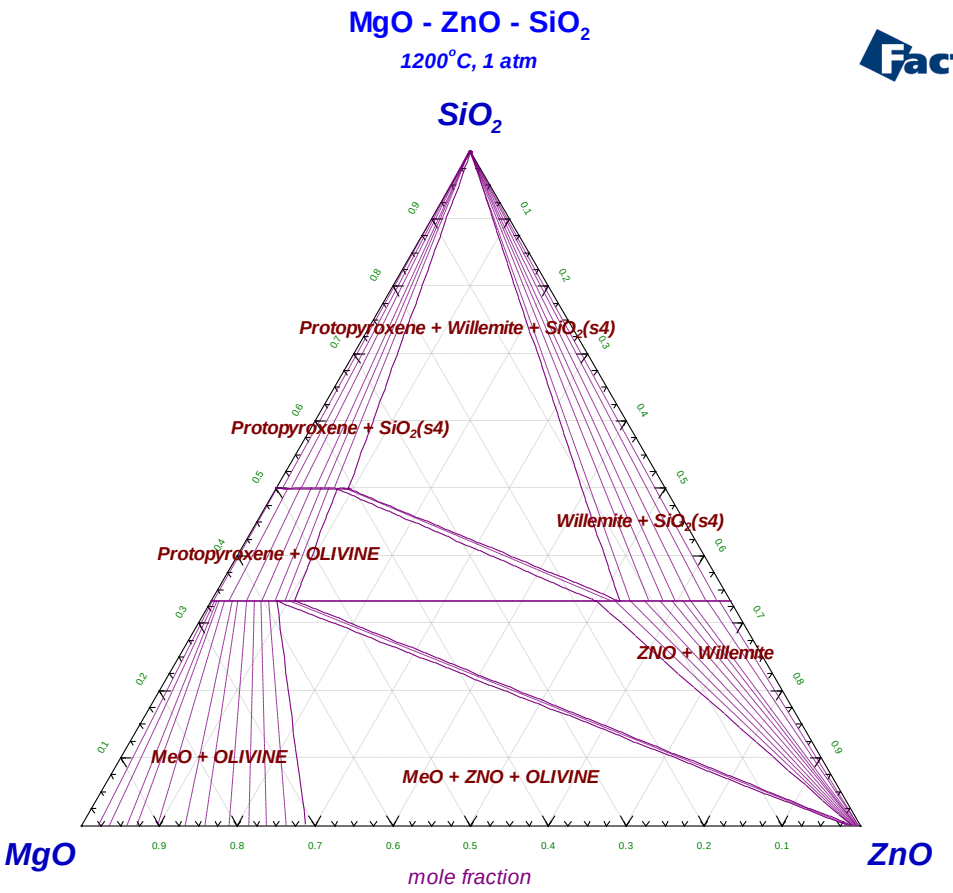

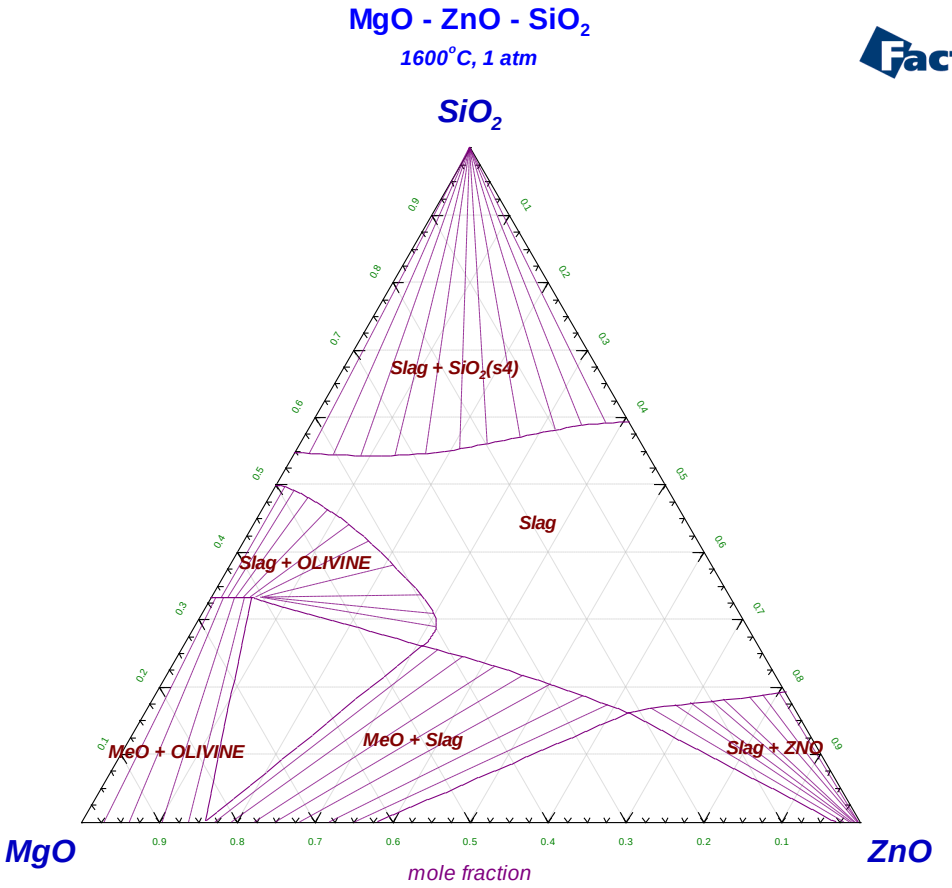
MgO - ZnO - SiO2
1600°C, 1 atm
FactSage™
SiO2
Slag + SiO2(s4)
Slag
Slag + OLIVINE
MeO + OLIVINE
MeO + Slag
Slag + ZNO
MgO
ZnO
mole fraction

Mole fraction, Isopleth Mg2SiO4-Zn2SiO4

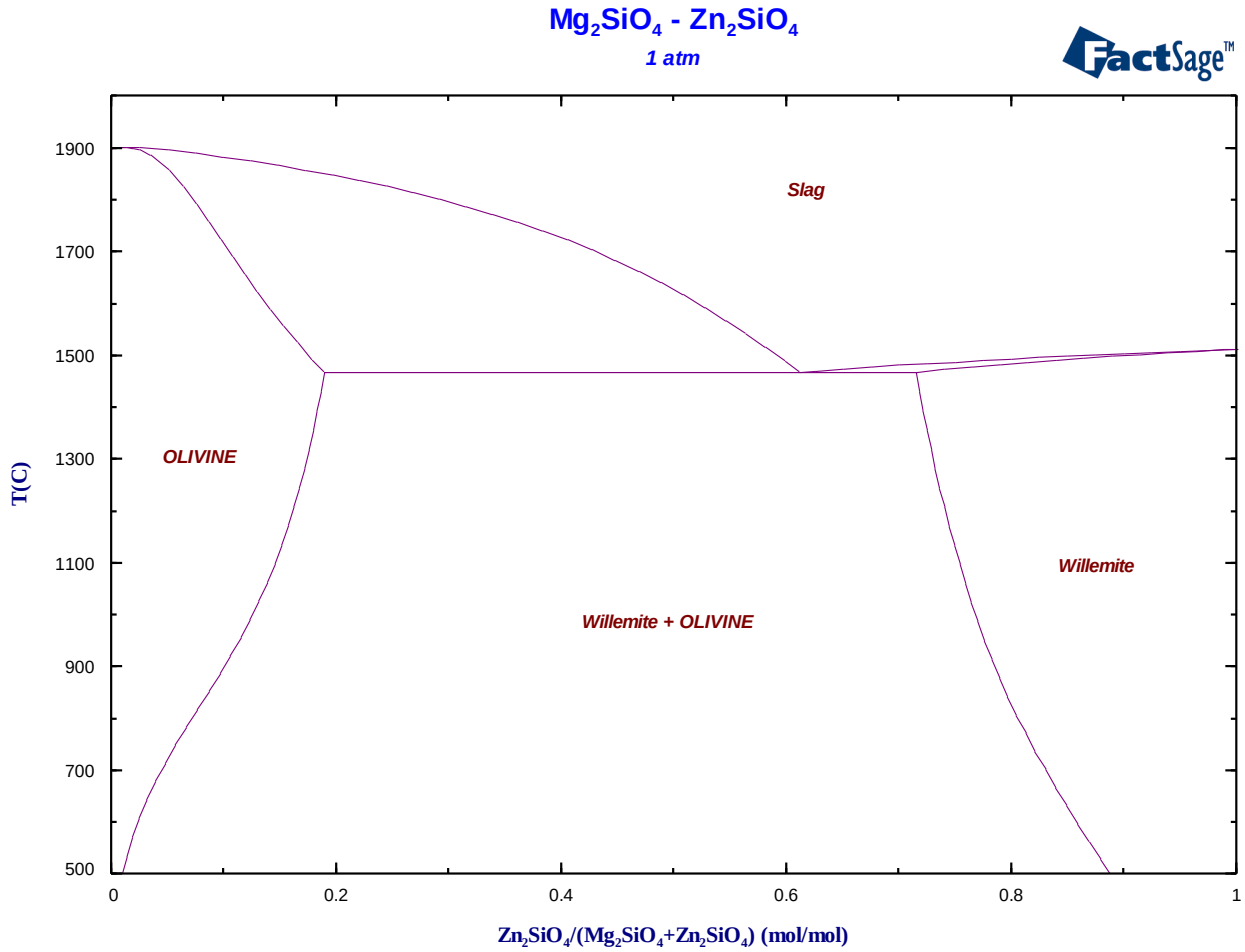

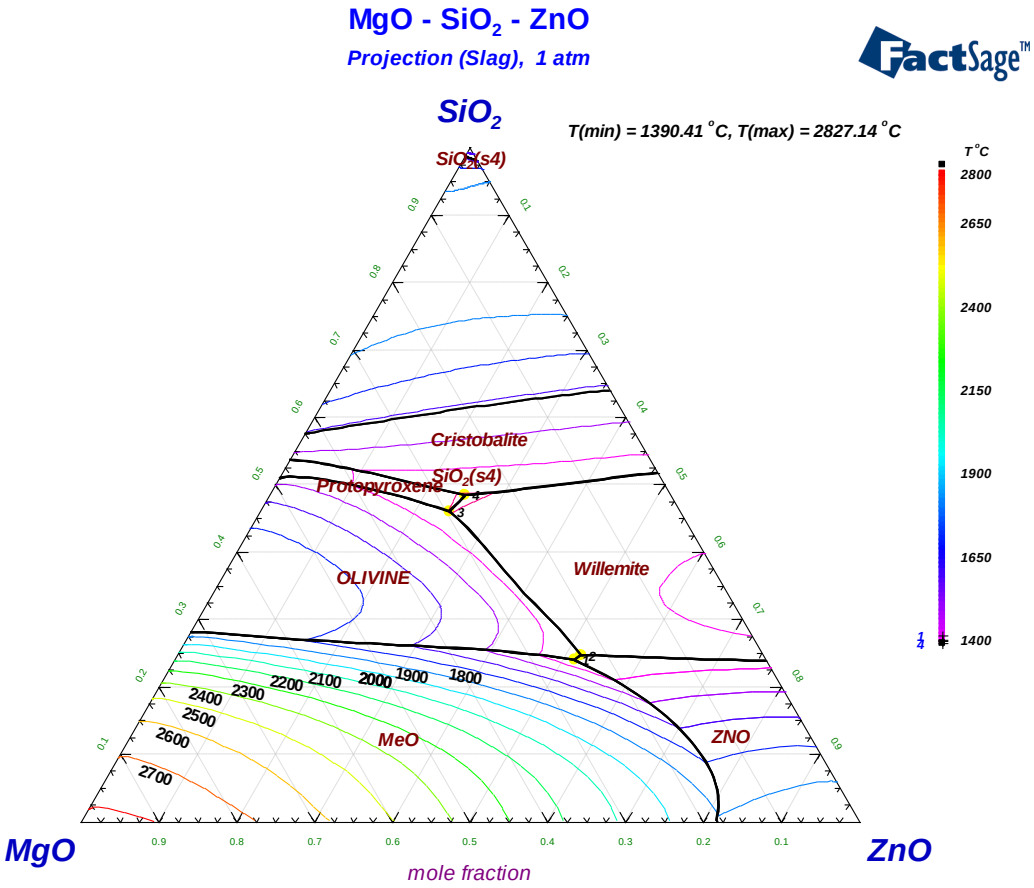
MgO - SiO2 - ZnO
Projection (Slag), 1 atm
FactSage™
SiO2
T(min) = 1390.41 °C, T(max) = 2827.14 °C
T°C
2800
2650
2400
2150
1900
1650
1400
SiO2(s4)
Cristobalite
SiO2(s4)
Protopyroxene
OLIVINE
Willemite
MeO
ZNO
2700
2600
2500
2400
2300
2200
2100
2000
1900
1800
MgO
ZnO
mole fraction

Weight percent, Liquidussurface compared with experimental data

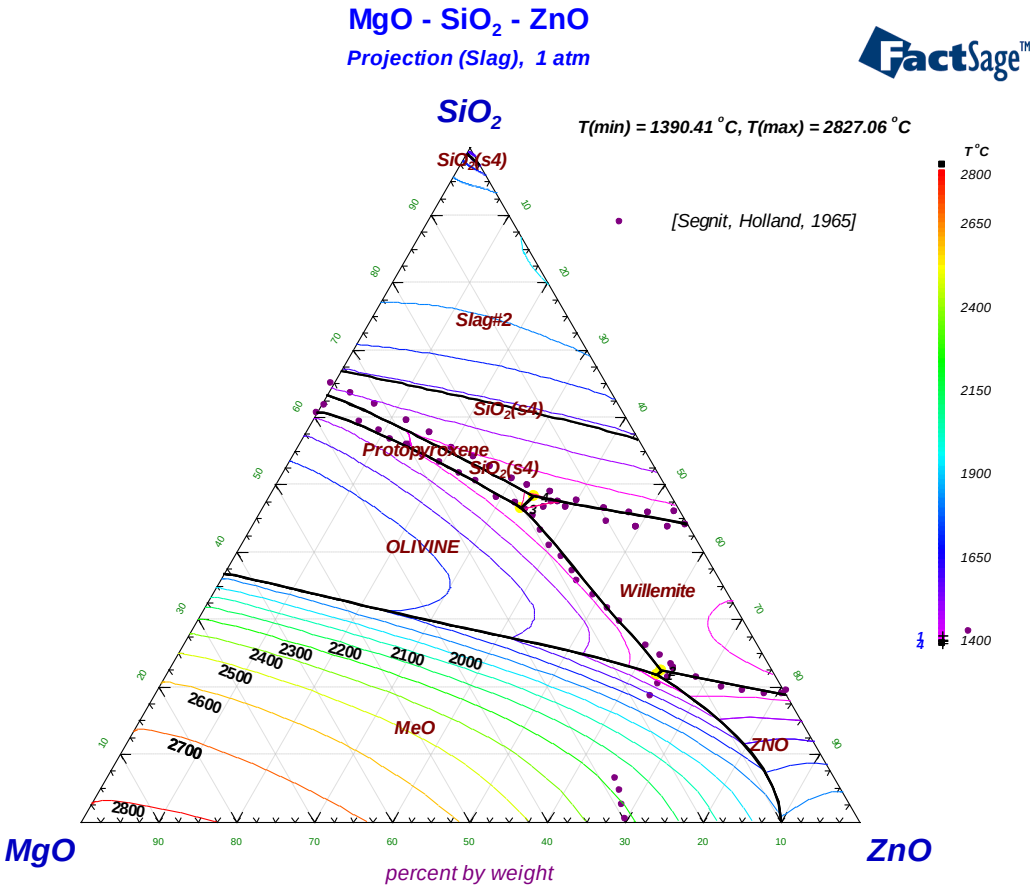

Invariant equilibria on the liquidus surface

Intersections with slag	Mole fraction				Weight percent			
	A = SiO2, B = MgO, C = ZnO				A = SiO2, B = MgO, C = ZnO			
	X(A)	X(B)	X(C)	T(C)	W(A)	W(B)	W(C)	T(C)
1: MeO / OLIVINE / ZNO	1: 0.23981	0.24600	0.51419	1415.70	1: 21.776	14.984	63.240	1415.70
2: OLIVINE / Willemite / ZNO	2: 0.24736	0.23351	0.51913	1401.07	2: 22.343	14.148	63.509	1401.07
3: OLIVINE / Protopyroxene / Willemite	3: 0.46043	0.29617	0.24340	1398.54	3: 46.566	20.093	33.341	1398.59
4: Protopyroxene / Cristobalite / Willemite	4: 0.48397	0.26394	0.25209	1390.42	4: 48.278	17.662	34.060	1390.41

MgO-TiO2-Ti2O3,
Mole fraction, 1500°C

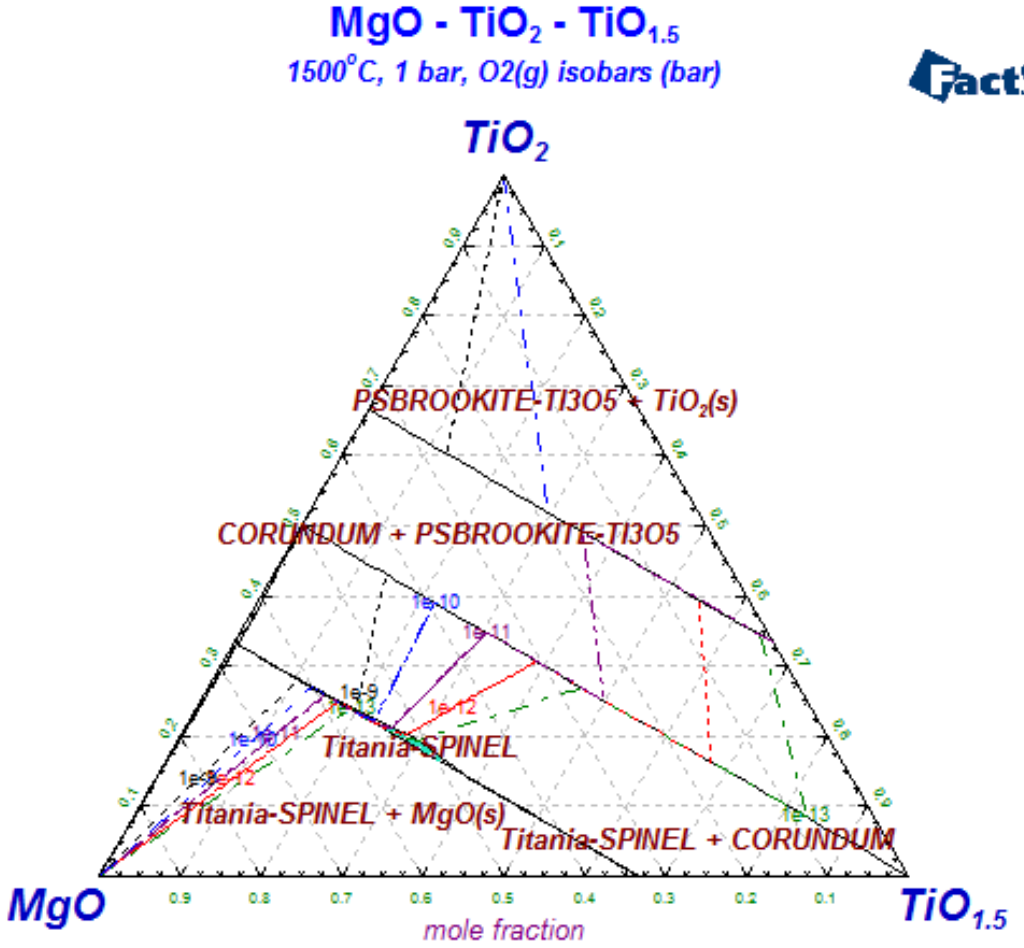

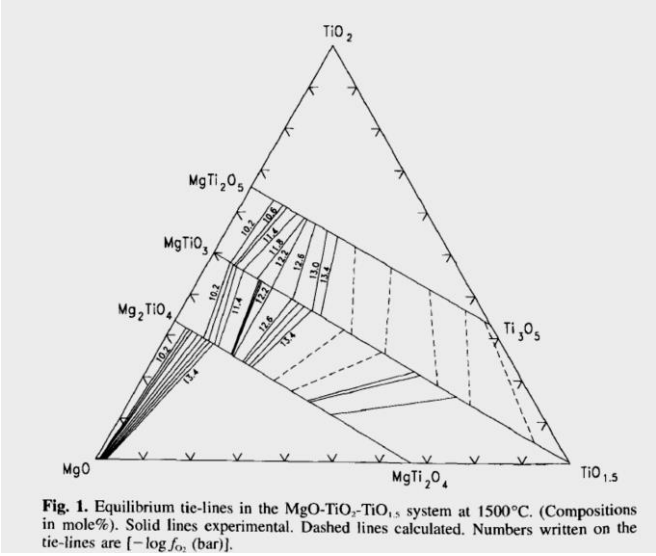

Fig. 1. Equilibrium tie-lines in the MgO-TiO_2-$TiO_{1.5}$ system at 1500°C. (Compositions in mole%). Solid lines experimental. Dashed lines calculated. Numbers written on the tie-lines are $[-\log f_{O_2}$ (bar)].

A.D. Pelton, G. Eriksson, D. Krajewski, M.Göbbels, E. Woermann, Z. Phys. Chem., 207 (1998), pp. 163-180.

MgO-TiO2-Ti2O3,
Mole fraction, Liquidus surface

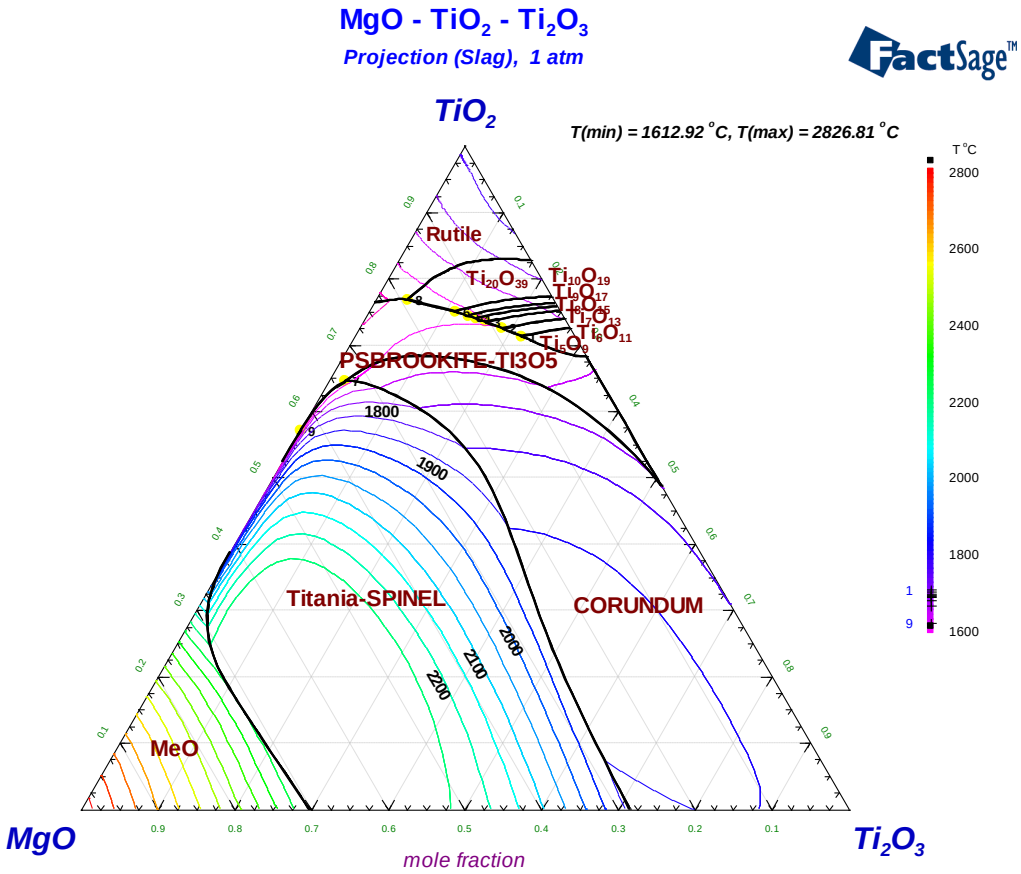

MgO-TiO2-Ti2O3,
Weight percent, Liquidus surface

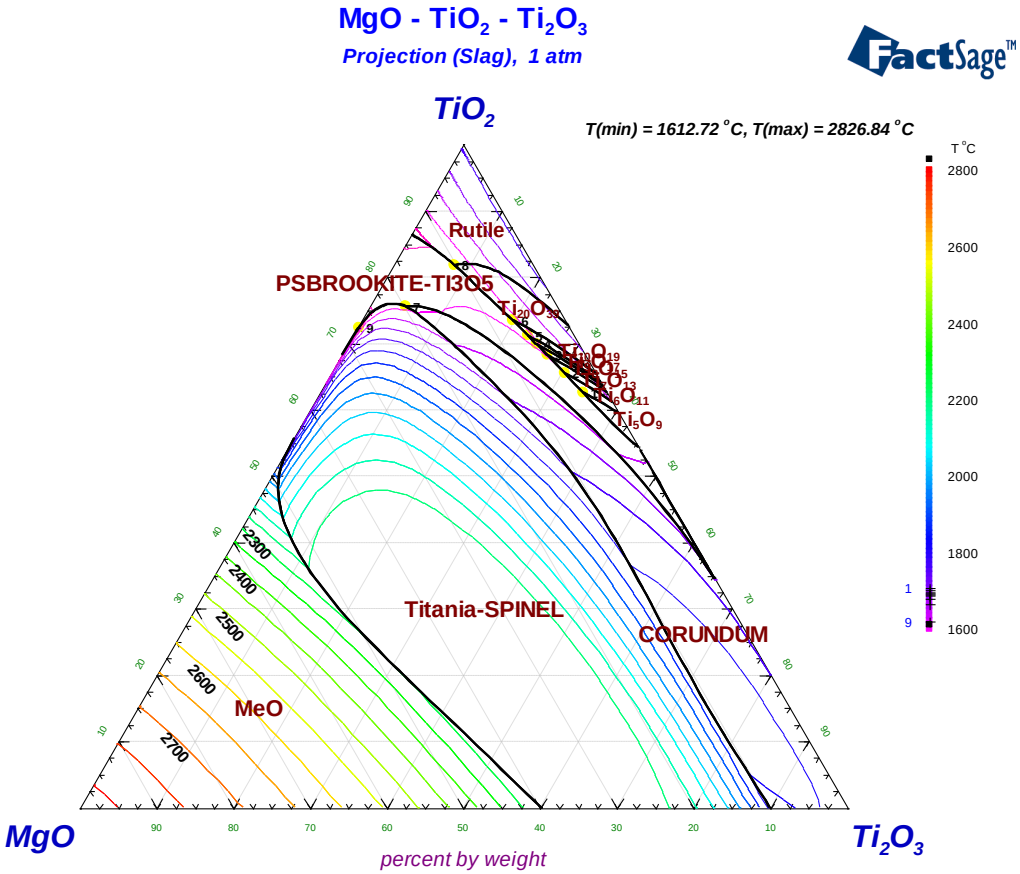

Invariant equilibria on the liquidus surface

Intersections with slag	Mole fraction A = TiO2, B = MgO, C = Ti2O3				Weight percent A = TiO2, B = MgO, C = Ti2O3			
	X(A)	X(B)	X(C)	T(C)	W(A)	W(B)	W(C)	T(C)
1: PSBROOKITE-TI3O5 / Ti5O9 / Ti6O11	0.71330	0.06905	0.21765	1708.81	62.579	3.057	34.364	1708.81
2: PSBROOKITE-TI3O5 / Ti6O11 / Ti7O13	0.72497	0.08855	0.18648	1702.35	65.593	4.043	30.364	1702.35
3: PSBROOKITE-TI3O5 / Ti7O13 / Ti8O15	0.73456	0.10562	0.15982	1697.03	68.301	4.956	26.743	1697.03
4: PSBROOKITE-TI3O5 / Ti8O15 / Ti9O17	0.74004	0.11585	0.14411	1693.86	69.956	5.527	24.518	1693.86
5: PSBROOKITE-TI3O5 / Ti10O19 / Ti9O17	0.74403	0.12373	0.13224	1691.44	71.236	5.978	22.786	1691.44
6: PSBROOKITE-TI3O5 / Ti10O19 / Ti20O39	0.75074	0.13720	0.11206	1686.97	73.483	6.777	19.740	1686.97
7: CORUNDUM / PSBROOKITE / Titania-SPINEL	0.64511	0.33343	0.02146	1680.83	75.717	19.749	4.533	1680.83
8: PSBROOKITE-TI3O5 / Rutile / Ti20O39	0.76845	0.19027	0.04128	1664.49	81.858	10.229	7.913	1664.49
9: CORUNDUM / PSBROOKITE / Titania-SPINEL	0.57125	0.42823	0.00052	1620.25	72.466	27.414	0.119	1620.22

MnO-Mn2O3-TiO2,
Mole fraction, 1200°C

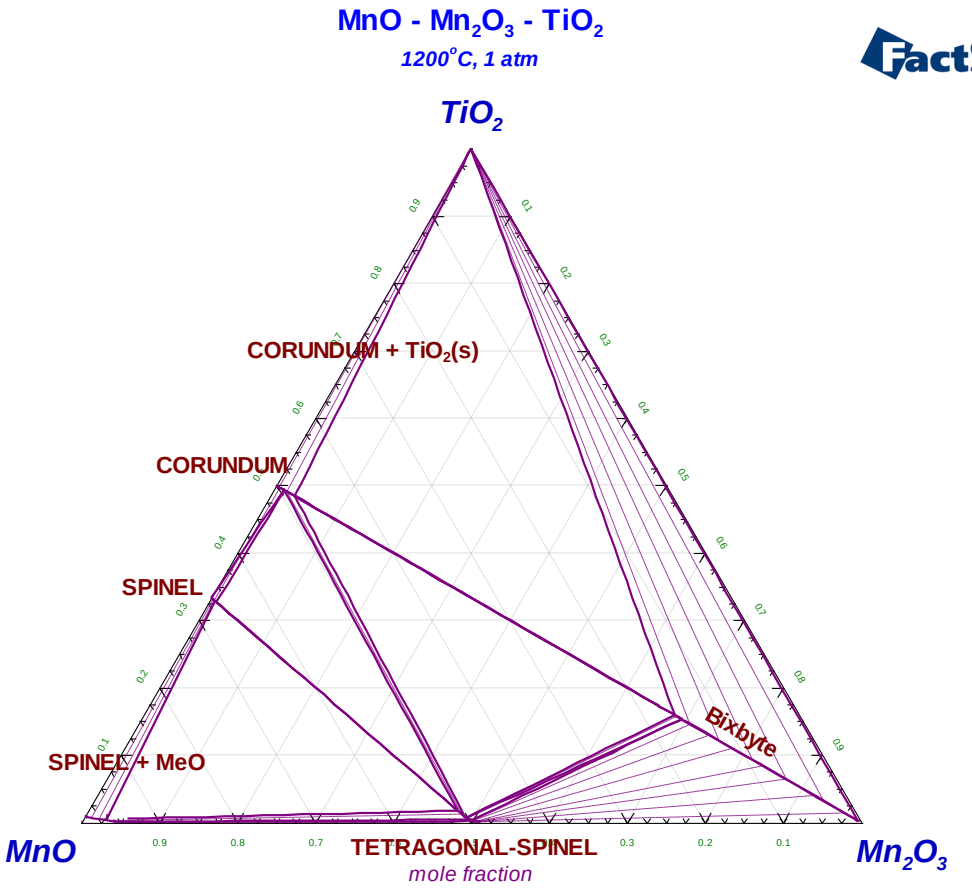

MnO-Mn2O3-TiO2, Mole fraction, 1400°C

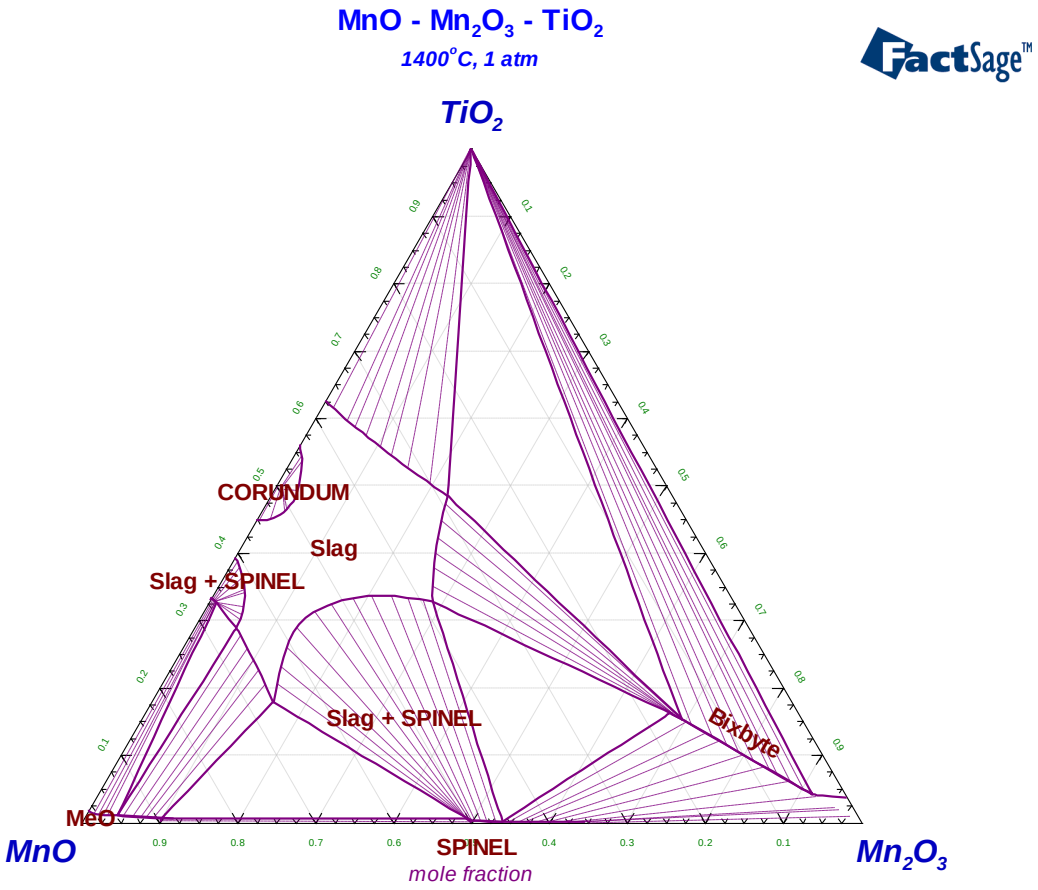

MnO-MnS-SiO2, Weight percent, 1200°C

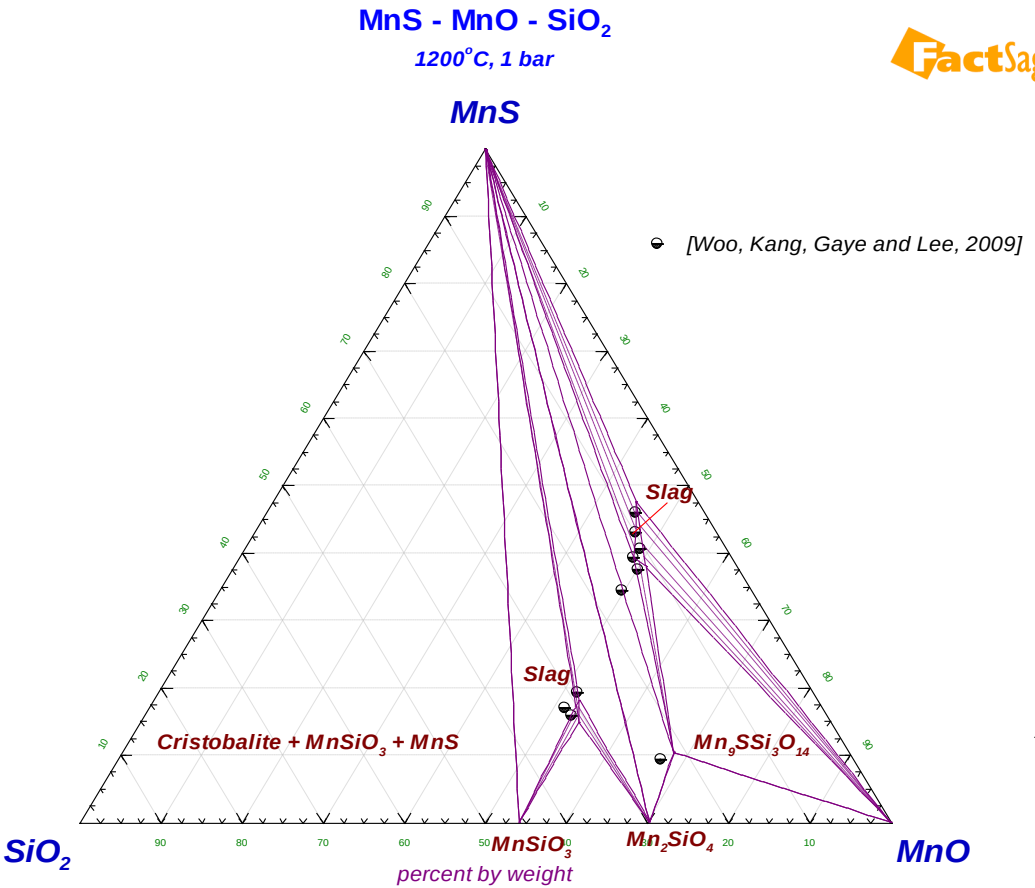

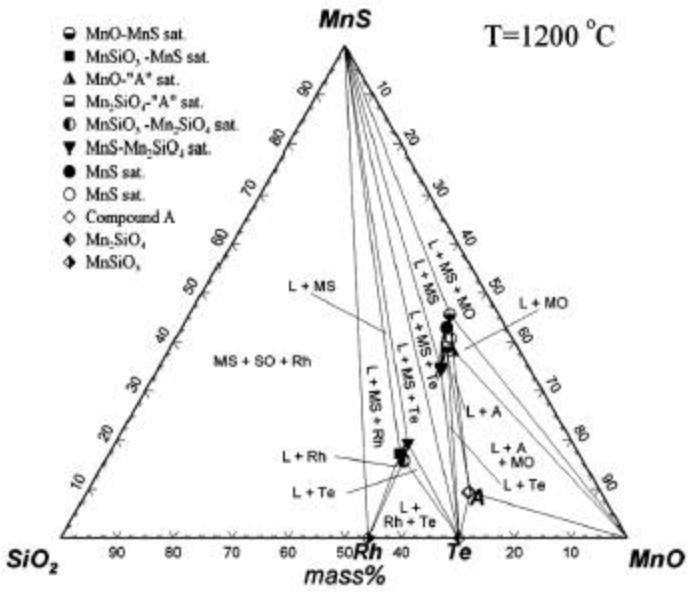

D.-H. Woo, Y.-B. Kang, H.Gaye and H.-G. Lee, ISIJ Intern., 49 (2009), pp. 1490-1497.

MnO-MnS-SiO2,
Weight percent, 1250°

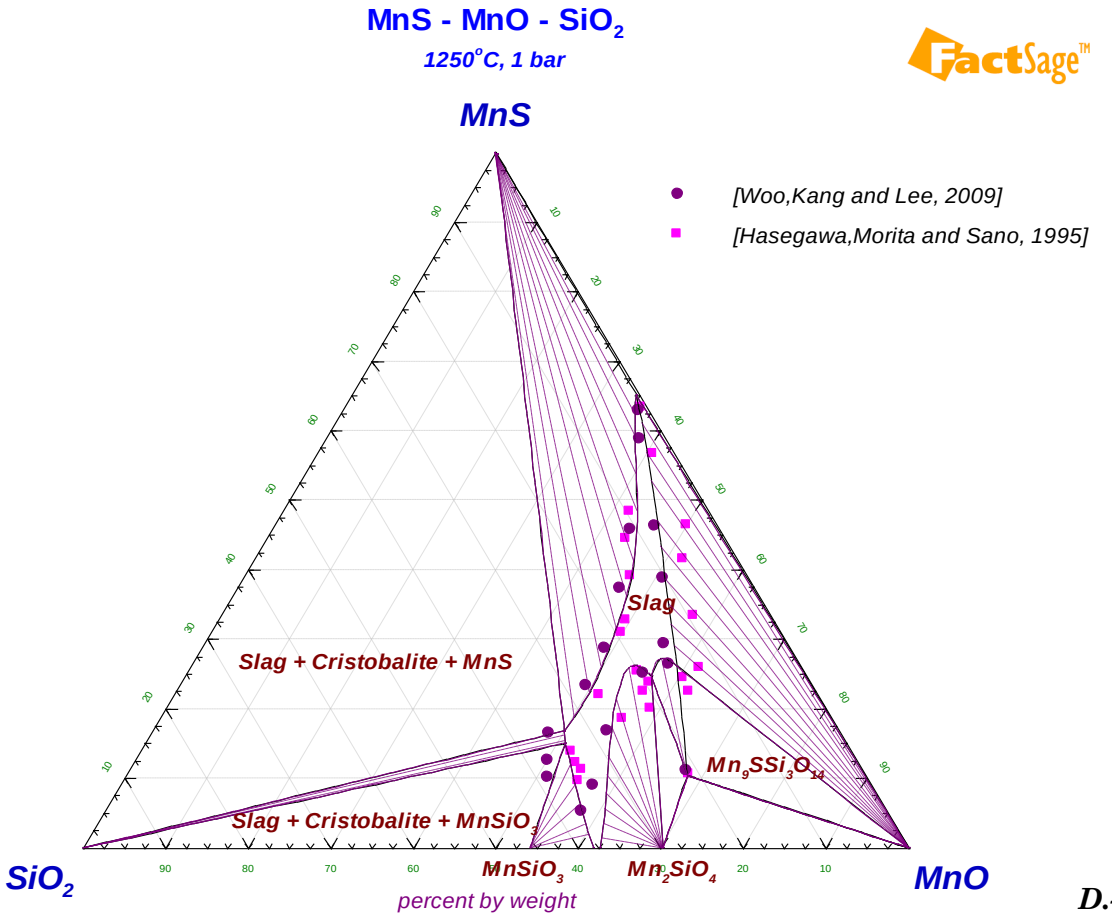

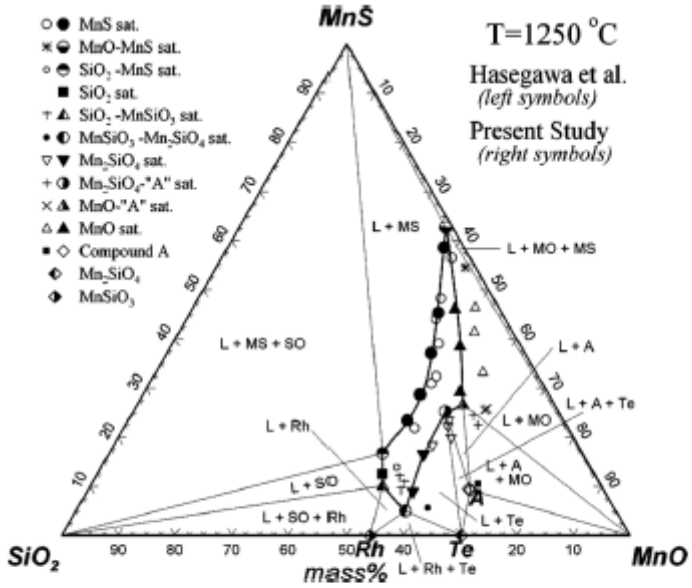

Fig. 12. Phase diagram of the MnO–SiO_2–MnS system with experimentally determined phase equilibrium data at 1 250°C. Composition of compound A was determined to be 67.0 mass% MnO, 23.6 mass% SiO_2 and 9.4 mass% MnS by EPMA analysis in the present study. Legend: MS=MnS, SO=SiO_2, MO=MnS, L=Liquid.

D.-H. Woo, Y.-B. Kang, H.Gaye and H.-G. Lee, ISIJ Intern., 49 (2009), pp. 1490-1497.

MnO-MnS-SiO2,
Weight percent, 1300°C

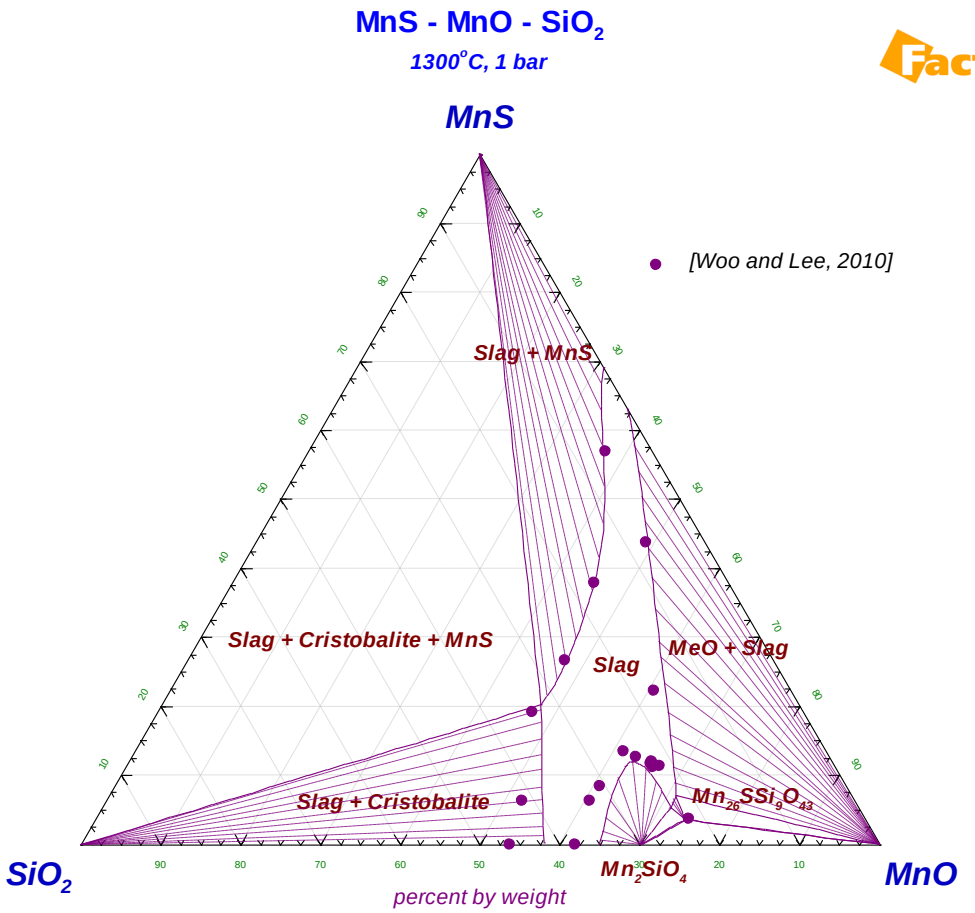

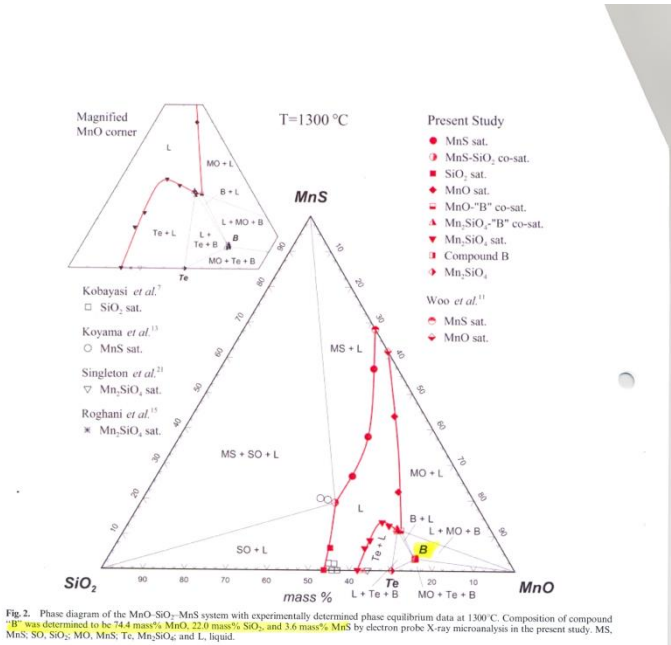

Fig. 2. Phase diagram of the MnO–SiO_2–MnS system with experimentally determined phase equilibrium data at 1300°C. Composition of compound "B" was determined to be 74.4 mass% MnO, 22.0 mass% SiO_2, and 3.6 mass% MnS by electron probe X-ray microanalysis in the present study. MS, MnS; SO, SiO_2; MO, MnS; Te, Mn_2SiO_4; and L, liquid.

D.-H. Woo and H.-G. Lee, J. Am. Ceram. Soc., 93 [7], (2010), pp. 20098-2106.

Weight percent, Isopleth MnS-MnSiO3 compared with experimental data

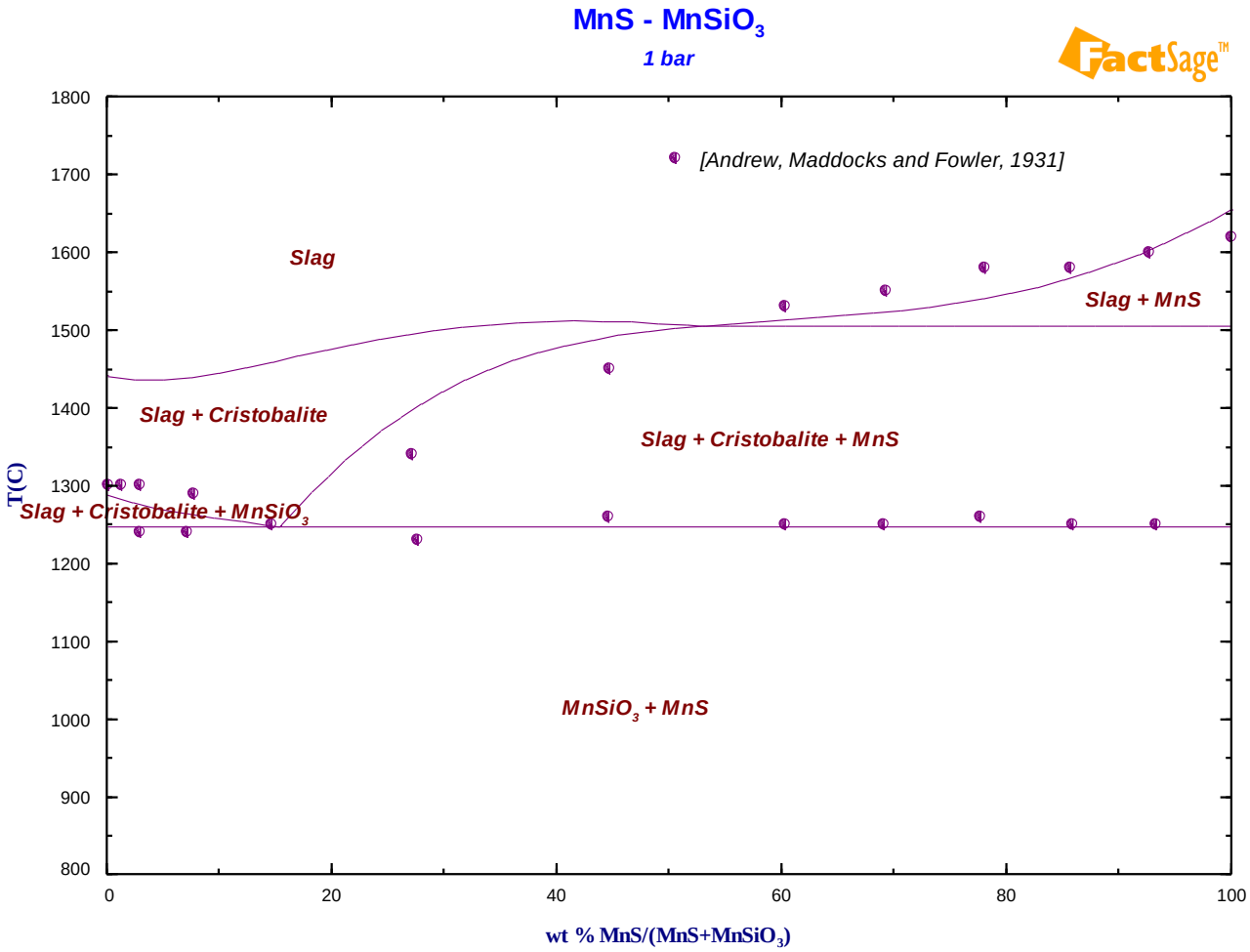

Mole fraction, Liquidussurface

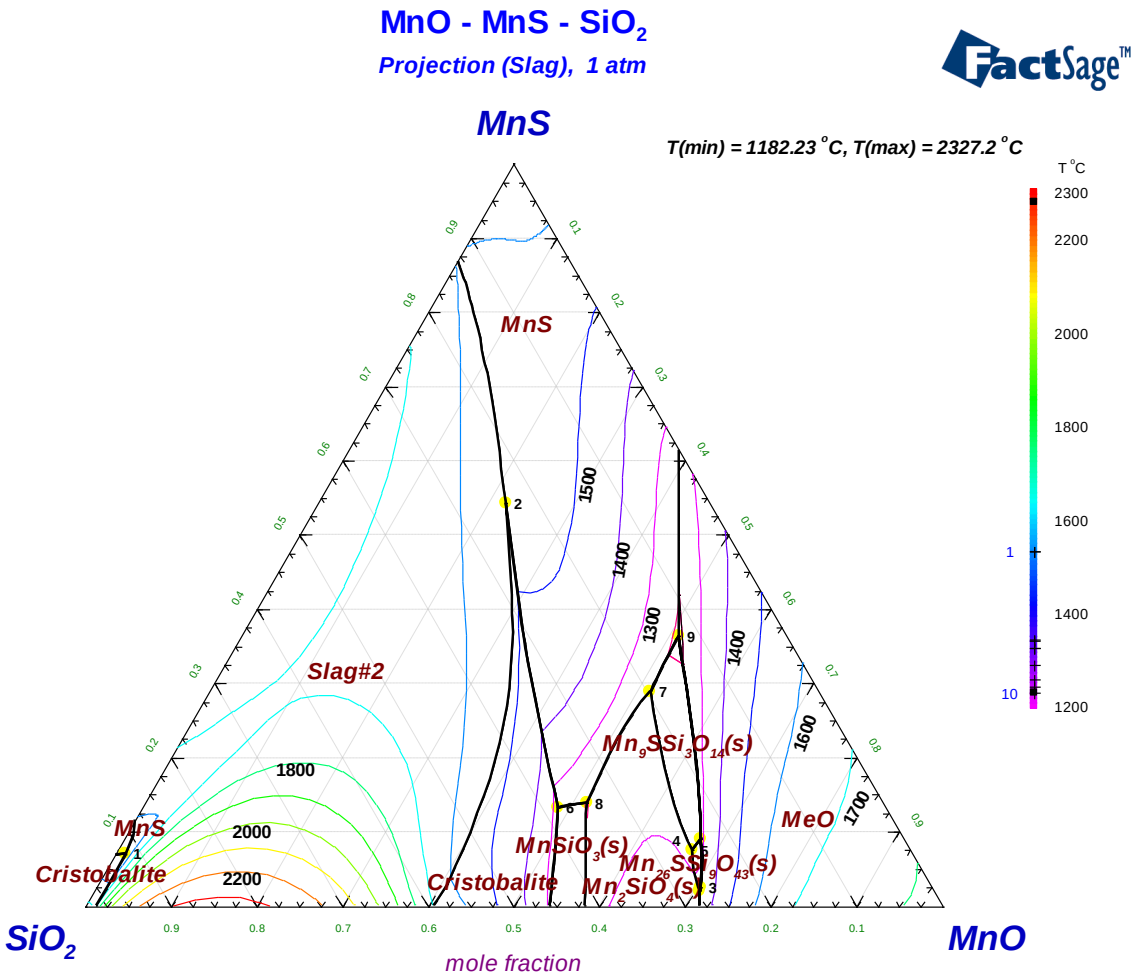

Weight percent, Liquidussurface

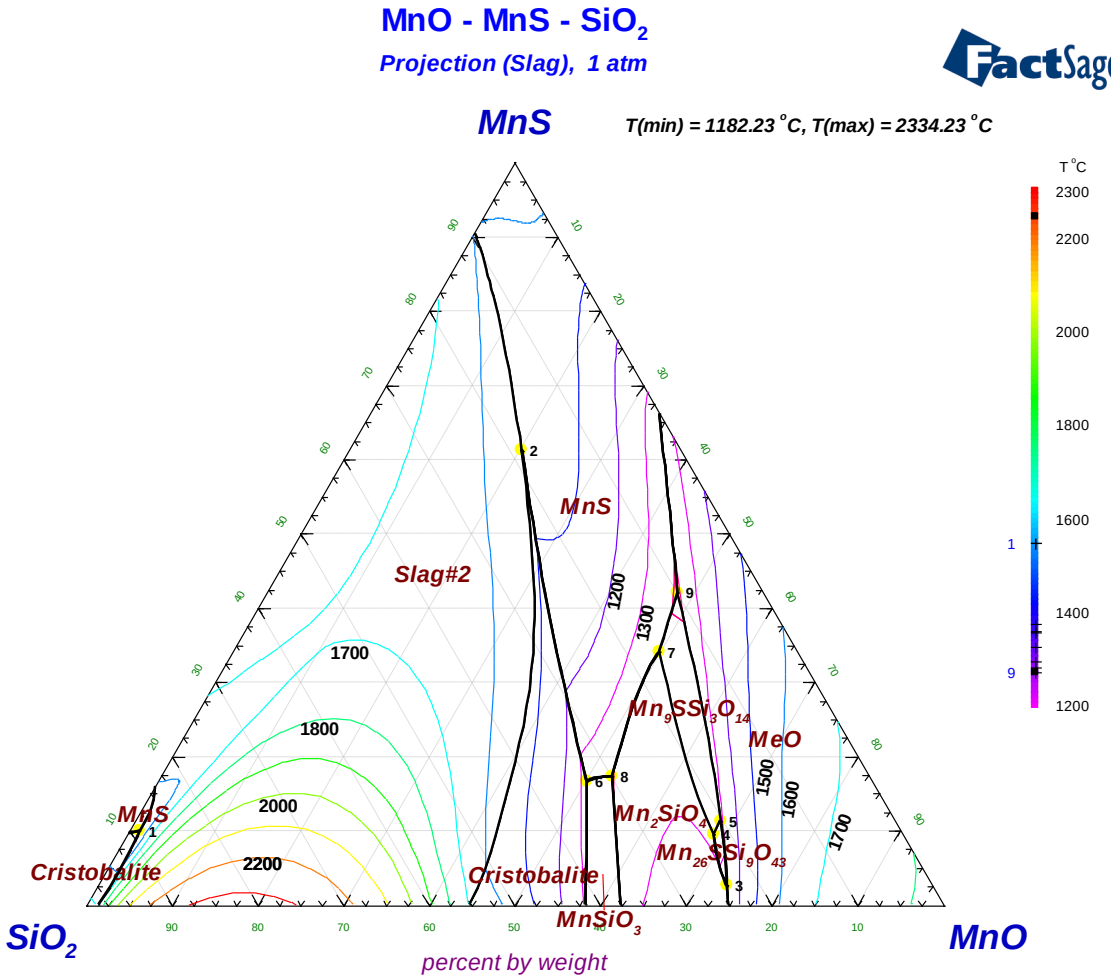

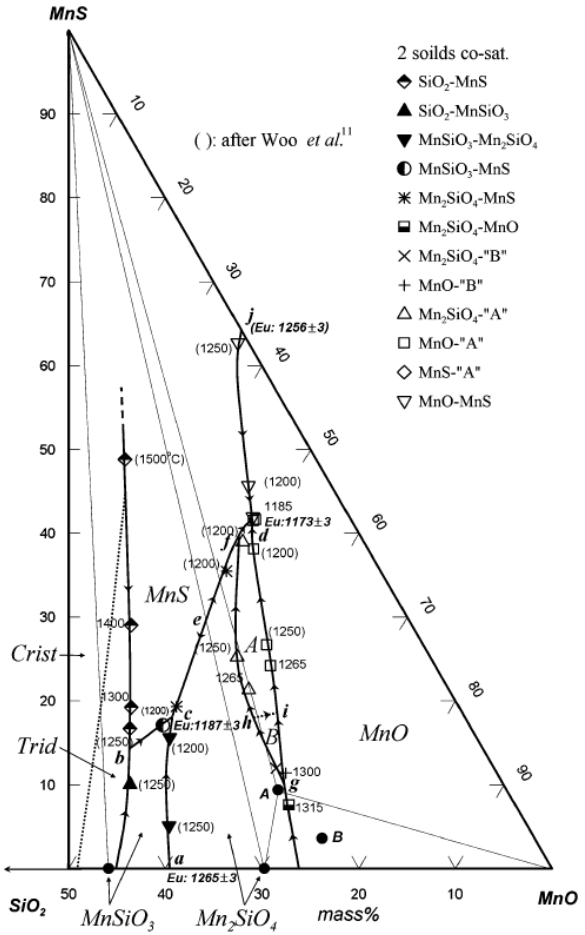

D.-H. Woo and H.-G. Lee, J. Am. Ceram. Soc., 93 [7], (2010), pp.2098-2106.

Invariant equilibria on the liquidus surface

Intersections with slag	Mole fraction A = MnS, B = SiO2, C = MnO				Weight percent A = MnS, B = SiO2, C = MnO				
		X(A)	X(B)	X(C)	T(C)		W(A)	W(B)	W(C)	T(C)
1: MnS(s) / Cristobalite / Slag#2	1:	0.07162	0.91766	0.01072	1511.32	1:	10.029	88.747	1.224	1511.32
2: MnS(s) / Cristobalite / Slag#2	2:	0.54388	0.23741	0.21871	1511.31	2:	61.375	18.502	20.123	1511.31
3: MeO / Mn26SSi9O43 / Mn2SiO4(s)	3:	0.02058	0.27249	0.70692	1304.53	3:	2.622	23.968	73.411	1304.53
4: Mn26SSi9O43 / Mn2SiO4(s) / Mn9SSi3O14	4:	0.07577	0.25448	0.66975	1286.38	4:	9.499	22.035	68.466	1286.38
5: MeO / Mn26SSi9O43 / Mn9SSi3O14	5:	0.09100	0.23635	0.67265	1284.92	5:	11.337	20.335	68.327	1284.92
6: MnS(s) / MnSiO3(s) / Cristobalite	6:	0.13244	0.38184	0.48573	1247.34	6:	16.718	33.288	49.994	1247.34
7: Mn2SiO4(s) / Mn9SSi3O14 / MnS(s)	7:	0.28853	0.19627	0.51520	1211.65	7:	34.180	16.057	49.763	1211.65
8: Mn2SiO4(s) / MnS(s) / MnSiO3(s)	8:	0.13882	0.34590	0.51529	1195.30	8:	17.399	29.941	52.660	1195.30
9: MeO / Mn9SSi3O14 / MnS(s)	9:	0.36430	0.12559	0.51010	1182.24	9:	42.021	10.004	47.974	1182.23

Mole fraction, 1200°C

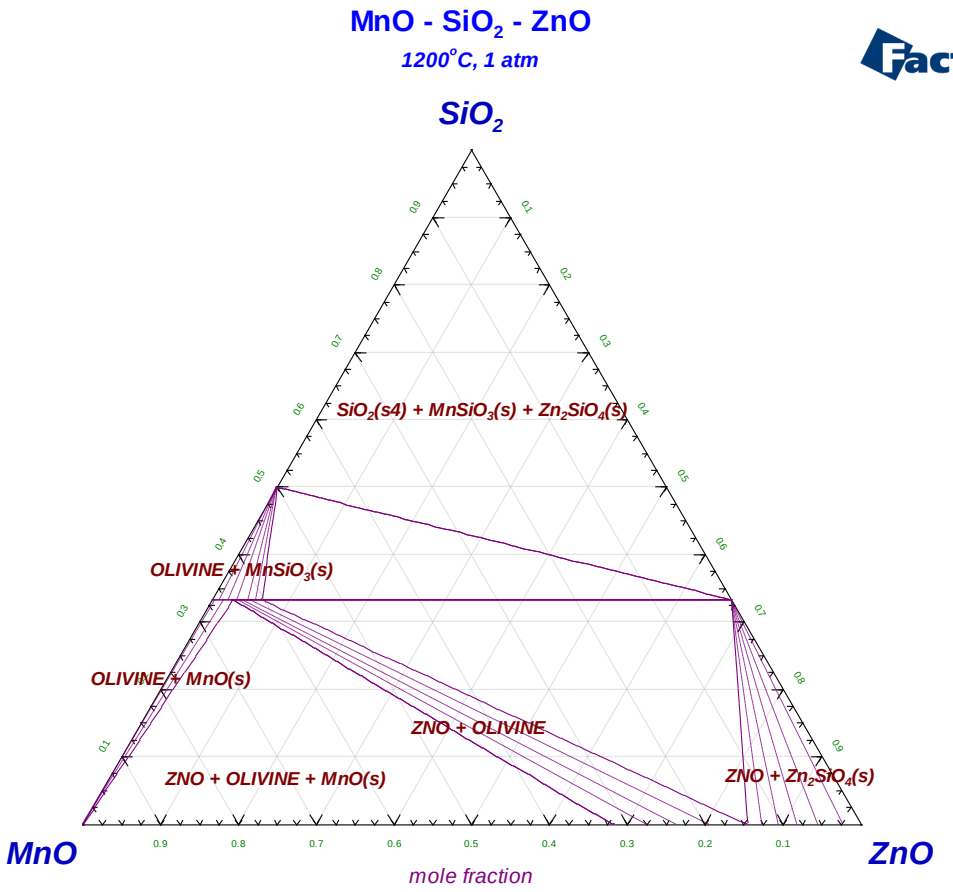

Mole fraction, Isopleth Mn2SiO4-Zn2SiO4

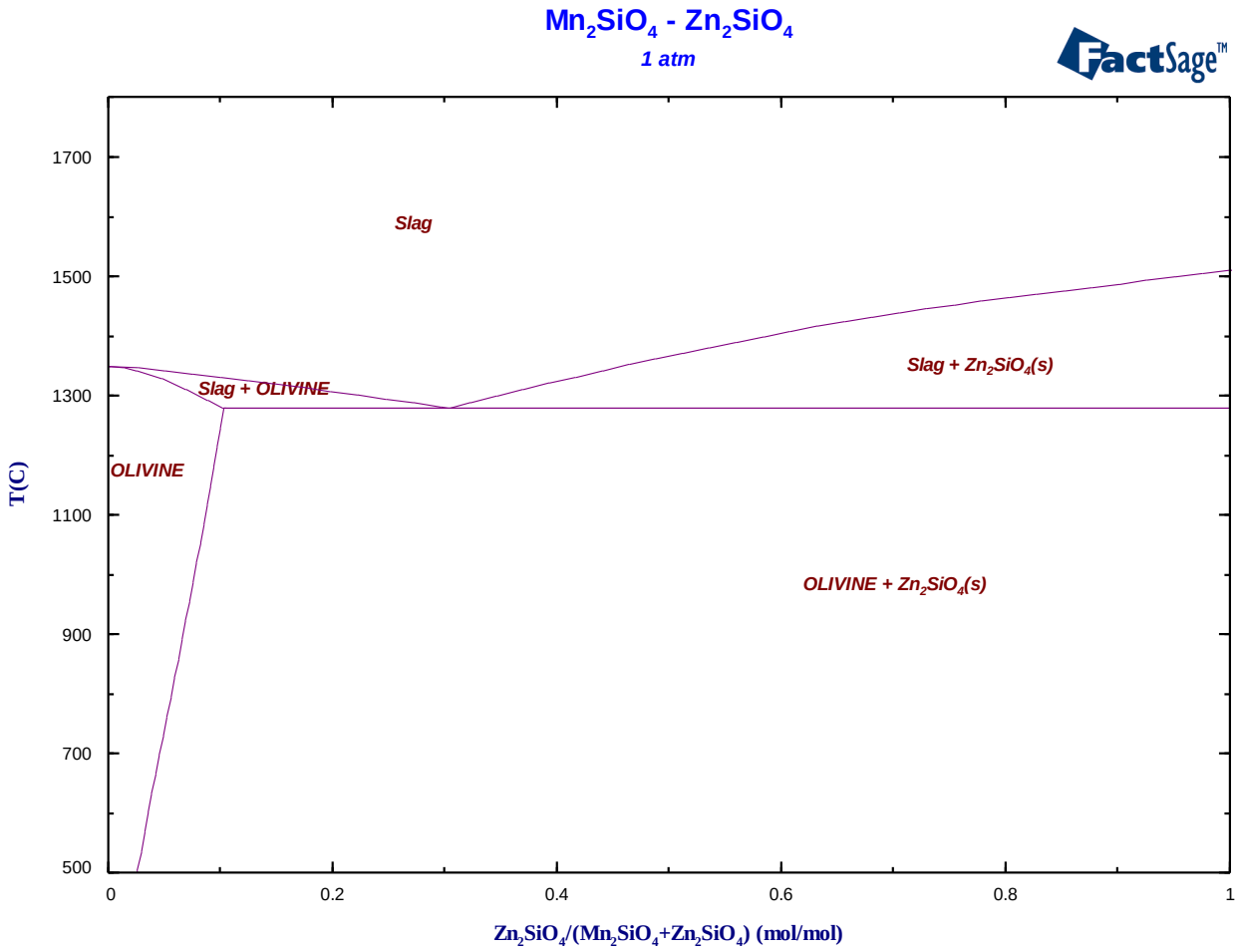

Mole fraction, Liquidussurface

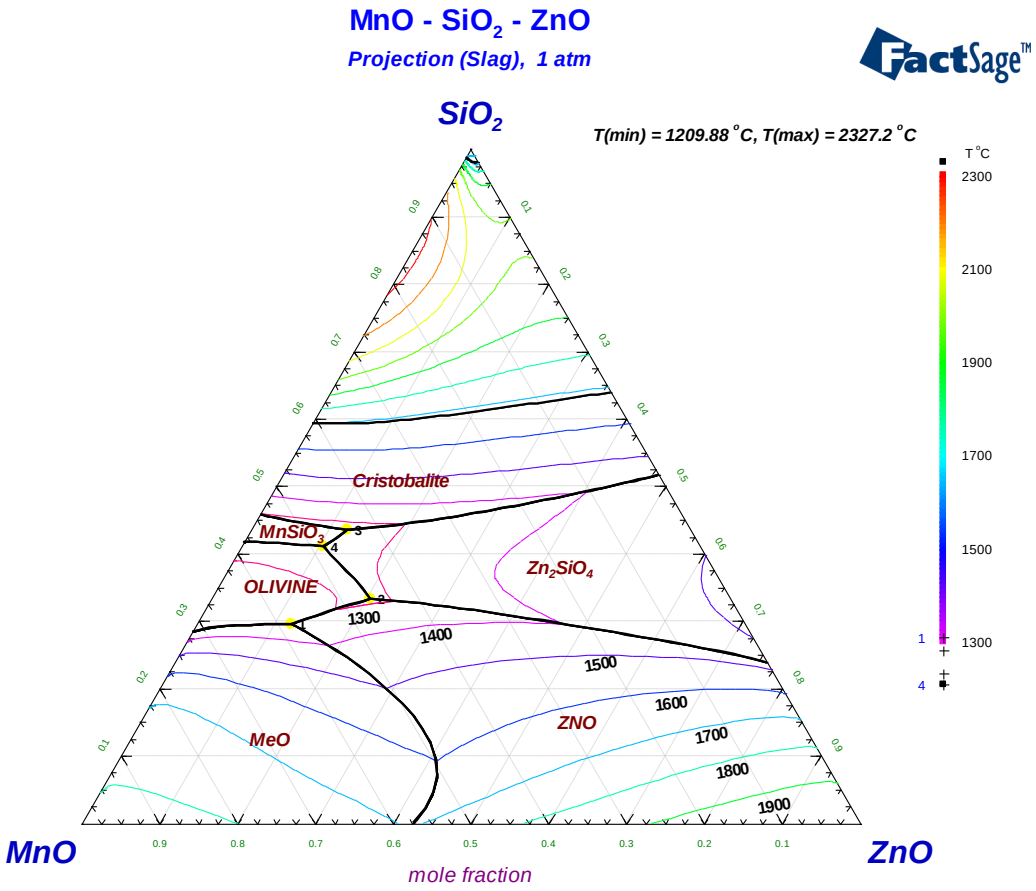

Weight percent, Liquidussurface

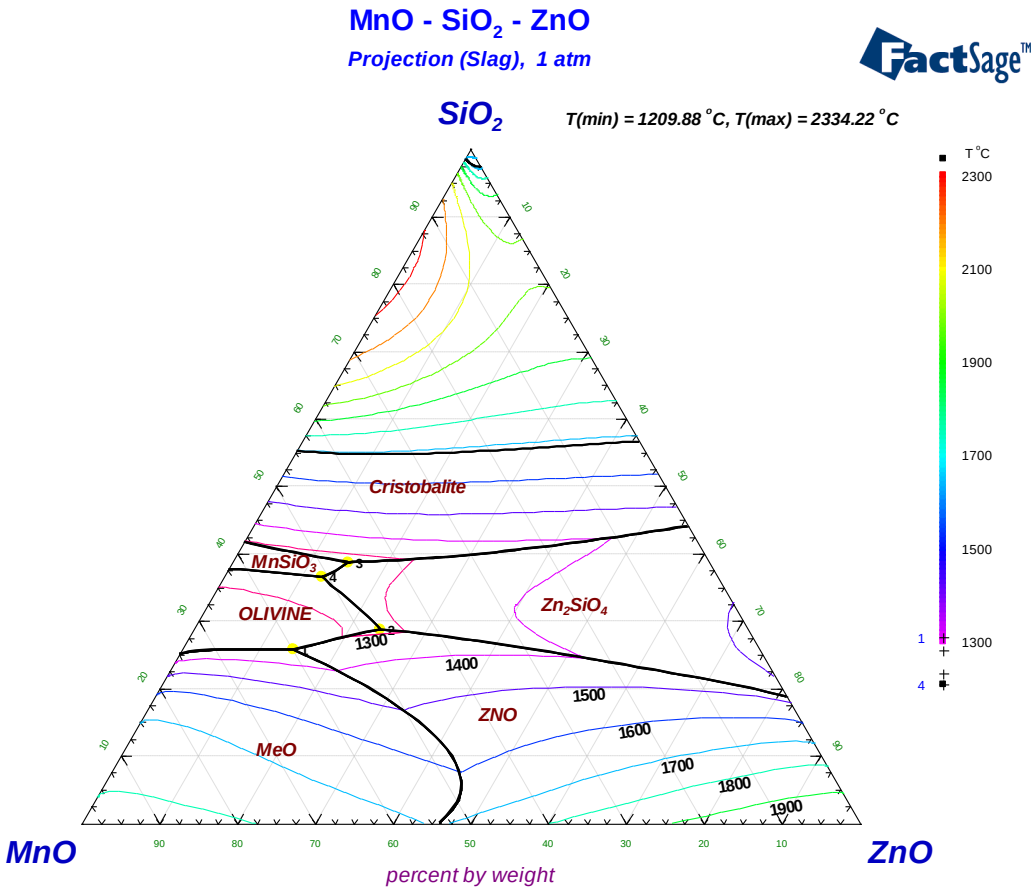

Invariant equilibria on the liquidus surface

Intersections with slag	Mole fraction A = SiO2, B = MnO, C = ZnO				Weight percent A = SiO2, B = MnO, C = ZnO			
	X(A)	X(B)	X(C)	T(C)	W(A)	W(B)	W(C)	T(C)
1: MeO / OLIVINE / ZNO	1: 0.29561	0.58254	0.12185	1309.25	1: 25.741	59.889	14.370	1309.22
2: OLIVINE / ZNO / Zn2SiO4	2: 0.33302	0.46205	0.20493	1281.21	2: 28.806	47.186	24.009	1281.21
3: MnSiO3 / Cristobalite / Zn2SiO4	3: 0.43533	0.44135	0.12333	1232.57	3: 38.750	46.382	14.868	1232.69
4: MnSiO3 / OLIVINE / Zn2SiO4	4: 0.41100	0.48390	0.10511	1209.88	4: 36.544	50.798	12.658	1209.88

MnO-TiO2-Ti2O3,
Mole fraction, 1200°C

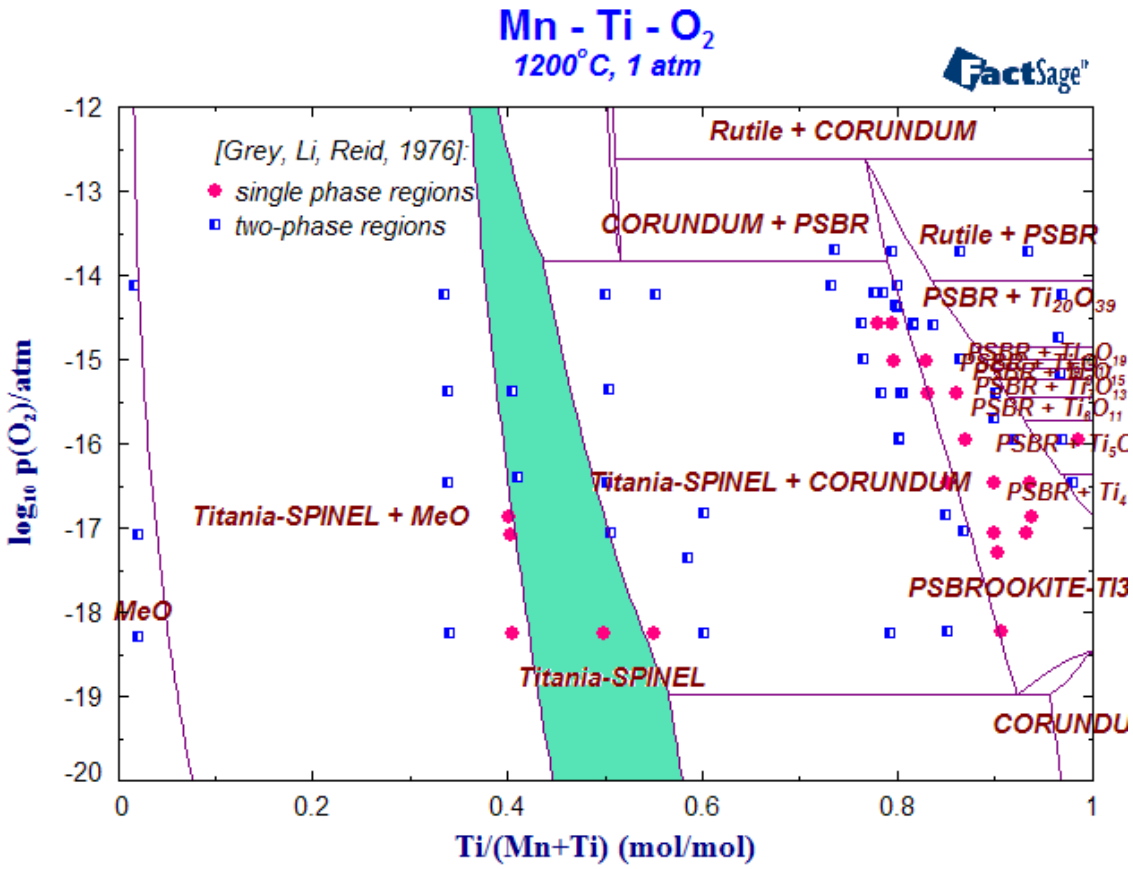

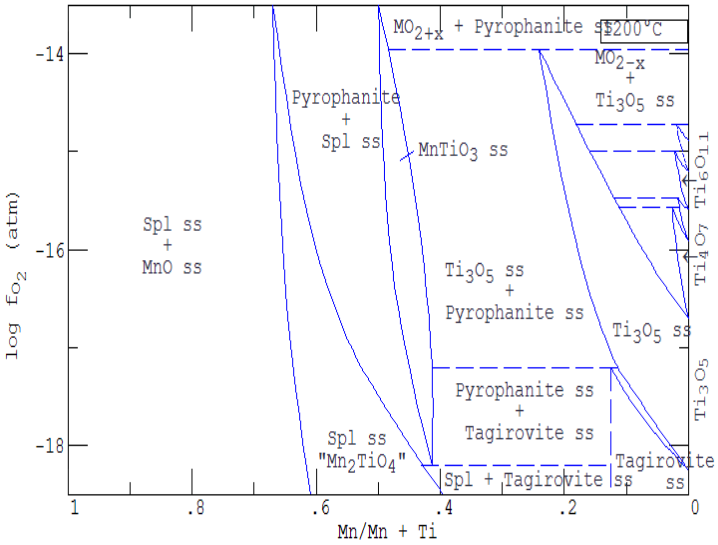

I.E. Grey, C. Li, A.F. Reid, J. Solid State Chem., 17 [4], (1976), pp. 343-352.

MnO-TiO2-Ti2O3,
Mole fraction, TiO2-TiO1.6-Mn.33Ti.67O1.6, 1200°C

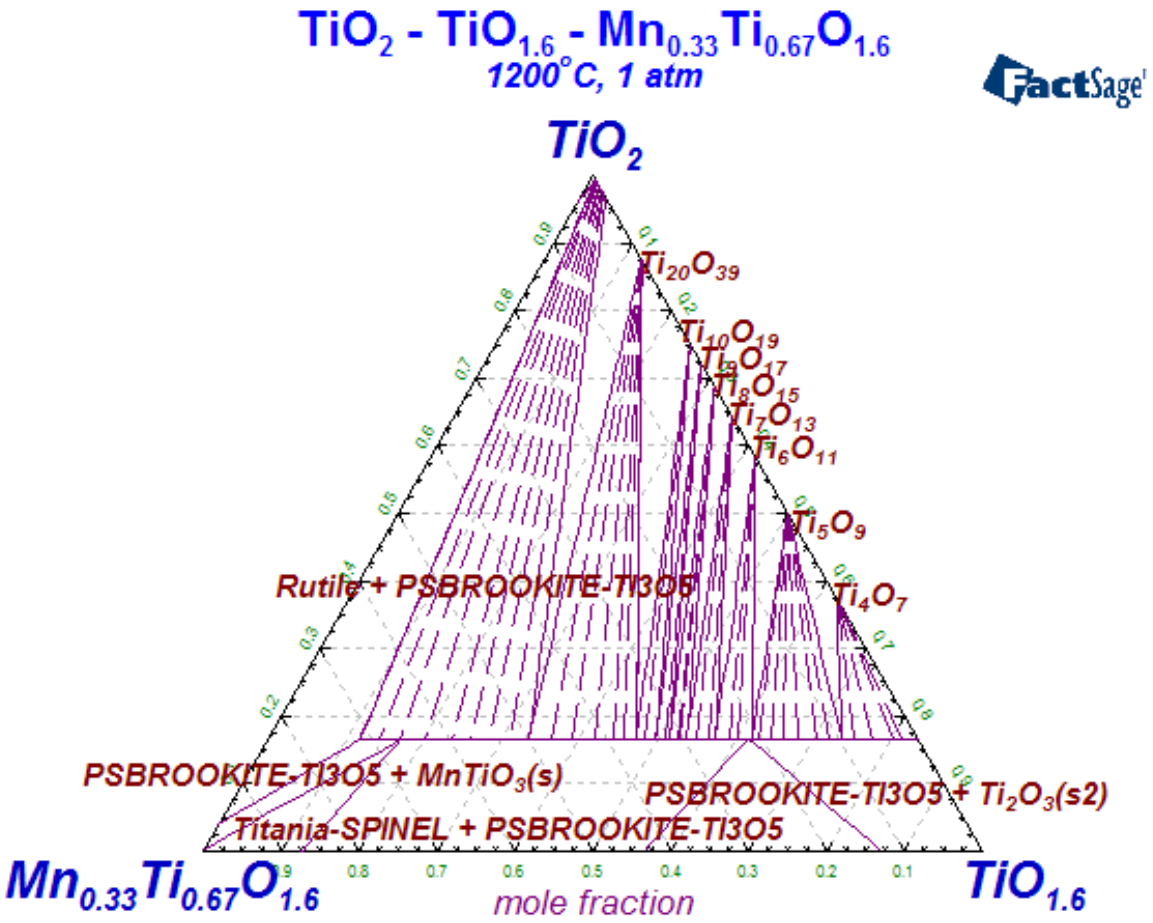

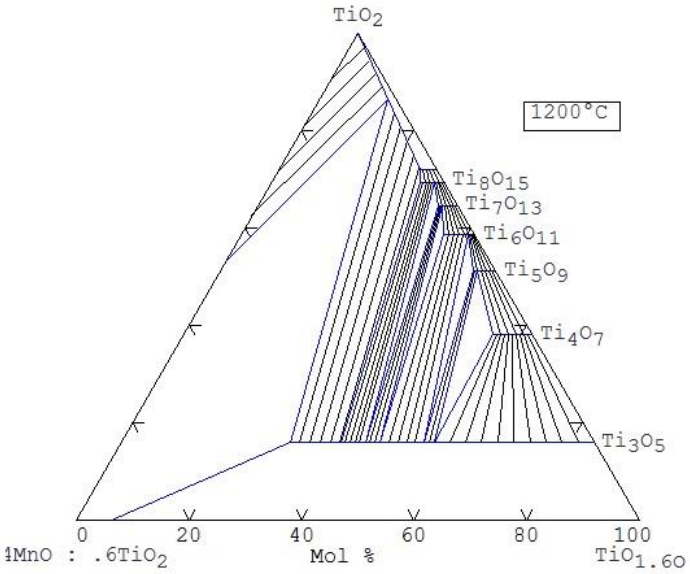

I.E. Grey, C. Li, A.F. Reid, J. Solid State Chem., 17 [4], (1976), pp. 343-352.

MnO-TiO2-Ti2O3,
Mole fraction, 1400°C

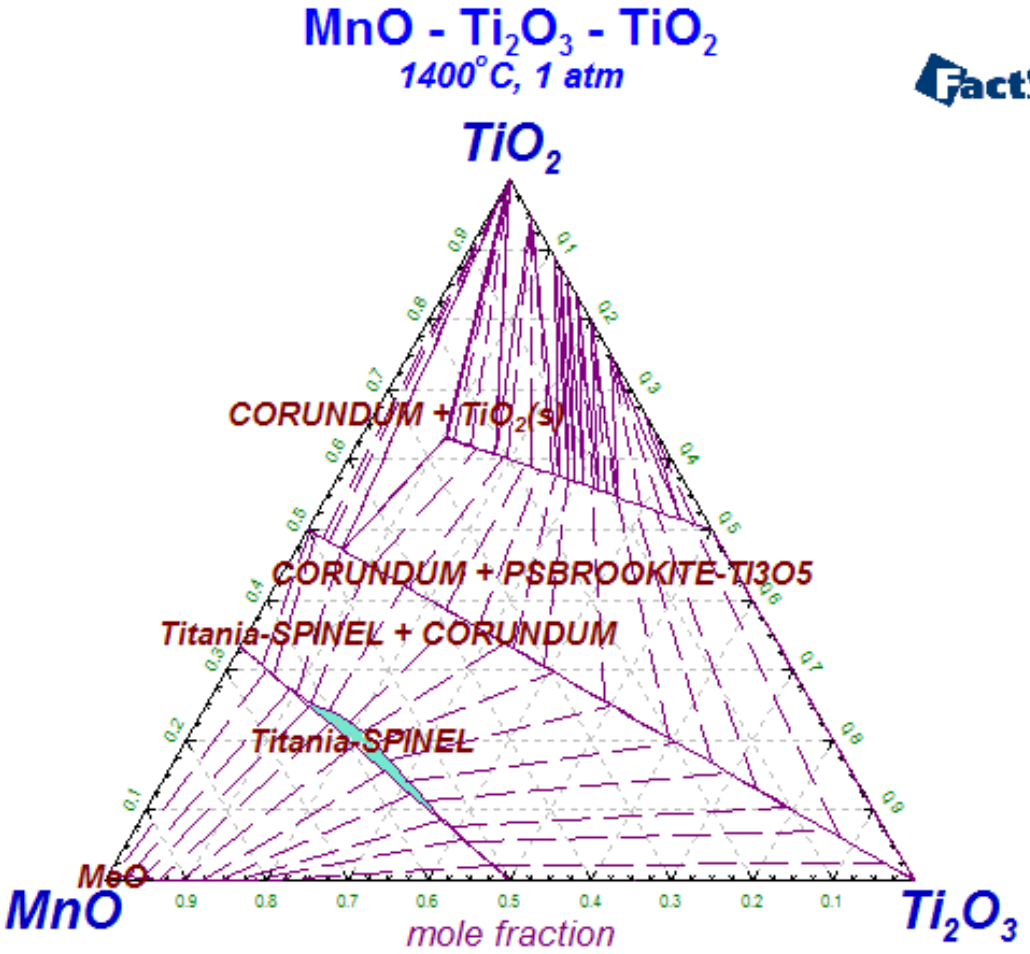

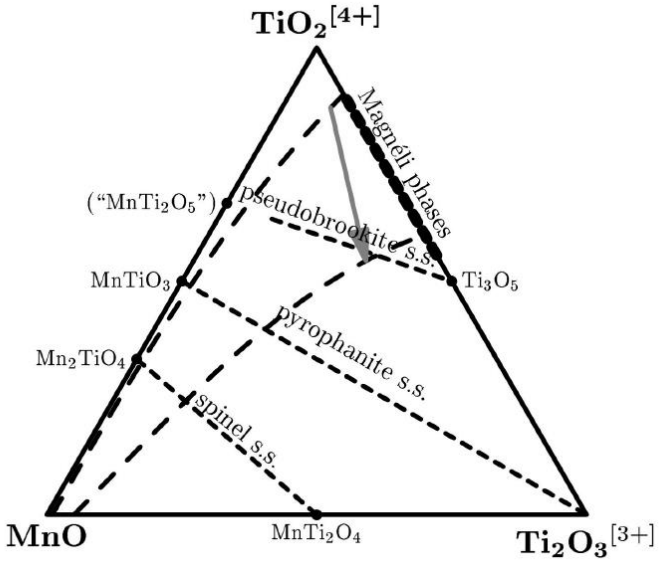

J.-B. Kang, H.-B. Lee, ISIJ Intern., 45 (2005), pp. 1543-1551.

MnO-TiO2-Ti2O3,
Mole fraction, Liquidussurface

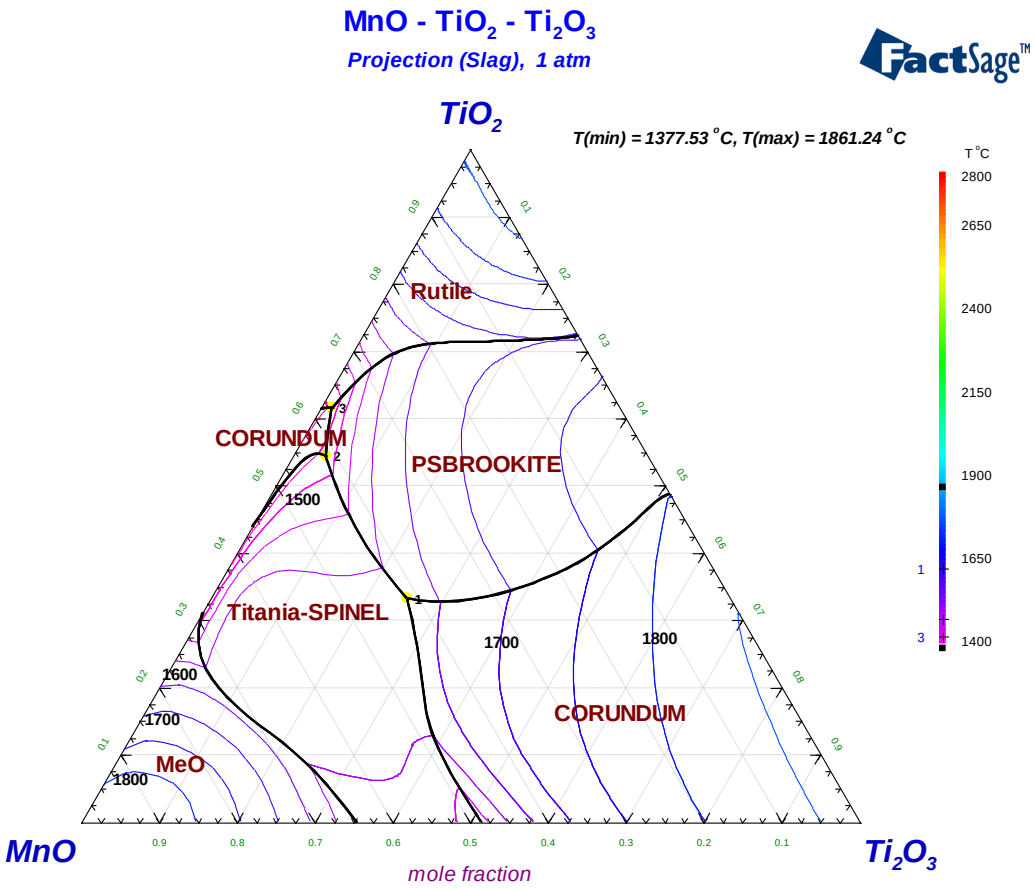

MnO-TiO2-Ti2O3,
Weight percent, Liquidussurface

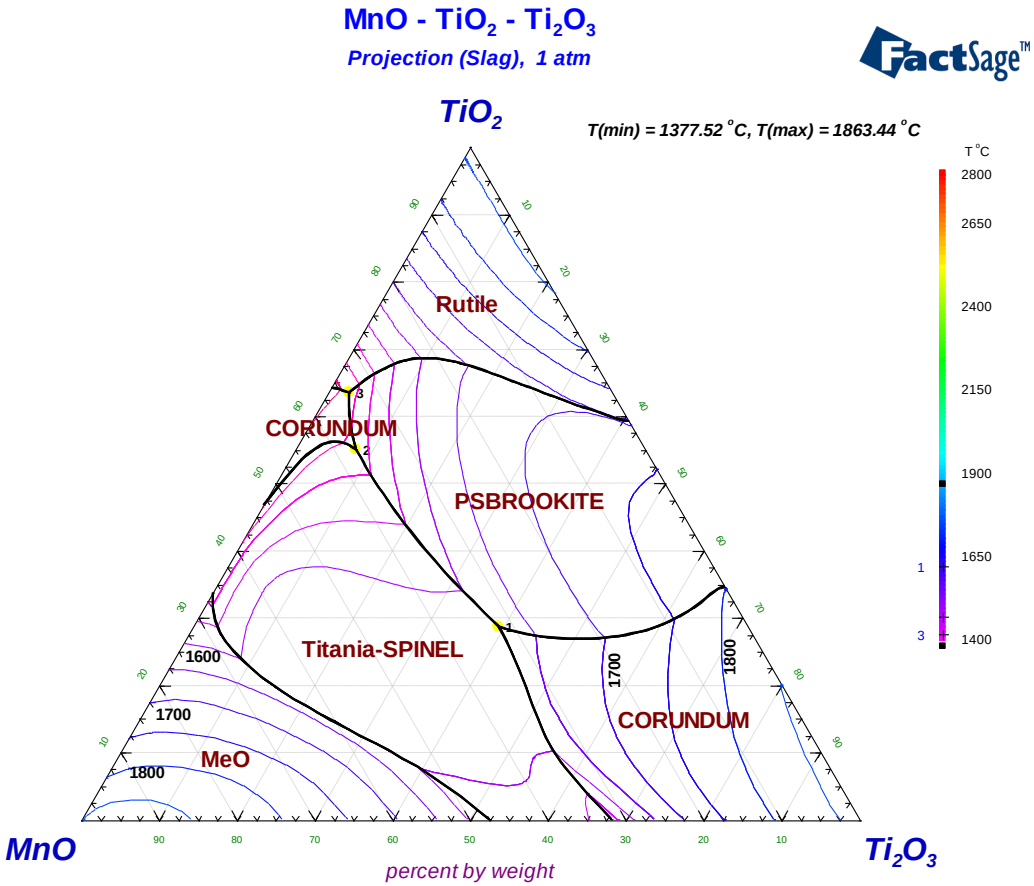

Invariant equilibria on the liquidus surface

Intersections with slag	Mole fraction				Weight percent			
	A = TiO2, B = MnO, C = Ti2O3				A = SiO2, B = MnO, C = ZnO			
	X(A)	X(B)	X(C)	T(C)	W(A)	W(B)	W(C)	T(C)
1: CORUNDUM / PSBROOKITE / Titania-SPINEL	1: 0.33261	0.41551	0.25188	1618.96	1: 28.798	31.954	39.248	1618.96
2: CORUNDUM / PSBROOKITE / Titania-SPINEL	2: 0.54404	0.41335	0.04261	1466.40	2: 55.072	37.165	7.763	1466.40
3: CORUNDUM / PSBROOKITE-TI3O5 / Rutile	3: 0.61621	0.36991	0.01388	1415.70	3: 63.544	33.881	2.575	1415.70

Na2O-P2O5-SiO2,
Mole fraction, ternary phases

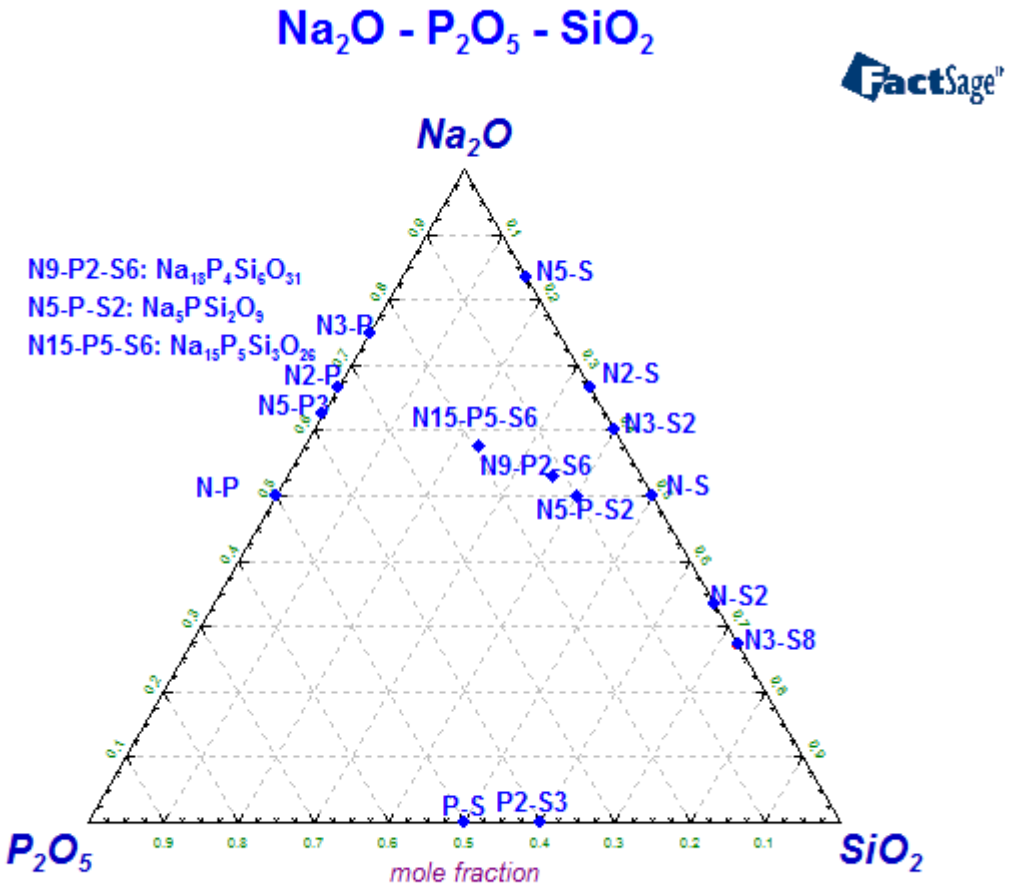

Mole fraction Isopleth $2Na_3PO_4$-Na_2SiO_3 compared with experimental data

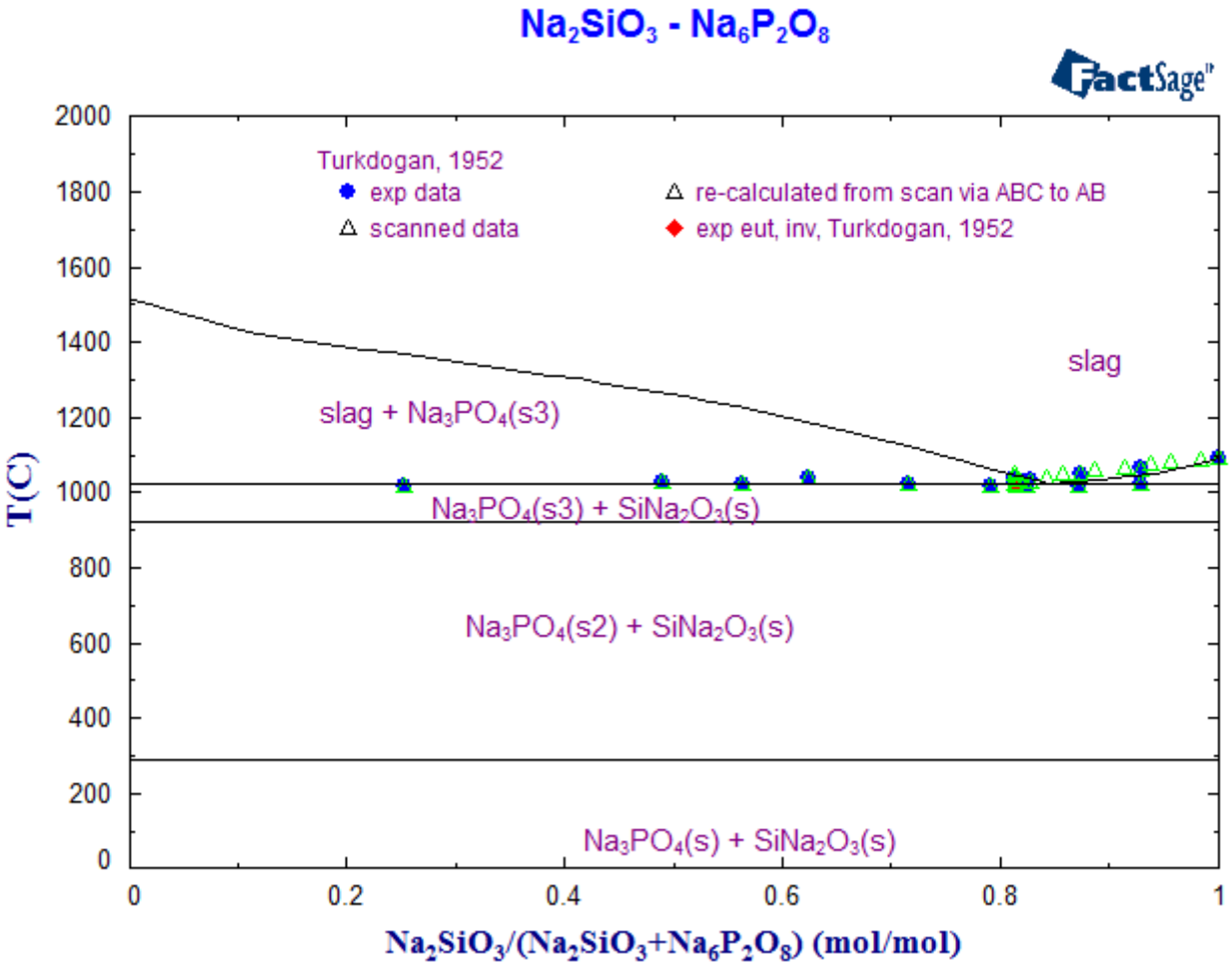

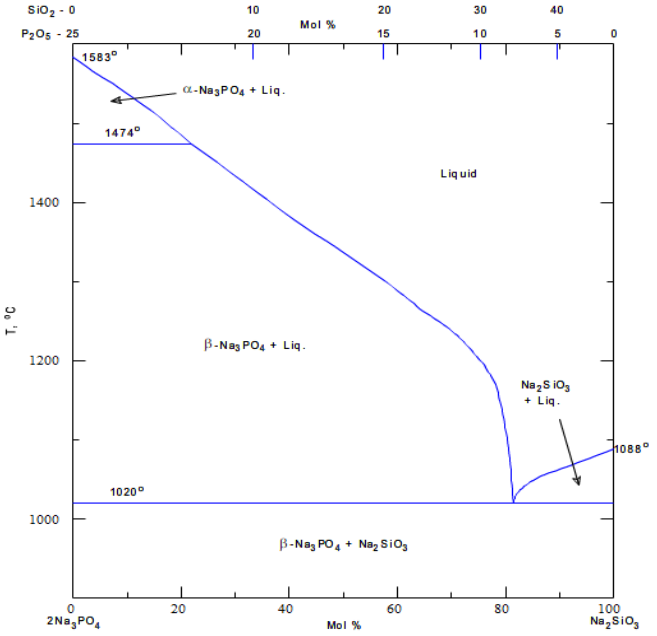

Na_3PO_4 Na_2SiO_3

E. T. Turkdogan and W. R. Maddocks, J. Iron Steel Inst., London, 172 [Pt. 1] 1-15 (1952).

Mole fraction Isopleth $2Na_3PO_4$-$Na_2Si_2O_5$ compared with experimental data

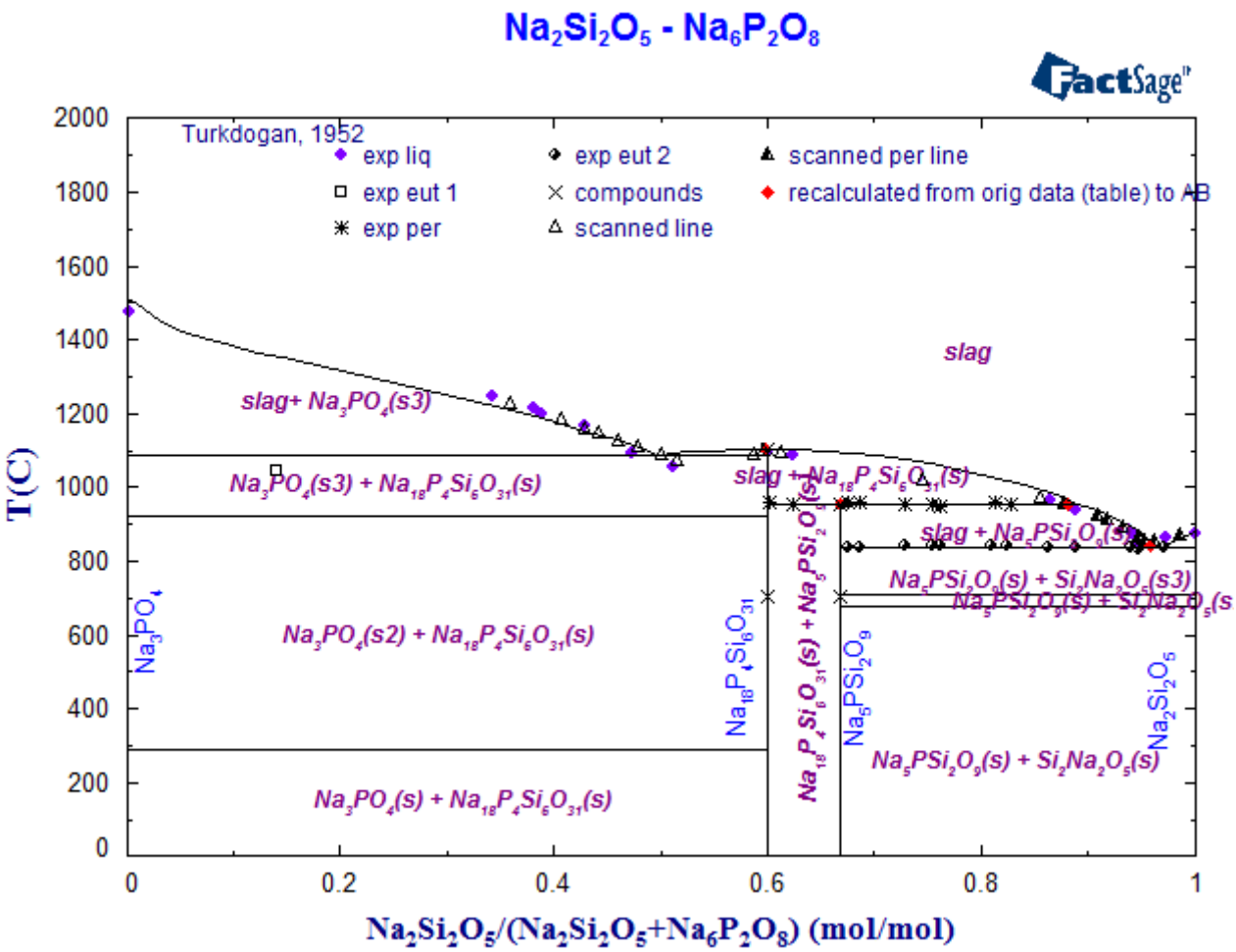

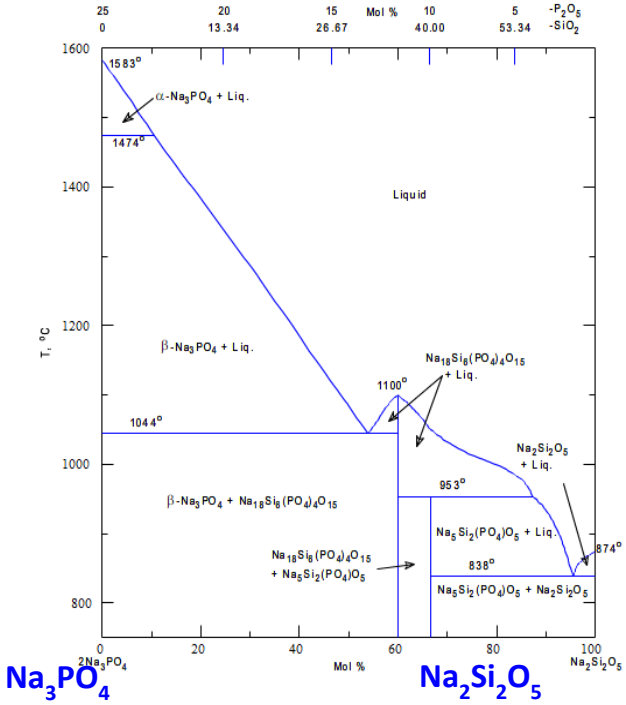

E. T. Turkdogan and W. R. Maddocks, J. Iron Steel Inst., London, 172 [Pt. 1] 1-15 (1952).

Mole fraction Isopleth $Na_{18}P_4Si_6O_{31}$-$Na_4P_2O_7$ compared with experimental data

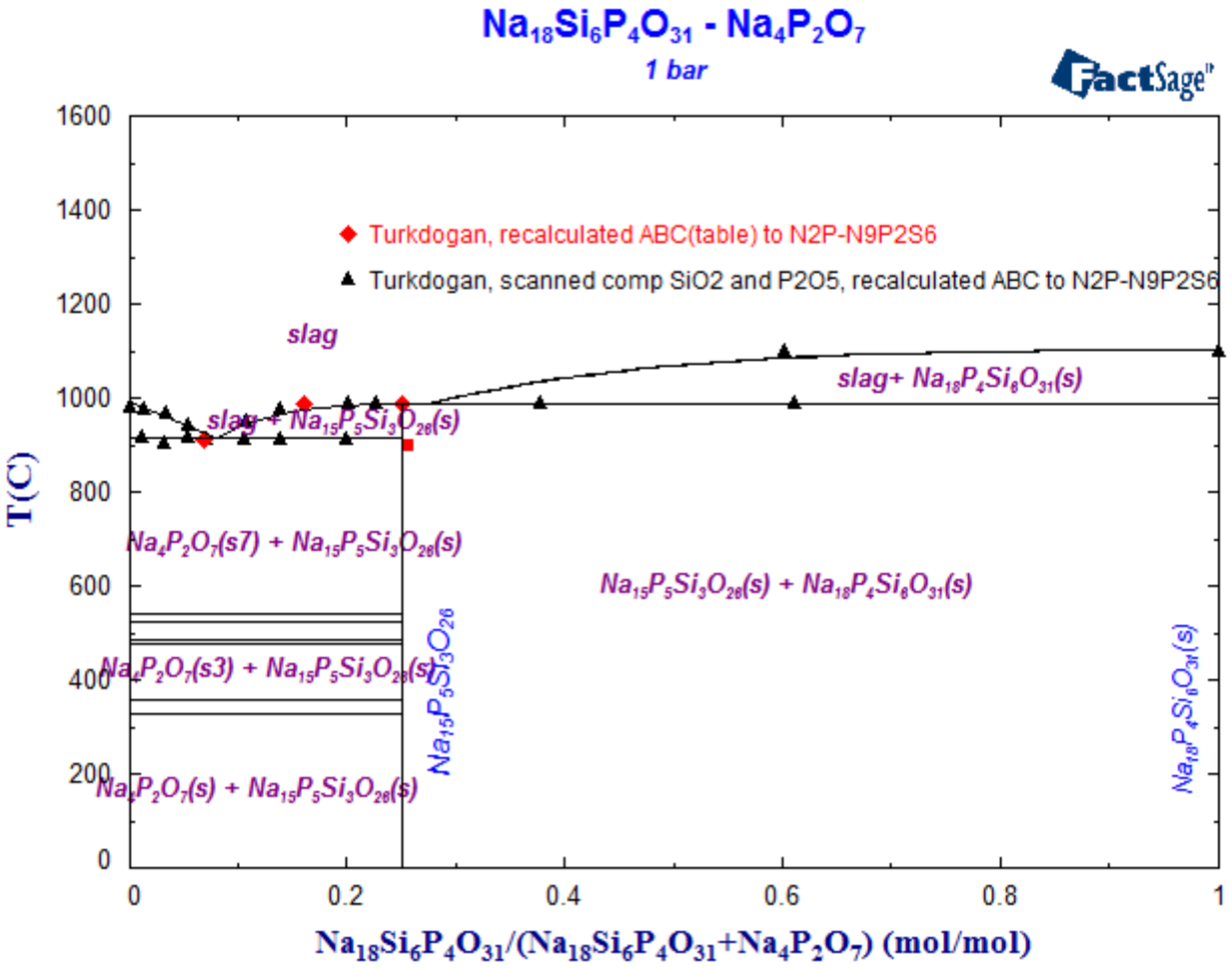

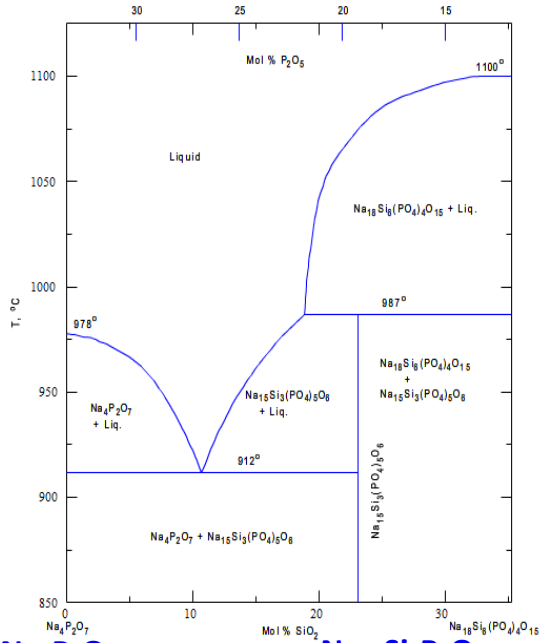

E. T. Turkdogan and W. R. Maddocks, J. Iron Steel Inst., London, 172 [Pt. 1] 1-15 (1952).

Mole fraction Isopleth $Na_4P_2O_7$-SiO_2 compared with experimental data

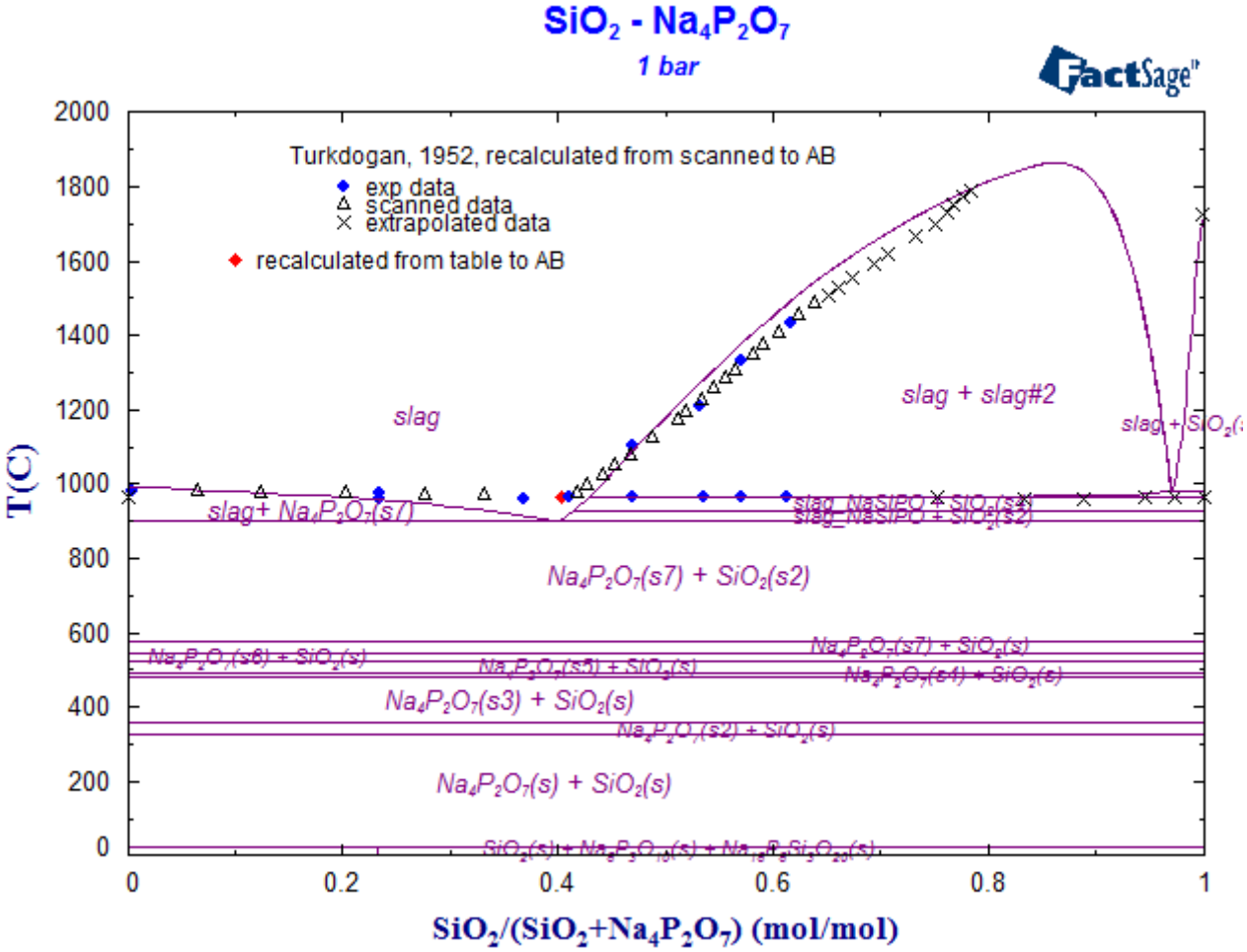

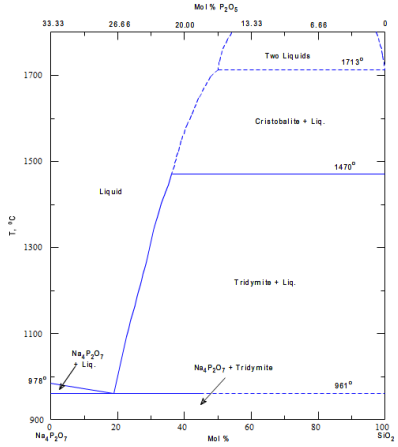

E. T. Turkdogan and W. R. Maddocks, J. Iron Steel Inst., London, 172 [Pt. 1] 1-15 (1952).

Mole fraction Isopleth $NaPO_3$-SiO_2 compared with experimental data

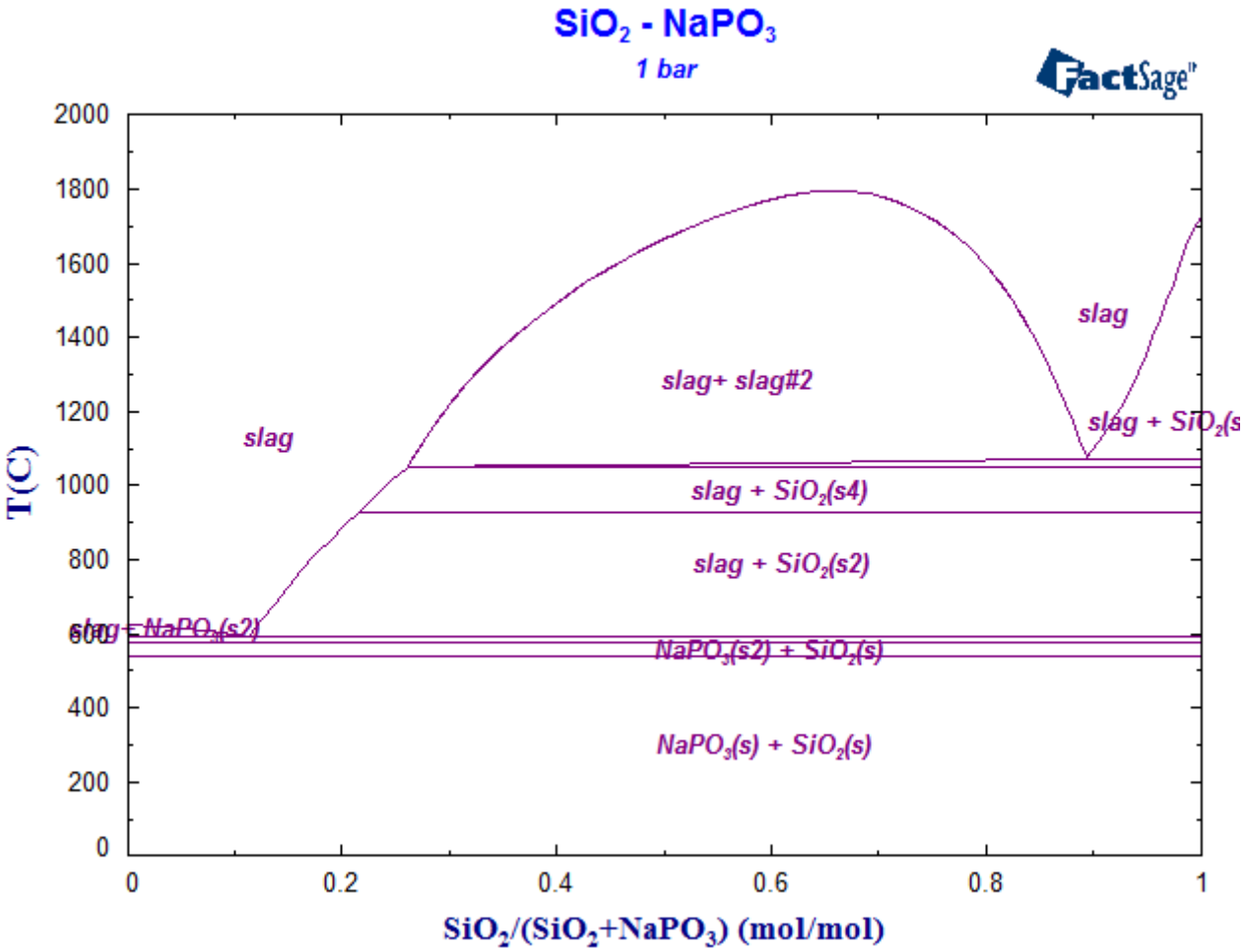

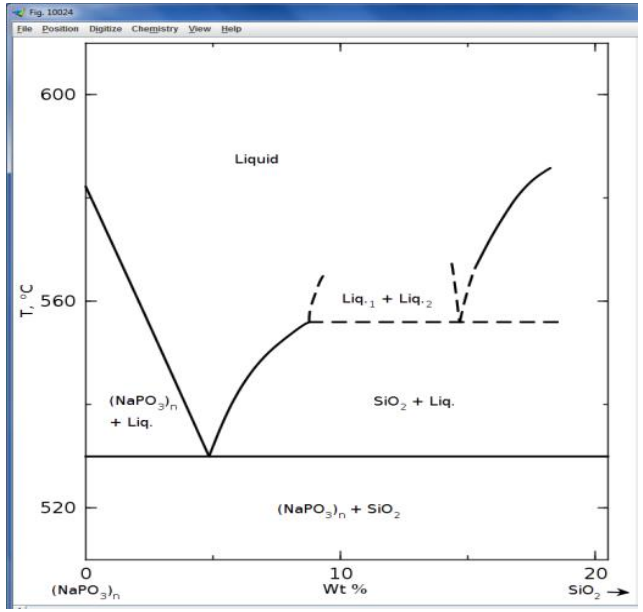

$NaPO_3$ SiO_2

V. P. Kochergin, L. V. Paderova, E. G. Viskova, S. S. Nokhrin, and N. N. Anikina, Rasplavy, 1 [3] 102-109 (1987).

Mole fraction Isopleth $Na_{18}P_4Si_6O_{31}$-Na_2SiO_3 compared with experimental data

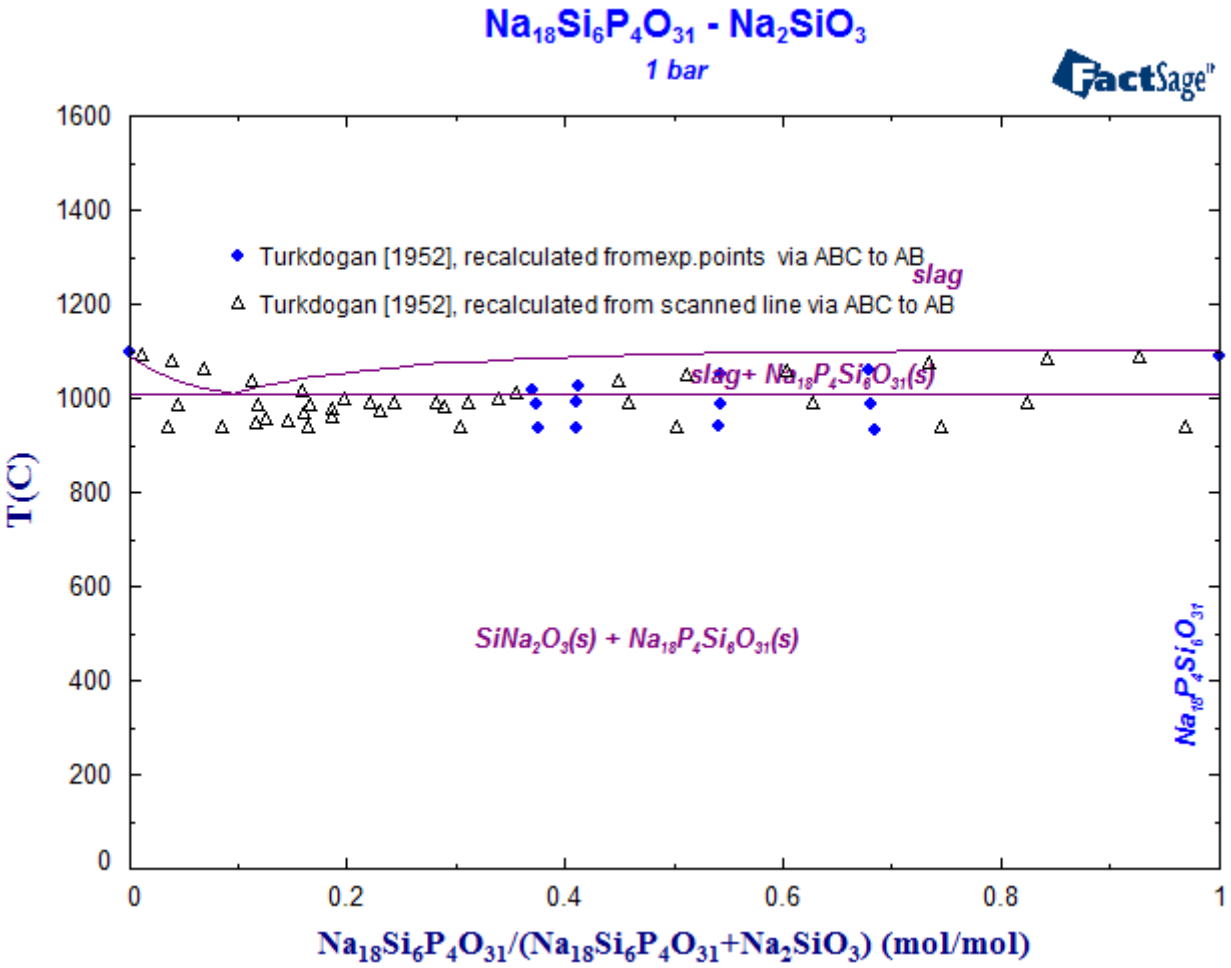

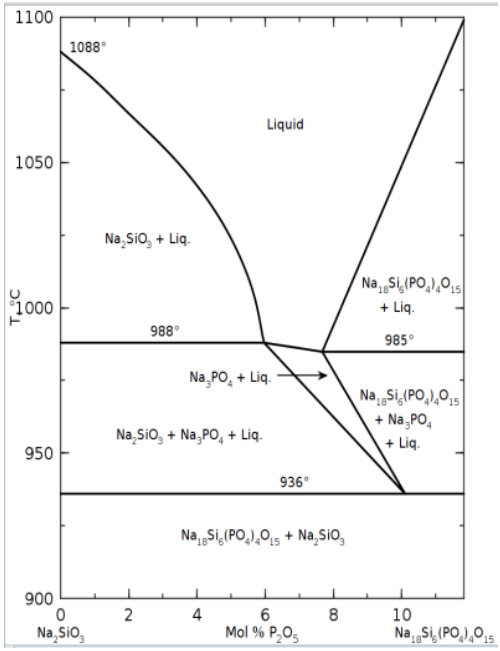

Na_2SiO_3 $Na_{18}Si_6P_4O_{31}$

E. T. Turkdogan and W. R. Maddocks, J. Iron Steel Inst., London, 172 [Pt. 1] 1-15 (1952).

Mole fraction, Subsolidus surface

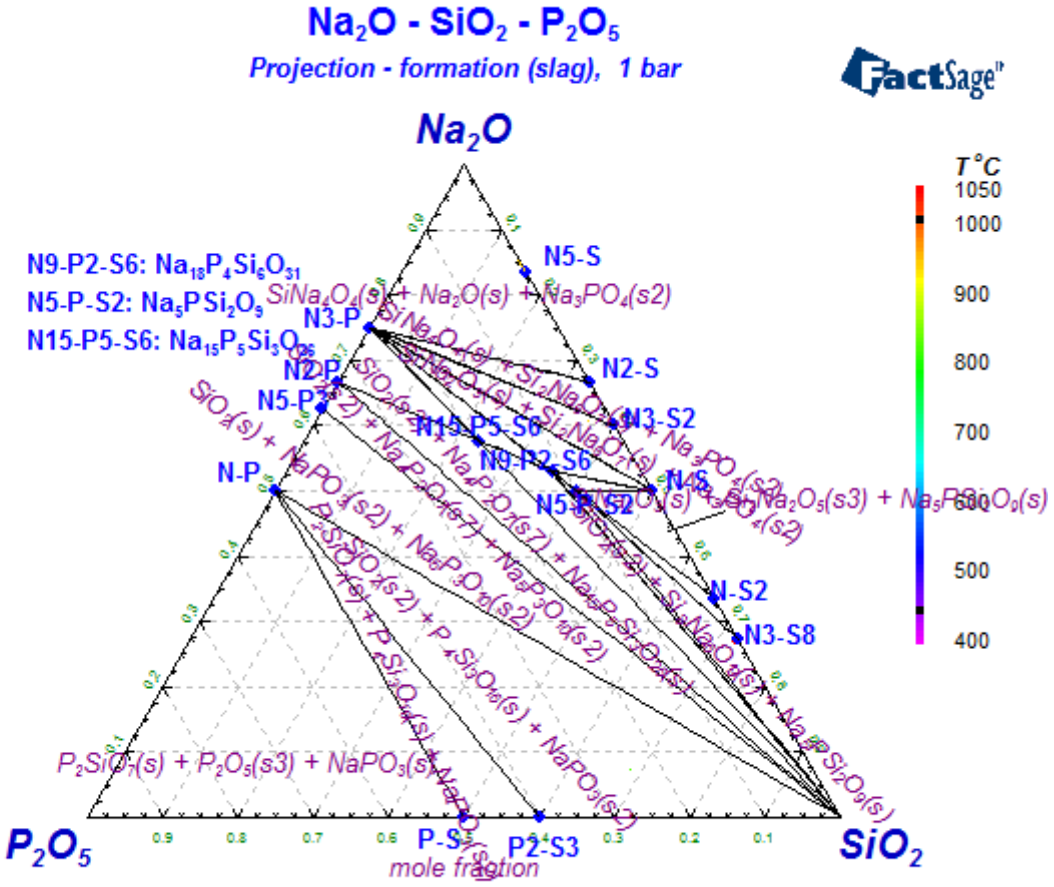

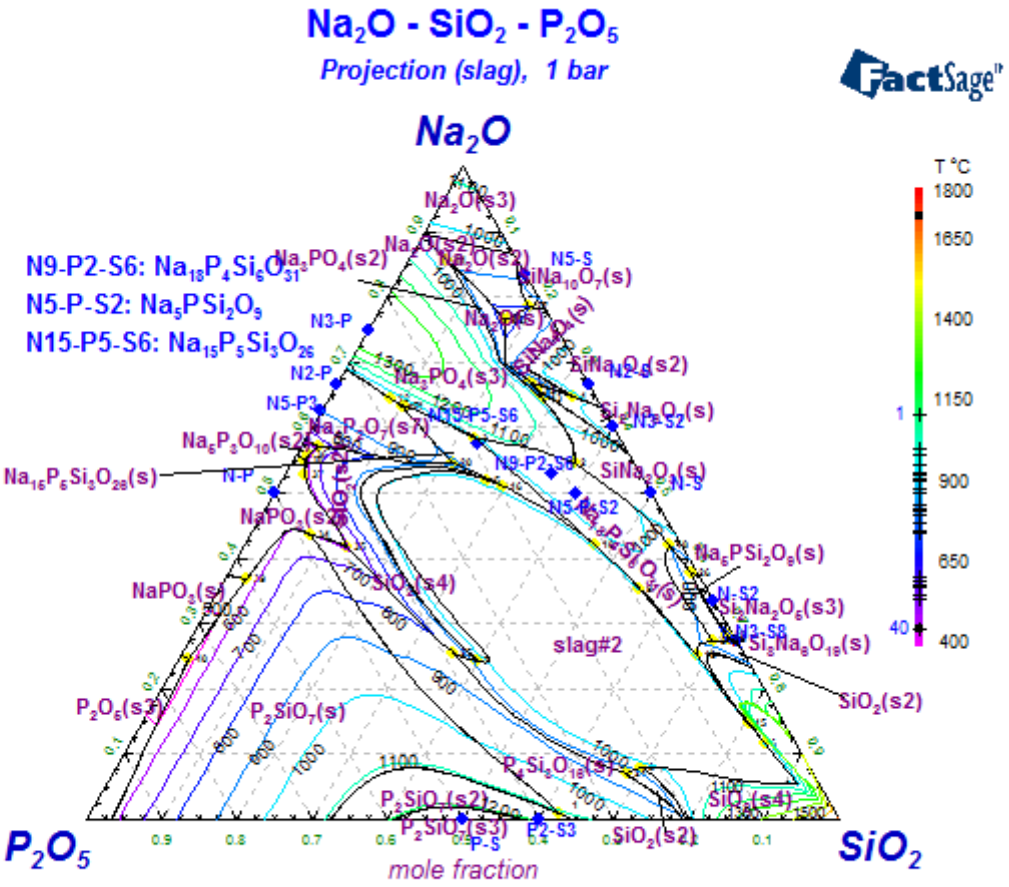

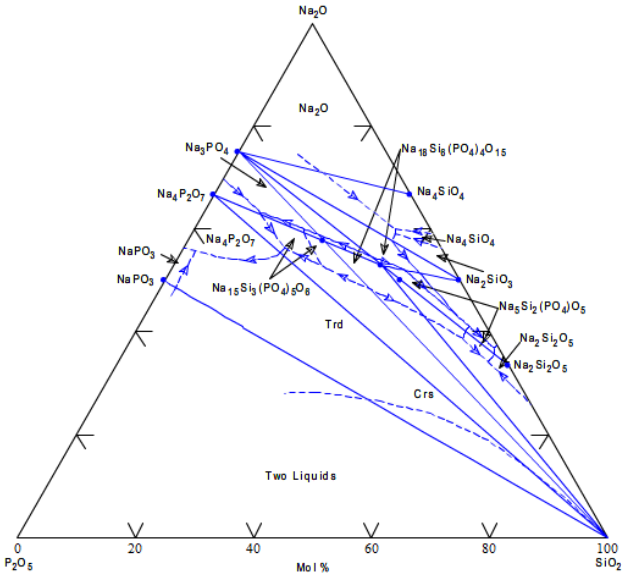

E. T. Turkdogan and W. R. Maddocks, J. Iron Steel Inst., London, 172 [Pt. 1] 1-15 (1952).

Weight percent, Liquidus surface

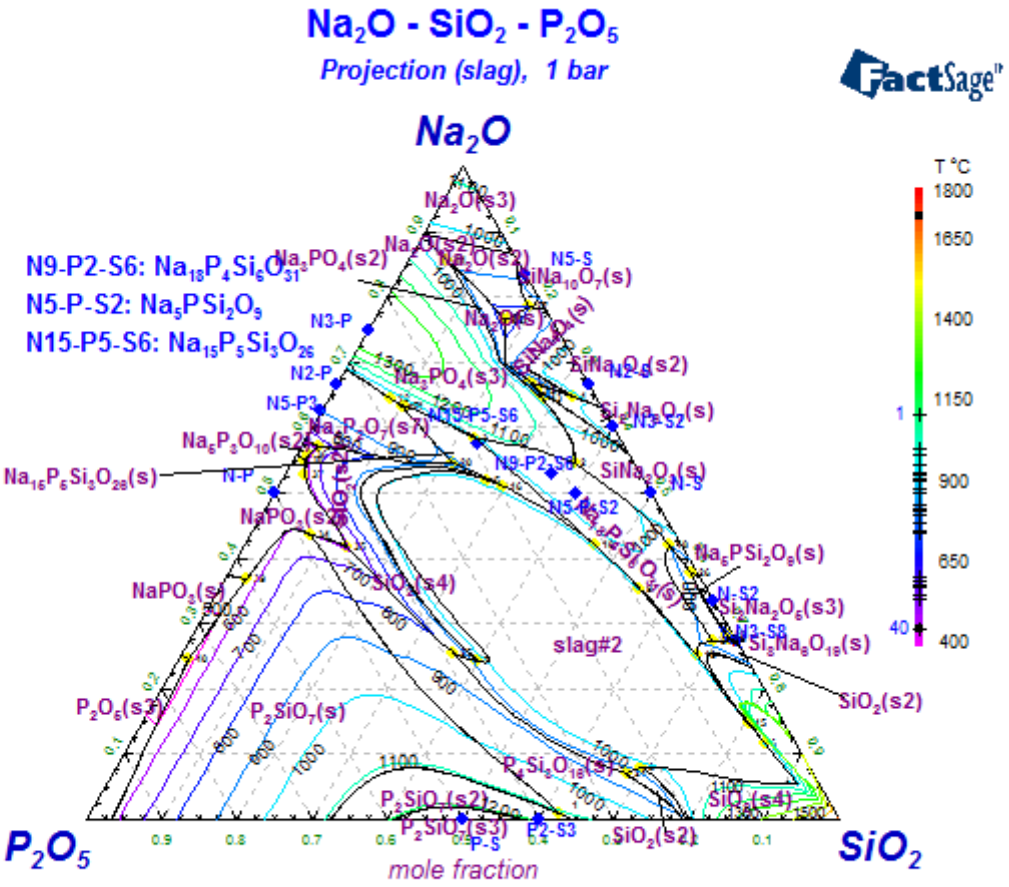

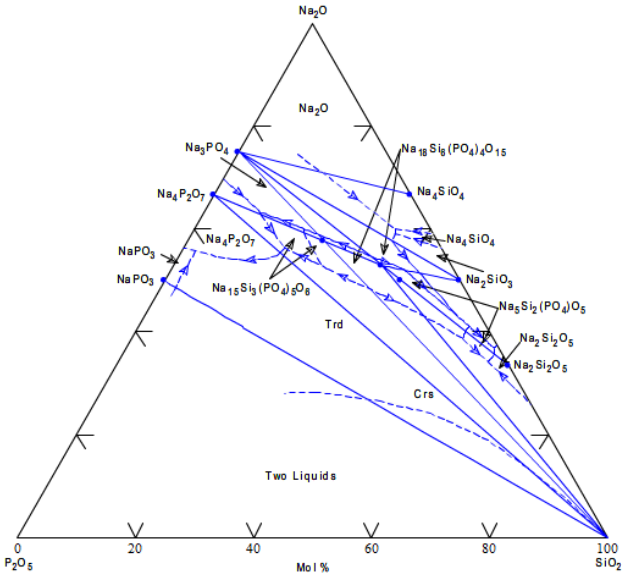

E. T. Turkdogan and W. R. Maddocks, J. Iron Steel Inst., London, 172 [Pt. 1] 1-15 (1952).

Invariant equilibria on the liquidus surface

Intersections with slag	Mole fraction A = Na2O, B = P2O5, C = SiO2				Weight percent A = Na2O, B = P2O5, C = SiO2			
	X(A)	X(B)	X(C)	T(C)	W(A)	W(B)	W(C)	T(C)
1: P2SiO7(s) / P2SiO7(s2) / P4Si3O16(s)	0.00927	0.36673	0.62399	1106.85	0.638	57.761	41.601	1106.85
2: Na18P4Si6O31 / Na3PO4(s3) / SiNa2O3(s)	0.54560	0.07950	0.37490	1005.32	50.004	16.687	33.309	1005.32
3: Na15P5Si3O26 / Na18P4Si6O31 / Na3PO4(s3)	0.58443	0.19216	0.22340	985.19	47.090	35.460	17.450	985.19
4: Si2Na6O7(s) / SiNa4O4(s2) / SiNa4O4(s)	0.64715	0.03037	0.32247	954.76	62.871	6.758	30.371	954.75
5: SiO2(s4) / SiO2(s2) / slag#2	0.51964	0.20743	0.27293	926.29	6.217	40.392	53.391	926.29
6: SiO2(s4) / SiO2(s2) / slag#2	0.11679	0.04097	0.84224	926.28	41.265	37.725	21.011	926.28
7: SiO2(s4) / SiO2(s2) / slag#2	0.24329	0.36023	0.39648	926.28	16.748	56.792	26.459	926.28
8: SiO2(s4) / SiO2(s4) / SiO2(s2)	0.07877	0.22345	0.69778	926.26	11.371	9.136	79.494	926.28
9: Na15P5Si3O26 / Na18P4Si6O31 / slag#2	0.35407	0.08879	0.55715	922.72	32.261	18.527	49.213	922.69
10: Na15P5Si3O26 / Na15P5Si3O26 /Na18P4Si6O31	0.41958	0.11376	0.46666	922.69	37.049	23.005	39.947	922.69
11: Na15P5Si3O26 / Na3PO4(s3) / Na3PO4(s2)	0.63150	0.26034	0.10816	922.41	59.348	15.203	25.449	922.40
12: Na3PO4(s3) / Na3PO4(s2) / Na4P2O7(s7)	0.64477	0.27388	0.08135	922.40	76.561	19.079	4.361	922.40
13: Na3PO4(s3) / Na3PO4(s2) / SiNa2O3(s)	0.64343	0.07197	0.28460	922.40	47.389	44.742	7.869	922.40
14: Na2O(s2) / Na3PO4(s3) / Na3PO4(s2)	0.85648	0.09319	0.05032	922.40	47.730	46.432	5.838	922.40
15: Na15P5Si3O26 / SiO2(s2) / slag#2	0.14639	0.04764	0.80597	919.71	14.119	10.524	75.358	919.71
16: Na15P5Si3O26 / SiO2(s2) / slag#2	0.50946	0.19111	0.29943	919.71	41.171	35.371	23.458	919.71
17: Na15P5Si3O26 / Na3PO4(s2) / Na4P2O7(s7)	0.63250	0.26464	0.10286	912.82	47.262	45.287	7.451	912.82
18: Na18P4Si6O31 / Na5PSi2O9 / SiNa2O3(s)	0.41969	0.01679	0.56352	906.37	41.783	3.829	54.388	906.39
19: Na15P5Si3O26 / Na18P4Si6O31 / SiO2(s2)	0.25126	0.06383	0.68490	902.14	23.672	13.773	62.555	902.14
20: Na15P5Si3O26 / Na4P2O7(s7) / SiO2(s2)	0.54526	0.24024	0.21450	879.85	41.834	42.212	15.954	879.88
21: Na18P4Si6O31 / Na5PSi2O9 / SiO2(s2)	0.27201	0.03195	0.69604	869.77	26.669	7.173	66.157	869.81
22: Na3PO4(s2) / Si2Na6O7(s) / SiNa2O3(s)	0.65671	0.07193	0.27136	864.10	60.554	15.189	24.257	864.08
23: Na3PO4(s2) / Si2Na6O7(s) / SiNa4O4(s)	0.66936	0.07576	0.25488	832.21	61.412	15.919	0.22.669	832.22
24: P4Si3O16(s) / SiO2(s2) / slag#2	0.06915	0.24759	0.68326	815.91	5.325	43.666	0.51.009	815.93
25: P4Si3O16(s) / P4Si3O16 / SiO2(s2)	0.25543	0.38536	0.35921	815.91	17.187	59.383	0.23.431	815.91
26: Na5PSi2O9 / Si2Na2O5(s3) / SiNa2O3(s)	0.37674	0.00839	0.61487	812.87	37.977	1.936	0.60.087	812.88
27: Na2O(s2) / SiNa10O7(s) / SiNa4O4(s)	0.78515	0.01859	0.19626	797.16	77.127	4.183	0.18.690	797.16
28: Na5PSi2O9 / Si2Na2O5(s3) / Si8Na6O19(s)	0.28146	0.00844	0.71010	775.00	28.454	1.955	0.69.592	775.00
29: Na5PSi2O9 / Si8Na6O19(s) / SiO2(s2)	0.27726	0.00860	0.71415	774.04	28.027	1.990	0.69.983	774.06
30: Na2O(s) / Na2O(s2) / Na3PO4(s2)	0.76801	0.06324	0.16875	750.05	72.025	11.907	0.16.068	750.06
31: Na2O(s) / Na2O(s2) / SiNa4O4(s)	0.76787	0.05543	0.17671	750.05	71.348	13.455	0.15.198	750.05
32: Na2O(s) / Na3PO4(s2) / SiNa4O4(s)	0.76427	0.06268	0.17305	739.79	71.056	13.347	0.15.597	739.78
33: Na4P2O7(s7) / Na5P3O10(s2) / SiO2(s2)	0.56940	0.40742	0.02318	607.46	37.339	61.187	0.01.473	607.47
34: NaPO3(s2) / P2SiO7(s) / P4Si3O16(s)	0.43675	0.48372	0.07954	593.84	26.932	68.313	0.04.755	593.81
35: NaPO3(s2) / P4Si3O16(s) / SiO2(s2)	0.41646	0.44558	0.13796	581.23	26.515	64.970	0.08.515	581.23
36: Na5P3O10(s2) / SiO2(s) / SiO2(s2)	0.55936	0.42413	0.01651	574.85	33.564	64.778	0.01.658	574.85
37: NaPO3(s2) / SiO2(s) / SiO2(s2)	0.52807	0.44502	0.02691	574.85	36.164	62.801	0.01.035	574.85
38: Na5P3O10(s2) / NaPO3(s2) / SiO2(s)	0.54983	0.43502	0.01515	552.91	35.227	63.832	0.00.941	552.94
39: NaPO3(s2) / NaPO3(s) / P2SiO7(s)	0.36893	0.60190	0.02917	539.40	20.777	77.631	0.01.593	539.41
40: NaPO3(s) / P2O5(s3) / P2SiO7(s)	0.24444	0.74250	0.01306	443.18	12.487	86.867	0.00.647	443.18

Mole fraction, Ternary phases

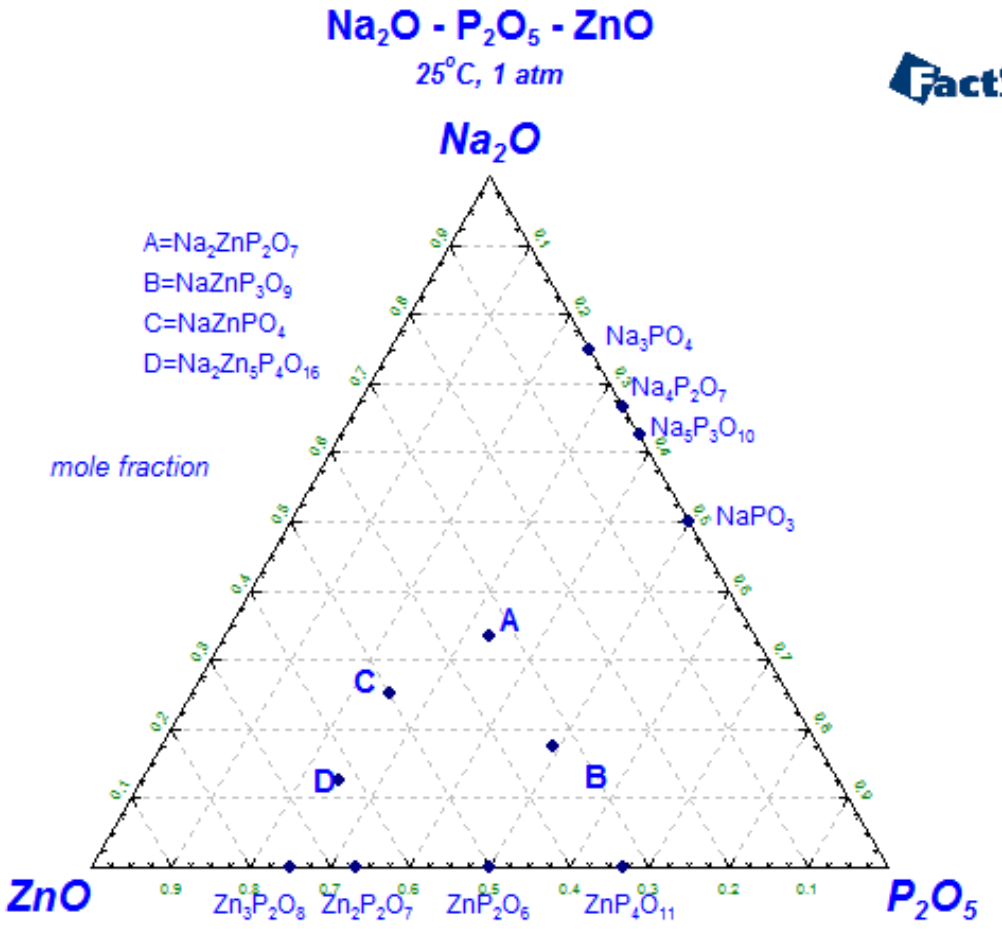

Mole fraction, Isopleth $ZnO\text{-}Na_2Zn_5P_4O_{16}$

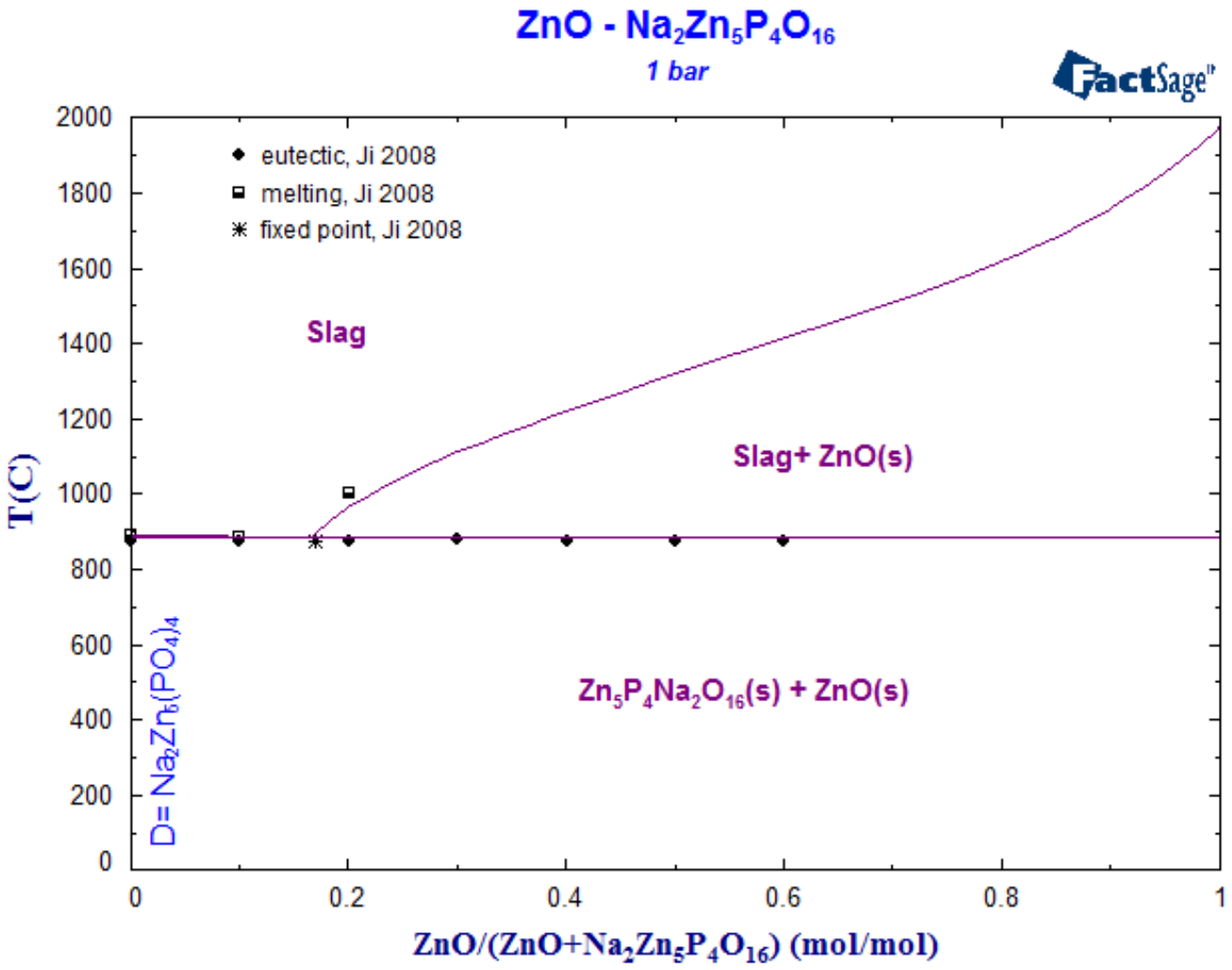

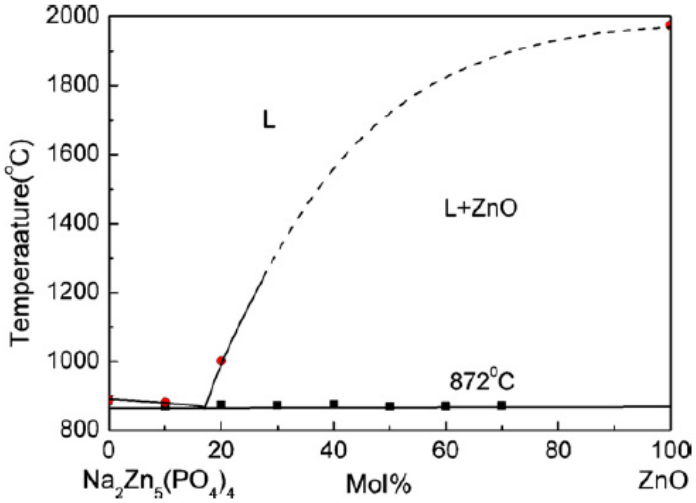

L.N. Ji, J.B. Li, J. Luo, J.K. Liang, J.Y. Zhang, Y.H. Liu, G.H. Rao, Phase relations and flux research for zink oxidy crystal growth in the $ZnO\text{-}Na_2O\text{-}P_2O_5$ system, J. Alloys Compd. 465 (2008) 436-441.

Mole fraction, Isopleth ZnO-$NaPO_3$

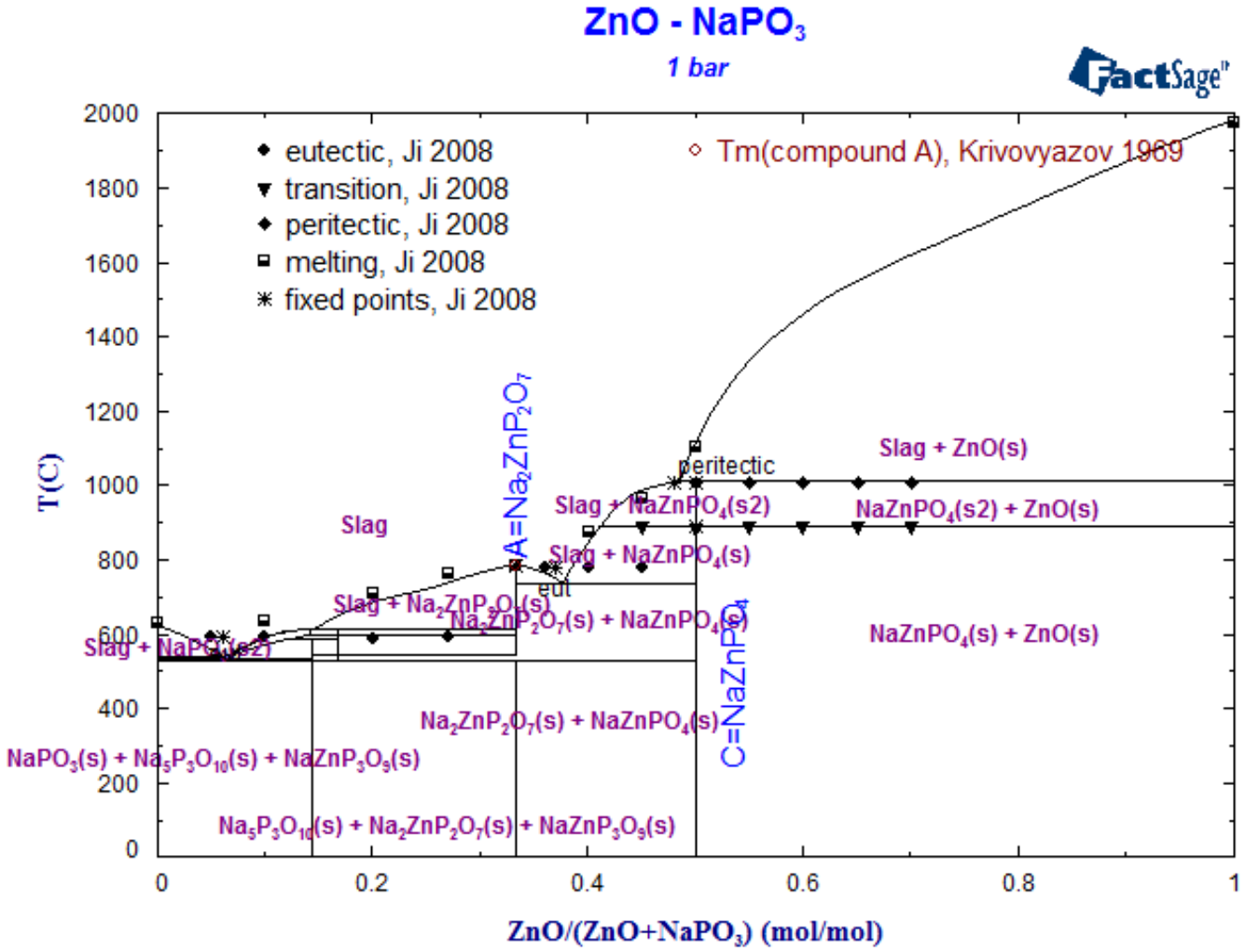

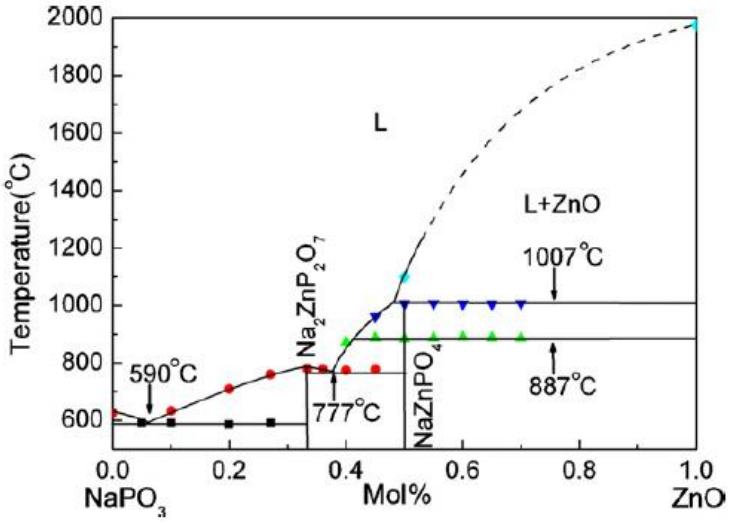

L.N. Ji, J.B. Li, J. Luo, J.K. Liang, J.Y. Zhang, Y.H. Liu, G.H. Rao, Phase relations and flux research for zink oxidy crystal growth in the ZnO-Na_2O-P_2O_5 system, J. Alloys Compd. 465 (2008) 436-441.

Mole fraction, Isopleth ZnP_2O_6-$NaPO_3$

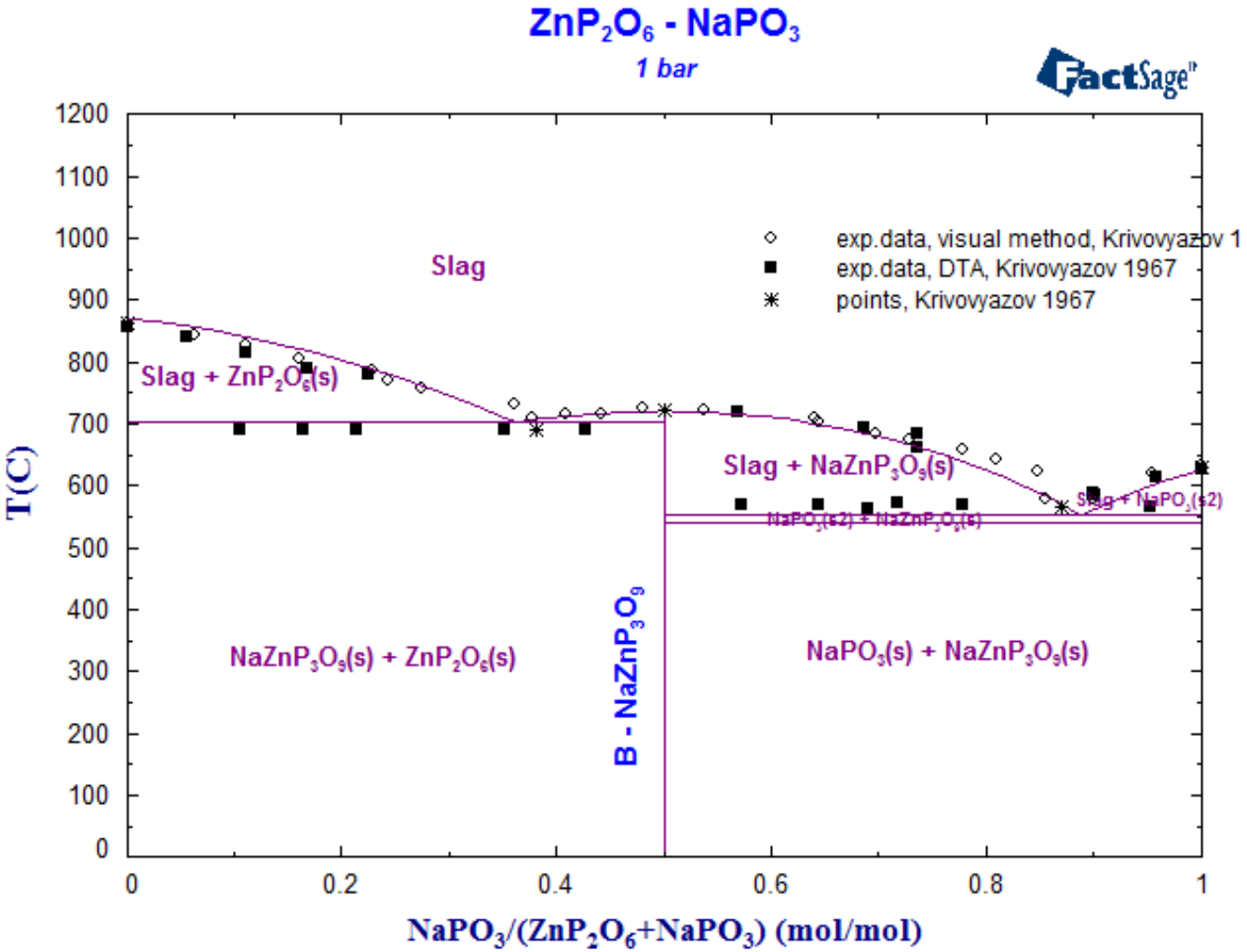

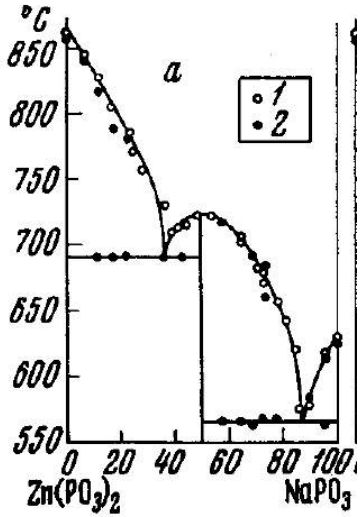

E.L. Krivovjasov, K.K. Palkina, N.K. Voskresenskaja, Dokl. Akad. Nauk, UdSSR, Chem., 174 [3] 610-613 (1967)

Mole fraction, Isopleth $Zn_3P_2O_8$-Na_3PO_4

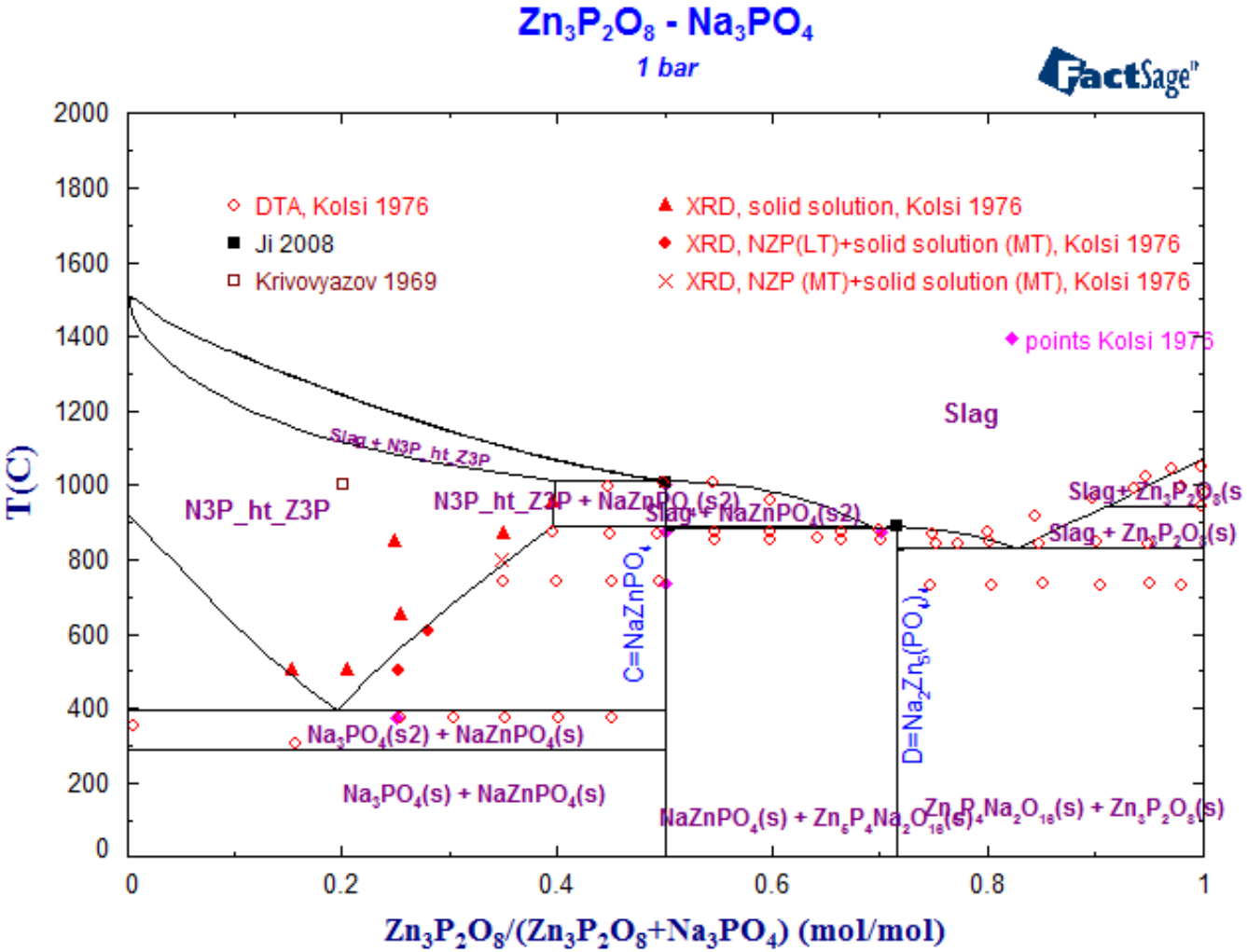

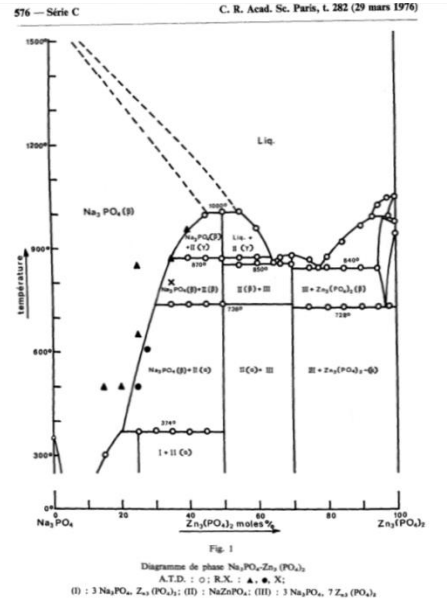

A.-W. Kolsi, A. Erb, W. Freundlich, C. R. Acad. Sc. Paris 282(serie C) (1976) 575-577.

Mole fraction, Isopleth $Na_4P_2O_7$-$Zn_2P_2O_7$

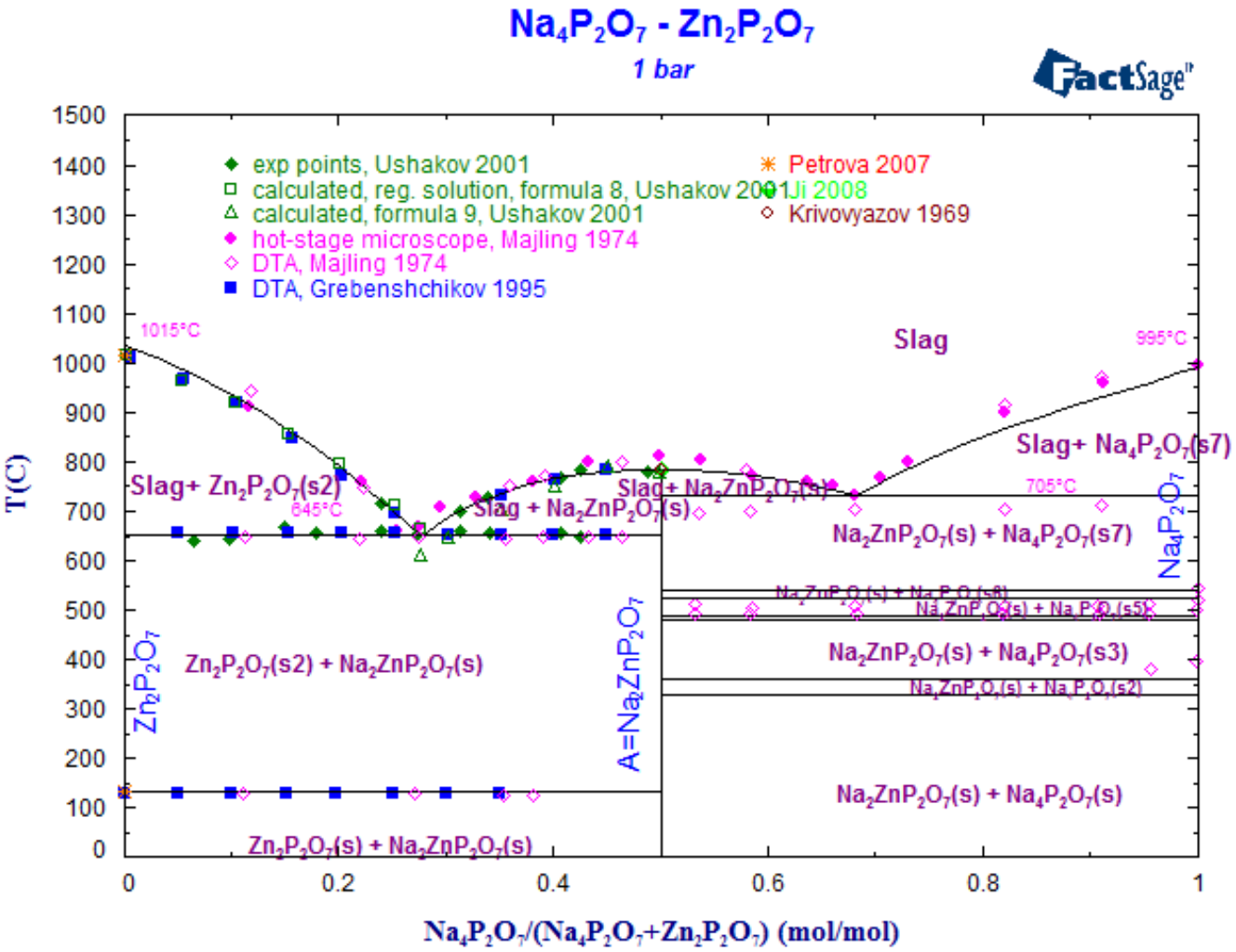

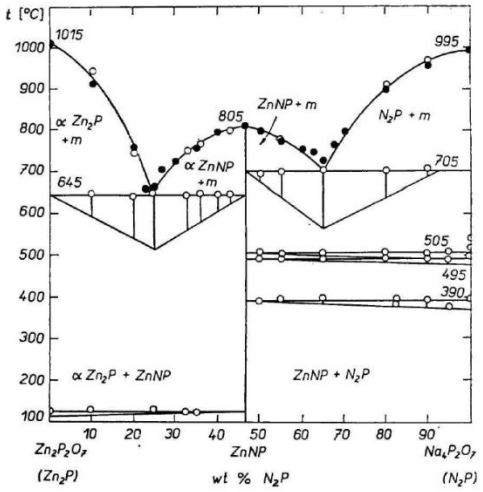

J. Majling, S. Palco, F. Hanic, J. Petrovic, Chem. zvesti 28(3) (1974) 294-297

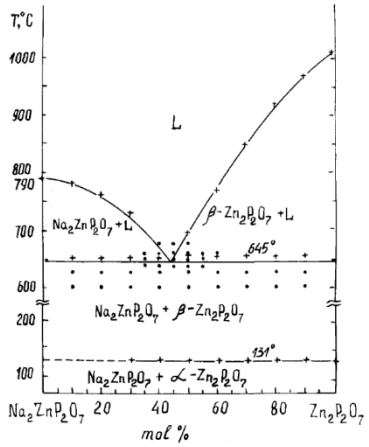

R.G. Grebenshchikov, et al., J. Mater. Res. 10(8) (1995) 2017-2023.

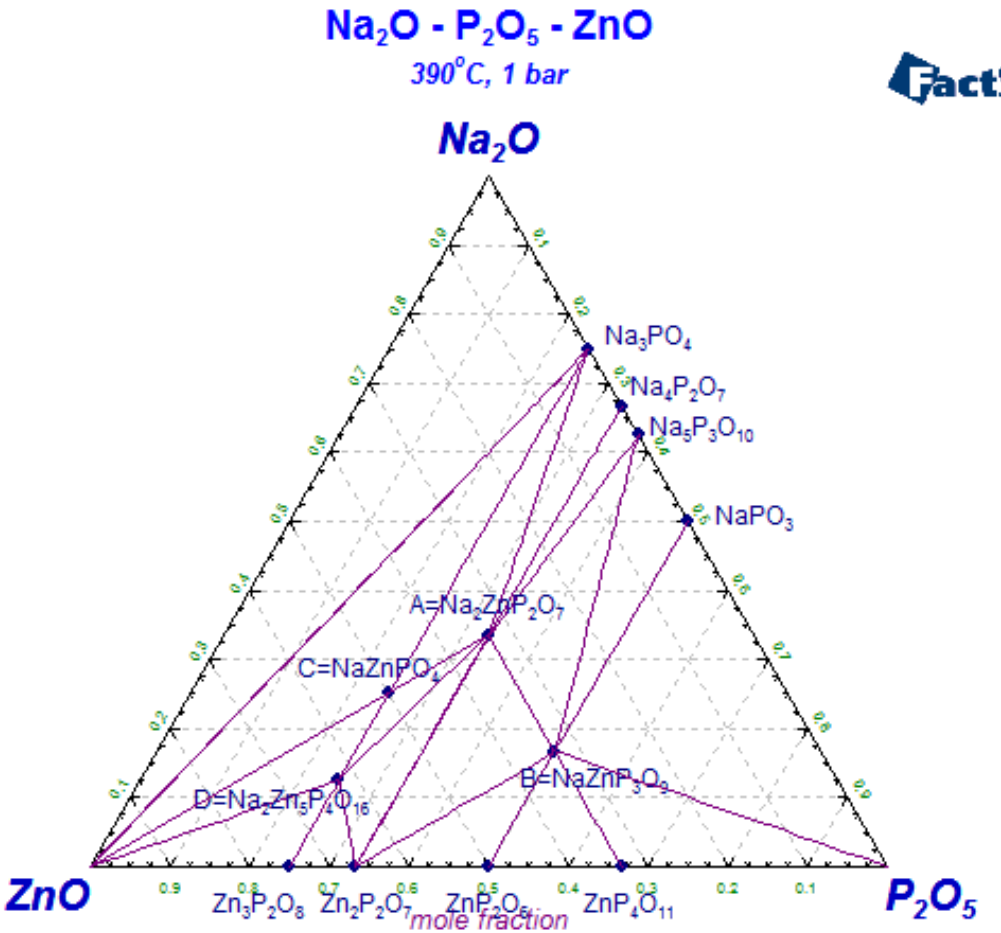

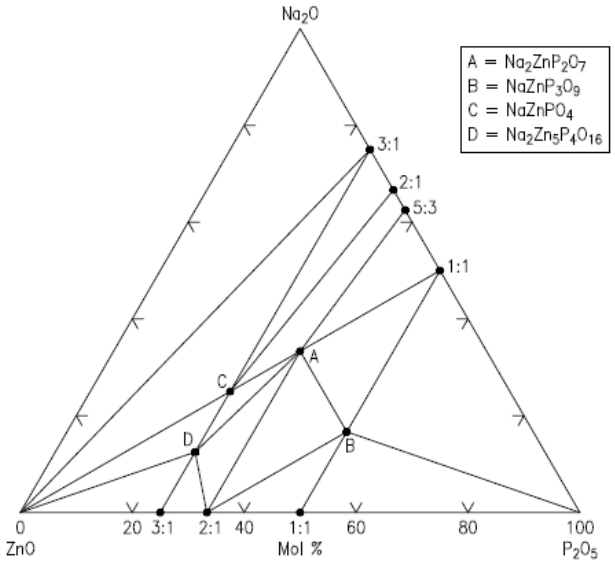

L.N. Ji, J.B. Li, J. Luo, J.K. Liang, J.Y. Zhang, Y.H. Liu, G.H. Rao, Phase relations and flux research for zink oxidy crystal growth in the ZnO-Na_2O-P_2O_5 system, J. Alloys Compd. 465 (2008) 436-441

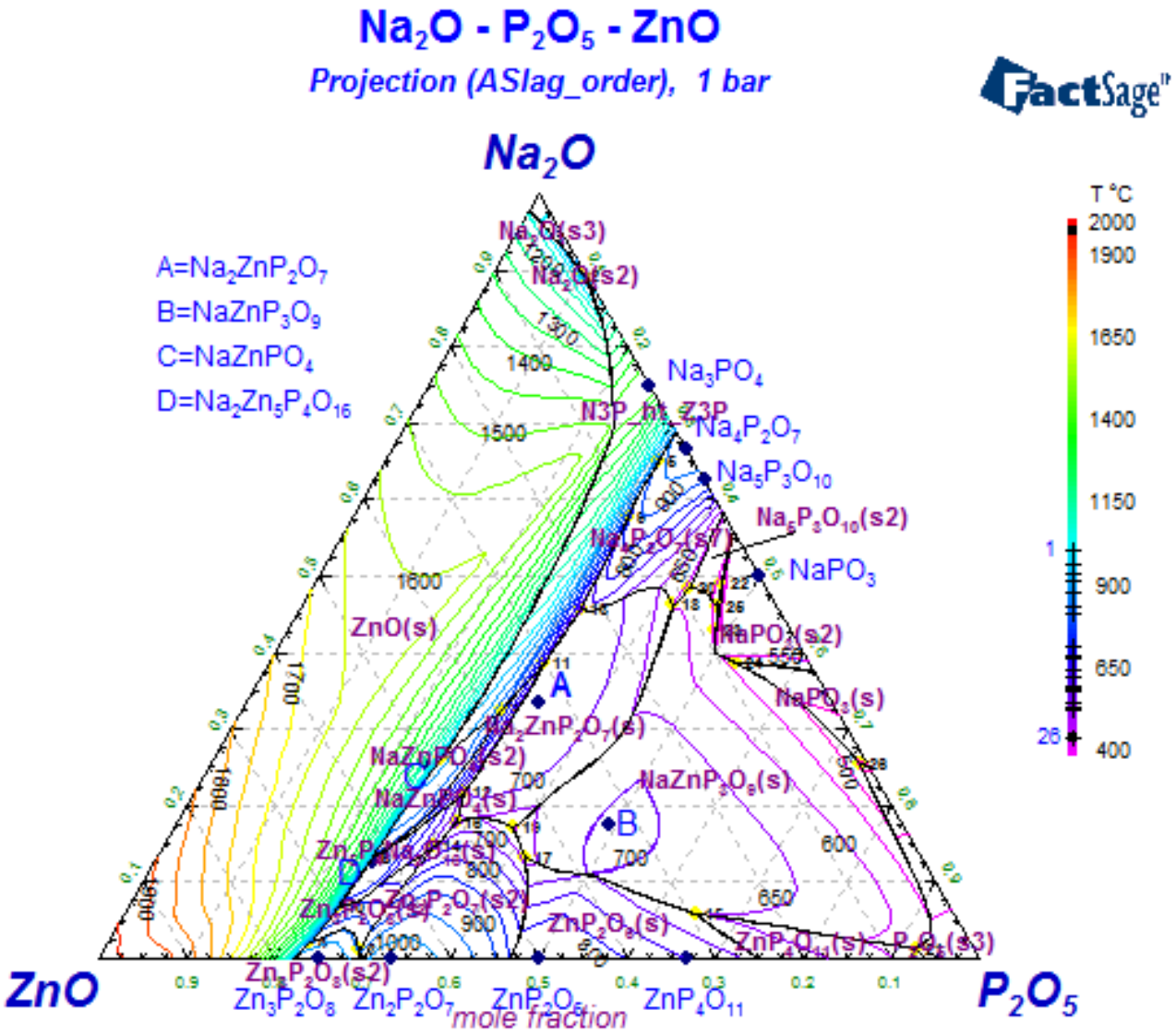
Na2O - P2O5 - ZnO
Projection (ASlag_order), 1 bar
FactSage
Na2O
ZnO
P2O5
mole fraction
A=Na2ZnP2O7
B=NaZnP3O9
C=NaZnPO4
D=Na2Zn5P4O16
T °C
2000
1900
1650
1400
1150
900
650
400
Na2O(s3)
Na2O(s2)
Na3PO4
N3P_ht
Z3P
Na4P2O7
Na5P3O10
Na5P3O10(s2)
NaPO3
NaPO3(s2)
NaPO3(s)
ZnO(s)
A
Na2ZnP2O7(s)
NaZnPO4(s2)
NaZnPO4(s)
NaZnP3O9(s)
B
D
Zn2P2O7(s2)
ZnP2O3(s)
ZnP4O11(s)
P2O5(s3)
Zn3P2O8(s2)
Zn3P2O8
Zn2P2O7
ZnP2O6
ZnP4O11

Weight percent, Liquidus surface

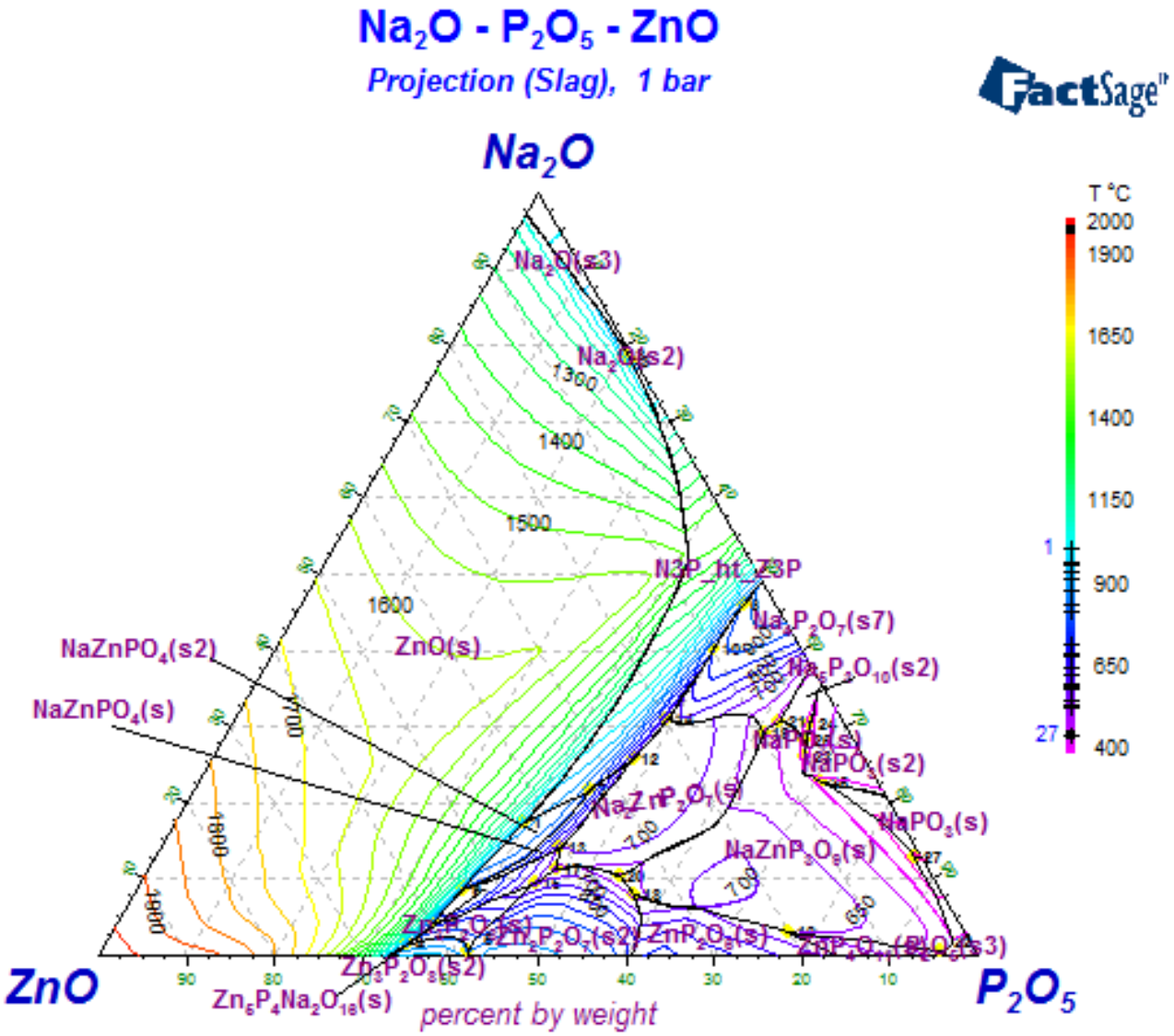

Invariant equilibria on the liquidus surface

Intersections with slag	Mole fraction A = Na2O, B = ZnO, C = P2O5				Weight percent A = Na2O, B = ZnO, C = P2O5				
		X(A)	X(B)	X(C)	T(C)		W(A)	W(B)	W(C)	T(C)
1: N3P_HT / NaZnPO4(s2) / ZnO(s)	1:	0.25914	0.48303	0.25783	1008.94	1:	17.464	42.742	39.794	1008.98
2: Na2O(s2) / Na2O(s3) / ZnO(s)	2:	0.89452	0.00307	0.10241	970.05	2:	78.945	0.355	20.699	970.05
3: Zn2P2O7(s2) / Zn3P2O8(s) / Zn3P2O8(s2)	3:	0.01067	0.69845	0.29089	941.86	3:	1.394	64.215	34.391	941.85
4: Zn3P2O8(s) / Zn3P2O8(s2) / ZnO(s)	4:	0.02134	0.74876	0.22990	941.86	4:	0.669	57.535	41.795	941.85
5: N3P_HT / Na3PO4(s2) / Na4P2O7(s7)	5:	0.64912	0.03994	0.31094	915.71	5:	45.918	3.710	50.373	915.71
6: NaZnPO4(s) / NaZnPO4(s2) / ZnO(s)	6:	0.13286	0.62198	0.24517	887.02	6:	8.793	54.048	37.160	887.01
7: N3P_HT / NaZnPO4(s) / NaZnPO4(s2)	7:	0.32489	0.37949	0.29562	887.00	7:	21.657	33.214	45.130	886.99
8: NaZnPO4(s) / Zn5P4Na2O16(s) / ZnO(s)	8:	0.13136	0.62362	0.24502	883.50	8:	8.691	54.179	37.130	883.50
9: N3P_HT / Na3PO4(s2) / Na4P2O7(s7)	9:	0.57738	0.10962	0.31300	839.50	9:	40.148	10.008	49.844	839.48
10: Zn3P2O8(s) / Zn5P4Na2O16(s) / ZnO(s)	10:	0.06546	0.69476	0.23978	822.21	10:	4.287	59.747	35.966	822.24
11: N3P_HT / Na2ZnP2O7(s) / NaZnPO4(s)	11:	0.38611	0.30045	0.31344	718.66	11:	25.767	26.327	47.906	718.66
12: Na2ZnP2O7(s) / NaZnPO4(s) / Zn5P4Na2O16	12:	0.21596	0.47710	0.30694	693.31	12:	13.975	40.537	45.489	693.31
13: N3P_HT / Na2ZnP2O7(s) / Na4P2O7(s7)	13:	0.45748	0.22372	0.31881	690.27	13:	30.882	19.829	49.288	690.27
14: Zn2P2O7(s2) / Zn3P2O8(s) / Zn5P4Na2O16	14:	0.14712	0.54506	0.30782	685.36	14:	9.384	45.649	44.966	685.33
15: NaZnP3O9(s) / ZnP2O6(s) / ZnP4O11(s)	15:	0.05875	0.29288	0.64836	651.91	15:	3.047	19.944	77.009	651.91
16: Na2ZnP2O7(s) / Zn2P2O7(s2) / Zn5P4Na2O16(s)	16:	0.17715	0.50558	0.31727	630.81	16:	11.301	42.347	46.352	630.76
17: NaZnP3O9(s) / Zn2P2O7(s2) / ZnP2O6(s)	17:	0.13156	0.44941	0.41903	628.87	17:	7.825	35.097	57.079	628.86
18: Na2ZnP2O7(s) / Na4P2O7(s7) / NaZnP3O9(s)	18:	0.46221	0.11659	0.42120	597.19	18:	29.255	9.689	61.056	597.21
19: Na2ZnP2O7(s) / NaZnP3O9(s) / Zn2P2O7(s2)	19:	0.17064	0.44341	0.38595	595.01	19:	10.425	35.571	54.004	595.01
20: Na4P2O7(s7) / Na5P3O10(s2) / NaZnP3O9_S1(s)	20:	0.48374	0.08697	0.42929	584.92	20:	30.596	7.222	62.182	584.93
21: NaZnP3O9(s) / P2O5(s3) / ZnP4O11(s)	21:	0.01293	0.06562	0.92145	552.55	21:	0.585	3.900	95.515	552.61
22: Na5P3O10(s2) / NaPO3(s2) / NaPO3(s)	22:	0.49070	0.04667	0.46263	539.40	22:	25.897	6.750	67.353	539.40
23: NaPO3(s2) / NaPO3(s) / NaZnP3O9(s)	23:	0.42842	0.08505	0.48653	539.40	23:	30.450	3.803	65.747	539.40
24: NaPO3(s2) / NaPO3(s) / NaZnP3O9(s)	24:	0.38644	0.08347	0.53008	539.40	24:	22.598	6.409	70.992	539.40
25: Na5P3O10(s2) / NaPO3(s) / NaZnP3O9(s)	25:	0.45855	0.06850	0.47295	532.32	25:	28.103	5.512	66.384	532.32
26: NaPO3(s) / NaZnP3O9(s) / P2O5(s3)	26:	0.25381	0.00940	0.73680	444.21	26:	12.992	0.631	86.377	444.21

Na2O-SiO2-ZnO,
Mole fraction, 700°C

,

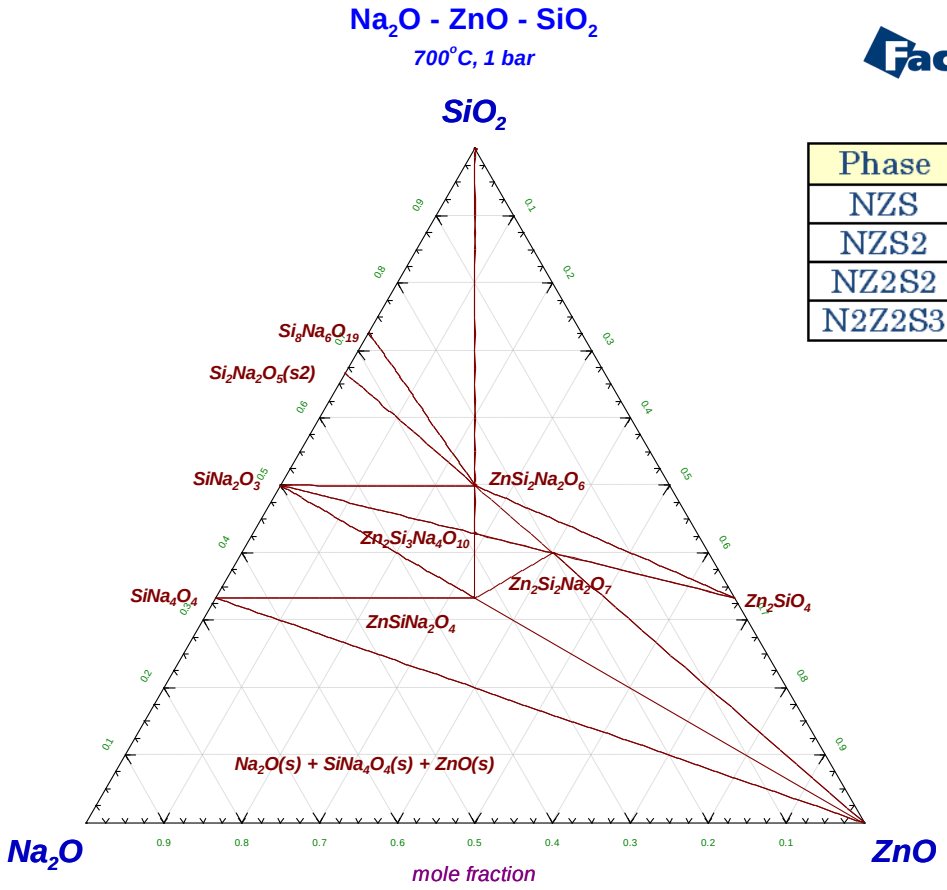

FactSage™

Phase	Formula	Tm,°C [1966Holland]	Tm,calc.
NZS	Na_2ZnSiO_4	1340	1339
NZS2	$Na_2ZnSi_2O_6$	860	859
NZ2S2	$Na_2Zn_2Si_2O_7$	1090	1088
N2Z2S3	$Na_4Zn_2Si_3O_{10}$	975	968

Na2O-SiO2-ZnO,
Mole fraction, 900°C
,

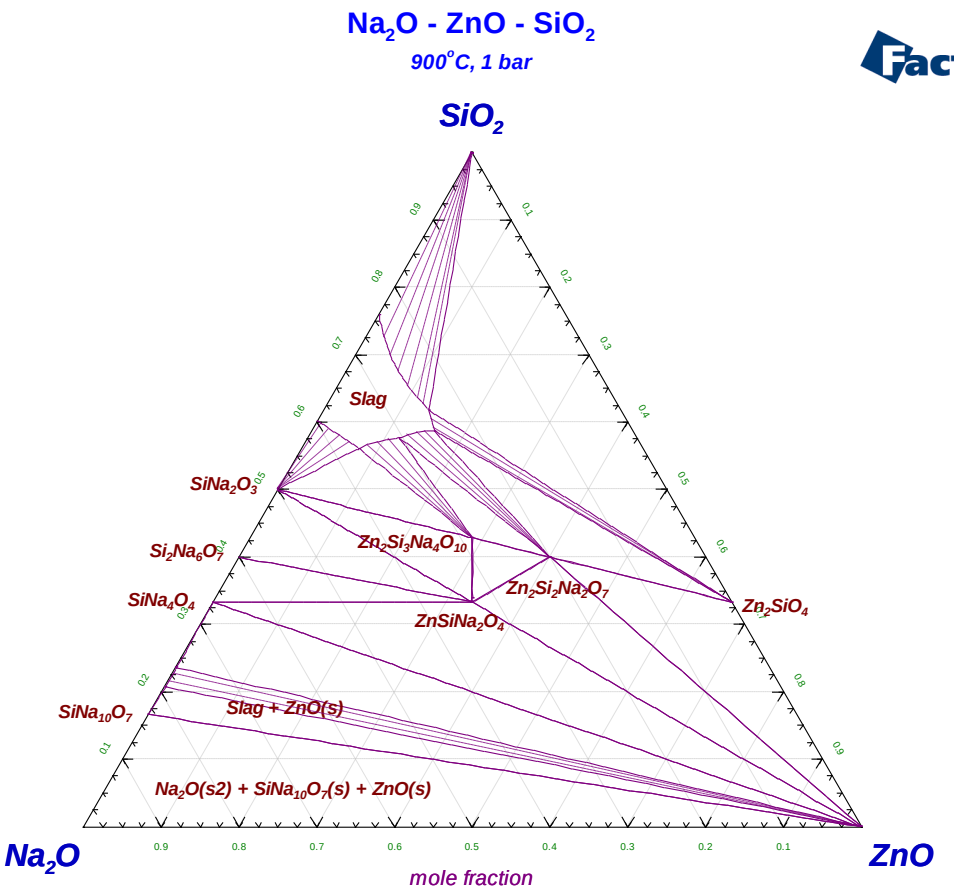

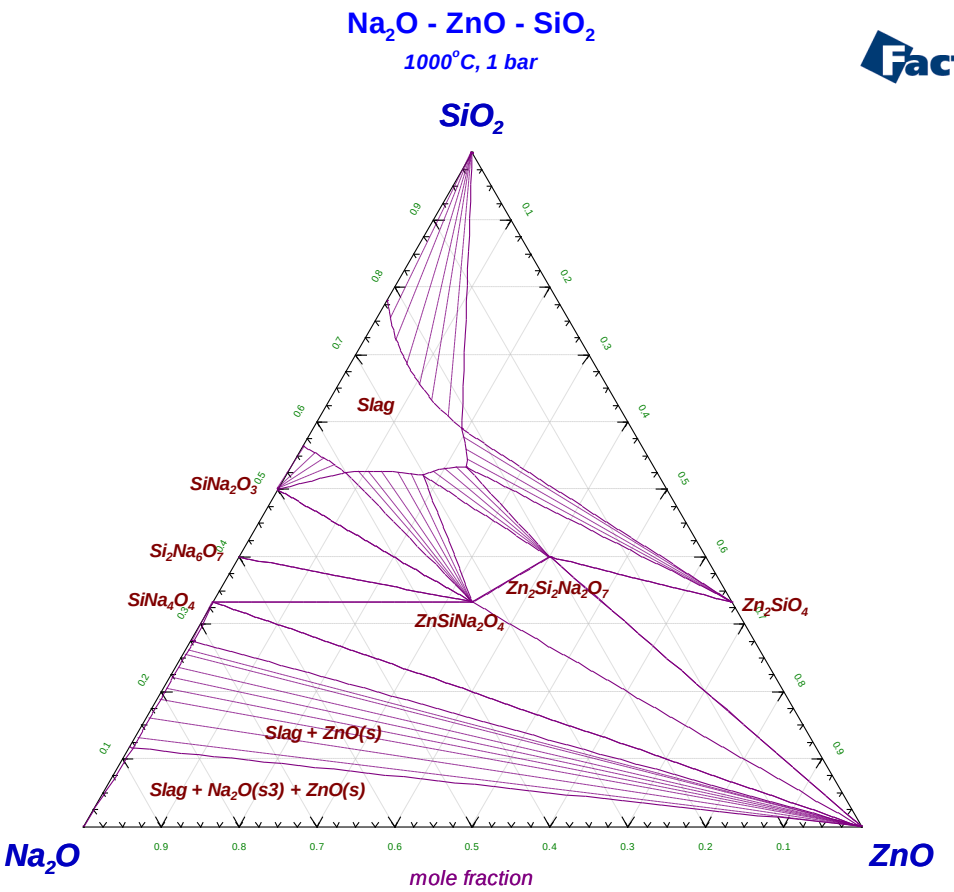
Na2O - ZnO - SiO2
1000°C, 1 bar
FactSage™
SiO2
Slag
SiNa2O3
Si2Na6O7
SiNa4O4
Zn2Si2Na2O7
ZnSiNa2O4
Zn2SiO4
Slag + ZnO(s)
Slag + Na2O(s3) + ZnO(s)
Na2O
ZnO
mole fraction

Na2O-SiO2-ZnO,
Mole fraction, 900°C
,

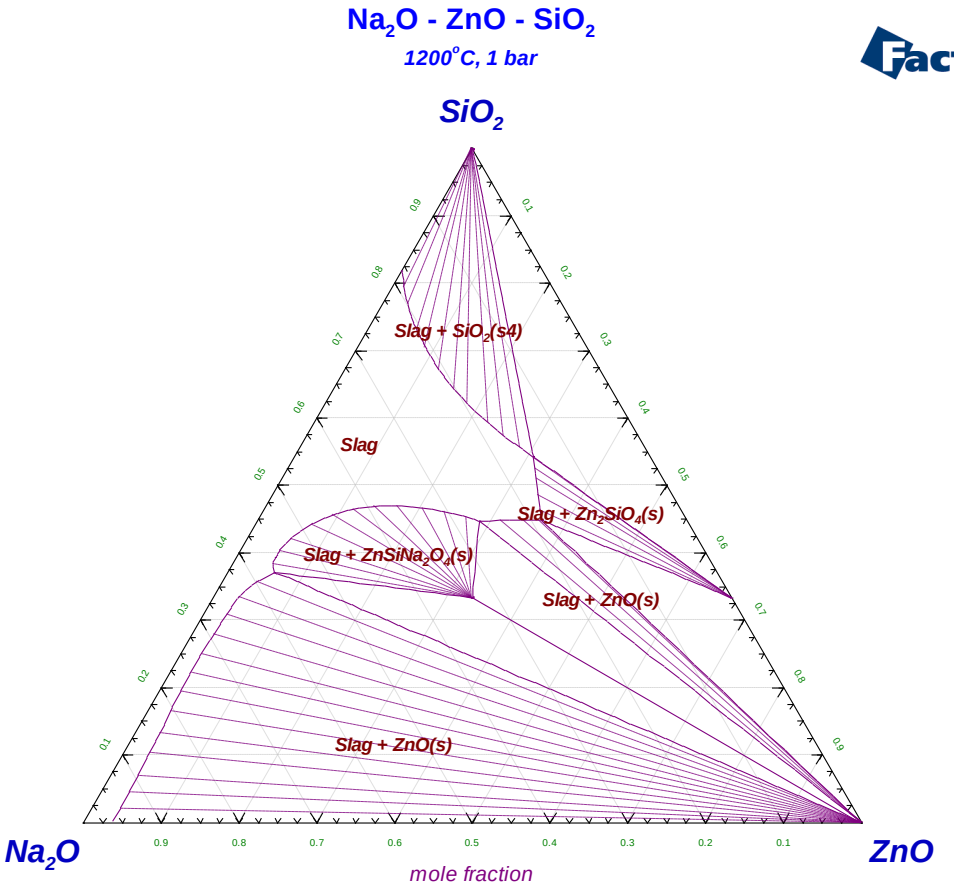

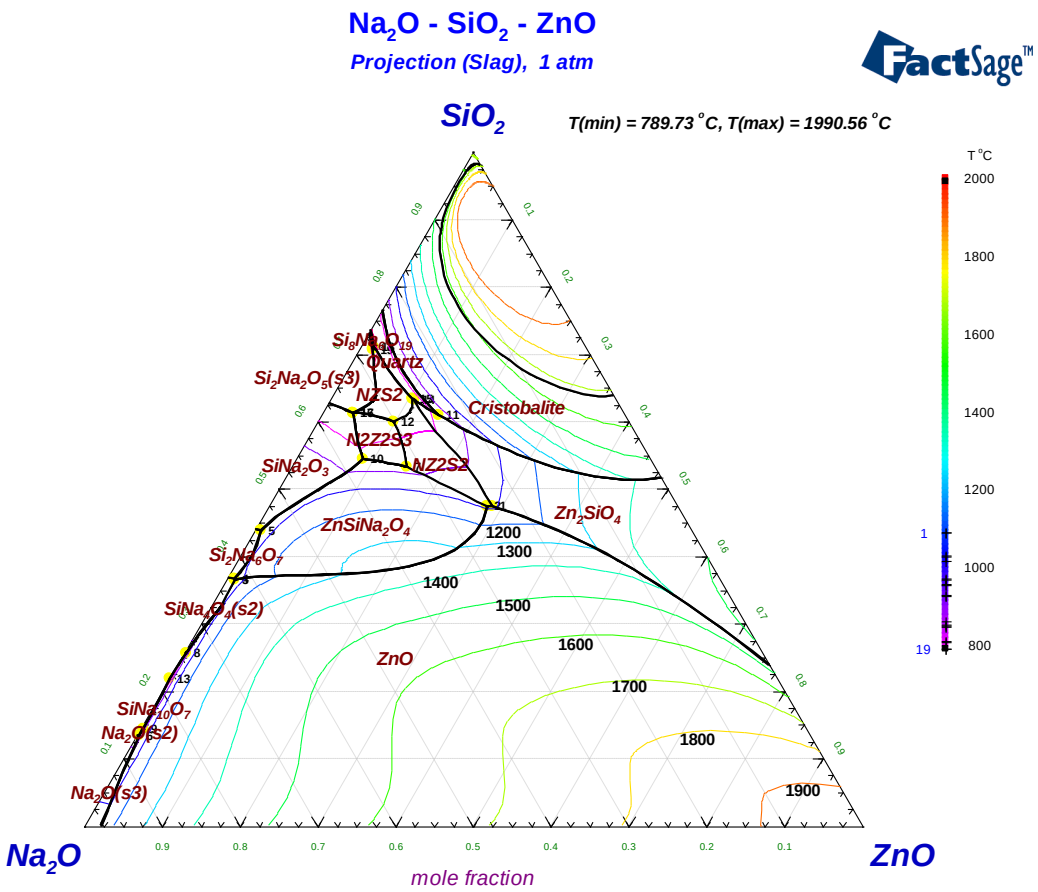
Na2O - SiO2 - ZnO
Projection (Slag), 1 atm
FactSage™
SiO2
T(min) = 789.73 °C, T(max) = 1990.56 °C
T °C
2000
1800
1600
1400
1200
1000
800
Si8Na2O19
Quartz
Si2Na2O5(s3)
NZS2
Cristobalite
NZ2S3
SiNa2O3
NZ2S2
Zn2SiO4
ZnSiNa2O4
Si2Na6O7
SiNa4O4(s2)
ZnO
SiNa10O7
Na2O(s2)
Na2O(s3)
1200
1300
1400
1500
1600
1700
1800
1900
Na2O
ZnO
mole fraction

Weight percent, Liquidussurface

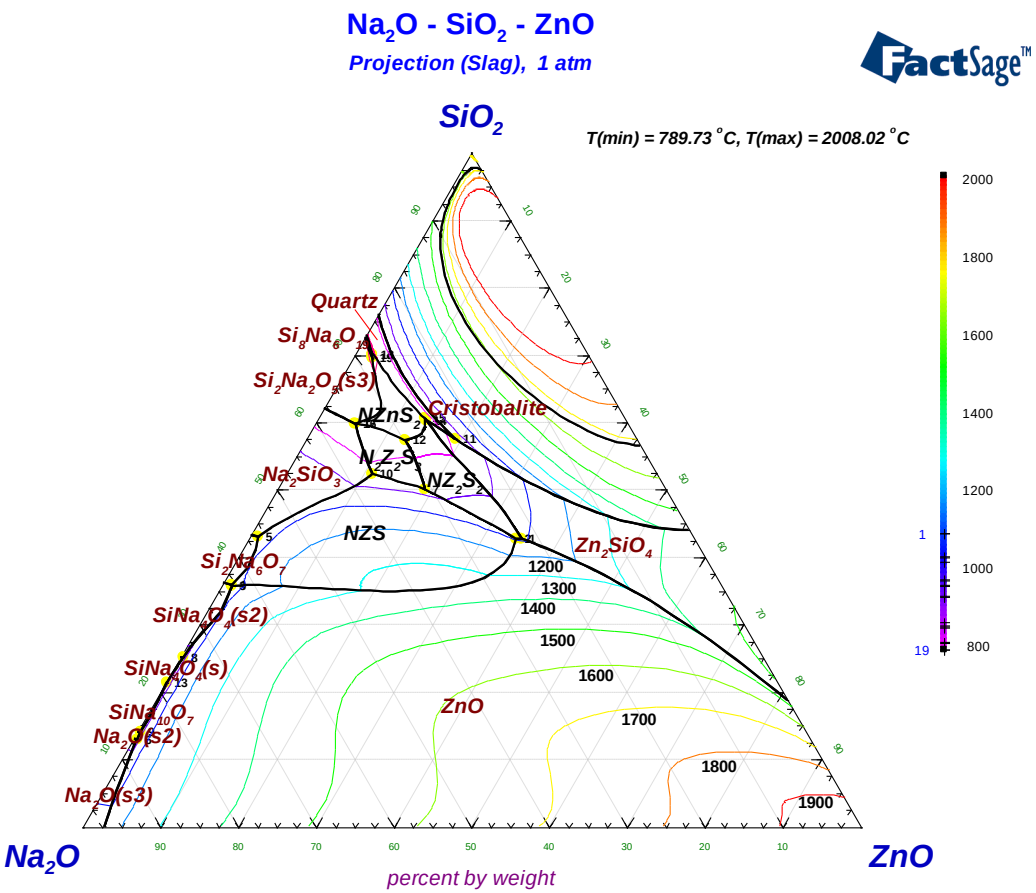

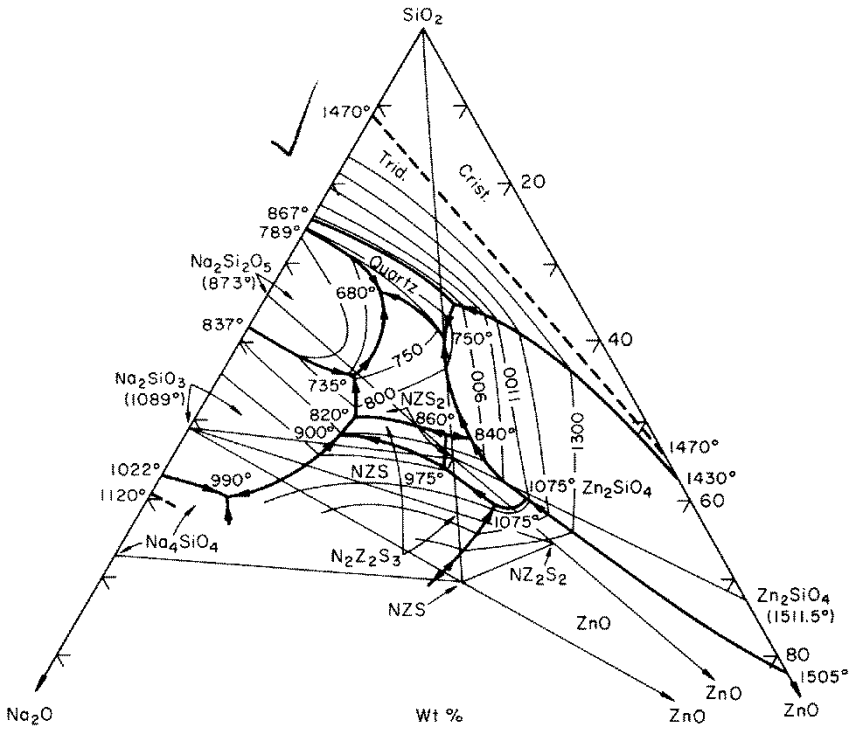

A.E. Holland. E.R. Segnit, Aust. J. Chem., 19 [6], (1966), pp. 905-913.

Invariant equilibria on the liquidus surface

Intersections with slag	Mole fraction A = SiO2, B = Na2O, C = ZnO				Weight percent A = SiO2, B = Na2O, C = ZnO			
	X(A)	X(B)	X(C)	T(C)	W(A)	W(B)	W(C)	T(C)
1: Zn2Si2Na2O7 / Zn2SiO4 / ZnO	1: 0.47441	0.23848	0.28711	1088.31	1: 42.768	22.177	35.056	1088.31
2: Zn2Si2Na2O7 / ZnO / ZnSiNa2O4	2: 0.47414	0.24481	0.28104	1088.00	2: 42.819	22.806	34.376	1087.97
3: SiNa4O4_HT(s2) / ZnO / ZnSiNa2O4	3: 0.36503	0.62450	0.01046	1030.40	3: 35.669	62.946	1.385	1030.34
4: Si2Na6O7 / SiNa4O4_HT(s2) / ZnSiNa2O4	4: 0.36700	0.62388	0.00912	1026.71	4: 35.878	62.914	1.208	1026.71
5: Si2Na6O7 / SiNa2O3 / ZnSiNa2O4	5: 0.43896	0.55353	0.00751	1015.08	5: 43.031	55.972	0.997	1015.07
6: Na2O(s2) / Na2O(s3) / ZnO	6: 0.13390	0.86263	0.00347	970.05	6: 13.019	86.523	0.458	970.05
7: Zn2Si2Na2O7 / Zn2Si3Na4O10 / ZnSiNa2O4	7: 0.53298	0.31897	0.14805	968.12	7: 50.162	30.966	18.872	968.11
8: SiNa4O4(s2) / SiNa4O4(s) / ZnO	8: 0.25722	0.74021	0.00257	954.75	8: 25.114	74.546	0.340	954.80
9: Na2O(s2) / SiNa10O7 / ZnO	9: 0.14487	0.85235	0.00278	952.88	9: 14.095	85.540	0.366	952.88
10: SiNa2O3 / Zn2Si3Na4O10 / ZnSiNa2O4	10: 0.54528	0.36926	0.08546	927.97	10: 52.333	36.558	11.109	927.97
11: Cristobalite / Quartz_beta / Zn2SiO4	11: 0.61064	0.23965	0.14972	926.28	11: 57.574	23.307	19.119	926.28
12: Zn2Si2Na2O7 / Zn2Si3Na4O10 / ZnSi2Na2O6	12: 0.59985	0.30228	0.09787	858.86	12: 57.445	29.860	12.695	858.84
13: SiNa10O7 / SiNa4O4(s) / ZnO	13: 0.21894	0.78036	0.00070	853.02	13: 21.363	78.545	0.092	853.02
14: Quartz_beta / Zn2Si2Na2O7 / Zn2SiO4	14: 0.63205	0.25990	0.10805	847.39	14: 60.397	25.619	13.984	847.39
15: Quartz_beta / Zn2Si2Na2O7 / ZnSi2Na2O6	15: 0.63391	0.26082	0.10527	844.99	15: 60.630	25.733	13.637	844.99
16: SiNa2O3 / Zn2Si3Na4O10 / ZnSi2Na2O6	16: 0.61277	0.34806	0.03917	808.45	16: 59.790	35.033	5.177	808.46
17: Si2Na2O5(s3) / SiNa2O3 / ZnSi2Na2O6	17: 0.61350	0.34799	0.03851	807.49	17: 59.876	35.034	5.090	807.48
18: Si8Na6O19 / Quartz_beta / ZnSi2Na2O6	18: 0.71171	0.27171	0.01658	789.89	18: 70.158	27.629	2.213	789.89
19: Si2Na2O5(s3) / Si8Na6O19 / ZnSi2Na2O6	19: 0.70709	0.27516	0.01775	789.73	19: 69.666	27.965	2.369	789.73

NiO-V2O5-ZnO,

NiO-V2O5-ZnO,
Mole fraction, 600°C
,

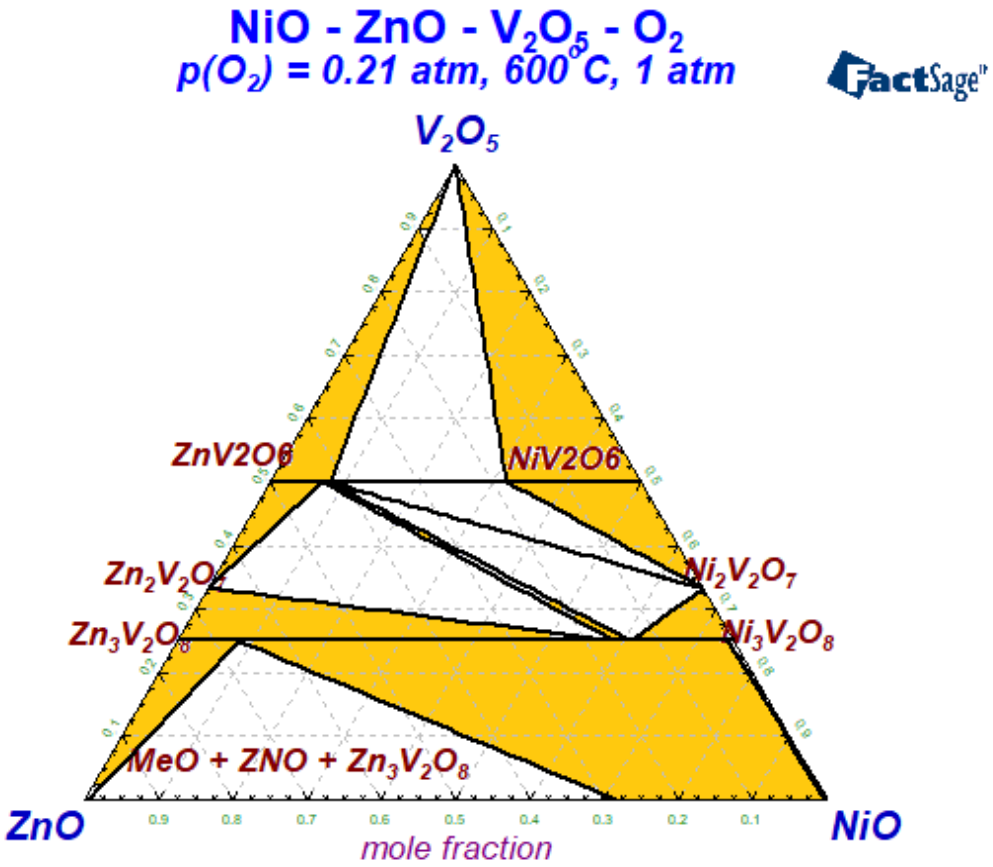

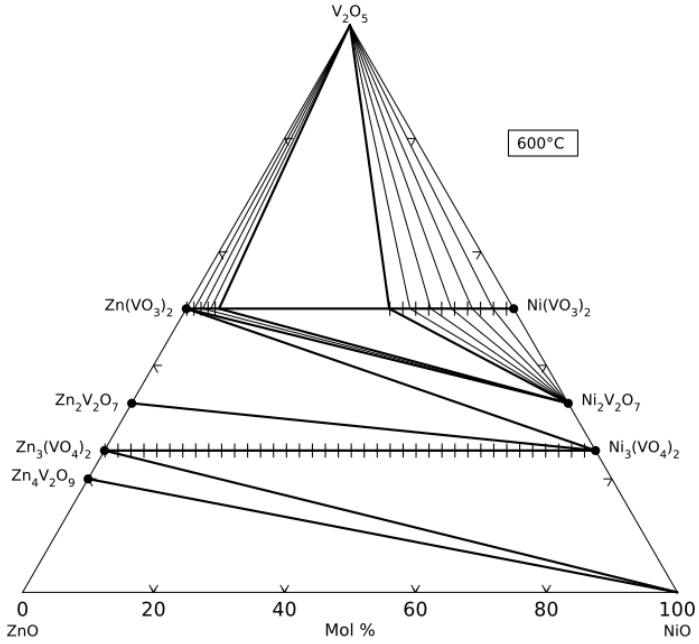

L. L. Surat, V. D. Zhuravlev, A. A. Fotiev, Yu. A. Velikodnyi, Zh. Neorg. Khim., 41 [8] 1370-1372 (1996).

NiO-V2O5-ZnO,
Mole fraction, Liquidussurface
,

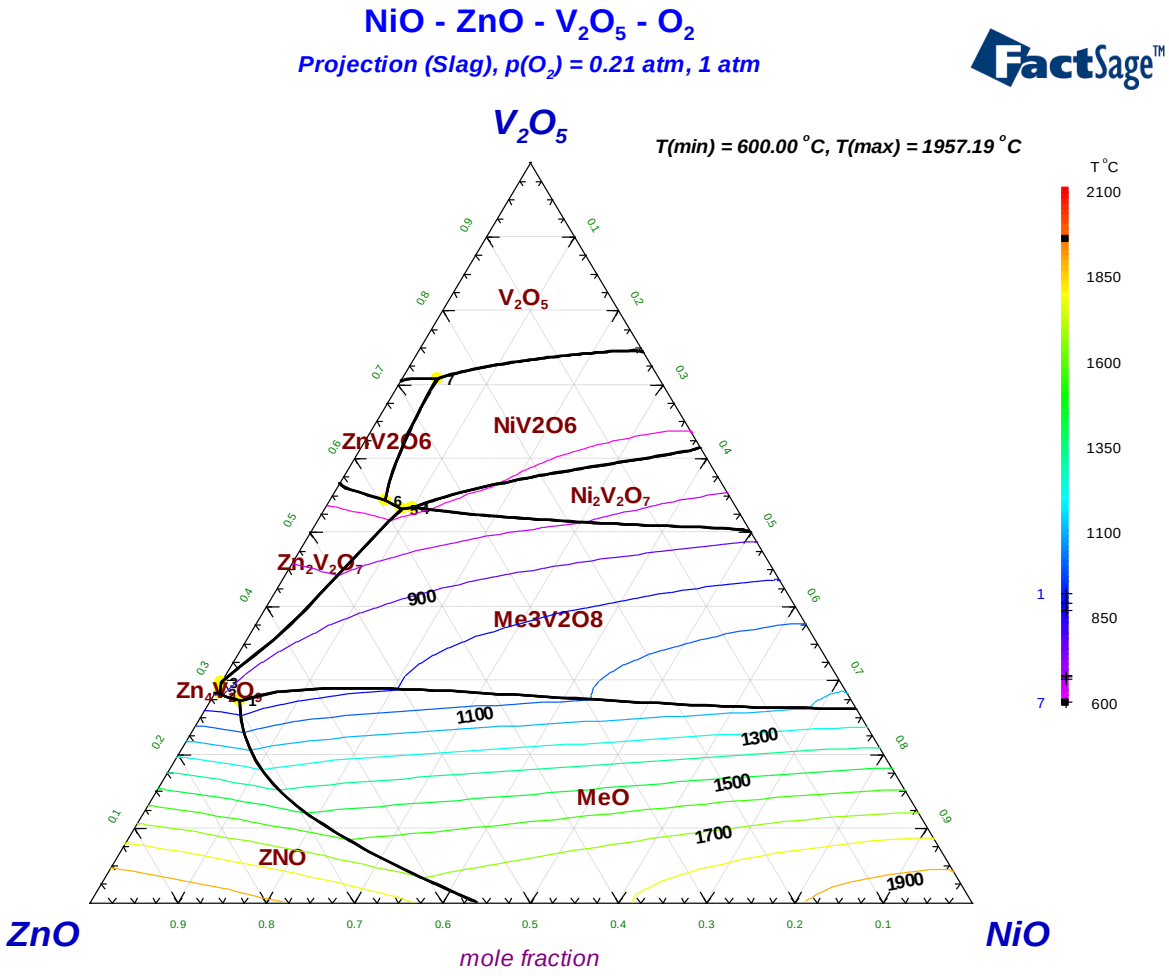

NiO-V2O5-ZnO,
Weight percent, Liquidussurface
,

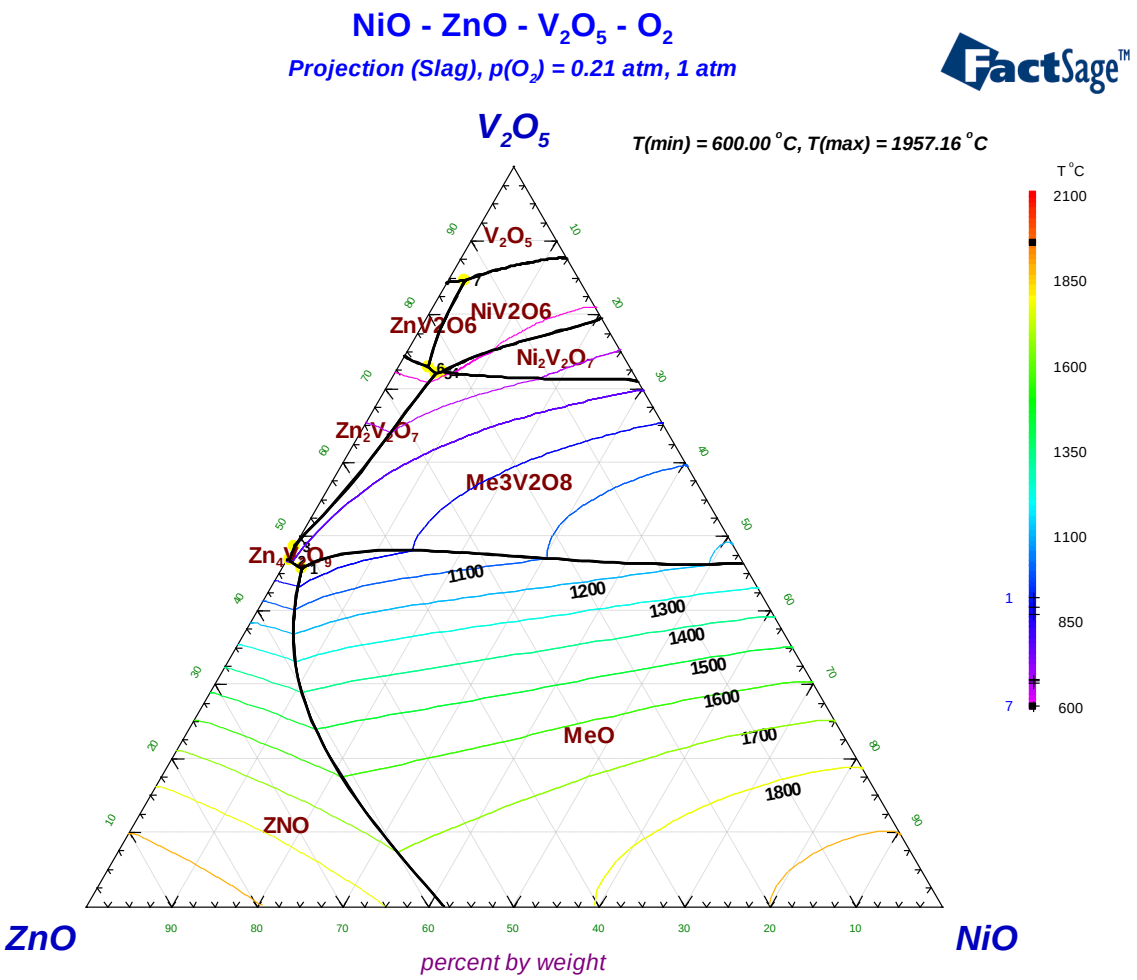

Invariant equilibria on the liquidus surface

Intersections with slag	Mole fraction A = V2O5, B = ZnO, C = NiO				Weight percent A = V2O5, B = ZnO, C = NiO			
	X(A)	X(B)	X(C)	T(C)	W(A)	W(B)	W(C)	T(C)
1: MeO / Me3V2O8 / ZNO	1: 0.27212	0.69313	0.03475	920.32	1: 45.618	51.990	2.393	920.33
2: Me3V2O8 / ZNO / Zn4V2O9	2: 0.28206	0.71110	0.00683	894.80	2: 46.774	52.761	0.465	894.81
3: Me3V2O8 / Zn2V2O7 / Zn4V2O9	3: 0.29730	0.70191	0.00079	873.91	3: 48.603	51.344	0.053	873.90
4: Ni2V2O7 / Me3V2O8 / NiV2O6	4: 0.53390	0.36598	0.10011	682.75	4: 72.269	22.166	5.565	682.75
5: Me3V2O8 / NiV2O6 / Zn2V2O7	5: 0.53143	0.38047	0.08809	679.01	5: 72.025	23.072	4.903	679.01
6: NiV2O6 / Zn2V2O7 / ZnV2O6	6: 0.54352	0.39243	0.06405	670.51	6: 72.915	23.556	3.529	670.51
7: NiV2O6 / V2O5 / ZnV2O6	7: 0.70777	0.25183	0.04040	604.13	7: 84.556	13.461	1.982	604.12

P2O5-SiO2-ZnO,
Mole fraction, 500°C
,

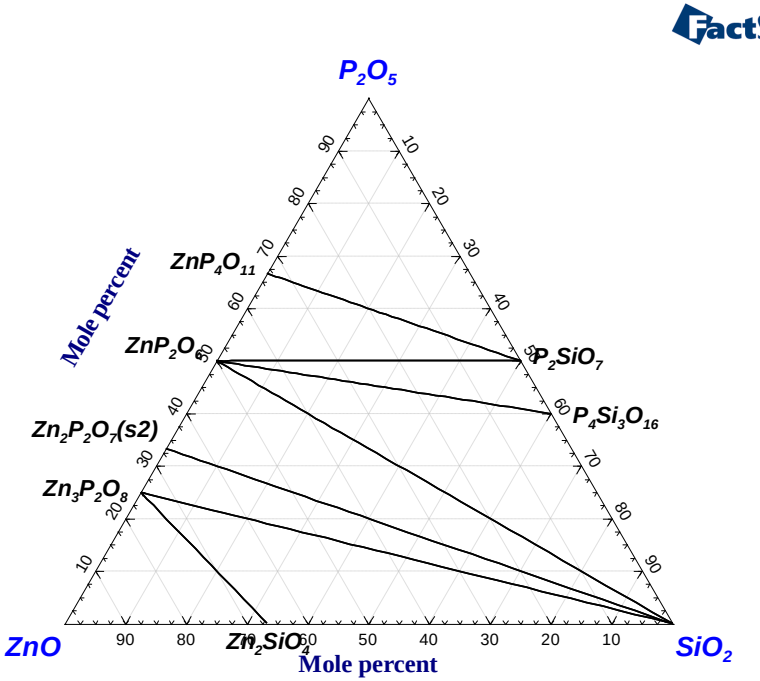

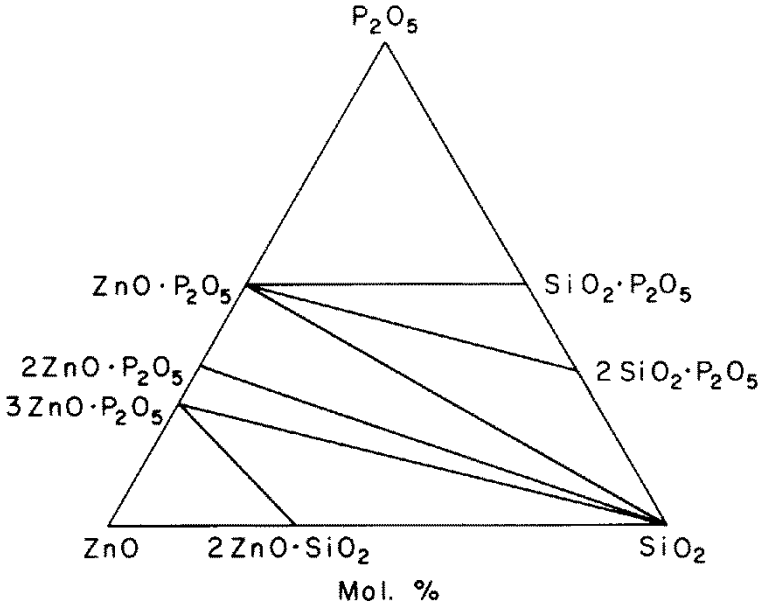

H.G. Huckenholz, D. Knittel, Contrib. Mineral. Petrol, 49 [3], (1975), pp.211-232.

P2O5-SiO2-ZnO,
Mole fraction, Liquidus surface
,

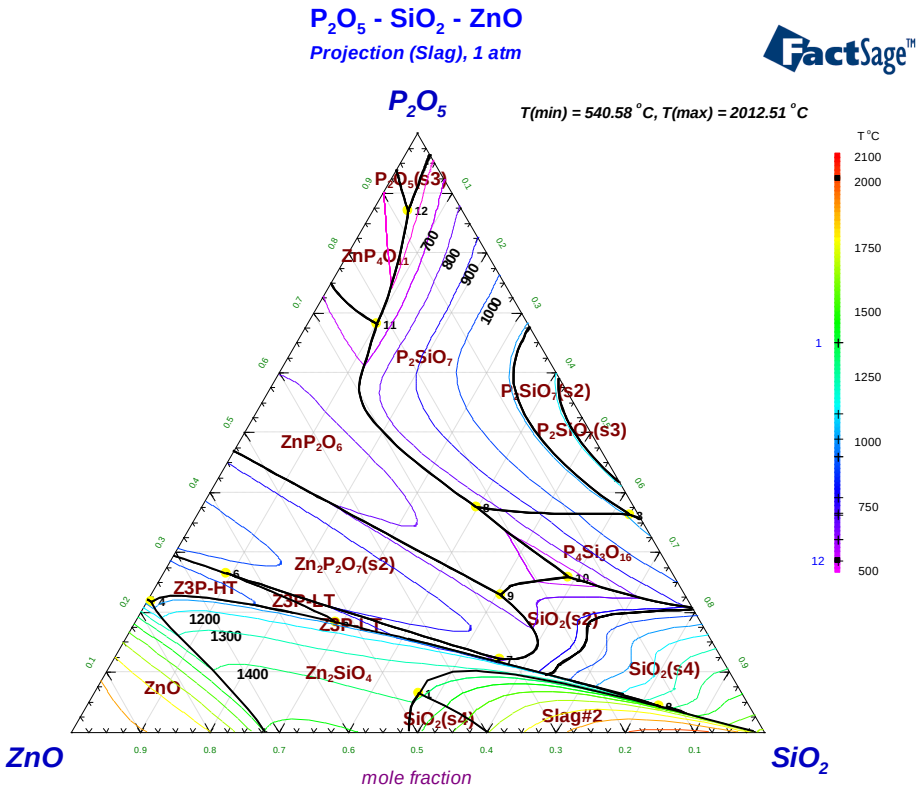

P2O5-SiO2-ZnO,
Weight percent, Liquidus surface
,

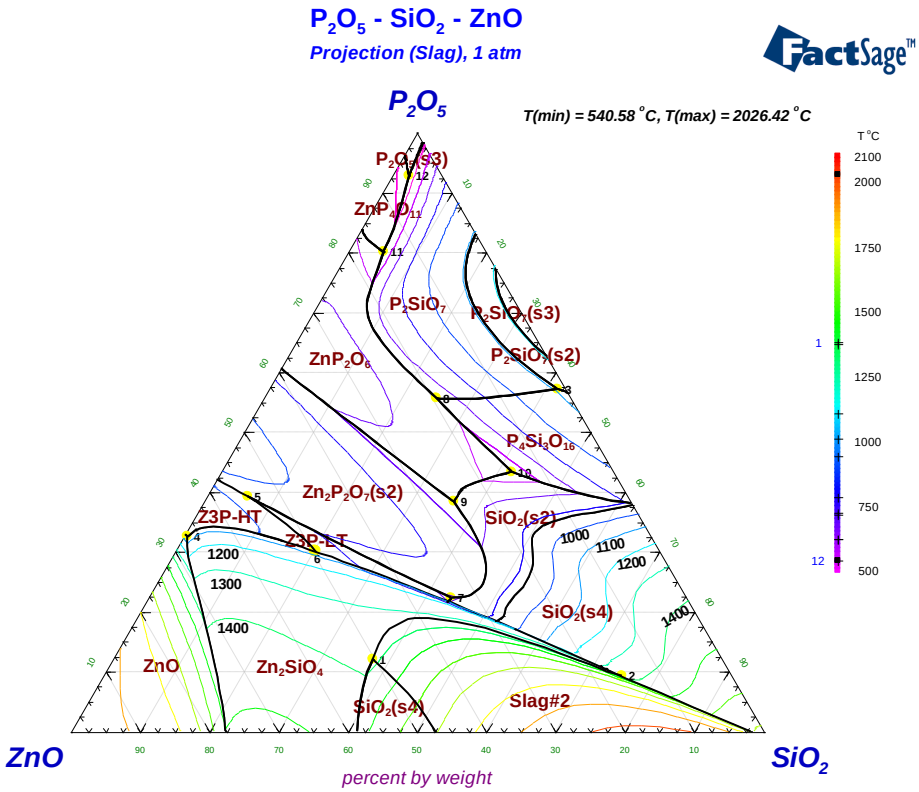

Invariant equilibria on the liquidus surface

Intersections with slag	Mole fraction				Weight percent			
	A = P2O5, B = ZnO, C = SiO2				A = P2O5, B = ZnO, C = SiO2			
	X(A)	X(B)	X(C)	T(C)	W(A)	W(B)	W(C)	T(C)
1. SiO2(s4) / Slag#2 / Zn2SiO4(s)	1: 0.06418	0.46534	0.47048	1380.56	1: 12.106	50.326	37.568	1380.54
2. SiO2(s4) / Slag#2 / Slag#2	2: 0.04255	0.12975	0.82770	1371.98	2: 9.331	15.794	74.875	1371.98
3. P2SiO7(s) / P2SiO7(s2) / P4Si3O16	3: 0.36317	0.01184	0.62499	1106.85	3: 57.237	1.070	41.694	1106.85
4. Z3P-HT / Zn2SiO4 / ZnO	4: 0.21697	0.77553	0.00750	1007.71	4: 32.638	66.884	0.478	1007.69
5. Z3P-HT / Z3P-LT / Zn2SiO4	5: 0.18249	0.52719	0.29031	941.85	5: 39.352	54.861	5.787	941.85
6. Z3P-HT / Z3P-LT / Zn2P2O7(s2)	6: 0.26462	0.64345	0.09193	941.85	6: 30.139	49.681	20.220	941.85
7. SiO2(s2) / Z3P-LT / Zn2P2O7(s2)	7: 0.12123	0.32081	0.55796	784.88	7: 22.395	33.976	43.629	784.88
8. P2SiO7(s) / P4Si3O16 / ZnP2O6(s)	8: 0.37538	0.22756	0.39706	721.76	8: 55.701	19.359	24.940	721.76
9. SiO2(s2) / Zn2P2O7(s2) / ZnP2O6(s)	9: 0.22868	0.26511	0.50620	715.25	9: 38.437	25.547	36.015	715.25
10. P4Si3O16 / SiO2(s2) / ZnP2O6(s)	10: 0.25884	0.15184	0.58932	623.25	10: 43.477	14.622	41.901	623.25
11. P2SiO7(s) / ZnP2O6(s) / ZnP4O11	11: 0.68083	0.21838	0.10079	622.32	11: 80.221	14.752	5.027	622.48
12. P2O5(s3) / P2SiO7(s) / ZnP4O11	12: 0.86984	0.07795	0.05221	540.58	12: 92.869	4.771	2.359	540.58

SiO2-TiO2-Ti2O3,
Mole fraction, Liquidus surface

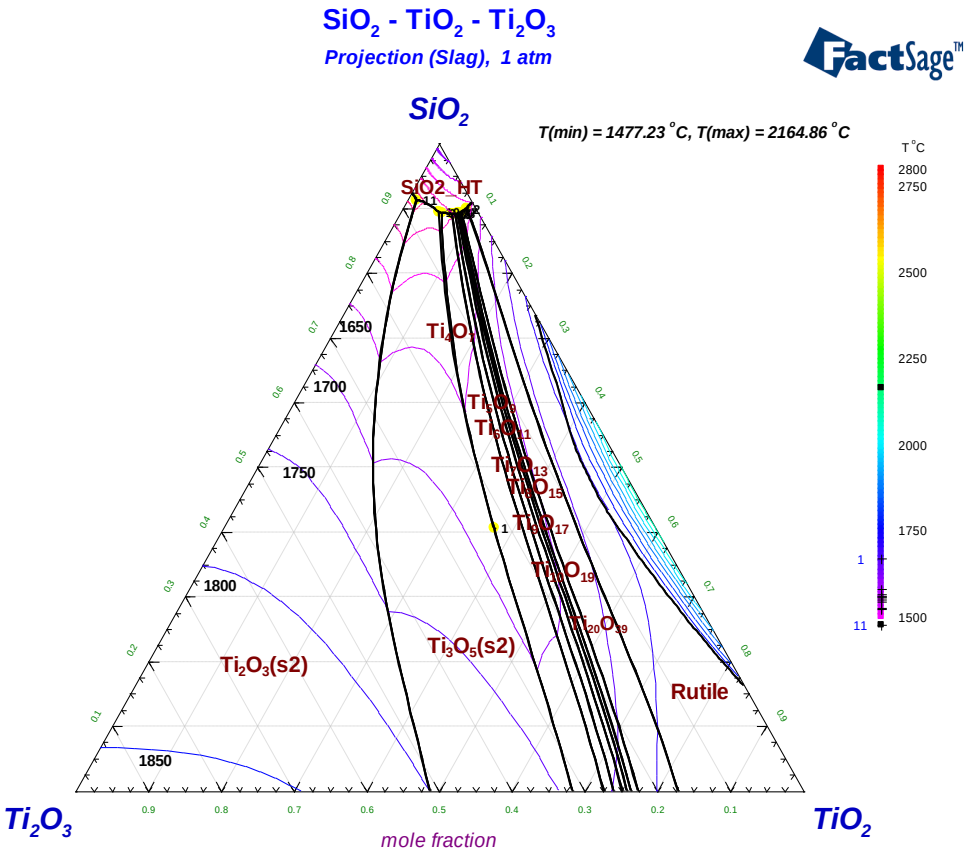

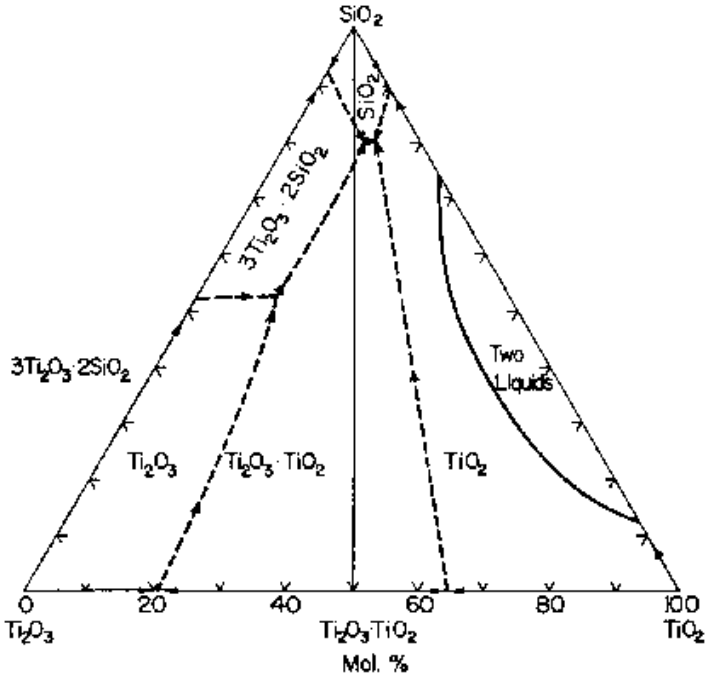

R. Roy, R.C. DeVries, D.E. Rase, M.W. Shafer, E.F. Osborn, Pennsylvania State College Quarterly Report, 1.10-31.12, Contract No. DA36-039 sc-5594, (1952).

SiO2-TiO2-Ti2O3,
Weight percent, Liquidus surface

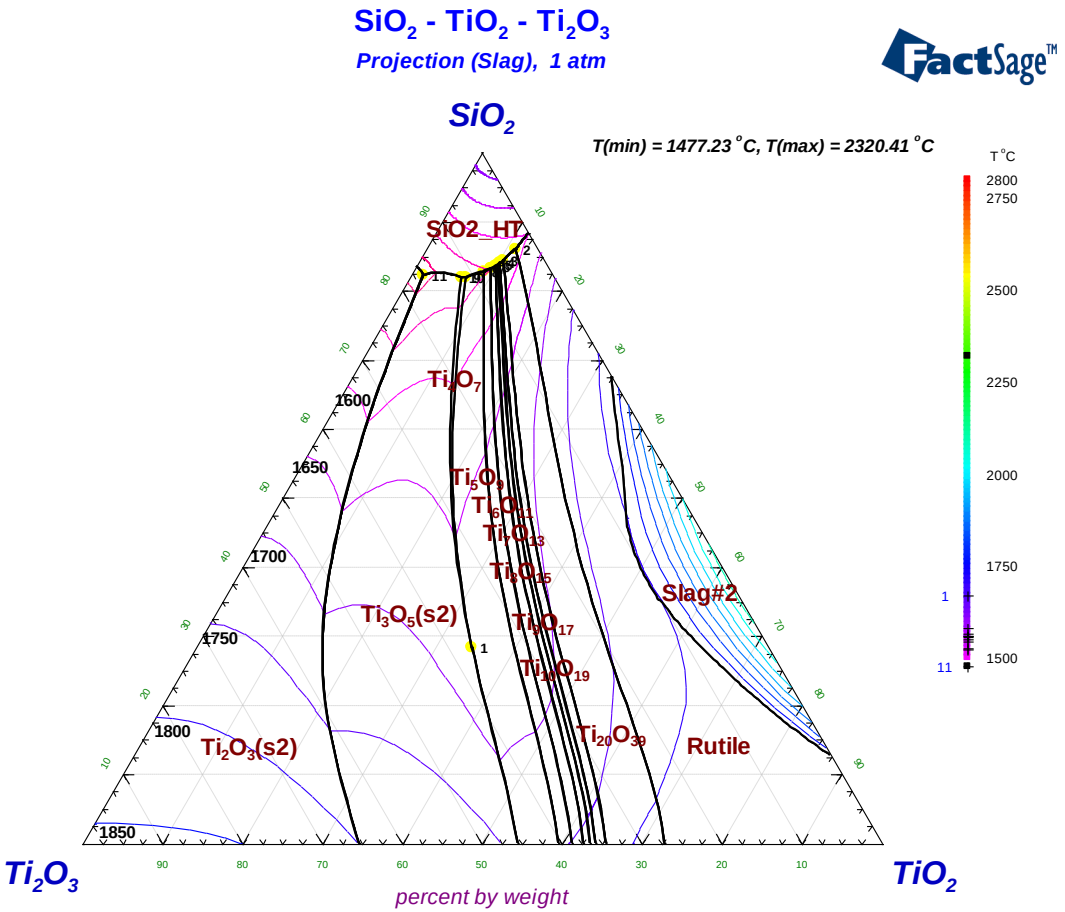

Invariant equilibria on the liquidus surface

Intersections with slag	Mole fraction A = SiO2, B = Ti2O3, C = TiO2				Weight percent A = SiO2, B = Ti2O3, C = TiO2			
	X(A)	X(B)	X(C)	T(C)	W(A)	W(B)	W(C)	T(C)
1: Ti3O5(s2) / Ti4O7 / Ti5O9	1: 0.40699	0.22158	0.37143	1669.74	1: 28.448	37.047	34.506	1669.75
2: Rutile / SiO2_HT / Ti20O39	2: 0.90043	0.01210	0.08747	1580.66	2: 86.113	2.768	11.119	1580.66
3: SiO2_HT / Ti10O19 / Ti20O39	3: 0.89390	0.02312	0.08298	1563.62	3: 84.370	5.219	10.411	1563.62
4: SiO2_HT / Ti10O19 / Ti9O17	4: 0.89299	0.02566	0.08134	1560.11	4: 84.045	5.778	10.176	1560.11
5: SiO2_HT / Ti8O15 / Ti9O17	5: 0.89252	0.02722	0.08027	1557.98	5: 83.858	6.118	10.024	1557.98
6: SiO2_HT / Ti7O13 / Ti8O15	6: 0.89203	0.02929	0.07868	1555.22	6: 83.626	6.569	9.805	1555.22
7: SiO2_HT / Ti6O11 / Ti7O13	7: 0.89150	0.03287	0.07563	1550.52	7: 83.267	7.344	9.390	1550.58
8: SiO2_HT / Ti5O9 / Ti6O11	8: 0.89140	0.03729	0.07131	1544.71	8: 82.890	8.296	8.814	1544.71
9: SiO2_HT / Ti4O7 / Ti5O9	9: 0.89318	0.05040	0.05642	1525.36	9: 82.037	11.074	6.889	1525.36
10: SiO2_HT / Ti3O5(s2) / Ti4O7	10: 0.89438	0.05298	0.05264	1521.40	10: 81.971	11.616	6.413	1521.41
11: SiO2_HT / Ti2O3(s2) / Ti3O5(s2)	11: 0.91289	0.07487	0.01224	1477.23	11: 82.372	16.160	1.468	1477.23

Sr-Fe-O,

Sr-Fe-O,
Mole fraction, 400°C

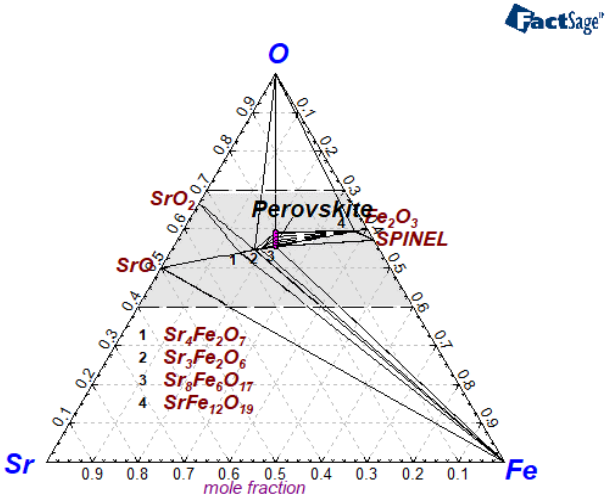

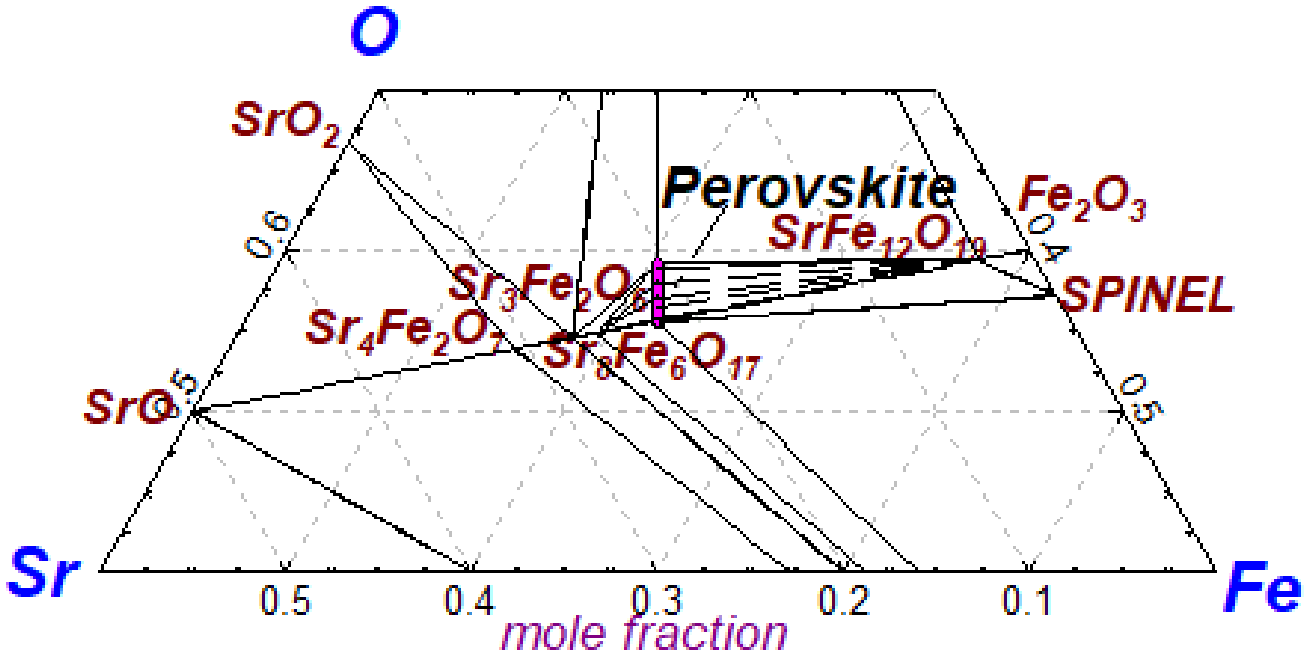

Sr-Fe-O,
Mole fraction, 800°C

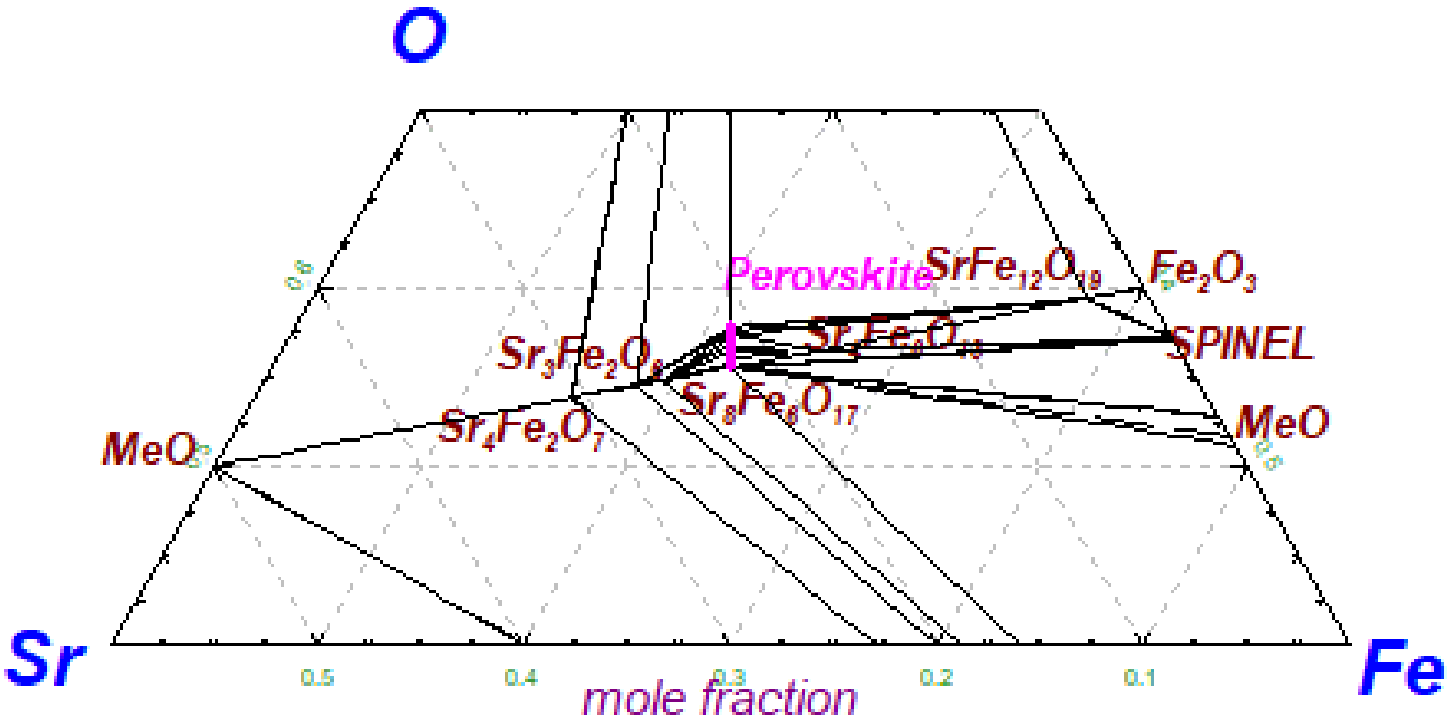

TiO2-Ti2O3-V2O3, Mole fraction, 1200°C

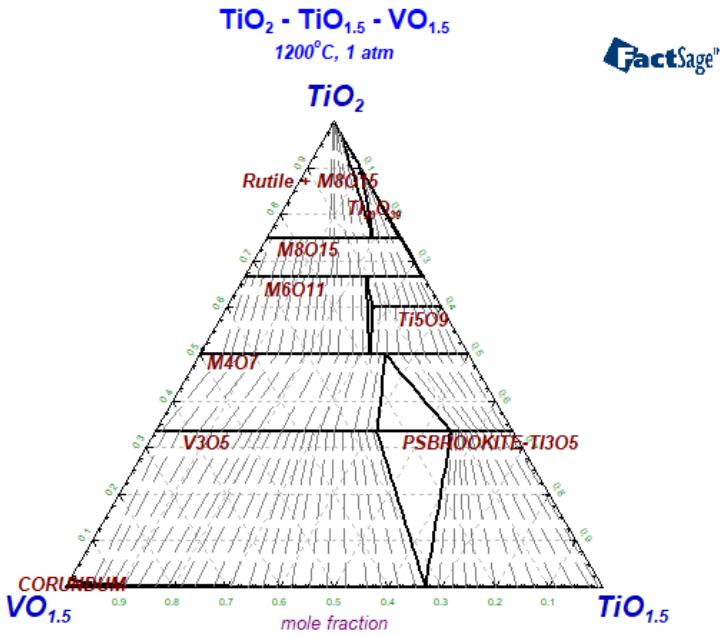

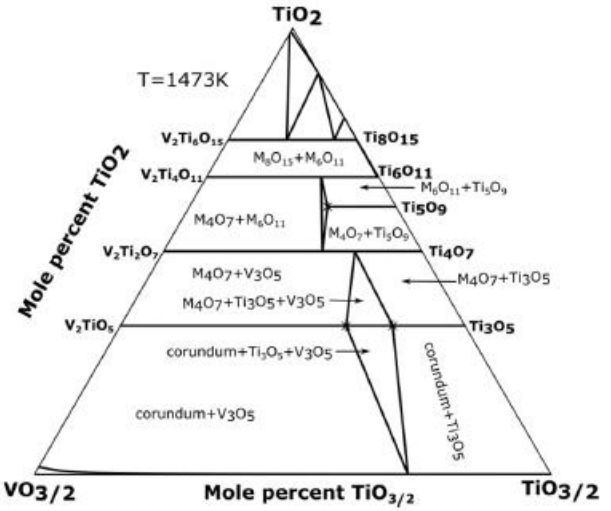

Fig. 5. Calculated isothermal section of the V_2O_3-Ti_2O_3-TiO_2 system at 1473 K. (The star symbols are the reported composition ranges for solid solutions, *viz*, $V_{0.69}Ti_{2.31}O_5$ for V_3O_5, $V_{0.42}Ti_{2.58}O_5$ for Ti_3O_5, $V_{0.665}Ti_{4.335}O_9$ for Ti_5O_9 [28].)

Phase	Description	Used data
Corundum	$(Ti^{+3},V^{+3},V^{+4})_2\,(Va)_1(O^{-2})_3$	Present work
Pseudobrookite	$(Ti, V)_1(Ti)_1(Ti)_1(O)_5$	Present work
Rutile	$(Ti, V)\,(O, Va)_2$	[Yang17]
V_3O_5	$(Ti, \underline{V})_3(O)_5$	[Yang17]
M_4O_7	$(Ti, V)_4(O)_7$	[Yang17]
V_5O_9	$(Ti, \underline{V})_5(O)_9$	[Yang17]
M_6O_{11}	$(Ti, V)_6(O)_{11}$	[Yang17]
M_8O_{15}	$(Ti, V)_8(O)_{15}$	[Yang17]

TiO2-Ti2O3-V2O3,
Mole fraction, Liquidus surface

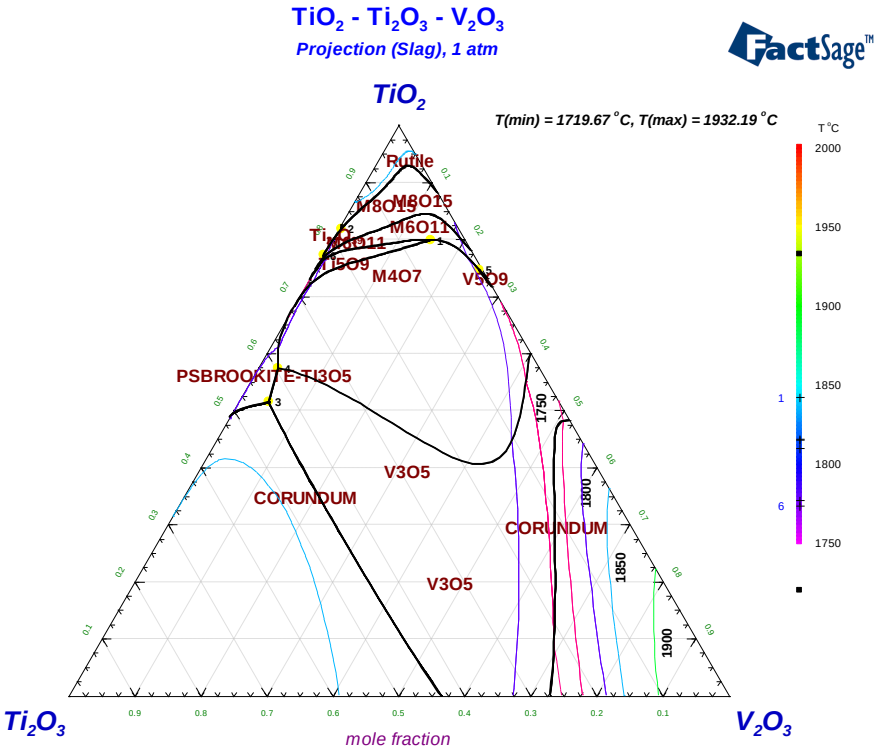

TiO2-Ti2O3-V2O3,
Weight percent, Liquidus surface

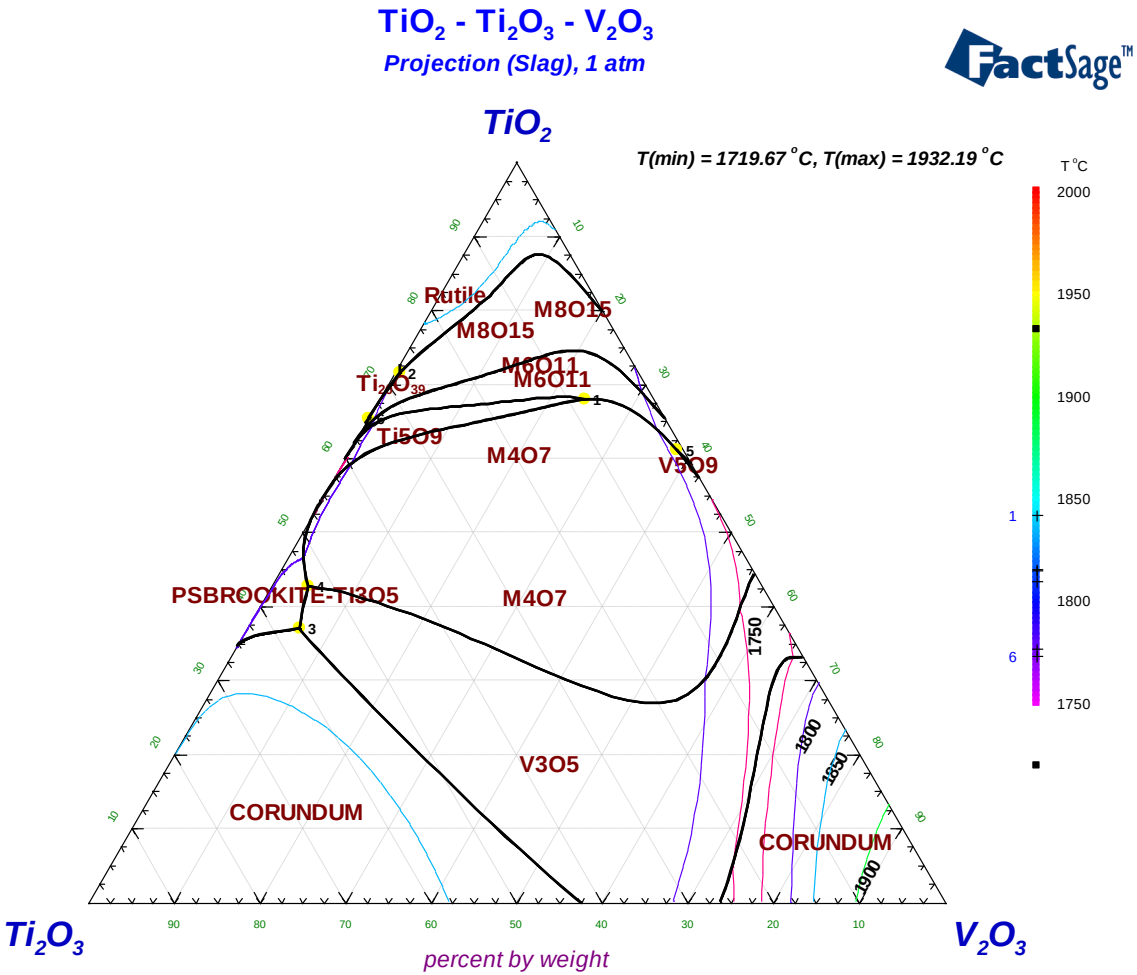

Invariant equilibria on the liquidus surface

Intersections with slag	Mole fraction A = TiO2, B = Ti2O3, C = V2O3				Weight percent A = TiO2, B = Ti2O3, C = V2O3			
	X(A)	X(B)	X(C)	T(C)	W(A)	W(B)	W(C)	T(C)
1: M4O7 / M6O11 / Ti5O9	1: 0.79820	0.05251	0.14929	1841.83	1: 68.056	8.057	23.887	1841.83
2. M8O15 / Rutile / Ti20O39(s)	2: 0.81890	0.17751	0.00359	1815.21	2: 71.514	27.898	0.588	1815.21
3. CORUNDUM#1 / PSBROOKITE-TI3O5 / V3O5	3: 0.51476	0.43986	0.04538	1814.60	3: 36.992	56.888	6.120	1814.60
4. M4O7 / PSBROOKITE-TI3O5 / V3O5	4: 0.57383	0.39532	0.03085	1809.51	4: 42.722	52.968	4.310	1809.51
5. M4O7 / M6O11 / V5O9	5: 0.74656	0.00468	0.24876	1776.47	5: 61.102	0.689	38.209	1776.47
6. M8O15 / Ti10O19(s) / Ti20O39(s)	6: 0.77307	0.22690	0.00002	1772.92	6: 65.433	34.563	0.004	1773.02

Quaternary systems:

Mole fraction,
Isopleth Uvarovite-Grossularite

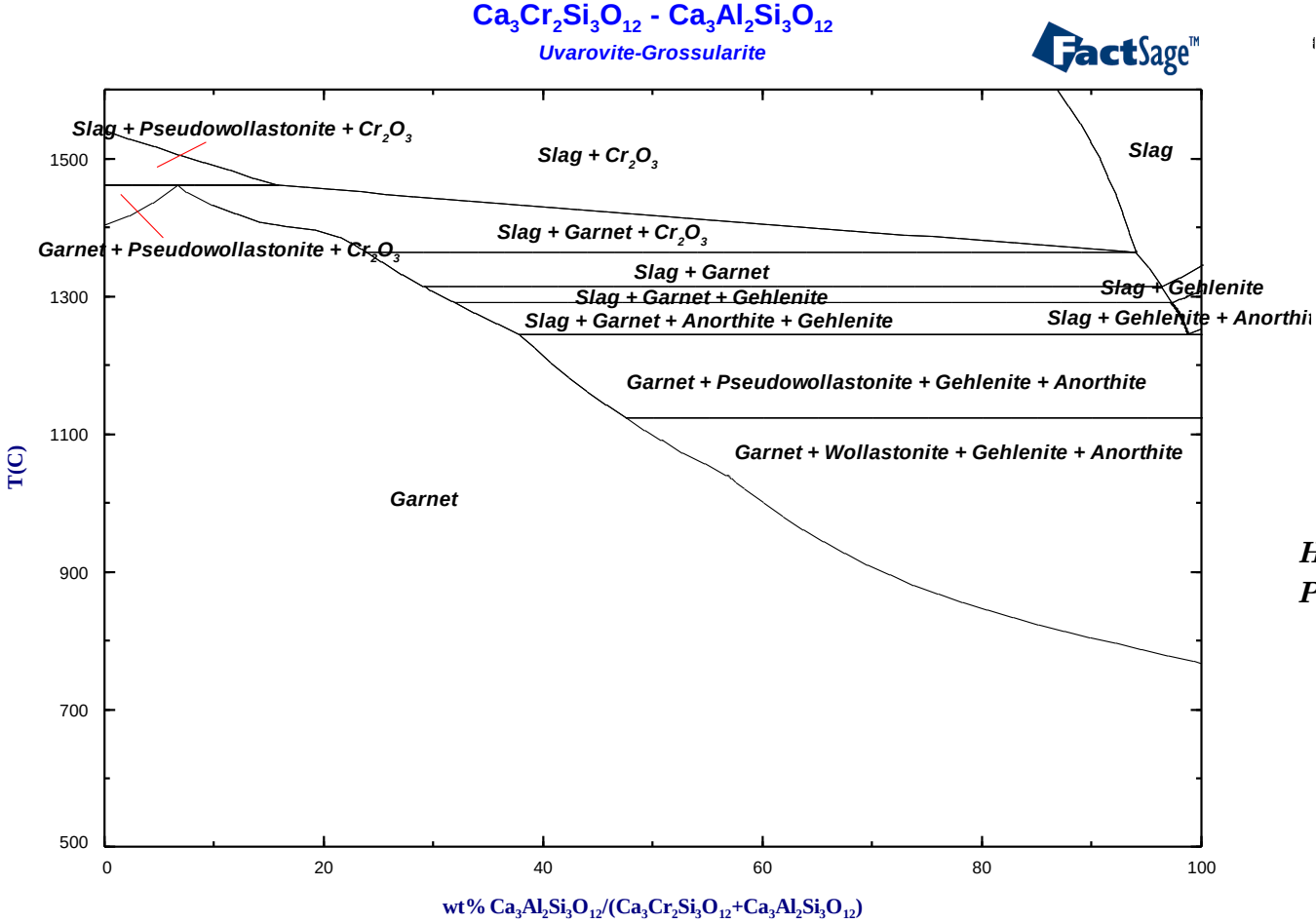

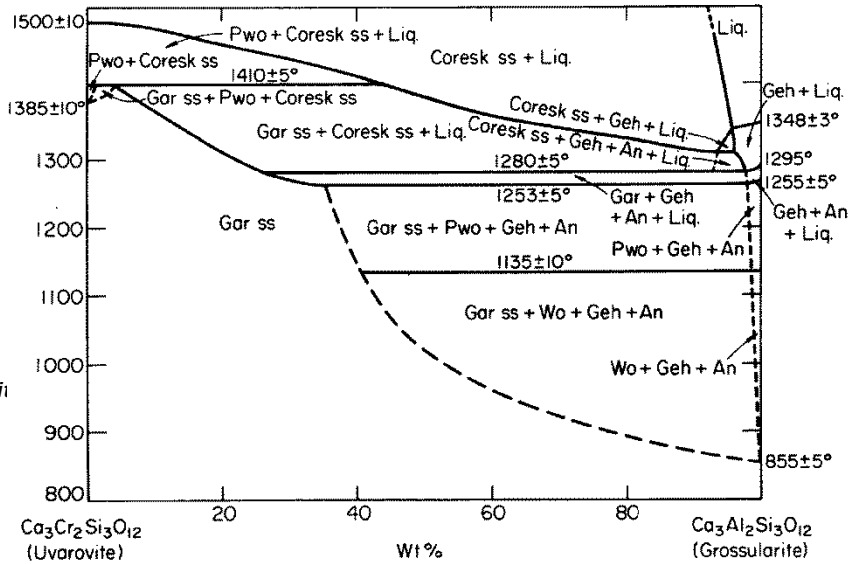

H.G. Huckenholz, D. Knittel, Contrib. Mineral. Petrol, 49 [3], (1975), pp.211-232.

Mole fraction 600°C,
Isothermischer Schnitt im AlKO2-AlNaO2-CaAl2O4 System

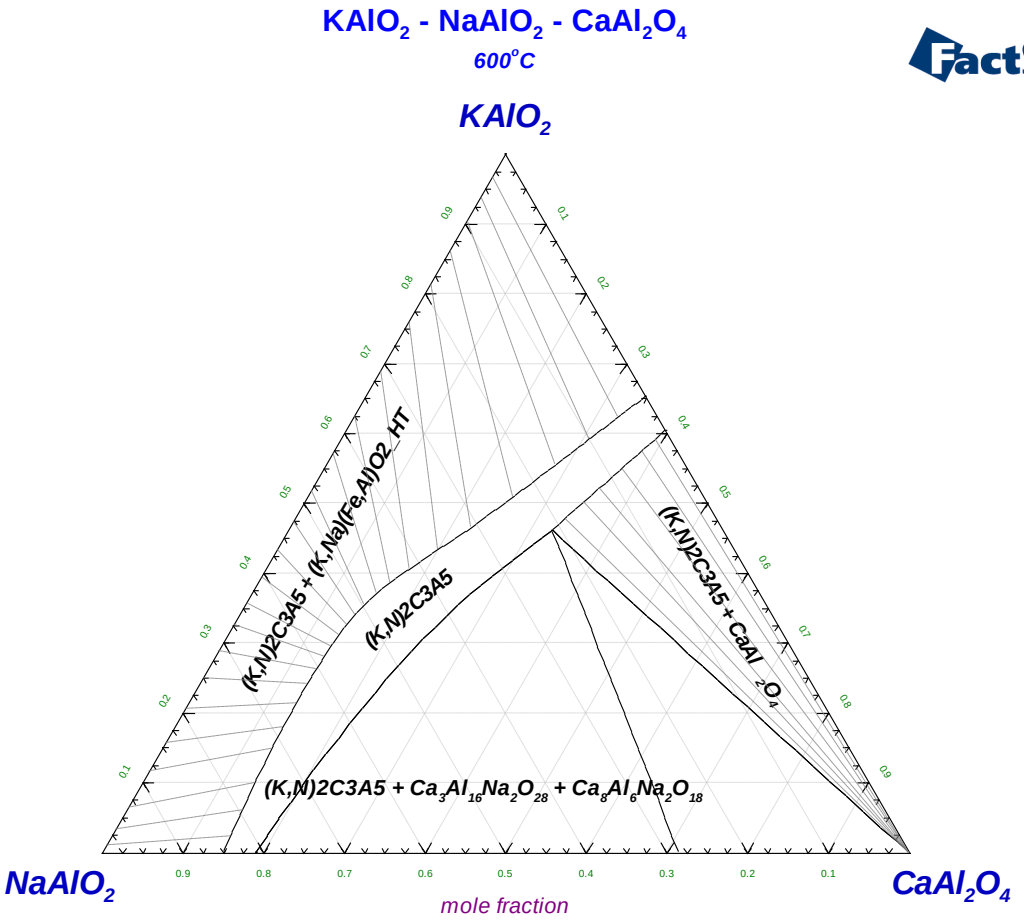

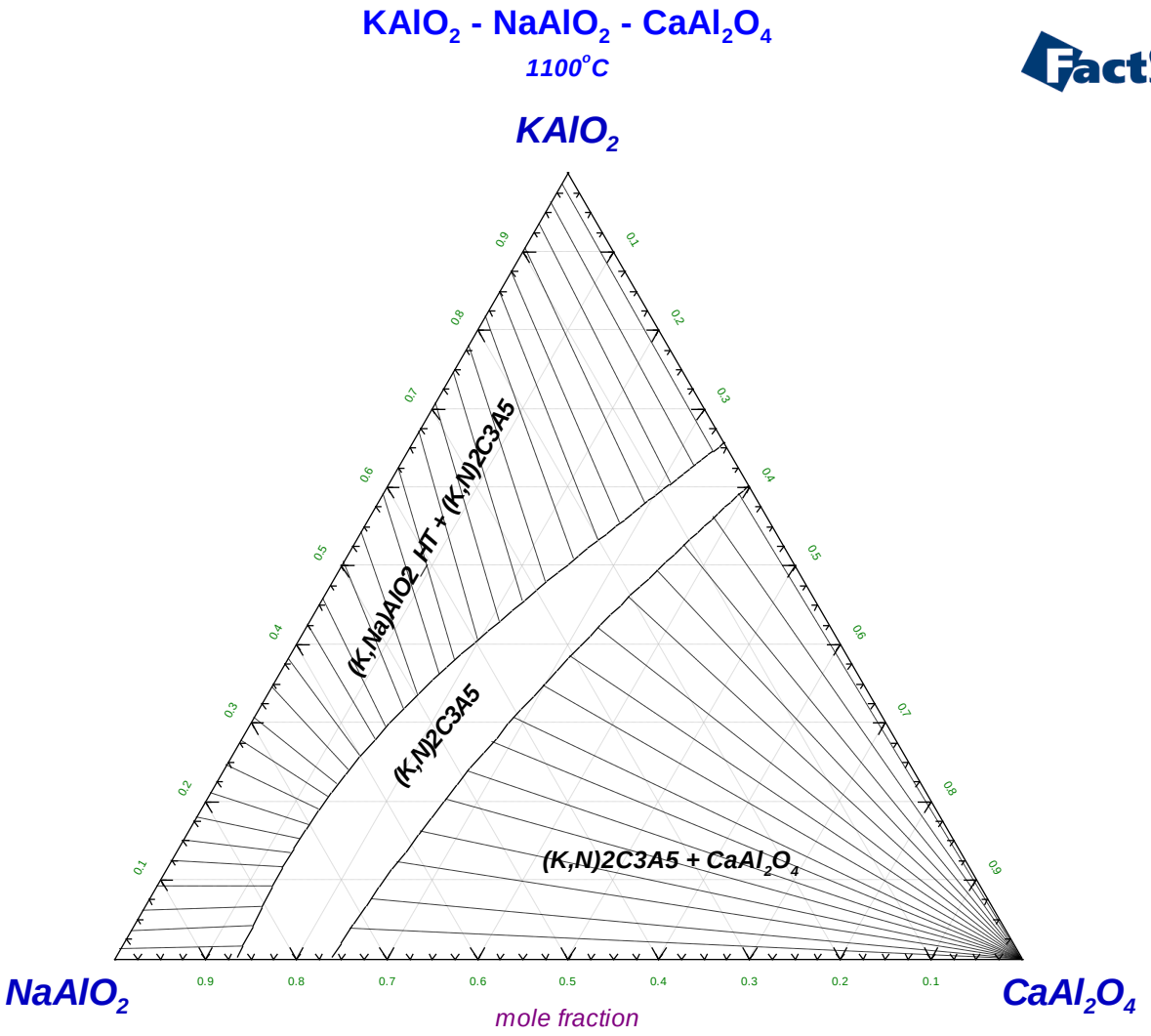
KAlO2 - NaAlO2 - CaAl2O4
1100°C
KAlO2
(K,Na)AlO2_HT + (K,N)2C3A5
(K,N)2C3A5
(K,N)2C3A5 + CaAl2O4
NaAlO2
CaAl2O4
mole fraction

Mole fraction 1700°C,
Isothermischer Schnitt im AlKO2-AlNaO2-CaAl2O4 System

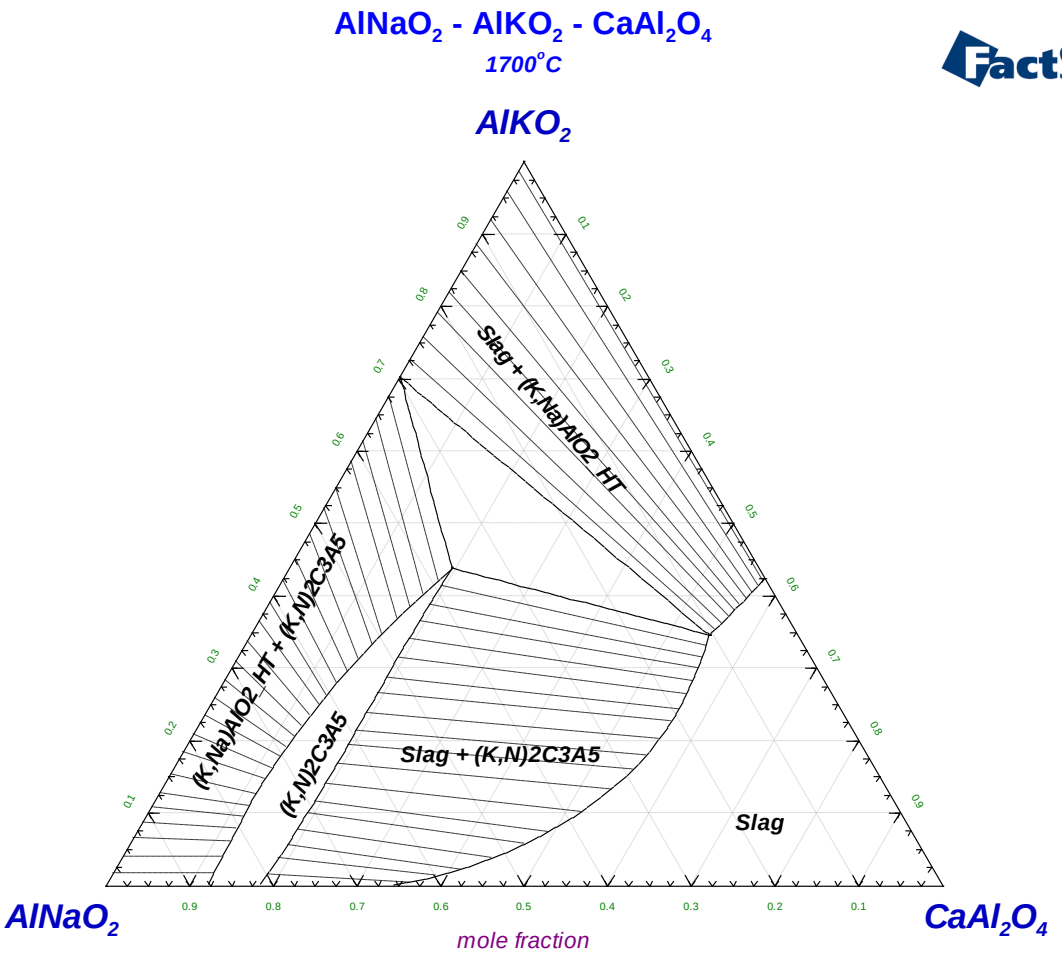

Weight percent,
Isopleth MgAl2O4-CaAl2Si2O7

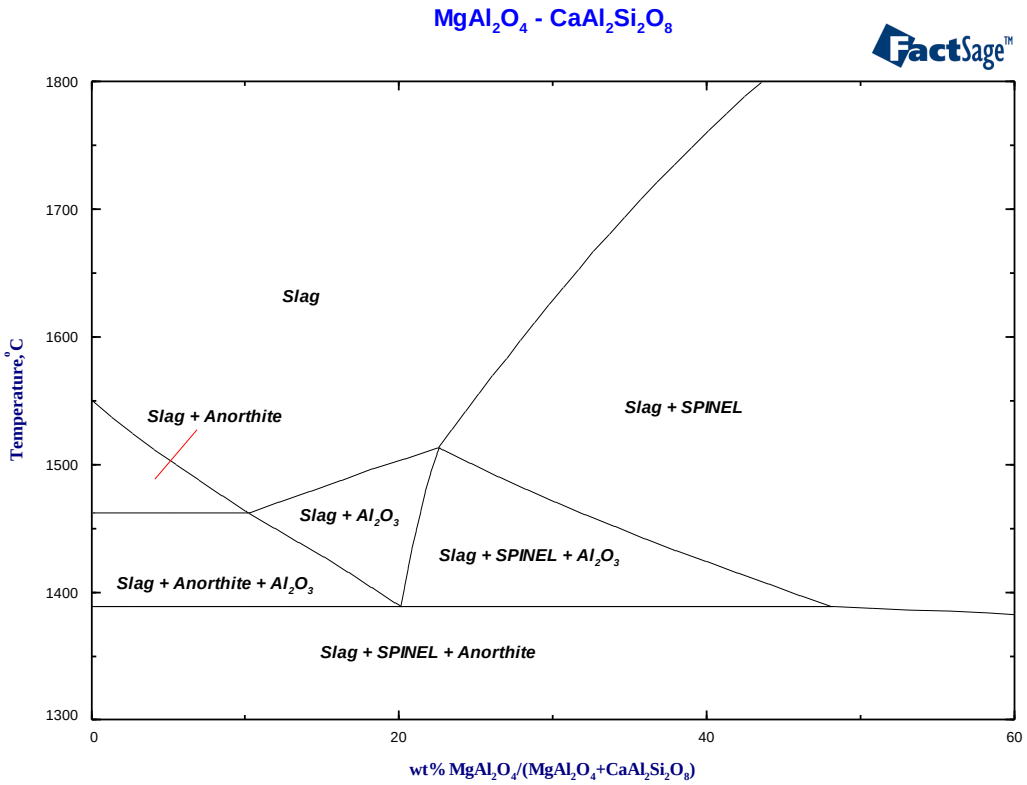

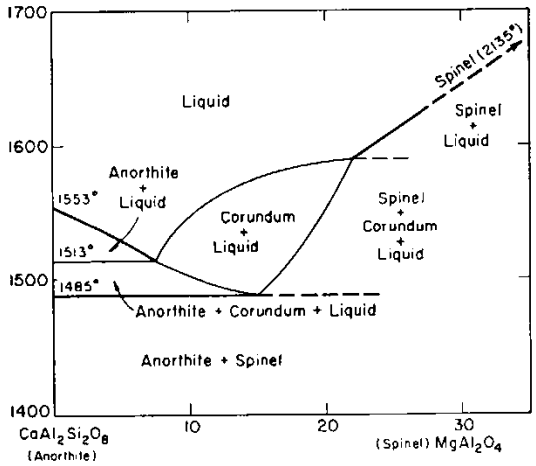

E.F. Osborn, R.C. DeVries, K.H. Gee, H.M. Kramer, Trans. Am. Inst. MIn., Metall. Pet. Eng., 200 (1954), pp.33-45.

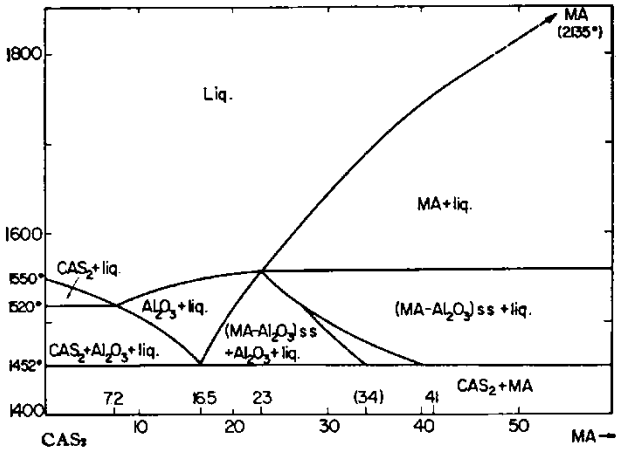

J.H. Welch, J. Iron Steel Inst., London, 183 [pt.3], (1956), pp.275-283.

Weight percent,
Isopleth MgAl2O4-Ca2Al2SiO7

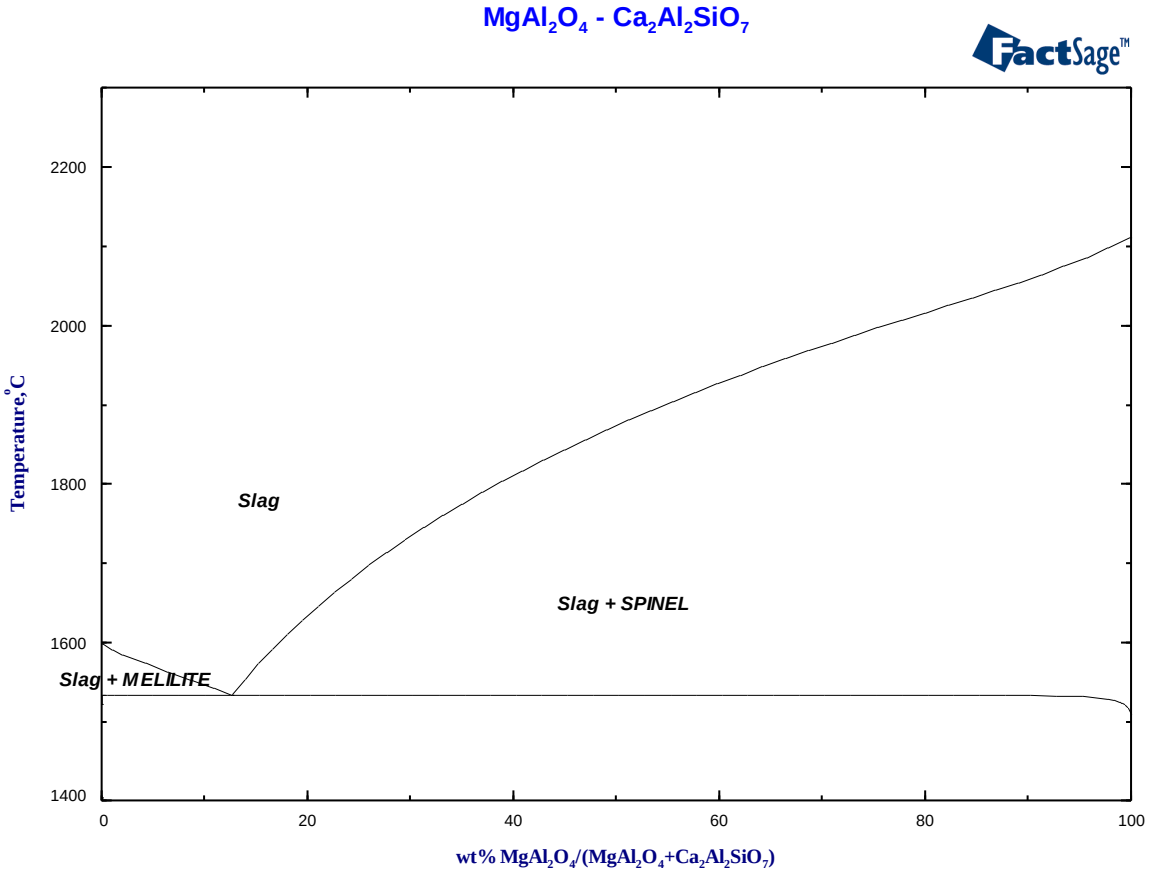

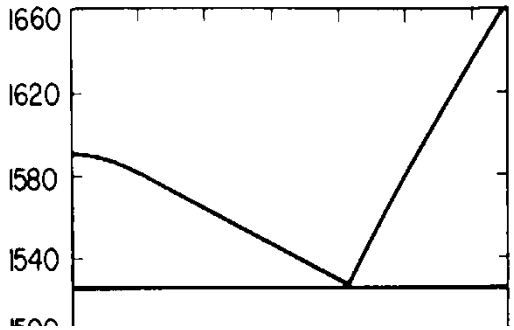

W.K. Gummer, J. Geol., 51 [8], (1943), pp.503-531.

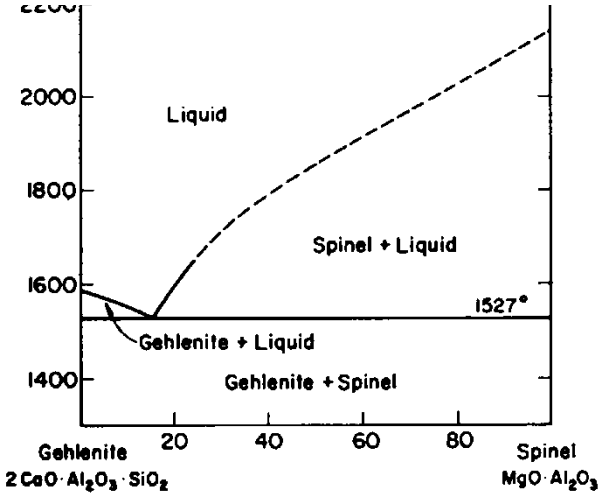

J.H. Welch, J. Iron Steel Inst., London, 183 [pt.3], (1956), pp.275-283.

Weight percent,
Liquidusoberfläche bei 10 mass.% Al2O3

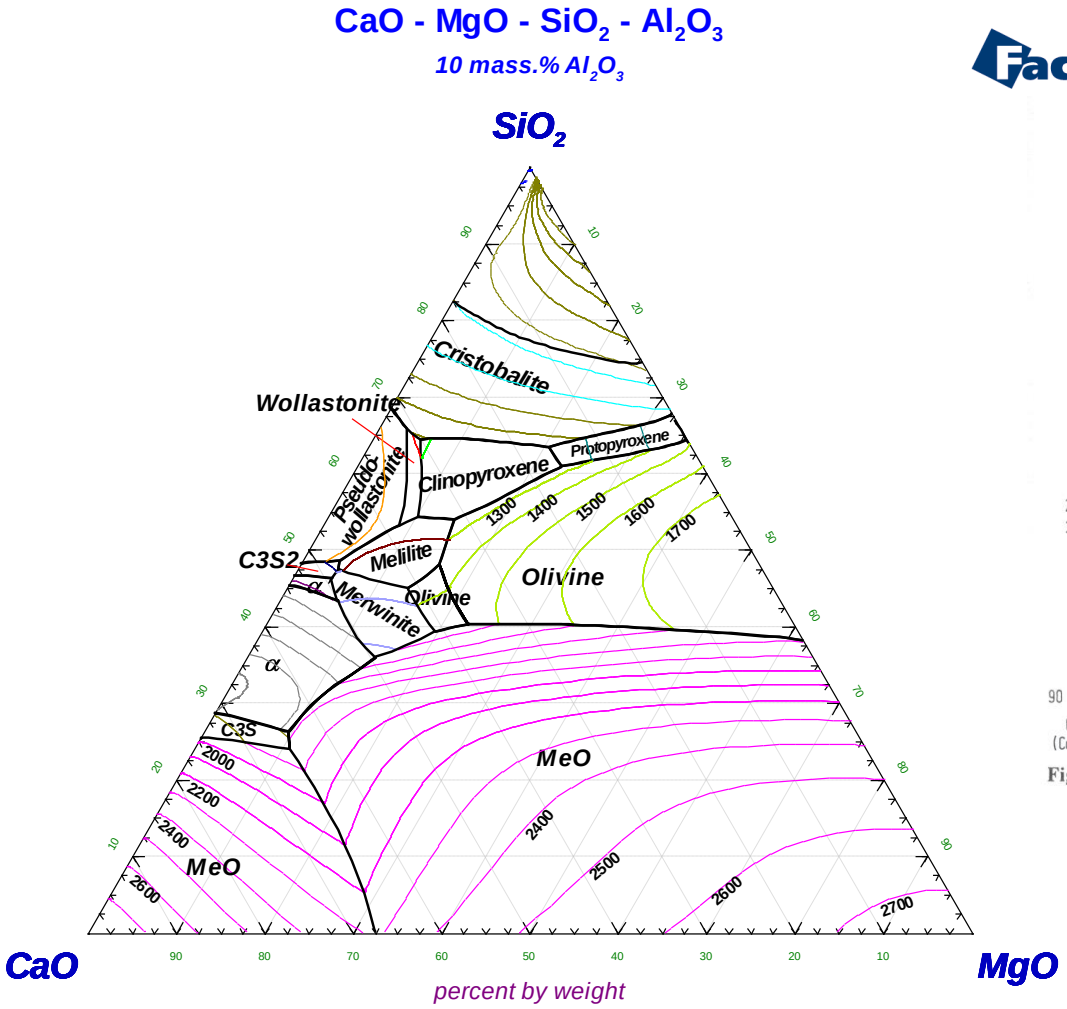

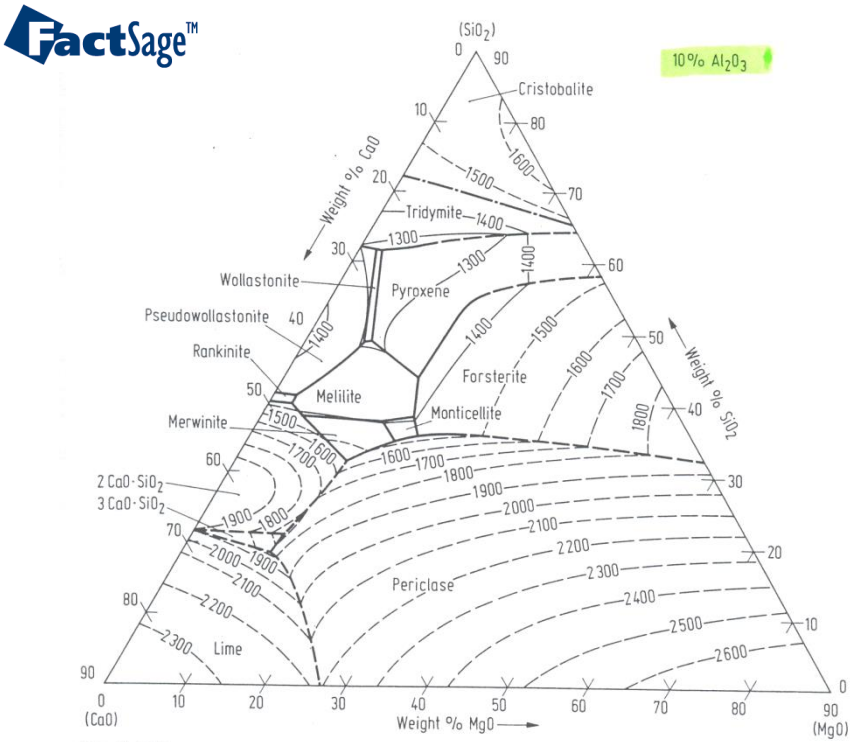

Fig. 3.318.

E. F. Osborn, R.C. DeVries, K.H. Gee, H.M. Kraner,Trans. Am. Inst. MIn., Metall. Pet. Eng., 200, (1954), pp.33-45.

Weight percent,
Liquidusoberfläche bei 15 mass.% Al2O3

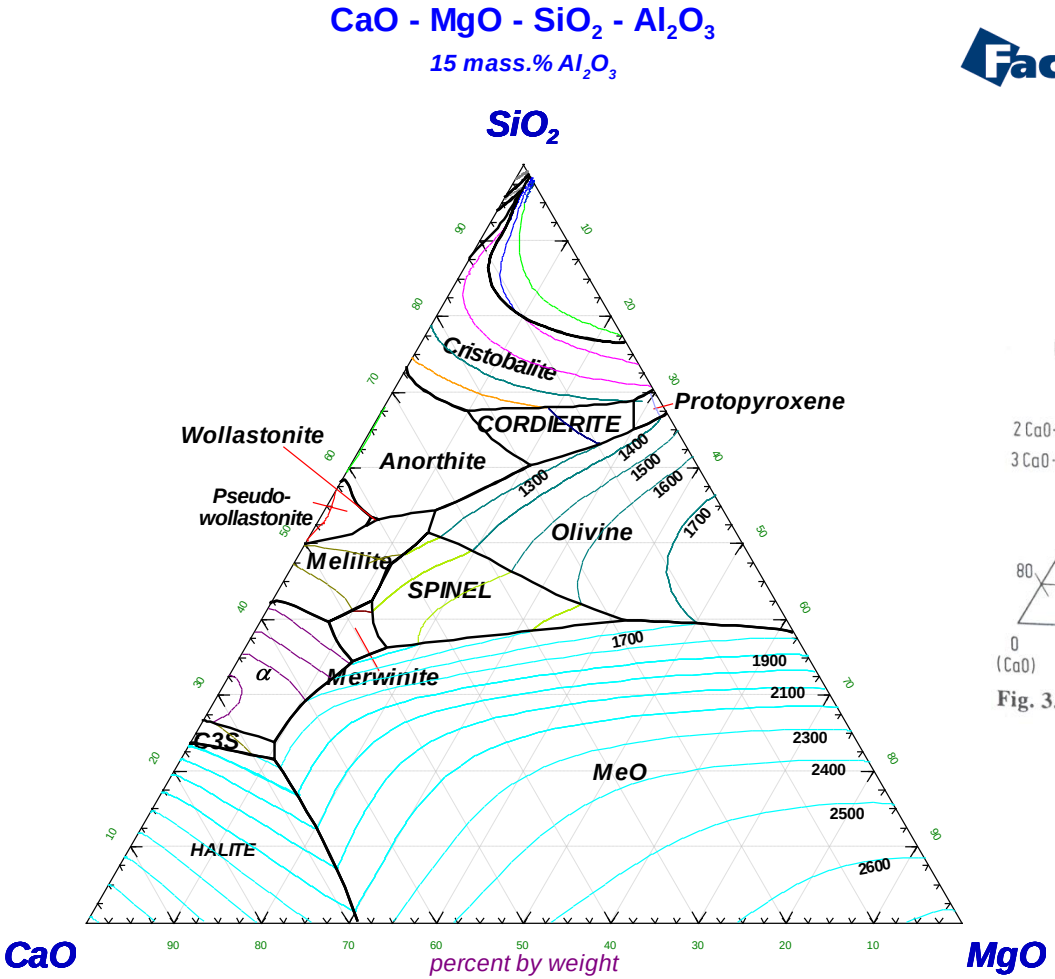

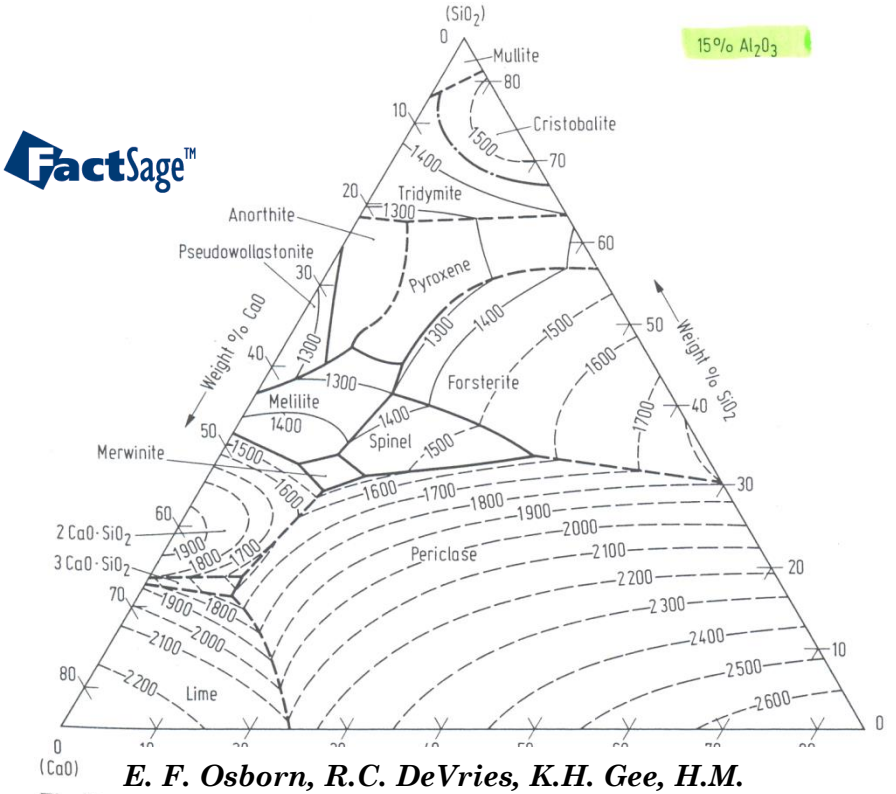

Fig. 3. *E. F. Osborn, R.C. DeVries, K.H. Gee, H.M. Kraner,Trans. Am. Inst. MIn., Metall. Pet. Eng., 200, (1954), pp.33-45.*

Weight percent,
Liquidusoberfläche bei 5 mass.% MgO

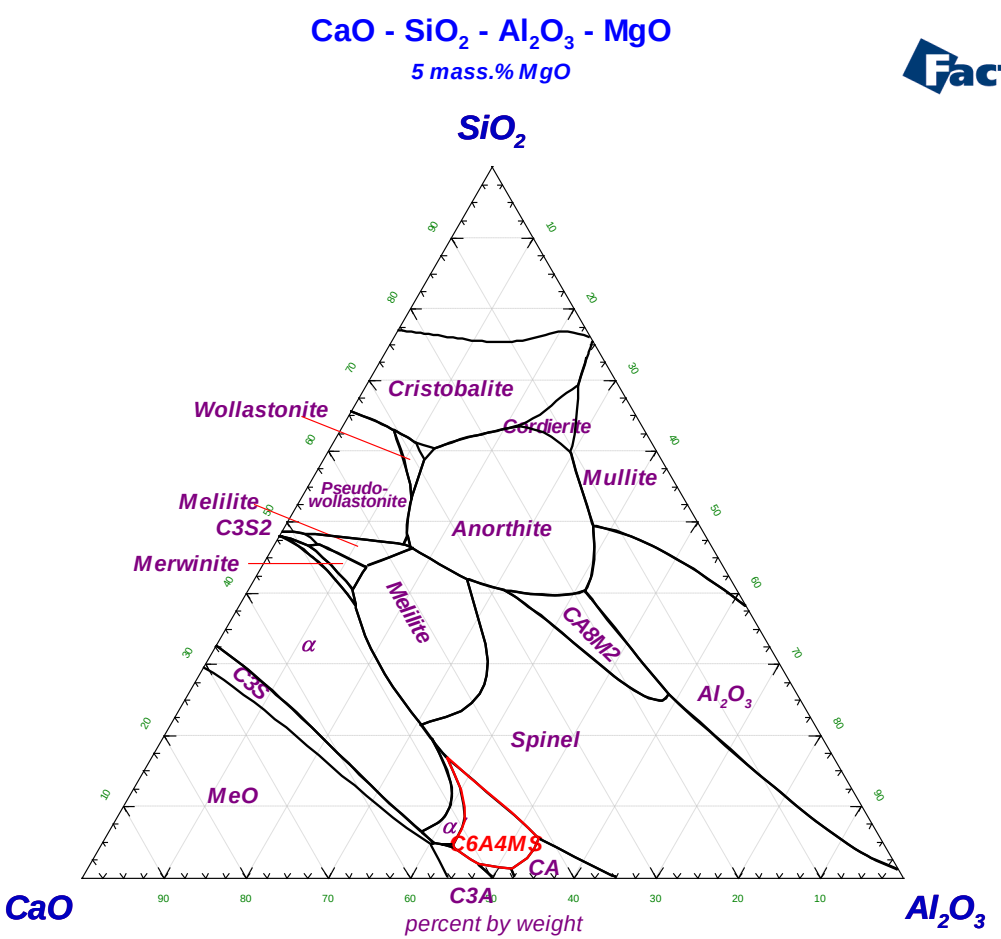

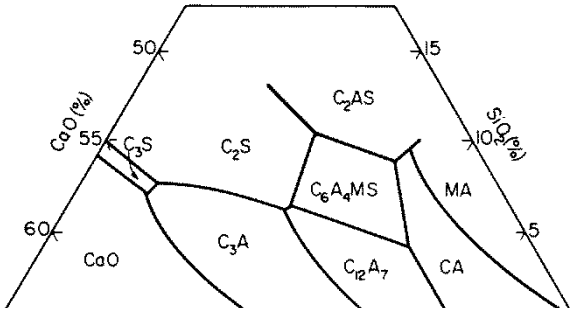

F.M. Lea, C.H. Desch, "The chemistry of cement and concrete", New York, (1956), pp.1-637.

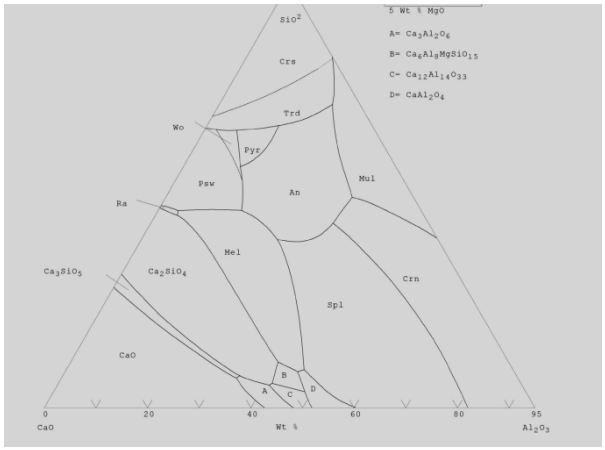

W.H. Gutt, A.D. Russell, J. Mater.Sci., 12 [9], (1977), pp.1869-1878.

Weight percent,
Liquidusoberfläche bei 10 mass.% MgO

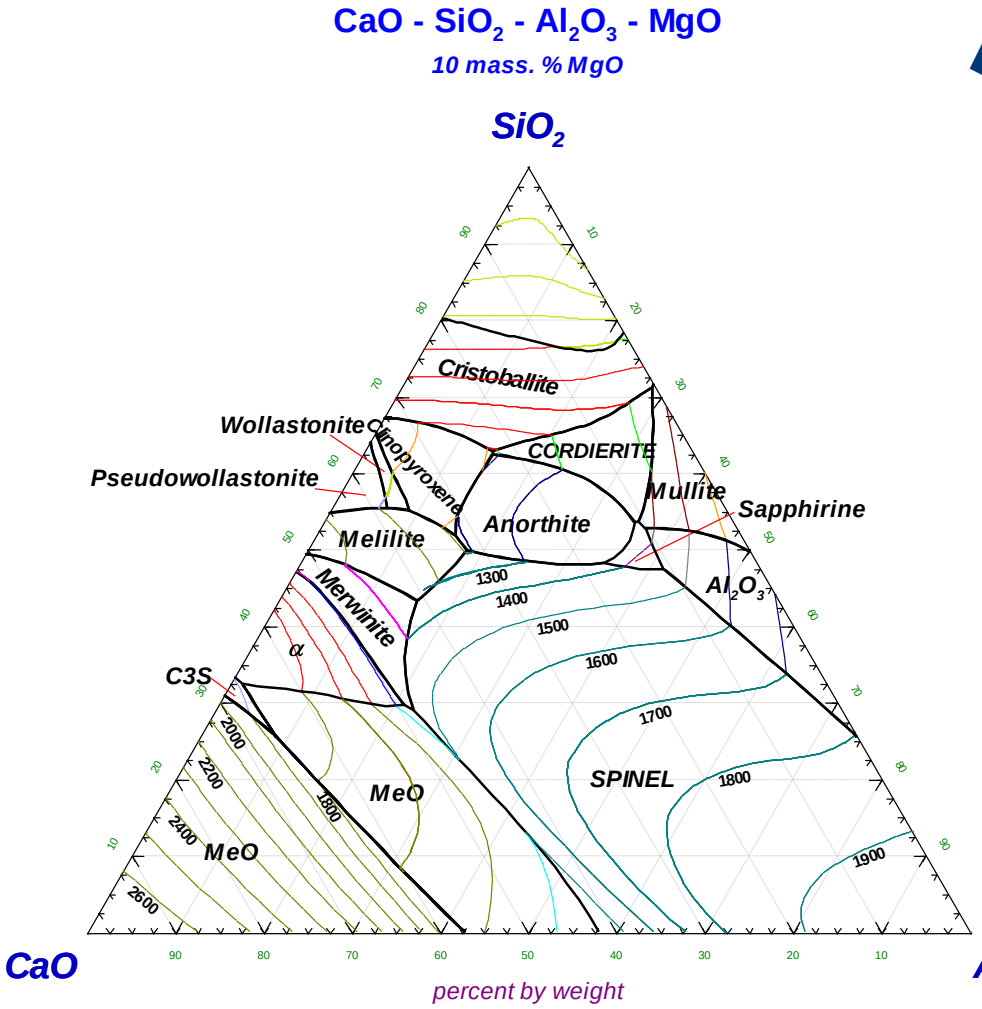

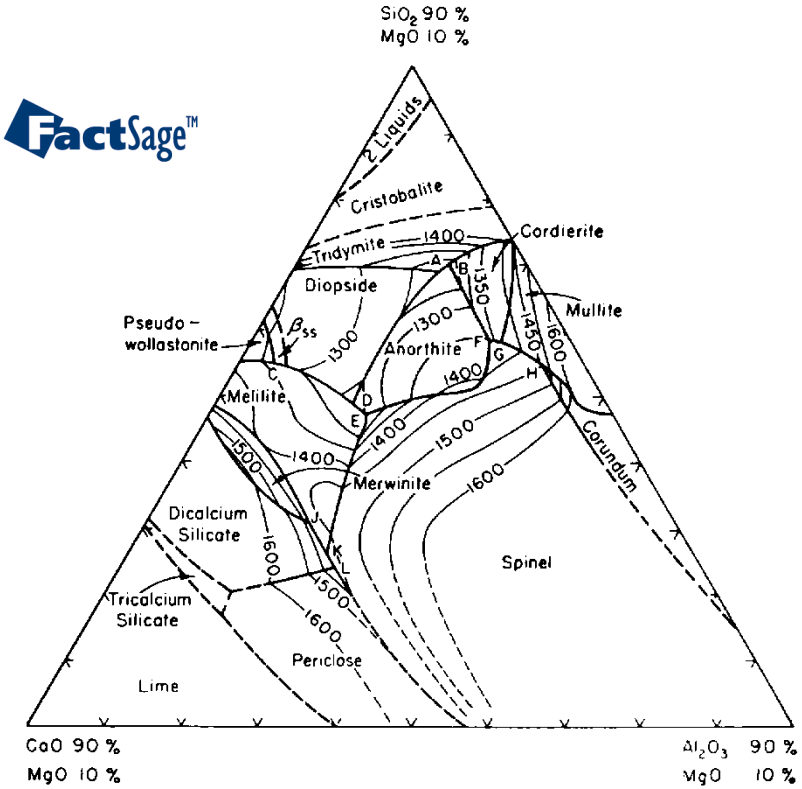

A.T. Prince, J. Am. Ceram. Soc., 37 [9],(1954), pp.402-408.

Weight percent,
Liquidusoberfläche im Ca2SiO4-Al2O3-Mg2SiO4 System

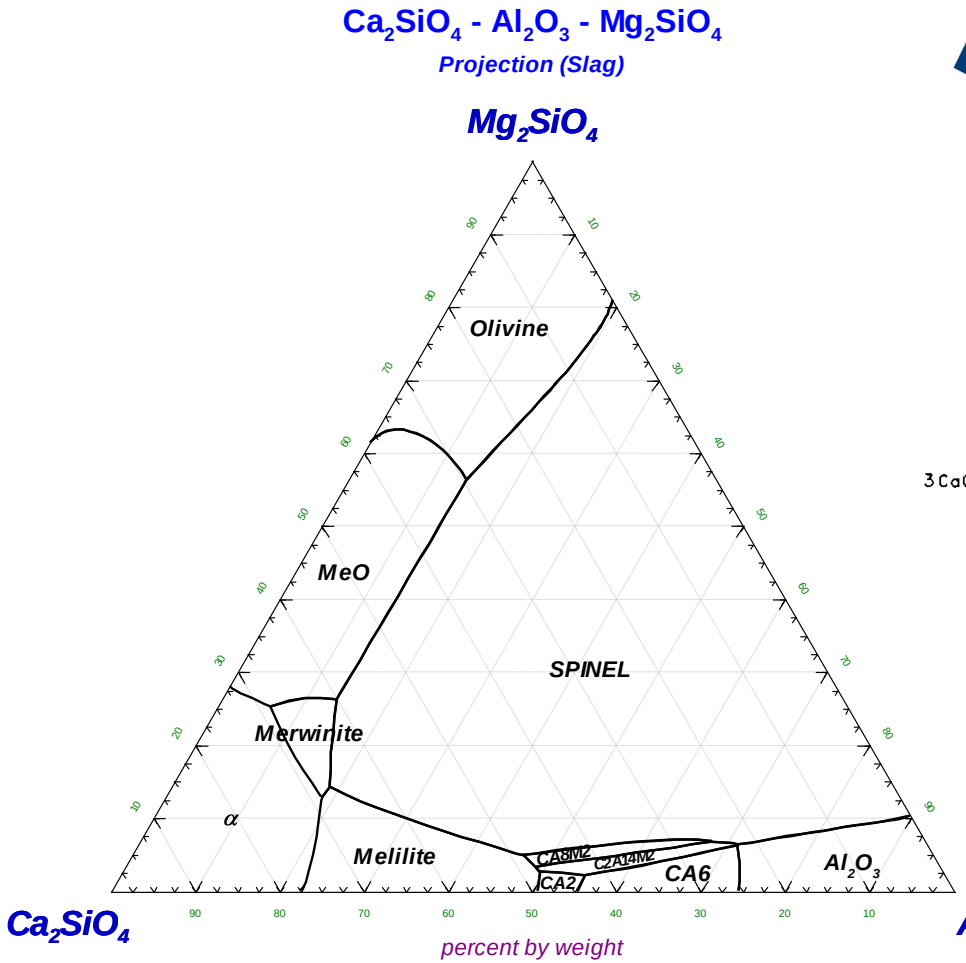

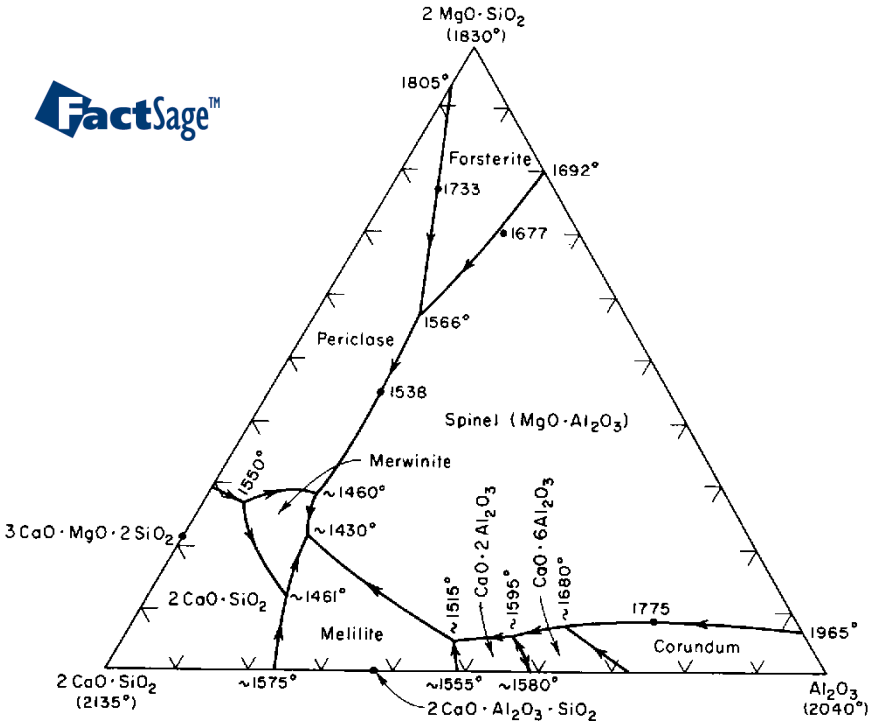

W. H. Gutt, J. Iron Steel Inst., London, 201 [Pt6], (1963), pp.532-536.

Weight percent,
Liquidusoberfläche im Al2CaSi2O8-CaMgSi2O6-CaSiO3 System

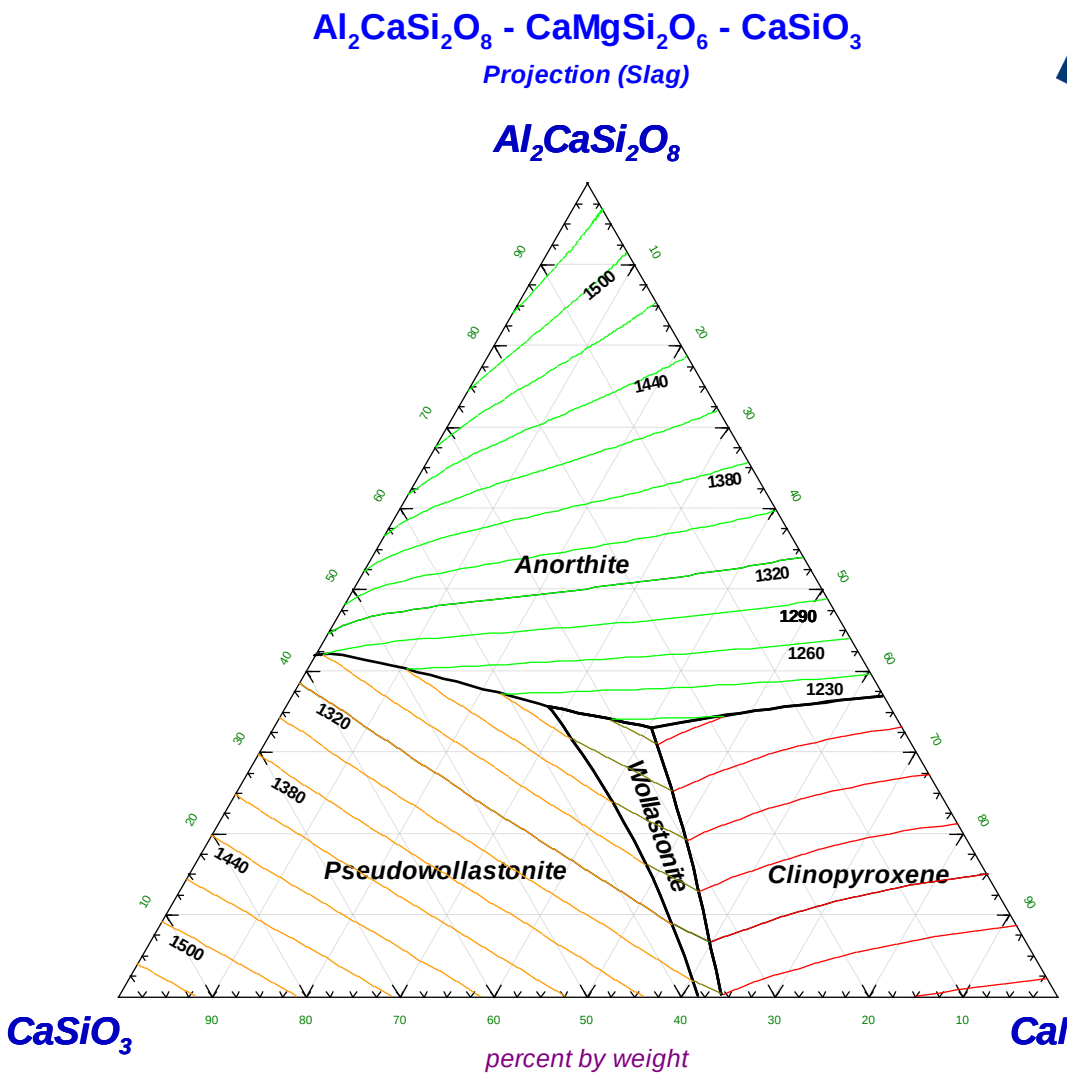

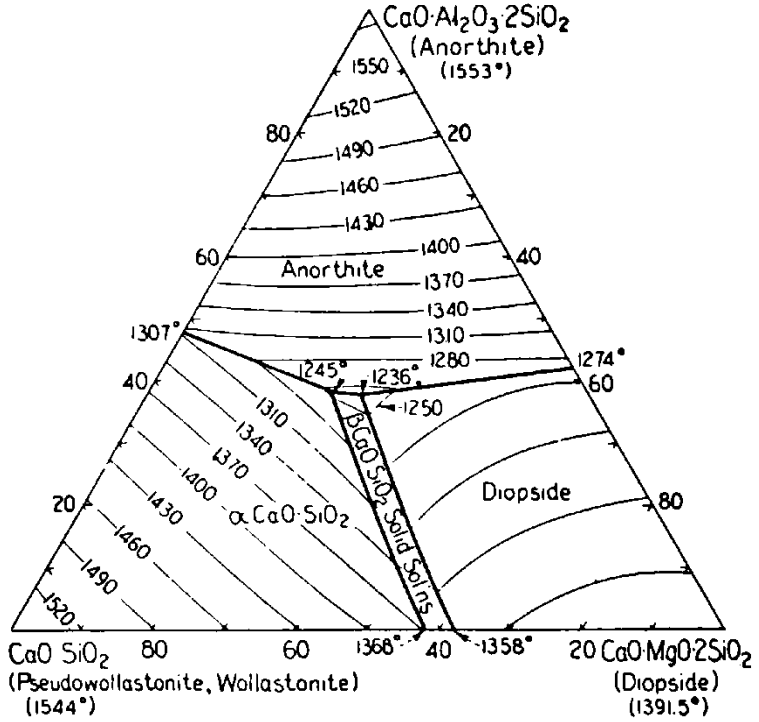

E.F. Osborn, Am. J. Sci., 240 [11], (1942), pp. 751-788.

$Al_2CaSi_2O_8$ - $CaMgSi_2O_6$ - Mg_2SiO_4

Projection (Slag)

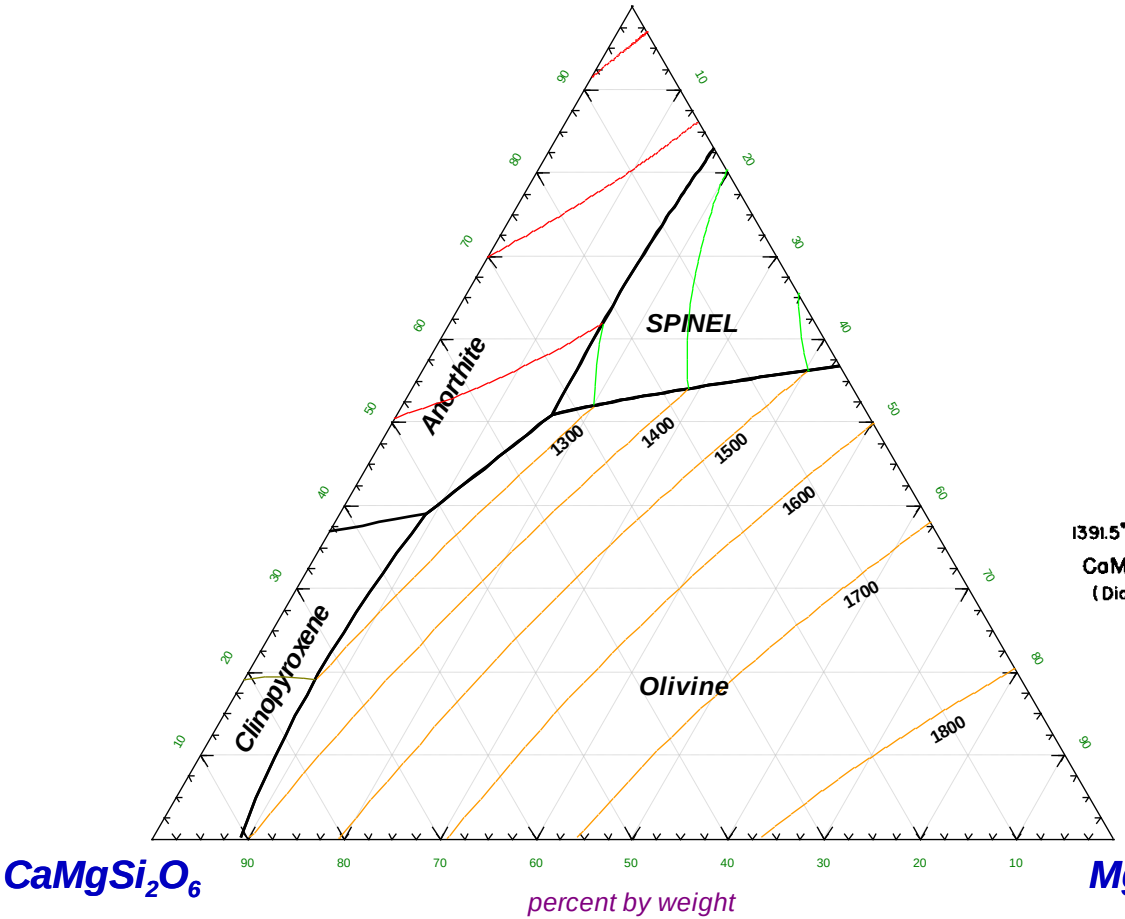

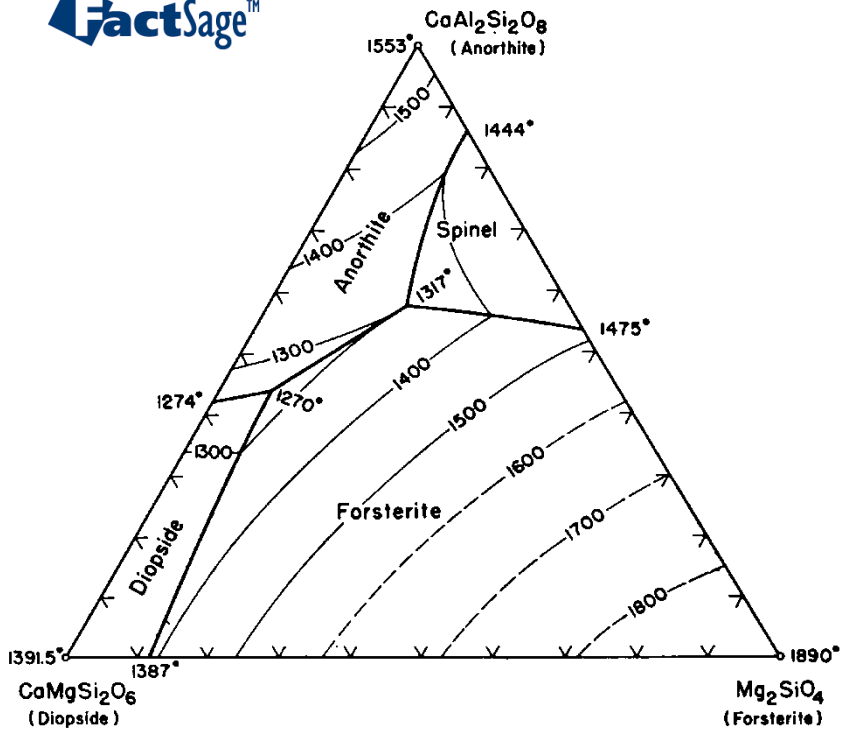

E.F. Osborn, D.B. Tait, Am. J. Sci., 250A [Bowen Vol.], (1952), pp. 413-433.

Weight percent,
Liquidusoberfläche im Al2O3-Al2Ca2SiO7-MgAl2O4 System

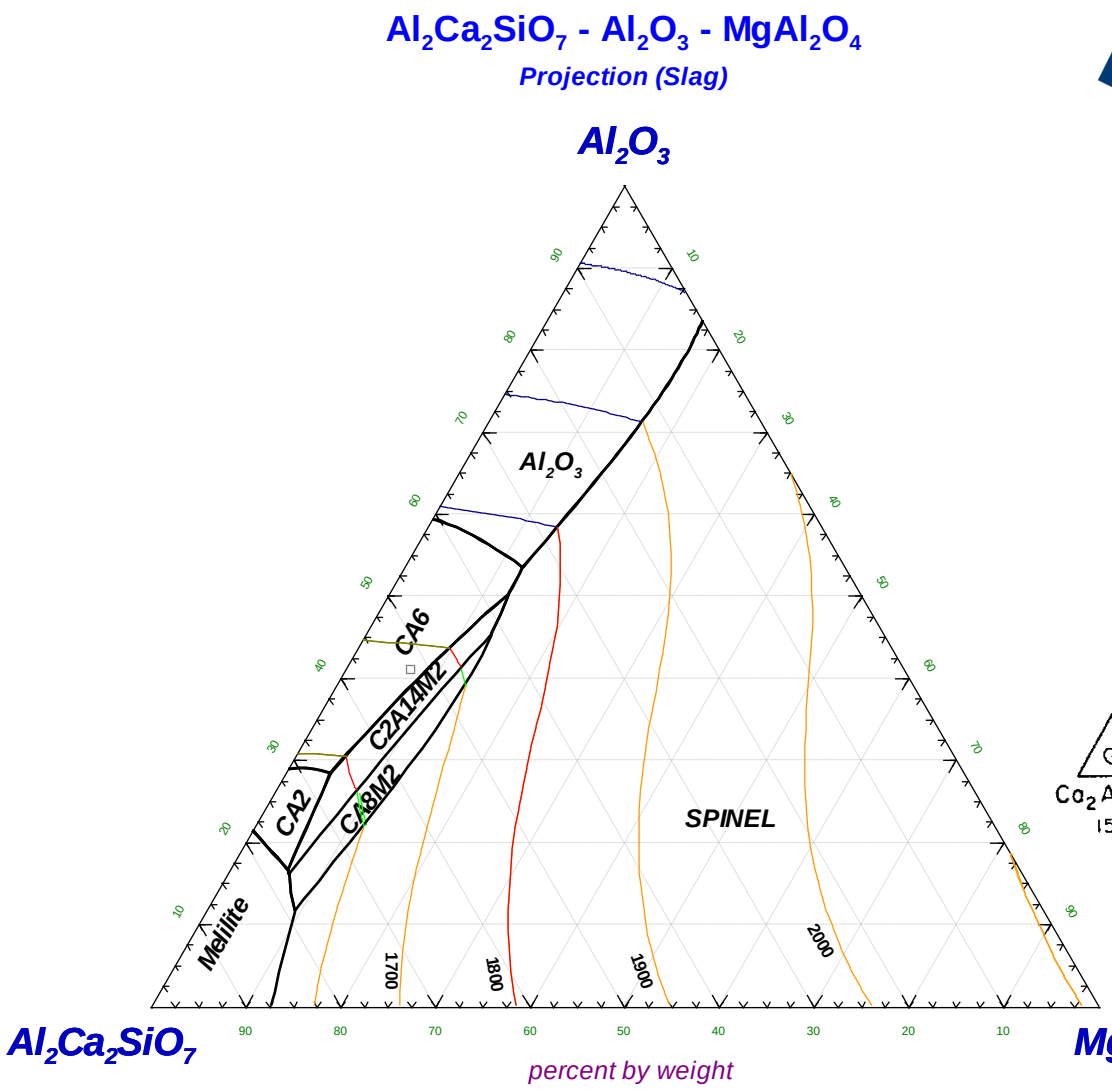

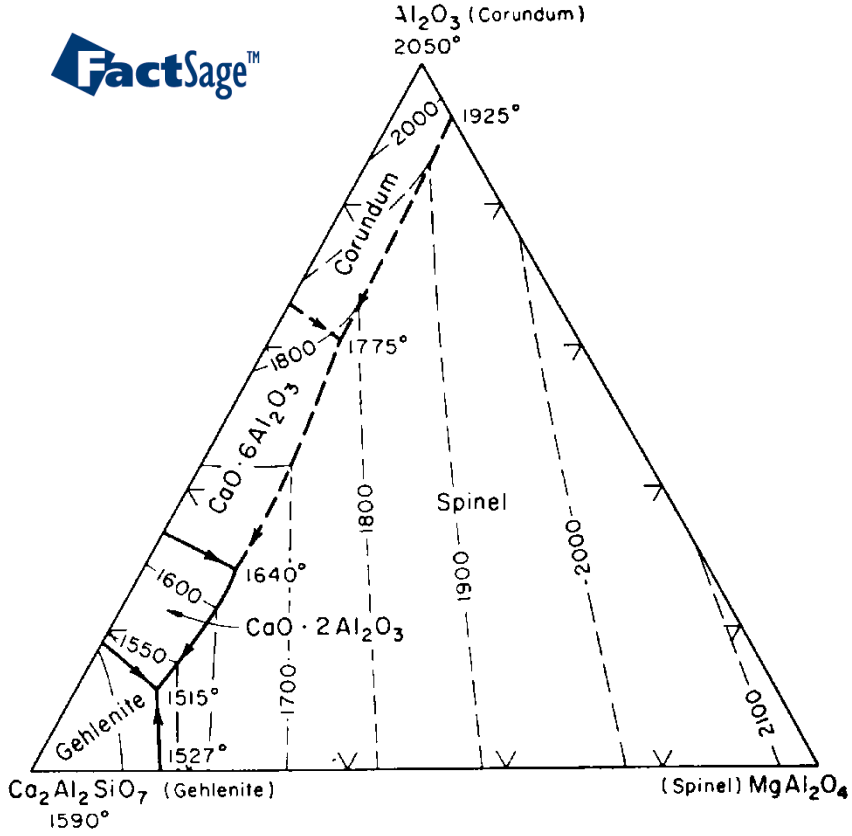

R.C. DeVries, E.F. Osborn, J. Ceram. Soc., 40[1], (1957), pp.6-15.

Al2O3-CaO-V2O3-SiO2,

Mole fraction, Isopleth Ca3V2Si3O12-Ca3Al2Si3O12

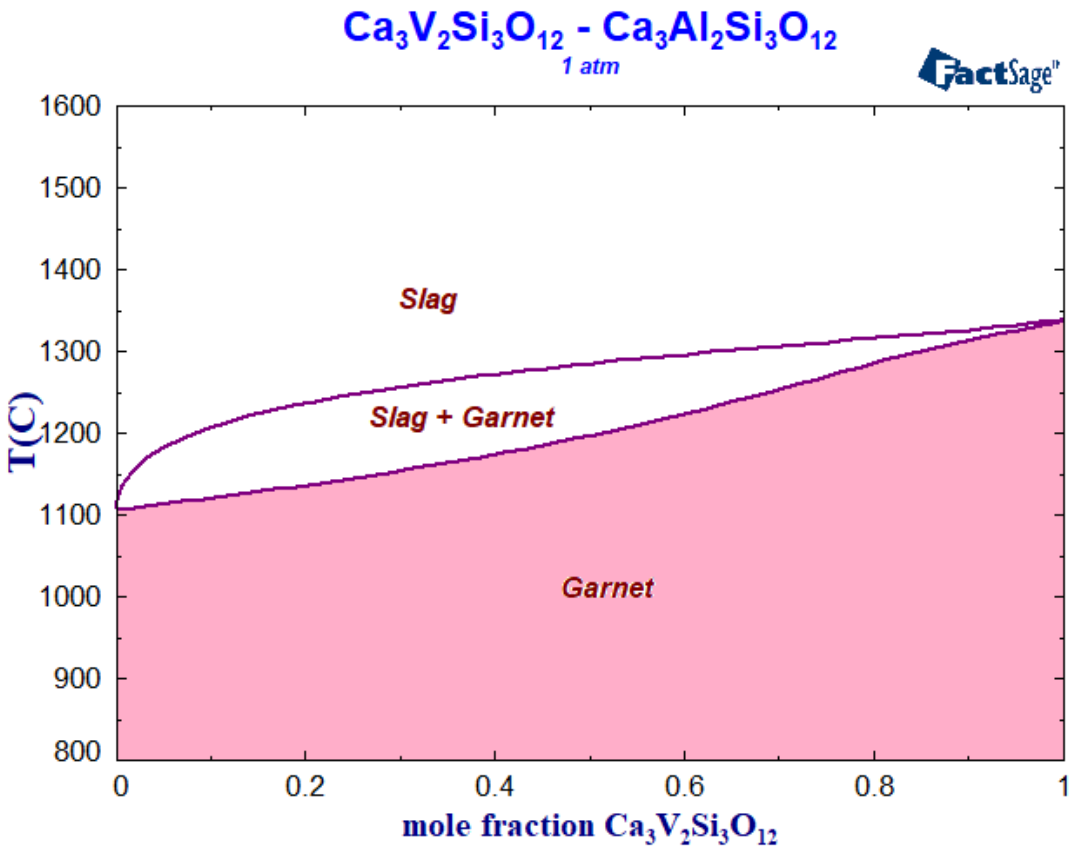

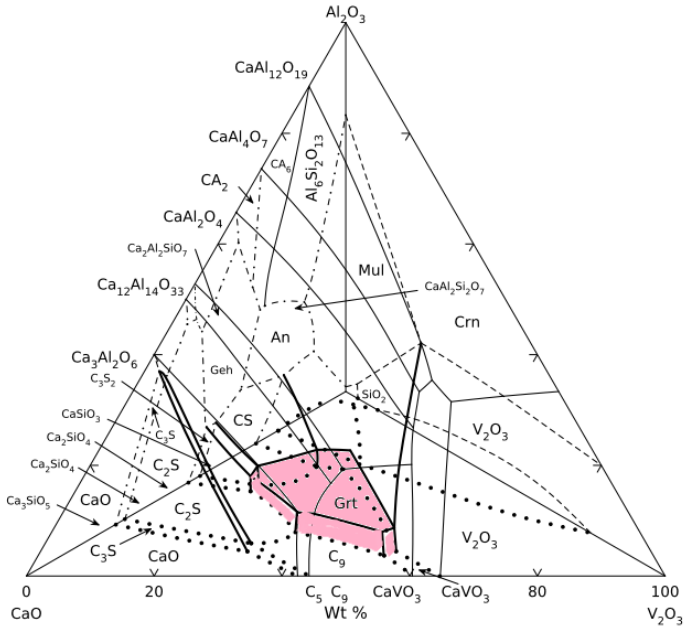

M. S. Najjar, Texaco Inc., White Plains, New York; private communication, 1992.

$Ca_3Al_2Si_3O_{12}$	Grossularite	**Garnet**
$Ca_3Cr_2Si_3O_{12}$	Uvarovite	
$Ca_3Fe_2Si_3O_{12}$	Andradite	
$Ca_3V_2Si_3O_{12}$	Goldmanite	

Mole fraction,
Isopleth KFeSiO4-KAlSiO4

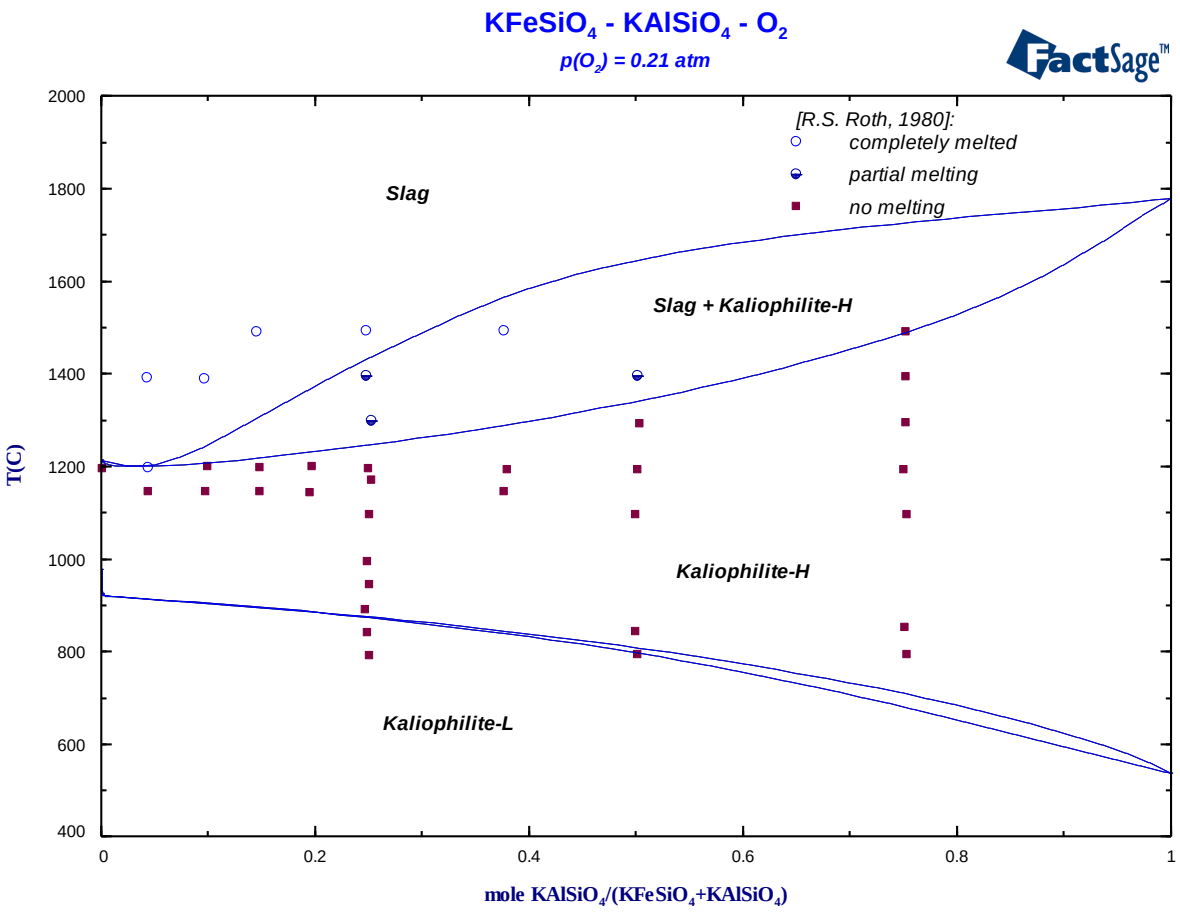

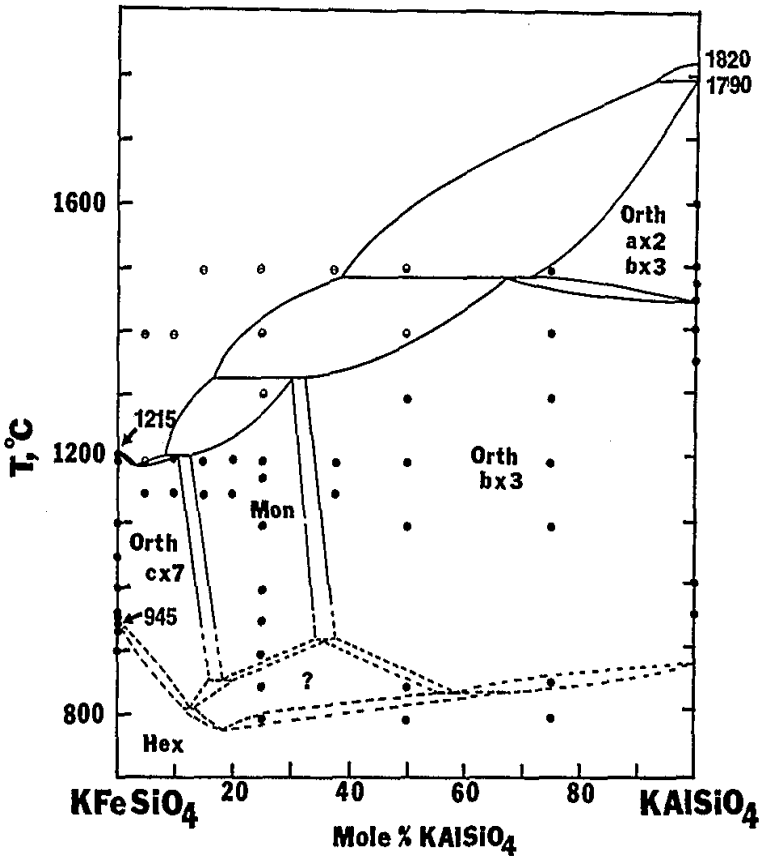

R.S. Roth, Amer. Chem. Soc., [20], pp. 391-408 (1980).

Mole fraction

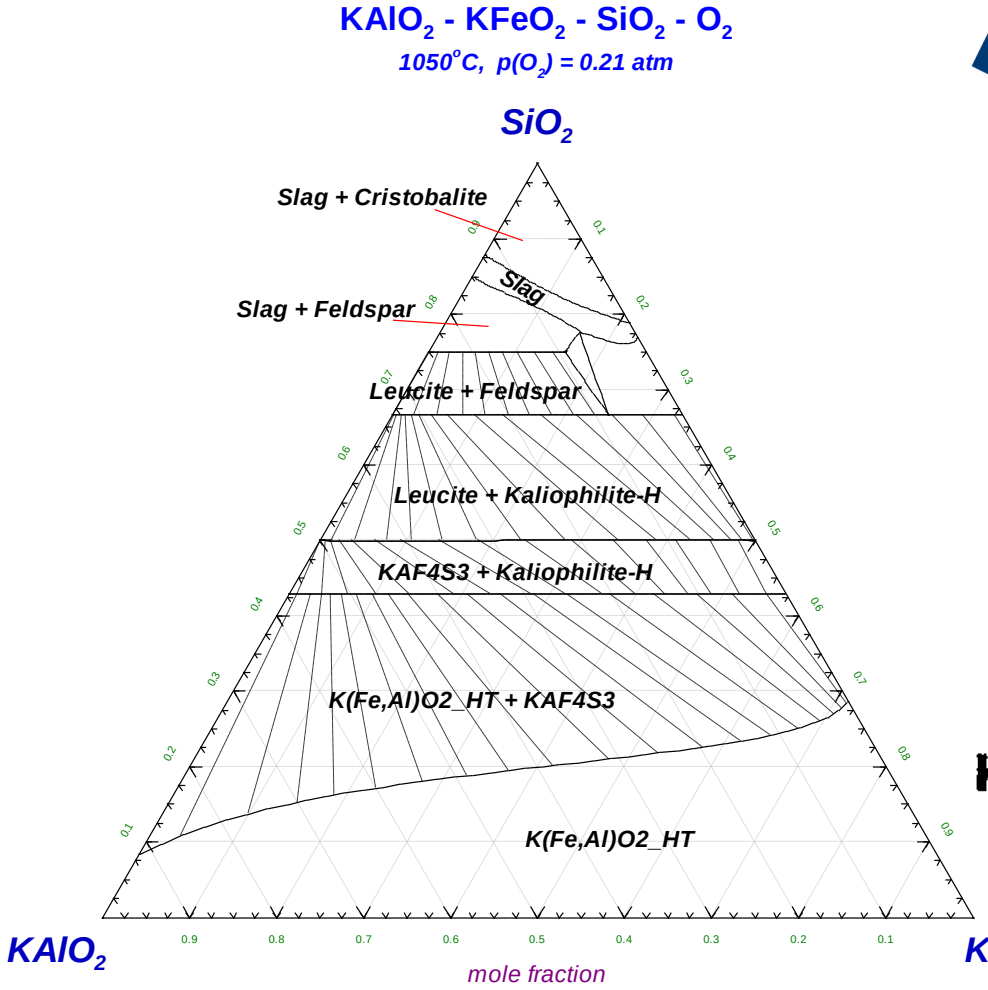

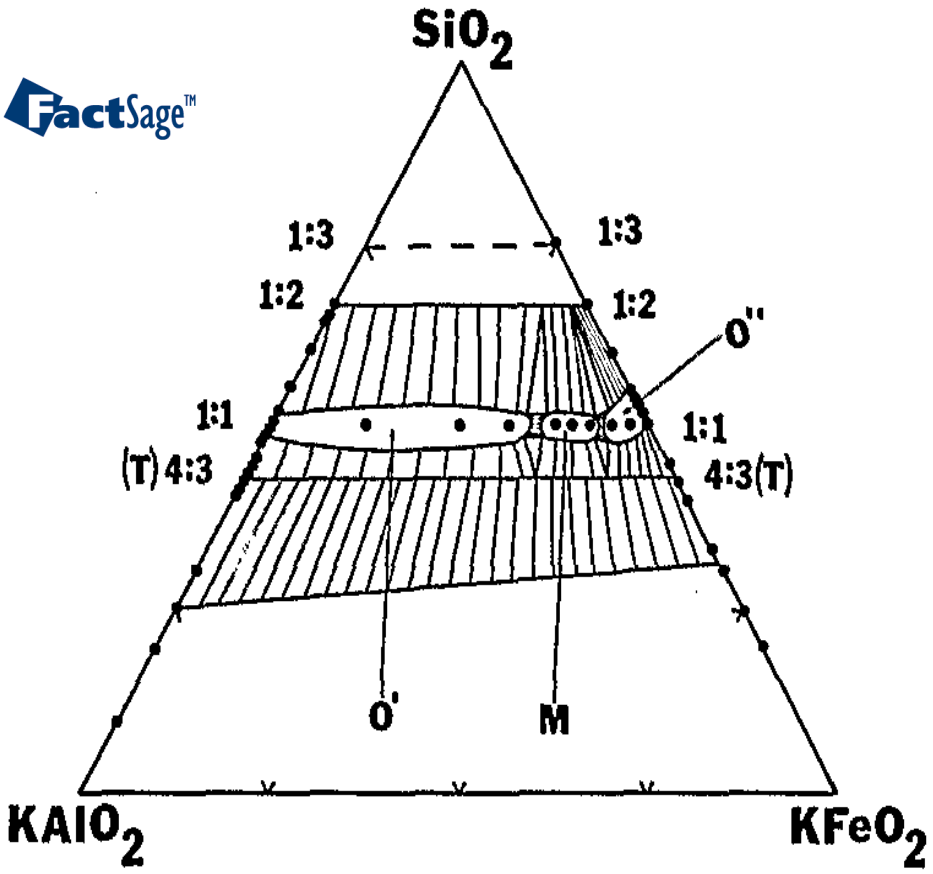

R.S. Roth, Amer. Chem. Soc., [20], pp. 391-408 (1980).

Weight percent,
Isopleth AlNaSi3O8-AlKSi3O8

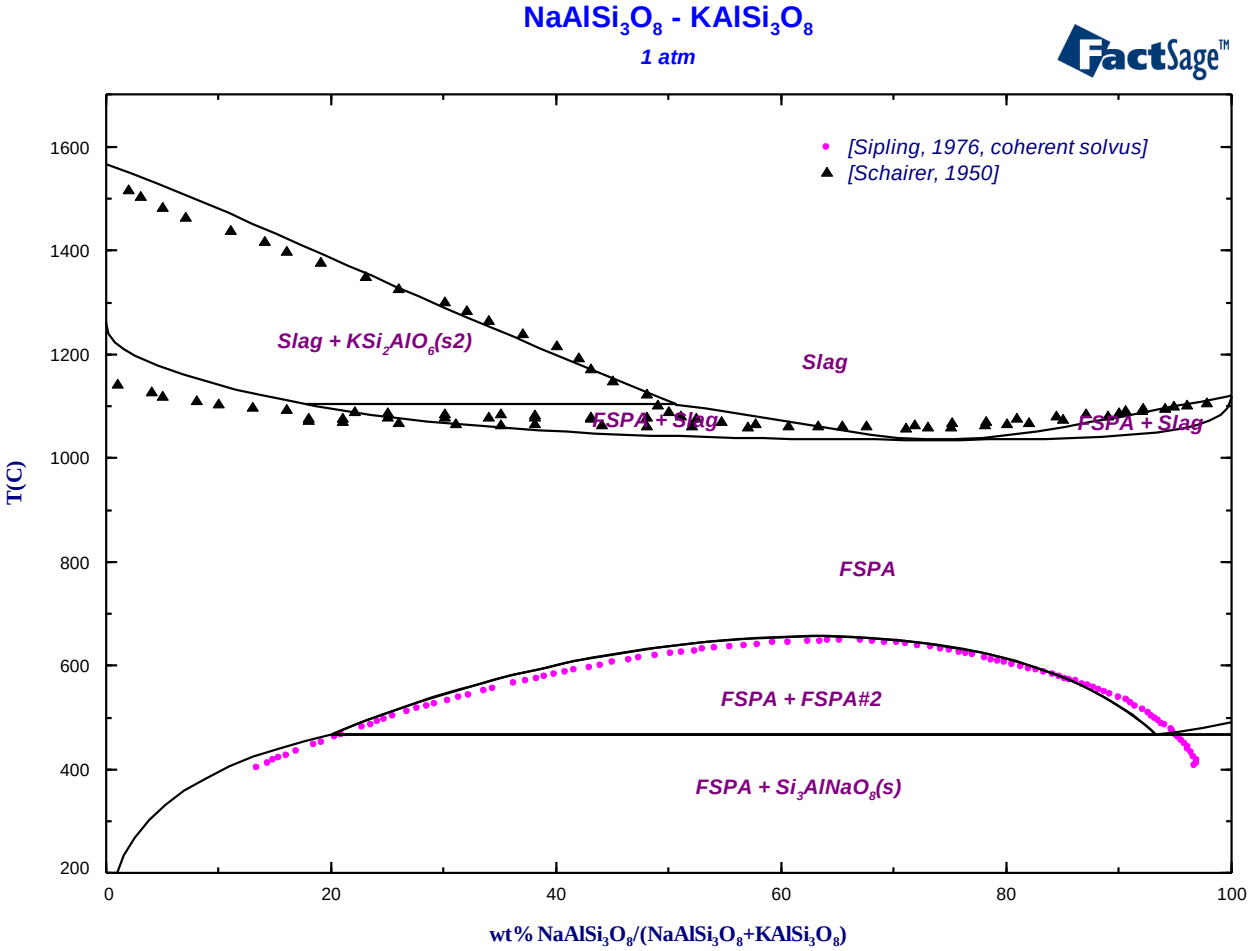

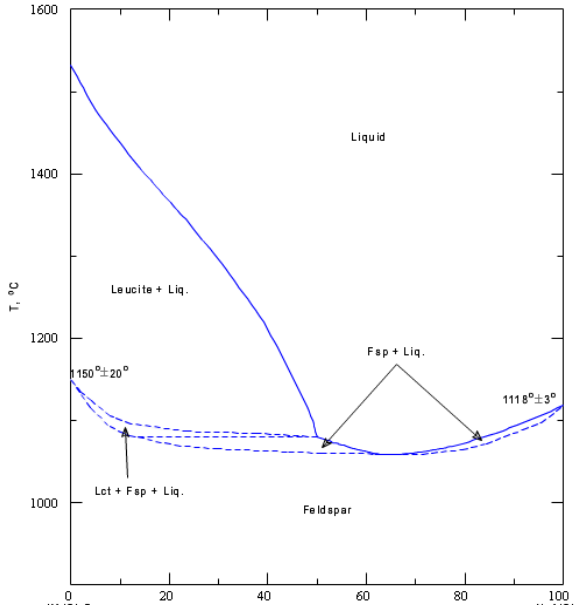

Schairer, J.F., The alkali-feldspar join in the system NaAlSiO4-KAlSiO4-SiO2, J. Geol. 58 (5) (1950)512-517.

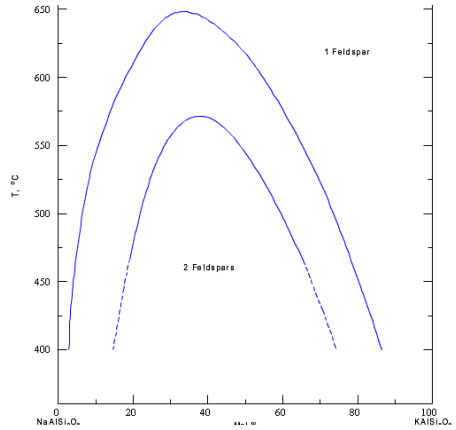

P. J. Sipling and R. A. Yand, Am. Mineral., 61 [9-10] 897-906 (1976).

Weight percent,
Isopleth NaAlSiO4-KAlSiO4,
(proposed calculation)

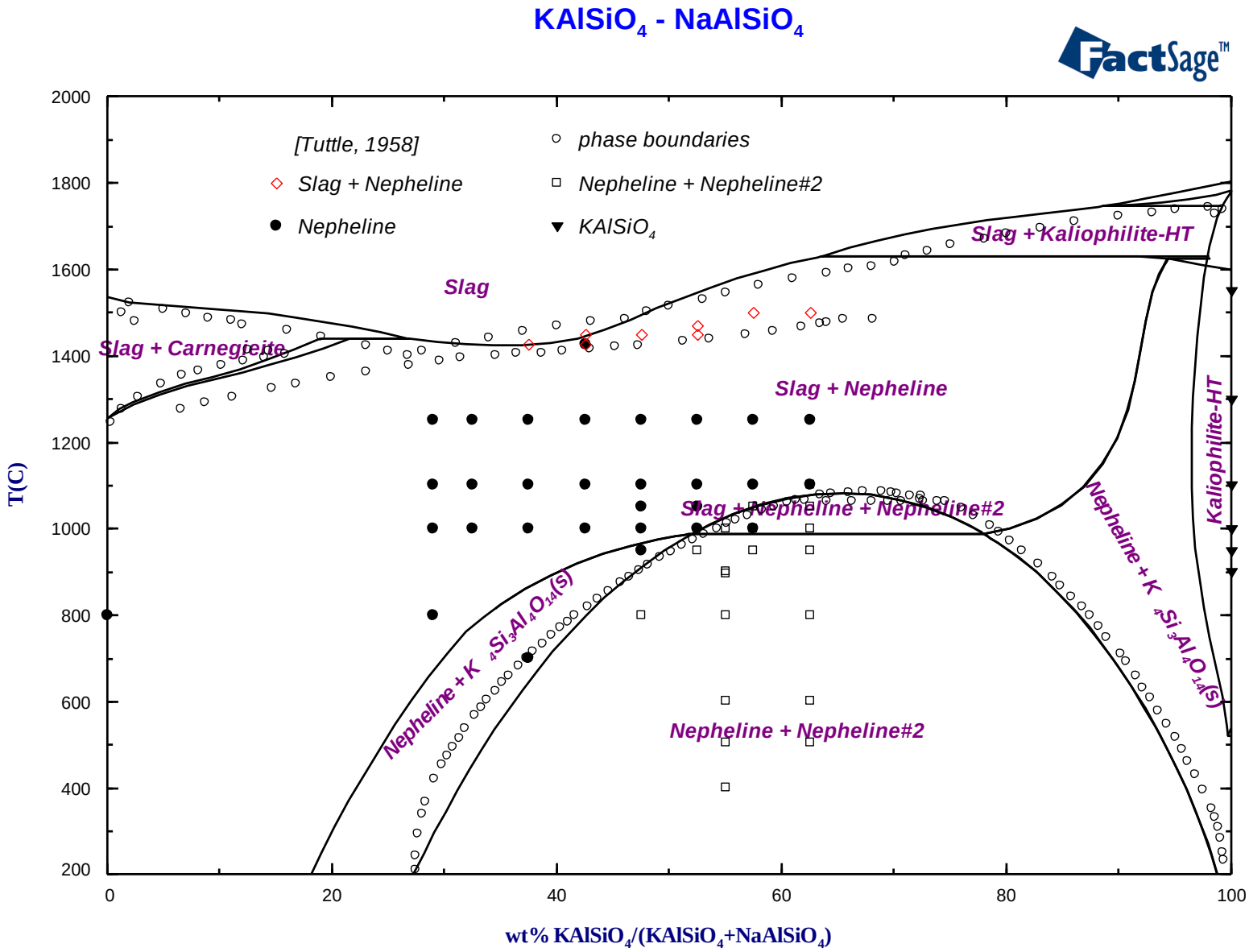

Weight percent,
Liquidussurface NaAlSiO4-KAlSiO4-SiO2

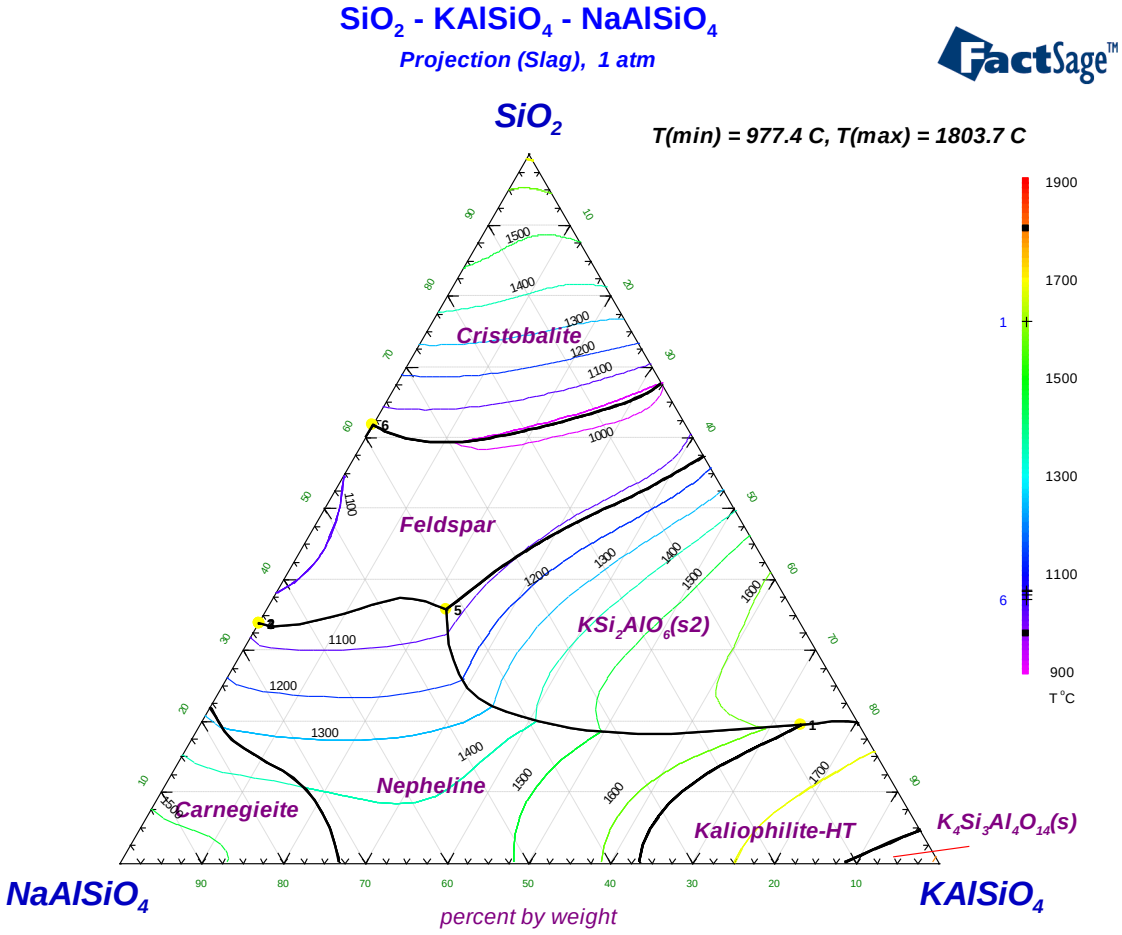

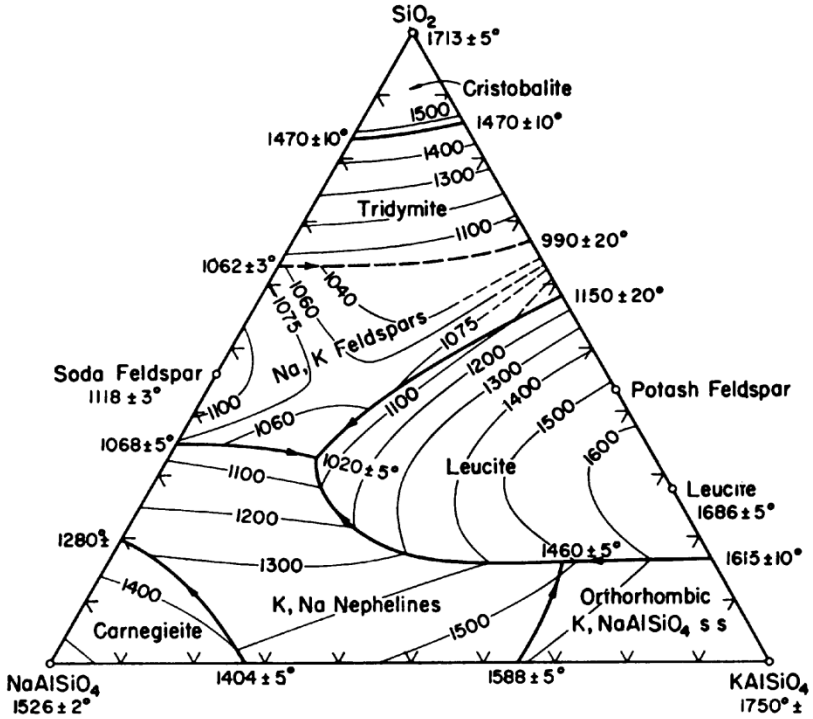

Schairer, J.F., The alkali-feldspar join in the system NaAlSiO4-KAlSiO4-SiO2, J. Geol. 58 (5) (1950)512-517.

Mole fraction, 1200°C in NaAlSiO4-KAlSiO4-SiO2 (proposed calculation)

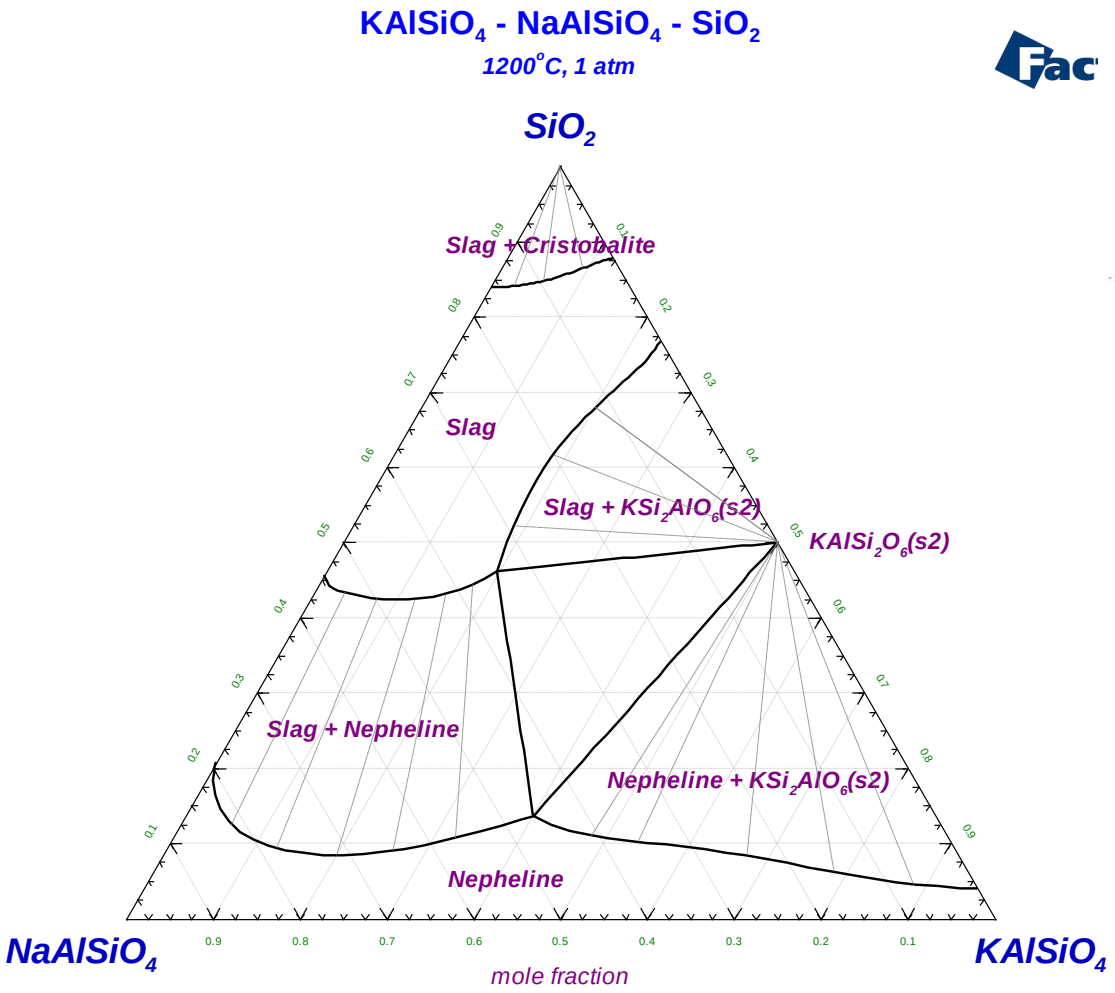

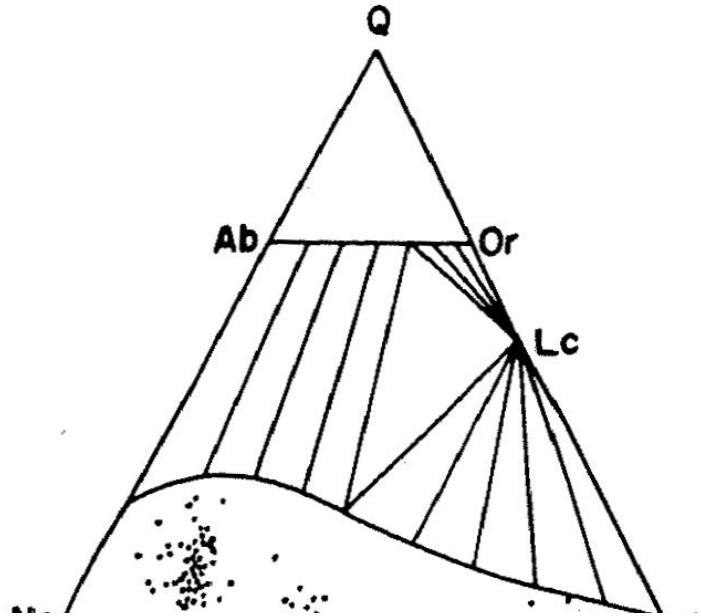

O.F. Tuttle, J.V. Smith, The nepheline-kalsilite system, II Phase relations; Am. J. Sci., 256 (1958) 571-589.

Mole fraction, 600°C in NaAlSiO4-KAlSiO4-SiO2 (proposed calculation)

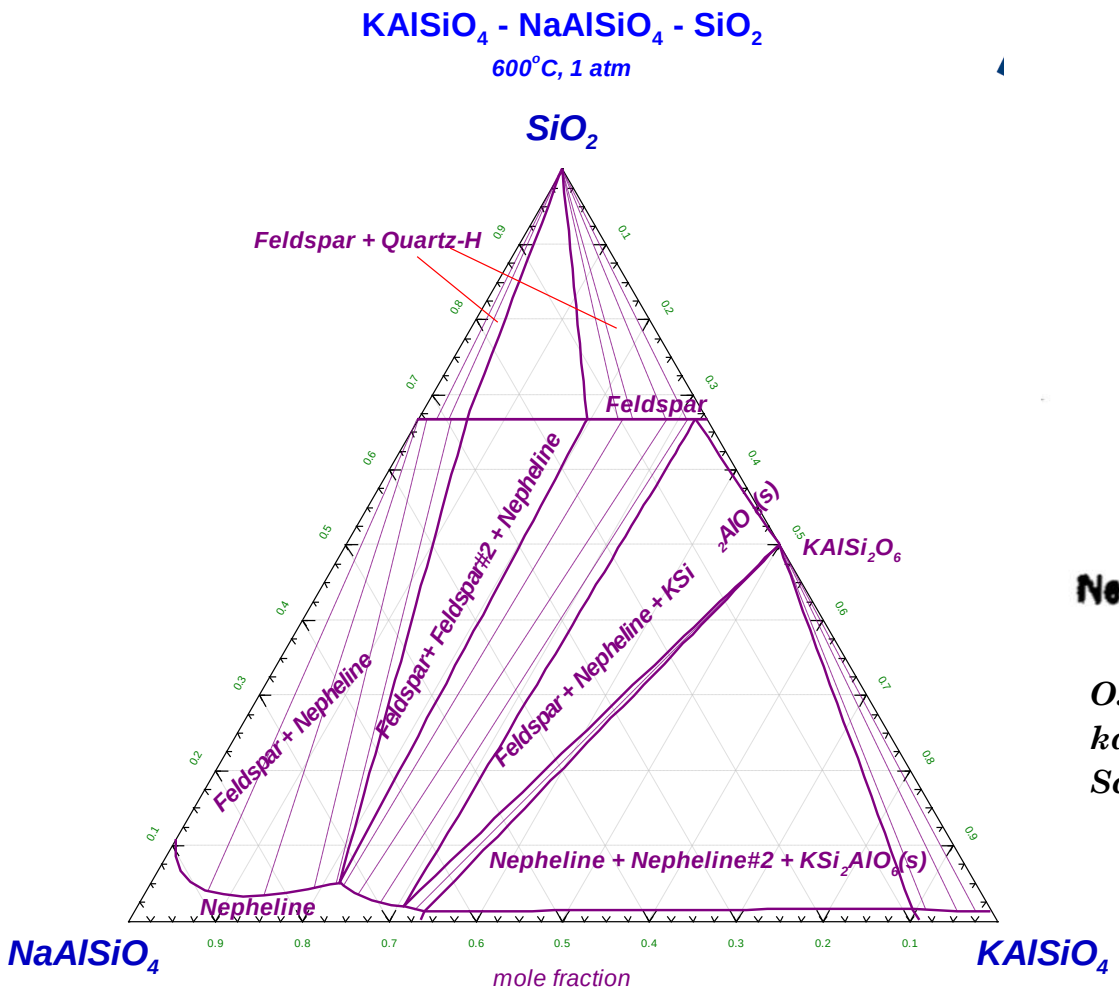

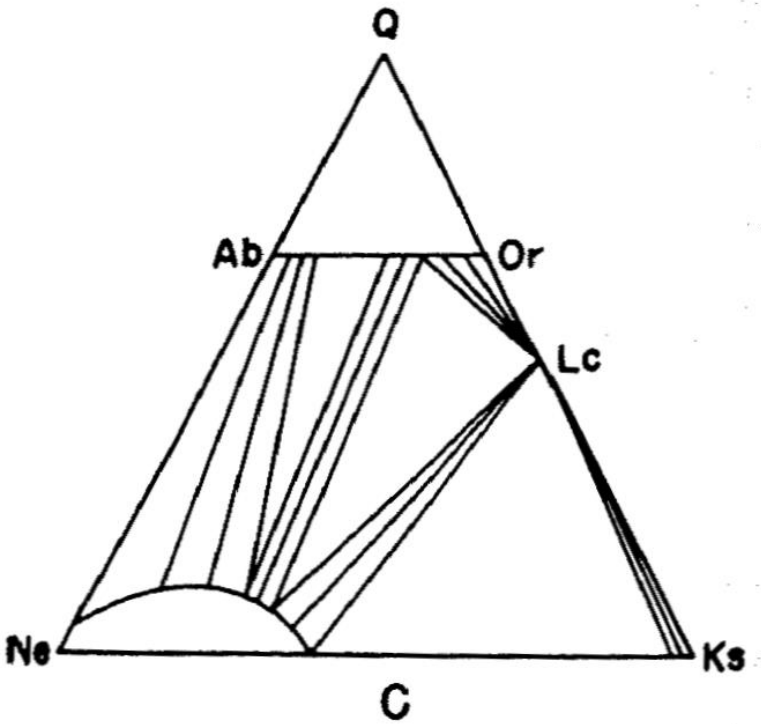

O.F. Tuttle, J.V. Smith, The nepheline-kalsilite system, II Phase relations; Am. J. Sci., 256 (1958) 571-589.

Mole fraction,
Liquidussurface NaAlSiO4-KAlSiO4-SiO2
(proposed calculation)

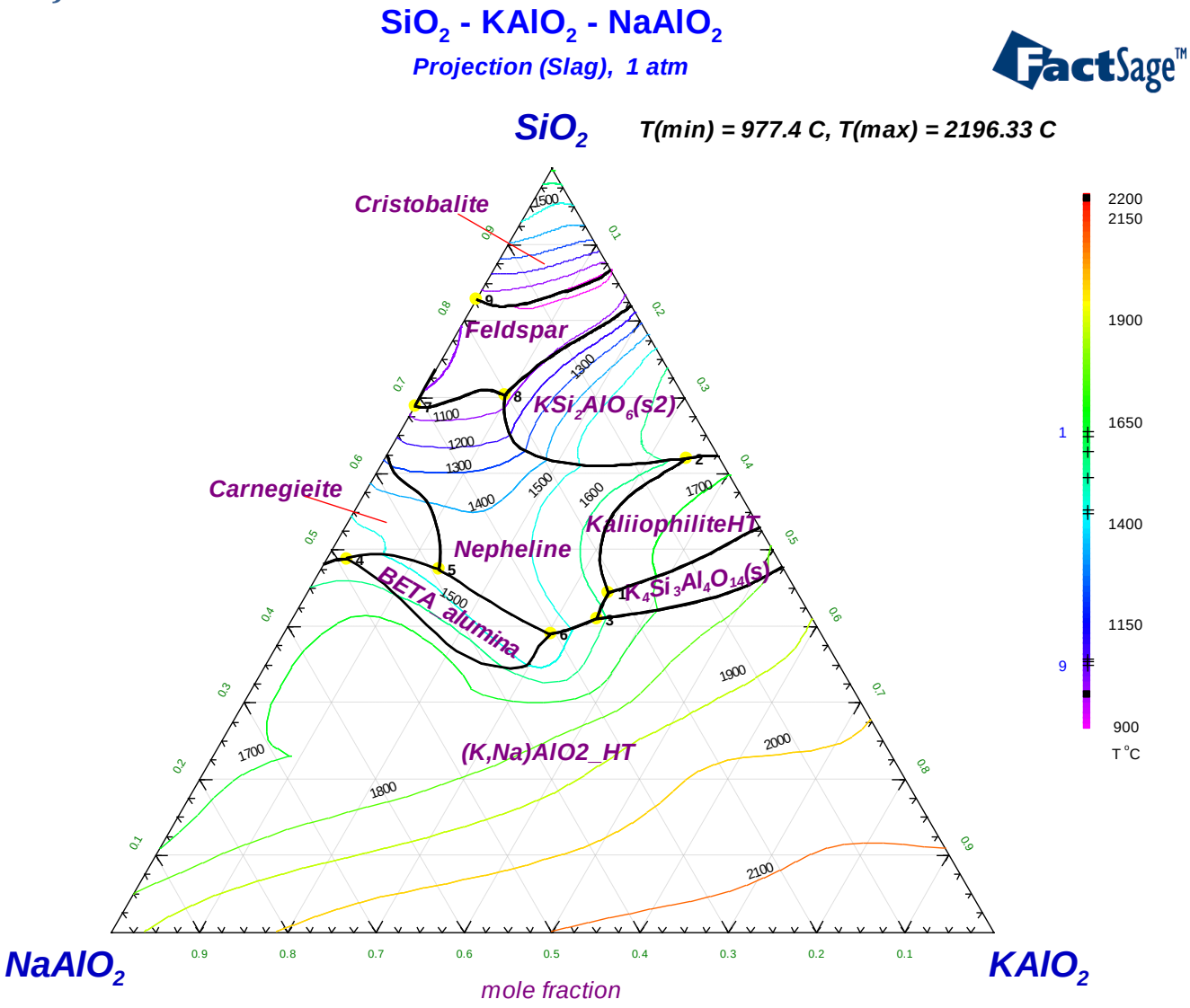

Weight percent,
MnS saturation boundaries at 1200°C with various wt pct Al2O3

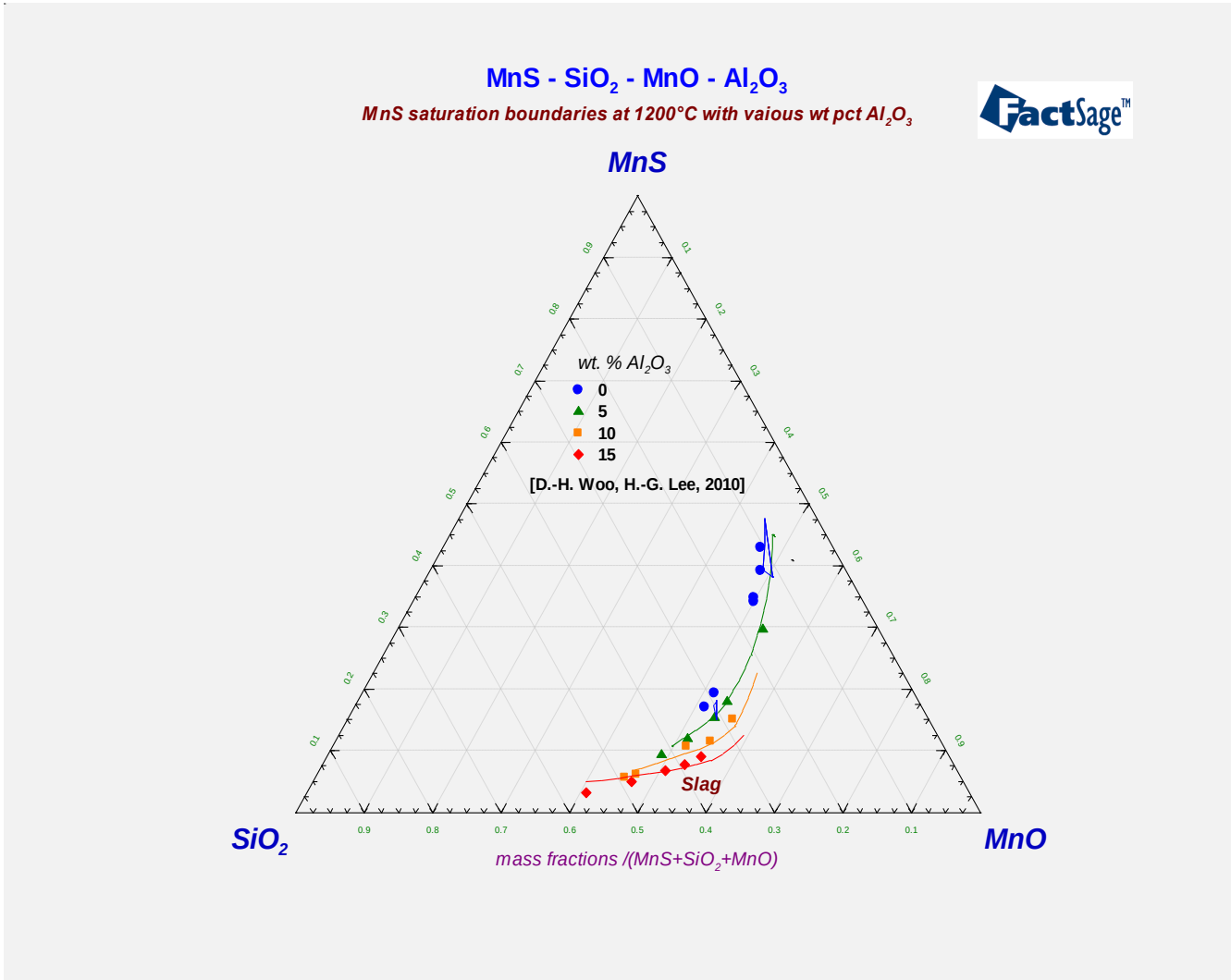

Cr-Fe-Mn-S,

Mole fraction,
Isopleth section FrCr2S4-MnCr2S4

